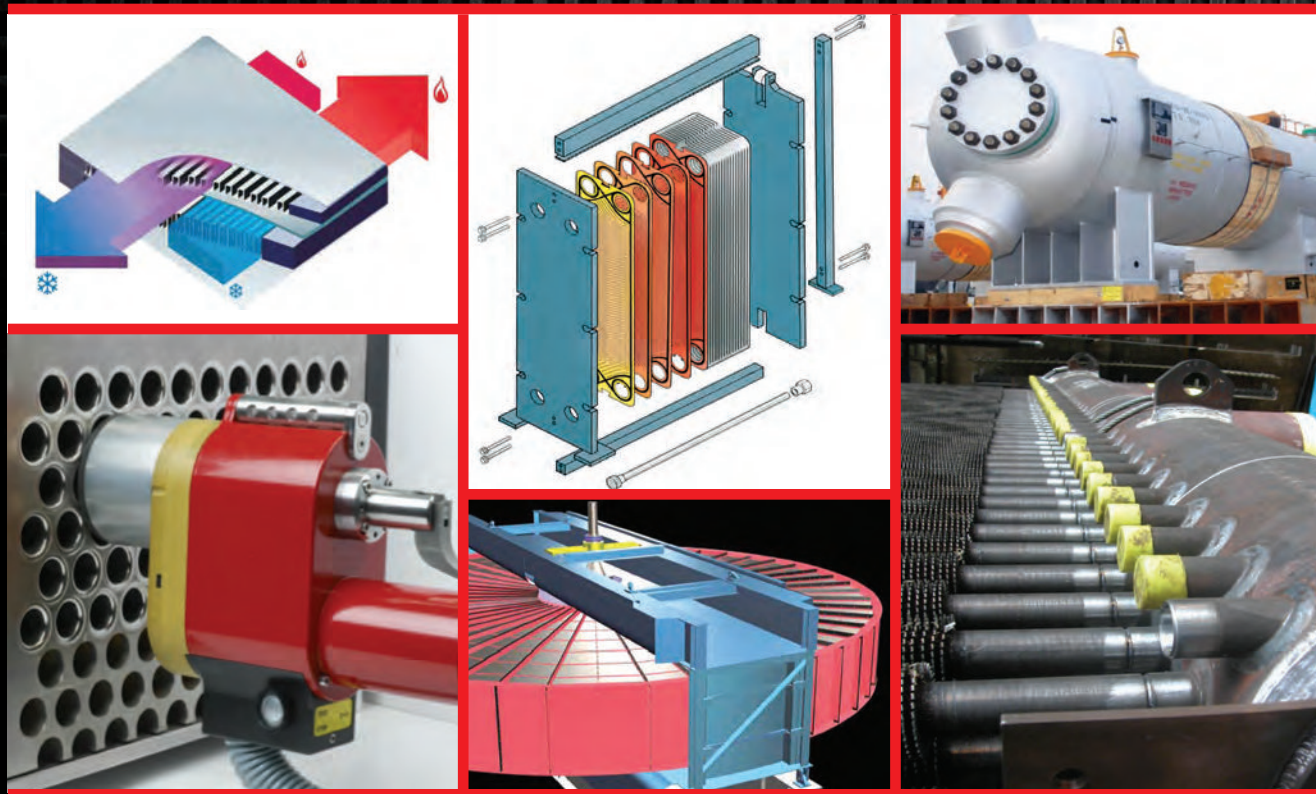


Heat Exchanger Design Handbook

SECOND EDITION



Kuppan Thulukkanam



CRC Press
Taylor & Francis Group

Heat Exchanger Design Handbook

S E C O N D E D I T I O N

MECHANICAL ENGINEERING

A Series of Textbooks and Reference Books

Founding Editor

L. L. Faulkner

*Columbus Division, Battelle Memorial Institute
and Department of Mechanical Engineering
The Ohio State University
Columbus, Ohio*

RECENTLY PUBLISHED TITLES

Heat Exchanger Design Handbook, Second Edition,
Kuppan Thulukkanam

Vehicle Dynamics, Stability, and Control, Second Edition,
Dean Karnopp

*HVAC Water Chillers and Cooling Towers: Fundamentals, Application,
and Operation, Second Edition,*
Herbert W. Stanford III

Ultrasonics: Fundamentals, Technologies, and Applications, Third Edition,
Dale Ensminger and Leonard J. Bond

Mechanical Tolerance Stackup and Analysis, Second Edition,
Bryan R. Fischer

Asset Management Excellence,
John D. Campbell, Andrew K. S. Jardine, and Joel McGlynn

*Solid Fuels Combustion and Gasification: Modeling, Simulation, and Equipment
Operations, Second Edition, Third Edition,*
Marcio L. de Souza-Santos

Mechanical Vibration Analysis, Uncertainties, and Control, Third Edition,
Haym Benaroya and Mark L. Nagurka

Principles of Biomechanics,
Ronald L. Huston

Practical Stress Analysis in Engineering Design, Third Edition,
Ronald L. Huston and Harold Josephs

*Practical Guide to the Packaging of Electronics, Second Edition:
Thermal and Mechanical Design and Analysis,*
Ali Jamnia

Friction Science and Technology: From Concepts to Applications, Second Edition,
Peter J. Blau

Design and Optimization of Thermal Systems, Second Edition,
Yogesh Jaluria

Heat Exchanger Design Handbook

S E C O N D E D I T I O N

Kuppan Thulukkanam



CRC Press

Taylor & Francis Group

Boca Raton London New York

CRC Press is an imprint of the
Taylor & Francis Group, an **informa** business

CRC Press
Taylor & Francis Group
6000 Broken Sound Parkway NW, Suite 300
Boca Raton, FL 33487-2742

© 2013 by Taylor & Francis Group, LLC
CRC Press is an imprint of Taylor & Francis Group, an Informa business

No claim to original U.S. Government works
Version Date: 20130204

International Standard Book Number-13: 978-1-4398-4213-3 (eBook - PDF)

This book contains information obtained from authentic and highly regarded sources. Reasonable efforts have been made to publish reliable data and information, but the author and publisher cannot assume responsibility for the validity of all materials or the consequences of their use. The authors and publishers have attempted to trace the copyright holders of all material reproduced in this publication and apologize to copyright holders if permission to publish in this form has not been obtained. If any copyright material has not been acknowledged please write and let us know so we may rectify in any future reprint.

Except as permitted under U.S. Copyright Law, no part of this book may be reprinted, reproduced, transmitted, or utilized in any form by any electronic, mechanical, or other means, now known or hereafter invented, including photocopying, microfilming, and recording, or in any information storage or retrieval system, without written permission from the publishers.

For permission to photocopy or use material electronically from this work, please access www.copyright.com (<http://www.copyright.com/>) or contact the Copyright Clearance Center, Inc. (CCC), 222 Rosewood Drive, Danvers, MA 01923, 978-750-8400. CCC is a not-for-profit organization that provides licenses and registration for a variety of users. For organizations that have been granted a photocopy license by the CCC, a separate system of payment has been arranged.

Trademark Notice: Product or corporate names may be trademarks or registered trademarks, and are used only for identification and explanation without intent to infringe.

Visit the Taylor & Francis Web site at
<http://www.taylorandfrancis.com>

and the CRC Press Web site at
<http://www.crcpress.com>

Dedicated to

*my parents, S. Thulukkanam and T. Senthamarai,
my wife, Tamizselvi Kuppan,
and my mentor, Dr. Ramesh K. Shah*

Contents

Preface.....	li
Acknowledgments.....	liii
Author	lv

Chapter 1	Heat Exchangers: Introduction, Classification, and Selection.....	1
1.1	Introduction	1
1.2	Construction of Heat Exchangers	1
1.3	Classification of Heat Exchangers	1
1.3.1	Classification According to Construction	2
1.3.1.1	Tubular Heat Exchanger	2
1.3.1.2	Plate Heat Exchangers	10
1.3.1.3	Extended Surface Exchangers	15
1.3.1.4	Regenerative Heat Exchangers	15
1.3.2	Classification according to Transfer Process	16
1.3.2.1	Indirect Contact Heat Exchangers	16
1.3.2.2	Direct Contact-Type Heat Exchangers.....	17
1.3.3	Classification according to Surface Compactness.....	17
1.3.4	Classification According to Flow Arrangement.....	18
1.3.4.1	Parallelflow Exchanger	18
1.3.4.2	Counterflow Exchanger	19
1.3.4.3	Crossflow Exchanger	19
1.3.5	Classification According to Pass Arrangements	20
1.3.5.1	Multipass Exchangers	20
1.3.6	Classification According to Phase of Fluids	21
1.3.6.1	Gas-Liquid	21
1.3.6.2	Liquid-Liquid	21
1.3.6.3	Gas-Gas.....	21
1.3.7	Classification According to Heat Transfer Mechanisms	21
1.3.7.1	Condensers.....	21
1.3.7.2	Evaporators	21
1.3.8	Other Classifications	22
1.3.8.1	Micro Heat Exchanger	22
1.3.8.2	Printed Circuit Heat Exchanger.....	23
1.3.8.3	Perforated Plate Heat Exchanger as Cryocoolers	25
1.3.8.4	Scraped Surface Heat Exchanger	25
1.3.8.5	Graphite Heat Exchanger.....	27
1.4	Selection of Heat Exchangers	28
1.4.1	Introduction	28
1.4.2	Selection Criteria.....	29
1.4.2.1	Materials of Construction	30
1.4.2.2	Operating Pressure and Temperature	30
1.4.2.3	Flow Rate.....	31
1.4.2.4	Flow Arrangement.....	31
1.4.2.5	Performance Parameters: Thermal Effectiveness and Pressure Drops.....	31

1.4.2.6	Fouling Tendencies	32
1.4.2.7	Types and Phases of Fluids	32
1.4.2.8	Maintenance, Inspection, Cleaning, Repair, and Extension Aspects	32
1.4.2.9	Overall Economy	32
1.4.2.10	Fabrication Techniques	33
1.4.2.11	Choice of Unit Type for Intended Applications	33
1.5	Requirements of Heat Exchangers	34
	References	34
	Suggested Readings	35
	Bibliography	35
Chapter 2	Heat Exchanger Thermohydraulic Fundamentals	39
2.1	Heat Exchanger Thermal Circuit and Overall Conductance Equation	39
2.2	Heat Exchanger Heat Transfer Analysis Methods	41
2.2.1	Energy Balance Equation	41
2.2.2	Heat Transfer	41
2.2.3	Basic Methods to Calculate Thermal Effectiveness	42
2.2.3.1	ϵ -NTU Method	42
2.2.3.2	P -NTU _i Method	43
2.2.3.3	Log Mean Temperature Difference Correction Factor Method	45
2.2.3.4	ψ - P Method	48
2.2.4	Some Fundamental Relationships to Characterize the Exchanger for “Subdesign” Condition	49
2.3	Thermal Effectiveness Charts	50
2.4	Symmetry Property and Flow Reversibility and Relation between the Thermal Effectiveness of Overall Parallel and Counterflow Heat Exchanger Geometries	52
2.4.1	Symmetry Property	52
2.4.2	Flow Reversibility	52
2.5	Temperature Approach, Temperature Meet, and Temperature Cross	54
2.5.1	Temperature Cross for Other TEMA Shells	56
2.6	Thermal Relation Formulas for Various Flow Arrangements and Pass Arrangements	56
2.6.1	Parallelflow	57
2.6.2	Counterflow	57
2.6.3	Crossflow Arrangement	57
2.6.3.1	Unmixed–Unmixed Crossflow	57
2.6.3.2	Unmixed–Mixed Crossflow	57
2.6.3.3	Mixed–Mixed Crossflow	57
2.6.3.4	Single or Multiple Rows in Crossflow	57
2.6.4	Thermal Relations for Various TEMA Shells and Others	72
2.6.4.1	E Shell	74
2.6.4.2	TEMA F Shell	79
2.6.4.3	TEMA G Shell or Split-Flow Exchanger	79
2.6.4.4	TEMA H Shell	81
2.6.4.5	TEMA J Shell or Divided-Flow Shell	81
2.6.4.6	TEMA X Shell	90
2.6.5	Thermal Effectiveness of Multiple Heat Exchangers	90

2.6.5.1	Two-Pass Exchangers	92
2.6.5.2	<i>N</i> -Pass Exchangers.....	92
2.6.6	Multipass Crossflow Exchangers.....	92
2.6.6.1	Multipassing with Complete Mixing between Passes	93
2.6.6.2	Two Passes with One Fluid Unmixed throughout, Cross-Counterflow Arrangement.....	94
2.6.6.3	Two Passes with Both Fluids Unmixed–Unmixed in Each Pass and One Fluid Unmixed throughout, Cross-Counterflow Arrangement.....	98
2.6.6.4	Two Passes with Both Fluids Unmixed throughout, Cross-Counterflow Arrangement.....	101
2.6.7	Thermal Effectiveness of Multiple-Pass Shell and Tube Heat Exchangers	108
	Acknowledgment.....	113
	References	113
	Bibliography	115
Chapter 3	Heat Exchanger Thermal Design	117
3.1	Fundamentals of Heat Exchanger Design Methodology	117
3.1.1	Process/Design Specifications	117
3.1.1.1	Problem Specification	117
3.1.1.2	Exchanger Construction.....	118
3.1.1.3	Surface Selection	119
3.1.2	Thermohydraulic Design.....	119
3.1.2.1	Basic Thermohydraulic Design Methods	119
3.1.2.2	Thermophysical Properties.....	119
3.1.2.3	Surface Geometrical Properties	119
3.1.2.4	Surface Characteristics	119
3.2	Design Procedure	120
3.3	Heat Exchanger Design Problems	120
3.3.1	Rating	120
3.3.1.1	Rating of a Compact Exchanger	120
3.3.1.2	Rating of a Shell and Tube Exchanger.....	121
3.3.2	Sizing.....	121
3.3.2.1	Size of a Heat Exchanger	121
3.3.2.2	Sensitivity Analysis	122
3.3.2.3	Sizing of a Compact Heat Exchanger	122
3.3.2.4	Sizing of a Shell and Tube Heat Exchanger.....	122
3.3.2.5	Heat Exchanger Optimization	122
3.3.3	Solution to the Rating and Sizing Problem	122
3.3.3.1	Rating.....	122
3.3.3.2	Solution to the Sizing Problem	123
3.4	Computer-Aided Thermal Design	123
3.4.1	Overall Structure of a Thermal Design Computer Program.....	123
3.4.1.1	Guidelines on Program Logic.....	124
3.4.2	Program Structure for a Shell and Tube Exchanger.....	125
3.5	Pressure-Drop Analysis, Temperature-Dependent Fluid Properties, Performance Failures, Flow Maldistribution, Fouling, and Corrosion	125
3.5.1	Heat Exchanger Pressure-Drop Analysis	125
3.5.1.1	Pressure-Drop Evaluation for Heat Exchangers	125

3.5.1.2	Pressure Drop through a Heat Exchanger	126
3.5.1.3	Shell and Tube Heat Exchangers	127
3.5.1.4	Pressure Drop due to Flow Turning.....	127
3.5.1.5	Pressure Drop in the Nozzles	128
3.5.2	Temperature-Dependent Fluid Properties Correction.....	128
3.5.2.1	Gases.....	128
3.5.2.2	Liquids	129
3.5.3	Performance Failures	130
3.5.4	Maldistribution	131
3.5.5	Fouling	131
3.5.6	Corrosion Allowance.....	132
3.6	Cooperative Research Programs on Heat Exchanger Design	132
3.6.1	HTRI	132
3.6.2	HTFS	132
3.7	Uncertainties in Thermal Design of Heat Exchangers.....	133
3.7.1	Uncertainties in Heat Exchanger Design	133
3.7.1.1	Uncertainty in Process Conditions	134
3.7.1.2	Uncertainty in the Physical Properties of the Process Fluids	134
3.7.1.3	Flow Nonuniformity	134
3.7.1.4	Nonuniform Flow Passages	135
3.7.1.5	Uncertainty in the Basic Design Correlations	135
3.7.1.6	Uncertainty due to Thermodynamically Defined Mixed or Unmixed Flows for Crossflow Heat Exchangers, after Digiovanni and Webb	136
3.7.1.7	Nonuniform Heat Transfer Coefficient.....	136
3.7.1.8	Bypass Path on the Air Side of Compact Tube-Fin Exchangers.....	137
3.7.1.9	Uncertainty in Fouling	137
3.7.1.10	Miscellaneous Effects.....	137
3.7.2	Determination of Uncertainties.....	137
3.7.2.1	Computational Procedures	137
3.7.3.2	Additional Surface Area Required due to Uncertainty	139
3.7.3.3	Additional Pressure Drop due to Uncertainty	139
	Nomenclature	140
	References	141
	Bibliography	143

Chapter 4 Compact Heat Exchangers 145

4.1	Classification and Construction Details of Tube-Fin Compact Heat Exchangers.....	145
4.1.1	Characteristics of Compact Heat Exchangers	145
4.1.2	Construction Types of Compact Heat Exchangers.....	146
4.1.3	Tube-Fin Heat Exchangers	146
4.1.3.1	Specific Qualitative Considerations for Tube-Fin Surfaces.....	147
4.1.3.2	Applications	148
4.1.3.3	Individually Finned Tubes	148
4.1.4	Continuous Fins on a Tube Array	151
4.1.4.1	Tube: Primary Surface	151
4.1.4.2	Fin: Secondary Surface.....	151

4.1.4.3	Headers.....	152
4.1.4.4	Tube-to-Header Joints	152
4.1.4.5	Casings or Tube Frame.....	152
4.1.4.6	Circuiting	152
4.1.4.7	Exchangers for Air Conditioning and Refrigeration.....	152
4.1.4.8	Radiators	153
4.1.4.9	Effect of Fin Density on Fouling	153
4.1.4.10	One-Row Radiator	154
4.1.4.11	Manufacture of Continuous Finned Tube Heat Exchangers	155
4.1.5	Surface Selection.....	156
4.1.5.1	Qualitative Considerations	156
4.1.5.2	Quantitative Considerations	157
4.2	Plate-Fin Heat Exchangers	157
4.2.1	PFHE: Essential Features.....	158
4.2.2	Application for Fouling Service	158
4.2.3	Size	159
4.2.4	Advantages of PFHEs	159
4.2.5	Limitations of PFHEs.....	159
4.2.6	Applications.....	159
4.2.7	Economics	160
4.2.8	Flow Arrangements	160
4.2.9	Fin Geometry Selection and Performance Factors	160
4.2.9.1	Plain Fin	160
4.2.9.2	Plain-Perforated Fin	161
4.2.9.3	Offset Strip Fin	162
4.2.9.4	Serrated Fins	163
4.2.9.5	Herringbone or Wavy Fin	163
4.2.9.6	Louver Fins	163
4.2.9.7	Pin Fins	164
4.2.9.8	FIN Corrugation Code	165
4.2.10	Corrugation Selection.....	166
4.2.11	Materials of Construction.....	166
4.2.11.1	Aluminum	166
4.2.11.2	Other Metals.....	166
4.2.12	Mechanical Design.....	166
4.2.13	Manufacture, Inspection, and Quality Control	166
4.2.14	Brazed Aluminum Plate-Fin Heat Exchanger (BAHX)	166
4.2.14.1	ALPEMA Standard.....	166
4.2.14.2	Applications	169
4.2.14.3	Heat Exchanger Core	169
4.2.14.4	Flow Arrangement	169
4.2.14.5	Rough Estimation of the Core Volume	171
4.2.14.6	Provisions for Thermal Expansion and Contraction.....	173
4.2.14.7	Mechanical Design of Brazed Aluminum Plate-Fin Heat Exchangers.....	173
4.2.14.8	Codes.....	173
4.2.14.9	Materials of Construction	173
4.2.14.10	Manufacture	174
4.2.14.11	Quality Assurance Program and Third Party Inspection	174

	4.2.14.12	Testing of BAHX	174
	4.2.14.13	Guarantees	174
	4.2.14.14	ALEX: BrazeD ALuminum EXchanger	174
	4.2.15	Comparison of Salient Features of Plate-Fin Heat Exchangers and Coil-Wound Heat Exchanger	175
	4.2.16	Heat Exchanger Specification Sheet for Plate-Fin Heat Exchanger	175
4.3	Surface Geometrical Relations		175
	4.3.1	Surface Geometrical Parameters: General	175
	4.3.1.1	Hydraulic Diameter, D_h	175
	4.3.1.2	Surface Area Density α and σ	177
	4.3.2	Tubular Heat Exchangers	177
	4.3.2.1	Tube Inside	177
	4.3.2.2	Tube Outside	178
	4.3.3	Compact Plate-Fin Exchangers	184
	4.3.3.1	Heat Transfer Area	184
	4.3.3.2	Components of Pressure Loss	186
4.4	Factors Influencing Tube-Fin Heat Exchanger Performance		187
	4.4.1	Tube Layout	187
	4.4.2	Equilateral Layout versus Equivelocity Layout	187
	4.4.3	Number of Tube Rows	187
	4.4.4	Tube Pitch	188
	4.4.5	Tube-Fin Variables	188
	4.4.5.1	Fin Height and Fin Pitch	188
	4.4.6	Finned Tubes with Surface Modifications	188
	4.4.7	Side Leakage	189
	4.4.8	Boundary-Layer Disturbances and Characteristic Flow Length	189
	4.4.9	Contact Resistance in Finned Tube Heat Exchangers	190
	4.4.9.1	Continuous Finned Tube Exchanger	190
	4.4.9.2	Tension-Wound Fins on Circular Tubes	190
	4.4.9.3	Integral Finned Tube	190
	4.4.10	Induced Draft versus Forced Draft	191
	4.4.10.1	Induced Draft	191
	4.4.10.2	Forced Draft	191
4.5	Thermohydraulic Fundamentals of Finned Tube Heat Exchangers		191
	4.5.1	Heat Transfer and Friction Factor Correlations for Crossflow over Staggered Finned Tube Banks	191
	4.5.2	The j and f Factors	192
	4.5.2.1	Bare Tube Bank	192
	4.5.2.2	Circular Tube-Fin Arrangement	193
	4.5.2.3	Continuous Fin on Circular Tube	196
	4.5.2.4	Continuous Fin on Flat Tube Array	198
4.6	Correlations for j and f factors of Plate-Fin Heat Exchangers		198
	4.6.1	Offset Strip Fin Heat Exchanger	198
	4.6.2	Louvered Fin	200
	4.6.3	Pin Fin Heat Exchangers	201
4.7	Fin Efficiency		202
	4.7.1	Fin Length for Some Plate-Fin Heat Exchanger Fin Configurations	202
	4.7.2	Fin Efficiency	202
	4.7.2.1	Circular Fin	202
	4.7.2.2	Plain Continuous Fin on Circular Tubes	204

4.8	Rating of a Compact Exchanger	206
4.8.1	Rating of Single-Pass Counterflow and Crossflow Exchangers	207
4.8.2	Shah's Method for Rating of Multipass Counterflow and Crossflow Heat Exchangers	209
4.9	Sizing of a Compact Heat Exchanger	210
4.9.1	Core Mass Velocity Equation	210
4.9.2	Procedure for Sizing a Compact Heat Exchanger	211
4.9.3	Optimization of Plate-Fin Exchangers and Constraints on Weight Minimization	211
4.10	Effect of Longitudinal Heat Conduction on Thermal Effectiveness	212
4.10.1	Longitudinal Conduction Influence on Various Flow Arrangements	213
4.10.2	Comparison of Thermal Performance of Compact Heat Exchangers	213
4.11	Air-Cooled Heat Exchanger (ACHE)	213
4.11.1	Air versus Water Cooling	214
4.11.1.1	Air Cooling	215
4.11.2	Construction of ACHE	216
4.11.2.1	Tube Bundle Construction	216
4.11.3	American Petroleum Institute Standard API 661/ISO 13706	224
4.11.4	Problems with Heat Exchangers in Low-Temperature Environments ..	225
4.11.4.1	Temperature Control	225
4.11.5	Forced Draft versus Induced Draft	225
4.11.5.1	Forced Draft	225
4.11.5.2	Induced Draft	225
4.11.6	Recirculation	226
4.11.7	Design Aspects	226
4.11.7.1	Design Variables	226
4.11.7.2	Design Air Temperature	227
4.11.8	Design Tips	228
4.11.8.1	Air-Cooled Heat Exchanger Design Procedure	228
4.11.8.2	Air-Cooled Heat Exchanger Data/Specification Sheet	229
4.11.8.3	Performance Control of ACHEs	230
	Nomenclature	230
	References	232
	Bibliography	236
Chapter 5	Shell and Tube Heat Exchanger Design	237
5.1	Construction Details for Shell and Tube Exchangers	237
5.1.1	Design Standards	237
5.1.1.1	TEMA Standard	237
5.1.1.2	ANSI/API Standard 660	237
5.2	Tubes	238
5.2.1	Tube Diameter	239
5.2.2	Tube Wall Thickness	239
5.2.3	Low-Finned Tubes	240
5.2.4	Tube Length	240
5.2.5	Means of Fabricating Tubes	240
5.2.6	Duplex or Bimetallic Tubes	240
5.2.7	Number of Tubes	241

5.2.8	Tube Count	241
5.2.9	U-Tube	241
5.2.9.1	U-Tube U-Bend Requirements as per TEMA.....	241
5.3	Tube Arrangement.....	242
5.3.1	Tube Pitch.....	242
5.3.2	Tube Layout.....	242
5.3.2.1	Triangular and Rotated Triangular Arrangements	242
5.3.2.2	Square and Rotated Square Arrangements.....	243
5.4	Baffles.....	243
5.4.1	Classification of Baffles.....	243
5.4.2	Transverse Baffles	243
5.4.2.1	Segmental Baffles	243
5.4.3	Disk and Doughnut Baffle.....	247
5.4.4	Orifice Baffle.....	248
5.4.5	No Tubes in Window	248
5.4.6	Longitudinal Baffles.....	249
5.4.7	Rod Baffles	249
5.4.8	NEST Baffles and Egg-Crate Tube Support.....	249
5.4.8.1	Non-Segmental Baffles	250
5.4.9	Grimmas Baffle	251
5.4.10	Wavy Bar Baffle	251
5.4.11	Baffles for Steam Generator Tube Support	251
5.5	Tubesheet and Its Connection with Shell and Channel	252
5.5.1	Clad and Faced Tubesheets	253
5.5.2	Tube-to-Tubesheet Attachment.....	253
5.5.3	Double Tubesheets.....	253
5.5.3.1	Types of Double Tubesheet Designs	253
5.5.4	Demerits of Double Tubesheets.....	256
5.6	Tube Bundle.....	256
5.6.1	Bundle Weight.....	256
5.6.2	Spacers, Tie-Rods, and Sealing Devices	256
5.6.3	Outer Tube Limit	256
5.7	Shells	258
5.8	Pass Arrangement.....	258
5.8.1	Tubeside Passes	258
5.8.1.1	Number of Tube Passes.....	258
5.8.1.2	End Channel and Channel Cover.....	260
5.8.2	Shellside Passes	262
5.8.2.1	Expansion Joint.....	263
5.8.2.2	Drains and Vents.....	263
5.8.2.3	Nozzles and Impingement Protection	263
5.9	Fluid Properties and Allocation	266
5.10	Classification of Shell and Tube Heat Exchangers	266
5.11	TEMA System for Describing Heat Exchanger Types.....	266
5.11.1	Fixed Tubesheet Exchangers	269
5.11.2	U-Tube Exchangers.....	270
5.11.2.1	Shortcomings of U-Tube Exchangers	270
5.11.3	Floating Head Exchangers	271
5.11.3.1	Sliding Bar/Surface.....	271
5.11.3.2	Kettle-Type Reboiler.....	272

5.12	Differential Thermal Expansion.....	272
5.13	TEMA Classification of Heat Exchangers Based on Service Condition.....	272
5.14	Shell and Tube Heat Exchanger Selection.....	272
5.14.1	Shell Types	272
5.14.1.1	TEMA <i>E</i> Shell	274
5.14.1.2	TEMA <i>F</i> Shell	274
5.14.1.3	TEMA <i>G, H</i> Shell.....	275
5.14.1.4	TEMA <i>G</i> Shell or Split Flow Exchanger.....	275
5.14.1.5	TEMA <i>H</i> Shell or Double Split Flow Exchanger	275
5.14.1.6	TEMA <i>J</i> Shell or Divided Flow Exchanger	276
5.14.1.7	TEMA <i>K</i> Shell or Kettle Type Reboiler	276
5.14.1.8	TEM <i>X</i> Shell.....	277
5.14.1.9	Comparison of Various TEMA Shells.....	278
5.14.2	Front and Rear Head Designs	278
5.14.2.1	Designations for Head Types	278
5.14.3	TEMA Specification Sheet.....	279
5.15	Shellside Clearances.....	279
5.15.1	Tube-to-Baffle-Hole Clearance	279
5.15.2	Shell-to-Baffle Clearance	279
5.15.3	Shell-to-Bundle Clearance	279
5.15.4	Bypass Lanes.....	282
5.16	Design Methodology	282
5.16.1	Shellside Flow Pattern.....	282
5.16.1.1	Shell Fluid Bypassing and Leakage	282
5.16.1.2	Bypass Prevention and Sealing Devices.....	282
5.16.1.3	Shellside Flow Pattern	284
5.16.1.4	Flow Fractions for Each Stream	285
5.16.1.5	Shellside Performance	285
5.16.2	Sizing of Shell and Tube Heat Exchangers	285
5.16.3	Guidelines for STHE Design.....	285
5.16.3.1	Heat Transfer Coefficient and Pressure Drop.....	286
5.16.4	Guidelines for Shellside Design	286
5.16.4.1	Specify the Right Heat Exchanger.....	287
5.16.5	Design Considerations for a Shell and Tube Heat Exchanger.....	287
5.16.5.1	Thermal Design Procedure.....	288
5.16.5.2	Detailed Design Method: Bell–Delaware Method	291
5.16.5.3	Auxiliary Calculations, Step-by-Step Procedure	293
5.16.6	Shellside Heat Transfer and Pressure-Drop Correction Factors	297
5.16.6.1	Step-by-Step Procedure to Determine Heat Transfer and Pressure-Drop Correction Factors	298
5.16.6.2	Shellside Heat Transfer Coefficient and Pressure Drop	301
5.16.6.3	Tubeside Heat Transfer Coefficient and Pressure Drop	304
5.16.6.4	Accuracy of the Bell–Delaware Method	308
5.16.6.5	Extension of the Delaware Method to Other Geometries	308
5.17	Shell and Tube Heat Exchangers with Non-Segmental Baffles	310
5.17.1	Phillips RODbaffle Heat Exchanger.....	310
5.17.1.1	RODbaffle Exchanger Concepts	310
5.17.1.2	Important Benefit: Elimination of Shellside Flow-Induced Vibration.....	311
5.17.1.3	Proven RODbaffle Applications	311

5.17.1.4	Operational Characteristics	311
5.17.1.5	Thermal Performance	311
5.17.1.6	Design and Rating Program Available	312
5.17.2	EMBaffle® Heat Exchanger	312
5.17.2.1	Application of EMBaffle Technology	312
5.17.2.2	Design	312
5.17.2.3	Benefits of EMBaffle Technology	314
5.17.3	Helixchanger® Heat Exchanger	314
5.17.3.1	Merits of Helixchanger Heat Exchanger.....	315
5.17.3.2	Applications	315
5.17.3.3	Helixchanger Heat Exchanger: Configurations	315
5.17.3.4	Performance.....	317
5.17.4	Twisted Tube® Heat Exchanger	318
5.17.4.1	Applications	318
5.17.4.2	Advantages.....	318
5.17.4.3	Merits of Twisted Tube Heat Exchanger.....	319
5.17.5	End Closures	319
5.17.5.1	Breech-Lock™ Closure	319
5.17.5.2	Easy Installation and Dismantling Jig	320
5.17.6	Taper-Lok® Closure.....	320
5.17.7	High-Pressure End Closures	320
5.A	Appendix A	321
5.A.1	Reference Crossflow Velocity as per Tinker	321
5.A.2	Design of Disk and Doughnut Heat Exchanger	323
5.A.2.1	Design Method.....	323
5.A.2.2	Heat Transfer	324
5.A.2.3	Shellside Pressure Drop.....	326
5.A.2.4	Shortcomings of Disk and Doughnut Heat Exchanger.....	326
5.A.3	NORAM RF™ Radial Flow Gas Heat Exchanger	326
5.A.3.1	Tube Layout	327
5.A.4	Closed Feedwater Heaters	327
5.A.4.1	Low-Pressure Feedwater Heaters	328
5.A.4.2	High-Pressure Feedwater Heaters	328
5.A.5	Steam Surface Condenser	329
5.A.5.1	Mechanical Description.....	330
5.A.5.2	Parts of Condenser.....	330
5.A.5.3	Condenser Tube Material.....	331
5.A.5.4	Condenser Support Systems	332
	Nomenclature	332
	References	333
	Suggested Readings.....	336
Chapter 6	Regenerators	337
6.1	Introduction	337
6.1.1	Regeneration Principle	337
6.1.2	Regenerators in Thermodynamic Systems and Others	337
6.1.3	Gas Turbine Cycle with Regeneration	337
6.1.4	Waste Heat Recovery Application.....	338
6.1.5	Benefits of Waste Heat Recovery	338
6.1.5.1	Direct Benefits	338

	6.1.5.2	Indirect Benefits.....	339
	6.1.5.3	Fuel Savings due to Preheating Combustion Air.....	339
6.2		Heat Exchangers Used for Regeneration	339
	6.2.1	Recuperator	339
	6.2.1.1	Merits of Recuperators	339
	6.2.2	Regenerator.....	340
	6.2.3	Types of Regenerators	340
	6.2.4	Fixed-Matrix or Fixed-Bed-Type Regenerator.....	341
	6.2.4.1	Fixed-Matrix Surface Geometries.....	342
	6.2.4.2	Size	342
	6.2.4.3	Merits of Fixed-Bed Regenerators.....	342
	6.2.5	Rotary Regenerators.....	343
	6.2.5.1	Salient Features of Rotary Regenerators	343
	6.2.5.2	Rotary Regenerators for Gas Turbine Applications.....	345
	6.2.5.3	Types of Rotary Regenerators	345
	6.2.5.4	Drive to Rotary Regenerators	345
	6.2.5.5	Operating Temperature and Pressure	345
	6.2.5.6	Surface Geometries for Rotary Regenerators.....	345
	6.2.5.7	Influence of Hydraulic Diameter on Performance.....	345
	6.2.5.8	Size	346
	6.2.5.9	Desirable Characteristics for a Regenerative Matrix.....	346
	6.2.5.10	Total Heat Regenerators.....	346
	6.2.5.11	Merits of Regenerators.....	347
6.3		Rotary Regenerative Air Preheater	347
	6.3.1	Design Features	348
	6.3.2	Heating Element Profiles.....	349
	6.3.3	Enameled Elements	349
	6.3.4	Corrosion and Fouling.....	349
	6.3.5	Heat Exchanger Baskets	349
	6.3.6	Seals and Sealing System Components.....	350
	6.3.6.1	Radial Seals and Sector Plates.....	350
	6.3.6.2	Axial Seals and Sealing Plates	351
	6.3.6.3	Circumferential Seals and Circumferential Sealing Ring	351
	6.3.7	Leakage	351
	6.3.8	Alstom Power Trisector Ljungström® Air Preheater.....	351
6.4		Comparison of Recuperators and Regenerators	352
6.5		Considerations in Establishing a Heat Recovery System	352
	6.5.1	Compatibility with the Existing Process System	352
	6.5.2	Economic Benefits.....	353
	6.5.2.1	Capital Costs.....	353
	6.5.3	Life of the Exchanger	353
	6.5.4	Maintainability	353
6.6		Regenerator Construction Material	353
	6.6.1	Strength and Stability at the Operating Temperature	354
	6.6.2	Corrosion Resistance.....	355
	6.6.3	Ceramic Heat Exchangers	355
	6.6.3.1	Low Gas Permeability	355
	6.6.4	Ceramic–Metallic Hybrid Recuperator.....	355
	6.6.5	Regenerator Materials for Other than Waste Heat Recovery.....	355

6.7	Thermal Design: Thermal-Hydraulic Fundamentals	356
6.7.1	Surface Geometrical Properties	356
6.7.2	Correlation for j and f	357
6.8	Thermal Design Theory	358
6.8.1	Regenerator Solution Techniques	359
6.8.1.1	Open Methods: Numerical Finite-Difference Method	359
6.8.1.2	Closed Methods	359
6.8.2	Basic Thermal Design Methods	359
6.8.3	Coppage and Longon Model for a Rotary Regenerator	360
6.8.3.1	Thermal Effectiveness	362
6.8.3.2	Heat Transfer	364
6.8.4	Parameter Definitions.....	364
6.8.5	Classification of Regenerator.....	365
6.8.6	Additional Formulas for Regenerator Effectiveness	365
6.8.6.1	Balanced and Symmetric Counterflow Regenerator	366
6.8.7	Reduced Length–Reduced Period (Λ – Π) Method.....	367
6.8.7.1	Counterflow Regenerator.....	367
6.8.8	Razelos Method for Asymmetric-Unbalanced Counterflow Regenerator.....	370
6.8.9	Influence of Longitudinal Heat Conduction in the Wall.....	371
6.8.9.1	Bahnke and Howard Method.....	372
6.8.9.2	Romie’s Solution	372
6.8.9.3	Shah’s Solution to Account for the Longitudinal Conduction Effect	373
6.8.10	Fluid Bypass and Carryover on Thermal Effectiveness.....	374
6.8.11	Regenerator Design Methodology.....	374
6.8.12	Primary Considerations Influencing Design	374
6.8.13	Rating of Rotary Regenerators.....	374
6.8.14	Sizing of Rotary Regenerators	374
6.9	Mechanical Design.....	375
6.9.1	Single-Bed and Dual-Bed Fixed Regenerators	375
6.9.2	Rotary Regenerators.....	375
6.9.2.1	Leakages	375
6.9.2.2	Seal Design.....	376
6.9.2.3	Drive for the Rotor.....	376
6.9.2.4	Thermal Distortion and Transients.....	377
6.9.2.5	Pressure Forces	377
6.10	Industrial Regenerators and Heat Recovery Devices	377
6.10.1	Fluid-Bed Regenerative Heat Exchangers.....	377
6.10.2	Fluidized-Bed Waste Heat Recovery	378
6.10.3	Vortex-Flow Direct-Contact Heat Exchangers.....	379
6.10.4	Ceramic Bayonet Tube Heat Exchangers	379
6.10.5	Regenerative Burners	379
6.10.6	Porcelain-Enameled Flat-Plate Heat Exchangers.....	380
6.10.7	Radiation Recuperators	380
6.10.8	Heat-Pipe Heat Exchangers.....	381
6.10.8.1	Merits of Heat-Pipe Heat Exchanger	382
6.10.8.2	Application.....	382
6.10.9	Economizer	382
6.10.10	Thermocompressor.....	382
6.10.11	Mueller Temp-Plate® Energy Recovery Banks	383

6.11	Rotary Heat Exchangers for Space Heating	383
6.11.1	Working Principle	384
6.11.2	Construction	385
6.11.3	Rotor Materials.....	385
6.11.3.1	Construction.....	385
6.11.3.2	Carryover	385
6.11.3.3	Seals.....	385
6.11.4	Drive System and Control Unit	386
6.11.5	Cleaning Devices	386
	Nomenclature	386
	References	388
	Bibliography	391
Chapter 7	Plate Heat Exchangers and Spiral Plate Heat Exchangers	393
7.1	Plate Heat Exchanger Construction: General	393
7.1.1	Flow Patterns and Pass Arrangement	394
7.1.2	Useful Data on PHE	396
7.1.3	Standard Performance Limits	397
7.2	Benefits Offered by Plate Heat Exchangers.....	397
7.3	Comparison between a Plate Heat Exchanger and a Shell and Tube Heat Exchanger	399
7.4	Plate Heat Exchanger: Detailed Construction Features	399
7.4.1	Plate.....	399
7.4.1.1	Plate Pattern.....	399
7.4.1.2	Types of Plate Corrugation	400
7.4.1.3	Intermating Troughs Pattern.....	400
7.4.1.4	Chevron or Herringbone Trough Pattern.....	400
7.4.1.5	Plate Materials	400
7.4.2	Gasket Selection	400
7.4.3	Bleed Port Design.....	400
7.4.4	Frames	402
7.4.5	Nozzles	402
7.4.6	Tie Bolts	402
7.4.7	Connector Plates.....	403
7.4.8	Connections.....	403
7.4.9	Installation.....	403
7.5	Brazed Plate Heat Exchanger	403
7.6	Other Forms of Plate Heat Exchangers	403
7.6.1	All-Welded Plate Exchangers.....	403
7.6.2	Supermax® and Maxchanger® Plate Heat Exchangers.....	404
7.6.3	Wide-Gap Plate Heat Exchanger.....	406
7.6.4	GEABloc Fully Welded Plate Heat Exchanger	407
7.6.5	Free-Flow Plate Heat Exchanger.....	407
7.6.6	Flow-Flex Tubular Plate Heat Exchanger.....	407
7.6.7	Semiwelded or Twin-Plate Heat Exchanger	409
7.6.8	Double-Wall Plate Heat Exchanger	411
7.6.9	Diabon F Graphite Plate Heat Exchanger	411
7.6.10	Glue-Free Gaskets (Clip-On Snap-On Gaskets)	411
7.6.11	AlfaNova 100% Stainless Steel Plate Heat Exchanger	412
7.6.12	Plate Heat Exchanger with Electrode Plate	412

7.6.13	Plate Heat Exchanger with Flow Rings.....	412
7.6.14	AlfaRex™ Gasket-Free Plate Heat Exchanger	412
7.6.15	Alfa Laval Plate Evaporator	413
7.6.16	Sanitary Heat Exchangers	413
7.6.17	EKasic® Silicon Carbide Plate Heat Exchangers	413
7.6.18	Deep-Set Gasket Grooves	413
7.7	Where to Use Plate Heat Exchangers	413
7.7.1	Applications for Which Plate Heat Exchangers Are Not Recommended.....	413
7.8	Thermohydraulic Fundamentals of Plate Heat Exchangers	414
7.8.1	High- and Low-Theta Plates.....	415
7.8.2	Thermal Mixing	416
7.8.2.1	Thermal Mixing Using High- and Low-Theta Plates.....	416
7.8.2.2	Thermal Mixing Using Horizontal and Vertical Plates	416
7.8.3	Flow Area.....	417
7.8.4	Heat Transfer and Pressure-Drop Correlations	419
7.8.4.1	Heat Transfer Correlations.....	419
7.8.4.2	Pressure Drop	420
7.8.5	Specific Pressure Drop or Jensen Number	421
7.9	PHE Thermal Design Methods	421
7.9.1	LMTD Method due to Buonopane et al.	422
7.9.2	ϵ -NTU Approach.....	422
7.9.3	Specification Sheet for PHE	423
7.9.3.1	Design Pressure	423
7.9.3.2	Plate Hanger.....	424
7.10	Corrosion of Plate Heat Exchangers.....	424
7.11	Fouling.....	425
7.12	Limitations of Plate Heat Exchangers	425
7.13	Spiral Plate Heat Exchangers	425
7.13.1	Flow Arrangements and Applications.....	426
7.13.2	Construction Material	426
7.13.3	Thermal Design of Spiral Plate Heat Exchangers.....	426
7.13.4	Mechanical Design of Spiral Plate Heat Exchangers.....	427
7.13.5	Applications for Spiral Plate Heat Exchangers	427
7.13.6	Advantages of Spiral Plate Exchangers.....	428
7.13.7	Limitations	428
7.14	Platecoil® Prime Surface Plate Heat Exchangers	428
	Nomenclature	429
	References	430
	Bibliography	431

Chapter 8	Heat Transfer Augmentation	433
8.1	Introduction	433
8.1.1	Benefits of Heat Transfer Augmentation	433
8.2	Application of Augmented Surfaces.....	433
8.3	Principle of Single-Phase Heat Transfer Enhancement.....	434
8.3.1	Increase in Convection Coefficient without an Appreciable Area Increase.....	434

8.3.2	Enhancement in Turbulent Flow	434
8.3.3	Enhancement in Laminar Flow	435
8.4	Approaches and Techniques for Heat Transfer Enhancement.....	435
8.5	Heat Transfer Mode	437
8.6	Passive Techniques	437
8.6.1	Extended Surfaces	437
8.6.1.1	Extended Surfaces for Gases	437
8.6.1.2	Extended Surfaces for Liquids.....	438
8.6.2	Treated Surfaces	441
8.6.3	Rough Surfaces	442
8.6.4	Tube Inserts and Displaced Flow Enhancement Devices	444
8.6.4.1	Enhancement Mechanism.....	444
8.6.4.2	Forms of Insert Device	444
8.6.4.3	Displaced Flow Enhancement Devices	444
8.6.5	Swirl Flow Devices	450
8.6.5.1	Twisted Tape Insert.....	450
8.6.5.2	Corrugated Surfaces	450
8.6.5.3	Doubly Enhanced Surfaces.....	452
8.6.5.4	Turbulators	453
8.6.6	Surface Tension Devices	453
8.6.7	Additives for Liquids	453
8.6.8	Additives for Gases	453
8.7	Active Techniques	454
8.8	Friction Factor	454
8.9	Pertinent Problems	454
8.9.1	Testing Methods	454
8.9.2	Fouling	455
8.9.3	Performance Evaluation Criteria.....	455
8.9.3.1	Webb's PECs: Performance Comparison with a Reference.....	456
8.9.3.2	Shah's Recommendation for Surface Selection of Compact Heat Exchanger with Gas on One Side	456
8.9.4	Market Factors.....	457
8.9.4.1	Alternate Means of Energy Savings	457
8.9.4.2	Adoptability to Existing Heat Exchanger	457
8.9.4.3	Proven Field/Performance Trials.....	457
8.9.5	Mechanical Design and Construction Considerations	458
8.10	Phase Change.....	458
8.10.1	Condensation Enhancement	458
8.10.1.1	Horizontal Orientation.....	459
8.10.1.2	Shellside Condensation on Vertical Tubes.....	459
8.10.2	Evaporation Enhancement.....	459
8.10.3	Heat Transfer Augmentation Devices for the Air-Conditioning and Refrigeration Industry	459
8.10.3.1	Shellside Evaporation of Refrigerants	459
8.10.3.2	Shellside Condensation of Refrigerants.....	460
8.10.3.3	In-Tube Evaporation of Refrigerants.....	460
8.11	Major Areas of Applications	460
	Nomenclature	461
	References	461
	Bibliography	463

Chapter 9	Fouling	465
9.1	Effect of Fouling on the Thermohydraulic Performance of Heat Exchangers	465
9.2	Costs of Heat Exchanger Fouling	467
9.2.1	Oversizing	467
9.2.2	Additional Energy Costs	467
9.2.3	Treatment Cost to Lessen Corrosion and Fouling	467
9.2.4	Lost Production due to Maintenance Schedules and Down Time for Maintenance	467
9.3	Fouling Curves/Modes of Fouling	467
9.4	Stages of Fouling	468
9.5	Fouling Model	468
9.6	Parameters That Influence Fouling Resistances	469
9.6.1	Properties of Fluids and Usual Propensity for Fouling	469
9.6.2	Temperature	469
9.6.3	Velocity and Hydrodynamic Effects	470
9.6.4	Tube Material	470
9.6.5	Impurities	470
9.6.6	Surface Roughness	471
9.6.7	Suspended Solids	471
9.6.8	Placing More Fouling Fluid on the Tubeside	471
9.6.9	Shellside Flow	471
9.6.10	Type of Heat Exchanger	472
9.6.10.1	Low-Finned Tube Heat Exchanger	472
9.6.10.2	Heat Transfer Augmentation Devices	472
9.6.10.3	Gasketed Plate Heat Exchangers	472
9.6.10.4	Spiral Plate Exchangers	472
9.6.11	Seasonal Temperature Changes	472
9.6.12	Equipment Design	472
9.6.13	Heat Exchanger Geometry and Orientation	472
9.6.14	Heat Transfer Processes like Sensible Heating, Cooling, Condensation, and Vaporization	473
9.6.15	Shell and Tube Heat Exchanger with Improved Shellside Performance	473
9.6.15.1	EMBaffle® Heat Exchanger	473
9.6.15.2	Twisted Tube Heat Exchanger	473
9.6.15.3	Helixchanger Heat Exchanger	473
9.7	Mechanisms of Fouling	474
9.7.1	Particulate Fouling	474
9.7.2	Chemical Reaction Fouling (Polymerization)	475
9.7.3	Corrosion Fouling	475
9.7.4	Crystallization or Precipitation Fouling	476
9.7.4.1	Modeling for Scaling	476
9.7.5	Biological Fouling	476
9.7.6	Solidification Fouling or Freezing Fouling	477
9.8	Fouling Data	477
9.9	How Fouling Is Dealt while Designing Heat Exchangers	477
9.9.1	Specifying the Fouling Resistances	477
9.9.2	Oversizing	477
9.10	TEMA Fouling Resistance Values	478
9.10.1	Research in Fouling	478

9.11	Fouling Monitoring	478
9.11.1	Fouling Inline Analysis	478
9.11.2	Tube Fouling Monitors	481
9.11.3	Fouling Monitor Operation	482
9.11.3.1	Instruments for Monitoring of Fouling	482
9.11.3.2	Gas-Side Fouling Measuring Devices	482
9.12	Expert System	482
9.13	Fouling Prevention and Control	483
9.13.1	Measures to Be Taken during the Design Stages	483
9.14	Cleaning of Heat Exchangers	484
9.14.1	Cleaning Techniques	484
9.14.2	Deposit Analysis	485
9.14.3	Selection of Appropriate Cleaning Methods	485
9.14.3.1	Precautions to Be Taken while Undertaking a Cleaning Operation	485
9.14.4	Off-Line Mechanical Cleaning	485
9.14.4.1	Manual Cleaning	486
9.14.4.2	Jet Cleaning	486
9.14.4.3	Drilling and Roding of Tubes	487
9.14.4.4	Turbining	487
9.14.4.5	Hydro Drilling Action	487
9.14.4.6	Passing Brushes through Exchanger Tubes	487
9.14.4.7	Scraper-Type Tube Cleaners	487
9.14.4.8	Blast Cleaning	488
9.14.4.9	Soot Blowing	488
9.14.4.10	Thermal Cleaning	488
9.14.5	Merits of Mechanical Cleaning	488
9.14.6	Chemical Cleaning	489
9.14.6.1	Clean-in-Place Systems	489
9.14.6.2	Choosing a Chemical Cleaning Method	489
9.14.6.3	Chemical Cleaning Solutions	489
9.14.7	General Procedure for Chemical Cleaning	489
9.14.8	Off-line Chemical Cleaning	490
9.14.8.1	Integrated Chemical Cleaning Apparatus	491
9.14.9	Merits of Chemical Cleaning	491
9.14.10	Disadvantages of Chemical Cleaning Methods	491
9.14.11	Online Cleaning Methods	491
9.14.12	Online Mechanical Cleaning Methods	492
9.14.12.1	Upstream Filtration (Debris Filter)	492
9.14.12.2	Flow Excursion	492
9.14.12.3	Air Bumping	492
9.14.12.4	Reversing Flow in Heat Exchangers	492
9.14.12.5	Automatic Tube Cleaning Systems	493
9.14.12.6	Insert Technology	494
9.14.12.7	Grit Cleaning	496
9.14.12.8	Self-Cleaning Heat Exchangers	497
9.14.13	Merits of Online Cleaning	499
9.15	Foulant Control by Chemical Additives	499
9.16	Control of Fouling from Suspended Solids	501
9.17	Cooling-Water Management for Reduced Fouling	501
9.17.1	Forms of Water-Side Fouling	501

9.17.2	Influence of Surface Temperature on Fouling.....	502
9.17.3	Foulant Control versus Type of Cooling-Water System	502
9.17.3.1	Once-Through System	502
9.17.3.2	Open Recirculating System	502
9.17.3.3	Closed Recirculating Systems	502
9.17.3.4	Online Chemical Control of Cooling-Water Foulants	502
9.17.4	Control of Scale Formation and Fouling Resistances for Treated Cooling Water	503
9.17.4.1	Chemical Means to Control Scaling.....	503
9.17.4.2	Electrostatic Scale Controller and Preventer	504
9.17.5	Cleaning of Scales.....	504
9.17.5.1	Chemical Cleaning	504
9.17.6	Iron Oxide Removal	504
	Nomenclature	504
	References	505
	Bibliography	507

Chapter 10 Flow-Induced Vibration of Shell and Tube Heat Exchangers 509

10.1	Principles of Flow-Induced Vibration	509
10.1.1	Principles of Flow-Induced Vibration	509
10.1.2	Possible Damaging Effects of FIV on Heat Exchangers.....	510
10.1.3	Most Probable Regions of Tube Failure	510
10.1.4	Failure Mechanisms	510
10.1.5	Flow-Induced Vibration Mechanisms	511
10.1.6	Tube Response Curve.....	511
10.1.7	Dynamical Behavior of Tube Arrays in Crossflow	511
10.1.8	Hydrodynamic Forces	512
10.1.9	FIV Mechanisms versus Flow Mediums	512
10.1.10	Approaches to FIV Analysis	512
10.1.11	Empirical Nature of Flow-Induced Vibration Analysis	512
10.2	Discussion of Flow-Induced Vibration Mechanisms.....	513
10.2.1	Vortex Shedding.....	513
10.2.1.1	Single Tube	513
10.2.1.2	Strouhal Number	513
10.2.1.3	Vortex Shedding for Tube Bundles.....	514
10.2.1.4	Avoiding Resonance	515
10.2.1.5	Calculation of Strouhal Number for Tube Arrays	515
10.2.1.6	Criteria to Avoid Vortex Shedding	516
10.2.1.7	Response due to Vortex Shedding Vibration Prediction by Dynamic Analysis	517
10.3	Turbulence-Induced Excitation Mechanism.....	518
10.3.1	Turbulence	518
10.3.2	Turbulent Buffeting	518
10.3.3	Owen's Expression for Turbulent Buffeting Frequency	518
10.3.4	Turbulent Buffeting Excitation as a Random Phenomenon	519
10.4	Fluid Elastic Instability	519
10.4.1	Fluid Elastic Forces	520
10.4.2	General Characteristics of Instability	520
10.4.3	Connors' Fluid Elastic Instability Analysis	520
10.4.4	Analytical Model.....	521

10.4.5	Unsteady Model.....	521
10.4.5.1	Displacement Mechanism.....	521
10.4.5.2	Velocity Mechanism	521
10.4.5.3	Unsteady Model	522
10.4.6	Design Recommendations.....	522
10.4.6.1	Chen's Criterion	522
10.4.6.2	Au-Yang et al. Criteria	523
10.4.6.2	Guidelines of Pettigrew and Taylor.....	523
10.4.7	Acceptance Criteria.....	523
10.4.8	Stability Diagrams	524
10.5	Acoustic Resonance.....	524
10.5.1	Principle of Standing Waves	524
10.5.1.1	Effect of Tube Solidity on Sound Velocity	525
10.5.2	Expressions for Acoustic Resonance Frequency.....	526
10.5.2.1	Blevins Expression.....	527
10.5.3	Excitation Mechanisms	528
10.5.3.1	Vortex Shedding Mechanism.....	528
10.5.3.2	Turbulent Buffeting Mechanism.....	528
10.5.4	Acceptance Criteria for Occurrence of Acoustic Resonance.....	529
10.5.4.1	Vortex Shedding.....	529
10.5.4.2	Turbulent Buffeting.....	530
10.6	Vibration Evaluation Procedure	530
10.6.1	Steps of Vibration Evaluation.....	530
10.6.1.1	Step 6 for Liquid Flow	531
10.6.1.2	Step 6 for Gas Flow	531
10.6.2	Caution in Applying Experimentally Derived Values for Vibration Evaluation	531
10.7	Design Guidelines for Vibration Prevention	531
10.7.1	Methods to Increase Tube Natural Frequency	531
10.7.1.1	FIV of Retubed Units.....	533
10.7.2	Methods to Decrease Crossflow Velocity.....	534
10.7.3	Suppression of Standing Wave Vibration.....	535
10.7.3.1	Antivibration Baffles.....	535
10.7.3.2	Helmholtz Cavity Resonator.....	537
10.7.3.3	Concept of Fin Barrier	537
10.7.3.4	Concept of Helical Spacers.....	538
10.7.3.5	Detuning	538
10.7.3.6	Removal of Tubes.....	538
10.7.3.7	Surface Modification.....	539
10.7.3.8	Irregular Spacing of Tubes.....	539
10.7.3.9	Change the Mass Flow Rate	539
10.8	Baffle Damage and Collision Damage	539
10.8.1	Empirical Checks for Vibration Severity	539
10.9	Impact and Fretting Wear.....	539
10.9.1	Tube Wear Prediction by Experimental Techniques.....	540
10.9.2	Theoretical Model.....	540
10.10	Determination of Hydrodynamic Mass, Natural Frequency, and Damping.....	541
10.10.1	Added Mass or Hydrodynamic Mass.....	541
10.10.2	Determination of Added Mass Coefficient, C_m , for Single-Phase Flow.....	541

10.10.2.1	Blevins Correlation	541
10.10.2.2	Experimental Data of Moretti et al.	542
10.10.3	Natural Frequencies of Tube Bundles	542
10.10.3.1	Estimation of Natural Frequencies of Straight Tubes	543
10.10.3.2	U-Tube Natural Frequency.....	544
10.10.4	Damping	544
10.10.4.1	Determination of Damping.....	545
10.10.5	Other Values	546
10.11	New Technologies of Antivibration Tools	546
10.11.1	Antivibration Tube Stakes.....	546
10.11.2	ExxonMobil Research and Engineering	548
10.12	Software Programs for Analysis of FIV.....	548
10.A	Appendix A: Calculation Procedure for Shellside Liquids	549
	Nomenclature	556
	References	558
	Suggested Readings.....	562

Chapter 11	Mechanical Design of Shell and Tube Heat Exchangers	563
11.1	Standards and Codes	563
11.1.1	Standards	563
11.1.1.1	Company Standards.....	563
11.1.1.2	Trade or Manufacturer's Association Standards	564
11.1.1.3	National Standards.....	564
11.1.2	Design Standards Used for the Mechanical Design of Heat Exchangers	564
11.1.2.1	TEMA Standards Scope and General Requirements (Section B-1, RCB-1.1).....	564
11.1.2.2	Scope of TEMA Standards.....	564
11.1.2.3	Differences among TEMA Classes R, C, and B	565
11.1.2.4	TEMA Engineering Software	565
11.1.2.5	When Do the TEMA Standards Supplement or Override the ASME Code Specification?.....	565
11.1.2.6	Heat Exchange Institute Standards.....	566
11.1.3	Codes.....	566
11.1.3.1	ASME Codes	567
11.1.3.2	CODAP	572
11.1.3.3	AD Merkblatter 2000—German Pressure Vessel Code	572
11.1.3.4	UPV: The European Standards EN 13445	573
11.2	Basics of Mechanical Design	573
11.2.1	Fundamentals of Mechanical Design.....	574
11.2.1.1	Information for Mechanical Design	574
11.2.1.2	Content of Mechanical Design of Shell and Tube Heat Exchangers.....	575
11.2.1.3	Mechanical Design Procedure.....	577
11.2.1.4	Design Loadings.....	577
11.2.1.5	Topics Covered in the Next Sections	577
11.3	Stress Analysis, Classes, and Categories of Stress.....	577
11.3.1	Stress Analysis	577
11.3.2	Classes and Categories of Stresses.....	577
11.3.2.1	Stress Categories.....	578

11.3.2.2	Stress Classification	578
11.3.2.3	Membrane Stress	578
11.3.2.4	Primary Stress	578
11.3.3	Stress Classification.....	578
11.3.3.1	Primary Membrane Stress, P_m	578
11.3.3.2	Primary Bending Stress, P_b	579
11.3.3.3	Local Membrane Stress, P_L	579
11.3.3.4	Secondary Stress.....	579
11.3.3.5	Thermal Stresses.....	580
11.3.3.6	Peak Stress, F	580
11.3.3.7	Discontinuity Stresses.....	580
11.3.4	Fatigue Analysis	580
11.3.5	Design Methods and Design Criteria	581
11.3.5.1	ASME Code Section VIII Design Criteria.....	581
11.3.6	Allowable Stress	581
11.3.7	Combined-Thickness Approach for Clad Plates	581
11.3.8	Welded Joints.....	582
11.3.8.1	Welded Joint Efficiencies.....	582
11.3.8.2	Joint Categories.....	582
11.3.8.3	Weld Joint Types.....	583
11.3.9	Key Terms in Heat Exchanger Design	583
11.3.9.1	Design Pressure	583
11.3.9.2	Design Temperature.....	584
11.3.9.3	Maximum Allowable Working Pressure	584
11.3.9.4	Operating Temperature or Working Temperature	584
11.3.9.5	Operating Pressure or Working Pressure	584
11.4	Tubesheet Design.....	585
11.4.1	Fundamentals	585
11.4.1.1	Tubesheet Connection with the Shell and Channel	585
11.4.1.2	Supported Tubesheet and Unsupported Tubesheet.....	585
11.4.1.3	Tubesheet Thickness.....	585
11.4.1.4	Tubesheet Design Procedure: Historical Background.....	586
11.4.1.5	Assumptions in Tubesheet Analysis	587
11.4.2	Basis of Tubesheet Design.....	590
11.4.2.1	Analytical Treatment of Tubesheets	590
11.4.2.2	Design Analysis	591
11.4.3	Tubesheet Design as per TEMA Standards	595
11.4.3.1	Tubesheet Formula for Bending	595
11.4.3.2	Parameter F	596
11.4.3.3	Shear Formula RCB-7.133	597
11.4.3.4	Stress Category Concept in TEMA Formula	598
11.4.3.5	Determination of Effective Design Pressure, P (RCB-7.16)	598
11.4.3.6	Equivalent Differential Expansion Pressure, p_d (RCB 7.161).....	598
11.4.3.7	Differential Pressure Design, after Yokell.....	600
11.4.3.8	Longitudinal Stress Induced in the Shell and Tube Bundle.....	601
11.4.3.9	TEMA Fixed Tubesheet Design with Different Thickness	603

11.4.4	Tubesheet Design Method as per ASME, CODAP and UPV:EN 13443 and Comparison with TEMA Rules.....	603
11.4.4.1	Effect of Ligament Efficiency in Tubesheet Thickness and Tube-to-Tubesheet Joint Strength Calculation.....	604
11.4.4.2	Tubesheet Design Rules.....	605
11.4.5	Methodology to Use ASME Rules.....	608
11.4.6	Flanged Tubesheets: TEMA Design Procedure.....	609
11.4.6.1	Fixed Tubesheet or Floating Tubesheet.....	609
11.4.6.2	U-Tube Tubesheet.....	610
11.4.7	Rectangular Tubesheet Design.....	610
11.4.7.1	Methods of Tubesheet Analysis.....	610
11.4.8	Curved Tubesheets.....	611
11.4.8.1	Advantages of Curved Tubesheets.....	611
11.4.9	Conventional Double Tubesheet Design.....	611
11.5	Cylindrical Shell, End Closures, and Formed Heads under Internal Pressure.....	612
11.5.1	Cylindrical Shell under Internal Pressure.....	612
11.5.1.1	Thin Thick Cylindrical Shells.....	612
11.5.1.2	Design for External Pressure and/or Internal Vacuum.....	613
11.5.2	End Closures and Formed Heads.....	613
11.5.2.1	Flat Cover.....	614
11.5.2.2	Hemispherical.....	614
11.5.2.3	Ellipsoidal.....	614
11.5.2.4	Torispherical.....	615
11.5.2.5	Conical.....	615
11.5.3	Minimum Thickness of Heads and Closures.....	616
11.5.3.1	Flat Cover.....	617
11.5.3.2	Ellipsoidal Heads.....	617
11.5.3.3	Torispherical Heads.....	617
11.5.3.4	Hemispherical Heads.....	617
11.5.3.5	Conical Heads and Sections (without Transition Knuckle).....	618
11.5.4	Comparison of Various Heads.....	619
11.6	Bolted Flanged Joint Design.....	619
11.6.1	Construction and Design.....	619
11.6.1.1	Flanged Joint Types.....	619
11.6.1.2	Constructional Details of Bolted Flange Joints.....	619
11.6.1.3	Design of Bolted Flange Joints.....	620
11.6.1.4	Gasket Design.....	623
11.6.1.5	Bolting Design.....	626
11.6.1.6	Flange Design.....	629
11.6.2	Step-by-Step Procedure for Integral/Loose/Optional Flanges Design.....	633
11.6.2.1	Data Required.....	633
11.6.2.2	Step-by-Step Design Procedure.....	633
11.6.2.3	Taper-Lok® Heat Exchanger Closure.....	637
11.6.2.4	Zero-Gap Flange.....	638
11.6.2.5	Long Weld Neck Assembly.....	639
11.7	Expansion Joints.....	640
11.7.1	Flexibility of Expansion Joints.....	640

11.7.2	Classification of Expansion Joints.....	640
11.7.2.1	Formed Head or Flanged-and-Flued Head.....	640
11.7.2.2	Bellows or Formed Membrane	642
11.7.2.3	Deciding between Thick- and Thin-Walled Expansion Joints	644
11.7.3	Design of Expansion Joints	644
11.7.3.1	Formed Head Expansion Joints	644
11.7.3.2	Finite Element Analysis.....	645
11.7.3.3	FEA by Design Consultants	645
11.7.3.4	Singh and Soler Model.....	646
11.7.3.5	Procedure for Design of Formed Head Expansion Joints.....	647
11.7.3.6	Design Procedure as per ASME Code	648
11.7.4	Design of Bellows or Formed Membranes.....	649
11.7.4.1	Shapes and Cross Section	649
11.7.4.2	Bellows Materials	649
11.7.4.3	Bellows Design: Circular Expansion Joints.....	649
11.7.4.4	Limitations and Means to Improve the Operational Capability of Bellows	649
11.7.4.5	Fatigue Life.....	652
11.8	Opening and Nozzles.....	653
11.8.1	Openings	653
11.8.1.1	Reinforcement Pad.....	653
11.8.1.2	Reinforced Pad and Air–Soap Solution Testing	653
11.8.2	Nozzles	654
11.8.3	Stacked Units.....	655
11.9	Supports.....	655
11.9.1	Design Loads.....	655
11.9.2	Horizontal Vessel Supports	656
11.9.2.1	Saddle Supports	656
11.9.2.2	Ring Supports	656
11.9.2.2	Leg Supports.....	657
11.9.3	Vertical Vessels	657
11.9.3.1	Skirt Supports	657
11.9.3.2	Lug Supports.....	657
11.9.3.3	Ring Support.....	658
11.9.4	Procedure for Support Design.....	658
11.9.4.1	TEMA Rules for Supports Design (G-7.1).....	658
11.9.4.2	ASME Code.....	659
11.9.5	Lifting Devices and Attachments.....	659
	References	659
	Bibliography	663

Chapter 12 Corrosion..... 665

12.1	Basics of Corrosion.....	665
12.1.1	Reasons for Corrosion Studies	665
12.1.2	Corrosion Mechanism	666
12.1.2.1	Basic Corrosion Mechanism of Iron in Aerated Aqueous System.....	667

12.1.3	Forms of Electrochemical Corrosion	668
12.1.3.1	Bimetallic Cell	668
12.1.3.2	Concentration Cell	668
12.1.3.3	Differential Temperature Cells	669
12.1.4	Corrosion Potential and Corrosion Current	669
12.1.5	Corrosion Kinetics	669
12.1.5.1	Polarization Effects	669
12.1.5.2	Passivation.....	670
12.1.6	Factors Affecting Corrosion of a Material in an Environment	672
12.1.6.1	Environmental Factors	672
12.2	Forms of Corrosion.....	673
12.2.1	Uniform Corrosion versus Localized Corrosion	673
12.2.2	Factors That Favor Localized Attack	674
12.2.3	Forms of Corrosion	674
12.2.3.1	Uniform or General Corrosion.....	675
12.2.3.2	Galvanic Corrosion	680
12.2.3.3	Pitting Corrosion	684
12.2.3.4	Crevice Corrosion	689
12.2.3.5	Intergranular Corrosion.....	691
12.2.3.6	Dealloying or Selective Leaching	692
12.2.3.7	Erosion–Corrosion	694
12.2.3.8	Stress Corrosion Cracking	701
12.2.3.9	Hydrogen Damage.....	705
12.2.3.10	Fretting Corrosion	706
12.2.3.11	Corrosion Fatigue.....	706
12.2.3.12	Microbiologically Influenced Corrosion.....	707
12.3	Corrosion of Weldments	711
12.4	Corrosion Prevention and Control	712
12.4.1	Principles of Corrosion Control	712
12.4.2	Corrosion Control by Proper Engineering Design.....	713
12.4.2.1	Design Details.....	713
12.4.2.2	Preservation of Inbuilt Corrosion Resistance	713
12.4.2.3	Design to Avoid Various Forms of Corrosion.....	713
12.4.2.4	Weldments, Brazed and Soldered Joints	713
12.4.2.5	Plant Location	714
12.4.2.6	Startup and Shutdown Problems.....	714
12.4.2.7	Overdesign	714
12.4.3	Corrosion Control by Modification of the Environment (Use of Inhibitors)	714
12.4.3.1	Inhibitors	715
12.4.4	Corrosion-Resistant Alloys	717
12.4.5	Bimetal Concept.....	717
12.4.5.1	Cladding	718
12.4.5.2	Bimetallic or Duplex Tubing.....	718
12.4.6	Protective Coatings	719
12.4.6.1	Plastic Coatings	720
12.4.6.2	Effectiveness of Coatings.....	720
12.4.6.3	Surface Treatment	720
12.4.7	Electrochemical Protection (Cathodic and Anodic Protection)	720
12.4.7.1	Principle of Cathodic Protection.....	720
12.4.7.2	Anodic Protection	721

12.4.8	Passivation.....	722
12.5	Corrosion Monitoring.....	722
12.5.1	Benefits.....	722
12.5.2	Approaches to Corrosion Monitoring	722
12.5.3	Corrosion Monitoring Techniques	723
12.5.3.1	Online Monitoring Techniques.....	723
12.5.3.2	Corrosion Monitoring of Condensers by Systematic Examination of the State of the Tubes.....	724
12.5.4	Limitations of Corrosion Monitoring.....	724
12.5.5	Requirements for Success of Corrosion Monitoring Systems.....	724
12.6	Cooling-Water Corrosion.....	725
12.6.1	Corrosion Processes in Water Systems	725
12.6.2	Causes of Corrosion in Cooling-Water Systems	725
12.6.2.1	Dissolved Solids and Water Hardness	726
12.6.2.2	Chloride	728
12.6.2.3	Sulfates	728
12.6.2.4	Silica	728
12.6.2.5	Oil	728
12.6.2.6	Iron and Manganese	728
12.6.2.7	Suspended Matter	729
12.6.2.8	Dry Residue	729
12.6.2.9	Dissolved Gases.....	729
12.6.3	Cooling Systems.....	732
12.6.3.1	Once-Through System	732
12.6.3.2	Open Recirculating Systems.....	733
12.6.3.3	Closed Recirculating Systems	733
12.6.4	Corrosion Control Methods for Cooling-Water Systems	733
12.6.4.1	Material Selection.....	734
12.6.4.2	Water Treatment	735
12.6.4.3	Corrosion Inhibitors.....	735
12.6.4.4	Ferrous Sulfate Dosing	735
12.6.4.5	Passivation	735
12.6.5	Influence of Cooling-Water Types on Corrosion.....	736
12.6.5.1	Fresh Water.....	736
12.6.5.2	Seawater Corrosion.....	736
12.6.5.3	Brackish Waters.....	736
12.6.5.4	Boiler Feedwaters	736
12.6.6	Corrosion of Individual Metals in Cooling-Water Systems	736
12.6.7	Forms of Corrosion in Cooling Water.....	737
12.6.7.1	Uniform Corrosion.....	737
12.6.7.2	Galvanic Corrosion.....	737
12.6.7.3	Pitting Corrosion.....	737
12.6.7.4	Crevice Corrosion	738
12.6.7.5	Stress Corrosion Cracking	738
12.6.7.6	Corrosion Fatigue and Fretting Wear	738
12.6.7.7	Erosion of Tube Inlet	738
12.6.7.8	Dezincification.....	738
12.6.7.9	Microbiologically Induced Corrosion.....	738
12.6.8	Material Selection for Condenser Tubes	738
12.6.9	Operational Maintenance of Condensers and Feedwater Heaters ...	739
12.6.10	Preventing Corrosion in Automotive Cooling Systems.....	739

12.7	Material Selection for Hydrogen Sulfide Environments	739
12.7.1	Effects of Hydrogen in Steel (ASTM/ASME A/SA 516 Grades 60/65/70).....	739
12.7.2	Sources of Hydrogen in Steel	740
12.7.3	Hydrogen-Induced Cracking	740
12.7.3.1	Stress-Oriented Hydrogen-Induced Cracking	740
12.7.3.2	Susceptibility of Steels to HIC	741
12.7.3.3	Prevention of HIC	741
12.7.4	Hydrogen Embrittlement	741
12.7.4.1	Mechanism of Hydrogen Embrittlement	741
12.7.4.2	Hydrogen Embrittlement of Steel Weldments	742
12.7.5	Hydrogen-Assisted Cracking.....	742
12.7.5.1	Prevention of HSCC	742
12.7.6	Hydrogen Blistering	743
12.7.6.1	Susceptible Materials.....	743
12.7.6.2	Prevention of Blistering.....	743
12.7.6.3	Detection of Blisters in Service.....	743
12.7.6.4	Correction of Blistered Condition in Steel Equipment.....	743
12.7.7	Pressure Vessel Steels for Sour Environments.....	743
12.7.8	HIC Testing Specification	743
	References	744
	Bibliography	748

Chapter 13 Material Selection and Fabrication 749

13.1	Material Selection Principles.....	749
13.1.1	Material Selection	750
13.1.2	Review of Operating Process	750
13.1.3	Review of Design	750
13.1.4	Selection of Material	750
13.1.4.1	ASME Code Material Requirements.....	750
13.1.4.2	Functional Requirements of Materials	751
13.1.5	Evaluation of Materials	760
13.1.5.1	Material Tests	761
13.1.5.2	Materials Evaluation and Selection to Resist Corrosion	761
13.1.6	Cost.....	761
13.1.6.1	Cost-Effective Material Selection.....	761
13.1.7	Possible Failure Modes and Damage in Service	762
13.2	Equipment Design Features.....	762
13.2.1	Maintenance	762
13.2.2	Failsafe Features.....	762
13.2.3	Access for Inspection	762
13.2.4	Safety.....	763
13.2.5	Equipment Life.....	763
13.2.5.1	Component Life	763
13.2.6	Field Trials.....	763
13.3	Raw Material Forms Used in the Construction of Heat Exchangers	763
13.3.1	Castings	764
13.3.2	Forgings.....	764
13.3.3	Rods and Bars	764
13.3.3.1	Pipe Fittings and Flanges.....	764

13.3.4	Bolts and Studs.....	764
13.3.4.1	Materials for Corrosion-Resistant Fasteners	764
13.3.5	Handling of Materials	765
13.3.6	Material Selection for Pressure Boundary Components	765
13.3.6.1	Shell, Channel, Covers, and Bonnets.....	765
13.3.6.2	Tubes.....	765
13.3.6.3	Tubesheet	765
13.3.6.4	Baffles	766
13.4	Materials for Heat Exchanger Construction	766
13.5	Plate Steels.....	767
13.5.1	Classifications and Designations of Plate Steels: Carbon and Alloy Steels	767
13.5.1.1	How Do Plate Steels Gain Their Properties?	767
13.5.1.2	Changes in Steel Properties due to Heat Treatment	767
13.5.1.3	ASTM Specifications on Plate Steels Used for Pressure Vessel Fabrications and Heat Exchangers.....	768
13.5.2	Processing of Plate Steels.....	770
13.6	Pipes and Tubes	771
13.6.1	Tubing Requirements	771
13.6.2	Selection of Tubes for Heat Exchangers.....	772
13.6.3	Specifications for Tubes	772
13.6.4	Defect Detection.....	772
13.6.5	Standard Testing for Tubular Products.....	772
13.6.5.1	Hydrostatic Pressure Testing	772
13.6.5.2	Pneumatic Test.....	773
13.6.5.3	Corrosion Tests	773
13.6.5.4	Dimensional Tolerance Tests	773
13.6.6	Mill Scale	773
13.6.7	ASTM Specifications for Ferrous Alloys Tubings	773
13.7	Weldability Problems	774
13.7.1	Cold Cracking	774
13.7.1.1	Hydrogen-Induced Cracking.....	775
13.7.1.2	Underbead Cracking	780
13.7.1.3	Lamellar Tearing	780
13.7.1.4	Fish-Eye Cracking	783
13.8	Hot Cracking	783
13.8.1	Factors Responsible for Hot Cracking.....	784
13.8.1.1	Segregation of Low-Melting-Point Elements.....	784
13.8.1.2	Stress States That Induce Restraint	784
13.8.1.3	Mode of Solidification	784
13.8.2	Susceptible Alloys	784
13.8.3	Types of Hot Cracking	784
13.8.3.1	Solidification Cracking	784
13.8.3.2	Heat-Affected Zone Liquation Cracking.....	786
13.8.3.3	Reheat Cracking or Stress-Relief Cracking.....	786
13.8.3.4	Ductility Dip Cracking	788
13.8.3.5	Chevron Cracking.....	788
13.8.3.6	Crater Cracks	788
13.9	Laboratory Tests to Determining Susceptibility to Cracking	788
13.9.1	Weldability Tests	788
13.9.2	Varestraint (Variable Restraint) Test.....	789

13.9.3	MultiTask Vareststraint Weldability Testing System	790
13.10	Service-Oriented Cracking.....	790
13.10.1	Temper Embrittlement or Creep Embrittlement	790
13.11	Welding-Related Failures	790
13.12	Selection of Cast Iron and Carbon Steels	791
13.12.1	Cast Iron	791
13.12.2	Steels.....	791
13.12.2.1	Process Improvements	792
13.12.2.2	Carbon Steels	792
13.12.2.3	Types of Steel.....	792
13.12.2.4	Product Forms	792
13.12.2.5	Use of Carbon Steels	793
13.12.2.6	Fabrication	794
13.13	Low-Alloy Steels	795
13.13.1	Selection of Steels for Pressure Vessel Construction	795
13.13.2	Low-Alloy Steels for Pressure Vessel Constructions	796
13.13.2.1	Applications of Low-Alloy Steel Plates.....	796
13.13.2.2	Carbon–Molybdenum Steels	796
13.13.2.3	Carbon–Manganese Steels	796
13.13.2.4	Carbon–Manganese–Molybdenum Steels	797
13.14	Quenched and Tempered Steels.....	797
13.14.1	Compositions and Properties	798
13.14.2	Weldability.....	799
13.14.3	Joint Design	799
13.14.4	Preheat	799
13.14.5	Welding Processes	799
13.14.6	Postweld Heat Treatment	799
13.14.7	Stress-Relief Cracking	800
13.15	Chromium–Molybdenum Steels.....	800
13.15.1	Composition and Properties	800
13.15.2	Applications	801
13.15.3	Creep Strength	801
13.15.4	Welding Metallurgy	802
13.15.4.1	Joint Design	802
13.15.4.2	Joint Preparation	802
13.15.4.3	Preheating	802
13.15.4.4	Welding Processes	802
13.15.4.5	Filler Metal	802
13.15.5	Temper Embrittlement Susceptibility	802
13.15.6	Step-Cooling Heat Treatment	803
13.15.7	CVN Impact Properties	804
13.15.8	Temper Embrittlement of Weld Metal	804
13.15.8.1	Control of Temper Embrittlement of Weld Metal.....	804
13.15.9	Postweld Heat Treatment (Stress Relief)	804
13.15.9.1	Larson–Miller Tempering Parameter	805
13.15.10	Reheat Cracking in Cr–Mo and Cr–Mo–V Steels	805
13.15.11	Modified 9Cr–1Mo Steel	805
13.15.12	Advanced 3Cr–Mo–Ni Steels.....	805
13.16	Stainless Steels	805
13.16.1	Classification and Designation of Stainless Steels	806
13.16.1.1	Designations	806

	13.16.1.2	ASTM Specification for Stainless Steels.....	806
	13.16.1.3	Guidance for Stainless Steel Selection	806
13.16.2		Martensitic Stainless Steel.....	806
13.16.3		Austenitic Stainless Steel Properties and Metallurgy	807
	13.16.3.1	Types of Austenitic Stainless Steel.....	807
	13.16.3.2	Alloy Development	807
	13.16.3.3	Stainless Steel for Heat Exchanger Applications	808
	13.16.3.4	Properties of Austenitic Stainless Steels	808
	13.16.3.5	Alloying Elements and Microstructure	809
	13.16.3.6	Alloy Types and Their Applications.....	809
13.16.4		Mechanism of Corrosion Resistance	810
	13.16.4.1	Sigma Phase.....	811
	13.16.4.2	Passive versus Active Behavior.....	811
	13.16.4.3	Resistance to Chemicals	811
	13.16.4.4	Stainless Steel in Seawater	811
	13.16.4.5	Resistance to Various Forms of Corrosion	811
	13.16.4.6	Galvanic Corrosion.....	811
	13.16.4.7	Localized Forms of Corrosion.....	812
	13.16.4.8	Pitting Corrosion.....	812
	13.16.4.9	Crevice Corrosion	813
	13.16.4.10	Stress Corrosion Cracking	814
	13.16.4.11	Intergranular Corrosion	817
	13.16.4.12	Knifeline Attack	818
13.16.5		Austenitic Stainless Steel Fabrication.....	819
	13.16.5.1	Pickling.....	819
	13.16.5.2	Passivation	819
	13.16.5.3	Mechanical Cutting Methods	819
	13.16.5.4	Gas Cutting Method	819
13.16.6		Austenitic Stainless Steel Welding	820
	13.16.6.1	Welding Processes	820
	13.16.6.2	Welding Methods	820
	13.16.6.3	Filler Metal Selection	821
	13.16.6.4	Shielding Gases	822
	13.16.6.5	Weld Preparation	822
	13.16.6.6	Joint Design	822
	13.16.6.7	Preweld Cleaning.....	822
	13.16.6.8	Welding Considerations	823
	13.16.6.9	TIG Welding Techniques to Overcome Carbide Precipitation.....	830
	13.16.6.10	Gas Coverage.....	830
	13.16.6.11	Welding Practices to Improve the Weld Performance.....	831
	13.16.6.12	Protection of Weld Metal against Oxidation and Fluxing to Remove Chromium Oxide	831
	13.16.6.13	Protecting the Roots of the Welds against Oxidation	831
	13.16.6.14	Welding Processes Generate Different Weld Defects.....	832
	13.16.6.15	Postweld Heat Treatment	832
	13.16.6.16	Welding Stainless Steels to Dissimilar Metals.....	833
	13.16.6.17	Postweld Cleaning	833
	13.16.6.18	Corrosion Resistance of Stainless Steel Welds.....	834
13.17		Ferritic Stainless Steels	834
	13.17.1	Conventional Ferritic Stainless Steels	834

13.17.2	“New” and “Old” Ferritic Stainless Steels	835
13.17.2.1	Superferritic Stainless Steels, Superaustenitic Stainless Steels, and Duplex Stainless Steels	835
13.17.3	Superferritic Stainless Steel	835
13.17.3.1	Characteristics	835
13.17.3.2	Alloy Composition	835
13.17.3.3	Applications	837
13.17.3.4	Physical Properties	837
13.17.3.5	Corrosion Resistance	838
13.17.3.6	Fabricability	839
13.17.3.7	Welding	839
13.18	Duplex Stainless Steels	840
13.18.1	Composition of Duplex Stainless Steels	841
13.18.2	Comparison with Austenitic and Ferritic Stainless Steels	842
13.18.3	Corrosion Resistance of Duplex Stainless Steels	843
13.18.4	Process Applications	843
13.18.5	Welding Methods	843
13.18.5.1	Weldability	843
13.18.5.2	Postweld Stress Relief	845
13.18.6	Nondestructive Testing of Duplex SS	845
13.19	Superaustenitic Stainless Steels with Mo + N	845
13.19.1	4.5% Mo Superaustenitic Steels	846
13.19.2	6% Mo Superaustenitic Stainless Steel	846
13.19.2.1	Corrosion Resistance	847
13.19.2.2	Applications	847
13.19.2.3	Welding	848
13.19.3	Corrosion Resistance of Superaustenitic Stainless Steel Welds	849
13.20	Aluminum Alloys: Metallurgy	850
13.20.1	Properties of Aluminum	850
13.20.1.1	Aluminum for Heat Exchanger Applications	850
13.20.1.2	Wrought Alloy Designations	851
13.20.1.3	Temper Designation System of Aluminum and Aluminum Alloys	853
13.20.1.4	Product Forms and Shapes	853
13.20.2	Corrosion Resistance	853
13.20.2.1	Surface Oxide Film on Aluminum	853
13.20.2.2	Chemical Nature of Aluminum: Passivity	854
13.20.2.3	Resistance to Waters	854
13.20.2.4	Forms of Corrosion	855
13.20.2.5	Corrosion Prevention and Control Measures	858
13.20.3	Fabrication	859
13.20.3.1	Parameters Affecting Aluminum Welding	859
13.20.3.2	Surface Preparation and Surface Cleanliness	861
13.20.3.3	Plate Cutting and Forming	861
13.20.3.4	Joint Design	861
13.20.3.5	Joint Geometry	861
13.20.3.6	Preheating	861
13.20.3.7	Wire Feeding	862
13.20.3.8	Push Technique	862
13.20.3.9	Travel Speed	862
13.20.3.10	Shielding Gas	862

13.20.3.11	Welding Wire	862
13.20.3.12	Convex-Shaped Welds	862
13.20.3.13	Corrosion Resistance: Welded, Brazed, and Soldered Joints	862
13.20.3.14	Welding Filler Metals	862
13.20.3.15	Welding Methods	863
13.21	Copper	864
13.21.1	Copper Alloy Designation	864
13.21.1.1	Wrought Alloys	864
13.21.1.2	Heat Exchanger Applications	864
13.21.1.3	Copper in Steam Generation	865
13.21.1.4	Wrought Copper Alloys: Properties and Applications	865
13.21.1.5	Product Forms	868
13.21.2	Copper Corrosion	868
13.21.2.1	Corrosion Resistance	868
13.21.2.2	Galvanic Corrosion	868
13.21.2.3	Pitting Corrosion	870
13.21.2.4	Intergranular Corrosion	870
13.21.2.5	Dealloying (Dezincification)	871
13.21.2.6	Erosion–Corrosion	872
13.21.2.7	Stress Corrosion Cracking	872
13.21.2.8	Condensate Corrosion	873
13.21.2.9	Deposit Attack	873
13.21.2.10	Hot-Spot Corrosion	874
13.21.2.11	Snake Skin Formation	874
13.21.2.12	Corrosion Fatigue	874
13.21.2.13	Biofouling	874
13.21.2.14	Cooling-Water Applications	874
13.21.2.15	Resistance to Seawater Corrosion	874
13.21.2.16	Sulfide Attack	874
13.21.2.17	Exfoliation	875
13.21.2.18	Copper and Aquatic Life	875
13.21.3	Copper Welding	875
13.21.3.1	Weldability	875
13.21.3.2	Alloy Classification from Weldability Considerations ..	877
13.21.3.3	PWHT	879
13.21.3.4	Dissimilar Metal Welding	879
13.22	Nickel and Nickel-Base Alloys Metallurgy and Properties	880
13.22.1	Classification of Nickel Alloys	881
13.22.1.1	Commercially Pure Nickel	881
13.22.1.2	Nickel–Copper Alloys and Copper–Nickel Alloys	882
13.22.1.3	Inconel and Inco Alloy	882
13.22.1.4	Nickel–Iron–Chromium Alloys and Inco Nickel–Iron–Chromium Alloys for High-Temperature Applications	884
13.22.1.5	Magnetic Properties and Differentiation of Nickels	885
13.22.2	Nickel and Nickel-Base Alloys: Corrosion Resistance	885
13.22.2.1	Galvanic Corrosion	885
13.22.2.2	Pitting Resistance	886
13.22.2.3	Intergranular Corrosion	886
13.22.2.4	Stress Corrosion Cracking	887

13.22.3	Nickel and Nickel-Base Alloys: Welding.....	888
13.22.3.1	Considerations while Welding Nickel	888
13.22.3.2	Welding Methods	891
13.22.3.3	Postweld Heat Treatment	892
13.22.4	Hastelloy®	892
13.23	Titanium: Properties and Metallurgy	892
13.23.1	Properties That Favor Heat Exchanger Applications	892
13.23.2	Alloy Specification	893
13.23.3	Titanium Grades and Alloys.....	893
13.23.3.1	Unalloyed Grades.....	893
13.23.3.2	Alloy Grades	894
13.23.3.3	ASTM and ASME Specifications for Mill Product Forms	894
13.23.4	Titanium Corrosion Resistance	895
13.23.4.1	Surface Oxide Film	895
13.23.4.2	General Corrosion	895
13.23.4.3	Resistance to Chemicals and Solutions.....	896
13.23.4.4	Resistance to Waters	896
13.23.4.5	Forms of Corrosion	896
13.23.4.6	Thermal Performance	897
13.23.4.7	Fouling	898
13.23.4.8	Applications	898
13.23.5	Titanium Fabrication	899
13.23.5.1	Welding Titanium	899
13.23.5.2	In-Process Quality Control and Weld Tests.....	903
13.23.5.3	Heat Treatment.....	904
13.23.5.4	Forming of Titanium-Clad Steel Plate.....	904
13.24	Zirconium	904
13.24.1	Properties and Metallurgy	904
13.24.1.1	Alloy Classification	904
13.24.1.2	Limitations of Zirconium.....	905
13.24.2	Corrosion Resistance	905
13.24.2.1	Resistance to Chemicals	906
13.24.2.2	Forms of Corrosion	906
13.24.3	Fabrication	906
13.24.3.1	Welding Method.....	906
13.24.3.2	Weld Metal Shielding.....	907
13.24.3.3	Weld Preparation.....	907
13.24.3.4	Surface Cleaning.....	907
13.24.3.5	Filler Metals	907
13.24.3.6	Weld Inspection.....	907
13.24.3.7	Welding of Dissimilar Metals	907
13.25	Tantalum	907
13.25.1	Corrosion Resistance	909
13.25.1.1	Hydrogen Embrittlement.....	909
13.25.1.2	Resistance to Chemicals	909
13.25.2	Product Forms and Cost	909
13.25.3	Performance versus Other Materials	909
13.25.4	Heat Transfer	909
13.25.5	Welding.....	910
13.26	Graphite, Glass, Teflon, and Ceramics	910

13.27	Graphite	910
13.27.1	Applications of Impervious Graphite Heat Exchangers	910
13.27.2	Drawbacks Associated with Graphite	911
13.27.3	Forms of Graphite Heat Exchangers	911
13.27.4	Shell-and-Tube Heat Exchanger	911
13.27.5	Graphite Plate Exchanger	912
13.28	Glass	912
13.28.1	Applications	912
13.28.2	Mechanical Properties and Resistance to Chemicals	912
13.28.3	Construction Types	912
13.28.3.1	Shell-and-Tube Heat Exchangers	913
13.28.3.2	Coil Heat Exchangers	913
13.28.3.3	Hybrid Heat Exchangers	913
13.28.3.4	Glass-Lined Steel	913
13.28.3.5	Drawbacks of Glass Material	913
13.29	Teflon	913
13.29.1	Teflon as Heat Exchanger Material	913
13.29.2	Heat Exchangers of Teflon in the Chemical Processing Industry	914
13.29.3	Design Considerations	914
13.29.4	Size/Construction	914
13.29.5	Heat Exchanger Fabrication Technology	914
13.29.6	Fluoropolymer Resin Development	915
13.30	Ceramics	915
13.30.1	Suitability of Ceramics for Heat Exchanger Construction	915
13.30.2	Classification of Engineering Ceramics	915
13.30.3	Types of Ceramic Heat Exchanger Construction	916
13.31	Hexoloy® Silicon Carbide Heat Exchanger Tube	916
13.32	Alloys for Subzero Temperatures	917
13.32.1	Ductile–Brittle Transition Temperature	917
13.32.2	Crystal Structure Determines Low-Temperature Behavior	917
13.32.3	Requirements of Materials for Low-Temperature Applications	918
13.32.4	Notch Toughness	918
13.32.4.1	Notch Toughness: ASME Code Requirements	918
13.32.5	Selection of Material for Low-Temperature Applications	918
13.32.6	Materials for Low-Temperature and Cryogenic Applications	918
13.32.6.1	Aluminum for Cryogenic Applications	919
13.32.6.2	Copper and Copper Alloys	920
13.32.6.3	Titanium and Titanium Alloys	920
13.32.6.4	Nickel and High-Nickel Alloys	920
13.32.6.5	Carbon Steels and Alloy Plate Steels	920
13.32.6.6	Products Other than Plate	922
13.32.6.7	Austenitic Stainless Steel	922
13.32.7	Fabrication of Cryogenic Vessels and Heat Exchangers	922
13.32.8	9% Nickel Steel	923
13.32.8.1	Merits of 9% Nickel Steel	923
13.32.8.2	Forming of 9% Nickel Steel	923
13.32.8.3	Surface Preparation and Scale Removal for Welding	923
13.32.8.4	Edge Preparation	923
13.32.8.5	Welding Procedures	923
13.32.8.6	Electrodes	924

13.32.8.7	Guidelines for Welding of 9% Ni Steel.....	924
13.32.8.8	Welding Problems with 9% Ni Steel.....	925
13.32.8.9	Postweld Heat Treatment	925
13.32.9	Welding of Austenitic Stainless Steels for Cryogenic Application.....	925
13.32.9.1	Charpy V-Notch Impact Properties	925
13.32.9.2	Problems in Welding.....	926
13.32.10	Safety in Cryogenics.....	926
13.32.10.1	Checklist	926
13.33	Cladding	927
13.33.1	Clad Plate.....	927
13.33.2	Cladding Thickness	927
13.33.3	Methods of Cladding	927
13.33.3.1	Loose Lining	928
13.33.3.2	Resistance Cladding.....	928
13.33.3.3	Lining Using Plug Welding.....	928
13.33.3.4	Thermal Spraying	928
13.33.3.5	Weld Overlaying or Weld Surfacing	928
13.33.3.6	Roll Cladding	932
13.33.3.7	Explosive Cladding	933
13.33.4	Processing of Clad Plates	936
13.33.4.1	Forming of Clad Steel Plates	936
13.33.5	Failure of Clad Material	938
13.33.6	ASME Code Requirements in Using Clad Material	938
13.34	Postweld Heat Treatment of Welded Joints in Steel Pressure Vessels and Heat Exchangers	938
13.34.1	Objectives of Heat Treatment	939
13.34.2	Types of Heat Treatment	939
13.34.3	Effects of Changes in Steel Quality and PWHT	940
13.34.4	ASME Code Requirements for PWHT	940
13.34.4.1	Charts for Heat Treatment as per ASME Code	940
13.34.5	PWHT Cycle.....	940
13.34.6	Quality Control during Heat Treatment	941
13.34.7	Methods of PWHT	941
13.34.8	Effectiveness of Heat Treatment.....	942
13.34.9	Defects due to Heat Treatment	942
13.34.10	Possible Welding-Related Failures	942
13.34.11	NDT after PWHT.....	942
	References	942
	Bibliography	953

Chapter 14 Quality Control and Quality Assurance, Inspection, and Nondestructive Testing.....955

14.1	Quality Control and Quality Assurance	955
14.1.1	Quality Management in Industry	955
14.1.2	Quality and Quality Control	955
14.1.2.1	Aim of Quality Control	956
14.1.3	Quality Assurance.....	956
14.1.3.1	Need for QA.....	956
14.1.3.2	Essential Elements of Quality Assurance Program.....	956
14.1.3.3	Requirements of QA Programs for Success	956

14.1.3.4	Quality Assurance in Fabrication of Heat Exchangers and Pressure Vessels	956
14.1.3.5	Contents of QAP for Pressure Vessels and Heat Exchangers	957
14.1.4	Quality System	957
14.1.4.1	ASME Code: Quality Control System.....	959
14.1.5	Quality Manual	959
14.1.5.1	Details of QA Manuals	960
14.1.6	Main Documents of the Quality System	960
14.1.6.1	Quality Assurance Program	960
14.1.6.2	Operation Process Sheet	960
14.1.6.3	Checklist	961
14.1.7	Economics of Quality Assurance	961
14.1.8	Review and Evaluation Procedures	962
14.1.8.1	Auditing	962
14.1.8.2	Auditing Procedure.....	962
14.1.8.3	Contents of an Audit Plan.....	962
14.1.9	Documentation	962
14.1.10	ISO 9000	963
14.1.10.1	What Is the ISO 9000 Series?.....	963
14.1.10.2	Principles of ISO 9000	963
14.1.10.3	Why ISO 9000?	963
14.1.10.4	Benefits of ISO 9000	963
14.1.10.5	Listing of Selected ISO 9000 Quality Standards	963
14.1.10.6	Total Quality Management	963
14.2	Inspection	964
14.2.1	Definitions	964
14.2.2	Objectives of Inspection	964
14.2.3	Design and Inspection	964
14.2.4	Inspection Guidelines.....	964
14.2.5	Scope of Inspection of Heat Exchangers.....	964
14.2.5.1	Material Control and Raw Material Inspection.....	965
14.2.5.2	Positive Material Identification.....	965
14.2.6	Detailed Checklist for Components	966
14.2.6.1	Checklist for Tubesheet	966
14.2.7	TEMA Standard for Inspection.....	966
14.2.8	Master Traveler.....	966
14.2.9	Scope of Third-Party Inspection	967
14.2.9.1	Hold Points and Witness Points.....	967
14.3	Welding Design	968
14.3.1	Parameters Affecting Welding Quality.....	968
14.3.2	Welding Quality Design	968
14.3.2.1	Variables Affecting Welding Quality	969
14.3.3	Scheme of Symbols for Welding	970
14.3.4	Standard for Welding and Welding Design.....	970
14.3.4.1	ASME Code Section IX	970
14.3.5	Selection of Consumables	970
14.3.6	P Numbers	970
14.3.7	Filler Metals	970
14.3.7.1	F Numbers	971
14.3.7.2	A Numbers.....	971

14.3.8	Welding Procedure Qualification: Welding Procedure Specification and Procedure Qualification Record	971
14.3.8.1	Welding Procedure Specification	971
14.3.8.2	Procedure Qualification Record	972
14.3.8.3	Welder's Performance Qualification.....	972
14.3.8.4	Welder Requalification	972
14.3.8.5	Welding Positions and Qualifications.....	972
14.3.9	Weld Defects and Inspection of Weld Quality	973
14.3.9.1	Weld Defects (Discontinuities)	973
14.3.9.2	Causes of Discontinuities	973
14.3.9.3	General Types of Defects and Their Significance	973
14.3.9.4	Approach to Weld Defect Acceptance Levels	975
14.4	Nondestructive Testing Methods	976
14.4.1	Selection of NDT Methods	976
14.4.1.1	Capabilities and Limitations of Nondestructive Testing Methods.....	976
14.4.1.2	Acceptance Criteria	976
14.4.1.3	Cost	976
14.4.1.4	Personnel.....	979
14.4.2	Inspection Equipment.....	980
14.4.3	Reference Codes and Standards	980
14.4.3.1	ASME Code Section V: Nondestructive Examination	980
14.4.4	NDT Symbols.....	980
14.4.5	Written Procedures.....	980
14.4.5.1	Content of NDT Procedures	981
14.4.5.2	General Details of Requirements in the NDT Procedure Document	981
14.4.5.3	Deficiencies in NDT Procedures	982
14.4.6	Visual Examination.....	982
14.4.6.1	Principle of VT	982
14.4.6.2	Merits of Visual Examination	983
14.4.6.3	VT Written Procedure	983
14.4.6.4	Reference Document.....	983
14.4.6.5	Visual Examination: Prerequisites	983
14.4.6.6	Visual Examination Equipment.....	983
14.4.6.7	NDT of Raw Materials	983
14.4.6.8	Visual Examination during Various Stages of Fabrication by Welding.....	984
14.4.6.9	Developments in Visual Examination Optical Instruments	984
14.4.7	Liquid Penetrant Inspection	986
14.4.7.1	Principle.....	986
14.4.7.2	Applications	987
14.4.7.3	Merits of PT.....	987
14.4.7.4	Limitations.....	987
14.4.7.5	Written Procedure.....	987
14.4.7.6	Standards	988
14.4.7.7	Test Procedure	988
14.4.7.8	Penetrants.....	988
14.4.7.9	Method.....	989

14.4.7.10	Selection of Developer.....	989
14.4.7.11	Penetrant Application	989
14.4.7.12	Surface Preparation	989
14.4.7.13	Excess Penetrant Removal.....	989
14.4.7.14	Standardization of Light Levels for Penetrant and Magnetic Inspection	990
14.4.7.15	Evaluation of Indications	990
14.4.7.16	Acceptance Standards.....	990
14.4.7.17	Postcleaning.....	990
14.4.7.18	Recent Developments in PT.....	990
14.4.8	Magnetic Particle Inspection.....	990
14.4.8.1	Principle.....	991
14.4.8.2	Applications	991
14.4.8.3	Reference Documents	991
14.4.8.4	Test Procedure	991
14.4.8.5	Factors Affecting the Formation and Appearance of the Magnetic Particles Pattern.....	991
14.4.8.6	Merits of Magnetic Particle Inspection	992
14.4.8.7	Limitations of the Method	992
14.4.8.8	Written Procedure.....	992
14.4.8.9	Magnetizing Current	992
14.4.8.10	Equipment for Magnetic Particle Inspection	993
14.4.8.11	Magnetizing Technique	993
14.4.8.12	Inspection Medium (Magnetic Particles)	994
14.4.8.13	Inspection Method	995
14.4.8.14	Surface Preparation	995
14.4.8.15	Evaluation of Indications	996
14.4.8.16	Demagnetization	996
14.4.8.17	Record of Test Data	996
14.4.8.18	Interpretation	996
14.4.8.19	Acceptance Standards.....	996
14.4.8.20	MT Accessories	996
14.4.9	Radiographic Testing.....	996
14.4.9.1	Principle of Radiography	997
14.4.9.2	Application.....	997
14.4.9.3	Radiation Sources (X-Rays and Gamma Rays)	997
14.4.9.4	Merits and Limitations	998
14.4.9.5	Radiographic Test Written Procedure	998
14.4.9.6	Requirements of Radiography	999
14.4.9.7	General Procedure in Radiography	999
14.4.9.8	Reference Documents	999
14.4.9.9	Safety	999
14.4.9.10	Identification Marks.....	999
14.4.9.11	Location Markers.....	999
14.4.9.12	Processing of X-Ray Films	999
14.4.9.13	Surface Preparation	999
14.4.9.14	Radiographic Techniques for Weldments of Pressure Vessels	1000
14.4.9.15	Full Radiography	1001
14.4.9.16	Radiographic Quality	1002
14.4.9.17	Recent Developments in Radiography.....	1004

14.4.10	Ultrasonic Testing	1007
14.4.10.1	Test Method	1008
14.4.10.2	Application of Ultrasonic Technique in Pressure Vessel Industry	1008
14.4.10.3	Written Procedure	1009
14.4.10.4	Code Coverage.....	1009
14.4.10.5	Advantages of Ultrasonic Inspection	1009
14.4.10.6	Limitations of Ultrasonic Inspection.....	1010
14.4.10.7	Examination Procedure.....	1010
14.4.10.8	Surface Preparation	1012
14.4.10.9	Probes	1012
14.4.10.10	Couplant.....	1012
14.4.10.11	Ultrasonic Testing of Welds	1012
14.4.10.12	Examination Coverage	1014
14.4.10.13	UT Calculators	1014
14.4.10.14	Acceptance Criteria	1014
14.4.10.15	Reference Blocks	1014
14.4.10.16	Calibration	1015
14.4.10.17	Phased Array Ultrasonic Testing.....	1015
14.4.10.18	Fracture Mechanics	1019
14.4.10.19	What Is New in UT?.....	1020
14.4.11	Acoustical Holography	1021
14.4.11.1	Merits and Comparison of Acoustical Holography with Radiography and Ultrasonic Testing	1021
14.4.11.2	Holographic and Speckle Interferometry	1021
14.4.12	Acoustic Emission Testing	1021
14.4.12.1	Principle of Acoustic Emission	1021
14.4.12.2	Emission Types and Characteristics.....	1022
14.4.12.3	Kaiser Effect.....	1022
14.4.12.4	Reference Code.....	1023
14.4.12.5	Written Procedure	1023
14.4.12.6	AE Testing Instrument	1023
14.4.12.7	Signal Analysis	1023
14.4.12.8	Factors Influencing AE Data	1023
14.4.12.9	Applications: Role of AE in Inspection and Quality Control of Pressure Vessels and Heat Exchangers	1023
14.4.12.10	Merits of Acoustic Emission Testing.....	1024
14.4.13	Eddy Current Testing	1024
14.4.13.1	Principles of Eddy Current Testing	1025
14.4.13.2	Written Procedure	1026
14.4.13.3	ASTM Specifications.....	1026
14.4.13.4	Probes	1026
14.4.13.5	Eddy Current Test Equipment	1027
14.4.13.6	Signal Processing	1027
14.4.13.7	Inspection or Test Frequency and Its Effect on Flaw Detectability	1028
14.4.13.8	Operating Variables.....	1028
14.4.13.9	Inspection Method for Tube Interior	1029
14.4.13.10	Tube Inspection with Magnetic Flux Leakage	1030
14.4.13.11	Remote Field Eddy Current Testing.....	1030
14.4.13.12	Tube Inspection with Near Field Testing.....	1030

14.4.13.13	Tube Inspection with Internal Rotating Inspection System for Ferrous and Nonferrous Materials	1033
14.4.13.14	Instrumentation	1033
14.4.13.15	Testing of Weldments	1033
14.4.13.16	Calibration	1033
14.4.13.17	Merits of ET and Comparison with Other Methods.....	1034
14.4.13.18	Limitations of Eddy Current Testing.....	1034
14.4.13.19	Recent Advances in Eddy Current Testing.....	1034
14.4.13.20	Tubesheet Diagram for Windows	1035
14.4.14	Leak Testing	1035
14.4.14.1	Written Procedure	1036
14.4.14.2	Methods of Leak Testing.....	1036
	References	1041
	Bibliography	1044

Chapter 15 Heat Exchanger Fabrication 1045

15.1	Introduction to Fabrication of the Shell and Tube Heat Exchanger	1045
15.2	Details of Manufacturing Drawing	1045
15.2.1	Additional Necessary Entries.....	1046
15.3	Stages of Heat Exchanger Fabrication.....	1046
15.3.1	Identification of Materials	1046
15.3.2	Edge Preparation and Rolling of Shell Sections, Tack Welding, and Alignment for Welding of Longitudinal Seams	1047
15.3.2.1	General Discussion on Forming of Plates	1047
15.3.2.2	Fabrication of Shell.....	1049
15.3.3	Plate Bending Machines, PWHT, and Manipulative Equipment	1051
15.3.3.1	Roll Bending Machine	1051
15.3.3.2	Vertical Plate Bending Machine.....	1051
15.3.3.3	PWHT of Shells.....	1051
15.3.3.4	Manipulative Equipment	1051
15.3.4	Welding of Shells, Checking the Dimensions, and Subjecting Pieces to Radiography	1051
15.3.5	Checking the Circularity of the Shell and the Assembly Fit, Including Nozzles and Expansion Joints	1052
15.3.5.1	Welding of Nozzles.....	1053
15.3.5.2	Supports	1053
15.3.5.3	Attachment of Expansion Joints	1053
15.3.6	Tubesheet and Baffle Drilling	1054
15.3.6.1	Tubesheet Drilling	1054
15.3.6.2	Tube Hole Finish.....	1054
15.3.6.3	Drilling of Baffles.....	1055
15.3.7	Tube Bundle Assembly.....	1056
15.3.7.1	Assembly of Tube Bundle outside the Exchanger Shell.....	1056
15.3.7.2	Assembly of Tube Bundle inside the Shell	1058
15.3.7.3	Tube Nest Assembly of Large Steam Condensers	1059
15.3.7.4	Cautions to Exercise while Inserting Tubes	1059
15.3.7.5	Assembly of U-Tube Bundle.....	1059
15.3.8	Tubesheet to Shell Welding	1060

15.3.9	Tube-to-Tubesheet Joint Fabrication	1061
15.3.9.1	Quality Assurance Program for Tube-to-Tubesheet Joint	1062
15.3.9.2	Mock-Up Test	1062
15.3.9.3	Tube Expansion	1063
15.3.9.4	Requirements for Expanded Tube-to-Tubesheet Joints	1063
15.3.9.5	Tube-to-Tubesheet Expansion Methods	1063
15.3.9.6	Rolling Equipment	1064
15.3.9.7	Basic Rolling Process.....	1064
15.3.9.8	Optimum Degree of Expansion	1065
15.3.9.9	Methods to Check the Degree of Expansion.....	1066
15.3.9.10	Criterion for Rolling-in Adequacy	1066
15.3.9.11	Length of Tube Expansion	1074
15.3.9.12	Full-Depth Rolling	1075
15.3.9.13	Size of Tube Holes.....	1076
15.3.9.14	Factors Affecting Rolling Process	1079
15.3.9.15	Strength and Leak Tightness of Rolled Joints	1079
15.3.9.16	Expanding in Double Tubesheets.....	1081
15.3.9.17	Leak Testing.....	1081
15.3.9.18	Residual Stresses in Tube-to-Tubesheet Joints.....	1081
15.3.10	Tube-to-Tubesheet Joint Welding	1082
15.3.10.1	Various Methods of Tube-to-Tubesheet Joint Welding	1083
15.3.10.2	Tube-to-Tubesheet Joint Configuration	1083
15.3.10.3	Welding of Sections of Unequal Thickness	1092
15.3.10.4	Seal-Welded and Strength-Welded Joints.....	1093
15.3.10.5	Considerations in Tube-to-Tubesheet Welding.....	1094
15.3.10.6	Welding of Titanium Tubes to Tubesheet.....	1096
15.3.10.7	Merits of Sequence of Completion of Expanded and Welded Joints	1096
15.3.10.8	Full-Depth, Full-Strength Expanding after Welding	1099
15.3.10.9	Ductility of Welded Joint in Feedwater Heaters	1099
15.3.10.10	Welded Mock-Ups	1100
15.3.10.11	Inspection of Tube-to-Tubesheet Joint Weld	1100
15.3.10.12	Leak Testing of Tube-to-Tubesheet Joint	1102
15.3.10.13	Brazing Method for Tube-to-Tubesheet Joints	1102
15.3.11	Heat Treatment	1103
15.3.11.1	With Tubes Welded in One Tubesheet and Left Free in the Other Tubesheet	1103
15.3.11.2	Both Ends of the Tubes Welded with Tubesheets	1103
15.3.11.3	Heat Treatment: General Requirements.....	1103
15.3.12	Assembly of Channels/End Closures	1104
15.3.12.1	Bolt Tightening	1104
15.3.13	Hydrostatic Testing.....	1104
15.3.13.1	ASME CODE Requirement	1104
15.3.13.2	TEMA Standard Requirement	1105
15.3.13.3	Hydrostatic Testing: Prerequisites.....	1105
15.3.13.4	Improved Method for Hydrostatic Testing of Welded Tube-to-Tubesheet Joint of Feedwater Heaters	1106
15.3.13.5	HydroProof™.....	1106
15.3.13.6	Plate-Fin Heat Exchanger	1107

15.3.14	Preparation of Heat Exchangers for Shipment	1108
15.3.14.1	Painting	1108
15.3.14.2	Nitrogen Filling.....	1108
15.3.15	Making Up Certificates	1108
15.3.15.1	Foundation Loading Diagrams/Drawings	1109
15.3.15.2	Schematics or Flow Diagrams	1109
15.3.15.3	Installation, Maintenance, and Operating Instructions.....	1109
15.4	Forming of Heads and Closures	1109
15.4.1	Forming Methods.....	1109
15.4.2	Spinning	1109
15.4.3	Pressing	1110
15.4.4	Crown-and-Segment (C and S) Technique.....	1112
15.4.5	PWHT of Dished Ends.....	1112
15.4.6	Dimensional Check of Heads.....	1114
15.4.7	Purchased End Closures.....	1114
15.5	Brazing	1114
15.5.1	Definition and General Description of Brazing	1114
15.5.2	Brazing Advantages	1114
15.5.3	Disadvantages of Brazing.....	1115
15.6	Elements of Brazing	1115
15.6.1	Joint Design.....	1115
15.6.1.1	Joint Types.....	1116
15.6.2	Brazing Filler Metals	1116
15.6.2.1	Composition of Filler Metals.....	1116
15.6.2.2	Aluminum Filler Metals.....	1116
15.6.2.3	Copper Fillers	1117
15.6.2.4	Nickel-Based Filler Metals	1117
15.6.2.5	Silver-Based Filler Metals	1117
15.6.2.6	Gold-Based Fillers.....	1117
15.6.2.7	Forms of Filler Metal	1118
15.6.2.8	Placement of Filler Metal	1118
15.6.2.9	ASME Code Specification for Filler Metals	1118
15.6.3	Precleaning and Surface Preparation.....	1118
15.6.3.1	Precleaning.....	1118
15.6.3.2	Scale and Oxide Removal.....	1118
15.6.3.3	Protection of Precleaned Parts.....	1119
15.6.4	Fluxing	1119
15.6.4.1	Selection of a Flux.....	1119
15.6.4.2	Composition of the Flux	1119
15.6.4.3	Demerits of Brazing Using Corrosive Fluxes.....	1119
15.6.5	Fixturing.....	1119
15.6.6	Brazing Methods	1120
15.6.6.1	Torch Brazing.....	1120
15.6.6.2	Dip Brazing.....	1120
15.6.6.3	Furnace Brazing.....	1122
15.6.6.4	Vacuum Brazing.....	1124
15.6.7	Postbrazing Cleaning.....	1125
15.6.7.1	Braze Stopoffs.....	1125
15.7	Fundamentals of Brazing Process Control.....	1125
15.7.1	Heating Rate.....	1125

15.7.2	Brazing Temperature	1125
15.7.3	Brazing Time	1125
15.7.4	Temperature Uniformity	1126
15.7.5	Control of Distortion during the Furnace Cycle	1126
15.8	Brazing of Aluminum	1126
15.8.1	Need for Closer Temperature Control	1126
15.8.2	Aluminum Alloys That Can Be Brazed	1127
15.8.3	Elements of Aluminum Brazing	1127
15.8.3.1	Joint Clearance	1127
15.8.3.2	Precleaning	1127
15.8.3.3	Surface Oxide Removal	1127
15.8.3.4	Aluminum Filler Metals	1127
15.8.3.5	Fluxing	1127
15.8.4	Brazing Methods	1128
15.8.4.1	Aluminum Dip Brazing	1128
15.8.4.2	Furnace Brazing	1128
15.8.4.3	Brazing Process	1130
15.8.4.4	Vacuum Brazing of Aluminum	1132
15.9	Brazing of Heat-Resistant Alloys and Stainless Steel	1135
15.9.1	Brazing of Nickel-Based Alloys	1135
15.9.1.1	Brazing Filler Metals	1135
15.9.2	Brazing of Cobalt-Based Alloys	1136
15.9.3	Brazing of Stainless Steel	1136
15.9.3.1	Brazeability of Stainless Steel	1136
15.10	Quality Control, Inspection, and NDT of Brazed Heat Exchangers	1137
15.10.1	Quality of the Brazed Joints	1138
15.10.1.1	Discontinuities	1138
15.10.2	Inspection	1139
15.10.2.1	Visual Examination	1139
15.10.2.2	Leak Testing	1139
15.10.3	Brazing Codes and Standards	1139
15.11	Soldering of Heat Exchangers	1139
15.11.1	Elements of Soldering	1139
15.11.1.1	Joint Design	1140
15.11.1.2	Tube Joints	1140
15.11.1.3	Tube-to-Header Solder Joints	1140
15.11.1.4	Solders	1140
15.11.1.5	Cleaning and Descaling	1141
15.11.1.6	Soldering Fluxes	1141
15.11.1.7	Soldering Processes	1141
15.11.1.8	Flux Residue Removal	1142
15.11.2	Ultrasonic Soldering of Aluminum Heat Exchangers	1142
15.11.2.1	Material That Can Be Ultrasonically Soldered	1143
15.11.2.2	Basic Processes for Soldering All-Aluminum Coils	1143
15.11.3	Quality Control, Inspection, and Testing	1146
15.11.4	Nondestructive Testing	1146
15.11.4.1	Visual Inspection	1146
15.11.4.2	Discontinuities	1146
15.11.4.3	Removal of Residual Flux	1146
15.11.4.4	Pressure and Leak Testing	1147
15.11.4.5	Destructive Testing	1147

15.12	Corrosion of Brazed and Soldered Joints	1147
15.12.1	Factors Affecting Corrosion of Brazed Joints.....	1147
15.12.2	Corrosion of the Aluminum Brazed Joint.....	1147
15.12.2.1	Galvanic Corrosion Resistance.....	1147
15.12.2.2	Influence of Brazing Process	1148
15.12.3	Corrosion of Soldered Joints	1149
15.12.3.1	Solder Bloom Corrosion.....	1149
15.12.3.2	Manufacturing Procedures to Control Solder Bloom Corrosion	1149
15.13	Evaluation of Design and Materials of Automotive Radiators.....	1149
15.13.1	Mechanical Durability Tests	1150
15.13.2	Tests for Corrosion Resistance	1150
15.13.2.1	External Corrosion Tests.....	1150
15.13.2.2	Internal Corrosion Tests	1150
15.14	CuproBraz Heat Exchanger	1151
15.14.1	Round Tube versus Flat Tube	1151
15.14.1.1	Tube Fabrication.....	1151
15.14.1.2	High-Performance Coatings	1151
15.A	Appendix	1151
	References	1162
	Suggested Reading	1165

Chapter 16	Heat Exchanger Installation, Operation, and Maintenance	1167
16.1	Storage.....	1168
16.2	Installation.....	1168
16.3	Operation	1168
16.4	Maintenance	1169
16.5	Periodical Inspection of Unit.....	1169
16.6	Indications of Fouling.....	1169
16.7	Deterioration of Heat Exchanger Performance	1170
16.7.1	Air-Cooled Heat Exchangers.....	1170
16.7.1.1	Determine the Original Design Performance Data of the ACHE.....	1170
16.7.1.2	Inspect the Heat Exchanger Unit	1170
16.7.1.3	Determine the Current ACHE Performance and Set Baseline.....	1170
16.7.1.4	Install Upgrades.....	1170
16.7.1.5	Tube Bundle	1171
16.7.2	Shell and Tube Heat Exchanger.....	1171
16.7.2.1	Quality Auditing of Existing Heat Exchanger.....	1171
16.7.2.2	Leak Detection: Weep-Hole Inspection	1171
16.7.2.3	Tube Bundle Removal and Handling.....	1172
16.7.3	Brazed Aluminum Plate-Fin Heat Exchanger.....	1181
16.7.3.1	Leak Detection.....	1181
16.7.3.2	Repair of Leaks	1181
16.8	NDT Methods to Inspect and Assess the Condition of Heat Exchanger and Pressure Vessel Components	1182
16.8.1	Ultrasonic Internal Rotary Inspection System.....	1182
16.8.2	Remote Field Eddy Current Testing.....	1182

16.8.3	Eddy Current Testing	1182
16.8.4	Tubes	1183
16.9	Residual Life Assessment of Heat Exchangers by NDT Techniques	1183
16.9.1	Creep Waves	1184
16.9.2	Ultrasonic Method Based on Backscatter and Velocity Ratio Measurement	1184
16.9.3	Pulsed Eddy Currents.....	1184
16.9.4	Flash Radiography.....	1184
16.9.5	Low-Frequency Electromagnetic Test.....	1184
16.9.6	Photon-Induced Positron Annihilation and Distributed Source Positron Annihilation	1185
	16.9.6.1 Replication Techniques.....	1185
	16.9.6.2 Creep Determinations by Nondestructive Testing Method	1185
16.10	Pressure Vessel Failure.....	1185
	16.10.1 Failure Modes.....	1185
16.11	Professional Service Providers for Heat Exchangers	1185
	References	1186

Preface

INTRODUCTION

The advances in heat exchanger technology since the publication of the first edition and the topics that had been missed have necessitated a second edition of this book. This edition showcases recent advances in the selection, design, construction, operation, and maintenance of heat exchangers. The errors in the previous edition have been corrected, and the quality of figures including thermal effectiveness charts has been improved. This book provides up-to-date information on the single-phase heat transfer problems encountered by engineers in their daily work. It will continue to be a centerpiece of information for practicing engineers, research engineers, academicians, designers, and manufacturers involved in heat exchange between two or more fluids. Permission was sought from leading heat exchanger manufacturers and research organizations to include figures of practical importance, and these have been added in this edition. Care has been taken to minimize errors.

COVERAGE

In the chapter on the classification of heat exchangers, topics such as scrapped surface heat exchanger, graphite heat exchanger, coil wound heat exchanger, microscale heat exchanger, and printed circuit heat exchanger have been included. The construction and performance features of various types of heat exchangers have been compared.

Concepts like ALEX core for PFHE, radial flow heat exchanger for waste heat recovery, and rotary regenerator for HVAC applications have been added. Breach-Lock™ and Taper-Lok™ end closures have also been included.

Construction details and performance features of nonsegmental baffles heat exchangers such as EMbaffle®, Helixchanger®, and Twisted Tube® heat exchangers have been added. Design features of feedwater heater, steam surface condenser, and tantalum heat exchanger for pharmaceutical applications have also been included.

Information on pressure vessel codes, manufacturer's association standards, and ASME codes has been updated. ALPEMA standards for PFHE have been dealt with in depth.

Performance features of coil wound heat exchangers have been compared with brazed aluminum heat exchangers. The construction, selection, design, and concepts of manufacture of ACHE have been updated.

Recent advances in PHE concepts such as all welded, shell type, wide gap, free flow, semi-welded, and double-wall have been discussed and their construction and performance features compared.

The chapter on heat transfer augmentation has been thoroughly revised. Underlying the principle of heat transfer enhancement, devices such as hiTRAN thermal system and wire matrix turbulators have been described.

Fouling control concepts, such as back flushing, heat exchangers, such as self-cleaning, and liquid fluidized bed technology, fluidized bed units, and fouling control devices, such as Spirelf®, Fixotal®, and Turbotal®, have been added.

A new chapter on heat exchanger installation, operation, and maintenance covers the commissioning of new units, operation, their maintenance, repair practices, tube bundle removal, handling and cleaning, leak testing and plugging of tubes, condition monitoring, quality audit, and residual life assessment by NDT methods.

The tubesheet design procedure as per the latest ASME code, CODAP, PD 5000, and UPV has been discussed and compared with TEMA standards. The software program structure for design

of ACHE and STHE has been updated. Recent trends in NDT methods such as ECT, UT, and leak testing have been included.

The chapter on fabrication of heat exchangers has now been revised, covering the recent advances in tube expansion and tube-to-tubesheet welding practices, rolling equipment, accessories, adequacy of rolling, cold working principle, configuration of tube-to-tubesheet joints for welding, modern equipment for tube hole preparation, and internal bore welding tubes. The section on heat exchanger heads has now been updated by incorporating various hot/cold working methods, and manufacturing procedures and PWHT have been discussed. New topics like CAB brazing of compact heat exchanger, cupro-braze radiators, and flat tube versus round tube concept for radiator tubings have also been added.

Due to their content and coverage, chapters 2, 5, 13 and 15 can be treated as individually self-contained units, as they do not require other chapters to be understood. This edition is abundantly illustrated with over 600 drawings, diagrams, photos, and tables. The *Heat Exchanger Design Handbook*, Second Edition is an excellent resource for mechanical, chemical, and petrochemical engineers; process equipment and pressure vessel designers, consultants, and heat exchanger manufacturers; and upper-level undergraduate and graduate students in these disciplines.

Acknowledgments

A large number of my colleagues from Indian Railways, well-wishers, and family members had contributed immensely toward the preparation of the book. Though I could not acknowledge them individually in the first edition, I mention a few of them here, as follows: Jothimani Gunasekaran, V. R. Ventakaraman, P. Subramani, Rajasri Anandan, and P. Gajapathy of ICF; Amitab Chakraborty (ADG), O. P. Agarwal (ED), M. Vijayakumar (Director), R. S. Madhukar, Suresh Prakash, Ashok Krishan, P. A. Rehman, and V. P. Gupta of RDSO, Lucknow; S. Bangaru Lakshman (then MOSR) and S. Dasarathy (then member mechanical, Railway Board, Ministry of Railways); Lilly Ravi, Renuka Devi Balasubramanian, Sukanya Balakrishnan, Sardha Balasubramaniam, and T. Adikesavan of Southern Railway; Amarnath, GM (retd.), and Radhey Shyam, GM, CLW; Cittaranjan, Ministry of Railways; Shanka Sinha of CLW; K. Kamaraj of IIT-Madras Library; M. Krishnasamy, Member of Parliament; my sisters, Anjala Manoharan, Maya Pannerselvam, and Indira Mari; my family members, Dr. K. Kalai (alias Vasanth), Dr. K. Kumudhini, and Er. K. Praveen; and Arunkumar Aranganathan, project manager, and Anithajohny Mariasusai, assistant director at SPi Global, Puducherry, India, who oversaw the production of the second edition on behalf of Taylor & Francis Group. I have immensely benefited from the contributions of scholars such as Dr. K. P. Singh, Dr. J. P. Gupta, and Dr. Ramesh K. Shah, the Donald Q. Kern awardee for the year 2005 by the American Society of Mechanical Engineers and the American Institute of Chemical Engineers. I also acknowledge the computer facilities of the Engine Development Directorate of RDSO, Lucknow, Ministry of Railways, and the library facilities of IIT-M, IIT-K, IIT-D, and RDSO, Lucknow. A large number of heat exchanger manufacturers and research organizations had spared photos and figures, and their names are acknowledged in the respective figure captions.

Author

Thulukkanam Kuppan, Indian Railway Service of Mechanical Engineers (IRSME), Ministry of Railways, is the chief mechanical engineer (senior administrative grade) in a rolling stock production unit. He has authored an article in the *ASME Journal of Pressure Vessel Technology*. His various roles have included being an experienced administrator, staff recruitment board chairman for a zonal railway, and joint director of the Engine Development Directorate of RDSO, Lucknow. He was also involved in design and performance evaluation of various types of heat exchangers used in diesel electric locomotives and has served as chief workshop engineer for the production of rolling stocks and as Director of Public Grievances (DPG) to the Minister of State for Railways, Railway Board, Government of India. Kuppan received his BE (hons) in 1980 from the PSG College of Technology, Coimbatore, Madras University, and his MTech in production engineering in 1982 from the Indian Institute of Technology, Madras, India.

1 Heat Exchangers

Introduction, Classification, and Selection

1.1 INTRODUCTION

A heat exchanger is a heat transfer device that is used for transfer of internal thermal energy between two or more fluids available at different temperatures. In most heat exchangers, the fluids are separated by a heat transfer surface, and ideally they do not mix. Heat exchangers are used in the process, power, petroleum, transportation, air-conditioning, refrigeration, cryogenic, heat recovery, alternate fuels, and other industries. Common examples of heat exchangers familiar to us in day-to-day use are automobile radiators, condensers, evaporators, air preheaters, and oil coolers. Heat exchangers can be classified into many different ways.

1.2 CONSTRUCTION OF HEAT EXCHANGERS

A heat exchanger consists of heat-exchanging elements such as a core or matrix containing the heat transfer surface, and fluid distribution elements such as headers or tanks, inlet and outlet nozzles or pipes, etc. Usually, there are no moving parts in the heat exchanger; however, there are exceptions, such as a rotary regenerator in which the matrix is driven to rotate at some design speed and a scraped surface heat exchanger in which a rotary element with scraper blades continuously rotates inside the heat transfer tube. The heat transfer surface is in direct contact with fluids through which heat is transferred by conduction. The portion of the surface that separates the fluids is referred to as the primary or direct contact surface. To increase heat transfer area, secondary surfaces known as fins may be attached to the primary surface. Figure 1.1 shows a collection of few types of heat exchangers.

1.3 CLASSIFICATION OF HEAT EXCHANGERS

In general, industrial heat exchangers have been classified according to (1) construction, (2) transfer processes, (3) degrees of surface compactness, (4) flow arrangements, (5) pass arrangements, (6) phase of the process fluids, and (7) heat transfer mechanisms. These classifications are briefly discussed here. For more details on heat exchanger classification and construction, refer to Shah [1,2], Gupta [3], and Graham Walker [4]. For classification and systematic procedure for selection of heat exchangers, refer to Larowski et al. [5a,5b]. Table 1.1 shows some types of heat exchangers, their construction details, and performance parameters.

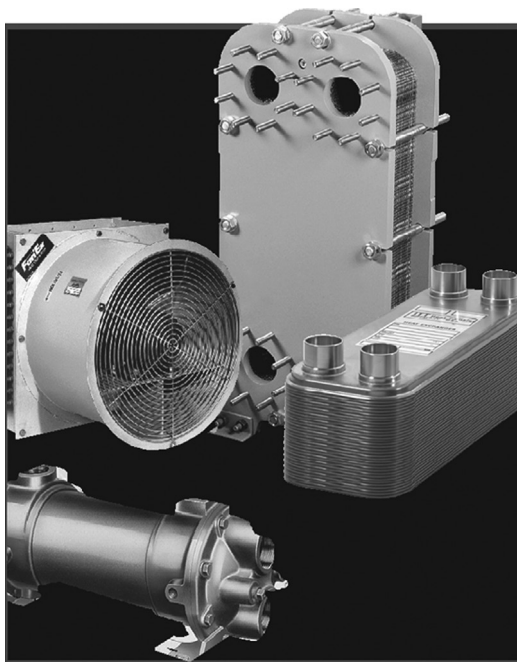


FIGURE 1.1 Collection of few types of heat exchangers. (Courtesy of ITT STANDARD, Cheektowaga, NY.)

1.3.1 CLASSIFICATION ACCORDING TO CONSTRUCTION

According to constructional details, heat exchangers are classified as [1] follows:

Tubular heat exchangers—double pipe, shell and tube, coiled tube

Plate heat exchangers (PHEs)—gasketed, brazed, welded, spiral, panel coil, lamella

Extended surface heat exchangers—tube-fin, plate-fin

Regenerators—fixed matrix, rotary matrix

1.3.1.1 Tubular Heat Exchanger

1.3.1.1.1 Double-Pipe Exchangers

A double-pipe heat exchanger has two concentric pipes, usually in the form of a U-bend design. Double-pipe heat exchangers with U-bend design are known as hairpin heat exchangers. The flow arrangement is pure countercurrent. A number of double-pipe heat exchangers can be connected in series or parallel as necessary. Their usual application is for small duties requiring, typically, less than 300 ft² and they are suitable for high pressures and temperatures and thermally long duties [5]. This has the advantage of flexibility since units can be added or removed as required, and the design is easy to service and requires low inventory of spares because of its standardization. Either longitudinal fins or circumferential fins within the annulus on the inner pipe wall are required to enhance the heat transfer from the inner pipe fluid to the annulus fluid. Design pressures and temperatures are broadly similar to shell and tube heat exchangers (STHEs). The design is straightforward and is carried out using the method of Kern [6] or proprietary programs. The Koch Heat Transfer Company LP, USA, is the pioneer in the design of hairpin heat exchangers. Figures 1.2 through 1.4 show double-pipe heat exchangers.

1.3.1.1.1.1 Application When the process calls for a temperature cross (when the hot fluid outlet temperature is below the cold fluid outlet temperature), a hairpin heat exchanger is the most efficient design and will result in fewer sections and less surface area. Also, they are commonly used for high-fouling services such as slurries and for smaller heat duties. Multitube heat

TABLE 1.1
Heat Exchanger Types: Construction and Performance Features

Type of Heat Exchanger	Constructional Features	Performance Features
Double pipe(hair pin) heat exchanger	A double pipe heat exchanger has two concentric pipes, usually in the form of a U-bend design. U-bend design is known as hairpin heat exchangers. The flow arrangement is pure countercurrent. The surface area ranges from 300 to 6000 ft ² (finned tubes). Pressure capabilities are full vacuum to over 14,000 psi (limited by size, material, and design condition) and temperature from –100°C to 600°C (–150°F to 1100°F).	Applicable services: The process results in a temperature cross, high-pressure stream on tubeside, a low allowable pressure drop is required on one side, when the exchanger is subject to thermal shocks, when flow-induced vibration may be a problem.
Shell and tube heat exchanger (STHE)	The most commonly used heat exchanger. It is the “workhorse” of industrial process heat transfer. They are used as oil cooler, surface condenser, feed water heater, etc. The major components of a shell and tube exchanger are tubes, baffles, shell, front head, rear head, and nozzles. Shell diameter: 60 up to 2000 mm. Operating temperature: –20°C up to 500°C. Operating pressure max. 600 bar.	Advantages: Extremely flexible and robust design, easy to maintain and repair. Disadvantages 1. Require large site (footprint) area for installation and often need extra space to remove the bundle. 2. Construction is heavy. 3. PHE may be cheaper for pressure below 16 bar (230 psi) and temperature below 200°C (392°F).
Coiled tube heat exchanger (CTHE)	Construction of these heat exchangers involves winding a large number of small-bore ductile tubes in helix fashion around a central core tube, with each exchanger containing many layers of tubes along both the principal and radial axes. Different fluids may be passed in counterflow to the single shellside fluid.	Advantages, especially when dealing with low-temperature applications where simultaneous heat transfer between more than two streams is desired. Because of small bore tubes on both sides, CTHEs do not permit mechanical cleaning and therefore are used to handle clean, solid-free fluids or fluids whose fouling deposits can be cleaned by chemicals. Materials are usually aluminum alloys for cryogenics, and stainless steels for high-temperature applications.
Finned-tube heat exchanger	Construction 1. Normal fins on individual tubes referred to as individually finned tubes. 2. Longitudinal fins on individual tubes, which are generally used in condensing applications and for viscous fluids in double-pipe heat exchangers. 3. Flat or continuous (plain, wavy, or interrupted) external fins on an array of tubes (either circular or flat tube). 4. The tube layout pattern is mostly staggered.	Merits: small inventory, low weight, easier transport, less foundation, better temperature control Applications Condensers and evaporators of air conditioners, radiators for internal combustion engines, charge air coolers and intercoolers for cooling supercharged engine intake air of diesel engines, etc.

(continued)

TABLE 1.1 (continued)
Heat Exchanger Types: Construction and Performance Features

Type of Heat Exchanger	Constructional Features	Performance Features
Air cooled heat exchanger (ACHE)	<p>Construction</p> <ol style="list-style-type: none"> 1. Individually finned tube bundle. The tube bundle consists of a series of finned tubes set between side frames, passing between header boxes at either end. 2. An air-pumping device (such as an axial flow fan or blower) across the tube bundle which may be either forced draft or induced draft. 3. A support structure high enough to allow air to enter beneath the ACHE. 	<p>Merits: Design of ACHE is simpler compared to STHE, since the airside pressure and temperature pertain to ambient conditions. Tubeside design is same as STHE. Maintenance cost is normally less than that for water-cooled systems. The fouling on the air side can be cleaned easily.</p> <p>Disadvantages of ACHEs</p> <p>ACHEs require large heat transfer surfaces because of the low heat transfer coefficient on the air side and the low specific heat of air. Noise is a factor with ACHEs.</p>
Plate-fin heat exchanger (PFHE)	<p>Plate fin heat exchangers (PFHEs) are a form of compact heat exchanger consisting of a stack of alternate flat plates called “parting sheets” and fin corrugations, brazed together as a block. Different fins (such as the plain triangular, louver, perforated, or wavy fin) can be used between plates for different applications.</p> <p>Plate-fin surfaces are commonly used in gas-to-gas exchanger applications. They offer high area densities (up to about 6000 m²/m³ or 1800 ft²/ft³).</p> <p>Designed for low-pressure applications, with operating pressures limited to about 1000 kPa g (150 psig) and operating temperature from cryogenic to 150°C (all-aluminum PFHE) and about 700°C–800°C (1300°F–1500°F) (made of heat-resistant alloys).</p>	<ol style="list-style-type: none"> 1. PFHE offers superior in thermal performance compared to extended surface heat exchangers. 2. PFHE can achieve temperature approaches as low as 1°C between single-phase streams and 3°C between multiphase streams. 3. With their high surface compactness, ability to handle multiple streams, and with aluminum’s highly desirable low-temperature properties, brazed aluminum plate fins are an obvious choice for cryogenic applications. 4. Very high thermal effectiveness can be achieved; for cryogenic applications, effectiveness of the order of 95% and above is common. <p>Limitations:</p> <ol style="list-style-type: none"> 1. Narrow passages in plate-fin exchangers make them susceptible for fouling and they cannot be cleaned by mechanical means. This limits their use to clean applications like handling air, light hydrocarbons, and refrigerants.
Regenerator	<p>The heat exchanger used to preheat combustion air is called either a recuperator or a regenerator. A recuperator is a convective heat transfer type heat exchanger like tubular, plate-fin and extended surface heat exchangers. The regenerator is classified as (1) fixed matrix or fixed bed and (2) rotary regenerators. The matrix is alternatively heated by hot fluid and cooled by the cold fluid. Features:</p> <ol style="list-style-type: none"> 1. A more compact size ($\beta = 8800 \text{ m}^2/\text{m}^3$ for rotating type and $1600 \text{ m}^2/\text{m}^3$ for fixed matrix type). 2. Application to both high temperatures (800°C–1100°C) for metal matrix, and 2000°C for ceramic regenerators for services like gas turbine applications, melting furnaces or steam power plant heat recovery, and low-temperature applications like space heating (HVAC). 	<p>Usage</p> <ol style="list-style-type: none"> 1. Reheating process feedstock. 2. Waste heat boiler and feed water heating for generating steam (low-temperature recovery system). 3. Air preheater—preheating the combustion air (high temperature heat recovery system). 4. Space heating—rotary heat exchanger (wheel) is mainly used in building ventilation or in the air supply/discharge system of air conditioning equipment.

TABLE 1.1 (continued)
Heat Exchanger Types: Construction and Performance Features

Type of Heat Exchanger	Constructional Features	Performance Features														
	<p>3. Operating pressure of 5–7 bar for gas turbine applications and low pressure of 1–1.5 bar for air dehumidifier and waste heat recovery applications.</p> <p>4. The absence of a separate flow path like tubes or plate walls but the presence of seals to separate the gas stream in order to avoid mixing due to pressure differential.</p>															
Plate heat exchanger (PHE)	<p>A plate heat exchanger is usually comprised of a stack of corrugated or embossed metal plates in mutual contact, each plate having four apertures serving as inlet and outlet ports, and seals designed so as to direct the fluids in alternate flow passages.</p> <p>Standard performance limits</p> <table><tr><td>Maximum operating pressure</td><td>25 bar (360 psi)</td></tr><tr><td>Maximum temperature</td><td>160°C (320°F)</td></tr><tr><td>With special gaskets</td><td>200°C (390°F)</td></tr><tr><td>Maximum flow rate</td><td>3600 m³/h (950,000 USG/min)</td></tr><tr><td>Temperature approach</td><td>As low as 1°C</td></tr><tr><td>Heat recovery</td><td>As high as 93%</td></tr><tr><td>Heat transfer coefficient (water–water duties with normal fouling resistance)</td><td>3000–7000 W/m².°C</td></tr></table> <p>Other varieties include, brazed plate heat exchanger (BPHE), shell and plate heat exchanger, welded plate heat exchanger, wide-gap plate heat exchanger, free-flow plate heat exchanger, semi-welded or twin-plate heat exchanger, double-wall plate heat exchanger, biabon F graphite plate heat exchanger, etc.</p>	Maximum operating pressure	25 bar (360 psi)	Maximum temperature	160°C (320°F)	With special gaskets	200°C (390°F)	Maximum flow rate	3600 m ³ /h (950,000 USG/min)	Temperature approach	As low as 1°C	Heat recovery	As high as 93%	Heat transfer coefficient (water–water duties with normal fouling resistance)	3000–7000 W/m ² .°C	<p>Merits: True counterflow, high turbulence and high heat transfer performance. Close approach temperature.</p> <p>Reduced fouling: Cross-contamination eliminated. Multiple duties with a single unit. Expandable. Easy to inspect and clean, and less maintenance. Low liquid volume and quick process control.</p> <p>Lower cost.</p> <p>Disadvantages</p> <ol style="list-style-type: none">1. The maximum operating temperature and pressure are limited by gasket materials. The gaskets cannot handle corrosive or aggressive media.2. Gasketed plate heat exchangers cannot handle particulates that are larger than 0.5 mm.3. Gaskets always increase the leakage risk.
Maximum operating pressure	25 bar (360 psi)															
Maximum temperature	160°C (320°F)															
With special gaskets	200°C (390°F)															
Maximum flow rate	3600 m ³ /h (950,000 USG/min)															
Temperature approach	As low as 1°C															
Heat recovery	As high as 93%															
Heat transfer coefficient (water–water duties with normal fouling resistance)	3000–7000 W/m ² .°C															
Spiral plate heat exchanger (SPHE)	<p>SPHE is fabricated by rolling a pair of relatively long strips of plate to form a pair of spiral passages. Channel spacing is maintained uniformly along the length of the spiral passages by means of spacer studs welded to the plate strips prior to rolling.</p>	<p>Advantages: To handle slurries and liquids with suspended fibers, and mineral ore treatment where the solid content is up to 50%. The SPHE is the first choice for extremely high viscosities, say up to 500,000 cp, especially in cooling duties.</p> <p>Applications: SPHEs are finding applications in reboiling, condensing, heating or cooling of viscous fluids, slurries, and sludge.</p>														
Printed circuit heat exchangers (PCHes)	<p>HEATRIC printed circuit heat exchangers consist of diffusion-bonded heat exchanger core that are constructed from flat metal plates into which fluid flow channels are either chemically etched or pressed. They can withstand pressure of 600 bar (9000 psi) with extreme temperatures, ranging from cryogenic to 700°C (1650°F).</p>	<p>Merits: fluid flow can be parallelflow, counterflow, crossflow, or a combination of these to suit the process requirements. Thermal effectiveness is of the order of 98% in a single unit. They can incorporate more than two process streams into a single unit.</p>														

(continued)

TABLE 1.1 (continued)**Heat Exchanger Types: Construction and Performance Features**

Type of Heat Exchanger	Constructional Features	Performance Features
Lamella heat exchanger (LHE)	A lamella heat exchanger normally consists of a cylindrical shell surrounding a number of heat transferring lamellas. The design can be compared to a tube heat exchanger but with the circular tubes replaced by thin and wide channels, lamellas. The lamella heat exchanger works with the media in full counter current flow. The absence of baffle plates minimizes the pressure drop and makes handling of most media possible.	Merits: Since the lamella bundle can be easily dismantled from the shell, inspection and cleaning is easy. Applications Cooking fluid heating in pulp mills. Liquor preheaters. Coolers and condensers of flue gas. Oil coolers.
Heat pipe heat exchanger	The heat-pipe heat exchanger used for gas–gas heat recovery is essentially bundle of finned tubes assembled like a conventional air-cooled heat exchanger. The heat pipe consists of three elements: (1) a working fluid inside the tubes, (2) a wick lining inside the wall, and (3) vacuum sealed finned tube. The heat-pipe heat exchanger consists of an evaporative section through which the hot exhaust gas flows and a condensation section through which the cold air flows. These two sections are separated by a separating wall.	Application: The heat pipes are used for (i) heat recovery from process fluid to preheating of air for space heating, (ii) HVAC application-waste heat recovery from the exhaust air to heat the incoming process air It virtually does not need mechanical maintenance, as there are no moving parts. The heat pipe heat recovery systems are capable of operating at a temperature of 300°C–315°C with 60%–80% heat recovery capability.
Plate coil heat exchanger (PCHE)	Fabricated from two metal sheets, one or both of which are embossed. When welded together, the embossings form a series of well-defined passages through which the heat transfer media flows.	A variety of standard PLATECOIL® fabrications, such as pipe coil, half pipe, jacketed tanks and vessels, clamp-on upgrades, immersion heaters and coolers, heat recovery banks, storage tank heaters, etc., are available. Easy access to panels and robust cleaning surfaces reduce maintenance burdens.
Scraped surface heat exchanger	Scraped surface heat exchangers are essentially double pipe construction with the process fluid in the inner pipe and the cooling (water) or heating medium (steam) in the annulus. A rotating element is contained within the tube and is equipped with spring-loaded blades. In operation the rotating shaft scraper blades continuously scrape product film from the heat transfer tube wall, thereby enhancing heat transfer and agitating the product to produce a homogenous mixture.	Scraped surface heat exchangers are used for processes likely to result in the substantial deposition of suspended solids on the heat transfer surface. Scraped surface heat exchangers can be employed in the continuous, closed processing of virtually any pumpable fluid or slurry involving cooking, slush freezing, cooling, crystallizing, mixing, plasticizing, gelling, polymerizing, heating, aseptic processing, etc. Use of a scraped surface exchanger prevents the accumulation of significant buildup of solid deposits.

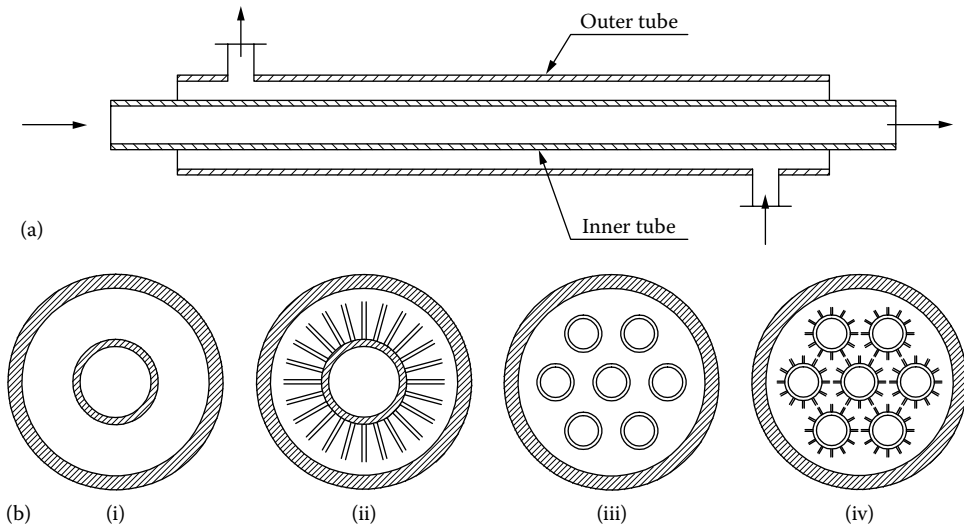


FIGURE 1.2 Double pipe/twin pipe hairpin heat exchanger. (a) Schematic of the unit, (b): (i) double pipe with bare internal tube, (ii) double pipe with finned internal tube, (iii) double pipe with multibare internal tubes, and (iv) double pipe with multifinned internal tubes. (Courtesy of Peerless Mfg. Co., Dallas, TX, Makers of Alco and Bos-Hatten brands of heat exchangers.)

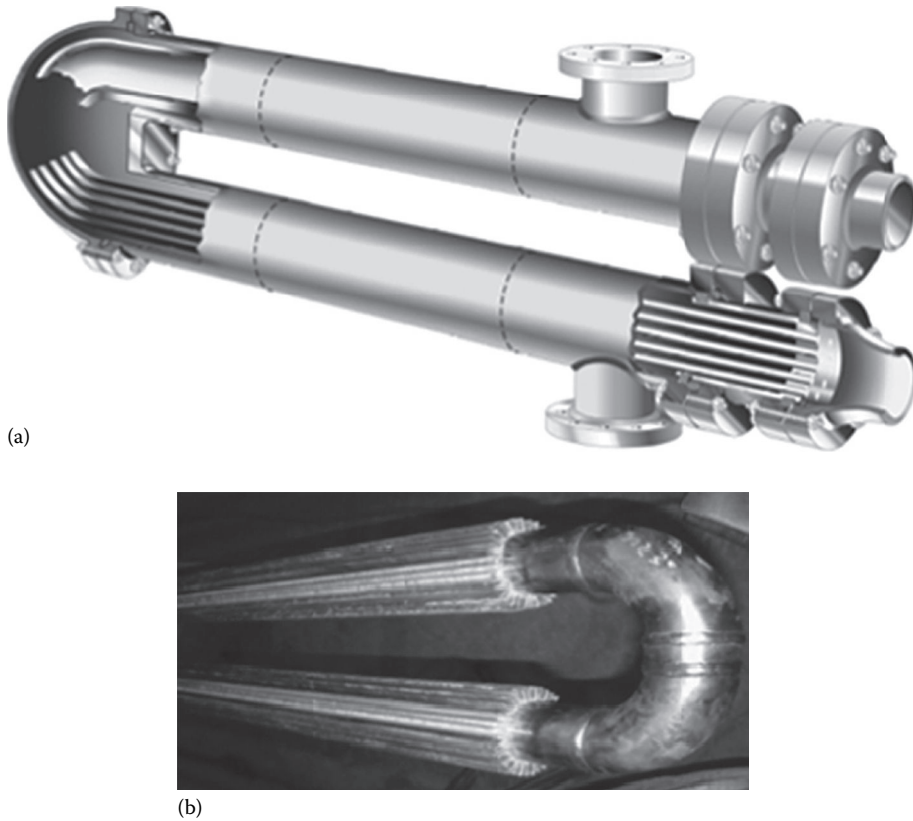


FIGURE 1.3 Double pipe/hairpin heat exchanger. (a) 3-D view and (b) tube bundle with longitudinal fins. (Courtesy of Peerless Mfg. Co., Dallas, TX, Makers of Alco and Bos-Hatten brands of heat exchangers.)

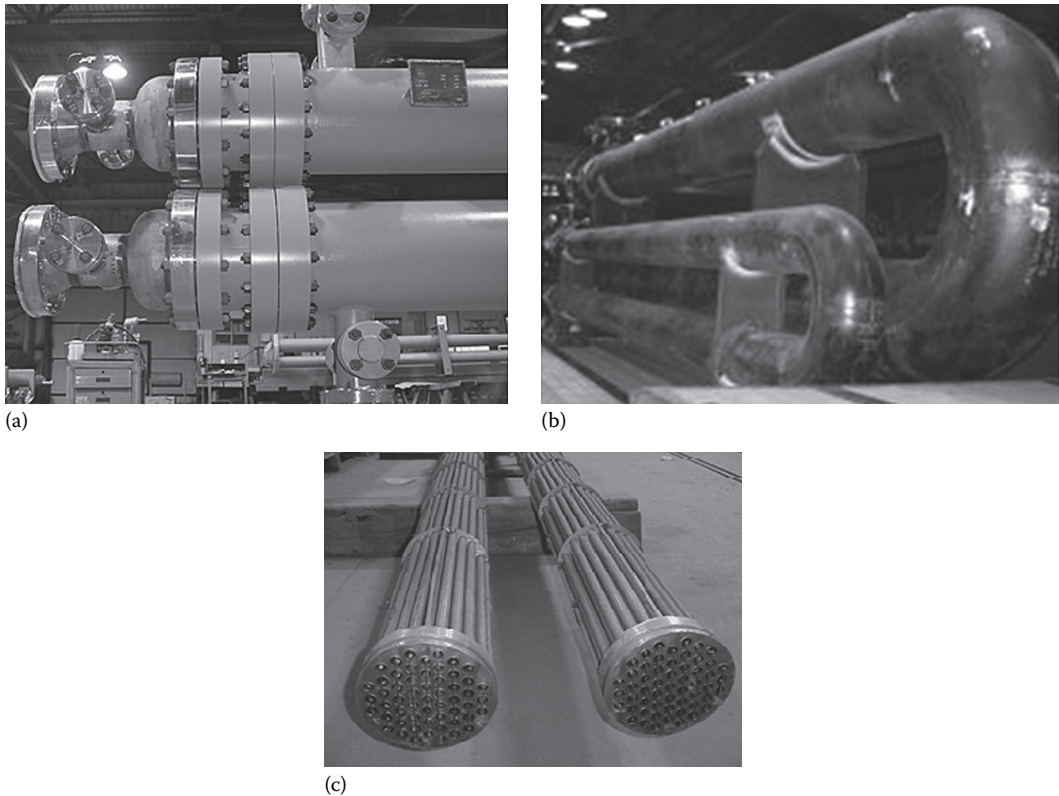


FIGURE 1.4 Hairpin heat exchanger. (a) Separated head closure using separate bolting on shellside and tube-side and (b) Hairpin exchangers for high-pressure and high-temperature applications and (c) multitubes (bare) bundle. (Photo courtesy of Heat Exchanger Design, Inc., Indianapolis, IN.)

exchangers are used for larger heat duties. A hairpin heat exchanger should be considered when one or more of the following conditions exist:

- The process results in a temperature cross
- High pressure on tubeside application
- A low allowable pressure drop is required on one side
- When an augmentation device to enhance the heat transfer coefficient is desired
- When the exchanger is subject to thermal shocks
- When flow-induced vibration may be a problem
- When solid particulates or slurries are present in the process stream

1.3.1.1.2 Shell and Tube Heat Exchanger

In process industries, shell and tube heat exchangers are used in great numbers, far more than any other type of exchanger. More than 90% of heat exchangers used in industry are of the shell and tube type [7]. STHes are the “workhorses” of industrial process heat transfer [8]. They are the first choice because of well-established procedures for design and manufacture from a wide variety of materials, many years of satisfactory service, and availability of codes and standards for design and fabrication. They are produced in the widest variety of sizes and styles. There is virtually no limit on the operating temperature and pressure. Figure 1.5 shows STHes.

1.3.1.1.3 Coiled Tube Heat Exchanger

Construction of these heat exchangers involves winding a large number of small-bore ductile tubes in helix fashion around a central core tube, with each exchanger containing many layers of tubes

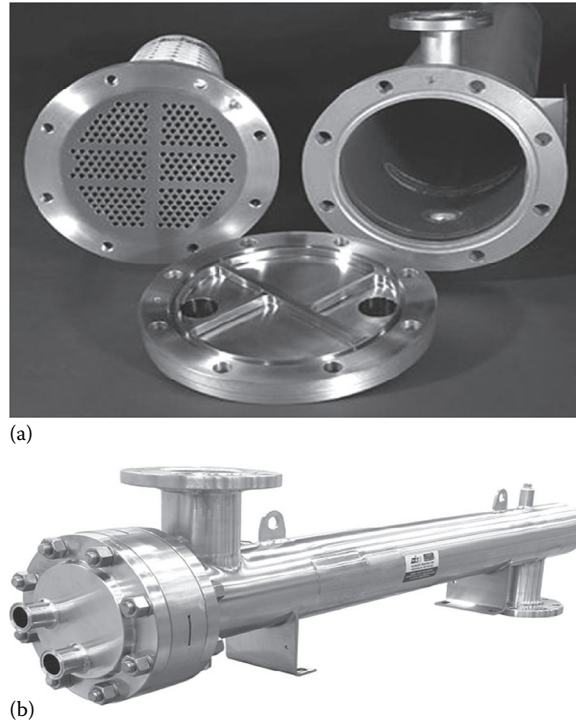


FIGURE 1.5 Shell and tube heat exchanger. (a) Components and (b) heat exchanger. (Courtesy of Allegheny Bradford Corporation, Bradford, PA.)

along both the principal and radial axes. The tubes in individual layers or groups of layers may be brought together into one or more tube plates through which different fluids may be passed in counterflow to the single shellside fluid. The construction details have been explained in Refs. [5,9]. The high-pressure stream flows through the small-diameter tubes, while the low-pressure return stream flows across outside of the small-diameter tubes in the annular space between the inner central core tube and the outer shell. Pressure drops in the coiled tubes are equalized for each high-pressure stream by using tubes of equal length and varying the spacing of these in the different layers. Because of small-bore tubes on both sides, CTHEs do not permit mechanical cleaning and therefore are used to handle clean, solid-free fluids or fluids whose fouling deposits can be cleaned by chemicals. The materials used are usually aluminum alloys for cryogenics and stainless steel for high-temperature applications.

CTHE offers unique advantages, especially when dealing with low-temperature applications for the following cases [9]:

- Simultaneous heat transfer between more than two streams is desired. One of the three classical heat exchangers used today for large-scale liquefaction systems is CTHE.
- A large number of heat transfer units are required.
- High-operating pressures are involved.

CTHE is not cheap because of the material costs, high labor input in winding the tubes, and the central mandrel, which is not useful for heat transfer but increases the shell diameter [5].

1.3.1.1.3.1 Linde Coil-Wound Heat Exchangers Linde coil-wound heat exchangers are compact and reliable with a broad temperature and pressure range and suitable for both single- and two-phase streams. Multiple streams can be accommodated in one exchanger. They are known for their

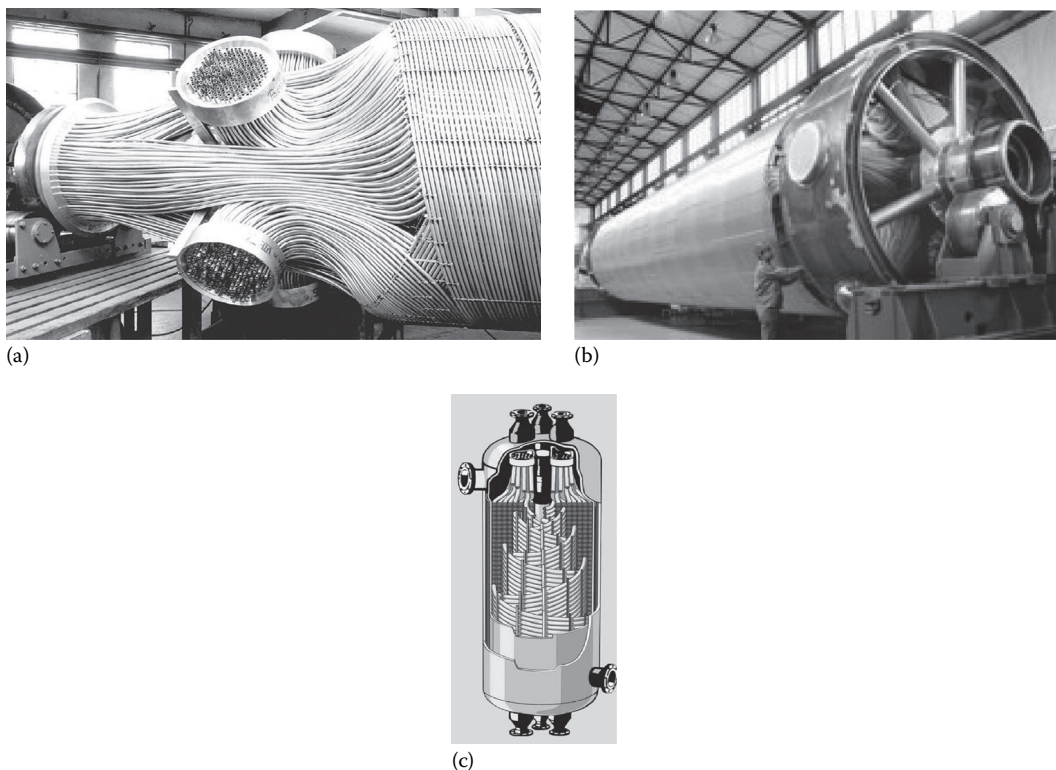


FIGURE 1.6 Coiled tube heat exchanger. (a) End section of a tube bundle, (b) tube bundle under fabrication, and (c) construction details. (From Linde AG, Engineering Division. With permission.)

robustness in particularly during start-up and shut-down or plant-trip conditions. Both the brazed aluminum PFHEs and CTHEs find application in liquefaction processes. A comparison of salient features of these two types of heat exchangers is shown in Chapter 4. Figure 1.6 shows Linde coil-wound heat exchangers.

Glass coil heat exchangers: Two basic types of glass coil heat exchangers are (i) coil type and (ii) STHE with glass or MS shells in combination with glass tube as standard material for tube. Glass coil exchangers have a coil fused to the shell to make a one-piece unit. This prohibits leakage between the coil and shellside fluids [10]. The reduced heat transfer coefficient of boro silicate glass equipment compares favorably with many alternate tube materials. This is due to the smooth surface of the glass that improves the film coefficient and reduces the tendency for fouling. More details on glass heat exchangers are furnished in Chapter 13.

1.3.1.2 Plate Heat Exchangers

PHEs are less widely used than tubular heat exchangers but offer certain important advantages. PHEs can be classified into three principal groups:

1. Plate and frame or gasketed PHEs used as an alternative to tube and shell exchangers for low- and medium-pressure liquid–liquid heat transfer applications
2. Spiral heat exchanger used as an alternative to shell and tube exchangers where low maintenance is required, particularly with fluids tending to sludge or containing slurries or solids in suspension
3. Panel heat exchangers made from embossed plates to form a conduit or coil for liquids coupled with fins

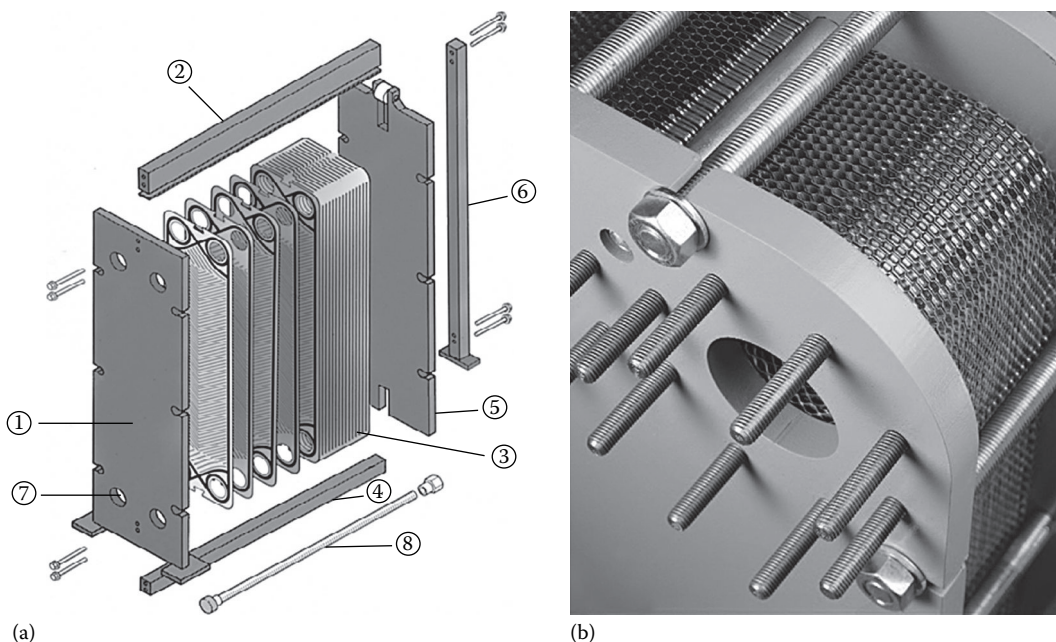


FIGURE 1.7 Plate heat exchanger. (a) Construction details—schematic (Parts details: 1, Fixed frame plate; 2, Top carrying bar; 3, Plate pack; 4, Bottom carrying bar; 5, Movable pressure plate; 6, Support column; 7, Fluids port; and 8, Tightening bolts.) and (b) closer view of assembled plates. (Courtesy of ITT STANDARD, Cheektowaga, NY.)

1.3.1.2.1 Plate and Frame or Gasketed Plate Heat Exchangers

A PHE essentially consists of a number of corrugated metal plates in mutual contact, each plate having four apertures serving as inlet and outlet ports, and seals designed to direct the fluids in alternate flow passages. The plates are clamped together in a frame that includes connections for the fluids. Since each plate is generally provided with peripheral gaskets to provide sealing arrangements, PHEs are called gasketed PHEs. PHEs are shown in Figure 1.7 and are covered in detail in Chapter 7.

1.3.1.2.2 Spiral Plate Heat Exchanger

SPHEs have been used since the 1930s, when they were originally developed in Sweden for heat recovery in pulp mills. They are classified as a type of welded PHE. An SPHE is fabricated by rolling a pair of relatively long strips of plate around a split mandrel to form a pair of spiral passages. Channel spacing is maintained uniformly along the length of the spiral passages by means of spacer studs welded to the plate strips prior to rolling. Figure 1.8 shows an SPHE. For most applications, both flow channels are closed by alternate channels welded at both sides of the spiral plate. In some services, one of the channels is left open, whereas the other closed at both sides of the plate. These two types of construction prevent the fluids from mixing.

The SPHE is intended especially for the following applications [5]:

- To handle slurries and liquids with suspended fibers and mineral ore treatment where the solid content is up to 50%.

- SPHE is the first choice for extremely high viscosities, say up to 500,000 cp, especially in cooling duties, because of maldistribution, and hence partial blockage by local overcooling is less likely to occur in a single-channel exchanger.

- SPHEs are finding applications in reboiling, condensing, heating, or cooling of viscous fluids, slurries, and sludge [11].

More details on SPHE are furnished in Chapter 7.

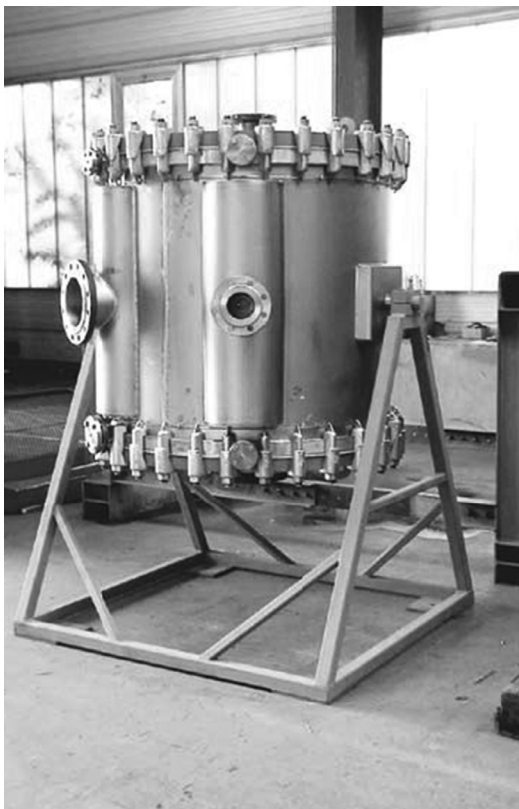


FIGURE 1.8 Spiral plate heat exchanger. (Courtesy of Tranter, Inc., Wichita Falls, TX.)

1.3.1.2.3 Plate or Panel Coil Heat Exchanger

These exchangers are called panel coils, plate coils, or embossed panel or jacketing. The panel coil serves as a heat sink or a heat source, depending upon whether the fluid within the coil is being cooled or heated. Panel coil heat exchangers are relatively inexpensive and can be made into any desired shape and thickness for heat sinks and heat sources under varied operating conditions. Hence, they have been used in many industrial applications such as cryogenics, chemicals, fibers, food, paints, pharmaceuticals, and solar absorbers.

Construction details of a panel coil: A few types of panel coil designs are shown in Figure 1.9. The panel coil is used in such industries as plating, metal finishing, chemical, textile, brewery, pharmaceutical, dairy, pulp and paper, food, nuclear, beverage, waste treatment, and many others. Construction details of panel coils are discussed next. M/s Paul Muller Company, Springfield, MO, and Tranter, Inc., TX, are the leading manufacturers of panel coil/plate coil heat exchangers.

Single embossed surface: The single embossed heat transfer surface is an economical type to utilize for interior tank walls, conveyor beds, and when a flat side is required. The single embossed design uses two sheets of material of different thickness and is available in stainless steel, other alloys, carbon steel, and in many material gages and working pressures.

Double embossed surface: Inflated on both sides using two sheets of material and the same thickness, the double embossed construction maximizes the heating and cooling process by utilizing both sides of the heat transfer plate. The double embossed design is commonly used in immersion applications and is available in stainless steel, other alloys, carbon steel, and in many material gages and working pressures.

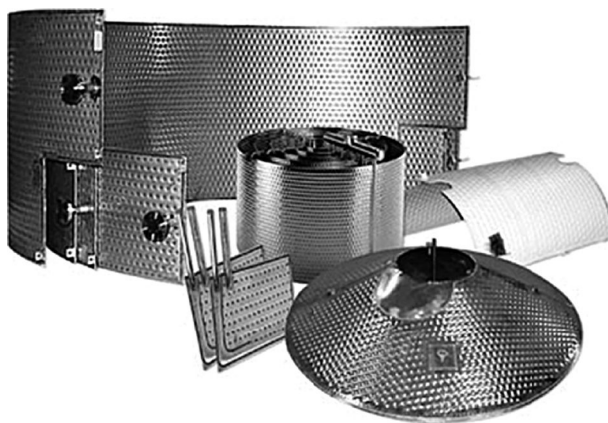


FIGURE 1.9 Temp-Plate® heat transfer surface. (Courtesy of Mueller, Heat Transfer Products, Springfield, MO.)

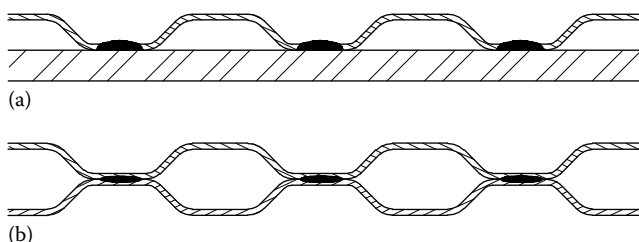


FIGURE 1.10 Welded dimpled jacket template. (a) Gas metal arc welded and (b) resistance welded.

Dimpled surface: This surface is machine punched and swaged, prior to welding, to increase the flow area in the passages. It is available in stainless steel, other alloys, carbon steel, in many material gages and working pressures, and in both MIG plug-welded and resistance spot-welded forms.

Methods of manufacture of panel coils: Basically, three different methods have been used to manufacture the panel coils: (1) they are usually welded by the resistance spot-welding or seam-welding process. An alternate method now available offers the ability to resistance spot-weld the dimpled jacket-style panel coil with a perimeter weldment made with the GMAW or resistance welding. Figure 1.10 shows a vessel jacket welded by GMAW and resistance-welding process. Other methods are (2) the die-stamping process and (3) the roll-bond process. In the die-stamping process, flow channels are die-stamped on either one or two metal sheets. When one sheet is embossed and joined to a flat (unembossed sheet), it forms a single-sided embossed panel coil. When both sheets are stamped, it forms a double-sided embossed panel coil.

Types of jackets: Jacketing of process vessels is usually accomplished by using one of the three main available types: conventional jackets, dimple jackets, and half-pipe coil jackets [12].

Advantages of panel coils: Panel coils provide the optimum method of heating and cooling process vessels in terms of control, efficiency, and product quality. Using a panel as a means of heat transfer offers the following advantages [12]:

- All liquids can be handled, as well as steam and other high-temperature vapors.
- Circulation, temperature, and velocity of heat transfer media can be accurately controlled.
- Panels may often be fabricated from a much less expensive metal than the vessel itself.
- Contamination, cleaning, and maintenance problems are eliminated.

- Maximum efficiency, economy, and flexibility are achieved.
- In designing reactors for specific process, this variety gives chemical engineers a great deal of flexibility in the choice of heat transfer medium.

1.3.1.2.4 Lamella Heat Exchanger

The lamella heat exchanger is an efficient, and compact, heat exchanger. The principle was originally developed around 1930 by Ramens Patenter. Later Ramens Patenter was acquired by Rosenblads Patenter and the lamella heat exchanger was marketed under the Rosenblad name. In 1988, Berglunds acquired the product and continued to develop it. A lamella heat exchanger normally consists of a cylindrical shell surrounding a number of heat-transferring lamellas. The design can be compared to a tube heat exchanger but with the circular tubes replaced by thin and wide channels, lamellas. Sondex Tapiro Oy Ab Pikkupurontie 11, FIN-00810 Helsinki, Finland, markets lamella heat exchangers worldwide.

The lamella is a form of welded heat exchanger that combines the construction of a PHE with that of a shell and tube exchanger without baffles. In this design, tubes are replaced by pairs of thin flat parallel metal plates, which are edge welded to provide long narrow channels, and banks of these elements of varying width are packed together to form a circular bundle and fitted within a shell. The cross section of a lamella heat exchanger is shown schematically in Figure 1.11. With this design, the flow area on the shellside is a minimum and similar in magnitude to that of the inside of the bank of elements; due to this, the velocities of the two liquid media are comparable [13]. The flow is essentially longitudinal countercurrent “tubeside” flow of both tube and shell fluids [4]. Due to this, the velocities of the two liquid media are comparable. Also, the absence of baffles minimizes the pressure drop. One end of the element pack is fixed and the other is floating to allow for thermal expansion and contraction. The connections fitted at either end of the shell, as in the normal shell and tube design, allow the bank of elements to be withdrawn, making the outside surface accessible for inspection and cleaning. Opposed from an STHE, where the whole exchanger has to be replaced in case of damage, it is possible just to replace the lamella battery and preserve the existing shell. Lamella heat exchangers can be fabricated from carbon steel, stainless steel, titanium, Incolloy, and Hastelloy. They can handle most fluids, with large volume ratios between fluids. The floating nature of the bundle usually limits the working pressure to 300 psi. Lamella heat exchangers are generally used only in special cases. Design is usually done by the vendors.

Merits of lamella heat exchanger are as follows:

1. Strong turbulence in the fluid
2. High operation pressure

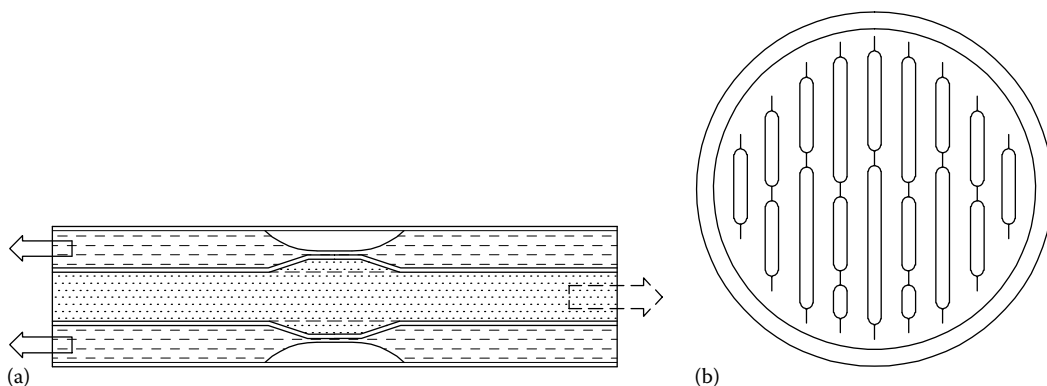


FIGURE 1.11 Lamella heat exchanger. (a) Counterflow concept and (b) lamella tube bundle.



FIGURE 1.12 Air-cooled condenser. (Courtesy of GEA Iberica S.A., Vizcaya, Spain.)

Applications

- Cooking fluid heating in pulp mills
- Liquor preheaters
- Coolers and condensers of flue gas
- Oils coolers

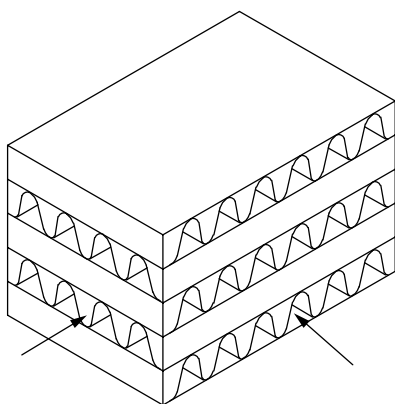
1.3.1.3 Extended Surface Exchangers

In a heat exchanger with gases or some liquids, if the heat transfer coefficient is quite low, a large heat transfer surface area is required to increase the heat transfer rate. This requirement is served by fins attached to the primary surface. Tube-fin heat exchangers (Figure 1.12) and plate-fin heat exchangers (Figure 1.13) are the most common examples of extended surface heat exchangers. Their design is covered in Chapter 4.

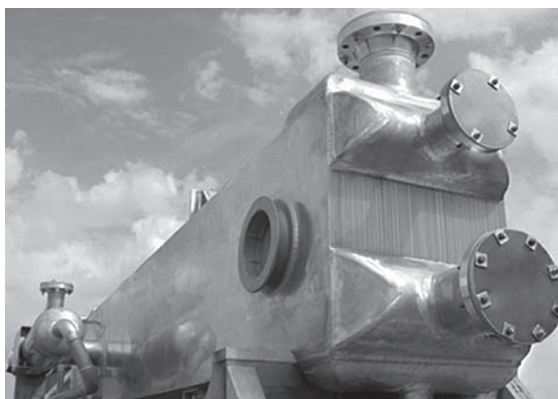
1.3.1.4 Regenerative Heat Exchangers

Regeneration is an old technology dating back to the first open hearths and blast furnace stoves. Manufacturing and process industries such as glass, cement, and primary and secondary metals account for a significant fraction of all energy consumed. Much of this energy is discarded in the form of high-temperature exhaust gas. Recovery of waste heat from the exhaust gas by means of heat exchangers known as regenerators can improve the overall plant efficiency [14].

Types of regenerators: Regenerators are generally classified as fixed-matrix and rotary regenerators. Further classifications of fixed and rotary regenerators are shown in Figure 1.14. In the former,



(a)



(b)

FIGURE 1.13 Plate-fin heat exchanger. (a) Schematic of exchanger and (b) brazed aluminum plate-fin heat exchanger. (From Linde AG, Engineering Division. With permission.)

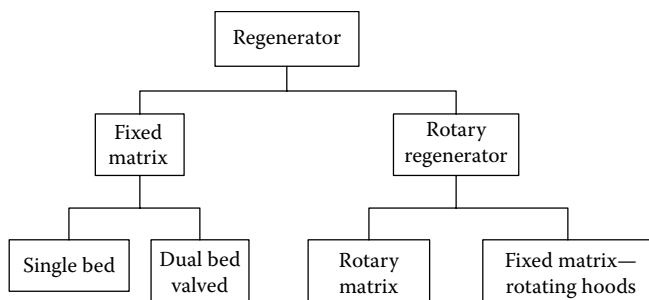


FIGURE 1.14 Classification of regenerators.

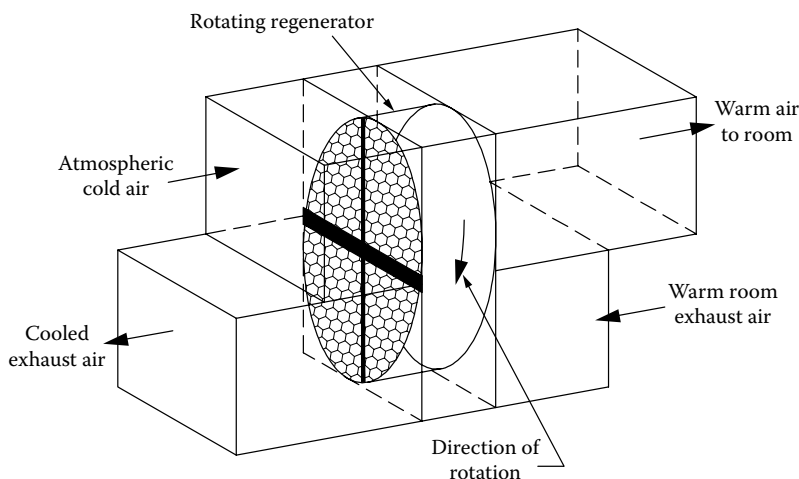


FIGURE 1.15 Rotary regenerator: working principle.

regeneration is achieved with periodic and alternate blowing of hot and the cold stream through a fixed matrix. During the hot flow period, the matrix receives thermal energy from the hot gas and transfers it to the cold stream during the cold stream flow. In the latter, the matrix revolves slowly with respect to two fluid streams. The rotary regenerator is commonly employed in gas turbine power plants where the waste heat in the hot exhaust gases is utilized for raising the temperature of compressed air before it is supplied to the combustion chamber. A rotary regenerator (rotary wheel for HVAC application) working principle is shown in Figure 1.15, and Figure 1.16 shows the Rothemuhle regenerative air preheater of Babcock and Wilcox Company. Rotary regenerators fall in the category of compact heat exchangers since the heat transfer surface area to regenerator volume ratio is very high. Regenerators are further discussed in detail in Chapter 6.

1.3.2 CLASSIFICATION ACCORDING TO TRANSFER PROCESS

These classifications are as follows:

- Indirect contact type—direct transfer type, storage type, fluidized bed
- Direct contact type—cooling towers

1.3.2.1 Indirect Contact Heat Exchangers

In an indirect contact-type heat exchanger, the fluid streams remain separate and the heat transfer takes place continuously through a dividing impervious wall. This type of heat exchanger can be further classified into direct transfer type, storage type, and fluidized bed exchangers. Direct transfer type is dealt with next, whereas the storage type and the fluidized bed type are discussed in Chapter 6.

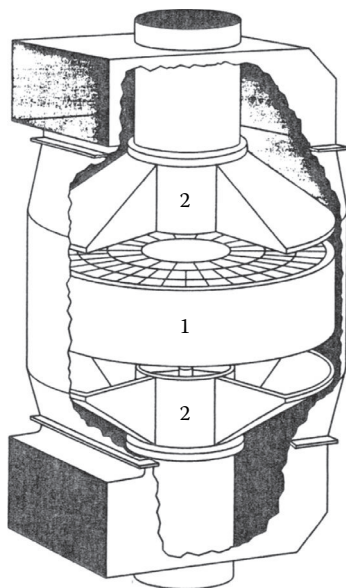


FIGURE 1.16 Rothemuhle regenerative air preheater of Babcock and Wilcox Company—stationary matrix (part 1) and revolving hoods (part 2). (Adapted from Mondt, J.R., *Regenerative heat exchangers: The elements of their design, selection and use*, Research Publication GMR-3396, General Motors Research Laboratories, Warren, MI, 1980.)

1.3.2.1.1 Direct Transfer-Type Exchangers

In this type, there is a continuous flow of heat from the hot fluid to the cold fluid through a separating wall. There is no direct mixing of the fluids because each fluid flows in separate fluid passages. There are no moving parts. This type of exchanger is designated as a recuperator. Some examples of direct transfer-type heat exchangers are tubular exchangers, PHEs, and extended surface exchangers. Recuperators are further subclassified as prime surface exchangers, which do not employ fins or extended surfaces on the prime surface. Plain tubular exchangers, shell and tube exchangers with plain tubes, and PHEs are examples of prime surface exchangers.

1.3.2.2 Direct Contact-Type Heat Exchangers

In direct contact-type heat exchangers, the two fluids are not separated by a wall and come into direct contact, exchange heat, and are then separated.

Owing to the absence of a wall, closer temperature approaches are attained. Very often, in the direct contact type, the process of heat transfer is also accompanied by mass transfer. Various types of direct contact heat exchangers include (a) immiscible fluid exchanger, (b) gas-liquid exchanger, and (c) liquid-vapor exchanger. The cooling towers and scrubbers are examples of a direct contact-type heat exchanger.

1.3.3 CLASSIFICATION ACCORDING TO SURFACE COMPACTNESS

Compact heat exchangers are important when there are restrictions on the size and weight of exchangers. A compact heat exchanger incorporates a heat transfer surface having a high area density, β , somewhat arbitrarily $700 \text{ m}^2/\text{m}^3$ ($200 \text{ ft}^2/\text{ft}^3$) and higher [1]. The area density, β , is the ratio of heat transfer area A to its volume V . A compact heat exchanger employs a compact surface on one or more sides of a two-fluid or a multifluid heat exchanger. They can often achieve higher thermal effectiveness than shell and tube exchangers (95% vs. the 60%–80% typical for STHes), which

makes them particularly useful in energy-intensive industries [15]. For least capital cost, the size of the unit should be minimal. There are some additional advantages to small volume as follows:

- Small inventory, making them good for handling expensive or hazardous materials [15]
- Low weight
- Easier transport
- Less foundation
- Better temperature control

Some barriers to the use of compact heat exchangers include [15] the following:

- The lack of standards similar to pressure vessel codes and standards, although this is now being redressed in the areas of plate-fin exchangers [16] and air-cooled exchangers [17].
- Narrow passages in plate-fin exchangers make them susceptible for fouling and they cannot be cleaned by mechanical means. This limits their use to clean applications like handling air, light hydrocarbons, and refrigerants.

1.3.4 CLASSIFICATION ACCORDING TO FLOW ARRANGEMENT

The basic flow arrangements of the fluids in a heat exchanger are as follows:

- Parallelflow
- Counterflow
- Crossflow

The choice of a particular flow arrangement is dependent upon the required exchanger effectiveness, fluid flow paths, packaging envelope, allowable thermal stresses, temperature levels, and other design criteria. These basic flow arrangements are discussed next.

1.3.4.1 Parallelflow Exchanger

In this type, both the fluid streams enter at the same end, flow parallel to each other in the same direction, and leave at the other end (Figure 1.17). (For fluid temperature variations, idealized as one-dimensional, refer Figure 2.2 of Chapter 2.) This arrangement has the lowest exchanger effectiveness among the single-pass exchangers for the same flow rates, capacity rate (mass \times specific heat) ratio, and surface area. Moreover, the existence of large temperature differences at the inlet end may induce high thermal stresses in the exchanger wall at inlet. Parallelflows are advantageous. (a) In heating very viscous fluids, parallelflow provides for rapid heating. The quick change in viscosity results in reduced pumping power requirements through the heat exchanger, (b) where the more moderate mean metal temperatures of the tube walls are required, and (c) where the improvements in heat transfer rates compensate for the lower LMTD. Although this flow arrangement is not used widely, it is preferred for the following reasons [2]:

1. When there is a possibility that the temperature of the warmer fluid may reach its freezing point.
2. It provides early initiation of nucleate boiling for boiling applications.
3. For a balanced exchanger (i.e., heat capacity rate ratio $C^* = 1$), the desired exchanger effectiveness is low and is to be maintained approximately constant over a range of NTU values.
4. The application allows piping only suited to parallelflow.

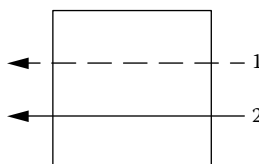


FIGURE 1.17 Parallelflow arrangement.

5. Temperature-sensitive fluids such as food products, pharmaceuticals, and biological products are less likely to be “thermally damaged” in a parallelflow heat exchanger.
6. Certain types of fouling such as chemical reaction fouling, scaling, corrosion fouling, and freezing fouling are sensitive to temperature. Where control of temperature-sensitive fouling is a major concern, it is advantageous to use parallelflow.

1.3.4.2 Counterflow Exchanger

In this type, as shown in Figure 1.18a, the two fluids flow parallel to each other but in opposite directions, and its temperature distribution may be idealized as shown in Figure 1.18b. Ideally, this is the most efficient of all flow arrangements for single-pass arrangements under the same parameters. Since the temperature difference across the exchanger wall at a given cross section is the lowest, it produces minimum thermal stresses in the wall for equivalent performance compared to other flow arrangements. In certain types of heat exchangers, counterflow arrangement cannot be achieved easily, due to manufacturing difficulties associated with the separation of the fluids at each end, and the design of inlet and outlet header design is complex and difficult [2].

1.3.4.3 Crossflow Exchanger

In this type, as shown in Figure 1.19, the two fluids flow normal to each other. Important types of flow arrangement combinations for a single-pass crossflow exchanger include the following:

- Both fluids unmixed
- One fluid unmixed and the other fluid mixed
- Both fluids mixed

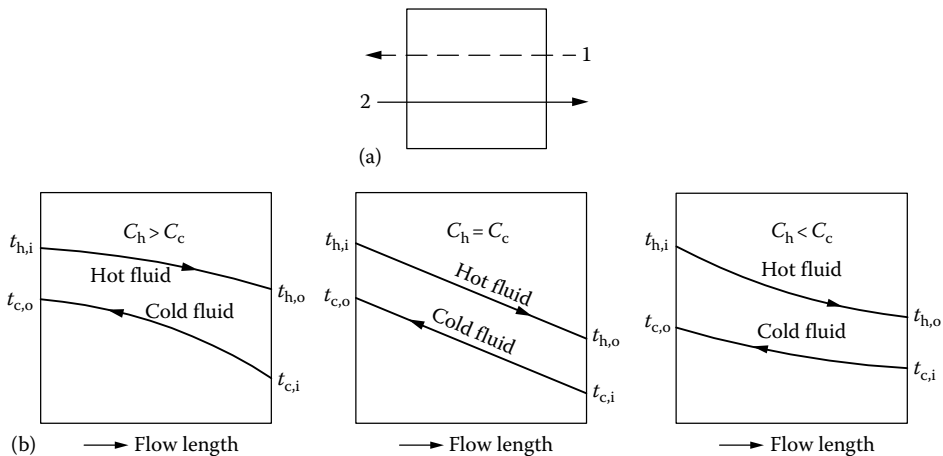


FIGURE 1.18 (a) Counterflow arrangement (schematic) and (b) temperature distribution (schematic). (Note: C_h and C_c are the heat capacity rate of hot fluid and cold fluid respectively, i refers to inlet, o refers to outlet conditions and t refers to fluid temperature.)

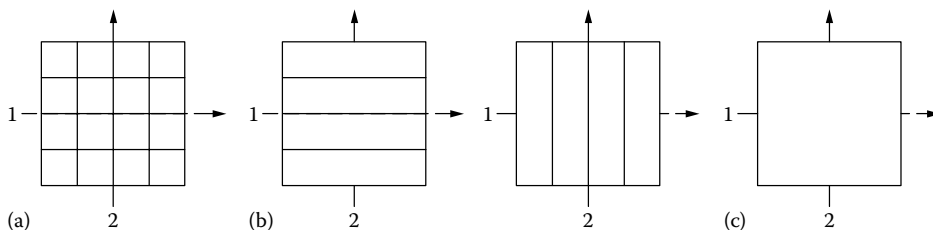


FIGURE 1.19 Crossflow arrangement: (a) unmixed-unmixed, (b) unmixed-mixed, and (c) mixed-mixed.

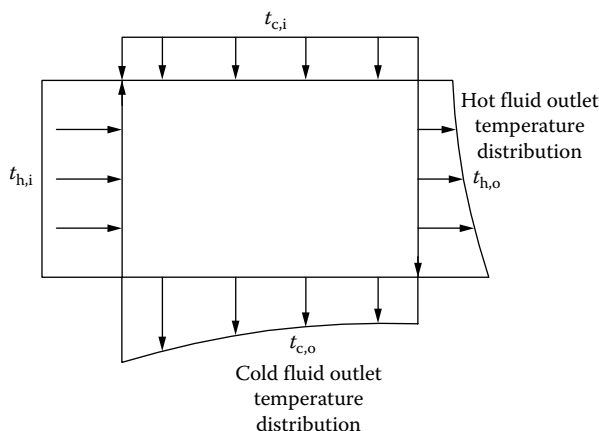


FIGURE 1.20 Temperature distribution for unmixed–unmixed crossflow arrangement.

A fluid stream is considered “unmixed” when it passes through individual flow passage without any fluid mixing between adjacent flow passages. Mixing implies that a thermal averaging process takes place at each cross section across the full width of the flow passage. A tube-fin exchanger with flat (continuous) fins and a plate-fin exchanger wherein the two fluids flow in separate passages (e.g., wavy fin, plain continuous rectangular or triangular flow passages) represent the unmixed–unmixed case. A crossflow tubular exchanger with bare tubes on the outside would be treated as the unmixed–mixed case, that is, unmixed on the tubeside and mixed on the outside. The both fluid mixed case is practically a less important case and represents a limiting case of some multipass shell and tube exchangers (TEMA E and J shell).

For the unmixed–unmixed case, fluid temperature variations are idealized as two-dimensional only for the inlet and outlet sections; this is shown in Figure 1.20. The thermal effectiveness for the crossflow exchanger falls in between those of the parallelflow and counterflow arrangements. This is the most common flow arrangement used for extended surface heat exchangers because it greatly simplifies the header design. If the desired heat exchanger effectiveness is generally more than 80%, the size penalty for crossflow may become excessive. In such a case, a counterflow unit is preferred [2]. In shell and tube exchangers, crossflow arrangement is used in the TEMA X shell having a single tube pass.

1.3.5 CLASSIFICATION ACCORDING TO PASS ARRANGEMENTS

These are either single pass or multipass. A fluid is considered to have made one pass if it flows through a section of the heat exchanger through its full length once. In a multipass arrangement, a fluid is reversed and flows through the flow length two or more times.

1.3.5.1 Multipass Exchangers

When the design of a heat exchanger results in either extreme length, significantly low velocities, or low effectiveness, or due to other design criteria, a multipass heat exchanger or several single-pass exchangers in series or a combination of both is employed. Specifically, multipassing is resorted to increase the exchanger thermal effectiveness over the individual pass effectiveness. As the number of passes increases, the overall direction of the two fluids approaches that of a pure counterflow exchanger. The multipass arrangements are possible with compact, shell and tube, and plate exchangers.

1.3.6 CLASSIFICATION ACCORDING TO PHASE OF FLUIDS

1.3.6.1 Gas–Liquid

Gas–liquid heat exchangers are mostly tube-fin-type compact heat exchangers with the liquid on the tubeside. The radiator is by far the major type of liquid–gas heat exchanger, typically cooling the engine jacket water by air. Similar units are necessary for all the other water-cooled engines used in trucks, locomotives, diesel-powered equipment, and stationery diesel power plants. Other examples are air coolers, oil coolers for aircraft, intercoolers and aftercoolers in compressors, and condensers and evaporators of room air-conditioners. Normally, the liquid is pumped through the tubes, which have a very high convective heat transfer coefficient. The air flows in crossflow over the tubes. The heat transfer coefficient on the air side will be lower than that on the liquid side. Fins will be generally used on the outside of the tubes to enhance the heat transfer rate.

1.3.6.2 Liquid–Liquid

Most of the liquid–liquid heat exchangers are shell and tube type, and PHEs to a lesser extent. Both fluids are pumped through the exchanger, so the principal mode of heat transfer is forced convection. The relatively high density of liquids results in very high heat transfer rate, so normally fins or other devices are not used to enhance the heat transfer [4]. In certain applications, low-finned tubes, microfin tubes, and heat transfer augmentation devices are used to enhance the heat transfer.

1.3.6.3 Gas–Gas

This type of exchanger is found in exhaust gas–air preheating recuperators, rotary regenerators, intercoolers, and/or aftercoolers to cool supercharged engine intake air of some land-based diesel power packs and diesel locomotives, and cryogenic gas liquefaction systems. In many cases, one gas is compressed so that the density is high while the other is at low pressure and low density. Compared to liquid–liquid exchangers, the size of the gas–gas exchanger will be much larger, because the convective heat transfer coefficient on the gas side is low compared to the liquid side. Therefore, secondary surfaces are mostly employed to enhance the heat transfer rate.

1.3.7 CLASSIFICATION ACCORDING TO HEAT TRANSFER MECHANISMS

The basic heat transfer mechanisms employed for heat transfer from one fluid to the other are (1) single-phase convection, forced or free, (2) two-phase convection (condensation or evaporation) by forced or free convection, and (3) combined convection and radiation. Any of these mechanisms individually or in combination could be active on each side of the exchanger. Based on the phase change mechanisms, the heat exchangers are classified as (1) condensers and (2) evaporators.

1.3.7.1 Condensers

Condensers may be liquid (water) or gas (air) cooled. The heat from condensing streams may be used for heating fluid. Normally, the condensing fluid is routed (1) outside the tubes with a water-cooled steam condenser or (2) inside the tubes with gas cooling, that is, air-cooled condensers of refrigerators and air-conditioners. Fins are normally provided to enhance heat transfer on the gas side.

1.3.7.2 Evaporators

This important group of tubular heat exchangers can be subdivided into two classes: fired systems and unfired systems.

Fired systems: These involve the products of combustion of fossil fuels at very high temperatures but at ambient pressure (and hence low density) and generate steam under pressure. Fired systems are called boilers. A system may be a fire tube boiler (for small low-pressure applications) or a water tube boiler.

Unfired systems: These embrace a great variety of steam generators extending over a broad temperature range from high-temperature nuclear steam generators to very-low-temperature cryogenic gasifiers for liquid natural gas evaporation. Many chemical and food processing applications involve the use of steam to evaporate solvents, concentrate solutions, distill liquors, or dehydrate compounds.

1.3.8 OTHER CLASSIFICATIONS

1.3.8.1 Micro Heat Exchanger

Micro- or microscale heat exchangers are heat exchangers in which at least one fluid flows in lateral confinements with typical dimensions below 1 mm and are fabricated via silicon micromachining, deep x-ray lithography, or nonlithographic micromachining [18]. The plates are stacked forming “sandwich” structures, as in the “large” plate exchangers. All flow configurations (cocurrent, countercurrent, and crossflow) are possible.

Typically, the fluid flows through a cavity called a microchannel. Microheat exchangers have been demonstrated with high convective heat transfer coefficient. Investigation of microscale thermal devices is motivated by the single-phase internal flow correlation for convective heat transfer:

$$h = \frac{\text{Nu } k}{D_h}$$

where

h is the heat transfer coefficient

Nu is the Nusselt number

k is the thermal conductivity of the fluid

D_h is the hydraulic diameter of the channel or duct

In internal laminar flows, the Nusselt number becomes a constant. As the Reynolds number is proportional to hydraulic diameter, fluid flow in channels of small hydraulic diameter will predominantly be laminar. This correlation therefore indicates that the heat transfer coefficient increases as the channel diameter decreases. Heat transfer enhancement in laminar flow is further discussed in Chapter 8 Section 8.3.3.

1.3.8.1.1 Advantages over Macroscale Heat Exchangers

- Substantially better performance
- Enhanced heat transfer coefficient with a large number of smaller channels
- Smaller size that allows for an increase in mobility and uses
- Light weight reduces the structural and support requirements
- Lower cost due to less material being used in fabrication

1.3.8.1.2 Applications of Microscale Heat Exchangers

Microscale heat exchangers are being used in the development of fuel cells. They are currently used in automotive industries, HVAC applications, aircraft, manufacturing industries, and electronics cooling.

1.3.8.1.3 Demerits of Microscale Heat Exchangers

One of the main disadvantages of microchannel heat exchangers is the high-pressure loss that is associated with a small hydraulic diameter.

1.3.8.2 Printed Circuit Heat Exchanger

PCHE, developed by Heatric Division of Meggitt (UK) Ltd., is a promising heat exchanger because it is able to withstand pressures up to 50 MPa and temperatures from cryogenic to 700°C. It is extremely compact (the most common design feature to achieve compactness has been small channel size) and has high efficiency, of the order of 98%. It can handle a wide variety of clean fluids. The flow configuration can be either crossflow or counterflow. It will maintain parent material strength and can be made from stainless steel, nickel alloys, copper alloys, and titanium. Fluid flow channels are etched chemically on metal plates. It has a typical plate thickness of 1.6 mm, width 600 mm, and length 1200 mm. The channels are semicircular with 1–2 mm diameter. Etched plates are stacked and diffusion bonded together to fabricate as a block. The blocks are then welded together to form the complete heat exchanger core, as shown in Figure 1.21a.

HEATRIC PCHEs consist of diffusion-bonded heat exchanger core that are constructed from flat metal plates into which fluid flow channels are either chemically etched or pressed. The required configuration of the channels on the plates for each fluid is governed by the operating temperature and pressure-drop constraints for the heat exchange duty and the channels can be of unlimited variety and complexity. Fluid flow can be parallelflow, counterflow, crossflow, or a combination of these to suit the process requirements. Figure 1.21b through f shows HEATRIC PCHE.

The etched plates are then stacked and diffusion-bonded together to form strong, compact, all metal heat exchanger core. Diffusion bonding is a “solid-state joining” process entailing pressing metal surfaces together at temperatures below the melting point, thereby promoting grain growth between the surfaces. Under carefully controlled conditions, diffusion-bonded joints reach parent metal strength and stacks of plates are converted into solid blocks containing the fluid flow passages. The blocks are then welded together to form the complete heat exchange core. Finally, headers and nozzles are welded to the core in order to direct the fluids to the appropriate sets of passages. Welded and diffusion-bonded PCHEs employ no gaskets or braze material, resulting in superior integrity compared to other technologies that may use gaskets or brazing as part of their construction. (Gaskets or braze material can be potential sources of leakage, fluid incompatibility, and temperature limitations.) The mechanical design is normally of ASME VIII Division 1. Other design codes can be employed as required.

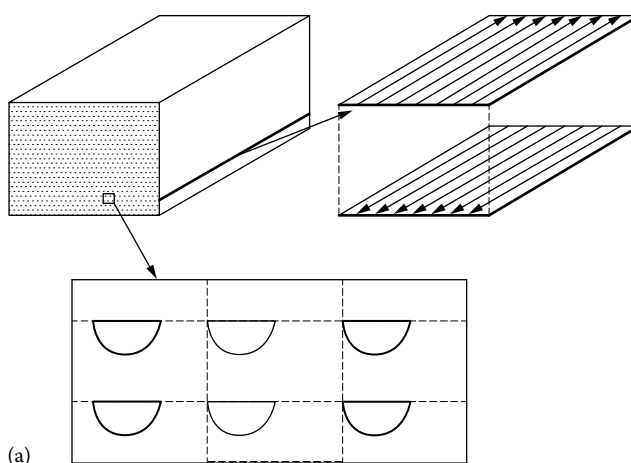


FIGURE 1.21 Printed circuit heat exchanger. (a) Heat exchanger block with flow channel.

(continued)

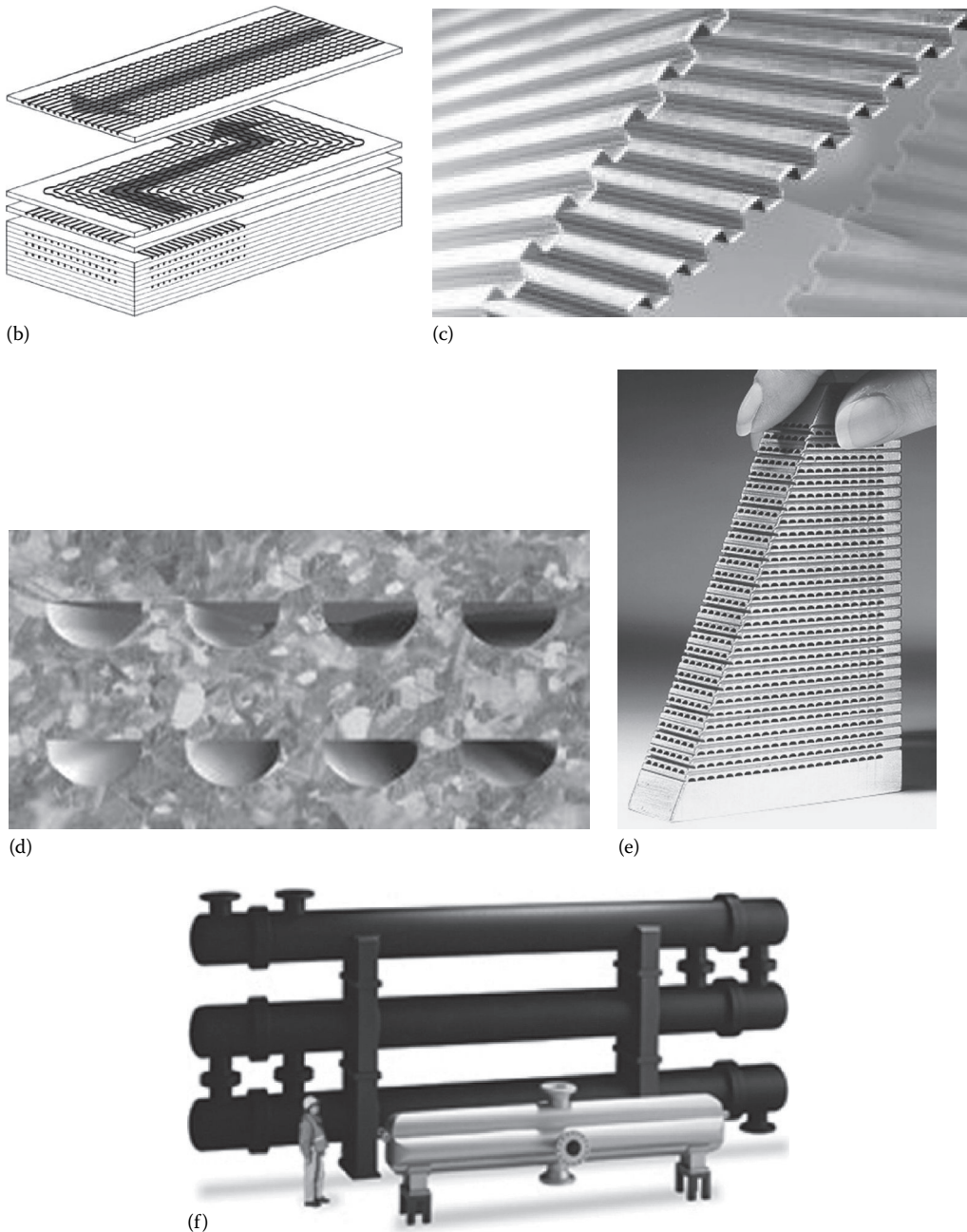


FIGURE 1.21 (continued) Printed circuit heat exchanger. (b) Flow channel, (c) and (d) section through flow channel, (e) diffusion bonded core, (f) comparison of size of PCHE shell and tube heat exchanger (smaller size) with a conventional exchanger (bigger size) for similar duty. (Courtesy of Heatric UK, Dorset, U.K.)

1.3.8.2.1 Materials of Construction

The majority of diffusion-bonded heat exchangers are constructed from 300 series austenitic stainless steel. Various other metals that are compatible with the diffusion-bonded process and have been qualified for use include 22 chromeduplex, copper–nickel, nickel alloys, and titanium.

1.3.8.2.2 Features of PCHE

Diffusion-bonded heat exchangers are highly compact and robust that are well established in the upstream hydrocarbon processing, petrochemical and refining industries. Various salient constructional and performance features are given next:

1. Compactness: Diffusion-bonded heat exchangers are 1/4–1/6th the conventional STHs of the equivalent heat duty. This design feature has space and weight advantages, reducing exchanger size together with piping and valve requirements. The diffusion-bonded heat exchanger in the foreground of Figure 1.21e undertakes the same thermal duty, at the same pressure drop, as the stack of three shell and tube exchangers behind. PCHE might be judged as a promising compact heat exchanger for the high efficiency recuperator [19].
2. Process capability: They can withstand pressures of 600 bar (9000 psi) or excess and can cope with extreme temperatures, ranging from cryogenic to 900°C (1650°F).
3. Thermal effectiveness: Diffusion-bonded exchangers can achieve high thermal effectiveness of the order of 98% in a single unit.
4. They can incorporate more than two process streams into a single unit.
5. The compatibility of the chemical etching and diffusion-bonding process with a wide range of materials ensure that they are suitable for a range of corrosive and high purity streams.

1.3.8.3 Perforated Plate Heat Exchanger as Cryocoolers

High-efficiency compact heat exchangers are needed in cryocoolers to achieve very low temperatures. One approach to meet the requirements for compact and efficient cooling systems is the perforated PHE. Such heat exchangers are made up of a large number of parallel, perforated plates of high-thermal conductivity metal in a stacked array, with gaps between plates being provided by spacers. Gas flows longitudinally through the plates in one direction and other stream flows in the opposite direction through separated portions of the plates. Heat transfer takes place laterally across the plates from one stream to the other. The operating principles of this type of heat exchanger are described by Fleming [20]. The device employs plates of 0.81 mm thickness with holes of 1.14 mm in diameter and a resulting length-to-diameter ratio in the range of 0.5–1.0. The device is designed to operate from room temperature to 80 K. In order to improve operation of a compact cryocooler, much smaller holes, in the low-micron-diameter range, and thinner plates with high length-to-diameter ratio are needed. As per US Patent 5101894 [21], uniform, tubular perforations having diameters down to the low-micron-size range can be obtained. Various types of heat exchange devices including recuperative and regenerative heat exchangers may be constructed in accordance with the invention for use in cooling systems based on a number of refrigeration cycles such as the Linde–Hampson, Brayton, and Stirling cycles.

1.3.8.4 Scraped Surface Heat Exchanger

Scraped surface heat exchangers are used for processes likely to result in the substantial deposition of suspended solids on the heat transfer surface. Scraped surface heat exchangers can be employed in the continuous, closed processing of virtually any pumpable fluid or slurry involving cooking, slush freezing, cooling, crystallizing, mixing, plasticizing, gelling, polymerizing, heating, aseptic processing, etc. Use of a scraped surface exchanger prevents the accumulation of significant buildup of solid deposits. The construction details of scraped surface heat exchangers are explained in Ref. [4]. Scraped surface heat exchangers are essentially double pipe construction with the process fluid in the inner pipe and the cooling (water) or heating medium (steam) in the annulus. A rotating element is contained within the tube and is equipped with spring-loaded blades. In operation, the rotating shaft scraper blades continuously scrape product film from the heat transfer tube wall, thereby enhancing heat transfer and agitating the product to produce a homogenous mixture. For most applications, the shaft is mounted in the center of the heat transfer tube. An off-centered shaft mount or *eccentric* design is recommended for viscous and sticky

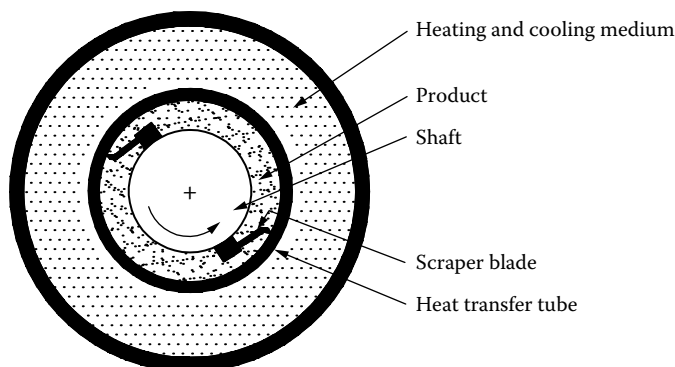


FIGURE 1.22 Scraped surface heat exchanger: principle.

products. This shaft arrangement increases product mixing and reduces the mechanical heat load. Oval tubes are used to process extremely viscous products. All pressure elements are designed in accordance with the latest ASME code requirements. The principle of working of scraped surface heat exchangers is shown in Figure 1.22. For scraped surface exchangers, operating costs are high and applications are highly specific [5]. Design is mostly done by vendors. The leading manufacturers include HRS Heat Exchangers, Ltd., UK, and Waukesha Cherry-Burrell, USA.

1.3.8.4.1 Unicus Scraped Surface Heat Exchanger

Unicus™ is the trade name for scraped surface heat exchanger of HRS Heat Exchangers Ltd., UK, for high-fouling and viscous fluid applications. The design is based on STHE with scraping elements inside each interior tube. The scrapers are moved back and forth by hydraulic action. The scraping action has two very important advantages: any fouling on the tube wall is removed and the scraping movement introduces turbulence in the fluid increasing heat transfer.

1.3.8.4.1.1 Elements of the Unicus Unicus consists of three parts: a hydraulic cylinder that moves the scraper bars, the STHE part, and a chamber that separates both the elements. The hydraulic cylinder is connected to a hydraulic power pack. The smaller models of the Unicus range can be supplied with a pneumatic cylinder. The scraping system consists of a stainless steel rod to which the scraping elements are fitted, as shown in Figure 1.23, and Figure 1.24 shows Unicus scraped surface heat exchangers. The pictures show the various types of scrapers that can be applied. For each application, the optimal scraper is selected and fitted.

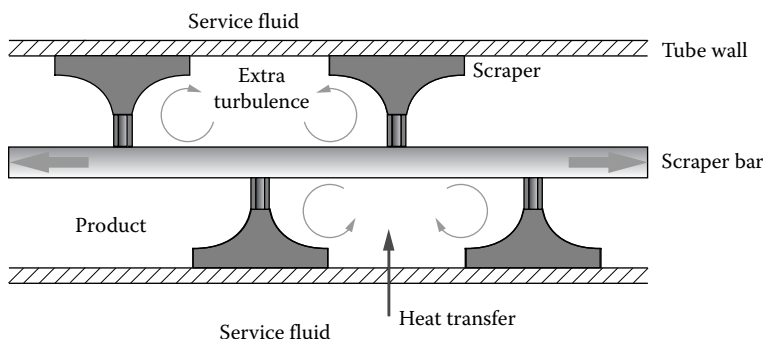


FIGURE 1.23 Principle of Unicus scraped surface heat exchanger working. (Courtesy of HRS Heat Exchangers Ltd, Herts, U.K.)

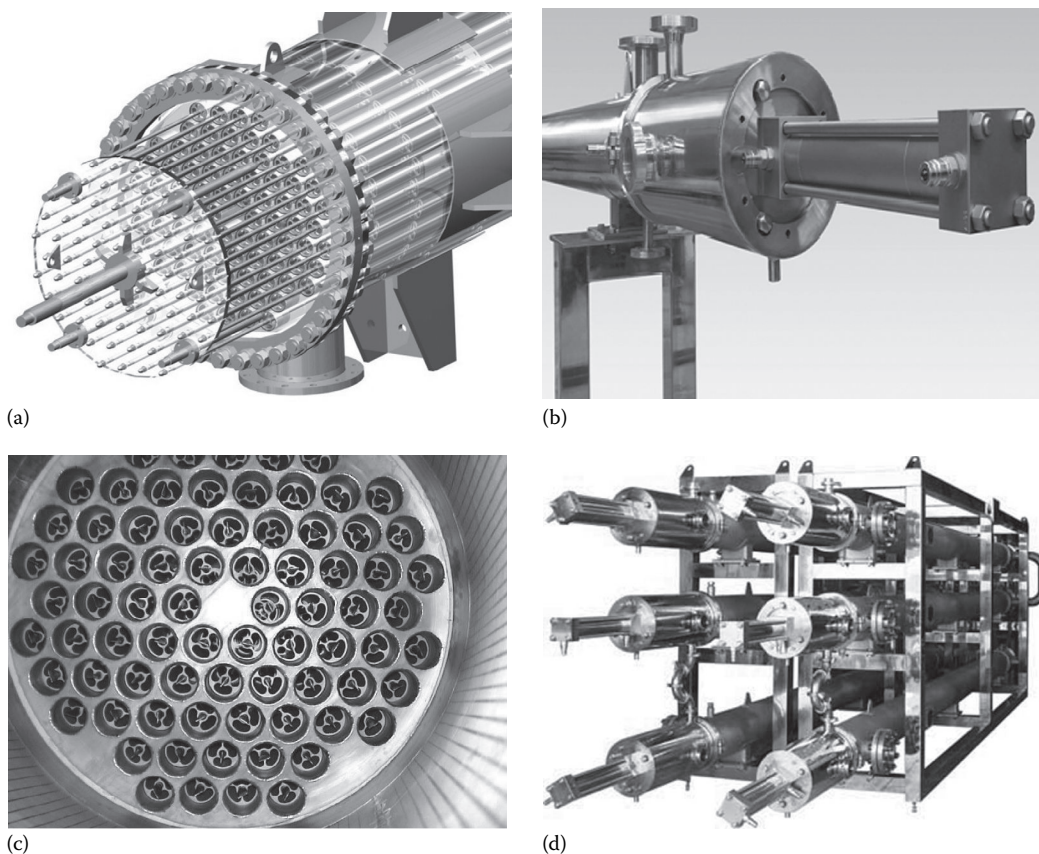


FIGURE 1.24 Unicus dynamic scraped surface heat exchanger. (a) 3-D model, (b) hydraulic cylinder head, (c) a unit of Unicus, and (d) multiple Unicus units. (Courtesy of HRS Heat Exchangers Ltd, Herts, U.K.)

1.3.8.5 Graphite Heat Exchanger

Impervious graphite as a heat exchanger material is used for the construction of various types of heat exchangers such as STHE, cubic block heat exchanger, and plate and frame or gasketed heat exchangers (PHEs). Graphite tubes are used in STHE (refer to Chapter 13) and plates are used in PHEs (refer to Chapter 7) for special purpose applications. It resists a wide variety of inorganic and organic chemicals. Graphite heat exchangers are employed as boilers and condensers in the distillation by evaporation of hydrochloric acid and in the concentration of weak sulfuric acid and of rare earth chloride solutions. Since cubic heat exchanger cannot be treated in categorization of extended surface heat exchanger, the same is covered next.

Cubic heat exchanger: It is similar to the compact crossflow heat exchanger, consisting of drilled holes in two perpendicular planes. They are suitable when both the process streams are corrosive. With a cubic exchanger, a multipass arrangement is possible. It is manufactured by assembling of accurately machined and drilled graphite plates bonded together by synthetic resins, oven cured and sintered. Gasketed headers with nozzles are assembled on both sides to the block to form a block heat exchanger and are clamped together, as shown in Figure 1.25.

Modular-block cylindrical exchanger: In this arrangement, solid impervious graphite blocks have holes drilled in them. These blocks can be multistacked in a cylindrical steel shell that has

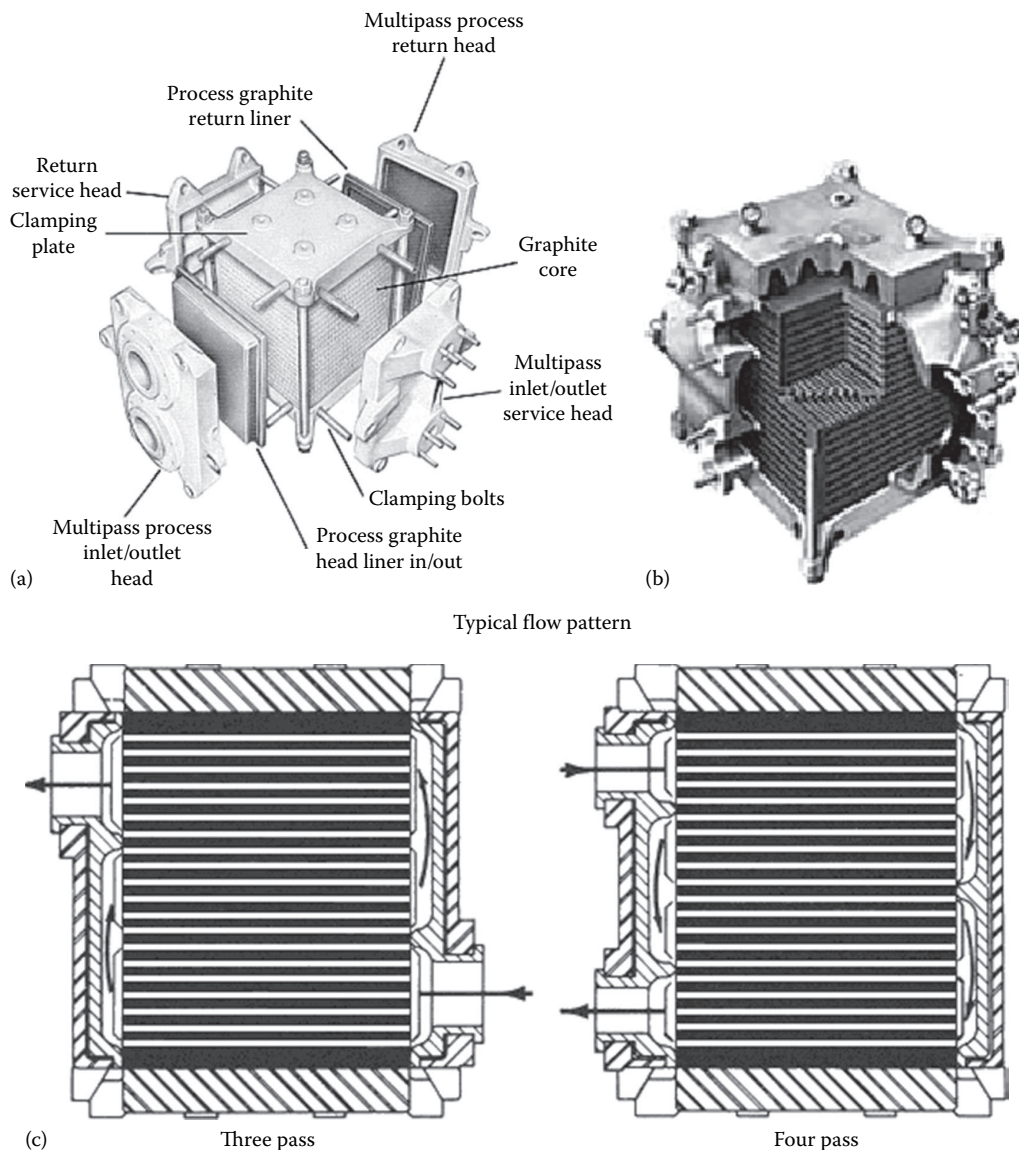


FIGURE 1.25 NK series multipass cubic graphite heat exchanger. (a) Construction details, (b) cut section, and (c) multipass flow pattern. (Courtesy of MERSEN, Paris La Défense, France.)

gland fittings. The process holes are axial and the service holes are transverse. The units are designed as evaporators and reboilers. A modular block Graphilor® exchanger is shown in Figure 1.26.

1.4 SELECTION OF HEAT EXCHANGERS

1.4.1 INTRODUCTION

Selection is the process in which the designer selects a particular type of heat exchanger for a given application from a variety of heat exchangers. There are a number of alternatives for selecting heat transfer equipment, but only one among them is the best for a given set of conditions. The heat exchanger selection criteria are discussed next.

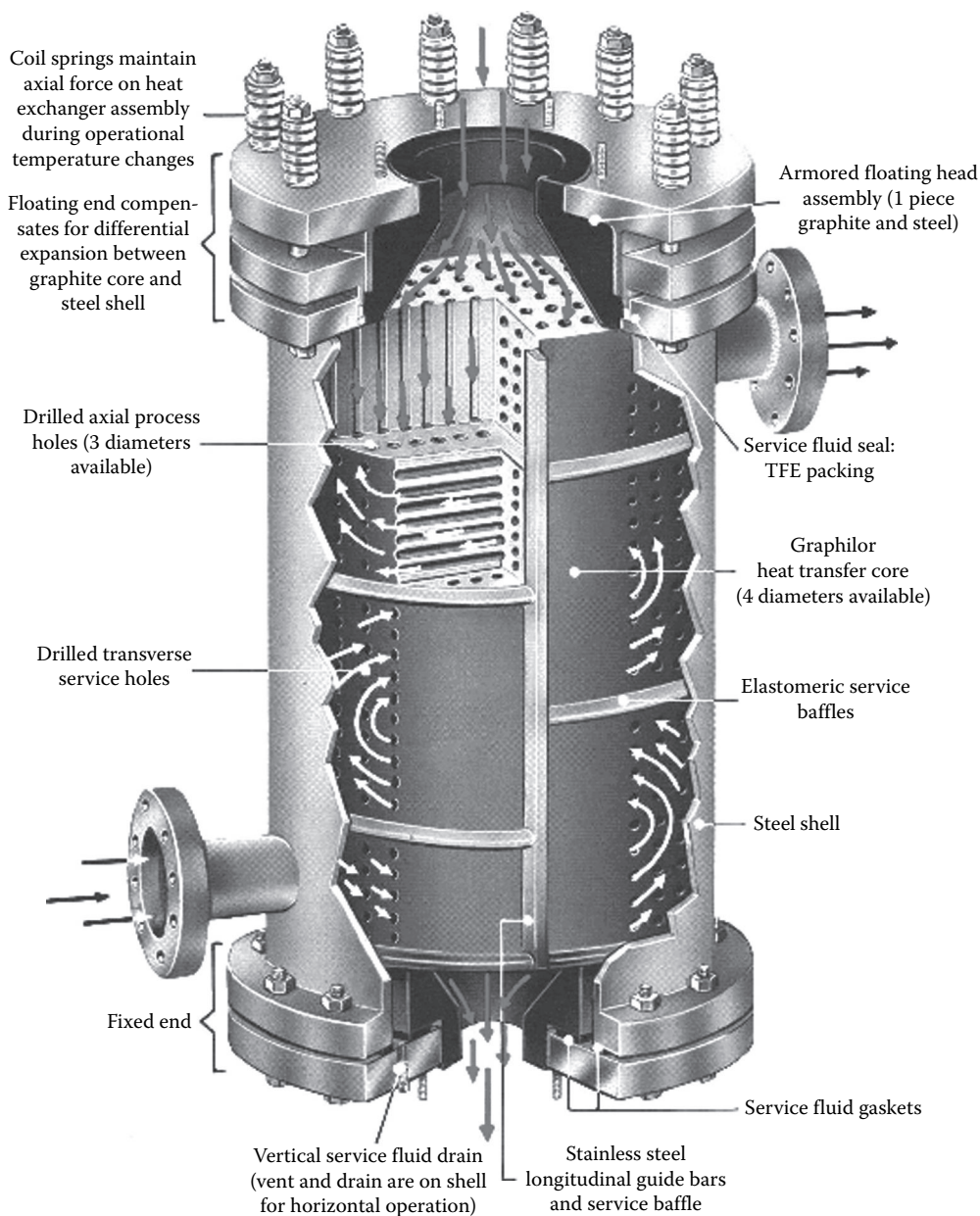


FIGURE 1.26 GRAPHILOR® cylindrical tubes (in block) heat exchanger. (Courtesy of MERSEN, Paris La Défense, France.)

1.4.2 SELECTION CRITERIA

Selection criteria are many, but primary criteria are type of fluids to be handled, operating pressures and temperatures, heat duty, and cost (see Table 1.1). The fluids involved in heat transfer can be characterized by temperature, pressure, phase, physical properties, toxicity, corrosivity, and fouling tendency. Operating conditions for heat exchangers vary over a very wide range, and a broad spectrum of demands is imposed for their design and performance. All of these must be

considered when assessing the type of unit to be used [22]. When selecting a heat exchanger for a given duty, the following points must be considered:

- Materials of construction
- Operating pressure and temperature, temperature program, and temperature driving force
- Flow rates
- Flow arrangements
- Performance parameters—thermal effectiveness and pressure drops
- Fouling tendencies
- Types and phases of fluids
- Maintenance, inspection, cleaning, extension, and repair possibilities
- Overall economy
- Fabrication techniques
- Mounting arrangements: horizontal or vertical
- Intended applications

1.4.2.1 Materials of Construction

For reliable and continuous use, the construction materials for pressure vessels and heat exchangers should have a well-defined corrosion rate in the service environments. Furthermore, the material should exhibit strength to withstand the operating temperature and pressure. STHes can be manufactured in virtually any material that may be required for corrosion resistance, for example, from nonmetals like glass, Teflon, and graphite to exotic metals like titanium, zirconium, tantalum, etc. Compact heat exchangers with extended surfaces are mostly manufactured from any metal that has drawability, formability, and malleability. Heat exchanger types like PHEs normally require a material that can be pressed or welded.

1.4.2.2 Operating Pressure and Temperature

1.4.2.2.1 Pressure

The design pressure is important to determine the thickness of the pressure-retaining components. The higher the pressure, the greater will be the required thickness of the pressure-retaining membranes and the more advantage there is to placing the high-pressure fluid on the tubeside. The pressure level of the fluids has a significant effect on the type of unit selected [22].

At low pressures, the vapor-phase volumetric flow rate is high and the low-allowable pressure drops may require a design that maximizes the area available for flow, such as crossflow or split flow with multiple nozzles.

At high pressures, the vapor-phase volumetric flow rates are lower and allowable pressure drops are greater. These lead to more compact units.

In general, higher heat transfer rates are obtained by placing the low-pressure gas on the outside of tubular surfaces.

Operating pressures of the gasketed PHEs and SPHEs are limited because of the difficulty in pressing the required plate thickness, and by the gasket materials in the case of PHEs. The floating nature of floating-head shell and tube heat exchangers and lamella heat exchangers limits the operating pressure.

1.4.2.2.2 Temperature

Design temperature: This parameter is important as it indicates whether a material at the design temperature can withstand the operating pressure and various loads imposed on the component. For low-temperature and cryogenic applications, toughness is a prime requirement, and for high-temperature applications the material has to exhibit creep resistance.

Temperature program: Temperature program in both a single-pass and multipass STHes decides (1) the mean metal temperatures of various components like shell, tube bundle, and tubesheet, and

(2) the possibility of temperature cross. The mean metal temperatures affect the integrity and capability of heat exchangers and thermal stresses induced in various components.

Temperature driving force: The effective temperature driving force is a measure of the actual potential for heat transfer that exists at the design conditions. With a counterflow arrangement, the effective temperature difference is defined by the log mean temperature difference (LMTD). For flow arrangements other than counterflow arrangement, LMTD must be corrected by a correction factor, F . The F factor can be determined analytically for each flow arrangement but is usually presented graphically in terms of the thermal effectiveness P and the heat capacity ratio R for each flow arrangement.

Influence of operating pressure and temperature on selection of some types of heat exchangers: The influence of operating pressure and temperature on selection of STHE, compact heat exchanger, gasketed PHE, and spiral exchanger is discussed next.

Shell and tube heat exchanger: STHE units can be designed for almost any combination of pressure and temperature. In extreme cases, high pressure may impose limitations by fabrication problems associated with material thickness, and by the weight of the finished unit. Differential thermal expansion under steady conditions can induce severe thermal stresses either in the tube bundle or in the shell. Damage due to flow-induced vibration on the shellside is well known. In heat-exchanger applications where high heat transfer effectiveness (close approach temperature) is required, the standard shell and tube design may require a very large amount of heat transfer surface [23]. Depending on the fluids and operating conditions, other types of heat-exchanger design should be investigated.

Compact heat exchanger: Compact heat exchangers are constructed from thinner materials; they are manufactured by mechanical bonding, soldering, brazing, welding, etc. Therefore, they are limited in operating pressures and temperatures.

Gasketed plate heat exchangers and spiral exchangers: Gasketed PHEs and spiral exchangers are limited by pressure and temperature, wherein the limitations are imposed by the capability of the gaskets.

1.4.2.3 Flow Rate

Flow rate determines the flow area: the higher the flow rate, the higher will be the crossflow area. Higher flow area is required to limit the flow velocity through the conduits and flow passages, and the higher velocity is limited by pressure drop, impingement, erosion, and, in the case of shell and tube exchanger, by shellside flow-induced vibration. Sometimes, a minimum flow velocity is necessary to improve heat transfer to eliminate stagnant areas and to minimize fouling.

1.4.2.4 Flow Arrangement

As defined earlier, the choice of a particular flow arrangement is dependent upon the required exchanger effectiveness, exchanger construction type, upstream and downstream ducting, packaging envelope, and other design criteria.

1.4.2.5 Performance Parameters: Thermal Effectiveness and Pressure Drops

Thermal effectiveness: For high-performance service requiring high thermal effectiveness, use brazed plate-fin exchangers (e.g., cryogenic service) and regenerators (e.g., gas turbine applications), use tube-fin exchangers for slightly less thermal effectiveness in applications, and use shell and tube units for low-thermal effectiveness service.

Pressure drop: Pressure drop is an important parameter in heat exchanger design. Limitations may be imposed either by pumping cost or by process limitations or both. The heat exchanger should be designed in such a way that unproductive pressure drop is avoided to the maximum extent

in areas like inlet and outlet bends, nozzles, and manifolds. At the same time, any pressure-drop limitation that is imposed must be utilized as nearly as possible for an economic design.

1.4.2.6 Fouling Tendencies

Fouling is defined as the formation on heat exchanger surfaces of undesirable deposits that impede the heat transfer and increase the resistance to fluid flow, resulting in higher pressure drop. The growth of these deposits causes the thermohydraulic performance of heat exchanger to decline with time. Fouling affects the energy consumption of industrial processes, and it also decides the amount of extra material required to provide extra heat transfer surface to compensate for the effects of fouling. Compact heat exchangers are generally preferred for nonfouling applications. In a shell and tube unit, the fluid with more fouling tendencies should be put on the tubeside for ease of cleaning. On the shellside with cross baffles, it is sometimes difficult to achieve a good flow distribution if the baffle cut is either too high or too low. Stagnation in any regions of low velocity behind the baffles is difficult to avoid if the baffles are cut more than about 20%–25%. PHEs and spiral plate exchangers are better chosen for fouling services. The flow pattern in PHE induces turbulence even at comparable low velocities; in the spiral units, the scrubbing action of the fluids on the curved surfaces minimizes fouling. Also consider Philips RODbaffle heat exchanger, TWISTED TUBE® heat exchanger, Helixchanger® heat exchanger or EMbaffle® heat exchanger to improve flow velocity on shellside, enhance heat transfer performance and reduce fouling tendencies on shellside.

1.4.2.7 Types and Phases of Fluids

The phase of the fluids within a unit is an important consideration in the selection of the heat exchanger type. Various combinations of fluid phases dealt in heat exchangers are liquid–liquid, liquid–gas, and gas–gas. Liquid-phase fluids are generally the simplest to deal with. The high density and the favorable values of many transport properties allow high heat transfer coefficients to be obtained at relatively low-pressure drops [4].

1.4.2.8 Maintenance, Inspection, Cleaning, Repair, and Extension Aspects

Consider the suitability of various heat exchangers as regards maintenance, inspection, cleaning, repair, and extension. For example, the pharmaceutical, dairy, and food industries require quick access to internal components for frequent cleaning. Since some of the heat exchanger types offer great variations in design, this must be kept in mind when designing for a certain application. For instance, consider inspection and manual cleaning. Spiral plate exchangers can be made with both sides open at one edge, or with one side open and one closed. They can be made with channels between 5 and 25 mm wide, with or without studs. STHE can be made with fixed tubesheets or with a removable tube bundle, with small- or large-diameter tubes, or small or wide pitch. A lamella heat exchanger bundle is removable and thus fairly easy to clean on the shellside. Inside, the lamella, however, cannot be drilled to remove the hard fouling deposits. Gasketed PHEs are easy to open, especially when all nozzles are located on the stationary end-plate side. The plate arrangement can be changed for other duties within the frame and nozzle capacity.

Repair of some of the shell and tube exchanger components is possible, but the repair of expansion joint is very difficult. Tubes can be renewed or plugged. Repair of compact heat exchangers of tube-fin type is very difficult except by plugging of the tube. Repair of the plate-fin exchanger is generally very difficult. For these two types of heat exchangers, extension of units for higher thermal duties is generally not possible. All these drawbacks are easily overcome in a PHE. It can be easily repaired, and plates and other parts can be easily replaced. Due to modular construction, PHEs possess the flexibility of enhancing or reducing the heat transfer surface area, modifying the pass arrangement, and addition of more than one duty according to the heat transfer requirements at a future date.

1.4.2.9 Overall Economy

There are two major costs to consider in designing a heat exchanger: the manufacturing cost and the operating costs, including maintenance costs. In general, the less the heat transfer surface area and less

the complexity of the design, the lower is the manufacturing cost. The operating cost is the pumping cost due to pumping devices such as fans, blowers, and pumps. The maintenance costs include costs of spares that require frequent renewal due to corrosion, and costs due to corrosion/fouling prevention and control. Therefore, the heat exchanger design requires a proper balance between thermal sizing and pressure drop.

1.4.2.10 Fabrication Techniques

Fabrication techniques are likely to be the determining factor in the selection of a heat transfer surface matrix or core. They are the major factors in the initial cost and to a large extent influence the integrity, service life, and ease of maintenance of the finished heat exchanger [24]. For example, shell and tube units are mostly fabricated by welding, plate-fin heat exchangers and automobile aluminum radiators by brazing, copper–brass radiators by soldering, most of the circular tube-fin exchangers by mechanical assembling, etc.

1.4.2.11 Choice of Unit Type for Intended Applications

According to the intended applications, the selection of heat exchangers will follow the guidelines given in Table 1.2.

TABLE 1.2
Choice of Heat Exchanger Type for Intended Applications

Application	Remarks
Low-viscosity fluids	For high temperature/pressures, use STHE or double-pipe heat exchanger. Use PHE or LHE for low temperature/pressure applications.
Low-viscosity liquid to steam	Use STHE in carbon steel.
Medium-viscosity fluids	Use PHE or with high solids content, use SPHE.
High-viscosity fluids	PHE offers the advantages of good flow distribution. For extreme viscosities, the SPHE is preferred.
Fouling liquids	Use STHE with removable tube bundle. SPHE or PHE is preferred due to good flow distribution. Use PHE if easy access is of importance. Also consider Philips RODbaffle heat exchanger, <i>TWISTED TUBE® heat exchanger</i> and Helixchanger® heat exchanger, and EMbaffle® heat exchanger to improve flow velocity on the shellside, enhance heat transfer performance, and reduce fouling tendencies on shellside.
Slurries, suspensions, and pulps	SPHE offers the best characteristics. Also consider free flow PHE or wide gap PHE, or scraped surface heat exchanger.
Heat-sensitive liquids	PHE fulfills the requirements best. Also consider SPHE.
Cooling with air	Extended surface types like tube-fin heat exchanger or PFHE.
Gas or air under pressure	Use STHE with extended surface on the gas side or brazed plate-fin exchanger made of stainless steel or nickel alloys.
Cryogenic applications	Brazed aluminum plate-fin exchanger, coiled tube heat exchangers, or PCHE.
Vapor condensation	Surface condensers of STHE in carbon steel are preferred. Also consider SPHE or brazed plate heat exchanger.
Vapor/gas partial condensation	Choose SPHE.
Refrigeration and air conditioning applications	Finned tube heat exchangers, special types of PHEs, brazed PHE up to 200°C.
Air–air or gas–gas applications	Regenerators and plate-fin heat exchangers. Also consider STHE.
Viscous products, aseptic products, jam, food and meat processing, heat sensitive products and particulate laden products	Scraped surface heat exchanger.

Note: STHE, shell and tube heat exchanger; PHE, gasketed plate heat exchanger; SPHE, spiral plate heat exchanger; LHE, lamella heat exchanger; PCHE, printed circuit heat exchangers; CTHE, coiled tube heat exchanger; PFHE, plate-fin heat exchanger.

1.5 REQUIREMENTS OF HEAT EXCHANGERS

Heat exchangers have to fulfill the following requirements:

- High thermal effectiveness
- Pressure drop as low as possible
- Reliability and life expectancy
- High-quality product and safe operation
- Material compatibility with process fluids
- Convenient size, easy for installation, reliable in use
- Easy for maintenance and servicing
- Light in weight but strong in construction to withstand the operational pressures and vibrations especially heat exchangers for military applications
- Simplicity of manufacture
- Low cost
- Possibility of effecting repair to maintenance problems

The heat exchanger must meet normal process requirements specified through problem specification and service conditions for combinations of the clean and fouled conditions, and uncorroded and corroded conditions. The exchanger must be maintainable, which usually means choosing a configuration that permits cleaning as required and replacement of tubes, gaskets, and any other components that are damaged by corrosion, erosion, vibration, or aging. This requirement may also place limitations on space for tube bundle pulling, to carry out maintenance around it, lifting requirements for heat exchanger components, and adaptability for in-service inspection and monitoring.

REFERENCES

1. Shah, R. K., Classification of heat exchangers, in *Heat Exchangers: Thermal-Hydraulic Fundamentals and Design* (S. Kakac, A. E. Bergles, and F. Mayinger, eds.), Hemisphere, Washington, DC, 1981, pp. 9–46.
2. Shah, R. K. and Sekulic, D. P., *Fundamentals of Heat Exchanger Design*, John & Wiley, New York, 2003.
3. Gupta, J. P., *Fundamentals of Heat Exchanger and Pressure Vessel Technology*, Hemisphere, Washington, DC, 1986.
4. Walker, G., *Cryocoolers, Part 2: Applications*, Plenum Press, New York, 1983.
- 5a. Larowski, A. and Taylor, M. A., *Systematic Procedures for Selection of Heat Exchangers*, C58/82, Institution of Mechanical Engineers, London, U.K., 1982, pp. 32–56.
- 5b. Larowski, A. and Taylor, M. A., *Systematic Procedure for Selection of Heat Exchangers*, *Proc. Inst. Mech. Eng.*, 197A, 51–69 (1983).
6. Kern, D. Q., *Process Heat Transfer*, McGraw-Hill, New York, 1950.
7. Chisholm, D. (ed.), *Developments in Heat Exchanger Technology—I*, Applied Science Publishers, London, England, 1980.
8. Minton, P., Process heat transfer, *Proceedings of the 9th International Heat Transfer Conference*, Heat Transfer 1990–Jerusalem, Israel, Paper No. KN–2, 1, 355–362 (1990).
9. Timmerhaus, K. D. and Flynn, T. M., *Cryogenic Progress Engineering*, Plenum Press, New York, 1989.
10. Muoio, J. M., Glass as a material of construction for heat transfer equipment, *Industrial Heat Exchangers Conference Proceedings* (A. J. Hayes, W. W. Liang, S. L. Richlen, and E. S. Tabb, eds.), American Society for Metals, Metals Park, OH, 1985, pp. 385–390.
11. Yilmaz, S. and Samuelson, B., Vertical thermosyphon boiling in spiral plate heat exchangers, in *Heat Transfer—1983, Seattle, Chem. Eng. Prog. Symp. Ser.*, 79(225), 47–53 (1983).
12. Markovitz, R. E., Picking the best vessel jacket, *Chem. Eng.*, 78(26), 156–162 (1971).
13. Usher, J. D. and Cattell, G. S., Compact heat exchangers, in *Developments in Heat Exchanger Technology—I* (D. Chisholm, ed.), Applied Science Publishers Ltd., London, U.K., 1980, pp. 127–152.

14. Reay, D. A., Heat exchangers for waste heat recovery, International Research and Development Co., Ltd., New Castle upon Tyne, U.K., in *Developments in Heat Exchanger Technology—I* (D. Chisholm, ed.), Applied Science Publishers Ltd., London, U.K., 1980, pp. 233–256.
15. Butterworth, D. and Mascone, C. F., Heat transfer heads into the 21 century, *Chem. Eng. Prog.*, September, 30–37 (1991).
- 16a. Taylor, M. A. (ed), *Plate-Fin Heat Exchangers, Guide to Their Specification and Use*, HTFS (Harwell Laboratory), Oxon, U.K., 1980.
- 16b. ALPEMA, The standards of the Braze Aluminium Plate-Fin Heat Exchanger Manufacturer's Association, 3rd ed., Didcot, Oxon, U.K., 2010. (www.alpema.org).
17. API Standard 660, *Shell and Tube Exchangers for General Refinery Services*, 7th edn., American Petroleum Institute, Washington, DC, 2002.
- 18a. Steinke, M. E. and Kandlikar, G., Single-phase heat transfer enhancement techniques in microchannel and minichannel flows, in *Microchannels and Minichannels—2004*, ASME, Rochester, NY, June 17–19, 2004.
- 18b. Tuckerman, D. B. and Pease, R. F. W., High-performance heat sinking for VLSI, *IEEE Electron Device Letters*, Vol. 2 (5), May 1981, pp. 126–129.
19. Nikitin, K., Kato, Y. and Ngo, L., Thermal-Hydraulic Performance of Printed Circuit Heat Exchanger in Supercritical CO₂ Cycle, Research Laboratory for Nuclear Reactors, Tokyo Institute of Technology, Okayama, Tokyo, Japan, 2005.
20. Fleming, R. B., A Compact Perforated Plate Heat Exchanger, in *Advances in Cryogenic Engineering*, Vol. 14, Plenum Press, New York, 1969, pp. 196–204.
21. Hendricks, J. B., Perforated plate heat exchanger and method of fabrication, Patent number: 5101894, Apr 7, 1992.
22. Gollin, M., Heat exchanger design and rating, in *Handbook of Applied Thermal Design* (E. C. Guyer, ed.), Chapter 2, Part 7, McGraw-Hill, New York, 1984, pp. 7-24–7-36.
23. Caciula, L. and Rudy, T. M., Prediction of plate heat exchanger performance, *D Symp. Ser., Heat Transfer—1983*, Seattle, WA, pp. 76–89.
24. Fraas, A. P. and Ozisik, M. N., *Heat Exchanger Design*, John Wiley & Sons, New York, 1965.

SUGGESTED READINGS

- Bell, K. J. and Mueller, A. C., *Wolverine Heat Transfer Data Book II*, Wolverine Division of UOP Inc., Decatur, AL, 1984.
- Scaccia, C. and Theoclitus, G., Types, performance and applications, in *The Chemical Engineering Guide to Heat Transfer, Volume I: Plant Principles* (K. J. McNaughton and the Staff of Chemical Engineering, eds.), Hemisphere/McGraw-Hill, New York, 1986, pp. 3–14.
- Shah, R. K., Classification of heat exchangers, in *Low Reynolds Number Flow Heat Exchangers* (S. Kakac, R. K. Shah, and A. E. Bergles, eds.), Hemisphere, Washington, DC, 1983, pp. 9–19.
- Shah, R. K., What's new in heat exchanger design, *ASME, Mech. Eng.*, 106, 50–59 (1984).
- Sukhatme, S. P. and Devotta, S., Classification of heat transfer equipment, in *Heat Transfer Equipment Design* (R. K. Shah, E. C. Subbarao, and R. A. Mashelikar, eds.), Hemisphere, Washington, DC, 1988, pp. 7–16.
- Thome, R. T., *Wolverine Heat Transfer Engineering Data Book III*, Wolverine Division of UOP Inc., Decatur, AL, 2004.

BIBLIOGRAPHY

- Afgan, N. H. and Schlunder, E. U. (eds.), *Heat Exchangers: Design and Theory Sourcebook*, McGraw-Hill, New York, 1974.
- Applett, W. R. (ed.), *Shell and Tube Heat Exchangers*, American Society for Metals, Metals Park, OH, 1982.
- Bhatia, M. V. and Cheremisinoff, N. P., *Heat Transfer Equipment*, Process equipment series, Vol. 2, Technomic, Westport, CT, 1980.
- Bryers, R. W. (ed.), *Fouling of Heat Exchanger Surfaces*, Engineering Foundation, New York, 1983.
- Chen, S. S., *Flow Induced Vibration of Circular Cylindrical Structures*, Hemisphere, Washington, DC, 1987.
- Cheremisinoff, N. (ed.), *Handbook of Heat and Mass Transfer, Vol. 1—Heat Transfer Operation & Vol. 2—Mass Transfer and Reactor Design*, Gulf Publishing Company, Houston, TX, pp. 767–805, 1986.

- Cheremisinoff, N. P., *Heat Transfer Pocket Handbook*, Gulf Publishing Company, Books Division, Houston, TX, 1984.
- Chisholm, D. (ed.), *Heat Exchanger Technology*, Elsevier Applied Science, New York, 1988.
- Effectiveness Ntu Relationships for Design and Performance Evaluation of Multi-pass Crossflow Heat Exchangers, Engineering Sciences Data Unit Item 87020, ESDU International, McLean, VA, October 1987.
- Effectiveness Ntu Relationships for Design and Performance Evaluation of Two-Stream Heat Exchangers, Engineering Sciences Data Unit Item 86018, ESDU International, McLean, VA, July 1986.
- Foster, B. D. and Patton, J. B. (eds.), *Ceramic Heat Exchangers*, American Ceramic Society, Columbus, OH, 1985.
- Fraas, A. P., *Heat Exchanger Design*, 2nd edn., John Wiley & Sons, New York, 1989.
- Ganapathy, V., *Applied Heat Transfer*, PennWell Publishing Co., Tulsa, OK, 1982.
- Garrett-Price, B. A., Smith, S. A., Watts, R. L., Knudsen, J. C., Marner, W. J., and Suito, J. W., *Fouling of Heat Exchangers*, Noyes, Park Ridge, NJ, 1985.
- Hayes, A. J., Liang, W. W., Richlen, S. L., and Tabb, E. S. (eds.), *Industrial Heat Exchangers Conference Proceedings*, American Society for Metals, Metals Park, OH, 1985.
- Hewitt, G. F. (coordinating editor), *Hemisphere Handbook of Heat Exchanger Design*, Hemisphere, New York, 1990.
- Hewitt, G. F., Shires, G. L., and Bott, T. R., *Process Heat Transfer*, CRC Press, Boca Raton, FL, 1994.
- Hewitt, G. F. and Whalley, P. B., *Handbook of Heat Exchanger Calculations*, Hemisphere, Washington, DC, 1989.
- Hrynyszak, W., *Heat Exchangers: Application to Gas Turbines*, Butterworth Scientific Publications, London, U.K., 1958.
- Hussain, H., *Heat Transfer in Counterflow, Parallel Flow and Cross Flow*, McGraw-Hill, New York, 1982.
- Jakob, M., *Heat Transfer*, John Wiley & Sons, New York, 1957.
- Kakac, S., Bergles, A. E., and Fernandes, E. O. (eds.), *Two-Phase Flow Heat Exchangers: Thermal Hydraulic Fundamentals and Design*, Kluwer Academic Publishers, Dordrecht, the Netherlands, 1988.
- Kakac, S., Bergles, A. E., and Mayinger, F. (eds.), *Heat Exchangers: Thermal-Hydraulic Fundamentals and Design*, Hemisphere/McGraw-Hill, Washington, DC, 1981.
- Kakac, S., Shah, R. K., and Aung, W. (eds.), *Handbook of Single Phase Convective Heat Transfer*, John Wiley & Sons, New York, 1987.
- Kakac, S., Shah, R. K., and Bergles, A. E. (eds.), *Low Reynolds Number Flow Heat Exchangers*, Hemisphere, Washington, DC, 1983.
- Kays, W. M. and London, A. L., *Compact Heat Exchangers*, 3rd edn., McGraw-Hill, New York, 1984.
- Kern, D. Q. and Kraus, A. D., *Extended Surface Heat Transfer*, McGraw-Hill, New York, 1972, pp. 439–641.
- Kraus, A. D., *Analysis and Evaluation of Extended Surface Thermal Systems*, Hemisphere, Washington, DC, 1982.
- Levenspiel, O., *Engineering Flow and Heat Exchange*, Plenum Press, New York, 1984.
- Mahajan, K. K., *Design of Process Equipments*, Pressure Vessel Handbook Publishing Company, Tulsa, OK, 1985.
- Manzoor, M., *Heat Flow through Extended Surface Heat Exchangers*, Springer-Verlag, Berlin, Germany, 1984.
- Martin, H., *Heat Exchangers*, Hemisphere, Washington, DC, 1992.
- McNaughton, K. J. and the Staff of Chemical Engineering (eds.), *The Chemical Engineering Guide to Heat Transfer: Vol. I: Plant Principles, Vol. II: Equipment*, Hemisphere/McGraw-Hill, New York, 1986.
- Melo, L. F., Bott, T. R., and Bernardo, C. A. (eds.), *Advances in Fouling Science and Technology*, Kluwer Academic Publishers, Dordrecht, the Netherlands, 1988.
- Mondt, J. R., Regenerative Heat Exchangers: The Elements of Their Design, Selection and Use, Research Publication GMR-3396, General Motors Research Laboratories, Warren, MI, 1980.
- Mori, Y., Sheindlin, A. E., and Afgan, N. H. (eds.), *High Temperature Heat Exchangers*, Hemisphere, Washington, DC, 1986.
- Palen, J. W. (ed.), *Heat Exchanger Sourcebook*, Hemisphere, Washington, DC, 1987.
- Perry, R. H. and Chilton, C. H. (eds.), *Chemical Engineers' Handbook*, 5th edn., McGraw-Hill, New York, 1973.
- Reay, D. A., *Heat Recovery Systems*, E. and F. N. Spon Ltd., London, U.K., 1979.
- Rohsenow, W. M., Hartnett, J. P., and Ganic, E. N. (eds.), *Handbook of Heat Transfer Applications*, McGraw-Hill, New York, 1985.
- Saunders, E. A. D., *Heat Exchangers: Selection, Design and Construction*, Addison Wesley Longman, Reading, MA, 1989.

- Schlunder, E. U. (editor-in-chief), *Heat Exchanger Design Handbook*, in five volumes (Vol. 1—*Heat Exchanger Theory*, Vol. 2—*Fluid Mechanics and Heat Transfer*, Vol. 3—*Thermal and Hydraulic Design of Heat Exchangers*, Vol. 4—*Mechanical Design of Heat Exchangers*, and Vol. 5—*Physical Properties*), Hemisphere, Washington, DC, 1983.
- Schmidt, F. W. and Willmott, A. J., *Thermal Energy Storage and Regeneration*, Hemisphere/McGraw-Hill, Washington, DC, 1981.
- Shah, R. K., Kraus, A. D., and Metzger, D. (eds.), *Compact Heat Exchangers—A Festschrift for A. L. London*, Hemisphere, Washington, DC, 1990, pp. 31–90.
- Shah, R. K. and London, A. L., *Laminar Flow Forced Convection in Ducts*, Supplement 1 to advances in heat transfer series, Academic Press, New York, 1978.
- Shah, R. K. and Mueller, A. C., Heat exchanger, in *Ullmann's Encyclopedia of Industrial Chemistry*, Unit Operations II, Vol. B3, Chapter 2, VCH Publishers, Weinheim, Germany, 1989.
- Shah, R. K., Subbarao, E. C., and Mashelkar, R. A. (eds.), *Heat Transfer Equipment Design*, Hemisphere, Washington, DC, 1988.
- Sheindlin, A. E. (ed.), *High Temperature Equipment*, Hemisphere, Washington, DC, 1986.
- Singh, K. P. and Soler, A. I., *Mechanical Design of Heat Exchangers and Pressure Vessel Components*, Arcturus Publishers, Cherry Hill, NJ, 1984.
- Somerscales, E. F. C. and Knudsen, J. G. (eds.), *Fouling of Heat Transfer Equipment*, Hemisphere/McGraw-Hill, Washington, DC, 1981.
- Stasiulevicius, J. and Skrinska, A., *Heat Transfer of Finned Tube Bundles in Crossflow*, Hemisphere, Washington, DC, 1987.
- Taborek, J., Hewitt, G. F., and Afgan, N. (eds.), *Heat Exchangers: Theory and Practice*, Hemisphere/McGraw-Hill, Washington, DC, 1983.
- Walker, G., *Industrial Heat Exchangers—A Basic Guide*, Hemisphere/McGraw-Hill, New York, 1982.
- Yokell, S., *A Working Guide to Shell and Tube Heat Exchangers*, McGraw-Hill, New York, 1990.
- Zukauskas, A. A., *High Performance Single-Phase Heat Exchangers* (J. Karni, English edition editor), Hemisphere, Washington, DC, 1989.
- Zukauskas, A. and Ulinskas, R., *Heat Transfer in Tube Banks in Crossflow*, Hemisphere, Washington, DC, 1988.

2 Heat Exchanger Thermohydraulic Fundamentals

2.1 HEAT EXCHANGER THERMAL CIRCUIT AND OVERALL CONDUCTANCE EQUATION

In order to develop relationships between the heat transfer rate q , surface area A , fluid terminal temperatures, and flow rates in a heat exchanger, the basic equations used for analysis are the energy conservation and heat transfer rate equations [1]. The energy conservation equation for an exchanger having an arbitrary flow arrangement is

$$q = C_h(t_{h,i} - t_{h,o}) = C_c(t_{c,o} - t_{c,i}) \quad (2.1)$$

and the heat transfer rate equation is

$$q = UA\Delta t_m = \frac{\Delta t_m}{R_o} \quad (2.2)$$

where

Δt_m is the true mean temperature difference (MTD), which depends upon the exchanger flow arrangement and the degree of fluid mixing within each fluid stream

C_c is the capacity rate of the cold fluid, $(Mc_p)_c$

C_h is the capacity rate of the hot fluid, $(Mc_p)_h$

$t_{c,i}$ and $t_{c,o}$ are cold fluid terminal temperatures (inlet and outlet)

$t_{h,i}$ and $t_{h,o}$ are hot fluid terminal temperatures (inlet and outlet)

The heat exchanger thermal circuit variables and overall conduction described here are based on Refs. [1,2].

The inverse of the overall thermal conductance UA is referred to as the overall thermal resistance R_o , and it is made up of component resistances in series as shown in Figure 2.1:

$$R_o = R_h + R_1 + R_w + R_2 + R_c \quad (2.3)$$

where the parameters of the right-hand side of Equation 2.3 are R_h , hot side film convection resistance, $1/(\eta_o h A)_h$; R_1 , thermal resistance due to fouling on the hot side given in terms of fouling resistance $R_{f,h}$ (i.e., values tabulated in standards or textbooks), $R_{f,h}/(\eta_o A)_h$; R_w , thermal resistance of the separating wall, expressed for a flat wall by

$$R_w = \frac{\delta}{A_w k_w} \quad (2.4a)$$

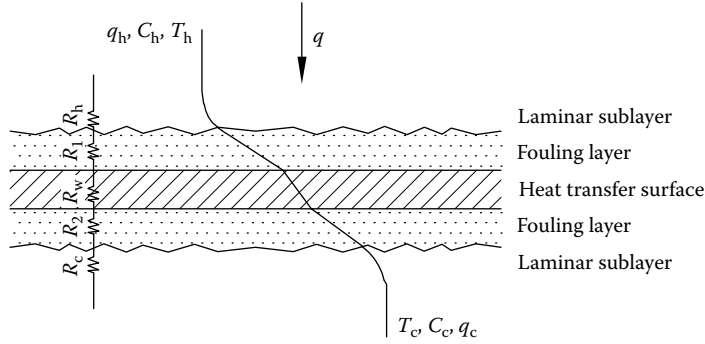


FIGURE 2.1 Elements of thermal resistance of a heat exchanger.

and for a circular wall by

$$R_w = \frac{\ln(d/d_i)}{2\pi k_w L N_t} \quad (2.4b)$$

where

δ is the wall thickness

A_w is the total wall area for heat conduction

k_w is the thermal conductivity of the wall material

d is the tube outside diameter

d_i is the tube inside diameter

L is the tube length

N_t is the number of tubes, and total wall area for heat conduction is given by

$$A_w = L_1 L_2 L_p \quad (2.5)$$

where

L_1, L_2 , and N_p are the length, width, and total number of separating plates, respectively

$R_{f,c}$ is the thermal resistance due to fouling on the cold side, given in terms of cold side fouling resistance $R_{f,c}/(\eta_o A)_c$

R_c is the cold side film convection resistance, $1/(\eta_o h A)_c$

In these definitions, h is the heat transfer coefficient on the side under consideration, A represents the total of the primary surface area, A_p , and the secondary (finned) surface area, A_f , on the fluid side under consideration, η_o is the overall surface effectiveness of an extended surface, and the subscripts h and c refer to the hot and cold fluid sides, respectively. The overall surface effectiveness η_o is related to the fin efficiency η_f and the ratio of fin surface area A_f to total surface area A as follows:

$$\eta_o = 1 - \frac{A_f}{A} (1 - \eta_f) \quad (2.6)$$

Note that η_o is the unity for an all prime surface exchanger without fins. Equation 2.3 can be alternately expressed as

$$\frac{1}{UA} = \frac{1}{(\eta_o h A)_h} + \frac{R_{f,h}}{(\eta_o A)_h} + R_w + \frac{1}{(\eta_o h A)_c} + \frac{R_{f,c}}{(\eta_o A)_c} \quad (2.7)$$

Since $UA = U_h A_h = U_c A_c$, the overall heat transfer coefficient U as per Equation 2.7 may be defined optionally in terms of either hot fluid surface area or cold fluid surface area. Thus, the option of A_h or A_c must be specified in evaluating U from the product, UA . For plain tubular exchangers, U_o based on tube outside surface is given by

$$\frac{1}{U_o} = \frac{1}{h_o} + R_{f,o} + \frac{d \ln(d/d_i)}{2k_w} + \frac{R_{f,i}d}{d_i} + \frac{d}{h_i d_i} \quad (2.8)$$

The knowledge of wall temperature in a heat exchanger is essential to determine the localized hot spots, freeze points, thermal stresses, local fouling characteristics, or boiling and condensing coefficients. Based on the thermal circuit of Figure 2.1, when R_w is negligible, $T_{w,h} = T_{w,c} = T_w$ is computed from [1,2] as

$$T_w = \frac{T_h + T_c [(R_h + R_1)/(R_c + R_2)]}{1 + [(R_h + R_1)/(R_c + R_2)]} \quad (2.9)$$

When $R_1 = R_2 = 0$, Equation 2.9 further simplifies to

$$T_w = \frac{T_h/R_h + T_c/R_c}{1/R_h + 1/R_c} = \frac{(\eta_o hA)_h T_h + (\eta_o hA)_c T_c}{(\eta_o hA)_h + (\eta_o hA)_c} \quad (2.10)$$

2.2 HEAT EXCHANGER HEAT TRANSFER ANALYSIS METHODS

2.2.1 ENERGY BALANCE EQUATION

The first law of thermodynamics must be satisfied in any heat exchanger design procedure at both the macro and microlevels. The overall energy balance for any two-fluid heat exchanger is given by

$$m_h c_{p,h} (t_{h,i} - t_{h,o}) = m_c c_{p,c} (t_{c,o} - t_{c,i}) \quad (2.11)$$

Equation 2.11 satisfies the “macro” energy balance under the usual idealizations made for the basic design theory of heat exchangers [3].

2.2.2 HEAT TRANSFER

For any flow arrangement, heat transfer for two fluid streams is given by

$$q = C_h (t_{h,i} - t_{h,o}) = C_c (t_{c,o} - t_{c,i}) \quad (2.12)$$

and the expression for maximum possible heat transfer rate q_{\max} is

$$q_{\max} = C_{\min} (t_{h,i} - t_{c,i}) \quad (2.13)$$

The maximum possible heat transfer rate would be obtained in a counterflow heat exchanger with very large surface area and zero longitudinal wall heat conduction, and the actual operating conditions are the same as the theoretical conditions.

2.2.3 BASIC METHODS TO CALCULATE THERMAL EFFECTIVENESS

There are four design methods to calculate the thermal effectiveness of heat exchangers:

1. ϵ -NTU method
2. P -NTU_i method
3. LMTD method
4. ψ - P method

The basics of these methods are discussed next. For more details on these methods, refer to Refs. [1,2].

2.2.3.1 ϵ -NTU Method

The formal introduction of the ϵ -NTU method for the heat exchanger analysis was in 1942 by London and Seban [4]. In this method, the total heat transfer rate from the hot fluid to the cold fluid in the exchanger is expressed as

$$q = \epsilon C_{\min}(t_{h,i} - t_{c,i}) \quad (2.14)$$

where ϵ is the heat exchanger effectiveness. It is nondimensional and for a direct transfer type heat exchanger, in general, it is dependent on NTU, C^* , and the flow arrangement:

$$\epsilon = \phi(\text{NTU}, C^*, \text{flow arrangement}) \quad (2.15)$$

These three nondimensional parameters, C^* , NTU, and ϵ , are defined next.

Heat capacity rate ratio, C^ :* This is simply the ratio of the smaller to larger heat capacity rate for the two fluid streams so that $C^* \leq 1$.

$$C^* = \frac{C_{\min}}{C_{\max}} = \frac{(mc_p)_{\min}}{(mc_p)_{\max}} \quad (2.16)$$

where

C refers to the product of mass and specific heat of the fluid
the subscripts min and max refer to the C_{\min} and C_{\max} sides, respectively

In a two-fluid heat exchanger, one of the streams will usually undergo a greater temperature change than the other. The first stream is said to be the “weak” stream, having a lower thermal capacity rate (C_{\min}), and the other with higher thermal capacity rate (C_{\max}) is the “strong” stream.

Number of transfer units, NTU: NTU designates the nondimensional “heat transfer size” or “thermal size” of the exchanger. It is defined as a ratio of the overall conductance to the smaller heat capacity rate:

$$\text{NTU} = \frac{UA}{C_{\min}} = \frac{1}{C_{\min}} \int_A U dA \quad (2.17)$$

If U is not a constant, the definition of the second equality applies. For constant U , substitution of the expression for UA results in [1,2]

$$\text{NTU} = \frac{1}{C_{\min}} \left[\frac{1}{1/(\eta_o hA)_h + R_1 + R_w + R_2 + 1/(\eta_o hA)_c} \right] \quad (2.18)$$

where R_1 and R_2 are the thermal resistances due to fouling on the hot side and the cold side, respectively, as defined in Equation 2.7. In the absence of the fouling resistances, NTU can be given by the expression

$$\frac{1}{NTU} = \frac{1}{NTU_h(C_h/C_{\min})} + R_w C_{\min} + \frac{1}{NTU_c(C_c/C_{\min})} \quad (2.19)$$

and the number of heat transfer units on the hot and cold sides of the exchanger may be defined as follows:

$$NUT_h = \frac{(\eta_o hA)_h}{C_h} \quad NUT_c = \frac{(\eta_o hA)_c}{C_c} \quad (2.20)$$

Heat exchanger effectiveness, ϵ : Heat exchanger effectiveness, ϵ , is defined as the ratio of the actual heat transfer rate, q , to the thermodynamically possible maximum heat transfer rate (q_{\max}) by the second law of thermodynamics:

$$\epsilon = \frac{q}{q_{\max}} \quad (2.21)$$

The value of ϵ ranges between 0 and 1. Using the value of actual heat transfer rate q from Equation 2.12 and q_{\max} from Equation 2.13, the exchanger effectiveness ϵ of Equation 2.21 is given by

$$\epsilon = \frac{C_h(t_{h,i} - t_{h,o})}{C_{\min}(t_{h,i} - t_{c,i})} = \frac{C_c(t_{c,o} - t_{c,i})}{C_{\min}(t_{h,i} - t_{c,i})} \quad (2.22)$$

For $C^* = 1$, $\epsilon_h = \epsilon_c$

Dependence of ϵ on NTU: At low NTU, the exchanger effectiveness is generally low. With increasing values of NTU, the exchanger effectiveness generally increases, and in the limit it approaches the maximum asymptotic value. However, there are exceptions such that after reaching a maximum value, the effectiveness decreases with increasing NTU.

2.2.3.2 P -NTU_t Method

This method represents a variant of the ϵ -NTU method. The origin of this method is related to shell and tube exchangers. In the ϵ -NTU method, one has to keep track of the C_{\min} fluid. In order to avoid possible errors, an alternative is to present the temperature effectiveness, P , of the fluid side under consideration as a function of NTU and heat capacity rate of that side to that of the other side, R . Somewhat arbitrarily, the side chosen is the tubeside regardless of whether it is the hot side or the cold side.

General P -NUT_t functional relationship: Similar to the exchanger effectiveness ϵ , the thermal effectiveness P is a function of NTU_t, R , and flow arrangement:

$$P = \phi(NTU_t, R, \text{flow arrangement}) \quad (2.23)$$

where P , NTU_t, and R are defined consistently based on the tubeside fluid variables. In this method, the total heat transfer rate from the hot fluid to the cold fluid is expressed by

$$q = PC_t(T_1 - t_1) \quad (2.24)$$

Thermal effectiveness, P : For a shell and tube heat exchanger, the temperature effectiveness of the tubeside fluid, P , is referred to as the “thermal effectiveness.” It is defined as the ratio of the temperature rise (drop) of the tubeside fluid (regardless of whether it is hot or cold fluid) to the difference of inlet temperature of the two fluids. According to this definition, P is given by

$$P = \frac{t_2 - t_1}{T_1 - t_1} \quad (P \text{ is referred to tubeside}) \quad (2.25)$$

where

t_1 and t_2 refer to tubeside inlet and outlet temperatures, respectively

T_1 and T_2 refer to shellside inlet and outlet temperatures, respectively

Comparing Equations 2.25 and 2.22, it is found that the thermal effectiveness P and the exchanger effectiveness ε are related as

$$\begin{aligned} P &= \frac{C_{\min}}{C_t} \varepsilon = \varepsilon \quad \text{for } C_t = C_{\min} \\ &= \varepsilon C^* \quad \text{for } C_t = C_{\max} \end{aligned} \quad (2.26)$$

Note that P is always less than or equal to ε . The thermal effectiveness of the shellside fluid can be determined from the tubeside values by the relationship given by

$$P_s = P \frac{C_t}{C_s} = PR \quad (2.27)$$

$$\text{For } R^* = 1, \quad P_s = P \text{ (tubeside)}$$

(For TEMA shell types, the thermal effectiveness charts given in this chapter 2, depicts thermal effectiveness referred to tubeside only)

Heat capacity ratio, R : For a shell and tube exchanger, R is the ratio of the capacity rate of the tube fluid to the shell fluid. This definition gives rise to the following relation in terms of temperature drop (rise) of the shell fluid to the temperature rise (drop) of the tube fluid:

$$R = \frac{C_t}{C_s} = \frac{T_1 - T_2}{t_2 - t_1} \quad (2.28)$$

where the right-hand-side expressions come from an energy balance and indicate the temperature drop/rise ratios. The value of R ranges from zero to infinity, zero being for pure vapor condensation and infinity being for pure liquid evaporation. Comparing Equations 2.28 and 2.16, R and C^* are related by

$$\begin{aligned} R &= \frac{C_t}{C_s} = C^* \quad \text{for } C_t = C_{\min} \\ &= \frac{1}{C^*} \quad \text{for } C_t = C_{\max} \end{aligned} \quad (2.29)$$

Thus R is always greater than or equal to C^* .

Number of transfer units, NTU_t : For a shell and tube exchanger, the number of transfer units NTU_t is defined as a ratio of the overall conductance to the tubeside fluid heat capacity rate:

$$NTU_t = \frac{UA}{C_t} \quad (2.30)$$

Thus, NTU_t is related to NTU based on C_{\min} by

$$\begin{aligned} NTU_t &= NTU \frac{C_{\min}}{C_t} = NTU \quad \text{for } C_t = C_{\min} \\ &= NTUC^* \quad \text{for } C_t = C_{\max} \end{aligned} \quad (2.31)$$

Thus NTU_t is always less than or equal to NTU .

2.2.3.3 Log Mean Temperature Difference Correction Factor Method

The maximum driving force for heat transfer is always the log mean temperature difference (LMTD) when two fluid streams are in countercurrent flow. However, the overriding importance of other design factors causes most heat exchangers to be designed in flow patterns different from true countercurrent flow. The true MTD of such flow arrangements will differ from the logarithmic MTD by a certain factor dependent on the flow pattern and the terminal temperatures. This factor is usually designated as the log MTD correction factor, F . The factor F may be defined as the ratio of the true MTD to the logarithmic MTD. The heat transfer rate equation incorporating F is given by

$$q = UA\Delta t_m = UAF\Delta t_{lm} \quad (2.32)$$

where

Δt_m is the true MTD

Δt_{lm} is the LMTD

The expression for LMTD for a counterflow exchanger is given by

$$LMTD = \Delta t_{lm} = \frac{\Delta t_1 - \Delta t_2}{\ln(\Delta t_1 / \Delta t_2)} \quad (2.33a)$$

where $\Delta t_1 = t_{h,i} - t_{c,o} = T_1 - t_2$ and $\Delta t_2 = t_{h,o} - t_{c,i} = T_2 - t_1$ for all flow arrangements except for parallelflow; for parallelflow $\Delta t_1 = t_{h,i} - t_{c,i} (=T_1 - t_1)$ and $\Delta t_2 = t_{h,o} - t_{c,o} (=T_2 - t_2)$. Therefore, LMTD can be represented in terms of the terminal temperatures, that is, greater terminal temperature difference (GTDD or GTD) and smaller terminal temperature difference (STTD or STD) for both pure parallel- and counterflow arrangements. Accordingly, LMTD is given by

$$LMTD = \Delta t_{lm} = \frac{GTDD - STTD}{\ln(GTDD/STTD)} \quad (2.33b)$$

The terminal temperature distribution to calculate LMTD is shown in Figure 2.2a.

2.2.3.3.1 LMTD Correction Factor, F

Charts to determine LMTD from the terminal temperature differences are shown in Figure 2.2b. (Note: While referring the nomogram of Figure 2.2b, use GTD in place of GTDD and STD in place of STTD.)

From its definition, F is expressed by

$$F = \frac{\Delta t_m}{\Delta t_{lm}} \quad (2.34)$$

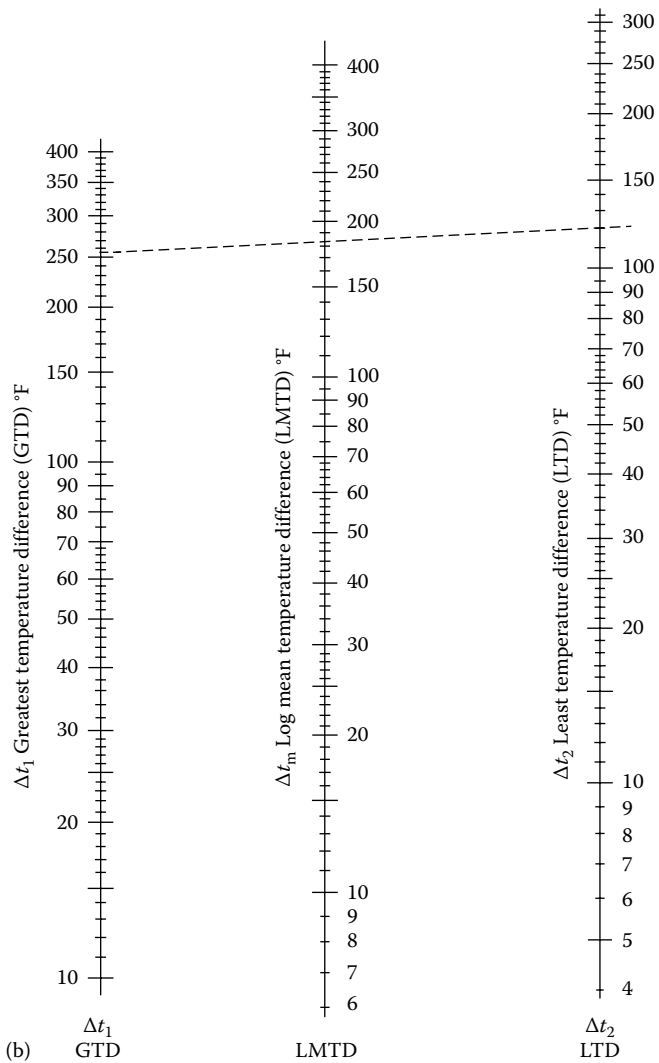
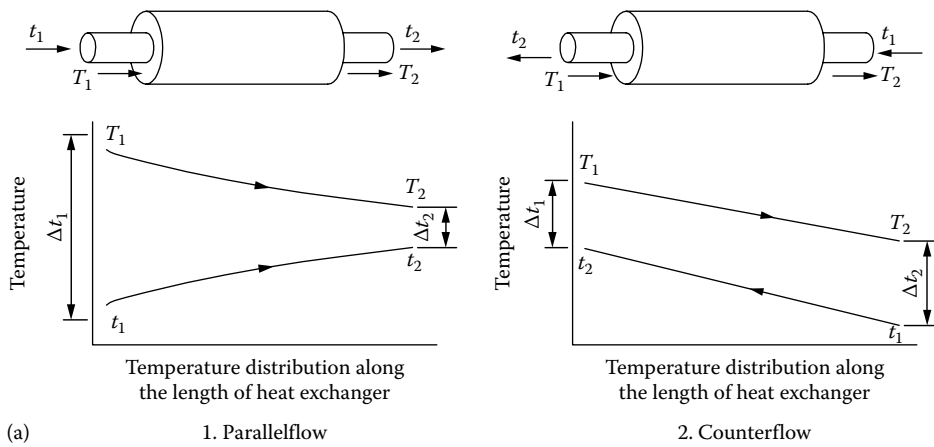


FIGURE 2.2 (a) Terminal temperature to calculate LMTD; (b) nomogram to find LMTD. (Courtesy of Paul-Muller Company, Springfield, MO.)

In situations where the heat release curves are nonlinear, the approach just described is not applicable and a “weighted” temperature difference must be determined.

It can be shown that, in general, F is dependent upon the thermal effectiveness P , the heat capacity rate ratio R , and the flow arrangement. Therefore, F is represented by

$$F = \phi(P, R, NTU_i, \text{flow arrangement}) \quad (2.35)$$

and the expression for F in terms of P , R , and NTU is given by

$$\begin{aligned} F &= \frac{1}{(R-1)NTU} \ln \left[\frac{1-P}{1-PR} \right] \quad \text{for } R \neq 1 \\ &= \frac{P}{(1-P)NTU} \quad \text{for } R = 1 \end{aligned} \quad (2.36a)$$

$$\begin{aligned} F &= \frac{1}{(1-C^*)NTU} \ln \left[\frac{1-\epsilon C^*}{1-\epsilon} \right] \quad \text{for } C^* \neq 1 \\ &= \frac{\epsilon}{(1-\epsilon)NTU} \quad \text{for } C^* = 1 \end{aligned} \quad (2.36b)$$

The factor F is dimensionless.

The value of F is unity for a true counterflow exchanger, and thus independent of P and R . For other arrangements, F is generally less than unity, and can be explicitly presented as a function of P , R , and NTU_i by Equation 2.36. The value of F close to unity does not mean a highly efficient heat exchanger, but it means a close approach to the counterflow behavior for the comparable operating conditions of flow rates and inlet fluid temperatures. Because of a large capital cost involved with a shell and tube exchanger, generally it is designed in the steep region of the P - NTU_i curve (ϵ - NTU relation for the compact heat exchanger) (ϵ or $P < 60\%$), and as a rule of thumb, the F value selected is 0.80 and higher. However, a better guideline for F_{\min} is provided in the next section. For more details on heat exchanger thermal design methods, refer to Shah and Sekulic [5] and Ref. [6].

2.2.3.3.2 Approximate F Value for Heat Exchanger Sizing Purpose

This correction factor accounts for the two streams not in counterflow. At the estimation stage, we do not know the detailed flow and pass arrangement so we can assume the following for preliminary sizing:

- $F = 1.0$ for true counterflow, e.g., double-pipe heat exchanger in counterflow arrangement, F shell type of shell and tube heat exchanger
- $F = 0.7$ for crossflow heat exchanger
- $F = 0.7$ for TEMA E shell with single pass on both shellside and tubeside
- $F = 0.80$ for E_{1-2} shell and tube heat exchanger (refer Figure 2.28)
- $F = 0.95$ for G_{1-2} (refer Figure 2.34), H_{1-2} shell and tube heat exchanger (refer Figure 2.36)
- $F = 0.79$ for J_{1-2} shell and tube heat exchanger (refer Figure 2.38)
- $F = 0.9$ for multi-pass compact heat exchanger and multiple passes on both shellside and tubeside of TEMA E shell
- $F = 1.0$ if one stream is isothermal, $C^* = 0$, $R = 0$ or ∞ (typically boiling or condensation)

Applicability of ϵ - NTU and LMTD methods: Generally, the ϵ - NTU method is used for the design of compact heat exchangers. The LMTD method is used for the design of shell and tube heat exchangers. It should be emphasized that either method will yield the identical results within the convergence tolerances specified.

2.2.3.4 ψ - P Method

The ψ - P method was originally proposed by Smith [7] and modified by Mueller [8]. In this method, a new term ψ is introduced, which is expressed as the ratio of the true MTD to the inlet temperature difference of the two fluids:

$$\psi = \frac{\Delta t_m}{t_{h,i} - t_{c,i}} = \frac{\Delta t_m}{T_1 - t_1} \quad (2.37)$$

and ψ is related to ε and NTU and P and NTU_t as

$$\psi = \frac{\varepsilon}{\text{NTU}} = \frac{P}{\text{NTU}_t} \quad (2.38)$$

and the heat transfer rate is given by

$$q = UA\psi(t_{h,i} - t_{c,i}) \quad (2.39a)$$

$$= UA\psi(T_1 - t_1) \quad (2.39b)$$

Since ψ represents the nondimensional Δt_m , there is no need to compute Δt_m in this method.

Functional relationship between the various thermal design methods: The general functional relationship for the ε -NTU, P -NTU_t, LMTD, and ψ - P methods is shown in Table 2.1, which has been adapted and modified from Ref. [1], and the relationship between the dimensionless groups of these methods is given in Table 2.2.

Thermal design methods for the design of shell and tube heat exchangers: Any of the four methods (ε -NTU, P -NTU_t, LMTD, and ψ - P) can be used for shell and tube exchangers.

TABLE 2.1
General Functional Relationship between Dimensionless Groups of the ε -NTU, P -NTU_t, and LMTD

Heat Transfer Parameters	ε -NTU Method	P -NTU _t Method	LMTD Method
Heat capacity rate ratio	$C^* = \frac{C_{\min}}{C_{\max}} = \frac{(mc_p)_{\min}}{(mc_p)_{\max}}$	$R = \frac{C_t}{C_s} = \frac{T_1 - T_2}{t_2 - t_1}$	$\text{LMTD} = \frac{\Delta t_1 - \Delta t_2}{\ln \left[\frac{\Delta t_1}{\Delta t_2} \right]}$
NTU	$\text{NTU} = \frac{UA}{C_{\min}} = \frac{1}{C_{\min}} \int_A U dA$	$\text{NTU}_t = \frac{UA}{C_t}$	$\text{LMTD} = \Delta t_{\text{lm}}$ $F = \phi(P, R, \text{NTU}_t, \text{flow arrangement})$
Thermal effectiveness	$\varepsilon = \phi(\text{NTU}, C^*, \text{flow arrangement})$ $\varepsilon = \frac{C_h(t_{h,i} - t_{h,o})}{C_{\min}(t_{h,i} - t_{c,i})} = \frac{C_c(t_{c,o} - t_{c,i})}{C_{\min}(t_{h,i} - t_{c,i})}$	$P = \phi(\text{NTU}_t, R, \text{flow arrangement})$ $P = \frac{t_2 - t_1}{T_1 - t_1}$ $P_s = P \frac{C_t}{C_s} = PR$	$F = \frac{\Delta t_m}{\Delta t_{\text{lm}}}$ $F = \frac{1}{(R-1)\text{NTU}} \ln \left[\frac{1-P}{1-PR} \right]$ for $R \neq 1$ $= \frac{P}{(1-P)\text{NTU}}$ for $R = 1$ $q = UA\Delta t_m = UAF\Delta t_{\text{lm}}$
Heat transfer	$q = C_h(t_{h,i} - t_{h,o}) = C_c(t_{c,o} - t_{c,i})$	$q = PC_t(T_1 - t_1)$	

TABLE 2.2
Relationship between Dimensionless Groups
of the ε -NTU, P -NTU, and LMTD Methods

$$\begin{aligned}
 R &= \frac{C_t}{C_s} = C^* \quad \text{for } C_t = C_{\min} \\
 &= \frac{1}{C^*} \quad \text{for } C_t = C_{\max} \\
 NTU_t &= NTU \frac{C_{\min}}{C_t} = NTU \quad \text{for } C_t = C_{\min} \\
 &= NTUC^* \quad \text{for } C_t = C_{\max} \\
 F &= \frac{1}{(R-1)NTU} \ln \left[\frac{1-P}{1-PR} \right] \quad \text{for } R \neq 1 \\
 &= \frac{P}{(1-P)NTU} \quad \text{for } R = 1 \\
 \Psi &= \frac{\varepsilon}{NTU} = \frac{P}{NTU_t}
 \end{aligned}$$

2.2.4 SOME FUNDAMENTAL RELATIONSHIPS TO CHARACTERIZE THE EXCHANGER FOR “SUBDESIGN” CONDITION

The partial derivatives of the temperature efficiency P with respect to NTU and R enable complete characterization of the exchanger performance around an operating point. Thus, the exchanger performance can be readily predicted for the “subdesign” conditions [9]. Singh [9] developed derivatives of P , F , and NTU . Derivatives for P and F are discussed next.

Dependence of thermal effectiveness: Thermal performance P and thermal effectiveness ε can be represented through R by [9]

$$\begin{aligned}
 \varepsilon &= P \quad R \leq 1 \\
 &= PR \quad R > 1
 \end{aligned} \tag{2.40}$$

$$P = f(NTU, R) \tag{2.41}$$

$$\varepsilon = \phi(NTU, R^*) \tag{2.42}$$

Thus,

$$d\varepsilon = d\phi = \frac{\partial \phi}{\partial NTU} dNTU + \frac{\partial \phi}{\partial R} dR \tag{2.43}$$

$$d\varepsilon = dP = \frac{\partial P}{\partial NTU} dNTU + \frac{\partial P}{\partial R} dR \quad \text{for } R \leq 1 \tag{2.44}$$

$$d\varepsilon = PdR + RdP \tag{2.45}$$

$$= PdR + R \left(\frac{\partial P}{\partial NTU} dNTU + \frac{\partial P}{\partial R} dR \right) \tag{2.46}$$

or

$$d\varepsilon = \left(P + R \frac{\partial P}{\partial R} \right) dR + R \frac{\partial P}{\partial \text{NTU}} d\text{NTU} \quad \text{for } R \geq 1 \quad (2.47)$$

Dependence of LMTD correction factor, F: The derivatives of F with respect to ε , P , and R are given by [9]

$$\frac{\partial F}{\partial \text{NTU}} = -\frac{1}{\text{NTU}^2(R-1)} \ln \left[\frac{1-P}{1-PR} \right] = \frac{-F}{\text{NTU}} \quad (2.48)$$

$$\frac{\partial F}{\partial P} = \frac{1}{\text{NTU}(1-P)(1-PR)} \quad (2.49)$$

$$\frac{\partial F}{\partial R} = \frac{-F}{(R-1)} + \frac{1}{\text{NTU}(R-1)(1-PR)} \quad (2.50)$$

and

$$dF = \frac{\partial F}{\partial P} dP + \frac{\partial F}{\partial \text{NTU}} d\text{NTU} + \frac{\partial F}{\partial R} dR \quad (2.51)$$

2.3 THERMAL EFFECTIVENESS CHARTS

Broadly speaking, there are two types of heat exchanger problems: rating and sizing. To solve either type of problem from first principles is laborious and time-consuming. However, sizing and rating of heat exchangers are solved with the use of performance charts easily. The graphical charts were introduced many years ago and have gained wide acceptance throughout the industry. Five types of heat exchanger design charts are found in the literature, and the salient features of these charts are discussed by Turton et al. [10]. These charts are shown schematically in Figure 2.3a–f. The dimensionless variables used in these charts (ε , P , R , C^* , F , NTU , NTU_1) have been defined in Section 2.2.

Figure 2.3a is the most widely used of these charts and was introduced by Bowman et al. [11] in 1940. In this chart, the LMTD correction factor, F , is presented as a function of the effectiveness, P , and the heat capacity rate ratio, R . Using this chart, the design problem where terminal temperatures and flow rates are usually specified but overall U and/or A are unknown can be solved; however, the rating problem can be solved by a trial-and-error solution. Since F compares the true MTD of a given flow arrangement with that of the counterflow arrangement, these charts provide a well-suited means of finding out the best of several possible flow arrangements. The one with the higher F will require the lower NTU , that is, the lower area if U remains constant, operating with the same R and P . Underwood [12] first derived the expression for true MTD for E_{1-2} , E_{1-4} , and E_{2-4} shell and tube exchangers in 1934. Bowman et al. [11] published a summary of correction factors for exchangers of different flow arrangements. Ten Broeck [13] further constructed charts using dimensionless groups, $UA/(mc_p)$, $P = (t_2 - t_1)/(T_1 - t_1)$, and $R = (T_1 - T_2)/(t_2 - t_1)$ for direct calculation of terminal temperatures with known surface area of a heat exchanger. At present, F charts are available for all TEMA shells.

Figure 2.3b and c are due to Kays and London [14] and TEMA [15], respectively. Figure 2.3c is plotted on a semilog paper, since the most useful NTU and NTU_1 design range for compact heat exchangers and shell and tube exchangers, respectively, is 0.2–3.0. A careful look at the linear graphical presentation of the ε - NTU results of Figure 2.3b indicates that the NTU scale in this range is short and hence one cannot obtain the accurate values of ε or NTU from graphs.

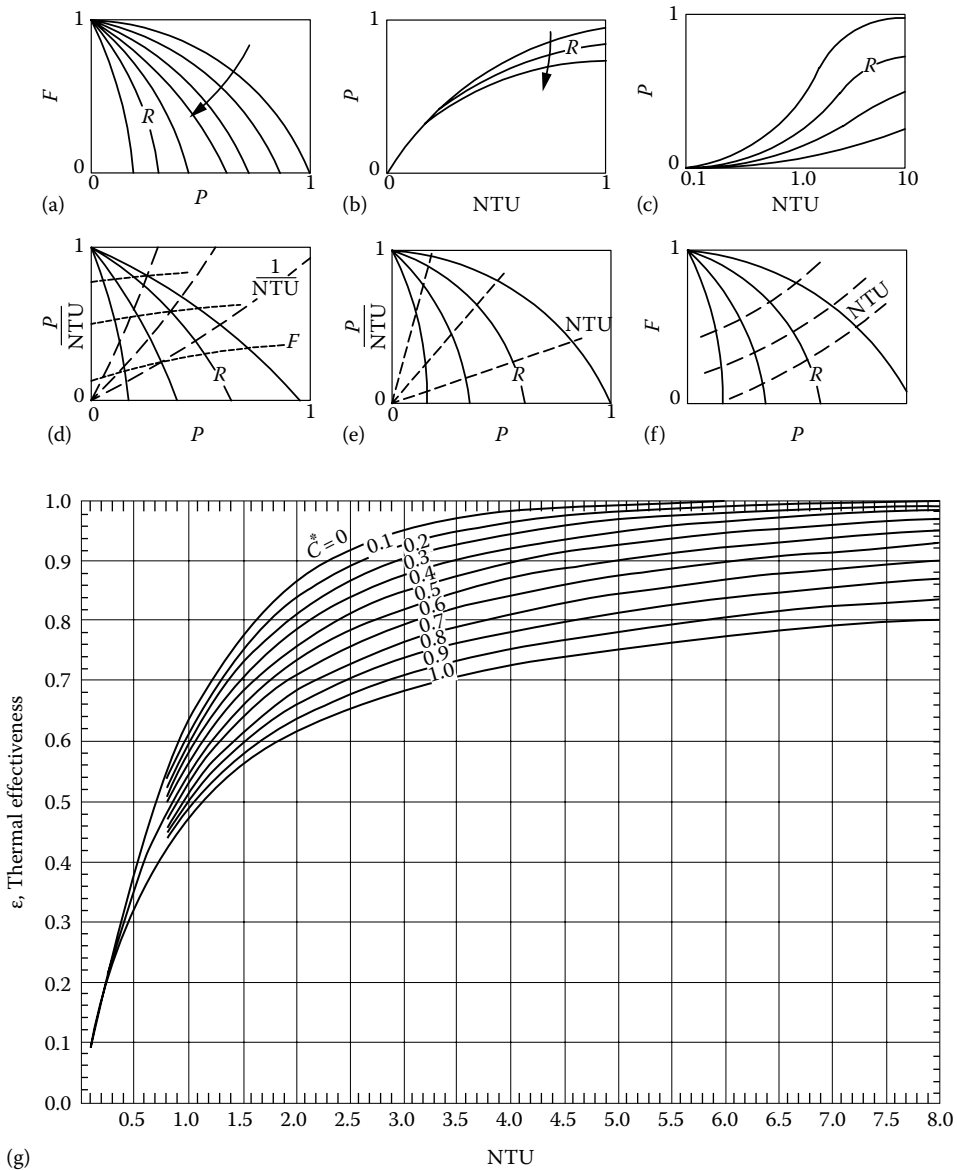


FIGURE 2.3 Thermal effectiveness charts. (a) Bowman chart; (b) Kays and London chart; (c) TEMA chart; (d) F - P - R -chart; (e) ψ chart; (f) F - P - R -NTU chart (From Turton, R. et al., *Trans. ASME J. Heat Transfer*, 106, 893, 1984); (g) ϵ -NTU chart for unmixed-unmixed crossflow, as per Eq. T4 of Table 2.4.

For better appreciation, this is illustrated through the thermal relation chart (ϵ -NTU) for crossflow heat exchanger in Figure 2.3. An alternative is to stretch the NTU scale in the range 0.2–3.0 by using a logarithmic scale. Thus, the P -NTU_i results are generally presented on a semilog paper, as shown for example in Figure 2.3c, in order to obtain more accurate graphical values of P or NTU_i. Using these charts, both the sizing and rating problem can be solved. However, the LMTD correction factor F is not shown in these charts. Hence, it is to be calculated additionally.

Muller [8] proposed the charts of Figure 2.3d with its triple family of curves. This chart can be used to solve both the sizing and rating problems and in addition gives the F values. However, Figure 2.3d is somewhat cramped and difficult to read accurately and introduces yet another parameter,

P/NTU_i . The Muller charts have been redrawn recently by Taborek and included in HEDH [16]. The present form of this chart is shown in Figure 2.3e. The main difference between Figure 2.3d and e is that the F parameter curves have been omitted in the latter, and thus the problem of having to separately calculate the F values has been retained.

In a system with four variables, F , P , R , and NTU or NTU_i , any chart displays just one family of curves, such as Figure 2.3a–c, and does not give all the interrelationships directly. On the other hand, a chart with three families of curves, as in Figure 2.3d, has one set that is redundant. To show all the interrelationships between these four variables requires a chart with two families of curves. This is satisfied by Figure 2.3e.

In the graphical presentation, ψ is plotted against P and R as a parameter as shown in Figure 2.3e. The lines of constant R originate at $\psi = 1$ and terminate at $\psi = 0$ so that the asymptotic values of P for NTU tend to infinity. Thus the curves of constant R are similar to those for the F - P charts. In order to tie in with the P - NTU_i and LMTD methods, the lines of constant NTU_i and constant F are also superimposed on this chart. Figure 2.3e also has one limitation: It does not show directly the four parameters of interest.

Constraints due to the charts in Figure 2.3a–e are overcome by a chart, shown in Figure 2.3f, proposed by Turton et al. [10]. The chart in Figure 2.3f extends the easy-to-read Bowman charts of Figure 2.3a to include a second family of curves representing the variable NTU . Both the sizing and rating problems can be solved using this form of chart, and F values can be found directly for both types of problems. Thus to find exchanger surface area, use P and R to evaluate F and NTU . To find terminal temperature, use NTU and R to evaluate P and F . Most of the charts included in this book are of the type of Figure 2.3f.

2.4 SYMMETRY PROPERTY AND FLOW REVERSIBILITY AND RELATION BETWEEN THE THERMAL EFFECTIVENESS OF OVERALL PARALLEL AND COUNTERFLOW HEAT EXCHANGER GEOMETRIES

2.4.1 SYMMETRY PROPERTY

The symmetry property relates the thermal behavior of a heat exchange process to that of the reverse process, in which the directions of flow of both fluids are reversed [17]. Figure 2.4 shows four different flow arrangements for the TEMA E_{1-2} shell and tube heat exchanger that are equivalent if complete transverse mixing of the shell fluid is satisfied.

2.4.2 FLOW REVERSIBILITY

Flow reversibility establishes a relation between the thermal effectiveness of two heat exchanger configurations that differ from each other in the inversion of either one of the two fluids [18].

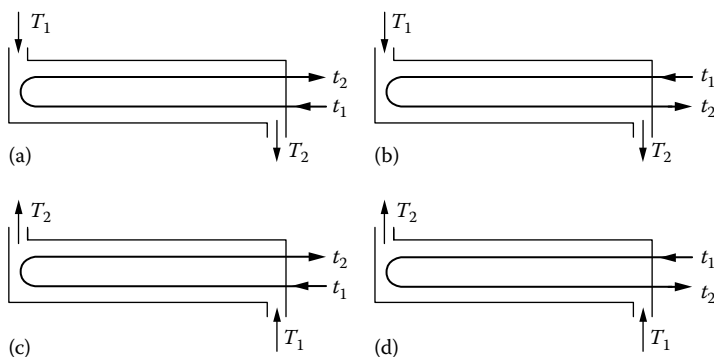


FIGURE 2.4 Flow reversibility principle. (a) Basic E_{1-2} case, (b) basic case with tube fluid reversed, (c) basic case with shell fluid reversed, and (d) basic case with both shell and tube fluids reversed. (Symmetry operations performed on the TEMA E_{1-2} shell.) (From Pignotti, A., *Trans. ASME, J. Heat Transfer*, 106, 361, 1984.)

Although the inversion of both fluids often does not alter the configuration, the inversion of only one of them usually leads from one configuration to an entirely different one, as is the case in going from a pure parallelflow to a pure counterflow arrangement or vice versa. Using this relation, if the expression for the effectiveness, P , of a configuration as a function of the heat capacity rate ratio, R (or C^*), and the number of heat transfer units NTU is known, the corresponding expression for the “inverse” configuration is immediately obtained from the simple relation [18]:

$$P_i(R, NTU) = \frac{P(-R, NTU)}{1 + RP(-R, NTU)} \quad (2.52)$$

where P denotes the effectiveness of a given arrangement, and P_i , that of the same one with fluid direction reversed. The relation is valid under the assumptions of temperature independence of the heat transfer coefficient and heat capacity rates, when one of the fluids proceeds through the exchanger in a single, mixed stream. In some cases with special symmetry, the inversion of both fluids does not alter the geometry, and therefore this property is trivially satisfied. Pignotti [18] illustrates the property of flow reversibility with several examples from the available literature. An example to clarify the meaning of Equation 2.52 is given next. Consider the well-known expression for the effectiveness of a parallelflow configuration:

$$P(R, NTU) = \frac{[1 - \exp[-NTU(1 + R)]]}{(1 + R)} \quad (2.53)$$

Let us derive from it the expression for the effectiveness of a pure counterflow configuration, which we denote $P_c(R, NTU)$. Equation 2.52 is applicable, because the counterflow geometry is obtained from parallelflow by inverting the direction of flow of one of the fluids, and the condition that at least one of the fluids should be mixed throughout the exchanger is satisfied. After replacing R by $-R$ in Equation 2.53 and performing the elementary algebraic operations indicated in Equation 2.52, we obtain the expression for the effectiveness of the counterflow configuration:

$$P_c(R, NTU) = \frac{\{1 - \exp[-NTU(1 - R)]\}}{\{1 - R \exp[-NTU(1 - R)]\}} \quad (2.54)$$

Observe also that the inversion of one fluid leads from a parallelflow connection to a counterflow one, and likewise, from the latter to the former; therefore, Equation 2.52 can be used to go from parallelflow to counterflow and vice versa.

The transformation property of Equation 2.52 can also be expressed in terms of the variables referred to the mixed fluid. For example, if the thermal relation on the shellside or tubeside is known in terms of P_x , R_x , and NTU_x , the thermal relation for the other side P_y , R_y , and NTU_y may be obtained from the relation

$$P_y = R_x P_x, \quad R_y = \frac{1}{R_x}, \quad NTU_y = R_x NTU_x \quad (2.55)$$

For example, let the tubeside values of an H_{1-2} exchanger be $P = 0.752$, $R = 0.7$, and $NTU = 2.5$. Then the shellside values will be $P = 0.7 \times 0.752$, $R = 1/0.7$, and $NTU = 0.7 \times 2.5$. For $R = 1.0$, both the tubeside and shellside values are the same.

When the thermal effectiveness is the same for the original case and the inverted case, it is referred to as stream symmetric. Typical examples for stream symmetric are parallelflow, counterflow, and crossflow unmixed–unmixed and mixed–mixed cases.

2.5 TEMPERATURE APPROACH, TEMPERATURE MEET, AND TEMPERATURE CROSS

The meanings of temperature approach, temperature meet, and temperature cross are as follows. Temperature approach is the difference of the hotside and coldside fluid temperature at any point of a given exchanger. In a counterflow exchanger or a multipass exchanger, (1) if the cold fluid outlet temperature $t_{c,o}$ is less than the hot fluid outlet temperature $t_{h,o}$, then this condition is referred to as temperature approach; (2) if $t_{c,o} = t_{h,o}$, this condition is referred to as temperature meet; and (3) if $t_{c,o}$ is greater than $t_{h,o}$, the difference $(t_{c,o} - t_{h,o})$ is referred to as the temperature cross or temperature pinch. In this case, the temperature approach $(t_{h,o} - t_{c,o})$ is negative and loses its meaning. Temperature cross indicates a negative driving force for heat transfer between the fluids. It requires either a large area for heat transfer or the fluid velocity to increase overall heat transfer coefficient. The underlying meanings of these three cases are brought out in Table 2.3 and the same are shown in Figure 2.5a.

The temperature cross is undesirable, particularly for shell and tube exchangers, because the tube surface area is not utilized effectively and hence there is wastage of capital cost. If outlet

TABLE 2.3
Temperature Approach, Temperature Meet,
and Temperature Cross

Temperature Approach	Temperature Meet	Temperature Cross
$t_{h,i} \rightarrow t_{h,o}$	$t_{h,i} \rightarrow t_{h,o}$	$t_{h,i} \rightarrow t_{h,o}$
$t_{c,o} \leftarrow t_{c,i}$	$t_{c,o} \leftarrow t_{c,i}$	$t_{c,o} \leftarrow t_{c,i}$
$t_{c,o} < t_{h,o}$	$t_{c,o} = t_{h,o}$	$t_{c,o} > t_{h,o}$

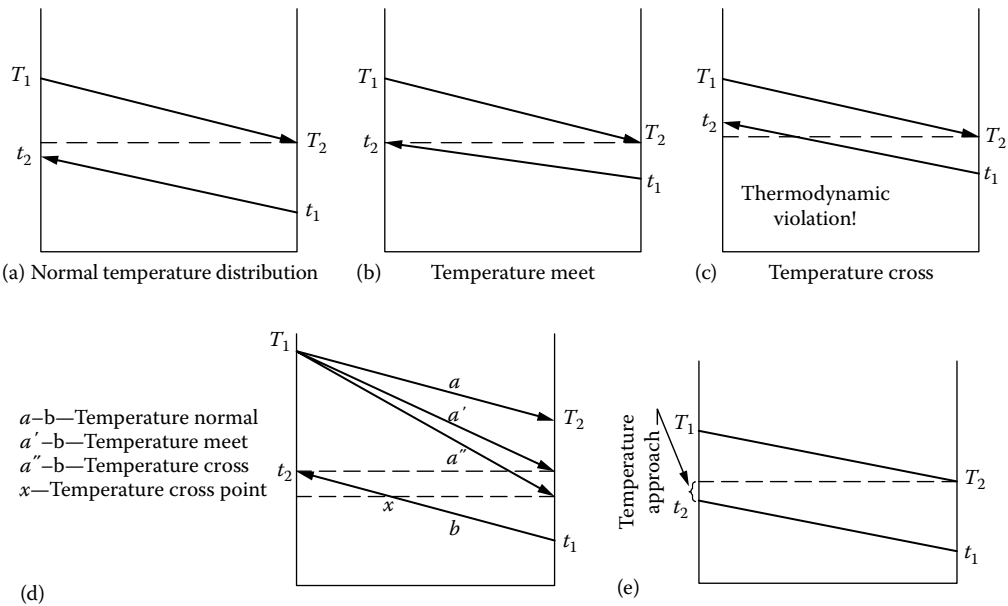


FIGURE 2.5 Principle of temperature approach, temperature meet, and temperature cross. (a) Normal temperature distribution; (b) temperature meet; (c) temperature cross; (d) temperature approach, meet, and cross superimposed; (e) temperature distribution in an E_{1-2} exchanger without temperature cross;

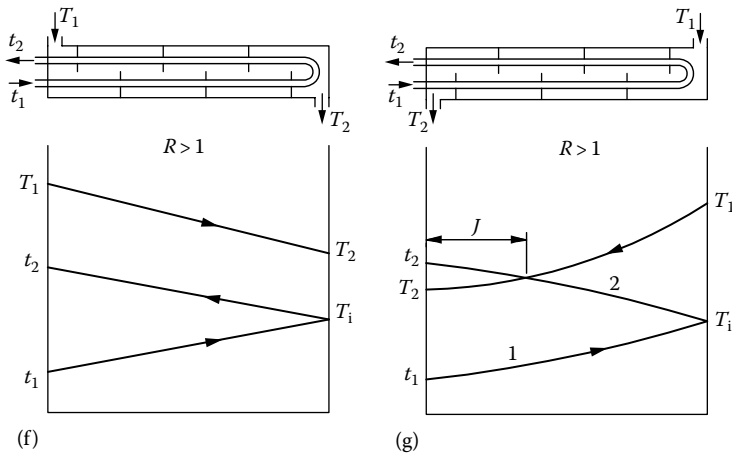


FIGURE 2.5 (continued) Principle of temperature approach, temperature meet, and temperature cross. (f) with temperature cross.

temperatures form a temperature cross in a multiple tube pass heat exchanger, a lower than desirable LMTD correction factor will occur. A simple way to avoid this is to use more exchanger shells in series. Other engineers suggest that a small temperature cross may be acceptable and may provide a less expensive design than the more complex alternatives. For a E_{1-2} heat exchanger, the temperature cross occurs around a relatively narrow range of F value about 0.78–0.82. Lower values of F may be taken as an indication that temperature cross will occur.

The concept of the temperature cross or meet at the exchanger outlet can be utilized to determine the number of shells in series required to meet the heat duty without having a temperature cross in any individual shell. Temperature cross is undesirable for shell and tube heat exchanger because the tube surface area is not utilized cost-effectively. An optimum design would mean that the temperature cross or meet point lies just at the end of the second tube pass. This phenomenon is explained in detail by Shah [2] and is briefly dealt with here with reference to an E_{1-2} exchanger.

For E_{1-2} two possible shell fluid directions with respect to the tube fluid direction are shown in Figure 2.5b. The temperature distributions of Figure 2.5b reveal that there is a temperature cross. In region X, the second tube pass transfers heat to the shell fluid. This is contrary to the design objective, in which ideally the heat transfer should have taken place only in one direction (from the shell fluid to the tube fluid, as shown in Figure 2.5a) throughout the two passes. The reason for this temperature cross is as follows: Although an addition of surface area (a high value of NTU_t , or a low value of LMTD correction factor F) is effective in raising the temperature of the tube fluid and rises in the second pass up to point X, beyond this point the temperature of the shell fluid is lower than that of the tube fluid, since we have considered the shell fluid mixed at a cross section and it is cooled rapidly by the first pass. Thus, the addition of the surface area in the second tube pass left of point X is useless from the thermal design point of view. A “good” design avoids the temperature cross in a shell and tube exchanger. Theoretically, the optimum design would have the temperature cross point just at the end of the second tube pass, which will satisfy the following condition:

$$t_{t,o} = t_{s,o} \quad \text{or} \quad t_{t,o} - t_{s,o} = 0 \quad (2.56)$$

This condition leads to the following formula:

$$P = \frac{1}{1+R} \quad (2.57)$$

Thus for a given R , Equation 2.57 provides the limiting (maximum) value of P . Corresponding to P and R , the limiting (maximum) value of NTU_t beyond which there will be a temperature cross can be determined from its thermal relation formula. Therefore, from P , R , and NTU , F can be calculated. This F value is known as the F_{\min} value beyond which there will be a temperature cross. This is illustrated for an E_{1-2} exchanger here. For a known value of R , determine the limiting value of P from Equation 2.57 and NTU from the following equation:

$$NTU_{E_{1-2}} = \frac{1}{(1+R^2)^{0.5}} \ln \left[\frac{2-P \left[R+1-(1+R^2)^{0.5} \right]}{2-P \left[R+1+(1+R^2)^{0.5} \right]} \right] \quad (2.58)$$

For known values of P , R , and NTU , determine F from Equation 2.36.

2.5.1 TEMPERATURE CROSS FOR OTHER TEMA SHELLS

Temperature cross for other TEMA shells such as G_{1-2} , H_{1-2} , and J_{1-2} can be evaluated from Equation 2.57 [19]. The F_{\min} curves for G_{1-2} , H_{1-2} , and J_{1-2} cases are given in the next section.

2.6 THERMAL RELATION FORMULAS FOR VARIOUS FLOW ARRANGEMENTS AND PASS ARRANGEMENTS

The heat exchanger effectiveness is defined as the ratio of the overall temperature drop of the weaker stream to the maximum possible temperature difference between the fluid inlet temperatures. The following assumptions are commonly made in deriving thermal effectiveness:

1. The overall heat transfer coefficient is constant throughout the exchanger.
2. Each pass has the same heat transfer area; that is, unsymmetrical pass arrangements are not considered.
3. There is no phase change.
4. The specific heat of each fluid is constant and independent of temperature.
5. The flow rates of both streams are steady.
6. The flow of both fluids is evenly distributed over both the local and the total transfer area.
7. Heat losses from the system are negligible.

In this section, thermal relation formulas for (1) various flow arrangements—parallelflow, counterflow, and crossflow—(2) various types of heat exchangers—compact and shell and tube—and (3) multipass arrangements or multiple units of both compact and shell and tube heat exchangers are presented. Most of the formulas are tabulated and the thermal effectiveness charts are given. Mostly counterflow arrangements are considered. For shell and tube exchangers, formulas are given for both parallelflow and counterflow, but thermal effectiveness charts are given only for counterflow arrangements referred to tubeside (similar to TEMA Standards [15]). For stream symmetric cases, thermal effectiveness relations referred to the shellside can be derived from the “flow reversibility” principle. From counterflow thermal effectiveness relations, thermal effectiveness relations for parallelflow arrangements can be easily derived (for stream symmetric cases only) from the “flow reversibility” principle. Customarily, the ϵ -NTU method is employed for compact heat exchangers. In this method, the capacity ratio C^* is always ≤ 1 . Hence, thermal effectiveness charts are given in terms of ϵ - C^* -NTU, and wherever possible, the thermal effectiveness charts are also given in terms of P - R - F -NTU, instead of ϵ - C^* -NTU.

2.6.1 PARALLELFLOW

For a given set of values of C^* or R , and NTU, (1) the thermal effectiveness is much lower for parallelflow than for counterflow arrangement, except in the limiting case $C^* = R = 0$, where it is the same for both cases and approaches unity as NTU increases to infinity, and (2) at a given value of NTU, the effectiveness increases with decreasing capacity ratio, C^* or R . The formula for thermal effectiveness is given by Equation T1 in Table 2.4, and the thermal effectiveness chart is given in Figure 2.6.

2.6.2 COUNTERFLOW

Among the various flow arrangements, counterflow has the highest thermal effectiveness. For counterflow exchangers, at a given value of NTU, the effectiveness increases with decreasing capacity ratio, C^* or R . The formula for thermal effectiveness is given by Equation T2, and the thermal effectiveness chart is given in Figure 2.7.

2.6.3 CROSSFLOW ARRANGEMENT

2.6.3.1 Unmixed–Unmixed Crossflow

This is an industrially important arrangement representing the case of a large number of unmixed channels in both sides. The original solution was due to Nusselt [20] and was later reformulated into a more manageable equation by Mason [21]. Mason's formula is given by Equation T3, and this equation can be used for P –NTU– R relation. Baclic [22] presents Nusselt's equation in terms of a modified Bessel function of the first kind as given in Equation T4; Eckert [23] provides a simplified formula without involving Bessel function as given by Equation T5, and this equation predicts ϵ within $\pm 1\%$ of ϵ from Equation T4 for $1 < NTU < 7$; Equations T4 and T5 can be used for formulas involving $C^* \leq 1$ only. The thermal effectiveness chart as per Equation T3 is given in Figure 2.8 and as per Equation T4 is given in Figure 2.9.

2.6.3.2 Unmixed–Mixed Crossflow

In this arrangement, one fluid is mixed and the other is unmixed. A typical example is a bare tube compact heat exchanger in which the fluid outside the tube is mixed, whereas the tubeside fluid is unmixed. There are two possible cases: (1) weaker fluid (C_{\min}) is mixed and (2) stronger fluid (C_{\max}) is mixed. Formulas for thermal effectiveness for the weaker fluid mixed are given by Equation T6 and for the stronger fluid mixed by Equation T7. The thermal effectiveness charts are given in Figure 2.10 for the weaker fluid mixed and Figure 2.11 for the stronger fluid mixed. For $R = 1$ or $C^* = 1$, the thermal effectiveness is the same for both cases.

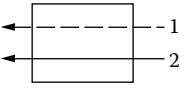
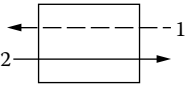
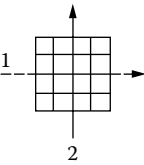
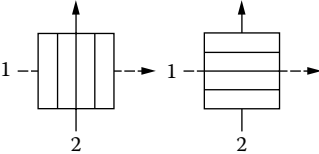
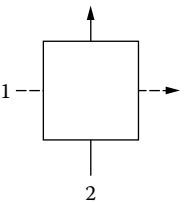
2.6.3.3 Mixed–Mixed Crossflow

This case has no industrial application and is shown here only as an extreme of the crossflow arrangement. The solution is identical to the TEMA J shell with infinite tubeside passes. The formula for thermal effectiveness is given by Equation T8.

2.6.3.4 Single or Multiple Rows in Crossflow

Many process heat exchangers provide a crossflow arrangement between the hot (or cold) process fluid that flows through the tubes and the external coolant (or hot air such as supercharged engine intake air), usually air. Because this flow arrangement is not strictly countercurrent, the MTD must be corrected by applying a correction factor, F . The factor F depends on the terminal temperatures, the number of tube rows per pass, and the number of passes. The basic unmixed–unmixed case shown in Figure 2.12 assumes a large number of flow channels in both streams. For a single tubeside pass with one or more tube rows, the thermal effectiveness formula is different from that of the basic unmixed–unmixed case. Thermal relations for single-pass tube rows arrangements are discussed next.

TABLE 2.4
Thermal Effectiveness Relations for Basic Cases

Flow Arrangement	Equation No./Reference	General Formula	Value for $R = 1$ and Special Cases
 <p>Parallelflow; stream symmetric</p>	T1	$P = \frac{1 - e^{-NTU(1+R)}}{1 + R}$	$P = \frac{1}{2} [1 - e^{(-2NTU)}] \quad \text{for } R = 1$ $= 1 - e^{-NTU} \quad \text{for } R = 0$ $P_{\max} = 50\% \quad \text{for } R = 1$
 <p>Counterflow; stream symmetric</p>	T2	$P = \frac{1 - e^{-NTU(1-R)}}{1 - R e^{-NTU(1-R)}}$	$P = \frac{NTU}{1 + NTU} \quad \text{for } R = 1$ $= 1 - e^{-NTU} \quad \text{for } R = 0$
	T3 [21]	$P = \frac{1}{RNTU} \sum_{k=0}^{\infty} \left\{ \left[1 - e^{-NTU} \sum_{m=0}^k \frac{NTU^m}{m!} \right] \left[1 - e^{-RNTU} \sum_{m=0}^k \frac{(RNTU)^m}{m!} \right] \right\}$	
		For $R = 1$, this equation holds.	
	T4 [22]	$\varepsilon = 1 - e^{[-(1+C^*)NTU]} \left[I_0(2NTU\sqrt{C^*}) + \sqrt{C^*} I_1(2NTU\sqrt{C^*}) - \frac{1 - C^*}{C^*} \sum_{n=2}^{\infty} C^{*n/2} I_n(2NTU\sqrt{C^*}) \right]$	
Crossflow; both the fluids unmixed; stream symmetric		For $C^* = 1$.	
		$\varepsilon = 1 - e^{-2NTU} [I_0(2NTU) + I_1(2NTU)]$	
	T5 [23]	$\varepsilon = 1 - \exp \left\{ \frac{NTU^{0.22}}{C^*} [\exp(-C^* NTU^{0.78}) - 1] \right\}$	
Crossflow; one fluid mixed and the other fluid unmixed (1) weaker (C_{\min}) fluid mixed; (2) stronger (C_{\max}) fluid mixed	T6	<p>Weaker (C_{\min}) fluid mixed</p> $P_1 = 1 - e^{-(1-e^{-NTU})}$ $P_1 = [1 - \exp(-K/R)]$ $K = 1 - \exp(-RNTU)$	
	T7	<p>Stronger (C_{\max}) fluid mixed</p> $P_1 = \frac{[1 - \exp(-KR)]}{R}$ $K = 1 - \exp(-NTU)$	$P_1 = 1 - e^{-(1-e^{-NTU})}$
	T8	$P = \frac{1}{\left(\frac{1}{K_1} + \frac{R}{K_2} - \frac{1}{NTU} \right)}$ $K_1 = 1 - e^{(-NTU)}$ $K_2 = 1 - e^{(-RNTU)}$	$P = \frac{1}{\frac{2}{K_1} - \frac{1}{NTU}}$
Crossflow; mixed-mixed flow; stream symmetric same as $J_{1-\infty}$			
<p>Note: P_2 can be found using Equation 2.55;</p> <p>I_0, I_1 and I_n are modified Bessel functions of the first kind.</p>			

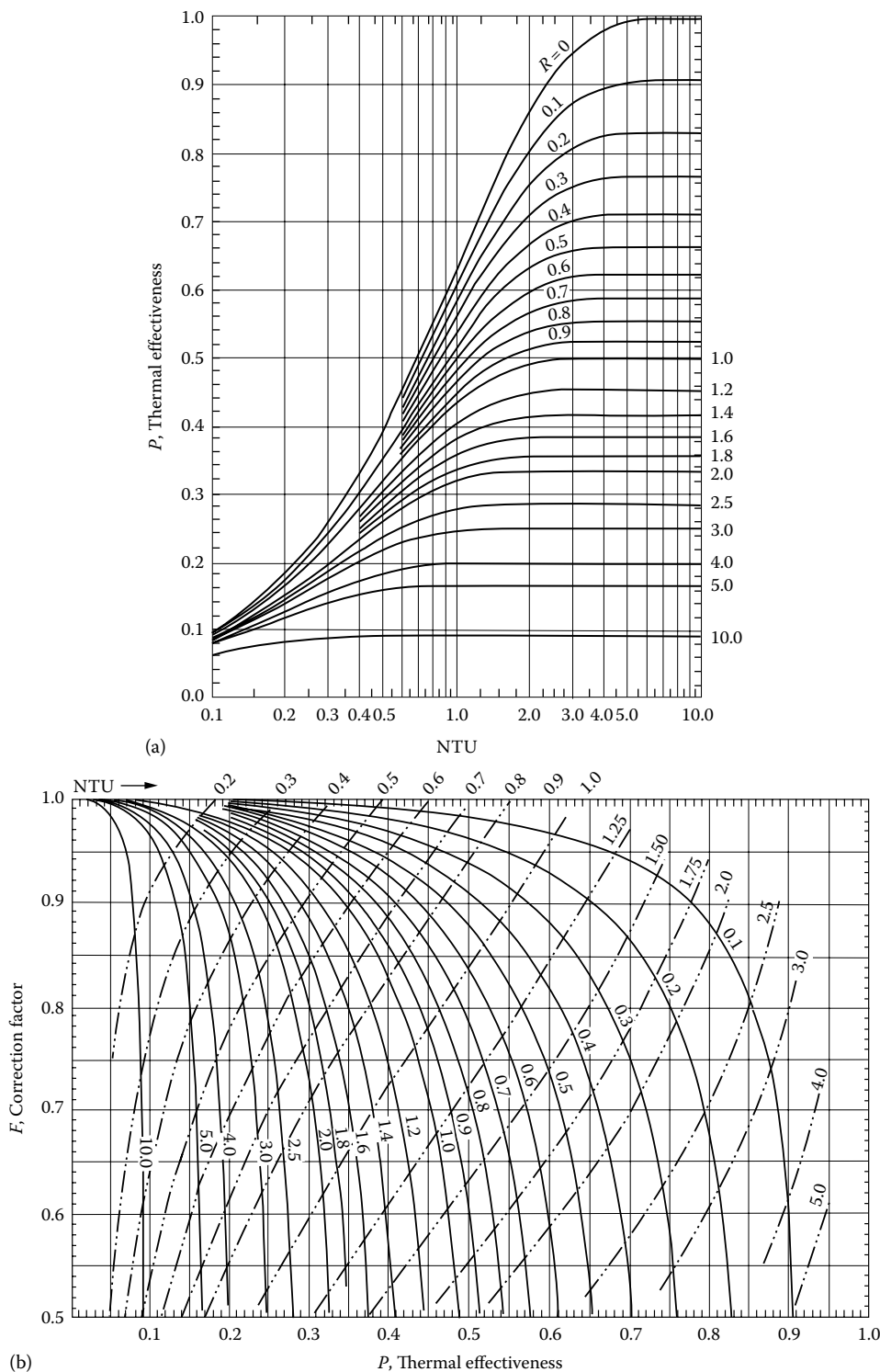


FIGURE 2.6 (a) Thermal effectiveness chart—parallelflow; stream symmetric, R - P - NTU chart (as per Equation T1, Table 2.4); (b) parallelflow; stream symmetric, F - R - P - NTU chart; F as a function of P for constant R (solid lines) and constant NTU (dashed lines) (Equation T1, Table 2.4).

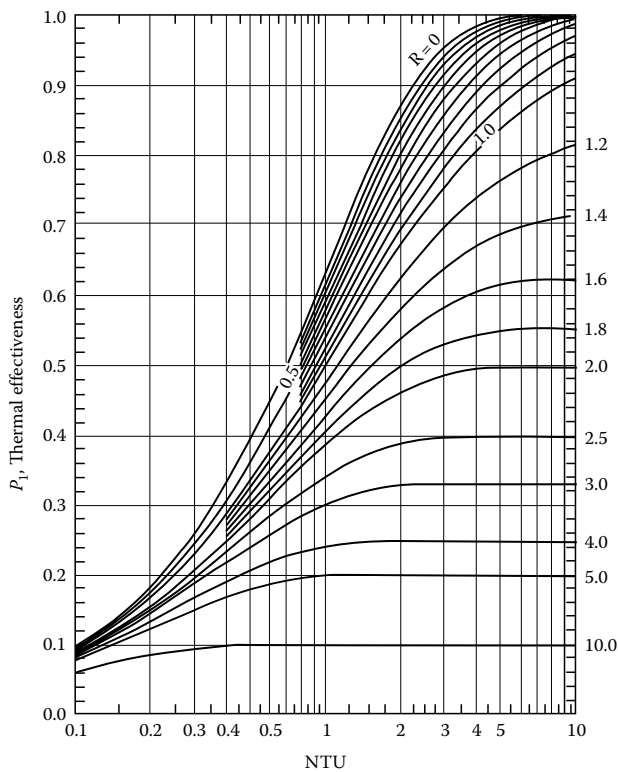


FIGURE 2.7 Thermal effectiveness chart—counterflow; stream symmetric, R - P - NTU chart (as per Equation T2, Table 2.4).

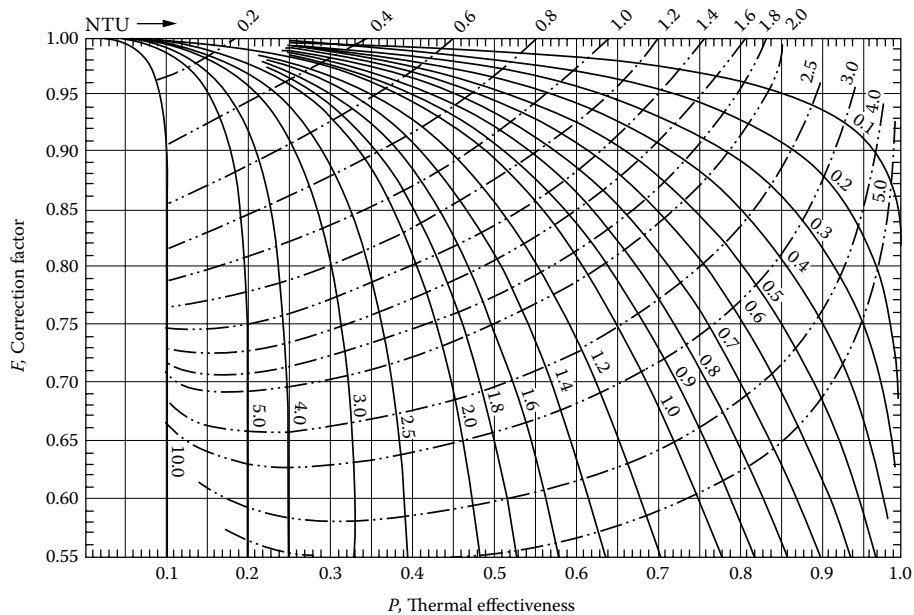


FIGURE 2.8 Thermal effectiveness chart—crossflow; both the fluids unmixed; stream symmetric; F - R - P - NTU chart; F as a function of P for constant R (solid lines) and constant NTU (dashed lines) (as per Equation T3, Table 2.4).

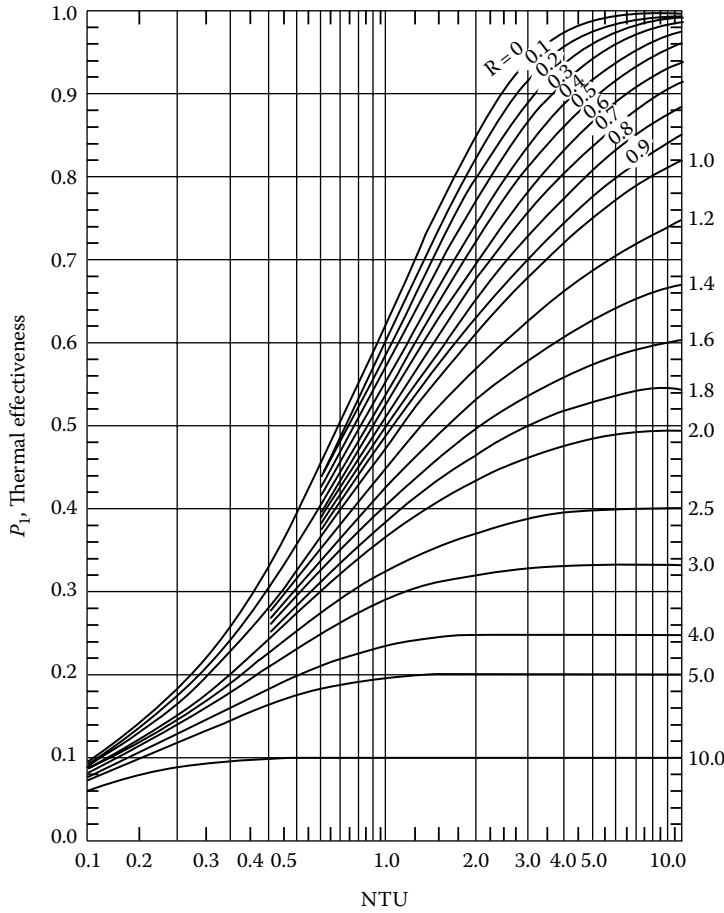


FIGURE 2.9 Thermal effectiveness chart—crossflow; both the fluids unmixed; stream symmetric; R – P – NTU chart (as per Equation T4, Table 2.4).

2.6.3.4.1 Single Tubeside Pass, N Rows per Pass, Both Fluids Unmixed

A common header at one end of the tubes distributes the tubeside fluid into a single pass having N rows in parallel. A similar header at the other end collects tubeside fluid. For given terminal temperatures, F increases with the number of rows per pass and the number of passes being increased and is more sensitive to the latter. Taborek [24], Pignotti and Cordero [25], and Pignotti [26] present values of F for a variety of crossflow configurations, applicable to air-cooled heat exchangers.

Schedwill's formula for the thermal effectiveness of N rows is given by [27]

$$P = \frac{1}{R} \left\{ 1 - \left[\frac{Ne^{NKR}}{1 + \sum_{i=1}^{N-1} \sum_{j=0}^i \binom{i}{j} K^j e^{-(i-j)NTU/N} \sum_{k=0}^j \frac{(NKR)^k}{k!}} \right] \right\}^{-1} \quad (2.59)$$

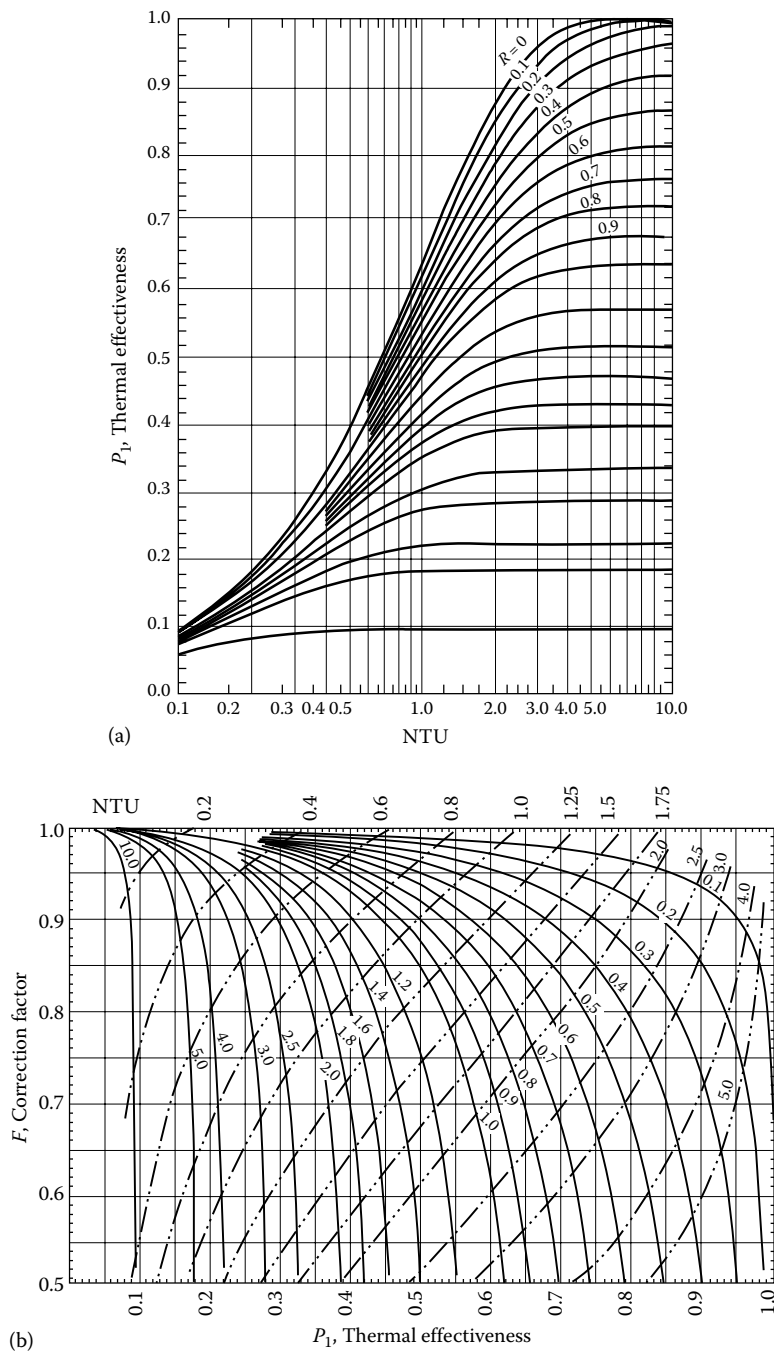


FIGURE 2.10 (a) Thermal effectiveness chart—crossflow: unmixed-mixed—the weaker (C_{min}) fluid mixed, R - P - NTU chart (as per Equation T6, Table 2.4); (b) F - R - P - NTU chart; F as a function of P for constant R (solid lines) and constant NTU (dashed lines) (as per Equation T6, Table 2.4).

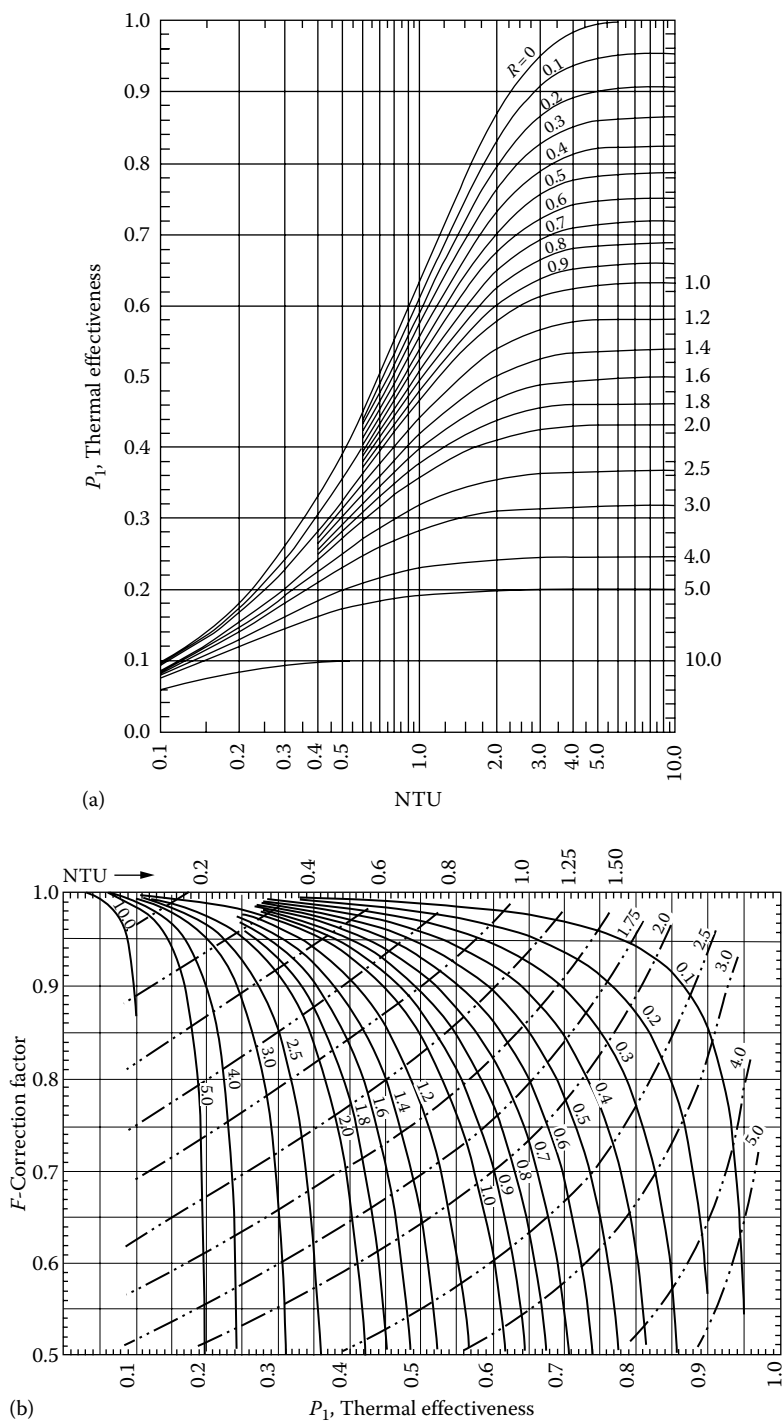


FIGURE 2.11 (a) Thermal effectiveness chart—crossflow: unmixed–mixed—the stronger (C_{\max}) fluid mixed, ϵ - C^* -NTU chart (as per Equation T7, Table 2.4); (b) Thermal effectiveness chart: F - R - P -NTU chart; F as a function of P for constant R (solid lines) and constant NTU (dashed lines) (as per Equation T7, Table 2.4).

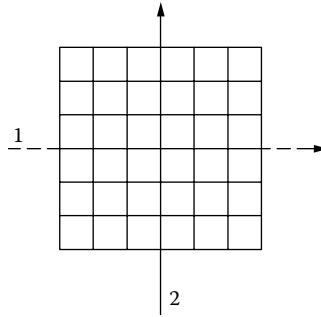


FIGURE 2.12 Unmixed–unmixed crossflow arrangement.

where

$$\binom{i}{j} = \frac{i!}{(i-j)!j!} \quad (2.60)$$

that is, the number of combinations of i and j taken j at a time, and

$$K = 1 - \exp\left(-\frac{NTU}{N}\right) \quad (2.61)$$

By substituting $N = 1, 2, 3, \dots$ in Equations 2.59 and 2.61, equations for thermal relations are obtained for the specific arrangements by Nicole [28], and this is given in Table 2.5 (Equations T9 through T12) for one row, two rows, three rows, and four rows. For a larger number of tube rows (for all practical purposes, when N exceeds 5), the solution approaches that of unmixed–unmixed crossflow arrangement. Values of F for $N = 1, 2, 3, 4$ are shown in Figures 2.13 through 2.16 and are always less than the basic case of unmixed–unmixed crossflow (Figure 2.8).

2.6.3.4.2 *Multipass Tube Rows Cross-Counterflow Arrangements, Both Fluids Unmixed, and Multiple Tube Rows in Multipass Tube Rows, Cross-Counterflow Arrangements*

This would apply to a manifold-type air cooler in which the tubes in one row are connected to the next by U-bends. The solutions are based on Ref. [28]. Solutions for the 2 rows-2 pass and 3 rows-3 pass cases are based on Stevens et al. [29]. The general formula for thermal effectiveness referred to the air side (fin side) is given by [28]

$$P_1 = \frac{1}{R} \left(1 - \frac{1}{\zeta} \right) \quad (2.62)$$

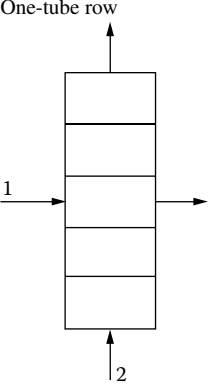
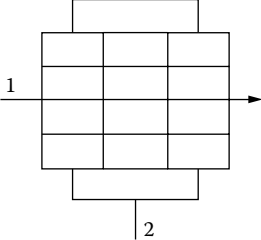
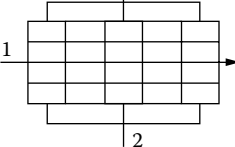
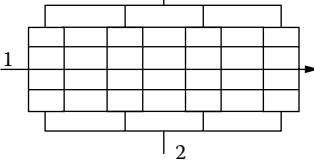
The expressions for ζ for various cases are as follows:

1. Two-tube rows, two passes, as shown in Figure 2.17a [29]

$$\zeta = \frac{K}{2} + \left(1 - \frac{K}{2} \right) e^{2KR} \quad (2.63a)$$

$$K = 1 - \exp\left(-\frac{NTU}{2}\right) \quad (2.63b)$$

TABLE 2.5
Thermal Effectiveness Relations for Tube Rows with Single Pass Arrangement

Flow Arrangement	Equation No./ Reference	General Formula, Ref. [28]. Note: These Formulas Are Valid for $R = 1$
<p>One-tube row</p> 	T9 [28]	$P_1 = \frac{1}{R}(1 - e^{-KR})$ $K = 1 - \exp(-NTU)$
<p>Two-tube rows</p> 	T10 [28]	$P_1 = \frac{1}{R} \left[1 - e^{-2KR} (1 + RK^2) \right]$ $K = 1 - \exp\left(-\frac{NTU}{2}\right)$
<p>Three-tube rows</p> 	T11 [28]	$P_1 = \frac{1}{R} \left\{ 1 - \left[\frac{e^{3KR}}{1 + RK^2(3 - K) + (3/2)R^2K^4} \right]^{-1} \right\}$ $K = 1 - \exp\left(-\frac{NTU}{3}\right)$
<p>Four-tube rows</p> 	T12 [28]	$P_1 = \frac{1}{R} \left\{ 1 - \left[\frac{e^{4KR}}{[1 + RK^2(6 - 4K + K^2) + 4R^2K^4(2 - K) + (8/3)R^3K^6]} \right]^{-1} \right\}$ $K = 1 - \exp(-NTU/4)$

Note: To find P_2 , use Equation 2.55.

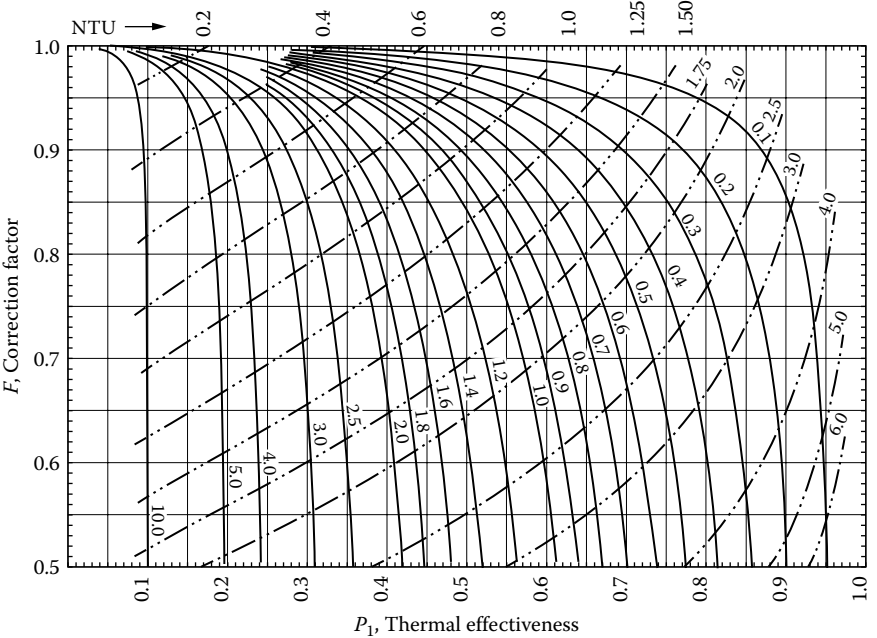


FIGURE 2.13 Thermal effectiveness chart—one-tube row; F as a function of P for constant R (solid lines) and constant NTU (dashed lines) (as per Equation T9, Table 2.5).

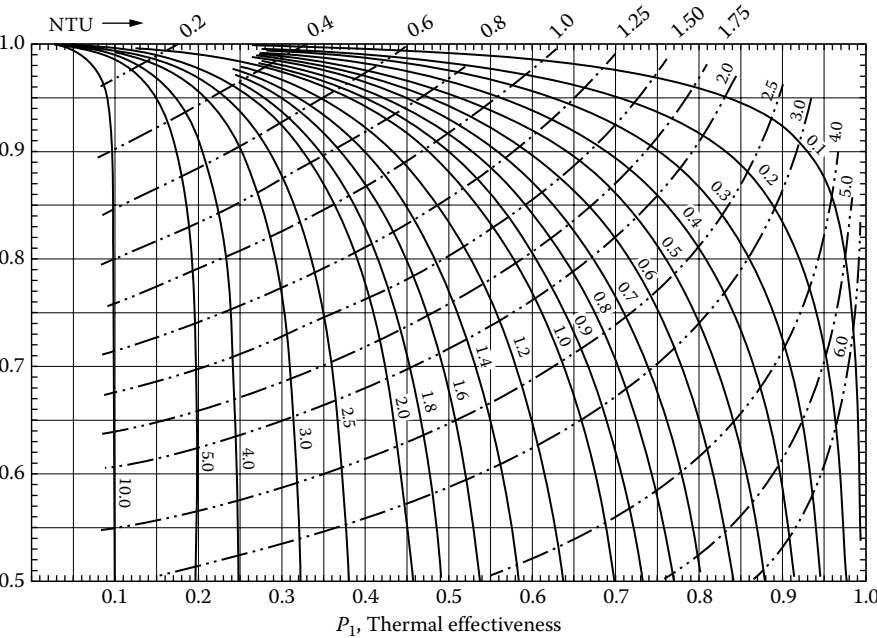


FIGURE 2.14 Thermal effectiveness chart—two-tube rows; F as a function of P for constant R (solid lines) and constant NTU (dashed lines) (as per Equation T10, Table 2.5).

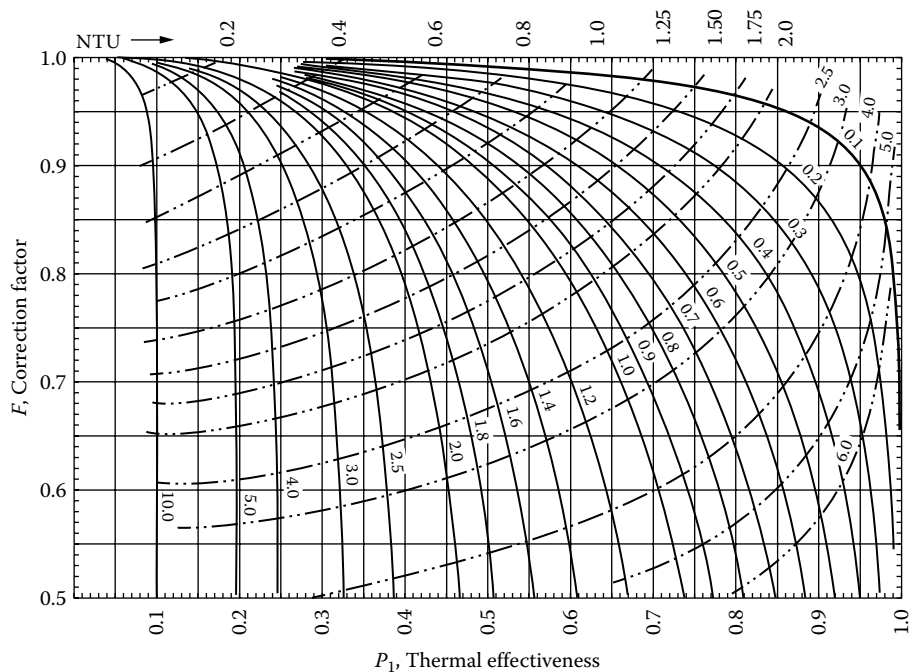


FIGURE 2.15 Thermal effectiveness chart—three-tube rows; F as a function of P for constant R (solid lines) and constant NTU (dashed lines) (as per Equation T11, Table 2.5).

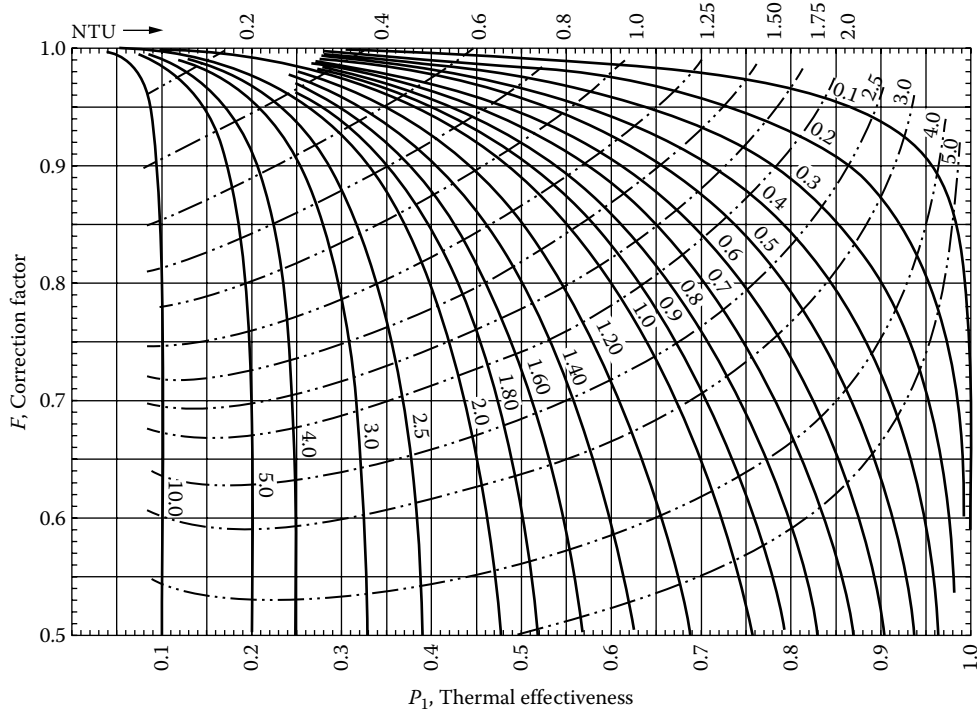


FIGURE 2.16 Thermal effectiveness chart—four-tube rows; F as a function of P for constant R (solid lines) and constant NTU (dashed lines) (as per Equation T12, Table 2.5).

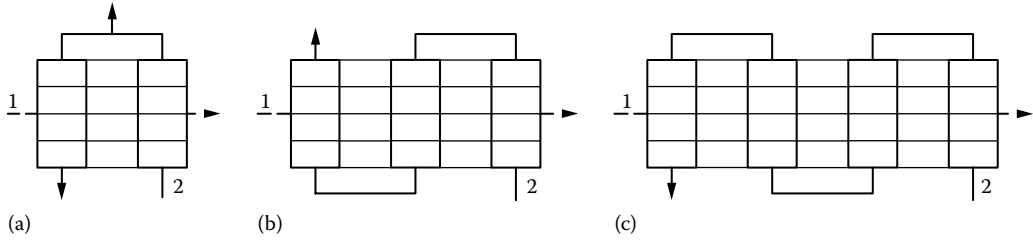


FIGURE 2.17 Multipass tube rows. (a) Two rows-two pass; (b) three rows-three pass; (c) four rows-four pass.

2. Three-tube rows, three passes, as shown in Figure 2.17b [29]

$$\zeta = K \left[1 - \frac{K}{4} - RK \left(1 - \frac{K}{2} \right) \right] e^{KR} + e^{3KR} \left(1 - \frac{K}{2} \right)^2 \quad (2.64a)$$

$$K = 1 - \exp \left(-\frac{NTU}{3} \right) \quad (2.64b)$$

3. Four-tube rows, four passes, as shown in Figure 2.17c [28]

$$\zeta = \frac{K}{2} \left(1 - \frac{K}{2} + \frac{K^2}{4} \right) + K \left(1 - \frac{K}{2} \right) \left[1 - \frac{R}{8} K \left(1 - \frac{K}{2} \right) e^{2KR} \right] + e^{4KR} \left(1 - \frac{K}{2} \right)^3 \quad (2.65a)$$

$$K = 1 - \exp \left(-\frac{NTU}{4} \right) \quad (2.65b)$$

4. Five-tube rows, five passes [28]

$$\begin{aligned} \zeta = & \left\{ K \left(1 - \frac{3}{4} K + \frac{K^2}{2} - \frac{K^3}{8} \right) - RK^2 \left[1 - K + \frac{3}{4} K^2 - \frac{1}{4} K^3 - \frac{R}{2} K^2 \left(1 - \frac{K}{2} \right)^2 \right] \right\} e^{KR} \\ & + \left[K \left(1 - \frac{3}{4} K + \frac{1}{16} K^3 \right) - 3RK^2 \left(1 - \frac{K}{2} \right)^3 \right] e^{3KR} + \left(1 - \frac{K}{2} \right)^4 e^{5KR} \end{aligned} \quad (2.66a)$$

$$K = 1 - \exp \left(-\frac{NTU}{5} \right) \quad (2.66b)$$

5. Six-tube rows, six passes [28]

$$\begin{aligned} \zeta = & \frac{K}{2} \left(1 - K + K^2 - \frac{1}{2} K^3 + \frac{1}{8} K^4 \right) + K \left(1 - K + \frac{3}{4} K^2 - \frac{5}{16} K^3 + \frac{1}{32} K^4 \right) e^{2KR} \\ & - RK^2 \left[2 - 3K + 3K^2 - \frac{7}{4} K^3 + \frac{3}{8} K^4 - RK^2 \left(2 - 3K + \frac{3}{2} K^2 - \frac{1}{4} K^3 \right) \right] e^{2KR} \\ & + \left[\frac{K}{2} \left(2 - 2K + \frac{1}{2} K^3 - \frac{1}{8} K^4 \right) - 4RK^2 \left(1 - \frac{K}{2} \right)^4 \right] e^{4KR} + \left(1 - \frac{K}{2} \right)^5 e^{6KR} \end{aligned} \quad (2.67a)$$

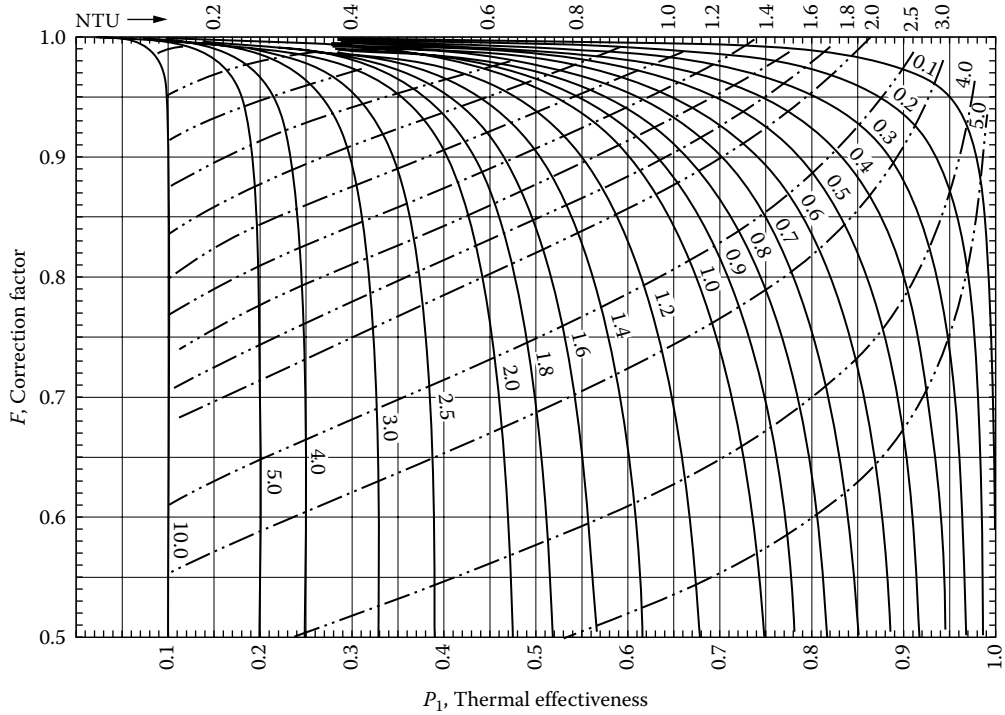


FIGURE 2.18 Thermal effectiveness chart—two-tube rows, two passes. Both fluids unmixed throughout; fluid 1 inverted coupling between passes (for the flow arrangement shown in Figure 2.17a). F as a function of P for constant R (solid lines) and constant NTU (dashed lines) (as per Equations 2.62 and 2.63).

$$K = 1 - \exp\left(-\frac{NTU}{6}\right) \quad (2.67b)$$

Values of F referred to the fluid outside the tubeside (air side) for $N = 2, 3, 4, 5$, and 6 are shown in Figures 2.18 through 2.22, respectively. The F values are always higher than the basic case (Figure 2.8). When N becomes greater than 6 , F approaches 1, that is, pure counter current flow.

6. Multiple tube rows in multipass cross-counterflow arrangements; one fluid unmixed throughout; other fluid (tube fluid) unmixed in each pass but mixed between passes:
 - a. Four rows, two passes, with two rows per pass. Tubeside fluid mixed at the header and the other fluid is unmixed throughout, coupling in inverted order (Figure 2.23a) [28]:

$$P_1 = \frac{1}{R} \left(1 - \frac{1}{\zeta}\right) \quad \text{from Equation 2.62}$$

$$\zeta = \left\{ \frac{R}{2} K^3 [4 - K + 2RK^2] + e^{4KR} + K \left[1 - \frac{K}{2} + \frac{K^2}{8} \right] [1 - e^{4KR}] \right\} \frac{1}{(1 + RK^2)^2} \quad (2.68a)$$

$$K = 1 - \exp\left(-\frac{NTU}{4}\right) \quad (2.68b)$$

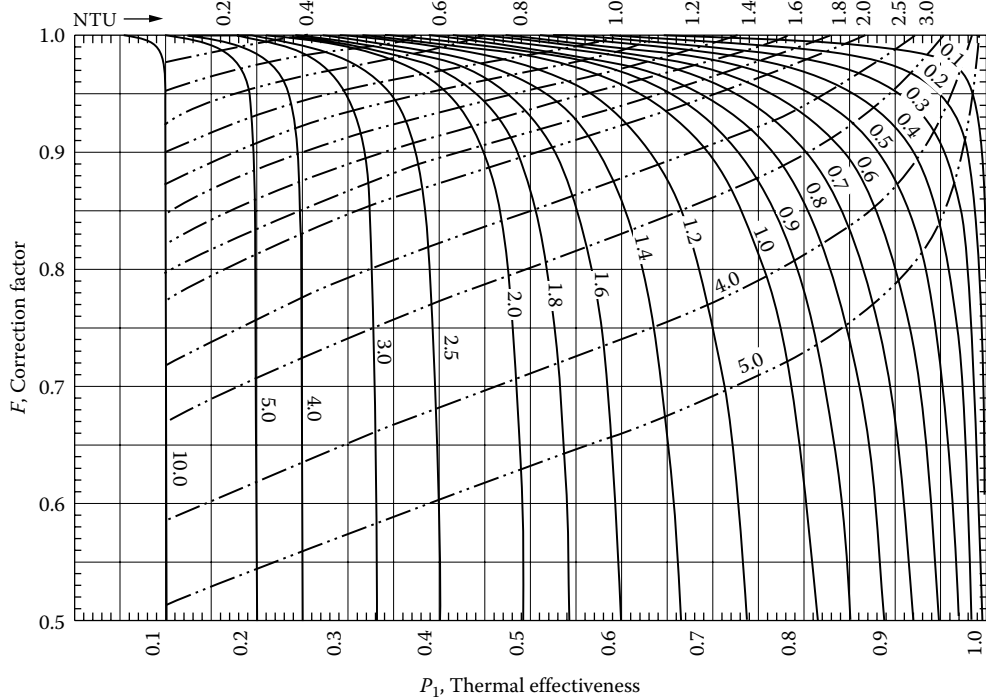


FIGURE 2.19 Thermal effectiveness chart—three-tube rows, three passes. Both fluids unmixed throughout; fluid 1 inverted coupling between passes (for the flow arrangement shown in Figure 2.17b). F as a function of P for constant R (solid lines) and constant NTU (dashed lines) (as per Equations 2.62 and 2.64).

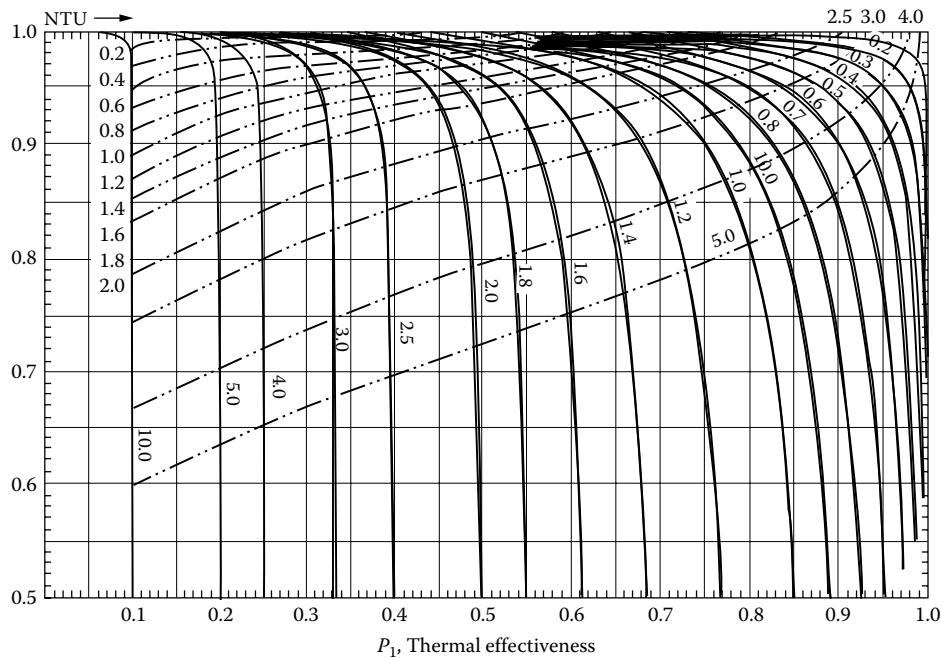


FIGURE 2.20 Thermal effectiveness chart—four-tube rows, four passes. Both fluids unmixed throughout; fluid 1 inverted between passes (for the flow arrangement shown in Figure 2.17c). F as a function of P for constant R (solid lines) and constant NTU (dashed lines) (as per Equations 2.62 and 2.65).

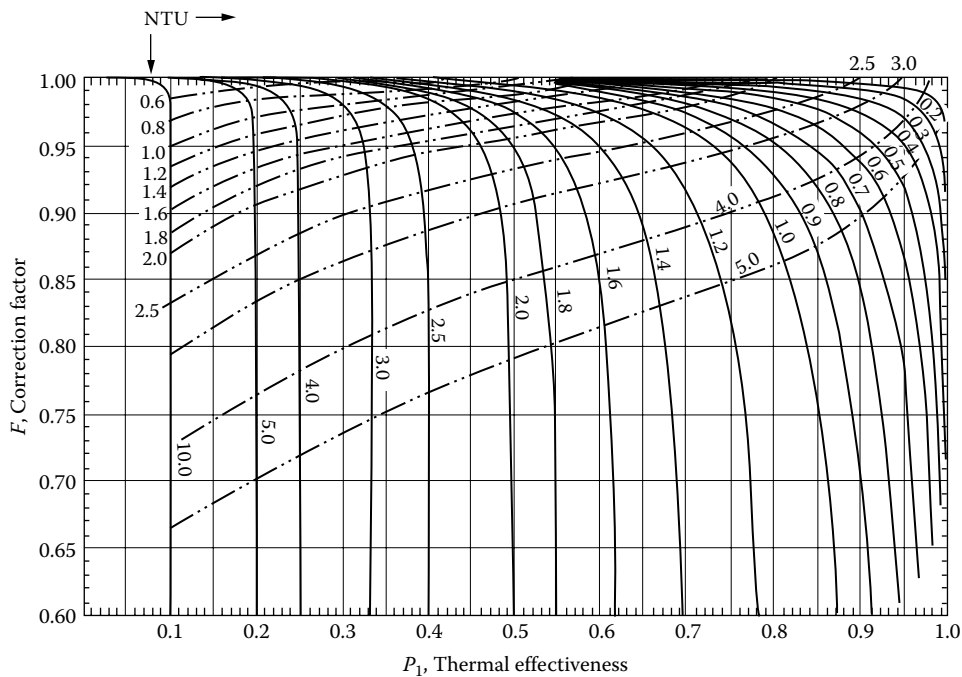


FIGURE 2.21 Thermal effectiveness chart—five-tube rows, five passes. Both fluids unmixed throughout; fluid 1 inverted coupling between passes. F as a function of P for constant R (solid lines) and constant NTU (dashed lines) (as per Equations 2.62 and 2.66).

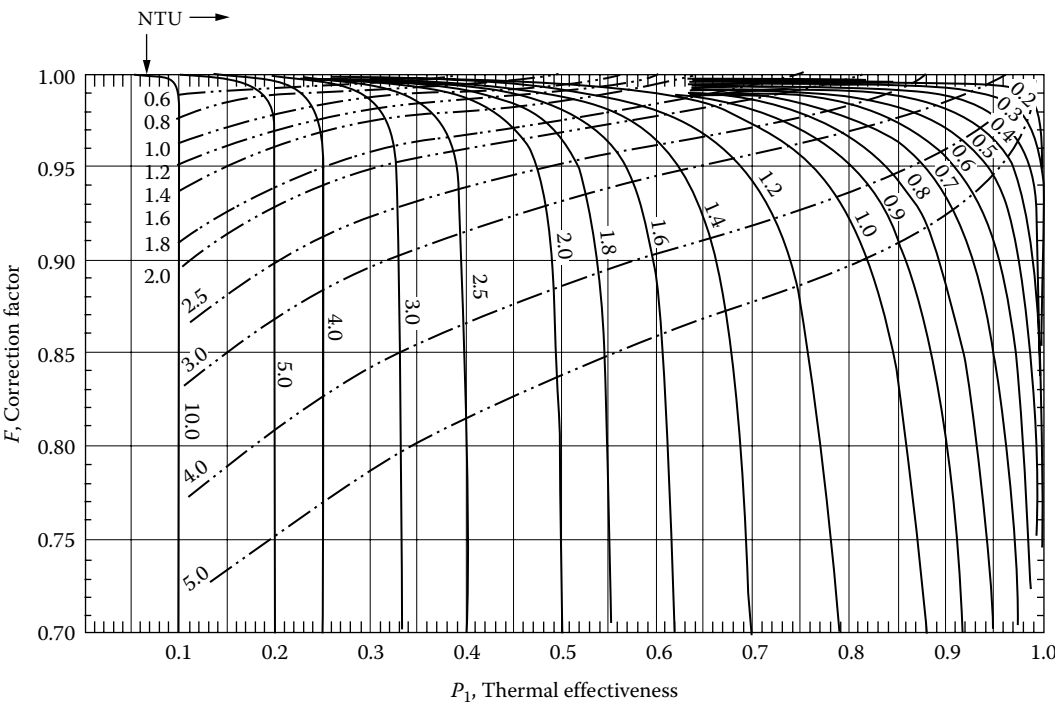


FIGURE 2.22 Thermal effectiveness chart—six-tube rows, six passes. Both fluids unmixed throughout; fluid 1 inverted coupling between passes. F as a function of P for constant R (solid lines) and constant NTU (dashed lines) (as per Equations 2.62 and 2.67).

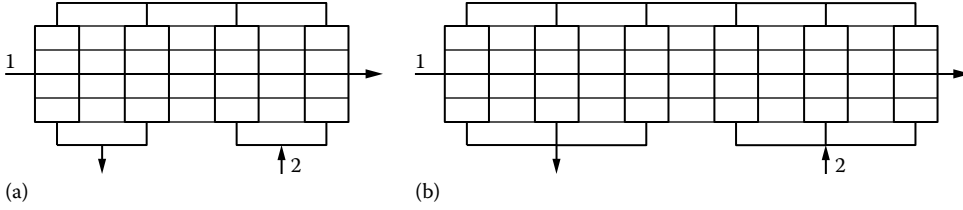


FIGURE 2.23 Tube rows multiples arrangement: (a) four rows-two pass; (b) six rows-two pass.

- b. Six rows, two passes, with three rows per pass. Tubeside fluid is mixed between passes, that is, at the header, and the other fluid is unmixed throughout, coupling in inverted order (Figure 2.23b) [26]:

$$P_1 = \frac{2A - RA^2 - \delta}{1 - R\delta} \quad (2.69a)$$

$$A = a_0 C_0(3KR) + a_1 C_1(3KR) + a_2 C_2(3KR)$$

$$a_0 = 1 - (1 - K)^3$$

$$a_1 = 3RK^3(3 - 2K)$$

$$a_2 = \frac{9R^2 K^5}{2}$$

$$\delta = a_0^2 C_0(6KR) + 2a_0 a_1 C_1(6KR) + (a_1^2 + 2a_0 a_2) C_2(6KR) + 2a_1 a_2 C_3(6KR) + a_2^2 C_4(6KR)$$

$$C_n(z) = \frac{n!}{z^{n+1}} \left[1 - e^{-z} \left(1 + z + \frac{z^2}{2!} + \cdots + \frac{z^n}{n!} \right) \right]$$

$$K = 1 - \exp\left(-\frac{NTU}{6}\right) \quad (2.69b)$$

Values of F for four rows, two passes (2 rows in a pass) and six rows, two passes (3 rows in a pass) are shown in Figures 2.24 and 2.25, respectively.

2.6.4 THERMAL RELATIONS FOR VARIOUS TEMA SHELLS AND OTHERS

The thermal effectiveness relations for various TEMA shells and others are presented next, using the following simplifying assumptions given at the beginning of this section and the additional assumption of perfect transverse mixing of the shell fluid. Since the shellside flow arrangement is unique with each shell type, the exchanger effectiveness is different for each shell even though the number of tube passes may be the same. The P -NTU_i or LMTD method is commonly used for the thermal analysis of shell and tube exchangers. Therefore, thermal relation formulas and effectiveness charts are presented as for the P -NTU_i method.

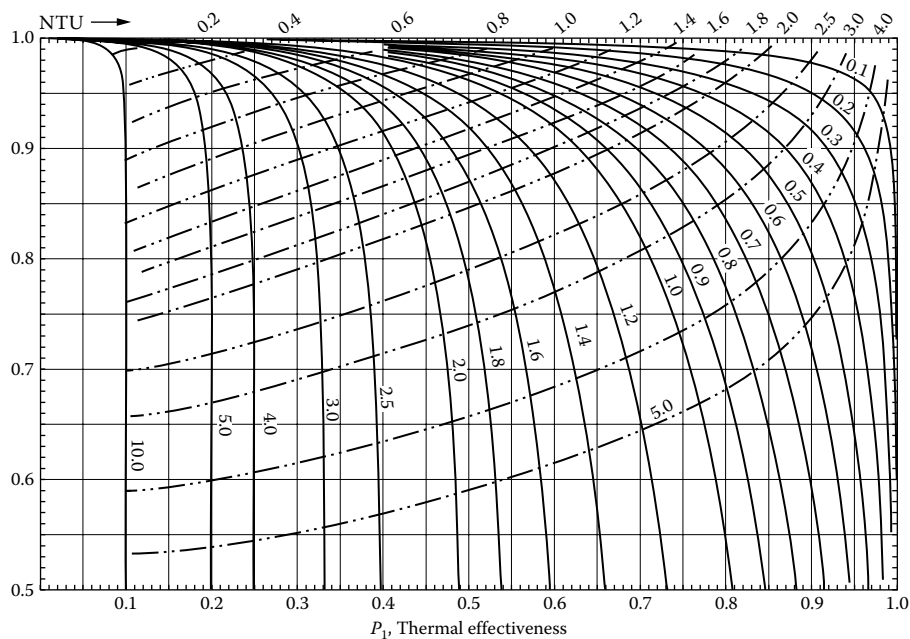


FIGURE 2.24 Thermal effectiveness chart—four rows-two passes with two rows per pass. One fluid is unmixed throughout; tubside fluid mixed between passes and in each pass unmixed; fluid 1 inverted coupling between passes (for the flow arrangement shown in Figure 2.23a). F as a function of P for constant R (solid lines) and constant NTU (dashed lines) (as per Equations 2.62 and 2.68).

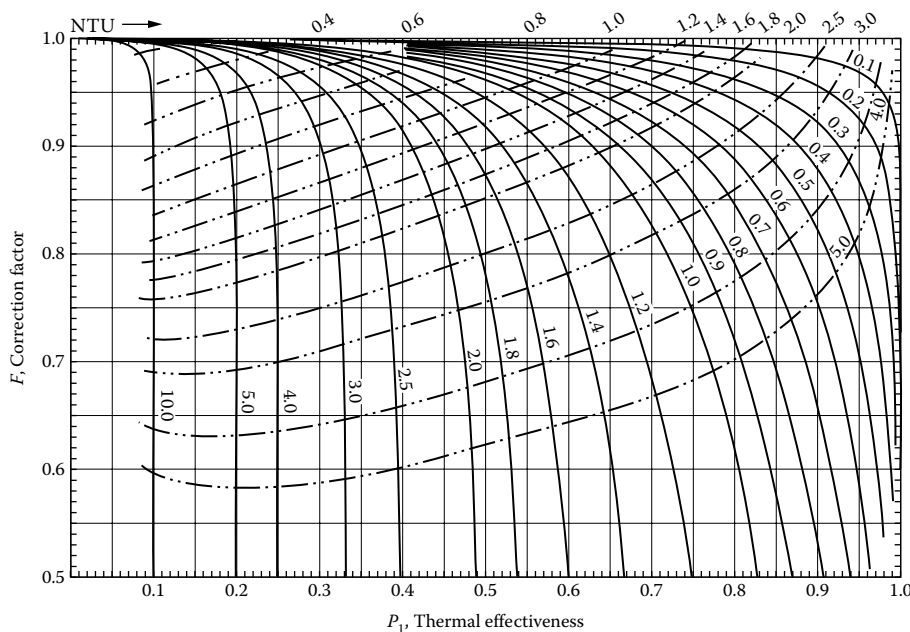


FIGURE 2.25 Thermal effectiveness chart—six rows-two passes with three rows per pass. One fluid is unmixed throughout; tubside fluid mixed between passes and in each pass unmixed; fluid 1 inverted coupling between passes (for the flow arrangement shown in Figure 2.23b). F as a function of P for constant R (solid lines) and constant NTU (dashed lines) (as per Equations 2.62 and 2.69).

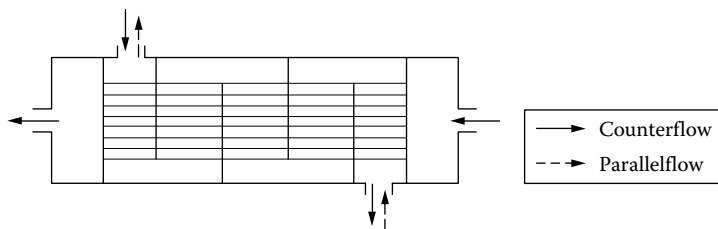


FIGURE 2.26 *E* shell single-pass arrangement—parallelflow/counterflow. (Note: For a large number of segmental baffles, the flow approaches true parallelflow and counterflow.)

2.6.4.1 *E* Shell

The basic case of the *E* shell, one shell pass and one tube pass with parallelflow and counterflow arrangement, is shown in Figure 2.26. For the counterflow case with more than five baffles, the F value can be taken as 1. Thermal effectiveness charts shown in Figure 2.6 can be used for parallelflow arrangement and Figure 2.7 for counterflow arrangement.

2.6.4.1.1 *Multipassing on the Tubeside*

On the tubeside, any number of odd or even passes is possible. Increasing the even number of tube passes from two to four, six, etc. decreases the exchanger effectiveness slightly, and in the limit when the number of tube passes approaches infinity with one shell pass, the exchanger effectiveness approaches that for a single-pass crossflow exchanger with both fluids mixed. The odd number of tube passes per shell has slightly better effectiveness when the shell fluid flows countercurrent to

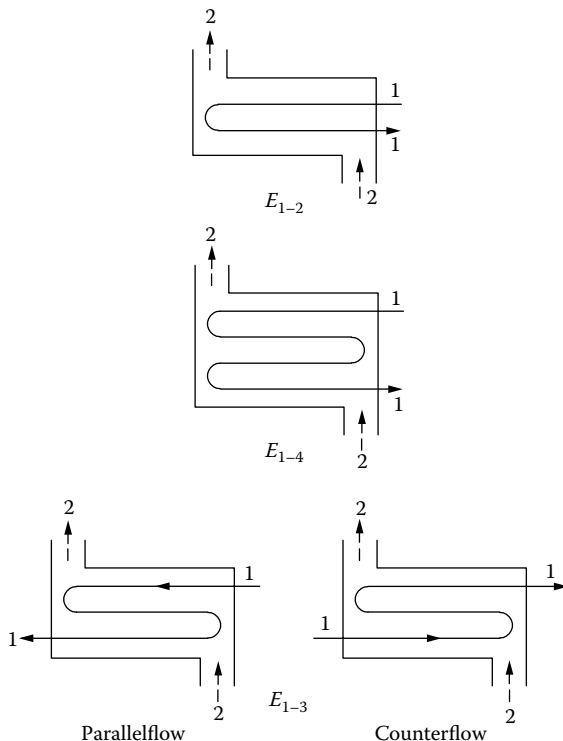


FIGURE 2.27 Common tube pass arrangement for E_{1-2} , E_{1-4} , and E_{1-3} shells.

the tube fluid for more than half the tube passes. However, this is an uncommon design and may result in structural and thermal problems in manufacturing and design. Common tubeside multipass arrangements for TEMA E_{1-2} , E_{1-3} , and E_{1-4} shells are shown in Figure 2.27.

2.6.4.1.2 Even Number of Tube Passes

One shell pass and two tube passes as shown in Figure 2.4 using a U-tube bundle is one of the most common flow arrangements used in the single-pass TEMA E shell. The heat exchanger with this arrangement is also simply referred to as a conventional 1–2 heat exchanger. If the shell fluid is idealized as well mixed, its temperature is constant at any cross section. In this case, reversing the tube fluid flow direction will not change the idealized temperature distribution and the exchanger thermal effectiveness. Possible flow patterns of the E_{1-2} shell were already shown in Figure 2.4. This is referred as “stream symmetric.”

The 1–2 and 1–4 cases were solved long ago by Bowman [11], Underwood [12], and Nagle [30]. The 1– N geometry for even number of passes was solved by Baclic [31]. The thermal effectiveness formula for the E_{1-2} case is given by Equation T13 in Table 2.6 and the thermal effectiveness chart is given in Figure 2.28 along with F_{\min} curve. The thermal effectiveness formulas for 4 and N tubeside passes are given by Equations T14 and T15, respectively. The thermal effectiveness chart for the E_{1-4} case is shown in Figure 2.29, and this figure may be used for even $N \geq 6$ cases also without loss of much accuracy. Alternate relation (approximate) to find out F factor for even number of tubeside passes of E Shell (E_{1-2} , E_{1-4} , E_{1-6} , E_{1-2n}) is given (Equation 2.70) as follows:

$$F = \frac{\sqrt{R^2 + 1} \ln \left[\frac{1 - P}{1 - PR} \right]}{(R - 1) \ln \left[\frac{2 - P[R + 1 - (1 + R^2)^{0.5}]}{2 - P[R + 1 + (1 + R^2)^{0.5}]} \right]} \quad (2.70)$$

2.6.4.1.3 Odd Number of Tube Passes

With the TEMA E shell, an odd number of tube passes can have both parallelflow and counterflow arrangements. The thermal effectiveness relations for overall parallelflow and counterflow arrangements are discussed next.

In an E_{1-3} overall counterflow arrangement, two tube passes are in counterflow and one tube pass is in parallelflow, whereas in an E_{1-3} overall parallelflow arrangement, two tube passes are in parallelflow and one tube pass is in counterflow. Similarly, in an E_{1-5} overall counterflow arrangement, three tube passes are in counterflow and two tube passes are in parallelflow. The flow arrangement for E_{1-3} is already shown in Figure 2.27 and for E_{1-5} is shown in Figure 2.30. Pignotti and Tamborenea [32] obtained an analytical solution for the 1– N (odd N) case and obtained effectiveness for the 1–3 and 1–5. Explicit thermal relations are given by Pignotti [18] for E_{1-3} parallelflow and counterflow cases.

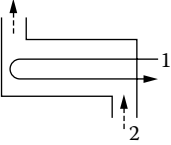
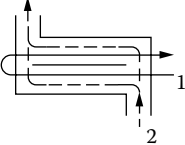
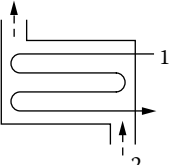
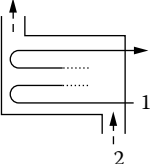
For $N = 3$. Thermal effectiveness formulas for E_{1-3} parallelflow arrangement are given by Equation T16 and for E_{1-3} counterflow arrangement by Equation T17 in Table 2.7. The thermal effectiveness chart for E_{1-3} counterflow arrangement is given in Figure 2.31.

For $N = 5$. For the overall counterflow arrangement or opposite end case, the thermal effectiveness is given by Equation T18 in Table 2.8 and the thermal effectiveness chart is given in Figure 2.32.

For the overall parallelflow arrangement or same end case, the configuration can be obtained from that of the opposite end case (T18) by just the inversion of the direction of flow of the tube fluid, which leads to the following expression [32]:

$$P_1 = \left(1 - X_5^* \right) \quad (2.71a)$$

TABLE 2.6 **E_{1-3} Shell (N Even) (Referred to Tubeside)**

Flow Arrangement	Equation No./ Reference	General Formula	Value for $R = 1$ and Special Cases
 <p>TEMA E_{1-2} shell: shell fluid mixed, tube fluid mixed between passes; stream symmetric</p>	T13 [30]	$P = \frac{2}{1 + R + A \coth(ANTU/2)}$ $A = \sqrt{1 + R^2}$	$P = \frac{1}{1 + \coth(NTU/\sqrt{2})/\sqrt{2}}$
 <p>E_{1-2} shell: shell fluid divided into two streams, individually mixed; tube fluid mixed between passes</p>	Same as J_{1-1} shell		Same as J_{1-1} shell
 <p>TEMA E_{1-4} shell: shell fluid mixed, tube fluid mixed between passes</p>	T14 [30]	$P_1 = \frac{4}{2(1 + R) + \gamma \coth\left(\frac{\gamma NTU}{4}\right) + \tanh\left(\frac{NTU}{4}\right)}$ $\gamma = \sqrt{(4R^2 + 1)}$	$P = \frac{4}{[4 + \sqrt{5}A + B]}$ $A = \coth(\sqrt{5}NTU/4)$ $B = \tanh(NTU/4)$
 <p>TEMA E_{1-N} (even N) shell: shell fluid mixed and tube fluid mixed between passes</p>	T15 [31]	$P_1 = \frac{2}{A + B + C}$ $A = 1 + R + \coth(NTU/2)$ $B = \frac{-1}{N_1} \coth\left(\frac{NTU}{2N_1}\right)$ $C = \frac{1}{N_1} \sqrt{1 + N_1^2 R^2} \coth\left(\frac{NTU}{2N_1} \sqrt{1 + N_1^2 R^2}\right)$ $N_1 = \frac{N}{2}$ <p>$N \rightarrow \infty$ results in well-known single-pass crossflow exchanger with both fluids mixed</p>	Same as Equation T15 with $R = 1$

Note: $P_2(P_s) = P_1 R_1$, $R_2 = 1/R_1$, $NTU_2 = R_1 NTU_1$; Equation 2.55.

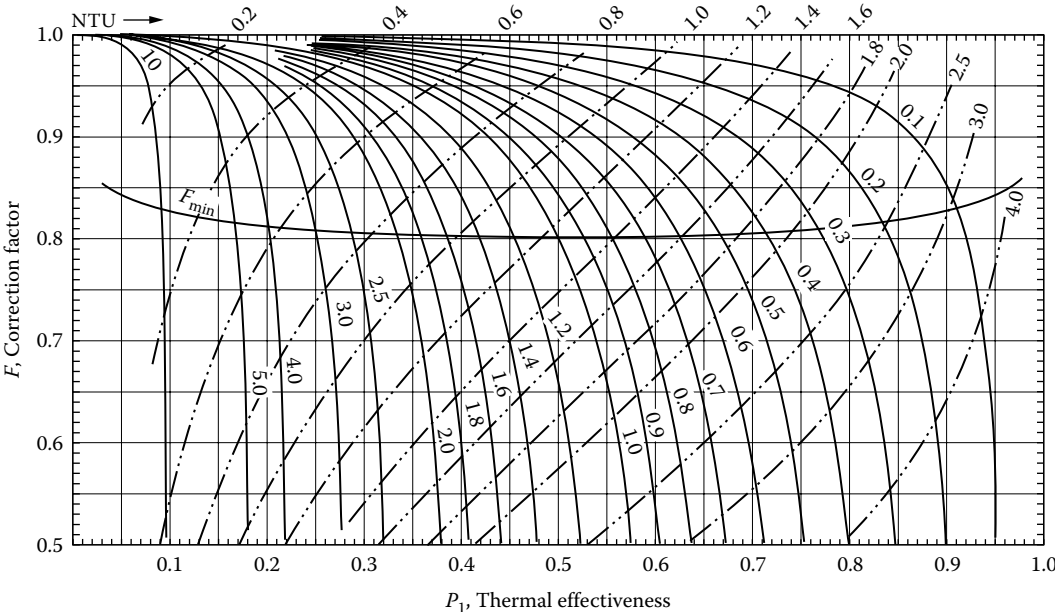


FIGURE 2.28 Thermal effectiveness chart—TEMA E_{1-2} shell; shell fluid mixed, tube fluid mixed between passes. Stream symmetric. F as a function of P for constant R (solid lines) and constant NTU (dashed lines) F_{min} line is also shown (as per Equation T13 and Table 2.6).

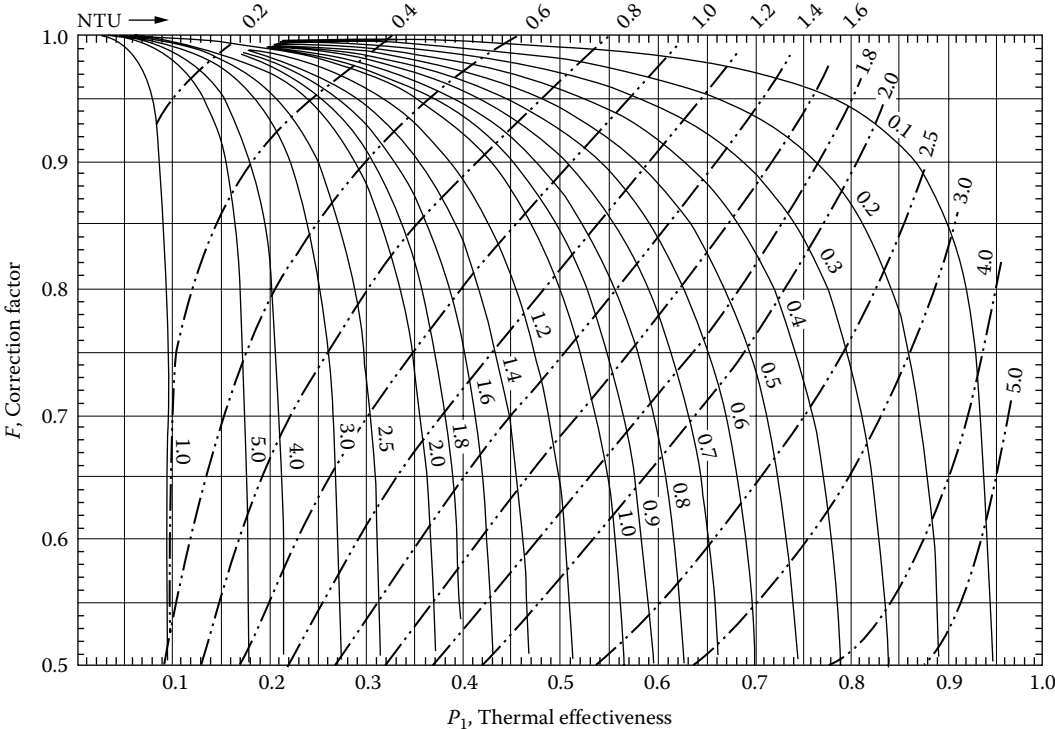


FIGURE 2.29 Thermal effectiveness chart—TEMA E_{1-4} shell. Shell fluid mixed, tube fluid mixed between passes. F as a function of P for constant R (solid lines) and constant NTU (dashed lines) (as per Equation T14, Table 2.6).

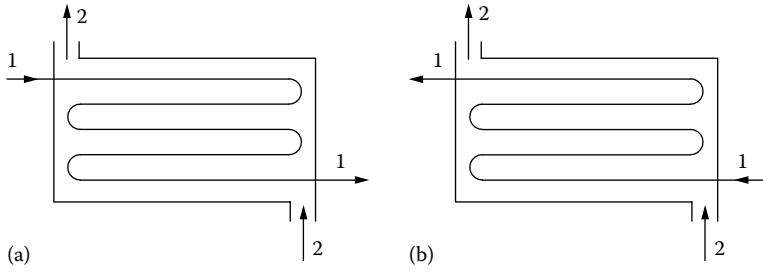
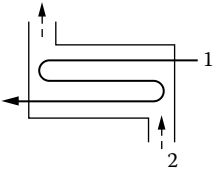
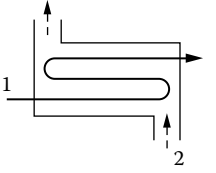


FIGURE 2.30 Flow arrangement of E shell with one shell pass and five tube passes (E_{1-5}). (a) Counterflow; (b) parallelflow.

TABLE 2.7

E_{1-3} Shell (Referred to Tubeside)

Flow Arrangement	Equation No./Reference	General Formula	Value for $R = 1$
<p>1-3 TMA E shell: two parallelflow and one counterflow passes; shell fluid mixed, tube fluid mixed between passes</p> 	T16 [18]	$P_1 = \left[1 - \frac{AC + B^2}{C} \right]$ $A = \chi_1(1 - R\lambda_1)(1 + R\lambda_2)/2R^2\lambda_1 - E$ $- \chi_2(1 - R\lambda_2)(1 + R\lambda_1)/2R^2\lambda_2 + R/(1 + R)$ $B = -\chi_1(1 + R\lambda_2)/R + \chi_2(1 + R\lambda_1)/R + E$ $C = \chi_1(3 - R\lambda_2)/R - \chi_2(3 - R\lambda_1)/R + E$ $E = 0.5e^{(-NTU/3)}$ $\lambda_{1,2} = (-3 \pm \delta)/2$ $\delta = \frac{[9R^2 + 4(R+1)]^{0.5}}{R}$ $\chi_{1,2} = \frac{e^{(\lambda_{1,2}RNTU/3)}}{2\delta}$	Same as Equation T16 with $R = 1$
<p>1-3 TEMA E shell: one parallelflow and two counterflow passes; shell fluid mixed between passes</p> 	T17 [18]	$P_1 = \left[1 - \frac{C}{(AC + B^2)} \right]$ $A = \chi_1(1 + R\lambda_1)(1 - R\lambda_2)/2R^2\lambda_1 - E$ $- \chi_2(1 + R\lambda_2)(1 - R\lambda_1)/2R^2\lambda_2 + R/(R - 1)$ $B = \chi_1(1 - R\lambda_2)/R - \chi_2(1 - R\lambda_1)/R + E$ $C = -\chi_1(3 + R\lambda_2)/R + \chi_2(3 + R\lambda_1)/R + E$ $E = 0.5e^{(NTU/3)}$ $\lambda_{1,2} = (-3 \pm \delta)/2$ $\delta = \frac{[9R^2 + 4(1 - R)]^{0.5}}{R}$ $\chi_{1,2} = \frac{e^{(\lambda_{1,2}RNTU/3)}}{2\delta}$	<p>Same as Equation T17 with $R = 1$ and</p> $A = -\frac{e^{-NTU}}{18} - \frac{e^{NTU/3}}{2} + \frac{(5 + NTU)}{9}$

Note: $P_2(P_s) = P_1R_1$, $R_2 = 1/R_1$, $NTU_2 = R_1NTU_1$; Equation 2.55.

with

$$X_5^*(R, NTU) = \frac{1}{X_5(-R, NTU)} \quad (2.71b)$$

2.6.4.2 TEMA F Shell

For the TEMA *F* shell, as is usual with two tube passes, the arrangement results in pure counterflow with $F = 1$. For four tube passes, the configuration would be treated as two E_{1-2} exchangers in series. As the longitudinal baffle is exposed on the one side to the hot stream and on the other side to the cold stream, there is a conduction heat exchange that reduces the thermal effectiveness and hence the F factor has to be corrected. The effect of thermal leakage by conduction across the baffle has been analyzed by Whistler [33] and in nondimensional form by Rozenman and Taborek [34], with proposed baffle correction methods. The baffle correction factor based on Ref. [34] is presented in Ref. [35].

2.6.4.3 TEMA G Shell or Split-Flow Exchanger

Possible flow arrangements for the TEMA *G* shell are G_{1-1} , G_{1-2} , and G_{1-4} . The solution of the G_{1-2} counterflow case is due to Schindler and Bates [36] and that of the parallelflow case is due to Pignotti [18]. The thermal effectiveness P of this shell with two tube passes is higher than that of the conventional E_{1-2} exchanger for a given NTU_i and R . It is also possible to have only a single pass on the tubeside, which is stream symmetric [37]. The thermal effectiveness formula for G_{1-1} is given by Equation T19 in

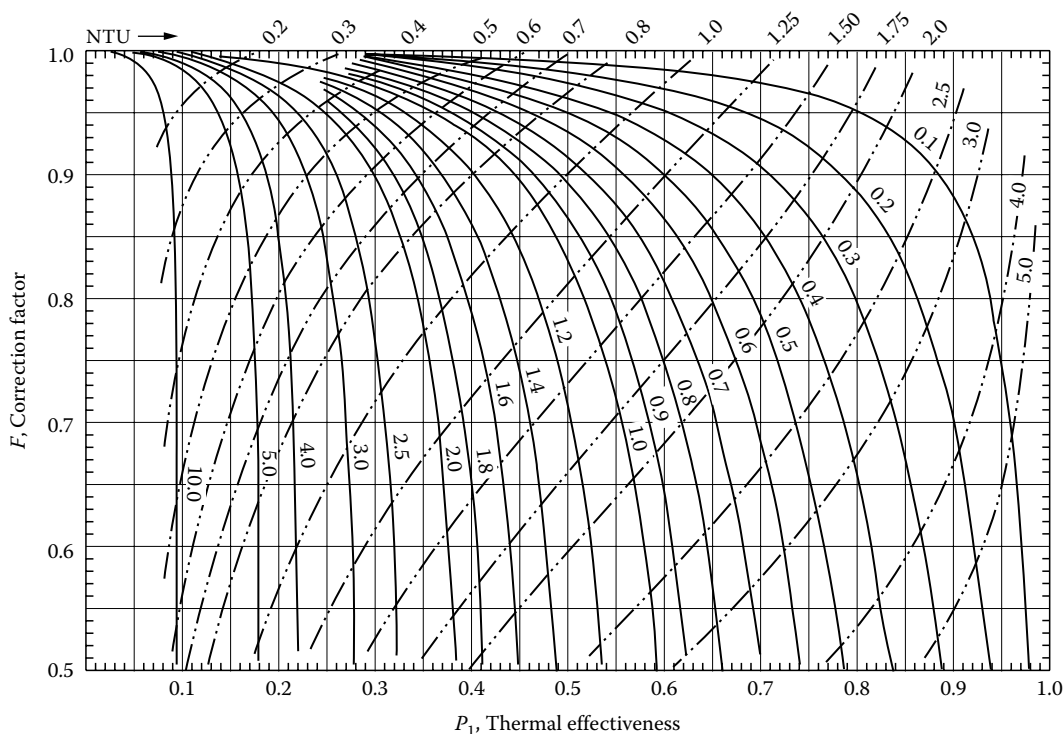
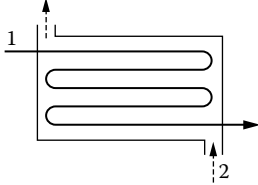


FIGURE 2.31 Thermal effectiveness chart—TEMA E_{1-3} shell. One parallelflow and two counterflow passes (overall counterflow arrangement); shell fluid mixed, tube fluid mixed between passes. F as a function of P for constant R (solid lines) and constant NTU (dashed lines) (as per Equation T17, Table 2.7).

TABLE 2.8

Formula for E_{1-5} Shell and Tube Exchanger with Three Tube Two Tube Passes in Parallelfow Arrangement; Shell Fluid Mixed, Passes (Referred to Tubeside)

where



$$P_1 = (1 - X_N)/R \quad \text{for } N = 5$$

$$X_N = X_5 = \frac{(\alpha\gamma - \beta^2)}{[(\alpha\gamma - \beta^2)H_{13} + \alpha\xi^2 + \gamma\eta^2 - 2\beta\xi\eta]}$$

$$\alpha = H_{24} - H_{11} - 2H_{12}$$

$$\beta = H_{22} - H_{13} - 2H_{12}$$

$$\gamma = H_{24} - H_{13} - 2H_{12}$$

$$\xi = H_{11} + H_{12}$$

$$\eta = H_{13} + H_{12}$$

T18

$$H_{11} = \frac{(1 + R\lambda_1)(1 - R\lambda_2)}{R^2(N+1)\lambda_1\delta} X_1 - \frac{(1 - R\lambda_1)(1 + R\lambda_2)}{R^2(N+1)\lambda_2\delta} X_2 + \frac{N-1}{N+1} X_3 + \frac{R}{R-1} \quad \text{for } R \neq 1$$

$$= \frac{2N-1+NTU}{N^2} + \frac{1-N}{(N+1)N^2} X_2 + \frac{N-1}{N+1} X_3 \quad \text{for } R = 1$$

$$H_{12} = \frac{(1 + R\lambda_1)(1 + R\lambda_2)}{R^2(N-1)\lambda_1\delta} X_1 - \frac{(1 + R\lambda_1)(1 + R\lambda_2)}{R^2(N-1)\lambda_2\delta} X_2 - \frac{R}{R-1} \quad \text{for } R \neq 1$$

$$= \frac{1-NTU}{N^2} - \frac{X_2}{N^2} \quad \text{for } R = 1$$

$$H_{13} = \frac{(1 + R\lambda_1)(1 - R\lambda_2)}{R^2(N+1)\lambda_1\delta} X_1 - \frac{(1 - R\lambda_1)(1 + R\lambda_2)}{R^2(N+1)\lambda_2\delta} X_2 - \frac{2}{N+1} X_3 + \frac{R}{R-1} \quad \text{for } R \neq 1$$

$$= \frac{2N-1+NTU}{N^2} + \frac{1-N}{(N+1)N^2} X_2 - \frac{2}{N+1} X_3 \quad \text{for } R = 1$$

$$H_{22} = \frac{(1 - R\lambda_1)(1 + R\lambda_2)}{R^2(N-1)\lambda_1\delta} X_1 - \frac{(1 + R\lambda_1)(1 - R\lambda_2)}{R^2(N-1)\lambda_2\delta} X_2 + \frac{N-3}{N-1} X_4 - \frac{R}{R-1} \quad \text{for } R \neq 1$$

$$= \frac{2N+1-NTU}{N^2} + \frac{1+N}{(N-1)N^2} X_2 + \frac{N-3}{N-1} X_4 \quad \text{for } R = 1$$

$$H_{24} = \frac{(1 - R\lambda_1)(1 + R\lambda_2)}{R^2(N-1)\lambda_1\delta} X_1 - \frac{(1 + R\lambda_1)(1 - R\lambda_2)}{R^2(N-1)\lambda_2\delta} X_2 - \frac{2X_4}{N-1} - \frac{R}{R-1} \quad \text{for } R \neq 1$$

$$= \frac{2N+1-NTU}{N^2} + \frac{1+N}{(N-1)N^2} X_2 - \frac{2X_4}{N-1} \quad \text{for } R = 1$$

Sources: Pignotti, A. and Tamborenea, P.I., *Trans. ASME, J. Heat Transfer*, 111, 54, 1988.

Note: Expressions for δ , λ_1 , λ_2 , X_1 , X_2 , X_3 and X_4 are $\lambda_{1,2} = -\frac{N}{2} \pm \left[\frac{N^2}{4} + \frac{1}{R^2} (1-R) \right]^{0.5}$; $\lambda_3 = 1/R$; $\lambda_4 = 1/R$; $\delta = \lambda_1 - \lambda_2$;

$$X_1 = e^{(\lambda_1 R NTU/5)}; X_2 = e^{(\lambda_2 R NTU/5)}; X_3 = e^{(\lambda_3 R NTU/5)}; X_4 = e^{(\lambda_4 R NTU/5)};$$

$P_2(P_s)$ can be found using Equation 2.55.

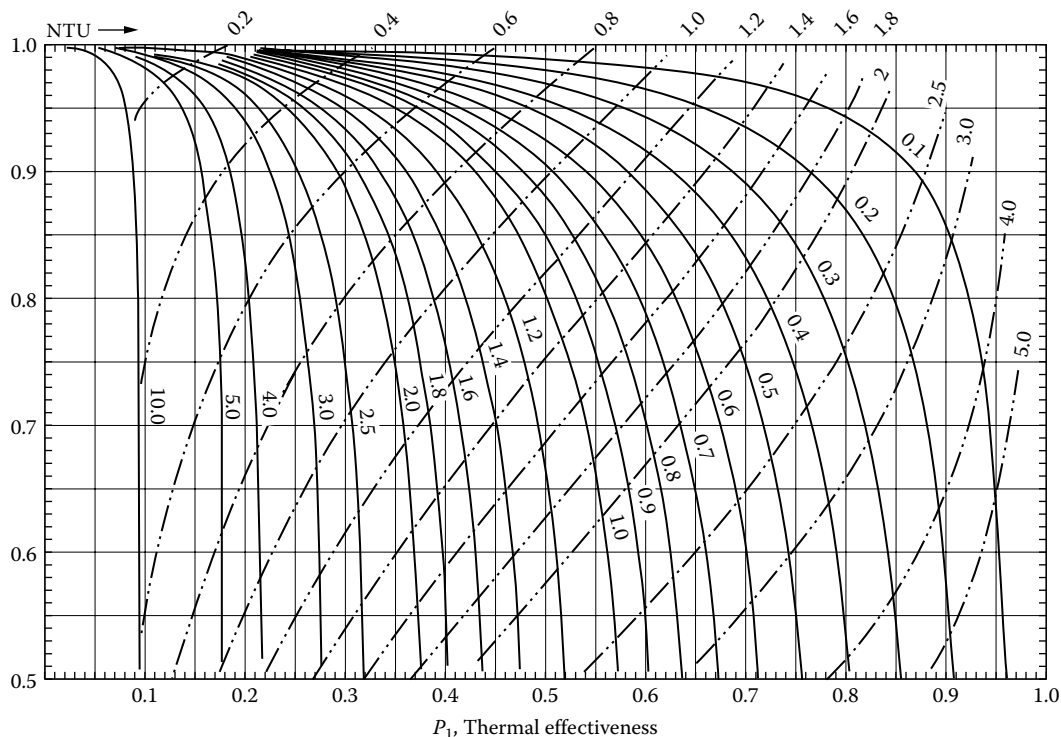


FIGURE 2.32 Thermal effectiveness chart—TEMA E_{1-5} shell. Two parallelflow and three counterflow passes (overall counterflow arrangement); shell fluid mixed, tube fluid mixed between passes. F as a function P for constant R (solid lines) and constant NTU (dashed lines) (as per Equation T18, Table 2.8).

Table 2.9, and the thermal effectiveness chart is given in Figure 2.33. For the G_{1-2} arrangement, the thermal relations for the parallelflow and counterflow arrangements are given by Equations T20 and T21, respectively, and the thermal effectiveness chart for the counterflow arrangement is given in Figure 2.34. G_{1-4} arrangement was analyzed by Singh et al. [38], and the thermal effectiveness chart is given at the end of this chapter.

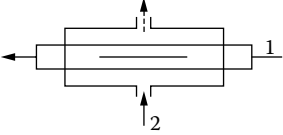
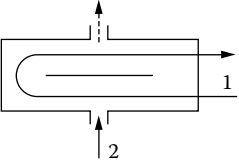
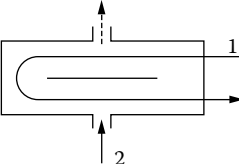
2.6.4.4 TEMA H Shell

The arrangement of the TEMA H shell exchanger resembles a configuration in which two TEMA G shell exchangers are connected side by side. The solution for the TEMA H shell with 1–2 flow arrangement was analytically derived by Kohei Ishihara and Palen [39]. It is also possible to have only a single pass on the tubeside [40]. The thermal effectiveness relation referred to the shellside for H_{1-1} is given by Equation T22 in Table 2.10, and the thermal effectiveness chart referred to the shellside is given in Figure 2.35. For the H_{1-2} arrangement, the thermal relations for the parallelflow and counterflow arrangements are given by Equations T23 and T24, respectively, and the thermal effectiveness chart for the counterflow arrangement is given in Figure 2.36.

2.6.4.5 TEMA J Shell or Divided-Flow Shell

The use of divided-flow exchangers with one shell pass and one or more tube passes is very common. If the shellside heat transfer resistance is not a limiting factor, and entrance and exit losses

TABLE 2.9
G Shell (Referred to Tubeside)

Flow Arrangement	Equation No./ Reference	General Formula	Value for $R = 1$ and Special Cases
 <p>1-1 G shell: tube fluid split into two streams; shell fluid mixed. Stream symmetric</p>	T19 [37]	$P = \frac{1}{R} [A + B - AB(1 + 1/R) + AB^2/R]$ $A = \frac{1 - e^{-NTU(1+R)/2}}{(1+R)/R}$ $B = \frac{(1-D)}{(1-D/R)}$ $D = e^{-NTU(R-1)/2}$	$B = \frac{NTU}{2 + NTU}$ for $R = 1$
 <p>1-2 TEMA G shell: overall parallelflow arrangement; shell fluid mixed, tube fluid mixed between passes</p>	T20 [18]	$P_1 = \frac{(B - \alpha^2)}{R(A - \alpha^2/R + 2)}$ $A = \frac{(1 - \alpha)^2}{(R - 0.5)}$ $B = \frac{4R - \beta(2R - 1)}{(2R + 1)}$ $\alpha = e^{\frac{-NTU(2R-1)}{4}}$ $\beta = e^{\frac{-NTU(2R+1)}{2}}$	<p>For $R = 0.5$</p> $P_1 = \frac{1 + 2RNTU - \beta}{R(4 + 4RNTU + R^2NTU^2)}$ $\beta = e^{(-2RNTU)}$
 <p>1-2 TEMA G shell: overall counterflow arrangement; shell fluid mixed, tube fluid mixed between passes</p>	T21 [36]	$P_1 = \frac{(B - \alpha^2)}{R(A + 2 + B/R)}$ $A = \frac{-(1 - \alpha)^2}{(R + 0.5)}$ $B = \frac{4R - \beta(2R + 1)}{(2R - 1)}$ $\alpha = e^{\frac{-NTU(2R+1)}{4}}$ $\beta = e^{\frac{-NTU(2R-1)}{2}}$	<p>For $R = 0.5$</p> $P_1 = \frac{1 + 2RNTU - \alpha^2}{R[4 + 4RNTU - (1 - \alpha)^2]}$ $\alpha = e^{(-RNTU)}$

Note: $P_2(P_s)$ can be found using Equation 2.55.

are neglected, the shellside pressure loss is approximately one-eighth of that same heat exchanger arranged as the conventional E_{1-2} or E_{1-4} exchanger. The possible flow arrangements are

1. Divided-flow shell with one tube pass. This arrangement is equivalent to the E_{1-2} exchanger with unmixed shell fluid.
2. Divided-flow shell with two tube passes.
3. Divided-flow shell with four tube passes.
4. Divided-flow shell with infinite number of tube passes.

Jaw [41] analyzed the cases with two and four tube passes. Extending the number of tube passes to infinity, the case becomes identical to that of mixed-mixed crossflow, as derived by Gardner [42a]. Divided flow shell with one tube pass arrangement is equivalent to E_{1-2} exchanger with

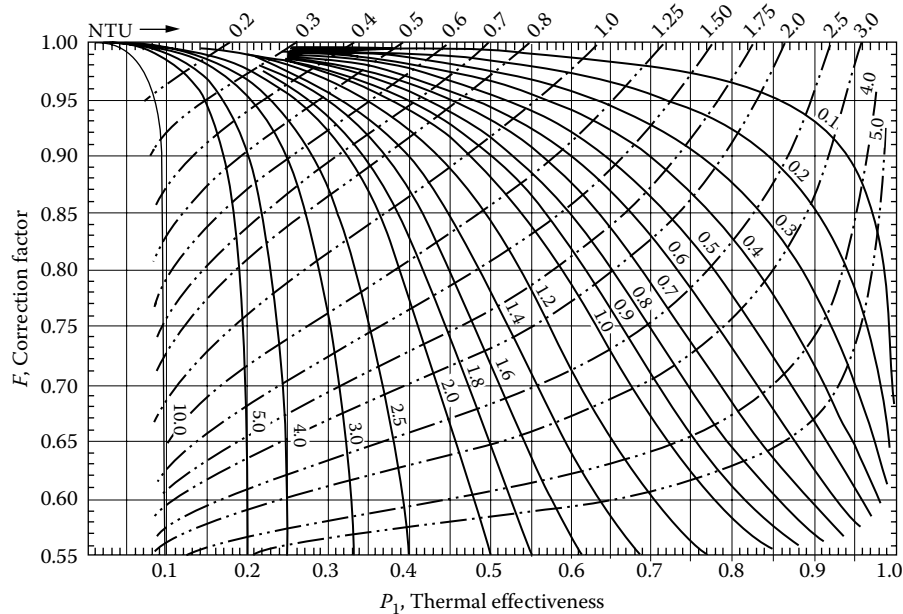


FIGURE 2.33 Thermal effectiveness chart— G_{1-1} shell. Tube fluid split into two streams with shell of mixed fluid. Stream symmetric. F as a function of P for constant R (solid lines) and constant NTU (dashed lines) (as per Equation T19, Table 2.9).

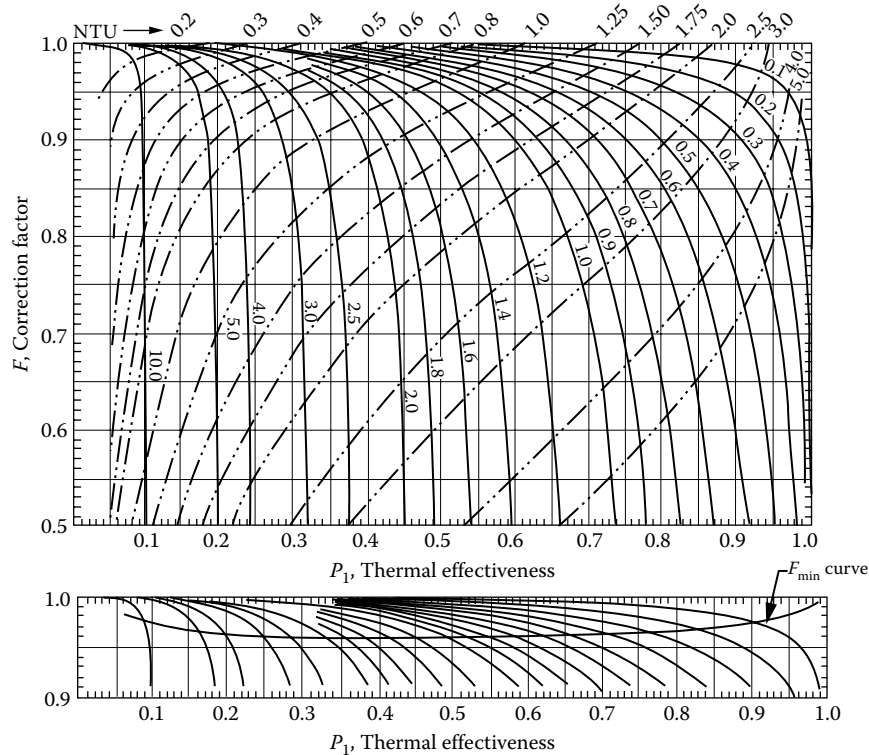
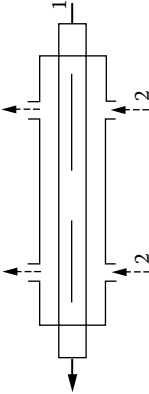
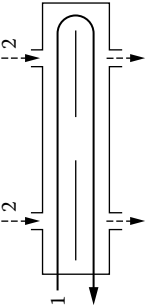
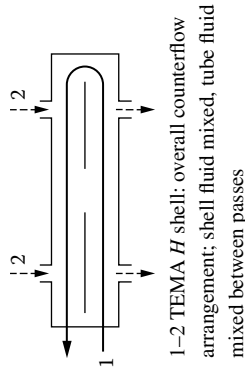


FIGURE 2.34 Thermal effectiveness chart—TEMA G_{1-2} shell. Overall counterflow arrangement; shell fluid mixed, tube fluid mixed between passes. F as a function of P for constant R (solid lines) and constant NTU (dashed lines). F_{min} curve is also shown (as per Equation T21, Table 2.9).

TABLE 2.10
H Shell (Referred to Tubeside)

Flow Arrangement	Equation No./Reference	General Formula	Value for $R = 1$ and Special Cases
	T22 [37]	$P_1 = \frac{1}{R} \left\{ E \left[1 + (1 - B/2R)(1 - A/2R + AB/R) \right] - AB(1 - B/2R) \right\}$ $A = \frac{1}{1 + 1/2R} (1 - \exp[-RNTU(1 + 1/2R)/2])$ $B = (1 - D)/(1 - D/2R)$ $D = e^{1 - RNTU(1 + 1/2R)/2}$ $E = (A + B - AB/2R)/2$	Same as Equation T22 with $R = 0.5$ $B = \frac{RNTU}{(2 + RNTU)}$
1-1 H shell: tube fluid split into two streams; shell fluid mixed			
	T23 [39]	$P_1 = \left[1 - \frac{B + 4GR}{(1 - D)^4} \right]$ $B = (1 + H)(1 + E)^2$ $G = (1 - D)^2 (D^2 + E^2) + D^2 (1 + E)^2$ $D = \frac{1 - e^{-\alpha}}{1 - 4R}$ $E = \frac{e^{-\beta} - 1}{4R + 1}$ $H = \frac{e^{-2\beta} - 1}{4R + 1}$ $\alpha = \frac{NTU}{8} (4R - 1)$ $\beta = \frac{NTU}{8} (4R + 1)$	For $R = 0.25$ $P_1 = \left[1 - \frac{B + 4GR}{(1 - D)^4} \right]$ $D = -NTU/8$
1-2 TEMA H shell: overall parallelflow arrangement; shell fluid mixed, tube fluid mixed between passes			



T24 [39]

$$P_1 = \left[1 - \frac{(1-D)^4}{(B-4RG)} \right]$$
$$B = (1+H)(1+E)^2$$
$$G = (1-D)^2(D^2 + E^2) + D^2(1+E)^2$$
$$D = \frac{1-e^{-\alpha}}{4R+1}$$
$$E = \frac{1-e^{-\beta}}{4R-1}$$
$$H = \frac{1-e^{-2\beta}}{4R-1}$$
$$\alpha = \frac{NTU}{8} (4R+1)$$
$$\beta = \frac{NTU}{8} (4R-1)$$

For $R = 0.25$

$$P_1 = \left[1 - \frac{(1-D)^4}{(B-G)} \right]$$
$$B = (1+\alpha)(1+\alpha/2)^2$$
$$G = (1-D)^2 x$$
$$(D^2 + \alpha^2/4) + D^2(1+\alpha/2)^2$$

Note: $P_2(P_3)$ can be found using Equation 2.55.

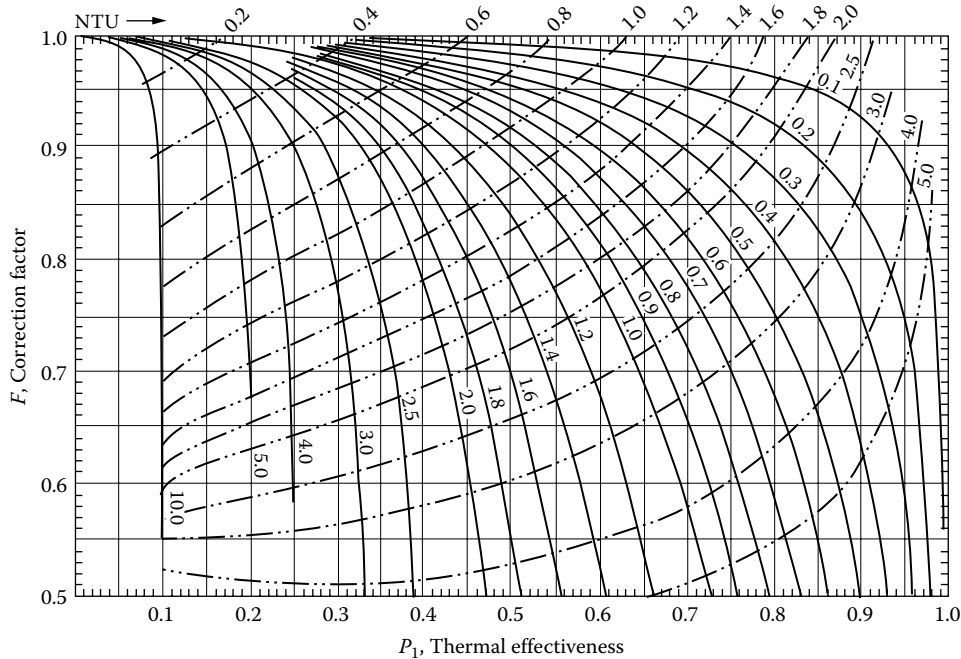


FIGURE 2.35 Thermal effectiveness chart— H_{1-1} shell. Tube fluid split into two streams. Shell mixed. F as a function of P for constant R (solid lines) and constant NTU (dashed lines) referred to shellside (as per Equation T22, Table 2.10).

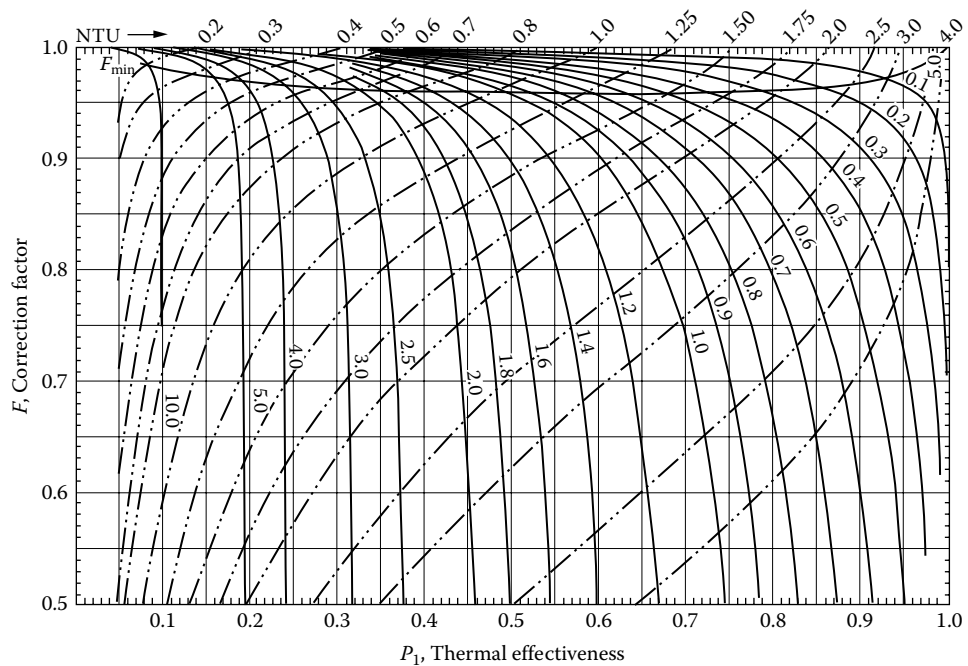
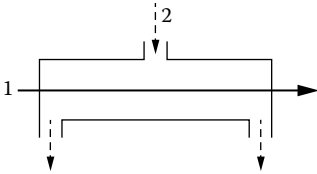
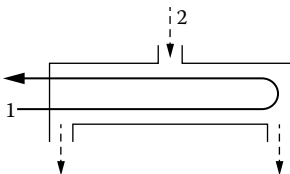
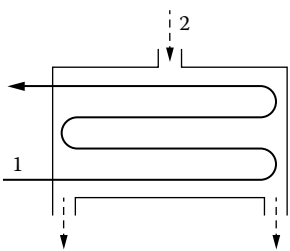


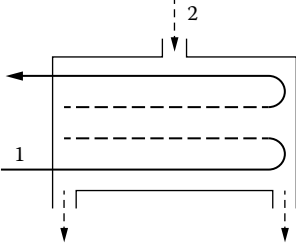
FIGURE 2.36 Thermal effectiveness chart—TEMA H_{1-2} shell. Overall counterflow arrangement; shell fluid mixed, tube fluid mixed between passes. F as a function of P for constant R (solid lines) and constant NTU (dashed lines). F_{min} curve is also shown (as per Equation T24, Table 2.10).

TABLE 2.11**J Shell (Referred to Tubeside)**

Flow Arrangement	Equation No./ Reference	General Formula	Values for $R = 1$ and Special Cases
 <p>1-1 TEMA J shell: shell fluid mixed</p>	T25 [40]	$P_1 = 1 - \frac{(2R-1)}{(2R+1)} \left[\frac{2R + \phi^{-(R+0.5)}}{2R - \phi^{-(R-0.5)}} \right] G$ $\phi = e^{NTU}$	For $R = 0.5$, $P_1 = 1 - \frac{1 + \phi^{-1}}{2 + NTU}$
 <p>1-2 TEMA J shell: shell fluid mixed and tube fluid mixed between passes</p>	T26 [41]	$P_1 = \frac{2}{1 + 2R[1 + \lambda A - 2B\lambda(1 + C)]}$ $A = \frac{\phi^{R\lambda} + 1}{\phi^{R\lambda} - 1}$ $B = \frac{\frac{\phi^{R(1+\lambda)/2}}{\phi^{R\lambda} - 1}}{1 + \lambda \left(\frac{\phi^{R\lambda} + 1}{\phi^{R\lambda} - 1} \right)}$ $C = 1 + \frac{\lambda \phi^{R(\lambda-1)/2}}{\phi^{R\lambda} - 1}$ $\phi = e^{NTU}$ $\lambda = \frac{\sqrt{1 + 4R^2}}{2R}$	Same as Equation T26
 <p>1-4 J shell: shell fluid mixed and tube mixed between passes</p>	T27 [41]	$P_1 = \frac{4}{1 + A + 4R[1 + \lambda B - 2C\lambda(1 + D)]}$ $A = \frac{2\sqrt{\phi}}{1 + \sqrt{\phi}}$ $B = \frac{\phi^{R\lambda} + 1}{\phi^{R\lambda} - 1}$ $C = \frac{\frac{\phi^{R(1+\lambda)/2}}{\phi^{R\lambda} - 1}}{1 + \lambda \left(\frac{\phi^{R\lambda} + 1}{\phi^{R\lambda} - 1} \right)}$ $D = 1 + \frac{\lambda \phi^{R(\lambda-1)/2}}{\phi^{R\lambda} - 1}$ $\phi = e^{NTU}$ $\lambda = \frac{\sqrt{1 + 16R^2}}{4R}$	Same as Equation T27

(continued)

TABLE 2.11 (continued)
J Shell (Referred to Tubeside)

Flow Arrangement	Equation No./ Reference	General Formula	Values for $R = 1$ and Special Cases
	T28 [42]	$P = \frac{1}{\frac{R\phi^R}{(\phi^R - 1)} + \frac{\phi}{\phi - 1} - \frac{1}{NTU}}$ $\phi = e^{NTU}$	Same as Equation T28
Line of 1-N J shell for $N \rightarrow \infty$: shell fluid mixed and tube fluid mixed between passes; stream symmetric			
Note: $P_2(P_s)$ can be found using Equation 2.55.			

unmixed shell fluid as presented by Gardner [42b]. The difference in P is negligible for four or more passes compared to the two passes arrangement in the region of interest, i.e., $F > 0.5$. The thermal effectiveness relations for J_{1-1} , J_{1-2} , J_{1-4} , and $J_{1-\infty}$ arrangements are given by Equations T25 through T28, respectively, in Table 2.11. The thermal effectiveness charts for J_{1-1} , J_{1-2} , and J_{1-4} are given in Figures 2.37 through 2.39, respectively.

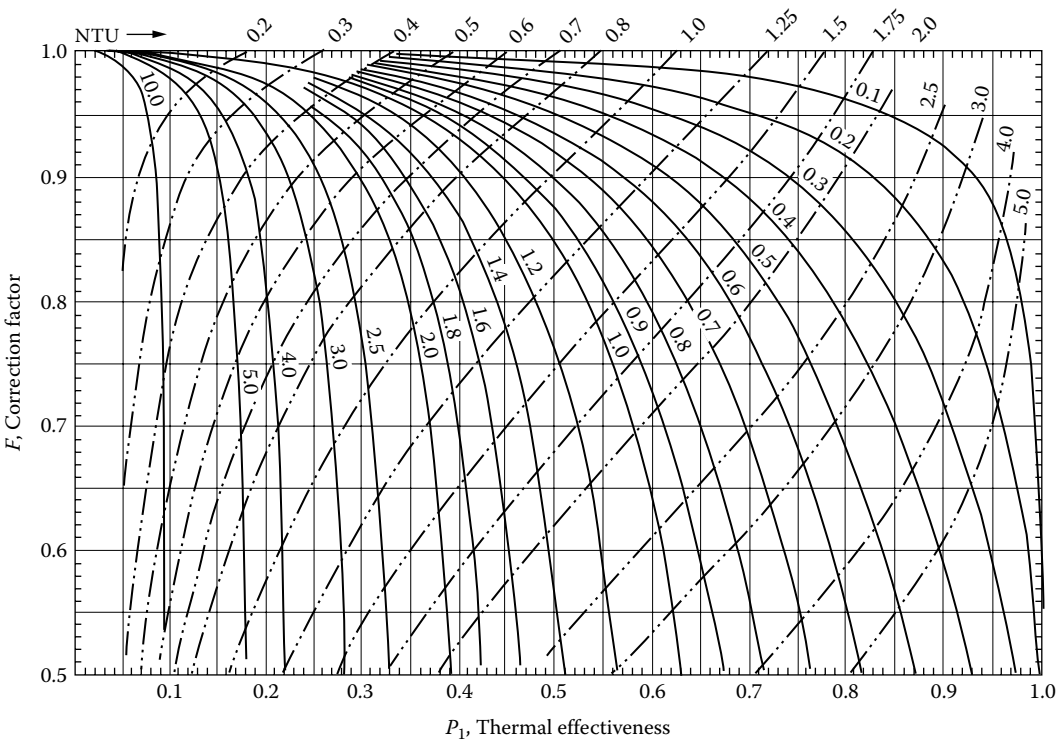


FIGURE 2.37 Thermal effectiveness chart—TEMA J_{1-1} shell. Shell fluid mixed. F as a function of P for constant R (solid lines) and constant NTU (dashed lines) (as per Equation T25, Table 2.11).

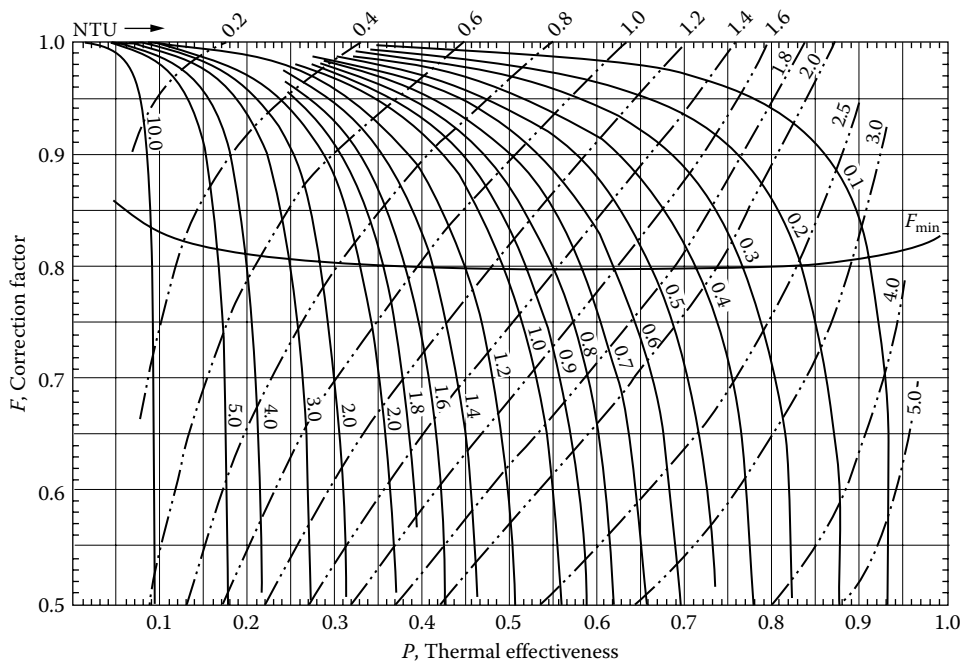


FIGURE 2.38 Thermal effectiveness chart—TEMA J_{1-2} shell. Shell fluid mixed and tube fluid mixed between passes. F as a function of P for constant R (solid lines) and constant NTU (dashed lines), with F_{\min} to avoid temperature cross (horizontal bowl-shaped curve) (as per Equation T26, Table 2.11).

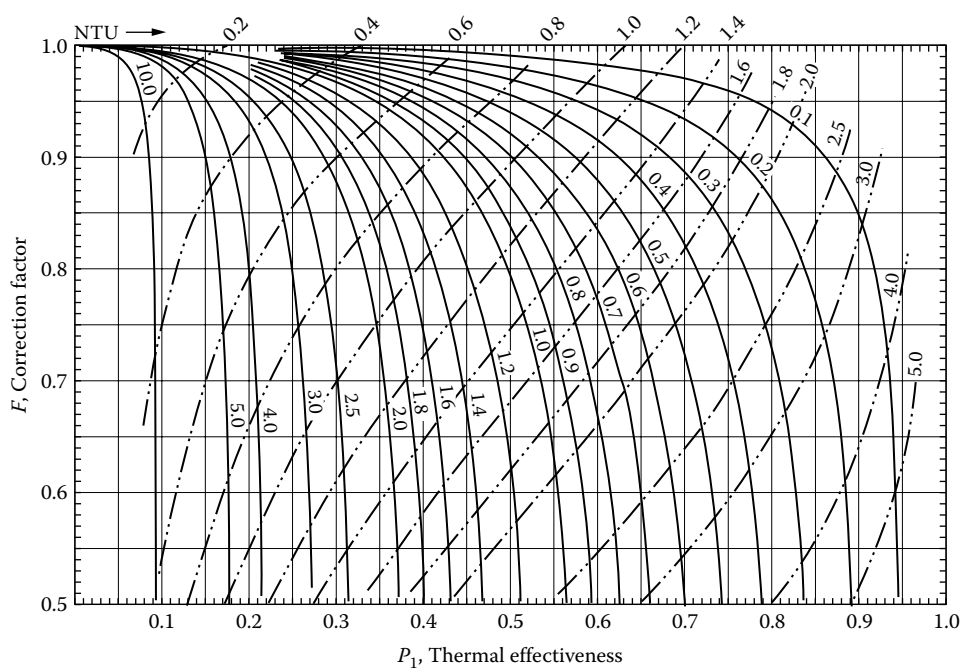


FIGURE 2.39 Thermal effectiveness chart—TEMA J_{1-4} shell. Shell fluid mixed and tube fluid mixed between passes. F as a function of P for constant R (solid lines) and constant NTU (dashed lines) (as per Equation T27, Table 2.11).

2.6.4.6 TEMA X Shell

This exchanger is for very-low-pressure applications. For an X_{1-1} exchanger, the thermal effectiveness is same as single-pass crossflow with both fluids unmixed, that is, the unmixed–unmixed case [1]. An X_{1-2} crossflow shell and tube exchanger is equivalent to Figure 2.40a for both fluids unmixed throughout with overall parallelflow (shell fluid entering at the tube inlet pass end) and Figure 2.40b for overall counterflow (shell fluid entering at the tube exit pass end), respectively. The thermal relation formulas are discussed in Section 2.6.6.

2.6.5 THERMAL EFFECTIVENESS OF MULTIPLE HEAT EXCHANGERS

A multiple exchanger assembly consists of two or more exchangers piped or manifolded together into a single assembly with the exchangers arranged either in a parallel, series, or combination of parallel/series arrangement. Multiple exchanger assemblies are used when the customer's heat transfer requirements are too large for either single piece or modular heat exchanger construction. Sometimes, to utilize the allowable pressure drop effectively, multipassing is also employed; this in turn enhances the thermal effectiveness. Multipassing by multiple units is possible with both compact exchangers and shell and tube exchangers. With multipassing, two or more exchangers can be coupled either in an overall parallel or in an overall countercurrent scheme as shown in Figure 2.41. Multipassing is also possible in a single unit of a compact exchanger (Figure 2.42).

The fundamental formulas for the global effectiveness of multiple units are given next. These equations are not valid for multiple tubeside passes of various TEMA shells. The following idealizations are employed, in addition to those already listed at the beginning of this section:

1. Each pass has the same effectiveness, although any basic flow arrangement may be employed in any pass. If each pass has the same flow arrangement, then NTU is equally distributed between N passes, and NTU per pass (NTU_p) is given by NTU/N .
2. The fluid properties are idealized as constant so that C^* or R is the same for each pass. The final results of this analysis are valid regardless of which fluid is being C_{\max} or C_{\min} .

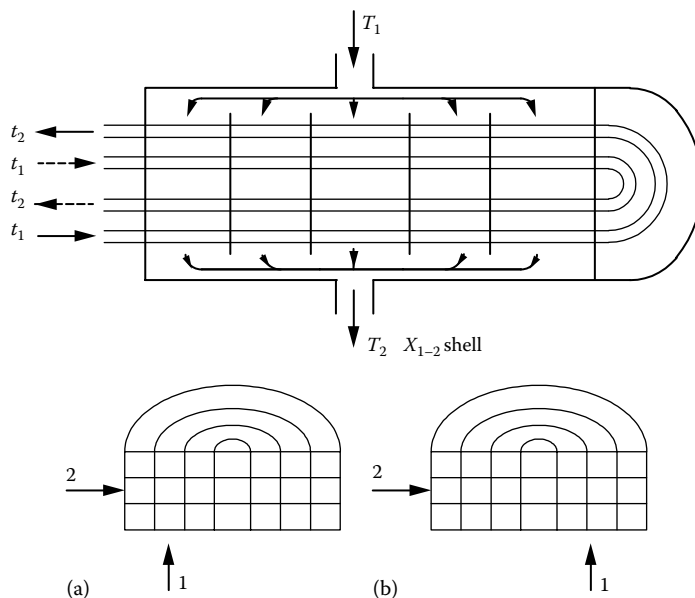


FIGURE 2.40 X_{1-2} shell arrangement equivalent with two-pass crossflow heat exchanger: (a) parallelflow; (b) counterflow.

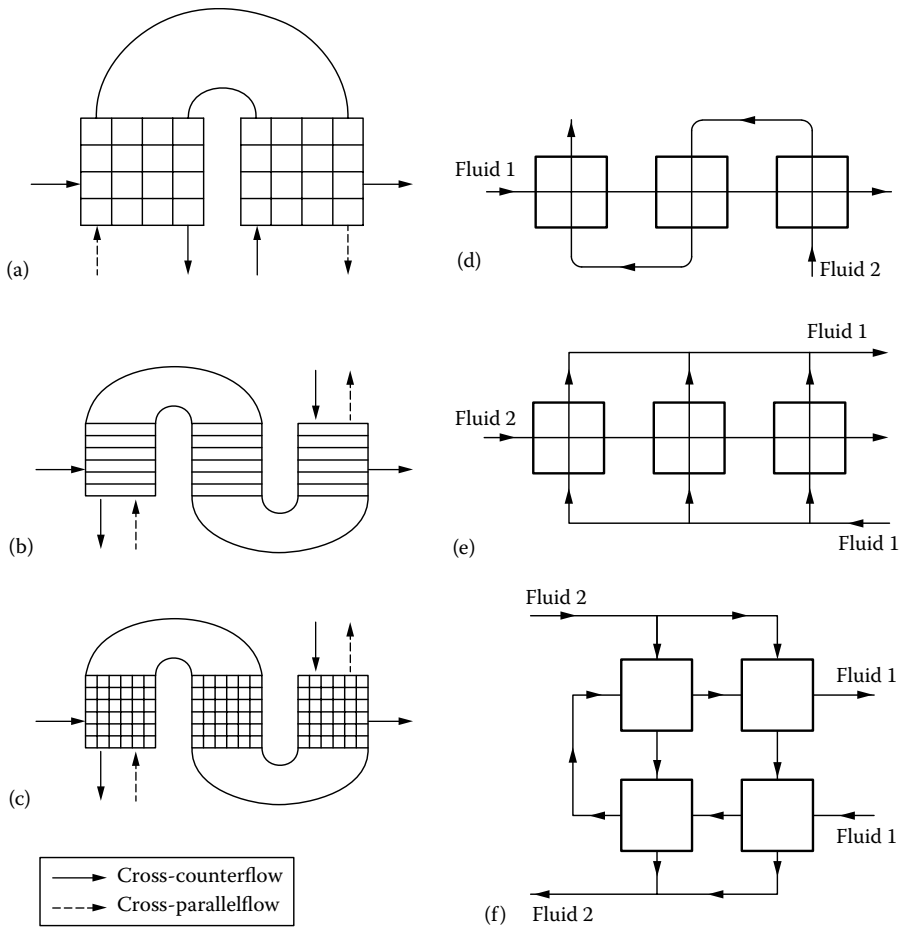


FIGURE 2.41 Multipass assemblies. (a) Two-pass assembly, both the fluids unmixed in each pass and mixed between passes; (b) three-pass assembly, one fluid is unmixed in each pass and mixed between passes, and the other fluid is mixed throughout; (c) three-pass assembly, both the fluids unmixed in each pass and mixed between passes; (d) three-pass counterflow assembly, both the fluids mixed between passes; (e) three-pass parallel-crossflow assembly, fluid 1 is split into three streams-single pass, fluid 2 in three passes mixed between passes; (f) complex multipass assembly, fluid 2 is split into two streams and each stream is in two passes and fluid 1 is in four passes.

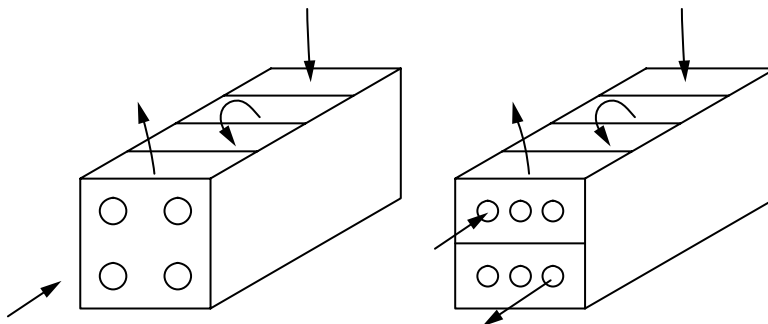


FIGURE 2.42 Multipassing in the same unit.

2.6.5.1 Two-Pass Exchangers

The expression for the global effectiveness for the parallelflow case is given by Pignotti [43] in the following equation:

$$P_2 = P_A + P_B - P_A P_B (1 + R) \quad (2.72)$$

and for the counterflow case by

$$P_2 = \frac{P_A + P_B - P_A P_B (1 + R)}{(1 - R P_A P_B)} \quad (2.73)$$

where

P_A and P_B are the thermal effectiveness of individual heat exchanger

R is the capacity rate ratio

2.6.5.2 N-Pass Exchangers

Counterflow arrangement: The effectiveness P_N of an N -pass assembly, in terms of the effectiveness P_i of each unit, which is equal for all units, has been described by Domingos [44]. For overall countercurrent connection, the effectiveness is given by

$$P_N = \frac{1 - \left[\frac{(1 - P_i R)}{(1 - P_i)} \right]^N}{R - \left[\frac{(1 - P_i R)}{(1 - P_i)} \right]^N} \quad \text{for } R \neq 1 \quad (2.74a)$$

$$= \frac{N P_i}{1 + (N - 1) P_i} \quad \text{for } R = 1 \quad (2.74b)$$

where R is the heat capacity rate ratio, which is the same for the individual unit, as for the overall assembly. Alternately, if P_N is known, then the individual component effectiveness can be determined from the following formulas:

$$P_i = \frac{1 - \left[\frac{(1 - P_N R)}{(1 - P_N)} \right]^{1/N}}{R - \left[\frac{(1 - P_N R)}{1 - P_N} \right]^{1/N}} \quad \text{for } R \neq 1 \quad (2.75a)$$

$$= \frac{P_N}{N - P_N(N - 1)} \quad \text{for } R = 1 \quad (2.75b)$$

2.6.6 MULTIPASS CROSSFLOW EXCHANGERS

Two or more crossflow units can be coupled in two or more passes either in an overall parallelflow or in an overall counterflow arrangement. When both fluids are mixed in the interpass, mixing the resulting flow arrangement can be differentiated only by the flow arrangements in each pass (unmixed–mixed or mixed–mixed). However, if one fluid is unmixed throughout, the order in which the streams enter the next pass must be differentiated. The coupling of the unmixed fluid from one pass to the other pass can be of

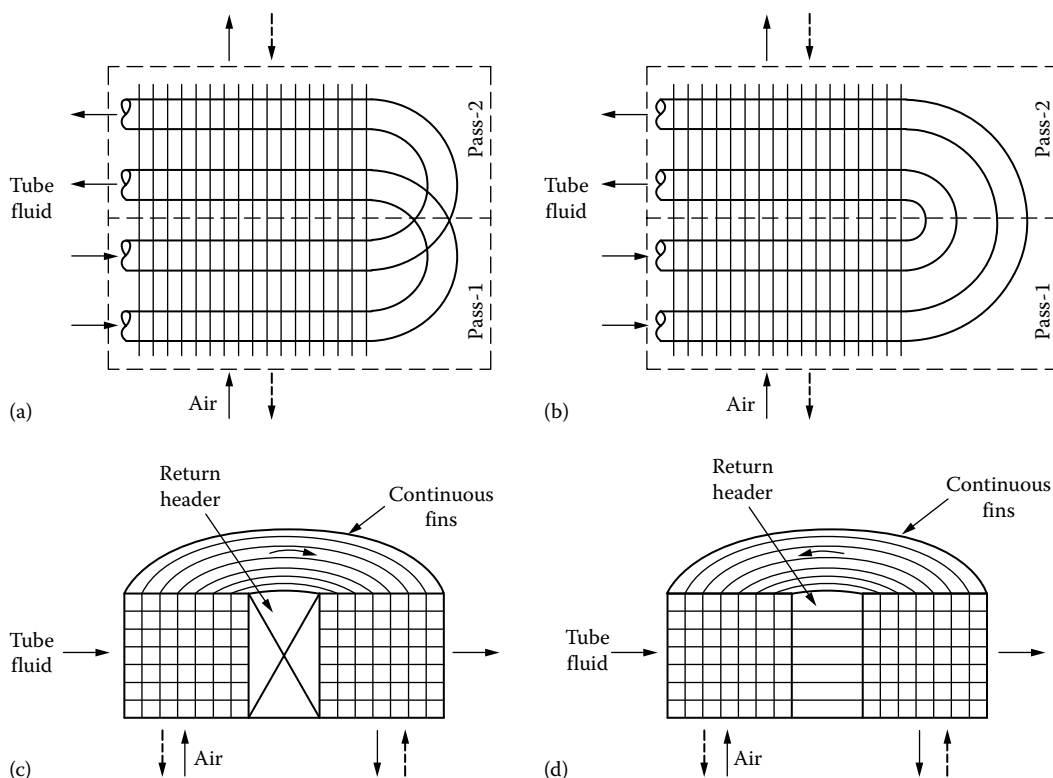


FIGURE 2.43 Two-pass parallel-crossflow and counter-crossflow with both fluids unmixed throughout; coupling of tube fluid between passes: (a) identical order coupling; (b) inverted order coupling. The cases (c) and (d) are symbolic representations of cases (a) and (b), respectively. (Adapted from Shah, R.K. and Mueller, A.C., Heat exchanger basic thermal design methods, in *Handbook of Heat Transfer Applications*, 2nd edn. [W.M. Rohsenow, J.P. Hartnett, and E.N. Ganic, eds.], McGraw-Hill, New York, pp. 4-1–4-77, 1985.)

two types as shown in Figure 2.43 [1]: (1) identical order coupling and (2) inverted order coupling. The coupling is referred to an identical order if the stream leaving one pass enters the next pass from the same side as in the previous pass, as in Figure 2.43a, whereas a coupling is considered to be in an inverted order if the stream leaving one pass enters the next pass from the opposite side of the previous pass, as in Figure 2.43b. Inverted-order coupling is very convenient for manufacturing and installation of heat exchangers. Thermal effectiveness must decrease for constant NTU whenever irreversibilities take place, which may be due to mixing between passes, or due to higher local temperature difference between the fluids, which occurs when the order of the flow arrangement is inverted [28]. Some of the possible cases of two-pass heat exchangers are shown in Figure 2.44a and 2.44b. All these cases were analyzed by Stevens et al. [29], some analytically and others by numerical integration, whereas Baclic [3] solved all possible flow arrangements of two passes units analytically. Multipass crossflow arrangements with complete mixing between passes were analyzed by Domingos [44], and the formulas are also presented in Ref. [2].

2.6.6.1 Multipassing with Complete Mixing between Passes

The thermal effectiveness charts are given for the following cases of two- and three-pass cross-counterflow arrangements with complete mixing between passes:

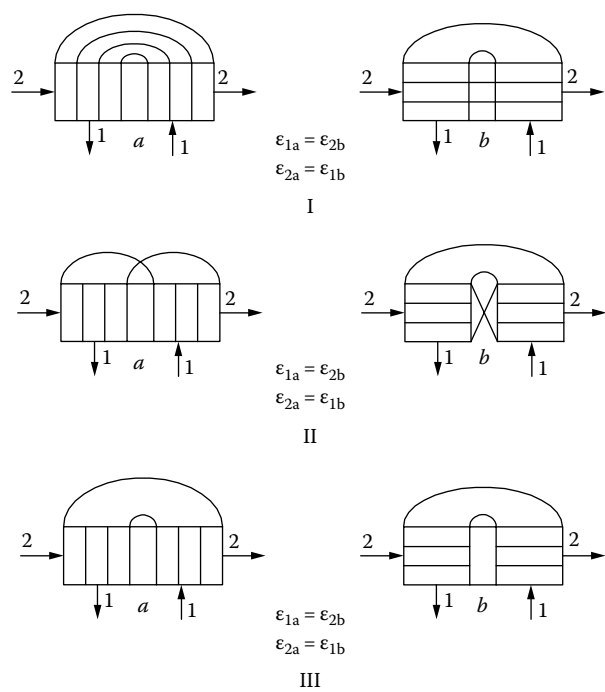
1. Weaker fluid is mixed in all the passes: For the two-pass arrangement (I-a or I-b of Figure 2.44a), the thermal effectiveness chart is given in Figure 2.45, and in Figure 2.46 for the three-pass arrangements.

- 2. Stronger fluid is mixed in all the passes: For the two-pass arrangement (I-a or I-b of Figure 2.44a), the thermal effectiveness chart is given in Figure 2.47, and in Figure 2.48 for the three-pass arrangements.
- 3. Both the fluids unmixed–unmixed in all the passes: For the two-pass arrangements (IV-b of Figure 2.44b), the thermal effectiveness chart is given in Figure 2.49, and in Figure 2.50 for the three-pass arrangements.

2.6.6.2 Two Passes with One Fluid Unmixed throughout, Cross-Counterflow Arrangement

Some of the possible cases of two passes with one fluid unmixed throughout with cross-counterflow arrangements are given here, and these cases were solved by Stevens et al. [29]:

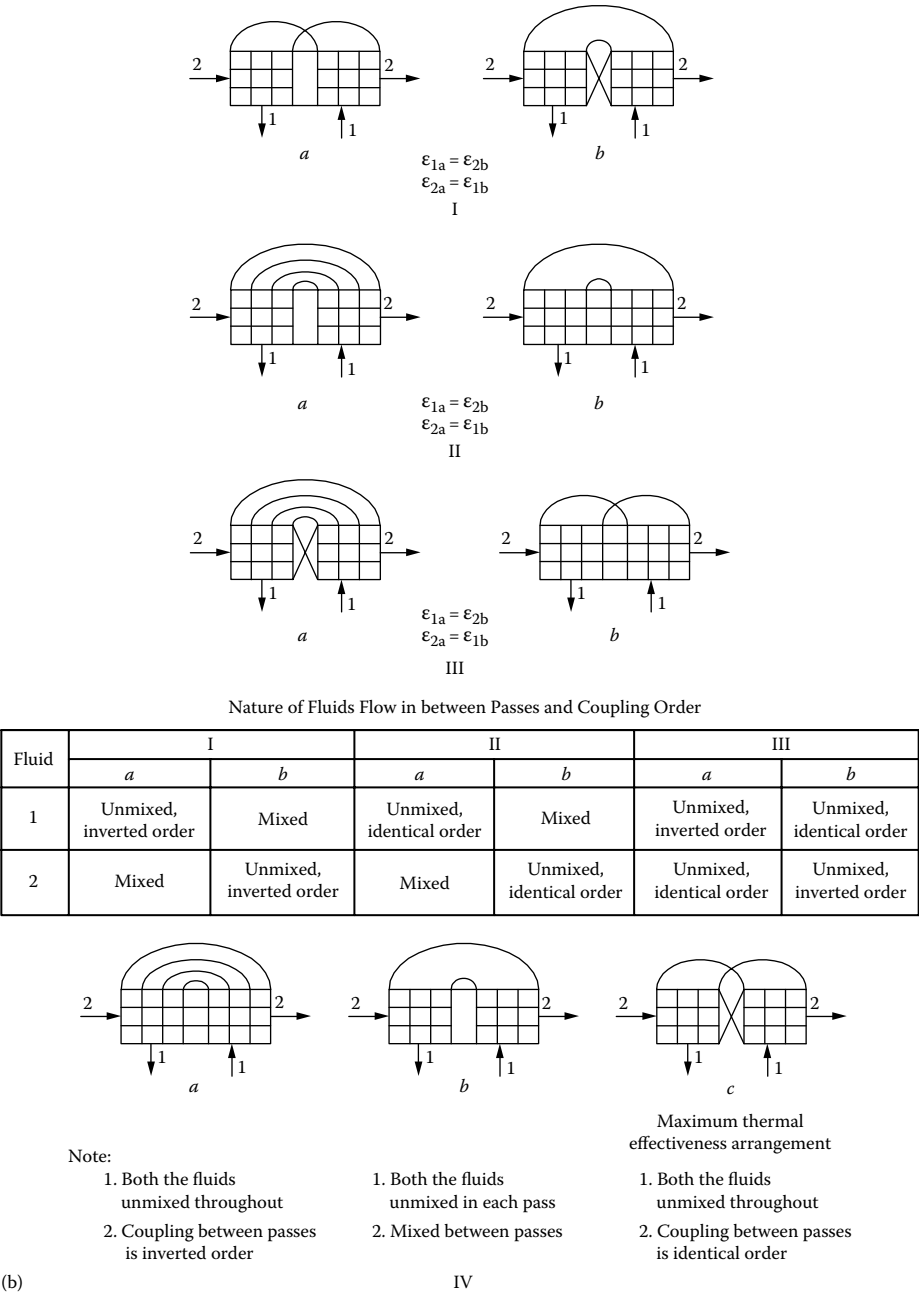
- 1. Two-pass cross-counterflow arrangement: Fluid 1 unmixed throughout, inverted-order coupling; fluid 2 mixed throughout (I-a of Figure 2.44a). Refer Equation T29 of Table 2.12.
- 2. Two-pass cross-counterflow arrangement: Fluid 1 mixed throughout; fluid 2 unmixed throughout, inverted-order coupling (I-b of Figure 2.44a). Refer Equation T30 of Table 2.12.



Nature of Fluids Flow in between Passes and Coupling Order				
Fluid	Case	I	II	III
Fluid 1	a	Unmixed, inverted order	Unmixed, identical order	Mixed
Fluid 2	b	Unmixed, inverted order	Unmixed, identical order	Mixed

(a)

FIGURE 2.44 (a) Some of the possible cases of two-pass heat exchangers with one fluid mixed throughout and the other fluid is unmixed in each pass. *Note:* $\epsilon_{II-a} > \epsilon_{III-a} > \epsilon_{I-a}$



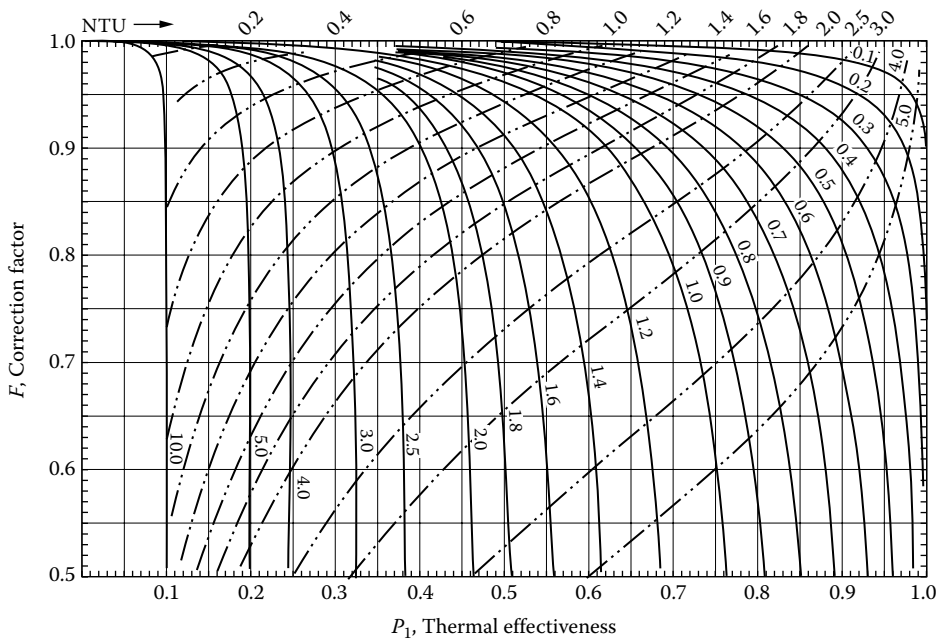


FIGURE 2.45 Thermal effectiveness chart—two-pass cross-counterflow arrangement with complete mixing between passes. Each pass is unmixed–mixed arrangement with weaker fluid mixed (as per Equation T6 of Table 2.4 for single pass; for the flow arrangement shown in III-a or b of Figure 2.44a); F – R – P – NTU chart; F as a function of P for constant R (solid lines) and constant NTU (dashed lines).

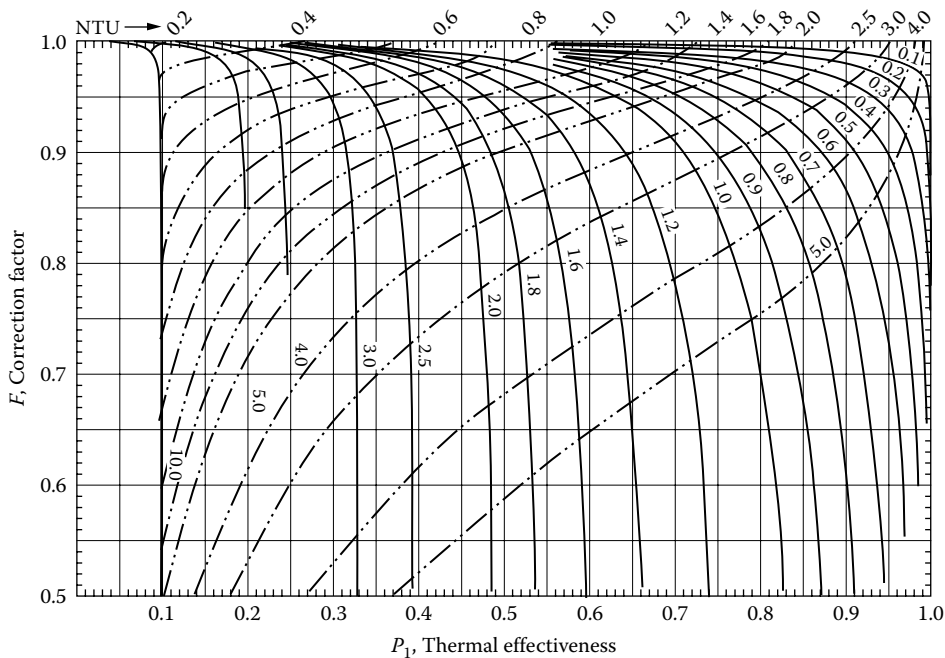


FIGURE 2.46 Thermal effectiveness chart—three-pass cross-counterflow arrangement with complete mixing between passes. Each pass is unmixed–mixed arrangement with weaker fluid mixed (as per Equation T6 of Table 2.4 for single pass; similar to the flow arrangement shown in III-a or b of Figure 2.44a); F – R – P – NTU chart; F as a function of P for constant R (solid lines) and constant NTU (dashed lines).

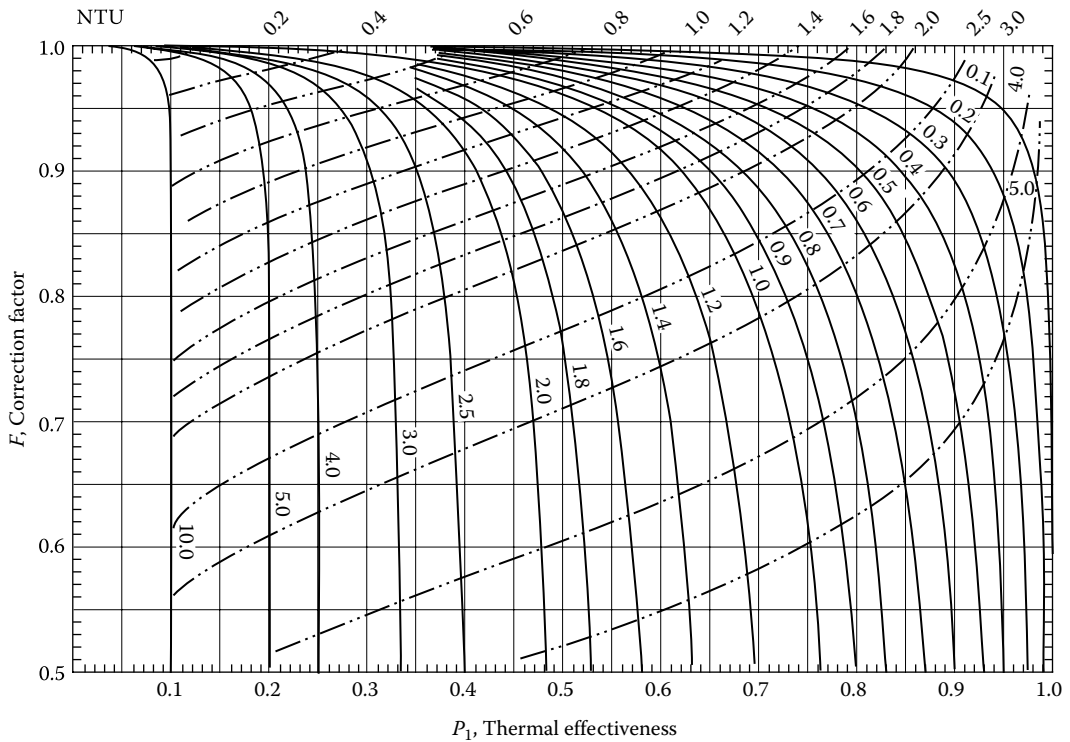


FIGURE 2.47 Thermal effectiveness chart—two-pass cross-counterflow arrangement with complete mixing between passes. Each pass is unmixed–mixed arrangement with stronger fluid mixed (as per Equation T7 of Table 2.4 for single pass; for the flow arrangement shown in III-a or b of Figure 2.44a); F – R – P – NTU chart; F as a function of P for constant R (solid lines) and constant NTU (dashed lines).

3. Two-pass cross-counterflow arrangement: Fluid 1 unmixed throughout, identical-order coupling; fluid 2 mixed throughout (II-a of Figure 2.44a). Refer Equation T31 of Table 2.12.
4. Two-pass cross-counterflow arrangement: Fluid 1 mixed throughout; fluid 2 unmixed throughout, identical-order coupling (II-b of Figure 2.44a). Refer Equation T32 of Table 2.12.

Thermal relation formulas (T29 through T32) for these cases are given in Table 2.12, and thermal effectiveness charts are given in Figures 2.51 through 2.54, respectively.

Comparison of thermal effectiveness of two-pass crossflow cases:

For the possible cases of two-pass exchangers shown in Figure 2.44a, the thermal reflectiveness comparison is given by

$$\epsilon_{II-a} > \epsilon_{III-a} > \epsilon_{I-a} \text{ of Figure 2.44a.}$$

For $NTU = 4$ and $C^* = 1$ [29], the thermal effectiveness of cases a, b, and c of Figure 2.44a is less about 5%–7%.

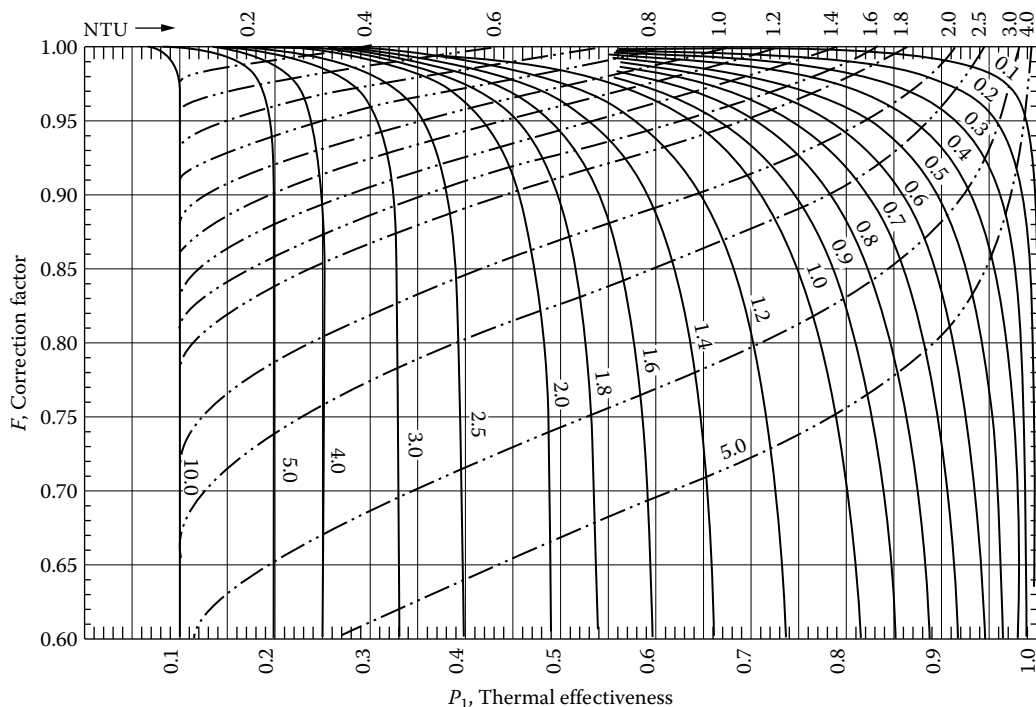


FIGURE 2.48 Thermal effectiveness chart—three-pass cross-counterflow arrangement with complete mixing between passes. Each pass is unmixed–mixed arrangement with stronger fluid mixed (as per Equation T7 of Table 2.4 for single pass; similar to the flow arrangement shown in to III-a or b of Figure 2.44a); F – R – P – NTU chart; F as a function of P for constant R (solid lines) and constant NTU (dashed lines).

2.6.6.3 Two Passes with Both Fluids Unmixed–Unmixed in Each Pass and One Fluid Unmixed throughout, Cross-Counterflow Arrangement

Possible cases of two passes with both fluids unmixed–unmixed in each pass and one fluid unmixed throughout with cross-counterflow arrangements are the following:

1. Two-pass cross-counterflow arrangement: fluid 1 unmixed throughout, inverted-order coupling; fluid 2 unmixed in each pass and mixed between passes (II-a of Figure 2.44b). (Refer Equation T33 of Table 2.13 [45].)
2. Two-pass cross-counterflow arrangement: fluid 1 unmixed in each pass and mixed between passes; fluid 2 unmixed throughout, inverted-order coupling (II-b of Figure 2.44b). (Refer Equation T34 of Table 2.13 [45].)
3. Two-pass cross-counterflow arrangement: fluid 1 unmixed throughout, identical-order coupling; fluid 2 mixed between passes and unmixed in each pass (I-a of Figure 2.44b). (Refer Equation T35 of Table 2.13 [46].)
4. Two-pass cross-counterflow arrangement: fluid 1 mixed between passes and unmixed in each pass; fluid 2 unmixed throughout, identical-order coupling (II-b of Figure 2.44b). (Refer Equation T36 of Table 2.13 [46].)

Thermal relation formulas (T33 through T36) for these cases are given in Table 2.13. The thermal effectiveness chart for case 2 is given in Figure 2.55 and for case 3 in Figure 2.56.

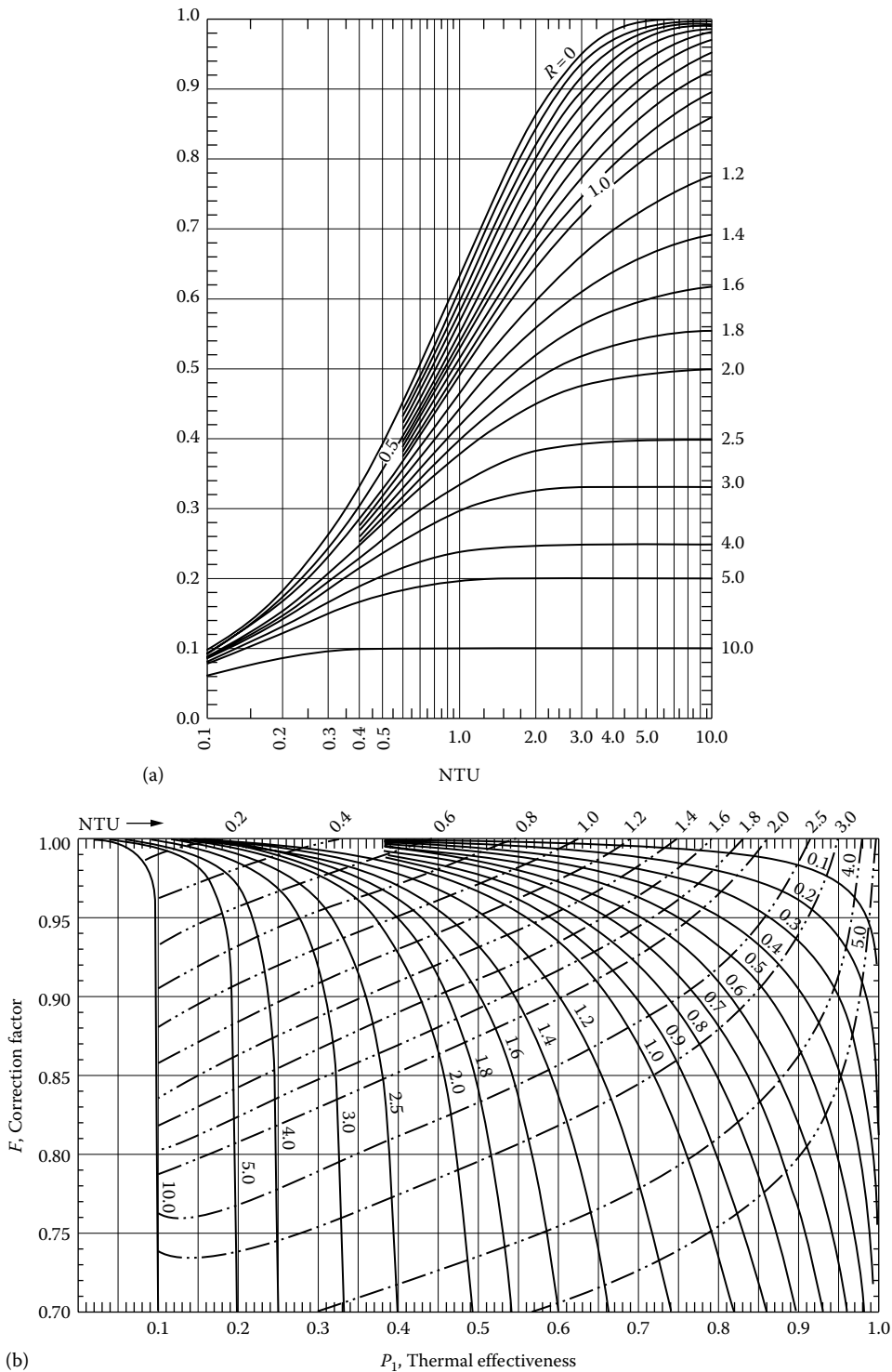


FIGURE 2.49 (a) Thermal effectiveness chart—two-pass cross-counterflow arrangement with complete mixing between passes. In each pass, both the fluids unmixed; R - P -NTU chart; (b) F - R - P -NTU chart; F as a function of P for constant R (solid lines) and constant NTU (dashed lines) (for the flow arrangement shown in IV-b of Figure 2.44b).

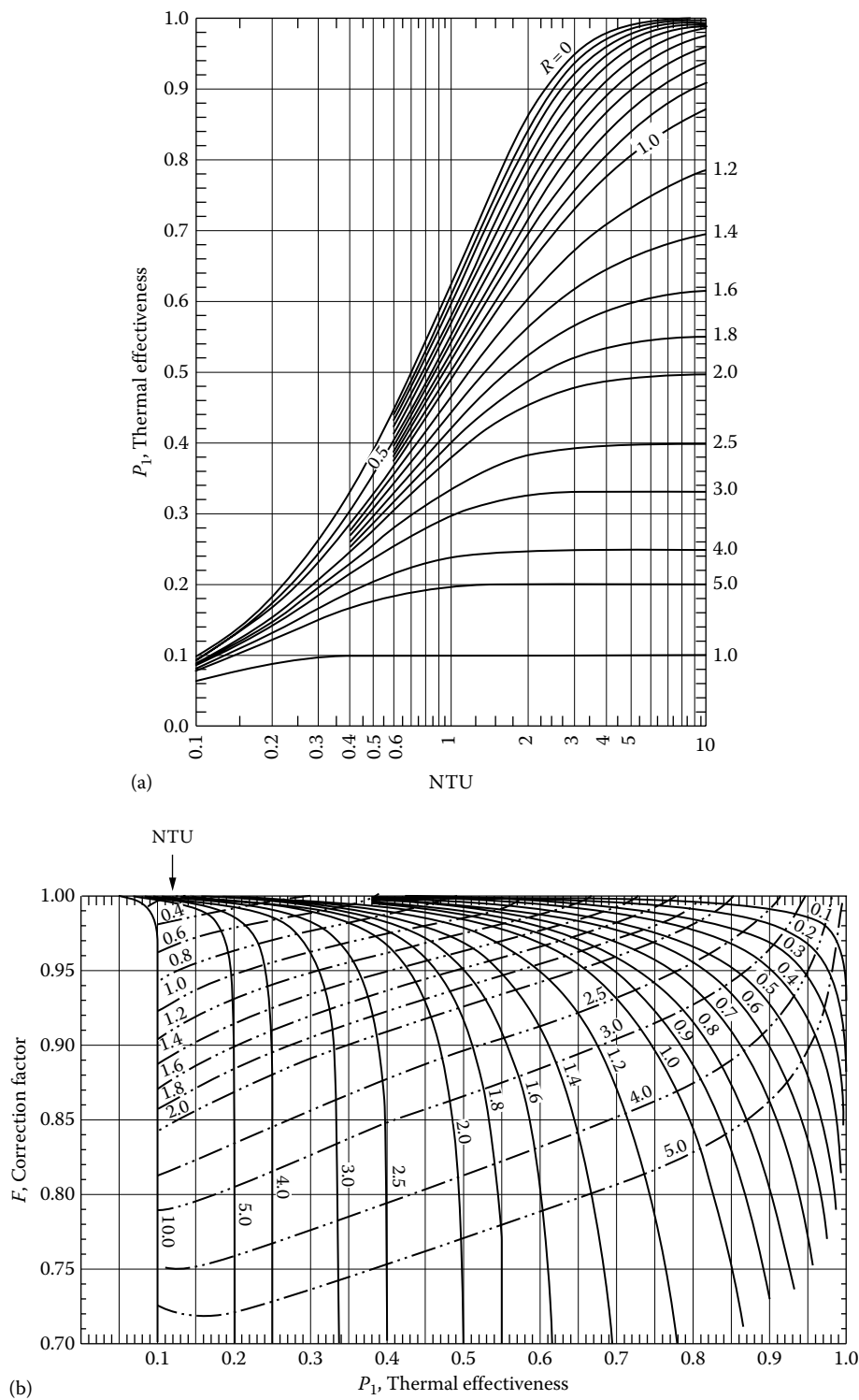
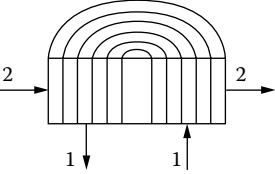
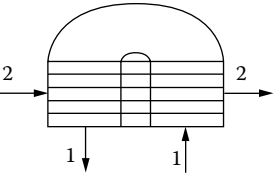
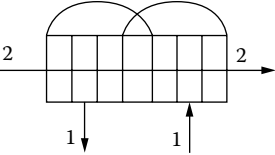
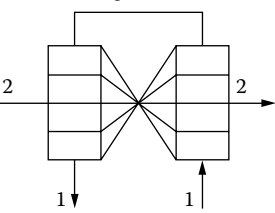


FIGURE 2.50 (a) Thermal effectiveness chart—three-pass cross-counterflow arrangement with complete mixing between passes. In each pass, both the fluids unmixed (for the flow arrangement shown in Figure 2.41c); R - P -NTU chart; (b) F - R - P -NTU chart; F as a function of P for constant R (solid lines) and constant NTU (dashed lines) (for the flow arrangement shown in Figure 2.41c).

TABLE 2.12**Thermal Effectiveness Relations for Two-Pass Assemblies of Heat Exchangers Arrangement with One Fluid Unmixed Throughout**

Flow Arrangement	Equation No./ Reference	Formula for Overall Cross-Counterflow Exchangers
 <p>Fluid 1 unmixed throughout; fluid 2 mixed throughout</p>	T29 [28]	$P_1 = \frac{1}{R} \left[1 - \frac{1}{\frac{K}{2} + \left(1 - \frac{K}{2}\right) e^{2KR}} \right]$ $K = 1 - e^{(-NTU/2)}$ <p>Equation for P_2 = Equation T30</p>
 <p>Fluid 1 mixed throughout; fluid 2 unmixed throughout</p>	T30 [28]	$P_1 = \left[1 - \frac{1}{\frac{K}{2} + \left(1 - \frac{K}{2}\right) e^{(2K/R)}} \right]$ $K = 1 - e^{(-RNTU/2)}$ <p>Equation for P_2 = Equation T29</p>
 <p>Fluid 1 unmixed throughout, identical order; fluid 2 mixed throughout</p>	T31 [28]	$P_1 = \frac{1}{R} \left[1 - \frac{e^{-KR}}{e^{KR} - K^2/R} \right]$ $K = 1 - e^{(-NTU/2)}$ <p>Equation for P_2 = Equation T32</p>
 <p>Fluid 1 mixed throughout; fluid 2 unmixed throughout, identical order</p>	T32 [28]	$P_1 = \left[1 - \frac{e^{-K/R}}{e^{K/R} - K^2/R} \right]$ $K = 1 - e^{(-RNTU/2)}$ <p>Equation for P_2 = Equation T31</p>

Note: For an individual case, at $R = 1$, $P_1 = P_2$.

2.6.6.4 Two Passes with Both Fluids Unmixed throughout, Cross-Counterflow Arrangement

1. Fluid 1 unmixed throughout; fluid 2 unmixed throughout. Both fluids coupling in inverted order (IV-a of Figure 2.44b). The thermal effectiveness chart is given in Figure 2.57. This is also equivalent to the TEMA X-shell, two passes on the tubeside with counterflow arrangement.

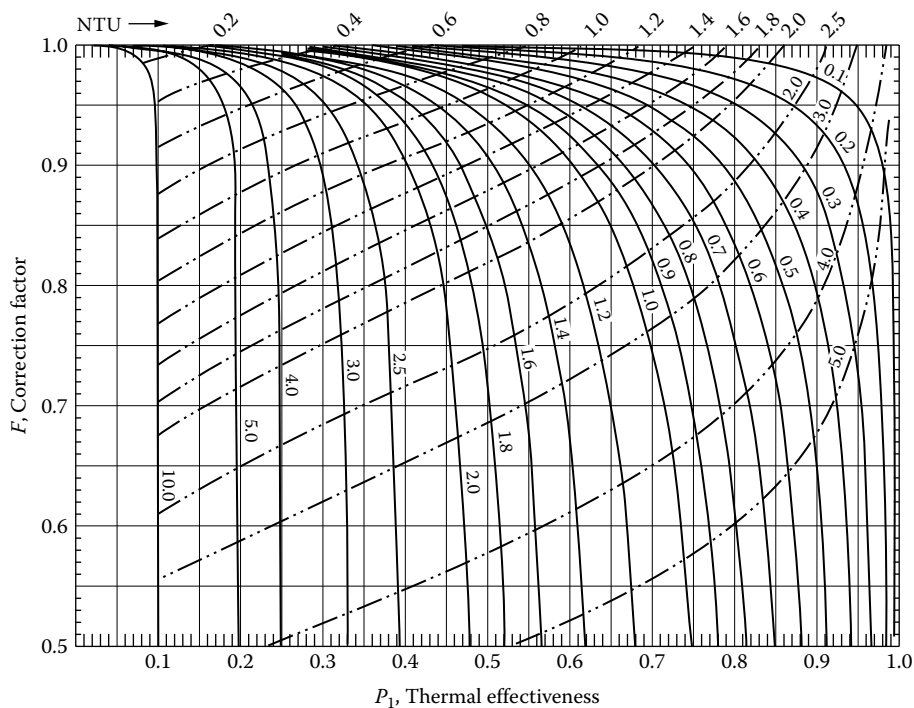


FIGURE 2.51 Thermal effectiveness chart—two-pass cross-counterflow arrangement. Fluid 1 unmixed throughout, inverted order coupling; fluid 2 mixed throughout. F as a function of P for constant R (solid lines) and constant NTU (dashed lines) (as per Equation T29 of Table 2.12, for the configuration shown in I-a of Figure 2.44a).

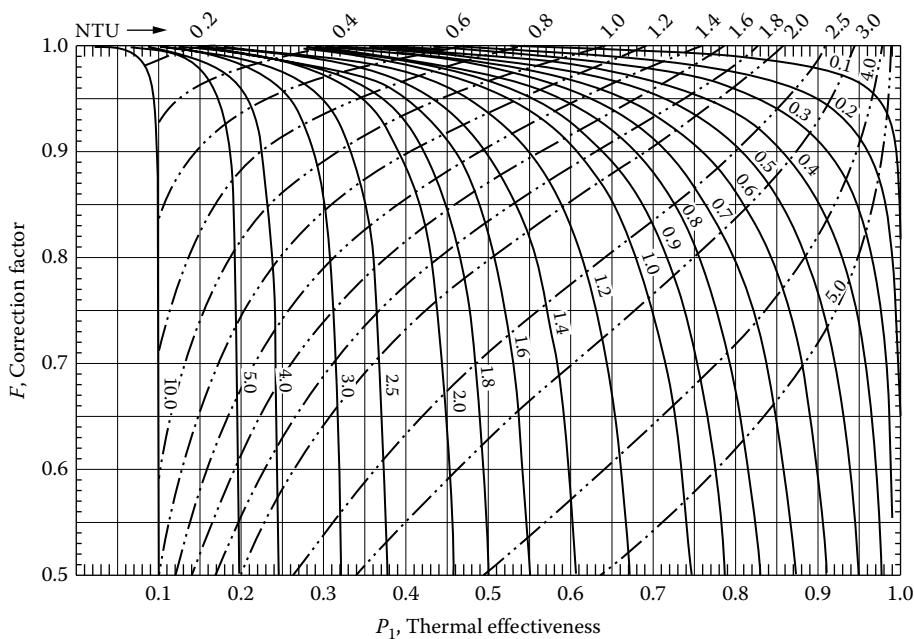


FIGURE 2.52 Thermal effectiveness chart—two-pass cross-counterflow arrangement. Fluid 1 mixed throughout; fluid 2 unmixed throughout, inverted order coupling. F as a function of P for constant R (solid lines) and constant NTU (dashed lines) (as per Equation T30 of Table 2.12, for the configuration shown in I-b of Figure 2.44a).

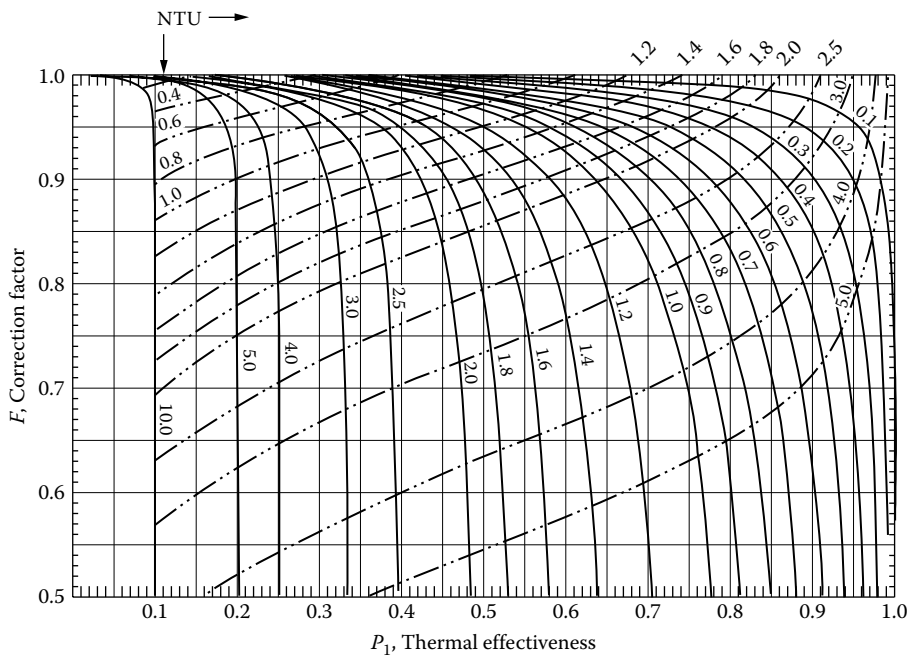


FIGURE 2.53 Thermal effectiveness chart—two-pass cross-counterflow arrangement. Fluid 1 unmixed throughout, identical order coupling; fluid 2 mixed throughout. F as a function of P for constant R (solid lines) and constant NTU (dashed lines) (as per Equation T31 of Table 2.12, for the configuration shown in II-a of Figure 2.44a).

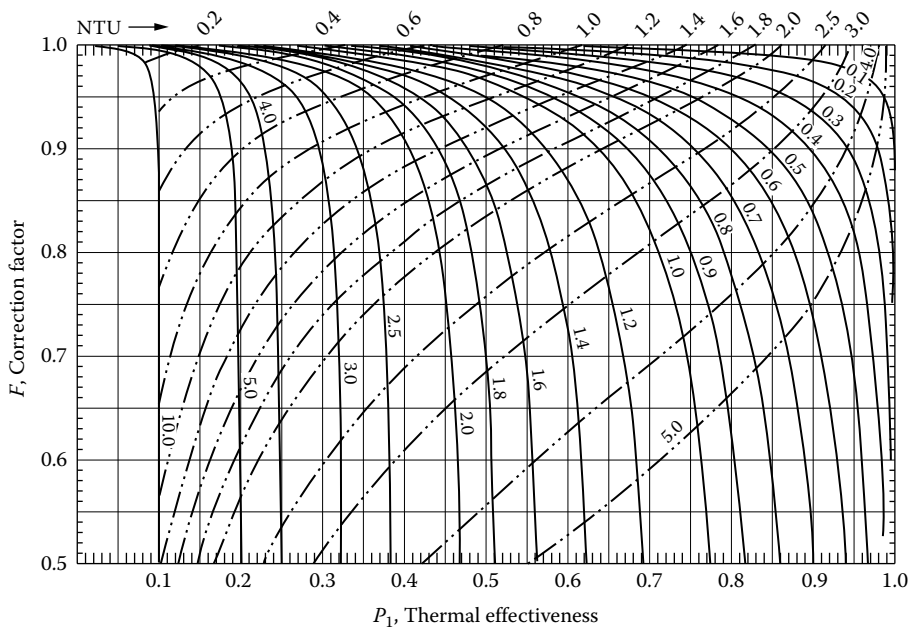
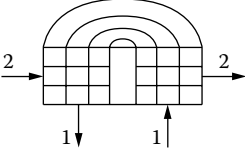
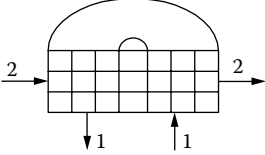
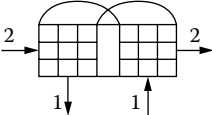
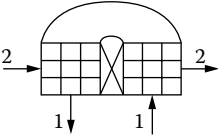


FIGURE 2.54 Thermal effectiveness chart—two-pass cross-counterflow arrangement. Fluid 1 mixed throughout; fluid 2 unmixed throughout, identical order coupling. F as a function of P for constant R (solid lines) and constant NTU (dashed lines) (as per Equation T32 of Table 2.12, for the configuration shown in II-b of Figure 2.44a).

TABLE 2.13

Thermal Effectiveness Relations for Two-Pass Assemblies of Heat Exchangers
Arrangement with Both Fluids Unmixed in the Passes

Flow Arrangement	Equation No./ Reference	Formula for Overall Cross-Counterflow Exchangers
	T33 [45]	$\epsilon_1 = \frac{1}{C^*} \left[1 - \frac{\bar{v}_{1/2}^2}{\bar{v}_{1/2} + \bar{\mu}_{1/2}} \right]$ <p>Equation for $\epsilon_2 = \text{T34}$</p>
<p>Fluid 1 unmixed throughout; fluid 2 unmixed in each pass and mixed between passes</p> 	T34 [45]	$\epsilon_1 = 1 - \frac{\bar{v}_{1/2}^2}{\bar{v}_{1/2} + \bar{\mu}_{1/2}}$ <p>Equation for $\epsilon_2 = \text{T33}$</p>
<p>Fluid 1 unmixed in each pass and mixed between passes; fluid 2 unmixed throughout</p> 	T35 [46]	$\epsilon_1 = \frac{1}{C^*} \left[1 - \frac{\bar{v}_{1/2}^2}{1 + 2\bar{v}_{1/2} - 2\bar{v}_{2/2}} \right]$ <p>Equation for $\epsilon_2 = \text{T36}$</p>
<p>Fluid 1 unmixed throughout, identical order; fluid 2 mixed between passes and unmixed in each pass</p> 	T36 [46]	$\epsilon_1 = 1 - \frac{\bar{v}_{1/2}^2}{1 + 2\bar{v}_{1/2} - 2\bar{v}_{2/2}}$ <p>Equation for $\epsilon_2 = \text{T35}$</p>

Fluid 1 mixed between passes and unmixed in each pass; fluid 2 unmixed throughout, identical order

Note: For individual case at $C^* = 1$, $\epsilon_1 = \epsilon_2$.

Terms of the equations:

$$\bar{\mu}_{1/2} = \frac{2}{C^* NTU} \sum_{m=0}^{\infty} \sum_{n=0}^{\infty} \frac{(-1)^m (n+m)!}{n! m!} V_{m+2} \left(\frac{C^* NTU}{2}, \frac{NTU}{2} \right) V_{n+2} \left(\frac{NTU}{2}, \frac{C^* NTU}{2} \right) \quad (\text{A})$$

Set $C^* = 1/C^*$, $NTU = C^* NTU$ and $C^* NTU = NTU$ in Equation (A), then, Equation (B) is obtained by

$$\bar{\mu}_{1/2} = \frac{2}{NTU} \sum_{n=0}^{\infty} \sum_{m=0}^{\infty} \frac{(-1)^m (n+m)!}{n! m!} V_{m+2} \left(\frac{NTU}{2}, \frac{C^* NTU}{2} \right) V_{n+2} \left(\frac{C^* NTU}{2}, \frac{NTU}{2} \right) \quad (\text{B})$$

in which

$$V_0(\xi, \eta) = e^{-(\xi+\eta)} I_0(2\sqrt{\xi\eta}) \quad (\text{C})$$

$$V_m(\xi, \eta) = e^{-(\xi+\eta)} \sum_{n=m-1}^{\infty} \binom{n}{m-1} \left(\frac{\eta}{\xi} \right)^{n/2} I_n(2\sqrt{\xi\eta}) \quad m \geq 1 \quad (\text{D})$$

$$v(a, b) = e^{-(a+b)} \left[I_0(2\sqrt{ab}) + \sqrt{(b/a)} I_1(2\sqrt{ab}) - \left(\frac{a}{b} - 1 \right) \sum_{n=2}^{\infty} \left(\frac{b}{a} \right)^{n/2} I_n(2\sqrt{ab}) \right] \quad (\text{E})$$

TABLE 2.13 (continued)

**Thermal Effectiveness Relations for Two-Pass Assemblies of Heat Exchangers
Arrangement with Both Fluids Unmixed in the Passes**

Flow Arrangement	Equation No./ Reference	Formula for Overall Cross-Counterflow Exchangers
The expressions for $v_{1/2}$ and $\bar{v}_{1/2}$ are given by		
$v_{1/2} = \exp \left[-(1 + C^*) \frac{NTU}{2} \right]$ $\times \left[I_0(NTU\sqrt{C^*}) + \sqrt{C^*} I_1(NTU\sqrt{C^*}) - \frac{1 - C^*}{C^*} \sum_{n=2}^{\infty} (C^*)^{n/2} I_n(NTU\sqrt{C^*}) \right]$		(F)
$\bar{v}_{1/2} = \exp \left[-\frac{1 + C^*}{C^*} \frac{C^* NTU}{2} \right]$ $\times \left[I_0(NTU\sqrt{C^*}) + \sqrt{\frac{1}{C^*}} I_1(NTU\sqrt{C^*}) - (C^* - 1) \sum_{n=2}^{\infty} (C^*)^{-n/2} I_n(NTU\sqrt{C^*}) \right]$		(G)

Various forms of Equation (E): $\bar{v} = \bar{v}_{1/1} = v(NTU, C^*NTU)$; $\bar{v}_{1/2} = v(NTU/2, C^*NTU/2)$;
 $\bar{v}_{2/2} = v(NTU/2, C^*NTU)$; $\bar{v} = \bar{v}_{1/1} = v(C^*NTU, NTU)$; $\bar{v}_{1/2} = v(C^*NTU/2, NTU/2)$;
 $\bar{v}_{2/2} = v(C^*NTU/2, NTU)$.

Sources: Shah, R.K. and Mueller, A.C., Heat exchanger basic thermal design methods, in *Handbook of Heat Transfer Applications*, 2nd edn., W.M. Rohsenow, J.P. Hartnett, and E.N. Ganic, eds., McGraw-Hill, New York, pp. 4-1-4-77, 1985; Baclic, B.S. and Gvozdenac, D.D., Exact explicit equations for some two- and three-pass cross-flow heat exchanger effectiveness, in *Heat Exchangers; Thermal-Hydraulic Fundamentals and Design*, S. Kakac, A.E. Bergles, and F. Mayinger, eds., Hemisphere, Washington, DC, pp. 481-494, 1981; Baclic, B.S. and Gvozdenac, D.D., NTU relationships for inverted order flow arrangements of two-pass crossflow heat exchangers, in *Regenerative and Recuperative Heat Exchangers*, Vol. 21, R.K. Shah and D.E. Metzger, eds., ASME, New York, pp. 27-41, 1981.

For cross-parallelflow, the thermal effectiveness is given by [45]

$$\varepsilon = \mu_{1/2} + \frac{1}{C^*} \bar{\mu}_{1/2} \quad (2.76)$$

where the terms of the equation were defined earlier. This is also equivalent to the TEMA X-shell, two passes on the tubeside with parallelflow arrangement.

- Fluid 1 unmixed throughout, coupling in identical order; fluid 2 unmixed throughout, coupling in inverted order (III-b of Figure 2.44b).
- Fluid 1 unmixed throughout, coupling in inverted order; fluid 2 unmixed throughout, coupling in identical order (III-a of Figure 2.44b). The thermal effectiveness chart is shown in Figure 2.58.
- Fluid 1 unmixed throughout; fluid 2 unmixed throughout. Both fluids coupling in identical order (I-b of Figure 2.44b).

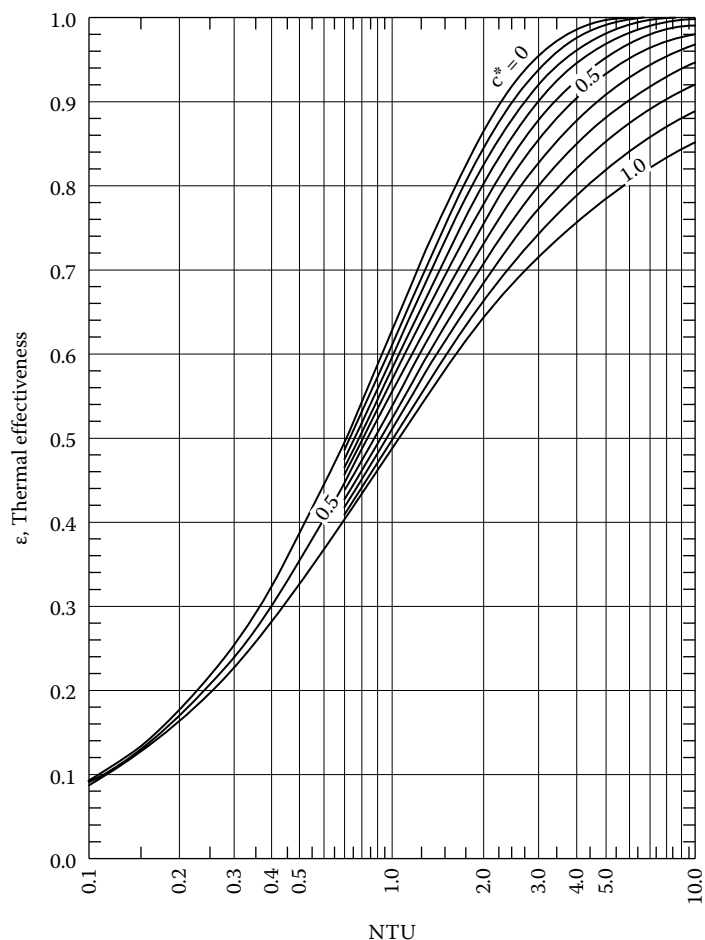


FIGURE 2.55 Thermal effectiveness chart—two-pass cross-counterflow arrangement. Fluid 1 unmixed in each pass mixed between passes; fluid 2 unmixed throughout, inverted order coupling (as per Equation T34 of Table 2.13, for the configuration shown in II-b of Figure 2.44b).

The thermal effectiveness charts shown in Figures 2.57 and 2.58 were arrived at by a numerical method as described by Stevens et al. [29]. For all these four cases, a closed-form solution is given by Baclic [3].

For the flow arrangement of IV-c of Figure 2.44b, *the most efficient case*, the thermal effectiveness for $C^* = 0.5$ is less by 1.8% (approx.) compared to the corresponding counterflow case. The maximum difference is in the NTU range 3.5–4.0, and for other values of NTU, the difference is fast decreasing and approaches zero. Also, for $0.0 < C^* < 0.5$, the difference is decreasing with C^* and it is zero for $C^* = 0.0$. For $C^* = 1.0$, the thermal effectiveness is less by 2.9% (approx.) compared to the corresponding counterflow case. The maximum difference is in the NTU range 4–6, and for other values of NTU, the difference is fast decreasing and approaches to zero. Also, for $0.5 < C^* < 1$, the difference is decreasing with decrease in C^* .

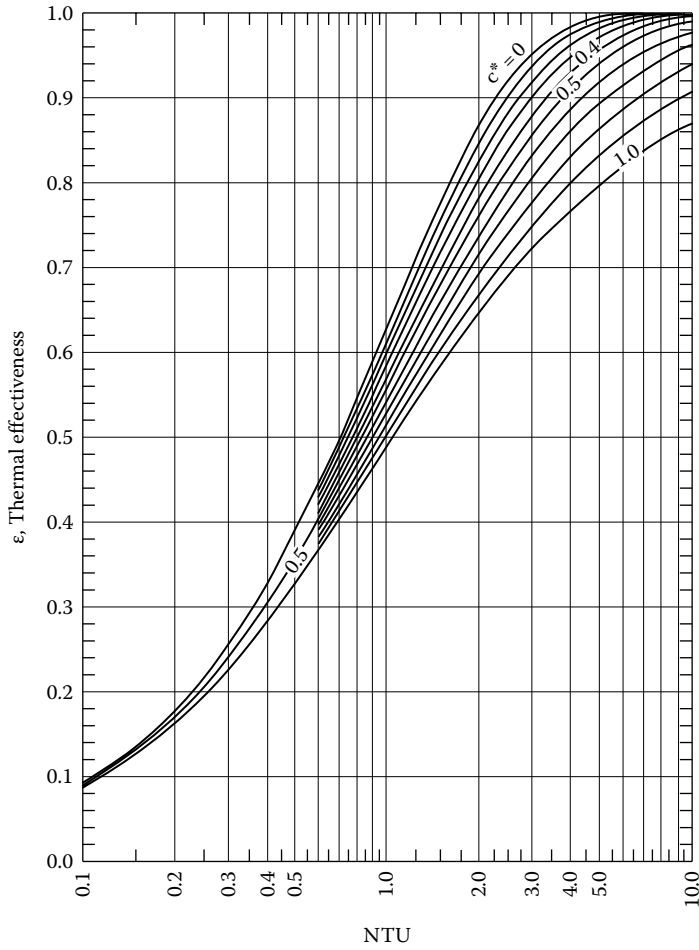


FIGURE 2.56 Thermal effectiveness chart—two-pass cross-counterflow arrangement. Fluid 1 unmixed throughout, identical order coupling; fluid 2 mixed between passes and unmixed in each pass (as per Equation T35 of Table 2.13, for the configuration shown in I-a of Figure 2.44b).

Comparison of thermal effectiveness of two-pass crossflow cases:

For the possible cases of two pass exchangers shown in Figure 2.44b, the thermal reflectiveness comparison is given by

$$\epsilon_{IV-c} > \epsilon_{I-a} > \epsilon_{IV-b} > \epsilon_{III-a} > \epsilon_{II-a} > \epsilon_{IV-a}$$

For $NTU = 4$ and $C^* = 1$ [29],

$$\epsilon_{IV-c}/\epsilon_{IV-a} = 1.038 \quad \text{and} \quad \epsilon_{IV-c}/\epsilon_{I-a} = 1.012$$

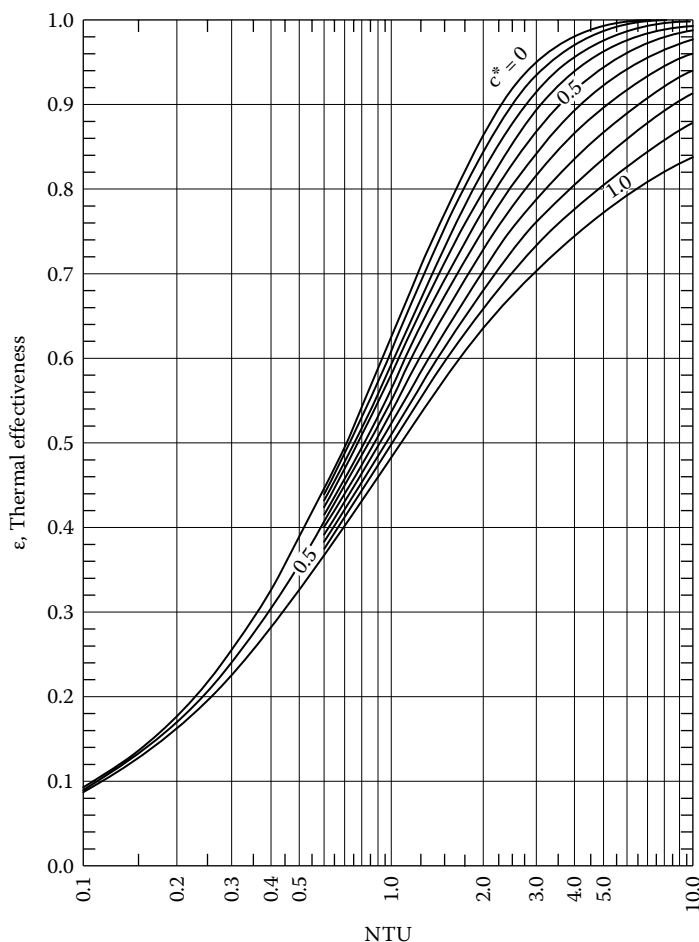


FIGURE 2.57 Thermal effectiveness chart—two-pass cross-counterflow arrangement. Fluid 1 unmixed throughout; fluid 2 unmixed throughout, both the fluids coupling in inverted order (equivalent to TEMA X_{1-2} shell with two passes on the tubeside, counterflow arrangement) (for the configuration shown in IV-a of Figure 2.44b).

2.6.7 THERMAL EFFECTIVENESS OF MULTIPLE-PASS SHELL AND TUBE HEAT EXCHANGERS

Since the $1 - N$ exchanger has lower effectiveness, multipassing on the shellside may be employed to approach the counterflow effectiveness. With this concept, the heat exchanger would have M shell passes and N tube passes. Figure 2.59 represents few such multipassing arrangements for E_{1-2} and E_{1-3} shells [32]. But multipassing on the shellside decreases the transfer area on the shellside, it is very difficult to fit the partition walls, and the possibility of leakage through the partition plates cannot be ruled out. Therefore, this difficulty is overcome by multiple shells with basic shell arrangements. A configuration with M shell passes, each one with N tube passes (similar to Figure 2.59), is equivalent to a series assembly of M shells each with N tube passes. This is illustrated in Figure 2.60 for E_{1-2} .

Multiple E shells in series, each with two tube passes, E_{1-2} : The thermal effectiveness charts for $2E_{1-2}$, $3E_{1-2}$, $4E_{1-2}$, $5E_{1-2}$, and $6E_{1-2}$ are given in Figures 2.61 through 2.65.

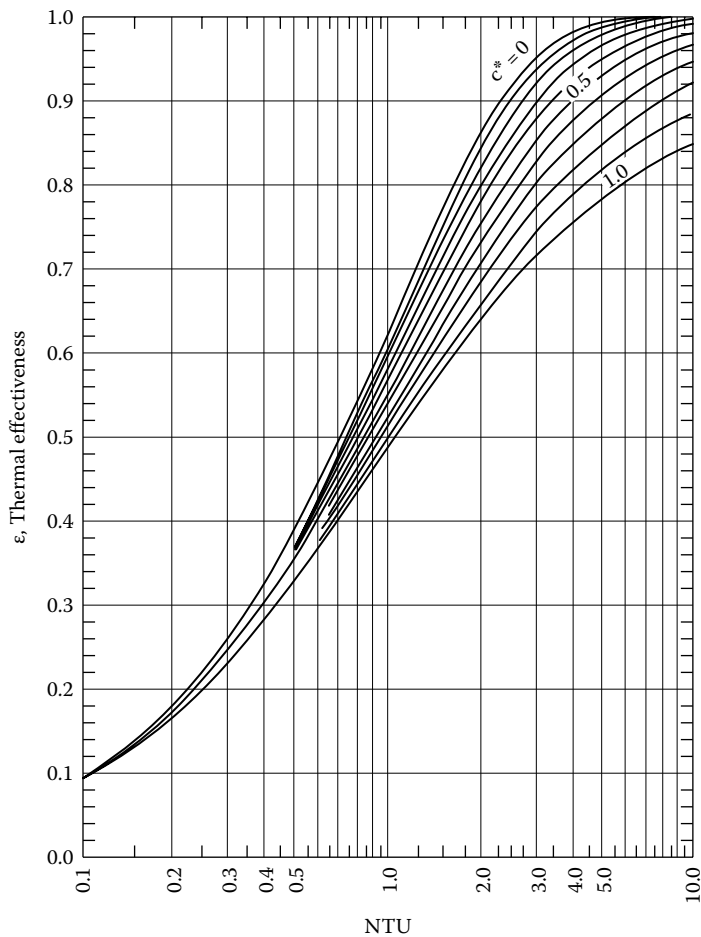


FIGURE 2.58 Thermal effectiveness chart—two-pass cross-counterflow arrangement. Fluid 1 unmixed throughout; fluid 2 unmixed throughout, coupling in identical order (for the configuration shown in III-a of Figure 2.44b).

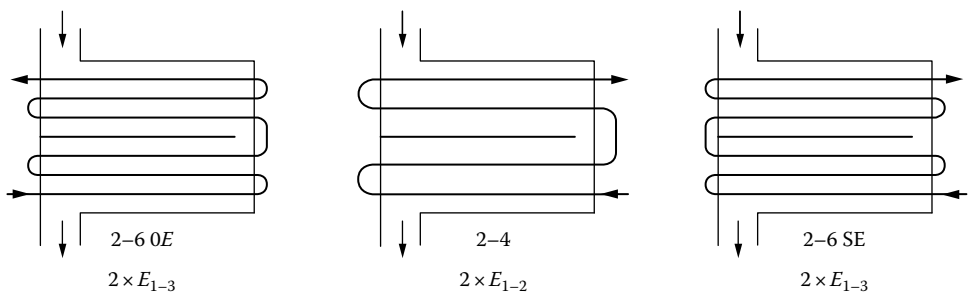


FIGURE 2.59 Shellside multipass arrangement for *E* shell. (From Pignotti, A. and Tamborenea, P.I., *Trans. ASME, J. Heat Transfer*, 111, 54, 1988.)

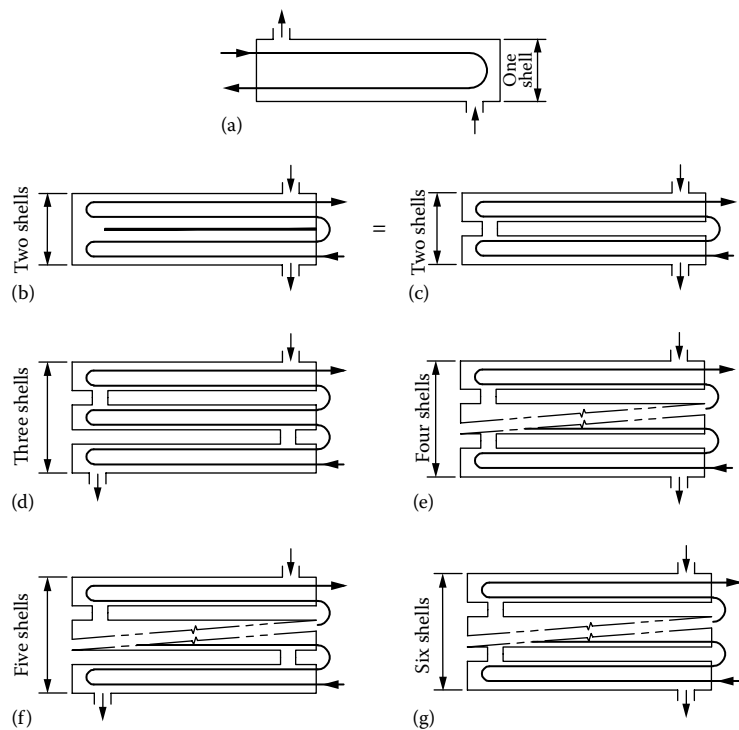


FIGURE 2.60 M -shell passes and each shell with N -tube pass is equivalent to M -shells in series, each with N -tube passes. (a) Basic E_{1-2} shell; (b) and (c) two E_{1-2} shells in series; (d) three E_{1-2} shells in series; (e) four E_{1-2} shells in series; (f) five E_{1-2} shells in series; (g) six E_{1-2} shells in series.

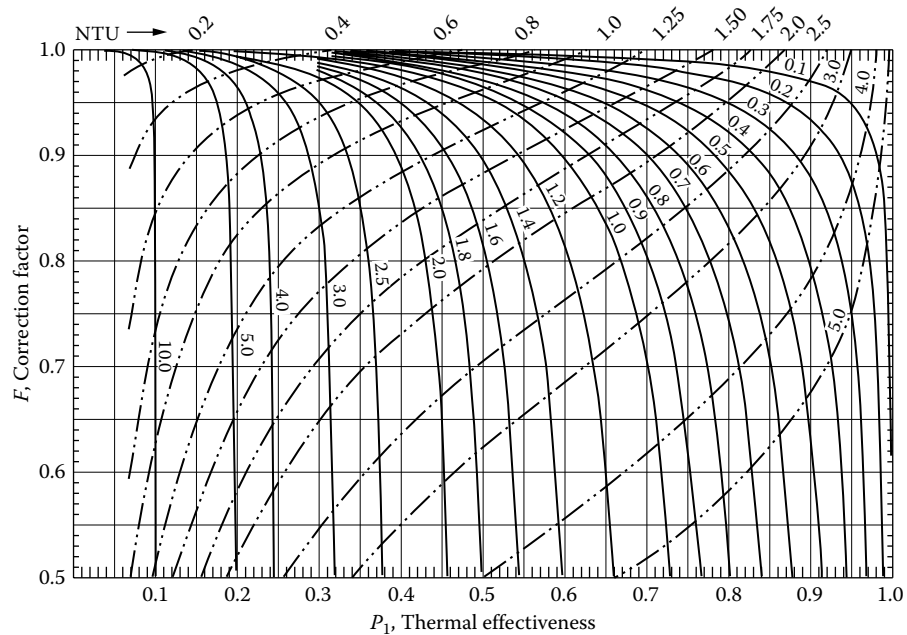


FIGURE 2.61 Two E_{1-2} shells in series; shell fluid mixed, tube fluid mixed between passes with stream symmetric (for the flow arrangement shown in Figure 2.60b). F as a function of P for constant R (solid lines) and constant NTU (dashed lines).

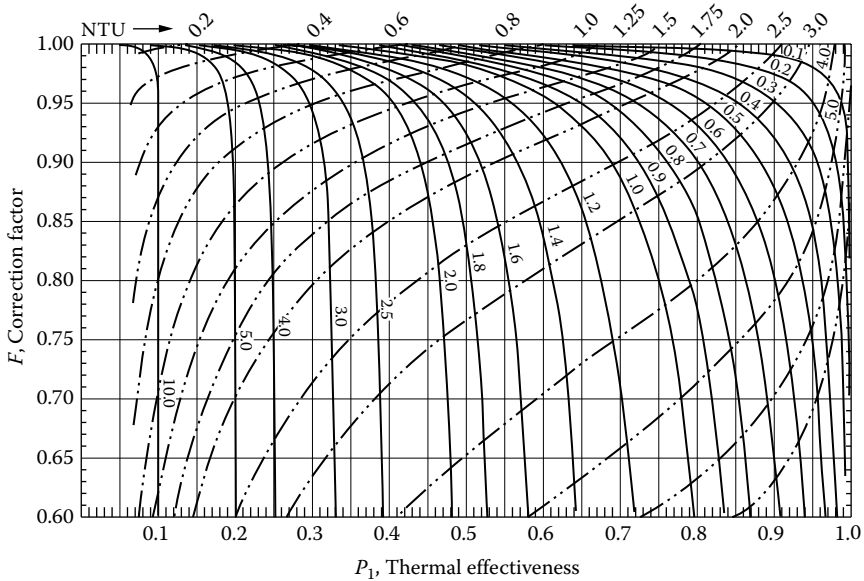


FIGURE 2.62 Three E_{1-2} shells in series; shell fluid mixed, tube fluid mixed between passes with stream symmetric (for the flow arrangement shown in Figure 2.60d). F as a function of P for constant R (solid lines) and constant NTU (dashed lines).

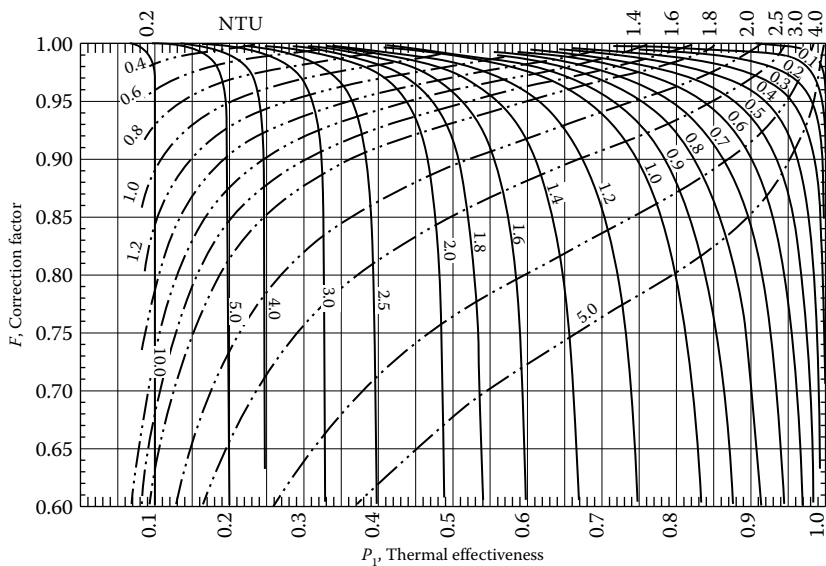


FIGURE 2.63 Four E_{1-2} shells in series; shell fluid mixed, tube fluid mixed between passes with stream symmetric (for the flow arrangement shown in Figure 2.60e). F as a function of P for constant R (solid lines) and constant NTU (dashed lines).

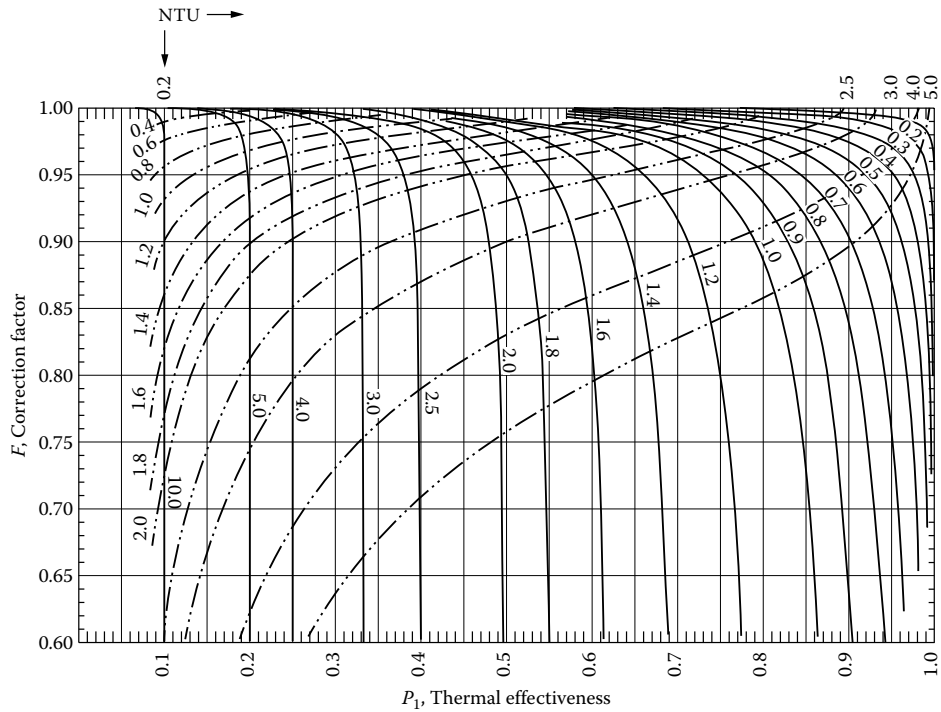


FIGURE 2.64 Five E_{1-2} shells in series; shell fluid mixed, tube fluid mixed between passes with stream symmetric (for the flow arrangement shown in Figure 2.60f). F as a function of P for constant R (solid lines) and constant NTU (dashed lines).

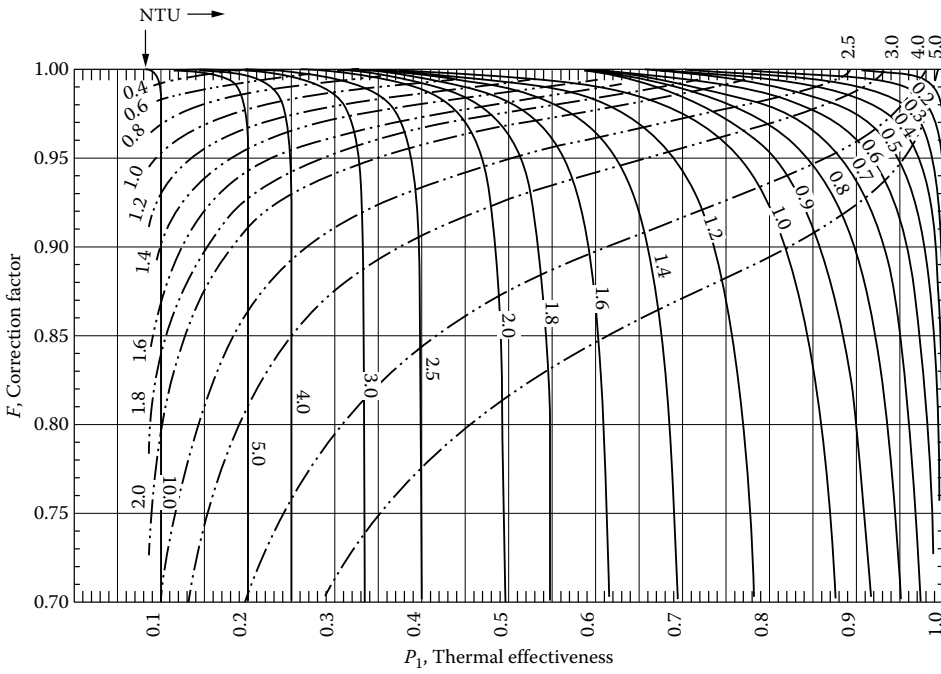


FIGURE 2.65 Six E_{1-2} shells in series; shell fluid mixed, tube fluid mixed between passes with stream symmetric (for the flow arrangement shown in Figure 2.60g). F as a function of P for constant R (solid lines) and constant NTU (dashed lines).

ACKNOWLEDGMENT

The author acknowledges Dr. R.K. Shah for providing the thermal relation formulas for various cases of crossflow arrangements and shell and tube heat exchangers.

REFERENCES

1. Shah, R. K. and Mueller, A. C., Heat exchanger basic thermal design methods, in *Handbook of Heat Transfer Applications*, 2nd edn. (W. M. Rohsenow, J. P. Hartnett, and E. N. Ganic, eds.), McGraw-Hill, New York, 1985, pp. 4-1-4-77.
2. Shah, R. K., Heat exchanger basic design methods, in *Low Reynolds Number Flow Heat Exchangers* (S. Kakac, R. K. Shah, and A. E. Bergles, eds.), Hemisphere, Washington, DC, 1983, pp. 21-71.
3. Baclic, B. S., ϵ -NTU analysis of complicated flow arrangements, in *Compact Heat Exchangers—A Festschrift for A. L. London* (R. K. Shah, A. D. Kraus, and D. Metzger, eds.), Hemisphere, Washington, DC, 1990, pp. 31-90.
- 4a. London, A. L. and Seban, R. A., A generalization of the methods of heat exchanger analysis, Mechanical Engineering Department, Stanford University, Stanford, CA, 1942.
- 4b. London, A. L. and Seban, R. A., A generalization of the methods of heat exchanger analysis, *Int. J. Heat Mass Transfer*, 23, 5-16, 1980.
5. Shah, R. K. and Sekulic, D., *Fundamentals of Heat Exchanger Design*, Wiley, New York, NY, 2003.
6. Kraus, A. D., Heat exchangers, Chapter 11, in *Heat Transfer Handbook* (A. Bejan and A.D. Kraus, eds.), John Wiley & Sons, pp. 797-911, 2003.
7. Smith, D. M., Mean temperature difference in crossflow, *Engineering*, 138, 479-481; 138, 606-607 (1934).
8. Mueller, A. C., Heat Exchangers, Section 18 in *Handbook of Heat Transfer* (W. H. Rohsenow and J. P. Hartnett, eds.), McGraw-Hill, New York, pp. 634-793, 1973.
9. Singh, K. P., Some fundamental relationships for tubular heat exchanger thermal performance, *Trans. ASME, J. Heat Transfer*, 103, 573-578 (1981).
10. Turton, R., Ferguson, C. D., and Levenspiel, O., Performance and design charts for heat exchangers, *Trans. ASME, J. Heat Transfer*, 106, 893-895 (1984).
11. Bowman, R. A., Mueller, A. C., and Nagle, W. M., Mean temperature difference, *Trans. ASME*, 62, 283-294 (1940).
12. Underwood, A. J. V., The calculation of the mean temperature difference in multipass heat exchangers, *J. Inst. Petrol. Technol.*, 20, 145-158 (1934).
13. Ten Broeck, H., Multipass heat exchanger calculations, *Ind. Eng. Chem.*, 30, 1041-1042 (1938).
14. Kays, W. M. and London, A. L., *Compact Heat Exchangers*, 2nd edn., McGraw-Hill, New York, 1964.
15. *Standards of Tubular Exchanger Manufacturers Association*, 9th edn., Tubular Exchanger Manufacturers Association, Tarrytown, NY, 2007.
16. Schlinder, E. V. editor-in-chief, *Heat Exchanger Design Handbook*, Vol. 1, Hemisphere, Washington, DC, 1983.
17. Pignotti, A., Flow reversibility of heat exchangers, *Trans. ASME, J. Heat Transfer*, 106, 361-368 (1984).
18. Pignotti, A., Relation between the thermal effectiveness of overall parallel and counterflow heat exchangers, *Trans. ASME, J. Heat Transfer*, 111, 294-299 (1989).
19. Shah, R. K. and Sekulic, D. P., Heat exchangers, in *Handbook of Heat Transfer Applications*, Rohsenow, W. M., Hartnett, J. P., and Ganic, E. N. (eds.), 3rd edn., McGraw-Hill, New York, 1998, pp. 17.1-17.169, Chapter 17.
20. Nusselt, W., A new formula for heat transfer in crossflow [in German], *Tech. Mech. Thermodyn.*, 1, 417-422 (1930).
21. Mason, J. L., Heat transfer in crossflow, *Proceedings of the Second U.S. National Congress of Applied Mechanics*, Ann Arbor, MI, ASME, New York, 1955, pp. 801-803.
22. Baclic, B. S., A simplified formula for crossflow heat exchanger effectiveness, *Trans. ASME, J. Heat Transfer*, 100, 746-747 (1978).
23. Eckert, E. R. G., *Heat Transfer*, 2nd edn., McGraw-Hill, New York, 1959, p. 483.
24. Taborek, J., F and θ charts for crossflow arrangements, in *Heat Exchanger Design Handbook*, Vol. 1, Section 1.5.3 (E. V. Schlunder, editor-in-chief), Hemisphere, Washington, DC, 1983, pp. 1.5.3-1-1.5.3-15.

25. (a) Pignotti, A. and Cordero, G. O., Mean temperature difference in multipass crossflow, *Trans. ASME, J. Heat Transfer*, 105, 584–591 (1983); (b) Pignotti, A. and Cordero, G. O., Mean temperature difference charts for air coolers, *Trans. ASME, J. Heat Transfer*, 105, 592–597 (1983).
26. (a) Pignotti, A., Analytical techniques for basic thermal design of complex heat exchanger configurations, *Heat Transfer, Eighth International Conference*, San Francisco, CA, 1986; (b) Pignotti, A., Matrix formalism for complex heat exchangers, *Trans. ASME, J. Heat Transfer*, 106, 352–360 (1984).
27. Schedwill, H., Thermische Auslegung von Kreuzstromwärmeaustauschern, Fortschr-Ber. VDI-Z Reihe 6 Nr. 19, VDI-Verlag, Dusseldorf, Germany, 1968.
28. Nicole, F. J. L., Mean temperature difference for heat exchanger design, Council for Scientific and Industrial Research, Special Report Chem. 223, Pretoria, South Africa, 1972.
29. Stevens, R. A., Fernandez, J., and Woolf, J. R., Mean temperature difference in one, two, three-pass crossflow heat exchangers, *Trans. ASME*, 79, 287–297 (1957).
30. Nagle, W. M., Mean temperature difference in multipass heat exchanger, *Ind. Eng. Chem.*, 25, 604–609 (1933).
31. Baclic, B. S., 1–2N shell and tube exchanger effectiveness: A simplified Kraus-Kern equation, *Trans. ASME, J. Heat Transfer*, 111, 181–182 (1989).
32. Pignotti, A. and Tamborenea, P. I., Thermal effectiveness of multiple shell and tube pass TEMA E heat exchangers, *Trans. ASME, J. Heat Transfer*, 111, 54–59 (1988).
33. Whistler, A. M., Correction for heat conduction through longitudinal baffle of heat exchanger, *Trans. ASME*, 69, 683–685 (1947).
34. Rozenmann, T. and Taborek, J., The effect of leakage through the longitudinal baffle on the performance of two pass shell exchangers, *Heat Transfer—Tulsa*, 1972, AIChE Symposium Series No. 118, 68, 12–20 (1972).
35. Taborek, J., F and θ charts for shell and tube exchangers, in *Heat Exchanger Design Handbook*, Vol. 1, Section 1.5.2 (E. V. Schlunder, editor-in-chief), Hemisphere, Washington, DC, 1983, pp. 1.5.2-1–1.5.2-15.
36. Schlinder, D. L. and Bates, H. T., True temperature difference in a 1–2 divided flow heat exchanger, heat transfer—Starrs, *Chem. Eng. Prog. Symp. Ser.*, 56, 203–206 (1960).
37. Murty, K. N., Heat transfer characteristics of one- and two-pass split flow heat exchangers, *Heat Transfer Eng.*, 4(3–4), 26–34 (1983).
38. Singh, K. P. and Holtz, M. J., Generalization of the split flow heat exchanger geometry for enhanced heat transfer, heat transfer—San Diego, *AIChE Symp. Ser.*, 75, 219–226 (1979).
39. Ishihara, K. and Palen, J. W., Mean temperature difference correction factor for the TEMA H shell, *Proceedings of the Eighth International Heat Transfer Conference*, San Francisco, CA (C. L. Tien, V. P. Carey, and J. K. Ferrel, eds.), Hemisphere, Washington, DC, 1986, pp. 2709–2714.
40. Shah, R. K. and Pignotti, A., Heat exchanger basic design theory and results, A report prepared under NSF Grant No. INT-8513531, Buffalo, NY, 1989. TEMA G_{1-1} exchanger results are also derived in this report by the chain rule methodology.
41. Jaw, L., Temperature relations in shell and tube exchangers having one pass splitflow shells, *Trans. ASME, J. Heat Transfer*, 86, 408–416 (1964).
42. (a) Gardner, K. A., Mean temperature difference in multipass exchangers—Correction factors with shell fluid unmixed, *Ind. Eng. Chem.*, 33, 1495–1500 (1941); (b) Gardner, K. A., Mean temperature difference in multipass exchangers, *Ind. Eng. Chem.*, 33, 1215–1223 (1941).
43. Pignotti, A., Effectiveness of series assemblies of divided-flow heat exchanger, *Trans. ASME, J. Heat Transfer*, 108, 141–146 (1986).
44. Domingos, J. D., Analysis of complex assemblies of heat exchangers, *Int. J. Heat Mass Transfer*, 12, 537–548 (1969).
45. Baclic, B. S. and Gvozdenac, D. D., Exact explicit equations for some two- and three-pass cross-flow heat exchanger effectiveness, in *Heat Exchangers; Thermal-Hydraulic Fundamentals and Design* (S. Kakac, A. E. Bergles, and F. Mayinger, eds.), Hemisphere, Washington, DC, 1981, pp. 481–494.
46. Baclic, B. S. and Gvozdenac, D. D., NTU relationships for inverted order flow arrangements of two-pass crossflow heat exchangers, in *Regenerative and Recuperative Heat Exchangers*, Vol. 21 (R. K. Shah and D. E. Metzger, eds.), ASME, New York, 1981, pp. 27–41.

BIBLIOGRAPHY

- Cho, S. M., Basic thermal design methods for heat exchangers, in *Heat Transfer Equipment Design* (R. K. Shah, E. C. Subbarao, and R. A. Mashelkar, eds.), Hemisphere, Washington, DC, 1988, pp. 23–38.
- Effectiveness-Ntu Relationships for Design and Performance Evaluation of Two-Stream Heat Exchangers*, Engineering Sciences Data Unit Item No. 86018, July 1986, ESDU International Ltd., McLean, VA.
- Effectiveness-Ntu Relationships for the Design and Performance Evaluation of Multi-Pass Crossflow Heat Exchangers*, Engineering Sciences Data Unit Item No. 87020, October 1987, ESDU International Ltd., McLean, VA.
- Gardner, K. A. and Taborek, J., Mean temperature difference: A reappraisal, *AIChE J.*, 23, 777–786 (1977).
- Kays, W. M. and London, A. L., *Compact Heat Exchangers*, 3rd edn., McGraw-Hill, New York, 1984.

3 Heat Exchanger Thermal Design

3.1 FUNDAMENTALS OF HEAT EXCHANGER DESIGN METHODOLOGY

Heat exchanger design methodology, shown in Figure 3.1, involves the following major design considerations [1]:

1. Process/design specifications
2. Thermohydraulic design to ensure the required heat exchanger performance and to satisfy the pressure-drop requirements for each stream
3. Flow-induced vibration in the case of shell and tube heat exchanger and individual fin-tube and bare tube bank compact heat exchanger
4. Mechanical design to provide the mechanical integrity required by design codes and operating conditions
5. Cost and manufacturing considerations
6. Trade-off factors and system-based optimization

Most of these considerations are dependent on each other and should be considered simultaneously to arrive at the optimum exchanger design. Of these design considerations, items 1 and 2 are discussed in this chapter, flow-induced vibration and mechanical design are discussed in Chapters 10 and 11, respectively, and item 5 was discussed earlier in Chapter 1. The remaining item, trade-off factors and system-based optimization, is not within the scope of this book.

3.1.1 PROCESS/DESIGN SPECIFICATIONS

Process or design specifications include all the necessary information to design and optimize the exchanger for a specific application. It includes the following information [1]: (1) problem specification; (2) exchanger construction type; (3) flow arrangement; (4) construction materials; (5) design considerations like preferred tube sizes, tube layout pattern, maximum shell dimensions and maintenance consideration; (6) design standard and construction code; (7) safety and protection, high product purity; and (8) special operating considerations such as cycling, upset conditions, etc.

3.1.1.1 Problem Specification

The problem specification involves the process parameters, operating conditions, and environment in which the heat exchanger is going to be operated. Typical details pertaining to problem specification include design parameters such as inlet temperatures and pressures; flow rates (including composition for mixtures); vapor quality, heat duty, allowable pressure drops, and fluctuations in the process parameters; overall size, layout, weight, etc.; and corrosiveness and fouling characteristics of fluid. Other factors that must be considered are

1. Climatic conditions—minimum ambient, frost, snow, hail, and humidity
2. Operating environment—maritime, desert, tropical, seismic, cyclonic, and dust
3. Site layout—proximity to buildings or other cooling equipment, prevailing wind directions, duct allowances, length of pipe runs, and access

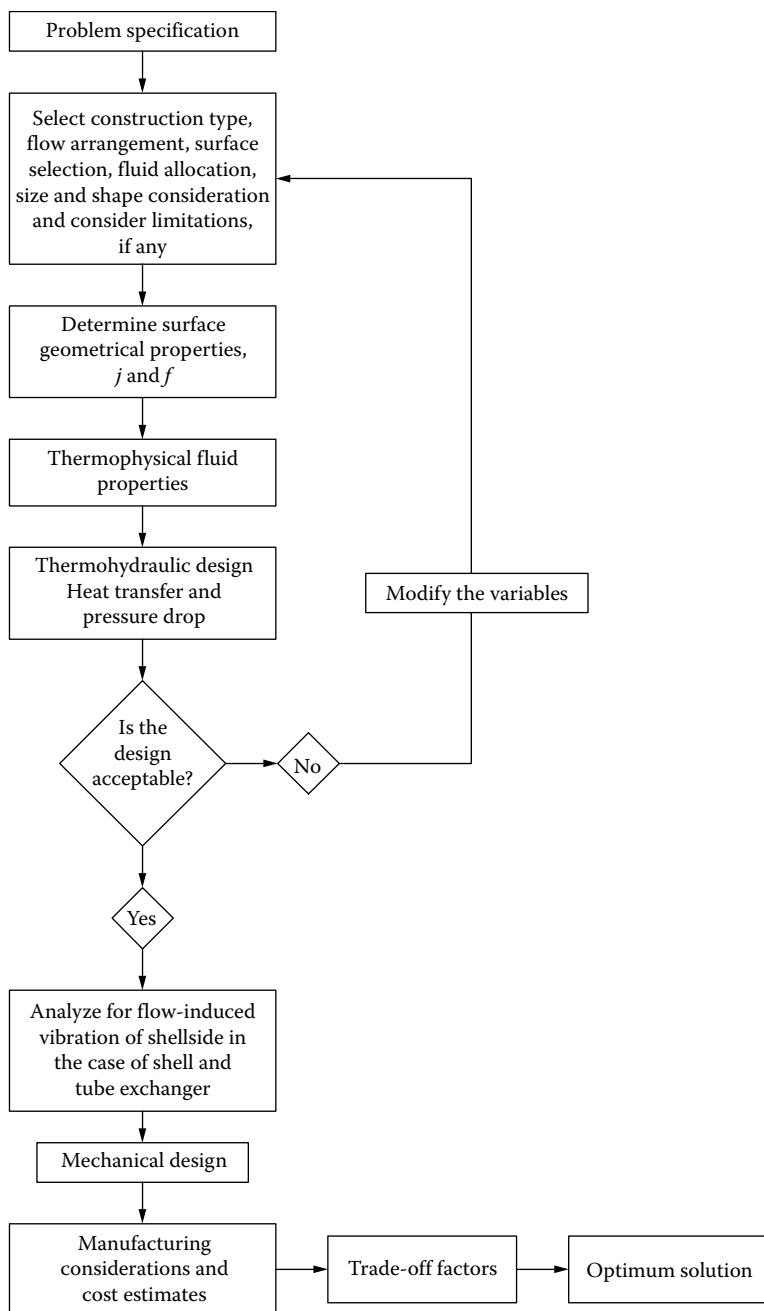


FIGURE 3.1 Heat exchanger design methodology.

3.1.1.2 Exchanger Construction

Based on the problem specifications and experience, the exchanger construction type and flow arrangement are first selected. Selection of the construction type depends upon the following parameters [1]:

1. Fluids (gas, liquids, or condensing/evaporating) used on each side of a two-fluid exchanger
2. Operating pressures and temperatures

3. Fouling
4. Whether leakage or contamination of one fluid to the other is allowed or not
5. Cost and available heat exchanger manufacturing technology

3.1.1.3 Surface Selection

Compact heat exchanger: Factors that influence the surface selection include the operating pressures, fouling, maintenance requirements, erosion, fabricability, cost, etc.

Shell and tube heat exchanger: For shell and tube exchangers, the criteria for selecting core geometry or configurations are the desired heat transfer performance within specified pressure drops, fouling, corrosion, maintenance, repair, cleanability by mechanical means, minimal operational problems (flow-induced vibrations), safety, and cost; additionally, the allocation of fluids on the shellside and the tubeside is an important consideration.

3.1.2 THERMOHYDRAULIC DESIGN

Heat exchanger thermohydraulic design involves quantitative heat transfer and pressure-drop evaluation or exchanger sizing. Basic thermohydraulic design methods and inputs to these analyses are as follows.

3.1.2.1 Basic Thermohydraulic Design Methods

As discussed in Chapter 2, the ϵ -NTU, P -NTU, LMTD, or ψ - P method can be used for solving the thermal design problem.

3.1.2.2 Thermophysical Properties

For heat transfer and pressure-drop analysis, the following thermophysical properties of the fluids are needed: dynamic viscosity μ , density, specific heat c_p , surface tension, and thermal conductivity k . For the conduction wall, thermal conductivity is needed.

3.1.2.3 Surface Geometrical Properties

For heat transfer and pressure-drop analyses, at least the following surface geometrical properties are needed on each side of a two-fluid compact heat exchanger:

- Heat transfer area, A , which includes both primary and secondary surface area if any
- Core frontal area, A_{fr}
- Minimum free flow area, A_o
- Hydraulic diameter, D_h
- Flow length, L
- Fin thickness and fin conduction length
- Core volume, V and core dimensions L_1 , L_2 , and L_3

These quantities are computed from the basic dimensions of the core and heat transfer surface. On the shellside of a shell and tube heat exchanger, various leakage and bypass flow areas are also needed. The procedure to compute these quantities is presented elsewhere.

3.1.2.4 Surface Characteristics

Surface characteristics for heat transfer, j , and flow friction, f , are key inputs for the exchanger heat transfer and pressure-drop analysis, respectively. Experimental results for a variety of exchanger surfaces are presented in Kays and London [2], and correlations in Shah and Bhatti [3]. More references on j and f factors are furnished in Chapter 4.

3.2 DESIGN PROCEDURE

The design of heat exchangers requires the consideration of the factors just outlined. It is unlikely that any two designers will arrive at exactly the same design for a given set of conditions, as the design process involves many judgments while carrying out the design [4]. Gollin [4] describes the step-by-step design procedure for a heat exchanger. Important steps in the heat exchanger design procedure include the following:

1. Assess the heat transfer mechanisms involved
2. Select the heat exchanger class
3. Determine the construction details and select the surface geometry
4. Determine size and layout parameters keeping in mind the constraints imposed by the purchaser/client
5. Perform preliminary thermal design known as approximate sizing
6. Perform the detailed design
7. Check the design
8. Optimize the design
9. Perform the check for flow-induced vibration in the case of shell and tube heat exchanger, individually finned tube, and bare tube bank compact heat exchangers
10. Perform mechanical design
11. Estimate cost and finalize the design as per trade considerations

3.3 HEAT EXCHANGER DESIGN PROBLEMS

In a broad sense, the design of a new heat exchanger means the selection of exchanger construction type, flow arrangement, tube and fin material, and the physical size of an exchanger to meet the specified heat transfer and pressure-drop requirements. Two most common heat exchanger design problems are the rating and sizing. For an existing exchanger, the performance evaluation problem is referred to as the rating problem. The sizing problem is also referred to as the design problem. Rating and sizing problems are discussed here. For more details on the rating and sizing problems, refer to Refs. [2,5] and Bell [6].

3.3.1 RATING

Determination of heat transfer and pressure-drop performance of either an existing exchanger or an already sized exchanger is referred to as a rating problem. Inputs to the rating problem include [1] (1) heat exchanger construction details, (2) flow arrangement, (3) overall dimensions, (4) material details, (5) surface geometries and surface characteristics (j and f factors), (6) fluid flow rates, (7) inlet temperatures, and (8) fouling factors. The designer's task is to predict the fluid outlet temperatures, total heat transfer rate, and pressure drop on each side.

3.3.1.1 Rating of a Compact Exchanger

The rating problems for a two-fluid direct-transfer type compact heat exchanger that has gas as a working fluid at least on one side is discussed briefly here, and the detailed rating of a cross-flow and counter-crossflow exchanger is described separately. Customarily, the ϵ -NTU method is employed for compact heat exchangers. Hence, the solution procedure is outlined here using the ϵ -NTU method. The basic steps involved in the analysis of a rating problem are the determination of

1. Surface geometrical parameters
2. Thermophysical fluid properties
3. Reynolds numbers
4. Surface characteristics, j and f

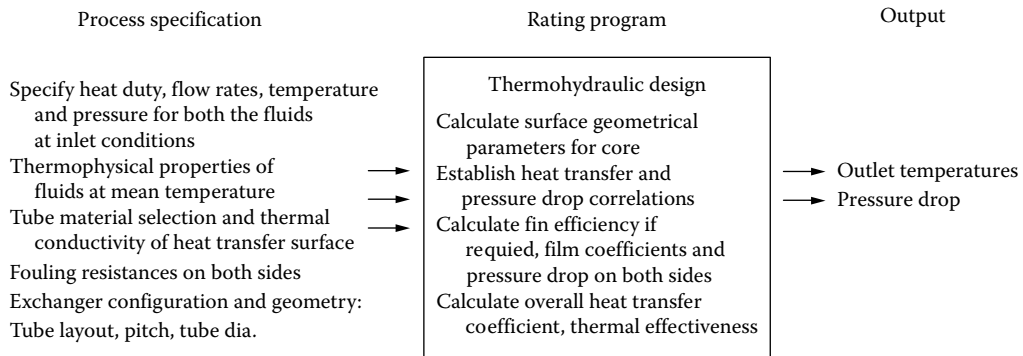


FIGURE 3.2 Rating of shell and tube heat exchanger (Modified from Bell, K. J., Overall design methodology for shell and tube exchangers, in *Heat Transfer Equipment Design* [R. K. Shah, E. C. Subbarao, and R. A. Mashelkar, eds.], Hemisphere, Washington, DC, 1988, pp. 131–144).

5. Corrections to the temperature-dependent fluid properties
6. Heat transfer coefficients
7. Fin effectiveness and overall surface effectiveness
8. Thermal resistance due to conduction wall
9. Overall heat transfer coefficient
10. NTU, C^* , and exchanger effectiveness, ϵ
11. Heat transfer rate, outlet temperatures, and pressure drop on each side

3.3.1.2 Rating of a Shell and Tube Exchanger

“Rating” implies that a specific heat exchanger is fairly completely described geometrically (with the possible exception of the length) and the process specifications for the two streams are given. The Bell-Delaware method is a rating method. The basic rating program of the Bell-Delaware method is shown in Figure 3.2, and the method is described in detail in Chapter 5.

3.3.2 SIZING

In a sizing or design problem, we determine the physical size (length, width, height, and surface area on each side) of an exchanger. Inputs to the sizing problem are the fluid inlet and outlet temperatures, flow rates, fouling factors, and the pressure drop on each side. The designer’s task is to select construction type, flow arrangement, materials, and surface geometry on each side. With the selection of construction types and surface geometries on each side, the problem then reduces to the determination of the core dimensions for the specified heat transfer and pressure-drop performance. However, one can reduce the sizing problem to the rating problem by tentatively specifying the dimensions, then predicting the performance [1]. If the computed results do not agree with the specified values, a new size is assumed and the calculations are repeated.

3.3.2.1 Size of a Heat Exchanger

For a given heat duty, the size of the heat exchanger is a function of the following parameters:

1. Thermal effectiveness
2. Fluid flow rate
3. Secondary surface area per unit volume
4. Heat transfer surface performance parameters
5. Heat transfer augmentation devices, if any
6. Conductance ratio of the process fluids

3.3.2.2 Sensitivity Analysis

In a sizing problem, sometimes one is interested in determining the sensitivity of certain variables individually. For example, how does the heat transfer vary when changing the fin density in a compact heat exchanger with secondary surface? In such a case, one inputs a series of values of fin densities at one time, runs the performance (rating) calculations, obtains a series of results, and analyzes them.

3.3.2.3 Sizing of a Compact Heat Exchanger

The principle of compact heat exchanger sizing is discussed in Chapter 4.

3.3.2.4 Sizing of a Shell and Tube Heat Exchanger

Shell and tube heat exchanger design or sizing is based upon (1) design conditions, that is, fluid flow rates, terminal temperatures, thermophysical fluid properties, and allowable pressure drop; (2) assumptions, heat transfer surface area, overall heat transfer coefficient, or size, length, or number of tubes; and (3) pressure drop across the heat exchanger [7]. The design conditions are fixed by overall plant design and determine the expected performance of the exchanger. Trial-and-error calculations of the film coefficients are used to check the assumptions, which are also checked by an overall heat balance. Finally, the pressure drop is calculated and compared with the allowable values. If the calculated pressure drop is too high, a new set of assumptions is made and rechecked as before.

3.3.2.5 Heat Exchanger Optimization

The solution to the sizing problem in general is not adequate for the design of a new exchanger, since other constraints in addition to pressure drop are imposed on the design, and the objective of the design is to minimize the weight, volume, and heat transfer surface, and minimum pumping power, pressure drop, or other considerations in addition to meeting the required heat transfer. This is achieved by heat exchanger optimization. Shah et al. [8] reviewed various methods used in the literature for heat exchanger optimization and described numerical nonlinear programming techniques.

3.3.3 SOLUTION TO THE RATING AND SIZING PROBLEM

Now let us discuss the basic steps involved in the solution of the two design problems, the rating and sizing.

3.3.3.1 Rating

The basic steps involved in the solution to the rating problem are as follows [9].

ϵ -NTU method:

1. Compute C^* and NTU from the input specifications.
2. Determine ϵ for known NTU, C^* , and the flow arrangement.
3. Compute q from

$$q = \epsilon C_{\min}(t_{h,i} - t_{c,i})$$

and outlet temperatures from

$$t_{h,o} = t_{h,i} - \frac{q}{C_h}$$

$$t_{c,o} = t_{c,i} + \frac{q}{C_c}$$

and compare with those of step 2.

LMTD method:

1. Compute R from $R = C_c/C_h$.
2. Assume the outlet temperatures to determine P , or assume P and calculate outlet temperatures. Also calculate LMTD.
3. Determine LMTD correction factor, F .
4. Determine q from $q = UAF(\text{LMTD})$.
5. Evaluate the outlet temperatures from known q , C_c , and C_h , and compare with those of step 2.
6. Repeat steps 2–5 until the desired convergence is achieved.

3.3.3.2 Solution to the Sizing Problem

In a sizing problem, U , C_c , C_h , and the terminal temperatures are specified, and the surface area A is to be determined. Or U may be calculated from the specified convective film coefficients and the fouling resistances. The basic steps involved in sizing by the ϵ -NTU and LMTD methods are as follows [9].

ϵ -NTU method:

1. Compute ϵ from the specified inlet and outlet temperatures and calculate C^* .
2. Determine NTU from known ϵ , C^* , and the flow arrangement.
3. Calculate the required surface area A from $A = (\text{NTU})C_{\min}/U$ and from terminal temperatures.

LMTD method:

1. Compute P and R from the specified inlet and outlet temperatures.
2. Determine F from F - P curves for known P , R , and the flow arrangement.
3. Calculate the heat transfer rate q and LMTD.
4. Calculate A from $A = q/[UF(\text{LMTD})]$.

A trial-and-error approach is needed for the solution of the rating problem by the LMTD method.

3.4 COMPUTER-AIDED THERMAL DESIGN

In the present computer era, thermal design is almost exclusively performed by industry using computers. Chenoweth et al. [10], Bell [11], and Palen [12] discuss computer-aided design methods for shell and tube exchangers. Shah [13] discusses in detail the computer-aided thermal design methodology for both compact and shell and tube exchangers. Although there are similarities in the overall structure of the computer programs, the details vary significantly between compact and shell and tube exchangers. In the following sections, we discuss the structure of a computer design method for thermal design of (1) compact heat exchangers and (2) shell and tube heat exchangers. Salient features of this computer program are discussed.

3.4.1 OVERALL STRUCTURE OF A THERMAL DESIGN COMPUTER PROGRAM

The overall structure of a thermal design computer program for a compact heat exchanger consists at a minimum of the following subroutines [13]: (1) input subroutines, (2) geometry subroutine, (3) fluid properties subroutine, (4) surface characteristics subroutine, (5) fin efficiency subroutine, (6) ϵ -NTU subroutine, (7) pressure-drop subroutine, (8) rating problem subroutine, (9) sizing problem subroutine, (10) optimization subroutines, and (11) output subroutines.

Input subroutines: These serve (1) to feed the problem specifications/process data, and (2) to convert the given unit from one system to other.

Geometry subroutine: The geometry subroutine calculates the various surface geometrical parameters for commonly used surfaces. For uncommon surfaces, calculated values are fed through the input subroutine or the terminal.

Fluid properties subroutine: This subroutine provides fluid properties for commonly used fluids in the form of specific or generalized correlations together with heat release/added curve. For others, they may be transferred through input data. Methods or correlations should be incorporated for evaluating properties of fluid mixtures.

Surface characteristics subroutine: For common surfaces, j and f versus Reynolds number data may be stored in the subroutine, or correlations may be built in. For uncommon surfaces, such information may be transferred through the input subroutine or through the terminal.

Fin efficiency subroutine: This subroutine calculates the fin efficiency and overall surface effectiveness for various types of extended surfaces.

ϵ -NTU subroutine: ϵ -NTU formulas for all flow arrangements of interest are built into this subroutine. The subroutine could be used for solving both the rating and sizing problems. That means, for a rating problem, it computes ϵ when NTU and C^* are given, and for a sizing problem it computes NTU when ϵ and C^* are given.

Pressure-drop subroutine: The friction factor f is fed through the surface characteristic subroutine. Provisions must be made to compute the pressure drop in manifolds, headers, turns, or sudden area changes at manifold/header inlet/outlet sections.

Rating problem subroutine: Since outlet temperatures are not known initially, they are therefore guessed, and the solution to the rating problem is iterated on the fluid properties once or twice until the desired convergence is achieved.

Sizing problem subroutine: All of the subroutines (except the rating problem subroutine) discussed so far are used in sizing problem. The sizing problem is solved by first determining an approximate mass velocity G that accounts for both specified heat transfer and pressure drop. The sizing problem is iterated on G until the desired convergence is met.

Optimization subroutines: In a sophisticated computer program, not only are the options of solving straightforward rating and sizing problems available, but also optimization procedures are incorporated. Such a program logically searches among feasible solutions and arrives at an optimum objective function.

Output subroutines: These serve to print all the output results in the desired units along with the desired input data and error messages. All important output results should be verified for their basic validity.

3.4.1.1 Guidelines on Program Logic

Shah [13] lists several points that should be taken into account in the initial organization and writing of the program:

1. The program should be written in a modular form containing many subroutines rather than one big main program. This allows flexibility in thorough debugging and modification of the program while running the program.
2. Error messages subroutines should be inbuilt that monitor the warning and minor and major errors for the input data and throughout the problem execution.
3. All of the iterative calculations should have a maximum number of iterations specified.
4. For a sophisticated computer program to be good, it must satisfy the requirements of individuals with diverse yet specific interests. The program should provide correct answers and ease of use, and it will be viable only as long its developers provide user support [10].

3.4.2 PROGRAM STRUCTURE FOR A SHELL AND TUBE EXCHANGER

For a shell and tube exchanger, most of the structures of the subroutines mentioned so far are common but the contents slightly vary as follows:

1. *Geometry subroutine*: This should include the auxiliary calculations on the shellside and a range of geometries including the shell type, number of shells in series, number of shells in parallel, shell diameter, tube length, baffles and baffle cut, various shellside clearances, tube count, and nozzles.
2. Various shellside correction factors calculated for heat transfer and pressure drop.
3. *The thermal effectiveness subroutine*: P -NTU_t relations should be built in for all possible flow arrangements and TEMA shells, including the check for “temperature cross.”

3.5 PRESSURE-DROP ANALYSIS, TEMPERATURE-DEPENDENT FLUID PROPERTIES, PERFORMANCE FAILURES, FLOW MALDISTRIBUTION, FOULING, AND CORROSION

3.5.1 HEAT EXCHANGER PRESSURE-DROP ANALYSIS

The term “pressure drop” refers to the pressure loss that is not recoverable in the circuit. The determination of pressure drop in a heat exchanger is essential for many applications for at least two reasons [9]:

1. The operating cost of a heat exchanger is primarily the cost of the power to run fluid-moving devices such as pumps, fans, and blowers. This pumping power, P_p , is proportional to the exchanger pressure drop as given by

$$P_p = \frac{M\Delta p}{\rho} \quad (3.1)$$

where

M is the mass flow rate

Δp is the pressure drop

ρ is the fluid density

2. The heat transfer rate can be significantly influenced by the saturation temperature change for a condensing/evaporating fluid for a large pressure drop.

The principle of pressure-drop analysis for a heat exchanger is described by Kays [14] and is extended to all types of heat exchangers. In this section, pressure-drop analysis for various types of heat exchangers as per Ref. [10] is discussed.

3.5.1.1 Pressure-Drop Evaluation for Heat Exchangers

The pressure drop associated with a heat exchanger may be considered as having two major components: (1) pressure drop associated with the core or matrix, and (2) pressure drop in inlet and outlet headers, manifolds, nozzles, or ducting due to change in flow area, flow turning, etc. In this section, core pressure drop for extended surface exchangers, regenerators, and tubular exchangers is presented, followed by the pressure drop associated with bends and flow turnings.

3.5.1.2 Pressure Drop through a Heat Exchanger

The pressure drop on any one side consists of pressure losses due to sudden contraction at the core inlet, Δp_{1-2} , core pressure drop, Δp_{2-3} , and the pressure rise due to sudden expansion at the core outlet, Δp_{3-4} . Therefore, the total pressure drop on any one side of the exchanger is given by

$$\Delta p = \Delta p_{1-2} + \Delta p_{2-3} - \Delta p_{3-4} \quad (3.2)$$

Pressure drop for various compact heat exchangers: Pressure drop for various compact heat exchangers on the fin side is given in the following [9,10].

1. Plate-fin heat exchangers

$$\frac{\Delta p}{p_i} = \frac{G^2}{2g_c} \frac{1}{p_i \rho_i} \left[(1 - \sigma^2 + K_c) + 2 \left(\frac{\rho_i}{\rho_0} - 1 \right) + f \frac{L}{r_h} \rho_i \left(\frac{1}{\rho} \right)_m - (1 - \sigma^2 - K_e) \frac{\rho_i}{\rho_0} \right] \quad (3.3)$$

1.1 For simplified formula, refer to Chapter 4, Section 4.3.3.2.

2a. Tube-fin heat exchangers (individually finned)

$$\frac{\Delta p}{p_i} = \frac{G^2}{2g_c} \frac{1}{p_i \rho_i} \left[2 \left(\frac{\rho_i}{\rho_0} - 1 \right) + f \frac{L}{r_h} \rho_i \left(\frac{1}{\rho} \right)_m \right] \quad (3.4)$$

2b. Tube-fin heat exchangers (continuously finned)

$$\frac{\Delta p}{p_i} = \frac{G^2}{2g_c} \frac{1}{p_i \rho_i} \left[2 \left(\frac{\rho_i}{\rho_0} - 1 \right) + f \frac{4L}{D_h} \rho_i \left(\frac{1}{\rho} \right)_m \right] + \frac{G'^2}{2g_c} \frac{1}{p_i \rho_i} \left[(1 - \sigma'^2 + K_c) - (1 - \sigma'^2 - K_e) \frac{\rho_i}{\rho_0} \right]$$

where $G\sigma = G'\sigma'$ (3.5)

3. Regenerator both plate-fin type and randomly staked matrix—same as Equations 3.3 and 3.4.

4. For plate heat exchanger, refer to Chapter 7, Section 7.8.4.2.

5. For shell and tube heat exchanger, refer to Chapter 5, Section 5.16.6.

Generally, the core frictional pressure drop is a dominating term, accounting for about 90% or more of the pressure drop. The entrance and exit losses are important at low values of σ (short flow length) and L (i.e., short core), high values of Reynolds number and for gases. They are negligible for liquids. The values of K_c and K_e are presented in Ref. [14]. The definitions of terms used in Equations 3.3 through 3.5 are as hereunder:

1. K_c is the contraction loss coefficient. Values of K_c are given in Ref. [14] for four different entrance flow passage geometries.

2. $\left(\frac{1}{\rho} \right)_m$ is defined as

$$\left(\frac{1}{\rho} \right)_m = v_m = \frac{v_i + v_0}{2} = \frac{1}{2} \left(\frac{1}{\rho_i} + \frac{1}{\rho_0} \right) \quad (3.6)$$

where v denotes specific volume, ρ_i denotes density of the fluid at inlet conditions and ρ_o at the outlet conditions. For a perfect gas,

$$\left(\frac{1}{\rho}\right)_m = \frac{R_c T_{lm}}{P_{ave}} \quad (3.7)$$

where

R_c is the gas constant

$P_{ave} = (p_i + p_o)/2$

$T_{lm} = T_m \pm \text{LMTD}$

Here, T_m is the average temperature of the fluid on the other side of the exchanger.

3. K_e is the expansion coefficient. Values of K_e for four different flow passage geometries are presented in Ref. [4].
4. Mass velocity G is given by

$$G = \frac{M}{A_o} \quad (3.8)$$

where A_o is the minimum free flow area.

5. σ' for continuously finned tube-fin heat exchangers (Figure 4.25) is given by [15]:

$$\sigma' = \frac{L_3 L_1 - L_3 \delta N_f L_1}{L_3 L_1} \quad (3.9a)$$

and

$$G\sigma = G'\sigma' \quad (3.9b)$$

3.5.1.3 Shell and Tube Heat Exchangers

The pressure drop on the tubeside is determined from Equation 3.3 with proper values of f , K_c , and K_e . However, in shell and tube exchangers, K_c and K_e for the tube flow are generally neglected since their contribution is small compared to the losses associated with inlet and outlet headers/channels. If U-tubes or hairpins are used in a multipass unit, additional pressure drop due to a 180° bend needs to be included. The pressure drop associated with such a bend is discussed next.

3.5.1.4 Pressure Drop due to Flow Turning

The pressure drop associated with flow turning, Δp_t is expressed in the general form as

$$\Delta p_t = K \left(\frac{1}{2} \rho U^2 \right) \quad (3.10)$$

where

K is the turning loss coefficient

U is the upstream velocity based on unaffected flow area

ρ is the fluid density at the bulk mean temperature

For a 180° turning, Δp_t is expressed in terms of mass velocity G by

$$\begin{aligned} \Delta p_t &= \frac{4G^2}{2g_c \rho} \\ &= 4 \times \text{Velocity head} \end{aligned} \quad (3.11)$$

3.5.1.5 Pressure Drop in the Nozzles

Pressure drop in the inlet nozzle, $\Delta p_{n,i}$, in terms of mass velocity through nozzle, G_n is given by

$$\begin{aligned}\Delta p_{n,i} &= \frac{1.0 G_n^2}{2 g_c \rho} \\ &= 1.0 \times \text{Velocity head}\end{aligned}\quad (3.12)$$

Pressure drop in the outlet nozzle, $\Delta p_{n,e}$, is given by

$$\begin{aligned}\Delta p_{n,e} &= \frac{0.5 G_n^2}{2 g_c \rho} \\ &= 0.5 \times \text{Velocity head}\end{aligned}\quad (3.13)$$

Total pressure drop associated with the inlet and outlet nozzles, Δp_n , is given by

$$\begin{aligned}\Delta p_n &= \frac{1.5 G_n^2}{2 g_c \rho} \\ &= 1.5 \times \text{Velocity head}\end{aligned}\quad (3.14)$$

where G_n is the mass velocity through nozzle.

3.5.2 TEMPERATURE-DEPENDENT FLUID PROPERTIES CORRECTION

One of the basic idealizations made in the theoretical solutions for Colburn j factor and friction factor f is that the fluid properties are constant. Most of the experimental j and f data obtained involve small temperature differences so that the fluid properties do not vary significantly. For those problems that involve large temperature differences, the constant-property results would deviate substantially and need to be modified [2,5]. Two schemes for such correction commonly used are

1. The property ratio method, which is extensively used for the internal flow problem
2. The reference temperature method, which is most common for the external flow problem

One of the two methods, the property ratio method, is described next. In the property ratio method, all properties are evaluated at the bulk mean temperature, and then all of the variable properties effects are lumped into a function. Shah's approach [5] to temperature-dependent fluid properties correction via the property ratio method is discussed here.

3.5.2.1 Gases

For gases, the viscosity, thermal conductivity, and density are functions of the absolute temperature T ; they generally increase with temperature. The temperature-dependent property effects for gases in terms of Stanton number St are correlated by the following equations:

$$\frac{Nu}{Nu_{cp}} = \frac{St}{St_{cp}} = \left(\frac{T_w}{T_m} \right)^n \quad (3.15)$$

$$\frac{f}{f_{cp}} = \left(\frac{T_w}{T_m} \right)^m \quad (3.16)$$

where

T_w is the tube wall temperature

T_m is the bulk mean temperature of the fluid

where the subscript cp refers to the constant property variable and all temperatures are absolute. All of the properties in dimensionless groups of Equations 3.15 and 3.16 are evaluated at the bulk mean temperature. The values of the exponents n and m depend upon the flow regime, namely, laminar or turbulent.

Laminar flow: For laminar flow, the exponents n and m are given by [16]

$$n = 0.0, \quad m = 1.00 \quad \text{for } 1 < \frac{T_w}{T_m} < 3 \quad (\text{heating}) \quad (3.17)$$

$$n = 0.0, \quad m = 0.81 \quad \text{for } 0.5 < \frac{T_w}{T_m} < 1 \quad (\text{cooling}) \quad (3.18)$$

Turbulent flow:

Gas heating: For gas heating, Sleicher and Rouse [17] recommend the following correlations:

$$Nu = 5 + 0.012 Re^{0.83} (Pr + 0.29) \left(\frac{T_w}{T_m} \right)^n \quad (3.19)$$

where

$$n = - \left[\log_{10} \left(\frac{T_w}{T_m} \right) \right]^{0.25} + 0.3 \quad (3.20)$$

Equations 3.19 and 3.20 are valid for $0.6 < Pr < 0.9$, $10^4 < Re < 10^6$, $1 < T_w/T_m < 5$, $L/D_h > 40$. All the fluid properties in Nu , Re , and Pr are evaluated at the bulk mean temperature. (Nu is Nusslet number, Re is Reynolds number and Pr is Prandtl number.)

Further, $m = -0.10$ for $1 < T_w/T_m < 2.4$.

Gas cooling: Kays and Crawford [18] recommend $n = 0.0$ and $m = -0.10$.

3.5.2.2 Liquids

For liquids, only the viscosity varies greatly with temperature. Thus, the temperature-dependent effects for liquids are correlated by the following equations:

$$\frac{Nu}{Nu_{cp}} = \left(\frac{\mu_w}{\mu_m} \right)^n \quad (3.21)$$

$$\frac{f}{f_{cp}} = \left(\frac{\mu_w}{\mu_m} \right)^m \quad (3.22)$$

where

μ_w is the viscosity of the fluid at tube wall temperature

μ_m is the bulk mean temperature of the fluid

Laminar flow: For laminar flow through a circular tube, the exponents n and m are given by Deissler [19] for heating and by Shannon and Depew [20] for cooling as

$$n = -0.14, \quad m = 0.58 \quad \text{for } \frac{\mu_w}{\mu_m} < 1 \quad (\text{heating}) \quad (3.23)$$

$$n = -0.14, \quad m = +0.54 \quad \text{for } \frac{\mu_w}{\mu_m} > 1 \quad (\text{cooling}) \quad (3.24)$$

Turbulent flow: Petukhov [21] recommends the following values for the exponents n and m :

$$n = -0.11 \quad \text{for } 0.8 < \frac{\mu_w}{\mu_m} < 1 \quad (\text{heating}) \quad (3.25)$$

$$n = -0.25 \quad \text{for } 40 > \frac{\mu_w}{\mu_m} > 1 \quad (\text{cooling}) \quad (3.26)$$

which are valid for $2 \leq \text{Pr} \leq 140$, $10^4 \leq \text{Re} \leq 1.25 \times 10^5$. Also,

$$m = 0.25 \quad \text{for } 0.35 < \frac{\mu_w}{\mu_m} < 1 \quad (\text{heating}) \quad (3.27)$$

$$m = 0.24 \quad \text{for } 2 > \frac{\mu_w}{\mu_m} > 1 \quad (\text{cooling}) \quad (3.28)$$

which are valid for $1.3 \leq \text{Pr} \leq 10$, $10^4 \leq \text{Re} \leq 2.3 \times 10^5$.

For liquid heating, Petukhov [21] correlates the variable property friction data in the following forms:

$$\frac{f}{f_{cp}} = \frac{1}{6} \left(7 - \frac{\mu_m}{\mu_w} \right) \quad \text{for } 0.35 < \frac{\mu_w}{\mu_m} < 1 \quad (3.29)$$

Equation 3.29 is based on the following data: $1.3 \leq \text{Pr} \leq 10$, $10^4 \leq \text{Re} \leq 2.3 \times 10^5$, and $0.35-2$ for μ_w/μ_m .

3.5.3 PERFORMANCE FAILURES

Satisfactory performance of heat exchangers can be obtained only from units that are properly designed and have built-in quality. Correct installation and preventive maintenance are user responsibilities. The failure of heat exchanger equipment to perform satisfactorily may be caused by one or more factors:

1. Improper thermal design
2. Operating conditions differing from design conditions
3. Uncertainties in the design parameters
4. Excessive fouling
5. Air or gas blanketing
6. Flow maldistribution
7. Deterioration in the geometrical parameters that cause bypassing the main fluids

3.5.4 MALDISTRIBUTION

A serious deterioration in performance results for a heat exchanger when the flow through the core is not uniformly distributed. This is known as maldistribution. Maldistribution of flow takes place when the flow is not uniformly distributed over the frontal area of the core. This is due to inherent design constraints in accommodating the distributor. Due to maldistribution, the flow passages nearer to the distributor will be flush with more fluids, whereas the passages further away will have lean flow or starve for want of fluids. Maldistribution causes the following:

1. Thermal performance deterioration
2. Enhanced pressure drop
3. Erosive wear of flow passages with high mass velocity

Typical causes of maldistribution are the following:

1. Poor header design; for example, too small header or distributor located in one end of the core; flow commences from one end of the core and flows perpendicular to the core
2. Blocking of fin passages due to fouling, mechanical damage of core passages
3. Damage of flow passages either at the entrance or at the exit

Maldistribution due to unfavorable nozzle location can be corrected either by relocating the nozzles (Figure 3.3) or using deflecting vanes (for side entry nozzle), or baffle plates or perforated plates in the header to direct the fluid uniformly through the tubes [22]. The baffle plate/perforated plate should be installed parallel to the tubesheet.

3.5.5 FOULING

Fouling of the shellside heat transfer surfaces is common. Generally, the effects of fouling are to reduce the leakage of fluid between baffles and tubes by blocking these gaps, and it also results in less leakage paths [23]. Industrial practice is generally to evaluate the heat transfer in the clean condition and apply appropriate fouling resistances (refer Chapter 9) to arrive at the heat transfer surface area required in the fouled condition. Pressure drop is lower during commissioning and start-up after cleaning and gradually increases to values those predicted in the fouled condition.

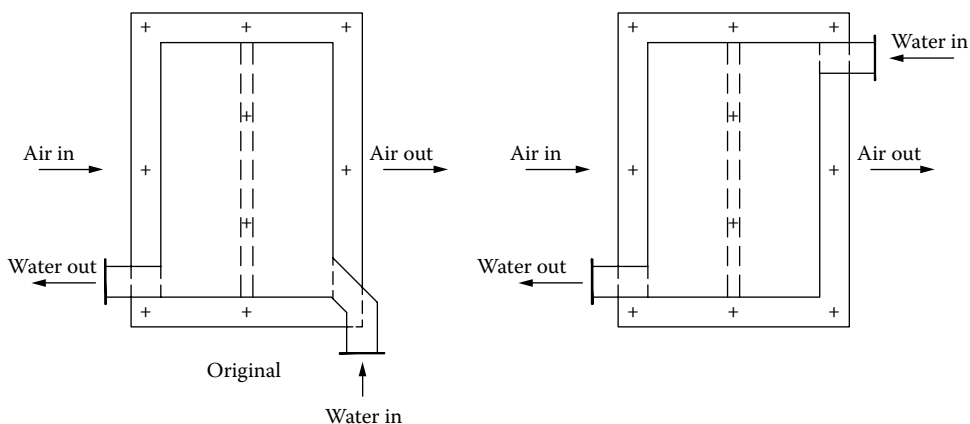


FIGURE 3.3 Maldistribution due to nozzle location with 2 passes on the tubeside corrected by relocating the nozzles.

3.5.6 CORROSION ALLOWANCE

Corrosion allowances are required for the various heat exchanger components to allow for the material loss due to corrosion in service. Corrosion allowances are specified according to the severity of corrosion and the corrosion resistance property of the material. Corrosion allowance is usually specified by the purchaser and goes hand-in-hand with the material selection.

3.6 COOPERATIVE RESEARCH PROGRAMS ON HEAT EXCHANGER DESIGN

Nowadays, thermal design of most of the exchangers are carried out using commercially available software such as those developed by cooperative research organizations like Heat transfer Research Inc. (HTRI) and Heat transfer and Fluid Flow Services (HTFS). Other softwares are Advanced Pressure Vessel of Computer Engineering, Inc., Blue Springs, MO, Intergraph® PV Elite™, Houston, TX, and COMPRESS of CODEWARE, Houston, TX (www.codeware.com). These programs offer design and cost analysis for all primary heat exchanger types and incorporate multiple design codes and standards. However, these programs are application oriented and contain company proprietary data.

3.6.1 HTRI

Heat Transfer Research, Inc. (HTRI), Alhambra, CA, is a cooperative research organization whose membership includes many of the leading users of heat exchangers, engineering contractors, and heat exchanger manufacturers. One of the major activities of HTRI is the development of computer programs that enable its members to design and rate heat exchangers. The scope of HTRI software HTRI Xchanger Suite6® includes design, rating, and simulation of (a) air-cooled heat exchangers, heat recovery bundles, and air preheaters, (b) hairpin heat exchangers, (c) single- and two-phase shell and tube heat exchangers, including kettle and thermosiphon, reboilers, falling film evaporators, and reflux condensers, (d) plate heat exchangers, and (e) spiral plate heat exchangers; graphical stand-alone tube layout software and flow-induced vibration analysis of individual tubes in a heat exchanger bundle.

3.6.2 HTFS

Heat transfer and fluid flow service (HTFS) is a cooperative venture between industry and the United Kingdom and Canadian governments. Aspen Technology, Inc., is a leading supplier of software and services for the analysis, design, and automation of process manufacturing plants in industries such as chemical, petroleum, pharmaceuticals, electric power, pulp and paper, and metals. Process manufacturers use AspenTech's solutions to improve the way they design, operate, and manage their plants. These solutions enable customers to reduce their raw material, energy, and capital expenses, meet environmental and safety regulations, improve product quality, and shorten the time required to get new production processes on stream. The headquarters of Aspen Technologies is at Cambridge, MA. HTFS software, Aspen, will simulate and design and rate the shell and tube heat exchanger, crossflow heat exchanger, plate heat exchanger, etc. The scope of various HTFS ASPEN software includes mechanical design, rating of shell, and tube heat exchangers or basic pressure vessels, design checking and simulation of air-cooled or other crossflow heat exchangers, of multi-stream plate-fin heat exchanger, plate heat exchangers, or brazed plate heat exchanger—it models both single-phase and two-phase streams and multistream plate-fin heat exchanger made of aluminum, stainless steel, and titanium. Simulation covers thermosiphon and crossflow pattern and also detailed layer-by-layer analysis.

3.7 UNCERTAINTIES IN THERMAL DESIGN OF HEAT EXCHANGERS

A major problem constantly faced by heat exchanger designers is to predict accurately the performance of a given heat exchanger or a system of heat exchangers for a given set of service conditions. The problem is complicated by the fact that uncertainties exist in most of the design parameters and in the design procedures themselves [24]. The design parameters that are used in the basic thermal design calculations of a heat exchanger include process parameters, heat transfer coefficients, tube dimensions (e.g., tube diameter and wall thickness), thermal conductivity of the tube material, and thermophysical properties of the fluids. Nominal or mean values of these parameters are used in the design calculations. However, uncertainties in these parameters prevent us from predicting the exact performance of the unit.

The effect of the uncertainties is mostly in the performance degradation in service. Hence, there is an imperative need to consider all the uncertainties and to critically evaluate them and correctly predict the thermal performance of a heat exchanger. This is particularly true for critical applications. In this section, various uncertainties that influence the thermal performance and a method to account for these uncertainties in the design calculations are presented.

3.7.1 UNCERTAINTIES IN HEAT EXCHANGER DESIGN

Uncertainties in the design parameters are summarized by Al-Zakri et al. [24], Cho [25], and Mahbub Uddin and Bell [26]. Various uncertainties and their reasons are the following:

1. Fluid flow rates, temperatures, pressures, and compositions vary from the design conditions.
2. Temperatures of cooling water and air used to cool process fluids vary with seasonal temperature changes.
3. Physical properties of the process fluids are often poorly known, especially for mixtures.
4. Heat transfer and pressure-drop correlations from which one computes convective heat transfer coefficients and pressure drop have data spreads around the mean values.
5. Manufacturing of heat transfer tubes and other component dimensions influencing thermal performance does not produce precise tube dimensions.
6. Manufacturing tolerances in equipment lead to significant differences in thermohydraulic performance between nominally identical units.
7. Fouling of heat transfer surface is poorly predictable.
8. Miscellaneous factors influence the thermal performance.

In this section, the following uncertainties are discussed:

1. Uncertainty in process conditions
2. Uncertainty in the physical properties of the process fluids
3. Flow nonuniformity
4. Nonuniform flow passages
5. Uncertainty in the basic design correlations
6. Uncertainty due to thermodynamically defined mixed or unmixed flows for crossflow heat exchangers
7. Bypass path on the air side of compact fin-tube exchangers
8. Nonuniform heat transfer coefficient
9. Uncertainties in fouling
10. Miscellaneous effects

Items 1–3, 5, and 8–10 are common both for shell and tube exchangers and compact heat exchangers. Items 4, 6, and 7 pertain to compact heat exchangers only.

3.7.1.1 Uncertainty in Process Conditions

Heat exchangers are designed for a nominal set of operating conditions chosen to represent a relatively ideal state of a system. In general, a heat exchanger will not operate under the ideal design conditions. Process stream flow rates, compositions, and temperatures can all be expected to vary during the lifetime of the exchanger, and seasonal changes in weather constantly change cooling water and air temperatures.

3.7.1.2 Uncertainty in the Physical Properties of the Process Fluids

Correlations for heat transfer coefficients and pressure drops, and the heat transfer rate equation, require values of one or more of the following physical properties: density, specific heat, viscosity, thermal conductivity, latent heat, etc. There are substantial uncertainties in the physical properties of all but a few fluids. Uncertainties in these physical properties are due to the following reasons [27]:

1. Measure error.
2. Extrapolation and interpolation errors—interpolation errors may be very small, whereas extrapolation errors may be substantial.
3. Estimation errors.
4. Errors in estimated temperatures and pressures.
5. Mixture properties calculated from component properties.
6. Physical properties closer to the critical temperature and pressure change rapidly and significantly. Any attempt to get mixture properties via individual properties of components around their critical points needs great care.
7. If the fluid is a mixture, the uncertainties will normally be larger than those for a pure component.

3.7.1.3 Flow Nonuniformity

To obtain maximum thermal performance, the flow should be uniform across the entire frontal area of the core. However, the flow may not be uniform due to unfavorable header design, nozzle location, and nonuniform flow passages in the case of tube-fin and plate-fin heat exchangers. For example, automobile radiators are usually designed with the assumptions that the cooling air is uniformly distributed over the radiator core, and the cooling water is uniformly distributed over the radiator tubes [28]. According to Chiou [28], these assumptions are normally not met due to these reasons: flow nonuniformity on the cooling airside is usually due to unfavorable location of fan with respect to the radiators and due to crowded radiator compartment. The flow nonuniformity on the engine coolant side is the result of the unfavorable arrangement and configuration of the inlet manifold of the coolant to the radiator. Nonuniform flow distribution adversely affects the thermal performance and also could produce high-velocity regions leading to erosion–corrosion of flow passages. Chiou presents a mathematical method to determine the thermal effectiveness of the engine radiator accounting for two-dimensional nonuniform fluid flow distribution on both cooling air and engine coolant sides. Flow nonuniformity due to header design and due to unfavorable location of radiator fan of a diesel electric locomotive are discussed next.

Flow nonuniformity due to header design: Normally the frontal area of a compact heat exchanger is very large compared to the dimensions of the nozzles and the core depth. The large frontal area requires turning the streams in a system of headers. The turnings have marked area changes through the headers, leading to nonuniform flow through the core (Figure. 3.4), even though there may be uniform flow passages. Therefore, the header design has a profound effect on the thermal performance of the core. The main objective in designing the header is to ensure uniform distribution of fluids over the entire frontal area of the core and to have minimum pressure drop due to flow turning. Maldistribution due to unfavorable nozzle location can be corrected as discussed earlier. The thermal

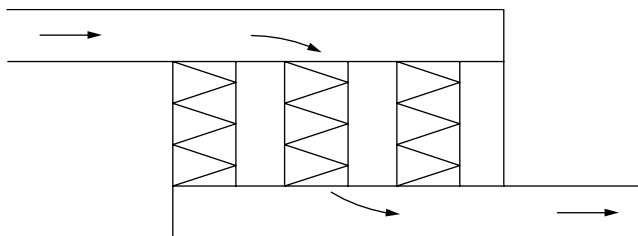


FIGURE 3.4 Nonuniform flow due to flow turning in a header.

performance degradation due to unfavorable nozzle location on the tubeside can be evaluated as discussed by Muller [29]. If the tubeside film coefficient is not controlling the overall thermal resistance, the effect of maldistribution on the overall heat transfer coefficient will be negligible.

Maldistribution due to unfavorable location of radiator fan in a diesel electric locomotive: Flow nonuniformity on diesel locomotive radiators is usually due to inherent problems on the air side due to unfavorable location of the fan with respect to the radiators. In diesel locomotives, the left and right radiators are mounted vertically; the radiator fan is mounted at the top but at the center of the radiators, which results in nonuniform flow distribution over the radiators. Other reasons for flow nonuniformity are crowded radiator compartment fitted with lube oil cooler and filter, and radiator fan drives.

3.7.1.4 Nonuniform Flow Passages

For high-surface-density compact heat exchangers such as tube-fin and plate-fin units with parallel fins, the identified nonuniform flow passages are due to [30] (1) nonuniform fin spacing, (2) recurved fin, and (3) open fin. For mechanically bonded tube-fin cores, there is ample scope for bunching of fins due to deficiency in bullet expansion, thermal fatigue, and cracking of fin collars. Maldistribution due to nonuniform flow passages as shown in Figure 3.5 does not adversely affect the thermal performance in the case of either turbulent flow or highly interrupted laminar flow surfaces like offset strip fins and louvered fins, but can have a marked effect in fully developed laminar flow in continuous cylindrical passage geometries, such as those employed in disk-type rotary regenerators [31]. As a result, the reduction in Colburn j factor is substantial, with a slight reduction in friction factor f . The theoretical analysis of this problem for low Reynolds number laminar flow surfaces is discussed in Refs. [30–32]. To a certain extent, nonuniform flow passages due to fin bunching of mechanically bonded cores or soldered radiator cores can be overcome by combing of fins during maintenance schedules.

3.7.1.5 Uncertainty in the Basic Design Correlations

All of the correlations for the basic fluid flow and heat transfer mechanisms in heat exchangers show scatter when compared to experimental data. Some processes such as nucleate boiling are only very crudely predictable a priori [24].

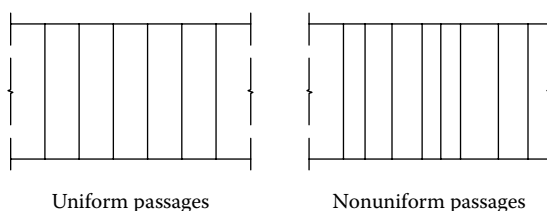


FIGURE 3.5 Nonuniform flow passages of a compact heat exchanger.

3.7.1.6 Uncertainty due to Thermodynamically Defined Mixed or Unmixed Flows for Crossflow Heat Exchangers, after Digiovanni and Webb

The thermal effectiveness of crossflow heat exchangers is evaluated for known values of NTU and capacity rate ratio C^* , from the thermodynamically defined fluid mixedness and unmixedness and/or both through the core. The typical patterns of flow mixedness across the core are the following:

1. Unmixed–unmixed; for example, brazed plate-fin exchanger with plain fins and continuously finned tube compact heat exchanger
2. Unmixed–mixed
3. Mixed–mixed

However, the thermodynamic definitions do not tell whether a specific geometry will provide mixed or unmixed flow. For any values of NTU and C^* , the unmixed–unmixed arrangement yields the highest thermal effectiveness and the mixed–mixed arrangement has the lowest, and the unmixed–mixed case offers the intermediate values.

Generally there is always some mixedness on the air side in the cases of individually finned tube banks and offset strip fins. During the design stage if these cases are assumed to act as a thermodynamically unmixed case, the actual thermal effectiveness will be less than the predicted value. For a tube bank, the level of mixedness depends on the tube layout patterns, pitch ratios, Reynolds number, size of the eddies in the transverse direction, etc.

Correction for partial mixing. Digiovanni and Webb [33] developed a procedure to calculate the effectiveness of crossflow heat exchangers for partially mixed flow. To calculate the correction factor, it is necessary to provide a quantitative definition of the “percent mixing,” which is designated as 100y. The partially mixed condition is defined by linear interpolation between the unmixed and the mixed flow effectiveness values. If $y = 0$, the flow stream is unmixed, and $y = 1$ represents the fully mixed stream. There are three possible cases of interest for the partially mixed condition:

1. Partially mixed flow on one stream and unmixed in the other stream
2. One stream partially mixed and the other stream mixed
3. Both streams partially mixed

They presented equations to define y for the three cases of interest. For case 1, y has been defined; for the other two cases refer to Ref. [33].

Case 1: If the measured effectiveness of the partially mixed exchangers is $\epsilon_{pm,u}$, then

$$y = \frac{\epsilon_{u,u} - \epsilon_{pm,u}}{\epsilon_{u,u} - \epsilon_{m,u}} \quad (3.30)$$

From Equation 3.30, for $y\%$ mixedness, $\epsilon_{pm,u}$ is given by

$$\epsilon_{pm,u} = \epsilon_{u,u} - y(\epsilon_{u,u} - \epsilon_{m,u}) \quad (3.31)$$

3.7.1.7 Nonuniform Heat Transfer Coefficient

The idealization that the heat transfer coefficient, h , is constant throughout its flow length is not correct. It varies with location, the entrance length effect (due to the boundary layer development), surface temperature, maldistribution, fouling, manufacturing imperfections, fluid physical properties, etc. [34]. Thermal performance degradation due to uncertainties in heat transfer will be felt more in the case of highly viscous fluids and units in which phase change takes place. Temperature effects and thermal entry length effect are significant in laminar flows; the latter effect is generally not significant in turbulent flow except for low Prandtl number fluids. Approximate methods to account for specific variations in heat transfer coefficient for counterflow are analyzed by Colburn [35]

and Butterworth [36], for crossflow by Sider-Tate [37] and Roetzel [38], and for 1 – 2N shell flow by Bowman et al. [39]. These methods are summarized in Refs. [33,34]. The state of the art on nonuniform heat transfer coefficient is reviewed in Ref. [34].

3.7.1.8 Bypass Path on the Air Side of Compact Tube-Fin Exchangers

Owing to the construction requirements, there are various clearances on the shellside of a shell and tube exchanger leading to various bypass paths. Modern procedures for shellside heat transfer calculations do take care of various leakages and bypass streams while evaluating shellside performance. In the case of finned-tube banks, the bypass paths are inevitable between (1) the sidesheet assembly and the outermost tubes, and (2) the core assembly and the housing in which the core is housed. The thermal performance deterioration due to these clearances can be overcome by the following means:

1. Attach seals to the sidesheet assembly to block the clearance between the sidesheet assembly and the outermost tubes
2. Permanently weld strips to the housing (without hindering the fitment of the core), which will block the bypass path between the core assembly and the housing in which the core is housed

These measures will be discussed in Chapter 4.

3.7.1.9 Uncertainty in Fouling

The influence of uncertainties inherent in fouling factors is generally greater than that of uncertainties in physical properties, flow rates, or temperatures, such as in heat exchange between dirty aqueous fluids, in which fouling resistances can completely dominate the thermal design [40]. Planned fouling prevention, maintenance, and cleaning schedules make it possible to allow lower resistance values.

3.7.1.10 Miscellaneous Effects

Depending upon the individual design/constructional features, there exist certain miscellaneous effects that add uncertainties on thermal performance. Such effects include stagnant regions, radiation effects, allowance for in-service tube plugging due to leakages that cannot be corrected, influence of brazing/soldering, etc. Compact soldered finned-tube cores and brazed PFHEs will suffer from soldering/brazing-induced surface roughness/partial blockage due to melting of brazing filler metal. This may reduce the j factor slightly but increase the f factor substantially.

3.7.2 DETERMINATION OF UNCERTAINTIES

The method usually used by heat exchanger designers is to ignore in the original calculations uncertainties in the design parameters. After the area has been calculated, it is multiplied by a safety factor assigned by the designer to ensure that the exchanger will perform adequately. The safety factor is based mostly upon the designer's experience and judgment and can vary from 15% to 100%. Such methods can unnecessarily add to the cost of the equipment in capital investment [24].

3.7.2.1 Computational Procedures

Buckley [41] was the first to use a statistical approach to the sizing of process equipment. His approach was to first size the unit with nominal values of design parameters. Then, based on the assumption that uncertainties follow the normal distribution, he determined the standard deviation for each variable. From the individual uncertainty (standard deviation), its effect on the overall uncertainty of the area was determined. Once the effects of all uncertain parameters on the overall heat transfer area are known, the oversizing can be determined according to the desired confidence level.

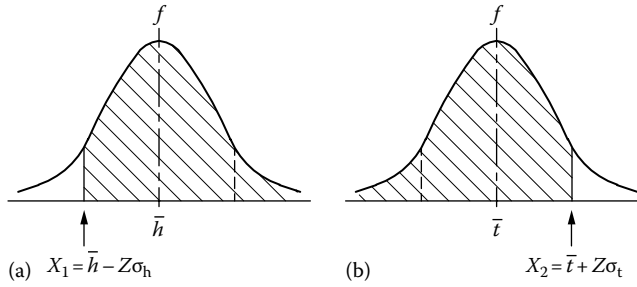


FIGURE 3.6 Normal distribution of (a) heat transfer coefficient, h , and (b) tube-wall thickness, t .

Mahbub Uddin and Bell [26] presents a Monte Carlo procedure for dealing with the effect of uncertainties on the design, performance, and operation of systems of process heat exchangers.

Cho [25] presents a simple method of assessing the uncertainties in the design of heat exchangers assuming a Gaussian form of data distribution for “uncertain” parameters, which leads to the root sum square (RSS) method of establishing the probability, or confidence level, that the heat exchanger design will meet its performance requirements. This method is briefly discussed next.

Cho’s method of uncertainty analysis [25]: The degree of data spread around the mean value may be quantified using the concept of standard deviation, σ . Suppose that the distribution of data points for a certain parameter has a Gaussian or normal distribution. Then the procedure to incorporate the effect of data spread into the design of a heat exchanger is as follows. For example, consider the convective heat transfer coefficient, h , which has a data spread as shown in Figure 3.6a. The probability of the value of h falling below the mean value is of concern. Therefore, if one takes

$$X_1 = \bar{h} - Z\sigma_h \quad \text{and} \quad X_2 = \infty \quad (3.32a)$$

or

$$Z_1 = -Z \quad \text{and} \quad Z_2 = \infty \quad (3.32b)$$

then the probability that h will attain a value greater than $\bar{h} - Z\sigma_h$ is

$$P(X_1 = \bar{h} - Z\sigma_h, X_2 = \infty) = \frac{1}{\sqrt{2\pi}} \int_{-Z}^{\infty} e^{-Z^2/2} dZ \quad (3.33)$$

where

$$Z = \left(\frac{Z - \bar{X}}{\sigma} \right) \quad (3.34)$$

This probability is known as the cumulative probability or one-sided confidence level and the numerical values are given in Ref. [25]. Here, Z indicates the degree of the design confidence level; for example, if one desires a 90% confidence level, the value of Z becomes 1.282. This means the value of h should be reduced to $\bar{h} - 1.282\sigma_h$ to obtain a 90% level of design confidence. Due to

the reduction in the heat transfer coefficient, the surface area is to be increased to get the desired thermal performance. Equations 3.32 and 3.33 are applicable to uncertain parameters whose lower values are of design concern, like heat transfer coefficients and tube-wall thermal conductivity.

Now consider the effect of tube-wall thickness, t , which has a data spread as shown in Figure 3.6b. The value of t greater than the mean value is of concern here. Therefore, if one takes

$$X_1 = -\infty^* \quad \text{and} \quad X_2 = \bar{t} + Z\sigma_t \quad (3.35a)$$

or

$$Z_1 = -\infty \quad \text{and} \quad Z_2 = +Z \quad (3.35b)$$

then the probability that \bar{t} will attain a value less than $\bar{t} + Z\sigma_t$ is

$$P(X_1 = -\infty, X_2 = \bar{t} + Z\sigma_t) = \frac{1}{\sqrt{2\pi}} \int_{-\infty}^{\infty} e^{-Z^2/2} dZ \quad (3.36)$$

Again, Z indicates the degree of the design confidence level. A 90% level of design confidence requires the use of an increased thickness, $\bar{t} + 1.282\sigma_t$ in the sizing calculation. The reduction in heat transfer rate due to increased thickness is to be compensated by increase in heat transfer surface area. Equations 3.35 and 3.36 are applicable to uncertain parameters whose upper values are of design concern, like tube-wall thickness and fouling resistance.

The effects of data spreads have been discussed for individual parameters. These individual effects usually take place simultaneously, and the combined effect can be assessed for normally distributed parameters, using the RSS method [25]:

$$\Delta X = \sqrt{\sum_{i=1}^N (\Delta X_i)^2} \quad (3.37)$$

3.7.3.2 Additional Surface Area Required due to Uncertainty

The effects of data spread have been discussed for individual parameters. These individual effects usually take place simultaneously and the combined effect is assessed using the RSS method. The total additional surface area ΔA_i required to obtain a certain level of design confidence is calculated from [25]

$$\Delta A = \sqrt{\sum_{i=1}^N (\Delta A_i)^2} \quad (3.38)$$

3.7.3.3 Additional Pressure Drop due to Uncertainty

Equation 3.37 can also be applied to determine the additional pressure drop, $\Delta(\Delta p)$, required to obtain a certain level of design confidence, as given by the following equation [25]:

$$\Delta(\Delta p) = \sqrt{\sum_{i=1}^N [\Delta(\Delta p)_i]^2} \quad (3.39)$$

NOMENCLATURE

A	total heat transfer area, m^2 (ft^2)
A_o	minimum free flow area, m^2 (ft^2)
c_p	specific heat, $\text{J/kg } ^\circ\text{C}$ ($\text{Btu/lbm.}^\circ\text{F}$)
C	specific heat of cold fluid, $\text{J/kg } ^\circ\text{C}$ ($\text{Btu/lbm.}^\circ\text{F}$)
C_c	specific heat of cold fluid, $\text{J/kg } ^\circ\text{C}$ ($\text{Btu/lbm.}^\circ\text{F}$)
C_h	specific heat of hot fluid, $\text{J/kg } ^\circ\text{C}$ ($\text{Btu/lbm.}^\circ\text{F}$)
$C^* =$	heat capacity rate ratio $= (mc_p)_{\min}/(mc_p)_{\max}$
D_h	hydraulic diameter, $(4r_h)$, m (ft)
F	LMTD correction factor
f	Fanning friction factor
G	mass velocity, $\text{kg/m}^2\cdot\text{s}$ ($\text{lbm/h}\cdot\text{ft}^2$)
g_c	acceleration due to gravity or proportionality constant 9.81 m/s^2 (32.17 ft/s^2)
$=$	1 and dimensionless in SI units
h	convective heat transfer coefficient, $\text{W/m}^2\cdot^\circ\text{C}$ ($\text{Btu/ft}^2 \text{ h}\cdot^\circ\text{F}$)
j	Colburn heat transfer factor
K_c	fluid entrance contraction coefficient
K_e	fluid exit expansion coefficient
k	thermal conductivity of the fluid, $\text{W/m}\cdot^\circ\text{C}$ ($\text{Btu/h}\cdot\text{ft}\cdot^\circ\text{F}$)
L	length in the fluid flow direction, m (ft)
L_1, L_2, L_3	heat exchanger core dimensions of a tube bank, m (ft)
M	mass flow rate of the fluid, kg/s (lbm/h)
m	exponent
NTU	number of transfer units,
Nu	Nusselt number
n	exponent
P_p	fluid pumping power
p	pressure, Pa (lbf/ft^2)
Pr	Prandtl number
Q	total heat duty of the exchanger, $\text{W}\cdot\text{s}$ (Btu)
q	heat transfer rate, W (Btu/h)
R	heat capacity rate ratio of shell and tube heat exchanger fluids
Re	Reynolds number
r_h	hydraulic radius, m (ft) $= D_h/4$
P	thermal effectiveness of shell and tube heat exchanger
P	fluid friction power
p	pressure, Pa (lbf/ft^2)
St	Stanton number
T	Temperature, $^\circ\text{C}$ ($^\circ\text{F}$)
t	Temperature, $^\circ\text{C}$ ($^\circ\text{F}$)
U	upstream fluid velocity, m/s (ft/s)
U	overall heat transfer coefficient, $\text{W/m}^2\cdot^\circ\text{C}$ ($\text{Btu/h}\cdot\text{ft}^2\cdot^\circ\text{F}$)
Δp	pressure drop, Pa (lbf/ft^2)
ϵ	thermal effectiveness
μ_m	viscosity of the fluid at bulk mean temperature, $\text{kg/m}\cdot\text{s}$ or $\text{Pa}\cdot\text{s}$ ($\text{lbm/h}\cdot\text{ft}$)
μ_w	viscosity of the fluid at wall temperature, $\text{kg/m}\cdot\text{s}$ or $\text{Pa}\cdot\text{s}$ ($\text{lbm/h}\cdot\text{ft}$)
ρ	fluid density, kg/m^3 (lbm/ft^3)
β	area density, m^2/m^3 (ft^2/ft^3)
$\Delta p =$	pressure drop

η_o fin efficiency or the overall surface efficiency
 $\sigma =$ the ratio of minimum free flow area to frontal area

Subscripts

ave average
 c cold
 h hot
 cp constant property
 e exit
 i inlet
 lm log mean
 m mean
 n nozzle
 o outlet
 s shell
 t tube
 m,u mixed, unmixed
 pu,u partially unmixed, unmixed
 u,u unmixed, unmixed
 w wall temperature conditions
 1 inlet of the exchanger
 2 outlet of the exchanger
 min minimum
 max maxim

REFERENCES

1. Shah, R. K., Heat exchanger design methodology, in *Heat Transfer Equipment Design* (R. K. Shah, E. C. Subbarao, and R. A. Mashelkar, eds.), Hemisphere, Washington, DC, 1988, pp. 17–22.
2. Kays, W. M. and London, A. L., *Compact Heat Exchangers*, 3rd edn., McGraw-Hill, New York, 1984.
3. Shah, R. K. and Bhatti, M. S., Assessment of correlations for single-phase heat exchangers, in *Two-Phase Flow Heat Exchangers—Thermal-Hydraulic Fundamentals and Design* (S. Kakac, A. E. Bergles, and F. E. Oliveira, eds.), Kluwer Academic Publishers, London, U.K., 1988, pp. 81–122.
4. Gollin, M., Heat exchanger design and rating, in *Handbook of Applied Thermal Design* (E. C. Guyer, ed.), McGraw-Hill, New York, 1984, pp. 7-24–7-36.
5. Shah, R. K., Compact heat exchanger design procedures, in *Heat Exchangers: Thermal Hydraulic Fundamentals and Design* (S. Kakac, A. E. Bergles, and F. Mayinger, eds.), Hemisphere, Washington, DC, 1981, pp. 495–536.
6. Bell, K. J., Delaware method for shellside design, in *Heat Transfer Equipment Design* (R. K. Shah, E. C. Subbarao, and R. A. Mashelkar, eds.), Hemisphere, Washington, DC, 1988, pp. 145–166.
7. Cardwell, Optimum tube size for shell and tube type heat exchangers, *Trans. ASME*, 72, 1061–1065 (1950).
8. Shah, R. K., Afimiwala, K. A., and Mayne, R. W., Heat exchanger optimization, in *Heat Transfer*, Vol. 4, Hemisphere, Washington, DC, 1978, pp. 185–191.
9. Shah, R. K. and Mueller, A. C., Heat exchanger basic thermal design methods, in *Handbook of Heat Transfer Applications*, 2nd edn. (W. M. Rohsenow, J. P. Hartnett, and E. N. Ganic, eds.), McGraw-Hill, New York, 1985, pp. 4-1–4-77.
10. Shah, R. K., Heat exchanger basic design methods, in *Low Reynolds Number Flow Heat Exchangers* (S. Kakac, R. K. Shah, and A. E. Bergles, eds.), Hemisphere, Washington, DC, 1983, pp. 21–71.
11. Chenoweth, J. M. and Kistler, R. S., Computer program as a tool for heat exchanger rating and design, ASME Paper No. 76-WA/HT-4, 1976.

12. Taborek, J., Evolution of heat exchanger design techniques, *Heat Transfer Eng.*, 1, 15–29 (1979).
13. Shah, R. K., Compact heat exchanger surface selection, optimization, and computer aided thermal design, in *Low Reynolds Number Flow Heat Exchangers* (S. Kakac, R. K. Shah, and A. E. Bergles, eds.), Hemisphere, Washington, DC, 1983, pp. 983–998.
14. Kays, W. M., Loss coefficients for abrupt changes in flow cross section with low Reynolds number flow in single and multiple tube system, *Trans. ASME*, 1067–1074 (1950).
15. Shah, R. K., Personal Communication, dt. 3.1.1998. Senior Staff Research Scientist, Heat Exchanger Development, DELPHI Harrison Thermal Systems, Lockport, NY.
16. Kays, W. K. and Perkins, H. C., Forces convection, internal flow in ducts, in *Handbook of Heat Transfer* (W. M. Rohsenow and J. P. Hartnett, eds.), McGraw-Hill, New York, 1973.
17. Sleicher, C. A. and Rouse, M. W., A convenient correlation for heat transfer to constant and variable property fluids in turbulent pipe flow, *Int. J. Heat Mass Transfer*, 18, 677–683 (1975).
18. Kays, W. M. and Crawford, M. E., *Convective Heat and Mass Transfer*, 2nd edn., McGraw-Hill, New York, 1980.
19. Deissler, R. G., Analytical investigation of fully developed laminar flow in tubes with heat transfer with fluid properties variable along the radius, NACA TN 2410, NACA, Washington, DC, 1951.
20. Shannon, R. L. and Depew, C. A., Forced laminar flow convection in a horizontal tube with variable viscosity and free convection effects, *Trans. ASME J. Heat Transfer*, 91, 251–258 (1969).
21. Petukhov, B. S., Heat transfer and friction in turbulent pipe flow with variable physical properties, in *Advances in Heat Transfer*, Vol. 6, Academic Press, New York, 1970, pp. 503–564.
22. Shah, R. K., Compact heat exchangers, in *Handbook of Heat Transfer Applications* (W. M. Rohsenow, J. P. Hartnett, and E. N. Ganic, eds.), McGraw-Hill, New York, 1985, pp. 4-174–4-312.
23. Minton, P. E., Process heat transfer, *Proceedings of the Ninth International Heat Transfer Conference*, Heat Transfer 1990-Jerusalem, Paper No. KN-22, Vol. 1, 1990, pp. 355–362.
24. Al-Zakir, A. S. and Bell, K. J., Estimating performance when uncertainties exist, *Chem. Eng. Prog.*, 77, 39–49 (1981).
25. Cho, S. M., Uncertainty analysis of heat exchanger thermal hydraulic design, in *Proceedings of the Thermal/Mechanical Heat Exchanger Design—Karl Gardner Memorial Session*, Vol. 64, (K. P. Singh and S. M. Shenkman, eds.), American Society of Mechanical Engineers Winter Meeting, Anaheim, CA, December 7, 1986, 1985, pp. 33–41.
26. Mahbub Uddin, A. K. M. and Bell, K. J., Effect of uncertainties on the design and operation of systems of heat exchangers, in *Heat Transfer Equipment Design* (R. K. Shah, E. C. Subbarao, and R. A. Mashlikar, eds.), Hemisphere, Washington, DC, 1988, pp. 39–47.
27. Haseler, L. E., Owen, R. G., and Sardesai, R. G., The sensitivity of heat exchanger calculations to uncertainties in the physical properties of the process fluids, in *Practical Application of Heat Transfer*, IMechE Conference Publications, 1982–1984, C56/82, IMechE, London, U.K., pp. 11–20.
28. Chiou, J. P., The effect of flow nonuniformity on the sizing of the engine radiator, 800035 SAE, 1981, pp. 222–230.
29. Mueller, A. C., An inquiry of selected topics on heat exchanger design, *Chem. Eng. Prog. Symp. Ser.*, 73, 273–287 (1976).
30. London, A. L., Laminar flow gas turbine regenerators—The influence of manufacturing tolerances, *Trans. ASME J. Eng. Power Ser. A*, 92, 46–56 (1970).
31. Shah, R. K. and London, A. L., Effect of nonuniform passages on compact heat exchanger performance, *Trans. ASME J. Eng. Power*, 102, 653–659 (1980).
32. Mondt, J. R., Effects of nonuniform passages on deepfold heat exchanger performance, *Trans. ASME J. Eng. Power*, 99, 657–663 (1977).
33. Digiovanni, M. A. and Webb, R. L., Uncertainty in effectiveness for crossflow heat exchangers, *Heat Transfer Eng.*, 10, 61–69 (1989).
34. Shah, R. K., Nonuniform heat transfer coefficient for heat exchanger thermal design, in *Aerospace Heat Exchanger Technology* (R. K. Shah and A. Hashemi, eds.), Elsevier Science Publishers, Amsterdam, the Netherlands, 1993, pp. 417–445.
35. Colburn, A. P., Mean temperature difference and heat transfer coefficient in liquid heat exchangers, *Ind. Eng. Chem.*, 25, 873–877 (1933).
36. Butterworth, D., Condensers: Thermal-hydraulic design, in *Heat Exchangers: Thermal-Hydraulic Fundamentals and Design* (S. Kakac, A. E. Bergles, and F. Mayinger, eds.), Hemisphere/McGraw-Hill, Washington, DC, 1981, pp. 647–679.
37. Sieder, E. N. and Tate, G. E., Heat transfer and pressure drop of liquids in tubes, *Ind. Eng. Chem.*, 28, 1429–1435 (1936).

38. Roetzel, W., Heat exchanger design with variable transfer coefficient for crossflow and mixed flow arrangements, *Int. J. Heat Mass Transfer*, 17, 1037–1049 (1974).
39. Bowman, R. A., Muller, A. C., and Nagle, W. M., Mean temperature difference, *Trans. ASME*, 62, 283–294 (1940).
40. Larowski, A. and Taylor, M. A., *Systematic Procedures for Selection of Heat Exchangers*, C58/82, Institution of Mechanical Engineers, London, U.K., 1982, pp. 32–56.
41. Buckley, P. S., Statistical methods in process design, *Chem. Eng.*, September, 112–114 (1950).

BIBLIOGRAPHY

- Bell, K. J., Overall design methodology for shell and tube exchangers, in *Heat Transfer Equipment Design* (R. K. Shah, E. C. Subbarao, and R. A. Mashelkar, eds.), Hemisphere, Washington, DC, 1988, pp. 131–144.
- Breber, G., Computer programs for design of heat exchangers, in *Heat Transfer Equipment Design* (R. K. Shah, E. C. Subbarao, and R. A. Mashelkar, eds.), Hemisphere, Washington, DC, 1988, pp. 167–178.
- Cho, S. M., Basic thermal design methods for heat exchangers, in *Heat Transfer Equipment Design* (R. K. Shah, E. C. Subbarao, and R. A. Mashelkar, eds.), Hemisphere, Washington, DC, 1988, pp. 23–38.
- Lord, R. C., Minton, P. E., and Sulusser, R. P., Guide to trouble free heat exchangers, in *Process Heat Exchange, Chemical Engineering Magazine* (V. Cavaseno, ed.), McGraw-Hill, New York, 1979, pp. 60–67.
- Palen, J. W., Design of process heat exchanger by computers—A short history, *Heat Transfer, Eighth International Conference*, San Francisco, CA, 1986, pp. 239–248.
- Pase, G. K., Computer programs for heat exchanger design, *Chem. Eng. Prog.*, 70, 53–56 (1986).

4 Compact Heat Exchangers

4.1 CLASSIFICATION AND CONSTRUCTION DETAILS OF TUBE-FIN COMPACT HEAT EXCHANGERS

Compact heat exchangers are used in a wide variety of applications. Typical among them are the heat exchangers used in automobiles, air conditioning, electronics cooling, waste and process heat recovery, cryogenics, aircraft and spacecraft, ocean thermal energy conservation, solar, and geothermal systems. The need for light-weight, space-saving, and economical heat exchangers has driven the development of compact surfaces.

4.1.1 CHARACTERISTICS OF COMPACT HEAT EXCHANGERS

Specific characteristics of compact heat exchangers are discussed by Shah [1–4] and include the following:

1. Usually with extended surfaces.
2. A high heat transfer surface area per unit volume of the core, usually in excess of $700 \text{ m}^2/\text{m}^3$ on at least one of the fluid sides, which usually has gas flow.
3. Small hydraulic diameter.
4. Usually at least one of the fluids is a gas.
5. Fluids must be clean and relatively nonfouling because of small hydraulic diameter (D_h) flow passages and difficulty in cleaning; plain uninterrupted fins are used when “moderate” fouling is expected.
6. The fluid pumping power (i.e., pressure drop) consideration is as important as the heat transfer rate.
7. Operating pressures and temperatures are limited to a certain extent compared to shell and tube exchangers due to thin fins and/or joining of the fins to plates or tubes by brazing, mechanical expansion, etc.
8. The use of highly compact surfaces results in an exchanger with a large frontal area and a short flow length; therefore, the header design of a compact heat exchanger is important for a uniform flow distribution.
9. Fluid contamination is generally not a problem.
10. Variety of surfaces are available having different order of magnitudes of surface area density.
11. Flexibility in distributing surface area on the hot or cold side as desired by the designer.

Other features of compact heat exchangers are as follows:

Materials for the manufacture of fins are limited by the operating temperature of certain applications. For low- to moderate-temperature applications, fins can be made from aluminum, copper, or brass and thus maintain high-fin efficiency. For high-temperature applications, stainless steel and heat-resistant alloys may be used with possibly a reduction in the fin efficiency. Consequently, suitable high-performance surfaces may be selected to offset the reduction in fin efficiency or the fin thickness should be reduced.

Manufacture is by brazing or welding. For low- or moderate-temperature applications, the fins can be mechanically bonded. Low-fin tubes are extruded.

Flow arrangements: Compact exchangers are mostly used as single-pass crossflow or multipass cross-counterflow exchangers.

4.1.2 CONSTRUCTION TYPES OF COMPACT HEAT EXCHANGERS

Basic construction types of compact heat exchangers are

1. Tube-fin
2. Plate-fin
3. Regenerators

Tube-fin and plate-fin heat exchangers are discussed in this chapter. Regenerators, exclusively used in gas-to-gas applications, could have more compact surface area density compared to plate-fin or tube-fin surfaces. They are covered in detail in a separate chapter. The unique characteristics of compact extended-surface plate-fin and tube-fin exchangers that favor them as compared with the conventional shell and tube exchangers include the following [1,3,4]:

1. Many surfaces are available having different orders of magnitude of surface area density.
2. Flexibility in distributing surface area on the hot and cold sides as warranted by design considerations.
3. Generally substantial cost, weight, or volume savings.

The following factors mainly determine the choice among the three types of compact heat exchangers:

1. Operating pressure and temperature
2. Phases of the fluids dealt with
3. Fouling characteristics of the fluid
4. Allowable pressure drop
5. Strength and ruggedness
6. Restrictions on size and/or weight
7. Acceptable intermixing of the fluids dealt with

4.1.3 TUBE-FIN HEAT EXCHANGERS

Tube-fin heat exchangers are widely used throughout the industry in a variety of applications. They are employed when one fluid stream is at a higher pressure and/or has a significantly higher heat transfer coefficient compared to the other fluid stream. For example, in a gas-to-liquid exchanger, the heat transfer coefficient on the liquid side is generally very high compared to the gas side. Fins are used on the gas side to increase surface area. In a tube-fin exchanger, round and rectangular tubes are most commonly used (although elliptical tubes are also used), and fins are employed either on the outside or on the inside, or on both sides of the tubes, depending upon the application. Fins on the outside of the tubes (Figure 4.1) may be categorized as follows:

1. Normal fins on individual tubes (Figure 4.1a), referred to as individually finned tubes.
2. Longitudinal fins on individual tubes (Figure 4.1b), which are generally used in condensing applications and for viscous fluids in double-pipe heat exchangers.
3. Flat or continuous (plain, wavy, or interrupted) external fins on an array of tubes (either circular or flat tube) as shown in Figure 4.1c,d. Since interrupted fins are more prone to fouling, many users prefer plain continuous fins in situations where fouling, particularly by fibrous matter, is a serious problem.

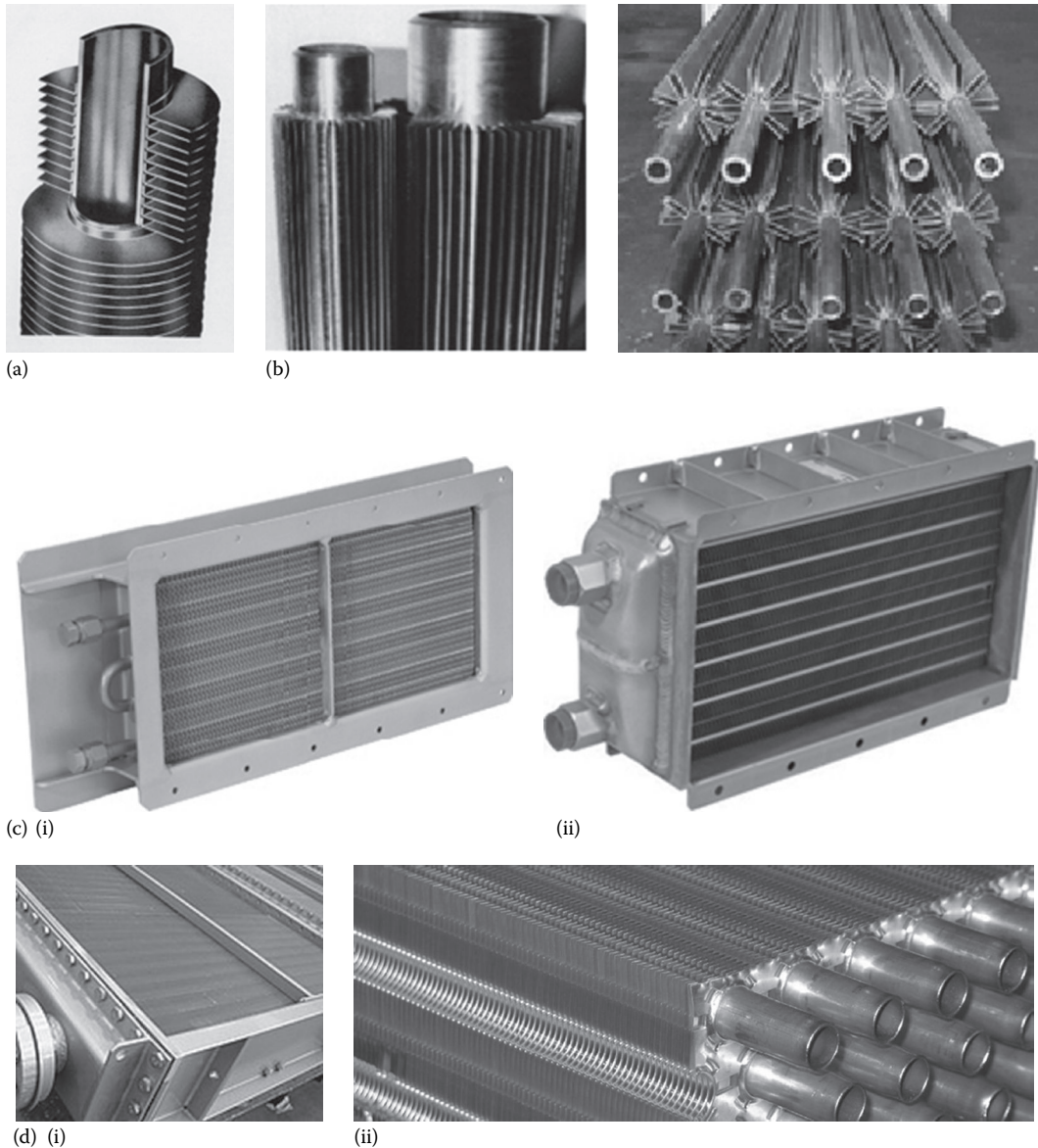


FIGURE 4.1 (a) Aluminum L foot tube fin and (b) welded longitudinal fin. (Courtesy of Vulcan Finned Tubes, Tomball, TX.) (c) *Continuous finned* tube heat exchanger—(i) cupronickel tube-fin heat exchanger and (ii) flat-tube heat exchanger to cool hydraulics (ALEX Core). (Courtesy of Lytron Inc., Woburn, MA.) (d) Continuous finned compact cooler. (Courtesy of GEA Heat Exchangers, Catoosa, OK.)

4.1.3.1 Specific Qualitative Considerations for Tube-Fin Surfaces

Specific qualitative considerations for the tube-fin surfaces include the following:

- Tube-fin exchangers usually have lower compactness than plate-fin units.
- A tube-fin exchanger may be designed for a wide range of tube fluid operating pressures, with the other fluid being at low pressure.
- Reasonable fouling can be tolerated on the tubeside if the tubes can be cleaned.

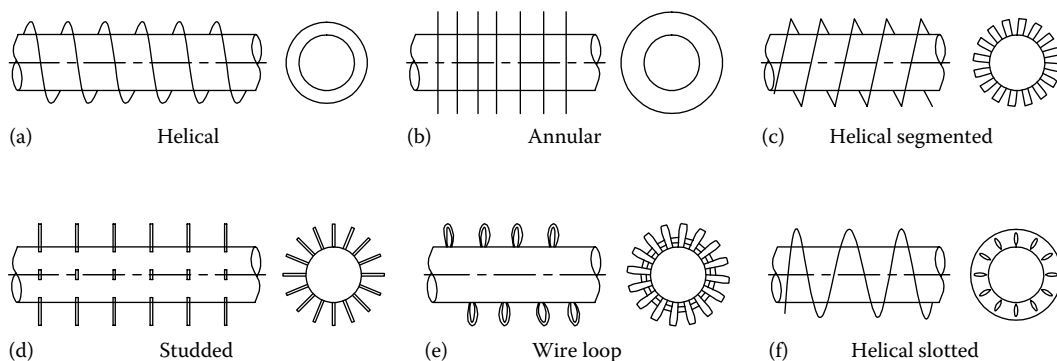


FIGURE 4.2 Forms of individually finned tubes. (a) Helical, (b) annular, (c) helical segmented, (d) studded, (e) wire loop, and (f) helical slotted.

4.1.3.2 Applications

Tube-fin exchangers are extensively used as condensers and evaporators in air-conditioning and refrigeration applications, for cooling of water or oil of vehicular or stationary internal combustion engines, and as air-cooled exchangers in the process and power industries. The usual arrangement is that water, oil, or refrigerant flows in the tubes, while air flows across the finned tubes.

4.1.3.3 Individually Finned Tubes

Individually finned tube geometry is much more rugged than the continuous fin geometry, but has lower compactness. The most common individual finned tubes are with plain circular, helical, or annular enhanced fin geometries like segmented, studded, slotted, or wire-loop fins [5]. Figure 4.2 shows some of the fin geometries (schematic) that have been used on circular tubes (few of these geometries are discussed as heat transfer enhancement fins in Chapter 8), Figure 4.3 shows photos of fin-tube geometries, and Figure 4.4 shows circular fin-tube geometrical parameters. Fins are attached to the tubes by a tight mechanical fit, tension winding, adhesive bonding, soldering, brazing, welding, or extrusion or sleeving a liner containing extruded fins on a base metal. Figure 4.5 shows common circular tube-fin classification and manufacturing techniques. Details of various fin geometries are discussed next.

4.1.3.3.1 Plain Circular Fins

Plain circular fins are the simplest and most common. They are manufactured by tension wrapping the fin strip around a tube, forming a continuous helical fin, or by mounting circular fin disks on the tube. Helically wrapped and extruded fins on circular tubes are frequently used in the process industries and in heat recovery applications. Classification of plain circular fin tubes in terms of fin height is discussed next.

4.1.3.3.2 Fin Height and Classification of Finned Tubes

Fin height and classification of finned tubes are discussed by Wen-Jei Yan [6]. According to fin height, the finned tubes are called low-fin tubes, medium-fin tubes, and high-fin tubes as follows:

1. In low-fin tubes, fins are extruded from the tube material with fin heights on the order of 1–2 mm. Fins of nominal 1.6 mm (1/16 in.) height have become standard for the low-fin type of duty usually required in shell and tube exchangers. Low-fin tubes are generally manufactured by raising the fin from base tube metal by a fabrication operation (possibly by an extrusion process). Integral fining ensures the maximum thermal efficiency of the tube since there is no possibility of fins becoming loose (and hence increase in thermal contact resistance) due to corrosion, thermal expansion and contraction, or by mechanical damage in handling.

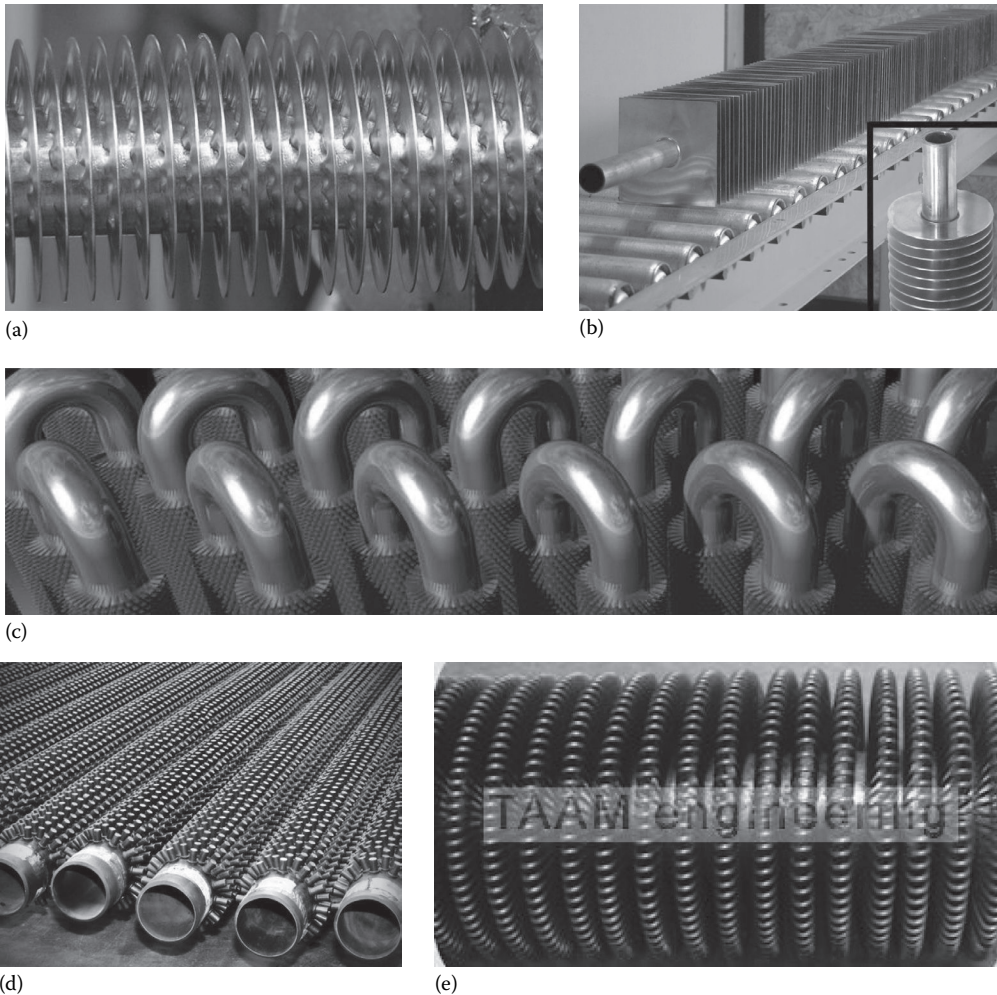


FIGURE 4.3 (a) Helical spiral wound crimped finned tube. (b) Annular fin or stamped fin tube. (a and b Courtesy of Fin Tube Products, Inc., Wadsworth, OH.) (c) TURB-XHF (serrated or segmented fin). (d) Stud welded tube. (c and d Courtesy of Fin Tube, LLC, Tulsa, OK; www.fintubellc.com) (e) Wire loop fin tube. (TAAM Engineering, Maharashtra, India.)

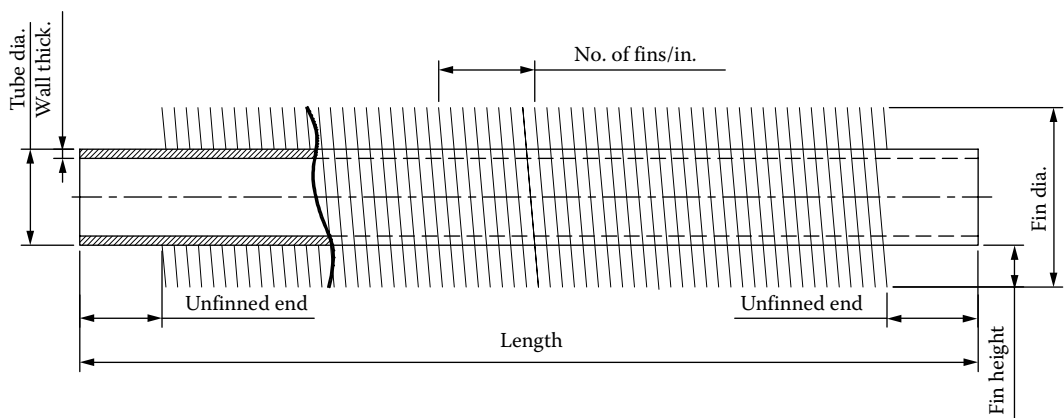


FIGURE 4.4 Individually finned tube details.

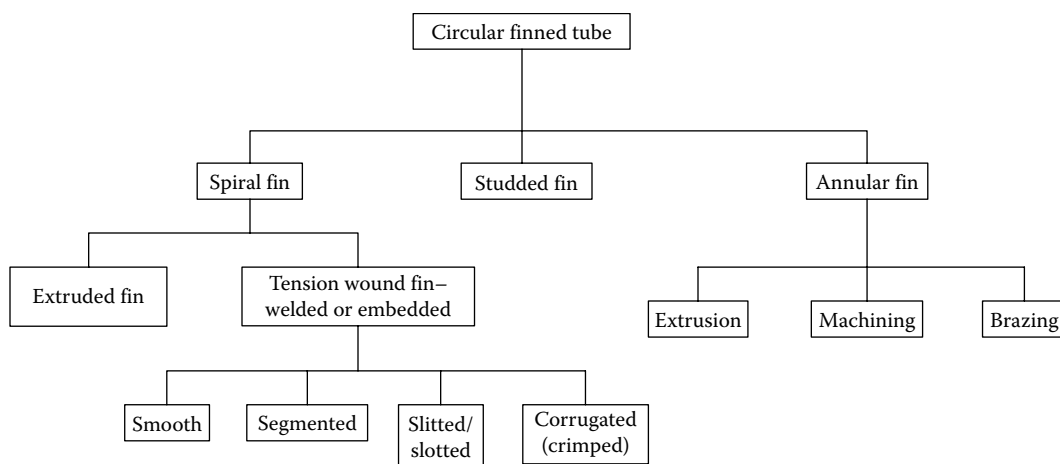


FIGURE 4.5 Tube-fin classification.

2. Fins of approximately 3.2 mm (1/8 in.) are referred to as medium fins and are usually employed in shell and tube exchangers.
3. Air-cooled exchangers require high fins, which have the height of 6.4–25 mm (1/4–1.0 in.). Heat recovery systems prefer medium to high fins in tube banks of inline arrangement.

However, Rabas and Taborek [7] classify low-fin tubes as having a fin height less than 6.35 mm (0.25 in.). The major reasons for using low-finned tubes in various types of heat exchangers are [7] as follows:

1. To balance heat transfer resistance
2. To maintain fin bond integrity
3. To reduce fouling
4. To satisfy the tube material specification

4.1.3.3.3 Enhanced Fin Geometries

Segmented or spine fins: Segmented or spine fins are made by helically winding a continuous strip of metal that has been partially cut into narrow sections. Upon winding, the narrow sections separate and form the narrow strip fins that are connected at the base.

Studded fins: A studded fin is similar to the segmented fin, but individual studs are welded to the tubes.

Slotted fins: Slotted fins have slots in the radial direction; when radially slitted material is wound on a tube, the slits open.

Wire loops around the tube: The wire loops are held in the tube by a tensioned wire within the helix or by soldering. The enhancement characteristic of small-diameter wires is important at low flows where the enhancement of other interrupted fins diminishes.

All of these geometries provide enhancement by the periodic development of thin boundary layers on small-diameter wires or flat strips, followed by their dissipation in the wake region between elements [8].

4.1.3.3.4 Construction Materials

The materials to be used for the tubes, headers, and water tanks depend on the specific requirements of the application. The most common materials for tubes and fins are copper, aluminum, and steel.

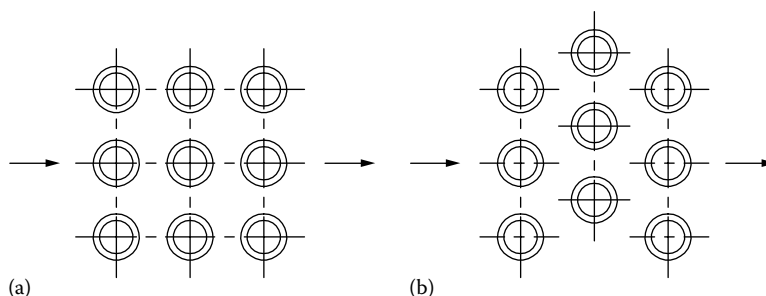


FIGURE 4.6 Tube-fin layout: (a) inline and (b) staggered.

For open-circuit installations, the tubes are made from copper, phosphorus-deoxidized copper, aluminum, brass, and copper–nickel–iron alloys, that is, cupronickels, and carbon steel for heat recovery applications. Fins are mostly from aluminum and copper; for heat recovery applications they are made from carbon steel. Headers and tube plates are made of carbon steel.

4.1.3.3.5 Tube Layout

The two basic arrangements of the tubes in a tube bank are staggered and inline. These arrangements are shown in Figure 4.6. The only construction difference between these two is that in the staggered arrangement each alternate row is shifted half a transverse pitch, and the two arrangements differ in flow dynamics. Due to compactness and higher heat transfer, the staggered layouts are mostly used. However, if the air stream is laden with dust, abrasive particles, etc., inline layout is preferred, being less affected and having ease of cleaning.

4.1.4 CONTINUOUS FINS ON A TUBE ARRAY

This type of tube-fin geometry is most commonly used in (1) air-conditioning and refrigeration exchangers known as coils, in which high-pressure refrigerant is contained on the tubeside, (2) as radiators for internal combustion engines, and (3) for charge air coolers and intercoolers for cooling supercharged engine intake air of diesel locomotives, etc. The tube layout pattern is mostly staggered.

4.1.4.1 Tube: Primary Surface

All tubes feature seamless tubes supplied to ASTM/ASME specifications. Return bends can be supplied of heavier wall tubing to ensure adequately formed thickness in applications where erosion is a concern. Round or flat tubes (rectangular tubes with rounded corners) usually with a staggered tube arrangement are used. Elliptical tubes are also being used. Round tubes are used for high-pressure applications and also when considerable fouling is anticipated. The use of flat tubes is limited to low-pressure applications, such as vehicular radiators. Flat or elliptical tubes, instead of round tubes, are used for increased heat transfer in the tube and reduced pressure drop outside the tubes [2,9]. High-parasitic-form drag is associated with flow normal to the round tubes. In contrast, the flat tubes yield lower pressure loss for flow normal to the tubes due to lower form drag and avoid the low-performance wake region behind the tubes.

4.1.4.2 Fin: Secondary Surface

All coils or continuous fin exchangers feature die formed, flat or patterned plate-fins of either aluminum or copper. The fins are attached to the tubes by mechanical expansion of the tube, ensuring

a permanent fin-to-tube bond. Full fin collars allow for both precise fin spacing and maximum fin-to-tube contact. Fin pattern is optimized to produce highly energy efficient operation, resistance to airflow and cleanability.

Flat fin: Flat fin has no corrugation, which provides the lowest possible air pressure drop and lowest fan horsepower.

Star fin: Star fin pattern corrugation around the tubes provides higher heat transfer than the flat fin with a slight increase in air pressure drop.

Wavy fin: Wave fin corrugation across the fin provides the maximum heat transfer rate for a given surface area.

Louvered fin: Heat exchangers with flat tubes and louver fins are widely used due to higher heat transfer and reduced size.

4.1.4.3 Headers

Coils feature either steel or nonferrous manifold headers with threaded pipe connections. Cooling coils are supplied with vents and drains. Header tube holes are drilled. Headers provide proper joint clearances and to allow optimum braze metal application. Coils have steel or copper tubesheets and removable steel headers with threaded connections. Header thickness, gasket surface area, and bolt area are designed and tested to provide a leak tight gasket seal.

4.1.4.4 Tube-to-Header Joints

Tube-to-header joints are either roller-expanded or brazed or soldered.

4.1.4.5 Casings or Tube Frame

The coil incorporates a heavy-duty rectangular structural tube frame, which improves rigidity, squareness, and long-term stability and double flanged for coil stacking. Coil casings are either galvanized or stainless steel. Casing supports are provided on various centers for extra support during handling. Coil casings are furnished without mounting holes unless required.

4.1.4.6 Circuiting

Each coil is individually circuited for specific applications in recirculated, flooded, direct expansion, or control pressure receiver refrigeration systems along with water, glycols, or brines.

4.1.4.7 Exchangers for Air Conditioning and Refrigeration

Evaporators and condensers for air conditioning and refrigeration are usually the tube-fin type when air is one of the fluids. These exchangers are referred to as coils (Figure 4.7) when air is one of the

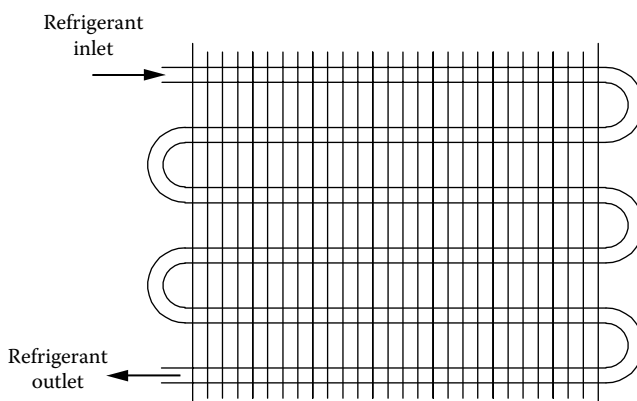


FIGURE 4.7 Heating/cooling coils—schematic.

fluids. Tube-fin geometry is becoming widespread in the current energy conservation era, because the bond between the fin and tube is made by mechanically or hydraulically expanding the tube against the fin, instead of employing welding, brazing, or soldering [2]. Formation of a mechanical bond requires very little energy compared to the energy required to solder, braze, or weld the fin to the tube. Because of the mechanical bond, the operating temperature is limited.

To specify a continuous fin-tube heat exchanger or coil, the following parameters are required:

1. Coil type
2. Fin details
 - a. Fins per inch (fpi)
 - b. Material—aluminum, copper, stainless steel, carbon steel
 - c. Fin size
 - d. Fin pattern/type—flat, star, wavy, louvered
3. Rows
4. Header material (copper, brass, carbon steel or stainless steel)
5. Tube material and tube wall thickness
6. Casing material, either galvanized steel or stainless steel (also specify if mounting holes are required)
7. Connection type (MPT, Butt Weld, or Flanged) (also specify if top or bottom supply)
8. Horizontal or vertical airflow

Tube-fin details for air-conditioning and refrigeration applications are furnished by Shah [2]: Evaporator coils for small-capacity systems (less than 20 tons) use 7.9, 9.5, and 12.7 mm (5/16, 3/8, and 1/2 in.) tubes and fin densities in the range of 315–551 fins/m (8–14 fins/in.). For refrigeration applications, lower fin densities (157–315 fins/m or 4–8 fins/in.) are used due to the possibility of frosting and blockage. For condenser coils, tube diameters used are 7.9, 9.5, and 12.7 mm (5/16, 3/8, and 1/2 in.), and fin densities range from 394 to 787 fins/m (10–20 fins/in.) and fin thickness from 0.09 to 0.25 mm (0.0035–0.10 in.).

4.1.4.8 Radiators

Radiators are compact liquid-to-air heat exchangers widely used in automotive vehicles. Major construction types used for radiators include (1) soldered design with flat brass tubes with flat plain or louvered copper fins—tubes and header sheets are made from brass and the water tank from brass or plastics—and (2) brazed aluminum design with flat tube and corrugated fins, usually louvered fins or flat tube continuous fins. These construction types are shown in Figure 4.8. Louvered cores are preferred as they allow a lower fin density than a nonlouvered core of the same area for the same thermal performance. The soldered brass tubes and copper fins were primarily used before the 1980s. Because of lightweight and significantly better durability and operating life, brazed aluminum tubes and aluminum corrugated multilouver fin radiators have almost replaced the copper-brass radiators [2]. Typical fin density ranges from 400 to 1000 fins/m (10–25 fins/in.), and the surface area density (β) ranges from 900 to 1650 m²/m³ (275–500 ft²/ft³).

4.1.4.9 Effect of Fin Density on Fouling

A major question in the choice of detailed dimensions for a core is the appropriate fin spacing. As the number of fins per inch (or per meter) is increased, the unit can be made progressively more compact. At the same time, it becomes more sensitive to clogging by dirt, soot, airborne dirt, insects, and the like, and more sensitive to nonuniformity in the fin spacing. In practice, it has been found that for most automotive applications, radiators can have 10–12 fins/in. Fourteen fins per inch can be fabricated with little increase in cost per unit surface area, and this closer fin spacing may be justified for installations where space is a constraint and fouling of the surfaces is not a problem [9].

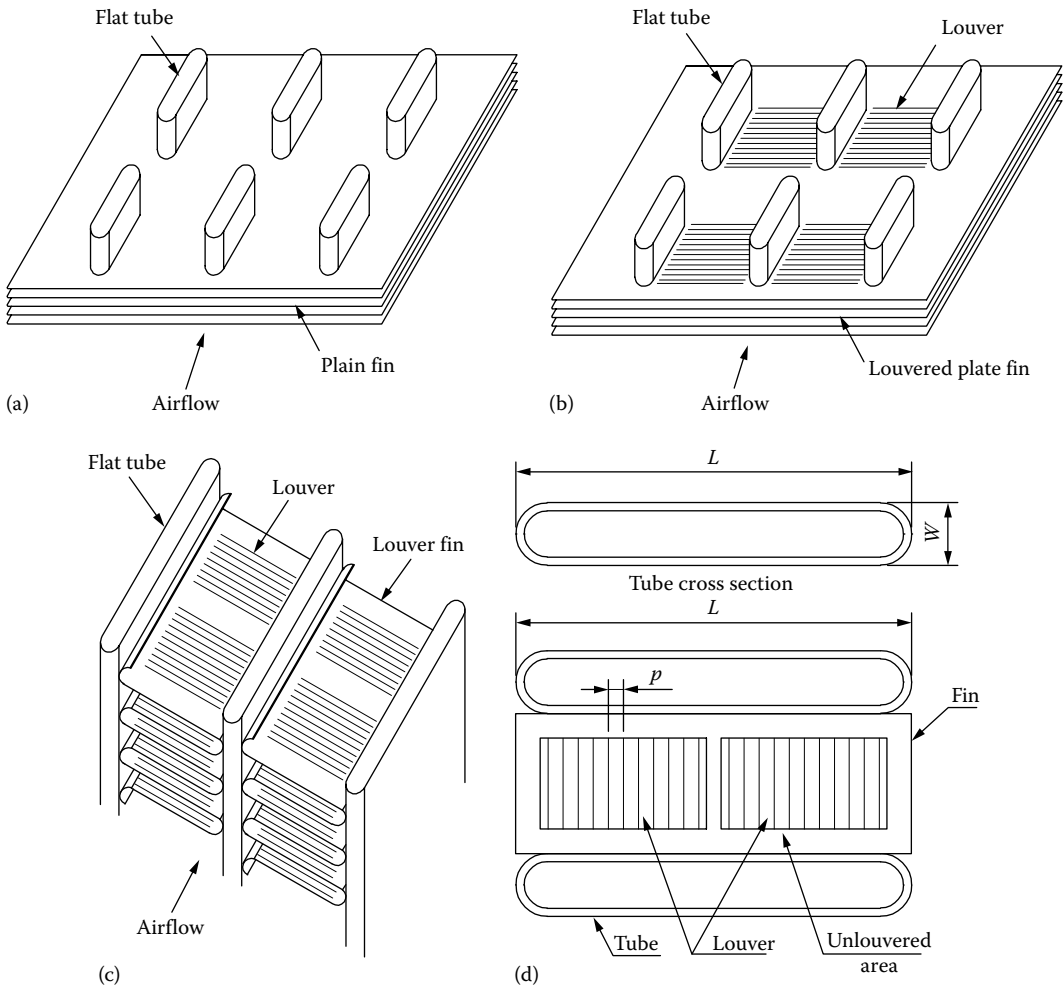


FIGURE 4.8 Tube-fin details of radiator: (a) continuous plain fin-flat tube radiator, (b) continuous louvered fin-flat tube design, (c) single flat tube row louvered fin radiator design, and (d) tube-fin details.

4.1.4.10 One-Row Radiator

In conventional multirow radiators, the fin array is not in contact with the tubes over the full fin depth. The region of no contact occurs between the tube rows and is illustrated in Figure 4.9. This hinders heat conduction from the tubes to the fin region between the tube rows. If the fins are louvered in this region, the conduction path is further impaired. Hence the thermal performance per unit fin depth is low compared to the fin region in contact with the tubes. Remedies for this problem are as follows [10]:

1. Use a one-row core (Figure 4.10) in place of the multirow design. This design eliminates the low-performance fin area between tube rows, and offers either material savings and lower air pressure drop, or increased thermal performance. In the United States, manufacturers usually make 19.1 mm (3/4 in.) tubes in 0.152 mm (0.006 in.) thick brass. To prevent the tube wall from becoming concave during core assembly, heavier wall thickness is usually adopted. Another method followed to prevent the tube wall from becoming concave during assembly is to use cross-ribbed turbulator tubes. The indented cross ribs increase the cross-sectional moment of inertia of the tube wall, increasing its stiffness. The indentations in the wall of turbulator tubes may be beneficial for low-flow-rate applications, where

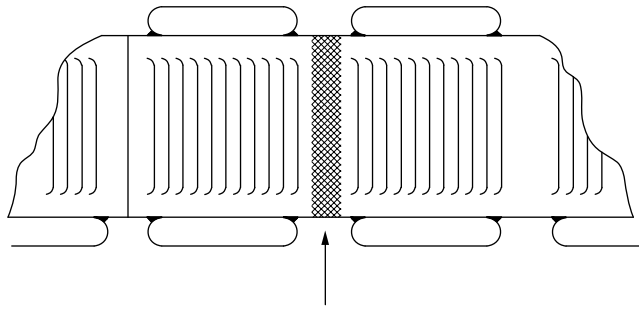


FIGURE 4.9 Region of no contact between flat tube rows of a radiator.

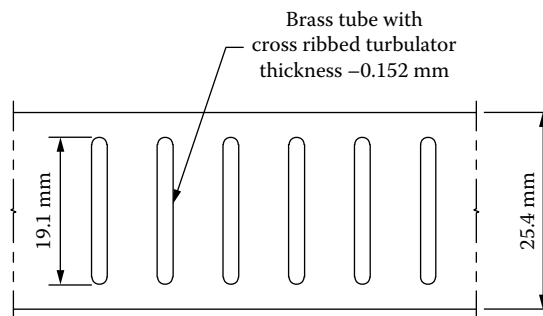


FIGURE 4.10 Single tube row radiator design.

the flow may be laminar. For turbulent flow, the increase in coolant-side heat transfer coefficient will be marginal, because the dominant thermal resistance is typically on the airside, and the ribs or indentations produce large increase in pressure drop.

2. An alternative method of eliminating the ineffective fin area is to eliminate the space between the tube rows. In other words, have the tubes touching in the axial direction. This is referred to as the “tubes-touching” design. To achieve tubes-touching design, the ends of the tubes must be shaped to provide the requirement of minimum ligament between the tubes in the header plate. For the same fin depth in the airflow direction, the tubes-touching design should provide the same thermal performance as a one-row design.

4.1.4.11 Manufacture of Continuous Finned Tube Heat Exchangers

The manufacturing procedure for continuous finned tube heat exchanger is discussed next. Detailed manufacturing practices are further described in the chapter on Heat Exchanger Fabrication: Brazing and Soldering.

Mechanically bonded core: In a rounded hole design, the flat fins are formed with holes larger than the tubes to be inserted. Tubes are assembled in a fixture and fins are inserted. The fin gap (i.e., the fin density) is controlled by the ferrule height (Figure 4.11). After assembly, the tubes are

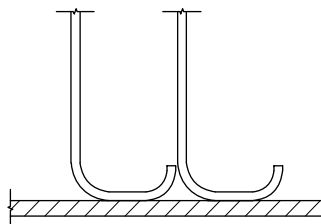


FIGURE 4.11 Ferrule height of a tube-fin heat exchanger.

expanded so that metal-to-metal contact is being achieved. The tube ends are generally expanded into the header plates. Sometimes, on thinner tube plates, the tubes are brazed. The tubes, fins, and headers together form the core, which is then attached to the side sheet assembly and the header for the tubeside fluid or water tank, as the case may be, and tightly sealed with gaskets.

Soldered core: In a soldered design, which is mostly followed for flat tube-fin exchangers, the radiator cores are built from tinned brass tubes and copper fin sheets. The fins are punched with holes slightly larger than the tube dimension, and tubes are inserted through the holes. The tube outer surfaces and fin surfaces are solder coated for achieving bonding. After the header plates are assembled, the core is baked in an oven. During baking the solder metal on the tube outer surface and on the fin surface melts and give perfect metal-to-metal contact. Alternately, a fluxed core assembly is dip soldered.

4.1.5 SURFACE SELECTION

Various surfaces are being used in compact heat exchanger applications. A proper selection of a surface is one of the most important considerations in compact heat exchanger design. The selection criteria for these surfaces are dependent upon (1) the qualitative and (2) the quantitative considerations [11].

4.1.5.1 Qualitative Considerations

The qualitative considerations include the following:

1. Heat transfer requirements
2. Operating temperature and pressure
3. Flow resistance
4. Size or compactness and weight
5. Mechanical integrity
6. Fouling characteristics
7. Availability of surfaces, manufacturing considerations
8. Low capital cost, and low operating cost, especially low pumping cost
9. Designer's experience and judgment
10. Maintenance requirements, reliability, and safety

Heat transfer requirements with low flow resistance to minimize the pumping cost and a compact, low-weight unit are the important criteria for selecting a surface for a compact heat exchanger. These aspects are common for all types of heat exchangers and have been covered earlier. Surface selection influenced by fouling, manufacturing considerations, and cost are discussed next with additional details.

Fouling of compact exchangers: Fouling is one of the major problems in compact heat exchangers, particularly with various fin geometries and fine flow passages that cannot be cleaned mechanically. Hence, compact heat exchangers may not be applicable in highly fouling applications. There is a belief and some evidence that integral and low-finned tubes foul either at essentially the same rate or in some cases at a lower rate than plain tubes and also they are easier to clean the most types of fouling [7]. Other than low-finned tubes, if fouling is a problem, with the understanding of the problem and applying innovative means to prevent/minimize fouling, compact heat exchangers may be used in at least low to moderate fouling applications. Methods to reduce fouling are discussed in Chapter 9.

Manufacturing considerations: Most of the heat exchanger manufacturing industries make only a limited number of surfaces due to limited availability of tools and to market potential. Select a surface that a company can manufacture, even though theory and analysis can be used to arrive at some high-performance surfaces that may pose problems to manufacture.

Cost: Cost is one of the most important factors in the selection of surfaces, such that the overall heat exchanger is least expensive either in initial cost or in both initial and operating costs. If a plain fin surface can do the job for an application, a plain surface is preferable to expensive complicated surface geometries.

4.1.5.2 Quantitative Considerations

The quantitative considerations include performance comparison of surfaces with some simple “yardsticks.” Surface selection by a quantitative method is made by comparing performance of various heat exchanger surfaces and choosing the best under some specified criteria for a given heat exchanger application. Shah [11] categorizes the surface selection method as follows:

1. Comparisons based on j and f factors
2. Comparison of heat transfer as a function of fluid pumping power
3. Miscellaneous direct comparison methods
4. Performance comparisons with a reference surface

These methods are discussed in Chapter 8.

4.2 PLATE-FIN HEAT EXCHANGERS

Two important sources on PFHE and brazed aluminum plate-fin heat exchanger are ALPEMA Standard [12] and *The Plate-Fin Heat Exchangers Guide to Their Specification and Use* [13]. The definition for PFHE given in Ref. [13] is as follows: Plate-fin heat exchangers (PFHE) are a form of compact heat exchanger consisting of a stack of alternate flat plates called “parting sheets” and fin corrugations, brazed together as a block. The basic elements of PFHE, two types of crossflow arrangements are shown in Figure 4.12 and counterflow arrangement is shown in Figure 4.13. Fluid streams flow along the passages made by the corrugations between the parting sheets.

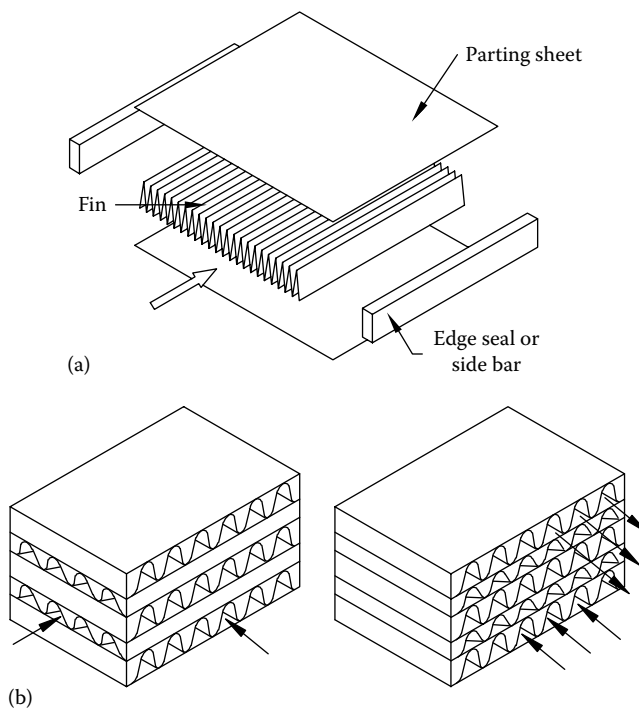


FIGURE 4.12 Plate-fin heat exchanger: (a) basic elements, (b) two types of flow arrangements.

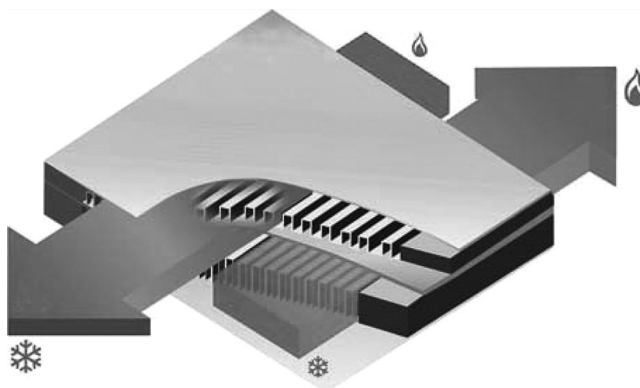


FIGURE 4.13 Counterflow plate-fin heat exchanger—schematic. (Photo courtesy of Fives Cryo, Golbey, France.)

The corrugations serve as both secondary heat transfer surfaces and mechanical supports for the internal pressures between layers. In liquid or phase-change (to gas) applications, the parting sheets may be replaced by flat tubes on the liquid or phase-change side. Further, PFHEs are widely used in various industrial applications because of their compactness. For many years, PFHEs have been widely used for gas separation in cryogenic applications and for aircraft cooling duties. In aerospace applications weight saving is of paramount importance. In the following sections, first the salient features of PFHE are covered followed by specific features of brazed aluminum PFHEs as per ALPEMA Standard [12].

4.2.1 PFHE: ESSENTIAL FEATURES

Salient features of PFHE as discussed by Shah include the following [1,2]:

1. Plate-fin surfaces are commonly used in gas-to-gas exchanger applications. They offer high area densities (up to about $6000 \text{ m}^2/\text{m}^3$ or $1800 \text{ ft}^2/\text{ft}^3$).
2. The passage height on each side could be easily varied. Different fins (such as [a] rectangular or triangular fin either plain or with louver or perforation, [b] offset strip fin (OSF), and [c] wavy fin) can be used between plates for different applications.
3. Plate-fin exchangers are generally designed for low-pressure applications, which operating pressures limited to about 1000 kPag (150 psig).
4. The maximum operating temperatures are limited by the type of fin-to-plate bonding and the materials employed. Plate-fin exchangers have been designed from low cryogenic operating temperatures (all-aluminum PFHE) to about 800°C (1500°F) (made of heat-resistant alloys).
5. Fluid contamination (mixing) is generally not a problem since there is practically zero fluid leakage from one side to the other of the exchanger.

4.2.2 APPLICATION FOR FOULING SERVICE

The PFHE is limited in application to relatively clean streams because of its small flow passages. It is generally not designed for applications involving heavy fouling since there is no easy method of cleaning the exchanger. If there is a risk of fouling, use wavy fins and avoid serrated fins. Upstream strainers should be employed where there is any doubt about solids in the feed. Measures to overcome fouling problems with PFHE are described by Shah [2].

4.2.3 SIZE

Maximum size is limited by the brazing furnace dimensions, and by the furnace lifting capacity. The heating characteristics of denser blocks also impose limitations on the maximum size which can be brazed. Typical maximum dimensions for low-pressure aluminum PFHEs are 1.2 m × 1.2 m in cross section × 6.2 m along the direction of flow [1,2,13], and 1.0 m × 1.0 m × 1.5 m for nonaluminum PFHEs [13]. Higher pressure units, being heavier per volume, make both handling and brazing more difficult, thus reducing the economic maximum size. Duties that call for larger units are met by welding together several blocks, or by manifolding pipework.

4.2.4 ADVANTAGES OF PFHEs

The principal advantages of PFHEs over other forms of heat exchangers are summarized in Ref. [13] and include the following:

1. Plate-fin heat exchangers, in general, are superior in thermal performance to those of the other type of heat exchangers employing extended surfaces.
2. PFHE can achieve temperature approaches as low as 1°C between single-phase streams and 3°C between multiphase streams. Typically, overall mean temperature differences of 3°C–6°C are employed in aluminum PFHE applications [13].
3. With their high surface compactness, ability to handle multiple streams, and with aluminum's highly desirable low temperature properties, brazed aluminum plate-fins are an obvious choice for cryogenic applications.
4. Very high thermal effectiveness can be achieved; for cryogenic applications, effectiveness of the order of 95% and above is common.
5. Provided the streams are reasonably clean, PFHEs can be used to exchange heat in most processes, for the wide range of stream compositions and pressure/temperature envelopes [13].
6. Large heat transfer surface per unit volume is possible.
7. Low weight per unit heat transfer.
8. Possibility of heat exchange between many process streams.
9. Provided correct materials are selected, the PFHE can be specified for temperatures ranging from near absolute zero to more than 800°C, and for pressures up to at least 140 bar [1]. According to Shah [1], usually PFHEs do not involve both high temperature and high pressure together.
10. PFHE offers about 25 times more surface area per equipment weight than the shell and tube heat exchanger [13].

4.2.5 LIMITATIONS OF PFHEs

Limitations other than fouling and size include the following [1]:

1. With a high-effectiveness heat exchanger and/or large frontal area, flow maldistribution becomes important.
2. Due to short transient times, a careful design of controls is required for startup compared with shell and tube exchangers.
3. Flow oscillations could be a problem.

4.2.6 APPLICATIONS

Current areas of application include [13] the following:

1. Cryogenics/air separation
2. Petrochemical production

3. Syngas production
4. Aerospace
5. Land transport (automotive, locomotive)
6. Oil and natural gas processing

PFHEs are used in all modes of heat duty, including [13] the following:

1. Heat exchange between gases, liquids, or both
2. Condensing
3. Boiling
4. Sublimation (“reversing” heat exchangers)
5. Heat or cold storage

4.2.7 ECONOMICS

The PFHE is not necessarily cheaper for a given heat duty than other forms of heat exchangers, because the method used for constructing PFHEs is complex and energy-intensive [13].

4.2.8 FLOW ARRANGEMENTS

The fins on each side can be easily arranged such that overall flow arrangement of the two fluids can result in crossflow, counterflow, cross-counterflow, or parallelflow, though parallelflow is mostly not used. Properly designed, the PFHE can be made to exchange heat in perfect counterflow, which permits PFHEs to satisfy duties requiring a high thermal effectiveness. The construction of a multifluid plate-fin exchanger is relatively straightforward except for the inlet and outlet headers for each fluid. Some of the possible flow arrangements are shown in Figure 4.14.

4.2.9 FIN GEOMETRY SELECTION AND PERFORMANCE FACTORS

Plate-fin surfaces have plain triangular, plain rectangular, wavy, offset strip, louver, perforated, or pin fin geometries. These fin geometries are shown in Figure 4.15 [8]. PFHEs are superior to tube-fin heat exchangers from heat transfer and pressure-drop points of view for the given total packaging space. Fin density varies from 120 to 700 fins/m (3–18 fins/in.), thickness from 0.05 to 0.25 mm (0.002–0.01 in.), and fin heights may range from 2 to 25 mm (0.08–1.0 in.) [2].

4.2.9.1 Plain Fin

Plain fin corrugation is the simplest type of fining. These surfaces are straight fins that are uninterrupted (uncut) in the fluid flow direction. Triangular and rectangular passages are more common. The triangular fin is generally not structurally as strong as the rectangular fin for the same passage size and fin thickness. When the fins are straight along the flow length, the boundary layers tend to be thick resulting in lower values of the heat transfer coefficient. When they are wavy or off-set strip fin along the flow length, the boundary layers are thinner or the growth of boundary layers is disrupted periodically, respectively, resulting in a higher heat transfer coefficient.

Plain fin surfaces have pressure-drop and heat transfer characteristics similar to flow through small-bore tubes, i.e., relatively low pressure drop and heat transfer, but a high ratio of heat transfer to pressure drop [13]. For a flow channel with rectangular or triangular cross section, under turbulent flow conditions, standard equations for turbulent flow in circular tubes may be used to calculate j and f , provided the Reynolds number (Re) is based on the hydraulic diameter, D_h . If the Re based on hydraulic diameter is less than 2000, one may use theoretical laminar flow solutions for j and f .

Plain fins are preferred for very low Reynolds number applications and in applications where the pressure drop is very critical. Condensing duties require minimal pressure drop or else the

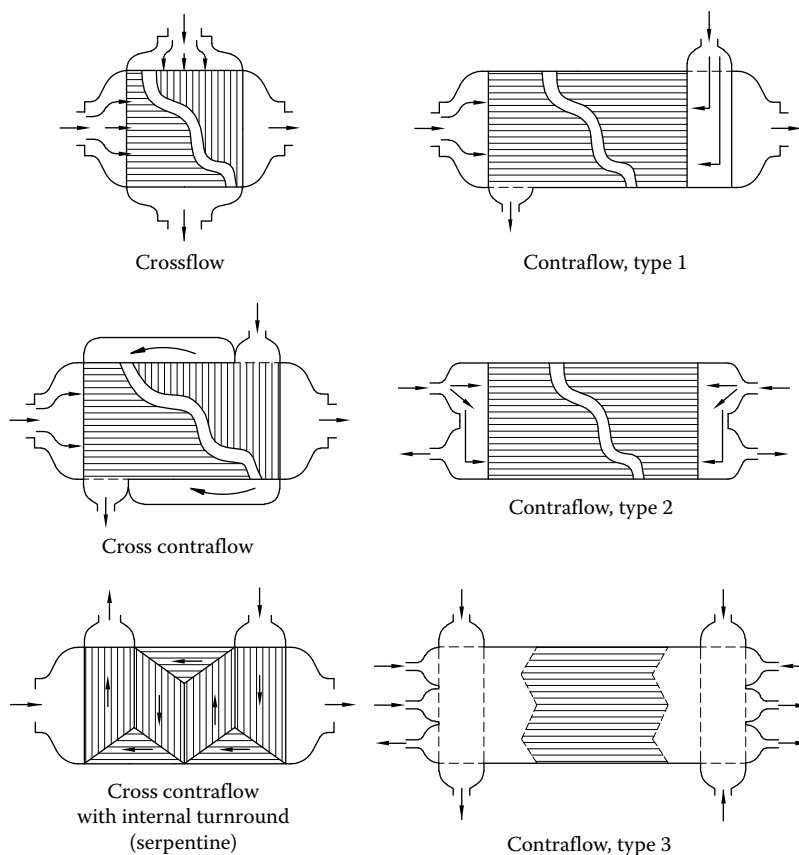


FIGURE 4.14 Fluid flow arrangement through PFHE. (Note: contraflow is to be read as counterflow). (Courtesy of Chart Industries Inc., Garfield Heights, OH.)

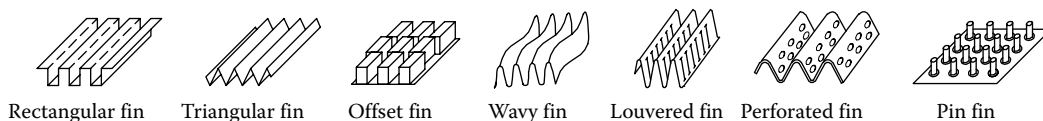


FIGURE 4.15 PFHE fin geometries.

heat release curve can significantly alter and the overall duty may not be met. Therefore, for condensation, plain fins are normally specified.

4.2.9.2 Plain-Perforated Fin

Perforated fins have either round or rectangular perforations, having the size and longitudinal and transverse spacings as major perforation variables. The flow passages are either triangular or rectangular. A metal strip is first perforated, then corrugated. Perforated areas vary from about 5% to 25% of the sheet area [13]. When the corrugations are laid across the flow, the stream is forced to pass through these small holes. Salient performance features include:

1. The perforated holes promote turbulence, which increases the local heat transfer coefficient compared to plain fins, but as the percentage of perforated holes increase, the loss of heat transfer surface offsets this advantage [13].
2. The perforated surface is prone to flow-induced noise and vibration.

Applications: Perforated fins are now used in only a limited number of applications [14].

Typical applications include the following:

1. “Turbulators” in oil coolers.
2. In boiling applications to maintain a wetted surface and minimize depositions/concentrations [13]. Perforated corrugations permit interchannel fluid migration, which evens out surges and vibration and avoids localized concentrations or depositions.
3. Perforated fins were once used in two-phase cryogenic air separation exchangers, but now they have been replaced by OSFs.

Shah [15] provides a very detailed evaluation of the perforated fin geometries.

4.2.9.3 Offset Strip Fin

The offset strip fin (OSF) is the commonly used geometry in PFHEs. The fin has a rectangular cross section; it is cut into small strips of length l , and every alternate strip is offset by about 50% of the fin pitch in the transverse direction as schematically shown in Figure 4.16a. Fin spacing, fin height, fin thickness, and strip length in the flow direction are the major variables of OSFs.

OSF geometry is characterized by high heat transfer area per unit volume, and high heat transfer coefficients. The heat transfer mechanism in OSFs is described by Joshi and Webb [16] and is as follows. The heat transfer enhancement is obtained by periodic growth of laminar boundary layers on the fin length, and their dissipation in the fin wakes as shown in Figure 4.16b. This enhancement is accompanied by an increase in pressure drop because of increased friction factor. A form drag force, due to the finite thickness of the fins, also contributes to the pressure drop. Fluid interchange between channels is possible. OSFs are used in the

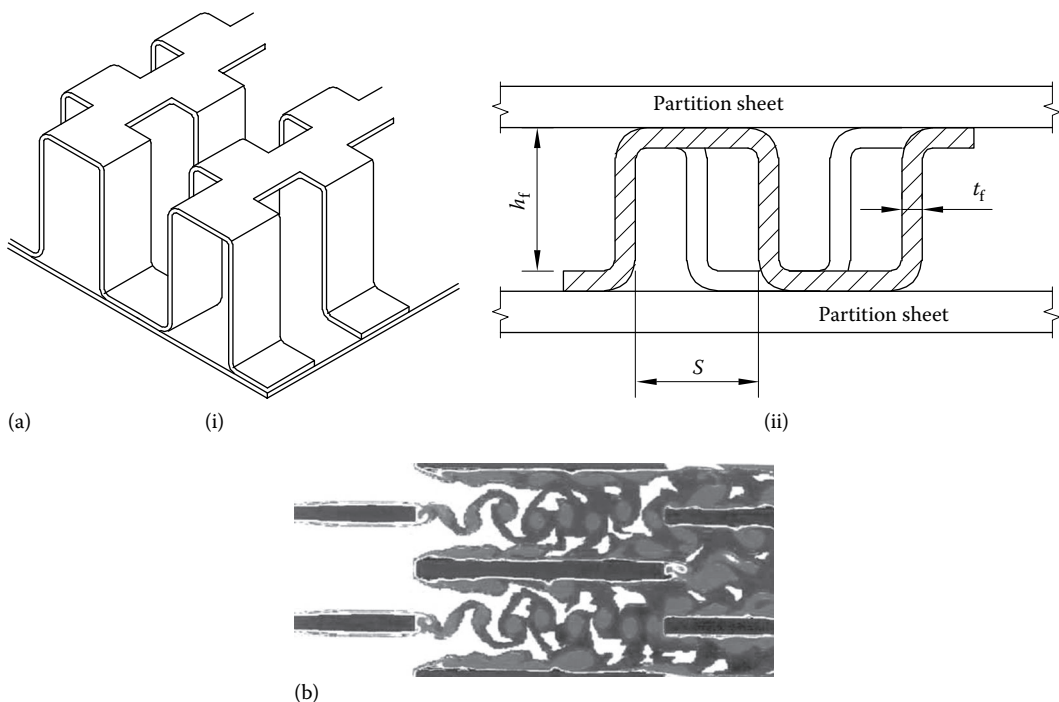


FIGURE 4.16 (a) Offset strip fin—schematic. (b) Flow past offset strip fin—formation of turbulence behind the fin. (Photo courtesy of Fives Cryo, Golbey, France.)

approximate Reynolds number range of 500–10,000 [14]. Salient features pertaining to thermal performance include the following [13]:

1. Commonly used in air separation plants where high thermal effectiveness at low mass velocities is required [13].
2. The heat transfer performance of OSFs is increased by a factor of about 1.5–4 over plain fins of similar geometry, but at the expense of higher pressure drop [14].
3. At high Reynolds numbers, the j factor decreases, while the friction factor remains constant because of the high form drag. Therefore, offset fins are used less frequently for very high Reynolds number applications.
4. They are used at low Reynolds number applications calling for accurate performance predictions, such as some aerospace applications; other fin performance data are not as repeatable.

4.2.9.4 Serrated Fins

It is similar to OSF. Serrated fin is formed by simultaneously folding and cutting alternative sections of fins (Figure 4.23a and 4.24d). These fins are also known as lanced fins.

4.2.9.5 Herringbone or Wavy Fin

Since wavy fins have noninterrupted walls in each flow channel, they are less likely to catch particulates and foul than are OSFs. Their performance is competitive with that of the OSF, but the friction factor continues to fall with increasing Reynolds numbers [13]. The waveform in the flow direction provides effective interruptions to flow and induces very complex flows. The augmentation is due to Goertler vortices, which form as the fluid passes over the concave wave surfaces. These are counterrotating vortices, which produce a corkscrew-like pattern and probable local flow separation that will occur on the downstream side of the convex surface [8,14]. In the low-turbulence regime (Re of about 6000–8000), the wall corrugations increase the heat transfer by about nearly three times compared with the smooth wall channel. Therefore, wavy fins are often a better choice at the higher Reynolds numbers typical of the hydrocarbon industry; the smooth surface allows the friction factor to fall with increasing Reynolds number. Kays and London [17] provide curves of j and f versus Reynolds number for two wavy-fin geometries.

4.2.9.6 Louver Fins

The louvers are essentially formed by cutting the sheet metal of the fin at intervals and by rotating the strips of metal thus formed out of the plane of the fin. Louvers can be made in many different geometries, some of which are shown in Figure 4.17. Note that the parallel louver fin and OSF both have small strips aligned parallel to the flow. The louvered fin geometry bears a similarity to the offset strip (Figure 4.16a). Rather than offsetting slit strips, the entire slit fin is rotated 20°–60° relative to the airflow direction. As such, they are similar in principle to the OSF. Louvered fins enhance heat transfer by providing multiple flat plate leading edges with their associated high values of heat transfer coefficient. Salient features of louver fins are as follows:

- The louvered fin strip length is usually longer than that of OSF, e.g., 6–18 mm, versus 3–9 mm for the OSF [8]; the louvered fin gage is generally thinner than that of an offset strip of the fin.
- The fin corrugations normally form a triangular passage. Hence, it is generally not as strong as an OSF, since the latter has a “large” flat area for brazing, thus providing strength [14].
- The louver fins may have a slightly higher potential of fouling compared to the OSFs [14].
- The louvered fin can provide heat transfer coefficients comparable to the OSF. However, the ratio of j/f tends to be lower because of the considerable form drag on the bent fins [8].

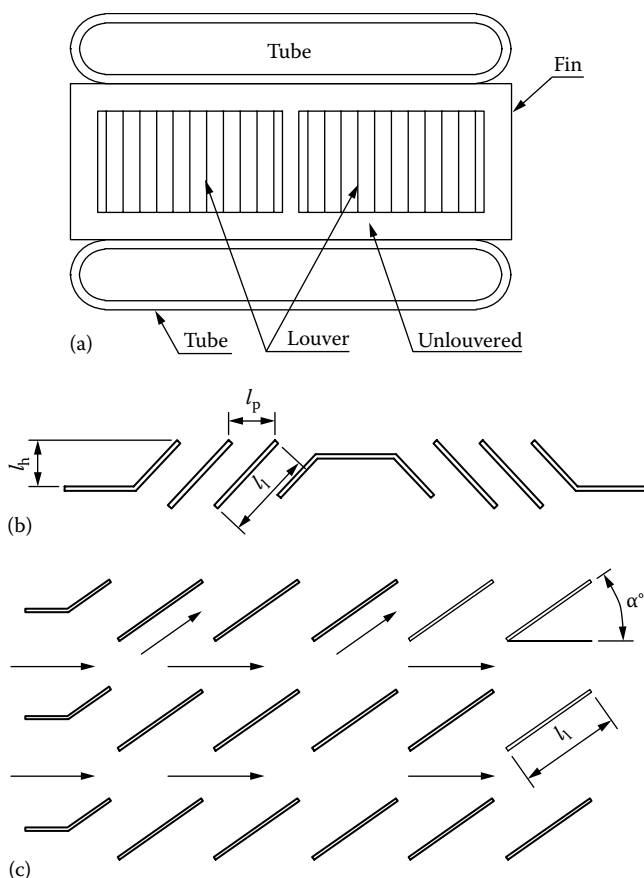


FIGURE 4.17 Louvered fin details. (a) Tube-louver fin arrangement, (b) louver fin geometry, and (c) fluid flow through louver. (Note: l_h is louver height, l_p is louver pitch, l_l is louver length and α is louver angle.)

- Louver fins can enhance heat transfer by a factor of two or three compared with the equivalent unlouvered surfaces [13].
- A wide range in performance can be achieved by varying the louver angle, louver width, and louver form.

The operating Reynolds number range is 100–5000, depending upon the type of louver geometry employed [14].

Applications: Their attractive thermal performance characteristics in terms of compactness, light weight, and low pumping power for a given heat transfer duty make louver fins a potential candidate for aerospace applications [18]. They are recognized as very effective heat transfer surfaces, leading to compact solutions to cooling problems. Louvered fin surfaces are now used widely for engine cooling equipment, air-conditioning heat exchangers (evaporators and condensers), and aircraft oil and air coolers. They share this quality with the OSF surfaces [19]. The louvered surface is the standard geometry for automotive radiators. For the same strip width, the louvered fin geometry provides heat transfer coefficients comparable to the OSF.

4.2.9.7 Pin Fins

An array of wall-attached cylinders (e.g., rods, wires) mounted perpendicular to the wall is known as pin fins. They can be manufactured at a very high speed continuously from a thin wire. After the wire is

formed into rectangular passages, the top and bottom horizontal wire portions are flattened for brazing or soldering with the plates. Pins can be of circular or elliptical shapes. The enhancement mechanism due to a pin array is the same as that of the OSF, namely, repeated boundary-layer growth and wake dissipation [8]. The potential application for pin fins is at very low Reynolds number ($Re < 500$) for which the pressure drop is of no major concern. Present applications for pin fins include [14] (1) electronic cooling devices with generally free convective flows over the pin fins and (2) to cool turbine blades.

Limitations of pin fins:

1. The surface compactness achieved by the pin fin geometry is much lower than that achieved by the strip fin or louver fin surfaces.
2. Due to vortex shedding behind the circular pins, noise and flow-induced vibrations can take place.

Table 4.1 shows commonly used plate-fin geometries and their relative merits.

4.2.9.8 FIN Corrugation Code

A commonly encountered code for fin corrugation is [13] 350S1808. The first three digits give the fin height in thousandths of an inch ($350 = 0.35$ in.). The letter gives the type of corrugation

TABLE 4.1
Commonly Used Plate-Fin Geometries and Their Relative Merits

Corrugation	Description	Application	Features	
			Relative Heat Transfer	Relative Pressure Drop
Plain	Straight fins (rectangular or triangular)	Low Reynolds number applications and in applications where the pressure drop is very critical, e.g., condensation	Lowest	Lowest
Perforated	Straight fin with small holes	For general use	Low	Low
Herringbone or wavy fin	Smooth but wavy, about 10 mm pitch	In the Re range of 6000–8000, the wall corrugations increase the heat transfer by about three times compared with the smooth wall channel due to Goertler vortices. Less likely to catch particulates and foul than are OSFs	High	High
Louvered fin	The louvers are formed by cutting the sheet metal of the fin at intervals and by rotating the strips of metal thus formed out of the plane of the fin	Radiators, air conditioning heat exchangers (evaporators and condensers), and aircraft oil and air coolers	Highest	Highest
OSF	Straight but offset by half a pitch (usually about every 3–4 mm)	Air separation plants and low Reynolds number applications calling for accurate performance predictions, e.g., aerospace applications	Highest	Highest

(S = serrated). Other types are P = plain, R = perforated, H = herringbone. The next two digits give the fins per inch (18 = 18 fpi). The following two digits give the fin thickness in thousandths of an inch (08 = 0.008 in.). The time following the oblique stroke (if any) is used only for perforated fin and it is the porosity, σ .

4.2.10 CORRUGATION SELECTION

Corrugations, edge bars, and parting sheets are chosen primarily to contain the appropriate pressure. Corrugation selection depends on factors such as [13] compactness, pressure, mechanical integrity, manufacture, performance, velocity limits, and fouling.

4.2.11 MATERIALS OF CONSTRUCTION

PFHEs are made in a variety of materials to suit a wide range of process streams, temperatures and pressures. Material specifications should comply with the appropriate section of the ASME or to other applicable codes.

4.2.11.1 Aluminum

Aluminum is preferred for cryogenic duties, because of its relatively high thermal conductivity, strength at low temperatures, and low cost. For cryogenic services, aluminum alloy 3003 is generally used for the parting sheets, fins, and edge bars that form the rectangular PFHE block. Headers and nozzles are made from aluminum alloy 3003, 5154, 5083, 5086, or 5454 [13]. Above ambient temperature, with increase in temperature, most aluminum alloys rapidly lose their strength. For land-based transport vehicles, aluminum PFHEs are used up to 170°C–180°C to cool supercharged engine intake air.

4.2.11.2 Other Metals

Stainless steels and most nickel alloys are used for PFHEs, particularly for high-temperature services. Stainless steels have poor thermal conductivity, but their higher strength allows thinner parting plates and fins than with aluminum, which offsets some of the reduction in heat transfer.

4.2.12 MECHANICAL DESIGN

The PFHE is a pressure vessel. It is required to be designed and constructed in accordance with a recognized Pressure Vessel Code. The mechanical design of a PFHE can be divided into the conventional pressure vessel area of header tanks, nozzle, nozzle reinforcements, lifting devices, pipe loads, etc., and the less familiar area of the block itself. Details on mechanical design of vessel components are given in Chapter 11.

4.2.13 MANUFACTURE, INSPECTION, AND QUALITY CONTROL

PFHEs are manufactured by brazing. Heat exchanger manufacture by brazing is described in Chapter 15. The manufacturer is responsible for the mechanical design and for the thermal design where the latter is not specified by the purchaser. Salient features of quality control and inspection of PFHE are detailed in Refs. [13,14].

4.2.14 BRAZED ALUMINUM PLATE-FIN HEAT EXCHANGER (BAHX)

4.2.14.1 ALPEMA Standard

Though most of the details on PFHE are covered before, specific details on aluminum PFHE are discussed here. Over the past 40 years, brazed aluminum plate-fin heat exchangers (BAHXs) have become the preferred type of exchanger for a variety of applications, mainly in heating

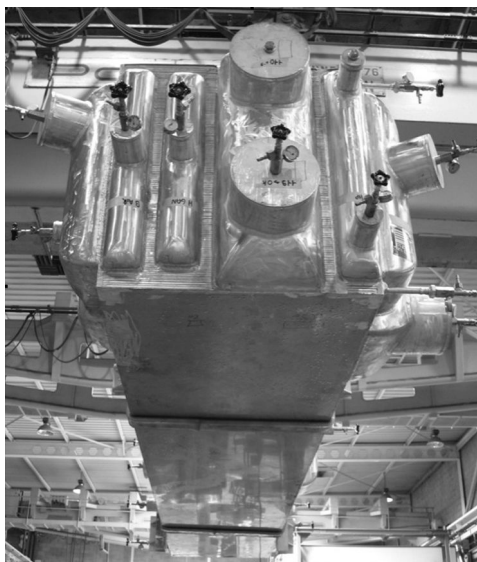


FIGURE 4.18 Brazed aluminum plate-fin heat exchanger. (Courtesy of Fives Cryo, Golbey, France.)

and cooling of liquids and gases, and condensing and boiling with single and multicomponent streams. BAHXs are capable of handling a wide variety of noncorrosive streams, up to a pressure of 100 bar (1450 psi) and from cryogenic temperature of -269°C to 204°C (-452°F to 400°F). BAHXs can handle several streams in the same exchanger. A brazed aluminum PFHE is shown in Figure 4.18 and a collection of different shapes/configuration of PFHEs are shown in Figures 4.19 and 4.20. Brazed aluminum PFHEs are designed and manufactured as per the guidelines of ALPEMA Standard, 3rd edition, 2010 [12]. Members of ALPEMA Standards are (in alphabetical order)

1. Chart Energy and Chemicals Inc., 2191 Ward Avenue, La Crosse, WI
2. FivesCryo, 25, Rue du Fort BP 8788194 Golbey, Cedex, France
3. Kobe Steel Ltd., Energy System Center, Takasago Equipment Plant, 2-3-1, Shinhamma, Arai-cho, Takasago-Shi, Hyogo-Ken, 676-8670, Japan
4. LINDE AG, Engineering Division, Works Schalchen, D-83342 Tacherting, Germany
5. Sumitomo Precision Products Co Ltd., Thermal Energy Systems Engineering Department, 1-10 Fuso-cho, Amagasaki, Hyogo Pref. 660-0891, Japan

Other PFHE manufacturer among others include, 1. Lytron Inc., 55 Dragon Court, Woburn, MA. The ALPEMA standards comprise the following chapters:

1. General description and nomenclature
2. Tolerances
3. General fabrication and contractual information
4. Installation, operation, and maintenance
5. Mechanical standards
6. Materials
7. Thermal and hydraulic design
8. Recommended good practice

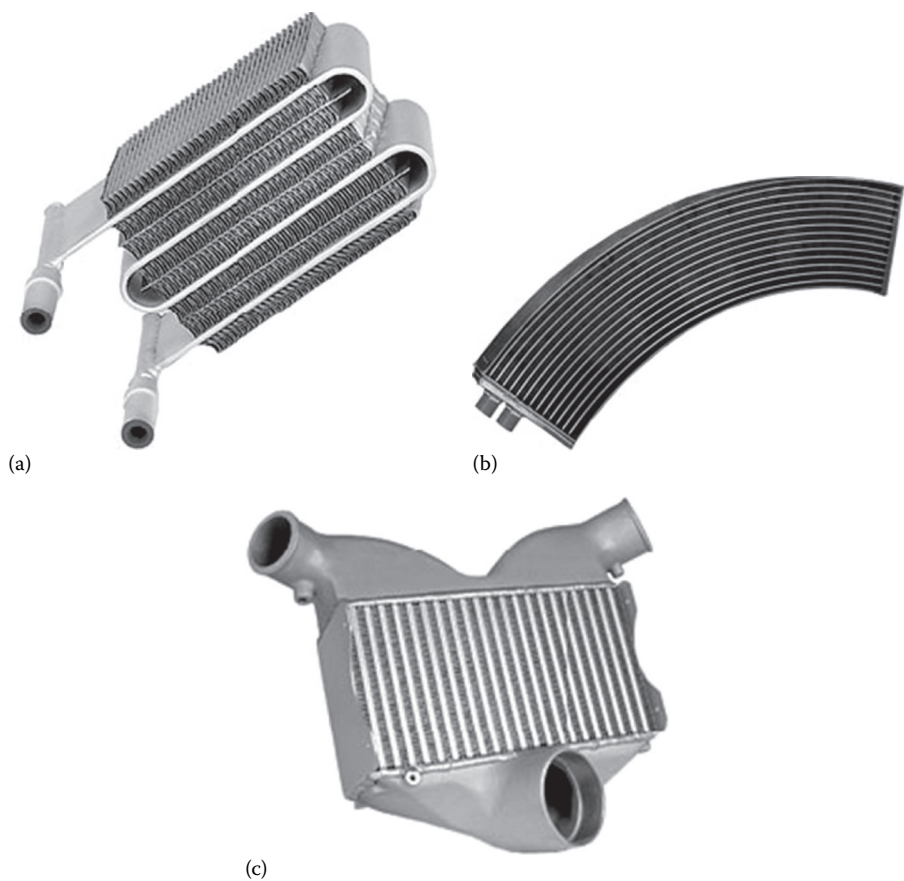


FIGURE 4.19 Varieties of brazed aluminum PFHEs configuration—(a) heat exchanger with single continuous piece of aluminum flat tube, (b) flat tube heat exchanger with curved tubes, and (c) plate-fin heat exchanger for air-to-air application. (Courtesy of Lytron Inc., Woburn, MA.)

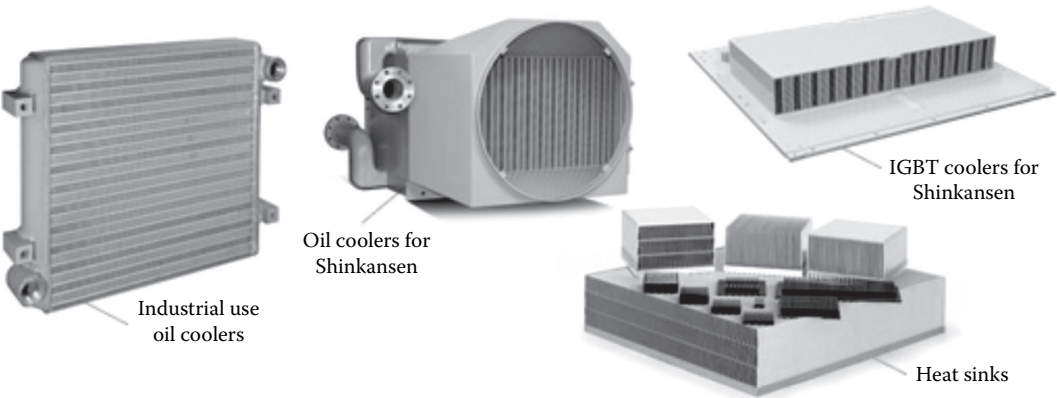


FIGURE 4.20 Varieties of brazed aluminum plate-fin heat exchangers. (Courtesy of Sumitomo Precision Products Co. Ltd., Thermal Energy Systems Engineering Department, Japan.)

4.2.14.2 Applications

PFHEs can be used for a wide range of applications, especially for low temperature services and treatment of clean fluids. Such applications among others include, petrochemical plants, gas treatment plants, natural gas liquefaction plants, air separation plants, and helium liquefaction plants.

4.2.14.3 Heat Exchanger Core

Each heat exchanger is built by stacking layers of fins separated by parting sheets and sealed along the edges with side bars. The matrix assembly is brazed in a vacuum/controlled atmosphere brazing (CAB) furnace to form an integral, rigid heat exchanger block. Headers and supports welded onto the brazed matrix complete the unit. Design variations in the configuration of the heat exchanger matrix can accommodate an almost unlimited range of flow options, including counterflow, crossflow, parallelflow, multipass and multistreams formats. The structure and components of brazed aluminum heat exchangers (BAHXs) is shown in Figure 4.21.

4.2.14.4 Flow Arrangement

A simple crossflow layout is generally suitable for low to moderate duties. It is used extensively for gas/liquid applications and is especially effective when handling a low pressure gas stream on one side of the heat exchanger. For heavier duty tasks, where the mean effective temperature difference in crossflow may be significantly reduced, the counterflow pattern offers an efficient solution. The higher levels of efficiency achieved by counterflow units are essential to most low-temperature applications.

A heat exchanger's size, number of layers, type of fins, stacking arrangement, and stream circuiting will vary depending on the application requirements. The basic components of a BAHX are as follows [14].

- Fins
- Fins types

The herringbone and serrated fins provide the greatest surface area and the highest heat transfer performance. They are particularly suitable for applications involving close temperature approaches.

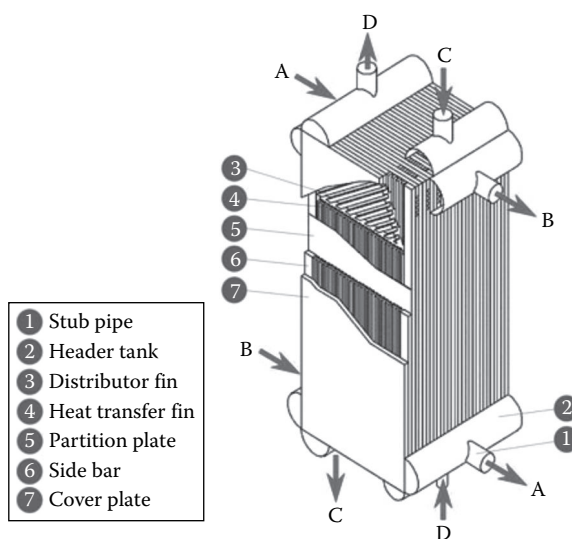


FIGURE 4.21 Brazed aluminum plate-fin heat exchanger structure. (Note: A, B, C, D are fluids.) (From Linde AG, Engineering Division. With permission.)

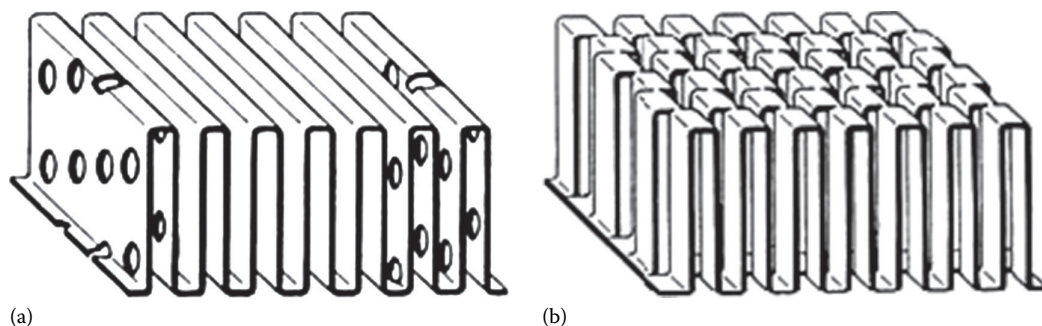


FIGURE 4.22 Brazed aluminum plate-fin heat exchanger fin profiles—(a) perforated fin and (b) offset strip fin (schematic). (From Linde AG, Engineering Division. With permission.)



FIGURE 4.23 Brazed aluminum plate-fin heat exchanger fin profiles—(a) serrated fins (b) OSF and (c) perforated fins. (Courtesy of Fives Cryo, Golbey, France.)

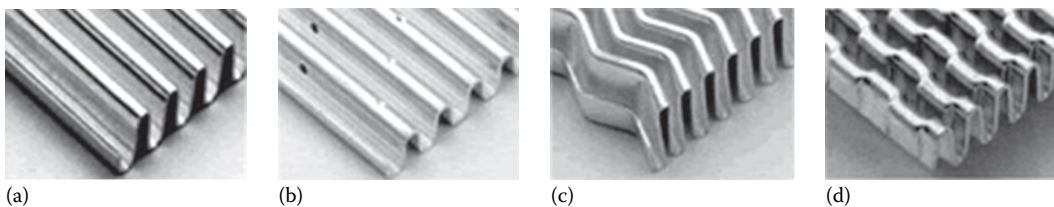


FIGURE 4.24 Brazed aluminum plate-fin heat exchanger fin profiles: (a) plain fin, (b) perforated fin, (c) herringbone fin, and (d) serrated fin. (Courtesy of Chart Industries Inc., Garfield Heights, OH.)

Where there are critical pressure drop requirements, the plain and perforated fins can be used. Fins, also known as secondary surface, provide an extended heat transfer surface. Fins provide a connecting structure between the parting sheets, thereby creating the essential structural and pressure holding integrity of the heat exchanger. Various fin types are shown in Figures 4.22 through 4.24. Typical fin height, thickness, and density are

- Fin height: 3.8–12 mm
- Fin thickness: 0.15–0.61 mm
- Fin pitch: 1.15–4.5 mm (i.e., fin density is 22–6 fpi)
- Surface area density, area/volume: $1500 \text{ m}^2/\text{m}^3$
- Design pressure up to a maximum of 110 bar (1600 psig)
- The size is available up to (W × H × L)— $1.5 \times 3.0 \times 8.2 \text{ M}$

4.2.14.5 Rough Estimation of the Core Volume

To obtain a quick indication of the heat exchanger volume required for a certain duty, the following simple relation as per ALPEMA standard may be used

$$V = \frac{Q/MTD}{\Gamma}$$

where

V is the required volume of heat exchanger (without headers)

Q is the overall heat duty

MTD is the mean temperature difference between streams

Γ is the coefficient: 100,000 for hydrocarbon applications

50,000 for air separation application

The values of 100,000 and 50,000 represent the product, UA_d , assuming an overall heat transfer coefficient of 200 W/m² and 100 W/m² K, respectively, and a mean geometric heat transfer surface density of 500 m²/m³.

The weight of a complete heat exchanger may be assumed to be 1000 kg per unit core volume (m³). This value varies in practice between 650 and 1500 kg/m³.

Distributor fins: Distributor fins distribute the fluid between the port and the heat transfer fins. The distributor fin used adjacent to a port is called a port fin. The distributor fin used between a port fin and a heat transfer fin is called a turning fin. The typical distributor fin thickness is 0.45 mm (0.016 in.).

Parting sheets: Parting sheets (sometimes referred to as separator sheets) contain the fluids within individual layers in the exchanger and also serve as primary heat transfer surface. Their selection is mainly based on design pressures. Parting sheets are normally clad on both sides with a brazing alloy. However, unclad parting sheets are available, where brazing is performed using brazing foils (filler material). Standard parting sheet thicknesses typically vary between 0.8 and 2.0 mm. Typical parting sheet thicknesses are 1.0, 2.0, and 3.0 mm (0.040, 0.080, and 0.125 in.).

Cap sheet or outside sheets: Cap sheets serve as the outside parting sheets. Standard cap sheet thicknesses are typically 5 or 6 mm. However, thicknesses from 2 to 10 mm are also used for special applications.

Side and end bars: Side and end bars enclose individual layers and form the protective perimeter of the exchanger. Solid extruded forms are used. Side bar heights are the same as the fin heights, and width is selected by the manufacturer according to the design pressure and typically varies between 10 and 25 mm.

Permissible temperature differences between adjacent streams: Aluminum PFHEs are produced by brazing. To maintain the thermal stresses within the acceptable limits for the material used, the maximum permissible temperature difference between streams shall be about 50°C.

Support angles: Support angles are typically 90° extruded aluminum angles welded to the exchanger bar face for the purpose of supporting or securing an exchanger in its installed position. Other support configurations, such as pedestal bases, are also available.

Lifting lugs: Lifting lugs (aluminum) are lift attachment points strategically welded to the exchanger block assembly for the specific purpose of lifting the exchanger into its installed position.

Header/nozzle configurations: Streams to and from the heat exchanger enter and leave by means of various header/nozzle configurations. Nozzles are the pipe sections used to connect the heat

exchanger headers to the customer piping. Headers are the half cylinders which provide for the distribution of fluid from the nozzles to or from the ports of each appropriate layer within the heat exchanger.

Ports: Ports are the openings in either the side bar or the end bar, located under the headers, through which the fluids enter or leave individual layers.

Materials of construction: Typical materials of construction for the BAHX components are hereunder.

Cap sheets—AA 3003	Headers and nozzles, flanges-AA
Parting sheets—AA 3003	5083/5454
Side and end bars—AA 3003	Support angles—AA 6061-T6
Heat transfer fins—AA 3003	Lifting lugs—AA 5083
Distributor fins—AA 3003	

Life: A design life similar to tubular heat exchangers can be expected from them.

Construction code: The design, construction, and testing of BAHXs are governed by the existing national rules applying to pressure vessels.

Modular exchanger assembly: A modular exchanger assembly consists of two or more exchanger blocks, welded together prior to attaching the headers, to form a single piece exchanger. This form of construction is used when the customer's heat exchange requirements exceed the maximum block size which can be furnace brazed. Modular construction eliminates the need for costly piping to interconnect separate, individual exchangers.

Cold box: The installation of different exchangers in a steel containment (cold box), usually rectangular in shape. Interconnecting piping, vessels, valves, and instrumentation are included in this packaged unit to form, after filling with insulation material, a ready-to-operate unit.

Block-in-shell: One or more heat exchanger blocks installed in a shell instead of a tube bundle. This is a highly efficient and economical alternative to standard shell and tube heat exchangers. The benefits include tighter approach temperatures, smaller in size and weight, lower capital costs, and lower operating costs. A typical block-in-shell is shown in Figure 4.25.

Transition joint: A transition joint is a bimetallic coupling used to make the transition from aluminum to stainless steel piping. Transition joints are available in various configurations.

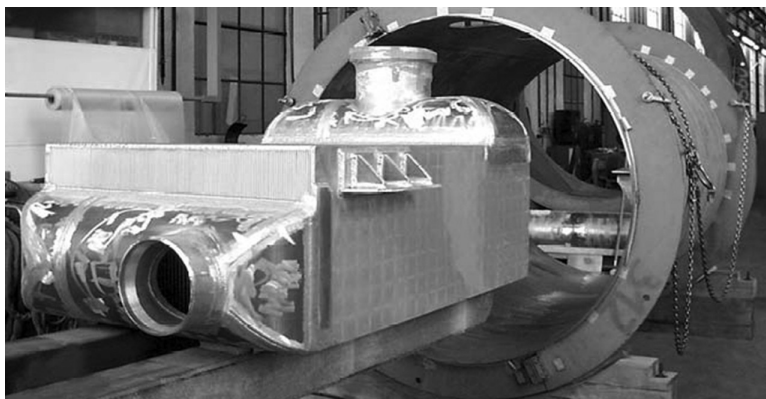


FIGURE 4.25 Brazed aluminum heat exchanger: block-in-shell. (From Linde AG, Engineering Division. With permission.)

4.2.14.6 Provisions for Thermal Expansion and Contraction

Provisions for thermal expansion and contraction of the heat exchanger in the horizontal plane at the support location must be provided. The expected thermal movement should be calculated in both horizontal directions by the following equation:

$$\Delta L = 12.6 \times 10^{-6} \times L \times \Delta T \text{ in. (in FPS units)}$$

$$\Delta L = 97.1 \times 10^{-6} \times L \times \Delta T \text{ m (in SI units)}$$

where

L is the distance in m/in. between extreme bolts in the direction under consideration

ΔT is the change in temperature in °C(°F) at the support location from the installed (ambient) temperature to the coldest possible operating temperature

ΔL is the expected thermal movement in m/in. which will result from this calculation

If the expected thermal movement in both directions is 12.7 mm (0.5") or less, the bolt hole diameters in the aluminum support angles should be oversized by adding the maximum expected thermal movement to the bolt diameter. If the expected thermal movement exceeds 12.7 mm (0.5 in.) in one of the horizontal directions, a slotted hole should be used with a slot length equal to the bolt diameter plus the maximum expected thermal movement.

4.2.14.7 Mechanical Design of Brazed Aluminum Plate-Fin Heat Exchangers

The design of a brazed aluminum PFHEs is the result of the mechanical strength analysis of

- The plate-fin structure under pressure
- The influence of headers on the plate-fin structure
- The header/nozzle assembly

Pressure vessel codes generally do not contain formulae for the fins. The calculation methods used by manufacturers have been approved by the applicable Code Authority. The calculated stresses are compared with the maximum allowable stress as per the code.

4.2.14.8 Codes

BAHXs are normally designed and manufactured in accordance with Section VIII, Division I of the ASME Pressure Vessel Code, carry the "U" stamp, and are registered with the National Board of Boiler and Pressure Vessel Inspectors. Manufacturers can manufacture to other international standards, such as PED European Pressure Equipment Directive, AD-Merkblätter, Australian Standard, British Standard, Chinese Standard, CODAP, Japanese Industrial Standards, Raccolta/VSR, Stoomwezen Grondslagen, Swedish Pressure Vessel Code, Russian Gost, etc.

Associated piping is normally designed and manufactured in accordance with the ASME B31.3 Piping Code. The ASME pressure vessel and piping code boundaries are indicated on the drawing. Heat exchangers and piping are sometimes designed and manufactured to other national codes. The governing national code is specified on the drawing and exchanger nameplate.

4.2.14.9 Materials of Construction

Typical materials for use on the construction of brazed aluminum PFHEs are (1) core matrix (fins, plates, side bars) is aluminum alloy AA 3003 and (2) headers/nozzles is aluminum alloy AA 5083 and their mean metal temperature limitations as per ASME code are alloy AA 3003 is -269/+204°C and that of AA 5083 is -269/+65°C.

4.2.14.10 Manufacture

After forming, cutting, and cleaning of the single parts, the block is stacked and prepared for high vacuum brazing at about 600°C. For welding of headers and nozzles to the core, proven welding procedures, such as GTAW and GMAW, are used.

4.2.14.11 Quality Assurance Program and Third Party Inspection

Quality management is an essential part of all manufacturers' strategy. The companies are certified to various national and international standards. Acceptance inspection is carried out by firm's own specialists and further by experts from various international inspection organizations/agencies, such as TÜV, Lloyd's Register, Stoomwezen, ISPESL, Bureau Veritas, Det Norske Veritas, etc.

4.2.14.12 Testing of BAHX

Extensive test procedures are carried out on the completely assembled heat exchangers. These include radiographic and dye penetrant testing of weld seams, pressure test, and helium leak tests and if requested, flow tests. A BAHX is first structurally tested. For hydrostatic test methods, each stream is pressurized, with the other streams at zero pressure, to 1.3 times the design pressure as per the requirements of ASME. The unit remains pressurized for stipulated period as per the code. Pneumatic test methods can be used with the pressure level being adjusted to 1.1 times design pressure. Leak testing is performed after the structural test has been successfully performed. Internal leak testing is performed by pressurizing each stream individually and monitoring small nozzle valves on the unpressurized streams using soap film solution. External leak testing is performed using soap solution on the exchanger external joints. For critical applications, helium vacuum leak testing may also be used to validate the leak tightness of an exchanger.

4.2.14.13 Guarantees

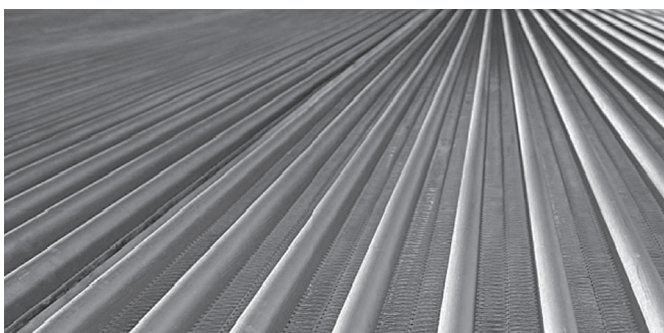
Manufacturers shall offer a thermal performance guarantee and a mechanical guarantee. Details shall be agreed upon by the purchaser and the manufacturer.

4.2.14.14 ALEX: BraZed ALuminum EXchanger

ALEX is the trade name of a BAHX developed independently by Kobe Steel in 1963 for use as the regenerator in air separation plants. Core tube is steel with aluminum coated in flat shape with parallel sides and smooth fins having a reduced tendency for fouling. Kobe Steel is one of the members of ALPEMA standards and is the top user of ALEX for cold box for LNG applications, core-in-drum type heat exchangers, etc. A small ALEX core is shown in Figure 4.26a, and an air-cooled condenser made of ALEX core is shown in Figure 4.26b.



(a)



(b)

FIGURE 4.26 Aluminum Exchanger (ALEX) core—(a) mini core and (b) aircooled heat exchanger with single row type with steel tubes and ALEX core. (Courtesy of GEA Power Cooling, Inc., Lakewood, CO.)

TABLE 4.2
Comparison of Salient Features of Plate-Fin Heat Exchangers and Coil-Wound Heat Exchangers

	Plate-Fin Heat Exchangers	Coil-Wound Heat Exchangers
Characteristics	Extremely compact, multiple streams, single- and two-phase streams	Compact, multiple streams, single and two-phase streams
Fluid	To be very clean	To be clean
Flow types	Counterflow, crossflow	Cross counterflow
Heating surface compactness	300–1400 m ² /m ³	20–300 m ² /m ³
Materials	Aluminum	Aluminum, stainless steel (SS), carbon steel (CS), special alloys
Temperature	–269°C to +65°C (150°F)	All
Pressure	Up to 115 bar (1660 psi)	Up to 250 bar (3625 psi)
Applications	Cryogenic plants, noncorrosive fluids. Very limited installation space	Also for corrosive fluids and thermal shocks

Source: Linde AG, Engineering Division, Germany. With permission.

4.2.15 COMPARISON OF SALIENT FEATURES OF PLATE-FIN HEAT EXCHANGERS AND COIL-WOUND HEAT EXCHANGER

Both the brazed aluminum PFHEs and coiled tube heat exchangers find application in liquefaction processes. Salient features of these two types of heat exchangers are compared in Table 4.2 for the intended service.

4.2.16 HEAT EXCHANGER SPECIFICATION SHEET FOR PLATE-FIN HEAT EXCHANGER

Heat exchanger specification sheet for PFHE is shown in Figure 4.27.

4.3 SURFACE GEOMETRICAL RELATIONS

4.3.1 SURFACE GEOMETRICAL PARAMETERS: GENERAL

The following are some of the basic relationships between the surface and core geometries on one side of the compact heat exchangers.

4.3.1.1 Hydraulic Diameter, D_h

The generalized relation for hydraulic diameter is given by

$$D_h = \frac{4A_o L}{A} \quad (4.1)$$

where

A is the total heat transfer area

A_o is the free flow area

L is the flow length

The hydraulic radius r_h is given by $D_h/4$.



CUSTOMER :	PROJECT :	N.C. ORDER N° :
ITEM N° :	LOCATION :	CUST. JOB N° :
	PLANT SERVICE :	CONSTRUCTION CODE :

[illegible]

FIGURE 4.27 PFHE specification sheet N°. (Courtesy of Fives Cryo, Golbey, France.)

4.3.1.2 Surface Area Density α and σ

For a compact heat exchanger with secondary surface on one side, it is customary to designate the ratio of the total heat transfer surface area on one side of the exchanger to total volume of the exchanger by α , and the ratio of the free flow area to the frontal area by σ . Thus,

$$\alpha_1 = \frac{A_1}{V} \quad \text{and} \quad \alpha_2 = \frac{A_2}{V} \quad (4.2)$$

$$\sigma_1 = \frac{A_{0,1}}{A_{fr,1}} = \left(\frac{AD_h/4}{A_{fr}L} \right)_1 = \frac{(AD_h/4)_1}{V} \quad (4.3a)$$

$$\sigma_2 = \frac{A_{0,2}}{A_{fr,2}} = \left(\frac{AD_h/4}{A_{fr}L} \right)_2 = \frac{(AD_h/4)_2}{V} \quad (4.3b)$$

From the definition of hydraulic diameter D_h , the relation between hydraulic diameter, surface area density α , and σ is given by

$$\left(\frac{D_h}{4L} \right)_1 = \left(\frac{A_o}{A} \right)_1 = \left(\frac{\sigma}{L\alpha} \right)_1 \quad (4.4a)$$

$$\left(\frac{D_h}{4L} \right)_2 = \left(\frac{A_o}{A} \right)_2 = \left(\frac{\sigma}{L\alpha} \right)_2 \quad (4.4b)$$

and

$$D_{h,1} = 4 \frac{\sigma_1}{\alpha_1}, \quad D_{h,2} = 4 \frac{\sigma_2}{\alpha_2} \quad (4.5)$$

4.3.2 TUBULAR HEAT EXCHANGERS

Geometrical relations are derived for the inline and staggered tube arrangements with bare tubes, individually finned circular tubes, and circular tubes with plain continuous fins. The header dimensions for the tube bank is $L_2 \times L_3$, the core length for flow normal to the tube bank is L_2 , and the no-flow dimension is L_3 . The lateral pitch is given by P_t , and longitudinal pitch by P_l . Flow is idealized as being normal to the tube bank on the outside. Surface geometrical relations for tube-fin heat exchangers are derived from first principles by Shah [20,21], and for individually finned tubes by Idem et al. [22]. The surface geometrical relations given here are based on Shah [21].

4.3.2.1 Tube Inside

Tubes have inside diameter d_i , length between headers L_l , header thickness T_h , and total length including header plates thickness as $L_l + 2T_h$. The total number of tubes, N_t , is given by

$$N_t = \frac{L_2 L_3}{P_t P_l} \quad (4.6)$$

The geometrical properties of interest for analysis are

$$\text{Total heat transfer area } A = \pi d_i L_1 N_t \quad (4.7)$$

$$\text{Minimum free flow area } A_o = \left(\frac{\pi}{4} \right) d_i^2 N_t \quad (4.8)$$

$$\text{Hydraulic diameter } D_h = d_i \quad (4.9)$$

$$\text{Tube length for heat transfer} = L_1 \quad (4.10)$$

$$\text{Tube length for pressure drop} = L_1 + 2T_h \quad (4.11)$$

The geometrical properties given by Equations 4.7 through 4.11 also hold good for other types of arrangements discussed next.

4.3.2.2 Tube Outside

4.3.2.2.1 Bare Tube Bank

Inline arrangement: The geometrical properties of the inline tube bank as shown in Figure 4.28 are summarized here. The number of tubes in one row (in the flow direction) is

$$N_1 = \frac{L_3}{P_t} \quad (4.12)$$

The total heat transfer area consists of the area associated with the tube outside surface given by

$$A = \pi d_o L_1 N_t \quad (4.13)$$

The minimum free flow area A_o , frontal area A_{fr} , the ratio of free flow area to frontal area σ , and hydraulic diameter D_h are given by

$$A_o = (P_t - d_o) N_t' L_1 \quad (4.14)$$

$$A_{Fr} = L_1 L_3 \quad (4.15)$$

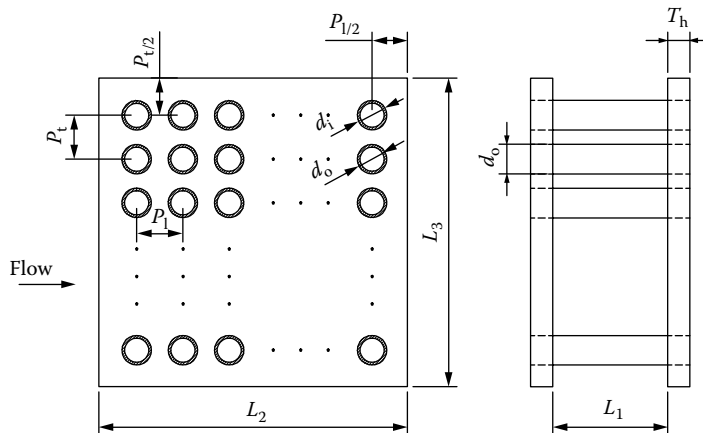


FIGURE 4.28 Inline tube bank geometry (bare tube).

$$\sigma = \frac{(P_t - d_o)}{P_t} \quad (4.16)$$

$$D_h = \frac{4A_o L_2}{A} \quad (4.17)$$

$$\text{Flow length for pressure drop calculation} = L_2 \quad (4.18)$$

$$\text{Heat exchanger volume } V = L_1 L_2 L_3$$

It must be emphasized that the foregoing definition of the hydraulic diameter is used by Kays and London [17] for tube banks. However, many correlations use the tube outside diameter or fin root diameter as the characteristic dimension in the heat transfer and pressure-drop correlations. So it is essential to find out first the specific definition of the characteristic length before using a particular correlation.

The geometrical properties given by Equations 4.14 through 4.18 also hold good for other types of arrangements discussed later.

Staggered arrangement: A staggered tube bank layout and its unit cell are shown in Figure 4.29. The total number of tubes with half tubes in the alternate row is given by Equation 4.6. If the half tubes are eliminated from the alternate intermediate tube rows, then the number of tubes in the first row will be L_3/X_t , and in the second row $L_3/X_t - 1$. The minimum free flow area occurs either at the front or through the diagonals (refer to Figure 4.29b). The minimum free flow area is then given by [20,21]

$$A_o = \left[\left(\frac{L_3}{P_t} - 1 \right) z + (P_t - d_o) \right] L_1 \quad (4.19a)$$

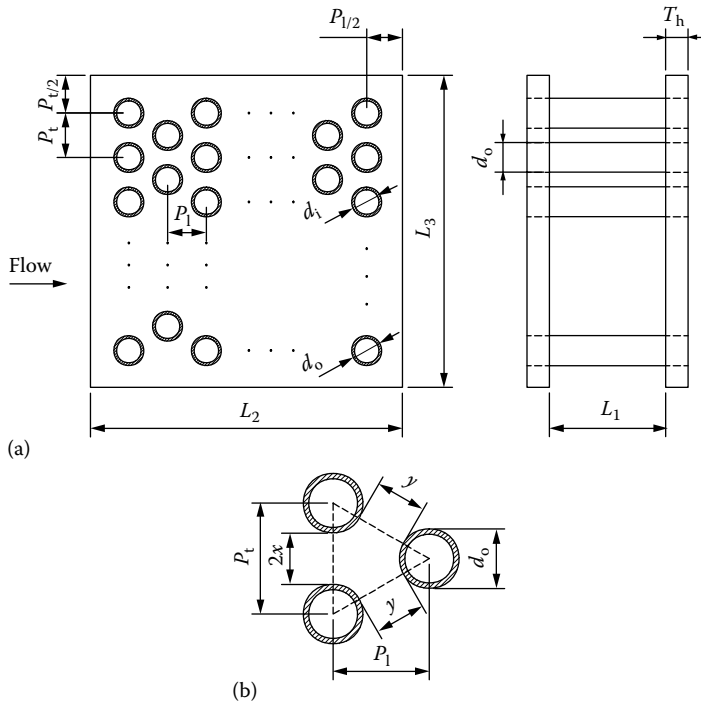


FIGURE 4.29 Staggered tube bank (bare tube): (a) layout and (b) unit cell.

where

$$z = 2x \quad \text{if } 2x < 2y \quad (4.19b)$$

$$z = 2y \quad \text{if } 2y < 2x \quad (4.19c)$$

in which $2x$ and y are defined as

$$2x = (P_t - d_o) \quad (4.20a)$$

$$y = \left[\left(\frac{P_t}{2} \right)^2 + (P_t)^2 \right]^{0.5} - d_o \quad (4.20b)$$

In Equation 4.19a, the last term $(P_t - d_o)L_1$ corresponds to the free flow area between the last tube at each end in the first row and the exchanger wall.

4.3.2.2.2 Circular Fins on Circular Tubes

The basic core geometry of an idealized single-pass crossflow exchanger for an inline arrangement is shown in Figure 4.30. The total number of tubes in this exchanger is given by Equation 4.6. It is idealized that the root of a circular fin has an effective diameter d_r and the fin tip has a diameter d_f . Depending upon the manufacturing techniques, d_r may be the tube outside diameter or tube outside diameter plus two fin collar thickness. The total heat transfer area consists of the area associated

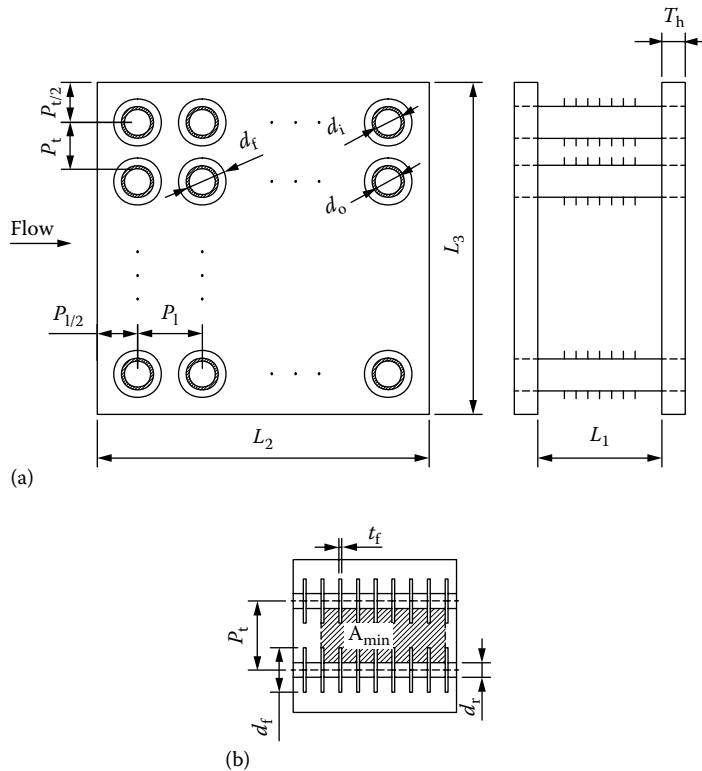


FIGURE 4.30 Individually finned circular fin tube. (a) Inline layout and (b) diagram showing frontal area (dotted lines) and free flow area (hatched area).

with the exposed tubes (primary area) and fins (secondary area). The primary area, A_p , is the tube surface area minus the area blocked by the fins. It is given by

$$A_p = \pi d_r (L_1 - t_f N_f L_1) N_t \quad (4.21)$$

where

t_f is the fin thickness

N_f is the number of fins per unit length

The fin surface area, A_f , is given by

$$A_f = \left[\frac{2\pi(d_f^2 - d_r^2)}{4} + \pi d_r t_f \right] N_f L_1 N_t \quad (4.22)$$

and therefore, the total heat transfer surface area A is equal to $A_p + A_f$, given by

$$A = \pi d_r (L_1 - t_f N_f L_1) N_t + \left[\frac{2\pi(d_f^2 - d_r^2)}{4} + \pi d_r t_f \right] N_f L_1 N_t \quad (4.23)$$

Minimum free flow area: Inline arrangement: The minimum free flow area for the inline arrangement is that area for a tube bank, Equation 4.13, minus the area blocked by the fins:

$$A_o = [(P_t - d_r)L_1 - (d_f - d_r)t_f N_f L_1] \left(\frac{L_3}{P_t} \right) \quad (4.24)$$

Minimum free flow: Staggered arrangement: The basic core geometry of an idealized single-pass crossflow exchanger for staggered arrangement is given in Figure 4.31. The total number of tubes in this exchanger is given by Equation 4.6. For the staggered tube arrangement, the minimum free flow area could occur either through the transverse pitch or through the diagonals similar to those of the unit cell shown in Figure 4.31b. The minimum free flow area is given by [19,20]

$$A_o = \left[\left(\frac{L_3}{P_t} - 1 \right) z' + (P_t - d_r) - (d_f - d_r)t_f N_f \right] L_1 \quad (4.25)$$

where

$$z' = 2x' \quad \text{if } 2x' < 2y' \quad (4.26a)$$

$$z' = 2y' \quad \text{if } 2y' < 2x' \quad (4.26b)$$

in which $2x'$ and y' are given by

$$2x' = (P_t - d_r) - (d_f - d_r)t_f N_f \quad (4.27a)$$

$$y' = \left[\left(\frac{P_t}{2} \right)^2 + (P_t)^2 \right]^{0.5} - d_r - (d_f - d_r)t_f N_f \quad (4.27b)$$

Dimensions $2x'$ and y' cannot be depicted in the figure.

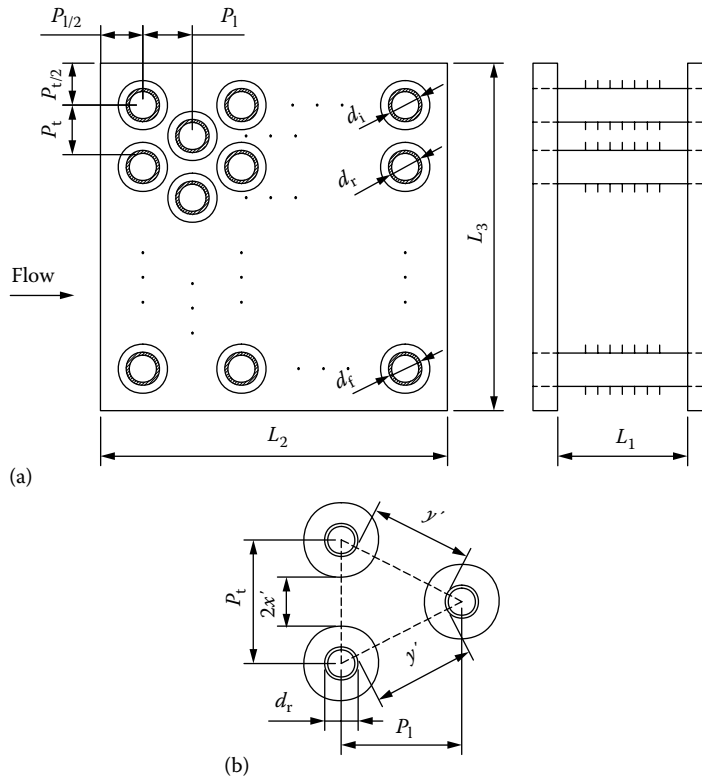


FIGURE 4.31 Individually finned tube staggered arrangement. (a) Geometry and (b) unit cell. (After Shah, R.K., Compact heat exchangers, in *Handbook of Heat Transfer Applications*, W.M. Rohsenow, J.P. Harnett, and E.N. Ganic, eds., McGraw-Hill, New York, 1985, pp. 4-176–4-312.)

4.3.2.2.3 Continuous Plain Fins on Circular Tubes

The tube-fin arrangement is shown in Figure 4.32. The total heat transfer area consists of the area associated with the exposed tubes (primary area) and the fins (secondary area). The primary area is the same as that given by Equation 4.13, minus the area blocked by the fins. Therefore, A_p is given by [14,20]

$$A_p = \pi d_r (L_1 - t_f N_f L_1) N_t \quad (4.28)$$

The total fin surface area, A_f , consists of (1) the fin surface area, and (2) the area with leading and trailing edges, given by

$$A_f = 2[(L_2 L_3 - \pi d_r^2 N_f)/4] N_t L_1 + 2 L_3 t_f N_f L_1 \quad (4.29)$$

and

$$\text{Total heat transfer surface area } A = A_p + A_f \quad (4.30)$$

Minimum free flow area for the inline arrangement: The minimum free flow area for an inline arrangement is that area for a tube, Equation 4.13, minus the area blocked by the fins [14,20]

$$A_o = [(P_t - d_r) L_1 - (P_t - d_r) t_f N_f L_1] \left(\frac{L_3}{P_t} \right) \quad (4.31)$$

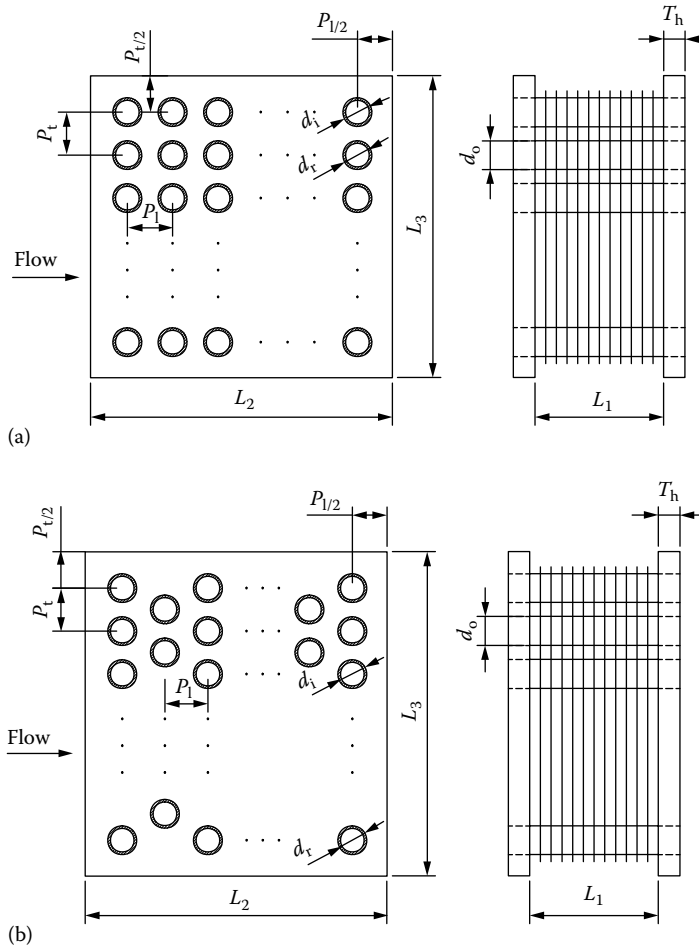


FIGURE 4.32 Continuous flat fin-tube heat exchanger: (a) inline layout and (b) staggered layout.

Minimum free flow area for the staggered arrangement: For the staggered tube arrangement as shown in Figure 4.32b, the minimum free flow area could occur either through the transverse pitch or through the diagonals. The minimum free flow area is given by [20,21] as follows:

$$A_o = \left\{ \left(L_3/P_t - 1 \right) z'' + \left[(P_t - d_r) - (P_t - d_o)t_f N_f \right] \right\} L_1 \quad (4.32)$$

In Equation 4.32, z'' is defined as

$$z'' = 2x'' \quad \text{if } 2x'' < 2y'' \quad (4.33a)$$

$$z'' = 2y'' \quad \text{if } 2y'' < 2x'' \quad (4.33b)$$

where $2x''$ and y'' are given by

$$2x'' = (P_t - d_r) - (P_t - d_r)t_f N_f \quad (4.34a)$$

$$y'' = \left[\left(\frac{P_t}{2} \right)^2 + (P_l)^2 \right]^{0.5} - d_r - (P_t - d_r)t_f N_f \quad (4.34b)$$

Minimum free flow area for pressure drop: For the determination of entrance and exit pressure losses, the area contraction and expansion ratio σ' is needed at the leading and trailing fin edges. It is given by [14,20] as follows:

$$\sigma' = \frac{L_3 L_1 - L_3 t_f N_f L_1}{L_3 L_1} \quad (4.35)$$

4.3.3 COMPACT PLATE-FIN EXCHANGERS

The following geometrical properties on each side are needed for the heat transfer and pressure-drop analysis of a PFHE:

1. The primary and secondary surface area (if any) A_p and A_s , respectively
2. Minimum free flow area A_o
3. Frontal area A_{fr}
4. Hydraulic diameter D_h
5. Flow length L
6. Fin dimensions—thickness and length (height)

4.3.3.1 Heat Transfer Area

The total heat transfer area consists of sum of the primary and secondary heat transfer areas and their calculation method is given later. The primary heat transfer surface within the heat exchanger consists of the bare parting sheet and the fin base directly brazed to the parting sheet and the secondary heat transfer surface is provided by the fins. The cross-sectional view of fin and parting sheet is shown in Figure 4.33. The effectiveness of the secondary surface to transfer heat is given by the fin efficiency. Per unit area of the each parting sheet is given by

- a. Primary surface area, A_p is given by $2(1 - nt_f)$
- b. Secondary surface, A_s is given by $2n(l_f - 1)$

where

n is the fin density (m^{-1}), i.e. number of fins per unit length

t_f is the fin thickness (m)

l_f is the fin height (m)

The effective heat transfer surface area for a passage can be estimated by the following equation:

$$A = A_p + \eta \phi A_s \quad (4.36)$$

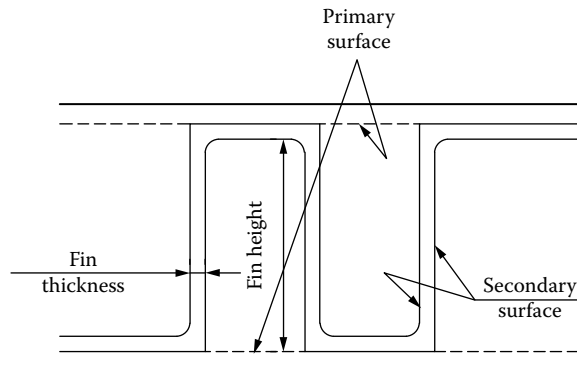


FIGURE 4.33 Primary and secondary heat transfer area for a unit flow passage.

single blanking (Figure 4.33) and fin efficiency, η is given by

$$\eta = \frac{\tan h(\beta/2)}{\beta/2} \quad (4.37a)$$

where

A_p is the primary heat transfer surface of a stream (Figure 4.33)

A_s is the secondary heat transfer surface of a stream (Figure 4.33)

η is the passage fin efficiency for single banking

l_f is the fin height

t_f is the fin thickness

n is the fin density

$$\beta = h \left(\frac{2\alpha}{k_f t_f} \right)^{0.5} \quad (4.37b)$$

α is the effective heat transfer coefficient of a stream

ϕ is the unperforated fraction ($1 - \text{ratio of perforated area to the total fin area}$)/100

k_f is the thermal conductivity of fin material

h is the heat transfer coefficient

The thermal length of a brazed aluminum PFHE is defined as the effective length of the finned region between, but not including, the distributors.

The information not specified directly is computed based on the specified surface geometries and core dimensions. Consider a PFHE as shown in Figure 4.34 in which L_1 and L_2 are the flow lengths, N_p and $N_p + 1$ are the number of flow passages on sides 1 and 2, respectively, and V is the total core volume. The following formulas define some of the geometrical properties on any one side of the PFHE. These geometrical relations are derived in Refs. [17,23,24].

The volume between plates on each side is given by

$$V_{p,1} = L_1 L_2 (b_1 N_p) \quad V_{p,2} = L_1 L_2 b_2 (N_p + 1) \quad (4.38)$$

Heat transfer area on each side is given by

$$A_1 = \beta_1 V_{p,1} \quad A_2 = \beta_2 V_{p,2} \quad (4.39)$$

where β_1 and β_2 are the surface area density on each side per unit volume between plates.

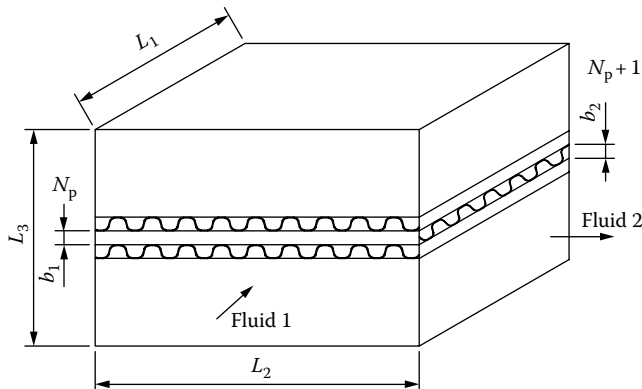


FIGURE 4.34 Plate-fin heat exchanger core to calculate surface geometrical parameters.

The ratio of minimum free flow area to frontal area (σ) on side 1 is given by

$$\sigma_1 = \frac{A_{0,1}}{A_{fr,1}} = \frac{A_{0,1}L_1}{A_{fr,1}L_1} = \frac{A_1D_{h,1}/4}{V} = \frac{V_{p,1}\beta_1D_{h,1}/4}{V} \quad (4.40a)$$

$$= \frac{b_1N_p\beta_1D_{h,1}/4}{b_1N_p + b_2(N_p + 1) + 2a(N_p + 1)} \approx \frac{b_1\beta_1D_{h,1}/4}{b_1 + b_2 + 2a} \quad (4.40b)$$

$$\sigma_2 = \frac{b_2(N_p + 1)\beta_2D_{h,2}/4}{b_1N_p + b_2(N_p + 1) + 2a(N_p + 1)} \approx \frac{b_2\beta_2D_{h,2}/4}{b_1 + b_2 + 2a} \quad (4.40c)$$

where a is the thickness of parting plates. The ratio is given similarly for side 2. Here, the last approximate equality is for the case when N_p is very large or the numbers of passages on the two sides are the same.

The heat transfer surface area on one side divided by the total volume V of the exchanger, designated as α_1 , is

$$\alpha_1 = \frac{A_1}{V} = \frac{4\sigma_1}{D_{h,1}} = \frac{b_1\beta_1}{b_1 + b_2 + 2a} \quad (4.41a)$$

Similarly, α_2 is given by

$$\alpha_2 = \frac{A_2}{V} = \frac{4\sigma_2}{D_{h,2}} = \frac{b_2\beta_2}{b_1 + b_2 + 2a} \quad (4.41b)$$

4.3.3.2 Components of Pressure Loss

The individual pressure losses within a heat exchanger typically consist of [12]

1. Expansion loss into the inlet header
2. Contraction loss at the entry to the core
3. Loss across the inlet distributor
4. Loss across the heat transfer length
5. Loss across the outlet distributor
6. Expansion loss into the outlet header
7. Contraction loss into the outlet nozzle

4.3.3.2.1 Single-Phase Pressure Loss

The frictional pressure loss across a plate-fin passage and at any associated entry, exit, and turning losses can be expressed by [12]

$$\Delta p = 4f \left(\frac{L}{D_h} \right) \left(\frac{G_m^2}{2\rho} \right) + K \left(\frac{G_m^2}{2\rho} \right) \quad (4.42)$$

where

f is the fanning friction factor

L is the passage length

D_h is the hydraulic diameter of passage

G_m is the mass velocity (mass flux) of stream

ρ is the density of a stream

K is the expansion, contraction, or turning loss coefficient

Δp is the overall pressure drop

4.4 FACTORS INFLUENCING TUBE-FIN HEAT EXCHANGER PERFORMANCE

Important factors that influence the heat transfer performance of tube-fin heat exchangers include the following:

1. Tube layout (staggered vs. inline arrangement)
2. Equilateral layout versus equivelocity layout
3. Number of rows
4. Tube pitch
5. Finned tube variables (fin height, spacing, thickness)
6. Fin tubes with surface modifications
7. Side leakage
8. Boundary-layer disturbances and characteristic flow length
9. Contact resistance in finned tube heat exchangers
10. Induced draft versus forced draft

Johnson [25] and Rabas and Taborek [7] discuss the effect of various tube-fin parameters on thermohydraulic performance.

4.4.1 TUBE LAYOUT

The two basic arrangements of the tubes in a tube bank are (1) staggered arrangement with equilateral triangular pitch and (2) inline arrangement. The extent of transverse flow in the inline layout is small in comparison to the staggered arrangement. The most commonly used is the staggered layout. There are very few applications of low-finned tubes with the inline arrangement. It may be used when airside fouling problems are encountered. For identical operating conditions, the inline arrangement has low heat transfer, of the order of 70%, and pressure drop is also of this order.

4.4.2 EQUILATERAL LAYOUT VERSUS EQUIVELOCITY LAYOUT

In the conventional equilateral staggered layout, the area available for airflow in the transverse direction is half of that available in the diagonal direction; therefore, energy is lost in accelerating and decelerating the air stream as it flows through the bank. In the equivelocity layout, these two areas are made equal by adjusting the transverse (P_t) and longitudinal (P_l) pitches, thus minimizing these losses. In general, for applications where horsepower is evaluated at a high premium and a reduced pressure drop is attractive, even at the expense of some loss of thermal performance, an expanded pitch layout type should be strongly considered.

4.4.3 NUMBER OF TUBE ROWS

The addition of tube rows in the crossflow direction is the common way of increasing heat transfer area when the frontal area of the tube bank is fixed. Such an addition of tube rows increases the flow length for the air and may affect the fluid dynamics with a possible effect on heat transfer and pressure drop. Pressure drop through the tube bundle increases with the number of tube rows. The temperature drop through the tube bundle also increases with the number of tube rows, though the effect is very large with the first few tube rows and for a very large number of tube rows the effect is small. Temperature drop through a multirow tube bank is shown schematically in Figure 4.35. The row effect on heat transfer coefficient is discussed by Johnson [25]. A basic difference exists between the row effects for the inline and the staggered arrangements. For an inline arrangement, the heat transfer coefficient decreases with an increase in the number of rows. Brauer [27] shows that the one-row tube bank heat transfer coefficient is approximately 50%–80% higher than the average for four rows, whereas for a staggered arrangement the four-row tube bank has approximately 30% higher heat transfer coefficient (average) than a one-row tube bank.

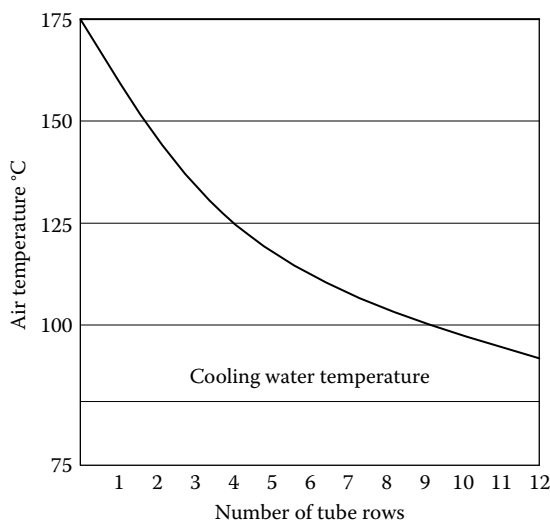


FIGURE 4.35 Temperature drop through a multi-tube row heat exchanger—schematic (for a typical case).

4.4.4 TUBE PITCH

Tube pitch is commonly used in heat-exchanger design to affect compactness of the core and flow conditions. The hydraulic diameter increases with the pitch. Based on comparable air velocities, the pitch has no effect on the heat transfer coefficient. However, increasing the pitch strongly affects the pressure drop, as it decreases the pressure drop through the bundle [25].

4.4.5 TUBE-FIN VARIABLES

The tube-fin variables that affect the thermal performance include fin height, fin spacing, and thickness and thermal conductivity of the fin material. Surface area of the tube bank can be increased by employing fin tubes with high (longer) fins and denser spacing. However, increasing the fin height will decrease the fin effectiveness, and may lower heat transfer compared with the short fins. Denser fins may lower the heat transfer because of laminarization of the flow conditions between the fins [25]. Fin efficiency increases with a reduction in fin height and an increase in fin thickness. Thermal conductivity is usually not a problem in selecting the material of a primary surface, but it is important in extended surfaces because of the relatively long and narrow heat flow path, which affects their heat transfer performance [6].

4.4.5.1 Fin Height and Fin Pitch

The fin height and fin pitch that can be used effectively are fundamentally related to the boundary-layer thickness [6]. Wen-Jei Yang [6] states the rule of thumb: (1) For large thermal boundary-layer thickness, the heat transfer coefficient, h , is low and thus high fins are employed; (2) low fins are employed in the case of a thin boundary layer where h is high; and (3) if the fin spacing is too small, the main stream cannot penetrate the spaces between the fins, resulting in no increase in thermal boundary area and an excessive pressure drop.

4.4.6 FINNED TUBES WITH SURFACE MODIFICATIONS

The term “surface modification” refers to fin tubes that have extended surfaces that are mechanically deformed to various shapes by crimping, corrugating, cutting, slotting, or serrating the fins; for continuous plate-fins, surface interruptions constitute surface modification [25]. Any surface modification will increase the heat transfer and pressure drop as compared with the identical smooth fin. Common surface modifications for circular fins are discussed further in Chapter 8.

4.4.7 SIDE LEAKAGE

The heat transfer and pressure-drop performance of a tube bank is affected by the leakage flow between the outermost tube and the side walls. This is equivalent to the bundle-to-shell bypass stream (C-stream) leakage in a shell and tube exchanger. The effect of bypass flow can be minimized by attaching side seals to the exchanger in every even row as shown in Figure 4.36. Clearance between the core and the housing can be minimized by welding metal strips to the housing or attaching metal strips to the header as shown in Figure 4.36b.

4.4.8 BOUNDARY-LAYER DISTURBANCES AND CHARACTERISTIC FLOW LENGTH

Periodic interruption of the boundary layer is achieved by breaking the total flow length into many characteristic lengths by means of OSFs, louvered fins, wavy fins, etc. [28]. The characteristic flow length, L_f , is illustrated in Figure 4.37. The characteristic flow length and the hydraulic diameter, D_h , are responsible for the numerical merits of a surface geometry. The representative length of finned heat exchangers as parameters to represent their performance suggests that it would be possible

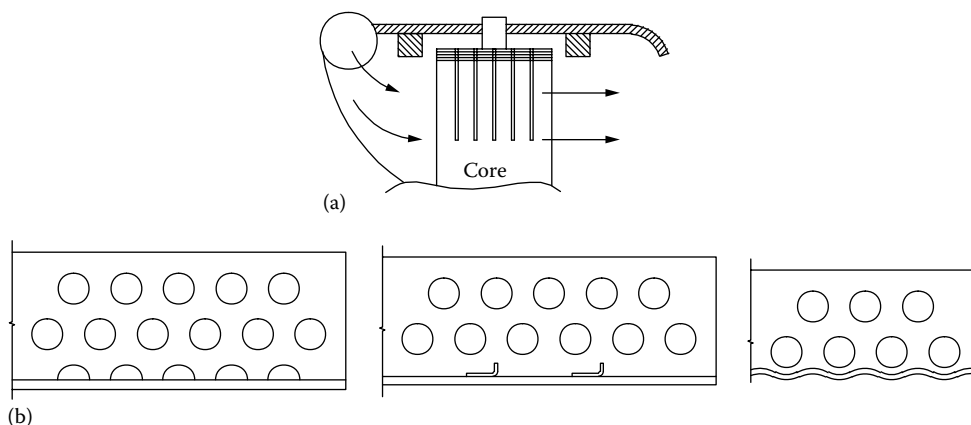


FIGURE 4.36 Sealing strips to arrest bypass flow: (a) between the core and the housing and (b) between the tubes and side sheets.

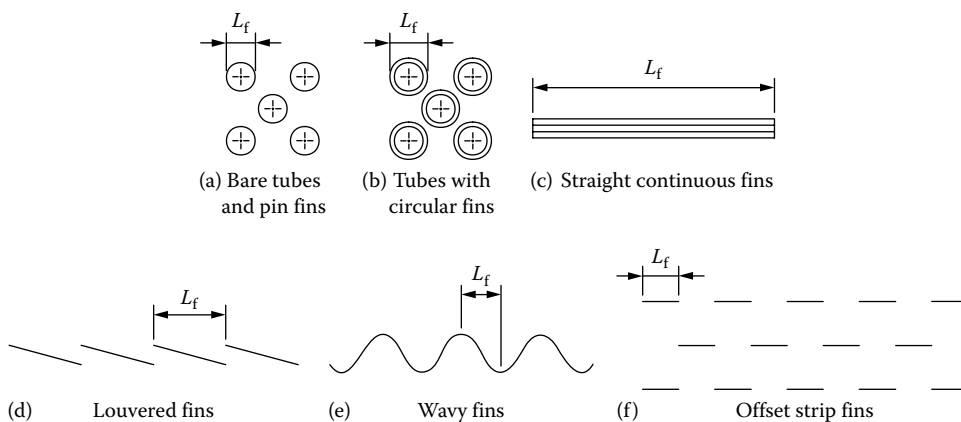


FIGURE 4.37 Characteristic flow length between major boundary layer disturbance for various heat exchanger surfaces. (Adapted from LaHaye, P.G. et al., *Trans. ASME, J. Heat Transfer*, 96, 511, 1974.)

to enhance their performance by shortening the representative length of the fin and using finer segmentation than the regions of louvered or OSFs [29]. The application of the pin finned surface can be considered one of the best candidates.

4.4.9 CONTACT RESISTANCE IN FINNED TUBE HEAT EXCHANGERS

4.4.9.1 Continuous Finned Tube Exchanger

In the design of finned tube heat exchangers, the contribution of contact resistance at the interface between the tube and fin collar is not always negligible compared with the total heat transfer resistance, Figure 4.38 [29]. This is particularly true for mechanically bonded tube-fin exchangers used in low-pressure applications such as air-conditioning industries and air coolers for supercharged engine intake air. In the heat exchanger assembly process, the initial interference, the microhardness of the softer material at the interface, contact area, and contact pressure are parameters that determine the contact resistance [30]. Selection of the proper bullet size can optimize the degree of contact at the interface. During the last three decades, many researchers have developed experimental methods to measure thermal contact resistance accurately. An experimental method to measure contact resistance in a vacuum environment is described by Nho et al. [30]. In a typical experimental setup, they found that the contact resistance at the tube and fin interface was 17.6%–31.5% of the overall resistance in a vacuum environment.

4.4.9.2 Tension-Wound Fins on Circular Tubes

For round-fin tubes with aluminum fins wrapped on steel tubes under tension, the contact resistance increases quickly with the operating temperature so that their application is limited to temperatures of 100°C or less [31]. Otherwise, the tension would be reduced, leading to fin loosening, due to the higher thermal expansion of aluminum.

4.4.9.3 Integral Finned Tube

With an integral finned tube, there is no concern at the fin bond about heat transfer resistance and the integrity of tubing, regardless of temperature and pressure levels. However, only certain fin geometries can be obtained with an extrusion process.

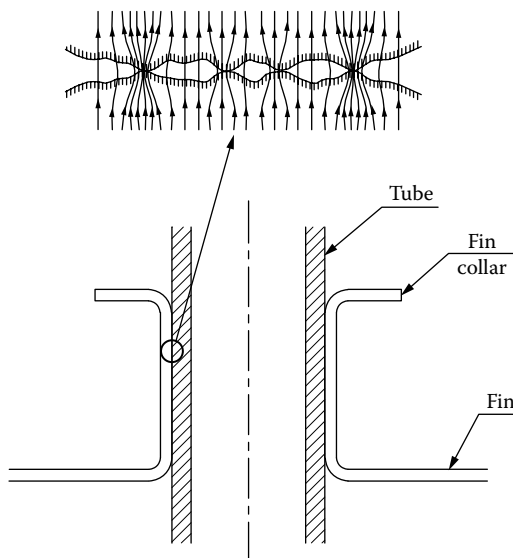


FIGURE 4.38 Metal-to-metal contact between the tube and the fin.

4.4.10 INDUCED DRAFT VERSUS FORCED DRAFT

The heat transfer and pressure drop depend on the method used to generate the flow on the tube bank, namely, induced draft or forced draft. When a fluid enters the tube bank, the level of turbulence can change with penetration into the bundle. The tube bundle heat transfer coefficient and pressure-drop performance vary for each additional row for a shallow exchanger, and become independent of the number of rows only for the deep bundles with a very large number of tube rows [7]. Common practice is to apply a row correction multiplier to the deep bundle correlations (ideal bundle) to account for these variations. Recommendations by Rabas et al. [7] for the mode of flow are discussed next.

4.4.10.1 Induced Draft

For induced draft, the recommended approach is to use the heat transfer row correction for plain tube banks. For the plain tube, bundle row corrections refer to Giedt [32] and ESDU [33]. The value varies from 0.65 for a single row to about 0.98–1.0 for an eight tube rows bundle. The bundle pressure-drop variation with row number is smaller than the heat transfer coefficient variation and hence the row effect is usually ignored.

4.4.10.2 Forced Draft

A conservative approach suggested is to neglect the row correction for the forced draft mode of operation for low-finned tube banks [7].

4.5 THERMOHYDRAULIC FUNDAMENTALS OF FINNED TUBE HEAT EXCHANGERS

It is a common practice to use the Colburn j factor to characterize the heat transfer performance and the Fanning friction factor f to characterize the pressure drop of the tube banks as functions of Reynolds number. This section provides empirical correlations for j and f factors. With these correlations, the performance of geometrically similar heat exchangers can be predicted, within the parameter range of the correlations.

4.5.1 HEAT TRANSFER AND FRICTION FACTOR CORRELATIONS FOR CROSSFLOW OVER STAGGERED FINNED TUBE BANKS

During the last 50 years, many investigations have been carried out to determine the heat transfer and pressure drop over the tube banks. One of the first correlations was established by Grimson [34] for bare tube banks. A standard reference for the heat transfer and friction data of PFHE surfaces is the book by Kays and London [17]. This book presents j and f versus Reynolds number plots for tube banks, tube-fin heat exchangers, and 52 different plate-fin surface geometries. Some of these data were published in *Transactions of the ASME*. Shah and Bhatti [35] summarize important theoretical solutions and correlations for simple geometries that are common in compact heat exchangers. Most of the experimental data have been obtained with air as the test fluid. The j factor and fanning f factor are defined rather consistently in the literature by the following equations:

$$j = \frac{h(\text{Pr})^{2/3}}{Gc_p} \quad (4.43a)$$

$$= \frac{h}{Gc_p} \left(\frac{\mu c_p}{k} \right)^{2/3} \quad (4.43b)$$

$$h = jGc_p \left(\frac{\mu c_p}{k} \right)^{-2/3} \quad \text{or} \quad h = \frac{Nuk}{D_h} \quad (4.43c)$$

$$\Delta p = 4f \frac{L}{D_h} \left(\frac{G_{\max}^2}{2g_c \rho} \right) \quad (4.44)$$

where G_{\max} is given by

$$G_{\max} = \rho U_f \left(\frac{A_{fr}}{A_o} \right) \quad (4.45)$$

and is based on the minimum free flow area within the tube bundle. This minimum free flow area includes the gaps between the outermost tubes and the side walls of the tube bundle. In Equation 4.44, contraction and expansion losses and momentum losses are neglected; only flow friction effect is taken into account.

The Reynolds number is defined as

$$Re = \frac{Gd_r}{\mu} \quad \text{or} \quad Re = \frac{Gd_o}{\mu} \quad \text{or} \quad Re = \frac{GD_h}{\mu} \quad (4.46)$$

where

d_r is the fin root diameter or the tube outside diameter, which depends on the tube manufacturing techniques

D_h is the hydraulic diameter

The j factor is related to Stanton number and Prandtl number by

$$j = St(Pr)^{2/3} \quad (4.47)$$

where the Stanton number is given by

$$St = \frac{Nu}{Re(Pr)} \quad (4.48)$$

From Equations 4.47 and 4.48, the expression for j is given by

$$j = \frac{Nu}{Re(Pr)^{1/3}} \quad (4.49)$$

4.5.2 THE j AND f FACTORS

4.5.2.1 Bare Tube Bank

Experimental heat transfer and fluid friction data for six staggered circular tube patterns and one inline arrangement are given in Ref. [36]. The results of Ref. [36] have been presented in Kays and London [17].

The Giedt [32] correlation states that the thermal performance of a bare tube bank is given by

$$j = \frac{0.376}{Re^{0.4}} \quad (4.50)$$

4.5.2.1.1 Inline Tube Bank

For a 10-row-deep inline tube bank, the correlation for j is given by [37]

$$j = \frac{0.33}{\text{Re}^{0.4}} \quad (4.51)$$

This correlation is valid for tube diameter from 1/4 to 2 in., and Reynolds number range 100–80,000.

4.5.2.2 Circular Tube-Fin Arrangement

The basic geometry is shown in Figure 4.39.

Experimental heat transfer and fluid friction data for three circular finned tube surfaces are given in London et al. [38]. The results of Ref. [38] have been presented in Kays and London [17].

4.5.2.2.1 Briggs and Young Correlations [39]

For low-fin tube banks, the correlation based on experimental heat transfer data is

$$\text{Nu} = 0.1507 \text{Re}_d^{0.667} \text{Pr}^{1/3} \left(\frac{s}{l_f} \right)^{0.164} \left(\frac{s}{t_f} \right)^{0.075} \quad (4.52)$$

where $[s = (l - N_f t_f)/N_f]$ with a standard deviation of 3.1%. This is applicable for a circular finned tube with low-fin height and high-fin density, Re_d (based on tube outer diameter) = 1000–20,000, $N_r \geq 6$, and equilateral triangular pitch.

For high-fin tube banks, the correlation based on experimental heat transfer data is

$$\text{Nu} = 0.1378 \text{Re}_d^{0.718} \text{Pr}^{1/3} \left(\frac{s}{l_f} \right)^{0.296} \quad (4.53)$$

with a standard deviation of 5.1%.

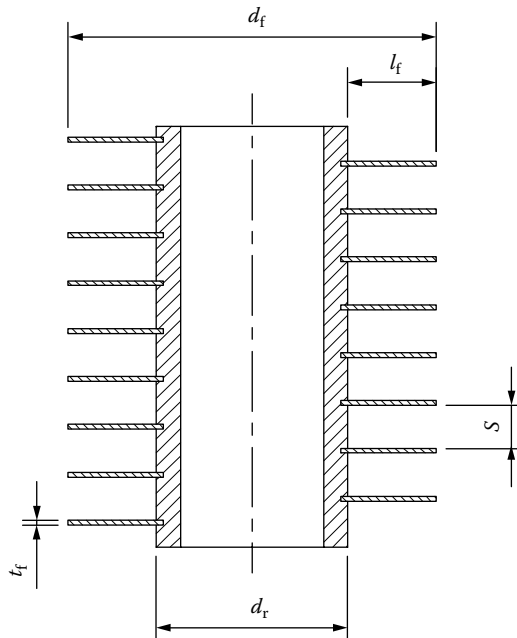


FIGURE 4.39 Tube-fin details.

For all tube banks, the correlation based on regression analysis is

$$\text{Nu} = 0.134 \text{Re}_d^{0.681} \text{Pr}^{1/3} \left(\frac{s}{l_f} \right)^{0.200} \left(\frac{s}{t_f} \right)^{0.1134} \quad (4.54)$$

$$j = 0.134 \text{Re}_d^{-0.319} \left(\frac{s}{l_f} \right)^{0.200} \left(\frac{s}{t_f} \right)^{0.1134} \quad (4.55)$$

with a standard deviation of 5.1%.

4.5.2.2.2 Robinson and Briggs Correlations [40]

For equilateral triangular pitch with high-finned tubes,

$$f = 9.465 \text{Re}_d^{-0.316} \left(\frac{P_t}{d_o} \right)^{-0.927} \quad (4.56)$$

with a standard deviation of 7.8%. This is applicable for the following parameter definitions:

$$\text{Re}_d = 2000\text{--}50,000$$

$$d_f = 1.562\text{--}2.750$$

$$P_t = 1.687\text{--}4.50$$

For isosceles triangular layout,

$$f = 9.465 \text{Re}_d^{-0.316} \left(\frac{P_t}{d_r} \right)^{-0.927} \left(\frac{P_t}{P_l} \right)^{0.515} \quad (4.57)$$

This is applicable for

$$d_o(\text{mm}) = 18.6\text{--}40.9$$

$$l_f/d_o = 0.35\text{--}0.56$$

$$l_f/s = 4.5\text{--}5.3$$

$$\sigma = 13.3\text{--}17.4$$

$$P_t/d_o = 1.8\text{--}4.6$$

$$P_l/d_o = 1.8\text{--}4.6$$

$$N_r \geq 6$$

4.5.2.2.3 Rabas, Eckels, and Sabatino Correlation [41]

For tube banks arranged on an equilateral triangular pitch with low-finned tubes,

$$j = 0.292 \text{Re}_d^{-m} \left(\frac{s}{d_f} \right)^{1.116} \left(\frac{s}{l_f} \right)^{0.257} \left(\frac{t_f}{s} \right)^{0.666} \\ \times \left(\frac{d_f}{d_r} \right)^{0.473} \left(\frac{d_f}{t_f} \right)^{0.7717} \alpha_h \alpha_n \quad (4.58a)$$

$$m = 0.415 - 0.0346 \ln \left(\frac{d_f}{s} \right) \quad (4.58b)$$

$$f = 3.805 Re_d^{-0.234} \left(\frac{s}{d_f} \right)^{0.251} \left(\frac{l_f}{s} \right)^{0.759} \\ \times \left(\frac{d_r}{d_f} \right)^{0.729} \left(\frac{d_r}{P_t} \right)^{0.709} \left(\frac{P_t}{P_l} \right)^{0.379} \quad (4.59)$$

where α_h and α_n are a temperature-dependent fluid properties correction factor and a row correction factor, respectively. The row correction factor has been covered earlier. Rabas and Taborek [7] recommend the following correlations for α_h :

$$\alpha_h = \left(\frac{T_b + 273}{T_w + 273} \right)^{0.25} \quad (4.60a)$$

$$\alpha_h = \left(\frac{Pr(T_b)}{Pr(T_w)} \right)^{0.26} \quad (4.60b)$$

Equation 4.60a is from Weierman [42], and Equation 4.60b is from ESDU [33]. However, the Prandtl number format is recommended by Rabas and Taborek [7] for liquids and there is no fluid property correction term for the friction factor f . These are applicable for $l_f < 6.35$ mm, $1000 < Re_d < 25,000$, 4.76 mm $\leq d \leq 31.75$ mm, $246 \leq N_f \leq 1181$ fins/m, 15.08 mm $\leq P_t \leq 111$ mm, 10.32 mm $\leq P_l \leq 96.11$ mm, $P_l \leq P_t$, $d_f/s < 40$, and $N_r > 6$.

4.5.2.2.4 ESDU Correlation [33]

$$j = 0.183 Re_d^{+0.3} Pr^{0.027} \left(\frac{s}{l_f} \right)^{0.36} \left(\frac{l_f}{d_f} \right)^{0.11} \left(\frac{P_t}{d_f} \right)^{0.06} \alpha_h \alpha_n \quad (4.61a)$$

$$f = 4.71 Re_d^{(-0.286)} \left(\frac{X_t}{d_r} - 1 \right)^{(-0.36)} \left(\frac{l_f}{s} \right)^{0.51} \left(\frac{X_t - d_r}{X_l - d_r} \right)^{0.536} \quad (4.61b)$$

This is applicable for $1000 < Re_d < 80,000$ or $100,000$ and $N_t > 10$.

4.5.2.2.5 Ganguly et al. [43] Correlation

$$j = 0.255 Re_d^{-0.3} \left(\frac{d_f}{s} \right)^{-0.3} \quad (4.62)$$

$$f = F_s f_p \quad (4.63a)$$

where

$$F_s = 2.5 + \frac{3}{\pi} \tan^{-1} [0.5(A/A_p - 5)] \quad (4.63b)$$

$$f_p = 0.25\beta \left(\text{Re}_d^{-0.25} \right) \quad (4.63c)$$

$$\beta = 2.5 + 1.2(X_t - 0.85)^{-1.06} + 0.4 \left(\frac{X_1}{X_t} - 1 \right)^3 - 0.01 \left(\frac{X_t}{X_1} - 1 \right)^3 \quad (4.63d)$$

For both j and f factors, 95% of the data correlated within 15% and 100% of the data correlated within 20%. This is applicable for $l_f \leq 6.35$ mm, $800 \leq \text{Re}_d \leq 800,000$, $20 \leq \theta \leq 40$, $X_t \leq 4$, and $N_r \geq 4$.

4.5.2.2.6 Elmahdy and Biggs Correlation [44]

For a multirow staggered circular or continuous fin-tube arrangement,

$$j = C_1 \text{Re}_h^{C_2} \quad (4.64a)$$

where

$$C_1 = 0.159 \left(\frac{t_f}{l_f} \right)^{0.141} \left(\frac{D_h}{t_f} \right)^{0.065} \quad (4.64b)$$

$$C_2 = -0.323 \left(\frac{t_f}{l_f} \right)^{0.049} \left(\frac{s}{t_f} \right)^{0.077} \quad (4.64c)$$

This correlation is also valid for circular fin-tube arrangement. The experimentally determined j factor is 3%–5% lower than that predicted analytically.

This correlation is applicable for the following:

$$\text{Re}_d = 200\text{--}2000$$

$$D_h/t_f = 3.00\text{--}33.0$$

$$t_f/l_f = 0.01\text{--}0.45$$

$$d_f/P_1 = 0.87\text{--}1.27$$

$$s/t_f = 2.00\text{--}25.0$$

$$d_f/P_t = 0.76\text{--}1.40$$

$$d/d_f = 0.37\text{--}0.85$$

$$\sigma = 0.35\text{--}0.62$$

4.5.2.3 Continuous Fin on Circular Tube

4.5.2.3.1 Gray and Webb Correlation [45]

Four-row array:

$$j_4 = 0.14 \text{Re}_d^{-0.328} \left(\frac{P_t}{P_1} \right)^{-0.502} \left(\frac{s}{d_o} \right)^{0.0312} \quad (4.65)$$

For this form, 89% of data were correlated within $\pm 10\%$.

Up to three rows:

$$\frac{j_N}{j_4} = 0.991 \left[2.24 \text{Re}_d^{-0.092} \left(\frac{N_r}{4} \right)^{-0.031} \right]^{0.607(4-N_r)} \quad (4.66)$$

This is used for $N_r = 1-3$ (for $N_r > 4$, the row effect is negligible). The standard deviation is -4% to $+8\%$.

Pressure drop correlation: Gray and Webb correlation is based on a superposition model that was initially proposed by Rich [46]. The basic model is written as

$$\Delta p = \Delta p_f + \Delta p_t \quad (4.67)$$

where

Δp_t , is the pressure-drop component due to the drag force on the tubes

Δp_f is the pressure-drop component due to the friction factor on the fins

Accordingly, the expressions for Δp_t and Δp_f are given by

$$\Delta p_f = f_f \frac{A_f}{A_c} \frac{G^2}{2g_c \rho} \quad (4.68a)$$

$$\Delta p_t = f_t \frac{A_t}{A_{c,t}} \frac{G^2}{2g_c \rho} \quad (4.68b)$$

$$f = f_f \frac{A_f}{A} + f_t \left(1 - \frac{A_f}{A} \right) \left(1 - \frac{t_f}{s} \right) \quad (4.69a)$$

$$f_f = 0.508 \text{Re}_d^{-0.521} \left(\frac{P_t}{d_o} \right)^{1.318} \quad (4.69b)$$

The mass velocity G used in Equations 4.68a and 4.68b is evaluated as the same G that exists in the finned-tube exchanger. Several correlations are available for the friction factor of flow normal to tube banks [32,36,47]. Parameters are

$$N_r = 1-8 \text{ or more}$$

$$\text{Re}_d = 500-24,700$$

$$P_t/d_o = 1.97-2.55$$

$$P_l/d_o = 1.70-2.58$$

$$s/d_o = 0.08-0.64$$

$$\text{Re} = Gd_o/\mu$$

4.5.2.3.2 McQuiston Correlation [48]

Continuous-fin tube heat exchanger with four rows:

$$j_4 = 0.0014 + 0.2618 \text{Re}_d^{-0.4} \left(\frac{A}{A_t} \right)^{-0.15} \quad (4.70)$$

where A/A_t is the ratio of the total surface area to the area of the bone tube. Here, 90% of data were correlated within $\pm 10\%$.

Less than four rows:

$$\frac{j_N}{j_4} = \frac{1.0 - 128 N_r \text{Re}_L^{-1.2}}{1.0 - 5120 \text{Re}_L^{-1.2}} \quad (4.71)$$

for $N_r = 1-3$ with a standard deviation of -9% to $+18\%$.

$$f = 4.904 \times 10^{-3} + 1.382 \alpha^2 \quad (4.72a)$$

$$\alpha = \text{Re}_d^{-0.25} \left(\frac{R}{R^*} \right)^{0.25} \left[\frac{(X_a - 2R)N_f}{4(1 - n_f t_f)} \right]^{-0.4} \left(\frac{P_t}{2R^*} - 1 \right)^{-0.5} \quad (4.72b)$$

$$\left(\frac{R^*}{R} \right) = \frac{A/A_t}{(P_t - 2R)n_f + 1} \quad (4.72c)$$

$$\frac{A}{A_t} = \frac{4}{\pi} \frac{P_t}{D_h} \frac{P_t}{d_o} \sigma \quad (4.72d)$$

$$R = \frac{d_o}{2}$$

Parameters are

$$P_1, P_t = 1-2 \text{ in.}$$

$$\alpha = 0.08-0.24$$

$$d_o = \frac{3}{8} - \frac{5}{8} \text{ in.}$$

$$\text{Tube spacing} = 1-2 \text{ in.}$$

$$N_f = 4-14 \text{ fin/in.}$$

$$t_f = 0.006-0.010 \text{ in.}$$

4.5.2.4 Continuous Fin on Flat Tube Array

Performance figures for three geometries are given in Kays and London [17]. New data are presented for two new types of rippled fin by Maltson et al. [49]. For these types of layouts, fin length for calculating fin efficiency is half the spanwise length of fin between tubes. Kroger [50] presented

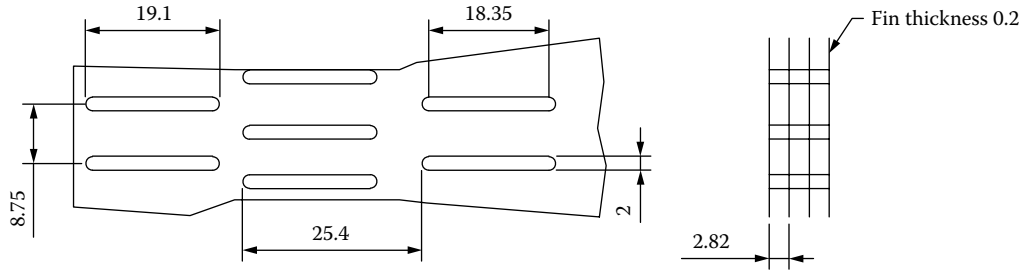


FIGURE 4.40 Geometrical details of a flat tube-fin radiator to calculate j and f factors as per Equation 4.73. (Parameters are in mm.)

performance characteristics for a six rows deep (3×2) core geometry given in Figure 4.40, whose j and f factors are given by

$$j = \frac{0.174}{\text{Re}_h^{0.387}}, \quad f = \frac{0.3778}{\text{Re}_h^{0.3565}} \quad (4.73)$$

These equations were also found to correlate the data for having eight rows deep (4×2).

4.6 CORRELATIONS FOR j AND f FACTORS OF PLATE-FIN HEAT EXCHANGERS

4.6.1 OFFSET STRIP FIN HEAT EXCHANGER

Wieting correlations [51] consist of power-law curve fits of the j and f values for 22 heat exchanger surface geometries over two Reynolds number ranges: $\text{Re}_h \leq 1000$, which is primarily laminar, and $\text{Re}_h \geq 2000$, which is primarily turbulent.

For $\text{Re}_h \leq 1000$,

$$j = 0.483 \left(\frac{l_f}{D_h} \right)^{-0.162} \xi^{-0.184} \text{Re}_h^{-0.536} \quad (4.74)$$

$$f = 7.661 \left(\frac{l_f}{D_h} \right)^{-0.384} \xi^{-0.092} \text{Re}_h^{-0.712} \quad (4.75)$$

For $\text{Re}_h \geq 2000$,

$$j = 0.242 \left(\frac{l_f}{D_h} \right)^{-0.322} \left(\frac{t_f}{D_h} \right)^{0.089} \text{Re}_h^{-0.368} \quad (4.76)$$

$$f = 1.136 \left(\frac{l_f}{D_h} \right)^{-0.781} \left(\frac{t_f}{D_h} \right)^{0.534} \text{Re}_h^{-0.198} \quad (4.77)$$

where Re_h is the Reynolds number based on hydraulic diameter D_h given by

$$D_h = \frac{2sh_f}{s + h_f} \quad (4.78)$$

and α is the aspect ratio, s/h_f (Figure 4.41).

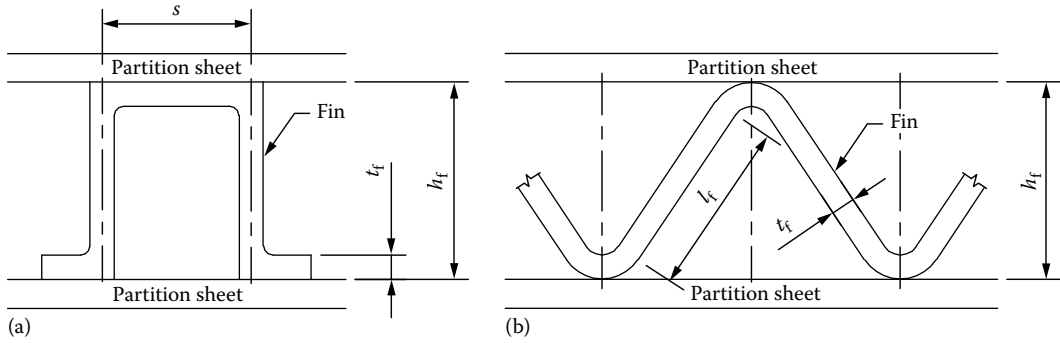


FIGURE 4.41 Details of offset strip fin. (a) Rectangular fin and (b) triangular fin.

Joshi and Webb [16] have developed a more sophisticated theoretical model to predict the characteristics of j and f versus Reynolds number for the OSF. This model preferably includes all geometrical factors of the array (s/d , t_f/l_f , t_f/s) and heat transfer to the base surface area to which the fins are attached.

Manglik and Bergles [52] reviewed the available j and f data and developed improved correlations for j and f , with a single predictive equation representing the data continuously from laminar to turbulent flow. Their correlations for j and f are as follows:

$$j = 0.6522 \text{Re}_h^{-0.5403} \xi^{-0.1541} \delta^{0.1499} \eta^{-0.0678} \times \left\{ 1 + 5.269 \times 10^{-5} \text{Re}_h^{1.340} \xi^{0.504} \delta^{0.456} \eta^{-1.055} \right\}^{0.1} \quad (4.79)$$

and

$$f = 9.6243 \text{Re}_h^{-0.7422} \xi^{-0.1856} \delta^{0.3053} \eta^{0.2659} \times \left\{ 1 + 7.6669 \times 10^{-8} \text{Re}_h^{4.429} \xi^{0.92} \delta^{3.767} \eta^{0.236} \right\}^{0.1} \quad (4.80)$$

where ξ is the aspect ratio = s/h_s ; $\delta = t_f/l_f$; $\eta = t_f/s$; and Re_h is based on the hydraulic diameter D_h given by the following equation:

$$D_h = \frac{4sh_f l_f}{2(sl_f + h_f l_f + t_f h_f) + t_f s} \quad (4.81)$$

These equations correlate the experimental data for the 18 cores within $\pm 20\%$.

4.6.2 LOUVERED FIN

Based on tests of 32 louvered-fin geometries, Davenport [19] developed multiple regression correlations for j and f versus Re as follows:

$$j = 0.249 \text{Re}_{lp}^{-0.42} l_h^{0.33} H_1^{0.26} \left(\frac{l_l}{H_1} \right)^{1.1} \quad 300 < \text{Re} < 4000 \quad (4.82)$$

$$f = 5.47 \text{Re}_{\text{lp}}^{-0.72} l_{\text{h}}^{0.37} H_1^{0.23} l_{\text{p}}^{0.2} \left(\frac{l_1}{H_1} \right)^{0.89} \quad 70 < \text{Re} < 1000 \quad (4.83a)$$

$$f = 0.494 \text{Re}_{\text{lp}}^{-0.39} H_1^{0.46} \left(\frac{l_{\text{h}}}{H_1} \right)^{0.33} \left(\frac{l_1}{H_1} \right)^{1.1} \quad 1000 < \text{Re} < 4000 \quad (4.83b)$$

where

Re_{lp} is the Reynolds number based on louver pitch

l_{h} is the louver height

l_1 is the louver length

l_{p} is the louver pitch

H_1 is the fin height

Here, 95% of the data could be correlated within $\pm 6\%$ for heat transfer, and within $\pm 10\%$ for the friction factor. The required dimensions are millimeters. Figure 4.17 defines the terms in the equations. The characteristic dimension in the Reynolds number is louver pitch, l_{p} and not D_{h} .

4.6.3 PIN FIN HEAT EXCHANGERS

For the heat transfer characteristics of pin-finned surfaces, refer to Kays [53], Norris et al. [54] and Kanzaka et al. [55], among others. The results of Ref. [53] were presented in Kays and London [17]. The works of Kays [53] and Norris [54] are limited to the heat transfer characteristics of pin fins having their representative length comparable to those of louvered or offset fins currently used [55]. To materialize a heat exchanger that has thermal performance superior to those of offset or louvered fins requires a more finely segmented surface of less than 1 mm at maximum. Kanzaka et al. [55] studied the heat transfer and fluid dynamic characteristics of pin-finned surfaces of various profiles, namely, circular, square, and rectangular, and both inline and staggered arrangements.

Staggered arrangements: For their test element, the expression for the Nusselt number is

$$\text{Nu}_{\phi} = 0.662 \text{Re}_{\phi}^{0.5} \text{Pr}^{1/3} \quad (4.84)$$

Inline arrangements: The expression for the Nusselt number is

$$\text{Nu}_{\phi} = 0.440 \text{Re}_{\phi}^{0.5} \text{Pr}^{1/3} \quad (4.85)$$

where ϕ is the characteristic length. The expressions for Nusselt number and d_{ϕ} are

$$\text{Nu}_{\phi} = \frac{hd_{\phi}}{k} \quad \text{Re}_{\phi} = \frac{Gd_{\phi}}{\mu} \quad (4.86)$$

$$d_{\phi} = \frac{\pi d_{\text{p}}}{2} \quad \text{for circular fins} \quad (4.87a)$$

$$d_{\phi} = \frac{a_{\text{p}} + b_{\text{p}}}{2} \quad \text{for rectangular fins} \quad (4.87b)$$

where

a_{p} and b_{p} are the rectangular pin fin dimensions (i.e., cross section is $a_{\text{p}} \times b_{\text{p}}$)

d_{p} is the circular fin diameter

4.7 FIN EFFICIENCY

Fins are primarily used to increase the surface area and consequently to enhance the total heat transfer rate. Both conduction through the fin cross section and convection from the surface area take place. Hence, the fin surface temperature is generally lower than the base (prime surface) temperature if the fin convects heat to the fluid. Due to this, the fin transfers less heat than if it had been at the base temperature. This is described by the fin temperature effectiveness or fin efficiency η_f . The fin temperature effectiveness is defined as the ratio of the actual heat transfer, q , through the fin to that which would be obtained, q_i , if the entire fin were at the base metal temperature:

$$\eta_f = \frac{q}{q_i} \quad (4.88)$$

The fin efficiency for plate-fin surfaces in heat exchanger design can be determined from Gardner [56], Kern and Kraus [57], Scott and Goldschmidt [58], Schmidt [59], Zabronsky [60], Lin and Sparrow [61], Shah [19,62], and others. Fin efficiency of a plain rectangular profile cross section is discussed in this section.

4.7.1 FIN LENGTH FOR SOME PLATE-FIN HEAT EXCHANGER FIN CONFIGURATIONS

The two most commonly used plate-fin geometries are rectangular and triangular passages, shown in Figure 4.41. From a review of Figure 4.41, the fin length l_f for a rectangular passage is

$$l_f = \frac{h_f - t_f}{2} \approx \frac{h_f}{2} \quad (4.89)$$

Note that no effect of the fin inclination is taken into account in Equation 4.89 for the triangular fin. Numerous fin geometries and corresponding fin lengths for various flow passage configuration are presented by Shah [24].

4.7.2 FIN EFFICIENCY

4.7.2.1 Circular Fin

Kern and Kraus [57], formula for rectangular-profile circular fin: For circular fins (Figure 4.42), the fin efficiency is given by

$$\eta_f = \frac{2r_o}{m(r_c^2 - r_o^2)} \left[\frac{I_1(mr_c)K_1(mr_o) - K_1(mr_c)I_1(mr_o)}{I_o(mr_o)K_1(mr_c) + I_1(mr_c)K_o(mr_o)} \right] \quad (4.90)$$

where

$$m = (2h/k_f t_f)^{0.5}$$

I_n is the modified Bessel function of the first kind (n th order)

K_n is the modified Bessel function of the second kind (n th order)

k_f is the fin material thermal conductivity

r_c is the fin radius

r_o is the tube outer radius

t_f is the fin thickness

h is the heat transfer coefficient

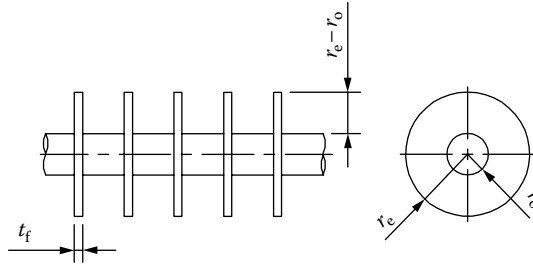


FIGURE 4.42 Circular fin details to calculate fin efficiency as per Equations 4.90, 4.94, and 4.95.

The fin efficiency expressed by Equation 4.90 does not lend itself to comparison with the efficiencies of fins of other radial profiles but can be adjusted by expressing the efficiency in terms of the radius ratio r_o/r_e and a parameter ϕ :

$$\rho = \frac{r_o}{r_e} \quad (4.91)$$

$$\phi = (r_e - r_o)^{3/2} \left(\frac{2h}{k_f A_p} \right)^{0.5} \quad (4.92)$$

where A_p is the profile area of the fin

$$A_p = t_f(r_e - r_o) \quad (4.93)$$

Substituting the values of ρ and ϕ in Equation 4.90, the resulting formula for fin efficiency is given by

$$\eta_f = \frac{2\rho}{\phi(1+\rho)} \left[\frac{I_1[\phi/(1-\rho)]K_1[\rho\phi/(1-\rho)] - K_1[\phi/(1-\rho)]I_1[\rho\phi/(1-\rho)]}{I_o[\rho\phi/(1-\rho)]K_1[\phi/(1-\rho)] + I_1[\phi/(1-\rho)]K_o[\rho\phi/(1-\rho)]} \right] \quad (4.94)$$

Scott and Goldschmidt: An excellent approximation of Equation 4.94 has been provided by Scott and Goldschmidt [58] as follows:

$$\eta_f = x(ml_e)^{-y} \quad \text{for } \phi > 0.6 + 2.257(r^*)^{-0.445} \quad (4.95a)$$

$$\eta_f = \frac{(\tanh \phi)}{\phi} \quad \text{for } \phi \leq 0.6 + 2.257(r^*)^{-0.445} \quad (4.95b)$$

where

$$x_1 = (r^*)^{-0.246} \quad (4.96)$$

$$\phi = ml_e(r^*)^{\exp(0.13ml_e - 1.3863)} \quad (4.97)$$

$$y_1 = 0.9107 + 0.0893r^* \quad \text{for } r^* \leq 2 \quad (4.98a)$$

$$= 0.9706 + 0.17125 \ln r^* \quad \text{for } r^* > 2 \quad (4.98b)$$

$$r^* = \frac{r_e}{r_o}, \quad (4.99)$$

$$l_e = l_f + \frac{t_f}{2} \quad (4.100)$$

Schmidt method: The Schmidt [59] formula for the efficiency of a plane circular fin is given by

$$\eta = \frac{\tanh ml^*}{ml^*} \quad (4.101)$$

where l^* is given by

$$l^* = (r_e - r_o) \left[1 + \frac{t_f}{2(r_e - r_o)} \right] [1 + 0.35 \ln(\rho)] \quad (4.102)$$

in which $\rho = r_e/r_o$. It was shown that for $0.5 \leq \rho \leq 1$ and $1 \leq \rho \leq 8$, the error using Equation 4.101 is less than 1% of the exact value of the fin efficiency. Because the fin efficiency is very close to unity for typical low-finned tube geometries, Rabas and Taborek [7] do not recommend any corrections to this method to account for departure from a rectangular profile and for the nonuniformity of the heat transfer coefficient over the height of the fin.

4.7.2.2 Plain Continuous Fin on Circular Tubes

A recurring arrangement of extended surface is that of a single sheet of metal pierced by round tubes in either a square or equilateral triangular array. For polygonal fins, methods suggested in Refs. [19,59–61] can be used.

Schmidt method: Schmidt [59] extended the circular fin efficiency formula expressed in Equation 4.101 to rectangular and hexagonal layout fin surfaces as shown in Figure 4.43. The extension was made by analyzing these surfaces on the basis of equivalent circular fins. The expression for the ratio of the equivalent fin radius to the tube radius, ρ_e , is expressed as follows:

For rectangular fins,

$$\rho_e = 1.28\lambda_1(\beta_1 - 0.2)^{0.5} \quad (4.103)$$

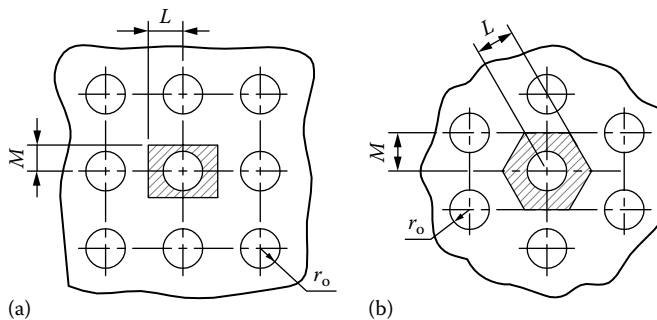


FIGURE 4.43 Geometrical details of continuous fin-tube heat exchanger layouts. (a) Rectangular tube array and (b) hexagonal tube array.

For hexagonal fins,

$$\rho_e = 1.27\lambda_1(\beta_1 - 0.3)^{0.5} \quad (4.104)$$

where

$$\lambda_1 = \frac{M}{r_o} \quad (4.105)$$

$$\beta_1 = \frac{L}{M} \quad (4.106)$$

and where L and M are defined in Figure 4.43. Of these two, L must always be the larger dimension. The fin efficiencies calculated in this way always fall within the known upper and lower limits defined by the inner and outer circumscribing circles and are very close to that of a circular fin of equal area. The accuracy of this method is especially good for square or regular hexagonal fins, where $L = M$.

Sparrow and Lin method: The Sparrow and Lin method [61] considered both the square fin and hexagonal fin formed by tubes on equilateral triangular pitch as shown in Figure 4.44. For the fins shown in Figure 4.44, the fin efficiency is obtained from the numerical temperature solution and is

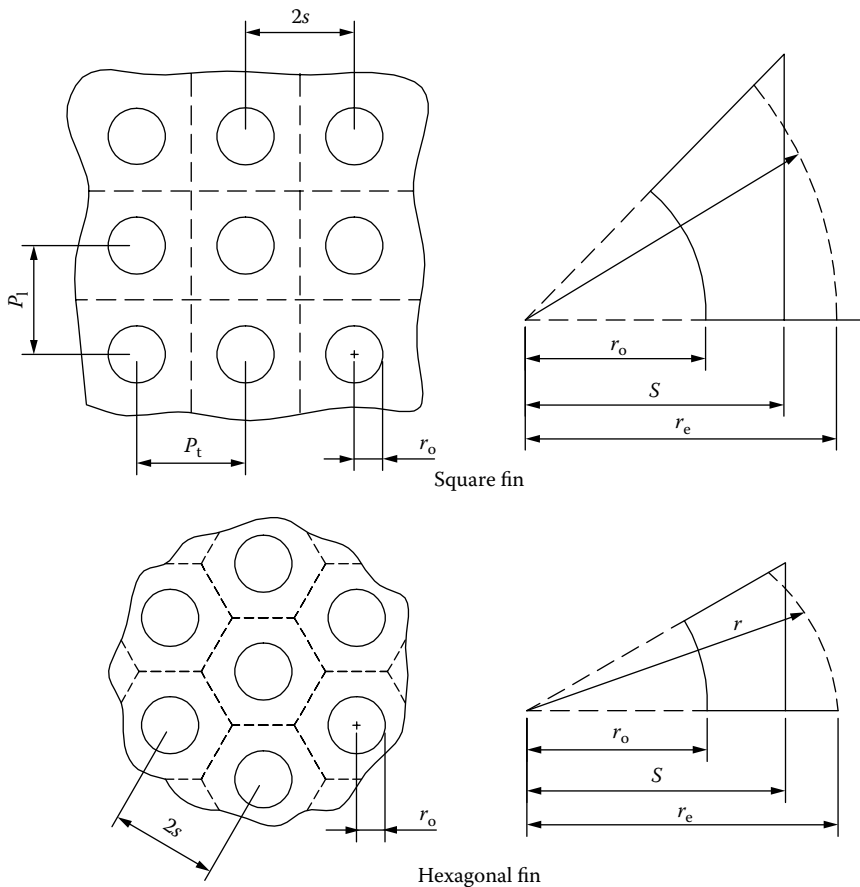


FIGURE 4.44 Fictitious edge radius for unit fin surface of continuous fin with circular tube. (a) Square layout (i.e., square fin) and (b) staggered layout (60°) (i.e., hexagonal fin).

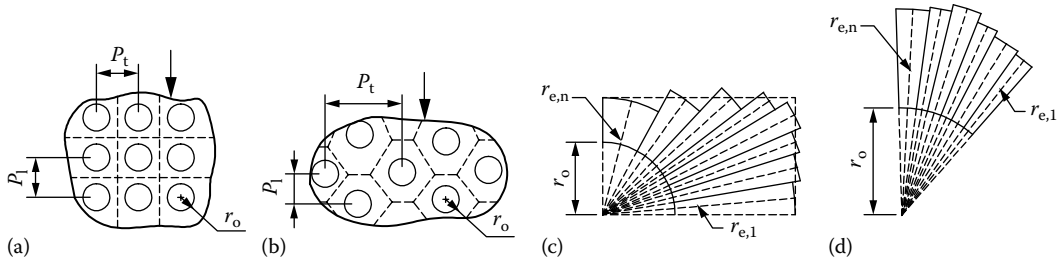


FIGURE 4.45 Fin sectors to determine fin efficiency of continuous finned-tube heat exchanger. (a) Inline layout, (b) staggered layout, (c) fin sectors for inline layout, and (d) fin sectors for staggered layout.

conveniently represented in terms of a fictitious edge radius r_e^* that corresponds to a radial fin having the same surface area as the square and hexagonal fins under consideration. This fictitious edge radius for the square fin is given by

$$r_e^* = \left(\frac{2}{\sqrt{\pi}} \right) s \quad (4.107)$$

and for the hexagonal fin

$$r_e^* = \left(\frac{2\sqrt{3}}{\pi} \right)^{1/2} s \quad (4.108)$$

The Sparrow and Lin method satisfies exactly the isothermal boundary condition at the fin base and fulfills approximately to any desired accuracy the adiabatic boundary condition at the fin edge.

Sector method: The fin efficiency of the polygonal fin is obtained by an approximate method referred to as the “sector method” [24]. The flat fin is broken down into n sectors bounded by idealized adiabatic planes as indicated by the dotted lines for the inline and staggered tube arrangements in Figure 4.45. The radius of each circular sector is determined by the length of a construction line originating from the tube center and passing through the midpoint of each line segment. The fin efficiency of each sector is then determined by use of Equations 4.94, 4.95, or 4.101. The fin efficiency for the entire surface can then be determined by the summation as [24]

$$\eta_f = \frac{\sum_{i=1}^n \eta_{f,i} A_{f,i}}{\sum_{i=1}^n A_{f,i}} \quad (4.109)$$

where $A_{f,i}$ is the area of each fin sector. The approximation improves as n becomes very large, but for practical purposes, only a few segments will suffice to provide η_f within a desired accuracy of 0.1%. The fin efficiency calculated by the sector method is lower than that for the actual flat fin, whereas the equivalent annulus method yields η_f values that are higher than those by the sector method for highly rectangular fin geometry around the tubes [24].

4.8 RATING OF A COMPACT EXCHANGER

The rating problems for a two-fluid direct transfer type compact crossflow and counterflow exchanger with gas as a working fluid at least on one side is discussed in this section. The surface employed on the gas side of this exchanger has a high surface area density and low hydraulic diameter. Customarily, the ε -NTU

method is employed for compact heat exchangers. Hence, the solution procedure is outlined using the ϵ -NTU method. The rating procedure given here is as in Refs. [24,63].

4.8.1 RATING OF SINGLE-PASS COUNTERFLOW AND CROSSFLOW EXCHANGERS

The basic steps of the rating problem are shown in Figure 4.46 and involve the determination of the following parameters.

1. Surface geometrical properties. These include

A_o minimum free flow area

A heat transfer surface area (total of primary surface area, A_p , and secondary surface area, A_f)

L flow length

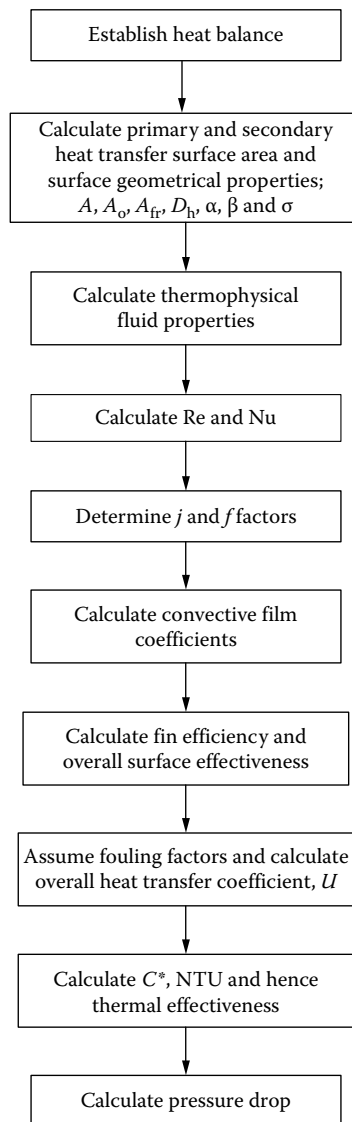


FIGURE 4.46 Flowchart for rating of a compact heat exchanger. (Note: Wherever applicable the calculation is to be done for both fluid 1 and fluid 2.)

- D_h hydraulic diameter
 β heat transfer surface area density
 σ ratio of minimum free flow area to frontal area
 l_f fin length
 t_f fin thickness

Also included are specialized dimensions used for heat transfer and pressure-drop correlations.

- Fluid physical properties. Determine the thermophysical properties at bulk mean temperature for each fluid, namely, hot and cold fluids. The properties needed for the rating problem are μ , c_p , k , and Pr . Since the outlet temperatures are not known for the rating problem, they are guessed initially. Unless it is known from the past experience, assume an exchanger effectiveness as 60%–75% for most single-pass crossflow exchangers, and 80%–85% for single-pass counterflow and two-pass cross-counterflow exchangers. For the assumed effectiveness, calculate the fluid outlet temperatures by

$$t_{h,o} = t_{h,i} - \varepsilon \frac{C_{\min}(t_{h,i} - t_{c,i})}{C_h} \quad (4.110)$$

$$t_{c,o} = t_{c,i} + \varepsilon \frac{C_{\min}}{C_c}(t_{h,i} - t_{c,i}) \quad (4.111)$$

Initially, assume $C_c/C_h \approx M_c/M_h$ for a gas-to-gas exchangers, or $C_c/C_h = (Mc_p)_c/(Mc_p)_h$ for a gas-to-liquid exchanger with approximate values of c_p . For exchangers with $C^* \geq 0.5$ (usually gas-to-gas exchangers), the bulk mean temperature on each side will be the arithmetic mean of the inlet and outlet temperatures on each side. For exchangers with $C^* < 0.5$ (usually gas-to-liquid exchangers), the bulk mean temperature for C_{\max} as the hot fluid is $t_{h,m} = (t_{h,i} + t_{h,o})/2$, $t_{c,m} = t_{h,m} - \text{LMTD}$ and for C_{\max} as the cold fluid $t_{c,m} = (t_{c,i} + t_{c,o})/2$, $t_{h,m} = t_{c,m} + \text{LMTD}$ [24,63].

Once the bulk mean temperatures are obtained on each side, obtain the fluid properties from thermophysical property tables or from standard thermal engineering books.

- Reynolds numbers. Calculate the Reynolds number and/or any other pertinent dimensionless groups needed to determine j or Nu and f of heat transfer surfaces on each side of the exchanger.
- Compute j or Nu and f factors.
- Correct Nu (or j) and f for variable fluid property effects in the second and subsequent iterations.
- From Nu or j , determine heat transfer coefficient for both the fluid streams.

$$h = \frac{Nuk}{D_h} \quad (4.112a)$$

or

$$h = jG C_p Pr^{-2/3} \quad (4.112b)$$

- Determine the fin efficiency η_f and the overall surface efficiency η_o given by

$$\eta_f = \frac{\tanh ml}{ml} \quad (4.113)$$

where l is the fin length.

$$\eta_o = 1 - \frac{A_f}{A}(1 - \eta_f) \quad (4.114)$$

8. Overall conductance. Calculate the wall thermal resistance, R_w . Knowing the fouling resistances $R_{f,h}$ and $R_{f,c}$ on the hot and cold fluid sides, respectively, calculate the overall thermal conductance UA from

$$\frac{1}{UA} = \frac{1}{(\eta_o hA)_h} + \frac{R_{f,h}}{(\eta_o hA)_h} + R_w + \frac{1}{(\eta_o hA)_c} + \frac{R_{f,c}}{(\eta_o hA)_c} \quad (4.115a)$$

$$= R_h + R_l + R_w + R_2 + R_c \quad (4.115b)$$

9. Calculate NTU, C^* , and exchanger effectiveness, ϵ . If the thermal effectiveness is above 80%, correct for wall longitudinal conduction effect.
10. Compute the outlet temperature from Equations 4.110 and 4.111. If these outlet temperatures differ significantly from those assumed in step 2, use these outlet temperatures in step 2 and continue iterating steps 2–9 until the assumed and computed outlet temperatures converge within the desired degree of accuracy. For a gas-to-gas exchanger, probably one or two iterations will be sufficient.
11. Compute the heat duty from

$$q = \epsilon C_{\min}(t_{h,i} - t_{c,i}) \quad (4.116)$$

12. Calculate the core pressure drop. The friction factor f on each side is corrected for the variable fluid properties as discussed in Chapter 3. The wall temperature T_w is computed from

$$T_{w,h} = t_{m,h} - q(R_h + R_l) \quad (4.117)$$

$$T_{w,c} = t_{m,c} - q(R_c + R_2) \quad (4.118)$$

4.8.2 SHAH'S METHOD FOR RATING OF MULTIPASS COUNTERFLOW AND CROSSFLOW HEAT EXCHANGERS

The rating procedure for multipass crossflow exchangers with fluids mixed between passes is described by Shah [63]. The solution procedure for rating problem for the two-pass crossflow exchangers with flows unmixed in the passes but mixed between passes is also very similar to the sizing of single-pass crossflow. Only some of the calculations on the two pass side need to be modified, and only those points are summarized here.

1. In order to compute fluid bulk mean temperature and thermophysical properties of fluids, first guess the overall thermal effectiveness, ϵ_N . Assume it to be 80%–85% unless it is known from the past experience. Assume that the NTU per pass is same. The individual pass effectiveness ϵ_p is related to overall effectiveness ϵ_N for the case of fluids mixed between passes. Compute approximate values of C_c and C_h since we don't know yet the accurate values of the specific heats.
2. Determine the intermediate and outlet temperature by solving the following individual pass effectiveness and overall effectiveness equations:

$$\epsilon_{p1} = \frac{C_c(t_{c,o} - t_{c,int})}{C_{\min}(t_{h,i} - t_{c,int})} \quad (4.119)$$

$$\varepsilon_{p2} = \frac{C_c(t_{c,int} - t_{c,i})}{C_{min}(t_{h,int} - t_{c,i})} \quad (4.120)$$

$$\varepsilon = \frac{C_c(t_{c,o} - t_{c,i})}{C_{min}(t_{h,i} - t_{c,i})} \quad (4.121)$$

In the foregoing three equations, there are three unknowns: $t_{c,o}$, $t_{c,int}$, and $t_{h,int}$. Hence, they can be evaluated exactly and then from the overall energy balance $t_{h,o}$ is calculated.

$$C_c(t_{c,o} - t_{c,i}) = C_h(t_{h,i} - t_{h,o}) \quad (4.122)$$

Since we know all terminal temperatures for each pass, we can determine the bulk mean temperature for each fluid in each pass and subsequently the fluid properties separately for each pass.

4.9 SIZING OF A COMPACT HEAT EXCHANGER

The basis of sizing involves coupling of heat transfer and flow friction in the derivation of the core mass velocity G on each side of a two-fluid exchanger. Subsequently, the sizing problem is carried out in a manner similar to the rating problem.

4.9.1 CORE MASS VELOCITY EQUATION*

The dominant term in the expression for the pressure drop is the core friction term. The entrance and exit effects are generally relatively small and are of the opposite sign. Similarly, the flow acceleration term is relatively small in most heat exchangers, being generally less than 10% of the core friction term [24], so their elimination is usually warranted in a first approximation. With these approximations and $L/r_h = A/A_o$, the expression for pressure drop may be written after rearrangement as

$$\frac{G^2}{2g_c p_i \rho_i} = \frac{\Delta p}{p_i} \frac{A_o}{A} \frac{1}{\rho_i (1/\rho)_m} \frac{1}{f} \quad (4.123)$$

In the absence of fouling resistances, the overall NTU is related to NTU_h , NTU_c , and the wall resistance, R_w , by

$$\frac{1}{NTU} = \frac{1}{NTU_h(C_h/C_{min})} + C_{min}R_w + \frac{1}{NTU_c(C_c/C_{min})} \quad (4.124)$$

The wall resistance term is generally small and hence neglected in the first-approximation calculation. Hence, the number of transfer units on one side of interest (either hot or cold), designated as NTU_1 , may be estimated from the known overall NTU as given next.

If both fluids are gases, one can start with the estimate that the design is “balanced” by a selection of the hot and cold side surfaces so that $R_h = R_c = R_o/2$, that is, $NTU_h = NTU_c = 2NTU$. Then

$$NTU_1 = NTU_2 = 2NTU \quad (4.125)$$

For a gas–liquid heat exchanger, one might estimate

$$NTU_{gas\ side} = 1.1(NTU) \quad (4.126)$$

* After Shah, R.K., Compact heat exchanger design procedures, in *Heat Exchangers: Thermal-Hydraulic Fundamentals and Design*, Kakac, S., Bergles, A.E., and Mayinger, F., eds., Hemisphere, Washington, DC, pp. 495–536, 1981.

The term NTU_1 is related to the Colburn factor j on side 1 by

$$NTU_1 = \left(\frac{\eta_o h A}{MC_p} \right)_1 = \left(\frac{\eta_o h A}{GC_p A_o} \right)_1 = \left(\eta_o j Pr^{-2/3} \frac{A}{A_o} \right)_1 \quad (4.127)$$

Eliminating (A/A_o) from Equations 4.123 and 4.127, and simplifying the expression, we get the core mass velocity G for one side:

$$G = \left[\left(\frac{2g_c \eta_o}{(1/\rho)_m Pr^{2/3}} \right) \left(\frac{\Delta p}{NTU} \right) \left(\frac{j}{f} \right) \right]^{0.5} \quad (4.128)$$

The feature that makes this equation so useful is that the ratio j/f is a relatively flat function of the Reynolds number. Thus, one can readily estimate an accurate magnitude of j/f based on a “ballpark” estimate of Re . If there are no fins, overall surface efficiency $\eta_o = 1$. For a “good design,” the fin geometry is chosen such that η_o is in the range 70%–90%. Therefore, $\eta_o = 0.8$ is suggested as a first approximation to determine G from Equation 4.128.

4.9.2 PROCEDURE FOR SIZING A COMPACT HEAT EXCHANGER

The procedure for sizing any of the compact heat exchangers (Figure 4.47) is almost inevitably an iterative one and thus lends itself very conveniently to computer calculations. Kays and London [17] illustrate the procedure for sizing a crossflow heat exchanger. To illustrate this, a simple crossflow heat exchanger is considered as shown in Figure 4.34. It is assumed that each fluid is unmixed throughout. The two fluids are designated by h and c . The problem is to determine the three dimensions L_1 , L_2 , and L_3 . The first step after choosing the two surfaces is to assemble the geometric characteristics of the surface— D_h , σ , α , β , A_f/A , and A_w/A for the hot side and cold fluids side. A first estimate of G_h and G_c can be made using Equation 4.128. After the determination of mass velocity, carry out the calculations similar to a rating problem. The sequence of parameters to be calculated after determination of mass velocity include Re , η_f , η_o , j , f , h , UA , A_o , A_f , flow length, K_c , K_e , and $(\Delta p/p)$, both on the hot side and cold side. The pressure drop results are then compared with those specified for the design, and the procedure is repeated until the two pressure drops are within the specified value.

4.9.3 OPTIMIZATION OF PLATE-FIN EXCHANGERS AND CONSTRAINTS ON WEIGHT MINIMIZATION [64]

Minimizing the material volume, or weight, of the PFHE core does not necessarily represent the optimum solution, even for weight-sensitive aerospace applications; size and shape can be important design considerations [64]. Minimum weight core could be longer than is desirable because of the low-fin efficiency implied. If the fin is too thin, its efficiency will be low, and to compensate both core length and flow area will be high, giving an excessively high weight. On the other hand, a very thick fin giving high-fin efficiency will yield a low core length but with low porosity (free flow area) and weight. Minimizing the components' thickness can also contribute to low weight. But there are limitations in reducing components beyond certain limits as follows:

The thicknesses of fin material and separating plates have lower limits set by pressure-retaining capability.

Plate-fin cores are usually made from sheet stock of a fixed range of thickness; rolling finstock to a special “optimum” thickness could be uneconomic.

It may not be possible to form fins of sufficient dimensional accuracy if they are too thin; if they can be made, they might deform unsatisfactorily on brazing.

There may also be lower thickness limits set by erosion and corrosion problems.

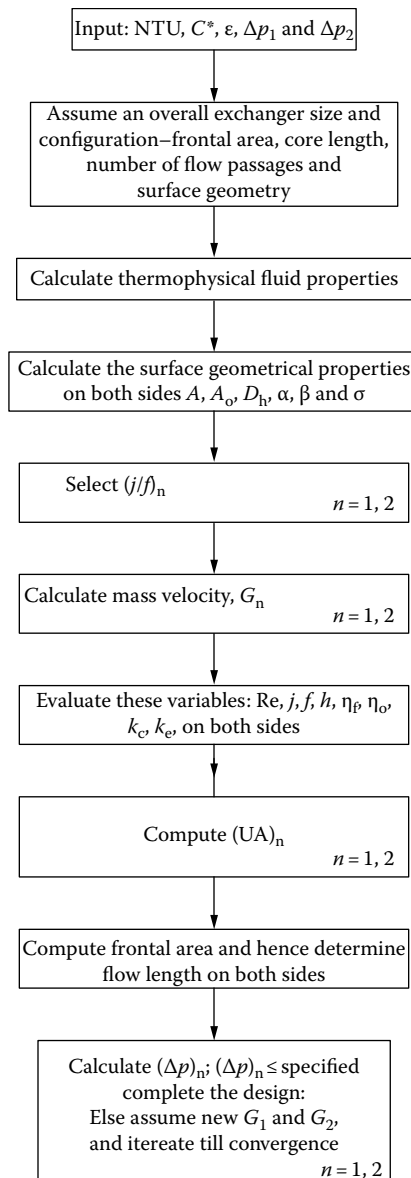


FIGURE 4.47 Flowchart for sizing of a compact heat exchanger. (Note: 1, 2 are both sides fluids designation.)

4.10 EFFECT OF LONGITUDINAL HEAT CONDUCTION ON THERMAL EFFECTIVENESS

The ϵ -NTU and LMTD methods discussed are based on the idealization of zero longitudinal heat conduction in the wall in the fluid flow direction. If a temperature gradient is established in the wall in the fluid flow direction, heat transfer by conduction takes place from the hotter to the colder region of the wall in the longitudinal direction. This longitudinal conduction in the wall flattens the temperature distributions, reduces the mean outlet temperature of the cold fluid, increases the mean outlet temperature of the hot fluid, and thus reduces the thermal effectiveness [63,65]. The reduction in the effectiveness at a specified NTU may be quite significant for a compact exchanger

designed for high thermal effectiveness (above ~80%) and a short flow length, L . The shell and tube exchangers and plate exchangers are usually designed for effectiveness of 60% or less per pass. Therefore, the influence of heat conduction in the wall in the flow direction is negligible for these effectiveness levels. The presence of longitudinal heat conduction in the wall is incorporated into the thermal effectiveness formula by an additional parameter, λ , referred to as the longitudinal conduction parameter. Another parameter that influences the longitudinal wall heat conduction is the convection conduction ratio, $\eta_o hA$. Thus, in the presence of longitudinal heat conduction in the wall, the exchanger thermal effectiveness is expressed in a functional form [65]:

$$\varepsilon = \phi\{NTU, C^*, \eta_o hA, \lambda\} \quad (4.129)$$

4.10.1 LONGITUDINAL CONDUCTION INFLUENCE ON VARIOUS FLOW ARRANGEMENTS

The influence of longitudinal conduction in the case of parallelflow is not discussed because high-performance exchangers are not designed as for parallelflow arrangements. For high-performance exchangers, the effect is discussed in Chapter 7. In a crossflow arrangement, the wall temperature distributions are different in the two perpendicular flow directions. This results in a two-dimensional longitudinal conduction effect, and is accounted for by the cold-side and hot-side parameters defined as [65]:

$$\lambda_c = \left(\frac{k_w A_k}{LC} \right)_c \quad \text{and} \quad \lambda_h = \left(\frac{k_w A_k}{LC} \right)_h \quad (4.130)$$

Note that the flow lengths L_c and L_h are independent in a crossflow exchanger. If the separating wall thickness is a , and the total number of parting sheets is N_p , then the transfer area for longitudinal conduction is given by [65] as follows:

$$A_{k,c} = 2N_p L_h a \quad \text{and} \quad A_{k,h} = 2N_p L_c a \quad (4.131)$$

Chiou [66] analyzed the problem for a single-pass crossflow heat exchanger with both fluid unmixed and tabulated values for the reduction in thermal effectiveness due to longitudinal wall heat conduction.

4.10.2 COMPARISON OF THERMAL PERFORMANCE OF COMPACT HEAT EXCHANGERS

Among the three types of compact heat exchangers, viz., tube-fin, continuous fin, and PFHE, PFHE has maximum heat transfer capacity compared to the other two types of heat exchangers. Figure 4.48 shows comparison of thermal performance of PFHEs, flat tube heat exchangers (oil coolers), and tube-fin heat exchangers. Performance is shown as Q/ITD , the heat load divided by the difference in incoming temperature of the liquid and air.

4.11 AIR-COOLED HEAT EXCHANGER (ACHE)

Air-cooled heat exchangers (ACHEs), or “fin-fans,” are an alternate heat rejection method that is used frequently in place of the conventional water-cooled shell and tube heat exchanger to cool a process fluid. They can be used in all climates. ACHE are increasingly found in a wide spectrum of applications including chemical, process, petroleum refining, and other industries. A fan located below the tube bundle forces air up through the bundle, or a fan above draws the air through the bundle. The fans are axial low fans varying from 4 to 12 ft diameter and having

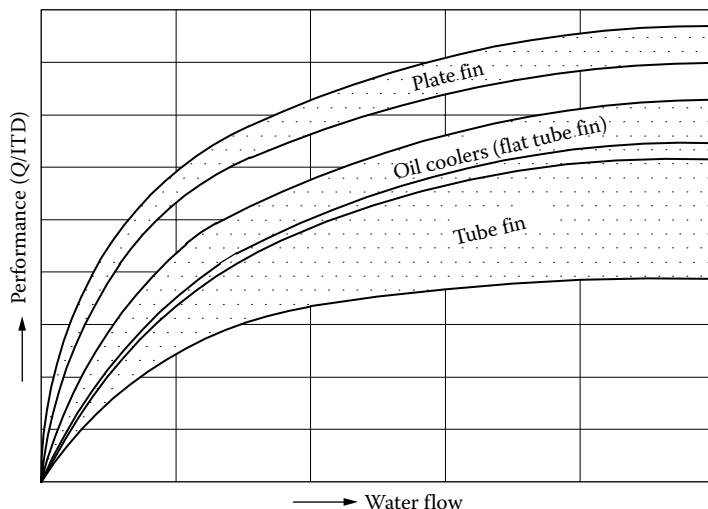


FIGURE 4.48 Chart for comparison of thermal performance of PFHEs, flat tube heat exchangers (oil coolers), and tube-fin heat exchangers performance is shown as Q/ITD , the heat load divided by the difference in incoming temperature of the liquid and air. (Courtesy of Lytron Inc., Woburn, MA.)

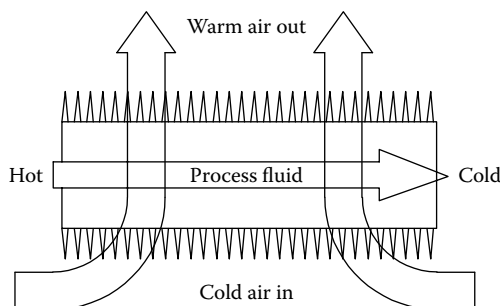


FIGURE 4.49 Principle of ACHE.

four to six blades. The fan blades may be of aluminum, plastic, or, in the case of corrosive atmospheres, stainless steel. The drive can be an electric motor with gears or V-belts. Before discussing the construction details and design aspects, the factors that favor air cooling over water cooling are discussed. For generic/specific details on design, manufacture, and operation of ACHEs, refer to references [67–86]. An important guide book for design of ACHEs is American Petroleum Institute Standard 661 [70]. The principle of ACHE is shown in Figure 4.49 and a forced draft ACHE is shown in Figure 4.50.

4.11.1 AIR VERSUS WATER COOLING

Two primary methods of process cooling are (1) water cooling and (2) air cooling. The choice between air or water as coolant depends on many factors like (1) cooler location; (2) space for cooling system; (3) effect of weather; (4) design pressure and temperature; (5) danger of contamination; (6) fouling, cleaning, and maintenance; and (7) capital costs. Environmental concerns such as shortage of makeup water, blowdown disposal, and thermal pollution have become an additional factor in cooling system selection.

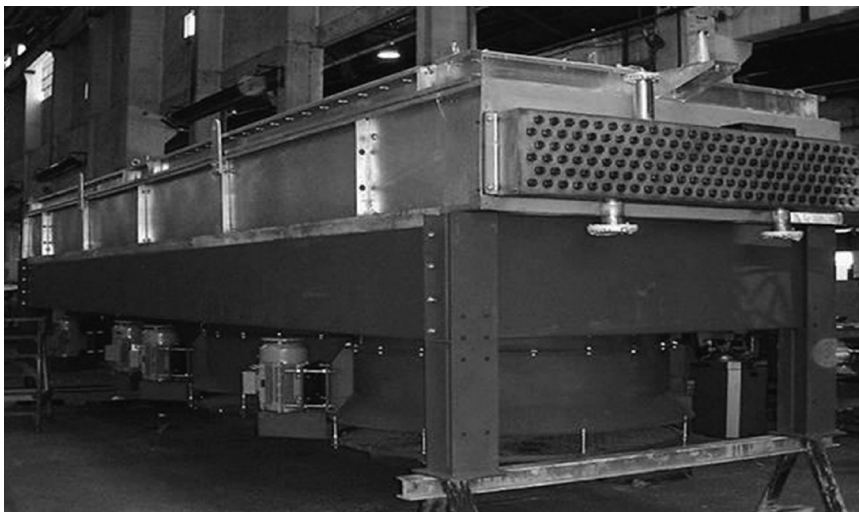


FIGURE 4.50 A bank of ACHes. (Courtesy of GEA Iberica S.A., Vizcaya, Spain.)

4.11.1.1 Air Cooling

Air cooling is increasing in use, particularly where water is in short supply. Factors that favor air cooling include the following:

1. Air is available free in abundant quantity with no preparation costs.
2. ACHE design is well established, and can perform well with a reasonable degree of reliability.
3. Water is corrosive and requires treatment to control both scaling and deposition of dirt, whereas air is mostly noncorrosive. Therefore, material selection is governed by process fluids routed through the tubeside.
4. Mechanical design problems are eased with ACHes since the process fluid is always on the tubeside.
5. Danger of process fluid contamination is much greater with water-cooled system.
6. Air-side fouling can be periodically cleaned by air blowing, and chemical cleaning can be carried out either during half-yearly or yearly attention. Water-cooled systems may require frequent cleaning.
7. Maintenance costs for ACHes are about 20%–30% of those for water-cooled system [68]. Operating costs for water coolers are higher, because of higher cooling water circulation pump horsepower and water treatment costs.
8. Air cooling eliminates the environmental problems like heating up of lakes, rivers, etc., blowdown, and washout.

Air cooling has the following disadvantages:

1. ACHes require large surfaces because of their low heat transfer coefficient on the airside and the low specific heat of air. Water coolers require much less heat transfer surface.
2. ACHes cannot be located next to large obstructions if air recirculation is to be avoided.
3. Because of air's low specific heat, and dependence on the dry-bulb temperature, air cannot usually cool a process fluid to low temperatures. Water can usually cool a process fluid from 10°F to 5°F lower than air, and recycled water can be cooled to near the wet-bulb temperature of the site in a cooling tower [68].

4. The seasonal variation in air temperatures can affect performance and make temperature control more difficult. Low winter temperatures may cause process fluids to freeze.
5. ACHEs are affected by hailstorms and may be affected by cyclonic winds.
6. Noise is a factor with ACHEs. Low noise fans can reduce this problem but at the cost of fan efficiency and higher energy costs.
7. May need special controls for cold weather protection.
8. Cannot cool the process fluid to the same low temperature as cooling water

4.11.2 CONSTRUCTION OF ACHE

A typical ACHE consists of the following components:

1. Tube bundle.
2. An air pumping device, such as an axial flow fan or blower driven by an electric motor and power transmission device such as belt (up to 50 hp) or gear (above 50 hp) to mechanically rotate the air moving device.
3. The moving of air across the tube bundle may be either forced draft (fan is located below the tube bundle and air is forced through the fin tubes) or induced draft (fan is located above the bundle and air is induced or pulled through the fin tubes).
4. A support structure high enough to allow air to enter beneath the ACHE at a reasonable flow rate.
5. Optional features like (i) header and fan maintenance walkways with ladders to climb (Figure 4.51), (ii) louvers for process outlet temperature control, (iii) recirculation ducts and chambers for protection against freezing or solidification of high pour point fluids in cold weather, and (iv) variable pitch fan hub or frequency drive for temperature control.

4.11.2.1 Tube Bundle Construction

An ACHE tube bundle consists of a series of finned tubes set between side frames, passing between header boxes at either end. The number of passes on the tubeside (the process fluid side) is made possible by internal baffling of the header boxes. For horizontal bundles, vertical baffles result in a side-by-side crossflow arrangement, whereas horizontal baffles result in a counter-crossflow arrangement relative to airflow. Inlet and outlet nozzles may or may not be on the same header box. Tubes are attached to the tubesheet by expansion or welding.

4.11.2.1.1 Tube Bundle Fin Geometry

The tube-fin geometries, viz., attachment of fins to the tubes, include extruded, embedded, and welded—single footed or double footed (Figure 4.52). These fins can be solid or serrated, tension wound or welded, and of a variety of metals. For higher process temperatures, most customers

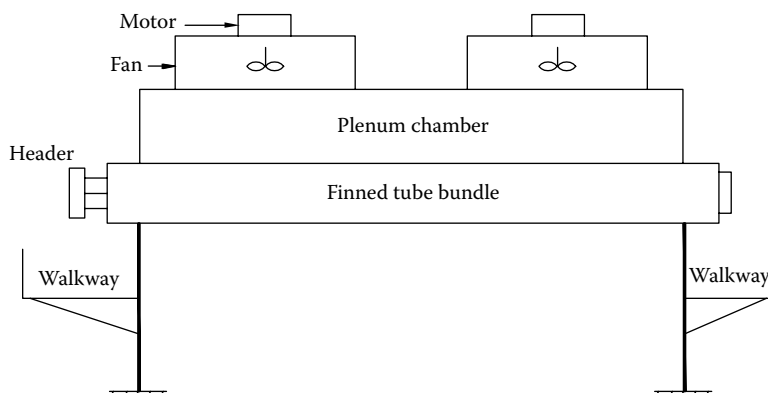


FIGURE 4.51 Layout of ACHE showing tube bank with walkways. (*Note:* Induced draft design.)

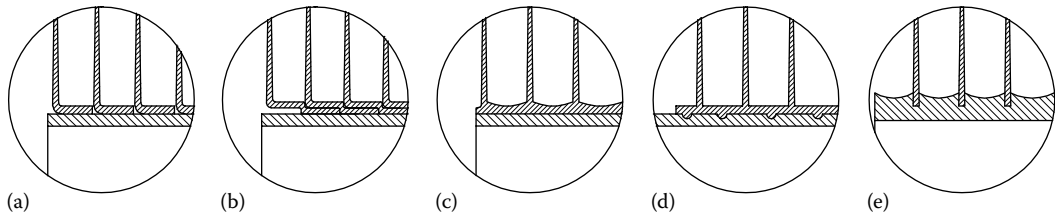


FIGURE 4.52 Tube-fin geometry—(a) welded single L footed, (b) welded double L footed, (c) extruded, (d) serrated, and (e) embedded.

prefer either embedded 400°C (750°F) or extruded fins 310°C (590°F). Extruded fins are made by putting an aluminum sleeve (sometimes called a muff) over the tube, then passing the tube through a machine which has rollers which squish the aluminum to form fins. The process is similar to a thread-rolling. This results in a fin tube which has extremely good metal-to-metal contact between the tube and fin sleeve. Extruded fins are often used in coastal regions or on offshore platforms for this reason. Extruded fins typically have the maximum ability to transfer heat due to absence of contact resistance at the fin and tube base. High finned (extruded) monometallic fin-tube and bimetallic fin-tubes are shown in Figure 4.53. Serrations or slitting the fin tips help to increase the airside heat transfer coefficient. However, this improvement is accompanied by higher airside pressure drop and hence will require higher motor power and depending on the physical location of the ACHE,

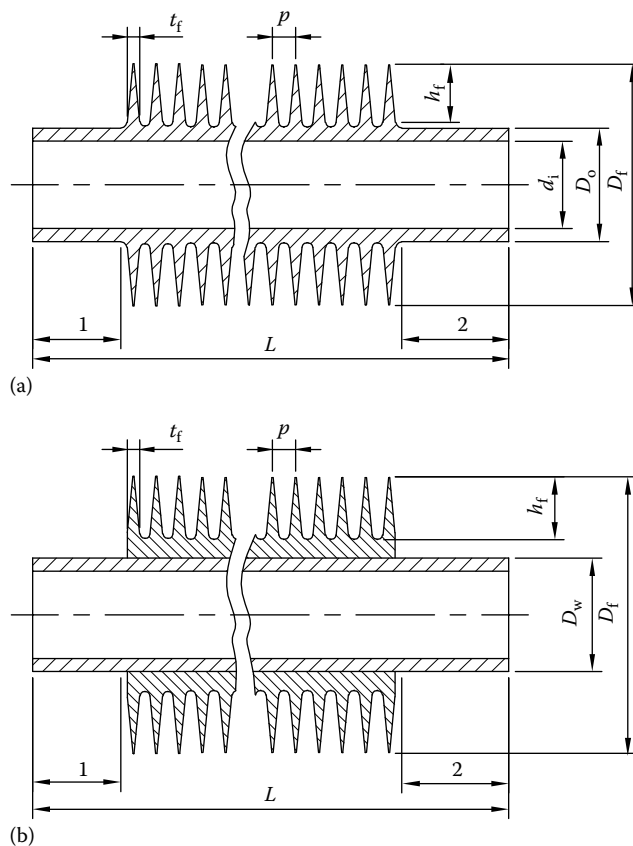


FIGURE 4.53 High finned tube—(a) extruded monometallic fin tube and (b) bimetallic fin tube. *Note:* Sections 1 and 2 are unfinned sections. d_i is tube inner diameter, D_o or D_w is tube outer diameter, D_f is fin diameter, L is tube length and h_f is fin height, p is fin pitch and t_f is fin thickness..

serrated fins will have a greater propensity for fouling. To check the adequacy of bonding between the fin and tube, manufacturers subject the fin to a tensile test by pulling the fin using a spring balance. Other tests involve such aspects as fin spacing, diameter, and thickness.

The fin most commonly used for ACHEs is aluminum, tension wound and footed. These are used where the process temperatures are below about 177°C (350°F). The API 661 specification calls for cast zinc bands at the ends of the tubes to prevent the fins from unwrapping. It is cheaper but susceptible to damage due to thermal upsets and airside corrosion. The embedded fins have the highest temperature capabilities. They are made by a process which cuts a helical groove in the outer diameter of the tube, wraps the fin into the groove, then rolls the upset metal from the tube back against the fin to lock it into place. Embedded fins have less contact resistance to heat transfer than do tension-wound fins, but corrosion is likely to be induced at the groove between fin and tube. Additionally, embedded fin tubes require tubes that are nominally one gauge heavier in wall thickness to account for the mechanical attachment of fin in to the groove [68].

The tubes are usually 1 in. (25.4 mm) diameter; fin density varies from 7 to 16 fins/in. (276–630 fins/m), fin height from 3/8 to 5/8 in. (9.53–15.88 mm), and fin thickness from 0.012 to 0.02 in. (0.3–0.51 mm). The tubes are arranged in standard bundles ranging from 4 to 40 ft (1.22–12.20 m) long and from 4 to 20 ft (1.22–6.10 m) wide, but usually limited to 9.90–10.8 ft (3.2–3.5 m).

4.11.2.1.2 *Fin Materials*

Aluminum fins are used because of high thermal conductivity, light weight, and formability, but their use is limited to low-temperature applications. Either SO₂-containing or marine atmospheres may corrode aluminum fins, so carbon steel might be preferred for such conditions. As the base tube is usually carbon or low-alloy steel, galvanic corrosion at the fin/tube junction is expected. Hence, finned tubes of carbon steel can be hot-dip galvanized to protect against galvanic corrosion and also to provide a metallic bond between the fin and the bare tube [68]. Carbon steel tubes with carbon steel or alloy steel fins are used in boiler and fired heater applications.

4.11.2.1.3 *Header*

Headers are the boxes at the ends of the tubes which distribute the fluid from the piping to the tubes. Tube-to-header joints are either welded or expanded depending on header design. A wide range of header designs has been developed for different applications and requirements. Almost all headers on air-cooled exchangers are welded rectangular boxes. Headers are usually constructed of carbon steel or stainless steel, but sometimes more exotic alloys are used for corrosion resistance. The selection of materials is usually made by the customer. Standard header configurations are presented next. Major types of headers with finned tube bundle are shown in Figure 4.54. Cross section of commonly used headers are shown in Figures 4.55 and 4.56 shows finned tubes positioned with the header for welding.

4.11.2.1.3.1 *Cover Plate Header* Either with removable cover or with bonnet, a cover plate header is typically used in chemical applications or services with severe fouling conditions. This design is available for low to medium pressure (<300 psi) installations and where fouling is a potential problem and hence the tube bundle may require internal cleaning. As the name implies, these have a removable plate on the back side of the header opposite the tubes. The cover plate is attached to the header by a set of studs or through-bolts to a flange around the perimeter of the header. A bonnet header is similar, but opposite in construction. The whole header or bonnet bolts to the tubesheet end comes off. Bonnet headers are sometimes used where the process fluid is very highly corrosive and the tubesheet material is exotic alloy, such as titanium.

4.11.2.1.3.2 *Cover Plate Header (with Stud Bolts)* The cover plate header with stud bolts features top or bottom nozzles to allow cover removal without disassembly of the piping (Figure 4.54a). Nozzles may alternatively be integrated in the cover. The header is fit for a maximum pressure of

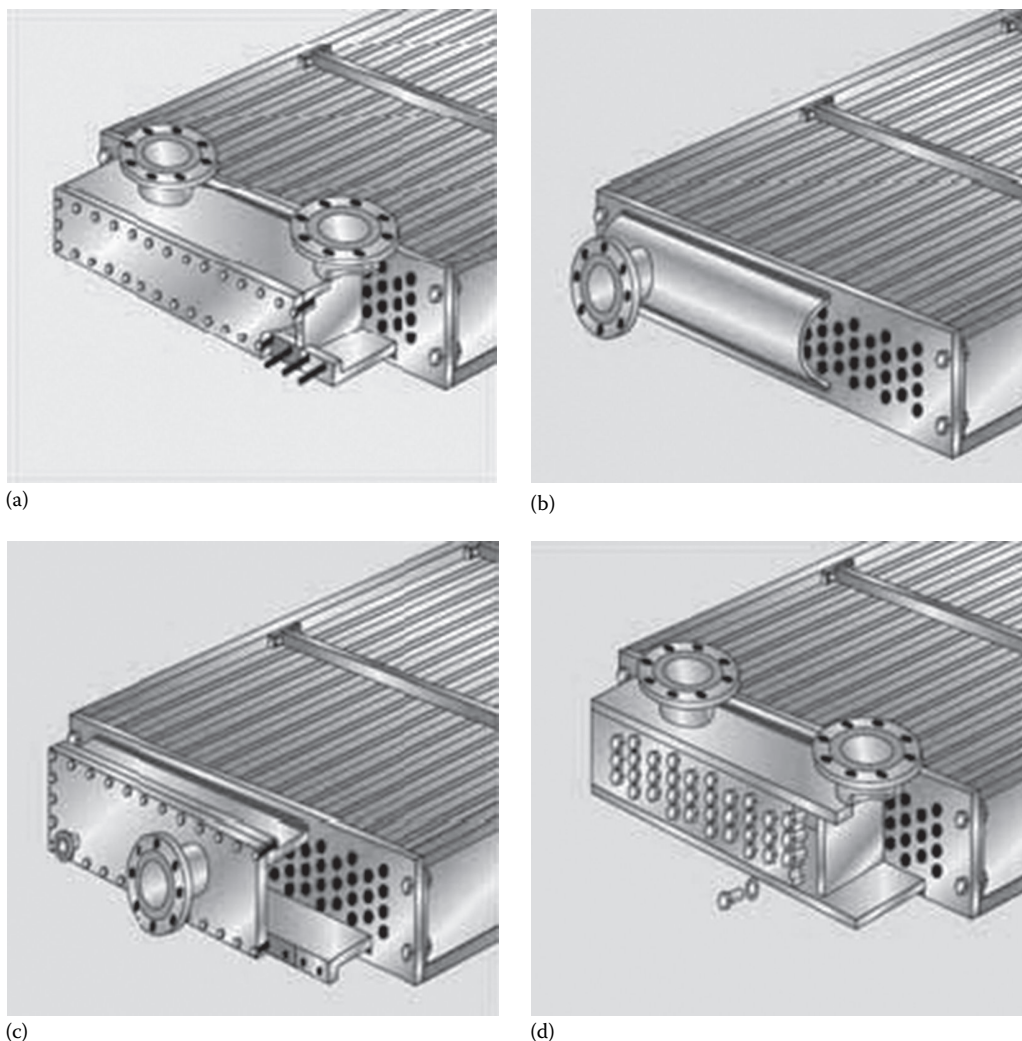


FIGURE 4.54 ACHE header types—(a) cover plate header with stud bolts, (b) welded header (D type), (c) cover plate header with through-bolts, and (d) plug type header. (Courtesy of GEA Luftkühler GmbH, Bochum, Germany.)

50 bar depending on fluid temperature and the type of sealing. A nonstandard header design is required for higher pressures. Tubes may be weld connected or expanded.

4.11.2.1.3.3 Welded Header (D-Type) The welded header is mainly used for clean products or vacuum pressure conditions. The tubes are welded into tube sheets to which the bonnet-type header with the necessary nozzles is welded (Figure 4.54b).

4.11.2.1.3.4 Cover Plate Header (with Through-Bolts) The header features a removable cover plate with through-bolts for easy inspection and tube cleaning (Figure 4.54c). It is normally sufficient to remove a pipe bend for inspection, since the removal of the bend allows the examination of part of the tube array. Tubes may be weld connected or expanded.

4.11.2.1.3.5 Plug Header A vast majority of the headers are of the plug type. The design consists of a shoulder plug opposite each tube which allows access for inspection and cleaning of individual tube (Figure 4.54d). This general purpose design is used for most refinery and power processes with

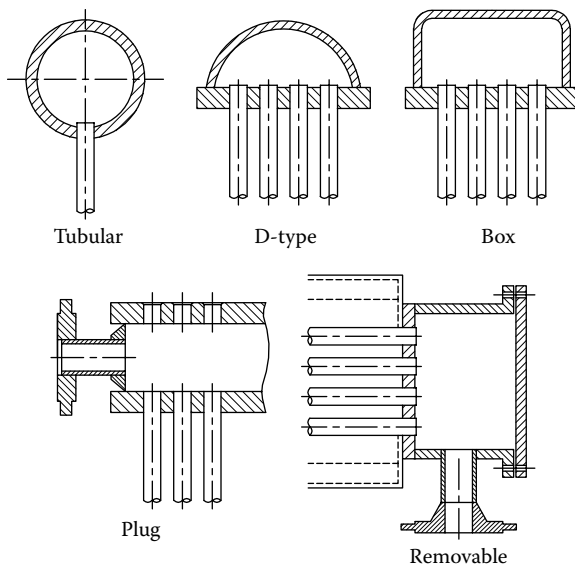


FIGURE 4.55 Cross section of commonly used headers.



FIGURE 4.56 Finned tubes positioned with the header for welding. (Courtesy of Polysoude S.A.S, Cedex, France.)

low to moderately high pressures. They can also be used to plug a leaking tube. The plug holes are used in the manufacturing process for access to roller expand the tubes into the headers.

4.11.2.1.3.6 Pipe Manifold or Billet Header Pipe manifold headers are common for all pressures, including full vacuum. Billet headers, machined from a solid piece of material, are used in extremely high pressure ($>10,000$ psig) applications.

4.11.2.1.3.7 High-Pressure Header with Return Segments A threaded plug with a soft iron gasket is located opposite each tube. The plug may be removed for further tube expansion or for tube cleaning.

Number of passes on the tubeside: On the tubeside, ACHEs can be designed with up to 10 or more passes. But normally, the number of passes adopted is up to four. Figure 4.57 shows front and rear headers with three passes arrangement on the tubeside. Figure 4.58 shows a four pass rectangular tubeplate.

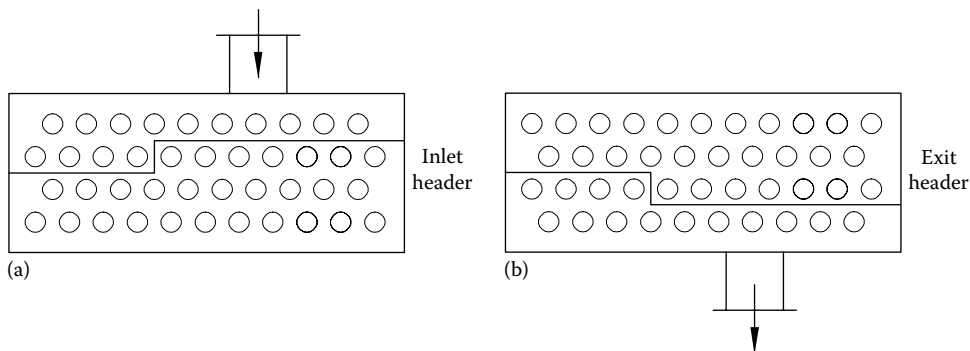


FIGURE 4.57 ACHE: (a) inlet or front header and (b) exit or rear headers with three passes arrangement on the tubeside.



FIGURE 4.58 Four pass rectangular tube plate of an energy recuperator. (From Thermofin, www.thermofin.net)

Number of tube rows: A minimum of three rows is used in the tube bank. The usual maximum limit is eight rows, though occasionally up to 12 rows are used.

4.11.2.1.4 Orientation of Tube Bundle

ACHE bundles can be installed either vertically or horizontally. Various orientations of ACHEs are shown in Figure 4.59. The most common orientation is in the horizontal plane. A considerable reduction in ground area can be made if bundles are vertically mounted, but the performance of the unit is greatly influenced by the prevailing wind direction. In general, the use of vertically mounted bundles is confined to small, packaged units. A compromise, which requires about half the ground area of the horizontal unit, is the A- or V-frame unit. In this type, two bundles sloped at 45° – 60° from the horizontal are joined by their headers at top or bottom to form the sloping side of the A (i.e., roof type) or V, respectively. The A-frame type with forced draft fans below (Figure 4.60) is the more common and is used in steam condensing applications. Specification sheet for ACHE is shown in Figure 4.61.

4.11.2.1.4.1 Fan Ring Design Fan ring design varies among manufacturers. The common configurations for fan rings are [83] the following: (1) eased inlet, (2) taper fan ring, (3) straight inlet, (4) flanged inlet, and (5) channel rings, and they are indicated in Figure 4.62. Due to the cost of manufacture, the eased or taper fan rings are generally not utilized in standard products; however, they are available when required for special applications.

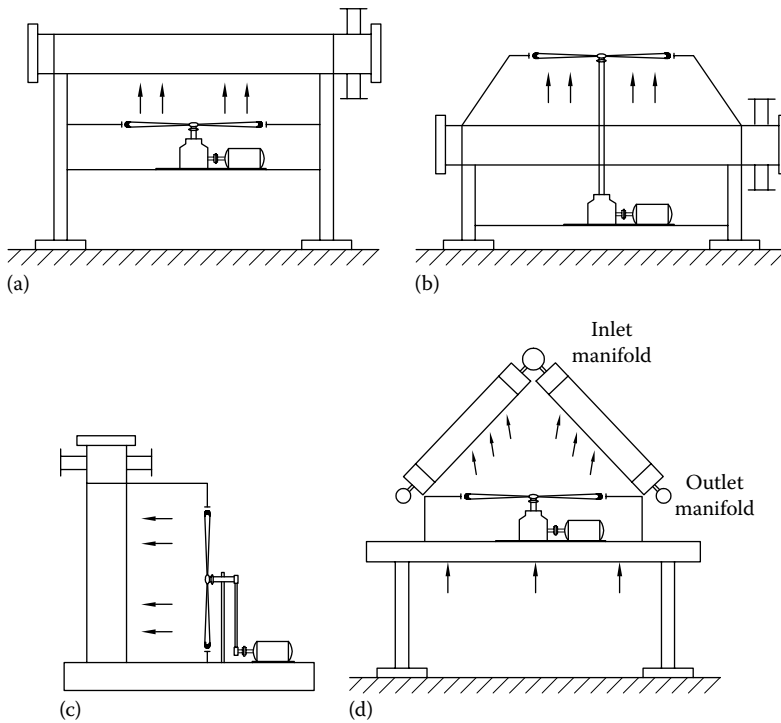


FIGURE 4.59 Orientation of ACHE tube bundle—(a) horizontal, forced draft, (b) horizontal, induced draft, (c) vertical, and (d) A-frame.

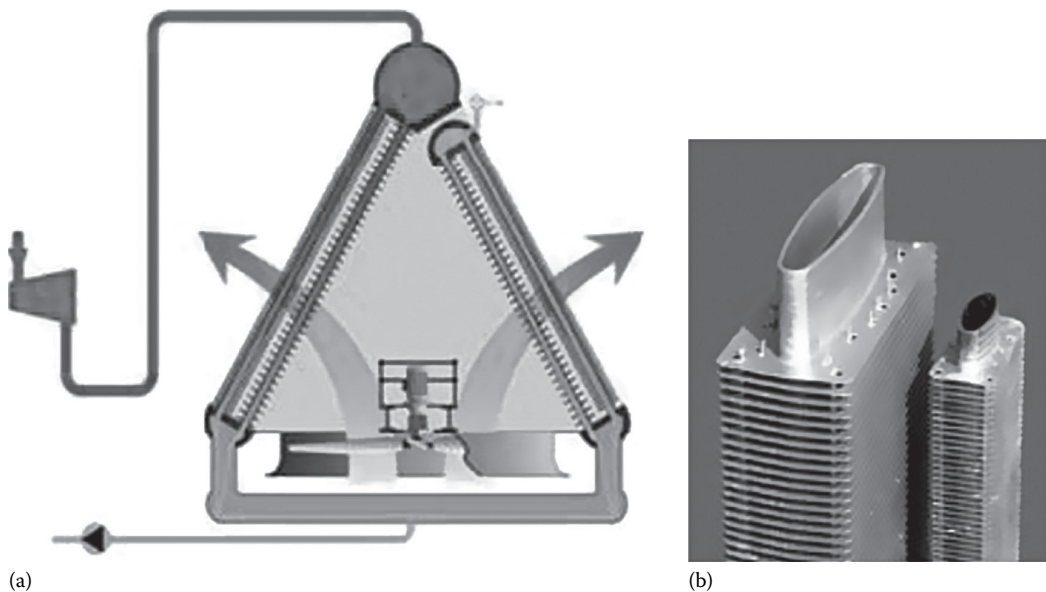


FIGURE 4.60 Air-cooled condensers (A-type orientation)—(a) two tube row design with hot dip galvanized elliptical fin tubes with rectangular fins and (b) hot dip galvanized elliptical fin tube. (Courtesy of GEA Iberica S.A., Vizcaya, Spain.)

Air-Cooled Heat Exchanger Specification Sheet						
Customer:	Equip. Tag No:					
Plant Location:	Manufacturer					
Service:	Size:					
Job Number:	Surface area per bundle					
Model No:	Type: Forced or Induced Draft					
Heat duty	Orientation: A- or V-frame					
Process Data						
Fluid Circulated:				Tubeside		
	In	Out		In	Out	
Fluid quantity, total			Molecular Weight, Vapor			
Liquid			Molecular Weight, Non condensable			
Vapor			Viscosity			
Non condensable			Thermal Conductivity			
Steam /water			Latent heat			
Temperature			Inlet Pressure (specify gauge or absolute)			
Dew Point			Outlet Pressure			
Freezing point –Bubble point			Maximum Allowable Pressure Drop			
Pour point			Calculated pressure drop			
Density			Fouling resistance (min.)			
Specific heat						
Air Side Data						
Air quantity			Altitude			
Air quantity/fan			Temperature in			
Static Fouling resistance:		Pressure:	Temperature out			
Mass Velocity	Face velocity	Min. ambient temp.				
Design pressure	Test pressure	Design Temperature				
Tube bundle	Headers	Tubes details				
Size	Type	Material				
No./bay	Material	ASTM: Seamless/Welded				
Arrangement:	Passes:	O.D./Min. Thk.				
Bundles in Parallel	Plug design	Tubes/bundle				
Bays in Parallel	Material	Tube pitch				
Bundle Frame	Gasket material	Fin Type				
Miscellaneous	Corrosion Allow.	Fin Material				
Structure	Inlet nozzle(s)	Fin O.D.				
Surface Prep.: Galvanised/Painted	Outlet nozzle(s)	Fin Thickness				
Louvers Auto/Manual	Nozzle Rating/Type	Fin density(Fins/inch):				
Standards/Code		API-661/ASME Code				

FIGURE 4.61 ACHE specification sheet.

(continued)

Mechanical Drive Equipment		
Fan -Constant- or Variable pitch	Drive	Speed Reducer
Mfg/Model	Type: Belt/Gear	Type
No./bay	No./bay	No./bay
HP/fan	HP/Drive motor	Model
Fan Diameter/RPM	RPM	HP rating
No. blades	Enclosure	Speed ratio
Pitch: Adjustable or Auto	Volt/Ph/Cycles	Manufacturer
Blade/Hub Material	Manufacturer	Coupling Model
Vibration switch	Louvers	Control: Open/Closed
Noise: dB	Motor- Constant- or variable freq.	Fan- Install Inlet bells- and Fan seal disc
Remarks: 1. Recirculation ducts and chambers- 2. Support structure height- 3. Maintenance walkways-		

FIGURE 4.61 (continued) ACHE specification sheet.

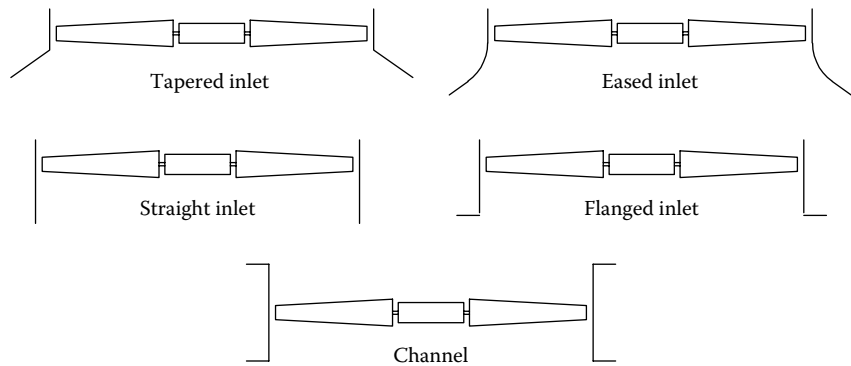


FIGURE 4.62 Fan ring design.

Tapered or eased rings: The tapered inlet and eased rings both allow for a more uniform exit of the air from the fan ring. Most fan design programs will indicate slightly less airside pressure drop and less horsepower required for this configuration. In addition, these fan rings allow for better air dispersion since the air is directed when it leaves the ring. In most ACHEs, the cost of producing this configuration outweighs the increased savings in horsepower, or in airflow efficiency.

Straight, flanged inlet or channel rings: These are the most common fan rings utilized by manufacturers. This ring is easily produced, and provides good air movement if close tip clearance between the ring and the fan is maintained. The depth of this ring will vary with the fan selected.

4.11.3 AMERICAN PETROLEUM INSTITUTE STANDARD API 661/ISO 13706

American Petroleum Institute Standard 661/ISO 13706 [70] is meant for ACHEs for general refinery service. The scope of the standard includes minimum requirements for design, materials selection,

fabrication, inspection, testing, and preparation for shipment of refinery process ACHEs. The standard specifies that the pressure parts shall be designed in accordance with ASME Code, Section VIII, Division 1 [71]. API Standard 661 should be specified and used as a guide in preparing the requisition/specification. When the customer's requirements deviate from API 661, the exceptions or special requirements should be listed as "Specific Requirements" [72].

4.11.4 PROBLEMS WITH HEAT EXCHANGERS IN LOW-TEMPERATURE ENVIRONMENTS

ACHEs are designed to perform at ambient temperatures ranging from 130°F to -60°F. In extremely cold environments, overcooling of the process fluid may cause freezing. This may lead to tube burst, and hence freeze protection is required to prevent plugging or damage to the tubes. The minimum temperature also affects material selection for construction of the cooler.

4.11.4.1 Temperature Control

Several methods are used to control the performance of ACHEs to meet variations in weather and process requirements. The current practice for ACHE design in cold climates for problem services include (1) recirculation of hot air through the tube bundle; (2) steam coils provided to preheat air for start-up conditions—these may be mounted at the cooler base to warm up the inlet air, and according to the recommendation of API 661, this steam coil should be separate from the main cooler bundle; (3) control devices that enable part of the process fluid to bypass the unit; (4) for some units, particularly viscous oil coolers, concurrent design is appropriate, where the hot fluid enters nearest the cold ambient wall, and the outlet where wall temperature is critical is in the warm air stream [69]; and (5) in certain cases, simply controlling the process outlet temperature with fan switching, two-speed fan drives, variable-speed motor automatic louvers, variable pitch fans, or autovaryable-pitch fans is sufficient. Each case must be considered on its merits to decide on the best method of control.

4.11.5 FORCED DRAFT VERSUS INDUCED DRAFT

One of the design criteria affecting the performance of ACHEs is the type of draft: forced draft or induced draft. Both these arrangements are shown in Figure 4.59.

4.11.5.1 Forced Draft

The majority of air-cooled exchangers is of forced draft construction. A common problem with forced draft coolers is accidental warm air recirculation. Forced draft fans have the advantage of handling cold air entering the exchanger, requiring smaller volumes of air and less horsepower. They generally offer better arrangements for maintenance and they are easily accessible. They are best adapted for cold-climate operation with warm air recirculation. Also, forced draft fans afford a higher heat transfer coefficient relative to induced draft, because forced draft fans cause turbulence across the tube bundle [68].

4.11.5.2 Induced Draft

Compared with the forced draft design, induced draft design has the following advantages:

1. Easier to shop assemble, ship, and install
2. The hoods offer protection from weather and hailstone protection
3. Easier to clean the underside when covered with lint, bugs, and debris
4. Better air distribution over the tube bundle
5. Less likely to be affected by hot air recirculation

The disadvantages of induced draft design are

1. More difficult to remove bundles for maintenance
2. High-temperature service limited due to effect of hot air on the fans
3. More difficult to work on the fan assembly, due to heat from the bundle and due to their location

4.11.6 RECIRCULATION

Recirculation of hot plume air occurs in most forced draft ACHEs. The resultant increase in inlet cooling air reduces the effectiveness of the heat exchanger. To reduce the amount of recirculation, wind walls may be erected along the periphery of the heat exchanger. This problem has been analyzed experimentally and numerically by Kroger [67].

4.11.7 DESIGN ASPECTS

Proper design of ACHEs for cold climate service requires a well-balanced consideration of fluid flow, heat transfer, structural design, air movement, wind effects, temperature control in cold climate, and economics [73].

4.11.7.1 Design Variables

Modern ACHEs are designed thermally by computers, which are capable of examining all design variables to produce the optimum unit. In view of the increased size and cost of these units in large plants and the competitive nature of the industry, improved and more sophisticated designs are essential to satisfy the needs of the industry and the society [67]. Important design variables pertaining to the tube bundle include

- Tube (diameter, length and wall thickness, number of tube rows)
- Fins (height, spacing, thickness)
- Space (length, width, and depth)
- Number of tube rows
- Number of passes
- Face area
- Horsepower availability
- Plot area

Designers usually optimize criteria such as [78]

- Capital versus running cost
- Forced versus induced draft fan
- Type and spacing of fins
- Number of tube rows
- Fan design and noise level
- Some of the governing factors in the design of the ACHE and hence the thermal design program structure is shown in Table 4.3

4.11.7.1.1 Air Velocity

If the airflow rate is known, the tentative air velocity may be chosen, which establishes the cooler face area. In air-cooled heat exchanges, face velocity is usually in the range of 1.5–4 m/s [75]. Face velocity is based on the gross cross-sectional area for airflow (face area), as though the tubes were absent.

TABLE 4.3**Program Structure for Design of Air-Cooled Heat Exchanger**

Input Parameters	Heat Duty, Process Parameters, Fouling Resistances, Allowable Pressure Drop, Minimum Ambient Temperature
Code	ASME Code, Section VIII, Div. 1
Standard	API 661
Header types	Plug, studded cover, flanged confined cover, flanged full face cover, bonnet, U-tube, pipe(dished), header gasket type
Tube parameters	Diameter (internal, outer), length and wall thickness and material
Bundle parameters	Size (length, width, and depth) Tubes per row, tube rows per pass, passes per bundle, bundle connection and bay connection
Tube layout pattern	Triangular, rotated triangular, square, diamond
Fin size	High- fin (fin height, spacing/fin density, thickness, diameter of fin)
Fin configuration	Circular, tension wound
Fin attachment	Extruded, L-type weld, L-type tension, embedded, sleeve, metal coated, etc.
Nozzle details	Number of inlet and outlet nozzles, inlet and outlet nozzle diameter
Type of flange	Slip-on, weld neck, lap joint, ring type joint, long weld neck
Bundle orientation	Horizontal, vertical or inclined
Fan	Horse power rating, size, number of blades, rpm, fan pitch control, noise level and type of drive
Draft type	Forced, induced draft
Others	Recirculation, operation of louvers, controls for winter operation

4.11.7.1.2 Airside Pressure Losses, Fan Power, and Noise

The total air-side pressure loss is the sum of pressure loss through the finned-tube bundle and the pressure loss due to the fan and plenum. Bundle pressure loss is calculated from makers' test data or correlations.

4.11.7.1.3 Capital versus Running Cost

A total cost evaluation usually consists of the following four elements [79]:

1. Project equipment cost
2. Field installation cost
3. Electrical distribution cost
4. Operating cost

ACHE costs are influenced by the type of airside flow and the temperature control requirements. Those process fluids that do not require controlled outlet temperature and do not have freeze problems require minimal airflow control [77]. Consider the preferred drive and cost of horsepower, and the payback time for balancing capital investment for adding surface area, against operating costs of fan horsepower.

4.11.7.2 Design Air Temperature

The following data are needed for realistic estimates of the design air temperature [68]:

- An annual temperature probability curve
- Typical daily temperature curves
- Duration frequency curves for the occurrence of the maximum dry-bulb temperature

4.11.8 DESIGN TIPS

A list of points to help to create the most economical design of ACHE for process industries as suggested by GEA Heat Exchangers/GEA Rainey Corporation, Catoosa, OK, are as follows:

- a. Maximize tube length while maintaining 40% or more fan coverage.
- b. Design aircooler with a 1:3 ratio (width to core length ratio) which helps reduce the header size, the most expensive portion of an aircooler, and maintain proper fan coverage.
- c. Minimize tube rows to increase heat transfer effectiveness of area, minimize header thickness. Typically between four and six tube rows (maximum).
- d. Try to use 25.4 mm (1 in.) tube diameter, depending on service. Even high viscosity services that appear to benefit from larger diameter tubes can typically be designed cheaper with more 25.4 mm (1 in.) diameter tubes. Minimum thickness of tubeplate shall be 20 mm for carbon and low alloy steel tubes and 15 mm for high alloy steel or other material [70].
- e. Utilize allowable pressure drop. This allows more passes in the bundle reducing the cooler size.

Other design tips are as follows [83]:

- i. A general rule of thumb for the airside face velocity through the coils is as follows:
- ii. Three row coil 800–850 fpm, four row coil 500–700 fpm, five row coil 450–600 fpm, and six row coil 350–500 fpm.
- iii. On new construction, good design practice would normally restrict the number of tube rows to 4.
- iv. This allows for some modification, if need later, to allow for higher heat load applications. Normally, on gas compressor applications, the air is at such a high temperature after the four rows, that additional cooling from additional rows is minimal.
- v. A minimum fan to coil face area of 40%.
- vi. Air dispersion angle of 45° should not be exceeded, without compensating for this in the design.
- vii. Fans should be operated in the mid range of the fan performance, this should be applied to tip speed, ability to handle the static pressure, and blade angle.
- viii. The fan tip speed shall not exceed the maximum value specified by the fan manufacturer for the selected fan type. Fan tip speed shall not exceed 60 m/s (12,000 ft/min) unless approved by the purchaser. The radial clearance between the fan tip and the fan orifice ring shall be as specified by the design.
- xi. More surface area is always better than more airflow.

4.11.8.1 Air-Cooled Heat Exchanger Design Procedure

Preliminary sizing by Brown's method: Once the inlet temperature is known, a reliable first approximation of the cooler design may be obtained. There are several short-cut manual methods available in the literature. One such method is that of Brown [74]. Brown considers his method will establish a size within 25% of optimum. The method can be stated by the following simple steps:

First, an overall heat transfer coefficient is assumed, depending on the process fluid and its temperature range. Approximate overall heat transfer coefficient, for ACHEs are tabulated in Ref. [74].

Second, the air temperature rise ($t_2 - t_1$) is calculated by the following empirical formula:

$$t_2 - t_1 = 0.005U \left(\frac{T_1 + T_2}{2} - t_1 \right) \quad (4.132)$$

where T_1 and T_2 are hot process fluid terminal temperatures.

Third, the estimate is based on bare tubes, with a layout and fan horsepower estimated from that, so as to avoid the complexity of fin types. Approximate bare tube surface versus unit sizes are tabulated in Ref. [74].

Sizing: The procedure to follow in ACHE design includes the following steps:

1. Specify process data and identify site data.
2. Assume the layout of the tube bundle (from preliminary sizing), fin geometry, and air temperature rise.
3. Calculate film coefficients and overall heat transfer coefficient, mean temperature difference and correction F , and surface area. Check this surface against the assumed layout.
4. If the required surface matches with the assumed layout, calculate the tubeside pressure drop and verify with the specified value.
5. If the surface area and tubeside pressure drop are verified, calculate the airside pressure drop and fan horsepower.

4.11.8.2 Air-Cooled Heat Exchanger Data/Specification Sheet

An ACHE data/specification sheet is shown in Figure 4.61. It should be submitted to the vendor along with the job “specific requirements” as follows [72]:

1. Location of the plant and elevation above sea level
2. Location of the unit in the plant
3. Temperature variation due to weather conditions
4. Seismic and wind loads
5. Variations in operation
6. Process control instrumentation
7. Fire protection
8. Pumping power. The fan power (P_p) required is given by

$$P_p = \frac{M \Delta p}{\rho} \quad (4.133a)$$

or

$$P_p = \frac{G A_{min} \Delta p}{\rho} \quad (4.133b)$$

9. Special surface finish

The condition for dispersion angle of the fan is shown in Figure 4.63. Each fan shall be located such that its dispersion angle shall not exceed 45° at the bundle centerline [70].

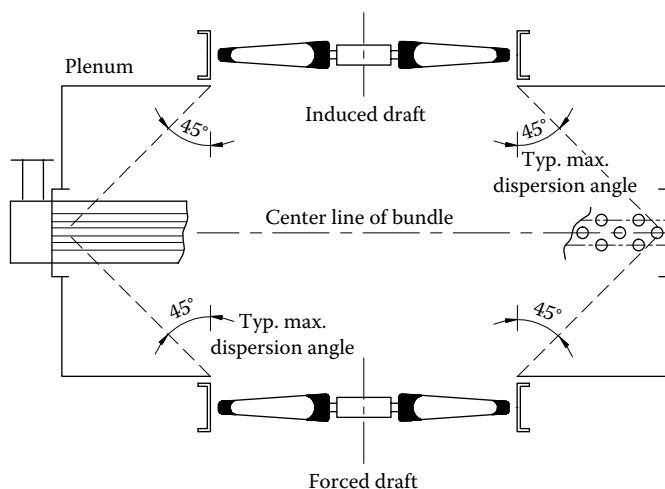


FIGURE 4.63 Condition for dispersion angle of the fan.



FIGURE 4.64 *HI-MAX™ all stainless steel all welded fin tube.* (Courtesy of Holtec International, Marlton, NJ.)

4.11.8.3 Performance Control of ACHes

In addition to the fact that the process flow rate, composition, and inlet temperature of the fluid may vary from the design conditions, the ambient air temperature varies throughout a 24 h day and from day to day. Since ACHes are designed for maximum conditions, some form of control is necessary when overcooling of the process fluid is detrimental, or when saving fan power is desired. Although control could be accomplished using by-passing of process fluid, this is rarely done, and the usual method is airflow control [79].

4.11.8.3.1 Varying Airflow

Varying airflow can be accomplished by [79]

- Adjustable louvers on top of the bundles
- Two-speed fan motors
- Fan shut-off in sequence for multifan units
- AUTO-VARIABLE® fans
- Variable frequency fan motor control

4.11.8.3.1.1 Holtec's HI-MAX™ All Stainless Steel All Welded Fin Tube HI-MAX's stainless steel fin tubes (Figure 4.64) eliminate the thermal stresses associated with aluminized carbon steel tubes and aluminum fins (used in peer systems), thus extending the performance life of the air-cooled condenser. The stainless steel bundles also provide a superior internal and external corrosion protection, which mitigates two significant problems with today's ACHes—(1) flow accelerated corrosion and (2) iron carryover into the condensate. The HI-MAX fin-to-tube bond is made by laser welding and hence stronger in construction. HI-MAX do not have a galvanic coating to combat against corrosion.

NOMENCLATURE

A	total heat transfer area, m^2 (ft^2)
A_f	fin surface area, m^2 (ft^2)
A_{fr}	frontal area, m^2 (ft^2)
A_o	minimum free flow area, m^2 (ft^2)
A_p	primary heat transfer surface area, m^2 (ft^2)
A_s	secondary heat transfer surface area, m^2 (ft^2)
C, c_p	specific heat, $\text{J/kg } ^\circ\text{C}$ ($\text{Btu/lbm.}^\circ\text{F}$)

C_c	specific heat of cold fluid, J/kg °C (Btu/lbm.°F)
C_h	specific heat of hold fluid, J/kg °C (Btu/lbm.°F)
C^*	heat capacity rate ratio for a compact exchanger= $(mc_p)_{\min}/(mc_p)_{\max}$
D_h	hydraulic diameter, $(4r_h)$, m (ft)
d_i	inside diameter of the tueb, m (ft)
d_f	fin diameter of circular fin, m (ft)
d_o	outside diameter of the tube, m (ft)
d_r	effective fin diameter at the collar, m (ft)
F	LMTD correction factor
f	Fanning friction factor
f_f	friction factor on the fin surfaces
f_t	friction factor due to drag force on the tubes
G, G_m	mass velocity, kg/m ² ·s (lbm/h·ft ²)
G_{max}	mass velocity based on free flow area, kg/m ² ·s (lbm/h·ft ²)
g_c	acceleration due to gravity or proportionality constant 9.81 m/s ² (32.17 ft/s ²)
$=$	1 and dimensionless in SI units
h	convective heat transfer coefficient, W/m ² ·°C (Btu/ft ² h·°F)
j	Colburn heat transfer factor
j_N	Colburn heat transfer factor for N number of tube rows
K	fluid entrance contraction or exit expansion coefficient
k	thermal conductivity of the fluid, W/m°C (Btu/h·ft·°F)
k_f	thermal conductivity of the fin material, W/m°C (Btu/h·ft·°F)
L	length in the fluid flow direction, m (ft)
L_f	characteristic fin length, m (ft)
l_f	fin length, m (ft)
L_1, L_2, L_3	heat exchanger core dimensions of a tube bank, m (ft)
M	mass flow rate of the fluid, kg/s (lbm/h)
N_1	number of tubes in one row
N_t	total number of tubes
N_f	fin density of a tubular exchanger
N_p	Number of flow passages on side 1 of PFHE
$N_p + 1$	Number of flow passages on side 2 of PFHE
NTU	number of transfer units,
Nu	Nusselt number
N_r	number of tube rows,
n	fin density of PFHE
P_p	fluid pumping power
P_l	longitudinal pitch, m ² (ft ²)
P_T, P_t	lateral pitch, m ² (ft ²)
p	pressure, Pa (lbf/ft ²)
Pr	Prandtl number
Q	total heat duty of the exchanger, W·s (Btu)
q	heat transfer rate, W (Btu/h)
R	heat capacity rate ratio of shell and tube heat exchanger fluids
Re	Reynolds number
Re_d	Reynolds number based on tube outer diameter
Re_h	Reynolds number based on hydraulic diameter
r_h	hydraulic radius, m (ft) = $D_h/4$
St	Stanton number
s	gap between two fins, m (ft)
t_f	thickness, m (ft)

T	Temperature, °C (°F)
t	Temperature, °C (°F)
T_h	header plate thickness, m (ft)
U_f	upstream fluid velocity on the fin side, m/s (ft/s)
U	overall heat transfer coefficient, W/m ² ·°C (Btu/h·ft ² ·°F)
V_p	volume between plates on one side, m ³ (ft ³)
α	Surface area density of PFHE, m ² /m ³ (ft ² /ft ³)
α	the effective heat transfer coefficient of a stream (Eq. 4.37b), W/m ² ·°C (Btu/ft ² h·°F)
Δp	pressure drop, Pa (lbf/ft ²)
ϵ	thermal effectiveness
μ	viscosity of the fluid, kg/m·s or Pa·s (lbm/h·ft)
ρ	fluid density, kg/m ³ (lbm/ft ³)
β	surface area density, m ² /m ³ (ft ² /ft ³)
η_f	fin efficiency
η_o	overall surface efficiency
$\sigma =$	the ratio of minimum free flow area to frontal area

Subscripts

ave	average
b	bulk mean temperature
c	cold
h	hot
e	exit
i	inlet
lm	log mean
m	mean
n	nozzle
o	outlet
w	wall temperature conditions
1	side 1 or inlet of the exchanger
2	side 2 or outlet of the exchanger
min	minimum
max	maximum

REFERENCES

1. Shah, R. K. and Robertson, J. M., Compact heat exchangers for the process industry, in *Energy Efficiency in Process Technology* (P. A. Pilavachi, ed.), Elsevier Applied Science, London, U.K., pp. 565–580, 1993.
2. Shah, R. K., Compact heat exchanger technology, and applications, in *Heat Exchange Engineering, Vol. 2, Compact Heat Exchangers: Techniques of Size Reduction* (E. A. Foumeny and P. J. Heggs, eds.), Ellis Horwood, New York, 1991, pp. 1–29.
3. Shah, R. K., Classification of heat exchangers, in *Low Reynolds Number Flow Heat Exchangers* (S. Kakac, R. K. Shah, and A. E. Bergles, eds.), Hemisphere, Washington, DC, 1983, pp. 9–14.
4. Shah, R. K., Classification of heat exchangers, in *Heat Exchangers: Thermal-Hydraulic Fundamentals and Design* (S. Kakac, A. E. Bergles, and F. Mayinger, eds.), Hemisphere, Washington, DC, 1981, pp. 9–46.
5. Webb, R. L., Enhancement of single phase heat transfer, in *Handbook of Single Phase Convective Heat Transfer* (S. Kakac, R. K. Shah, and W. Aung, eds.), Chapter 17, John Wiley & Sons, Inc., New York, 1987, pp. 17.1–17.62.
6. Yang, W.-J., High performance heat transfer surfaces: Single phase flows, in *Heat Transfer in Energy Problems*, pp. 109–116.
7. Rabas, T. J. and Taborek, J., Survey of turbulent forced convection heat transfer and pressure drop characteristics of low finned tube banks in crossflow, *Heat Transfer Eng.*, 8, 49–61 (1987).

8. Webb, R. L., Enhancement for extended surface geometries used in air cooled heat exchangers, in *Low Reynolds Number Flow Heat Exchangers* (S. Kakac, R. K. Shah, and A. E. Bergles, eds.), Hemisphere, Washington, DC, 1983, pp. 721–734.
9. Fraas, A. P. and Ozisik, M. N., *Heat Exchanger Design*, John Wiley & Sons, New York, 1965.
10. Webb, R. L. and Farrell, P. A., Improved thermal and mechanical design of copper/brass radiators, SAE, 900724, SAE, Warrendale, PA, 1990, pp. 737–748.
11. Shah, R. K., Compact heat exchanger surface selection methods, in *Heat Transfer*, Vol. 4, Hemisphere, Washington, DC, 1978, pp. 193–199.
12. ALPEMA Standard, *The Brazed Aluminium Plate-Fin Heat Exchanger Manufacturer's Association*, 3rd edn., Didcot, Oxon, U.K., 2010.
13. Taylor, M. A., ed., *Plate-Fin Heat Exchangers, Guide to Their Specification and Use*, HTFS (Harwell Laboratory), Oxon, U.K., 1980.
14. Shah, R. K., Compact heat exchanger surface selection, optimization, and computer aided thermal design, in *Low Reynolds Number Flow Heat Exchangers* (S. Kakac, R. K. Shah, and A. E. Bergles, eds.), Hemisphere, Washington, DC, 1983, pp. 983–998.
- 15a. Shah, R. K., Perforated heat exchanger surfaces part 1—Flow phenomena, noise and vibration characteristics, ASME Paper No. 75-WA/HT-8, 1975.
- 15b. Shah, R. K., Perforated heat exchanger surfaces part 2—Heat transfer and flow friction characteristics, ASME Paper No. 75-WA/HT-9, 1975.
16. Joshi, H. M. and Webb, R. L., Heat transfer and friction in the offset strip-fin heat exchanger, *Int. J. Heat Mass Transfer*, 30, 69–84 (1987).
17. Kays, W. M. and London, A. L., *Compact Heat Exchangers*, 3rd edn., McGraw-Hill, New York, 1984.
18. Cowell, T. A., Heikal, M. R., and Achaichia, A., Flow and heat transfer in compact louvered fin surfaces, in *Aerospace Heat Exchanger Technology* (R. K. Shah and A. Hashemi, eds.), Elsevier Science Publishers, Amsterdam, the Netherlands, 1993, pp. 549–560.
19. Davenport, C. J., Correlations for heat transfer and flow friction characteristics of louvered fin, *Heat Transfer—Seattle, AIChE Symp. Ser.*, 79(225), 19–27 (1983).
20. Shah, R. K., Surface geometrical properties—Tube-fin heat exchangers, Class notes for course no. MEA 522, Spring 1993, pp. 413–418.
21. Shah, R. K., Compact heat exchangers, in *Handbook of Heat Transfer Applications* (W. M. Rohsenow, J. P. Harnett, and E. N. Ganic, eds.), McGraw-Hill, New York, 1985, pp. 4-176–4-312.
- 22a. Idem, S. A., Jung, C., Gonzalez, G. J., and Goldschmidt, V. W., Performance of air-to-water copper finned tube heat exchangers at moderately low airside Reynolds numbers, including the effects of baffles, *Int. J. Heat Mass Transfer*, 30, 1733–1741 (1987).
- 22b. Idem, S. A., Jacobi, A. M., and Goldschmidt, V. W., Heat transfer characterization of a finned tube heat exchanger (with and without condensation), *Trans. ASME, J. Heat Transfer*, 112, 64–70 (1990).
- 22c. Hedderich, P. C., Kelleher, M. D., and Vanderplasts, G. N., Design and optimization of air cooled heat exchangers, *Trans. ASME, J. Heat Transfer*, 104, 683–690 (1982).
23. Kays, W. M. and London, A. L., Heat transfer and flow friction characteristics of some compact heat exchanger surfaces, Part 2—Design data for thirteen surfaces, *Trans. ASME*, 72, 1087–1097 (1950).
24. Shah, R. K., Compact heat exchanger design procedures, in *Heat Exchangers: Thermal-Hydraulic Fundamentals and Design* (S. Kakac, A. E. Bergles, and F. Mayinger, eds.), Hemisphere, Washington, DC, 1981, pp. 495–536.
25. Johnson, B. M., The performance of extended surface heat exchangers, in *Handbook of Heat and Mass Transfer, Vol. 1, Heat Transfer Operation* (N. P. Cheremisinoff, ed.), Gulf Publishing Company, Houston, TX, pp. 767–805.
26. Monheit, M. and Freim, J., Experimental performance of staggered equilateral and equivelocity tube layouts in air cooled heat exchangers, *Industrial Heat Exchangers Conference Proceedings* (A. J. Hayes, W. W. Liang, S. L. Richlen, and E. S. Tabb, eds.), American Society for Metals, Metals Park, OH, 1985, pp. 181–190.
27. Brauer, H., *Kalttechnik*, 13 Jahrgang, Heft 8, 1961, pp. 274–279.
28. LaHaye, P. G., Neugebauer, F. J., and Sakhuja, R. K., A generalized prediction of heat transfer surfaces, *Trans. ASME, J. Heat Transfer*, 96, 511–517 (1974).
29. Fletcher, L. S., Recent developments in contact conductance heat transfer, *Trans. ASME, J. Heat Transfer*, 110, 1059–1070, (1988).
30. Nho, K. M. and Yovanovich, M. M., Effect of oxide layers on measured and theoretical contact conductances in finned tube heat exchangers, in *Compact Heat Exchangers* (R. K. Shah, A. D. Kraus, and D. Metzger, eds.), Hemisphere, Washington, DC, 1990, pp. 397–419.

31. Paikert, P., Air cooled heat exchangers, in *Heat Exchanger Design Handbook* (E. U. Schlunder, editor-in-chief), Vol. 3, Hemisphere, Washington, DC, 1983, Section 3.8.
32. Giedt, W. H., *Principles of Engineering Heat Transfer*, Van Nostrand, New York, 1957.
33. ESDU, Engineering sciences data unit convective heat transfer during crossflow of fluid over plain tube banks, ESDU, Item number 73031, 1973.
34. Grimson, E. D., Correlation and utilization of new data on flow resistance and heat transfer for cross flow of gases over tube banks, *Trans. ASME*, 59, 583–594 (1937).
35. Shah, R. K. and Bhatti, M. S., Assessment of correlations for single-phase heat exchangers, in *Two-Phase Flow Heat Exchangers—Thermal-Hydraulic Fundamentals and Design* (S. Kakac, A. E. Bergles, and F. E. Oliveira, eds.), Kluwer Academic Publishers, London, U.K., 1988, pp. 81–122.
36. Kays, W. M., London, A. L., and Shah, R. K., Heat transfer and friction characteristics of gas flow normal to tube banks—Use of a transient test technique, *Trans. ASME*, 76, 387–396 (1954).
37. Gram, A. J., Mackey, C. O., and Monroe, E. S., Convection heat transfer and pressure drop of air flowing across inline tube banks II—Correlation of data for ten row deep tube banks, *Trans. ASME*, 80, 25–35 (1958).
38. London, A. L., Kays, W. M., and Johnson, D. W., Heat transfer and flow-friction characteristics of some compact heat exchanger surfaces, *Trans. ASME*, 74, 1167–1178 (1952).
39. Briggs, D. E. and Young, E. H., Convection heat transfer and pressure drop of air flowing across triangular pitch banks of finned tubes, *Chem. Eng. Prog. Symp. Ser.*, 59, 1–10 (1963).
40. Robinson, K. K. and Briggs, D. E., Pressure drop of air flowing across triangular pitch banks of finned tubes, *Chem. Eng. Prog. Symp. Ser.*, 62, 177–184 (1966).
41. Rabas, T. J., Eckels, P. W., and Sabatino, R. A., The effect of fin density on the heat transfer and pressure drop performance of low finned tube banks, *Chem. Eng. Commun.*, 10, 127–147 (1981).
42. Weierman, C., Pressure drop data for heavy duty finned tubes, *Chem. Eng. Prog.*, 73, 69–72 (1977).
43. Ganguli, A., and Yilmaz, S. B., New heat transfer and pressure drop correlations for cross flow over low finned tube banks, *AIChE Symp. Ser. Heat Transfer—Pittsburg*, 83, 9–19 (1987).
44. Elmahdy, A. H. and Biggs, R. C., Finned tube heat exchanger: Correlation of dry surface heat transfer data, ASHRAE, No. 2544, 1978, pp. 262–273.
45. Gray, D. L. and Webb, R. L., Heat transfer and friction correlations for plate fin and tube heat exchangers having plain fins, *Proceedings of the Eighth International Heat Transfer Conference*, Vol. 6, San Francisco, CA, 1986, pp. 2745–2750.
46. Rich, D. G., The effect of fin spacing on the heat transfer and friction performance of multirow, smooth plate fin tube heat exchanger, *ASHRAE Trans.*, 79, 137–145 (1973).
47. Zukauskas, A. A., *High Performance Single-Phase Heat Exchangers* (J. Karni, ed., English edition), Hemisphere, Washington, DC, 1989.
- 48a. McQuiston, F. C., Finned tube heat exchangers—State of the art for the air side, *Trans. ASHRAE*, 87, 1077–1085 (1981).
- 48b. McQuiston, F. C., Heat, mass and momentum transfer data for five plate fin tube heat transfer surfaces, *Trans. ASHRAE*, 84, 266–281 (1978).
49. Maltson, J. D., Wilcock, D., and Davenport, C. J., Comparative performance of rippled fin plate fin and tube heat exchangers, *Trans. ASME J. Heat Transfer*, 111, 21–28 (1989).
50. Kroger, D. G., Radiator characterisation and optimization, SAE 840380, 1985, pp. 2.984–2.990.
51. Weiting, A. R., Empirical correlations for heat transfer and flow friction characteristics of rectangular offset-fin plate-fin heat exchangers, *Trans. ASME, J. Heat Transfer*, 97, 488–490 (1975).
52. Manglik, R. M. and Bergles, A. E., The thermal hydraulic design of the rectangular offset strip-fin compact heat exchanger, in *Compact Heat Exchangers—A Festschrift for A. L. London* (R. K. Shah, A. D. Kraus, and D. Metzger, eds.), Hemisphere, Washington, DC, 1990, pp. 123–149.
53. Kays, W. M., Pin-fin heat exchanger surfaces, *Trans. ASME*, May, 471–483 (1955).
54. Norris, R. H. and Spofford, W. A., High-performance fins for heat transfer, *Trans. ASME*, 64, 489–496 (1942).
55. Kanzaka, M., Iwabuchi, M., Aoki, Y., and Ueda, S., Study on heat transfer characteristics of pin finned plate type heat exchangers, *Heat Transfer—Philadelphia*, 85, 306–311 (1989).
56. Gardner, K. A., Efficiency of extended surface, *Trans. ASME*, 67, 621–632 (1945).
57. Kern, D. Q. and Kraus, A. D., *Extended Surface Heat Transfer*, McGraw-Hill, New York, 1972.
58. Scott, T. C. and Goldschmidt, I., Accurate, simple expressions for the fin efficiency of single and composite extended surfaces, *Adv. Enhanced Heat Transfer; ASME Symp.*, 100–122, 79–85 (1979).
59. Schmidt, T. E., Heat transfer calculations for extended surfaces, *J. ASHRAE*, April, 351–357 (1949).
60. Zabronsky, H., Temperature distribution and efficiency of a heat exchanger using square fins on round tubes, *ASME J. Appl. Mech.*, 22, 119–122, (1955).

61. Sparrow, E. M. and Lin, S. H., Shorter communication, *Int. J. Heat Mass Transfer*, 7, 951–953 (1964).
62. Shah, R. K., Temperature effectiveness of multiple sandwich rectangular plate-fin surfaces, *Trans. ASME, J. Heat Transfer*, 91, 471–473 (1971).
63. Shah, R. K., Plate-fin and tube-fin heat exchanger design procedures, in *Heat Transfer Equipment Design* (R. K. Shah, D. C. Subbarao, and R. M. Mashelekar, eds.), Hemisphere, Washington, DC, 1988, pp. 255–266.
64. Hesselgraves, J. E., Optimizing size and weight of plate fin heat exchangers, in *Aerospace Heat Exchanger Technology* (R. K. Shah and A. Hashemi, eds.), Elsevier Science Publishers, Amsterdam, the Netherlands, 1993, pp. 391–399.
65. Shah, R. K. and Mueller, A. C., Heat exchanger basic thermal design methods, in *Handbook of Heat Transfer Applications* (W. M. Rohsenow, J. P. Hartnett, and E. N. Ganic, eds.), 2nd edn., McGraw-Hill, New York, 1985, pp. 4-1–4-77.
66. Chiou, J. P., The advancement of compact heat exchanger theory considering the effects of longitudinal heat conduction and flow nonuniformity, in *Symposium on Compact Heat Exchanges—History, Technological Advancement and Mechanical Design Problems*, Vol. 10, (R. K. Shah, C. F. McDonald, and C. P. Howard, eds.), ASME, New York, 1980, pp. 101–121.
67. Kroger, D. G., Experimental heat transfer, fluid mechanics and thermodynamics in the development of large air cooled heat exchangers, in *Experimental Heat Transfer, Fluid Mechanics and Thermodynamics* (M. D. Kelleher et al., eds.), Elsevier Science Publishers, Amsterdam, the Netherlands, 1993, pp. 135–141.
68. Ganapathy, V., Design of aircooled exchangers—Process design criteria, in *Process Heat Exchange, Chemical Engineering Magazine*, (V. Cavaseno, ed.), McGraw-Hill, New York, 1979, pp. 418–425.
69. North, C. D. R., Air coolers, in *Developments in Heat Exchanger Technology-I* (D. Chisholm, ed.), Applied Science Publishers, London, U.K., 1980, pp. 155–177.
70. ANSI/API Standard 661, *Air Cooled Heat Exchangers for General Refinery Service*, 5th edn./ISO 13706, American Petroleum Institute, Washington, DC, 2002.
71. ASME Boiler and Pressure Vessel Code, Section VIII, *Division 1—Rules for Construction of Pressure Vessels*, American Society of Mechanical Engineers, New York, 2010.
72. Baker, W. J., Selecting and specifying air cooled heat exchangers, *Hydrocarbon Process.*, May, 173–177 (1980).
73. Shipes, K. V., Air cooled exchangers in cold climates, *Chem. Eng. Prog.*, 70, 53–58 (1974).
74. Brown, R., Design of aircooled exchangers—A procedure for preliminary estimates, in *Process Heat Exchange, Chemical Engineering Magazine* (V. Cavaseno, ed.), McGraw-Hill, New York, 1979, pp. 414–417.
75. Saunders, E. A. D., Air cooled heat exchangers, in *Heat Exchangers: Selection Design and Construction*, Addison Wesley Longman, Reading, MA, 1989.
76. Larowski, A. and Taylor, M. A., *Systematic Procedures for Selection of Heat Exchangers*, C58/82, Institution of Mechanical Engineers, London, U.K., 1982, pp. 32–56.
77. Mukherjee, R., Avoid operating problems in air cooled heat exchangers, *Hydrocarbon Process.*, March, 69–76 (1997).
78. Brown, J. W. and Benkley, G. J., Heat exchangers in cold service—A contractor's view, *Chem. Eng. Prog.*, 70, 59–62 (1974).
79. Hudson Products Corporation, The basics of air-cooled heat exchanger, August 2010, pp. 1–16.
80. American Institute of Chemical Engineers, Air-cooled heat exchangers—A guide to performance evaluation, AIChE Equipment Testing Procedure, August 26, 1978.
81. Marc Ellmer, *A Practical Guide for Identifying and Solving Air-Cooled Heat Exchanger Performance Problems in the Field*, Reprinted from *Hydrocarbon Engg.*, April 2008, pp. 1–6.
82. Jim Stone, *Air-Cooled Heat Exchangers—General Information*, Stone Process Equipment Co., Akron, OH, pp. 1–4, <http://www.stoneprocess.com/acooler.htm>
83. Amercool Manufacturing Inc., *Basics of Air Cooled Heat Exchangers*, Amercool Manufacturing Inc., Tulsa, OK, www.amercool.com
84. Bell, K. J. and Mueller, A. C., *Wolverine Heat Transfer Data Book II*, Wolverine Division of UOP Inc., Decatur, AL, 1984.
85. Thome, R. T., *Wolverine Heat Transfer Engineering Data Book III*, Wolverine Division of UOP Inc., Decatur, AL, 2004.
86. Giammaruti, R., Performance improvement to existing air-cooled heat exchangers, Paper No. TP04-13, Presented at the *Cooling Technology Institute Annual Conference*, Houston, TX, February 2–11, 2004. August 2010, pp. 1–16.

BIBLIOGRAPHY

- Agarwal, R. S., Ramaswamy, M., and Srivastava, V. K., Simulation of air-cooled condensers, *J. Energy, Heat Mass Transfer (India)*, 13, 145–164 (1991).
- Bell, K. J., Application of plate-fin heat exchangers in the process industries, in *Compact Heat Exchangers* (R. K. Shah, A. D. Kraus, and D. Metzger, eds.), Hemisphere, Washington, DC, 1990, pp. 591–602.
- Bergles, A. E., Blumenkrantz, A. R., and Taborek, J., Performance evaluation criteria for enhanced heat transfer surfaces, in *Heat Transfer*, Vol. II, JSME, Tokyo, Japan, 1974, pp. 239–243.
- Fletcher, L. S., Experimental techniques for thermal contact resistance measurements, in *Experimental Heat Transfer, Fluid Mechanics and Thermodynamics* (M. D. Kelleher et al., eds.), Elsevier Science Publishers, Amsterdam, the Netherlands, 1993, pp. 195–206.
- Ganguli, A., Tung, S. S., and Taborek, J., Parametric study of air cooled heat exchanger finned tube geometry, *Heat Transfer—Denver*, 81, 122–128 (1985).
- Glass, J., Design of aircooled exchangers—Specifying and rating fans, in *Process Heat Exchange, Chemical Engineering Magazine* (V. Cavaseno, ed.), McGraw-Hill, New York, 1979, pp. 426–430.
- GPSA, *Gas Processors Suppliers Association Engineering Data Book*, Vol. 1, 10th edn., 1987.
- Huang, L. J. and Shah, R. K., Assessment of calculation methods for efficiency of straight fins of rectangular profile, *Int. J. Heat Fluid Flow*, 13, 282–293 (1992).
- Kern, M. J. and Wallner, R., *Water Cooled Charge Air Coolers for Heavy Diesel Engines*, C116/86, 1986, IMechE, London, U.K., pp. 261–268.
- London, A. L. and Shah, R. K., Offset rectangular plate-fin surfaces—Heat transfer and flow friction characteristics, *Trans. ASME, J. Eng. Power*, 90A, 218–228 (1968a).
- McQuiston, F. C., Heat transfer and flow friction data for fin-tube surfaces, *Trans. ASME, J. Heat Transfer*, 93C, 249–250 (1971).
- McQuiston, F. C. and Tree, D. R., Optimum space envelopes of the finned tube heat transfer surface, *ASHRAE*, 78, 144–152 (1972).
- Mueller, A. C., Air cooled heat exchangers, in *Heat Transfer Equipment Design* (R. K. Shah, E. C. Subbarao, and R. A. Mashelikar, eds.), Hemisphere, Washington, DC, 1988, pp. 179–190.
- Nir, A., Heat transfer and friction factor correlations for crossflow over staggered finned tube banks, *Heat Transfer Eng.*, 12, 43–58 (1991).
- Rich, D. G., The efficiency and thermal resistance of annular and rectangular fins, *Proc. 3rd Int. Heat Transfer Conf.*, 111, 281–289 (1966).
- Shah, R. K. and London, A. L., Influence of brazing on very compact heat exchanger surfaces, ASME Paper No. 71-HT-29, 1971.
- Shah, R. K. and Webb, R. L., Compact and extended heat exchangers, in *Heat Exchangers: Theory and Practice* (J. Taborek, G. F. Hewitt, and N. Afgan, eds.), Hemisphere/McGraw-Hill, Washington, DC, 1983, pp. 425–468.
- Soland, J. G., Mack, W. M. Jr., and Rohsenow, W. M., Performance ranking of plate-fin heat exchanger surfaces, *Trans. ASME, J. Heat Transfer*, 100, 514–519 (1978).
- Sunden, B. and Svantesson, J., Thermal hydraulic performance of new multilouvered fins, *Heat Transfer—Jerusalem*, Paper No. 14-HX-16, 1990, pp. 91–96.
- Taborek, J., Bond resistance and design temperatures for high finned tubes—A reappraisal, *Proceedings of the ASME, Thermal/Mechanical Heat Exchanger Design, Karl Gardner Memorial Session* (K. P. Singh and S. M. Shenkman, eds.), Vol. 118, 1985, pp. 49–57.
- Ward, D. J. and Young, E. H., Heat transfer and pressure drop of air in forced convection across triangular pitch banks of finned tubes, *Chem. Eng. Prog. Symp. Ser.*, 55, 37 (1959).
- Ward, D. J. and Young, E. H., Heat transfer and pressure drop of air in forced convection across triangular pitch banks of finned tubes, *Chem. Eng. Prog. Symp. Ser.* 59, 37–44 (1963).
- Webb, R. L., Air side heat transfer in finned tube heat exchangers, *Heat Transfer Eng.*, 1, 33–49 (1980).
- Webb, R. L., Compact heat exchangers, in *Heat Exchanger Design Handbook* (E. U. Schlunder, editor-in-chief), Vol. 3, Hemisphere, Washington, DC, 1983, Section 3.9.
- Zukauskas, A., Heat transfer from tubes in cross flow, in *Advances in Heat Transfer* (J. P. Hartnett and T. Irvine, Jr., eds.), Vol. 8, Academic Press, New York, 1972, pp. 93–160.

5 Shell and Tube Heat Exchanger Design

The most commonly used heat exchanger is the shell and tube type. It is the “workhorse” of industrial process heat transfer. It has many applications in the power generation, petroleum refinery, chemical industries, and process industries. They are used as oil cooler, condenser, feedwater heater, etc. Other types of heat exchangers are used when economical. Though the application of other types of heat exchangers is increasing, the shell and tube heat exchanger will continue its popularity for a long time, largely because of its versatility [1].

5.1 CONSTRUCTION DETAILS FOR SHELL AND TUBE EXCHANGERS

The major components of a shell and tube exchanger are tubes, baffles, shell, front head, rear head, and nozzles. Expansion joint is an important component in the case of fixed tubesheet exchanger for certain design conditions. Other components include tie-rods and spacers, impingement plates, sealing strips, supports, and lugs. The selection criteria for a proper combination of these components are dependent upon the operating pressures, temperatures, thermal stresses, corrosion characteristics of fluids, fouling, cleanability, and cost. Expansion joints, nozzles, and supports are discussed in detail in Chapter 11. A large number of geometrical variables are associated with each component, and they are discussed in detail in this chapter. Major components of shell and tube heat exchangers and a cut section of a heat exchanger are shown in Figure 5.1.

5.1.1 DESIGN STANDARDS

5.1.1.1 TEMA Standard

TEMA standards [2] are followed in most countries of the world for the design of shell and tube heat exchangers. The TEMA standards are applicable to unfired shell and tube heat exchangers with inside diameters not exceeding 60 in. (1524 mm). Each section is identified by an uppercase letter symbol, which precedes the paragraph numbers of the section and identifies the subject matter. TEMA classes R, C, and B have been combined into one section titled class RCB. The differences in design practices among the classes have been to some extent simplified. Details of R, C, and B classification are as follows:

1. TEMA B—generally for chemical process services, more stringent than TEMA C, but not as stringent as R
2. TEMA C—for generally moderate commercial and process application requirements, the most commonly used in industries
3. TEMA R—the highest integrity design

5.1.1.2 ANSI/API Standard 660

ANSI/API Standard 660 [3] is the national adoption of ISO 16812:2002—Petroleum and natural gas industries—Shell and tube heat exchangers. This International Standard specifies requirements and gives recommendations for the mechanical design, material selection, fabrication, inspection, testing, and preparation for the shipment of shell and tube heat exchangers for the petroleum and natural gas industries.

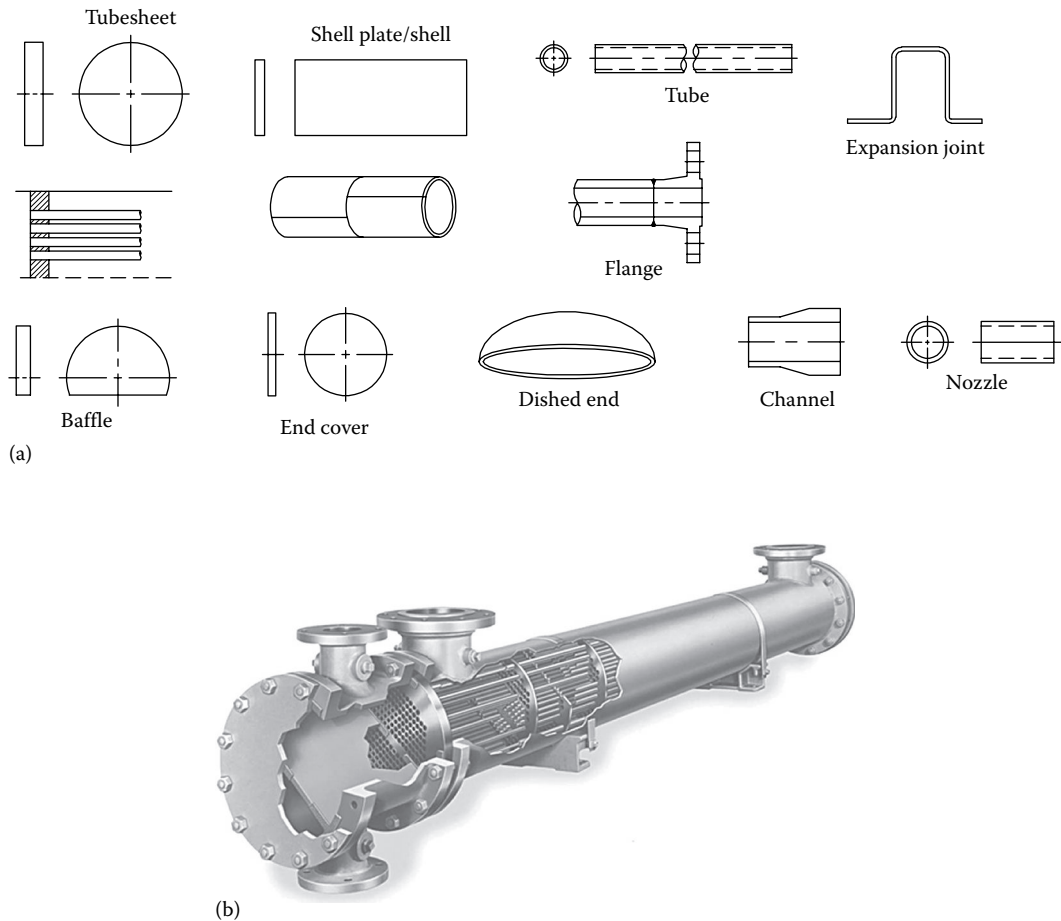


FIGURE 5.1 (a) Major components of a shell and tube heat exchanger. (b) Cut section of a shell and tube heat exchanger. (Courtesy of API Heat Transfer Inc., Buffalo, NY.)

5.2 TUBES

Tubes of circular cross section are exclusively used in exchangers. Since the desired heat transfer in the exchanger takes place across the tube surface, the selection of tube geometrical variables is important from the performance point of view [4]. Important tube geometrical variables include tube outside diameter, tube wall thickness, tube pitch, and tube layout patterns (Figure 5.2). Tubes should be able to withstand the following:

1. Operating temperature and pressure on both sides
2. Thermal stresses due to the differential thermal expansion between the shell and the tube bundle
3. Corrosive nature of both the shellside and the tubeside fluids

There are two types of tubes: straight tubes and U-tubes. The tubes are further classified as

1. Plain tubes
2. Finned tubes
3. Duplex or bimetallic tubes
4. Enhanced surface tubes

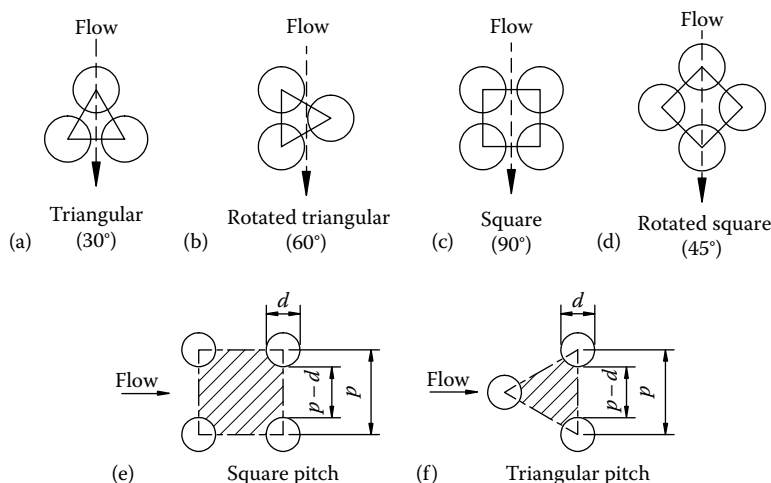


FIGURE 5.2 Tube layout patterns: (a) 30°; (b) 60°; (c) 90°; (d) 45°; (e) flow area for square pitch; and (f) flow area for triangular pitch.

Extended or enhanced surface tubes are used when one fluid has a substantially lower heat transfer coefficient than the other fluid. Doubly enhanced tubes with enhancement both on inside and outside of the tubes are available that can reduce the size and cost of the exchanger. Extended surfaces of finned tubes types can provide 2–4 times as much heat transfer area on the outside as the corresponding bare tube, and this enhanced area helps to offset a lower outside heat transfer coefficient. More recent developments include corrugated tube, which has both inside and outside heat transfer enhancement, a finned tube, which has integral inside turbulators as well as extended outside surface, and tubing, which has outside surfaces designed to promote nucleate boiling [5].

5.2.1 TUBE DIAMETER

Tube size is specified by outside diameter and wall thickness. From the heat transfer point of view, smaller diameter tubes yield higher heat transfer coefficients and result in a compact exchanger. However, larger diameter tubes are easier to clean, more rugged, and they are necessary when the allowable tubeside pressure drop is small. Almost all heat exchanger tubes fall within the range of $\frac{1}{4}$ in. (6.35 mm) to 2 in. (50.8 mm) outside diameter. TEMA tube sizes in terms of outside diameter are $\frac{1}{4}$, $\frac{3}{8}$, $\frac{1}{2}$, $\frac{5}{8}$, $\frac{3}{4}$, $\frac{7}{8}$, 1, 1.25, 1.5, and 2 in. (6.35, 9.53, 12.70, 15.88, 19.05, 22.23, 25.40, 31.75, 38.10, and 50.80 mm). Standard tube sizes and gauges for various metals are given in TEMA Table RCB-2.21. These sizes give the best performance and are most economical in many applications. Most popular are the $\frac{3}{8}$ -in. and $\frac{3}{4}$ -in. sizes, and these sizes give the best all-around performance and are most economical in most applications [6]. Use $\frac{1}{4}$ in. (6.35 mm) diameter tubes for clean fluids. For mechanical cleaning, the smallest practical size is $\frac{3}{4}$ in. (19.05 mm). Tubes of diameter 1 in. are normally used when fouling is expected because smaller ones are not suitable for mechanical cleaning, and falling film exchangers and vaporizers generally are supplied with 1.5- and 2-in. tubes [7].

5.2.2 TUBE WALL THICKNESS

The tube wall thickness is generally identified by the Birmingham wire gauge. Standard tube sizes and tube wall thickness in inches are presented in TEMA Table RCB-2.21. Tube wall thickness must be checked against the internal and external pressures separately, or maximum pressure differential across the wall. However, in many cases, the pressure is not the governing factor in determining the wall thickness. Except when pressure governs, the wall thickness is selected on these bases [8]: (1) providing an adequate margin against corrosion, (2) fretting

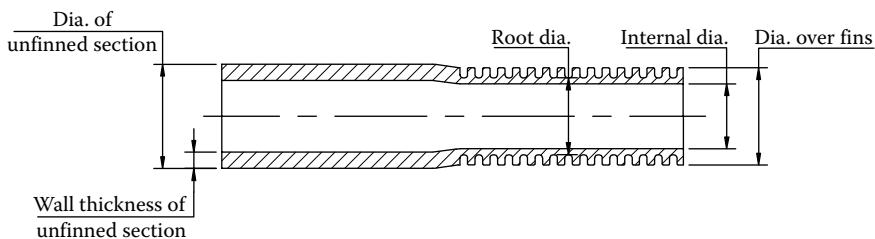


FIGURE 5.3 Low-finned tube.

and wear due to flow-induced vibration, (3) axial strength, particularly in fixed exchangers, (4) standardized dimensions, and (5) cost.

5.2.3 LOW-FINNED TUBES

Shell and tube exchangers employ low-finned tubes (Figure 5.3) to increase the surface area on the shellside when the shellside heat transfer coefficient is low compared to the tubeside coefficient—e.g., when shellside fluid is highly viscous liquids, gases, or condensing vapors. The low-finned tubes are generally helical or annular fins on individual tubes.

Fin tubes for a shell and tube exchanger are generally “low-fin” type with fin height slightly less than $\frac{1}{16}$ in. (1.59 mm). The most common fin density range is 19–40 fins/in. (748–1575 fins/m). The surface area of such a fin tube is about 2.5–3.5 times that of a bare tube [4]. The finned tube has bare ends having conventional diameters of bare tubing; the diameter of the fin is either slightly lower than or the same as the diameter of the bare ends, depending upon the manufacturer. In addition to the geometrical variables associated with bare tubes, the additional geometrical dimensions associated with a fin tube are root diameter, fin height, and fin pitch.

5.2.4 TUBE LENGTH

For a given surface area, the most economical exchanger is possible with a small shell diameter and long tubes, consistent with the space and the availability of handling facilities at site and in the fabricator’s shop [8]. Therefore, minimum restrictions on length should be observed. However, for offshore applications, long exchangers, especially with removable bundles, are often very difficult to install and maintain economically because of space limitations [9]. In this case, shorter and larger shells are preferred despite their higher price per unit heat transfer surface. Standard lengths as per TEMA standard RCB-2.1 are 96, 120, 144, 196, and 240 in. Other lengths may be used.

5.2.5 MEANS OF FABRICATING TUBES

Tubing used for heat exchanger service may be either welded or seamless. The welded tube is rolled into cylindrical shape from strip material and is welded automatically by a precise joining process. A seamless tube may be extruded or hot pierced and drawn. Copper and copper alloys are available only as seamless products, whereas most commercial metals are offered in both welded and seamless. More details on tubing are given in Chapters 8 and 13.

5.2.6 DUPLEX OR BIMETALLIC TUBES

Duplex or bimetallic tubes are available to meet the specific process problem pertaining to either the shellside or the tubeside. For example, if the tube material is compatible with the shellside fluid, but not compatible with the tubeside fluid, a bimetallic tube allows it to satisfy both the corrosive conditions.

5.2.7 NUMBER OF TUBES

The number of tubes depends upon the fluid flow rate and the available pressure drop. The number of tubes is selected such that the tubeside velocity for water and similar liquids ranges from 3 to 8 ft/s (0.9–2.4 m/s) and the shellside velocity from 2 to 5 ft/s (0.6–1.5 m/s) [4]. The lower velocity limit is desired to limit fouling; the higher velocity is limited to avoid erosion–corrosion on the tubeside, and impingement attack and flow-induced vibration on the shellside. When sand, silt, and particulates are present, the velocity is kept high enough to prevent settling down.

5.2.8 TUBE COUNT

To design a shell and tube exchanger, one must know the total number of tubes that can fit into the shell of a given inside diameter. This is known as tube count. Factors on which the tube count depends are discussed in Ref. [8] and in Phadke [10] and Whitley et al. [11]. Such factors include the following:

- Shell diameter
- Outside diameter of the tubes
- Tube pitch
- Tube layout pattern—square, triangular, rotated square, or rotated triangular
- Clearance between the shell inside diameter and the tube bundle diameter
- Type of exchanger, i.e., fixed tubesheet, floating head, or U-tube
- Number of tubeside passes
- Design pressure
- Nozzle diameter
- Tie-rods and sealing devices that block space
- Type of channel baffle, i.e., ribbon, pie shape, vertical, etc. [11]

The conventional method of obtaining tube count by plotting the layout and counting the tubes (thus the tube count) is cumbersome, time-consuming, and prone to error. Tables of tube count are available in references like Ref. [10,12], and others, which often cover only certain standard combinations of pitch, tube diameter, and layout parameters. A mathematical approach using number theory is suggested by Phadke [10] to predict the tube count and presented tube count for various combinations of tube layout parameters. His method eliminates the disadvantages of drawing the tube layout pattern and can accommodate any configuration.

5.2.9 U-TUBE

5.2.9.1 U-Tube U-Bend Requirements as per TEMA

When U-bends are formed, it is normal for the tube wall at the outer radius to thin. As per TEMA section RCB-2.33, the minimum tube wall thickness in the bent portion before bending shall be [2]

$$t_o = t_1 \left(1 + \frac{d}{4R_b} \right) \quad (5.1)$$

where

t_o is the original tube wall thickness

t_1 the minimum tube wall thickness calculated by code rules for a straight tube subjected to the same pressure and metal temperature

d the tube outer diameter

R_b the mean radius of bend

5.3 TUBE ARRANGEMENT

5.3.1 TUBE PITCH

The selection of tube pitch is a compromise between a close pitch for increased shellside heat transfer and surface compactness, and a larger pitch for decreased shellside pressure drop and fouling, and ease in cleaning. In most shell and tube exchangers, the minimum ratio of tube pitch to tube outside diameter (pitch ratio) is 1.25. The minimum value is restricted to 1.25 because the ligament (a ligament is the portion of material between two neighboring tube holes) may become too weak for proper rolling of the tubes into the tubesheet. The ligament width is defined as the tube pitch minus the tube hole diameter; this is shown in Figure 5.4.

5.3.2 TUBE LAYOUT

Tube layout arrangements (Figure 5.2) are designed so as to include as many tubes as possible within the shell to achieve maximum heat transfer area. Sometimes a layout is selected that also permits access to the tubes for cleaning as required by process conditions. Four standard types of tube layout patterns are triangular (30°), rotated triangular (60°), square (90°), and rotated square (45°). (Note that the tube layout angle is defined in relation to the flow direction and is not related to the horizontal or vertical reference line arrangement, and that the 30° , 60° , and 45° arrangements are “staggered,” and 90° is “in-line.”) For identical tube pitch and flow rates, the tube layouts in decreasing order of shellside heat transfer coefficient and pressure drop are 30° , 45° , 60° , and 90° . Thus, the 90° layout will have the lowest heat transfer coefficient and pressure drop. The selection of the tube layout pattern depends on the following parameters, which influence the shellside performance and hence the overall performance:

1. Compactness
2. Heat transfer
3. Pressure drop
4. Accessibility for mechanical cleaning
5. Phase change if any on the shellside

5.3.2.1 Triangular and Rotated Triangular Arrangements

Triangular and rotated triangular layouts (30° and 60°) provide a compact arrangement, better shellside heat transfer coefficients, and stronger tubesheets for a specified shellside flow area. For a given tube pitch/outside diameter ratio, about 15% more tubes can be accommodated within a given shell diameter using these layouts [8]. These layout patterns are satisfactory for clean services, but have the disadvantage of making the lanes between tubes rather inaccessible for mechanical cleaning. It is difficult to insert a rigid tool between the tubes. Only chemical cleaning or water jet cleaning is possible.

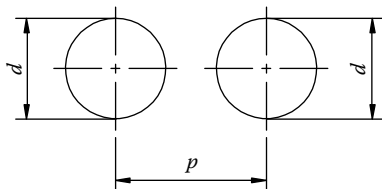


FIGURE 5.4 Tube pitch and ligament width ($p-d$).

5.3.2.2 Square and Rotated Square Arrangements

When mechanical cleaning is necessary on the shellside, 45° and 90° layouts must be used with a minimum gap between tubes of 6.35 mm. There is no theoretical limit to tube outer diameter for mechanical cleaning, but the 6.35 mm clearance limits the tubes to a minimum of $\frac{5}{8}$ or $\frac{3}{4}$ in outer diameter in practice [9]. The square pitch is generally not used in the fixed design because of no need of mechanical cleaning on the shellside. These layout patterns offer lower pressure drops and lower heat transfer coefficients than triangular pitch. The 45° layout is preferred for single-phase laminar flow or fouling service, and for condensing fluid on the shellside. Shah [4] suggests a square layout for the following applications:

1. If the pressure drop is a constraint on the shellside, the 90° layout is used for turbulent flow, since in turbulent flow, the 90° has superior heat transfer rate and less pressure drop.
2. For reboilers, a square layout will be preferred for stability reasons. The 90° layout provides vapor escape lanes.

5.4 BAFFLES

Baffles must generally be employed on the shellside to support the tubes, to maintain the tube spacing, and to direct the shellside fluid across or along the tube bundle in a specified manner. There are a number of different types of baffles, and these may be installed in different ways to provide the flow pattern required for a given application.

5.4.1 CLASSIFICATION OF BAFFLES

Baffles are either normal or parallel to the tubes. Accordingly, baffles may be classified as transverse or longitudinal. The transverse baffles direct the shellside fluid into the tube bundle at approximately right angles to the tubes and increase the turbulence of the shell fluid. Every shell and tube exchanger has transverse baffles except the X and K shells, which have only support plates. The longitudinal baffles are used to control the direction of the shellside flow. For example, F, G, and H shells have longitudinal baffles. In the F shell, an overall counterflow is achieved.

5.4.2 TRANSVERSE BAFFLES

Transverse baffles are of two types: (1) plate baffles and (2) rod baffles. Three types of plate baffles are (1) segmental, (2) disk and doughnut, and (3) orifice baffles.

5.4.2.1 Segmental Baffles

The segmental baffle is a circular disk (with baffle holes) having a segment removed. Predominantly, a large number of shell and tube exchangers employ segmental baffles. This cutting is denoted as the baffle cut, and it is commonly expressed as a percentage of the shell inside diameter as shown in Figure 5.5. Here the percent baffle cut is the height, H , given as a percentage of the shell inside diameter, D_s . The segmental baffle is also referred to as a single segmental baffle. The heat transfer and pressure drop of crossflow bundles are greatly affected by the baffle cut. The baffle cuts vary from 20% to 49% with the most common being 20%–25%, and the optimum baffle cut is generally 20%, as it affords the highest heat transfer for a given pressure drop. Baffle cuts smaller than 20% can result in high pressure (HP) drop. As the baffle cut increases beyond 20%, the flow pattern deviates more and more from crossflow [7] and can result in stagnant regions or areas with lower flow velocities; both of these reduce the thermal effectiveness of the bundle [1].

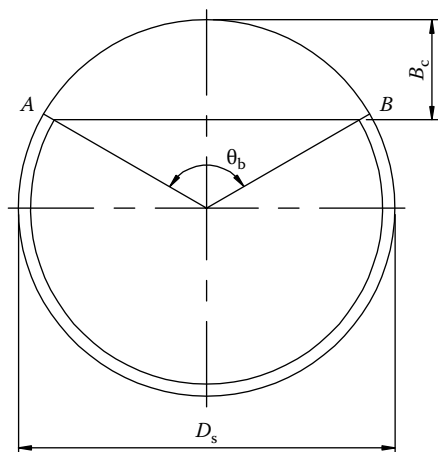


FIGURE 5.5 Baffle cut.

Baffle spacing: The practical range of single segmental baffle spacing is $\frac{1}{5}$ –1 shell diameter [1], though optimum could be 40%–50% [1]. TEMA Table RCB-4.52 [2] provides maximum baffle spacing for various tube outer diameters, tube materials, and the corresponding maximum allowable temperature limit. The baffles are generally spaced between the nozzles. The inlet and outlet baffle spacings are in general larger than the “central” baffle spacing to accommodate the nozzles, since the nozzle dimensions frequently require that the nozzle should be located far enough from the tubesheets.

Baffle thickness: TEMA Tables R-4.41 and CB-4.41 [2] provide the minimum thickness of transverse baffles applying to all materials for various shell diameters and plate spacings.

Shellside flow distribution: Segmental baffles have a tendency to poor flow distribution if spacing or baffle cut ratio is not in correct proportion, as shown in Figure 5.6 [13]. Too low or too high a ratio results in maldistribution and produces inefficient heat transfer and also favors fouling. For low-pressure (LP)-drop designs, choose baffles that ensure a more uniform flow such as multisegmental, disk and doughnuts, and rod baffles.

Orientation of baffles: Alternate segmental baffles are arranged at 180° to each other, which cause shellside flow to approach crossflow through the bundle and axial flow in the baffle window zone. All segmental baffles have horizontal baffle cuts as shown in Figure 5.7a. Unless the shellside fluid is condensed, the horizontal baffle cut should be used for single-phase application, to reduce accumulation of deposits on the bottom of the shell and to prevent stratification of the shellside fluid [7]. The direction of the baffle cut is selected as vertical (Figure 5.7b) for the following shellside applications [8]:

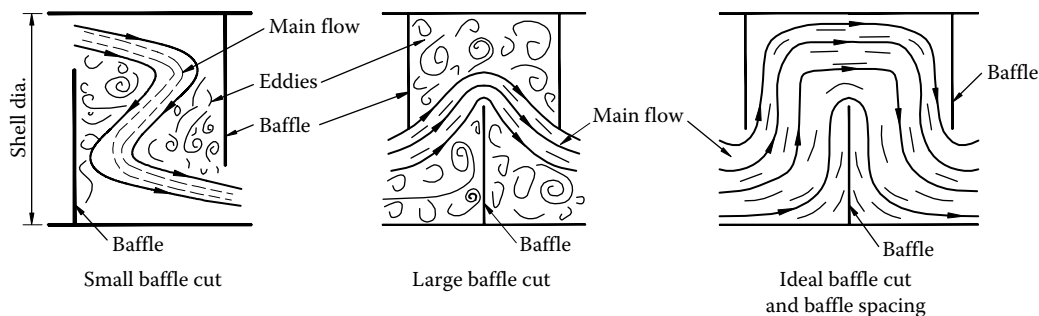


FIGURE 5.6 Shellside flow distribution influenced by baffle cut.

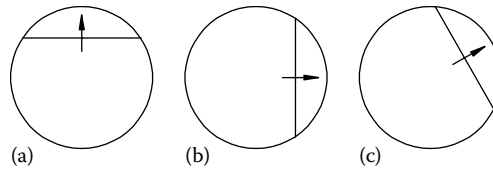


FIGURE 5.7 Baffle cut orientation: (a) horizontal; (b) vertical; and (c) rotated.

(1) for condensation, to allow the condensate to flow freely to the outlet without covering an excessive amount of tubes [4,7]; (2) for boiling or condensing fluids, to promote more uniform flow; and (3) for solids entrained in liquid (to provide least interference for the solids to fall out).

5.4.2.1.1 Double Segmental and Multiple Segmental Baffles

Various multi-segmental baffles can be used to reduce baffle spacing or to reduce crossflow because of pressure limitations. The multi-segmental baffles are characterized by large open areas and some allow the fluid to flow nearly parallel to the tubes, offering a much lower pressure drop [14].

Double and triple segmental baffle layout are shown in Figure 5.8a, Figure 5.8b shows design requirement to ensure adequate tube support [5], idealized fluid flow fraction through the baffles is shown in Figure 5.8c, and fluid flow stream pattern is shown in Figure 5.8d. In an exchanger with

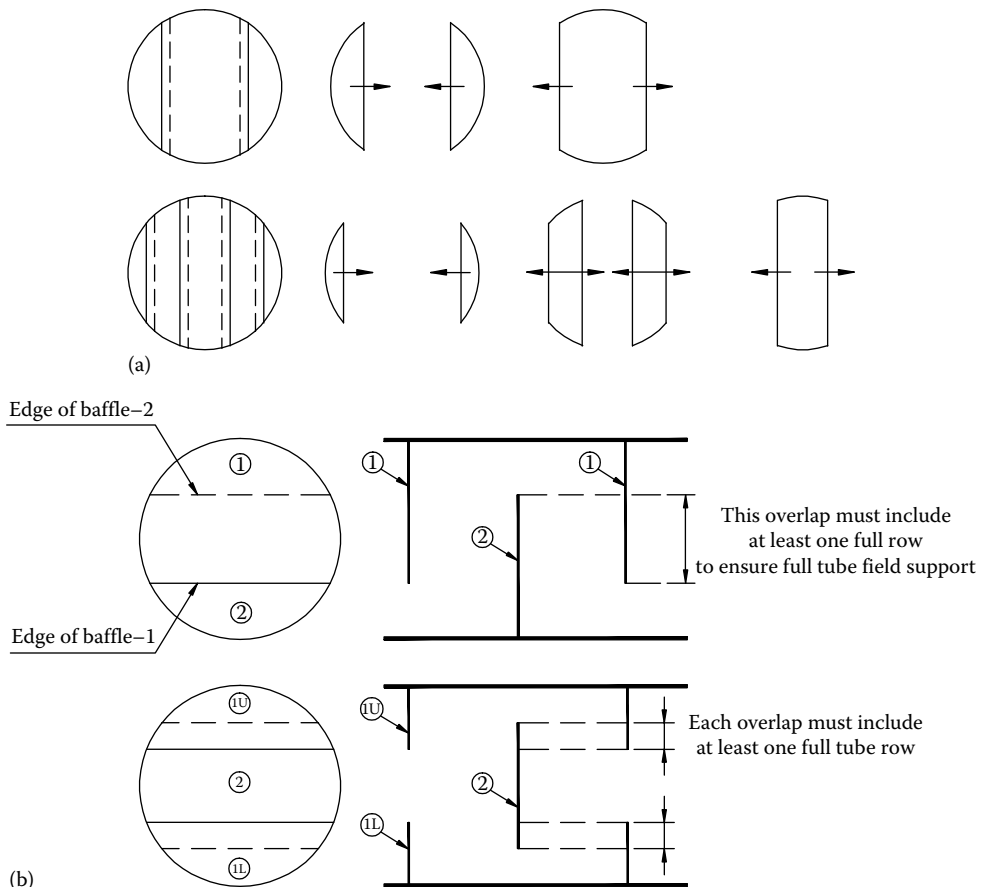


FIGURE 5.8 Segmental baffles layout. (a) Double and triple segmental baffles with end view flow pattern, (b) design requirement to ensure adequate tube support with double and triple segmental baffles.

(continued)

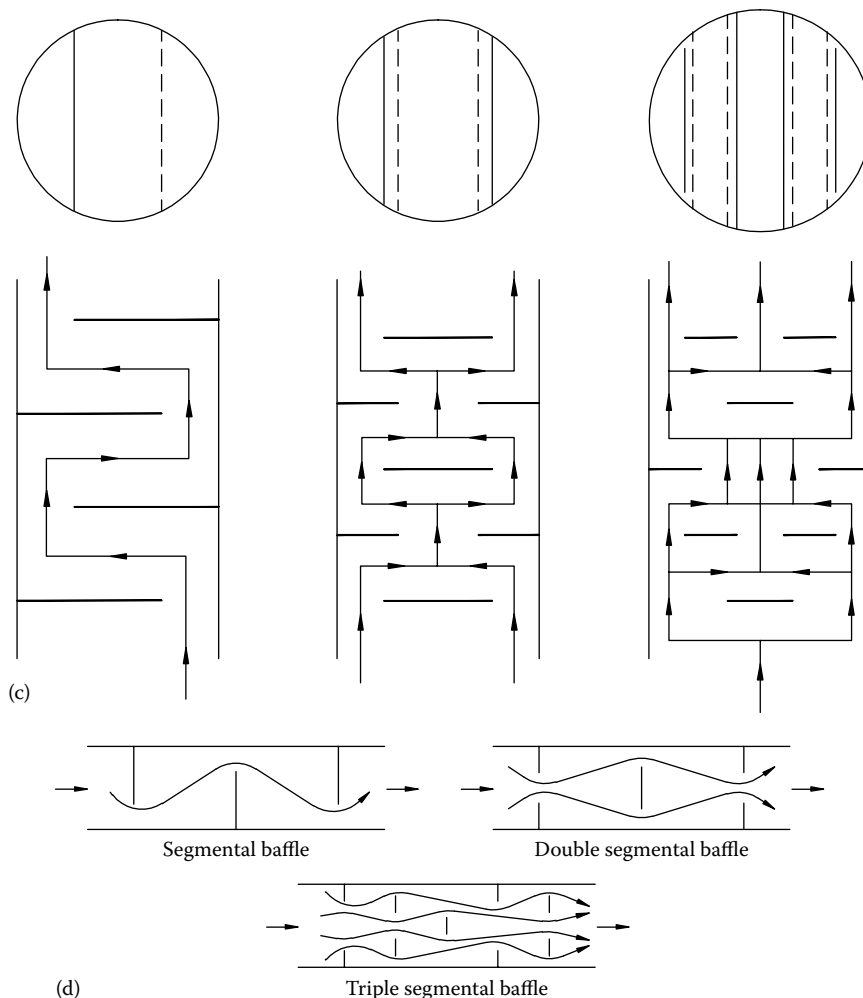


FIGURE 5.8 (continued) Segmental baffles layout. (c) idealized flow fraction with segmental baffles, and (d) stream flow distribution with segmental baffles.

single segmental baffles the total flow, except for leakages and bypass streams, passes through the tube bank between baffles in crossflow, whereas with double segmental baffles barring the leakages, the flow divides into two streams on either side of the baffle, and in triple segmental baffles, the flow divides into three streams as shown in Figure 5.8c and d. Due to this, heat exchangers with double or multiple segmental baffles can handle larger fluid flows on the shellside. Other features of double segmental or multiple segmental baffles are as follows [4]:

1. The flow on the shellside is split into two or more streams as per the number of baffle segments, namely, double, triple, multiple, etc.; hence, the danger of shellside flow-induced vibration is minimal.
2. The baffle spacing should not be too small; otherwise, it results in a more parallel (longitudinal) flow with significant low stagnant areas.

Double segmental and triple segmental baffle heat exchanger units under fabrication are shown in Figure 5.9a and b, respectively.

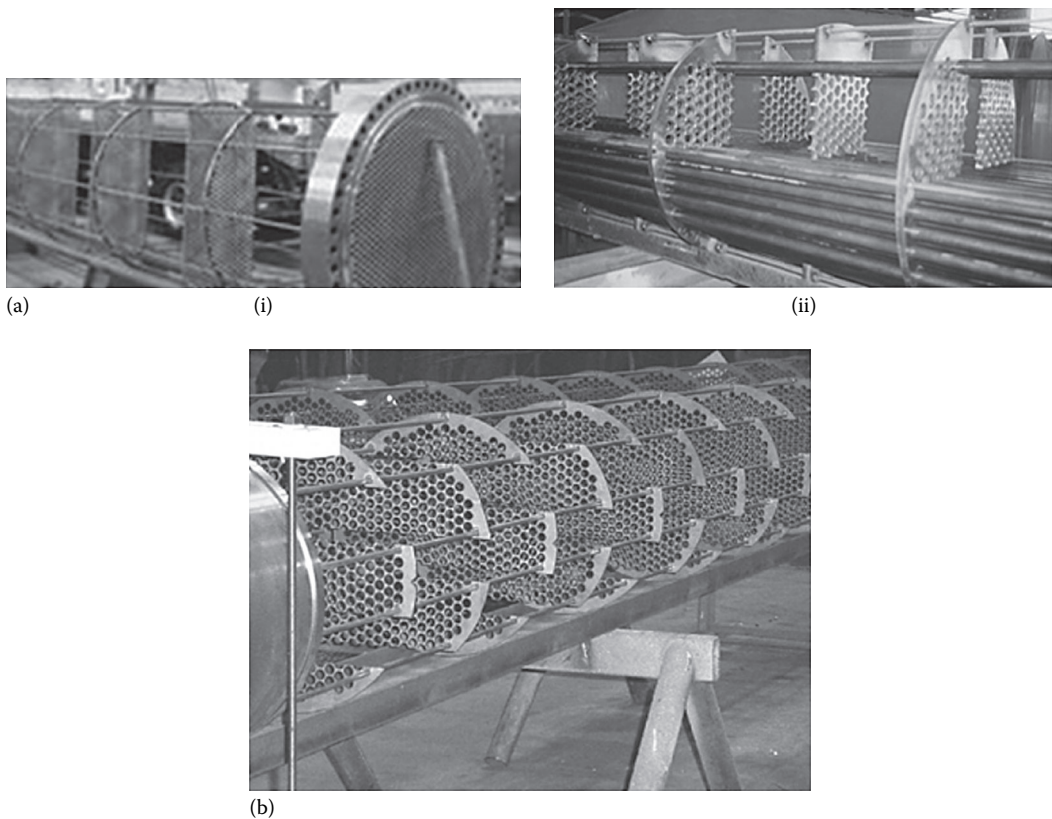


FIGURE 5.9 (a) Heat exchanger with double segmental baffles. (i) Cage assembly (Courtesy of Brembana Costruzioni Industriali S.p.A., Milan, Italy), and (ii) tube bundle under assembly. (Courtesy of Peerless Mfg. Co. of Dallas, TX, Makers of Alco and Bos-Hatten brands of heat exchangers.) (b) Shell and tube heat exchanger tube bundle cage with triple segmental baffles. (Courtesy of Heat Exchanger Design, Inc., Indianapolis, IN.)

5.4.2.1.2 Window Baffles

These are considered when crossflow is not practical because of pressure-drop limitations. Window baffles allow the fluid to flow parallel to the tubes, offering much lower pressure drop [7].

5.4.3 DISK AND DOUGHNUT BAFFLE

The disk and doughnut baffle is made up of alternate “disks” and “doughnut” baffles as shown in Figure 5.10. Disk and doughnut baffle heat exchangers are primarily used in nuclear heat exchangers [4].

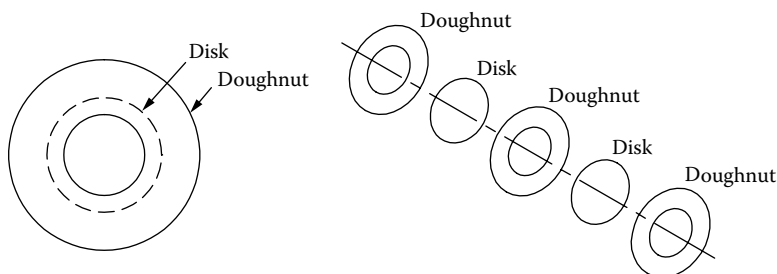


FIGURE 5.10 Disk and doughnut baffles.

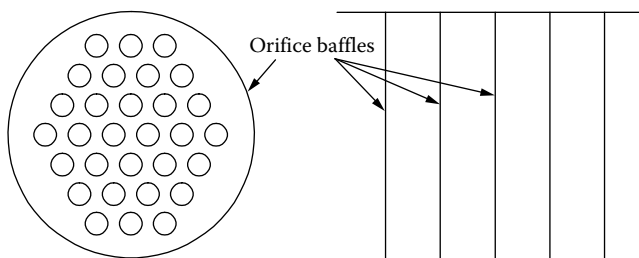


FIGURE 5.11 Orifice baffle.

This baffle design provides a lower pressure drop compared to a single segmental baffle for the same unsupported tube span and eliminates the tube bundle to shell bypass stream.

5.4.4 ORIFICE BAFFLE

In an orifice baffle, the tube-to-baffle hole clearance is large so that it acts as an orifice for the shellside flow (Figure 5.11). These baffles do not provide support to tubes, and, due to fouling, the annular orifices plug easily and cannot be cleaned. This baffle design is rarely used.

5.4.5 NO TUBES IN WINDOW

The baffle cut area, or baffle window region, is generally filled with tubes. Since the tubes in the window zone are supported at a distance of two times the central baffle spacing, they are most susceptible to vibration. To eliminate the susceptibility of tube vibrations, the tubes in the window zone are removed and therefore all tubes pass through all baffles. Additional support plates are introduced between main baffles to reduce the unsupported span of the tubes as shown in Figure 5.12, thus providing an increase in the natural frequency of the tubes. The resultant design is referred to as the segmental baffle with no-tubes-in-window (NTIW) design. NTIW design has the following characteristics [15]:

1. Pressure drop about one-third that of single segmental baffle design
2. Uniform shellside flow pattern resembling that of an ideal tube bank, which offers high shellside heat transfer coefficient and low fouling tendency
3. The baffle cut and the number of tubes removed vary from 15% to 25%
4. Very LP drop in the window and correspondingly lower bypass and leakage streams

Since the loss in heat transfer surface is considerable in an NTIW design, this can be minimized by having small baffle cuts and possibly by an increase in the shellside fluid velocity or larger shell

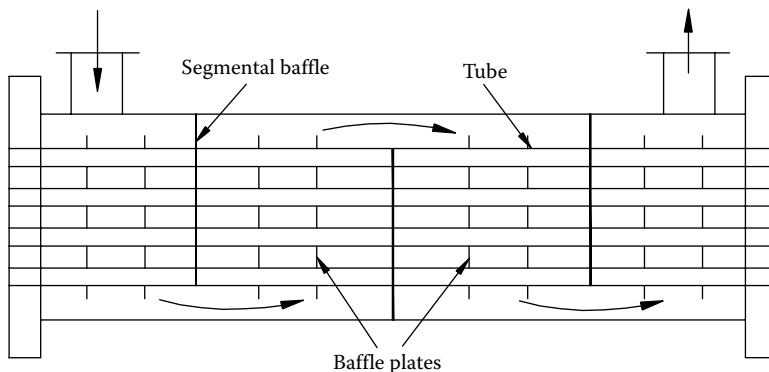


FIGURE 5.12 NTIW design.

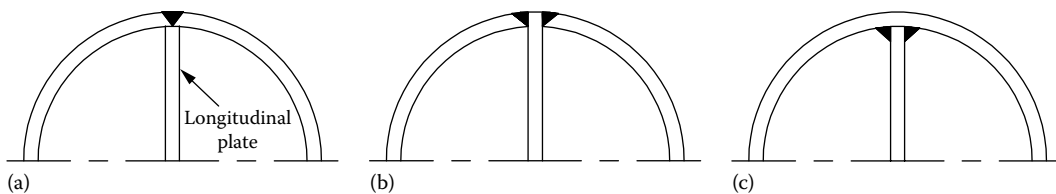


FIGURE 5.13 Longitudinal baffle weld joint with shell. (a) Shell gouged and welded, (b) baffle passes through shell and welded, and (c) baffle welded to inside of the shell.

diameter to contain the same number of tubes. It may be noted that the design of tubesheet of NTIW does not fall within TEMA Standard.

5.4.6 LONGITUDINAL BAFFLES

Longitudinal baffles divide the shell into two or more sections, providing multipass on the shellside. But this type should not be used unless the baffle is welded to the shell and tubesheet. Nevertheless, several sealing devices have been tried to seal the baffle and the shell, but none has been very effective [7]. Gupta [16] lists some sealing devices that are used to seal the baffle and shell. They are the following:

- Sealing strips or multiplex arrangement
- Packing arrangement
- Slide-in or tongue-and-groove arrangement

If the baffle is not welded, bypassing occurs from one side to the other, which adversely affects the heat transfer coefficient and makes its accurate prediction rather difficult. Hence, it is better to weld than to prefer this design. Common methods to weld the longitudinal baffle to the shellside are shown in Figure 5.13 [17]. When multipass shells are required, it is economical to use a separate shell, unless the shell diameter is large enough to easily weld a longitudinal baffle to the shell [7].

5.4.7 ROD BAFFLES

Phillips RODbaffle design uses alternate sets of rod grids instead of plate baffles, enabling the tubes to be supported at shorter intervals without resulting in a large pressure drop. Flow-induced vibration is virtually eliminated by this design. The flow is essentially parallel to tube axis; as a result of the longitudinal flow, it has LP drop to heat transfer conversion characteristics. The tube layout is usually 45° or 90° . Design of rod baffle heat exchanger is covered separately in this chapter.

5.4.8 NEST BAFFLES AND EGG-CRATE TUBE SUPPORT

NEST™ baffle: This is a patented design intended to overcome the danger of flow-induced vibration of tubes. In this design, each tube rests in a V-shaped cradle and is supported at line segments (Figure 5.14a). These elements are preformed to the desired tube pitch and ligament size. The flow is parallel to the tube bundle, and hence the vibration problem is greatly reduced [18]. It is claimed that the pressure drop is lower for the same amount of heat transfer compared to a segmentally baffled exchanger.

EGG-CRATE-GRID™ support (Figure 5.14b) is a simple and economical support for heat exchanger tubes, which can droop or collapse under stress and elevated temperature. This support is fabricated from commercial flat strip material, typically of stainless steel; strip ends are tack welded to the heat exchanger shell and tubes are welded to strips at specified intervals. This design eliminates conventional s, which requires tube insertion through drilled holes.

Figure 5.14c shows patented baffles similar to EGG-CRATE baffle but with a square tube layout.

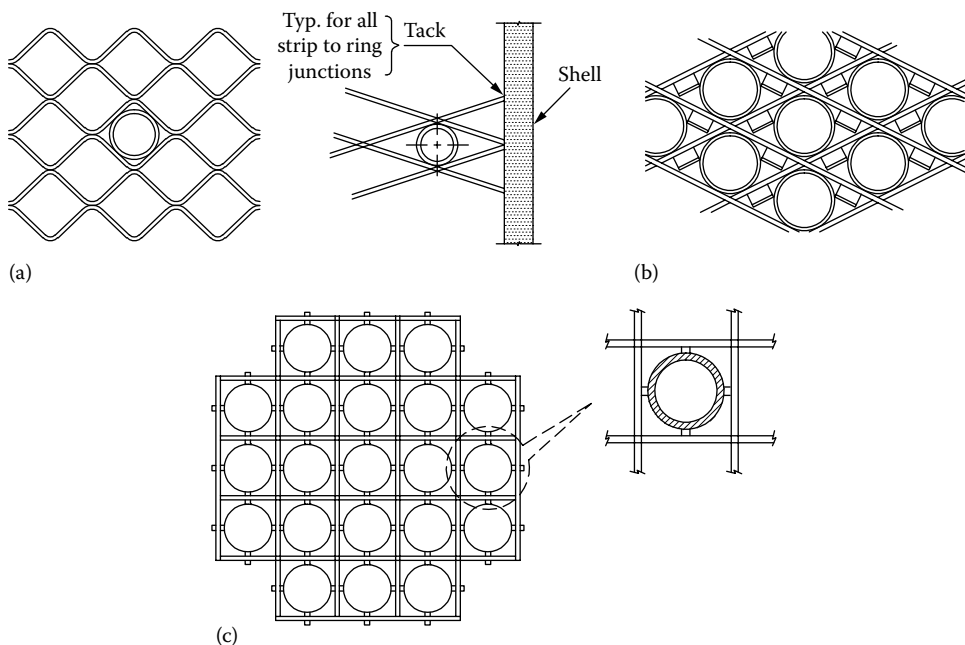


FIGURE 5.14 Special types of plate baffles. (a) NEST™, (b) EGG-CRATE baffle support, and (c) patented baffles with a square tube layout.

5.4.8.1 Non-Segmental Baffles

The non-segmental baffle as shown in Figure 5.15 is a Holtec patented tube support system used to promote axial flow in a tube bundle. Holtec's non-segmental baffle eliminates the problems associated with high-volume shellside flows, since it provides total tube support while offering minimal obstruction to the passing fluid. Furthermore, non-segmental baffles have been used by in a variety of applications involving phase change (boiling or condensing), and thermosiphon flows. In addition, the use of these baffles virtually eliminates flow-induced vibrations and premature tube failure. These non-segmental baffles are made from a flat metal strip that emulates the surface quality of typical heat exchanger tubing. Each strip is laser cut to ensure a precise lattice-like structure. Typical materials of construction are 304 and 316 stainless steel; however, other material can be used upon request. Tube hole clearances are within the TEMA and HEI limits.

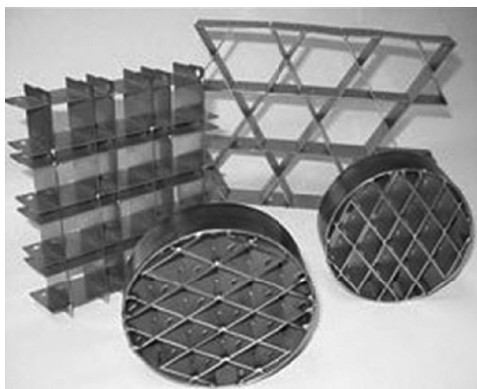


FIGURE 5.15 Non-segmental baffles. (Courtesy of Holtec International, Marlton, NJ.)



FIGURE 5.16 LP drop baffles. (Courtesy of Holtec International, Marlton, NJ.)

5.4.8.1.1 Low-Pressure Drop Baffles

Another type of non-segmental baffle made of rods (Figure 5.16) was developed by Koch Heat Transfer, USA, and Holtec International, USA, and to ensure LP drop on the shellside since the shellside flow is longitudinal in nature. This baffle type is different from Phillips RODbaffle heat exchanger.

5.4.9 GRIMMAS BAFFLE

The Grimmas baffle is a patented version of the plate baffle, which ensures an axial flow and improves heat transfer [19]. The design is shown in Figure 5.17.

5.4.10 WAVY BAR BAFFLE

Wavy bar baffle design, as shown in Figure 5.18, is similar to Grimmas baffle but made of wavy bar. This design ensures axial flow and improves heat transfer and ensures LP drop on the shellside.

5.4.11 BAFFLES FOR STEAM GENERATOR TUBE SUPPORT

Figure 5.19 shows five types of baffles—four with plate baffles and one with lattice bars similar to EGG-CRATE baffle used in applications of steam generators [20].

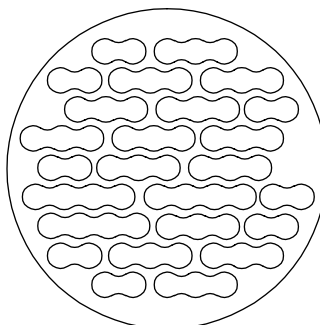


FIGURE 5.17 Grimmas baffle.

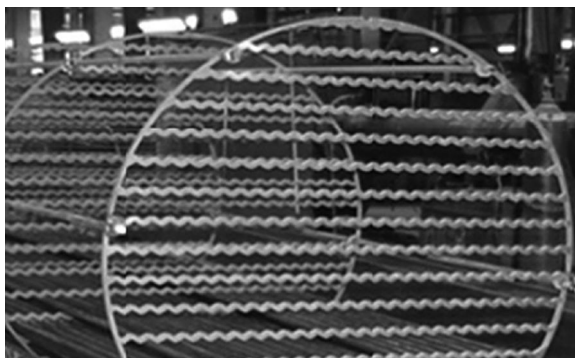


FIGURE 5.18 Wavy bar baffle design. (Courtesy of Peerless Mfg. Co. of Dallas, TX, Makers of Alco and Bos-Hatten brands of heat exchangers.)

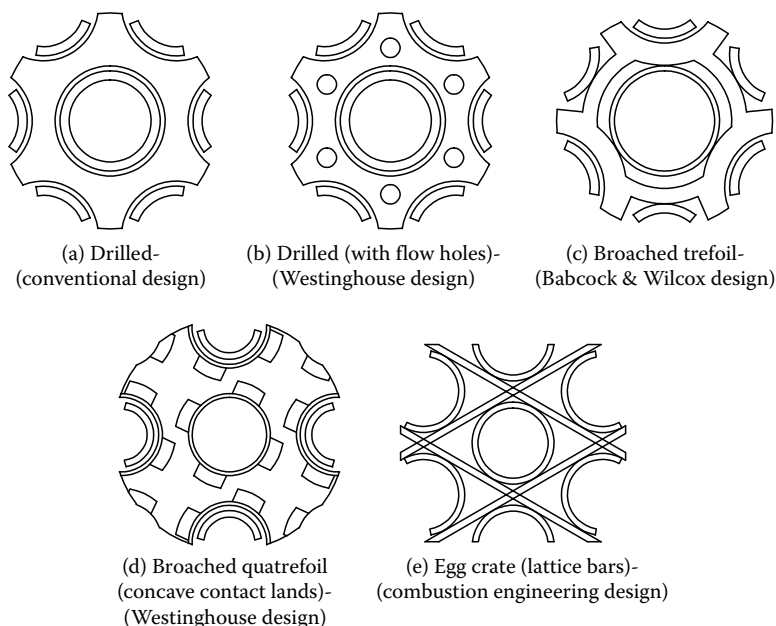


FIGURE 5.19 Types of baffle plates for a steam generator. (a) Drilled, (b), drilled (with flow holes), (c) broached trefoil, (d) broached quatrefoil (concave contact lands), and (e) egg crate (lattice bars).

5.5 TUBESHEET AND ITS CONNECTION WITH SHELL AND CHANNEL

A tubesheet is an important component of a heat exchanger. It is the principal barrier between the shellside and tubeside fluids. Proper design of a tubesheet is important for safety and reliability of the heat exchanger. Tubesheets are mostly circular with uniform pattern of drilled holes as shown in Figure 5.20. Tubesheets of surface condensers are rectangular shape. Tubesheets are connected to the shell and the channels either by welds (integral) or with bolts (gasketed joints) or with a combination thereof in six possible types:

1. Both shellside and tubeside are integral with tubesheet (Figure 11.2a)
2. Shellside integral and gasketed on tubeside, tubesheet extended as a flange (Figure 11.2b)
3. Shellside integral and tubeside gasketed construction (Figure 11.2c)
4. Both shellside and tubeside gasketed construction (Figure 11.2d)
5. Tubesheet gasketed on shellside and integral with channel, extended as a flange (Figure 11.2e)
6. Shellside gasketed and tubeside integral construction (Figure 11.2f)

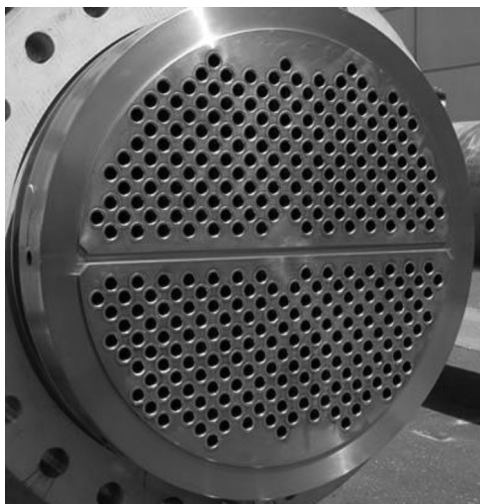


FIGURE 5.20 Drilled titanium tubesheet. (Courtesy of TITAN Metal Fabricators Inc, Camarillo, CA.)

5.5.1 CLAD AND FACED TUBESHEETS

As per TEMA RB 7.8, the nominal clad thickness on tubeside face of tubesheet shall be 5/16 in. (7.8 mm) when tubes are expanded and minimum clad thickness of 1/8 in. (3.2 mm) when tubes are welded to tubesheet. As per C 7.8, the nominal clad thickness on tubeside face of tubesheet shall be 3/16 in. (4.8 mm) when tubes are expanded and a minimum clad thickness of 1/8 in. (3.2 mm) when tubes are welded to tubesheet.

5.5.2 TUBE-TO-TUBESHEET ATTACHMENT

Tubes are attached to the tubesheet by (1) rolling, (2) welding, (3) rolling and welding, (4) explosive welding, and (5) brazing. Schematic sketches of tube to tubesheet attachment are given in Chapter 15. Expansion of the tubes into the tubesheet is most widely used and is satisfactory for many services. However, when stresses are higher, or where pressures are such that significant leakage could occur, or where contamination between fluids is not permitted, the tubes are welded to the tubesheet. Explosion welding can be used instead of conventional welding where there is incompatibility between tube and tubesheet materials and for tube plugging under hazardous conditions.

5.5.3 DOUBLE TUBESHEETS

No known method of making tube to tubesheet joints can completely eliminate the possibility of mixing of shellside and tubeside fluids due to leakage. When the possibility of intermixing of the shellside and tubeside fluids cannot be tolerated, double tubesheet construction will offer positive assurance against one fluid leaking into the other at a tube to tubesheet joint.

5.5.3.1 Types of Double Tubesheet Designs

Two designs of double tubesheets are available: (1) the conventional double tubesheet design, which consists of two individual tubesheets at each end of the tubes, and (2) the integral double tubesheet design [21].

5.5.3.1.1 Conventional Double Tubesheet Design

In a conventional double tubesheet design, the tubesheets are installed with a small space between them. The space is usually open to the atmosphere. Sometimes a thin strip is welded to avoid ingress of dusts and dirt, or an expansion joint is welded with vent at the top and a drain at the bottom.

These patterns are shown schematically in Figure 5.21 and double tubesheet heat exchangers are shown in Figure 5.22 through 5.24. While selecting material for double tubesheet design, the outer should be compatible with the tubeside fluid and the inner should be compatible with the shellside fluid. The most important consideration is the differential radial expansion of the two s , which will stress the tubes. The double tubesheet can be installed only in the U-tube, fixed tubesheet, and floating head, outside packed stuffing box exchangers. It is not feasible to use the double tubesheet

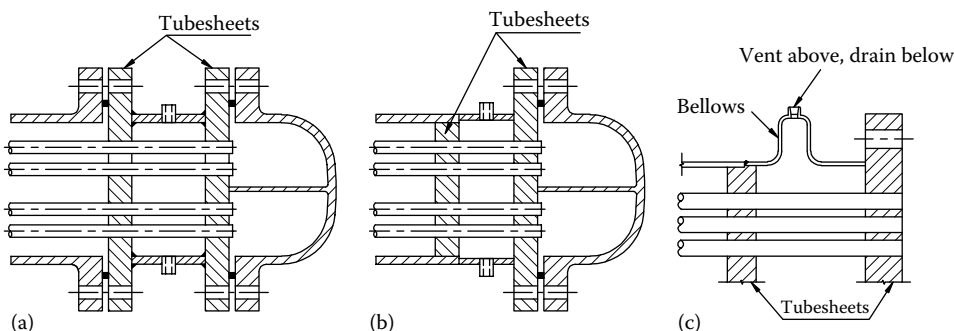


FIGURE 5.21 Double tubesheet shell and tube heat exchanger—schematic. (a) Removable tube bundle with light gauge shroud between two tubesheets, (b) fixed tubesheets with light gauge shroud, and (c) fixed tubesheet with bellows.

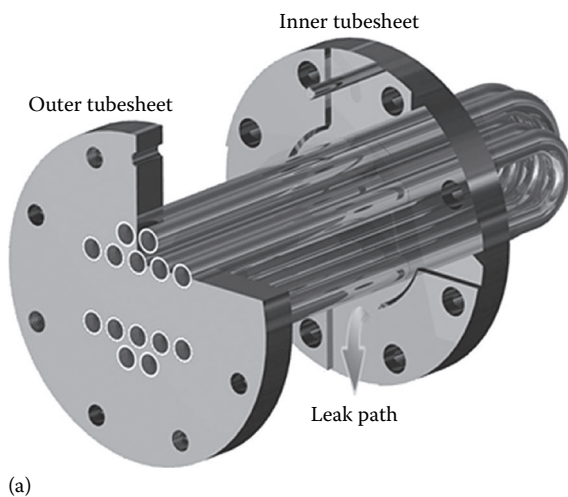


FIGURE 5.22 Double tubesheet shell and tube heat exchanger. (a) Schematic and (b) heat exchanger. (Courtesy of Allegheny Bradford Corporation, Bradford, PA.)



FIGURE 5.23 Double tubesheet shell and tube heat exchanger. (Courtesy of GEA Heat Exchangers Ltd, Brazil/GEA do Brasil Intercambiadores Ltd, Brazil.)

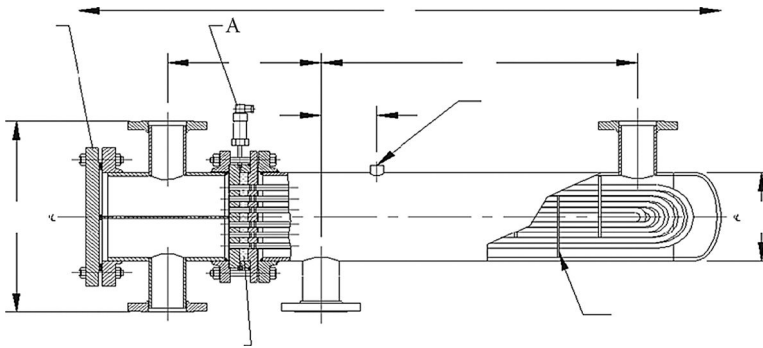


FIGURE 5.24 Double tubesheet shell and tube heat exchanger with real-time leak indicator (A). (Courtesy of Alstrom Corporation, Bronx, NY.)

in heat exchanger types such as [6] (1) floating head, pull-through bundle, (2) floating head with split backing ring, and (3) floating head, outside packed lantern ring exchangers. An expression for the space between the s pairs, l_g , which is widely used in the industry, is a special case of the more complex analysis of Urgami et al. [22]. The expression is given by [21]

$$l_g = \frac{\sqrt{1.5E_t d \delta}}{S_t} \quad (5.2)$$

where δ is the free differential in-plane movement in inches (mm) given by

$$\delta = 0.5D_{out} [\alpha_h (T_h - T_{amb}) - \alpha_c (T_c - T_{amb})] \quad (5.3)$$

and where

d is the tube outer diameter, inches (mm)

E_t is Young's modulus for the tube, psi (Pa)

D_{out} is the tube outer limit, inches (mm)

T_{amb} the ambient (assembly) temperature, °F (°C)

T_c the temperature of the colder tubesheet, °F (°C)

T_h the temperature of the hotter tubesheet, °F (°C)

α_c the coefficient of thermal expansion of the colder tubesheet between the assembly temperature and temperature T_c , in./in. (°F) [mm/(mm °C)]

α_h the coefficient of thermal expansion of the hotter tubesheet between the assembly temperature and temperature T_h , in./in. (°F) [mm/(mm °C)]

S_t the allowable stress in the tubes, psi (Pa)

The provision of a double tubesheet has been mandatory for UK power-station condensers in past years to eliminate any possibility of cooling water entering the steam space of the condenser [23]. The tubesheet interspace is drained to a low-level vessel, which is maintained at the condenser absolute pressure by means of a connection to the air pump suction line.

5.5.3.1.2 Integral Double Tubesheets

The patented integral double tubesheet design consists of a single tubesheet made from a single plate or forging, drilled to the desired tube layout pattern. Then the annular grooves are machined into the tube holes about midway between the faces to interconnect the adjacent tubes. This construction in effect minimizes differential expansion problems, but it is expensive and not effective like conventional double tubesheets to avoid fluid mixing [24].

5.5.4 DEMERITS OF DOUBLE TUBESHEETS

If at all practical, double tubesheets should be avoided. However, some conditions dictate their use along with the problems such as [24] the following:

1. Wasted tube surface.
2. Increased fabrication cost due to additional drilling and rolling requiring special equipment.
3. Differential radial expansion. This limits the length of the gap between the tubesheets to prevent overstressing the tubes in bending or shear. Very short gaps can result in outer tubes being sheared off at the face.
4. Differential longitudinal expansion. (This is a problem if the tubesheets are restrained across the gap and increases as the gap increases.)
5. All conditions of start-up, shutdown, and steam out (in the case of condenser) must be considered since they will generally be more severe on the double tubesheet section than in the operating condition.

5.6 TUBE BUNDLE

A tube bundle is an assembly of tubes, baffles, tubesheets, spacers and tie-rods, and longitudinal baffles, if any. Spacers and tie-rods are required for maintaining the space between baffles. Refer to TEMA for details on the number of spacers and tie-rods. A straight tube bundle and a U-tube bundle are shown in Figure 5.25.

5.6.1 BUNDLE WEIGHT

The maximum bundle weight that can conveniently be pulled should be specified and should allow for the buildup of fouling and scaling deposits. Offshore applications are particularly sensitive to weight.

5.6.2 SPACERS, TIE-RODS, AND SEALING DEVICES

The tube bundle is held together and the baffles are located in their correct positions by a number of tie-rods and spacers. The tie-rods are screwed into the stationary tubesheet and extend the length of the bundle up to the last baffle, where they are secured by locknuts (refer to Figure 5.25a). Between baffles, tie-rods have spacers fitted over them. Tie-rods and spacers may also be used as a sealing device to block bypass paths due to pass partition lanes or the clearance between the shell and the tube bundle. A baffle cage assembly showing the tie-rods and spacers is shown schematically in Figure 5.26.

5.6.3 OUTER TUBE LIMIT

The outer tube limit (OTL) is the diameter of the largest circle, drawn around the tubesheet center, beyond which no tube may encroach. OTL is shown schematically in Figure 5.27.

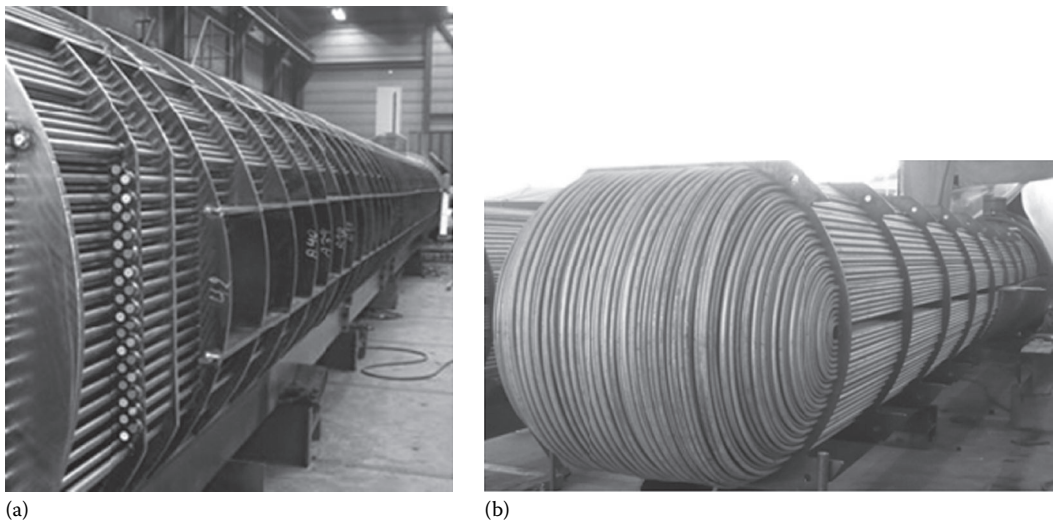


FIGURE 5.25 Shell and tube heat exchanger tube bundle assembly. (a) Straight tube bundle (Courtesy of Vermeer Eemhaven B.V., Rotterdam, the Netherlands) and (b) U-tube bundle. (Courtesy of Holtec International, Marlton, NJ.)

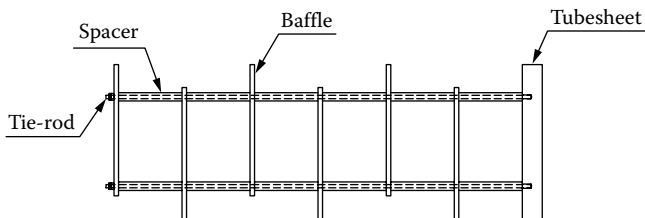


FIGURE 5.26 Baffle cage assembly.

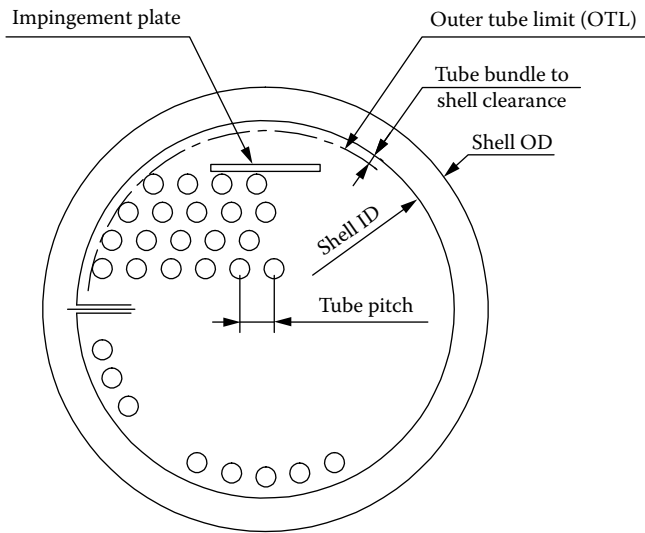


FIGURE 5.27 Definition of OTL.

5.7 SHELLS

Heat exchanger shells are manufactured in a large range of standard sizes, materials, and thickness. Smaller sizes are usually fabricated from standard size pipes. Larger sizes are fabricated from plate by rolling. The cost of the shell is much more than the cost of the tubes; hence, a designer tries to accommodate the required heat transfer surface in one shell. It is found that a more economical heat exchanger can usually be designed by using a small diameter shell and the maximum shell length permitted by such practical factors as plant layout, installation, servicing, etc. [6]. Up to six shorter shells in series is common, and this arrangement results in countercurrent flow close to performance as if one long single shell design was used. Nominal shell diameter and shell thickness are furnished in TEMA Tables R-3.13 and CB-3.13 [2]. Roundness and consistent shell inner diameter are necessary to minimize the space between the baffle edge and the shell as excessive space allows fluid bypass and reduced performance.

5.8 PASS ARRANGEMENT

5.8.1 TUBESIDE PASSES

The simplest flow pattern through the tubes is for the fluid to enter at one end and exit at the other. This is a single-pass tube arrangement. To improve the heat transfer rate, higher velocities are preferred. This is achieved by increasing the number of tubeside passes. The improvements achievable with multipass heat exchangers are sufficiently large, and hence they have become common in industry than the counterflow designs. Tubeside multiple passes are normally designed to provide roughly equal number of tubes in each pass to ensure an even fluid velocity and pressure drop throughout the bundle. In a two-tube-pass arrangement, the fluid flows through only half of the total tubes, so that the Reynolds number is high. Increasing the Reynolds number results in increased turbulence and Nusselt number and finally increase in overall heat transfer coefficient.

5.8.1.1 Number of Tube Passes

The number of tubeside passes generally ranges from one to eight. The standard design has one, two, or four tube passes. The practical upper limit is 16. Partitions built into heads known as partition plates or pass ribs control tubeside passes. This is shown schematically in Figure 5.28. The pass partitions may be straight or wavy rib design. The maximum number of tubeside passes is limited by workers' abilities to fit the pass partitions into the available space and the bolting and flange design to avoid interpass leakages on the tubeside. In multipass designs, an even number of passes is generally used; odd numbers of passes are uncommon and may result in mechanical and thermal problems in fabrication and operation. The number of tube passes depends upon the available pressure drop, since higher velocity in the tube results in higher heat transfer coefficient, at the cost of increased pressure drop. Larowski et al. [9] suggest the following guidelines for tubeside passes:

1. Two-phase flow on the tubeside, whether condensing or boiling, is best kept in a single straight tube run or in a U-tube.
2. If the shellside heat transfer coefficient is significantly lower than that on the tubeside, it is not advisable to increase the film coefficient on the tubeside at the cost of higher tubeside pressure drop, since this situation will lead to a marginal improvement in overall heat transfer coefficient.

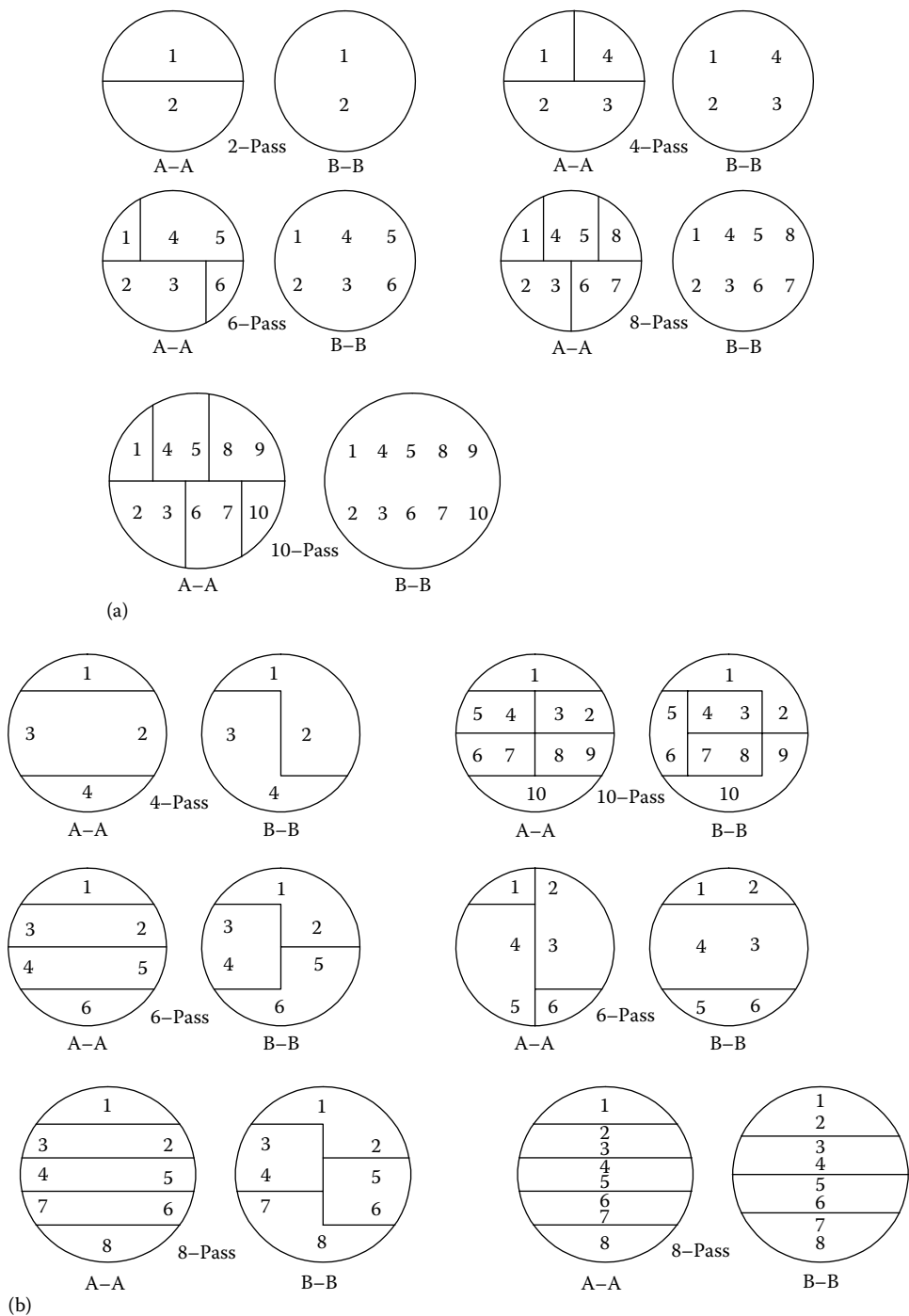


FIGURE 5.28 Typical tubeside partitions for multipass arrangement. (a) U-tube and (b) straight tubes. *Note:* A-A: Front view and B-B: Rear view.

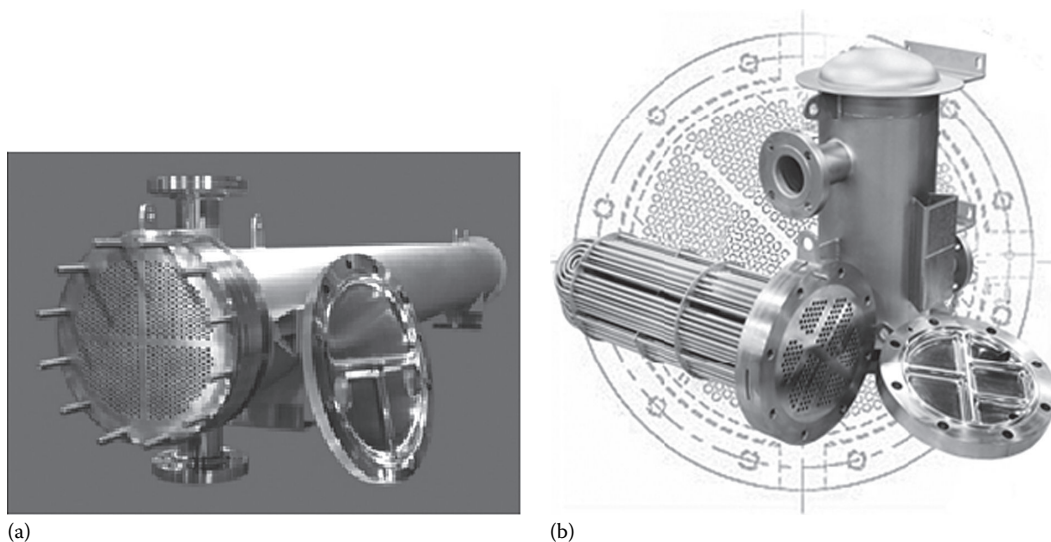


FIGURE 5.29 Shell and tube heat exchanger tube bundle assemblies. (a) Four-pass arrangement and (b) eight-pass arrangement. (Courtesy of Allegheny Bradford Corporation, Bradford, PA.)

There are some limitations on how the different types of heat exchangers can be partitioned to provide various numbers of passes. They are summarized here.

1. Fixed tubesheet exchanger—any practical number of passes, odd or even. For multipass arrangements, partitions are built into both front and rear heads.
2. U-tube exchanger—minimum two passes; any practical even number of tube passes can be obtained by building partition plates in the front head.
3. Floating head exchangers:
 - a. With pull-through floating head (*T* head) type and split backing ring exchanger (*S* head), any practical even number of passes is possible. For single-pass operation, however, a packed joint must be installed on the floating head.
 - b. With outside packed floating head type (*P* head), the number of passes is limited to one or two.
 - c. With externally sealed floating (*W* head), no practical tube pass limitation.
4. Two-phase flow on the tubeside, whether condensing or boiling, is best kept within a single-pass or in U-tubes to avoid uneven distribution and hence uneven heat transfer.

Figures 5.29 through 5.31 shows tube bundle assemblies with multipasses on the tubeside.

5.8.1.2 End Channel and Channel Cover

Tubeside enclosures are known as end channels or bonnets. They are typically fabricated or cast. They are attached to the tubesheet the by bolting with a gasket between the two metal surfaces. Cast heads are typically used up to 250 mm (14 in.) and are made from cast iron, steel, bronze, or stainless steel. They typically have pipe thread connection. Fabricated heads can be made in a wide variety of configurations. They can have metal cover that allows servicing the tubes without disturbing the shell or tube piping. Heads can have axially or tangentially oriented nozzles, which are typically ANSI flanges. Flanged nozzles or threaded bonnets are used in smaller exchangers.

Channel covers: These are round plates that tend to be bolted to the channel flanges. Figure 5.32 shows heat exchanger with bonnet and channel cover.

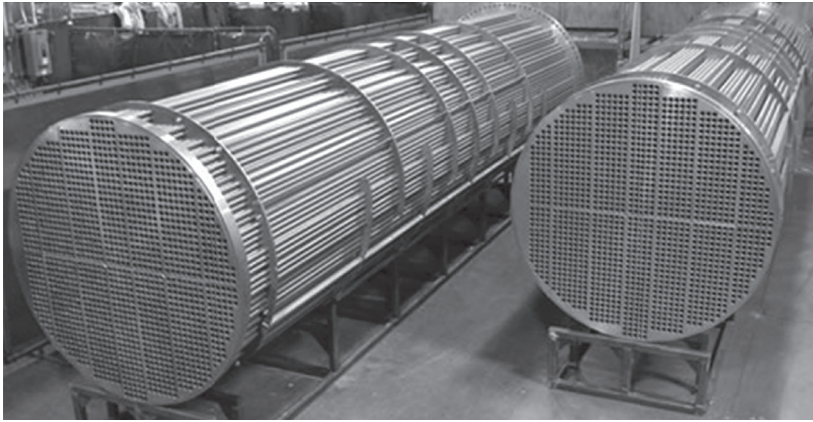


FIGURE 5.30 Multipass titanium tube bundle assemblies. (Courtesy of TITAN Metal Fabricators Inc, Camarillo, CA.)



FIGURE 5.31 Eight-pass shell and tube heat exchanger tube bundle showing a few top rows of tubes not incorporated to avoid erosion due to high impingement velocity. (Courtesy of Riggins Company, Hampton, VA.)

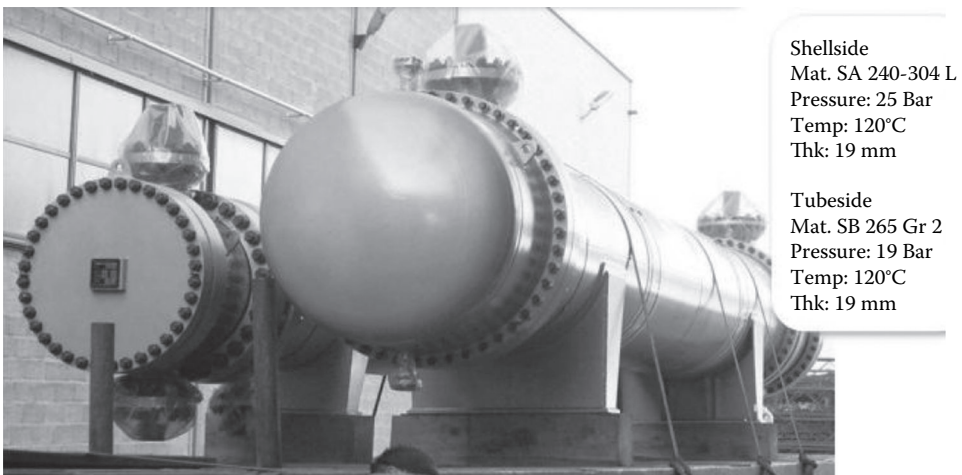


FIGURE 5.32 U-tube shell and tube heat exchangers showing bonnet and channel cover plate. (Courtesy of Brembana Costruzioni Industriali S.p.A., Milan, Italy.)

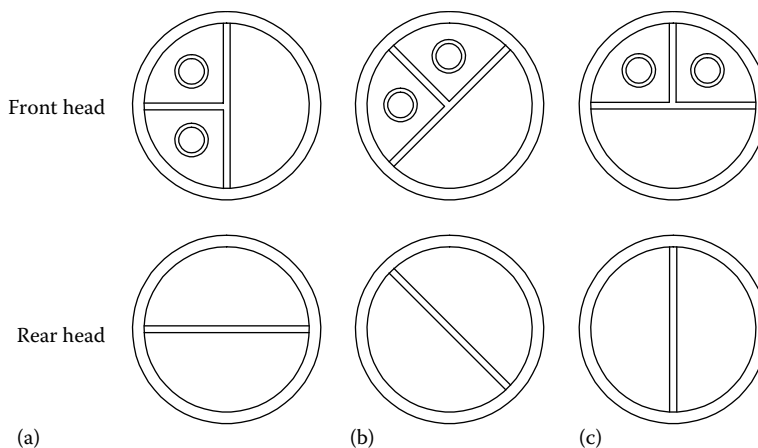


FIGURE 5.33 Four-pass partitions in front channel. (a) Pass partition plate is vertical, (b) pass partition plate is inclined, and (c) horizontal and rear channel.

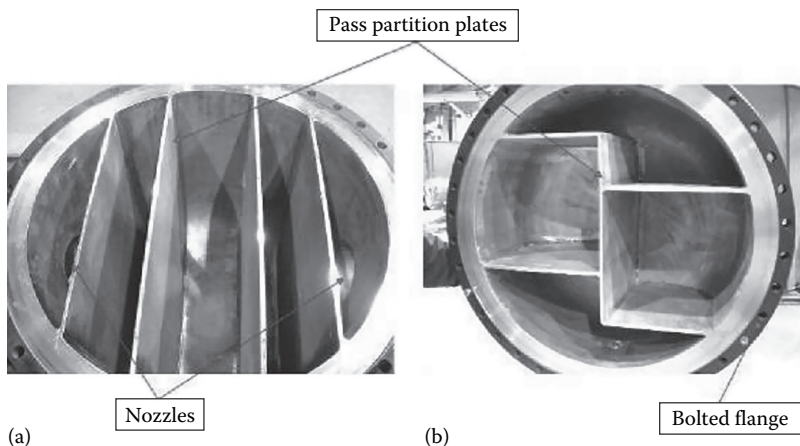


FIGURE 5.34 Six-pass partitions in (a) front channel and (b) rear channel. (Courtesy of Festival City Fabricators, div. of CSTI, Stratford, Ontario, Canada.)

Pass divider or ribs: This is required in exchanger with two or more tubeside passes. The divider is required in both bonnets and channels (Figures 5.33 and 5.34). Front and rear head pass ribs and gaskets are matched. Pass ribs in cast heads are integrally cast and then machined to sizes; in fabricated heads, they are welded in place. On the tubesheet, pass rib(s) requires either removing tubes to allow a straight pass rib or machining the pass rib with curves around the tubes, which is costlier to manufacture. Where a full bundle tube count is required to satisfy the thermal requirements, the pass rib approach may lead to consider the next larger shell diameter.

5.8.2 SHELLSIDE PASSES

For exchangers requiring high effectiveness, multipassing is the only alternative. Shellside passes could be made by the use of longitudinal baffles. However, multipassing on the shell with longitudinal baffles will reduce the flow area per pass compared to a single pass on the shellside. This drawback is overcome by shells in series (Figures 5.35), which is also equivalent to multipassing on the shellside. For the case of the overall direction of two fluids in counterflow, as the number of shellside passes is increased to infinity

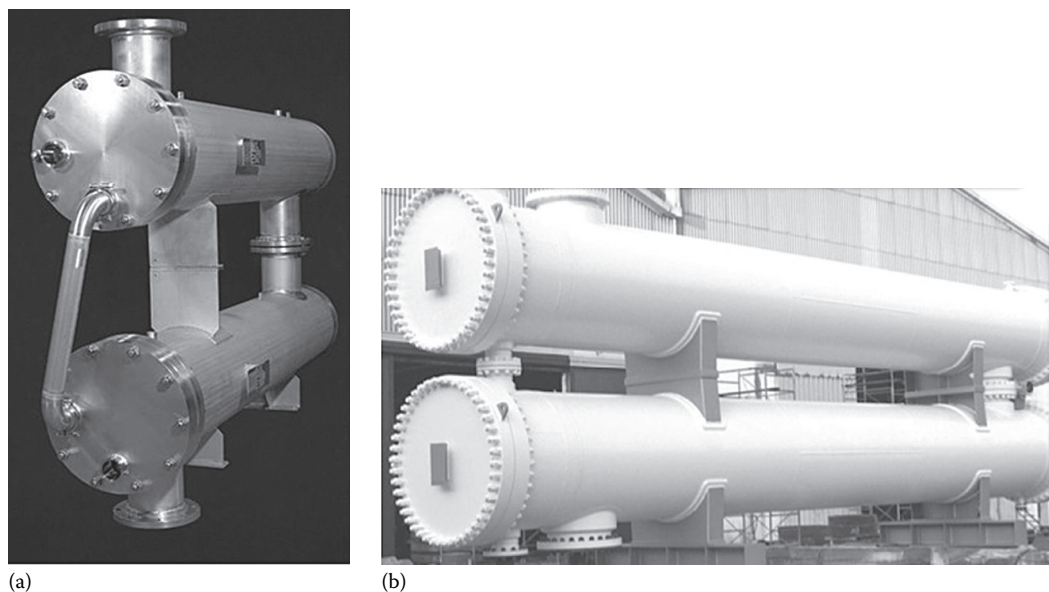


FIGURE 5.35 (a and b) Stack of two shells in series/shell and tube heat exchangers stack. (Photo a: Courtesy of Allegheny Bradford Corporation, Bradford, PA and photo b: Courtesy of Brembana Costruzioni Industriali S.p.A., Milan, Italy.)

(practically above four), its effectiveness approaches that of a pure counterflow exchanger. In heat recovery trains and some other applications, up to six shells in series are commonly used.

5.8.2.1 Expansion Joint

Since the shellside fluid is at a different temperature than the tubeside fluid, there will be a corresponding difference in the expansion of shell and tube. If the temperature difference is high, the differential thermal expansion will be excessive, and hence the thermal stresses induced in the shell and the tube bundle will be high. This is particularly true for fixed tubesheet exchangers. In fixed tubesheet exchangers, the differential thermal expansion problem is overcome by incorporating an expansion joint into the shell. A heat exchanger with an expansion joint is shown in Figure 5.36. Alternatively, an expansion bellow fitted on one end of the tube bundle as shown in Figure 5.37 can be devised to overcome the thermal expansion problem [5]. For U-tube exchangers and floating head exchangers, this is taken care of by the inherent design. Types of expansion joints, selection procedure, and design aspects are discussed in Chapter 11.

5.8.2.2 Drains and Vents

All exchangers need to be drained and vented; therefore, care should be taken to properly locate and size drains and vents. Additional openings may be required for instruments such as pressure gauges and thermocouples.

5.8.2.3 Nozzles and Impingement Protection

Nozzles are used to convey fluids into and out of the exchanger. These nozzles are pipes of constant cross section welded to the shell and the channels. The nozzles must be sized with the understanding that the tube bundle will partially block the opening. Whenever a high-velocity fluid is entering the shell, some type of impingement protection is required to avoid tube erosion and vibration. As per TEMA standard, impingement protection is mandatory if the inlet fluid is a gas with abrasive particles and in heat exchanger that receives liquid–vapor mixtures or vapor with entrained liquid where the erosive effects are intense. For single-phase fluid,

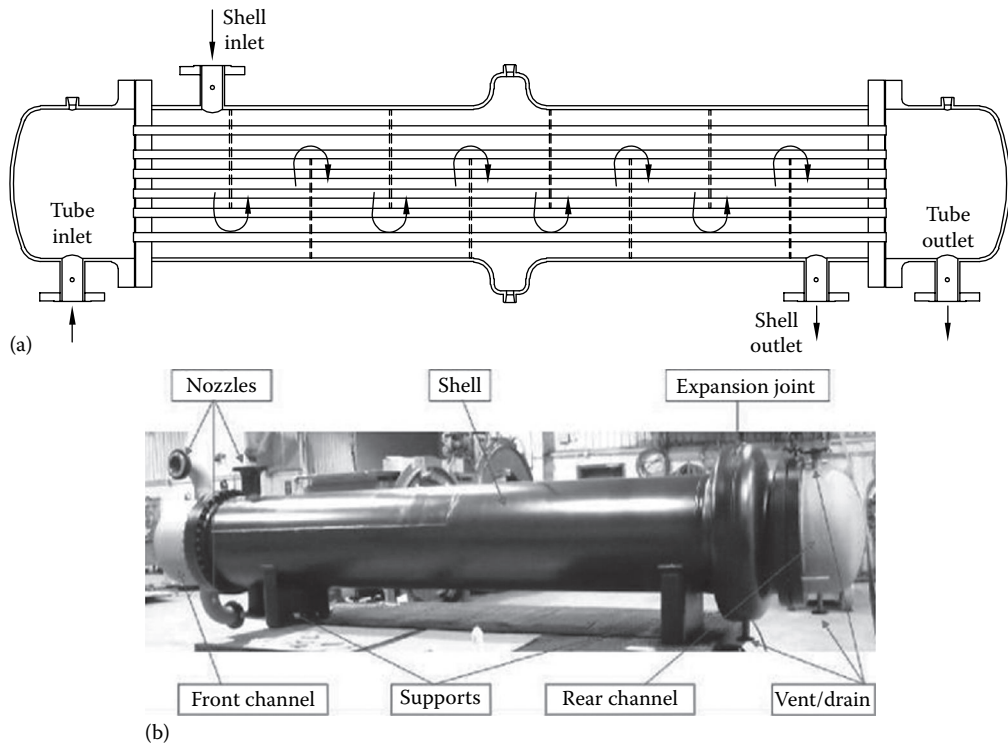


FIGURE 5.36 (a) Cross-sectional view of a fixed tubesheet shell and tube heat exchanger with an expansion joint (schematic). (b) Fixed tubesheet shell and tube heat exchanger with an expansion joint. (Courtesy of Festival City Fabricators, div. of CSTI, Stratford, Ontario, Canada.)

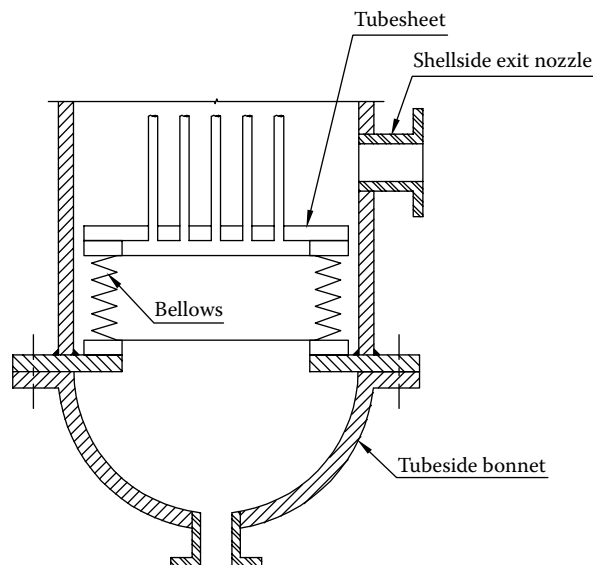


FIGURE 5.37 Shell and tube heat exchanger with an expansion bellow on one end of the tube bundle to overcome thermal expansion problem. (Adapted from Bell, K.J. and Mueller, A.C. *Wolverine Heat Transfer Data Book II*, Wolverine Division of UOP Inc., Decatur, AL, 1984.)

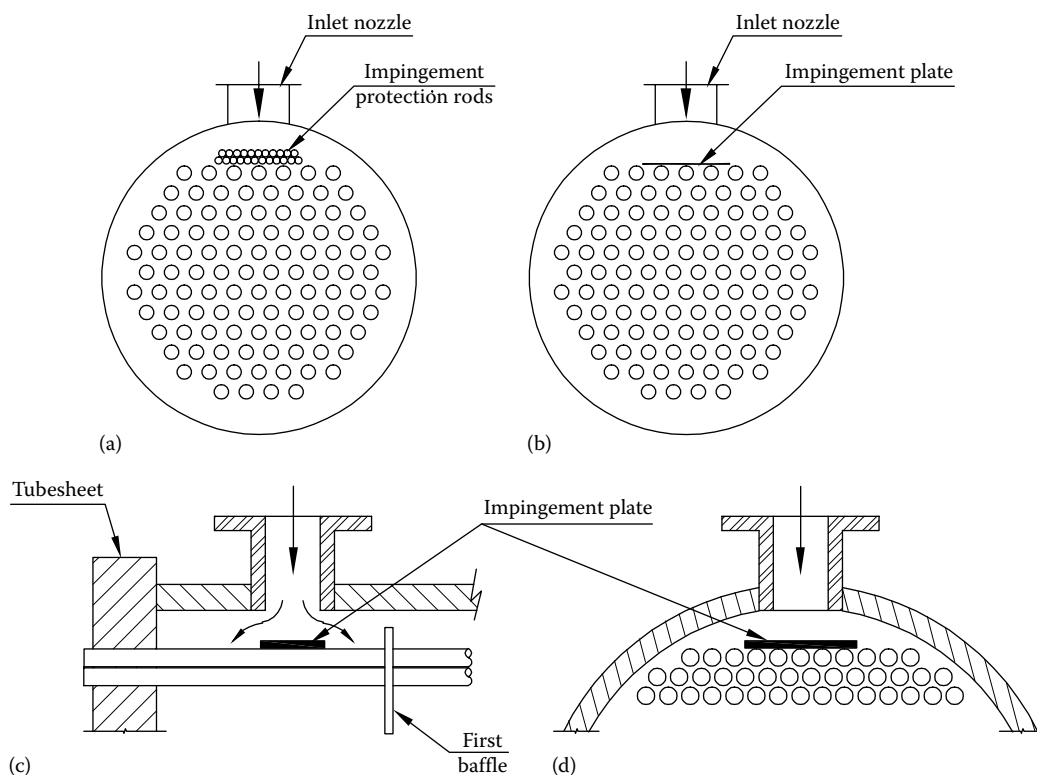


FIGURE 5.38 Impingement protection arrangement. (a) Rod arrangement, (b) plate arrangement, (c) and (d) plate view in the inlet baffle zone.

TEMA standards define when the installation of impingement protection is required, depending on the kinetic energy of the fluid entering the shell. For liquids with abrasive particles, impingement protection is required if the inlet mass velocity ρV^2 exceeds 744 kg/m^2 , and for clean single-phase fluids, impingement protection is required if the inlet mass velocity ρV^2 exceeds $2,230 \text{ kg/m}^2$. Some forms of impingement protection include (1) impingement plate (Figure 5.38a), (2) impingement rods (Figure 5.38b), and (3) annular distributors. Criteria for the requirement of the impingement protection are covered in Chapter 12.

5.8.2.3.1 Minimum Nozzle Size

Gollin [25] presents a methodology for determining the minimum inside diameter of a nozzle for various types of fluid entering or leaving the unit. The actual size of nozzle used will depend on the pressure, material, corrosion allowance, and pipe schedule.

The minimum inside diameter, d_{\min} , is calculated from

$$d_{\min} = \sqrt[4]{\frac{M^2}{3.54 \times 10^6 \times \Delta p_v \rho}} \quad (5.4)$$

where

M is the mass flow rate of fluid through nozzle (lb/h)

ρ the density of fluid (lb/ft³)

Δp_v the velocity head loss through the nozzle (psi)

5.9 FLUID PROPERTIES AND ALLOCATION

To determine which fluid should be routed through the shellside and which fluid on the tubeside, consider the following factors. These factors are discussed in detail in Refs. [5,26,27].

Corrosion: Fewer corrosion-resistant alloys or clad components are needed if the corrosive fluid is placed on the tubeside.

Fouling: This can be minimized by placing the fouling fluid in the tubes to allow better velocity control; increased velocities tend to reduce fouling.

Cleanability: The shellside is difficult to clean; chemical cleaning is usually not effective on the shellside because of bypassing and requires the cleaner fluid. Straight tubes can be physically cleaned without removing the tube bundle; chemical cleaning can usually be done better on the tubeside.

Temperature: For high-temperature services requiring expensive alloy materials, fewer alloy components are needed when the hot fluid is placed on the tubeside.

Pressure: Placing a HP fluid in the tubes will require fewer costly HP components and the shell thickness will be less.

Pressure drop: If the pressure drop of one fluid is critical and must be accurately predicted, then that fluid should generally be placed on the tubeside.

Viscosity: Higher heat transfer rates are generally obtained by placing a viscous fluid on the shellside. The critical Reynolds number for turbulent flow in the shell is about 200; hence, when the flow in the tubes is laminar, it may be turbulent if the same fluid is placed on the shellside. However, if the flow is still laminar when in the shell, it is better to place the viscous fluid only on the tubeside since it is somewhat easier to predict both heat transfer and flow distribution [27].

Toxic and lethal fluids: Generally, the toxic fluid should be placed on the tubeside, using a double tubesheet to minimize the possibility of leakage. Construction code requirements for lethal service must be followed.

Flow rate: Placing the fluid with the lower flow rate on the shellside usually results in a more economical design and a design safe from flow-induced vibration. Turbulence exists on the shellside at much lower velocities than on the tubeside.

5.10 CLASSIFICATION OF SHELL AND TUBE HEAT EXCHANGERS

There are four basic considerations in choosing a mechanical arrangement that provides for efficient heat transfer between the two fluids while taking care of such practical matters as preventing leakage from one into the other [6]:

1. Consideration for differential thermal expansion of tubes and shell
2. Means of directing fluid through the tubes
3. Means of controlling fluid flow through the shell
4. Consideration for ease of maintenance and servicing

Heat exchangers have been developed with different approaches to these four fundamental design factors. Three principal types of heat exchangers—(1) fixed tubesheet exchangers, (2) U-tube exchangers, and (3) floating head exchangers—satisfy these design requirements.

5.11 TEMA SYSTEM FOR DESCRIBING HEAT EXCHANGER TYPES

Major components of a shell and tube heat exchanger are the front head, shell section, and rear head. Each of these components is available in a number of standard designs. In TEMA standards, they are identified by an alphabetic character. A heat exchanger unit is designated using

the designations of front head, shell, and rear head. It consists of three alphabetic characters, such as AES, AKT, AJW, BEM, AEP, and CFU. Seven major types of shells, five types of front heads, and eight types of rear heads known as heat exchanger nomenclature as per TEMA are shown in Figure 5.39. In addition to these types, special types of shells and heads are also available depending upon the applications and customer needs. Figure 5.40a through f illustrates various types of heat exchangers.

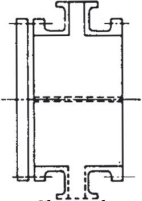
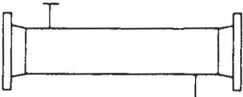
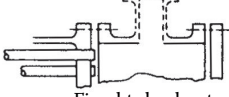
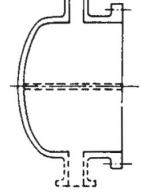
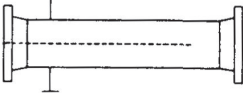
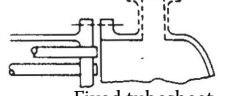
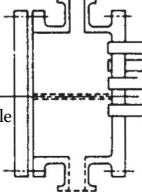
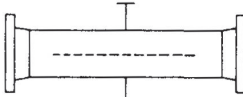
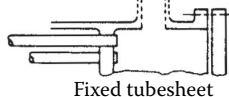
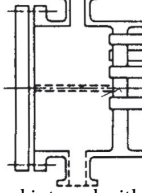
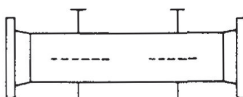
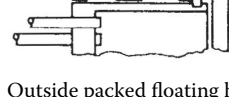
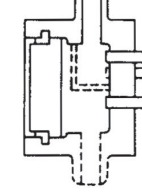

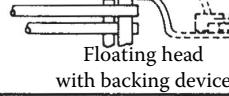
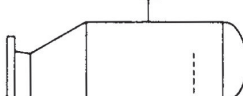
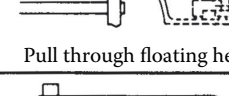

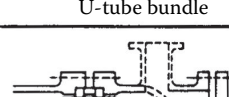
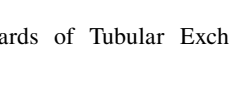
	Front End Stationary Head Types		Shell Types		Rear End Head Types
A	 <p>Channel and removable cover</p>	E	 <p>One pass shell</p>	L	 <p>Fixed tubesheet like "A" stationary head</p>
B	 <p>Bonnet (integral cover)</p>	F	 <p>Two pass shell with longitudinal baffle</p>	M	 <p>Fixed tubesheet like "B" stationary head</p>
C	 <p>Removable tube bundle only</p>	G	 <p>Split flow</p>	N	 <p>Fixed tubesheet like "N" stationary head</p>
N	 <p>Channel integral with tube sheet and removable cover</p>	H	 <p>Double split flow</p>	P	 <p>Outside packed floating head</p>
D	 <p>Special high pressure closure</p>	J	 <p>Divided flow</p>	S	 <p>Floating head with backing device</p>
		K	 <p>Kettle type reboiler</p>	T	 <p>Pull through floating head</p>
		X	 <p>Cross flow</p>	U	 <p>U-tube bundle</p>
				W	 <p>Externally sealed floating tubesheet</p>

FIGURE 5.39 Nomenclature for heat exchanger components. (© Standards of Tubular Exchanger Manufacturers Association, Inc., 9th edn., 2007.)

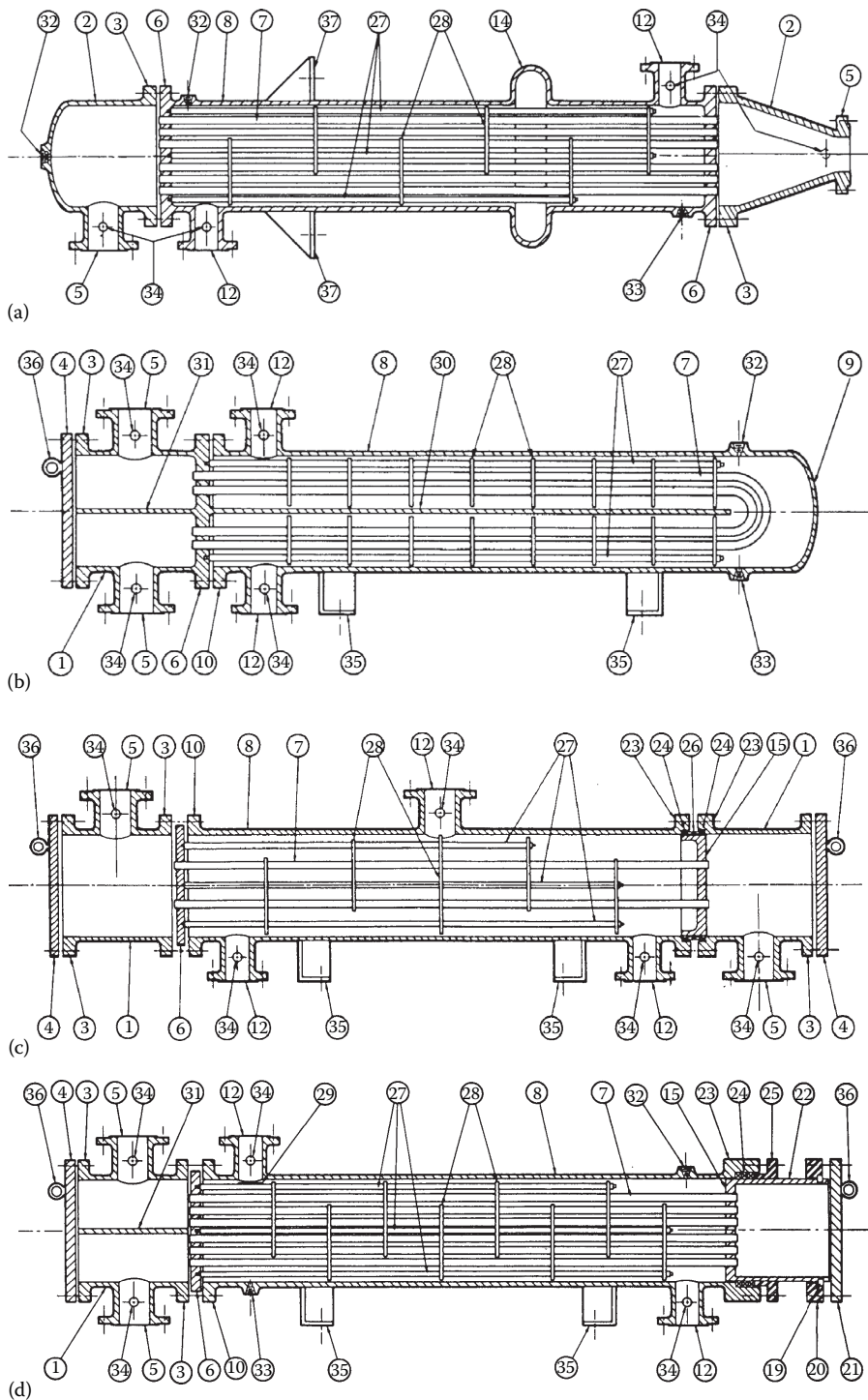


FIGURE 5.40 Heat exchanger types as per TEMA designation. (a) Fixed tubesheet heat exchanger, (b) U-tube heat exchanger, (c) divided flow—externally sealed floating tubesheet heat exchanger, (d) floating head—outside packed floating head heat exchanger.

(continued)

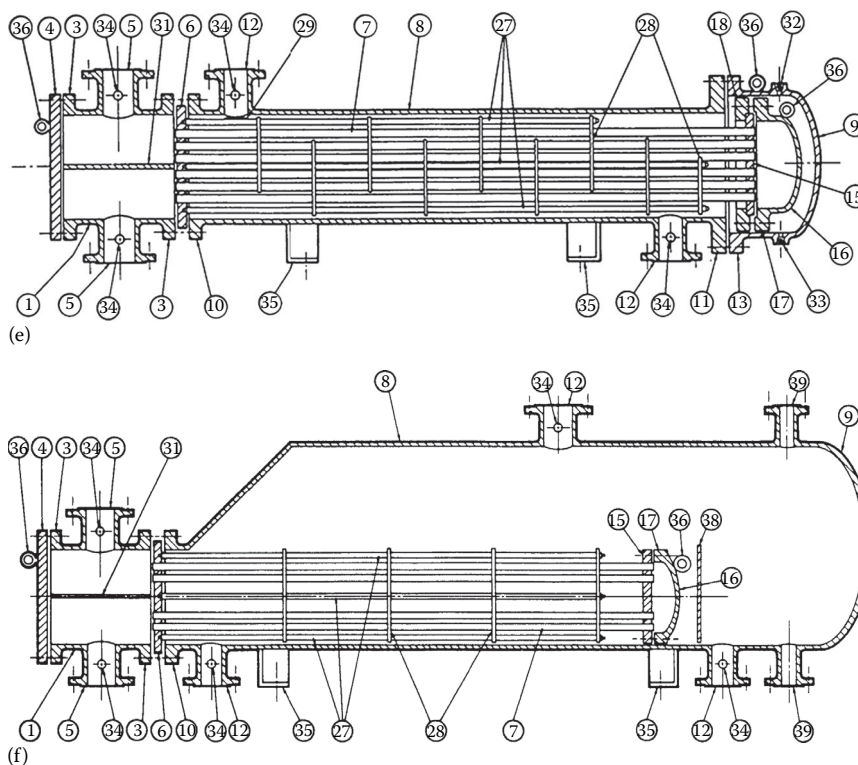


FIGURE 5.40 (continued) Heat exchanger types as per TEMA designation. (e) floating head heat exchanger with a backing device, and (f) Kettle reboiler—pull through floating head. Nomenclature of heat exchanger components: (1) Stationary head—channel; (2) stationary head—bonnet; (3) stationary head flange—channel or bonnet; (4) channel cover; (5) stationary head nozzle; (6) stationary; (7) tubes; (8) shell; (9) shell cover; (10) shell flange—stationary head end; (11) shell flange—rear head end; (12) shell nozzle; (13) shell cover flange; (14) expansion joint; (15) floating; (16) floating head cover; (17) floating head cover flange; (18) floating head backing device; (19) split shear ring; (20) slip-on backing flange; (21) floating head cover—external; (22) floating skirt; (23) packing box; (24) packing; (25) packing gland; (26) lantern ring; (27) tie-rods and spacers; (28) transverse baffles or support plates; (29) impingement plate; (30) longitudinal baffle; (31) pass partition; (32) vent connection; (33) drain connection; (34) instrument connection; (35) support saddle; (36) lifting lug; (37) support bracket; (38) weir; and (39) liquid level connection. (a) BEM, (b) CFU, (c) AJW, (d) AEP, (e) AES, and (f) AKT. (© Standards of Tubular Exchanger Manufacturers Association, Inc., 9th edn., 2007.)

5.11.1 FIXED TUBESHEET EXCHANGERS

This is the most popular type of shell and tube heat exchanger. These units are constructed with the tubesheets integral with the shell. The fixed tubesheet heat exchanger uses straight tubes secured at both ends into tubesheets, which are firmly welded to the shell. Hence, gasketed joints are minimized in this type, and thereby least maintenance is required. They may be used with *A*-, *B*-, or *N*-type front head and *L*-, *M*-, or *N*-type rear head. A BEM-type fixed tubesheet heat exchanger is shown in Figure 5.40a. Fixed tubesheet heat exchangers are used where [28]

1. It is desired to minimize the number of joints
2. Temperature conditions do not represent a problem for thermal stress
3. The shellside fluid is clean and tube bundle removal is not required
4. High degree of protection against contamination of streams
5. Double tubesheet is possible
6. Mechanical tubeside cleaning is possible

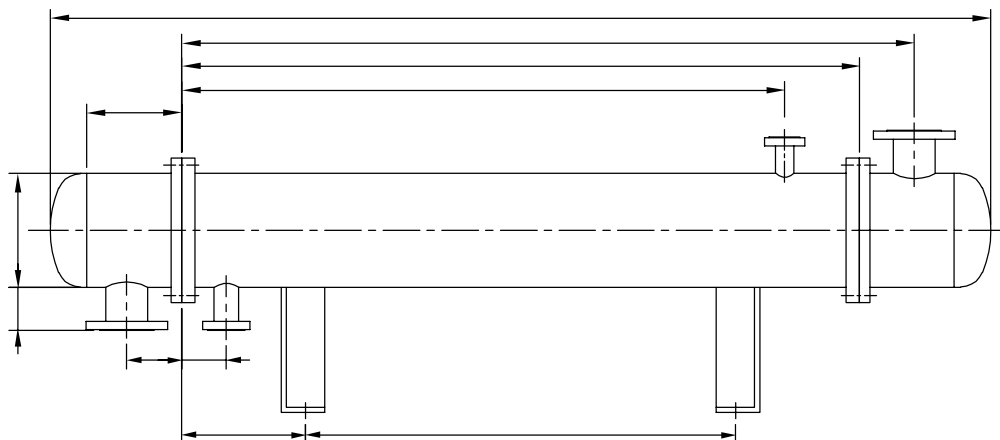


FIGURE 5.41 Important dimensions of a fixed tubesheet heat exchanger.

Provision is to be made to accommodate the differential thermal expansion of the shell and the tubes when the thermal expansion is excessive. Fixed tubesheet exchangers can be designed with removable channel covers, “bonnet”-type channels, integral tubesheets on both sides, and tubesheets extended as shell flanges. They can be designed as counterflow one-to-one exchangers (i.e., single pass on the tubeside and on the shellside) or with multipasses on the tubeside. Where three or five passes have been specified for the tubeside, the inlet and outlet connections will be on opposite sides. For fixed tubesheet exchangers, a temperature analysis must be made considering all phases of operation (i.e., start-up, normal, upset, abnormal) to determine if thermal stress is a problem and how to relieve it [28].

Figure 5.41 shows important dimensions of a fixed tubesheet heat exchanger.

5.11.2 U-TUBE EXCHANGERS

In this type of construction, tube bundle and individual tubes are free to expand and the tube bundle is removable. A U-tube exchanger, CFU type, is shown in Figure 5.40b. U-tube exchangers can be used for the following services [28]:

1. Clean fluid on the tubeside
2. Extreme HP on one side
3. Temperature conditions requiring thermal relief by expansion
4. For H_2 service in extreme pressures, utilizing an all-welded construction with a nonremovable bundle
5. To allow the shell inlet nozzle to be located beyond the bundle
6. High degree of protection against contamination of streams
7. Double tubesheet is possible

5.11.2.1 Shortcomings of U-Tube Exchangers

Some of the drawbacks associated with U-tube exchangers are the following:

1. Mechanical cleaning from inside tubes is difficult; the chemical cleaning is possible.
2. Flow-induced vibration can also be a problem in the U-bend region for the tubes in the outermost row because of long unsupported span.
3. Due to the bend radius, U-tube bundles have less heat transfer area compared to straight tube bundles.

4. Interior tubes are difficult to replace, many times requiring the removal of outer layers or plugging the leaking tube.
5. Erosion damage of U-bends is seen with high tubeside velocity.
6. Tubeside pressure drop will be on the higher side due to flow reversals in the U-end.

U-tube exchangers may be used with A-, B-, C-, N-, or D-type front head.

5.11.3 FLOATING HEAD EXCHANGERS

The floating head exchanger consists of a stationary tubesheet and one floating tubesheet that is free to accommodate the thermal expansion of the tube bundle. A floating head exchanger with TEMA designations AES, AJW, and AEP are shown in Figure 5.40c through e. They may be used with A-, B-, or C-type front head. There are four basic types of floating head exchangers. They are discussed next.

Floating head, outside packed floating head: The floating head (*P* head), outside packed stuffing box heat exchanger uses the outer skirt of the floating tubesheet as part of the floating head. The packed stuffing box seals the shellside fluid while allowing the floating head to move. The tube bundle is removable. Maintenance is also very easy since all bolting is from outside only. With this floating head, any leak (from either the shellside or the tubeside) at the gaskets is to the outside, and there is no possibility of contamination of fluids. Since the bundle-to-shell clearance is large (about 1.5 in. or 38 mm), sealing strips are usually required. The earlier types are recommended for LP, low-temperature, nonhazardous fluids.

Floating head, externally sealed floating tubesheet: In the floating head (*W* head), externally sealed floating tubesheet, or outside packed lantern ring heat exchanger uses a lantern ring around the floating tubesheet to seal the two fluids as the floating tubesheet moves back and forth. The lantern ring is packed on both sides and is provided with vent or weep holes so that leakage through either should be to the outside. Number of tube passes is limited to one or two. The tube bundle is removable. This is the lowest cost of the floating head design and can be used with type A, B, or C front head. This type is recommended for LP, low-temperature, and nonhazardous fluids.

Floating head, pull-through head: In the floating head (*T* head), pull-through head exchanger, a separate head or cover is bolted to the floating tubesheet within the shell. In this design, the tube bundle can be removed without dismantling the joints at the floating end. Due to the floating head bonnet flange and bolt circle, many tubes are omitted from the tube bundle at the tube bundle periphery, and hence it accommodates the smallest number of tubes for a given shell diameter. This results in the largest bundle-to-shell clearance or a significant bundle-to-shell bypass stream *C*. To overcome the reduction in thermal performance, sealing devices are normally required, and the shell diameter is somewhat increased to accommodate a required amount of surface area. An ideal application for the *T* head design is as the kettle reboiler, in which there is ample space on the shellside and the flow bypass stream *C* is of no concern.

Floating head with backing device: In the floating head (*S* head) with backing device, the floating head cover (instead of being bolted directly to the floating tubesheet as in the pull-through type) is bolted to a split backing ring. The shell cover over the floating head has a diameter larger than the shell. As a result, the bundle to shell clearance is reasonable, and sealing strips are generally not required. The tube bundle is not removable. Both ends of the heat exchanger must be disassembled for cleaning and maintenance. This type is recommended for HP, nonhazardous process fluids.

5.11.3.1 Sliding Bar/Surface

All removable tube bundles whose mass exceeds 5,450 kg (12,000 lb) shall be provided with a continuous sliding surface to facilitate removal of tube bundle. If sliding bars are provided, they should be welded to the transverse baffles and the support plate to form a continuous sliding surface. For more details, refer to TEMA standard.

5.11.3.2 Kettle-Type Reboiler

Kettle-type reboiler is shown Figure 5.40f, and it is described later.

5.12 DIFFERENTIAL THERMAL EXPANSION

Means should be identified to accommodate the thermal expansion or contraction between the shell and the tube bundle due to high mean metal temperature differentials between the shell and the tube bundle. This is particularly true for fixed tubesheet exchangers. Differential thermal expansion is overcome by the following means in the shell and tube heat exchangers:

U-tube design: The U-bend design allows each tube to expand and contract independently.

Fixed tubesheet design: For fixed tubesheet exchangers, when the difference between shell and tube mean metal temperatures becomes large (greater than approximately 50°C for carbon steel), the tubesheet thickness and tube end loads become excessive [29]. When a thermal expansion problem exists, an expansion joint is incorporated in the shell. This permits the shell to expand and contract.

Floating head designs: The floating head exchangers solve the expansion problem by having one stationary tubesheet and one floating tubesheet that is free to accommodate the thermal expansion of the tube bundle.

5.13 TEMA CLASSIFICATION OF HEAT EXCHANGERS BASED ON SERVICE CONDITION

TEMA has set up mechanical standards for three classes of shell and tube heat exchangers: *R*, *C*, and *B*. Class *R* heat exchangers specify design and fabrication of unfired shell and tube heat exchangers for the generally severe requirements of petroleum and related processing applications, class *C* for the generally moderate requirements of commercial and general process applications, and class for chemical process service. Salient features of TEMA standards are discussed in Chapter 11. Table 5.1 shows some major differences between TEMA classes *R*, *C*, and *B*. For more details on TEMA classes, consult Ref. [30].

5.14 SHELL AND TUBE HEAT EXCHANGER SELECTION

The fixed tubesheet exchanger is usually the cheapest. If, however, an expansion joint has to be used, then a U-tube exchanger may prove cheaper. If the bundle has to be removable, a U-tube will be the cheapest.

5.14.1 SHELL TYPES

Seven types of shells are standardized by TEMA [2]. They are as follows:

1. *E* One-pass shell
2. *F* Two-pass shell with longitudinal baffle
3. *G* Split flow
4. *H* Double split flow
5. *J* Divided flow
6. *K* Kettle type reboiler
7. *X* Crossflow

Shellside flow for *E*, *F*, *G*, *H*, and *J* shells are shown schematically in Figure 5.42. A brief description of each type is provided next.

TABLE 5.1
Major Differences between TEMA Classes R, C, and B

Item	Description	Classes	Remarks
RCB 1.5	Corrosion allowances	R,C + B	1/8 in. (3.2 mm), 1/16 in. (1.6 mm)
RCB 2.5	Tube pitch	R,C,B	1.25; 1.25/1.2, 1.2 times tube OD
	Minimum cleaning lanes		1/4 in., 3/16 in./1/4 in.
RCB 4.3	Baffle thickness	R,C+B	1/8 in. (3.2 mm), 1/16 in. (1.6 mm)
RCB 4.3	Longitudinal baffle thickness	R,C+B	Min.1/4 in. (6.4 mm), 1/4 in. (6.4 mm) but not less than 1/8 in. (3.2 mm)
RCB4.71	Tie-rod size	R,C+B	3/8 in. (9.5 mm), 1/4 in. (6.4 mm)
RCB 5.11	Floating head covers minimum depth vs. tube area in one pass	R,C + B	1.3 times flow area through tubes of one pass one time flow area through tubes of one pass
RCB 5.3	Lantern ring design	C,R + B	Design pressure limitation
RCB 6.2	Gasket material—metal jacketed or solid metal	R,C + B	300 psi and above: int. float. head and all types of joints, int. float. head
RCB 6.3	Minimum width of gaskets	R + C,B	Full face gasket
RCB 6.32	Gasket surface flatness	R,C + B	Tolerances
RCB 6.5	Pass partition gasket	R,C + B	Confined; confined or unconfined
RCB 7.13	Minimum tubesheet thickness	R,C,B	Function of tube diameter
RCB 7.44	Tube hole grooving	C,R + B	C only above 300 psi; two grooves 1/8 in. (3.2 mm) wide and 1/64 in. (0.4 mm) deep
RCB 7.51	Length of tube-to-tubesheet joints	C,R + B	Length not less than 2 in. or two tube diameter or the tubesheet thickness minus 1/8 in.; lesser of 2 in. or tubesheet thickness minus 1/8 in.
RCB 7.6	Pass partition grooves	R,C + B	Pressure limit for C, B
RCB 7.8	Clad thickness of tubesheet (expanded tubes)	C,R + B	3/16 in. (4.8 mm), 5/16 in. (7.8 mm)
RCB 7.8	Clad thickness tubesheet (welded tubes)	C,R + B	1/8 in. (3.2 mm)
RCB 9.11	Channels and bonnets	R,C + B	Minimum thickness
RCB 11.1	End-flange minimum bolt size	R,C,B	$\frac{3}{4}$, $\frac{1}{2}$, $\frac{5}{8}$ in. M20, M12, M16

Note: Refer to [2] for details.

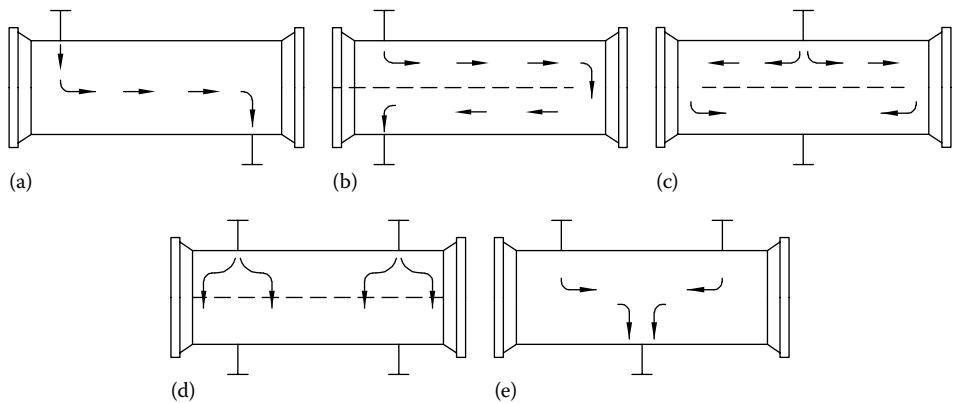


FIGURE 5.42 TEMA shell types and shellside flow distribution pattern. (a) Single-pass shell, (b) two-pass shell with longitudinal baffle, (c) split flow, (d) double split flow, and (e) crossflow.

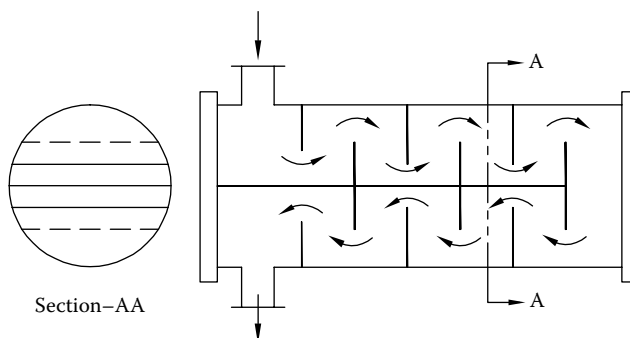


FIGURE 5.44 TEMA *F* shell.

Although ideally this is a desirable flow arrangement, it is rarely used because of many problems associated with the shellside longitudinal baffle. They include the following:

1. There will be a conduction heat transfer through the longitudinal baffle because of the temperature gradient between the shellside passes.
2. If the longitudinal baffle is not continuously welded to the shell, or if seals are not provided effectively between the longitudinal baffle and the shell, there will be fluid leakage from the HP to LP side.

Both the factors will reduce the mean temperature difference and the exchanger effectiveness more than the gain by achieving the pure counterflow arrangement. The welded baffle construction has a drawback: It does not permit the withdrawal of the tube bundle for inspection or cleaning. Hence, if one needs to increase the mean temperature difference, multiple shells in series are preferred over the *F* shell.

5.14.1.3 TEMA *G*, *H* Shell

TEMA *G* and *H* shell designs are most suitable for phase change applications where the bypass around the longitudinal plate and counterflow is less important than even flow distribution. In this type of shell, the longitudinal plate offers better flow distribution for vapor streams and helps to flush out noncondensables. They are frequently specified for use in horizontal thermosiphon reboilers and total condensers.

5.14.1.4 TEMA *G* Shell or Split Flow Exchanger

In this exchanger, there is one central inlet and one central outlet nozzle with a longitudinal baffle. The shell fluid enters at the center of the exchanger and divides into two streams. Hence, it is also known as a split flow unit. Possible flow arrangements (G_{1-1} , G_{1-2} , and G_{1-4}) are shown in Figure 5.45. *G* shells are quite popular with heat exchanger designers for several reasons. One important reason is their ability to produce “temperature correction factors” comparable to those in an *F* shell with only a fraction of the shellside pressure loss (same as *E* shell) in the latter type [31].

5.14.1.5 TEMA *H* Shell or Double Split Flow Exchanger

This is similar to the *G* shell, but with two inlet nozzles and two outlet nozzles and two horizontal baffles resulting in a double split flow unit. It is used when the available pressure drop is very limited. Possible pass arrangements are H_{1-1} and H_{1-2} (Figure 5.46). The *H* shell approaches the crossflow arrangement of the *X* shell, and it usually has low shellside pressure drop compared to *E*, *F*, and *G* shells [4], i.e., compared to *E* shell, the shellside velocity is 1/2 times and pressure drop is 1/8 times.

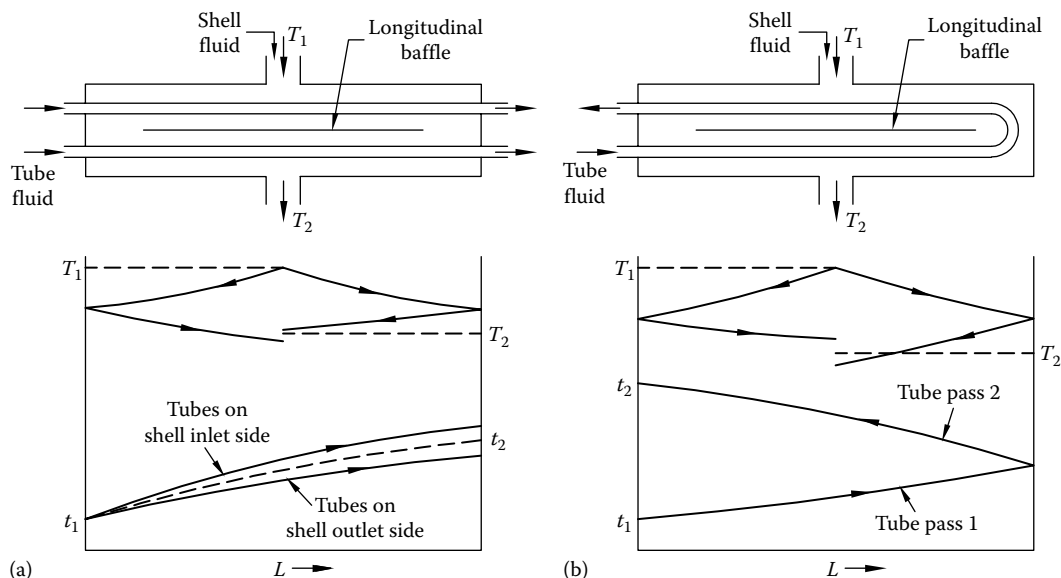


FIGURE 5.45 G shell flow arrangement and temperature distribution. (a) G_{1-1} and (b) G_{1-2} .

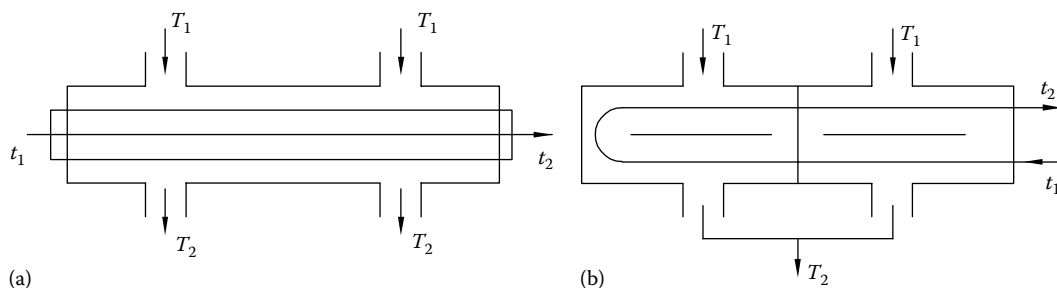


FIGURE 5.46 H shell flow arrangement. (a) H_{1-1} and (b) H_{1-2} .

5.14.1.6 TEMA J Shell or Divided Flow Exchanger

The divided flow J shell has two inlets and one outlet or one inlet and two outlet nozzles (i.e., a single nozzle at the midpoint of shell and two nozzles near the tube ends). With a single inlet nozzle at the middle, the shell fluid enters at the center of the exchanger and divides into two streams. These streams flow in longitudinal directions along the exchanger length and exit from two nozzles, one at each end of the exchanger. The possible pass arrangements are one shell pass, and one, two, four, N (even) or infinite tube passes. J shell pass arrangements with temperature distribution are shown in Figure 5.47 [32]. With a TEMA J shell, the shellside velocity will be one-half that of the TEMA E shell and hence the pressure drop will be approximately one-eighth that of a comparable E shell. Due to this reason, it is used for LP-drop applications like condensing in vacuum [4]. For a condensing shell fluid, the J shell is used with two inlets for the gas phase and one central outlet for the condensates and leftover gases.

5.14.1.7 TEMA K Shell or Kettle Type Reboiler

The K shell is used for partially vaporizing the shell fluid. It is used as a kettle reboiler in the process industry and as a flooded chiller in the refrigeration industry. Usually, it consists of a horizontal bundle of heated U tubes or floating head placed in an oversized shell. The tube bundle is

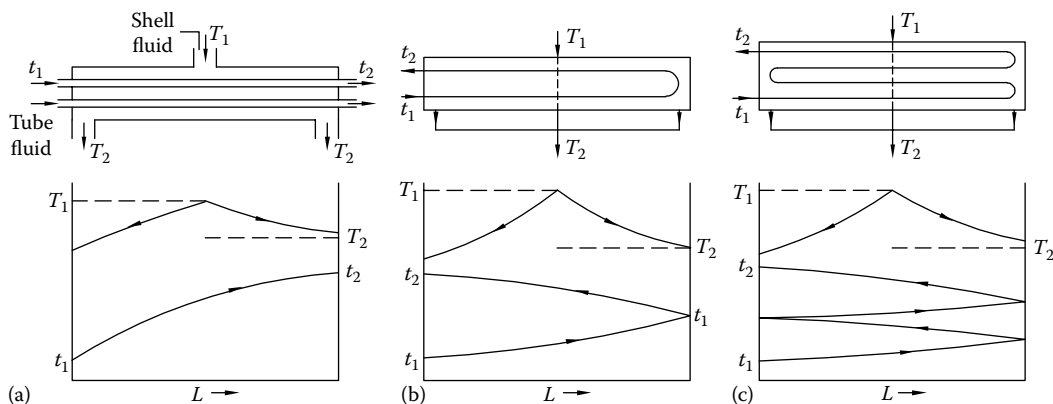


FIGURE 5.47 TEMA *J* shell flow arrangement and temperature distribution. (a) J_{1-1} , (b) J_{1-2} , and (c) J_{1-4} . (From Jaw, L., *Trans. ASME, J. Heat Transfer*, 56C, 408, 1964.)



FIGURE 5.48 Kettle-type reboilers. (Courtesy of Brembana Costruzioni Industriali S.p.A., Milan, Italy.)

free to move and it is removable. Its diameter is about 50%–70% of the shell diameter. The large empty space above the tube bundle acts as a vapor-disengaging space. Kettle boiler heat exchanger of TEMA-type AKT is shown in Figure 5.41f. The liquid to be vaporized enters at the bottom, near the tubesheet, and covers the tube bundle; the vapor occupies the upper space in the shell, and the dry vapor exits from the top nozzle(s), while a weir (the vertical unperforated baffle shown in Figure 5.41f) helps to maintain the liquid level over the tube bundle. The bottom nozzle in this space is used to drain the excess liquid. Kettle boiler heat exchanger is shown in Figure 5.48.

5.14.1.8 TEM X Shell

The X shell (Figure 5.49) is characterized by pure shellside crossflow. No transverse baffles are used in the X shell; however, support plates are used to suppress the flow-induced vibrations. It has nozzles in the middle as in the *G* shell. The shellside fluid is divided into many substreams, and each substream flows over the tube bundle and leaves through the bottom nozzle. Flow maldistributions on the shellside can be a problem unless a proper provision has been made to feed the fluid uniformly at the inlet. Uniform flow distribution can be achieved by a bathtub nozzle, multiple nozzles, or keeping a clear lane along the length of the shell near the nozzle inlet [4]. The tubeside can be single pass, or two passes, either parallel crossflow or counter-crossflow. For a given set of conditions, the X shell has the lowest shellside pressure drop compared to all other shell types (except the *K* shell). Hence, it is used for gas heating and cooling applications and for condensing under vacuum.

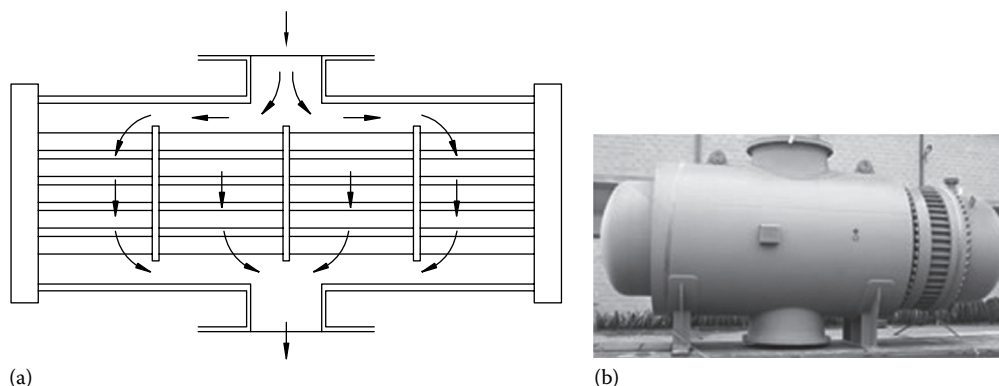


FIGURE 5.49 (a) Cross section of TEMA X shell—schematic and (b) tube heat exchanger.

5.14.1.9 Comparison of Various TEMA Shells

In general, *E*- and *F*-type shells are suited to single-phase fluids because of the many different baffle arrangements possible and the relatively long flow path [9]. When the shellside pressure drop is a limiting factor, *G* and *H* shells can be used. The *G* and *H* shells are not used for shellside single-phase applications, since there is no edge over the *E* or *X* shells. They are used as horizontal thermosiphon reboilers, condensers, and in other phase-change applications. The longitudinal baffle serves to prevent flashing out of the lighter components of the shell fluid, helps flushing out noncondensables, provides increased mixing, and helps flow distribution [4]. Velocity head and pressure drop for various TEMA shells are given in Ref. [33].

5.14.2 FRONT AND REAR HEAD DESIGNS

Head designs can vary from plain standard castings to fabricated assemblies with many special features. Two of the major considerations in the choice of heads are [6] (1) accessibility to the tubes and (2) piping convenience. Where fouling conditions are encountered or where frequent access for inspection is desired, a head or cover plate that can be easily removed is an obvious choice. In this head, connections are located on the sides, not on the ends of removable heads. Typical open-end heads used for this purpose are called channels. They are fabricated from cylindrical shells and fitted with easily removable cover plates so that the tubes can be cleaned without disturbing piping.

5.14.2.1 Designations for Head Types

Front head: For the variable front head, the constants and their meanings are thus:

- A* Channel with removable cover
- B* Bonnet with integral cover
- C* Channel integral with the tubesheet and removable cover when the tube bundle is removable
- N* Channel integral with the tubesheet and having a removable cover but the tube bundle is not removable
- D* Special HP closure

Rear head:

- L* Fixed tubesheet like “A” stationary head
- M* Fixed tubesheet like “B” stationary head
- N* Fixed tubesheet like “N” stationary head
- P* Outside packed floating head
- S* Floating head with backing device
- T* Pull-through floating head
- U* U-tube bundle
- W* Externally sealed floating tubesheet

Salient features of these heads are discussed and tabulated by Larowski et al. [9]. Few of the possible combinations of front and rear heads result in the following removable bundle exchanger:

1. BEU/AEU, 2. CEU, 3. BEW/AEW, 4. AEP/BEP, 5. AES/AET, 6. NEU, 7. NEN, 8. AEM/BEM/AEL, etc.

5.14.3 TEMA SPECIFICATION SHEET

TEMA specification sheet (both in metric and in FPS-English units) for shell and tube heat exchanger is shown in Figure 5.50. It is used as a basic engineering document in the thermal design, purchasing, and construction of shell and tube heat exchangers.

5.15 SHELLSIDE CLEARANCES

Even though one of the major functions of the plate baffle is to induce crossflow over the tube bundle, this objective is achieved partially. Various clearances on the shellside partially bypass the fluid. Bypassing is defined as a leakage flow where fluid from the crossflow stream, intended to flow through the tube bundle, avoids flowing through it by passing through an alternative, low-resistance flow path [34]. A major source of bypassing is the shellside clearances. Clearances are required for heat exchanger fabrication. Fabrication clearances and tolerances have been established by the TEMA, and these have become widely accepted around the world and are enforced through inspection during fabrication. Three clearances are normally associated with a plate baffle exchanger. They are (1) tube-to-baffle hole, (2) baffle to shell, and (3) bundle to shell. Additionally, in a multipass unit, the tube layout partitions may create open passages for the bypass of the crossflow stream. Since bypassing reduces heat transfer on the shellside, to achieve good shellside heat transfer, bypassing of the fluid must be reduced. These clearances and their effect on the shellside performance are discussed in detail next.

5.15.1 TUBE-TO-BAFFLE-HOLE CLEARANCE

The holes in the baffles must be slightly larger than the tube outer diameter to ensure easy tube insertion. The resultant clearance is referred to as the tube-to-baffle-hole clearance (Figure 5.51). It should be kept at a minimum (1) to reduce the flow-induced vibration and (2) to minimize the A leakage stream (various shellside bypass streams are discussed next). As per TEMA RCB-4.2, where the maximum unsupported tube length is 36 in. (914.4 mm) or less, or for tubes larger than 1.25 in. (31.8 mm) outer diameter, the clearance is 1/32 in. (0.80 mm); where the unsupported tube length exceeds 36 in. for tube outer diameter 1.25 in. or smaller, the clearance is 1/62 in. (0.40 mm).

5.15.2 SHELL-TO-BAFFLE CLEARANCE

The clearance between the shell inner diameter and baffle outer diameter is referred to as the baffle-to-shell clearance. It should be kept to a minimum to minimize the E leakage stream. TEMA recommends that maximum clearance as per RCB-4.3 [2] varies from 0.125 in. (3.175 mm) for 6 in. (152.4 mm) shell inner diameter to 0.315 in. (7.94 mm) for 60 in. (1524 mm) shell inner diameter.

5.15.3 SHELL-TO-BUNDLE CLEARANCE

Since the tube bundle does not fill the shell, there is a shell-to-bundle clearance. This allows the so-called bypass stream C flowing around the bundle. Sealing strips are used to block this space and force the bypass stream to flow across the tubes. The use of sealing strips is recommended every five to seven rows of tubes in the bypass stream direction.

1					Job No.	
2	Customer				Reference No.	
3	Address				Proposal No.	
4	Plant Location				Date	Rev.
5	Service of Unit				Item No.	
6	Size	Type	(Hor/Vert)	Connected in	Parallel	Series
7	Surf/Unit (Gross/Eff.)		Sq m; Shells/Unit	Surf/Shell (Gross/Eff.)		sq m
8	PERFORMANCE OF ONE UNIT					
9	Fluid Allocation		Shell Side		Tube Side	
10	Fluid Name					
11	Fluid Quantity total		kg/Hr			
12	Vapor (In/Out)					
13	Liquid					
14	Steam					
15	Water					
16	Noncondensable					
17	Temperature (In/Out)		°C			
18	Specific Gravity					
19	Viscosity, Liquid		Cp			
20	Molecular Weight, Vapor					
21	Molecular Weight, Noncondensable					
22	Specific Heat		J/kg °C			
23	Thermal Conductivity		W/m °C			
24	Latent Heat		J/kg @ °C			
25	Inlet Pressure		kPa(abs.)			
26	Velocity		m/sec			
27	Pressure Drop, Allow. /Calc		kPa	/		/
28	Fouling Resistance (Min.)		Sq m °C / W			
29	Heat Exchanged		W	MTD (Corrected)		°C
30	Transfer Rate, Service		Clean			W/Sq m °C
31	CONSTRUCTION OF ONE SHELL				Sketch (Bundle/Nozzle Orientation)	
32			Shell Side	Tube Side		
33	Design / Test Pressure		kPag	/	/	
34	Design Temp. Max/Min		°C	/	/	
35	No. Passes per Shel					
36	Corrosion Allowance		mm			
37	Connections		In			
38	Size &		Out			
39	Rating		Intermediate			
40	Tube No.	OD	mm;Thk (Min/Avg)	mm;Length	mm;Pitch	mm
41	Tube Type		Material			
42	Shell	ID	OD	mm	Shell Cover	(Integ.) (Remov.)
43	Channel or Bonne		Channel Cover			
44	Tubesheet-Stationary		Tubesheet-Floating			
45	Floating Head Cove		Impingement Protection			
46	Baffles-Cross	Type	%Cut (Diam/Area)	Spacing: c/c	Inlet	mm
47	Baffles-Long		Seal Type			
48	Supports-Tube	U-Bend			Type	
49	Bypass Seal Arrangemen		Tube-to-Tubesheet Joint			
50	Expansion Joint		Type			
51	pv ² -Inlet Nozzle	Bundle Entrance		Bundle Exit		
52	Gaskets-Shell Side		Tube Side			
53	Floating Head					
54	Code Requirements		TEMA Class			
55	Weight / Shell	Filled with Water		Bundle		kg
56	Remarks					
57						
58						
59						
60						
61						

(a)

FIGURE 5.50 (a) TEMA specification sheet for shell and tube heat exchanger—metric units.

1					Job No.	
2	Customer				Reference No.	
3	Address				Proposal No.	
4	Plant Location				Date	Rev.
5	Service of Unit				Item No.	
6	Size	Type	(Hor/Vert)	Connected in	Parallel	Series
7	Surf/Unit (Gross/Eff.)	sq ft; Shells/Unit		Surf/Shell (Gross/Eff.)	sq ft	
8	PERFORMANCE OF ONE UNIT					
9	Fluid Allocation		Shell Side		Tube Side	
10	Fluid Name					
11	Fluid Quantity Total		lb/hr			
12	Vapor (In Out)					
13	Liquid					
14	Steam					
15	Water					
16	Noncondensable					
17	Temperature		°F			
18	Specific Gravity					
19	Viscosity, Liquid		cP			
20	Molecular Weight, Vapor					
21	Molecular Weight, Noncondensable					
22	Specific Heat		BTU / lb °F			
23	Thermal Conductivity		BTU ft / hr sq ft °F			
24	Latent Heat		BTU / lb @ °F			
25	Inlet Pressure		psia			
26	Velocity		ft / sec			
27	Pressure Drop, Allow. /Calc		psi		/	
28	Fouling Resistance (Min.)		hr sq ft °F / BTU			
29	Heat Exchanged		BTU / hr MTD (Corrected)		°F	
30	Transfer Rate, Service		Clean		BTU / hr sq ft °F	
31	CONSTRUCTION OF ONE SHELL				Sketch (Bundle/Nozzle Orientation)	
32			Shell Side		Tube Side	
33	Design / Test Pressure		psig		/	
34	Design Temp. Max/Min		°F		/	
35	No. Passes per Shel					
36	Corrosion Allowance		in			
37	Connections		In			
38	Size &		Out			
39	Rating		Intermediate			
40	Tube No.	OD	in;Thk (Min/Avg)	in;Length	ft;Pitch	in $\leftarrow 30 \rightarrow 60 \rightarrow 90 \rightarrow 45$
41	Tube Type		Materia			
42	Shell	ID	OD	in	Shell Cover	(Integ.) (Remov.)
43	Channel or Bonne			Channel Cover		
44	Tubesheet-Stationary			Tubesheet-Floating		
45	Floating Head Cove			Impingement Protection		
46	Baffles-Cross	Type	%Cut (Diam/Area)		Spacing: c/c	Inlet in
47	Baffles-Long			Seal Type		
48	Supports-Tube	U-Bend		Type		
49	Bypass Seal Arrangement			Tube-to-Tubesheet Joint		
50	Expansion Joint			Type		
51	pv ² -Inlet Nozzle	Bundle Entrance		Bundle Exit		
52	Gaskets-Shell Side			Tube Side		
53	Floating Head					
54	Code Requirements			TEMA Class		
55	Weight / Shell	Filled with Water		Bundle		lb
56	Remarks					
57						
58						
59						
60						
61						

(b)

FIGURE 5.50 (continued) (b) TEMA specification sheet for shell and tube heat exchanger—FPS system units. (© Standards of Tubular Exchanger Manufacturers Association, Inc., 9th edn., 2007.)

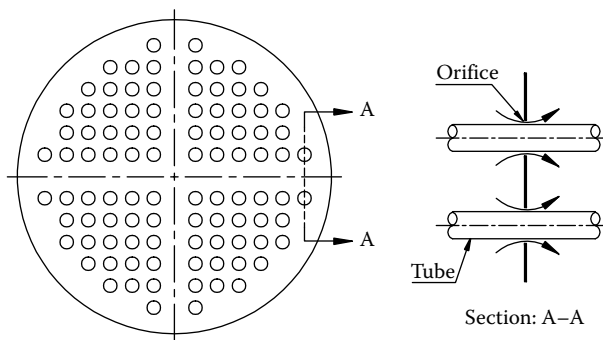


FIGURE 5.51 Tube-to-baffle leakage stream.

5.15.4 BYPASS LANES

The lanes provided for the tubeside partition ribs are a source of bypass on the shellside. The pass partition lanes are, however, placed perpendicular to the crossflow whenever possible, or the bypass lanes are usually blocked by tie-rods, which act similar to the sealing strips. Hence, the effect of the bypass lanes on thermal performance usually can be neglected.

5.16 DESIGN METHODOLOGY

5.16.1 SHELLSIDE FLOW PATTERN

5.16.1.1 Shell Fluid Bypassing and Leakage

In shell and tube exchangers with segmental plate baffles, the shellside flow is very complex due to a substantial portion of the fluid bypassing the tube bundle through various shellside constructional clearances defined earlier. Another contributing factor for bypassing is due to notches made in the bottom portion of the baffles for draining purposes. Notches are usually not required for draining because the necessary fabrication tolerances provide ample draining [4]. To achieve good shellside heat transfer, bypassing of the fluid must be reduced.

5.16.1.2 Bypass Prevention and Sealing Devices

Sealing devices can be employed to minimize the bypassing of fluid around the bundle or through pass partition lanes [34]. If tube bundle-to-shell bypass clearance becomes large, such as for pull-through bundles, resulting in decreased heat transfer efficiency, the effectiveness can be restored by fitting “sealing strips.” As a rule of thumb, sealing strips should be considered if the tube bundle-to-shell diameter clearance exceeds approximately 2.25 in. (30 mm). Fixed tubesheet and U-tube heat exchangers usually do not require sealing strips, but split ring and pull-through floating head designs usually require sealing strips.

Types of sealing devices: Sealing devices are strips that prevent bypass around a bundle by “sealing” or blocking the clearance area between the outermost tubes and the inside of the shell. Some common types include [7] tie-rods, sealing devices, and tie-rods.

1. Tie-rods and spacers hold the baffles in place but can be located at the periphery of the baffle to prevent bypassing.
2. Sealing strips. These are typically longitudinal strips of metal between the outside of the bundle and the shell and fastened to the baffles (Figure 5.52); they force the bypass flow back into the tube field. A typical flow pattern with sealing strips in an effective penetration area is shown in Figure 5.52.

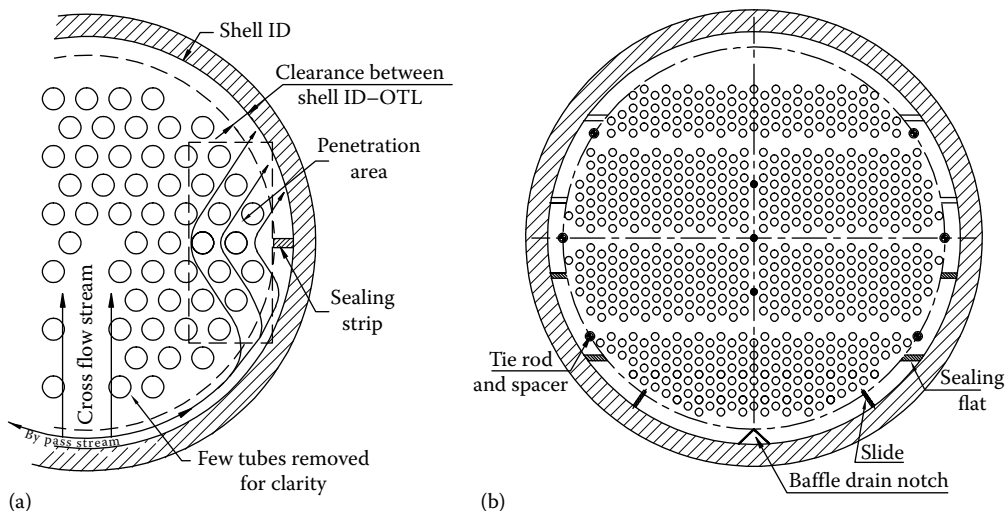


FIGURE 5.52 Sealing strips. (a) Typical flow pattern with sealing strips. (Adapted from Palen, J.W. and Taborek, J., *Chem. Eng., Symp. Ser.*, No. 92, *Heat Transfer—Philadelphia*, 65, 53, 1969.) (b) Shows attachment of sealing strip, baffle drain notch, tie-rod, and slide plate attached to the tube bundle.

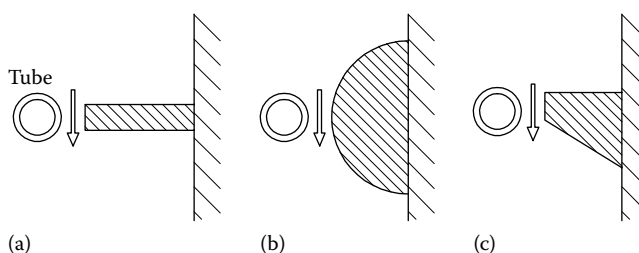


FIGURE 5.53 Forms of sealing strips. (a) Rectangular, (b) semicircular, and (c) triangular. (From Taylor, C.E. and Currie, I.G., *Trans. ASME J. Heat Transfer*, 109, 569, 1987.)

Number of sealing strips pair in between two baffles: Bypassing of the shellside fluid can be adequately controlled by providing one sealing device for every four tube rows on the bundle periphery and by providing one sealing device for every two tube rows at bypass lanes internal to the bundle such as pass partition lanes [1]. The use of sealing strips to divert flow within heat exchangers was studied by Taylor et al. [35]. They examined the variation of sealing strip shape (Figure 5.53), location, and gap size, i.e., the distance between the sealing device and the nearest tube. According to their study, (1) rectangular-shaped sealing strips are preferred, (2) sealing strips placed close together (3.6 rows apart) will provide optimum heat transfer characteristics, and (3) most significant results were obtained when the gap size = $p - d$.

3. Tie-rods with “winged” spacers. The wings are extended longitudinal strips attached to the spacers.

Dummy tubes: Usually closed at one end, dummy tubes are used to prevent bypassing through lanes parallel to the direction of fluid flow on the shellside (Figure 5.25a). They do not pass through the tubesheet. In moderate to large exchangers, one dummy tube is as effective in promoting heat transfer as 50 process tubes [7].

5.16.1.3 Shellside Flow Pattern

An ideal tube bundle (the term introduced by Heat Transfer Research, Incorporated (HTRI), CA refers to segmentally baffled circular bundles with no clearance between tubes and baffles, baffles and shell, or outer tubes and the shell, so that all fluid must flow across the tube bundle [13]. In a practical tube bundle, the total shellside flow distributes itself into a number of distinct partial streams due to varying flow resistances through the shellside clearances. This stream distribution pattern is now well established and is shown schematically in Figure 5.54. Figure 5.54a shows three regions of flow over the tube bundle, Figure 5.54b shows regions of parallelflow, and Figure 5.54c shows different streams flow through the tube bundle. This flow model was originally proposed by Tinker [36] and later modified by Palen et al. [13] for a segmentally baffled exchanger. Various streams in order of decreasing thermal effectiveness are discussed next.

A stream: This is a tube-to-baffle-hole leakage stream through the clearance between the tubes and the tube holes in the baffles (Figure 5.54c). This stream is created by the pressure difference on the sides of the baffle. As heat transfer coefficients are very high in the annular spaces, this stream is considered fully effective.

B stream: This is a crossflow stream through tube bundle. This stream is considered fully effective for both heat transfer and pressure drop.

C stream: This is a bundle-to-shell bypass stream through the annular spaces between the tube bundle and the shell. It flows between successive baffle windows. This stream is only partially effective for heat transfer as it contacts the tubes near the tube bundle periphery.

E stream: This is a shell-to-baffle leakage stream through the clearance between the edge of a baffle and the shell. This stream is the least effective for heat transfer, particularly in laminar flow, because it may not come in contact with any tubes.

F stream: This is a tube pass partition bypass stream through open passages created by tube layout partition lanes (when placed in the direction of the main crossflow stream) in a multipass unit.

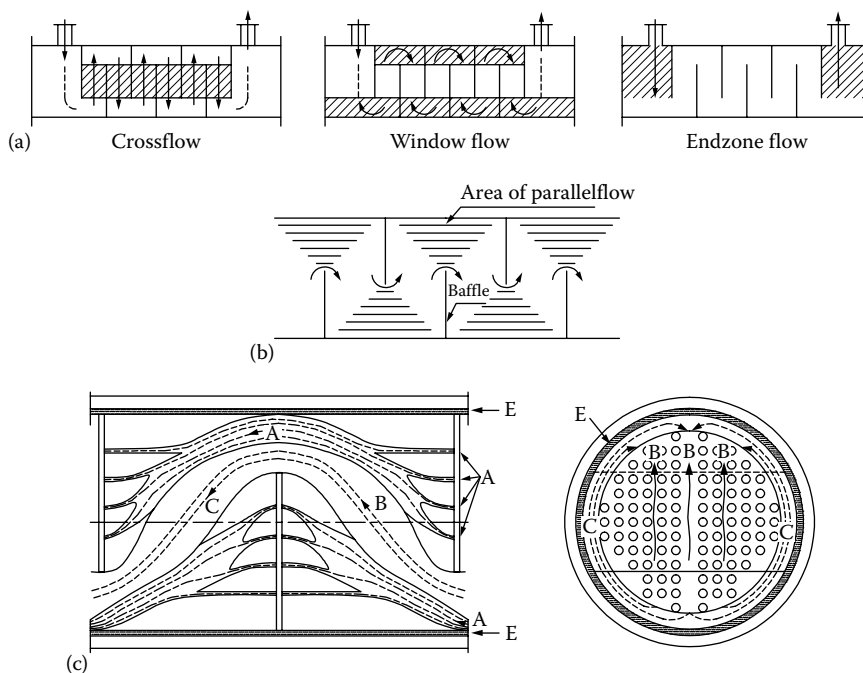


FIGURE 5.54 Shellside flow distribution. (a) Three regions of flow over the tube bundle, (b) regions of parallel flow, and (c) shows different streams flow through the tube bundle.

This stream is less effective than the *A* stream because it comes into contact with less heat transfer area per unit volume; however, it is slightly more effective than the *C* stream.

From the earlier discussion, the fluid in streams *C*, *E*, and *F* bypasses the tubes, which reduces the effective heat transfer area. Stream *C* is the main bypass stream and will be particularly significant in pull-through bundle exchangers, where the clearance between the shell and the bundle is of necessity large. Stream *C* can be considerably reduced by using sealing strips.

5.16.1.4 Flow Fractions for Each Stream

Each of the streams has a certain flow fraction of the total flow such that the total pressure drop for each stream is the same. Each stream undergoes different frictional processes and has different heat transfer effectiveness as discussed earlier. The design of the plate baffle shell and tube exchanger should be such that most of the flow (ideally about 80%) represents the crossflow *B* stream. However, this is rarely achieved in practice. Narrow baffle spacing will result in higher pressure drop for the *B* stream and forces more flow into the *A*, *C*, and *E* streams.

Based on extensive test data, Palen et al. [13] arrived at the flow fractions for various streams both for laminar flow and for turbulent flow. Even for a good design, the crossflow stream represents only 65% of the total flow in turbulent flow and 50% in laminar flow. Hence, the predicted performance based on the conventional LMTD method will not be accurate in general. As a result, there is no need to compute very accurate *F* factors for the various exchanger configurations [13]. If the computed values of the *B* stream are lower than those indicated, the baffle geometry and various clearances should be checked.

5.16.1.5 Shellside Performance

Many investigators have studied the shellside thermal performance. One of the earliest was Tinker [36,37]. Perhaps the most widely accepted and recognized study is known as the Bell–Delaware method [38]. The original method has been further refined by Bell [39] and presented also in Ref. [40], and other modifications and improvements have been made by Taborek [15]. For generic details on shell and tube heat exchangers, their classification, stream analysis and guidance for thermal design refer to Mukurjee [41] and Hewitt et al. [42].

5.16.2 SIZING OF SHELL AND TUBE HEAT EXCHANGERS

The design of shell and tube heat exchanger involves the determination of the heat transfer coefficient and pressure drop on both the tubeside and the shellside. A large number of methods [37,43–45] are available for determining the shellside performance. Since the Bell–Delaware method is considered the most suitable open-literature method for evaluating shellside performance, the method is described here. Before discussing the design procedure, tips for thermal design, and heat transfer coefficient and pressure drop are discussed, some guidelines for shellside design and points to be raised while specifying a heat exchanger are listed, followed by preliminary sizing of a shell and tube heat exchanger.

5.16.3 GUIDELINES FOR STHE DESIGN

Tips for thermal design

1. Always specify counterflow operation for maximum performance.
2. The heat exchanger can be mounted vertically if required; however, this may require special mounting brackets.

3. If the sizing procedure suggests a nonstandard shell length, use the next larger size or consider using two shorter heat exchangers.
4. Consider using two or more heat exchangers when the heat duty is on the higher side or space for locating the heat exchanger is limited, or temperature and flow parameters are outside the recommended range for a single heat exchanger.

5.16.3.1 Heat Transfer Coefficient and Pressure Drop

5.16.3.1.1 Heat Transfer Coefficient

The tubeside heat transfer coefficient is a function of the Reynolds number, the Prandtl number, and the tube diameter. The earlier-mentioned nondimensional numbers are based on the fundamental parameters such as fluid physical properties (i.e., viscosity, thermal conductivity, and specific heat), tube diameter, and mass velocity. For turbulent flow, the tubeside heat transfer coefficient varies to the 0.8 power of tubeside mass velocity. Also the variation in liquid viscosity has a dramatic effect on heat transfer coefficient.

The shellside heat transfer coefficient is dependent on shellside parameters like fluid velocity, shell inside diameter, baffle cut, baffle spacing, tube hole clearance in the baffle plate, various shellside clearances other than the desired fluid flow path, number of passes on shellside, shell type, etc.

5.16.3.1.2 Pressure Drop

Fluid pressure drop is controlled by a wide variety of design variables and the process fluid flow parameters. For the tubeside stream, the controlling variables are tube diameter, tube length, tube geometry (straight or U-tubes), number of tube passes and number of shells in series or parallel, and nozzle size. For turbulent flow, tubeside pressure drop is proportional to the square of velocity. Consequently, there will be an optimum mass velocity above which it will be wasteful to increase the velocity further. In addition to higher pumping costs, very high velocities lead to erosion. However, the pressure-drop limitation usually becomes the controlling factor long before the erosive velocity limits are attained. The minimum recommended liquid velocity inside tubes is 1.0 m/s, while the maximum is 2.5–3.0 m/s. Since pressure drop depends on the total length of travel, as the number of tube passes increases, for a given number of tubes and a given tubeside flow rate, the pressure drop rises dramatically. Shellside fluid pressure drop is influenced by equipment design variables such as tube diameter, tube pitch, tube layout, shell diameter, baffle type, baffle cut, baffle spacing, number and size of shellside nozzles, and the exchanger shell type.

5.16.4 GUIDELINES FOR SHELLSIDE DESIGN

Recommended guidelines for shellside design include the following [1]:

1. Accept TEMA fabrication clearances and tolerances and enforce these standards during fabrication.
2. For segmental baffles employ 20% baffle cuts.
3. Employ NTIW design to eliminate the damage from flow-induced vibration.
4. Evaluate heat transfer in the clean condition and pressure drop in the maximum fouled condition.
5. Employ sealing devices to minimize bypassing between the bundle and shell for pull-through floating heat exchanger and through pass partition lanes.
6. Ratio of baffle spacing to shell diameter may be restricted to values between 0.2 and 1.0. Baffle spacing much greater than the shell diameter must be carefully evaluated.
7. Avoid shell longitudinal baffles that are not welded to the shell; all other sealing methods are inadequate.

5.16.4.1 Specify the Right Heat Exchanger

When specifying an exchanger for design, various factors to be considered or questions that should be raised are listed by Gutterman [28]. A partial list includes the following:

1. Type of heat transfer, i.e., boiling, condensing, or single-phase heat transfer.
2. Since the heat exchanger has two pressure chambers, which chamber should receive the cold fluid?
3. More viscous fluid shall be routed on the shellside to obtain better heat transfer.
4. It is customary to assign the higher pressure to the tubeside to minimize shell thickness.
5. Consider various potential and possible upset conditions in assigning the design pressure and/or design temperature.
6. Pass arrangements on the shellside and tubeside to obtain maximum heat transfer?
7. Have you considered the tube size and the thickness?
8. What is the acceptable pressure drop on the tubeside and the shellside? Is the sum of the pumping cost and the initial equipment cost minimized?
9. Have you considered the maximum allowable pressure drop to obtain the maximum heat transfer?
10. Are the tubeside and shellside velocities high enough for good heat transfer and to minimize fouling but well below the limits that can cause erosion–corrosion on the tubeside, and impingement attack and flow-induced vibration on the shellside?
11. Have you considered the nozzle sizes and adequate shell escape area? Are the nozzle orientations consistent with tube layout pattern?
12. Is the baffle arrangement designed to promote good flow distribution on the shellside and hence good heat transfer, and to minimize fouling and flow-induced vibration?
13. Does the design provide for efficient expulsion of noncondensables that may degrade the performance? (A prime example in this category is surface condensers.)
14. Is the service corrosive or dirty? If so, have you specified corrosion-resistant materials and reasonable fouling factors?
15. Does the design minimize fouling?
16. Do you want to remove the bundle? If so, are adequate space and handling facilities available for tube bundle removal?
17. Is leakage a factor to be considered? If so, did you specify (a) seal-welded tube joint, (b) rolled joint, (c) strength welded joint? Is the tube wall thickness adequate for welding? Are you specifying tube holes with grooves or without grooves?
18. What kind of tests do you specify to prove the tube-to-tubesheet joint integrity?

All of these and numerous other factors determine the type of exchanger to be specified.

5.16.5 DESIGN CONSIDERATIONS FOR A SHELL AND TUBE HEAT EXCHANGER

The basic criterion that a given or designed heat exchanger should satisfy is that it should perform the given heat duty within the allowable pressure drop. The design is also to satisfy additional criteria such as [46]

1. Withstand operating conditions, start-up, shutdown, and upset conditions that influence the thermal and mechanical design
2. Maintenance and servicing
3. Multiple shell arrangement
4. Cost
5. Size limitations

In terms of the five factors just mentioned, multishell arrangement needs some comments on it. Consider the advantages of a multishell arrangement to allow one unit to be taken out of service

for maintenance without severely upsetting the rest of the plant. For part load operations, multiple shells will result into an economical operation. Shipping and handling may dictate restrictions on the overall size or weight of the unit, resulting in multiple shells for an application.

5.16.5.1 Thermal Design Procedure

The overall design procedure of a shell and tube heat exchanger is quite lengthy, and hence it is necessary to break down this procedure into distinct steps:

1. Approximate sizing of shell and tube heat exchanger
2. Evaluation of geometric parameters also known as auxiliary calculations
3. Correction factors for heat transfer and pressure drop
4. Shellside heat transfer coefficient and pressure drop
5. Tubeside heat transfer coefficient and pressure drop
6. Evaluation of the design, i.e., comparison of the results with the design specification

In this section, approximate sizing of the shell and tube exchanger by Bell's method is discussed first; then this is extended to size estimation, and subsequently the rating is carried out as per the Bell–Delaware method. Finally, the rated unit is evaluated.

Bell's method [46] for approximate sizing of a shell and tube heat exchanger: The approximate design involves arriving at a tentative set of heat exchanger parameters, and if the design is accepted after rating, then this becomes the final design. Various stages of approximate design include the following:

1. Compute overall heat transfer coefficient
2. Compute heat transfer rate required
3. Compute the heat transfer area required
4. Design the geometry

A flowchart for approximate sizing is given in Figure 5.55.

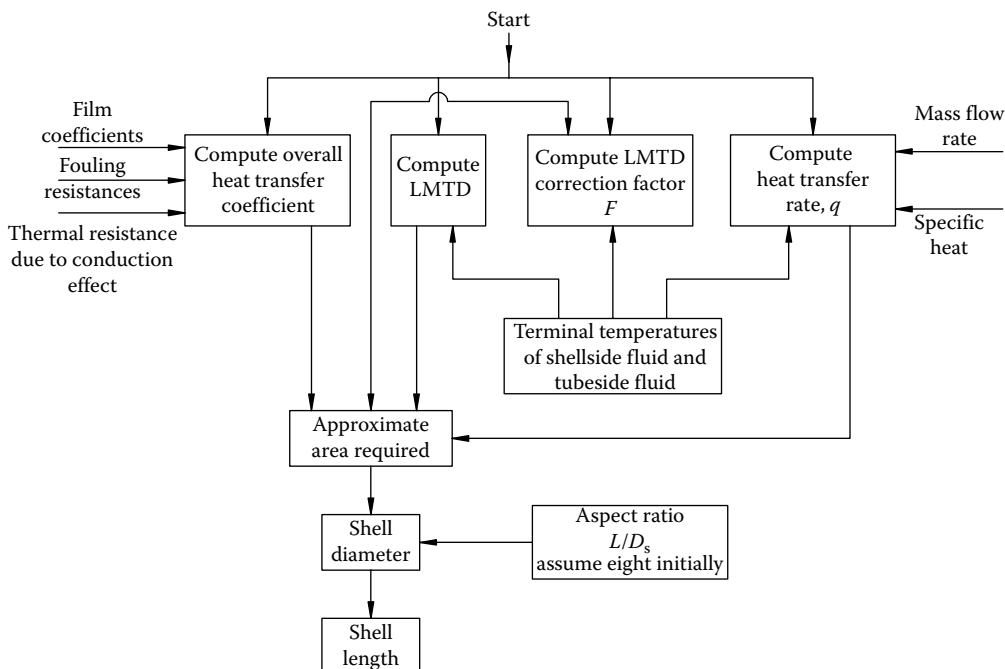


FIGURE 5.55 Flowchart for approximate sizing of STHE.

Estimation of heat load: The heat load is calculated in the general case from

$$q = M_h c_{p,h} (T_{h,i} - T_{h,o}) = M_c c_{p,c} (T_{c,o} - T_{c,i}) \quad (5.5)$$

where

$c_{p,h}$ and $c_{p,c}$ are the specific heats of the hot and cold fluids
 $T_{h,i}$ and $T_{h,o}$ are the inlet and outlet temperatures of the hot stream
 $T_{c,i}$ and $T_{c,o}$ are the inlet and outlet temperatures of the cold stream

Estimation of log mean temperature difference: Determine the logarithmic mean temperature difference for countercurrent flow using the temperatures as defined earlier:

$$\text{LMTD} = \frac{(T_{h,i} - T_{c,o}) - (T_{h,o} - T_{c,i})}{\ln[(T_{h,i} - T_{c,o}) / (T_{h,o} - T_{c,i})]} \quad (5.6)$$

LMTD correction factor: Values of F can be found from the thermal relation charts given in Chapter 2 for a variety of heat exchanger flow configurations. However, for estimation purposes, a reasonable estimate may often be obtained without restoring to the charts.

1. For a single tube pass, purely countercurrent heat exchanger, $F = 1.0$.
2. For a single shell with any even number of tubeside passes, F should be between 0.8 and 1.0. (For other shell types refer to Chapter 2, Section 2.2.3.3).

Method to determine number of shells: Quickly check the limits:

$$2T_{h,o} \geq T_{c,i} + T_{c,o} \quad \text{hot fluid on the shell side}$$

$$2T_{c,o} \leq T_{h,i} + T_{h,o} \quad \text{cold fluid on the shell side}$$

If these limits are approached, it is necessary to use multiple $1 - 2N$ shells in series. There is a rapid graphical technique for estimating a sufficient number of $1 - 2N$ shells in series. The procedure is discussed here. The terminal temperatures of the two streams are plotted on the ordinates of an arithmetic graph paper sheet as shown in Figure 5.56. The distance between the ordinates is arbitrary. Starting with the cold fluid outlet temperature, a horizontal line is laid off until it intercepts the hot fluid line. From that point, a vertical line is drawn to the cold fluid temperature. The process is repeated until a vertical line intercepts the cold fluid operating line at or below the cold fluid inlet temperature. The number of horizontal lines (including the one that intersects the right-hand

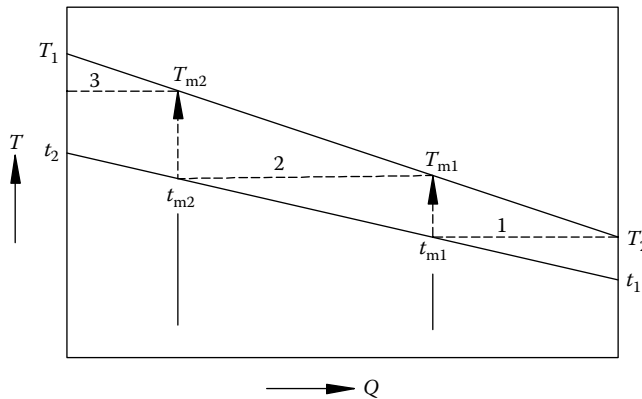


FIGURE 5.56 Procedure to determine the number of shells. *Note:* T_1 and T_2 are shellside terminal temperatures and t_1 and t_2 are tubeside terminal temperatures.

ordinate) is equal to the number of shells in series that is clearly sufficient to perform the duty. Following this procedure will usually result in a number of shells having an overall F close to 0.8.

Estimation of U : The greatest uncertainty in preliminary calculations is estimating the overall heat transfer coefficient. Approximate film coefficients for different types of fluids are given by Bell [43]. Thus, U can be calculated from the individual values of heat transfer coefficient on the shellside (h_s) and the tubeside (h_t), wall resistance (k_w), and fouling resistance (R_{fo} and R_{fi}), using the following equation:

$$U = \frac{1}{\left[(1/h_s) + R_{fo} + (t_w/k_w)(A_o/A_m) + (R_{fi} + (1/h_t)) A_o/A_i \right]} \quad (5.7)$$

where t_w is the wall thickness and A_m is the effective mean wall heat transfer area, which is approximated by the arithmetic mean, using the outside and inside radii, r_o and r_i :

$$A_m = \pi L(r_o + r_i) \quad (5.8a)$$

$$\text{For a bare tube } \frac{A_o}{A_i} \rightarrow \frac{r_o}{r_i} \quad (5.8b)$$

$$\frac{A_o}{A_m} \rightarrow \frac{r_o}{r_o + r_i} \quad (5.8c)$$

Heat transfer coefficient for finned tubes: Bell [46] suggests that the values given for plain tubes can be usually used with caution for low-finned tubes if the controlling resistance is placed on the shellside; the values should be reduced by 10%–30% if the shellside fluid is of medium or high viscosity, and by 50% if the shellside fluid is of high viscosity and is being cooled. Whitley et al. [11] suggest reducing the value for finned tubes to 90% of those of plain tubes.

Fouling resistance: Fouling resistance values may be chosen from TEMA Table RGP-T-2.4. Also refer to Chapter 9 for more details on fouling resistances.

Calculation of A_o : Once q , U , LMTD, and F are known, the total outside heat transfer area (including fin area) A_o is readily found from the following equation:

$$A_o = \frac{q}{UF(\text{LMTD})} \quad (5.9)$$

Determination of shell size and tube length from heat transfer area, A_o (after Taborek [26]): The problem now arises of how to interpret the value of A in terms of tube length and shell diameter, when both values are not known. If the problem specification specifies the limitation on shell length and diameter, the problem can be simplified. In the absence of these values, A_o is given by

$$A_o = \pi d L_{ta} N_t \quad (5.10)$$

and for estimation purposes, the tube count N_t is given in terms of tube pitch, L_{tp} , by

$$N_t = \frac{0.78 D_{cl}^2}{C_1 L_{tp}^2} \quad (5.11)$$

where C_1 is the tube layout constant given by

$$C_1 = 0.86 \quad \text{for } \theta_{tp} = 30^\circ \quad (5.12)$$

$$C_1 = 1.0 \quad \text{for } \theta_{tp} = 45^\circ \text{ and } 90^\circ$$

Substituting Equation 5.11 into Equation 5.10, the resulting equation is given by

$$A_o = (0.78\pi) \frac{d}{C_1 L_{tp}^2} [L_{ta} D_{ct}^2] \quad (5.13)$$

In Equation 5.13, the first term is a constant; the second term reflects the tube size and the tube layout geometry; and the third term includes the values of tube length and shell diameter (known as aspect ratio), which are the items to be determined. Heat transfer surface A_o can be obtained by various combinations of the parameter L_{ta} and D_{ct} for any given tube layout pattern. An initially assumed aspect ratio of 8 is suggested. Some tube count tables are available in Refs. [10,12,21], and there is a tube count chart in Ref. [46] for various tube layout patterns, tube diameters, and shell diameters. This helps to calculate A_o easily. If such a source is not available, the designer must assume a rational tube length and calculate the corresponding diameter D_{ct} and finally the shell inside diameter D_s .

5.16.5.2 Detailed Design Method: Bell–Delaware Method

Designing a shell and tube heat exchanger with the Bell–Delaware method is explained here. A flowchart for designing with the Bell–Delaware method is shown in Figure 5.57.

5.16.5.2.1 Evaluation of Geometric Parameters

After the determination of shell inside diameter and tube length, the next step is the evaluation of geometric parameters, such as

1. Baffle and bundle geometry
2. Flow areas
3. Various flow areas for calculating various correction factors

The calculation of various geometric parameters is known as auxiliary calculations in the Bell–Delaware method [41]. These calculations are required for the determination of shellside heat transfer coefficient and pressure drop. The auxiliary calculations are defined in the following steps.

5.16.5.2.2 Input Data

The Bell–Delaware method assumes that the flow rate and the inlet and the outlet temperatures (also pressures for a gas or vapor) of the shellside fluid are specified and that the density, viscosity, thermal conductivity, and specific heat of the shellside fluid are known. The method also assumes that the following minimum set of shellside geometry data is known or specified:

- Tube outside diameter, d
- Tube layout pattern, θ_{tp}
- Shell inside diameter, D_s
- Tube bank OTL diameter, D_{otl}
- Effective tube length (between tubesheets), L_{ti}
- Baffle cut, B_c , as a percent of D_s
- Central baffle spacing, L_{bc} (also the inlet and outlet baffle spacing, L_{bi} and L_{bo} , if different from L_{bc})
- Number of sealing strips per side, N_{ss}

From this geometrical information, all remaining geometrical parameters pertaining to the shellside can be calculated or estimated by methods given here, assuming that the standards of TEMA are met with respect to various shellside constructional details.

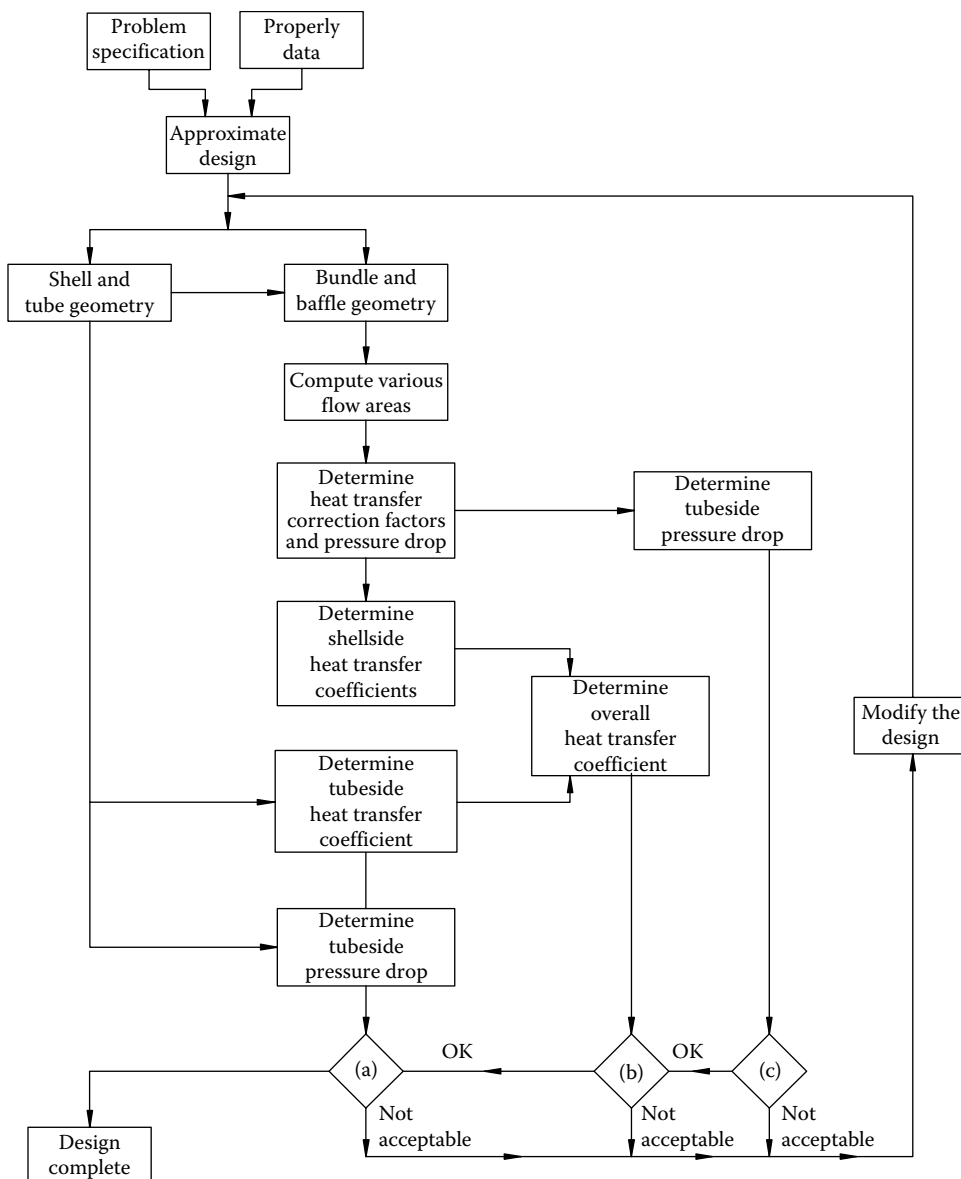


FIGURE 5.57 Flowchart for detailed design of STHE. (a) $\Delta P_t \leq$ allowed pressure drop, (b) compare area required with area available for heat transfer, and (c) $\Delta P_s \leq$ allowable pressure drop.

5.16.5.2.3 Shellside Parameters

Bundle-to-shell clearance, L_{bb} : A suitable tube bundle is selected based on the user's requirement, and the bundle-to-shell clearance is calculated based upon these equations:

For a fixed tubesheet heat exchanger,

$$L_{bb} = 12.0 + 0.005 D_s \text{ (mm)}$$

For a U-tube exchanger,

$$L_{bb} = 12.0 + 0.005 D_s \text{ (mm)}$$

Bundle diameter (D_{cl}): This is computed from the equation

$$\begin{aligned} D_{otl} &= D_s - L_{bb} \\ &= D_{cl} + d \end{aligned}$$

Shell length: This is taken as the overall nominal tube length, L_{to} , given by

$$L_{to} = L_{ta} + 2L_{ts}$$

where L_{ts} is tubesheet thickness. Its value may be assumed initially as 1 in. (25.4 mm) for calculation purposes.

Central baffle spacing, L_{bc} . The number of baffles N_b is required for calculation of the total number of cross passes and window turnarounds. It is expressed as

$$N_b = \frac{L_{ti}}{L_{bc}} - 1 \quad (5.14)$$

where L_{ti} and L_{bc} are the tube length and central baffle spacing, respectively. Tube length L_{ti} is defined in Figure 5.58. A uniform baffle spacing (L_{bc}) is assumed initially, equal to the shell diameter, D_s . To determine L_{ti} , we must know the tubesheet thickness. If drawings are not available, the tubesheet thickness, L_{ts} , can be roughly estimated as $L_{ts} = 0.1D_s$ with limit $L_{ts} = 25$ mm. Otherwise assume the minimum tubesheet thickness as specified in TEMA [2]. For all bundle types except U-tubes, $L_{ti} = L_{to} - L_{ts}$, whereas for U-tube bundles, L_{to} is nominal tube length.

The number of baffles is rounded off to the lower integer value, and the exact central spacing is then calculated by

$$L_{bc} = \frac{L_{ta}}{N_b + 1} \quad (5.15)$$

5.16.5.3 Auxiliary Calculations, Step-by-Step Procedure

Step 1: Segmental baffle window calculations. Refer to Figure 5.59, which reveals the basic segmental baffle geometry in relation to the tube field. Calculate the centriangle of baffle cut, θ_{ds} , and upper centriangle of baffle cut, θ_{cl} .

The centriangle of baffle cut, θ_{ds} , is the angle subtended at the center by the intersection of the baffle cut and the inner shell wall as shown in Figure 5.59. It is given by

$$\theta_{ds} = 2 \cos^{-1} \left(1 - \frac{2B_c}{100} \right) \quad (5.16)$$

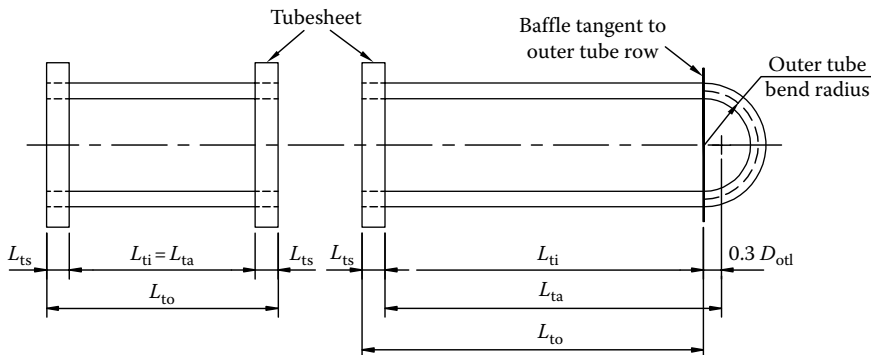


FIGURE 5.58 Shell and tube heat exchanger tube length definition.

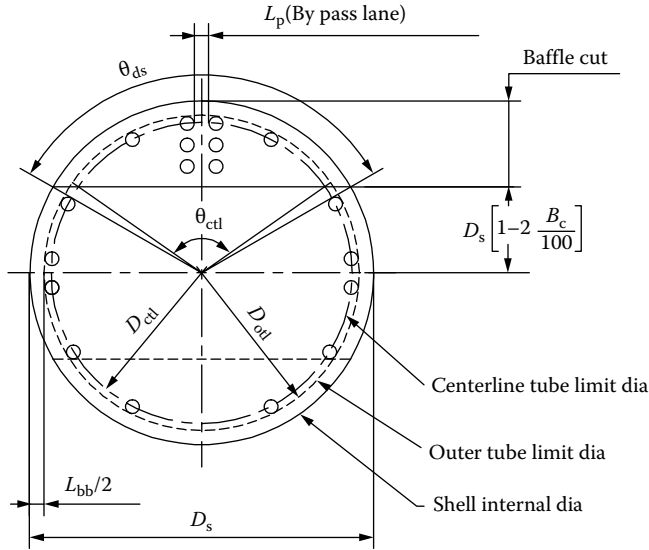


FIGURE 5.59 Basic segmental baffle geometry.

The upper centriangle of baffle cut, θ_{ctl} , is the angle subtended at the center by the intersection of the baffle cut and the tube bundle diameter, as shown in Figure 5.59. It is given by

$$\theta_{ctl} = 2 \cos^{-1} \left[\frac{D_s}{D_{ctl}} \left(1 - \frac{2B_c}{100} \right) \right] \quad (5.17)$$

Step 2: Shellside crossflow area. The shellside crossflow area, S_m , is given by

$$S_m = L_{bc} \left[L_{bb} + \frac{D_{ctl}}{L_{tp,eff}} (L_{tp} - d) \right] \quad (5.18)$$

where

$$L_{bb} = D_s - D_{otl}$$

$$D_{ctl} = D_{otl} - d$$

$$L_{tp,eff} = L_{tp} \quad \text{for } 30^\circ \text{ and } 90^\circ \text{ layouts}$$

$$= 0.707 L_{tp} \quad \text{for } 45^\circ \text{ layouts}$$

$$L_{tp} = \text{tube pitch}$$

Basic tube layout parameters are given in Table 5.2.

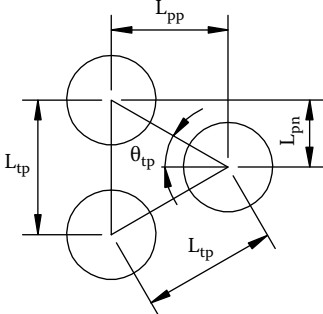
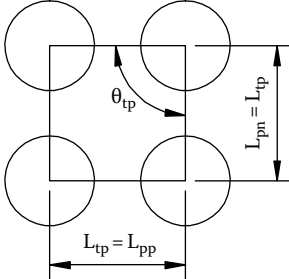
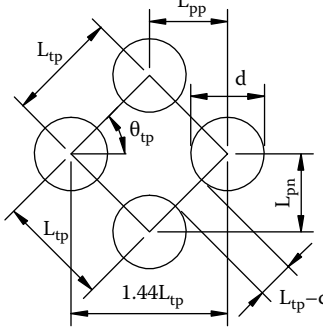
Step 3: Baffle window flow areas. The gross window flow area, i.e., without tubes in the window, S_{wg} , is given by

$$S_{wg} = \frac{\pi}{4} D_s^2 \left(\frac{\theta_{ds}}{2\pi} - \frac{\sin \theta_{ds}}{2\pi} \right) \quad (5.19)$$

From the calculations of centriangle and gross window flow area, calculate the fraction of tubes in baffle window, F_w , and in pure crossflow, F_c , i.e., between the baffle cut tips as indicated in Figure 5.59 by distance $D_s[1 - 2(B_c/100)]$:

$$F_c = 1 - 2F_w \quad (5.20)$$

TABLE 5.2
Tube Layout Basic Parameters

Crossflow →	θ_{tp}	L_{pn}	L_{pp}
	30°	$0.5L_{tp}$	$0.866L_{tp}$
	90°	L_{tp}	L_{tp}
	45°	$0.707L_{tp}$	$0.707L_{tp}$

where F_w is the fraction of number of tubes in the baffle window, given by

$$F_w = \frac{\theta_{ctl}}{2\pi} - \frac{\sin \theta_{ctl}}{2\pi} \quad (5.21)$$

The segmental baffle window area occupied by the tubes, S_{wt} , can be expressed as

$$S_{wt} = N_{tw} \frac{\pi}{4} d^2 \quad (5.22a)$$

$$= N_t F_w \frac{\pi}{4} d^2 \quad (5.22b)$$

The number of tubes in the window, N_{tw} , is expressed as

$$N_{tw} = N_t F_w \quad (5.23)$$

The net crossflow area through one baffle window, S_w , is the difference between the gross flow area, S_{wg} , and the area occupied by the tubes, S_{wt} . Net crossflow area through one baffle window, S_w , is given by

$$S_w = S_{wg} - S_{wt} \quad (5.24)$$

Step 4: Equivalent hydraulic diameter of a segmental baffle window, D_w . The equivalent hydraulic diameter of a segmental baffle window, D_w , is required only for pressure-drop calculations in laminar flow, i.e., if $Re_s < 100$. It is calculated by classical definition of hydraulic diameter, i.e., four times the window crossflow area S_w divided by the periphery length in contact with the flow. This is expressed in the following equation:

$$D_w = \frac{4S_w}{\pi d N_{tw} + \pi D_s \theta_{ds}/2\pi} \quad (5.25)$$

Step 5: Number of effective tube rows in crossflow, N_{tcc} and baffle window, N_{tcw} . The number of effective tube rows crossed in one crossflow section, i.e., between the baffle tips, is expressed as N_{tcc} :

$$N_{tcc} = -\frac{D_s}{L_{pp}} \left(1 - \frac{2B_c}{100} \right) \quad (5.26)$$

where L_{pp} is the effective tube row distance in the flow direction, which is given in Table 5.2. The effective number of tube rows crossed in the baffle window, N_{tcw} , is given by

$$N_{tcw} = \frac{0.8}{L_{pp}} \left[\frac{D_s B_c}{100} - \frac{D_s - D_{ctl}}{2} \right] \quad (5.27)$$

Step 6: Bundle-to-shell bypass area parameters, S_b and F_{sbp} . The bypass area between the shell and the tube bundle within one baffle, S_b , is given by

$$S_b = L_{bc}(D_s - D_{otl} + L_{pl}) \quad (5.28)$$

where L_{pl} expresses the effect of the tube lane partition bypass width (between tube walls) as follows: L_{pl} is 0 for all standard calculations; L_{pl} is half the dimension of the tube lane partition L_p . For estimation purposes, assume that $L_p = d$.

For calculations of the correction factors J_1 and R_1 , the ratio of the bypass area, S_b , to the overall crossflow area, S_m , designated as F_{sbp} , is calculated from the expression

$$F_{sbp} = \frac{S_b}{S_m} \quad (5.29)$$

Step 7: Shell-to-baffle leakage area for one baffle, S_{sb} . The shell-to-baffle leakage area, S_{sb} , is a factor for calculating baffle leakage effect parameters J_1 and R_1 . The diametral clearance between the shell diameter D_s and the baffle diameter D_b is designated as L_{sb} and given by

$$L_{sb} = 3.1 + 0.004D_s \quad (5.30)$$

The shell-to-baffle leakage area within the circle segment occupied by the baffle is calculated as

$$S_{sb} = \pi D_s \frac{L_{sb}}{2} \left(\frac{2\pi - \theta_{ds}}{2\pi} \right) \quad (5.31)$$

Step 8: Tube-to-baffle-hole leakage area for one baffle, S_{th} . The tube-to-baffle-hole leakage area for one baffle, S_{th} , is required for the calculation of the correction factors J_1 and R_1 . The total tube-to-baffle leakage area is given by

$$S_{tb} = \frac{\pi}{4} [(d + L_{tb})^2 - d^2] N_t (1 - F_w) \quad (5.32)$$

where L_{tb} is diametral clearance between tube outside diameter and baffle hole. TEMA standards specify recommended clearances as a function of tube diameter and baffle spacing. Its value is either 0.8 or 0.4.

Step 9: Calculate shellside crossflow velocity, U_s . The shellside crossflow velocity U_s from shellside mass flow rate M_s is given by

$$U_s = \frac{M_s}{\rho_s S_m} \quad (5.33)$$

where ρ_s is the mass density of the shellside fluid. Equation 5.33 gives shellside crossflow velocity as per the Bell–Delaware method. Since flow-induced vibration guidelines given in the TEMA Standards are based on crossflow velocity as per Tinker [37], the procedure to calculate crossflow velocity is given in Appendix 5.A.

5.16.6 SHELLSIDE HEAT TRANSFER AND PRESSURE-DROP CORRECTION FACTORS

Heat transfer correction factors: In the Bell–Delaware method, the flow fraction for each stream is found by knowing the corresponding flow areas and flow resistances. The heat transfer coefficient for ideal crossflow is then modified for the presence of each stream through correction factors. The shellside heat transfer coefficient, h_s , is given by

$$h_s = h_i J_c J_1 J_b J_s J_r \quad (5.34)$$

where h_i is the heat transfer coefficient for pure crossflow of an ideal tube bank. The correction factors in Equation 5.34 are thus:

J_c is the correction factor for baffle cut and spacing. This correction factor is used to express the effects of the baffle window flow on the shellside ideal heat transfer coefficient h_i , which is based on crossflow.

J_1 is the correction factor for baffle leakage effects, including both shell-to-baffle and tube-to-baffle leakage.

J_b is the correction factor for the bundle bypass flow (C and F streams).

J_s is the correction factor for variable baffle spacing in the inlet and outlet sections.

J_r is the correction factor for adverse temperature gradient buildup in laminar flow.

The combined effect of all of these correction factors for a reasonably well-designed shell and tube heat exchanger is typically of the order of 0.6; i.e., the effective mean shellside heat transfer coefficient for the exchanger is of the order of 60% of that calculated if the flow took place across an ideal tube bank corresponding in geometry to one crossflow section. It is interesting to note that this value was suggested by McAdams [47] in 1933 and has been used as a rule of thumb [1].

Pressure-drop correction factors: The following three correction factors are applied for pressure drop:

1. Correction factor for bundle bypass effects, R_b
2. Correction factor for baffle leakage effects, R_1
3. Correction factor for unequal baffle spacing at inlet and/or outlet, R_s

5.16.6.1 Step-by-Step Procedure to Determine Heat Transfer and Pressure-Drop Correction Factors

Step 10: Segmental baffle window correction factor, J_c . For the baffle cut range 15%–45%, J_c is expressed by

$$J_c = 0.55 + 0.72F_c \quad (5.35)$$

This value is equal to 1.0 for NTIW design, increases to a value as high as 1.15 for small baffle cut, and decreases to a value of about 0.52 for very large baffle cuts. A typical value for a well-designed heat exchanger with liquid on the shellside is about 1.0.

Step 11: Correction factors for baffle leakage effects for heat transfer, J_1 , and pressure drop, R_1 . The correction factor J_1 penalizes the design if the baffles are put too close together, leading to an excessive fraction of the flow being in the leakage streams compared to the crossflow stream. R_1 is the correction factor for baffle leakage effects. For computer applications, the correction factors are curve-fitted as follows:

$$J_1 = 0.44(1 - r_s) + [1 - 0.44(1 - r_s)]e^{-2.2n_m} \quad (5.36)$$

$$R_1 = \exp[-1.33(1 + r_s)]r_{lm}^x \quad (5.37)$$

where

$$x = [-0.15(1 + r_s) + 0.8] \quad (5.38)$$

The correlational parameters used are

$$r_s = \frac{S_{sb}}{S_{sb} + S_{tb}} \quad (5.39)$$

$$r_{lm} = \frac{S_{sb} + S_{tb}}{S_m} \quad (5.40)$$

where

S_{sb} is the shell-to-baffle leakage area

S_{tb} the tube-to-baffle leakage area

S_m the crossflow area at bundle centerline

A well-designed exchanger should have a value of J_1 , not less than 0.6, preferably in the range 0.7–0.9. If a low J_1 value is obtained, modify the design with wider baffle spacing, increase tube pitch, or change the tube layout to 90° or 45°. More drastic measures include change to double or triple segmental baffles, TEMA J shell type, or both. A typical value for R_1 is in the range of 0.4–0.5, though lower values may be found in exchangers with closely spaced baffles.

Step 12: Correction factors for bundle bypass effects for heat transfer, J_b , and pressure drop, R_b . To determine J_b and R_b , the following parameters must be known:

1. N_{ss} , the number of sealing strips (pairs) in one baffle spacing
2. N_{tce} , the number of tube rows crossed between baffle tips in one baffle section

The expression for J_b is correlated as

$$J_b = \exp\left\{-C_{bh}F_{sbp}\left[1 - (2r_{ss})^{1/3}\right]\right\} \quad (5.41)$$

where

$$C_{bh} = 1.25 \text{ for laminar flow, } Re_s \leq 100, \text{ with the limit of } J_b = 1, \text{ at } r_{ss} \geq 0.5$$

$$= 1.35 \text{ for turbulent and transition flow, } Re_s > 100$$

The expression for R_b is given by

$$R_b = e^{[-C_{bp}F_{sbp}\{1-(r_{ss})^{1/3}\}]} \quad (5.42)$$

where

$$r_{ss} = \frac{N_{ss}}{N_{tcc}} \quad (5.43)$$

with the limits of

$$R_b = 1 \quad \text{at } r_{ss} \geq 0.5$$

$$C_{bp} = 4.5 \quad \text{for laminar flow, } Re_s \leq 100$$

$$= 3.7 \quad \text{for turbulent and transition flow, } Re_s > 100$$

For the relatively small clearance between the shell and the tube bundle, J_b is about 0.9; for the much larger clearance required by pull-through floating head construction, it is about 0.7. J_b can be improved using sealing strips.

A typical value for R_b ranges from 0.5 to 0.8, depending upon the construction type and number of sealing strips. The lower value would be typical of a pull-through floating head with only one or two pairs of sealing strips, and the higher value typical of a fully tubed fixed tubesheet exchanger.

Step 13: Heat transfer correction factor for adverse temperature gradient in laminar flow, J_r . J_r applies only if the shellside Reynolds number is less than 100 and is fully effective only in deep laminar flow characterized by Re_s less than 20. For $Re_s < 20$, J_r can be expressed as

$$J_r = \frac{1.51}{N_c^{0.18}} \quad (5.44)$$

where N_c is the total number of tube rows crossed in the entire exchanger. N_c is given by

$$N_c = (N_{tcc} + N_{tcw})(N_b + 1) \quad (5.45)$$

For Re_s between 20 and 100, a linear proportion is applied resulting in

$$J_r = \frac{1.51}{N_c^{0.18}} + \left(\frac{20 - Re_s}{80} \right) \left(\frac{1.51}{N_c^{0.18}} - 1 \right) \quad (5.46)$$

with the limit

$$J_r = 0.400 \quad \text{for } Re_s \leq 100$$

$$J_r = 1 \quad \text{for } Re_s > 100$$

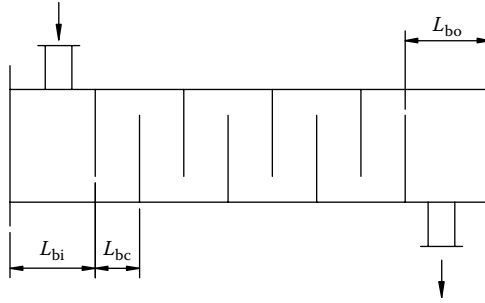


FIGURE 5.60 Typical layout of baffle spacing.

Step 14: Heat transfer correction for unequal baffle spacing at inlet and/or outlet, J_s . Figure 5.60 shows a schematic sketch of an exchanger where the inlet and outlet baffle spacing L_{bi} and L_{bo} are shown in comparison to the central baffle spacing, L_{bc} :

$$J_s = \frac{(N_b - 1) + \left(L_i^*\right)^{1-n} + \left(L_o^*\right)^{1-n}}{(N_b - 1) + \left(L_i^* - 1\right) + \left(L_o^* - 1\right)} \quad (5.47)$$

where

$$L_i^* = \frac{L_{bi}}{L_{bc}} \quad L_o^* = \frac{L_{bo}}{L_{bc}} \quad (5.48)$$

J_s will usually be between 0.85 and 1.0. If $L_{bi} = L_{bo} = L_{bc}$ or $L^* = L_i^* = L_o^* = 1.0$, $J_s = 1.0$. For turbulent flow, $n = 0.6$, and values of L^* larger than 2 would be considered poor design, especially if combined with a few baffles only, i.e., low N_b . In such a case, an annular distributor or other measures should be used. Typical arrangements for increasing effectiveness of end zones are presented by Tinker [36]. For laminar flow, the correction factor is about halfway between 1 and J_s computed for turbulent conditions.

Step 15: Pressure-drop correction for unequal baffle spacing at inlet and/or outlet, R_s . R_s is given by

$$R_s = \left(\frac{1}{L_i^*}\right)^{2-n} + \left(\frac{1}{L_o^*}\right)^{2-n} \quad (5.49)$$

with $n = 1$ for laminar flow, $Re_s \leq 100$, and $n = 0.2$ for turbulent flow.

1. For $L_{bc} = L_{bo} = L_{bi}$, $R_s = 2$.
2. For the reasonable extreme case $L_{bo} = L_{bi} = 2L_{bc}$, $R_s = 1.0$ for laminar flow, and $R_s = 0.57$ for turbulent flow.
3. For a typical U-tube, $L_{bi} = L_{bc}$ and $L_{bo} = 2L_{bc}$, $R_s = 1.5$ for laminar flow, and $R_s = 3.0$ for turbulent flow.

5.16.6.2 Shellside Heat Transfer Coefficient and Pressure Drop

5.16.6.2.1 Shellside Heat Transfer Coefficient

1. Calculate the shellside mass velocity G_s , Reynolds number Re_s , and Prandtl number Pr_s :

$$G_s = \frac{M_s}{S_m} \text{ kg}/(\text{m}^2 \cdot \text{s}) \quad \text{or} \quad \text{lb}_m/(\text{h} \cdot \text{ft}^2) \quad (5.50)$$

$$Re_s = \frac{dG_s}{\mu_s} \quad Pr_s = \frac{\mu_s C_{ps}}{k_s} \quad (5.51)$$

2. Calculate the ideal heat transfer coefficient h_i given by

$$h_i = \frac{j_i C_{ps} G_s (\phi_s)^n}{Pr_s^{2/3}} \quad (5.52)$$

where j_i and $(\phi_s)^n$ are defined next.

The term j_i is the ideal Colburn j factor for the shellside and can be determined from the appropriate Bell–Delaware curve for the tube layout and pitch and a typical curve. For example, $d = 0.75$ in. (19.05 mm), pitch = 1.0 in. (25.4 mm), and $\theta_{tp} = 30^\circ$; curve fits for j_i are given by Bell [40]:

$$j_i = 1.73 Re_s^{(-0.694)} \quad 1 \leq Re_s < 100 \quad (5.53a)$$

$$= 0.717 Re_s^{(-0.574)} \quad 100 \leq Re_s < 1000 \quad (5.53b)$$

$$= 0.236 Re_s^{(-0.346)} \quad 1000 \leq Re_s \quad (5.53c)$$

The term $(\phi_s)^n$ is the viscosity correction factor, which accounts for the viscosity gradient at the tube wall (μ_w) versus the viscosity at the bulk mean temperature (μ_s) of the fluid and is given by [48]:

$$(\phi_s)^n = \left(\frac{\mu_s}{\mu_w} \right)^{0.14} \quad (5.54)$$

For liquids, ϕ_s is greater than 1 if the shellside fluid is heated and less than 1 if shellside fluid is cooled. In order to determine μ_w , it is essential to determine T_w , which is estimated as follows using the approximate values of h_t and h_s [48]:

$$T_w = T_{t,av} + \frac{T_{s,av} - T_{t,av}}{1 + h_t/h_s} \quad (5.55)$$

where $T_{s,av}$ and $T_{t,av}$ denote the average mean metal temperatures of shell and tube, both of them being the arithmetic means of inlet and outlet fluid temperatures on the shellside and tubeside, respectively. The mean temperature calculation method for shellside and tubeside fluids and mean

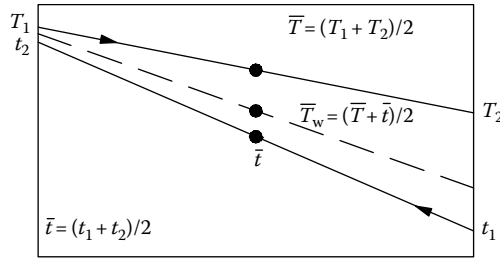


FIGURE 5.61 Mean temperature calculation method for shellside and tubeside fluids and mean metal temperature for conduction wall.

metal temperature for conduction wall is shown graphically in Figure 5.61. An accurate equation to calculate tube mean metal temperature is given by TEMA. For gases, the viscosity is a weak function of temperature. The correction factor ϕ_s is formulated as follows:

$$\text{For gases being cooled: } (\phi_s)^n = 1.0 \quad (5.56)$$

$$\text{For gases being heated } (\phi_s)^n = \left[\frac{(T_{s,av} + 273.15)}{(T_w + 273.15)} \right]^{0.25} \quad (5.57)$$

For a gas being heated, T_w is always higher than $T_{s,av}$ and hence the correction factor is less than 1.0. Calculate the shellside heat transfer coefficient given by

$$h_s = h_i J_c J_1 J_s J_b J_r \quad (5.58)$$

5.16.6.2.2 Shellside Pressure Drop

The shellside pressure drop is calculated in the Delaware method by summing the pressure drop for the inlet and exit sections, and the internal sections after applying various correction factors. The total shellside pressure drop Δp_s consists of the pressure drop due to (1) crossflow Δp_c , (2) window regions Δp_w , and (3) entrance and exit sections Δp_e as given by Refs. [39,40]:

$$\Delta p_s = \Delta p_c + \Delta p_w + \Delta p_e \quad (5.59)$$

The elements of shellside pressure drop are shown schematically in Figure 5.62. The crossflow pressure drop and the entrance and exit region pressure drop depend on the ideal tube bank pressure drop, given by

$$\Delta p_{b,i} = 2 f_s N_{icc} \frac{G_s^2}{g_c \rho_s} (\phi_s)^{-n} \quad (5.60)$$

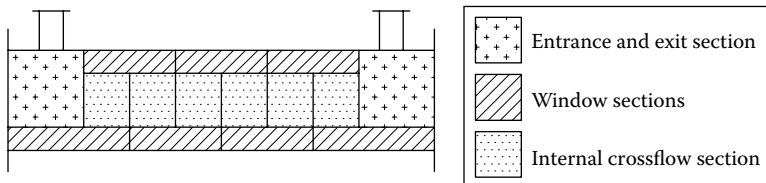


FIGURE 5.62 Elements of shellside pressure drop of a TEMA E shell.

The friction factor f_s can be determined from the appropriate Bell–Delaware curve for the tube layout and pitch under consideration. For example, for $d = 0.75$ in. (19.05 mm), pitch = 1.0 in. (25.4 mm), and $\theta_{ip} = 30^\circ$, curve fits for f_s are given by Bell [40]:

$$f_s = \frac{52}{Re_s} + 0.17 \quad 1 \leq Re_s < 500 \quad (5.61a)$$

$$= 0.56 Re_s^{(-0.14)} \quad 500 \leq Re_s \quad (5.61b)$$

Calculate the various terms of shellside pressure drop as given next and finally calculate the overall heat transfer coefficient.

1. The pressure drop in the interior crossflow sections is affected by both bypass and leakage. Therefore, the combined pressure drop of all the interior crossflow sections is given by

$$\Delta p_c = (N_b - 1)(\Delta p_{b,i} R_b R_l) \quad (5.62)$$

2. The pressure drop in the entrance and exit sections is affected by bypass but not by leakage, and by variable baffle spacing. Therefore, the combined pressure drop for the entrance and exit sections is

$$\Delta p_e = 2(\Delta p_{b,i}) \left(1 + \frac{N_{tcw}}{N_{tcc}} \right) R_b R_s \quad (5.63)$$

3. The pressure drop in the windows is affected by leakage but not by bypass. Therefore, the combined pressure drop of all the window sections is given by

$$\Delta p_w N_b R_l \quad (5.64)$$

where Δp_w is given as follows:

For $Re_s \geq 100$,

$$\Delta p_w = \frac{(2 + 0.6 N_{tcw}) G_w^2}{2 g_c \rho_s} \quad (5.65)$$

For $Re_s < 100$,

$$\Delta p_w = 26 \frac{G_w \mu_s}{g_c \rho_s} \left(\frac{N_{tcw}}{L_{ip} - d} + \frac{L_{bc}}{D_w^2} \right) + 2 \frac{G_w^2}{g_c \rho_s} \quad (5.66)$$

in which the window mass velocity G_w is given by

$$G_w = \frac{M_s}{\sqrt{S_m S_w}} \quad (5.67)$$

Summing these individual effects, we obtain the equation for the total nozzle-to-nozzle shellside pressure drop:

$$\Delta p_s = [(N_b - 1)(\Delta p_{b,i} R_b) + N_b(\Delta p_w)] R_l + 2(\Delta p_{b,i}) \left(1 + \frac{N_{tcw}}{N_{tcc}} \right) R_b R_s \quad (5.68)$$

The total shellside pressure drop of a typical shell and tube exchanger is of the order of 20%–30% of the pressure drop that would be calculated for flow through the corresponding heat exchanger without baffle leakage and without tube bundle bypass effects [39].

5.16.6.3 Tubeside Heat Transfer Coefficient and Pressure Drop

5.16.6.3.1 Tubeside Heat Transfer Coefficient

1. Calculate the tubeside mass velocity G_t , Reynolds number Re_t , and Prandtl number, Pr_t :

$$G_t = \frac{M_t}{A_t} \quad \text{for single pass} \quad (5.69a)$$

$$= \frac{M_t}{A_t/N_p} \quad \text{for } N_p \text{ passes} \quad (5.69b)$$

where

$$A_t = \frac{\pi}{4} d_i^2 N_t$$

and where A_t is the tubeside flow area, N_p the number of tubeside passes, N_t the number of tubes, and

$$Re_t = \frac{G_t d_i}{\mu_i} \quad Pr_t = \frac{\mu_i C_{pt}}{k_t} \quad (5.70)$$

2. Calculate the tubeside heat transfer coefficient, h_t : For laminar flow with Re_t of 2100 and less, the heat transfer coefficient is determined from the Sider–Tate (1936) empirical equation for both heating and cooling of viscous liquids:

$$\frac{h_t d_i}{k_i} = 1.86 \left[Re_t Pr_t \frac{d_i}{L} \right]^{0.5} Pr_t^{1/3} \left(\frac{\mu_t}{\mu_w} \right)^{0.14} \quad (5.71)$$

For those cases where the Grashof number Na_r exceeds 25,000, the value of h_t obtained from Equation 5.71 must be corrected for the increase in heat transfer due to natural convection effects by multiplying by the term

$$0.8 \left(1 + 0.015 Na_r^{1/3} \right) \quad (5.71a)$$

$$Na_r = \frac{\beta \Delta t d_i^2 \rho_i^2 g_c}{\mu_t^2} \quad (5.71b)$$

where

β is the thermal coefficient of cubical expansion, $1/^\circ\text{F}$

Δt is the temperature difference, $^\circ\text{F}$

Na_r is the Grashof number

ρ_i is the tubeside fluid density, lb/ft^3

g_c is the acceleration of gravity, $4.17 \times 10^8 \text{ ft/h}^2$

μ_t is the viscosity at bulk mean temperature, lb/h ft

At values above 10,000, turbulent flow occurs and the heat transfer coefficient is determined from the following correlation:

Sieder–Tate equation modified by McAdams:

$$\frac{h_i d_i}{k_t} = 0.027 \text{Re}_t^{0.8} \text{Pr}_t^{1/3} \left(\frac{\mu_t}{\mu_w} \right)^{0.14} \quad (5.72)$$

In the intermediate region where Reynolds number varies from 2,100 to 10,000, the relation does not follow a straight line.

Colburn equation

$$\frac{h_i d_i}{k_t} = 0.023 \text{Re}_t^{0.8} \text{Pr}_t^{0.4} \left(\frac{\mu_t}{\mu_w} \right)^{0.14} \quad (5.73a)$$

Dittus–Boelter equation

$$\frac{h_i d_i}{k_t} = 0.023 \text{Re}_t^{0.8} \text{Pr}_t^n \quad (5.73b)$$

where

$n = 0.4$ for heating

$= 0.3$ for cooling

In the intermediate region where Re_t varies between 2,100 and 10,000, the relation does not follow a straight line. In this region, Kern [40] recommends the following formula:

$$\frac{h_i d_i}{k_t} = 0.116 \left[\text{Re}_t^{2/3} - 125 \right] \left[1 + \left(\frac{d_i}{L} \right)^{2/3} \right] \text{Pr}_t^{1/3} \left(\frac{\mu_t}{\mu_w} \right)^{0.14} \quad (5.74)$$

5.16.6.3.2 Tubeside Pressure Drop

Pressure drop in tubes and pipes—general: For tubes and pipes, the pressure drop in steady flow between any two points may be expressed by the following Weisbach–Darcy equation:

$$\Delta p_t = f_t \left(\frac{L}{d_i} \right) \frac{G_t^2}{2g_c \rho_t} \frac{1}{(\varphi_t)^f} \quad (5.75)$$

where

$$(\phi_t)^r = \left(\frac{\mu_t}{\mu_w} \right)^{0.14} \quad \text{for } Re_t > 2100 \quad (5.76a)$$

$$= \left(\frac{\mu_t}{\mu_w} \right)^{0.25} \quad \text{for } Re_t < 2100 \quad (5.76b)$$

and where L is the length of pipe between two points, d_i the inside diameter of the pipe, ρ_t the mass density of the tubeside fluid, G_t the mass velocity of the fluid inside the pipe, k_i or k_t is thermal conductivity of the tubeside fluid, and f_t the friction factor. To determine the pressure drop through the tube bundle, multiply the pressure drop by the number of tubes. For multipass arrangements, multiply by the number of tubeside passes.

The total pressure drop for a single pass consists of the following items:

1. Pressure drop in the nozzles, Δp_n , which is the sum of pressure drop in the inlet ($\Delta p_{n,i}$) and outlet nozzle ($\Delta p_{n,o}$):

$$\Delta p_n = \frac{1.5 G_n^2}{2 g_c \rho_t} \quad (5.77)$$

2. Sudden contraction and expansion losses at the tube entry and exit, $\Delta p_{c,e}$, is given by

$$\Delta p_{c,e} = \frac{G_t^2}{2 g_c \rho_t} (K_c + K_e) N_p \quad (5.78)$$

where K_c and K_e are the contraction and expansion loss coefficients.

3. Pressure drop through the tube bundle, Δp_t :

$$\Delta p_t = \frac{f L_{tp} G_t^2 N_p}{2 g_c \rho_t d_i} \frac{1}{\phi_t^r} \quad (5.79)$$

4. Pressure drop associated with the turning losses, Δp_r , given by

$$\begin{aligned} \Delta p_r &= \frac{4 N_p G_t^2}{2 g_c \rho_t} \\ &= 4 N_p \times \text{Velocity head per pass} \end{aligned} \quad (5.80)$$

Total tubeside pressure drop, Δp_t , is given by

$$\Delta p_t = \frac{G_t^2}{2 g_c \rho_t} \left[\frac{1.5}{N_p} + \frac{f L_{tp}}{d_i} \frac{1}{(\phi_t)^r} + K_c + K_e + 4 \right] N_p \quad (5.81)$$

Determination of friction factor f on the tubeside: The friction factor f has been found to depend upon Reynolds numbers only. For laminar flow in smooth pipes, the value of f can be derived from the well-known Hagen–Poiseuille equation.

Accordingly, f for laminar flow is given by

$$f = \frac{64}{\text{Re}_t} \quad (5.82)$$

For turbulent flow in smooth pipes, f can be determined from the Blasius empirical formula given by

$$f = \frac{0.3164}{\text{Re}_t^{0.25}} \quad (5.83)$$

This equation is valid for Reynolds numbers up to 1,000,000. Another formula to determine f for smooth-walled conduits in the Reynolds number range 10,000–120,000 is given by [49]

$$f = \frac{0.184}{\text{Re}_t^{0.2}} \quad (5.84)$$

Calculate the overall heat transfer coefficient, U , as per Equation 5.7 using the values of h_s and h_t from Equations 5.53 and 5.71, respectively.

Calculate heat transfer area, A_o , required using Equation 5.9 using the U value calculated earlier.

5.16.6.3.3 Evaluation and Comparison of the Results with the Specified Values

In the evaluation stage, the calculated values of the film coefficients and the pressure drop, for both the streams, are compared with the specified values. If the values match, the design is complete. If the calculated values and the specified values do not match, repeat the design with new design variables. Sometimes, even after many iterations, the design may not meet the specified performance limits in the following parameters [26]:

1. Heat transfer coefficient
2. Pressure drop
3. Temperature driving force
4. Fouling factors

Taborek [26] describes various measures to overcome limitations in these parameters. For the heat transfer-limited cases, utilize the permissible pressure drop effectively. The film coefficients can be increased by increasing the flow velocities, changing the baffle spacing, changing the number of the tubeside passes, etc. Attempts to increase the heat transfer coefficient also results in pressure-drop increase. Designs with inherently low heat transfer coefficients, such as laminar flow or LP gases, may deserve special attention. For pressure-drop-limited cases, try alternate designs such as [26] the following:

- Double or multiple segmental baffles
- Use TEMA J or X shell
- Reduce tube length
- Increase tube pitch
- Change tube layout pattern

For the temperature-driving-force-limited cases, methods to improve the LMTD correction factor have been discussed while describing various shell types and pass arrangements. Fouling-limited

cases are dealt with during the design stage by making sure that the factors promoting fouling are suppressed and/or designed for periodic cleaning.

5.16.6.4 Accuracy of the Bell–Delaware Method

It should be remembered that this method, though apparently generally the best in the open literature, is not extremely accurate [13]. Palen et al. [13] compare the thermohydraulic performance prediction error of Bell–Delaware methods [38,39], stream analysis methods [13], and Tinker [37].

5.16.6.5 Extension of the Delaware Method to Other Geometries

The Delaware method, as originally developed and as it exists in the open literature, is more or less explicitly confined to the design of fully tubed *E* shell configurations using plain tubes. Extension of this method to other geometries is discussed in Refs. [15,27], and these are discussed in this subsection.

Applications to low-finned tubes: It is possible to apply the Delaware method to the design of such heat exchangers in a fairly straightforward way by making use of the results of Brigs and Young [50] and Briggs, Katz, and Young [51]. As shown by Briggs et al. [51], the Colburn *j* factor for low-finned tubes is slightly less than that for a plain tube in the Reynolds number range about 2–1000; the difference is larger in the lower Reynolds number range. The fin-tube *j* factor j_f can be represented in terms of plain-tube-bank *j* factor as j_i as [15]

$$j_f = K_f j_i \quad (5.85)$$

where K_f is the correction factor whose values, taken from Ref. [50], are presented in Ref. [15]. Its approximate values at discrete points are as follows:

Re	20	70	100	200	400	600	800–1000
K_f	0.575	0.65	0.675	0.75	0.885	0.975	1.0

For the fin tube friction factor, Bell [39,40] suggests a conservative value that is 1.5 times those for the corresponding plain tube bank, whereas Taborek [15] recommends 1.4 times the friction factor of the plain tube bank. The adaptation of the Bell–Delaware method to finned tubes is explained in Refs. [15,27].

Application to the no-tubes-in-window configuration: In calculations, use $N_{cw} = 0$ and the baffle configuration correction factor $J_c = 1$. Otherwise, the calculation is essentially identical to a fully tubed bundle. It is suggested that one choose a smaller baffle cut so that the free flow area through the window corresponds reasonably closely to the free crossflow area through the tube bank itself.

*Application to *F* shells:* Since the shellside is essentially split into two, it is possible to adopt the Delaware method by reducing all of the areas for flow by half compared to the case for a single shellside pass. It is assumed that the flow leakage and conduction across the longitudinal baffle are minimized.

*Application to *J* shells:* The adaptation of the method to a *J* shell is straightforward. Take one-half the length of the exchanger as a “unit” equivalent to an *E* shell and take one-half the mass flow rate.

Application to double segmental and disk and doughnut exchangers: According to Taborek [15], the Bell–Delaware method cannot be easily adapted to these baffle types, as the driving forces for bypass and leakage flow are much smaller than for segmental baffles.

Software for thermal design of shell and tube heat exchanger: Nowadays most of the exchangers are designed using commercially available software such as Xchanger Suite6® of HTRI [52] and Aspen Shell & Tube Mechanical of HTFS, Oxon, UK [53], among others. Typical features of thermal design program structure of shell and tube heat exchanger are shown in Table 5.3, and output program in Table 5.4. These methods are generally restricted for use by members of the organizations.

TABLE 5.3
Typical Features of Thermal Design Program Structure of Shell and Tube Heat Exchanger

Specification	Description
Process parameters	Heat duty, inlet parameters, pressure drop, fouling resistances
TEMA class	TEMA <i>R, B, C</i>
TEMA exchanger types	Front head: <i>A, B, C, D, N</i> Shell: <i>E, F, G, H, J, K, X</i> Rear head: <i>L, M, N, P, S, T, U, W</i>
Tubesheet	Single tubesheet (also OTL, untubed area), double tubesheet
Tube details	Plain tube, integral low finned tube, tube material, tube diameters, and tube length. For U-tubes, U-bend details
Baffle types	Single segmental, double segmental, triple segmental, no tubes in window, disk and doughnut, RODbaffles, EMBaffle®, etc.
Plate baffle details	Inlet, central, and outlet baffle spacings
Impingement protection	Plate or rod type on shellside
Baffle cuts	Horizontal, vertical, rotated, % baffle cut, baffle spacing
Tube patterns	Triangular, rotated triangular, square, rotated square, and pitch
Tube passes	Possible: 1–16 (odd or even). Specify the number of tube passes
Pass layout types	Quadrant, mixed, ribbon
Shell details	Diameter, length, number of shells in series/parallel
Nozzles	Number, inside diameter, orientation, etc.
Tubeside heat transfer calculation (sensible heat)	Laminar flow, turbulent flow—colburn
Single-phase frictional pressure drop	Method, Dittus–Boelter equation Blasius equation or others
Method to calculate shellside pressure drop and film coefficients for single-phase sensible flow	Stream-analysis method, Bell–Delaware method
Special operating conditions	Start-up, transient, and shutdown

TABLE 5.4
Typical Features of Output of Thermal Design Program of Shell and Tube Heat Exchanger

Design summary	An overview of the most important variables: shell and tubeside temperatures, flow rates, heat transfer coefficients, velocities, and pressure drops. Description of key heat exchanger dimensions and geometry
TEMA specification sheet	Filling up of TEMA specification sheet (English/Metric units)
Performance evaluation	Required area and distribution of resistances in clean, specified fouling, and maximum fouling conditions
Heat transfer coefficients	Film coefficients and their components
MTD and heat flux	LMTD, <i>F</i> -correction factors, heat fluxes, and heat flux limitations. Heating curves
Pressure drop	Clean and dirty conditions, velocity and pressure-drop distribution from inlet to outlet zone
Shellside flow data	Stream analysis—flow fractions and pV^2 analysis (per TEMA)
Construction of tube bundle	Baffle and tube layout details, tube count, bundle diameter, shell-to-tube-bundle clearances, etc.
Flow-induced vibration analysis details	Critical velocity and natural frequency, fluid elastic instability and turbulent buffeting analysis, frequency matching for acoustic and vortex shedding at inlet, bundle, outlet, and user specified spans
Recap of design cases	Concise summary of alternative solutions that have been explored and their costs

5.17 SHELL AND TUBE HEAT EXCHANGERS WITH NON-SEGMENTAL BAFFLES

5.17.1 PHILLIPS RODBAFFLE HEAT EXCHANGER

The RODbaffle exchanger is a shell and tube heat exchanger that uses an improved support system for the tubes. It consists of rods located in a predisposed manner such that they confine tube movement. RODbaffle heat exchangers are used in process industries to enhance thermohydraulic performance, eliminate flow-induced tube vibration occurrence, minimize shellside pressure losses, increase shellside flow-field uniformity, and reduce shellside fouling [54]. The RODbaffle concept and design came about as a result of tube vibration failures in three shell and tube exchanger bundles resulting in frequent plant shutdowns in a Phillips Petroleum plant in 1970. The emergency repairs made included the substitution of rod tube supports for the plate baffles, resulting in significantly improved operating characteristics. This was the starting point of the RODbaffle concept. References [54–59] provide general and specific information on RODbaffle heat exchanger design.

5.17.1.1 RODbaffle Exchanger Concepts

The RODbaffle exchangers (Figure 5.63) use rods, with a diameter equal to the clearance between tube rows, inserted between alternate tube rows in the bundle in both the horizontal and vertical directions. The support rods are laid out on a square pitch with no nominal clearance between tubes and support rods. Support rods are welded at each end to a fabricated circumferential baffle ring. Major components of each individual RODbaffle are support rods, baffle ring, cross-support strips, partition blockage plate, and longitudinal slide bars. Concept of RODbaffle heat exchanger is shown in Figure 5.63a. Four different RODbaffle configurations, W–X–Y–Z are welded to longitudinal

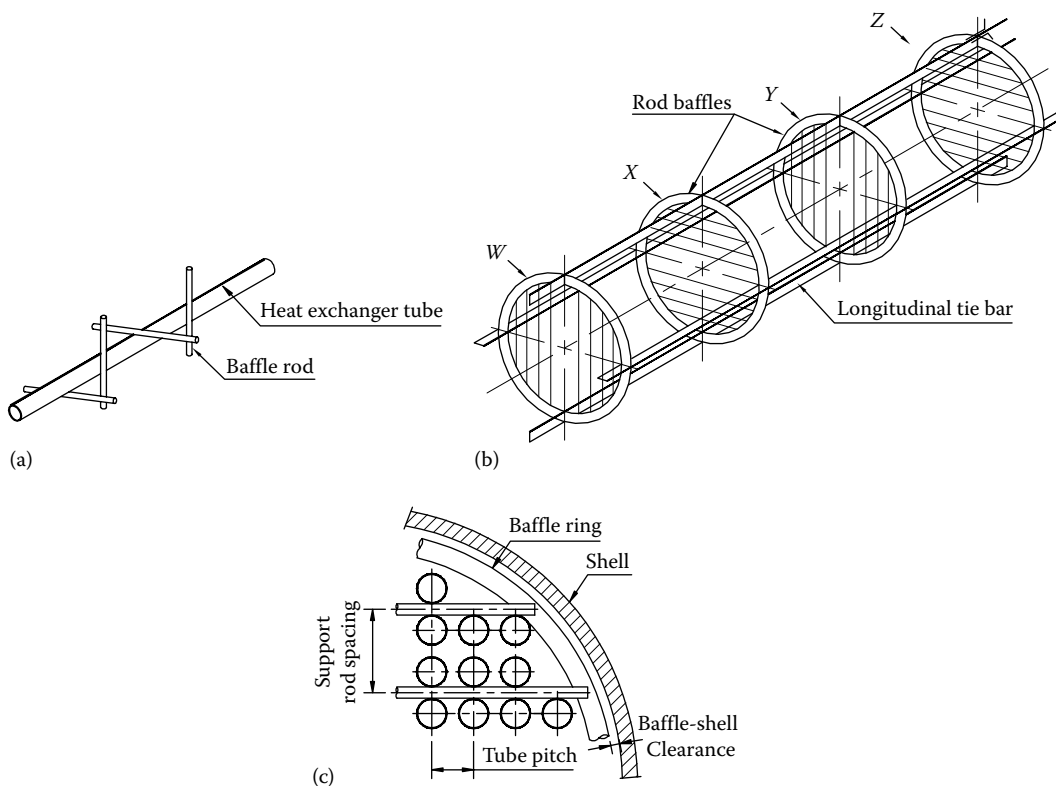


FIGURE 5.63 RODbaffle heat exchanger and support. (a) Concept—schematic, (b) RODbaffle cage assembly, and (c) tube and rod layout.

slide bars to form the RODbaffle cage assembly as shown in Figure 5.63b. Tube and rod layout is shown in Figure 5.63c.

5.17.1.2 Important Benefit: Elimination of Shellside Flow-Induced Vibration

Although RODbaffle heat exchangers are being increasingly used because of thermohydraulic advantages, flow-induced vibration protection of tubes remains one of the major design considerations. The RODbaffle bundle eliminates harmful flow-induced vibration by using these major design innovations:

1. Each tube is supported in all four directions
2. Positive four-point confinement of the tubes
3. Minimum convex point contact between rods and tubes

Since these exchangers have longitudinal flow fields, vortex shedding and fluid elastic instability mechanisms (which lead to flow-induced tube vibration in crossflow exchangers) are not present. Similarly, because zero nominal clearance exists between tubes and support rods, fretting wear and collision damage that may occur in plate baffle units are not evident in RODbaffle exchangers. Under design conditions where plate baffles are required and positive tube support is critical, combination RODbaffle–plate–baffle exchangers may be used [55].

5.17.1.3 Proven RODbaffle Applications

Typical applications for RODbaffle exchangers include gas–gas exchangers, compressor after-coolers, gas–oil coolers, reactor feed–effluent exchangers, condensers, kettle reboilers, waste heat boilers, HF acid coolers, and carbon black air preheaters.

5.17.1.4 Operational Characteristics

The unobstructed flow path created by the support rod matrix makes the flow field in a RODbaffle heat exchanger predominantly longitudinal. Longitudinal flow fields produce the highest thermohydraulic effectiveness of any commercial heat exchanger geometry. The main characteristics of longitudinal flow on the outside of tube bundles include the following [60]:

1. Extremely LP drop and a very high effectiveness of pressure drop to heat transfer conversion, compared to baffled crossflow pattern. In longitudinal flow, the friction occurs directly at the heat transfer surface, and there are no parasitic pressure losses due to window turnarounds.
2. Uniformity of flow distribution, without any stagnant areas characteristic of segmental baffle exchangers, results in uniform local heat transfer rates and less fouling.
3. The grid baffles not only increase pressure drop through the flow contraction process, but also enhance heat transfer.

As reported in Refs. [55,56], RODbaffle exchanger heat transfer rates compare favorably with double segmental plate baffle exchangers and are generally higher than that in comparable triple segmental plate baffle and “NTIW” designs. Shellside pressure losses in RODbaffle exchangers are lower because neither bundle crossflow form drag nor repeated flow reversal effects are present.

5.17.1.5 Thermal Performance

For shellside, the expressions for Nusselt number, Nu , for laminar flow and turbulent flow are given by [59]

$$Nu = C_L Re_h^{0.6} Pr^{0.4} (\phi_s)^n \quad \text{for laminar flow} \quad (5.86a)$$

$$Nu = C_T Re_h^{0.8} Pr^{0.4} (\phi_s)^n \quad \text{for turbulent flow} \quad (5.86b)$$

where C_L and C_T are RODbaffle exchanger geometric coefficient functions for laminar flow and turbulent flow, respectively.

Pressure drop: Shellside pressure loss for flow through a RODbaffle heat exchanger bundle, excluding inlet and exit nozzles, is defined as the sum of an unbaffled frictional component, Δp_L , and a baffle flow contribution Δp_b as [54]:

$$\Delta p = \Delta p_L + \Delta p_b \quad (5.87)$$

According to Gentry [54], shellside pressure losses in RODbaffle exchangers are generally less than 25% of shellside losses produced in comparable double segmental plate baffle exchangers.

5.17.1.6 Design and Rating Program Available

Phillips Petroleum engineers have an ongoing development and testing program on RODbaffle exchangers from which they have developed basic correlations to predict heat transfer and pressure drop. The correlations are based on experimental data obtained from different bare and low-finned tube test bundles using water, light oil, and air as test fluids. The program is available for use on an IBM mainframe or IBM PC or equivalent.

5.17.2 EMbaffle® HEAT EXCHANGER*

The patented EMbaffle design uses expanded metal baffles made of plate material that has been slit and expanded. Figure 5.64a shows a section of EMbaffle. The open structure results in a low hydraulic resistance and enhanced heat transfer. With this new EMbaffle technology, the shell-side fluid flows axially along the tubes, but in the vicinity of the baffles, the flow area is reduced. This creates local turbulence in the flow while breaking up the boundary layer over the tubes. The shape of the grid induces a local crossflow component on top of the longitudinal flow pattern, which together improve the heat transfer characteristics at the surface of the tubes. The breakup of the boundary layer occurs repeatedly at each expanded metal baffle along the length of the heat exchanger, resulting in lower hydraulic resistance while maintaining higher heat transfer [61]. Pressure loss is effectively converted into improved heat transfer, and compared with the segmental baffle, heat transfer at the same fluid velocity is significantly higher. Figure 5.64 shows the concept of EMbaffle, heat exchanger tube bundle assembly and completed tube bundle assembly.

As a direct consequence of the longitudinal flow on the shellside, tube vibration in an EMbaffle heat exchanger is effectively eliminated, significantly reducing the risk of mechanical damage. The longitudinal direction of the shellside liquid in EMbaffle heat exchangers approaches pure countercurrent flow; as a result, they can deliver higher heat duty at the same approach temperature.

5.17.2.1 Application of EMbaffle Technology

Initially developed as a potential solution for fouling services, EMbaffle technology has been proven in a wide range of applications from liquid/liquid and gas/gas to condensing and boiling. In fouling services, for instance, in crude preheat trains, the dead zones typically found with conventional segmental designs reduce the performance of the heat exchanger with an increasing pressure drop during operation. However, with EMbaffle, due to the longitudinal flow, no dead zones are created behind the EMbaffle, and in-service thermal performance has been shown to improve by more than 50% [61]. It eliminates vibration by virtue of all tubes being fully supported on every baffle.

5.17.2.2 Design

The thermal design parameters for EMbaffle technology have been embedded in the industry standard HTRIX Changer™ software suite, enabling licensees and users to carry out their own thermal engineering designs. A complete range of standard and customized grid designs is available for

* EMbaffle® is a registered trademark of EMbaffle B.V., Alphen a/d Rijn, the Netherlands.

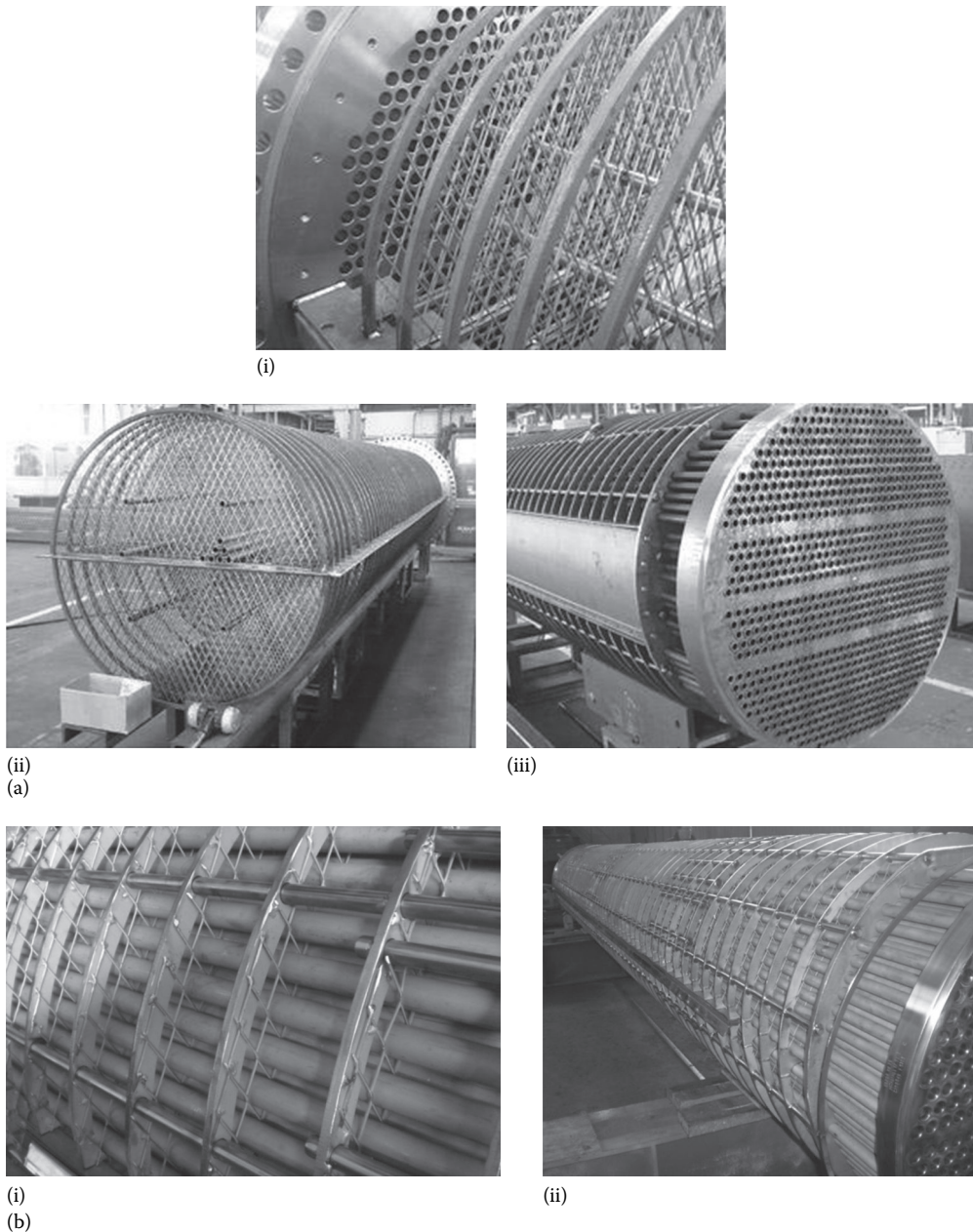


FIGURE 5.64 EMbaffle heat exchanger. (a) (i) Sectional view of tube bundle cage assembly, (ii) Tube bundle under assembly, and (iii) Assembled tube bundle (2 passes on the tubeside). (b) (i–ii) EMbaffle heat exchanger tube bundle under assembly. (Courtesy of EMbaffle B.V., LionsParc, A. van Leeuwenhoekweg 38A10, 2408 Amsterdam, the Netherlands.)

all conventional tube sizes and most applications. Baffles are available in most sizes and materials from carbon steel, stainless, duplex and superduplex steels, high-nickel alloys and copper alloys, including bronze, brass, and cupronickels. EMbaffle heat exchanger utilizes TEMA tolerances and the same pressure parts as conventional segmental designs. It is compliant with all relevant international standards [61].

5.17.2.3 Benefits of EMbaffle Technology

The benefits of EMbaffle technology compared with conventional designs include the following [61]

- a. Improved heat transfer capabilities
- b. Elimination of flow-induced tube vibration
- c. Uniform flow pattern on the shellside
- d. Lower shellside pressure drop
- e. Reduced fouling rates
- f. Lower energy consumption

5.17.3 HELIXCHANGER® HEAT EXCHANGER*

The Helixchanger heat exchanger is a high-efficiency heat exchanger and a proprietary product of Lummus Technology Heat Transfer, a division of Lummus Technology. In a Helixchanger heat exchanger, the conventional segmental baffle plates are replaced by quadrant-shaped baffle plates positioned at an angle to the tube axis in a sequential arrangement to create a helical flow pattern creating a uniform velocity through the tube bundle. Figures 5.65 through 5.67 show helical flow pattern on the shellside and orientation of helical baffles of a tube bundle. Shellside helical flow offers higher thermal efficiency as well as lower fouling rates as compared to the conventional segmental baffled heat exchangers [62]. Effective protection against flow-induced vibrations is achieved by both

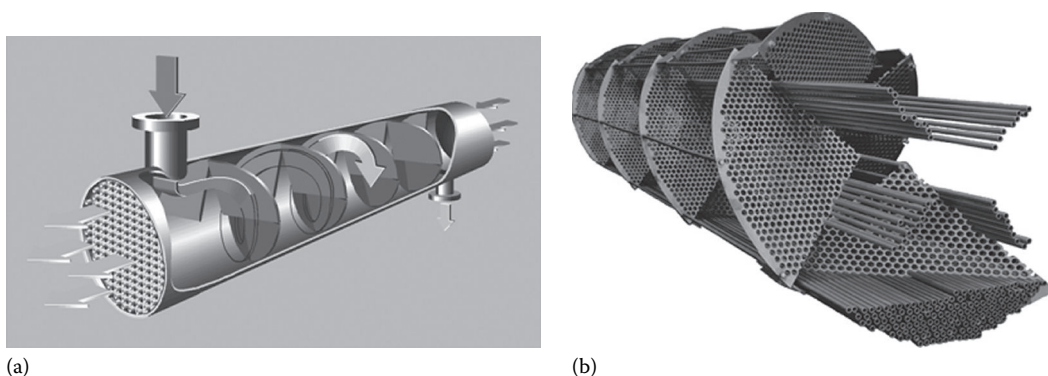


FIGURE 5.65 Helixchanger heat exchanger. (a) Shellside flow pattern (schematic) and (b) helical baffle orientation. (Courtesy of Lummus Technology Heat Transfer, A Division of Lummus Technology Inc., Bloomfield, NJ.)

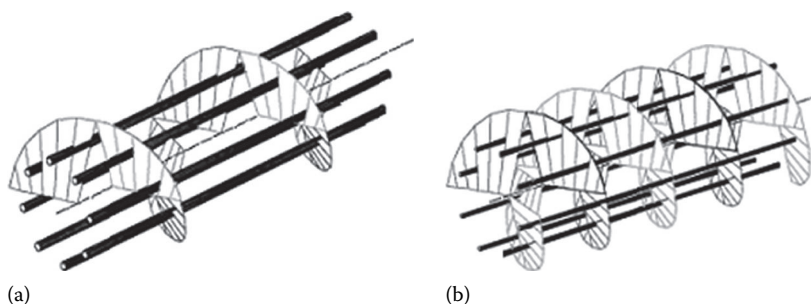


FIGURE 5.66 Helical baffles. (a) Single helical baffle and (b) double helical baffles (schematic). (Courtesy of Lummus Technology Heat Transfer, A Division of Lummus Technology Inc., Bloomfield, NJ.)

* HELIXCHANGER and HELIFIN are registered trademarks of Lummus Technology Inc.

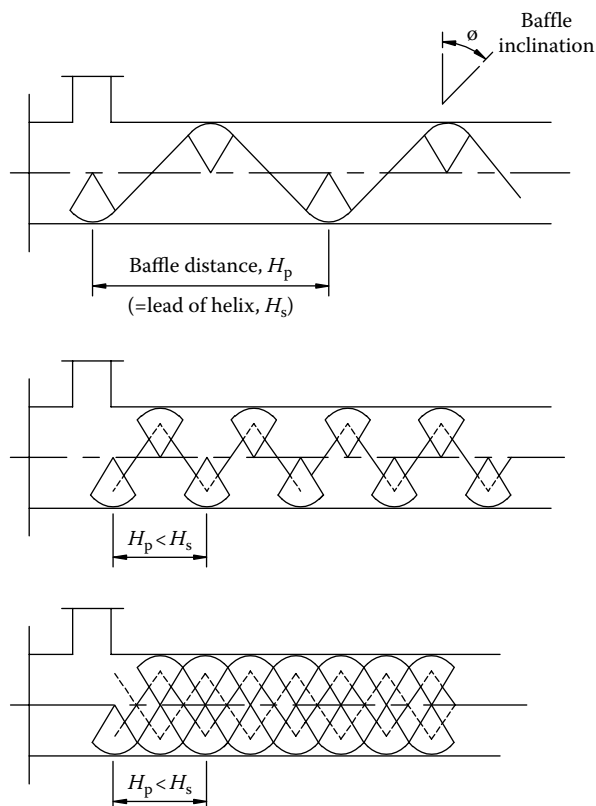


FIGURE 5.67 Orientation of single helical and double helical baffles.

the single- and the double-helix baffle arrangement. In a double-helix arrangement, two strings of helical baffles are intertwined to reduce the unsupported tube spans offering greater integrity against vibrations without compromising the thermohydraulic performance.

5.17.3.1 Merits of Helixchanger Heat Exchanger

In a conventional shell and tube heat exchanger with segmental baffles, uneven velocity profiles, back flows and eddies results in higher fouling and hence shorter run lengths. In a Helixchanger heat exchanger, the helical flow offers improved thermal effectiveness, enhanced heat transfer, reduced pressure drop, lower fouling, and significantly reduced flow-induced vibration hazards [62].

5.17.3.2 Applications

More than 2300 Helixchanger heat exchangers are in operation worldwide, for varied applications in the oil and gas, refining, petrochemical, and chemical industries. The applications range from crude preheat exchangers, feed preheat exchangers in delayed cokers, feed/effluent exchangers in refinery and petrochemical processes, bitumen exchangers in oil sands, major equipment in ethylene plants, to polymer solution coolers in the chemical industry.

5.17.3.3 Helixchanger Heat Exchanger: Configurations

5.17.3.3.1 Helixchanger Heat Exchanger

In a Helixchanger heat exchanger, quadrant-shaped plate baffles are used on the shellside, placed at an angle to the tube axis in a successive arrangement to create a helical flow pattern. Figure 5.68 shows the Helixchanger heat exchanger tube bundle assembly.

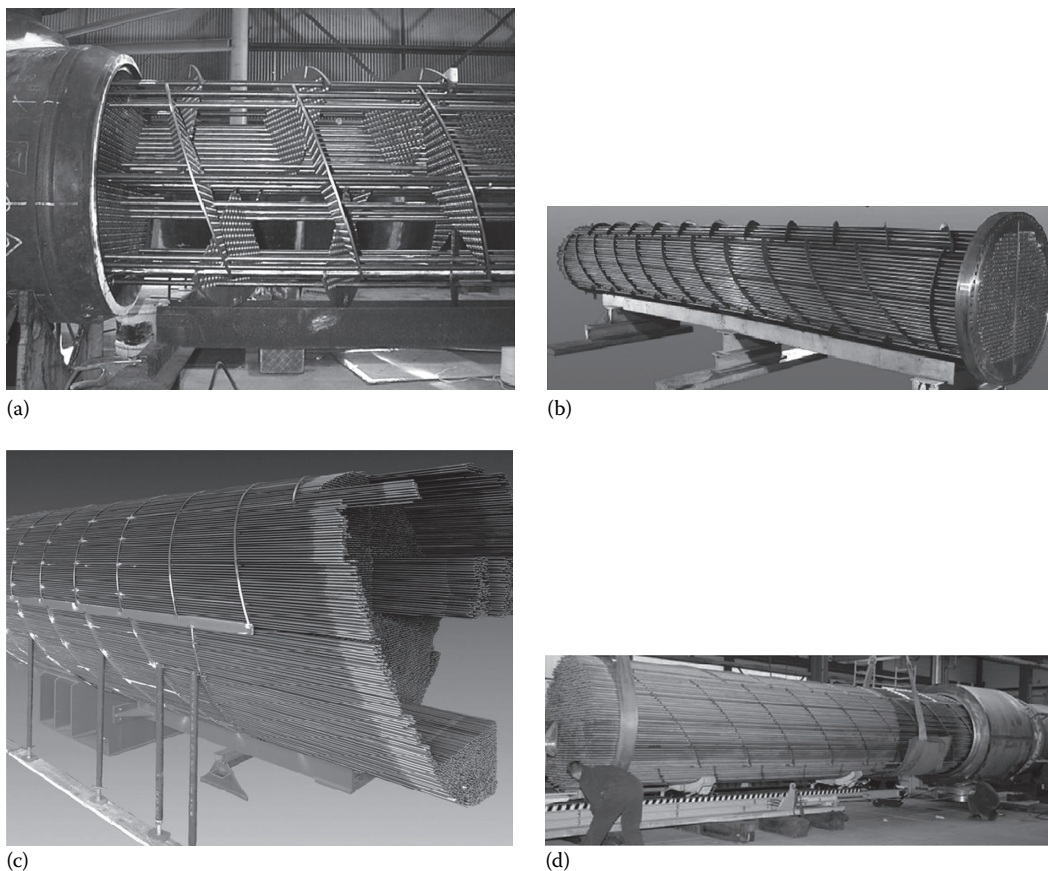


FIGURE 5.68 Helixchanger heat exchanger tube bundle assembly. (a) A section of tube bundle under assembly and (b) completed tube bundle assembly. (a and b: Courtesy of Lummus Technology Heat Transfer, A Division of Lummus Technology Inc., Bloomfield, NJ.) (c) Helixchanger tube bundle under assembly and (d) Helixchanger tube bundle assembly is inserted into the shell. (c and d: Courtesy of Vermeer Eemhaven B.V., Rotterdam, the Netherlands.)

5.17.3.3.2 *Helifin[®] Heat Exchanger*

When a Helixchanger heat exchanger is built with low-fin tubes for the tube bundle, it is called a Helifin heat exchanger. Low-fin tubes offer extended heat transfer surface on the outside of the tubes. For process conditions where low-fin tubes are suitable, the Helifin heat exchanger offers a more economical solution with increased reliability against flow-induced vibrations.

5.17.3.3.3 *Helitower[™] Heat Exchanger**

In certain processes where high-temperature effluent is used to preheat the feed stream, a large bank of horizontal heat exchangers is required in series arrangement. A more economical option using one or two heat exchangers with longer tubes in a vertical orientation is often better suited in achieving the desired performance. When Helixchanger heat exchangers are employed in such a vertical orientation using long tube bundles, they are called Helitower heat exchangers. Figure 5.69 shows a Helitower heat exchanger.

* Helitower is a trademark of Lummus Technology Inc.

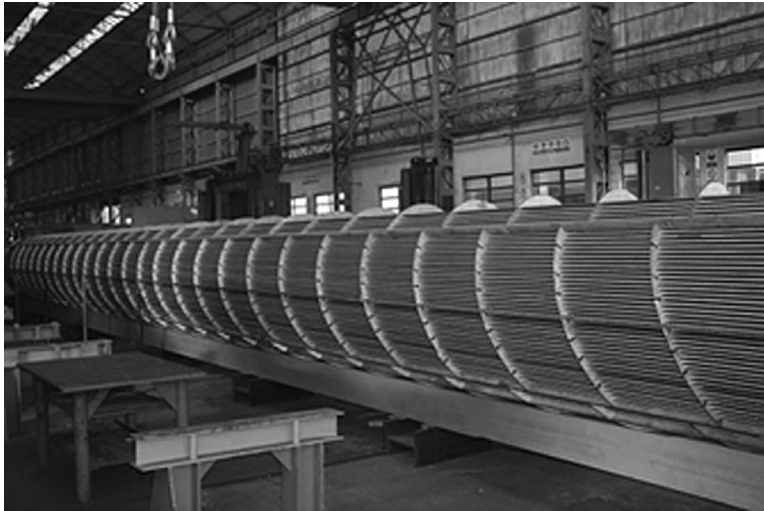


FIGURE 5.69 Helitower™ heat exchanger. (Courtesy of Lummus Technology Heat Transfer, A Division of Lummus Technology Inc., Bloomfield, NJ.)

5.17.3.4 Performance

Frequently, the fouling mechanism responsible for the deterioration of heat exchanger performance is maldistribution of flow, wakes, and eddies caused by poor heat exchanger geometry on the shellside. In a shell and tube heat exchanger, the conventional segmental baffle geometry is largely responsible for higher fouling rates. Uneven velocity profiles, backflows, and eddies generated on the shellside of a segmental baffled heat exchanger result in higher fouling and shorter run lengths between periodic cleaning and maintenance of tube bundles. In a Helixchanger heat exchanger, the quadrant-shaped baffle plates are arranged at an angle to the tube axis creating a helical flow pattern on the shellside. Near-plug flow conditions are achieved in a Helixchanger heat exchanger with little backflow and eddies, often responsible for fouling and corrosion. Figure 5.70 shows the flow patterns of a conventional shell and tube heat exchanger compared with a Helixchanger heat exchanger. The absence of backflows and eddies on the shellside of Helixchanger heat exchangers significantly reduces fouling while in operation. Figure 5.71 shows a comparison of typical run lengths between periodic cleaning and maintenance of the tube

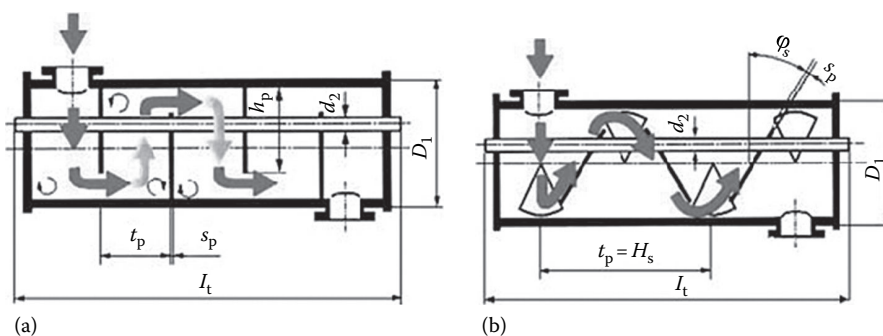


FIGURE 5.70 Shellside flow pattern. (a) Conventional shell and tube heat exchanger and (b) Helixchanger heat exchanger. (Courtesy of Lummus Technology Heat Transfer, A Division of Lummus Technology Inc., Bloomfield, NJ.)

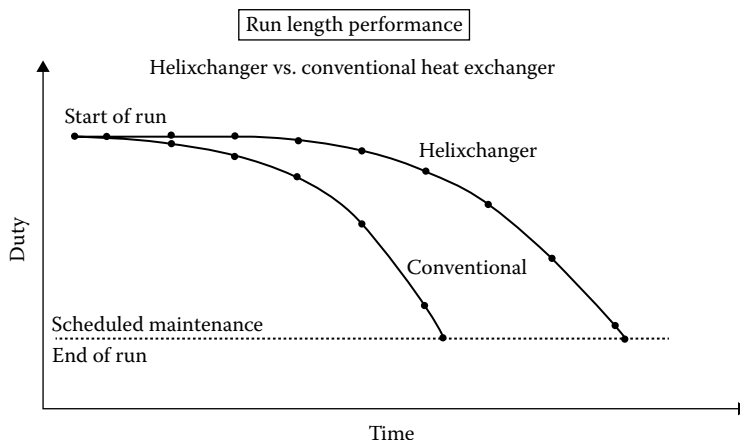


FIGURE 5.71 Comparison of run lengths between periodic cleaning and maintenance of tube bundle of conventional shell and tube heat exchanger with that of Helixchanger heat exchanger. (Courtesy of Lummus Technology Heat Transfer, A Division of Lummus Technology Inc., Bloomfield, NJ.)

bundle of a conventional shell and tube heat exchanger (shorter run length) and the Helixchanger heat exchanger (longer run length). (Figure 9.6b shows the comparison of the level of fouling of a conventional shell and tube heat exchanger with a Helixchanger heat exchanger in a typical feed/effluent exchanger application. The conventional segmental baffle exchanger is fouled heavily compared to the Helixchanger bundle.)

5.17.4 TWISTED TUBE® HEAT EXCHANGER*

Koch Heat Transfer Company's innovative Twisted Tube tube design avoids the need for baffles. The unique helix-shaped tubes are arranged in a triangular pattern. Each tube is firmly and frequently supported by adjacent tubes, yet fluid swirls freely along its length. This support system eliminates crossflow-induced tube vibration, which is a common problem in conventional shell and tube heat exchanger services. The twist arrangement for baffle-free support with gaps aligned between the tubes also provides for easier cleaning on the shellside. The Twisted Tube heat exchangers are round at each end, allowing for conventional tube-to-tubesheet joints to be used [63,64].

5.17.4.1 Applications

Crude preheat, feed/effluent for—reformer (CCR and semi-regeneration), hydrotreater, hydrocracker, alkylation, etc., overhead condensers, reboilers (kettle and *J* shell), lean/rich amine, compressor interstage coolers, etc.

5.17.4.2 Advantages

Twisted Tube tubing offers benefits such as increased heat transfer, smaller exchangers or fewer shells, elimination of flow-induced vibration, and reduced fouling. *When used as retrofit bundles or exchangers*, Twisted Tube tubings *also offer* increased capacity, lower installed costs, lower pressure drop, and extended run time between cleanings.

* Twisted Tube is a registered trademark of Koch Heat Transfer Company, LP, and is registered in the United States and other countries worldwide.

5.17.4.3 Merits of Twisted Tube Heat Exchanger

Twisted Tube heat exchangers provide a higher heat transfer coefficient than the conventional tubular heat exchanger due to the following reasons [63]:

- a. Uniform fluid distribution combined with interrupted swirl flow on the shellside induces the maximum turbulence to improve heat transfer.
- b. On the tubeside, swirl flow creates turbulence resulting in higher tubeside heat transfer coefficient.
- c. *High localized velocities scrub tube wall to combat fouling and offers 40% higher tube-side heat transfer coefficient.*
- d. *Lower pressure drop:* The longitudinal swirl flow of Twisted Tube tubing reduces the high pressure drop associated with segmental baffles. Twisted Tube heat exchangers are usually shorter in length and have fewer number of passes, for a lower pressure drop on the tubeside.
- e. *Baffle-free tube support and elimination of flow-induced vibration.*

5.17.5 END CLOSURES

5.17.5.1 Breech-Lock™ Closure

Breech-Lock closure is used to seal the tubeside of shell and tube heat exchangers in specific applications (Figure 5.72). Breech-Lock heat exchangers are fabricated and supplied by heat exchanger manufacturers under fabrication license from ABB Lummus Heat Transfer and the Breech-Lock is a registered trademark of ABB LHT.

The tubesheet for the Breech-Lock heat exchanger is designed for a differential pressure. The internal bolts are used to apply the seating load to the gasket at the tubesheet and shell interface. The pressure load is absorbed by the threaded closure and the outer row of external bolts applies the seating load to the channel gasket. The inner row of external bolts is used to increase the seating load between the tubesheet and shell gasket in the event of relaxation of the inner bolts. Since the hydrostatic pressure load is taken by the channel body and not by heavy bolting (bolts are only sized for gasket compression loading), the design results in a relatively thin channel (no edge bending due to bolting) with consequent reduction in the exchanger's size and weight. These exchangers are easy to operate and comparatively easy to dismantle and reassemble, which results in more reliable

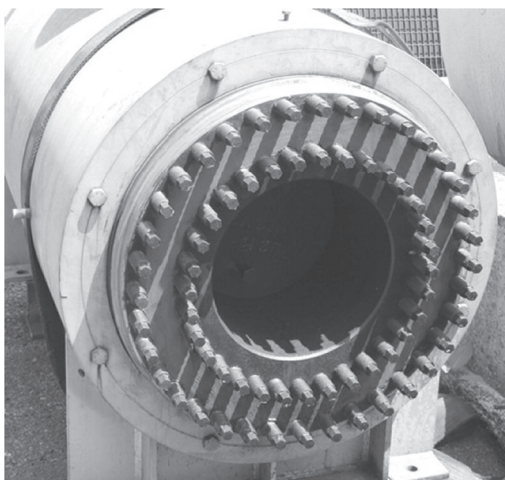


FIGURE 5.72 Breech-Lock end closure. (Courtesy of Brembana Costruzioni Industriali S.p.A., Milan, Italy.)

operation and shorter shut down time. Koch Heat Transfer Company, LP, Houston, Texas, is one of the leading manufacturers of Breech-Lock Closure heat exchangers. The main features of the Breech-Lock Closure are hereunder:

1. Extremely reliable high-pressure sealing
2. Seating of gaskets by small-diameter bolts
3. Absence of threaded holes in forging or in cladding
4. Easy dismantling/reassembly for inspection
5. No need of welding during reassembly
6. Reduced maintenance times and craneage costs with special dismantling jig

5.17.5.2 Easy Installation and Dismantling Jig

IMB™ has developed a unique proprietary jig assembly designed to facilitate dismantling and reassembling operations. With the IMB jig, it is possible to open the channel, remove the internals, and then reassemble and reclose of the Breech-Lock exchangers in a very short time *without the need for heavy craneage*.

5.17.6 TAPER-LOK® CLOSURE

The Taper-Lok closure is typically used for high pressure up to 15,000 psi (1,055 kg/cm²) applications. The Taper-Lok closure uses separate tubeside and shellside flanges, bolting, and gasketing. The unique feature of this closure offers a reusable Taper-Lok ring that acts as a self-energizing seal. More details on Taper-Lok closure are given in Chapter 11.

5.17.7 HIGH-PRESSURE END CLOSURES

Construction, fabrication, qualification and design of high-pressure vessels, heat exchangers, separators, and reactors up to 250 bar(g) on the shellside and up to 1000 bar(g) on the tubeside are treated as high-pressure heat exchangers. A typical high-pressure heat exchanger is shown in Figure 5.73.



FIGURE 5.73 High pressure heat exchanger for hydrocracking plant. (Courtesy of Brembana Costruzioni Industriali S.p.A., Milan, Italy.)

5.A APPENDIX A

5.A.1 REFERENCE CROSSFLOW VELOCITY AS PER TINKER

Reference crossflow velocity as per Tinker [37] is given by

$$U_s = \frac{F_h M_s}{M A_x \rho_s} \quad (5.88)$$

where

A_x is the crossflow area within the limits of the tube bundle

F_h is the fraction of total fluid flowing through A_x of clean unit

M is the A_x multiplication factor

M_s is the mass flow rate of shellside fluid

ρ_s is the mass density of shellside fluid

$$A_x = a_x L_{bc} D_3 \quad (5.89)$$

$$F_h = \frac{1}{1 + N_h \sqrt{S}} \quad (5.90)$$

$$M = \left[\frac{1}{1 + \frac{0.7 L_{bc}}{D_1} \left[\frac{1}{M_w^{0.6}} - 1 \right]} \right]^{1.67} \quad (5.91)$$

The list of expressions required to evaluate N_h , M_w , is

$$a_1 = \frac{D_1}{D_3} \quad (5.92)$$

For units with sealing strips, a_1 is given by

$$a_1 = 1 + \left[\frac{D_1/D_3 - 1}{4} \right] + 1.5 \left[\frac{D_1 - D_2}{D_1} \right] \quad (5.93)$$

$$a_2 = \frac{d_B - d}{d} \quad (5.94)$$

$$a_3 = \frac{D_1 - D_2}{D_1} \quad (5.95)$$

$$b_1 = \frac{(a_1 - 1)^{1.5}}{\sqrt{a_1}} \quad (5.96)$$

$$b_2 = \frac{a_2}{a_1^{1.5}} \quad (5.97)$$

$$b_3 = a_3 \sqrt{a_1} \quad (5.98)$$

The terms a_x , a_4 , a_5 , a_6 , and m are dependent on the tube layout pattern, and they are given in Table 5.5.

The expression for a_7 is

$$a_7 = a_4 \left(\frac{p}{p-d} \right)^{1.5} \quad (5.99)$$

Values for a_8 are given in Table 5.6.

$$A = a_5 a_8 \left(\frac{D_1}{L_{bc}} \right) \left(\frac{d}{p} \right)^2 \left(\frac{p}{p-d} \right) \quad (5.100)$$

$$E = a_6 \left(\frac{p}{p-d} \right) \left(\frac{D_1}{L_{bc}} \right) \left(1 - \frac{h}{D_1} \right) \quad (5.101)$$

$$N_h = a_7 b_1 + A b_2 + b_3 E \quad (5.102)$$

$$M_w = m a_1^{0.5} \quad (5.103)$$

TABLE 5.5
Terms to Find Crossflow Velocity

	30°	90°	45°	60°
a_x	$\frac{0.97(p-d)}{p}$	$\frac{0.97(p-d)}{p}$	$\frac{1.372(p-d)}{p}$	$\frac{0.97(p-d)}{p}$
a_4	1.26	1.26	0.90	1.09
a_5	0.82	0.66	0.56	0.61
a_6	1.48	1.38	1.17	1.28
M	0.85	0.93	0.80	0.87

Source: Tinker, T., *Trans. ASME*, vol. 80, 36, 1958.

Note: Values for 60° have been taken from TEMA [2].

TABLE 5.6
Baffle Cut Ratio and the Term a_8 for Crossflow Velocity

h/D_1	0.10	0.15	0.20	0.25	0.30	0.35	0.40	0.45	0.50
a_8	0.94	0.90	0.85	0.80	0.74	0.68	0.62	0.54	0.49

Source: Tinker, T., *Trans. ASME*, vol. 80, 36, 1958.

5.A.2 DESIGN OF DISK AND DOUGHNUT HEAT EXCHANGER

In shell and tube heat exchangers with baffle disks and rings, known as disk and doughnut heat exchanger (Figure 5.74), the flow inside the shell is made to alternate between longitudinal and transverse (or crossflow) directions in relation to the tube bundle. This type of heat exchanger is used in some European countries. Occasionally, oil coolers at thermal power stations are of this type. It has been reported that for the same pressure drop in shellside fluid, the heat transfer coefficient obtained with disk and doughnut baffles is approximately 15% more than that obtained with segmental baffles [65]. Exchangers are fabricated for horizontal or vertical installation.

5.A.2.1 Design Method

The effect of clearance between segmental baffles and the shell on the performance of a heat exchanger has been reasonably well studied, but there is hardly any corresponding published literature available for the disk-and-doughnut-type heat exchangers. Very few open literature methods are available for the thermal design of disk and doughnut heat exchangers. Notable among them are Donohue [66], Slipcevic [67,68], and Goyal et al. [69]. Donohue's thermal design method was recently discussed by Ratnasamy [70]. In this section, the Slipcevic and Donohue's method is discussed.

5.A.2.1.1 Slipcevic Method

5.A.2.1.1.1 Design Considerations

Follow these design guidelines on the shellside [67]:

1. The spacing between the baffle disks and rings usually amounts to 20%–45% of the inside shell diameter. Less than 15% is not advisable.
2. Since the heat transfer coefficient for flow parallel with the tubes is lower than that for flow normal to the tubes, space the baffle plates so that the velocity in the baffle spacing opening is higher than that of the flow normal to the tubes.
3. It is advisable to make the annular area between the disk and the shell, S_{k1} , the same as the area inside the ring, S_{k2} , such that

$$S_{k1} = \frac{\pi}{4} (D_s^2 - D_1^2) \quad (5.104)$$

$$S_{k2} = \frac{\pi}{4} D_2^2 \quad (5.105)$$

$$S_{k1} = S_{k2} \rightarrow D_s^2 = D_1^2 + D_2^2 \quad (5.106)$$

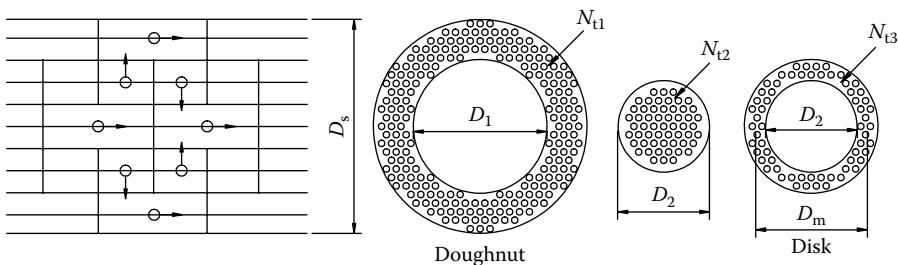


FIGURE 5.74 Disk and doughnut heat exchanger with tubes in various flow areas. Note: $D_m = 0.5(D_1 + D_2)$, where D_1 is disk diameter.

5.A.2.2 Heat Transfer

Step 1: Calculate the individual flow area for longitudinal flow:

1. Flow area in the annular region between the disk and the shell, S_1 :

$$S_1 = \frac{\pi}{4} (D_s^2 - D_1^2 - N_{t1} d^2) \quad (5.107)$$

2. Flow area in the ring opening, S_2 :

$$S_2 = \frac{\pi}{4} (D_2^2 - N_{t2} d^2) \quad (5.108)$$

Step 2: Calculate the effective crossflow area, S_q :

$$S_q = L_s \Sigma x \quad (5.109)$$

where Σx is the sum of the clear distances between the neighboring tubes closest to the mean diameter, $D_m = 0.5(D_1 + D_2)$. Determine the sum of clear distances between neighboring tubes closest to D_m , either from a drawing (as shown in Figure 5.75) or by computational methods.

The number of tubes in the flow areas S_1 , S_2 , and crossflow area S_3 (to be defined later) is N_{t1} , N_{t2} and N_{t3} , respectively. They are shown in Figure 5.74.

Step 3: Calculate the hydraulic diameter for the longitudinal flow in the annulus, D_{h1} , and in the ring opening, D_{h2} :

$$D_{h1} = \frac{4S_1}{\pi(N_{t1}d + D_s + D_1)} \quad (5.110)$$

$$D_{h2} = \frac{4S_2}{\pi(N_{t2}d + D_2)} \quad (5.111)$$

Step 4: Calculate the heat transfer coefficients h_1 and h_2 for the longitudinal flow through the cross section S_1 and S_2 from the equation of Hausen [71]:

$$\text{Nu}_1 = 0.024 \text{Re}_1^{0.8} \text{Pr}^{0.33} \left(\frac{\mu_b}{\mu_w} \right)^{0.14} \quad (5.112)$$

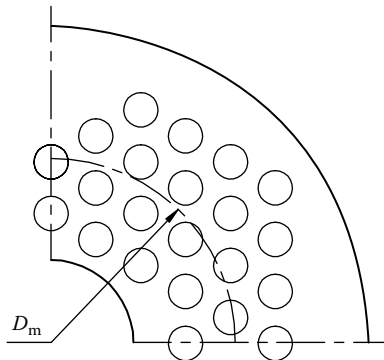


FIGURE 5.75 Mean diameter to calculate effective crossflow area of a disk and doughnut heat exchanger.

$$\text{Nu}_2 = 0.024 \text{Re}_2^{0.8} \text{Pr}^{0.33} \left(\frac{\mu_s}{\mu_w} \right)^{0.14} \quad (5.113)$$

where

$$\text{Nu}_1 = \frac{h_1 D_{h1}}{k} \quad (5.114)$$

$$\text{Nu}_2 = \frac{h_2 D_{h2}}{k}$$

$$\text{Re}_1 = \frac{U_1 D_{h1}}{\mu_s} \quad (5.115a)$$

$$\text{Re}_2 = \frac{U_2 D_{h2}}{\mu_s} \quad (5.115b)$$

and U_1 and U_2 are based on S_1 and S_2 , respectively.

Step 5: Calculate the heat transfer coefficient h_3 for crossflow across the bundle from McAdams [47] for the turbulent range:

$$\text{Nu}_3 = K \text{Re}_3^{0.6} \text{Pr}^{0.33} \left(\frac{T_b}{T_w} \right)^{0.14} \quad (5.116)$$

where $K = 0.33$ for the staggered tube arrangement and $K = 0.26$ for the in-line tube arrangement.

To calculate Re_3 , use U_3 calculated using the crossflow area S_q :

$$\text{Re}_3 = \frac{U_3 d}{\mu_s} \quad (5.117)$$

Alternately, Slipcevic recommends calculating the heat transfer coefficient of the individual tube row with the corresponding flow cross section. From these heat transfer coefficients, calculate the weighted mean average of heat transfer coefficients.

Step 6: Calculate the heat transfer area in the longitudinal flow section A_1 , A_2 , crossflow section A_3 , and total heat transfer area, A :

$$A_1 = \pi d L N_{t1} \quad (5.118a)$$

$$A_2 = \pi d L N_{t2} \quad (5.118b)$$

$$A_3 = \pi d L N_{t3} \quad (5.118c)$$

where

$$N_{t3} = N_{t2} - (N_{t1} + N_{t2}) \quad (5.119)$$

$$A = A_1 + A_2 + A_3 \quad (5.120a)$$

$$= \pi d N_t L \quad (5.120b)$$

Step 7: Calculate the heat transfer coefficient h referred to the entire heat transfer surface A :

$$h = \frac{h_1 A_1 + h_2 A_2 + h_3 A_3}{A} \quad (5.121)$$

5.A.2.3 Shellside Pressure Drop

Refer to Slipcevic [68] for pressure-drop calculation.

5.A.2.4 Shortcomings of Disk and Doughnut Heat Exchanger

The disadvantages of this design include the following [4]: (1) All the tie-rods to hold baffles are within the tube bundle, and (2) the central tubes are supported by the disk baffles, which in turn are supported only by tubes in the overlap of the larger diameter disk over the doughnut hole.

5.A.3 NORAM RF™ RADIAL FLOW GAS HEAT EXCHANGER

The NORAM RF radial flow gas heat exchanger (by NORAM Engineering and Constructors Limited, Vancouver, British Columbia, Canada) offers a fundamental improvement in gas heat exchanger performance over designs traditionally used in the sulfuric acid industry. The RF design far surpasses existing single and double segmental heat exchanger design in heat transfer rates, at a significantly lower pressure loss.

In the RF gas exchanger, tubes are arranged in an annular pattern using disk and doughnut baffles (Figure 5.76). Flow is directed from an inner core outward across the tube bundle and from

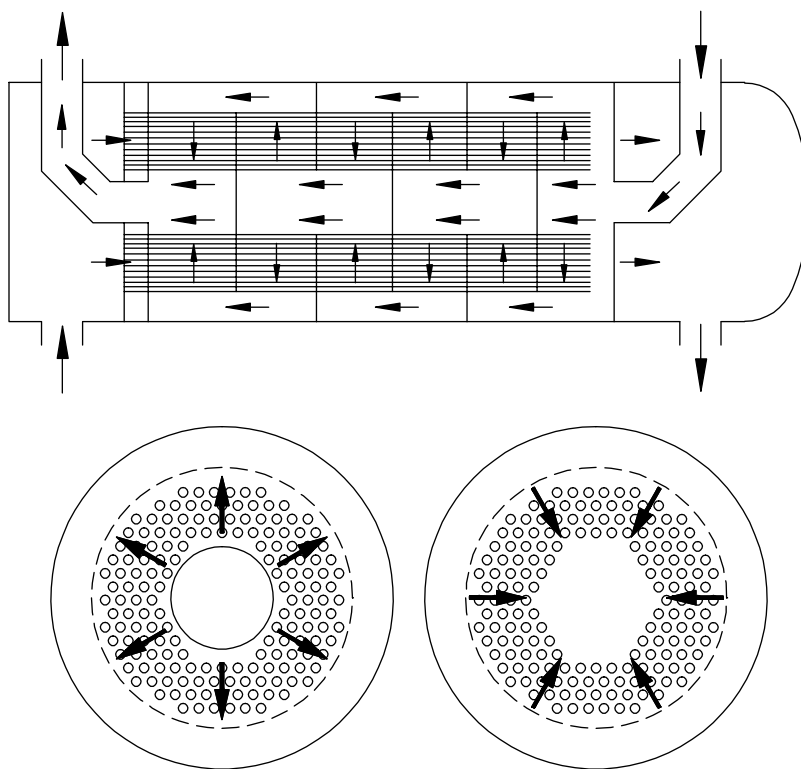


FIGURE 5.76 NORAM RF radial flow gas heat exchanger. (Courtesy of NORAM Engineering and Constructors Limited, Vancouver, British Columbia, Canada.)

an outer annulus inward across the tube bundle. The gas turns in the inner core and outer annulus are not restricted by tubes so that pressure losses are minimized. The flow resistance across the tube bundle is uniform, resulting in uniform flow and LP losses due to minimal gas acceleration and deceleration. Also the radial design minimizes the number of tube rows that have to be crossed by the gas, resulting in a low shellside pressure drop. Steps are taken in the design to maintain uniform velocity through the core, the bundle, and the annulus to minimize overall flow resistance. Heat transfer rates in the RF gas exchanger are maximized because all the heat transfer surface is fully utilized. Shell gas flow is always perpendicular to the tubes providing the maximum heat transfer coefficients.

5.A.3.1 TUBE LAYOUT

The RF design makes effective use of the heat transfer surface by placing tubes only in areas of crossflow. The gas flows radially across the tube bundle between an open core and an open outer annulus, directed by disk and doughnut baffles. All tubes are located in an annular domain between the core and the outer annulus.

5.A.4 CLOSED FEEDWATER HEATERS

A feedwater heater is an unfired heat exchanger designed to preheat feedwater by means of condensing steam extracted or bleed from a steam turbine. Feedwater heaters are used in regenerative water-system cycle to improve the thermodynamics efficiency, resulting in a reduction of fuel consumption and thermal pollution. The boiler feedwater is heated up by steam extracted from suitable turbine stages. The heater is classified as closed, since the tubeside fluid remains in a closed circuit and does not mix with the shellside condensate, as is the case with open feedwater heaters. They are unfired since the heat transfer within the vessel does not occur by means of combustion, but by convection and by condensation.

Leading feedwater heaters manufacturers include Alstrom, Holtec International, Balcke-Durr, an SPX Company, and Westinghouse among others. Most feedwater heaters are of a standard shell and tube configuration, although some are of header type. The majority uses U-tubes, which are relatively tolerant to the thermal expansion during operation. They are designed as per HEI Standard for closed feedwater heaters [72] or other national standards. For design of power plant heat exchangers, refer to Ref. [73].

Based on operating pressure, it is as classified as

- i. LP heater
- ii. HP heater
- iii. Intermediate pressure heater (if present).
- iv. Orientation shall be either horizontal or vertical channel down or vertical channel up

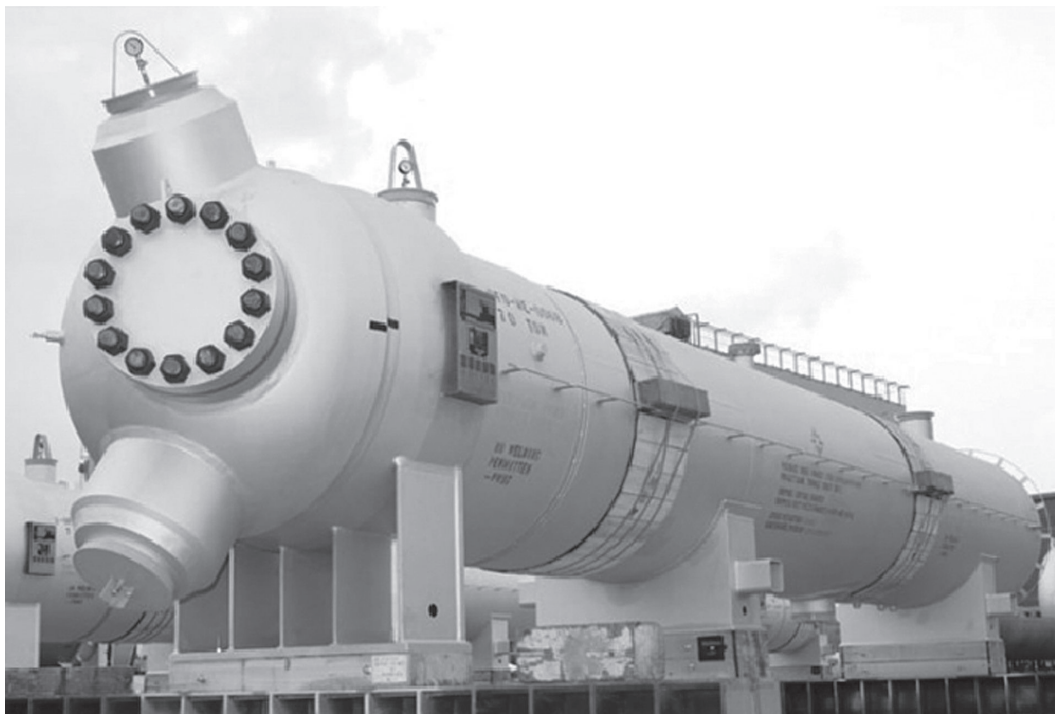
Figure 5.77 shows LP feedwater heater and HP feedwater heater.

There are three separate zones within the shell in a feedwater heater and their details are given hereunder:

1. Condensing zone: All of the steam is condensed in this area, and any remaining noncondensable gases must be removed. A large percentage of the energy added by the heater occurs here. All feedwaters have this zone.
2. The condensed steam subcooling zone (optional).
3. Desuperheating zone (optional): The incoming steam enters this zone, giving up most of its superheat to the feedwater.



(a)



(b)

FIGURE 5.77 Feedwater heater. (a) LP feedwater heater and (b) HP feedwater heater. (Courtesy of Holtec International, Marlton, NJ.)

5.A.4.1 Low-Pressure Feedwater Heaters

The feedwater heaters placed between the main condensate pumps and the boiler feedwater pumps are named LP feedwater heaters. They are U-tube bundle heat exchangers. The recommended tube material is stainless steel. The advantage is the resistance to corrosion and erosion. The tubes are longitudinally welded, which allows small tube wall thickness to be realized. The LP feedwater heaters are arranged horizontally.

5.A.4.2 High-Pressure Feedwater Heaters

The feedwater heaters placed between boiler feedwater pump and boiler are named high-pressure feedwater heaters. The tube material is mostly specified by the consumer. The standard is using seamless low-alloy carbon steel tubes. The advantages are the good thermal conductivity and its

good mechanical properties at high temperatures. In special cases, austenitic or ferritic stainless steel are also utilized since these materials offer high resistance to erosion–corrosion. HP heaters are either installed vertically (channel/waterbox down as a rule) or horizontally.

5.A.5 STEAM SURFACE CONDENSER

The condenser is simply a large heat exchanger with tubes usually horizontally mounted. The condenser has thousands of small tubes that are made out of admiralty brass, copper, ferritic/super austenitic stainless steel, titanium, etc. The function of a surface condenser is to create the lowest possible turbine or process operating back pressure while condensing steam. The condensate generated is usually recirculated back into the boiler and reused. Steam enters the condenser shell through the steam inlet connection usually located at the top of the condenser. It is distributed longitudinally over the tubes through the space designated as dome area. When the steam contacts the relatively cold tubes, it condenses. This condensing effect is a rapid change in state from a gas to a liquid. This change in state results in a great reduction in specific volume, and it is this reduction in volume that creates the vacuum in the condenser. The vacuum produced by condensation will be maintained as long as the condenser is kept free of air. A vacuum venting system is utilized to support the condenser vacuum by continually removing any air entering the system. The condensate is continually removed from the hotwell by condensate pump(s) and is discharged into the condensate system. The air in the system, generally due to leakage in piping, around shaft seals, valves, etc., enters the condenser and mixes with the steam. The saturated air is removed from the condenser by the vacuum venting equipment such as steam jet air ejectors, liquid ring vacuum pumps, or a combination of both. It is necessary to continuously remove air from the system in order to maintain the desired vacuum. An increasing amount of air in the condenser would reduce its capacity and cause the pressure to rise. For standards on steam surface condensers refer to Ref. [74]. A typical steam surface condenser is shown in Figure 5.78. Figure 5.79 shows air-removing section of a surface condenser.

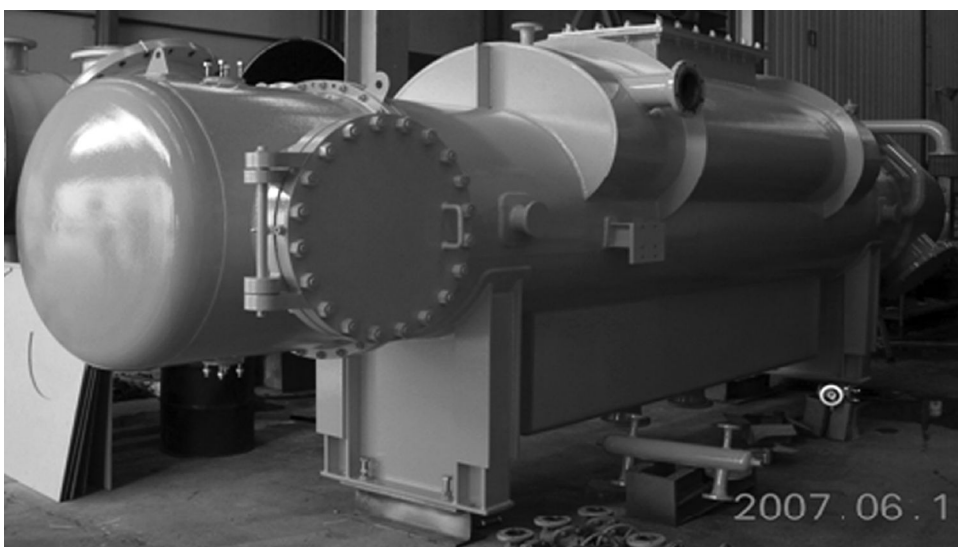


FIGURE 5.78 Steam surface condenser. (Courtesy of GEA Iberica S.A., Barrio de San Juan, Vizcaya, Spain.)

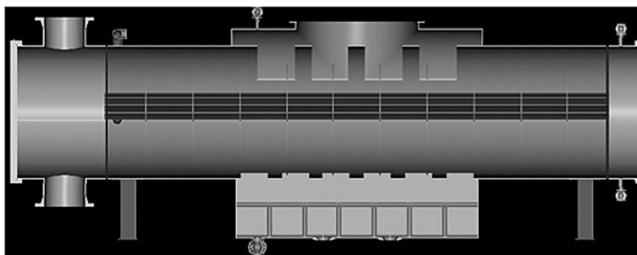


FIGURE 5.79 Steam surface condenser showing dome for steam entry at the top, air removal section in the middle of the core, and condensate collection well at the bottom. (Courtesy of GEA Iberica S.A., Barrio de San Juan, Vizcaya, Spain.)

5.A.5.1 Mechanical Description

The tubes in the condenser are normally expanded into the tubesheets at both ends. The tubes are supported by properly located baffle plates to help prevent deflection and flow-induced vibration of the tubes. The tube holes in the supports are de-burred on each side to prevent damage to the tubes. The waterbox/tubesheet/shell joints are fastened together in three ways, depending upon the tubesheet design.

1. *Tubesheet is flanged to the shell*—The waterboxes on either end of the shell are bolted to the tubesheets and shell flanges utilizing staked studs and stud bolts. Stake studs can be identified by the double nuts included on the shellside. The stake studs are threaded into the tubesheet. The stud bolts are through bolts with no threads in the tubesheet. The staked studs permit the operator to remove the waterboxes without disturbing the seal between the tubesheets and shell flanges.
2. *Tubesheet is welded to the shell*—The tubesheet outside diameter is larger than the shell, and it extends to form a flange. In this case, the waterbox is simply bolted to the tubesheet with through bolts. All of the through bolts must be removed in this type of design in order to remove the waterboxes.
3. *Tubesheet is welded to the shell and to the waterbox*—The waterboxes are not removable. The waterbox covers can be removed by simply removing all of the through bolts.

Figure 5.80 shows a circular shell surface condenser under fabrication.

5.A.5.2 Parts of Condenser

(1) Steam inlet; (2) exhaust connection for turbine; (3) impingement protection—a plate (perforated or solid), dummy tubes, or solid rods used to protect the tubes against high entrance impingement velocity; (4) condenser shell—cylindrical or rectangular body; (5) baffle plate; (6) shell expansion joint; (7) tubes; (8) dome area—an open area above the tubes that permits the steam to easily distribute throughout the length of the bundle without stagnant or overloaded zones; (9) shell flange; (10) air removal section; (11) air ejector; (12) hotwell-storage area with volume sufficient to contain all the condensate produced in the condenser in a given time period. Normally 1 min retention time is specified under design operating conditions. Bath tub or cylindrical types may be used, depending upon the volume and deaeration requirements; (13) condensate outlet(s); (14) support saddles; (15) tubesheets; (16) waterbox—commonly referred to as inlet waterbox, outlet waterbox, return waterbox, return bonnet: provides a directional pathway for circulating water through the tube bundle; (17) waterbox cover flat plate bolted to the ends of channel type waterboxes; (18) waterbox flanges; (19) pass partitions ribs.

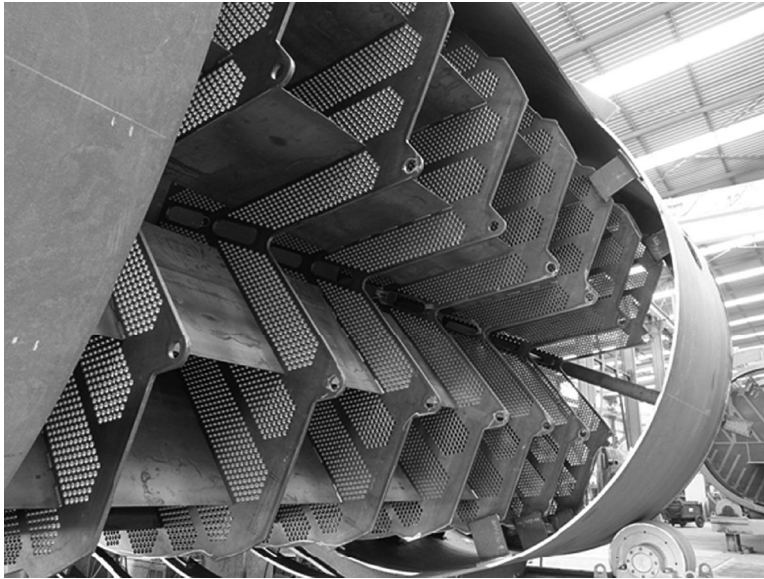


FIGURE 5.80 Circular shell surface condenser under fabrication. (Courtesy of Caldemon Iberica, S.A., a unit of GEA Heat Exchangers, Cantabria, Spain.)

5.A.5.3 Condenser Tube Material

Condenser tube material selection is one of the most important decisions faced by designers. Typical criteria for evaluating condenser tube materials include waterside erosion–corrosion resistance, steam side corrosion resistance and resistance against impingement attack, resistance to pitting due to chlorides and sulfate-reducing bacteria, resistance to ammonia attack and SCC, compatibility with other system materials to avoid galvanic corrosion, heat transfer capability, economics, etc. A partial list of condenser tube material is given as follows:

Tube Material	ASTM Spec.
Titanium Gr1, 2, 3	B-338
304L	A249
304N	A249
316L	A249
2205	A789
904L	B674
254SMO™	B676
AL-6XN™	B676
Sea-Cure™	A268
AL29-4C™	A268
Copper (iron bearing)	B111/B543
Admiralty brass (inhibited)	B111/B543
Al brass	B111/B543
Al bronze	B111/B543
Arsenical copper	B111/B543
CuNi 70/30	B111/B543
CuNi 90/10	B111/B543
Carbon steel	A179
Carbon steel	A214

5.A.5.4 Condenser Support Systems

1. Clean the condenser tubes—the tubes are generally kept clean by an automatic tube cleaning system that injects small abrasive sponge like balls or periodical manual cleaning.
2. Maintain the water level in the condenser so that efficiency is not degraded.
3. Generally, the colder the circulating water, the more efficient the plant. Power plants become less efficient when the condenser tubes are fouled.
4. The waterboxes are kept full using an air ejector or other system that keeps water level in the column from the waterbox as high as needed—above the tubes.
5. Maintain condenser vacuum—vacuum in the condenser is maintained by either a mechanical vacuum pump or steam-driven air ejectors that suck gases (not steam) from the condenser.

NOMENCLATURE

A	total heat transfer area on the shellside
A_n	crossflow area within the limits of tube bundle
A_w	area of one baffle window
A_1	heat transfer area for longitudinal flow in the annulus between the shell and the disk
A_2	heat transfer area for longitudinal flow through the ring opening
A_3	heat transfer area for crossflow
a_1	bypass clearance constant
a_2	baffle hole clearance constant
a_3	baffle edge clearance constant
a_1 – a_8	factors required to determine F_h
b_1, b_2, b_3	factors required to determine F_h
C_L	laminar heat transfer bundle geometry function
C_T	turbulent heat transfer bundle geometry function
D_1	disk diameter
D_1	shell inside diameter (D_s)
D_2	diameter of ring opening
D_2	baffle diameter
D_3	diameter of OTL (D_{otl})
d_B	baffle hole diameter
D_m	mean diameter for calculating the crossflow area = $0.5 (D_1 + D_2)$
D_s	shell inside diameter
d	tube outer diameter (for finned tubes, equal to fin root diameter)
F_h	fraction of total fluid flowing within the limits of tube bundle
g_c	acceleration due to gravity
h	baffle cut
h_1	heat transfer coefficient for the longitudinal flow corresponding to Nu_1
h_2	heat transfer coefficient for the longitudinal flow corresponding to Nu_2
h_3	heat transfer coefficient for the crossflow corresponding to Nu_3
K	heat transfer correlation coefficient
L	tube length
L_{bc}	baffle spacing
M	multiplication factor in Equation 5.86
M_s	mass flow rate of shellside fluid
$M_w A_x$	multiplier to obtain geometric mean of A_x and A_w
N_1	total number of tubes

N_{t1}	number of tubes in annulus between the shell and the disk
N_{t2}	number of tubes in the ring opening
N_{t3}	number of tubes in crossflow
Nu	Nusselt number
Nu_1	Nusselt number to calculate h_1
Nu_2	Nusselt number to calculate h_2
Nu_3	Nusselt number to calculate h_3
p	tube pitch
Pr	Prandtl number
Re_n	Reynolds number
Re_1	Reynolds number in the longitudinal flow area S_1
Re_2	Reynolds number in the longitudinal flow area S_2
Re_3	Reynolds number in the longitudinal flow area S_3
S	exchanger size ratio = D_1/p
S_1	cross-sectional area for longitudinal flow through the annulus between the shell and the disk
S_2	cross-sectional area for longitudinal flow through the ring opening
S_{k1}	annular area between the disk and the shell
S_{k2}	area inside the ring
S_q	crossflow area through tube bundle
S_s	mean longitudinal flow area = $0.5(S_1 + S_2)$
T_b	bulk mean temperature of the shellside fluid
T_w	tube wall temperature
U_1	shellside velocity through the cross-sectional area S_1
U_2	shellside velocity through the cross-sectional area S_2
U_3	shellside velocity through the cross-sectional area S_3
Δp_L	pressure drop due to unbaffled frictional component
Δp_b	pressure drop due to baffle flow contribution
μ_s	viscosity at bulk mean temperature of the shellside fluid (kg/m s)
μ_w	viscosity at tube wall temperature of the shellside fluid (kg/m s)
$(\phi_s)^n$	bulk-to-wall viscosity correction $(\mu_s/\mu_w)^{0.14}$
ρ_s	density of shellside fluid

REFERENCES

1. Minton, P. E., Process heat transfer, *Proceedings of the 9th International Heat Transfer Conference, Heat Transfer 1990*, Jerusalem, Israel, Paper No. KN-22, 1990, Vol. 1, pp. 355–362.
2. TEMA, *Standards of Tubular Exchanger Manufacturers Association*, 9th edn., Tubular Exchanger Manufacturers Association, Tarrytown, NY, 2007.
3. API Standard 660, *Shell and Tube Heat Exchangers-for Petroleum and Natural Gas Industries*, 7th edn., American Petroleum Institute, Washington, DC, 2003.
4. Shah, R. K. and Sekulic, D. P., Heat Exchangers in *Handbook of Heat Transfer Applications*, Rohsenow, W. M., Hartnett, J. P., and Ganic, E. N. (eds.), 3rd edn., McGraw-Hill, New York, 1998, pp. 17.1–17.169, Chapter 17.
5. Bell, K. J. and Mueller, A. C., *Wolverine Heat Transfer Data Book II*, Wolverine Division of UOP Inc., Decatur, AL, 1984.
6. Drake, C. E. and Carp, J. R., Shell and tube heat exchangers, *Chem. Eng.*, 36, 165–170 (1960).
7. Lord, R. C., Minton, P. E., and Sulusser, R. P., Design of exchangers, *Chem. Eng.*, January, 96–118 (1970).
8. Saunders, E. A. D., Features relating to thermal design, in *Heat Exchanger Design Handbook*, Vol. 4 (E. U. Schlunder, editor-in-chief), Hemisphere, Washington, DC, 1983, Section 4.2.5.
9. (a) Larowski, A. and Taylor, M. A., *Systematic Procedures for Selection of Heat Exchangers*, C58/82, Institution of Mechanical Engineers, London, U.K., 1982, pp. 32–56; (b) Larowski, A. and Taylor, M. A., Systematic procedure for selection of heat exchangers, IMechE, *Proc. Inst. Mech. Eng.*, 197A, 51–69 (1983).

10. Phadke, P. S., Determining tube counts for shell and tube exchangers, *Chem. Eng.*, September, 91, 65–68 (1984).
11. Whitly, D. L. and Ludwig, E. E., Rate exchangers this computer way, *Petrol. Refiner*, 147–156 (1961).
12. Fraas, A. P. and Ozisik, M. N., *Heat Exchanger Design*, John Wiley & Sons, New York, 1965.
13. Palen, J. W. and Taborek, J., Solution of shellside flow, pressure drop and heat transfer by stream analysis method, *Chem. Eng., Symp. Ser.*, No. 92, *Heat Transfer—Philadelphia*, 65, 53–63 (1969).
14. Fanaritis, J. P. and Bevevino, J. W., How to select the optimum shell and heat exchanger, in *Process Heat Exchange, Chemical Engineering Magazine* (V. Cavaseno, ed.), McGraw-Hill, New York, 1979, pp. 5–13.
15. Taborek, J., Shell and tube heat exchanger design—Extension of the method to other shell, baffle, and tube bundle geometries, in *Heat Exchanger Design Handbook*, Vol. 3 (E. U. Schlunder, editor-in-chief), Hemisphere, Washington, DC, 1983, Section 3.3.11.
16. Gupta, J. P., *Fundamentals of Heat Exchanger and Pressure Vessel Technology*, Hemisphere, Washington, DC, 1986.
17. Singh, K. P., Mechanical design of tubular heat exchangers—An appraisal of the state-of-the-art, in *Heat Transfer Equipment Design* (R. K. Shah, C. Subbarao, and R. M. Mashelekar, eds.), Hemisphere, Washington, DC, 1988, pp. 71–87.
18. Boyer, R. C. and Pase, G. K., The energy saving NESTS concept, *Heat Transfer Eng.*, 2, 19–27 (1980).
19. Butterworth, D., New twists in heat exchange, *Chem. Eng.*, September, 23–28 (1992).
20. IAEA, Assessment and management of aging of major nuclear power plant components important for the Safety Steam Generator, IAEA-TEC DOC 981, International Atomic Energy Agency, Vienna, Austria, 1999, pp. 1–181.
21. Yokell, S., *A Working Guide to Shell and Tube Heat Exchangers*, McGraw-Hill, New York, 1990.
22. Yokell, S., Double tubesheet heat exchanger design stops shell-tube leakage, *Chem. Eng.*, May, 133–136 (1973).
23. Woodward, A. R., Howard, D. L., and Andrews, E. F. C., Condensers, pumps and cooling water plant, in *Modern Power Station Practice, Vol. C, Turbines, Generators, and Associated Plant* (D. J. Littler, E. J. Davies, H. E. Johnson, F. Kirkby, P. B. Myerscough, and W. Wright, eds.), 3rd edn., Chapter 4, Pergamon Press, New York, 1991.
24. Spencer, T. C., Mechanical design and fabrication of exchangers in the United States, *Heat Transfer Eng.*, 8, 58–61 (1987).
25. Gollin, M., Heat exchanger design and rating, in *Handbook of Applied Thermal Design* (E. C. Guyer, ed.), McGraw-Hill, New York, 1989, pp. 7-24–7-36.
26. Taborek, J., Design procedures for segmentally baffled heat exchangers, in *Heat Exchanger Design Handbook*, Vol. 3 (E. U. Schlunder, editor-in-chief), Hemisphere, Washington, DC, 1983, pp. 3.3.10-1–3.3.10-8.
27. Mueller, A. C., Process heat exchangers, in *Handbook of Heat Transfer Applications*, 2nd edn. (W. M. Rohsenow, J. P. Hartnett, and E. N. Ganic, eds.), McGraw-Hill, New York, 1985, pp. 4-78–4-173.
28. Gutterman, G., Specify the right heat exchanger, *Hydrocarbon Process.*, April, 161–163 (1980).
29. Schlunder, E. U. (editor-in-chief), Mechanical design codes, in *Heat Exchanger Design Handbook, Vol. 4, Expansion Joints*, Hemisphere, Washington, DC, 1983, Section 4.1.6.
30. Taborek, J. and Auriolles, G., Effect of 1988 TEMA standards on mechanical and thermo hydraulic design of shell and tube heat exchangers, in *Heat Transfer*, Philadelphia, PA, 1989, pp. 79–83.
31. Singh, K. P. and Soler, A. I., *Mechanical Design of Heat Exchangers and Pressure Vessel Components*, Arcturus Publishers, Cherry Hill, NJ, 1984.
32. Jaw, L., Temperature relations in shell and tube exchangers having one pass splitflow shells, *Trans. ASME, J. Heat Transfer*, 86C, 408–416 (1964).
33. Grant, I. D. R., Shell and tube exchangers for single phase applications, in *Developments in Heat Exchanger Technology—1* (D. Chisholm, ed.), Applied Science Publishers, London, U.K., 1980, pp. 11–40.
34. Martin, D. J., Haseler, L. E., Hollingsworth, M. A., and Mathew, Y. R., The use of sealing strips to block bypassing flow in a rectangular tube bundle, *Heat Transfer*, Jerusalem, Israel, Paper No. 14-HX-23, 1990, pp. 33–138.
35. Taylor, C. E. and Currie, I. G., Sealing strips in tubular heat exchangers, *Trans. ASME, J. Heat Transfer*, 109, 569–573 (1987).
36. Tinker, T., Shellside characteristics of shell and tube heat exchangers—Proceedings on General discussion on heat transfer, Parts I, II and III, *Inst. Mech. Eng. Lond.*, 97–116 (1951).
37. Tinker, T., Shellside characteristics of shell and tube heat exchangers—A simplified rating system for commercial heat exchangers, *Trans. ASME*, 80, 36–52 (1958).

38. Bell, K. J., Final report of the cooperative research program on shell and tube heat exchangers, Bull. No. 5, University of Delaware Engineering Experiment Station, New York, June 1963.
39. Bell, K. J., Delaware method for shellside design, in *Heat Exchangers—Thermal Hydraulic Fundamentals and Design* (S. Kakac, A. E. Bergles, and F. Mayinger, eds.), Hemisphere/McGraw-Hill, Washington, DC, 1981, pp. 581–618.
40. Bell, K. J., Delaware method for shellside design, in *Heat Transfer Equipment Design* (R. K. Shah, E. C. Subbarao, and R. A. Mashelkar, eds.), Hemisphere, Washington, DC, 1988, pp. 145–166.
41. Mukherjee, R., Effectively design shell and tube heat exchangers, *Chem. Eng. Prog., Am. Inst. Chem. Eng.*, 94(2), 21–37, February, 1998.
42. Hewitt, G. F., Shires, G. L., and Bott, T. R., *Process Heat Transfer*, CRC Press, Boca Raton, FL, 1994.
43. Kern, D. Q., *Process Heat Transfer*, McGraw-Hill, New York, 1950.
44. Donohue, D. A., Heat exchanger design, in *Petroleum Refiner: Part 1, Types and Arrangements*, Vol. 34, pp. 94–100; *Part 2, Heat Transfer*, Vol. 34, pp. 9–8; *Part 3, Fluid Flow and Thermal Design*, Vol. 34, 1955, pp. 175–184; *Part 4, Mechanical Design*, Vol. 35, 1956, pp. 155–160.
45. Devore, A., Try this simplified method for rating baffled heat exchangers, *Hydrocarbon Process. Petrol. Refining*, 40, 221–233 (1961).
46. Bell, K. J., Approximate sizing of shell and tube heat exchangers, in *Heat Exchanger Design Handbook*, Vol. 3 (E. U. Schlunder, editor-in-chief), Hemisphere, Washington, DC, 1983, Section 3.1.4.
47. McAdams, W. H., *Heat Transmission*, 3rd edn., McGraw-Hill, New York, 1954, p. 229.
48. Taborek, J., Ideal tube bank correlations for heat transfer and pressure drop, in *Heat Exchanger Design Handbook*, Vol. 3 (E. U. Schlunder, editor-in-chief), Hemisphere, Washington, DC, 1983, Section 3.3.7.
49. Kays, W. M. and London, A. L., *Compact Heat Exchangers*, 3rd edn., McGraw-Hill, New York, 1984.
50. Briggs, D. E. and Young, E. H., Convection heat transfer and pressure drop of air flowing across triangular pitch bank of finned tubes, *Chem. Eng. Prog. Symp. Ser.*, No. 41, *Heat Transfer—Houston*, 59, 1–10 (1963).
51. Briggs, D. E., Katz, D. L., and Young, E. H., How to design finned tube heat exchangers, *Chem. Eng. Prog.*, 59, 49–59 (1963).
52. Xchanger Suite6® software, Heat Transfer Research, Inc. (HTRI), Alhambra, CA.
53. Aspen Shell & Tube Exchanger software, Heat transfer and fluid flow service (HTFS), Oxon, U.K.
54. Gentry, C. C., ROD baffle heat exchanger technology, *Chem. Eng. Prog.*, July, 48–57 (1990).
55. Gentry, C. C., ROD baffle heat exchanger design methods, *Sixth International Symposium on Transport Phenomena in Thermal Engineering*, Seoul, Korea, May 9–13, 1993, pp. 301–306.
56. Gentry, C. C., Young, R. K., and Small, W. M., RODbaffle heat exchanger thermal and hydraulic predictive methods, *Proceedings of the 7th International Heat Transfer Conference*, Munich, Germany, Vol. 6, Hemisphere, Washington, DC, 1982, pp. 197–202.
57. Gentry, C. C., Young, R. K., and Small, W. M., RODbaffle heat exchanger thermal and hydraulic predictive methods for bare and low finned tubes, *Proceedings of the 22nd National Heat Transfer Conference, Heat Transfer*, Niagara Falls, NY, 1984, *AIChE Symp. Ser.*, 80, 104–109 (1984).
58. Gentry, C. C., Young, R. K., and Small, W. M., A conceptual RODbaffle nuclear steam generator design, *1982 ASME Joint Power Generation Conference, Nuclear Heat Exchanger Sessions*, Denver, CO, October 17–21, 1982.
59. Hesselgraeves, J. E., *Proceedings of the 2nd UK National Conference on Heat Transfer*, Glasgow, U. K., Vol. 1, Institution of Mechanical Engineers, London, U.K., 1988, pp. 787–800.
60. Taborek, J., Longitudinal flow in tube bundles with grid baffles, in *Heat Transfer*, Philadelphia, PA, 1989, pp. 72–78.
61. (a) EMbaffle® Technology, a major advance in heat exchanger technology, (www.shellglobalsolutions.com/EMbaffle); (b) EMbaffle® Technology, Shell Global Solutions, (www.shellglobalsolutions.com/EMbaffle).
62. (a) Chunangad, K. S., Master, B. I., Thome, J. R., and Tolba, M. B., Helixchanger heat exchanger: Single-phase and two-phase enhancement, *Proceedings of the International Conference on Compact Heat Exchangers and Enhancement Technology for the Process Industries*, Begell House, New York, 1999, pp. 471–477; (b) Zhang, Z. and Fang, X., Comparison of heat transfer and pressure drop for the helically baffled heat exchanger combined with three-dimensional and two-dimensional finned tubes, *Heat Transfer Eng.*, Taylor & Francis Group, LLC, 27(7), 17–22 (2006).
63. (a) Design and Application of TWISTED TUBE® Heat Exchangers, Koch Heat Transfer Company, Houston, TX. (www.kochheattransfer.com); (b) Heat Transfer Innovators, Byron Black, Brown fintube innovators, pp. 1–9.
64. Butterworth, D., Guy, A. R., and Welkey, J. J., Design and application of twisted tube heat exchangers, advances in industrial heat transfer, *ICHEME*, 87–95 (1996).

65. Short, B. E., *Heat Transfer and Pressure Drop in Heat Exchangers*, Publication No. 4324, University of Texas, Austin, TX, 1943, pp. 1–55.
66. Donohue, D. A., Heat transfer and pressure drop in heat exchangers, *Ind. Eng. Chem.*, **41**, 2499–2511 (1969).
67. Slipcevic, B., Designing heat exchangers with disk and ring baffles, *Sulzer Tech. Rev.*, **3**, 114–120 (1976).
68. Slipcevic, B., Shellside pressure drop in shell and tube heat exchangers with disk and ring baffles, *Sulzer Tech. Rev.*, **60**, 28–30 (1978).
69. Goyal, K. P. and Gupta, B. K., An experimental performance evaluation of a disk and doughnut type heat exchanger, *Trans. ASME J. Heat Transfer*, **106**, 759–765 (1984).
70. Ratnasamy, K., Exchanger design using disc and donut baffles, *Hydrocarb. Process.*, April, 63–65 (1987).
71. Hausen, H., *Wärmeübertragung im Gegenstrom und Kreuzstrom*, Springer-Verlag, Berlin, Germany, 1950.
72. Heat Exchange Institute, *Standards for Closed Feedwater Heaters*, 8th edn., Heat Exchange Institute, Cleveland, OH, 1984, 2008.
73. Heat Exchange Institute, *Standards for Power Plant Heat Exchangers*, 4th edn., Heat Exchange Institute, Cleveland, OH, 2004.
74. Heat Exchange Institute, *Standards for Surface Condensers*, 10th edn., Heat Exchange Institute, Cleveland, OH, 2006.

SUGGESTED READINGS

- Bell, K. J., Overall design methodology for shell and tube exchangers, in *Heat Transfer Equipment Design* (R. K. Shah, E. C. Subbarao, and R. A. Mashelkar, eds.), Hemisphere, Washington, DC, 1988, pp. 131–144.
- Escoe, K. A., *Mechanical Design of Process Systems, Vol. 2, Shell and Tube Heat Exchangers, Rotating Equipment, Bins, Silos, Stacks*, Gulf Publishing Company, Houston, TX, 1995.
- Gentry, G. C., Gentry, M. C., and Scanlon, G. E., *Heating the Process and Fluid Flow, Shell and Tube Heat Exchanger Applications*, PTQ Autumn, 1999, pp. 95–101.
- Gulley, D., Troubleshooting shell and tube heat exchangers, *Hydrocarbon Process.*, September, 91–98, 1996.
- McNaughton, K. J. (ed.), *The Chemical Engineering Guide to Heat Transfer, Vol. I. Plant Principles*, Hemisphere/McGraw-Hill, New York, 1986.
- Mehra, D. K., Shell and tube exchangers, in *The Chemical Engineering Guide to Heat Transfer, Vol. I, Plant Principles* (K. J. McNaughton and the staff of Chemical Engineering, eds.), Hemisphere/McGraw-Hill, New York, 1986, pp. 43–52.
- Saunders, E. A. D., *Heat Exchangers: Selection, Design and Construction*, Addison Wesley Longman, Reading, MA, 1989.
- Soler, A. I., Expert system for design integration—Application to the total design of shell and tube heat exchangers, *Proceedings of the ASME, Thermal/Mechanical Heat Exchanger Design, Karl Gardner Memorial Session*, Vol. 118 (K. P. Singh and S. M. Shenkman, eds.), ASME PVP, Washington, DC, 1985, pp. 135–138.
- Taborek, J., Heat exchanger design, *Heat Transfer*, **4**, 269–285 (1978).
- Yokell, S., Heat exchanger tube-to-tubesheet connections, *The Chemical Engineering Guide to Heat Transfer, Vol. I, Plant Principles* (K. J. McNaughton, ed.), Hemisphere, New York, 1986, pp. 76–92.

6 Regenerators

6.1 INTRODUCTION

Waste heat recovery is an old technology dating back to the first open hearths and blast furnace stoves. The drastic escalation of energy prices has made waste heat recovery more attractive over the past two decades. Manufacturing and process industries such as glass, cement, primary and secondary metals, etc., account for a significant fraction of all energy consumed. Much of this energy is discarded in the form of high-temperature flue gas exhaust streams. Recovery of waste heat from flue gas by means of heat exchangers known as regenerator can improve the overall plant efficiency and serves to reduce the national energy needs and conserve fossil fuels. Figure 6.1 shows the cross section of a regenerative furnace [1]. Currently, interest in storage-type regenerators has been renewed due to their applications of heat recovery, heat storage, and general energy-related problems [2]. The objective of this chapter is to acquaint the readers with various types of regenerators, construction details, and thermal and mechanical design. Additionally, some industrial heat recovery devices for waste heat recovery are discussed.

6.1.1 REGENERATION PRINCIPLE

For many years, the regeneration principle has been applied to waste heat recovery by preheating the air for blast furnaces and steam generation. In the former, the regeneration is achieved with periodic and alternate blowing of the hot and the cold stream through a fixed matrix of checkered brick. During the hot flow period, the matrix receives thermal energy from the hot gas and transfers it to the cold stream during the cold stream flow. In the latter, the metal matrix revolves slowly with respect to two fluid streams. The two gas streams may flow either in parallel directions or in opposite directions. However, counterflow is mostly preferred because of high thermal effectiveness. The inclusion of an air preheater in a steam power plant improves the boiler efficiency and overall performance of the power plant.

6.1.2 REGENERATORS IN THERMODYNAMIC SYSTEMS AND OTHERS

The addition of regeneration as a thermodynamic principle improves the overall performance of the gas turbine power plants, steam power plants, and the heat exchangers embodying the thermodynamic cycle of Stirling, Ericsson, Gifford, McMohan, and Vuilleumier [3]. Regenerators are also used as a dehumidifier for air-conditioning applications, cryogenic separation processes, and in non-catalytic chemical reactors such as the Wisconsin process for the fixation of nitrogen and the Wulff process for pyrolysis of hydrocarbon feedstocks to produce acetylene and ethylene. The principle of regeneration applied to a gas turbine plant is described next.

6.1.3 GAS TURBINE CYCLE WITH REGENERATION

The simple gas turbine plant consisting only of compressor, combustion chamber, and turbine has the advantages of light weight and compactness. However, it is known for high specific fuel consumption compared to the modern steam power plant and reciprocating internal combustion engines. The single improvement that gives the greatest increase in thermal efficiency is the addition of a regenerator for transferring thermal energy from the hot turbine exhaust gas to the air leaving the compressor, especially when it is employed in conjunction with intercooling during compression.

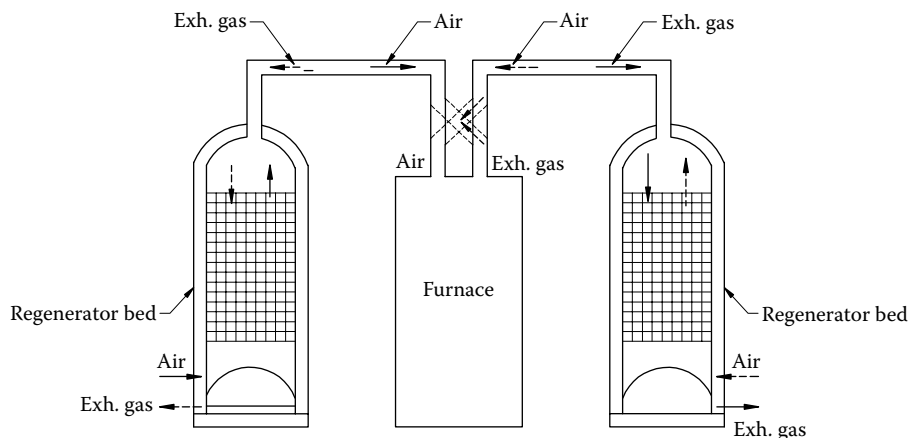


FIGURE 6.1 Regenerative furnace.

The addition of a regenerator results in a flat fuel economy versus load characteristic, which is highly desirable for the transportation-type prime movers like the gas turbine locomotives, marine gas turbine plant, and the aircraft turboprop.

6.1.4 WASTE HEAT RECOVERY APPLICATION

Substantial gains in fuel efficiency can be achieved by recovering the heat contained in the flue gas by the following four means [4]:

1. Reheating process feedstock.
2. Waste heat boiler and feed water heating for generating steam (low-temperature recovery system).
3. Preheating the combustion air (high-temperature recovery system).
4. Space heating—Rotary heat exchanger (wheel) is mainly used in building ventilation or in the air supply/discharge system of conditioning equipment. The wheel transfers the energy (cold or heat) contained in exhaust air to the fresh air supply to indoor. It is one important equipment and key technology in the field of construction energy saving.

Each of these methods of heat recovery has its own merits. According to Liang et al. [4], feedstock preheating is often best suited for continuous counterflow furnaces. Applications of this method, however, are often limited by high capital costs and large space requirements. Steam generation is an effective means for heat recovery when the demand for steam corresponds well to the availability of flue gas. Typical methods of steam generation include simple forced recirculation cycle, exhaust heat recovery with economizer, and exhaust heat recovery with superheater and economizer. Combustion air preheating is the most adaptable of heat recovery systems because it requires minimum modification to the existing system. This improves the system efficiency, and preheating the cold combustion air reduces the fuel requirement.

6.1.5 BENEFITS OF WASTE HEAT RECOVERY

Benefits of waste heat recovery can be broadly classified into two categories as follows.

6.1.5.1 Direct Benefits

Recovery of waste heat has a direct effect on the efficiency of the process. This is reflected in fuel savings.

6.1.5.2 Indirect Benefits

1. Reduction in pollution: A number of toxic combustible wastes such as carbon monoxide gas, sour gas, oil sludge, plastic chemicals, etc., released to atmosphere if burnt in the incinerators are avoided.
2. Reduction in sizes of flue gas handling equipment such as fans, stacks, ducts, and burners since waste heat recovery reduces the fuel consumption, which leads to reduction in the flue gas produced.
3. Reduction in energy consumption by auxiliary equipment due to reduction in equipment sizes.

6.1.5.3 Fuel Savings due to Preheating Combustion Air

Recuperators of high-temperature furnaces can provide and increase the process efficiency. Fuel savings depends on parameters such as [5]

1. Exhaust gas temperature
2. Preheat combustion air temperature
3. Effectiveness of the recuperator

The higher the percentage of exhaust gas temperature, the higher the percentage of fuel that can be saved. For a flue gas temperature of 1350°C and an air preheated temperature of 1100°C, the theoretical fuel savings achievable is approximately 65% of fuel consumption of an unrecuperated furnace operating at the same temperature levels.

6.2 HEAT EXCHANGERS USED FOR REGENERATION

The heat exchanger used to preheat combustion air is called either a recuperator or a regenerator. Thermodynamically, the exhaust gas thermal energy is in part recuperated or regenerated, and this same thermodynamic function is served regardless of the type of heat exchanger employed. The thermodynamic principle of regeneration is discussed in the following.

6.2.1 RECUPERATOR

A recuperator is a convective heat transfer-type heat exchanger where the two fluids are separated by a conduction wall through which heat transfer takes place due to convection or a combination of radiation and convective design. The fluids flow simultaneously and remain unmixed. There are no moving parts in the recuperator. Some examples of recuperators are tubular, plate-fin, and extended surface heat exchangers. Recuperators are used when the flue gas is clean and uncontaminated. An integral bypass solution can be applied to the waste heat recovery units. The system consists of louvre-type dampers, which can be either pneumatic actuated or hydraulic operated depending on individual customer requirements. The gas flow over the heat convection bank is modulated depending on the outlet fluid temperature. A convective recuperator is shown in Figure 6.2.

6.2.1.1 Merits of Recuperators

The recuperators have the advantages of (1) ease of manufacture, (2) stationary nature, (3) uniform temperature distribution and hence less thermal shock, and (4) absence of sealing problem. However, their use is limited due to the requirement of temperature-resistant material to withstand the high-temperature flue gas and to retain its shape under operating temperature and pressure. Also, recuperators are subject to degradation in heat recovery performance by fouling from exhaust-gas-borne volatiles and dust.



FIGURE 6.2 Waste heat recovery recuperative heat exchanger. (Courtesy of GEA Iberica S.A., Vizcaya, Spain.)

6.2.2 REGENERATOR

A regenerator consists of a matrix through which the hot stream and cold stream flow periodically and alternatively. First the hot fluid gives up its heat to the regenerator. Then the cold fluid flows through the same passage, picking up the stored heat. The passing of hot fluid stream through a matrix is called the hot blow and the cold flow is called the cold blow. Thus, by regular reversals, the matrix is alternatively exposed to the hot and cold gas streams, and the temperature of the packing, and the gas, at each position fluctuates with time. Under steady-state operating conditions, a number of cycles after the start-up of the regenerator, a condition of cyclic equilibrium is reached where the variations of temperature with time are the same during successive cycles and the period of hot blow and the cold blow should ensure sufficient time to absorb and release heat. From this, the regenerators can be distinguished from recuperators. In the case of recuperators, heat is transferred between two fluid streams across some fixed boundary, and conditions at any point depend, during steady-state operation, only on the position of that point, whereas in the case of regenerators, the heat transport is transient and conditions depend on both position and time.

Figure 6.3 shows the temperature field in a regenerator, for both the fluid and matrix at the instant of flow reversal. The upper curve represents the temperature of the fluid and matrix at the end of the hot blow and the start of the cold blow. The lower curves represent temperature conditions at the end of the cold blow and the start of hot blow. At any particular station along the length of the matrix, the temperatures may fluctuate between the upper and lower curves in a time-dependent relationship.

6.2.3 TYPES OF REGENERATORS

Since the matrix is alternatively heated by the hot fluid and cooled by the cold fluid, either the matrix must remain stationary and the gas streams must be passed alternatively or the matrix must be rotated between the passages of the hot and cold gases. Hence, the regenerator may be classified according to its position with respect to time as (1) fixed-matrix or fixed-bed and (2) rotary regenerators.

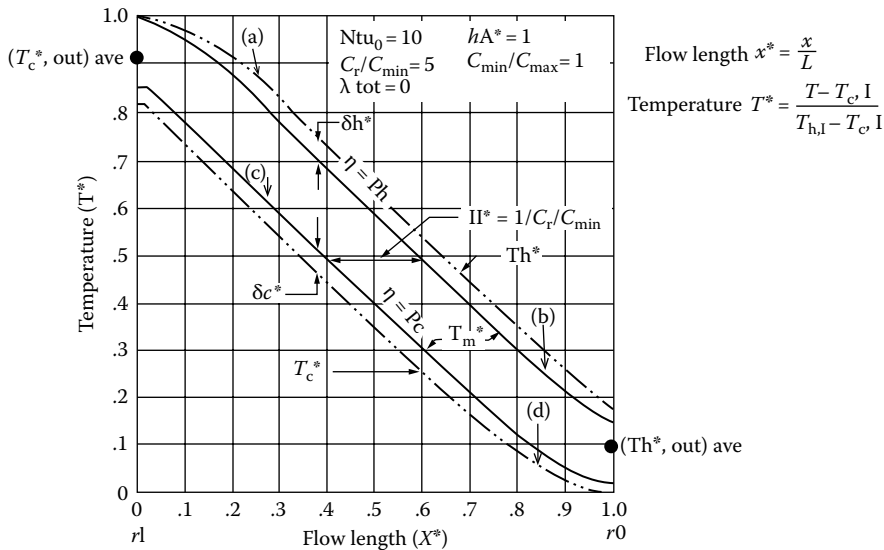


FIGURE 6.3 Balanced regenerator temperature distribution at switching instants. (a) Hot fluid temperature at end of the hot blow; (b) matrix temperature at end of the hot blow and start of the cold blow, (c) hood arrangements and (d) matrix temperature at the end of the cold blow; and (d) cold fluid temperature at the end of cold blow. (From Mondt, J.R., *Trans. ASME J. Eng. Power*, 86, 121, 1964.)

6.2.4 FIXED-MATRIX OR FIXED-BED-TYPE REGENERATOR

The fixed-matrix or fixed-bed or storage-type regenerator is a periodic-flow heat transfer device with high thermal capacity matrix through which the hot fluid stream and cold fluid stream pass alternatively. To achieve continuous flow, at least two matrices are necessary as shown in Figure 6.1. The flow through the matrix is controlled by valves. According to the number of beds employed, the fixed matrix regenerators are classified into two categories: (1) single-bed and (2) dual-bed valved. In a dual-bed valved type, shown in Figure 6.4, initially matrix A is heated by the hot fluid

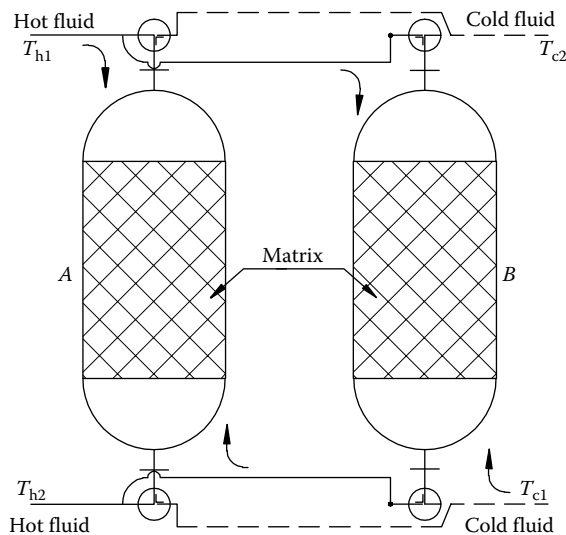


FIGURE 6.4 Dual-bed valved-type regenerator. (Adapted from Mondt, J.R., *Regenerative heat exchangers: The elements of their design, selection and use*, Research Publication GMR-3396, General Motors Research Laboratories, Warren, MI, 1980.)

and matrix B is cooled by the cold fluid. After a certain interval of time, the valves are operated so that the hot fluid flows through B and transfers heat to it. Cold fluid, however, flows through A and the fluid is being heated. The switching process continues periodically. Some examples of storage-type heat exchangers are fixed-bed air preheaters for blast furnace stoves, glass furnaces, and open hearth furnaces.

Shape: The shape of matrix used for the construction of a fixed-matrix regenerator is dependent upon the application. For example, in the glass-making industry, the matrix is often constructed from ceramic bricks arranged in patterns such as pigeonhole setting, closed basket weave setting, and open basket weave setting. In the steel-making industry, the gases are much cleaner and a variety of proprietary configurations such as Andco checkers, McKee checkers, Kopper checkers, and Mohr checkers are used in place of the brick arrangements. Most of these types of checkers employ tongue-and-groove shapes, which provide a bonded structure of higher stability, because regenerators in the steel-making industry are normally much taller than in the glass industry.

Construction features: A fixed regenerator is generally constructed of either a porous matrix or checkers. The porous matrix forms a long, tortuous path for the flowing fluid in order to provide the largest possible contact surface between the regenerator matrix and the fluid. Checkers are blocks with holes pierced through them. Additional details on checkers and settings are given next.

Checkers: Checkers are the tools of heat recovery; they consist of a large quantity of bricks properly arranged in an orderly setting creating many small flues and offering a large surface area for heat absorption and release. The design of the brick, their proper setting, and flow of turbulent gases in the flues are the keys to efficient heat recovery.

Settings: The development of special strapped bricks and their setting in checkers potentially yield higher efficiencies through improved heat transfer features. The open basket weave setting has been popular in the glass industry. The brick checkers geometry commonly used in the valved-type glass furnace regenerator are essentially an offset strip fin having a large fin thickness.

6.2.4.1 Fixed-Matrix Surface Geometries

Noncompact surface geometry: The commonly used checker shapes have a surface area density range of 25–42 m²/m³ (8–13 ft²/ft³). The checker flow passage (referred to as flue) size is relatively large primarily due to the fouling problem. A typical heat transfer coefficient in such a passage is about 5 W/m² K (1 Btu/h ft²°F) [3].

Compact surface geometry: The surface geometries used for the compact fixed-matrix regenerator are similar to those used for rotary regenerators, but in addition quartz pebbles, steel, copper, or lead shots, copper wool, packed fibers, powders, randomly packed woven screens, and crossed rods are used.

6.2.4.2 Size

The fixed-bed regenerators are usually very large heat exchangers, some having spatial dimensions up to 50 m height and having unidirectional flow periods of many hours.

6.2.4.3 Merits of Fixed-Bed Regenerators

Fixed-bed regenerators consisting of a packed bed of refractory offer the following inherent advantages:

1. If loosely packed, the bed material is free to expand thermally; hence, thermal stresses are low.
2. Regenerators of this type are easily equipped so that the bed materials can be removed, cleaned, and replaced.
3. Unlike a recuperator, accumulated fouling does not reduce the heat exchanger capability of a regenerator; it merely increases the resistance to flow [6].

The major disadvantages of fixed-bed regenerators are the additional complexity and cost associated with the flow-switching mechanisms.

6.2.5 ROTARY REGENERATORS

A rotary regenerator (Figure 6.5), also known as heat wheel, consists of a rotating matrix through which the hot and cold fluid streams flow continuously. The rotary regenerator is also called a periodic-flow heat exchanger since each part of the matrix, because of its continuous rotation, is exposed to a regular periodic flow of hot and cold gas streams. The rotary regeneration principle is achieved by two means: (1) the flow through the matrix is periodically reversed by rotating the matrix, and (2) the matrix is held stationary whereas the headers are rotated continuously. Both the approaches are rotary because for either design approach, heat transfer performance, pressure drop, and leakage considerations are the same, and rotary components must be designed for either system. The examples for rotary regenerators are (1) the Rothemuhle type and (2) the Ljungstrom type. In the Rothemuhle type, the connecting hood rotates while the heat transfer matrix is stationary (Figure 6.5c(ii)), whereas in Ljungstrom type the matrix rotates and connecting hood is stationary (Figure 6.5c(i)). The rotary regenerators are also used in vehicular gas turbine engines and as a dehumidifier in HVAC applications.

6.2.5.1 Salient Features of Rotary Regenerators

The periodic flow rotary regenerator is characterized by the features such as those given in the following:

1. A more compact size ($\beta = 8800 \text{ m}^2/\text{m}^3$ for rotating type and $1600 \text{ m}^2/\text{m}^3$ for fixed matrix type), shape, desired density, porosity, and low hydraulic diameter can be achieved by pressing the metal strips, wire mesh, or sintered ceramic and hence less expensive surface per unit transfer area.
2. The porous matrix provides a long, tortuous path and hence large area of contact for the flowing fluids.
3. The absence of a separate flow path like tubes or plate walls but the presence of seals to separate the gas stream in order to avoid mixing due to pressure differential.
4. The presence of moving parts like the rotary core in rotary regenerators and alternate closing and opening of valves in a fixed regenerator.
5. With rotary regenerators, high effectiveness can be obtained since the matrix can be heated up to nearly the full exhaust gas temperature.
6. To achieve very high thermal effectiveness approaching unity, the thermal capacity of the matrix should be very large compared to the working fluids. This requirement restricts the use of regenerators exclusively to gaseous applications.
7. Bypass leakage from the high-pressure cold stream to the low-pressure hot stream and carryover loss from one stream to the other with flow reversal or rotary nature of the matrix. However, the bypass leakage problem is less in a dehumidifier for an air-conditioning application.
8. Application to both high temperatures (800°C – 1100°C) for metal matrix, and 2000°C for ceramic regenerators for services like gas turbine applications, melting furnaces or steam power plant heat recovery, and cryogenic applications (-20°).
9. Operating pressure of 5–7 bar for gas turbine applications and low pressure of 1–1.5 bar for air dehumidifier and waste heat recovery applications.
10. Regenerators have self-cleaning characteristics because the hot and cold gases flow in the opposite directions periodically through the same passage. As a result, compact regenerators have minimal fouling. If heavy fouling is anticipated, regenerators are not used.
11. Normally a laminar flow condition prevails, due to the small hydraulic diameter.

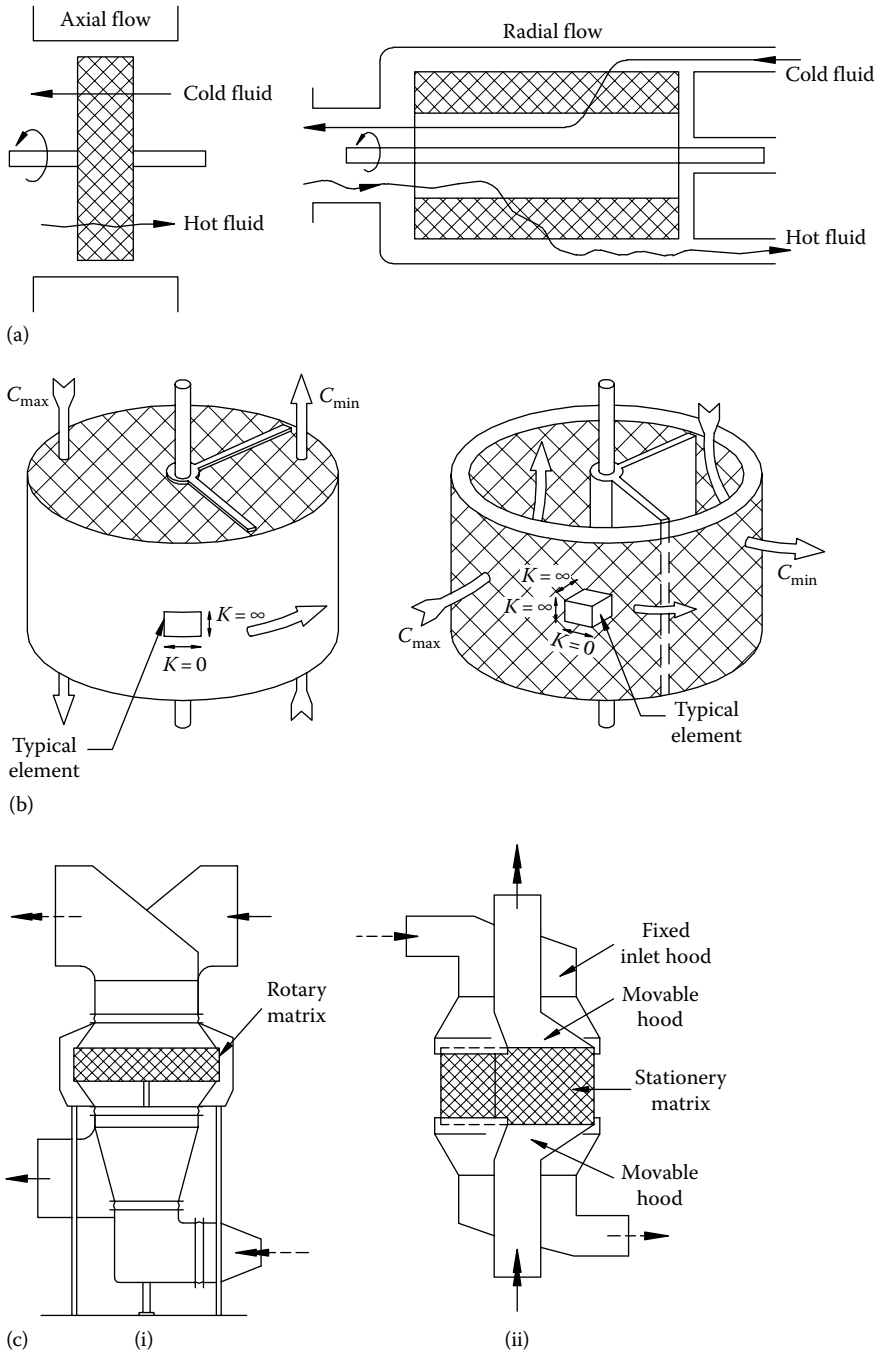


FIGURE 6.5 Rotary regenerator. (a) Disk and drum type (From Coppage, J.E. and London, A.L., *Trans. ASME*, 75, 779, 1953), (b) illustrative arrangement of matrix (From Bahnke, G.D. and Howard, C.P., *Trans. ASME J. Eng. Power*, 86, 105, 1964), and (c) two alternative forms of disk-type rotary regenerator: (i) Ljungstrom type and (ii) Rothenmuhle type.

6.2.5.2 Rotary Regenerators for Gas Turbine Applications

One of the important areas of rotary regenerator applications is in vehicular gas turbine engines. Starting in the 1950s, the vehicle industry intensively researched gas turbine power plants, which included rotary regenerators. Both disk and drum regenerators were developed by General Motors and other vehicle builders for gas turbine engines. Their engine programs significantly advanced all facets of regenerator technology such as improved modeling, heat transfer surfaces for the matrix, sealing designs, and materials, both metals and ceramics [2].

6.2.5.3 Types of Rotary Regenerators

Though two types of rotary regenerators—(1) disk and (2) drum types (shown in Figure 6.5a)—the most commonly used configuration is of disk type. The disk-type matrix consists of alternate layers of corrugated, flat, thin metal strips wrapped around a central hub or ceramic pressing in a disk shape. Gases flow normal to the disk. In an ideal circumstance without maldistribution, the single-disk design is favored due to less seal length and lower seal leakage. Depending upon the applications, disk-type regenerators are variously referred to as heat wheel, thermal wheel, Muntz wheel, or Ljungstrom wheel. The schematic of disk-type rotary regenerator with ducts is shown in Figure 6.5c. The drum-type matrix consists of heat exchanger material in a hollow drum shape. Gases flow radially through the drum. The cost of fabricating a drum-type regenerator is much higher than that for a disk-type regenerator, and hence the drum is not used in any applications.

6.2.5.4 Drive to Rotary Regenerators

The matrix in the regenerator is rotated by a hub shaft or a peripheral ring gear drive. Most ceramic regenerators have been driven at the periphery, probably because of their brittleness.

6.2.5.5 Operating Temperature and Pressure

The regenerators are designed to cover an operating temperature range from cryogenic to very high temperatures. Metal regenerators are used for operating temperatures up to about 870°C (1600°F). Ceramic regenerators are used for higher temperature, up to about 2000°C (3600°F). Regenerators are usually designed for a low-pressure application. Rotary regenerators are limited to operating pressures about 615 kPa or 90 psi and even lower pressures for fixed-matrix regenerators.

6.2.5.6 Surface Geometries for Rotary Regenerators

The rotary regenerator surfaces consist of many uninterrupted passages in parallel. The most common are triangular, rectangular, circular, or hexagonal smooth continuous passages. Details on the foregoing surface geometries are provided in Ref. [2]. Interrupted passage surfaces (such as strip fins, louver fins) are not used because a transverse flow leakage will be present if the two fluids are at different pressures. Hence, the matrix generally has continuous, uninterrupted flow passages and the fluid is unmixed at any cross section for these surfaces. Some surface geometries for rotary regenerator are shown in Figure 6.6.

6.2.5.7 Influence of Hydraulic Diameter on Performance

Packings having small hydraulic diameter will provide the highest heat transfer coefficients; for laminar flow, $h \propto 1/D_h$. However, the associated fouling by the hot gas may limit the size of the flow passages. Very small passage size may be used in air ventilation heat recovery regenerators compared to in those used for exhaust gas heat recovery, particularly from coal-fired exhaust gases or glass furnace exhausts. As passage size is reduced, the number of passages required increases, while the passage length must decrease if the pressure drop is to be maintained constant. The conventional shell and tube heat exchanger cannot exploit this characteristic very far as a large number of small tubes introduce fabrication difficulties and short tube lengths prevent the use of counterflow.

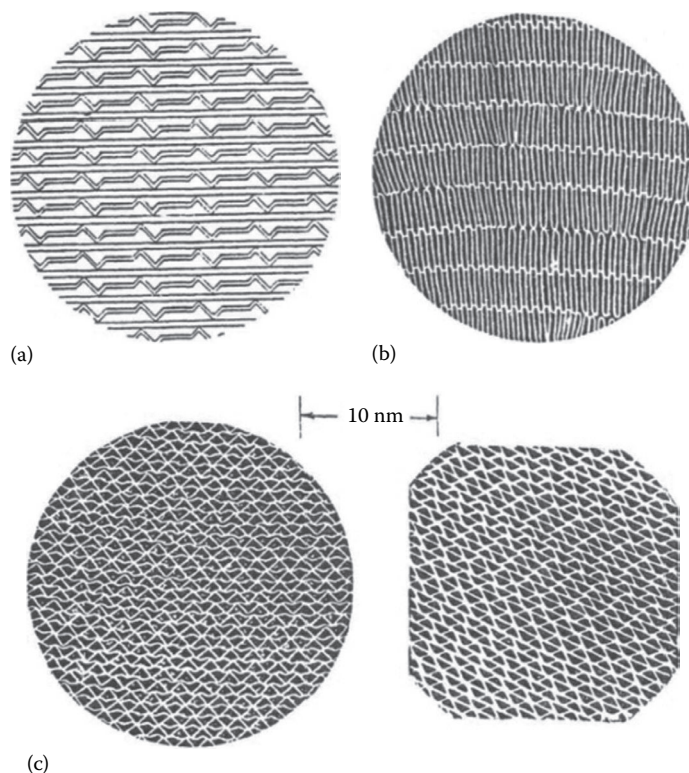


FIGURE 6.6 Surface geometries for rotary regenerator matrix. (a) Nonuniform complex profile, (b) rectangular, and (c) triangular. (From Mondt, J.R., *Regenerative heat exchangers: The elements of their design, selection and use*, Research Publication GMR-3396, General Motors Research Laboratories, Warren, MI, 1980.)

6.2.5.8 Size

Typical power-plant regenerators have the rotor diameter up to 10 m (33 ft) and rotational speeds in the range of 0.5–3 rpm. The air ventilating regenerators have the rotors with 0.25–3 m (0.8–9.8 ft) diameters and rotational speeds up to 10 rpm. The vehicular regenerators have diameters up to 0.6 m (24 in.) and rotational speeds up to 18 rpm [3].

6.2.5.9 Desirable Characteristics for a Regenerative Matrix

Desirable characteristics of a regenerator matrix include the following [7]:

1. A large and solid matrix, for maximum heat capacity.
2. A porous matrix without obstruction, to minimize the possible blocking and contamination.
3. A large, finely divided matrix, to achieve maximum heat transfer rate.
4. A small, highly porous matrix, for minimum flow losses.
5. A small, dense matrix, for minimum dead space.

Other desirable matrix properties include negligible thermal conduction in the direction of fluid flow, to minimize longitudinal conduction, and maximum specific heat, for high thermal capacity.

6.2.5.10 Total Heat Regenerators

Up to this point, consideration has only been given to the transfer of sensible heat between two fluid streams and the intermittent storage of thermal energy, as sensible heat, in a solid matrix. A number of variations on these conditions are possible; for example, rotary regenerators are designed to

transfer both sensible heat and latent heat of vapors mixed with the gas stream, known as total regenerators. They are intended mainly for air-conditioning applications and can employ both absorbent fibrous materials and nonabsorbent materials like plastics.

6.2.5.11 Merits of Regenerators

Among their advantages, regenerators

1. Can use compact heat transfer materials
2. Can use less expensive heat transfer surfaces
3. Are self-cleaning because of periodic flow reversals
4. Can use simpler header designs

In contrast, there are several major disadvantages of the periodic flow regenerators. They are as follows:

1. Seals suitable for pressure differentials of 4–7 bar represent a major problem; the necessity of provision of seals between the hot fluids due to high-pressure differential, and the leakage problem enhanced due to the thermal expansion and contraction of the matrix.
2. Many more changes of flow direction are required as compared to the recuperators, resulting in flow losses and requiring expensive ducting.
3. Restrictions in pressure drop make necessary a large flow area with the usual matrix surface. As a consequence, the advantage of small matrix volume is somewhat nullified by the requirement of bulky approach ducting.
4. Carryover and leakage losses, especially for the high-pressure compressed air that has absorbed the compressor work.
5. Always some amount of mixing of the two fluids due to carryover and bypass leakages. Where this leakage and subsequent fluid contamination is not permissible (e.g., cryogenic systems), the regenerator is not used.
6. The high thermal effectiveness, approaching unity, provided by the regenerator demands a heat capacity of the matrix considerably larger than that of the working fluid. This requirement restricts the use of regenerators to gases only.
7. The rotary designs require a drive and support system.

6.3 ROTARY REGENERATIVE AIR PREHEATER

An air preheater is a general term used to describe any heat transfer device designed to heat air before it is used in another process, for example, combustion in a boiler. Air preheaters may also be used as process gas heat exchangers, which recover waste heat from one gas stream and use it to heat or preheat another. Available in a broad range of sizes, arrangements, and materials, Ljungström® rotary regenerative air preheater finds applications in electrical power generating plants, fluidized bed boilers, large industrial boilers, hydrocarbon and chemical processes, waste incinerators and drying systems, flue gas and other reheating systems, etc., due to its high thermal effectiveness, proven performance and reliability, effective leakage control, compactness of its design, and its adaptability to various fuel burning process. Construction types of regenerative air preheaters include traditional two sector type, three sector, four sector, and concentric types. A picture of Howden air preheater is shown in Figure 6.7. Air preheaters and gas-to-gas heat exchangers function similarly. Regenerative gas–gas heater is a special type of regenerative heater by design and material, and it is adapted to hard conditions of power plant desulphurization. Leading air preheater manufacturers include Howden, UK, ALSTOM Power Air Preheater Company and Balcke-Dürr GmbH, Germany. Salient features of air preheater are discussed later.

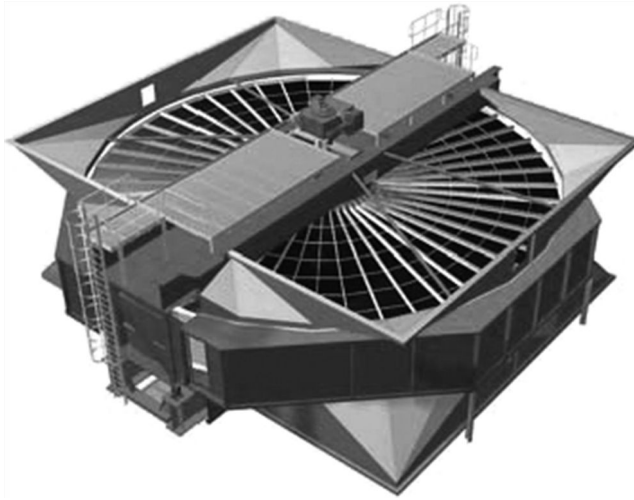


FIGURE 6.7 Picture of air preheater. (© Howden Group Limited.)

6.3.1 DESIGN FEATURES

Metallic heat transfer surfaces are contained in the rotor that turns at 1–3 rpm, depending on the size of the unit. A typical rotor under refurbishment is shown in Figure 6.8. The rotor housing and rotor have sealing members to form separate gas and air passages through the heat exchanger. The rotor drive unit, cleaning device mechanism, rotor bearing assemblies, and sealing surface adjuster



FIGURE 6.8 Refurbishment of air preheater rotor matrix. (© Howden Group Limited.)

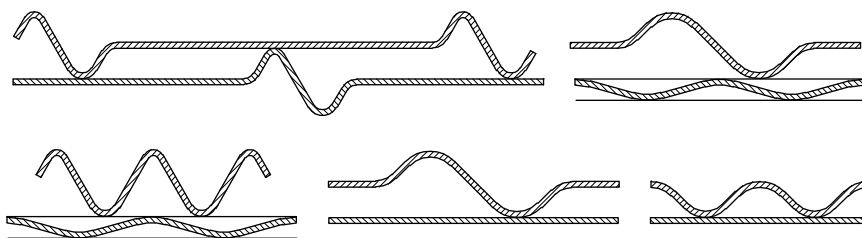


FIGURE 6.9 Regenerator heating elements profile.

are all located externally and are readily accessible while the unit is in operation. The overall design of the rotary regenerative heat exchanger lends itself to modularization. This helps reduce the time and effort required for on-site erection and maintenance.

6.3.2 HEATING ELEMENT PROFILES

The selection of the optimum heat transfer surface configuration for each application results in the highest level of thermal efficiency for the available pressure drop, which is cleanable and otherwise compatible with the fuel that is being fired. With a range of individual profiles, simple “open” profiles that have a lower tendency for fouling but correspondingly lower heat transfer properties to more complex profiles which are more compact and induce turbulence in the gas flow to improve heat transfer. The choice of heating element is vital to ensure that the optimum combination of heat transfer and pressure drop is achieved. Few profiles of heating elements are shown in Figure 6.9.

6.3.3 ENAMELED ELEMENTS

In applications where heat transfer surfaces are exposed to highly corrosive atmospheres and low exit gas temperatures, alloy steels or porcelain enamel coatings can be utilized. Selective enameled heat exchanger elements of Howden make are shown in Figure 6.10. It was found that porcelain enamel coatings are the most cost-effective means of providing an extremely high level of acid resistance for this application. Additionally, this enamel coating has been found to provide a highly smooth glass-like surface, more readily facilitating the cleaning of ash deposits.

6.3.4 CORROSION AND FOULING

All air preheaters on coal- and oil-fired plants are subject to some degree of corrosion and fouling caused by the approach to either the sulfuric acid or water dew point. Cold end fouling can be caused by the high sulfur content in the fuel oil in combination with very low combined cold end temperatures or due to insufficient ash in the flue gas to absorb the condensing acid formed from the sulfur in the fuel. Cold end corrosion can be minimized by the use of a cold end layer of higher grade steel or enamel coating. Hot end elements are prone to fouling as a result of large particles of fused ash becoming lodged in the element passages and smaller particles compacting behind them. These large particles generally arise as a result of less than optimum combustion conditions in the furnace. This can be overcome by the use of an element profile that is less prone to fouling and easier to clean and/or by the installation of hot end soot blowers.

6.3.5 HEAT EXCHANGER BASKETS

Baskets are designed and manufactured to ensure that the elements remain tightly packed to avoid damage caused by vibration while the air preheater or gas–gas heater is operating. A typical heat exchanger basket of Howden air preheater is shown in Figure 6.11.

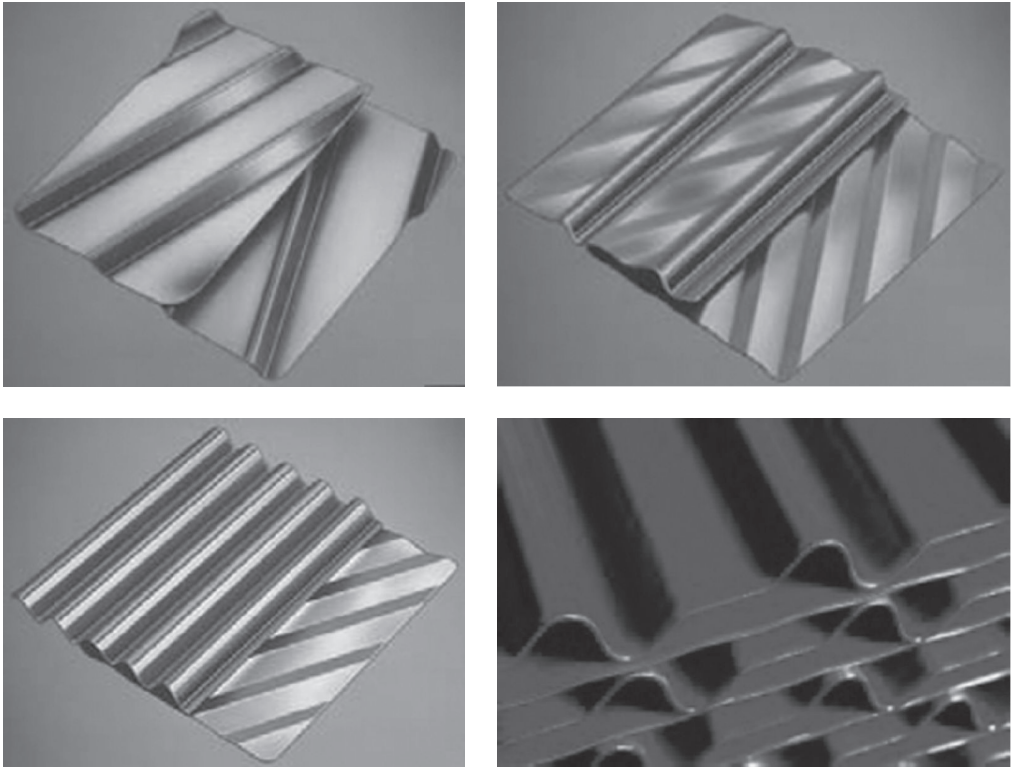


FIGURE 6.10 Enameled elements of rotary regenerative heat exchanger. (© Howden Group Limited.)



FIGURE 6.11 Rotary regenerator heat exchanger elements basket. (© Howden Group Limited.)

6.3.6 SEALS AND SEALING SYSTEM COMPONENTS

6.3.6.1 Radial Seals and Sector Plates

Radial seals and sector plates are located at the hot and cold ends of the air preheater. The radial seals that separate the individual rotor compartments, and as the rotor turns the seals pass in close proximity to the sector plates located between the air and gas sides of the air preheater. The purpose of these seals is to reduce the area available for leakage from the air to the gas side between the rotor and the air preheater housing.

6.3.6.2 Axial Seals and Sealing Plates

Axial seals, used in conjunction with bypass seals, minimize leakage passing radially around the rotor shell. The axial seals are mounted on the outside of the rotor shell and seal against the axial seal plates mounted on the air preheater housing.

6.3.6.3 Circumferential Seals and Circumferential Sealing Ring

Circumferential seals are mounted on the rotor and the sealing ring connected to the housing. The circumferential seals and sealing ring prevent air and gas from bypassing the heating surface through the space between the rotor and the housing shell. They also prevent air and gas from flowing axially around the rotor.

6.3.7 LEAKAGE

Air preheaters suffer from leakage drift, i.e., the significant increase in leakage over a period of time. This can affect boiler operation in a number of ways, such as increasing fan power, increasing velocities in the precipitators, reducing the flow of hot air to the mills, or shrinking the draught fan margins. Hence, reducing and maintaining low air preheater leakage is vital for the overall performance of the thermal system. Seals can wear due to soot blowing, corrosion, erosion, and contact with the static sealing surfaces on start-up and/or shutdown. Seal wear and seal settings should be checked as per schedule so that seals can be reset to proper clearances or replaced should they exhibit excessive wear. Sealing plate surfaces may also wear due to contact with the seals and erosion, and they may also become out of level and out of plane. Seal plate wear should also be repaired, plate alignments should be verified as soon as the need is detected. By fitting the sealing as that of Howden VN sealing system, these problems can be reduced or eliminated. Figure 6.12 shows computer model of Howden VN air preheater. The system improves the seal design on both the rotor and the casing, and dispenses with the need for actuated sector plates. In addition to better heat recovery and improved thermal performance, a peripheral benefit of using the Howden VN sealing system is a reduction in maintenance requirements on the air preheater.

6.3.8 ALSTOM POWER TRISECTOR LJUNGSTRÖM® AIR PREHEATER

Designed for coal-fired applications, the *Alstom Power* trisector Ljungström® air preheater permits a single heat exchanger matrix to perform two functions: coal drying and combustion air heating. Because only one gas duct is required, the need for ductwork, expansion joints, and insulation

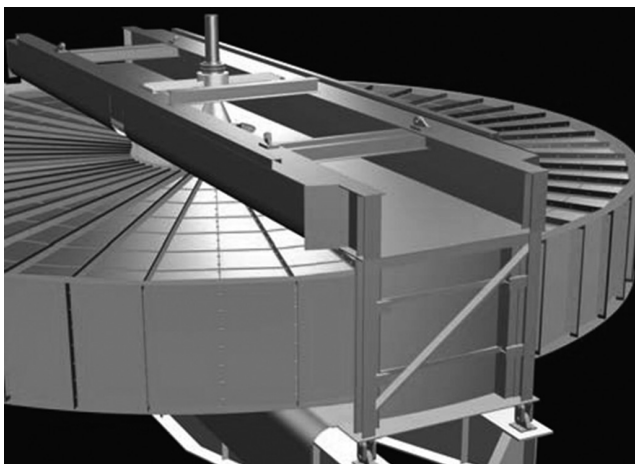


FIGURE 6.12 Computer model of Howden VN air preheater-ducting removed. (© Howden Group Limited.)

is greatly reduced when compared with a separate air heating system. Equipment layout is simplified, less structural steel is needed to install the system, and less cleaning equipment is required. The design has three sectors: one for flue gas, the second sector for primary air that dries the coal in the pulverizer, and the third sector is for preheating the secondary air that goes to the boiler for combustion.

6.4 COMPARISON OF RECUPERATORS AND REGENERATORS

1. A recuperator is easier to build and rugged in design. For a given size, the recuperator is less effective than the regenerator due to lower overall mean temperature difference. The regenerator, on the other hand, is smaller and, for its size, a much more efficient heat exchanger. Much higher surface area, higher heat transfer coefficients because of random nature of flow through the packing, and a higher overall temperature difference as the top of the packing is heated to the exhaust gas temperature [7] are found.
2. Because a recuperator is not rotating and is at a constant temperature, there is less thermal shock and many normal materials can be used. Because of periodic flow, regenerators are subjected to thermal shock.
3. A recuperator does not have the problem of sealing between the hot and cold gas streams.

6.5 CONSIDERATIONS IN ESTABLISHING A HEAT RECOVERY SYSTEM

Although the addition of a regenerator is highly attractive from a thermodynamic point of view, its bulk, shape, mass, or cost may be such as to nullify the thermodynamic advantages. Optimum design therefore will call for a careful consideration of the following factors [4]:

1. Heat recovery—Quality and quantity
Quality: Depending upon the type of process, waste heat can be recovered at virtually from that of chilled cooling water to high temperature waste gases from an industrial furnace or kiln. Usually higher the temperature, higher the quality and more cost effective is the heat recovery.
Quantity: In any heat recovery situation, it is essential to know the amount of heat recoverable and also how it can be used.
2. Compatibility with the existing process [8].
3. Initial capital cost.
4. Economic benefits.
5. Life of the equipment.
6. Maintenance and cleaning requirement.
7. Controllability and production scheduling.

Other limitations include manufacturing limitations, and weight, space, and shape limitations.

6.5.1 COMPATIBILITY WITH THE EXISTING PROCESS SYSTEM

In order for a heat exchanger to be integrated into a process, the system design must be compatible with the process design parameters. One key area of compatibility is pressure drop. Many combustion processes are designed to use the natural draft of a stack to remove the products of combustion from the process. The heat recovery equipment designed for such a process either must be designed within the pressure drop limitations imposed by natural draft or must incorporate an educator to overcome these pressure-drop restrictions [8].

6.5.2 ECONOMIC BENEFITS

It is necessary to evaluate the selected waste heat recovery system on the basis of financial analysis such as investment, depreciation, payback period, fuel savings, rate of return, etc.

6.5.2.1 Capital Costs

The capital costs include the heat exchanger costs and the ancillary equipment required for the functioning of the system. Such ancillary equipment includes the following:

Blowers: Both the flue gas and the preheat air streams would require blowers to overcome pressure losses in the system.

Ducting: Ducting is between the furnace and the heat exchanger to conduit the flue gas and the preheat air.

Controls: The proposed heat recovery system would be operated in conjunction with the demand of the furnace. A control mechanism would be established for this purpose.

Energy savings: The benefits of energy savings due to the heat recovery system should offset the capital costs on heat exchanger, blowers, ducting and control mechanisms, and maintenance cost. A break-even analysis (capital costs vs. fuel savings) will help in this regard. The desired economic benefits can be accomplished by designing a heat exchanger to [8]

1. Maximize the equipment life
2. Maximize the energy cost savings
3. Minimize the equipment capital costs

6.5.3 LIFE OF THE EXCHANGER

The success of waste heat recovery depends on the maximum equipment life against the hostile environment of exhaust gases. The factors that affect the heat exchanger life are [8]

1. Excessive thermal stress
2. Creep
3. Thermal fatigue and thermal shock
4. High-temperature gaseous corrosion

Corrosion and stress cause accelerated failure in both metal and ceramic recuperators, resulting in leakage, which degrades the performance.

6.5.4 MAINTAINABILITY

Ideally, a heat exchanger should provide long service life and the equipment installation should facilitate easy maintenance. Where necessary, the design should incorporate provisions to isolate the heat exchanger from the system so that inspection, maintenance, repairs, and replacement can be made without interrupting the process, and the ability to clean the fouling deposits from the heat transfer surfaces should be provided for those processes in which fouling will take place [8].

6.6 REGENERATOR CONSTRUCTION MATERIAL

An important requirement of a regenerator for waste heat recovery is life and extended durability. Regenerators are to work under hostile environments including (1) elevated temperatures, (2) fouling particulates, (3) corrosive gases and particulates, and (4) thermal cycling [9]. To achieve

this requirement, proper material selection is vital. Much of the waste heat is in the form of high temperature (1900°F – 3000°F), and the exhaust gases are corrosive in nature. Therefore, the two important considerations for selecting material for heat exchangers of a heat recovery system are (1) strength and stability at the operating temperature, and (2) corrosion resistance. Other parameters include low cost, formability, and availability.

6.6.1 STRENGTH AND STABILITY AT THE OPERATING TEMPERATURE

Metals are ideal for recuperator and regenerator construction because of their ductility and ease of fabrication. But the metallic units lack the ability to withstand high temperatures and are susceptible to corrosion from exhaust gases. Stainless steels and certain nickel- and iron-based alloys are the conventionally preferred materials. Generally, carbon steel at temperatures above 425°C (800°F) and stainless steel at temperatures above 650°C (1200°F) begin to rapidly oxidize, and if the exhaust stream contains corrosive constituents, there will be a severe corrosion attack [10]. Approximate temperature ranges for various heat exchanger materials are shown in Figure 6.13 [11]. In general, above 1600°F , metal heat exchangers have limitations due to excessive costs from the expensive alloys required, requirements of temperature control devices or loss of effectiveness due to air dilution, and maintenance problems due to high thermal stresses [12]. In some cases, the high-temperature problem is overcome by diluting the flue gas with a portion of cold air to be preheated. However, dilution lowers the heat transfer from the flue gas stream.

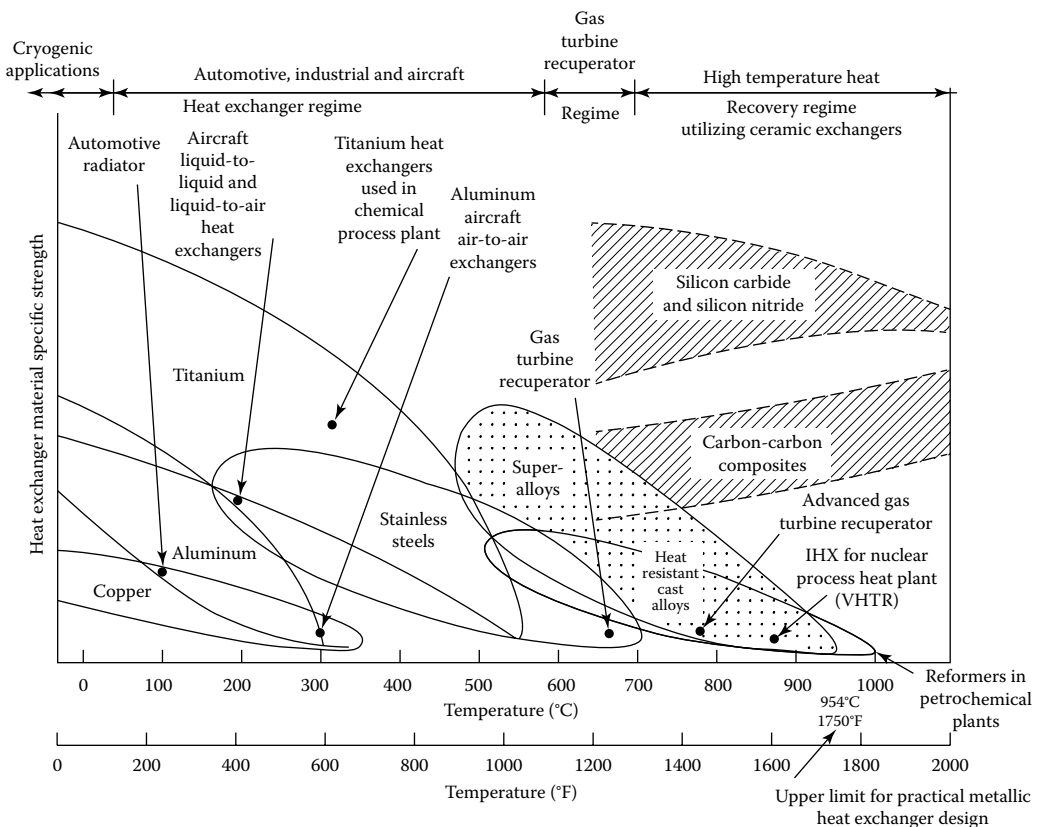


FIGURE 6.13 Approximate temperature range for various heat exchanger materials. (From McDonald, C.F., *Trans. ASME J. Eng. Power*, 102, 303, 1980.)

6.6.2 CORROSION RESISTANCE

Materials for high-temperature heat exchangers should exhibit high-temperature gaseous and liquid corrosion resistance to the carburizing, sulfidizing, oxidizing, and other effects of combustion products, and to the coal ash slag and fuel impurities. Regenerators used for heat recovery from the gases generated by boiler, furnaces, heaters, etc., should be protected against “cold end corrosion” caused by condensation of sulfuric acid and water on the heat transfer surface and the volatiles and corrosive fluxes in the exhaust gas. This problem is overcome either by ceramic units or with the use of the porcelain enameled exchanger.

6.6.3 CERAMIC HEAT EXCHANGERS

Ceramic units can be very cost effective above 1600°F since they have the potential for greater resistance to creep and oxidation at very high temperatures, and do not require temperature controls or air dilution because of their high melting points [12]. At present, a ceramic heat exchanger is probably the most economical solution for high temperature in excess of 800°C (1475°F) applications where the specific strength of metallic materials decreases very rapidly. The ceramic recuperators are available as plate-fin and bayonet tube exchangers. Material properties that favor ceramic as regenerator materials are

Moderate strength, generally inexpensive, high thermal shock resistance and lower high temperature creep, good corrosion resistance, and excellent erosion resistance properties.

Low thermal expansion characteristics; this simplifies the sealing problem. About one-fifth the density of steel, high specific heats, and higher thermal conductivity.

6.6.3.1 Low Gas Permeability

The inability to join ceramic shapes reliably, once the parts have been densified, is a serious impediment to the design of large assemblies such as heat exchangers. Among the other drawbacks, the application of ceramic materials in recuperators is limited by the inherent brittleness, the higher fabrication costs associated with producing ceramic heat exchangers, and the low thermal conductivity of many oxide ceramics [13]. According to McNallan et al. [13], because of their higher thermal conductivities and corrosion resistance compared with other ceramics, silicon carbide-based ceramics have received the most attention as heat exchanger materials.

6.6.4 CERAMIC–METALLIC HYBRID RECUPERATOR

To overcome the high-temperature heat recovery problem, a ceramic-metallic hybrid recuperator is used. It consists of a ceramic recuperator operating in series with a conventional plate-fin metallic recuperator. An air dilution system is employed between the two recuperators to overcome the high-temperature oxidation problem of the metallic recuperator. This system is capable of handling flue gas temperatures up to 1370°C (2520°F).

6.6.5 REGENERATOR MATERIALS FOR OTHER THAN WASTE HEAT RECOVERY

The regenerator construction materials used for applications other than waste heat recovery are discussed by Shah [3]. They include the following:

1. In the air-conditioning and industrial process heat recovery applications, rotary regenerators are made from knitted aluminum or stainless steel wire matrix.
2. For cryogenic applications, ordinary carbon steels become brittle, so materials such as austenitic stainless steels, copper alloys, certain aluminum alloys, nickel, titanium, and a few other metals that retain ductility at cryogenic temperatures must be used. Cryogenic materials are covered in the chapter on material selection and fabrication (Chapter 13).
3. Plastics, paper, and wool are used for regenerators operating below 65°C (150°F).

6.7 THERMAL DESIGN: THERMAL-HYDRAULIC FUNDAMENTALS

6.7.1 SURFACE GEOMETRICAL PROPERTIES

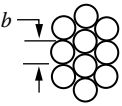
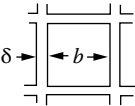
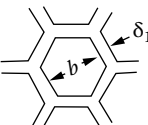
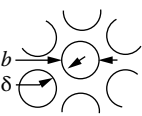
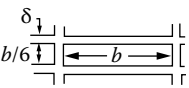
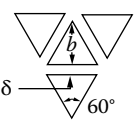
A consistent set of geometry-related symbols and factors facilitates comparative studies. The following factors can be used for all geometries, either bluff or laminar [2].

1. Porosity, σ = void volume/total volume
2. Area density, β = surface area/total volume
3. Hydraulic radius, r_h = flow area/wetted perimeter = σ/β
4. Flow area, A_x = porosity \times frontal area = σA_{fr}
5. Cell density, N_c = number of holes or cells per unit frontal area

Reference [2] presents these surface geometrical factors for several surface geometries—square, hexagonal, circular, rectangular, and triangular and the same is given in Table 6.1. The surface geometrical properties, D_h ($4r_h$), L (flow length), σ , and β are the same on both fluid sides. They are related to each other as follows:

$$D_h = \frac{4A_o L}{A} = \frac{4\sigma}{\beta} \quad \sigma = \frac{A_o}{A_{fr}}, \quad \beta = \frac{4\sigma}{D_h} \quad (6.1)$$

TABLE 6.1
Surface Geometrical Properties for Rotary Regenerators Matrix

	Cell Density N_c (Cells/ In^2)	Porosity p_{or}	Area Density β (1/m)	Hydraulic Radius r_h (m)
	—	0.37–0.39	$\frac{6(1-p_{or})}{b}$	$\frac{b(p_{or})}{6(1-p_{or})}$
	$\frac{1}{(b+\delta)^2}$	$\frac{b^2}{(b+\delta)^2}$	$\frac{4b}{(b+\delta)^2}$	$\frac{b}{4}$
	$\frac{2}{\sqrt{3}(b+\delta)^2}$	$\frac{b^2}{(b+\delta)^2}$	$\frac{4b}{(b+\delta)^2}$	$\frac{b}{4}$
	$\frac{2}{\sqrt{3}(b+\delta)^2}$	$\frac{\pi b^2}{2\sqrt{3}(b+\delta)^2}$	$\frac{2\pi b}{\sqrt{3}(b+\delta)^2}$	$\frac{b}{4}$
	$\frac{1}{\left(\frac{b}{6}+\delta\right)(b+\delta)}$	$\frac{b^2/6}{\left(\frac{b}{6}+\delta\right)(b+\delta)}$	$\frac{7b/3}{\left(\frac{b}{6}+\delta\right)(b+\delta)}$	$\frac{b}{14}$
	$\frac{4\sqrt{3}}{(2b+3\delta)^2}$	$\frac{4b^2}{(2b+3\delta)^2}$	$\frac{24b}{(2b+3\delta)^2}$	$\frac{b}{6}$

If the frontal area is not 50% for each fluid, the disk frontal area, minimum free flow area, and heat transfer area on each side will not be the same. The method to calculate frontal area and heat transfer surface area on the hot and cold sides, area for longitudinal conduction, and mass is described by Shah [14], and various parameters are explained as per Shah's method. If the flow area ratio split for both fluids is in the ratio $x:y$, where $x + y = 1$, and if the face seal and hub coverage are specified as $a\%$ of the total face area $A_{fr,t}$, then the frontal areas on each side, namely, $A_{fr,h}$ and $A_{fr,c}$, are given by

$$A_{fr,t} = \frac{\pi}{4}(D^2 - d^2) \quad A_{fr} = A_{fr,t} \left(1 - \frac{a}{100}\right) \quad (6.2)$$

$$A_{fr,h} = \frac{x}{x+y} A_{fr} \quad A_{fr,c} = \frac{y}{x+y} A_{fr} \quad (6.3)$$

where

$$A_{fr} = A_{fr,h} + A_{fr,c}$$

D is the regenerator disk outer diameter at the end of the heat transfer surface

d is the hub diameter

The effective total volume of the regenerator is given by

$$V = (A_{fr,h} + A_{fr,c})L \quad (6.4)$$

With the known porosity σ , the minimum free flow area on each side is calculated from $A_o = \sigma A_{fr}$. The heat transfer surface areas on the hot and cold sides are given by

$$A_h = \frac{x}{x+y} \beta V \quad A_c = \frac{y}{x+y} \beta V \quad (6.5)$$

The matrix mass M_r is calculated from the following equation for known matrix material density, ρ_r :

$$M_r = \rho_r V(1 - \sigma) = \rho_r (1 - \sigma) A_{fr,t} L \quad (6.6)$$

6.7.2 CORRELATION FOR j AND F

For j and f values of commonly used surface geometries, refer to Mondt [2] and Kays and London [15]. Basic heat transfer and flow friction design data are presented for three straight, triangular-passage, glass ceramic heat exchanger surfaces in London et al. [16]. These surfaces have heat transfer area density ratios ranging from 1300 to 2400 ft^2/ft^3 corresponding to a passage count of 526 to 2215 passages/in.² Table 6.2 provides a comparison of the surface geometrical characteristics. Figure 6.14 provides a description of the idealized triangular geometry used to calculate D_h and α . Glass ceramic heat exchangers are of importance to vehicular gas turbine technology as they give promise of allowing low mass production costs for the high-effectiveness rotary regenerator required for most of the vehicular turbine engine concepts now under development.

If manufacturing tolerances are controlled as specified, the recommended j factor for $\text{Re} < 1000$ is given by

$$j = \frac{3.0}{\text{Re}} \quad (6.7)$$

TABLE 6.2
Surface Geometrical Properties for Triangular
Geometry Glass Ceramic Heat Exchangers

Core Description/Case No.	505A	503A	504A
Passage count, N_c	526	1008	2215
Number/in. ²			
Porosity, σ	0.794	0.708	0.644
Hyd. diam., D_h , 10 ⁻³ ft	2.47	1.675	1.074
Area density, α ft ² /ft ³	1285	1692	2397
Cell height/width, d^*	0.731	0.709	0.708
L/D_h	101	149.5	233

Source: London, A.L. et al., *Trans. ASME J. Eng. Power*, 92A, 381, 1970.

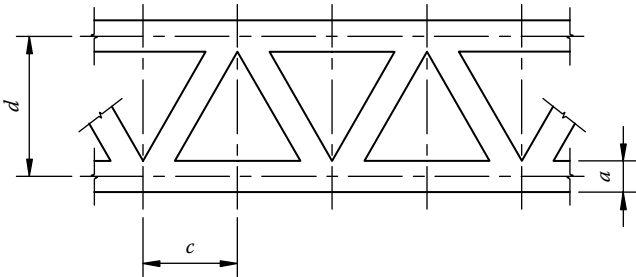


FIGURE 6.14 Idealized triangular geometry for glass ceramic heat exchanger. (From London, A.L. et al., *Trans. ASME J. Eng. Power*, 92A, 381, 1970.)

This is approximately 10% lower than the theory to allow for some passage nonuniformity ($\pm 20\%$ of flow area).

The recommended j factor for $Re < 1000$ is given by

$$j = \frac{14.0}{Re} \tag{6.8}$$

This is 5% higher than the theory to allow a small margin for the walls and the variation of passage cross section along flow length.

6.8 THERMAL DESIGN THEORY

The thermal design theory of recuperators is simple and quite straightforward. The effectiveness-number of transfer units (ϵ -NTU) method is used to analyze heat transfer in recuperators. In contrast, the theory of the periodic-flow-type regenerator is much more difficult. Despite the simplicity of the differential equations under classical assumptions, their solution has proved to be challenging, and performances of counterflow regenerators have been widely investigated numerically as well as analytically [17]. Various solution techniques have been tried for solving the thermal design problem, and they are discussed here.

6.8.1 REGENERATOR SOLUTION TECHNIQUES

For the steady-state behavior of a regenerator, Nusselt [18] has given an exact solution, which consists of an infinite series of integrals. However, this solution is complicated for practical purposes, and hence several solution techniques were developed. They are

1. Approximate solution methods by simplifying the parameters defining the regenerator behavior; examples include Hausen's [19] heat pole method, which approximates the integral equation for the initial temperature distribution of the matrix. Hausen expressed the performance result in terms of two dimensionless parameters called the *reduced length* and the *reduced period*.
2. Empirical effectiveness relation correlated by treating the regenerator by an equivalent recuperator, e.g., that of Coppage and London [20].

6.8.1.1 Open Methods: Numerical Finite-Difference Method

Prior to the availability of general-purpose digital computers, regenerator thermal behavior was analyzed by restricting the range of parameters. With the availability of digital computers, Lamberston [21], Bahnke and Howard [22], Mondt [23], and Chung-Hsiung Li [24], among others, used a numerical finite-difference method for the calculation of the regenerator thermal effectiveness. In this approach, the regenerator and the gas streams are represented by two separate but dependent heat exchangers with the matrix stream in crossflow with each gas stream as shown in Figure 6.15.

6.8.1.2 Closed Methods

In the closed methods, the reversal condition is implicitly incorporated in the mathematical model for solving the differential equations both for the hot period and the cold period. The closed methods used to solve the Nusselt integral equation are

1. Collocation method of Nahavandi and Weinstein [25] and Willmott and Duggan [26]
2. Galerkin method of Baclic [17] and Baclic et al. [27]
3. Successive integral method (SIM) of Romie and Baclic [28]

6.8.2 BASIC THERMAL DESIGN METHODS

For design purposes, a regenerator is usually considered to have attained regular periodic flow conditions. The solution to the governing differential equations is presented in terms of the regenerator effectiveness as a function of the pertinent dimensionless groups. The specific form of these

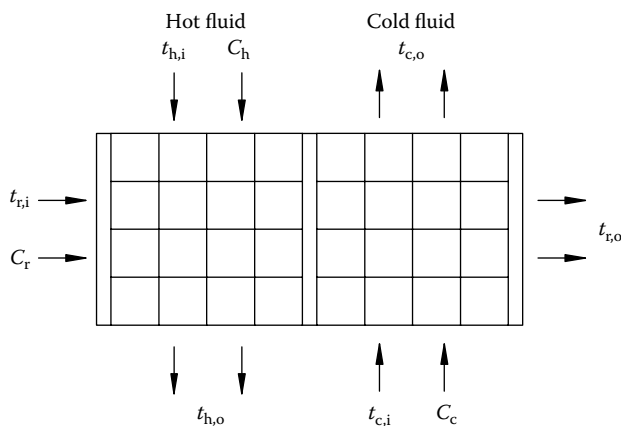


FIGURE 6.15 Regenerator matrix as the third stream. (From Lambertson, T.J., *Trans. ASME*, 80, 586, 1958.)

dimensionless groups is to some extent optional, and the two most common forms are (1) the effectiveness and modified number of transfer units (ε -NTU_o) method (generally used for rotary regenerators), whereby

$$\varepsilon = \phi[\text{NTU}_o, C^*, C_r^*, (hA)^*] \quad (6.9)$$

and (2) the reduced length-reduced period (Λ - Π) method (generally used for fixed matrix regenerators) in which

$$\varepsilon = \phi[\Lambda_h, \Lambda_c, \Pi_h, \Pi_c] \quad (6.10)$$

These two methods are equivalent as shown in Ref. [20] and Shah [29]; that is, the thermal effectiveness of a single fixed regenerator is equal to that of the rotary regenerator with the same values of the four parameters. This one-to-one correspondence between the two dimensionless methodologies, as shown in Table 6.3, allows the results obtained in the form of either Equation 6.9 or 6.10 to be used for both types of regenerators.

The ε -NTU_o method is mainly used for rotary regenerator design and analysis, and was first developed by Coppage and London [20]. Their model is explained next.

6.8.3 COPPAGE AND LONGON MODEL FOR A ROTARY REGENERATOR

The ε -NTU_o method was used for the rotary regenerator design and analysis by Coppage and London [20] with the following idealizations.

1. The thermal conductivity of the matrix is zero in the gas and air flow directions, and infinite in the direction normal to the flow.
2. The specific heats of the fluids and the matrix material are constant with temperature.
3. No mixing of the fluids occurs during the switch over from hot to cold flow.
4. The convective conductances between the fluids and the matrix are constant with flow length.
5. The fluids flow in counterflow directions.
6. Entering fluid temperatures are uniform over the flow cross section and constant with time.

TABLE 6.3
Equivalence between the ε -NTU_o and Λ - Π Design Methods

ε -NTU _o Method	Λ - Π Method
$\text{NTU}_o = \frac{\Lambda_c / \Pi_c}{1 / \Pi_c + 1 / \Pi_h}$	$\Lambda_h = C^* \left[1 + \frac{1}{(hA)^*} \right] \text{NTU}_o$
$C^* = \frac{\Pi_c / \Lambda_c}{\Pi_c / \Lambda_h}$	$\Lambda_c = [1 + (hA)^*] \text{NTU}_o$
$C_r^* = \frac{\Lambda_c}{\Pi_c}$	$\Pi_h = \frac{1}{C_r^*} \left[1 + \frac{1}{(hA)^*} \right] \text{NTU}_o$
$(hA)^* = \frac{\Pi_c}{\Pi_h}$	$\Pi_c = \frac{1}{C_r^*} [1 + (hA)^*] \text{NTU}_o$

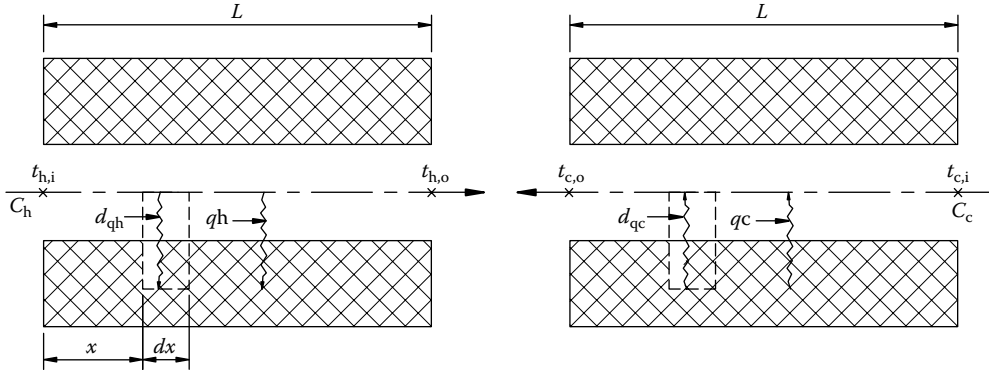


FIGURE 6.16 Regenerator basic heat transfer model. Regenerator elemental flow passage and associated matrix during (a) hot flow period and (b) cold gas flow period. (From Coppage, J.E. and London, A.L., *Trans. ASME*, 75, 779, 1953.)

7. Regular periodic conditions are established for all matrix elements, and heat losses to the surroundings are negligible.
8. Fluid carryover during the switching operation and the pressure leakage effects are negligible.

On the basis of these idealizations, the following differential equations and boundary conditions may be expressed. For the hot gas flow, energy balance on the element dx , as shown in Figure 6.16, is given by

$$\frac{dq_h}{dx} = \frac{M_r C_r}{L} \frac{\partial t_r}{\partial \tau} \quad (6.11)$$

$$\frac{dq_h}{dx} = - \left(M_h c_{p,h} \frac{\partial t_h}{\partial x} + \frac{m'_h c_{p,h}}{L} \frac{\partial t_h}{\partial \tau} \right) \quad (6.12)$$

Equation 6.11 represents the energy received by the matrix in terms of its thermal capacitance. The right-hand side of Equation 6.12 represents the energy given up by the hot gas, and m'_h/L represents the mass of the hot gas retained in a flow length dx . The convective heat transfer rate equation is

$$dq_h = \frac{h_h A_h}{L} (t_h - t_r) dx \quad (6.13)$$

Elimination of dq_h yields the equation

$$M_h c_{p,h} \frac{\partial t_h}{\partial x} + \frac{m'_h c_{p,h}}{L} \frac{\partial t_h}{\partial \tau} = \frac{M_r c_r}{L} \frac{\partial t_r}{\partial \tau} = \frac{-h_h A_h}{L} (t_h - t_r) \quad (6.14)$$

For the cold gas flow, a similar equation results as follows:

$$M_c c_{p,c} \frac{\partial t_c}{\partial x} + \frac{m'_c c_{p,c}}{L} \frac{\partial t_c}{\partial \tau} = - \frac{M_r c_r}{L} \frac{\partial t_r}{\partial \tau} = \frac{-h_c A_c}{L} (t_c - t_r) \quad (6.15)$$

The boundary conditions are as follows:

For interval of hot flow: $t_{h,i} = \text{constant at } x = 0$

For interval of cold flow: $t_{c,i} = \text{constant at } x = L$

6.8.3.1 Thermal Effectiveness

The overall heat transfer performance of the regenerator is most conveniently expressed as the heat transfer “effectiveness” ε , which compares the actual heat transfer rate to the thermodynamically limited maximum possible heat transfer rate. With this definition, the regenerator thermal effectiveness is simply the dimensionless time-average cold fluid outlet temperature. This is true under the condition that the cold stream is weaker, that is, it has the lower heat capacity rate. This definition (for $C_c \leq C_h$ as is the case for the recuperator) results in

$$\varepsilon = \frac{t_{c,o} - t_{c,i}}{t_{h,i} - t_{c,i}} \quad (6.16)$$

where $t_{c,o}$ is the bulk average temperature of the cold air stream after passage through the regenerator. The effectiveness is expressed as a function of four nondimensional parameters given by

$$\varepsilon = \phi \left[C^*, C_r^*, (hA)^*, NTU_o \right] \quad (6.17)$$

Definition of $NTU_o, C^, C_r^*, (hA)^*$*

NTU_o is the modified number of transfer units, defined as

$$NTU_o = NTU_c \left[\frac{1}{1 + (hA)^*} \right] \quad (6.18)$$

The heat capacity rate ratio C^* is simply the ratio of the smaller to larger heat capacity rate of the fluid streams so that C^* should be less than or equal to 1.

$$C^* = \frac{C_{\min}}{C_{\max}} = \frac{(Mc_p)_{\min}}{(Mc_p)_{\max}} = \frac{C_c}{C_h} \quad (6.19)$$

C_r^* is the matrix heat capacity rate C_r normalized with respect to C_{\min}

$$C_r^* = \frac{C_r}{C_{\min}} = \frac{M_r c_r N}{(Mc_p)_{\min}} \quad (6.20)$$

where

M_r is the mass of the matrix

c_r is the specific heat of the matrix material

N is the speed of the matrix in revolution per unit time

$(hA)^*$ is the ratio of the convective conductance on the C_{\min} side to that on the C_{\max} side:

$$(hA)^* = \frac{(hA) \text{ on the } C_{\min} \text{ side}}{(hA) \text{ on the } C_{\max} \text{ side}} = \frac{(hA)_c}{(hA)_h} \quad (6.21)$$

Various terms used here are defined as follows:

- A_c = matrix transfer area on cold side
- A_h = matrix transfer area on hot side
- C_c = fluid stream capacity rate (Mc_p) for cold gas flow
- C_h = fluid stream capacity rate (Mc_p) for hot gas flow
- C_r = capacity rate of the rotor matrix ($M_r c_r N$)
- $(hA)^*$ = thermal conductance
- h_c = convective conductance for cold gas
- h_h = convective conductance for hot gas
- M_c = mass flow rate of cold gas
- M_h = mass flow rate of hot gas
- M_r = matrix mass
- $(Mc_p)_c$ = capacity rate of cold gas
- $(Mc_p)_h$ = capacity rate of hot gas
- $M_r c_r$ = thermal capacitance of matrix
- m'_c = mass of cold gas retained in the matrix length L
- m'_h = mass of hot gas retained in the matrix length L
- L = matrix flow length
- N = rpm of the matrix
- t_c = temperature of the cold gas
- t_h = temperature of the hot gas
- t_r = temperature of the matrix
- $t_{c,i}, t_{c,o}$ = cold fluid terminal temperatures
- $t_{h,i}, t_{h,o}$ = hot fluid terminal temperatures
- τ = flow period

For the special case of $C_r/C_c = \infty$, the behavior becomes identical in form to that of a counterflow direct-type exchanger and its effectiveness is given by

$$\varepsilon_{cf} = \frac{1 - e^{[-NTU_o(1-C^*)]}}{1 - C^* e^{[-NTU_o(1-C^*)]}} \quad \text{for } C^* < 1 \quad (6.22a)$$

$$= \frac{NTU_o}{(1 + NTU_o)} \quad \text{for } C^* = 1 \quad (6.22b)$$

The following formula for thermal effectiveness was first empirically correlated by Lambertson [21] and later modified by Kays and London [15]:

$$\varepsilon = \varepsilon_{cf} \left[1 - \frac{1}{9 C_r^{*1.93}} \right] \quad (6.23)$$

Equation 6.23 agrees with accurate numerical results within $\pm 1\%$ for the following ranges [14]: (1) $3 \leq NTU_o \leq 9$, $0.90 \leq C^* \leq 1$, $1.25 \leq C_r^* \leq 5$; (2) $2 \leq NTU_o \leq 14$, $C^* = 1$, $C_r^* \geq 1.5$; (3) $NTU_o \leq 20$, $C^* = 1$, $C_r^* \geq 2$; and (4) the complete range of NTU_o , $C^* = 1$, $C_r^* \geq 5$. In all cases, $0.25 \leq (hA)^* \leq 4$. Note that the value of C^* is limited to between 0.9 and 1.0.

The regenerator effectiveness increases with NTU_o asymptotically and approaches unity for specified values of C^* and C_r^* . Thus, in this case, the periodic-flow-type regenerator would have the same performance as a counterflow direct-type unit possessing the same hot-side and cold-side

transfer areas and the same convection heat transfer coefficients, providing only negligible thermal resistance offered by the wall structure. To provide a sense of magnitude for these parameters, the following tabulations were presented by these authors to indicate extreme ranges of values to be expected in gas turbine design work:

$$\varepsilon = 50\% - 90\%$$

$$\frac{C_c}{C_h} = 0.90 - 1.00$$

$$\frac{C_r}{C_c} = 1 - 10$$

$$(hA)^* = \frac{(hA)_c}{(hA)_h} = 0.2 - 1$$

$$NTU_c = 2 - 20 \text{ (}\approx \text{twice } NTU_o \text{)}$$

$$NTU_o = 1 - 10$$

6.8.3.2 Heat Transfer

For rotary regenerators, the magnitude of the heat transfer rate between the gas and the matrix during a flow period is necessarily the same for both flow periods, and therefore

$$q = \varepsilon (Mc_p)_c (t_{h,i} - t_{c,i}) \quad (6.24a)$$

in which $t_{h,i}$ and $t_{c,i}$ are constant inlet temperatures of the hot and cold gases. For stationary regenerators, the heat transfer rate is

$$q = \varepsilon (Mc_p \tau)_c (t_{h,i} - t_{c,i}) \quad (6.24b)$$

6.8.4 PARAMETER DEFINITIONS

Various parameters definitions and their equivalents for the stationary and rotary regenerators are given in Table 6.4.

TABLE 6.4
Parameter Definitions and
Equivalents for Stationary and Rotary Regenerators

	Stationary	Rotary
NTU_o	$\frac{\Lambda_c}{1 + (hA)^*}$	$NTU_c \left[\frac{1}{1 + (hA)^*} \right]$
C^*	$\frac{(Mc_p \tau)_c}{(Mc_p \tau)_h}$	$\frac{(Mc_p)_c}{(Mc_p)_h}$
C_r^*	$\frac{M_r c_r}{(Mc_p \tau)_c}$	$\frac{M_r c_r N}{(Mc_p)_c}$
$(hA)^*$	$\frac{(hA \tau)_c}{(hA \tau)_h}$	$\frac{(hA)_c}{(hA)_h}$

Note: While defining various parameters, throughout this chapter, it is assumed that the cold fluid is the C_{\min} fluid and accordingly, subscripts c for cold fluid and h for hot fluid are allotted. However, parameter definition can be generalized to subscripts a and b such that the term

$$\frac{C_a}{C_b} \leq 1 \quad \text{or} \quad \frac{\Lambda_b \Pi_a}{\Lambda_a \Pi_b} \leq 1 \quad (6.25)$$

6.8.5 CLASSIFICATION OF REGENERATOR

Based on the values of C^* and $(hA)^*$, or $\Lambda-\Pi$, regenerators are classified into eight types [29,30]: (1) balanced regenerator, (2) unbalanced regenerator, (3) symmetric regenerator, (4) unsymmetric regenerator, (5) symmetric and balanced regenerator, (6) unsymmetric and balanced regenerator, (7) symmetric and unbalanced regenerator, and (8) unsymmetric and unbalanced regenerator. For a balanced regenerator, the heat capacity of the fluids blown through the regenerator is equal and a regenerator is termed symmetric if the reduced length of each period is equal. The unsymmetric and unbalanced regenerator operation is the most general one, and the others are merely subsets [30]. These designations are shown in Table 6.5. The utilization factor U_h on the hot side and U_c on the cold side are given by

$$U_c = \left(\frac{\Lambda}{\Pi} \right)_c = \frac{C_r}{C_c} \quad (6.26a)$$

$$U_h = \left(\frac{\Lambda}{\Pi} \right)_h = \frac{C_r}{C_h} \quad (6.26b)$$

6.8.6 ADDITIONAL FORMULAS FOR REGENERATOR EFFECTIVENESS

Tables of thermal effectiveness are given by many sources: Kays and London [15], Baclic [17], Lamberston [21], Bhanke and Howard [22], and Romie [31], among others. Methods of computing the thermal effectiveness are described by, for example, Baclic [17], Willmott and Duggan [26], Baclic et al. [27], Romie and Baclic [28], Ref. [32], and many others. Additional formulas and closed form solutions from a few of these references are given next.

TABLE 6.5
Designation of Regenerators

Terminology	$\Lambda-\Pi$ Method	NTU _o Method
1. Balanced regenerator (defined in terms of utilization factor U or heat capacity rate ratio C^*)	$U_h = U_c$ $U_h/U_c = 1$ $\Lambda_h/\Pi_h = \Lambda_c/\Pi_c$	$C_h = C_c$ $C_h/C_c = 1$ $C^* = 1$
2. Unbalanced regenerator	$U_h \neq U_c$ $U_h/U_c \neq 1$ $\Lambda_h/\Pi_h \neq \Lambda_c/\Pi_c$	$C_h \neq C_c$ $C_h/C_c \neq 1$ $C^* \neq 1$
3. Symmetric regenerator (defined in terms of (i) reduced length Λ or reduced period Π or (ii) thermal conductance ratio $(hA)^*$)	$\Lambda_h = \Lambda_c$ $\Pi_h = \Pi_c$	$(hA)_h = (hA)_c$ $(hA)^* = 1$
4. Unsymmetric regenerator	$\Lambda_h \neq \Lambda_c$ $\Pi_h \neq \Pi_c$	$(hA)_h \neq (hA)_c$ $(hA)^* \neq 1$
5. Symmetric and balanced regenerator	$\Lambda_h = \Lambda_c, \Pi_h = \Pi_c$ $U_h = U_c$ i.e., $\Lambda_h/\Pi_h = \Lambda_c/\Pi_c$	$(hA)^* = 1$ $C^* = 1$

6.8.6.1 Balanced and Symmetric Counterflow Regenerator

Baclic [17] obtained a highly accurate closed form expression for the counterflow regenerator effectiveness for the balanced and symmetric regenerator; that is, for $C^* = 1$ and $(hA)^* = 1$ by the Galerkin method:

$$\varepsilon = \frac{\Lambda}{\Pi} \left[\left(2 \sum_{j=0}^N B_j - 1 \right) \right] \quad (6.27)$$

where B_j is determined by solving the set of equations of the form

$$\sum_{j=0}^N a_{jk} B_j = 1 \quad (6.28)$$

where

$$a_{jk} = \frac{(k+1)!(j+1)!}{(k+j+1)!} \left[1 + (k+j+1)! \sum_{m=0}^k \frac{(-1)^m}{(k-m)!} V_{j+m+2} \left(\Pi, \frac{\Lambda}{\Lambda^{j+m+1}} \right) \right] \quad (6.29)$$

$$V_m(x, y) = e^{[-(x+y)]} \sum_{n=m-1}^{\infty} \binom{n}{m-1} \left(\frac{y}{x} \right)^{n/2} I_n(2\sqrt{xy}) \quad m \geq 1 \quad (6.30a)$$

$$\binom{n}{m-1} = \frac{n!}{(m-1)!(n-m+1)!} \quad (6.30b)$$

For $N = 2$, the equation for ε simplifies to the following equation:

$$\varepsilon = C_r^* \frac{1 + 7\beta_2 - 24\{B - 2[R_1 - A_1 - 90(N_1 + 2E)]\}}{1 + 9\beta_2 - 24\{B - 6[R - A - 20(N - 3E)]\}} \quad (6.31)$$

where

$$B = 3\beta_3 - 13\beta_4 + 30(\beta_5 - \beta_6) \quad (6.32)$$

and

$$R = \beta_2[3\beta_4 - 5(3\beta_5 - 4\beta_6)] \quad (6.33)$$

$$A = \beta_3[3\beta_3 - 5(3\beta_4 + 4\beta_5 - 12\beta_6)] \quad (6.34)$$

$$N = \beta_4[2\beta_4 - 3(\beta_5 + \beta_6)] + 3\beta_5^2 \quad (6.35)$$

$$E = \beta_2\beta_4\beta_6 - \beta_2\beta_5^2 - \beta_5^2\beta_6 + 2\beta_3\beta_4\beta_5 - \beta_4^3 \quad (6.36)$$

$$N_1 = \beta_4[\beta_4 - 2(\beta_5 + \beta_6)] + 2\beta_5^2 \quad (6.37)$$

$$A_1 = \beta_3[\beta_3 - 15(\beta_4 + 4\beta_5 - 12\beta_6)] \quad (6.38)$$

$$R_1 = \beta_2[\beta_4 - 15(\beta_5 - 2\beta_6)] \quad (6.39)$$

$$\beta_i = V_i \frac{\left(2NTU_o, 2 \frac{NTU_o}{C_r^*} \right)}{(2NTU_o)^{i-1}} = \frac{V_i(\Pi, \Lambda)}{\Lambda^{i-1}} \quad \text{for } i = 2, 3, \dots, 6 \quad (6.40)$$

$$V_i(x, y) = e^{[-(x+y)]} \sum_{n=i-1}^{\infty} \binom{n}{i-1} \left(\frac{y}{x} \right)^{n/2} I_n(2\sqrt{xy}) \quad i \geq 1 \quad (6.41)$$

Regenerator effectiveness ε , computed from Equation 6.31, as a function of NTU_o and C_r^* is presented in Table 6.6. Note that the results are valid for $C^* = 1$ and $(hA)^* = 1$. It is emphasized again that the regenerator effectiveness ε from Equation 6.23 is valid for $0.9 \leq C^* \leq 1$ and $C_r^* > 1.25$ while that of Equation 6.31 is valid not only for $C^* = 1$ but for all values of C_r^* . Exact asymptotic values of ε for $\Lambda \rightarrow \infty$ and $\Pi/\Lambda \rightarrow 0$, when $\varepsilon = \Lambda/(2 + \Lambda)$ holds, are also included in Table 6.6.

6.8.7 REDUCED LENGTH–REDUCED PERIOD (Λ – Π) METHOD

6.8.7.1 Counterflow Regenerator

The asymmetric-unbalanced counterflow regenerator problem is solved by Baclic et al. [27] by adopting Galerkin model. Based on these assumptions, an energy balance provides two equations applicable during the hot gas flow period and two equations during the cold gas flow period:

$$\frac{1}{\Lambda_h} \frac{\partial t_h}{\partial \xi} = - \frac{1}{\Pi_h} \frac{\partial t_r}{\partial \eta} = t_r - t_h \quad (6.42)$$

$$\pm \frac{1}{\Lambda_c} \frac{\partial t_c}{\partial \xi} = - \frac{1}{\Pi_c} \frac{\partial t_r}{\partial \eta} = t_r - t_c \quad (6.43)$$

The regenerator can operate with either parallelflow (plus sign in Equation 6.43) or counterflow arrangement (minus sign in Equation 6.43). In Equations 6.42 and 6.43, ξ is the fractional distance along the flow path in the regenerator matrix of length L and η is the fractional completion of a respective gas flow period. Temperatures of the hotter gas, colder gas, and the solid matrix are denoted by t_h , t_c , and t_r , respectively. The expressions for four parameters Λ_h and Λ_c (reduced lengths), Π_h and Π_c (reduced periods) are given in Table 6.7.

The differential equations (6.42) and (6.43) describe the regenerator operation when the appropriate boundary conditions are specified. These are constant gas inlet temperatures $t_{h,i}$ and $t_{c,i}$ at the opposite ends ($\xi = 0$ and 1) of the regenerator matrix, and the condition stating that the matrix temperature field at the end of one gas flow period is the initial matrix temperature distribution for the subsequent gas flow period.

The subscript 1 is assigned to the weaker gas flow period such that the respective $U_1 = (\Lambda/\Pi)_1$ ratio is smaller of the two ratios $U_h = (\Lambda/\Pi)_h$ and $U_c = (\Lambda/\Pi)_c$. The ratio (Λ/Π) is termed the *utilization factor*. The main advantage of the utilization factors is the fact that these parameters do not contain the fluid to matrix heat transfer coefficients of the respective flow periods. Thus, U_1 is defined as

$$U_1 = \min\{U_c, U_h\} \quad (6.44)$$

TABLE 6.6
Symmetric and Balanced Counterflow Regenerator Effectiveness $\varepsilon = \varphi(\Lambda, \Pi)$ (as Calculated from Equation 6.31)

$\Lambda \backslash \Pi/\Lambda$	0.0	0.1	0.2	0.3	0.4	0.5	0.6	0.7	0.8	0.9	1.0
1.0	1/3	0.3332	0.3329	0.3323	0.3315	0.3304	0.3292	0.3277	0.3260	0.3241	0.3221
1.5	3/7	0.4283	0.4276	0.4264	0.4248	0.4227	0.4202	0.4173	0.4139	0.4102	0.4061
2.0	1/2	0.4996	0.4986	0.4968	0.4943	0.4912	0.4874	0.4830	0.4780	0.4725	0.4665
2.5	5/9	0.5551	0.5537	0.5513	0.5481	0.5440	0.5391	0.5333	0.5269	0.5197	0.5120
3.0	3/5	0.5994	0.5977	0.5949	0.5910	0.5861	0.5802	0.5733	0.5655	0.5570	0.5477
3.5	7/11	0.6357	0.6338	0.6305	0.6261	0.6204	0.6137	0.6058	0.5970	0.5872	0.5766
4.0	2/3	0.6659	0.6638	0.6602	0.6553	0.6490	0.6416	0.6329	0.6232	0.6124	0.6006
4.5	9/13	0.6915	0.6892	0.6853	0.6800	0.6732	0.6652	0.6559	0.6454	0.6337	0.6210
5.0	5/7	0.7134	0.7109	0.7068	0.7011	0.6940	0.6855	0.6756	0.6645	0.6521	0.6385
5.5	11/15	0.7324	0.7293	0.7255	0.7195	0.7121	0.7032	0.6928	0.6811	0.6681	0.6537
6.0	3/4	0.7491	0.7463	0.7418	0.7356	0.7279	0.7187	0.7080	0.6958	0.6822	0.6672
6.5	13/17	0.7637	0.7609	0.7562	0.7498	0.7419	0.7324	0.7215	0.7089	0.6948	0.6792
7.0	7/9	0.7768	0.7738	0.7690	0.7625	0.7544	0.7447	0.7335	0.7206	0.7061	0.6900
7.5	15/19	0.7884	0.7854	0.7804	0.7738	0.7656	0.7558	0.7444	0.7313	0.7164	0.6997
8.0	4/5	0.7989	0.7958	0.7908	0.7840	0.7757	0.7658	0.7543	0.7409	0.7257	0.7036
8.5	17/21	0.8084	0.8052	0.8001	0.7933	0.7849	0.7749	0.7633	0.7497	0.7342	0.7167
9.0	9/11	0.8171	0.8138	0.8086	0.8017	0.7933	0.7833	0.7715	0.7578	0.7421	0.7242
9.5	19/23	0.8250	0.8216	0.8164	0.8094	0.8010	0.7909	0.7791	0.7653	0.7493	0.7311
10.0	5/6	0.8322	0.8288	0.8235	0.8165	0.8080	0.7980	0.7862	0.7722	0.7560	0.7375
10.5	21/25	0.8388	0.8354	0.8300	0.8230	0.8146	0.8046	0.7927	0.7787	0.7623	0.7435
11.0	11/13	0.8450	0.8415	0.8361	0.8290	0.8206	0.8106	0.7988	0.7847	0.7681	0.7491
11.5	23/27	0.8506	0.8471	0.8417	0.8346	0.8262	0.8163	0.8044	0.7903	0.7736	0.7543
12.0	6/7	0.8559	0.8524	0.8469	0.8398	0.8315	0.8216	0.8098	0.7956	0.7788	0.7592
12.5	25/29	0.8603	0.8573	0.8517	0.8447	0.8364	0.8266	0.8147	0.8005	0.7836	0.7638
13.0	13/15	0.8654	0.8618	0.8562	0.8492	0.8410	0.8312	0.8194	0.8052	0.7882	0.7682
13.5	27/31	0.8697	0.8661	0.8605	0.8535	0.8453	0.8356	0.8239	0.8096	0.7925	0.7723
14.0	7/8	0.8737	0.8701	0.8644	0.8575	0.8494	0.8397	0.8280	0.8138	0.7966	0.7762
14.5	29/33	0.8775	0.8738	0.8682	0.8612	0.8532	0.8436	0.8320	0.8177	0.8004	0.7799
15.0	15/17	0.8811	0.8773	0.8717	0.8648	0.8568	0.8473	0.8358	0.8215	0.8041	0.7834
15.5	31/35	0.8844	0.8807	0.8750	0.8681	0.8602	0.8508	0.8393	0.8251	0.8076	0.7868
16.0	8/9	0.8876	0.8838	0.8781	0.8713	0.8635	0.8542	0.8427	0.8285	0.8110	0.7900
17.0	17/19	0.8934	0.8896	0.8839	0.8771	0.8695	0.8604	0.8490	0.8348	0.8172	0.7959
18.0	9/10	0.8967	0.8948	0.8891	0.8824	0.8749	0.8660	0.8548	0.8406	0.8229	0.8014
19.0	19/21	0.9034	0.8995	0.8938	0.8872	0.8799	0.8711	0.8601	0.8459	0.8282	0.8065
20.0	10/11	0.9077	0.9038	0.8981	0.8916	0.8844	0.8758	0.8649	0.8509	0.8331	0.8111
25	25/27	0.9245	0.9205	0.9148	0.9087	0.9024	0.8947	0.8844	0.8707	0.8528	0.8302
30	15/16	0.9360	0.9319	0.9263	0.9207	0.9151	0.9081	0.8984	0.8851	0.8673	0.8442
35	35/37	0.9445	0.9403	0.9347	0.9295	0.9246	0.9182	0.9090	0.8961	0.8785	0.8552
40	20/21	0.9509	0.9467	0.9411	0.9363	0.9320	0.9261	0.9174	0.9048	0.8875	0.8640
45	45/47	0.9559	0.9517	0.9462	0.9417	0.9379	0.9325	0.9241	0.9119	0.8948	0.8713
50	25/26	0.9600	0.9557	0.9503	0.9461	0.9427	0.9378	0.9297	0.9177	0.9009	0.8775
60	30/31	0.9662	0.9619	0.9565	0.9529	0.9502	0.9459	0.9383	0.9269	0.9106	0.8874
70	35/36	0.9707	0.9663	0.9611	0.9578	0.9558	0.9519	0.9447	0.9337	0.9180	0.8951
80	40/41	0.9740	0.9697	0.9645	0.9616	0.9600	0.9565	0.9497	0.9390	0.9239	0.9014
90	45/46	0.9767	0.9723	0.9672	0.9646	0.9634	0.9602	0.9536	0.9432	0.9236	0.9065

TABLE 6.6 (continued)

Symmetric and Balanced Counterflow Regenerator Effectiveness $\varepsilon = \varphi(\Lambda, \Pi)$ (as Calculated from Equation 6.31)

$\Lambda \backslash \Pi/\Lambda$	0.0	0.1	0.2	0.3	0.4	0.5	0.6	0.7	0.8	0.9	1.0
100	50/51	0.9788	0.9744	0.9693	0.9670	0.9662	0.9632	0.9568	0.9467	0.9325	0.9109
150	75/76	0.9852	0.9808	0.9759	0.9744	0.9747	0.9726	0.9667	0.9574	0.9452	0.9258
200	100/101	0.9835	0.9840	0.9792	0.9782	0.9791	0.9774	0.9719	0.9629	0.9520	0.9348
300	150/151	0.9917	0.9873	0.9826	0.9821	0.9837	0.9824	0.9772	0.9686	0.9592	0.9456
400	200/201	0.9934	0.9889	0.9843	0.9841	0.9860	0.9850	0.9799	0.9714	0.9629	0.9522
500	250/251	0.9944	0.9899	0.9853	0.9853	0.9874	0.9865	0.9815	0.9731	0.9651	0.9568
600	300/301	0.9950	0.9905	0.9860	0.9861	0.9884	0.9876	0.9826	0.9743	0.9665	0.9602
800	400/401	0.9959	0.9914	0.9869	0.9871	0.9896	0.9889	0.9840	0.9758	0.9682	0.9650
1000	500/501	0.9964	0.9919	0.9874	0.9877	0.9903	0.9897	0.9848	0.9766	0.9692	0.9634
2000	1000/1001	0.9974	0.9928	0.9884	0.9890	0.9917	0.9912	0.9865	0.9784	0.9711	0.9770
∞	1.0000	1.0000	1.0000	1.0000	1.0000	1.0000	1.0000	1.0000	1.0000	1.0000	1.0000

Source: Baclic, B.S., *Trans. ASME J. Heat Transfer*, 107, 214, 1985.

Note: For the ε -NTU_o method, $\frac{\Pi}{\Lambda} = \frac{1}{C_r^*}$ and $\Lambda = 2\text{NTU}_o$.

TABLE 6.7

Expressions for Λ_h , Λ_c , Π_c , and Π_h

$$\Pi_c = \frac{(hA\tau)_c}{M_r C_r} \quad \Pi_h = \frac{(hA\tau)_h}{M_r C_r} \quad \Lambda_c = \frac{(hA)_c}{(Mc_p)_c} \quad \Lambda_h = \frac{(hA)_h}{(Mc_p)_h}$$

The effectiveness is given by

$$\varepsilon = \frac{1}{U_1} \sum_{m=0}^M \frac{x_{2m} - x_{1m}}{(m+1)!} \quad \text{for } m = 0, 1, 2, 3, \dots, M \quad (6.45)$$

The unknown coefficients x_{1m} and x_{2m} are determined from the following set of algebraic equations:

$$\sum_{m=0}^M [-A_{mk}(\Pi_1, \Lambda_1)x_{1m} + B_{mk}x_{2m}] = C_k \quad k = 0, 1, 2, 3, \dots, M \quad (6.46)$$

$$\sum_{m=0}^M [B_{mk}x_{1m} - A_{mk}(\Pi_2, \Lambda_2)x_{2m}] = 0 \quad k = 0, 1, 2, 3, \dots, M \quad (6.47)$$

where

$$A_{mk}(\Pi_j, \Lambda_j) = \sum_{j=0}^M \frac{(-1)^i}{(k-i)!} \frac{V_{i+m+2}(\Pi_j, \Lambda_j)}{\Lambda_j^{i+m+1}} \quad j = 1, 2 \quad (6.48)$$

$$B_{mk} = \frac{1}{(m+k+1)!} \quad (6.49)$$

$$C_k = \frac{1}{(k+1)!} - \sum_{j=0}^k \frac{(-1)^j}{(k-j)!} \frac{V_{j+2}(\Pi_1, \Lambda_1)}{\Lambda_1^{j+1}} \quad (6.50)$$

For any fixed M , one needs $2(M+1)$ equations for $M+1$ unknowns x_{1m} and for $M+1$ unknowns x_{2m} . For any practical purpose $M=2$ will be adequate.

6.8.8 RAZELOS METHOD FOR ASYMMETRIC-UNBALANCED COUNTERFLOW REGENERATOR

The forms produced by the Galerkin method of Baclic et al. [27] are not amenable for hand calculation methods. They can be solved by either a computer or a programmable calculator. A hand calculation method was presented by Razelos [33]. In this approach, the unsymmetric regenerator is approximated using an “equivalent” symmetric regenerator. The Razelos approximate method can be used to calculate the counterflow regenerator effectiveness for the complete range of C^* and NTU_o , and $C_r^* \geq 1$, $0.25 \leq (hA)^* \leq 4$. The method follows the following steps:

1. For the $\varepsilon\text{-NTU}_o$ method, compute the range of $\text{NTU}_{o,m}$ and $C_{r,m}^*$ for an equivalent balanced regenerator as follows from the specified values of NTU_o , C_r^* , and C^* .

$$\text{NTU}_{o,m} = \frac{2\text{NTU}_o(C^*)}{1+C^*} \quad (6.51)$$

$$C_{r,m}^* = \frac{2C_r^*C^*}{1+C^*} \quad (6.52)$$

2. For the $\Lambda\text{-}\Pi$ method, calculate Λ_m and Π_m as

$$\Pi_m = \frac{2}{(\Pi_h^{-1} + \Pi_c^{-1})} \quad \Lambda_m = \frac{2\Pi_m}{[(\Pi/\Lambda)_h + (\Pi/\Lambda)_c]} \quad (6.53)$$

3. The equivalent balanced regenerator effectiveness ε_r is evaluated from Equation 6.23 or 6.31 for $\text{NTU}_{o,m}$ and $C_{r,m}^*$ or from Table 6.6 for Λ_m and Π_m . For example, the equivalent form of Equation 6.23 is given by

$$\varepsilon_r = \frac{\text{NTU}_{o,m}}{1+\text{NTU}_{o,m}} \left[1 - \frac{1}{9(C_{r,m}^*)^{1.93}} \right] \quad (6.54)$$

4. The actual regenerator effectiveness ε is then given by

$$\varepsilon = \frac{1 - e^{\{\varepsilon_r(C^{*2}-1)/[2C^*(1-\varepsilon_r)]\}}}{1 - C^* e^{\{\varepsilon_r(C^{*2}-1)/[2C^*(1-\varepsilon_r)]\}}} \quad (6.55)$$

or

$$\varepsilon = \frac{1 - e^{[\phi \varepsilon_r / (1 - \varepsilon_r)]}}{1 - [(\Lambda/\Pi)_h / (\Lambda/\Pi)_c] e^{\phi \varepsilon_r / (1 - \varepsilon_r)}} \quad (6.56)$$

where

$$\phi = \frac{[(\Lambda/\Pi)_h^2 - (\Lambda/\Pi)_c^2]}{2(\Lambda/\Pi)_h(\Lambda/\Pi)_c} \quad (6.57)$$

where C^* is the original specified value, which is less than unity.

A sample calculation [17] for $\Lambda_h = 18$, $\Lambda_c = 15.5$, $\Pi_h = 16$, and $(\Lambda/\Pi)_c = 1.2$ yields $\Pi_m = 4960/347$ and $\Lambda_m = 5760/347$. From Table 6.6, by linear interpolation, one obtains $\varepsilon_r = 0.8215$, since $(\Lambda/\Pi)_m = 31/36$ for this case, while $\phi = -0.0645833$ from the equation. With these values, $\varepsilon = 0.847047$ from the equation. The exact value of the effectiveness for this example is 0.847311, which is just 0.03% higher than the result obtained from this approximate procedure.

6.8.9 INFLUENCE OF LONGITUDINAL HEAT CONDUCTION IN THE WALL

In the foregoing analysis, the influence of longitudinal heat conduction was neglected. For a high-thermal-effectiveness regenerator with a large axial temperature gradient in the wall, longitudinal heat conduction reduces the regenerator effectiveness and the overall heat transfer rate. Bahnke and Howard [22] showed that an additional parameter λ , the longitudinal conduction parameter, would account for the influence of longitudinal heat conduction in the wall. Here, λ is defined as

$$\lambda = \frac{k_w A_{k,t}}{LC_{\min}} \quad (6.58)$$

where

k_w is the thermal conductivity of the matrix wall

$A_{k,t}$ is the total solid area available for longitudinal conduction

$A_{k,t}$ is given by [14]

$$A_{k,t} = A_{k,h} + A_{k,c} = A_{fr} - A_o = A_{fr}(1 - \sigma) \quad (6.59)$$

Introducing the longitudinal conduction parameter, a generalized expression for thermal effectiveness in the functional form is given by

$$\varepsilon = \{NTU_o, C^*, C_r^*, (hA)^*, \lambda\} \quad (6.60)$$

Lowered effectiveness because of longitudinal conduction, $\Delta\varepsilon$, can be calculated in several ways. Parameter definitions for λ and its equivalents for the stationary and rotary regenerators are given in Table 6.8.

TABLE 6.8
Parameter Definitions for λ

	Stationary	Rotary
λ	$\frac{k_w A_{k,t}}{L(MC_p)_c} \left(\frac{\tau_c + \tau_h}{\tau_c} \right)$	$\frac{k_w A_{k,t}}{L(MC_p)_c}$

6.8.9.1 Bahnke and Howard Method

Bahnke and Howard [22] illustrated the influence of the thermal conductivity on thermal effectiveness by a factor called the *conduction effect*. The conduction effect is defined as the ratio of the difference between effectiveness with no conduction effect and with conduction effect to the no conduction effectiveness, as given by

$$\frac{\Delta \epsilon}{\epsilon} = \frac{\epsilon_{\lambda=0} - \epsilon_{\lambda}}{\epsilon_{\lambda=0}} \quad (6.61)$$

Bahnke and Howard tabulated results for ϵ for a wide range of NTU_o , C_r^* , C_r , and λ . Their results are valid over the following range of dimensionless parameters:

$$\begin{aligned} 1 &\geq \frac{C_{\min}}{C_{\max}} \geq 0.90 \\ 1.0 &\leq \frac{C_r}{C_{\min}} \leq \infty \\ 1 &\leq NTU_o \leq 100 \\ 1.0 &\geq (hA)^* \geq 0.25 \\ 1.0 &\geq A_s^* \geq 0.25 \\ 0.01 &\leq \lambda \leq 0.32 \end{aligned}$$

Bahnke and Howard's results for $C^* = 1$ can be accurately expressed by [29]:

$$\epsilon = C_{\lambda} \epsilon_{\lambda=0} \quad (6.62)$$

where $\epsilon_{\lambda=0}$ is given by Equation 6.23 or 6.31, and C_{λ} is given by

$$C_{\lambda} = \frac{1 + NTU_o}{NTU_o} \left[1 - \frac{1}{1 + NTU_o(1 + \lambda\psi)/(1 + \lambda NTU_o)} \right] \quad (6.63)$$

in which

$$\psi = \left(\frac{\lambda NTU_o}{1 + \lambda NTU_o} \right)^{0.5} \tanh \left[\frac{NTU_o}{[\lambda NTU_o/(1 + \lambda NTU_o)]^{0.5}} \right] \quad (6.64a)$$

$$\approx \left(\frac{\lambda NTU_o}{1 + \lambda NTU_o} \right)^{0.5} \quad \text{for } NTU_o \geq 3 \quad (6.64b)$$

6.8.9.2 Romie's Solution

Romie [34] expressed the effects of longitudinal heat conduction on thermal effectiveness in terms of a parameter G_L . The factor G_L is derived from the analysis of axial conduction in counterflow recuperators by Hahnemann [35]. G_L is given by

$$G_L = 1 - \left[1 - \frac{\tanh(b)}{b} \right] \left(\frac{NTU}{b} \right)^2 \quad \text{for } C^* = 1, (hA)^* = 1 \quad (6.65)$$

where

$$b = NTU_o \left[1 + \frac{1}{(\lambda NTU_o)} \right]^{0.5} \quad (6.66)$$

The expression for $\epsilon_{\lambda=0}$ is given by

$$\epsilon_{\lambda \neq 0} = \frac{1 - e^{-G_L NTU_o (1 - C^*)}}{1 - C^* e^{-G_L NTU_o (1 - C^*)}} \quad C^* < 1 \quad (6.67a)$$

$$= \frac{G_L NTU_o}{(1 + G_L NTU_o)} \quad C^* = 1 \quad (6.67b)$$

Figure 6.17 shows G_L as a function of the product NTU_o for several values of NTU_o . The curves are for $(hA)^* = 1$ and $C^* = 0.9$ and 1. The same curves were obtained using $(hA)^* = 0.5$, thus indicating that G_L is a very weak function of $(hA)^*$ [34].

6.8.9.3 Shah's Solution to Account for the Longitudinal Conduction Effect

For $0.9 \leq C^* \leq 1$, Shah [36] has provided a closed-form formula to take into account the longitudinal conduction effect. However, the following more general method is recommended for $C^* < 1$ by Shah [14]:

1. Use the Razelos method to compute $\epsilon_{r,\lambda=0}$ for an equivalent balanced regenerator using the procedure from Equations 6.51, 6.52, and 6.54.
2. Compute C_λ from Equation 6.63 using $NTU_{o,m}$ and λ .
3. Calculate $\epsilon_{r,\lambda \neq 0} = C_\lambda \epsilon_{r,\lambda=0}$.
4. Finally, ϵ is determined from Equation 6.55 or 6.56 with ϵ_λ replaced by $\epsilon_{r,\lambda \neq 0}$.

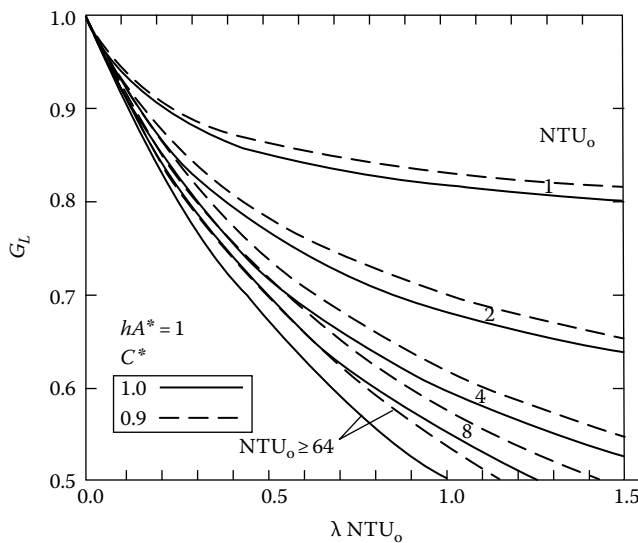


FIGURE 6.17 Parameter G_L for longitudinal conduction effect. (From Romie, F.E., *Trans. ASME J. Heat Transfer*, 113, 247, 1991.)

This procedure yields a value of ϵ accurate within 1% for $1 \leq NTU_o \leq 20$ and $C_r^* \geq 1$ when compared to Bahnke and Howard's results.

6.8.10 FLUID BYPASS AND CARRYOVER ON THERMAL EFFECTIVENESS

Fluid bypass and carryover on thermal effectiveness are discussed in Refs. [14,37].

6.8.11 REGENERATOR DESIGN METHODOLOGY

To design a successful regenerator, the engineer must consider many design factors including the following [2]:

1. Describe the different types of regenerative heat exchangers
2. Discuss the basic heat transfer process and the correlation of cyclic temperature distributions resulting from storage of thermal energy
3. Relate the regenerator to classical counterflow arrangements to enable trade-offs of heat transfer, pressure drop, size, and alternative surfaces
4. Discuss the effects of leakage on both performance and design
5. Consider the effects of pressure loads, leakage control, and rotation on mechanical design

6.8.12 PRIMARY CONSIDERATIONS INFLUENCING DESIGN

Primary considerations influencing the design of a regenerator especially for aircraft/vehicular gas turbine applications may be summarized as follows [38]:

1. Manufacturing limitations
2. Cost limitations
3. Maintenance and cleaning requirements
4. Mechanical design problems
5. Weight, shape, and size limitations
6. Limitations on flow friction-power expenditure
7. Desired exchanger heat transfer effectiveness

6.8.13 RATING OF ROTARY REGENERATORS

The basic steps involved in the analysis of a rating problem are the determination of surface geometrical properties, matrix wall properties, fluid physical properties, Reynolds numbers, j (or Nu) and f factors corrected for property variations, heat transfer coefficients, NTU_o , C^* , C_r^* , and pressure drops. The procedure presented for regenerators parallels that for a compact heat exchanger. Therefore, the rating procedure is not repeated here. However, for details on a rating procedure from first principles consult Shah [14].

6.8.14 SIZING OF ROTARY REGENERATORS

The sizing problem for a rotary regenerator is more difficult. Similar to recuperator design, the sizing of a regenerator involves decisions on material, surface geometry selection, and mechanical design considerations. Once these are decided, the problem reduces to the determination of the disk diameter, division of flow area, disk depth, and disk rotational speed to meet the specified heat transfer and pressure drops [14]. Sometimes a limitation on the size is also imposed. One method for a new design would be to assume a regenerator size, consider it as a rating

problem, and evaluate the performance as outlined for compact recuperators. Iterate on the size until the computed performance matches the specified performance. A detailed sizing procedure is outline in Ref. [14].

6.9 MECHANICAL DESIGN

After the heat transfer surface has been chosen, sizing studies completed, and the regenerator selected to be compatible with the overall system requirements, the next step involves mechanical design. Mechanical designs must consider items such as [2] (1) thermal distortions, (2) leakages, (3) pressure loadings, and in the case of the rotary types, (4) a drive system, and (5) sealing. An important source book on regenerator mechanical design is Mondt [2].

6.9.1 SINGLE-BED AND DUAL-BED FIXED REGENERATORS

Single-bed and dual-bed regenerators can be relatively simple to design. If the bed is composed of loose pellets, grids or screens are necessary to retain the pellets within a container. The grid mesh must be fine enough to retain the smallest pellet in the bed, yet the mesh must be porous enough to keep pressure drops low. If the retaining grids are not strong enough at the operating temperature, the bed will “sag” and loosen the packing.

Leakages: Both the single-bed and dual-bed valved regenerators have displacement leakage, that is, displacement of the fluid entrained in the matrix voids at the switching instant. This fluid is trapped and “displaced” into the other fluid stream and hence is known as displacement leakage. In addition to displacement leakage, fixed-bed regenerators may have small primary leakage of one fluid into the other through leaks in closed switching valves.

6.9.2 ROTARY REGENERATORS

The mechanical design of a rotary regenerator requires (additionally to the recuperator) the following items [39]:

1. A subdivision of the casing into a rotor and a stator
2. Leakage and an effective seal between the two gases
3. Means for supporting the rotor in the stator
4. A drive for the rotor

Items (2) and (4) are discussed next.

6.9.2.1 Leakages

Primary leakages in a rotary regenerator can be classified as (1) labyrinth leakage, (2) carryover or displacement leakage, and (3) structural leakage.

Labyrinth or seal leakage: This is leakage through the seal stem from the fact that the cold gases are at much higher pressures than the hot gases. This is especially true in the case of gas turbine with high-pressure ratio.

Carryover or displacement leakage: In addition to direct leakage through seals, there is inevitably a “carryover” or displacement leakage due to air trapped in the matrix as it passes through the gas side.

Structural primary leakage: Structural leakages take place through any gaps existing in the matrix and the housing.

Any leakage is a serious loss, because it is the air that has absorbed compressor work but escapes to the atmosphere without passing through the turbine. It is more important than pressure loss, as it affects the net work severely [40]. Leakage is dependent mainly on pressure ratio and carryover on matrix rpm. Leakage due to seal leakage and displacement leakage can amount to 3%–4% of the

airflow out of the compressor [41]. The effect of a given fractional leakage depends on the values of exchanger effectiveness and cycle pressure ratio. As an example, for a cycle with typical temperatures, component efficiencies, and regenerator effectiveness of 90%, a leakage of 5% will reduce the net output by about 11% while a leakage of 10% will reduce it by twice that amount [40].

6.9.2.2 Seal Design

In a rotary regenerator, the stationary seal locations control the desired frontal areas for each fluid and also serve to minimize the primary leakage from the high-pressure side to the low-pressure side. The sealing arrangement must adequately prevent leakage flow, and at the same time not introduce high frictional resistance for rotation. Because the matrix is alternately exposed to hot and cold gases, thermal expansion and contraction add to the sealing problem. Typical seals used in rotary regenerator include radial seals, axial seals, and circumferential seals. While designing seals, the pressure forces under the seal faces, which must be balanced, and allowances to be made for the thermal distortion of the rotor [42]. Sealing arrangements are illustrated diagrammatically in Figure 6.18. Certain considerations for seal design are [43] as follows:

1. The seals must be efficient at very high temperature and pressures but still allow freedom of movement.
2. The seals must accommodate the expansion and contraction accompanying temperature variations and still prevent leakage.

6.9.2.3 Drive for the Rotor

A design problem encountered with the regenerator is that of supporting and driving the matrix at low speed. The regenerator usually rotates at a speed of approximately 20–30 rpm [41]. An electric drive will be ideal, because of its low rpm and small power requirement.

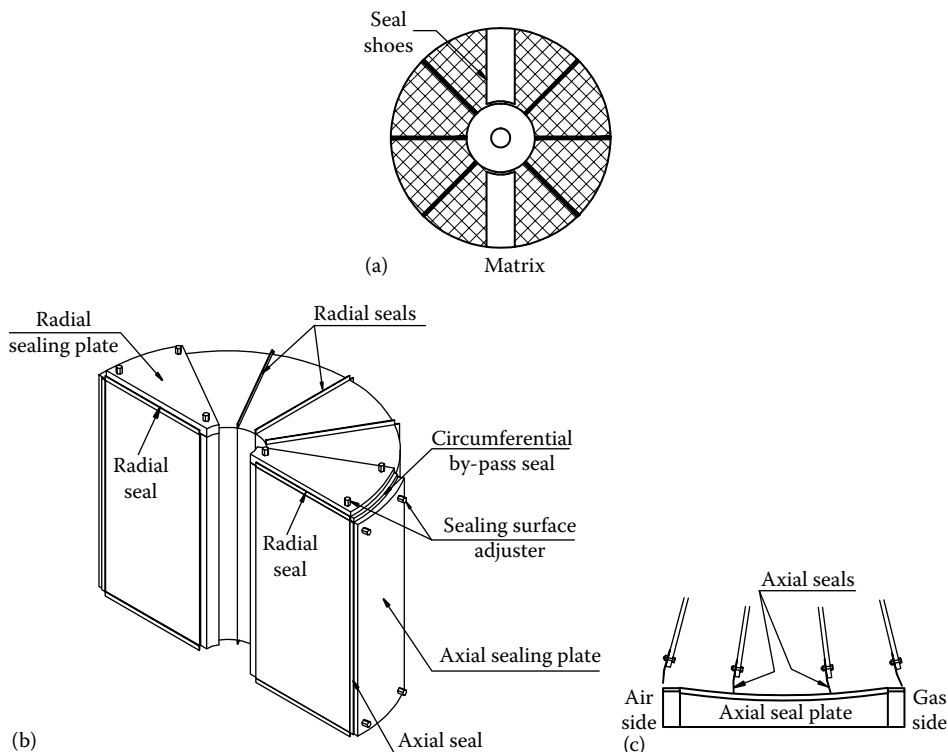


FIGURE 6.18 Seals for rotary regenerator.

6.9.2.4 Thermal Distortion and Transients

A regenerator is subjected to thermal shock and thermal distortion due to unsteady thermal conditions. However, this can be minimized by the use of ceramic material. A regenerator cannot be designed assuming that all operations will be at steady-state conditions. In vehicular gas turbines system, transients are common. Even industrial regenerators are occasionally exposed to starting and stopping transients. Gentle or long-duration transients are desirable to minimize thermal distortions and potential thermal stresses [2]. More problems are usually faced during the warm-up of a regenerator than during stopping because on starting, the matrix and rotor respond much faster than the surrounding housing. If the housing does not accommodate the matrix and the rotor to expand during warm-up, the housing may constrain the matrix growth and cause thermal stresses.

6.9.2.5 Pressure Forces

Pressures in the regenerator system exert forces on the matrix or structure. There are two sources of pressure forces in a rotary regenerator [2]: One source of pressure forces is due to pressure difference between the high-pressure cold air and the low-pressure hot gases. This pressure force depends on the seal arrangement. The seals for a disk can be arranged so that the net force on the support is essentially zero. The second source results from pressure drop of the fluids flowing through the matrix. This pressure force is the product of the total pressure drop and the frontal area.

6.10 INDUSTRIAL REGENERATORS AND HEAT RECOVERY DEVICES

Apart from recuperators and regenerators, various types of heat recovery devices are available for many years. Commercially available heat recovery devices for combustion air preheaters include the following [44]:

1. Fluid-bed regenerative heat exchanger
2. Fluidized-bed waste heat recovery system
3. Vortex-flow direct-contact heat exchanger
4. Ceramic bayonet tube heat exchanger or high-temperature burner duct recuperators
5. Regenerative burner
6. Porcelain-enameled flat-plate heat exchanger
7. Radiation recuperators
8. Heat-pipe exchangers
9. Economizer
10. Thermocompressor
11. Plate heat exchanger energy bank

Because of the multitude of different industrial heating processes and exhaust system designs, there is no one universal type of heat transfer device best suited for all applications. Various types of industrial air preheaters are discussed here under and readers may refer for more details to Ref. [44].

6.10.1 FLUID-BED REGENERATIVE HEAT EXCHANGERS

In fluid-bed regenerative heat exchangers, fluidized beds of pellets recover heat from hot exhaust gas and transfer this heat to cold combustion air [45]. The basic fluid-bed heat exchanger consists of an insulated cylindrical tower incorporating an upper and a lower chamber as shown in Figure 6.19. Each chamber is fitted with several horizontal perforated trays. Hot exhaust gases enter the upper chamber near its base and rise to the outlet near the top, heating counterflow alumina pellets as they fall. The heated pellets pass through an aperture into the lower chamber, where they give up their heat to the cold air. Air enters the lower chamber near the base and exits near the top. Direct

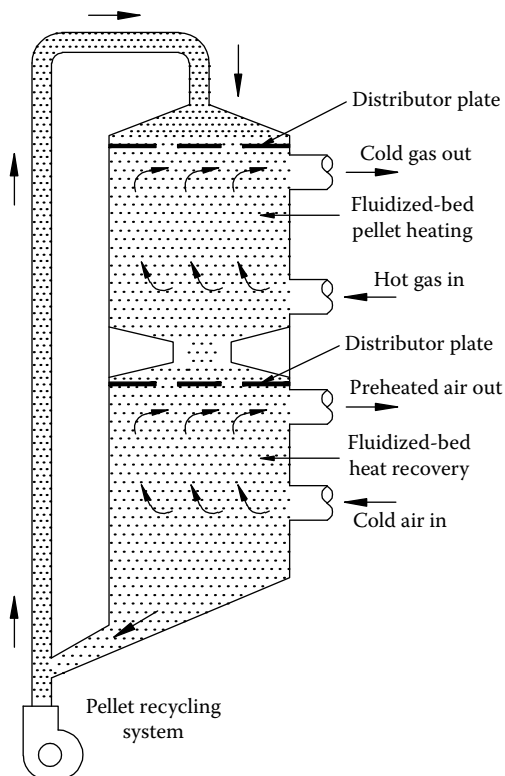


FIGURE 6.19 Fluid-bed regenerator.

contact of gas and air streams with the heat exchange media, namely, the alumina pellets, coupled with controlled dwell time at the trays, results in high heat transfer rates. By controlling the rate of pellet recycling, the temperature of the air being heated can be held constant within wide variations of gas inlet temperature and volume. As a part of this heat exchange system, an auxiliary pneumatic system is incorporated for recycling alumina pellets.

6.10.2 FLUIDIZED-BED WASTE HEAT RECOVERY

Fluidized-bed waste heat recovery (FBWHR) systems are being developed to preheat combustion air for industrial furnaces. FBWHR systems employ a heat transfer particulate media, which is heated as it falls through the upward-flowing flue gases in a raining bed heat exchanger [9,46]. This type of heat exchanger is known as a fluidized-bed heat exchanger (FBHE). FBHE offer the potential for economic recovery of high-temperature (2000°F–3000°F) heat from the flue gases of industrial processes such as steel soaking pits, aluminum remelt furnaces, and glass melting furnaces.

An FBHE consists of horizontal finned heat exchanger tubes with a shallow bed of fine inert particles, which move upward with gas flow and give up the heat to the finned tubes, which in turn transfer heat to cold air passing through them. A thin steel plate with small perforations supports the bed and distributes the hot gas evenly. The perforations are uniform with a hole size of 1.5 mm diameter or less, and the holes are spaced to provide a free flow area of 3%–10%. For many applications, only ceramic distributor plates will withstand the temperatures and corrosive environments of flue gases. Among the FBHE advantages are enduring the hostile environments such as elevated temperature, fouling particulates, corrosive gases, corrosive particulates, and thermal cycling [9]. Most surfaces are kept clean by fluidizing action.

6.10.3 VORTEX-FLOW DIRECT-CONTACT HEAT EXCHANGERS

The vortex-flow direct-contact heat exchanger represents a new approach for high-temperature (2500°F) heat recovery from industrial waste heat flue gas with a simple payback period. In the vortex-flow direct-contact heat exchanger, the heat conduction material wall of conventional metal or high-temperature ceramic material is replaced by a vortex-induced fluid dynamic gas boundary, which separates the tangentially rotating hot and cold gas flows between which heat exchange is desired [47].

The VFHE is a cylindrical cavity into which separate hot flue gas and cold preheat air gas flows are injected. Injection of the gases is such that a vortex-flow pattern is established in the cavity, providing confinement of hot fluid to the central region of the cavity surrounded by cold air stream. Solid particles of 20–200 μm diameters as a medium to exchange heat between hot and cold streams are injected into the hot spiraling gas stream. Due to centrifugal action, these particles pass into the surrounding cold gas rotating flow, to which the particles transfer heat. Upon reaching the outside cavity surface, the particles are entrained in the outermost region of the vortex flow and removed with a portion of the cold flow, which exits at the periphery (exhaust end wall). The VFHE requires a particle injection and separation subsystem to collect and recycle the particle to the vortex chamber for continued heating and cooling cycles.

6.10.4 CERAMIC BAYONET TUBE HEAT EXCHANGERS

Babcock and Wilcox (B&W) and the Department of Energy (DOE) developed high-temperature burner duct recuperator (HTBDR) systems capable of recovering waste heat from high-temperature flue gas using ceramic bayonet elements [48,49]. The HTBDRs consist of silicon carbide ceramic bayonet tubes suspended into the exhaust gas flow stream, where they recover the heat from the exhaust and preheat the combustion air up to a temperature of 1090°C (2000°F). The ceramic bayonet elements consist of an assembly of two concentric tubes of each bayonet element suspended from metallic, air-cooled tubesheets at the top end of the element. Combustion air is directed through the elements at the inner tube or the annulus from heavily insulated plena located above the tubesheets. The tubes of each element are free to expand or contract under the influence of temperature variations. The ceramic bayonet elements are also expected to ease maintenance and to best deal with problems associated with thermal stress, leakage, and stress-related corrosion.

6.10.5 REGENERATIVE BURNERS

The reGen regenerative burner, an all-ceramic high-temperature burner, close coupled to a compact, fast-cycle, ceramic regenerator, provides air preheats in excess of 85% of the process temperature in fuel-fired applications up to 1399°C (2550°F) [7]. Figure 6.20 shows one complete regenerative

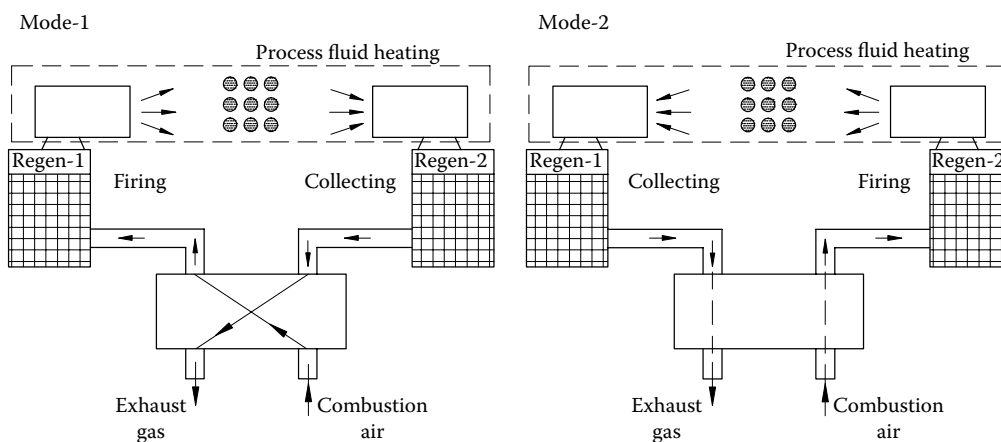


FIGURE 6.20 Regenerative burner.

unit comprised of two burners, two regenerators, a reversing valve, and the related pipings. While one of the burners fires, drawing the preheated air fed through its regenerator, exhaust gas is drawn through the other burner and down into its associated regenerator, then discharged to the atmosphere. After a sufficient interval, the reversing operation takes place.

6.10.6 PORCELAIN-ENAMELED FLAT-PLATE HEAT EXCHANGERS

Porcelain-enameled heat exchangers offer cost-effective solutions to problems of heat recovery from extremely corrosive gases that preclude the use of carbon steel or common types of stainless steels [50]. Porcelain enamel is a glass coating material that is applied to a metal substrate to protect the base metal. The base metal gives strength and rigidity; the metal can be steel, cast iron, aluminum, or copper, but mostly steel is used on a larger scale. The glass coating offers significant corrosion resistance to the corrosive flue gas. The porcelain-enameled coating finds application in flat-plate heat exchangers of the open channel air preheater (OCAP) type for advanced heat recovery. The OCAP is a plate-type exchanger characterized by a nonweld construction of the heat transfer core. The enameled plates are assembled into a floating construction. Elastic springs are used between all adjacent plates to ensure a uniform distribution of the dead weights and to allow for the thermal expansion and contraction in operation. This floating core is enclosed in a rigid frame, again without any welding or any damage to the porcelain enamel layer.

6.10.7 RADIATION RECUPERATORS

Metallic recuperators for industrial furnaces are generally of the following types [51]:

1. Convective units, operating at flue gas temperatures up to a maximum of 1100°C (2000°F).
2. Radiation-type units, that is, the heat transfer mode is by radiation, operating at temperature ranges of nearly 900°C–1500°C (2700°F). In radiation-type recuperators, parallelflow is essential to control the operating temperatures of the heating surface. A combination of parallelflow and counterflow is required to reach the highest recuperator efficiencies of air temperature of above 800°C (1500°F). Typical radiation recuperators include a double-shell parallelflow radiation recuperator consisting of two concentric cylinders (Figure 6.21)—through the inner shell the flue gas flows and through the annulus the cold air flows in a parallel direction—as well as cage-type radiation recuperators for very large high-temperature furnaces, with a combination of parallelflow and counterflow units.

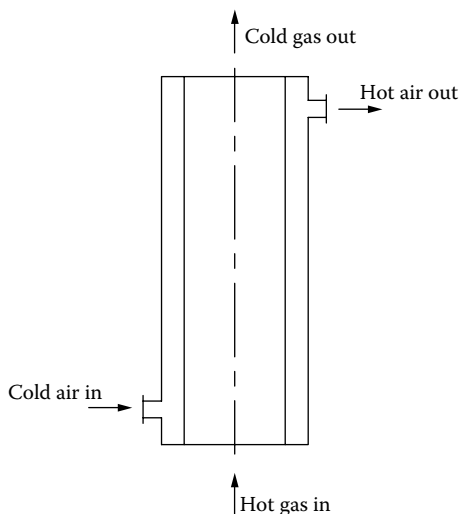


FIGURE 6.21 Radiation recuperator.

6.10.8 HEAT-PIPE HEAT EXCHANGERS

The heat-pipe heat exchanger used for gas–gas heat recovery is essentially a bundle of finned heat pipes assembled like a conventional air-cooled heat exchanger. The heat pipe consists of three elements (1) a working fluid inside the tubes, (2) a wick lining inside the wall, and (3) a vacuum sealed finned tube. Because the pipe is sealed under a vacuum, the working fluid is in equilibrium with its own vapor. The purpose of the wick is to transport the working fluid contained within the heat pipe, from one end to the other by capillary action.

The heat-pipe heat exchanger consists of an evaporative section through which the hot exhaust gas flows and a condensation section through which the cold air flows. These two sections are separated by a separating wall as shown in Figure 6.22 [52]. The working of a heat-pipe heat exchanger is as follows. Heat transfer by the hot flue gas at the evaporative section causes the working fluid contained within the wick to evaporate and the increase in pressure causes the vapor to flow along the central vapor region to the condensation section, where it condenses, and gives up the latent heat to the cold air. The condensate then drains back to the evaporative section by capillary action in the wick. Figure 6.23 shows heat-pipe heat exchanger finned U-tube. In cases where gravity aids return of the condensate to the evaporative section, it is possible to operate without a wick; the device then becomes a simple two-phase thermosiphon.

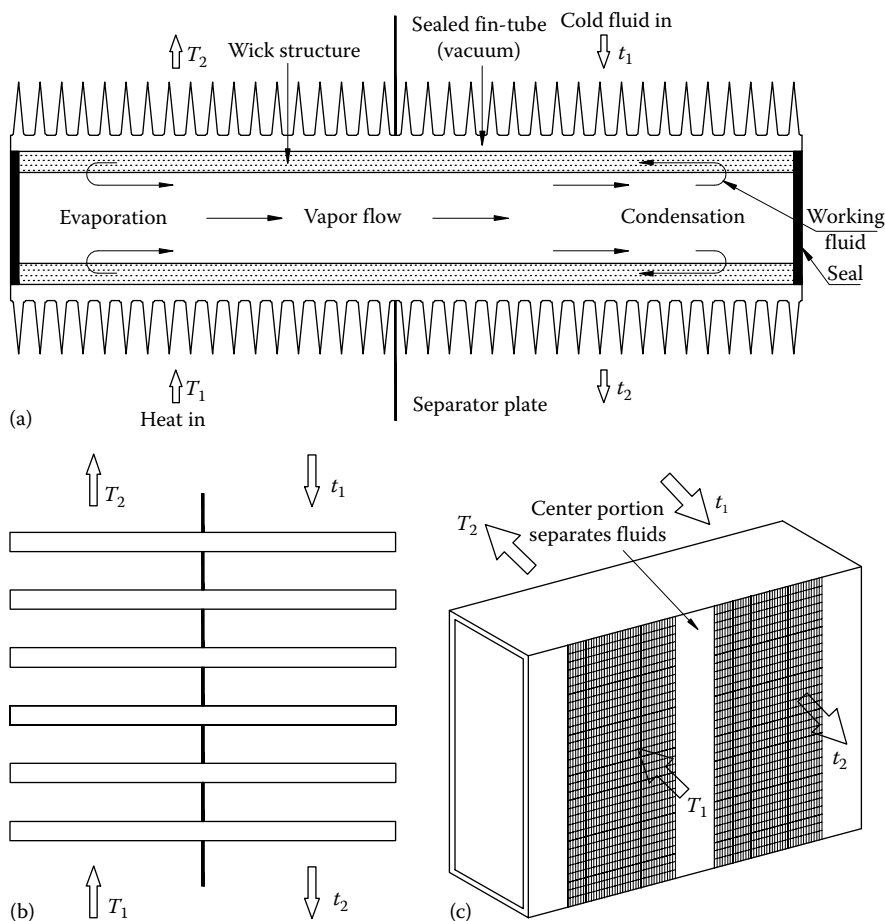


FIGURE 6.22 Heat-pipe heat exchanger. (a) Principle of working, (b) heat-pipe tube arrangement, and (c) heat-pipe heat exchanger (schematic).



FIGURE 6.23 Heat-pipe heat exchanger finned U-tube. (From Thermofin, www.thermofin.net)

6.10.8.1 Merits of Heat-Pipe Heat Exchanger

The heat-pipe exchanger is a lightweight compact heat recovery system. It does not need mechanical maintenance, as there are no moving parts. It does not need input power for its operation.

6.10.8.2 Application

The heat pipes are used in following industrial applications such as (1) process fluid to preheating of air; (2) preheating of boiler combustion air; (3) heating, ventilating, and air-conditioning (HVAC) systems; (4) recovery of waste heat from furnaces; (5) reheating of fresh air for hot air driers; (6) preheating of boiler feed water with waste heat recovery from flue gases in the heat-pipe economizers; and (7) reverberatory furnaces (secondary recovery).

6.10.9 ECONOMIZER

In case of boiler system, economizer is provided to utilize the flue gas heat either for preheating the boiler feed water or the combustion air. In both the cases, there is a corresponding reduction in the fuel requirements of the boiler. For every 22°C reduction in flue gas temperature by passing through an economizer or a preheater, there is 1% saving of fuel in the boiler. In other words, for every 6°C rise in feed water temperature through an economizer or 20°C rise in combustion air temperature through an air preheater, there is 1% saving of fuel in the boiler [52]. Few types of industrial economizers are shown in Figure 6.24.

6.10.10 THERMOCOMPRESSOR

In many cases, very low-pressure steams are reused as water after condensation for lack of any better option of reuse. Also, it becomes feasible to compress low-pressure steam by very high-pressure steam and reuse it as a medium pressure steam. The major energy in steam is its latent heat value and thus thermocompressing would give a large improvement in waste heat recovery. The thermocompressor is a simple equipment with a nozzle where high-pressure steam is accelerated into a high-velocity fluid (Figure 6.25). This entrains the low-pressure steam by momentum transfer and then recompresses in a divergent venturi. It is typically used in evaporators where the boiling steam is recompressed and used as heating steam.

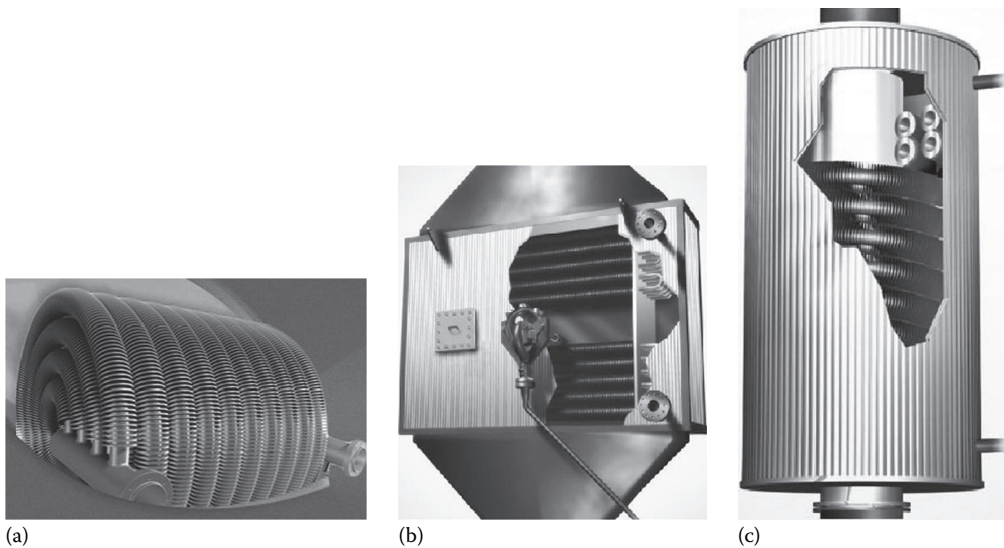


FIGURE 6.24 Economizer. (a) Coiled-tube economizer, (b) rectangular economizer, and (c) cylindrical economizer. (Courtesy of Fintube, LLC, Tulsa, OK; www.fintubellc.com)

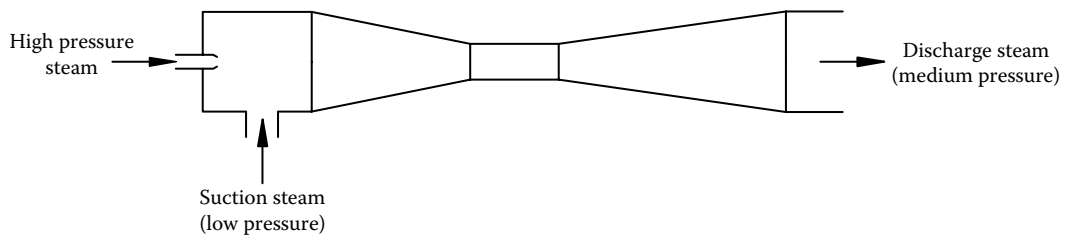


FIGURE 6.25 Thermocompressor.

6.10.11 MUELLER TEMP-PLATE® ENERGY RECOVERY BANKS

A Mueller Temp-Plate energy recovery bank (Figure 6.26) transfers the heat content of the waste gas to the media used in the process or to an intermediate heat transfer solution. High grade heat can be efficiently recovered using a Mueller Temp-Plate energy recovery bank.

6.11 ROTARY HEAT EXCHANGERS FOR SPACE HEATING

The ventilation losses account for the major part of energy use in HVAC, it is imperative to reduce these losses as much as possible. Rotary heat exchangers are well-proven means of high efficiency energy recovery, typically recovering up to 80% in typical HVAC (space heating and ventilation) applications. The combination of heat and humidity recovery by rotary heat exchangers is a highly efficient energy-saving method. Typical summer application is dehumidification of warm and humid supply air to reduce the energy consumption of the downstream cooling equipment. During winter, operation of this feature recovers moisture from the exhaust air to reduce the humidification load.

Leading rotary heat exchanger manufacturers for HVAC applications include Hovalwerk AG, 9490 Vaduz, Liechtenstein, Reznor UK Ltd, Klingenburg GmbH, Germany, Munters International Inc., FL and Fläkt Woods AB, SE-551 84 Jönköping.

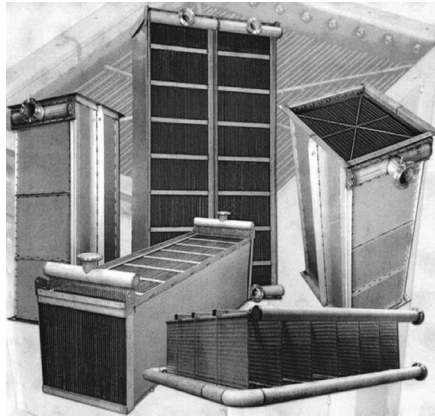


FIGURE 6.26 Mueller Temp-Plate energy recovery banks. (Courtesy of Mueller, Heat Transfer Products, Springfield, MO.)

6.11.1 WORKING PRINCIPLE

The rotor with its axial, smooth air channels serves as a storage mass, half of which is heated by the warm air stream and half of which is cooled by the cold air stream, in a counterflow arrangement. Consequently, the temperature of the storage mass varies depending on the rotor depth in the axial direction and on the angle of rotation. In a counterflow arrangement, the rotating, air permeable storage mass is heated and cooled alternately by the heat-releasing and heat-absorbing air streams. Depending on the air conditions and on the surface of the storage mass, also moisture may be transferred in this process. The supply and extract air streams must be adjacent and pass through the heat exchanger simultaneously. A typical rotary wheel for HVAC applications is shown in Figure 6.27. (Also refer to Figure 1.15.)

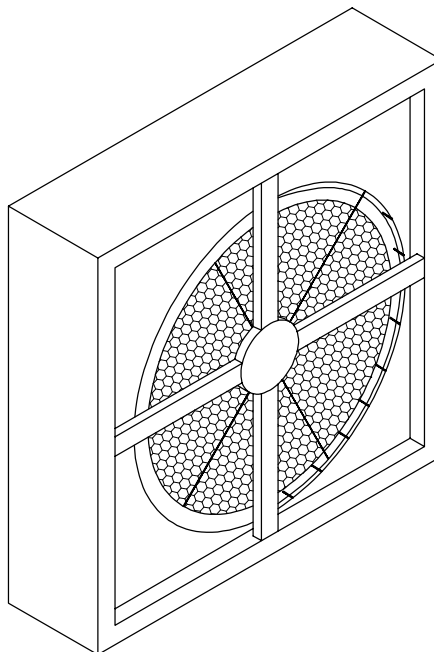


FIGURE 6.27 Rotary wheel for HVAC application.

6.11.2 CONSTRUCTION

Rotor wheel—The rotor wheel shall be made of layers of corrugated and intervening flat composite material or aluminum foil of uniform width to ensure a smooth surface. This wheel material is bonded together to form a rigid heat transfer matrix forming a multitude of narrow triangular air channels in an axial direction. Rotors with straight oriented waves guarantee a laminar flow through the heat exchanger with an optimum degree of efficiency and favorable pressure drops as well as a high level of self-cleaning. The thickness of the material (usually aluminum) is 0.06–1.2 mm. The standard range of airway wave height available is 1.6–2.9 mm depending on the application. Depending on the heights of the waves in the aluminum foil, air channels of different sizes can be supplied, smaller air channels increase operating efficiency but increase the pressure drop. The depth of the storage mass in the direction of air flow is usually 200 mm. Rotors are available from 0.25 to 6.0 m diameter and it can handle air flow rates up to 150,000 m³/h.

The wheel can be fully wound or on larger units, sectorized, i.e., assembled in segments for the ease of transport, stability, and insertion into building. The segments are assembled between rigid spokes, thus ensuring structural rigidity and longevity and allowing replacement of one or specific segments or all of the segments without having to remove any spokes. The segments need to be installed inside the divided casing at the final site. At the perimeter the rotor is enclosed by a welded aluminum shell, ensuring true running and allowing maximum use of the wheel face area. The wheels shall be tested in accordance with ASHRAE-78 method. Rotary heat exchangers can transfer moisture as well as heat. The decisive criterion for the transfer of moisture is the material or surface of the storage mass. The following are the major designs available in the market:

1. Condensation rotor or non-hygroscopic aluminum wheel for recovering principally sensible heat. The storage mass consists of smooth untreated aluminum foil transferring moisture only when condensation occurs on the warm air side and (part of) this is taken up by the cold air. Condensation may be carried along with the air flow.
2. Enthalpy rotors or hygroscopic aluminum wheel for recovering sensible and latent heat.
3. Sorption wheel consisting of aluminum backing foil which is coated with a sorbent (e.g., silicagel) to accomplish vapor transfer without condensation.

6.11.3 ROTOR MATERIALS

Normally, the rotor wheel shall be made of aluminum foil. Operating conditions with high degrees of fouling and corrosion have led to the development of aluminum plated steel foil, chrome steel, and chrome nickel steel foils of various thicknesses. Rotors are also available with epoxy-coated aluminum matrix in order to increase the corrosion resistance.

6.11.3.1 Construction

Casing: The casing shall be constructed as a single skin, self-supporting from galvanized steel and include rotary wheel support beams and a purging sector.

6.11.3.2 Carryover

To a minor degree, the two air flows mix due to the rotating storage mass. Depending on the air velocity and rotation speed, carryover amounts to about 2%–4% of the airflow rate. Carryover of exhaust air to the fresh air side can be minimized by installing a purge sector.

6.11.3.3 Seals

The casing shall be equipped with adjustable brush seals which minimize carryover loss. Sealing at the periphery is important for the internal leakage of the rotary heat exchanger. A plastic seal tape

being pressed onto the storage mass by means of springs. This design keeps cross-contamination via the inside of the rotor casing to a minimum. Transverse seal is also required between the warm air and the cold air. Manufacturers use an adjustable threefold lip seal, ensuring a minimal air gap to the storage mass. This reduces direct carryover from warm air to cold air (and vice versa) to a minimum.

6.11.4 DRIVE SYSTEM AND CONTROL UNIT

The rotor shall be belt or gear driven along its periphery. A constant speed or variable speed drive motor shall be used. The motor shall be mounted on a self-adjusting base to provide correct belt tension. The drive unit shall be available with a differential thermostat for summer/winter changeover, a speed detector with alarm function, an interface for central energy management control system and for climate zones a frequency converter to control and regulate the efficiency of fan by varying its rpm. Rotary heat exchangers have optimized efficiency around 12–20 rpm.

6.11.5 CLEANING DEVICES

For the regenerative heat exchangers, there are several types of cleaning devices. They are selected according to the degree of fouling of the rotor. Under normal conditions, the rotor has a high self-cleaning effect, on account of the continuously changing directions of air flow. The cleaning methods include (1) compressed air cleaning, (2) compressed air and water cleaning, (3) steam cleaning, and (4) compressed air and warm water cleaning.

NOMENCLATURE

A_C	matrix transfer area on cold side, m^2 (ft^2)
A_{fr}	frontal area, m^2 (ft^2) = $A_{fr,h} + A_{fr,c}$
$A_{fr,c}$	frontal area on cold side, m^2 (ft^2)
$A_{fr,h}$	frontal area on hot side, m^2 (ft^2)
$A_{fr,t}$	total face area, m^2 (ft^2)
A_h	matrix transfer area on hot side, m^2 (ft^2)
$A_{k,l}$	total solid area for longitudinal conduction, m^2 (ft^2)
A_{mk}	constants defined by Equation 6.48
a_{jk}	constants defined by Equation 6.29
A_o	minimum free flow area, m^2 (ft^2) = σA_{fr}
$\%a$	face seal and hub coverage
B_j	constants defined by Equation 6.28
B_{mk}	constants defined by Equation 6.49
b	cell geometry dimension, m (ft); or function defined by Equation 6.66
C	heat capacity rate (Mc_p), $J/^\circ C$ ($Btu/h \cdot ^\circ F$)
C^*	heat capacity rate ratio (it should be less than or equal to 1) = C_{min}/C_{max}
C_c	fluid stream capacity rate (Mc_p) for cold gas, $W/^\circ C$ ($Btu/h \cdot ^\circ F$)
C_h	fluid stream capacity rate (Mc_p) for hot gas, $W/^\circ C$ ($Btu/h \cdot ^\circ F$)
C_k	constant defined by Equation 6.50
C_{max}	maximum of C_c or C_h , $W/^\circ C$ ($Btu/h \cdot ^\circ F$)
C_{min}	minimum of C_c or C_h , $W/^\circ C$ ($Btu/h \cdot ^\circ F$)
$c_{p,c}$	specific heat of cold gas, $J/kg \cdot ^\circ C$ ($Btu/lbm \cdot ^\circ F$)
$c_{p,h}$	specific heat of hot gas, $J/kg \cdot ^\circ C$ ($Btu/lbm \cdot ^\circ F$)
$C_r =$ $= M_{r,c_r} N$	capacity rate of the rotor matrix (M_{r,c_r}), $W/^\circ C$ ($Btu/h \cdot ^\circ F$) for rotary regenerator, $W/^\circ C$ ($Btu/h \cdot ^\circ F$)
c_r	specific heat of the matrix material, $J/kg \cdot ^\circ C$ ($Btu/lbm \cdot ^\circ F$)

C^*	matrix heat capacity rate ratio
$C_{r,m}^* =$	matrix heat capacity rate ratio $= (M_r c_r)/C_{\min}$
$C_{r,m}^* = C_r^*$	for equivalent balanced regenerator
C_λ	longitudinal conduction correction factor
D	regenerator disk outer diameter at the end of the heat transfer surface, m (ft)
D_h	hydraulic diameter, $(4r_h)$, m (ft)
d	hub diameter, m (ft)
d^*	cell height/width
f	Fanning friction factor
G_L	parameter to account the effects of longitudinal heat conduction on thermal effectiveness as defined in Equation 6.65
hA	thermal conductance $W/^\circ C$ (Btu/h \cdot $^\circ F$)
$(hA)^*$	ratio of the convective conductance on the C_{\min} side to C_{\max} side $= (hA)_c/(hA)_h$
h_c	convective conductance for cold gas, $W/m^2 \cdot ^\circ C$ (Btu/h $ft^2 \cdot ^\circ F$)
h_h	convective conductance for hot gas, $W/m^2 \cdot ^\circ C$ (Btu/h $ft^2 \cdot ^\circ F$)
$I_n(\cdot)$	modified Bessel function of the first kind and n th order
j	Colburn factor for heat transfer
i, j, k, n	integers
k_w	thermal conductivity of the matrix wall
L	matrix flow length, m (ft)
M	order of the trial solution, Equation 6.45
M_c	mass flow rate of cold gas, kg/s (lbm/h)
m_c	mass of the cold gas retained in the matrix flow length dx , kg (lbm)
$(Mc_p)_c$	capacity rate of cold gas, $W/^\circ C$ (Btu/h \cdot $^\circ F$)
$(Mc_p)_h$	capacity rate of hot gas, $W/^\circ C$ (Btu/h \cdot $^\circ F$)
M_h	mass flow rate of hot gas, kg/s (lbm/h)
m'_h	mass of the hot gas retained in the matrix flow length dx , kg (lbm)
M_r	matrix mass, kg (lbm)
$M_r c_r$	thermal capacitance of matrix, $W/^\circ C$ (Btu/h \cdot $^\circ F$)
N	rpm of the rotary matrix
N_c	cell density
Nu	Nusselt number, hD_h/k
NTU	number of transfer units, hA/C
NTU_c	number of transfer units on the cold side (\approx twice NTU_o)
NTU_h	number of transfer units on the hot side (\approx twice NTU_o)
NTU_o	modified number of transfer units
$NTU_{o,m}$	NTU_o for an equivalent balanced regenerator
Q	total heat duty of the exchanger, W s (Btu)
q	heat transfer rate, W (Btu/h)
Re	Reynolds number
r_h	hydraulic radius, m (ft) $= D_h/4$
t_c	temperature of the cold gas, $^\circ C$ ($^\circ F$)
t_h	temperature of the hot gas, $^\circ C$ ($^\circ F$)
t_r	temperature of the matrix, $^\circ C$ ($^\circ F$)
$t_{c,i}, t_{c,o}$	cold fluid terminal temperatures, $^\circ C$ ($^\circ F$)
$t_{h,i}, t_{h,o}$	hot fluid terminal temperatures, $^\circ C$ ($^\circ F$)
U_c	utilization factor on the cold side $(\Lambda/\Pi)_c$
U_h	utilization factor on the cold side $(\Lambda/\Pi)_h$
U_1	$(\Lambda/\Pi)_1$, the smaller of the two ratios U_c and U_h

x_{1m}, x_{2m}	unknown coefficients defined by Equation 6.45
x, y	variables as defined in Equation 6.2
$V =$	$(A_{fr,h} + A_{fr,c})L$, m^3 (ft^3), volume of regenerator
$V_i(x, y)$	special functions defined by Equation 6.41
β	area density, m^2/m^3 (ft^2/ft^3)
δ	matrix stock thickness, m (ft)
ϵ	thermal effectiveness
ϵ_{cf}	counterflow regenerator thermal effectiveness
ϵ_r	thermal effectiveness of reference regenerator
$\Delta\epsilon$	lowered effectiveness because of longitudinal conduction
$\epsilon_{r,\lambda=0}$	equivalent balanced regenerator neglecting longitudinal heat conduction
$\epsilon_{r,\lambda\neq 0} =$	$C_\lambda \epsilon_{r,\lambda=0}$
ξ	fractional distance along the flow path in the regenerator matrix of length L
η	fractional completion of a respective gas flow period
Λ	reduced length
Λ_m	mean reduced length
λ	longitudinal conduction parameter
λ_c	longitudinal conduction on the cold side
λ_h	longitudinal conduction on the hot side
Π	reduced period
Π_m	mean reduced period
ρ_r	matrix material density
φ	function defined by Equation 6.57
ψ	function defined by Equation 6.64
σ	porosity $= A_o/A_{fr}$
τ	flow period, s
τ_c	duration of cold flow period, s
τ_h	duration of hot flow period, s
τ_L	time for one revolution, $\tau_c + \tau_h$, s

Subscripts

c	cold
h	hot
i	in
m	mean
o	hot
r	matrix

REFERENCES

1. Denniston, D. W., Waste recovery in the glass industry, in *Industrial Heat Exchangers Conference Proceedings* (A. J. Hayes, W. W. Liang, S. L. Richlen, and E. S. Tabb, eds.), American Society for Metals, Metals Park, OH, 1985, pp. 13–20.
2. Mondt, J. R., Regenerative heat exchangers: The elements of their design, selection and use, Research Publication GMR-3396, General Motors Research Laboratories, Warren, MI, 1980.
3. Shah, R. K. and Sekulic, D. P., Heat Exchangers, in *Handbook of Heat Transfer Applications*, Rohsenow, W. M., Hartnett, J. P., and Ganic, E. N. (eds.), 3rd edn., McGraw-Hill, New York, 1998, pp. 17.1–17.169, Chapter 17.
4. Liang, W. W. and Tabb, E. S., CRI's advanced heat transfer systems program, in *Industrial Heat Exchangers Conference Proceedings* (A. J. Hayes, W. W. Liang, S. L. Richlen, and E. S. Tabb, eds.), American Society for Metals, Metals Park, OH, 1985, pp. 29–36.

5. Coombs, M. G., Strumpf, H. J., and Kotchick, D. M., A ceramic finned plate recuperator for industrial applications, in *Industrial Heat Exchangers Conference Proceedings* (A. J. Hayes, W. W. Liang, S. L. Richlen, and E. S. Tabb, eds.), American Society for Metals, Metals Park, OH, 1985, pp. 63–68.
6. Newby, J. N., The Regen regenerative burner—Principles, properties and practice, in *Industrial Heat Exchangers Conference Proceedings* (A. J. Hayes, W. W. Liang, S. L. Richlen, and E. S. Tabb, eds.), American Society for Metals, Metals Park, OH, 1985, pp. 143–152.
7. Walker, G., *Cryocoolers, Part 2: Applications*, Plenum Press, New York, p. 44, 1983.
8. Bugyis, E. J. and Taylor, H. L., Heat exchange in the steel industry, in *Industrial Heat Exchangers Conference Proceedings* (A. J. Hayes, W. W. Liang, S. L. Richlen, and E. S. Tabb, eds.), American Society for Metals, Metals Park, OH, 1985, pp. 3–12.
9. Hoffman, L. C. and Williams, H. W., Fluid bed waste recovery performance in a hostile environment, in *Industrial Heat Exchangers Conference Proceedings* (A. J. Hayes, W. W. Liang, S. L. Richlen, and E. S. Tabb, eds.), American Society for Metals, Metals Park, OH, 1985, pp. 87–94.
10. Hayes, A. J. and Richlen, S. L., The Department of Energy's advanced heat exchangers program, in *Industrial Heat Exchangers Conference Proceedings* (A. J. Hayes, W. W. Liang, S. L. Richlen, and E. S. Tabb, eds.), American Society for Metals, Metals Park, OH, 1985, pp. 21–28.
11. McDonald, C. F., The role of the ceramic heat exchanger in energy and resource conservation, *Trans. ASME J. Eng. Power*, 102, 303–315 (1980).
12. Kleiner, R. N. and Coubrough, L. E., Advanced high performance ceramic heat exchanger designs for industrial heat recovery applications, in *Industrial Heat Exchangers Conference Proceedings* (A. J. Hayes, W. W. Liang, S. L. Richlen, and E. S. Tabb, eds.), American Society for Metals, Metals Park, OH, 1985, pp. 51–56.
13. McNallan, M. J., Liang, W. W., and Rothman, M. F., An investigation of the hot-corrosion of metallic and ceramic heat exchanger materials in chlorine contaminated environments, in *Industrial Heat Exchangers Conference Proceedings* (A. J. Hayes, W. W. Liang, S. L. Richlen, and E. S. Tabb, eds.), American Society for Metals, Metals Park, OH, 1985, pp. 293–298.
14. Shah, R. K., Counterflow rotary regenerator thermal design procedures, in *Heat Transfer Equipment Design* (R. K. Shah, E. C. Subbarao, and R. M. Mashelikar, eds.), Hemisphere, Washington, DC, 1988, pp. 267–296.
15. Kays, W. M. and London, A. L., *Compact Heat Exchangers*, 3rd edn., McGraw-Hill, New York, 1984.
16. London, A. L., Young, M. B. O., and Stang, J. H., Glass-ceramic surfaces, straight triangular passages—Heat transfer and flow friction characteristics, *Trans. ASME J. Eng. Power*, 92A, 381–389 (1970).
17. Baclic, B. S., The application of the Galerkin method to the solution of the symmetric and balanced counterflow regenerator problem, *Trans. ASME J. Heat Transfer*, 107, 214–221 (1985).
18. Nusselt, W., Die Theorie des Winderhitzers [Theory of the air heater], *Z. Ver. Dt. Ing.*, 71, 85–91 (1927).
19. Hausen, H., Über die Theorie des Wärmeaustausches in Regeneratoren, *Z. Angew. Math. Mech.*, 9, 173–200 (1929). Also, in *Vervollständigte Berechnung des Wärmeaustausches in Regeneratoren*, *Z. Ver. Dtsch. Ing.*, 2 (1942).
20. Coppage, J. E. and London, A. L., The periodic-flow regenerator—A summary of design theory, *Trans. ASME*, 75, 779–787 (1953).
21. Lambertson, T. J., Performance factors of a periodic flow heat exchanger, *Trans. ASME*, 80, 586–592 (1958).
22. Bahnke, G. D. and Howard, C. P., The effect of longitudinal heat conduction on periodic flow heat exchanger performance, *Trans. ASME J. Eng. Power*, 86, 105–120 (1964).
23. Mondt, J. R., Vehicular gas turbine periodic flow heat exchanger solid and fluid temperature distributions, *Trans. ASME J. Eng. Power*, 86, 121–126 (1964).
24. Li, C.-H., A numerical finite difference method for performance evaluation of a periodic flow heat exchanger, *Trans. ASME J. Heat Transfer*, 105, 611–617 (1983).
25. Nahavandi, A. H. and Weinstein, A. S., A solution to the periodic flow regenerative heat exchanger problem, *Appl. Sci. Res.*, 10, 335–348 (1961).
26. Willmott, A. J. and Duggan, R. C., Refined closed methods for the contra-flow thermal regenerator problem, *Int. J. Heat Mass Transfer*, 23, 655–662 (1980).
27. Baclic, B. S. and Dragutinovic, G. D., Asymmetric-unbalanced counterflow thermal regenerator problem: Solution by the Galerkin method and meaning of dimensionless parameters, *Int. J. Heat Mass Transfer*, 34, 483–498 (1991).
28. Romie, F. E. and Baclic, B. S., Methods for rapid calculation of the operation of asymmetric counterflow regenerator, *Trans. ASME J. Heat Transfer*, 110, 785–788 (1988).

29. Shah, R. K., Thermal design theory for regenerators, in *Heat Exchangers: Thermal-Hydraulic fundamentals and Design* (S. Kakac, A. E. Bergles, and F. Mayinger, eds.), Hemisphere/McGraw-Hill, New York, 1981, pp. 721–763.
30. Heggs, P. J., Calculation of high temperature regenerative heat exchangers, in *High Temperature Equipment* (A. E. Sheindlin, ed.), Hemisphere, Washington, DC, 1986, pp. 115–149.
31. Romie, F. E., A table of regenerator effectiveness, *Trans. ASME J. Heat Transfer*, 112, 497–499.
- 32a. Hill, A. and Willmott, A. J., A robust method for regenerative heat exchanger calculations, *Int. J. Heat Mass Transfer*, 30, 241–249 (1987).
- 32b. Hill, A. and Willmott, A. J., Accurate and rapid thermal regenerator calculations, *Int. J. Heat Mass Transfer*, 32, 465–476 (1989).
33. Razelos, P., An analytical solution to the electric analog simulation of the regenerative heat exchanger with time varying fluid inlet temperatures, *Warme Stoffubertrag*, 12, 59–71 (1979).
34. Romie, F. E., Treatment of transverse and longitudinal heat conduction in regenerators, *Trans. ASME J. Heat Transfer*, 113, 247–249 (1991).
35. Hahnemann, H. N., Approximate calculations of thermal ratios in heat exchangers including conduction in the direction of flow, National Gas Turbine Establishment Memorandum No. M36, TPA3/TIB, Ministry of Supply, Millbank, London, U.K., 1948.
36. Shah, R. K., A correlation for longitudinal heat conduction effects in periodic-flow heat exchangers, *Trans. ASME J. Eng. Power*, 97A, 453–454 (1975).
37. Shah, R. K., Compact heat exchangers, in *Handbook of Heat Transfer Applications*, 2nd edn. (W. M. Rohsenow, J. P. Hartnett, and E. N. Ganic, eds.), McGraw-Hill, New York, 1985, pp. 4-174–4-311.
38. London, A. L. and Ferguson, C. K., Test results of high performance heat exchanger surfaces used in aircraft intercoolers and their significance for gas turbine regenerator design, *Trans. ASME*, 71, 17–26 (1949).
39. Bowden, A. T. and Hrynyszak, W., The rotary regenerative air preheater for gas turbines, *Trans. ASME*, 769–777 (1953).
40. Shepherd, D. G., *Introduction to the Gas Turbines*, 2nd edn., Constable and Company, London, U.K., 1960.
41. Bathe, W. W., *Fundamentals of Gas Turbines*, John Wiley & Sons, New York, 1984.
42. Harper, D. B., Seal leakage in the rotary regenerator and its effect on rotary regenerator design for gas turbines, *Trans. ASME*, 79, 233–245 (1957).
43. Vincent, E. J., *The Theory and Design of Gas Turbines and Jet Engines*, McGraw-Hill, New York, 1956.
44. Hayes, A. J., Liang, W. W., Richlen, S. L., and Tabb, E. S., eds., *Industrial Heat Exchangers Conference Proceedings*, American Society of Metals, Metals Park, OH, 1985.
45. Schadt, H. F., High-efficiency fluid-bed heat exchanger recovers heat from combustion gases, in *Industrial Heat Exchangers Conference Proceedings* (A. J. Hayes, W. W. Liang, S. L. Richlen, and E. S. Tabb, eds.), American Society for Metals, Metals Park, OH, 1985, pp. 71–80.
46. Williams, H. W., Fluid bed waste heat recovery operating experience on aluminum melting furnace, in *Industrial Heat Exchangers Conference Proceedings* (A. J. Hayes, W. W. Liang, S. L. Richlen, and E. S. Tabb, eds.), American Society for Metals, Metals Park, OH, 1985, pp. 241–248.
47. Rodgers, R. J., Vortex flow direct contact heat exchanger conceptual design and performance, in *Industrial Heat Exchangers Conference Proceedings* (A. J. Hayes, W. W. Liang, S. L. Richlen, and E. S. Tabb, eds.), American Society for Metals, Metals Park, OH, 1985, pp. 101–108.
48. Godbole, S. S., Gilbert, M. L., and Snyder, J. E., Design verification of the DOE/B&W HTBDR control system using interactive simulation, in *Industrial Heat Exchangers Conference Proceedings* (A. J. Hayes, W. W. Liang, S. L. Richlen, and E. S. Tabb, eds.), American Society for Metals, Metals Park, OH, 1985, pp. 45–50.
49. Luu, M. and Grant, K. W., Thermal and fluid design of a ceramic bayonet tube heat exchanger for high temperature waste heat recovery, in *Industrial Heat Exchangers Conference Proceedings* (A. J. Hayes, W. W. Liang, S. L. Richlen, and E. S. Tabb, eds.), American Society for Metals, Metals Park, OH, 1985, pp. 159–174.
50. Hackler, C. L. and Dinulescu, M., Porcelain enamelled flat plate heat exchangers—Engineering and application, in *Industrial Heat Exchangers Conference Proceedings* (A. J. Hayes, W. W. Liang, S. L. Richlen, and E. S. Tabb, eds.), American Society for Metals, Metals Park, OH, 1985, pp. 381–384.
51. Seehausen, J. W., Thermal-hydraulic performance of radiation recuperators, in *Industrial Heat Exchangers Conference Proceedings* (A. J. Hayes, W. W. Liang, S. L. Richlen, and E. S. Tabb, eds.), American Society for Metals, Metals Park, OH, 1985, pp. 175–180.
52. Reay, D. A., Heat exchangers for waste heat recovery, International Research and Development Co., Ltd., New Castle upon Tyne, U.K., in *Developments in Heat Exchanger Technology—1* (D. Chisholm, ed.), Applied Science Publishers, London, U.K., 1980, pp. 233–256.

BIBLIOGRAPHY

- Atthey, D. R. and Chew, P. E., Calculation of high temperature regenerative heat exchangers, in *High Temperature Equipment* (A. E. Sheindlin, ed.), Hemisphere, Washington, DC, 1986, pp. 73–113.
- Hausen, H., *Heat Transfer in Counterflow, Parallel Flow and Cross Flow*, 2nd edn., McGraw-Hill, New York, 1983.
- Iliffe, C. E., Thermal analysis of the contra-flow regenerative heat exchanger, *Proc. Inst. Mech. Eng.*, 159, 363–371 (1948).
- Jakob, M., *Heat Transfer*, Vol. II, John Wiley & Sons, New York, 1957.
- Johnson, J. E., Regenerator heat exchangers for gas turbines, R. A. E. Report Aero. 2266 S.D. 27, 1948, pp. 1–72.
- Kroger, P. G., Performance deterioration in high effectiveness heat exchangers due to axial heat conduction effects, *Adv. Cryogen. Eng.*, 12, 363–372 (1967).
- London, A. L. and Kays, K. M., The liquid-coupled indirect-transfer regenerator for gas-turbine plants, *Trans. ASME*, 73, 529–542 (1951).
- Romie, F. E., Periodic thermal storage: The regenerator, *Trans. ASME J. Heat Transfer*, 101, 726–731 (1979).
- Romie, F. E., Transient response of rotary regenerators, *Trans. ASME J. Heat Transfer*, 110, 836–840, 1988.
- Schmidt, F. W. and Willmott, A. J., *Thermal Energy Storage and Regeneration*, McGraw-Hill, New York, 1981.
- Shah, R. K., Compact heat exchanger design procedures, in *Heat Exchangers: Thermal-Hydraulic Fundamentals and Design* (S. Kakac, A. E. Bergles, and F. Mayinger, eds.), Hemisphere, Washington, DC, 1981, pp. 495–536.
- Shah, R. K., Compact heat exchanger technology and applications, Key Note Lecture, *Eleventh Heat and Mass Transfer Conference*, Indian Society for Heat and Mass Transfer, Madras, India, 1992, pp. 1–25.
- Willmott, A. J., The regenerative heat exchanger computer representation, *Int. J. Heat Mass Transfer*, 12, 997–1014 (1969).

7 Plate Heat Exchangers and Spiral Plate Heat Exchangers

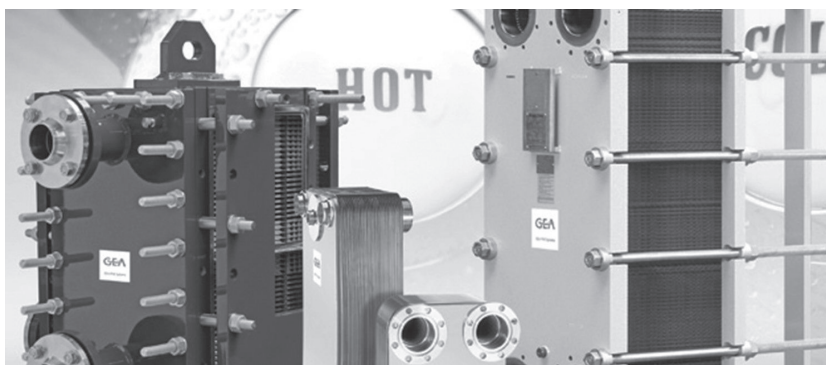
Dr. Richard Seligman, the founder of APV International, introduced the first commercially successful gasketed plate heat exchanger design in 1923. A plate heat exchanger essentially consists of a number of corrugated metal plates provided with gaskets and corner ports to achieve the desired flow arrangement. Each fluid passes through alternate channels. The plates are clamped together in a frame that includes connections for the fluids. Since each plate is generally provided with peripheral gaskets to provide sealing arrangements, the plate heat exchangers are called gasketed plate heat exchangers. Extensive information on the plate heat exchanger is provided by Focke [1], Cooper et al. [2], Raju et al. [3,4], and Shah et al. [5], and in the website of leading manufacturers like Alpha Laval, Pune, India, APV Co., Tonawanda, NY, Paul-Muller Company, Springfield, MO, GEA PHE Systems, Sarstedt, Germany, Tranter, Inc., Wichita Falls, TX, HRS Heat Exchangers Ltd, Herts, United Kingdom, ITT STANDARD, Cheektowaga, NY, Polaris Plate Heat Exchangers, Tinton, Falls, NJ.

7.1 PLATE HEAT EXCHANGER CONSTRUCTION: GENERAL

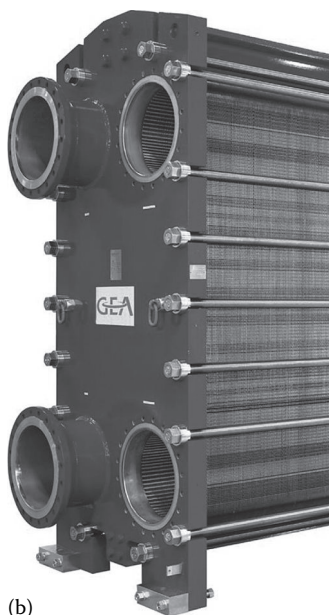
A plate heat exchanger (PHE), as shown in Figure 7.1, is usually comprised of a stack of corrugated or embossed metal plates in mutual contact, each plate having four apertures serving as inlet and outlet ports, and seals designed so as to direct the fluids in alternate flow passages. The flow passages are formed by adjacent plates so that the two streams exchange heat while passing through alternate channels. When assembled, the spacing between adjacent plates ranges from 1.3 to 6.4 mm. The number and size of the plates are determined by the flow rate, physical properties of the fluids, pressure drop, and temperature program. The plate corrugations promote fluid turbulence and support the plates against differential pressure. The stack of plates is held together in a frame by a pressure arrangement.

The periphery of each plate is grooved to house a molded gasket, each open to the atmosphere. Gaskets are generally cemented in, but snap-on gaskets are available that do not require cement. Gasket failure cannot result in fluid intermixing but merely in leakage to the atmosphere. Proper selection of gasket material and operating conditions will eliminate the leakage risk. Frame assembly tightly holds the plates pack. It ensures optimum compression and leak tightness (Figure 7.2; for more details on construction, refer to Figure 1.7). If the plates are correctly assembled, the edges form a “honeycomb” pattern, as shown in Figure 7.3.

The elements of the frame are fixed plate, compression plate, pressing equipment, and connecting ports. Every plate is notched at the center of its top and bottom edges so that it may be suspended from the top carrier bar and guided by the bottom guide bar, and the plates are free to slide along the bars. The movable head plate is similarly notched and free to slide along both bars. Both the upper carrying bar and the lower guiding bar are fixed to the support columns. The plate pack is tightened by means of either a mechanical or hydraulic tightening device. Connections are located in the frame cover or, if either or both fluids make more than a single pass within the unit, the frame and pressure plates. By including intermediate separating/connecting plates, three or



(a)



(b)

FIGURE 7.1 (a) Collection of different types of PHE. (b) NT series plate heat exchanger. (Courtesy of GEA PHE Systems, Sarstedt, Germany).

more separate fluid streams can be handled. Frames are usually free standing; for smaller units, they are attached to structural steel work. Salient constructional features of PHE and the resulting advantages and benefits are given in Table 7.1.

7.1.1 FLOW PATTERNS AND PASS ARRANGEMENT

In a PHE, several types of flow patterns can be achieved:

1. Series flow arrangement, in which a stream is continuous and changes direction after each vertical path, that is, n pass– n pass with individual passes per channel, as shown in Figure 7.4a.
2. Single-pass looped arrangement: U-arrangement, Z-arrangement. Both fluids flow counter-currently through parallel passages that make up a single pass, as shown in Figure 7.4b.

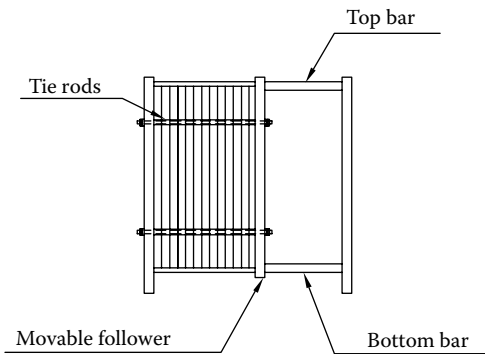


FIGURE 7.2 Plate heat exchanger construction details.

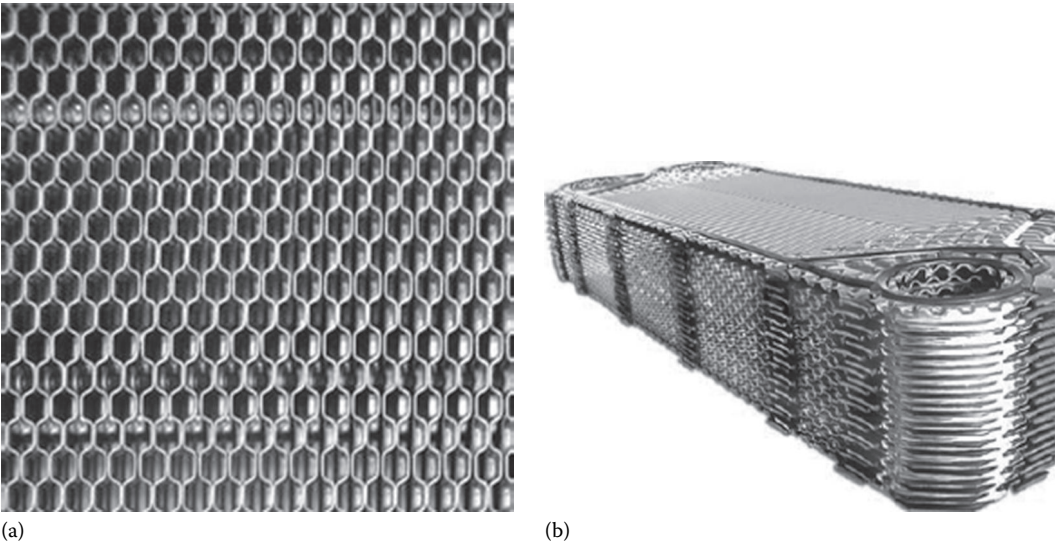


FIGURE 7.3 PHE plate pack shows a continuous honeycomb pattern. (Courtesy of HRS Heat Exchangers Ltd, Herts, U.K.)

TABLE 7.1
Construction Features of Plate Heat Exchangers and Their Benefits

Feature	Advantage
PHE concept	High turbulence, true counterflow and hence efficient heat transfer and very close approach temperature; reduced fouling. Low weight and smaller foundations
Modular construction	Flexibility for future expansion and easy to modify for altered duties
Fixed frame and movable pressure plates	Easy accessibility for maintenance
Metallic contact between plates	Rigidity of plate pack is enhanced and hence minimized vibrations and less noise
Thin channels	Quick process control and low hold-up volume. Light weight
Each plate is individually gasketed	Cross contamination is eliminated. Easy to inspect
Glue-free gaskets	Simplified regasketing while still in frame, maintenance friendly feature, Lesser gasket changing time

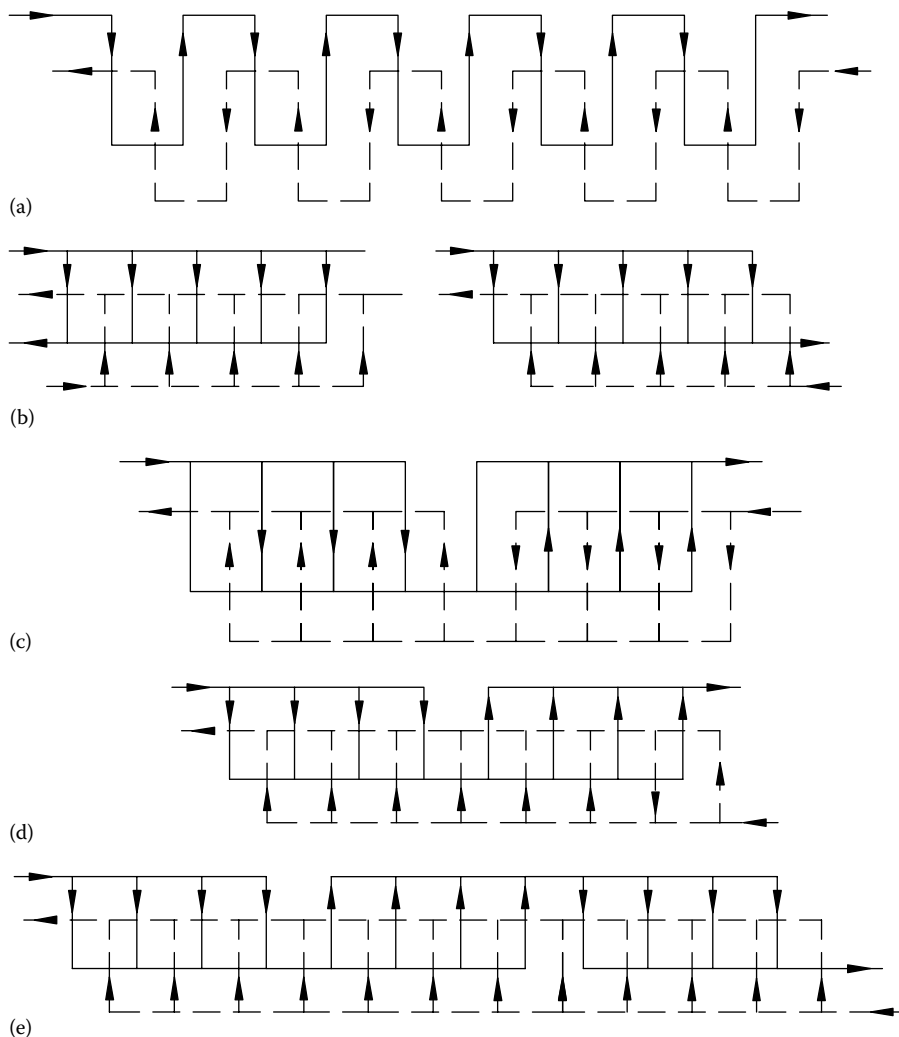


FIGURE 7.4 PHE flow arrangements. (a) Series flow n pass- n pass; (b) single-pass looped: U-arrangement, Z-arrangement; (c) multipass with equal pass (n pass- n pass); (d) multipass with unequal pass, 2 pass-1 pass; and (e) multipass with unequal pass, 3 pass-1 pass.

3. Multipass with equal passes (series flow pattern), wherein the stream divides into a number of parallelflow channels and then recombines to flow through the exit in a single stream, that is, n pass- n pass, as shown in Figure 7.4c.
4. Multipass with unequal pass, such as 2 pass-1 pass, and 3 pass-1 pass, as shown in Figure 7.4d.

7.1.2 USEFUL DATA ON PHE

Useful data on plate exchangers are given in Table 7.2.

TABLE 7.2
Useful Data on PHE

Unit		Plates	
Size	1540–2500 m ²	Thickness	0.5–1.2 mm
Number of plates	Up to 700	Size	0.03–2.2 m
Port size	Up to 39 cm	Spacing	1.5–5.0 mm
		Corrugation depth	3–5 mm

7.1.3 STANDARD PERFORMANCE LIMITS

Standard performance limits for Alpha-Laval 1 PHE are [6]

Maximum operating pressure	25 bar (360 psi)
With special construction	30 bar (435 psi)
Maximum temperature	160°C (320°F)
With special gaskets	200°C (390°F)
Maximum flow rate	3,600 m ³ /h (950,000 USG/min)
Heat transfer coefficient	3500–7500 W/m ² ·°C (600–1,300 BTU/ft ² ·h·°F)
Heat transfer area	0.1–2,200 m ² (1–24,000 ft ²)
Maximum connection size	450 mm (18 in.)
Thermohydraulic data	
Temperature approach	As low as 1°C
Heat recovery	As high as 93%
Heat transfer coefficient	3,000–7,000 W/m ² ·°C (water–water duties with normal fouling resistance)
NTU	0.3–4.0
Pressure drop	30 kPa per NTU
<i>Note:</i> Refer to manufacturers catalogue for current performance lists.	

7.2 BENEFITS OFFERED BY PLATE HEAT EXCHANGERS

High turbulence and high heat transfer performance: The embossed plate pattern promotes high turbulence at low fluid velocities (Figure 7.5). On plates with the washboard pattern, turbulence is promoted by the continuously changing flow direction and velocity [7]. Plates with the herringbone pattern are assembled with the corrugations pointing in alternate directions, which imparts a swirling motion to the fluids. This high turbulence results in very high heat transfer coefficients.

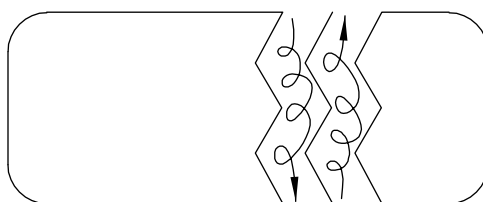


FIGURE 7.5 PHE—turbulence promoted by embossed plate pattern.

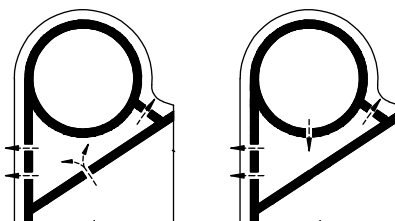


FIGURE 7.6 PHE—elimination of cross-contamination by venting of gasket space.

Reduced fouling: High turbulence, absence of stagnant areas, uniform fluid flow, and the smooth plate surface reduce fouling and the need for frequent cleaning.

Cross-contamination eliminated: In PHE, each medium is individually gasketed. The space between gaskets is vented to atmosphere, eliminating the possibility of any cross-contamination of fluids (Figure 7.6).

True counterflow: In PHE, fluids can be made to flow in opposite directions, resulting in greater effective temperature difference.

Close approach temperature: In PHE, very close approach temperatures of 1°F – 2°F are possible because of the true counterflow, advantageous flow rate characteristics, and high heat transfer efficiency of the plates.

Multiple duties with a single unit: It is possible to heat or cool two or more fluids within the same unit by simply installing intermediate divider sections between the heat transfer plates (Figure 7.7).

Expandable: Due to modular construction, true flexibility is unique to the PHE both in initial design and after installation (Figure 7.8).

Easy to inspect and clean, and less maintenance: A PHE can be easily opened for inspection, cleaning, and gasket replacement. By simply removing the compression bolts and sliding away the movable end frame, one can visually inspect the entire heat transfer surface. Easy cleanability and

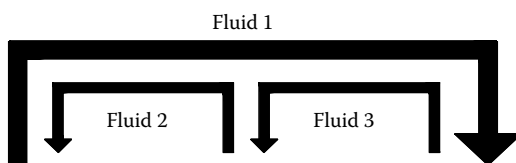


FIGURE 7.7 PHE—capability of handling of multiple duties.

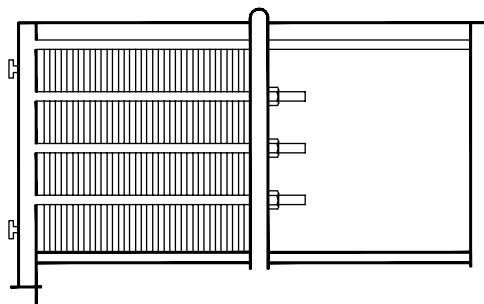


FIGURE 7.8 PHE—flexibility of expansion.

thin layer of product to ensure a good bacteriological effect during pasteurization are advantages in the dairy industry, where PHE are cleaned once a day.

Lightweight: The PHE unit is lighter in total weight than other types of heat exchangers because of reduced liquid volume space and less surface area for a given application.

High-viscosity applications: Because the PHE induces turbulence at low fluid velocities, it has practical application for high-viscosity fluids. Note that a fluid sufficiently viscous to produce laminar flow in a shell and tube heat exchanger may well be in turbulent flow in PHE.

Saves space and servicing time: The PHE fits into an area one-fifth to one-half of that required for a comparable shell and tube heat exchanger. The PHE can be opened for inspection, maintenance, or rebuilding all within the length of the frame, while the shell and tube heat exchanger with removable tube bundle requires double its length to remove the tube bundle.

Lower liquid volume: Since the gap between the heat transfer plates is relatively small, a PHE contains only low quantities of process fluids. The benefit is reduced cost due to lower volume requirements for often costly refrigerants, coolants, or process fluids. Since the product remains in the heat exchanger for a short period of time, the process can be easily stopped or the temperature can be changed quickly with minimum impact on the product.

Less operational problems: In PHEs, flow-induced vibration, noise, and erosion–corrosion due to impingement attack are not present as in shell and tube heat exchangers.

Lower cost: PHEs are generally more economical than other types of equivalent duty heat exchangers due to the higher thermal efficiency and lower manufacturing costs.

Quick process control: Owing to the thin channels created between the two adjacent plates, the volume of fluid contained in PHE is small; it quickly reacts to the new process condition and is thereby easier to control.

7.3 COMPARISON BETWEEN A PLATE HEAT EXCHANGER AND A SHELL AND TUBE HEAT EXCHANGER

In many applications, the PHE has replaced the shell and tube heat exchanger (STHE) for services within the former's operational limits. For identical duties (liquid–liquid service) and in those cases when the working limits of the gaskets are not exceeded, the merits of the PHE over the STHE are hereunder: (a) Can handle multiple duties and future expansion is possible (20%–30%), (b) high heat transfer ratio, (c) low operating weight ratio, (d) low hold up volume, (e) no welds, (e) no flow induced vibrations, (f) access for inspection is easy and less time consuming, (g) true countercurrent flow is achieved, (h) very close approach temperature can be achieved, (i) due to high turbulence/swirl motion, less fouling is encountered, and (j) leakage is easily detected and easy to replace plate and/or gasket. (*Note:* For a typical rail road application, a shell and tube oil cooler with an operating pressure of 8 bar and temperature of 135°C (approx.) was replaced by a gasketed PHE which solved the problem of frequent tube failure and hence the mixing of cooling water with lube oil).

7.4 PLATE HEAT EXCHANGER: DETAILED CONSTRUCTION FEATURES

With a brief discussion of PHE construction, additional construction features and materials of construction for components such as plates, gaskets, frame, and connectors are discussed next.

7.4.1 PLATE

7.4.1.1 Plate Pattern

Plates are available in a variety of corrugated or embossed patterns. The basic objective of providing corrugation to the plates is to impart high turbulence to the fluids, which results in a very high heat transfer coefficient compared to those obtainable in a shell and tube heat exchanger for

similar duties. These embossing patterns also result in increased effective surface areas and provide additional strength to the plates by means of many contact points over the plates to withstand differential pressure that exists between the adjacent plates. Plate thickness as low as 0.6 mm (0.024 in.) can therefore be used for working pressures as high as 230 psig, particularly when using the cross-corrugated, herringbone pattern [8].

7.4.1.2 Types of Plate Corrugation

Over 60 different plate patterns have been developed worldwide. The pattern and geometry are proprietary. The most widely used corrugation types are the *intermating troughs* or *wash board* and the *chevron* or *herringbone* pattern. Figure 7.9 shows the chevron pattern that is most widely used. The construction features of these two patterns are discussed next.

7.4.1.3 Intermating Troughs Pattern

In the intermating troughs or washboard pattern, the corrugations are usually pressed deeper than the plate spacing. The plates nestle into one another when the plate pack is assembled. The plate spacing is maintained by dimples, which are pressed into the crests and troughs and contact one another on adjacent plates. Since the washboard type has fewer contact points, and due to its greater corrugation depth than the herringbone type, it operates at lower pressures. The maximum channel gap varies from 3 to 5 mm and the minimum channel gap varies from 1.5 to 3 mm. Typical liquid velocity range in turbulent flow is from 0.2 to 3 m/s, depending upon the required pressure drop [5].

7.4.1.4 Chevron or Herringbone Trough Pattern

In the herringbone pattern (Figure 7.9a), the corrugations are pressed to the same depth as the plate spacing. It is the most common type in use today. The corrugation depth generally varies from 3 to 5 mm. Typical liquid velocities (in turbulent flow) range from 0.1 to 1 m/s [5]. The chevron angle is reversed on adjacent plates so that when the plates are clamped together the corrugations cross one another to provide numerous contact points. Possible profiles of two adjoining plates in contact

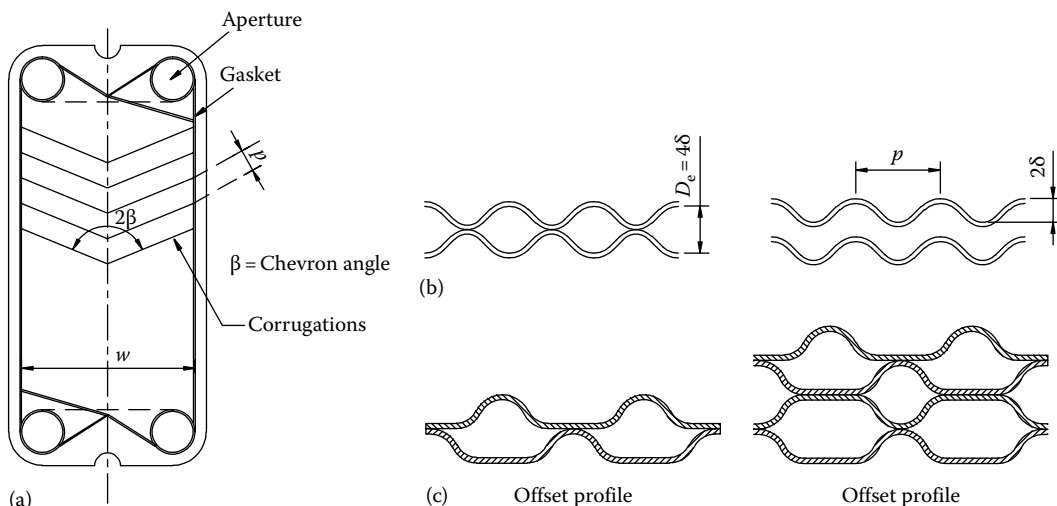


FIGURE 7.9 (a) Chevron plate—schematic showing Chevron angle, (b) gap between two plates-chevron troughs, and (c) two adjoining plates with different corrugation profile in contact.

TABLE 7.3
Common PHE Plate Materials

Stainless steel AISI 304	Incoloy 825
Stainless steel AISI 316	Monel 400
Avesta SMO 254	Hastelloy B
Titanium, titanium–0.2%	Hastelloy C-276
Palladium stabilized	Aluminum brass 76/22/2
Tantalum	Cupronickel (70/30)
Inconel 600	Cupronickel (90/10)
Inconel 625	Diabon F 100

are shown in Figure 7.9d. The herringbone type therefore has greater strength than the washboard type, which enables it to withstand higher pressures with smaller plate thickness [9].

7.4.1.5 Plate Materials

Materials that are suitable for cold pressing and corrosion resistant are the standard materials of construction. Table 7.3 gives a list of most common materials used for fabrication of plates. Carbon steel is rarely used due to its poor corrosion resistance.

7.4.2 GASKET SELECTION

When selecting the gasket material, the important requirements to be met are chemical and temperature resistance coupled with good sealing properties and shape over an acceptable period of life [3]. Much work has been done to develop elastomer formulations that increase the temperature range and chemical resistance of gaskets. Typical gasket materials and their maximum operating temperatures are given in Table 7.4.

7.4.3 BLEED PORT DESIGN

With gasket/bleed port design, fluids will not intermix (other than a through-plate failure) when the plates are properly gasketed and the unit is assembled in accordance with prescribed instructions and design specifications. Liquid flowing on the surface of each plate flows on the inside of the boundary gasket. Should one of the liquids leak beyond a boundary gasket, it will flow to the outside of the unit through the bleed ports, preventing intermixing.

TABLE 7.4
Gasket Materials and Maximum Operating Temperature

Styrene butadiene rubber (80°C)
Nitrile rubber (140°C)
Ethylene propylene rubber, EPDM (150°C)
Resin-cured butyl rubber (140°C)
Fluorocarbon rubbers (180°C)
Fluoroelastomer (Viton) (100°C)
Compressed asbestos fiber (CAF) (260°C)
Silicon elastomers (low-temperature applications)

7.4.4 FRAMES

Frames are classified [7] as (1) B frame, suspension-type frame used with larger PHEs, (2) C frame, compact cantilever-type frame used with smaller PHEs, and (3) F frame, an intermediate size suspension-type frame. The frame is usually constructed in carbon steel and painted for corrosion resistance. Where stringent cleanliness requirements apply, such as in pharmaceuticals and in dairy, food, and soft drinks industries, the frame may be supplied in stainless steel. Stainless steel clad frames are available for highly corrosive environments. The units are normally floor mounted, but small units may be wall mounted.

7.4.5 NOZZLES

Nozzles are located in one or both end plates. In single-pass arrangement, both the inlet and outlet ports for both fluids are located in the fixed head end, and hence the unit may be opened up without disturbing the external piping. But with multipass arrangements, the ports must always be located on both heads. This means that the unit cannot be opened up without disturbing the external piping at the movable head end. To be corrosion resistant, nozzles are usually same as plate material. Typical nozzle materials include stainless steel type 316, rubber clad, titanium, Incoloy 825, and Hastelloy C-276.

7.4.6 TIE BOLTS

The tie bolts are usually made of 1% Cr-0.5% Mo low-alloy steel. The packing of large units may be compressed by hydraulic, pneumatic, or electric tightening devices.

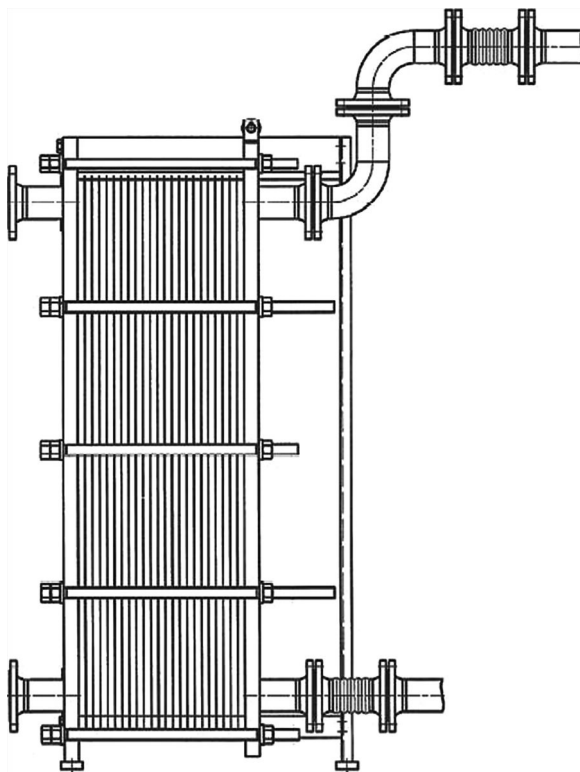


FIGURE 7.10 The opening space of the PHE, which is between the pressure plate and support, should not be obstructed by fixed piping. (Courtesy of HRS Heat Exchangers Ltd, Herts, U.K.)

7.4.7 CONNECTOR PLATES

It is possible to process three or more fluids in a single gasketed PHE. This is being achieved by means of connector plates. This practice is widely used in food processing and permits heating, cooling, and heat recovery of the fluids in a single unit [9].

7.4.8 CONNECTIONS

Connections are usually made of the same material as the plates to avoid the galvanic corrosion damage. Rubber-lined connections can be used for some duties.

7.4.9 INSTALLATION

PHE is to be mounted vertically on the floor with a level foundation and be strong enough so no settling occurs that can cause a loading strain on the connections. The heat exchanger must be installed with clearance on both sides for maintenance (Figure 7.10). The foundation for the heat exchanger must be level and firm enough so that no settling occurs, which could put forces and strain on the piping connected to it.

7.5 BRAZED PLATE HEAT EXCHANGER

Brazed PHE evolved from the conventional PHE in answer to the need for a compact PHE for high-pressure and high-temperature duties. Like the gasketed PHE, the brazed PHE is constructed of a series of corrugated metal plates but without the gaskets, tightening bolts, frame, or carrying and guide bars. It consists of stainless steel plates and two end plates. The plates are brazed together in a vacuum oven to form a complete pressure-resistant unit. The two fluids flow in separate channels. This compact design can easily be mounted directly on piping without brackets and foundations. Brazed PHEs accommodate a wide range of temperatures, from cryogenic to 200°C. Because of the brazed construction, the units are not expandable but get their reputation from their relatively compact size. Available with copper or nickel brazing, these units give a number of critical advantages: a sealed, compact system, high temperature and pressure capability, gasket-free construction, high thermal efficiency, and ideal for refrigeration and process applications. Figure 7.11 shows brazed PHEs, and overall dimensions of a brazed PHE are shown in Figure 7.12.

7.6 OTHER FORMS OF PLATE HEAT EXCHANGERS

Continued developments and product innovations are taking place among various manufacturers to overcome limitations of pressure and temperatures, and to handle products of high viscosity, high fibrous contents, and high corrosivity. As a result, various forms of PHEs have come into the market. Some new forms of PHEs are discussed next.

7.6.1 ALL-WELDED PLATE EXCHANGERS

This design entirely eliminates the gaskets and by developing a fully welded plate exchanger further enhances the reliability as well as the temperature and pressure limits of the gasketed plate exchanger. Welded plate exchangers, unlike gasketed and semiwelded models, can neither be expanded in surface area nor be cleaned readily by mechanical methods. Only chemical cleaning is possible.

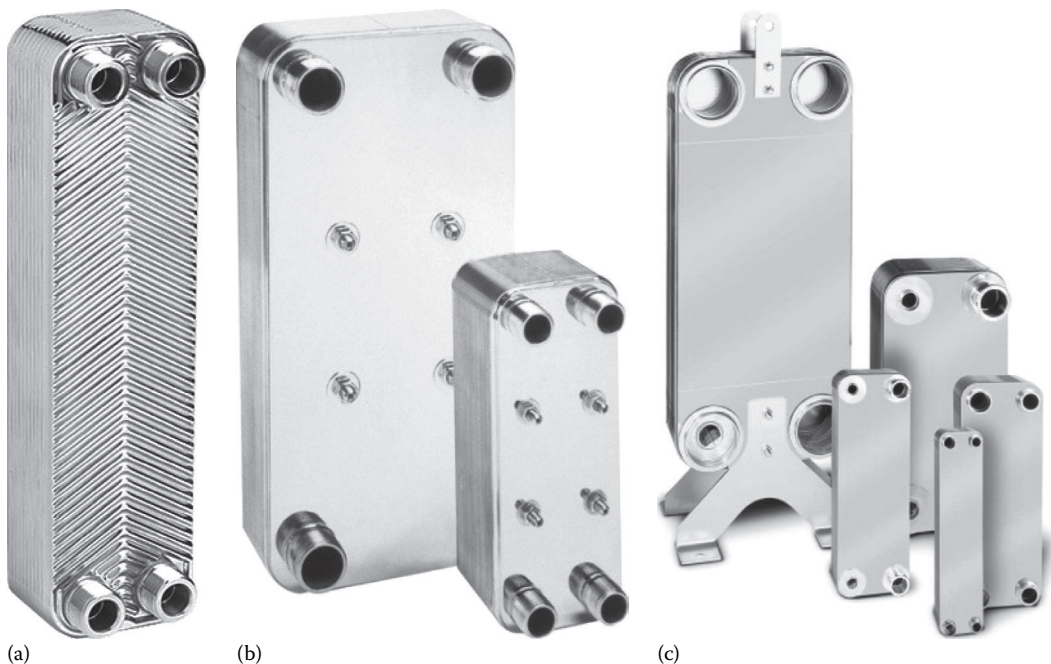


FIGURE 7.11 Brazed plate heat exchangers. (Courtesy of GEA PHE Systems, Sarstedt, Germany.)

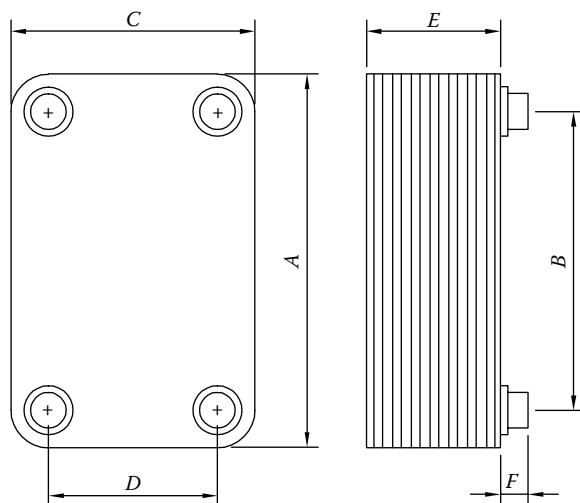


FIGURE 7.12 Overall dimensions of brazed plate heat exchanger.

7.6.2 SUPERMAX[®] AND MAXCHANGER[®] PLATE HEAT EXCHANGERS

Tranter's Supermax shell & plate heat exchanger and Maxchanger welded plate heat exchangers require less space of the equivalent shell and tube exchangers. Turbulent flow induced by the corrugated and dimpled plate patterns produces high heat transfer rates. This high efficiency allows compact exchangers with a 1°C (2°F) temperature approach. Another benefit is the small hold-up volume that offers fast start-up times and close following of process changes.

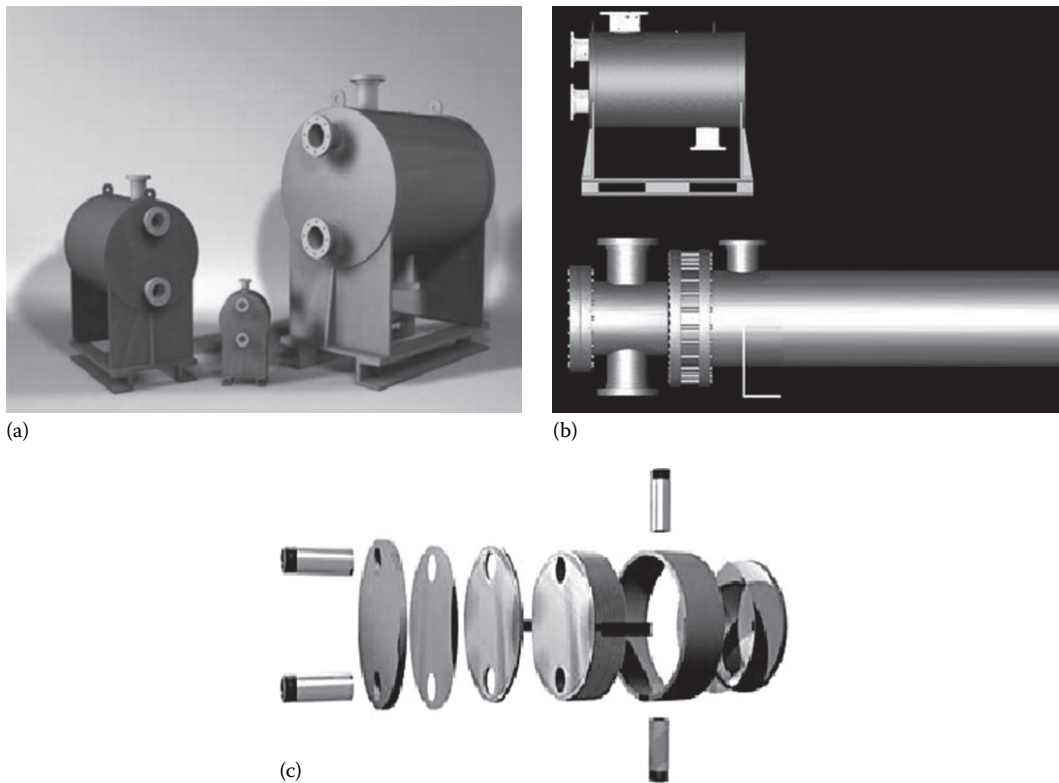


FIGURE 7.13 Supermax shell and plate heat exchanger. (a) Units, (b) comparison with a shell and tube heat exchanger, and (c) details. (Courtesy of Tranter, Inc., Wichita Falls, TX.)

Supermax (shown in Figure 7.13) and Maxchanger (shown in Figure 7.14) exchangers can be applied to applications involving liquids, gases, steam, and two-phase mixtures. This includes aggressive media, which are beyond the capability of traditional gasketed plate and frame heat exchangers. In addition to efficiency, the units offer cost effectiveness and minimal maintenance. The Supermax shell & plate heat exchanger is designed for pressures up to 100 barg (1450 psig) and at temperatures up to 538°C (1000°F) for standard range units. In refrigeration and cryogenic service, the exchangers require a low refrigerant charge. They are also resistant to freezing because of high fluid turbulence induced by the corrugated plate pattern. Supermax wide temperature/pressure ratings offer good performance with natural refrigerants such as ammonia and carbon dioxide. Fluids can undergo phase change on either the plate or shellside.

Pairs of chevron-type plates are placed back-to-back and fabricated into a cassette by full automatic perimeter welding of adjacent port holes. Cassettes are then placed together and perimeter welded to each other, producing an accordion-like core that is highly tolerant to thermal expansion. The plate pack is then inserted in a cylindrical shell. Fluid diverters positioned between the shell and the plate pack ensure proper flow through the shell side channels. End plates, nozzles, and top and bottom covers are welded to the shell to form a pressure vessel of high integrity. Extra-large nozzle sizes can be accommodated on the shell side of the exchanger. Plates can also be arranged to form multiple passes. Figure 7.15 shows collection of Tranter plate heat exchangers—Maxchanger (foreground) and Supermax (right), welded plate heat exchangers spiral (left), Superchanger® gasketed P&F (back), and Platecoil® prime surface.



FIGURE 7.14 Maxchanger welded plate heat exchanger. (Courtesy of Tranter, Inc., Wichita Falls, TX.)



FIGURE 7.15 Collection of Tranter plate heat exchangers: Maxchanger (foreground) and Supermax (right), welded plate heat exchangers spiral (left), Superchanger gasketed PHE (back), and Platecoil prime surface bank. (Courtesy of Tranter, Inc., Wichita Falls, TX.)

7.6.3 WIDE-GAP PLATE HEAT EXCHANGER

Wide-gap PHE provides a free-flow channel for liquids and products containing fibers or coarse particles or high-viscosity liquids that normally clog or cannot be satisfactorily treated in shell and tube heat exchangers. These plates have a draw depth two to five times greater than conventional plates, permitting unrestricted passage of coarse particles and fibers. Plates can be

arranged in a wide/narrow configuration when only one fluid with large particulates requires a wide gap or placed in a medium/medium position. Wide-gap plates economically recover heat from hard-to-handle waste streams in a variety of industries, including pulp and paper, sugar processing, alcohol production, grain processing, chemicals, latex, polymer slurries, textiles, and ethanol distilling. The plate design is also excellent for low-pressure steam since the wide gap will more readily accommodate the high volumetric flows typical of low-pressure steam applications. Like conventional plates, the wide-gap PHE plates provide additional strength to the plates by means of many contact points over the plates to withstand differential pressure that exists between the adjacent plates.

7.6.4 GEABLOC FULLY WELDED PLATE HEAT EXCHANGER

GEABloc combines two different plate corrugations in an innovative way (Figure 7.16). The plates are rotated through 90° to one another and then welded together to produce two different cross-flow channels. The frame is made of four pillars, a bottom plate and a top plate together with four side pressure plates, and connections mounted in the pressure plates. All frame components are bolted together for easy dismantling to clean and maintain the plate pack. GEABloc is available in various corrugation designs and sizes for a wide range of applications. Adjustable deflectors allow the heat exchanger to be adapted to its operating points delivering these features:

- Maximum operating temperature: 315°C, on both sides
- Maximum operating pressure: 32 bar, on both sides
- Material: SMO, titanium, etc.
- Surface area: 1–320 m²
- Max. flow rate: 3860 m³/h
- Corrugation patterns: Herringbone, dimple

7.6.5 FREE-FLOW PLATE HEAT EXCHANGER

Free-flow PHEs feature a special plate geometry that offers an uninterrupted wide flow path for fouling fluids, viscous fluids, or those containing fibrous materials (fruit juices containing fibers and pulps, waste water in the paper and pulp, textile, and sugar industries, as well as highly viscous products). Their special features include the constant width gap cross section between the individual plates and the rough-wave profiling of the plates. The clearance between the plates is up to 12/15 mm. The free-flow design is an improved design compared to the conventional wide-gap plate exchanger, since there are no contact points in the flow path of free-flow plates that restrict the flow. The corrugation pattern provides the right balance of high-efficiency heat transfer, clogging resistance, and low pressure drop, providing a cost advantage over larger, more expensive shell and tube technology. The constant width gaps reduce clogging and hence extended service life. Various patterns of free-flow plates are shown in Figure 7.17. A comparison of plate patterns and flow path of conventional and Mueller free-flow plate is shown in Figure 7.18.

7.6.6 FLOW-FLEX TUBULAR PLATE HEAT EXCHANGER

The Alfa Laval Flow-Flex, the tubular PHE, the plate pattern builds the tube channels with a free cross section on one side and conventional plate channels on the other. This allows Flow-Flex to handle asymmetrical duties, that is, dissimilar flow rates at a ratio of at least two to one (for the same fluid properties and pressure drop). This vibration-free construction is also suitable for low-pressure condensing and vaporizing duties and for fibrous and particle-laden fluids.

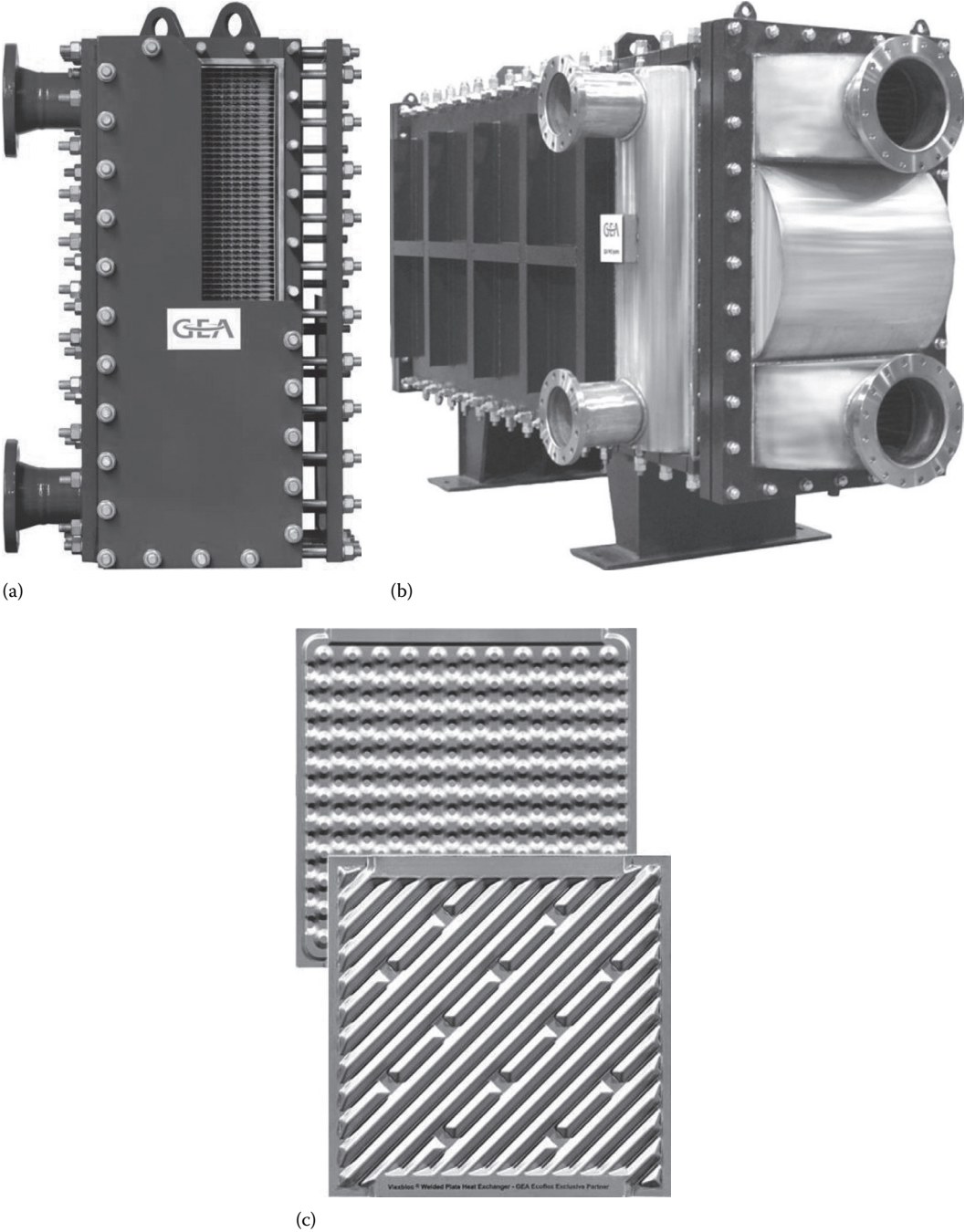


FIGURE 7.16 (a) GEABloc welded plate heat exchanger, (b) GEABox fully welded PHE, and (c) Chevron and free flow plate corrugations pattern. (Courtesy of GEA PHE Systems, Sarstedt, Germany.)

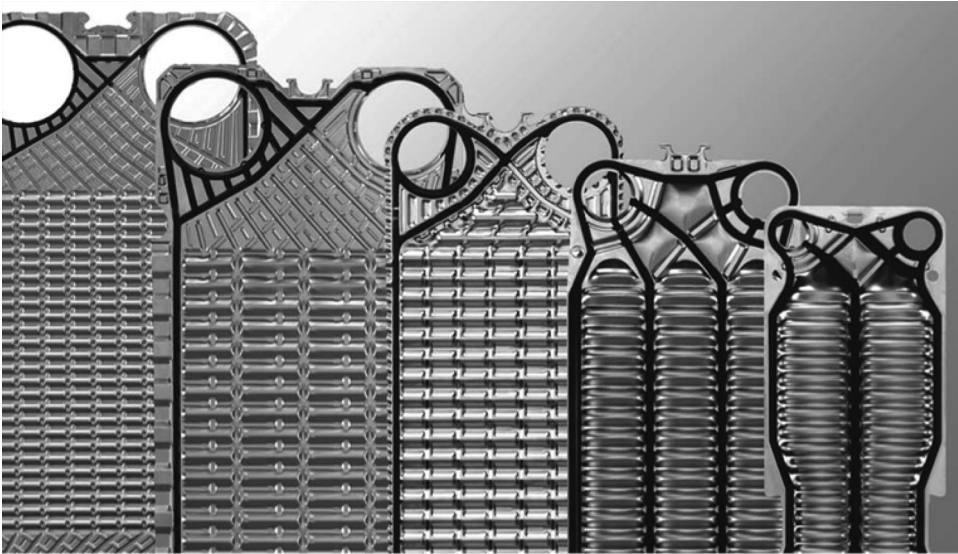


FIGURE 7.17 A collection of free flow plates. (Courtesy of GEA PHE Systems, Sarstedt, Germany.)

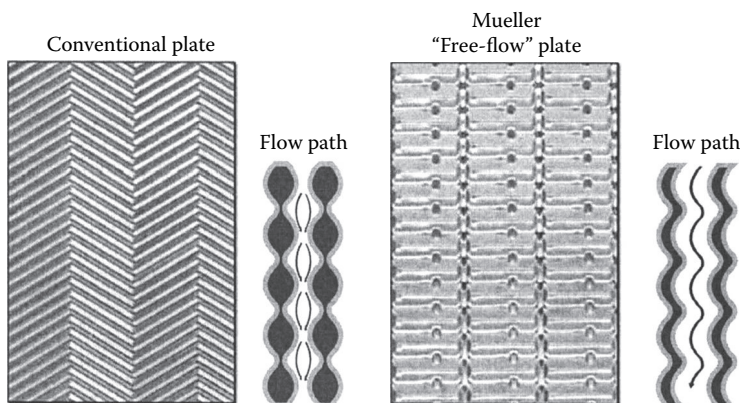


FIGURE 7.18 Comparison of plate patterns and flow path of conventional and Mueller Accu-Therm™ free flow plate. (Courtesy of Mueller, Heat Transfer Products, Springfield, MO.)

7.6.7 SEMIWELDED OR TWIN-PLATE HEAT EXCHANGER

The semiwelded or twin-plate heat exchanger plates offer the same advantages as standard PHE units, yet overcome pressure limitations and avoid chemical resistance to gaskets. Semiwelded plates are formed from two cassettes that are laser welded together. The cassettes are separated by standard gaskets, such as EPDM, NBR, or Viton, as shown in Figures 7.19 and 7.20. The welded pairs allow for aggressive fluids or refrigerants between plates and the only gaskets in contact with the aggressive medium are two circular porthole gaskets between the welded plate pair. The porthole gaskets are available in highly resistant elastomer and nonelastomeric materials. The other medium flows across gasketed channels. Semilaser welded PHEs offer superior sealing capability easy cleaning and comply with sanitary standards on the welded side. Use of semiwelded units is increasing in the chemical, petroleum refining, and refrigeration industries [10].

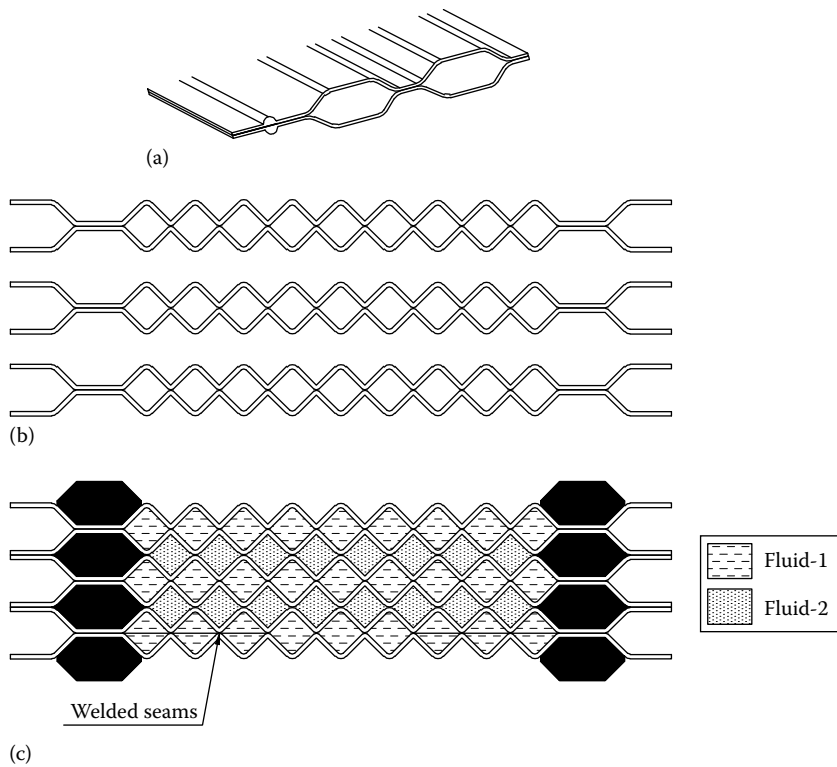


FIGURE 7.19 Semiwelded plateflow design: (a) and (b) concept and (c) assembly.

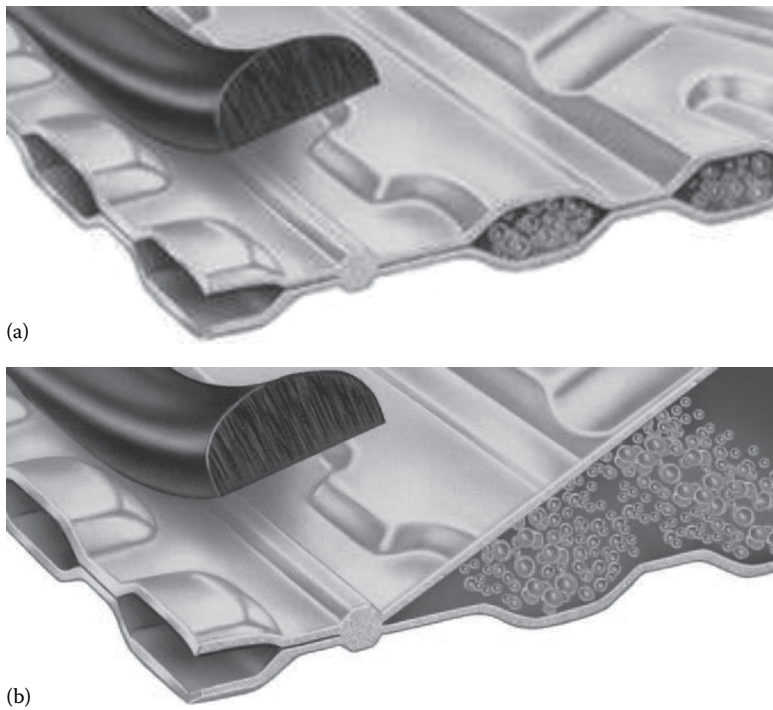


FIGURE 7.20 Semi-welded plateflow design: (a) light duty and (b) heavy duty. (Courtesy of ITT Standard, Cheektowaga, NY.)

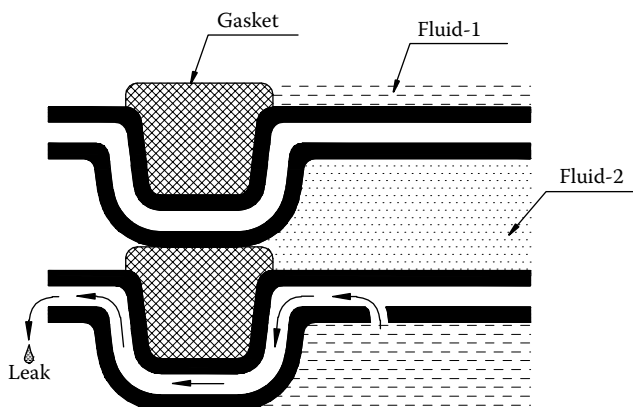


FIGURE 7.21 Double-wall units prevent intermixing of fluids due to a plate failure.

7.6.8 DOUBLE-WALL PLATE HEAT EXCHANGER

The double-wall PHE is intended for use where the two fluids on each side of the plates should not mix due to possible contamination, an undesirable reaction, environmental effects, or it would be hazardous. The double-wall PHE consists of two plates with a small air gap in between them (Figure 7.21). This gap is open to atmosphere and is not in contact with either of the media helping guard against intermixing of the media. The double-wall heat exchanger plates are designed for use in cooling/heating duties in dairy, pharmaceutical, brewery, and beverage installations where it is crucial to prevent any cross-contamination between the two media. A gasket defect causes an external leak, either directly from the peripheral gasket or from between the plates at the site of the failure. In addition to the major advantage of preventing intermixing of the two media used, double-wall PHEs are also superior to any comparable solutions, including double-wall shell and tube heat exchangers in terms of enhanced thermal performance and compactness.

7.6.9 DIABON F GRAPHITE PLATE HEAT EXCHANGER

The Alfa Laval Diabon F graphite PHE is a heat exchanger with graphite plates developed for use with media normally too corrosive for exotic metals and alloys. The Diabon F 100 graphite plates are made of a composite material composed of graphite and fluoroplastics. The material is compressed into corrugated plates fitted with thin, flat, corrosion-resistant gaskets. The graphite plates offer excellent corrosion resistance and good heat transfer properties in combination with low thermal expansion and high pressure.

7.6.10 GLUE-FREE GASKETS (CLIP-ON SNAP-ON GASKETS)

The clip-on snap-on gaskets are glue-free gaskets designed to perform in heavy industrial applications in the same manner as traditional glued gaskets and recommended wherever regular cleaning is necessary or aggressive fluids shorten gasket life. The glue-free gaskets (Figure 7.22) are attached to the plate by fasteners situated at regular intervals around the plate periphery. The gaskets simply slip into place during fitting and slip out for regasketing procedures, eliminating gluing procedures. All these contribute to reduced service costs and downtime. Typical ratings are 338°F (170°C) at low pressures and 357 psig (25 barg) at moderate temperatures, depending on application conditions.



FIGURE 7.22 Glueless gasket. (Courtesy of ITT Standard, Cheektowaga, NY.)

7.6.11 ALFANOVA 100% STAINLESS STEEL PLATE HEAT EXCHANGER

AlfaNova is a 100% stainless steel PHE. It comprises a number of corrugated stainless steel plates, a frame plate, and a pressure plate. The plate pack is brazed by AlfaFusion, a new technology patented by Alfa Laval. The fusion-brazed PHE, a new class of PHE, offers extremely high mechanical strength and thermal fatigue resistance than conventional brazed units. It is also hygienic, corrosion resistant, and fully recyclable. Its 100% stainless steel construction enables AlfaNova to withstand temperatures up to 550°C (1020°F).

7.6.12 PLATE HEAT EXCHANGER WITH ELECTRODE PLATE

A recent innovation is a standard construction of PHE but includes at least one electrode plate for cooling applications by a refrigerant. The electrode plate includes outer electrode surfaces on each side thereof to produce an electric field. The effect of the electric field is an increase in the heat transfer rate between the refrigerant and the heat transfer fluid.

7.6.13 PLATE HEAT EXCHANGER WITH FLOW RINGS

A design similar to a standard PHE includes flow rings. The design consists of a plurality of stamped plates but on each plate a flow ring and an extended surface fin structure is present. Each of the flow rings includes radial flow openings for evenly distributing the fluid between the plates. The plates are stacked with additional fin structure and ring pairs between each pair of plates to achieve the thermal requirements of the particular application. The advantages of this design are compactness, low cost, and thermal efficiency.

7.6.14 ALFAREX™ GASKET-FREE PLATE HEAT EXCHANGER

The AlfaRex is a gasket-free welded PHE for high-pressure and high-temperature applications where gaskets are unacceptable. Its working temperature can be from -58°F to 650°F and pressure up to 600 psig. The AlfaRex is ideal for batch reactor temperature control systems, aggressive media, and cyclical applications. Though it overcomes the gasket problem, it cannot be opened up for cleaning.

7.6.15 ALFA LAVAL PLATE EVAPORATOR

Plate evaporators are used for condensing in chemical, sugar, fats, and oil industries. They can be configured as a booster in existing systems.

7.6.16 SANITARY HEAT EXCHANGERS

For food, dairy, and pharmaceutical processing, sanitary heat exchangers combine low maintenance, high efficiency, and reliable separation of fluids. Plate gaps in these exchangers are sized to reduce fouling; the main pattern creates the necessary turbulence for effective heat transmission.

7.6.17 EKASIC® SILICON CARBIDE PLATE HEAT EXCHANGERS

EKasic silicon carbide PHEs are used in the chemical industry or similar sectors, especially where highly corrosive media must be heated and cooled, or evaporated and condensed. EKasic silicon carbide PHEs are also used in applications that must withstand the wear of particle-laden liquids. The very compact PHEs offer very high transfer performance in a small space. EKasic PHEs permit long service lives, high reliability, and improved product quality. The heat exchangers are further characterized by outstanding thermal shock resistance and resistance to cavitation.

7.6.18 DEEP-SET GASKET GROOVES

Polaris gasket grooves cut the risk of gasket failure. In traditional designs, grooves are shallow, which exposes more of the gasket to pressure exerted by the product. The deep-set Polaris groove exposes less gasket area to product pressure, which dramatically increases the gasket's reliability.

7.7 WHERE TO USE PLATE HEAT EXCHANGERS

The characteristics of PHEs are such that they are particularly well suited to liquid–liquid duties in turbulent flow [8]. Incidentally, a fluid sufficiently viscous to produce laminar flow in a shell and tube heat exchanger may be in turbulent flow in a PHE. In the 1930s, PHEs were introduced to meet the hygienic demands of the dairy industry. Today, PHE is universally used in many fields, including heating and ventilating, breweries, dairy, food processing, pharmaceuticals and fine chemicals, petroleum and chemical industries, power generation, offshore oil and gas production, onboard ships, pulp and paper production, etc. PHEs also find applications in water-to-water closed-circuit cooling-water systems using a potentially corrosive primary cooling water drawn from sea, river, lake, or cooling tower to cool a clean, noncorrosive secondary liquid flowing in a closed circuit [8]. In this application, titanium (99.8%)–palladium (0.2%) stabilized titanium is used because of its outstanding corrosion resistance.

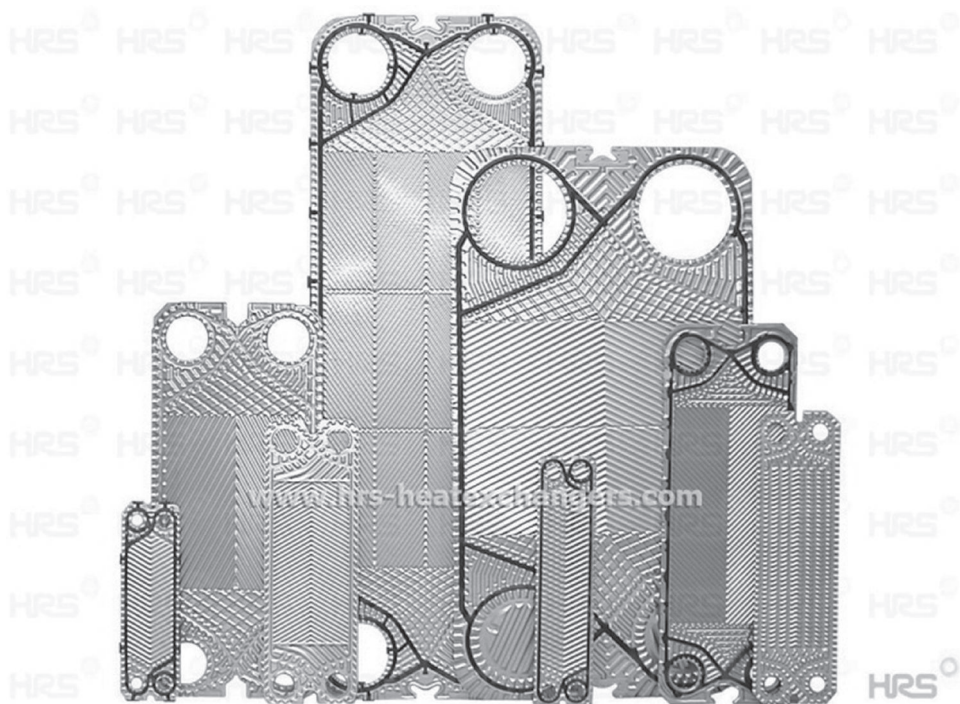
7.7.1 APPLICATIONS FOR WHICH PLATE HEAT EXCHANGERS ARE NOT RECOMMENDED

PHEs are not recommended for the following services [3]:

1. Gas-to-gas applications.
2. Fluids with very high viscosity may pose flow distribution problems, particularly when cooling is taking place; flow velocities less than 0.1 m/s are not used because they give low heat transfer coefficients and low heat exchanger efficiency.
3. Less suitable for vapors condensing under vacuum.

7.8 THERMOHYDRAULIC FUNDAMENTALS OF PLATE HEAT EXCHANGERS

The design of PHEs is highly specialized in nature, considering the variety of plate corrugations (there are more than 60 different plate) available to suit varied duties. Typical plate patterns are shown in Figure 7.23. The plate design varies from manufacturer to manufacturer, and hence the thermohydraulic performance. Unlike tubular heat exchangers, for which design data and methods are easily available, PHE design continues to be proprietary in nature. Manufacturers have developed their own empirical correlations for the prediction of thermal performance applicable to the exchangers marketed by them. Therefore, specific and accurate characteristics of specific plate patterns are not available in the open literature. In recent years, some correlations have been reported in many references. These correlations are mostly approximate in nature, to suit preliminary sizing of the units for a given duty. No published information is available on accurate heat transfer correlations. Hence, it is better to leave the thermal and also mechanical design aspects to a plate manufacturer who offers an optimum design for the process parameters submitted by the consignee. In the following paragraphs, the salient features of the thermal design methods for approximate sizing are presented.



(a)



(b)

FIGURE 7.23 (a) Collection of plate heat exchanger plates. (Courtesy of HRS Heat Exchangers Ltd, Herts, U.K.) (b) Collection of plate heat exchanger plates. (Courtesy of GEA PHE Systems, Sarstedt, Germany.)

TABLE 7.5
Salient Features of Few Newer Types of PHE

Description	Features
<i>Brazed plate heat exchanger (BHE)</i> —It is constructed of a series of corrugated metal plates brazed together in a vacuum oven to form a complete pressure-resistant unit. Absence of gaskets, tightening bolts, frame or carrying and guide bars.	A sealed, compact system, high temperature and pressure capability, gasket-free construction, high thermal efficiency and ideal for refrigeration and process applications. The units are not expandable.
<i>Shell and plate heat exchanger</i> —Pairs of chevron-type plates are placed back-to-back and fabricated into a cassette. Cassettes are then placed together and perimeter welded to each other. The plate pack is then inserted in to the cylindrical shell.	Can handle liquids, gases, steam, and two-phase mixtures. In addition to efficiency, the units offer cost effectiveness and minimal maintenance. Designed for pressures up to 100 barg (1450 psig) and temperatures up to 538°C (1000°F).
<i>Welded plate heat exchanger</i> —This design entirely eliminates the gaskets and by developing a fully welded plate exchanger.	It enhances the reliability as well as the temperature and pressure limits of the gasketed plate exchanger. Like gasketed PHE, it can neither be expanded in surface area nor be cleaned readily by mechanical methods. Only chemical cleaning is possible.
<i>Wide-gap plate heat exchanger</i> —It provides a free-flow channel for liquids and products containing fibers or coarse particles or high viscosity liquids that normally clog or cannot be satisfactorily treated in shell and tube heat exchangers.	Wide-Gap plates economically recovers heat from hard-to-handle waste streams in a variety of industries, including pulp and paper, sugar processing, alcohol production, grain processing, chemicals, latex, polymer slurries, textiles, and ethanol distilling.
<i>Free-flow plate heat exchanger</i> —Compared to the conventional wide gap plate exchanger, there is no contact points in the flow path of free flow plates which restricts the flow otherwise. Hence, it offers an uninterrupted wide flow path for fouling or viscous fluids or those containing fibrous materials.	The corrugation pattern provides the right balance of high efficiency in heat transfer, clogging resistance and low pressure drop, providing a cost advantage over larger, more expensive shell and tube heat exchanger.
<i>Semi-welded or twin-plate heat exchanger</i> —Semi-welded plates are formed from two cassettes that are laser welded together. The cassettes are separated by standard gaskets. The welded pairs allow for aggressive fluids or refrigerants between plates. The other medium flows across gasketed channels.	It offers superior sealing capability, easy cleaning and complies with sanitary standards on the welded side. Use of semi welded units is increasing in the chemical, petroleum refining, and refrigeration industries.
<i>Double-wall plate heat exchanger</i> —It consists of two plates with a small air gap in between them. This gap is open to atmosphere and not in contact with either of the media helping guard against intermixing of the media.	The double wall PHEs are designed for use in cooling/heating duties in dairy, pharmaceutical, brewery and beverage installations where it is crucial to prevent any cross contamination between the two media.
<i>Diabon F graphite plate heat exchanger</i> —The Alfa Laval Diabon F graphite PHE is with graphite plates developed for use with media normally too corrosive for exotic metals and alloys.	The graphite plates offer excellent corrosion resistance and good heat transfer properties in combination with low thermal expansion.

7.8.1 HIGH- AND LOW-THETA PLATES

A plate having high chevron angle (about 60°–65°) provides high heat transfer combined with high pressure drop, whereas a plate having a low chevron angle, β (about 25°–30°), provides a low heat transfer combined with low pressure drop [8]. Figure 7.24 shows schematic of high- and low-theta plates. Manufacturers specify the plates having low values of chevron angle as low-*theta* plates and

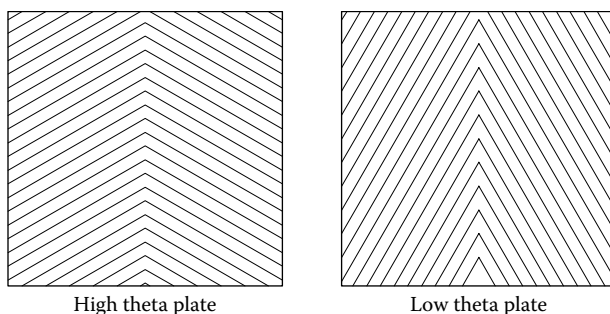


FIGURE 7.24 High-theta and low-theta plates (schematic).

plates having high values of chevron angle as high-*theta* plates. Theta is used by manufacturers to denote the number of heat transfer units (NTU). The expression for theta is given by

$$\theta_c = \text{NTU}_c = \frac{(UA)_c}{(mc_p)_c} \quad (7.1a)$$

$$\theta_h = \text{NTU}_h = \frac{(UA)_h}{(mc_p)_h} \quad (7.1b)$$

The values of θ achieved per pass for various plate types vary enormously (1.15 to about 4), and NTU for high-theta plates is of the order of 3.0 and for low-theta plates 0.5.

Salient features of high- and low-theta plates are hereunder:

- a. *High-theta plates*: Corrugated with obtuse chevron angles, generate very high turbulence, extremely high heat transfer rates, high pressure loss, etc.
- b. *Low-theta plates*: Corrugated with acute chevron angles, generate lower turbulence, lower heat transfer rates, and less pressure loss.

7.8.2 THERMAL MIXING

One of the thermal design problems associated with PHE is the exact matching of the thermal duties; it is very difficult to achieve the required thermal duty and at the same time utilize the available pressure drop fully [3]. This problem is overcome through a procedure known as thermal mixing. Thermal mixing provides the designers with a better opportunity to utilize the available pressure drop without excessive surface, and with fewer standard plate patterns [9]. Thermal mixing is achieved by two methods:

1. Using high- and low-theta plates
2. Using horizontal and vertical plates

7.8.2.1 Thermal Mixing Using High- and Low-Theta Plates

In this method, the pack of plates may be composed of all high-theta plates (say, $\beta = 30^\circ$) or all low-theta plates (say, $\beta = 60^\circ$), or a combination of high- and low-theta plates arranged alternatively in the pack to provide an intermediate level of performance. Thus, two-plate configurations provide three levels of performance plates, as shown in Figure 7.25.

7.8.2.2 Thermal Mixing Using Horizontal and Vertical Plates

In this method, two combinations of geometric patterns are selected to provide three levels of performance plates, as shown in Figure 7.26 [7]:

1. *Horizontal-style plates*: Accu-Therm™ “H” style plates have a horizontal herringbone embossing. These plates have higher heat transfer coefficients and slightly larger pressure drop.

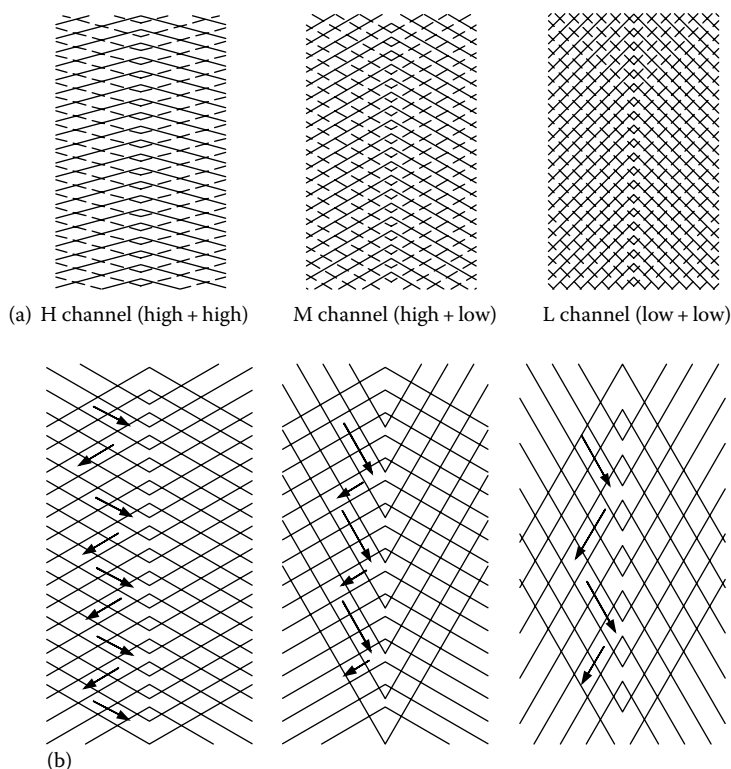


FIGURE 7.25 Thermal mixing (a) combination of high-theta and low-theta plate arrangements and (b) flow pattern.

2. Vertical-style plates: Accu-Therm™ “V” style plates have a vertical herringbone embossing. These plates have lower pressure drop and slightly lower heat transfer coefficients.
3. Combination-style plates: Accu-Therm™ “H” and “V” style plates have been combined to obtain an intermediate thermal and pressure-drop performance.

7.8.3 FLOW AREA

Close spacing of the plates with nominal gaps ranging from 2 to 5 mm (0.08 to 0.02 in.) gives hydraulic mean diameters in the range of 4–10 mm (0.15–0.4 in.) [9]. The plates are embossed so that very high degrees of turbulence are achieved. Critical Reynolds numbers are in the range of 10–400, depending on the geometry. These factors contribute to produce very high heat transfer coefficients. Nominal velocities for “waterlike” liquids in turbulent flow are usually in the range 0.3–1.0 m/s (1–3.1 ft/s), but true velocities may be higher by a factor three or four due to the effect of the corrugations [8]. All heat transfer and pressure-drop relationships are, normally, based on channel velocity. The channel velocity is calculated by dividing the flow per channel by the channel cross-sectional area [11]. The channel cross-sectional area, A_s , is given by

$$A_s = Wb \quad (7.2)$$

where

b is the mean plate gap

W is the effective plate width (gasket to gasket)

Dimension W is shown schematically in Figure 7.27.

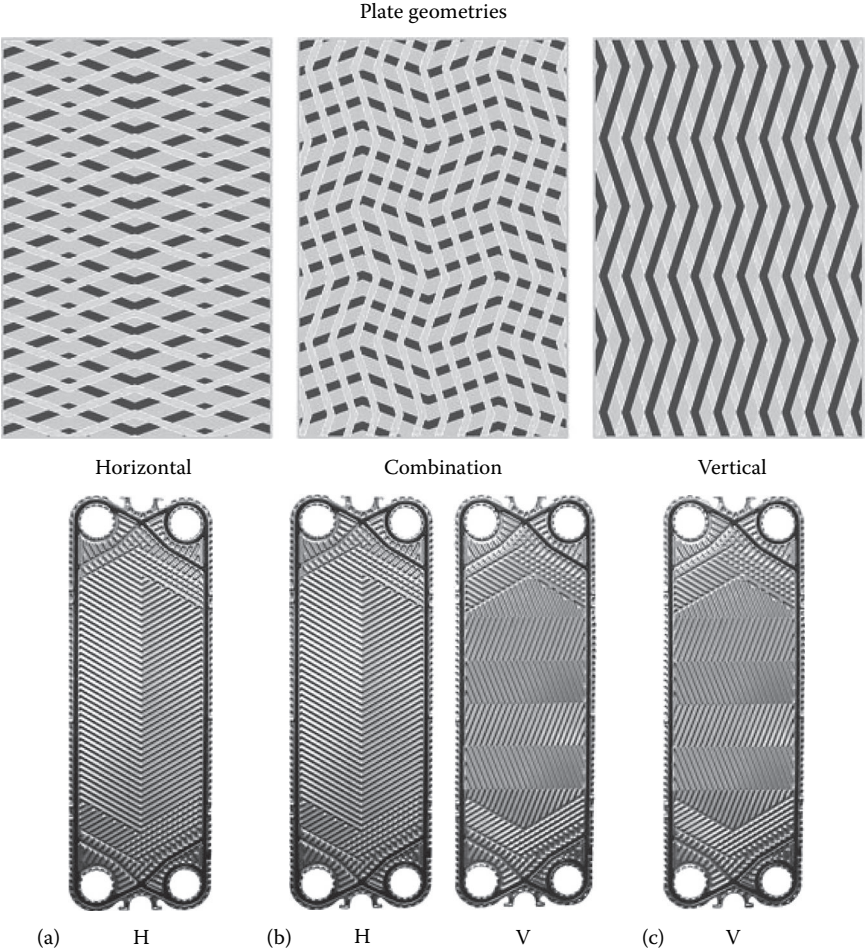


FIGURE 7.26 Thermal mixing using combination of plate geometries. (a) Horizontal–horizontal, (b) horizontal–vertical, and (c) vertical–vertical. (Courtesy of Mueller, Heat Transfer Products, Springfield, MO.)

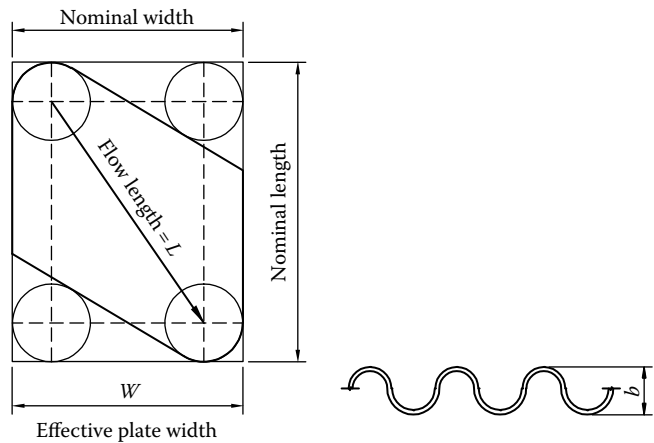


FIGURE 7.27 PHE, major plate dimensions: W –Plate width and L –Effective flow length.

7.8.4 HEAT TRANSFER AND PRESSURE-DROP CORRELATIONS

7.8.4.1 Heat Transfer Correlations

A general correlation for turbulent flow is given by [8]

$$\text{Nu} = C \text{Re}^n \text{Pr}^m \left(\frac{\mu_b}{\mu_w} \right)^x \quad (7.3)$$

Typical reported values are

$$C = 0.15\text{--}0.40$$

$$n = 0.65\text{--}0.85$$

$$m = 0.30\text{--}0.45 \quad (\text{usually } 0.333)$$

$$x = 0.05\text{--}0.20$$

One of the most widely used plates has the following relationship [8]:

$$\text{Nu} = 0.374 \text{Re}^{0.668} \text{Pr}^{0.33} \left(\frac{\mu_b}{\mu_w} \right)^{0.15} \quad (7.4)$$

where the Reynolds number is based on equivalent diameter, D_e , defined by

$$D_e = \frac{4Wb}{2(W+b)} \quad (7.5a)$$

$$= 2b \text{ since } b \text{ is very small compared to } W \quad (7.5b)$$

The expression for hydraulic diameter D_h for PHE is given by

$$D_h = \frac{4 \times \text{minimum free flow area}}{\text{wetted perimeter}} \quad (7.6a)$$

$$\approx \frac{2b}{\phi^*} \quad (7.6b)$$

where ϕ^* is the ratio of actual (developed) surface area to projected surface area.

But to calculate Reynolds number, the hydraulic diameter expressed by Equation 7.6 is not used because it is difficult to measure the parameter ϕ^* [5].

Buonopane and Troupe [12] present generalized relationships for a number of geometries for laminar flow. It seems that the following Sieder–Tate type relationship applies [8]:

$$\text{Nu} = C_1 \left(\text{Re} \text{Pr} \frac{D_h}{L} \right)^{0.333} \left(\frac{\mu_h}{\mu_w} \right)^{0.14} \quad (7.7)$$

where

$C_1 = 1.86\text{--}4.50$ depending on geometry, replace D_h by D_e

L is the effective plate length (as shown in Figure 7.27)

More correlations are summarized in Refs. [4,5,7,11].

7.8.4.2 Pressure Drop

Friction factor, f : The fanning friction factor, f , is of the form [13]

$$f = \frac{C_2}{\text{Re}^y} \quad (7.8)$$

where

C_2 is a constant characterizing each type of plate
 y covers different ranges

For a typical plate, the f factor is given by [13]

$$f = \frac{2.5}{\text{Re}^{0.3}} \quad (7.9)$$

Usher [14] reported that the friction factor for plate exchangers is 10–60 times that developed inside tubular exchangers at similar Reynolds numbers for turbulent flow. Marriott [8] observed that this value can be up to 400 times. Though the friction factors are high compared to that of the tubular units, the pressure drop will be less due to the following reasons [8]:

1. The nominal velocities are low, and nominal plate lengths do not exceed about 6 ft (1829 mm), so that the term $(G^2/2g_c)L$ in the pressure-drop equation is very much smaller than would be the case in a tubular unit.
2. Only a few passes will achieve the required NTU value, so that the pressure drop is effectively utilized for heat transfer and losses due to unfruitful flow reversals are minimized.

7.8.4.2.1 Expression for Pressure Drop

Generalized equation for pressure drop: The pressure drop in a PHE consists of the following components [5]:

1. Empirically, the pressure drop associated with the inlet and outlet manifolds and ports, Δp_m , is approximately 1.5 times the inlet velocity head per pass,

$$\Delta p_m = 1.5 \left(\frac{\rho U_m^2}{2g_c} \right)_i N_p \quad (7.10)$$

where

N_p is the number of fluid ports
 U_m the velocity through the ports

2. The pressure drop associated within the plate passages is given by

$$\Delta p_c = \underbrace{\frac{4fLG^2}{2g_c D_c} \left(\frac{1}{\rho} \right)_m}_{\text{friction effect}} + \underbrace{\left(\frac{1}{\rho_o} - \frac{1}{\rho_i} \right) \frac{G^2}{g_c}}_{\text{momentum effect}} \quad (7.11)$$

where

$$\left(\frac{1}{\rho}\right)_m = \frac{1}{2} \left(\frac{1}{\rho_o} + \frac{1}{\rho_i} \right) \quad (7.12)$$

and where G is the mass velocity and L is the flow passage length. The flow passage length is equal to the distance (diagonal) between the centers of inlet and outlet ports [11]. For liquids, the momentum effect is negligible, and $(1/\rho)_m \approx 1/\rho_m$.

3. The pressure drop due to an elevation change is given by

$$\Delta p_n = \pm \frac{\rho_m g L}{g_c} \quad (7.13)$$

where

the + stands for vertical upward flow

the – stands for vertical downward flow

g is the gravitational acceleration

g_c the proportionality constant in Newton's second law of motion, $g_c = 1$ and dimensionless in SI units, or $g_c = 32.174 \text{ lbf ft/lbf s}^2$

The total pressure drop on one side of the plate exchanger is the sum of Δp 's of Equations 7.10, 7.11, and 7.13.

Approximate equation for pressure drop: The general correlation for calculating pressure drop in a plate exchanger after accounting for Sieder–Tate viscosity correction factor has the general form

$$\Delta p = \frac{4fLG^2}{2g_c\rho D_e} \left(\frac{\mu_w}{\mu_b} \right)^{0.14} \quad (7.14)$$

7.8.5 SPECIFIC PRESSURE DROP OR JENSEN NUMBER

In assessing the performance of any heat exchanger, the *specific pressure drop* (J) can be used [15]. This is defined as the pressure drop per NTU, that is,

$$J = \frac{\Delta p}{\text{NTU}} = \frac{\Delta p}{\theta} \quad (7.15)$$

Jensen [15] reports that optimum values for J for water–water duties of commercially available plates are close to 4.5 psi/NTU.

7.9 PHE THERMAL DESIGN METHODS

There are two different aspects of PHE design [2]:

1. The design of individual plate types so that they conform to specific performance and operational characteristics
2. The calculation of the number and arrangement of such plates in order to satisfy the thermal and pressure-drop requirements

The thermal design method can be based on either the LMTD or ϵ -NTU method. Buonopane et al. [16] described the LMTD design method, and Jackson and Troupe [17] described the ϵ -NTU method, and both methods are described in Ref. [4] with the ϵ -NTU method in Ref. [5].

7.9.1 LMTD METHOD DUE TO BUONOPANE ET AL. [16]

This method gives the heat transfer area needed in a PHE for both looped and series flow arrangements, given the temperature program, flow rates, and physical characteristics of the plates. The steps involved in the method are given next.

For series flow (Figure 7.4a):

1. Determine the inlet and outlet temperatures for both the fluids.
2. Estimate LMTD for counterflow arrangement.
3. Estimate Reynolds number for the each stream, assuming an exchanger containing one thermal plate, one pass for each stream, as given:

$$Re = \frac{(G/n_s)D_e}{\mu} \quad (7.16)$$

where n_s is the number of substreams. For series flow, $n_s = 1$.

4. Estimate heat transfer coefficient on both sides
5. Estimate overall heat transfer coefficient taking into account the wall thermal resistance.
6. Estimate the total heat transfer area from $A = q/U \text{ LMTD } F$.
7. Estimate the number of plates from, $N = A/A_p$, where A_p is the area of a plate and $2A_p$ is the area per channel.

For parallelflow or looped flow (Figure 7.4b):

Repeat steps 1–7 already given.

8. From the number of thermal plates calculated in step 7, n_s is determined for both the fluids. For odd N , values of n_s will be equal for both fluids, whereas for even N , n_s will be different for both the fluids, and one fluid will have an additional substream compared to the other.
9. The values of n_s determined in step 8 are compared with the corresponding values assumed in step 3. If the calculated values do not agree with the assumed values, steps 3–9 are to be repeated, replacing the assumed values with the values calculated from step 8 until there is agreement between the two.

7.9.2 ϵ -NTU APPROACH

Jackson and Troupe [17] presented an ϵ -NTU method for the design of PHEs. The following steps illustrate the method:

1. Calculate the heat load, q , and from it determine the inlet and outlet temperatures for both the fluids.
2. Calculate the bulk mean temperature and determine the thermo physical fluid properties. Estimate the heat capacity rate ratio, C^* .
3. Estimate the heat transfer effectiveness, ϵ , using the relation

$$\epsilon = \frac{C_h(t_{h,i} - t_{h,o})}{C_{\min}(t_{h,i} - t_{c,i})} = \frac{C_c(t_{c,o} - t_{c,i})}{C_{\min}(t_{h,i} - t_{c,i})} \quad (7.17)$$

4. Assume an exchanger containing an infinite number of channels and find the required NTU using the appropriate ϵ -NTU relation.
5. Estimate Reynolds number for the each stream, assuming an exchanger containing one thermal plate, and one pass for each stream.
6. Calculate the heat transfer coefficient on both sides. Estimate the overall heat transfer coefficient, taking into account the wall thermal resistance.

For series flow (Figure 7.4a):

7. Estimate the approximate number of thermal plates using the equation

$$N = \frac{NTU(mc_p)_{\min}}{UA_p \Delta t_m} \quad (7.18)$$

where Δt_m is the mean temperature difference.

8. Assuming an exchanger of $N + 1$ channels, determine NTU from the appropriate ϵ -NTU relationship.
9. Recalculate N from Equation 7.18.
10. Repeat calculations in steps 8 and 9 until the calculated value of N in step 9 matches the assumed value in step 8.

For parallelflow or looped flow (Figure 7.4b): In a design involving looped flow patterns, the overall coefficient requires recalculation during each iteration because the channel flow rates become less with the addition of channels in parallel. The calculation procedure for looped flow is as follows:

1. Assuming an exchanger of N thermal plates, calculate the overall heat transfer coefficient as in step 6.
2. Estimate the approximate number of thermal plates using Equation 7.18.
3. Assuming an exchanger of $N + 1$ channels, determine NTU from the appropriate ϵ -NTU relationship for looped flow.
4. Recalculate the overall heat transfer coefficient as per step 6 and recalculate N with Equation 7.18.
5. Repeat calculations in steps 9 and 10 until the calculated value of N matches with the assumed value.

7.9.3 SPECIFICATION SHEET FOR PHE

The specification sheet for PHE is given in Table 7.6. The thermal design parameters and construction details of PHE adapted from Mueller, Heat Transfer Products, Springfield, USA, product literature are discussed next.

7.9.3.1 Design Pressure

The PHE shall be designed, fabricated, and tested in accordance with the requirements of ASME Code Section VIII, Division 1. The exchanger shall be code stamped for— — MPa (psi) design pressure at the maximum— — °C (°F) and minimum— — — °C(°F) fluid temperatures specified. The test pressure will be 130% of the design pressure. The exchanger shall be designed to withstand full design pressure in one circuit with zero pressure in the opposite circuit.

Design requirements: The heat exchanger performance, in clean condition, shall be in accordance with ARI 400-2001.

Plates: Plates shall be fabricated of ____ material (Type 304 or 316 stainless steel, titanium, Incoloy, Hastalloy, or other material) with a minimum plate thickness of 0.5 mm (nominal).

Gaskets: Gaskets shall be ____ (nitrile butadiene rubber, hypalon, viton, neoprene, or other material) as specified by the user.

TABLE 7.6
Specification Sheet for PHE

Description	Hot Side	Cold Side
Fluid circulated		
Flow rate		
Temperature in		
Temperature out		
Operating pressure		
Maximum pressure drop		
Specific heat		
Specific gravity or density		
Thermal conductivity		
Viscosity in		
Viscosity out		
Required gasket material		
Required plate material		
ASME code requirement		

Connections: All inlet and outlet connections shall be designed to accept either ANSI flanged or IPS threaded connections. Studded port connections shall be lined with metal or the same elastomer as provided on the plates.

Frame: Fixed and movable end frames shall each be constructed as to eliminate any need for adding stiffeners to provide reinforcement for less frame thickness. Frames shall be made from SA-516 or SA-515-70. The frame assembly shall be coated with corrosion-resistant paint.

Compression bolts: Compression bolts, nuts, and washers shall be galvanized, low-alloy steel (SA-193-B7/SA-194-2H).

Future expansion: The exchanger shall have frame capacity for future expansion of a minimum of 20%.

7.9.3.2 Plate Hanger

Plates shall be of one-piece design, without need of loose removable plate hanger components. The plates shall be supported by a Type 304 stainless steel plate hanger. The heat exchanger shall have a plate-positioning system that will prevent shifting during tightening of the plate pack and during unit operation.

Shroud: The top and sides of the plate pack shall be entirely enclosed within a protective shroud.

Overall size: The exchanger shall not exceed— — — mm (in.) height,— — — mm (in.) width, and— — — mm (in.) length.

7.10 CORROSION OF PLATE HEAT EXCHANGERS

It is general practice for plate exchanger manufacturers to use only corrosion-resistant materials for a PHE, dictated by factors such as product purity and to minimize corrosion fouling. Erosion is not a governing factor, since pressure-drop limitations will generally determine the maximum permissible fluid velocities. As the plates are very thin (0.6–1.2 mm) compared to the tube thickness (maximum permitted up to 4.2 mm in the case of 19.5 mm diameter tube dimensions, conforming to TEMA Standards [18]), corrosion allowances normally recommended for tubular units are not relevant for plate units. In the design of a tubular unit, a corrosion allowance of 0.125 mm/year is used; for plate units the corrosion rate should not exceed 0.05 mm/year [3].

7.11 FOULING

The types of fouling generally that occur in the plate fin heat exchanger include sedimentation (solids in suspension), biological (marine or organic), scaling or deposition (calcium carbonate), and corrosion. But high degrees of turbulence, uniform fluid flow and the smooth plate surface, and application of corrosion-resistant material for manufacture of plates reduce fouling and the need for frequent cleaning. Additionally, water treatment program and dosing of biocides and inhibitors are in place mostly in many heat exchanger applications. Strainers for the inlet port or the inspection port in the movable cover are available to protect the plate pack from large particulates clogging the channels. Clean-in-Place (CIP) systems are another option for cleansing the PFHX. CIP systems circulate a pre-heated detergent through the PFHX at a suitable flow rate to dissolve deposits. Back-flushing in reverse flow with a diverter valve is also an effective method for cleaning the port area without opening the heat exchanger unit. Fibers that can pose a problem for standard PHEs can be dealt by wide-gap or free-flow plate designs. Hence, the fouling factors required in PHEs are small compared with those commonly used in shell and tube designs [8]. They should be normally 20%–25% of those used in shell and tube exchangers. For design purposes, fouling values not greater than one-fifth of the published tubular figures are recommended by Cooper et al. [2]. Fouling factors for PHEs are tabulated by Marriott [8]. Marriott states that under no circumstances, even under low pressure-drop conditions, is a total fouling resistance exceeding $0.00012 \text{ m}^2\cdot\text{C}/\text{W}$ or $0.0006 \text{ ft}^2\cdot\text{F}\cdot\text{h}/\text{Btu}$ recommended.

7.12 LIMITATIONS OF PLATE HEAT EXCHANGERS

While plate exchangers have pressure drops comparable to those found in shell and tube units, they are generally confined to operation at lower pressures and temperatures due to the use of elastomer gaskets for sealing. Commonly stated limits have been 300°F (149°C) and 300 psi [14]. The maximum allowable working pressure is also limited by the frame strength and plate deformation resistance. Manufacturers produce a low-cost frame for low-pressure duties, say up to 85 psig (6 atm), and a more substantial frame for higher pressures, for a given plate size. All PHEs used in the chemical and allied industries are capable of operating at 85 psig, most at 142 psig, many at 230 psig, and some at pressures as high as 300 psig [8]. The limitations of temperature and pressure are overcome in heat exchangers with the lamella heat exchanger or by brazed plate exchanger or by welded heat exchangers. Other limitations of PHEs include the following:

1. Upper plate size is limited by the available press capacity to stamp out the plates from the sheet metal [3].
2. Because of the narrow gap (or the flow passages) between the plates, high liquid rates will involve excessive pressure drops, thus limiting the capacity.
3. Frequent gasket removal (gaskets are numerous) during cleaning of plates can lower the gasket life.
4. Large differences in fluid flow rates of two streams cannot be handled.
5. The gaskets cannot handle corrosive or aggressive media.
6. The standard PHEs cannot handle particulates that are larger than 0.5 mm. This restricts the use of heat exchangers with multiphase flow. If free-flowing-style plates are used, a slightly larger particulate size of 12 mm can be managed.
7. Gaskets always increase the leakage risk.

7.13 SPIRAL PLATE HEAT EXCHANGERS

A spiral plate heat exchanger (SPHE) is fabricated by rolling a pair of relatively long strips of plate to form a pair of spiral passages (Figure 7.28). Channel spacing is maintained uniformly along the length of the spiral passages by means of spacer studs welded to the plate strips prior to rolling. It can be made with channels 5–25 mm wide, with or without studs. The spiral channels are welded shut on their ends

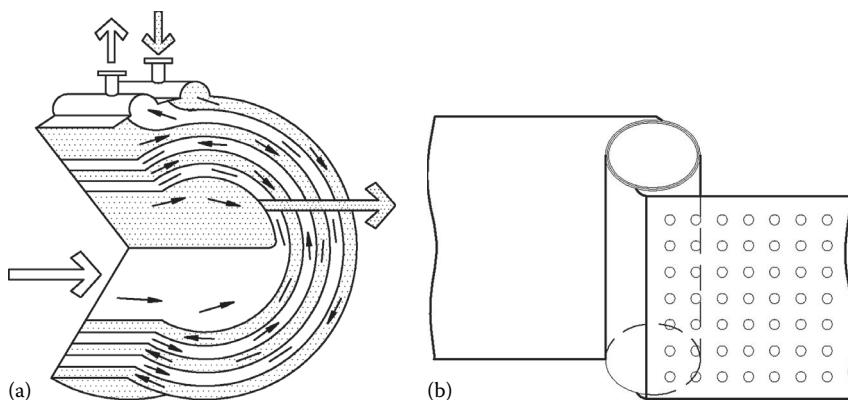


FIGURE 7.28 Spiral plate heat exchanger. (a) Unit and (b) two plates design (with studded or plain design).

in order to contain respective fluids. An overall gasket is applied to the cover. The covers are attached to the spiral element by means of forged hook bolts and adapters. The hook bolt engages the bevel at the back of the flange ring and the adapter engages the rim at the edge of the cover. A header is welded on the outer end of each passage to accommodate the respective peripheral nozzle. For most services, both fluid flow channels are closed by alternate channels welded at both sides of the spiral plate. In some applications, one of the channels is left completely open, and the other closed at both sides of the plate. These two types of construction prevent the fluids from mixing.

7.13.1 FLOW ARRANGEMENTS AND APPLICATIONS

The spiral assembly can be fitted with covers to provide three flow pattern types:

1. Both fluids in spiral flows; this arrangement can accommodate the media in full counter-flow. General uses are for liquid to liquid, condensers, and gas coolers.
2. One fluid in spiral flow and the other in axial flow across the spiral; general uses are as condensers, reboilers, and gas coolers and heaters.
3. One fluid in spiral flow and the other in a combination of axial and spiral flow; general uses are as condensers (with built-in aftercoolers) and vaporizers.

These flow arrangements are shown schematically in Figure 7.29.

7.13.2 CONSTRUCTION MATERIAL

Spiral plate exchangers are fabricated from any material that can be cold worked and welded. Typical construction materials include carbon steel, stainless steels, Hastelloy B and C, nickel and nickel alloys, aluminum alloys, titanium, and copper alloys. To protect against corrosion from cooling water, the surface is given baked phenolic resin coatings, among others. Anodic elements may also be wound into the assembly to anodically protect surfaces against corrosion [19].

7.13.3 THERMAL DESIGN OF SPIRAL PLATE HEAT EXCHANGERS

Thermal design procedures of SPHEs are covered by Minton [19]. The system of ordinary differential equations for the temperature distribution in SPHEs has been solved numerically by Chaudhury et al. [20] to obtain the efficiency,

LMTD correction factor F is a function of number of transfer units, number of turns n , and the heat capacity rate ratio. They found that the LMTD correction factors, when plotted versus NTU

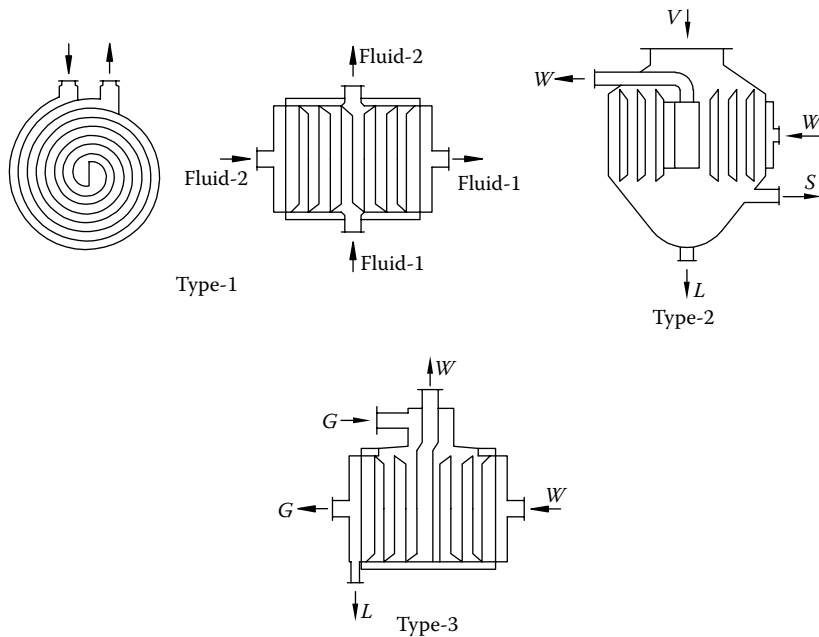


FIGURE 7.29 Alfa Laval SPHE flow arrangements (L, condensate; G, gas; W, liquid; V, vapor; and S, noncondensables).

per turn, fall approximately on a single curve and that curve can be represented by the simple formula [20]

$$F = \frac{n}{NTU} \tanh\left(\frac{NTU}{n}\right) \quad (7.19)$$

7.13.4 MECHANICAL DESIGN OF SPIRAL PLATE HEAT EXCHANGERS

Spiral exchangers can be furnished in accordance with most pressure vessel codes. Sizes range from 0.5 to 350 m² of heat transfer surface in one single spiral body. The maximum design pressure is normally limited to 150 psi due to the following reasons, although for smaller diameters the pressure may sometimes be higher [19]:

1. They are normally designed for the full pressure of each passage.
2. Because the turns of the spiral are of relatively large diameter, each turn must contain its design pressure.
3. The plate thickness is somewhat restricted.

Limitations of materials of constructions govern design temperature.

7.13.5 APPLICATIONS FOR SPIRAL PLATE HEAT EXCHANGERS

The SPHE is particularly suited for such liquid-to-liquid duties as

Clogging slurries such as PVC slurries

Clogging particle-laden and fibrous media such as TMP condensate in pulp and paper production

Clogging and erosive media such as alumina, hydrate slurries, etc.
 Fouling media such as waste water or sewage sludge
 High-viscosity media such as heavy oil
 Non-Newtonian fluids such as fermenting froth in pharmaceuticals processing

7.13.6 ADVANTAGES OF SPIRAL PLATE EXCHANGERS

SPHEs have a number of advantages over conventional shell and tube exchangers:

1. The spiral heat exchanger approaches the ideal in heat exchanger design. Media can be arranged in full counterflow. Flow characteristics are the same for each medium. The long passages on each side permit close temperature approaches. Radiation losses are negligible.
2. The exchanger is well suited for heating or cooling viscous fluids because its L/D ratio is lower than that of tubular exchangers [19].
3. At a velocity that would be marginal and approaching streamline flow in straight tubes, good turbulence is realized because of the continuously curving passages.
4. The scrubbing action of the fluids in each side of the passage tends to flush away deposits as they form and hence permits the use of low fouling resistance values.
5. Media cannot intermix; they are isolated by the welded closing on one side of each passage.
6. The spiral exchanger is compact and requires less installation and servicing space than conventional exchangers of equivalent surface.
7. They are easily maintainable. By removing the covers of the spiral exchanger, the entire lengths of the passages are easily accessible for inspection or mechanical cleaning, if necessary. Similarly, because of the single passage on each side, the spiral heat exchanger is readily cleaned with cleaning solutions without opening the unit.
8. Spiral plate exchangers avoid problems associated with differential thermal expansion in non-cyclic service [19].
9. In axial flow, a large flow area affords a low pressure drop, which becomes especially important when condensing under vacuum [19].

7.13.7 LIMITATIONS

Besides the pressure limitation noted earlier, the spiral plate exchanger also has the following disadvantages [19]:

1. Repairing an SPHE in the field is difficult; however, the possibility of leakage in a spiral is less because it is generally fabricated from much thicker plate than tube walls.
2. Spiral plate exchangers are not recommended for service in which thermal cycling is frequent. When used for such services, the unit sometimes must be designed for higher stresses.
3. The SPHE usually should not be used when a hard deposit forms during operation, because the spacer studs prevent such deposits from being easily removed by drilling.

7.14 PLATECOIL® PRIME SURFACE PLATE HEAT EXCHANGERS

Platecoil designates a group of heat transfer products (as shown in Figure 7.30) fabricated from two metal sheets, one or both of which are embossed. When welded together, the embossings form a series of well-defined passages through which the heat transfer media flows. Panels are then fabricated into pre-engineered modules, complete with piping, supporting structure and manifolds, or formed into vessel shells or jackets. Two embossed sheets welded together form a double embossed Platecoil. One embossed sheet welded to a flat companion plate is known as a single

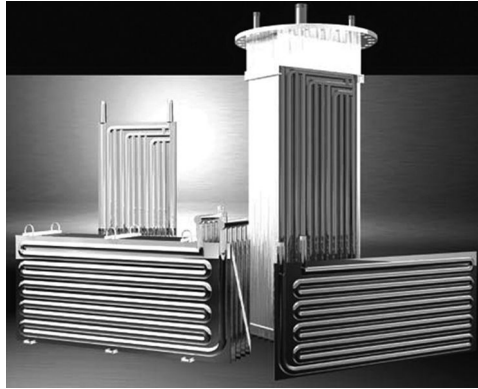


FIGURE 7.30 Tranter Platecoil. (Courtesy of Tranter, Inc., Wichita Falls, TX.)

embossed Platecoil. The passages formed by the embossings are designed to provide Platecoil users with a choice of two basic flow patterns, depending on the application. Platecoil's Multi-Zone flow configuration is ideal for use when steam is the heating medium. The serpentine flow configuration finds wide application with liquid heat transfer media such as water, oil, and liquid refrigerants. A variety of standard Platecoil fabrications, such as pipecoil, half pipe, jacketed tanks and vessels, clamp-on upgrades, immersion heaters and coolers heat recovery banks, storage tank heaters, drum warmers, vessels, suction heaters, and screw conveyor troughs are also available. Easy access to panels and robust cleaning surfaces reduce maintenance burdens.

NOMENCLATURE

A	total heat transfer area, m^2 (ft^2)
A_p	heat transfer area of a plate, m^2 (ft^2)
b	mean plate gap, m (ft)
C	constant in Equation 7.3
C_1	constant in Equation 7.7
C_2	constant in Equation 7.8
C_{\min}	minimum of $(mc_p)_h$, and $(mc_p)_c$, $\text{W}/^\circ\text{C}$ ($\text{Btu}/\text{h}\cdot^\circ\text{F}$)
C_c	specific heat of cold fluid, $\text{J}/\text{kg}\cdot^\circ\text{C}$ ($\text{Btu}/\text{lbm}\cdot^\circ\text{F}$)
C_h	specific heat of hold fluid, $\text{J}/\text{kg}\cdot^\circ\text{C}$ ($\text{Btu}/\text{lbm}\cdot^\circ\text{F}$)
c_p	specific heat, $\text{J}/\text{kg}\cdot^\circ\text{C}$ ($\text{Btu}/\text{lbm}\cdot^\circ\text{F}$)
C^*	heat capacity rate ratio = $(mc_p)_{\min}/(mc_p)_{\max}$
D_e	equivalent diameter of flow passages, m (ft)
D_h	hydraulic diameter, m (ft)
F	LMTD correction factor
f	Fanning friction factor
G	mass velocity based on minimum flow area, $\text{kg}/\text{m}^2\cdot\text{s}$ ($\text{lbm}/\text{h}\cdot\text{ft}^2$)
g_c	acceleration due to gravity or proportionality constant 9.81 m/s^2 (32.17 ft/s^2) = 1 and dimensionless in SI units
h	convective heat transfer coefficient, $\text{W}/\text{m}^2\cdot^\circ\text{C}$ ($\text{Btu}/\text{ft}^2\cdot\text{h}\cdot^\circ\text{F}$)
J	Jenson number (of specific pressure drop), Pa/NTU ($\text{lbf}/\text{ft}^2/\text{NTU}$)
j	Colburn heat transfer factor
k	thermal conductivity, $\text{W}/\text{m}\cdot^\circ\text{C}$ ($\text{Btu}/\text{h}\cdot\text{ft}\cdot^\circ\text{F}$)
L	effective flow passage length, m (ft)
LMTD	log mean temperature difference, $^\circ\text{C}$ ($^\circ\text{F}$)

m	mass flow rate of fluid, kg/s (Lb/s)
m, n	exponents in Equation 7.3
N	number of plates
n	number of turns of spiral plate heat exchanger, Equation 7.19
Nu	Nusselt number
N_p	number of fluid ports, Equation 7.10
n_s	number of substreams
Pr	Prandtl number
p	pressure, Pa (lbf/ft ²)
Q	total heat duty of the exchanger, W·s (Btu)
p	centre distance between two troughs or chevron pitch as per Figure 7.9
q	heat transfer rate, W (Btu/h)
Re	Reynolds number
R_r	Fouling resistance, m ² ·°C/W (ft ² ·°F·h/Btu)
t	fluid static temperature, °C (°F)
U	overall heat transfer coefficient, W/m ² ·°C (Btu/h·ft ² ·°F)
U_m	fluid velocity through port or manifold, m/s (ft/h)
W	width of the plate (gasket to gasket), m (ft)
x	exponent in Equation 7.3
y	exponent in Equation 7.8
β	chevron angle
Δp	pressure drop, Pa (lbf/ft ²)
Δp_c	pressure drop within the plate passages, Pa (lbf/ft ²)
Δp_h	pressure drop due to elevation, Pa (lbf/ft ²)
Δp_m	pressure drop associated with the inlet and outlet manifolds and ports, Pa (lbf/ft ²)
Δt_{lm}	log mean temperature difference, °C (°F)
Δt_m	mean temperature difference, °C (°F)
ϵ	thermal effectiveness
μ_b	viscosity at bulk mean temperature, Pa·s (lbm/h·ft)
μ_w	viscosity at wall temperature, Pa·s (lbm/h·ft)
ϕ^*	ratio of actual (developed) surface area to projected surface area.
ρ	fluid density, kg/m ³ (lbm/ft ³)
θ	number of transfer units (NTU)

Subscripts

c	cold
h	hot
i	inlet
m	mean
o	outlet
min	minimum
max	maximum

REFERENCES

1. Focke, W. W., Plate heat exchangers: Review of transport phenomena and design procedures, CSIR Report CENG 445, CSIR, Pretoria, South Africa, 1983.
2. Cooper, A. and Usher, J. D., Plate heat exchangers, in *Heat Exchanger Design Handbook*, Vol. 3, (E. U. Schlunder, editor-in-chief), Hemisphere, Washington, DC, 1983, Section 3.7.
3. Raju, K. S. N. and Bansal, J. C., Plate heat exchangers and their performance, in *Low Reynolds Number Flow Heat Exchangers* (S. Kakac, R. K. Shah, and A. E. Bergles, eds.), Hemisphere, Washington, DC, 1983, pp. 899–912.

4. Raju, K. S. N. and Bansal, J. C., Design of plate heat exchangers, in *Low Reynolds Number Flow Heat Exchangers* (S. Kakac, R. K. Shah, and A. E. Bergles, eds.), Hemisphere, Washington, DC, 1983, pp. 913–932.
5. Shah, R. K. and Focke, W. W., Plate heat exchangers and their design theory, in *Heat Transfer Equipment Design* (R. K. Shah, D. C. Subbarao, and R. M. Mashelekar, eds.), Hemisphere, Washington, DC, 1988, pp. 227–255.
6. Alpha-Laval product literature, M/s, Alpha-Laval (India) Limited, Pune, India.
7. Mueller Accu-Therm Plate heat exchangers, AT-1601–4, Paul Muller Company, Springfield, MO.
8. Marriott, J., Where and how to use plate heat exchangers, in *Process Heat Exchange, Chemical Engineering Magazine* (V. Cavaseno, ed.), McGraw-Hill, New York, 1979, pp. 156–162.
9. Saunders, E. A. D., Gasketed plate heat exchangers, in *Heat Exchangers: Selection, Design and Construction*, Addison Wesley Longman, Reading, MA, 1989, Chapter 16.
10. Trom, L., Heat exchangers: Is it time for a change? *Chem. Eng.*, February, 70–73 (1996).
11. Caeiula, L. and Rudy, T. M., Prediction of plate heat exchanger performance, in *AiChE Symposium Series Heat Transfer*, Seattle, WA, 1983, pp. 76–89.
12. Buonopane, R. A. and Troupe, R. A., A study of the effects of internal rib and channel geometry in rectangular channels, Part I: Pressure drop & Part II: Heat transfer, *AiChE J.*, July, 585–596 (1969).
13. *APV Heat Transfer Handbook, A History of Excellence*, APV Co., Getzville, NY, 2008.
14. Usher, J. D., Evaluating plate heat exchangers, in *Process Heat Exchange, Chemical Engineering Magazine* (V. Cavaseno, ed.), McGraw-Hill, New York, 1979, pp. 145–149.
15. Jenson, S., Assessment of heat transfer data, *Chem. Eng. Prog. Symp. Ser., Heat Transfer—1960*, 56, 195–201 (1960).
16. Buonopane, R. A., Troupe, R. A., and Morgan, J. C., Heat transfer design method for plate heat exchangers, *Chem. Eng. Prog.*, 59, 57–61 (1963).
17. Jackson, B. W. and Troupe, R. A., Plate exchanger design by ϵ -NTU method, *Heat Transfer Los Angeles, Chem. Eng. Prog. Symp. Ser.*, 62, 185–190 (1966).
18. *Standards of the Tubular Exchanger Manufacturers Association*, 9th edn., Tubular Exchanger Manufacturers Association, Tarrytown, NY, 2007.
19. Minton, P. E., Designing spiral plate heat exchangers, *Chem. Eng.*, 77, 103–112 (1970).
20. Chowdhury, K., Linkmeyer, H., Bassiouny, M. K., and Martin, H., Analytical studies on the temperature distribution in spiral plate heat exchangers, *Chem. Eng. Prog.*, 19, 183–190 (1985).

BIBLIOGRAPHY

- Bond, M. P., Plate heat exchangers for effective heat transfer, *Chem. Eng.*, 367, 162–166 (1981).
- Cowan, C. T., Choosing materials of construction for plate heat exchangers—I, in *Process Heat Exchange, Chemical Engineering Magazine* (V. Cavaseno, ed.), McGraw-Hill, New York, 1979, pp. 165–167.
- Cowan, C. T., Choosing materials of construction for plate heat exchangers—II, in *Process Heat Exchange, Chemical Engineering Magazine* (V. Cavaseno, ed.), McGraw-Hill, New York, 1979, pp. 168–169.
- Cross, P. H., Preventing fouling in plate heat exchangers, in *Process Heat Exchange, Chemical Engineering Magazine* (V. Cavaseno, ed.), McGraw-Hill, New York, 1979, pp. 211–214.
- Edwards, M. F., Heat transfer in plate heat exchangers at low Reynolds numbers, in *Low Reynolds Number Flow Heat Exchangers* (S. Kakac, R. K. Shah, and A. E. Bergles, eds.), Hemisphere, Washington, DC, 1983, pp. 933–947.
- Marriott, J., Where and how to use plate heat exchangers, *Chem. Eng.*, 78, 127–133 (1971).
- Saunders, E. A. D., Thermal appraisal: Gasketed plate heat exchangers, in *Heat Exchangers: Selection, Design and Construction*, Addison Wesley Longman, Reading, MA, 1989, Chapter 16.
- Shah, R. K. and Kandlikar, S. G., The influence of the number of thermal plates on plates heat exchanger performance, in *Current Researches in Heat and Mass Transfer, A Compendium and a Festschrift for Professor Arcot Ramachandran*, Hemisphere, Washington, DC, 1986, pp. 267–288.

8 Heat Transfer Augmentation

8.1 INTRODUCTION

The study of improved heat transfer performance is referred to as heat transfer enhancement or augmentation. The enhancement of heat transfer has concerned researchers and practitioners since the earliest documented studies of heat transfer [1]. In recent years, increasing energy and material costs have provided significant incentives for development of energy efficient heat exchangers. As a result, considerable emphasis has been placed on the development of various augmented heat transfer surfaces and devices [2,3]. Heat transfer enhancement today is characterized by vigorous activity in both research and industrial practice. This can be seen from the exponential increase in world technical literature published in heat transfer augmentation devices, growing patents, and hundreds of manufacturers offering products ranging from enhanced tubes to entire thermal systems incorporating enhancement technology [1]. In this chapter, single-phase heat transfer augmentation devices are discussed in detail without specific correlations for j and f factors and two-phase heat transfer augmentation devices are briefly dealt. An important reference source on heat transfer augmentation devices is Bergles [4].

8.1.1 BENEFITS OF HEAT TRANSFER AUGMENTATION

An enhanced surface is more efficient in transferring heat than what might be called the standard surface. The application of enhancement device can result in benefits such as

1. A decrease in heat transfer surface area, size, and hence weight of a heat exchanger for a given heat duty and pressure drop
2. An increase in heat transfer for a given size, flow rate, and pressure drop
3. A reduction in pumping power for a given size and heat duty
4. A reduction in the approach temperature difference
5. An appropriate combination of these points

While considering these benefits, the associated flow friction changes is also to be taken into account [2].

8.2 APPLICATION OF AUGMENTED SURFACES

For a two-fluid exchanger, augmentation should be considered for the fluid stream that has the controlling thermal resistance. If both resistances are approximately equal, augmentation may be considered for both sides of the exchanger. The majority of two-fluid exchanger applications are served by four basic exchanger types [5]: (1) shell and tube, (2) tube-fin, (3) brazed plate-fin, and (4) plate heat exchangers (PHEs). If enhancement is employed, it must be applied to the following three basic flow geometries [5]:

1. Internal flow in circular tubes
2. External flow normal to tubes and tube banks
3. Channel flow in closely spaced parallel plate channels, e.g., brazed plate-fin heat exchangers and PHEs

8.3 PRINCIPLE OF SINGLE-PHASE HEAT TRANSFER ENHANCEMENT

Single-phase flow can be classified as internal flow or external flow. It can be further classified as turbulent or laminar flow. The principal methods of enhancement in laminar or turbulent flow are the use of a secondary heat transfer surface and the disruption of the velocity gradient and temperature profile [6]. The three possible mechanisms for the single-phase heat transfer enhancement are decreasing the thermal boundary layer, increasing flow interruptions, and increasing the velocity gradient. The rate of heat transfer between a fluid and finned surface can be expressed in a general form as [7]

$$q = h\eta_o A \Delta T \quad (8.1)$$

where

h is the heat transfer coefficient

η_o is the overall surface efficiency

A is the total heat transfer area

ΔT is the surface–fluid temperature difference

In Equation 8.1, $h\eta_o A$ represents the surface conductance. Obviously, high performance may be achieved by using a heat transfer surface with high value of $\eta_o A$, h , or both. Special surface geometries provide enhancement by establishing a higher $h\eta_o A$ per unit surface area. Three basic principles are employed to increase $h\eta_o A$ or hA [5,7,8]:

1. Increase of A without appreciably changing h , e.g., finned tubes.
2. Increase in h without an appreciable area A increase, e.g., surface roughness or turbulence promoters. This principle is further explained in the next section.
3. Increase of both h and A , e.g., extended surfaces in compact heat exchangers have increased heat transfer coefficient by means of surface promoters such as perforations, louvers, and corrugations or displaced promoters such as canted tubes.

8.3.1 INCREASE IN CONVECTION COEFFICIENT WITHOUT AN APPRECIABLE AREA INCREASE

A surface that results in performance enhancement due to increase in the heat transfer coefficient h without an appreciable transfer area is known as an enhanced heat transfer (EHT) surface. EHT surfaces are vital to the development of heat transfer augmentation devices. The underlying principle of the EHT surface is as follows. As a reasonable approximation, the heat transfer coefficient is given by [7]

$$h = \frac{k}{\Delta} \quad (8.2)$$

where

k is the thermal conductivity of the fluid

Δ is the thermal boundary layer thickness

From Equation 8.2, it can be seen that h can be increased by altering the flow pattern near the surface in order to reduce the thermal boundary layer thickness.

8.3.2 ENHANCEMENT IN TURBULENT FLOW

Turbulent flow in a tube (after [6]) exhibits a low velocity flow region known as the laminar sublayer immediately adjacent to the wall, with velocity approaching zero at the wall. Most of the thermal resistance occurs in this low velocity region. Any roughness or enhancement technique (e.g., swirl

flow devices such as wire coil inserts, spiral inserts, and protrusions) that disturbs the laminar sublayer will enhance the heat transfer. For fully developed flow in a smooth tube, the dimensionless laminar sublayer thickness, y^* is given by

$$y^* = \frac{y\sqrt{G_c\tau_o/\rho}}{\nu} = 5 \quad (8.3)$$

Using the shear stress τ_o and ν for a smooth tube, the ratio of laminar sublayer thickness y^* to tube diameter d_i is given by

$$\frac{y}{d_i} = 25\text{Re}^{-0.875} \quad (8.4)$$

For example, if $\text{Re} = 30,000$ and $d_i = 1.0$ in. (25.4 mm), the laminar sublayer thickness is 0.003 in. (0.0762 mm). Any roughness or enhancement technique that disturbs the laminar sublayer will enhance the heat transfer.

8.3.3 ENHANCEMENT IN LAMINAR FLOW

Laminar flow generally results in low heat transfer coefficients. The fluid velocity and temperature vary across the entire flow channel width so that the thermal resistance is not just in the region near the wall as in turbulent flow. The most commonly used methods for predicting fully developed laminar flow heat transfer coefficients inside smooth, round tubes can be derived from first principles. For a uniform heat flux wall boundary condition (H) of fully developed laminar flow (both thermally and hydrodynamically), the Nusselt number is given by [9]

$$\text{Nu}_H = \frac{hd_i}{k} = 4.364 \quad (8.5)$$

The Nusselt number Nu_H is based on the hydraulic diameter, d_H (where d_i is tube inside diameter, h is convective heat transfer coefficient for a plain tube and k is thermal conductivity of the fluid). As can be seen, the heat transfer coefficient is not a function of the Reynolds number or the Prandtl number.

Similarly, for a uniform wall temperature wall boundary condition (T) of fully developed laminar flow, the Nusselt number, Nu_T , is given by [9]

$$\text{Nu}_T = \frac{hd_i}{k} = 3.657 \quad (8.6)$$

It can be seen from Eq. 8.6, the heat transfer coefficient is not a function of the Reynolds number or the Prandtl number.

To overcome the fact that laminar flow heat transfer coefficients are almost independent of fluid velocity and performance is difficult to improve using plain tubes, either inserts or external low fins or the enhancement techniques that employ swirling the flow or creating turbulence is required [6].

8.4 APPROACHES AND TECHNIQUES FOR HEAT TRANSFER ENHANCEMENT

Heat transfer enhancement mechanisms can improve the heat exchanger effectiveness of internal and external flows. Typically, they increase fluid mixing by increasing flow vorticity, unsteadiness, turbulence or by limiting the growth of thermal boundary layer close to the heat transfer surface.

The approaches followed to enhance heat transfer include heat transfer surface modifications/place-ment of displaced flow devices such as

- a. *Interruption such as slits or offset fins that interrupt the boundary layer, restarting it, creating secondary flows, etc.*
- b. *Roughness which accelerates transition from laminar flow to turbulent flow*
- c. Heat transfer surface modifications by introducing protuberances such as ridges or 3D shapes (profiles such as circular or semi circular, cube, pyramid, etc.) which generate secondary or unsteady flows
- d. Inserts placed inside flow channel so as to improve the fluid flow near the heat transfer surface or devices which create rotating and/or secondary flow inside tubes

Enhancement techniques based on these approaches may be classified as (1) passive methods, which require no direct application of external power, and (2) active methods, which require external power. The passive methods include extended surfaces, treated surfaces, rough surface or surface protuberances, displaced enhancement devices, swirl flow devices, surface tension devices, additives for fluids, additives for gases, etc. The active methods include mechanical aids, surface vibration, fluid vibration, *electrohydrodynamic (EHD) fields*, boundary layer injection, boundary layer suction, etc. The devices/methods adopted for heat transfer enhancement typically increase fluid mixing by increasing flow velocity, unsteadiness or turbulence, by limiting the growth of boundary layers close to the heat transfer surfaces. These methods are discussed in detail in Ref. [1]. Table 8.1 gives the working principle and heat transfer enhancement devices of few of the most widely used active methods. Two or more of the methods may be used to provide a “compound enhancement” greater than that of the individual method. Each method

TABLE 8.1
Passive Enhancement Techniques, Underlying Mechanism of Heat Transfer Enhancement and Enhancement Devices

Technique	Principle of Heat Transfer Enhancement	Devices
Extended surfaces	Interrupts the boundary layer, restarting it, creating secondary flows.	Tube-fin exchangers with external or internal short fins, plate-fin exchangers such as wavy fin, offset strip fin, perforated fin and louvered fin, microfin tube, <i>integral low-fin tubes (external)</i> .
Treated surfaces	Promotes turbulence.	Fine-scale alternation of the surface finish or provision of either continuous or discontinuous coating.
Surface roughness	Accelerates transition from laminar flow to turbulent flow.	Random sand-grain type roughness to discrete protuberances.
Surface protuberances	Generates secondary or unsteady flows; the ribs cause flow separation and reattachment.	Protuberances such as ridges or 3D shapes (profiles such as circular or semicircular, cube, pyramid, etc.).
Displaced enhancement devices	Interrupting the development of boundary layer of the fluid flow and increasing the degree of turbulence; causes periodic mixing of the gross flow.	Tube inserts such as wire turbulator, swirl strips, and twisted tapes. Displaced flow enhancement devices, such as streamline shape, disks, static mixer, and meshes or brushes, and wire coil inserts.
Swirl flow devices	Creates rotating and/or secondary flow inside tube.	Inlet vortex generators, twisted tape inserts, and axial core inserts with screw-type windings. Corrugated surfaces, corrugated tubes with circumferential indentations.

has its own merits and demerits. According to Bergles [4], the effectiveness of these methods depends strongly on the mode of heat transfer, which might range from single-phase free convection to dispersed-flow film boiling.

Although many enhancement techniques have been proposed and tested, only a small number are currently used in heat exchangers [1]. Of these, passively enhanced tubes are relatively easy to manufacture, cost-effective for many applications, and can be used for retrofitting existing units, whereas active methods, such as vibrating tubes, are costly and complex [10].

8.5 HEAT TRANSFER MODE

The heat transfer augmentation techniques can be applied for various heat transfer modes such as

1. Single-phase natural convection
2. Single-phase forced convection
3. Pool boiling
4. Forced convection boiling
5. Condensation

8.6 PASSIVE TECHNIQUES

8.6.1 EXTENDED SURFACES

Extended surfaces are routinely employed in compact heat exchangers and shell and tube exchangers either for liquids or for gases. The application of extended surfaces for liquid and gas service are discussed next.

8.6.1.1 Extended Surfaces for Gases

In forced convection heat transfer between a gas and a liquid, the heat transfer coefficient of the gas may be of the order of $1/50$ – $1/10$ that of the liquid, Ref. [8]. The use of extended surfaces will reduce the gas side thermal resistance. However, the resulting gas side resistance may still exceed that of the liquid.

Enhanced surface geometries on tube-fin exchangers: Enhanced surface geometries that have been used on circular tube-fin heat exchangers include [8] (1) plain circular fin, (2) slotted fin, (3) punched and bent triangular projections, (4) segmented fin, and (5) wire-loop extended surface. Some of the enhanced fin geometries of individual fins are shown in Figure 8.1 and a serrated fin tube is shown in Figure 8.2. All of these geometries provide enhancement by the periodic development of thin boundary layers on small diameter wires or flat strips, followed by their dissipation in the wake region between elements.

Enhanced surface geometries for plate-fin exchangers: Many enhanced surface geometries such as wavy fin, offset strip fin, perforated fin, and louvered fin are used on plate-fin exchangers. To be

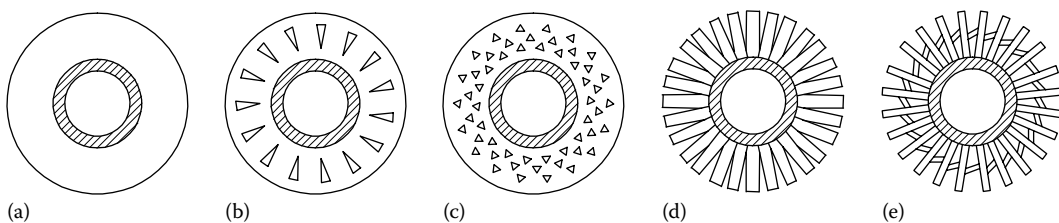


FIGURE 8.1 Externally enhanced finned tube geometries: (a) plain circular fin, (b) slotted fin, (c) punched and triangular projections, (d) serrated or segmented fin, and (e) wire-loop extended surface.



FIGURE 8.2 External enhancement-serrated fin. (Courtesy of Fintube, LLC, Tulsa, OK; www.fintubellc.com)

effective, the enhancement technique must be applicable to low Reynolds number flows. Two basic concepts have been extensively employed to provide enhancement [5,8]:

Special channel shapes, such as the wavy channel, which provide mixing due to secondary flows or boundary layer separation within the channel

Repeated growth and wake destruction of boundary layers, e.g., offset strip fin, louvered fin, pin fin, and to some extent the perforated fin

8.6.1.2 Extended Surfaces for Liquids

Extended surfaces used with liquids may be on the inner or outer surface of the tubes. Because liquids have higher heat transfer coefficients than gases, fin efficiency considerations require shorter fins with liquids than with gases.

Internally extended surfaces: Widely varied integral internally finned tubes (Figures 8.3 and 8.4) have been developed for tubeside heat transfer augmentation, and they are commercially available in copper and aluminum. Most of them are for single-phase flows. In recent years, tubes with special internal geometries for augmentation of boiling in refrigeration systems have been developed. Typical, commercial names include Thermofin tubes A, B, EX, and HEX. Other possible methods for tubeside augmentation include internal roughness geometries and inserts such as twisted tape inserts and wire coil inserts. Few forms of internal enhancement tubes are shown in Figure 8.5.

Microfin tube: The current trend for enhancement of in tube evaporation of refrigerants is toward the use of *internal microfin tubes*. The reasons for their popularity are the fact that (1) they increase heat transfer significantly while only slightly increasing pressure drop and (2) the amount of extra material required for microfin tubing is much less than that required for other types of internally finned tubes [11]. Consider microfin tubes when shellside heat transfer is controlling, expensive materials of construction are required, debottlenecking an existing exchanger, retrofitting or upgrading with new tube material, and meeting a stringent space or weight requirement.

Microfin tubes are available primarily in copper and also becoming available in other materials, such as aluminum, carbon steel, steel alloys, etc. For instance, Wolverine Tube Inc., HPT, *High performance tube* (Fine-Fin® types include 30FPISmoothBore, 28FPISmoothBore, 26FPISmoothBore, 36FPISmoothBore, 43FPISmoothBore) are few of the major manufacturers of microfin tubes for the air-conditioning and refrigeration industries/chemical process industries. Possible tube materials are carbon steels, titanium, zirconium, nickel alloys, stainless steel, monel alloy400, copper nickel, etc. Wolverine seamless microfin tubes are produced by drawing a plain copper tube over a mandrel to form helical fins. This production method allows microfins to be produced from about 0.1 to 0.4 mm

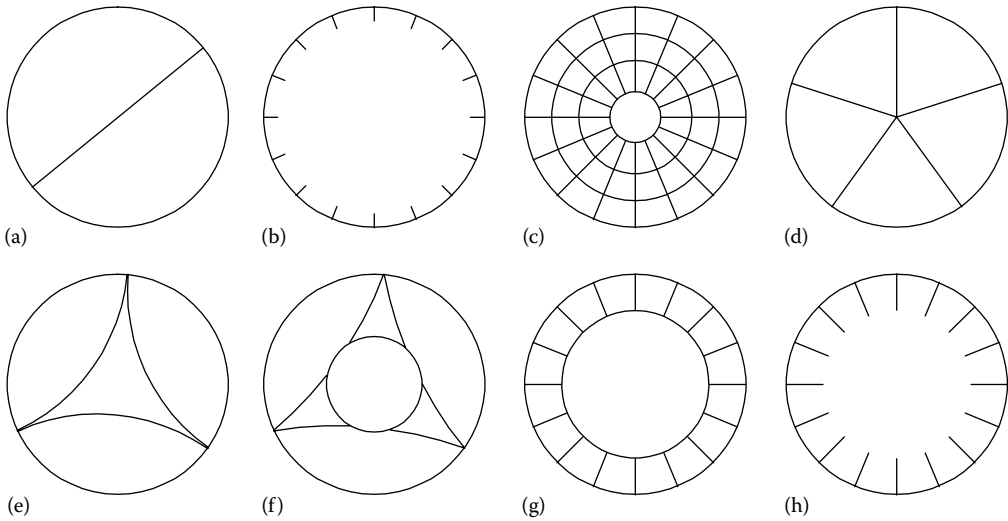


FIGURE 8.3 Representative commercially available tubes with internal enhancement. (a) Twisted tape insert in plain tube, (b) spiral internally finned tube, (c) quintuplex finned tube, (d) star-shaped insert in plain tube, (e) amatron internally finned tube, (f) corrugated tube, (g) duplex internally finned tube, and (h) straight internally finned tube. (Adapted from Marner, W.J. et al., *Trans. ASME J. Heat Transfer*, 105, 358, 1983.)

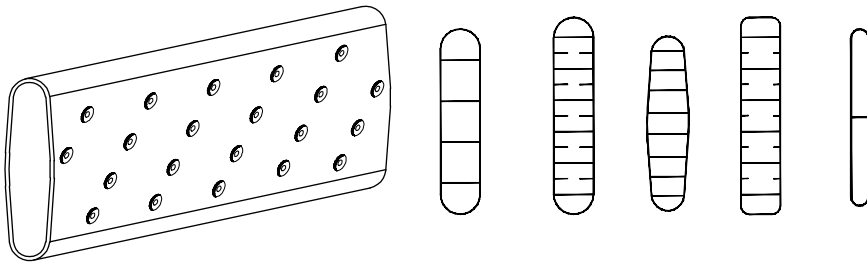


FIGURE 8.4 Representative commercially available aluminum tubes with internal enhancement.



FIGURE 8.5 Internal enhancement tubes—X-ID tubes (shows microfin tube, repeated rib roughness, and spirally fluted tube). (Courtesy of Fintube, LLC, Tulsa, OK; www.fintubellc.com)

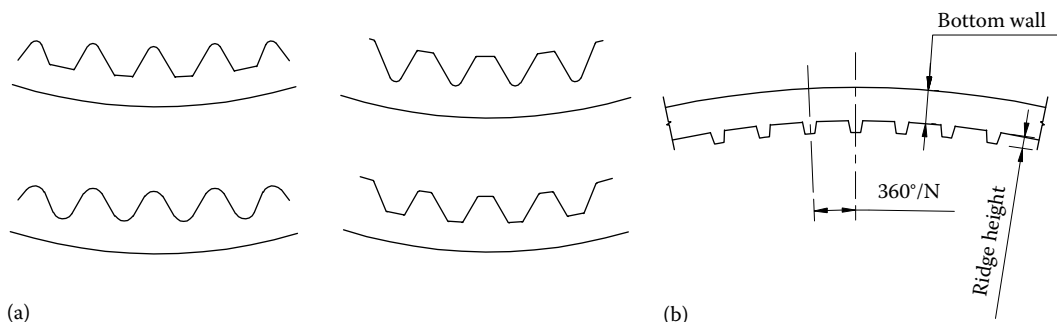


FIGURE 8.6 Fin profiles of microfin tubes used in refrigerant evaporators and condensers. (a) Fin profiles—triangular, wavy, and trapezoidal and (b) fin details. *Note:* N is integral fins density.

(0.004–0.016 in.) in height. The most favorable helix angles for heat transfer and pressure drop range from about 7° to 23° , but 18° seems to be most popular [1,12]. Instead, welded microfin tubes are formed from copper strip, whose microfin geometry has been embossed by a rolling operation. This manufacturing method allows a much wider range of microfin geometries to be produced, including 3D fin geometries. Figure 8.6 shows the fin profile of a microfin tube. The parameters which define its geometry are outside diameter, maximum internal diameter, helix angle, fin height and fin thickness, and fin's cross-sectional shape. Most microfins have approximately a trapezoidal cross section with a rounded top and rounded corners at the root. Other shapes are triangular, rectangular, and screw type, and fin height is about 0.2–0.3 mm (0.008–0.012 in.).

Integral low-fin tubes: Low-fin tubes are generally 0.75, 1 in. (19.2, 25.4 mm) OD with a typical maximum fin height of 0.059 in. (1.5 mm), the fin thickness is of 0.3 mm (0.012 in.), and fin densities are 11, 16, 19, 26, 28, 30, 32, 36 fpi, etc. Up to 19 fpi, the fin profiles are deeper made of softer materials and from 26 to 36 fpi shallow fin profiles made in materials such as stainless steels, titanium, nickel, zirconium, etc. Tube materials include carbon steel, austenitic stainless steels such as 304, 304L, 316, 316L, 321, etc.; duplex stainless steel; 6 Mo super austenitic stainless steel such as AL-6XN, copper alloys; nickel alloys such as Monel and cupronickel; titanium; and zirconium. An integral low-fin tube is ideally suited for a shell and tube exchanger. The outside surface of the low-fin tube is typically three times that of a plain tube. Tube diameters are the same as plain tubes; this permits low-fin and plain tubes to be interchangeable. Typical integral low-fin tube is shown in Figure 8.7. The general thermodynamic criteria for applying low-finned integral fin tube are [9] as follows:

1. Low shellside heat transfer coefficient—wherever the shellside heat transfer coefficient is approximately one third or less that of tubeside.
2. Large heat duty.
3. If the process stream on shellside involves condensation, evaporation, or gas cooling and the tubeside has cooling water or condensing steam.

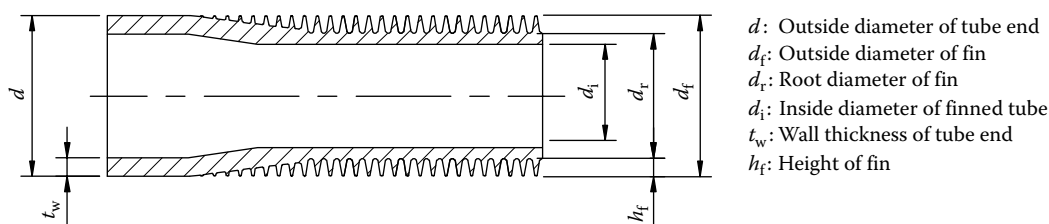


FIGURE 8.7 Integral low-fin tube.

4. Cases involving sensible heating or cooling of viscous fluids on the shellside.
5. In applications where corrosive fluid necessitates the use of titanium, zirconium, nickel alloys, hastelloy, etc. tubing, minimizing the cost of heat transfer surface area is a critical concern.
6. Debottlenecking existing heat exchanger performance.

The integral low-fin tube is also effective with compressed gases, namely, in intercoolers and after-coolers and they are employed in condensing and evaporating duties, particularly with refrigerants and hydrocarbons [7]. Low-fin tubes are used for applications such as [13]

1. Sensible heat applications like cooling of gases or viscous fluids.
2. Condensing fluids with relatively low surface tension; low-fin tubes can enhance condensing heat transfer typically by about 30%.
3. Boiling—low-fin tubes permit nucleate boiling at lower temperature differences than can be achieved with plain tubes.
4. Fouling fluids—fouling is not accelerated with low-fin tubes; it is often reduced. Low-fin tubes are more easily cleaned by chemical or mechanical means than are plain tubes.

8.6.2 TREATED SURFACES

Treated surfaces involve fine-scale alternation of the surface finish or provision of either continuous or discontinuous coating. Treated surfaces such as hydrophobic coatings and porous coatings (Figure 8.8) are most effective for phase changes but are not applicable to single-phase convection. The roughness height is below that which affects single-phase heat transfer [1].

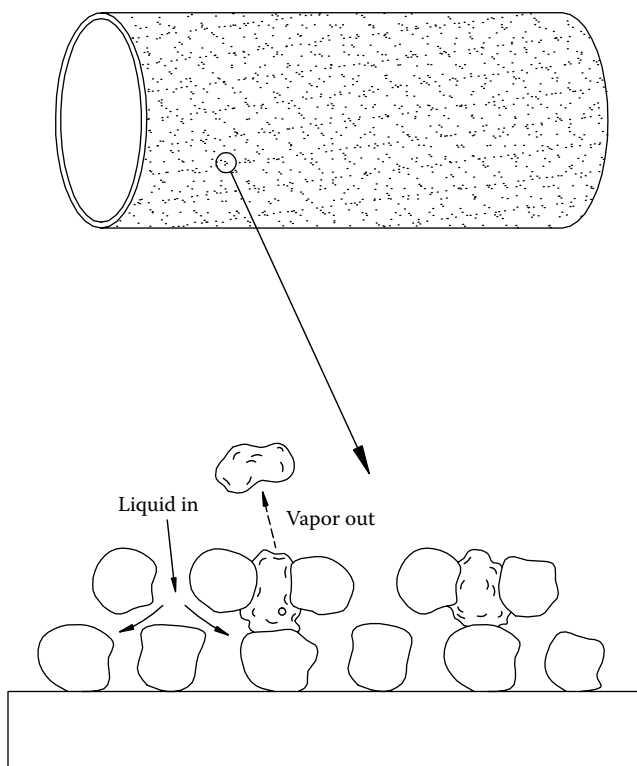


FIGURE 8.8 Treated heat transfer surface.

8.6.3 ROUGH SURFACES

Rough surfaces refer to tubes and channels having roughness elements in the form of regularly repeated ridge-like protrusions perpendicular to the stream direction. The configuration is generally chosen to promote turbulence rather than to increase the heat transfer surface area. The surface roughness may be applied to any of the usual prime or extended heat exchange surfaces [1,8]:

1. Flat plates
2. Circular tubes
3. Annuli having roughness on the outer surface of the inner tube
4. Fins

Rough surfaces are produced in many configurations, ranging from random sand-grain type roughness to discrete protuberances. Helical repeated rib roughness as shown in Figure 8.9 is readily manufactured and results in good heat transfer performance in single-phase turbulent flow without severe pressure drop [14]. The principal parameters are ridge height e , pitch p , and *helix angle* β (Figure 8.9a). The internal area ratio relative to a plain tube of the same diameter ranges from about 1.3 to 2.0. The internal fins can be of various cross-sectional shapes such as square, rectangle, triangular, semicircular, arc, sine wave, etc. [15]; Figure 8.9 shows square, semicircle, and round profile repeated rib ridges. Few of the leading helical internal fin tube manufacturers are Fintube LLC and Wolverine Tube Inc. (Helical internal fins or ribs are referred to as ridges in Wolverine Tube literature which includes low-finned tubes such as Turbo-Chil[®] and S/T Trufin[®] and to enhanced boiling and condensing tubes, such as the various versions of Turbo-B[®] and Turbo-C[®].)

Repeated rib roughness tubes are shown in Figure 8.10. The main effect on heat transfer is that the ribs cause flow separation and reattachment (as shown in Figure 8.11a) and flow pattern over helical ribs (as shown in Figure 8.11b). Both 2D and 3D integral roughness elements are also possible. Within the category of surface roughness, a 3D roughness of the sand-grain type appears to offer the highest performance [15]. Roughness elements have been produced by the traditional processes of machining,

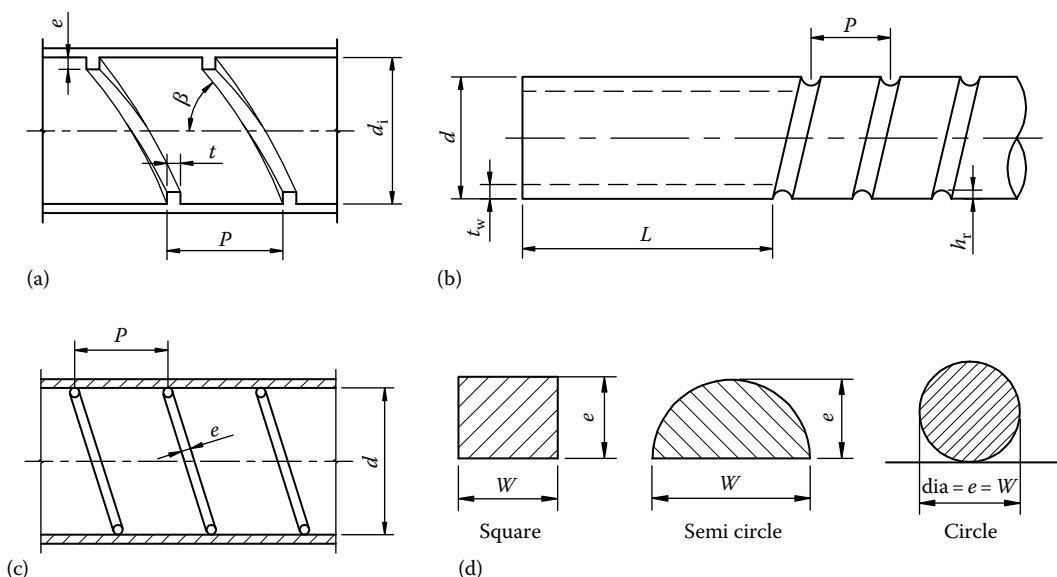


FIGURE 8.9 Internal enhancement by repeated rib roughness. (a) Square ridge, (b) semi circle, (c) circular, and (d) details of repeated rib roughness. *Note:* d -tube outer diameter or coil diameter, d_i -tube inner diameter- d of item c is to be read as d_i , e -protuberance thickness, h_r -rib depth, L -unfinned tube length, p -rib pitch, t -rib thickness, t_w -tube wall thickness, W -protuberance width and β helix angle of the rib.)

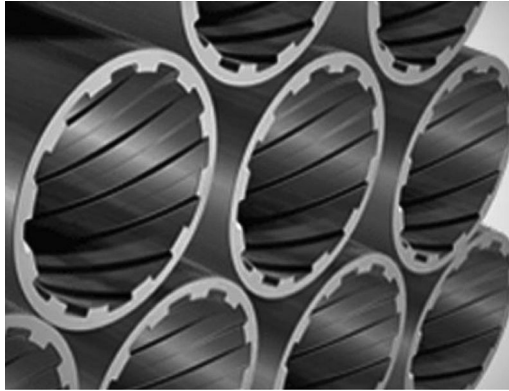


FIGURE 8.10 Internal enhancement by repeated rib roughness—X-ID tubes with repeated rib roughness. (Courtesy of Fintube, LLC, Tulsa, OK; www.fintubellc.com)

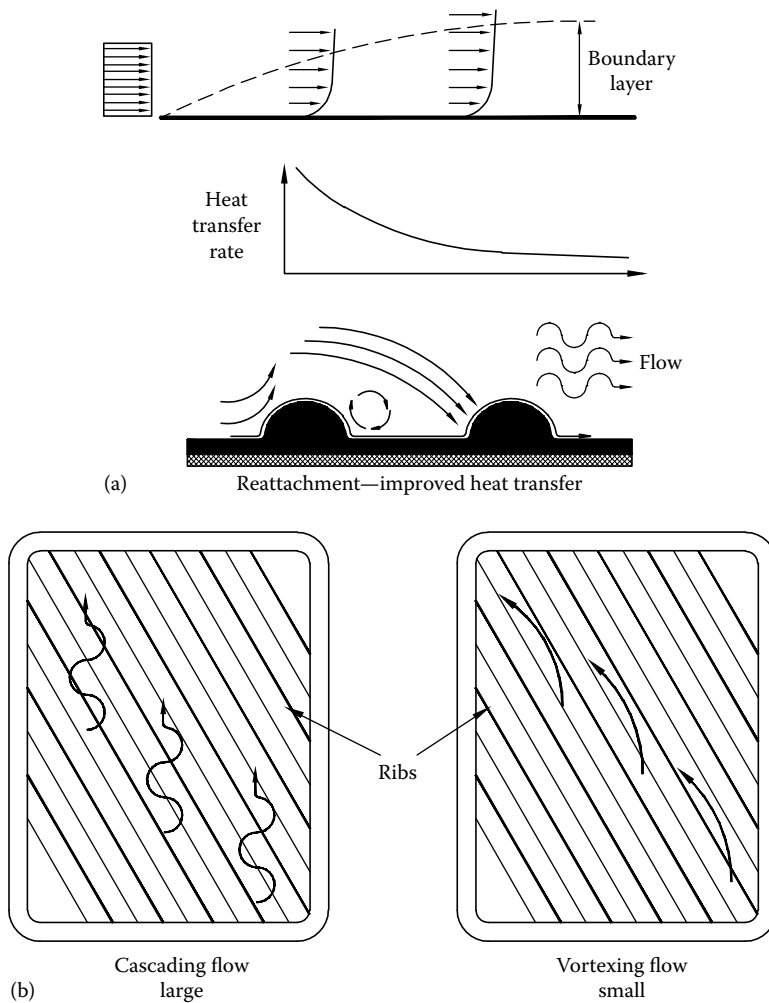


FIGURE 8.11 Principle of heat transfer enhancement of an X-ID tube: (a) developing boundary layer over smooth surface and disruption of boundary layer over ribs and (b) flow pattern over ribs. (Courtesy of Fintube, LLC, Tulsa, OK; www.fintubellc.com)

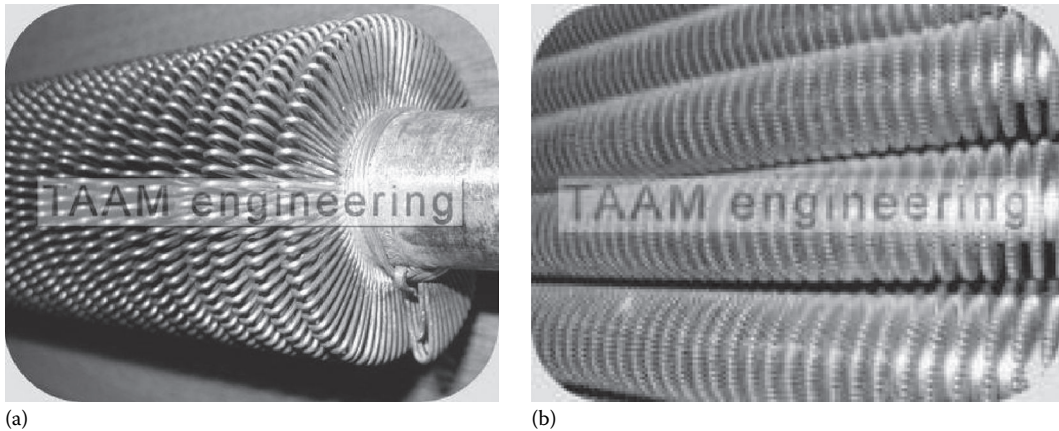


FIGURE 8.12 (a and b) Wire-loop wound fin tube. (Courtesy of TAAM Engineering, Sinnar, Maharashtra, India.)

forming, casting, or welding [7]. Various inserts or wrap-around structures such as wire-wound fin tube (Figure 8.12) can also provide surface protuberances [1].

Applications: Surface roughness is attractive for turbulent-flow applications with high Prandtl number fluids [15]. In laminar-flow applications, small-scale roughness is not effective, but twisted tape inserts and internally finned tubes appear to be the favored augmentation techniques [5].

8.6.4 TUBE INSERTS AND DISPLACED FLOW ENHANCEMENT DEVICES

This class refers to devices that are inserted inside a smooth tube. The tube inserts are relatively low in cost, relatively easy to insert and to take out of the tubes for cleaning operations.

8.6.4.1 Enhancement Mechanism

Tube inserts can create one of or some combinations of the following conditions, which are favorable for enhancing the heat transfer with a consequent increase in the flow friction [16]:

1. Interrupting the development of boundary layer of the fluid flow and increasing the degree of flow turbulence
2. Increasing the effective heat transfer area if the contact between the tube inserts and the tube wall is excellent
3. Generating rotating and/or secondary flow

8.6.4.2 Forms of Insert Device

Various forms of insert devices are [8] as follows:

1. Devices that cause the flow to swirl along the flow length, e.g., swirl strips and twisted tapes
2. Extended surface insert devices that provide thermal contact with the tube wall (this may also swirl the flow), e.g., star inserts
3. Wall-attached insert devices that mix the fluid at the tube wall
4. Displaced insert devices that are displaced from the tube wall and cause periodic mixing of the gross flow

8.6.4.3 Displaced Flow Enhancement Devices

Displaced flow enhancement devices are inserted into the flow channel so as to improve the fluid flow near the heat transfer surface [17]. These devices include [8] streamline shape, disks, static mixer, and meshes or brushes, and wire coil inserts.

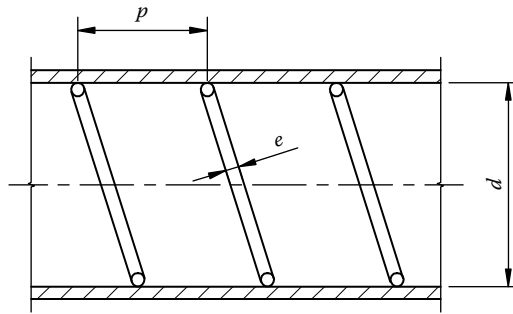
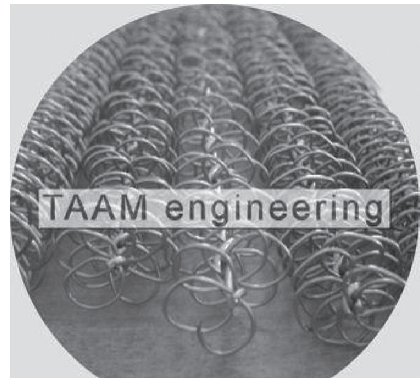


FIGURE 8.13 Wire coil insert details. *Note:* d is to be read as d_i .

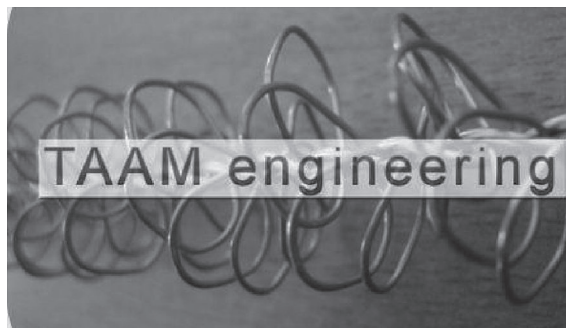
Coil inserts: Coil inserts provide an efficient and inexpensive way to enhance the heat transfer inside heat exchanger tubes [18]. Figure 8.13 shows schematic of coil insert and Figure 8.14 shows wire coil matrix as turbulator. In applications that require frequent cleaning, their easy-to-retrofit characteristic offers a significant advantage over integrally enhanced tube types; however, the coil inserts can have an inherent disadvantage if imperfect contact exists between the coil and the tube wall. For inserts, the parameters that affect the enhancement are the disruption height, the disruption spacing or pitch, the helix angle, and the disruption shape [10]. Wire coil enhances the heat transfer in turbulent flow efficiently. It performs better in turbulent flow than in laminar flow. Tube inserts normally have pull rings or attachments to install them, fix them in place, and to remove them for cleaning.



(a)



(b)



(c)

FIGURE 8.14 Wire matrix turbulators. (Courtesy of TAAM Engineering, Sinnar, Maharastra, India.)

8.6.4.3.1 hiTRAN Thermal Systems

Poor tubeside performance can usually be avoided by considering the use of heat transfer enhancement devices. Engineered devices such as hiTRAN Matrix Elements as shown in Figure 8.15a invariably provide increased heat transfer coefficients relative to plain tubes. Graphical representation of plain tube and hiTRAN Matrix Elements—enhanced performance range is shown in Figure 8.15b. When fluid flows through a plain tube, the fluid nearest to the wall is subjected to frictional drag, which has the effect of slowing down the fluid at the wall. This laminar boundary layer can significantly reduce the tubeside heat transfer coefficient and consequently, the performance of the heat exchanger. Inserting correctly profiled hiTRAN Matrix Elements which consists of a unique

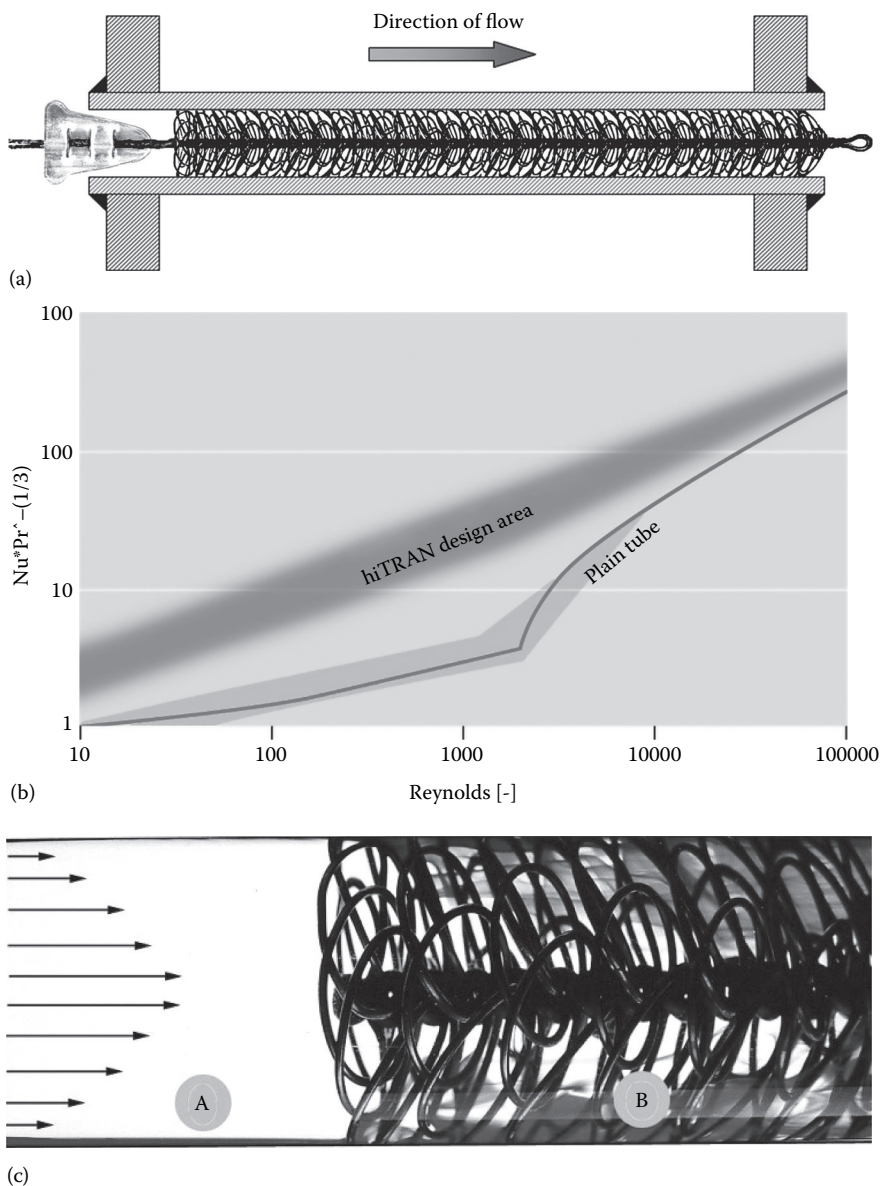
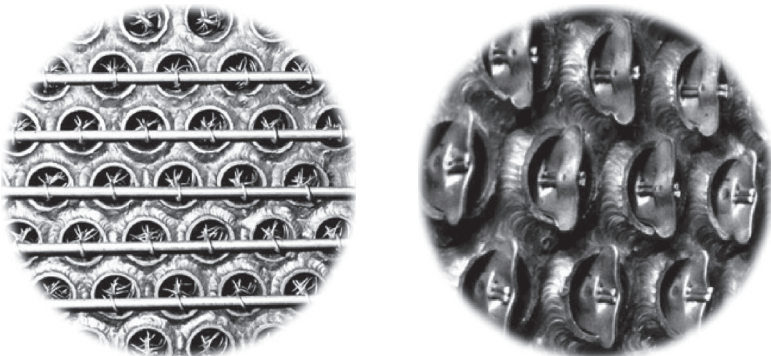


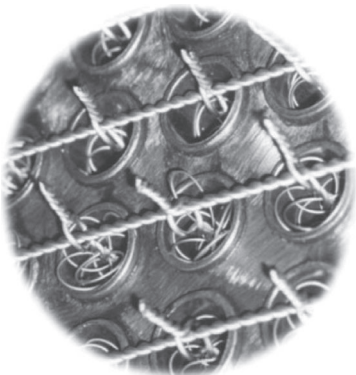
FIGURE 8.15 hiTRAN Matrix Elements—wire matrix turbulator. (a) Placement of hiTRAN matrix element in a tube; (b) hiTRAN system performance graph; (c) flow disruption caused by hiTRAN Matrix Elements; (A) laminar flow conditions; (B) turbulence caused by the use of hiTRAN matrix element tube inserts.



(d)



hiTRAN Matrix Elements held in place with key wire hiTRAN Matrix Elements held in place with core anchors



(e)

hiTRAN Matrix Elements held in place with fixing rods

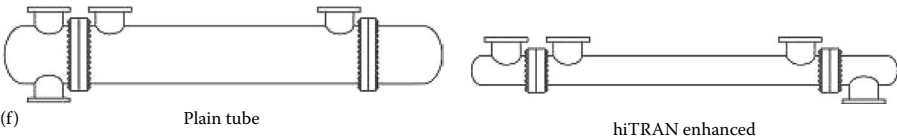
FIGURE 8.15 (continued) hiTRAN Matrix Elements—wire matrix turbulator. (d) Placement of hiTRAN Matrix Elements in a shell and tube heat exchanger; (e) hiTRAN Matrix Elements being held in place with key wire, core anchor, or fixing rods.

(continued)

Improved Design for the Shell and Tube Heat Exchanger Cooling Heavy Cycle Gas Oil Fluid
Catalytic Cracking Unit of an Oil Refinery

Design Comparison	Plain Tube	hiTRAN Enhanced
TEMA designation	BEM	BEM
Shell diameter (mm)	1524	689
Number of tubes	1828	371
Number of tube passes	8	1
Tube length (mm)	6096	6096
Length of flow path (m)	48.8	6.1
Tube diameter (mm)	25.4	25.4
Effective surface area (m ²)	874	178.5

Performance Details	Plain Tube	hiTRAN Enhanced
Prandtl number (in/out)	170/3800	170/3800
Reynolds number (in/out)	306/14	190/8
Overall service co-efficient (W/m ²)	40	182
Tubeside co-efficient (W/m ²)	51	295
Tubeside pressure drop (kPa)	70	70



Improved Design for an Air-Cooled Lube Oil Cooler Installed on a Gas Turbine-Driven Compressor

Design Comparison	Plain Bore-Finned Tube	hiTRAN System
Number of tubes/row	46	30
Number of rows of tubes	6	3
Tube length (mm)	7925	3350
Number of tube passes	6	1
Flow length (m)	47.55	3.35
Heat transfer rate (W/m ² K) finned surface	3.29	20.95
Number and size off fans (mm)	2 × 2250	2 × 1250
Approximate total fan power (kW)	11.8	5.0
Plot area (m ²)	23.40	8.12
Finned surface (m ²)	3058.3	563.2
Oil pressure drop (kPa)	71	71
Weight (kg)	8500	2200

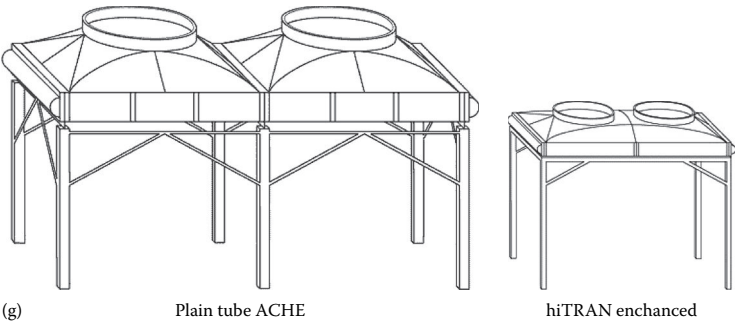


FIGURE 8.15 (continued) hiTRAN Matrix Elements—wire matrix turbulator. (f) Shell and tube heat exchanger comparison with and without hiTRAN systems; (g) air-cooled lube oil cooler comparison with and without hiTRAN System. (Courtesy of Cal Gavin Ltd, Alcester, Warwickshire, U.K; www.calgavin.com)

wire turbulator into the tube will disrupt the laminar boundary layer, creating additional fluid shear and mixing, thereby minimizing the effects of frictional drag. The working principle of hiTRAN Matrix Elements is shown in Figure 8.15c, hiTRAN Matrix Elements are particularly effective at enhancing heat transfer efficiency in tubes operating at low Reynolds numbers (laminar to transitional flow); although the heat transfer increase is greatest in the laminar flow region (up to 20 times), significant benefits can be obtained in the transitional flow regime (up to 15 times), and turbulent flow regime (up to 3 times). Cal Gavin has installed hiTRAN Systems in heat exchangers operating with Reynolds numbers from 1 to over 100,000. While there is an increase in frictional resistance associated with hiTRAN systems, the amount of enhancement is such that solutions can be found which offer increased heat transfer at equivalent or lower pressure drop than a plain tube.

8.6.4.3.2 New Heat Exchanger Design

Many tubular heat exchanger designs can be improved by the application of hiTRAN Thermal Systems. The best results are obtained where the tubeside heat transfer is limiting, and substantial reductions in required surface area can be achieved. hiTRAN Thermal Systems can provide a practical and economical solution to problems such as fouling mitigation, maldistribution, turndown, performance, energy savings, etc.

8.6.4.3.3 Maldistribution

Where tubeside maldistribution is suspected to be a problem, hiTRAN Thermal Systems have proved beneficial, both in new designs and in retrofit. In retrofits, the increased flow resistance of the hiTRAN Thermal System can be used to correct an existing maldistribution problem. In addition to correcting the maldistribution, the retrofit will also increase the heat transfer rate leading to significantly improved performance at very modest cost.

8.6.4.3.4 Turndown Operation

For fully turbulent flow, the performance of a heat exchanger will be proportional to the flowrate. If, however, turndown conditions are such that the tubeside flow regime drops into the transitional or laminar region, the performance can become more difficult to predict and control. Small changes in throughput can lead to large changes in heat exchanger outlet temperatures.

8.6.4.3.5 Installation of hiTRAN Matrix Elements

hiTRAN Matrix Elements are easily fitted and removed. Elements are specially designed to be flexible for ease and speed of installation, even where access is very confined. This flexibility also allows the system to adjust to any tube diameter tolerances. For new equipments, the exchanger fabricator will carry out the installation after completion of the bundle. In respect to U-tubes, hiTRAN Elements can be fitted into the straight leg by pushing instead of being pulled into place. The elements will be manufactured with a looser fit and one leg of each tube will have the element fitted in the opposite direction. hiTRAN Matrix Elements can be easily fitted (Figure 8.15d) in the field provided the tubeside has been effectively cleaned and held in place with fixing rods as shown in Figure 8.15e.

8.6.4.3.6 Benefits

The enhanced performance of hiTRAN Thermal Systems brings a range of benefits in the design and operation of tubular heat exchangers. This, in turn, delivers benefits to the process plant as a whole. A selection of the benefits provided are described next: reduced number of shells in series, lower weight due to smaller shell diameters, and reduced plot space due to shorter tube lengths. As far as air-cooled heat exchangers are concerned, the benefits are reduced plot space requirement, fewer tube rows and tube passes, lower fan power requirement, and reduced fan noise. Figure 8.15f shows reduction in shell size and Figure 8.15g shows reduction in size of air-cooled heat exchanger for typical cases due to installation of hiTRAN Thermal Systems.

8.6.4.3.7 Materials of Construction

hiTRAN Matrix Elements can be manufactured from a wide range of materials, including most grades of stainless steel, low carbon steel, hastelloy, titanium, tantalum, monel, inconel, and copper-based alloys for general corrosion resistance; the most common material used is stainless steel Grades 304 and 316.

Inserts for heating/cooling mode operation: In the heating mode operation, the rotating flow is noted to have favorable centrifugal convection effect, which can increase the heat transfer coefficient, whereas in the cooling mode operation, the rotating flow may have an adverse centrifugal convection effect, which even may decrease the convection heat transfer coefficient [16]. Thus tube inserts that can generate rotating flow, such as swirl strips or twisted tapes, are generally not used in oil coolers; instead, coil or spiral springs are used, since spiral springs usually do not generate rotating flow.

8.6.5 SWIRL FLOW DEVICES

Swirl flow devices include a number of geometric arrangements or tube inserts for forced flow that create rotating and/or secondary flow inside tube. Such devices include inlet vortex generators, twisted tape inserts, and axial core inserts with screw-type windings [1,16]. The augmentation is attributable to several effects [1]: increased path length of flow, secondary flow effects, and, in the case of tapes, fin effects.

8.6.5.1 Twisted Tape Insert

In the design of a laminar flow heat exchanger, twisted tape (Figure 8.16) can be used effectively to enhance the heat transfer. Twisted tapes are simple enhancement devices which can be installed into new or existing tubular exchangers. Twisted tape enhancement is achieved by inducing swirl flow in the tubeside fluid and offers a modest increase in heat transfer at low additional pressure loss. The width of the metal strip of twisted tape is equal to or less than the internal diameter of the duct depending upon whether the tape is loosely, snugly, or tightly fitted inside the tube. The twist ratio is defined as the axial length of tape necessary to make a 180° turn divided by the tube internal diameter. A twisted tape insert mixes the bulk flow well and therefore performs better in a laminar flow than any other insert. Compared with wire coil, twisted tape is not effective in turbulent flow because it blocks the flow and therefore the pressure drop is large. They are fully removable for cleaning. They are secured at the tube ends by rods or thick wires as shown in Figure 8.17.

8.6.5.2 Corrugated Surfaces

Corrugated tubes (e.g., Wolverine Korodense®) are associated with circumferential indentation (as shown in Figures 8.18 and 8.19) or spiral indentation (spirally fluted) tubes as shown in Figure 8.20. Figure 8.21 shows a collection of fluted enhanced fin tubes. Corrugated tubes are manufactured from copper, copper alloys, carbon steels, stainless steels, and titanium. The corrugations are defined by the corrugation pitch, corrugation depth, and the number of corrugations. Multistart corrugated tubes with large corrugation depths are typically referred to as fluted tubes. Most corrugated tubes have a

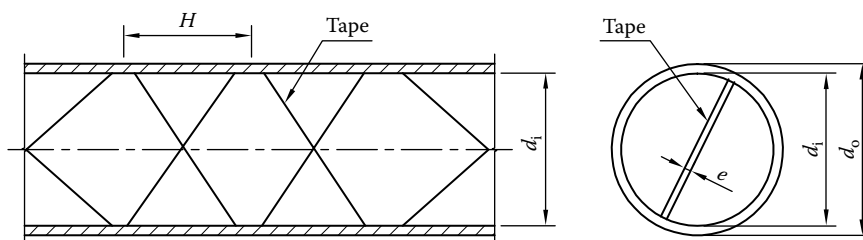


FIGURE 8.16 Twisted tape details. (Note: H is tape twist pitch length.)

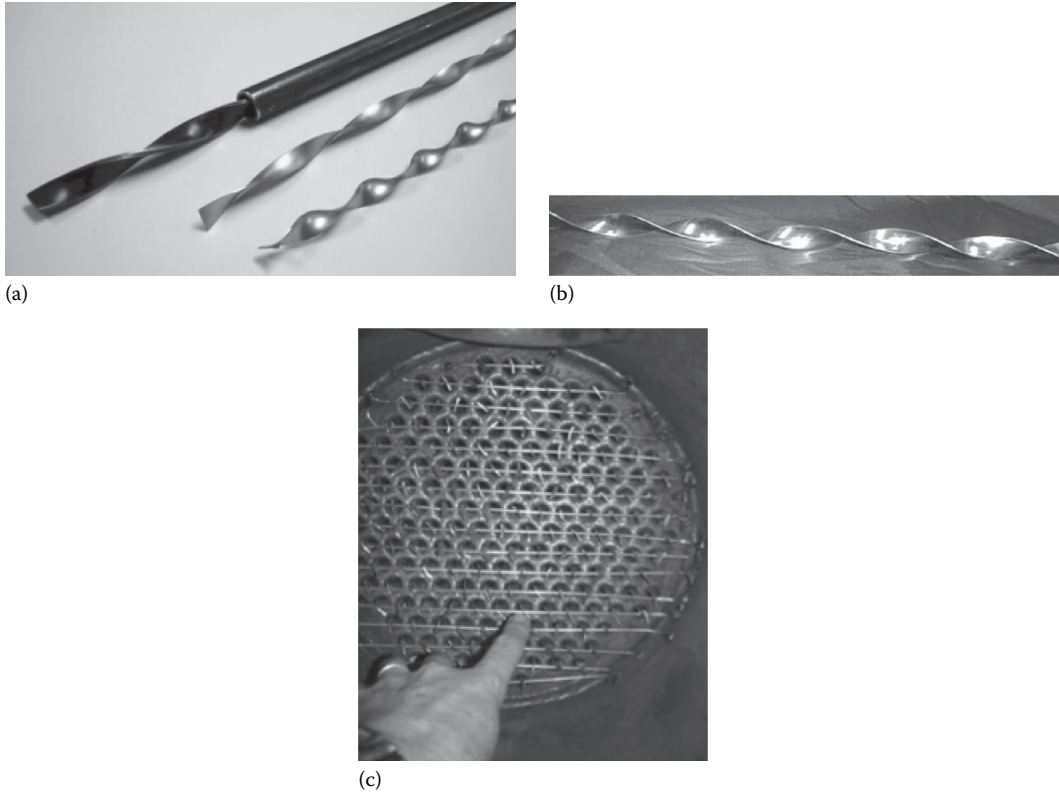


FIGURE 8.17 Twisted tapes installation. (a) Twisted tapes and (b) twisted tapes installed on tubeside held by fixing rods. (Courtesy of Peerless Mfg. Co. of Dallas, TX, makers of Alco and Bos-Hatten brands of heat exchangers.)

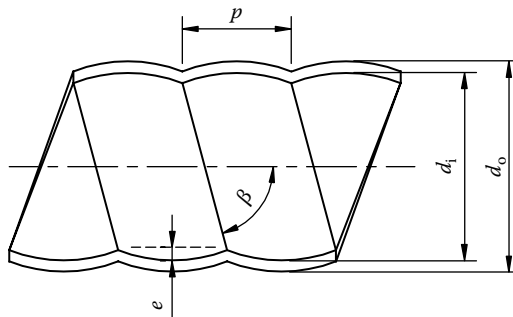


FIGURE 8.18 Corrugated tube details.

single start of corrugation that is defined by its depth e and its axial pitch p and helix angle β , as shown in Figure 8.18. The axial corrugation pitch is related to the internal diameter d_i , helix angle β relative to the axis of the tube, and the number of starts n_s , by the following equation

$$p = \pi d_i / n_s \tan \beta \quad (8.7)$$

The external diameter over the corrugations on the outside of the tube is equal to that of the plain ends of the tube. The internal diameter is taken as the external diameter less twice the tube wall thickness. The maximum internal diameter is typically used to define the internal heat transfer coefficient.



FIGURE 8.19 Corrugated tube—TEK tube—SA-214 heat exchanger tubes. (Courtesy of Fintube, LLC, Tulsa, OK; www.fintubellc.com)

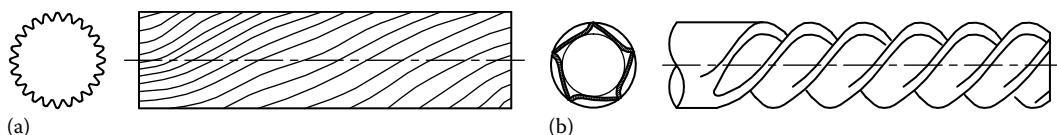


FIGURE 8.20 Spirally fluted tubes. (a) External helical rib and (b) both internally and externally corrugated tube (schematic).

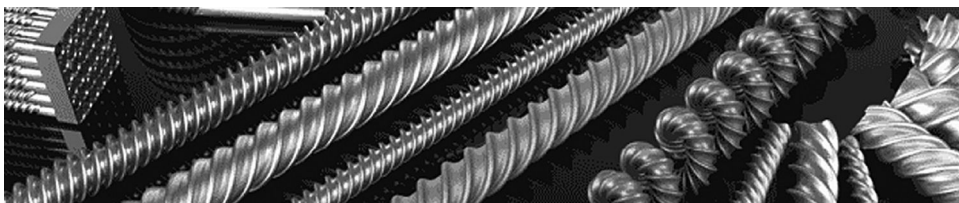


FIGURE 8.21 Spirally fluted tubes—a collection of enhanced fin tubes. (Courtesy of Turbotec Products, Inc., Windsor, CT.)

Among the corrugated tubes, spirally corrugated tubes provide several advantages over other rough surfaces. They have easier fabrication, limited fouling, and higher enhancement in the heat transfer rate compared to increase in the friction factor [19].

Flows in corrugated channels are associated with secondary flows, suppression of the secondary flow by counteracting centrifugal forces, and destruction of the secondary flow by the onset of turbulence [7]. In condensing services, corrugated tubes increase the heat transfer coefficient because only a thin film of the liquid condensate is left on the crests, while most of it drains into the troughs due to the surface tension and gravity effects. The thin film offers very little resistance, and hence the condensing coefficient is very high.

8.6.5.3 Doubly Enhanced Surfaces

If enhancement is applied to both the inner and outer tube surfaces, doubly enhanced tube results. Doubly enhanced tubes are beneficial in cases where maximum reduction of heat exchanger size is of critical importance. The ID fins with helical rib contribute added surface area (30%–40% approximately) but more significantly the change in the fluid flow pattern, viz., promotes mixing and turbulent flow. Applications for such doubly enhanced tubes include heat exchangers using sea water as a cooling medium, chemical industries, and condenser and evaporator tubes. Typical forms of doubly enhanced tubes include [8] the following: (1) helical rib roughness on inner surface and integral fins on outer surface, (2) internal fins on inner surface and porous boiling coating on outer surface, (3) twisted tape insert on inner surface and integral fins on outer surface, (4) corrugated roughness on inner and outer surfaces, and (5) corrugated tubes. Figure 8.22 shows few of the doubly enhanced tubes.

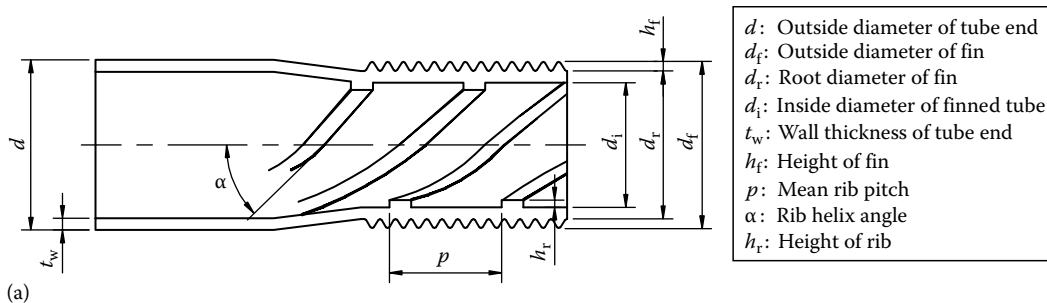


FIGURE 8.22 Doubly enhanced tubes: (a) integral fin tube with helical ribs on the inside and (b) thermofin integral turbulator. (From Thermofin; www.thermofin.net)

8.6.5.4 Turbulators

Turbulators are made from a narrow, thin metal strip bent and twisted in zig-zag fashion to allow periodic contact with the tube wall. A popular technique for enhancement of heat transfer in fire tube boilers is to introduce turbulators into the boiler tubes to increase the gas side heat transfer coefficients, thereby increasing heat recovery from flue gases [20]. This will reduce fuel consumption and improve boiler efficiency.

8.6.6 SURFACE TENSION DEVICES

Surface tension devices consist of relatively thick wicking material or grooved surfaces on heat transfer devices to direct the flow of liquid in boiling and condensing.

8.6.7 ADDITIVES FOR LIQUIDS

Additives for liquids are liquid droplets for boiling, solid particles in single-phase flow, and gas bubbles for boiling.

8.6.8 ADDITIVES FOR GASES

Additives for gases are liquid droplets or solid particles, either dilute phase (gas–solid suspensions) or dense phase (fluidized beds).

8.7 ACTIVE TECHNIQUES

The active techniques are (after Bergles [1,21]) described next.

1. *Mechanical aids* stir the fluid by mechanical means or by rotating the surface or by surface scraping. Surface scraping is widely used for viscous liquids in the chemical process industry.
2. *Surface vibration* (which thins or restarts boundary layer and/or induces secondary flows) at either low or high frequency has been used primarily to improve single-phase heat transfer. Possible modes of heat transfer applications are single-phase flow, boiling, and condensing.
3. *Fluid vibration* is the most practical type of vibration enhancement, given the mass of most heat exchangers. The vibrations range from pulsations of about 1 Hz to ultrasound. Single-phase fluids are primary concern. Possible modes of heat transfer applications are single-phase flow, boiling, and condensing.
4. *Electrostatic fields* (dc or ac) are applied in many different ways to dielectrics to cause greater bulk mixing of fluid in the vicinity of the heat transfer surface. An electrical field and a magnetic field may be combined to provide forced convection via electromagnetic pumping.
5. *Boundary layer injection* involves supplying gas to a flowing liquid through a porous heat transfer surface or injecting similar fluid upstream of the heat transfer section. (Enhancement is primarily for multiphase flows.) [21]
6. *Boundary layer suction* (it involves removal of boundary layer and restarts boundary layer downstream) involves either vapor removal through a porous heated surface in nucleate or film boiling, or fluid withdrawal through a porous heated surface in single-phase flow [21].
7. *Electrohydrodynamic(EHD): High voltage (>1 kV) applied to an electrode near a plate which induces secondary flows in boundary layer (applicable for liquid flows only)* [21].

The active techniques have not found commercial interest because of the capital and operating cost of the enhancement devices, complex nature, and problems associated with vibration or noise [10] or high voltage.

8.8 FRICTION FACTOR

Due to the form drag and increased turbulence caused by the disruption, the pressure drop with flow inside an enhanced tube always exceeds that obtained with a plain tube for the same length, flow rate, and diameter (after [18]). In most cases, the increase over that of plain tube is about 70%–500%, and usually exceeds the increase in heat transfer, which is about 50%–200%. However, for Reynolds number in the range of 5,000–10,000 and for fluids with Prandtl numbers greater than about 2, the heat transfer enhancement can exceed the pressure drop increase.

8.9 PERTINENT PROBLEMS

The problems related to enhanced surfaces in respect of their applications are (1) testing methods, (2) fouling, (3) performance evaluation criteria (PEC) [7], (4) market factors, and (5) mechanical design and construction considerations [21].

8.9.1 TESTING METHODS

The basis for selecting an “optimum” heat transfer surface is easy, provided generalized heat transfer and friction correlations and quantitative relations for performance evaluation are available. The multitude of augmentation devices with various surface geometries made it impossible to generalize specific correlations for j and f factors. However, this can be overcome, by devising a reliable experimental technique to determine the performance. A common method for determining turbulent-flow,

single-phase coefficients from heat-exchanger tests is the Wilson method [6]. In this method, the coefficient on one side is held constant, while the coefficient to be determined is varied by making a series of tests at different flow rates. The equation for Nusselt number describing the coefficient to be measured is of the form

$$\text{Nu} = k_1 \text{Re}^{k_2} \text{Pr}^{k_3} \quad (8.8)$$

where the constants k_2 and k_3 are known in advance. The objective of the test is to determine k_1 . As shown next, the total resistance R_T is composed of a constant resistance R_c and a variable resistance R_v , which is to be determined:

$$R_T = R_c + R_v = R_c + \frac{1}{k_1} \left(\frac{1}{k \text{Re}^{k_2} \text{Pr}^{k_3} / D_h} \right) \quad (8.9)$$

where D_h is the tube hydraulic diameter and k is the thermal conductivity of the fluid. Equation 8.6 is that of a straight line with slope $1/k_1$ and an intercept R_c .

8.9.2 FOULING

An important consideration for whether enhanced surfaces should be used is the effect of fouling on the heat exchanger performance. Fouling is a very difficult phenomenon to model and predict in general terms since its exact mechanism is specific to the process conditions. Many research programs are ongoing to study the fouling of enhanced surfaces. There are some techniques that are not affected by fouling; in some applications, fouling can be reduced by using enhanced surfaces. In general, the same factors that influence fouling on unenhanced surfaces will influence fouling of high performance surfaces [6].

8.9.3 PERFORMANCE EVALUATION CRITERIA

The basic thermohydraulic characteristic of an enhanced surface is defined by curves of the j and f versus Reynolds number. Numerous factors decide the merit of enhanced surfaces developed for augmentation of heat transfer. A PEC establishes a quantitative statement to account for the heat transfer enhancement, taking into account the pressure drop characteristics of the enhanced surface. Possible performance objectives of interest include [5,8] the following:

1. Reduced heat transfer size and hence low material requirement for fixed heat duty and pressure drop.
2. Increased UA; this may be exploited in two ways: to obtain increased heat duty and to secure reduced LMTD for fixed heat duty.
3. Reduced pumping power for fixed heat duty.

A PEC is established by selecting one of the operational variables, namely, geometry, flow rate, heat transfer rate, and fluid inlet temperature, for the performance objective subject to design constraints on the remaining variables. So far, there is no universally accepted criterion for evaluating performance, although numerous criteria have been in practice. Bergles et al. [22] reviewed these criteria, which were classified into the following three objectives: (1) increase in heat transfer, (2) reduced pumping power for fixed heat duty, and (3) reduce exchanger size for fixed heat duty and pressure drop. Shah [23] also critically reviewed more than 30 dimensional or nondimensional comparison methods.

8.9.3.1 Webb's PECs: Performance Comparison with a Reference

Webb [24] developed a number of PECs of interest with flow inside enhanced and smooth tubes of the same envelope diameter. Generally, these PECs are defined by the following three different geometry constraints:

1. *FG criteria*: The cross-sectional envelope area and tube length are held constant.
2. *FN criteria*: These criteria maintain fixed-flow frontal area and allow the length of the heat exchange to be a variable. These criteria seek reduced surface area or reduced pumping power for constant heat duty.
3. *VG criteria*: These criteria maintain constant exchanger flow rate.

The concepts of PEC analysis are explained for the case of a prescribed wall temperature or a prescribed heat flux in Ref. [8]. The heat transfer enhancement, $hA/h_p A_p = K/K_p$, in terms of Stanton number St and mass velocity G , is given by [8]

$$\frac{K}{K_p} = \frac{St}{St_p} \frac{A}{A_p} \frac{G}{G_p} \quad (8.10)$$

or

$$\frac{K}{K_p} = \frac{j}{j_p} \frac{A}{A_p} \frac{G}{G_p} \quad (8.11)$$

where the subscript p refers to the reference, or plain smooth surface and St is Stanton number, G is mass velocity and A is flow area. The relative friction power (P) is

$$\frac{P}{P_p} = \frac{f}{f_p} \frac{A}{A_p} \left(\frac{G}{G_p} \right)^3 \quad (8.12)$$

It is assumed that the smooth tube operating conditions (G_p , f_p , j_p , and St_p) are known.

The advantages of this comparison method for compact heat exchangers include [23] the following: (1) the designer can select his or her own criteria for comparison, (2) then the performance of a surface can be compared with the reference surface, and (3) there is no need to evaluate the fluid properties since they drop out in computing the comparison ratios.

8.9.3.2 Shah's Recommendation for Surface Selection of Compact Heat Exchanger with Gas on One Side

Four of the criteria recommended by Shah [23] are discussed here. These criteria require the j and f factors, and Reynolds number, together with the geometry specification. These criteria are employed for comparison of flat-tube radiators with plain fin and ruffled fin performances by Maltson et al. [25].

1. *Flow area goodness factor comparison*: The ratio of j factor to the friction factor f , against Reynolds number, generally known as the "flow area goodness factor," was suggested by London [26],

$$\frac{j}{f} = \frac{Nu Pr^{-1/3}}{f Re} = \frac{1}{Ac^2} \left[\frac{Pr^{1/3}}{2g_c} \frac{NTU M^2}{\Delta p} \right] \quad (8.13)$$

A surface having a higher j/f factor is "good" because it will require a lower free flow area and hence a lower frontal area for the exchanger.

2. *Volume goodness factor (E_{std}) comparison*: This is the standardized heat transfer coefficient against the pumping power per unit of heat transfer surface area, suggested by London and Ferguson [27]. Two types of comparison are suggested: (1) h_{std} versus E_{std} , and (2) $\eta_o h_{std} \beta$ versus $E_{std} \beta$ as given in the following:

$$h_{std} = \frac{j \text{Re} \mu_{std} C_{p, std}}{D_h \text{Pr}_{std}^{2/3}} \quad (8.14)$$

and

$$E_{std} = \frac{P_p}{A} = \frac{f \text{Re}^3 \mu_{std}^3}{2 g_c \rho_{std}^2 D_h^3} \quad (8.15)$$

3. The performance of the heat exchanger per unit volume, the criterion suggested by Shah [23]. This method includes the effect of the fin effectiveness. A good performance using this criterion gives the best heat exchanger to use where the size of the unit is an important consideration. Two types of comparison are suggested as follows: (1) h_{std} versus E_{std} , and (2) $\eta_o h_{std} \beta$ versus $E_{std} \beta$ as given in the following:

$$\eta_o h_{std} \beta = \frac{j \text{Re} (4\sigma) \eta_o C_{p, std} \mu_{std}}{\text{Pr}_{std}^{2/3} D_h^2} \quad (8.16)$$

and

$$E_{std} \beta = \frac{f \text{Re}^3 (4\sigma) \mu_{std}^3}{2 g_c \rho_{std}^2 D_h^4} \quad (8.17)$$

4. The actual heat transfer rate performance versus the gas side fan power, suggested by Bergles et al. [28].

8.9.4 MARKET FACTORS

8.9.4.1 Alternate Means of Energy Savings

The extent to which the EHT devices and techniques that affect design variables such as heat transfer efficiency and pressure drop and maintenance issues such as corrosion and fouling as compared with other performance enhancement options ultimately affects its ability to penetrate the market and appear in products. For example, heat transfer enhancement options may compete with the use of larger conventional heat exchangers and higher efficiency compressors to increase unit efficiency [21].

8.9.4.2 Adoptability to Existing Heat Exchanger

Manufacturers may be cautious about introducing novel heat transfer enhancement approaches/techniques into products. If approaches require appreciable modifications and hence to incur heavy costs to existing heat exchangers in service, the technique may not be acceptable to industries [21].

8.9.4.3 Proven Field/Performance Trials

To avoid deterioration of performance in service, manufacturers must carry out extensive laboratory and field testing to verify that the enhancements perform reliably over the range of expected operating conditions.



FIGURE 8.23 Enhanced tubes (TRU-TWIST™ tubes) with plain length at end. (Courtesy of Turbotec Products, Inc., Windsor, CT.)

8.9.5 MECHANICAL DESIGN AND CONSTRUCTION CONSIDERATIONS

Mechanical stress calculations: Burst tests with internal pressure on integral low-finned tubes have shown that the plain ends of the tube are the weakest point along the tube because the external helical fins act as reinforcement rings [21]. For most applications, the base wall thickness under the augmentation must be used for the mechanical stress calculations defined by various pressure vessel codes, such as that of ASME.

Heat exchanger fabrication: Enhanced tubes normally have plain length at each end, as shown in Figure 8.23. This allows these tubes to be rolled and/or welded into the tubesheet. The outside diameter over the finned section is equal to or slightly less than that of the plain ends. Hence, these tubes can be drawn into the tube bundle during assembly without any problems.

U-tubes: Nearly all integral heat transfer augmentations can be bent into U's-tube heat exchangers. For the minimum bending radius of a particular type of tube, one should refer to the manufacturer's recommendations.

8.10 PHASE CHANGE

Even though heat transfer with phase change is not within the scope of this book, for the sake of completion, EHT surfaces used for condensation and evaporation are mentioned. References [1,5,6] detail heat transfer enhancement techniques for phase change. One major area of application of EHT surfaces for phase change applications is in refrigeration and air-conditioning. Pate et al. [11], Bergles [1], and Ref. [9] detail the application of heat transfer enhancement techniques in refrigeration and air-conditioning industry.

8.10.1 CONDENSATION ENHANCEMENT

The heat transfer resistance in condensation of pure components is primarily due to conduction across the condensate film thickness. Condensation enhancement is generally obtained by taking advantages of surface tension forces to obtain thin condensate film or to strip condensate from the heat transfer surface. Special surface geometries or treated surfaces are effective in attaining this goal. Heat transfer enhancement is possible on either the shellside or tubeside of a condenser. Since the tube orientation will affect its condensate drainage characteristics, one must distinguish between horizontal and vertical orientations.

8.10.1.1 Horizontal Orientation

Shellside:

1. Short radial fins, fluted tubes, wires attached to tubes, modified annular fins with sharp tips on tubes [6].
2. Surfaces of doubly augmented tube geometries like helically corrugated tubes, helically deformed tubes having spiral ridges on outer surface and grooves on inner surface, or corrugated tubes formed by rolling in helical shape followed by seam welding are used [5].
3. Recent developments in extended surfaces for film condensation on horizontal tubes include Hitachi Thermoexcel-C, and the spine fin surface.

Tubeside: Closely spaced helical internal fin, twisted tape insert, repeated rib roughness, and sand-grain type roughness may be used.

8.10.1.2 Shellside Condensation on Vertical Tubes

Shellside condensation enhancement on a vertical surface can be achieved by finned tubes, fluted surfaces, and loosely attached spaced vertical wires [5].

8.10.2 EVAPORATION ENHANCEMENT

The mechanisms important for evaporation enhancement are thin film evaporation, convective boiling, and nucleate boiling [6]. Nucleate and transition pool boiling are usually dependent on the surface condition as characterized by the material, the surface finish, and the surface chemistry. Certain types of roughness have been shown to reduce wall superheats, increase peak critical heat flux, and destabilize film boiling [1]. Heat transfer augmentation techniques for thin film evaporation and nucleation are as follows:

1. Thin film vaporization: fluted vertical tubes.
2. Nucleation: For nucleation enhancement, structured surfaces are used. Structured surface refers to fine-scale alteration of the surface finish. A coating may be applied to the plain tube, or the surface may be deformed to produce subsurface channels or pores [1]. Typical structured surfaces are *enhanced surface cavities*—a pore or reentrant cavity within a critical size range, interconnected cavities, and nucleation sites of a re-entrant shape; and *integral roughness*—the three commercially used boiling surface of this type are Trane bent fins, Hitachi bent sawtooth fins, and Weiland flattened fins (T-shaped fin forming) [5].
3. Convective boiling: On the shellside, integral fins and enhanced boiling surfaces are used. On the tubeside, there are internal ridges, and axial and helical fins.
4. Flow boiling inside tubes: Linde porous coating and special internal roughness geometries.

8.10.3 HEAT TRANSFER AUGMENTATION DEVICES FOR THE AIR-CONDITIONING AND REFRIGERATION INDUSTRY

8.10.3.1 Shellside Evaporation of Refrigerants

Enhanced tubes and their commercial names include (1) modified structured surfaces with porous coatings—High Flux (Union Carbide) and (2) modified low-fin tubes such as are used for shellside evaporation of refrigerants: GEWA-T (Weiland Werke), GEWA-TX, GEWA-TXY, Thermoexcel-E (Hitachi), Turbo-B (Wolverine) [11], EverFin-40 (Furukawa Electric), and Thermoexcel-HE.

8.10.3.2 Shellside Condensation of Refrigerants

Recognition of surface tension as the dominant force for determining condensate thickness has led to the development of surfaces designed to produce thin films, and to remove condensate from the heat transfer surface. The profiles such as Thermoexcel-C (Hitachi) and Turbo-V shaped fin with a steep angle help in maintaining a thin refrigerant film.

8.10.3.3 In-Tube Evaporation of Refrigerants

In-tube enhancement devices for evaporation of refrigerants include (1) rough surfaces like helical wire inserts, internal thread, and corrugated tubes, (2) extended surfaces like microfin tubes and high-profile fins, and (3) swirl flow devices such as twisted tape inserts.

8.11 MAJOR AREAS OF APPLICATIONS

Refinery and process industries—single-phase exchangers [9]:

1. Use of integral low-finned tubes in heat exchangers when the limiting thermal resistance is on the shellside
2. Use of tube inserts (wire mesh or twisted tape types) is highly effective in laminar flows inside tubes
3. Installation of inserts on the tubeside of heat recovery units

Heating, ventilating, and refrigeration and air-conditioning: As the condensing or evaporating refrigerant temperature approaches that of the outdoor air temperature for an air-cooled condenser, the vapor compression cycle temperature difference (also referred to as the lift) decreases. This, in turn, decreases the pressure ratio across the compressor and increases its operational coefficient of performance (COP) and hence reduction in its energy consumption [21]. In the common evaporator or condenser coil, airside heat transfer is improved with louvered, corrugated, or serrated fins. Microfin configurations are usually found in evaporator or condenser applications.

Automotive industries: Radiators, charge air coolers, and intercoolers of automobiles have been provided with various forms of extended surfaces: louvered fin, offset strip fin, and low-fin tubes. On the tubeside, twisted tape inserts have received considerable attention for oil cooler applications [1].

Power sector: Integral low-finned tubes are widely used in power plant main condensers. Use of external fins shifts the controlling thermal resistance to the cooling waterside. Low-finned tubes with internal ribs are particularly suitable for this application. Installation of inserts on the tubeside (i.e., water side) of an existing steam condenser (plain or low-finned tube) increases the overall heat transfer coefficient and the vacuum in the steam chest; thus the steam turbine's power output can sometimes be increased by 0.5%–2% [9].

Process industries: The chemical process industry has sparingly adopted enhancement technology because of concerns about fouling. Wire loop inserts and vapor sphere matrix fluted spheres (tubeside) or solid spheres (shellside) not only improve heat transfer, but reduce fouling with typical process fluids [1].

Industrial heat recovery: Ceramic tubes that are enhanced externally and/or internally for high-temperature waste heat recovery are used.

Aerospace: Improved gas turbine blade cooling is achieved by transverse repeated ribs and pin fins cast into the blade, thereby reducing the wall temperature.

NOMENCLATURE

A	total heat transfer area, m^2 (ft^2)
A_c	minimum free flow area, m^2 (ft^2)
C_p	specific heat, $\text{J/kg} \cdot ^\circ\text{C}$ ($\text{Btu/lbm} \cdot ^\circ\text{F}$)
D_h	hydraulic diameter, $(4r_h)$, m (ft)
$E_{\text{std}} =$	P_p/A , Volume goodness factor or the standardized heat transfer coefficient against the pumping power per unit of heat transfer surface area as defined by Eq. 8.15
f	Fanning friction factor
G	mass velocity based on minimum flow area, $\text{kg/m}^2 \cdot \text{s}$ ($\text{lbm/h} \cdot \text{ft}^2$)
g_c	acceleration due to gravity or proportionality constant 9.81 m/s^2 (32.17 ft/s^2)
$=$	1 and dimensionless in SI units
h	convective heat transfer coefficient, $\text{W/m}^2 \cdot ^\circ\text{C}$ ($\text{Btu/ft}^2 \cdot \text{h} \cdot ^\circ\text{F}$)
hA	thermal conductance $\text{W}/^\circ\text{C}$ ($\text{Btu/h} \cdot ^\circ\text{F}$)
j	Colburn heat transfer factor
$K =$	the heat transfer enhancement factor or thermal conductance, hA as defined by Eq. (8.10)
k	thermal conductivity of the fluid, $\text{W/m} \cdot ^\circ\text{C}$ ($\text{Btu/h} \cdot \text{ft} \cdot ^\circ\text{F}$)
$k_1, k_2, k_3 =$	constants in Equation 8.9
M	mass flow rate of the fluid, kg/s (lbm/h)
NTU	number of transfer units, hA/C_p
Nu	Nusselt number
$P =$	fluid friction power
p	pressure, Pa (lbf/ft^2)
Pr	Prandtl number
Q	total heat duty of the exchanger, $\text{W} \cdot \text{s}$ (Btu)
q	heat transfer rate, W (Btu/h)
Re	Reynolds number
r_h	hydraulic radius, m (ft) $= D_h/4$
St	Stanton number
U	overall heat transfer coefficient, $\text{W/m}^2 \cdot ^\circ\text{C}$ ($\text{Btu/h} \cdot \text{ft}^2 \cdot ^\circ\text{F}$)
Δp	pressure drop, Pa (lbf/ft^2)
μ	viscosity of the fluid at bulk mean temperature, $\text{kg/m} \cdot \text{s}$ or $\text{Pa} \cdot \text{s}$ ($\text{lbm/h} \cdot \text{ft}$)
ρ	fluid density, kg/m^3 (lbm/ft^3)
β	area density, m^2/m^3 (ft^2/ft^3)
$\Delta p =$	pressure drop
η_o	fin efficiency or the overall surface efficiency
$\sigma =$	the ratio of minimum free flow area to frontal area

Subscripts

p	the reference or plain smooth heat transfer surface
std	standardized parameter

REFERENCES

- 1a. Bergles, A. E., Some perspective on enhanced heat transfer—Second generation heat transfer technology, *Trans. ASME J. Heat Transfer*, 110, 1082–1096 (1988).
- 1b. Bergles, A. E., High-flux Processes through enhanced heat transfer, keynote at the *Fifth International Conference on Boiling Heat Transfer*, Montego Bay, Jamaica, May 4–8, 2003, pp. 1–13.
2. Webb, R. L. and Bergles, A. E., Heat transfer enhancement: Second generation technology, *Mech. Eng.*, 115(6), 60–67 (1983).
3. Marner, W. J., Bergles, A. E., and Chenoweth, J. M., On the presentation of performance data for enhanced tubes used in shell and tube heat exchangers, *Trans. ASME J. Heat Transfer*, 105, 358–365 (1983).

4. Bergles, A. E., Techniques to augment heat transfer, in *Handbook of Heat Transfer Applications* (W. M. Rohsenow, J. P. Haitnett, and E. N. Ganic, eds.), McGraw-Hill, New York, 1985, pp. 3-1-3-79.
5. Webb, R. L., Special surface geometries for heat transfer augmentation, in *Developments in Heat Exchanger Technology—I* (D. Chisholm, ed.), Applied Science Publishers, London, U.K., 1980, pp. 179-215.
6. Kohler, J. A. and Staner, K. E., High performance heat transfer surfaces, in *Handbook of Applied Thermal Design* (E. C. Guyer, ed.), McGraw-Hill, New York, 1984, pp. 7-37-7-49.
7. Yang, W.-J., High performance heat transfer surfaces: Single phase flows, in *Heat Transfer in Energy Problems*, Mizushima, T. and Yang, W.J., (eds.) Hemisphere Publications, Washington, DC, 1983, pp. 109-116.
8. Webb, R. L., Enhancement of single phase heat transfer, in *Handbook of Single Phase Convective Heat Transfer* (S. Kakac, R. K. Shah, and W. Aung, eds.), John Wiley & Sons, New York, 1987, pp. 17.1-17.62.
9. Thome, R. T. Enhanced single phase laminar tube side flows and heat transfer, Chapter 4, pp. 4.1-4.27. *Wolverine Heat Transfer Engineering Data Book III*, Wolverine Division of UOP Inc., Decatur, AL, 2004.
10. Ravigururajan, T. S. and Rabas, T. J., Turbulent flow in integrally enhanced tubes, Part 1: Comprehensive review and database development, *Heat Transfer Eng.*, 17, 19-29 (1996).
11. Pate, M. B., Ayub, Z. H., and Kohler, J., Heat exchangers for the airconditioning and refrigeration industry, in *Compact Heat Exchangers—A Festschrift for A. L. London* (R. K. Shah, A. D. Kraus, and D. Metzger, eds.), Hemisphere, Washington, DC, 1990, pp. 567-590.
12. Khanpara, J. C., Bergles, A. E., and Pate, M. B., Augmentation of R-113 intube evaporation with microfin tubes, *ASHRAE Trans.*, 92(Part 2B), 506-524 (1986).
13. Thomas, Craig, Recent developments in the manufacturing and application of integral low fin tubing in titanium and zirconium, *Proceedings of Zirconium/Organics Conference*, Gleneden Beach, OR, 1997, pp. 169-177.
14. Minton, P. E., Process heat transfer, *Proceedings of the 9th International Heat Transfer Conference on Heat Transfer 1990—Jerusalem*, Paper No. KN-22, Vol. 1, Jerusalem, Israel, 1990, pp. 355-362.
15. Ravigururajan, T. S. and Bergles, A. E., General correlations for pressure drop heat transfer for single phase turbulent flow in internally ribbed tubes, *Conference Proceedings of the Augmentation of Heat Transfer in Energy Systems*, ASME, Miami Beach, FL, 1985.
16. Chiou, J. P., Experimental investigation of the augmentation of forced convection heat transfer in a circular tube using spiral spring inserts, *Trans. ASME J. Heat Transfer*, 109, 300-307 (1987).
17. Bergles, A. E. and Joshi, S. D., Augmentation techniques for low Reynolds number in-tube flow, in *Low Reynolds Number Flow Heat Exchangers* (S. Kakac, R. K. Shah, and A. E. Bergles, eds.), Hemisphere, Washington, DC, 1982, pp. 695-720.
18. Ravigururajan, T. S. and Rabas, T. J., Turbulent flow in integrally enhanced tubes, Part 2: Analysis and performance comparison, *Heat Transfer Eng.*, 17, 30-40 (1996).
19. Sethumadhavan, R. and Rao, R., Turbulent flow friction and heat transfer characteristics of single and multistart spirally enhanced tubes, *Trans. ASME J. Heat Transfer*, 108, 55-61 (1986).
20. Junkhan, G. H., Bergles, A. E., Nirmalan, V., and Ravigururajan, T., Investigation of turbulators for fire tube boilers, *Trans. ASME J. Heat Transfer*, 107, 354-360 (1985).
21. Westphalen, D., Roth, K., and Brodrick, J., Heat transfer enhancement—Emerging technologies, *ASHRAE J.* 48, 68-71 (2006).
22. Bergles, A. E., Webb, R. L., Junkhan, G. H., and Jensen, M. K., *Bibliography on Augmentation of Convective Heat and Mass Transfer*, Engineering Research Institute, Iowa State University, Ames, IA, May 1979.
23. (a) Shah, R. K., Compact heat exchanger surface selection methods, in *Heat Transfer*, Vol. IV, Hemisphere, Washington, DC, 1978, pp. 193-199. (b) Shah, R. K., Compact heat exchanger surface selection methods, in *Heat Transfer*, Vol. 4, Hemisphere, Washington, DC, 1978, pp. 279-284.
24. Webb, R. L., Performance evaluation criteria for use of enhanced heat transfer surfaces in heat exchanger design, *Int. J. Heat Mass Transfer*, 24, 715-726 (1981).
25. Maltson, J. D., Wilcock, D., and Davenport, C. J., Comparative performance of rippled fin plate fin and tube heat exchangers, *Trans. ASME J. Heat Transfer*, 111, 21-28 (1989).
26. London, A. L., Compact heat exchangers, Part 2: Surface geometry, *Mech. Eng.*, 86, 31-34 (1964).
27. London, A. L. and Ferguson, C. K., Test results of high performance heat exchanger surfaces used in aircraft intercoolers and their significance for gas turbine regenerator design, *Trans. ASME*, 71, 17-26 (1949).
28. Bergles, A. E., Blumenkrantz, A. R., and Taborek, J., Performance evaluation criteria for enhanced heat transfer surfaces, in *Heat Transfer*, Vol. II, JSME, 1974, pp. 239-243.

BIBLIOGRAPHY

- Arshad, J. and Thome, J. R., Enhanced boiling surfaces—Heat transfer mechanism and mixture boiling, *ASME/JSME Joint Thermal Engineering Conference Proceedings*, Vol. 1, Honolulu, HI, March 1983, pp. 191–197.
- Bergles, A. E., Enhancement of heat transfer, in *Heat Transfer—1978*, Vol. VI, Hemisphere, Washington, DC, 1978, pp. 89–108.
- Bergles, A. E., Junkhan, G. H., and Webb, R. L., Energy conservation via heat transfer enhancement, Paper No. EGY205, *1978 Midwest Energy Conference*, Chicago, IL, November 19–21, 1978, pp. 10–21.
- Carnavos, T. C., Some recent developments in augmented heat exchange elements, in *Heat Exchangers: Design and Theory Source Book*, Scripta, Washington, DC, 1974, pp. 441–489.
- Dewan, A., Mahanta, P., Sumithra Raju, K., and Suresh Kumar, P., Review of passive heat transfer augmentation techniques, *Proc. Inst. Mech. Eng. Part A: J. Power Ener.*, 218, 509–527, A04804 # IMechE 2004.
- Fujie, K., Nakayama, W., Kuwahara, H., and Kakizaki, K., Heat transfer wall for boiling liquids, U.S. Patent 4060125, November 29, 1977.
- Gupta, J. P., *Fundamentals of Heat Exchanger and Pressure Vessel Technology*, Hemisphere, Washington, DC, 1986.
- Song-Jiu Deng et al., Heat transfer enhancement and energy conservation, Hemisphere Publishing Corporation, New York.
- Takahashi, K., Nakayama, W., Senshu, T., and Yoshida, H., Heat transfer analysis of shell-and-tube condensers with shell-side enhancement, *ASHRAE Trans.*, 90(Part IB), 60 (1984).
- Thome, J. R., *Enhanced Boiling Heat Transfer*, Hemisphere, Washington, DC, 1990.
- Webb, R. L., Heat transfer surface having a high boiling heat transfer coefficient, U.S. Patent 3696861, October 10, 1972.
- Webb, R. L., Toward a common understanding of the performance and selection of roughness for forced convection, in *A Festschrift for E. R. G. Eckert* (J. P. Hartnett, T. F. Irvine, Jr., E. Pfender, and E. M. Sparrow, eds.), Hemisphere, Washington, DC, 1979.
- Webb, R. L., Enhancement for extended surface geometries used in air cooled heat exchangers, in *Low Reynolds Number Flow Heat Exchangers* (S. Kakac, R. K. Shah, and A. E. Bergles, eds.), Hemisphere, Washington, DC, 1983, pp. 721–734.
- Webb, R. L. and Bergles, A. E., Performance evaluation criteria for selection of heat transfer surface geometries used in low Reynolds number heat exchangers, in *Low Reynolds Number Flow Heat Exchangers* (S. Kakac, R. K. Shah, and A. E. Bergles, eds.), Hemisphere, Washington, DC, 1982, pp. 735–752.

9 Fouling

Fouling is defined as the formation of undesired deposits on heat transfer surfaces which impede the heat transfer and increase the resistance to fluid flow, resulting in higher pressure drop. Industrial heat exchangers rarely operate with nonfouling fluids. Low-temperature cryogenic heat exchangers are perhaps the only exception [1]. The growth of the deposits causes the thermohydraulic performance of heat exchanger to degrade with time. Fouling affects the energy consumption of industrial processes, and it can also decide the amount of extra material required to provide extra heat transfer surface employed in heat exchangers to compensate for the effects of fouling. In addition, where the heat flux is high, as in steam generators, fouling can lead to local hot spots and ultimately it may result in mechanical failure of the heat transfer surface [2]. Bott [3] and Chenoweth [4] give general and specific information on fouling. Figure 9.1 shows a fouled heat exchanger.

9.1 EFFECT OF FOULING ON THE THERMOHYDRAULIC PERFORMANCE OF HEAT EXCHANGERS

Effects can include the following:

1. The fouling layers on the inside and the outside surfaces are known generally to increase with time as the heat exchanger is operated. Since the fouling layers normally have lower thermal conductivity than the fluids or the conduction wall, they increase the overall thermal resistance. For the common case of a cylindrical tube with flow and fouling at both the inside and outside surface represented in Figure 9.2, the total resistance R_T to heat transfer between the two streams is given by

$$R_T = \frac{1}{U_o A_o} = \frac{1}{h_i A_i} + \frac{R_i}{A_i} + \frac{\Delta t_w}{k_w A_m} + \frac{R_o}{A_o} + \frac{1}{h_o A_o} \quad (9.1)$$

where the symbols have the usual meaning, and R_i and R_o are fouling resistance on the inside and outside surfaces, respectively. The overall heat transfer coefficient in fouled conditions may be expressed in terms of the overall heat transfer coefficient in clean condition and an overall fouling resistance R_f involving the terms related to fouling:

$$\frac{1}{U_{o,f}} = \left[\frac{1A_o}{h_i A_i} + \frac{\Delta t_w A_o}{k_w A_m} + \frac{1}{h_o} \right] + \left[R_i \frac{A_o}{A_i} + R_o \right] \quad (9.2a)$$

$$= \frac{1}{U_{o,c}} + R_f \quad (9.2b)$$

or

$$R_f = \frac{1}{U_{o,f}} - \frac{1}{U_{o,c}} \quad (9.3)$$

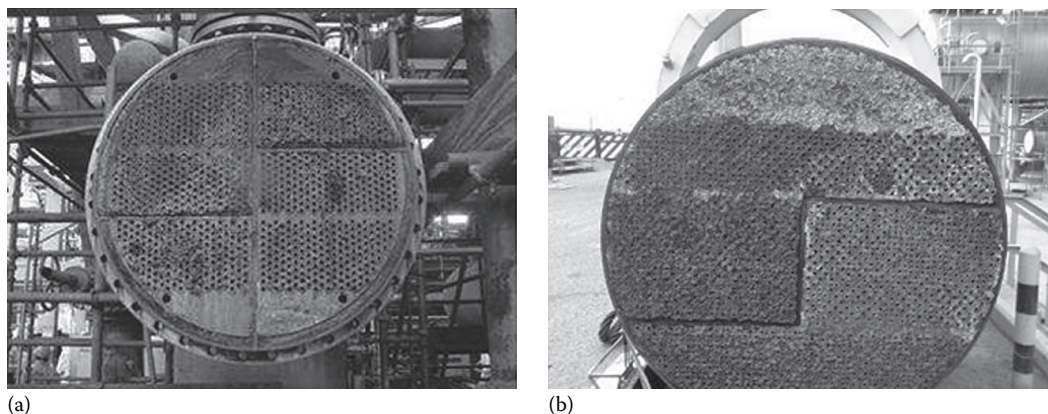


FIGURE 9.1 (a and b) Fouled shell and tube heat exchangers. (Courtesy of Merusonline, MERUS GmbH, Sindelfingen, Germany, Also MERUS California LLC.)

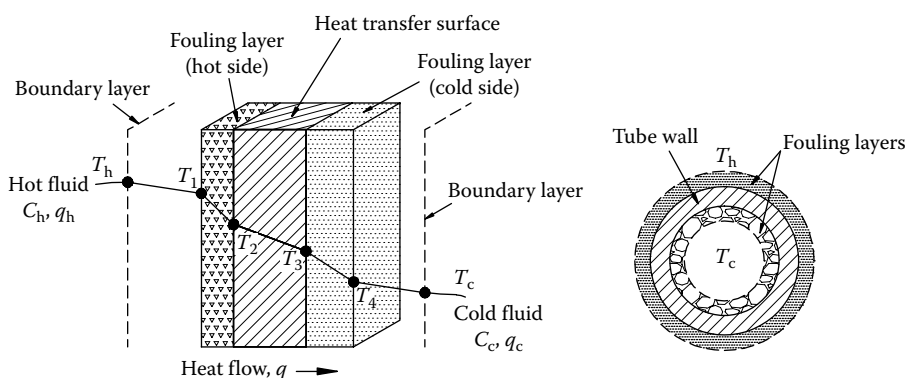


FIGURE 9.2 Fouling deposits build up on heat transfer surface.

2. There is an increase of the surface roughness, thus increasing frictional resistance to flow, and fouling blocks flow passages; due to these effects, the pressure drop across the heat exchanger increases.
3. Fouling may create a localized environment where corrosion is promoted.
4. Fouling will reduce the thermal effectiveness of heat exchangers, which in turn affect the subsequent processes or will increase the thermal load on the system.
5. An additional goal becomes prevention of contamination of a process fluid or product.

9.2 COSTS OF HEAT EXCHANGER FOULING

Fouling of heat exchangers has been estimated to represent an annual expense in the United States of somewhere between \$4.2 and \$10 billion [4]. Fouling is something that is unwanted and counterproductive. The presence of fouling on heat exchange surfaces causes additional costs due to the following reasons:

1. Increased capital expenditure due to oversizing
2. Energy losses associated with poor performance of the equipment
3. Treatment cost to lessen corrosion and fouling
4. Lost production due to maintenance schedules
5. Reduction of time in service

Economic considerations should be among the most influential parameters for determining appropriate allowances for fouling. It is important to determine a strategy as to whether first cost, operating and maintenance cost, or total cost over a period of years is the objective.

9.2.1 OVERSIZING

While sizing a heat exchanger, it is a normal practice to oversize the heat transfer surface area to account for fouling, and the oversizing is normally of the order of 20%–40%.

9.2.2 ADDITIONAL ENERGY COSTS

Since fouling reduces the heat transfer rates, additional energy is expended to increase the heat transfer rate; fouling also increases the pressure drop across the core and hence more pumping power is required to meet the heat load.

9.2.3 TREATMENT COST TO LESSEN CORROSION AND FOULING

The formation of fouling deposits on heat transfer surfaces necessitates periodical cleaning, which costs money for cleaning materials and process, personnel required, and recently environmental problems to discharge the effluents.

9.2.4 LOST PRODUCTION DUE TO MAINTENANCE SCHEDULES AND DOWN TIME FOR MAINTENANCE

Periodical cleaning requires plant shutdown and hence the unavailability of system for productive purposes. Critical industries that cannot afford for downtime and loss in production will maintain standby units, which again raises additional capital costs for spares.

9.3 FOULING CURVES/MODES OF FOULING

The amount of material deposited per unit area m_f is related to the fouling resistance R_f and the density of the foulant ρ_f , thermal conductivity k_f , and thickness of the deposit x_f by the following equation [1]:

$$m_f = \rho_f x_f = \rho_f k_f R_f \quad (9.4)$$

The incidence of fouling with reference to time is normally defined by the following three modes [1]:

1. Linear mode—Increase of m_f (or R_f) with time t .
2. Falling rate mode—The rate of deposition decreases with increasing time.
3. Asymptotic mode—The value of m_f (or R_f) is not time variant after initial fouling.

The representation of various modes of fouling with reference to time is known as a fouling curve. Typical fouling curves are shown in Figure 9.3. This figure also shows deterioration of U due to on set of fouling and U value when automatic tube cleaning system is installed (U_{ATC})-schematic. The linear modes and falling rate modes may be the incidence of fouling in the early stages of asymptotic behavior. The asymptotic mode is of particular interest to heat exchangers, since the incidence of fouling raises the possibility of continued operation of the equipments without additional fouling. The time delay period, t_d , is time required for the formation of initial

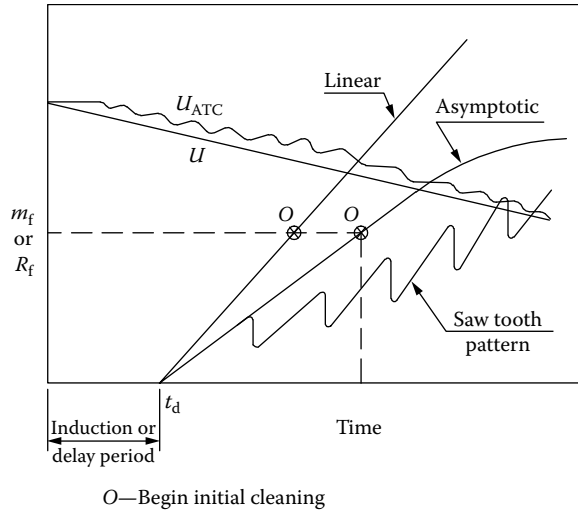


FIGURE 9.3 Fouling curves. (Modified from Collier, J.G., Heat exchanger fouling and corrosion, in *Heat Exchangers: Thermal-Hydraulic Fundamentals and Design*, Kakac, S., Bergles, A.E., and Mayinger, F., eds., Hemisphere, Washington, DC, pp. 999–1011, 1981.)

fouling substrata. Smooth and nonwetting surfaces like glass and Teflon will extend the delay period. Figure 9.3 also shows the falling rate of overall heat transfer coefficient with incidence of time but its increase with automatic tube cleaning system instituted in the system.

9.4 STAGES OF FOULING

For all the categories of fouling, the successive events that commonly occur in most situations are up to five in number. They are initiation of fouling, transport to surface, attachment to surfaces, removal from surfaces, and aging of deposit [5].

9.5 FOULING MODEL

Fouling is usually considered to be the net result of two simultaneous processes: a deposition process and a removal (re-entrainment process) [6]. A schematic representation of fouling process is given in Figure 9.4. The net rate of fouling can be expressed in terms of the rate of deposition of fouling mass (\dot{m}_d) and the rate of removal (\dot{m}_r) from the heat transfer surface. Thus,

rate of fouling = rate of deposition of fouling mass – rate of removal from the heat transfer surface

$$\frac{dm_f}{dt} = \dot{m}_d - \dot{m}_r \quad (9.5)$$

One of the earliest models of fouling was that by Kern and Seaton [7]. In this model, it was assumed that \dot{m}_d remained constant with time t but that \dot{m}_r was proportional to m_f and therefore increased with time to approach \dot{m}_d asymptotically. Thus $\dot{m}_d = \beta m_f$; then integration of Equation 9.5 from the initial condition $m_f = 0$ at $t = 0$ gives

$$m_f = m_f^* (1 - e^{-\beta t}) \quad (9.6)$$

where

m_f^* is the asymptotic value of m_f

$\beta = 1/t_c$

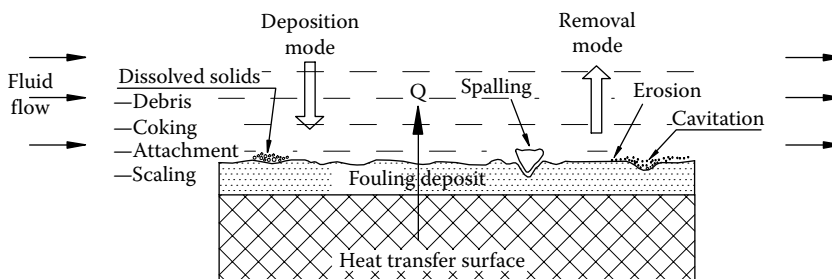


FIGURE 9.4 Schematic representation of fouling process. (Modified from O’Callaghan, M., Fouling of heat transfer equipment: Summary review, in *Heat Exchangers: Thermal-Hydraulic Fundamentals and Design*, S. Kakac, A. E. Bergles, and F. Mayinger, eds., Hemisphere, Washington, DC, pp. 1037–1047, 1981.)

The time constant t_c represents the average residence time for an element of fouling material at the heating surface. Equation 9.6 can be expressed in terms of fouling resistance R_f at time t in terms of the asymptotic value R_f^* by

$$R_f = R_f^* (1 - e^{-\beta t}) \quad (9.7)$$

9.6 PARAMETERS THAT INFLUENCE FOULING RESISTANCES

Many operational and design variables have been identified as having most pronounced and well-defined effects on fouling. These variables are reviewed here in principle to clarify the fouling problems and because the designer has an influence on their modification. These parameters include the following:

1. Properties of fluids and their propensity for fouling
2. Surface temperature
3. Velocity and hydrodynamic effects
4. Tube material
5. Fluid purity and freedom from contamination
6. Surface roughness
7. Suspended solids
8. Placing the more fouling fluid on the tubeside
9. Shellside flow
10. Type of heat exchanger
11. Heat exchanger geometry and orientation
12. Equipment design
13. Seasonal temperate changes
14. Heat transfer processes like sensible heating, cooling, condensation, vaporization, etc.
15. Shell and tube heat exchanger with improved shellside performance

9.6.1 PROPERTIES OF FLUIDS AND USUAL PROPENSITY FOR FOULING

The most important consideration is the fluid and the conditions conducive for fouling. At times a process modification can result in conditions that are less likely to cause fouling.

9.6.2 TEMPERATURE

A good practical rule to follow is to expect more fouling as the temperature rises. This is due to a “baking on” effect, scaling tendencies, increased corrosion rate, faster reactions, crystal formation

and polymerization, and loss in activity by some antifoulants [8]. Lower temperatures produce slower fouling buildup, and usually deposits that are easily removable [4]. However, for some process fluids, low surface temperature promotes crystallization and solidification fouling. For those applications, it is better to use an optimum surface temperature to overcome these problems. For cooling water with a potential to scaling, the desired maximum surface temperature is about 140°F (60°C). Biological fouling is a strong function of temperature. At higher temperatures, chemical and enzyme reactions proceed at a higher rate with a consequent increase in cell growth rate [9]. According to Mukherjee [9], for any biological organism, there is a temperature below which reproduction and growth rate are arrested and a temperature above which the organism becomes damaged or killed. If, however, the temperature rises to an even higher level, some heat-sensitive cells may die.

9.6.3 VELOCITY AND HYDRODYNAMIC EFFECTS

Hydrodynamic effects such as flow velocity and shear stress at the surface influence fouling. Within the pressure drop considerations, the higher the velocity, higher will be the thermal performance of the exchanger and less will be the fouling. Uniform and constant flow of process fluids past the heat exchanger favors less fouling. Foulants suspended in the process fluids will deposit in low-velocity regions, particularly where the velocity changes quickly, as in heat exchanger water boxes and on the shellside [8]. Higher shear stress promotes dislodging of deposits from surfaces. Maintain relatively uniform velocities across the heat exchanger to reduce the incidence of sedimentation and accumulation of deposits.

9.6.4 TUBE MATERIAL

The selection of tube material is significant to deal with corrosion fouling.

Carbon steel is corrosive but least expensive.

Copper exhibits biocidal effects in water. However, its use is limited in the following applications:

1. Copper is attacked by biological organisms including sulfate-reducing bacteria; this increases fouling.
2. Copper alloys are prohibited in high-pressure steam power plant heat exchangers, since the corrosion deposits of copper alloys are transported and deposited in high-pressure steam generators and subsequently block the turbine blades.
3. Environmental protection limits the use of copper in river, lake, and ocean waters, since copper is poisonous to aquatic life.

Noncorrosive materials such as titanium and nickel will prevent corrosion, but they are expensive and have no biocidal effects.

Glass, graphite, and Teflon tubes often resist fouling and/or improve cleaning.

Although the construction material is more important to resist fouling, surface treatment by plastics, vitreous enamel, glass, and some polymers will minimize the accumulation of deposits [3].

9.6.5 IMPURITIES

Seldom are fluids pure. Intrusion of minute amounts of impurities can initiate or substantially increase fouling. They can either deposit as a fouling layer or act as catalysts to the fouling processes [4]. For example, chemical reaction fouling or polymerization of refinery hydrocarbon streams is due to oxygen ingress and/or trace elements such as Va and Mo. In crystallization fouling, the presence of small particles of impurities may initiate the deposition process by seeding. The properties of the impurities form the basis of many antifoulant chemicals. Sometimes impurities such as sand or other suspended particles in a cooling water may have a scouring action, which will reduce or remove deposits [3].

9.6.6 SURFACE ROUGHNESS

The surface roughness is supposed to have the following effects [3]:

1. The provision of “nucleation sites” that encourage the laying down of the initial deposits
2. The creation of turbulence effects within the flowing fluid and, probably, instabilities in the viscous sublayer

Better surface finish has been shown to influence the delay of fouling and ease cleaning. Similarly, nonwetting surfaces delay fouling. Rough surfaces encourage particulate deposition. After the initiation of fouling, the persistence of the roughness effects will be more a function of the deposit itself [3]. Even smooth tubes may become rough in due course due to scale formation, formation of corrosion products, or erosion.

9.6.7 SUSPENDED SOLIDS

Suspended solids promote particulate fouling by sedimentation or settling under gravitation onto the heat transfer surfaces. Since particulate fouling is velocity dependent, prevention is achieved if stagnant areas are avoided. For water, high velocities (above 1 m/s) help prevent particulate fouling. Often it is economical to install an upstream filtration.

9.6.8 PLACING MORE FOULING FLUID ON THE TUBESIDE

As a general guideline, the fouling fluid is preferably placed on the tubeside for ease of cleaning. Also, there is less probability for low-velocity or stagnant regions on the tubeside.

9.6.9 SHELLSIDE FLOW

Velocities are generally lower on the shellside than on the tubeside, less uniform throughout the bundle, and limited by flow-induced vibration. Zero or low velocity regions on the shellside serve as ideal locations for the accumulation of foulants. If fouling is expected on the shellside, then attention should be paid to the selection of baffle design. Segmental baffles have the tendency for poor flow distribution if spacing or baffle cut ratio is not in correct proportions. Too low or too high a ratio results in an unfavorable flow regime that favors fouling (Figure 9.5).

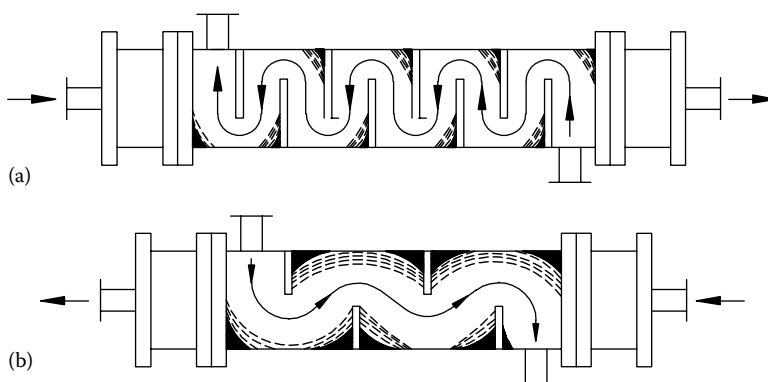


FIGURE 9.5 Effect of baffle spacing and baffle cut on fouling: (a) moderate baffle spacing and baffle cut and (b) wide baffle spacing and large baffle cut. Note: dark areas represent stagnant areas with heavy fouling.

9.6.10 TYPE OF HEAT EXCHANGER

9.6.10.1 Low-Finned Tube Heat Exchanger

There is a general apprehension that low Reynolds number flow heat exchangers with low-finned tubes will be more susceptible to fouling than plain tubes. Fouling is of little concern for finned surfaces operating with moderately clean gases. According to Silvestrini [10], fin type does not affect the fouling rate, but the fouling pattern is affected for waste heat recovery exchangers. Plain and serrated fin modules with identical densities and heights have the same fouling thickness increases in the same period of time. As far as fouling pattern is concerned, for plain fin tubes, soot deposits are equally distributed between fin and tube surfaces when buildup first begins. Subsequently, the distribution becomes uneven, as the fin fouling thickness reach a maximum and the fin gaps are filled with soot that builds up from the tube walls. This pattern also occurs in certain areas of the serrated fin tubes, but another pattern evident is localized bridging of the serrated fin tips across both the fin gaps and serrations.

9.6.10.2 Heat Transfer Augmentation Devices

Fouling is an important consideration in whether enhanced surface tubes should be used on heat exchangers to enhance the performance. Experimental evidence favors most of the heat transfer augmentation devices for improved heat transfer without penalty due to fouling. Fouling aspects of heat transfer augmentation devices are covered in the chapter on heat transfer augmentation (Chapter 8).

9.6.10.3 Gasketed Plate Heat Exchangers

High turbulence, absence of stagnant areas, uniform fluid flow, and the smooth plate surface reduce fouling, and the need for frequent cleaning. Hence the fouling factors required in plate heat exchangers are normally 10%–25% of those used in shell and tube heat exchangers.

9.6.10.4 Spiral Plate Exchangers

High turbulence and scrubbing action minimize fouling on the spiral plate exchanger. This permits the use of low fouling factors.

9.6.11 SEASONAL TEMPERATURE CHANGES

When cooling-tower water is used as coolant, considerations are to be given for winter conditions where the ambient temperature may be near zero or below zero on the Celsius scale. The increased temperature driving force during the cold season contributes to more substantial overdesign and hence overperformance problems, unless a control mechanism has been instituted to vary the water/air flow rate as per the ambient temperature.

9.6.12 EQUIPMENT DESIGN

Careful equipment design can contribute to reduction in fouling. Heat exchanger tubes that extend beyond tubesheet, for example, can cause rapid fouling.

9.6.13 HEAT EXCHANGER GEOMETRY AND ORIENTATION

Heat exchanger geometry influences the uniformity of flows on the shellside and tubeside. Orientation of heat exchangers eases cleaning [4]. Finned tube heat exchanger geometry and surface characteristics like tube layout, tube pitch, secondary surface density, etc. influence fouling. The influences of surface modification and fin density on fouling were discussed in Chapter 4.

9.6.14 HEAT TRANSFER PROCESSES LIKE SENSIBLE HEATING, COOLING, CONDENSATION, AND VAPORIZATION

The fouling resistances for the same fluid can be considerably different depending upon whether heat is being transferred through sensible heating or cooling, boiling, or condensing [4].

9.6.15 SHELL AND TUBE HEAT EXCHANGER WITH IMPROVED SHELLSIDE PERFORMANCE

More often, the fouling mechanism responsible for the deterioration of heat exchanger performance is flow-velocity dependent. Maldistribution of flow, stagnant zones, wakes, and eddies caused by poor heat exchanger geometry can have detrimental effect on heat exchanger performance and reliability. Over two decades, different kinds of shell and tube heat exchangers have been developed to improve shellside performance. Many baffle types such as Philips RODbaffle heat exchanger, Twisted Tube® Heat Exchanger and Helixchanger® heat exchanger, and EMbaffle® heat exchanger have been designed to improve flow velocity, enhance heat transfer performance, and reduce fouling on shellside. Few of these types from fouling reduction point of view are discussed next.

9.6.15.1 EMbaffle® Heat Exchanger*

The EMbaffle heat exchanger is an innovation designed to improve performance and simultaneously reduce operating costs by reducing fouling losses. The patented EMbaffle design uses expanded metal baffles made of plate material that has been slit and expanded. In fouling services, for instance in crude preheat trains, the dead zones typically found with conventional segmental designs reduce the performance of the heat exchanger with an increasing pressure drop during operation. However, with EMbaffle, due to the longitudinal flow, no low shellside velocity “dead zones” are created behind the EMbaffle, and there is a reduction in fouling. Consequently, the maintenance, cleaning, and refurbishment schedules can be optimized [11].

9.6.15.2 Twisted Tube Heat Exchanger†

Sedimentary-type fouling is enhanced in areas of low velocity or “dead” spots. Turbulent flow and the elimination of dead spots are needed to minimize this type of fouling. On the tubeside, higher velocities can be obtained with multiple tube passes and devices that enhance swirl flow to keep particles in suspension, such as Twisted Tubes. On the shellside, elimination of dead spots is most effective. With traditional segmental baffles, fouling occurs in the dead zones on each side of a baffle up against the shell. Baffle free Twisted Tube bundles have no such dead spots and the constant and uniform shellside velocity have ensures considerable reduction in fouling while in service [12].

9.6.15.3 Helixchanger Heat Exchanger‡

Helixchanger heat exchangers have demonstrated significant improvements in the fouling behavior of heat exchangers in operation. Uniform velocities and near plug flow conditions achieved in a Helixchanger provide low fouling characteristics offering much longer heat exchanger run-lengths between scheduled cleaning of tube bundles. Figure 9.6 shows a heavily fouled conventional segmental baffle shell and tube heat exchanger with a lightly fouled Helixchanger heat exchanger.

* EMbaffle is a registered trademark of EMbaffle B.V., Alphen a/d Rijn, the Netherlands.

† Twisted Tube is a registered trademark of Koch Heat Transfer Company.

‡ Helixchanger is a registered trademark of Lummus Technology Inc.

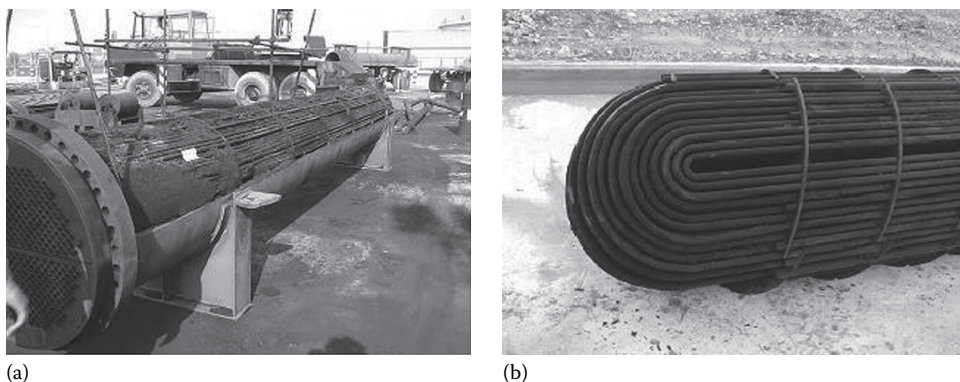


FIGURE 9.6 Comparison of level of fouling of conventional shell and tube heat exchanger and Helixchanger heat exchanger: (a) heavily fouled segmental baffle exchanger and (b) lightly fouled Helixchanger heat exchanger. (Courtesy of Lummus Technology Inc., Bloomfield, NJ.)

9.7 MECHANISMS OF FOULING

It is of great importance to understand the fouling mechanisms in principle, as they will indicate the causes and conditions of fouling and hence give clues how fouling can be minimized. Based on the mechanism of fouling, Epstein [5] classifies fouling into six types:

1. Particulate fouling
2. Reaction fouling
3. Corrosion fouling
4. Precipitation fouling
5. Biological fouling
6. Solidification fouling

9.7.1 PARTICULATE FOULING

Particulate fouling may be defined as the accumulation of particles suspended in the process streams onto the heat transfer surfaces. This type of fouling includes sedimentation of settling under gravitation as well as deposition of colloidal particles by other deposition mechanisms on to the heat transfer surfaces. Various forms of particulate fouling are as follows:

1. Fouling that occurs in once-through cooling-water systems using sea, river, and lake water containing mud, silt, and sediments. They are capable of depositing in low-flow areas, forming a physical barrier, and preventing oxygen from reaching the metal/solution interface. The deposit buildup will promote localized corrosion.
2. Gas-side fouling: Gas-side fouling is mostly by particulate fouling by dirty gas streams, airborne contaminants, and the leakage and mixing of one process stream with the other, in addition to its own contaminants—carbon soot in the case of combustion gases and exhaust gases. In some cases, gas-side fouling may also be accompanied by corrosion, particularly when condensation of corrosive acids take place from combustion gases. Level of gas-side fouling depends on features such as
 - a. Tube layout pattern—in-line or staggered
 - b. Tube pitch
 - c. Fin density
 - d. Fin surface characteristic such as plain fin, surface-modified fin

3. Another important area of particulate fouling is due to the aluminum transport phenomenon. The problem consists of corrosion of heat-rejecting aluminum surfaces (engine block) followed by deposition of insoluble aluminum salts in the radiator. The corrosion process can be prevented by the inclusion of silicate inhibitors in the coolant formulation.

9.7.2 CHEMICAL REACTION FOULING (POLYMERIZATION)

Deposits formed by chemical reactions at the heat transfer surface in which the surface material itself is not a reactant are known as chemical reaction fouling. Polymerization, cracking, and coking of hydrocarbons are prime examples of reaction fouling. The factors likely to affect reaction fouling include the following [3,13]:

Temperature is the most sensitive variable. It is usual that below a certain surface temperature polymerization does not initiate, but increases rapidly above that. The reaction rate is related to the temperature by the following Arrhenius law:

$$K_r = A_{cr}e^{E/RT_s} \quad (9.8)$$

where

E is the activation energy

R is the gas constant

A_{cr} is the rate constant

T_s is the heat transfer surface temperature

The presence of most sulfur compounds, nitrogen compounds, and the presence of trace elements (metallic impurities) such as Mo and Va in hydrocarbon streams significantly increases the fouling rates.

Composition of the process stream, including contaminants and, especially, oxygen ingress will affect reaction fouling.

Sound prevention measures for chemical reaction fouling should include the following [3,13]:

1. Avoidance of feed contact with air or oxygen by nitrogen blanketing.
2. Elimination or reduction of unsaturates, which are particularly high in cracked stocks.
3. Caustic scrubbing to remove sulfur compounds.
4. Desalting, which reduces trace metal contamination.
5. The use of antioxidation additives that inhibit the polymerization reaction, along with steps taken to minimize oxygen ingress.
6. Use of additives known as metal coordinators, which react with the trace elements and prevent them from functioning as fouling catalysts. Other additives recommended are corrosion inhibitors and dispersion agents [3].

9.7.3 CORROSION FOULING

Corrosion fouling is due to the deposition of corrosion products on heat transfer surfaces. In this category of fouling process, the heat transfer surface material itself reacts to produce corrosion products, which foul the heat transfer surface. The most common forms of this type of fouling are material loss due to general thinning, iron oxide on carbon steel tubes in cooling-water systems, and fouling of soldered radiator tube ends on the water side by solder bloom corrosion. Corrosion

fouling is highly dependent upon the choice of material of construction and the environment. Hence, it is possible to overcome corrosion fouling if the right choice of material has been made to resist the environment. Measures such as the use of inhibitors, cathodic protection, and surface treatment such as passivation of stainless steel will minimize corrosion and hence corrosion fouling.

9.7.4 CRYSTALLIZATION OR PRECIPITATION FOULING

This type of fouling mostly takes place in cooling-water systems, when water-soluble salts, predominantly calcium carbonates, become supersaturated and crystallize on the tube wall to form scaling. Such scaling occurs because many of the dissolved salts in water exhibit inverse solubility effects, a condition that reverses the normal solubility (increasing with temperature) into one that decreases with temperature. Thus an inverse solubility solution will crystallize when heated (e.g., cooling water), while normal solubility salts will crystallize when cooled. Chemical additives can be helpful to reduce fouling problems due to crystallization and freezing in a number of ways. Broadly there are four groups of chemicals to control crystallization [3]: distortion agents, dispersants, sequestering agents, and threshold chemicals.

9.7.4.1 Modeling for Scaling

According to Hasson [14], scaling is due to diffusion of calcium and carbonate ions from the bulk of the fluid, followed by crystallization of CaCO_3 on the hot wall surfaces. Their model for predicting CaCO_3 scaling rates is given by

$$m_s = K_R \left[(\text{Ca}^{2+})_i (\text{CO}_3^{2-})_i - K_{sp} \right] \quad (9.9)$$

where

m_s is the scale deposition rate ($\text{kg/m}^2 \cdot \text{s}$)

K_R the constant for crystallization rate

K_{sp} the solubility product of CaCO_3 (mol/m^3)²

The principle of fouling and the factors promoting scaling are discussed in the section on cooling water corrosion are discussed at the end of this chapter.

9.7.5 BIOLOGICAL FOULING

The attachment of microorganisms (bacteria, algae, and fungi) and macro organisms (barnacles, sponges, fishes, seaweed, etc.) on heat transfer surfaces where the cooling water is used in as drawn condition from river, lake, sea and coastal water, etc., is commonly referred to as biological fouling. On contact with heat transfer surfaces, these organisms can attach and breed, sometimes completely clogging the fluid passages, as well as entrapping silt or other suspended solids and giving rise to deposit corrosion. Concentration of microorganisms in cooling-water systems may be relatively low before problems of biofouling are initiated. For open recirculating systems, bacteria concentrations of the order of 1×10^5 cells/mL and fungi of 1×10^3 cells/mL may be regarded as limiting values [3]. Corrosion due to biological attachment to heat transfer surfaces is known as microbiologically influenced corrosion (MIC). MIC is discussed in detail in Chapter 12 on corrosion. The techniques that can be effective in controlling biological fouling include the following:

1. Select materials that possess good biocidal properties.
2. Mechanical cleaning techniques like upstream filtration, air bumping, backflushing, passing brushes, sponge rubber balls, grit coated rubber balls, and scrapers [4].
3. Chemical cleaning techniques that employ biocides such as chlorine, chlorine dioxide, bromine, ozone, surfactants, pH changes, and/or salt additions.

4. Thermal shock treatment by application of heat, or deslugging with steam or hot water.
5. Some less well-known techniques like ultraviolet radiation.

9.7.6 SOLIDIFICATION FOULING OR FREEZING FOULING

The freezing of a liquid or of higher-melting constituents of a multicomponent solution on a sub-cooled heat transfer surface is known as solidification fouling. Notable examples include frosting of moisture in the air, freezing of cooling water in low-temperature processes, and paraffin wax deposition during cooling of hydrocarbon streams. There are various remedies for dealing with duties where solidification occurs on the product side:

1. Do not include very large fouling resistances in the design. This will result in an oversized unit, which presents problems in the clean condition.
2. Use concurrent flow instead of counterflow.

9.8 FOULING DATA

Allowance for fouling is largely a matter of experience. There are tables of typical values for various services, e.g., TEMA Standards [15], and there is a proprietary correlation available for cooling water. However, fouling behavior is strongly dependent upon many variables and these interactions are very complex, so each problem needs to be examined for its special considerations. In choosing the fouling resistances to be used in a given heat exchanger, the designer has sources as follows:

1. Past experience of heat exchanger performance in the same or similar environments
2. Results from fouling monitoring
3. TEMA [15] values, which are overall values for a very limited number of environments
4. Rules of thumb (i.e., 20%–25% overdesign)
5. Model analysis/bench scale measurements under accelerated conditions
6. Empirical correlations based on laboratory experiments
7. Numerical simulations (i.e., CFD)

9.9 HOW FOULING IS DEALT WHILE DESIGNING HEAT EXCHANGERS

9.9.1 SPECIFYING THE FOULING RESISTANCES

Values of the fouling resistances are specified that are intended to reflect the values at the point in time just before the exchanger is to be cleaned. This implies that the exchanger is oversized for clean condition and barely adequate for conditions just before it should be cleaned. The fouling resistances result in higher heat transfer surface area. Planned fouling prevention, maintenance, and cleaning can justify lower fouling resistances, but at higher ongoing costs [4].

9.9.2 OVERSIZING

Another approach to heat exchanger design is to arbitrarily increase the heat transfer surface area to allow for fouling. This approach usually assumes zero fouling resistance in the fundamental overall heat transfer equation. The overall heat transfer coefficient is determined for clean conditions, and subsequently, the surface area required for clean condition is increased by a certain percentage. Based upon experience, the oversurface specified can range from 15% to 50% depending on the service [4]. In effect, the fouling for the exchanger is combined and no longer can be identified as belonging to one side or another.

9.10 TEMA FOULING RESISTANCE VALUES

The influence of the TEMA Fouling Resistance values [15] on design of heat exchangers has been enormous. In practice, some thought the TEMA values too high, others too low, since the tendency to fouling in a heat exchanger is dependent upon parameters such as local flow velocities, heat fluxes, etc., rather than overall values or point values as given for most cases in TEMA. Fouling types and effects of fouling are included in the RGP section of TEMA fouling resistance values taken from Ref (4) is shown in Table 9.1.

9.10.1 RESEARCH IN FOULING

Much research is in underway for fouling. This research will some day enable us to understand the parameters responsible for fouling and hence to devise means to control or eliminate fouling.

9.11 FOULING MONITORING

Exchangers subject to fouling or scaling should be monitored for their efficient functioning. A light fouling on the tube greatly reduces its efficiency. A marked increase in pressure drop and/or reduction in performance usually indicates fouling. The unit should first be checked for air or vapor binding to confirm that this is not the cause for the reduction in performance.

9.11.1 FOULING INLINE ANALYSIS

Guidelines are available to assist the heat exchanger user in determining the extent of fouling. By using these industry guidelines, cleaning and maintenance tasks can be better assigned.

EPRI heat exchanger performance monitoring: The EPRI *Heat Exchanger Performance Monitoring Guidelines*, EPRI NP-7552 lists several methods to evaluate the in-line heat transferring ability of heat exchangers. That document presents the details of each method and explains the strengths and weaknesses of each one. Few of the methods are hereunder [16]:

Heat transfer method: In this method, the fouling resistance can be determined from the reduction in heat transfer during the deposition process. The data may be reported in terms of changes in overall heat transfer coefficient or temperature variation compared to the design values. This is a reliable method because it is a direct test of heat transfer ability.

Pressure drop method: The pressure drop is increased for a given flow rate by virtue of the reduced flow area in the fouled condition and due to the increased roughness of the deposit. It is most challenging to measure small pressure drop changes and then make a determination regarding heat transfer ability.

In addition to the EPRI report, various heat exchanger monitoring techniques are presented in ASME OM-S/G-1994, *Standards and Guides for Operation and Maintenance of Nuclear Power Plants*, April 1995. A few of the techniques are given next.

1. *Functional test method:* Temperature is measured and compared to the acceptance criterion. An advantage to this method is that the parameter of interest is directly measured.
2. *Heat transfer coefficient test method (without phase change):* The fouling is computed directly based on conventional heat transfer analysis. An assumption is that the shellside flow is kept in the same flow regime.
3. *Heat transfer coefficient test method (with condensation).*
4. *Transient test method.*

TABLE 9.1
Fouling Resistance Values for Various Liquid Streams

Fluid	Fouling Resistance $r_f \times 10^4$ (M ² K/W)
<i>Industrial water streams</i>	
Seawater	1.75–3.5
Brackish water	3.5–5.3
Treated cooling tower water	1.75–3.5
Artificial spray pond	1.75–3.5
Closed loop treated water	1.75
River water	3.5–5.3
Engine jacket water	1.75
Distilled water or closed cycle condensate	0.9–1.75
Treated boiler feed water	0.9
Boiler blow down water	3.5–5.3
<i>Industrial liquid streams</i>	
No. 2 fuel oil	3.5
No. 6 fuel oil	0.9
Transformer oil, engine lube oil	1.75
Refrigerants, hydraulic fluid, ammonia	1.75
Industrial organic HT fluids	1.75–3.5
Ammonia (oil bearing)	5.3
Methanol, ethanol, ethylene glycol solutions	3.5
<i>Process liquid streams</i>	
MEA and DEA solutions	3.5
DEG and TEG solutions	3.5
Stable side draw and bottom products	1.75–3.5
Caustic solutions	3.5
<i>Crude oil refinery streams</i>	
Temperature (°C)	
120	3.5–7
120 to 180	5.3–7
180 to 230	7–9
>230	9–10.5
<i>Petroleum streams</i>	
Lean oil	3.5
Rich oil	1.75–3.5
Natural gasoline, liquefied petroleum gases	1.75–3.5
<i>Crude and vacuum unit gases and vapors</i>	
Atmospheric tower overhead	
Vapors, naphthas	1.7
Vacuum overhead vapors	3.5
<i>Crude and vacuum liquids</i>	
Gasoline	3.5
Naphtha, light distillates, kerosene, light gas oil	3.5–5.3
Heavy gas oil	5.3–9
Heavy fuel oil	5.3–12.3
Vacuum tower bottoms	17.6
Atmospheric tower bottoms	12.3
<i>Cracking and coking unit streams</i>	
Overhead vapors, light liquid products	3.5

(continued)

TABLE 9.1 (continued)
Fouling Resistance Values for Various Liquid Streams

Fluid	Fouling Resistance $r_f \times 10^4$ (M² K/W)
Light cycle oil	3.5–5.3
Heavy cycle oil, light coker gas oil	5.3–7
Heavy coker gas oil	7–9
Bottoms slurry oil	5.3
<i>Catalytic reforming, hydrocracking, and hydrosulfurization streams</i>	
Reformer charge, reformer effluent	2.6
Hydrocharger charge and effluent	3.5
Recycle gas, liquid product over 50°C	1.75
Liquid product 30°C to 50°C (API)	3.5
<i>Light ends processing streams</i>	
Overhead vapors, gases, liquid products	1.75
Absorption oils, reboiler streams	3.5–5.3
Alkylation trace acid streams	3.5
<i>Visbreaker</i>	
Overhead vapor	5.3
Visbreaker bottoms	17.5
<i>Naphtha hydrotreater</i>	
Feed	5.3
Effluent, naphthas	3.5
Overhead vapor	2.6
<i>Catalytic hydro desulfurizer</i>	
Charge	7–9
Effluent, HT separator overhead, liquid products	3.5
Stripper charge	5.3
<i>HF alky unit</i>	
Alkylate, depropanizer bottoms	5.3
Main fractional overhead and feed	5.3
Other process streams	3.5
<i>Industrial gas or vapor streams</i>	
Stream (non-oil-bearing)	9
Exhaust steam (oil-bearing)	2.6–3.5
Refrigerant (oil-bearing)	3.5
Compressed air	1.75
Ammonia	1.75
Carbon dioxide	3.5
Coal flue gas	17.5
Natural gas flue gas	9
<i>Chemical process streams</i>	
Acid gas	3.5–5.3
Solvent vapor	1.75
Stable overhead products	1.75
<i>Natural gas processing streams</i>	
Natural gas	1.75–3.5
Overheat products	1.75–3.5

Source: Adapted from Chenoweth, J.M., Final report of the HTRI/TEMA joint committee to review the fouling section of the TEMA Standards, Heat Transfer Research, Inc., Alhambra, CA, 1988 also reproduced from *Journal of Heat Transfer Engineering*, 11(1), 73–107, 1990.

5. *Temperature effectiveness test method*: It is applicable to single-phase fluid streams monitoring. The result is a projected temperature that is compared to its acceptance criterion.
6. *Batch test method*
7. *Temperature difference monitoring method*: The relationship between inlet cooling fluid and outlet process fluid temperatures is determined.
8. *Pressure loss monitoring method*.
9. *Visual inspection monitoring method*.

9.11.2 TUBE FOULING MONITORS

The ASME Condenser Performance Test Code (PTC 12.2–1998), released in September 1998, requires extensive use of a device to measure and determine the fouling characteristics of the tube bundle by monitoring individual tubes. A typical fouling monitors of Powerfect, USA, is shown in Figure 9.7 and its working principle is briefly discussed next.

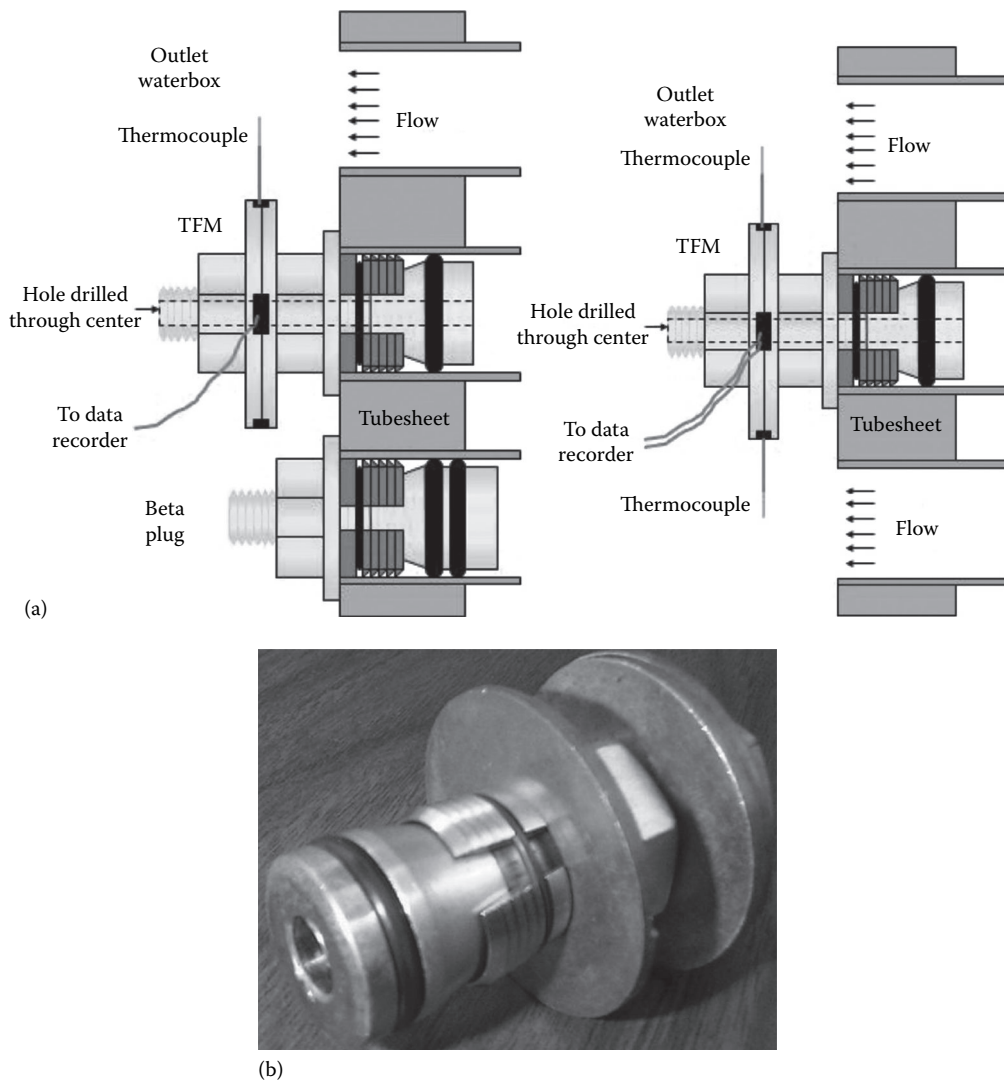


FIGURE 9.7 Tube fouling monitoring: (a) monitoring mechanism (illustration) and (b) monitoring plug. (Courtesy of Powerfect, Brick, NJ.)

9.11.3 FOULING MONITOR OPERATION

1. After tube cleaning or retube, Tube Fouling Monitor (TFM) is installed with one thermocouple lead positioned to measure outlet temperature of unplugged tube.
2. A control tube adjacent to TFM is plugged with removable plug on both ends.
3. Condenser is placed in service.
4. Outlet temperature data is recorded.
5. After designated period of time, control tube plugs are removed.
6. Second thermocouple lead is installed to measure outlet temperature of control tube.

9.11.3.1 Instruments for Monitoring of Fouling

Instruments have been developed to monitor conditions on a tube surface to indicate accumulation of fouling deposits and, in some cases, to indicate the effect on heat exchanger performance. Various fouling monitors are described in Ref. [17]. The following is a summary of the different fouling monitors [2].

1. Removable sections of the fouled surface, which may be used for microscopic examination, mass measurements, and chemical and biological analysis of the deposits.
2. Increase in pressure drop across the heat exchanger length. This method provides a measure of fluid frictional resistance, which usually increases with buildup of fouling deposits. This device is relatively inexpensive and is easy to operate.
3. Thermal resistance monitors are used to determine the effect of the deposit on overall heat transfer resistance. The thermal method of monitoring has the advantage over the others of giving directly information that is required for predicting or assessing heat transfer performance.

9.11.3.2 Gas-Side Fouling Measuring Devices

Marnier and Henslee [18] carried out a comprehensive review of gas-side fouling measuring devices. They classified the devices into the five groups: heat flux meters, mass accumulation probes, optical devices, deposition probes, and acid condensation probes. A heat flux meter uses the local heat transfer per unit area to monitor the fouling. The decrease in heat flux as a function of time is thus a measure of the fouling buildup. A mass accumulation device measures the fouling deposit under controlled conditions. Optical measuring devices use optical method to determine the deposition rate. Acid condensation probes are used to collect liquid acid that accumulates on a surface that is at a temperature below the acid dew point of the gas stream.

9.12 EXPERT SYSTEM

A computerized, consultative expert system has been developed that can simulate human reasoning, perform water treatment diagnoses, and recommend procedures to minimize corrosion and fouling in cooling water system [19]. In this work, a basic model adopted for knowledge representation is in the form of a fault tree. The expert system has been developed as a useful tool to accomplish the following:

1. Integrate myriad data from monitoring programs
2. Provide a diagnosis
3. Organize a logical stepwise approach to problem solving
4. Serve as a valuable tool for training

9.13 FOULING PREVENTION AND CONTROL

Specifying the fouling resistances or oversizing result in added heat transfer surface. The excess surface area can result in problems during startup and bring about conditions that can, in fact, encourage excess fouling due to low velocity [20]. There are a number of techniques that can overcome or mitigate the effects of fouling in heat exchangers, and they include the following:

1. Designing the plant or process in such a way that the condition leading to the fouling is limited or reduced
2. Instituting an online mechanical cleaning system, or cleaning the equipment when the effects of the fouling can no longer be tolerated to restore its effectiveness by various off-line cleaning techniques
3. Using chemical additives or antifoulants in the fouling stream

These aspects are discussed in detail next.

9.13.1 MEASURES TO BE TAKEN DURING THE DESIGN STAGES

No hard and fast rules can be applied for heat exchanger design in relation to fouling, but the following points should be kept in mind during the conception and design of a heat exchanger:

1. Make the design simple.
2. Select the heat exchanger type with point 1 in mind. Heat exchangers other than shell and tube units may be better suited to fouling applications. Gasketed plate exchangers and spiral plate exchangers offer better resistance to fouling because of increased turbulence, higher shear, or other factors. Before commissioning a heat exchanger, carry out design checks and ensure that all constructional details and clearances conform to specification.
3. Prevent the possibility of corrosion and fouling during and subsequent to hydrostatic testing.
4. Startup conditions should avoid temperatures higher or velocities lower than the design values [3].
5. Maximize the flow velocities of process fluids to enhance the removal of the fouling deposits, provided that the fluid velocity is not high enough to cause excessive pressure drop or flow-induced vibration on the shellside. Ensure that velocities in tubes are in general above 2 m/s and about 1 m/s on the shellside [3]. Avoid stagnant areas where the flow velocities are less than those in the bulk of the core.
6. Assume nominal fouling resistance either from past experience or from published standards and design the heat exchanger with nominal oversizing. The oversizing may be of the order of 20%–40%. It is generally prudent to avoid large fouling factors, which result in larger equipment. Larger equipment generally results in lower velocities and hence may accelerate fouling.
7. To minimize fouling of finned tube or plate fin heat exchangers, use optimum fin density. Otherwise the initial benefit of increased heat transfer will be offset by fouling in the long run. This is most appropriate for industrial air coolers, radiators of automobiles, and diesel locomotives. Compact heat exchangers functioning in outdoor unit are most prone to fouling due to airborne dirt, flying objects, leaves, and fibrous objects. Other considerations are in-line layouts to provide cleaning lanes for soot blowers, and wide pitches for dirty flue gases.
8. Fouling fluid on the tubeside: When the fouling fluid is on the tubeside, Mukherjee [9] recommends measures such as (1) using larger diameter tubes (a minimum of 25 mm OD), (2) maintaining high velocity (for cooling water, a minimum velocity of 1.5 m/s for

- mild steel, 1.2 m/s for nonferrous tubes, and as high as 5 m/s for titanium tubes is recommended), (3) leaving sufficient margin in pressure drop (for high fouling services, leave a margin of 30%–40% between the allowable and calculated pressure drop), (4) using a spare tube bundle or spare exchanger, (5) using two shells in parallel (each with 60%–70% of total capacity), (6) using wire-fin tube inserts, and (7) using online cleaning methods.
9. Fouling mitigation by installing hiTRAN[®] wire matrix elements
 - a. Fouling characteristics are dictated largely by the properties of the thermal and hydrodynamic boundary layers. hiTRAN wire matrix elements are a useful tool for controlling the conditions near the tube wall, especially in the laminar and transition flow regions and they have proven successful for direct fouling mitigation in the following scenarios.
 - b. In services where low tubeside heat transfer coefficients yield high wall temperatures leading to increased chemical reaction fouling and coking, hiTRAN wire matrix elements are used to reduce excessive wall temperatures in these tubeside controlled scenarios.
 - c. In cooling duties where low tube wall temperatures lead to crystallization fouling, hiTRAN thermal systems can raise the wall temperature above critical levels, and have been especially successful in the winterization of air cooled heat exchangers handling hydrocarbon streams with high pour points.
 - d. In exchangers operating at low flow velocities with increased risk of particulate and sedimentation fouling cases the increased shear resulting from the application of hiTRAN thermal systems will assist solid particles to pass through the heat exchanger without deposition.
 10. Fouling fluid on the shellside: When the fouling fluid is on the shellside, use a square or rotated square tube layout, minimize dead spaces by optimum baffle design, and maintain high velocity [9]. Or use non-segmental baffle heat exchangers as discussed in Section 9.6.15.
 11. If severe fouling is inevitable, it is frequently better to install spare units. Installed spares will permit cleaning while the other unit is in service.
 12. Proper selection of cooling medium can frequently avoid problems associated with fouling. For example, air cooling in place of cooling water solves many of the corrosion and fouling problems such as scaling, biological growth, and many of the aqueous corrosion. The cleaning of bare tube or finned tube surfaces fouled by air is easier than surfaces fouled by water.
 13. Particulate fouling, scaling, and trace-metal-catalyzed hydrocarbon reaction fouling can often be prevented by pretreatment of the feed streams to a heat exchanger by filtration, softening, and desalting, respectively [21].
 14. Once the unit is on-stream, operate at the design conditions of velocity and temperature.

9.14 CLEANING OF HEAT EXCHANGERS

In most applications, fouling is known to occur in spite of good design, effective operation, and maintenance. Hence, heat exchangers and associated equipment must be cleaned. The time between cleaning operations will depend upon the severity of the fouling problem. In some instances, cleaning can be carried out during periodical maintenance programs—say, twice yearly or annually—but in other cases frequent cleaning will be required, perhaps as frequently as monthly or quarterly. For example, locomotive radiators are air blown during their fortnightly schedules.

9.14.1 CLEANING TECHNIQUES

In general, the techniques used to remove the foulants from the heat exchanger surfaces, both on the shellside and on the tubeside, can be broadly classified into two categories: mechanical and chemical.

The cleaning process may be employed while the plant is still operating, that is, *online*, but in most situations it will be necessary to shutdown the plant to clean the heat exchangers, known as *off-line* cleaning. In some instances combinations of these cleaning methods may be necessary. Each method of cleaning has advantages and disadvantages with specific equipment types and materials of construction.

9.14.2 DEPOSIT ANALYSIS

Information about the composition of fouling deposits through deposit analysis is extremely helpful to identify the source of the major foulants, to develop proper treatment, and as an aid in developing a cleaning method for a fouling control program [8]. The sample should represent the most critical fouling area. For heat exchangers and boilers, this is the highest heat transfer area [22]. Many analytical techniques are used to characterize deposit analysis. Typical methods include x-ray diffraction analysis, x-ray spectrometry, and optical emission spectroscopy.

9.14.3 SELECTION OF APPROPRIATE CLEANING METHODS

Before attempting to clean a heat exchanger, the need should be carefully examined. Consider the following factors for selecting a cleaning method:

Degree of fouling.

Nature of the foulant, known through deposit analysis.

Chemical cleaning is associated with pumping hot corrosives through temporary connections and therefore the compatibility of the heat exchanger material and system components in contact with the cleaning chemicals.

Regulations against environmental discharges.

Accessibility of the surfaces for cleaning.

Cost factors.

9.14.3.1 Precautions to Be Taken while Undertaking a Cleaning Operation

Precautions to be taken while undertaking a cleaning operation are listed in TEMA [15] paragraph E-4.32 and Ref. [22]:

1. Individual tubes should not be steam blown because this heats the tube and may result in severe thermal strain and deformation of the tube, or loosening of the tube to tubesheet joint.
2. When mechanically cleaning a tube bundle, care should be exercised to avoid damaging the tubes. Tubes should not be hammered with a metallic tool.

Various cleaning methods are discussed next. (Cleaning of heat exchangers is also discussed in Chapter 16.)

9.14.4 OFF-LINE MECHANICAL CLEANING

Techniques using mechanical means for the removal of deposits are common throughout the industry. The various off-line mechanical cleaning methods are

1. Manual cleaning
2. Jet cleaning
3. Drilling and roding of tubes
4. Turbining
5. Hydro drilling action
6. Passing brushes through exchanger tubes
7. Scraper-type tube cleaners

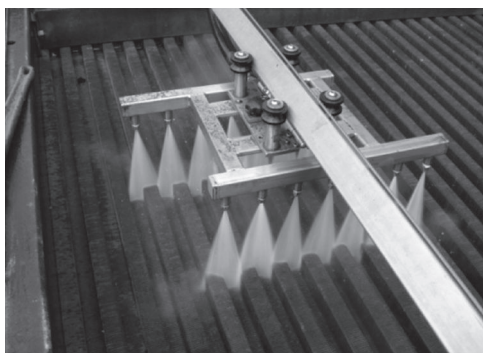
8. Blasting
9. Soot blowing
10. Thermal cleaning

9.14.4.1 Manual Cleaning

Where there is good access, as with a plate or spiral heat exchanger, or a removable tube bundle, and the deposit is soft, hand scrubbing and washing may be employed, although the labor costs are high.

9.14.4.2 Jet Cleaning

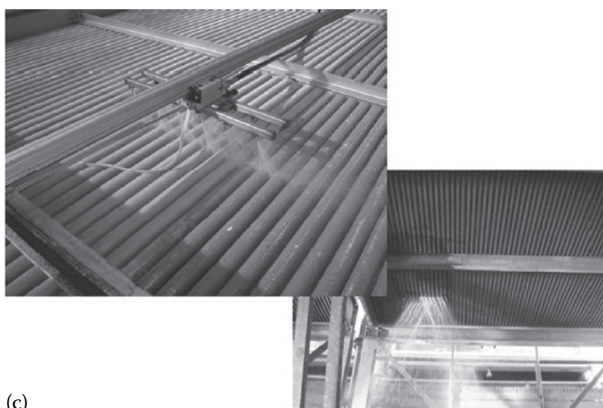
Jet cleaning or hydraulic cleaning with high-pressure water jets can be used mostly on external surfaces where there is an easy accessibility for passing the high pressure jet. Jet washing can be used to clean foulants such as [23]: (1) airborne contaminants of air-cooled exchangers at a pressure of 2–4 bar, (2) soft deposits, mud, loose rust, and biological growths in shell and tube exchangers at a pressure of 40–120 bar, (3) heavy organic deposits, polymers, tars in condensers and other heat exchangers at a pressure of 300–400 bar, and (4) scales on the tubeside and fire side of boilers, preheaters, and economizers at a pressure of 300–700 bar. This method consists of directing powerful water jets at fouled surfaces through special guns or lances. A variety of nozzles and tips is used to make most effective use of the hydraulic force. The effectiveness of this cleaning procedure depends on accessibility, and care is needed in application to prevent damage to the tubes and injury to the personnel. Similar to water jet cleaning, pneumatic descaling is employed on the fire side of coal-fired boiler tubes. Typical water jet cleaning of air cooled heat exchanger is shown in Figure 9.8.



(a)



(b)



(c)

FIGURE 9.8 (a-c). Cleaning of air cooler/air cooled condenser by water jet showing unique top-side cleaning. (Courtesy of ACC-Team B.V., Nieuwdorp, the Netherlands).

Traditionally, Fin-Fan Cooling Units were cleaned from the underside which simply forces the dirt further into the tube bundle. ACC Team's new and unique system cleans from above and forces the dirt out from where it came resulting in a 25%–40% improvement in cooling performance.

9.14.4.3 Drilling and Roding of Tubes

Drilling is employed for tightly plugged tubes and roding for lightly plugged tubes. Drilling of tightly plugged tubes is known as bulleting. For removing deposits, good access is required, and care is again required to prevent damage to the equipment. A typical example is roding of radiator tubes plugged by solder bloom corrosion products.

9.14.4.4 Turbining

Turbining is a tubeside cleaning method that uses air, steam, or water to send motor-driven cutters, brushes, or knockers in order to remove deposits.

9.14.4.5 Hydro Drilling Action

Through a water flushing and rotary drilling action, the hydro drilling system is the fastest and most effective way to remove difficult deposits from the inside of heat exchanger tubes, chemical reactors, condensers, reboilers, and absorbers. High torque drilling action removes obstructions from any type of tube ranging from 3/8" to 6" in diameter and up to 40' in length. It can effectively clean hard deposits such as coke, calcium, sulfur, bauxite, asphalt, oxides, and baked-on hard polymers. Typical hydro drilling by CONCO tube cleaning system is shown in Figure 9.9.

9.14.4.6 Passing Brushes through Exchanger Tubes

The unit consists of a long plastic dowel wrapped with nylon bristles. The brushes are propelled through the tube by a flexible shaft and the debris expelled by air/water shot right through the tube.

9.14.4.7 Scraper-Type Tube Cleaners

Scraper-type tube cleaners such as CONCO tube cleaner is an all purpose tube cleaner for condensers and heat exchangers with tube sizes 1/2"–1.25". This metal cleaner is effective on all types of deposits, including micro/macro fouling, organic-type scales, corrosion and pitting by-products, and all types of obstructions. The spring loaded tube cleaners are shot through the tubes with the Water Gun at 200–300 psi water pressure. The tube cleaner travels through the tube at 10–20 ft/s, plowing off deposits and corrosion and removing obstructions. Water flushes the removed matter out ahead of the cleaner, leaving a clean, polished bare metal inside diameter for optimum heat

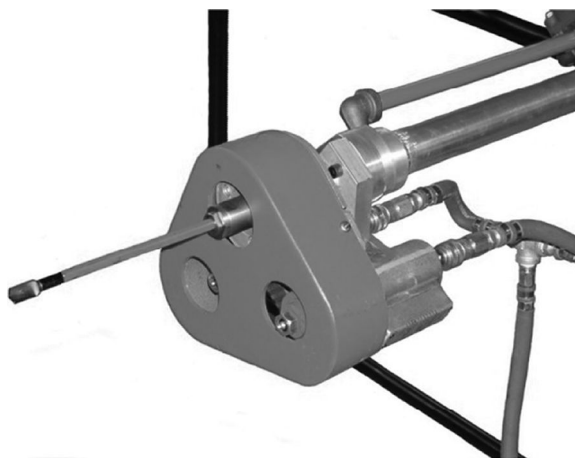


FIGURE 9.9 Hydro drilling system for dislodging fouling deposits. (Courtesy of Conco Systems, Inc., Verona, PA.)

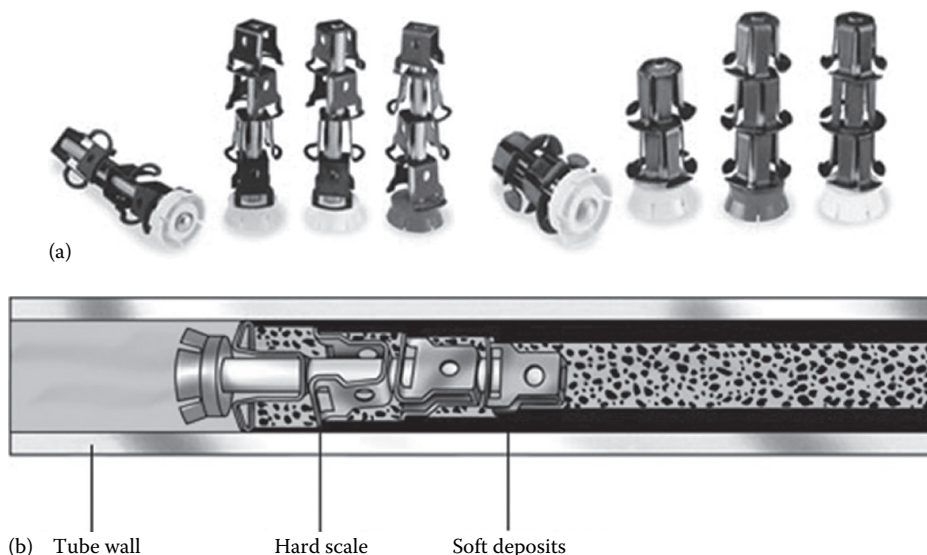


FIGURE 9.10 Scraper-type tube cleaners: (a) various models of tube cleaners and (b) tube cleaner in action—positioned inside a fouled tube. (Courtesy of Conco Systems, Inc., Verona, PA.)

transfer efficiency. Typical CONCO tube cleaners is shown in Figure 9.10. Plastic or metal cleaner capable of navigating U-tube configurations in heat exchangers and feedwater heaters is also marketed by Conco Systems.

9.14.4.8 Blast Cleaning

Blast cleaning involves propelling suitable abrasive material at high velocity by a blast of air or water (hydroblasting) to impinge on the fouled surface. Hydroblasting is seldom used to clean tube bundles because the tubes are very thin. However, the technique is suitable to descale and clean tubesheet faces, shells, channel covers, bonnets, and return covers inside and outside.

9.14.4.9 Soot Blowing

Soot blowing is a technique employed for boiler plants, and the combustion or flue gas heat exchangers of fired equipment. The removal of particles is achieved by the use of air or steam blasts directed on the fin side. Water washing may also be used to remove carbonaceous deposits from boiler plants. A similar cleaning procedure is followed for air blowing of radiators on the fin side during periodical schedule attention.

9.14.4.10 Thermal Cleaning

Thermal cleaning involves steam cleaning, with or without chemicals. This method is also known as hydrosteaming. It can be used to clean waxes and greases in condensers and other heat exchangers.

9.14.5 MERITS OF MECHANICAL CLEANING

The merits of mechanical cleaning methods include simplicity and ease of operation, and capability to clean even completely blocked tubes. However, this method may damage the equipment, particularly tubes, it does not produce a chemically clean surface, and the use of high-pressure water jet or air jet may cause injury and/or accidents to personnel engaged in the cleaning operation—hence the personnel are to be well protected against injuries.

9.14.6 CHEMICAL CLEANING

The usual practice is to resort to chemical cleaning of heat exchangers only when other methods are not satisfactory. Chemical cleaning involves the use of chemicals to dissolve or loosen deposits. The chemical cleaning methods are mostly off-line known as clean-in-place systems.

9.14.6.1 Clean-in-Place Systems

Clean-in-place systems using chemicals such as detergents and sterilizing agents have come into broad use due to a number of advantages:

- Time saving
- Cost savings resulting from the use of less chemical solution
- Elimination of unit openings on hazardous duties, etc.

9.14.6.2 Choosing a Chemical Cleaning Method

Chemical cleaning methods must take into account a number of factors as given in the following:

1. Compatibility of the system components with the chemical cleaning solutions. If required, inhibitors are added to the cleaning solutions.
2. Information relating to the deposit must be known beforehand.
3. Chemical cleaning solvents must be assessed by a corrosion test before beginning cleaning operation.
4. Adequate protection of personnel employed in the cleaning of the equipment must be provided.
5. Chemical cleaning poses the real possibility of equipment damage from corrosion. Precautions may be taken to reduce the corrosion rate to acceptable levels. Online corrosion monitoring during cleaning is necessary [22]. Postcleaning inspection is extremely important to check for corrosion damage due to cleaning solvents and to gauge the cleaning effectiveness.
6. Disposal of the spent solution.

9.14.6.3 Chemical Cleaning Solutions

Chemical cleaning solutions include mineral acids, organic acids, alkaline bases, complexing agents, oxidizing agents, reducing agents, and organic solvents. Inhibitors and surfactant are added to reduce corrosion and to improve cleaning efficiency [22]. Common foulants and cleaning solvents are given in Table 9.2 and common solvents and the compatible base materials are given in Table 9.3.

9.14.7 GENERAL PROCEDURE FOR CHEMICAL CLEANING

The majority of chemical cleaning procedures follow the following steps [23]:

1. Flush to remove loose debris.
2. Heating and circulation of water.
3. Injection of cleaning chemical and inhibitor if necessary in the circulating water.
4. After sufficient time, discharge cleaning solution and flush the system thoroughly.
5. Passivate the metal surfaces.
6. Flush to remove all traces of cleaning chemicals.

It is suggested that one employ qualified personnel or a qualified organization for cleaning services.

TABLE 9.2
Foulants and Common Solvents

Foulant	Cleaning Solvent
Iron oxides	Inhibited hydrofluoric acid, hydrochloric acid, monoammoniated citric acid or sulfamic acid, EDTA
Calcium and magnesium scale	Inhibited hydrochloric acid, citric acid, EDTA
Oils or light greases	Sodium hydroxide, trisodium phosphate with or without detergents, water-oil emulsion
Heavy organic deposits such as tars, asphalts, polymers	Chlorinated or aromatic solvents followed by a thorough rinsing
Coke/carbonaceous deposits	Alkaline solutions of potassium permanganate or steam air decoking

Sources: Compiled and modified from Lester, G. D. and Walton, R., Cleaning of heat exchangers, in *Practical Application of Heat Transfer*, C55/82, IMechE, London, U.K., pp. 1–10, 1982; Garverick, L., Corrosion in the chemical processing industry, *Corrosion in the Petrochemical Industry*, ASM International, OH, 163–224, 1994.

TABLE 9.3
Solvent and Compatible Base Metals

Solvent	Base Metal/Foulant
Hydrochloric acid	Water-side deposits on steels. Inhibited acid can be used for cleaning carbon steels, cast iron, brasses, bronzes, copper-nickels, and Monel 400. This acid is not recommended for austenitic stainless steels, Inconel 600, Incoloy 800, and aluminum
Hydrofluoric acid	To remove mill scale
Inhibited sulfuric acid	Carbon steel, austenitic stainless steels, copper-nickels, admiralty brass, aluminum bronze, and Monel 400. It should not be used on aluminum
Nitric acid	Stainless steel, titanium, and zirconium
Sulfamic acid	To remove calcium and other carbonate scales and iron oxides. Inhibited acid can be used on carbon steel, copper, admiralty brass, cast iron, and Monel 400
Formic acid with citric acid or HCl	To remove iron oxide deposit. Can be used on stainless steels
Acetic acid	To remove calcium carbonate scale
Citric acid	To clean iron oxide deposit on aluminum or titanium
Chromic acid	To remove iron pyrite and certain carbonaceous deposits that are insoluble in HCl on carbon steel and stainless steels. It should not be used on copper, brass, bronze, aluminum, and cast iron

Source: Compiled and modified from Deghan, T.F., Corrosion in the chemical processing industry, in *Metals Handbook*, Vol. 13, *Corrosion*, 9th edn., American Society for Metals, Metals Park, OH, pp. 1134–1185.

9.14.8 OFF-LINE CHEMICAL CLEANING

Major off-line chemical cleaning methods are

1. Circulation
2. Acid cleaning
3. Fill and soak cleaning
4. Vapor-phase organic cleaning
5. Steam injection cleaning

Circulation: This method involves the filling of the equipment with cleaning solution and circulating it by a pump. While cleaning is in progress, the concentration and temperature of the solution are monitored.

Acid cleaning: Scales due to cooling water are removed by circulating a dilute hydrochloric acid solution. This is discussed in detail with the discussion of cooling-water fouling.

Fill and soak cleaning: In this method, the equipment is filled with a chemical cleaning solution and drained after a period of time. This may be repeated several times until satisfactory results are achieved. However, this method is limited to small units only.

Vapor-phase organic cleaning: This method is used to remove deposits that are organic in nature.

Steam injection cleaning: This method involves an injection of a concentrated mix of cleaning solution and steam into a fast-moving stream. The steam atomizes the chemicals, increasing their effectiveness and ensuring good contact with metal surfaces.

9.14.8.1 Integrated Chemical Cleaning Apparatus

Generally, chemical cleaning is performed in four stages: degreasing, pickling, passivating, and flushing. Each of these stages ordinarily requires a separate and distinct setup of apparatus to complete the job adding considerable extra expense for additional man hours taken by pipefitters and other skilled labor. As per this invention, an integral chemical cleaning apparatus for supplying and recirculating chemical cleaning solutions used in the process of removing scale, rust, grease and dirt coatings from internal metallic surfaces of closed industrial equipment where the stages of pickling, passivating and flushing are performed consecutively without change-over to separate devices for each of such stages of the process and further it eliminates the need for virtually all auxiliary pumping requirements.

9.14.9 MERITS OF CHEMICAL CLEANING

Chemical cleaning offers the following advantages over the mechanical cleaning:

1. Uniform cleaning and sometimes complete cleaning.
2. Sometimes chemical cleaning is the only possible method.
3. No need to dismantle the unit, but it must be isolated from the system.
4. Capable of cleaning inaccessible areas.
5. Moderate cleaning cost and longer intervals between cleaning.

9.14.10 DISADVANTAGES OF CHEMICAL CLEANING METHODS

Chemicals used for cleaning are often hazardous to use and require elaborate disposal procedures. Noxious gases can be emitted from the cleaning solution from unexpected reactions. Chemical cleaning corrodes the base metal and the possibility of excess corrosion cannot be ruled out. Complete washing of the equipment is a must to eliminate corrosion due to residual chemicals.

9.14.11 ONLINE CLEANING METHODS

There is an obvious need for an industrial online cleaning procedure that can remove fouling deposits without interfering with a plant's normal operation. Online cleaning methods can be either mechanical or chemical. Online chemical cleaning is normally achieved by dosing with chemical additives.

9.14.12 ONLINE MECHANICAL CLEANING METHODS

Various online mechanical cleaning methods to control fouling in practice are as follows:

1. Upstream filtration
2. Flow excursion
3. Air bumping of heat exchangers
4. Reversing flow in heat exchangers
5. Automatic tube cleaning systems such as
 - a. Sponge rubber balls cleaning system
 - b. Brush and cage system
6. Insert technology
7. Grit cleaning
8. Self-cleaning fluidized-bed exchangers

9.14.12.1 Upstream Filtration (Debris Filter)

Cooling-water fouling can be controlled, and in some cases eliminated, by adequately filtering the intake water. Power-station condensers are more vulnerable to the intake of debris and biological organisms. One solution to prevent the blockage of condenser tubes is the installation of an upstream filtration system [24].

Fouling control of cooling water system by Automatic Debris Filter System (ADFS).

Despite all of the prescreening technology employed at raw cooling water intake sites, additional filtration is often required to avoid macro fouling of the units served. The solution to this problem is provided by the Automatic Debris Filter System (ADFS). The ADFS is designed to effectively prevent macro fouling by fibrous, coarse and marine life debris (larger than the selected filter perforation size), by capturing and ejecting all debris in an optimal manner. The optimal cleaning capability is achieved through the incorporation of dedicated suction ports for the two basic classes of water borne debris (course and fibrous).

9.14.12.2 Flow Excursion

In this method the instantaneous flow is increased to remove the fouling deposits. This method is particularly applicable to a heat exchanger fouled badly due to the effects of low velocity either on the shellside or the tubeside.

9.14.12.3 Air Bumping

This technique involves the creation of slugs of air, thereby creating localized turbulence as slugs pass through the equipment. The technique has been applied to the liquid system on the shellside of heat exchangers. Care has to be taken to avoid the possibility of producing explosive mixtures of gases if the process fluid is volatile and flammable [3].

9.14.12.4 Reversing Flow in Heat Exchangers

Reversing of flow or backflushing or back wash system is followed on the water side of the cooling water system by intermittent reversal of flow. Backflushing is an easy and efficient method to prevent clogging and fouling of heat exchangers. The cleaning effect is achieved by changing the flow direction in the heat exchanger so that the dirt accumulated in the inlet region and the heat exchanging channels is flushed out. Unlike filters, regular backflushing can prevent biological fouling. The algae and organisms that have entered the heat exchanger are flushed out before they can establish themselves. The heart of the system includes (1) A backflushing valve and (2) control panel. To avoid "water hammer" the valves must be opened and closed in a certain sequence, hence a control system is absolutely necessary. A typical backflushing valve and its working principle is shown in Figure 9.11. The merits of backflushing include *energy savings because* the backflushing valve does not

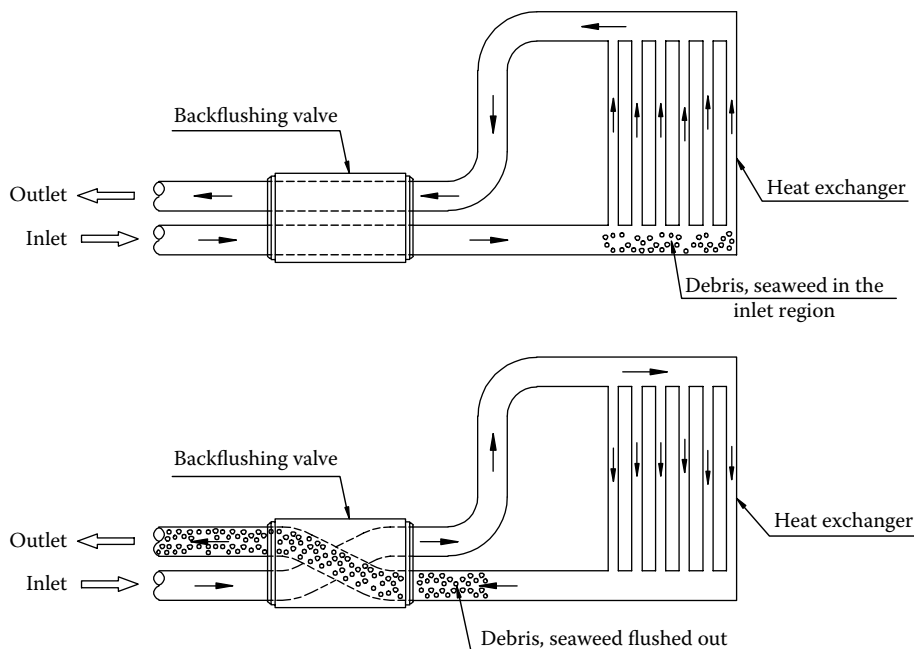


FIGURE 9.11 Backflushing—working principle.

affect the standard operation, and hence no extra pumping energy costs, and it is *nonpolluting and* ecologically harmless. By regular backflushing of heat exchangers in open cooling systems, the use of chemical cleaners can be reduced considerably.

9.14.12.5 Automatic Tube Cleaning Systems

Automatic tube cleaning systems (ATCS) such as sponge rubber balls cleaning system and brush and cage system have ideal applications on steam surface and overhead condensers, large chiller systems and auxiliary heat exchangers. These two types of systems are briefly explained next.

9.14.12.5.1 *Sponge Rubber Ball Cleaning System*

Major parts of a ball-type cleaning system include ball circulation pump, ball strainer, ball collector vessel, ball injector, control panel, and balls cleaning systems. A large number of sponge rubber balls, slightly larger in diameter than the inner diameter of the tubes and having about the same specific gravity as seawater, are passed continuously into the inlet water box as shown in Figure 9.12 (for instance, the Beaudrey or Taprogge system) [24]. The cooling-water flow forces the balls through the tubes and the deposits on the tube walls are wiped out. The method may not be effective on longer runs once hard deposits are formed, or pitted. The balls used for normal operation should have the right surface roughness to gently clean the tubes, without scoring the tube surface. To remove heavy deposits, special abrasive balls that have a coating of carborundum are available [25].

9.14.12.5.2 *Brush and Cage System Automatic Online Tube Cleaning System*

The brush and cage or the Mesroc automatic online tube cleaning system used for cleaning heat exchangers consists of (1) a four-way flow diverter, (2) a control panel, and (3) one lot of brushes and basket sets. The four-way flow diverter is installed between the tubeside piping to and from the unit. A specifically selected brush is inserted into each tube, and catch baskets are semi-permanently installed at both ends of each of the tubes as shown in Figure 9.13. By reversing the flow direction, every brush is being moved from one end of the tube to the other, where it is retained by the basket. It remains there until the next cleaning cycle. The brushes moving to and fro keep the inner walls

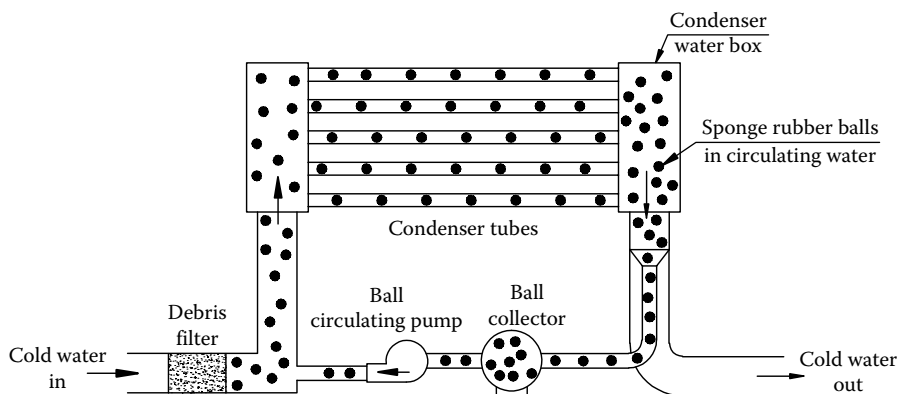


FIGURE 9.12 Sponge rubber ball cleaning system of a water-cooled condenser.

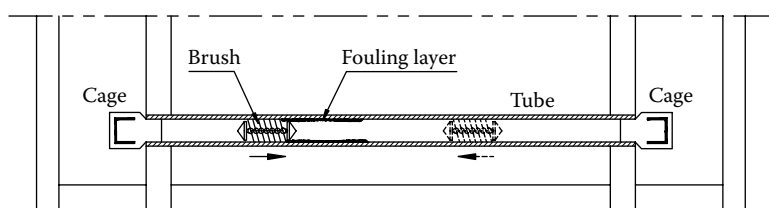


FIGURE 9.13 Brush and cage ATCS—schematic representation.

clean. An actuator and a control system initiate the cleaning cycles. Because this is done no less than every 6–8 h, even hardenable deposits are yet in a soft state and are easily removed. A major advantage of the system is that it does not require a recirculation system as for rubber ball system and an important disadvantage is the interruption of the flow in the heat exchanger and consequent disturbance of steady state conditions [3].

9.14.12.6 Insert Technology

Inserts are devices installed in tubular heat exchangers as a means of heat transfer augmentation device. Few types of inserts continuously reduce fouling and improve heat transfer by means of mechanical effects. Three inserts resulting from research by Total are available: Turbotal®, Fixotal®, and Spirelf® (Spirelf, Fixotal, and Turbotal are registered trademarks of Total, the French oil company, and Petroval, France, is the exclusive licensee of Total for the design and the commercialization of these inserts). Today they are widely used in preheat trains in oil refineries.

9.14.12.6.1 Spirelf System

In the Spirelf system shown in Figure 9.14, fine wire springs are threaded through the tubes and held in place by straight wires at the ends of the tubes as fluid flows through the tubes. After installation, the insert stays under tension. The springs vibrate radially and axially under the influence of fluid flow. This action reduces buildup of fouling inside the tube walls and break the boundary layer in the tubeside flow. These two effects achieves an improvement of

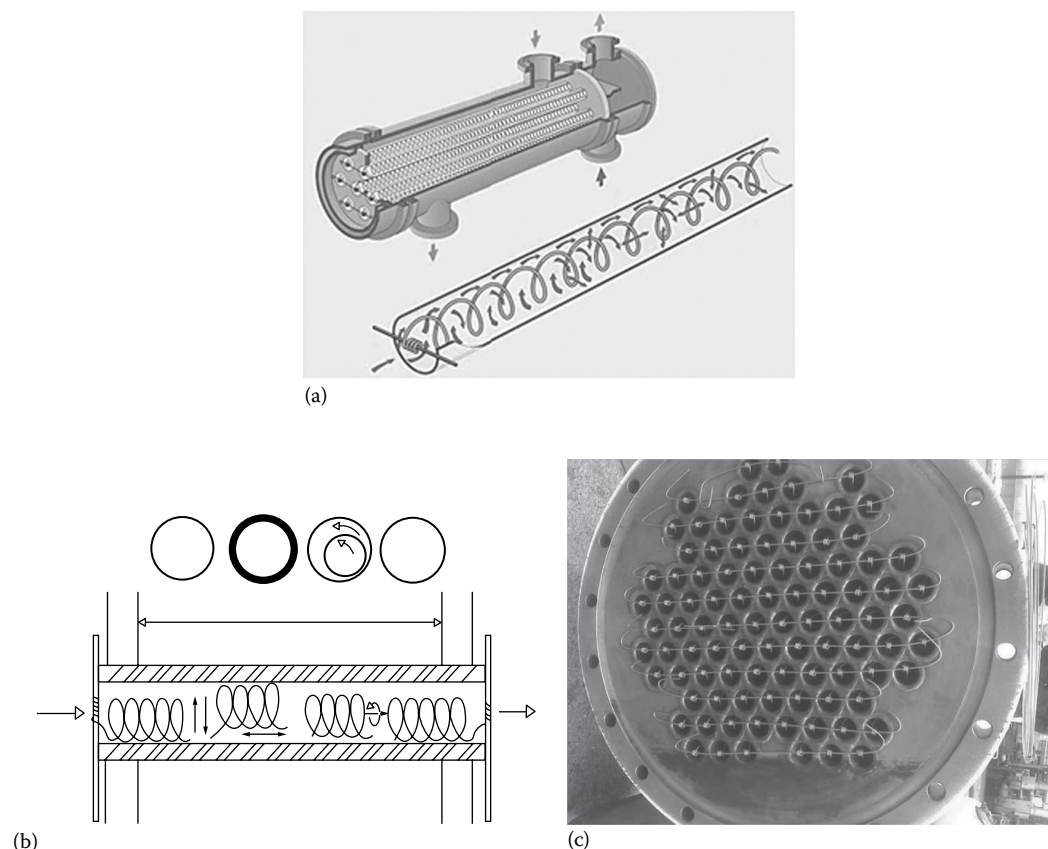


FIGURE 9.14 Spirelf: (a) schematic, (b) principle of working, and (c) spirelf placed inside tubes, application in reboilers.

the heat transfer rate. The effect of Spirelf system on thermohydraulic performance of a heat exchanger is shown in Figure 9.15.

9.14.12.6.2 *Turbotal*

The principle is based on the insertion of rotating metal devices, in rigid helicoidal form, into the tubes of shell and tube heat exchangers (Figure 9.16). Turbotal device is held at the inlet of tubes by a fixing device allowing the device to rotate around its axis by means of the fluid flow. This rotation causes a high turbulence in the flow and improves thus the internal heat transfer coefficient. As the boundary layer is continuously renewed, the wall temperature is lowered and fouling is slower. To get optimum performance, proper installation is essential, operate over limited velocity range—minimum velocity 0.7 m/s and maximum velocity 1.6 m/s and replace every 2 years. Typical applications include crude preheat train, hydrotreaters, and feed-effluent exchangers.

9.14.12.6.3 *Fixotal*

The purpose of this fixed device is mainly to increase the rate of heat transfer. Fixotal consists of a wire coil, which is inserted inside every tube, with the wire in firm contact with the inside tube wall. Once in place, the device has no possibility of the slightest displacement (no vibration, no rotation, and no translation), the device can be easily removed if necessary.

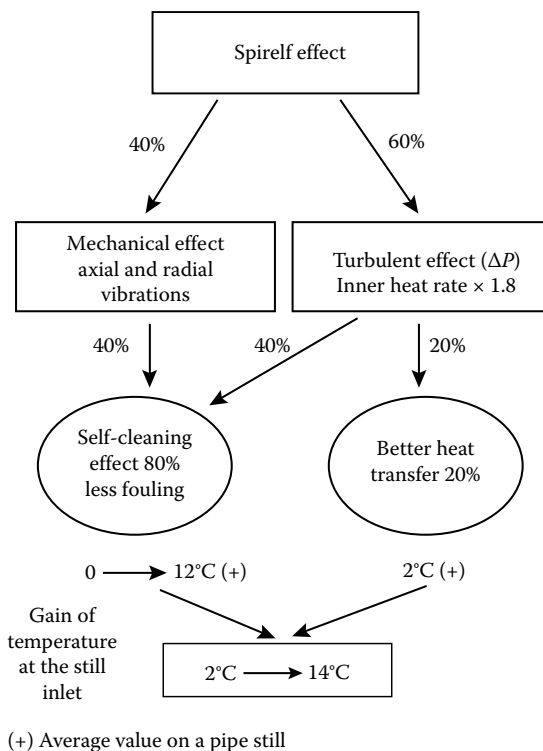


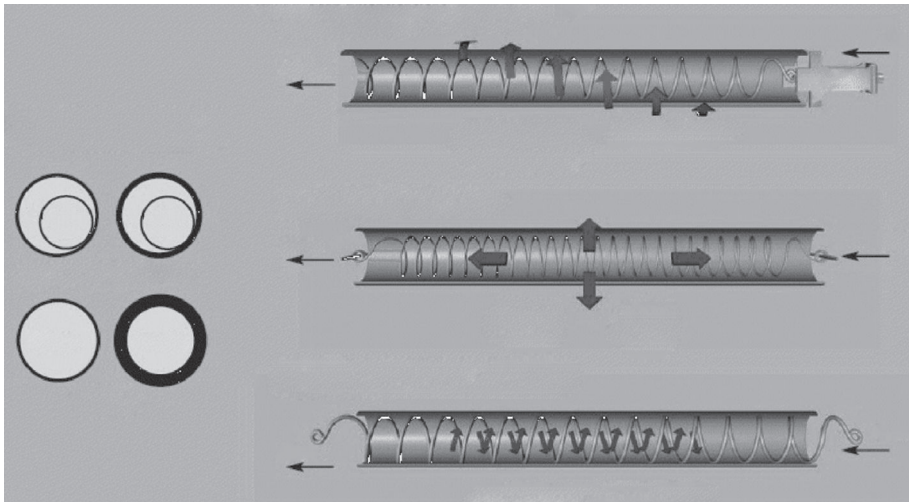
FIGURE 9.15 Spirelf effect.

Fixotal acts as a source of turbulence in contact with the internal walls of the tube, preventing the stagnation of products in the layer adjacent to the tube. The result is a significant increase of the tubeside heat transfer coefficient and a moderate increase of pressure drop through the tube and decrease in temperature gradient between tube wall and the bulk fluid. This leads to a decrease of the tubeside surface fouling rate, especially with fouling which is wall temperature dependant (polymerization, solidification of paraffin, scaling, etc.). Typical applications include air coolers, cooling water system, U-tubes, and mixed phase flow.

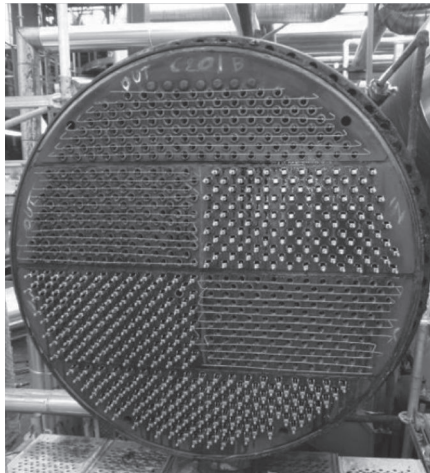
9.14.12.7 Grit Cleaning

In this method, abrasive materials, such as sand, glass, or metal spheres, are passed through the tubes. The scouring action removes the deposits from the inside of the tubes. The method has found application in cooling-water systems, but it could be used in conjunction with any fouling fluids. A special grit blasting nozzle accelerates the grit and causes it to follow a sinusoidal path through the tube, dislodging the deposits [24]. Velocities more than 3 m/s are probably required for the technique to be effective. The demerits of this method are [3] as follows:

1. The risk of settlement of particles in the low-velocity regions, as in the water boxes of exchangers where the local velocities are much lower than in the tubes.
2. The possibility of erosion–corrosion.
3. It is also necessary to filter out the particles from the liquid stream effectively, to avoid problems downstream from the exchanger.



(a)



(b)

FIGURE 9.16 Turbotal: (a) turbotal effect (schematic) and (b) turbotals placed inside tubes.

9.14.12.8 Self-Cleaning Heat Exchangers

The operating principle of the self-cleaning exchangers is shown in Figure 9.17.

The fouling liquid is fed upward through a vertical shell and tube exchanger that incorporates specially designed inlet and outlet channels. Solid particles are also fed at the inlet, where a flow distribution system uniformly provides the liquid and suspended particles throughout the internal surface of the bundle. The particles are transported by the upward flow of liquid through the tubes, where they create a mild scraping effect on the wall of the heat exchange tubes, thereby removing any deposit at an early stage of fouling formation. These particles consist of cut metal wire, glass or ceramic balls with diameters varying from 1 to 4 mm. At the top, inside the separator connected to the outlet channel, the particles disengage from the liquid and are returned to the inlet channel through an external downcomer, and the cycle is repeated. The process liquid fed to the exchanger is divided into a main flow and a control flow that transport the particles into the exchanger. By varying the control flow, it is possible to control the amount of particles in the

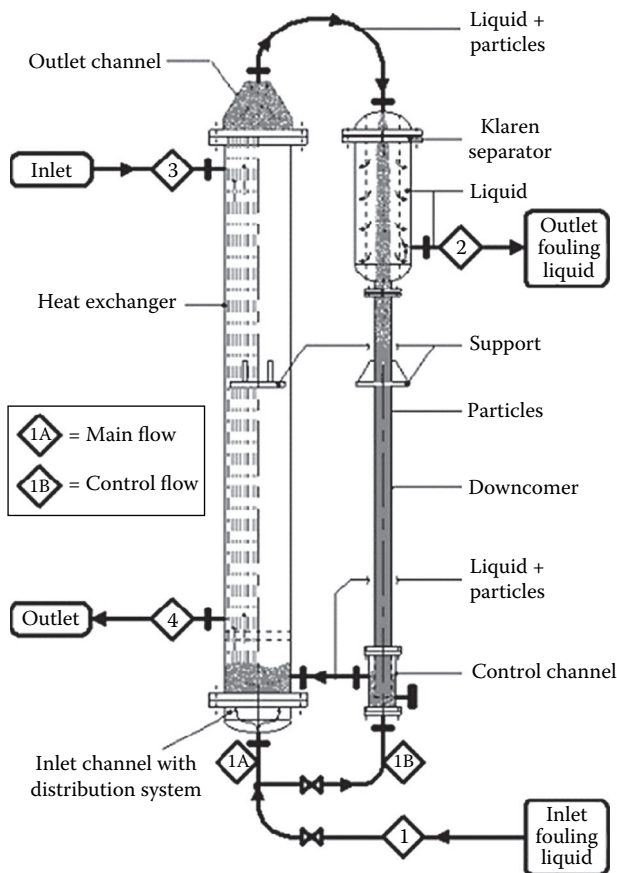


FIGURE 9.17 Principle of self-cleaning heat exchanger. (Courtesy of Klaren BV, Rotterdam, the Netherlands.)

tubes. This controls the efficiency of the cleaning mechanism, allowing the particle circulation to be either continuous or intermittent. It can be seen from Figure 9.18, the process liquid fed to the exchanger is divided into a main flow and a control flow that transport the particles into the exchanger.

A variation of the abrasive cleaning method is to use a fluidized bed of particles to control fouling on the outside tubular exchangers; its working of the same is briefly discussed next.

9.14.12.8.1 Liquid Fluidized-Bed Technology

Shellside application: Liquid fluidized-bed technology offers the potential for scale control and increased heat transfer coefficients in heat exchangers. Fluidized beds consist of a bed of solid particles (e.g., sand) with fluid passing upward through them, Figure 9.18. When the fluid reaches a velocity which causes the drag force on the individual particles to equal the particle weight, the particles are suspended or fluidized. The bed of particles will continue to expand as the velocity is increased and it will behave as a fluid until the terminal velocity is reached. At terminal velocity, the particles will be entrained in the fluid. This process of fluidization has been applied to liquid heat exchangers to eliminate the common problem of heat transfer surface scaling on shellside. The primary fluid may be used to fluidize a bed material such as sand. The fluidizing action of the bed creates two distinct advantages over conventional shell and tube flow arrangements: (1) the

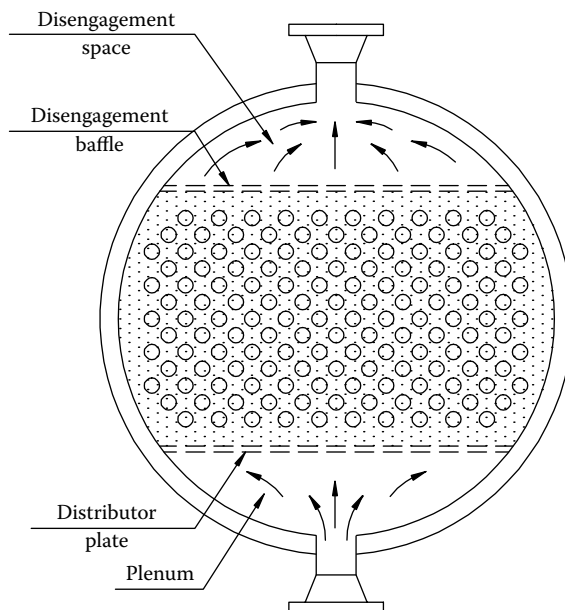


FIGURE 9.18 Liquid bed regenerator principle applied to shellside of a heat exchanger.

scouring action of the bed prevents scaling and limits corrosion on the tubes and (2) the heat transfer coefficient for the fluidized bed is almost double the coefficient for a conventional exchanger, Cole et al. [26].

Tubeside application: Liquid fluidized-bed technology offers the potential for scale control and increased heat transfer coefficients on the tubeside of shell and tube heat exchangers. Figure 9.19 shows schematic of the fluidized-bed principle applied to tubeside of a heat exchanger.

9.14.13 MERITS OF ONLINE CLEANING

The merits of online cleaning are as follows:

1. Increased heat transfer rate due to higher flow turbulence on tubeside
2. Reduction in maintenance cost due to reduced tubeside fouling
3. Extended run time between cleaning intervals
4. Convenient to install
5. Does not require any plant shutdown
6. Can save time and labor

However, the initial cost may be very high in certain cases.

9.15 FOULANT CONTROL BY CHEMICAL ADDITIVES

If fouling cannot be tackled adequately either by process design or equipment design, it can be further reduced by periodical online injection of additives into the process stream [21]. Chemical additives find wider use in cooling-water systems and to control fouling due to crystallization and freezing, chemical reaction or polymerization, precipitation, particulate, and scaling. The use of additives to prevent chemical reaction or polymerization fouling in liquids

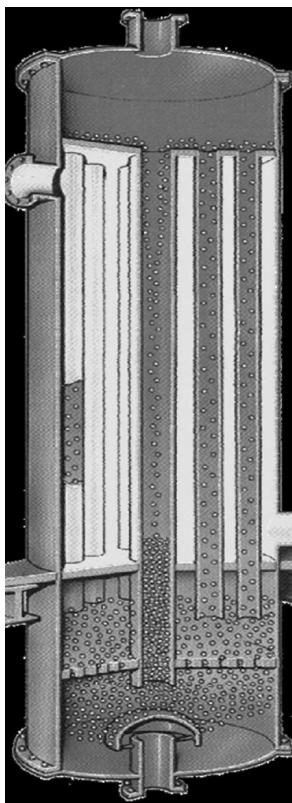


FIGURE 9.19 Schematic of the fluidized-bed principle applied to tubeside of heat exchanger. (Courtesy of Klaren BV, Rotterdam, the Netherlands.)

is well known in the petroleum refining industry, where a particular feedstock is a complex mixture of hydrocarbon and other organic materials [3]. Various types of additives and their functions are as follows:

1. *Alkali or acid dosing*: By dosing either alkali or acid, pH may be controlled. This may be effective to control precipitation fouling. Acid dosing controls the hardness of hard or brackish water.
2. *Complexing agents*: Agents such as chelants complex the metallic ion into a ring structure that is difficult to ionize.
3. *Chemical reactants*: These are used to complex or tie up the active foulants. They can solubilize or condition the foulants to prevent deposition.
4. *Sequestrant*: This additive complexes the metallic ions into a water-soluble structure, thus preventing its adhesion to the heat exchanger surface. A sequestrator physically surrounds and isolates particles (e.g., EDTA).
5. *Oxidizing agents*: These oxidize the deposits, making them suitable for dissolution (e.g., chromic acid, sodium nitrite, potassium permanganate).
6. *Reducing agents*: Reduce the compounds in deposits and make them suitable for dissolution and to prevent the formation of hazardous by-products.
7. *Inhibitors*: Control cooling-water corrosion. Corrosion inhibitors such as filming amines stifle chemical reaction fouling [3].
8. *Surfactant*: Added to chemical cleaning solution to improve the wetting characteristics.
9. *Antiscalants*: In aqueous system, these additives chemically combine the scales to form soluble compounds.

10. *Distortion agents*: These interfere with the crystal structure so that it becomes more difficult for coherent crystal structures to form on surfaces.
11. *Dispersants*: Dispersants impart an electrical charge to the particles so that they are held in suspension in the bulk of the liquid and the particles pass through the equipment without deposition on heat transfer surfaces. Dispersants are helpful to control chemical reaction fouling.
12. *Depressants*: Depressants lower the freezing point of the solution such that the potential forming solids is brought down (e.g., glycols, alcohols).
13. *Flocculating agent*: causes the particles to agglomerate so that they may be settled out of the cooling water or suitably filtered.
14. *Threshold agents* that prevent the creation of crystal nuclei around which the larger crystals form. They also arrest the growth of nuclei (e.g., polyphosphates). In cooling-water systems, threshold agents retard the precipitation of scale-forming salts.
15. *Stabilizers*: On reaching the solubility limit, stabilizers are able to retard the nucleation of individual low-solubility compounds and prevent any existing crystals from forming adhesive deposits.
16. Metal coordinators react with the trace metals and prevent them from functioning as fouling catalysts in the case of chemical reaction or polymerization fouling.
17. Biocides kill the micro or macroorganism. Biostats arrest the growth of microorganisms.

9.16 CONTROL OF FOULING FROM SUSPENDED SOLIDS

Methods of control of fouling from suspended solids include [3] the following:

1. Pretreatment of process fluids by means such as filtration, softening, and desalting to control precipitation fouling, particulate fouling, and scaling
2. Chemical treatment using dispersants and flocculating agents

9.17 COOLING-WATER MANAGEMENT FOR REDUCED FOULING

Many industries use cooling water for one purpose or another. It is appropriate to include a section devoted to cooling-water management for fouling control. Traditionally, the treatment of cooling water has often been oriented toward corrosion control followed by foulant control. However, it is impossible to separate these twin problems in any treatment program, since one can lead to the other, and since both can occur simultaneously [8]. In addition to some of the online foulant control measures discussed already, specific features of cooling-water fouling control are discussed here. Cooling-water corrosion control measures are discussed in Chapter 12 on corrosion.

9.17.1 FORMS OF WATER-SIDE FOULING

Water is by far the most common fluid subject to fouling. The quality of water used in the cooling system varies depending on its sources, like sea, river, ocean, lake, etc., and on the three forms of cooling water systems: once through, open recirculating, and closed systems. Cooling-water quality factors that contribute to fouling include turbidity, salinity, dissolved solids and hardness, biological organisms, airborne contaminants, etc. The quality of raw water changes according to weather conditions also. In general, fouling associated with cooling water can be classified under the following headings [3]:

Scaling due to crystallization of inverse solubility salts, mainly in cooling-tower water and sometimes in water drawn from a river, lake, or well.

Biological fouling of water drawn from a river, lake, sea, or the ocean; algae growth in open recirculating water.

Particulate fouling—Deposition of silts, sediments and suspended solids when water is drawn from a lake, river, or nearby seashore and due to airborne objects when water is exposed to the atmosphere.

Corrosion fouling due to cooling-water quality.

9.17.2 INFLUENCE OF SURFACE TEMPERATURE ON FOULING

The maximum tube surface temperature (the average between the temperature of the inlet fluid and the exchanger outlet water) on the water side at the tube–water interface is usually the critical concern. The recommended design surface temperature is 145°F (63°C) with 160°F (71°C) as a practical maximum. Heat exchangers with surface temperature above 160°F are prone to localized boiling. Boiling allows concentration of even the most soluble salts, with the threat of severe deposition and subsequent corrosion. For such a situation, water quality is to be improved by full softening or demineralization. (This material is based on Chenoweth [4].)

9.17.3 FOULANT CONTROL VERSUS TYPE OF COOLING-WATER SYSTEM

Fouling problems and their control in each of the three basic types of cooling systems (once-through, open recirculating, and closed) are often quite different and thus require different techniques. Cooling-system operation and specific characteristics should be analyzed constantly as a continuing part of the foulant control program.

9.17.3.1 Once-Through System

In once-through cooling-water systems, usually the major foulants are biological organisms, mud, silt, debris, or other suspended matter, and pollutants [8]. This type of cooling-water system generally needs only upstream filtration and a mechanical online cleaning method of passing plugs or sponge rubber balls as in condensers cooled by seawater. Generally, economics favor the chemical treatment. The chemical additives most generally used are mud fluidizers, dispersants, and biocides, particularly chlorination. Environmental regulations may restrict certain chemical additives.

9.17.3.2 Open Recirculating System

In open recirculating systems with cooling towers or spray ponds, foulants originate in the makeup water, air or process contamination, and from lack of good corrosion control [8]. Hence, this system is frequently treated for foulant control. Both mechanical and chemical methods are used singly or jointly to overcome fouling problems. Remove solid particles through sedimentation ponds and/or continuous filtration such as automatic debris filter system (ADFS). Mud fluidizers, dispersants, flocculating chemicals and foulant solubilizers, biocides, and other chemicals are added to control fouling.

9.17.3.3 Closed Recirculating Systems

The source of foulants is usually the corrosion products from heat exchangers and piping components. Corrosion control is mostly by inhibitors.

9.17.3.4 Online Chemical Control of Cooling-Water Foulants

Foulant control through some of the chemical additives include the following:

- Threshold chemicals

- Sequestrant and chelating chemicals, such as ethylenediamine tetraacetic acid (EDTA) and derivatives, nitrilotriacetic acid (NTA), organic phosphate esters, and organic phosphonates [8]

- Dispersants (e.g., lignins, tannins, alginates, cellulose, starch products, sodium polymethacrylate, and polyvinyl pyridinium butyl bromide) [8]

- Sludge fluidizers

- Biocides

9.17.4 CONTROL OF SCALE FORMATION AND FOULING RESISTANCES FOR TREATED COOLING WATER

The following values for cooling water assume that corrosion is under control and that biological growth does not represent a significant portion of fouling [4]:

1. Since scaling in cooling water system is due to inverse solubility phenomena, which normally take place about 140°F (60°C), keep the surface temperature below this temperature.
2. The cooling-water velocity is at least 4 ft/s on the tubeside for most nonferrous alloy tubes and 6 ft/s for carbon steel tubes. Velocities as high as 15 ft/s have been used inside titanium tubes.
3. The velocity of cooling water on the shellside is at least 2 ft/s. Higher velocities are permitted if erosion can be tolerated or flow-induced vibration is not possible.
4. Under the preceding conditions, a reasonable design value for the cooling-water-side fouling resistance is $0.001 \text{ h} \cdot \text{ft}^2 \cdot ^\circ\text{F}/\text{Btu}$.
5. The fouling resistance for a clean heat exchanger should be taken as $0.0005 \text{ h} \cdot \text{ft}^2 \cdot ^\circ\text{F}/\text{Btu}$.

9.17.4.1 Chemical Means to Control Scaling

Calcium carbonate formation can be controlled by adding acids or specific chemicals, including sulfuric acid, polymeric inorganic phosphates, phosphonates, and organic polymers like polycarboxylates [27].

Removal of the hardness salts: Removal of the scaling chemical species such as magnesium and calcium from water prior to use in the system, by ion exchange and lime softening procedures, is effective in scaling control. The large volumes of water usually encountered in many cooling-water systems are likely to make the treatment costs of these methods very high. The modern trend toward very small volumes and high recirculation rates may offer cost restrictions [3].

Conversion of hardness salts to a more soluble form: Control of scale formation involves conversion of hardness salts to a more soluble form. Since the solubility of scale-forming species in cooling water generally increases with decreasing pH, the addition of acid to maintain the pH in the range 6.5–7.5 (with 6.5 as the recommended minimum) may reduce the scaling. These effects are shown schematically in Figure 9.20. However, corrosion may be involved if the treatment is not carried out carefully. If large concentrations of sulfate are present, the use of sulfuric acid may cause sulfate scale to appear. Hydrochloric acid may be preferable under these circumstances [3].

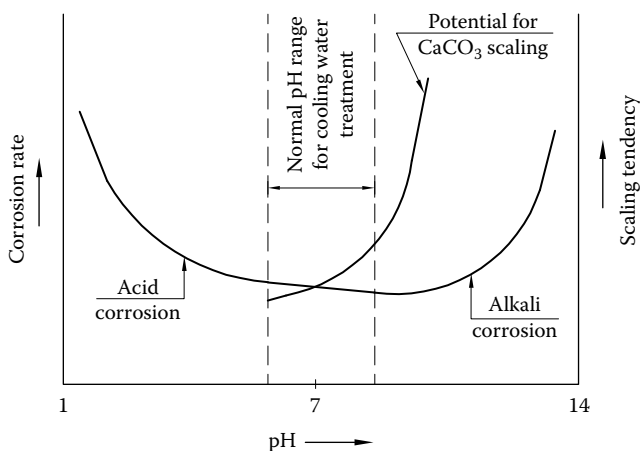


FIGURE 9.20 Cooling water corrosion and scaling control.

Alkaline cooling water operation for scale control: Alkaline cooling water treatment can also help in scale control. When the organic phosphorous compounds, including the well-known phosphates and polyol esters, and low-molecular-weight acrylic-acid-based polymers and copolymers are used properly, they completely prevent calcium carbonate deposition under alkaline conditions [28].

9.17.4.2 Electrostatic Scale Controller and Preventer

This is online equipment designed as a one-time fitment that performs the dual function of scale prevention and scale removal without using chemical additives. The equipment enables the use of untreated water. By subjecting the hard water to a carefully controlled electrostatic field, hardness ions are kept in suspension and prevented from depositing onto heat transfer surfaces. The merits of this system include (1) elimination of the use of expensive chemicals for descaling, (2) absence of corrosion of heat transfer surfaces from the use of chemicals for cleaning, and (3) eliminating the need to shut down the equipment for scale cleaning.

9.17.5 CLEANING OF SCALES

9.17.5.1 Chemical Cleaning

Chemical cleaning has been the most common method of scale removal. Mineral acids such as inhibited hydrochloric, ammonium bifluoride, sulfamic acid, and phosphoric acid are strong scale dissolvers. Organic acids are much weaker. They are often used in combination with other chemicals to complex scales. Refer to Table 9.3 for solvents and compatible base metals for scale removal.

9.17.6 IRON OXIDE REMOVAL

Conventional cleaning methods: Two common procedures generally followed in the industries for iron deposit removal are mechanical cleaning and chemical cleaning [29]:

1. Mechanical cleaning methods include water hydroblasting, lancing, and passing abrasive sponges, which remove most of the soft deposits but can leave hard, baked-on deposits.
2. Chemical cleaning with strong mineral acids or high concentrations of chelants up to 10% is used for temperatures up to 180°F (82°C).

Refer to Tables 9.2 and 9.3 for solvents and compatible base metals for iron oxide removal.

With the chemical cleaning methods, the possibility of corrosion of underlying metal surfaces as they dissolve away from the iron deposits cannot be ruled out. To overcome this problem, a new online procedure for removing iron-based deposits from cooling water systems has been developed. This is explained next.

Online removal of iron deposits [29]: The first step of the online cleaning process is the addition of a tannin-based, iron conditioning agent, which penetrates and softens the deposits. Later, a mild organic acid and dispersants are added and cause sloughing of the conditioned deposits. Postcleaning passivation of all metal surfaces can be accomplished by the normal corrosion inhibitor or by addition of online passivators to prevent flash corrosion. The process cleans transfer lines as well as heat exchangers and usually can be completed in 3–5 days.

NOMENCLATURE

A_{cr}	rate constant
A_i	surface area on the tube inside, m^2 (ft^2)
A_m	tube wall surface at the mid plane, m^2 (ft^2)
A_o	surface area on the tube outside, m^2 (ft^2)
A_r	chemical reaction fouling rate constant
A_w	total wall area for heat conduction, m^2 (ft^2)

d	tube outside diameter, m (ft)
d_i	tube inside diameter, m (ft)
E	activation energy for chemical reaction fouling
h_i	heat transfer coefficient on the tube inside, $\text{W/m}^2 \cdot ^\circ\text{C}$ ($\text{Btu/h} \cdot \text{ft}^2 \cdot ^\circ\text{F}$)
h_o	heat transfer coefficient on the tube outside, $\text{W/m}^2 \cdot ^\circ\text{C}$ ($\text{Btu/h} \cdot \text{ft}^2 \cdot ^\circ\text{F}$)
L	tube length, m (ft)
k_f	thermal conductivity of fouling deposit, $\text{W/m} \cdot ^\circ\text{C}$ ($\text{Btu/h} \cdot \text{ft} \cdot ^\circ\text{F}$)
K_R	constant for crystallization rate
K_r	chemical reaction fouling (polymerization) rate
K_{sp}	solubility product of CaCO_3 , $(\text{mol/m}^3)^2$
k_w	thermal conductivity of the conduction wall material, $\text{W/m} \cdot ^\circ\text{C}$ ($\text{Btu/h} \cdot \text{ft} \cdot ^\circ\text{F}$)
\dot{m}_d	rate of deposition of fouling mass on the heat transfer surface, $\text{kg/m}^2 \cdot \text{s}$ ($\text{lbm/ft}^2 \cdot \text{h}$)
m_f	net rate of fouling mass deposition per unit area, $\text{kg/m}^2 \cdot \text{s}$ ($\text{lbm/ft}^2 \cdot \text{h}$)
m_f^*	asymptotic value of m_f
\dot{m}_r	rate of removal of fouling mass from the heat transfer surface, $\text{kg/m}^2 \cdot \text{s}$ ($\text{lbm/ft}^2 \cdot \text{h}$)
m_s	CaCO_3 scaling rate, $\text{kg/m}^2 \cdot \text{s}$ ($\text{lbm/ft}^2 \cdot \text{h}$)
R	gas constant
R_f	thermal resistance due to fouling on both sides of a heat exchanger surface, $^\circ\text{C/W}$ ($^\circ\text{F} \cdot \text{h/Btu}$)
R_f	thermal resistance of fouling deposit for a unit surface area, m^2/W ($\text{ft}^2 \cdot ^\circ\text{F} \cdot \text{h/Btu}$)
R_f^*	asymptotic value of thermal resistance due to fouling, $^\circ\text{C/W}$ ($^\circ\text{F} \cdot \text{h/Btu}$)
R_i	fouling resistance on tube inside surface, $\text{m}^2 \cdot ^\circ\text{C/W}$ ($\text{ft}^2 \cdot ^\circ\text{F} \cdot \text{h/Btu}$)
R_o	fouling resistance on tube outside surface, $\text{m}^2 \cdot ^\circ\text{C/W}$ ($\text{ft}^2 \cdot ^\circ\text{F} \cdot \text{h/Btu}$)
R_T	total thermal resistance to heat transfer, $^\circ\text{C/W}$ ($\text{h} \cdot ^\circ\text{F/Btu}$)
R_w	thermal resistance of the separating wall, $^\circ\text{C/W}$ ($\text{h} \cdot ^\circ\text{F/Btu}$)
t	time, s
t_c	time constant
t_d	time delay period, s
T_s	heat transfer temperature, $^\circ\text{C}$ ($^\circ\text{F}$)
T_w	conduction wall temperature, $^\circ\text{C}$ ($^\circ\text{F}$)
U_o	overall heat transfer coefficient based on tube outside surface, $\text{W/m}^2 \cdot ^\circ\text{C}$ ($\text{Btu/h} \cdot \text{ft}^2 \cdot ^\circ\text{F}$)
$U_{o,c}$	overall heat transfer coefficient based on tube outside surface in clean condition, $\text{W/m}^2 \cdot ^\circ\text{C}$ ($\text{Btu/h} \cdot \text{ft}^2 \cdot ^\circ\text{F}$)
$U_{o,f}$	overall heat transfer coefficient based on tube outside surface in fouled condition, $\text{W/m}^2 \cdot ^\circ\text{C}$ ($\text{Btu/h} \cdot \text{ft}^2 \cdot ^\circ\text{F}$)
x_f	thickness of fouling deposit, m (ft)
β	constant = $1/t_c$
Δt_w	tube wall thickness, m (ft)
ρ_f	density of the foulant, kg/m^3 (lbm/ft^3)

REFERENCES

1. Collier, J. G., Heat exchanger fouling and corrosion, in *Heat Exchangers: Thermal-Hydraulic Fundamentals and Design* (S. Kakac, A. E. Bergles, and F. Mayinger, eds.), Hemisphere, Washington, DC, 1981, pp. 999–1011.
2. Zelter, N., Roe, F. L., and Characklis, W. G., Monitoring of fouling deposits in heat transfer tubes: Case studies, in *Industrial Heat Exchangers Conference Proceedings* (A. J. Hayes, W. W. Liang, S. L. Richlen, and E. S. Tabb, eds.), American Society for Metals, Metals Park, OH, 1985, pp. 201–208.
3. Bott, T. R., *Fouling Notebook*, Institution of Chemical Engineers, London, U.K., 1990.
4. Chenoweth, J. M., Final report of the HTRI/TEMA joint committee to review the fouling section of the TEMA standards, Heat Transfer Research, Inc., Alhambra, CA, 1988 also reproduced in *Journal of Heat Transfer Engineering*, 11(1), 73–107, 1990.

5. Epstein, N., Fundamentals of heat transfer surface fouling: With special emphasis on laminar flow, in *Low Reynolds Number Flow Heat Exchangers* (S. Kakac, R. K. Shah, and A. E. Bergles, eds.), Hemisphere, Washington, DC, 1982, pp. 951–964.
6. O'Callaghan, M., Fouling of heat transfer equipment: Summary review, in *Heat Exchangers: Thermal-Hydraulic Fundamentals and Design* (S. Kakac, A. E. Bergles, and F. Mayinger, eds.), Hemisphere, Washington, DC, 1981, pp. 1037–1047.
7. Kern, D. Q. and Seaton, R. E., A theoretical analysis of thermal surface fouling, *Br. Chem. Eng.*, **4**, 258–262 (1959).
8. Puckorius, P. R., Controlling deposits in cooling water systems, *Mater. Protect. Perform.*, **77**, 19–22 (November, 1972).
9. Mukherjee, R., Conquer heat exchanger fouling, *Hydrocarbon Processing*, **75**, 121–127 (January, 1996).
10. Silvestrini, R., Waste heat recovery: Heat exchanger fouling and corrosion, *Chem. Eng. Prog.*, **25**, 29–35 (December, 1979).
11. EMbaffle® technology, a major advance in heat exchanger technology, (www.embaffle.com).
12. Twisted Tube® heat exchangers, Koch Heat Transfer Company, Houston, Texas. (www.kochheattransfer.com)
13. Epstein, N., Fouling in heat exchangers, in *Proceedings of the Sixth International Heat Transfer Conference*, Toronto, Canada, August, Vol. 4, Hemisphere, Washington, DC, 1978, pp. 279–284.
14. Hasson, D., Precipitation fouling, in *Fouling of Heat Transfer Equipment* (E. F. C. Somerscales, and J. G. Knudson, eds.), *Proceedings of the International Conference on the Fouling of Heat Transfer Equipment*, 1979, Hemisphere, Washington, DC, 1981, pp. 569–586.
15. *Standards of Tubular Exchanger Manufacturers Association*, 9th edition, Tubular Exchanger Manufacturers Association, Inc., Tarrytown, NY, 2007.
16. *Heat Exchanger Performance Monitoring Guidelines*, Electric Power Research Institute, Palo Alto, CA, December 1991, Report NP-7552.
17. Knudsen, J. G., Apparatus and techniques for measurement of fouling of heat transfer surface, in *Fouling of Heat Transfer Equipment Proceedings of the International Conference on the Fouling of Heat Transfer Equipment*, 1979, (E. F. C. Somerscales and J. G. Knudson, eds.), Hemisphere, Washington, DC, 1981, pp. 57–81.
18. Marner, W. J. and Henslee, S. P., A survey of gas side fouling measuring devices, in *Industrial Heat Exchangers Conference Proceedings* (A. J. Hayes, W. W. Liang, S. L. Richlen, and E. S. Tabb, eds.), American Society for Metals, Metals Park, OH, 1985, pp. 209–226.
19. Feltzin, A. E., Garcia, H., and Alberto, I. L., Fouling and corrosion in open recirculating cooling water systems: The expert system approach, *Mater. Perform.*, **44**, 57–61 (June, 1988).
20. Knudsen, J. G., Conquer cooling-water fouling, *Chem. Eng. Prog.*, **87**, 42–48 (April, 1991).
21. Epstein, N., On minimizing fouling of heat transfer surfaces, in *Low Reynolds Number Flow Heat Exchangers* (S. Kakac, R. K. Shah, and A. E. Bergles, eds.), Hemisphere, Washington, DC, 1982, pp. 973–979.
22. Deghan, T. F., Corrosion in the chemical processing industry, in *Metals Handbook*, Vol. 13, *Corrosion*, 9th edn., (L. J. Korb and D. L. Olson, eds.), American Society for Metals, Metals Park, OH, pp. 1134–1185, 1987.
23. Lester, G. D. and Walton, R., Cleaning of heat exchangers, in *Practical Application of Heat Transfer*, C55/82, IMechE, London, U.K., pp. 1–10, 1982.
24. Woodward, A. R., Howard, D. L., and Andrews, E. F. C., Condensers, pumps and cooling water plant, in *Modern Power Station Practice*, Vol. C, *Turbines, Generators, and Associated Plant* (D. J. Littler, E. J. Davies, H. E. Johnson, F. Kirkby, P. B. Myerscough, and W. Wright, eds.), 3rd edn., Pergamon Press, New York, 1991.
25. Stegelman, A. F. and Renffltlen, R., On line mechanical cleaning of heat exchangers, *Hydrocarb. Process.*, **82**, 95–97 (1983).
26. L. T. Cole, L. T., Allen, C. A., Liquid-fluidized bed heat exchanger flow distribution models, ICP 1151. 1979. National Technical Information Service, Alexandria, VA,
27. Boffardi, P., Control of environmental variables in water-recirculating systems, in *Metals Handbook*, Vol. 13, *Corrosion*, 9th edn., American Society for Metals, Metals Park, OH, pp. 487–497.
28. Freedman, A. J., Cooling water technology in the 1980s, *NACE Mater. Perform.*, **11**, 9–16 (1984).
29. Kaplan, R. I. and Ekis, E. W., Jr., The on-line removal of iron deposits from cooling water systems, *NACE Mater. Perform.*, **40**, 40–44 (1984).

BIBLIOGRAPHY

- Branch, C. A. and Muller-Steinhagen, H. M., Influence of scaling on the performance of shell and tube heat exchangers, *Heat Transfer Eng.*, 12, 37–45 (1991).
- Characklis, W. G., Microbial fouling: A process analysis, in *Fouling of Heat Transfer Equipment* (E. F. C. Somerscales and J. G. Knudson, eds.), Proceedings of the International Conference on the Fouling of Heat Transfer Equipment, 1979, Hemisphere, Washington, DC, 1981, pp. 251–292.
- de Deus, J. and Pinheiro, R. S., Fouling of heat transfer surfaces, in *Heat Exchangers: Thermal-Hydraulic Fundamentals and Design* (S. Kakac, A. E. Bergles, and F. Mayinger, eds.), Hemisphere, Washington, DC, 1981, pp. 1013–1035.
- Epstein, N., Fouling models: Laminar flow, in *Low Reynolds Number Flow Heat Exchangers* (S. Kakac, R. K. Shah, and A. E. Bergles, eds.), Hemisphere, Washington, DC, 1982, pp. 965–971.
- Fassbender, L. L., Industrial fouling data base development, in *Industrial Heat Exchangers Conference Proceedings* (A. J. Hayes, W. W. Liang, S. L. Richlen, and E. S. Tabb, eds.), American Society for Metals, Metals Park, OH, 1985, pp. 227–238.
- Gudmundsson, J. S., Particulate fouling, in *Fouling of Heat Transfer Equipment* (E. F. C. Somerscales and J. G. Knudson, eds.), Proceedings of the International Conference on the Fouling of Heat Transfer Equipment, 1979, Hemisphere, Washington, DC, 1981, pp. 357–388.
- Klaren, D. G., Fluid bed heat exchangers—A new approach in severe fouling heat transfer, *Resour. Conserv.*, 7, 301–314 (1981).
- Sheikholeslami, R. and Watkinson, A. P., Scaling of plain and externally finned heat exchanger tubes, *Trans. ASME J. Heat Transfer*, 108, 147–152 (1986).
- Smith, S. A. and Dirks, J. A., Costs of heat exchanger fouling in the U.S. industrial sector, in *Industrial Heat Exchangers Conference Proceedings* (A. J. Hayes, W. W. Liang, S. L. Richlen, and E. S. Tabb, eds.), American Society for Metals, Metals Park, OH, 1985, pp. 339–344.
- Somerscales, E. F. C., Introduction and summary, in *Fouling of Heat Transfer Equipment* (E. F. C. Somerscales and J. G. Knudson, eds.), Proceedings of the International Conference on the Fouling of Heat Transfer Equipment, 1979, Hemisphere, Washington, DC, 1981, pp. 1–30.
- Suitor, J. W., Precipitation fouling, in *Fouling of Heat Transfer Equipment* (E. F. C. Somerscales, and J. G. Knudson, eds.), Proceedings of the International Conference on the Fouling of Heat Transfer Equipment, 1979, Hemisphere, Washington, DC, 1981.
- Marner, W. J., Progress in gas-side fouling of heat transfer surfaces, in *Compact Heat Exchangers—A Festschrift for A. L. London* (R. K. Shah, A. D. Kraus, and D. Metzger, eds.), Hemisphere, Washington, DC, 1990, pp. 421–490.
- Pritchard, A. M., Fouling—Science or art? An investigation of fouling and antifouling measures in the British Isles, in *Fouling of Heat Transfer Equipment* (E. F. C. Somerscales and J. G. Knudson, eds.), Proceedings of the International Conference on the Fouling of Heat Transfer Equipment, 1979, Hemisphere, Washington, DC, 1981, pp. 513–527.

10 Flow-Induced Vibration of Shell and Tube Heat Exchangers

10.1 PRINCIPLES OF FLOW-INDUCED VIBRATION

Flow-induced vibration of shell and tube heat exchangers (STHEs) has been known for a long time. Heat exchanger tubes tend to vibrate under the influence of crossflow velocities, and if the amplitude of vibration becomes large enough, the tubes can be damaged by one or more of several mechanisms: (1) thinning due to repeated midspan collision, (2) impact and fretting wear at baffle plate and tube interface, and (3) fatigue or corrosion fatigue due to high wear rate. Tube failures are costly because they result in plant shutdown to effect expensive repairs. These problems can be very serious in nuclear heat exchangers. Therefore, it is important to ensure that the modern STHEs are free from FIV problems at all operating conditions.

In the past, heat exchangers were designed conservatively. With the success of the state-of-the-art computer programs, the trend is to design an efficient and compact heat exchanger. Higher thermal performance and the desirability of low fouling generally require higher flow velocities, while fewer baffle plates are desirable to minimize pressure drop. Higher flow velocities and reduced structural supports can lead to severe FIV problems. In addition to these, the incorporation of new materials and processes without adequate considerations of the effects on the structural dynamics contributed to more FIV problems, many of which led to tube failures [1]. It is essential to avoid such costly tube failures by a detailed FIV analysis, preferably at the design stage after thermal design is over.

The FIV phenomenon and the mechanism responsible have been studied extensively over the past 25–30 years. As a result, considerable literature has been developed, and there have been efforts to define guidelines for vibration prevention. The subject continues to receive increasing attention because of its significance in heat exchanger applications, since as much as 60% of the heat exchangers in process industries are shell and tube type. References [1–18] bring about a better understanding of the FIV phenomenon in STHEs. In this chapter, the mechanisms that cause FIV and their evaluation, acceptance criteria, and design guidelines for vibration prevention are presented. Design guidelines included in TEMA Standards [19] and ASME Code Section III [20] are presented at appropriate places.

10.1.1 PRINCIPLES OF FLOW-INDUCED VIBRATION

To excite vibration, energy must be fed to the tubes. The shellside flow represents a source of energy that can induce and sustain tube vibration. The tubes, which are slender elastic beams among the heat exchanger components, are disturbed from their equilibrium position and undergo vibratory motion. Tube vibration is manifested by the periodic movement of the tube from its equilibrium position. With increasing crossflow velocity, the tube movement has the following three manifestations [1]:

1. At low crossflow velocities, the tubes vibrate with low-amplitude random motion.
2. As the flow velocity is increased, rattling of tubes within the baffle holes takes place.
3. As the flow velocity exceeds a threshold value, high-amplitude motion takes place.

When the natural frequencies of the tubes are closer to the exciting frequency, resonance takes place. The relative motion between the tubes and the rigid structures like baffle supports and shell boundary can cause impact and fretting wear of tubes.

10.1.2 POSSIBLE DAMAGING EFFECTS OF FIV ON HEAT EXCHANGERS

FIV can cause severe damage to the tubes and other structural components of the heat exchanger. Mechanical failure as a result of tube vibration can occur from fatigue, collision damage, baffle damage, or tube joint failures [11,12]. These failures are discussed next.

Midspan collision: If the amplitude of response at the midspan is greater enough, collision with adjacent tubes takes place. The resulting wear causes failure of the tube wall under pressure.

Wear damage at the tube interface with the baffle support: Heat exchangers are generally designed with a clearance between the tube and the baffle plates. This clearance is required for ease of manufacture and design considerations. Tubes that suffer lower amplitude vibration close to baffle plates may fail by impact and fretting wear or fatigue.

Fatigue failures: If the contact stress due to impact or collision is greater than the allowable fatigue stress, fretting wear takes place.

Excessive operating noise level: When the shellside medium is a gas, steam, or air, acoustic vibration will be induced within the tube bank containment. The acoustic vibration is characterized by pure-tone, low-frequency intense noise.

Severe pressure drop: Since the vibration of tube requires the energy from the shellside fluid, the shellside pressure drop increases. If the vibration is severe, destructive pressure fluctuations take place.

Intensified stress corrosion: Due to repeated impact with the baffle supports, intensive tensile stresses are induced on the tube surface. Susceptible tube material can fail due to the accelerated stress corrosion cracking in the shellside medium. However, corrosion due to FIV is second to the failure of tube material due to the corrosive nature of shellside fluid and/or tubeside fluid.

10.1.3 MOST PROBABLE REGIONS OF TUBE FAILURE

Although the tubes can fail anywhere in the exchanger, the regions more susceptible for FIV are the high-velocity regions such as the following:

Largest unsupported midspan between two baffles.

Tubes located in the baffle window region at periphery of the tube bundle.

U-bend regions of U-tube bundle.

Tubes located beneath the inlet nozzle.

Tubes located in the tube bundle bypass area, next to pass partition lanes.

Regions/interfaces where there is a relative movement between the tube and the heat exchanger structural components. Such regions include tube and baffle support interfaces and tube and tubesheet interfaces.

10.1.4 FAILURE MECHANISMS

The primary failure mechanisms that cause tube failure are [1]:

1. Impact wear (tube-to-tube and tube-to-baffle)
2. Fretting wear at the tube–baffle interfaces as a result of impact and/or sliding motion at the support
3. Combination of impact and fretting wear

10.1.5 FLOW-INDUCED VIBRATION MECHANISMS

The excitation mechanisms generally regarded as responsible for FIV are

1. Vortex shedding or flow periodicity
2. Turbulent buffeting
3. Fluid elastic instability (FEI)
4. Acoustic resonance

Vortex shedding, turbulent buffeting, and acoustic excitation are due to resonance phenomena. Resonance occurs when the excitation frequency synchronizes with the natural frequency of the tubes. FEI sets in for tubes in a crossflow at a critical flow velocity or threshold velocity resulting in the amplitude of tube response large enough to collide with the adjacent tubes and cause failure. Below the critical velocity, FEI will not take place. Instability attains when the energy input to the tube mass-damping system exceeds the energy dissipated by the system.

10.1.6 TUBE RESPONSE CURVE

Figure 10.1 shows the tube response due to FIV of tubes in tube bundles as a result of the three excitation mechanisms, namely, vortex shedding, turbulent buffeting, and FEI [3]. Each of them manifests itself only over a given range of flow parameters. However, it is believed that turbulent buffeting is operative in the entire range of flow parameters.

10.1.7 DYNAMICAL BEHAVIOR OF TUBE ARRAYS IN CROSSFLOW

Flow of fluid over an array of elastic tubes results in (1) hydrodynamic effects or fluid oscillation (acoustic vibration) and (2) fluid–structure coupling. These effects cause hydrodynamic forces and fluid structure coupling forces. The dynamical behavior of an array of cylinders in increasing cross-flow velocity (U) is considered to have three distinct manifestations as follows [3]:

1. At low flow velocities, the cylinder responds principally to turbulent buffeting; with increasing flow velocity, the amplitude of tube vibration goes up roughly as U^2 .
2. At higher flow velocities, various kinds of resonance conditions may arise, such as vortex shedding, turbulent buffeting, and acoustical oscillation of gas column.
3. At sufficient high flow velocities, FEI will generally develop, and the amplitude of vibration increases rapidly with the flow velocity without a limit.

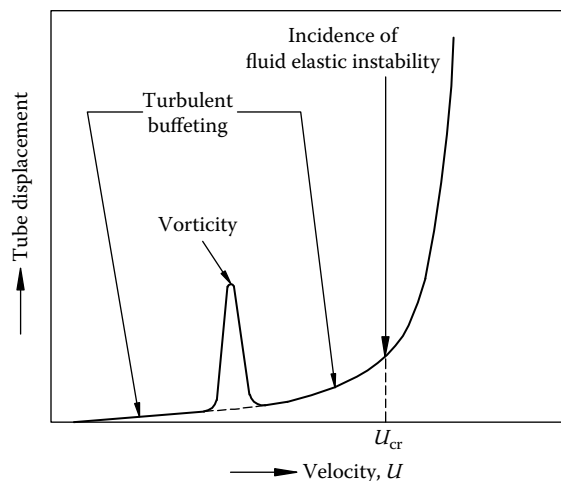


FIGURE 10.1 Tube response due to FIV mechanism—ideal diagram. (Adapted from Paidoussis, M.P., *J. Sound Vib.* 76, 329–359, 1981.)

10.1.8 HYDRODYNAMIC FORCES

The hydrodynamic forces that contribute to FIV mainly fall into three groups:

1. Forces arising due to turbulent fluctuations of the pressure field
2. Forces resulting from periodic vortex shedding from tubes and formation of Von Karman's streets in their wakes
3. Motion-dependent fluid forces arising when the tubes are shifted elastically from their equilibrium within the bundle due to interaction with the flow

10.1.9 FIV MECHANISMS VERSUS FLOW MEDIUMS

Of the different excitation mechanisms of FIV, only FEI is a primary concern in all flow mediums. Vortex shedding is possible in liquid and gas medium but unlikely in two-phase medium. Other mechanisms have less importance in certain flow media. Turbulent buffeting is possible in liquid and gas medium, which may result in fretting wear.

Hence, design restrictions are imposed to limit acoustic resonance and FEI [9].

10.1.10 APPROACHES TO FIV ANALYSIS

Two approaches are normally followed to predict FIV effects of STHes:

1. Finite-element modeling technique. This model simulates the time-dependent motion of a multispan heat exchanger tube in the presence of tube and baffle plate clearance, and the resulting wear is determined. This approach is normally followed for heat exchangers and steam generators used in very critical services such as nuclear energy generation.
2. Limiting amplitude of vibration. This approach linearizes the structural model by assuming tubes as classical beams with support plates offering simple support at the intermediate points and clamped at the tubesheet ends. The designer then predicts the amplitude of vibration or instability thresholds and selects an acceptance criterion that will conservatively limit the vibration. This approach is used in this chapter. This procedure can be used to provide conservative designs or troubleshoot an existing heat exchanger and is widely accepted in the field.

10.1.11 EMPIRICAL NATURE OF FLOW-INDUCED VIBRATION ANALYSIS

Before discussing FIV excitation mechanisms in detail, it is important to note that FIV of STHes is a physical phenomenon that cannot be explained by simple empirical correlations [9,13]. It is most difficult to analyze [1,7] due to reasons like the following:

1. Tube bank dynamics is a multibody problem. The tubes are supported by multiple baffles with holes slightly larger than the tube diameter.
2. The interaction between the tube and the support plates is characterized by impacting as well as sliding motion. This makes the system nonlinear in nature.
3. The tubes and the surrounding fluid form a fluid-structure coupling that results in motion-dependent fluid forces that give rise to added mass, coupled modes, and damping.
4. Generally, the flow field is quite complex, nonuniform, and quite unsteady, and the incidence of flow on the tubes is at variable angles to the longitudinal axis [21].

5. Structural complexity arises due to time-variant flow-dependent boundary conditions. Mechanical tolerances, initial straightness, fit-up, and tube buckling due to manufacturing process add complexities in defining boundary conditions [22].
6. Effects of tube bundle parameters such as transverse and longitudinal pitches, tube layout pattern, pass partition lanes, shell to tube bundle clearance, number of tube rows, etc., on the occurrence of FIV cannot be correctly evaluated. The effects of some parameters have been studied by Gorman [23].

For these reasons, most of the methods in the analysis of tube bank dynamics are semiempirical in nature. To render the problem amenable for most analytical studies and experimental investigations, the flow conditions are idealized as follows:

1. The flow is uniform and steady.
2. The incident of the flow is either axial or normal to the tubes.
3. The tube motion is linearized, and it is assumed that the frequencies are well defined.
4. The baffle supports provide a simply supported condition.

10.2 DISCUSSION OF FLOW-INDUCED VIBRATION MECHANISMS

10.2.1 VORTEX SHEDDING

10.2.1.1 Single Tube

Consider a bluff body such as a circular cylinder in crossflow with the tube axis perpendicular to the flow. As the fluid flows past the tube, the wake behind the tube is no longer regular, but contains distinct vortices of the pattern shown in Figure 10.2. The periodic shedding of vortices alternately from each side of the body in a regular manner gives rise to alternating lift and drag forces. This causes periodic movement of the tube. The familiar example is the von Karman vortex street behind a circular cylinder in crossflow.

10.2.1.2 Strouhal Number

The vortex shedding phenomenon can be characterized by a nondimensional parameter known as the Strouhal number S_u , and it is related to vortex shedding frequency f_v by

$$S_u = \frac{f_v D}{U_\infty} \quad (10.1)$$

where

D is the tube outer diameter

U_∞ the upstream velocity

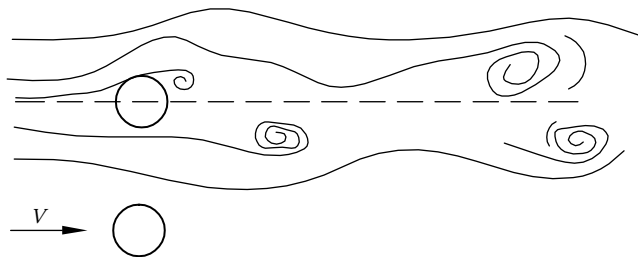


FIGURE 10.2 Vortex shedding past a single cylinder.

When the vortex shedding frequency f_v is sufficiently close to the natural frequency of the tubes f_n , the following will occur [4]:

1. The vortex shedding frequency shifts to the structural natural frequency, developing the condition called “lock-in” or “synchronization.” The lock-in phenomenon leads to high-amplitude vibration with substantial energy input to the tube.
2. The lift force becomes a function of structural amplitude.
3. The drag force on the structure increases. However, the magnitude of the oscillating drag force is smaller than the oscillating lift force. Also the drag force occurs at twice the vortex shedding frequency.
4. The strength of the shed vortices increases.

When the vortex shedding frequency coincides with the tube natural frequency or close to the natural frequency, resonance takes place. Resonance is characterized by large amplitudes of tube motion with possible damage to the tube. This mechanism has been variously referred to as vortex shedding, periodic wake shedding, Strouhal periodicity, or Strouhal excitation.

Since the vortex shedding drag force in the streamwise direction (drag) occurs at twice the vortex shedding frequency and the magnitude of drag force is smaller than the oscillating lift force, normally the analysis is carried out for lift forces only.

The vortex shedding phenomenon for a single cylinder with a peak response is well defined and has been dealt with by various researchers. Information on the lift and drag force coefficients and the Strouhal number over the complete range of Reynolds numbers of interest has been reviewed and presented by Chen and Weber [24]. For crossflow over a single tube, the Strouhal number is an almost constant value of 0.2 for Reynolds numbers starting from 300 to the lower critical Reynolds number of 2×10^5 . After this point, the Strouhal number seems to increase due to the narrowing of the wake. But as the Reynolds number exceeds the value of 3.5×10^5 and when the supercritical range is reached, the wakes become completely turbulent. No regular vortex shedding exists any more. This exceptional case lasts only to a Reynolds number of 3.5×10^6 . After exceeding this value, a Von Karman vortex can be formed again. In the transcritical range, the Strouhal number is about 0.27 [25].

10.2.1.3 Vortex Shedding for Tube Bundles

Traditionally, it has been thought that for multiple tube arrays or ideal tube banks subjected to crossflow, vortex shedding will occur similar to that of a single isolated cylinder. However, research to date shows that vortex shedding produces a peak response similar to that observed for isolated cylinders for the first few tube rows in a tube array, and a clear resonant peak does not occur for most of the tube arrays. Vortex shedding past a tube bank is shown in Figure 10.3. Owen [26] disputed the existence of vortices deep within a tube bank. Deep within the tube bank, the dominant spectral frequency for both lift and drag forces of vortex shedding and turbulent buffeting coincides. According to Blevins [8] and Zukauskas [13], within a closely spaced tube arrays with pitch ratio less than 2.0, the vortex shedding degenerates into broadband turbulent eddies rather than a single distinct frequency. Such a mechanism is referred to as turbulent buffeting and is described in the next section. In the light of this discussion, it may be concluded that vortex shedding is a potential design problem in the front tube rows of a tube bank in liquid flows or may be a source of acoustic noise in gas flows [6]. Hence, the possibility of the first few tube rows being excited by vortex shedding must be determined. Within the array, vortex shedding can be regarded as a special case of turbulent buffeting and analyzed by the method of random vibration, as explained in the next section.

The expression for the Strouhal number for a tube bank is same as Equation 10.1, but the velocity term U_∞ should be replaced by the crossflow velocity. The crossflow velocity is calculated by Tinker's method [27], Bell's method [28], the stream analysis method [29], proprietary programs such as HTRI [30] and HTFS [31,32], or by any other standard programs.

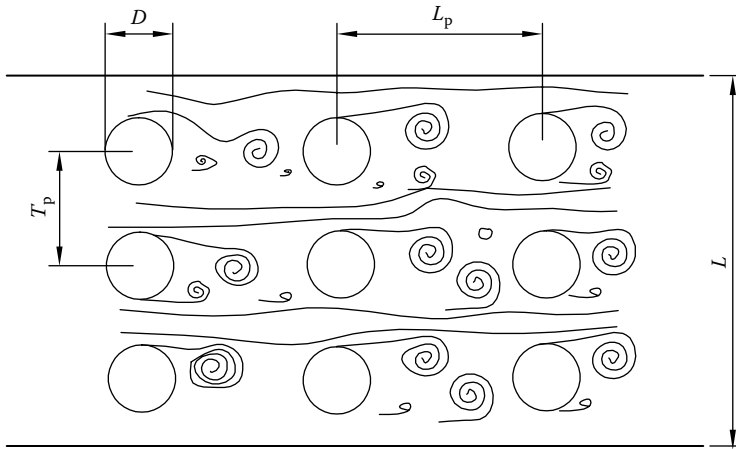


FIGURE 10.3 Vortex shedding in a tube array.

10.2.1.4 Avoiding Resonance

The design criterion for the possibility of vortex shedding as an excitation source involves the parameter of reduced frequency ($f_n D/U$) and/or the determination of Strouhal number, S_u . Determination of the Strouhal number is discussed next.

10.2.1.5 Calculation of Strouhal Number for Tube Arrays

The Strouhal number may be determined from Chen's Strouhal maps [25] and Fitz-Hugh [33]. These maps are plotted with various pitch ratios. Alternately, it can be determined from correlations of Zukauskas [13] or Zukauskas and Katinas [34] and Weaver et al. [35]. The correlation of Weaver et al. is given next. Blevins [8] presents Fitz-Hugh's map and TEMA presents Chen's map.

Correlations of Weaver et al. [35]: The expressions for Strouhal number S_u for various tube layout patterns (Figure 10.4) are given by

$$S_u = \frac{1}{1.73X_p} \quad \text{for } 30^\circ \text{ layout} \quad (10.2a)$$

$$= \frac{1}{1.16X_p} \quad \text{for } 60^\circ \text{ layout} \quad (10.2b)$$

$$= \frac{1}{2X_p} \quad \text{for } 90^\circ \text{ and } 45^\circ \text{ layout} \quad (10.2c)$$

where X_p is the pitch ratio, p/D . The original expressions were in terms of upstream velocity. They were corrected for gap velocity by multiplying the expressions by $(p - D)/p$.

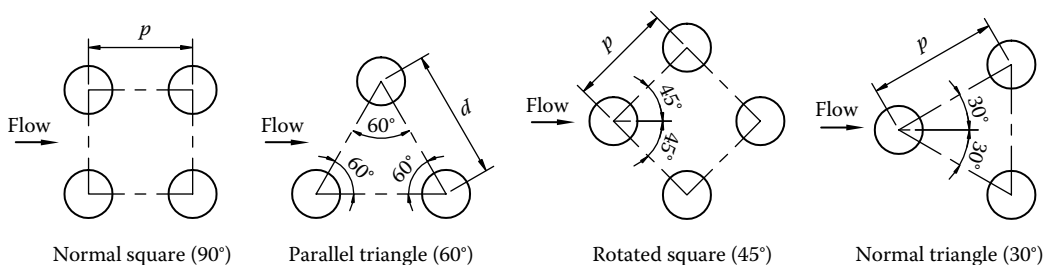


FIGURE 10.4 Tube layout patterns.

10.2.1.6 Criteria to Avoid Vortex Shedding

Criterion of Pettigrew and Gorman: The criterion to avoid resonance due to vortex shedding is expressed in terms of reduced frequency, $(f_n D/U)$, by Pettigrew and Gorman [36] as

$$\frac{f_n D}{U} > 2S_u \quad (10.3)$$

Criterion of Au-Yang [4]: To avoid resonance, the Strouhal number S_u must be less than 20% of the reduced frequency [7]:

$$\frac{f_n D}{U} < 0.2S_u \quad (10.4)$$

Criteria of Au-Yang et al. [4]: The criteria for avoiding lock-in due to vortex shedding in the first two to three rows in a tube bank are given by Au-Yang et al. [4]. They are the following:

1. If the reduced velocity for the fundamental vibration mode ($n = 1$) is satisfied by the relation

$$\frac{U}{f_n D} < 1 \quad \text{for } n = 1 \quad (10.5)$$

both lift and drag direction lock-in are avoided.

2. For a given vibration mode, if the reduced damping C_n is large enough,

$$C_n > 64$$

then lock-in will be suppressed in that vibration mode.

3. If for a given vibration mode

$$\frac{U}{f_n D} < 3.3 \quad (10.6)$$

and $C_n > 1.2$, then lift direction lock-in is avoided and drag direction lock-in is suppressed. The reduced damping C_n is calculated by the equation

$$C_n = \frac{4\pi\xi_n M_n}{\rho_s D^2 \int_0^{L_e} \phi_n^2(x) dx} \quad (10.7)$$

where

M_n is the modal mass

L_e is the tube length subjected to vortex shedding

$\phi_n(x)$ is the mode shape

The expression for M_n is given by

$$M_n = \int_0^{L_e} m(x) \phi_n^2(x) dx \quad (10.8)$$

where $m(x)$ is the tube mass per unit length. Substituting the expression for the modal mass and normalizing the mode shape, the expression for reduced damping C_n is given by

$$C_n = \frac{4\pi\xi_n m}{\rho_s D^2} \quad \text{when } M_n = m(x) = m \quad (10.9)$$

These guidelines are included in ASME Code Section III.

In the preceding equations, f_n is the tube natural frequency, m is the effective tube mass per unit length, and ξ_n is the critical damping ratio. The effective tube mass is the sum of structural mass, fluid-added mass due to the contribution of shellside fluid displaced by the vibrating tube, and the mass of the contained fluid per unit length. In simple terms,

$$\begin{aligned} m &= \text{added mass} + \text{contained fluid mass} + \text{structural mass} \\ &= m_a + m_i + m_t \end{aligned} \quad (10.10)$$

$$= \frac{\pi D^2 C_m \rho_s}{4} + \frac{\pi D_i^2 \rho_i}{4} + \frac{\pi (D^2 - D_i^2) \rho}{4} \quad (10.11)$$

where

- m_a is the added mass per unit length
- m_i the contained fluid mass per unit length
- m_t the structural mass per unit length

The terms ρ_i , ρ_s , and ρ are density of tubeside fluid, shellside fluid, and tube metal, respectively. The added mass involves a term called added mass coefficient, C_m . The determination of f_n , C_m , and critical damping ratio ξ_n are discussed at the end of this section.

10.2.1.7 Response due to Vortex Shedding Vibration Prediction by Dynamic Analysis

If resonance occurs, the maximum tube response can be obtained by a forced response analysis as described in Refs. [4,36]. Sandifer [9] describes this from first principles. The generalized equation for the tube response $y(x)$ for any mode number j is given by [36]

$$y(x) = \frac{C_L \rho_s D}{16\pi^2 \xi_{n,j} f_{n,j}^2 M_j} \phi_j(x) \int_0^{L_j} U^2(x) \phi_j(x) dx \quad (10.12)$$

The mode shape in Equation 10.12 is normalized by

$$\int_0^{L_i} \phi^2(x) dx = 1 \quad (10.13)$$

and evaluation of this integral gives

$$\begin{aligned} \phi(x) &= \sqrt{\frac{2}{L_i}} \sin\left(\frac{\pi x}{L_i}\right) \\ &= \sqrt{\frac{2}{L_i}} (\text{maximum value}) \end{aligned} \quad (10.14)$$

After normalizing the modal mass, the maximum response y_{\max} is given by

$$y_{\max} = \frac{C_L \rho_s D U^2}{4\pi^3 \xi_n f_n^2 M} \quad \text{where } M = m \quad (10.15)$$

The peak lift coefficients C_L (peak) for various tube layout patterns are tabulated in Refs. [9,37]. A conservative design can be obtained with $C_L(\text{peak}) = 0.091$. According to these, as long as the peak amplitude of tube response is less than 2% of the tube diameter D , it is unlikely that the tube motion would be sufficient to control and correlate wake shedding along the tube. Accordingly, the acceptance criterion is given by

$$y_{\max} < 0.02D \quad (10.16)$$

This procedure is included in ASME Code Section III.

10.3 TURBULENCE-INDUCED EXCITATION MECHANISM

10.3.1 TURBULENCE

In general, higher flow rates promote and maintain high turbulence in the fluid, which is desirable for enhanced heat transfer, but the high turbulence is a source of structural excitation. Heat exchanger tubes respond in a random manner to turbulence in the flow field. In addition to structural excitation, turbulence in the flow can affect the existence and strength of other excitation mechanism, namely, vortex shedding.

10.3.2 TURBULENT BUFFETING

Turbulent buffeting in a tube bank, sometimes called subcritical vibration, refers to the low-amplitude response before the critical velocity is reached and away from the vortex lock-in velocity region due to unsteady forces developed on a body exposed to a high turbulence in the flow field.

The turbulent flow has been characterized by random velocity perturbations associated with turbulent eddies spread over a wide range of frequencies distributed around a central dominant frequency. When the dominant central frequency in the flow field coincides with the lowest natural frequency of the tube, a considerable amount of energy transfer takes place, leading to resonance and high-amplitude tube vibration. Even in the absence of resonance, turbulent buffeting can cause fretting wear and fatigue failure. With a design objective of 40 years codal life for nuclear power plant steam generators and heat exchangers, even relatively small tube wear rates cannot be acceptable [6,38]. Hence, turbulence excitation becomes an important design consideration in the design of reliable heat exchangers.

10.3.3 OWEN'S EXPRESSION FOR TURBULENT BUFFETING FREQUENCY

Based on experimental study of gas flow normal to a tube bank, Owen [26] correlated an expression for the central dominant frequency of the turbulent buffeting, f_{tb} , as

$$f_{tb} = \frac{U}{DX_1 X_t} \left[3.05 \left(1 - \frac{1}{X_t} \right)^2 + 0.28 \right] \quad (10.17)$$

where

X_1 = longitudinal pitch ratio = L_p/D (L_p is longitudinal pitch)

X_t = transverse pitch ratio = T_p/D (T_p is transverse pitch)

Weaver and Grover [39] reviewed various works and observed that Owen's approach is most reliable for predicting the peak frequency in the turbulence, provided the minimum gap velocity is used in the expression. The preceding correlation is applicable for a tube bank with transverse pitch ratio more than 1.25. Since this correlation has not been tested for liquids, it should be restricted to gases only. TEMA has included this expression.

10.3.4 TURBULENT BUFFETING EXCITATION AS A RANDOM PHENOMENON

By assuming that the tube vibrations represent steady-state random process, expression for rms amplitude of tube response has been developed by Au-Yang et al. [4], Au-Yang [7], and Pettigrew and Gorman [36]. Sandifer [9] describes the equation for tube response from first principles. The mean square resonant response of a lightly damped structure is given by

$$\bar{y}^2(x) = \frac{\rho_s^2 D^2 L_i}{256\pi^3} \sum_j \frac{[C_R(f_j) U_j^2 \phi_j(x)]^2}{\xi_{n,j} f_{n,j}^3 M_j^2} \quad (10.18)$$

After normalizing the mode shape over the span length and for the first mode of vibration, the maximum mean square response is given by

$$\bar{y}_{\max}^2 = \frac{L_i [C_R(f) \rho_s U^2 D \sqrt{2/L_i}]^2}{256\pi^3 \xi_{n,j} f_{n,j}^3 M^2} \quad \text{where } M = m \quad (10.19a)$$

$$\bar{y}_{\max}^2 = \frac{[C_R(f) \rho_s U^2 D]^2}{128\pi^3 \xi_{n,j} f_{n,j}^3 M^2} \quad \text{where } M = m \quad (10.19b)$$

$$y_{\text{rms}} = \sqrt{\bar{y}_{\max}^2} \quad (10.19c)$$

A recommended acceptance criterion is

$$y_{\text{rms}} \leq 0.010 \text{ in.} \quad \text{or} \quad 0.254 \text{ mm} \quad (10.20)$$

The parameter $C_R(f)$ can be determined from Ref. [36].

10.4 FLUID ELASTIC INSTABILITY

A group of circular cylinders submerged in crossflow can be subjected to dynamic instability, typically referred to as FEI. Fluid elastic vibration sets in at a critical flow velocity and can become of large amplitude if the flow is increased further. The familiar examples of FEI vibration are aircraft wing flutter, transmission line galloping, and vibration of tube arrays in heat exchangers.

A sudden change in vibration pattern within the tube array indicates instability and is attained when the energy input to the tube mass-damping system exceeds the energy dissipated by the system. FEI has been recognized as a mechanism that will almost lead to tube failure in a relatively short period of time, and this is to be avoided at any cost by limiting the crossflow velocity [40]. However, some tube responses due to turbulent buffeting or vortex shedding cannot be avoided, and this may lead to long-term fretting failure [41]. If vortex shedding resonances are predicted at velocities above the fluid elastic critical velocity, then vortex shedding is not a concern, and it is not necessary to predict the associated amplitudes of vibration.

10.4.1 FLUID ELASTIC FORCES

Flow of fluid over an array of elastic tubes results in the following fluid elastic forces or fluid damping forces with or without fluid–structure coupling. The forces induced on the tube fall into the following three major groups [4,5]:

1. Forces that vary approximately linearly with displacement of a tube from its equilibrium position. The resulting instability mechanism is known as displacement mechanism.
2. Velocity-dependent fluid forces such as fluid inertia, fluid damping, and fluid stiffness forces. The resulting instability mechanism is known as velocity mechanism.
3. The combination of the foregoing forces.

Instability may result from any or all of these fluid forces, which are functions of the tube motion.

10.4.2 GENERAL CHARACTERISTICS OF INSTABILITY

Before understanding the FEI mechanism, it is pertinent to know the features of instability. A sudden change in vibration pattern within the tube array is indicative of instability. The general characteristics of tube vibrations during instability include

1. Large vibration amplitude
2. Synchronization between adjacent tubes
3. Fluid structure coupling

10.4.3 CONNORS' FLUID ELASTIC INSTABILITY ANALYSIS

The pioneering work on FEI was initiated by Connors [42]. In 1970, Connors studied a tube row in a wind tunnel using a quasi-static model. The model, using fluid dynamic coefficients obtained from tests on a stationary body to determine the fluid dynamic forces acting on a vibrating body, is generally called a quasi-static model. According to Connors, the FEI results when the amount of energy input to tubes in crossflow exceeds the amount of energy that can be dissipated by the system damping. As a result of energy imbalance, the tube vibration will intensify to the point that clashing with adjacent tubes takes place. From his model, he measured quasi-steady force coefficients and developed a semiempirical stability criterion for predicting the onset of FEI of tube arrays. The stability criterion relates the critical flow velocity U_{cr} to the properties of the fluid and structures of the form

$$\frac{U_{cr}}{f_n D} = K \left(\frac{m\delta}{\rho_s D^2} \right)^a \quad (10.21)$$

where

U_{cr} is the critical velocity

δ is equal to $2\pi\xi_n$

For his single-row experimental model with $p/D = 1.41$, the value of K is 9.9 and $a = 0.5$. Accordingly, the expression for instability is given by

$$\frac{U_{cr}}{f_n D} = 9.9 \left(\frac{m\delta}{\rho_s D^2} \right)^{0.5} \quad (10.22)$$

In this expression, the two main parameters are $U_{cr}/f_n D$, the reduced velocity, and $m\delta/\rho_s D^2$, the mass-damping parameter. The Connors' vibration mechanism was later referred to as a displacement mechanism, and the model is known as a quasi-static model.

For tube bundles, the parameter $K = 9.9$ does not hold good, and hence numerous investigators conducted extensive experiments to form a more appropriate instability parameter K . Several new models—the analytical model [43–45] and the unsteady model [15,16,46,47]—have been proposed. A few researchers [48–50] refined the quasi-static model. A mechanism called the velocity mechanism was suggested by Blevins [8]. Many reviews [3,6,14] and the state of the art [6] have been presented. However, most of the researchers proposed a stability criterion similar to the Connors' stability equation form. In the following sections, various instability models are discussed briefly. Subsequently, the design guidelines and acceptance criteria are presented. Wherever these criteria are common with TEMA and ASME Code, this is specified.

10.4.4 ANALYTICAL MODEL

The analytical model was proposed by Lever and Weaver [43–45]. From a series of flow visualization experiments conducted in airflow to investigate the underlying mechanism responsible for the FEI of tube arrays in crossflow, the authors assumed that a single elastic tube surrendered by rigid tubes becomes independently unstable; the effect of neighboring tubes is primarily to define the flow field unique to each array pattern. The model is known as tube-in-channel model.

10.4.5 UNSTEADY MODEL

Prior to 1980, the mechanism thought to cause FEI was a displacement mechanism, and the dominant force causing instability was referred as fluid elastic stiffness force. From the unsteady fluid dynamic forces of Tanaka and Takahara [46,47] and Refs. [15,16,51–53], it is known that the instability is caused not only by a displacement mechanism but also by an additional mechanism called the velocity mechanism. This instability model is called the unsteady model. The existence of velocity mechanism was demonstrated analytically and verified experimentally by Chen et al. [54,55]. In this model, the FEI is caused by the following mechanisms:

1. Position-dependent FEI, which occurs at relatively high flow velocities. The instability mechanism is called displacement mechanism.
2. Fluid-damping-type instability occurring at low flow velocities. The instability mechanism is called velocity mechanism.

In most cases, either the velocity mechanism or the displacement mechanism or a combination of both will be dominant. The displacement mechanism and velocity mechanism are discussed in detail in Refs. [5,16,55]. They are briefly explained next.

10.4.5.1 Displacement Mechanism

According to this mechanism, the instability is due to fluid elastic force, which is proportional to the displacement of tubes. This mechanism is dominant for high values of reduced flow velocity corresponding to gas flows. The instability criterion is given by [5]

$$\frac{U_{cr}}{f_n D} = \alpha_d \left(\frac{m \delta}{\rho_s D^2} \right)^{0.5} \quad (10.23a)$$

where α_d is a function of fluid elastic stiffness coefficients.

10.4.5.2 Velocity Mechanism

According to this mechanism, the dominant fluid force is a flow velocity-dependent damping force that is proportional to the velocity of the tubes. At low reduced velocity, the fluid damping force may

act as an energy dissipation mechanism, whereas, at high reduced velocities, it acts as an excitation mechanism. When it acts as an excitation mechanism, the system damping is reduced. The tube loses stability once the modal damping of a mode becomes negative. This type of instability is called fluid-damping-controlled instability, and it is dominant for low values of reduced velocities that correspond to liquid flow. The instability criterion is given by [5]

$$\frac{U_{cr}}{f_n D} = \alpha_v \left(\frac{m\delta}{\rho_s D^2} \right)^{0.5} \quad (10.23b)$$

where α_v is a function of fluid elastic stiffness coefficients.

10.4.5.3 Unsteady Model

Based on the displacement mechanism and velocity mechanism, the dynamics of the tube array in simple form is written as [16]

$$[M_s + M_f]\{\ddot{q}\} + [C_s + C_f + C_v]\{\dot{q}\} + [K_s + K_f]\{q\} = [F] \quad (10.24)$$

where

- $[M_s]$ is the structural mass
- $[M_f]$ is the added mass of the fluid
- $[C_s]$ is the structural damping of the system
- $[C_f]$ is the viscous damping of the still fluid
- $[C_v]$ is the velocity-dependent damping of the fluid
- $[K_s]$ is the structural stiffness
- $[K_f]$ is the fluid elastic stiffness
- $[F]$ is the fluid forces independent of the tube motion
- $\{q\}$ is the structural displacement
- $\{\dot{q}\}$ is the structural velocity
- $\{\ddot{q}\}$ is the structural acceleration

In the preceding expression, the terms in square brackets are matrices and those in braces are vectors. The constituents of fluid dynamic forces are

1. $[M_f]\{\ddot{q}\}$, fluid inertia force
2. $[C_f + C_v]\{\dot{q}\}$, fluid damping force
3. $[K_f]\{q\}$, fluid elastic force

The major obstacle in the analysis of the instability mechanism by the unsteady model is to determine the flow-velocity-dependent damping $[C_v]$ and fluid stiffness $[K_f]$ for every tube layout pattern and for the entire range of reduced flow velocity of interest, either analytically or experimentally. These forces were measured experimentally by Tanaka and Takahara [47].

10.4.6 DESIGN RECOMMENDATIONS

10.4.6.1 Chen's Criterion

From the data of many investigators, Chen [5] recommended a criterion for the lower bound of critical velocity. Later, Chen [56] revised the criteria and the same is included in TEMA [19]. For 45° layout and $0.1 \leq \chi \leq 300$, the equation is given by

$$U_{cr}/f_n D = 4.13\{(p/D) - 0.5\} \chi^{0.5} \quad (10.25a)$$

where the expression for χ (same as damping parameter included in Equation 10.21) is given by

$$\chi = \frac{m\delta}{\rho_s D^2} \quad (10.25b)$$

The notable feature of Chen's criterion is the presence of pitch ratio (p/D) in the equation for 30° and 45° layouts.

10.4.6.2 Au-Yang et al. Criteria

From the instability database of Ref. [5], Au-Yang et al. [4] developed the following criteria:

$$\frac{U_{cr}}{f_n D} = K \left(\frac{m\delta}{\rho_s D^2} \right)^a \quad (10.26)$$

1. For the displacement mechanism where $m\delta/\rho_s D^2 > 0.7$, the stability equation is similar to Connors' equation with $a = 0.5$. The values for K are given in Table 10.1.
2. For the velocity mechanism where $m\delta/\rho_s D^2 < 0.7$, the criteria of displacement mechanism may be used. However, this will give a conservative value.

These guidelines are included in ASME Code, Section III.

Conservative guideline: If the crossflow velocity is less than the critical velocity calculated using $K = 2.1$ and $a = 0.5$ with $\xi_n = 0.5\%$ in gas flow and 1.5% in liquid flow, instability is almost certainly not a problem.

10.4.6.2 Guidelines of Pettigrew and Taylor

From a parametric study of nearly 300 data points on FEI of the flexible tube bundles subjected to single-phase crossflow, a design criterion was evolved by Pettigrew and Taylor [14]. The criterion is

$$\frac{U_{cr}}{f_n D} = 3.0 \left(\frac{m\delta}{\rho_s D^2} \right)^{0.5} \quad (10.27)$$

The reasons for variation among the various acceptance criteria are discussed in Ref. [14].

10.4.7 ACCEPTANCE CRITERIA

To avoid FEI, the acceptance criteria are thus:

1. Normal criterion

$$U_{cr} > U \quad (10.28a)$$

2. Conservative criterion [9]

$$\frac{U}{U_{cr}} = < 0.5 \quad (10.28b)$$

TABLE 10.1

Au-Yang et al. [4] Criteria for FEI

Pitch Angle	30°	60°	45°	90°	All Arrays
K	4.5	4.0	5.8	3.4	4.0

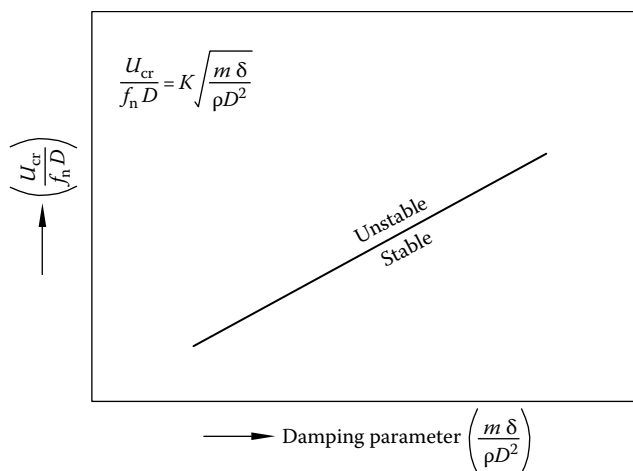


FIGURE 10.5 Stability diagram.

10.4.8 STABILITY DIAGRAMS

The presentation of the stability criteria in a graphical form (log-log plot) with mass-damping parameter on the x -axis and reduced velocity on the y -axis is referred to as a stability diagram. It shows relatively distinct “stable” and “unstable” regions [48]. A typical stability diagram is shown in Figure 10.5.

10.5 ACOUSTIC RESONANCE

Acoustic resonance is excited by the crossflow of air, gas, or steam. It is due to the vibration of the standing waves surrounding the tubes. The existence of standing waves is described as follows. The gas flow across the tube bank has, in addition to its mean velocity in the flow direction, a fluctuating velocity transverse to the mean flow direction. This fluctuating velocity is associated with the standing waves (gas column). Standing waves (Figure 10.6) occur transverse to both the tube axis and the flow direction. The resonant vibration of the standing waves surrounding the tubes is commonly called acoustic resonance or acoustic vibration. It is usually characterized with intense, low-frequency, pure-tone noise. When the excitation frequency is closer to the standing wave frequency or both coincide in a heat exchanger, there is a possibility of acoustic vibration. Also, if the standing wave frequency coincides with natural frequencies of structural components such as casing, tubes, etc., it may be structurally harmful [57], and it can affect the performance characteristics of the heat exchanger by increasing the pressure drop. Acoustic resonance occurred in-line and staggered tube banks, single rows of tubes, helically coiled tubular heat exchangers, air heater economizers, superheaters, ducts of rectangular and circular shells, and others [58–61].

10.5.1 PRINCIPLE OF STANDING WAVES

Standing waves will develop if the distance L_a between the bounding walls is $\lambda/2$ or a multiple of $\lambda/2$, i.e., $L_a = n\lambda/2$ where $n = 1, 2, 3, \dots$ and λ is the wavelength of the standing wave. The standing wave frequencies are given by

$$f_a = \left(\frac{nC}{2L_a} \right) \quad \text{for } n = 1, 2, 3, \dots \quad (10.29)$$

where

C is the velocity of sound in the shellside medium

L_a is the characteristic dimension (normally the enclosing walls of the flow passages)

n is the mode number

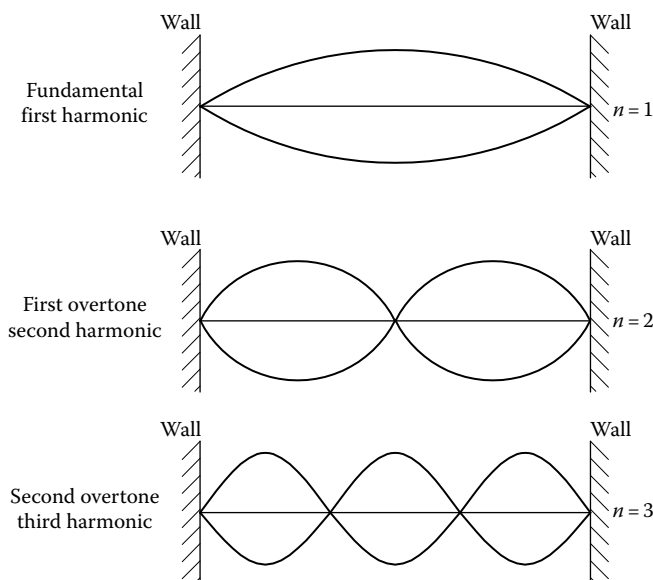


FIGURE 10.6 Variation of the fluctuating transverse velocity associated with standing waves with one, two, and three half waves.

The velocity of sound C in the shellside medium is given by

$$C = \sqrt{\frac{g_c Z \gamma R_c T}{M_g}} \quad (10.30)$$

where

g is the acceleration due to gravity (32.174 ft/s² or 9.81 m/s²)

Z is the gas compressibility factor

R_c is the universal gas constant, 1545.32 lbf·ft/lb mole or 847.6 kgf·m/kg mole°K

T is the absolute temperature of the gas, °R/°K

= °F + 459.69 or °C + 273.16

M_g is the molecular weight of the gas, lb mol or kg mol

γ is the ratio of specific heat of gas at constant pressure to constant volume

The value of M_g (molecular weight of the gas) for air or flue gas is 28.97 lb mol and for steam 18.02 lb mol, and γ , the ratio of the specific heat of the gas at constant pressure to that at constant volume, is 1.4 for air or flue gas and 1.328 for steam [62].

Typical standing waves with fundamental and second modes are shown in Figure 10.6. Normally, the standing wave will form in open lanes of 45° or 90° layout angle geometries, since the least exciting energy is required to form in these tube layout patterns. According to Barrington [63], acoustic vibration occurs most frequently with a rotated square (45°) tube layout compared to other tube layouts. Although the rotated square geometry exhibited the greatest resistance to FEI, this was marred by the presence of intense acoustic standing waves. Hence, they may not be suitable for shellside gaseous medium [40].

10.5.1.1 Effect of Tube Solidity on Sound Velocity

For STHEs, Parker [64] and Burton [65] have shown that the actual speed of sound C in the shellside fluid is reduced due to the presence of the tubes. The rate of decrease in the sound speed is mainly

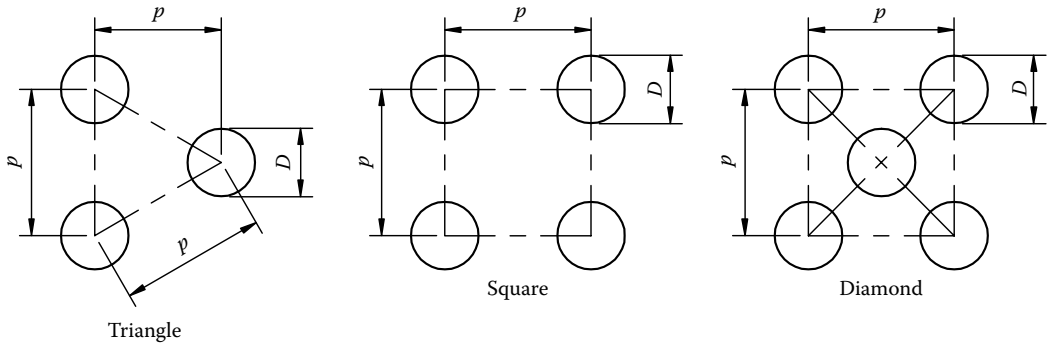


FIGURE 10.7 Tube layout parameters to calculate solidity factor. (From Blevins, R.D. and Bressler, M.M., *Trans. ASME J. Pressure Vessel Technol.*, 109, 275, 1987.)

dependent on the solidity ratio σ of the tube layout and a weak function of added mass coefficient, C_m . Accordingly, formulas for effective speed of sound C_{eff} through the tube bundle are given by

$$C_{\text{eff}} = \frac{C}{\sqrt{(1 + \sigma)}} \quad \text{Parker} \quad (10.31a)$$

$$C_{\text{eff}} = \frac{C}{\sqrt{(1 + C_m \sigma)}} \quad \text{Burton} \quad (10.31b)$$

For widely spaced arrays, $C_m = 1$ (approximately).

The solidity ratio σ is defined as the ratio of free flow area to the frontal area of the tube layout. The expression for σ for the various tube layout patterns shown in Figure 10.7 is given by Blevins [8]:

$$\begin{aligned} \sigma &= 0.9069 \left(\frac{D}{p} \right)^2 \quad \text{for } 30^\circ \text{ or } 60^\circ \text{ layout} \\ &= 0.7853 \left(\frac{D}{p} \right)^2 \quad \text{for } 90^\circ \text{ layout} \\ &= 1.5707 \left(\frac{D}{p} \right)^2 \quad \text{for } 45^\circ \text{ layout} \end{aligned} \quad (10.32)$$

In heat exchangers of normal size, either the fundamental mode or the second mode is most likely to occur. However, in large exchangers with shell diameter of the order of 20–30 m, the acoustic vibration can be excited up to fifth or sixth mode.

Principles of acoustic vibration, their evaluation, and prediction methods are discussed by Grotz and Arnold [66], in Refs. [24,25,57–62], by Barrington [63,67], and by Fitzpatrick [68]. The better understanding of acoustic resonance is mostly due to Dr. Blevins. In this section, the excitation mechanisms are discussed and acceptance criteria are defined.

10.5.2 EXPRESSIONS FOR ACOUSTIC RESONANCE FREQUENCY

Two versions of expression, one in terms of shellside pressure and shellside fluid density (TEMA) and the other in terms velocity of sound through shellside medium and shell dimensions, are given next for calculating the acoustic vibration frequency f_a .

TEMA expression

$$f_a = \frac{483.2}{L_a} \left(\frac{p_s}{\rho_s} \right)^{0.5} \quad (\text{use TEMA dimensional units}) \quad (10.33)$$

10.5.2.1 Blevins Expression

Circular shell: For a circular shell of radius R , the expression for standing wave frequency is given by [8,62]

$$f_a = \frac{C_{\text{eff}} \lambda_i}{2\pi R} \quad (10.34)$$

where

$$\lambda_1 = 1.84$$

$$\lambda_2 = 3.054$$

Rectangular shell: Consider a closed rectangular volume of dimension L_x , L_y , and L_z with tubes as shown in Figure 10.8. The indices i, j , and k give the number of acoustic waves in the flow direction (x), transverse direction (y), and tube axial (z) direction, respectively. The acoustic modes typically excited by crossflow are the transverse modes (modes $j = 1, 2, 3, \dots$) in the y direction, which are perpendicular to the flow direction and tube axis. Longitudinal modes i in the flow direction x and transverse modes k in the direction of the tube axis z are rarely excited by crossflow. Assuming that both the tubes and the duct are rigid structures and the dimension of the wavelength of the standing waves is of comparable size to the duct width and much higher than the tube diameters, the expression for acoustical frequency of the duct is given by [8]

$$f_a = \frac{C_{\text{eff}}}{2} \left[\left(\frac{i}{L_x} \right)^2 + \left(\frac{j}{L_y} \right)^2 + \left(\frac{k}{L_z} \right)^2 \right]^{0.5} \quad (10.35)$$

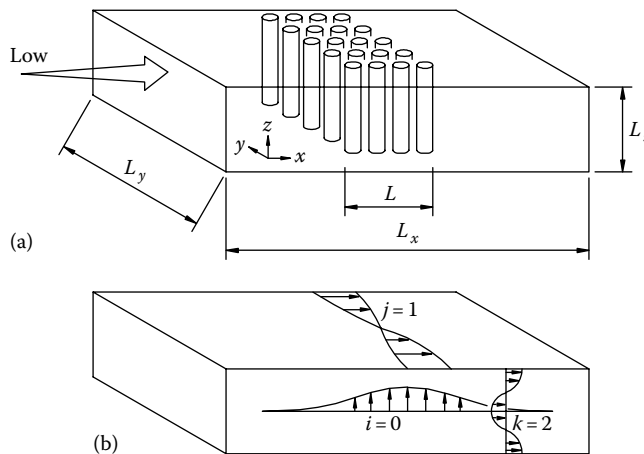


FIGURE 10.8 Acoustic modes in a closed rectangular chamber with tubes. (a) Tube bundle in duct and (b) typical mode shape of pressure in cutoff mode. (From Blevins, R.D. and Bressler, M.M., *Trans. ASME J. Pressure Vessel Technol.*, 109, 275, 1987.)

In the absence of any standing waves in x and z directions ($i = k = 0$), the equation simplify to the following [62]:

$$f_a = \frac{jC_{\text{eff}}}{2L_y} \quad (10.36)$$

where L_y is the chamber dimension in the y direction, which is equal to the shell width.

10.5.3 EXCITATION MECHANISMS

The occurrence of acoustic resonance in tubular heat exchangers is caused by either a vortex shedding mechanism or turbulent buffeting.

10.5.3.1 Vortex Shedding Mechanism

According to vortex shedding theory, if the frequency of vortex shedding coincides with the standing wave frequency, a strong acoustic oscillation of the gas column is possible and resonance is said to occur. Thus the resonance criterion is

$$f_a = f_v \quad (10.37)$$

The mechanism of vortex shedding is shown schematically in Figure 10.9, which shows an in-line heat exchanger tube bank with its containment; and f_{a1} and f_{a2} represent the frequencies of the first and second acoustical modes of the containment [69]. Normally it is considered that for the lock-in phenomenon to occur, the acoustic resonance should be within $\pm 20\%$ of vortex shedding frequency.

10.5.3.2 Turbulent Buffeting Mechanism

According to this theory, acoustic resonance takes place if the dominant frequency of the turbulent eddies coincides with the standing wave frequency of the gas column. Thus, the criterion for resonance is given by

$$f_a = f_{tb} \quad (10.38)$$

The turbulent buffeting frequency f_{tb} for fundamental mode is determined using the criteria of Owen [26] or Fitzpatrick [68]. TEMA included Owen's buffeting frequency criteria.

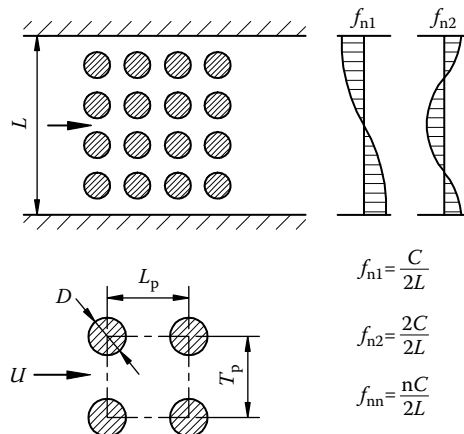


FIGURE 10.9 Acoustic resonance due to vortex shedding.

10.5.4 ACCEPTANCE CRITERIA FOR OCCURRENCE OF ACOUSTIC RESONANCE

10.5.4.1 Vortex Shedding

Eisinger criterion [25,57]. Eisinger expressed a criterion in terms of the Chen number, ψ , for in-line arrays (Figure 10.10a). The Chen number is a function of the Reynolds number, Strouhal number, and longitudinal and transverse pitch ratios. The expression for the Chen number is

$$\psi = \frac{\text{Re}}{S_u} \frac{(2X_l - 1)^2}{4X_l^2 X_t} \quad (10.39)$$

where the Reynolds number is given by

$$\text{Re} = \frac{UD}{\nu} \quad (10.40)$$

Acoustic resonance criteria are as follows:

- $\psi < 2000$ No vibration
- $\psi = 2000\text{--}4000$ low likelihood of vibration
- $\psi > 4000$ high likelihood of vibration

The TEMA condition is as follows: Acoustic resonance is possible if $\psi > 2000$.

For staggered arrays as shown in Figure 10.10b, replace L_p by $2L_p$ [60].

Blevins criterion: Acoustic resonance is possible if [8]

$$\frac{(1 - \alpha)S_u U}{D} < f_a < \frac{(1 + \beta)S_u U}{D} \quad (10.41)$$

where the parameters α and β take their values as follows.

Normal criterion: For normal design criteria, $\alpha = \beta = 0.2$, and the resulting expression for the Blevins criterion is

$$\frac{0.8S_u U}{D} < f_a < \frac{1.2S_u U}{D} \quad (10.42)$$

Conservative criterion: For the conservative criterion, $\alpha_{\max} = 0.40$ and $\beta_{\max} = 0.48$, and the resulting expression for the Blevins criterion is

$$\frac{0.6S_u U}{D} < f_a < \frac{1.48S_u U}{D} \quad (10.43)$$

TEMA prescribes $\alpha = \beta = 0.2$ in the conditionality equation.

The acoustical Strouhal number due to vortex shedding is determined either from Chen's plot [25] or from the Fitz-Hugh [33] map or from the correlations of Weaver et al. [35]. TEMA included Chen's plot.

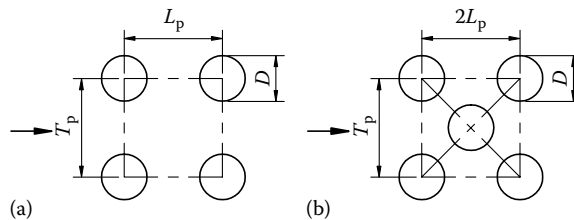


FIGURE 10.10 Tube layout parameters for calculating SPL as per Equation 10.39 (a) Inline array and (b) staggered array.

Blevins [8] sound pressure level (SPL) at resonance: If resonance is predicted, calculate SPL from the following equation [8]:

$$\text{SPL} = 20 \log_{10} \left(\frac{P_{\text{rms}}}{0.00002} \right) \quad (10.44)$$

or determine from the SPL maps of Blevins [8]. These maps are valid for Reynolds number up to 95.1×10^3 .

Check: If $\text{SPL} < 140$ dB, there is no damage either to the structural components or to the surroundings.

10.5.4.2 Turbulent Buffeting

Owen [26] criterion for resonance:

$$0.8f_{\text{tb}} < f_a < 1.2f_{\text{tb}} \quad (10.45)$$

Criterion of Rae and Murray [70]: Resonance will not occur for

$$\frac{U}{f_a D} < 2(X_1 - 0.5) \quad (10.46)$$

This criterion is included in TEMA.

Grotz and Arnold [66] criterion for in-line arrays: Calculate the slenderness ratio τ from the following equation:

$$\tau = \frac{L_a}{Dn(X_1 - 1)} \quad (10.47)$$

where

L_a is the duct width

n is the mode number

Resonance will occur for $\tau = 62\text{--}80$. Application to staggered arrays is questionable [62].

Other methods for prediction of acoustic resonance have been suggested by Fitzpatrick et al. [71] and Zaida et al. [72].

10.6 VIBRATION EVALUATION PROCEDURE

Basically, the vibration evaluation procedure involves an estimation of certain parameters for various flow-induced excitation mechanisms. The estimated parameters are compared with their respective limiting values to check whether or not vibrations from such excitation mechanisms can cause potential damage to the tubes and the shell. There is a need to individually examine various zones of interest, namely, the nozzle inlet zone, U-bend region, and baffle window region, since there is a likelihood of high turbulence and high crossflow velocity in these regions and the variations of span lengths between baffle supports compared to the central baffle region.

10.6.1 STEPS OF VIBRATION EVALUATION

1. Calculate the effective mass per unit length.
2. Identify the zones of interest (inlet, baffle window, central baffle zones, U-bend, etc.) to calculate the natural frequency.

3. Calculate the natural frequency for spans in various regions of interest.
4. Calculate the damping parameter.
5. Calculate crossflow velocity for the TEMA shell under consideration.

10.6.1.1 Step 6 for Liquid Flow

Vortex shedding:

- a. Calculate vortex shedding frequency. Check for the acceptance criteria.
- b. If resonance takes place, calculate tube response and check whether it is not exceeding the limiting value.

Turbulent buffeting: If resonance is predicted, calculate tube response due to random excitation and check for the acceptance criterion.

Fluid elastic instability: Calculate the critical velocity and compare with crossflow velocity. Keep the maximum crossflow velocity below the critical velocity.

10.6.1.2 Step 6 for Gas Flow

In addition to the criteria given for liquid flow, the following check for acoustic resonance due to standing waves may be carried out.

- a. Calculate acoustic resonance frequency.
- b. Calculate vortex shedding frequency. Check for various vortex shedding criteria.
- c. Calculate turbulent buffeting frequency. Check for various turbulent buffeting criteria.

Fill these values into the FIV specification sheet for acoustic resonance given in Table 10.2.

10.6.2 CAUTION IN APPLYING EXPERIMENTALLY DERIVED VALUES FOR VIBRATION EVALUATION

The vibration prediction methods are mostly based on linearized models that require input data reflecting a particular flow pattern and a structural configuration. The guidelines are derived from simplified test conditions, and they cannot be generalized for actual heat exchangers. The parameters such as damping, Strouhal number, FEI constant, etc., are mostly known for idealized test conditions and may be different in the real environment of the heat exchanger due to interaction between various mechanisms of excitation [57]. If the outcome of the experimentally derived design criteria is applied to specific heat exchangers, it may lead to conservative or marginal designs.

Accurately predicting the critical velocity requires testing a single-tube mock-up with end conditions and supports as nearly identical as possible to the actual heat exchanger unit, or a part scale model [73] or a full scale model if it is economically feasible. Hence, it can be concluded that the judgment of the designer, precautions taken by the heat exchanger fabricator, and model test conducted by the researchers are the means available to provide reasonable assurance that a design will not fail due to FIV [73].

10.7 DESIGN GUIDELINES FOR VIBRATION PREVENTION

FIV problems are better prevented rather than corrected. After the thermal design stage, a check for FIV is carried out, and if the tubes are susceptible to FIV, excitation sources are identified and corrective action is taken. Tube vibration can be reduced to within limits by either increasing the tube natural frequency or reducing the crossflow velocity or suppressing the source of excitation as discussed next.

10.7.1 METHODS TO INCREASE TUBE NATURAL FREQUENCY

Tube natural frequency is represented by

$$f_n \propto \frac{1}{L_i^2} \left(\frac{EI g_c}{m} \right)^{0.5} \quad (10.48)$$

TABLE 10.2**Flow-Induced Vibration Specification Sheet for Gases—Acoustic Resonance**

1. Effective sound velocity

a. Sound velocity

$$C = \sqrt{g_c Z \gamma R T / M_g}$$

b. Solidity ratio

$$\sigma = 0.9060 \left(\frac{D}{p} \right)^2 \quad \text{for } 30^\circ \text{ or } 60^\circ \text{ layout}$$

$$= 0.7853 \left(\frac{D}{p} \right)^2 \quad \text{for } 90^\circ \text{ layout}$$

$$= 1.5707 \left(\frac{D}{p} \right)^2 \quad \text{for } 45^\circ \text{ layout}$$

c. Effective sound velocity

$$C_{\text{eff}} = \frac{C}{\sqrt{(1 + \sigma)}}$$

or

$$C_{\text{eff}} = \frac{C}{\sqrt{(1 + C_m \sigma)}}$$

3. Check for vortex shedding lock-in

a. Normal criteria

SPL

If SPL < 140, safe

$$0.8 \frac{S_u U}{D} < f_a < 1.2 \frac{S_u U}{D}$$

b. Conservative criteria

$$0.6 \frac{S_u U}{D} < f_a < 1.48 \frac{S_u U}{D}$$

4. Check for turbulent excitation own

$$f_{\text{tb}} = \frac{U}{D X_1 X_1} \left[3.05 \left(1 - \frac{1}{X_1} \right)^2 + 0.28 \right]$$

for resonance: $0.8 f_{\text{tb}} < f_a < 1.2 f_{\text{tb}}$

2. Acoustic resonance frequency

a. Blevins

i. For circular shell

$$f_a = \frac{C_{\text{eff}} \lambda_i}{2\pi R} \quad (\lambda = 1.84, \lambda_2 = 3.054)$$

ii. For rectangular shell

$$f_a = \frac{j C_{\text{eff}}}{2L_y} \quad j = 1, 2, 3 \dots$$

$$\text{b. } f_a = \frac{483.2 (p_s / \rho_s)^{0.5}}{L_a} \quad (\text{TEMA units})$$

Chen No. Ψ and Eisinger criteria

$$\text{Re} = \frac{U D \rho_s}{\mu}, \quad \Psi = \frac{\text{Re} (2X_1 - 1)^2}{S_u^2 4X_1^2 X_t}$$

 $\Psi < 2000$ no vibration $\Psi < 2000$ –4000 low likelihood of vibration $\Psi > 4000$ high likelihood of vibration

Bryce criteria

$$\frac{U}{f_a D} < 2(X_1 - 0.5)$$

No resonance

Blevins

for $U/f_a D > 2$

resonance will occur

Arnold's slenderness ratio

$$\tau = \frac{L_a}{D n (X_1 - 1)}$$

If, $\tau < 62$ –80,

resonance will occur

A careful review of this natural frequency equation indicates that the tube natural frequency can be increased by reducing the tube span L_i , increasing the ratio l/m , or increasing Young's modulus E . Since the moment of inertia and tube mass are limited by the standard tube dimensions and E is limited by the material chosen, in most of the cases, the only option available to increase the natural frequency is to reduce the tube span L_i [11]. For single-segmental baffles, reducing the

tube span will increase the natural frequency proportionally to $1/L_i^2$ and increase the crossflow velocity proportionally to $1/L_i$. Hence, the tube span may be reduced to an optimum level [17]. The influence of E and thin tubing on FIV is explained next with reference to a retubed unit.

10.7.1.1 FIV of Retubed Units

The importance of tube support spacing and Young's modulus has often come to light when a condenser that was initially fitted with copper alloy tubes is retubed with thin titanium tubes, which have a relatively low modulus of elasticity. The thin-wall titanium tubing is not as stiff as the copper tubing it replaces, so that it usually requires supplementary support to avoid FIV problems.

1. If the tube vibration problem is anticipated in the window zone due to longer tube span between baffles ($2L_{bc}$) and higher velocity than the tubes at central zone, eliminate the tubes in the window zone, resulting in a no-tubes-in window design (NTIW). To offset any loss in heat transfer, introduce support plates to divert the fluid across the bundle.
2. An alternative to the NTIW design is to employ strip baffles in the window zone. This additional support given to the tubes in this zone increases the stiffness of the tubes and hence increases the natural frequency.
3. Increase the structural damping of the tube bundle by means of thicker baffle plates and reduce the fretting wear by employing softer baffle material.
4. Lace the tube bundle using wire laces to increase the tube bundle stiffness.
5. U-bend support: The natural frequency of the U-bend is considerably increased by providing a support known as antivibration bars (AVB) to the U-bend. Principal types of U-bend support configurations are (a) scalloped bars, (b) wiggle bars, (c) lattice bars, and (d) flat bars, and they are as shown in Figure 10.11 [41].

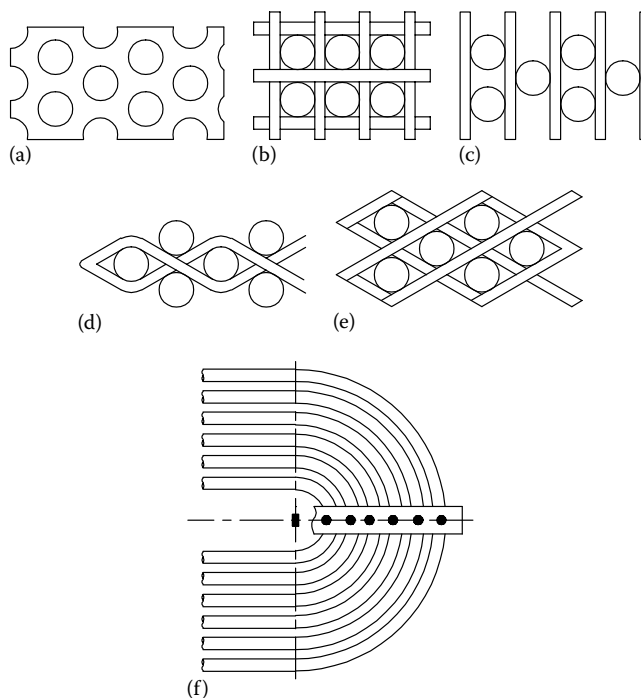


FIGURE 10.11 U-bend supports. (Based on Weaver, D.S. and Schneider, W. *Trans. ASME J. Eng. Power*, 105, October, 775, 1983.)

6. Tubes are likely to be under some axial loading as a result of fabrication and operation. Tensile stresses increase the natural frequency, whereas compressive stress decreases the natural frequency. Since axial compressive stress in the tube decreases the tube natural frequency, rolling-in of the tubes into the tubesheet should be done carefully. Care should be also taken to allow for the free thermal expansion of the tubes. When significant compressive axial loads are induced on the tubes in a multipass exchanger, these tubes shall be located in the baffle overlap regions to minimize the unsupported span length [11].
7. When only few tubes are exposed to high localized velocities, sealing strips may be applied to provide flow resistance and reduce flow in critical areas [74].

Plugging of tubes: The affected tubes may be omitted or plugged if proper precautions are taken to ensure that collision will not endanger the adjacent tubes [74].

Detuning of tubes: Detuning is defined as the method of producing differences among the natural frequencies of the neighboring tubes in a tube array. The tubes are detuned by installation of additional supports such as clips, wedges, flat bars, helical spacers, strip baffles, or any other means of increasing the tube fixity. Detuned tube arrays lose stability at a higher flow velocity; the incidence of instability is more gradual in a tube bank with differences in tube-to-tube frequency than in a bank with identical tube frequency [8].

Detuning effect: For the displacement mechanism associated with the coupled motion of adjacent tubes, detuning will have a significant effect, whereas, for the velocity mechanism, the effect is little since the individual tube motion is independent of neighboring tubes and the instability is controlled by fluid damping forces [55]. Lever and Weaver [43] found that for airflow, detuning of neighboring tubes produced a maximum increase in critical velocity about 40% at a frequency difference of 3%. For frequency differences greater than about 10%, there was no significant improvement in threshold instability. Tanaka et al. [46] report that detuning has increased the critical velocities for airflow by about 60%.

Avoid longer unsupported tube spans. Follow maximum unsupported tube length as specified in TEMA, RCB-4.52 [19].

10.7.2 METHODS TO DECREASE CROSSFLOW VELOCITY

The following methods may be employed to reduce the crossflow velocity, which in turn will decrease the vibration excitation potential (refer to Chapter 5 for more details on this topic):

1. Reduce the crossflow velocity either by decreasing the flow rate or by increasing the shell diameter. However, this will reduce the heat transfer rate. Even though testing has indicated that controlling an instability usually requires lowering of the flow rate below its initial threshold value, hysteresis suggests that instability may be initiated by flow pulses that are caused by operational transients. Hence, while evaluating the critical velocity, if such operational transients are anticipated, it may be desirable to reduce the allowable flow rate significantly below the instability threshold [74].
2. Increase the tube pitch such that crossflow area is increased. However, this will be at the cost of lower shellside heat transfer.
3. If vibration damage to the tubes located beneath the nozzle is predicted, increase the nozzle openings to decrease the mass velocity or install impingement plate.
4. If the vibration potential is predicted in the middle zone of an E shell, change the shell design into either an X shell or J shell. Theoretically speaking, for the same mass flow rate, the crossflow velocity on the shellside of a J shell will be half that of the E shell [75].
5. Use double or multiple segmental baffles to divide the flow into two or more streams. In an exchanger with single segmental baffles, the total flow, except for leakages and bypass streams, passes through the tube bank between baffles, whereas in an exchanger with double segmental baffles barring the leakages, the flow divides into two streams on either side of the

shell and into three streams in triple segmental baffles. Under ideal conditions, the crossflow velocity in a double-segmental baffle unit is half that of a comparable single-segmental baffle unit and one-third with triple-segmental baffles. Hence, it is expected that double-segmental baffles will double the critical velocity compared to single-segmental baffles. However, experiments on an industrial-size heat exchanger at Argonne National Laboratory [76] show that the threshold velocity increased by 24%–67%. The full theoretical potential of approximately doubled threshold velocities was not realized. This was attributed to the effects of localized end zone conditions, which were probably not eliminated.

6. Since the crossflow velocity is the major cause of FIV, one of the design alternatives is to substitute the existing window baffle supports to Grid baffle or RODbaffle supports [77]. In a rod baffle exchanger, the shellside fluid is parallel to the tubes and the rod baffles offer very high stiffness to the tube bundle.
7. Like RODbaffle supports, other tube support arrangements or heat exchangers that produces axial flow over the tubes include NESTS™ [78], EMBaffle® design (which uses expanded metal baffles made of plate material that has been slit and expanded), Helixchanger® heat exchanger (which uses helical baffles), and Twisted Tube® heat exchanger without baffle (baffle-free tube support) eliminates flow induced vibration.
8. Limit the high localized velocities in the bundle bypass flow region or in the pass partition lanes by carefully selecting the sealing strips and pass portion lane widths, respectively, without introducing a penalty on heat transfer on the shellside.
9. Avoid too small or too large baffle cuts, since both yield poor velocity distribution and high localized velocities.
10. Maintain small tube-to-baffle hole clearances; follow TEMA Standard RCB-4.2 [19].
11. Ensure uniform baffle spacings.

10.7.3 SUPPRESSION OF STANDING WAVE VIBRATION

The acoustic standing waves can be suppressed by any of the following devices or methods:

1. Antivibration baffles, solid or porous baffle
2. Resonators
3. Fin barriers
4. Helical spacers
5. Detuning or structural modification
6. Removal of tubes
7. Surface modification
8. Irregular lateral spacing of tubes
9. Changing the mass flow rate

10.7.3.1 Antivibration Baffles

Solid baffle: The occurrence of acoustic resonance in a crossflow heat exchanger is related to the development of standing waves. If the standing waves are inhibited from developing, then the associated acoustic resonance will not take place. This is achieved by incorporation of either a solid baffle or a porous baffle inside the heat exchanger, in a direction parallel to the flow and perpendicular to the direction of standing waves. The baffles are also called detuning baffles. The placement of solid baffles is shown schematically in Figure 10.12.

Number of solid baffles: As per theory, if solid baffles are to be installed in a tubular heat exchanger in which the maximum number of half-waves that can occur between the walls is N_w , then N_w solid baffles should be installed to prevent the acoustic vibration. The major drawback associated with the solid baffles is that the number of baffles required is very high for a heat exchanger

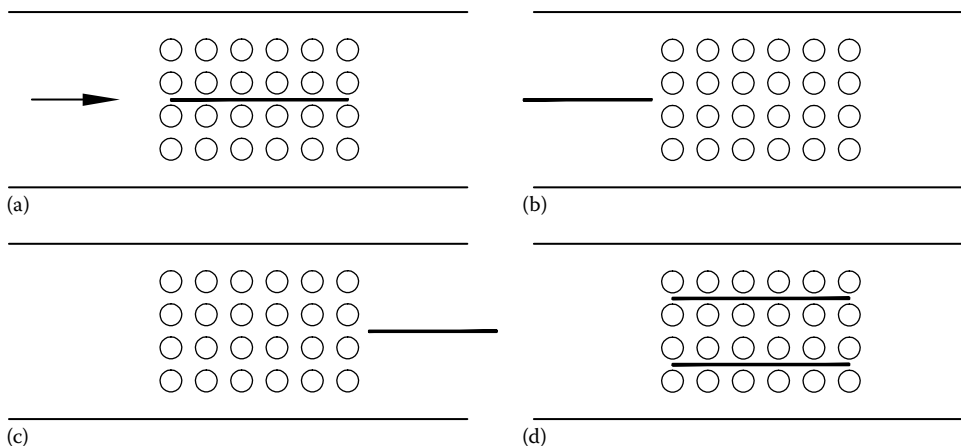


FIGURE 10.12 Detuning solid baffle arrangement. (a) Central baffle, (b) upstream baffle, (c) downstream baffle, and (d) two baffles at 1/3 and 2/3 transverse locations. (From Blevins, R.D. and Bressler, M.M., *Trans. ASME J. Pressure Vessel Technol.*, 109, 282, 1987.)

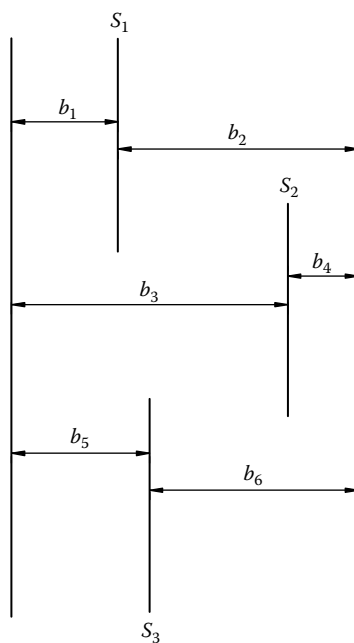


FIGURE 10.13 Chen's method of solid baffle arrangement to prevent acoustic vibration. Insertion of the slightly overlapped detuning baffles into the heat exchanger to make the natural frequencies of the transverse gas columns in the spaces, b_1 , b_2 , b_3 , b_4 , b_5 , and b_6 as different as possible from one another. (From Chen, Y.N., *Trans. ASME J. Eng. Industry*, February, 134, 1968.)

of spatial size of 20–30 m used in the fossil fuel utilities, like an economizer, reheater, etc. However, the number of baffles requirement can be minimized by following Chen's method [25]. The method consists of placing solid baffles in preferred locations as shown in Figure 10.13. The distances b_1 , b_2 , b_3 , b_4 , b_5 , and b_6 are all to be kept different from each other and their ratios b_2/b_1 , b_4/b_3 , and b_6/b_5 should deviate much from the integers corresponding to the modes of the vibrations to be expected. While placing the baffles, the length of the baffle should be large in comparison with the wavelength

of the standing waves to be expected in the heat exchanger. The shortcomings associated with the solid baffles are discussed by Eisinger [57]. They include

1. Expensive for retrofitting
2. Inhibition of periodical inspection and maintenance operations
3. Limited life if the medium of flow is corrosive in nature
4. Tendency to vibrate and susceptible to thermal distortion in service

Porous baffle: The porous baffle concept consists of a single flow-resistive element inserted between the tubes so that it is parallel to the flow direction [79]. Byrne [79] has shown that, in general, if the maximum number of half-waves between the walls is N_w , then a single porous baffle should be located at a distance from one wall equal to the wall-to-wall span divided by $2N_w$. The advantage of a porous baffle over that of solid baffles is that a single porous baffle can be used to inhibit the development of a number of standing waves, whereas the number of solid baffles required is equal to the maximum number of half-waves that can develop between the walls.

10.7.3.2 Helmholtz Cavity Resonator

Installation of an acoustic damper such as a tuned Helmholtz cavity resonator on the shellside will suppress the acoustic vibration. A simple Helmholtz resonator is shown in Figure 10.14. The damping is maximum when the resonator is tuned with the acoustic mode of interest [62]. When tuned, there is a large oscillating mass flow through the resonator neck that expends energy by passing through the neck and/or the screen placed in the neck. An approximate formula for the resonator natural frequency is given by [62]

$$f = \frac{C}{2\pi} \left(\frac{A}{V_h l_h} \right)^{0.5} \quad (10.49)$$

where

A is the area of cross section of opening in the resonator

V_h the volume of the cavity resonator

l_h the length of the opening in the resonator

10.7.3.3 Concept of Fin Barrier

To overcome the drawbacks associated with solid baffles, a new method of solving standing wave vibration was suggested by Eisinger [57]. The method consists of using fin barriers welded to the heat exchanger

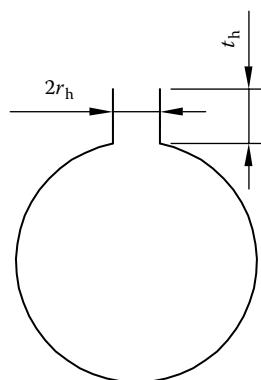


FIGURE 10.14 Helmholtz resonator.

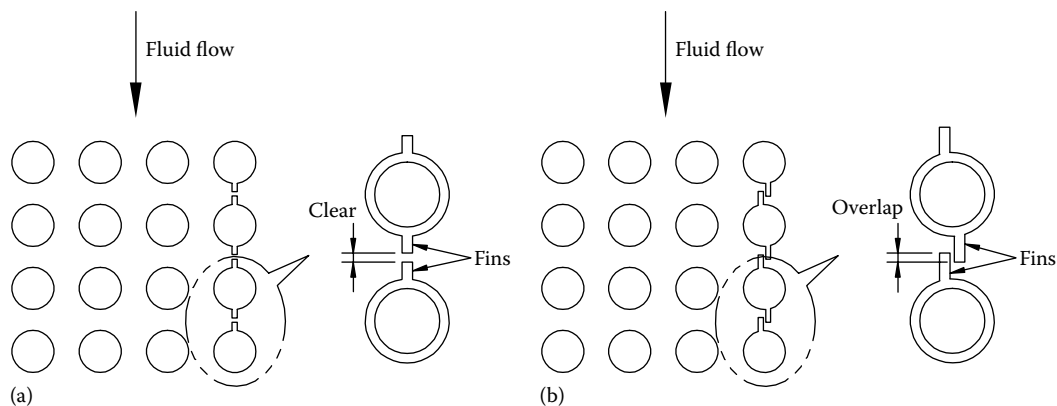


FIGURE 10.15 Arrangements of fin barriers for in-line array to solve standing wave problem. (a) Inline layout and (b) staggered layout. (From Eisinger, F.L., *Trans. ASME J. Pressure Vessel Technol.*, 102, 138, 1980.)

tubes, forming a thin wall parallel to the flow direction and perpendicular to the direction of propagation of standing waves. The various forms of fin barriers are shown schematically in Figure 10.15.

10.7.3.4 Concept of Helical Spacers

A novel idea for overcoming FIV in a closely spaced tube array is to introduce helical spacers inside the tube bank area [57]. This method is well suited to the initial design stage or for use in field modifications. The method is applicable both for staggered and for in-line tube layout, and spacer placement is shown schematically in Figure 10.16.

10.7.3.5 Detuning

This has been already discussed.

10.7.3.6 Removal of Tubes

Selective removal of a few tubes at the displacement antinodes of the standing waves will eliminate the vortex shedding and thus avoid the coupling between vortex shedding and acoustic resonance.

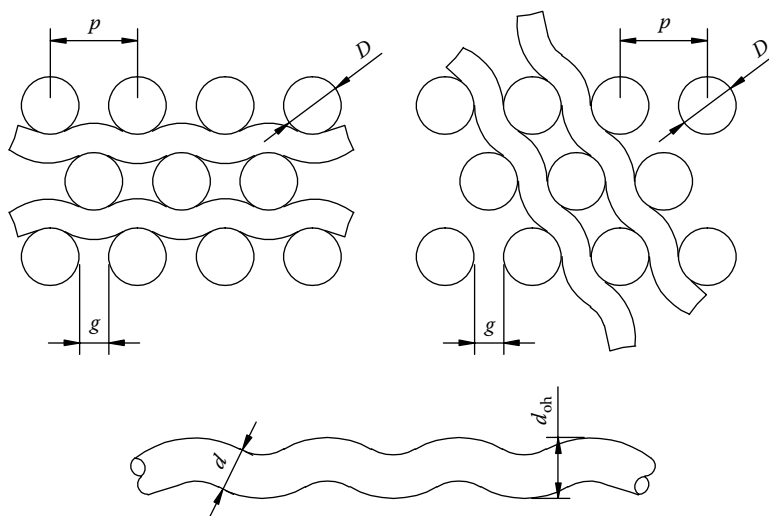


FIGURE 10.16 Helical spacers to overcome FIV of a staggered tube array. (From Eisinger, F.L., *Trans. ASME J. Pressure Vessel Technol.*, 102, 138, 1980.)

This also upsets the vortex shedding regularity at pressure nodes. Walker and Reising [80] and Barrington [63,67] have observed that by removing 3%–10% of tubes near the center of the tube bank, acoustic resonance can be diminished or eliminated.

10.7.3.7 Surface Modification

Fouling of heat exchanger tubes by dirt and carbon soot has been associated with the reduction in sound level, and hence the deposition increases the acoustic damping [8,81].

10.7.3.8 Irregular Spacing of Tubes

Destroy the phasing of vortex streets by having irregular spacing of tubes. This will scramble the vortex shedding frequency. Zdravkovich and Nuttal [82] found the nonoccurrence of standing waves by displacing the susceptible tubes either laterally or longitudinally. However, this method is attractive only if the thermal performance is not affected.

10.7.3.9 Change the Mass Flow Rate

Modify vortex shedding frequency by changing the mass flow rate. This may not be very attractive from a thermal performance point of view.

10.8 BAFFLE DAMAGE AND COLLISION DAMAGE

10.8.1 EMPIRICAL CHECKS FOR VIBRATION SEVERITY

From the prevalent pattern of tube failures occurring at the baffle supports and at the midspan, Thorngren [83] has attributed tube failures mainly to (1) baffle-type damage and (2) collision-type damage. He proposed two empirical correlations, called baffle damage number, n_{BD} , and collision damage number, N_{CD} , to check the severity of tube damage due to FIV. The expressions for these damage numbers can be easily deduced similar to Connors' instability equation. Therefore, they are not discussed here.

10.9 IMPACT AND FRETTING WEAR

Heat exchanger tubes are supported at regular intervals by passing through oversized holes in baffle plates (Figure 10.17). When the tube vibrates against the baffle plates, material can be fretted away from both the tube and the support plate as shown in Figure 10.18. If the fretting

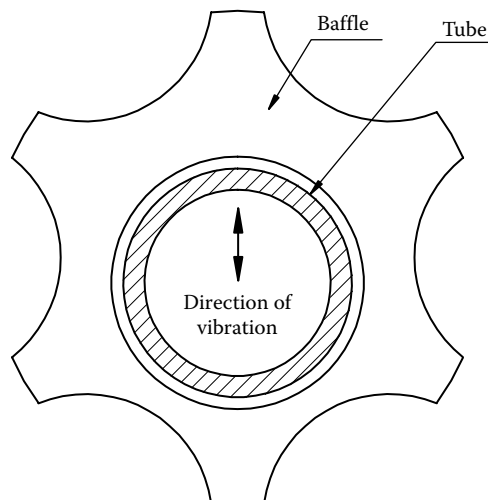


FIGURE 10.17 Vibrating tube in baffle hole.

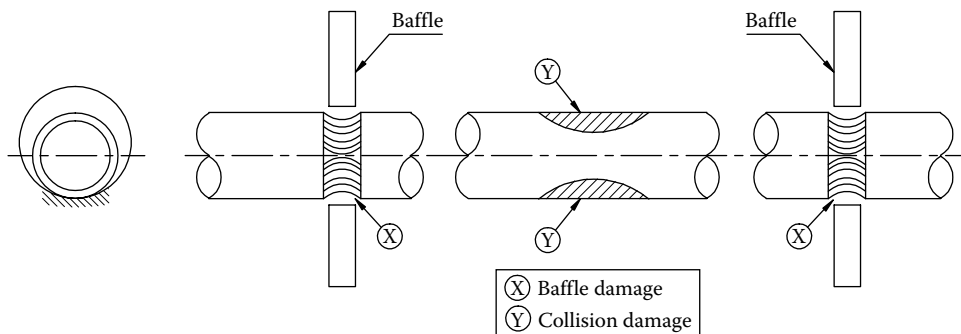


FIGURE 10.18 Fretting wear of tube.

wear of tube is sufficiently large, the tubes will eventually rupture due to the fluid pressure [38]. When one considers that a design objective for a nuclear power plant steam generator or a heat exchanger is a 40 year codal life, even relatively small tube wear rates cannot be tolerated [6,38]. Hence in recent years, significant attention has been given to study the effect of tube-to-tube support plate clearances on tube vibration and wear, by (1) laboratory experiments, (2) theoretical simulations, and (3) analytical models. Vibration excitation mechanisms responsible for fretting wear are (1) vortex shedding, (2) turbulent buffeting, and (3) FEI. References [38,84–93] brought about a greater understanding of the tube-to-tube support plate interaction characteristics and resultant tube wear.

10.9.1 TUBE WEAR PREDICTION BY EXPERIMENTAL TECHNIQUES

Among the experimental techniques, the notable are that of Blevins [84,85] and Haslinger et al. [86]. The fundamental assumption of the Blevins [84] experimental fretting wear model is that fretting wear is the result of relative motion between the tube and the support plates. Blevins assumed that the fretting wear is a function of parameters such as (1) tube geometry; (2) baffle plate geometry; (3) tube and baffle plate material properties; (4) amplitude, frequency, and mode shape of tube vibration; (5) preload between the tube and support plate; and (6) nature of environment and operating temperature.

Recently, Blevins [94] conducted experiments to predict that wear induced by vibration on a heat exchanger model with alloy 800H and 2.25Cr–1Mo steel heat exchanger tubes loosely held supports in a helium environment at temperatures up to 650°C (1200°F). From the conclusions derived from his experiments, it is seen that (1) impact wear can be minimized by reducing the impact contact stresses below the fatigue allowable stress, (2) decreasing the vibration amplitude or baffle hole clearance markedly decreases wear rate and subsurface deformation at all temperatures, and (3) application of chromium coating both to the tube and the plate specimens greatly reduces the surface self-adhesion and surface deformation that would otherwise occur above 500°C (930°F). Below this temperature, a coating is probably not required.

10.9.2 THEORETICAL MODEL

Nonlinear finite-element modeling techniques to predict tube wear due to turbulence excitation, FEI, or vortex shedding are discussed in Refs. [38,89–93]. The wear parameters central for the theoretical models are (1) sliding distance, (2) contact time, (3) average contact time, (4) threshold crossings, and (5) work rate.

10.10 DETERMINATION OF HYDRODYNAMIC MASS, NATURAL FREQUENCY, AND DAMPING

FIV analysis of heat exchangers requires the knowledge of damping, hydrodynamic mass, and natural frequency of tube bundle. Their determination is discussed next.

10.10.1 ADDED MASS OR HYDRODYNAMIC MASS

During FIV, the vibrant tubes displace the shellside fluid. When the fluids involved are liquids or very dense gases, the inertia of the fluid will have substantial effect on natural frequency of the tubes. Hence, while calculating the natural frequency of the tube, the influence of the displaced fluid is taken care of by augmenting the mass of the vibrating tube by including hydrodynamic mass or added mass. The added mass is defined as the displaced fluid mass times an added mass coefficient C_m . Since the added mass augments the vibrating tube mass, the natural frequency of the tube will be reduced compared to when the tube is vibrating in vacuum or very low-density gas.

10.10.2 DETERMINATION OF ADDED MASS COEFFICIENT, C_m , FOR SINGLE-PHASE FLOW

The added mass coefficient is estimated either by the analytical method of Blevins [8] or from the experimental database of Moretti et al. [95].

10.10.2.1 Blevins Correlation

Blevins [8] gave an analytical formula to determine added mass coefficient of a single flexible tube surrounded by an array of rigid tubes as shown in Figure 10.19. This is a reasonable approximation of the more complex case of all flexible cylinders. The expression for added mass coefficient C_m is given as

$$C_m = \frac{(D_e/D)^2 + 1}{(D_e/D)^2 - 1} \quad (10.50)$$

where $D_e/D = ((1 + 0.5 p/D)p/D)$ in which D_e is the equivalent diameter of a tube array. The equivalent diameter D_e is used to represent the confinement due to surrounding tubes.

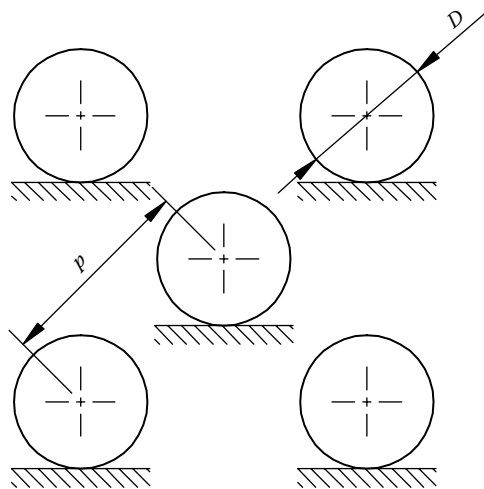


FIGURE 10.19 Tube arrangement for determining added mass coefficient. (From Moretti, P.M. and Lowery, R.L., *Trans. ASME J. Pressure Vessel Technol.*, 98, 190 1976.)

10.10.2.2 Experimental Data of Moretti et al.

The experimental results of Moretti et al. [95] for a single flexible tube surrounded by rigid tubes in a hexangular array or in a square array with a pitch-to-diameter ratio from 1.25 to 1.50 are given in Figure 10.20. Their test results for C_m for four pitch-to-diameter ratios are given in Table 10.3. TEMA included this figure (Figure 10.20) for determination of added mass coefficient [19].

10.10.3 NATURAL FREQUENCIES OF TUBE BUNDLES

The tubes in a heat exchanger are slender beams and the most flexible members. They vibrate at discrete frequencies when they are excited. The natural frequency depends on their geometry, material properties like Young’s modulus, density and material damping, tube-to-support interactions, etc.

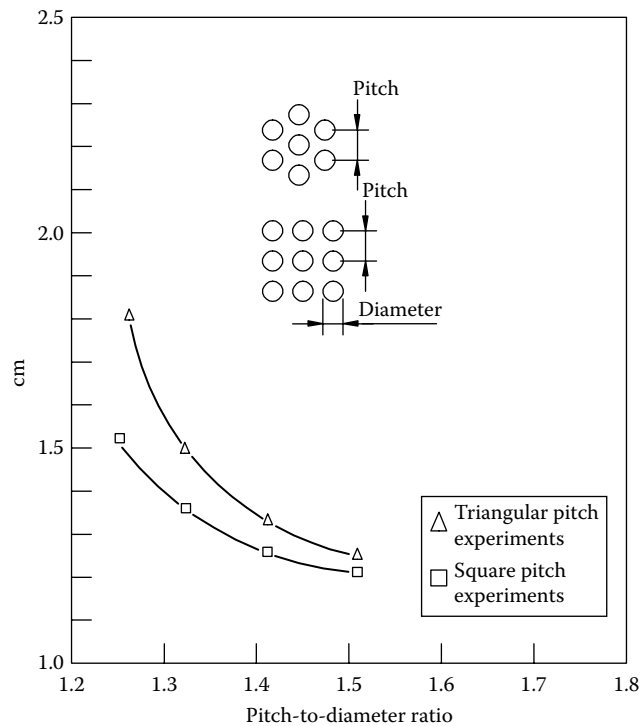


FIGURE 10.20 Determination of added mass coefficient. (From Moretti, P.M. and Lowery, R.L., *Trans. ASME, J. Pressure Vessel Technol.*, 98, 190 1976.)

TABLE 10.3
Added Mass Coefficient, C_m

Pitch-to-Diameter Ratio	C_m	
	Triangular Pitch	Square Pitch
1.25	1.1756	1.519
1.33	1.429	1.381
1.42	1.347	1.286
1.50	1.274	1.272

Source: Interpreted from Moretti, P.M. and Lowery, R.L., *Trans. ASME J. Pressure Vessel Technol.*, 98, 190–193, 1976.

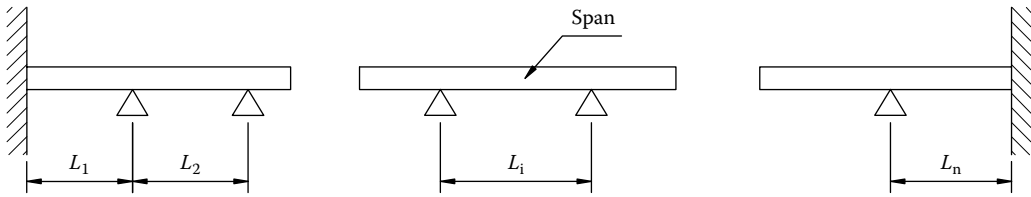


FIGURE 10.21 Heat exchanger tube span modeling—multispan uniform beam with fixed ends.

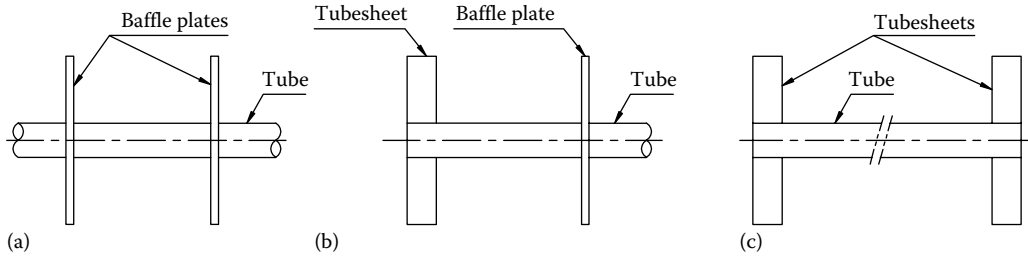


FIGURE 10.22 Individual tube span. (a) Pinned–pinned, (b) fixed–pinned, and (c) fixed–fixed end conditions.

The lowest frequency at which the tubes vibrate is known as the natural frequency. The coincidence of the exciting frequency with the natural frequency is called resonance. The conventional STHs have either straight tubes or U-tubes with baffle supports at intermediate points and fixed at their ends. The determination of the natural frequencies of the straight tubes and U-tubes is dealt with next.

10.10.3.1 Estimation of Natural Frequencies of Straight Tubes

Hand calculation method: Though a rigorous analysis considering the multispan (Figure 10.21) modeling is possible, the state of the art on vibration prediction method recommends a simpler but a slightly conservative approach treating the individual spans separately [11]. For example, the simpler hand calculation methods of Timoshenko and Young [96] basically consider a tube as a continuous elastic beam on multiple supports with fixed end conditions and simply supported at the intermediate points (baffle locations). The individual spans (Figure 10.22) are each treated as a separate beam with its own end conditions (fixed–pinned, pinned–pinned, etc.). Natural frequencies of the individual spans are calculated, and the lowest frequency of the spans is taken as the representative figure for the whole tube and hence for the tube bundle.

The Timoshenko and Young method of treating the individual spans separately to find the natural frequency is recommended by Singh and Soler [11], Zukaskus [13], TEMA, and others. The frequency equation in a generalized form including the effect of axial stress is given by

$$f_n = \frac{1}{2\pi} \frac{\chi_B \lambda_n^2}{L_i^2} \left(\frac{EI g_c}{m} \right)^{0.5} \quad n = 1, 2, 3, \dots \quad (10.51)$$

The expression for axial stress factor χ_B in terms of tube axial load F and Euler's critical buckling load F_{cr} is given by

$$\chi_B = \sqrt{1 \pm \frac{F_a}{F_{cr}}} \quad (10.52)$$

where

$$F_a = A_t \sigma_t \quad (10.53)$$

TABLE 10.4
Frequency Constant, λ_n , and Euler
Buckling Load, F_{cr}

	Pinned–Pinned	Fixed–Pinned	Fixed–Fixed
λ_n	$n\pi$	$0.25(4n+1)\pi$	$0.5(2n+1)\pi$
F_{cr}	$\pi^2 EI/L^2$	$2\pi^2 EI/L^2$	$4\pi^2 EI/L^2$

TABLE 10.5
Numerical Values for Frequency Constant λ_n up to Fifth Mode

End Conditions	First Mode	Second Mode	Third Mode	Fourth Mode	Fifth Mode
Pinned–pinned	3.1416	6.2832	9.4248	12.5664	15.7080
Fixed–pinned	3.9269	7.0686	10.2102	13.3518	16.4934
Fixed–fixed	4.7124	7.8540	10.9956	14.1372	17.2788

In Equation 10.53, F_a is tube axial load, A_t is tube metal cross-sectional area, and σ_t is tube longitudinal stress. In Equation 10.52, the plus sign is for tensile load and the negative sign is for compressive load included in the tubes. The expressions for frequency constant λ_n for the n th mode and for Euler's buckling load for various end conditions are given in Table 10.4, and the values of λ_n up to fifth mode are given in Table 10.5.

Rigorous approaches to calculate straight-tube natural frequencies: These include the methods of Timoshenko and Young [96] and ABAQUS [97].

Natural frequencies of low-finned tubes: These may be calculated by the TEMA method.

10.10.3.2 U-Tube Natural Frequency

The expression for the lower bound of the natural frequency of U-tubes included in TEMA for various forms of tube symmetry and U-bend support configuration is of the form

$$f_{n,u} = 68.06 \frac{C_u}{R^2} \left(\frac{EI}{m} \right)^{0.5} \quad (10.54)$$

Detailed charts are given in TEMA [19] to determine C_u for various U-bend support geometries.

10.10.4 DAMPING

Damping plays an important role on the stability of the tube array. It limits the tube response when the tube is excited by any one of the excitation mechanisms. The higher the damping, the lower will be the tube response. Damping determines the critical flow velocity for FEI. The critical velocity increases with increasing damping. Damping in a vibrating system is due to several possible energy dissipation mechanisms. According to Pettigrew et al. [98], various energy dissipation mechanisms are

- Internal or material damping
- Viscous damping
- Squeeze film damping in the baffle hole clearance

Flow-dependent damping
 Frictional damping
 Joint damping at the tube and tubesheet interface
 Energy dissipated by tube impact on the support and by the traveling waves

10.10.4.1 Determination of Damping

Determination of damping by experimental methods is very difficult. Empirical correlations for determining damping for gases and liquids are given next.

Gases: From the review and analysis of the available data on damping of multispan heat exchanger tubes in gases, Pettigrew et al. [98] recommended empirical correlations to calculate damping ratio ξ_n . The damping ratio is defined as the ratio of actual damping over critical damping. The logarithmic decrement of damping δ is equal to $2\pi\xi_n$. According to these authors, for gas flow, frictional damping and impacting are the dominant energy dissipation mechanisms, with baffle thickness a dominant parameter, whereas diametral clearance between the tube and baffle support is much less significant.

Liquids: According to Pettigrew et al. [99], the most important damping mechanisms in liquid flow are viscous damping (tube to fluid), squeeze film damping, and friction damping. They fitted experimental data with an empirical model considering viscous and squeeze film damping resulting in the following empirical correlation. The semiempirical expressions recommended to estimate damping for design purposes in single-phase fluids, gases, and liquids are given.

Gas flow on the shellside [98]:

$$\xi_n = \frac{0.7}{100} \frac{N-1}{2N} \frac{t_b}{12.7} \quad \text{for } t_b < 12.7 \quad (10.55)$$

$$\therefore \delta = 3.463 \times 10^{-3} \frac{N-1}{N} t_b \quad (10.56)$$

$$\xi_n = \frac{5}{100} \frac{N-1}{N} \left(\frac{t_b}{L_i} \right)^{0.5} \quad \text{for } t_b \geq 12.7 \quad (10.57)$$

$$\therefore \delta = 0.314 \frac{N-1}{N} \left(\frac{t_b}{L_i} \right)^{0.5} \quad (10.58)$$

where

t_b is the tube support thickness

L_i the characteristic span length

N the number of tube supports for the tube under consideration

These expressions are valid for $D = 12\text{--}15$ mm, $t_b = 6\text{--}25$ mm, $f = 20\text{--}600$ Hz, and baffle hole clearances $0.4\text{--}0.8$ mm.

TEMA included Equation 10.57 for all baffle thicknesses.

Liquid flow on the shellside: The determination of δ involves either dynamic (absolute) viscosity μ in the expression suggested in TEMA or kinematic viscosity ν in the expression of Pettigrew et al. [99]. The relation between them is

$$\text{Kinematic viscosity } \nu = \frac{\text{absolute viscosity } \mu}{\text{specific gravity}}$$

$$\therefore \mu = \nu \times \text{specific gravity}$$

The units are centistokes for ν and centipoise for μ . *Note:* TEMA uses the symbol ν instead of μ .

Pettigrew et al. [99] give the equation

$$\xi_n = \frac{\pi}{\sqrt{8}} \frac{1 + (D/D_e)^3}{[1 - D/D_e]^2} \left(\frac{\rho_s D^2}{m} \right) \left(\frac{2\nu}{\pi f_n D^2} \right)^{0.5} + \left(\frac{N-1}{N} \right) \left(\frac{22}{f_n} \right) \left(\frac{\rho_s D^2}{m} \right) \left(\frac{t_b}{L_i} \right)^{0.6} \quad (10.59)$$

where

$$\frac{D_e}{D} = 1.7 \frac{P}{D} \quad \text{for triangular arrays} \quad (10.60a)$$

$$= 1.9 \frac{P}{D} \quad \text{for square arrays} \quad (10.60b)$$

Note: If ξ_n is less than 0.006, assume $\xi_n = 0.006$ [9] to account for friction damping.

TEMA included the following expressions for liquid flow. The damping parameter δ is the greater of δ_1 and δ_2 :

$$\delta_1 = \frac{3.41D}{mf_n} \quad (10.61a)$$

$$\delta_2 = \frac{0.012D}{m} \left(\frac{\rho_s \mu}{f_n} \right)^{0.5} \quad (10.61b)$$

$$\therefore \delta = \max\{\delta_1, \delta_2\} \quad (10.62)$$

Note: Use TEMA dimensional units, $D = \text{in.}$, $\rho_s = \text{lbm/ft}^3$, $\mu = \text{centipoise}$, and $m = \text{lbm/ft}$.

10.10.5 OTHER VALUES

Fill the values of added mass coefficient, natural frequency, and damping parameter into the format given in Table 10.6.

10.11 NEW TECHNOLOGIES OF ANTIVIBRATION TOOLS

10.11.1 ANTIVIBRATION TUBE STAKES

Holtec's antivibration tube stakes as shown in Figure 10.23 prevent collisions between adjacent tubes in condenser and heat exchanger bundles that may be susceptible to FIVs. These tube stakes can be used in new heat exchanger bundles or installed in existing equipment to negate harmful vibrations occurring during a unit's operating life. Holtec's tube stakes are precisely formed from thin 304 stainless steel strips to develop a U-shaped cross section that matches the tube lane gap and provides the necessary rigidity for inserting the stakes deep into this tube bundle. The stakes are fabricated with a "Shepard's Crook" at one end, which locks onto the peripheral tubes to prevent any movement of the stakes during operation. These precision formed stakes do not require any lubrication or special tools for installation. Introduced in 1986, Holtec stakes have proved their effectiveness in numerous power plant condensers and a variety of tubular heat exchangers.

TABLE 10.6**Hydrodynamic Mass Coefficient, Mass per Unit Length, and Damping Parameter**1. Hydrodynamic mass coefficient, C_m

(a) Blevins correlation, Equation 10.50

$$\frac{D_c}{D} = \left(1 + 0.5 \frac{p}{D}\right) \frac{p}{D}$$

$$C_m = \frac{(D_c/D)^2 + 1}{(D_c/D)^2 - 1}$$

(b) Moretti et al.

Read from Figure 10.20 or from Table 10.3

2. Mass per unit length

$$m = \frac{\pi D^2 C_m \rho_m}{4} + \frac{\pi D_i^2 \rho_i}{4} + \frac{\pi (D^2 - D_i^2) \rho}{4}$$

3. Tube natural frequency

i. For straight tube (Equation 10.51)

$$L_i = \dots, A_i = \dots, \sigma_i = \dots, F = A_i \sigma_i,$$

$$F_{cr} = \dots, \chi_B = \dots, I = \dots, \lambda_n = \dots$$

$$f_n = \frac{1}{2\pi} \frac{\chi_B \lambda_n^2}{L_i^2} \left(\frac{EI g_c}{m} \right)^{0.5} \quad n = 1, 2, 3, \dots$$

ii. U-tube

$$l_q/r =$$

$$s/r =$$

$$R =$$

$$I =$$

$$C_u =$$

$$f_{n,u} = \frac{68.06 C_u}{R^2} \left[\frac{EI}{m} \right]^{0.5} \quad (\text{use TEMA dimensional units})$$

4. Damping parameter

TEMA (Equation 10.61a and 10.61b)

$$\delta_1 = \frac{3.41D}{mf_n} \quad \text{and} \quad \delta_2 = \frac{0.012D}{m} \left(\frac{\rho_s \mu}{f_n} \right)^{0.5}$$

$$\delta = \max\{\delta_1, \delta_2\}$$

Others

Gases

$$\delta = 3.463 \times 10^{-3} \frac{N-1}{N} t_b \quad \text{for } t_b < 12.7$$

$$\delta = 0.314 \frac{N-1}{N} \left(\frac{t_b}{L_i} \right)^{0.5} \quad \text{for } t_b \geq 12.7$$

Liquid

$$i. \quad \frac{D}{D_c} = (1.7p/D)^{-1} \quad \text{for triangular array}$$

$$= (1.9p/D)^{-1} \quad \text{for square array}$$

$$\xi_n = \frac{\pi}{\sqrt{8}} \frac{1 + (D/D_c)^3}{[1 - D/D_c]^2} \left(\frac{\rho_s D^2}{m} \right) \left(\frac{2v}{\pi f_n D^2} \right)^{0.5} \\ + \left(\frac{N-1}{N} \right) \left(\frac{22}{f_n} \right) \left(\frac{\rho_s D^2}{m} \right) \left(\frac{t_b}{L_i} \right)^{0.6}$$

$$ii. \quad \delta = 2\pi \xi_n$$

Note: TEMA dimensional units are $E = \text{psi}$, $I = \text{in.}^4$, $m = \text{lbm/ft}$, $R = \text{in.}$; If δ is less than 0.0377, then assume $\delta = 0.0377$.

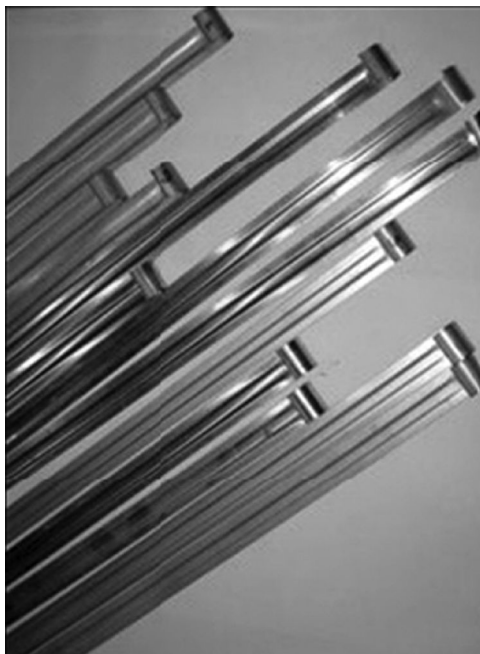


FIGURE 10.23 Antivibration tube stakes. (Courtesy of Holtec International, Marlton, NJ).

10.11.2 EXXONMOBIL RESEARCH AND ENGINEERING

ExxonMobil Research and Engineering has developed a suite of new technologies to [100]

1. Improve the reliability of existing equipment that may have already suffered vibration damage.
2. Provide tube vibration mitigation to an existing bundle predicted to have vibration problems at a future/planned increased throughput.
3. Modify baffle design to decrease shellside pressure drop while also providing vibration mitigation. Their tools/kits to overcome antivibration measures are hereunder:
 - a. Dimpled tube supports (DTS™)
 - b. Saddled tube supports (STS™)
 - c. Slotted baffle exchangers (SBX™)

Dimpled tube support is shown in Figure 10.24.

10.12 SOFTWARE PROGRAMS FOR ANALYSIS OF FIV

Proprietary programs of HTRI [30] and HTFS [32], among others, perform flow-induced vibration analysis of a single tube in a heat exchanger bundle. The program uses a rigorous structural analysis approach to calculate the tube natural frequencies for various modes and offers flexibility in the geometries it can handle. The analysis can be performed for straight or U-tubes. Results of flow-induced vibration analysis for each mode normally include (1) natural frequency of the tube, (2) maximum ratio of fluid gap velocity and critical velocity, and (3) maximum tube deflections due to vibration by vortex shedding or other mechanisms.

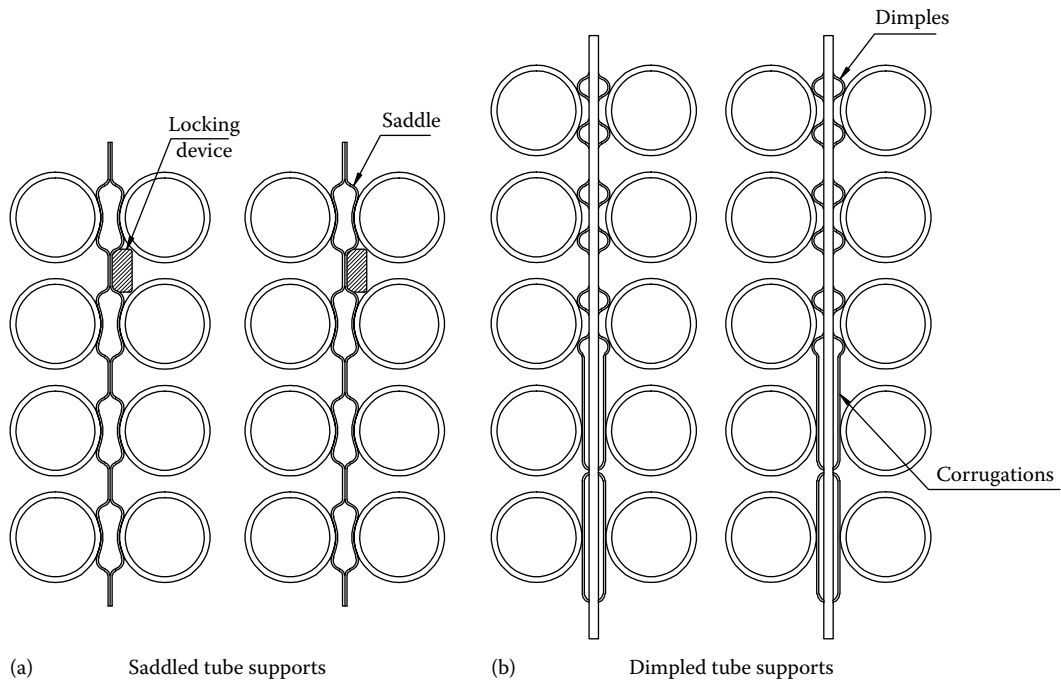


FIGURE 10.24 ExxonMobil Research and Engineering antivibration tube support-dimpled tube supports. (Adapted from Amar W. and Ruzek, Z.F., Antivibration technologies for heat exchangers, ExxonMobil Research and Engineering and EPRI, August 31, 2009.)

10.A APPENDIX A: CALCULATION PROCEDURE FOR SHELLSIDE LIQUIDS

Draw a sketch of the exchanger and identify the most probable zone susceptible for FIV. Then follow these steps.

Step 1: Calculate tube mass per unit length, m

a. Calculate hydrodynamic mass coefficient, C_m by TEMA method (read C_m from Figure 10.20):

$$C_m =$$

or by Blevins method

$$\frac{D_e}{D} = \left(1 + 0.5 \frac{P}{D}\right) \frac{P}{D}$$

$$C_m = \frac{(D_e/D)^2 + 1}{(D_e/D)^2 - 1}$$

b. Calculate the tube mass per unit length, $m = \frac{\pi D^2 C_m \rho_m}{4} + \frac{\pi D_i^2 \rho_i}{4} + \frac{\pi (D^2 - D_i^2) \rho}{4}$

Step 2: Calculate tube natural frequency, f_n

For straight tube

a. Calculate the area moment of inertia of the tube cross section, I

$$I = \frac{\pi}{64} (D^4 - D_i^4)$$

- b. Calculate cross section of the tube, A_t

$$A_t = \frac{\pi(D^2 - D_i^2)}{4}$$

- c. Calculate tube axial longitudinal load, F_a

$$F_a = \sigma_t A_t$$

(positive for tensile load and negative for compressive, σ_t tube longitudinal stress calculated as per TEMA RCB-7.23 or by any other method).

- d. Identify the span with pinned–pinned condition between two baffles in window zone. Find out the tube span length, L_i , to calculate f_n and other parameters. L_i is given by

$$L_i = L_{BC} + L_{BC} \quad (\text{for central window zone})$$

- e. Calculate the buckling load for the tube span

$$F_{cr} = \frac{\pi^2 EI}{L^2} \quad \text{for pinned-pinned condition}$$

- f. Calculate natural frequency multiplier

$$\chi_B = \frac{F}{a F_{cr}}$$

- g. From Table 10.4, choose the value of frequency constant λ_n for central window span:

$$\lambda_n =$$

- h. Calculate natural frequency, f_n

$$f_n = \frac{1}{2\pi} \frac{\chi_B \lambda_n^2}{L_i^2} \left(\frac{EI g_C}{m} \right)^{0.5} \quad \text{for } L_i = L_{BC} + L_{BC}$$

Note: f_n is calculated for the central baffle window region. If it is suspected that the tube span between the tubesheet and the first baffle in the window zone will be controlling, then calculate f_n with $L_i = L_{BI} + L_{BC}$ (inlet window zone).

For U-tube

- Draw a sketch of the U-bend section and identify the configuration with TEMA figures. Calculate $I_b/r = \dots$, $s/r = \dots$
- Determine C_u from TEMA charts.
- Calculate the natural frequency for the first mode.

$$f_{n,u} = 68.06 \frac{C_u}{R^2} \left(\frac{EI}{m} \right)^{0.5} \quad (\text{use TEMA dimensional units})$$

Note: TEMA dimensional units are $E = \text{psi}$, $I = \text{in}^4$, $m = \text{lbm/ft}$, $R = \text{in}$.

Step 3: Calculate damping parameter δ

TEMA method

$$\delta_1 = \frac{3.41D}{mf_n} \quad \text{and} \quad \delta_2 = \frac{0.012D}{m} \left(\frac{\rho_s \mu}{f_n} \right)^{0.5}$$

$$\delta = \max\{\delta_1, \delta_2\}$$

Correlations of Pettigrew, Rogers, and Axisa

$$\frac{D}{D_e} = \left(\frac{1.7p}{D} \right)^{-1} \quad \text{for triangular array}$$

$$= \left(\frac{1.9p}{D} \right)^{-1} \quad \text{for square array}$$

$$\xi_n = \frac{\pi}{\sqrt{8}} \frac{1 + (D/D_e)^3}{[1 - D/D_e]^2} \left(\frac{\rho_s D^2}{m} \right) \left(\frac{2v}{\pi f_n D^2} \right)^{0.5} + \left(\frac{N-1}{N} \right) \left(\frac{22}{f_n} \right) \left(\frac{\rho_s D^2}{m} \right) \left(\frac{t_b}{L_i} \right)^{0.6}$$

$$\delta = 2\pi\xi_n$$

Note: If δ is less than 0.0377, then assume $\delta = 0.0377$.

Step 4: Calculate the crossflow velocity, U

Calculate U for the shell under consideration by TEMA/Bell/other methods. Otherwise, take the value from the TEMA thermal specification sheet.

Step 5: Check for vortex shedding

TEMA criterion: Not available for liquids, only available for gas flow.

Correlations of Weaver and Fitzpatrick:

a. Calculate Strouhal number, S_u

$$S_u = \frac{1}{1.73X_t} \quad \text{for } 30^\circ \text{ layout}$$

$$= \frac{1}{1.16X_t} \quad \text{for } 60^\circ \text{ layout}$$

$$= \frac{1}{2X_t} \quad 90^\circ \quad \text{and} \quad 45^\circ \text{ layout}$$

b. Calculate vortex shedding frequency, f_s

$$f_s = \frac{S_u U}{D}$$

c. Check

$$0.8f_s < f_n < 1.2f_s \quad \text{Resonance}$$

$$\frac{f_n D}{U} > 2S_u \quad \text{Acceptable}$$

$$\frac{f_n D}{U} < 0.2S_u \quad \text{Acceptable}$$

Au-Yang et al. criteria: Calculate the reduced damping C_n :

$$C_n = \frac{4\pi\xi_n m}{\rho_s D^2}$$

a. Both lift and drag direction lock-in are avoided if

$$\frac{U}{f_n D} < 1 \quad \text{Check: OK or not OK}$$

b. For a given vibration mode, if the reduced damping satisfies the following condition, then lock-in will be suppressed in that vibration mode:

$$C_n > 64 \quad \text{Check: OK or not OK}$$

c. For a given vibration mode, if $C_n > 1.2$ and the following condition is satisfied, then lift direction lock-in is avoided and drag direction lock-in is suppressed:

$$\frac{U}{f_n D} < 3.3 \quad \text{Check: OK or not OK}$$

Maximum deflection due to vortex shedding at resonance

- Determine lift coefficient C_L . If C_L for the pitch ratio under consideration is not available, assume the conservative value of 0.091.
- Calculate the maximum response, y_{\max} , of the tube span between two baffles.

$$y_{\max} = \frac{C_L \rho_s D U^2}{4\xi_n \pi^3 f_n^2 m^2}$$

c. Check: If $y_{\max} < 0.02D$, OK.

Step 6: Turbulence-induced excitation

a. Determine $C_R(f)$ from Ref. [36].

(Note: For $f_n = 10-40$, C_L for upstream tubes, is to be assumed as 2.6×10^{-3})

b. The mean square response for a pinned-pinned span is given by

$$\bar{y}_{\max}^2 = \frac{[C_R(f) \rho_s U^2 D]^2}{128 \pi^3 \xi_n f_n^3 m^2}$$

$$y_{\text{rms}} = \sqrt{\bar{y}_{\max}^2}$$

c. Check: If $y_{\text{rms}} < 0.01$ in (0.254 mm), OK.

Step 7: FEI

TEMA criterion

- a. Calculate reduced velocity parameter, χ :

$$\chi = \frac{m\delta}{\rho_s D^2}$$

- b. Calculate critical velocity by referring to [19].

$$U_{cr} =$$

- c. Check: If $U < U_{cr}$ or $U/U_{cr} < 0.5$, OK.

Au-Yang et al. criteria: Choose K_{mean} from Table 10.1 (a) for the particular tube layout pattern and (b) for all arrays.

- a. For the particular tube layout pattern

$$\frac{U_{cr}}{f_n D} = K \left(\frac{m\delta}{\rho_s D^2} \right)^a$$

$$U_{cr} =$$

Check: If $U < U_{cr}$ or $U/U_{cr} < 0.5$, OK.

- b. $K_{mean} = 4.0$ for all arrays:

$$\frac{U_{cr}}{f_n D} = 4.0 \left(\frac{m\delta}{\rho_s D^2} \right)^{0.5}$$

$$U_{cr} =$$

Check: if $U < U_{cr}$ or $U/U_{cr} < 0.5$, OK.

- c. Check as per conservative criteria. Assume $\delta = 0.09425$ and $K = 2.1$.

$$\frac{U_{cr}}{f_n D} = 2.1 \left(\frac{m\delta}{\rho_s D^2} \right)^{0.5}$$

$$U_{cr} =$$

Check: If $U < U_{cr}$, certainly FIV will not be a problem.

Pettigrew and Taylor criterion

$$\frac{U_{cr}}{f_n D} = 3.0 \left(\frac{m\delta}{\rho_s D^2} \right)^{0.5}$$

Check: If $U < U_{cr}$ or $U/U_{cr} < 0.5$, OK.

Calculation procedure for shellside vapors

Step 8: Repeat steps 1–7 as already described. For gases, the damping parameter is calculated by this correlation:

$$\delta = 3.463 \times 10^{-3} \frac{N-1}{N} t_b \quad \text{for } t_b < 12.7$$

$$\delta = 0.314 \frac{N-1}{N} \left(\frac{t_b}{L_i} \right)^{0.5} \quad \text{for } t_b \geq 12.7$$

and the criterion for amplitude at peak resonance due to turbulent buffeting may be neglected.

Step 9: Check for acoustic resonance

Calculate the acoustic vibration frequency, f_a :

TEMA method (for cylindrical volume only)

$$f_a = \frac{483.2}{L_a} \left(\frac{p_s}{\rho_s} \right)^{0.5} \quad (\text{use TEMA dimensional units})$$

Blevins method

a. Calculate velocity of sound C through the tube bank.

$$C = \sqrt{\frac{g_c Z \gamma R_c T}{M_g}}$$

b. Calculate tube layout solidity factor, σ :

$$\sigma = 0.9069 \left(\frac{D}{p} \right)^2 \quad \text{for } \theta = 30^\circ \text{ or } \theta = 60^\circ$$

$$= 0.7853 \left(\frac{D}{p} \right)^2 \quad \text{for } \theta = 90^\circ$$

$$= 1.5707 \left(\frac{D}{p} \right)^2 \quad \text{for } \theta = 45^\circ$$

c. Calculate effective velocity of sound through the tube bank:

$$C_{\text{eff}} = \frac{C}{\sqrt{1 + \sigma}} \quad \text{Parker}$$

$$C_{\text{eff}} = \frac{C}{\sqrt{1 + C_m \sigma}} \quad \text{Burton}$$

Note: Choose C_{eff} by Burton method for conservative values.

d. Calculate the acoustic resonance frequency, f_a :

For a cylindrical volume,

$$f_a = \frac{C_{\text{eff}} \lambda_i}{2\pi R}$$

where $\lambda_1 = 1.84$ and $\lambda_2 = 3.054$.

For a rectangular volume,

$$f_n = \frac{1}{2\pi} \frac{\chi_B \lambda_n^2}{L_i^2} \left(\frac{EIgc}{m} \right)^{0.5} \quad \text{for } L_i = L_{BC} + L_{BC}$$

where $i = 0, j = 1$, and $k = 0$. *Note:* In heat exchangers of normal size, the fundamental or the second mode is the most likely to occur. For large exchangers with shell diameter of the order of 20–30 m, the acoustic vibration can be excited up to fifth or sixth mode.

Step 10: Criteria for occurrence of acoustic resonance

Criteria for vortex shedding mechanism: Calculate Strouhal number due to vortex shedding:

$$S_u = \frac{f_v D}{U}$$

a. Chen number and Eisinger criteria: Calculate Reynolds number, Re:

$$\text{Re} = \frac{UD}{\nu}$$

Calculate Chen number, ψ :

$$\psi = \frac{\text{Re}(2X_1 - 1)^2}{S_u(4X_1^2 X_1)}$$

Check:

$\psi < 2000$	No vibration
$\psi = 2000\text{--}4000$	Low likelihood of vibration
$\psi > 4000$	High likelihood of vibration

TEMA condition: Acoustic resonance is possible if $\psi = 2000$.

b. Blevins criteria

Normal criteria

$$\text{Check : If } \frac{0.8S_u U}{D} < f_a < \frac{1.2S_u U}{D} \quad \text{resonance will occur}$$

Conservative criteria

$$\text{Check : If } \frac{0.6S_u U}{D} < f_a < \frac{1.48S_u U}{E} \quad \text{resonance will occur}$$

- c. SPL at resonance: Calculate SPL from the following equation or determine from the SPL maps of Blevins [8] or empirically:

$$\text{SPL} = 20 \log_{10} \left(\frac{p_{\text{rms}}}{0.00002} \right)$$

Check: If $\text{SPL} < 140$ dB, there is no damage either to the structural components or to the surroundings. *Note:* Sound level maps are valid for Reynolds numbers up to 95.1×10^3 .

- d. Resonance will occur if $U/f_a D > 2$

Criteria for turbulent buffeting

- a. Owen's criterion for the central dominant frequency when $p/D > 1.25$ is

$$f_{\text{tb}} = \frac{U}{DX_t X_1} \left[3.05 \left(1 - \frac{1}{X_t} \right)^2 + 0.28 \right]$$

Check : If $0.8 f_{\text{tb}} < f_a < 1.2 f_{\text{tb}}$ resonance will occur.

- b. Criterion of Rae and Murray

$$\text{Check : If } \frac{U}{f_a D} < 2(X_1 - 0.5), \quad \text{OK.}$$

This criterion is included in TEMA.

- c. Grotz and Arnold criterion (for in-line arrays): Calculate the slenderness ratio τ .

$$\tau = \frac{L_a}{Dn(X_1 - 1)}$$

Check: Resonance will occur for $\tau = 62-80$.

Step 11: Fill the parameters and design criteria into the acoustic resonance specification sheet of Table 10.2.

NOMENCLATURE

A	area of cross section of opening in the Helmholtz cavity resonator
A_1	tube cross-sectional area, m^2 (in.^2)
C	speed of sound in the shellside medium
C_{eff}	effective speed of sound in the shellside fluid
C_L	lift coefficient for vortex shedding
C_m	added mass coefficient
C_n	reduced damping in n th mode
$C_R(f)$	turbulence force coefficient
C_u	constant to determine U-tube natural frequency
D	tube outside diameter

D_B	baffle diameter
D_e	equivalent confinement diameter in a tube array ($1 + 0.5p/D$) p to calculate C_m
D_e/D	1.7 p/D for triangular array to calculate ξ_n 1.9 p/D for square array to calculate ξ_n
D_i	tube inside diameter
E	modulus of elasticity of the tube material
F_a	axial load on tubes
F_{cr}	critical buckling load of the tube span analyzed
f	Helmholtz cavity resonator resonance frequency, s^{-1}
f_a	acoustic resonance frequency, s^{-1}
f_n	tube natural frequency, s^{-1}
$f_{n,u}$	frequency of U-bend region
f_s	vortex shedding frequency, s^{-1}
f_{tb}	turbulent buffeting frequency in a tube array, s^{-1}
g_c	proportionality constant, 9.81 m/s^2 1.0 in SI units and dimensionless 32.174 $lbm\ ft/lbf\ s$
I	moment of inertia of the cross section
j, n	vibration mode number; $j = n = 1$ is fundamental mode
i, j, k	acoustic modal indices
K	FEI constant
L_a	characteristic dimension for acoustic standing wave
L	unsupported tube span length for FIV
L_i	unsupported tube span for FIV or characteristic tube span length, m (in.)
L_{BC}	central baffle spacing
L_{BI}	baffle spacing inlet
L_{BO}	baffle spacing outlet
L_e	characteristic tube length
L_p	longitudinal tube pitch, mm (in.)
L_t	total tube length
L_x, L_y, L_z	acoustic chamber dimensions
l_h	length of Helmholtz cavity resonator neck
M, M_n	modal mass
M_g	molecular weight of shellside gas or vapor
M	mass per unit length of tube, $m_a + m_c + m_s$
$m(x)$	mass per unit length of tube at a distance x along the tube axis
m_a	fluid-added mass per unit length
m_i	contained fluid mass per unit length
m_t	structural mass per unit length
N	number of tube spans for the tube being analyzed
N_w	number of solid baffles
n	mode number
p_s	shellside pressure, Pa (psi)
p_{rms}	rms value of shellside pressure Pa (psi)
p	tube pitch, m (in.)
Q_g	volume flow rate of gas phase in two-phase flow
Q_L	volume flow rate of liquid phase in two-phase flow
R	U-tube bend radius, shell radius, m (in.)

R_c	universal gas constant
Re	Reynolds number based on the tube outside diameter, dimensionless, UD/ν
r, s	U-bend dimensions
r_h	Helmholtz cavity resonator neck radius, m (ft)
SPL	sound pressure level, dB
S_u	Strouhal number, dimensionless
T	absolute temperature of shellside gas, ($^{\circ}R/^{\circ}K$)
T_p	transverse tube pitch
t	time
t_b	baffle support plate thickness
U, U_{Bell}, U_{Tinker}	
U_{others}	reference crossflow velocity
U_{cr}	critical fluid velocity for fluid elastic excitation
$U(x)$	crossflow velocity distribution
U_{∞}	upstream velocity
V_h	volume of Helmholtz cavity resonator
ν	kinematic viscosity of the fluid, centistokes
X_l	longitudinal pitch ratio, L_p/D
X_p	pitch ratio = p/D
X_t	transverse pitch ratio, T_p/D
x	axial distance
$y(x)$	amplitude of vibration
y_{rms}	rms amplitude of tube vibration
\bar{y}_{rms}^2	mean square amplitude of vibration
y_{max}	maximum tube response due to resonance due to vortex shedding
Z	shellside gas or vapor compressibility factor
λ_n, λ_t	frequency constant
σ	tube bank solidity, dimensionless
δ	logarithmic decrement of damping = $2\pi\xi_n$
Ψ	Chen number
χ	nondimensional parameter
χ_B	factor to account for tube axial load on tube natural frequency
$\phi_n(x)$	mode constant for tube natural frequency, dimensionless
ξ_n	critical damping ratio
ρ	density of tube material
ρ_i	density of tubeside fluid
ρ_s	density of shellside fluid
σ_T	shell longitudinal stress + for tensile stress – for compressive stress
τ	Arnold's slenderness ratio
γ	ratio of specific heat of gas at constant pressure to constant volume
μ	absolute viscosity, centipoise

REFERENCES

1. Wambsganss, M. W., Tube vibration and flow distribution in shell and tube heat exchangers, *Heat Transfer Eng.*, 8, 62–71 (1987).
2. Paidoussis, M. P., Flow induced vibrations in nuclear reactors and heat exchangers: Practical experiences and state of knowledge, in *Practical Experiences with Flow Induced Vibration* (E. Naudascher and D. Rockwell, eds.), Springer-Verlag, Berlin, Germany, 1980, pp. 1–18.
3. Paidoussis, M. P., Fluid elastic vibration of cylinder arrays in axial and crossflow: State of art, *J. Sound Vib.*, 76, 329–359 (1981).

4. Au-Yang, M. K., Blevins, R. D., and Mulcahy, T. M., Flow induced vibration analysis of tube bundles—A proposed Section III Appendix N nonmandatory code, *Trans. ASME J. Pressure Vessel Technol.*, 113, 257–267 (1991).
5. Chen, S. S., Guidelines for the instability flow velocity tube arrays in crossflow, *J. Sound Vib.*, 93(3), 439–455 (1984).
6. Weaver, D. S. and Fitzpatrick, J. A., A review of flow induced vibration in heat exchangers, in *International Conference on Flow Induced Vibration*, sponsored by BHRA, Bowness-on-Windermere, England, May 12–14, 1987, pp. 1–17.
7. Au-Yang, M. K., Flow induced vibration: Guidelines for design, diagnosis and troubleshooting of common power plant components, *Trans. ASME J. Pressure Vessel Technol.*, 107, November, 326–334 (1985).
8. Blevins, R. D., *Flow Induced Vibration*, 2nd edn., Van Nostrand Reinhold, New York, 1990.
9. Sandifer, J. B., Guidelines for flow induced vibration prevention in heat exchangers, Welding Research Council Bulletin 372, Welding Research Council, New York, May 1992.
10. Chen, S. S., *Flow Induced Vibration of Circular Cylindrical Structures*, Hemisphere, New York, 1987.
11. Singh, K. P. and Soler, S. I., *Mechanical Design of Heat Exchangers and Pressure Vessel Components*, Arcturus, Cherry Hill, NJ, 1984.
12. Gupta, J. P., *Fundamentals of Heat Exchanger and Pressure Vessel Technology*, Hemisphere, Washington, DC, 1984.
13. Zukauskas, A. A., Vibration of tubes in heat exchangers, in *High Performance Single Phase Heat Exchangers*, Hemisphere, Washington, DC, 1989, pp. 316–348.
14. Pettigrew, M. J. and Taylor, C. E., Fluid elastic instability of heat exchanger tube bundles: Review and design recommendations, *Trans. ASME J. Pressure Vessel Technol.*, 113, 242–255 (1991).
15. Chen, S. S. and Jendrzeczyk, J. A., Stability of tube arrays in crossflow, *Nucl. Eng. Des.*, 75(3), 351–374 (1983).
16. Chen, S. S., Some issues concerning fluid elastic instability of a group of circular cylinders in crossflow, *Trans. ASME J. Pressure Vessel Technol.*, 111, 507–518 (1989).
17. Shah, R. K., Flow induced vibration and noise in heat exchangers, *Proceedings of Seventh National Heat and Mass Conference*, Kharagpur, India, 1983, pp. 89–108.
18. Chenoweth, J. M. and Kistler, R. S., Tube vibration in shell and tube heat exchangers, *AIChE Symposium Series*, No. 174, *Heat Transfer: Research and Application*, vol. 74, 1978, pp. 6–14.
19. *Standards of the Tubular Exchanger Manufacturers Association*, 9th edn., Tubular Exchanger Manufacturers Association, Inc., Tarrytown, NY, 2007.
20. *ASME Boiler and Pressure Vessel Code, Section III, Nonmandatory Code*, American Society of Mechanical Engineers, New York, 2010.
21. Paidoussis, M. P. and Besancon, P., Dynamics of arrays of cylinders with internal and external axial flow, *J. Sound Vib.*, 76(3), 361–379 (1981).
22. Goyder, H. G. D., The structural dynamics of tube bundle vibration problem, in *International Conference on Flow Induced Vibrations*, Bowness on Windermere, England, U.K., May 12–14, 1987.
23. Gorman, D. J., Experimental study of peripheral problems in heat exchangers and steam generator, Paper V.F4/g, *Proceedings of the Fourth International Conference on Structural Mechanics in Reactor Technology*, San Francisco, CA, 1977.
24. Chen, Y. N. and Weber, M., Flow induced vibrations in tube bundle heat exchangers with crossflow and parallel flow, in *Flow Induced Vibrations in Heat Exchangers, Proceedings of a Symposium Sponsored by the ASME*, New York, 1970, pp. 57–77.
25. Chen, Y. N., Flow induced vibration and noise in tube bank heat exchangers due to Von Karman streets, *Trans. ASME J. Eng. Ind.*, 90, February, 134–146 (1968).
26. Owen, P. R., Buffeting excitation of boiler tube vibration, *J. Mech. Eng. Sci.*, 4, 431–439 (1965).
27. Tinker, T., Shellside characteristics of shell and tube heat exchangers—A simplified rating system for commercial heat exchangers, *Trans. ASME*, 80, 36–52 (1958).
28. Bell, K. J., Delaware method for shellside design, in *Heat Transfer Equipment Design* (R. K. Shah, E. C. Subbarao, and R. A. Mashelkar, eds.), Hemisphere, Washington, DC, 1988, pp. 145–166.
29. Palen, J. W. and Taborek, J., Solution of shellside flow pressure drop and heat transfer by stream analysis method, *Chemical Engineering Progress Symposium Series*, No. 92, *Heat Transfer*, Philadelphia, PA, vol. 65, 1969, pp. 53–63.
30. Xvib, HTRI Xchanger Suite 6.0, Heat Transfer Research, Inc., Alhambra, CA.
31. Aspen Shell & Tube Mechanical, Heat Transfer and Fluid Flow Services, Oxon, U.K.
32. Sing, K. P. and Soler, A. I., *HEXDES User Manual*, Arcturus, Cherry Hill, NJ, 1984. B-JAC International, Inc., Midlothian, VA.

33. Fitz-Hugh, J. S., Flow induced vibration in heat exchangers, in *International Symposium on Vibration Problems in Industry*, Keswick, U.K., April 10–12, 1973.
34. Zukauskas, A. and Katinas, V., Flow induced vibration in heat exchanger tube banks, in *Proceedings of Symposium of Practical Experiences with Flow Induced Vibration*, (eds. E. Naudascher and D. Rockwell), Springer, New York, 1980, pp. 188–196.
35. Weaver, D. S., Fitzpatrick, J. A., and El Kashlan, M. L., Strouhal numbers of heat exchanger tube arrays in crossflow, in *ASME Symposium on Flow Induced Vibration*, (S. S. Chen, J. C. Simonis, and Y. S. Shin, eds.), Chicago, IL, Vol. 104, 1986.
36. Pettigrew, M. J. and Gorman, D. J., Vibration of heat exchanger tube bundles in liquid and two phase crossflow, in *Flow Induced Vibration Guidelines* (P. Y. Chen, ed.), PVP Vol. 52, ASME, New York, 1981.
37. Pettigrew, M. J. and Gorman, D. J., Vibration of heat exchanger components in liquid and two phase crossflow, presented at *British Nuclear Society International Conference on Vibration in Nuclear Plant*, Keswick, U.K., May 9–12, 1978.
38. Rao, M. S. M., Gupta, G. D., Eisinger, F. L., Hibbitt, H. D., and Steininger, D. A., Computer modelling of vibration and wear of multispan tubes with clearances at the supports, presented at *Flow Induced Vibration Conference*, sponsored by BHRA, Bowness-Windermere, England, May 12–14, 1987, pp. 437–448.
39. Weaver, D. S. and Grover, L. K., Crossflow induced vibration in a tube bank—Turbulent buffeting and fluid elastic instability, *J. Sound Vib.*, 59(2), 277–294 (1978).
40. Soper, B. M. H., The effect of tube layout on the fluid elastic instability of tubes bundle in cross-flow, *Trans. ASME J. Heat Transfer*, 105, 744–750 (1983).
41. Weaver, D. S. and Schneider, W., The effect of flat bar supports on the crossflow induced response of heat exchanger U-tubes, *Trans. ASME J. Eng. Power*, 105, 775–781 (October, 1983).
42. Connors, H. J. Jr., Fluid elastic vibration of tube arrays excitation by crossflow, in *Flow Induced Vibration in Heat Exchangers* (D. D. Reill, ed.), ASME, New York, 1970, pp. 42–56.
43. Lever, J. H. and Weaver, D. S., A theoretical model for fluid elastic instability in heat exchangers tube bundles, *Trans. ASME J. Pressure Vessel Technol.*, 104, 147–158 (1982).
44. Lever, J. H. and Weaver, D. S., On the stability of heat exchanger tube bundles: Part 1—Modified theoretical model, *J. Sound Vib.*, 107(3), 375–392 (1986).
45. Lever, J. H. and Weaver, D. S., On the stability of heat exchanger tube bundles: Part 2—Numerical results and comparison with experiments, *J. Sound Vib.*, 107(3), 393–411 (1986).
46. Tanaka, H. and Takahara, S., Fluid elastic vibration of a tube array in crossflow, *J. Sound Vib.*, 77, 19–37 (1981).
47. Tanaka, H. and Takahara, S., Unsteady fluid dynamic force on tube bundle and its dynamic effects on vibration, in *Flow Induced Vibration of Power Plant Components*, ASME Special Publication No. PVP 141 (M. K. Au-Yang, ed.), ASME, New York, 1980, pp. 77–92.
48. Price, S. J. and Paidoussis, M. P., Fluid elastic instability of a double row of circular cylinders subject to a crossflow, *Trans. ASME J. Vib. Acoust. Stress Reliab. Des.*, 105, 59–66 (1983).
49. Price, S. J. and Paidoussis, M. P., An improved mathematical model for the stability of cylinder rows subjected to crossflow, *J. Sound Vib.*, 97(4), 615–640 (1984).
50. Whiston, G. S. and Thomas, G. D., Whirling instabilities in heat exchanger tube arrays, *J. Sound Vib.*, 81(1), 1–31 (1982).
51. Chen, S. S., Instability mechanisms and stability criteria of a group of circular cylinders subjected to crossflow, Part I, ASME Paper No. 81-Det 21, ASME, New York.
52. Chen, S. S., Instability mechanisms and stability criteria of group of circular cylinders subjected to crossflow, Part II: Numerical Results and Discussions, ASME Paper No. 81-Det 22, New York.
53. Chen, S. S., Instability mechanism and stability criteria of a group of cylinders subjected to crossflow, Part I: Theory; Part II: Numerical results and discussions, *J. Vibration Acoustics Stress Reliability Designs*, 105, 253–260 (1983).
54. Chen, S. S. and Jendrzejczyk, J. A., Experiments and analysis of instability of tube rows subjected to liquid crossflow, *Trans. ASME J. Appl. Mech.*, 49, 704–709 (1982).
55. Chen, S. S. and Jendrzejczyk, J. A., Experiments on fluid elastic instability in tube banks subjected to liquid crossflow, *J. Sound Vib.*, 78, 355–381.
56. Chen, S. S., Flow induced vibration of circular cylindrical structures, Argonne National Laboratory, Report No. ANL-CT-85-51, Argonne, IL.
57. Eisinger, F. L., Prevention and cure of flow induced vibration problems in tubular heat exchangers, *Trans. ASME J. Pressure Vessel Technol.*, 102, 138–145 (1980).

58. Blevins, R. D., Review of sound induced by vortex shedding from cylinders, *J. Sound Vib.*, 92(4), 455–470 (1984).
59. Blevins, R. D., Acoustic modes of heat exchanger tube bundles, *J. Sound Vib.*, 109(1), 19–30 (1986).
60. Blevins, R. D. and Bressler, M. M., Acoustic resonance in heat exchanger tube bundles, Part I: Physical nature of the phenomenon, *Trans. ASME J. Pressure Vessel Technol.*, 109, 275–281 (1987).
61. Blevins, R. D. and Bressler, M. M., Acoustic resonance in heat exchanger tube bundles—Part II: Prediction and suppression of resonance, *Trans. ASME J. Pressure Vessel Technol.*, 109, 282–288 (1987).
62. Blevins, R. D., Acoustic resonance in heat exchanger tube bundles, Welding Research Bulletin No. 389, Welding Research Council, New York, 1994.
63. Barrington, E. A., Experience with acoustic vibration in tubular heat exchangers, *Chem. Eng. Prog.*, 69(7), 62–68 (1973).
64. Parker, R., Acoustic resonance in passages containing bank of heat exchanger tubes, *J. Sound Vib.*, 57, 245–260 (1978).
65. Burton, T. E., Sound speed in a heat exchanger tube bank, *J. Sound Vib.*, 71, 157–160 (1980).
66. Grotz, B. J. and Arnold, F. R., Flow induced vibration in heat exchangers, Department of Mechanical Engineering Tech. Rep. No. 31, DTIC No. 104568, Stanford University, Stanford, CA, 1956.
67. Barrington, E. A., Cure exchanger acoustic vibration, *Hydrocarbon Process.*, 193–198 (1978).
68. Fitzpatrick, J. A., The prediction of flow induced noise in heat exchanger tube arrays, *J. Sound Vib.*, 99, 425–435 (1985).
69. Ziada, S. and Oengoren, A., Flow induced acoustical resonances of in-line tube bundles, *Sulzer Tech. Rev.*, 45–47 (1990).
70. Rae, G. J. and Murray, B. G., Flow induced acoustic resonances in heat exchangers, *International Conference on Flow Induced Vibrations*, Bowness-on-Windermere, England, May 12–14, 1987, pp. 221–231.
71. Fitzpatrick, J. A. and Donaldson, J. A., Effects of scale on parameters associated with flow induced noise in tube arrays, in *Symposium on Flow Induced Vibrations* (M. P. Paidoussis, ed.), American Society of Mechanical Engineers, New York, pp. 243–250.
72. Ziada, S., Oengoren, A., and Buhlmann, E. T., Acoustical resonance in tube arrays, in *International Symposium on Flow Induced Vibration and Noise* (M. P. Paidoussis et al., eds.), American Society of Mechanical Engineers, New York, 1988, pp. 219–254.
73. Kerner Smith, H., Vibration in nuclear reactor heat exchangers—One manufacturers viewpoint, in *Flow Induced Vibration in Heat Exchangers*, *Proceedings of ASME* (D. D. Reill, ed.), 1987, pp. 1–7.
74. Halle, H., Chenoweth, J. M., and Wambsganss, M. W., Shellside water flow induced tube vibration in heat exchanger configurations with tube pitch to diameter ratio of 1.42, *Trans. ASME J. Pressure Vessel Technol.*, 111, 441–449 (1989).
75. Saunders, E. A. D., Shellside flow induced tube vibration, in *Heat Exchangers: Design, Selection and Construction*, Addison Wesley Longman, Reading, MA, pp. 245–273, 1989.
76. Halle, H., Chenoweth, J. M., and Wambsganss, M. W., Flow induced vibration in shell and tube heat exchanger with double segmental baffles, in *Heat Transfer 1986, Proceedings of Eighth International Heat Transfer Conference*, San Francisco, CA, Vol. 6, 1986, pp. 2763–2768.
77. Gentry, C. C., Young, R. K., and Small, M. W., RODbaffle heat exchanger thermal-hydraulic predictive methods, in *Heat Transfer 1982*, Vol. 6, Hemisphere, Washington, DC, 1982, pp. 197–202.
78. Boyer, R. C. and Pase, G. K., The energy saving NESTS concept, *Heat Transfer Eng.*, 2, 19–27 (1980).
79. Byrne, K. P., The use of porous baffles to control acoustic vibration in crossflow tubular heat exchangers, *Trans. ASME, J. Heat Transfer*, 105, 751–757 (1983).
80. Walker, E. M. and Reising, G. F. S., Flow induced vibrations in crossflow heat exchangers, *Chem. Process Eng.*, 49, 95–103 (1968).
81. Rogers, J. D. and Penterson, C. A., Predicting sonic vibration in crossflow heat exchangers—Experience and model testing, American Society of Mechanical Engineers, New York, Paper 77-FE-7, 1977.
82. Zdravkovich, M. and Nuttal, J. A., On elimination of aerodynamic noise in staggered tube bank, *J. Sound Vib.*, 34, 173–177 (1974).
83. Thorngren, J. T., Predict exchanger tube damage, *Hydrocarbon Process.*, Vol. 49, April, 129–131 (1970).
84. Blevins, R. D., Fretting wear of heat exchanger tubes, Part I: Experiments, *Trans. ASME J. Eng. Power*, 101, 625–629 (1979).
85. Blevins, R. D., Fretting wear of heat exchanger tubes, Part II: Models, *Trans. ASME J. Eng. Power*, 101, 630–633 (1979).
86. Haslinger, K. H., Martin, M. L., and Steininger, D. A., Pressurized water reactor steam generator tube wear prediction utilizing experimental techniques, in *Proceedings of the International Conference on Flow Induced Vibration*, Bowness-on-Windermere, England, May 12–14, 1987, pp. 437–448.

87. Ko, P. L. and Basista, H., Correlation of support impact force and fretting wear for heat exchanger tube, *Trans. ASME J. Pressure Vessel Technol.*, 106, 69–77 (1984).
88. Cha, J. H., Wambsganss, M. W., and Jendrzeycyk, J. A., Experimental study of impact/fretting wear in heat exchanger tubes, Argonne National Laboratory Publication ANL-85-38, Argonne, IL., 1985.
89. Hofmann, P. J., Schettler, T., and Steininger, D. A., Pressurized water reactor steam generator tube fretting and fatigue wear characteristics, in *Proceedings of the ASME Pressure Vessel and Piping Conference*, ASME 86PVP-2, Chicago, IL, July 1986.
90. Fisher, N. J., Olsen, M., Rogers, R. J., and Ko, P. L., Simulation of tube-to-support dynamic interaction of heat exchange equipment, *Trans. ASME J. Pressure Vessel Technol.*, 111, 378–384 (1989).
91. Eisinger, F. L., Rao, M. S. M., Steininger, D. A., and Haslinger, K. H., Numerical simulation of fluid elastic vibration and comparison with experimental results, in *Flow Induced Vibration and Wear Book* No. H00632, 1991, pp. 101–111. Reprinted from PVP Vol. 206.
92. Rao, M. S. M., Steininger, D. A., and Eisinger, F. L., Computer simulation of vibration and wear of steam generator and tubular heat exchanger tubes, in *International Symposium on Advanced Computers for Dynamics and Design '89*, Tsuchiura, Japan, Mechanical Division, JSME, September 6–8, 1989.
93. Rao, M. S. M., Steininger, D. A., and Eisinger, F. L., Numerical simulation of fluid elastic vibration and wear of multispan tubes with clearances at supports, in *Flow Induced Vibration in Heat Transfer Equipment* (J. M. Paidoussis, S. S. Chenoweth, J. R. Chen, Stenner, and W. J., Bryan, eds.), Vol. 5, Book No. G00445, 1988, pp. 235–251.
94. Blevins, R. D., Vibration induced wear of heat exchanger tubes, *Trans. ASME J. Eng. Mater. Technol.*, 107, 61–67 (1985).
95. Moretti, P. M. and Lowery, R. L., Hydrodynamic inertia coefficients for a tube surrounded by rigid tube, *Trans. ASME J. Pressure Vessel Technol.*, 98, 190–193 (1976).
96. Timoshenko, S. P. and Young, D. H., Vibration problems in engineering, in *Vibration of Elastic-Bodies*, Van Nostrand Reinhold, Toronto, Canada, 1965, Chapter 5.
97. SIMULIA 6.2 (Formerly known as ABAQUS), Dassault Systèmes Simulia Corp., 2005, *Providence, RI*.
98. Pettigrew, M. J., Goyder, H. G. D., Qiao, Z. L., and Axisa, F., Damping of multispan heat exchanger tubes, Part 1: In gases, in *Flow Induced Vibration 1986* (S. S. Chen, J. C. Simon, and Y. S. Shin, eds.), ASME PVP Vol. 104, ASME, New York, 1986, pp. 81–87.
99. Pettigrew, M. J., Rogers, R. J., and Axisa, F., Damping of multispan heat exchanger tubes, Part 2: In liquids, in *Flow Induced Vibration 1986* (S. S. Chen, J. C. Simon, and Y. S. Shin, eds.), ASME, New York, PVP Vol. 104, pp. 89–98.
100. Amar W. and Ruzek, Z. F, Antivibration technologies for heat exchangers, ExxonMobil Research and Engineering and EPRI, August 31, 2009.

SUGGESTED READINGS

- Bolleter, U. and Blevins, R. D., Natural frequencies of finned heat exchanger tubes, *J. Sound Vibration*, 80, 367–371 (1982).
- Chenoweth, J. M., Flow induced vibration phenomena, in *Heat Exchanger Design Handbook* (E. U. Schlunder, ed.), Vol. 4, Hemisphere, Washington, DC, 1983, Section 4.6.4.
- Gorman, D. J., *Free Vibration Analysis of Beam and Shafts*, John Wiley & Sons, New York, 1975.
- Lowery, R. L. and Moretti, P. M., Natural frequencies and damping of tubes on multiple supports, ed. J.C. Chen, *AIChE Symposium Series*, No. 174, *Heat Transfer: Research and Application*, vol. 74, 1978, pp. 1–5.
- MacDuff, J. N. and Felgar, R. P., Vibration design charts, *Trans. ASME*, 79, 1459–1474 (1957).
- Moretti, P. M., Fundamental frequencies of U-tubes in tube bundles, *Trans. ASME J. Pressure Vessel Technol.*, 107, 207–209 (1985).
- Naguyen, D. C., Lester, T., Good, J. K., Lowery, R. L., and Moretti, P. M., Lowest natural frequencies of multiply supported U-tubes, *Trans. ASME J. Pressure Vessel Technol.*, 106, 414–416 (1984).

11 Mechanical Design of Shell and Tube Heat Exchangers

11.1 STANDARDS AND CODES

Standards and codes were established primarily to ensure safety against failure. The need for safety standards is obvious in a world growing increasingly aware of the hazards posed to people, property, and the environment due to failures of pressure vessels and heat exchangers in any industrial plant [1]. Failures may occur due to design inadequacies, use of inferior materials for construction, poor workmanship in fabrication and welding, and inadequate quality control checks. Hence, it is essential that due consideration is given at all stages of design, manufacturing, and installation. The codes and standards give guidance and in some cases govern the design, manufacture, construction, operation, and maintenance of heat exchangers and pressure vessels. The codes and standards are published periodically by issuing organizations or associations. They have committees consisting of representatives from industries, professional groups, users, government agencies, insurance companies, and other interest groups for maintaining, updating, and revising the codes and standards based on technological developments, research, experience and feedback, and changes in specifications and regulations. The present-day codes have their origin in the rules laid down by the insurance companies in the past for the safe operation of boilers and pressure vessels against explosions or accidents and consequential damage to the human lives and property.

11.1.1 STANDARDS

A standard can be defined as a set of technical definitions and guidelines, or how-to instructions for designers and manufacturers [2]. Standards are mostly voluntary in nature. They serve as guidelines but do not themselves have a force of law. Standards are universally adopted in manufacturing, procurement, and operation of thousands of devices and products, including raw materials, equipment, etc. Many standards have been adopted as a means of satisfying the regulatory or procurement requirements. Standards help to reduce the cost of products and processes in the following manner:

At the design level, rationalization of design procedure, drawings, and specifications takes place. This avoids the repetition of detailed design analysis for either identical or similar jobs.

Standards help in complete interchangeability and uniformity of fundamental design, tools, gauges, tool accessories, etc.

The standards can be of the following major four types:

1. Company standards
2. Trade or manufacturer's association standards
3. National standards
4. International standards

11.1.1.1 Company Standards

Company standards are followed by individual companies, subcontractors to the companies, and the license holders.

11.1.1.2 Trade or Manufacturer's Association Standards

Trade or manufacturer's association standards are the rules and the recommendations of various manufacturers of common interest, developed based on experience in design, manufacture, installation, and operation. While making the standards, feedback from users is normally included. Manufacturer's association standards that are most famous among heat exchanger manufacturers are Tubular Exchanger Manufacturers Association (TEMA) [3], Heat Exchange Institute (HEI) [4–6], and API Standards [7]. There are also Expansion Joint Manufacturers Association (EJMA) Standards [8] for the design of membrane-type expansion joints and American National Standards Institute (ANSI) standards for design of fittings, flanges, valves, piping, and piping components.

11.1.1.3 National Standards

National standards are followed in the country where the standard has been issued by subcontractors or license holders in other countries or complied with when the purchasers have so specified. Few national standards are BSI (Britain) [9], JIS (Japan) [10], and DIN (Germany) [11].

11.1.2 DESIGN STANDARDS USED FOR THE MECHANICAL DESIGN OF HEAT EXCHANGERS

Some design standards used for the mechanical design of heat exchangers include the following: TEMA-USA, HEI-USA, and API-USA,

TEMA Standards founded in 1939, the Tubular Exchanger Manufacturers Association, Inc., is a group of leading manufacturers of shell and tube heat exchangers who have pioneered the research and development of heat exchangers for over 60 years. TEMA Standards are followed in most countries of the world for the design of shell and tube heat exchangers. Some noteworthy features of the ninth edition (2007) include the following:

- New rules for flexible shell elements (FSEs; expansion joints), which are based on a finite element analysis (FEA) approach.
- Tables for tube hole drilling have been expanded to 3 in. diameter tubes.
- Guidelines for performing FEA have been added.
- Rules for the design of shell intersections (with large nozzle-to-cylinder ratios) subjected to pressure and external loadings have been added.
- Foreign material cross-reference linking material specifications from various international codes have been added.
- Rules for the design of longitudinal baffles have been added.

11.1.2.1 TEMA Standards Scope and General Requirements (Section B-1, RCB-1.1)

The TEMA mechanical standards are applicable to unfired shell and tube heat exchangers with inside diameters not exceeding 60 in. (1524 mm), a maximum product of nominal diameter (in.) and design pressure (psi) of 60,000 lb/in., or a maximum design pressure of 3,000 psi. The intent of these parameters is to limit the maximum shell wall thickness to approximately 2 in. (50.8 mm) and the maximum stud diameter to approximately 3 in. (76.2 mm). Criteria contained in these standards can be applied to units constructed with larger diameters. For units outside this scope, refer to TEMA Standards Section 11.10, Recommended Good Practice.

11.1.2.2 Scope of TEMA Standards (Table 11.1)

11.1.2.2.1 Contents

The contents of TEMA Standards are given here (Table 11.1). Each section is identified by an upper-case letter symbol, which precedes the paragraph numbers of the section and identifies the subject matter. TEMA classes R, C, and B have been combined into one section titled class RCB. The differences in design practices among the classes have been to some extent simplified. Section 11.5 has mechanical standards that apply to three classes of heat exchangers R, C, and B.

TABLE 11.1
Scope of TEMA Standards

Parameter	Limit
Inside diameter	60 in. (1524 mm)
Nominal diameter \times pressure	60,000 lb/in. (10,500 N/mm)
Pressure	3,000 psi (20,670 kPa)
Shell wall thickness	2 in. (50.8 mm)
Stud diameters (approx.)	3 in. (76.2 mm)
Construction code	ASME Section VIII, Div. 1
Pressure source	Indirect (unfired units only)

TEMA Standards Contents

Section	Symbol	Paragraph
1	N	Nomenclature
2	F	Fabrication tolerances
3	G	General fabrication and performance information
4	E	Installation, operation, and maintenance
5	RCB	Mechanical standards TEMA class RCB heat exchangers
6	V	Flow-induced vibration
7	T	Thermal relations
8	P	Physical properties of fluids
9	D	General information
10	RGP	Recommended good practice

11.1.2.2.2 Construction Code

According to Section RCB-1.13, the construction of heat exchangers shall comply with the ASME boiler and pressure vessel code (BPVC), Section VIII, Div. 1.

11.1.2.3 Differences among TEMA Classes R, C, and B

Differences among TEMA classes R, C, and B have been summarized by Taborek et al. [12] and are listed in Chapter 5.

11.1.2.4 TEMA Engineering Software

The TEMA has made available user-friendly, state-of-the-art engineering software for the IBM PC and compatibles. This software complements the TEMA Standards, ninth edition, in the areas of

1. FSEs (expansion joints) analysis
2. Flow-induced vibration analysis
3. Fixed tubesheet design and analysis

The programs handle the complex calculations of their respective sections of the seventh edition TEMA Standards.

11.1.2.5 When Do the TEMA Standards Supplement or Override the ASME Code Specification?

ASME Code provides rules for the design of the pressure boundary components like the shell, front and rear heads, flanges and covers, openings, nozzle, and reinforcements, and rules for

construction, manufacturer's inspection, and hydrostatic testing. Formulas are also included for tubesheet design, design of membrane-type expansion joints, and flanged and flued-type expansion joints (procedures for the determination of spring rate and stress analysis are not given). The rest of the information comes from the TEMA Standards. This includes the minimum thickness of shell and end closures; thickness of the pass partition plates and baffles; baffle spacing; tube-to-baffle hole clearance; drill drift; tolerance on ligaments; shell-to-baffle clearance; dimensional tolerances; standard clearances and tolerances applying to tubesheets, partitions, covers, and flanges; impingement protection; tubesheet design; stress induced in the shell and the tube bundle; tube-to-tubesheet joints; design criteria for flat cover deflection; fabrication tolerances; standard tolerances on external dimensions; nozzle and support locations; nozzle extension into the shell and angularity, etc. TEMA Standards also includes formulas to determine the minimum thickness of the tubesheet extended as a flange and a section on flow-induced vibration guidelines. In situations where the specifications are provided both by the codes and by the TEMA Standards, the latter generally override the former [13]. However, the following points warrant comment here: (1) Maximum allowable stresses in the components designed according to TEMA Standards are limited to ASME Code values and (2) tubesheets shall be designed as per TEMA only, even though separate procedures are included in the nonmandatory section of ASME Code.

11.1.2.6 Heat Exchange Institute Standards

The HEI, Cleveland, Ohio, is an association of manufacturers of heat transfer equipment used in power generation. The association promotes improved designs by developing equipment design standards. It publishes standards for tubular heat exchangers used in power generation. Such exchangers include surface condensers, feedwater heaters, and other power plant heat exchangers. Among these standards are

1. Standards for Steam Surface Condenser, 10th Edition 2006 [4]
2. Standards for Power Plant Heat Exchangers, 4th Edition 2004 [5]
3. Standards for Closed Feedwater Heaters, 8th Edition 2008 [6]

11.1.2.6.1 API Standard 660

API Standard 660, Shell and Tube Heat Exchangers for General Refinery Services [7], covers technical sections that exceed or supplement the TEMA Standards R class heat exchangers. This standard is a purchaser's specification intended for removable bundle floating head or U-tube construction. It does not discuss sections concerned with commercial matters.

11.1.2.6.2 EJMA Standards

The Expansion Joint Manufacturers Association Inc. [8] is a group of leading manufacturers of bellows-type expansion joints. This association issues standards on the design of bellows-type expansion joints known as EJMA Standards. The bellows-type expansion joints are employed primarily in piping systems to absorb differential thermal expansion while containing the system under pressure. Other applications include pressure vessels and heat exchangers. Typical service conditions range from pressures of 25 μm to 1000 psig and -420°F to 1800°F (-251°C to 982°C).

11.1.3 CODES

A code is a system of regulations or a systematic book of law often given statutory force by state or legislative bodies [14]. A code becomes a legal document in a state, a province, or a country if the government concerned passes appropriate legislation making it a legal requirement. Codes provide rules/specific design criteria (i) in respect of permissible materials of construction, allowable working stresses, and load sets that must be considered in design; (ii) to determine the minimum wall thickness

TABLE 11.2
International Design Codes Used for the Mechanical
Design of Heat Exchangers

Code Name	Country
ASME Code, Section III, Section VIII, Divs. 1 and 2	The United States
PD 5500	The United Kingdom
CODAP	France
AD Merkblatter 2000	Germany
UPV Code EN 13445	Europe
ANNC	Italy
Stoomwezen	Dutch
ISO/DIS-2694	International
IS:2825-1969	India
GOST	USSR
Pressure Vessel Code ^a	Japan
Regels voor Toetsellen Onder Druck	The Netherlands

^a Dai Isshu Atsuryouk Youki Kousou Kikahu.

and structural behavior due to the effects of internal pressure, thermal expansion, dead weight, live loads, or other imposed internal or external loads; (iii) for design requirement for components such as valves, flanges, standard fittings, and non-standard fittings; and (iv) for reinforcement of the openings in a pressure vessel. Among the codes, the ASME Code [15–17] for the construction of boilers and pressure vessels including heat exchangers is the most widely used and is referred to code in the world today. Apart from ASME Code, many other codes are issued by various countries such as CODAP [18], PED European Pressure Equipment Directive, PD 5500 [19] and AD Merkblatter [20]. Codes followed by few other countries are shown in Table 11.2. Basically, the codes differ in their legal status in their own countries. Range of applicability varies with regard to the scope of the codes, which includes basis of design and stress analysis, design pressure and temperature, diameter, volume, materials of constructions, fabrication, and inspection. There is no specific code available exclusively for the construction of heat exchangers in the world. Generally, heat exchanger standards quote certain codes to be followed for construction of the heat exchangers. In the following paragraphs, codes like ASME Code, PD 5000, CODAP, and AD Merkblatter are discussed.

11.1.3.1 ASME Codes

11.1.3.1.1 What Is the ASME Boiler and Pressure Vessel Code?

ASME Code establishes minimum rules of safety governing the design, fabrication, inspection, and testing of boilers, pressure vessels, and nuclear power plant components. It covers new construction and rerating the existing equipment. Before an ASME vessel can be fabricated, a manufacturer must apply for and receive a certificate of authorization from the Boiler and Pressure Vessel Committee of the American Society of Mechanical Engineers. Thereafter, in conformance with this certificate of authorization, an ASME Code vessel must be designed, fabricated, and inspected in accordance with the rules of the ASME Code.

Either of the symbols “U” or “UM” may be used to identify an ASME Code vessel. The symbol used must be stamped either on the vessel itself or on the manufacturer’s data plate attached to the vessel. When the “U” symbol is used, it indicates that a manufacturer has complied with all the provisions of the ASME Code for pressure vessels. In addition, it means that the vessel has passed inspection by an authorized inspector commissioned by the National Board of Boiler and

Pressure Vessel Inspectors. The Form U-1 Data Report furnished, on request, with each vessel contains the signature of the inspector. This certifies that the vessel has met the requirements of the ASME Code. When the “UM” symbol is used, a certificate (Form U-3) is also furnished only on request. The ASME Code requires that the “UM” vessel must be inspected only by the company inspector. The existence of the code stamp on a pressure vessel, with the indicated pressure and temperature, establishes the design conditions, new and old. The service conditions such as corrosion, erosion, change in operating pressure, and/or temperature may be the reasons to rerate the unit, but the original stamping remains valid. Supplemental stamping is a requirement to address rerating [21].

11.1.3.1.2 ASME Code: Historical Background

The steady increase in boiler explosions in the 40 years from 1870 to 1910 excited public feeling to make rules and regulations for safe operation of steam boilers. In 1911, ASME formed a Boiler Committee, now called as Boiler and Pressure Vessel Code Committee, to devise a uniform code to protect life, limb, equipment, and property. With the publication of the ASME Code for Construction of Boiler and Pressure Vessels in 1914, serious boiler explosions steadily decreased despite the fact that the number of boilers in use has increased enormously. Primarily as a result of the ASME Boiler Code, boiler explosions and the consequent loss of life and damage to property are a rarity today [22]. To become familiar with the important aspects of ASME Codes, refer to Refs. [1,23], Nichols [24] and Refs. [25–27]. Readers are advised to refer the latest codes and standards to know the state of the art. Unless otherwise mentioned, the mention of ASME Code throughout this book refers to ASME Code Section VIII, Div. 1, only.

11.1.3.1.3 ASME Codes

ASME Codes consist of 11 sections, and Section VIII deals with unfired pressure vessels. The various sections are as follows:

- I. Power boilers
- II. Material specifications
 - Part A—Ferrous materials
 - Part B—Nonferrous materials
 - Part C—Welding rods, electrodes, and filler metals
 - Part D—Material properties(customary/metric)
- III. Rules for construction of nuclear power plant components
 - Subsection NCA—General requirements for Division 1, Division 2, and Division 3
 - Division 1
 - Subsection NB—Class 1 components
 - Subsection NC—Class 2 components
 - Subsection ND—Class 3 components
 - Subsection NE—Class MC components
 - Subsection NF—Component supports
 - Subsection NG—Core support structures
 - Subsection NH—Class 1 components in elevated temp service
 - Appendices
 - Division 2—Code for concrete reactor vessels and containments
 - Division 3—Containment systems and transportation and packaging of spent nuclear fuel
- IV. Heating boilers
- V. Nondestructive examination

- VI. Recommended rules for care and operation of heating boilers limited to the operating ranges of heating boilers (Section IV)
- VII. Recommended rules for care of power boilers
- VIII. Pressure vessels, Division 1
 - Pressure vessels, Division 2 alternative rules
 - Pressure Vessels, Division 3 alternative rules for construction of high pressure Vessels
- IX. Welding and brazing qualifications
- X. Fiberglass-reinforced plastic pressure vessels
- XI. Rules for in-service inspection of nuclear power plant components
- XII. Rules for construction and continued service of transport tanks
 - Addenda
 - Interpretations
 - Code cases
 - Boilers and pressure vessels
 - Nuclear components
 - Address trade inquiries to the following address:
ANSI/ASME—Boiler and pressure vessel codes
American National Standards Institute
11 West 42nd Street
New York, NY 10036

Sections relevant for the fabrication of heat exchangers other than nuclear power plant units (i.e., unfired pressure vessels) are Section II, Section V, Section VIII, and Section IX. The ASME Code does not dictate what section of the code to use. The law or regulatory body at the point of installation determines what section to use.

11.1.3.1.4 Scope of the ASME Code Section VIII

Pressure vessels are typically designed in accordance with the ASME Code Section VIII. Section VIII is divided into three divisions: Division 1, Division 2, and Division 3. Division 1 is used most often since it contains sufficient requirements for the majority of pressure vessel applications. The main objective of ASME Code rules is to establish the minimum requirements that are necessary for safe construction and operation. The ASME Code protects the public by defining the material, design, fabrication, inspection, and testing requirements that are needed to achieve a safe design.

11.1.3.1.4.1 Division 1 The ASME Code Section VIII, Division 1, applies for pressures that exceed 15 psig and through 3000 psig. At pressures below 15 psig, the ASME Code is not applicable. Above 3000 psig pressure, additional design rules are required to cover the design and construction requirements that are needed [28]. The ASME Code is not applicable for piping system components that are attached to pressure vessels. Therefore, at pressure vessel nozzles, ASME Code rules apply only through the first junction that connects to the pipe. This junction may be at the following locations:

1. Welded end connection through the first circumferential joint
2. First threaded joint for screwed connections
3. Face of the first flange for bolted, flanged connections
4. First sealing surface for proprietary connections or fittings

The code also does not apply to non-pressure-containing parts that are welded, or not welded, to pressure-containing parts. However, the weld that makes the attachment to the pressure part must meet code rules. Therefore, items such as pressure vessel internal components or external supports do not need to follow code rules, except for any attachment weld to the vessel.

11.1.3.1.4.2 Division 2, Alternative Rules The scope of Division 2 is identical to that of Division 1; however, Division 2 contains requirements that differ from those that are contained in Division 1. Several areas where the requirements between the two divisions differ are highlighted in the following.

Stress: The maximum allowable primary membrane stress for a Division 2 pressure vessel is higher than that of a Division 1 pressure vessel. The Division 2 vessel is thinner and uses less material. A Division 2 vessel compensates for the higher allowable primary membrane stress by being more stringent than Division 1 in other respects.

Stress calculations: Division 2 uses a complex method of formulas, charts, and design-by-analysis (DBA) that results in more precise stress calculations than that are required in Division 1.

Design: Some design details that are allowed in Division 1 are not permitted in Division 2.

Quality control: Material quality control is more stringent in Division 2 than in Division 1.

Fabrication and inspection: Division 2 has more stringent requirements than Division 1.

The choice between using Division 1 and Division 2 is based on economics. The areas where Division 2 is more conservative than Division 1 add to the cost of a vessel. The lower costs that are associated with the use of less material (because of the higher allowable membrane stress) must exceed the increased costs that are associated with the more conservative Division 2 requirements in order for the Division 2 design to be economically attractive.

A Division 2 design is more likely to be attractive for vessels that require greater wall thickness, typically over approximately 2 in. thick. The thickness break point is lower for more expensive alloy material than for plain carbon steel and will also be influenced by current market conditions. A Division 2 design will also be attractive for very large pressure vessels where a slight reduction in required thickness will greatly reduce shipping weights and foundation load design requirements.

11.1.3.1.4.3 Division 3, Alternative Rules for Construction of High-Pressure Vessels Division 3 applies to the design, fabrication, inspection, testing, and certification of unfired or fired pressure vessels operating at internal or external pressures generally above 10,000 psi. This pressure may be obtained from an external source, from a process reaction, by the application of heat, or any combination thereof. Division 3 does not establish either maximum pressure limits for Division 1 or Division 2 or minimum pressure limits for Division 3.

11.1.3.1.5 Structure of Section VIII, Division 1

The ASME Code, Section VIII, Division 1, is divided into three subsections as follows:

1. *Subsection A* consists of Part UG, the general requirements that apply to all pressure vessels, regardless of fabrication method or material.
2. *Subsection B* covers requirements that apply to various fabrication methods. Subsection B consists of Parts UW, UF, and UB that deal with welded, forged, and brazed fabrication methods, respectively.
3. *Subsection C* covers requirements that apply to several classes of materials. Subsection C consists of Parts UCS (carbon and low-alloy steel), UNF (nonferrous metals), UHA (high-alloy steel), UCI (cast iron), UCL (clad and lined material), UCD (cast ductile iron), UHT (ferritic steel with properties enhanced by heat treatment), ULW (layered construction), and ULT (low-temperature materials).

Division 1 also contains the following appendices:

Mandatory Appendices address subjects that are not covered elsewhere in the code. The requirements that are contained in these appendices are mandatory when the subject that is covered is included in the pressure vessel under consideration. Examples of mandatory appendices are as follows:

1. Supplementary Design Formulas
2. Rules for Bolted Flange Connections with Ring Type Gaskets
3. Vessels of Noncircular Cross Section
4. Design Rules for Clamped Connections

Nonmandatory Appendices provide information and suggested good practices. The use of these nonmandatory appendices is not required unless their use is specified in the vessel purchase order. Examples of nonmandatory appendices are the following:

1. Basis for establishing allowable loads for tube-to-tubesheet joints
2. Suggested good practice regarding internal structures
3. Rules for the design of tubesheets
4. Flanged-and-flued or flanged-only expansion joints
5. Half-pipe jackets

11.1.3.1.6 *Addenda*

Colored sheet addenda, which include additions and revisions to individual sections of the code, are published annually and will be sent automatically to the purchasers of the applicable sections up to the publication of the next edition/revision.

11.1.3.1.7 *Interpretations*

The ASME issues written replies to inquiries concerning interpretation of technical aspects of the code. The interpretations for each individual section will be published separately and will be included as part of the update service to that section.

11.1.3.1.8 *Code Cases, Boilers, and Pressure Vessels*

This contains provisions that have been adopted by the Boiler and Pressure Vessel Committee that cover all sections of the code other than Section III, Divs. 1 and 2, Section XI, to provide, when the need is urgent, rules for materials, or constructions not covered by existing code rules. Case revisions in the form of supplements will be sent automatically to purchasers up to the publication of the 1995 Code. Code cases may be used in the construction of components to be stamped with the ASME Code symbol beginning with the date of their approval by ASME.

11.1.3.1.9 *Technical Inquiries*

When a user of the code has difficulty in understanding a part of the code, a technical inquiry may be sent to the ASME Code Committee for an interpretation of the provisions or requirements of the code. The letter should be addressed to the secretary to the following address:

Secretary
Boiler and Pressure Vessel Code Committee
American Society of Mechanical Engineers
345 East Forty Seventh Street
New York, NY 10017, USA

TABLE 11.3
Contents of PD 5500

Section 1	Section 4: Manufacture and workmanship
Foreword	Section 5: Inspection and testing
Scope	Annexes
Interpretation	Figures
Definitions	Tables
Information and requirements to be agreed and to be documented	Aluminum supplement
	Copper supplement
	Nickel supplement
	List of references
Section 2: Materials	Enquiry cases
Section 3: Design	

There are several reasons why an inquiry will not be handled by the committee, and the inquirer is so informed. The reasons for rejection include [29] (1) basis of code rules; (2) indefinite question with no reference to code paragraphs, figures, or rules; (3) semicommercial question with doubt as to whether question is related to code requirements or is asking approval of design; and (4) approval of specific design.

PD 5500 British Standards for unfired fusion welded pressure vessels

PD 5500 specifies requirements for the design, manufacture, inspection, testing, and verification of compliance for unfired fusion welded pressure vessels manufactured from carbon steel, ferritic steels, and austenitic stainless steels, aluminum, copper, and nickel used in a wide range of process and energy industry applications. PD 5500 is applicable to vessels subject to electrical heating or heated process streams. It excludes, however, those that are subject to direct generated heat or flame impingement from a fired process. The 2009 edition includes all the corrigendum and amendments made to the 2006 edition. This specification can be used

- To support equipment and systems previously designed and manufactured to PD 5500
- For pressure vessels intended for use outside the European Union (Table 11.3)

11.1.3.2 CODAP

CODAP is the French Code for Construction of Unfired Pressure Vessels. The evolution of the demand to the manufacturers and the regular modifications in the international, European, and French standards have led the SNCT to prepare new editions of the Codes of Construction, reflecting the French professionalism. Consisting of two divisions, this new edition meets the requirements of the future standard ISO 16528. The Division 1 is essentially intended for the construction of the most common vessels to be manufactured from common materials. The Division 2 intended for the construction of more complex vessels offers all the possibilities set out in the former versions of the code, largely supplemented with a great number of innovations. Rules for tubesheets are codified in part C7 of the CODAP Code. Contents of CODAP rules are shown in Table 11.4.

11.1.3.3 AD Merkblätter 2000—German Pressure Vessel Code

The AD 2000 Code of practice for pressure vessels is drawn up by the German Pressure Vessel Association. It contains regulations and generally accepted rules of technology regarding pressure vessels, steam boilers, pipes, and fittings and contain safety requirement for these equipment design,

TABLE 11.4
General Structure of the CODAP Code

Part G	General provisions
Part M	Material
Part C	Design rules
Part F	Fabrication
Part I	Control and inspection
Part S	Protection against overpressure

material selection, manufacture, and testing. These regulations are complied by seven trade associations of Germany, who together form the AD. Contents of the code are the following:

- Equipment, installation and marketing (Series A)
- Design (Series B)
- Fundamentals (Series G)
- Manufacturing and testing (Series HP)
- Non-metallic materials (Series N)
- Special cases (Series S)
- Materials (Series W)
- Additional notes (Series Z)

11.1.3.4 UPV: The European Standards EN 13445

The Unified Pressure Vessel code EN 13445 [30] provides the definitive European Standards for unfired pressure vessels. Part 3 of EN 13445 gives the rules to be used for design and calculation under internal and/or external pressures (as applicable) of pressure-bearing components of pressure vessels, such as shells of various shapes, flat walls, flanges, heat exchanger tubesheets, and calculation of reinforcement of openings. Rules are also given for components subjected to local loads and to actions other than pressure.

For all these components, design-by-formula (DBF) method is generally followed, i.e., appropriate formulas are given in order to find stresses that have to be limited to safe stress values. These formulas are generally intended for predominantly noncyclic loads, which means for a number of full pressure cycles not exceeding 500. However, general prescriptions are also given for DBA as an alternative to DBF. Methods are also given for fatigue evaluation if the number of load cycles exceeds 500.

11.2 BASICS OF MECHANICAL DESIGN

The structural integrity of pressure vessels and heat exchangers depends on proper mechanical design arrived at after detailed stress analysis keeping in view all the static, dynamic, steady, and transient loads. Heat transfer efficiency and fabrication costs of a tubular exchanger are directly influenced by proper functional and mechanical design. Therefore, an optimum mechanical design of various components of heat exchangers is of paramount importance. Mechanical design of various pressure-retaining components and some non-pressure-retaining components of heat exchangers is discussed in this section. Also discussed in this section are the fundamentals of mechanical design and stress analysis, classification of stresses and stress category concept, allowable stress, weld joint efficiency and joint category, and various design terms. Important source books on mechanical design of heat exchangers and pressure vessels are Singh and Soler [31] and Escoe [32] and on pressure vessels Moss [33], Brownell and Young [34], Bednar [35], Harvey [36], and Chuse [37], among others.

11.2.1 FUNDAMENTALS OF MECHANICAL DESIGN

Mechanical design involves the design of pressure-retaining and non-pressure-retaining components and equipments to withstand the design loads and the deterioration in service so that the equipment will function satisfactorily and reliably throughout its codal life. Mechanical design is done as per the procedure given in the construction codes and standards. Where no guidance is provided by the codes and standards, the procedure may be arrived at by mutual agreement between the purchaser and the fabricator.

11.2.1.1 Information for Mechanical Design

For mechanical design of shell and tube heat exchangers, certain minimum information is required [13]. The following listing summarizes the minimum information required:

1. Thermohydraulic design details in the form TEMA or an equivalent specification sheet.
2. TEMA class, type of TEMA shell, channels/heads.
3. Shellside and tubeside passes.
4. Number, type, size, and layout of tubes.
5. Diameter and length of shell, channel/head, and its configuration.
6. Design temperatures and pressures.
7. External pressure if the equipment is under external pressure or is under internal vacuum.
8. Worst-case coincident conditions of temperature and pressure.
9. Nozzle, wind, and seismic loads, impact loads (including water hammer, if any).
10. Superimposed loads due to insulation, piping, stacked units, etc.
11. Corrosion properties of the fluids and the environment in which the unit will be installed and the expected service life. This will help to specify corrosion allowances or better material selection to reduce the material loss due to corrosion.
12. Materials of construction except tube material, which is arrived at the thermal design stage.
13. Fouling characteristics of the streams to be handled by the exchanger. This will determine if closures are required for frequent cleaning of internal parts of the exchanger. Many fixed tubesheet heat exchangers, if not specified otherwise, may be of welded head and shell construction.
14. Flow rate to size the nozzles and to determine whether impingement protection is required.
15. Special restrictions imposed by the purchaser on available space, piping layout, location of supports, type of material, servicing conditions, etc.
16. Construction Code and Standard to be followed.
17. Installation—vertical or horizontal.
18. Installation and operation considerations like startup, transients, shutdown and upset conditions that decide tubesheet thickness [38].
19. Handling of lethal or toxic fluids, which demand more stringent welding and NDT requirements.

When high-pressure fluid is routed through the tubeside, the effect of tube failure on the low-pressure shellside should be considered. It is essential to provide excess pressure protection on the shellside.

11.2.1.1.1 Sequence of Decisions to Be Made during Mechanical Design

In addition to the information required at the mechanical design stage as mentioned already, certain decisions are also to be made at the mechanical design stage. Soler [39] summarizes a typical

sequence of decisions that must be made at the mechanical design stage of a heat exchanger design. Some of the points are as follows:

1. What kind of connections (welded, flanged, or packed) should be provided at the front head, tubesheet, and rear head?
2. What style of flanged joint should be used—e.g., ring-type gasket or full-face gasket?
3. What kind of closures (hemispherical, ellipsoidal, torispherical, conical, etc.) should be used?
4. What combination of load will govern the pressure part design? (Typical loads are shell-side pressure, tubeside pressure, differential thermal expansion, self-weight, mechanically transmitted vibration, seismic vibration, etc.)
5. Type and style of openings.
6. Type of nozzle connections, such as self-reinforcing forging stock versus pipe schedule.
7. Details of vent and drain design.
8. Minimum bend radii for U-tubes.
9. Whether an expansion joint is required. If so, what is the best type and style of the expansion joint?
10. Whether installation is horizontal or vertical, to decide the type/style of heat exchanger supports.
11. Evaluation of the ability of the exchanger to withstand operational transients, startup, and pressure testing.

Each of these decisions and evaluation steps requires a proper adjudication among various possibilities; many of these considerations require and/or are amenable to mathematical analysis, while others are derived from past experience or experimental data [39].

11.2.1.2 Content of Mechanical Design of Shell and Tube Heat Exchangers

Mechanical design of shell and tube heat exchangers involves at a minimum the following components design and the determination of stresses induced in that component:

1. Shell thickness.
2. Shell flange and channel flange design.
3. Dished end calculation.
4. Design of openings and nozzles.
5. Tubesheet thickness. If the differential expansion between shell and tubes is excessive, then an expansion joint is to be designed and thus final tubesheet thickness is arrived at.
6. Shell longitudinal stress and bending stress.
7. Tube longitudinal stress, both at the tube bundle inside and at the periphery.
8. Channel longitudinal stress and bending stress.
9. Tube-to-tubesheet joint load.
10. Flat cover thickness.
11. Design of supports.
12. Additionally consider the cost of material, fabrication and labor.

11.2.1.2.1 Software for Mechanical Design of Heat Exchanger

Nowadays most of the mechanical design of heat exchangers and pressure vessels are done by software. Typical software for mechanical design include Advanced Pressure Vessel of Computer Engineering, Inc., MO, Intergraph® PV Elite™, Houston, TX, and COMPRESS of CODEWARE, Houston, TX (www.codeware.com). Typical software program structure and output of mechanical design of shell and tube heat exchanger is shown in Table 11.5.

TABLE 11.5**Typical Software Program Structure and Output of Mechanical Design of Shell and Tube Heat Exchanger**

Design conditions	Concise summary of design pressures, temperatures, corrosion allowances, weights (empty, full, bundle)
Cylinder	Diameters, Code calculated thickness, TEMA minimum thickness, external pressure minimum thickness, actual thickness, maximum external pressure, maximum length for external pressure, materials of construction. Vessel cross sectional areas and moment of inertia checks. Vessel longitudinal stress check-Stress analysis due to the combined effect of pressure, live loads, dead weights, etc.
Heads/covers	Calculations are performed using the ID or OD for Flanged and Dished, Braced and Stayed, Torispherical, Ellipsoidal, Hemispherical, Conical, Flat, and Toriconical heads
Nozzles	Diameters, Code calculated thickness, actual thickness, reinforcement pad diameter and thickness, materials of construction. Nozzle weld load, stress, strength of connection, shear and path of failure
Flanges	ANSI B 16.5 flange: Computes pressure rating based on Class, Grade and design temperature. Custom flange calculations as per Appendix 2 and Taylor Forge method for min. thickness and MAWP. Flange outer diameter, bolt circle, bolt diameter, bolt number, gasket outer diameter, gasket width, gasket thickness, Code calculated flange thickness, actual flange thickness, lap joint ring dimensions, hub dimensions, materials of construction
Tubesheets	Diameters (front and rear), TEMA bending thickness, shear thickness, flange extension thickness, effective thickness, recesses, actual thickness, clad thickness, tubing details, outer tube limit, materials of construction
Expansion joints	Number of joints, diameter, flexible element thickness, dimensions, spring rates, cycle life, materials of construction
Supports	Support dimensions, gussets, hole dimensions, wear plate thickness, Zick stress analysis; For vertical vessel base ring or legs and/or lugs analyzed. materials of construction.
Maximum allowable working pressures (MAWP)	MAWP for all code components at design and ambient conditions, with controlling components flagged
Minimum design metal temperature (MDMT)	Calculations performed per UCS-66 for all pressure components composed of UCS-23 materials
External loadings on nozzles	Local stresses in cylinders with applied loads, design conditions, maximum loads and moments, interaction diagram
Lifting lug design	Calculation for both horizontal and vertical lifting lugs as per standard engineering methods
Rigging analysis	Bending and shear stresses generated in a vessel while its being lifted are computed. These stresses are compared to their allowable values
Vessel natural frequency	Computes natural frequency of the vessel in filled, empty and operating conditions
Vortex shedding loads	Computes fatigue stresses and number of hours of safe operation, based on loads generated by dynamic wind vibration
Wind deflection	Computes the elemental deflection, angular rotation and critical speed
Calculation and documentation	Formulas used and intermediate results for verification of Code and TEMA calculations
Tubesheet layout details	Number of tubes per row, distances offset from horizontal and vertical center lines for each row, tie rod locations, pass partition locations, balance of tubes per pass, baffle cut dimensions
Drawings	Setting plan, sectional drawing, bundle layout, tubesheet layout, etc.
Others	Fatigue analysis, Seismic loads, graphics, thermal and mechanical design interface, material database, supporting Standards and Codes
Bill of materials	Quantity of all components, their dimensions and specifications, costing

11.2.1.3 Mechanical Design Procedure

A typical sequence of mechanical design procedures is discussed by Singh [40]. They are the following:

1. Identify applied loadings
2. Determine applicable codes and standards
3. Select materials of construction (except for tube material, which is selected during the thermal design stage)
4. Compute pressure part thickness and reinforcements
5. Select appropriate welding details
6. Establish that no thermohydraulic conditions are violated
7. Design non-pressure parts
8. Design supports
9. Select appropriate inspection procedure

11.2.1.4 Design Loadings

A list of loadings to be considered in designing a heat exchanger or a pressure vessel part is given in UG-22 of ASME Code Section VIII, Div. 1. They include the following:

1. Internal and/or external design pressure (as defined in UG-21)
2. Weight of vessel and normal contents including the static head of liquid
3. Local loadings on the shell, such as those due to internals, vessel supports, lugs, etc.
4. Cyclic and dynamic reactions due to pressure or thermal variations, mechanical loadings, etc.
5. Wind, seismic, and snow loadings where required
6. Impact loadings, such as those due to fluid shock

11.2.1.5 Topics Covered in the Next Sections

In the next sections, the following topics are covered:

1. Stress analysis, classes, and categories of stress.
2. Calculation or design of (a) shell thickness, (b) dished end thickness, flat cover thickness, (d) flange thickness, (e) tubesheet thickness, (f) shell longitudinal stress, (g) tube longitudinal stress, (h) tube-to-tubesheet joint loads at the periphery of the tube bundle, (i) expansion joint, (j) nozzle openings and reinforcement of nozzle openings, and (k) supports.

11.3 STRESS ANALYSIS, CLASSES, AND CATEGORIES OF STRESS

11.3.1 STRESS ANALYSIS

Stress analysis is the determination of the relationship between external forces applied to a vessel and the corresponding stress. The stress analysis of heat exchangers and pressure vessels is similar to other structural members in that it involves mathematical operations with unknown forces and displacements. In the evaluation of the stress field in heat exchangers and pressure vessels, the problem is considerably simplified due to these reasons [31]: (1) The pressure-retaining components such as shell, heads, and cones are surfaces of revolution; (2) pressure loading—the primary mechanical loading is spatially uniform; (3) the thickness of a pressure vessel is small compared to its characteristic dimensions; and (4) with little accuracy loss, we can assume that the meridian, tangential, and through-thickness directions are principal directions.

11.3.2 CLASSES AND CATEGORIES OF STRESSES

Classes of stress, categories of stress, and allowable stresses as permitted by codes are based on the type of loading that produced them and on the hazard they cause to the structure.

11.3.2.1 Stress Categories

The combined stresses due to a combination of loads acting simultaneously are called stress categories.

11.3.2.2 Stress Classification

The stresses that are present in pressure vessels are separated into various classes in accordance with the types of loads that produced them and the hazard they pose to the vessel. The reason for classifying stresses into various groups is that not all types of stresses require the same safety factors in protection against failure. Limit analysis theory indicates that some stresses may be permitted to a higher level than other stresses. Before discussing stress classification, membrane stress and primary stress are defined.

11.3.2.3 Membrane Stress

When the thickness is small in comparison with other dimensions ($R_m/t > 10$), vessels are referred to as membranes, and the resulting stresses due to contained pressure are called membrane stresses [33]. The membrane is assumed to offer no resistance to bending. When the wall offers resistance to bending, bending stresses occur in addition to membrane stresses.

11.3.2.4 Primary Stress

Primary stress is a normal stress or a shear stress developed by the imposed loading that is necessary to satisfy the laws of equilibrium. The basic characteristic of a primary stress is that it is not self-limiting. Primary stresses that exceed the yield strength will result in plastic deformation, gross distortion, or failure. Thermal stress is not classified as a primary stress. It is classified as a secondary stress only.

Classes of stress and categories of stress are dealt in detail by Refs. [31,33,35], among others.

11.3.3 STRESS CLASSIFICATION

In the design codes, stresses are classified into five types. They are as follows:

1. Primary membrane stress, P_m
2. Primary bending stress, P_b
3. Local membrane stress, P_L
4. Secondary stress, Q
5. Peak stress, F

11.3.3.1 Primary Membrane Stress, P_m

The component of primary stress that is obtained by averaging the stress distribution across the thickness of the pressure vessel is referred to as the primary membrane stress. It is the most significant stress class. An important characteristic of the primary membrane stress is that beyond the yield point, redistribution of stresses in the structure does not take place. It is remote from discontinuities such as head-shell intersections, nozzles, and supports. Design codes limit its value to the allowable stress for the component material. Examples for primary membrane stresses are as follows:

1. Circumferential (hoop) and longitudinal (meridian) stresses due to internal or external pressures
2. Stress due to vessel weight
3. Longitudinal stress due to the bending of the horizontal vessel over the supports

4. Membrane stress in the nozzle wall within the area of reinforcement due to pressure or external loads
5. Stress caused by wind and seismic forces

11.3.3.2 Primary Bending Stress, P_b

In contrast to a cylindrical shell, certain structural shapes cannot resist external loadings without bending, and the resulting stress is known as primary bending stress. Primary bending stress is capable of causing permanent distortion or collapse of the vessel. Some examples of primary bending stress are the following:

1. Bending stress due to pressure in a flat cover
2. Bending stress in the crown of a torispherical head due to internal pressure
3. Bending stress in the ligaments of closely spaced openings, such as bending stress in the tubesheet averaged across the ligament

Primary general stresses are divided into primary membrane and primary bending stresses, and the reason for such a division is that the calculated value of a primary bending stress may be allowed to go higher than that of a primary membrane stress.

11.3.3.3 Local Membrane Stress, P_L

Local (primary) membrane stress is produced either by pressure load alone or by other mechanical loads. It has some self-limiting characteristics. Since the loads are localized, once the yield strength of the material is reached, the load is redistributed to stiffer portions of the vessel. Typical examples for local primary membrane stress are stresses at supports and stresses due to internal pressure at structural discontinuities [35].

11.3.3.4 Secondary Stress

Secondary stress is a normal or shear stress arising because of the constraint of adjacent material or by self-constraint of the structure. These stresses arise solely to satisfy compatibility conditions and are not required to satisfy laws of equilibrium. They are self-limiting in nature. Local yielding can relieve the conditions that lead to the development of these stresses and limit their maximum value. Failure from secondary stress is not to be expected. The concept of primary and secondary stresses is not relevant for brittle materials. Two sources of secondary stresses are (1) temperature and (2) gross structural discontinuity.

Secondary stresses can be subdivided into two major categories: (1) load-actuated secondary stresses and (2) temperature-actuated secondary stresses. Examples for these classes are given next.

Some examples of load-actuated secondary stresses are the following:

1. Bending stress in a shell where it is connected to a head or to a flange
2. Bending stress in a shell or a head due to nozzle loads
3. Bending stress in the knuckle at a head-to-shell joint

Some examples of temperature-actuated secondary stresses are the following:

1. Stresses caused by axial temperature variation in a shell
2. Both membrane and bending stresses due to differential thermal expansion between two adjoining parts of a structure such as nozzle to shell or shell to head

Moss [33] additionally classifies secondary stresses into two groups: membrane and bending. Examples of secondary membrane stress, Q_m , are as follows:

11.3.3.5 Thermal Stresses

Membrane stress in the knuckle area of the head

Examples of secondary bending stress, Q_b , are the following:

1. Bending stress at a gross structural discontinuity due to relenting loads only, such as nozzles and lugs
2. The nonuniform portion of the stress distribution in a thick-walled vessel due to internal pressure

11.3.3.6 Peak Stress, F

Peak stresses are the additional stresses due to stress concentration in highly localized areas. They are caused by mechanical and thermal loads, and they apply to both limiting and self-limiting loads. Peak stresses are added to the primary and secondary stresses to give the total stress at a point. A peak stress does not cause any noticeable distortion. The determination of peak stress is necessary only for fatigue analysis or a source of stress corrosion cracking, or it can be a possible source of brittle fracture [35]. Peak stress applies to membrane, bending, and shear stresses. Examples for peak stresses due to thermal and mechanical loads are given next.

Some examples of peak stresses due to thermal loads are as follows:

1. Thermal stress in the cladding or weld overlay of a tubesheet, shell, or vessel head
2. Thermal stresses in a wall caused by a sudden change in the surface temperature (thermal shock)

Some examples of load-actuated peak stresses for specific situations are as follows:

1. Peak stress in a ligament (uniform ligament pattern)
2. Stress at a local structural discontinuity
3. Stress at corner of a discontinuity
4. Stress due to notch effect or stress concentration or small radius fillet, hole, or incomplete penetration [35]
5. Additional stresses developed at the fillet at a nozzle-to-shell junction due to internal pressure or external loads

11.3.3.7 Discontinuity Stresses

Pressure vessel components and sections usually contain regions of different thickness, material, diameter, and abrupt changes in geometry. The juncture at these locations is known as “discontinuity” areas. Examples include the skirt junction with the shell/vessel and head and shell. The stresses induced in the respective parts at or near discontinuity areas are called discontinuity stresses. Discontinuity stresses are necessary to satisfy compatibility conditions at discontinuity regions. They are not serious under static loads such as internal pressure with ductile materials if they are kept within limits by the design, but they are important under cyclic loads [35]. The characteristics of discontinuity stresses are [33] as follows:

1. These stresses are local in extent but can be of very high magnitude.
2. Discontinuity stresses are considered as “secondary stresses” and self-limiting, if their extent along the length is limited.
3. In average application, discontinuity stresses will not lead to failure. However, they may be a major consideration for (1) brittle materials and (2) high-pressure applications (>1500 psi).

11.3.4 FATIGUE ANALYSIS

When a vessel is subjected to repeated loading that could cause failure by the development of a progressive fracture, the vessel is said to be in cyclic service.

11.3.5 DESIGN METHODS AND DESIGN CRITERIA

There are two basic design methods used by the codes for the design of heat exchangers and pressure vessels; these are termed, “design-by-rule” and “design-by-analysis.” The first is based on experience and does not require a detailed evaluation of all stresses. It gives formulas for sizing the majority of widely used components. The latter is based on criteria requiring detailed stress analysis.

11.3.5.1 ASME Code Section VIII Design Criteria

In general, pressure vessels conforming to the ASME Code, Section VIII, Div. 1, are designed by “design-by-rules” and do not require a detailed stress analysis. It is recognized that high localized and secondary bending stresses may exist, but they are allowed for by use of a higher safety factor. However, as per code rules, all loadings applied to a vessel or its structural attachments must be considered (UG-22). The code establishes allowable stresses by stating in Paragraph UG-23 that the maximum primary membrane stress must not exceed the maximum allowable stress value in tension. Further, it states that the maximum primary membrane stress plus primary bending stress may not exceed 1.5 times the allowable stress of the material in tension. It also recognizes that high localized discontinuity stresses may exist, but the design rules have been written to limit such stresses to a safe level consistent with experience.

Design criteria: Comparison of ASME Code Section VIII Div. 1 versus Div. 2

Salient features and differences among code rules between Div. 1 and Div. 2 are discussed in Ref. [33], and the differences are given in Table 11.6.

11.3.6 ALLOWABLE STRESS

Allowable stresses are used in the design of pressure vessels, heat exchangers, structures, machine elements, etc. The code gives tables for allowable stresses in tension for most structural materials at discrete temperatures. The allowable stresses in compression depend on the slenderness of the pressure components and are therefore presented in terms of slenderness ratio. The basis of the ASME Code allowable stress values is discussed in Ref. [40].

11.3.7 COMBINED-THICKNESS APPROACH FOR CLAD PLATES

In general, the code does not permit using the clad thickness as additional thickness to resist pressure but rather treats it only as a corrosion allowance. As an exception, for clad material conforming to SA-263, SA-264, and SA-265, the cladding thickness after deducting the corrosion allowance can

TABLE 11.6
Comparison of Design Criteria of ASME Code Section VIII

Division 1	Division 2
Design is by “design-by-rules” principle and does not require a detailed evaluation of all stresses. It gives formulas for sizing the majority of widely used components	Design is by “DBA” and requires an all much more rigorous design analysis
Does not explicitly consider the effects of combined stress and does not give detailed methods on how stresses are combined	Provides specific guidelines on classes of stresses, stresses categories, and how they are combined
Stress analysis considers a biaxial state of stress combined in accordance with the maximum principal stress theory	Considers all stresses in a triaxial state combined in accordance with the maximum shear stress theory
Does not specifically provide for design of vessels in fatigue	Criteria for determining when a vessel must be analyzed for fatigue are specified

be used for the thickness calculation purpose. As per Paragraph UCL-23(c), if the nominal thickness of base plate is t_b , then the allowable combined thickness, t_t , that can be used for pressure calculations is given by

$$t_t = t_b + \left(\frac{S_c}{S_b} \right) t_c \quad (11.1)$$

where

S_c is the maximum allowable stress of cladding at design temperature

S_b is the maximum allowable stress of the base material at design temperature

t_c is the nominal thickness of cladding less corrosion allowance

Where S_c is greater than S_b , the multiplier S_c/S_b shall be taken equal to unity.

Example: Given the base plate thickness is 1.0 in., clad plate thickness is 0.25 in., allowable stress for the base plate is 17,500 lb/in.², and allowable stress for the clad material is 11,200 lb/in.², what is the allowable combined thickness t_t that can be used for pressure calculations if the corrosion allowance on the cladding is 0.050 in.?

$$t_t = 1.0 + \left(\frac{11,200}{17,500} \right) (0.25 - 0.05) = 1.128 \text{ in.}$$

11.3.8 WELDED JOINTS

The most common way to fabricate a pressure vessel is by welding. For vessel members with weld joints, all thickness formulas shall contain the weld joint efficiency term E inserted into the equation. The multiplication of the efficiency term E with the code allowable stress, S , gives the effective allowable stress, SE , for the weld seam. If no E term is contained in the formula, the allowable stress may have to be modified by a quality factor of 80% [28]. Special restrictions prevail at the weld joint for the following cases:

1. The vessel contains a lethal substance
2. The vessel will operate at a temperature lower than -20°F
3. The vessel is an unfired steam boiler with design pressure exceeding 50 psi
4. The vessel is subjected to direct firing

In these cases, all joints are restricted to butt joints and full penetration welds.

11.3.8.1 Welded Joint Efficiencies

In industry, radiographic examination (RT) is the most common technique to establish soundness of the weld joints. Depending on the type of weld joint (single or double butt, double full fillet lap, single-welded butt joint without backing strip, etc.), and also on the extent of RT used to check the soundness of the joint, most of the pressure vessel codes prescribe a “joint efficiency” E to be used in the thickness formulas. The code recognizes full radiography, spot radiography, and none. As per ASME Code Table UW-12, for a double-welding butt joint, the corresponding efficiencies would then be fully radiographed 100%, spot radiographed 85%, and none 70%. The decrease in joint efficiency from 100% to 70% when no spot radiographic examinations are made on the welded joints means that a fabricator must provide more thickness.

11.3.8.2 Joint Categories

As per Paragraph UW-3 of ASME Code Section VIII, Div. 1, the term “category” is used to define the location of a joint in a vessel, but not the type of the joint. Categories are established for the

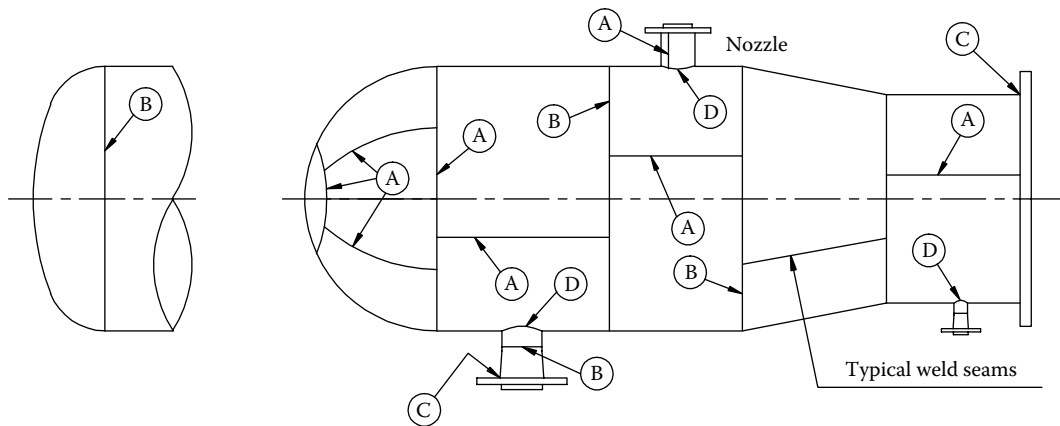


FIGURE 11.1 ASME Code joint category designation.

purpose of specifying special requirements regarding joint type and degree of inspections of certain welded pressure vessels. ASME Code categorizes various joint locations into the following four types: Category A locations, Category B locations, Category C locations, and Category D locations. These locations are schematically shown in Figure 11.1. Some examples for Category A, B, C, and D are given next. For complete details, refer to ASME Code Section VIII, Div. 1.

11.3.8.2.1 Category A Locations

Category A locations are longitudinal welded joints within a main shell, and welded joints within a sphere, within a formed or flat head, or within the side plates of a flat-sided vessel; circumferential welded joints connect hemispherical heads to main shells and several other locations.

11.3.8.2.2 Category B Locations

Category B locations are circumferential welded joints within the main shell, and circumferential welded joints connecting formed heads other than hemispherical to main shells, to transitions in diameter, to nozzles, or to communicating chambers and several other locations.

11.3.8.2.3 Category C Locations

Category C locations are welded joints connecting flanges, tubesheets, or flat heads to the main shell, to formed heads, to transitions in diameter, and to nozzles; any welded joints connect one side plate to another side plate of a flat-sided vessel and several other locations.

11.3.8.2.4 Category D Locations

Category D locations are welded joints connecting communicating chambers or nozzles to main shells, to spheres, to heads, or to flat-sided vessels, those joints connecting nozzles to communicating chambers, and several other locations.

11.3.8.3 Weld Joint Types

The category of the weld joint determines permissible joint types, weld examination requirements, and associated weld joint efficiencies used in pressure part thickness calculation. The code defines six weld joint types (UW-2); their definitions are given in Table 11.7.

11.3.9 KEY TERMS IN HEAT EXCHANGER DESIGN

11.3.9.1 Design Pressure

Design pressure for a pressure vessel or a heat exchanger is the gauge pressure at the top of the vessel and, together with the coincident design metal temperature, used in the design calculations

TABLE 11.7
Weld Joint Types

Type	Description
Joint type 1	Double-welded butt joint, or by other means that produce the same quality of weld on the inside and outside. Welds using metal backing strips that remain in place are excluded
Joint type 2	Single-welded butt joints with backing strip which remains in place after welding
Joint type 3	Single-welded butt joints without backing strip
Joint type 4	Double full fillet lap joint
Joint type 5	Single full fillet lap joints with plug welds
Joint type 6	Single full fillet lap joint without plug welds

of a pressure vessel for the purpose of determining the minimum thickness of the various pressure-retaining components of the vessel. Since a heat exchanger is made of two different pressure zones—tubeside and shellside—at least two design pressures shall be defined. ASME Code encourages (UG-21) that the design pressure be higher than the normal operating pressure with a suitable safe margin to allow for probable pressure surges in the vessel up to the setting of pressure relief valves (UG-134). When vessels are subjected to inside vacuum and external positive pressure on the outside, then the maximum difference between the inside and outside of the vessel shall be taken into account.

11.3.9.2 Design Temperature

This is the temperature stamped on the nameplate along with the design pressure. This temperature shall not be less than the mean metal temperature expected across the thickness, under the operating conditions for the parts under consideration (UG-20). Design temperature can be different for the different pressure parts if the operating conditions ensure a defined temperature variation [40]. For example, in a multipass shell and tube heat exchanger in which there is an appreciable temperature drop or rise on the tubeside, the inlet headers and outlet headers can have different design temperatures. In no case shall the design temperature exceed the temperature corresponding to the code allowable stress for the material used in the thickness calculations or the allowable working temperature for the material specified in the code.

11.3.9.3 Maximum Allowable Working Pressure

The maximum allowable working pressure (MAWP) is the gauge pressure for a specified operating temperature that is permitted for the vessel in operation, such that, together with any other likely loadings other than pressure, the stresses computed using code formulas do not exceed the code allowable stress values. Metal thickness specified as corrosion allowance is not considered for the calculation of thickness. It is the basis for the pressure setting of the pressure-relieving devices that protect the vessel. The MAWP is normally specified for two conditions—new (uncorroded) and old (corroded).

11.3.9.4 Operating Temperature or Working Temperature

As per ASME Code, this is defined as the temperature that will be maintained in the metal of the part of the vessel being considered for the specified operation of the vessel.

11.3.9.5 Operating Pressure or Working Pressure

As per ASME Code, this is defined as the pressure at the top of the vessel at which it normally operates. It shall not exceed the MAWP, and it is kept at a suitable level below the setting of the pressure-relieving devices to prevent their frequent opening.

11.4 TUBESHEET DESIGN

11.4.1 FUNDAMENTALS

A tubesheet is an important component of a heat exchanger. It is the principal barrier between the shellside and tubeside pressures. The cost of drilling and reaming the tube holes as well as the overall cost of the tubesheet of a given dimension will have direct bearing on the heat exchanger cost. Additionally, proper design of a tubesheet is important for safe and reliable operation of the heat exchanger. In this section, fundamentals of tubesheet design such as classification of tubesheets and constructional features are discussed.

11.4.1.1 Tubesheet Connection with the Shell and Channel

Tubesheets are mostly flat circular plates with uniform pattern of drilled holes. Tubesheets of surface condensers are rectangular in shape. The tubesheet is connected to the shell and the channel either by welding (integral) or bolts (gasketed joints) or a combination thereof. Six possible types of tubesheet connection with the shell and channel are given hereunder:

1. Tubesheet integral with shell and channel (Figure 11.2a)
2. Tubesheet integral with shell and gasketed with channel, extended as a flange (Figure 11.2b)
3. Tubesheet integral with shell and gasketed with channel, not extended as a flange (Figure 11.2c)
4. Both shellside and tubeside gasketed construction (Figure 11.2d)
5. Tubesheet gasketed on shellside and integral with channel, extended as a flange (Figure 11.2e)
6. Shellside gasketed and tubeside integral construction, not extended as a flange (Figure 11.2f)

11.4.1.2 Supported Tubesheet and Unsupported Tubesheet

Heat exchanger tubes other than a U-tube heat exchanger may be considered to act as stays that support or contribute to the strength of the tubesheets in which they are attached. In the case of fixed and floating head heat exchangers, the tube bundle behaves like an elastic foundation. However, the floating nature of one of the tubesheets makes the staying action partial. This is especially true for an outside packed floating-type heat exchanger. In the case of U-tube heat exchangers, tubes provide only a reactive bending moment to the tubesheet bending. According to the level of support provided by the tubes, TEMA classifies the tubesheets as (1) supported tubesheet and (2) unsupported tubesheet; examples are as follows:

1. Unsupported tubesheets, e.g., U-tube tubesheets
2. Supported tubesheets, e.g., fixed tubesheets and floating tubesheets

11.4.1.3 Tubesheet Thickness

Being a plate-type structure, the tubesheet resists the lateral pressure by bending, and the membrane loads are negligible. Hence, the limiting stress is the primary bending stress only. The factors that control the tubesheet thickness are the following:

1. Tube pitch and layout pattern, which define the ligament efficiency of perforated tubesheets.
2. The manner in which the deformation of tubesheet is influenced by the support being provided by the tube bundle to the tubesheets. For the same process conditions and tubesheet diameter, tubesheet thickness decreases in the order of the following exchanger types:
 - a. U-tube heat exchanger
 - b. Floating head exchanger
 - c. Fixed tubesheet exchanger

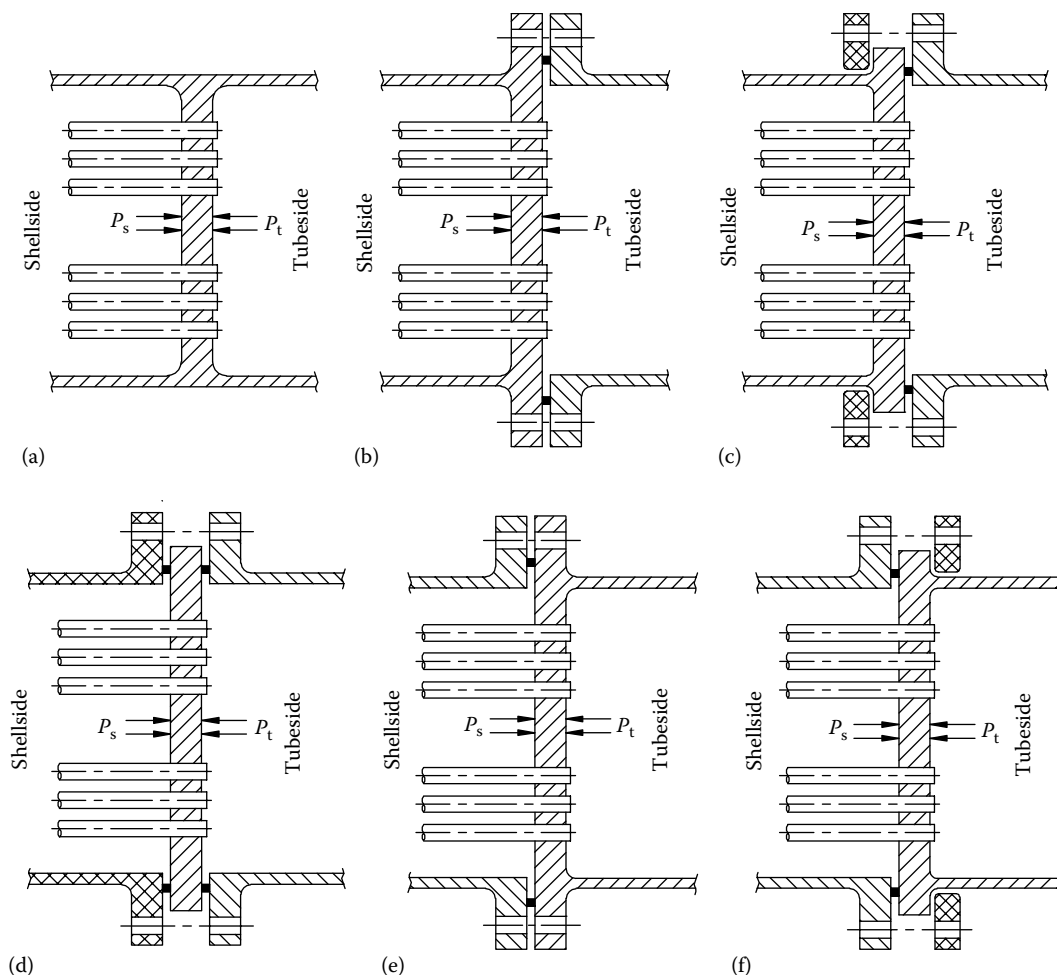


FIGURE 11.2 Six possible connections of tubesheet with shell and channel. (a) Tubesheet integral with shell and channel, (b) tubesheet integral with shell and gasketed with channel, extended as a flange, (c) tubesheet integral with shell and gasketed with channel, not extended as a flange, (d) tubesheet both shellside and tube-side gasketed construction, not extended as a flange (e) tubesheet gasketed on shellside and integral with channel, extended as a flange, and (f) tubesheet shellside gasketed and tubeside integral construction, not extended as a flange.

3. Mean metal temperatures of tubesheet, tube, and shell.
4. Number of tubes.
5. Limits of the tube field and the extent of untubed portion.
6. Method of joining the tubes to the tubesheets, e.g., rolled, seal welded, or strength welded.
7. Shell and the channel connection with the tubesheets, e.g., gasketed and integral.
8. Shell and the channel thickness.

11.4.1.4 Tubesheet Design Procedure: Historical Background

TEMA set up rules for the design of U-tube and floating head heat exchangers in 1941. These rules were simple but do not ensure an overall safety for all heat exchangers. Hence, many researchers [41–72] published papers on tubesheet design and interpreted code rules from 1948 onward.

The codes and standards periodically updated the procedure for tubesheet design as and when better methods were published. In recent years, new tubesheet design procedures have been

incorporated in TEMA, British Standards PD 5500, ASME Section VIII Div. 1, UPV-EN13443, CODAP, and others. Historical background of tubesheet analysis is covered in Ref. [60].

Among the heat exchanger standards and codes, the tubesheet design procedures of the standards of the TEMA have been used successfully for the last 60 years, partly due to simplicity and partly due to satisfactory performance of the heat exchangers designed as per these standards, and during this period, TEMA Standards have been modified several times. TEMA with its seventh edition (1988) revised its original formula by including a term for mean ligament efficiency η in the tubesheet bending formula. The required effective tubesheet thickness for any type of heat exchanger shall be determined for both tubeside and shellside conditions with or without the thermal load, using whichever thickness is greater.

Design procedure for tubesheets varies among the code rules and standards, and hence designers get different thickness for the same design condition due to reasons such as the following:

1. Assumptions that tubesheets are either simply supported or clamped or elastically restrained at its edges
2. Local stresses developed at the shell/tubesheet and channel/tubesheet junction are neither calculated nor required to be limited
3. Failure to consider the effect of untubed annular rim

With this background knowledge, tubesheet design procedure is explained next. First, the assumptions made in various tubesheet design models are discussed, followed by the basis of fixed tubesheet design procedure. Subsequently, the tubesheet design procedure for fixed, floating head, and U-tubesheet procedure included in TEMA is dealt with. Finally, the unified tubesheet formula of ASME Code Section VIII Div. 1, CODAP and UPV is discussed. Design aspects of double tubesheets, rectangular tubesheets, and curved tubesheets are covered at the end.

11.4.1.5 Assumptions in Tubesheet Analysis

While analyzing the tubesheets, certain assumptions are made in their models by many researchers. The tubesheets are treated as thin plates compared to their radial dimension, both circumferential and radial stresses vary linearly through the thickness of the tubesheets, and shear stresses vary parabolically from zero at one face to zero at the other face with a maximum at the center. Other assumptions include the following:

1. The tubesheet is uniformly perforated over its whole area; the unperforated annular rim is not considered by some standards. For example, TEMA Standards do not consider the unperforated tubesheet portion for all classifications of tubesheets.
2. The membrane loads in the tubesheets are negligible as compared to the bending loads [44].
3. No slip occurs at the junction between the tubes and the tubesheet.
4. The tubes are adequately stayed by baffle plates to enable them to stand up to the calculated loads without sagging.
5. The bending moments in the tubes at their attachment with the tubesheet are neglected.
6. The exchanger is axis symmetrical and symmetric about the plane midway between the tubesheets.
7. Modeling of the tube bundle: The tubes are assumed uniformly distributed over the whole tubesheet and in sufficient number (N_t) so as to act as a uniform elastic foundation of modulus K_w . The expression for K_w is

$$K_w = \frac{N_t K_t}{\pi R^2} \quad (11.2a)$$

where K_t represents the axial rigidity of one tube as given by

$$K_t = \frac{\pi E_t t (d - t)}{L} \quad (11.2b)$$

Note: The elastic modulus for a half bundle, k_w , is equal to $2K_w$, and the axial rigidity of one half tube, k_t , is equal to $2K_t$.

8. Modeling of the tubesheet: The perforated tubesheet is replaced by an equivalent solid plate of effective elastic constants E^* and ν^* (the determination of effective elastic constants is discussed separately). The flexural rigidity of the perforated plate D^* , in terms of the flexural rigidity of unperforated plate D and deflection efficiency η , is given by

$$\eta = \frac{D^*}{D} \quad (11.3)$$

where D^* and D are given by

$$D = \frac{ET^3}{12(1 - \nu^2)} \quad \text{and} \quad D^* = \frac{E^*T^3}{12(1 - \nu^{*2})} \quad (11.4)$$

One of the drawbacks of the work of Gardner [42,43] and Miller [44] is the assumption that the Poisson ratio of the perforated tubesheet is the same as that for the unperforated tubesheet; accordingly, a constant value of $\nu^* = 0.3$ was assumed in their treatment.

9. The maximum stress in the perforated plate will be the maximum stress in the homogeneous plate divided by the ligament efficiency, μ .
10. The analysis is based on the optimum design of tubesheets within their elastic behavior of all components attached to the tubesheet. If the temperatures are high enough, creep becomes of primary importance [47].
11. The deflection of the tubesheet is small, and hence the angular distortion of the tube ends due to the bending of the tubesheet can be neglected.
12. The effect of rotational resistance of the tubes is negligible since it is minor in nature.
13. Boundary restraint and parameters X and Z .

Tubesheets are weakened due to drilling holes, whereas they are stiffened by the tube bundle and tubesheet edge restraint offered by the shell and the channel connected with the tubesheet by welding. Based on the tubesheet connection with the shell and the channel, the edge-restraint condition is treated as simply supported, clamped, and an intermediate case. The stresses induced in the shell, channel, and tubesheet depend on a dimensionless parameter, X (which is equal to the ratio of the axial tube bundle rigidity to the bending rigidity of the tubesheet) that accounts for the support afforded by the tube bundle to the tubesheet and the perforations that weaken it. It may vary from almost zero as in U-tube heat exchanger to about 50 (very stiff tube bundle as compared to the tubesheet). Common values generally lie between 2 and 8. A second parameter Z , which represents the degree of rotational restraint of the tubesheet by the shell and channel, is also important. However, the complication of the combined effects of discontinuity stresses due to shellside and tubeside pressures and differential thermal expansion between the shell and the tube bundle, and the tubesheet and the channel head, makes the determination of boundary restraint an uncertain factor in the estimation of

the tubesheet stresses, Gardner [43]. In view of these factors, Gardner [43] suggests that the designer be guided by judgment and experience in determining the relative fixity of the tubesheet periphery as between the simply supported and the clamped. According to Miller [44], the boundary restraints may be treated as (1) a simply supported case, (2) a clamped case, and (3) the intermediate to these two cases. The examples suggested by Miller for these cases are the following:

- a. Simply supported case: a narrow joint face or trapped ring gasket.
- b. Clamped case, e.g., full-face gasketed joint.

Hence in codes and standards, a parameter, F is introduced in all the tubesheet thickness calculation formulas to take into account the boundary restraint condition, viz., the connection of shell and channel with the tubesheet.

14. *Treatment of boundary restraint and perforation in tubesheet in TEMA Standards.*

In the seventh edition of TEMA [3], the weakening effect of the tube hole drilling is taken into account by including the mean ligament efficiency term η in the tubesheet bending formula. However, the tubesheet edge restraint offered by the shell and the channel connection with the tubesheet is not taken care of adequately. As in the earlier editions, the F -factor used to account for the simply supported condition, fixed (clamped) condition, and intermediate condition is retained. Due to this reason, the TEMA formula is not safe for all sizes and all operating pressures, Osweller [61,64]. This is especially true for large units with high operating pressures. For certain values of the parameter X (used to represent the relative rigidity of the tube bundle with respect to the tubesheet), the TEMA formula is safe, but for lower values, it is not adequate and hence unsafe. The TEMA fixed tubesheet formula is compared with CODAP by Osweiller [61,64]. TEMA F -factor is further compared with F -factor of ASME, CODAP, and UPV CODES in the later section.

15. *Effective elastic constants of perforated plates:* While designing the perforated tubesheets, the weakening effect due to the tube hole perforations has been taken into account by replacing the plate by an equivalent solid plate with new elastic constants known as the effective Young's modulus, E^* , and effective Poisson's ratio, ν^* . The values of E^* and ν^* are such that the equivalent plate has the same deflection as that of the original unperforated plate. This is known as the equivalent solid plate concept. The equivalent solid plate concept has been found to be quite useful in the design and analysis of perforated plates by equating strains in the equivalent solid material to the average strains in the perforated material [67]. These effective elastic constants must be evaluated correctly, especially in fixed tubesheet heat exchangers [68]. If they are too low, the stresses at the junction with the shell and the head will be lower than that in real units. If they are too high, the stress at the center of the plate, which may be a maximum, will be too low.

16. *Determination of effective elastic constants:* The effective elastic constants depend on the pattern, size, and pitch of the perforations. During the last two decades, many researchers have proposed theoretical and experimental methods to determine the effective elastic constants. However, there are disparities in the values obtained by these methods. Modern pressure vessel codes such as ASME, CODAP, and UPV present curves to determine effective elastic constants. TEMA does not determine the effective elastic constants. It assumes a constant value of 0.178 for deflection efficiency. An excellent review of about 60 papers on the elastic constants was done by Osweiller [68]. Osweiller proposed curves for the determination of effective elastic constants that have been adopted in CODAP.

17. *Ligament efficiency:* The ligament efficiency is a very useful dimensionless parameter for the analysis of perforated plates. The ligament efficiency, defined in terms of the tube layout pattern and pitch ratio in TEMA, is known as mean ligament efficiency, η (Figure 11.3), and in terms of pitch ratio is known as minimum ligament efficiency, μ in codes such as

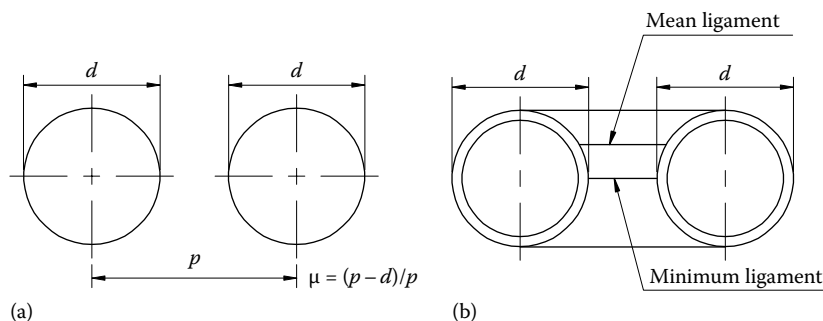


FIGURE 11.3 Minimum ligament width definition.

CODAP (Figure 11.3) and ligament efficiency in ASME Code Section VIII, Div. 1. The general expression for ligament efficiency is

$$\mu = \frac{p - d}{p} \quad (11.5)$$

where

d is the tube outer diameter

p is the tube pitch

$p - d$ is the minimum ligament width

The effect of ligament efficiency in the calculations of tubesheet thickness and tube-to-tubesheet joint strength is discussed in the later section.

11.4.2 BASIS OF TUBESHEET DESIGN

The basis of tubesheet design procedure is discussed here. This discussion closely follows the method of Galletly [47] and Ref. [58], which was further expanded by Osweiler [61,64] for inclusion in CODAP.

11.4.2.1 Analytical Treatment of Tubesheets

The analytical treatment has the same basis in UPV, CODAP, and ASME rules and has been widely presented in papers, Soler [58] and Osweiler [61,64]. The same is summarized later (see Figure 11.4):

1. Thin circular plate on elastic foundation. Most tubesheet design analysis treats the tubesheet as a thin circular plate on an elastic foundation. The elastic foundation is provided by the tube bundle.
2. The tubesheet is disconnected from the shell and channel. A shear force V_E and a moment M_E are applied at the tubesheet edge as shown in Figure 11.4b.
3. The perforated tubesheet is treated as a solid equivalent circular plate of effective elastic constants E^* (effective modulus of elasticity) and ν^* (effective Poisson's ratio) depending on the ligament efficiency μ^* of the tubesheet.
4. The tubes are replaced by an equivalent elastic foundation of modulus k_w . In U-tube heat exchangers, the tubes do not act as an elastic foundation and hence $k_w = 0$.
5. Classical thin plate theory is applied to this equivalent tubesheet to determine the maximum stresses in the tubesheet, tubes, shell, and channel.
6. The maximum stresses are limited to a set of maximum allowable stresses derived from the concept of primary and secondary stresses, based on stress analysis of ASME Code Section VIII, Div. 2 Appendix 4 [16] or UPV-EN 13445 Part 3 Appendix C [30] as the case may be.
7. Tubesheet parameters.

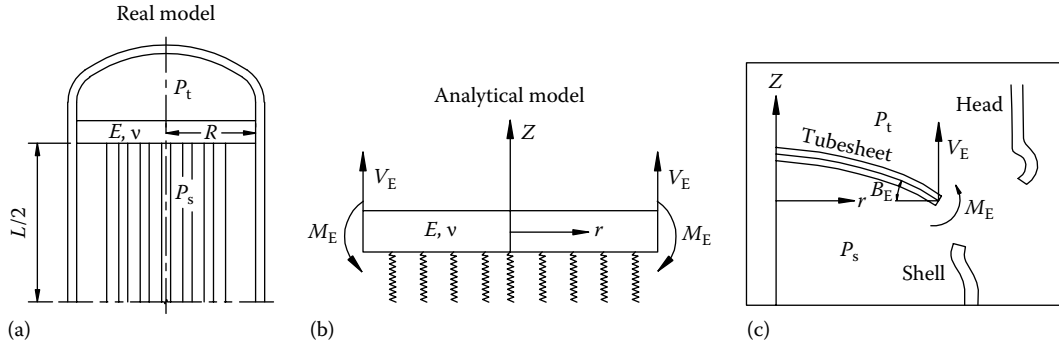


FIGURE 11.4 Basis of tubesheet analysis. (a) Half heat exchanger, (b) circular plate on an elastic foundation, and (c) force and moment at the tubesheet edge. (From Osweiller, F., *ASME J. Press. Vessel Technol.*, 114, 124–131, 1992.)

The analytical aspect is based on the following terms:

a. *Ligament efficiency, μ^**

ASME ligament efficiency μ^* has been adopted by UPV. It accounts for an untubed diametral lane of width U_L (through the effective tube pitch p^*) and for the degree of tube expansion ρ (through the effective tube diameter d^*). UPV has improved this concept by proposing a more general formula for p^* , which accounts for more than one untubed lane.

b. *Effective elastic constants E^* and ν^**

CODAP and UPV effective elastic constants E^* and ν^* given by curves as a function of μ^* have been adopted by ASME.

c. *Local thickening of the shell*

When the tubesheet is integral with the shell, the UPV method allows thickening of the shell at its connection to the tubesheet when the bending stress in the shell exceeds the allowable limit. This is also an efficient mean of reducing the tubesheet thickness significantly, even if the shell is not overstressed.

d. *Parameters X and Z*

11.4.2.2 Design Analysis

The heat exchanger is assumed to be of revolution and symmetrical about a plane midway between the tubesheets, so as to analyze a half exchanger as shown in Figure 11.4a. Figure 11.4b shows a circular plate of thickness T resting on an elastic foundation. To minimize the complexity, the untubed tubesheet portion is neglected, and the tubesheet is integral with both the shell and the channel. The tubesheet is disconnected from the remainder of the exchanger, i.e., from shell and channel. The plate is elastically restrained against deflection and rotation around its periphery, θ_c by (1) an axial reaction V_E due to the end load acting on the head and to the axial displacement Δ_s of the half shell, and (2) a reactive bending moment M_E ($-K_\theta \theta_c$) as shown schematically in Figure 11.4c. The plate is subjected to a uniform net effective pressure $q(r)$ given by [46,47,60]

$$q(r) = p_s f_s - p_t f_t - v_t \left[\frac{N_t}{R^2} \frac{(p_t - p_s)(d - t)^2}{2} \right] + 2v_s p_s Q - k_w \left[w(r) - \frac{\gamma}{2} + \Delta_s \right] \quad (11.6)$$

In the expression for $q(r)$, the first term takes into account the differential pressure acting on the equivalent plate, which is corrected for the tube hole areas by the shellside drilling coefficient, f_s , and tubeside drilling coefficient, f_t , respectively; the second and third terms take into account the loads resulting from the axial displacements of tubes and shell by the Poisson effect of shellside pressure, p_s , and tubeside pressure, p_t , respectively (Q is the ratio of rigidity of tube bundle to the shell); and the fourth term traduces the reactive effect of the elastic foundation. In this, the term $w(r)$ is the deflection of the plate at a distance r from the center axis, and $\gamma/2$ is the differential thermal expansion between the tubes and the shell, which is given for the half exchanger by

$$\frac{\gamma}{2} = \left[\alpha_t (\theta_t - \theta_{\text{amb}}) - \alpha_s (\theta_s - \theta_{\text{amb}}) \right] \frac{L}{2} \quad (11.7)$$

The expressions for f_s , f_t , and Q are

$$f_s = 1 - \frac{N_t d^2}{4R^2} \quad (11.8)$$

$$f_t = 1 - \frac{N_t (d - 2t)}{4R^2} \quad (11.9)$$

$$Q = \frac{N_t K_t}{K_s} \quad (11.10)$$

$$= \frac{1}{K} \quad (11.11)$$

where K is the ratio of axial rigidity of the shell (K_s) to the axial rigidity of the tube bundle ($N_t K_t$). The parameter K signifies the ratio of the force required to produce a given strain in the shell to the force necessary to produce the same strain in the tube bundle. It is thus the measure of the ability of the shell to resist movement of the two tubesheets relative to the tube bundle [41]. However, when there is a considerable thermal expansion between the shell and the tube bundle, the high rigidity of the shell may induce very high thermal stresses in the tube bundle and the shell. This ability is reduced by the introduction of an expansion joint into the shell. An externally packed floating head exchanger for purposes of tubesheet design is considered as a perfect expansion joint, and for exchangers so constructed, the value of K is zero. The expression for the axial rigidity of the shell K_s is given by

$$K_s = \frac{\pi t_s (D_o - t_s) E_s}{L} \quad (11.12)$$

From the expression for K_t (Equation 11.2) and K_s (Equation 11.12), the resulting expression for K is given by

$$K = \frac{E_s t_s (D_o - t_s)}{E_t N_t t (d - t)} \quad (11.13)$$

where D_o is the shell outside diameter. The expression for axial rigidity of the half shell, k_s , is equal to $2K_s$, and axial rigidity of the half tube, k_t , is equal to $2K_t$.

11.4.2.2.1 Deflection, Slope, and Bending Moment

From classical thin-plate theory, the deflection of a solid circular plate of elastic constants E^* , ν^* , and flexural rigidity D^* resting on elastic foundation k_w , subjected to net effective pressure $q(r)$ and elastically restrained at its periphery, is given by

$$\frac{d^4 w}{dr^4} + \frac{2}{r} \frac{d^3 w}{dr^3} - \frac{1}{r^2} \frac{d^2 w}{dr^2} + \frac{1}{r^3} \frac{dw}{dr} = \frac{q(r)}{D^*} \quad (11.14)$$

The solution of this equation is of the form

$$w(r) = A\text{Ber}(x) + B\text{Bei}(x) + \frac{P^*}{k_w} - \Delta_s + \frac{\gamma}{2} \quad (11.15)$$

Deflection, slope, and bending moment

$$p^* = p_s f_s - p_t f_t - \nu_t \left[\frac{N_t}{R^2} \frac{(p_t - p_s)(d-t)^2}{2} \right] + 2\nu_s p_s Q \quad (11.16)$$

$$x = kr = \sqrt[4]{\frac{k_w}{D^*}} r \quad (11.17)$$

In Equation 11.15, $\text{Ber}(x)$ and $\text{Bei}(x)$ are the modified Bessel functions of the first kind, and A and B are unknown constants.

At the periphery of the tubesheet (i.e., $r = R$), x becomes X . It represents the relative rigidity of the tube bundle with respect to the tubesheet. It may vary from 0 (no tube in the bundle) to above 50 for very stiff tube bundle. The expression for X is as follows:

$$X = kR = \sqrt[4]{\frac{k_w}{D^*}} R \quad (11.18)$$

$$= \sqrt[4]{\frac{\pi N_t E_t t (d-t)}{\pi R^2 L / 2} \frac{12(1-\nu^{*2}) R^4}{E^* T^3}} \quad (11.19)$$

Substituting for $N_t E_t (d-t)$ by $E_s t_s (D_o - t_s)/K$ and for $E^*/(1-\nu^{*2})$ by $\eta E/(1-\nu^2)$ and $D_o - t_s \approx 2R$, X becomes

$$X = \sqrt[4]{\frac{24 E_s t_s (D_o - t_s)}{KL} \frac{R^2 (1-\nu^2)}{\eta E}} \quad (11.20a)$$

$$= \sqrt[4]{\frac{6(1-\nu^2)}{\eta} \frac{E_s t_s}{KLE} \left(\frac{2R}{T} \right)^3} \quad (11.20b)$$

From $w(r)$, one may determine the shear forces, the bending moment, and the slope at any point in the tubesheet. By employing the Kirchoffs–Kelvin equation, the expressions for slope, dw/dr , and bending moment, M , are given by

$$\theta = \frac{dw}{dr} \quad (11.21)$$

$$M = D^* \left(\frac{d^2 w}{dr^2} + \frac{\nu^*}{r} \frac{dw}{dr} \right) \quad (11.22)$$

The two constants of integration A and B and the axial displacement of the half shell, Δ_s , are determined by the following three boundary conditions:

1. At $r = R$, the deflection $w(r)$ at the edge of the plate due to bending is zero.
2. At $r = R$, the radial bending moment at the edge of the plate equals the moment exerted by the rotational spring, i.e.,

$$D^* \left(\frac{d^2 w}{dr^2} + \frac{\nu^*}{r} \frac{dw}{dr} \right) \Big|_{r=R} = -K_\theta \frac{dw}{dr} \Big|_{r=R} \quad (11.23)$$

where K_θ is the spring constant for half shell. Its value is the sum of the bending rigidities of the shell and the channel.

3. The vertical force at the edge, V_E , is given by the net effective force acting on the plate in terms of net effective pressure $q(r)$:

$$2\pi \int_0^R q(r) dr = 2\pi R V_E \quad (11.24a)$$

where

$$V_E = \frac{\pi R^2 p_t - k_s \Delta_s}{2\pi R} \quad (11.24b)$$

11.4.2.2.2 Parameter Z

Though the parameter Z is not figuring in the earlier relations, it is required to find equivalent pressure in CODAP and other rules. The expression for Z [47,60] is given by

$$Z = \frac{K_\theta}{kD^*} = \frac{K_\theta}{\sqrt[4]{k_w D^{*3}}} \quad (11.25)$$

where K_θ is the edge moment coefficient. It depends on the bending rigidities of the shell (δ_s) and the channel (δ_c). It represents the degree of elastic restraint of the tubesheet offered to it by the shell and the channel connected to it. Its value varies between the two extreme values: 0, which corresponds to the simply supported case, and ∞ , which corresponds to the clamped case.

$$K_{\theta} = 2[\delta_s + \delta_c]$$

$$K_{\theta} = 2 \left[\frac{E_s t_s^{2.5}}{[12(1-\nu^2)]^{0.75} (D_s + t_s)^{0.5}} + \frac{E_c t_c^{2.5}}{[12(1-\nu^2)]^{0.75} (D_c + t_c)^{0.5}} \right] \quad (11.26)$$

11.4.3 TUBESHEET DESIGN AS PER TEMA STANDARDS

Design loading cases: TEMA considers the following seven loading cases:

1. Tubeside pressure acting only, without thermal expansion
2. Shellside pressure acting only, without thermal expansion
3. Tubeside and shellside pressures acting simultaneously, without thermal expansion
4. Thermal expansion acting alone
5. Tubeside pressure acting only, with thermal expansion
6. Shellside pressure acting only, with thermal expansion
7. Tubeside and shellside pressures acting simultaneously, with thermal expansion

11.4.3.1 Tubesheet Formula for Bending

As per RCB-7.131, the formula for minimum tubesheet thickness to resist bending is given by

$$T = \frac{FG}{3} \sqrt{\frac{P}{\eta S}} \quad (11.27)$$

where

F is the parameter used to account for the elastic restraint at the edge of the tubesheet due to shell and channel connections

G is the diameter over which the pressure is acting

P is the effective design pressure

S is the ASME Code allowable stress

η is the mean ligament efficiency (it depends on the mean width of the ligament), given in terms of tube layout pattern angle θ and pitch ratio p/d whose expression is given by

$$\eta = 1 - \frac{\pi}{4(\sin \theta)(p/d)^2}$$

$$= 1 - \frac{0.785}{(p/d)^2} \quad \text{for } \theta = 90^\circ \quad \text{and} \quad 45^\circ$$

$$= 1 - \frac{0.907}{(p/d)^2} \quad \text{for } \theta = 60^\circ \quad \text{and} \quad 30^\circ \quad (11.28)$$

The minimum values of η are 0.42 (triangular pitch) and 0.50 (square pitch); therefore, for a given value of ligament efficiency, the tubesheet thickness is lower for square pitch than for triangular pitch. But in real cases, η will generally range between 0.45 and 0.60, which leads to a decrease of T by about 10%–15%. TEMA ligament efficiency η is significantly higher than ASME ligament efficiency μ^* (generally $0.25 \leq \mu^* \leq 0.35$). ASME ligament efficiency μ^* is based on the minimum width of the ligament, which leads to lower values than TEMA. For these reasons, tubesheet thickness obtained by ASME is generally thicker than TEMA, Osweiller [61].

The values of F , P , and G differ for supported and unsupported tubesheets. For a fixed tubesheet exchanger, G shall be the shell inside diameter. For other types of exchangers, refer to TEMA for the definition of G . For a fixed tubesheet exchanger, the effective design pressure, P , shall be calculated as per Sections RCB-7.163, RCB-7.164, and RCB-7.165. The definition of F for supported and unsupported tubesheets is discussed next. For all types of tubesheets, the thickness shall be calculated both for uncorroded and for corroded conditions.

11.4.3.2 Parameter F

1. Supported tubesheet

Gasketed both sides, e.g., stationary tubesheet and floating tubesheet and floating head exchanger:

$$F = 1.0$$

2. Clamped or integral tubesheet

Integral on both sides or a single side, e.g., stationary tubesheet of fixed tubesheet exchanger and floating head exchanger: When the tubesheet is integral with both sides or a single side, F is determined by curve H in Fig. RCB-7.132. The curve is presented in terms of the ratio of wall thickness to internal diameter (ID) of the shell or channel, i.e., (t/ID) , whichever yields the smaller value of F . For the shellside integral condition, use the shell ID to find F . The H curve can be represented by

$$\begin{aligned} F &= 1.0 \quad \text{for} \quad \frac{t}{ID} \leq 0.02 \\ &= \frac{17 - 100(t/ID)}{12} \quad \text{for} \quad 0.05 \geq \frac{t}{ID} > 0.02 \\ &= 0.8 \quad \text{for} \quad \frac{t}{ID} > 0.05 \end{aligned} \quad (11.29)$$

As per this condition, the minimum value of F is 0.8 and the maximum value is 1.0.

Both the tubesheets of the fixed tubesheet exchanger are satisfied by this condition, and both the tubesheets shall have the same thickness, unless the provisions of RCB-7.166 are satisfied.

Note: The F value for the tubesheet at the floating head for all configurations is 1.0. *Unsupported tubesheet, for example, U-tubesheet*

1. When gasketed at both sides, $F = 1.25$.

2. For tubesheets integral on both sides or a single side, F shall be determined by curve U in Fig. RCB-7.132. The curve is presented in terms of the ratio of wall thickness to ID of the integral side, i.e., (t/ID) . The U curve can be represented by

$$\begin{aligned} F &= 1.25 \quad \text{for} \quad \frac{t}{ID} \leq 0.02 \\ &= \frac{17 - 100(t/ID)}{15} \quad \text{for} \quad 0.05 \geq \frac{t}{ID} > 0.02 \\ &= 1.0 \quad \text{for} \quad \frac{t}{ID} > 0.05 \end{aligned} \quad (11.30)$$

As per this condition, the maximum value of F is 1.25 and the minimum value is 1.0.

Effective Design Pressure: The term P is the effective design pressure where $P = p_s + p_b$ or $p_t + p_b$; p_b is defined as equivalent bolting pressure when the tubesheet is extended as a flange. The expression for p_b is given by

$$p_b = \frac{-6.2M^*}{F^2G^3} \quad (11.31)$$

where M^* is defined in Paragraph RCB-7.1342. Expression for M^* is furnished in the section on 3.6 flanged tubesheet—TEMA design procedure.

11.4.3.3 Shear Formula RCB-7.133

The effective tubesheet thickness T to resist shear is given by

$$T = \frac{0.31D_e}{(1-d/p)} \frac{P}{S} \quad (11.32)$$

where

D_e is the equivalent diameter of the perforated tubesheet ($4A_p/C$)

C is the perimeter of the tube layout measured stepwise in increments of one tube pitch from center to center of the outermost tubes (Figure 11.5 shows the application to typical triangular and square tube patterns; only a portion is shown)

A_p is the total area enclosed by the perimeter C

The shear stress formula was derived by limiting the maximum allowable shear stress to 0.8 times the code allowable stress S . The shear formula controls the tubesheet thickness only in high-pressure and small-diameter cases. Since the quantities C and A_p are available after the tube layout is finalized, TEMA provides a formula to check whether shear stress will be controlling the tubesheet thickness or not. Shear formula will not control the tubesheet thickness if

$$\frac{P}{S} < 1.6 \left(1 - \frac{d}{p} \right)^2 \quad (11.33)$$

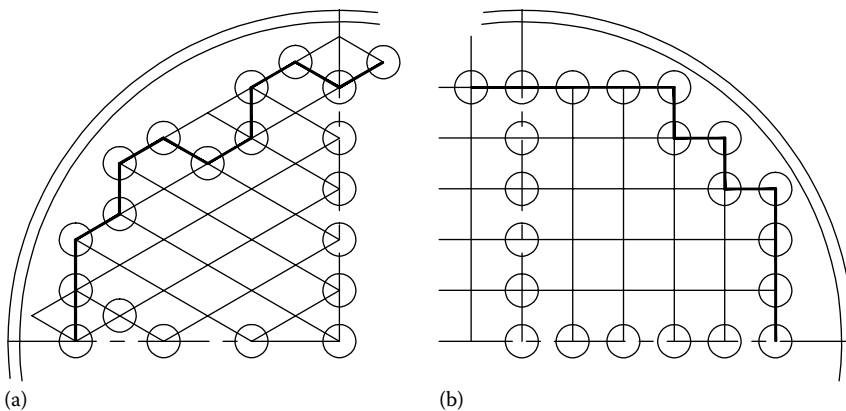


FIGURE 11.5 Perimeter of tube layout for shear stress calculation as per TEMA method. (a) Triangular layout and (b) square layout.

11.4.3.4 Stress Category Concept in TEMA Formula

The primary stress in the tubesheet is limited to ASME Code Section VIII, Div. 1, allowable stress S , and the primary stress plus the thermal stress (secondary stress) is limited to $2S$. Accordingly, the expression for effective pressure is halved before being used in the thickness formula.

11.4.3.5 Determination of Effective Design Pressure, P (RCB-7.16)

The determination of (1) effective shellside design pressure involves the terms p'_s , equivalent differential expansion pressure p_d , and equivalent bolting pressure (p_{bs} and/or p_{bt}) and (2) effective tubeside design pressure involves p'_t , p_d , and p_{bs} , and/or p_{bt} . The expressions for p_d equivalent bolting pressure (p_{bs} , p_{bt}), p'_s , and p'_t are given next.

11.4.3.6 Equivalent Differential Expansion Pressure, p_d (RCB 7.161)

The equivalent differential expansion pressure, p_d , is given by [63]

$$p_d = \frac{4Jt_s E_s [\alpha_s (\theta_s - \theta_{amb}) - \alpha_t (\theta_t - \theta_{amb})] (D_o - t_s) (D_o - 2t_s)^2}{1 + JK F_q} \quad (11.34)$$

where D_o is the shell outer diameter, F_q a parameter that is a function of X (G_4 of Miller [44] and H_4 of Galletly [46,47]),

$$\theta_l = \theta_{l,m} - \theta_{amb}$$

$$\theta_s = \theta_{s,m} - \theta_{amb}$$

and where J is the expansion joint flexibility parameter ($=1.0$ for shells without expansion joint).

The expressions for J and F_q and the final expression for p_d follow.

1. The expansion joint flexibility parameter J is given by

$$J = \frac{1}{1 + (K_s/S_j)} \quad (11.35)$$

Substituting the expression for K_s , J is given by

$$J = \frac{S_j L}{S_j L + \pi (D_o - t_s) E_s t_s} \quad (11.36)$$

J can be assumed equal to zero for a shell with expansion joints if the following condition is satisfied:

$$S_j < \frac{(D_o - t_s) t_s E_s}{10L} \quad (11.37)$$

where S_j is the spring rate of the expansion joint.

2. From Osweiller [63], the expression for F_q in terms of X is given by

$$F_q = 0.25 + \alpha X \quad (11.38)$$

where α is a function of the tubesheet correction factor F . By substituting the expression for α , the resulting expression for F_q is given by

$$\alpha = (F - 0.6) \frac{\sqrt{2}}{0.8} \quad (11.39)$$

$$\therefore F_q = 0.25 + (F - 0.6) \frac{\sqrt{2}}{0.8} \left[\frac{6(1 - \nu^2)}{\eta} \frac{E_s t_s}{KLE} \left(\frac{G}{T} \right)^3 \right]^{0.25} \quad (11.40)$$

By assuming that the tubesheet deflection efficiency η is 0.178 and ν is 0.3, we get an expression for F_q similar to the TEMA form:

$$F_q = 0.25 + (F - 0.6) \sqrt[4]{\frac{300 E_s t_s}{KTE} \left(\frac{G}{T} \right)^3} \quad (11.41)$$

where G is the shell inside diameter ($2R$, where R is the shell inside radius). Note: use the calculated value of F_q or 1.0 whichever is greater. By approximating

$$\frac{D_o - t_s}{(D_o - 2t_s)^2} \approx \frac{1}{(D_o - 3t_s)} \quad (11.42)$$

and replacing $\alpha_s(\theta_s - \theta_{amb})$ and $\alpha_t(\theta_t - \theta_{amb})$ by $\Delta L/L$, the expression for p_d is given by

$$p_d = \frac{4JE_s t_s (\Delta L / L)}{(D_o - 3t_s)(1 + JFKF_q)} \quad (11.43)$$

where ΔL is the differential thermal expansion between the shell and the tube bundle.

Equivalent bolting pressure (RCB 7-162): When the tubesheet is extended as a flange for bolting to head or channel with a ring-type gasket, the effect of the flange moment acting upon the tubesheet is accounted for in effective design pressure in terms of equivalent tubeside bolting pressure, p_{bt} , and equivalent shellside bolting pressure, p_{bs} , as given by

$$p_{bt} = \frac{6.2M_1}{F^2 G^3} \quad (11.44a)$$

$$p_{bs} = \frac{6.2M_2}{F^2 G^3} \quad (11.44b)$$

where

M_1 is the bolting moment acting under the operating condition, as defined by the ASME Code as M_o under flange design

M_2 is the bolting moment acting under the gasket seating condition, as defined by the ASME Code as M_o under flange design

G is the inside diameter of the shell

Expression for p'_s . The expression for p'_s is given by [63]

$$p'_s = \frac{p_s \left[JK [2v_t + f_s(1 - 2v_t)] + 2v_s J - ((1 - J)/2) \left((D_j^2 - G^2)/G^2 \right) \right]}{1 + JK F_q} \quad (11.45)$$

By substituting $v_s = v_t = 0.3$, and rearranging the terms, p'_s is given in TEMA form:

$$p'_s = \frac{p_s \left[0.4J [1.5 + K(1.5 + f_s)] - ((1 - J)/2) \left((D_j^2/G^2) - 1 \right) \right]}{1 + JK F_q} \quad \text{for } v_s = v_t = 0.3 \quad (11.46)$$

Expression for P'_t . The expression for P'_t is given by [63]

$$p'_t = \frac{p_t \left[1 + JK \{ f_t + 2v_t(1 - f_t) \} \right]}{1 + JK F_q} \quad (11.47)$$

$$= \frac{p_t [1 + 0.4 JK(1.5 + f_t)]}{1 + JK F_q} \quad (\text{for } v_t = 0.3) \quad (11.48)$$

where

- D_j is the expansion joint diameter
- G is the inside diameter of the shell
- p_{bt} is the equivalent bolting pressure when tubeside pressure is acting
- p_s is the shellside design pressure
- p_t is the tubeside design pressure

11.4.3.7 Differential Pressure Design, after Yokell [23]

In differential pressure design, the pressure parts exposed to both fluids are designed for the difference in operating pressures between the two fluids, i.e., simultaneous action of both the shellside and tubeside pressures. Differential pressure design is seldom used when the simultaneous design pressures are less than 1000 psi (6895 kPa). The operating circumstances that favor differential pressure design are

1. A common source of supply of the shellside and tubeside fluids
2. Shellside and tubeside operating pressures in the range of 1000 psi (6895 kPa) and above, when the pressure in one side is directly controlled by the other
3. High pressure on both sides in which the differential pressure can be measured and controlled

11.4.3.7.1 Merits of Differential Pressure Design

Differential pressure design reduces the tubesheet thickness below what would be required for conventional design. However, this design involves certain safety and protection devices to be incorporated into the system, in the event of failure on one side [23]. To justify this design, the reduction in capital cost due to thin tubesheet and the associated machining cost savings must exceed any operating cost associated with differential pressure design and safety devices to be provided. TEMA and BS 5500 recognize differential pressure design when it is mutually agreed between the purchaser and the seller.

11.4.3.7.2 Effective Differential Design Pressure, P (RCB 7.165)

For differential pressure design, the effective differential design pressure is calculated as per RCB 7.165. For practical use, TEMA considers the seven combined design loading cases where pressure acts on the shellside ($p_t = 0$), on the tubeside ($p_s = 0$), on both sides, and in each case with and without thermal expansion; the seventh case is obtained for thermal expansion acting alone ($p_s = 0$ and $p_t = 0$).

11.4.3.8 Longitudinal Stress Induced in the Shell and Tube Bundle

After arriving at the tubesheet thickness, it is necessary to determine the stresses induced in the shell, channel, and tubes located at the periphery and interior of the tube bundle in the case of fixed and floating tubesheet exchangers. The check for longitudinal stress induced in the shell is calculated as per RCB-7.22. However, there is no procedure in TEMA to calculate the bending stresses induced in the shell and both the longitudinal stress and the bending stress in the channel. The check for tube longitudinal stress both in tension and in compression in the tubes located at the periphery of fixed tubesheet exchangers is calculated as per RCB-7.23 and RCB-7.24, respectively. This is discussed next.

11.4.3.8.1 Shell Longitudinal Stress, $\sigma_{s,l}$ (RCB-7.22)

The maximum longitudinal stress induced in the shell, $\sigma_{s,l}$ is given by

$$\sigma_{s,l} = \frac{p_s^* (D_o - t_s) Z_s}{4t_s} \quad (11.49)$$

Seven loading cases are examined, which lead to seven values of p_s^* . The value of parameter Z_s depends on the stress category concept. Its value is either 0.5 or 1.0; p_s^* is determined as per TEMA definition.

11.4.3.8.2 Longitudinal Stress Induced in the Tubes Located at the Periphery of the Tube Bundle, $\sigma_{t,l}$ (RCB-7.23)

The maximum longitudinal stress induced on the tubes located at the periphery of tube bundle is given by

$$\sigma_{t,l} = \frac{F_q G^2 p_t^* Z_t}{4N_t t (d - t)} \quad (11.50)$$

As for the shell longitudinal stress case, seven loading cases are examined, which lead to seven values of p_t^* . The value of parameter Z_t depends on the stress category concept. Its value is either 0.5 or 1.0; p_t^* is determined as per TEMA definition.

11.4.3.8.3 Longitudinal Stresses inside the Tube Bundle

Although the tubes located at the interior of the bundle can become loaded both in tension and in compression, longitudinal stresses inside the tube bundle are not calculated in TEMA. Tensile forces are generally not a problem if the requirements of RCB-7.22 are met. However, compressive forces might create unstable conditions for tubes at the interior of the bundle. Typical conditions that can cause this are loading and geometry, as follows:

Loading: Tubeside pressure and/or differential thermal expansion where the shell, if unrestrained, would lengthen more than the tubes (positive P_d per RCB-7.161).

Geometry: Flexible tubesheet systems. Generally, those that are simply supported at the edge ($F = 1$) and have a value of F_q greater than 2.5.

Methods similar to those provided in the references cited in TEMA and others such as in Refs. [47,58,60,63] can be used to predict loadings on tubes at the interior of the bundle.

11.4.3.8.4 Compressive Stress Induced in the Tubes Located at the Periphery of the Tube Bundle (RCB 7-24)

The compressive stress acting on the tubes located at the periphery is limited to the allowable compressive stress S_c based on the Euler critical buckling load for a column as given by

$$\sigma_c = \frac{\pi^2 E_t}{F_s (kl/r_G)^2} \quad \text{when } \Lambda \leq \frac{kl}{r_G} \quad (11.51)$$

$$= \frac{S_y}{F_s} \left[1 - \frac{kl/r_G}{2\Lambda} \right] \quad \text{when } \Lambda > \frac{kl}{r_G} \quad (11.52)$$

where

$$\Lambda = \sqrt{\frac{2\pi^2 E_t}{S_y}} \quad (11.53)$$

r_G is the radius of gyration of the tubes,

$$r_G = 0.25 \sqrt{d^2 + (d - 2t)^2} \quad (11.54)$$

where

kl is the equivalent unsupported buckling length of the tube

k is a factor that takes into account the tube span end conditions

l is the unsupported tube span between two baffles

F_s is the factor of safety

11.4.3.8.5 Tube-to-Tubesheet Joint Loads (RCB-7.25)

The maximum effective tube-to-tubesheet joint load, F_j , acting on the tubes located at the periphery of the tube bundle is given by

$$F_j = \frac{\pi F_q p_t^* G^2}{4N_t} \quad (11.55)$$

where p_t^* is determined as per TEMA definition. This joint load is to be less than the maximum allowable joint load calculated as per ASME Code Section VIII, Div. 1.

11.4.3.8.6 Maximum Allowable Joint Loads

In the design of shell and tube heat exchangers other than U-tube construction, the maximum allowable axial load on tube-to-tubesheet joints shall be determined in accordance with the code formula. The basis for establishing allowable loads for tube-to-tubesheet joints loads is given in ASME Code

Appendix AA. In ASME Code, various joints types are identified by a, b, c, d, e, f, g, h, i, j, and k. The maximum allowable joint load F_{\max} is calculated as follows:

1. For joint types a, b, c, d, e

$$F_{\max} = A_t S_a f_r \quad (11.56)$$

2. For joint types f, g, h, i, j, k

$$F_{\max} = A_t S_a f_e f_r f_y \quad (11.57)$$

where

A_t is the nominal transverse cross-sectional area of tube wall

S_a is the code allowable stresses in tension of tube material at design temperature

f_e is a factor for the percentage of tube expansion length

f_c is 1.0 for joints made with expanded tubes in grooved tube holes

d is the tube outer diameter

f_r is the factor for efficiency of joint

f_y is the ratio of tubesheet material yield stress to tube material yield stress

Refer to ASME Code Section VIII, Div. 1, for complete details including joint types on the nomenclature.

11.4.3.9 TEMA Fixed Tubesheet Design with Different Thickness

Fixed tubesheets of different thickness in the same unit are designed as per RCB-7.166. Considerable savings may be realized when a process dictates a high-quality material at only one end of a unit where the temperature is very high.

11.4.4 TUBESHEET DESIGN METHOD AS PER ASME, CODAP AND UPV:EN 13443 AND COMPARISON WITH TEMA RULES

During the last six decades, TEMA Standards have been extensively used for the design of tubesheets of heat exchangers. Due to their simplicity, TEMA rules do not account for and do not treat rigorously several effects (e.g., perforated tubesheet, unperforated rim, tube expansion, the connection of the tubesheet with shell and channel) that have a significant impact on the thickness of the tubesheet [64]. Hence, TEMA design rules do not ensure the same safety level for all heat exchangers—they often lead to tubesheet over-thickness or occasionally to under-thickness, which may be detrimental to the safety of the heat exchanger. UPV, CODAP, and ASME developed a more rational approach based on the works of [61] and reconciled their heat exchanger design rules on both the analytical and editorial aspects. The reconciliation work is published in

1. ASME Code Section VIII—Div. 1 Appendix AA, Section UHX, in July 2002 Addenda
2. UPV—EN 13443 Part 3-Clause 13 in July 2002
3. CODAP Section C7 in January 2000

These rules propose a better treatment of the mechanical behavior of various components of the heat exchanger. They lead to tubesheet thicknesses that will ensure a consistent safety margin for all types of heat exchangers. Use of common notations, tubesheet configurations, and terminology

will facilitate an easy correspondence among these three codes. English notations, based on TEMA, have been adopted by UPV, CODAP, and ASME—subscripts t for tubes, s for shell, c for channel, and no subscripts for tubesheet. However, the following notations will remain different in U.S. Codes/Standard (ASME, TEMA) and European Codes (CODAP, UPV):

Tubesheet thickness: h in the United States; e in Europe

Shell and channel thickness, t_s , t_c in the United States; e_s , e_c in Europe

Nominal design stress: S in the United States; f in Europe

Structure and presentation of the rules have been made consistent as far as possible. In these three codes, each of the three types of heat exchangers (U-tube, floating head, fixed tubesheets) is covered by independent and self-supporting rules.

The basis of design rules for U-tube tubesheet, fixed tubesheets, and floating heads and a discussion of the differences between the ASME Code requirements and those of TEMA Standards and other international codes like CODAP and UPV are outlined by Osweiller [61,64]. On similar lines, a white paper is included in ASME Sec VIII, Div. 1, to describe the basis of requirements contained in Mandatory Section UHX of Section VIII Division 1 of the BPVC [15].

Tubesheet configurations: Six tubesheet configurations have been adopted independently of the heat exchanger type (see Figure 11.2).

Design loading cases: Seven design loading cases are considered based on TEMA. ASME and TEMA loading cases are correlated as follows using P_t (p_t) for the tubeside pressure, P_s (p_s) for the shellside pressure, and P_γ (p_d) for the pressure due to the differential thermal expansion γ (Table 11.8).

11.4.4.1 Effect of Ligament Efficiency in Tubesheet Thickness and Tube-to-Tubesheet Joint Strength Calculation

The TEMA and ASME Part UHX tubesheet design methods both define and use a ligament efficiency. The TEMA method is based on the average width of the ligament between the tube holes, and it is different for triangular pitch and square pitch. The Part UHX method uses the minimum ligament width

TABLE 11.8
ASME and TEMA Loading Cases

Loading Cases	ASME Load Cases	TEMA Loading Cases RCB-7.23, p_t^* ; p_s^* , RCB-7.22
1. Tubeside pressure acting only, without thermal expansion	P_t	p_t
2. Shellside pressure acting only, without thermal expansion	P_s	p_s
3. Tubeside and shellside pressures acting simultaneously, without thermal expansion	P_t, P_s	$p_t - p_s$
4. Thermal expansion acting alone	P_γ	p_d
5. Shellside pressure acting only, with thermal expansion	P_t, P_γ	$p_t + p_d$
6. Tubeside pressure acting only, with thermal expansion	P_s, P_γ	$p_s + p_d$
7. Tubeside and shellside pressures acting simultaneously, with thermal expansion	P_t, P_s	$p_t - p_s + p_d$

- Note:*
1. Loading cases 1, 2, and 3 consider only the effects of pressure loading, and they are referred to as the pressure loading cases. Elastic moduli, yield strength, and allowable stresses shall be taken at design temperature.
 2. Loading cases 4, 5, 6, and 7 also include the effects of thermal expansion P_γ (TEMA = p_d) and are referred to as the thermal loading cases. Elastic moduli, yield strength, and allowable stresses shall be taken at operating temperature.
 3. For U-tube tubesheets and floating heads, only the first three loading cases are to be considered.

(Figure 11.3). However, if the tubes are expanded into the tubesheet, then tube wall may be considered as part of the effective ligament. For this purpose, the Part UHX calculation procedure defines the effective tube hole diameter d^* , used to calculate μ^* (the effective ligament efficiency) as follows:

$$\mu^* = \frac{p - d^*}{p} \quad (11.58)$$

$$d^* = \text{Max} \left\{ \left[d_t - 2t_t \left[\frac{E_t}{E} \frac{S_t}{S} \right] \right] \rho, [d_t - 2t_t] \right\} \quad (11.59)$$

where

μ^* is the effective ligament efficiency

p is the tube pitch, mm (in.)

d^* is the effective tube hole diameter, mm (in.)

d_t is the nominal outside diameter of tubes, mm (in.)

t_t is the nominal tube wall thickness, mm (in.)

E_t is the modulus of elasticity for tube material at design temperature, MPa (psi)

E is the modulus of elasticity for tubesheet material at design temperature, MPa (psi)

S_t is the allowable stress for tube material at design temperature, MPa (psi) (for a welded tube, use the allowable stress for an equivalent seamless tube, MPa [psi])

S is the allowable stress for tubesheet material at design temperature, MPa (psi)

ρ is the tube expansion depth ratio = l_{tx}/h , ($0 < \rho < 1$)

where

l_{tx} is the expanded length of tube in tubesheet ($0 < l_{tx} < h$), mm (in.)

h is the tubesheet thickness, mm (in.)

The Part UHX calculation procedure also takes into account differences in material properties of the tube and the tubesheet. It allows the heat exchanger manufacturer to take advantage of the stiffening effect of a tube expanded into a tubesheet for all tubesheet configurations, whether U-tube or straight tube.

The ligament efficiency has a direct bearing on the calculated tubesheet stress. A smaller ligament efficiency results in a larger predicted tubesheet stress and a larger ligament efficiency results in a smaller predicted tubesheet stress. In other words, tubesheet thickness obtained by ASME is generally thicker than TEMA.

In order to maintain joint integrity, the heat exchanger manufacturer's design and tube expanding procedure shall ensure that the tube is in contact with the hole under all operating conditions such as startups, shutdowns, normal operation, and upsets. Therefore, the manufacturers shall have written qualified expanding procedures for tube-to-tubesheet joints—as per ASME Code Sec. VIII, Div. 1 (whether welded and expanded or expanded only) to demonstrate that the expanded joint is capable of providing the required properties for its intended application. It is also desired that the manufacturer shall demonstrate to the authorized inspector a record of having produced satisfactory expanded joints using an existing written procedure or by shear load testing of specimens produced using written procedure.

11.4.4.2 Tubesheet Design Rules

11.4.4.2.1 U-Tube Heat Exchanger

11.4.4.2.1.1 ASME Code Appendix AA-1 for U-tube tubesheet appeared in Section VIII Div. 1 for the first time in 1982. The rules were based on Gardner's method [49]. The same method was adopted in BS 5500 in 1976 and CODAP in 1982, used for the allowable bending stress in the

tubesheet: $\Omega S = 2S$ as recommended by Gardner (where Ω is a multiplier of the basic code allowable stress). The method was improved in 1990 by ASME, based on works of Soler et al. [58] to account for the configurations b and e (tubesheet gasketed on one side and integral on the other side) (see Figure 11.2). In the year 2000, Osweiller [61] proposed a more refined approach to provide an analysis model to cover the six configurations of tubesheets shown in Figure 11.2. This method follows the stress analysis of ASME Code Section VIII Div. 2 Appendix 4. In addition to the same analytical basis mentioned earlier, in U-tubesheet analysis, the unperforated tubesheet rim is treated as a rigid ring. This method has been adopted by all the three codes—ASME Code Section VIII, Div. 1, Appendix AA-1, UHX, by CODAP in Chapter C7, and European Standard (UPV) Design Part, Clause 13 in 2002. This is also the basis of Part UHX-12 of ASME Code Section VIII, Div. 1. For more details of the specific derivation, refer [64].

11.4.4.2.1.2 ASME, CODAP, and UPV Rules There is no straight forward formula to calculate tubesheet thickness, and iterative calculations are necessary to obtain the optimized tubesheet thickness. As the calculation procedure is iterative, a value of h (or T) shall be assumed for the tubesheet thickness to calculate and check that the maximum stresses induced in tubesheet, tubes, shell, and channel are within the maximum permissible stress limits. The designer shall consider the effect of deflections in the tubesheet design, especially when the tubesheet thickness is less than the tube diameter.

11.4.4.2.1.3 Fixed Tubesheet Heat Exchanger

1. Analytical treatment of tubesheets

Configurations a, b, c, and d of Figure 11.2 are covered. The stresses are calculated according to the analytical basis explained earlier.

11.4.4.2.1.4 Differences between UPV and ASME Code Rules Some theoretical differences remain between the two design rules, although they rest on the same analytical treatment [61]:

1. The tubesheet unperforated rim is treated as a solid ring in ASME method. In the UPV method, the tubes are assumed to be uniformly distributed over the whole tubesheet. Hence, the fundamental parameter X of the tubesheet will always be higher in UPV rule than in ASME rule.
2. In UPV method, the radial displacement of the tubesheet at its connection with shell and channel is ignored.
3. When the tubesheet is extended as a flange, ASME method considers the loads due to the gasket and the bolts, while UPV ignores it.

For more details, see Osweiller [61].

11.4.4.2.1.5 ASME, CODAP, and UPV Rules for Fixed Tubesheet Heat Exchanger Similar to TEMA formula, the fixed tubesheet formula as per ASME, CODAP, and UPV can be represented by

$$T = \frac{F_{\text{TEMA}} G}{3} \sqrt{\frac{P}{\eta S}}$$

where $F_{\text{TEMA}} = 1.0$ for simply supported = 0.8 for clamped

$$T = \frac{F_{\text{ASME}} G}{3} \sqrt{\frac{P}{\eta S}} \quad (11.60)$$

$$T = \frac{F_{UPV}G}{3} \sqrt{\frac{P}{\eta S}}$$

where

$$F_{UPV} = \sqrt{12F_m(X)}$$

$$F_{ASME} = \sqrt{12F_m(X)}$$

The coefficient F_{UPV} depends strongly on the fundamental parameter X . It can be shown that [61]

1. For low values of X ($X < 3$), the tubesheet thickness obtained by TEMA will be lower than UPV, CODAP, or ASME thickness
2. For high values of X ($X > 6$), the tubesheet thickness obtained by TEMA will be higher than UPV, CODAP, or ASME thickness. The discrepancy will increase appreciably when X is very high (i.e., $X > 12$)
3. In the intermediate range ($3 \leq X \leq 6$), UPV, CODAP, and TEMA thicknesses will be about the same

11.4.4.2.1.6 Comparison with TEMA Rules TEMA rules are based on the same basic approach as ASME and CODAP, but simplifications have been made as given later:

1. Unperforated rim is not considered.
2. Connection of tubesheet with shell and channel is not treated rigorously (ratio e_s/D_s where e_s is shell thickness and D_s is the shell diameter) in coefficient F ; it cannot account for the rotational stiffness of the shell and/or channel.
3. The coefficient F that appears in the TEMA tubesheet formula has a constant value:
 $F = 1$, 0 if the tubesheet is simply supported.
 $F = 0$, 8 if the tubesheet is clamped.
 - a. Coefficient F accounts *neither* for the stiffening effect of the tube bundle (i.e., axial tube bundle rigidity), nor for the holes that weaken the tubesheet (i.e., reduced tubesheet rigidity). But TEMA assumes that these two effects are counterbalanced, whereas the design of the heat exchanger tubesheet is significantly affected by the stiffness ratio X . Due to simplifications mentioned earlier, TEMA rules do not provide the same design margin for all heat exchanger types, leading to over-thickness when the X value is high and under-thickness when the X value is low. However, it must be pointed out that the value of coefficient F of TEMA has been remarkably well chosen as it represents approximately the mean value of coefficient F_{ASME} . For more details, see Soler et al. [58] and Osweiller [61].

11.4.4.2.2 Tubesheets of Floating Head Heat Exchanger

11.4.4.2.2.1 UPV Rule The CODAP 95 rule for floating heads was based on Gardner [49] method. This method has the following drawbacks:

1. The connection of the tubesheet with shell and channel is not treated correctly (the tubesheet is considered as either simply supported or clamped)
2. Tubesheet thicknesses obtained are generally high
3. Some of the charts provided for the calculation of tube stresses were not usable in certain ranges of X

It was therefore decided to adapt the fixed tubesheet approach to cover floating tubesheet heat exchangers, with the following benefits, [61]:

1. Better consistency with the fixed tubesheet rules
2. Correct treatment of tubesheet connection with shell and channel
3. Reduced tubesheet thickness

However, this method does not account for the unperforated rim, and the two tubesheets are assumed identical. Three types of heat exchangers are covered:

1. Immersed floating head
2. Externally sealed floating head
3. Internally sealed floating tubesheet

The stationary tubesheet may have any of the configurations (Figure 11.2a through f). The floating tubesheet may be gasketed (extended as a flange, or not) or integral with the floating head.

The design procedure is similar to the fixed tubesheet design procedure.

11.4.4.2.2.2 ASME Rule Like UPV, ASME rule is based on the same analytical approach for fixed tubesheet method with the simplification that the equivalent pressures, $P_e(X) = P_s - P_t$.

11.4.4.2.2.3 Tube Stresses ASME: The ASME calculation for the tube longitudinal stress $\sigma_{t,o}$ is given in UHX-13.5.9 for fixed tubesheet heat exchangers and UHX-14.5.9 for floating tubesheet heat exchangers. The ASME equation does not require a Ct because $\sigma_{t,o}$ is compared to 1.0 time the allowable stress for the pressure loading cases and to 2.0 times the allowable stress for thermal loading cases. When the tubes are in compression ($\sigma_{t,o}$ negative), the stress must not exceed the buckling stress limit $S_{t,b}$ calculated in UHX-13.5.9(b) or UHX-14.5.9(b). The calculated tube stresses as per the TEMA and ASME Code will not be the same due to the differences in their tube loading models, but both compare these stresses to the same allowable stress limits.

11.4.4.2.3 Tube-to-Tubesheet Joint Loads

11.4.4.2.3.1 ASME Code The tube joint load W_j can easily be calculated from the formula

$$W_j = \sigma_{t,o} A_t \quad (11.61)$$

where

W_j is the tube-to-tubesheet joint load, lb (N)

$\sigma_{t,o}$ is the axial tube stress from UHX-13.5.9 or UHX-14.5.9, psi (MPa)

A_t is the tube cross-sectional area, mm² (in.²)

The ASME Code specifies the allowable tube joint load L_{max} in either UHX-15 (formerly UW-20) for strength welded tube joints or Appendix A for all other tube joints. The ASME method permits the designer to calculate the tube joint load for every loading case, whereas the TEMA method requires this calculation only for pressure loading.

11.4.5 METHODOLOGY TO USE ASME RULES

Based on the earlier discussion, the rules of Part UHX for tubesheet should generally be used in the following manner [61]:

1. Establish the geometry for the initial set of calculations.
2. Calculate the tubesheet stress based on the full support of an integrally attached shell and/or channel using loading cases 1, 2, and 3.

3. If the tubesheet stress is acceptable using an allowable stress based on 1.5 S (where S is the basic allowable stress from Section II Part D), calculate the shell/channel stresses as appropriate for loading cases 1, 2, and 3.
4. If the shell/channel stresses do not exceed their respective allowable stress based on 1.5 S , then the geometry is acceptable for load cases 1, 2, and 3, and it is not necessary to conduct a plastic analysis.
5. If the shell/channel stress exceeds its primary stress allowable of 1.5 S , but less than the secondary stress allowable (greater of 3 S or 2 S_y), then the simplified elastic-plastic analysis may be used for loading cases 1, 2, and 3.
 - a. If the tubesheet stress from the elastic-plastic analysis exceeds the allowable primary bending stress, then a new geometry shall be established and redo the calculation from the first step.
6. If the shell/channel stress exceeds its primary plus secondary stress limit (larger of 3 S or 2 S_y), then the geometry is not acceptable and must be revised. It will then be necessary to start over and return to the first step.
7. Determine the tube loading for loading cases 1, 2, and 3. The maximum tube stress shall not exceed its allowable value in either tension or compression using the primary stress limits.
 - a. For loading cases 4, 5, 6, and 7 (which consider pressure plus restrained differential thermal expansion), determine tubesheet, shell, channel, and tube stresses using the unaltered elastic properties for the shell and/or channel (use the elastic analysis parameters). If any of the stresses exceed their respective allowable stress of the larger of 3 S or 2 S_y , then the geometry is not acceptable, and it is necessary to redo the calculation from the first step.
8. Use the allowable buckling stress for determining the tube allowable compressive stresses. If the allowable stresses are satisfied, then the design is considered acceptable.

11.4.6 FLANGED TUBESHEETS: TEMA DESIGN PROCEDURE

Formulas are included in the TEMA seventh edition for the calculation of the minimum thickness required on the flanged portion of the tubesheet of fixed, floating, and U-tube exchangers. The calculation procedure is based on the work of Singh et al. [65]. The purpose of this new method is to insure that there is sufficient tubesheet thickness to withstand bending moments transmitted by the adjoining flange.

11.4.6.1 Fixed Tubesheet or Floating Tubesheet

The thickness of the portion of the tubesheet extended as a flange, t_F , is given by [65]

$$T_f = 0.98 \left[\frac{M \{ r_f^2 - 1 + 3.72 \ln(r_f) \}}{S(D_T - G)(1.0 + 1.86 r_f^2)} \right]^{0.5} \quad (11.62)$$

where M is the bolting moment due either to gasket seating condition or to operating condition, whichever is greater; if a joint is integral (welded connection), then the corresponding edge moment is zero; D_T and G are the tubesheet outer diameter and effective gasket diameter as defined in TEMA RCB-7.132, respectively; and S is the code allowable stress at the design temperature. The quantity r_f is the ratio of D_T to G :

$$r_f = \frac{D_T}{G} \quad (11.63)$$

11.4.6.2 U-Tube Tubesheet

The minimum thickness of the portion of the tubesheet of thickness T extended as a flange, T_f , is given by [65]

$$T_f = 1.38 \left[\frac{M^* + M + 0.39 PG^2 W}{(D_T - G)S} \right]^{0.5} \quad (11.64)$$

where

$$M^* = \frac{(0.069w/\eta)F^3 PG^3 (T_f/T)^3 - MG - 0.39wPG^3}{G + (1.37/\eta)(T_f/T)^3 w} \quad (11.65)$$

where M is the bolting moment either due to gasket seating condition or due to operating condition whichever is greater (if a joint is integral, such as welded connection, then the corresponding edge moment is zero); G has different values for different styles of construction (e.g., G is the inside diameter of the pressure part for the pressure acting on an integral side of a tubesheet; it is the location of the gasket load reaction as defined in the code for the pressure acting on the gasketed side of a tubesheet, TEMA RCB-7.132); $P = p_s$ or p_t or maximum differential pressure or as defined in TEMA; and $w = 0.5 (D_T - G)$.

For each pressure loading, the calculation procedure is as follows:

1. Compute M^* from Equation 11.65, assuming $T_f = T$ (rim and interior tubesheet thickness equal).
2. Assume $P = p_s$ or p_t or maximum differential pressure, as applicable.
3. Compute the required tubesheet rim thickness T_f from Equation 11.64. If $T > T_f$ and both are set equal to the computed T , then the calculation may be terminated at this point.
4. If it is desired to reduce the rim thickness below T , the value of T_f arrived at in step 3 is used to calculate a new M^* in Equation 11.65. Next, the calculation returns to step 2.

11.4.7 RECTANGULAR TUBESHEET DESIGN

The rectangular tubesheet of a surface condenser is designed as per HEI Standards [4]. The basis of the rectangular tubesheet design as per HEI standards is discussed by Bernstein et al. [69].

11.4.7.1 Methods of Tubesheet Analysis

A condenser tubesheet is assumed to be a partially perforated plate on an elastic foundation, with the tubes comprising the foundation. The hydrostatic pull from the water box and surface pressure on the tubesheets are the dominant loads. Irregular tube patterns and variations in edge boundary conditions make solutions of the plate problem difficult. The HEI Standards mention the following four methods by which the structural integrity of the tubesheet and tubes may be demonstrated [69]:

1. Interaction analysis using plate and shell formulas
2. Experimental modeling techniques or prior services
3. FEA (elastic or elastic-plastic)
4. Beam strip on elastic foundation (single or multiple strips)

Of these four methods, the basis of the beam strip method is discussed next.

11.4.7.1.1 *Beam Strip Method*

In the beam strip method, the problem of an elastically restrained perforated rectangular plate on an irregular elastic foundation is replaced by several more readily solved beams on an elastic foundation. The beams represent narrow strips of tubesheets supported by tubes, loaded by hydrostatic pressure and water box pull. The loading on each beam strip must be estimated, taking into account forces and moments acting on the water box and the type of end fixity.

The standard explains the steps in the beam strip method, with an example. Briefly, these steps cover the choice of the beam strip models (width, length, reduced stiffness of perforated zones), the loading to be applied, and an estimate of the edge restraint against rotation provided to the beam strip by the water box flange.

The notable features of HEI Standards on tubesheet design include features such as consideration of pressure surges, pump shutoff, head circulating water system characteristics, and adequate means for provision of expansion. Allowable stress and loads are to be chosen similar to the DBA approach of Appendix 4 in the ASME Code, Section VIII, Div. 2.

11.4.8 CURVED TUBESHEETS

Traditionally, heat exchangers use thick flat tubesheets. The problem of replacing thick flat tubesheets by thinner curved tubesheets was suggested first by Rachkov and Morozov [70]. They designed a much thinner semi-ellipsoidal curved tubesheet based on membrane theory of shells. The design of shallow spherical curved tubesheets for heat exchangers is discussed by Paliwal et al. [71]. Similar to a flat tubesheet treated as a thin flat plate on an elastic foundation, the curved tubesheet model uses the theory of a thin elastic shallow spherical shell on an elastic foundation and replaces the curved plate by an equivalent plate having effective elastic constants; the nominal bending and membrane stresses and deflections are determined.

11.4.8.1 **Advantages of Curved Tubesheets**

As compared with thick flat tubesheets, elliptical tubesheets have many advantages [72]:

1. Material savings due to thin tubesheet.
2. Because the sheet is thin, the thermal stresses developed in the tubesheet will be less.
3. Because the elliptical tubesheets are perforated elliptical shells, their stress levels will be far lower than those of flat tubesheets of the same thickness under the same operating conditions.
4. The deformation ability of a thin-walled shell is larger than that of flat plates, so the elliptical tubesheet can compensate for larger thermal deformations produced by temperature differences between the tubeside and the shellside.

11.4.9 CONVENTIONAL DOUBLE TUBESHEET DESIGN

In a conventional double tubesheet construction, in addition to the usual thermal loading, a new thermal condition arises due to in-plane differential thermal loading of the two tubesheets. This differential radial expansion of the adjacent tubesheets may be caused by the two tubesheets having different coefficients of thermal expansion and/or differences in mean metal temperatures. The portion of tube bundle between the two tubesheets induces coupling between out-of-plane bending and direct radial expansion of the two tubesheets. Therefore, in contrast to the single tubesheet analyses, any double tubesheet analysis must encompass both tubesheet bending and radial growth. These requirements make the solution procedure amenable to computer analysis only. Design of double tubesheets is discussed by Singh and Soler [31].

11.5 CYLINDRICAL SHELL, END CLOSURES, AND FORMED HEADS UNDER INTERNAL PRESSURE

The following symbols are used in the formulas required to calculate the minimum thickness of a cylindrical shell and various end closures:

t is the minimum required thickness of shell or heads or end closures

P is the internal design pressure, psi (see UG-21) (or MAWP, see UG-98)

C is a factor depending upon the method of attachment of head, shell dimensions, and other items as listed in ASME Code

D is the inside length of the major axis of an ellipsoidal head, or inside diameter of a torispherical head, or inside diameter of a conical head at the point under consideration measured perpendicular to the longitudinal axis

D_o is the outside length of the major axis of an ellipsoidal head, or outside diameter of a conical head at the point under consideration measured perpendicular to the longitudinal axis

d is the dimension of the short span for flat heads

G is the mean gasket diameter (not the effective gasket diameter as defined in the ASME Code)

h is the maximum inside depth of the ellipsoidal head, exclusive of the flange

h_G is the gasket moment arm (i.e., radial offset between the circle and the bolt circle)

IDD is the inside depth of torispherical head

K is the factor in the formulas for ellipsoidal heads depending on the head proportion $D/2h$

L is the inside spherical radius or crown radius

L_o is the outside spherical radius or crown radius

M is the factor in the formulas for torispherical heads depending on the head proportion L/r

R is the inside radius of the shell course under consideration

R_o is the outside radius of the shell course under consideration

r is the inside knuckle radius

S is the maximum allowable stress value, psi (see UG-23 and the stress limitations specified in UG-24)

E is the joint efficiency, or the efficiency of appropriate joint in cylindrical or spherical shells, or the efficiency of ligaments between openings, whichever is less (in decimal form)

W is the total bolt load

α is the one-half of the included (apex) angle of the cone at the centerline of the head

11.5.1 CYLINDRICAL SHELL UNDER INTERNAL PRESSURE

Design of cylindrical shell is carried out as per UG-27 or UG-29 of the ASME Code. The design formulas in the code are based on equating the maximum membrane stress to the allowable stress corrected for weld joint efficiency. As per ASME Code procedure, the thickness of shells under internal pressure shall not be less than that computed by the following formulas. In addition, provision shall be made for any of the other loadings listed in UG-22, when such loadings are expected (see UG-16).

11.5.1.1 Thin Thick Cylindrical Shells

11.5.1.1.1 Circumferential Stress (Longitudinal Joints)

When the thickness does not exceed one-half of the inside radius, or P does not exceed $0.385SE$, the following formulas shall apply:

$$t = \frac{PR}{SE - 0.6P} \quad \text{or} \quad P = \frac{SEt}{R + 0.6t} \quad (11.66)$$

TABLE 11.9
ASME Code Formulas for Minimum Thickness of Thin Cylindrical
Shell to Withstand Internal Pressure

Member	Thickness, t	Maximum Internal Pressure, P	Limitation
Longitudinal joints	$t = \frac{PR}{SE - 0.6P}$	$P = \frac{SEt}{R + 0.6t}$	$P \leq 0.385SE$ $t \leq 0.5R$
Circumferential joints ^a	$t = \frac{PR}{2SE + 0.4P}$	$P = \frac{2SEt}{R - 0.4t}$	$P \leq 1.25SE$ $t \leq 0.5R$
In terms of outside radius R_o	$t = \frac{PR_o}{SE + 0.4P}$	$P = \frac{SEt}{R_o - 0.4t}$	$P \leq 0.385SE$ $t \leq 0.5R$

Source: ASME Boiler and Pressure Vessel Code, Section VIII, Division 1—Pressure, American Society of Mechanical Engineers, New York, 2010.

^a Formulas based on stress across circumferential joint will govern only if circumferential joint (Category B) efficiency is less than one-half of the longitudinal joint efficiency.

11.5.1.1.2 Longitudinal Stress (Circumferential Joints)

When the thickness does not exceed one-half of the inside radius, or P does not exceed $1.25SE$, the following formulas shall apply:

$$t = \frac{PR}{2SE + 0.4P} \quad \text{or} \quad P = \frac{2SEt}{R - 0.4t} \quad (11.67)$$

The minimum thickness or MAWP of cylindrical shell shall be the greater thickness or lesser pressure as given by Equations 11.66 and 11.67.

These formulas are presented in Table 11.9 along with the formulas based on shell outside dimension; Table 11.10 gives formulas for thick cylindrical shells.

11.5.1.2 Design for External Pressure and/or Internal Vacuum

There is no straightforward formula as in the case for the design under internal pressure, because buckling has to be taken into account. The procedure to be followed is given in the ASME Code Section VIII, Div. 1, Paragraph UG-28, and requires the use of various charts given in Appendix 5.

11.5.2 END CLOSURES AND FORMED HEADS

End closures for heat exchangers and pressure vessels are in the form of either flat covers or formed heads. ASME Code Section VIII, Div. 1, recognizes the following end closures:

1. Flat cover
2. Hemispherical cover
3. Ellipsoidal cover
4. Torispherical cover (flanged and dished)
5. Conical/torispherical cover

These end closures are shown schematically in Figure 11.6, and few formed heads are shown in Figure 11.7. TEMA designates the front and rear covers by B and M , respectively. Closures other

TABLE 11.10
ASME Code Formulas for Minimum Thickness of Thick
Cylindrical Shells to Withstand Internal Pressure

Member	Thickness, t	Maximum Internal Pressure, P	Limitation
Longitudinal joint	$t = R(\sqrt{z} - 1)$ $= R_0 \frac{(\sqrt{z} - 1)}{\sqrt{z}}$ <p>where</p> $z = \left(\frac{SE + P}{SE - P} \right)$	$P = SE \frac{(z_1 - 1)}{(z_1 + 1)}$ <p>where</p> $z_1 = \left(\frac{R + t}{R} \right)^2$ $= \frac{R_0^2}{(R_0 - t)^2}$	$P > 0.385SE$ $t > 0.5R$
Circumferential joint ^a	$t = R(\sqrt{z_2} - 1)$ $= R_0 \frac{\sqrt{z_2} - 1}{\sqrt{z_2}}$ <p>where</p> $z_2 = \left(\frac{P}{SE} + 1 \right)$	$P = SE(z_1 - 1)$ where z_1 is as defined earlier	$P > 1.25SE$ $t > 0.5R$

Source: ASME Boiler and Pressure Vessel Code, Section VIII, Division 1—Pressure Vessels, American Society of Mechanical Engineers, New York, 2010.

^a Formulas based on stress across circumferential joint will govern only if circumferential joint (Category B) efficiency is less than one-half of the longitudinal joint efficiency.

than flat heads are normally formed type; sometimes for low-pressure application, cast heads are also used. Closures are designed as per UG-32 or UA-4 of the ASME Code. First, a brief description of various end closures is presented and then the determination of minimum thickness to retain internal pressure is presented.

11.5.2.1 Flat Cover

Flat covers are easy to fabricate in any thickness from plates or forgings. They are widely used from low- to high-pressure applications. Since a flat cover resists pressure load only by bending, its thickness is significantly greater than that of the cylindrical section to which these are attached as a closure.

11.5.2.2 Hemispherical

Hemispherical heads are used for high-pressure service since their thickness is about half that of a cylindrical shell. The degree of forming and accompanying costs are greater than any other heads, and the available sizes from single plates are limited [34].

11.5.2.3 Ellipsoidal

These are widely used for low- to intermediate-pressure services. When the minor-to-major axis ratio is 0.5 (most common), the head thickness is almost the same as that of the cylindrical shell. This simplifies the joining of these two and minimizes the discontinuity stresses at the joint. Another popular ellipsoidal head is with minor axis 25% of D .

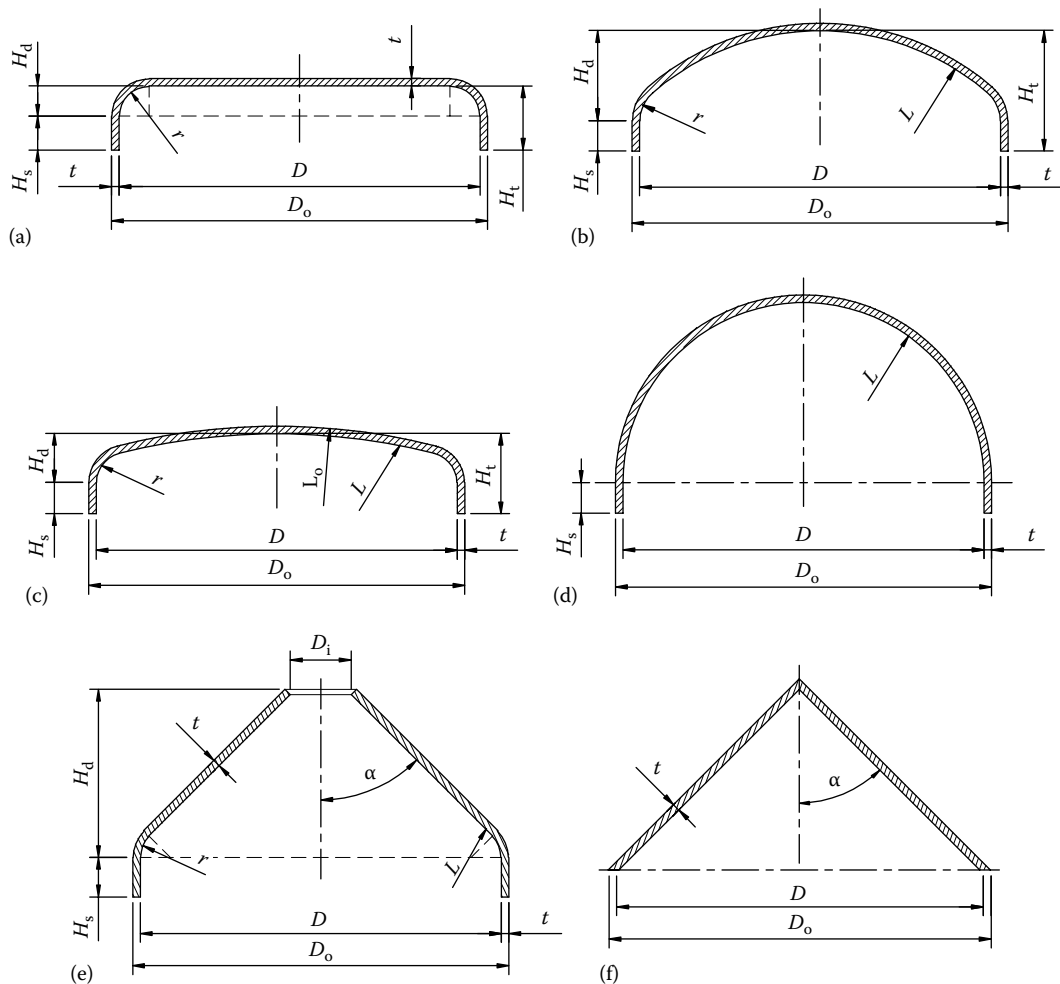


FIGURE 11.6 End closures: (a) Flat head; (b) ellipsoidal head; (c) torispherical head; (d) hemispherical head; (e) toriconical head; and (f) conical head.

11.5.2.4 Torispherical

Among the various types of formed heads, the torispherical head is the most widely used in the industries, particularly for low-pressure service, i.e., up to 200 psi [40]. For pressures over 200 psi gauge, ellipsoidal heads are used. The torispherical head is characterized by four geometric parameters: inside head diameter D , crown radius L , knuckle radius r , and head thickness t . Figure 11.8 shows the details of the torispherical head geometry. In Figure 11.8, the depth of dish b is a geometric function of crown radius L and knuckle radius r , and the straight cylindrical flange is integral with the dished end. By varying the ratios of L/D and L/r , heads of different shapes can be manufactured. Heads wherein $L \approx D$, $L \approx 16\frac{2}{3}r$, and $r = 0.06D$ are referred to as ASME flanged and dished heads in the pressure vessel industry. Another popular variation is the 80:10 head where $L \approx 0.8D$ and $r = 0.1L$.

11.5.2.5 Conical

These are used for low- and intermediate-pressure service with the half apex angle generally not more than 30° . A knuckle portion is provided to minimize the discontinuity stresses where it joins the shell.

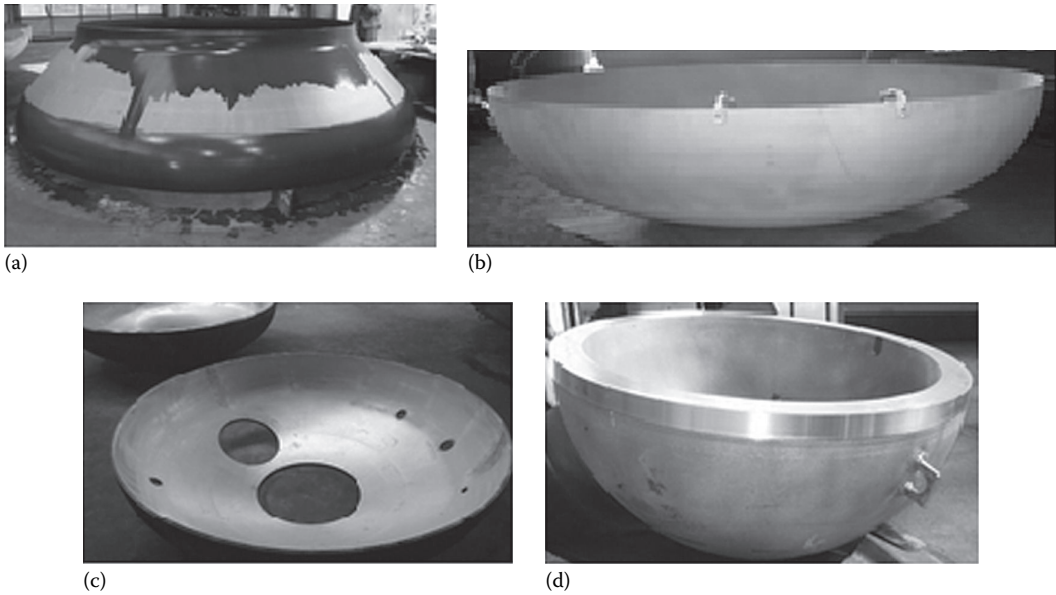


FIGURE 11.7 Few types of formed heads. (a) Cone made of Titanium Gr. 7, (b) elliptical head, (c) semi-elliptical head made of SA-516 Gr. 70, and (d) hemispherical head made of SA-533. (Courtesy of König + Co., GmbH, Netphen, Germany.)

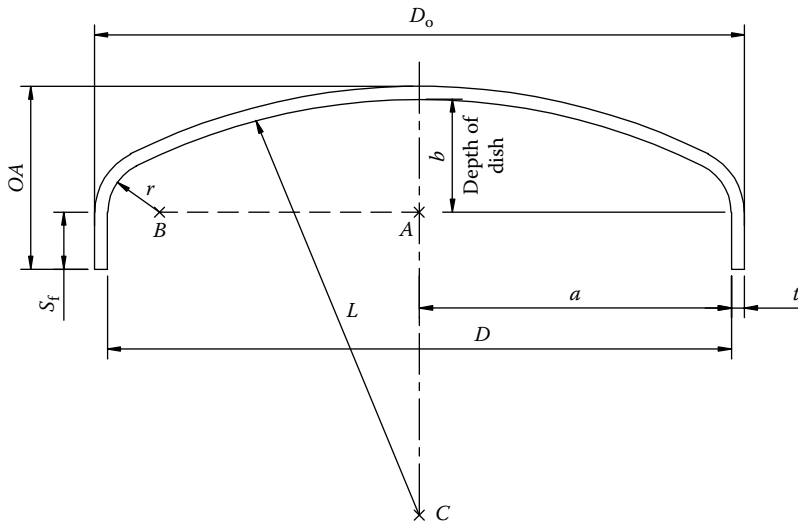


FIGURE 11.8 Dimensional details of flanged and dished torispherical head.

$$a = \frac{D}{2}; \quad b = L - \sqrt{(BC)^2 - (AB)^2}; \quad AB = \frac{D}{2} - r; \quad BC = L - r; \quad AC = \sqrt{(BC)^2 - (AB)^2}; \quad \text{and} \quad OA = t + b + S_f$$

11.5.3 MINIMUM THICKNESS OF HEADS AND CLOSURES

The required thickness at the thinnest point after forming of ellipsoidal, torispherical, hemispherical, conical, and toriconical heads under an internal pressure shall be computed by the appropriate formulas in UG-16 of the ASME Code. In addition, provision shall be made for any of the other loadings given in UG-22. The head design formulas in the code are based on equating the maximum membrane stresses to the allowable stresses corrected for weld joint efficiency.

11.5.3.1 Flat Cover

1. As per UG-34, the minimum required thickness of flat head, cover, and blind flanges shall be calculated by the formula

$$t = d \sqrt{\frac{CP}{SE}} \quad (11.68)$$

2. The minimum required thickness of flat head, cover, and blind flange attached by bolts causing an edge moment is given by the formula

$$t = d \left(\frac{CP}{SE} + \frac{1.9Wh_G}{SEd^3} \right)^{0.5} \quad (11.69)$$

11.5.3.1.1 TEMA Standards

The TEMA Standards have a deflection-based formula that seeks to limit the maximum deflection, d , of the flat cover of a multitube pass unit to 0.030 in. (0.762 mm) [40]. The resulting formula for flat cover thickness, t , in inches, is given by [40]

$$t = \left[\frac{1.425G^4P}{E} + \frac{0.5h_GA_bG \times 10^6}{Ed_b^{1/2}} \right]^{1/3} \quad (11.70)$$

11.5.3.2 Ellipsoidal Heads

The thickness or the MAWP of a dished head of semi-ellipsoidal form, in which half the minor axis equals one-fourth of the inside diameter of the head skirt, shall be determined by

$$t = \frac{PD}{2SE - 0.2P} \quad \text{or} \quad P = \frac{2SEt}{D + 0.2t} \quad (11.71)$$

11.5.3.3 Torispherical Heads

The required thickness or the MAWP of a torispherical head for the case in which the knuckle radius is 6% of the inside radius and the inside crown radius equals the inside diameter of the skirt (i.e., $L \approx D$, $L_1 \approx 16\frac{2}{3}r$, and $r = 0.06D$) shall be determined by

$$t = \frac{0.885PL}{SE - 0.1P} \quad \text{or} \quad P = \frac{SEt}{0.885L + 0.1t} \quad (11.72)$$

11.5.3.4 Hemispherical Heads

When the thickness or the MAWP of a hemispherical head does not exceed $0.356L$, or the internal pressure P does not exceed $0.665SE$, the required thickness or the MAWP of a hemispherical head is given by

$$t = \frac{PL}{2SE - 0.2P} \quad \text{or} \quad P = \frac{2SEt}{L + 0.2t} \quad (11.73)$$

11.5.3.5 Conical Heads and Sections (without Transition Knuckle)

The required thickness of conical heads or conical shell sections that have a half apex angle α not greater than 30° shall be determined by

$$t = \frac{PD}{2(\cos \alpha)(SE - 0.6P)} \quad \text{or} \quad P = \frac{2SEt(\cos \alpha)}{D + 1.2t(\cos \alpha)} \quad (11.74)$$

These formulas and formulas for minimum head thickness referred to outside head dimension are given in Table 11.11.

TABLE 11.11
ASME Code Formulas for Minimum Thickness of Heads/End
Closures to Withstand Internal Pressure

Head	Minimum Thickness, t	Maximum Pressure, p
Ellipsoidal	$t = \frac{PD}{2SE - 0.2P}$	$P = \frac{2SEt}{D + 0.2t}$
	$t = \frac{PDK}{2SE - 0.2P}$	$P = \frac{2SEt}{KD + 0.2t}$
	$t = \frac{PD_o K}{2SE + 2P(K - 0.1)}$	$P = \frac{2SEt}{KD_o - 2t(K - 0.1)}$
	where $K = \frac{1}{6} \left[2 + \left(\frac{D}{2h} \right)^2 \right]$	
Torispherical	$t = \frac{0.885PL}{SE - 0.1P}$	$P = \frac{SEt}{0.885L + 0.1t}$
	$t = \frac{PLM}{2SE - 0.2P}$	$P = \frac{2SEt}{LM + 0.2t}$
	$t = \frac{PL_o M}{2SE + P(M - 0.2)}$	$P = \frac{2SEt}{ML_o - t(M - 0.2)}$
	where $M = \frac{1}{4} \left[3 + \left(\frac{L}{r} \right)^{0.5} \right]$	
Hemispherical	$t = \frac{PL}{2SE - 0.2P}$	$P = \frac{2SEt}{L + 0.2t}$
Conical	$t = \frac{PD}{2(\cos \alpha)(SE - 0.6P)}$	$P = \frac{2SEt(\cos \alpha)}{D + 1.2t(\cos \alpha)}$
	$t = \frac{PD_o}{2(\cos \alpha)(SE + 0.4P)}$	$P = \frac{2SEt(\cos \alpha)}{D_o - 0.8t(\cos \alpha)}$

Source: ASME Boiler and Pressure Vessel Code, Section VIII, Division 1—Pressure Vessels, American Society of Mechanical Engineers, New York, 2010.

11.5.4 COMPARISON OF VARIOUS HEADS

1. Compared to a flat cover, which resists pressure load only by bending, a formed head resists pressure by developing membrane stress, and hence the thickness of formed heads will be less than the flat cover [40].
2. The formed head has the drawback of thinning out in areas of sharp curvature and thickening in adjacent regions of moderate curvature. Such a variation is more pronounced in spun heads, and more particularly in hot-formed heads than in cold-formed heads.
3. As far as the cost is concerned, the head that is the lowest in cost and meets the code requirements should be designed. The ellipsoidal and hemispherical heads have the least weight per unit volume.
4. Salient features of fabrication of various heads are discussed in Chapter 15, Heat Exchanger Fabrication.

11.6 BOLTED FLANGED JOINT DESIGN

11.6.1 CONSTRUCTION AND DESIGN

Flanges are often employed to connect two sections by bolting them together so that the sections can be assembled and disassembled easily. In heat exchangers, the flange joints are used to connect together the following components:

1. Channel and channel cover
2. Heads or channels with the shell/tubesheets
3. Inlet and outlet nozzles with the pipes carrying the fluids
4. To close various openings such as manholes, peepholes, and their cover plates

The flanged joints play an important role from the standpoint of integrity and reliability of heat exchangers. Improper design of flanges causes leakage of heat exchanger fluids. Therefore, preventing the liquid or gas leaks is one of the most important considerations while designing flanged joints.

11.6.1.1 Flanged Joint Types

From a conceptual standpoint, flanged joints may be subdivided into two major categories [31]:

1. Bolted joints
2. Pressure-actuated or self-energizing joints

The bolted joint is by far the most common type. The basic difference between these two joint types lies in the manner by which the pressure load is resisted and leak tightness is achieved. A bolted joint essentially consists of a gasket interposed between two structural members called flanges, which in turn are connected to other structural members like cylindrical shells or pipes, and a set of bolts for joining together the two flanges. To make the joint, the gasket is compressed to a desired value by prestressing the bolts. Pressure-actuated joints exploit the header pressure force to compress and to seal the gasket. Pressure-actuated joints find application in the higher pressure range, typically over 2000 psi [31].

11.6.1.2 Constructional Details of Bolted Flange Joints

11.6.1.2.1 Types of Bolted Flanges

Based on the width of gasket, flange joints are classified as (1) ring-type gasket joint and (2) full-face gasket joint. For very-low-pressure applications (100–300 psi), wide gaskets that span the entire

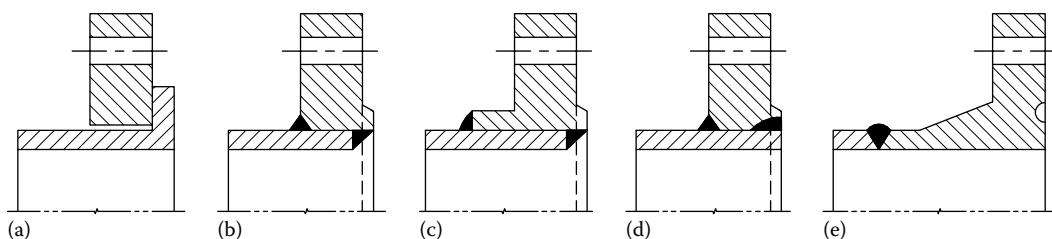


FIGURE 11.9 Flanged joint construction—types of bolted flanges. (a) Loose ring flange, (b) fusion lap welded ring flange, (c) fusion lap welded hubbed flange, (d) fusion through welded ring flange, and (e) fusion butt welded hubbed flange.

flange face may be used. This construction is known as “full-face gasket” design. A design method for flanges utilizing full-face gaskets is presented in Ref. [31]. In general, for high-pressure and medium- to high-pressure applications, only ring-type gaskets are used. Sometimes even for low-pressure applications, ring-type gaskets are used. Based on constructional details, flanged joints (Figure 11.9) are classified as

1. Ring flange
2. Weld neck integral flange or tapered hub flange
3. Lap joint flange
4. Reverse flange

11.6.1.2.1.1 Ring Flange The ring flange consists of an annular circular plate welded to the end of the cylindrical shell. A number of equidistant bolt holes are drilled on a uniform pitch circle, and the gasket is confined inside the bolt circle. This joint is utilized in low- to moderate-pressure applications. A ring-type gasket joint is shown schematically in Figure 11.9a.

11.6.1.2.1.2 Weld Neck Integral Flange The weld neck flange or a tapered hub flange, as shown in Figure 11.9b, may be viewed as a structural member consisting of an annular ring and a tapered hub butt welded to the cylindrical shell. This flange has the best characteristics for preventing failure from fatigue and thermal stresses. These flanges have been used at pressures as high as 5000 psi, although the flange becomes massive and heavy as pressure and diameter increase.

11.6.1.2.1.3 Lap Joint Flange The lap joint flange, shown in Figure 11.9c, finds use in low-pressure applications where economy of construction is an important consideration. The backing ring can be made from low-cost but strong structural material (e.g., carbon steel), whereas the “lap ring” may be made from expensive corrosion-resistant material. Furthermore, this flange design facilitates alignment of bolt holes in matching rings in opposing pipe ends. In outside packed floating head heat exchangers, the flange at the rear end is of the lap joint type.

Figure 11.10 shows types of flanges.

11.6.1.3 Design of Bolted Flange Joints

The objectives in flange design are to ensure that the residual gasket stress levels and the pressure induced in the flange during bolt preload, as well as under operating conditions, do not exceed allowable stress values in the structural members.

The earliest treatment of the problem of flange design to receive widespread recognition was that of Waters et al. [73], which gave the general basis for the design rules in the ASME Code. Design of flanged joints with ring-type gaskets is carried out as per Appendix 2 of ASME Code Section VIII, Div. 1. Appendix S of the code gives general guidelines for bolting requirements of flanges. The code method for the design of integral-type flange and ring flange is briefly described here.

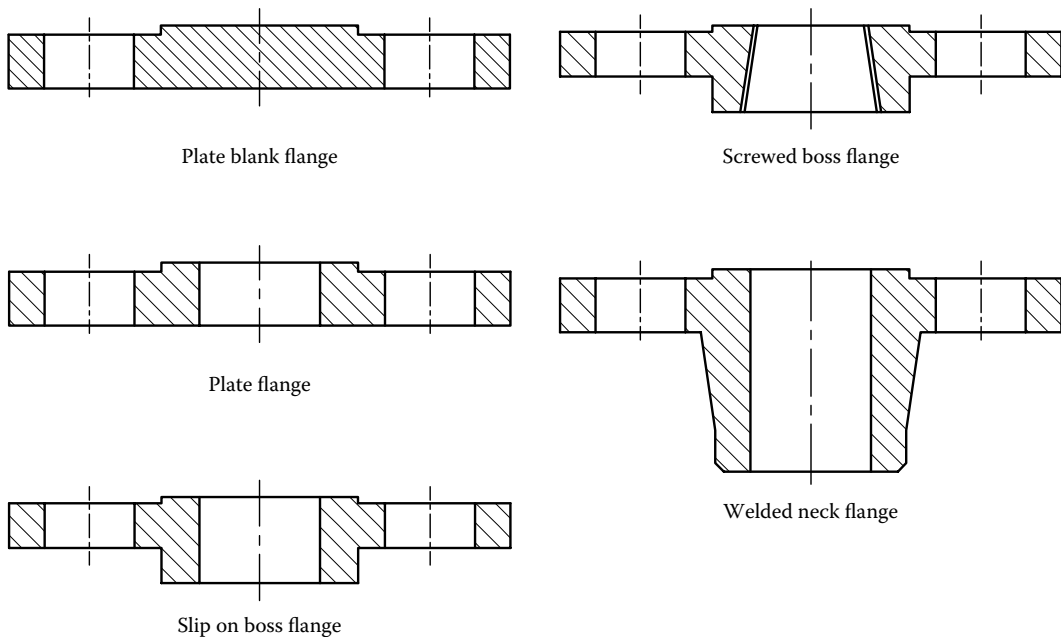


FIGURE 11.10 Types of flanges.

11.6.1.3.1 ASME Code Classification of Circular Flanges for Design Purposes

For computation purposes, ASME Code Section VIII, Div. 1, classifies circular flanges with ring-type gaskets as

1. Loose-type flanges
2. Integral-type flanges
3. Optional-type flanges
4. Flanges with nut stop
5. Reverse flanges

Salient constructional details, design features, and step-by-step design procedures of various flanged joint types except flanges with nut stop and reverse flanges are described in the following sections.

11.6.1.3.1.1 Loose-Type Flanges This type covers those designs in which the flange has no direct connection to the nozzle neck, vessel, or pipe wall and designs where the method of attachment is not considered to give the mechanical strength equivalent of integral attachment.

11.6.1.3.1.2 Integral-Type Flanges This type covers those designs in which the flange is cast or forged integrally with the nozzle neck, vessel, or pipe wall, butt welded thereto, or attached by other forms of arc or gas welding of such a nature that the flange and nozzle neck and vessel or pipe wall are considered to be the equivalent of an integral structure.

11.6.1.3.1.3 Optional-Type Flanges This type covers those designs in which the attachment of the flange to the nozzle neck, vessel, or pipe wall is considered to act as a unit, which shall be calculated as an integral flange, except that for simplicity the designer may calculate the construction as a loose-type flange provided none of the values given in the ASME Code are exceeded.

11.6.1.3.2 *Flange Materials*

1. Carbon Steel: SA105(N), SA765-GR2, SA105-HIC • A707-L3, SA350-LF1, SA350-LF2, SA266-GR4
2. Alloy Steel: SA350-LF3, SA182-F12, SA182-F5, SA182-F22, SA182-F9, SA182-F91, SA182-F11, A694-F65
3. Stainless Steel: SA182-F304 (L), SA182-F316(L), SA182-F304H, SA182-F347

11.6.1.3.3 *Material Test*

FVC, Houston, Texas, identifies the following testing capabilities for the forged vessel component such as nozzles and flanges: chemical analysis, tensile property tests, impact tests, hardness tests, nil-ductility testing, H.I.C. testing, metallurgical analysis (macroetch, microetch, grain, size, sulfur prints), nondestructive testing (ultrasonic, magnetic particle, liquid penetrant), and positive material identification.

11.6.1.3.4 *Custom-Designed Flanges*

Custom-designed flanges are used when diameter does not match that of a standard flange and when optimum design is desired, such as girth flanges in shell and tube heat exchangers and flanges for removable cover for vessels and other pressure equipments—whereas custom designed flanges are designed for specific design conditions and when there is a requirement to use special materials which may result in usually smaller and lighter than a standard flange. But demerits include the following: longer delivery time, design calculations are to be performed, and cost may be higher than the off-the-shelf standard flanges. Information required to develop a custom flange is as follows:

1. Applicable design code
2. Flange and bolting material specification
3. Gasket style, material, and thickness
4. Minimum neck thickness
5. Details of mating flange such as number of bolts and bolt circle diameter
6. Nozzle bore diameter
7. Design parameters such as maximum pressure and temperature, and corrosion allowance
8. Style of flange—tapered hub, loose ring, or straight hub, with or without nut relief

11.6.1.3.5 *Design Procedure*

The integrity and reliability of a bolted flanged joint depend to a large extent upon the correct choice of materials, dimensions, and loads on the gasket. The flange design procedure can be summarized as three separate elements:

1. Gasket design
2. Bolting design
3. Flange design

To start with, materials of construction of flange, bolting, and gasket, and gasket properties are chosen. Flange inner diameter and shell thickness to which the flange is to be welded are also known. A rough guess of the various dimensions of the flange is made, taking into account the permissible hub slope, and minimum hub length in the case of weld neck flange, and bolting dimensional requirements. Suitable gasket outer diameter and width are also chosen, keeping the minimum width requirements. Flange dimensions shall be such that the calculated stresses in the flange shall not exceed code stress values. In the following paragraphs, the detailed design procedures of the three elements of flange design are described.

11.6.1.4 Gasket Design

11.6.1.4.1 Gaskets and Their Characteristics

A leak-proof joint with metal-to-metal surfaces without a gasket is difficult to achieve even with the use of accurately machined fine-finish surfaces. Surface irregularities of only a few millionths of an inch will permit the escape of a fluid under pressure [34]. Being a semi-plastic material, the gasket deforms under load, which in turn seals the minute surface irregularities and prevents leakage of the fluid.

11.6.1.4.2 Selection of Gasket Material

A gasket is essentially an elastoplastic material that is softer than the flange faces. In the gasket seating condition, the entire bolt load is borne by the gasket. Hence, the gasket must be strong enough to withstand load due to bolting and operating conditions without crushing or extruding out. Therefore, soft materials like asbestos and organic fibers are precluded for high-pressure applications. Also the gasket material shall withstand the operating temperature and exhibit corrosion resistance to the fluid contained in the pressure vessel [74].

11.6.1.4.3 Gasket Materials

Gaskets are made out of a myriad variety of materials. Good references are available from many gasket manufacturers for the selection of proper gaskets for the intended applications. Table 2-5.1 of the ASME Code gives a list of many commonly used gasket materials. A partial list of gasket materials included in Table 2-5.1 of the ASME Code [15] are

- Elastomers without fabric or high percentage of asbestos fiber
- Asbestos with suitable binder
- Elastomers with cotton fabric insertion
- Elastomers with asbestos fabric insertion
- Spiral-wound asbestos-filled metal
- Corrugated metal with asbestos fill
- Corrugated metal
- Flat metal, jacketed asbestos fill
- Grooved metal
- Solid flat metal

11.6.1.4.4 Gasket Profile

Commonly used gasket profiles include (1) single jacketed, (2) double jacketed, (3) Double-jacketed corrugated, (4) double shell jacket, (5) solid metal, (6) solid profile, (7) Double-corrugated jacket with non-asbestos fill, and (8) two-piece French type. Figure 11.11 shows various gasket cross-sectional profiles and Figure 11.12 shows various forms of profiles for heat exchanger gaskets.

11.6.1.4.5 Gasket Size

The size restrictions for heat exchanger gaskets depend only on the available sizes of the materials. Heat exchanger gaskets are commonly made in diameters up to 120 in., with rib widths up to 31 mm

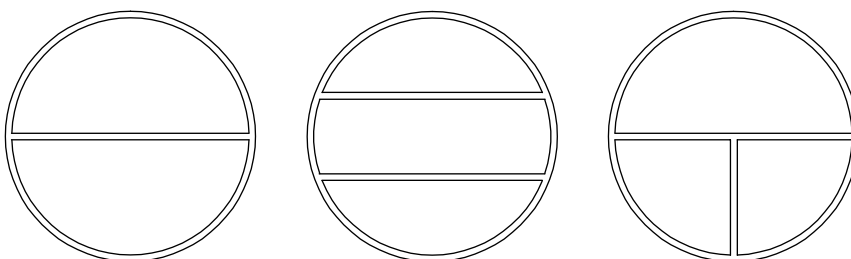


FIGURE 11.11 Heat exchanger gasket shapes.

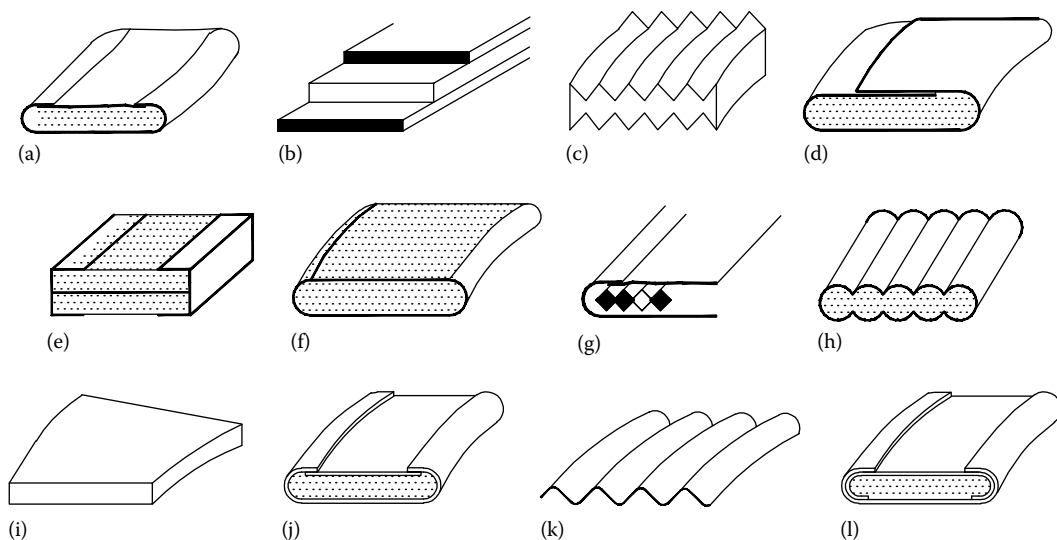


FIGURE 11.12 Heat exchanger gasket profiles. (a) Double jacketed, (b) solid metal with flexible graphite covering, (c) solid metal profiled, (d) single jacketed overlap, selected metal with felt, (e) selected metal and Cerafelt®, (f) single jacketed, (g) double jacketed profile, (h) single jacketed profile, (i) solid metal, (j) double jacketed covered, (k) solid metallic corrugated, and (l) double shell jacket.

(1.25 in.) and thicknesses up to 6.4 mm (1/4 in.). When ordering gaskets for heat exchangers, specify these information, (1) model/style number, shape, thickness, and material (metal or metal and filler) and (2) outside diameter, inside diameter, rib width, radius of rib, bolt circle radius, distance from centerline of gasket to centerline of ribs, radius around bolt, and size and number of bolt holes.

The choice of the gasket material is often based upon the required gasket width. If the gasket is made too narrow, the unit pressure on it may be excessive, whereas if the gasket is made too wide, the bolt load will be unnecessarily high [34]. Standard metals include 304 Stainless, 316L Stainless, Inconel® 600, Inconel® 625, Incoloy® 800, Incoloy® 825, Hastelloy® C276, and Monel® 400, and sealing elements include flexible graphite, ePTFE, and combination graphite and ePTFE.

Garlock Sealing Technologies, Palmyra, New York, manufactures a wide variety of heat exchanger gaskets and their trade names include GET™ gasket, Graphonic® gasket, Tephonic® gasket, Garlock Kammprofile Gasket, and Flexseal® spiral wound. Among the most requested styles are double-jacketed gaskets, Kammprofile, corrugated gaskets, and solid gaskets, all available in a choice of metals and filler materials. Custom configurations of heat exchanger gaskets are also available. Spiral windings can be designed with or without partitions welded to the winding, or inner and outer rings.

11.6.1.4.5.1 Gasket Factors The basic behavior of the gasket is defined by the gasket factor m and gasket or joint contact surface unit seating load y , which are tabulated in the ASME Code, Section VIII, Div. 1.

11.6.1.4.5.2 Gasket Factor, m This is the ratio of the residual stress on the gasket under operating pressure to that pressure. In other words, $m = (\text{bolt load} - \text{hydrostatic end load})/(\text{gasket area} \times \text{internal pressure})$.

11.6.1.4.5.3 Gasket or Joint Contact Surface Unit Seating Load, y This is the stress required to make the gasket surface take up the shape of the flange faces, or the gasket stress required to contain zero internal pressure. The factor y is usually expressed as a unit stress in pounds per square inch and is independent of the pressure in the vessel. Table 2-5.1 of the ASME Code gives suggested design values of gasket factor m and minimum design seating stress y .

11.6.1.4.5.4 *Gasket Dimensions* A relationship for making a preliminary estimate of the proportions of the gasket may be derived as follows [31]:

Residual gasket force = gasket seating force – hydrostatic pressure force

The residual gasket force cannot be less than that required to prevent leakage of the internal fluid under operating pressure. This condition results in the following expression:

$$\frac{d_o}{d_i} = \sqrt{\frac{y - pm}{y - p(m + 1)}}$$

(11.75)

where

- d_o is the gasket outside diameter
- m is the gasket factor
- y the minimum design seating stress

To determine m and y , refer to ASME code [15].

The inside diameter of the gasket (in inches) is normally as follows:

$$d_i = B + 0.01$$

where B equals the shell inside diameter for weld neck flange and shell outside diameter for ring flange.

11.6.1.4.5.5 *Gasket Width and Diametral Location of Gasket Load Reaction* The steps involved in arriving at the gasket width and diametral location of gasket load reaction are as follows:

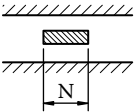
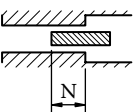
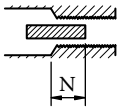
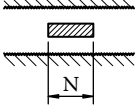
1. Calculate the gasket width, N , given by

$$N = \frac{(d_o - d_i)}{2}$$

(11.76)

2. Select the gasket width such that it is not less than the minimum specified width of the gasket as specified in Table 2-5.2 of the ASME Code, and a representative value for one case is shown in Table 11.12.
3. Calculate the basic gasket width, b_o , given by Table 2-5.2 of the ASME Code.

TABLE 11.12 Basic Gasket Seating Width

Facing sketch (exaggerated)		Basic gasket seating width, b_o	
		Column-I	Column-II
(1a)		N/2	N/2
			
(1b)		N/2	N/2
			

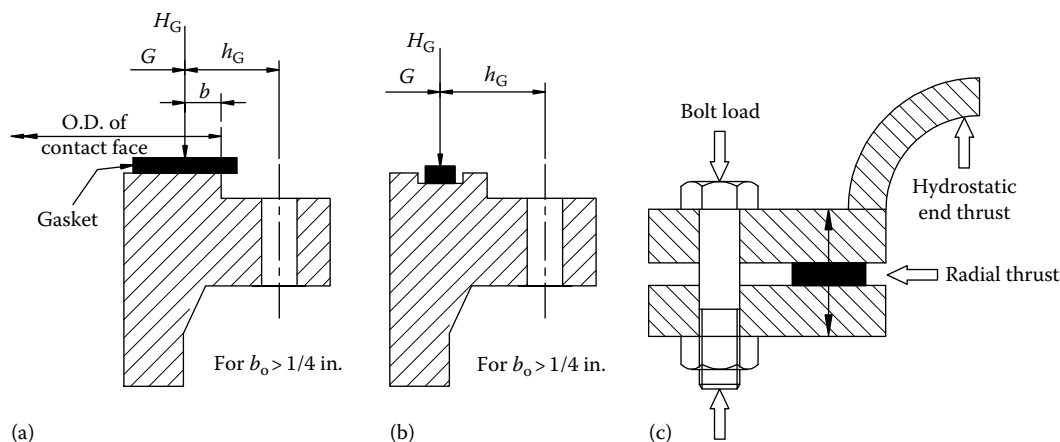


FIGURE 11.13 (a–c) Location of gasket load reaction.

11.6.1.5 Bolting Design

With the size and shape of the gasket established, next determine the bolting required. The bolting should be designed to maintain the required compression on the gasket with the internal pressure acting. Various design aspects of bolting are discussed next.

11.6.1.5.1 Determination of Bolt Loads

The bolt loads, W , required under the following conditions could be considered:

1. Gasket seating condition in the absence of internal pressure
2. Operating conditions

The thickness of flanges shall be determined as the greater required either by the operating or by the bolting-up conditions, and in all cases, both conditions shall be calculated in accordance with the following.

11.6.1.5.2 Gasket Seating Conditions

The gasket seating conditions are the conditions existing when the gasket or joint contact surface is seated by applying an initial load on the bolts when assembling the joint, at atmospheric pressure and temperature. The minimum initial load considered to be adequate for proper gasket seating is a function of the gasket material and the effective or contact area to be seated. The minimum initial bolt load required for this purpose, W_{m2} , shall be determined using the following formula:

$$W_{m2} = \pi b G y \quad (11.77)$$

The need for providing sufficient bolt load to seat the gasket or joint contact surfaces in accordance with this formula will prevail on many low-pressure designs and with facings and materials that require a high seating load, and the bolt load calculated for operating conditions is not sufficient to seat the joint. When formula (11.77) governs, flange dimensions will be a function of the bolting instead of internal pressure.

As per code formulas, for flange pairs used to contain a tubesheet (both sides gasketed) for a floating head or a U-tube type of heat exchanger, or for any other similar design, and where the flanges and/or gaskets are not the same, W_{m2} shall be the larger of the values obtained from formula (11.77) as individually calculated for each flange and gasket, and that value shall be used for both flanges.

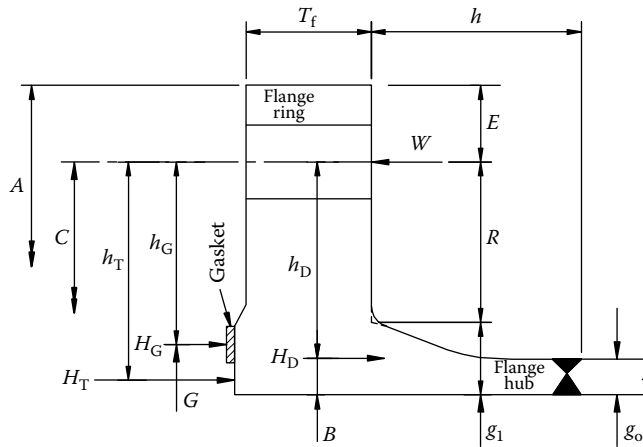


FIGURE 11.14 Dimensional data and flange forces—weld neck flange.

11.6.1.5.3 Operating Conditions

The operating conditions are the conditions required to resist the hydrostatic end force (H) of the design pressure, which tends to part the joint and to maintain on the gasket or joint contact surface sufficient compression force (H_p) to assure a tight joint at all operating conditions. The minimum load is a function of the design pressure, the gasket material, and the effective gasket area or the effective contact area to be kept tight under pressure. The required bolt load W_{m1} for the operating condition is given by

$$W_{m1} = H + H_p = \frac{\pi}{4} G^2 P + 2\pi b G m P \quad (11.78)$$

Various flange forces are shown schematically in Figure 11.14 and for more details on flange design refer to [75].

11.6.1.5.4 Bolt Area at the Root of the Threads

The necessary bolt area at the root of the threads, A_m , required for both the gasket seating and the operating conditions is the greater of the values W_{m1}/S_b and W_{m2}/S_a as given by the following expression:

$$A_m = \max \left| \frac{W_{m1}}{S_b}, \frac{W_{m2}}{S_a} \right| \quad (11.79)$$

From the required bolt area, determine the minimum number of bolts required (generally in multiples of 4) and observe the minimum sizes as recommended by TEMA, RCB-11. From the number of bolts chosen, find out the actual bolt area, A_b . In no case shall A_b be less than A_m . At this point, the designer should sketch a tentative layout showing the desired location and size of gasket or contact surface, hub thickness, and diameter of bolts and bolt circle, and from these set the outside diameter of the flange.

11.6.1.5.5 Flange Bolt Load W

The bolt loads used in the flange design shall be the values obtained from these formulas:

1. For the gasket seating condition,

$$W = \frac{(A_m + A_b)S_a}{2} \quad (11.80)$$

2. For the operating condition,

$$W = W_{m1} \quad (11.81)$$

11.6.1.5.6 Pitch Circle Diameter

In general, the pitch circle diameter for each particular size of bolt considered should be kept small, to keep the flange bending moment and flange outside diameter small [76].

11.6.1.5.7 Minimum Bolt Size

Small bolts should be avoided wherever possible, owing to the ease with which they may be overstressed by torsion applied with a wrench. Bolts, studs, nuts, and washers must meet the code requirements. Appendix 2 of the code recommends not using bolts and studs smaller than 0.5 in. (12.7 mm). If bolts or studs are smaller than 0.5 in. (12.7 mm), alloy steel bolting material must be used. Precautions must be taken to avoid overstressing small-diameter bolts.

TEMA Standards give guidelines for minimum bolt size in RCB-11. The minimum bolt size is 0.75 in. for R , 0.5 in. for C , and 0.625 in. for B class exchangers.

11.6.1.5.8 Minimum Recommended Bolt Spacing

Bolts should be spaced far enough apart to permit the clearance necessary for socket wrenches and to insure a uniform compression on the gasket. Likewise, the bolt circle on hubbed or integral flanges should have sufficient diameter to permit a generous fillet between the back of the flange and hub. Waters et al. [73] a bolt spacing of at least 2.25 times bolt diameters between centers to avoid high stress concentration.

In the TEMA guidelines, the minimum chordal pitch between adjacent bolts and minimum recommended wrench and nut clearances may be read from TEMA Table D-5.

11.6.1.5.9 Maximum Recommended Bolt Spacing

The bolt spacing should not be so great as to result in an appreciable reduction in gasket pressure between bolts. Waters et al. [73] recommends a spacing of $3.5d$ (d is the nominal diameter of bolt) between bolt hole centers as a reasonable maximum. An empirical expression given by Taylor Forge and Pipe Works [75] expresses the maximum bolt pitch in the form

$$B_{\max} = 2d + \frac{6T_f}{m + 0.5} \quad (11.82)$$

where

B_{\max} is the maximum bolt spacing for a tight joint (in.)

d is the nominal bolt diameter (in.)

T_f is the flange thickness (in.)

m is the gasket factor, which is obtained from ASME Code Table 2-5.1

This is included in TEMA, RCB-11.22.

11.6.1.5.10 Load Concentration Factor

As per TEMA RCB-11.23, when the distance between bolt centerlines exceeds the recommended B_{\max} , the total flange moment determined shall be multiplied by a load concentration factor equal to [3]

$$\sqrt{\frac{B}{B_{\max}}} \quad (11.83)$$

where B is the centerline-to-centerline bolt spacing.

Note: To prevent overstressing of bolted flanged connections, the designer should, wherever possible, set the lengths of wrench to be used.

11.6.1.5.11 Relaxation of Bolt Stress at Elevated Temperature

A rise in the temperature of a flanged joint causes the bolt and flange stresses to diminish, and on maintaining the joint at temperature, further reduction in stresses may occur due to creep as time elapses [76]. A multiphase PVRC elevated temperature program was initiated in 1982 by a task group of the PVRC Subcommittee on Gasket Testing Elevated Temperature Joint Behaviour, and the committee's report is published through WRC Bulletin 391 by Derenne et al. [77].

11.6.1.6 Flange Design

After the gasket and bolting design, next determine the flange dimensions required to withstand the bolt load without exceeding the allowable stress for the flange material. The outside diameter of the flange must be large enough to seat the bolt with manufacturing tolerance. In addition to bolting data, some more details on flange dimensions can be read from TEMA Table D-5. Since the flange design procedure is iterative in the case of integral weld neck flange and slip-on flange, initially assume a flange thickness. In the case of the ring flange, a closed-form solution for flange thickness is possible. The next step is to determine the moment arm of the various forces and reactions.

11.6.1.6.1 Flange Moments

In the calculation of flange stress, the moment of a load acting on the flange is the product of the load and the moment arm.

Various forces acting during the operating condition are the hydrostatic end force on area inside of the flange, H_D , the pressure force on the flange face, H_T , and the gasket load under operating conditions, H_G :

$$H_D = \frac{\pi B^2 P}{4} \quad (11.84)$$

$$H_T = H - H_D \quad (11.85)$$

$$H_G = W - H \quad (11.86)$$

where W is bolt load, W_{m1} or W_{m2} , whichever is greater. For the operating condition, the flange moment M_o is the sum of the three individual moments M_D , M_T , and M_G . Determine the moment arms h_D , h_T , and h_G for flange loads under operating conditions from Table 11.13 for the three

TABLE 11.13
Moment Arms for Flange Loads under Operating
Conditions

Type of Flange	h_D	h_T	h_G
Integral flange	$R + 0.5g_1$	$0.5(R + g_1 + h_G)$	$0.5(C - G)$
Loose or ring flange	$0.5(C - B)$	$0.5(h_D + h_G)$	$0.5(C - G)$
Lap flange	$0.5(C - B)$	$0.5(C - G)$	$0.5(C - G)$

types of flanges. Calculate M_D (moment due to H_D), M_T (moment due to H_T), and M_G (moment due to H_G) as given by

$$M_D = H_D h_D \quad (11.87)$$

$$M_T = H_T h_T \quad (11.88)$$

$$M_G = H_G h_G \quad (11.89)$$

and

$$M_o = M_D + M_T + M_G \quad (11.90)$$

For the gasket seating condition, the total flange moment M'_o (ASME Code uses the term M_o for moment due to gasket seating condition also), which is opposed only by the gasket load W , is given by

$$M'_o = \frac{W(C - G)}{2} \quad (11.91)$$

11.6.1.6.2 Flange Thickness

For a ring flange, the flange thickness t_f required is the greater of the gasket seating condition or operating condition, given by

$$T_f = \max \left(\sqrt{\frac{M_o Y}{S_{tb} B}}, \sqrt{\frac{M'_o Y}{S_{ta} B}} \right) \quad (11.92)$$

where Y is the shape constant, defined in Section 11.5.2, Step 5.

For the weld neck integral flange, as mentioned earlier, flange thickness is calculated by iterative process until such time as the flange stress falls within allowable stress for the flange material. If not within the limit, increase the flange thickness and continue the steps mentioned earlier. The stresses induced in the flange shall be determined for both the operating condition and the gasket seating condition, whichever controls. The procedure to determine flange stresses is listed in the step-by-step procedure given in the Appendix.

11.6.1.6.3 Flange Facings

The geometric details of the mating flange surfaces on which the gasket seats are known as flange facings (Figure 11.15). The ability of a flanged joint to maintain a leak-proof joint depends on a number of parameters, of which the gasket and flange facing details are the most important [31]. Flange facings

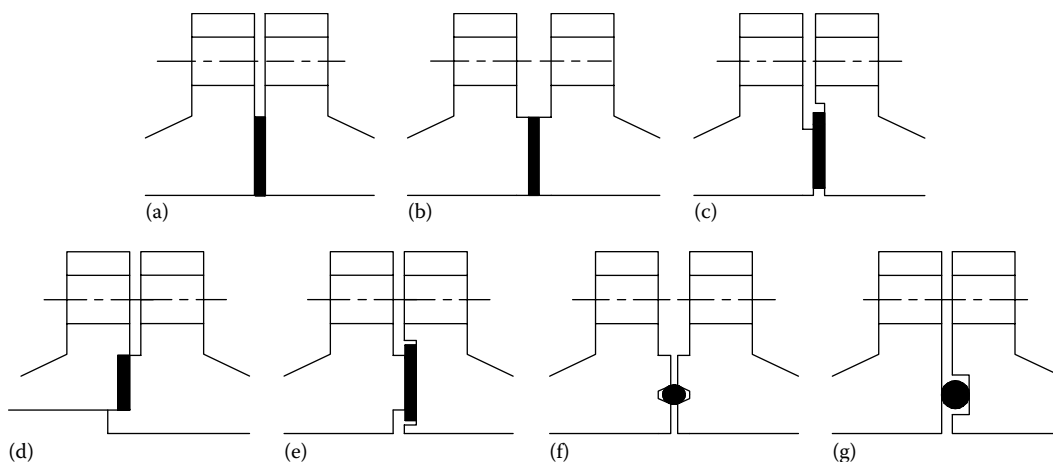


FIGURE 11.15 Flange facings. (a) Flat face, (b) raised face, (c) recessed face, (d) confined, (e) tongue and groove, (f) ring joint, and (g) O-ring.

are prepared to suit the gasket type, the kind of application, and the service conditions. Some of the classifications of the flange facings are as follows:

1. Unconfined and prestressed: flat face and raised face (RF)
2. Semiconfined and prestressed (male and female joint)
3. Confined and prestressed: tongue and groove, double step joint, ring joint
4. Self-energizing: O-rings, metallic, elastomer, etc.

The applicability of various flange facings is discussed in Refs. [31,34]. Flat face and RF are used for low-pressure applications; the male and female facings have the advantage of confining the gasket, thereby minimizing the possibility of blowout of gaskets. Since the mating flanges are nonidentical, male and female facings are widely used on heat exchangers and not on pipelines. Also the tongue-and-groove-type facings give protection against deforming soft gaskets into the interior of the vessel. Table 2-5.2 of the ASME Code gives a list of many commonly used contact facings.

11.6.1.6.4 Flange Facing Finish

The type and texture of surface finish are important for leak tightness of a flanged joint. There are five distinct styles of surface finish that are commonly used in the industry [31]: rounded nose spiral finish, spiral serrated finish, concentric serrated finish, smooth finish, and cold water finish.

11.6.1.6.4.1 Raised Face Flange RF flanges seal with a flat gasket, designed for installation between the RFs of two mating flanges (both with RFs). The RFs have a prescribed texture to increase their gripping and retaining force on this flat gasket. Some users of RF flanges specify the use of spiral wound gaskets.

11.6.1.6.4.2 Spiral Wound Gasket (SPWG) SPWG identifies a flat gasket used between two raised flanges (without ring grooves). SPWD gaskets contain a “spiral wound” metallic filler for reinforcement.

11.6.1.6.4.3 Ring-Type Joint Flange RTJ flanges have grooves cut into their faces that accept steel ring gaskets. RTJ flanges seal when tightened bolts compress the gasket between the flanges into the grooves, deforming (or coining) the gasket to make intimate contact inside the grooves, creating a metal-to-metal seal. An RTJ flange may have an RF with a ring groove machined into it.

11.6.1.6.5 Requirements for Flange Materials

The material used for flanges must meet the ASME Code general requirements for materials for pressure-retaining parts. Some specific ASME Code Section VIII, Div. 1 (Appendix 2), requirements for flange materials include the following:

1. Flanges made from ferritic steel must be given a normalizing or full annealing heat treatment when the thickness of the flange section exceeds 3 in. (76.2 mm)
2. Material on which welding is to be performed must be proved to be of good weldable quality
3. Welding shall not be performed on steel that has a carbon content higher than 0.35%
4. All welding on flange connections must comply with the code requirements for postweld heat treatment
5. Fabricated hubbed flanges may be machined from a hot-rolled or forged billet or a forged bar

11.6.1.6.6 Rating of Standard Flanges

Standard flanges are rated as 150, 300, 400, 600, 900, 1500, and 2500 lb flanges. TEMA Table D-3 provides dimensions of ANSI standard flanges and bores of welding neck flanges. Lengths of alloy steel stud bolts for various flange ratings are furnished in TEMA Table D-4.

11.6.1.6.7 Bolting Procedures

In a flanged connection, all components must be correct to achieve a seal. The most common cause of leaky gasketed joints is improper installation procedures. To ensure leak-free joint, the bolting procedures as recommended by Garlock Sealing Technologies, Palmyra, New York, are given as follows:

1. Place the gasket on the flange surface to be sealed. Bring the opposing flange into contact with the gasket.
2. Clean the bolts and lubricate them with a quality lubricant, such as an oil and graphite mixture.
3. Place the bolts into the bolt holes.
4. Finger-tighten the nuts.
5. Follow the bolting sequence as shown in Figure 11.16. During the initial tightening sequence, do not tighten any bolts more than 30% of the recommended bolt stress. Doing so will cause cocking of the flange, and the gasket will be crushed. Upon reaching the recommended torque requirements, do a clockwise bolt-to-bolt torque check to make certain that the bolts have been stressed evenly.
6. Due to creep and stress relaxation, it is essential to prestress the bolts to ensure adequate stress load during operation.

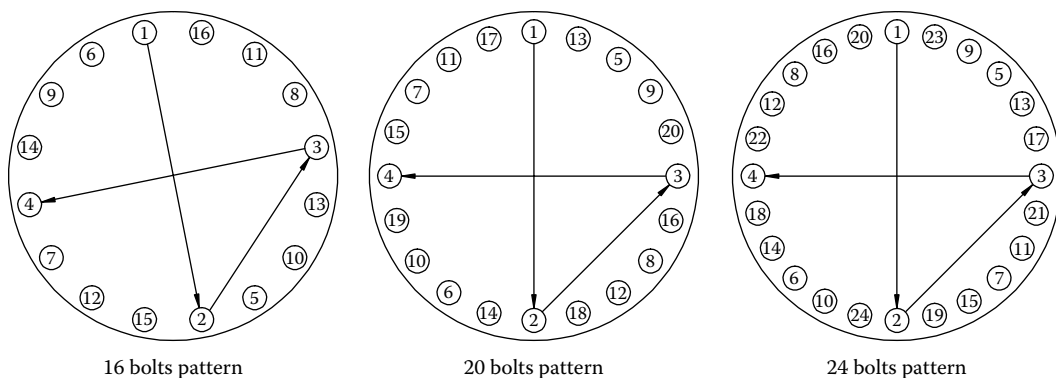


FIGURE 11.16 Flange bolt tightening sequence.

11.6.1.6.8 Bolted Joint Integrity and Intertube Pass Leakage in U-Tube Exchangers

An analysis technique to determine the structural behavior of the both sides gasketed U-tube tubesheet exchanger is studied in Ref. [78]. The method also provides procedure to compute the magnitude of the interpass leakage between the channel pass partition lanes. Some of the main conclusions of this study with reference to flange stresses are as follows:

1. The flange for the low-pressure chamber may be grossly overstressed if sized using the ASME Code.
2. The stresses in the high-pressure side flange are generally higher than those predicted by the ASME Code.
3. Increasing the bolt prestress increases the stresses in the flanged joint elements. It has, however, a minor effect in reducing the leakage area.

11.6.2 STEP-BY-STEP PROCEDURE FOR INTEGRAL/LOOSE/OPTIONAL FLANGES DESIGN

The ASME Code procedure for bolted flange joints for integral/loose/optional design is given here. The design procedure for reverse flange design is not covered. Certain steps may not be relevant for any one or two of these varieties. The procedure given here is similar to the ASME Code procedure detailed in the Taylor and Forge Company Bulletin on flange design [75]. The essential steps on bolted flange design are as follows:

1. Selection of material for flange, gasket, bolts
2. Calculation of load for gasket seating condition
3. Calculation of load to withstand hydrostatic pressure known as operating condition
4. Bolting design and number of bolts decided
5. Thickness of flange estimation to withstand governing moment
6. Calculation of stress in the flange and to verify that the calculated stresses are within code allowable stress

11.6.2.1 Data Required

1. Design pressure, P
2. Design temperature, T
3. Atmospheric temperature, T_a
4. Material specification for
 - a. Flange
 - b. Bolting
 - c. Gasket
5. Code allowable bolt stress
 - a. At design temperature, S_o
 - b. At atmospheric temperature, S_a
6. Code allowable flange stress
 - a. At design temperature, S_{fo}
 - b. At atmospheric temperature, S_{fa}

11.6.2.2 Step-by-Step Design Procedure

Step 1:

- a. Draw a sketch of the flange with dimensional details, including flange forces, and moment arms. It depicts the flange thickness as t .
- b. Select gasket material and choose the gasket factors m and y .

- c. Determine the gasket dimensions—ID, d_i , and outside diameter, d_o , as follows: The inside diameter of the gasket (in inches) is normally taken as

$$d_i = B + 0.01$$

where B equals the shell inside diameter for a weld neck flange and shell outside diameter for a ring flange.

From d_i , calculate d_o using the following formula:

$$\frac{d_o}{d_i} = \sqrt{\frac{y - pm}{y - p(m+1)}}$$

where m is the gasket factor and y the minimum design seating stress.

- d. Gasket width and gasket load reaction diameter.

Calculate the gasket width, N , given by

$$N = \frac{(d_o - d_i)}{2}$$

Calculate the basic gasket width, b_o .

Calculate gasket load reaction diameter, G :

$$\begin{aligned} G &= \text{mean diameter of gasket face (if } b_o \leq 0.25 \text{ in.)} \\ &= \text{OD of gasket contact face} - 2b \text{ (if } b_o > 0.25 \text{ in.)} \end{aligned}$$

Step 2:

- a. Calculate bolt load for gasket seating condition W_{m2} and operating condition W_{m1} :

$$W_{m2} = \pi b G y$$

$$W_{m1} = H + H_p$$

where

H is the total hydrostatic end force

H_p is the total joint contact surface compression load

They are given by

$$H = \frac{\pi}{4} G^2 P$$

$$H_p = 2\pi b G m P$$

- b. Calculate bolt cross-sectional area, A_m , required to resist the bolt load, which is the greater of

$$\frac{W_{m1}}{S_b} \quad \text{or} \quad \frac{W_{m2}}{S_a}$$

- c. From A_m determine the number of bolts required (normally in multiples of 4), keeping the minimum bolt size as recommended in TEMA.

Step 3: Calculation of flange forces and their moments:

a. Calculated various flange forces:

$$H_D = \frac{\pi B^2 P}{4}$$

$$H_T = H - H_D$$

For operating condition: $H_G = W - H$

For gasket seating condition: $H_G = W$

b. Determine the moment arms h_D , h_T , and h_G for flange loads under operating conditions from Table 11.13 for the three types of flanges.

c. Calculate M_D (moment due to H_D), M_T (moment due to H_T), and M_G (moment due to H_G):

$$M_D = H_D h_D \quad M_T = H_T h_T \quad M_G = H_G h_G$$

Step 4: Calculate flange moments.

a. For operating conditions, the total flange moment M_o is the sum of the three individual moments M_D , M_T , and M_G :

$$M_o = M_D + M_T + M_G$$

b. For gasket seating M'_o (ASME Code uses the term M_o for moment due to gasket seating condition also) as given by

$$M'_o = \frac{W(C - G)}{2}$$

Step 5: Calculate the parameters E and K , and hub factors T , U , Y , and Z as follows, or they may be read from Fig. 2-7.1 of the ASME Code.

$$E = 0.5(A - C) \quad (\text{shown in Figure 11.14.})$$

$$K = \frac{A}{B}$$

$$U = \frac{K^2(1 + 4.6052(1 + \nu / 1 - \nu) \log_{10} K) - 1}{1.0472(K^2 - 1)(K - 1)(1 + \nu)}$$

$$T = \frac{(1 - \nu^2)(K^2 - 1)U}{(1 - \nu) + (1 + \nu)K^2}$$

$$Y = (1 - \nu^2)U$$

$$Z = \frac{K^2 + 1}{K^2 - 1}$$

Refer to ASME Code[] for determining factors F , V , F_L , and V_L pertaining to loose flange.

Step 6: Calculate factor h_o :

$$h_o = \sqrt{Bg_o}$$

Step 7: Calculate factors d_1 and e .

$$d_1 \quad (\text{for loose flanges}) = \frac{Uh_o g_o^2}{V_L}$$

$$(\text{for integral flanges}) = \frac{Uh_o g_o^2}{V}$$

$$e \quad (\text{for loose flanges}) = \frac{F_L}{h_o}$$

$$(\text{for integral flanges}) = \frac{F}{h_o}$$

where g_o is the thickness of the hub at the small end.

Step 8: Determine flange thickness:

- For weld neck integral flange and loose flange, calculate the flange stresses as detailed in step 10 and check if they are within limit (step 11). If not within the limit, increase the flange thickness and continue from Step 9 onward.
- For ring flange, flange thickness required is the greater of gasket seating condition or operating condition, given by

$$t = \sqrt{\frac{M_o Y}{S_{fo} B}} \quad \text{or} \quad t = \sqrt{\frac{M'_o Y}{S_{fa} B}}$$

where Y is the ring flange shape factor.

Step 9: Calculate stress formula factors.

$$\alpha = te + 1$$

$$\beta = \frac{4}{3}te + 1$$

$$\delta = \frac{t^3}{d_1}$$

$$\gamma = \frac{\alpha}{t}$$

$$\lambda = \gamma + \delta$$

$$m_o = \frac{M_o}{B}$$

$$m'_o = \frac{M'_o}{B}$$

Step 10: Calculate flange stresses. Flange stresses shall be determined for the governing moment, namely, more severe of the operating or the bolting conditions.

For operating conditions, calculate

- a. Longitudinal hub stress, S_H

$$S_H = \frac{fm_o}{\lambda g_l^2}$$

- b. Radial flange stress, S_R

$$S_R = \frac{(1.33te + 1)m_o}{\lambda t^2}$$

- c. Tangential flange stress, S_T

$$S_T = \frac{Ym_o}{t^2} - ZS_R$$

For the gasket seating condition, repeat the stress calculations replacing m_o by m_o

Step 11: Allowable flange stress: The stresses as calculated earlier are compared with the allowable stresses for the flange material at the design temperature S_{fo} (equation follows), and if required, the thickness can be modified. These stresses shall be calculated separately both for the gasket seating condition and for operating condition. For the operating condition, the allowable stresses are given by

$$S_H = 1.5S_{fo}$$

$$S_R = S_{fo}$$

$$S_T = S_{fo}$$

$$S_{fo} = \max[0.5(S_H + S_R), 0.5(S_H + S_T)]$$

For the gasket seating condition, the flange stresses are compared with the allowable stresses for the flange material at the atmospheric temperature S_{fa} (equation follows), and if required, the thickness can be modified.

$$S_H = 1.5S_{fa}$$

$$S_R = S_{fa}$$

$$S_T = S_{fa}$$

$$S_{fa} = \max[0.5(S_H + S_R), 0.5(S_H + S_T)]$$

11.6.2.3 Taper-Lok® Heat Exchanger Closure

It is common practice to design and build large-diameter, high-pressure heat exchangers with a welded diaphragm plate to seal the channel opening. While this solution does provide a seal for the closure, there are a few inherent problems. Generally, there are several thermal cycles encountered during the

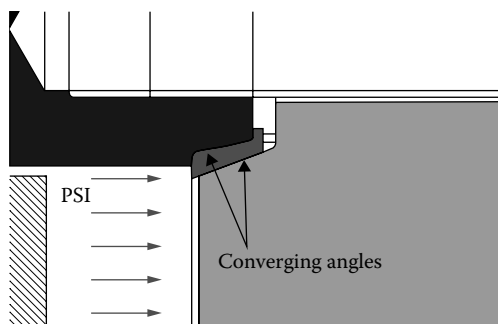


FIGURE 11.17 Taper-Lok closure metal-to-metal seal ring with dual converging tapered contact surfaces. (Courtesy Taper-Lok Corporation, Houston, TX.)

service of the heat exchanger. These cycles induce stress cracks due to thermal expansion at weld of the diaphragm plate, resulting in a leak. Leaks may also occur from less than perfect welds. *Leaking welded diaphragms of high-pressure heat exchangers in hydro treating and hydro processing service units are a serious problem for the petrochemical industry.* Repairing the weld to stop leaks is very costly. The reoccurring maintenance process to cut and reweld is cumbersome as it usually requires a nitrogen purge, stress relief at the weld, and nondestructive weld testing. The patented Taper-Lok seal (of Taper-Lok Corporation, Houston, Texas) offers the most simplified and reliable seal for high-pressure exchanger designs. Taper-Lok seals are a proven technology for durability in sealing heat exchangers, hard to hold or lethal fluids, especially in high-pressure or high-temperature environments.

Being “self energized” under operating conditions imparts an even tighter seal, as the internal pressure acts on the wedge-shape geometry of the seal ring creating greater tension on the wide area sealing surfaces, effectively creating a leak-free, zero fugitive emissions. Taper-Lok closure is typically used for high pressure up to 20,000 psi rating applications. Like a Separated-Head, the Taper-Lok connection uses independent tubeside and shellside flanges, bolting, and gasketing. The unique feature this closure offers is a reusable Taper-Lok ring that acts as a self-energizing seal connection.

Construction: The Taper-Lok seal is a metal-to-metal seal ring with dual converging tapered contact surfaces (Figure 11.17). The assembly consists of male flange, female flange, seal ring, studs, and nuts. The pressure-energized seal ring seats into a pocket in the female flange and is wedged and seated by a male nose located on the male flange. Utilizing this concept, the exchanger channel cylinder would contain the female pocket, while the channel cover would have the male nose geometry (Figure 11.18). In the pre-bolted condition, the Taper-Lok seal ring lip stands off of the face of the channel. The converging seal surfaces are brought together like a wedge during bolt up. This wedging motion forces the seal ring onto the male nose and into the female pocket forcing a compressive hoop stress. Minimal bolt load is required to achieve the required contact stress on the seal surfaces. The converging angles of the seal ring create a wedge or “doorstop” effect. As the equipment internal pressure increases, the seal seats tighter into this sealing wedge. The seals can be made from the same material as the process equipment (exchanger channel and cover) to ensure that thermal expansions are consistent across all components. The effects of bimetallic (galvanic) corrosion are eliminated. A baked-on molybdenum disulfide coating is applied to the seal to prevent galling.

11.6.2.4 Zero-Gap Flange

In polymer processing systems, the gap between conventional flanges can cause turbulence and/or stagnation in the flow of polymer materials that are transported through the pipelines. This, in turn, can cause the materials to solidify and build up in the pipeline at the connector. As the solidified material builds up, the flow through the pipeline is restricted. The flanges must be periodically dismantled and the solidified polymer removed. This is an extremely expensive

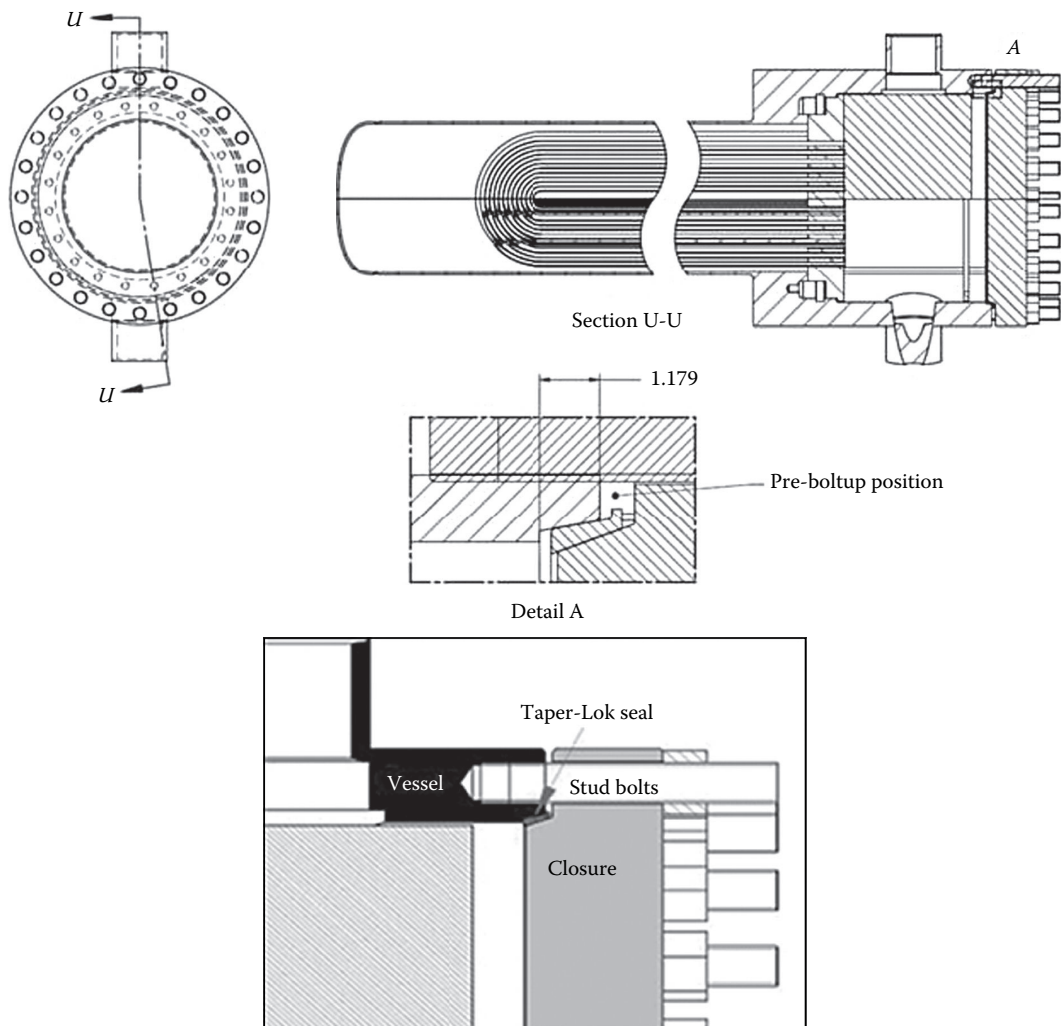


FIGURE 11.18 Taper-Lok closure for a high-pressure heat exchanger. (Courtesy Taper-Lok Corporation, Houston, TX.)

process, due to both the cost of dismantling/cleaning the connectors and the cost associated with downtime of the system.

Taper-Lok zero-gap connection consists of a through bore, as the male nose is landed onto the female flange to eliminate the gap between the two flanges (Figure 11.19). The resulting through bore significantly reduces problems with crevice corrosion and polymer solidification. The connector offers an advantage in critical services with crevice corrosion, such as alkylation units with hydrofluoric acid and sulfuric acid. Flanges in these highly corrosive environments suffer from significant corrosion specifically in the crevice between the two flanges.

11.6.2.5 Long Weld Neck Assembly

The long weld neck assembly comprises a male or female flange with an extra-long reinforced neck, a seal ring, a male or female blind flange, and a complete set of studs and nuts. The long weld neck is typically used in pressure vessel applications where the reinforced neck thickness is required to match or replace the material that removed from the shell of the pressure vessel. The blind flange can also be replaced with a weld neck flange if continuous piping is required.



FIGURE 11.19 Taper-Lok's zero-gap connection. (Courtesy Taper-Lok Corporation, Houston, TX.)

11.7 EXPANSION JOINTS

Expansion joints are promising for accommodating differential thermal expansion of heat exchanger shells, pressure vessels, and pipelines carrying high-temperature fluids. Differences in the axial expansion of the shell and the tube bundle due to high mean metal temperature differentials warrant incorporation of expansion joints in heat exchangers. This is particularly true for fixed tubesheet exchangers. For fixed tubesheet exchangers, when the difference between shell and tube mean metal temperatures becomes large (greater than approximately 50°C for carbon steel), the tubesheet thickness and tube end loads become excessive [26]. In most cases, the tubes are hotter than the shell; moreover, tube material is sometimes high alloy, i.e., stainless steel or nickel alloy, which expands about 50% more than carbon steel. Therefore, an expansion joint is incorporated into the shell. Expansion joints also find applications in floating head exchangers, in the pipe between the floating head cover and the shell cover to cushion the thermal expansion between the tube bundle and the shell.

11.7.1 FLEXIBILITY OF EXPANSION JOINTS

Expansion joints used as an integral part of heat exchangers or other pressure vessels shall be designed to provide flexibility for thermal expansion and also to function as a pressure-retaining structural element. Hence, an expansion joint must compromise between two contradictory loading conditions [79]: (1) pressure-retaining capacity and (2) flexibility to accommodate the differential thermal expansion. In many cases, the design for a particular application will involve a compromise of normally conflicting requirements. For example, to retain a high pressure, usually a thick-walled bellows is required, whereas high flexibility and high fatigue life require a thin-walled bellows.

11.7.2 CLASSIFICATION OF EXPANSION JOINTS

Expansion joints are broadly classified into two types:

1. Formed head or flanged-and-flued head
2. Bellows or formed membrane

11.7.2.1 Formed Head or Flanged-and-Flued Head

Formed head expansion joints, also called thick-walled expansion joints, are characterized by higher spring rates (i.e., force required for unit deflection of a bellow) and usually a lower cycle life than

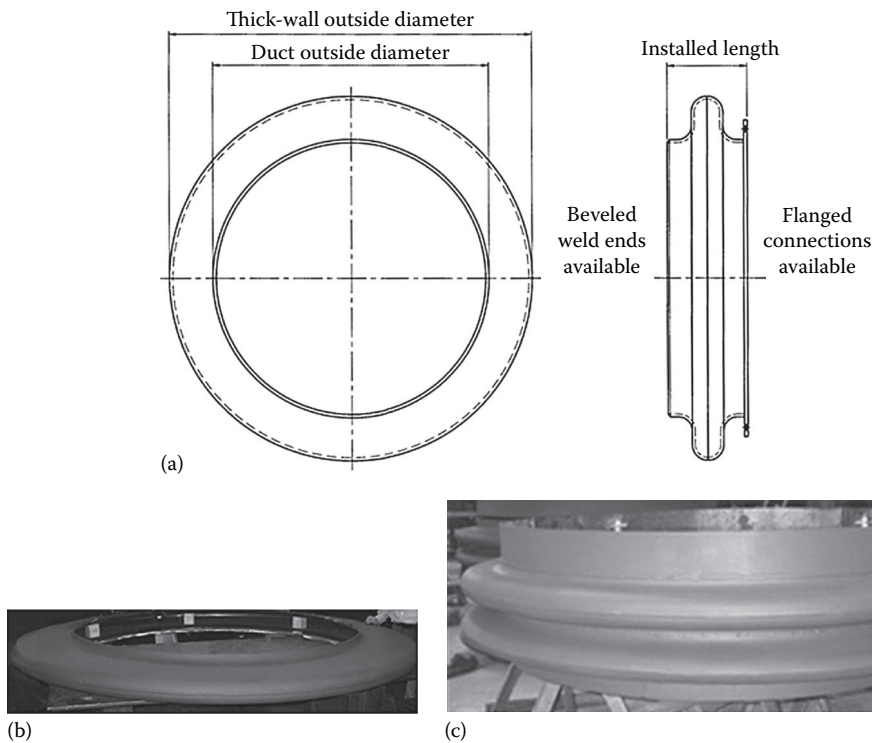


FIGURE 11.20 Thick-walled expansion joint. (a) Schematic, (b) expansion joint with a single convolution, and (c) expansion joint with double convolutions. (Courtesy of U.S. Bellows, Inc, Houston, TX, www.usbellows.com.)

thin-walled bellows. The convolutions on the bellows may be U-shaped or toroidal depending on the design conditions. Because of the higher wall thickness, this type of expansion joint is rugged and the most durable from the standpoint of abuse, but it has the disadvantage of very limited flexibility. Design of such bellows is covered by ASME Code Sec VIII Div 1, Appendix CC. Heavy wall bellows are rugged, generally having a wall thickness equal or near to the shell wall. Because of material thickness, no cover or shroud is necessary. The disadvantage is that a lot of fluid can be trapped in these corrugations, and a drain is sometimes required. Those bellows are formed by welding flanged-and-flued plates together, thus creating 1, 2, or 3 U-Shaped corrugations. ASME Code inspection and U-2 stamp are required. Construction details of formed head expansion joints are discussed in Refs. [31,40] and by Singh [80]. Thick-walled expansion joints are shown in Figures 11.20 and 11.21.



FIGURE 11.21 Expansion joint for a heat exchanger. (Courtesy of KE-Burgmann Expansion Joint Systems, Santee, CA.)

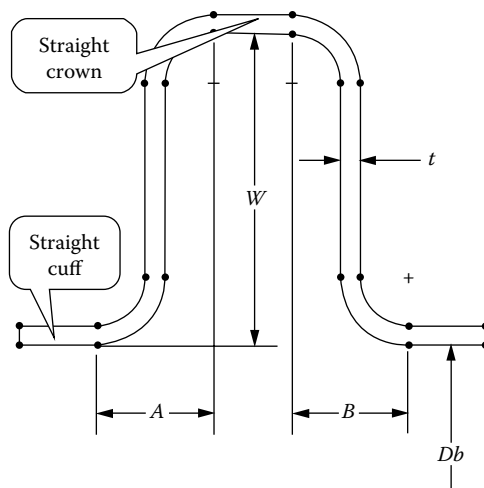


FIGURE 11.22 Cross section of a flanged-and-flued expansion joint. (Courtesy of Pressure Vessel Engineering Ltd., Waterloo, Ontario, Canada.)

Formed head expansion joints are made in two halves from flat annular plates. The outside edges of the plates are formed in one direction (flanged), and the inside edges are formed in the other direction (flued). The two halves are welded together and then welded into the heat exchanger shell (as shown in Figure 15.6 of Chapter 15). As a minimum, all code joints require 100% dye penetrant examination of the bellows longitudinal seams and attachment welds along with a hydrotest. Additional examination can be added such as x-rays, ultrasonics, helium leak test, and impact testing. All code joints are manufactured from a variety of ASME Code-approved SB materials. These materials require mill test reports and tracking so each part can be stamped with a unique serial number. This serial number contains a complete history of the expansion joints' materials and construction.

A flanged-and-flued head expansion joint consists of the following elements (Figure 11.22):

1. An outer shell or outer tangent
2. Two outer tori
3. Two annular plates
4. Two inner tori
5. Two inner shells or inner tangents butt welded to the main shell on both sides

The inner and outer tori serve to mitigate the stress concentration due to geometric discontinuities between the shell and the annular plates. The radii of the tori are seldom less than three times the expansion joint thickness [31]. The annular plate contributes to lower the spring rate of the joint. Where the flexibility requirement is rather feeble, annular plate and the outer shell are eliminated. This type of construction results in the semitorus construction (Figure 11.22b) [31,40]. The formed head type, i.e., without the inner tori, will lead to a flanged expansion joint as shown in Figure 11.22c.

11.7.2.2 Bellows or Formed Membrane

According to EJMA Standards [8], a bellows-type expansion joint is defined as a device containing one or more bellows used to absorb dimensional changes, such as those caused by thermal expansion or contraction of a pipeline, duct, or vessel. A bellows is defined as a flexible element of an expansion joint, consisting of one or more convolutions and the end tangents, if any. The bellows-type

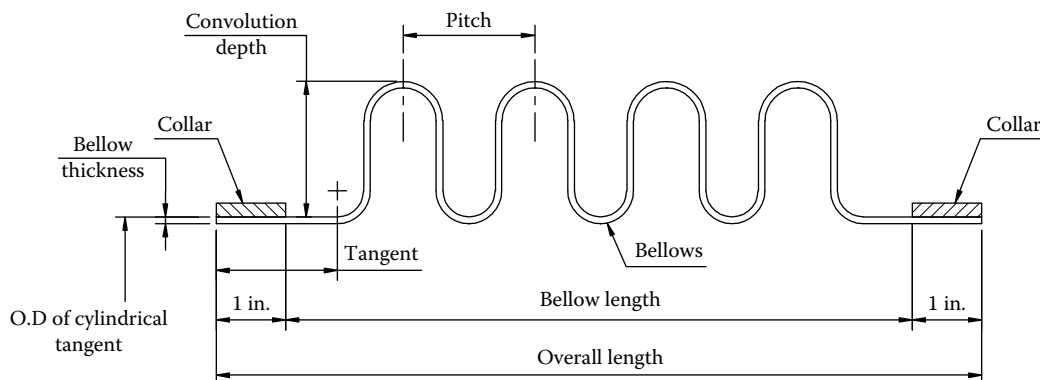


FIGURE 11.23 Bellows-type expansion joint (schematic).

expansion joint is also known as a “thin-walled expansion joint.” The name “thin-walled expansion joint” is used to mean any form of expansion joint whose thickness is less than the thickness of the heat exchanger shell. A part of bellows-type expansion joint is shown schematically in Figure 11.23.

Generally, the thin-walled bellows is formed from a thin plate whose thickness does not exceed 1/8 in. (3.2 mm) of corrosion-resistant material such as austenitic stainless steel or nickel-base alloys or high-alloy material using manufacturing processes like (1) disk or diaphragm forming, (2) elastomeric forming, (3) expansion forming, (4) hydraulic forming, and (5) pneumatic tube forming.

Bellows-type expansion joints are made primarily for piping applications. Figure 11.24 shows bellows-type expansion joints for piping applications. Heat exchanger shell bellows can also be thin-walled multi-convolution bellows, ring reinforced for higher pressures. When used in heat exchangers, they are costly and delicate [79]. The cost is derived from the fact that such vessels require special sizes and material. They are said to be delicate because a heat exchanger containing a thin-walled joint must be handled and supported carefully in order to avoid damage, puncture, and buckling of the joint. Thin-walled bellows have no circumferential welds. For this reason, a higher fatigue life is expected. These bellows are more compact in outer diameter than heavy-walled bellows. Design of thin-walled bellows is covered by ASME Code Sec VIII Div 1 mandatory Appendix 26.



FIGURE 11.24 Bellows-type expansion joint for piping applications. (Courtesy of U.S. Bellows, Inc, Houston, TX, www.usbellows.com.)

Thin-walled bellows can be formed by expanding mandrel, roll forming or hydro forming. An external cover or shroud is required for these bellows to protect against mechanical damage. Code inspection and U-2 stamp are required.

11.7.2.3 Deciding between Thick- and Thin-Walled Expansion Joints

11.7.2.3.1 Conditions That Favor Using Thick-Walled Joints

Some of the conditions that favor thick-walled expansion joints are [23] the following:

1. Shellside pressure is 300 psi (2070 kPa) or less
2. Deflections per flexible element are moderate, in the range arbitrarily set at 1/8–1/4 in. (3.2–6.3 mm)
3. Application is noncyclical
4. The joint must be capable of being vented and drained

11.7.2.3.2 Conditions That Favor Using Thin-Walled Joints

Some of the conditions that favor thin-walled expansion joints are [23] the following:

1. Shellside pressure exceeds 300 psi (2070 kPa)
2. Deflections per flexible element are high—arbitrarily greater than 1/4 in. (6.3 mm)
3. Application requires high cyclic life

11.7.3 DESIGN OF EXPANSION JOINTS

11.7.3.1 Formed Head Expansion Joints

Kopp and Sayre [81] are generally credited for the first comprehensive work to determine analytically the axial stiffness of “flanged-only” expansion joints. The method of analysis is based upon replacing the geometric configuration by an equivalent geometry. The outer torus (total length $\pi r/2$) is replaced by an equivalent corner end. One-half of the meridian of the outer torus is assigned to the annular plate and the other half to the outer shell. Figure 11.25 shows their idealized model. The structural characteristics of the annular plate are modeled by a unit width beam strip, the inner shell (heat exchanger main shell) is modeled using thin-shell bending equations, and the outer shell is not modeled using classical thin shell equations but instead an approximate relationship is used. Kopp and Sayre also conducted some experimental tests to verify their mathematical model.

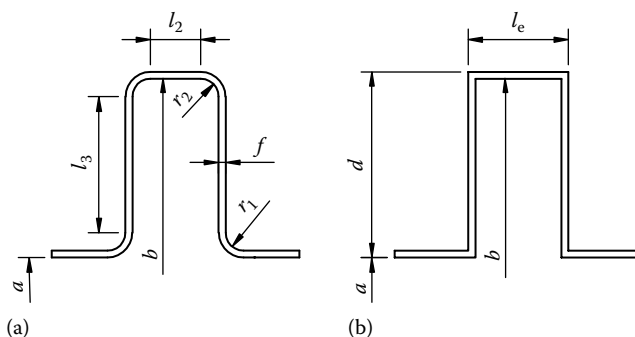


FIGURE 11.25 Kopp and Sayre model for flanged-and-flued expansion joint. (a) Actual model and (b) idealized model. *Note:* Dimensions a and b are radii. (From Kopp, S. and Sayre, M.F., *ASME Winter Annual Meeting*, New York, 1952.)

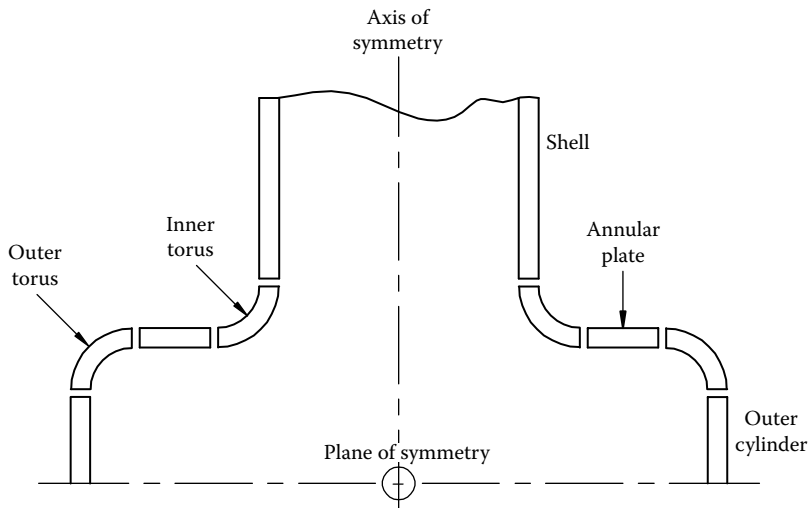


FIGURE 11.26 Finite element model for flanged-and-flued expansion joint. (From Wolf, L.J. and Mains, R.M., *Trans. ASME J. Eng. Ind.*, 145, 1973)

11.7.3.2 Finite Element Analysis

Wolf and Mains [79] applied FEA. The flanged-and-flued expansion joint is broken into its basic geometric components—a short cylinder, a toroidal segment, a flat annular plate, another toroidal segment, and a semi-infinite cylinder, as shown in Figure 11.26.

11.7.3.3 FEA by Design Consultants

FEA of Flanged-and-Flued Expansion Joint—The elements to be considered for FEA analysis are shown in Figure 11.26, and various possibilities to be considered to arrive at an appropriate/optimum design solution include bellow without straight crown and cuffs, bellow with straight crown but without straight cuffs, and bellow with straight crown and straight cuffs as shown in Figure 11.27.

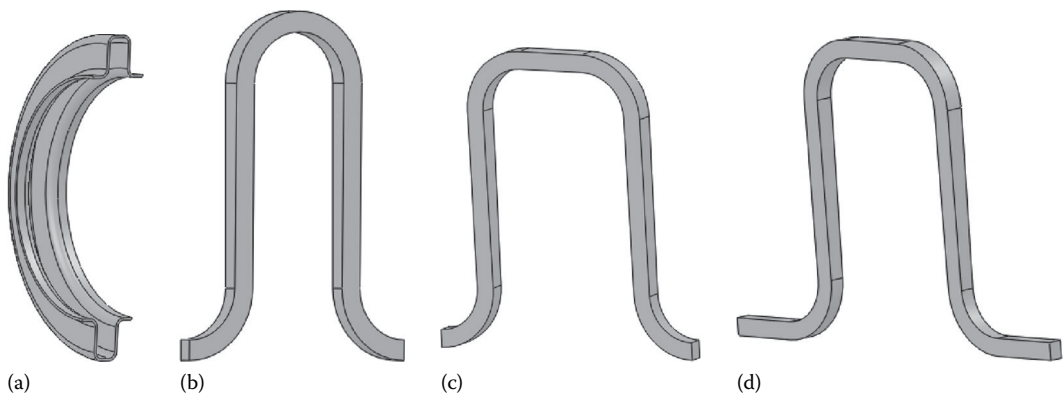


FIGURE 11.27 Various combinations of bellow elements considered for a typical design of case of a flanged-and-flued expansion joint by FEA. (a) Bellow profile, (b) bellow without straight crown and cuffs, (c) bellow with straight crown but without straight cuffs, and (d) bellow with straight crown and straight cuffs. (Courtesy of Pressure Vessel Engineering Ltd., Waterloo, Ontario, Canada.)

11.7.3.4 Singh and Soler Model

Singh and Soler [31] upgraded the Kopp and Sayre [81] solution by using classical plate and shell solutions in place of “beam” solutions. This model suffers from the limitation of considering one standard expansion joint geometry only. In practical applications, myriad variations of the standard flanged-and-flued configuration are employed. Hence, Singh [80] present generalized treatment of various forms of FSE geometry, while retaining its modeling assumptions, which were directly borrowed from Kopp and Sayre. This model is included in the TEMA seventh edition.

The basics of the Singh [80] model are discussed next without the details of stress analysis and determination of spring constant. The most general form of the FSE is shown in Figure 11.28. The FSE is one half of a standard expansion joint. Two flexible elements together make a standard expansion joint, such as the one shown in Figure 11.22a. The first step in the model simplification is to replace the circular segments with straight ones in the manner of Kopp and Sayre. By this step, the composite shells located at radii a and b are replaced by an equivalent shell of thickness t_1 and t_2 , respectively, with modified flexural rigidities. Since the chief contribution of the tori lies in reducing local bending stresses, which are secondary stresses, and since secondary stresses are of less importance, elimination of tori and replacement by sharp corners do not detract from the essence of developing a simple practical solution. The FSE is reduced to two concentric shells of radii a and b connected by an annular plate. The Young's moduli of the three elements can be different. The resulting idealized model has the appearance of Figure 11.28b. The three elements of the FSE can be characterized as follows:

1. Inner shell of thickness t_1 , equivalent Young's modulus E_1 , equivalent length l_1 , and radius a
2. Outer shell of thickness t_2 , equivalent Young's modulus E_2 , length l_2 , and radius b
3. Annular plate of thickness t_e , with inner and outer radii a and b , respectively

The equivalent lengths l_1 and l_2 warrant further comment. For the inner shell, l_1 should be taken sufficiently long such that the edge effects (at the annular plate and shell junction) die out. Taking $l_1 = 2.5 (at)^{0.5}$ will suffice, unless the shell is shorter, in which case the actual length should be used. Similarly, the length l_2 is actually the half-length of the top shell in the expansion joint.

11.7.2.4.1 Analysis for Axial Load and Internal Pressure

The resultant loading and internal stress acting on the elements along their inner junction A (the interface between the main shell element and annular plate) and outer junction B (the interface between the annular plate element and the outer shell) are shown in Figure 11.29.

11.7.2.4.2 Force due to Internal Shellside Pressure

The equilibrium of one-half of the joint, in the axial direction, gives F_2 in terms F_{ax} [31]:

$$2\pi F_2 b = 2\pi F_{ax} a + \pi(b^2 - a^2)p_s \quad (11.93)$$

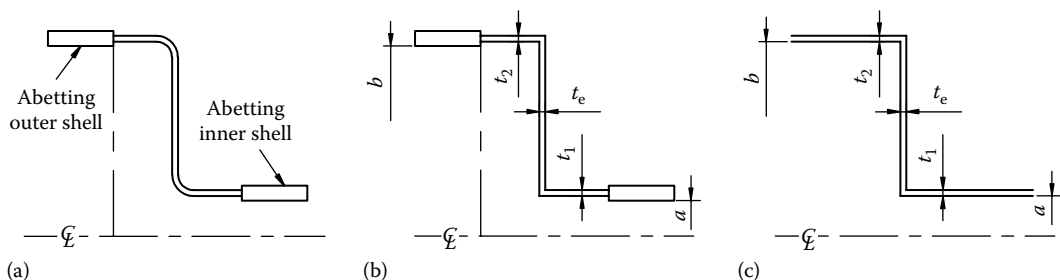


FIGURE 11.28 Singh and Soler model for flanged-and-flued expansion joint. (a) General model; (b) equivalent Kopp and Sayre model; and (c) final idealized model. (From Singh, K.P., *Trans. ASME, J. Pressure Vessel Technol.*, 113, 64, 1991.)

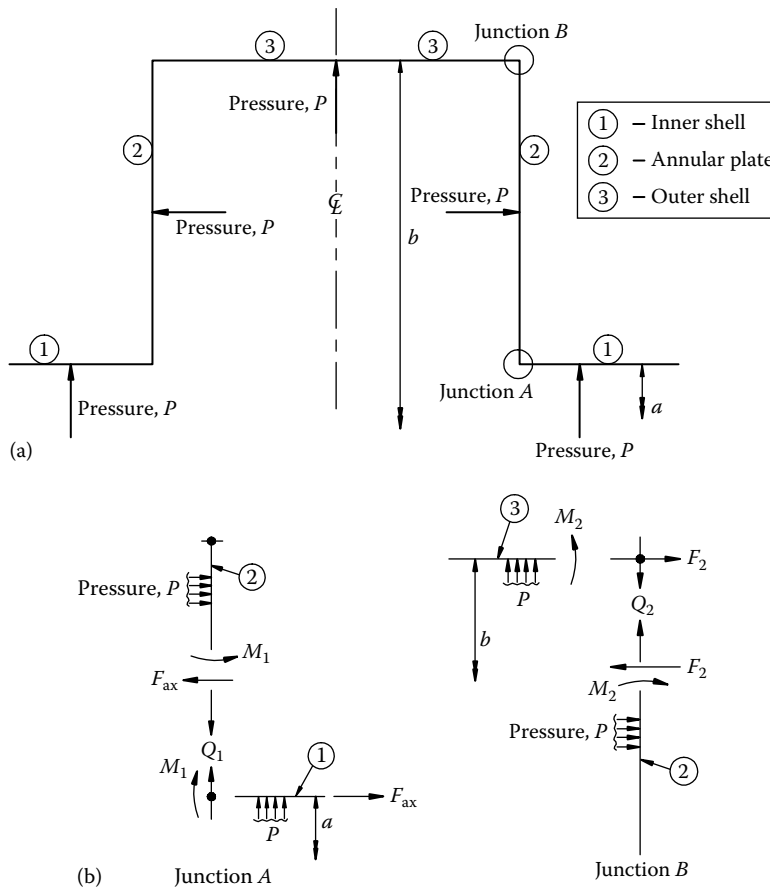


FIGURE 11.29 Loading and internal stress resultant acting on the flanged-and-flued expansion joint. (a) Loading pattern and (b) forces and moments acting at the joints. (Adapted and modified from Singh, K.P. and Soler, A.I., *Mechanical Design of Heat Exchangers and Pressure Vessel Components*, Arcturus, Cherry Hill, NJ, 1984.)

Equation 11.93 can be written as

$$F_2 = F_{ax} \frac{a}{b} + \frac{b^2 - a^2}{2b} p_s \quad (11.94)$$

The load deflection relations for short shell and annular plate elements to assemble the stiffness equations are derived in their work. They are not repeated here. Most of the formulas that are part of the TEMA procedure are arrived at after substituting $n = 0.3$ in the formulas of Singh and Soler [31] model.

11.7.3.5 Procedure for Design of Formed Head Expansion Joints

Rules for designing the formed head expansion joint currently exist in TEMA, ASME Code Section VIII, Div. 1, ANCC VSR1P, and AD Merkblatter, among others. HEDH [26] summarizes the salient features of flanged-and-flued-type expansion joint design.

ASME VIII-1 mandatory Appendix 5 provides guidelines for the design of flanged-and-flued expansion joints; ASME Code Appendix 26 (and EJMA Standard) provides rules to calculate these values, but the configuration of a flanged-and-flued expansion joint does not match that used in Appendix 26 or EJMA.

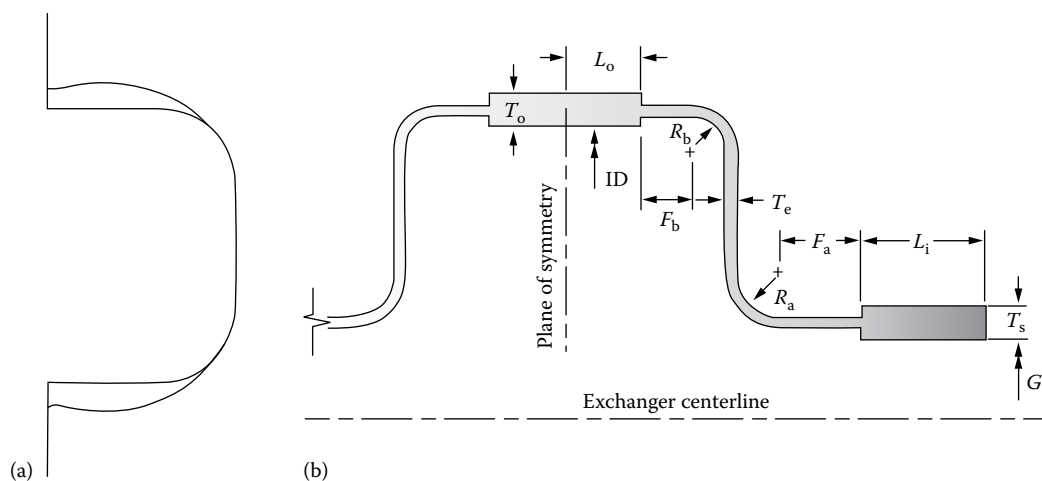


FIGURE 11.30 Expansion joint geometry (a) and deformed shape (b) as per TEMA software analysis for a typical case. (Courtesy of Paulin Research Group Houston, TX.)

The flanged-and-flued expansion joint has a straight crown and straight cuff neither of which is included in the ASME/EJMA stress and flexibility calculations.

11.7.2.5.1 TEMA Procedure

The seventh edition (1988) of the TEMA Standards includes a new section RCB-8 on FSEs (not light-gauge bellows-type expansion joints), to be used in conjunction with fixed tubesheet design. The paragraph encompasses several different shapes, such as flanged-and-flued heads, flanged-only heads, and others. Also included is a method to calculate the maximum stress for cycle life calculations. The shell flexible elements shall be analyzed in both corroded and uncorroded conditions and shall be evaluated for hydrostatic test conditions also.

Expansion joint geometry (right side) and deformed shape (left side) as per TEMA software analysis for a typical case by Paulin Research Group Houston, Texas, are shown in Figure 11.30.

11.7.2.5.2 Minimum Thickness

As per TEMA RCB-8.9, the minimum thickness of the FSEs shall be determined by the method of analysis. However, in no case shall the minimum uncorroded thickness be less than 3.2 mm (0.125 in.) for nominal diameters up to 18 in., 4.8 mm (3/16 in.) for nominal diameters in the range of 19–30 in. (482.6–762 mm), or 6.35 mm (0.25 in.) for nominal diameter greater than 30 in. (762 mm). The industry practice is to set the FSE thickness one gauge less than the shell thickness [31]. When required, use more than one set of formed heads.

11.7.2.5.3 Allowable Stress (TEMA RCB-8.8)

The allowable stresses in the flexible element, both in the corroded and in the uncorroded conditions, shall be as defined in the ASME Code using an appropriate stress concentration factor for the geometry.

11.7.3.6 Design Procedure as per ASME Code

ASME Code Section VIII, Div. 1, does not give formulas for sizing the formed head expansion joints. However, rules are given for materials of construction, stress limits, cycle life calculation, fabrication, inspection and pressure test, stamping, and reports. The design of expansion joints shall conform to the requirements of Appendix CC of the ASME Code. Design aspects of multilayer asymmetric geometries or loadings that differ from the basic concepts of Appendix CC are dealt in

Paragraph U-2(g). Details of fabrication and inspection of formed type expansion joints are covered in Chapter 15, Heat Exchanger Fabrication. Stamping details are covered here.

11.7.2.6.1 *Construction Materials and Minimum Thickness*

According to ASME Code Section VIII, Div. 1, the materials for pressure-retaining components shall conform to the requirements of UG-4. For thick-wall formed heads-type expansion joints, in general, the bellows are of the same material as the shell.

11.7.2.6.2 *Stamping and Reports*

Details of stamping and reports are outlined in Section CC-6. As per this section, the expansion joint manufacturer shall have a valid ASME Code U certification of authorization and shall complete a Form U-2 Manufacturer's Partial Data Report, as required by UG-120(c). The Manufacturer's Partial Data Report shall contain data and information like the following:

1. Maximum allowable working pressure and temperature
2. Spring rate and axial movement
3. Service conditions
4. Design life in cycles
5. A certification that the expansion joint has been constructed as per the rules of Appendix CC
6. Details of the vessel manufacturer

11.7.4 DESIGN OF BELLOWS OR FORMED MEMBRANES

Bellows-type expansion joint design shall conform to the requirements of EJMA Standards, the ANSI Piping Codes, and the ASME Codes as applicable. The design of structural attachment shall be in accordance with accepted methods, based on elastic theory. In addition to EJMA Standards, design analysis and rules are also included in Appendix BB, ASME Code Section VIII, Div. 1, for circular-type bellows with single-ply reinforced and nonreinforced bellows with thickness less than 3.2 mm (0.125 in.).

11.7.4.1 **Shapes and Cross Section**

The bellows are available both for circular shells and for rectangular shells. Rectangular shapes are used for surface condensers.

11.7.4.2 **Bellows Materials**

The bellows material shall be specified and must be compatible with the fluid handled, the external environment, and the operating temperature. Particular consideration shall be given to possible corrosion attack.

11.7.4.3 **Bellows Design: Circular Expansion Joints**

The design of bellows-type expansion joints involves an evaluation of pressure-retaining capacity, stress due to deflection, spring rate, fatigue life, and instability (squirm). The spring rate is a function of the dimensions of the bellows and the bellows material. The determination of an acceptable design further involves the bellows parameters such as material, diameter, thickness, number of convolutions, pitch, height, number of plies, method of reinforcement, manufacturing technique, and heat treatment. Specification sheet for circular bellows is shown in Figure 11.31.

11.7.4.4 **Limitations and Means to Improve the Operational Capability of Bellows**

Single-ply bellows are used for low-pressure applications. They are fragile and hence they are easily damaged; external covers to protect personnel against the hazards of bellows blowout due to failure

Customer:		Date:	Page:
Project:		Prepared by:	
Applicable codes and standards:			
Item or tag number:			
Quantity			
Size (specify inside or outside duct dimensions)			
Orientation (horizontal/vertical/inclined)			
Style or type			
Corner type			
End connections	Thickness/angle flange size		
	Material		
Pressure (in. water)	Design		
	Operating		
Temperature	Design		
	Operating		
	Installation		
Media	Media		
	Flow velocity		
	Flow direction		
Movements	Axial extension		
	Axial compression		
	Lateral (parallel to short side)		
	Lateral (parallel to long side)		
	Angular (parallel to short side)		
	Angular (parallel to long side)		
Materials	Bellows		
	Liner		
	Cover		
Dimensions	Overall length		
Maximum spring rates	Axial		
	Lateral (parallel to short side)		
	Lateral (parallel to long side)		
	Angular (parallel to short side)		
	Angular (parallel to long side)		
Quality assurance	Bellows corner welds		
	Bellows attachment weld		

FIGURE 11.31 Specification sheet for circular-type expansion joint. (Courtesy of U.S. Bellows, Inc., Houston, TX, www.usbellows.com.)

are necessary. Drainable varieties are expensive, and external supports may be required to maintain alignment of the shell sections welded to the expansion joint [23]. Additionally, single-ply bellows are susceptible to instability. Since a bellows is a thin shell of revolution with repeated U-shaped convolutions, there exist a large number of natural vibration modes. Basically, these vibration modes are classified into three types: axial accordion modes, lateral bending modes, and shell modes, among which the former two are easily excited [82]. Methods and improved designs to overcome various shortcomings are discussed in the EJMA Standards. The following measures are normally adopted by designers to improve the single-ply expansion joint:

1. Use of external reinforcement
2. Use of multi-ply construction and thicker convolutions

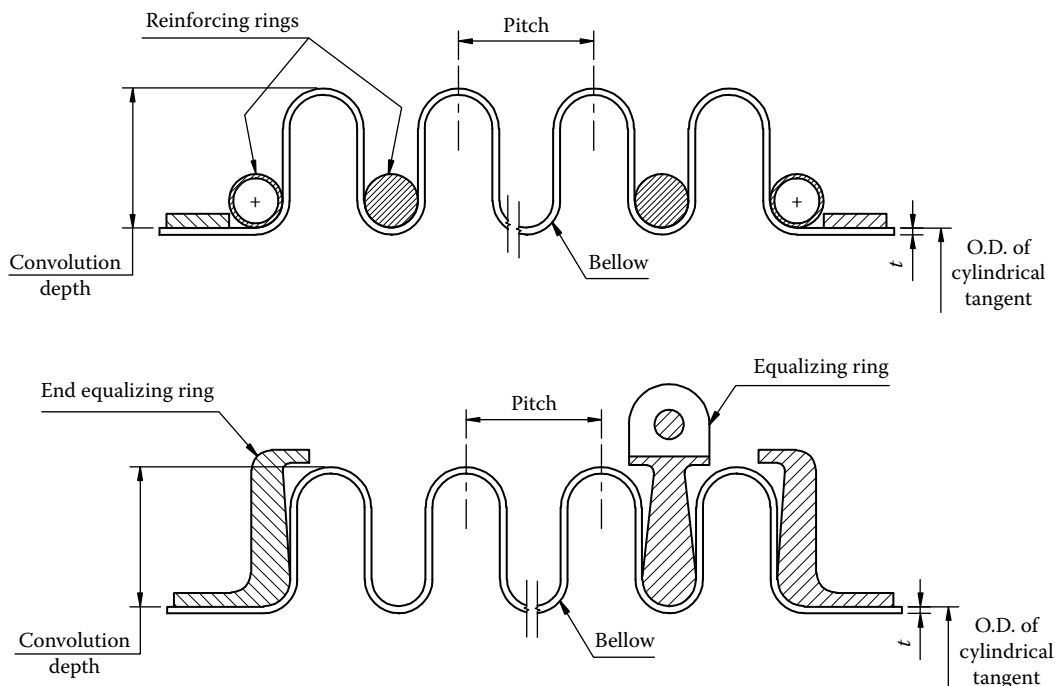


FIGURE 11.32 External reinforcement for bellows.

3. Pressure-balanced expansion joints
4. Flow sleeve inside the convolutions
5. Universal expansion joint assemblies

11.7.4.4.1 External Reinforcement

A combination of high internal pressure-retaining capacity and large deflection can be achieved by external reinforcement of the U-shaped bellows. The external reinforcement offers circumferential restraint and supports the root radius against collapse from internal pressure loading. Reinforcing rings are also added where instability or squirm of the bellows is a concern. Equalizing and reinforcing ring devices used on some expansion joints fitting snugly in the roots of the convolutions are shown in Figure 11.32. Equalizing rings are made of cast iron, carbon steel, stainless steel, or other suitable alloys and are approximately “T” shaped in cross section. Reinforcing rings are fabricated from tubing or solid round bars of carbon steel, stainless steel, or other suitable alloys.

11.7.4.4.2 Multi-Ply Construction and Thicker Convolutions

The pressure-retaining capacity of a bellows can be increased by the use of multi-ply construction and by increasing the thickness of the convolutions; however, the latter significantly reduces the bellows flexibility.

11.7.4.4.3 Pressure-Balanced Expansion Joints

The pressure-balanced expansion joints (Figure 11.33) are used for applications where pressure loading upon piping or equipment is considered excessive. The major advantage of the pressure-balanced expansion joint design is its ability to absorb externally imposed axial movement and/or lateral deflection while restraining the pressure thrust by means of tie devices interconnecting the flow bellows with an opposed bellows also subjected to line pressure. This type of expansion joint is normally used where a change of direction occurs in a run of piping but can be designed as an inline device where no change of direction is necessary. The flow end of a pressure-balanced



FIGURE 11.33 Inline pressure-balanced expansion joint. (Courtesy of U.S. Bellows, Inc., Houston, TX, www.usbellows.com.)

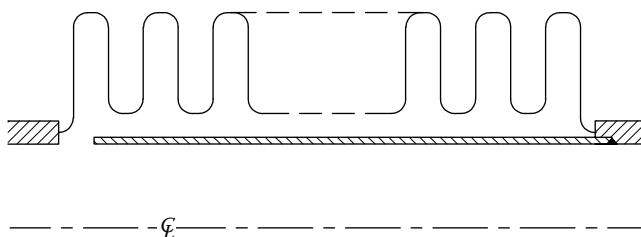


FIGURE 11.34 Flow sleeve to overcome FIV of bellows-type expansion joint (schematic).

expansion joint sometimes contains two bellows separated by a common connector, in which case it is called a universal pressure-balanced expansion joint. Their design should be as per EJMA Standards.

11.7.4.4.4 Flow Sleeve inside the Convolutions

To overcome flow-induced vibration, install a sleeve inside the convolutions as shown in Figure 11.34. In this case, the bellow is thought to be two coaxial cylinders consisting of the convolutions and the sleeve, and the coupled vibrations through the fluid in the annular region may significantly affect the lateral vibration of the convolutions.

Universal Expansion Joint Assemblies—A universal expansion joint is one containing two bellows connected by a common connector for the purpose of absorbing any combination of the three basic movements, i.e., axial movements, lateral deflection, and angular rotation. Universal expansion joints are usually furnished with control rods to distribute the movement between the two bellows of the expansion joint and stabilize the common connector.

Figure 11.35 shows expansion joints with flow sleeve inside the convolutions and universal expansion joint assembly.

11.7.4.5 Fatigue Life

For a given bellows configuration and material thickness, the fatigue life of the bellows will be proportional to the imposed pressure and deflection. Depending on its material of construction, the suitability of an expansion joint to withstand the required number of cycles shall be determined from equations given in EJMA Standards or Appendix BB of the ASME Code.

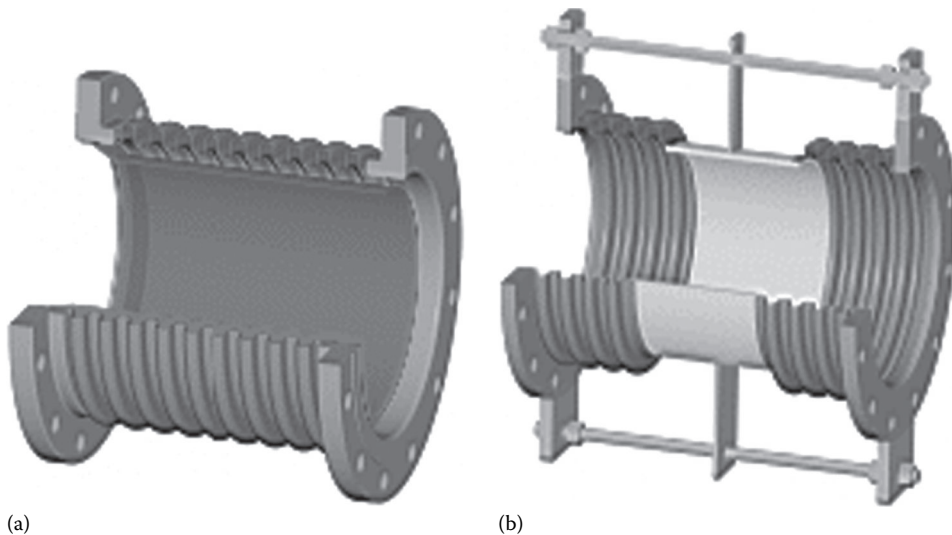


FIGURE 11.35 Expansion joints. (a) With an internal sleeve and (b) universal expansion joint. (Courtesy of KE-Burgmann Expansion Joint Systems, Santee, CA.)

11.8 OPENING AND NOZZLES

11.8.1 OPENINGS

Openings in pressure vessels and heat exchangers refer to the cuts made in shells, flat covers, channels, and heads for accommodating the nozzles and to provide manholes, peepholes, drains and vents, instrument connections, etc. Openings can be circular, elliptical, or oblong. Whenever an opening is made in the wall of the shell or in the head, the wall is weakened due to the discontinuity in the wall and decrease in cross-sectional area perpendicular to the hoop stress direction. To keep the local stresses within the permissible limits, reinforcements to the openings are made.

11.8.1.1 Reinforcement Pad

The design of reinforcement is covered in UG-36 to UG-42 of the ASME Code by an area-to-area method. Reinforced pads whenever required as per drawings/codes shall be of the same material or equivalent to the component to which they are welded. Even though a reinforcement pad can be applied on either the outside or the inside of the shell, it is the common practice to provide it at the outside due to easiness, and no need to meet the requirement of compatibility of the pad material with the process fluids, except that the pad should be resistant to general corrosion and of weldable equality. The factors to be kept in mind while considering the reinforcement pad are the following:

1. The pad should match the contour of the component to which it should be attached
2. Provide a telltale hole to release the entrapped gases during welding and to check the soundness of the welding

11.8.1.2 Reinforced Pad and Air–Soap Solution Testing

As per ASME Code UW-15, reinforcing plates and saddles of nozzles attached to the outside vessel shall be provided with at least one telltale tapped hole (maximum size NPS 1/4 tap) for compressed air–soap solution test for tightness of welds that seal off the inside of the vessel. Air pressure of 1.25 kg/cm²

is suggested for these tests or as per applicable Code. Higher test pressures are not recommended because the soap bubbles have a chance to blow off. Telltale holes in the reinforcing pads may be left open or plugged when the vessel is in service.

11.8.2 NOZZLES

Nozzles are incorporated to convey process fluids into the heat exchanger and out of it. Their sizes are arrived after calculating permissible fluid velocity limited by erosion–corrosion, impingement attack, pressure drop, etc. Minimum wall thickness is arrived using the cylindrical shell formula. Good nozzle design involves better distribution of process fluids, ability to withstand operating load and the other loads, and should provide easy accessibility to connect or disconnect the pipes. A well-designed nozzle should have a very low-pressure drop. Nozzle openings can be circular, elliptical, and oblong. Nozzles are connected by weldment to the shell by

1. Butt welding
2. Through type
3. Reinforcing pads

In addition to the welded-type connections, brazed, threaded, studded, and expanded connections are also employed. Nozzle design is carried out as per code. Considerations in nozzle design should include the inspectability of the nozzle-to-pipe and nozzle-to-vessel weld inspection [83].

Nozzle openings are reinforced by

1. Using thick forged-blank nozzle (Figure 11.36a)
2. Opening compensated by reinforcement pad (Figure 11.36b)
3. Welding of thick-walled nozzle pipe (Figure 11.36c)

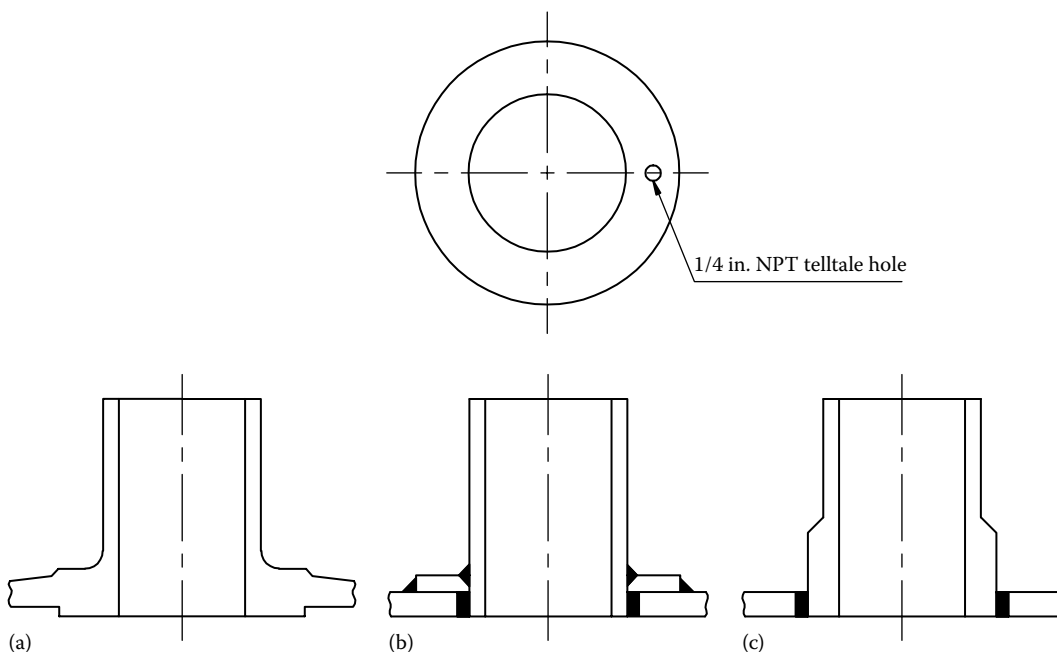


FIGURE 11.36 Nozzle opening reinforcement. (a) Thick forged-blank nozzle; (b) compensation by reinforcement pad; and (c) thick-walled nozzle.

Design aspects of various nozzle reinforcements are discussed by Schoessow et al. [84]. Requirements of reinforcement for openings in shells and formed heads are covered in UG-37 to UG-42, UG-82, and attachment welds in UW-15, and exemption from reinforcement in UG-36. As far as possible, nozzle design should avoid the separate reinforcement plate being welded to the shell, because the weld metal cracks at the interface between the reinforcement pad plate and the shell plate pose additional problems.

Nozzles are forged from hot-rolled bar, hot-rolled billet, or forged billet. All raw materials used are electric furnace, vacuum degassed and fully killed steel with stringent quality specifications. Heat treatment, machining, drilling, and contouring are standard controlled processes.

Information required to develop a self-reinforced nozzle is as follows:

1. Applicable design code
2. Material specification both for vessel and for nozzle
3. Vessel thickness at nozzle
4. Vessel ID and nozzle bore
5. Location of nozzle in vessel—shell, head, or cone
6. Internal projection allowed and external projection
7. Design parameters such as maximum pressure and temperature, and corrosion allowance
8. Style and rating of flange or pipe OD, for butt weld connection

11.8.3 STACKED UNITS

Stacked units with interconnecting nozzles are a source of many problems for the designer as well as the fabricator. Most of the trouble comes as a result of differential thermal expansion, either radial or longitudinal or both. Several general rules will help avoid trouble [85]:

1. Do not stack one-pass shells more than two deep, without thorough check of differentials
2. Keep intermediate shell nozzles as near-channel nozzles as possible
3. Avoid RTJ intermediate nozzles, if possible
4. Avoid offset direct interconnecting nozzles

11.9 SUPPORTS

All vessels shall be supported, and the supporting members shall be attached to the vessel wall. The design of supports shall normally conform to good engineering practice. The supports should be designed to resist internal and external pressures and accommodate the self-weight of the unit and contents, including the flooded weight during hydrostatic test. Based on their installation, the supports differ for horizontal vertical installation. The selection of the type of support for a pressure vessel is dependent on parameters such as the elevation of the vessel from the ground level, the materials of construction, and the operating temperature [34].

11.9.1 DESIGN LOADS

While designing the supports of a vessel, care should be taken to include all the external loads likely to be imposed on it. Such external loads include (1) wind loads, (2) loads due to connected piping, (3) superimposed loads, (4) shock loads due to surging or hydraulic hammer, and (5) seismic vibration. As per TEMA Standards, supports for a removable tube bundle heat exchanger should be designed to withstand a pulling force equal to 1.5 times the weight of the tube bundle, and when additional loads and forces from external nozzle loadings, wind loads, and seismic forces are assumed for the purposes of supports design, the combinations need not be assumed to occur simultaneously. Care should be taken that the thermal stresses in external supports do not exceed those permitted by the code.

11.9.2 HORIZONTAL VESSEL SUPPORTS

Horizontal vessels are subject to longitudinal bending moments and local shear forces due to the weight of their contents. They are generally supported by three types of supports: (1) saddle supports, (2) ring supports, and (3) leg supports. Saddle support is used most commonly for heat exchangers. It is shown in Figure 11.37. Whenever possible, horizontal vessels shall be supported by two supports only, with holes for anchor bolts. If more than two supports are used, the distribution of the reaction is affected by difference in support level, the straightness and local roundness of the vessel, and the relative stiffness of different parts of the vessel against local deflection [85].

11.9.2.1 Saddle Supports

Saddle supports may be used for vessels whose wall is not too thin. Horizontal vessels when supported on saddle supports such as in Figure 11.38 behave as beams, and with these kinds of supports, the maximum longitudinal bending stresses occur at the supports and at the mid span of the vessel. Hence, the location of supports from the mid span of the vessel or head tangent is critical to minimize the bending stresses at the supports. Consideration shall be given to ensure that the saddles should be preferably extended over at least 120° of the circumference of the vessel. The limitation, which is imposed by most codes of practice, is an empirical one based on experience with large vessels [85]. While designing, ensure that saddle supports can withstand a tube bundle pulling force equal to the weight of the removable bundle.

11.9.2.1.1 Zick Stress

Zick [86] developed a method for analyzing supports for the horizontal cylindrical shells. The analysis gives a detailed derivation of the equations for longitudinal bending stresses at the supports and at the mid span. These stresses are named as Zick stress. Zick's method is discussed in detail in Refs. [31,32,35], among others.

11.9.2.2 Ring Supports

Ring supports as shown in Figure 11.37b are preferred to saddle supports for large thin-walled vessels, vacuum vessels, and in the case of saddles located away from the head. Ring supports are also preferred when supporting a vessel at more than two cross sections becomes inevitable. The welds attaching ring supports should have a minimum leg length equal to the thickness of the thinner of the two parts being joined together.

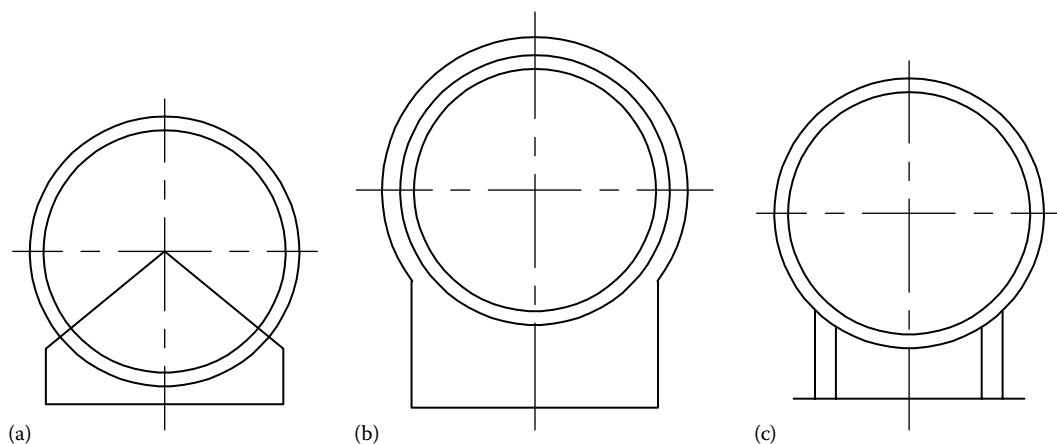


FIGURE 11.37 Examples of horizontal supports of pressure vessels, (a) Saddle support; (b) ring support; and (c) lug support.

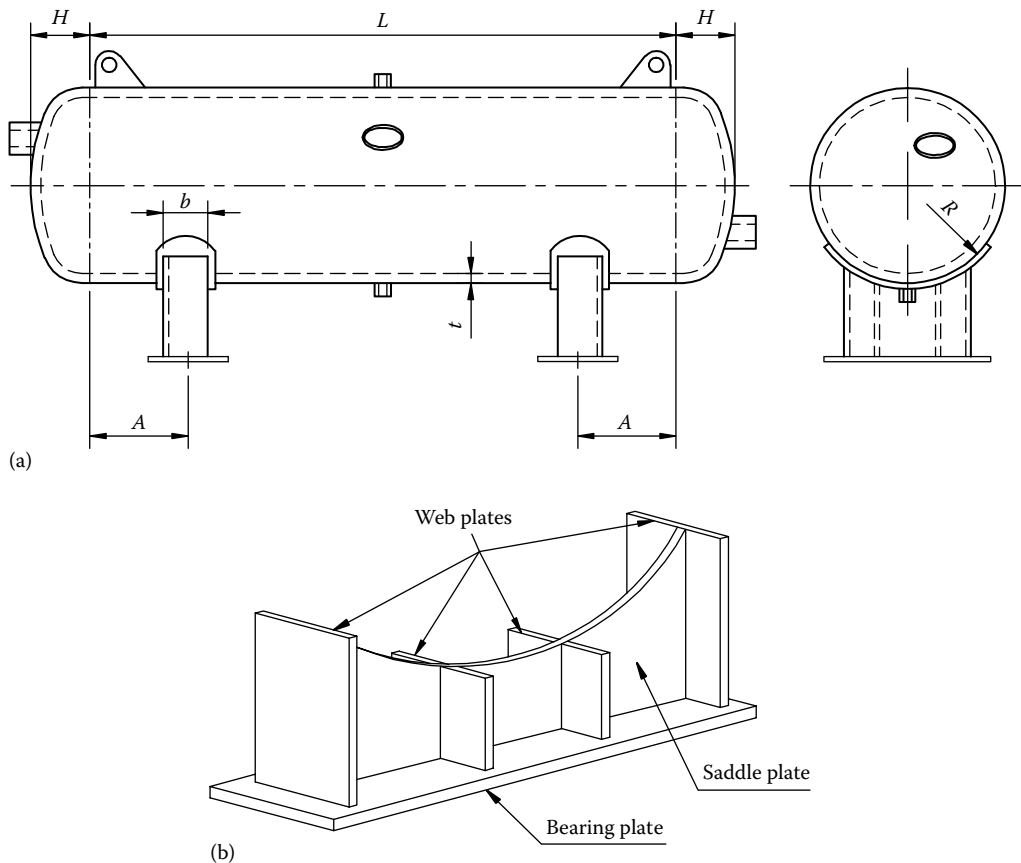


FIGURE 11.38 A vessel on horizontal saddle support. (a) Schematic and (b) details of the saddle support.

11.9.2.2 Leg Supports

Leg supports as shown in Figure 11.37c are usually permitted for small vessels by the usual code practice because of the severe local stresses that can be set up at the connection of the support to the vessel wall.

11.9.3 VERTICAL VESSELS

Supports for the vertical units may be skirt supports, ring supports, and lugs (columns). Some of these vertical supports are shown in Figure 11.39.

11.9.3.1 Skirt Supports

Skirt supports (Figure 11.39a) are recommended for large/tall vertical vessels. Skirt supports are preferred because they do not lead to concentrated local loads on the shell, offer less restraint against differential thermal expansion, and reduce the effect of discontinuity stresses at the junction of the cylindrical shell and the bottom [85]. The skirt supports shall be provided with at least one opening for inspection unless there is a provision to examine the bottom of the vessel accessible from below.

11.9.3.2 Lug Supports

Vertical vessels may be supported by a number of posts or lugs as shown in Figure 11.39b. Lug supports are ideal for thick-walled vessels. For thin-walled vessels, it is not convenient unless proper reinforcements are used or many lugs are welded. Brackets or lugs offer many advantages over

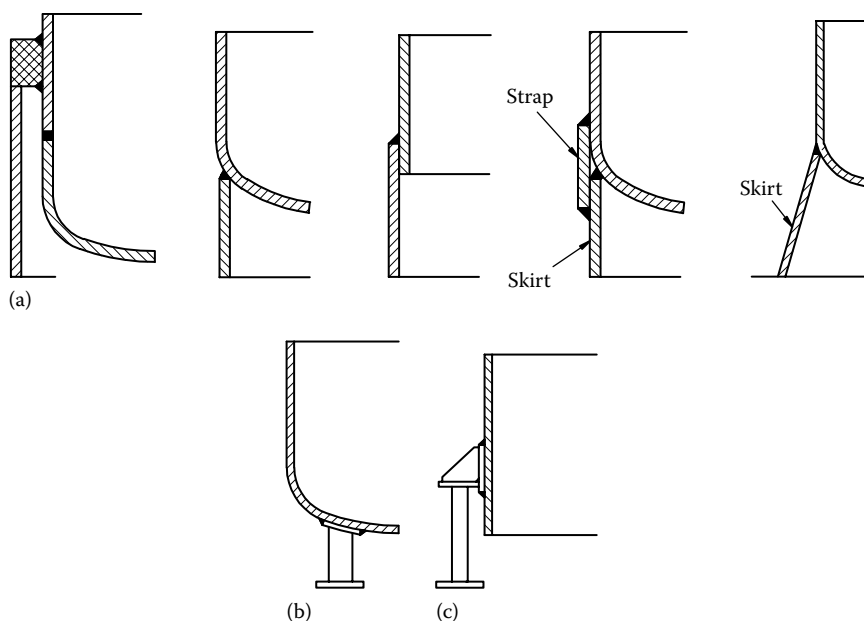


FIGURE 11.39 Examples of vertical supports of pressure vessels. (a) Skirt supports, (b) lug support, and (c) ring support.



FIGURE 11.40 Shell and tube heat exchanger with ring support for vertical mounting under transit. (Courtesy of Bronswerk Heat Transfer BV, Nijkerk, the Netherlands.)

other types of vessels [31]: They are inexpensive, can absorb diametrical expansion by sliding over greased or bronze plates, and requirements of welding are minimal.

11.8.3.3 Ring Support

Figure 11.40 shows a heat exchanger with ring supports for vertical mounting.

11.9.4 PROCEDURE FOR SUPPORT DESIGN

11.9.4.1 TEMA Rules for Supports Design (G-7.1)

TEMA rules for supports for horizontal units are listed in G-7.11 and for vertical units in G-7.12. For calculating resulting stresses due to the saddle supports, references are suggested under TEMA G-7.13. The “Recommended Good Practice” section of TEMA Standards provides additional information on support design.

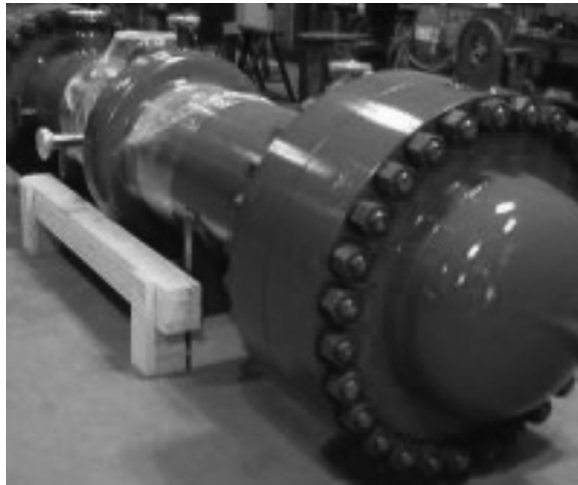


FIGURE 11.41 Shell and tube heat exchanger with an expansion joint (with a vent at the top) and bonnet with a lifting hook. (Courtesy of Heat Exchanger Design, Inc., Indianapolis, IN.)

11.9.4.2 ASME Code

ASME Code requirements for supports design are covered in UG-54. Appendix G contains suggested good practices for support design.

11.9.5 LIFTING DEVICES AND ATTACHMENTS

TEMA rules for the design of lifting devices are given in G-7.2. ASME Code rules for the construction of lifting devices and fitting attachments are covered in UG-82. Some of the TEMA Standards for design of lifting devices are as follows:

1. Channels, bonnets, and covers that weigh more than 60 lb are to be provided with lifting lugs (Figure 11.41).
2. Lifting devices are designed to lift the component to which they are directly attached. When lifting lugs are required by the purchaser to lift the complete unit, the device must be adequately designed.
3. The design load shall incorporate an appropriate impact factor.
4. Lifting devices and attachments shall be formed and fitted to conform to the curvature of the component surface to which they are attached.
5. The lifting lugs on shell shall be designed to take the weight of complete unit with full of content.

REFERENCES

1. (a) Hirschfeld, F., Codes, standards and certificate of authorization program: Part 1—Establishing safety standards, *Mech. Eng.*, January, 33–39 (1979); (b) Hirschfeld, F., Codes, standards and certificate of authorization program: Part 2—Policies, programs and organization, *Mech. Eng.*, February, 31–37 (1979).
2. Statement of the Council on Codes and Standards of the American Society of Mechanical Engineers on the Federal Role in International Standards, *Trans. ASME J. Pressure Vessel Technol.*, 112, 425–426 (1990).

3. TEMA, *Standards of the Tubular Exchanger Manufacturers Association*, 9th edn., Tubular Exchanger Manufacturers Association, Inc., Tarrytown, NY, 2007.
4. Heat Exchange Institute, *Standards for Surface Condensers*, 10th edn., Heat Exchange Institute, Cleveland, OH, 2006.
5. Heat Exchange Institute, *Standards for Power Plant Heat Exchangers*, 4th edn., Heat Exchange Institute, Cleveland, OH, 2004.
6. Heat Exchange Institute, *Standards for Closed Feedwater Heaters*, 8th edn., Heat Exchange Institute, Cleveland, OH, 1984, 2008.
7. American Petroleum Institute, *Shell and Tube Exchangers for General Refinery Services, API Standard 660*, 7th edn., American Petroleum Institute, Washington, DC, 2003.
8. EJMA, *Standards of the Expansion Joint Manufacturers Association*, 9th edn., Expansion Joint Manufacturers Association, Tarrytown, NY, 2008.
9. BSI, *British Standards (BSI)*, BSI Publications at Linford Wood, Milton Keynes, U.K., 1993.
10. JIS X 0208:1997, *Japanese Industrial Standards*, 1997.
11. DIN, *German Industrial Standards*, German Institute for Standardization Beuth, Beuth Verlag GmbH, Berlin, Germany.
12. Taborek, J. and Auriolles, G., Effect of 1988 TEMA standards on mechanical and thermohydraulic design of shell and tube heat exchangers, in *Heat Transfer*, Philadelphia, PA, 1989.
13. Gupta, J. P., *Fundamentals of Heat Exchanger and Pressure Vessel Technology*, Hemisphere, Washington, DC, 1986.
14. Codes, standards and the ASME: Part 3—Standards, safety standards, *Mech. Eng.*, August, 24–25 (1972).
15. ASME, *ASME Boiler and Pressure Vessel Code, Section VIII, Division 1—Pressure Vessels*, American Society of Mechanical Engineers, New York, 2010.
16. ASME, *ASME Boiler and Pressure Vessel Code, Section VIII, Division 2, Pressure Vessels—Alternative Rules*, American Society of Mechanical Engineers, New York, 2010.
17. ASME, *ASME Boiler and Pressure Vessel Code, Section VIII, Division 3, Pressure Vessels—Alternative Rules for High Pressure Vessels*, American Society of Mechanical Engineers, New York, 2007.
18. SNCT, ed., *CODAP, French Code for the Construction of Unfired Pressure Vessels*, Section C7, Paris, France, 2000.
19. PD 5500, *British Standard Specification for Fusion Welded Pressure Vessels*, 2000.
20. Merklatter, A. D., *German Pressure Vessel Code*, Carl Heymans Verlag KG, Koln, Germany.
21. Cepluch, R. J., The ASME Boiler and Pressure Vessel Code Committee—Challenges: Past and future, *Trans. ASME J. Pressure Vessel Technol.*, 112, 319–322 (1990).
22. Blackall, F. S., Jr., ASME standards save lives and dollars, *Mech. Eng.*, December, 979–981 (1953).
23. Yokell, S., *A Working Guide to Shell and Tube Heat Exchangers*, McGraw-Hill, New York, 1990.
24. Nichols, R. W. ed., *Pressure Vessel Codes and Standards: Developments in Pressure Vessel Technology—5*, Elsevier Applied Science, London, U.K., 1987.
25. (a) Codes, standards and the ASME: Part 1—Codes, *Mech. Eng.*, June, 24–25 (1972); (b) Codes, standards and the ASME: Part 2—ASME boiler and pressure vessel codes, *Mech. Eng.*, July, 16–18 (1972); (c) Codes, standards and the ASME: Part 4—International Standardization Committee, *Mech. Eng.*, September, 20–24 (1972).
26. Schlunder, E. U. (editor-in-chief), Mechanical design codes, in *Heat Exchanger Design Handbook*, Vol. 4, Hemisphere, Washington, DC, 1983, Section 4.1.6.
27. Mase, J. R. and Smolen, A. M., ASME pressure vessel code: Which division to choose, *Chem. Eng.*, January, 133–136 (1982).
28. Farr, J. R., The ASME boiler and pressure vessel code: Section VIII—Pressure vessels, in *Pressure Vessel Codes and Standards, Developments in Pressure Vessel Technology—5* (R. W. Nichols, ed.), Elsevier Applied Science, London, U.K., 1987, pp. 35–58.
29. Farr, J. R., The ASME boiler and pressure vessel code: Overview, in *Pressure Vessel Codes and Standards, Developments in Pressure Vessel Technology—5* (R. W. Nichols, ed.), Elsevier Applied Science, London, U.K., 1987, pp. 1–34.
30. EN 13445-2_2002(E), Unified Pressure Vessel Code, European Standards for Unfired Pressure Vessels, Part 3-Clause 13, 2002.
31. Singh, K. P. and Soler, A. I., *Mechanical Design of Heat Exchangers and Pressure Vessel Components*, Arcturus, Cherry Hill, NJ, 1984.
32. (a) Escoe, K. A., *Mechanical Design of Process Systems, Vol. 2—Shell and Tube Heat Exchangers, Rotating Equipment, Bins, Silos, Stacks*, Gulf Publishing Company, Book Division, Houston, TX, 1995; (b) Escoe, K. A., *Mechanical Design of Process Systems, Vol. 1, The Engineering Mechanics of Pressure Vessels*, Gulf Publishing Company, Book Division, Houston, TX, p. 19xx, Chapter 4

33. Moss, D. R., *Pressure Vessel Design Manual*, Gulf Publishing Company, Book Division, Houston, TX.
34. Brownell, L. E. and Young, E. H., *Process Equipment Design*, John Wiley & Sons, New York, 1968.
35. Bednar, H. H., *Pressure Vessel Design Handbook*, Von Nostrand Reinhold, New York, 1981.
36. Harvey, J. F., *Pressure Component Construction*, Von Nostrand Reinhold, New York, 1980.
37. Chuse, R., *Pressure Vessels—The ASME Code Simplified*, 6th edn., McGraw-Hill, New York, 1984.
38. Roach, G. H. and Wood, R. M., Shell and tube exchangers having improved design features, *Heat Transfer Eng.*, 7, 19–23 (1986).
39. Soler, A. I., Expert system for design integration—Application to the total design of shell and tube heat exchangers, in *Proceedings of the ASME, Thermal/Mechanical Heat Exchanger Design, Karl Gardner Memorial Session*, Vol. 118 (K. P. Singh and S. M. Shenkman, eds.), ASME PVP, 1985, pp. 135–138.
40. Singh, K. P., Mechanical design of tubular heat exchangers—An appraisal of the state-of-the-art, in *Heat Transfer Equipment Design* (R. K. Shah, C. Subbarao, and R. M. Mashelekar, eds.), Hemisphere, Washington, DC, 1988, pp. 71–87.
41. Gardner, K. A., Heat exchanger tubesheet design, *Trans. ASME J. Appl. Mech.*, 70A, 377–385 (1948).
42. Gardner, K. A., Heat exchanger tubesheet design—2, Fixed tubesheets, *Trans. ASME J. Appl. Mech.*, 74, 159–166 (1952).
43. Gardner, K. A., Heat exchanger tubesheet design—3, U-tube and bayonet tubesheets, *Trans. ASME J. Appl. Mech. Ser. E.*, 82, 25–33 (1960).
44. Miller, K. A. G., The design of tube plates in heat exchangers, in *Proceedings of Institution of Mechanical Engineers, Sect. B*, Vol. 1, London, U.K., 1952–1953, pp. 672–688.
45. Yu, Y. Y., Rational analysis of heat exchanger tubesheet stresses, *Trans. ASME J. Appl. Mech.*, 78, 468–473 (1956).
46. Galletly, G. D. and Garbett, C. R., Pressure vessels—Let the tubes support the tubesheet, *Ind. Eng. Chem.*, 50, 1227–1230 (1958).
47. Galletly, G. D., Optimum design of thin circular plates on an elastic foundation, *Proceedings of the Institution of the Mechanical Engineers, IMechE*, Vol. 173, London, U.K., 1959, pp. 689–698.
48. Boon, G. B. and Walsh, R. A., Fixed tubesheet heat exchangers, *Trans. ASME J. Appl. Mech.*, June, 175–180 (1964).
49. Gardner, K. A., Tubesheet design: A basis for standardization, in *Proceedings of the First International Conference on Pressure Vessel Technology: Part I, Design and Analysis*, Delft, the Netherlands, 1969, pp. 621–668.
50. Chiang, C. C., Closed form design solutions for box type heat exchangers, ASME publication 75-WA/DE, New York, 1975.
51. Hayashi, K., An analysis procedure for fixed tubesheet exchangers, in *Proceedings of the Third International Conference on Pressure Vessel Technology: Part I, Analysis, Design and Inspection*, Tokyo, Japan, 1977, pp. 363–373.
52. Malek, R. G., A new approach to exchanger tubesheet design, *Hydrocarb. Process.*, 165–169 (1977).
53. Singh, K. P., Analysis of vertically mounted through tube heat exchangers, *Trans. ASME J. Eng. Power*, 100, 380–390 (1978).
54. Soler, A. I. and Soehrens, J. E., Design curves for stress analysis of U-tube heat exchanger tubesheet with integral channel and head, *Trans. ASME J. Pressure Vessel Technol.*, 100, 221–232 (1978).
55. Soehrens, J. E., Tubesheet thicknesses and tube loads for floating head and fixed-tubesheet heat exchangers, *ASME J. Pressure Vessel Technol.*, 106, 289–299 (1984).
56. Cascales, D. H. and Militello, C., Tubesheet thicknesses and tube loads for fixed tubesheet heat exchangers [Letter to the editor], *Trans. ASME J. Pressure Vessel Technol.*, 107, 318–323 (1985).
57. Singh, K. P. and Soler, A. I., An elastic-plastic analysis of the integral tubesheet in U-tube heat exchangers—Towards an ASME code oriented approach, in *ASME Proceedings of the 1985 PVP Conference*, Vol. 98, New Orleans, LA, 1985, pp. 39–51.
58. Soler, A. I., Caldwell, S. M., and Singh, K. P., Tubesheet analysis—A proposed ASME design procedure, in *Proceedings of the ASME, Thermal/Mechanical Heat Exchanger Design—Karl Gardner Memorial Session*, Vol. 118 (K. P. Singh and S. M. Shenkman, eds.), ASME PVP, ASME, New York, 1985, pp. 93–101.
59. Soehrens, J. E., Stress analysis of heat exchangers, in *Proceedings of the ASME, PVP Vol. 118, Thermal/Mechanical Heat Exchanger Design—Karl Gardner Memorial Session*, Vol. 118 (K. P. Singh and S. M. Shenkman, eds.), ASME PVP, New York, 1985, pp. 79–91.

60. Osweiller, F., Basis of the tubesheet heat exchanger design rules used in the French pressure vessel code, *Trans. ASME J. Press. Vessel Technol.*, 114, 124–131 (1992).
61. Osweiller, F., Tubesheet heat exchangers: New common design rules in UPV, CODAP and ASME, *ASME J. Press. Vessel Technol.*, 12(3), 317–324 (August 2000).
62. ASME Section VIII—Div. 1—Appendix AA: July 2001 Edition (Addenda July 2002)—Section UHX, 2002.
63. Osweiller, F., Analysis of TEMA tubesheet design rules—Comparison with up to date code methods, in *Proceedings of the 1986 Pressure Vessel and Piping Conference*, Vol. 107, Chicago, IL, 1986, pp. 1–9.
64. Osweiller, F., New common design rules for U-tube heat exchangers in ASME, CODAP and UPV Codes, in *Proceedings of the ASME PVP Conference*, Vol. 439 (H01237), Vancouver, British Columbia, Canada, August 4–8, 2002.
65. Singh, K. P. and Marks, P., Proposed extension of the TEMA tubesheet design method to determine tubesheet rim thickness, in *Proceedings of the ASME, Thermal/Mechanical Heat Exchanger Design—Karl Gardner Memorial Session*, Vol. 118 (K. P. Singh and S. M. Shenkman, eds.), ASME PVP., ASME, New York, 1985, pp. 111–119.
66. Kuppan, T., Alternate design charts for fixed tubesheet design procedure included in ASME boiler and pressure vessel code, Section VIII, Div. 1, *Trans. ASME J. Pressure Vessel Technol.*, 117, 189–194 (1995).
67. O'Donnell, W. J. and Langer, B. F., Design of perforated plates, *ASME J. Eng. Ind.*, 84, 307–320 (1962).
68. Osweiller, F., Evolution and synthesis of the effective elastic constants concept for the design of tubesheets, *Trans. ASME J. Pressure Vessel Technol.*, 111, 209–217 (1989).
69. Bernstein, M. D. and Soler, A. I., The tubesheet analysis method in the new HEI condenser standards, *Trans. ASME J. Eng. Power*, 100, 363–368 (1978).
70. Rachkov, V. I. and Morozov, V. H., Designing curved tube plates, *Khim-i-reft. Masb*, 7, 14 (1968).
71. Paliwal, D. N. and Sinha, S. N., Design of shallow spherical curved tubesheet for heat exchangers, *Int. J. Press. Vessels Pip.*, 17, 185–192 (1984).
72. Sang, Z.-F. and Widera, G. E. O., Stress analysis of elliptical tube plates in heat exchangers, *Trans. ASME J. Press. Vessel Technol.*, 109, 310–314 (1987).
73. Waters, E. O., Westrom, D. B., and Williams, F. S. G., Design of bolted flanged connections, in *Pressure Vessel and Piping Design, Collected Papers 1927–959*, American Society of Mechanical Engineers, New York, 1960, pp. 58–61.
74. Bickford, J. H., Gasketed joints and leaks, in *An Introduction to the Design and Behavior of Bolted Joints*, 2nd edn., Marcel Dekker, New York, 1990, pp. 495–548.
75. *Modern Flange Design*, 7th edn., Taylor Forge International, Chicago, IL, Bull., 502, 1979.
76. Lake, G. F. and Boyd, G., Design of bolted, flanged joints of pressure vessels, *Proc. Inst. Mech. Eng.*, 171, 843–858 (1957).
77. Derenne, M., Marchand, L., Payne, J. R., and Bazergui, A., Elevated temperature testing of gaskets for bolted flanged connections, *WRC Bull.*, 391, 2003.
78. Singh, K. P., Study of bolted joint integrity and inter-tube pass leakage in U-tube heat exchangers—Part II: Analysis, *Trans. ASME J. Eng. Power*, 101, 16–22 (1979).
79. Wolf, L. J. and Mains, R. M., The stress analysis of heat exchanger expansion joints in the elastic range, *Trans. ASME J. Eng. Ind.*, 145–150 (1973).
80. Singh, K. P., A rational procedure for analyzing flanged and flued expansion joints, *Trans. ASME J. Pressure Vessel Technol.*, 113, 64–70 (1991).
81. Kopp, S. and Sayre, M. F., Expansion joints for heat exchangers, in *ASME Winter Annual Meeting*, New York, 1952.
82. Morishita, M., Ikahata, N., and Kitamura, S., Simplified dynamic analysis methods for metallic bellows expansion joints, *Trans. ASME J. Press. Vessel Technol.*, 113, 504–510 (1991).
83. Sattler, F. J., Forrer, G. R., and Parker, W. O., Jr., Inservice inspection of nuclear plants, *Mater. Eval.*, November, 18A–22A, 27A–29A (1972).
84. Schoessow, G. J. and Brooks, E., Analysis of experimental data regarding certain design features of pressure, in *Pressure Vessel and Piping Design, Collected Papers 1927–1959*, American Society of Mechanical Engineers, New York, 1960, pp. 24–34.
85. Spencer, T. C., Mechanical design and fabrication of exchangers in the United States, *Heat Transfer Eng.*, 8, 58–61 (1987).
86. Zick, L. P., Stresses in large horizontal cylindrical pressure vessels on two saddle supports, in *Pressure Vessel and Piping; Design and Analysis*, ASME, New York, 1972.

BIBLIOGRAPHY

- Baylac G. and Koplewicz D., EN 13445 Unfired pressure vessels, background to the rules in part 3 design, Issue 2, August 20, 2004, pp. 1–143.
- Osweiller, F., *Methode de calcul des exchangers a deux ictes fixés le CODAP*, Etude CETIM, No. 14B031, 1986.
- Cascales, D. H. and Militello, C., A model for fixed tubesheet heat exchanger, *Trans. ASME J. Press. Vessel Technol.*, 109, 289–296 (1987).
- Paliwal, D. N., Design of fixed tubesheet for heat exchangers, *Trans. ASME J. Press. Vessel Technol.*, 111, 79–85 (1989).

12 Corrosion

12.1 BASICS OF CORROSION

Most common metals and their alloys are attacked by environments such as the atmosphere, soil, water, or aqueous solutions. This destruction of metals and alloys is known as corrosion. It is generally agreed that metals are corroded by an electrochemical mechanism. With practically all commercial processes engineered on a continuous basis of operation, premature failure from corrosion of various types of equipments, including heat exchangers, piping, and others, may mean costly shutdowns and expensive maintenance operations. It is especially troublesome in oil refining, chemical industries, and electric power plants on land and sea, as well as in food and liquor processing, paper manufacture, refrigeration, air-conditioning, etc. Therefore, an understanding of corrosion principles and corrosion control should be of great interest to industry and the general public.

12.1.1 REASONS FOR CORROSION STUDIES

There are two main reasons for concern about and study of corrosion: (1) economics and (2) conservation of materials. Of these, the economic factors mostly favor study and research into the mechanisms of corrosion and the means of controlling corrosion. Economic reasons for corrosion study include the following:

1. Loss of efficiency: Corrosion can result in the buildup of corrosion products and scale, which can cause a reduction in heat transfer as well as an increase in the power required to pump the fluid through the system.
2. Loss of product due to leakage: High fuel and energy costs as a result of leakage of steam, fuel, water, compressed air, or process fluid that absorbed energy.
3. Possible impact on the environment: If the leaking fluid is corrosive in nature, it will attack its surroundings, and if lethal or poisonous, it will create hazards and environmental problems. Discharge of copper- and chromate-treated water is severely regulated to conserve aquatics and biosphere.
4. Lost production as a result of a failure.
5. High maintenance costs.
6. Warranty claims on corroded equipment and the consequent loss of customer confidence, sales, and reputation.
7. Contamination and loss of product quality, which can be detrimental to the product, such as foodstuffs, soap products, discoloration with dyes, etc.
8. Extra working capital to carry out maintenance operations and to stock spares to replace corroded components.
9. Overdesign: In many instances, when the corrosive effect of a system is known, additional thickness to components is provided for in the design. This is known as corrosion allowance and involves additional material cost and extra weight of new units.
10. Highly corrosive fluids may require the use of expensive materials such as titanium, nickel-base alloys, zirconium, tantalum, copper-nickels, etc. The use of these materials contributes to increased capital cost.
11. Damage to adjacent equipment and the system components.

12.1.2 CORROSION MECHANISM

According to electrochemical theory, the combination of anode, cathode, and aqueous solutions constitutes a small galvanic cell, and the corrosion reaction proceeds with a flow of current in a manner analogous to the way current is generated by chemical action in a primary cell or in a storage battery on discharge. Due to the electrochemical action, the anode is dissolved. For a current to flow, a complete electrical circuit is required. In a basic corroding system as shown in Figure 12.1, the circuit is made up of four components:

1. Anode
2. Electrolyte
3. Cathode
4. External circuit

1. Anode: The anode is the electrode at which oxidation (corrosion) takes place and current in the form of positively charged metal ions enters the electrolyte. At the anode, the metal atom loses an electron, oxidizing to an ion.
2. Electrolyte: The electrolyte is the solution that surrounds, or covers, both the anode and the cathode. The conductivity of the solution is the key to the speed of the corrosion process. A solution with low conductivity produces a slow corrosion reaction, while a solution with high conductivity produces rapid corrosion [1]. In the total absence of an electrolyte, little or no corrosion takes place. For example, iron exposed to dry desert air remains bright and shiny since water necessary to the rusting process is not available, and in arctic regions, no rusting is observed because ice is a nonconductor [2]. The electrolyte need not be liquid. It can be a solid layer also. For example, at elevated temperatures, corrosion of a metal can occur in the absence of water because a thick metal oxide scale acts as the electrolyte (Figure 12.2). The surface metal oxide is the cathode and the metal oxide and metal interface are the anode [2].
3. Cathode: The cathode is the electrode at which reduction takes place and current enters from the electrolyte.
4. External circuit: If there are two pieces of metal, they must either be in contact or have an external connection in order for the corrosion to take place. The external circuit is a metallic path between the anode and cathode that completes the circuit. Where the anode and cathode are on the metal surface, as shown in Figure 12.3, the metal itself acts as the external circuit.

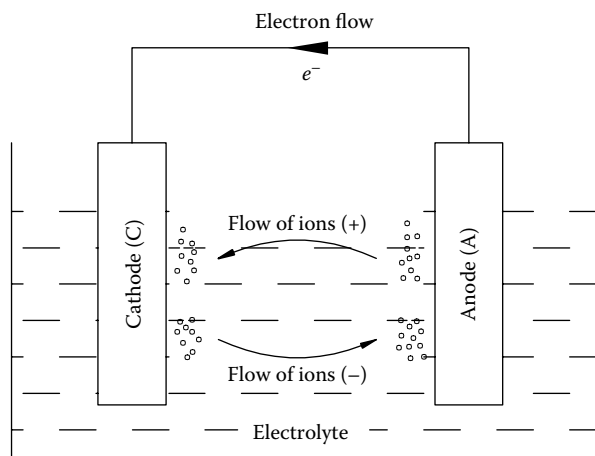


FIGURE 12.1 Galvanic cell—basic corroding system.

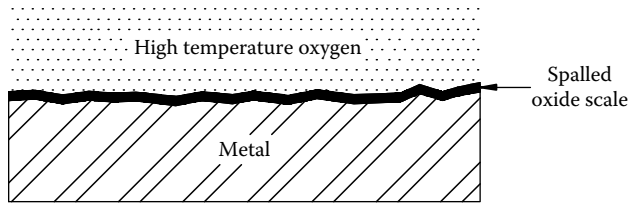


FIGURE 12.2 Thick metal oxide scale as the electrolyte. (Adapted from Pludek, R., *Design and Corrosion Control*, The Macmillan Press Ltd., London, U.K., 1977.)

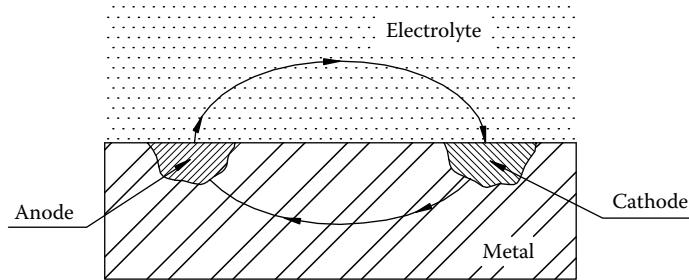


FIGURE 12.3 Anode and cathode on the same metal surface constituting a galvanic cell.

12.1.2.1 Basic Corrosion Mechanism of Iron in Aerated Aqueous System

The corrosion principle is explained by the basic corrosion mechanism of iron in an aerated aqueous system (Figure 12.4). In its simplest form, this reaction consists of two parts: (1) the dissolution of iron at the anode and (2) cathodic reaction in the absence of oxygen or the reduction of oxygen to form hydroxyl ions at the cathode. Hence, the overall theoretical corrosion reaction becomes

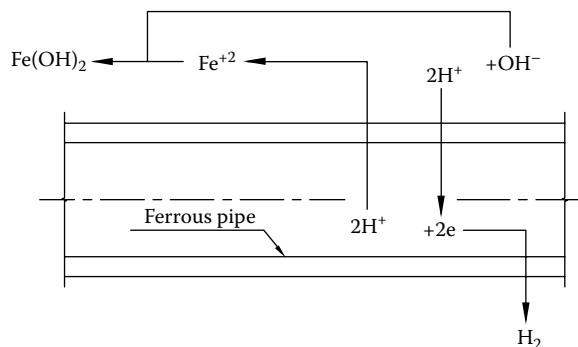


FIGURE 12.4 Corrosion of iron in water.

followed by



In practice, however, these reactions are much more complex. The rate of corrosion is governed by the rate of either the cathodic reaction or the anodic reaction or less frequently by the electrical resistance of the electrolyte [2]. When the anodic reaction is severely limited by films that form on the metal surface, as in the case of stainless steels, the metal is called passive.

12.1.3 FORMS OF ELECTROCHEMICAL CORROSION

Various forms of electrochemical corrosion are (1) bimetallic cell or dissimilar electrode cell, (2) concentration cell, and (3) differential temperature cells.

12.1.3.1 Bimetallic Cell

In a bimetallic cell, two dissimilar metals are in contact and are immersed in an electrolyte. The farther the two metals are apart in the electromotive series, the more severe is the corrosion. Bimetallic corrosion also takes place when a metal is nonhomogeneous. One part of a metallic structure may be anodic to another part if it is not exactly the same alloy. A bimetallic cell is also known as a dissimilar electrode cell.

12.1.3.2 Concentration Cell

A concentration cell is produced in an identical electrode, in contact with an electrolyte of a differing concentration. The area of metal in contact with the dilute solution will be anodic and it will corrode. It is often called crevice corrosion because a crevice acts as a diffusion barrier, and corrosion occurs most often within a crevice. There are mainly two kinds of concentration cell, as shown in Figure 12.5: (1) the salt concentration cell, formed due to differences in concentration of the salt in the electrolyte (Figure 12.5a), and (2) the differential aeration cell, where the oxygen concentration varies on the electrode

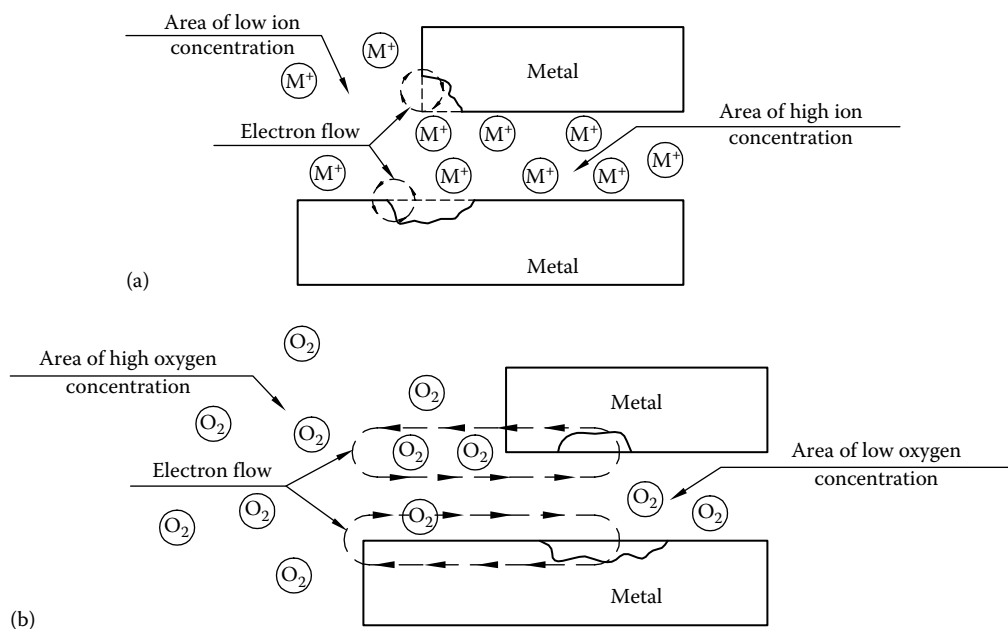


FIGURE 12.5 Concentration cell. (a) Salt concentration cell and (b) oxygen concentration cell. (Adapted from *Resistance to Corrosion*, 4th edn., Inco Alloys International, Huntington, WV, 1985.)

surface, with the anodic area being the one having lower oxygen concentration (Figure 12.5b). Such cells account for localized corrosion of metals at crevices formed by overlapping joints, threaded connections, or by microorganisms growing on metal surfaces [2]. The shielded area tends to be low in dissolved oxygen concentration and hence become anodic to the outside area with higher oxygen concentration.

12.1.3.3 Differential Temperature Cells

Components of these cells are electrodes of the same metal, each of which is at a different temperature, immersed in an electrolyte of the same initial composition. The surfaces at higher temperatures are generally anodic with respect to cooler ones.

12.1.4 CORROSION POTENTIAL AND CORROSION CURRENT

The driving force for current and corrosion is the potential developed between the metals. When no current flows between the anode and the cathode, the potential difference between them is at a maximum known as the open circuit potential. The current that flows between the anode and the cathode when a metal corrodes in an electrolyte is called the corrosion current, and the net potential of the corroding surface is the corrosion potential.

12.1.5 CORROSION KINETICS

The preceding discussion deals with the criteria leading to the formation of an electrolytic cell, which is the essential step in the corrosion process. However, the potential difference of the galvanic couple can change with time. As corrosion progresses, corrosion products may accumulate at the anode, cathode, or both. This reduces the speed at which corrosion proceeds. The phenomena affecting the corrosion kinetics are referred to as polarization and passivation. These two phenomena are also extremely important in the preventive measures that can be used for corrosion control.

12.1.5.1 Polarization Effects

The phenomenon that controls the rate of corrosion reaction is known as polarization, which is the ease with which anodic and cathodic reactions take place. The principle of polarization effects is as follows. As soon as current begins to flow through an electrolytic cell, it produces chemical changes at the electrodes, and these changes tend to set up a new voltaic cell with a voltage in the opposite direction to that of the main cell voltage. This new countervoltage is known as polarization, and it always opposes the main voltage of the cell; it never reinforces it. In simple terms, due to polarization, the potentials of the metals in a corrosion cell tend to approach each other. The decrease in anode potential is anodic polarization, and the decrease in cathode potential is cathodic polarization. This reduced voltage can drive less additional current through the cell. It is not always true that both anodic and cathodic polarization will take place to the same extent. In some cases, greater polarization is at the anode and in other cases at the cathode. In the former case, the reaction is said to be anodically controlled. In the latter case, it is said to be cathodically controlled.

Polarization in iron–water system: In the iron–water system, the reaction is cathodically controlled because hydrogen ions are available in small quantity. In other words, cathodic polarization limits the rate of reaction [3]. Oxygen is a depolarizer because it decreases the slope of one of the lines, thereby increasing the corrosion current and, in this reaction, the amount of corrosion. A little consideration of this will indicate the importance of polarization in limiting corrosion rate without it reaching an infinite value, which would have been the case in the absence of any polarization. It can take the form of slow ion movement in the electrolyte, slow combination of atoms to form gas molecules, or slow solvation of ions by electrolyte [1].

Factors affecting polarization: The degree of polarization is variable; some corrosion reactions proceed rapidly owing to high spontaneity and low polarization, and others proceed very

slowly owing to high polarization even though they have a pronounced tendency to corrode as shown by reversible EMF of the corrosion cell [4]. Factors affecting polarization include the following [1]:

1. Increasing the reaction area allows the corrosion to take place more readily and hence lowers the rate of polarization.
2. Agitation or electrolyte movement carries away the products of corrosion reaction from the surface and thereby provides a maximum number of ions contacting the electrodes, thus increasing the rate of corrosion and decreasing the polarization. On the other hand, if the cathodic reaction is activation controlled, agitation would have no effect on the corrosion rate.
3. Oxygen effectively depolarizes the electrode or makes the reaction go more rapidly by removing the reaction product atomic hydrogen.
4. Increasing the temperature increases the rate of most reactions and therefore lowers the polarization rate.

Polarization diagrams: Plots of anode and cathode potential versus current flow (E_p vs. I) are called polarization diagrams. By plotting current density on a logarithmic scale, the polarization lines will be linear, in accordance with the Tafel equation. These diagrams are also called Evans diagrams, after one of the founders of corrosion science, Ulick Evans. Idealized polarization diagrams are shown in Figure 12.6. Figure 12.6a shows a polarization diagram for a cathodically controlled corrosion cell and Figure 12.6b shows a polarization diagram for an anodically controlled corrosion cell. A polarization diagram for a passive metal anode is shown schematically in Figure 12.6c, and it can be seen from this figure that it does not polarize along a straight line as shown in an idealized diagram, but follows an S-shaped curve. The electrochemical behavior of active-passive transitions is illustrated by such curves. Such diagrams can be used to show the effects of cathodic polarization by hydrogen and anodic polarization by accumulated metal ions and corrosion products. In actual practice, the polarization curves would not be straight lines. The shapes of these curves will depend on the particular process responsible for the polarization [4].

Polarization measurement: Polarization measurements on the members of a galvanic couple can provide precise information regarding their behavior, particularly the prediction of localized corrosion. Polarization techniques and critical potentials are used to measure the susceptibility to pitting and crevice corrosion of metals and alloys in a chloride solution [5].

12.1.5.2 Passivation

Sometimes material corrodes, producing an adherent corrosion product that protects it from further corrosion. Such (passivated) material corrodes very little in a specific environment, even though it would otherwise corrode considerably [6]. For example, a look at the galvanic series will indicate that aluminum should corrode at a high rate. In practice, however, it is found that aluminum is highly resistant to attack in most of the media except halides. This phenomenon is known as passivation. Materials such as nickel, titanium, zirconium, chromium, and stainless steel owe their corrosion resistance to natural passivation.

Passivity can be understood through a study of polarization diagrams (schematic) presented by Roser et al. [7]. The anodic polarization curves of passive alloys shown in Figure 12.6b are distinctly different from those of nonpassive alloys. Comparison of anodic polarization curves for passive and nonpassive materials is shown in Figure 12.6c. Passivation is a result of marked anodic polarization whereby a barrier of thin protective film, either metal oxide or chemisorbed oxygen, is formed between the metal and the environment, preventing further contact with the electrolyte. In the case of iron, when more oxygen reaches the metal surface

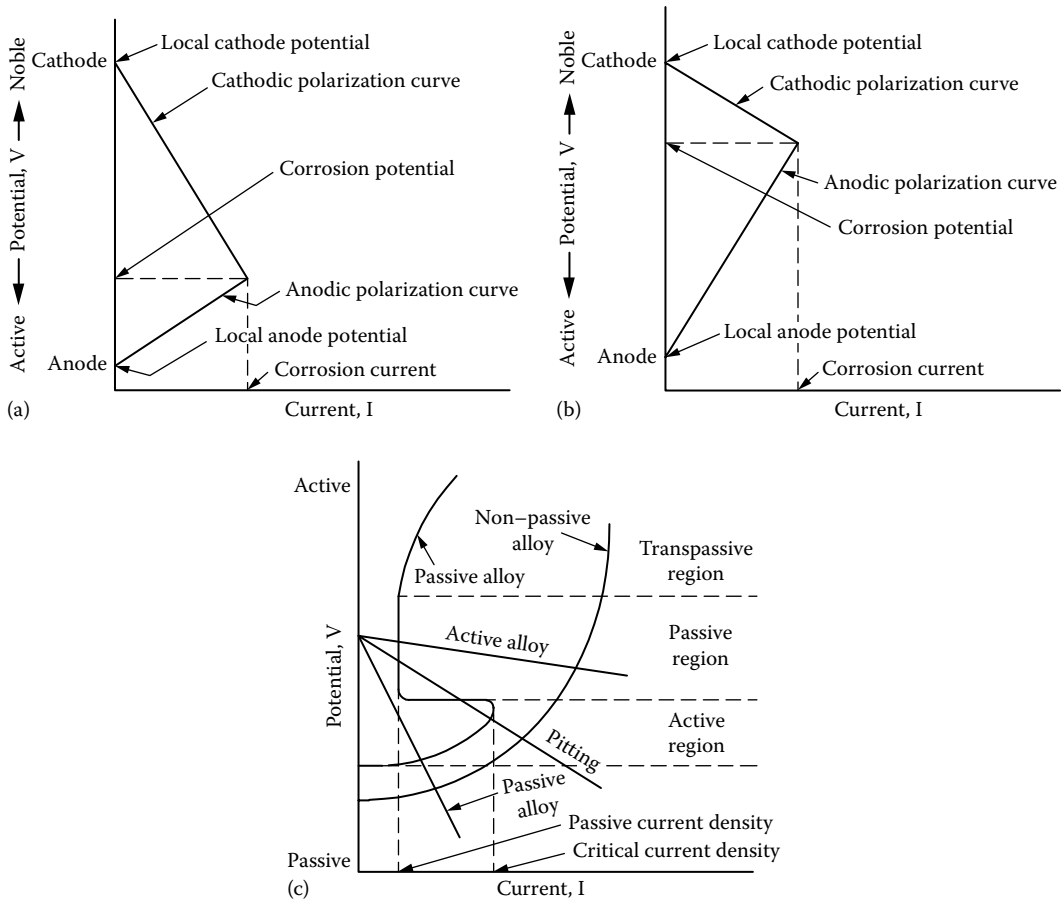


FIGURE 12.6 Polarization diagrams. (a) Cathodically controlled corrosion, (b) anodically controlled corrosion, and (c) comparison of anodic polarization curves for passive and nonpassive materials.

than that can be used in the cathodic reaction, a protective passive film is able to form [3]. Thus, the attainment of passivity is thus most important in avoiding accelerated corrosion. Whether a given alloy will be passive in a given situation depends on both the anodic and the cathodic polarization effects.

Passive alloys are widely used as corrosion-resistant materials for the construction of heat exchangers. The corrosion resistance of passive alloys depends on the chromium content, chloride and oxygen content in the environment, and the temperature [7]. Attainment of passivity in a given situation depends on the relative value of all factors rather than on any one of them. For example, high chromium aids passivity, low temperature aids passivity, depassivating ions such as chlorides hinder passivity, and oxygen aids passivity.

Behavior of passive alloys: Passive material corrodes very little in a specific environment, even though it would otherwise corrode considerably [6]. Conversely, alloys that commonly exhibit passivity are invariably quite active in the nonpassive state. Some elements break down passive films, causing the metal to corrode where the film is discontinuous. Chlorine ions, e.g., destroy the passivity of aluminum, iron, and the stainless steels, causing pitting corrosion. Therefore, the users of passive alloys should be particularly on guard for pitting, stress corrosion cracking (SCC), sensitization, and oxygen starvation-type corrosion [7].

12.1.6 FACTORS AFFECTING CORROSION OF A MATERIAL IN AN ENVIRONMENT

The corrosion process is affected by various parameters:

1. Environment factors such as concentration of chemicals, pH, velocity, impurities and suspended matter, and temperature of the medium.
2. Source of heat, if any. If the environment is heated through the material being selected, the effects of heat transfer and surface temperature may be the controlling factors.
3. Material factors like composition, alloying elements, passivity, tendency for fouling.
4. Design conditions and geometry of the joints, like gasketed surfaces, crevices, stagnant areas, and U-bends.
5. Fabrication techniques: corrosion due to welding, brazing, soldering, and heat treatment.

Factors influencing corrosion are shown schematically in Figure 12.7. Only the environmental factors are discussed next. The other factors are discussed while discussing various forms of corrosion.

12.1.6.1 Environmental Factors

Environmental factors that control corrosion of a material in an environment are as follows:

1. Presence of impurities
2. Temperature of the corrodent
3. Degree of aeration
4. Velocity of corrodent
5. Adherent deposits
6. Concentration of corrodent
7. Effects of pH

Presence of impurities: Impurities or contaminants in the corrosive environment can cause either general corrosion or localized attack within the system, or both. The presence of even minor amounts of impurities can alter the corrosion rate significantly. For example, chlorides above 30 ppm will increase the corrosion rate of austenitic stainless steel drastically.

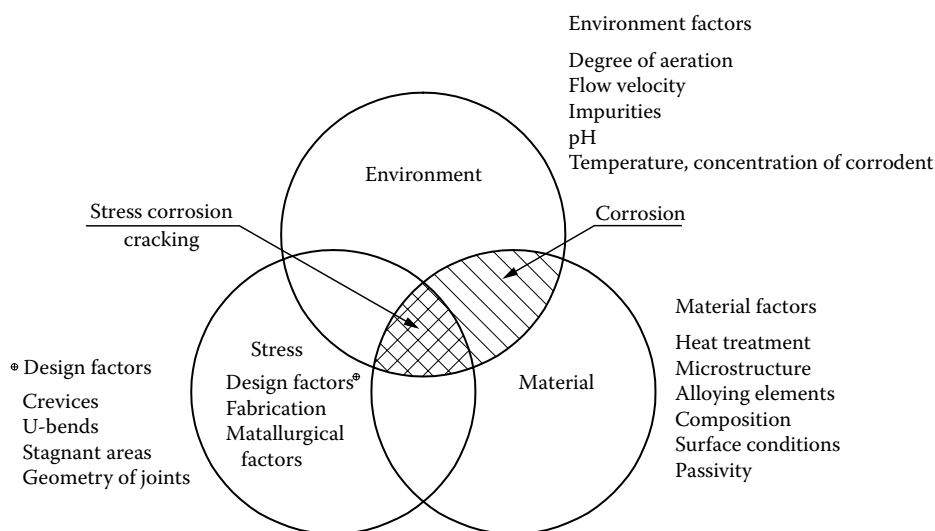


FIGURE 12.7 Factors influencing corrosion.

Temperature of the corrodent: As a rule, the degree of corrosion increases with increase in temperature, but increasing temperature also tends to drive dissolved gases out of solution so that a reaction that requires dissolved oxygen can often be slowed down by heating [2]. There are numerous cases where metals satisfactory for cold solutions are unsuitable for the same solutions at elevated temperatures. For instance, refrigerant-quality brine can be handled by a plate heat exchanger (PHE) in 18Cr-12N-2.5Mo (AISI 316) stainless steel, provided the surface temperature does not exceed 10°C (50°F). At higher temperatures, plate failure due to pitting and/or stress corrosion is inevitable.

Degree of aeration and oxygen content: The design of the plant and equipment selection in particular can influence the amount of air introduced into a process stream, which in turn may have an influence on corrosion. Oxygen can behave as a depolarizer and increase the rate of corrosion by speeding up the cathodic reaction. It can also act as a passivator because it promotes the formation of a stable passive film [2]. It also must be understood that the major contributor to the corrosion of all metals in the atmosphere is oxygen.

Velocity of corrodent: Velocity of the corrodent affects both the type and the severity of the corrosion and removal of fouling deposits. Corrosion is favored by too low or too high velocities. Uniform and constant flow of process fluids past heat exchanger favors less fouling and hence less corrosion. High velocity helps to prevent the accumulation and deposition of corrosion products, which might create anodic sites to initiate corrosion, to maintain clean surfaces free from fouling deposits, and to avoid crevices and stagnant areas. On the other hand, too high a velocity can destroy the protective surface film and result in erosion–corrosion, especially on metals such as copper and aluminum alloys.

Adherent deposits: Deposits on the metal surface cause crevices. These act as sites for accelerated corrosion. Adherent deposits cause localized hot spots, which in turn contribute to high-temperature corrosion.

Concentration of corrodent: In general, the corrosion rate increases with increasing concentration, including the concentration of the aggressive chemical species such as chloride ions. However, there are exceptions also. For example, iron is attacked vigorously in dilute nitric and sulfuric acids, but the corrosion rate is drastically reduced in concentrated acids due to passivation of the metal surfaces when once corrosion has begun.

Effects of pH: Increasing the acidity of a solution can result in a very large increase in general corrosion rate below a critical value or a range for a given alloy and environment. Since the reaction of a metal in an aqueous environment can be expressed as a simple displacement reaction



it is evident that where a greater number of hydrogen ions (low pH) are available, the corrosive reaction should occur more rapidly. Corrosion rate versus pH is presented schematically in Figure 12.8. The general shape of this curve may be considered as fairly typical for copper-base alloys. Such curves prepared for various metals and alloys could have their minima broadened or shortened, the slopes varied considerably, and the whole curve displaced in any direction, depending upon the characteristics of the alloy and the composition of the solution.

12.2 FORMS OF CORROSION

12.2.1 UNIFORM CORROSION VERSUS LOCALIZED CORROSION

Corrosion attack on the metal surfaces can be either uniform or localized, where the major part of the surface of the metal remains almost unaffected while certain localized areas are attacked at a very high rate with rapid penetration into the section of the metal. Uniform corrosion occurs during the corrosion of a metal in an acid, alkali, and during the exposure of certain metals to natural

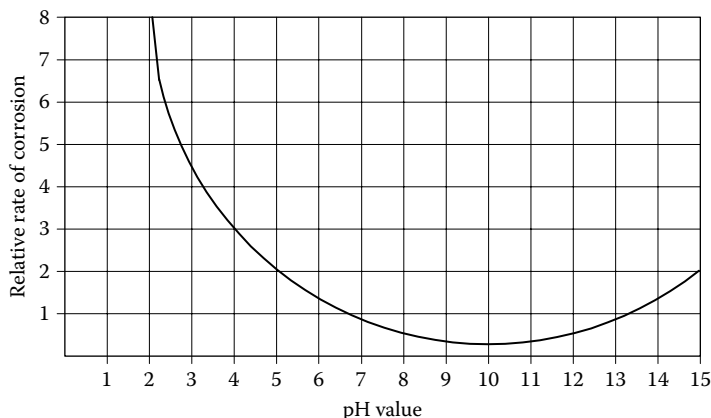


FIGURE 12.8 Corrosion rate versus pH (schematic).

environments like air and soil. In general, uniform corrosion takes place when the metal and environment system are homogeneous; that is, the metal is uniform in composition and structure and the nature of the environment (composition, oxygen concentration, acidity/alkalinity), temperature, velocity, etc., are the same at all parts of the metal surface [4]. Conversely, in many metals and environment systems, due to heterogeneities in the metal or variations in the environment or both, corrosive attack may be localized. Various forms of localized corrosion are pitting corrosion, crevice corrosion, intergranular corrosion, dealloying, erosion–corrosion, etc.

12.2.2 FACTORS THAT FAVOR LOCALIZED ATTACK

For metals and alloys, grain boundaries, intermetallic phases, inclusions, impurities, regions that differ in their mechanical or thermal treatments, discontinuities on metal surface such as cut edges or scratches, discontinuities in oxide or passive films or in applied metallic or nonmetallic coatings, and geometrical factors such as crevices favor localized attack [4]. Localized corrosion of a metal surface due to irregularities in metals is shown in Figure 12.9 [8].

12.2.3 FORMS OF CORROSION

Over the years, corrosion scientists and engineers have recognized that corrosion manifests itself in forms that have certain similarities and therefore can be categorized into specific groups. The most

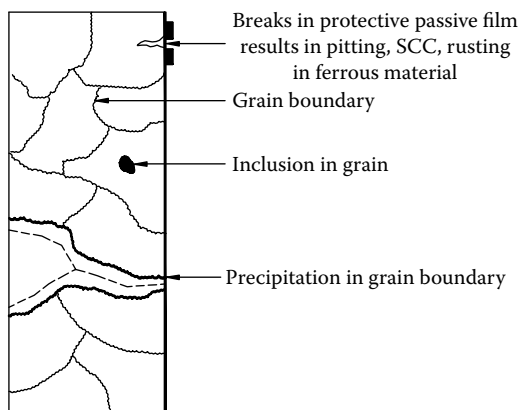


FIGURE 12.9 Localized corrosion of a metal surface due to irregularities in metals.

familiar and often used categorization of corrosion is probably the following eight forms presented by Fontana and Greene [9]:

1. Uniform corrosion
2. Galvanic corrosion
3. Pitting corrosion
4. Crevice corrosion
5. Intergranular corrosion
6. Dealloying or selective leaching
7. Erosion–corrosion
8. SCC

Hydrogen damage, although not a form of corrosion, often occurs indirectly as a result of corrosive attack [9]. This classification of corrosion was based on visual characteristics of the morphology of corrosion attack. Other forms of corrosion classified based on the mechanisms of attack rather than the visual characteristics are as follows:

Fretting corrosion
Corrosion fatigue
Microbiologically influenced corrosion (MIC)

All the corrosion types provided earlier can be grouped into

1. Uniform corrosion
2. Localized corrosion
3. Velocity-induced corrosion
4. Mechanically assisted corrosion

General corrosion takes place uniformly over a broad area. In galvanic corrosion, two dissimilar metals form a galvanic couple, and the less noble metal in the couple corrodes. Pitting is the localized attack that produces small pits, which may penetrate the metal thickness. Crevice corrosion is another form of localized corrosion and takes place under crevices or deposits. Intergranular corrosion takes place at grain boundaries in weld metal or in heat-affected zones (HAZs) of sensitized metals. In dealloying, an alloying element is preferentially corroded over others from the parent alloy, leaving behind a weak structure. Erosion–corrosion is a localized corrosion that occurs mostly on the tubeside, in areas where the turbulence intensity at the metal surface is high enough to remove the protective surface film. SCC results when the corrosive action of a susceptible metal and the tensile stress combine in a particular environment. Corrosion may combine with other forms of attack, such as fatigue, to produce severe damage. Corrosion fatigue is the reduction in the fatigue strength of a metal exposed to a corrosive environment. Various forms of corrosion are shown schematically in Figure 12.10, and forms of corrosion, factors influencing corrosion, susceptible metals, and corrosion control measures, are shown in Table 12.1. Forms of corrosion are discussed in detail in the following sections.

12.2.3.1 Uniform or General Corrosion

Uniform corrosion is the most common form of corrosive attack on metals and nonmetals. It refers to the corrosion process dominated by uniform thinning and proceeds without appreciable localized attack. Uniform corrosion is also referred to as general corrosion. Uniform corrosion results from prolonged contact with environments such as atmosphere, water, acids, alkalies, soil, etc. It is manifested by a chemical or electrochemical reaction. Uniform corrosion of the metal surface, as in the rusting of iron, results from anodes and cathodes rapidly interchanging sites at random; should the anode become fixed on the surface, a localized pitting corrosion will result instead [2].

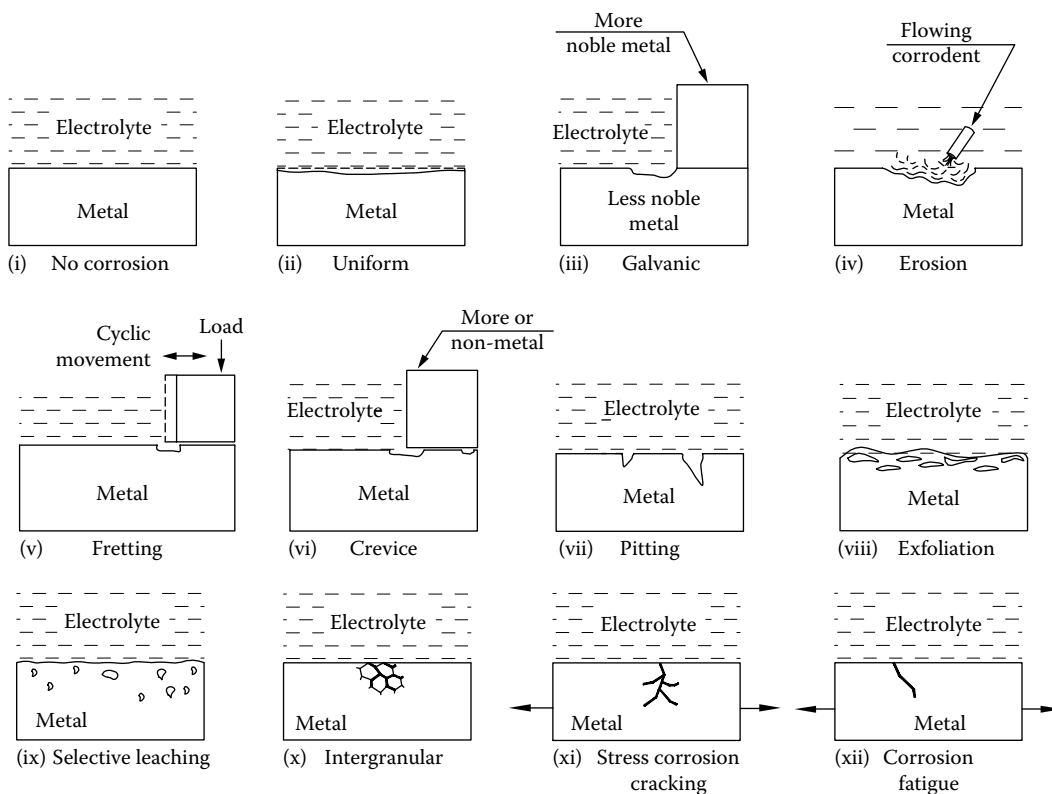


FIGURE 12.10 Schematic of various forms of corrosion.

Like other forms of corrosion, many factors influence general corrosion. The corrosive media is the most important factor governing corrosion. Environmental factors such as acidity, temperature, concentration, motion relative to metal surface, degree of oxidizing power and aeration, and presence or absence of inhibitors influence general corrosion [3].

Forms of uniform corrosion: Most general types of uniform corrosion are atmospheric corrosion and high-temperature (gaseous) corrosion. Although high-temperature attack in gaseous environments may manifest itself as various forms of corrosion, it has been incorporated into the category “general corrosion” because it is often dominated by uniform thinning [10]. Biological corrosion can manifest itself in a general or a localized form. It is covered at the end of this section.

Atmospheric corrosion: Atmospheric corrosion is defined as the corrosion of a material exposed to the air and its pollutants rather than immersed in a liquid. Many variables influence the atmospheric corrosion. Relative humidity, temperature, contents like sulfur dioxide, hydrogen sulfide, and chloride, amount of rainfall, dust, etc., influence corrosion behavior. Therefore, in an arid atmosphere, free of contaminants, only negligible corrosion would be expected. It also must be understood that the major contributor to the corrosion of all metals in the atmosphere is oxygen.

Types of corrosive atmospheres: A common practice is to divide atmospheres into categories such as rural, industrial, marine, and indoor [11]. Most of them are mixed and no clear lines of demarcation are present, and the type of atmosphere may vary with the wind pattern, particularly where corrosive pollutants are concentrated. Except for severe marine environments, there is no need to protect against atmospheric corrosion except with protective coatings [12].

Protection against atmospheric corrosion: Important considerations to protect against atmospheric corrosion should involve [12] (1) specific plant environment around the equipment,

TABLE 12.1**Forms of Corrosion, Factors Influencing Corrosion, Susceptible Metals, and Corrosion Control Measures**

Forms of Corrosion	Factors Influencing Corrosion	Susceptible Metals	Corrosion Prevention/Control Measures
Uniform corrosion (or general corrosion).	Corrosion process dominated by uniform thinning and proceeds without appreciable localized attack. Uniform corrosion results from prolonged contact with environments such as atmosphere, water, acids, alkalies, soil, etc.	Though all metals corrode/ tarnish in atmosphere, rusting of iron is most important	Proper material selection, alloying additions to the base metal, cathodic protection using sacrificial anodes, use of inhibitors, surface coatings, and corrosion allowances
Galvanic corrosion	When two dissimilar metals or alloys placed at different potentials in electromotive series are in contact with each other in a electrolyte, a galvanic couple is formed and results in corrosion of one of the metals (less noble metal), known as the anode of the couple	In seawater cooled condensers, tube materials such as copper–nickels, stainless steels, or titanium are more noble than tubesheet materials such as Muntz metal, naval brass, or aluminum bronze; consequently, the tubesheets may suffer galvanic attack	Choose the combination of metals as close together as possible in the galvanic series and avoid the unfavorable area effect
Pitting corrosion	Instead of a uniform corrosion in a corrosive environment, a metal very often suffers localized attack resulting in pitting. Metallurgical and structural factors, environmental factors, and polarization phenomena, breakdown of passive film, mill scale or applied coating. Compositional heterogeneity; inhomogeneities in the alloys	Aluminum, austenitic stainless steels, nickel, and their alloys, titanium in which surface film develops	Surface cleanliness and selection of materials resistant to pitting in the given environment: (a) For aqueous solutions of chlorides, choose AISI 316 or 317, Hastelloy G-3, Inconel alloy 625, and Hastelloy C-22, copper–nickel, Monel, or titanium. (b) In seawater and stagnant natural water applications, use copper–nickel, aluminum bronze, inhibited admiralty brass, titanium, superferritics, and duplex stainless steels. (c) Reduce the aggressiveness of the environment (the control of acidity, temperature, oxidizing agents, and chloride ions concentration)
Crevice corrosion	Localized form of corrosion that takes place at localized environments/areas that are distinctly different from the bulk environments	Metals or alloys that depend on protective surface film for corrosion resistance such as aluminum, stainless steels, and titanium	Materials can be alloyed to improve resistance to crevice corrosion. Design to minimize crevices and maintenance practices to keep surfaces clean and avoid deposits build up

(continued)

TABLE 12.1 (continued)**Forms of Corrosion, Factors Influencing Corrosion, Susceptible Metals, and Corrosion Control Measures**

Forms of Corrosion	Factors Influencing Corrosion	Susceptible Metals	Corrosion Prevention/Control Measures
Inter granular corrosion (IGC)	It takes place as the result of local cell action in the grain boundaries due to potential difference between second-phase micro constituents and the depleted solid solution from which the constituents are formed. The high cathode to anode area ratio results in rapid corrosion of the grain boundary material and the metal disintegrates	Austenitic stainless steels 304 (18-8), ferritic, superferritic, and duplex stainless steels. Nonferrous metals such as nickel 200 and nickel-base alloys like Inconel alloys 600 and 601, Incoloy alloys 800 and 800H, Hastelloys B and C and aluminum base alloys containing copper	Employ a suitable high-temperature solution heat treatment, commonly known as quench annealing or solution annealing. Ensure that the steel contains insufficient carbon to form Cr ₂₃ C ₆ and resulting alloy depletion. Such steels contain less than 0.03% C and are called extra-low-carbon (ELC) steels, signified by the suffix L (e.g., type 304L and 316L). Use stabilized steels such as type 347 (columbium stabilized) and type 321 (titanium stabilized) instead of type 304
Dealloying or selective leaching	Corrosion process in which an alloying element is preferentially corroded over others from the parent alloy, leaving behind a weak structure due to interaction of metallurgical, and environmental factors	Brasses-dezincification, cupronickels-denickelification, aluminum bronze-dealuminification, silicon bronze-destannification or desiliconification	Material substitution- use admiralty brass, inhibited admiralty brass, aluminum brass (inhibited), cupronickel, and titanium. Surface cleanliness and avoid stagnant fluid conditions
Erosion-corrosion	A form of localized corrosion which takes place due to the movement of a high velocity fluid over a material surface, Both mechanical and chemical factors such as turbulence, fluid velocity, impingement attack, level of suspended particles, aeration, bubble level, local partial pressure, cavitation, etc., affects	Normally restricted to copper and certain copper-base alloys and aluminum alloys.	Use filtered water. Use titanium or stainless steel or aluminum brasses or copper-nickel tubes which are resistant to erosion-corrosion. Installation of tube inserts made of wear-resistant materials; on the shellside use impingement plate protection beneath the inlet nozzle
Stress corrosion cracking (SCC)	The corrosion attack on a susceptible alloy due to combined and synergistic interaction of tensile stress, conducive environment and its temperature and susceptible material	Chloride cracking, of austenitic stainless steel and aluminum. Caustic cracking of carbon steel. Ammonia cracking of admiralty brass. Polythionic acid cracking of austenitic stainless steel. Sulfurous acid cracking of austenitic stainless steel	To avoid the metal and environment combinations that are favorable for SCC. To resist chloride SCC of Austenitic SS, use Inconel 600, Incoloy alloys 800 and 825; ferritic-, superferritic-, and duplex stainless steels or titanium

TABLE 12.1 (continued)**Forms of Corrosion, Factors Influencing Corrosion, Susceptible Metals, and Corrosion Control Measures**

Forms of Corrosion	Factors Influencing Corrosion	Susceptible Metals	Corrosion Prevention/Control Measures
Corrosion fatigue	Combined action of a cyclic stress, corrosive environment and metallurgical factors	Aluminum alloys exposed to chloride solution, Cu–Zn and Cu–Al alloys exposed to aqueous chloride solutions, and high-strength steel in a hydrogen atmosphere	Use of protective coatings, adding inhibitors to the environment, cathodic protection, and introduce residual compressive stresses by methods such as shot peening
Hydrogen attack or hydrogen damage. Other forms hydrogen attack are hydrogen induced cracking (HIC), hydrogen embrittlement (HE), hydrogen sulfide stress cracking (HSCC) or sulfide stress corrosion cracking (SSCC)	Degradation of steel by hydrogen sulfide (H ₂ S) in pressure vessels handling sour crude oil or gas in petroleum refinery equipment. Diffusion of mono atomic hydrogen into the steel and recombine to form molecular hydrogen at voids, laminations, discontinuities or around inclusions, generating extremely high pressure. It stiffens the metal, impairing its ductility. It also gives rise to blistering and cracking	High strength steels, titanium alloys and aluminum alloys. Steels with weldments are susceptible to hydrogen embrittlement. Use pressure vessel quality steels with 0.25%–0.35% C, in plate thickness 1–2 in (25.4–50.8 mm), such as ASTM A515 and A516	Selection of steel to resist high temperature and high pressure hydrogen/hydrogen sulfide environment. Follow the operating limits on temperature, partial pressure of hydrogen, and alloy composition set forth by Nelson curves. Cr–Mo steels are more resistant to hydrogen attack than plain carbon steel
Microbiologically influenced corrosion (MIC)	MIC occurs directly or indirectly as the result of metabolic activity of microorganisms on heat transfer surfaces	Common engineering metals and alloys such as carbon steel, lined steel, stainless steels, aluminum alloys, and copper alloys, 6% Mo stainless steels, and high-nickel alloys (Monel 400 and Alloy B-2)	Uptake filtration. Systematic cleaning and elimination of stagnant areas. Proper use of a biocide. Thermal shock treatments

(2) operating temperature, and (3) protection against ingress of rain water into crevices. Merrick discusses these factors in detail [12].

The specific plant environment around the equipment that involves releases of corrosive gases, such as hydrogen sulfide, sulfur dioxide, or ammonia, from nearby process plant will significantly increase atmospheric corrosion of equipment.

The operating temperature of the pressure vessels and heat exchangers has a significant effect on atmospheric corrosion. Units that operate below the dew point experience more corrosion than those operating at higher temperatures.

For protection against ingress of rain water into crevices, saddles and reinforcing pads for supports should be continuously welded to the vessel. Partial welding or stitch welds will act as a crevice. This will permit the ingress of rain water between the saddle and the vessel and can accelerate crevice corrosion.

Control of uniform corrosion: Uniform corrosion can be easily predicted and controlled by

- Proper material selection
- Small alloying additions to the base metal
- Cathodic protection using sacrificial anodes
- Use of inhibitors
- Surface coatings

Adding extra material known as corrosion allowances. Although uniform corrosion is obviously detrimental, it is least predictable, and corrosion allowances for losses are frequently made in the design of equipments. For corrosion-resistant materials, in general, no corrosion allowance is given.

Rating of metals subject to uniform corrosion: In contrast to localized forms of corrosion, uniform corrosion is rather predictable. The uniform attack on an entire area exposed to a corrosive environment is usually expressed in terms of an average loss of metal thickness for a given period of time in units of mils (1 mil = 1/1000 in.) per year (mpy), inches per month (ipm), or millimeter per year (mm/yr). Corrosion rate less than 5 mpy is excellent (for very critical application) and 5–20 mpy is satisfactory [13].

Determination of general corrosion: General corrosion is determined by immersion tests conducted according to ASTM G-31. Eight different boiling acid and alkali solutions—20% acetic acid, 45% formic acid, 10% oxalic acid, 20% phosphoric acid, 10% sodium bisulfate, 50% sodium hydroxide, 10% sulfamic acid, 10% sulfuric acid—are used to compare the performance of different alloys in a variety of solutions rather than to simulate a particular process industry environment. Duplicate samples are exposed for five 48 h periods, and an average corrosion rate is determined.

Material selection for general corrosion: Of the various forms of corrosion, general corrosion is the easiest to evaluate, and hence the material selection is straightforward; if a material shows only a general and uniform attack, a corrosion rate, 0.25 mm/yr (10 mils/yr) or less for low-cost material such as carbon steel, a negligible contamination of the process fluids, and availability, ease of fabrication etc., then that material favors the choice of selection. For more costly materials such as the 300 series austenitic stainless steels and copper- and nickel-base alloys, a maximum corrosion rate of 0.1 mm/year (4 mils/year) is generally acceptable [14]. The corrosion rate is multiplied by the nominal design life of the vessel (normally 20 years) to determine the corrosion allowance.

12.2.3.2 Galvanic Corrosion

When two dissimilar metals or alloys placed at different positions in electromotive series are in contact with each other in an electrolyte, a galvanic couple is formed and results in the corrosion of one of the metals, known as the anode of the couple. In other words, galvanic corrosion does not affect the cathode, which is known as a noble metal. This form of corrosive attack is known as galvanic corrosion since the entire system behaves as a galvanic cell. Galvanic corrosion can also take place even within the same group of metals due to local imperfections or heterogeneities on the metal surfaces or due to variation in local solution chemistry. Most often, galvanic corrosion shows up as furrows or troughs on the corroded metal at its point of contact with the more noble metal. For initiation of galvanic corrosion, four essential components are required: the anode, the cathode, the electrolyte, and a metallic path between the anode and the cathode, which completes the circuit. These four basic components were already discussed.

12.2.3.2.1 Heat Exchanger Locations Susceptible to Galvanic Corrosion

Components such as tubesheets, water box, bolts and flanges, and supports made of less noble metals will corrode at the following locations:

- Interfaces between the tube and baffle plates
- Between the tubes and tubesheet areas
- Welded joints, brazed joints, and soldered joints

Heat exchanger supports with the frame or shell bolts and fasteners if they are less noble than the flange materials.

In seawater-cooled condensers, tube materials such as copper–nickels, stainless steels, or titanium are more noble than tubesheet materials such as Muntz metal, naval brass, or aluminum bronze; consequently, the tubesheets may suffer galvanic attack when fitted with more noble tube materials. This is also true with tubes made of seawater-resistant stainless steels like superferritics and superaustenitics used to replace the copper alloy tubes in a Muntz metal tubesheet. Similarly, a cast iron water box may suffer galvanic attack because all other materials in the condenser are more noble than cast iron. In general, weld metal corrosion can be eliminated by using suitably balanced electrode; the remaining problems are discussed in the section on weld metal corrosion. Brazed joints are always at risk to galvanic corrosion because the fillers are invariably of different composition than that of the parent metals being joined. Fortunately, these fillers are normally noble than the metals being joined and hence the corrosion problem is not faced. Corrosion of brazed joints and corrosion of soldered joints are discussed in detail in Chapter 15, Heat Exchanger Manufacture, in the second part, Brazing and Soldering.

12.2.3.2.2 *Galvanic Corrosion Sources*

Two important sources of galvanic corrosion are (1) metallurgical sources and (2) environmental sources.

Metallurgical sources: Metallurgical sources are within the metal and/or in relative contact between dissimilar metals. Such sources include difference in potential of dissimilar materials, distance apart in galvanic series, relative areas of anode and cathode, oxide or mill scales, strained metal (cold work), inclusions in metal, and differences in microstructure, HAZ, and sensitization [15,16].

Environmental sources: Environmental sources include conductivity of the fluid, concentration differences in solution, changes in temperature, velocity, and direction of fluid flow, aeration, and ambient environment (seasonal changes) [15].

12.2.3.2.3 *Types of Galvanic Corrosion*

Among the various forms of electrochemical corrosion, (1) bimetal corrosion, (2) differential aeration corrosion, (3) differential concentration corrosion, and (4) work area corrosion belong to galvanic corrosion [17]. Items 1–3 have been discussed earlier. Only work area corrosion is defined here.

When a metal is cold worked so that it is denser in one place than another, a corrosion cell with the stressed area as an anode and the remaining area as cathode is set up if these two areas are immersed in an electrolyte [17]. This is called work area corrosion.

12.2.3.2.4 *Magnitude of Galvanic Effects*

The discussion given earlier deals with the criteria leading to the formation of an electrolytic cell, which is the essential step in the corrosion process. However, the extent of corrosion attack taking place is dependent on many factors as follows:

1. The polarization behavior of the metals or alloys
2. Passivation of the alloys
3. Potential difference between the metals or alloys, i.e., the distance effect
4. Area effect, i.e., the geometric relationships such as relative surface area

Items 1 and 2 have been discussed earlier, and the remaining points are discussed next.

Distance effect: Enhanced corrosion takes place when the metals in galvanic couple are placed further apart in the galvanic series. This is due to high electrochemical current density. In some cases, the separation between the two metals or alloys in the galvanic series gives an indication of the probable magnitude of the corrosive effect.

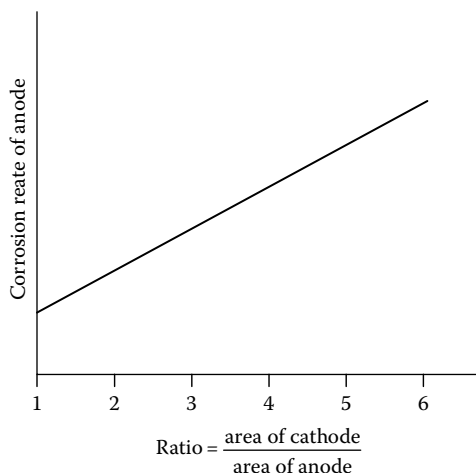


FIGURE 12.11 Galvanic corrosion due to area effect.

Area effect: Another important factor in galvanic corrosion is the area effect. As the ratio of the cathode-to-anode area increases, the corrosion rate of the anode metal rapidly accelerates (Figure 12.11). On the other hand, if the area of anode is large compared to the cathode area, the corrosion of the anode is so widely distributed that the amount of metal loss in terms of its thickness may be so small that it may be ignored. These observations suggest the well-established rule in corrosion engineering that when dissimilar metals are coupled, the anode area must be maintained as large as possible compared to cathode area. For example, the nuts and bolts that are critical to the flanged joints must always be noble (cathodic) to the larger area of the flange. The nuts and bolts (Figure 12.12) corrode at a rate well below normal at the negligible expense of the flange, which corrodes at only slightly above-normal rate over a large area.

12.2.3.2.5 Tools to Determine the Degree of Galvanic Corrosion

The degree of galvanic corrosion is normally known from the following two tools. They are the electromotive force (EMF) series and the galvanic series.

Electromotive force series: The EMF series is a list of elements arranged according to their standard electrode potentials, with the sign being positive for elements whose potentials are cathodic to hydrogen and negative for those anodic to hydrogen. In this listing, hydrogen is used as an arbitrary reference element, and metals such as gold and platinum have large positive values indicating little tendency for corrosion attack. Since the EMF series is of little value to the

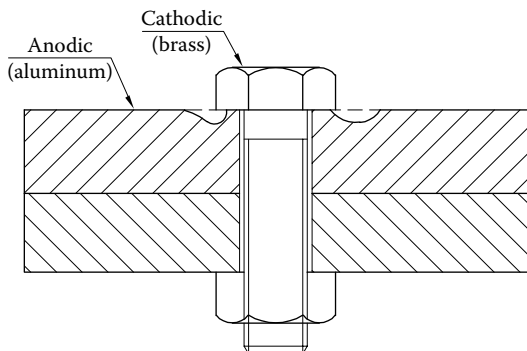


FIGURE 12.12 Nuts and bolts (cathodic) in a flanged joint (anodic).

practical corrosion scientist or technologist, it is necessary to develop some alternate system by which the relative corrodibility of a galvanic couple may be assessed [4]. Such a listing is known as the galvanic series.

Galvanic series: Whether a given metal or alloy is naturally anodic or cathodic with respect to another metal is judged by the galvanic series, which consists of an arrangement of metals and alloys in accordance with the measured potentials in flowing seawater at velocities ranging from 2.5 to 4 m/s. A typical tabulation is given in Table 12.2. With certain exceptions, this series is broadly applicable in other natural waters and in uncontaminated atmospheres. The galvanic series allows one to determine which metal or alloy in a galvanic couple is more active. The metals closer to the active end of the series will behave as the anode and will corrode, whereas those closer to the noble end will behave as the cathode and will be protected. The metals and alloys that are next to each other have little tendency to galvanic corrosion when connected together, so it is relatively safe to use such combinations in jointed assemblies [18].

TABLE 12.2
Galvanic Series in Seawater at 25°C (77°F)

Anodic (least noble) end or active end	Cartridge or yellow brass C27000
Magnesium	Admiralty brass C44300, C44400, C44500
Zinc	Aluminum bronze C60800, C61400
Galvanized iron	Red brass C23000
Aluminum alloy 5052H	ETP copper C11000
Aluminum alloy 3004	Silicon bronze C65100, C65500
Aluminum alloy 3003	Copper–nickel, 10%
Aluminum alloy 1100	Copper–nickel, 30%
Aluminum alloy 6053T	Nickel 200 (passive)
Alclad aluminum alloys	Inconel alloy 600 (passive)
Aluminum alloys, 2117	Monel alloy 400
Aluminum alloys, 2017T	Stainless steel type 410 (passive)
Aluminum alloys, 2024T	Stainless steel type 430 (passive)
Low-carbon steel	Stainless steel type 304 (passive)
Low-alloy steel	Stainless steel type 316 (passive)
Cast iron	E-Brite alloy
Stainless steel type 410 (active)	AL-29-4C alloy
Stainless steel type 430 (active)	AL-6XN alloy
50–50 Lead-tin solder	Inconel alloy 825
Stainless steel type 304 (active)	Inconel alloy 625, alloy 276
Stainless steel type 316 (active)	Hastelloy alloy C
Lead	Silver
Tin	Titanium
Muntz metal C28000	Graphite
Manganese bronze A—C67500	Zirconium
Naval brass: C46400, C46500, C46600, C46700	Tantalum
Nickel 200 (active)	Gold
Inconel alloy 600 (active)	Platinum
Hastelloy alloy B	Cathodic (most noble) end

Sources: Adapted from *Resistance to Corrosion*, 4th edn., Inco Alloys International, Huntington, WV, 1985; *AL-6XN[®] Alloy*, Allegheny Ludlum Steel Corporation, Pittsburgh, PA; Steven, P.L., General corrosion, in *Metals Handbook*, 9th edn., Vol. 13, Corrosion, American Society for Metals, Metals Park, OH, pp. 80–103, 1987.

12.2.3.2.6 Galvanic Corrosion Control

Design is a major factor in preventing or minimizing galvanic corrosion. Typical measures to control galvanic corrosion are as follows:

1. Choose the combination of metals as close together as possible in the galvanic series, unless the more noble metal is easily polarized.
2. Avoid the unfavorable area effect, i.e., small area of anode and a large cathode area. Otherwise small components such as bolts and fasteners should be of more noble metal.
3. Insulate or break the circuit between the two metals by applying coatings, introducing gas-kets, nonmetallic washers, etc., and make sure that metal-to-metal contact is not restored in service.
4. Add corrosion inhibitors to decrease the aggressiveness of the environment or to control the rate of cathodic and/or anodic reaction.
5. *Maintain coatings*: Coating is the most common method for combating corrosion.
6. Cathodic protection is one of the recommended methods of protecting the anode. Use a sacrificial anode such as Zn, Al, or Mg that is anodic to both the structural metals. Examples include sacrificial cladding (Alclad) applied in the internal aluminum tube surfaces of radiators to give protection to the tube core alloy and planting of Zn anode on the water box of condensers to protect both the tubes and the tubesheet. It is important to note that overprotection of the titanium tubesheet may result in the hydriding of the titanium tubes.

12.2.3.3 Pitting Corrosion

Instead of a uniform corrosion in a corrosive environment, a metal very often suffers localized attack resulting in pitting. Pitting usually occurs on metals that are covered with a very thin adherent protective surface film that formed on the metal surface during a surface treatment process or produced by reaction with an environment [19]. Thus, pitting corrosion occurs on aluminum, titanium, stainless steels, nickel, and their alloys, in which surface film develops. Pitting takes place when there is a breakdown of protective surface film. The protective film is an oxide layer in the case of carbon steel and ferritic stainless steel, whereas it is a passive film in the case of austenitic stainless steel. Once pits are initiated, they may continue to grow by a self-sustaining or autocatalytic process; that is, the corrosion process within a pit produces conditions that are both stimulating and self-propagating [9]. Pitting is the most aggressive form of corrosion and leads to premature failure due to perforation of the surfaces. Pitting corrosion is shown schematically in Figure 12.13.

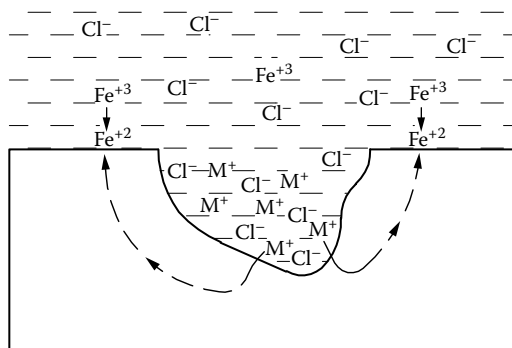


FIGURE 12.13 Schematic illustration of a growing pit. (Metal or alloy M is being attacked by a solution of ferric chloride. The dissolution reaction, $M \rightarrow M^+ + e^-$ is localized within a pit and cathodic reduction of the ferric ion, $Fe^{+3} + e^- \rightarrow Fe^{+2}$, occurs on the rest of the exposed metal surface.) (Adapted from *Resistance to Corrosion*, 4th edn., Inco Alloys International, Huntington, WV, 1985.)

12.2.3.3.1 Parameters Responsible for Pitting Corrosion

Pitting corrosion is caused by factors such as [20] (1) metallurgical and structural factors, (2) environmental factors, and (3) polarization phenomena. Other causes for pitting are the attachment of microorganisms, presence of corrosion products, deposits, etc. These parameters are explained next.

Metallurgical and structural factors: The following metallurgical and structural factors act as nucleation sites for initiation of pitting corrosion:

1. The breakdown of passive film, mill scale [21], or applied coating
2. Defect structures
3. A compositional heterogeneity; inhomogeneities in the alloys caused by segregation of alloys or by cold working [7]
4. Weld-related parameters [6]: Inclusions, multiple phases, compositional differences within the same phase, sensitization, arc strikes, spatter, and inhomogeneities in the base materials can act as potential pitting sites

Pits develop if there is a breakdown of passive film, mill scale, or applied coatings due to high turbulence in the flow, chemical attack, or mechanical damage or under deposits. Mill scale is cathodic to steel and is found to be one of the more common causes of pitting. Figure 12.14a illustrates the pit action due to breakdown of mill scale. A pit caused by broken mill scale becomes deeper, an oxygen concentration cell is formed by the depletion of oxygen in the pit, and this will accelerate the rate of penetration.

Studies show that the sites for initiation of pits on passive metal surfaces may be generally related to defect structures of the underlying metal such as dislocations, grain boundaries, or nonmetallic inclusions [20].

In terms of compositional heterogeneity, nonmetallic inclusions like sulfide inclusions, particularly manganese sulfides (MnS), are potential nucleation sites in austenitic stainless steels and ferritic stainless steels. Possible ways of eliminating the MnS inclusions in austenitic stainless steels are further explained in Chapter 13, Material Selection, in the section on austenitic stainless steels.

Environmental factors: Certain chemicals, mainly halide salts and particularly chlorides, are well-known pit producers. The passive metals are particularly susceptible to pitting in chloride environments. The chloride ions accumulate at anodic areas and either penetrate or dissolve the passive film at these points. Pitting can take place on stainless steel and other alloys exposed to marine life when natural water is left after hydrotesting. In this case, the marine life dies after a period of time. Due to the sulfides produced by the dying or decaying matter, the protective oxide film or passive film on the metal surface is destroyed, and pitting is initiated [1].

Influence of polarization on passive alloys, after Roser et al. [7]: Pitting can occur even in a relatively homogeneous alloy due to electrochemical causes. This is explained by polarization

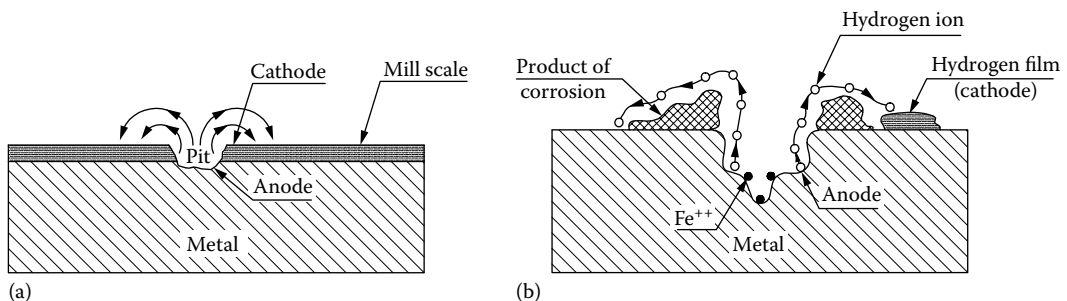


FIGURE 12.14 Pitting corrosion. (a) Pitting due to breakdown of mill scale and (b) pitting due to deposit on the base metal (galvanic cell).

curves as shown schematically in Figure 12.6c. If the cathodic polarization curve crosses the anodic polarization curve in the active region, the alloy will be active; if it crosses in the passive region, it will be passive; and if it passes in the intermediate region, the alloy will be partly active and partly passive. If the active regions are small and passive regions are large, the alloy can pit. Pitting can be avoided by either increasing or decreasing the polarization of the cathode to avoid the pitting region. Changes in alloy composition or structure can also be useful.

Attachment of microorganisms, presence of corrosion products, and deposits: Costly pitting failures of austenitic stainless steel components and weldments can take place by the attachment of microorganisms. Austenitic stainless steels form small tubercles from microbial action, under which severe pitting occurs. Or the sulfides produced by the dying microorganisms depassivate stainless steel, and pitting takes place underneath the fouling. Figure 12.14b illustrates the pit action due to the galvanic cell formed between the corrosion deposit and the base metal.

Basic condition for the initiation and propagation of pitting corrosion: A basic condition must be fulfilled for the initiation and propagation of pitting corrosion: "Pitting takes place when the anodic breakdown potential of the metal surface film is equal to or less than the corrosion potential under a given set of conditions."

12.2.3.3.2 Mechanisms and Theories of Pitting Corrosion

Nucleation and growth: The modern theory of pitting presupposes the formation of a pit at a minute area of a metal surface that suffers a breakdown in passivity [22]. This is known as the pit nucleation stage. The passive film breakdown is followed by formation of an electrolytic cell, which leads to growth and propagation of a pit rather than to spreading along the entire surface. The anode of this cell is a minute area of active metal, and the cathode is a considerable area of passive metal [23]. The large cathode-to-anode area ratio accounts for the considerable flow of current with rapid corrosion at the anode. Pits once initiated can propagate inside the pits. They stop propagating if the metal is polarized to (or below) the potential of metal inside the pits, which in the extreme is that of the active (nonpassive) state [24].

Growth and propagation of pit: A pit develops in stages: original attack, propagation, termination, and reinitiation [19]. Termination will occur with increase in internal resistance of the local cell.

12.2.3.3.3 Pitting Potential

For passive metals, pits are initiated at or above a specific potential. The potential at which pit initiation occurs is called the pitting potential. Resistance to pitting increases with the pitting potential. The pitting potential is an important criterion for evaluation of the stability of a passive film in an environment. The value of pitting potential depends on the material and its composition, the environment, and the concentration of aggressive ions, pH of the solutions, temperature, and history of heat treatment operation [24].

Determination of pitting potential: Pitting potential is determined by electrochemical techniques, which consist of measuring current and potential potentiostatically either stepwise or by applying a constant potential sweep rate in a standard chloride-containing solution. The recorded values of the current and potential are plotted. A theoretical curve obtained by electrochemical method is shown schematically in Figure 12.15 [13]. From such a curve, the following values are obtained and used to characterize alloys with respect to pitting and crevice corrosion: (1) pitting potential E_p where pits start to grow, (2) repassivation potential E_{rpp} below which already growing pits are repassivated, and (3) critical current densities characterizing the active/passive transition.

Morphology of pits: While the shapes of pits vary widely, they usually are roughly saucer shaped, conical, or hemispherical. If appreciable attack is confined to a relatively larger area and is not so deep, the pits are called shallow, whereas if the pit is confined in a small area, it is called deep pit. The depth of pitting is sometimes expressed by the term "pitting factor" [25]. This is the ratio of deepest metal penetration to average metal penetration as determined by the weight loss of the specimen. This is shown schematically in Figure 12.16.

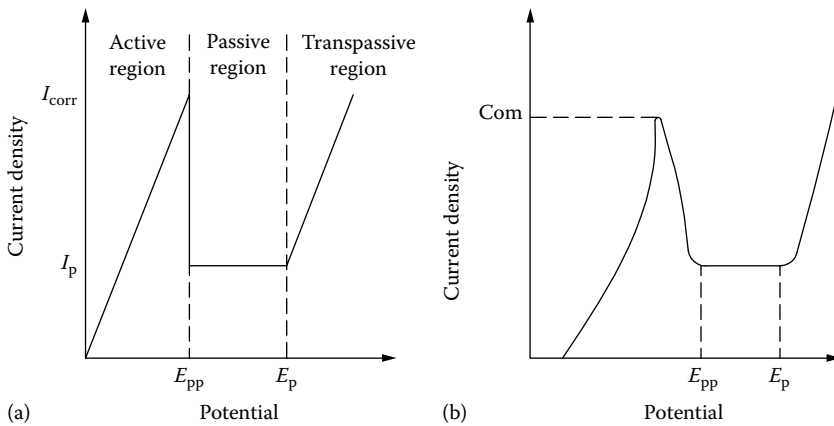


FIGURE 12.15 Pitting potential determined by electrochemical method. (a) Theoretical curve and (b) actual curve.

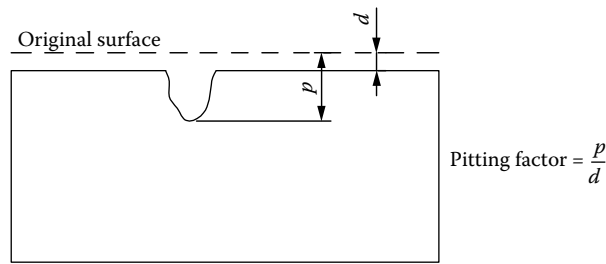


FIGURE 12.16 Pitting factor

Detection: Pitting is usually a slow process (taking several months or years to become visible) but still can cause unexpected failures. However, the small size of a pit and the small amount of metal dissolution make its detection difficult in the early stages.

12.2.3.3.4 Prevention of Pitting Corrosion

Surface cleanliness and selection of materials known to be resistant to pitting in the given environment are usually the safest ways of avoiding pitting corrosion. Details of these measures are as follows:

1. Reduce the aggressiveness of the environment, which includes the control of acidity, temperature, oxidizing agents, and chloride ion concentration [25].
2. Modify the design to avoid crevices, circulate/stir to eliminate zero velocity regions, and ensure proper drainage.
3. Systematic cleaning and elimination of stagnant areas: Since the presence of microorganisms, corrosion products, deposits, etc., stimulates pitting and, in particular, crevice corrosion in the tubes, keep the tubes clean [26].
4. Upgrade the materials of construction; chromium and nickel reduce pitting tendency very effectively, and these are often given a considerable boost with an alloy addition of molybdenum [6]. The resultant alloys are many superaustenitics highly resistant to pitting. Nitrogen improves the pitting resistance of wrought stainless steels but has the opposite effect in the weld metal, although either way the effect is fairly small compared to molybdenum [27]. Overlay with lining resistant to corrosion. Typical alternative materials that are resistant to pitting are (a) For aqueous solutions of chlorides, choose molybdenum-containing steels such as AISI 316 or 317, or alloys containing greater amounts of chromium and molybdenum

such as Hastelloy G-3, Inconel alloy 625, and Hastelloy C-22 [14], copper–nickel, Monel, or titanium. (b) In seawater and stagnant natural water applications, use materials such as copper–nickel, aluminum bronze, inhibited admiralty brass, titanium, superferritics, and duplex stainless steels. (c) Proven lower-cost nonmetallic coatings, linings, or cladding can be helpful. (d) The rating of certain stainless steel materials for pitting corrosion is discussed in Chapter 13, Material Selection, and in the section on stainless steels.

Avoid the metals and corrosive combinations that have the pitting tendencies [14]:

1. A1 and A1 alloys: electrolytes containing ions of heavy metals such as copper, lead, and mercury
2. Plain carbon and low-alloy steels: waters containing dissolved O₂ or sulfate-reducing bacteria (SRB)
3. Austenitic stainless steel weldment: exposed to stagnant natural waters that are infected with iron and/or manganese bacteria

12.2.3.3.5 How to Gauge Resistance to Pitting

The susceptibility of passive metals to pitting corrosion is usually investigated by experimental techniques: (1) simple immersion tests, (2) electrochemical methods, and (3) using empirical correlation for stainless steels. The methods are described next.

Critical pitting corrosion temperature: The formation of visible pits in specimens exposed to aqueous chloride containing solutions, at different temperatures, is frequently used as a measure of pitting resistance. The temperature at which the pits begin to form is known as the critical pitting temperature (CPT). This is determined as per ASTM G48.

ASTM G48 is a laboratory test method for determining the resistance of stainless steels and related alloys to pitting and crevice corrosion. The method uses a ferric chloride (FeCl₃) solution. The concentration of ferric chloride is usually 6%, but sometimes 10% is used instead and sometimes in an acidic mixture of chlorides and sulfates [4% NaCl + 1% Fe₂(SO₄)₃ + 0.01 M HCl]. The resulting indices are known as critical pitting corrosion temperature (CPT or CPCT) and critical crevice corrosion temperature (CCT or CCCT). These are the minimum temperatures at which these types of localized attack start in the FeCl₃ solution. CCT is determined with crevices.

To determine the CPT, a coupon of stainless steel is exposed for 24 h in the corrosive solution at a fixed temperature and then examined visually for pits on the rolled surface (edge pits are counted). If no pits exist, the temperature is increased by 2.5°C and the coupon is reimmersed. By stepwise increase in the temperature of 2.5°C, the pits initiated are to be noted for each step.

Pitting potential: Another laboratory test that is frequently used for ranking stainless steel is pitting potentials as measured using an electrochemical apparatus in a standard chloride-containing solution. The pitting potential indicates the relative susceptibility of an alloy to localized corrosion. Resistance to pitting increases with the pitting potential.

Pitting index number (PRE_N): Because the resistance of a stainless steel against pitting and crevice corrosion is primarily determined by the amount of chromium, molybdenum, and nitrogen in it, an index for comparing the resistance to these types of attack is often evaluated in terms of these elements. The index is called the pitting resistance equivalent number (PRE or PRE_N). It is defined, in weight percent, using the following equation:

$$\begin{aligned} \text{PRE}_N &= \% \text{Cr} + 3.3\% \text{Mo} + 16\% \text{N} && \text{for austenitic and duplex stainless steel} \\ &= \% \text{Cr} + 3.3\% \text{Mo} && \text{for ferritic stainless steel} \\ &= \% \text{Cr} + 3.3\% \text{Mo} + 30\% \text{N} && \text{for 6\% Mo superaustenitic stainless steel} \end{aligned}$$

The higher the PRE_N number, the better the performance of an alloy in chloride environments. For example, the PRE number for 6% Mo superaustenitic alloys containing nitrogen is 43, Alloy 2205 has 35, while for type 316L it is 24.

12.2.3.4 Crevice Corrosion

Crevice corrosion, similar to pitting, is a localized form of corrosion that takes place at localized environments/areas that are distinctly different from the bulk environments. Such localized environments include metal-to-metal joints (Figure 12.17), metal-to-nonmetal joints such as gasketed joints, shielding by corrosion products and fouling deposits, beneath biological growth, stagnant areas, and sharp corners. At these locations, the crevice corrosion is usually attributed to one or more of the following [28]: (1) changes in acidity in the crevice, (2) lack of oxygen in the crevice, (3) buildup of a detrimental ion species, (4) for passive metals, the loss of passivity within the crevices, and (5) depletion of inhibitors. This leads to concentration cells or aeration cells.

Susceptible alloys: Similar to pitting corrosion, metals or alloys that depend on protective surface film for corrosion resistance are particularly susceptible to crevice corrosion. Typical metals affected by crevice corrosion include aluminum, stainless steels, and titanium. In the case of passive metals like aluminum or the stainless steels, oxygen starvation within the crevice usually destroys the passive film responsible for the corrosion resistance and forms a passive–active cell. The passive–active cell exhibits a greater potential difference and hence induces higher current than that occurs within crevices formed by nonpassive metals like iron and copper [2].

Mechanism of crevice corrosion: Crevice corrosion takes place when a small volume of solution gets into a crack or a small opening. It stays there, stagnant, and its composition changes by the corrosion process so that its composition is different from the bulk solution. It may be oxygen depleted (oxygen concentration cell), enriched in metal ions (metal ion concentration cell), or enriched in chloride ions or at a lower pH than the rest of the solution. The corrosion rate increases as the crevice mouth narrows and as the external cathode area is increased. Crevices are particularly detrimental when alternate wetting and drying occurs, because corrosive liquids retained in the crevices are concentrated by evaporation [27,28]. To avoid crevice corrosion, the crevice must be wide open to allow the free movement of electrolyte. It usually occurs in gaps just a few micrometers wide, not in wide gaps or grooves [6].

Heat exchanger locations prone to crevice corrosion: Areas prone to crevice corrosion in a shell and tube heat exchanger and PHEs are as follows:

Shell and tube heat exchanger: clearance between the rolled tubes and the tubesheet, open welds at tubesheet, beneath deposits, water box gaskets, bolt holes, nuts, washer, disbonded water box linings, etc.

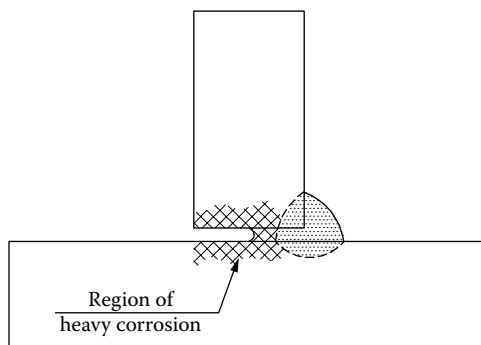


FIGURE 12.17 Crevice corrosion of a metal-to-metal welded joint.

Plate heat exchanger: beneath gaskets, plate contact points, and beneath deposits.

Crevice corrosion versus pitting corrosion: The mechanism of propagation of pits and crevice corrosion is identical; however, the mechanisms of initiation differ [24]. Crevice corrosion is initiated by differential concentration of oxygen or ions in the electrolyte, whereas pitting is initiated (on plane surfaces) by metallurgical factors and structural factors only [29]. These may include discontinuities in a protective film or coating, or compositional variations such as inclusions. The level of crevice corrosion occurring at crevices such as under deposits or gaskets or at joints between two metals is significantly greater than that of pitting on open surfaces. These two forms of corrosion are compared with reference to austenitic stainless steels in Chapter 13, Material Selection and Fabrication, in the section on austenitic stainless steel.

Crevice corrosion control: Like all forms of localized attack, crevice corrosion does not take place in all metal and corrodent combinations. Passive metals are more susceptible to it than others. These materials can be alloyed to improve resistance to crevice corrosion. This approach, together with designing to minimize crevices and maintenance practices to keep surfaces clean, is used to overcome crevice corrosion. Various practices recommended for safeguards against the occurrence of crevice corrosion include the following:

1. Structural designs should avoid any and all crevices. This is especially true for passive metals like aluminum, stainless steels, and various nickel-base alloys. Unavoidable crevices should be filled by weld metal or with nonconducting sealants or cements [2].
2. In a new equipment, specify butt welding joints and emphasize the necessity for complete penetration of the weld metal to guard against even minute crevices.
3. While designing the heat exchanger, avoid sharp corners, stagnant areas, or other sites favorable for the accumulation of precipitates or wherein the solute or O_2 concentration ion cell takes place.
4. Modify the design to avoid crevices. For example, projection of tubes beyond the tubesheet as shown in Figure 12.18 can lead to crevice corrosion.
5. For heat exchanger tubing, a minimum velocity of 5 ft/s is recommended to keep free of deposition. Also, regular cleaning will reduce susceptibility to crevice corrosion, as well as to pitting.
6. During the design stage and operation of tubular heat exchangers, endeavor to provide uniform velocity throughout the exchanger.

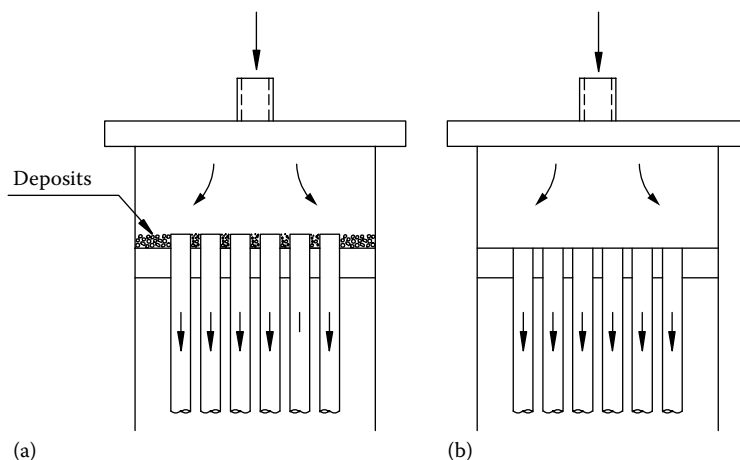


FIGURE 12.18 Projection of tubes beyond the tubesheet. (a) Original design with protrusion of tubes and hence prone for accumulation of deposits and (b) absence of crevices due to flush tube-to-tubesheet joint.

7. Upgrade the materials of construction. Use a higher alloy, which offers resistance to a broader range of conditions. Nitrogen combined with molybdenum has a beneficial effect on crevice corrosion resistance in chloride-bearing, oxidizing, and acid solutions. Use materials composed of these elements. High-molybdenum steels, particularly the superaustenitic stainless steels, give good corrosion resistance. Overlaying susceptible alloys with alloy that is resistant to crevice corrosion may also help.
8. Keep the crevices wide open or shallow to allow continued entry of the bulk fluid.
9. Reduce the aggressiveness of the environment, such as acidity, chloride ions concentration, oxidizing agents, or cathodic reactants.
10. Wherever possible, use solid nonabsorbent gaskets like Teflon for gasketed metal joints [9]. This prevents the entry of moisture.
11. Crevice corrosion is not initiated at a specific externally applied potential. Its propagation can be avoided by polarizing metal outside the crevice (cathode) to the potential of metal inside the crevice (anode) [24].

Prediction of crevice corrosion—Critical crevice corrosion temperature: Tests that establish the temperature of a ferric chloride solution at which crevice corrosion is first observed on mill-produced alloy samples with crevices, which is referred to as the CCCT, are often used to compare the crevice corrosion resistance of various alloys. CCCT is determined as per ASTM Practice G 48 B (6% or 10% FeCl₃, for 72 h with crevices).

12.2.3.5 Intergranular Corrosion

A localized and preferential form of corrosion attack in a narrow region along the grain boundaries or closely adjacent regions without appreciable attack on the grains is called intergranular corrosion. Due to this form of corrosion, the metal loses its strength and metallurgical corrosion. Intergranular corrosion generally takes place because the corrodent preferentially attacks the grain boundary phase or a zone adjacent to it that has lost an element necessary for adequate corrosion resistance. The depletion of a particular alloying element along the grain boundaries is usually caused by improper heat treatment or heat from welding or any other high-temperature operation that causes the precipitation of certain alloying element at the grain boundary. Conversely, alloys that do not form second-phase microconstituents at grain boundaries, or those in which the constituents have corrosion potentials similar to the matrix, are not susceptible to intergranular corrosion. It should be noted that the problem of sensitization seldom occurs in thin sheet metal [27].

12.2.3.5.1 Susceptible Alloys

In austenitic stainless steels (18-8), this form of attack is most common. Other susceptible alloys include ferritic, superferritic, and duplex stainless steels. Nonferrous metals such as nickel 200 and nickel-base alloys like Inconel alloys 600 and 601, Incoloy alloys 800 and 800 H, Hastelloys B and C, and aluminum-base alloys containing copper are susceptible to intergranular corrosion [14].

Sensitization of austenitic stainless steels: During heating of austenitic stainless steels between 800°F and 1500°F (450°C and 815°C) while the metal is subjected to welding, heat treatment, or high-temperature exposure, chromium carbides (Cr₂₃C₆) are precipitated along the grain boundaries. This precipitation causes the steel to lose chromium below 11% and makes the zone susceptible to corrosion, and this is known as sensitization. Compared to the rest of the grain, the chromium-depleted region is anodic, and severe attack occurs adjacent to the grain boundary if the metal comes into contact with an electrolyte. In the extreme case, whole grains become detached from the materials, which are considerably weakened.

Intergranular corrosion mechanism: Intergranular corrosion is an electrochemical corrosion that takes place as the result of local cell action in the grain boundaries. A galvanic cell is formed due to potential difference between second-phase microconstituents and the depleted solid solution

from which the constituents are formed. The carbide precipitate and the grain matrix are cathodic to the locally depleted grain boundary region. The high cathode-to-anode area ratio results in rapid corrosion of the grain boundary material and the metal disintegrates [27].

Weld decay: During welding, there will be a region of the HAZ at either side of the weld bead, which is inevitably sensitized, and these regions are susceptible to intergranular corrosion. Reheating a welded component during multipass welding is a common cause of this problem. This phenomenon is invariably termed weld decay, which is an unfortunate choice of words since, as discussed earlier, welding alone does not cause sensitization of stainless steels [27].

12.2.3.5.2 Control of Intergranular Corrosion in Austenitic Stainless Steel

There are three basic remedies for combating intergranular corrosion of austenitic stainless steel:

1. *Heat treatment:* Employ a suitable high-temperature solution heat treatment, commonly known as quench annealing or solution annealing. This involves heating the steel to 1976°F (1080°C) followed by rapid cooling. High-temperature heating causes decomposition of the Cr_{23}C_6 and homogenization of the chromium by diffusion. Rapid cooling is necessary to prevent the reformation of the carbide.
2. *Low-carbon steel:* Ensure that the steel contains insufficient carbon to form Cr_{23}C_6 and resulting alloy depletion. Such steels contain less than 0.03%C and are called extra-low-carbon steels, signified by the suffix L (e.g., type 304L and 316L). Type 304L (0.03%C max), the low-carbon version of type 304, is now used extensively in applications calling for resistance to intergranular attack in the welded condition. In a similar manner, type 316L is the low-carbon version of type 316. Lowering the carbon content below 0.03% is normally achieved by argon oxidation process (AOD) and other modern steel melting/refining processes.
3. *Stabilization:* It is possible to stabilize an austenitic stainless steel, such as the 18Cr–8Ni, by adding a potent carbide-forming element such as niobium (also known as columbium) or niobium plus tantalum or titanium. These elements fix the carbon so that it is unable to form Cr_{23}C_6 . The added elements are called stabilizers. It is usual to add titanium or niobium at about $5\text{--}10 \times \% \text{C}$ in order to ensure that no chromium carbides are formed. Typical stainless steels produced by adding stabilizers are type 347 (columbium stabilized) and type 321 (titanium stabilized).

Intergranular corrosion in ferritic stainless steels: Ferritic stainless steels are susceptible to intergranular corrosion after being heated to 1700°F–1800°F (925°C–982°C) due to welding or improper heat treatment. It appears that sensitization of ferritic stainless steel occurs under a wider range of conditions than for austenitic steels. This problem is overcome by alloying with titanium and/or columbium to form the carbides of these elements.

Test for detecting susceptibility of austenitic stainless steels to intergranular corrosion: ASTM A262, Standard Practices for Detecting Susceptibility to Intergranular Attack in Stainless Steels, is followed for evaluating austenitic stainless steel HAZ for sensitization. In this method, if the grain boundaries of the metallographic specimen are not preferentially attacked during etching, the material is said to be “nonsensitized.” On the other hand, if a preferentially attacked microstructure is developed, other tests must be performed to confirm sensitization of the microstructure. Detailed test methods for various stainless steel grades are given in Chapter 13, Material Selection and Fabrication.

12.2.3.6 Dealloying or Selective Leaching

Dealloying or selective leaching (sometimes called parting) is a corrosion process in which an alloying element is preferentially corroded over others from the parent alloy, leaving behind a weak structure.

TABLE 12.3
Combinations of Alloys and Environments Subject to Dealloying
and Elements Preferentially Removed

Alloy	Environment	Element
Brasses (includes beta-phase attack of Muntz metal and Naval brass)	Stagnant water, chlorides, under deposits, high temperature	Zinc (dezincification)
Aluminum bronzes	Hydrofluoric acid, acids containing chloride ions	Aluminum (dealuminification)
Silicon bronzes	High-temperature steam and acidic species	Silicon (desiliconification)
Copper–nickels	High heat flux and low water velocity (in refinery condenser tubes)	Nickel (denickelification)
Monel	Hydrofluoric acids and other acids	Copper in some acids and nickel in others
Nickel–molybdenum alloys	Oxygen at high temperature	Molybdenum

The corrosion is detrimental largely because it leaves a porous metal with poor mechanical properties. Dealloying takes place in specific alloy and environment combinations [30]. Combinations of alloys and environments subject to dealloying and elements preferentially removed are given in Table 12.3. The most common example is dealloying of zinc in brass (copper–zinc alloys), known as dezincification. Specific categories of the dealloying process normally carry the name of the alloying element that is selectively leached out in their titles, such as Brasses-dezincification, cupronickels-denickelification, aluminum bronze-dealuminification, silicon bronze-destannification or desiliconification.

12.2.3.6.1 Factors Influencing Dealloying

Dealloying is influenced by many critical factors; in general, factors that increase general corrosion will promote dealloying. However specific accelerating factors may be further classified into one of the three categories: (1) metallurgical, (2) environmental, and (3) water chemistry. These factors are explained while discussing dezincification of brasses.

Dealloying of zinc from brass containing more than 15% Zn (e.g., yellow brass 70% Cu: 30% Zn) under conditions of slow-moving water or stagnant water or under deposits is known as dezincification. Zinc is a chemically active element. Its standard electrode potential is very low (−0.763). Standard electrode potential of copper is much higher (+0.337).

The difference between the potentials is the driving force of dezincification. Alloys susceptible to dezincification include C 23000, C 26000, C 26800, C 27000, C 28000, C 36500, C 44300 (uninhibited), and C 46400.

12.2.3.6.2 Dezincification Types

Two major types of dezincification are (1) layer and (2) plug. The names are taken from the characteristic corrosion product morphologies.

In layer-type dezincification, the component surface is converted to corrosion product to roughly uniform depth. The alloying generally increases with increasing temperature and with increasing chloride content of the cooling water. Since the corrosive wear is normally slight, visual observation is difficult; only microscopic examination will reveal the damage.

When dealloying is generally restricted to localized areas such as beneath deposits, at hot spots, or in stagnant regions, it is called “plug-type” dealloying. Plug-type dezincification produces small pockets of plugs of almost pure copper.

12.2.3.6.3 Factors Influencing Dezincification

Metallurgical: Metallurgical factors cover the classes of copper alloys like brass, aluminum bronzes, and cupronickel susceptible to dealloying and the alloying elements parted from them.

This has been given in Table 12.3. One important metallurgical factor influencing dezincification is known as beta-phase attack.

For beta-phase attack, in the two-phase (alpha and beta) alloys such as Muntz and naval brasses, dezincification may be concentrated initially on the beta phase and may be sufficient to weaken the metal. If the attack spreads to both alpha and beta phases, complete dezincification may result with the formation of a layer of porous copper [31].

Environment: Stagnant conditions, deposits, high heat flux, crevice condition, and stresses accelerate dealloying. Porous or granular deposits further enhance the attack.

In common with many other types of corrosion and chemical reactions, an increase in temperature accelerates the rate of dezincification of brasses. At lower temperature, the rate of dezincification is low, and this explains the long life obtained from naval brass and Muntz metal piping, tubing, plates, sheets, etc., used in contact with cooling brine [31].

In terms of water chemistry, soft water, high concentration of dissolved carbon dioxide, acidic or high-pH conditions, and high chlorine concentrations promote dezincification.

Waters that deposit magnesium, calcium or iron silicates, or silica scale are protective to the underlying brass. Dense adherent calcium and iron carbonate scales are also effective in reducing or preventing dezincification. But thick scales are objectionable for well-known reasons [31].

Prevention of dealloying—General: Dealloying is overcome by material substitution, surface cleanliness, and chemical treatment. The most common method of preventing dealloying is to ensure that the tubes are kept clean and free of deposits by screening methods and cleaning procedures. Stagnant conditions should also be avoided.

Prevention of dezincification: Though dezincification can be minimized by reducing the aggressiveness of the environment, (e.g., oxygen removal) or by cathodic protection [9], it is mostly overcome by substituting alloys immune to or less susceptible to this form of attack. The resistance of brass is greatly increased by the addition of a little arsenic, antimony, and phosphorus, and the resulting alloy is known as inhibited admiralty brass. As a result, inhibited grades of brasses are routinely used in condensers. Typical alloys resistant to dezincification include the following:

Admiralty brass, developed by addition of tin.

Inhibited admiralty brass, developed by the addition of inhibitors such as phosphorus, antimony, or arsenic.

Alternate alloys like aluminum brass (inhibited), cupronickel, and titanium. Among the copper alloys resistant to dealloying, Cu–Ni alloys are considerably more resistant than Cu–Zn alloys.

12.2.3.7 Erosion–Corrosion

Erosion–corrosion, a form of localized corrosion, takes place due to the movement of a fluid over a material surface, as shown in Figure 12.19. It takes place mostly on the tubeside with water flowing through it. The corrosion damage involves both mechanical and chemical factors that allow the corrosion to proceed unhindered. The relative importance of mechanical wear (erosion) and corrosion is often difficult to assess and varies greatly from one situation to the other [28]. The role of erosion is usually attributed to the removal of protective surface film or adherent corrosion products by the fluid shear stress under high turbulence conditions.

Erosion–corrosion is usually accelerated when the fluid is entrained with air or abrasive solid particles, such as sand, but erosion–corrosion can also occur in filtered, bubble-free water [26]. The nature and properties of the protective films that form on some metals or alloys are very important from the standpoint of resistance to erosion–corrosion. A hard, dense, adherent, and continuous film would provide better protection than one that is easily removed by mechanical means or hydraulic force [9]. Erosion–corrosion is normally restricted to copper and certain copper-base alloys and aluminum alloys. In this section, erosion–corrosion is discussed in two different forms: (1) erosion–corrosion and (2) erosive wear.

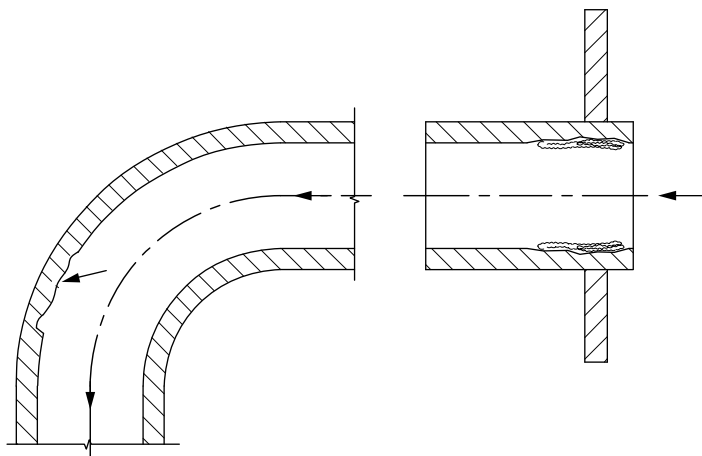


FIGURE 12.19 Tubeside erosion–corrosion.

12.2.3.7.1 Parameters Influencing Erosion–Corrosion

Erosion–corrosion is influenced by two parameters: (1) turbulence and parameters related to process fluids, such as fluid velocity, impingement attack, level of suspended particles, aeration, bubble level, local partial pressure, cavitation and (2) flow geometry. Turbulence increases with increasing velocity so that higher velocities favor the initiation of erosion–corrosion. Turbulence intensity is higher at tube inlets than downstream, resulting in the phenomenon of inlet-end erosion–corrosion. Similarly, on the shellside, the peripheral tubes located beneath the inlet nozzle without impingement plate protection are most affected by turbulence. Erosion–corrosion also occurs adjacent to a partial blockage in a tube where local velocities through the restricted opening are high or in the turbulent region just downstream of the blockage.

Pattern of erosion–corrosion: Erosion–corrosion mostly exhibits a directional property and is characterized by directional grooves, waves, valleys, gullies, holes, etc. [9], or pits in the shape of horseshoes at the site where the protective surface film is damaged [32], or crescent-shaped indentations facing upstream of the water flow that are often influenced by the local flow conditions; consequently, this form of attack has been sometimes referred as “horseshoe,” “star,” “crescent,” and “slot” attack [26]. The increased turbulence caused by pitting on the internal surfaces of a tube can result in rapidly increasing erosion rates and eventually a leak.

Condenser tube failure due to erosion–corrosion: The most common condenser tube failure is due to erosion–corrosion from impingement attack, which develops from a number of causes such as (1) general impingement attack, (2) lodged debris, (3) localized impingement attack due to blocking by iron oxide scale, (4) waterborne debris, and (5) mussel fouling [33]. Probability of impingement attack of various condenser tube materials in seawater in decreasing order is titanium < Cupronickel 70-30 < Aluminum brass < Cupronickel 95-5 < copper.

12.2.3.7.2 Erosive Wear

Four distinct forms of erosive wear have been listed by Paul Crook [34]:

1. Solid particle impingement erosion
2. Slurry erosion
3. Liquid droplet impingement erosion
4. Cavitation erosion

They have a common mechanism of attack, namely, damage to the surface film by mechanical action followed by localized corrosion.

Solid particle impingement erosion: Solid particle impingement erosion is associated with solid particle and surface interaction in gaseous environments. Relative velocities range from 2 to 500 m/s; particle sizes range in average diameter from 5 to 500 μm [34].

Slurry erosion: Slurry erosion refers to wear due to particle-laden fluid streams.

Liquid droplet impingement erosion: Impingement attack has been defined as localized erosion–corrosion caused by turbulence or impinging flow. Entrained solids and air bubbles accelerate this action. Liquid droplet impingement erosion or impingement attack takes place in pumps, valves, pipelines, elbows, heat exchanger tubes, and on the shellside underneath the inlet nozzle. The solution to impingement attack is the use of more resistant alloys like cupronickel containing 0.4%–1.0% Fe, titanium, and stainless steels [35]. Impingement attack has become one of the most frequently reported failure modes in condenser tubes primarily located beneath the inlet nozzle that receive the direct impact of the exhaust steam. This is discussed next.

Impingement attack or steam-side erosion of condenser: Impingement attack, so-called steam-side erosion, has been discussed in detail in ref. [26]. The problem arises when water droplets entrained in the steam enter the condenser and impact on the tubes at high velocity. While corrosion may play a small part in the overall process, purely mechanical processes are considered more important. To resist impingement attack, stainless steel and titanium tubes are superior to copper alloys. For this reason, it is common practice to install stainless steels or titanium tubes, at least in the peripheral sections of condensers where high erosion resistance is required. When thin-walled titanium tubes are used in the peripheral sections, adequate tube support must be provided to avoid the flow-induced vibration (FIV) problems. Properly designed condenser necks will reduce the collection and development of big droplets, which are especially harmful. Other popular method of controlling impingement attack is shown Figure 12.20 (also refer Figure 5.5), which shows clip-on or angle tube protectors made from a more erosion-resistant material [36].

TEMA [37] guidelines to limit impingement attack: On the shellside, an impingement plate or other means to protect the tube bundle against impinging fluids shall be provided when

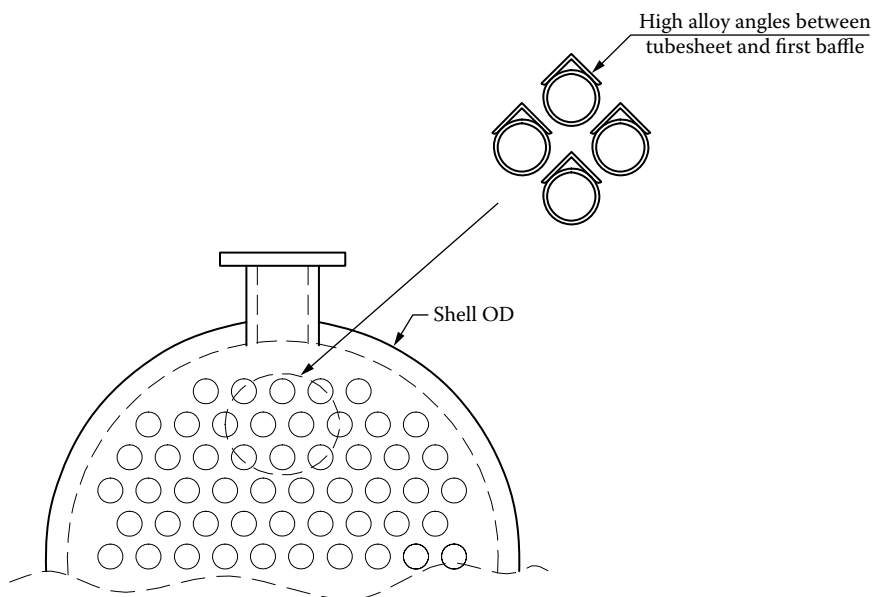


FIGURE 12.20 Impingement protection—angle tube protectors.

entrance line values of ρV^2 exceed the following (where V is the velocity of the fluid in ft/s and ρ is the fluid density in lb/ft³):

1. Noncorrosive, nonabrasive, single-phase fluids, 1500
2. All other liquids, including a liquid at its boiling point, 500

In no case shall the shell or bundle entrance or exit area produce a value of ρV^2 in excess of 4000.

On the tubeside, consideration shall be given to the need for special devices to prevent erosion of the tube ends under the following conditions:

1. Use of an axial inlet nozzle
2. Liquid ρV^2 is in excess of 6000

12.2.3.7.3 Cavitation

Cavitation damage, sometimes referred to as cavitation corrosion or cavitation erosion, is a form of localized corrosion combined with mechanical damage that occurs in turbulent flow or high-velocity fluids. It takes the form of areas or patches of pitted or roughened surface [38]. Cavitation is caused by rapid formation and collapse of vapor bubbles (i.e., voids or cavities), which exert high-pressure forces at the metal surface; these high-pressure forces can deform the underlying metal and remove protective surface films and form pits on surfaces. The occurrence of cavitation damage is shown schematically in Figure 12.21. The bubbles are created as a result of turbulence or when pressure in liquid falls below its vapor pressure. Collapse is caused by subsequent pressure increase. Among various factors, the surface finish plays an important role in the formation of bubbles. Smooth surfaces are beneficial since they reduce the number of sites for bubble formation [28].

Control of cavitation erosion: Cavitation damage involves both physical and electrochemical processes. Cavitation resistance increases as the grain size of a metal becomes smaller. Among the alloys, stainless steels is more resistant to cavitation damage because of its ductility, toughness, high corrosion fatigue limit, homogeneity, fine grain size, and ability to work harden (38). Preventing cavitation damage requires the use of the most resistant alloys and designing the system to avoid turbulence and cavitation.

12.2.3.7.4 Control of Erosion–Corrosion

Current engineering practice limits fluid velocities in tubes, pipes, and heat exchangers to some arbitrary value based on empirical tests or field experience [39]. The maximum allowable velocity is known as the threshold velocity or critical velocity. Below the critical velocity, the impingement attack does not occur, and above it, it increases rapidly. For example, the critical velocity for the protective film on aluminum brass and 70Cu–30Ni copper–nickel are 2.5 and 4 m/s, respectively [33]. However, not only is the fluid hydrodynamics important, but also the corrosiveness of the process stream and the use of inhibitors, if any, to control corrosion affects corrosion; therefore, a simple prediction based on velocity is not always valid [39]. Recent research demonstrates that it is possible to quantify and model flow-enhanced corrosion and erosion–corrosion phenomena in terms

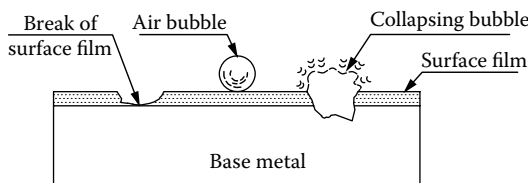


FIGURE 12.21 Cavitation damage.

of hydrodynamics, electrochemical corrosion kinetics, and film growth/removal phenomena [40]. Erosion–corrosion is mostly overcome by these measures [26]:

- Use filtered water.

- If susceptibility to erosion–corrosion is unusually high, it may be necessary to avoid the use of copper and certain copper alloys like brasses, and aluminum alloys, and to use titanium or stainless steel or aluminum brasses or copper–nickel tubes, since these alloys are essentially immune to erosion–corrosion.

- Installation of tube inserts made of wear-resistant materials like stainless steel or plastics at the tubes inlets. This aspect is further discussed in detail later. An alternative to inserts, sprayed-on epoxy coatings, is also preferred.

- Inlet-end erosion–corrosion can sometimes be prevented by streamlining the flow, redesigning the water box or inlet nozzle, or installing vanes and diffusers to reduce turbulence in the inlet region or eliminate low-pressure pockets.

- An important and even newer application of protective coatings is for the inlet end of tubes to prevent inlet-end erosion–corrosion [32].

- Install a cathodic protection system in the water box.

- On the shellside, use impingement plate protection beneath the inlet nozzle.

- Periodic injection of ferrous sulfate into the cooling water has proven to form protective surface film on brass that can be an effective method of controlling erosion–corrosion of power-plant condenser tubes.

- It has been shown for several multiphase alloys that if the ratio of surface hardness to abrasive hardness is less than 0.6, wear resistance is low, independent of microstructural conditions [34].

- Use alternate material; for brackish or sea water applications, use cupronickel (90:10) or Sea-Cure since both the materials are good resistance for erosion–corrosion [41].

Erosion–corrosion that takes place due to partial blockage of condenser tube ends can be overcome by [42]

- Installing an upstream filtration in the intake point

- Introducing an online cleaning method like sponge rubber ball cleaning to remove the fouling and corrosion deposits

- Periodical reversal of the flow

- Prevention of biological fouling by injection of biocides or subjecting to thermal shock

- Periodical off-line cleaning program

12.2.3.7.5 *Ferrules or Sleeves or Tube Inserts*

To overcome the tube inlet erosion–corrosion, metallic or plastic inserts, also known as sleeves, have been used in many applications. Some sleeves are leak limiting and others are designed to be sealable sleeves that can serve as a new pressure boundary should a through-wall penetration develop in the tube. Sleeves are typically 150–300 mm long, but are occasionally longer. They are fabricated from erosion-resistant materials like stainless steel, copper–nickels, plastics, etc. One important area where inserts are used is in steam generators that have caustic intergranular attack of tubing in the tubesheet or sludge pile, primary-side SCC of tubing in the tubesheet roller-expanded region, and pitting attack of tubing in the sludge pile [43]. While there is some loss of thermal transfer efficiency, a sleeved tube does little to diminish the overall effectiveness of the exchanger.

Sleeving has long been used in power generation heat exchangers to reduce the inlet end erosion. Because of the need to keep existing equipment operating as long as possible, sleeving the inlets of closed feedwater heaters and steam surface condensers is increasingly widespread in the power generation industry. The process of sleeving involves insertion of thin tubes (sleeve material) into the existing inlet tubes of a heat exchanger and then expanding the inserts into the tubes.

Typical sleeve thicknesses are in the range 0.01–0.03 in., depending upon the material of construction and the thickness of the original tubes.

Roller expanding: For many years, the principal method of fastening sleeves into tubes has been roller expanding. Some sleeves were also welded to the tubes at their sleeve outlet ends. Torque controls on rolling equipment produce less precise information than do controls on hydraulic sleeving equipment, and hydraulic methods have been developed to surmount this problem.

Hydraulic expanding: Control of hydraulic expanding pressure is far more precise than control of rolling torque. Consequently, there is less risk of overexpanding and causing the tube to bulge between supports and baffles. Hydraulic sleeve expanding pressure is best determined experimentally using mock-ups.

12.2.3.7.6 Sleeving (Expansion) Process

The Hydropro SleevePro® system is an electronically controlled means of hydraulically expanding sleeves into tubes, tubes into baffles, tubes into fins, and full-length liners into tubes by monitoring and controlling the growth or strain of the sleeve. Once the sleeve comes into contact with the parent tube, the SleevePro system controls additional tube growth to limit the radial expansion of the sleeve and parent tube, thus creating a tight interfacial fit by utilizing the elastic capacity of the parent tube. Figure 12.22a shows a sleeve placed inside a tube, and Figure 12.22b shows the pressure path during sleeving with the SleevePro system.

Seals for plugging leaking tubes: Patented seals known as Pop-A-Plug for plugging leaking tubes can serve as a new pressure boundary should a through-wall penetration develop in the heat exchanger; they have been patented by M/s. Expando Seal Tools Inc., PA, and marketed by Martin Engineering & Equipment Sales, NJ. The salient features of Pop-A-Plug are discussed next.

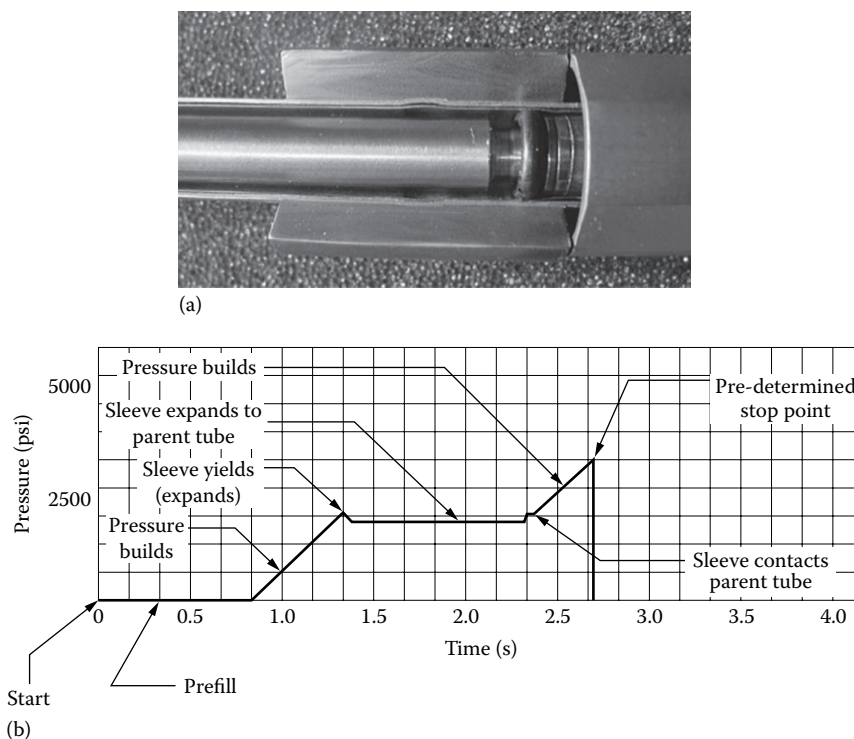


FIGURE 12.22 Sleeving of leaking/corroded tube. (a) Sleeve (SleevePro) and (b) pressure path during sleeving with the SleevePro system. (Courtesy of HydroPro, Inc., San Jose, CA.)

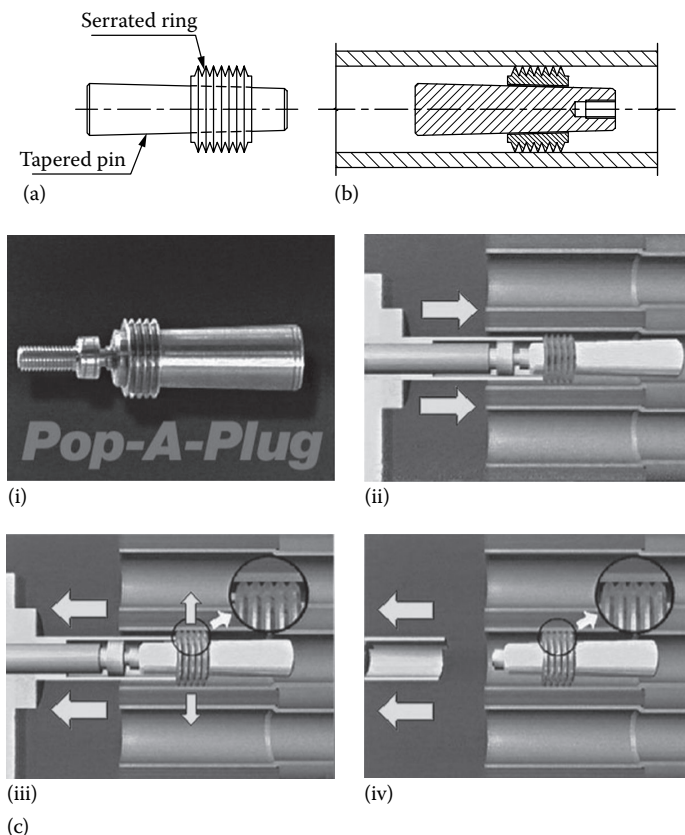


FIGURE 12.23 (a) Pop-A-Plug and (b) Pop-A-Plug positioned inside a tube (schematic). (c) Photo of a pop-a-plug. (i) Three mechanical parts: a threaded adapter, a sealing ring, and a tapered pin, (ii) insertion of Pop-A-Plug in to a tube, (iii) pulling of the Pop-A-Plug, and (iv) Pop-A-Plug positioned. (Courtesy of Maus Italia F. Agostino & C.s.a.s., Bagnolo Cremasco (Cr), Italy.)

The patented Pop-A-Plug System uses a 6600-lb or 17.5-ton hydraulic ram to expand a two-piece mechanical plug inside a leaking heat exchanger tube. The ram pulls a tapered center pin through an externally serrated ring. As the ring expands, the serrations compress against the tube wall. At a precise, predetermined pressure, a breakaway “pops,” sealing the tube and separating the plug from the ram. The plugs are available in brass, carbon steel, stainless steel, Monel, copper–nickel, aluminum bronze, and Inconel. Sizes fit tube inner diameters from 0.400 to 1.250 in. Pop-A-Plug and its installment is shown schematically in Figure 12.23.

Considerations while using inserts: While using metallic inserts, care should be exercised to avoid formation of galvanic couple between the tube metal and the insert metal. Also ensure a smooth transition between the end of the tube insert and the tube surface at the downstream to avoid turbulence, which will further enhance the erosion–corrosion in the downstream.

12.2.3.7.7 Stress Corrosion Cracking

Corrosion involving stressed materials: When the combined effects of corrosion and stresses are considered, they are usually divided into two classes [22]:

1. SCC, involving the effects of static stresses and corrosion
2. Corrosion fatigue, involving variable stresses and corrosion

Cracks resulting from the first phenomenon are predominantly intergranular, and those resulting from the latter phenomenon are transgranular.

Environmental effects on properties of materials: Certain environments drastically alter the strength and stability of engineering structures, whereas the same structures perform satisfactorily in air and other environments [44]. For example, a deep drawn brass fails spontaneously by cracking in air containing traces of ammonia, a stressed mild steel may crack when exposed to condensates of gaseous combustion products containing nitrates, and 18-8 stainless steel above room temperature on exposure to moist environment containing traces of chlorides. These are examples of what is called SCC.

12.2.3.8 Stress Corrosion Cracking

SCC is defined as the corrosion attack on a susceptible alloy due to combined and synergistic interaction of tensile stress and conducive environment. The stress required to cause SCC is normally low and usually below the yield stress, and it can be an applied or residual stress, but it is always a tensile stress. In simple terms, SCC requires the simultaneous occurrence of the following three conditions:

1. A susceptible material
2. A corrosive environment
3. Tensile stress

These conditions are shown schematically in Figure 12.24 and also refer to Figure 12.7.

Time for cracking ranges from few minutes under highly accelerated laboratory conditions to months or even years for resistant materials exposed to a mildly corrosive environment. SCC is much more insidious; the cracks propagate perpendicular to the tensile stress and may be transgranular (Figure 12.25a), common in stainless steels or intergranular (Figure 12.25b) as found in many aluminum alloys with little or no evidence of telltale corrosion products. There is little plastic deformation so that the material appears to behave in a brittle fashion. The characteristic appearance of SCC includes the lack of deformation and relatively small amounts of general corrosion [45]. SCC is the result of the interaction of a number of variables—mechanical, metallurgical, and environmental. The level of the corrosive attack depends on factors like the following:

1. Stress level and stress state
2. Aggressiveness of the corrosive environment
3. Temperature of the medium
4. Level of cold work and the level of stress relief treatment, grain structure, surface condition, etc.
5. Crack geometry
6. Electrode potential
7. Composition, metallurgical condition

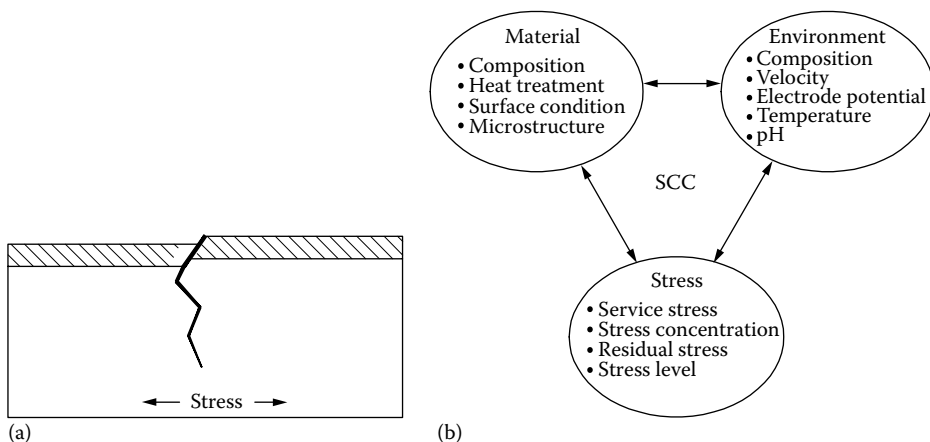


FIGURE 12.24 SCC. (a) Schematic and (b) factors influencing SCC.

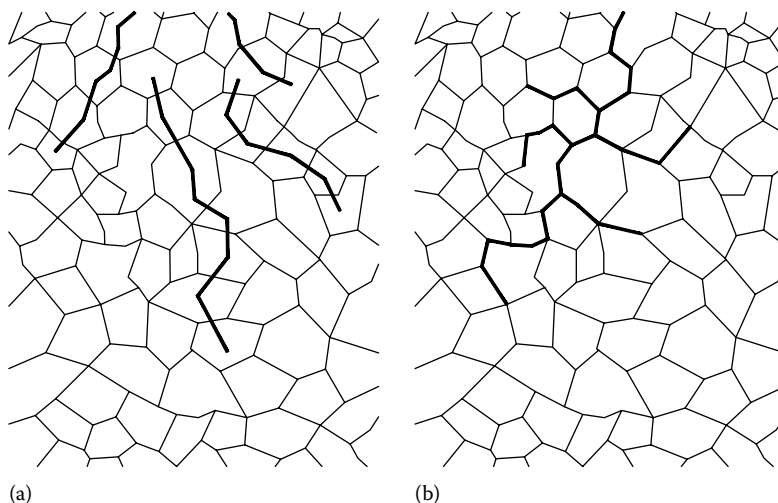


FIGURE 12.25 SCC cracking patterns. (a) Transgranular and (b) intergranular (schematic).

12.2.3.8.1 Heat Exchanger Components Susceptible to SCC

The most common places wherein SCC takes place include at (1) tube-to-tubesheet expanded joints, (2) U-tube bends, (3) indented locations by the baffle plates, and (4) bellows-type expansion joints.

Tube-to-tubesheet expanded joint: All tube-expanding methods leave residual stresses in the tube wall. To minimize residual stress, the tube expansion should not exceed certain percentage of the tube wall thickness, which varies from metal to metal (carbon steel 5%–8%, stainless steel 3%–5%, alloy steel 4%–6%). This value is to be controlled during rolling-in operation. The stresses are higher for these conditions [32]:

- Bigger tube hole in relation to the tube diameter
- Smaller tube diameter in relation to the bore hole
- Higher deformation of the tube after being rolled into the bore hole
- Rolling-in extending beyond the tubesheet (Figure 12.19)

U-bend: Cold forming of U-bend tubes induces severe residual tensile stress in the outer portion of the bend, which subsequently fails by SCC. Annealing of the bend tubes will prevent SCC. Other areas prone to SCC are near the U-bend apex for tubes of steam generators where the tube's legs were brought closer together via the denting forces and at nonsmooth transition region of U-bends [43]. Various regions of U-tube heat exchanger susceptible to SCC are shown in Figure 12.26.

Thin-walled expansion joints: SCC occurs in thin-walled expansion joint elements made of austenitic stainless steel materials on the bottom of horizontal units that are not drainable.

Classification of SCC failures: SCC failures may involve an electrochemical mechanism, attack by a molten phase, hydrogen embrittlement (HE), or some other factors. According to the environment causing cracking of metals and metal alloys, SCC can be categorized as follows:

- Chloride cracking, e.g., austenitic stainless steel, aluminum
- Caustic cracking, e.g., carbon steel
- Ammonia cracking, e.g., admiralty brass
- Polythionic acid cracking, e.g., austenitic stainless steel
- Sulfurous acid cracking, e.g., austenitic stainless steel

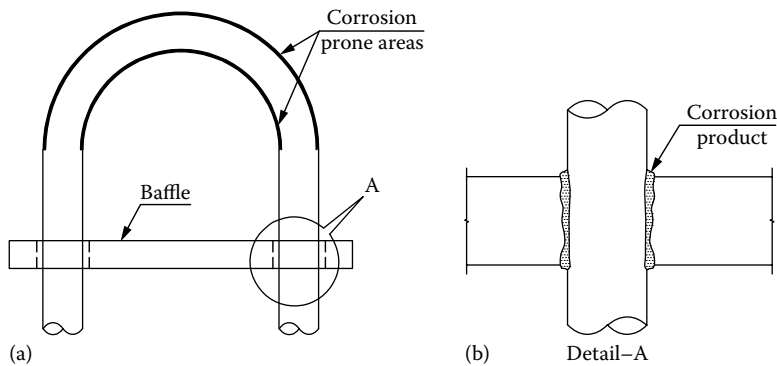


FIGURE 12.26 Some regions of U-tube heat exchanger susceptible to SCC. (a) Regions of U-bend and (b) tube indented locations by the baffle plate.

12.2.3.8.2 Discussion of Conditions Responsible for SCC

Susceptible alloys and the environment: SCC, like most forms of corrosion, is electrochemical and involves metals in contact with an electrolyte. The environments that cause SCC are specific for each metal. Except for ferritic stainless steel, virtually all metals and alloy systems are susceptible to SCC by a specific corrodent under conditions of temperature, stress level, etc. Chloride ions lead to SCC in 304 and 316 stainless steels when oxygen is present. Typical hostile environments for few of the most widely used metals are given in Table 12.4. Tables of environments and alloy combinations known to result in SCC are published by the National Association of Corrosion Engineers (NACE) [46], the Materials Technology Institute [47], and others for the chemical process.

Stress: Tensile stress at the surface of the metal is an essential factor in SCC. Cracking has never been found in metals under compression. The tensile stresses may be due to internal stress caused by metal deformation near welds and bolts, deformation caused by shrink fit, unequal cooling from high temperature, or volume changes in the material caused by phase change or rearrangement of crystal structure [48], or residual stress from some prior cold work or metal-forming operation or caused by an applied stress (i.e., service-induced external load). Residual and applied stresses are additive to evaluate the effect on cracking, and both must be known. Welding often leaves residual stresses that lead to SCC in susceptible environments.

SCC of welded joints: Welded joints are particularly prone to SCC for three reasons [27]: (1) The welding operation will leave a residual tensile stress in the weld area unless effective postweld stress relief is carried out, (2) stress concentrations are usually present, and (3) the thermal cycle can

TABLE 12.4
Environments That Cause SCC

Metal	Environment
Al and Al-base alloys	NaCl solution, seawater, H_2O_2 , chloride solution, and other halide solutions
Cu and Cu-base alloys	Ammonia and ammonium hydroxide, amines, mercury, sulfur dioxide, H_2S , steam
Carbon steel	Sodium hydroxide solutions, ammonia and sodium nitrate solutions, carbonate/bicarbonate
Austenitic stainless steel	Aqueous chlorides, seawater, sulfurous, and polythionic acid
Nickel and nickel-base alloys	Caustic above $315^\circ C$, fused caustic soda, hydrofluoric acid, polythionic acid
Titanium and titanium alloys	Reducing acids such as chlorides, iodides, fluorides, red fuming nitric acid, nitrogen tetroxide, methanol

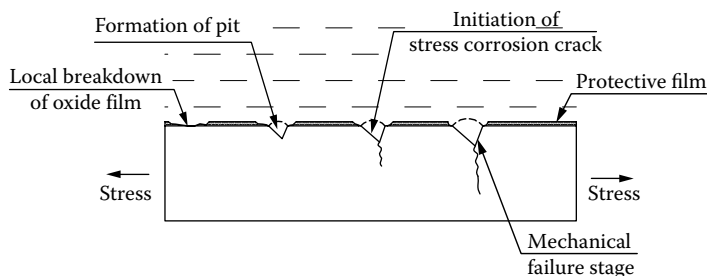


FIGURE 12.27 Growth and propagation of SCC.

produce a susceptible microstructure. SCC is overcome by shot peening after welding to induce compressive stress on the surface, stress-relief heat treatment, and use of alloys resistant to such cracking.

How to detect SCC: Some cracks may be visible to the naked eye and thus require no special detection means. Others may be seen after surface deposits are removed, particularly under magnification. Sophisticated microanalytical instruments such as the electron beam microprobe analyzer, scanning electron microscope, and mass spectrometer are being increasingly applied to failure analysis of power plant components [49]. Crack detection methods like magnetic particle testing, dye penetrant testing, x-rays, ultrasonics, and eddy current testing can also be used [48].

12.2.3.8.3 Theory of SCC

No unified theory for SCC is at present accepted. Theories attributed the failure to mechanical, chemical, fracture mechanics, surface energy, etc. The sequence of events involved in the SCC process is usually divided into three stages [50]:

- Crack initiation and propagation
- Steady-state crack propagation
- Crack propagation or final failure

Metallurgists at the Naval Research Laboratory, Physical Metallurgy Branch, have applied a fracture mechanics theory to SCC [51]. According to this theory, SCC occurs by nucleation and growth at the site of discontinuity in a protective surface oxide or passive film or at the site of pre-existing cracks or defects. Under stress or chemical action, pitting initiates at these sites, and pitting continues until the crack extends to its critical length and subsequent fracture. Growth and propagation of SCC are shown schematically in Figure 12.27.

12.2.3.8.4 Avoiding Stress Corrosion Cracking

Since SCC is due to the interaction of variables associated with (1) mechanical, (2) metallurgical, and (3) environmental factors, adjustment of these variables should minimize cracking [52]. To resist chloride SCC, use higher austenitic nickel-base alloys such as Inconel 600, Incoloy alloys 800 and 825, ferritic and superferritic stainless steels, duplex stainless steels such as ferralium 255, or titanium. Another important measure to prevent SCC is to avoid the metal and environment combinations that are favorable for SCC that are shown in Table 12.4. Other measures involving mechanical, metallurgical, and environmental aspects to control SCC are discussed as follows.

1. Mechanical

- a. Exercise control on the level of cold work and grain size. For example, adopt optimum clearance between the tube and the tube hole in the tubesheets to avoid excessive cold work.
- b. Reduce tensile stress by design change, reduce operating pressure, avoid misalignment of connections, prevent differential thermal expansion, etc. [48,53].

- c. Reduce residual stress to a safe level by thermal stress relief, which usually can be applied without significantly decreasing strength: mechanical surface treatment (shot peening to put metal surface in compression).
- d. Avoid stress concentrations.
2. Metallurgical
 - a. Replace the susceptible alloy by alternate alloys that show resistance or immune to SCC; e.g., replace type 304 SS by Inconel and superferritic stainless steels.
 - b. Use metallic or conversion coating.
 - c. Since SCC occurs by nucleation and growth at the site of discontinuity in protective surface oxide or passive film or at the site of preexisting cracks or defects, keep the surface free from these surface defects.
3. Environmental
 - a. Modify environment: If possible, reduce the aggressiveness of critical environment by de-gasification or demineralization or by any other method [9]. For example, elimination of chloride ions from water by an ion-exchange process may permit the use of stainless steels in high-temperature water [48], or it may be possible to lower the concentration less than 30 ppm for safe operation.
 - b. Exclude corrodents with protective coating.
 - c. SCC in aqueous solution can be prevented by cathodic protection.
 - d. Modify the environment by adding a corrosion inhibitor.
 - e. Modify the temperature.

Test for SCC: The sensitivity of a steel to SCC is determined by boiling a stressed sample in concentrated magnesium chloride or sodium chloride solutions. Stresses may come from a bead-on-plate weld or from plastic deformation of the specimen. The chlorine ions depassivate the steel and lead to SCC and eventual failure of the stressed specimen. ASTM B 154, mercurous nitrate test, is the standard test method for detecting the SCC of copper and copper alloys.

12.2.3.9 Hydrogen Damage

Monoatomic hydrogen can diffuse into steel and recombine to molecular hydrogen at voids, laminations, microcracks, or discontinuities around inclusions, generating extremely high pressures. As an interstitial element in the body-centered cubic ferritic lattice, hydrogen can cause a number of mechanical problems. It stiffens the metal and impairs its ductility. At higher temperatures, hydrogen diffused in a steel can react with carbon atoms to form methane. The accumulation of methane at certain locations in steels, such as grain boundaries and nonmetallic inclusions, causes the irreversible loss of strength and ductility. Elevated temperature exposure in hydrogen sometimes results in surface decarburization, followed by fissuring due to high gas pressure at localized sites. These changes in the steel are called hydrogen attack. The different forms of hydrogen damage are as follows:

1. HE
2. Hydrogen blistering
3. Hydrogen SCC
4. High-temperature attack

The development of hydrogen damage would presumably be hindered by anything present in the steel that would [54]

1. Decrease the rate of corrosion
2. Decrease the rate at which the hydrogen produced by corrosion entered the steel instead of escaping into the process stream
3. Speed up the passage of hydrogen through steel, thus reducing the time available for reaction
4. Decrease the rate of reaction of hydrogen with carbon in the steel

Other remedial measures include stress relief, the selection of material that does not harden so readily during the welding cycle, or the inhibition of the hydrogen evolution reaction causing the trouble. Hydrogen damage due to high temperature exposure is discussed in detail in Chapter 13, Material Selection, and hydrogen damage in the sour environment is discussed at the end of this chapter.

12.2.3.10 Fretting Corrosion

Fretting corrosion is the combined wear and corrosion process that takes place at locations where there is a relative movement between two components and the movement is restricted to very small amplitude. At the mating surfaces, the degree of deterioration increases because of repeated corrosion of the freshly abraded surface and the accumulation of abrasive corrosion products between these surfaces. A typical example is the wear of the heat exchanger tubes at the tube-baffle contacts. Various metallurgical, geometrical, and environmental factors influence the fretting wear of heat exchanger tubes. Factors that affect fretting wear include [55] contact load, amplitude, frequency, number of cycles, and temperature. Fretting wear of heat exchanger tubes has been covered in Chapter 10 on flow-induced vibration.

12.2.3.11 Corrosion Fatigue

Corrosion fatigue: Corrosion fatigue is the reduction in the fatigue strength of a metal as a result of exposure to a corrosive environment. When a metal is subjected to cyclic stress in a corrosive environment, a marked drop in or elimination of the endurance limit may occur even in a mildly corrosive environment. Surface film-protected alloy is especially susceptible to corrosion fatigue [56]. Corrosion fatigue is shown schematically in Figure 12.28a and the drop in endurance strength in Figure 12.28b. In film-protected alloys, stress reversals cause repeated cracking of the otherwise protective surface film, and this allows access of the corrodent to the unprotected metal, with resultant corrosion. The reduction in fatigue strength has a consequence on the life and reliability of a component. The reduction may be so severe that a detail that has been ignored at the design or inspection stage can lead to catastrophic failure in service [27]. In heat exchangers, corrosion fatigue can occur in any tube material; it is caused by steam buffeting in the case of the condenser or FIV in association with inadequate tube support [33]. Generally, failure occurs at tube mid span due to collision between adjacent tubes above critical velocity.

Factors influencing corrosion fatigue and crack growth: Corrosion fatigue occurs in metals as a result of the combined action of a cyclic stress, a corrosive environment, and metallurgical factors. The factors that influence corrosion fatigue include [55] stress intensity range, load frequency, stress state, environment, electrode potential, and metallurgical variables. The environmental factors

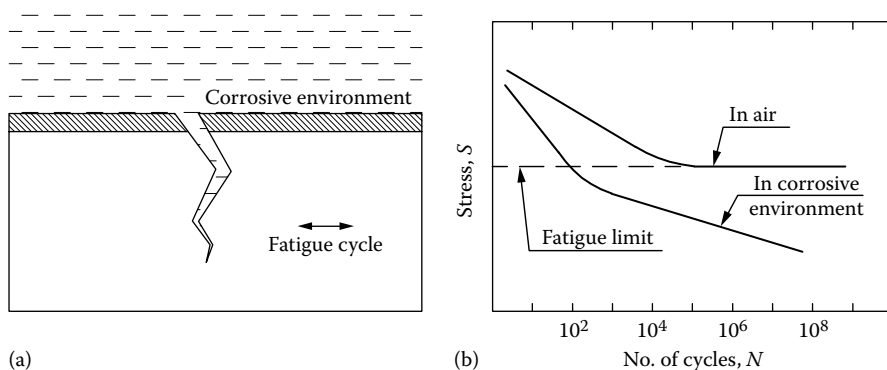


FIGURE 12.28 Corrosion fatigue. (a) Diagrammatic representative and (b) S–N curve for steels subjected to cyclical stress showing drop in endurance strength due to corrosion fatigue.

include pH, concentration of corrosive species, dissolved oxygen content, conductivity, pressure, temperature, and flow conditions. Corrosion fatigue cracks are always initiated at the surface unless there are nearby surface defects that act as stress concentration sites and facilitate subsurface crack initiation.

Intensity of corrosion fatigue: At any given time prior to failure, damage due to corrosion fatigue will be greater than the sum of corrosion damage plus fatigue damage [6]. Localized corrosion, such as pitting or intergranular corrosion, has a greater accelerating effect than the uniform corrosion [56]. The reduction in fatigue strength due to corrosion is sometimes expressed in terms of damage ratio, which is the ratio of corrosion fatigue strength in a particular environment divided by the air fatigue strength. The damage ratio for aluminum in seawater is 0.4, stainless steel 0.5, and mild steel 0.2 [27].

12.2.3.11.1 Corrosion Fatigue of Various Metals

The alloys that are generally affected by corrosion fatigue include aluminum alloys exposed to chloride solution, Cu–Zn and Cu–Al alloys exposed to aqueous chloride solutions, and high-strength steel in a hydrogen atmosphere.

Ferrous alloys: In a corrosive environment, ferrous alloys lose their fatigue limit, and hence the bottom of the standard stress-cycle curve (S–N) dips down from horizontal. As per theory, the drop in fatigue strength takes place as the cyclic stress causes progressive slip within metal grains, constantly producing clean metal surfaces that are anodic in nature and hence dissolve continuously [6].

Aluminum alloys: Aluminum alloys exposed to aqueous chloride solutions or humid air are subject to corrosion fatigue. Corrosion fatigue cracks originate at sites of pitting or intergranular corrosion, but pitting is not a requisite for crack initiation.

Copper and copper alloys: Corrosive environments have little additional effect on the fatigue life of pure copper. Copper–zinc and copper–aluminum alloys exhibit a marked reduction in fatigue strength, particularly in aqueous chloride solutions.

Corrosion fatigue of welded joints: Under normal circumstances, welded joints are likely to be associated with fatigue cracks associated with structural and mechanical discontinuities that are usually present in the welds [27]. The toes of fillet welds provide site for crack initiation, particularly in the presence of undercuts.

Relationship between corrosion fatigue and SCC: Corrosion fatigue is mostly interrelated to environmentally induced corrosive attack forms such as SCC and HE [55]. The relationship between corrosion fatigue and two other environmental cracking mechanisms, SCC and HE, is shown in Figure 12.29.

Prevention of corrosion fatigue: Corrosion fatigue can be prevented by several methods such as (1) using protective coatings, (2) adding inhibitors to the environment, (3) cathodic protection, and (4) introducing residual compressive stresses by methods such as shot peening.

12.2.3.12 Microbiologically Influenced Corrosion

MIC is the deterioration of metal by a corrosion process that occurs directly or indirectly as a result of metabolic activity of microorganisms on heat transfer surfaces. It also implies, however, that the corrosion would not have taken place in the absence of these organisms [57]. MIC is not a new form of corrosion, but some of the conditions created by microbes can lead to electrochemical reactions that make an environment much more corrosive. Certain microbes can metabolize nutrients (e.g., oxygen) and generate corrosive agents (e.g., organic acids) and other chemical compounds (e.g., sulfur and iron) or create a living crevice or active–passive cell due to biofouling [13]. Natural waters may contain several classes of microorganisms. Attack can be caused by SRB, biological slimes, mates, and tubercles by fungi and other microorganisms, including the iron bacterium [58]. Other synonyms

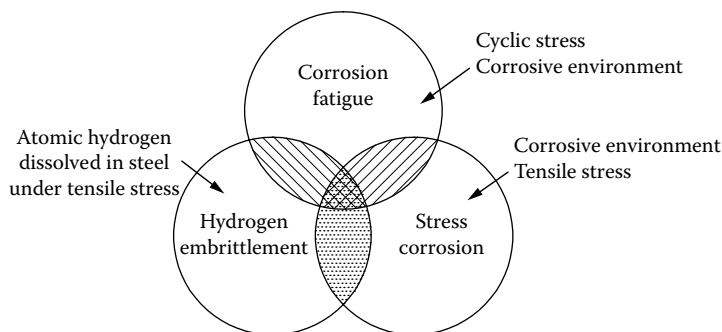


FIGURE 12.29 Relationship between corrosion fatigue, SCC, and HE. (Adapted from Glaser, W. and Wright, I. G., *Forms of corrosion—Mechanically assisted degradation*, in *Metals Handbook*, 9th edn., Vol. 13, Corrosion, American Society for Metals, Metals Park, OH, 1987, pp. 136–144.)

for MIC are microbial corrosion, biodeterioration, and biocorrosion. Since the concept of anaerobic MIC was introduced in 1934, scientists and engineers have recognized that MIC can be a significant contributor to component failures.

Susceptible metals: All but the higher nickel–chromium alloys and titanium have been found to be subject to microbiological corrosion. Common engineering metals and alloys such as carbon steel, lined steel, stainless steels, aluminum alloys, and copper alloys, 6% Mo stainless steels, and high–nickel alloys (Monel 400 and Alloy B-2) have exhibited susceptibility to MIC [59].

Sources of microorganisms: Microorganisms are widely distributed in nature, being present in streams, rivers, lakes, seawater, and coastal estuaries. Such microorganisms include bacteria, fungi, algae, and yeasts, depending on the sources of water.

12.2.3.12.1 Classification of Microbiological Organisms

Microbiological organisms, or microbes, known to cause corrosion of metals may be classified in four general flora groups [60]: (1) bacteria, (2) fungi, (3) algae, and (4) yeasts. According to their metabolic activities, corrosive microbes are classified into six general metabolic groups [60]: (1) acid producers, (2) mold growers, (3) slime formers, (4) sulfate reducers, (5) hydrocarbon feeders, and (6) metal ion concentrators/oxidizers. The three major types of microbes commonly associated with MIC are (1) SRB, (2) iron and manganese bacteria, and (3) sulfur-oxidizing bacteria [13].

Sulfate-reducing bacteria: The SRB seem to be involved in at least some form of the MIC of most of the susceptible alloys like iron and mild steels, aluminum alloys, and copper alloys [61]. They reduce sulfates to sulfides and depolarize cathodic sites on metal surfaces by consuming hydrogen.

Iron and manganese bacteria: Iron- and manganese-oxidizing bacteria, known as metal ion concentrators/oxidizers, are most often associated with the corrosion of stainless steels [13]. Such bacteria produce iron and manganese metabolites that form deposits that in turn create concentration cells or harbor other corrosive microbes.

Sulfur-oxidizing bacteria or acid producer: Some microbes can oxidize sulfur compounds to sulfuric acid; a pH as low as 2 has been recorded where sulfur-oxidizing microbes are active.

Attachment, growth, and influence of microorganisms on metal surfaces: On attachment to metal surfaces, microorganisms begin colonizing and produce a biofilm, known as slime or mat. Certain microbes can metabolize nutrients and other chemical compounds (e.g., sulfur and iron) to create corrosive environments or they can directly participate in electrochemical reactions. The metabolic processes of the microorganisms can influence the corrosion behavior of materials

by [60,62,63] (1) destroying protective surface films; (2) producing a localized acid environment; (3) creating corrosive deposits; (4) creating corrosion cells, notably differential aeration and ion concentration cells; and (5) altering anodic and cathodic reactions, depending on the environment and organisms involved. These processes may occur either alone or in combinations. The microorganisms tolerate elevated pressures and a wide temperature range, and oxygen content from 0 to almost 100%. Temperatures greater than 40°F (4°C) but less than 140°F (60°C) tend to promote MIC.

Categories of MIC: MIC can be divided into two categories: aerobic and anaerobic. Aerobic microbes exist in the presence of air. Anaerobic microbes can exist and multiply in the absence of air. SRB are the most important microorganisms in the anaerobic category, whereas slime-forming bacteria, sulfur bacteria, and iron bacteria are important microorganisms in the aerobic category.

12.2.3.12.2 MIC of Industrial Alloys

Mild steel: Due to MIC, carbon steels have experienced random pitting, general corrosion, and formation of tubercles on surfaces. MIC of carbon steels can be prevented by chemicals, coatings, or cathodic protection [61].

Austenitic stainless steel and weldments: Pitting failures of austenitic stainless steel components and weldments by MIC commonly result when residual natural water is left in stainless steel equipments after hydrotesting. MIC failures of austenitic stainless steel welds have been reviewed by Pope et al. [61] and in refs. [63,64]. The conditions/mechanisms responsible for the MIC of austenitic stainless steels include [64] the following:

1. Austenitic stainless steels form small tubercles from microbial action under which severe pitting occurs.
2. Oxygen concentration cells produce carbonic acid, which is corrosive to stainless steels.
3. Crevices are ideal sites for MIC to occur; perhaps the consumption of oxygen by the bio-film prevents the oxygen in the external environment from reaching the interior of the crevice.
4. Depassivation: Microbes, by forming a slime layer, produce a crevice in which regions of the normally passive film damaged by mechanical means or through halide attack go unrepaired.
5. Weldment surface conditions that are commonly associated with poor corrosion resistance, such as heat tint and conditions that are associated with residual stresses, such as gouges, may produce conditions that are susceptible to MIC.

Measures to overcome MIC in stainless steel include solution annealing and pickling, and a temporary measure, spraying the heat exchanger tube interior by a quick set epoxy to a distance of 5–6 ft instead of plugging [65].

Copper alloys: Copper and copper alloys are more resistant to the attachment of biofouling organisms than steel and most of the other common materials of construction [66]. This is due to the inherent characteristic of copper alloys and appears to be associated with copper ion formation within the corrosion product film. Therefore, coupling of steel or less noble materials or cathodic protection, which suppresses copper ion formation, allows biological fouling to occur [67]. Copper alloys are particularly sensitive to SRB and ammonia-producing bacteria and have exhibited failures by pitting, plug-type dealloying, SCC, and erosion–corrosion [61].

Titanium's resistance to MIC: Titanium and its alloys exhibit excellent resistance to MIC under both anaerobic and aerobic conditions. More than 30 years of extensive titanium alloy use in biologically active process and raw cooling waters, especially seawater, appears to substantiate

titanium's resistance to MIC [68]. Characteristic features of titanium alloys' resistance to MIC include the following [68]:

1. Titanium alloys are fully resistant to the reduced chemical species associated with anaerobic activity over the total range of concentrations and temperature as high as 212°F (100°C).
2. Titanium alloys are exceptionally resistant to the oxidizing and acidic conditions and compounds associated with aerobic activity.
3. The surface oxide film remains intact under fully deoxygenated, reducing conditions down to a pH of 2 at 100°C.
4. The surface oxide film exhibits excellent resistance to atomic and diatomic hydrogen absorption, the hydrogen being produced by the metabolism of SRB.
5. Both algae and fungi cannot produce conditions that affect titanium alloy passivity.

Nevertheless, titanium alloys are not biotoxic and permit growth or attachment of any micro or macro biofilm or organism on metal surfaces. However, in no case has localized corrosion ever been observed beneath these biofilms. Periodical cleaning to avoid the buildup of the biofouling is necessary or the water velocity should be sufficiently high.

12.2.3.12.3 Control of MIC

Prevention of MIC in most of the metals involves trying to prevent the occurrence, growth, and metabolic activities of MIC causing microbes in the vicinity of the metals. The important means of microbial control are as follows:

1. Uptake filtration
2. Systematic cleaning and elimination of stagnant areas
3. Proper use of a biocide
4. Thermal shock treatments

Uptake filtration: Intake screens are now available with mesh sizes down to 0.5 mm, small enough to filter out stringy debris and all but the smallest organisms [26].

Systematic cleaning and elimination of stagnant areas: Since the presence of scales, shellfish, corrosion products, etc., stimulates pitting and, in particular, crevice corrosion in the tubes, keep the tubes clean either continuously by online cleaning systems or intermittently by off-line cleaning methods [26].

Biocides: The most practical and efficient method of controlling microbiological activity in cooling waters is through chemicals known as biocides. These biocides kill the organism or inhibit their growth and reproductive cycles. Biocides used in cooling-water system include chlorides, chlorine dioxide, bromine, organo-bromide, methylene bithiocyanate, isothiazolinone, quaternary ammonium salts, organo-tin/quaternary ammonium salts [69], copper salts, chlorine donors (e.g., phenates), thiocyanates, and acrolein [70].

Limitations of biocides

1. Even though these chemicals can do a good job of killing organisms in the bulk water phase, they are much less effective in penetrating biofilms (slime) and killing the organisms therein.
2. While selecting biocides, consideration should be given for toxicity to plant and animal life exposed to the discharged water.
3. Hard-shelled organisms such as barnacles, mussels, and others possess the ability to tightly close their shells when first sensing a toxic substance such as chlorine in the water, to remain closed until it passes, and then to reopen and resume feeding [66].

Thermal shock: The thermal shock treatment involves recirculating the cooling water to allow the temperature to increase to 120°F (49°C), a condition that ensures the death of most organisms.

Microbiologically influenced corrosion failure analyses: MIC can be diagnosed by techniques such as in situ bacterial sampling of residual water, bacterial analysis of corrosion products using analytical chemistry, culture growth, and scanning electron microscopy, as well as nondestructive examination using ultrasonics and radiographic techniques. Metallographic examination can reveal MIC characteristics such as dendritic corrosion attack in weld metal [71]. If special techniques are not followed, they can be misdiagnosed as attack caused by conventional chloride crevice/pitting corrosion attack.

12.3 CORROSION OF WELDMENTS

Weld metal versus parent metal: Corrosion of weldments occurs in spite of proper selection of base metal and filler metal, codes and standards followed, and postweld heat treatment (PWHT) carried out. In welded joints, the weld metal is usually of matching composition to the parent material or overmatched, with its choice normally being dictated by the need to obtain a sound weld of mechanical properties comparable with those of the parent material and resistance to galvanic corrosion [72]. A survey of weld failures, reported at Corrosion 82, a forum on corrosion sponsored by the National Association of Corrosion Engineers, showed that poor welding practices such as poor fitups, misalignments, and incompletely fused root beads have caused many weld failures in process vessels. Incomplete fusion, particularly in root passes, is a common source of notches and crevices [6]. The factors that control the corrosion resistance of the weldments and how to optimize the weld quality are discussed in this section.

Causes of corrosion of weldments: In addition to the material composition, the following welding design/process-related features contribute to weld material corrosion [73]:

1. Weldment design
2. Fabrication technique
3. Heat input and welding practice
4. Protection of welding environment, carbon and nitrogen pickup during welding [6]
5. Formation of oxide film and scale
6. Weld slag and spatter
7. Welding defects like incomplete weld penetration or fusion, porosity, cracks, crevices, HAZ, and high residual stresses
8. Metallurgical factors like microsegregation, precipitation of intermetallic phases, formation of unmixed zones, recrystallization and grain growth in the weld HAZ, volatilization of alloying element(s) from the molten weld pool
9. PWHT
10. Postweld cleaning

The thermal cycle due to the welding process affects the microstructure and surface composition of welds and adjacent base metal. Often both crevice corrosion (Figure 12.30) and pitting corrosion are associated with the weld defects. The presence of secondary phases having different oxidation potential, and the attack on the phases of highest potential can be quite common. Weld deposits containing nonmetallic inclusions and porosity can accelerate the corrosion rate. Sometimes the weld metal may be deficient in corrosion resistance compared to the parent metal due to microsegregation of an important alloying element of the parent metal. This is especially true for welding 6-Mo super-austenitic stainless steel. This situation is overcome by overalloying the filler metal. Weld deposits containing entrapped slag particles or residues from fluxes act as sites for cathodic reaction and can lead to increased weld metal corrosion.

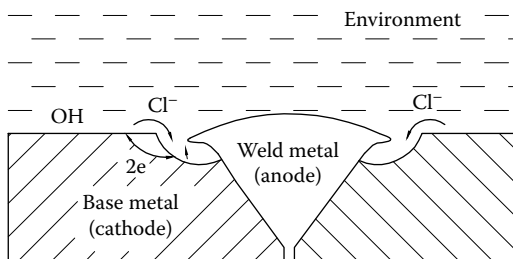


FIGURE 12.30 Crevice corrosion due to weld defect.

Measures to improve the corrosion resistance of weld metal: Corrosion resistance of the weld metal can be improved by

1. Shielding the molten and hot metal surfaces from reactive gases in the weld environment, including protection of underside of the root
2. Controlling grain growth in the HAZ
3. Controlling the precipitation of the intermetallic phases during welding/PWHT.
4. Proper PWHT
5. Postweld cleaning and passivating the surfaces in the case of stainless steels
6. Subjecting the weldments for thorough nondestructive testing (NDT) for weld defects

12.4 CORROSION PREVENTION AND CONTROL

The majority of the corrosion control techniques employed center around the ideas of either isolating the corroding metal from the environment or modifying the environment so that either the anodic or the cathodic reaction is brought under control [27]. Alternately, use corrosion-resistant metals in equipment construction. The last 40 years have seen the development of many specialized methods for improving the corrosion resistance of structural components in corrosive environments. These include coatings and cladding of alloy steels and minor alloy additions to the 300 series stainless steels, chromizing of internal surfaces of 2.25Cr–1Mo [74], and alonizing steel tubes. Corrosion control measures have been mentioned already briefly while discussing various forms of corrosion. However, some generalized procedures are explained in this section.

12.4.1 PRINCIPLES OF CORROSION CONTROL

Corrosion control can be divided into two principal approaches: (1) corrosion prevention and (2) corrosion protection. Corrosion prevention is based on the idea of designing equipment so that corrosion cannot occur, whereas corrosion protection aims at minimizing the corrosion attack. Since corrosion of a material takes place due to electrochemical reaction with its environment, in most practical situations, this attack cannot be prevented; it can only be controlled so that a useful life is obtained from the equipment. Various techniques for corrosion control are as follows:

1. Use of proper design
2. Changing the characteristics of the corrosive environment
3. Use of corrosion-resistant materials
4. Bimetal concept involving cladding and bimetallic tubes
5. Application of barrier coats, surface treatment
6. Providing electrochemical protection by cathodic or anodic protection
7. Passivation

There are advantages, disadvantages, and areas of the most economical use for each of these methods. No single method is a universal cure for all corrosion problems [1]. Each problem must be individually studied before implementing the corrosion control measure. The technical solution most suitable to these problems should be decided through cost–benefit analysis by the plant user.

12.4.2 CORROSION CONTROL BY PROPER ENGINEERING DESIGN

Design is an important aspect in the prevention of corrosion. In fact, in many engineering structures, the “weakest spot” is the lack of consideration given to corrosion control during the design stage.

12.4.2.1 Design Details

The design details of pressure vessels and heat exchangers can have a significant effect on corrosion. Design details to minimize corrosion are discussed in ref. [15]. During the design stage, give consideration to crevices, galvanic couples, drainage, and ventilation. Vessels should allow complete drainage. Inclined heat exchanger installation permits a dead space that may allow overheating if very hot gases are allowed on the tubeside (Figure 12.31). Disturbances to flow can create turbulence and cause impingement attack, and direct impingement should be avoided—introduce deflectors or protection devices. Nonaligned assembly distorts the fastener, which forms crevices. Supports should allow drainage; continuous welding is necessary for horizontal stiffeners and supports.

12.4.2.2 Preservation of Inbuilt Corrosion Resistance

The design details should preserve the inbuilt corrosion resistance, including the passivity of the materials. For metals like carbon steels, alloy steels, stainless steels, aluminum, titanium, zirconium, etc., corrosion resistance is inbuilt by means of an adherent protective surface film that separates the metal from the surrounding media. The designer must consider potential corrosion problems from fabrication practices and PWHT.

12.4.2.3 Design to Avoid Various Forms of Corrosion

Crevice and galvanic corrosion, erosion–corrosion, and SCC can be controlled by proper design. Figure 12.32 illustrates the insidious nature of crevices occurred in the tubesheet of a vertical condenser handling vapors of formic and acetic acid [75,76]. If there is a dead space (air pocket) at which chlorides are allowed to concentrate by alternate wetting and drying of tubing surfaces, the tubes will be attacked by SCC. This problem is overcome by air venting the dead space or allowing complete flooding of all tubing surfaces.

12.4.2.4 Weldments, Brazed and Soldered Joints

Corrosion in weldments and brazed and soldered joints is also controlled through proper design, fabrication, and joining techniques. Give attention to joint design, surface continuity, and concentration of stress and complete corrosive flux removal.

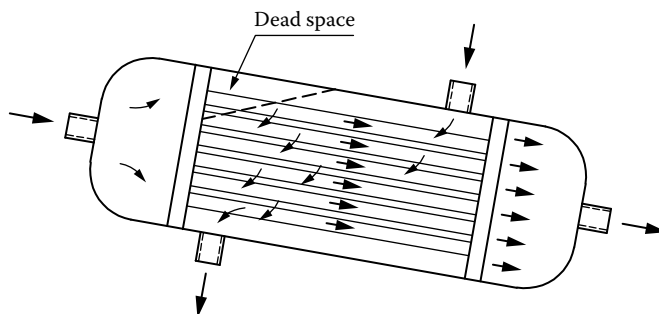


FIGURE 12.31 Inclined heat exchanger that permits a dead space at the top of the shell zone.

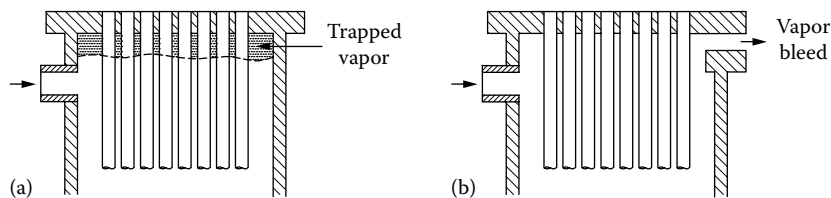


FIGURE 12.32 Crevice corrosion due to concentration of vapor phase and remedial measure. (a) Poor design and (b) correct design.

12.4.2.5 Plant Location

Nearby sources of exhaust and atmospheric pollution due to local industries have an important bearing on the materials of construction [76]. Plant structures should be located in the upwind direction. For example, placing stainless steel equipment just downwind of a hydrochloric acid scrubber can make the condenser susceptible to SCC [12,28].

12.4.2.6 Startup and Shutdown Problems

The construction materials should withstand not only the requirements at the design conditions but also the process upsets, startups, shutdowns, and standby. During these conditions, corrosion conditions can change significantly. Many corrosion problems do not originate when a plant is onstream. Rather, they can be traced to irregularities during startup or shutdown. Startup problems are often related to high temperature, difference in corrodent concentration, inadequate distribution of inhibitors, or incomplete oxygen removal [28]. Downtime problems are usually caused by residual process fluids or dry residues that result from prolonged shutdown periods or decaying of organic matter during shutdown periods. Residual fluids can promote localized corrosion such as pitting or crevice corrosion of stainless steel. Typical cases for shutdown problems are polythionic acid corrosion of stainless steel vessels in refinery applications, and SCC and sulfide attack of copper alloys due to ammonia liberated from putrefying organisms during shutdown periods.

12.4.2.7 Overdesign

In many instances, when the corrosive effect of a system is known, additional thickness to various components will be provided for in the design. This is known as a corrosion allowance. Because this thickness is in addition to that required for the design conditions, an extra cost is involved. Highly corrosive fluids may require the use of expensive corrosion-resistant metals such as stainless steel, titanium, nickel-base alloys, zirconium, tantalum, and nonmetals such as ceramics, graphite, glass, Teflon, etc. However, with the use of the special materials, normally the corrosion allowance is neglected or minimized.

Effect of the service environment: Code and regulatory requirements: The codes recognize that corrosion can occur and provide rules for including corrosion allowances to be specified by the designer in the calculation of required thickness.

12.4.3 CORROSION CONTROL BY MODIFICATION OF THE ENVIRONMENT (USE OF INHIBITORS)

Since corrosion is the reaction between a metal and its environment, any modification to the environment that makes it less aggressive will be beneficial in limiting the corrosion attack upon the metal. The corrosivity of a corroding medium can be changed by using various methods such as the following [77]:

1. Use a chemical additive, known as an inhibitor, that will have an effect on the electrochemical reaction to stifle corrosion.
2. Change the corrosivity of the environment by removing the active corrosive constituents. Some examples are removal of oxygen and carbon dioxide from boiler feed water, softening, demineralization of cooling waters, removal of chloride ions from a solution, and deaeration of acid solutions in contact with copper and nickel alloys.

12.4.3.1 Inhibitors

An inhibitor can be generally defined as a material that, when added to a corrodent (liquid), interferes with or retards the electrochemical reaction. To control corrosion, inhibitors are commonly added in small amounts to acids, cooling waters, steam, and other environments, periodically or continuously [78]. Inhibitors can be roughly classified according to the way in which they retard the electrochemical reaction to stifle corrosion. On this basis, if they inhibit the anodic reaction, they are called anodic inhibitors; those that inhibit the cathodic reaction are cathodic inhibitors; and if they inhibit both the anodic and cathodic reactions, they are called mixed inhibitors. The effect of an inhibitor in most cases is to form a barrier between the metal surface and the environment. Inorganic compounds such as chromates and nitrites interfere with the anodic reaction while the polyphosphates suppress the cathodic reaction. Another classification of inhibitors is single-component inhibitors and multicomponent inhibitors. The underlying principles of anodic and cathodic inhibitors are discussed next.

12.4.3.1.1 Anodic Inhibitors

During electrochemical reaction, a metal is dissolved at anodic areas to give metal ions and electrons that flow to cathodic areas. This may be represented as follows for a divalent metal:



A chemical that prevents or restricts action (in Equation 12.7) is called an anodic inhibitor and usually functions by combining with the M^{++} ions emerging from the corresponding area to form an insoluble compound on the metal surface. Typical anodic inhibitors include chromates, nitrites, phosphates, molybdates, orthophosphates, silicates, and some organic materials.

There are of three general types of anodic inhibitors:

1. Passivators
2. Oxidizing inhibitors
3. Nonoxidizing inhibitors such as orthophosphate

The passivators function by converting an anodic area to cathodic area, usually by means of impermeable oxide films. Oxidizing inhibitors function by increasing the oxidation potential at the anodic surfaces to increase the rate of formation of gamma-iron oxide [79] or are effective in repairing discontinuity in the passive film by quickly oxidizing iron wherever the surface is exposed. Chromate is the best known oxidizing anodic inhibitor in cooling-water systems. Its merits and demerits are discussed next.

Chromate: Chromate is probably the most effective corrosion inhibitor for water systems. Protection is afforded by a film consisting of alpha-ferric oxide and chromic oxide [8]. Chromates are the least expensive for use in water systems and are widely used in the recirculating cooling-water systems of internal combustion engines. However, chromates and heavy metals have recently become ecologically unacceptable in many places. To avoid toxic chemicals and meet regulations on effluent discharge, a large number of substitutes were developed, including zinc, poly- and orthophosphates, phosphonates, and a variety of polymers.

12.4.3.1.2 Cathodic Inhibitors

Cathodic inhibitors work by increasing the degree of cathodic polarization, thereby reducing the overall corrosion rate and current density, or they reduce corrosion by interfering with any of the steps of the oxygen reduction reaction. The cathodic reactions that complement the

anodic process (Equation 12.6) are Equations 12.2 and 12.3, and these reactions are necessary to absorb the electrons released by the dissolution of the metal at the anode. A compound that restricts reactions by Equations 12.2 or 12.3 is called a cathodic inhibitor. Reaction by Equation 12.2 will prevail in acid solutions. Reaction by Equation 12.3 will prevail over reaction by Equation 12.2 when there is an ample supply of dissolved oxygen and a low concentration of hydrogen ions as in alkaline solutions. By preventing absorption of the electrons released by the anodic reaction, corrosion must stop. Zinc is a well-known cathodic inhibitor [80]. Typical cathodic inhibitors are calcium bicarbonate, polyphosphates, phosphonates, metal cations, and organics. Cathodic inhibitors are often termed “safe” because they do not usually cause localized pitting attack [16]. Cathodic inhibitors are somewhat less effective than anodic inhibitors [81].

Adsorption inhibitors or organic (nonchromate) corrosion control polymers: Some organic compounds are effective as inhibitors because of adsorption mechanisms. Oil inhibitors are effective because of the physical adsorption process [82]. Organic inhibitors used in automotive diesel engine cooling-water systems include amines, benzoates, organic phosphates, mercaptans, triazoles, and polar type oils. Organic inhibitors such as starch quinoline and its derivatives and thiourea and its derivatives are commonly used for inhibition in acid media.

Multicomponent systems: Single-component inhibitors include chromates, sodium nitrite, silicates, sodium molybdate, and sodium phosphate. Multicomponent systems with many combinations have pronounced synergism in controlling steel corrosion in recirculating cooling-water systems compared with the individual components. Multicomponent systems can be either heavy metal treatments or non-heavy metal treatments (no zinc or chromate). Typical heavy metal multicomponent treatments include zinc chromate, zinc chromate/phosphonate, zinc polyphosphate, and zinc phosphonates. Non-heavy metal multicomponent systems (no zinc or chromium) in current use are [69,81] (1) combination of the phosphates (AMP/HEDP), (2) polyphosphate–phosphonate mixtures, and (3) the polyphosphate–orthophosphate.

Non-heavy metal treatment programs are receiving increased attention because of environmental regulations against discharge.

Passivation inhibitors: Passivation inhibitors, also known as film formers, work by depositing protective films over the entire surface, which provides a barrier to the dissolution of the metal in the corrosive environment. Typical passivation inhibitors include (1) chemical oxidizing substances, such as chromate and nitrate, and (2) organic substances such as tannin, gelatin, saponin, and beta-diketones, used in alkaline solutions.

Precipitation inhibitors: Precipitation inhibitors produce insoluble films on the cathode under conditions of locally high pH and isolate the cathode from the environment [69]. Sodium polyphosphate and zinc salts such as zinc sulfate and zinc chloride are examples of precipitation inhibitors.

Copper inhibitors: Though the previously mentioned ferrous inhibitors exert some control over corrosion of copper-base alloys, three specific inhibitors are extensively used on to protect copper-base alloys [69]: (1) mercaptobenzothiazole (MBT), (2) benzotriazole, and (3) polytriazone.

Requirements for effectiveness of inhibitors: The key to the success of an inhibitor is the maintenance of clean metal surfaces, which are essential for effective inhibitor film formation [83]. The inhibitors used should be compatible with the process fluids being used. Consideration should be given to avoid adverse effects such as foaming, decrease in catalytic activity, degradation of another material, and loss of heat transfer [78].

12.4.3.1.3 Inhibitor Evaluation

To determine the effectiveness of an inhibitor for use in a specific application, a comparison is made by using any of the corrosion testing techniques to determine the corrosion rate of the medium

without inhibitor, and the test is repeated with each inhibitor present in the medium. The effectiveness of each inhibitor can be calculated from the following equation:

$$\eta_i = \frac{m_o - m_i}{m_o} \times 100 \quad (12.8)$$

where

η_i is the inhibitor efficiency

m_o is the corrosion rate without inhibitor

m_i is the corrosion rate with inhibitor

Electrochemical techniques such as the galvanostatic pitting potential test can be used to determine the effectiveness of various corrosion inhibitors in the automobile cooling-water system. This method correlates the effectiveness of inhibitors in the prevention of pitting corrosion by measuring the inhibitor's effect on the pitting potential (E_p).

12.4.4 CORROSION-RESISTANT ALLOYS

Corrosion of certain metals is due to impurities in them. By controlling the impurities, the corrosion resistance can be improved markedly. Before the advent of the advanced refining techniques, ferritic stainless steels had relatively high levels of interstitials like carbon and nitrogen and, as a result, had serious limitations with respect to fabricability, toughness, and corrosion resistance. The newer ferritics, especially those with high chromium content and very low carbon content, have become possible through argon oxygen decarburization (AOD), vacuum induction melting, and vacuum oxygen decarburization [84]. On the other hand, a small addition of alloying element may have a profound effect on an alloy's resistance to certain types of corrosion. Addition of small amounts of copper to steel increases its atmospheric corrosion resistance; small amounts of phosphorus, antimony, and arsenic added to brasses inhibit dezincification; and small amounts of arsenic added to copper, and iron added to copper–nickel, increase the resistance to impingement attack and erosion–corrosion.

Besides changes in composition, metallurgical variations and mechanical effects may have an effect on reducing corrosion damage. Introduction of compressive stresses on the surface by shot peening will reduce corrosion fatigue or SCC. Annealing to reduce the internal stresses and solution annealing to remove the grain boundary segregation help in eliminating SCC and intergranular attack, respectively.

If corrosion of a metal in an environment is inevitable, use an alternate material, such as borosilicate glass, impervious graphite, zirconium, tantalum, Teflon, etc., that shows chemical inertness to most of the chemicals.

A recent focus to tackle severe corrosion is on three alloy families [85]: (1) duplex stainless steels, which exhibit good corrosion resistance to both pitting and SCC, and have about twice the yield strength of the typical austenitic stainless steel, (2) 6-Mo superaustenitic stainless steels, and (3) high-nickel alloys such as UNS NO 6625, UNS NO 4400, and UNS NO 7716.

12.4.5 BIMETAL CONCEPT

The term bimetal is applicable to any combination of two metals or alloys having nearly matching or widely dissimilar physical and chemical properties and bonded by one of a variety of processes. The bimetal concept is employed in (1) cladding and (2) duplex or bimetallic tubes.

12.4.5.1 Cladding

Cladding has been used for many years in pressure vessels, piping systems, and heat exchangers (Figure 12.33). Nuclear and petrochemical pressure vessels are weld overlay clad with 300 series stainless steels or high-chromium nickel-base alloys. The severe corrosion problems in various coal combustion and incineration environments have renewed interest in cladding technology for both Code-approved and enhanced-strength developmental alloys [74]. Typical cladding alloys include ferritic (straight chrome) and austenitic stainless steels, nickel-base alloys, titanium, zirconium, and tantalum. Clad steels satisfy severe service conditions at less cost than full-thickness sections of the costly corrosion-resistant material used for the cladding. Various cladding methods are discussed in detail in a separate section in Chapter 13.

12.4.5.2 Bimetallic or Duplex Tubing

Two dissimilar corrodents in a heat exchanger can cause havoc, with material having a propensity to corrosion to one fluid and virtually immune to the other fluid, or the problem of severe corrosion of different natures that sometimes attacks both sides of a tube can often be solved by treating such a condition as two separate corrosion problems. By selecting the specific kind of metal that is best for each condition, it is possible to combine two such metals into one tube, known as duplex tubing

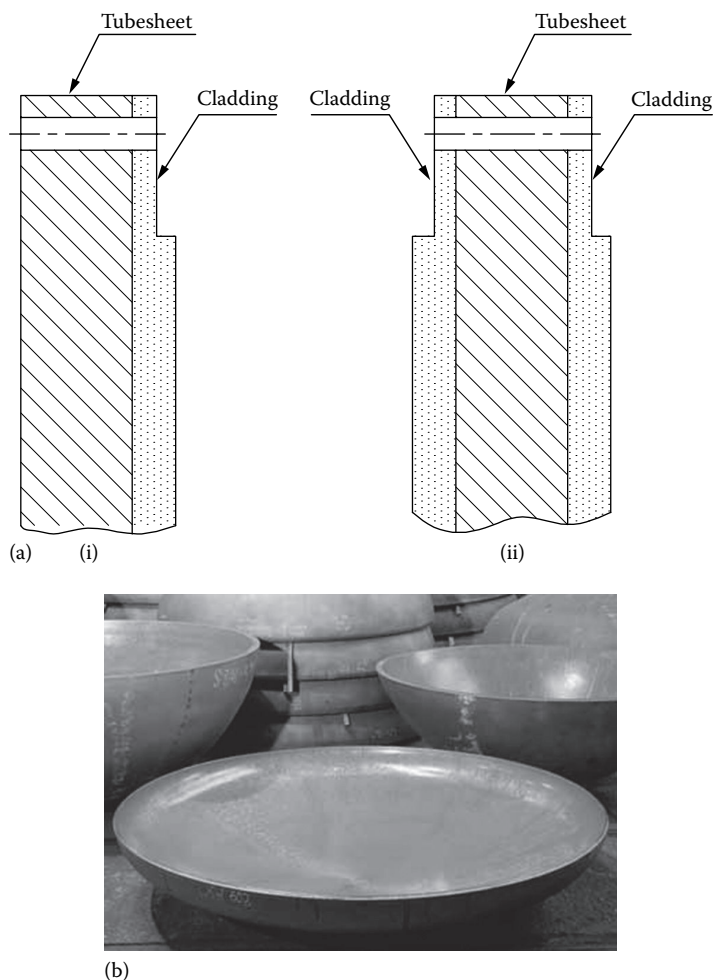


FIGURE 12.33 Cladded heat exchanger component. (a) Tubesheet and (b) heat exchanger heads. (Courtesy of Voestalpine Grobblech GmbH, Linz, Austria.)

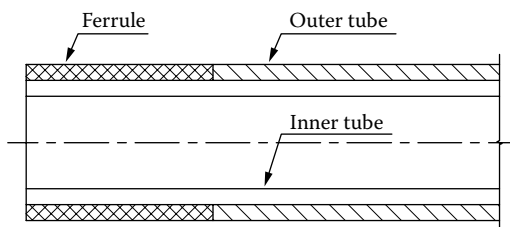


FIGURE 12.34 Duplex tubing.

or bimetallic tubing. Duplex tubing is shown schematically in Figure 12.34. Specific information on duplex tubing is given in Ref. [86].

The tube manufacturing method, mostly hot coextrusion, ensures close mechanical contact between the two metals without affecting the heat transfer properties. Duplex tubing is made up of various combinations of ferrous and nonferrous materials. Bimetallic tubes are available in a variety of stainless steel–carbon steel, Cu, brass, Al, and other combinations. Duplex tubings have been used in actual service for the past 25 years in oil refining, in production of synthetic rubber, and in process industries, chemical plants, coke by-product plants, refrigeration systems, and other applications. Typical metal combinations of bimetallic tubes used in refinery applications, high-temperature boiler corrosion, and condenser applications are discussed later.

Duplex tubing for refinery applications: For oil refining and in the natural gas industry, duplex tubing with the following combinations is used [31]:

- 1 Steel outside to resist various corrosive petroleum vapors and copper or copper alloy inside toward the fresh water
- 2 Steel outside toward the oil and admiralty, aluminum brass, or cupronickel inside toward circulating saltwater
- 3 Other applications in these industries call for the combinations of alloy steels with copper alloys or of aluminum with copper or brass either inside or outside

Duplex tubing in high-temperature boiler corrosion: C-Mn or low-alloy steels, clad with a stainless steel or superalloys, are used in parts of the boiler where loss is excessive due to high-temperature corrosion [87].

Duplex tubing in a condenser application: In a condenser with stainless steel tubing, hot corrosive vapors caused little trouble within the tubes. But brackish cooling water on the shellside caused a problem. This situation was overcome by installing Carpenter bimetallic tubing consisting of type 304 welded stainless on the inside and deoxidized copper tube on the outside. Ferrules at the tube ends facilitated expansion of the tubes into type 304 stainless tubesheets.

12.4.6 PROTECTIVE COATINGS

Coatings are generally relatively thin films separating the two reactive materials or a metal from an environment. Applying a protective barrier between a corrosive environment and the material to be protected is a fundamental method of corrosion control [88]. It is most widely used for the protection of steel and other metals. Coatings can be metallic, plastic, paints, or organic. Typical metallic coatings include nickel coatings, lead coatings, zinc coatings, cadmium coatings, tin coatings, and aluminum coatings. Mechanisms by which coatings protect can be summarized as follows [89]:

1. They isolate the metal substrate and the environment, as with nickel electroplating.
2. They limit contact between the environment and the substrate, as with most organic coatings.
3. They release substances that are protective or inhibit attack, as with chromate primers.
4. They produce an electrical current that is protective, as with galvanizing.

12.4.6.1 Plastic Coatings

Plastic coatings often represent the ideal solution to a cooling-water problem. Typical plastic materials used for coatings are polyethylene, polyvinyl chloride, epoxy resins, and polyamides. Under certain conditions, they allow a cheap and corrosion-susceptible metal to be covered with a high-grade corrosion-resistant plastic coating. To ensure satisfactory protection, these must be nonporous and sufficient thickness (0.150–0.250 mm) [90].

12.4.6.2 Effectiveness of Coatings

To be effective, the coating film must be completely continuous. Any breakdown of the coating film leads to corrosion. Resistance to water is the most important requirement of the coating, since all coatings will come in contact with water or moisture in one form or another [88,89].

12.4.6.3 Surface Treatment

Surface treatment is resorted to on certain metals to improve their corrosion resistance in specific applications. For example, (1) mild steel or low-alloy steel heat exchanger tubes are alonized or aluminized (aluminum vapor diffused) for high-temperature oxidation resistance and protection from sulfide corrosion in refinery applications [91], and (2) titanium tubes are anodized or thermally oxidized to form an inert surface oxide film for its corrosion resistance, especially where hydrogen uptake is of concern.

12.4.7 ELECTROCHEMICAL PROTECTION (CATHODIC AND ANODIC PROTECTION)

12.4.7.1 Principle of Cathodic Protection

Cathodic protection is defined as the reduction or elimination of corrosion by making a metal cathode by means of an impressed current or attachment to a more anodic metal (sacrificial anode) than the metal in the galvanic couple. These two methods are discussed next, and both the methods are shown schematically in Figure 12.35. Cathodic protection is one of the recommended methods of protecting the tubesheet.

12.4.7.1.1 Sacrificial Anode

A cathode is the electrode where practically no corrosion takes place. If follows, then, that if all anodic areas can be converted to cathodic areas, the entire structure will become a cathode, and corrosion will be eliminated. Corrosion control by this principle is known as cathodic protection by sacrificial anode. By coupling the structure with a less noble metal, it is allowed gradually to corrode but is replaced after an interval of time. Zinc or magnesium is often coupled with iron for this purpose and is termed a sacrificial anode (Figure 12.35a). This method is mostly followed in heat exchangers for protecting the end closures.

Galvanic combinations such as zinc or cadmium or magnesium coatings on steel, often used to avoid corrosion, are known as sacrificial anodic coatings, because they corrode in preference to steel and protect the latter from rusting. Galvanizing a steel heat exchanger of a tube bundle did not improve the life expectancy, and galvanizing is not sufficiently effective to be worth even the slight extra cost involved [92].

Impressed current method: Because the corrosive action is electrochemical, electric current can be applied to effectively stop the attack of metals exposed to corrosive media. This technique is called cathodic protection by impressed current. In this method, an impressed current from a dc source is passed on to the metal to be protected and coupled to an insoluble anode such as platinum, graphite, or ferrosilicon alloy or an expendable anode such as zinc, aluminum, or magnesium, thus forcing the structure that has to be protected to have as a large cathode so that it will not suffer attack. This method is presently employed in practice to protect buried pipelines carrying gas, oil, and water from corrosion by the surrounding soil. The principle of auxiliary anode method is shown in Figure 12.35b and protection of the tubesheet and the end closure when titanium tubes are installed in an exchanger is shown in Figure 12.35c [93].

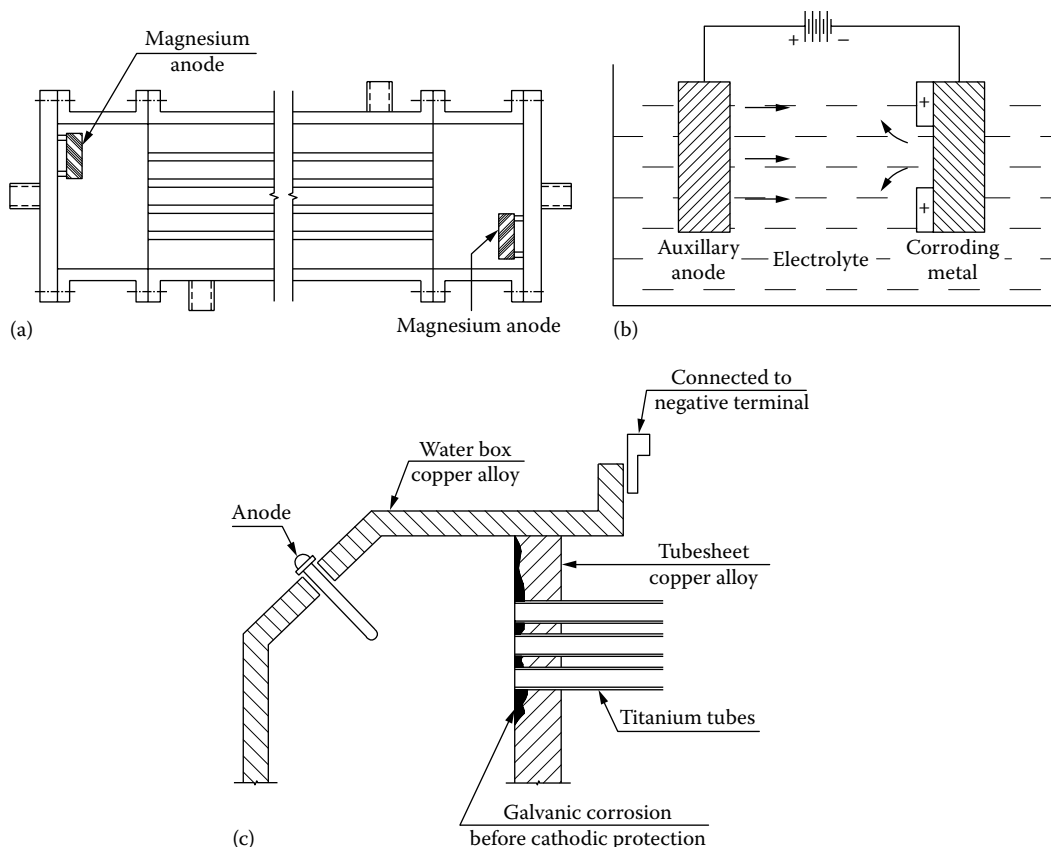


FIGURE 12.35 Cathodic protection. (a) Sacrificial anode, (b) auxiliary anode method, and (c) impressed current method.

Shortcomings of cathodic protection: With a cathodic protection system in seawater and in certain applications, if condenser and heat exchanger tubes happen to be cathodic, they may become covered with an undesirable thermal resistance layer. This may require a decrease in the amount of current flowing in the circuit or a change in the kind of anode, its location, or size [31]. Overprotection of a titanium tubesheet may result in the hydriding of the tubesheet.

12.4.7.2 Anodic Protection

If the potential of a metal is maintained in the range that leads to passivity, then the corrosion current density may be very low and will be stable. Consequently, the corrosion will be very low. This principle is employed in anodic protection. Anodic protection is an established, cost-effective method for corrosion control that can be applied in almost any electrically conductive solution in which a metal exhibits active-passive behavior [28,94]. The metals protected by anodic protection are iron, nickel, aluminum, titanium, zirconium, etc., and alloys containing major amounts of these metals. Electrolytes can vary from acid to alkaline. The pulp and paper industry was one of the first to investigate the use of anodic protection, particularly for carbon steel vessels containing alkaline solutions.

The advantages of using anodic protection are as follows [28]: (1) low operating costs, (2) applicability to a wide range of severe corrodents, (3) high throwing power (can protect complex structures, needs few auxiliary electrodes), (4) protection current can give an idea of the corrosion rate,

and (5) it is often possible to substitute for an expensive alloy in an unprotected plant a cheaper material that is anodically protected. The disadvantages of this method include the following [28]:

1. Anodic protection does not stop corrosion completely, but reduces it to a minimum level
2. The failure of the electrical supply may be hazardous because of depassivation
3. High installation costs: requires potentiostat, reference and auxiliary electrodes, and high starting current
4. The requirement for electrical current makes this measure unsuitable for protection in organic liquid environments, or for components that are not continuously immersed

12.4.8 PASSIVATION

“Passivation” is the conditioning of a metal surface to produce a protective surface film that blocks corrosive ions from reaching the metal, thereby retarding corrosion. To change a metal from an active to a passive state, the electrode potential must be raised above the passivation potential. Passivation can be achieved by methods such as the following [95]: (1) applying an external current of sufficient strength or (2) using agents of sufficient oxidizing power to give a mixed potential above the passivation potential of the metal.

12.5 CORROSION MONITORING

Continuous operation, associated with higher operating efficiency, is putting a heavier burden on heat exchangers operating in various process industries such as oil refining, chemical, electric power plants, food and liquor processing, pulp and paper industries, etc. Changes in process parameters such as temperature, pressure, velocity, and concentration can accelerate corrosion rates. When the process changes occur, it is imperative to monitor their effects on corrosion rates to prevent equipment failure caused by corrosion. Corrosion monitoring can be used to optimize process conditions to achieve the maximum capabilities without sacrificing the integrity of the equipment. Corrosion monitoring has been discussed in detail by Britton et al. [96] and in Ref. [97].

12.5.1 BENEFITS

Effective corrosion monitoring is justified economically for a large, complex plant at which production continuity is essential. The benefits of a successful corrosion monitoring program include the following [96]:

1. Corrosion problems can be predicted.
2. Plant maintenance and inspection can be scheduled.
3. Unscheduled shutdowns of plants can be avoided.
4. Improvements in reliability of equipments.
5. Better use of construction materials.
6. Detection of changes or abnormalities in the process affecting the corrosion rate.

12.5.2 APPROACHES TO CORROSION MONITORING

In general, there are three approaches for corrosion monitoring [98]: (1) local approach, (2) component approach, and (3) systems approach. The local approach involves investigations of corrosion in terms of local conditions. The component approach involves investigating plant components and their corrosion phenomena that arise due to the complex environmental and operational conditions. The systems approach considers the plant system in its totality. This approach deals with interrelations of phenomena occurring in different components of the system.

12.5.3 CORROSION MONITORING TECHNIQUES

Several techniques are used in corrosion monitoring, and the techniques are generally classified as either online or offline. Various online and offline techniques are described next.

12.5.3.1 Online Monitoring Techniques

Online corrosion monitoring is conducted to assess the corrosivity of the process stream and for detecting changes that may occur in operation. Online corrosion data are obtained from probes or sensors inserted into the system at accessible points that reproduce the particular area of interest. Various online monitoring techniques include corrosion coupons, electrical resistance principle, pitting potential, linear polarization principle and Tafel plots, hydrogen test probe, galvanic measurements, pH measurements, dimensional changes through online ultrasonic testing, radiography, and acoustic emission technique [96]. Some of these techniques are discussed next.

Corrosion coupons: The most common online monitoring technique is with corrosion coupons. Corrosion coupons can be made in any size or shape, such that they are retrievable from process equipment without shutting down the unit. Normally, the corrosion coupons are carefully weighed before insertion and weighed after retrieval.

Weight change: When results of other techniques are in question, they are usually verified with weight loss testing. However, weight loss determination would give misleading information in the case of localized attack such as pitting.

Hydrogen diffusion: Atomic hydrogen can diffuse into steel and form molecules. If hydrogen diffusion is detected, it shows imminent danger due to hydrogen damage/hydrogen attack. Hydrogen diffusion can be measured using either a hydrogen probe (pressure measurement) or a hydrogen monitoring system (electrochemical).

12.5.3.1.1 Electrochemical Techniques

Electrochemical techniques are particularly useful in determining the corrosion rate that is actually happening in a metal at any given time. The three techniques most often used involve (1) electrical resistance principles using zero-resistance ammeters, (2) polarization curves, and (3) linear polarization curves. In the electrical resistance technique, the change in resistance of a thin wire under consideration due to the corrosion process is measured. Polarization curves may be determined galvanostatically, potentiostatically, or potentiodynamically. Anodic polarization measurements (where the electrode potential is changed in the positive direction to show current variations over a wide range of oxidizing potentials) are used primarily to determine critical pitting potentials or breakdown potentials for localized corrosion. The principle of linear polarization technique, now referred to as the polarization technique, is as follows: The amount of externally applied current needed to change the corrosion potential of a freely corroding specimen by a few millivolts (approximately 10 mV) is measured. This current is related to the corrosion rate of the sample; that is, a linear relationship exists between the applied current and the resulting potential. If the metal is corroding rapidly, a large external current is needed to change its potential, and vice versa. This is the basis for the precise determination of corrosion rate.

Other methods include Tafel extrapolation (where the linear portion of the anodic or cathodic polarization curve is extrapolated back to the corrosion potential to locate the current density associated with corrosion rate at that potential) and current measurements at constant potential (where corrosion rate is monitored for a given oxidizing condition) [99].

Monitoring of pitting potential: The potential at which pit initiation occurs is called the pitting potential. Pitting potential is determined by electrochemical techniques, which consist of measuring current and potential potentiostatically, either stepwise or by applying a constant-potential sweep rate in a standard chloride-containing solution.

12.5.3.1.2 *Online Monitoring of Water Purity in Thermal Power Stations*

Corrosion inhibition in a cooling-water system involves monitoring calcium hardness, alkalinity, total solids, pH, dissolved gases (oxygen and hydrogen), total dissolved salts, etc. Automatic analyzers continuously monitor water and steam purities of thermal power stations. For more details on online monitoring of cooling water refer to Refs. [100,101].

Offline monitoring techniques: Offline monitoring techniques involve various nondestructive examination methods to determine the thickness and integrity of the heat exchanger and pressure vessel components. Various NDT methods employed are as follows:

1. Visual examination with or without optical aids such as borescopes
2. Eddy current testing
3. Magnetic particle examination
4. Liquid penetrant test
5. Ultrasonic examination
6. Radiography
7. Thermography

12.5.3.2 **Corrosion Monitoring of Condensers by Systematic Examination of the State of the Tubes**

This procedure involves extracting representative tubes and examining them in the laboratory with modern analytical equipment [101]. In a tube investigation procedure, one considers the three zones (inlet, center, and outlet) separately, because they are exposed to different conditions. On all samples, the following four criteria are checked:

1. Microscopic examination of the condition of the tube surface
2. Residual wall thickness
3. Weight of the surface layer
4. Composition of the surface layer

12.5.4 **LIMITATIONS OF CORROSION MONITORING**

It is important to be aware of the limitations of corrosion monitoring data. Some of the important limitations of corrosion monitoring are [96] the following:

1. The data are only a qualitative guide to the actual behavior of the plant or process.
2. A confidence factor is established only through experience, and particularly through comparison with other sources of information, notably that provided by NDT.

12.5.5 **REQUIREMENTS FOR SUCCESS OF CORROSION MONITORING SYSTEMS**

Many factors contribute to the success of a monitoring program. Some of the most important considerations include the following [96]:

1. Use of correct technique
2. Correct location of monitoring probes
3. Reliability of the equipment and instrumentation
4. Data obtained must be straightforward to interpret

12.6 COOLING-WATER CORROSION

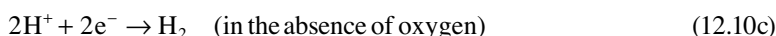
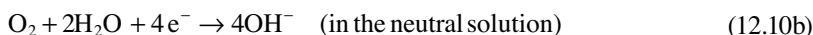
Water, the most commonly used cooling medium, removes unwanted heat from process fluids. Water is an excellent solvent for numerous substances: It washes the mineral elements out of the earth, it absorbs gases (O_2 , CO_2) from the atmosphere, it entrains suspended matter, and it promotes growth of microorganisms. If cooling water is used without treatment, it leads to the twin problems of fouling and corrosion [90]. Corrosion in cooling-water systems is electrochemical in nature, and the corrosion products may be either soluble or insoluble. The insoluble material that forms a deposit on the heat transfer surfaces retards heat transfer and promotes corrosion in long run.

12.6.1 CORROSION PROCESSES IN WATER SYSTEMS

Corrosion of metals in contact with water is electromechanical in nature. A generalized anodic oxidation reaction for ferrous metal has already been presented and copper and aluminum materials are represented by [69] the following:



where M represents the metal that has been oxidized to its ionic form having a valence of n^{+} and the release of n electrons. The reactions at the cathodic site on the metal surface are given by Ref. [69] as in the following:



12.6.2 CAUSES OF CORROSION IN COOLING-WATER SYSTEMS

Depending on the sources of water—river, lake, ocean, or sea—cooling-water corrosion that attacks heat exchangers is due to one or more of the following impurities [8,69,81,90]:

1. Dissolved solids and water hardness
2. Chloride
3. Sulfate
4. Silica
5. Oil
6. Iron and manganese
7. Suspended matter such as turbidity, dirt, clay, silt, sand, etc.
8. Dry residue
9. Dissolved gases such as O_2 , carbon dioxide, hydrogen sulfide, ammonia
10. Dissolved organic matter
11. Microbiological organisms

Apart from these factors, water temperature, pH, and flow velocity also influence corrosion. Effects of these factors on the cooling-water corrosion are discussed next.

12.6.2.1 Dissolved Solids and Water Hardness

All waters containing calcium and/or magnesium salts such as calcium carbonate (CaCO_3), calcium bicarbonate [$\text{Ca}(\text{HCO}_3)_2$], magnesium carbonate (MgCO_3), and magnesium bicarbonate [$\text{Mg}(\text{HCO}_3)_2$] in considerable amounts are called “hard.” The following classifications for hardness are often applied to freshwater [102]:

Soft: 0–50 ppm

Medium hard: 50–100 ppm

Hard: >100 ppm

The measure total dissolved solids (TDS) is the concentration of dissolved solids that cannot be removed by filtration. Seawater is many times higher in dissolved solids than freshwater.

Total hardness is the amount of calcium and magnesium salts, which may be present as bicarbonates (temporary hardness) or as sulfates, chlorides, nitrates, or carbonates (permanent hardness).

The overall aggressiveness of water is related to its hardness and alkalinity. Soft waters, which are low in calcium, are more corrosive than hard waters [69]. Hard water, high in calcium and magnesium, is less corrosive than soft water because of the tendency of the salts in the hard water to precipitate on the metal surface and form a protective film. However, increasing the dissolved solid contents of the waters increases its conductivity and hence a larger corrosion current can flow resulting in higher corrosion rate. The dissolved constituents can also have a variety of effects including increased scale and deposit formation. Hardness ions (Ca^{2+} and Mg^{2+}) and HCO_3^- ions are inhibitive and will suppress corrosion, but chloride (Cl^-) and sulfate (SO_4^{2-}) ions are deleterious and will increase the rate of some forms of corrosion [69].

Scale deposition: Water-formed deposits are commonly referred to as scale. This scale increases the resistance for heat transfer and increases pressure drop, and promotes localized hot corrosion spots. Some hardness in the water may be helpful if the pH and alkalinity can be controlled to permit formation of a thin protective scale (termed stabilization of the water). Unfortunately, the buildup of a thick scale on the tube surface seriously interferes with heat transfer. The normal scale-forming compounds commonly found in cooling-water systems are calcium carbonate, calcium sulfate, calcium phosphate, and silicates. Of these compounds, calcium carbonate has very low solubility and perhaps is the principal scale-forming material in cooling waters. Bicarbonate ions react with hydroxyl ions generated at the cathode to produce carbonate, which precipitates with calcium from the water as calcium carbonate. The equation for calcium carbonate scaling is given by



Prevention of calcium carbonate scale: Scale-forming tendencies of cooling water can be predicted by determining the Langelier saturation index (LSI), also known as the calcium carbonate saturation index, of the water. Some prefer the Ryznar stability index. The LSI is defined as the difference between the actual pH value of the water and the value of pH that the water would have if it was in equilibrium with CaCO_3 , also known as saturation pHs. Accordingly, the LSI is given by

$$\text{LSI} = \text{pH} - \text{pH}_s \quad (12.12)$$

The LSI is not applicable to seawater because of the high salt content [102].

Determination of LSI: The LSI is calculated from (1) the alkalinity, (2) the calcium hardness, (3) the ionic strength (total solids), (4) the pH value, and (5) the temperature. The index can also be found out by direct determination of the pH of water as such and after saturating it with calcium carbonate. A condition of carbonate equilibrium with the absence of scale can be accomplished by adjusting any of the variables of the LSI. The common practice is to lower the alkalinity and pH by adding sulfuric acid to the cooling water [70]. A chart for calculating the saturation index is shown in Figure 12.36.

Scaling control: If the LSI is positive, scale will be deposited and will probably stifle corrosion of the metal. If it is negative, the water is unsaturated with CaCO_3 , and it is likely to be corrosive and may dissolve existing hardness salts or may not be scale forming. In other words, for $\text{LSI} > 0$, water

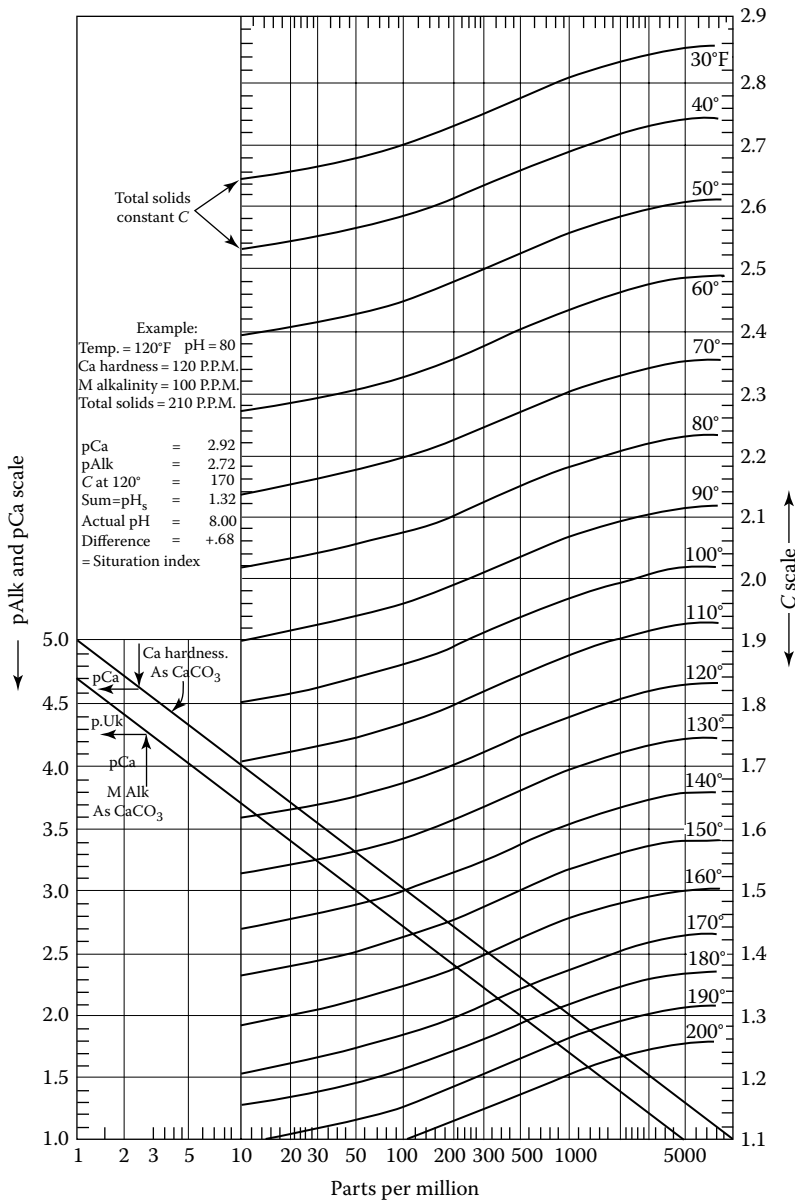


FIGURE 12.36 Chart for calculating saturation index. (Ca and alkalinity expressed as ppm CaCO_3 ; temperature in degrees F.) (From Powell, S. et al., *Ind. Eng. Chem.*, 37, 842, 1945.)

is super saturated and tends to precipitate a scale layer of CaCO_3 , and for $\text{LSI} = 0$, water is saturated (in equilibrium) with CaCO_3 . A scale layer of CaCO_3 is neither precipitated nor dissolved and, for $\text{LSI} < 0$, water is under saturated and tends to dissolve solid CaCO_3 . It is also worth noting that the LSI is temperature sensitive. The LSI becomes more positive as the water temperature increases. Conversely, systems that reduce water temperature will have less scaling. LSI and probable nature of water is given next [31]:

For $\text{LSI} = -2.0$, water is corrosive and non-scale forming

For $\text{LSI} = -0.5$, water is mildly corrosive and non-scale forming

For $\text{LSI} = 0.0$, water is mildly corrosive

For $\text{LSI} = +0.5$, water is mildly corrosive and scale forming

For $\text{LSI} = +2.0$, water is not corrosive but definitely scale forming

From these, the main choice appears to be between keeping the LSI low and controlling scale formation, or having a high index and controlling the corrosion. Methods to control scale formation are discussed in Chapter 9.

12.6.2.2 Chloride

Chlorides are the main salts in seawater, around 19,000 ppm [102]. High-chloride waters are usually corrosive. High chloride ion concentrations easily destroy the protective surface films including passive films on a large number of metals [90], or the chloride forms complex ions with dissolved iron, thereby preventing or interfering with the formation of protective corrosion product scales [16]. In the case of austenitic stainless steels, chloride ions will easily destroy the passive film and result in pitting corrosion or when the metal is subjected to simultaneous tensile stress can cause chloride SCC. Aluminum is also easily attacked by chloride.

12.6.2.3 Sulfates

Sulfates are not as corrosive as chlorides [102]. However, concrete cooling-water basins are endangered as soon as the water contains more than 250 ppm of sulfate ions [90].

12.6.2.4 Silica

Silica will react with magnesium or calcium to form deposits of insoluble magnesium or calcium silicates. Also it will form siliceous glassy scales. To avoid such deposits, the silica concentration must be limited.

12.6.2.5 Oil

Oil is one of the most undesirable contaminants of industrial cooling-water systems. Oils usually leak into the system as a result of poor maintenance. They interfere with the action of corrosion inhibitors; by forming a thin film on metal surfaces, oils retard heat transfer, and they become nutrients for biological organisms [8].

12.6.2.6 Iron and Manganese

Iron oxide is produced either by internal corrosion of steel heat exchanger surfaces and transmission lines or from precipitation of soluble iron brought into the cooling system from the earth by the makeup water. Less than 0.2 ppm of iron and manganese is desirable. With higher contents, sludge-type hydroxides are precipitated in the presence of oxygen [90]. Iron oxide scale, which forms as easily dislodged "plate-like" layers, becomes lodged in the tubes and leads to localized impingement attack. Iron oxide scale is prevented by applying cathodic protection or by protective coatings [33].

12.6.2.7 Suspended Matter

Suspended matter such as clays, silt, and corrosion products present in once-through or open cooling-water system is capable of depositing on metal surfaces in low-velocity areas (<1 m/s), forming a physical barrier. This buildup will contribute to the formation of differential aeration cells and will promote localized corrosion [69].

12.6.2.8 Dry Residue

Dry residue after evaporation includes all the dissolved substances in the water. If dry residue expressed as salt content is greater than 500 ppm, the conductivity of water when it comes in contact with the dry residue will increase, which in turn will enhance corrosion [90].

12.6.2.9 Dissolved Gases

The most common dissolved gases are oxygen, carbon dioxide, hydrogen sulfide, and ammonia. Their role in cooling-water corrosion is discussed next.

Oxygen: Cooling water saturated with oxygen will lead to increased corrosion. Oxygen can behave as a depolarizer and can increase the rate of corrosion by speeding up the cathodic reaction. It can also act as a passivator because it promotes the formation of a stable passive film. Dissolved oxygen is a major factor contributing to the natural corrosion of steel. Oxygen in traces promotes SCC of brass in the presence of ammonia; oxygen when coexisting with ammonia leads to the highest rate of sulfide attack; and oxygen also promotes condensate corrosion. Nevertheless, a minimum quantity of oxygen is needed to form the carbonate-rust protective film. This should amount to about 5–6 ppm at normal ambient temperature [31].

Removal of oxygen: Control of oxygen corrosion is critical to the reliability of a steam generator system. Mechanical deaeration and oxygen scavenging by chemical means effectively reduce oxygen levels in boiler feedwater systems [103]. Some of the successful devices to reduce the influence of oxygen on cooling-water corrosion are mentioned in ref. [31]. One of these methods is the mechanical method, which consists of raising the water temperature and lowering the pressure (vacuum) so that the gas is liberated (all gases are less soluble in water with increasing temperature and decreasing pressure). This method is applicable for removing other gases also from water. Another mechanical method consists of passing water over scrap iron, which removes the dissolved oxygen and is applicable to closed systems. There is also the chemical method that consists of adding a slight excess of sodium sulfite. The sodium sulfite reacts rapidly with the dissolved oxygen to form sodium sulfate:



This method has been economically used for years for the removal of the last traces of oxygen from boiler water.

Carbon dioxide: Natural cooling water always contains free carbon dioxide, in larger or smaller quantities. Dissolved free carbon dioxide makes water acidic. The free carbon dioxide is defined as the quantity that is required to retain the alkaline earth carbonate in accordance with the equation:



Cooling waters without excess free carbon dioxide lead to the formation of a protective carbonate-rust scale, which represents one of the most important protective surface layers [90]. However, excessive carbon dioxide will cause corrosion. Excess carbon dioxide is removed from cooling water by spraying water over a mass of coke or other inert material exposed to the air. Sometimes by this process the carbon dioxide content can be reduced to 5–10 ppm. The second method involves treating the water with lime [31].

Hydrogen sulfide: Hydrogen sulfide in cooling waters generally results from the action of bacteria on organic matter, particularly sewage. The presence of even few parts per million may change the corrosivity of water drastically. The presence of hydrogen sulfide in a water has the tendency to reduce inlet-end or impingement corrosion, but increases the probability of pitting corrosion occurring along the entire length of a tube [102]. Additionally, the salts created by this attack (copper sulfide, iron sulfide, etc.) are insoluble and precipitate on the metal surface as loose, noninhibitive deposits that promote galvanic couple and thus promote corrosion [8].

Ammonia: Ammonia is originally derived from the thermal degradation of various nitrogen-containing compounds added to the boiler feedwater to reduce corrosion. Ammonia does not cause excess corrosion on ferrous metals. However, traces of ammonia will cause both rapid general thinning and SCC in brasses. Pure copper and copper–nickel alloys are not susceptible to ammonia SCC, but a higher rate of uniform corrosion will take place with higher ammonia contents [90].

Dissolved organic matter: Dissolved organic matter in excess quantity tends to produce sludge-type deposits and fouling. Dissolved organic matter is detected indirectly by determining the potassium permanganate (KMnO_4) consumption. If the KMnO_4 consumption exceeds about 25 mg/L water, then the water is “dirty,” which tends to produce sludge-type deposits and fouling [90].

Microbiological organisms: Corrosion due to microbiological organisms has been discussed in the section on MIC.

pH value: The pH of the water can have several specific effects. High pH levels make the formation of heavy calcium carbonate and calcium phosphates scales likely. From Equation 12.6, it is evident that where a greater number of hydrogen ions (low pH) are available, the corrosion reaction should occur more rapidly. Natural waters produce more or less neutral solution (pH value about 7). Clean seawater has a pH of about 8. In general, the neutral and weakly alkaline waters usually cause no or only very slight corrosion on metallic materials, but weakly to strongly acidic water is always corrosive. Type of water also influences corrosion. The corrosiveness of a natural freshwater with a pH of 7–8 usually is much less than that of seawater with a similar pH. The difference is due to the presence of more mineral salts in seawater. Nevertheless, pH is not the only determining factor. Water hardness, particularly the carbonate hardness, is of decided importance [90]. An additional factor that decides the water corrosion is the dissolved mineral salts.

Temperature: In general, an increasing temperature will increase corrosion rates. Temperature plays a dual role with respect to oxygen corrosion. For an open system, beyond 175°F (80°C), increasing the temperature will reduce oxygen solubility, whereas for a closed system in which the oxygen cannot escape, corrosion continues to increase linearly with temperature [69]. Another effect of increased temperature is the increase in fermentation of organic materials with formation of sulfides, which promote corrosion [102]. In certain waters, the corrosion rate drops off with an increase in temperature because the water deposits a thin scale. Calcium carbonate forms as a result of the decomposition of calcium bicarbonate at elevated temperatures [31]:



Hot wall effect: Severe local corrosion or pitting can rapidly perforate condenser and heat exchanger tubes on the cooling-water side where bubbles of air or foreign material separate from the water (known as blanketing of base metal) and hence localized heating of heat transfer surface (Figure 12.37). Here the metal is hotter, and the corrosion proceeds at a correspondingly higher rate. This is known as the hot wall effect.

Flow velocities: Corrosion is favored by too low or too high cooling-water velocities. High velocity helps to prevent the accumulation and deposition of corrosion products, which might create anodic sites to initiate corrosion and helps to maintain clean surfaces free from fouling

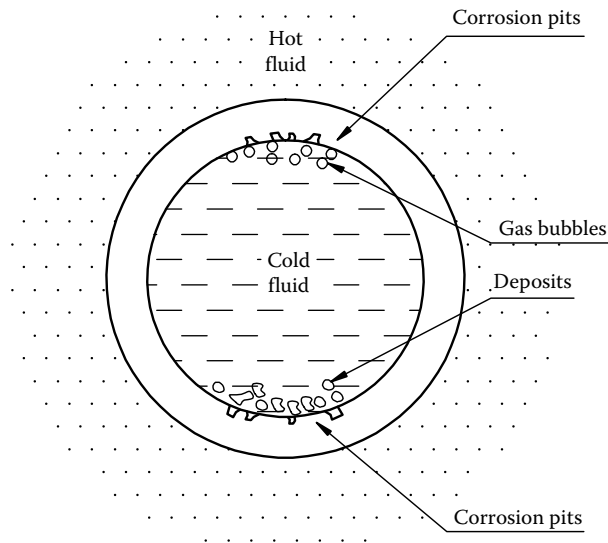


FIGURE 12.37 Hot wall effect. (Note: Read cold fluid as cooling water.)

deposits, stagnant areas, and hot wall effect. On the other hand, too high a velocity can destroy the protective surface film and result in erosion–corrosion or impingement corrosion, especially on metals such as copper and aluminum[90]. The velocity, in general, should not be less than about 1 m/s.

The following values apply in respect of the maximum admissible flow velocities for water, V_w :

Pure aluminum	1.2–1.8 m/s
Pure copper	1.8 m/s
Copper-containing arsenic	2.1 m/s
Aluminum brass	2.0–2.4 m/s
Naval brasses	2.0–2.4 m/s
CuNiFe 90/10	2.5–3.0 m/s
CuNiFe 70/30	3.0–4.5 m/s
Monel 400	4.0 m/s
Carbon steel	3 m/s
Austenitic stainless steel	4.0–5.0 m/s
Ni-Fe-Cr alloys	4.0–5.0 m/s
AL-6XN®	7.0–8.0 m/s
SEA-CURE®	9.0–10 m/s
Titanium	Up to 30.0 m/s

For other liquids, allowable velocity V_l is given by

$$V_l = V_w \left[\rho_w / \rho_l \right]^{0.5}$$

where

ρ_w is density of water

ρ_l is density of liquid

For gases and dry vapors, allowable velocity for steel tubing is given by

$$V_g = V_w \frac{1800}{\sqrt{p_a \times M_w}} \text{ ft/s}$$

where

V_g is gas/vapor velocity

p_a is absolute pressure of gas/vapor, psia

M_w is the molecular weight of gas/vapor

Allowable velocities for other metals may be taken to be in the same ratio as for water.

12.6.3 COOLING SYSTEMS

An understanding of the relationship between cooling water and the buildup of deposits and corrosion of heat transfer surfaces requires an awareness of cooling-system characteristics. There are basically three types of cooling systems:

Once-through cooling systems (Figure 12.38a)

Open recirculating or closed cycles with cooling towers (Figure 12.38b)

Closed recirculating systems (Figure 12.38c)

A choice among these depends on quantity and quality of water available, water temperature, type of process plant, heat exchanger size, and means for water disposal.

12.6.3.1 Once-Through System

In a once-through cooling-water system, the water is pumped from a water source and supplied through the equipment and discharged. This is used where cheap supplies of water in large quantity are available (e.g., river, lake, sea). The water may be hard or soft, may contain dissolved solids, iron and manganese, silica, oil, dissolved gases, chlorides, micro-or macroorganisms,

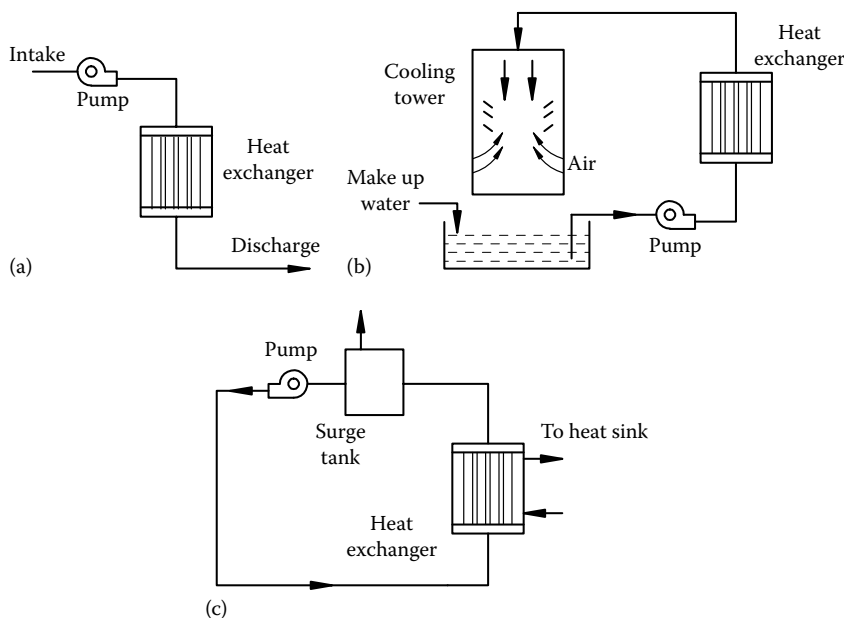


FIGURE 12.38 Cooling-water system. (a) Once through, (b) open recirculating, and (c) closed circulating.

and suspended matter such as turbidity, dirt, clay, silt, etc., either singly or jointly. The major advantage of this system is low initial cost. The possibilities of water treatment of the large quantity of water handled for corrosion control are practically nil due to economic reasons and environmental regulation on discharges [90]. Only upstream filtration or inoculation with dispersing agents or ferrous sulfate dosing can be considered. Additionally, cathodic protection control may be instituted.

12.6.3.2 Open Recirculating Systems

Open recirculating systems continuously reuse the water that passes through the heat exchanger. Circulated water can be drawn from spray ponds or cooling tower basins. Open recirculating cooling systems are oxygen saturated and may contain a high level of dissolved solids. The dissolved oxygen in water accelerates most corrosion processes. In closed-loop systems, the dissolved oxygen is consumed over time and no longer poses a corrosion risk. For open-loop systems, however, the continued exposure to air allows oxygen to dissolve into the coolant. Therefore, open-loop systems often suffer more corrosion problems compared to closed units. This type of system requires large quantities of treated fresh makeup water because of the high evaporation losses. The intensive contact between the cooling water and air, as well as the solar radiation, stimulates the growth of algae and microorganisms. The treatment of cooling water of this system calls for the following measures [90]:

- Monitoring and control of pH
- Adding a corrosion inhibitor
- Adding an algae-destroying agent
- An additive (stabilizer) to prevent calcium carbonate precipitations
- Possible makeup water treatment
- Partial filtration

12.6.3.3 Closed Recirculating Systems

Closed recirculating systems continuously recirculate the same water. This system has little water loss and is free from algal growth. Because there are no evaporation losses, the requirement for makeup water is minimal, and the mineral content remains essentially constant. However, corrosion by-products can foul the heat exchanger. Hence, fouling deposits should be removed periodically by suitable offline cleaning methods. The completely closed cycle represents the ideal possibility for a clean and effective water treatment. Corrosion control by inhibitors is the most important control measure.

12.6.4 CORROSION CONTROL METHODS FOR COOLING-WATER SYSTEMS

In principle, damage to cooling systems can be checked in many ways:

1. Proper material selection
2. Cooling-water system design
3. Continuous water treatment system
4. Use of inhibitors
5. Ferrous sulfate dosing
6. Protective coatings
7. Cathodic protection
8. Passivation
9. Biological control
10. Scale control
11. Systematic cleaning

Corrosion control measures such as protective coating and cathodic protection, biological control, and various scale control measures have been discussed earlier in this chapter. Additional measures to control scaling as a foulant were discussed in Chapter 9, Fouling.

12.6.4.1 Material Selection

Corrosion control by means of cooling-water design should take into account two possibilities: (1) the water treatment program and (2) selection of corrosion-resistant material. Proper material selection involves selecting a material that can be exposed to the cooling water without the danger of corrosion. The question of whether corrosion in cooling systems can be checked by means of suitable material selection at the design stage or by instituting a permanent water treatment program when the unit starts functioning must be considered on the basis of corrosion damage and economic considerations [90]. On the material side, cupronickel and titanium are costly compared to carbon steel, aluminum and copper, and certain copper alloys such as brasses. On the water treatment side, continuous online treatment including dosing of chemicals and additives involves money, especially when the quantity of water handled is large, as in once-through cooling-water system. The objectives of such a strategy are to ensure that the operating costs are minimized throughout the life of the plant. This can be established by studying the following technical and economic considerations [33]:

- Estimated life of candidate tube materials from trials, manufacturer's literature, and experience
- Predicted number of outages and associated costs
- Number of retubes required
- Capital costs of materials and retubing costs
- Heat transfer efficiency and thermal performance effects
- Compatibility with other cooling-water system materials
- Cooling-water system design

In planning a heat exchanger cooled by natural water, the first step is to obtain the following information about the water [32]:

- Analysis of water
- Water temperature upon entry
- Solids content
- Content of organic matter including H_2S

Certain guiding principles to be considered at the design stage are as follows [90,92]:

- Empty the cooling system completely when in the standstill condition. Many more cases of corrosion have taken place when the cooling system was at a standstill than in operation.
- When welding on the cooling-water side, care should be taken to avoid protruding weldments or crevices as a result of unsatisfactory weld penetration.
- Design sealing in such a way that seals cannot lift on the water side.
- Narrow gaps should be avoided in the design stage. If this is not possible, the gap width should preferably be large (>0.5 mm).
- The flow velocities should be neither too low nor too high. Except for coppers and brasses, maintain water velocities as high as practical. Velocities of 3–8 ft/s are the minimum desired.
- Beware of galvanic coupling.
- Always maintain vents on top tubesheets.
- Locate water inlet and outlet nozzles on the shellside as near the tubesheets as possible to reduce "dead pockets."
- Place water on the tubeside, and the process liquid on the shellside.

Additional guidelines were given by Forchhammer [32] as follows:

In the construction phase, check the integrity of system components for tightness with low-chloride water free from solids.

To form the first oxide layer in the tubes, the unit should run several weeks without interruption.

12.6.4.2 Water Treatment

By water treatment, we either remove the aggressive components to a great extent or add specific chemicals to the water. In this way, both corrosion and fouling are avoided. Water treatments can be generally subdivided into three main groups:

1. Chlorination/settling/filtration to remove the turbidity and microorganisms
2. Water softening to remove water hardness
3. Partial or full demineralization for the removal of hardness and all dissolved salts

Removal of hardness is effected by (1) the cold lime process, (2) the sodium cation exchange process, (3) demineralization, and (4) the acid process.

12.6.4.3 Corrosion Inhibitors

The use of corrosion inhibitors is one of the foremost methods of controlling corrosion in a cooling-water system. The main effect that corrosion inhibitors have in aqueous ferrous systems is to reduce the initial corrosion rate sufficiently to allow the gamma-iron oxide passive film to form and, in some cases, to take part directly in film formation. Corrosion control by inhibitors has been discussed in the section on corrosion prevention and control.

12.6.4.4 Ferrous Sulfate Dosing

It is difficult to form protective films on copper alloys such as aluminum brass while subjected to brackish water and seawater. The addition of ferrous sulfate offers a possibility of building up a protective film and diminishing the danger of erosion–corrosion [104]. Experience has shown that the best results are obtained under the following conditions [32,93]:

Ferrous sulfate dosing, tube cleaning by sponge balls or brushes, and deaeration must start working from the very beginning, as startup after the first corrosion attack has occurred cannot stop corrosion.

Cleanliness of tube surfaces is especially important while commissioning.

A water temperature above 8°C–10°C.

Association with continuous tube cleaning.

Solution injected at water box inlet.

Chlorination stopped during injection, since investigation shows that a synergistic effect between iron and chlorine can lead to rapid attack and early failure.

The optimum dose to form the protective film depends on the temperature and content of organic matter in seawater. Typical injection values range between 0.5 and 1 ppm of Fe^{2+} 1 h/day or continuous injection of 0.02–0.05 ppm [105].

12.6.4.5 Passivation

Donohue et al. [95] discussed passivation of clean metal surfaces in cooling-water system through pretreatment of surfaces by application of a polyphosphate–surfactant combination and prefilming with chromate or nonchromate zinc polyphosphate or polymer polyphosphates. Chromate, nitrite, and orthophosphate (in the presence of oxygen) can promote passivity on clean iron surfaces.

12.6.5 INFLUENCE OF COOLING-WATER TYPES ON CORROSION

Cooling waters may vary from the purest of distilled or demineralized waters to full-strength seawater. High-conductivity chloride-bearing water, saturated with oxygen, leads to concentration cell corrosion or deposit attack on almost all alloys, ferrous or nonferrous, regardless of their inherent resistance to water.

12.6.5.1 Fresh Water

In general, if fresh water is involved, no serious corrosion problems are likely to arise. Fresh waters are normally handled with tubes of arsenical copper, inhibited admiralty brass, inhibited aluminum brass, aluminum bronze, red brass, or copper–nickels [102].

12.6.5.2 Seawater Corrosion

Some of the key findings of 20 years of corrosion research on seawater are as follows [106]:

1. The presence of dissolved oxygen in seawater and desalting brine is the single most important factor in determining the performance of mild steel, low-alloy steels, copper alloys, and, to some extent, stainless steels.
2. For optimum performance of mild steel, low-alloy steel, copper alloys, and stainless steels in seawater and brine, the pH should be as high as possible without promoting calcium carbonate scale or precipitation of magnesium hydroxide.
3. Low-alloy steels can perform well, as much as 30% better than mild steels in typical desalination environments.

In seawater applications, arsenical copper and red brass 85:15 would not be used for tubes in power plant condensers cooled with seawater. Inhibited aluminum brass tubes are most widely used. Aluminum bronze (5%) would be suitable for acid-polluted seawater. Copper–nickels will give better service than other tubes in polluted waters [102].

12.6.5.3 Brackish Waters

Brackish waters are a mixture of seawater and fresh water. They are generally less corrosive than seawater except where contaminated with industrial wastes and sewage. In general, when contaminants are present, aluminum brass and aluminum bronze prove more satisfactory than other alloys. In the absence of contaminants, arsenical admiralty and the cupronickel alloys are satisfactory. The choice between these two depends upon water velocity [31]. Among ferrous alloys, the ferritic stainless steels, such as type 410 (12% chrome) and type 430 (18% chrome), are unsatisfactory in brackish cooling water due to insufficient alloy content to repair the passive films that are broken down by the deposit attack. Hence, the use of straight chrome stainless steel is to be avoided in brackish cooling water [92].

12.6.5.4 Boiler Feedwaters

Generally, boiler feedwaters are only slightly corrosive toward copper and its alloys due to deaeration and water treatment. The selection of the proper alloy is generally based on the temperature and pressure requirements. Copper and arsenical admiralty brass are most commonly used for the low-pressure and low-temperature feedwater heaters, whereas cupronickels are used for the higher-pressure and higher-temperature heaters because of their higher creep strength [31].

12.6.6 CORROSION OF INDIVIDUAL METALS IN COOLING-WATER SYSTEMS

Aluminum: For aluminum, pitting is the most common form of corrosion. Pitting is usually produced by the presence of halide ions, of which chloride (Cl^-) is most frequently encountered in liquid cooling loops. Waters containing small amounts of the heavy metal ions such as iron, copper, and mercury will also cause pitting corrosion. Waters that are essentially neutral offer no problem.

Pitting of aluminum may be experienced beneath deposits. Use of the Alclad products often makes aluminum usable in cooling-water services like automobile radiators and adds an inhibitor when using water with aluminum to maintain a clean heat transfer surface.

Copper and its alloys: Copper and its alloys are very important heat exchanger materials because of their generally high thermal conductivity and resistance to corrosion in waters. When copper corrodes, it is more often degraded by general corrosion than by pitting. General corrosion will often result when copper is exposed to ammonia, oxygen, or fluids with high sulfur content. Another source of corrosion affecting copper is dissolved salts in the fluid, such as chlorides, sulfates, and bicarbonates. Copper alloys too can suffer corrosion under deposits, erosion–corrosion, dezincification of the brasses, and sulfide attack.

Steel: The corrosion of steel in cooling water is governed mainly by the oxygen availability and water composition [92]. Corrosion attack is overcome by addition of inhibitors and cathodic protection.

Austenitic stainless steel: The corrosion resistance of chromium–nickel (18-8) stainless steels depends upon a passive surface film. This film is readily penetrated by the chloride ion. For this reason, the stainless steels are subject to pitting and SCC from the chlorides. The pitting rate of the 18-8 alloys is usually quite low in closed-cycle cooling waters and in inhibited water associated with periodic tube cleaning.

Superferritics and superaustenitics: These steels have been primarily developed for seawater applications.

Titanium: Titanium is an ideal material for seawater applications in the absence of fouling deposits.

12.6.7 FORMS OF CORROSION IN COOLING WATER

A wide spectrum of materials is used on the cooling-water side. These materials are affected by most forms of corrosion discussed earlier. The corrosion prevention and control measures discussed therein are equally applicable to combat cooling-water corrosion also. Various forms of corrosion, susceptible alloys or susceptible components, and remedial measures are mentioned very briefly in the following paragraphs.

12.6.7.1 Uniform Corrosion

All alloys, especially copper and its alloys, suffer uniform corrosion, which is controlled by pH adjustment, inhibition, and proper material selection.

12.6.7.2 Galvanic Corrosion

Less noble metals experience galvanic corrosion. Susceptible components are tubesheets, water boxes, bolts, and flanges. Alloys close to one another in the galvanic series should be used. Use insulation to separate the active metal from the noble metal.

12.6.7.3 Pitting Corrosion

Susceptible materials include aluminum, stainless steels, and copper alloys. Pitting corrosion takes place on the tubesheet and tube wall in the form of pits after local destruction of the protective film by deleterious chemical species such as chlorine or mercury ions. Additionally, at water speeds below about 3 ft/s, suspended solids tend to settle on the tube and may initiate pitting corrosion under the deposits due to differential cell action [104]. Causes for pitting on the tubeside include the following [32]:

- Nonhomogeneous tube surface
- Irregular sludge deposition from the water
- Local concentration of salt during standstill

- Putrescent products with H_2S
- Dry-out of protective layer followed by peeling off
- Small metallic inclusions like oxides and sulfides
- Foreign matter, such as sand, oil, barnacles, etc.

Most of these potential causes of pitting corrosion can be avoided by tube cleaning or removing chloride ions and others involving the water chemistry; use steel containing Mo.

12.6.7.4 Crevice Corrosion

Crevice corrosion takes place in the area between the tube and the tubesheet, at gasketed joints, beneath deposits, and at bolt holes. Proper tube expanding will prevent the circumferential tube crack in tube-to-tubesheet joints. While pitting and crevice corrosion normally occur fairly uniformly throughout the heat exchanger, the attack may predominate on the bottom of the internal surfaces of the tubes if mud or sediment has collected there and promotes crevice corrosion [26].

12.6.7.5 Stress Corrosion Cracking

Most common metals and alloys are susceptible to SCC. This form of corrosion takes place at the tube-to-tubesheet expanded joints and at U-tube bends.

12.6.7.6 Corrosion Fatigue and Fretting Wear

All alloys, at the tube and baffle interface, and tubes at midspan due to collision between adjacent tubes are susceptible to corrosion fatigue and fretting wear.

12.6.7.7 Erosion of Tube Inlet

When the cooling water contains large quantities of suspended abrasive solid particles, any protective film formed is rapidly removed and the tube is liable to thin [104]. The most common tube failures due to erosion–corrosion from impingement attack are discussed in Section 12.2.3.7. The problem of inlet-end tube erosion (erosion–corrosion) in high-pressure feedheaters with carbon steel tubes and condensers with copper alloy tubes is discussed here. In general, the factors governing erosion–corrosion in feedwater heaters are [107] the following:

- Feedwater velocity (turbulence)
- pH value of feedwater (protective layer of Fe_3O_4)
- O_2 content of feedwater (corrosion)
- Feedwater temperature (protective layer)

It has been suggested that at the usual pH values (9–9.5) and O_2 , contents (0.002–0.007 ppm), and with water chambers and tube inlets designed to promote uniform water flow, erosion at the tubes and tube inlets can be eliminated, even for high water velocity [107].

12.6.7.8 Dezincification

Tubes and tubesheets made of brasses are susceptible to dezincification.

12.6.7.9 Microbiologically Induced Corrosion

All but the higher nickel–chromium alloys and titanium have been found to be subject to microbiological corrosion. This form of failure was discussed earlier.

12.6.8 MATERIAL SELECTION FOR CONDENSER TUBES

The following main physical and chemical parameters revealed by water analysis are used to select the tube materials [105]: TDS, total suspended solids, sand content, chloride content, sulfur and NH_3 , content, and biochemical oxygen demand.

12.6.9 OPERATIONAL MAINTENANCE OF CONDENSERS AND FEEDWATER HEATERS

Important corrosion control measures for the maintenance of condensers and feedwater heaters include the following [108]:

1. The tubesheets are clad with stainless steel
2. All water boxes are fitted with sacrificial anodes
3. Depending on the water quality, ferrous sulfate is dosed
4. Upstream filtration ensures clean filtered water in association with an online cleaning system using sponge rubber balls to permit continuous cleaning of the tubes
5. Excessive biological growth is controlled with chlorine
6. Operation and shutdown based on many years of experience ensure correct treatment of the heat exchangers

12.6.10 PREVENTING CORROSION IN AUTOMOTIVE COOLING SYSTEMS

Water and water-and-glycol solutions are common heat transfer fluids used in automotive cooling systems. Quality of water needs to be considered to prevent corrosion. Chloride is corrosive, and use of tap water should be avoided if it contains more than 100 ppm of chloride. Hardness of water also needs to be considered because it forms scale on the metal surfaces. Deionized water or demineralized water is highly recommended in order to avoid chloride and scale buildup. A suitable corrosion inhibitor must be added to the deionized or demineralized water.

12.7 MATERIAL SELECTION FOR HYDROGEN SULFIDE ENVIRONMENTS

Degradation of steel by hydrogen sulfide (H_2S) is now recognized as a serious problem in pipelines handling sour crude oil or gas in petroleum refinery equipment. Sour environments are defined as fluids containing water as a liquid and hydrogen sulfide. Hydrogen sulfide-resistant steels for pressure vessels or pipelines in sour environments are often required to have both resistance to H_2S cracking and low-temperature toughness. Because iron-base alloys are principal materials of construction, these alloys have been the focus of study for many years. An important reference on hydrogen effects on steels is Warren [109].

12.7.1 EFFECTS OF HYDROGEN IN STEEL (ASTM/ASME A/SA 516 GRADES 60/65/70)

Hydrogen sulfide below dew point forms complex sulfides on metallic surfaces. Monoatomic hydrogen can then diffuse into the material and recombine to form molecular hydrogen at voids, laminations, microcracks, or discontinuities around inclusions, generating extremely high pressures [109]. As an interstitial element in the body-centered cubic (bcc) ferrite lattice, hydrogen can cause a number of mechanical problems for steels. It gives rise to blistering and cracking. It stiffens the metal, impairing its ductility. Spontaneous cracking of materials is possible if the material hardness is not limited. The effect of hydrogen absorbed by carbon steels is well known and extensively reported in the literature. The primary effects are the following:

1. Hydrogen-induced cracking (HIC) producing stepwise cracks to the metal surface
2. HE due to loss of ductility under a slow tensile loading
3. Cracking in high-strength or high-hardness steels, known as hydrogen induced stress corrosion cracking (HSCC) or sulfide stress corrosion cracking (SSCC)
4. Blister formation originating at nonmetallic inclusions, known as hydrogen blistering

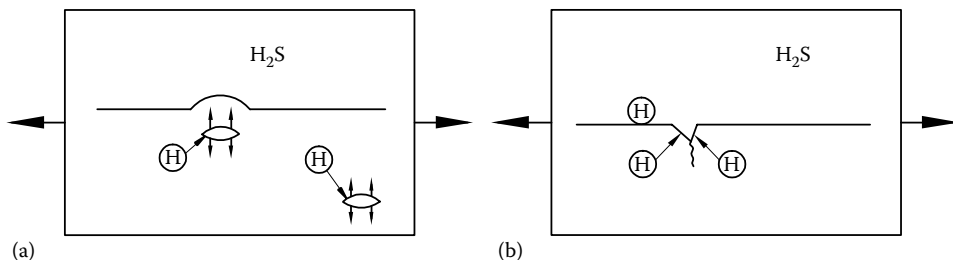


FIGURE 12.39 Schematic of hydrogen damage. (a) Blister and (b) HIC.

Figure 12.39 shows the effects of hydrogen on steel except HE. Requirements for the manufacture of pressure vessels for wet H_2S source are discussed in WRC Bulletin 374 [110]. It has been shown that the sound attenuation in hydrogen damaged steel can be used to quantify the level of degradation of the material's mechanical property and knowing this, the remaining life of an affected plant can be estimated.

12.7.2 SOURCES OF HYDROGEN IN STEEL

HE and other phenomena influenced by hydrogen require a susceptible material and a fabrication method or a process capable of promoting the entry of hydrogen into the steel. Before hydrogen can enter a metal, it must first adsorb on the metal surface as atomic hydrogen. Nascent or newly created atomic hydrogen can result from various operational processes [109]: initial melting, electroplating, acid pickling, high-pressure hydrogen environment, decomposition of gases (e.g., ammonia), hydrogen pickup during welding, corrosion with cathodic liberation of hydrogen, and hydrogen from cathodic protection. Acid corrosion, particularly in the presence of a “poison” such as sulfide, cyanide, arsenic, selenium, or antimony ions, promotes the entry of the hydrogen into the steel [3]. The nascent atomic hydrogen (H°) charged into the steel as a by-product of the corrosion reaction rather than gas evolution as H_2 is shown by the following equation [109]:



12.7.3 HYDROGEN-INDUCED CRACKING

Some of the atomic hydrogen evolved by the corrosion reaction diffuses into the steel and forms molecular hydrogen, which accumulates at discontinuities, principally inclusion metal interfaces [111]. When the internal pressure due to the molecular hydrogen buildup exceeds a critical level, HIC is initiated. It is recognized that HIC can occur in sour environments in the absence of external stress. Cracking can proceed along segregated bands containing lower temperature transformation products such as bainite and martensite. Cracking tends to be parallel to the surface but can be straight or stepwise.

12.7.3.1 Stress-Oriented Hydrogen-Induced Cracking

When the small hydrogen-induced cracks or stepwise cracks coalesce perpendicular to the axis of an applied tensile stress on a relatively low-hardness steel having a ferrite–pearlite microstructure, the phenomenon is known as stress-oriented hydrogen-induced cracking (SOHIC) [112]. It occurs around weldments in fabricated steel vessels and process equipment [113]. According to Kane et al. [113], the combination of stress concentration, residual tensile stress, hardness, and microstructure makes these locations prone to SOHIC.

12.7.3.2 Susceptibility of Steels to HIC

Metallurgy of steels: The susceptibility of steels to cracking is influenced strongly by inhomogeneities such as the nonmetallic inclusions, their shape and distribution, and segregation of alloying elements [111]. Voids, MnS stingers, oxide inclusions, and laminations present in the steels act as nucleation sites for blistering, stepwise cracking, and SOHIC [112].

Environmental factors: Environmental factors such as H_2S partial pressure, pH of the solutions, and other phenomena relevant to the absorption of hydrogen by the steel influence HIC [111].

Strength and alloying elements: The risk of cracking is increased by increasing the strength of steel as well as the partial pressure of H_2S .

Microstructure: In general, a nonhomogeneous microstructure such as pearlite banding can give high susceptibility to HE.

12.7.3.3 Prevention of HIC

Steels with resistance to HIC embody the following features:

1. The effects of segregation can be minimized by restricting the levels of elements such as C, S, Mn, and P and controlled rolling of plates, which enables high strengths to be obtained at low carbon levels. For wet H_2S systems, there are recommendations to use low-sulfur steels that have been qualified for HIC and SOHIC resistance using laboratory testing. The sulfur content is generally reduced to below 0.01%. In other words, use HIC-resistant steel that can reduce the effects of HIC in a wet H_2S or sour service environment. HIC resistant steels are fine-grain pressure vessel steels manufactured via electric arc furnace with desulfurization, dephosphorization, ladle refining, and vacuum degassing to provide an ultraclean and homogeneous steel.
2. Addition of calcium or rare earth metals to globularize the sulfide inclusions.
3. Low levels of oxide inclusions.
4. Mn is beneficial in improving toughness by refining the ferrite grain size, and therefore a minimum level of Mn must be maintained. Long elongated inclusions such as type II MnS are particularly favorable sites for crack initiation. Spheroidal inclusions are less susceptible to crack initiation except when they are in clusters [111].
5. Freedom from segregation so as to avoid bainitic or martensitic bands.
6. Reduced corrosion effects.
7. Periodic inspection of the wet H_2S refinery equipment even if it is made from HIC-resistant steel, as these steels may not provide total resistance to HIC and SOHIC in actual refinery service [113].
8. Use of stainless steel and stainless steel clad material for severe wet H_2S service as an alternative to reduce inspection and reinspection requirements. Clad products can be used for repair, replacement, or new construction [113].

12.7.4 HYDROGEN EMBRITTLEMENT

12.7.4.1 Mechanism of Hydrogen Embrittlement

HE involves two issues: (1) The crack has been formed by hydrogen and (2) the toughness changes because the material has been embrittled. Atomic hydrogen dissolved in steel can interfere with the normal process of plastic deformation. HE does not affect all metallic material. The most vulnerable are (i) high-strength steels, (ii) titanium alloys, and (iii) aluminum alloys. If a steel of initially limited notch ductility (e.g., a steel hardened to 175,000 psi) is charged with atomic hydrogen and strained at the appropriate rate and temperature, it cannot plastically deform to locally accommodate a notch or stress raiser. Consequently, a crack is initiated and brittle fracture can take place.

Severely cold-worked ferritic steels and welded steels of higher carbon content are similarly vulnerable to HE [109]. Plain carbon or alloy steels heat-treated to tensile strengths greater than 120,000 psi or hardness $>R_c$ 22–23 are susceptible to HE. However, the other forms of hydrogen damage such as hydrogen attack or hydrogen blistering are associated with unhardened low-alloy or carbon steel [14]. The susceptibility of steels to HE increases with [109] the following:

1. Increasing strength level (hardness) of the steel
2. Increasing amounts of cold work (plastic deformation)
3. Increasing residual or applied stress

The risk of cracking initiation should be reduced by avoiding notch effects, whether geometrical or “metallurgical.” Metallurgical notches include the formation of hard zones in the parent metal and in the weld areas. Crack propagation can be controlled by limiting operating and/or residual stresses and also by PWHT.

12.7.4.2 Hydrogen Embrittlement of Steel Weldments

Susceptible steels: Steels with weldments susceptible to HE include pressure vessel quality steels with 0.25%–0.35% C, in plate thickness 1–2 in (25.4–50.8 mm), such as ASTM A515 and A516 [109].

Prevention of hydrogen embrittlement and cracking of welds: Welding-related measures for the prevention of hydrogen cracking, such as use of dry electrode, joint surface cleanliness, sufficient preheat, and PWHT, will be helpful to prevent HE of welds. Hardness testing of weldments is a necessary requirement for most typical operating refinery or chemical plant environments. Limiting the weld hardness of carbon and low-alloy steels as indicated in NACE Standard MR-01-75 [114] can generally avoid this problem. Hardness of completed P-1 welds should be 200 BHN or less.

12.7.5 HYDROGEN-ASSISTED CRACKING

Hydrogen-assisted cracking, also known as hydrogen sulfide stress corrosion cracking (HSCC), is a special case of localized HE where the nascent atomic hydrogen is supplied to the steel as a by-product of the corrosion reaction. Acid corrosion of steel in the presence of a “poison” such as sulfide, cyanide, arsenic, antimony, or selenide ions is a prime example [109]. Examples for HSCC include sulfide stress cracking and cyanide stress cracking of hardened steel.

12.7.5.1 Prevention of HSCC

HSCC can be controlled or prevented by (1) selecting a material that is resistant to process corrosion and (2) avoiding the formation of hard and brittle microstructures. These two aspects are discussed next.

Material selection: HSCC can be controlled or prevented by selecting a material that is resistant to process corrosion; that is, if there is no corrosive attack on the material, there can be no cathodic liberation of hydrogen and, hence, no localized HE.

Avoiding the formation of hard and brittle microstructures: HSCC poses problems in weld zones. It can occur especially in HAZs with high hardness [111]. Attention should be given to composition, hardenability, and welding procedures to avoid the formation of hard and brittle microstructures. The occurrence of HSCC observed typically in high-strength steels having yield strength higher than 90,000 psi (620 MPa) is currently mitigated by imposing a restriction of maximum hardness of 22 Re or 225–235 BHN. Nevertheless, countermeasures similar to those described for the prevention of HIC are necessary to prevent HSCC in HAZ even with relatively low hardness [111].

12.7.6 HYDROGEN BLISTERING

Hydrogen blistering is a mechanism that involves hydrogen damage of unhardened steels near ambient temperature [14]. The blister originates at nonmetallic inclusion or other internal defects such as voids, laminations, or microcracks. Blistering requires a vulnerable material and a fabrication method or process condition that promotes the entry of atomic hydrogen into the steel as a by-product of the corrosion reaction rather than gas evolution as H_2 .

12.7.6.1 Susceptible Materials

Blistering is usually confined to the lower strength grades of steel, with tensile strength 70,000–80,000 psi, and Re 22 or less hardness, rimmed or semikilled steels because of laminations, and free machining steels with extensive sulfide or selenide stringers that can serve as blister sites.

12.7.6.2 Prevention of Blistering

Some of measures suggested by Warren [109] for the prevention of blistering include the following:

1. Selection of steel: (a) Where blistering is a concern, calcium-treated and argon-blown steels with 0.010% S maximum offer optimum resistance, (b) steels fully killed by silicon additions are preferable to aluminum-killed steel, (c) avoid susceptible steels such as rimmed, semikilled, and free machining steels, (d) hot-rolled or annealed material is preferable to cold-rolled material, and (e) apply cladding, lining, or protective coating with a more corrosion-resistant material.
2. Quality control and inspection of steel: To minimize blistering at planar defects, such as laminations and inclusion aggregates, steel plate should be ultrasonically inspected as per ASTM standards E114 and A578.
3. Venting of multilayer vessels.

12.7.6.3 Detection of Blisters in Service

Surface blisters may be detected by (1) visual inspection or by hand touch, (2) wet fluorescent magnetic particle inspection, (3) ultrasonic inspection to detect internal blisters within the steel, and (4) acoustic emission testing for locating active sites of SSC, HIC, and SOHIC [113]. Inspect both internal and external surfaces, including the less obvious items such as repair patch plate and unvented attachments (e.g., lifting lugs and support legs).

12.7.6.4 Correction of Blistered Condition in Steel Equipment

If blisters have jeopardized the vessel integrity, cut out the blistered areas and replace with ultrasonically inspected plate. Vent the blisters by careful drilling from the outside of the vessel. Avoid ignition of hydrogen within the blister; do not torch cut [109].

12.7.7 PRESSURE VESSEL STEELS FOR SOUR ENVIRONMENTS

Plates for Pressure Vessels in sour gas service are normally constructed of low-carbon steel ASME SA 516-70 normalized to ASTM Specification A300.

12.7.8 HIC TESTING SPECIFICATION

HIC testing is performed as per the standards of NACE TM-02-84 [115]. Refer to Figure 12.40 for the various parameters evaluated by this test method. Testing frequency by the manufacturer is one plate of each thickness rolled from each heat of steel. Melting practices by Lukens, one of the leading manufacturers of A 516-70, are mentioned here [116]. All “HIC-Tested A 516” steels are produced to the Lukens Fineline Double-O Two or more restrictive requirements, which utilize

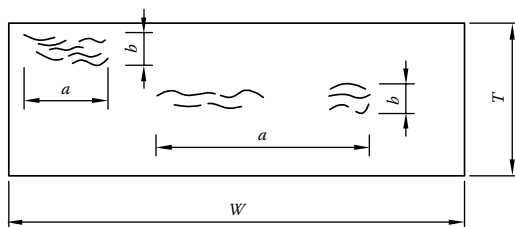


FIGURE 12.40 Determining hydrogen-induced cracking (HIC) resistance (NACE specification TM-02-84). Test specimen and crack dimensions to be used in calculating the following: crack sensitivity ratio (CSR) = $\frac{\Sigma(a \times b)}{(W \times T)} \times 100\%$; crack length ratio (CLR) = $\frac{\Sigma a}{W} \times 100\%$; crack thickness ratio (CTR) = $\frac{\Sigma b}{T} \times 100\%$ where a = crack length; b = crack thickness; W = section width; and T = test specimen thickness. Note: in the past CSR has been calculated by some investigators as $(\Sigma a \times \Sigma b)/(W \times T)$, which is simply the product of CLR \times CTR (i.e., $\Sigma a/W \times \Sigma b/T$). This does not give the same value as $\Sigma(a \times b)/(W \times T)$.

various maximum sulfur levels and calcium treatment for inclusion shape control. Phosphorus and oxygen level maximums may also be accepted. Two classes of chemistry control and HIC test guarantee levels may be specified for crack length ratio (CLR), crack thickness ratio (CTR), and crack sensitivity ratio (CSR).

REFERENCES

1. Munger, G. C., Corrosion as related to coatings, in *Corrosion Prevention by Protective Coatings*, National Association of Corrosion Engineers, Houston, TX, 1984, pp. 19–46.
2. Uhlig, H. H., Environmental effects on properties of materials, *Mater. Protect. Perform.*, July, 23–27 (1972).
3. *Resistance to Corrosion*, 4th edn., Inco Alloys International, Huntington, WV, 1985.
4. Jarman, R. A. and Shreir, L. L., The basic principles of corrosion, *Weld. Metal Fabr.*, October, 370–379 (1987).
5. Baboian, R. ed., *Corrosion Tests and Standards—Application and Interpretation*, ASTM, New York, 1995.
6. Brosilow, R., Can you weld to avoid corrosion, *Weld. Design Fabr.*, September, 67–74 (1982).
7. Roser, W. R. and Rizzo, F. E., The corrosion engineer's look at passive alloys, *Mater. Protect. Perform.*, April, 51–54 (1973).
8. Silverstein, M. R., Cooling water, *Client. Eng.*, August, 84–94 (1971).
9. Fontana, M. G. and Greene, N. D., *Corrosion Engineering*, 2nd edn., McGraw-Hill, New York, 1978.
10. Uhlig, H. H., *Corrosion and Corrosion Control*, John Wiley & Son, Inc., New York, 1963.
11. L. S. Van Delinder, ed., Atmospheric corrosion, in *Corrosion Basics—An Introduction*, NACE, Houston, TX, 1984, pp. 221–222.
12. Merrick, R. D., Design of pressure vessels and tanks to minimize corrosion, *Mater. Perform.*, January, 29–37 (1987).
13. AL-6XN® Alloy, Allegheny Ludlum Steel Corporation, Pittsburgh, PA.
14. Kobrin, G., Materials selection, in *Metals Handbook*, 9th edn., Vol. 13, Corrosion, American Society for Metals, Metals Park, OH, 1987, pp. 321–337.
15. Elliott, P., Design details to minimize corrosion, in *Metals Handbook*, 9th edn., Vol. 13, Corrosion, American Society for Metals, Metals Park, OH, 1987, pp. 338–343.
16. Freedman, A. J. and Boies, D. B., Causes and cures for cooling water corrosion problems, *Petroleum Refiner*, April, 157–162 (1961).
17. Stanfield, B. M., Polarization cell: A common cure for corrosion, *Mater. Protect. Perform.*, March, 32–35 (1973).
18. Steven, P. L., General corrosion, in *Metals Handbook*, 9th edn., Vol. 13, Corrosion, American Society for Metals, Metals Park, OH, 1987, pp. 80–103.
19. L. S. Van Delinder, ed., Open pitting corrosion, in *Corrosion Basics—An Introduction*, NACE, Houston, TX, 1984, p. 95.

20. Speidel, M. O. and Atrens, A. eds., *Brown Bowri Symposium on Corrosion in Power Generating Equipment*, Plenum Press, New York, 1983.
21. Lichtenstein, J., Fundamentals of corrosion causes and mitigation, *Mater. Perform.*, March, 29–31 (1978).
22. Wilten, H. M., Microscope speeds diagnosis of refinery corrosion, *Hydrocarb. Process. Petrol. Refiner*, 40, 151–280 (1961).
23. Asphahani, I. A., Corrosion resistance of high performance alloys, *Mater. Perform.*, 19, 33–43 (1980).
24. Uhlig, H. H., Discussion—An essay on pitting, crevice corrosion, and related potentials, *Mater. Perform.*, August, 35–36 (1983).
25. Dexter, C. S., Localized corrosion, in *Metals Handbook*, 9th edn., Vol. 13, Corrosion, American Society for Metals, Metals Park, OH, 1987, pp. 104–122.
26. Syrett, B. C. and Coit, R. L., Causes and prevention of power plant condenser tube failures, *Mater. Perform.*, February, 44–49 (1983).
27. Jarman, R. A. and Shreir, L. L., Corrosion of jointed structures—Part II, *Weld. Metal Fabr.*, 445–449 (1987).
28. Henthorne, M., Understanding corrosion, *Chem. Eng.*, Desk Book Issue, December 4, 19–33 (1972).
29. Guide to selecting engineered materials, metals, polymers, ceramics, composites, *Adv. Mater. Process.*, 137(6), (1990).
30. Stengerwald, R., Metallurgically influenced corrosion, in *Metals Handbook*, 9th edn., Vol. 13, Corrosion, American Society for Metals, Metals Park, OH, 1987, pp. 123–135.
31. *Condenser Tube Manual*, Bridgeport Brass Company, CT, USA, 1964.
32. Forchhammer, P., Results of damage research on corrosion failures in heat exchangers, *Heat Transfer Eng.*, 5, 19–32 (1984).
33. Woodward, A. R., Howard, D. L., and Andrews, E. F. C., Condensers, pumps and cooling water plant, in *Modern Power Station Practice, Vol. C, Turbines, Generators, and Associated Plant* (D. J. Littler, E. J. Davies, H. E. Johnson, F. Kirkby, P. B. Myerscough, and W. Wright, eds.), Pergamon Press, New York.
34. Crook, P., Practical guide to wear for corrosion engineers, *Mater. Perform.*, February, 64–66 (1991).
35. L. S. Van Delinder, ed., Erosion-corrosion, in *Corrosion Basics—An Introduction*, NACE, Houston, TX, 1984.
36. Yokell, S., *A Working Guide to Shell and Tube Heat Exchangers*, McGraw-Hill, New York, 1990.
37. TEMA, *Standards of Tubular Exchanger Manufacturers Association*, 9th edn., Tubular Exchanger Manufacturers Association, Tarrytown, NY, 2007.
38. L. S. Van Delinder, ed., Cavitation, in *Corrosion Basics—An Introduction*, NACE, Houston, TX, 1984.
39. Dawson, J. L., Shih, C. C., Gearey, D., and Miller, R. G., Flow effects on erosion-corrosion, *Mater. Perform.*, April, 57–60 (1991).
40. Dawson, J. L. and Shih, C. C., Corrosion under flowing conditions—An overview and model, *CORROSION/90*, Paper No. 21, Houston, TX, 1990.
41. 90/10 Copper-nickel vs Sea-Cure stainless steel—A functional comparison of two condenser tube alloys, FineweldR tube, Technical Letter, Olin Brass.
42. Syrett, B. C., Corrosion in fossil fuel power plants, in *Metals Handbook*, 9th edn., Vol. 13, Corrosion, American Society for Metals, Metals Park, OH, 1987, pp. 985–1010.
43. Theus, G. J. and Daniel, P. L., Corrosion in steam generating systems, in *Brown Bowri Symposium on Corrosion in Power Generating Equipment* (M. O. Speidel and A. Atrens, eds.), Plenum Press, New York, 1983, pp. 185–231.
44. Irving, B., Stress corrosion cracking: Welding's no. 1 nemesis, *Welding J.*, December, 37–40 (1992).
45. Kedzie, D. P. and Rizzo, F. E., The corrosion engineer's look at stress corrosion, *Mater. Protect. Perform.*, October, 53–56 (1972).
46. Logan, H. L., *The Stress Corrosion Cracking of Metals*, John Wiley & Sons, New York, 1966.
47. McIntyre, D. R. and Dillon, C. P., *Guidelines for Preventing Stress Corrosion Cracking in the Chemical Process Industries*, Publication 15, Materials Technology Institute, Columbus, OH, 1985, pp. 8–14.
48. Berry, W. E., Stress corrosion cracking—A nontechnical introduction to the problem, DMIC Report 144, Defence Metals Information Centre, Battelle Memorial Institute, Columbus, Ohio, January 6, 1961.
49. Pement, F. W., Wilson, I. L. W., Reynolds, S. D., and Fletcher, W. D., Microanalytical characterization of stress corrosion cracking in power plant heat exchanger tubing, *Mater. Perform.*, 26–39 (1977).
50. Craig, B., Environmentally induced cracking, in *Metals Handbook*, 9th edn., Vol. 13, Corrosion, American Society for Metals, Metals Park, OH, 1987, pp. 145–149.
51. Brown, B. F., *Stress Corrosion Cracking in High Strength Steels and in Titanium and Aluminum Alloys*, Naval Research Laboratory, Washington, DC, 1972.

52. Parkins, R. N., An overview: Prevention and control of stress corrosion cracking, *Materials Performance*, Vol. 24, No. 8, NACE, Houston, TX, August 1985, pp. 9–24.
53. McIntyre, D. R., How to prevent stress corrosion cracking in stainless steels—Part I, in *The Chemical Engineering Guide to Corrosion Control in the Process Industries* (R. W. Greene, ed.), McGraw-Hill Publications Co., New York, 1986, pp. 4–7.
54. Partridge, E. P., Hydrogen damage in power boilers, *Trans. ASME, J. Eng. Power*, July, 311–320 (1964).
55. Glaser, W. and Wright, I. G., Forms of corrosion—Mechanically assisted degradation, in *Metals Handbook*, 9th edn., Vol. 13, Corrosion, American Society for Metals, Metals Park, OH, 1987, pp. 136–144.
56. L. S. Van Delinder, ed., Corrosion fatigue, in *Corrosion Basics—An Introduction*, NACE, Houston, TX, 1984.
57. Tatnall, R. E., MIC: A corrosion engineer's enigma? *Mater. Perform.*, August, 56 (1988).
58. Pollock, W. I., What is MIC? *Mater. Perform.*, August, 56 (1988).
59. Scott, P. J. B., Goldie, J., and Davies, M., Ranking alloys for susceptibility to MIC—A preliminary report on high-Mo alloys, *Mater. Perform.*, January, 55–57 (1991).
60. Kobrin, G., Corrosion by microbiological organisms in natural waters, *Mater. Perform.*, July, 38–42 (1976).
61. Pope, D. H., Duquette, D. J., Arland, J. H., and Wayner, P. C., Microbiologically influenced corrosion of industrial alloys, *Mater. Perform.*, April, 14–18 (1984).
62. Pope, D. H., Soracco, R. J., and Wilde, E. W., Studies on biologically induced corrosion in heat exchanger system at the Savannah River Plant, Aiken, SC., *Mater. Perform.*, July, 43–50 (1982).
63. Borenstein, S. W., Microbiologically influenced corrosion of austenitic stainless steel weldments, *Mater. Perform.*, January, 52–54 (1991).
64. Borenstein, S. W., Microbiologically influenced corrosion failures of austenitic stainless steel welds, *Mater. Perform.*, August, 62–66 (1988).
65. Puckorius, P. R., Massive utility condenser failure caused by sulfide producing bacteria, *Mater. Perform.*, December, 19–22 (1983).
66. Powell, C. A., Preventing biofouling with copper alloys, Copper Development Association, Publication No. 113, U.K., 1995.
67. Tuthill, A. H., Guidelines for the use of copper alloys in seawater, *Mater. Perform.*, September, 12–22 (1987).
68. Schutz, R. W., A case for titanium's resistance to microbiologically influenced corrosion, *Mater. Perform.*, January, 58–61 (1991).
69. Boffardi, P., Control of environmental variables in water-recirculating systems, *Metals Handbook*, 9th edn., Vol. 13, Corrosion, American Society for Metals, Metals Park, OH, 1987, pp. 487–497.
70. Poole, J. S. and Bacon, H. E., Monitoring cooling water systems, *Mater. Protect. Perform.*, March, 16–25 (1972).
71. Borenstien, S. W. and Lindsay, P. B., Microbiologically influenced corrosion failure analyses, *Mater. Perform.*, March, 51–54 (1988).
72. Gooch, T. G., Stress corrosion cracking of welded austenitic stainless steel, *Weld. World*, 22, 64–76 (1984).
73. Corrosion of weldments, in *Metals Handbook*, 9th edn., Vol. 13, Corrosion, American Society for Metals, Metals Park, OH, 1987, pp. 344–368.
74. Swindeman, R. W. and Gold, M., Developments in ferrous alloy technology for high-temperature service, *Trans. ASME, J. Pressure Vessel Technol.*, 113, 133–140 (1991).
75. Collins, J. A., Effect of design, fabrication and installation in the performance of stainless steel equipment, *Corrosion*, 11(1), pp. 27–34, (1955).
76. Landrum, J. R., Designing equipment for corrosion resistance, in *Materials Engineering, Part I: Selecting Materials for Process Equipment* (K. J. McNaughton, ed.), McGraw-Hill, New York, 1980, pp. 157–164.
77. Shabin, H. I., Corrosion inhibition in a cooling water system, *Corros. Prevent. Control*, February, 9–12 (1982).
78. L. S. Van Delinder, ed., Inhibitors, in *Corrosion Basics—An Introduction*, NACE, Houston, TX, 1984, p. 127.
79. Freedman, A. J., Cooling water technology in the 1980s, *Mater. Perform.*, November, 9–16 (1984).
80. Kaplan, R. I. and Ekis, E. W., Jr., The on-line removal of iron deposits from cooling water systems, *Mater. Perform.*, November, 40–44 (1984).
81. Boffardi, B. P., Corrosion control of industrial cooling water systems, *Mater. Perform.*, November, 17–24 (1984).

82. Beynon, E., Cooper, N. R., and Haningan, H. J., Cooling system corrosion in relation to design and materials, in *Engine Coolant Testing: State of the Art, ASTM STP 705* (W. H. Ailor, ed.), American Society for Testing and Materials, Philadelphia, PA, 1980, pp. 310–326.
83. Hinchcliffe, D. and Town, J., Experience with nonchromate cooling water treatment (case histories), *Mater. Perform.*, September, 36–38 (1977).
84. Lula, R. A., Compiler, *Source Book on the Ferritic Stainless Steels*, American Society for Metals, Metals Park, OH.
85. Debold, T. A., Select the right stainless steel, *Chem. Eng. Prog.*, November, 38–43 (1991).
86. Saunders, E. A. D., *Heat Exchangers: Selection, Design and Construction*, Addison Wesley Longman, Reading, MA, 1989.
87. Llewellyn, D. T., *Steels, Metallurgy and Applications*, Butterworth-Heinemann, Oxford, U.K., 1992.
88. Munger, C. G., Corrosion prevention by protective coatings, *Mater. Perform.*, April, 57–58 (1987).
89. L. S. Van Delinder, ed., Coatings and linings, in *Corrosion Basics—An Introduction*, NACE, Houston, TX, 1984, pp. 47–48.
90. Weber, J., Corrosion and deposits in cooling systems—Their causes and prevention, *Sulzer Tech. Rev.*, 3, 219–232 (1972).
91. McGill, W. A. and Weinbaum, M. J., Aluminum vapor diffused steels resist refinery corrosion, *Mater. Protect. Perform.*, July, 28–32 (1972).
92. Asbaugh, W. G., Corrosion in heat exchangers using brackish water, *Chem. Eng.*, 5 July, 146–152 (1965).
93. Paren, J. and Pouzenc, C., Design of power station condensers, *GEC Alsthom Tech. Rev.*, 6, 19–38 (1991).
94. Singbell, D. and Garner, A., Anodic protection to prevent the stress corrosion cracking of pressure vessel steels in alkaline sulfide solutions, *Mater. Perform.*, April, 31–36 (1987).
95. Donohue, J. M. and James, E. W., Passivation and its application in cooling water systems, *Mater. Perform.*, October, 34–36 (1977).
96. Britton, C. F. and Tofield, B. C., Effective corrosion monitoring, *Mater. Perform.*, April, 41–44 (1988).
97. Schweitzer, P. A., ed., *Corrosion and Corrosion Protection Handbook*, 2nd edn., Marcel Dekker, New York, 1983.
98. Somm, E., Schlachter, W., and Schwarzenbach, A., Power generating equipment, in *Brown Bowri Symposium on Corrosion in Power Generating Equipment* (M. O. Speidel and A. Atrens, eds.), Plenum Press, New York, 1983, pp. 3–25.
99. Chance, R. L., Walker, M. S., and Rowe, L. C., Evaluation of engine coolants by electrochemical methods, in *Engine Coolant Testing: Second Symposium, ASTM STP 887* (R. E. Beal, ed.), American Society for Testing and Materials, Philadelphia, PA, 1986, pp. 99–122.
100. Cramer, S. D. and Covino, Jr., B. S. eds., *Corrosion: Fundamentals, Testing, and Protection*, Volume 13A, 10th edn., ASM International, Metals Park, OH, 2003.
101. Garverick, L., ed., *Corrosion in Petrochemical Industries*, 1st edn., ASM International, Metals Park, OH, 1994.
102. Tracy, A. W., Nole, V. F., and Duffy, E. J., Water analyses and their functions in selecting condenser tube alloys, *Trans. ASME, J. Eng. Power*, July, 329–332 (1965).
103. Cotton, I. J., Oxygen scavengers—The chemistry of sulfide under hydrothermal conditions, *Mater. Perform.*, March, 41–47 (1987).
104. Lockhart, A. M., Reducing condenser tube corrosion at Kincardine Generating Station with ferrous sulphate, *Proc. Inst. Mech. Eng.*, 495–512 (1964–1965).
105. Sato, S., Nagata, K., and Yamauchi, S., Evaluation of various preventive measures against corrosion of copper alloy condenser tubes by sea water, *NACE National Conference*, Unpublished Paper No. 195, Toronto, Ontario, Canada, 1981.
106. Schreiber, C. F. and Coley, F. H., *CORROSION/75*, Paper No. 36, NACE, Houston, TX, 1975.
107. Sonnenmoser, A., Design and operation of large high pressure feedheaters, *Brown Boveri Rev.*, 7/8–73, 352–359.
108. Sonnenmoser, A. and Wollschlegal, P., The design of extremely watertight condensers, *Brown Boveri Rev.*, 65, 505–515 (1978).
109. Warren, D., Hydrogen effects on steel, *Mater. Perform.*, January, 38–46 (1987).
110. Sauvage, M., Requirements for the manufacture of pressure vessels for wet H₂S service, *WRC Bulletin*, 374, 72–81.
111. Terasaki, F., Ohtani, H., Ikeda, A., and Nakanishi, M., Steel plates for pressure vessels in sour environment applications, *Proc. Inst. Mech. Eng.*, 200, 141–158.
112. Mirabal, E., Bhattacharjee, S., and Pazos, N., Carbonate-type cracking in an FCC wet gas compressor station, *Mater. Perform.*, July, 41–45 (1991).

113. Kane, R. D. and Cayard, M. S., Improve corrosion control in refining processes, *Hydrocarb. Process.*, November, 129–142 (1995).
114. *Methods and Controls to Prevent In-Service Cracking of Carbon Steel (P-I) Welds in Corrosive Petroleum Refinery Environments*, NACE RP-04–72 (1976 Rev.), National Association of Corrosion Engineers, Houston, TX, 1976.
115. Evaluation of pipeline and pressure vessel steels for resistance to hydrogen induced cracking, NACE Standard TM-02-84, NACE International, Houston, TX, 2011.
116. Tech. Services Bull. No. 778: A516 Steels Including HIC-Tested A516 Steels, Rev. November 1992, Lukens Steel Company, Coatesville, PA, 1992.

BIBLIOGRAPHY

- Bostwick, T. W., Reducing corrosion of power plant condenser tubing, *Corrosion*, Vol. 17, pp. 12-19, August (1961).
- Brittalan, O. J., Declerks, D. H., and Urhis, F. H., Linings, *Chem. Eng.*, Deskhook Issue, 12 October, 127–135 (1972).
- Coburn, S. K., ed., *Corrosion Source Book*, American Society for Metals, Metals Park, and National Association of Corrosion Engineers, Houston, TX, 1984.
- Craig, B., Forms of corrosion: Introduction, in *Metals Handbook*, 9th edn., Vol. 13, Corrosion, American Society for Metals, Metals Park, OH, 1987, p. 79.
- Greene, R. W., ed., *The Chemical Engineering Guide to Corrosion*, McGraw-Hill, New York, 1986.
- McDonald, M. M., Corrosion of brazed joints, in *Metals Handbook*, 9th edn., Vol. 13, Corrosion, American Society for Metals, Metals Park, OH, 1987, pp. 876–886.
- McNaughton, K. J., ed., *Materials Engineering, Part I: Selecting Materials for Process Equipment; Part II: Controlling Corrosion in Process Equipment*, McGraw-Hill, New York, 1980.
- Pludek, R. V., *Design and Corrosion Control*, Macmillan, London, U.K., 1977.

13 Material Selection and Fabrication

13.1 MATERIAL SELECTION PRINCIPLES

In engineering practice, the selection of materials of construction depends on the equipment being designed and the service requirements imposed on them. Selection of materials involves the thorough understanding of their availability, source, lead time, product forms, and size. In simple terms, the following factors are to be considered while selecting the materials for heat exchanger and pressure vessel components:

1. Compatibility of the materials with the process fluids
2. Compatibility of the materials with the other component materials
3. Ease of manufacture and fabrication by using standard methods like machining, rolling, forging, forming, and metal-joining methods such as welding, brazing, and soldering
4. Material strength and ability to withstand operating temperature and pressure
5. Cost
6. Availability

While selecting materials, one has to balance many requirements; these requirements include the following [1]:

- Expected total life of plant or process
- Expected service life of the material
- Reliability (safety, hazard, and economic consequences of failure)
- Material costs
- Fabrication costs
- Maintenance and inspection costs
- Availability in required size, shape, thickness, and so on, and delivery time
- Return on investment

Materials are selected based on past experience, corrosion tests, the literature, and the recommendations of material suppliers. The direct measure of success in material selection and fabrication is reflected in the behavior of the equipment in service. In order to assure safe, reliable, and uninterrupted service with monetary benefits, proper attention must be given to material selection commencing from the design stage and must continue through fabrication, installation, and maintenance. Once on stream, the equipment should be monitored for specified performance. With this background information, the logical sequence of material selection for the construction of pressure vessels and heat exchangers is discussed next.

13.1.1 MATERIAL SELECTION

While selecting materials for the construction of heat exchangers and pressure vessels, the following points may be considered for the desired performance and the life of the equipment [2]:

1. Review of operating process
2. Review of design
3. Selection of material
4. Evaluation of material
5. Specification

Finally, the material should be cost-effective. Do cost–benefit analysis for an optimum material selection.

13.1.2 REVIEW OF OPERATING PROCESS

The foremost step in the material selection is the thorough review of the process environment and equipment operating conditions like operating temperature, pressure, and phases of the fluids. The following operating data are required by the design engineer [3]:

- Environment—nature and composition of fluid handled, water chemistry, steam quality, constituents/concentration of a solution, conductivity, pH, aeration, impurities, and so on
- Pressure—average and range, constant or cyclic, internal and external loadings
- Temperature—average and range, constant or variable, thermal gradients, and thermal shock
- Velocity—flow rate, linear velocity, nominal and range, degree of agitation, turbulence, etc.

In addition to operating temperature and pressure, other factors such as the start-ups and shutdowns, intermittent operation, transients and pressure surges, and momentary failure of the system must be considered for the satisfactory performance of a material.

13.1.3 REVIEW OF DESIGN

After the review of the operating process, the type or design of the equipment and various assemblies and subassemblies, size, complexity, and criticality in service should be considered. Applicability of various fabrication techniques like forging, machining, welding, soldering, brazing, etc., is considered.

13.1.4 SELECTION OF MATERIAL

The selection of proper materials for wetted and nonwetted parts, pressure and nonpressure parts, and equipment support is an important design step. Material Standards like American Society for Testing and Materials (ASTM), DIN, BS, ISO, and JIS give data on a large number of ferrous and nonferrous materials. Many of these materials have been adopted in the Pressure Vessel Codes by the country of origin in the Material Standards. Data from these material standards are generally restricted to the physical properties, such as Young's modulus, yield strength, minimum tensile strength, maximum permissible operating temperature, elongation, coefficient of expansion, etc. But codes and standards do not explicitly express the suitability of the materials for the intended service environment, either internal or external. These details must be provided by the corrosion engineer or many sources are to be referred.

13.1.4.1 ASME Code Material Requirements

13.1.4.1.1 Pressure Parts

All materials used for pressure-retaining parts must meet the ASME Code (ASME Boiler and Pressure Vessel Code, Section II—Material Specifications, Part A—Ferrous Materials, Part B—Nonferrous Materials, Part C—Welding Rods, Electrodes, and Filler Metals, and Part D—Material

Properties, 1992, American Society of Mechanical Engineers, New York) general requirements for materials. Only code-specified material shall be used in the vessel construction or repair. The manufacturer should deliver the material after thorough inspection, with the chemical composition and metallurgy and properties as stipulated in the relevant specification. The allowable stresses for the different code-permitted materials should not be exceeded.

13.1.4.1.2 *Nonpressure Parts*

Materials used for nonpressure parts shall be compatible with the process fluids and ambient environment, and/or shall be of weldable quality.

13.1.4.2 **Functional Requirements of Materials**

Function of equipment has frequently been equated with long, trouble-free service [4]. Selected material has certain functional requirements, which ultimately reflect on the function of the equipment. Functional requirements of materials given in Ref. [5] have been enlarged to include additional information and presented in Table 13.1.

With reference to functional requirements, the following features/parameters are discussed.

1. Strength
2. Fatigue strength
3. Brittle fracture
4. Toughness
5. Creep
6. Resistance to temperature
7. Heat and corrosion
8. Corrosion resistance
9. Hydrogen attack
10. Fabricability

13.1.4.2.1 *Strength*

While the term “strength” applies to many mechanical properties, it most commonly refers to tensile strength and yield strength. These strengths are best understood by examining a stress–strain curve. Stress–strain diagram (schematic) for few of the heat exchanger materials is given in Figure 13.1. Other related strengths are compression, bending (flexural), shear, and torsional strength. It is better to use high-strength materials to keep the thickness of parts less.

TABLE 13.1
Functional Requirements of Materials

Characteristics	Functional Requirements
Strength	Tensile, torsion, bending, compression, shear, buckling, fatigue, creep, rupture strength, etc.
Physical properties	Design may require certain properties peculiar to the materials (thermal, electrical, acoustic, magnetic, etc.), coefficient of thermal expansion, thermal conductivity, modulus of elasticity, specific gravity (strength to weight ratio).
Temperature resistance	Low temperature: subzero and cryogenic; intermediate temperature; elevated temperature.
Geometric stability	Stiffness of the structure, effect of sustained loading, etc.
Toughness	Ability to cope with a sudden load, impact, low-temperature operation, etc.
Fabricability	Ability to be formed, forged, machined, joined, ease of heat treatment, etc.
Corrosion resistance	Compatibility of the materials with the process fluids, with the other component materials in contact; resistance to ambient environment; passivity; hydrogen attack.
Wear and abrasion	Loss of surface oxide film (passive films), which is helpful in corrosion resistance.

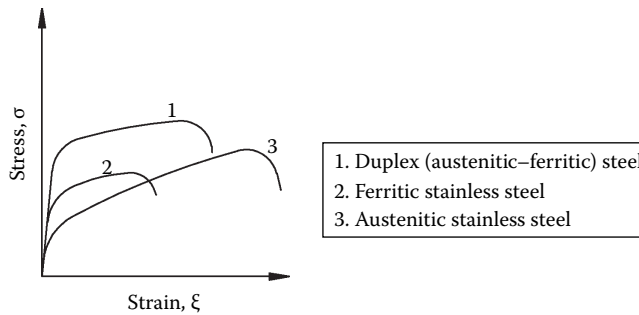


FIGURE 13.1 Stress–strain diagram of few common ferrous materials for heat exchanger.

13.1.4.2.2 Fatigue Strength

Fatigue is the failure of a metal by fracture when it is subjected to cyclic stress. The usual case involves rapidly fluctuating stresses that may be well below the tensile strength. As stress is increased, the number of cycles required to cause failure decreases. A stress–number of cycles (S–N) curve is conventionally plotted for a metal as shown in Figure 13.2a (creep curve is shown adjacently). The stress is plotted against the logarithm of the number of cycles. There is usually a stress level below which no failure will occur, for a specified large number of cycles, and this is called the endurance limit. Since the stress limits that are required to prevent distortion and bursting keep the nominal stresses at or below the endurance limit, the possibility of fatigue failure is almost always associated with discontinuities, notches, shocks, residual stresses, etc.

Fatigue failures are most likely to occur at welded joints, which, by virtue of their design, give rise to significant stress concentration effects. Some of the material and design characteristics favorable to fatigue resistance are as follows [6]: increased tensile strength via alloying or heat treatment, minimum workpiece thickness, polished surfaces, low design stress, smaller grain size, absence of metallurgical discontinuities and residual stresses, presence of surface compressive stress, minimizing environments conducive to corrosion and fatigue, and avoidance of metallic coating, such as Cr, Ni, or Cd plating, which can reduce fatigue strength due to microcracks in the plating. For pressure vessels, hydrostatic pressures that exceed the yield strength of the metal can relieve residual stresses and can improve fatigue strength [7].

13.1.4.2.3 Brittle Fracture

Brittle fracture is the term given to describe failure by rapid crack propagation at nominal stress below the yield strength. Brittle fracture has been mostly observed in body-centered cubic (bcc) crystal structure metals, notably ferritic steels, in which complete rupture takes place under certain

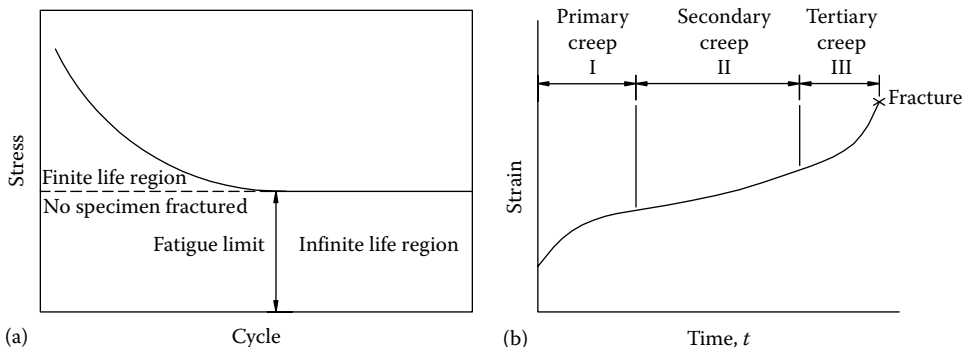


FIGURE 13.2 (a) S–N curve (stress–number of cycles of stress reversals) and (b) creep curve.

conditions at stress levels not only below the ultimate tensile strength but also even lower than yield strength. The conditions associated with brittle fracture of steels include the following [8,9]:

1. A preexisting defect
2. The presence of residual and/or applied tensile stress across the defect, which is more serious if triaxial
3. A sufficiently low temperature
4. Several metallurgical factors—deoxidation practice, composition, rolling practice, and subsequent heat treatment [8]

As per ASME Code Div-1, the following pressure vessel components must be considered in brittle fracture evaluation: shell, manways, head, reinforcing pad, nozzle, tubesheet, flanges, cover plates, etc. The minimum design metal temperature (MDMT) is the lowest temperature at which the component is designed to have adequate fracture toughness. Each component must be evaluated separately for impact test requirements based on its material thickness and MDMT.

The subject of brittle fracture is of interest to the designers of long-life pressure vessels for the following reasons [9]:

1. Even if the vessel is to operate at an elevated temperature, where the brittle fracture is not to be expected, there is a danger of failure of the vessel during the preservice cold hydrostatic test; another case of practical importance is the temper embrittlement of Cr–Mo steels, a condition caused by elevated temperature service after a long time in refinery service.
2. Cyclic variations of load and temperature during long service may enlarge small initial defects to the critical size and result in brittle fracture during start-up, shutdown, or cold periodic tests.
3. In the special case of nuclear vessels, neutron bombardment can produce large increase in the transition temperature (TT).

In welded structures, brittle fractures invariably initiate from weld defects. Weldment failure due to brittle fracture is dependent on through-thickness toughness, the critical defect/notch size, residual welding strains, mechanical constraints, grain size, inclusion content, and temperature [10]. It must not be overlooked that a normally ductile material can fail in a brittle manner at locations where complex and triaxial stress fields exist [11].

Measures to minimize brittle fracture: Brittle fracture may be prevented by selecting a notch-tough material and avoiding notches. The following design practices will help to minimize brittle fracture [12]:

1. Eliminate all defects, which is impracticable.
2. Employ design stress less than required for propagation, but this may not be justified economically.
3. Select materials whose TT is below operating temperature.
4. If the structures are not stress relieved, residual stresses may be superimposed on the applied stress and will cause local yielding in the vicinity of a defect and thus initiate a brittle crack.

Some simple practices to minimize the chance of nonservice failure have been suggested by Bravenec [13]. These recommendations include [13] the following:

1. Sheared and torched edges should be conditioned by grinding prior to forming.
2. Warm forming should be used whenever the ambient temperature is less than 75°F.
3. Material selection should meet end use requirements and code requirements; however, it must be recognized that code stipulates only a minimum standard.

13.1.4.2.4 Toughness

A material's toughness is its ability to absorb energy and deform plastically before fracture, and the amount of energy absorbed during both the deformation and the fracture is the measure of toughness. Toughness rather than strength is the most important low-temperature mechanical property. Notch toughness is influenced by chemical composition, microstructure, grain size, grain flow pattern, section size, hot and cold working temperature, method of fabrication, and surface conditions like carburization and decarburization [6].

Basic tests: The most common toughness tests use notched specimens and measure either notch toughness, usually by an impact test, or fracture toughness, which is measured at a relatively low strain rate. Impact tests reveal low-temperature strength, lack of ductility, and brittleness, and these tests are being particularly relevant to ferritic materials, which may show a transition from ductile-to-brittle (DBT) behavior. Two commonly used methods are the Charpy and Izod tests.

Charpy V-notch, CVN (ASTM E23): The Charpy V-notch test is considered the most appropriate because a part or structure will generally fail due to a notch or other stress concentration. This test is used to obtain absorbed energy, lateral expansion, and fracture appearance from a 10 mm × 10 mm × 55 mm piece of a material subjected to impact loading. The specimen has a 0.254 mm (0.010 in.) radius notch. Test results given in foot-pounds measure the capacity to absorb energy and thus signify the material ability to resist failure at points of local stress concentration.

Precracked Charpy V-notch: This is a test often used as a correlative measure of fracture toughness.

Nil-ductility transition temperature, NDTT (ASTM E208): This test defines the temperature at which a small flaw will initiate when subjected to yield loads. It is used with a Charpy V-notch test to establish the reference fracture toughness in ASME Code.

Fracture toughness: The notch toughness approach does not work well with high-strength steels and nonferrous metals because of the gradual transition from ductile to brittle behavior [6]. Also it is felt that CVN test results alone are not reliable enough to predict whether an existing crack of a certain size will grow slowly, causing leakage before failure, or fail catastrophically under the very slow strain rates likely to be encountered in liquefied natural gas (LNG) containment vessels [14]. In these situations, fracture toughness value is used to assess metal's toughness, and the approach is known as fracture mechanics approach. Plane-strain fracture toughness, or K_{Ic} , values are used to calculate the critical crack size in a stressed component that can result in an abrupt failure. K_{Ic} values, unlike notch toughness values, are independent of test specimen shape [6].

Fracture toughness (ASTM E399 and E813): These are the only two tests that yield "ASTM valid" fracture toughness values. E399 is for linear-elastic fracture toughness K_{Ic} , and E813 is for the "J-Integral," which can be converted to K_{Ic} .

13.1.4.2.5 Creep

Creep is defined as slow deformation of material with time, with the deformation taking place at elevated temperatures without increase in stress. Creep curve is shown in Figure 13.2b. At room temperature, creep is nonexistent in steel. Many pressure vessel steels have to operate in creep conditions, and the general basis of design is based on data from test specimens and involves the definition of stress below which failure will not occur within the expected life of the component. The phenomenon of creep is well understood, the basis of design is clear, and no special problems need be encountered. It is worth, however, sounding two notes of warning [15]:

1. If the design is poor so that unforeseen high local stresses occur, then the local creep deformation may exceed the creep ductility and lead to premature failure.
2. If the structures are not stress relieved, residual stresses may be superimposed on the applied stress and again lead to premature creep failure. This may well occur in welds around nozzles. It is thus important to remember that vessels operating under creep conditions should be stress relieved prior to service.

Creep test: Tests for resistance of a material to elevated temperature generally fall into three classes: short-time tests (tension, compression, bending, shear, torsion, and impact) run at elevated temperature, short-time tests run at room temperature after elevated-temperature exposure for various lengths of time, and longtime tests run at room temperature. Longtime strength tests, in turn, can be classified as constant load (creep, stress-rupture, and many fatigue tests) or constant deflection (stress relaxation and some fatigue tests) tests [6].

The standard test followed to determine creep is ASTM E139, “Standard practice for conducting creep, creep-rupture, and stress-rupture tests of metallic materials.” The Larsen–Miller parameter is considered reliable for using data from high-temperature tests to predict creep-rupture time. The Larson–Miller parameter P , used for predicting stress-rupture data for low-alloy steels is given by

$$P = 1.8T(k + \log t) \times 10^{-3}$$

where

T is temperature (K)

t is time in hours

k is a constant (≈ 20) for low-alloy steels

For temperature in $^{\circ}\text{R}$, eliminate the constant 1.8 in the equation.

13.1.4.2.6 Temperature Resistance

Temperature resistance of construction materials is discussed with reference to various temperatures of operation, since basic material behavior is intimately related to operating temperature. Accordingly, the temperature of operation is classified into the following four ranges:

1. Subzero and cryogenic operation
2. Low-temperature operation (up to 200°C)
3. Intermediate-temperature operation (200°C – 650°C)
4. High-temperature operation ($>650^{\circ}\text{C}$)

Subzero and cryogenic operation: A major requirement of materials for subzero applications is toughness at the handling temperature. Steels and nonferrous materials are used in cryogenic services for containment, handling, and transportation of liquefied gas and liquefaction of gases. Some metals display a marked loss of ductility in a narrow temperature range below room temperature or nil-ductility temperature (NDT). This is called the ductile–brittle transition temperature (DBTT). The application of metals below their NDT is avoided because of the danger created by brittle crack propagation. Below the NDT, very little energy is required for crack propagation [16].

Intermediate-temperature operation: The intermediate temperature category includes most of the vessels used in petroleum and petrochemical services. Here the most important consideration is that materials be used to best advantage. The principal criteria in this respect are design stress values, adequacy of design formulas, and ductility of material.

High-temperature operation: In high-temperature service, the materials operate in a pseudo-plastic or fully plastic state, and designs must be based on stresses that will keep the inelastic deformations below limits that would permit failure [12]. High-temperature design stress limits are established on the basis of longtime creep strength, as well as by the metal’s scaling resistance [17]. For the use of high-temperature applications, the selected materials should exhibit certain properties that are given in Table 13.2 [18]. At temperatures above 800°F (425°C), materials should be heat-resistant and must maintain corrosion resistance, mechanical strength, metallurgical stability, creep resistance, oxidation resistance, stress-rupture strength, toughness, and surface stability against combustion gas and chemicals handled [19].

TABLE 13.2**Mechanical Properties for High-Temperature Operation**

Tensile strength or yield strength

Creep and creep rupture strength

Thermal fatigue characteristics

Thermal shock characteristics

Temper embrittlement

Corrosion due to sulfides, high-temperature sulfidation for carbon steels above 260°C when sulfur content is above 0.2%

Metallurgical stability, grain growth, recrystallization, phase change, etc.

Resistance against surface oxidation and carburization

Precipitation of intermetallic phases at grain boundary, weld decay

Alloying elements for heat-resistant material: Heat-resisting materials must contain chromium for oxidation resistance. Cobalt, aluminum, silicon, and rare earths enhance the formation, stability, and tenacity of the oxide surface layer. Nickel provides strength, stability, toughness, and carburization resistance. Tungsten and molybdenum increase high-temperature strength [19].

Material groups and their service temperature: Approximate operating boundaries for various heat exchanger materials along with ceramic are shown in Chapter 6. For temperatures above 600°C, the following material groups are usually considered:

1. Ferritic steels with 17%–27% Cr and Mo addition
2. Austenitic high-temperature, high-strength steels (Cr–Ni–Mo steels having more than 8% Ni) like Type 321, 347, 316, and 310
3. Cast stainless steel (SS) heat-resistant alloys: HC, HK, HT, HP, HX
4. Solution-hardened nickel-base alloys with the addition of Cr and Fe, such as 800H, Incoloy 800HT, and 330
5. Precipitation-hardened nickel-base alloys with the addition of Cr, such as X-718 and X-750
6. Cobalt-base alloys: N-155, 188, L605, 25
7. Advanced ceramics and other highly refractory material (>1200°C)

Items 4–6 are often called superalloys.

Steels for high-temperature applications

1. Low-alloy steels for high-temperature service. C–Mo alloy steels, chromium–molybdenum alloy steels, and manganese–molybdenum–(nickel) alloy steels are regarded as steels for high-temperature service. When high-temperature strength (creep strength) is the principal consideration, molybdenum content in the steel composition is usually increased, but when high-temperature corrosion resistance is paramount, chromium content is increased. In the case of petroleum refinery equipment, which is subject to hydrogen attack, molybdenum and chromium are added to the steel to resist hydrogen attack [18].
2. SSs for elevated-temperature service. While carbon steels can be conveniently used at temperatures up to about 752°F (400°C) and low-alloy steels up to 1112°F–1200°F (600°C–650°C), their reliability ceases beyond these temperatures due to creep. While nickel-base and cobalt-base superalloys can withstand elevated temperatures without much loss of mechanical properties, their economics and availability may not permit their use for general applications such as in fossil fuel power plants operating in the middle temperature range of 1112°F–1247°F (600°C–675°C). For this temperature range, austenitic SS is preferred [20]. While selecting SSs for high-temperature applications, in addition to creep strength, consider high-temperature corrosion, oxidation, scaling and carburization, and

precipitation of secondary phases. Among the ferritics, E-Brite 26-1 (Allegheny Ludlum) appears to fill many gaps associated with the drawbacks of type 316 SS.

3. Developments in ferrous alloy technology for high-temperature service. During the past 25 years, new alloys with improved strength and corrosion resistance were developed for use in nuclear, fossil, and petrochemical industries. Specific groups of alloys include vanadium-modified low-alloy steels, 9Cr–1Mo–V steel, niobium-modified lean SSs, and high-chromium–nickel–iron alloys [21]. Alloying additions of vanadium, niobium, titanium, and nitrogen have been effective in strengthening both ferritic and austenitic alloys.

Nickel-base heat-resistant material: Inconel (nickel–chromium alloys) and Inco nickel–chromium alloys resist oxidation, carburization, and other forms of high-temperature deterioration. Typical heat-resistant alloys include (1) Inconel alloy 600, Inconel alloy 601, Inconel alloy 617, Inconel alloy 625, Inconel alloy 718, Inconel alloy X-750, and Inco alloy HX; (2) nickel–iron–chromium alloys and Inco nickel–iron–chromium alloys such as Incoloy alloy 800, and Incoloy alloy 800HT, and Incoloy alloy 825; and (3) other newer alloys such as 253MA, 556, HR-120, HR-160, 45TM 230, and 214. Table 13.3 shows material groups and their service temperatures.

Tests to evaluate steels at high temperature: Types of tests used to evaluate the mechanical properties of steels at elevated temperature include

- Short-term elevated temperature tests
- Long-term elevated temperature tests
- Short-term and long-term tests following long-term exposure to elevated temperature
- Fatigue tests (including thermal fatigue and thermal shock tests)
- Time-dependent fatigue tests
- Ductility and toughness tests

13.1.4.2.7 Heat and Corrosion

Alloys that have both heat and corrosion resistance are necessary for successful long-term operation of high-temperature processing equipment, particularly where the environment may be contaminated by corrosive constituents [22].

Mechanisms of high-temperature corrosion: Most high-temperature corrosion is due to the destruction of protective surface scale. Common impurities that increase the severity of high-temperature corrosion include carbon, nitrogen, halogens, sulfur and ash, and molten salt. High-temperature corrosion mechanisms include [22] the following: (1) carburization, which results in

TABLE 13.3
Material for High-Temperature Applications

Temperature Range	Alloys
Up to 1202°F (650°C)	Carbon steels having <1% Cr, or steels having 1%–12% Cr and Mo up to 1%.
1202°F–1472°F (650°C–800°C)	Carbon steels and low-alloy steels, Cr–Ni–Mo steels that can contain 12%–25% Cr and 5%–25% Ni, e.g., AISI type 310.
1472°F–1832°F (800°C–1000°C)	Steels with 17%–27% Cr and Mo addition, or higher Cr–Ni–Mo steels having more than 8% Ni.
1832°F–2192°F (1000°C–1200°C)	Higher alloyed nickel- or cobalt-base alloys with 18%–35% Cr; Al additions to these alloys improve resistance to high-temperature oxidation and cyclic oxidation.
>2192°F (1200°C)	Advanced ceramics and other highly refractory material.

Source: Compiled from Kane, R.D. and Cayard, M.S., *Hydrocarbon Process.*, November, 129, 1995.

internal carbide precipitates and embrittlement; (2) nitridization, which results in internal nitride precipitates and embrittlement; (3) formation of volatile metal halides on the surface; (4) deposits of hot ash and formation of molten deposits; and (5) corrosion due to the presence of sulfur in the process fluids, known as sulfidation. Alloy modifications to overcome these high-temperature corrosion problems involve the addition of Cr, Ni, Si, Al, and Mo, either individually or jointly. Various high-temperature corrosion mechanisms, the impurity or contaminant responsible for the corrosion, alloying modification, and process change to overcome the damage are discussed by Kane and Cayard [22].

13.1.4.2.8 Corrosion Resistance

Most common metals and their alloys, and nonmetals including plastic, glass, and graphite are attacked by environments such as atmosphere, water, or aqueous solutions. This destruction of metals and alloys is known as corrosion. With practically all commercial processes engineered on a continuous basis of operation, failure of equipment, heat exchangers, piping components, or other system components may mean costly shutdowns, expensive maintenance operations, and replacement of components. Therefore, the construction materials for pressure vessels and heat exchangers should have a well-defined corrosion rate in the service environment. Additional concern is corrosion due to surrounding atmosphere. Various forms of corrosion and their prevention and control are discussed in Chapter 12.

Selecting materials to resist corrosive conditions:

Favored combinations: In alloy selection, there are several natural metal and environment combinations. These combinations usually represent the maximum corrosion resistance at the lowest cost and should always be considered. A partial list includes the following combinations [3]:

- Carbon steels/concentrated sulfuric acid
- SSs/nitric acid
- Aluminum/nonstaining atmospheric exposure
- Copper–nickel/sea and brackish water
- Nickel and nickel alloys/caustic soda
- Monel 400/hydrofluoric acid
- Hastelloys/hot hydrochloric acid
- Titanium/hot strong oxidizing solutions
- Tantalum/most chemicals
- Additionally, consider the combination of superferritics/seawater

Avoid these combinations: There are some metal and environment combinations that are readily attacked by corrosion and must be avoided; a partial list is [3] as follows:

Ammonia and ammoniacal solutions/copper and copper alloys except copper–nickels
 Halogens and halides/austenitic SSs
 Mercury/aluminum and aluminum alloys, copper and copper alloys, Monel
 Sulfur and sulfides (at high-temperatures)/nickel and nickel alloys
 Caustic soda, other strong alkalies/aluminum

Sources of material data: To know the performance of a given material, the materials engineer must have information on corrosion of materials in various environments. There is a wide spectrum of corrosion data sources available. The following are identified as typical sources of corrosion data [4]:

1. Process licensors
2. Existing plants, that is plant experience
3. Pilot unit test data and plant corrosion monitoring
4. Technical publications

5. Internal databases collected by individual industrial companies (usually material suppliers), which may become available upon request to these companies—e.g., Inco Alloys, Allegheny Ludlum, Lukens Steels, US Steels, TIMET, RMI, Titanium Company, etc.
6. Publications of the trade

Other material sources include the following:

Publications from associations of common technical interest, like the National Association of Corrosion Engineers (NACE), ASTM, American Society for Metals (ASM), Aluminum Association (AA), Copper Development Association (CDA), Society of Automotive Engineers, etc.

Professional associations such as HTRI and HTFS

Government publications

Databases and abstract services, and expert systems

Corrosion Abstracts [23]

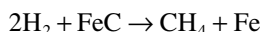
Corrosion Data Survey [24]

Corrosion failures: Even with careful material selection and corrosion prevention methods employed, there will always be a few unexpected failures, and we must have procedures for dealing with them. Unexpected corrosion failures result from one or more of the following [1]:

1. Defective material
2. Improper design
3. Abnormal operating conditions
4. Improper fabrication and inadequate inspection
5. Inadequate maintenance

13.1.4.2.9 Hydrogen Attack

Hydrogen attack is a damage mechanism that is associated with carbon and low-alloy steels exposed to hydrogen containing environments above 430°F–470°F (220°C–243°C) [25,26]. At room temperatures, even high-pressure hydrogen can be handled in steel cylinders. At higher temperatures, hydrogen diffused in a steel can react with carbon atoms to form methane gas as follows:



At elevated temperature/pressure, hydrogen can react with carbon in interstitial solid solution, resulting in initial decarburization, followed by destabilization of the carbides and the formation of methane bubbles at grain boundaries. Since methane cannot diffuse out of steel, its accumulation causes fissuring and blistering, resulting in loss of ductility, and in ultimate failure. Stable carbide compositions, morphologies, and distributions are required to reduce this problem [27].

Prevention of hydrogen attack: The only practical way to prevent hydrogen attack is to use steels that, based on plant experience, have been found to be resistant to this type of deterioration. The following general rules are applicable to hydrogen attack:

Carbide-forming alloying elements such as chromium and molybdenum, or carbide-stabilizing elements, such as chromium, titanium, and vanadium, increase the resistance of steel to hydrogen attack [28]. Molybdenum is four times as effective as chromium [29]. Vanadium is known to be a potent strengthener in low-alloy steels and to form a stable VC precipitate that is resistant to hydrogen attack [21].

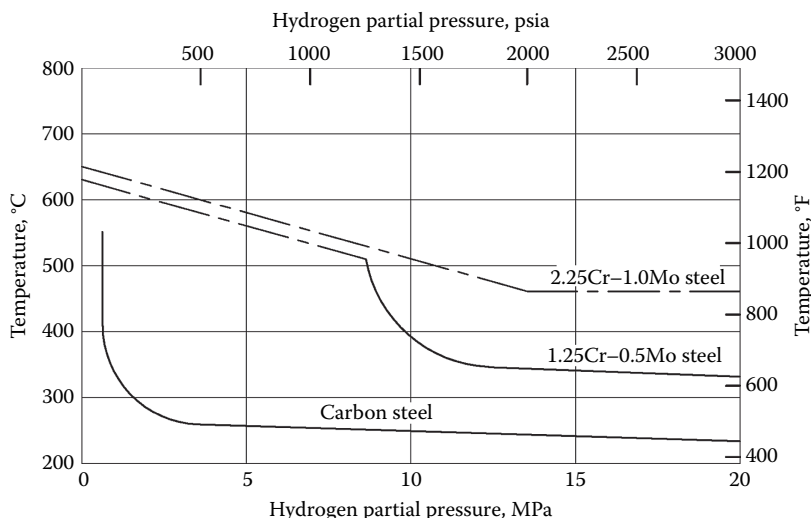


FIGURE 13.3 Nelson curve. (Adapted from API, *Steels for hydrogen service at elevated temperatures and pressures in petroleum refineries and petrochemical plants*, API Publication 941, Washington, DC, 1997.)

All of the austenitic SSs resist high-temperature hydrogen damage because of their high chromium content [25,28]. Hence, as an additional corrosion prevention measure, the inside surfaces of low-alloy steel vessels are often lined with SS overlay.

Heat-affected zones (HAZs) are more susceptible to hydrogen attack than the base metal or weld metal. Hence, limit the hardness of the HAZ.

Prevention of hydrogen attack: Nelson curves: Hydrogen attack is often an important consideration in the selection of steels for use in petroleum refinery equipment. Hydrogen attack on steel can best be avoided by following the operating limits on temperature, partial pressure of hydrogen, and alloy composition set forth by Nelson curves [30]. The Nelson curves are used throughout the world for the selection of materials for refinery applications. The curves are based on long experience in refinery operations rather than on laboratory studies. The curves are periodically revised by the API Subcommittee on Materials Engineering and Inspection, and the latest edition of API 941 [30] should be consulted.

The Nelson curves (partial) are shown schematically in Figure 13.3. Carbides of chromium and molybdenum are less reactive with hydrogen than iron carbide; therefore, Cr–Mo steels are more resistant to hydrogen attack than plain carbon steel. Austenitic SSs are completely resistant to hydrogen attack at all temperatures and hydrogen pressures.

13.1.4.2.10 Fabricability

Fabricability includes ease of forming, machining, welding and other metal-joining processes, and the subsequent heat treatment. Not all fabrication shops are technically qualified to handle the more sophisticated materials properly. Therefore, it is essential that a user know the capabilities of his or her fabricator [31]. Furthermore, advanced fabrication techniques require more sophisticated inspection criteria to judge the fabrication.

13.1.5 EVALUATION OF MATERIALS

Evaluation of materials involves testing the properties and metallurgy of the materials, fabricability, including metal joining, and the suitability of the material under lab tests or field tests. Material tests and material evaluation to resist corrosion are discussed further.

13.1.5.1 Material Tests

In addition to chemical analysis required to check the material composition, visual examination and mechanical tests of selected samples are usually called for to establish that the materials supplied are as per code requirements. Tests on welded samples are also needed to assess the quality of welds. Various mechanical tests employed for these purposes are the tensile test, bend test, impact test, etc. Metallographic examination of a sectioned specimen of the material provides information on the cleanliness of the material with respect to inclusions as well as metallurgical structure and grain size. In the case of welds, such examination may reveal weld defects such as inclusions, porosity, and cracks, and evidence of unsatisfactory welding techniques, etc. These tests are typically destructive in nature.

13.1.5.2 Materials Evaluation and Selection to Resist Corrosion

Materials engineers are increasingly using data from simulated environment tests as the basis for material selection to prevent corrosion including high-temperature corrosion. A partial list includes the following [22]: (1) corrosion coupons, (2) thermogravimetric analysis, (3) dynamic burner studies, (4) thermal cycling, (5) laboratory glassware tests, and (6) field tests.

13.1.6 Cost

13.1.6.1 Cost-Effective Material Selection

Two important strategies for selecting materials without paying attention to other factors are (1) minimum cost, that is selection of low-cost materials, followed by scheduled periodic replacements or follow corrosion control methods and (2) minimum corrosion, that is selection of the most corrosion-resistant material regardless of cost.

Low-cost material versus expensive material: The common belief that advanced construction materials are expensive is not entirely true. Manufacturers often deliberately select low-cost materials for their products, using the philosophy that manufacturing costs will be at a minimum and the product is therefore competitively priced. Plate steels with improved properties often cost a little more per unit weight, but the total vessel package is often less expensive. Savings are made possible because of the following factors [31]:

1. Less material required
2. Less welding time and less filler material required
3. Shorter heat-treatment cycles
4. Lower freight charges to destination
5. Easier handling requirements in the field during shipment and erection

Currently, the most common starting material is steel. About three-quarters of all pressure vessels are fabricated from carbon steel plate ranging from 0.2% to 0.3% in carbon content to provide easy forming and welding [32]. Although the strength-to-weight ratio of steel is not as favorable as those of certain aluminum alloys and titanium alloys, when combined with cost, steel often is quite favorable. The factors that favor steel as heat exchanger material are as follows:

Steel is relatively inexpensive

Available in standard shapes

Well-established mechanical properties, and these properties can be changed as a function of composition

Fabricable by a wide variety of methods

Easily joinable by a wide variety of welding processes, brazing, soldering to itself, and other materials

Its corrosion performance in most environments has been established, and techniques of protecting steel against corrosion in these environments are also widely developed

13.1.7 POSSIBLE FAILURE MODES AND DAMAGE IN SERVICE

Failure may take place in service either as a result of overloading, by the imposition of nominal service stresses that are above the safe stress of the material, or as a result of local deformation at stress concentration. Mostly, it is considered that the failure modes are based on the material properties in their final condition. Various possible modes of failure under pressure are [9] as follows:

1. Excessive elastic deformation and elastic instability
2. Plastic instability, deformation, and bursting
3. Brittle fracture
4. Fatigue failure
5. Creep deformation and creep rupture
6. Environmental damage such as corrosion and hydrogen damage

The great majority of service failures involve the initiation of cracking at defects situated in regions of stress concentrations. In welded structures, weld defects are quite common. It is therefore necessary not only to design against overload, but also to avoid the possibility of low-stress failures by brittle fracture, fatigue, creep, and corrosion. Excessive elastic deformation and elastic instability are overcome by the choice of material, limiting primary plus secondary stresses; plastic instability by limiting primary plus secondary stresses; and brittle fracture by proper material selection, manufacturing and inspection, verification of notch toughness, and so on. Failure due to general corrosion is a rarity in pressure vessels and heat exchangers since designers are well aware of the possibilities of general corrosion and normally introduce corrosion allowance and/or choose corrosion-resistant material. However, in certain environments, stress corrosion cracking (SCC) is a possibility, and design and material selection should prevent the possibility of this form of failure occurring.

13.2 EQUIPMENT DESIGN FEATURES

13.2.1 MAINTENANCE

To design for maintenance, the particular equipment should be well understood at the design stage. Some typical maintenance-related items that must be considered at the design stage include tube pull space required for retubing/space required for pulling the bundle, material handling facilities, proposed cleaning methods and facilities required for the purpose, ease of component replacement, ability to monitor corrosion and fouling, facility to perform in situ welding operations, and facilities and adoptability for in-service inspection.

13.2.2 FAILSAFE FEATURES

The failsafe design concepts employed not only recognize the limitations in manufacturing but also provide large safety margins for operations. This concept is relevant for fracture mechanics study. In designing the various parts of an equipment to have failsafe features, the following considerations are usually made [33]:

1. Determine points in the structure where fatigue cracks might develop.
2. Define a minimum detectable crack size.
3. Define the maximum detectable crack size, depending upon the maximum damage level and at any load between the minimum detectable crack and the critical crack size.

13.2.3 ACCESS FOR INSPECTION

The design of pressure vessels should provide access for plant personnel to enter the vessel to inspect for corrosion damage. Vessels that have a sufficient diameter for personnel entry should have internal components that can be removed to permit access to all parts of the vessel.

13.2.4 SAFETY

Safe operation of pressure vessels and heat exchangers requires conservative design and standard construction practices, and use of those materials permitted by the codes/standards. For heat exchangers and pressure vessels, the overriding reasons for safety are to avoid the consequences of failure, which can be catastrophic in human, monetary, and environmental terms. To ensure safety, the equipment should be fabricated properly and adequately inspected to prove compliance with the specifications. The equipment must be operated properly.

13.2.5 EQUIPMENT LIFE

To realize returns on the investment and for uninterrupted service, the equipment components and the equipment itself should have adequate life [4]. The life of a component is dependent on design, properties of the construction materials and their interaction with the service environments, effect of fabrication and inspection, operation, maintenance, etc. [34,35]. To get a satisfactory life, the equipment construction materials shall withstand (1) design stress, (2) wear, and (3) corrosion in service [35]. Corrosion problems should be as important during the design stage as other operational conditions and design parameters like pressure, temperature, and velocity. For best service life, the material selection should be based on the corrosion standpoint. Concise and clearly written specifications should be provided to the material supplier to ensure the proper material supply. The design details should preserve the built-in corrosion resistance of the materials.

13.1.5.1 Component Life

Exchanger shells, channels, and tubesheets should be designed for a minimum of 10 years or the original tube bundle life plus two additional retubings. The initial tubes should be chosen for a minimum of two run lengths or 5 years unless spare exchangers are provided, in which case a shorter expected life may be attractive [4]. However, this may not be relevant for nuclear heat exchangers and pressure vessels.

13.2.6 FIELD TRIALS

A number of accelerated tests are used to build and to increase confidence in heat exchanger design, particularly, radiator design, before large-scale fleet trials. Some of these tests were designed to represent worst field conditions and were later correlated with field service returns. These tests are primarily used to assess the mechanical durability and the internal and external corrosion resistance of aluminum radiators. This aspect is further discussed in detail in the chapter 15 on brazing, section 15.13.

13.3 RAW MATERIAL FORMS USED IN THE CONSTRUCTION OF HEAT EXCHANGERS

In the construction of heat exchangers, various forms of raw materials are used. The raw material forms include plates, sheets and strips, pipes and tubes, forgings, castings, bars and rods, etc. Major use for sheets and strips are in the construction of compact heat exchangers and plate heat exchangers. Tubes are used both in compact heat exchangers and in shell-and-tube heat exchangers (PHEs). The other forms are used extensively in the fabrication of shell-and-tube heat exchangers.

In this section, various raw material product forms are discussed with specific reference to ASTM specifications [36]. As far as the plates and tubes are concerned, plate steels and ferrous tubings are discussed here. Nonferrous plates and tubes are covered in their respective sections.

13.3.1 CASTINGS

Castings may be used in the construction of pressure vessels and vessel parts. Cast heads are used for feedwater heaters. Codes restrict maximum allowable stress values for acceptable casting materials. These allowable stress values should be multiplied by the applicable casting-quality factor for all materials except cast iron.

13.3.2 FORGINGS

Forged materials may be used in pressure vessel and heat exchanger construction provided the materials have been worked sufficiently to remove the coarse ingot structure. Tubesheets, channel covers, blind flange covers, etc., when made from forgings should be supplied as proof machined forgings. All further machine operations, drilling, etc., should be done by the fabricator. Before machining, the forging is to be examined ultrasonically. Most of the defects in a forging are caused by conditions produced in the ingot stage, such as segregation, piping or nonmetallic inclusions, laps or seam due to subsequent hot or cold forging, and excessive scale leading to surface flaws. For this reason, the acceptance standard for a forging is usually based on an ultrasonic test [37]. SA 388/ASTM A388/A388M covers standard practices for ultrasonic examination of heavy steel forgings.

Forgings are available in carbon steels, carbon–molybdenum steels, chromium–molybdenum steels, ferritic (straight chromium) SSs, austenitic, precipitation hardened, and other high-alloy steels, and nickel steels. According to Section VIII, Div. 1, the heat analysis of steel forgings to be fabricated by welding shall not exceed 0.35% carbon. When welding involves only minor nonpressure attachments or repairs, the carbon content shall not exceed 0.5% by heat analysis. When carbon exceeds 0.5% by heat analysis, no welding is permitted.

Some of ASTM specifications for pressure vessel forging steels are (1) A336—seamless drums, heads, and other components (ferritic steels and austenitic steels), (2) A372—thin-walled pressure vessel steels (carbon and alloy steels), (3) A508—quenched and tempered (Q&T) vacuum-treated carbon steels, (4) A541—Q&T forgings (carbon and alloy steels), and (5) A592—Q&T, high-strength, low-alloy (HSLA) steel, forged fittings, and parts.

13.3.3 RODS AND BARS

Rod and bar stock may be used in pressure vessel construction for pressure parts such as flange rings, stiffening rings, frames for reinforced openings, stays and staybolts, and similar parts. ASTM specification for bars includes A453, A479, A666, and A739.

13.3.3.1 Pipe Fittings and Flanges

ASTM standards A105, A182, A234, A403, A181, A182, etc.

13.3.4 BOLTS AND STUDS

Bolts and studs may be used for the attachment of removable parts.

13.3.4.1 Materials for Corrosion-Resistant Fasteners

Corrosion-resistant metallic fasteners are made of SSs and nonferrous alloys of copper, nickel, aluminum, and titanium. Fasteners can also be made from exotic materials such as tantalum. Orlando and Ballantine [38] discuss materials for corrosion-resistant fasteners. Standard corrosion-resistant fastener alloys and their ASTM specifications are as follows:

1. F593—Stainless bolts, hexagonal cap screws, and studs.
F594—SS nuts conforming to 17-4 PH, Types 302, 303, 304, 305, 309, 310, 316, 317, 321, 347, 410, 416, and 430.

2. F468—Nonferrous bolts, external cap screws and studs for general use and F467 non-ferrous nuts for general use: (a) copper and its alloys: electrolytic tough pitch copper, yellow brass, high-leaded brass, free cutting brass, naval brass 63.5%, uninhibited naval brass, silicon-bearing aluminum bronze, low-silicon bronze B, high-silicon bronze A; (b) nickel: Monel 400, 405, K-500, Inconel 600; (c) aluminum: 1100, 2024, 6061; and (d) titanium: ASTM Grades 1, 2, 3, and 4.

13.3.5 HANDLING OF MATERIALS

To preserve the quality and finish of the materials and to avoid any rusting and minimize additional cleaning, the following preventive measures should be taken:

1. Material should be kept in original cases or wrappers until fabrication actually begins. Cases or wrappers opened for initial inspection should again be carefully packed after inspection.
2. Store the materials/cases indoors on clean racks, which should be free from corrosive fumes.
3. Fabrication equipments should be cleaned of all residues, dirt, rust, and scales before being employed for a new operation on SSs and other materials where surface contamination can initiate corrosion or embrittlement during fabrication. Paper or other protective covering should be placed on all surfaces.

13.3.6 MATERIAL SELECTION FOR PRESSURE BOUNDARY COMPONENTS

Material for pressure boundary components such as shell, channel, tubesheet, and tubes should conform to material for pressure-retaining components. For item like baffles, corrosion-resistant material compatible with the process fluid should be chosen, whereas for supports, strength and corrosion resistance to the ambient environment shall be considered. Guidelines for selecting material for shell, channel, tubesheet, tubes, and baffles are discussed next. For more information, refer to Danis [39] and Ref. [40].

13.3.6.1 Shell, Channel, Covers, and Bonnets

Specify the materials with a corrosion allowance adequate for the design life of the exchanger. Often, this means selecting materials that should last for 15 years or more [39]. For corrosive service, consider clad material if it is economical. Materials such as chromium–molybdenum steels, Q&T steels, cryogenic materials, austenitics, duplexes, 6Mo steels, cupronickels, nickels, titanium, etc., should be carefully evaluated from a fabrication standpoint prior to their selection as a pressure boundary material.

13.3.6.2 Tubes

Specify a material and corrosion allowance for both the shellside and the tubeside of the exchanger. Tubes are often designed with a life span significantly shorter than that of the shell or channel, since they can be retubed. The tube material must be compatible with the tubesheet material. To avoid galvanic corrosion due to unfavorable area ratio, the tube must be cathodic to the tubesheet material.

13.3.6.3 Tubesheet

Most tubesheets are made from rolled plates or forged ingots. Tubesheets of small production line units may be cast. Carbon steel tubesheets less than about 5 in. (127 mm) thick are most often burned from plate. Thicker tubesheets are machined from forgings. Nonmetallic materials and composites of thin metals coated with epoxy resins have been used in small air-conditioning units. Commonly used tubesheet metals for corrosive applications are AISI Types

304 and 316, aluminum, bronze, Muntz metal, copper–nickels 10% and 30%, and titanium. Commonly used tubesheet materials are given as follows:

Titanium, Grade 2—TIMETAL®50A
 Titanium Grade 3—TIMETAL®65A
 Titanium Grade 9—TIMETAL®3-2.5
 Titanium Grade 12—TIMETAL®Code12
 SS, Type 304—S30400
 SS, Type 316—S31600
 Aluminum bronze—C61400
 Muntz metal—C36500
 90-10 Copper nickel—C70600
 70-30 Copper nickel—C71500

Specify a material with a corrosion allowance that reflects both the shellside and tubeside conditions. Cladding may often be required on the shellside, the tubeside, or both sides of the tubesheet. Solid alloy construction can be utilized if both sides of the tubesheet require cladding [39]. In general, if austenitic SS or titanium alloy tubing is required, a tubesheet with a matching alloy clad on the corrosive side should be specified. Some of the considerations to choose clad tubesheets are [41] the following:

1. A metal that is resistant to corrosion by the fluid on one side while it is corrosive to the other side fluid.
2. It is desirable to fusion-weld the tubes to the tubesheet, but the tube and tubesheet materials are not compatible.
3. The granular structure of the tubesheet is not uniform, making it unsuitable for fusion-welding the tubes to the tubesheet.

13.3.6.4 Baffles

Specify a material to match the nominal chemistry of the tube material and shellside fluid. If the shellside conditions favor galvanic coupling, or if shellside fluid is not conducive to baffles, corrosion rates would cause the baffles to fail before the tubes.

13.4 MATERIALS FOR HEAT EXCHANGER CONSTRUCTION

A wide spectrum of materials is used in the construction of heat exchangers. The materials may be metals or nonmetals like glass, graphite, ceramic, and plastics. The principles of selection of heat exchanger materials have been discussed earlier. In this section, the properties of the following common heat exchanger materials that favor them for heat exchanger construction, metallurgy, corrosion resistance, and fabrication including welding are discussed.

1. Cast iron
2. Carbon steel
3. Low-alloy steel
4. SS: martensitic, austenitic, ferritic, superferritic, duplex, superaustenitic
5. Aluminum and aluminum alloys
6. Copper and copper alloys
7. Nickel and nickel alloys
8. Titanium and titanium alloys
9. Zirconium
10. Tantalum

11. Graphite
12. Glass
13. Teflon
14. Ceramics
15. Silicon carbide

13.5 PLATE STEELS

Plates used in the construction of pressure parts of pressure vessels shall conform to one of the specifications in ASME Code Section II, for which allowable stress values are given in the tables referenced in UG-23. Important sources on the selection of pressure vessel quality plate steels include Weymueller [42,43], Ref. [18], and Hagel et al. [29], among others.

13.5.1 CLASSIFICATIONS AND DESIGNATIONS OF PLATE STEELS: CARBON AND ALLOY STEELS

Regular quality is the common designation for carbon steel plate sold only on the basis of a maximum carbon content of 0.33% by heat analysis. Plate of this quality can vary substantially in chemical composition due to the broad range of carbon content permitted and unspecified chemical composition limits for other elements.

Structural quality plate is intended for application in structures such as bridges, buildings, tanks, railroad cars, mobile equipment, and miscellaneous fabrications. General specifications for structural quality plate steels are covered by ASTM A6.

Pressure vessel quality plate is intended for applications in pressure vessels, heat exchangers, and similar end uses. The manufacturing practices for pressure vessel applications are set up to provide plate with improved quality. Additional testing is required, such as mechanical and nondestructive testing (NDT), including notch toughness tests, radiography, and ultrasonic inspection. General specifications for pressure vessel quality plate steels are covered by ASTM A20.

Forging quality plate is intended for forging, heat treating, or similar purposes or when uniformity of composition and freedom from injurious imperfections are essential.

13.5.1.1 How Do Plate Steels Gain Their Properties?

The primary function of alloying elements is to improve the mechanical properties and stability at moderately high temperatures and also to increase resistance to specific corrosive environment. Plate steels achieve strength and ductility through the following alloying elements [42]:

1. Carbon, manganese, nickel, chromium, boron, and molybdenum raise hardenability and hence increase strength
2. Silicon and aluminum remove oxygen, ensuring porosity-free microstructures
3. Aluminum, titanium, columbium, vanadium, and zirconium are used as grain refiners
4. Copper increases atmospheric corrosion resistance

One of the principal functions of alloying elements is to increase hardenability, which is the property that determines the depth to which the steel will harden. In addition to alloying elements, heat treatment is used to develop certain desirable properties.

13.5.1.2 Changes in Steel Properties due to Heat Treatment

Heat treatments that steel plates undergo at the fabricator's plant vary from fabricator to fabricator. To meet the heat-treatment requirements of individual fabricators, plate makers give, under simulated conditions, the same heat treatments that will be used by the fabricator to test specimens taken from each plate ordered [18]. This guarantees the required properties. Therefore, in the purchase

order, the fabricator must provide information on the heat treatments likely to be given while processing the plates in shop floor.

13.5.1.3 ASTM Specifications on Plate Steels Used for Pressure Vessel Fabrications and Heat Exchangers

Material specifications list, in order, topics pertaining to the material—scope of the specification, referenced documents, terminology, ordering information, materials and manufacture, responsibility for quality assurance, heat treatment, chemical requirements, metallurgical structure, mechanical requirements, certification, identification, marking of product, packaging and package marking, mill test report, and supplementary requirements. Each specification is unique to the material; committees add some topics and drop others to fit the material and its expected use. General ASTM specifications for pressure vessel quality plate steels are given in Table 13.4.

Carbon steels: ASTM specifications for carbon steels include A285, A299, A442, A455, A515, A516, A537, A562, A612, A662, A724, A738, and A841. Carbon steels lack the alloying elements that are required for heat and corrosion resistance. Carbon steels are mostly used for moderate-temperature applications. ASTM specifications for various carbon steels are given in Table 13.5.

HSLA grades: ASTM specifications A734 and A737 cover HSLA steels. A734 covers two steels, both quenched and tempered: Type A, a nickel-chromium-molybdenum steel, retains its properties down to -80°F . Type B finds uses at -20°F and above. Two HSLA steels, designated Grades B and C, are described in A737.

Alloy steel: Alloy steels for pressure vessels contain three major alloying additions: chromium, nickel, and molybdenum, and other elements such as carbon, manganese, and silicon, found in killed steels. Alloy steels exhibit mechanical properties superior to carbon steel as a result of chromium, nickel, and molybdenum. Various alloy steels are given in Table 13.6.

TABLE 13.4
General ASTM Specifications for Pressure Vessel Quality Plate Steels

ASTM Number	Content
A20/A20M	General requirements for pressure vessel quality steel plates: descriptive terms, ordering instructions, manufacture and quality control, material identification, packaging, and shipment
A370/A370M	Test methods and definitions of mechanical testing: requirements for tension, bend, hardness, and impact tests
A435/A435M	Specification for straight beam ultrasonic examination of steel plates to determine internal discontinuities such as pipes, ruptures, and laminations
A577/A577M	Specification for anglebeam ultrasonic examination of steel plates to locate and size interior defects
A673/A673M	Mechanical testing: sampling procedures for impact (Charpy V-notch) tests of steel products
A700/A700M	Practices for steel product handling: packaging, marking, and loading for shipment
A770/A770M	Specification for through thickness tension tests of steel plates to determine propensity to lamellar tearing
A578/A578M	Specification for straight beam ultrasonic examination of rolled steel plates for special applications
A941/A941M	Terminology relating to steel, stainless steel, and related alloys
E 208	Test method for conducting drop-weight test to determine nil-ductility transition temperature of ferritic steels
E709	Guide for magnetic particle testing

Source: Adapted from Weymueller, C.R., *Weld. Design Fabr.*, February, 42, 1992.

TABLE 13.5
ASTM Specifications for Carbon Steel Plate (Pressure Vessel Quality)

Title of Specification	ASTM No.
Low and intermediate tensile strength carbon steel plates	A285
Manganese–silicon carbon steel plates	A299
Improved transition properties of carbon steel plates	A442
High-strength manganese carbon steel plates	A455
Intermediate and higher temperature service carbon steel plates	A515
Moderate and lower temperature service carbon steel plates	A516
Heat-treated, carbon–manganese–silicon steel plates	A537
Manganese–titanium carbon steel plates for glass or diffused metallic coatings	A562
High strength, for moderate and lower temperature service, carbon steel plates	A612
Carbon–manganese steel plates for moderate- and lower-temperature service	A662
Carbon steel, Q&T, for welded layered pressure vessels	A724
Heat-treated, carbon–manganese–silicon steel plates	A738
Carbon steel plates produced by the thermomechanical control process	A841

Subzero and cryogenic applications: Steels for subzero and cryogenic applications include

TABLE 13.6
ASTM Specifications for Alloy Steel Plate (Pressure Vessel Quality)

Title of Specification	ASTM No.
Chromium–manganese–silicon alloy steel plates	A202
Nickel alloy steel plates	A203
Molybdenum alloy steel plates	A204
Manganese–vanadium–nickel alloy steel plates	A225
Heat-resisting chromium and chromium–nickel stainless steel plates	A240
Steel plate clad with corrosion resistance chromium alloy	A263
Steel plate clad with corrosion resisting stainless steel (Cr–Ni)	A264
Steel plate clad with corrosion resisting nickel-base alloy	A265
Manganese–molybdenum and manganese–molybdenum–nickel alloy steel plates	A302
9% nickel double normalized and tempered alloy steel plates	A353
Chromium–molybdenum alloy steel plates for elevated temperature services	A387
High tensile strength Q&T alloy steel plates	A517
Q&T manganese–molybdenum and manganese–molybdenum–nickel alloy plates	A533
Q&T chromium–molybdenum alloy steel plates	A542
Q&T nickel–chromium–molybdenum alloy steel plates	A543
Q&T 8% and 9% nickel alloy steel plates	A553
Q&T nickel–cobalt–molybdenum–chromium alloy steel plates	A605
Specially heat-treated 5% nickel alloy plates	A645
36% nickel plate for low thermal expansion	A658
High-strength and low-alloy, Q&T, alloy steel plates for cryogenic use	A734
Low-carbon manganese–molybdenum–columbium alloy steel for moderate- and lower-temperature service	A735
Low-carbon age hardening nickel–copper–chromium–molybdenum–columbium alloy plates	A736
HSLA steel plates	A737
Q&T, manganese–chromium–molybdenum–silicon–zirconium alloy steel plates	A782
Chromium–molybdenum–vanadium–titanium–boron alloy steel plates	A832
9% nickel alloy steel plates, produced by the direct-quenching process	A844

TABLE 13.7
ASTM Specification for Clad Steel Plate

Description	ASTM No.
Chromium steel clad plate, sheet, and strip	A263
Chromium–nickel SS clad plate, sheet, and strip	A264
Nickel and nickel-base alloy clad steel plate	A265

A203, A353, A442, A517, A537, A542, A543, A553, A612, A645, A662, A724, A735, A736, A782, and A844.

Specification for stainless steels: Most of the AISI Types—*austenitic* (Types 302, 304, 304L, 316, 316L, 317, 317L, 321, and 347), *duplex*, *ferritic* and *martensitic* SSs, plus some special stainless like *superferritic* and *superaustenitic* steels—are included in A240.

Clad steels and other grades: Clad steels are covered by ASTM A263, A264, and A265. The cladding material specifications A263 and A264, chromium and Cr–Ni cladding, respectively, must conform to ASTM A240. Clad steels listed in A265, nickel- and nickel-base alloys, are covered by a number of ASTM specs and trade designation, such as (1) Nickel 200, Monel 400, Inconel 625, Incoloy 800 and 800H, and Incoloy 825, produced by Inco Alloys International; (2) Hastelloy B and B-2, C4 and C276, and G and G2, produced by Haynes International, Inc.; and (3) Carpenter 20 CB-3, produced by Carpenter Technology. Descriptions of these clad steels are given in Table 13.7. Producers include Lukens Steel and du Pont.

Producers of steel plates in the United States: Major producers of plate steels include the following:

Bethlehem Steel Corporation
 Gulf States Steel Company
 Inland Steel Industries
 Oregon Steel Mills
 Lukens Steel Company
 USS Div., USX Corporation

Major producers of SS include the following:

Allegheny Ludlum Steel Corporation
 Eastern SS Division
 Cyclops Corporation
 Jessop Steel Company

13.5.2 PROCESSING OF PLATE STEELS

Various processing methods and cracking problems faced are hereunder:

1. Quenching and Tempering—Quench cracking.
2. Forming—Cracking during cold, warm, or hot forming.
3. Thermal cutting—Cracking from HAZ, stress cracking.
4. Welding—Hydrogen assisted cold cracking and hot cracking.

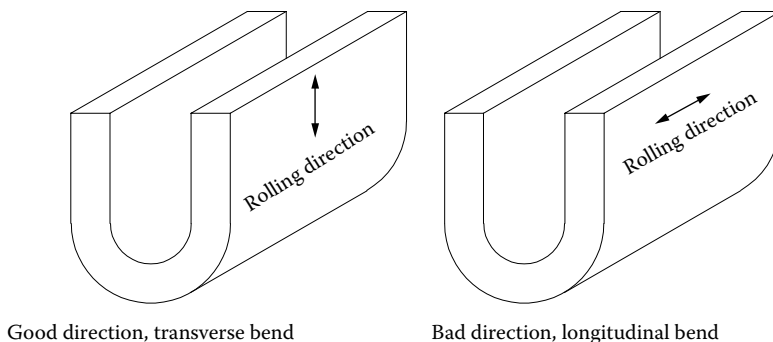


FIGURE 13.4 Optimum forming orientation for severe bending of plate steel.

5. Orientation—Hot rolling of plate steel results in directionality of properties being created. Nonmetallic inclusions in conventional steels are elongated in the primary rolling direction. These become sites for localized deformation and eventual cracking. Thus there is an optimum forming orientation for severe bending applications, as shown in Figure 13.4. For more details on the points discussed earlier, refer to “Guidelines for Fabricating and Processing Plate Steel,” Mittal Steel USA- Plate, 3/06, printed in the United States.

13.6 PIPES AND TUBES

ASME Code requirements are the following:

1. Pipes and tubes of seamless or welded construction conforming to one of the specifications given in ASME Code Section II may be used for shells and other parts of pressure vessels. Allowable stress values for the materials used in pipe and tubes are given in the tables referenced in UG-23.
2. Integrally finned tubes may be made from tubes that conform to one of the specifications given in Section II.

13.6.1 TUBING REQUIREMENTS

For heat exchanger applications, the tubing must meet four requirements [44]: (1) the tube must withstand the pressures from both the shellside and the tubeside at the operating temperature, (2) the tube must be corrosion resistant to both shellside and tubeside fluids, (3) the tube must be capable of being fixed into the tubesheets either by rolling or by welding, and (4) the tube must achieve optimum economy.

The tubes may be solid-drawn, electric resistance welded (ERW), or fusion-welded. It is a common practice to prefer solid-drawn tube to ERW tube for high-pressure duties. BS 3606, Steel Tubes for Heat Exchangers, identifies the following methods of manufacture [45]:

1. Cold-finished seamless
2. ERW and induction welded
3. Cold-finished ERW and induction welded
4. Longitudinally welded and heat-treated austenitic SS
5. Longitudinally welded, cold-finished, and heat-treated austenitic SS
6. Longitudinally welded, bead-conditioned, and heat-treated austenitic SS

13.6.2 SELECTION OF TUBES FOR HEAT EXCHANGERS

In addition to the choice of material for the tubes themselves, consideration must be given to the following factors [46]:

1. The tubesheet material.
2. The method of fixing the tubes into the tubesheet(s), e.g., roller expansion, explosive expansion, or fusion-welding.
3. Materials for ends/end closures.
4. In the case of water-cooled units, there may be a need for corrosion protection measures such as coatings on water boxes, and cathodic protection to protect the water boxes, tubesheets, and tube ends; also, water treatment may be necessary to prevent scaling, fouling, and corrosion.
5. In addition to compatibility with the environments concerned, they must be compatible with one another in any electrolyte involved so that excessive galvanic corrosion is avoided.

13.6.3 SPECIFICATIONS FOR TUBES

At minimum, specifications must require at least one method for leak detection, ductility test, and a check on the dimensional tolerances. Tubing used in corrosive environments may be further evaluated by one or more of the corrosion tests. Inspection and testing should also be carried out after any specified heat treatment or pickling operation. U-tubes usually cannot be inspected by electric test methods. Visual inspection and air-underwater tests should be performed on all U-tubes after bending. Tubes should be in fully heat-treated condition as received from the mill.

13.6.4 DEFECT DETECTION

Inspection to detect and eliminate defective tubes is the key to tubing reliability. All the defect testing methods can be applied to tubing at the mill. Different defect detection methods applied to tubing are discussed next. These methods detect mechanical-type defects that will produce leaks regardless of the corrosive environment [44]. Typical mechanical defects include through-wall defects, partial through-wall defects, delamination, ductility defects, and dimensional tolerance defects. Even mild and uniform corrosion may open up defects, causing premature leaks.

13.6.5 STANDARD TESTING FOR TUBULAR PRODUCTS

Standard tests for tubular products are visual examination; the eddy current test (ASTM E-426); hydrostatic pressure testing including pneumatic air-underwater testing (ASTM B-338/ASME SB-338); the magnetic particle test; an ultrasonic test (ASTM E-213); corrosion tests; mechanical tests, including tensile, flaring, flattening, and reverse flattening; metallographic testing; and dimensional tolerance testing. Hydrostatic pressure tests including pneumatic air-underwater tests, corrosion tests, and dimensional tolerance tests are discussed next.

13.6.5.1 Hydrostatic Pressure Testing

Hydrostatic testing is the most common test performed on tubing at the mill and is required on ASME Code exchangers. Test pressures are usually 6.9 MPa (1000 psi), but this may be decreased for large-diameter, thin-wall tubing. Most ASTM specifications allow testing at higher pressures as long as the hoop stress does not exceed a certain value; however, equipment limitations usually restrict pressures to about 38 MPa (5500 psi).

According to ASTM Standards, each tube shall withstand a hydrostatic pressure sufficient to subject the material to a fiber stress of 48 MPa (7000 psi) determined by the following equation for thin-walled cylinder under internal pressure:

$$P = \frac{2St}{D - 0.8t} \quad \text{or} \quad P = \frac{2Set}{D - 0.8t} \quad (\text{ASME Code procedure})$$

where

P is the hydrostatic pressure (MPa or psi)

S is the code allowable stress of the tube material (MPa or psi)

e is the weld joint efficiency that is equal to 0.85 for welded tube and 1.00 for seamless tube

D is the tube outer diameter (mm or in.)

t is the thickness of the tube wall (mm or in.)

The tube should not show any evidence of leakage. The tube need not be tested at a hydrostatic pressure more than 6.9 MPa (1000 psi), unless so specified.

13.6.5.2 Pneumatic Test

The pneumatic air–underwater test is a superior test for detecting through-wall defects that result from tube manufacturing, compared to the hydrostatic test. Air pressure up to 1.0 MPa (150 psi) is applied to the tubing submerged in water, and the tube is observed for leaks for 5 s. This test method is dependent solely on visual observation of leaks and not on pressure drop, which is an indication of leaks during hydrostatic testing. Extremely small through-wall defects may not be detected by air passage.

13.6.5.3 Corrosion Tests

Corrosion tests are used to evaluate tube material for its corrosion resistance. Usually, only a small section of tubes from a lot or heat is subjected to corrosion testing. Some of the most common corrosion tests include the uniform or general corrosion test, intergranular corrosion test, SCC test, critical pitting corrosion test, critical crevice corrosion test, and exfoliation corrosion test.

13.6.5.4 Dimensional Tolerance Tests

Dimensional tolerance tests, such as outer diameter and inner diameter, wall thickness, weld flash thickness, ovality, length, straightness, and squareness of end cut, are checked by use of measuring instruments such as micrometers, ring gauges, feeler gauges, and others.

13.6.6 MILL SCALE

Most carbon steel, irrespective of form, is manufactured by hot working. The hot-working operations produce a thin but rough film of black magnetic iron oxide (Fe_3O_4) on the surface of the steel. This film is commonly referred to as “mill scale” [47]. Mill scale is anodic to the base metal, and any discontinuity in the mill scale will induce pitting corrosion in a corrosive environment. For this reason, mill scale is regarded as a contaminant, and mostly this is removed prior to installation in a heat exchanger.

13.6.7 ASTM SPECIFICATIONS FOR FERROUS ALLOYS TUBINGS

ASTM specifications for some ferrous alloy tubings are given in Table 13.8. For nonferrous tubes, the specifications are given while discussing various nonferrous metals.

Ferrous tubing is further specified by A498, the specification for seamless and welded carbon, ferritic, and austenitic alloy steel heat exchanger tubes with integral fins. The finned tubes shall be

TABLE 13.8**ASTM Specifications for Some Ferrous Tubing for Heat Exchangers**

Description	ASTM No.
Seamless cold-drawn low-carbon steel heat exchanger and condenser tubes	A179
Seamless cold-drawn intermediate alloy (Cr–Mo and Cr–Mo–Si) steel heat exchanger and condenser tubes	A199
Seamless ferritic and austenitic alloy steel boiler superheater, and heat exchanger tubes	A213
ERW carbon steel heat exchanger and condenser tubes	A214
Welded austenitic steel boiler, superheater, heat exchanger, and condenser tubes	A249
Seamless and welded carbon, ferritic and austenitic alloy steel externally finned tubes	A498
Seamless cold-drawn carbon steel feedwater heater tubes, includes U-tubes	A556
ERW carbon steel tubes (straight and U-tubes) for feedwater applications	A557
Welded austenitic SS feedwater heater tubes, includes U-tubes	A688
Welded ferritic SS feedwater heater tubes, includes U-tubes	A803
High-frequency induction welded, unannealed, austenitic steel steam surface condenser tubes	A851
Seamless/welded ferritic, austenitic and duplex alloy steel condenser, and heat exchanger tubes with integral fins	A1012

manufactured from plain tubes that conform to one of the following ASTM specifications: A179, A199, A213, A214, A249, and A334.

13.7 WELDABILITY PROBLEMS

In the following pages, selection of various metals, the properties that favor them as heat exchanger materials, corrosion resistance, and fabrication by welding are discussed. Before that, certain weldability problems common to some or many metals are discussed in this section.

Weldability is defined as the degree of ease or difficulty of joining two metals to produce a weld that gives the required properties in service. De facto, weldability is the ease or difficulty of making a joint that is free of cracks [48]. Cracking of any nature cannot be allowed in a weld metal. Some important weldability considerations, such as cold cracking, hot cracking, and laboratory tests to determine susceptibility to cracking, are discussed in this section. References [49–57] provide general or specific information on weldability problem. Other important sources on weldability considerations include Brosilow [58] and the leading welding research institute publications.

13.7.1 COLD CRACKING

Cold cracking, also known as delayed cracking, occurs at lower temperatures, sometimes long after the weld has cooled to room temperature. These cracks go through the alloy grains.

Some forms of cold cracking of base metal are

- hydrogen-induced cracking
- toe crack
- root crack
- transverse crack
- underbead cracking
- lamellar tearing
- fish-eye cracking

Few forms of these cracks are shown in Figure 13.5.

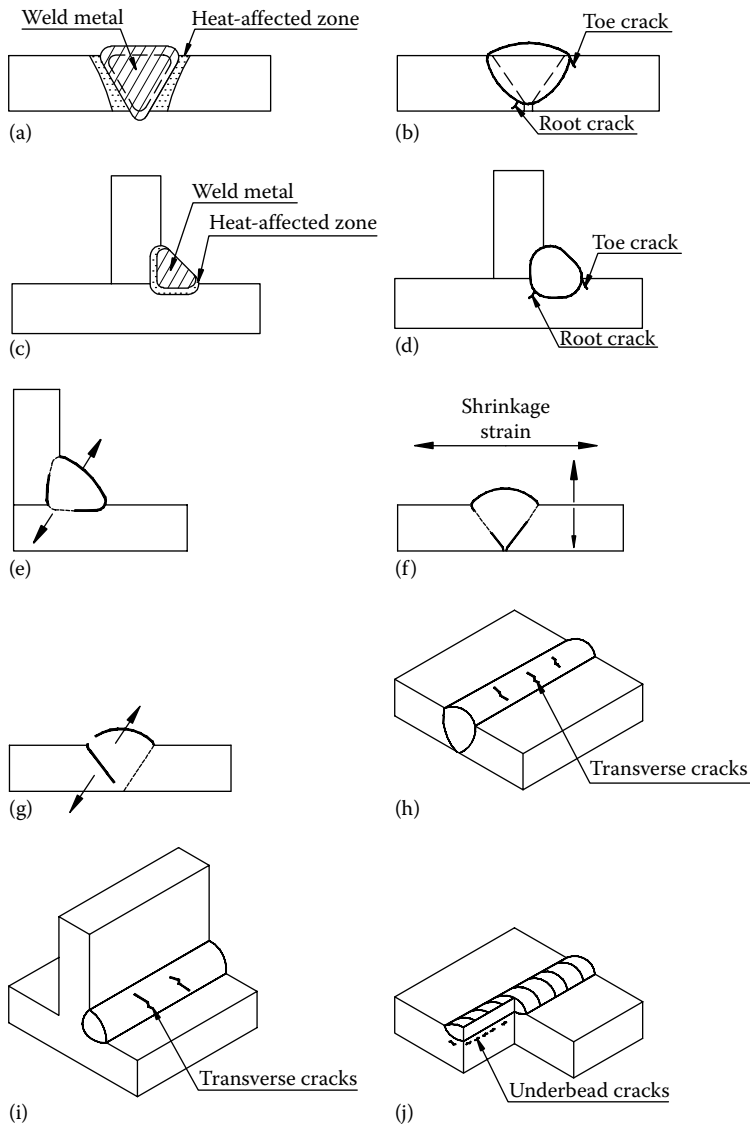


FIGURE 13.5 Forms of cold cracking. (a) Weld metal and HAZ, (b) toe and root crack, (c) weld metal and HAZ, (d) toe and root crack, (e, f, and g) hydrogen-induced cracking, (h and i) transverse crack, and (j) underbead crack.

13.7.1.1 Hydrogen-Induced Cracking

Hydrogen-induced cracking is the most common HAZ defect, but may also occur in the weld metal. It occurs after solidification, often showing up as zigzag transgranular fractures. Three conditions present simultaneously make a hydrogen-induced crack:

1. The presence of hydrogen in the steel
2. A susceptible microstructure that is partly or wholly martensitic
3. A tensile stress of significant magnitude at the sensitive location

Hydrogen-induced cracking will not take place if one or more of these conditions is not present or is at a low level. Also this form of cracking is generally not encountered in section thickness less than 0.4 in. (10.6 mm). Heavy sections rapidly draw heat from the weld zone and thereby intensify thermal stress.

13.7.1.1.1 Susceptible Materials

When other factors such as hydrogen, restraint, and thermal cycle are constant, a steel with higher carbon content and/or alloying elements level has a greater tendency to form a harder microstructure, which is more susceptible to hydrogen-induced cracking. Therefore, hydrogen-induced cracking is usually more prevalent when welding hardenable carbon and alloy steels than when welding plain carbon steels. Steels with 0.15% carbon or less are immune to this problem, especially when thick sections are welded.

13.7.1.1.2 Hydrogen Sources

Hydrogen is generally introduced during welding. The source may be the filler metal, moisture in the electrode coating, welding flux, the atmosphere or shielding gas, or a surface contaminant on the filler or base metal.

13.7.1.1.3 Stresses

Welding stresses arise from external restraint of the welded sections, unequal thermal expansion and contraction of the base metal and weld metal, volumetric expansion resulting from microstructural changes in the weld metal, and also from welding practices-related factors like low amperage, high welding speed, low heat input, fast cooling of weld metal, as well as from poor joint design and fitup, and from no preheating.

13.7.1.1.4 Avoiding Hydrogen Cracking

Hydrogen-induced cracking can be controlled using (1) hydrogen-free welding by using low-hydrogen electrodes (5–10 mL/100 g), clean wire, a wire brush, and/or a clean surface; (2) use of ductile nonmartensitic structure with low carbon equivalents (CEs)—the toughest and strongest welds contain acicular ferrite [58]; (3) welding methods incorporating preheating, high amperage, low speed, high weld heat, interpass temperature control, and slow cooling—preheating to reduce cooling rate and maintaining interpass temperature to let hydrogen diffuse out of the weld bead before a subsequent pass covers it, and when preheating is impractical, using austenitic filler metal; (4) use of a low-hydrogen process such as gas metal arc or gas tungsten arc welding (GTAW); (5) adoption of welding procedures that result in low welding stresses; (6) use of electrodes containing a deoxidizer like aluminum, manganese, or silicon; and (7) adoption of special welding techniques like the temper bead technique (Figure 13.6) in multipass welding to soften the final weld pass, and two-layer welding, which uses the second pass to refine the HAZ of the previous pass [58].

13.7.1.1.5 Preheating, Interpass Temperature, and Postheating

Preheating temperature: Preheating is specified primarily to prevent hydrogen-induced cracking. Preheat reduces the cooling rate of the HAZ of each weld bead, which in turn reduces hardness, hydrogen content in the vicinity of the weld, and stresses. Preheating of a joint is commonly done with torches or electrical strip heaters. If the part is small enough, it can be placed in a furnace. The temperature for preheating depends on the welding process, base metal thickness, composition, and properties.

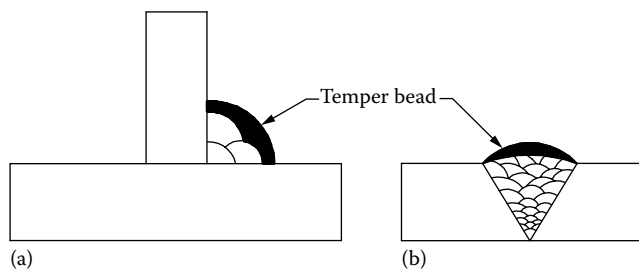


FIGURE 13.6 Temper bead technique.

1. Thumb rule: The preheating temperature t_p ($^{\circ}\text{F}$) is given by the following formula:

$$t_p = 1000(C - 0.1) + 18t$$

where

C is the percent C in the base material

t is the thickness of base material (in.)

2. An alternate formula to predict the preheating temperature t_p ($^{\circ}\text{F}$) is given by

$$t_p = 350\sqrt{(CE - 0.25)}$$

where CE is the carbon equivalent and it is calculated by the following formula:

$$CE = C + \frac{\text{Mn}}{6} + \frac{\text{Cr} + \text{Mo} + \text{V}}{5} + \frac{\text{Ni} + \text{Cu}}{16}$$

The CE is a measure of the tendency of the weld to form martensite on cooling and to suffer hydrogen cracking.

3. Yet another formula is recommended as follows [49]:

$$CE = \%C + \frac{\%Mn}{6} + \frac{\%Ni}{15} + \frac{\%Mo}{4} + \frac{\%Cr}{4} + \frac{\%Cu}{13}$$

With this formula,

$CE < 0.45\%$ preheat is generally not used.

$0.45\% < CE < 0.60\%$ preheat at 200°F – 400°F (93°C – 204°C).

$0.60\% < CE$ preheat at 400°F – 700°F (204°C – 371°C).

Interpass temperature: A preheat temperature that is maintained between weld beads throughout the welding cycle is known as the interpass temperature. Hydrogen-induced cracking can occur if the interpass temperature becomes too low. An upper limit also must be maintained because too high an interpass temperature may cause excessive grain growth in the HAZ, with a reduction in mechanical properties. Maximum interpass temperatures of about 250°C are usually specified for austenitic steel welds.

Postheating: The situation of heavy welding carried out in a localized area where the stress will be high and causing cracks can be avoided by postheating the weldment for 1 or 2 h immediately after welding. This is essential for high-thickness and low-alloy steel weldments.

Specification for preheating, interpass, and postheating temperatures: Specification of preheat and postweld heat-treatment (PWHT) conditions should generally follow the relevant code/standard for the particular parent materials.

Carbon equivalent to assess cold cracking: The tendency to hydrogen-induced cracking in carbon and low-alloy steels seems to correspond roughly to the composition of the steel. Therefore, calculation of the CE, an index figure that relates steel composition to cracking, is the usual first step to estimate weldability of the steel. The higher the CE and the thicker the components to be joined, the greater is the risk of hydrogen cracking. Several CE formulas have been proposed as parameters indicating a steel's susceptibility to hydrogen-induced cold cracking at the HAZ. These formulas reduce the significant composition variables to a single number, known as the CE.

1. *IIW formula*: Traditionally, the International Institute of Welding (IIW) formula has been used to assess the weldability of carbon steels:

$$CE(IIW) = C + \frac{Mn}{6} + \frac{Cu + Ni}{15} + \frac{Cr + Mo + V}{5}$$

Values of CE(IIW) below 0.42 denote a steel that is easy to weld without cracking; values above 0.5 are difficult. It is reported that CE(IIW) is a more appropriate parameter for evaluating the cold-working susceptibility of steels whose carbon content is more than 0.16%. A more accurate estimate will be obtained if the factor of Si/6 is added to the CE(IIW) formula [59]:

$$CE = C + \frac{Mn + Si}{6} + \frac{Cu + Ni}{15} + \frac{Cr + Mo + V}{15}$$

This formula is used by AWS.

2. *Low-carbon steels*: There is a general feeling that the IIW formula is not adequate to define the behavior of modern steels with low carbon contents (0.07%–0.22% C), and the following relationship by Ito and Bessoy is sometimes preferred [49]:

$$P_{cm} = CE = C + \frac{Si}{30} + \frac{Ni}{60} + \frac{Mn + Cu + Cr}{20} + \frac{Mo}{15} + \frac{V}{10} + 5B$$

CE is in the range 0.35–0.45 depending on the plate thickness, and restraint is susceptible to cold cracking. P_{cm} has been shown to be reliable for evaluating the cold-cracking tendency in low-carbon steels.

3. *Yurioka et al. formula [60]*: This is a general-purpose formula. Due to the reason given in item 2, it is not possible for one simple CE formula to describe, overall, the cold-working tendency of steels if their carbon contents range widely [60]. It is with this in mind that Yurioka et al. proposed the following CE formula, which has an accommodation factor $A(C)$ as a function of the CE:

$$CE = C + A(C) \left\{ \frac{Si}{24} + \frac{Mn}{6} + \frac{Cu}{15} + \frac{Ni}{20} + \frac{Cr + Mo + Nb + V}{5} + 5B \right\}$$

where $A(C) = 0.75 + 0.25 \tanh\{20(C - 0.12)\}$. $A(C)$ increases with an increase in carbon content. It approaches 0.5 as the carbon content decreases below 0.08% and 1.0 as it increases above 0.18%. As a parameter describing the probability of the occurrence of cold cracking in steel welding, a cracking index (CI) was proposed. It is expressed as

$$CI = CE + 0.15 \log H_{JIS} + 0.30 \log(0.017 K_t \sigma_w)$$

where

H_{JIS} is the hydrogen content in the deposited weld metal determined using JIS glycerin displacement method, $(H_{IIW} - 0.16)/1.3$

K_t is the stress concentration factor at root and toe weld positions where a crack is initiated— K_t is 1.5 for V (root), 4–5 for Y (root), and 3.5 for double V (root) (for others refer to Ref. [60])

σ_w is the mean stress acting on the weld metal

Yurioka et al. proposed the necessary preheating temperatures to avoid cold cracking by the following criterion:

$$t_{100} \geq (t_{100})_{cr}$$

where t_{100} is the cooling time to 100°C (212°F); this is influenced not only by the preheating temperature employed, but also by welding heat input, plate thickness, and preheating method. Critical time $(t_{100})_{cr}$ is given as

$$(t_{100})_{cr} = \exp(67.6 CI^3 - 182.0 CI^2 + 163.8 CI - 41.0)$$

4. *Stout and Doty formula for CE [48]*

$$CE = \%C + \frac{\%Mn}{6} + \frac{\%Ni}{20} + \frac{\%Cr + \%Mo}{10} + \frac{\%Cu}{40}$$

If CE is < 0.40, the steel may be insensitive to hydrogen cracking; over 0.50, cracking is sure, and low-hydrogen welding procedures are necessary.

5. *Hardenable carbon steels and alloy steels:* This formula takes into account the silicon content, and equation for CE is given by [56]

$$CE = \%C + \frac{\%Mn}{6} + \frac{\%Cr + \%Mo + \%V}{5} + \frac{\%Si + \%Ni + \%Cu}{15}$$

Using this formula, steels having CEs of less than 0.35% usually require no preheating or postheating. Steels with CEs between 0.35% and 0.55% usually require preheating, and steels with CEs greater than 0.55% may require both preheating and postheating.

6. Expressions that include fabrication conditions such as heat input, cooling rate, joint design, and restraint conditions have also been proposed. This includes the following:

$$P_H = P_{cm} + 0.075 \log_{10} H + R_f / 40,000$$

where

P_H is the cracking susceptibility parameter

H is the concentration of hydrogen (ppm)

R_f is the restraint stress (MPa)

P_{cm} was defined earlier

Maximum carbon equivalent as per ASTM A20: As per ASTM Specification A20, for weldability considerations, the plates shall be specified with a specific maximum CE value based on heat analysis. The CE shall be calculated using the following formula:

$$CE = C + \frac{Mn}{6} + \frac{Cr + Mo + V}{5} + \frac{Ni + Cu}{15}$$

The maximum values of the CE for C-steels, including C–Mn, C–Mn–Si, and C–Mn–Si–Al steels, are given in Table 13.9.

Caution about using the carbon equivalent formulas to predict preheating temperature: Because the CE is calculated from the base metal composition and includes no other variables related to filler metal and welding procedures, it is only an approximate measure of weldability or predicting susceptibility to hydrogen-induced cracking.

TABLE 13.9
Maximum CE of Plate Steels Conforming to ASTM A20
for Weldability

Specified Minimum UTS, ksi (MPa)	Maximum CE Value	
	Up to 2 in. Thick	>2 in. Thick
$60 \leq \text{UTS} < 70$ ($415 \leq \text{UTS} < 485$)	0.45	0.46
$70 \leq \text{UTS} < 80$ ($485 \leq \text{UTS} < 550$)	0.47	0.48
$\text{UTS} \geq 80$ ($\text{UTS} \geq 550$)	0.48	—

Note: For applicability of various conditions, refer ASTM Specification A20.

13.7.1.2 Underbead Cracking

Underbead cracks are cold cracks that are most frequently encountered when welding a hardenable base metal. This is found at the toes of weld deposits and is promoted by these factors [56]: (1) increased base metal hardenability contributed by high carbon and alloying element content; (2) depositing small welds so that the cooling rates after welding favor the formation of hard, brittle HAZ; (3) weld designs that impose a high degree of mechanical restraint on the weld metal; and (4) the presence of hydrogen. Underbead cracking can be minimized or prevented by using low-hydrogen electrodes or by preheating joints to the range of 250°F–400°F and avoiding the already mentioned factors that cause underbead cracking.

13.7.1.3 Lamellar Tearing

Lamellar tearing is a cold-cracking phenomenon that occurs beneath welds and is principally found in rolled steel plate fabrications (Figure 13.7). The tearing always lies within the parent plate, often outside the visible HAZ. It is characterized by step-like cracking parallel to the rolling plane [15,56,61,62]. Lamellar tearing is due to the presence of planar inclusions lying parallel to the plate surface, and it is shown schematically in Figure 13.7a.

For a given type of welded joint—T (Figure 13.7b), L, or cruciform configuration—the occurrence of lamellar tearing will be governed by the drop in strength and ductility of a plate in the through-thickness direction (z direction) as compared with the rolling direction. This anisotropy results in particular from the content and shape of the nonmetallic inclusions such as silicates, sulfides, and alumina, which in turn are influenced by degassing and the rolling technique. Such conditions usually are present in conventionally melted steels. When the ingot is rolled to form plates, the inclusions deform into platelets with resultant loss in through-thickness direction strength. All conventional steels are susceptible to lamellar tearing to some extent: mild and low-alloy steels whether semikilled or fully killed and including vacuum-degassed steels. For a given inclusion content, lamellar tearing is more likely as the strength of the steel increases. A considerable amount of rectification is usually necessary to repair the defect, and hence this is of considerable concern and trouble to the fabricator should it occur [63]. Because of this, lamellar tearing has attracted increasing interest from both the steel-making industry and the fabrication industry.

13.7.1.3.1 Conditions That Promote Lamellar Tearing

For lamellar tearing to occur, these conditions must be satisfied [56,62]:

1. Strains must develop in the short transverse direction of the plate. These strains arise from weld metal shrinkage in the joint, but can be greatly increased by strains developed from reaction with other joints in restrained structures.
2. The fusion boundary is roughly parallel to the plate surface.

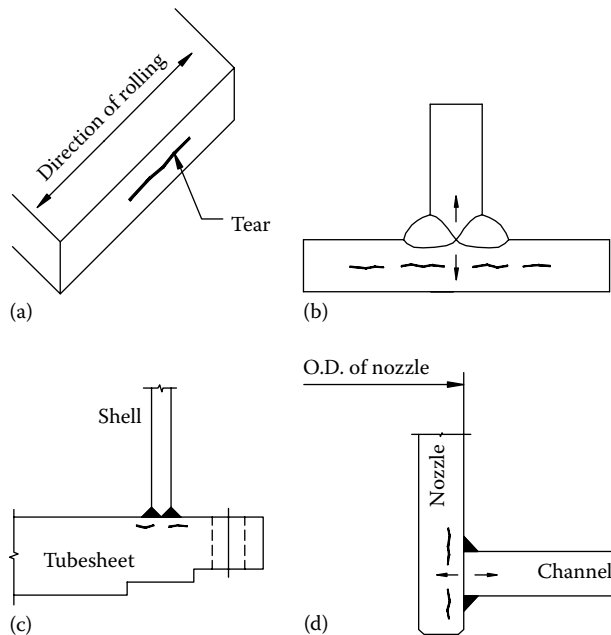


FIGURE 13.7 Lamellar tearing principle and susceptible welded joints: (a) Lamellar tearing due to planar inclusion lying parallel to the surface, (b) Lamellar tearing susceptible welded T-joint, (c) Shell to fixed tubesheet joint and (d) T-joint such as nozzle set through a rigid plane like channel.

3. Susceptible base material with a local concentration of inclusions, particularly those extended in planar directions.
4. Section thickness: Lamellar tearing does not normally occur in welds of lighter gauge plates because of insufficient constraint. Most reported occurrences of tearing are in plates greater than 25 mm in thickness [62].

Factors affecting weldment cracking due to lamellar tear (subcritical mode) include [10] through-thickness ductility, size, shape, and distribution of inclusions, matrix-inclusion cohesion, residual welding strains, mechanical constraints, and temperature.

13.7.1.3.2 Structures/Locations Prone to Lamellar Tearing

Any joint may be subject to lamellar tearing under certain conditions where a restrained weld is laid against a plate surface rather than the edge. From an analysis of fabrication failures, it appears that three major categories of structure type are commonly associated with the problem [62]:

1. Shell to tubesheet connection on fixed-tubesheet heat exchangers (Figure 13.7c)
2. Stiffeners or end closure plates in cylindrical structures
3. Nozzle or penetrator set through a rigid plate (T joint) (Figure 13.7d)

13.7.1.3.3 Prevention of Lamellar Tearing

The risk of lamellar tearing can be solved by directing attention toward steel quality, appropriate design, and welding and fabrication techniques (Figure 13.8). These approaches are discussed next.

Melting practice: The most reliable method of avoiding lamellar tearing involves special melting and solidification technique. Any steel-making technique that reduces the inclusion content of the steel will improve the steel properties in the through-thickness direction (z direction) and reduce the risk of tearing. Examples are deoxidation practices such as (1) low sulfur content accomplished

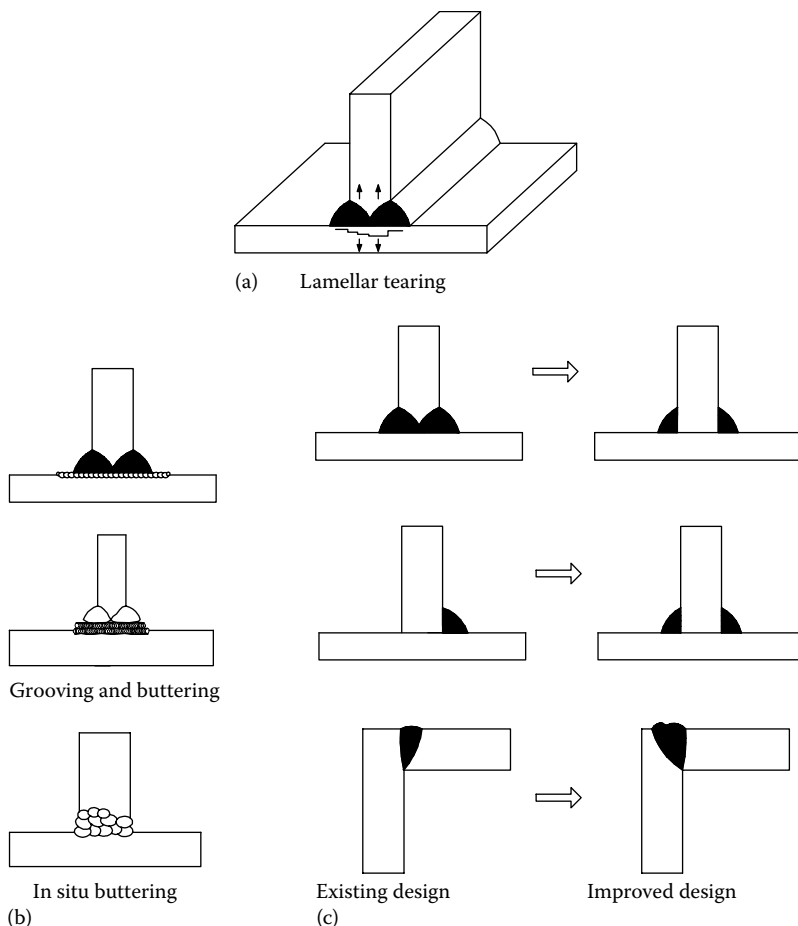


FIGURE 13.8 Lamellar tearing: (a) principle, (b) methods to overcome lamellar tearing-welding techniques and (c) methods to overcome lamellar tearing-T-joint design: original design and improved design. (Courtesy of TWI Ltd, UK, <http://www.twi.co.uk>.)

by ladle addition of cerium or calcium, (2) sulfide shape control, that is to “ball up” the sulfides into spheres that do not spread out into relatively large platelets during rolling, and (3) use of aluminum or other strong deoxidizers to protect the shape control and prevent silicate formation and improve through-thickness ductility; also (4) slabs may be continuously cast rather than being rolled from ingots, and (5) vacuum melting can reduce oxygen content and incremental rapid solidification to reduce segregation. These techniques are described in detail in Refs. [56,61,62] and by Gross-Wordemann and Dittrich [64].

Design improvements: Many instances of lamellar tearing can be avoided in practice by improvements in design:

- Replacement of cruciform joints by offset T configurations
 - Replacement of T or L joints by butt joints
 - Location of T joints in regions of lower restraint
 - Replacement of plates by forgings, castings, or extrusions in critical T and L joints, or to avoid fillet welds
- Design improvements to overcome lamellar tearing are shown in Figure 13.8c

Welding procedural factors: The following can be helpful measures:

Buttering or grooving and buttering, and in situ buttering of the plate surface [62]
Selection of sequence of turns to reduce strains in plates susceptible to lamellar tearing
Balanced welding
Control of preheating and interpass temperature to minimize tensile strains around the joint
Following low-hydrogen welding practice
Shot-peening the weld beads
Welding procedures such as buttering and balanced welding are shown in Figure 13.8b

Complementary information test for lamellar tearing: Conventional pulse echo techniques, although useful for detecting laminations in plate, cannot reliably detect small inclusions, which can give rise to lamellar tears [62]. Hence for further assurance, additional testing is conducted at room temperature, known as the through-thickness tensile test. In this test, the strain developed during weld cooling is simulated, and the material parameter associated with lamellar tearing resistance, through-thickness reduction of area (TTRA), is easily measured. A TTRA value of 20% or more is indicative of resistance to lamellar tearing. Steels are processed so as to achieve high TTRA values and thereby provide high resistance to lamellar tearing. ASTM Specification A770 covers procedures and acceptance standards for through-thickness tension tests. The room-temperature through-thickness tensile tests specimens of any one of the following can be used [65]:

1. Type 1. These tests are recommended for all thicknesses and fitted with welded extensions. They may be machined from friction-welded assemblies or stud-welded or fusion-welded extensions. Friction- or stud-welded extensions are recommended in order to test the plates as close to the surface as possible.
2. Type 2. Test pieces of this type are recommended for plates having a thickness over 25 mm.

13.7.1.3.4 Detection of Lamellar Tearing after Welding

For surface tears, visual, dye penetrant and magnetic particle testing will be satisfactory. For sub-surface tears, ultrasonics is probably the most widely used technique, but there may be problems in distinguishing true lamellar tears from inclusion bands and other forms of cracking. Therefore, pay particular attention to the position of the cracking in relation to the plate thickness and weld fusion boundary, to avoid confusion with lack of penetration defects, entrapped slags, etc. [62].

13.7.1.4 Fish-Eye Cracking

Fish-eye cracking is a form of hydrogen-induced cracking that occurs in weld metal and appears as small bright spots on the fractured faces of broken specimens of weld metal. These small bright spots are similar to fish eyes and hence the name fish-eye cracking. The fish eye usually surrounds some discontinuity in the metal, such as a hydrogen gas pocket or a nonmetallic inclusion, which gives the appearance of a “pupil in an eye.” The conditions that lead to fish-eye cracking can be minimized by using dry low-hydrogen electrodes or by heating the weldments for some period in the temperature range of 200°F–300°F. Longer times are required with lower temperatures.

13.8 HOT CRACKING

Hot cracking occurs during solidification and cooling of a weld, in the weld metal or in the HAZ. It occurs above solidus temperature of the lowest melting phase present. During the final stages of solidification, narrow solid bridges separating areas of low melting liquid are subject to the maximum proportion of the shrinkage-induced strains. An increase in the amount of low-melting phase or the inherent strain resulting from solidification shrinkage may cause fracture of these solid

bridges, thus resulting in hot cracks [66]. Hot cracking is the subject of most fabrication weldability testing, so much so that many fabricators equate the term “weldability” with “hot cracking” and use the terms interchangeably [48].

13.8.1 FACTORS RESPONSIBLE FOR HOT CRACKING

Most mechanisms proposed deal with the metallurgical factors that can lead to hot cracking. Hot cracking will occur due to (1) the segregation of low-melting-point elements, (2) the sufficient stress applied to a susceptible microstructure, and (3) the mode of solidification.

13.8.1.1 Segregation of Low-Melting-Point Elements

The segregation of low-melting-point elements, such as phosphorus and sulfur, or the presence of a eutectic can cause hot cracking by extending the temperature range over which liquid is present in the microstructure. By restricting the individual concentrations of sulfur and phosphorus, resistance to solidification cracking may be obtained.

13.8.1.2 Stress States That Induce Restraint

Stresses are invariably present in a solidifying weldment due to the complex thermomechanical transients that occur during welding. Thermal expansion and contraction, plastic strains, phase transformations involving volumetric changes, etc., contribute to the stress states that induce restraint [67].

13.8.1.3 Mode of Solidification

In certain cases, as in austenitic SS, the mode of solidification, whether as primary austenite or primary ferrite, strongly influences the sensitivity to hot cracking, presumably due to the differing distribution of minor elements between these two phases.

13.8.2 SUSCEPTIBLE ALLOYS

These include (1) copper-base alloys like silicon bronzes, aluminum bronzes, and copper-nickels, (2) aluminum alloys, (3) fully austenitic and superaustenitic SSs, and (4) nickel-base alloys.

13.8.3 TYPES OF HOT CRACKING

Various types of hot cracking are the following:

- Solidification cracking
- HAZ liquation cracking, microfissuring
- Reheat cracking (RC) or stress-relief cracking
- Ductility dip cracking
- Chevron cracks
- Crater cracks

13.8.3.1 Solidification Cracking

Solidification cracking of the weld metal takes place within a few hundred degrees of the nominal liquidus temperature of the weld metal. It is caused by welding stresses and the presence of low-melting-point constituents that form as a result of segregation during solidification. Solidification cracking is shown schematically in Figure 13.9.

13.8.3.1.1 Elements Contributing to Solidification Cracking

Increased amounts of carbon, phosphorus, and sulfur enhance the solidification cracking tendency. Resistance to solidification cracking may be obtained if the concentrations of sulfur and phosphorus

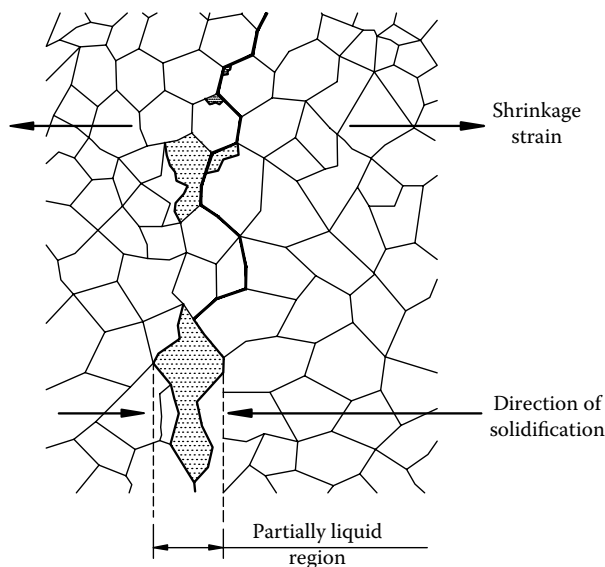


FIGURE 13.9 Solidification cracking (schematic).

are restricted. Cracking is less troublesome in carbon steel than in the high-alloy steel. Susceptibility to solidification cracking is given by the following empirical formula [48]:

$$UCS = 230C + 190S + 75P + 45Cb - 12.3Si - 5.4Mn - 1$$

As a rating of 20, a T fillet weld is likely to crack.

13.8.3.1.2 Welding Procedure-Related Factors Responsible for Solidification Cracking

These include the following:

1. Small electrode, excessive travel speed, high thermal stress, small weld, and low weld current.
2. No or low preheat, high restraint, poor joint preparation, poor weld profile, poor fitup, inadequate jigging or tacking, unbalanced heat input, and poor electrode manipulation.
3. Weld metal used is not chosen correctly to accommodate the impurity level in the plate.

13.8.3.1.3 Welding Procedure to Overcome Solidification Cracking

Eliminate or overcome the various welding-related factors responsible for solidification cracking discussed earlier. The degree of restraint should be reduced, and low-heat-input processes and procedures should be used. Susceptible solidification patterns, such as those with high weld pool depth-to-width ratios and those that include long columnar crystals, should be avoided. Measures such as low travel speed, use of larger electrode, improved joint design and fitup, improved joint cleanliness, modification of tacking and jigging procedures, and the use of welding procedures tolerant of impurities will minimize hot cracking tendency. For example, basic-coated electrodes are more tolerant of sulfur than rutile-coated electrodes, and manganese–silicon deoxidized CO_2 wires than manganese–silicon–aluminum deoxidized wires [15].

13.8.3.2 Heat-Affected Zone Liquation Cracking

HAZ liquation cracking is a type of high-temperature weld cracking that occurs in the HAZ adjacent to the fusion boundary during welding. In the region adjacent to the fusion boundary, where high peak temperatures are attained during welding, local melting may occur at the grain boundaries in ferritic steels due to the formation of a sulfide eutectic. The phenomenon has been known for many years to occur on steels heated at too high a temperature during processing and is known as “burning” [15].

The metallurgical basis for cracking involves the presence and persistence of liquid films at grain boundaries and the inability of these films to accommodate the thermal and/or mechanical strains experienced during weld cooling [68]. Impurity elements like sulfur and phosphorus promote hot cracking in ferrous alloys. The degree of HAZ liquation cracking will be affected by the welding process used. HAZ liquated cracking is illustrated schematically in Figure 13.10.

This problem can be controlled by restricting the sulfur level in the parent material and increasing the manganese, in sufficient concentrations [66]; usually a 20:1 ratio (manganese to sulfur) ties up most of the available sulfur as globular manganese sulfide and leaves no sulfur for the formation of low-melting intergranular sulfide films. Welding processes characterized by a relatively high heat input, such as submerged arc and electroslag welding, are likely to produce a greater degree of HAZ liquation cracking than processes such as the manual metal arc (MMA) and metal inert gas (MIG) welding processes [15]. Cleanliness and purity of the base material and welding consumables also lessen the tendency to hot cracking.

13.8.3.2.1 HAZ Liquation Cracking Susceptible Alloys

HAZ liquation cracking is often encountered during welding of austenitic SSs, nickel- and aluminum-base alloys [68], and superaustenitic SS and duplex SSs. HAZ liquation cracking in austenitic SS is known as microfissuring.

13.8.3.3 Reheat Cracking or Stress-Relief Cracking

RC is defined as intergranular cracking in the HAZ, and occasionally in the weld metal of a welded joint, being initiated during heat treatment in the temperature range of 950°F–1200°F or during service at a sufficiently high temperature [69]. The process is driven by the relaxation of residual welding stresses. The extent of cracking during heat treatment depends on composition, the microstructure of the HAZ, heat-treatment temperature, and time at temperature; for some steels, it is

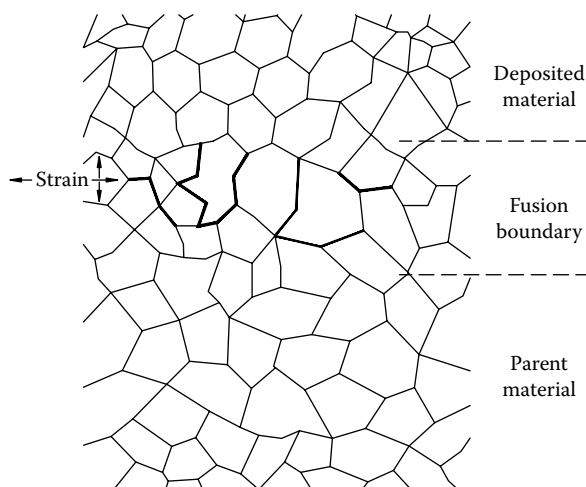


FIGURE 13.10 Liquation cracking (schematic).

greater with slow cooling, as in stress relieving. RC, stress-relief cracking (SRC), and stress-rupture cracking are equivalent forms of cracking.

Causes include poor creep ductility in HAZ coupled with thermal stress, accentuated by severe notches such as preexisting cracks or tear at weld toes, or in the fused root of a partial penetration weld.

13.8.3.3.1 *Susceptible Alloys*

RC is reported in low-alloy structural steels, Q&T steels, ferritic creep-resisting steels (Cr–Mo and Cr–Mo–V steels), nickel-base alloys, and austenitic SSs. Chromium, molybdenum, and vanadium contribute to this crack susceptibility. The appearance of the cracking and its position will depend on the local factors, such as [15] geometry of the joint, the relative properties of the weld metal and HAZ, and presence or absence of long-range stresses.

Phosphorus was found to enhance the RC susceptibility of Cr–Mo steels, as it segregates to some extent to the austenite grain boundaries during the weld thermal cycle. For a particular alloy, there exists a critical level of P above which embrittlement is apparent. The addition of a small amount of Ti (0.07%) decreases the RC susceptibility [69].

13.8.3.3.2 *Empirical Check for Reheat Cracking*

Nakamura et al. [70] observed that susceptibility to stress-rupture cracking (ΔG) in the HAZ of welds is related to composition as follows:

$$\Delta G = \%Cr + 3.3(\%Mo) + 8.1(\%V) - 2$$

According to this equation, cracking is possible if ΔG is greater than zero. However, experience has shown that this relationship does not always give a reliable estimate of crack susceptibility. Furthermore, factors other than chemical composition are known to affect crack susceptibility.

13.8.3.3.3 *Avoidance of Reheat Cracking*

It is possible to weld any steel without the risk of RC if proper design and welding procedures are followed. Some procedures that may be used to minimize SRC in the steels include [69] the following:

1. Welding process changes
 - Proper selection of consumables, joint cleanliness, and proper preheat
 - Use of lower strength weld metal than that of the HAZ
 - Buttering of susceptible alloys
 - Increasing heat input and/or preheat
 - Increasing the amount of grain refinement by overlapping of the HAZ
 - Use of temper beads, that is small stringer beads placed over the last pass to refine the grain structure of the HAZ
2. Complete normalization after welding
3. Use low PWHT temperatures and high heating rates (provided stresses due to temperature gradients can be avoided)
4. Dress weld to remove discontinuities at weld toes and minimize stress concentrations in the weld joint
5. Reduce weld stresses by weld sequencing, back stepping techniques, and interpass PWHT; shot-peen each layer of the weld metal to reduce residual tensile stresses at the surface of the weld
6. Lower the overall level of restraint
7. Control of sulfur level to avoid liquation cracking will also be beneficial since it has been established that liquation cracks can be potent initiation points for RC [15]

13.8.3.3.4 Underclad Cracking

RC taking place under clad surfaces is known as underclad cracking (UCC). UCC of low-alloy steels is a potential problem associated with the fabrication of internally clad pressure vessels, in particular nuclear reactor vessels [69]. The incidence of UCC has been reduced considerably by measures such as [71]

1. Avoid liquation and hydrogen-induced cracks
2. Use low-susceptibility alloys, such as SA508 C13
3. Use clean steels: restrict impurity levels and minimize residual solidification segregation remaining in the surfaces to be clad
4. Reduction of carbide and carbide-forming elements consistent with the compositional requirements to achieve adequate strength
5. Adopt cladding procedures that can ensure a fine-grained structure in the entire HAZ

13.8.3.4 Ductility Dip Cracking

Ductility dip cracking may occur in either weld metal or the HAZ of austenitic steels, cupronickels, aluminum bronzes, and some nickel-base alloys while the weld cools through a range of temperatures where the ductility of the particular metal is inherently low. Cracking occurs if sufficient restraint is present as the metal cools through the ductility dip temperature range. The ductility dip temperature for austenitic steels is 100°C–300°C (212°F–600°F) below the equilibrium solidus, and the cracks formed are generally much less extensive than solidification cracks [66].

13.8.3.5 Chevron Cracking

Transverse cracking in submerged arc welds has been observed when welding 2.25Cr–1Mo steel for pressure vessels, carbon–manganese–niobium steel, and 1Ni–0.5Cr–0.5Mo steel. This form of cracking lies at 45° to the weld surface in multipass welds in thick-walled plate. Due to the inclination of these cracks, they are called chevron cracks. Chevron cracking is associated with large weld beads resulting from high heat inputs [59], the moisture content in the submerged arc fluxes and when high-basicity (low-oxygen-potential) submerged arc fluxes are used. They are not easily detected by ultrasonic inspection method and usually found only with detailed metallographic examination.

13.8.3.6 Crater Cracks

These are cracks formed from a circular surface with a depression either in the weld or at the end of a weld. They are caused by a volume contraction of molten metal during solidification, usually the result of abrupt interruption of the welding arc in the root run. Crater cracks are avoided by taking back the electrode and keeping stationary for a moment at the weld pool while stopping the weld.

13.9 LABORATORY TESTS TO DETERMINING SUSCEPTIBILITY TO CRACKING

13.9.1 WELDABILITY TESTS

Tests are conducted to determine the susceptibility of metals and their alloys to various forms of cracking such as cold cracking, hot cracking, lamellar tearing, etc. They are also carried out by development laboratories for material development of steel, aluminum, and copper, and by fabricating shops for preliminary welding procedure qualification. The laboratory tests come in a wide range of sophistication. All tests restrain the welding during cooling by some means, then gauge the amount of cracking that occurs. Tests for lamellar tearing have been already discussed. Some tests used to determine hot cracking, cold cracking (delayed cracking), or underbead cracking are as follows:

- Spot Varestraint test, for hot cracking
- Longitudinal Varestraint test, for hot cracking
- Sigmajig, for hot cracking

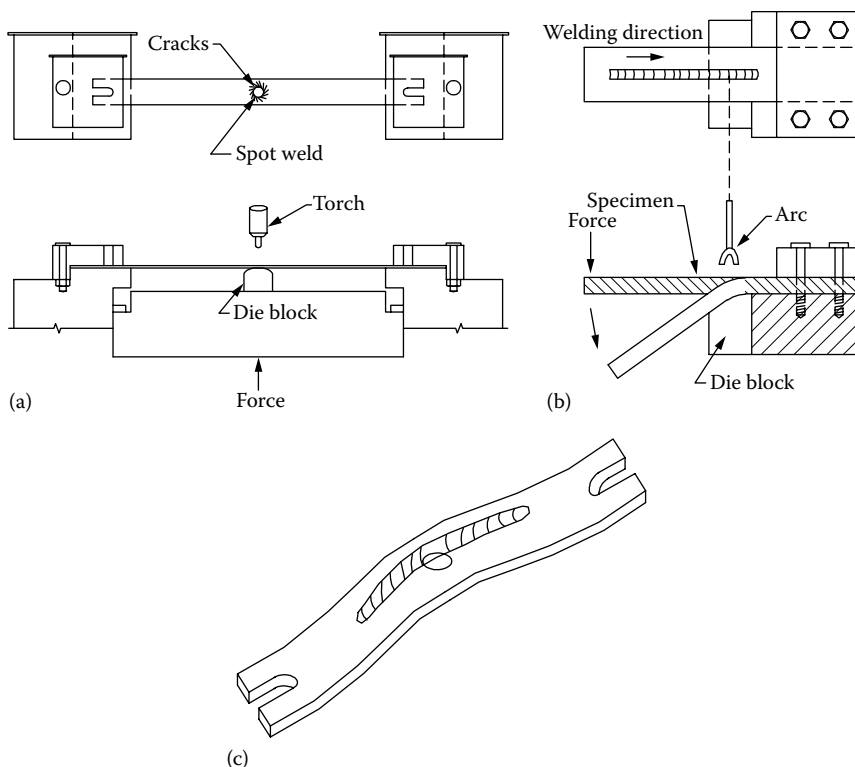


FIGURE 13.11 Configuration for testing weld cracking, (a) spot Varestraint test, (b) longitudinal Varestraint test, and (c) Varestraint test sample.

Hot ductility test, for hot cracking

Lehigh restraint test, for cold cracking

Controlled thermal severity test, for cold cracking

Cruciform cracking test, for cold cracking

Battelle underbead cracking test, for cold cracking

The HAZ liquation cracking susceptibilities of several commercial austenitic and duplex SSs were evaluated using the spot Varestraint test by Lippold et al. [72]. According to them, low ferrite potential (FP) heats (FP 0–1) of Type 304L were found to be more susceptible to cracking than a Type 304 alloy with FP 8, whereas duplex SSs, ferralium 255 and alloy 2205, were roughly equivalent to that of the low-FP austenitic SSs.

Tigamajig is the original name for the spot Varestraint test. Additional tests are discussed and detailed in Ref. [73]. The drawings in Figure 13.11 show some common tests for weld cracking [74,75]. Only the Varestraint test is discussed next.

13.9.2 VARESTRAINT (VARIABLE RESTRAINT) TEST

This test measures the hot-cracking tendency of a weld as it is being laid down on a specimen plate. The Varestraint is one of the few hot-cracking tests that tests for cracking by imposing an external stress. The strain can be calculated from the geometry of the test setup, and it can be reproduced time and time again, independent of the welding procedure. The applied augmented strain, ϵ , can be varied by adjusting the radius of the die block, R , using the equation $\epsilon = t/(2R + t)$, where t is the specimen thickness. In this method, the Varestraint test plate (Figure 13.11a) is bent to a preset radius while an autogenous weld bead is being arc-melted past point X .

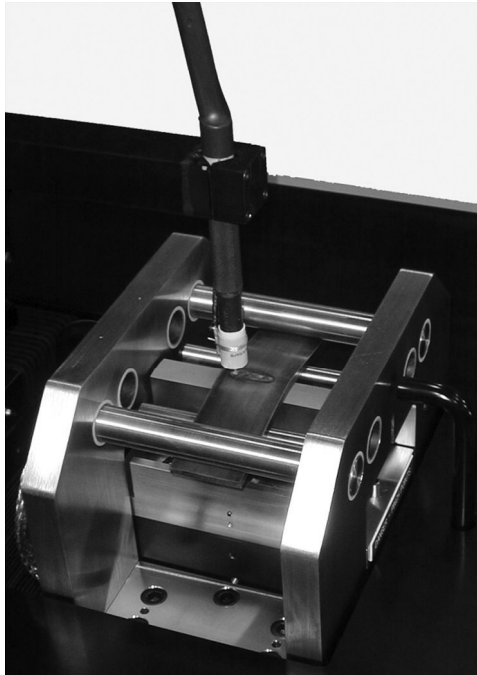


FIGURE 13.12 Multitask Vareststraint Weldability Testing System. (Courtesy of D. L. Wright, Inc., Zanesville, Ohio.)

13.9.3 MULTITASK VARESTRAINT WELDABILITY TESTING SYSTEM

The Multitask Vareststraint (MTV) Weldability Testing System (Figure 13.12) is used to evaluate the solidification, liquidation, and HAZ cracking susceptibility of materials. This system can perform both conventional (i.e., consecutive) and simultaneous Vareststraint tests for three types of welds: spot, transverse, and longitudinal. In the conventional or consecutive test method, strain is applied to the sample after the weld is completed. In the simultaneous test method, strain is applied to the sample as the weld is being produced. The graphical user interface allows the user to easily establish test parameters, which are controlled through a closed-loop system. The parameters include thus: welding torch position and speed (X, Y, Z), bend rate, bend delay time, and bend holding time.

13.10 SERVICE-ORIENTED CRACKING

13.10.1 TEMPER EMBRITTLEMENT OR CREEP EMBRITTLEMENT

Cr–Mo low-alloy steels are susceptible to temper embrittlement, a condition caused by long-term, elevated-temperature exposure in the 370°C–560°C (700°F–1050°F) range, coupled with the presence of impurity elements such as phosphorus, tin, antimony, and arsenic. The phenomenon results in the progressive reduction of the notch toughness of the material as embrittlement develops. As the material toughness decreases, its resistance to brittle fracture decreases. This phenomenon is discussed further in the Section 13.15.5 on Cr–Mo steels.

13.11 WELDING-RELATED FAILURES

Welding-related failures take place (1) during welding, e.g., lamellar tearing, cold cracking, and hot cracking; (2) during stress-relief annealing, e.g., temperature-induced embrittlement, elongation-induced embrittlement, and SRC; and (3) during operation, e.g., stress-induced corrosion,

intergranular corrosion, SCC, crack growth, and creep embrittlement [76]. Inadequate welding techniques often degrade the inherent corrosion resistance of parent metals.

13.12 SELECTION OF CAST IRON AND CARBON STEELS

13.12.1 CAST IRON

For low-pressure applications, cast-iron bonnets and covers are used. According to ASME Code Section VIII, Div. 1, cast-iron vessels shall not be used for the following services:

- To contain lethal or flammable substances, either liquid or gases
- For unfired steam boilers
- For direct firing

The design pressure and temperature limitations for the vessels and the vessel parts constructed of cast iron are listed in ASME Code Section VIII, Div. 1, UCI-3.

13.12.2 STEELS

Grades of steel may vary in chemical composition from almost pure iron to a material of complex composition made up of several elements. Widely dissimilar properties and qualities may be obtained from a carbon steel within specified chemical limits of a given grade by changes in steel making and mill processing. In the selection of the proper quality within a given grade, the end use and method of fabrication should be considered. Various practices are employed in all phases of steel production that determine the type and quality of the finished product.

Carbon steel is the steel for which no minimum content is specified or required for alloying elements such as, chromium, cobalt, columbium, molybdenum, nickel, titanium, tungsten, vanadium, or zirconium, or any other element added to obtain a desired effect; when the specified minimum for copper does not exceed 0.40%; or when the maximum content specified for any of the following elements does not exceed the percentages noted: manganese 1.65, silicon 0.60, and copper 0.60. Carbon steel depends on carbon and manganese in conjunction with proper processing to improve mechanical properties.

High-strength low-alloy (HSLA) steel comprises a group of steels with chemical composition specially developed to impart higher values of mechanical properties—in certain of these steels, greater resistance to atmospheric corrosion than that is obtainable from conventional carbon structural steels. It is not considered to be alloy steel, even though an intentionally added alloy would qualify it as such. The minimum yield point and tensile strength requirements most often specified are 42–80 ksi (290–550 MPa) yield point and 60–90 ksi (415–620 MPa) tensile strength. These steels achieve high strength, high toughness, good formability, and good weldability.

Low-alloy steels are divided into groups according to their chemical composition, that is molybdenum alloy steel, manganese–molybdenum–nickel alloy steel, and chromium–molybdenum alloy steel, and each group is further divided according to strength level. Steels are commercially classified as low-alloy steels when they have

1. Manganese content exceeding 1.65%
2. Silicon content exceeding 0.60%
3. Copper content in excess of 0.60%
4. A range or a minimum amount of any other alloying element such as nickel, molybdenum, vanadium, chromium, etc., specified or added to obtain any alloying effect

Alloy steels can utilize a wide variety of alloying elements and heat treatments to develop the most desirable combination of properties.

13.12.2.1 Process Improvements

Steel making has undergone considerable change in the last 25 years, resulting in various steels with changes in properties of the end product. Improved refining techniques, vacuum induction melting (VIM) technique, low-sulfur steel-making methods, refining processes such as argon–oxygen decarburization (AOD, process primarily used in stainless steel making and other high-grade alloys with oxidizable elements such as chromium and aluminum), and vacuum oxygen decarburization (VOD), electroslag remelting, ladle metallurgy, vacuum degassing, pressure casting, continuous casting, controlled rolling, etc., resulted in clean, low-carbon-equivalent steels of high design strengths and improved weldability, increased corrosion resistance, and increased toughness.

13.12.2.2 Carbon Steels

Carbon steels are alloys of iron and carbon in which carbon does not usually exceed 1%, manganese does not exceed 1.6%, and copper and silicon do not exceed 0.60%. Other alloying elements are normally not present in more than residual amounts. The properties and weldability of carbon steels mainly depend on carbon content. Carbon steel can be classified according to various deoxidation practices, as rimmed, capped, semikilled, or killed steel. Variations in carbon content will influence the mechanical properties. Carbon steels are normally used in the as-rolled condition, although some may be in the annealed or normalized condition.

13.12.2.3 Types of Steel

In steel making, the principal reaction is the combination of carbon and oxygen to form a gas. If the oxygen is not removed, the gaseous product continues to evolve as the steel changes from a liquid to a solid. Silicon and/or aluminum are added to remove the oxygen. Control of the amount of gas evolved during solidification determines the type of steel. If practically no gas is evolved, the steel is completely deoxidized and is termed “killed” because it lies quietly in the molds. Increasing degrees of gas evolution result in semikilled, capped, or rimmed steels [77].

Killed steels are fully deoxidized and are characterized by more uniform chemical composition and mechanical properties as compared with other types. In general, killed steel is specified when homogeneous structure and internal soundness are required. It may be made fine grained or coarse grained. Generally, most carbon specifications require that plate over 1.5 in. (38 mm) thick be made from killed steel.

Semikilled steels are characterized by variable degrees of uniformity in composition that are intermediate between those of killed and those of rimmed steel. They are deoxidized less than killed steels.

Rimmed and capped steels are characterized by marked difference in chemical composition across the section and from top to bottom of the ingot. There is a continuous evolution of gas during solidification resulting in a rim, or case of purer, cleaner solid metal free from blowholes and inclusions. They are, therefore, primarily used for making products requiring a very good surface. Most sheet and strip products are this type of steel. Steels that rim best contain no more than 0.15% carbon. Steels containing more than 0.30% carbon cannot be made to rim at all. Steels that are completely deoxidized cannot be rimmed [77].

13.12.2.4 Product Forms

Steels are available in plates, tubes, pipes, forgings, etc.

Carbon steels for pressure vessels

These are specified as A285, Grade A, B, C; A229; A442, Grade 55, 60; A515, Grade 55, 60, 65, 70; A516, Grade 55, 60, 65, 70; A537, Grade 1 (Q&T condition) and Grade 2 normalized and tempered condition

13.12.2.5 Use of Carbon Steels

Due to low cost, carbon steels are most widely used, despite their low corrosion resistance, in large quantities as heat exchanger material in the chemical industries, fossil fuel power plants, petroleum refining operations, etc. Apart from cost, the other properties that favor low-carbon steels are (1) easy availability and (2) ease of fabrication by conventional methods. Features that favor carbon steels for feedwater applications and refinery applications are discussed next.

13.12.2.5.1 Carbon Steel Tubes for Feedwater Applications

In recent years, manufacturers were forced to abandon copper alloy tubes for high-pressure feedwater heater tubing. At the elevated feedwater temperatures used in modern power-plant cycles, the corrosion of copper tubes by the feedwater, although very slight, gives rise to the problem of carryover of copper into the steam generator and possible blockage in turbine units [47,78]. Sometimes low-molybdenum alloy steel is also used. The factors that favor plain carbon steel or low-molybdenum alloy steel are better weldability, high strength, and low cost. The slightly lower thermal conductivity of carbon steel than the copper–nickel is of little significance in the small-bore thin-wall tubes used in high-pressure feed heaters. The fundamental deficiency of carbon steel tubing is its low resistance to corrosion. The general corrosion and pitting problems with carbon steel tubes can be minimized with improved handling and fabrication techniques, controlled water conditions, and proper shutdown practices. These materials require corrosion protection when the plant is idle for considerable periods.

13.12.2.5.2 Refinery Operations

In refinery operations, carbon steel is an acceptable material for crudes up to 260°C to resist hydrogen attack and sulfide corrosion. At higher temperatures, corrosion rates increase and alloy steels or ferritic or SS may be used.

13.12.2.5.3 Corrosion Resistance

The corrosion resistance of carbon steel is somewhat limited and is dependent on the formation of an oxide film on its surface. Carbon steel should not be used in contact with dilute acids.

Carbon steels are susceptible to SCC by several corrosives including aqueous solutions of amines, carbonates, acidified cyanides, hydroxides, ammonium nitrate, anhydrous ammonia, coal gas liquors [2,79], and sulfide cracking of steels used in sour oil fields containing hydrogen sulfide. The temperature and concentration limits for the susceptibility of carbon steel to SCC in caustic soda are fairly well defined and given in chart form [24]. Of all the metallic materials, carbon steel is the most economical for handling solutions of up to 50% concentration at temperatures up to 190°F (88°C). If iron contamination is permissible, steel can be used to handle caustic soda up to 75% concentration and up to 100°C (212°F). Stress relieving should be employed to reduce caustic embrittlement.

Brine and seawater corrode steel at a slow rate. Steel is little affected by neutral water and most organic chemicals. In general, the presence of oxygen and/or acidic conditions will promote the corrosion of carbon steel, while alkaline conditions will inhibit the corrosion of carbon steel.

General aqueous corrosion: Principal factors governing the overall corrosion of carbon steel include solution pH, dissolved oxygen in the solution, temperature, dissolved salts, and solution. The effects of these factors are well discussed by Kirby [80]. Salient features of carbon steel in aqueous solutions are discussed next [80]:

Effects of pH: Acidic solutions (pH less than 5) are highly corrosive to carbon steel. The protective oxide is soluble at pH values below 5.0 and above 13.0. Corrosion is low over a wide band of pH values [81].

Effects of dissolved oxygen: At ambient temperatures in near-neutral solutions, the overall corrosion rate is proportional to the oxygen concentration, up to air saturation.

Temperature effects: High temperatures increase the corrosion rate by accelerating the diffusion of oxygen through cathodic layers of hydrated iron oxide.

Effects of dissolved salts: The presence of acid or neutral salts may increase the corrosion rate, whereas the presence of alkaline salts may lower them.

Effects of velocity: In general, increasing the solution velocity steps up corrosion rates, especially if NaCl is present. To prevent failures due to the impingement of natural waters on equipment walls, velocities should be limited to a maximum of 8 ft/s.

Carbon steels exhibit passivity in alkaline environment and have minimal corrosion rates. This property is exploited in phosphating. Corrosion prevention measures for carbon steels include metallic coatings, painting, cathodic protection, addition of inhibitors, alloying additions, removal of oxygen from environment, elimination of galvanic couples, and organic coatings.

13.12.2.6 Fabrication

13.12.2.6.1 Plate Cutting

Carbon steel plates are to cut to size by flame cutting and/or machining. All plate edges after cutting must be examined for laminations and to ensure that the sheared edges are free from cracks. Dye penetrant and ultrasonic check of edges forming main weld seams is recommended, especially for higher thickness plates when these plates are used for low-temperature or hydrogen service.

13.12.2.6.2 Rating of Weldability

The weldability of a steel in terms of its susceptibility to cracking can be roughly estimated by CE. The influence of CE on weldability has already been covered in Section 13.7.

13.12.2.6.3 Weldability Considerations

While welding carbon steel, consider the following factors:

1. Hydrogen-induced cold cracking
2. Solidification cracking
3. Lamellar tear
4. Hardness limitation for refinery service and sour gas service

These problems are also discussed by Campbell [82] and in Ref. [83]. Factors 1–3 were discussed in Section 13.7.

13.12.2.6.4 Hardness Limitation for Refinery Service

The prevention of in-service weld cracking is of special concern to the refining industry because carbon steel is widely used for refinery pressure vessels, heat exchangers, tanks, and piping. Three primary factors are believed to be involved in producing in-service cracking of welds: corrosive environment, total stress, and hardness. NACE Standard RP-04-72 establishes a hardness limitation of 200 HB on completed P-I welds. Hardness limitation is further discussed in Chapter 12.

13.12.2.6.5 Welding Processes

Most carbon steels can be welded using covered electrodes and appropriate welding procedures including preheating when required. Welding processes used for carbon steel are gas metal arc welding (GMAW), flux-cored arc welding (FCAW), submerged arc welding (SAW), electroslag and electrogas welding, and oxyacetylene welding (OAW).

13.12.2.6.6 Arc Welding of Carbon Steels

Selection of welding electrodes is based on compatibility between base metals to be joined and the service requirements of the weldment. The essential factors in the selection of electrodes for the carbon steels are (1) mechanical properties, (2) material composition, (3) welding current, (4) position of welding, and (5) cost. Precautions should be taken to store electrodes in dry places.

TABLE 13.10**Carbon Steel Welding Defects Associated with Various Arc Welding Methods**

SMAW	FCAW	SAW	GMAW and GTAW
Slag inclusion	Due to excessive arc voltage:	Weld porosity	GMAW
Porosity		Contaminants in the flux	Weld-metal cracks
Wormhole porosity	Porosity		Porosity
Undercuts	Heavy spatter	Insufficient flux coverage	Inclusions
Hot cracking	Undercutting		Incomplete fusion
Cold cracking	Due to excessive current:	Excessive viscous fluxes	Lack of penetration
Centerline cracking			Undercutting
Underbead cracks	Convex weld beads	Arc blow	Excessive melt-through
Base metal cracks	Large droplet	Cracking	
Microfissuring	Due to travel speed:	Solidification cracking	Wire feed stoppage
Weld craters	Slag interference	Hydrogen cracking	Inadequate shielding
Arc strikes	Convex weld bead	Chevron cracking	GTAW
Oxidation		Underbead cracking	Contamination of tungsten electrodes
Gaps from incomplete fusion		Slag inclusions	Tungsten inclusion
Sink or concavity			Electrode extension
Weld reinforcement overlapping			
Excessive weld spatter			

Source: Compiled from Nippes, E.F. (ed.), *Metals Handbook, Vol. 6, Welding, Brazing, and Soldering*, 9th edn., American Society for Metals, Metals Park, OH, 1983, pp. 238–244.

The minimum thickness of low-carbon steel that can be welded by shielded metal arc welding (SMAW) depends on welder's skill, welding position, characteristic of the current, type of joint, fitup, class and size of electrode, amperage, arc length, and welding speed. Steel as thin as 0.036 in. (0.91 mm) has been successfully welded with flux-covered electrodes.

In terms of thick sections, all commercial thicknesses can be welded successfully by SMAW provided that the root of the joint can be reached with the electrode.

13.12.2.6.7 Welding Defects

Since carbon steels are used extensively, the welding defects associated with various arc welding methods are given in Table 13.10.

13.13 LOW-ALLOY STEELS

13.13.1 SELECTION OF STEELS FOR PRESSURE VESSEL CONSTRUCTION

The most important factors to be considered in the selection of steels for pressure vessels and heat exchangers are tensile strength, creep strength, notch toughness, weldability, and heat treatment. In general, thinner steel plates are preferred for these reasons [29]: low weight, ease of fabrication, and low foundation cost; ease of welding, heat treatment and stress relief, NDT, erection, higher fatigue strength, and resistance to brittle fracture. The inherently poorer properties of thicker sections of carbon steels are well known. For example, increased thickness offers greater internal restraint at a

defect and thus increases the likelihood of defect growth by brittle fracture. Therefore, the trend is to use high-strength steels in place of thicker plates.

13.13.2 LOW-ALLOY STEELS FOR PRESSURE VESSEL CONSTRUCTIONS

Low-alloy steels used in pressure vessel and heat exchanger construction are the following:

1. Carbon–molybdenum steels
2. Carbon–manganese steels
3. Carbon–manganese–molybdenum steels
4. Manganese–molybdenum–nickel alloy steels
5. Chromium–molybdenum steels or creep-resistant steels such as Cr–Mo, Cr–Mo–V, and modified Cr–Mo steels

Items 1–4 are covered here, and chromium–molybdenum steels are covered separately.

13.13.2.1 Applications of Low-Alloy Steel Plates

Principal applications for low-alloy steel plates include [18] the following:

1. Boiler drums for thermal power plants
2. Reactor pressure vessels, steam generators, and pressurizers for nuclear power plants
3. Various types of reactors, converters, steam drums, separators, pressurizers, heat exchangers, and hydrocrackers for chemical plants

Of all these types of equipment, large nuclear reactors and heavy oil desulfurizers require particularly heavy steel plates, ranging from 150 to 300 mm in thickness and 30 to 50 tons in unit weight.

13.13.2.2 Carbon–Molybdenum Steels

Carbon–molybdenum steels are similar to carbon steels except they have an addition of approximately 0.5% Mo. The addition of 0.5% Mo and a little boron to carbon steels has a considerable effect on the transformation to lower bainite at normal rates of cooling [84]. This has a relatively high strength, which is retained to a moderately high temperature. These steels include ASTM A204 Grades A, B, and C; A302 Grades A and B; and ASTM A182 Grade F1 forging. Steels with 0.5% Mo find considerable use in the petroleum industry, where they have replaced carbon steel because of their resistance to hydrogen at higher temperatures. The possibility of graphitization limits their use to a maximum temperature of 875°F (470°C) [29]. These steels are produced in the as-rolled or normalized condition. The weldments should be given PWHT.

13.13.2.3 Carbon–Manganese Steels

These steels find use in pressure vessels, ships, and other large fabrications. Manganese is added to steel for a number of reasons [15,85]:

1. Manganese combines preferentially with sulfur to form manganese-rich sulfide inclusions of high melting point that are not liquid during the hot working of the steel and hence have little effect on the toughness of the resulting product, since they are distributed more uniformly in the steel.
2. Manganese increases the strength of the steel by forming a solid solution with the iron.
3. Manganese retards the transformation of austenite to ferrite and pearlite. This means effectively that in thicker plates and sections, which cool more rapidly at the surface than in the interior, better and more uniform properties can be obtained.

The properties of carbon–manganese steels can be further improved in a number of ways [15,85]:

1. By grain refining: The addition of aluminum to a killed steel refines its grain size to produce greater toughness
2. By normalizing
3. By controlled rolling—this leads to relatively high strength and toughness
4. Quenching and tempering: If carbon–manganese steels are quenched, products with a good combination of strength and toughness can be obtained

Fabricators have not been able to join these steels by the most productive processes, like electroslag welding and SAW, because these steels cannot tolerate the high heat input of these processes. As heat input increases, austenite grains in these base metals and in weld HAZs grow large; slow cooling results in a grain-coarsened ferrite microstructure of low toughness [58]. For continuously cast steels of thickness 2 in. and less, titanium treatment involving titanium nitride additions provides inclusion sites for grain refinement, whereas thicker sections (>2 in./50.4 mm) and ingot-cast steels cool too slowly to achieve grain refinement.

To avoid the formation of hard constituents in weld metal susceptible to hydrogen cracking, slow the cooling rate by increasing heat input to the weld; in multipass welding, proper sequencing can reaustenize previous passes to form softer microconstituents and temper hard ones [58].

13.13.2.3.1 Application of Carbon–Manganese Steels

Carbon–manganese steels are cheaper, and they are relatively easy to produce in large quantities. They include the so-called mild steel boiler quality plate with yield strengths of about 15 tonf/in.² (230 N/mm²) and ultimate strengths of about 25 tonf/in.² (385 N/mm²). They are extensively used in boilers and high-pressure plants working at up to, say, 350°C (660°F). Above this temperature, however, they lose their strength very rapidly, and in addition, they have inadequate corrosion resistance and scaling resistance. The ambient temperature strength can be improved substantially by normalizing, by controlled rolling, and by quenching and tempering [15]. Controlled rolled steels are available with minimum yield strengths exceeding 25 tonf/in.² (385 N/mm²) and Q&T steels with even higher strength.

13.13.2.4 Carbon–Manganese–Molybdenum Steels

The addition of molybdenum to carbon–manganese steel increases the strength at ambient temperature slightly but has a marked effect on the strength at higher temperature. Carbon–manganese steels containing about 0.5% Mo have found extensive use in pressure vessels. However, their creep ductility is rather limited, and for that reason and for their improved resistance to high-temperature corrosion and oxidation, the chromium–molybdenum steels may be preferable in some cases.

13.14 QUENCHED AND TEMPERED STEELS

An important group of steels is those in which the hardenability is increased by alloy additions so as to produce martensite throughout the plate thickness when the steel is quenched or even air-cooled from the austenite range. The steels are then tempered to give the required properties. The total alloy content of such steels may be relatively high, but they have a very attractive combination of strength and toughness. These steels are known as Q&T steels. They are also relatively easy to weld since the carbon content to achieve a given strength can be kept low. The use of the term “quenched and tempered” is a little misleading since it may not always be applied to martensitic steels. Some “normalized and tempered” steels have to be quenched and tempered when used in thick sections to achieve the required rate of cooling and hence the desired properties [15]. Better properties can be obtained by quenching and tempering carbon–manganese steels as well as more highly alloyed steels.

13.14.1 COMPOSITIONS AND PROPERTIES

These steels contain not more than 0.25% carbon and a total content of alloying elements (not including Mn and Si) ranging from 0.85% to about 16%. Q&T steels are furnished in the heat-treated condition with yield strengths ranging from 50 to 150 ksi depending on chemical composition, thickness, and heat treatment. They have high strength in combination with good ductility. Various combinations of toughness, fatigue strength, and corrosion resistance can be developed to meet the requirements of pressure vessels for use in atmospheric conditions, at elevated temperature, or at cryogenic temperatures. Some Q&T steels fall within the ASTM carbon steel classification, and others within the alloy steel classification. Typical Q&T plate steels are given in Table 13.11. A brief description of some of these Q&T steels is given next, and important sources on Q&T steels include Refs. [18,43,86].

1. A517 Alloy steel: Fifteen grades, quenched and tempered to yield strengths (minimum) of 90 ksi (more than 2.5–6 in.) and 100–125 ksi (less than 2.5). Amounts of C, Mn, Si, and other minor alloying elements such as Ni, Cr, Mo, B, V, Ti, Zr, and Cu vary with grades.
2. A533 Alloy steel: Four types, quenched and tempered to three tensile strength ranges, 80–100 ksi, 90–115 ksi, and 100–125 ksi. Composition: 0.50Mo (Type A), 0.50Mo + 0.55Ni (Type B), 0.85Ni (Type C), and 0.30Ni (Type D). This steel, with a somewhat higher carbon content, has the least susceptibility to hot cracking because it has a high manganese-to-sulfur ratio, usually about 50:1. ASTM A533 Grade B steel is used in thick section for nuclear pressure vessels, and at its highest strength level (Class 3), it may be used for thin-walled or layered pressure vessels.

TABLE 13.11
Q&T Steel Plates, ASTM Specification

A203 Grade F	A542 Type A Cl. 1	A553 Type 1 (8% and 9% Ni steel)
	A542 Type A Cl. 2	
A517 (15 Grades)	A542 Type A Cl. 3	
	A542 Type A Cl. 4	A645 5% Ni steel
A533 Type A Cl. 1	A542 Type A Cl. 4a	
A533 Type A Cl. 2	A542 Type B Cl. 1	A724 Grade A
A533 Type A Cl. 3	A542 Type B Cl. 2	A724 Grade B
A533 Type B Cl. 1	A542 Type B Cl. 3	A724 Grade C
A533 Type B Cl. 2	A542 Type B Cl. 4	
A533 Type B Cl. 3	A542 Type B Cl. 4a	A734 HSLA Type A
A533 Type C Cl. 1	A542 Type C Cl. 1	A734 HSLA Type B
A533 Type C Cl. 2	A542 Type C Cl. 2	
A533 Type C Cl. 3	A542 Type C Cl. 3	A738 Grade A
A533 Type D Cl. 1	A542 Type C Cl. 4	A738 Grade B
A533 Type D Cl. 2	A542 Type C Cl. 4a	
A533 Type D Cl. 3		A782 Class 1
	A543 Type B Cl. 1	A782 Class 2
A537 Cl. 2	A543 Type B Cl. 2	A782 Class 3
	A543 Type B Cl. 3	
	A543 Type C Cl. 1	
	A543 Type C Cl. 2	
	A543 Type C Cl. 3	

Note: A543 Grade is: Q&T up to 4 in. A738 Grade A is N or Q&T up to 2.5 in.; Q&T over 2–5 in.

3. ASTM A537 (Class 2) carbon steel is used in pressure vessels where high notch toughness is required.
4. A542 Alloy steel: Five classes, quenched and tempered to tensile strengths (minimum) of 85, 95, 105, and 115 ksi. Two types of 2.25Cr–1Mo steels, one type of 3Cr–1Mo–0.25V–Ti–B steel.
5. A543 Alloy steel: Three classes, quenched and tempered to tensile strengths (minimum) of 90, 105, and 115 ksi. Two types of Ni–Cr–Mo steels.
6. A553 Alloy steel: Two types, quenched and tempered to 85 ksi yield strength (minimum).
7. ASTM A592 used as forgings where good notch toughness is needed in a steel having a yield strength of 100 ksi.

13.14.2 WELDABILITY

The carbon content of Q&T steels generally does not exceed 0.22% for good weldability. The alloying elements are carefully selected to ensure the most economically heat-treated steel with the desired properties and acceptable weldability. The development of good notch toughness in the HAZ of Q&T steels depends on the rapid dissipation of welding heat to permit the formation of martensite and bainite on cooling. This requirement may increase the susceptibility of the Q&T steel to hydrogen-induced cold cracking.

13.14.3 JOINT DESIGN

Appropriate joint design, good workmanship, and adequate inspection are needed to take advantage of the high strength of Q&T steels and to optimize the serviceability of weldments made from these steels. Weld joint design should avoid abrupt changes in sections to reduce stress concentrations, the welds must be located at sites where there is sufficient access for weld inspection, and fillet welds are preferred to butt welds. Joint preparation can usually be done by gas or arc cutting without preheating. Excessive weld reinforcement should be avoided.

13.14.4 PREHEAT

Preheat for welding Q&T steels must be used with caution because it reduces the cooling rate of the weld HAZ. If the cooling rate is too slow, the reaustenized zone adjacent to weld metal can transform to ferrite with regions of high-carbon martensite or coarse bainite, with loss of strength and toughness.

13.14.5 WELDING PROCESSES

Welding processes such as SMAW, SAW, GMAW, FCAW, and GTAW can be used to join Q&T steels having minimum yield strength up to 150 ksi and carbon content up to 0.25%. Filler metal should be selected with care. Adopt low-hydrogen welding practices: use properly dried low-hydrogen electrodes, clean and dry flux, moisture-free shielding gas, clean low-hydrogen electrode wire, etc.

13.14.6 POSTWELD HEAT TREATMENT

The heat treatment for most of these steels consists of austenitizing, quenching, and tempering. A few are given a precipitation hardening (PH; aging) treatment following hot rolling or a hardening treatment. Welded structures fabricated from these steels generally do not need further heat treatment except for a stress relief in special situations. Stress relief is necessary for these

circumstances: (1) The steel has inadequate notch toughness after cold forming or welding, (2) to maintain dimensional stability after fabrication, and (3) the weldment with high-residual stress is susceptible to SCC.

13.14.7 STRESS-RELIEF CRACKING

The weldments of many quenched and low-alloy steels are susceptible to SRC, also known as RC. Chromium, molybdenum, and vanadium contribute to this type of cracking, but other carbide-forming elements also contribute to SRC. Measures to overcome SRC have been discussed in the earlier Section 13.8.3.3 weldability consideration.

13.15 CHROMIUM–MOLYBDENUM STEELS

Chromium–molybdenum steels, also referred as creep-resistant low-alloy steels, are used for fabricating pressure vessels to be operated under high-temperature and high-pressure conditions. These steels contain varying amounts of chromium up to a nominal composition of 9%, and 0.5% or 1% molybdenum. The carbon content is normally less than 0.20% to achieve good weldability, but the alloys have high hardenability. The chromium provides improved oxidation and corrosion resistance, and the molybdenum increases strength at elevated temperatures. These steels usually come from the steel manufacturer in the annealed, normalized and tempered, or Q&T condition. The most popular grades of creep-resistant Cr–Mo steels are 0.5Cr–0.5Mo–0.25V, 1Cr–0.5Mo, and 1.25Cr–0.5Mo and 2.25Cr–1Mo (with or without vanadium). 1Cr–0.5Mo (Grade 11) and 2.25Cr–1Mo steel (Grade 22, Class 2) have long been used to fabricate heavy sections of pressure vessel and piping for fossil power, petroleum, and petrochemical applications. 2.25Cr–1Mo steel is frequently used for its superior hot strength; plates are covered by specification SA-387, Grade 22, Class 2, and forgings by specification SA-336, Grade F22. 5Cr–1Mo and 9Cr–1Mo are widely used in the petrochemical industry for their superior corrosion and oxidation resistance [87].

13.15.1 COMPOSITION AND PROPERTIES

ASTM specification A387, Grades 2, 5, 7, 9, 11, 12, 21, 22, and 91, cover plates, and ASTM A182 Grades F2, F5, F7, F9, F11, F12, F21, and F22 deal with forging. The nominal chemical compositions of certain grades of Cr–Mo steels are given in Tables 13.12 and 13.13. Some alloys may contain small additions of columbium, titanium, or vanadium, or increased amounts of carbon or silicon for specific applications. The structure of the chromium–molybdenum steels is usually a ferrite/bainite.

TABLE 13.12
ASTM A387/A387M Cr–Mo
Steel Nominal Composition

Grade	Cr%	Mo%
2	0.50	0.50
12	1.00	0.50
11	1.25	0.50
22.22L	2.25	1.00
21.21L	3.00	1.00
5	5.00	0.50
7	7.00	0.50
9	9.00	1.00
91	9.00	1.00

TABLE 13.13
Nominal Composition of ASTM A387/A387M Cr–Mo Steel Plate

Grade	Generic Name	Composition (%)				
		C	Mn	Si	Cr	Mo
12	1.00Cr	0.05–0.17	0.40–0.65	0.15–0.40	0.80–1.15	0.45–0.60
11	1.25Cr	0.05–0.17	0.40–0.65	0.50–0.80	1.00–1.50	0.45–0.65
22	2.25Cr	0.05–0.15	0.30–0.60	0.50 max	2.00–2.50	0.90–1.10
5	5.00Cr	0.15 max	0.30–0.60	0.50 max	4.00–6.00	0.45–0.65
91	9.00Cr	0.06–0.15	0.30–0.60	0.50–1.00	8.00–10.00	0.90–1.10

TABLE 13.14
ASTM Specification for Chromium–Molybdenum Steel Product Forms^a

Steel Type	Plate:ASTM Spec.	Tube:ASTM Spec.	Max. Service Temperature
0.5Cr–0.5Mo	A387–Gr2, Cl. 1,2	A213–T2	
1Cr–0.5Mo	A387–Gr12, Cl. 1,2	A213–T11, T12	450°C–475°C
1.25Cr–0.5Mo	A387–Gr11, Cl. 1,2	A199–T11, A200–T11, A213–T11	450°C–500°C
2.25Cr–1Mo	A387–Gr22, Cl. 1,2, A542	A199–T22, A200–T22 A213–T22	500°C–550°C
3Cr–1Mo	A387–Gr21	A199–T21, A200–T21 A213–T21	500°C–550°C
5Cr–0.5Mo	A387–Gr5, Cl. 1,2	A199–T5, A200–T5 A213–T5	550°C
7Cr–0.5Mo	A387–Gr7	A199–T7, A200–T7 A213–T7	550°C
9Cr–1Mo	A387–Gr9, Cl. 1,2	A199–T9, A200–T9 A213–T9	550°C–600°C

^a Forgings and bar–ASTM A182, Pipe A 335, Welded fittings A234.

These steels are used in pressure vessels as plates, tubes, pipes, forgings, and castings. ASTM specifications for various product forms are shown in Table 13.14.

13.15.2 APPLICATIONS

Chromium–molybdenum steels are primarily used for service at elevated temperatures up to about 1300°F (704°C) in applications such as power plants and petroleum refineries, and in chemical industries for pressure vessels and piping systems. However, the normal application temperature range is 400°C–550°C. These alloys exhibit excellent resistance to refinery corrosives like sulfur, elevated temperature, and hydrogen attack. For improved corrosion resistance, these alloys are often overlaid with SS.

13.15.3 CREEP STRENGTH

The optimum creep strength is developed in chromium–molybdenum steels by tempering following normalizing or quenching. In the more highly alloyed steels, the tempering treatment results in the precipitation of fine particles of alloy carbide, which are very effective in producing good

creep strength. It should be noted, however, that there is usually a corresponding decrease in the fracture toughness. A further increase in creep strength is achieved by the addition of vanadium to give normal compositions such as 1Cr–0.5Mo–0.25V and 0.5Cr–0.5Mo–0.25V. The presence of a fine dispersion of V carbides makes the steels more stable than other chromium and molybdenum carbides. Like other grades, vanadium is added to 2.25Cr–1Mo steel to improve creep strength.

13.15.4 WELDING METALLURGY

Cr–Mo steels are weldable, but they require a higher degree of welding design and control than low-carbon steel. The primary difference is the air hardenability of alloy steels. These steels are susceptible to cracking from inadequate ductility. Such types of cracking include lamellar tearing, hot cracking, and reheat or SRC. The welding procedures must incorporate low-hydrogen welding practices to prevent hydrogen-induced cracking in the weld metal and in the HAZ. They are welded in various heat-treated conditions: annealed, normalized and tempered, or quenched and tempered. Welded joints are often heat-treated prior to use to improve ductility and toughness and reduce welding stresses.

13.15.4.1 Joint Design

Joint design should provide adequate room for electrode manipulation to ensure root bead penetration and subsequent ease of slag removal. The joint geometry should minimize any notch conditions that act as stress raisers. Sharp corners and rapid changes in section size are to be avoided.

13.15.4.2 Joint Preparation

Joint edges can be prepared by shearing, machining, grinding, gas cutting, or arc cutting. Before welding, surface irregularities that act as stress raisers must be ground out. Surface contaminations and other foreign materials must be removed. Tenacious chromium oxides that form during thermal cutting and heating and that melt at higher temperatures than the base metal and scale should also be removed by suitable means.

13.15.4.3 Preheating

Preheating is extremely important when welding air-hardening Cr–Mo steels. Preheating is required to prevent hardening and cracking. Preheating reduces stresses, limits or tempers martensitic areas, and reduces the amount of hydrogen retained in the weld. A weld without preheat or even a small arc strike will cause localized hard spots that can initiate solidification or delayed cracking. Holding the joint at a postheat temperature (equal to the preheat temperature) after the weld is completed allows hydrogen to diffuse out of the weld.

13.15.4.4 Welding Processes

Most fusion-welding processes can be applied for joining Cr–Mo steels. Typical welding processes include SMAW, GTAW, plasma arc welding (PAW), SAW, electroslag welding, GMAW, and FCAW.

13.15.4.5 Filler Metal

The filler metal composition should be nearly the same as that of the base metal, except for carbon content to obtain uniform strength and resistance to heat and corrosion. The carbon content of the filler metal is usually lower than that of the base metal. A matching carbon content is required when the weldment is to be quenched and tempered or normalized and tempered.

13.15.5 TEMPER EMBRITTLEMENT SUSCEPTIBILITY

Cr–Mo steels, especially 2.25Cr–1Mo steels, are susceptible to temper embrittlement, a condition caused by long-term, elevated-temperature exposure in the 370°C–560°C (700°F–1050°F) range,

associated with the presence of impurity elements, such as phosphorous, tin, antimony, and arsenic [88–90]. The phenomenon results in the progressive reduction of the notch toughness of the material as embrittlement develops. In other words, due to embrittlement, steels ductile at room temperature tend to become brittle during service. Temper embrittlement susceptibility of 2.25Cr–1Mo steel is very high among Cr–Mo steels and ranks next to (but almost equal to) that of 3Cr–1Mo steel [91]. It has been established that higher silicon and manganese levels will have an even greater effect on toughness degradation.

Requirements for resistance against temper embrittlement and low-temperature toughness are becoming severer recently, especially for the Cr–Mo steel to be used for fabricating the pressure vessels, particularly in the petroleum industry, since it indicates that the potential for brittle fracture increases with service time in the critical temperature range. The resulting implication is that certain units may become susceptible to brittle failure during start-up or shutdown without any warning [92].

Temper embrittlement of all 2.25Cr–1Mo plates, forgings, and weld metal can be minimized by ordering all material to chemical specifications that limit the elements that cause temper embrittlement. All materials can also be subjected to special temper embrittlement testing prior to being used in the vessel. Modern steel-making practices produce steels of sufficiently high purity that temper embrittlement can be virtually eliminated. Temper embrittlement resistance is often specified by various factors that combine the effect of these and other elements. Two of these factors, Watanabe number or J factor and \bar{X} factor, for 2.25Cr–1Mo can be specified [95]:

$$J = (\%Si + \%Mn)(\%P + \%Sn) \times 10^4 \quad (\text{weight } \%)$$

$$\bar{X} = \frac{(10P + 5SP + 4Sn + As)}{100} \quad (\text{all elements in ppm})$$

The other known contributors to temper embrittlement, arsenic and antimony, are less effective in 2.5Cr–1Mo steel when they are controlled under 0.020% and 0.004%, respectively [91].

Good resistance to temper embrittlement is generally obtained with a J factor below 200 Shut in 40-ft-lb transition temp. [93]—most recent specifications require a J factor less than 150 [88]—but there is appreciable scatter in the correlation between the J factor and the shift in the 54-J (40 ft-lb) CVN TT for individual heats [94].

Temper embrittlement is measured by testing the notch toughness of the material before and after a slow cooling cycle from 595°C to 315°C. The shift in an energy TT, usually the 54-J transition, is the measure of embrittlement.

Modern ASTM A387 steels are most often fine grain, low silicon, low sulfur, calcium treated for inclusion shape control and occasionally quenched and tempered to provide the highest possible toughness levels. The resulting changes in chemistry over the past 15 years include the general reductions in silicon content from 0.25% to 0.1%, in sulfur from 0.02% to 0.002%, and in phosphorus from 0.015% to 0.005%. The finer grain sizes have allowed a shift in the typical DBT transition curve toward lower temperatures [90]. It can be stated with reasonable confidence that Q&T 2.25Cr–1Mo plate should not experience rapid embrittlement in vessels operating at or below 400°C (750°F) [92].

13.15.6 STEP-COOLING HEAT TREATMENT

Some specifications additionally require a step-cooled simulation treatment, which is an accelerated embrittling treatment used to predict temper embrittlement susceptibility in a relatively short test period. Manufacturers will perform this laboratory step-cooling treatment and meet commonly specified shifts in the 40 ft-lb CVN TT.

13.15.7 CVN IMPACT PROPERTIES

Improved Charpy V-notch properties can be met for A387 steels with Fineline Processing (0.010% or 0.005% maximum sulfur, vacuum degassed, with calcium treatment for inclusion shape control). When thick plates are specified with high CVN toughness requirements, a quenching and tempering heat treatment may be required. Multiple austenizations may also be utilized for increased toughness.

13.15.8 TEMPER EMBRITTLEMENT OF WELD METAL

Correlation of the J factor with the temper embrittlement of weld metal is poor. This is probably due to significantly different chemical composition and microstructure of weld metal compared to the wrought product. Therefore, the susceptibility of the weld metal to temper embrittlement is frequently determined by a direct measurement of CVN impact toughness using the following equation [94]:

$$vTr40 + 1.5\Delta vTr40 < 100^{\circ}F$$

where

$vTr40$ is the TT for embrittlement weld metal

$\Delta vTr40$ is the change in TT for weld metal that has been step-cooled to cause temper embrittlement

13.15.8.1 Control of Temper Embrittlement of Weld Metal

Control of temper embrittlement in weld metal of 2.25Cr–1Mo is considerably more difficult than that with plate and forgings. Higher silicon and manganese contents are necessary to sound weld metal. Basic fluxes generally provide the minimum susceptibility to temper embrittlement consistent with high-temperature strength requirements [88,96]. The other factors that may affect the low-temperature toughness and temper embrittlement are discussed next [88,96]:

1. It is well known that reduction of grain size is effective for improving the low-temperature toughness of the weld metal. Addition of nitrogen results in the reduction in grain size, which in turn improves low-temperature toughness.
2. It is known that reduction of oxygen content in weld metal leads to improved toughness. C, Si, Mn, and Ti are generally used as the deoxidants. Be cautious because extremely low oxygen content can cause a reduction in toughness.
3. Control of chemical compositions and impurities in the weld metal. The influencing elements are phosphorus, arsenic, antimony, and tin. In the case of manganese, the recommended range for the weld metal is 0.7%–1.0% Mn.
4. The best temperature range for the PWHT is 1250°F–1300°F (677°C–704°C). The CVN values can be improved by prolonging the time of PWHT.

13.15.9 POSTWELD HEAT TREATMENT (STRESS RELIEF)

ASME boiler and pressure vessel code requires PWHT, or stress relieving, primarily to soften the HAZ, minimizing the presence of hard zones and stabilizing its microstructure. Otherwise, hydrogen attack or creep embrittlement could occur in service. Various stress-relieving requirements are specified by end users and fabricators of A387 grade steels. Some specifications have increased the stress-relieving temperatures and hold times for these steels because of the interest in stabilizing the microstructure of the HAZs after fabrication and accounting for possible weld repairs of the vessels while in service. However, as stress-relieving temperatures and times are increased, the capability

of the chemical composition of each grade of steel to achieve the tensile requirements of the specification using a normalized and tempering heat treatment is limited [95]. It is found that there is deleterious influence of extensive stress-relief treatments on CVN toughness levels.

13.15.9.1 Larson–Miller Tempering Parameter

The Larson–Miller parameter is usually employed to obtain some idea of the change in a given property of a material during a heat-treatment process performed at different temperatures and with different holding times [8,96]. It is widely used because of its usefulness in summarizing the heat-treating characteristics of low-alloy steels and in estimating their longtime strengths at given temperatures [18].

Cr–Mo steel has a hardened structure in the as-welded condition. This is given PWHT for changing it to a softened structure (tempered bainite) before use. By softening the structure, the toughness recovers gradually, but the heat-treatment parameter commonly known as the Larson–Miller parameter, $P = T(20 + \log t)$, where T is the absolute temperature in Kelvin (K) and t is heat-treatment time in hours, becomes large. Excessive increase in this parameter causes reduction in the toughness. Therefore, it is necessary to carefully examine the heat-treatment conditions.

13.15.10 REHEAT CRACKING IN CR–MO AND CR–MO–V STEELS

Phosphorus and sulfur were found to enhance the RC susceptibility of Cr–Mo steels. For a particular alloy, there exists a critical phosphorus content below which embrittlement will not take place. Measures such as (1) reduction of P and S, (2) addition of a small quantity of titanium (0.07%), which decreases the RC susceptibility due to phosphorus effects, and (3) the addition of calcium or rare earth metals, in accordance with sulfur, improve resistance to RC.

13.15.11 MODIFIED 9Cr–1Mo STEEL

Small additions of niobium (0.06%–0.10%) and vanadium (0.18%–0.25%) to the standard 9Cr–1Mo elevated-temperature steel result in a steel that is stronger and more ductile. This new steel exhibits improved long-term creep properties, lower thermal expansion, higher thermal conductivity, and better resistance to SCC [97]. Proposed applications for the modified 9Cr–1Mo steel include boilers, reaction vessels, breeder reactor systems, pressure vessels for coal liquefaction and gasification, oil refining hydrotreating equipment, and geothermal energy systems.

13.15.12 ADVANCED 3Cr–Mo–Ni STEELS

Advanced 3Cr–Mo–Ni steels have been developed for use in thick-section pressure vessels, specifically for coal liquefaction and gasification, by minor alloy modifications to commercial 2.25Cr–1Mo (ASTM A387, Grade 22, Class 2 steel) [98]. Specifically, the new alloy shows improved hardenability (i.e., fully bainitic microstructures following normalizing of 400 mm plates), enhanced strength, superior hydrogen attack resistance, and better Charpy V-notch impact toughness, with comparable ductility, creep-rupture resistance, and temper embrittlement resistance.

13.16 STAINLESS STEELS

Stainless steels (SSs) are those alloy steels that have a normal chromium content of not less than 12%, with or without other alloy additions. SSs are more resistant to rusting and staining than plain carbon steel and low-alloy steels. They have superior corrosion resistance because of relatively high contents of chromium. These metals are available in both wrought and cast forms.

13.16.1 CLASSIFICATION AND DESIGNATION OF STAINLESS STEELS

SS may be classified into five families, according to metallurgical structure:

1. Martensitic SS
2. Austenitic SS
3. Ferritic SS
4. Duplex SS
5. PH SS

The first four groups are characterized by the predominant metallurgical phase present when the SS is placed in service. In iron and steel, the bcc lattice is called ferrite and the face-centered cubic (fcc) lattice is austenite, so the steels are described as ferritic or austenitic depending on their major structural constituent. As the name implies, duplex SS consists of both austenite and ferrite phases in 50:50 proportion. The fifth group contains those SSs that can be strengthened by an aging heat treatment. This steel is generally not used in heat exchanger applications. Therefore, it is not covered here.

13.16.1.1 Designations

Wrought SSs are assigned designations by the American Iron and Steel Institute (AISI) according to composition: the Cr–Ni–Mn austenitic SSs as 2xx series, and the Cr–Ni austenitic SSs as 3xx series and 4xx series. The PH grades are assigned designations based on their Cr and Ni contents.

13.16.1.2 ASTM Specification for Stainless Steels

Most of the AISI types— austenitic, duplex, ferritic, and martensitic SSs, plus some special stainless like superferritic and superaustenitic steels—are included in A240.

13.16.1.3 Guidance for Stainless Steel Selection

Guidelines for selection of the types of available SSs are discussed by Brown [99] and Debold [100]. According to Brown, the following guidelines will serve to select a proper grade for the service under consideration:

Select the level of corrosion resistance required for the application.

Select the level of strength required.

For special fabrication problems, select one of the basic alloy modifications that provides the best fabrication characteristics.

Do a cost–benefit analysis to include the initial raw material price, cost of installation, and the effective life expectancy of the finished product.

Determine the availability of the raw material at the most economical and practical choice.

Debold [100] discusses the approach to select SSs to meet corrosion resistance and strength.

13.16.2 MARTENSITIC STAINLESS STEEL

The martensitic SSs are on the lower scale of corrosion resistance, because they contain only 11%–18% Cr, with carbon content usually less than 0.4%. The lower limit on chromium is governed by corrosion resistance, and the upper limit by the requirement for the alloy to convert fully to austenite on heat treatment [101]. The key feature of this family is that it can be hardened by heat treatment. Its utility as heat exchanger material in aqueous environments is limited. But these steels do exhibit a useful combination of strength, ductility, toughness, and corrosion resistance in mild environments. Resistance to corrosion is obtained only when the material is fully hardened and tempered [102]. AISI 410 is the most widely used of the martensitic grades. It is occasionally used in heat exchangers.

13.16.3 AUSTENITIC STAINLESS STEEL PROPERTIES AND METALLURGY

Austenitic SSs make up approximately 80%–90% of the SSs in use today [103]. This class of SS includes both the 200 and 300 series alloys that are hardenable by cold working. The 200 series alloys are originally developed to conserve nickel by replacing it with manganese at a ratio of 2% manganese for each 1% of nickel replaced. The common austenitic SS Type 300 series are low carbon, iron, and chromium alloys sufficiently alloyed with nickel and sometimes manganese or nitrogen, or combinations of these elements, to have an austenitic structure, most or all of it when the steel is cooled rapidly to room temperature. The chromium content is between 15% and 32%, nickel between 8% and 37%, and carbon is restricted to a maximum of 0.03%. Chromium provides oxidation resistance and resistance to corrosion in certain media. An important source book on SSs is Llewellyn [104].

13.16.3.1 Types of Austenitic Stainless Steel

The conventional types of 3xx SS include types such as 304, 304L, 309, 310, 316, 316L, 321, 347, and 348. The basic alloy Type 304 SS contains 18% chromium and 8% nickel. It has moderate strength, excellent toughness, and moderate corrosion resistance. Additional resistance to chloride pitting was achieved by the addition of Mo, creating Types 316 and 317. Types 316 (18% Cr, 12% Ni, 2.5% Mo) and 317 (18% Cr, 15% Ni, 3.5% Mo) have greater resistance to corrosion in chloride environments than Type 304. The characteristics of austenitic SSs are as follows:

- Nonmagnetic, ductile, work hardenable
- Nonhardenable by heat treatment
- Single phase from 0 K to melting point
- Crystallographic form—face-centered cubic
- Easy to weld
- Not subject to 885°F (475°C) embrittlement and hydrogen embrittlement
- Not subject to DBT temperature transition

13.16.3.2 Alloy Development

The 18Cr–8Ni austenitic SSs have been successfully used in freshwater and mildly corrosive industrial conditions for more than 50 years. The corrosion resistance, weldability, and strength of the austenitic family of alloys have been constantly improved for more demanding industrial applications by changing the basic chemical composition [105]. Such features include the following:

1. Molybdenum is added to enhance corrosion resistance in chloride environments, such as AISI Types 316 and 317. These steels possess a greatly increased resistance to chemical attack as compared to that of the basic Cr–Ni Type 304.
2. Low-carbon steels (Types 304L, 316L, and 317L) are resistant to carbide precipitation in the 800°F–1600°F range and can thus undergo normal welding without reduction in corrosion resistance. These steels are generally recommended for use below 800°F.
3. Nitrogen is added to compensate for the reduced strength of the low-carbon-grade steels (L grades); it increases strength at all temperatures—cryogenic through elevated—improves localized corrosion resistance in acid chloride solutions, and improves pitting resistance and phase stability. Nitrogen addition also improves passivation characteristics and enhances the effects of other alloy element additions, particularly, Cr and Mo, which add corrosion resistance [106]. Nitrogen addition may be of the order of 0.1%–0.25%. Maximum nitrogen content in austenitic SSs is typically restricted to 0.25% by weight to avoid problems such as ingot porosity, hot workability, and nitride precipitation that are associated with excess nitrogen content. Nitrogen addition is denoted by the suffix N.
4. Chromium is increased to enhance pitting and crevice corrosion resistance.

5. Nickel is added to stabilize the austenitic microstructure and to improve resistance to SCC as well as general corrosion in reducing environments. The effect of nickel on SCC of SSs is explained by the Copson curve.
6. Stabilized grades: The addition of titanium and niobium forms stable carbides, which prevents chromium depletion by the formation of complex chromium carbides, thereby avoiding sensitization of weldments or heat-treated parts; examples are Type 321 (Ti stabilized) and Type 347 (Nb stabilized).
7. LR stands for low residuals, and in this case the restrictions are on carbon for corrosion resistance. Reducing the carbon also allows the Nb to be reduced and so minimizes the risk of Nb-rich interdendritic films. There is also restriction on Si, S, and P for liquation cracking resistance. Manganese is usually raised to improve resistance to solidification cracking.

13.16.3.3 Stainless Steel for Heat Exchanger Applications

Austenitic SSs are used primarily because of their low cost, corrosion resistance, and good mechanical properties over a broad temperature range from cryogenics to high temperature. They have been applied successfully in a large variety of environments including acids, freshwater, and seawater. On the other hand, the martensitic and ferritic SSs have acquired a more restricted field of application due to low toughness at room temperature. Factors that favor austenitic SS selection as heat exchanger material include the following [107,108]:

- High resistance to uniform corrosion, such as erosion corrosion
- Resistance to high-pH solutions
- Resistance to oxidation and sulfidation
- Suitability for intended fabrication techniques
- Can be easily maintained and cleaned to remove fouling deposits by most of the chemical and mechanical means without damage
- Compatible with other materials commonly used for fabrication of heat exchangers
- Stability of properties in service
- Generally compatible with the process fluids
- Toughness at cryogenic temperature and strength at elevated temperatures
- Resistance to galling and seizing
- Moderate thermal conductivity
- Dimensional stability

13.16.3.3.1 Newer Stainless Steels for Heat Exchanger Service

New steel-making technologies like AOD and VIM in the last two decades have introduced a variety of new grades of ferritic, austenitic, and duplex SSs with low-impurity elements and a wide range of alloying elements tailored to the requirements of specific applications.

Against these good properties, the following are the demerits of SSs [109]:

1. Sensitive to crevice corrosion under deposits
2. Sensitive to pitting corrosion and SCC in the presence of chloride ions if temperature exceeds 50°C
3. Sensitization leads to intergranular corrosion
4. Sensitive to fouling

13.16.3.4 Properties of Austenitic Stainless Steels

SSs are known for excellent fabricability, weldability, good mechanical properties (strength, toughness, and ductility) over a broad temperature range, and corrosion resistance in many environments. Other relevant properties are lower melting points, higher electrical resistance, lower thermal conductivity, and higher coefficients of thermal expansion than carbon steels.

13.16.3.4.1 Mechanical Properties at Cryogenic Temperature and Elevated Temperature

Although austenitic SSs are used primarily because of their high corrosion resistance, they also possess excellent mechanical properties over a wide range of temperature from cryogenic to elevated temperature.

Cryogenic applications: Unlike ferritic materials, austenitic SSs do not exhibit DBT transition. They maintain a high level of toughness at cryogenic temperatures. Austenitic SSs types such as 304, 304L, 316, 316L, and 347 are used in cryogenic applications for liquid gas storage and transportation vessels.

Elevated temperature strength: Austenitic SSs exhibit good creep-rupture strength at temperatures up to 600°C. If still higher creep strength and elevated temperature strength are required, addition of V, Nb, and Ti is necessary. Addition of these elements can lead to an increase in strength, but also a reduction in the low-temperature toughness. SSs also exhibit high-temperature oxidation resistance due to the oxide layer formed on the surface.

13.16.3.5 Alloying Elements and Microstructure

The microstructures most important in weldable SSs are ferrite and austenite. Although chromium and nickel are the principal alloying elements in austenitic SSs, other elements are added to meet specific requirements and therefore consideration must be given to their effects on microstructure. Molybdenum, columbium, and titanium promote the formation of delta ferrite in the austenitic matrix and also form carbides similar to that of chromium. These elements are known as ferrite-forming elements. On the other hand, copper, manganese, cobalt, carbon, and nitrogen have a similar effect to nickel and promote the formation of austenite. These elements are known as austenite-forming elements.

13.16.3.5.1 Composition of Wrought Alloys

The compositions of typical wrought austenitic SSs are given in Table 13.15. There are several variations for some of those listed.

13.16.3.6 Alloy Types and Their Applications

The workhorse materials for the process industries are Types 304, 304L, 316, and 347. SS is used as a heat exchanger material for condensers, feedwater heaters, and other heat exchangers and has wide use in refineries, chemical process industries, fertilizer industries, pulp and paper industries, food processing industries, etc. The properties and their usage of AISI Types 304, 310, 316, 321, and 347 are discussed next.

TABLE 13.15
Nominal Composition of Typical Wrought Austenitic SS

Grade	C (max)	Mn (max)	P (max)	S (max)	Si (max)	Cr	Ni	Mo	Other Elements
304	0.08	2.0	0.045	0.03	1.0	18.0–20.0	8.0–12.0	—	
304L	0.03	2.0	0.045	0.03	1.0	18.0–20.0	8.0–12.0		
316	0.08	2.0	0.045	0.03	1.0	16.0–18.0	10.0–14.0	2.0–3.0	
316L	0.03	2.0	0.045	0.03	1.0	16.0–18.0	10.0–14.0	2.0–3.0	
317	0.08	2.0	0.045	0.03	1.0	18.0–20.0	11.0–15.0	3.0–4.0	
317L	0.03	2.0	0.045	0.03	1.0	18.0–20.0	11.0–15.0	3.0–4.0	
321	0.08	2.0	0.045	0.03	1.0	17.0–19.0	9.0–12.0		Ti = 5C min (0.70 max)
347	0.08	2.0	0.045	0.03	1.0	17.0–19.0	9.0–13.0		Nb + Ta = 10C min (1.10 max)
348	0.08	2.0	0.045	0.03	1.0	17.0–19.0	9.0–13.0		Nb + Ta = 10C min (1.10 max)

13.16.3.6.1 Type 304

Type 304 (18Cr–8Ni) is the most popular grade in the series and is used in a wide variety of applications that require a good combination of corrosion resistance and formability. Its homogeneous structure, high ductility, and excellent strength ensure excellent performance in cold forming, deep drawing, and spinning. It is nonmagnetic in the annealed condition. Its excellent toughness at low temperature is utilized for the construction of cryogenic vessels. It is particularly well suited for applications where welded construction is required and where the finished product must resist the more severe forms of corrosion. The lighter sections can be welded with little trouble from carbide precipitation or loss of corrosion resistance. Hence, for this reason, PWHT is not necessary in most cases.

Type 304 is highly resistant to ordinary rusting and immune to foods, most of the organic chemicals, dyes, and a wide range of inorganic chemicals. It has excellent corrosion resistance in oxidizing solutions. It resists nitric acid very well but sulfuric acid only moderately and halogen acids poorly. For best results, it is recommended to passivate this grade of SS to retain its corrosion resistance. It resists scaling up to 1600°F. For intermittent heating and cooling applications, temperatures should not exceed 1500°F. The maximum temperature for continuous service is 1650°F [110].

13.16.3.6.2 Type 310

Type 310 (25Cr–20Ni) represents the most highly alloyed composition in the popular range of austenitic SSs and exhibits the greatest resistance to corrosion and oxidation.

13.16.3.6.3 Type 316

The addition of molybdenum gives this grade the highest resistance to pitting corrosion of any of the chromium–nickel grades, which makes this grade particularly suitable for applications involving severe chloride corrosion. Therefore, alloys 316 and 316L are “workhorse” materials in both the chemical industries and the pulp and paper industries [111]. Type 316 has excellent resistance to sulfates, chlorides, phosphates, and other salts. Nevertheless, the resistance of Types 316 and 316L to pitting and crevice corrosion is often not high enough, particularly in stagnant or slow-moving seawater (<1.5 m/s). For this reason, in the last two decades, several more highly alloyed grades have been developed. They are known as superferritic, duplex, superaustenitic SSs.

Type 316 is used for applications requiring high strength and creep resistance at elevated temperatures. Its molybdenum content provides higher creep strength than Type 304. Type 316 has excellent resistance to oxidation and has a low rate of scaling in ordinary atmosphere at temperatures up to 1650°F in continuous service and 1500°F when used intermittently (110). It can be welded without difficulty and usually does not require subsequent heat treatment. This steel is used for applications requiring high strength and creep resistance at the elevated temperatures. Its molybdenum content provides several times the resistance to creep that is available with Type 304. This grade is used for chemical and pulp handling equipment, and photographic and food processing equipment.

Because of their freedom from chromium carbide precipitation and intergranular attack, Type 321 (18% Cr, 10.5% Ni, Ti), Type 347 (18% Cr, 11% Ni, Nb), and Type 348 (18% Cr, 11% Ni, Nb) are often referred to as stabilized SSs.

13.16.4 MECHANISM OF CORROSION RESISTANCE

SSs owe their corrosion resistance to a relatively thin passive surface film that provides a physical barrier between the steel and the service environment. This layer, only 20–30 angstroms thick, of hydrated chromium oxide (Cr_2O_3), is extremely adherent and resistant to chemical attack [15]. The passive films are formed on the surface interacting with the environment, essentially containing O_2

or oxidizing conditions. If the passive film is damaged by abrasion or scratching, a healing process or repassivation occurs almost immediately in the presence of oxygen. On the other hand, SS will show rapid corrosion attack in reducing conditions or under crevices or local deposits, which produce an O_2 depleted zone [16].

Another reason for loss in corrosion resistance of SSs is the formation of oxide films on the surface due to bad cleaning after heat treatment. The oxide film is different from passive film. Cleaning of heat-treated components should be done in an inert solution to avoid the formation of oxide films, which render the SS susceptible to various forms of corrosion [107].

13.16.4.1 Sigma Phase

Sigma phase, an intermetallic compound, in SSs may significantly reduce their ductility and toughness, and renders SS susceptible to SCC and other forms of corrosion.

The sigma phase is one cause of low-ductility creep failure of certain austenitic welds [112]. When cooling a weld metal from 1800°F to 1000°F, the rate of cooling must be relatively rapid to avoid the formation of a sigma phase. Avoidance of prolonged time in this temperature range will usually result in a weld metal containing very small amounts of sigma phase, which is generally harmless. Like sensitization, precipitation of intermetallic phases can be corrected by solution annealing. In newer varieties of austenitic SSs, namely, superaustenitics, alloying with nitrogen retards sigma-phase formation and allows for the production of thicker plates [113].

13.16.4.2 Passive versus Active Behavior

In most natural environments, SS will remain in a passive state. When exposed to conditions that remove the passive film, SSs are subject to the active state. Change to an active state usually occurs when chloride concentrations are high, as in seawaters or in reducing solutions, or when there is oxygen starvation. Oxygen starvation occurs when there is no free access to oxygen, such as in crevices and beneath deposits.

13.16.4.3 Resistance to Chemicals

SS alloys have excellent resistance to nitric acid, particularly to all concentrations and temperatures. Type 304 is most widely used in nitric acid plants. To handle sulfuric acid without inhibitors, Type 316 SS has limited application.

13.16.4.4 Stainless Steel in Seawater

While Type 304 (18Cr–8Ni) alloys have been satisfactorily used in freshwater, the Mo-containing Type 316 is preferred in saltwater. Variable results have been obtained with Type 316 in seawater. In the case of seawater-cooled condenser tubes, satisfactory use was obtained where tubes were cleaned regularly in service to prevent fouling. However, the alloy content of Type 316 was found to be too lean to prevent pitting and crevice corrosion in stagnant seawater. This is because of the breakdown of the passive film by the chloride ions in the seawater under stagnant/low-velocity conditions.

13.16.4.5 Resistance to Various Forms of Corrosion

In general, the corrosion and oxidation resistance of SSs increases with chromium content, and the materials are used in a wide range of aggressive media in the chemical and process industries. They are resistant to uniform corrosion, erosion and erosion corrosion, and high-pH solution [109]. However, under certain conditions, SSs are attacked by localized corrosion forms.

13.16.4.6 Galvanic Corrosion

Consideration should be given to when SS is connected to a more noble metal. However, if the SS is passive in the environment, galvanic corrosion may not take place. The most important aspect for the prevention of galvanic corrosion of SS is to select the weldments and fasteners of adequate corrosion resistance in the bulk of the material and/or possessing larger exposed area.

13.16.4.7 Localized Forms of Corrosion

Under certain conditions, SSs are susceptible to highly localized forms of corrosion. For SSs, almost 60% of equipment failures in the chemical process industries are due to (1) pitting corrosion, (2) crevice corrosion, and (3) SCC [114]. Additionally, they also fail by intergranular corrosion. Operating parameters and environmental factors such as pH, temperature, and chloride and oxygen levels greatly affect alloy performance. Various forms of SS localized corrosion are discussed next.

13.16.4.8 Pitting Corrosion

The corrosion resistance of SSs relies on the stability and the maintenance of continuity of passive films on the exposed surfaces. The stability of the passive film to resist pitting initiation is controlled mainly by chromium and molybdenum contents in SSs. Another element that improves resistance to pitting and crevice corrosion is nitrogen [100,115]. Nitrogen addition is considerably cheaper than molybdenum steels. The breakdown of the passive films takes place due to imperfections in the films, mechanical damages, inhomogeneities in the metal surface such as inclusions or surface scale, precipitates, second phases, and the presence of chloride ions in the environment [116]. High chloride levels locally break down the passive film, as well as provide a good conductor that promotes corrosion [117]. The severity of attack is related to the chloride content and the acidity, pH, and presence of oxygen and oxidizers [114]. Welding-related factors/defects such as inclusions, secondary phases, compositional differences within the same phase, sensitization, arc strikes, spatter, and local inhomogeneities in the base material act as potential sites where pitting can initiate [118,119]. In terms of microstructure, MnS inclusions are important sites for pit initiation. Other features such as delta ferrite and sigma phase can also promote pitting corrosion.

13.16.4.8.1 Pitting Resistance Number

The resistance to pitting increases with chromium content, but major benefit is obtained from the addition of molybdenum in SS, such as Type 316 (18% Cr, 12% Ni, 2.5% Mo). The addition of nitrogen is also beneficial, and the combined effects of chromium, nitrogen, plus molybdenum are used as a measure of potential pitting resistance of SSs, often expressed in terms of a pitting index number, known as pitting resistance equivalence number (PRE_N). $Pitting\ index\ or\ PRE_N = Cr\% + 3.3Mo\% + 16N\%$. The ranking of various metals according to pitting resistance is given in Table 13.16.

13.16.4.8.2 Critical Pitting Corrosion Temperature

In addition to the surface condition and the presence of deposits, chloride ions, pitting initiation is also influenced by the environment temperature. For a given grade of SS, there is a single

TABLE 13.16
Pitting Resistance Number for Few Austenitic Stainless Steels

Alloy	UNS Designation	Composition Required to Calculate PRE_N			PRE_N^a
		Cr	Mo	N	
Type 304/304L	S30400/S30403	18	0.0	—	18.0
Type 316/316L	S30600/S30603	16.5	2.1	—	23.4
Type 317	S30700	18.5	3.1	0.06	29.7
AL-6XN		20.5	6.3	0.23	47.9

^a $PRE_N = Cr + 3.3Mo + 16N$.

temperature, or a very narrow range of temperature, of an environment at which pitting is first observed, known as the *critical pitting temperature* (CPT). It is therefore possible to select a grade that will not be subject to pitting attack if the environment temperatures do not exceed the critical levels [107]. CPT can be also used to rate the relative performance of various alloys. CPT values have been determined according to practice ASTM G 48A [120] in ferric chloride (10% $\text{FeCl}_3 \cdot 6\text{H}_2\text{O}$) and in an acidic mixture of chlorides and sulfates [4% NaCl + 1% $\text{Fe}_2(\text{SO}_4)_3$ + 0.01 M HCl]. CPT values have been determined in 10% $\text{FeCl}_3 \cdot 6\text{H}_2\text{O}$ by Garner [121] and in 4% NaCl + 1% $\text{Fe}_2(\text{SO}_4)_3$ + 0.01 M HCl by Bandy et al. [122]. However, laboratory tests on pitting behavior are now more generally based on electrochemical techniques.

Resistance to pitting corrosion is achieved by steel grades with higher chromium and molybdenum contents, such as austenitic SS in the progression of levels of Types 304, 316, and 317. Otherwise, use alternate materials such as nickel-base alloys (e.g., Inconel alloy 625, Hastelloy and G-3); certain proprietary steels like 317 LM, Jessop 700, and Alloy AL-6X; and titanium, copper-nickel, and nickel-copper alloys.

13.16.4.9 Crevice Corrosion

Crevices due to metal-to-metal joint, gasket, and fouling deposits, which tend to restrict oxygen access, result in crevice corrosion. For austenitic SSs, numerous factors affect both crevice corrosion initiation and propagation and include the following [123]:

1. Geometrical factors: crevice type (metal-to-metal, nonmetal-to-metal), crevice gap and depth, exterior-to-interior surface area ratio
2. Environmental factors: oxygen content, pH, chloride level, temperature, agitation, diffusion and convection, crevice solution, biological influences
3. Electrochemical reactions: metal dissolution, oxygen reduction, hydrogen evolution
4. Metallurgical factors: alloy composition impurities, passive film characteristics

Although it is unlikely that one can avoid design crevices, the problem can be minimized by maintaining uniform flow velocity in the bulk of the heat exchanger and using higher chromium and molybdenum grades, which are more resistant to crevice corrosion. Austenitic SS grades with higher Mo contents like 316L, 904L, and 254 SMO, ferritic grades like 18Cr-2Mo, and duplex steel like 2205 exhibit resistance to crevice attack.

13.16.4.9.1 Critical Crevice Corrosion Temperature

For a particular grade of SS, crevice corrosion is also influenced by the temperature of the environment. Above a critical temperature, crevice corrosion will initiate, and below this it will not initiate. It is therefore possible to select a grade that will not be subject to crevice corrosion, if the chemical environment temperature does not exceed the critical levels. Critical crevice corrosion temperature (CCCT) values have been determined according to practice ASTM G-48B in ferric chloride (6% FeCl_3 for 72 h with crevices). The critical crevice corrosion temperatures for some industrial alloys are given in Table 18 [105].

13.16.4.9.2 Comparison of Pitting and Crevice Corrosion of Stainless Steels

These two forms of corrosion are compared in Chapter 13 (Section 13.2.3.4). The mechanism of propagation of pits and crevice corrosion is identical; however, the mechanisms of initiation differ [124]. Crevice corrosion does not require the same aggressive conditions, that is not as high chloride content, as pitting. A steel that is resistant to pitting in a certain solution can, in the same solution, be attacked by crevice corrosion. Control measures of metallurgical nature that improve the resistance to pitting are also beneficial to crevice corrosion. If the manganese sulfides are eliminated, the resistance to both pitting and crevice corrosion will improve [111]. According to Blom and Degerbeck [111], the three possible ways of eliminating manganese sulfide inclusions include (1) decreasing Mn

content below the solubility product of MnS, (2) decreasing sulfur content to get below the solubility product of MnS, and (3) adding an element, like Ti, and Zr, that forms a stronger and more beneficial sulfide than MnS.

13.16.4.10 Stress Corrosion Cracking

It is well known that austenitic SS may be subject to SCC. A range of environmental conditions are associated with SCC, but these can be rationalized into two types, depending on whether they promote predominantly transgranular or intergranular cracking. Transgranular SCC is found mostly in media containing chloride ions and, less frequently, hydroxyl ions. Intergranular cracking occurs in a range of aqueous environments, but is dependent upon achieving a “sensitized” condition [125]. The important environments that cause SCC of SS are

1. Aqueous chlorides
2. Caustic (hydroxide) solutions
3. Polythionic acid

The stress below which SCC cannot occur is not well defined but must be assumed to be low; weld residual stresses are often significantly high [79].

13.16.4.10.1 Chloride SCC of Austenitic Stainless Steel

The usual failure mode of chloride SCC of austenitic SS is transgranular and highly branched. Factors that influence the rate and severity of cracking are chloride content, oxygen level, temperature, stress level, and pH of the aqueous solution. Generally, for SSs to suffer chloride SCC, chloride concentrations must be 30 ppm or higher, and 20 ppm is normally noncorrosive. However, when chlorides are present in trace amounts, high concentrations may develop locally that will lead to cracking. Proper design—e.g., venting—can often eliminate places where chlorides can concentrate. Most of the SCC failures occur above 170°F (75°C), and 120°F (50°C) is generally considered the threshold limit below which SCC is not a problem [114].

13.16.4.10.2 Caustic SCC

Caustic SCC of SS occurs at temperatures above 120°C. At higher temperatures, the newer ferrite SS, nickel, and high-nickel alloys are substituted for austenitic SS in caustic evaporators.

13.16.4.10.3 Influence of Nickel Content on SCC

The influence of nickel content on SCC of austenitic SS can be studied through the Copson curve [126], which is shown in Figure 13.13. Figure 13.13 shows that the maximum propensity for austenitic SSs to SCC is with the nickel content in the 8%–12% range, typical of those standard austenitic steels such as Types 302, 304, and 316 [127,128]. A reduction in nickel from these levels leads to an improvement in the SCC behavior, but this is associated with the progressive replacement of austenite by delta ferrite in the microstructure. With increasing nickel content, resistance to SCC improves until about 42%–45% nickel, where alloys are virtually immune. This includes Alloy 825, Alloy G, and Alloy 625. Thus, it can be stated as a practical guide that alloys with a nickel content above 22% seldom experience SCC, and this includes Alloy 904, Alloy 28, and Alloy 20 [114]. These materials have performed well in many industrial applications containing chlorides.

13.16.4.10.4 SCC of Welded Austenitic Stainless Steels

Austenitic SSs that contain surface tensile stresses either locked in during fabrication or externally applied may fail by transgranular cracking in chloride solutions. Welded joints are particularly prone to SCC for three reasons [79]: (1) The welding operation will leave a residual tensile stress in the weld area unless effective postweld stress relief is carried out, (2) stress concentrations are usually

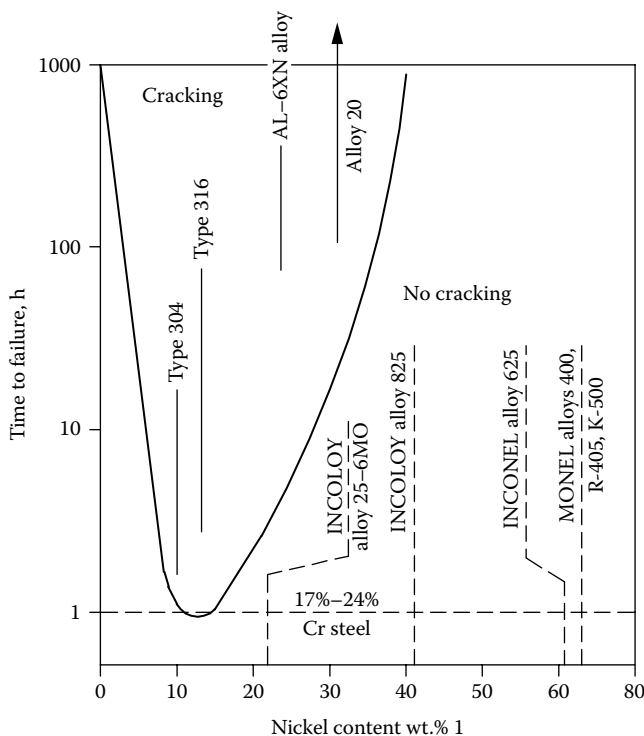


FIGURE 13.13 Copson curve. (Modified from AL-6XN[®] Alloy, Allegheny Ludlum Steel Corporation, Pittsburgh, PA.)

present, and (3) the thermal cycle can produce a susceptible microstructure. Postweld stress relief can be of substantial remedy in avoiding intergranular SCC. In this regard, full solution treatment at 1922°F (1050°C) may not be necessary, but a stabilizing anneal at 1598°F–1742°F (870°C–950°C) is frequently applied to welded components that find application in the petrochemical industry, to guard against polythionic acid corrosion.

13.16.4.10.5 Polythionic Acid Stress Corrosion Cracking (PASCC)

Intergranular SCC is specifically caused by the action of polythionic acids on sensitized materials, and such conditions can be present in some types of refinery equipment, particularly during shutdown periods. PASCC requires the presence of sensitized material, oxygen, water, tensile stress, and iron sulfide scale. Polythionic acid can form readily during shutdown as a result of the interaction of the sulfide with moisture and oxygen. Normal-grade SSs such as Type 304 and Type 316 and Incoloy alloy 800 can be sensitized due to welding; sulfide scales can form during service, and oxygen and water can be introduced during shutdown. Remedial measures to control PASCC include [89] the following:

- Nitrogen purging of components or assemblies exposed to atmosphere.

- Neutralizing the acid by ammonia and soda ash washing.

- Use of stabilized materials for the construction of heat exchangers. It is reported that even the stabilized SSs (321 or 347) are susceptible to PASCC, unless they have been heat-treated properly [129].

- Suitable procedures to overcome this form of corrosion attack are dealt with and well documented in NACE RP-01-70 [130].

13.16.4.10.6 *Laboratory Tests to Determine SCC*

Susceptibility of alloys to chloride SCC is assessed by laboratory corrosion testing as per ASTM 636 or by relating the rate of crack propagation to stress intensification at the crack tip, and polythionic SCC by laboratory corrosion test ASTM G 35.

13.16.4.10.7 *Evaluation of Sensitization of Austenitic SS to PASCC*

The electrochemical potentiokinetic reactivation method can be used during in-service periodic inspection for evaluating the degree of sensitization of austenitic SSs in high-temperature water [129].

13.16.4.10.8 *Methods to Prevent SCC of SS*

Typical methods to overcome SCC of austenitic SSs are discussed in Ref. [107] and by Fontana and Greene [131]. Such measures include thus:

1. Use of alternative materials that are more resistant to chloride SCC. Typical examples are new ferritics Type 430, superferritics such as E-Brite, Sea-Cure, etc., duplex SS, and titanium or higher nickel austenitic alloys. Ferritics are either immune to SCC or least attacked by SCC. Otherwise, grades such as 304 and 316L, which are susceptible to SCC, may be used when precautions are taken to eliminate one or more of the factors that cause SCC, namely, residual tensile stress, chloride environment, and temperature.
2. Method of safe ending: In vertical heat exchangers, SCC is overcome by a procedure known as *safe ending*. This method consists of butt welding of short lengths of resistant material to austenitic SS tubes at the place of greatest exposure to SCC conditions, that is under the top tubesheet.
3. If there is a dead space (air pocket) at which chlorides are allowed to concentrate by alternate wetting and drying of tubing surfaces, the tubes will be attacked by SCC. This problem can be overcome by air venting the dead space or allowing complete flooding of all tubing surfaces. (For more details, refer to Chapter 12.)
4. Bimetallic tubing.

13.16.4.10.9 *Prevention of SCC in Boiling Water Reactors*

Intergranular stress corrosion cracking (IGSCC) adjacent to girth welds in SS piping systems has been a serious problem in boiling water reactor (BWR) plants [132]. The pipe cracking remedies for BWRs and remedies for protection of internals and attachments are [132] the following:

1. Material-related remedies: The aim of the material-related remedies is to prevent contact between sensitized material and the BWR coolant, including (a) use of nuclear grade (NG) SSs, where the NG suffix signifies tightly controlled requirements for carbon and nitrogen contents to ensure that the materials do not sensitize due to welding; (b) solution heat treatment (SHT), where SHT following welding redissolves grain boundary carbides and restores the grain boundary chromium concentration; and (c) use of corrosion-resistant cladding (CRC). Fractographic observations, which showed the superior IGSCC resistance of duplex weld metals, provided the basis for the CRC remedy, in which the pipe inside surface adjacent to the girth weld is clad with weld metal. The result is enhancement of life by a factor of 6.5.
2. Stress-related remedies: These aim to prevent IGSCC by subjecting the sensitized material at the inside surface of the weld HAZ to large compressive residual stresses.
3. Adopt heat-sink welding and last pass heat-sink welding.
4. Adopt induction heating stress improvement and mechanical stress improvement process.
5. Environment related.

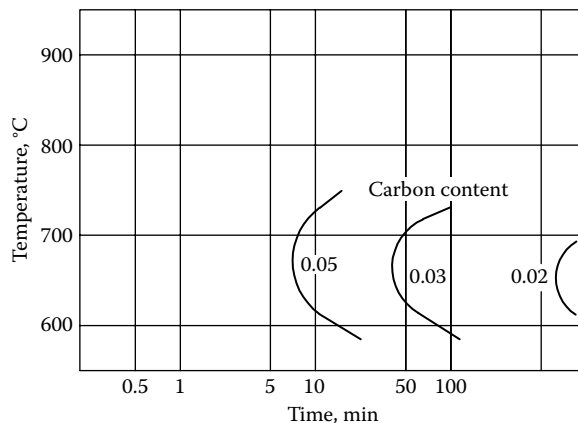


FIGURE 13.14 Typical time–temperature sensitization diagram for austenitic SSs.

The remedy called hydrogen water chemistry (HWC) consists of reducing the electrochemical potential of SS in the recirculation systems of operating BWRs to values below -230 mV standard hydrogen electrode (SHE) by injecting hydrogen into the feedwater (hence the name “hydrogen water chemistry”).

13.16.4.11 Intergranular Corrosion

Sensitization of SSs is covered in Chapter 12. Sensitization of SS with $C \geq 0.05\%$ that takes place in the temperature range 500°C – 900°C when exposed to high-temperature operations like welding (known as weld decay), heat treatment, or brazing. The degree of severity of sensitization depends on welding process variables and plate thickness, since these determine the time in the critical temperature range. The sensitization temperature range is schematically shown in Figure 13.14 [119,133], in which the curves show the times required for carbide precipitation in steels with various carbon contents. Carbides precipitate in the areas to the right of the various carbon content lines.

13.16.4.11.1 Factors Influencing Susceptibility to Weld Decay

The main factors that determine the sensitivity of austenitic SSs are [134] the following:

1. Metal composition and microstructure: The main compositional factor that determines the susceptibility to weld decay is the carbon content, with increasing carbon being detrimental; the presence of ferrite is beneficial in resisting weld decay, but a large grain size is deleterious.
2. Thermal history: Sensitization is mainly dependent on the maximum time spent at temperatures between 550°C and 850°C .
3. Internal or external stresses arising from prior deformation, welding, or service loads.
4. Environment: SS will be attacked by intergranular corrosion when a sensitized metal is exposed to a corrosive environment. Not all environments will cause weld decay. Weld decay can arise only in three distinct types of environments [134]: (a) marginally oxidizing, (b) moderately oxidizing, and (c) highly oxidizing. Risk of weld decay is most commonly encountered in moderately oxidizing conditions.

13.16.4.11.2 Measures to Overcome Weld Decay

Measures to overcome weld decay are discussed by Jarman and Shreir [79]. They are summarized here: (1) To ensure optimum corrosion resistance, especially in welded thick plate, subject the weldment to solution treatment followed by quenching. (2) The problem of sensitization is overcome for lower temperature heat exchanger materials by selection of extra-low-carbon (ELC) steels or

stabilized steels such as Type 321 (Ti stabilized) and Type 347 (Nb stabilized). Ti and Nb have a greater affinity for carbide formation than Cr, thus preventing the precipitation of Cr_{23}C_6 . The additions made to SSs are slightly in excess of those required by stoichiometry for complete precipitation of carbon and nitrogen, namely, [135], $\text{Ti} = 5(\text{C} + \text{N})\%$ and $\text{Nb} = 8(\text{C} + \text{N})\%$. Stabilized grades should be used whenever the steel is held for long periods in the temperature range 425°C – 800°C (800°F – 1500°F). Another measure is (3) low heat input ($<3 \text{ kJ/mm}$) and an interpass temperature maintained below 175°C . (4) Fillers and electrodes should also be stabilized or of ELC. (5) Increase the nickel and chromium contents of the filler to offset losses in the arc transfer. Note that titanium-stabilized fillers should not be used in argon arc welding, as titanium will be vaporized and its effectiveness as a stabilizer is lost.

Even though the problem of intergranular corrosion is overcome by the use of low-carbon grades or stabilized grades, these grades have some *drawbacks*:

1. Low-carbon grades have lower strength than stabilized grades.
2. Stabilized grades may be more hot-cracking sensitive and require more careful ferrite control, compared to nonstabilized grades.
3. Stabilized grades are susceptible to localized precipitation of carbides in narrow regions of the HAZ that can lead to intergranular corrosion known as knifeline attack [103,107,135]. Knifeline attack is further discussed next.

13.16.4.12 Knifeline Attack

While welding stabilized grades such as Types 321 and 347, the HAZ is raised to temperatures above 2102°F (1150°C), and this can result in the partial dissolution of TiC or NbC . Carbon is therefore taken into solution in a narrow region adjacent to the weld and can be available for the formation of chromium carbide on cooling through the sensitization temperature range. The susceptible region, being only a few grains in width, can give rise to a thin line of intergranular attack and hence the name knifeline attack. Nb-stabilized steels appear to be more resistant to knifeline attack than the Ti-stabilized steels. In both types, elevated-temperature solution treatment and quenching cannot adequately restore the original properties [79]. Knifeline attack differs from weld decay in the following ways [131]:

1. Knifeline attack occurs in a narrow band in the parent metal immediately adjacent to the weld, whereas weld decay develops at an appreciable distance from the weld.
2. Knifeline attack occurs in the stabilized steels.
3. The thermal history of the metal is different.

Knifeline attack can be avoided by the proper choice of welding variables and by the use of stabilizing heat treatments that allow diffusion to occur [135]. Therefore, the trend is to use low-carbon grades rather than the use of stabilized grades [136].

13.16.4.12.1 Prediction of IGC by Laboratory Tests

Two laboratory tests are most widely used to predict intergranular corrosion. They are described next.

1. *Direct exposure testing*: Direct exposure testing is the most satisfactory way of evaluating the risk of weld decay in a given environment [122]. The ASTM test method by direct exposure for detecting susceptibility to intergranular corrosion is given in Table 13.17. More details on tests for susceptibility to intergranular corrosion of SS are furnished in Ref. [107].
2. *Potentiostatic test method*: This technique involves exposing a polished weld sample to a suitable electrolyte at a constant potential, which can be varied over the entire range of passivity or corrosion. The potentiostatic test method offers advantages over conventional test methods in enabling quantitative assessment of the risk of weld decay and gives data relevant to a wide range of service conditions [134].

TABLE 13.17**ASTM Standard Test for Susceptibility to Intergranular Corrosion in Stainless Steels**

ASTM Test Method	Description
A262, Practice A, B, C, E, F	Standard practices for detecting susceptibility to intergranular attack in austenitic stainless steels
G28, Practice A, B	Standard test methods for detecting susceptibility to intergranular corrosion in wrought, nickel-rich, chromium-bearing alloys
A763, Practice W, X, Y, Z	Standard practices for detecting susceptibility to intergranular attack in ferritic stainless steels

13.16.5 AUSTENITIC STAINLESS STEEL FABRICATION

Austenitic SSs may be formed by the usual processes, such as drawing, bending, spinning, pressing, etc. They are extremely ductile and will accept a considerable amount of cold work, work harden rapidly, and with increasing thickness, severe forming operations may need subsequent or even interstage heat treatment [137]. Austenitic steels are difficult to machine because they work harden and gall. Rigid machines, heavy cuts, and high speeds are necessary.

Hot working may be carried out in the temperature range 2012°F–1652°F (1100°C–900°C), duly observing the susceptibility to the sensitization of unstabilized varieties. When heating for forming, electric furnaces are preferred to minimize scaling. Gas- or oil-fired furnaces are also used in the fabrication industry. Use fuels of low sulfur content, to reduce the possibility of sulfur contamination, which embrittles the material and reduces corrosion resistance. Flame selection is important; a slightly oxidizing flame is preferred, since reducing flames may lead to carbon pickup with loss of corrosion resistance, and highly oxidizing flames result in excessive scaling [137].

13.16.5.1 Pickling

Hot worked material will generally need to be descaled, usually by acid pickling. Pickling may be carried out in one of a number of suitable acids, e.g., hydrochloric, sulfuric, nitric, or various mixtures, either hot or cold.

13.16.5.2 Passivation

Passivation of SS consists of treating SS parts in a solution of HNO_3 and a combination of oxidizing salts. This treatment dissolves the embedded or smeared iron and restores the original corrosion-resistant surface. Passivate austenitic and ferritic grades for 20–30 min at 130°F. Rinse in clean hot water. Tests should be made to check on the extent of free iron removal.

13.16.5.3 Mechanical Cutting Methods

All SSs may be cut using friction saws with greater than 3/8 in. (9.5 mm) thickness. Heat removal becomes a problem, resulting in rapid deterioration of the saw blade and burning of the material. High-speed abrasive disks can be used for cutting tube and bar to length, although a coolant should be used and this should not be sulfur based. Rubber-bonded disks should also be avoided [137].

13.16.5.4 Gas Cutting Method

One of the major difficulties in the fabrication of SS is the gas cutting of the material. SS cannot be cut by the conventional oxyacetylene process because of the highly refractory chromium oxide that is formed on heating [137,138]. The powder cutting technique employed in the past involved the injection of iron powder into an oxyacetylene stream. This method is undesirable, because it

gives rise to considerable fumes, and the resulting cut is normally of poor quality and contaminated by iron powder, so that it is essential to machine an appreciable amount from a cut edge. Recent introduction of the plasma arc cutting technique has eliminated this difficulty. For thickness up to 15 mm, cold shearing may also be used.

13.16.6 AUSTENITIC STAINLESS STEEL WELDING

Two important objectives in making weld joints in austenitic SS are (1) preservation of corrosion resistance and (2) prevention of cracking. Good weldability is an attractive feature of SSs, and this contributes to the wider usage and versatility of these materials in the fabrication of pressure vessels, storage tanks, chemical plants, and domestic appliances. Welds in austenitic SSs usually have chemical compositions and mechanical properties, and toughnesses comparable to those of the parent metals. They are not prone to cold cracking. Due to a stable structure, there is no need to preheat or postheat the weldment. Normally, there is no heat input limitation, and high arc energies can be used without any adverse effects.

Being austenitic, these weldments are virtually nonmagnetic and not subject to arc blow while welding. Compared with plain carbon steels and low-alloy and 400 series SSs, the austenitic SSs have lower melting points, higher electrical resistance, 30%–50% lower thermal conductivity, and 50% higher coefficient of thermal expansion. For these reasons, less heat input (less current) and the heat concentration in a small zone adjacent to the weld arc are required for fusion. Even though SSs are ductile enough to accommodate a fair amount of shrinkage, welds may be cracked when restrained [139].

13.16.6.1 Welding Processes

SMAW, SAW, GMAW, GTAW, and PAW are used extensively for joining SSs. In general, those steels that contain aluminum or titanium or both can be arc welded only with the gas-shielded processes like SMAW and GTAW. For GTAW process, use direct current, straight polarity, employing 2% thoriated tungsten electrodes [140]. Austenitic SS poses distinct challenges when using TIG welding such as carbide precipitation and distortion specifically too hot of a TIG weld. SAW is not recommended when the austenitic SS weld deposit must be fully austenitic or low in ferrite content. However, it is suitable when a ferrite content of 4% is permissible in the weld metal. Demands for FCAW of SSs have markedly increased recently. This is because of excellent applicability of FCAW in satisfying the requirements for streamlining and productivity improvement in the welding of SS.

Oxyfuel welding of SS is to be avoided since the heat input is high and the gas combustion produces carbon monoxide and carbon dioxide, likely to carburize the weld metal and increase the chances of sensitization [119]. Therefore, OAW is not recommended except for emergency repairs where suitable arc welding equipment is not available. A neutral or a slightly reducing flame is recommended.

Carbon arc welding was never suitable due to the danger of carbon pickup. CO₂ consumable electrode welding can be used in applications in which corrosion can be tolerated. When corrosion resistance is a major factor, metal arc welding with covered electrodes or one of the inert gas processes can be used [137].

The welding of SSs has been reviewed extensively by Fenn [136], Banks [137], Weymueller [139], Beigay et al. [140,141], and Castro and DeCadenet [142], and the topic has been updated more recently by Castner [143]. Welding methods and various aspects of SS welding are discussed next.

13.16.6.2 Welding Methods

13.16.6.2.1 Shielded Metal Arc Welding

SMAW is a fast, versatile process that is very popular for welding SS, especially for joining shapes that cannot be easily set up for automatic welding methods. Choose electrodes on the basis of alloy composition and according to the coating. The electrode coatings are generally lime-based or

titania-based materials, depending on the type of welding to be done and the type of supply used. The handling and storage of coated electrodes is very important because coatings tend to absorb moisture and moisture in the weld zone during welding can lead to porosity.

13.16.6.2.2 GTAW

GTAW easily welds all SSs and used extensively in joining tubes-to-tubesheet welding of shell-and-tube heat exchanger. Generally, filler metal is fed manually by the welder, but this method is slow, especially for thick components. To achieve higher deposition rates, the process can be automated and the filler wire heated by resistance heating. This process is called hot-wire GTAW, and it can result in a 100% increase in welding speed. Another variation of GTAW is pulsed arc. In this process, the pulsing arc provides control of the molten weld puddle to increase penetration and to minimize porosity.

The use of a gas lens is highly recommended when TIG welding austenitic SS. A gas lens is a copper and brass component with layered SS mesh screens that replaces the collot body in a standard GTAW torch. The gas lens helps distribute gas more evenly around the arc and weld puddle and provides good cooling action.

Full penetration welds require back purging, that is covering the back of the weld with shielding gas. Back purging ensures that the underside of the weld is protected from atmospheric elements and can be done with commercial apparatuses or individually manufactured methods.

Finally, remember to maintain adequate gas after weld (postweld flow). The best practice is to maintain one second of post flow for every 10 amps of welding current used during welding.

13.16.6.2.3 GMAW

Generally speaking, GMAW is about four times faster than GTAW. Based on the method of transfer of metal, there are three basic variations of the GMAW process. These are (1) spray or free-flight transfer, (2) short-circuiting transfer, and (3) pulsed-type transfer. Spray arc welding is essentially a down hand welding process. Short-circuiting and pulsed-spray transfer are for all-position welding. The type of welding current used for GMAW depends primarily on the type of penetration desired. GTAW obtains its highest penetration on straight polarity whereas GMAW obtains its greatest penetration on reverse polarity (electrode positive).

13.16.6.3 Filler Metal Selection

In order to optimize the properties of stainless welds, careful selection of welding consumables and fabrication procedures is mandatory. AWS A5.4, Specification for Corrosion Resisting Chromium and Chromium-Nickel Steel Covered Welding Electrodes, lists types, compositions, and other data for standard electrodes. AWS ER 3xx filler metals or overmatching 300 series filler metals are used in over 90% of SS welding applications. Such welds exhibit good corrosion resistance, toughness, and excellent strength at both low and high temperatures, and a high degree of toughness in the as-welded condition. A few recommended filler metals and the austenitic steel base metals are given in Table 13.18.

TABLE 13.18
Filler Metals for Austenitic SS

Base Metal	Filler Metal
Types 301, 302, 304	AWS E308/308L
Type 304L	AWS E308L
Types 316, 316L	AWS E316L
Type 317	AWS E317L
Types 321, 347	AWS E347

13.16.6.4 Shielding Gases

Gas blends used to join SSs frequently contain argon because of its inert nature, its ability to support easy arc starting, and it helps spray-type metal transfer. For some welding processes, helium may be added to conduct more heat to the base metal, increase weld penetration, and improve the weld puddle fluidity. In GMAW and FCAW, oxygen or CO_2 is added to the shielding gas to improve arc stability and weld puddle fluidity. In special cases, nitrogen or hydrogen may be added in controlled amounts to refine weld properties and improve bead appearance in austenitic SS.

13.16.6.5 Weld Preparation

Weld preparations for SSs are similar to those used for carbon steels and may be obtained by machining, grinding, or plasma cutting.

13.16.6.6 Joint Design

Weld penetration is generally less in SSs than in carbon steels, so weld preparation angles are greater, root faces smaller, and root gaps wider; greater welding skill is required to ensure that adequate penetration is achieved without root defects [137]. A typical joint design for SS is shown in Figure 13.15.

13.16.6.7 Preweld Cleaning

To obtain sound welds free from cracks or embrittlements, the surfaces to be joined require cleaning prior to welding. The area to be cleaned should include the weld groove faces and the adjacent surfaces for at least 0.5 in. on each side. The most common forms of surface contaminants are iron contamination and organic contamination.

13.16.6.7.1 Iron Contamination

On occasion, forming equipment and tools made of carbon steel can cause embedding of iron particles on SS surfaces. Since rust is anodic to the bulk austenitic surface, galvanic corrosion will take place, resulting in pit formation. Hence, it is desired during fabrication to use cardboard or plastic sheets on carbon steel machinery and plants and handling equipment to avoid carbon embedding on SS surfaces. Remove the embedded iron by pickling. Always use aluminum oxide grinding wheels, not silicon carbide, for any dressing of weld surfaces. The carbide may react with the chromium, which decreases the corrosion resistance of the weld metal.

13.16.6.7.2 Organic Contamination

During the fabrication stage, organic contamination on the metal surfaces takes place as a result of grease, oil, cutting fluids, crayon markings, paint, and sticky substances. Even small amounts of these contaminants can crack or embrittle welds or HAZs. To avoid this, make sure both the base metal and the filler metals are clean. Removal of organic contaminants is best accomplished by

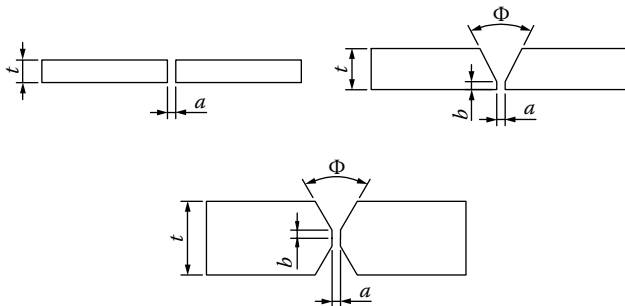


FIGURE 13.15 Joint design for austenitic SS welding.

degreasing using a nonchlorinated solvent. Oxide films can be removed by mechanical methods or by pickling with 10%–20% nitric acid solution. Mechanical cleaning techniques for surface oxide removal include (1) stainless wire brushing where the brushes have not been used for any other purpose, (2) sand or grit blasting, and (3) machining and grinding using chloride-free cutting fluid.

13.16.6.8 Welding Considerations

There are a number of welding processes and material considerations that are important to the production of sound welds with suitable properties in austenitic SSs. Here are some of the most important of those considerations:

1. Microfissuring or liquation cracking is the most frequently encountered problem.
2. Autogenous welds may be subject to variable penetration.
3. Sensitization of HAZ may affect corrosion resistance. Other factors that govern the corrosion resistance of weldment include microstructure in the vicinity of the surface, inclusions, surface oxides, residual weld stresses, spotter, and contaminations and geometric surface defects and crevices [118].
4. Type 304 requires less heat to produce fusion, which means faster welding for the same heat or less heat input for the same speed. This is of importance in electrical fusion-welding methods. The higher the resistance of austenitic SS results in the generation of more heat for the same current for the same heat with lower current as compared with carbon steel.
5. If multiple weld passes are required, maintain the interpass temperatures at less than 100°C (212°F) to prevent cracking and distortion, and less heating (30% less) is generally required. The welds take longer to cool, maintain short arc length, and use staggered beads for very long welds to reduce heat input.
6. Greater thermal expansion may result in warping or distortion, especially in thin sections, suggesting greater need for jiggling to maintain dimensional control.
7. Welding fumes present potential hazards to workers.
8. Several factors must be considered when PWHT is required.
9. Dissimilar metal weld joints require selection of proper filler metal and procedures.
10. Minimizing Hot Cracking. Some SSs during welding have a tendency toward hot shortness or tearing (e.g., Type 347), hence more welding passes may be needed. Weld metal hot cracking can be reduced by (i) adopting stringer bead techniques rather than weaving, (ii) short-circuiting welding because of the lower dilution of the base metal—excessive dilution sometimes produces a completely austenitic weld metal having strong cracking characteristics, and (iii) preheating to about 260°C (500°F), which helps to improve the bead contour and reduce hot cracking when using the stringer-bead technique on sections of 25.4 mm (1 in.) or higher thickness.
11. Because SS has lower heat conductivity than carbon steel, 30% less heat input generally is required. Also the welds take longer time to cool. Maintain short arc length and use staggered beads for very long welds to reduce heat input.
12. The coefficient of thermal expansion of austenitic SS is higher than carbon steel, ferritic, or martensitic SSs. Therefore, keep the base metal restraint to a minimum to prevent distortion and adding residual stress to the weldment.

13.16.6.8.1 Microfissuring or Liquation Cracking in Austenitic Stainless Steel Weld

The structures of most importance in the weldable SSs are ferrite and austenite. The structure of austenitic SS weld metals varies from fully austenitic in Type 310 to dual-phase austenitic–ferritic in Types 304, 308, 309, 312, and 316. Fully austenitic alloys tend to be hot short, and welds in these materials show fine cracking or microfissuring, also known as liquation cracking, either in the weld metal itself or in the HAZ, while those that solidify with delta ferrite as the primary solidification mode are the least susceptible to hot cracking.

Segregation of low-melting-point impurities like S, Si, and P between the grain boundaries can cause liquation cracking or microfissuring in the weldment, the HAZ, and weld overlays. Shrinkage stresses combined with high restraint (clamping is often used on SS during welding to prevent distortion) may cause these films to rupture prior to complete solidification [144]. Each element exhibits detrimental effects on hot cracking. Phosphorus content above 0.025%, sulfur content above 0.025%, or silicon content above 2.0% may cause the same length of solidification crack. The combined effect of these impurities may be much more disastrous [145].

HAZ liquation cracking-susceptible alloys: Austenitic SSs susceptible to HAZ liquation cracking include AISI 304, 304L, and the stabilized grades such as Type 321 and Type 347. HAZ liquation cracking has been reported in both cast and wrought versions of a wide variety of nickel-base alloys such as Incoloy Alloy 800, Alloy 718, and Hastelloy X [72].

Avoiding liquation cracking is the most important issue in fusion-welding of austenitic SSs. In general, alloys that solidified with ferrite as the primary phase and containing 4%–11% by volume of ferrite in the as-welded condition were more resistant to cracking than alloys solidified as austenite. Hence, in order to control microfissuring in stainless welding, the alloying elements are balanced in such a way as to attempt to produce a weld deposit containing ferrite in the order of 4–11 ferrite number (FN). The FN is a magnetically determined scale of ferrite measurement. This provides sufficient control in most applications where minimum ferrite content or a ferrite range is specified.

Benefits of ferrite in austenitic SS: Major benefits of ferrite to austenitic stainless weld metal are improved resistance to microfissuring and hot cracking, improved resistance to SCC, and good low-temperature impact strength [144].

Optimum weld metal ferrite content: It is a common practice today to specify a minimum ferrite content of about 3 or 4 FN in a nominal austenitic SS weld metal to provide assurance that the weld will be free of hot cracks and microfissures. Following are the minimum recommended levels of weld metal ferrite content (a range of 8–10 FN is considered optimum under most conditions) for various types of austenitic SSs [144]:

Type 308/308L, 3 FN
 Type 309/309L, 5 FN
 Type 316/316L, 3 FN
 Type 347, 6 FN

However, an FN in excess of 11 can have a detrimental effect in these applications [144,146]:

1. Weldments intended for cryogenic service where ferrite is less tough than austenite.
2. Weldments intended for certain special corrosive environments where ferrite is preferentially attacked, such as in the manufacture of urea.
3. Weldments that must experience PWHT or service at elevated temperatures where ferrite can transform to embrittling phases such as the sigma phase.
4. Duplex SS weldments with excessive ferrite can result in poor ductility, toughness, and corrosion resistance.

Industrial use of ferrite standards: In practice, standards and industrial measurement of ferrite have three areas of application [146]:

1. Certification and verification of filler metals
2. Development of qualified welding procedures for particular critical applications, using certified filler metals
3. Quality assurance examination of production weldments

Effects of alloying elements on microstructure: The addition of alloying elements to steel affects the stability of the various phases, with some stabilizing the ferrite and others the austenite. The amount of delta ferrite in the weld metal is largely, but not completely, controlled by a balance in the weld metal composition between the ferrite-promoting elements, expressed by chromium equivalent, and the austenite-promoting elements, expressed by nickel equivalent. Many workers have examined these effects, and Anton L. Schaeffler [147a] produced a diagram known as a *constitution diagram*, indicating the phase distribution in weld deposits of various compositions. Schaeffler expressed the empirical expressions for chromium equivalent and nickel equivalent as follows:

$$\text{Chromium equivalent} = \% \text{Cr} + \% \text{Mo} + 1.5 \times \% \text{Si} + 0.5 \times \% \text{Nb}$$

$$\text{Nickel equivalent} = \% \text{Ni} + 30 \times \% \text{C} + 0.5 \times \% \text{Mn}$$

The composition of the weld metal required to satisfy the ferrite content requirement is found to be fulfilled when $\text{Cr}_{\text{Eq}}/\text{Ni}_{\text{Eq}}$ is above 1.48 [103].

Schaeffler assumed that the level of nitrogen, a strong austenizer, was constant in his diagram. This has been taken into consideration by DeLong [147b] among others. DeLong developed a diagram that included the effects of nitrogen. The Welding Research Council (WRC) published modified diagrams in 1988 and 1992 [147c] that allow accurate prediction of the FN. According to the DeLong diagram, the chromium and nickel equivalents are expressed as

$$\text{Chromium equivalent} = \% \text{Cr} + \% \text{Mo} + 1.5(\% \text{Si}) + 0.5(\% \text{Nb})$$

$$\text{Nickel equivalent} = \% \text{Ni} + 30(\% \text{C}) + 30(\% \text{N}) + 0.5(\% \text{Mn})$$

As per the 1992 WRC constitution diagram for SSs, the chromium and nickel equivalents are expressed by [147c] as

$$\text{Chromium equivalent} = \% \text{Cr} + \% \text{Mo} + 0.7(\% \text{Nb})$$

$$\text{Nickel equivalent} = \% \text{Ni} + 35(\% \text{C}) + 20(\% \text{N}) + 0.25(\% \text{Cu})$$

Prevention of microfissuring: Influence of welding procedure and welding parameters on ferrite content: The FN of an arc weld made with filler metal is primarily a function of filler metal and base metal composition and base metal dilution, which are controlled by the welding procedure, whereas the FN of an autogenous arc weld is a function of the composition of the base metal and the welding procedure. Microfissuring can be minimized by selecting (1) welding consumables, (2) welding process parameters, and (3) welding procedure variations that ensure solidification as delta ferrite. These three parameters are discussed next.

13.16.6.8.2 Welding Consumables

The composition of electrodes and filler wires for welding the fully austenitic steels is normally adjusted to provide 3%–5% ferrite in the weld metal deposit to protect against microfissuring. Elements such as nickel, silicon, sulfur, and phosphorus increase the susceptibility to cracking, whereas chromium, nitrogen, and manganese reduce the cracking tendency. Therefore, filler metals can be designed that are completely austenitic and free from microfissuring. Such fillers are low in sulfur, phosphorus, and silicon but often contain 7%–10% Mn. The principle of prevention of microfissuring by increasing manganese content is made use of in the “zero ferrite electrode.”

13.16.6.8.3 Welding Process

High heat input welding procedures, deep and narrow weld beads, high interpass temperatures, and high levels of restraint may result in cracking even with 4 FN ferrite in the completed weld bead [143]. Certain welding process parameters can also help to prevent microfissuring. Such parameters are as follows:

1. A long arc tends to reduce the ferrite content due to chromium loss across the arc [137].
2. Due to dilution, root pass welding generally results in a low ferrite content in the root weld metal. To offset this effect, a filler metal with a higher FN should be used [144]. Hot wire GTAW is particularly good from this standpoint [112].
3. High welding speeds that result in teardrop-shaped weld pools increase the solidification rate at the weld centerline and promote primary austenite formation, which makes these welds more likely to crack [143].

13.16.6.8.4 Welding Procedure Variations

Any procedure variation that admits nitrogen into the arc will reduce weld FN, and very high welding heat input tends to reduce ferrite content. The influence of nitrogen pickup is further discussed next.

13.16.6.8.5 Nitrogen Pickup

Higher than normal nitrogen levels can reduce weld ferrite and cause hot cracking. Excessive nitrogen pickup can result from (1) poor shielding gas coverage for GTAW and GMAW, (2) loss of flux coverage during SAW, and (3) use of excessively long arc lengths during SMAW or self-shielded FCAW [143].

Mock-up test: Prior to production welding where ferrite content is critical, pretesting in a mock-up is necessary to ensure that the combination of process, consumable, technique, and cooling rate will produce the desired FN in the weld [144].

Standards for ferrite determination: Determination of ferrite at room temperature has taken four forms over the years. They are (1) metallographic examination, (2) constitution diagrams, (3) magnetic measuring instruments, and (4) x-rays.

1. *Metallographic examination:* In the metallographic method, the ferrite content is determined by microscopic analysis. This method provides a statistical determination of the amount of ferrite. One of the common statistical methods of metallographic examination is by point-count analysis, where evenly spaced points are superimposed on a field on the specimen and the points found on a constituent are counted. A large number of fields are sampled to ensure statistical accuracy. The drawbacks associated with this method include the following: Examination is destructive in nature, interpretation is subject to error, and due to variations in etching, lab-to-lab reproducibility is sometimes poor [144].
2. *Constitution diagrams:* As an alternative to metallographic examination, constitution diagrams have been developed that permit estimation of weld metal ferrite from deposit composition. The Schaeffler diagram [147a] has been used in purchase specifications for filler metals; the DeLong diagram not only is used in purchase specifications for filler metals but also has become part of standards such as the ASME Code [146]. Recently, with the Winter 1994–1995 Addendum to the ASME Code, the 1992 WRC diagram [147c] has replaced the DeLong diagram [147b] in that code.

The Schaeffler diagram shown in Figure 13.16a, the DeLong diagram shown in Figure 13.16b, and the 1992 WRC diagram shown in Figure 13.16c use an x axis of chromium equivalents versus a y axis of nickel equivalents. Carbon contents are 0.03% minimum unless otherwise indicated.

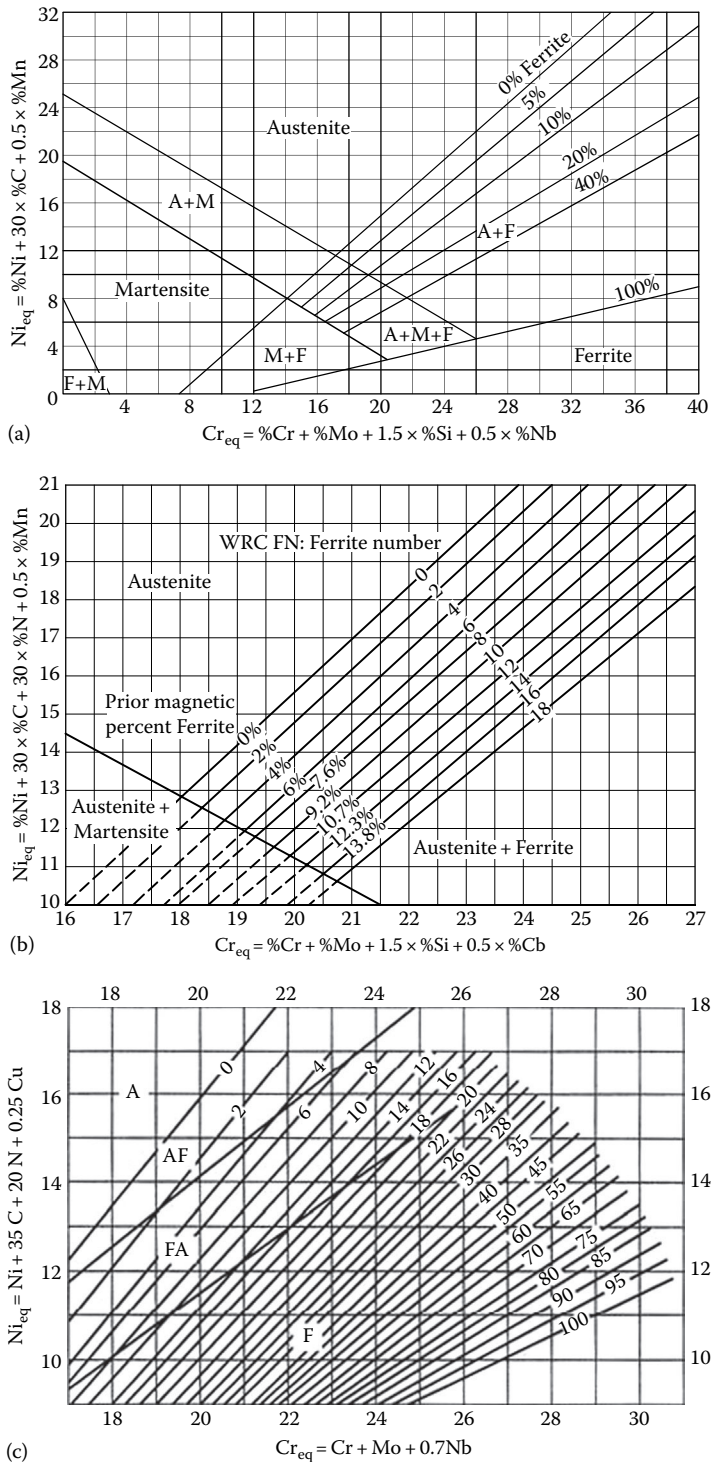


FIGURE 13.16 Constitution diagram. (a) Schaeffler diagram, (From Schaeffler, A.L., Constitution diagram for stainless steel weld metal, *Metal Prog* 56, 69, 1949.) (b) DeLong diagram, (From DeLong, W.T., Ferrite in austenitic stainless steel weld metal, *Weld. J.*, 53, 273-s–286-s, 1974.) (c) WRC 1992 diagram, (From Kotecki, D.J. and Siewet, T.A., WRC–1992 constitution diagram for stainless steel weld metals: A modification of the WRC–1988 diagram, *Weld J.*, May, 171-s–178-s, 1992.)

The Cr–Ni equivalents of the consumable and base material are plotted on a set of ferrite content lines that have been empirically derived. The dotted line indicates the approximate boundary of the austenite region for wrought alloys. Ferrite contents are determined by calculating specific chromium and nickel equivalents from alloy compositions and plotting the respective points on the diagram.

Caution is required in the use of these diagrams [144]:

1. These diagrams may not accurately reflect the effects of welding process, technique, dilution, or cooling rate on ferrite content; they are really applicable to welds made under conditions similar to those used by these researchers.
2. Neither the Schaeffler nor the DeLong diagram accounts adequately for the effects of manganese in amounts greater than 2.5% in a weld metal, in which case both the diagrams seriously underestimate ferrite content.

For these reasons, the constitution diagrams just described should be used only as guidance to choosing a particular consumable or for an approximation of ferrite content and never as a final word regarding weld metal ferrite content. Where accurate, ferrite measurement is required, magnetic instruments should be used, and the consumable manufacturer's recommendations followed.

3. *Magnetic measuring instruments or ferrite gauges:* Ferrite is ferromagnetic, while austenite is not; this provides the basis for magnetic determination of ferrite at room temperature. Ferrite determinations by magnetic means using ferrite gauges are reproducible, and this is a nondestructive test. Standard methods of ferrite determination by magnetic methods for industrial use are discussed in ANSI/AWS A4.2 and ISO 8249. Portable ferrite gauges or indicators are designed for on-site use. Various trade names for magnetic measuring instruments are Magne-Gage, Ferritescope, Severn gauge, Foerster gauge, and Elcometer [144]. Methods of measuring of ferrite as per magnetic properties of steels and their principles are given as follows:
 - a. Ferrite indicator: comparing the magnetic attraction between a standard ferrite percent insert and a test specimen
 - b. Ferrite scope: measuring the change of magnetic induction affected by the ferrite content of a test specimen
 - c. Magne-Gage: measuring the pull off force necessary to detach a standard permanent magnet from a test specimen.

13.16.6.8.6 Secondary Weld Metal Standards

The austenitic SS weld metal standards intended to be used for the calibration and a cross-referencing of instruments for measuring ferrite in weld metal are available from VEW-Bohler in Austria, among others. These samples have been prepared on behalf of Commission II on Arc Welding of the IIW and contain varying amounts of delta ferrite. FN s for the eight samples, in the approximate range 3–27 FN, have been determined using the IIW recommended procedure and are given on an accompanying card.

4. *X-rays:* This method of ferrite determination relies on the fact that all materials consist of different crystal structures. The intensities of diffraction lines of the different phases allow determination and measurement of their presence. This type of analysis is only possible on the surface thickness (approximately 2 mils) and can only measure amounts of ferrite in excess of 3 FN. Equipment of this type is costly, complicated, and not always practical [144].

13.16.6.8.7 Ferrite in Duplex Stainless Steels

HAZs in duplex SSs have a tendency to form a high level of ferrite, and this provides a special problem for ferrite measurement. The ferrite content can be kept within acceptance limits by controlling the composition of the base metal and by controlling the heat input, typically 0.5–2.5 kJ/mm, with more restrictive limits for higher alloyed “super duplex” SSs [146]. In duplex SSs, HAZ ferrite

content determination using a precisely defined metallographic point counting procedure is recommended. Ferrite content by magnetic means can be determined as per ANSI/AWS A4.2.

13.16.6.8.8 Variable Weld Penetration

Variable penetration refers to the marked differences in the depth of penetration observed when steels of nominally the same composition but produced from two different heats were welded under identical conditions. There is a tendency for the weld to deflect to one side of the joint when steels from different casts are welded together, and deviation to one side of the joint sometimes results in a lack of fusion. For this reason, the problem is also known as cast-to-cast or “heat-to-heat” variability [104,143]. Variable penetration is mostly experienced with the introduction of automatic autogenous welding processes, such as orbital TIG for tube-to-tubesheet joining, particularly with SSs grades such as AISI 304 and 316 [103].

Factors responsible for variable penetration: It is now generally agreed that variable penetration is associated with the influence of surface-active elements such as S, O, Se, Te, and Ce on the fluid flow in the weld pool [148]. In steels containing surface-active elements, the flow is toward the center of the liquid pool, giving downward axial flow and good penetration (Figure 13.17a). On the other hand, in high-purity steels with surface active elements absent, the penetration is shallow or off center (Figure 13.17b,c). Problems are particularly evident for heats containing less than 0.003% sulfur [149]. In high-purity steels such as calcium-treated steels, calcium forms sulfides, thus consuming the sulfur available to assist in producing the convergent flow. In order to achieve good weld penetrations, fabricators may specify a minimum of 0.01% S but with a caution that high sulfur content affects the corrosion resistance of SSs.

Measures to overcome variable penetration: Penetration can be achieved by increasing welding current or decreasing travel speed. However, it is difficult to implement these changes for individual heats in automatic welding operations [143]. Process tolerance can be increased by using short arc lengths and sharp-pointed electrodes, but these practices are often already in use when variable penetration is encountered. The following recommendations were given by Castner [143] and others to avoid variable penetration:

1. Avoid calcium- and rare-earth-treated steels; calcium and rare earth element content should not exceed 10 ppm [103].
2. Avoid steels with sulfur contents of less than 0.006% and steels with aluminum contents greater than 0.01%.
3. Change the shielding gases. Additions of helium and/or hydrogen to argon have been found to be effective in overcoming variable penetration. Argon with 5% hydrogen is very effective [143]. The influence of shielding gas on penetration in austenitic SS is shown schematically in Figure 13.18.
4. Massive copper alloy heat sinks surrounding the weld joint successfully overcome the problem [148].

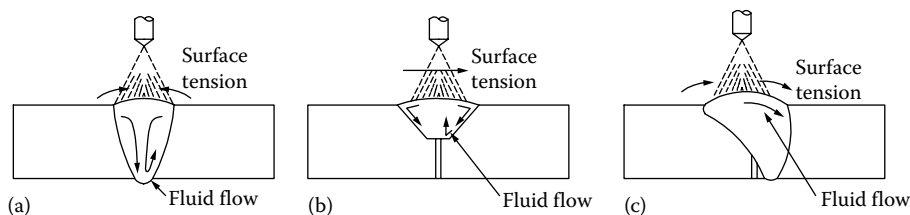


FIGURE 13.17 Weld metal penetration: (a) good penetration; (b) variable penetration due to absence of surface active elements, shallow penetration; and (c) off-center penetration. (After The Welding Institute, *Weld. J.*, December, 53, 1986. Excerpted from *Effects of Residual, Impurity, and Microalloying Elements on Weldability and Weld Properties*, The Welding Institute, 1985; adapted by Hallock C. Campbell.)

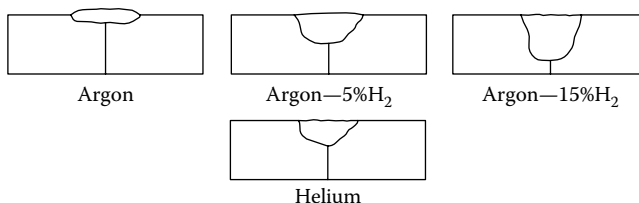


FIGURE 13.18 Shielding gas influencing austenitic SS weldment. (From Castner, H.R., *Weld. J.*, April, 53, 1993.)

13.16.6.8.9 Sensitization (Weld Decay) and Corrosion Resistance

Most widely used methods to prevent sensitization have already been discussed. Even stabilized grades are susceptible to localized precipitation of carbides in narrow regions of the HAZ, which can lead to intergranular corrosion known as knifeline attack. For welding purposes, the niobium-stabilized steel electrodes are preferred because less niobium is lost during transfer across the arc and thus more niobium is retained in the weld metal for carbide-forming purposes [136]. Residual stress from welding can cause SCC. Loss of corrosion resistance in austenitic SSs can be minimized by selecting the proper materials and welding procedure.

13.16.6.9 TIG Welding Techniques to Overcome Carbide Precipitation

Three main factors responsible for carbide precipitation are (1) excessive heat input, (2) too slow travel speed, and (3) inadequate shielding gas, or a combination of these factors cause the problem. Specifically, too hot of a TIG weld or too slow of travel speed and/or inadequate shielding gas coverage can individually or in combination cause the problem. Guidelines to avoid carbide precipitation thus include the following: (1) remember the rule of amperages—use one amp of welding current for every thousandths of an inch of material thickness and (2) maintain an appropriate travel speed helps prevent an excess amount of heat from entering the TIG weld. One way to monitor travel speed is to look for what is dubbed the “devil’s eye,” that is a fluid dot in the center of the weld puddle that is formed by foreign elements that continuously dance around in the center of the weld puddle. The presence of the “devil’s eye” is assurance that not only is travel speed appropriate, but also that other factors of the TIG welding (torch angle, filter rod position, penetration, and root opening) are all optimal.

13.16.6.10 Gas Coverage

Pure argon provides the best results when welding thinner austenitic SS, but the addition of small percentage of hydrogen is added when faster travel speeds are desired. Helium is preferred on heavier material as it produces deep penetration.

13.16.6.10.1 Control of Distortion

The relatively high coefficient of thermal expansion and the low thermal conductivity of austenitic SSs may result in more warping, especially in thin sections, than in other types of SSs, carbon steels, and alloy steels [137]. This suggests a greater need for jigging to maintain dimensional control. Measures to control distortion are discussed by Banks [137] and Castner [143]. They are the following:

1. More frequent tack welds are required to limit shrinkage.
2. Thin sections should be restrained with fixtures and strong backs.
3. Heat sinks can be used to minimize the size of the area affected by the heat of welding.
4. Fabrication of complex structures should employ the minimum permissible weld size and minimum weld heat input.
5. Heavy sections should be welded in as few passes as practical, using stringer beads and welding sequences that limit interpass temperature. Weld passes should be balanced around the neutral axis.

6. Too high of current setting and/or slow of travel speed contribute to this problem. Joint design and clamping are good defenses against distortion. The key to joint design is creating a joint that limits the number of weld passes and with it the amount of heat input. One way to limit these passes is to create a joint design consisting of a V-groove, modified V-groove, U-groove, or J-groove.

Mild steel jigs, strongbacks, etc., must not be directly attached to SS items that form part of the final fabrication, because this results in reduction in corrosion resistance, dilution effect, or air-hardening compositions susceptible to cracking.

13.16.6.10.2 Welding Fumes

Fumes from arc welding processes are a potential hazard to personnel. On-site measurements of fume concentrations are required to determine exposure for a given application. Local exhaust ventilation and/or respiratory protection are recommended to control exposure when welding austenitic SSs [143]. It may be possible to minimize fumes by selection of consumables and welding parameters as discussed in Ref. [143].

13.16.6.11 Welding Practices to Improve the Weld Performance

1. Minimize porosity in welds by using electrodes containing a deoxidizer like silicon or manganese [150].
2. Use lowest possible heat input to minimize the width of HAZ and minimize time at temperature in the range that can cause carbide precipitation. The degree of sensitization caused by welding is mostly related to the heat input processes. An arc welding process carried out at fast travel speeds, GTAW in particular, is better. A high heat input process, like SAW, is likely to sensitize SS unless travel speed is high and auxiliary cooling is applied [119].

13.16.6.12 Protection of Weld Metal against Oxidation and Fluxing to Remove Chromium Oxide

While welding SSs, the welding process must protect the molten weld metal from the atmosphere during transfer across the arc and during solidification. Some welding processes require fluxing to remove chromium and other oxides from the surfaces to be joined and from the molten weld metal. The presence of chromium oxide impairs the quality of SS weldments. Fluorides are the most effective agents for removing chromium oxide. Calcium and sodium fluorides are used in covered electrode coatings and SAW fluxes.

13.16.6.13 Protecting the Roots of the Welds against Oxidation

13.16.6.13.1 Gas Shielding

Oxidation of the underside surface of root beads of full penetration welds can occur if proper shielding is not provided. This oxidation is detrimental in corrosive environments because the oxide layer may reduce the corrosion resistance and facilitate preferential corrosion [118,143]. Therefore, protect the roots of welds from oxidation with argon; nitrogen also can be used as a backup gas. For multipass welds, the gas shield should be maintained during welding of the root pass and a few additional passes.

13.16.6.13.2 Root Flux

Root flux is a powder that, when made into paste and applied to the metallic surfaces to be protected, reacts with the heat from welding to form a thin slag that helps to protect the metal surface from oxidation [118]. However, root flux is not a substitute for gas shielding, but an improvement to welding with no root shielding.

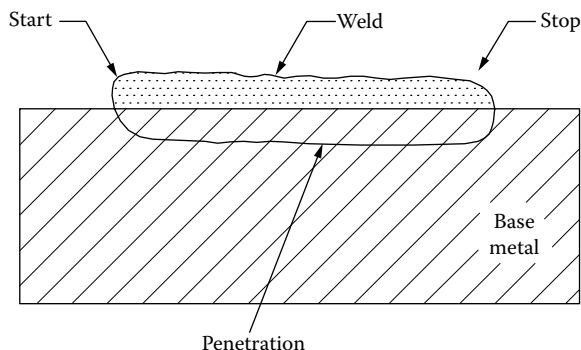


FIGURE 13.19 Beginning-and-end defect of welding of austenitic SS. (From Vackar, B.K., *Weld. Design Fabr.*, June, 86, 1977.)

13.16.6.13.3 Porosity: Beginning and End

One of the porosity problems of SS welding is known as “beginning and end.” It takes place at the beginnings and ends of welds (Figure 13.19) in SSs and nickel alloys due to hydrogen entrapped during solidification [150]. Preheating will help to reduce the amount of porosity in stainless and nickel alloy welds. According to Vackar [150], the probable causes of beginning-and-end defects are the following:

Base metal too cold.

Poor shielding at the start; poor shielding all along would produce porosity along the length of the weld.

Fast cooling at the end.

Once made, grind at least 1/16 in deep and get rid of front and back weld defects.

Underbead cracking: This can occur in the HAZ of the austenitic SS base metal immediately adjacent to the weld metal, especially in sections more than 0.75 in. thick.

13.16.6.14 Welding Processes Generate Different Weld Defects

The different arc welding processes typically generate different weld defects in SS. Among the gas-shielded arc welding methods, MIG process generates spatter and leaves slag residues on the weld-affected areas; TIG and plasma arc processes raise the risk of losing alloying elements from the weld pool and thereby locally decrease the pitting resistance of the weld metal; and slag shielding methods (SMAW, SAW, and FCAW) leave slag and spatter during the process and generate inclusions in the vicinity of the weld metal surface [118].

13.16.6.15 Postweld Heat Treatment

Austenitic SS weldments are normally placed in service in the as-welded condition. However, environments that can cause SCC due to residual stress from welding, or to overcome the susceptibility to intergranular corrosion due to carbide precipitation, or the need to assure dimensional stability may require a form of PWHT known as solution annealing. Solution annealing puts carbides back into solution and restores normal corrosion resistance. PWHT temperature ranges and heating and cooling rates must be selected to avoid the following potential problems [143]:

1. Heating in the range of 800°F–1650°F (425°C–900°C) can result in sensitization.
2. Heating welds between 1000°F and 1700°F (540°C–925°C) can transform ferrite to a hard, brittle sigma phase. Sigma-phase formation while carrying out PWHT can be minimized if the maximum weld metal FN is limited to 10–12 FN.
3. Stabilized SSs such as Types 321 and 347 will be susceptible to RC.

13.16.6.15.1 *Solution Annealing*

PWHT of SSs usually involve solution annealing at temperatures of 1950°F–2050°F (1065°C–1120°C) followed by rapid cooling or water quenching. Material not stabilized with columbium or titanium should be cooled through the range from 1700°F to 1000°F (927°C to 538°C) in not more than 3 min. The rapid cooling should be continued to below 800°F (427°C). Since the solution annealing temperature range is very high (1900°F minimum), unless SS is protected from air at these temperatures, it oxidizes rapidly, forming adherent oxide scale; if thin sections are not adequately supported, they may sag or warp.

13.16.6.15.2 *PWHT Cracking*

SSs may suffer cracking in the HAZ during PWHT or during high-temperature use. PWHT cracking is more likely to form in the stabilized grades containing niobium and titanium; it does not occur in molybdenum-bearing grades unless niobium is present, and therefore niobium additions should be avoided in molybdenum-bearing steels that are likely to be used in high-temperature applications [103].

13.16.6.16 **Welding Stainless Steels to Dissimilar Metals**

On many occasions, it is necessary to weld austenitic SSs to other materials, including carbon, low-alloy steel, martensitic and ferritic SS, copper alloys, and nickel alloys. Welding procedures for dissimilar metal joints must consider differences in strength, chemical composition, corrosion resistance, thermal expansion, and heat-treatment response [143]. Important weldability problems with dissimilar metals welding include (1) solidification cracking and (2) dilution of the weld metal, which can result in martensitic weld metal that is susceptible to hydrogen-induced cold cracking.

13.16.6.16.1 *Methods to Overcome Dilution Problems*

Dilution problems associated with the mixing of dissimilar metals in weld runs can be solved with reference to a Schaeffler constitutional diagram. This can be particularly helpful in choosing a proper filler metal and welding parameters to give adequate control of the delta ferrite and austenite phase. Methods to overcome dilution problems are [143] the following:

1. Base metal dilution should be minimized by use of low heat input and stringer bead techniques
2. When joining SS to mild steel, it is a usual practice to use a more highly alloyed filler metal in order to allow for the dilution on the mild steel side
3. Buttering the carbon steel base metal prior to completing the joint is an effective technique to minimize dilution

13.16.6.16.2 *Filler Metals for Welding SS with Dissimilar Metal*

Welding filler metals for joints between carbon or low-alloy steels and austenitic SSs must be selected to prevent solidification cracking. For dissimilar metal welding, particularly between carbon steels and austenitic SSs, Type 309 electrodes and filler metals are probably the most commonly used filler metals. Nickel-alloy filler metals are recommended for critical service conditions and service temperatures above 800°F. To weld one of the ELC unstabilized varieties, a correct choice is to use a matching electrode, rather than using a high-carbon stabilized electrode [137].

PWHT: If PWHT is required, the temperature and heat-treatment cycles must be carefully selected to avoid sigma-phase formation in the weld, sensitization of austenitic steels, or problems due to differences in thermal expansion.

13.16.6.17 **Postweld Cleaning**

Welding-related surface contamination and imperfections such as weld splatter, welding slag, arc strikes, heat tint, oxides, and other surface contaminants can be a source of corrosion initiation. Thorough postweld cleaning is necessary to remove the welding contaminations and to obtain optimum corrosion resistance of the parent metal. The cleaning procedure should avoid the formation

of oxide films, which render the SS susceptible to various forms of corrosion. Procedures should allow for repassivation [118].

Welding contamination is best removed by the use of a wire brush not used for other purposes, abrasive disks, flapper wheels, or pickling. Grinding should be avoided, since this procedure tends to overheat the surface, thereby reducing its corrosion resistance. Or subsequently, overheating or “bluing” of the surface must be avoided, or removed perfectly, preferably by acid pickling. Avoid chloride-bearing solvents for cleaning SSs. Generally, a nitric acid final wash oxidizes the surface and passivates the metal [119]. ASTM A380 details ways to clean SS.

13.16.6.18 Corrosion Resistance of Stainless Steel Welds

During all welding processes, the surfaces affected by welding will be subjected to various metal-lurgical and surface-related phenomena that locally weaken the passive film and make it susceptible to pitting corrosion. The general rules of good welding practice also apply to welding of SSs for corrosion resistance. Pitting corrosion resistance of SS welds depends on the following factors [118]:

1. Microstructure and chemical composition in the vicinity of the weld metal surface
2. Inclusions
3. Weld spatter, arc strikes, contaminations from fabrication and shop environment
4. Residual welding stresses
5. Geometric surface defects, notches, solidification cracks, and crevices
6. Surface oxides, inhomogeneous structure, and depletion of the alloying element from the underlying parent metal

Measures for optimization of the pitting corrosion resistance of SS welds are as follows:

1. Careful selection of welding consumables and fabrication procedures
2. Gas shielding to avoid surface oxide formation
3. Root fluxes to protect the metallic surfaces from oxidation
4. Postweld cleaning

13.17 FERRITIC STAINLESS STEELS

13.17.1 CONVENTIONAL FERRITIC STAINLESS STEELS

Ferritic SSs are basically Fe–Cr (conventional ferritics) or Fe–Cr–Mo (mostly superferritic) alloys containing approximately 11%–30% chromium, and when molybdenum is added, resistance to pitting corrosion increases. Conventional ferritic SSs are listed in the 400 series. Ferritic SS are magnetic. High-chromium ferritic SSs have good resistance to corrosion, including resistance to chloride SCC. Oxidation resistance of the ferritic steels is also very good, especially for the high-chromium grades such as Type 446, or when aluminum and rare earths are added. They cannot be hardened by heat treatment and only moderately by cold working. In spite of equivalent corrosion resistance and low-cost alloying elements, the ferritic steels have been surpassed by the austenitic SSs, primarily because of their lower formability and toughness and reduced weldability [151,152]. These drawbacks are minimized in light gauges, so the bulk of current use of ferritic steels is in light gauge tubular and sheet form. To improve the weld metal ductility, sometimes welding of Types 430 and 446 is done with austenitic filler metals. This solves the ductility problem but can lead to loss of corrosion resistance [119]. These alloys have higher thermal conductivity, lower thermal expansion, and lower cost. Types 430, 443, and 446 have become popular in low-pressure, high-temperature heat exchangers [153]. A new kind of ferritic SS, Type 444, has less carbon than L grades and is stabilized with titanium and columbium to prevent sensitization. This grade shows major improvements in as-welded ductility compared with conventional ferritics.

13.17.2 “NEW” AND “OLD” FERRITIC STAINLESS STEELS

When reviewing the various commercial ferritic SSs, it is appropriate to distinguish between the “old” and the “new” steels. The newer varieties are called as superferritics. The old ferritic SSs are represented by the standard AISI grades as such as Gr 405, 409, 429, 430, 434, 436, 442, etc.

13.17.2.1 Superferritic Stainless Steels, Superaustenitic Stainless Steels, and Duplex Stainless Steels

Type 316, which is generally considered one of the most corrosion resistant of the common austenitic SSs, has not performed consistently well under conditions of total immersion in seawater. Even though copper–nickels or nickel–base materials or titanium can serve the purpose, these materials are usually expensive than SSs. A need was recognized for less costly materials for use in seawater applications, with greater resistance to chloride SCC and crevice corrosion than Type 316. Thus, a new generation of austenitic SSs known as superaustenitics and ferritic SSs known as superferritics were developed, usually with Mo as an alloying element to stabilize the passive film in the chloride-bearing environment. Since 1980, the high-performance SSs have become the first choice for seawater-cooled steam condensers [101]. These steels are discussed in the next section.

13.17.3 SUPERFERRITIC STAINLESS STEEL

Superferritics refer to iron–chromium SS alloyed with molybdenum for improved pitting corrosion resistance and titanium or niobium for improved resistance to intergranular corrosion. Their major advantage is very high resistance to chloride SCC. The ferritic structure and low or zero nickel content also provide high resistance to SCC. They also exhibit better general corrosion resistance.

Before the advent of the advanced steel melting and refining methods, ferritic SSs had relatively high levels of interstitials—carbon and nitrogen—and as a result had serious limitations with respect to fabric ability, toughness, and corrosion resistance. The newer ferritics, especially those with high chromium content, have become possible through AOD, VIM, and VOD. All are capable of producing low interstitial content [154]. During the refining stage, care is taken to reduce interstitials to very low levels and/or to “tie up” carbon and nitrogen by stabilizing them with elements such as titanium or niobium.

13.17.3.1 Characteristics

- Magnetic, crystallographic form—body-centered cubic
- High ambient temperature strength
- Low work hardening
- Low carbon grades easy to weld
- Nonhardenable by heat treatment
- Resistant to chloride SCC, subject to 475°C (885°F) embrittlement as low as 315°C (600°F)
- Subject to hydrogen embrittlement, subject to DBT temperature transition

13.17.3.2 Alloy Composition

The superferritic grades contain up to 29% Cr (although grade 18Cr–2Mo is sometimes considered a superferritic material), 4% Mo, and in some alloys, 3.5% Ni, and have completely ferritic microstructures. The well-known superferritics include 18-SR (Armco), 18Cr–2Mo, 26-1S, E-Brite 26-1 (Airco, Allegheny Ludlum), and 29Cr–4Mo (du Pont), with UNS S44735, 29Cr–4Mo–2Ni (du Pont), and Sea-Cure (UNS S44660), containing 26% Cr, 3% Mo, and 1% Ni. They are primarily proprietary grades. Their compositions are given in Tables 13.19 and 13.20 and their product forms in Table 13.21. For the most part, the workhorses in the superferritics category have been Alloy 29-4 (UNS S44735) and Alloy Sea-Cure (UNS S44660) [115]. Both have titanium and niobium

TABLE 13.19
Nominal Composition of Selected Ferritic/Superferritic SSs

UNS No.	Alloy	C	Cr	Ni	Mo	N ₂	Others
S43035	18-SR	0.05	18	0.5	—	0.020	2Al, 0.4Ti, 1Si
S44400	18-2	0.02	18	—	2	0.020	0.4Ti, 0.3Cb
S44625	26-1	0.01	26	0.5	1	0.015	0.5Ti
S44627	E-Brite	0.003	26	—	1	0.015	0.10Cb
S44660	Sea-Cure	0.01	26	2.5	3	0.025	0.4Ti
S44635	Monit	0.025	25	4	4	0.025	Nb + Ti
S44735	29-4C	0.02	29	0.3	4	0.020	0.4Ti, 0.2Cb
S44800	29-4-2	0.01	29	2	4	0.020	—

Notes: (a) The ferritic content is not explicitly mentioned. (b) E-Brite is the registered trademark of Allegheny Ludlum Steel Corp. (c) Monit is a trademark registered to Nyby-Uddeholm. (d) Sea-Cure is a registered trademark of Plymouth Tube.

TABLE 13.20
Pitting Resistance Number for Selected Superferritic Stainless Steel

Alloy	UNS Designation	Composition Required to Calculate PRE _N		PRE _N ^a
		Cr	Mo	
26-1 TM	S44625	26	1	29.3
E-Brite TM	S44627	26	1	29.3
Sea-Cure TM	S44660	26	3	35.9
Monit TM	S44635	25	4	38.2
AL 29-4C TM	S44735	29	4	42.2
AL 29-4-2 TM	S44800	29	4	42.2

^a PRE_N = %Cr + 3.3(%Mo).

TABLE 13.21
ASTM/ASME Spec. for Superferritic Stainless Steel Grade Heat Exchanger Tubes^a

Grade	UNS No.	ASTM Spec. for Tubes	ASME Sec. VIII, Div. 1
Sea-Cure	S44660	A268, A803	SA268, SA803
AL29-4-2	S44800	A268	SA268
AL 29-4C	S44735	A268	Code case 1921
Monit	S44635	A268	Code case 1900
E-Brite	S44627	A268	SA268

^a ASTM/ASME Spec. for sheet/plate is covered under A/SA240.

TABLE 13.22
Superferritic and Superaustenitic Alloys UNS Designations, Trade Names, and Manufacturers

Alloy UNS No.	Registered Trade Name	Producers
S44635	Monit	Uddeholm Steel Corp.
S44627	E-Brite	Allegheny Ludlum Steel Corp.
S44735	AL 29-4C	Allegheny Ludlum Steel Corp.
S44660	Sea-Cure	Trent Tube Div. of Colt Ind., Crucible Steel Co.
S44800	AL 29-4-2C	Allegheny Ludlum Steel Corp.
S31254	254 SMO	Avesta Jarnverks AD
N08904	AL 904L	Allegheny Ludlum Steel Corp.
N08366	AL-6X	Allegheny Ludlum Steel Corp.
N08367	AL-6XN	Allegheny Ludlum Steel Corp.
N08925	1925hMo, 25-6MO	VDM Technologies, Inco-Alloys Internationals
N08026	20Mo-6	Carpenter Technology

Note: This table gives only partial information on various alloy manufactures.

E-Brite (S44627), AL-6X (N08366), AL-6XN (N08367), and AL29-4C (S44735) are registered trademarks of Allegheny Properties Inc.

Monit (S44635) is a trademark registered to Nyby-Uddeholm.

254SMO (S31254) is a registered trademark of Outokumpu.

Sea-Cure (S44660) is a registered trademark of Plymouth Tube.

(also known as columbium) added to stabilize their carbon and nitrogen contents. Alloy trade designations for various superferritics, superaustenitics, and duplexes to be discussed in next sections are given in Table 13.22.

13.17.3.3 Applications

Superferritics have found extensive applications as tubing for power-plant condensers and heat exchangers handling chloride solutions, seawater, and brine. Types 18Cr–2Mo, E-Brite 26-1, Sea-Cure, and AL 29-4 are used in the petrochemical and chemical industries and in seawater applications. Because of its high chromium content, E-Brite 26-1 offers substantial resistance to oxidation and sulfidation at elevated temperatures. The E-Brite alloy is being used in air preheaters and heat recuperators.

13.17.3.4 Physical Properties

The ferritic SSs offer the following two physical properties that are of particular importance [154]:

1. Their thermal conductivity is about 50% higher than that of the austenitics, or about half that of carbon steel.
2. Their thermal expansion coefficient is low, roughly equal to that of carbon steel and about 30% less than that of Type 304 SS.

13.17.3.4.1 Strength

The strength of ferritics is compared with austenitic SSs as follows [151]:

1. The room-temperature yield strength in the annealed condition is 20%–40% higher than that of the austenitic steels.
2. The rate of work hardening of the ferritic steels is lower.
3. At high temperature, the ferritic steels have lower strength than the austenitics, but their oxidation resistance is very good.

13.17.3.4.2 Toughness and Embrittling Phenomena

Toughness of the ferritic SSs is influenced by three embrittling mechanisms [151]: (1) “885°F (475°C) embrittlement,” (2) sigma-phase precipitation, and (3) high-temperature embrittlement. Each of these conditions lowers the ductility and toughness of the ferritic SSs at room temperature and hence imposes restriction on the fabricator and user in various operations such as hot forming, brazing, welding, and heat treating in order to minimize high-temperature exposure [155].

“885°F (475°C) Embrittlement”: All ferritic SSs, with the possible exception of Type 409, are susceptible to this embrittlement phenomenon when exposed in the temperature range of 720°F–950°F (400°C–540°C). Peak hardening and embrittlement occur at approximately 885°F as a result of the formation and precipitation of alpha prime, a coherent chromium-rich particle in the iron-rich matrix [151]. Consequently, an increase in hardness and tensile strength is observed, concurrent with substantial decrease in ductility and impact resistance [156]. The phenomenon is observed at chromium levels in excess of about 12%. In order to overcome this form of embrittlement during processing, fast cooling is recommended through the 700°F–950°F temperature range. Consequently, neither the new nor the old ferritics should be exposed to this temperature range [151,154]. The 475°C (885°F) embrittlement limits the thickness of many of these alloys to about 3 mm (0.125 in.), so as attractive as the properties, etc., they cannot be used for heavy sections. However, they can be used as thin-walled heat exchanger tubes, wall paper, or liners.

Sigma-phase precipitation: Sigma phase may form in the higher chromium ferritic steels (15%–20%) when they are exposed for prolonged periods at 1100°F–1500°F. The precipitation results in room-temperature embrittlement as well as loss of corrosion resistance [151]. Formation of sigma phase may be minimized or prevented by a proper selection of composition, or sigma phase may be transformed into austenite and ferrite by suitable heating, followed by water quenching or rapidly cooling by other means.

High-temperature embrittlement: When high-chromium SSs of intermediate and high interstitial content are heated normally above about 1000°C and cooled to room temperature, precipitation of carbide and nitride can result in embrittlement as well as susceptibility to intergranular corrosion, especially in alloys containing high interstitial elements [151].

13.17.3.4.3 Ductile–Brittle Transition

The superferritic SSs with bcc crystal structure exhibit a DBTT that for many grades is close to room temperature. The interstitial elements carbon and nitrogen have a potential effect on the DBTT; a low-interstitial element content is essential for a low DBTT and hence good toughness at room temperature. For this reason, all the new ferritic SSs have very low-interstitial element content, obtained by special melting techniques [151]. The new grades are acceptably tough as both sheet and tubing, and therefore these alloys are typically used in thin sections, such as tubing, light-wall pipe, sheet, and strip. However, VIM-produced superferritics have extremely low carbon and nitrogen levels and thus improved toughness. These materials are usually used in all product forms up to plate thickness of about 0.50 in. (12.7 mm) [101].

13.17.3.5 Corrosion Resistance

Because the chromium content of the ferritic SSs ranges from 11% to 29%, the general corrosion resistance can vary from moderate to excellent [151]. An important feature of the ferritic SSs is their resistance to chloride SCC. Because the austenitic steels are highly susceptible to SCC, the ferritic steels provide a more economical alternative than the nickel-base alloys for applications requiring resistance to SCC. Superferritic SSs offer outstanding resistance to chlorides, alkalis, nitric acid, urea/ammonium carbamate, amines, and organic acids [152]. Additions of molybdenum increase the resistance to pitting corrosion by producing a more stable passive film. The PRE number is calculated using the formula

$$\text{PRE} = \% \text{Cr} + 3.3(\% \text{Mo})$$

13.17.3.5.1 *Intergranular Corrosion in Ferritic Stainless Steels*

A major obstacle to the use of ferritic SSs has been their susceptibility to intergranular corrosion [157]. Ferritic SSs are sensitized when exposed to a temperature of about 1800°F (982°C) due to welding or improper heat treatment, and this makes them susceptible to intergranular corrosion. The mechanism responsible for intergranular corrosion is generally accepted as being the same as that in austenitic SSs [158]. This problem is overcome by alloying with titanium and/or columbium to form the carbides of these elements. Lowering the carbon content below 0.03%, as in austenitic SSs, is not effective. Even with 0.01% maximum carbon content, it is necessary to add carbide-stabilizing elements [151].

13.17.3.6 **Fabricability**

The ductility and toughness of the ferritic SSs are low at room temperature. The sequence of fabrication operations, and often the design, should consider the relatively low toughness and ductility of the material at room temperature. Cold-forming operations must also be commensurate with possibly reduced ductility and toughness [155].

13.17.3.7 **Welding**

The two most important factors in making good welds in the superferritics are (1) the maintenance of alloy purity and (2) that ferritic weld metal structure cannot be refined by heat treatment [103]. Superferritic SSs tend to retain the problem of conventional ferritic steels in relation to grain growth in HAZ, grain coarsening in the weld metal, and loss of toughness after welding and reduced corrosion resistance due to sensitization and sigma-phase precipitation. The problems faced while welding ferritic SSs are summarized by Walker [159]:

- Grain growth
- Coarse-grained weld metal
- Reduced impact strength
- Reduced corrosion resistance due to sensitization and precipitation of sigma phase

Being highly magnetic, they are subjected to arc blow during welding. The following measures will help to reduce some of these problems [159]:

- TIG welding with good shielding and backing
- Extreme cleanliness of weld preparation
- Autogenous welding or matching filler
- Low heat input to minimize grain growth

Since the high quality of these steels is based on low carbon and nitrogen contents, it is essential that the pickup of these elements during the welding process should be avoided due to the risk of chromium carbide and nitride formation, resulting in loss of corrosion resistance [103,140]. Avoid the pickup of oxygen and hydrogen also. Careful shielding, front and back, with dry argon or helium is necessary [154]. Cleanliness and extraordinary inert gas shielding are essential for successful welding, particularly when matching filler metal is used.

Low heat input is necessary to limit grain growth. The grain growth problems can also be minimized by using austenitic filler materials, and still there is some grain growth in the HAZ; this can be reduced by keeping preheat temperature below 200°C [137].

The ferritics are less prone to welding defects than the austenitics, but their notch sensitivity makes any defects that are present much more detrimental. Therefore, special care must be taken to avoid undercutting or poor penetration, and thorough inspection of welds is essential [154].

13.17.3.7.1 *Surface Preparation and Joint Design*

Surface preparation and cleaning before and after welding are important for assured weld quality and corrosion resistance. Edge preparation of weld joints includes removal of all contaminated metal by machining or grinding the thermally cut surfaces. Weld joints and filler metal surfaces must be free of surface contaminants. A nonchlorinated, residue-free solvent, such as methyl ethyl ketone (MEK), is useful for this purpose. Cleaning should immediately precede welding. Optimum corrosion resistance is obtained by mechanically or chemically removing the heat tint after welding.

13.17.3.7.2 *Good Practices for Welding Ferritic Stainless Steels*

Beigay and Lovejoy [140] discuss good practices for ferritic SS welding. Some of the good practices include the following:

1. Minimize contamination by running stringer beads. Stringer beads are preferred over a “weaving” technique.
2. Keep ends of filler rods protected in shielding gas. Filler metal must not be pulled in and out of the shielding gas. Once pulled away from the shielding gas, the contaminated tip must be removed before the wire is used again.
3. Welding techniques that minimize contamination must be employed.
4. Allow shielding gas to flow after extinguishing the arc, protecting the weld bead and filler tip until both cool sufficiently to prevent oxidation.
5. To protect weld puddles, shield with pure argon or helium, or by vacuum. Avoid shielding gases containing carbon dioxide, nitrogen, or oxygen. Prefer GMAW and GTAW, because they shield the welding area well.
6. Brush tack welds with an SS wire brush, then weld to complete the root pass. Finish the weld using the same shielding used for tack welds and root pass.
7. Between passes, remove oxides with brushes having bristles of SS, not ordinary carbon steel. Carbon steel bristles, or grinding wheels containing carbon, will carbonize and crack SS welds [150].

The GTAW process is required to achieve the degree of shielding necessary.

13.17.3.7.3 *Filler Metals*

Although matching filler metals have been used successfully in a few cases, the most satisfactory results are obtained with low-carbon, austenitic SS or nickel-base fillers.

13.17.3.7.4 *PWHT*

This structure cannot be refined by heat treatment; however, the use of low heat inputs during welding will restrict the amount of martensite formation, and following by an annealing heat treatment will be useful.

13.18 DUPLEX STAINLESS STEELS

As the name implies, duplex SSs have a mixed microstructure of ferrite and austenite in the approximate proportion of 50:50. The corrosion resistance of duplex alloys depends primarily on their composition especially the amount of chromium, molybdenum, and nitrogen content. For these steels, the chromium content may vary from 22% to 27% and molybdenum 2% to 4%, depending upon corrosion resistance required. Many of the duplex grades have become known by a number that reflects their typical chromium and nickel contents. For example, the 2205 grade will have 22% Cr and 5% Ni. These composition-based names, used by many producers, have recently been added to ASTM A240. Typical newer varieties of duplex SSs include Alloy 2205, known as Code Plus Two, 44LN, and Ferralium 255 (S32550), which also contain 2% copper, 7 Mo-PLUS (UNS S32950),

Atlas 948, and 253 ME. Of these varieties, Ferralium 225 is regarded as the only seawater duplex SS [101]. 7 Mo-PLUS is being used very successfully in both tubeside and shellside cooler condensers for nitric acid production [115]. Because of their higher strength and better resistance to SCC than conventional austenitic SSs, duplexes are now gaining acceptance.

13.18.1 COMPOSITION OF DUPLEX STAINLESS STEELS

Duplex SSs usually contain high chromium (22%–27%) and Mo (2%–4%). The compositions are carefully controlled to maintain the proper balance of austenites and ferrites. The high chromium content makes duplex alloys exhibit strong resistance to oxidation. The nickel content varies from 4% to 7%. Because of lower nickel content, duplexes cost less. The addition of 0.15%–0.25% nitrogen enhances strength and toughness, and improves pitting and chloride SCC. Nitrogen cannot be added to the filler material as it cannot transfer across the arc when welding and hence nitrogen can be added to the weld through the gas shielding. Their carbon content is low. Material compositions for some duplex SS are given in Table 13.23 and pitting resistance number for selected alloys is shown in Table 13.24. The specification for various product forms has been included both in the ASTM and in the ASME Code Section VIII, Div. 1. A partial list is shown in Tables 13.25 and 13.26.

TABLE 13.23

Nominal Composition of Some Duplex/Super Duplex Stainless Steels

UNS No.	Alloy	C Max.	Cr	Ni	Mo	N	Others
S31803	2205 TM	0.03	21–23	4.5–6.5	2.5–3.5	0.15	0.7Mn (2 max.)
S32520	UR52N+ TM	0.03	24–26	5.5–8.0	3–5	0.2–0.35	1.5Mn
S32550	Ferralium 255 TM	0.03	24–27	4.5–6.5	2.9–3.9	0.20	2Cu, 1.5Mn
S32760	Zeron 100 TM	0.03	25	7.5	3.5	0.23	—
S32950	7-Mo plus TM	0.03	26–29	3.5–5.2	1.0–2.5	0.20	2Mn
S32750	2507 TM	0.03	24–26	6–8	3–5	0.28	1.2Mn, 0.50Cu

Note: S32550, S32950, and S32750 are super duplex stainless steels.

Ferralium 255 Super duplex stainless steel available from Langley Alloys Ltd., Newcastle-under-Lyme.

TABLE 13.24

Pitting Resistance Number for Duplex Alloys

UNS Designation	Alloy	Composition Required to Calculate PRE _N			PRE _N ^a
		Cr	Mo	N ₂	
S31803	2205 TM	22	3.0	0.15	33.7
S32520	UR52N+ TM	25	4	0.28	41.68
S32550	Ferralium 255 TM	25	3.5	0.20	39.7
S32900	7 Mo TM	25			25.
S32950	7-Mo plus TM	27.5	1.8	0.20	34.64
S32750	2507 TM	25	4.0	0.28	42.84
S32760	Zeron 100 TM	25	3.5	0.23	40.23

^a PRE_N = %Cr + 3.3 (%Mo) + 16 (%N).

TABLE 13.25
ASTM Specification for Duplex Stainless Steels

Product Form	ASTM Spec.	ASME Spec.
Bar	A276	—
Sheet, strip, plate	A240	SA240
Pipe (welded and seamless)	A790	SA790
Tubing (welded and seamless)	A789	SA789

TABLE 13.26
ASTM/ASME Spec. for Various Product Forms of Duplex Alloy 2205(S31803)

Alloy Name	UNS Designation	Sheet, Plate, and Strip	Heat Exchanger Tube	Pipe	Pipe Fittings	Rod, Bar, and Wire
2205™	S31803	A/SA 240	A 270, A/SA 789	A 928, A/SA 790	A/SA 815	A/SA 182, 276, 479

Characteristics of Duplex SS

Magnetic

Contains both austenite and ferrite phases

High strength

Subject to 885°F (475°C) embrittlement as low as 600°F (315°C)

Subject to hydrogen embrittlement

Subject to ductile–brittle temperature embrittlement

13.18.2 COMPARISON WITH AUSTENITIC AND FERRITIC STAINLESS STEELS

Because the duplex SSs are balanced with the composition of austenitic and ferritic phases, their physical properties fall between the comparable properties of the austenitic and ferritic SSs. Salient features of their properties compared to austenitic and ferritic SSs are the following:

1. Duplexes offer higher strength and toughness, good corrosion resistance, and better resistance to chloride SCC than austenitics, and they are relatively low-cost material.
2. Duplexes have a higher yield strength than the austenitics; this provides an economic advantage due to the use of lighter gauge material compared to austenitic SS. But duplexes are not suitable for cryogenic service.
3. At higher temperatures, there is a change in phase balance, and their use is not recommended for high-temperature applications.
4. The large amount of ferrite phase present in the duplexes makes them magnetic.
5. Because of the segregation of the ferrite and austenite phases, various duplex alloys can show variability in pitting and crevice corrosion resistance.
6. Duplexes have better toughness than ferritic grades. Compared to ferritics, the DBTT of the duplex alloy is more gradual and occurs at a lower temperature (below room temperature), thus allowing the production of thick plates; this allows manufacture of tubesheets.
7. The thermal conductivity is less than half that of carbon steel, but about 25% more than that of austenitic SS.
8. The coefficient of thermal expansion is about 40% less than that of austenitic SS, but equal to that of carbon steel.

13.18.3 CORROSION RESISTANCE OF DUPLEX STAINLESS STEELS

Although their nickel contents (4%–7.5%) are less than those of austenitic SSs, their SCC resistance is much better than that would be expected from nickel content alone. Duplex SSs have two important advantages over Types 304 and 316 SSs [115]: (1) good resistance to chloride SCC and (2) higher mechanical properties with good ductility. Because the duplexes have a higher yield strength than the austenitics, SCC resistance may usually be maximized with a 50:50 microstructure. Because nickel is a factor for providing corrosion resistance in reducing environments, the duplexes show less resistance in these environments than the austenitics.

The high chromium and molybdenum contents of the duplex stainless are particularly important in providing resistance in oxidizing environments and are also responsible for the better pitting and crevice corrosion resistance, particularly in chloride environments. The PRE_N number is calculated using the following formula [116]:

$$PRE_N = \%Cr + 3.3(\%Mo) + 16(\%N)$$

Some alloys contain an addition of tungsten, which increases the pitting resistance of duplex SSs. For these alloys, the pitting resistance is expressed as PRE_w :

$$PRE_w = \%Cr + 3.3\%Mo + 1.65W + 16\%N$$

The PRE_N or PRE_w number is commonly used to classify the family to which an alloy belongs; in general, materials having a pitting resistance number in the low value of 30 such as duplex alloy 2205 are classified as standard duplex, and those which with PREs of 40 or more are known as superduplex alloys.

Duplexes are produced with low carbon contents, usually less than 0.03%, and hence intergranular corrosion due to sensitization of weld metal as a result of carbide precipitation generally is not a problem. Hydrogen-induced cracking will occur when the ferrite exceeds 55 FN.

Laboratory corrosion tests include CPT by ASTM G-48A, ASTM A262-C (Huey Test) for IGC, and ASTM G30 and G36 for SCC.

13.18.4 PROCESS APPLICATIONS

The duplex alloys have excellent resistance to oxidizing and reducing acids, sulfuric acid below 25% concentration, organic and acid mixtures, seawater and sour oil and gas wells, and alkali solutions [160]. Duplexes are applied successfully in vessels and heat exchangers containing corrosive chlorides, in applications like oil and gas plant components, pulp and paper mill plants, oil refinery heat exchangers, chemical processing heat exchangers, tanks, pressure vessels, columns, flue gas scrubbers, boiler tubes, digester preheaters, evaporators, etc.

13.18.5 WELDING METHODS

Welding methods used for austenitic SS can be used except for the use of pure argon shielding during welding to protect cerium addition. The welding processes most applicable are GTAW, GMAW, PAW, SMAW, and SAW [161].

13.18.5.1 Weldability

The goal in welding duplex SS is to obtain weld metal and HAZ having the same corrosion resistance, toughness, and absence of intermetallics. The trick in welding the duplex SS is avoiding the formation of excess ferrite. The advantage of corrosion resistance and mechanical properties can be

achieved in welded assemblies when the welding practice ensures formation of a 50:50 austenitic–ferrite phase both in the weld metal and in the HAZ. The following problems are normally faced while welding duplex SSs [159]:

- High ferrite phase and hence reduced toughness
- Liquation cracking
- Grain growth in HAZ
- Reduced corrosion resistance due to sigma phase, and carbonitride precipitates
- Precipitation of chromium nitrides, which reduce corrosion resistance
- Prolonged heating in the range 350°C–550°C can cause 475°C temper embrittlement and therefore mostly confined to application temperatures below 300°C

To overcome these problems, the following measures will help [159]:

- Overalloyed filler metal with higher Ni content and with a guaranteed PRE value of not less than 40 [162]
- Controlled heat input
- Controlled interpass temperature (limited to 200°C maximum)

13.18.5.1.1 Balancing the Austenite and Ferrite Phases

Balanced phases can be ensured only if the cooling rate is slow enough to allow austenite to reform as the weld cools. If the rate is too slow, embrittling phases may form; on the other hand, if it is too fast, intermetallics could form. Autogenous welding will increase the ferrite phase in the weldment and adjacent areas of the base metal. Subsequent annealing will tend to restore the balance of phases in the base metal.

13.18.5.1.2 Heat Input

High weld heat inputs, preheat, and interpass temperatures promote coarse-grained weld deposits and HAZ, and the tendency to precipitation is enhanced [161]. Welding heat input should be controlled to limit the ferrite level, whereas too low a heat input produces too much ferrite, and it has been suggested that heat inputs above 1.5 kJ/mm must be employed [163].

13.18.5.1.3 Liquation Cracking

Duplex SS is susceptible to HAZ liquation cracking due to the formation of low-melting-point films of S and P along the grain boundaries, and the effect is aggravated in the presence of restraint and residual stresses.

13.18.5.1.4 Precipitations of Secondary Phases

Duplexes are susceptible to the precipitation of sigma phase due to the higher concentration of ferrite-forming elements. Base metals with low carbon, balanced ferrite–austenite phases, and adequate nitrogen speed the reformation of austenite during cooling and avoid secondary sigma-phase formations.

13.18.5.1.5 Precipitation of Chromium Nitrides

Due to the increased amounts of nitrogen that are now used to strengthen the austenite, chromium nitrides (Cr_2N) are usually formed in the weldments intragranularly, along with sigma phase. This causes the formation of secondary austenite in the surrounding material due to reduction in concentration of ferrite-forming elements. This secondary austenite causes the localized loss of corrosion resistance due to its low chromium content [103].

13.18.5.1.6 *Welding Consumables*

When consumables that match the parent plate material compositions are used, the final weld metal microstructure may be low in austenite and high in ferrite, causing a loss in toughness unless a slow cooling rate is ensured. Satisfactory phase balance is obtained by use of consumables that are overmatched in nickel by 2%–3%.

13.18.5.1.7 *Welding Practices*

Welding practices should ensure cleanliness, provide inert gas shielding, and avoid carbon contamination. Since ferrite is susceptible for hydrogen embrittlement, low-hydrogen welding practices should be followed. It is recommended to achieve a ferrite content of approximately 22%–70%, which is equivalent to 30–100 FN. A corrosion test in ferric chloride is also carried out as per ASTM G48 to assess the corrosion resistance of the weldment. As per this test, the CPT is specified at 22°C for duplex and 35°C for superduplex steel.

13.18.5.1.8 *Welding Practices to Retain Corrosion Resistance*

Welding practices to retain corrosion resistance include the following [161]:

1. Special attention is needed to control weld spatter, slag residues, and oxide formation, since these have adverse effects on resistance to pitting and crevice corrosion.
2. As far as possible, postweld cleaning is to be done; when cleaning is not possible, restrict oxygen to values of 10 and 25 ppm maximum inert backing gases. To promote arc stability and penetration, small additions of CO₂ and O₂ may be made to argon shields when employing GMAW technique.

13.18.5.2 **Postweld Stress Relief**

Postweld stress relief for duplex is not necessary as duplex steels are sensitive to short exposure temperature of 300°C–1000°C (572°F–1832°F). In this temperature range, precipitation of alpha prime phase can take place, which in turn reduces toughness and corrosion resistance. Any heat treatment applied to duplex steel should be a PWHT of full solution anneal typically at temperature above 1000°C followed by water quenching.

13.18.6 **NONDESTRUCTIVE TESTING OF DUPLEX SS**

Radiographic and dye penetrant inspection procedures are readily applicable. NDT by conventional ultrasonic techniques with angle beam shear waves can be difficult, owing to the anisotropy of the parent materials and weld deposits, especially the tendency to epitaxial columnar structures in the latter [161]. Improved techniques using angle beam compression wave probes and creep wave probes at diminished frequencies are reported.

13.19 **SUPERAUSTENITIC STAINLESS STEELS WITH MO + N**

Superaustenitic SSs are alloys with an fcc structure, highly alloyed, usually containing substantial amounts of chromium, molybdenum, and nitrogen, along with sufficient nickel to stabilize a fully austenitic microstructure. They are classified by their molybdenum content, which is in the range of 4.5%–7%. The addition of 0.3%–0.5% nitrogen provides yield strength typically twice that of conventional SSs [116]. Relatively high nickel content (18%–31%) and high chromium content and Mo content give the alloys excellent resistance to SCC. Copper is intentionally added to some of the alloys and improves resistance to reducing media such as hot phosphoric acid, acetic acid, and dilute sulfuric acid. In this section, superaustenitics are covered under two headings: 4.5% Mo superaustenitic steels and 6% MO superaustenitic steels.

13.19.1 4.5% Mo SUPERAUSTENITIC STEELS

The 4.5% Mo austenitic alloys like AL 904L, Ciramet, 254SLX, and JS700 have demonstrated sufficient resistance to corrosion in seawater to perform reasonably well as tubing. They are readily weldable and workable, available in a wide range of product forms such as tubing, sheet, plate, and forgings. Nitrogen content in the range of 0.4%–0.5% gives good resistance to pitting and crevice corrosion [115]. The high nickel (25%) and molybdenum (4.5%) contents provide good resistance to chloride SCC. They also exhibit resistance to intergranular corrosion. Chlorination to control microbiological fouling is necessary to minimize under-deposit corrosion; flange faces and gasketed surfaces are subject to crevice corrosion in brackish water and seawater [164].

13.19.2 6% Mo SUPERAUSTENITIC STAINLESS STEEL

The 6% Mo superaustenitics are now well established in the chemical process industries. They contain about 20% chromium, nickel contents range from 18% to 25%, and they are enhanced with more than 0.10% nitrogen. Nitrogen addition serves to improve strength, stabilize the austenitic structure, and improve pitting corrosion resistance. The 6% Mo superaustenitics exhibit excellent toughness and ductility characteristic of the 300 series austenitics. Several 6% Mo superaustenitic SSs, their product forms, and ASTM/ASME Code references are listed in Table 13.27 and their compositions in Table 13.28 along with Types 304 and 316. Although there are differences in their chemistry to permit three different UNS numbers (UNS S31254, N08367, and N08926) for these 6% Mo superaustenitics, for most applications, they have similar corrosion resistance and are used more or less interchangeably [115]. Superaustenitics have an iron content less than 50% and therefore do not fall under the jurisdiction of ASTM Committee A1 on steel, SS, and related alloys, except for 254 SMO. More recently developed 6% Mo alloys include N08031, S32050, and URAUS® B26 (UR B26), which is a 25% Ni, 20% Cr, 6% Mo superaustenitic SS grade with 0.2% nitrogen.

TABLE 13.27

Nominal Composition of Selected Superaustenitic SS along with Types 304 and 316

UNS No.	Alloy	C	Cr	Ni	Mo	N	Others
S30400	304	0.03	18	8	—	—	—
S31600	316	0.03	17	12	2.5	—	—
S31254	254SMO	0.02	20.0	18	6.2	0.2	0.75Cu
N08367	AL-6XN 1925hMo	0.02	21	24.5	6.5	0.2	0.75Cu, max
N08926	25-6 MO	0.01	20	25	6.5	0.2	1.1Cu
N08366	AL-6X	0.018	21	24.5	6.5		1.39Mn, 0.41Si

TABLE 13.28

ASTM/ASME Spec. for Various Product Forms of AL-6XN N08367

Alloy Name	UNS Designation	Sheet, Plate, and Strip	Heat Exchanger Tube	Pipe	Forgings	Fittings	Rod, Bar, and Wire
AL-6XN	N08367	A 240, B/ SB688	A/SA 249	A312; B/ SB675, 690, 829	B/SB564, A 182 F62	B462	B/SB691

The 25% nickel version of the 6Mo SS has shown some advantages over the 18% nickel version of 6Mo austenitic SS. Some of these advantages are thus:

- Improved stability of austenite
- Improved resistance to SCC
- Improved passivation characteristics
- Slower formation of precipitates, even in the temperature range of 700°C–1000°C (1290°F–1830°F)
- Slower sensitization kinetics

13.19.2.1 Corrosion Resistance

In general, the high-alloy superaustenitic steels show superior resistance to uniform corrosion, pitting and crevice corrosion, and SCC [165]. The 6% Mo superaustenitics resist both localized corrosion and SCC in oxidizing chloride and sulfide/chloride-containing solutions, as well as a broad range of process chemicals. They are widely used in severe seawater applications. The corrosion performance of 6% Mo superaustenitics falls between Types 316 and 317 SSs and the nickel-based alloys 625 and C-276 [115]. In order to be resistant to some corrosive environments, some steels also contain additions of copper, which improves its resistance to acids in general. The fully austenitic 6% Mo steels are primarily characterized by a high (Cr + Mo) content, with a PRE given as [166] follows:

$$PRE_N = \%Cr + 3.3(\%Mo) + 30(\%N)$$

exceeding 35 in all of the steels. Pitting resistance number for selected superaustenitic stainless steels is given in Table 13.29

13.19.2.2 Applications

In process industries, the 6% Mo superaustenitic SSs have replaced common austenitic SSs that have failed by pitting, crevice corrosion, and chloride SCC [167]. They have been used extensively in the offshore and desalination industries, in seawater handling, in chlorine and chlorine dioxide stages and bleach plants in the pulp and paper industries, and in flue gas desulfurization plants. Equipment fabricated of 6% Mo austenitics includes pressure vessels, columns, seawater-cooled condensers, evaporators, heat exchangers, crystallizers, pumps, piping, and components.

TABLE 13.29
Pitting Resistance Number for Selected
Superaustenitic Stainless Steels

Alloy	UNS Designation	Composition Required to Calculate PRE_N			PRE_N^a
		Cr	Mo	N ₂	
S31254	254SMO™	20.0	6.2	0.2	46.46
N08367	AL-6XN™ / 1925hMo™	21	6.5	0.2	45.65
N08926	25-6 MO™	20.5	6.5	0.2	45.15
N08366	AL-6X	21	6.5	—	42.45
S31277	27-7Mo™	22	7.2	0.35	57.26

^a $PRE_N = \%Cr + 3.3 (\%Mo) + 30 (\%N)$.

13.19.2.3 Welding

In general, fully austenitic 6% Mo superaustenitic SSs exhibit satisfactory weldability. The main concern when using the superaustenitic SSs is adequate corrosion resistance in welds. During welding, particular concern has to be paid to the following three phenomena:

1. Hot cracking
2. Elemental microsegregation
3. Precipitation of intermetallic phases

Since the carbon content of the 6% Mo steels is low ($<0.03\%$), the risk of chromium carbide precipitation in the grain boundaries of HAZ and thus the susceptibility to intergranular corrosion is negligible [166].

13.19.2.3.1 Hot Cracking

Hot cracking occurs either directly during solidification and is referred to as liquation cracking or upon reheating of successive weld runs, known as RC. Both types of cracking are related to the solidification mode of weld deposit and the presence of impurities such as sulfur and phosphorus [165]. Steels that exhibit a primary austenitic solidification mode are more susceptible to hot cracking than those that exhibit ferritic or mixed phases. Susceptibility to hot cracking is overcome by measures such as the use of fillers that deposit weld metals with relatively low levels of trace elements like P, S, and Sn and keep stresses due to restraint during welding to a minimum [166]. Welding should be done with low arc energy.

13.19.2.3.2 Molybdenum Microsegregation

Six percent Mo steels with high molybdenum levels show large molybdenum microsegregations in autogenous weld metals. The areas depleted in molybdenum have a lower local pitting index, and hence they are less resistant to chloride pitting corrosion [165,166]. Therefore, autogenous welds are not recommended for these steels, unless the completed equipment is to receive subsequent homogenization and solution annealing. To overcome the reduction in corrosion resistance, fillers are overalloyed with molybdenum.

13.19.2.3.3 Precipitation of Intermetallic Phases

When exposed to high temperature, the relatively high Cr and Mo contents of these steels may stimulate the precipitation of intermetallic phases such as the χ or sigma phases. These intermetallics can reduce the steel's corrosion resistance. To overcome this problem, limit the heat input and interpass temperatures. The heat input should be limited to $<15,000$ J/cm, and the interpass temperature should be restricted to 100°C , with an absolute maximum of 150°C [166].

13.19.2.3.4 Arc Welding Filler Metals

If it is practicable to solution anneal and homogenize the weld metal, use a matching filler metal. For applications in severe pitting or crevice corrosion environments, use filler metals that are overalloyed with molybdenum so that the welds are more resistant to corrosion than the base metal [162]. The use of overalloyed filler metals compensates for the lean areas in the deposit caused by microsegregation. The filler metal most frequently used is alloy 625 with 9% molybdenum, but some fabricators prefer alloy C-276 or C-22 [115]. Welds made with these fillers can be used in the as-welded condition. In addition to proper filler selection, certain measures are to be taken to obtain weld metal of required qualities. They include the following [105,166]:

1. Keep the surface free from contaminations before and after welding. Vapor degreasing or scrubbing with a solvent should be effective in removing all but paint. Alkaline cleaners are required to remove paint.
2. When using nickel-base filler metals, the proper weld preparation is also necessary. Excessive dilution has to be prevented, especially in the root pass area. In order to ensure a sufficiently high proportion of filler metal in the root pass, the root gap should be 2–3 mm.

3. To inhibit the formation of oxidation during welding, gas shield the root side.
4. The shielding gas for 6% Mo superaustenitic SSs is 90%–95% hydrogen and 5%–10% pure nitrogen.
5. Cleaning and pickling are necessary.

13.19.2.3.5 Welding Processes

The main welding processes employed are SMAW and manual and automatic GTAW with filler metals. GTAW without filler should be considered only in cases where a subsequent solution anneal heat treatment is to be applied. GMAW, SAW, and automatic PAW with filler metals are also used. To weld the 6Mo austenitic steel, (1) use filler metals that are sufficiently overalloyed with molybdenum so that the welds are more resistant to corrosion than the base metal (the filler metal most frequently used has been Alloy 625 with 9% molybdenum. Welds made with these fillers can be used in the as-welded condition); (2) ensure cleanliness before and after welding; (3) ensure adequate gas shielding during welding; and (4) restrict heat inputs and weld sizes to avoid hot cracking of the weld metal.

13.19.2.3.6 Postweld Heat Treatment

If the 6% Mo superaustenitics need to be annealed or stress relieved, they must be given a full anneal and water quench. Solution annealing at temperatures of 2102°F–2282°F (1150°C–1250°C) followed by quenching is also commonly used; this helps in better homogenization of the material properties of the weldments. Heat treatments that permit the 6% Mo austenitics to spend time in the 1300°F–1900°F (705°C–1040°C) temperature range make the material susceptible to sigma-phase precipitation with loss of corrosion resistance and possibly toughness [167]. Depending on the alloy composition, stress relieving at a temperature up to 1112°F (600°C) for several hours may be used in special cases. In all these cases, the fabricator should follow the material manufacturer's recommendations.

13.19.3 CORROSION RESISTANCE OF SUPERAUSTENITIC STAINLESS STEEL WELDS

The factors that contribute to the loss of corrosion resistance of superaustenitic SS welds and the measures to overcome them are [105] as follows:

1. Microsegregation of molybdenum at localized regions, which most likely takes place when the GTAW process involves autogenous welds, filler metal that has the same composition as the base metal, and high heat input.
2. Unmixed zones. High heat input welding can leave narrow bands of base metal adjacent to the fusion line, which have been melted but not mixed with the overmatched filler metal. This problem is overcome by controlling heat input and avoiding undercutting.
3. Crevices, cracks, and microfissures. Crevice corrosion sites can also occur at the beginning or end of weld passes, between weld passes, or under weld spatter.
4. Sensitization and carbide precipitation. Low carbon content (<0.02%) provides an alloy that is not susceptible to this problem. Molybdenum and nitrogen content increase the level of carbon and/or heat input that can be tolerated.
5. Precipitation of intermetallic phases like sigma and chi phases.
6. Surface contamination by embedded iron, which is removed by acid pickling or abrasive blasting with clean sand or glass beads, and organic contamination, which is removed by suitable solvent.
7. Surface oxide scale or heat tint, which is to be removed by descaling.
8. Shielding gas composition. Adding nitrogen at 3%–5% by volume to the torch and backing shielding gases enhance corrosion resistance.
9. To impart optimum corrosion resistance to the weld metal, especially for the autogenous welds, follow these measures: postweld anneal, postweld clean the surfaces, pickle for optimum corrosion resistance, and passivate the surface.

13.20 ALUMINUM ALLOYS: METALLURGY

Aluminum is a reactive metal. It is known for its higher thermal conductivity (188 kcal/m °C h), lightweight (density, $\rho = 2.7$ g/cc), corrosion resistance, and moderate cost. Its density is about one-third that of steel, which provides a high strength to weight ratio. Untempered, commercially pure aluminum has a tensile strength of 13,000 lb/in.² (89,622 kPa), and cold working can double this strength. The low mechanical properties can also be improved by alloying. Typical alloying elements include magnesium, manganese, zinc, copper, and silicon. By taking advantage of cold working, heat treatment, and aging, the strength of aluminum can be raised to 100,000 lb/in.² (689,476 kPa) [7]. With the addition of copper at 1.9%–6% (2000 series), the heat-treated properties exceed those of mild steel. Designing in aluminum is much like designing in other metals. Publications from the Aluminum Association, Aluminum Welding Seminar Technical Papers, and others [168] will be of great help.

13.20.1 PROPERTIES OF ALUMINUM

Aluminum alloys have a high resistance to corrosion in most atmospheres, waters, and many chemicals. They are nontoxic, permitting applications with foods, beverages, and pharmaceutical, and they are colorless, permitting applications with chemicals and other materials without discoloration. Their corrosion products are not damaging to the ecology. Aluminum is fabricated and joined readily by most of the metal-joining processes. Aluminum is excellent for cryogenic applications; most aluminum alloys have higher ultimate and yield strengths at –350°F to –450°F (–212°C to –268°C) than they have at room temperature. Other properties of aluminum and its alloys for certain applications are high electrical conductivity, high reflectivity, and nonmagnetic (ensures arc stability).

13.20.1.1 Aluminum for Heat Exchanger Applications

The unique combinations of properties provided by aluminum and its alloys make aluminum one of the most versatile and economical materials for heat exchanger applications. The properties that favor aluminum for heat exchanger applications are as follows:

1. Lightweight and high specific strength. This offers automotive heat exchanger designers the potential for compact low-cost heat exchangers over the more traditional copper and brass materials [169].
2. High thermal conductivity. The thermal conductivity of pure aluminum is about 60% that of pure copper.
3. High resistance to atmospheric corrosion and environments like freshwater, saltwater, and many chemicals and their solutions.
4. Depending on temper, it can be hot or cold formed; it has the ability to be formed into various shapes, tubes, fin patterns, etc.
5. Ability to be joined by welding, brazing, and soldering.
6. Aluminum clad products protect pitting corrosion of the core alloys.
7. They retain toughness and strength, and exhibit high thermal conductivity at subzero temperature. Aluminum maintains excellent strength and ductility to temperatures as low as –321°F (–196°C). It also exhibits high thermal conductivity at cryogenic temperature. For cryogenic services, aluminum alloy 3003 is generally used for the parting sheets, corrugated fins, and edge bars that form the plate-fin heat exchanger (PFHE) block. Headers and nozzles are made from aluminum alloys 3003, 5154, 5083, 5086, or 5454.
8. It has hygienic and nontoxic qualities.
9. It is nonmagnetic and nonsparking.
10. There is availability in many product shapes and moderate cost.

Limitations of aluminum

1. Aluminum and its alloys rapidly lose strength at temperatures above 100°C; aluminum does not resist fire as well as other materials. It is not generally used for PFHE process temperatures above 150°C, particularly in high-pressure service [170].
2. Aluminum is susceptible to damage by rough handling, excessive vibration, and localized unrelieved stresses.

13.20.1.2 Wrought Alloy Designations

A system of four-digit numerical designations is used to identify the various wrought aluminum alloys, as shown in Table 13.30. The first digit indicates the alloy group. The second digit indicates a modification of the original alloy or the impurity limit in the case of unalloyed aluminum. The third and fourth digits identify the alloy or indicate the aluminum purity.

13.20.1.2.1 Classification of Wrought Alloys

Wrought alloys are of two types: not heat-treatable, of the 1xxx, 3xxx, 4xxx, and 5xxx series, and heat-treatable, of the 2xxx, 6xxx, and 7xxx series. In the non-heat-treatable type, strengthening is produced by strain hardening. All non-heat-treatable alloys have a high resistance to general corrosion. Aluminum alloys of the 1xxx series, representing unalloyed aluminum, have a relatively low strength. Alloys of the 3xxx series (Al–Mn, Al–Mn–Mg) have the same desirable characteristics as those of the 1xxx series and somewhat higher strength. Common wrought alloys and their compositions are given in Table 13.31. An important source book on aluminum alloys metallurgy, welding and fabrication is Ref [171].

1xxx series: This grade of aluminum, with minimum 99.00% purity, exhibits excellent corrosion resistance, high thermal and electrical conductivity, excellent formability, but low mechanical properties. They are readily brazed and welded by all methods, and non-heat-treatable. Moderate increase in strength may be obtained by strain hardening. They are used as fin stocks in heat exchangers.

2xxx series: These alloys are copper based. The copper content is in the range of 1.9%–6%. These alloys are heat-treatable and more susceptible to corrosive attack than other groups of wrought aluminum alloys. Heat-treated properties exceed those of mild steel. Fusion-welding is not recommended, but resistance welding is recommended.

3xxx series: The major alloying element is manganese, up to about 1.5%. These alloys are non-heat-treatable. They have moderate strength, good corrosion resistance, and good workability/formability,

TABLE 13.30
Wrought Aluminum Alloy Designations

Designation	Alloying Elements	Major Alloying Elements	Heat Treatable
1xxx	99% min. Al	None	No
2xxx	Al–Cu, Al–Cu–Mg–Si (3%–6%/Cu)	Copper	Yes
3xxx	Al–Si–Mn	Manganese	No
4xxx	Al–Si–Cu	Silicon	No
5xxx	Al–Si–Cu–Mg Al–Mg (1%–2.5% Mg) Al–Mg–Mn (3%–6% Mg)	Magnesium	No
6xxx	Al–Mg–Si	Magnesium–silicon	Yes
7xxx	Al–Zn–Mg Al–Zn–Mg–Cu	Zinc	Yes

TABLE 13.31
Nominal Composition of Some Common Wrought Alloys

Designation	Composition (%), Remainder Al and Impurities						
	Cu	Si	Mn	Mg	Zn	Cr	Al
1100	0.05	0.25	0.03	0.03	0.05	0.03	99% (min)
3003	0.12	0.6	1.2	—	0.1	—	Reminder
3004	0.25	0.30	1.2	1.0	0.25	—	Reminder
3005	0.30	0.60	1.2	0.4	—	—	Reminder
5005	0.20	0.30	—	0.8	—	—	Reminder
5050	0.20	0.40	—	1.2	—	—	Reminder
5052	0.10	0.25	0.10	2.5	0.10	0.25	Reminder
5083	0.10	0.40	0.70	4.5	0.25	0.15	Reminder
5154	0.10	0.25	0.10	3.5	0.20	0.25	Reminder
5454	0.10	0.25	0.75	2.7	—	0.12	Reminder
5456	0.10	0.25	0.8	5.1	0.25	0.1	Reminder
6061	0.25	0.6	0.15	1.0	0.25	0.20	Reminder
6063	0.10	0.4	0.10	0.7	0.10	0.10	Reminder
7005	0.10	0.35	0.45	1.4	4.5	0.13	Reminder
7072	1.00	0.50	0.40	0.10	1.0	—	

and are used in pressure vessels and brazed and soldered heat exchangers. These are readily brazed and welded by all methods. Alloys 3003, 3004, and 3105 are widely used as general-purpose alloys for moderate-strength applications requiring good formability and workability. The strength of 3003 is higher than that of 1100 alloy, and 3004 is stronger than 3003. Alloy 3004 is known for fine grain size and general freedom from critical grain growth.

4xxx series: The major alloying element is silicon. These are non-heat-treatable and are often used for welding and brazing as filler metal with enough silicon to lower the melting point. For example, 4343 containing 7.5% silicon and 4045 containing 10.5% silicon are used as the clad brazing sheet. The core alloy is either 3xxx or 6xxx series.

5xxx series: Alloys of the 5xxx series (Al–Mg) are the strongest non-heat-treatable aluminum alloys. In most products, they are more economical than alloys of the 1xxx and 3xxx series in terms of strength per unit cost. Alloys of the 5xxx series have high resistance to general corrosion and good resistance in marine atmospheres. The most widely specified weldable grades are alloys 5083, 5052, and 5454. Their applications are numerous in the pressure vessel fields, including cryogenic applications. They are typically available as sheet and plate product forms. These are most fusion-welded of any series with a minimum loss of strength. Alloys with more than 3.5% Mg are essentially free from hot cracking. Because of their heavy oxide films, extra care in surface preparation is necessary [172]. These alloys solder and braze poorly.

6xxx series: These alloys contain both silicon and magnesium, which make the alloys heat-treatable. Compared with other aluminum alloys, these have high resistance to rural atmospheres, and good resistance to industrial and marine atmospheres. They generally possess excellent SCC resistance. These alloys possess good formability, machinability, and weldability.

The mechanical properties of the heat-treatable 6xxx series alloys are superior to those of the 3xxx series alloys. Compared to 3xxx series, the yield strength of the 6xxx series is about four to five times as high after heat treatment. The higher strength is desirable from the radiator manufacturers' point of view; this helps to minimize tube wall thickness in order to save weight and material cost.

But the disadvantages of 6xxx series are their lower melting temperature and higher susceptibility to silicon penetration from the cladding to the core.

The 6xxx series alloys can be soldered, brazed, and resistance spot welded satisfactorily. Alloy 6061 is the most widely specified weldable grade. The most popular temper for 6061 is T6, although the T651, T4, and F tempers are also popular.

The 6xxx series alloys are prone to hot cracking. However, this problem can be overcome by correct choice of filler metal and proper joint design. Care in joint and component design is also needed because of losses in strength in the HAZs. The HAZs strength can be improved, however, through PWHT [172].

7xxx series: These alloys contain zinc in the range of 1%–8%, and smaller percentage of Mg, Cu, and Cr. They are heat-treatable alloys. 7072 is most widely used as the anodic coating of the tubes and brazing sheet made of 3003, 3003, 5505, 6061, 6951, 7075, and 7178, and as fin stock.

13.20.1.3 Temper Designation System of Aluminum and Aluminum Alloys

A temper designation system is used to indicate the condition of the product forms. The system is based on the sequences of mechanical or thermal treatments, or both, used to produce the various tempers. The temper designation follows the alloy designation and is separated from it by a hyphen. Aluminum alloys come in four tempers: F, O, H, and T. Another, W, is sometimes used to state the unstable condition following SHT. The digits designate the sequence of basic treatments (e.g., 1100–H14 and 7075–T651). The basic temper designations are shown in Table 13.32.

13.20.1.4 Product Forms and Shapes

Aluminum is available in many forms and shapes, which include heat exchanger tubes (plain and integral fin), plates and sheets, bars and rods, and extrusions. Some ASTM specifications for tubes, plates and sheets are given in Table 13.33 and pipes, bar, rods, extrusions, and forgings are given in Tables 13.34.

13.20.2 CORROSION RESISTANCE

13.20.2.1 Surface Oxide Film on Aluminum

Aluminum owes its excellent corrosion resistance to the presence of a thin, compact, adherent aluminum oxide film on its surface. In air, aluminum swiftly acquires a surface film that is self-healing and self-limiting in thickness. The normal surface film thickness in air is about 50 Å [173]. Even if the surface film is damaged, it readily forms on the surface whenever a fresh aluminum surface is created and exposed to either air or moisture/water. Generally, the oxide film is stable over the pH range of 4–9.0. In strong acids and alkali, the oxide dissolves and hence the metal corrodes rapidly

TABLE 13.32

Basic Temper Designations for Aluminum Alloys

Designation	Conditions
F	As fabricated
O	Annealed, the softest temper
H	Strain hardened
H1	Strain hardened only
H2	Strain hardened and partially annealed
H3	Strain hardened and thermally stabilized
T (T1–T12)	Heat-treated forms; heat treatment produces needed workability, dimensional stability, and strength
W	Solution heat-treated

TABLE 13.33**Aluminum Alloy Heat Exchanger Tubes and Plates and Sheets**

ASTM Spec.	Description	Alloys UNS No.
<i>Heat exchanger tubes</i>		
B234	Aluminum and aluminum alloy drawn seamless tubes for condensers and heat exchangers	1060, 3003, Alclad 3003, 5052, 5454, 6061, 7072
<i>Aluminum plates and sheets</i>		
B209	Aluminum and aluminum alloy plates and sheets	1060, 1100, 3003, Alclad 3003, 3004, Alclad 3004, 5050, 5052, 5083, 5086, 5154, 5254, 5454, 5456, 5652, 6061, Alclad 6061

TABLE 13.34**Pipes, Bars, Rods, Extrusions, and Forgings**

ASTM Specification	ASME Spec.
Aluminum and aluminum alloy drawn seamless tubes	SB210
Aluminum and aluminum alloy bar, rod, and wire	SB211
Aluminum and aluminum alloy extruded bars, rods, wire, shapes, and tubes	SB221
Aluminum and aluminum alloy seamless pipe and seamless extruded tube	SB241
Aluminum and aluminum alloy die forging, hand forging, and rolled ring forging	SB247
Aluminum alloy 6061—T6 standard structural shapes	SB308

by uniform dissolution, but there are exceptions, such as stability in concentrated nitric acid (pH 1) and concentrated ammonium hydroxide (pH 13).

13.20.2.2 Chemical Nature of Aluminum: Passivity

Aluminum is an active metal whose resistance to corrosion depends on the passivity exhibited by the protective surface film. In aqueous solutions, the thermodynamic conditions under which the film develops are expressed commonly by the potential–pH diagram (Figure 13.20) according to Pourbaix [174]. This diagram shows that aluminum is passive only in the pH range of about 4–9. Most of the aluminum alloys have good corrosion resistance to natural atmospheres, freshwater, seawater, many oils and chemicals, and most foods. Aluminum tubing is used to handle Freon refrigerants.

13.20.2.3 Resistance to Waters

Alloys of the 1xxx, 3xxx, 5xxx, and 6xxx series exhibit corrosion resistance in high-purity water, natural waters, and seawater. A mild reaction takes place when the alloys are first exposed to high-purity water, but it decreases to a low rate within a few days upon formation of a protective oxide film of equilibrium thickness on the alloys.

13.20.2.3.1 Natural Waters

Aluminum alloys of the 1xxx, 3xxx, 5xxx, and 6xxx series have good resistance to most natural freshwaters. If corrosion does occur, it takes the form of pitting. The main components of natural water that cause pitting of aluminum are copper ions, bicarbonate, chloride, sulfate, and oxygen. Hard waters have a higher tendency of pitting.

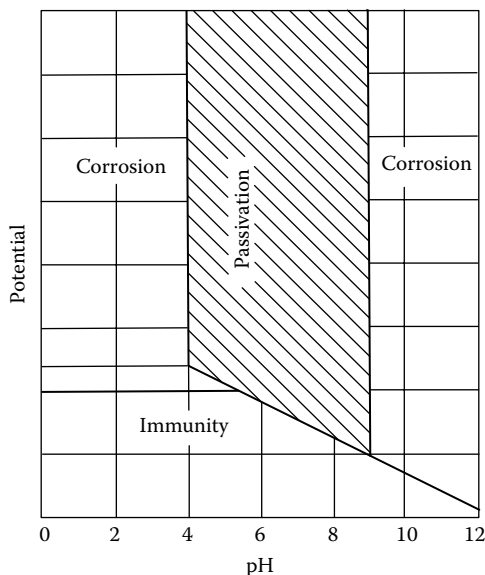


FIGURE 13.20 Pourbaix diagram for aluminum (schematic).

13.20.2.3.2 Seawater

Aluminum alloys of the 2xxx and 7xxx series are less resistant and should not be used in seawater unless protected or clad. Among wrought alloys, 1xxx, 5xxx, and 6xxx exhibit good resistance to seawater, and of these alloys, the aluminum–magnesium alloys (5xxx) series has the highest resistance to seawater; hence they are mostly used in seawater applications [175].

13.20.2.4 Forms of Corrosion

13.20.2.4.1 Uniform Corrosion

Most aluminum alloys have excellent resistance to atmospheric corrosion. If surface oxide film is soluble in the environment as in phosphoric acid or sodium hydroxide, aluminum dissolves uniformly and constantly.

13.20.2.4.2 Galvanic Corrosion

From its galvanic position, aluminum and its alloys are anodic to most other metals except zinc and magnesium. Contact of aluminum with more cathodic metals should be avoided in any environment in which aluminum by itself is subject to pitting [175]. The most common examples of galvanic corrosion of aluminum alloys in service will take place when they are joined to steel or copper and exposed to a wet saline environment. It is also undesirable to use copper components in aluminum vessels and heat exchangers used in cooling water systems; the presence of a few parts per million of copper in the supply water greatly increases the incidence of pitting attack on the aluminum [176]. Guidelines given to minimize galvanic corrosion in Chapter 12 are applicable for aluminum alloys also. The position of aluminum in galvanic series, which makes the aluminum and aluminum alloys anodic to most other metals and alloys, is utilized in Alclad products (sacrificial anode) to give cathodic protection to the core alloys.

13.20.2.4.3 Pitting Corrosion

Susceptible alloys: Of the commercial alloys, 1xxx, 3xxx, and 5xxx have excellent pitting resistance. However, with copper content higher than 0.04%, 3xxx alloys are susceptible to pitting. At 0.15% copper, they pit more extensively, especially in seawater. Alloys of the 2xxx, 6xxx, and 7xxx series are normally clad to protect against pitting.

Factors responsible for pitting corrosion: Pitting corrosion is mostly due to copper, mercury, and halide ions, of which chloride is the most damaging and often encountered in service. Pitting corrosion can be prevented by removal of the reducible species required for a cathodic reaction. In the absence of dissolved oxygen or other cathodic reactant, aluminum will not corrode by pitting since it is not polarized to its pitting potential. Pitting in neutral solutions is caused usually by oxygen.

Pitting behavior: The rate of pitting corrosion of aluminum depends on its polarization behavior. As with other passive metals, corrosion of aluminum in the passive range, that is pH range 4–9, may be of pitting corrosion. Pitting of aluminum diminishes beyond this range, and corrosion proceeds uniformly.

13.20.2.4.4 Stress Corrosion Cracking

SCC does not occur in commercial-purity alloys (1xxx), aluminum–manganese alloys (3xxx), and aluminum–magnesium alloys containing less than 3% magnesium (5xxx) and strengthened by cold work. On very rare occasions, SCC occurs in the aluminum–magnesium–silicon alloys (6xxx).

Susceptible alloys: SCC in wrought aluminum alloys is generally limited to those containing appreciable amounts of soluble alloying elements of copper, magnesium, silicon, and zinc [175]. Alloys that can be strengthened by cold work are relatively immune to SCC. The wrought alloys that are susceptible to SCC include the following [175,177]:

- The 2xxx series containing copper with smaller amounts of magnesium, manganese, and other elements
- The 7xxx series containing zinc with small amounts of magnesium, manganese, copper, and silicon, if any
- The 5xxx series containing more than 3% magnesium with or without other alloying elements

Factors affecting resistance to SCC: In aluminum alloys, this cracking is characteristically intergranular. Factors that affect SCC of aluminum alloys are given next.

Directional property of aluminum: SCC of an aluminum wrought alloy in a susceptible temper is determined by the magnitude and the duration of a tensile stress acting on its surface, and additionally, it is also determined by the direction of stressing. The effect of stressing in different directions is caused by the highly directional grain structure that is typical of many aluminum wrought products [173,175]. Resistance, which is measured by the magnitude of tensile stress required to cause cracking, is highest when the stress is applied in the longitudinal direction, lowest in the short transverse direction, and intermediate in the other direction. Resistance in the short transverse direction usually controls application of products that are of thick section or machined products with sustained tensile stresses in the short transverse direction.

Environment: Water or water vapor is a requisite for the SCC of aluminum, and in its absence, cracking does not occur. Among the species that accelerate cracking further, chlorides have the greatest effect [175].

Mitigation of SCC of aluminum alloys: In addition to the usual procedures for preventing SCC of materials, there are several methods specifically applicable to aluminum alloys [173]:

1. Forging and extrusions should be machined to their final dimensions prior to heat treatment.
2. Stressing of extrusions in the short transverse direction of extrusion should be avoided.
3. Cathodic protection in the form of Alclad layers on the surface of high-strength sheet material may be used to prevent general corrosion and SCC.
4. For most commercial alloys, stress-relieved tempers have been developed that provide a high degree of immunity to SCC.

Standard test method for determining susceptibility to SCC of high-strength aluminum alloy products: ASTM G47: This is the standard practice for determining the susceptibility to SCC of high-strength 2xxx (with 1.8%–7.0% Cu) and 7xxx (with 0.4%–2.8% Cu) aluminum alloy products, particularly when stressed in the short transverse direction relative to the grain structure.

13.20.2.4.5 Exfoliation Corrosion

Exfoliation is subsurface corrosion that begins on a clean surface but spreads below it. It is well known in aluminum alloys and to a certain extent to copper–nickels. The attack differs from pitting in that the attack has a laminated appearance. It proceeds generally along the grain boundaries, laterally from the sites of initiation along planes parallel to the surface. The corrosion attack causes a leafing or delamination and sometimes a blistered surface. Due to exfoliation, whole layers of materials are eaten away. The end of a sample looks like a pack of cards in which several cards have wasted away.

Susceptible alloys: In certain tempers, wrought products of some aluminum alloys are subject to exfoliation corrosion, which causes a leafing or delamination of the products. This type of corrosion develops in products that have a pronounced directional structure in which the grains are elongated highly and thin relative to their length and width. Alloys of the 2xxx, the 5xxx series with higher magnesium, and 7xxx series are most prone to exfoliation corrosion. It is rare in wrought alloys of the non-heat-treatable type (1xxx, 3xxx) and heat-treatable-type 6xxx. Exfoliation can be overcome by heat treatment and alloying [173,178].

Standard test method for determining exfoliation corrosion susceptibility: ASTM G34 is the immersion test method for determining exfoliation corrosion in 2xxx and 7xxx series aluminum alloys (EXCO test). This test method is applicable to wrought products such as plates, sheets, extrusions, and forgings. ASTM G66 is an immersion test of 5xxx series aluminum alloys for exfoliation corrosion, known as the ASSET test.

13.20.2.4.6 Intergranular Corrosion

Aluminum alloys that do not form second-phase microconstituents at grain boundaries, or those in which the constituents have corrosion potentials similar to the matrix, are not susceptible to intergranular corrosion. Aluminum alloys such as 1100, 3003, and 3004, aluminum–magnesium alloys (5xxx) containing less than 3% magnesium, are not affected by intergranular corrosion. The 6xxx series alloys generally resist this type of corrosion [175]. Thermal treatment in 2xxx, 5xxx with more than 3% Mg, and 7xxx series alloys that cause grain boundary precipitation is susceptible to intergranular corrosion. The level of susceptibility to corrosion increases with (1) magnesium content, (2) the amount of cold work, and (3) exposure time at temperature [173]. Resistance to intergranular corrosion is achieved by use of heat treatments that cause precipitation to be more uniform throughout the grain structure or by restricting the alloy element that causes the intergranular corrosion.

13.20.2.4.7 Crevice Corrosion

Crevice corrosion of aluminum is negligible in freshwater. In seawater, it takes the form of pitting, and the corrosion rate is low.

13.20.2.4.8 Erosion Corrosion, Cavitation, and Impingement Attack

Aluminum and its alloys are susceptible to cavitation, impingement, and erosion corrosion.

13.20.2.4.9 Corrosion Fatigue

Aluminum alloys, like many steels, have relatively low corrosion fatigue strength, about half the fatigue strength in air and about 25% of the original ultimate strength of material. Corrosion fatigue failures of aluminum alloys are characteristically transgranular and differ from SCC failures, which

are usually intergranular. Localized corrosion of the aluminum surface provides stress rises and greatly lowers fatigue strength and hence fatigue life [173].

13.20.2.4.10 Corrosion of Aluminum in Diesel Engine Cooling Water System

Uniform corrosion may take place in poorly inhibited or uninhibited glycol/water mixtures. Localized corrosion is initiated with the breakdown of the passive film by chloride ion. Pitting and crevice corrosion may be prevented by the use of inhibitors. Anions commonly used to reduce the effect of corrosion may be classified into two classes: (1) oxidizing, those that form a passive film on the metal surface; and (2) nonoxidizing, those that act as blocking agents by forming insoluble precipitates with aluminum ions [179]. Benzoate, phosphate, and silicate are examples of nonoxidizing inhibitors. Oxidizing inhibitors include nitrates and chromates.

13.20.2.5 Corrosion Prevention and Control Measures

A number of corrosion-preventive measures have already been described. Important methods of preventing corrosion of aluminum include [173,175] (1) alloy and temper selection, (2) design considerations of equipment, (3) inhibitors, (4) cathodic protection, (5) use of Alclad products, (6) modification of environment, and (7) thickened surface oxide film and organic coating. Some of these methods are discussed next.

13.20.2.5.1 Alloy and Temper Selection

In general, aluminum–magnesium alloys 5xxx series have the best corrosion resistance, followed by commercial-purity alloys series 1xxx and 3xxx, and 6xxx in that order. Alloys 2xxx and 7xxx are usually given a protective coating such as cladding. Temper selection gives better resistance to intergranular corrosion and exfoliation corrosion for alloys 5xxx, whereas in alloys 7xxx, improved resistance to SCC is being achieved [173].

13.20.2.5.2 Design Aspects

The design aspects that influence corrosion behavior include improper choice of alloy or temper, galvanic couple, failure to provide sealants in the crevices to avoid crevice corrosion, and selection of the joining method and filler metals.

13.20.2.5.3 Inhibitors

Phosphates, silicates, nitrates, fluorides, benzoates, etc., have been recommended for use with aluminum in some services. If copper is present in a closed system, use sodium mercaptobenzothiazole to prevent copper corrosion and subsequent deposition corrosion of the aluminum.

13.20.2.5.4 Cathodic Protection

In some applications, aluminum alloy parts are protected by cathodic protection, either by sacrificial anode or by impressed current method. Since cathodic reaction produces hydroxyl ions, the current on these alloys should not be high enough to make the solution sufficiently alkaline to cause significant corrosion [180].

13.20.2.5.5 Alclad Alloys

The use of Alclad products to resist corrosion has been well established. Alclad alloys is a composite product in which a thin surface layer of one aluminum alloy (anodic), usually 5%–10% of the total thickness, is metallurgically bonded to the main core alloy (cathodic), which was selected to provide the desired strength and the cladding to provide the maximum resistance, mostly to perforation by pitting. The difference in the potential between the core alloy and the cladding alloy provides cathodic protection to the core. The cladding generally used is alloy 7072, which contains 1% zinc and has a solution potential of -0.96 V, which is at least 100 mV more anodic than typical core alloys such as 3003 and 6951. Since the claddings are anodic to

TABLE 13.35
Alclad Alloys

Core Alloy	Cladding Alloy
3003	7072
3004, 6061	7072 or 7013
6951	7072
7075	7072, 7008, or 7011
7178	7072

the core, preferential corrosion of the cladding takes place until the core and cladding interface. After reaching the interface, it spreads laterally, avoiding localized corrosion. Alclad products are primarily available in the form of sheets and tubes, coated on one or both sides. For example, Alclad tubes are used in brazed aluminum radiators to avoid pitting corrosion of tubes on the water side. Typical combinations of Alclad products generally used in heat exchanger applications are given in Table 13.35.

13.20.2.5.6 *Modification of the Environment*

Such modifications are reducing the corrosivity of an environment, adjustment of pH of a solution, deaeration of water to minimize oxygen content and hence to reduce the tendency to pit aluminum, etc.

13.20.2.5.7 *Thickened Surface Oxide Film and Organic Coating*

Coatings by diffusion cladding or thermal spray will act in the same way as the cladding layer and corrode sacrificially to protect the core alloy [175].

13.20.2.5.8 *Aluminum Diffused Steels in Petroleum Refinery Heat Exchangers*

Aluminum vapor diffusion into the surface of iron-base or nickel-base alloys offers one method of protecting steel tubes (the process is known as alonizing) and other components in heat exchangers from the harmful effects of high-temperature oxidation, sulfidation, and carburization [181]. As a result, this process finds broad application for heat exchangers used in chemical plants and petroleum refineries.

13.20.3 FABRICATION

Aluminum alloys can be joined by most fusion and solid-state welding processes as well as by brazing and soldering. Fusion-welding is commonly done by GMAW, GTAW, FCAW, SMAW, resistance spot, and seam welding. Plasma and electron beam welding are used for special applications. Oxyfuel gas welding may be used for applications where high strength and quality are not essential for the intended service. Flux shielding is unsuitable for aluminum because flux tends to corrode the metal and produce spatter. Fusion-welding of aluminum is discussed next. Brazing and soldering are covered in Chapter 15.

13.20.3.1 **Parameters Affecting Aluminum Welding**

The parameters that influence welding aluminum and its alloys include surface oxide film, thermal conductivity, thermal expansion, reflectivity, lack of color change during melting, nonmagnetic, use of backing bars, surface preparation and cleanliness, gas shielding, welding heat on base metal properties, and hot cracking. These parameters are discussed in detail by Lancaster [176] and Young [182]. Salient features of these points are discussed here.

Surface oxide film: The surface oxide film on aluminum and its alloys is insoluble in the weld metal and inhibits wetting by molten filler metals. Additionally, the dielectric nature of the oxide film may prevent a stable starting of the welding arc. Therefore, to permit good wetting and fusion, the surface oxide must be removed from its surface before welding, brazing, and soldering.

Thermal conductivity: The higher thermal conductivity of aluminum (approximately three times that of steel) requires higher heat inputs. Thick sections may require preheating to reduce the heat input.

Thermal expansion: Higher thermal expansion diminishes the root gap in a butt joint; shrinkage during solidification (about 6%) narrows the root gap, and stresses try to crack the weld metal and warp the weldment. Measures to prevent cracking and distortion include clamping, fixturing, use of chill bars, and changing welding techniques.

Reflectivity: Aluminum sheets and plates reflect about 80% of light and heat rays. When employing arc welding, therefore, the welders must be protected against burns from reflected as well as direct rays. The intensity of burns is maximum when welding curved surfaces, such as the inside of a cylinder.

Lack of color change during melting: Aluminum does not assume a dark red color at 1200°F (649°F) just prior to melting, as does steel, but it appears to collapse suddenly at the melting point. The lack of color change makes it difficult to judge when the metal is approaching the molten state. Hence, practice in welding is required to learn to control the rate of heat input.

Nonmagnetic: Aluminum is nonmagnetic, and therefore, arc blow is not encountered when arc welding with direct current.

Backing bars: While welding, some form of backing for the molten pool is necessary. Removable backing bars of steel or cast iron are satisfactory, provided that the welding groove is of adequate depth [176]. Permanent backing bars are rarely used because they introduce undesirable notch effect, and welds are subjected to defects that originate at the root of the joint.

Root gaps: Large root gaps cannot be bridged.

Cleanliness: When fabricating aluminum, maintain a high standard of cleanliness. The method of edge preparation and cleaning determines weld quality.

Gas shielding: In a gas-shielded process, the maintenance of a satisfactory nonturbulent argon cover in the vicinity of arc and weld pool is essential [182]. Failure to observe this leads to weld defects like oxide inclusions, lack of fusion, and porosity. While employing GMAW, puckering and tunneling occur in welding at high currents due to turbulent conditions in the molten pool and entrainment of air in the gas shield. This is overcome by using an auxiliary gas shield or by increasing the primary gas coverage to prevent air being sucked in with argon.

Effect of welding heat on base metal: Welding heat weakens the base metal next to the weld; the weak zone is about an inch either side of the center of the butt or fillet welds. Heat-treatable alloys can be strengthened by heat treatment, but only cold working strengthens non-heat-treatable alloys [7].

Hot cracking: Aluminum welds are susceptible to hot cracking. Sensitivity to hot cracking is influenced by composition of the filler metal, the degree of dilution by the base metal, and restraint on the weldment. The following measures help to overcome hot cracking:

1. Avoid weld metal compositions known to be sensitive to cracking. Combining magnesium and copper in an aluminum weld metal is not desirable.
2. Use welding procedures that minimize restraint of the alloy being welded.
3. Select a filler metal of a composition whose solidus temperature is close to that of the base metal [48].
4. Use a filler metal of higher alloy content than the base metal.

13.20.3.2 Surface Preparation and Surface Cleanliness

Most porosity in aluminum welds is due to surface contaminants like shop dirt, cutting fluids, oils, grease, and marking crayons. Therefore, to obtain weld metal of desired quality, aluminum surfaces are to be clean. Surface cleaning may be done by these methods [7]:

Solvent decreasing: Wiping, spraying or dipping, and vapor degreasing remove oil, grease, dirt, and loose particles.

Mechanical cleaning: This is oxide removal by SS wire brushing, filing, milling, rubbing with steel wool, sanding, rotary planing.

Chemical cleaning: Use immersion in 5% sodium hydroxide (caustic soda) solution at 160°F (70°C) for 10–60 s, followed by rinse in commercial desmuting solution at room temperature for 10–30 s, followed by a hot-water rinse and air-dry.

13.20.3.3 Plate Cutting and Forming

Cut aluminum to size and shape and prepare its edges with most metal-working tools and methods. However, oxygas cutting will not work with aluminum. Care has to be taken while bending aluminum and its alloys with regard to scoring and mechanical damage because of their softness. It is essential to avoid iron and other foreign metallic embedments or inclusions into aluminum surfaces. To ensure this, cover the plates with plastic or sheets of paper and pasting paper over the rolls or by inserting a sheet of hardboard between the plate and the rolls. Lift large sheets or plates with vacuum lifters.

13.20.3.4 Joint Design

Joint design is important in selecting the joining method. If butt joints are required, the choice is limited preferably to an inert gas or vacuum-shielded fusion-welding process or a solid-state welding process.

13.20.3.5 Joint Geometry

In general, the recommended joint geometries for arc welding aluminum are similar to those for steel. However, smaller root openings and larger groove angles are generally used because aluminum is more fluid and welding gun nozzles are larger. Joint geometry for aluminum welding is shown in Figure 13.21.

13.20.3.6 Preheating

Preheating is usually avoided, because the properties and metallurgy of aluminum almost always suffer from high heat. If preheating is unavoidable, heat aluminum for a short while without exceeding 300°F (149°C). Welders should also preheat a thick piece of aluminum when welding it to a thin piece; if cold lapping occurs, try using run-on and run-off tabs.

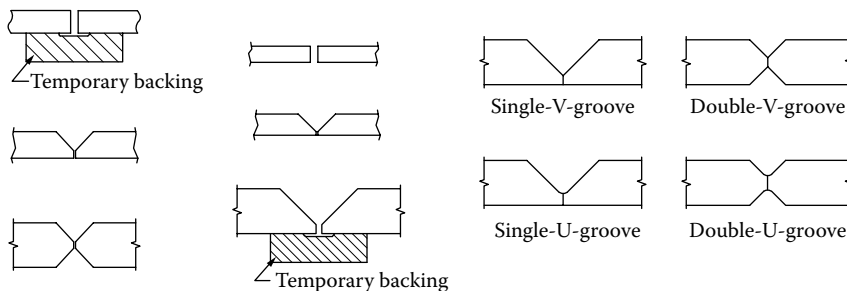


FIGURE 13.21 Typical joint design for arc welding of aluminum.

13.20.3.7 Wire Feeding

Feeding aluminum welding wire during GMAW presents a challenge because the wire is softer than steel, has a lower column strength, and tends to tangle at the drive roll.

13.20.3.8 Push Technique

With aluminum, pushing the gun away from the weld puddle rather than pulling it will result in better cleaning action, reduced weld contamination, and improved shielding gas coverage.

13.20.3.9 Travel Speed

Aluminum welding needs to be performed “hot and fast.” Unlike steel, the high thermal conductivity of aluminum dictates the use of higher amperage and voltage settings and higher weld travel speeds. If travel speed is too slow, excessive burn-through particularly on thin gauge aluminum sheet will result.

13.20.3.10 Shielding Gas

Argon, due to its good cleaning action and penetration effect, is the most common shielding gas used when welding aluminum.

13.20.3.11 Welding Wire

Select an aluminum filler wire that has a melting temperature similar to the base metal. The more the operator can narrow down the melting range of the metal, the easier it will be welded.

13.20.3.12 Convex-Shaped Welds

In aluminum welding, crater cracking causes most failures. Due to high thermal expansion and contraction of aluminum, considerable contraction takes place as weld metal cools. The risk of cracking is greatest with concave craters, since the surface of the crater contracts and tears as it cools. Therefore, welders should build up craters to form a convex or mound shape.

13.20.3.13 Corrosion Resistance: Welded, Brazed, and Soldered Joints

Most aluminum-base metal and filler metal combinations are satisfactory for service under normal conditions. For best performance in specific corrosive environments, the filler metal composition should nearly match the composition of the base metal. Some environments or chemicals may require the use of high-purity filler metals or tight limits on composition. For example, for some saltwater applications, weld 1100 plate with 1100 filler weld.

13.20.3.14 Welding Filler Metals

Aluminum welding rods and bare electrodes are generally used with the gas tungsten arc, gas metal arc, and oxyfuel gas welding processes. While selecting aluminum filler metal, consider these factors: (1) ease of welding, (2) corrosion resistance, (3) resistance to high temperatures, (4) response to anodic treatments, (5) enhanced strength or ductility, and (6) minimized chances for hot cracking. Choose a filler with higher alloy content than the base metal. To obtain the desired weld metal properties, the filler metals should be free from gas and nonmetallic inclusions and surface contamination. Keep the welding wire covered and store it in a dry area at even temperatures. Do not open a new box of wire until ready to use it. Filler metals for the most widely specified weldable-grade alloys 5052, 5083, 5454, and 6061 are given in Table 13.36.

TABLE 13.36
A Guide to Aluminum Welding Filler Metal Selection

Base Metal	Filler Metal
5052, 5056, 5083, 5086, 5154, 5254, 5454, 5456, 5652, 6005, 6061, 6063, 6070, 6151	4043 and 5356—Most preferred 5183, 5554, 5556, 5654

13.20.3.15 Welding Methods

13.20.3.15.1 Gas-Shielded Arc Welding

GMAW and GTAW have almost entirely replaced other arc welding processes for aluminum alloys. The workhorse welding process is GTAW, argon shielded for root passes, followed by GMAW fill passes, and in some cases a GTAW cover pass to dress the weld surface. Edge preparation is typically a 45°–73° opening with a 1/16-in. low.

13.20.3.15.2 Gas Tungsten Arc Welding Process

The GTAW process solves the two problems associated with aluminum, namely, high heat conductivity and aluminum oxide surface film, by concentrating large amounts of heat to remove the refractory oxide, then melting the base metal rapidly. It also produces smooth, high-quality spatter free welds. Since aluminum conducts heat well, it tends to absorb heat from the arc. Therefore, before GTAW deposits filler metal to the puddle, the welder should pause to let the arc clean the base metal and let it build up sufficient heat. Welders experienced in GTAW of steel will find this waiting period unusual since it is not required with steel. Infact, SS keeps all of the heat in the weld puddle. The GTAW process uses a consumable aluminum filler rod, and inert gas shielding (usually argon, which protects the electrode, filler, and weld metal from oxidation). An alternating current (AC) is most often used, because it not only provides heat input to the base metal but also removes the oxide surface film. Fluxes are not required. Welders usually restrict ac operation to thickness less than 0.25 in. (6.35 mm), handling heavier gases by direct current straight polarity (dcsp) GTAW or GMAW.

Power source selection for GTAW: Aluminum is one of the most demanding applications for GTAW. The best GTAW machines can operate at a wide range of outputs, from 5 to 350 A on ac. This differs greatly from welding on steel that typically calls for low dc current. For example, 1 in. thick steel can be welded with 90 A, but 1 in. aluminum requires 180 A.

High-amperage AC stabilization: The high-amperage requirements for welding aluminum call for a power source that produces a stable ac output over 200 A. Look for a consistent arc (one that does not wander, surge, or cause excessive tungsten consumption) from the tungsten to the workpiece.

GTAW by direct current: GTAW is performed with dcsp or dcrp. With straight polarity welding, current flows (electron) from the electrode to the work, and the oxide film is not removed. To remove the oxide film, electrons must flow from the joint, and this is achieved with dcrp.

Tungsten types: For improved current carrying capacity and to minimize tungsten transfer across the arc, zirconiated tungsten work better. For dc operation, ceriated and lanthanated tungsten electrodes is suggested.

13.20.3.15.3 Gas Metal Arc Welding

GMAW is probably the most popular method for welding aluminum in heavier gases other than GTAW. It is capable of much higher production rates than GTAW. Higher current density, coupled with efficient heat transfer in the arc, give deep penetration, high welding speeds, minimum distortion of base metal, and good mechanical strength. Weld metal transfer modes include spray (the most desirable), globular, short-circuit, and pulsed spray. In GMAW, dcrp is used to establish arc between the consumable electrode and the workpiece in a shield of inert gas (argon or helium).

Wire feeder: The preferred method for feeding soft aluminum long wire is the push–pull method, which employs an enclosed wire-feed cabinet to project the wire from the environment.

Welding guns: Use a separate gun liner for welding aluminum. To prevent wire chaffing, try to restrain both ends of the liner to eliminate gaps between the liner and the gas diffuser on the gun. Change liner often to minimize the potential for the abrasive aluminum oxide to cause wire-feeding problems.

13.20.3.15.4 Merits of Gas-Shielded Arc Welding Processes

GMAW and GTAW processes result in optimum weld quality and minimum distortion, and they require no flux. Since there is no flux is used, (1) difficult-to-reach places and completely inaccessible interiors are left without the danger of corrosion from residual corrosive flux, (2) welding can be done in all positions, because there is no slag to be removed out of the weld by gravity or by puddling, and (3) visibility is good because the gas envelope around the arc is transparent and the weld pool is clean.

13.21 COPPER

Metallurgy and physical properties: Copper is a noble metal. It has excellent electrical and thermal conductivity; it is malleable and machinable. Being a noble metal, it resists many corrosive environments. Other useful properties include ductility, formability, easy joinability by most conventional methods, nonmagnetic, availability in many products, proven service performance, and moderate cost. However, it has low mechanical properties and must be cold worked or alloyed to obtain strength. Typical alloying elements include zinc, aluminum, nickel, silicon, tin, iron, and so on. There are hundreds of copper alloys. Copper combines with zinc, tin, silicon, aluminum, and nickel to create the major copper alloy families. Copper is completely soluble in nickel and vice versa. Small additions of alloying elements ensure specific purposes—e.g., silver provides resistance to softening; beryllium, hardenability; lead, machinability; phosphorus deoxidizes; phosphorus, antimony, arsenic, and tin give resistance to dezincification; iron adds strength and resistance to erosion–corrosion; and nickel adds high strength and resistance to various corrosion types [183,184].

13.21.1 COPPER ALLOY DESIGNATION

To bring order and to identify the many alloys, the Copper Development Association [185], together with the American Society of Testing and Materials and the Society of Automotive Engineers, developed a five-digit system. This system is part of the Unified Numbering System (UNS) for metals and alloys. In this system, the numbers C10000 through C79999 denote the wrought alloys; cast copper and copper alloys are numbered from C80000 through C99999. Wrought copper alloys are divided in the UNS system in the following groups.

- Copper and high-copper alloys C1xxxx
- Zinc brasses (Cu–Zn) C2xxxx
- Zinc–lead brasses C3xxxx
- Zinc–tin brasses C4xxxx
- Tin bronzes C5xxxx
- Aluminum, manganese, silicon bronzes C6xxxx
- Copper–nickel alloys C7xxxx

For selecting copper cast products, refer to Peters and Kundig [186].

13.21.1.1 Wrought Alloys

In Table 13.37, the major alloy groupings used for pressure vessels and heat exchangers, the UNS number ranges, and the major alloying elements are given.

13.21.1.2 Heat Exchanger Applications

Heat exchanger materials require good thermal conductivity, strength, corrosion resistance, ease of formability into various shapes like tubes, tubesheets, and fins by processes like drawing, roll forming, bending, blanking, shearing, machining, etc., and joinability. Copper and copper alloys offer good combinations of these properties. In addition, copper alloys have a biostatic action,

TABLE 13.37
Alloy Groupings and UNS Number Ranges
Copper and Its Alloys

Coppers	C10100–C15760	>99% Cu
High-copper alloys	C16200–C19600	>96% Cu
Brasses	C20500–C28580	Cu–Zn
Leaded brasses	C40400–C38590	Cu–Zn–Pb
Tin brasses	C40400–C49080	Cu–Zn–Sn–Pb
Aluminum bronzes	C60600–C64400	Cu–Al–Ni–Fe–Si–Sn
Silicon bronzes	C64700–C66100	Cu–Si–Sn
Copper–nickels	C70000–C79900	Cu–Ni–Fe

which gives tube surface antifouling properties. The three major areas of applications of copper and copper alloys are in (1) steam condenser tubings, (2) automotive heat exchangers such as charge air coolers, radiators, and oil coolers, and (3) condensers and evaporators of refrigerators and air conditioners.

13.21.1.3 Copper in Steam Generation

Copper alloys such as admiralty brass, cupronickels, aluminum bronze, and the nickel-base alloy Monel have found wide use in feedwater heaters. Their subsequent corrosion by the feedwater, although minor, gives rise to the problem of carryover of copper into the steam generator and possible blockage in turbine units. With the advent of the high-pressure supercritical units, the use of carbon steel tubes in feedwater heaters became common practice in order to eliminate the main source of copper carryover into the steam generator [47,78].

13.21.1.4 Wrought Copper Alloys: Properties and Applications

In this section, wrought copper and copper alloys that are used for the construction of heat exchangers and pressure vessels are discussed.

13.21.1.4.1 Coppers

High-purity coppers such as C10100, C10200, C10400, C10500, C10700, C10800, C11000, C11300, C11400, C11500, and C11600 are included in this category. They contain at minimum 99.3% copper. The elements like silver, arsenic, antimony, sulfur, phosphorus, lead, nickel, cadmium, zirconium, magnesium, boron, and bismuth may be present singly or in combination. These are commercially available in various types (oxygen-bearing, oxygen-free, and deoxidized). Due to their high thermal conductivity, these metals are entirely used for fins and tubes for charge air cooler, inter-cooler, oil cooler, soldered radiator, and condenser and evaporator of air conditioner, refrigerator, and heater coils. They have good resistance to atmospheric corrosion and galvanic corrosion.

13.21.1.4.1.1 Oxygen-Free Coppers The oxygen-free coppers have mechanical properties similar to those of the oxygen-bearing coppers, but their microstructures are more uniform. They have excellent ductility and resistance to fatigue and can be joined readily by welding, brazing, and soldering. Silver is sometimes added to oxygen-free copper to increase the strength at elevated temperature.

13.21.1.4.1.2 Phosphorus-Deoxidized Copper (C12000–C12300) C12000 (DLP), C12200 (DHP), and C12300 (DHP) belong to this category. Due to good thermal conductivities, they are extensively used as tubes in charge air coolers, condensers, and evaporators in sugar and fertilizer industries, refrigerators, and air conditioners. Deoxidized copper is popular in the construction of

process equipment because it can be oxyacetylene welded, silver brazed, and soldered. Deoxidized coppers suffer embrittlement when heated in a reducing atmosphere at 370°C or above.

13.21.1.4.1.3 Fire-Refined Copper C12500, C12700, C12800, C12900, and C13000 are used for radiator manufacture.

13.21.1.4.2 High-Copper Alloys

The wrought high-copper alloys C19200 and C19400 contain a minimum of 96% copper. C19400 is essentially copper with the addition of about 2.4% iron. Iron addition enhances strength and corrosion resistance. These alloys are known for good formability, excellent soldering, brazing, and shielded arc welding, and good OAW. They are resistant to SCC. The alloys are primarily used as seam-welded condenser tubing in desalting service.

13.21.1.4.3 Brasses (Copper–Zinc Alloys)

Brasses contain zinc as their principal alloying element. C23000, C24000, C26000, C26800, C27000, and C28000 belong to this category. Other major alloying elements are lead, tin, and aluminum. The addition of zinc to copper decreases the melting point, density, thermal conductivity, and modulus of elasticity, among others. It increases the strength, hardness, ductility, and coefficient of thermal expansion. These alloys are susceptible to dezincification and SCC. Lead is added to improve machinability. The addition of tin, nominally about 1%, increases strength and resistance to dezincification. Aluminum is added to stabilize the protective surface film.

13.21.1.4.3.1 Muntz Metal (60Cu–40Zn), C28000 This has generally better resistance to sulfur-bearing compounds than higher copper alloys. It shows poor cold-working but excellent hot-working properties and is the strongest of Cu–Zn alloys.

13.21.1.4.4 Leaded Brasses (Cu–Zn–Pb), C31200–C38590

Leaded Muntz metal or leaded brasses such as C36500, C36600, C36700, and C36800 belong to this series, with good resistance to corrosion in both fresh- and saltwater. C36500 is an uninhibited alloy and susceptible to dezincification. Others, C36600, C36700, and C36800, are inhibited alloys containing As, Sb, or P as an inhibitor element (0.02%–0.1%), which imparts high resistance to dezincification.

13.21.1.4.5 Tin Brasses (Cu–Zn–Sn–Pb), C40400–C49080

Admiralty brass, C44300, is extensively used in water-cooled condensers and coolers of petroleum refining and petrochemical operations. It is attacked by pitting, and ammonia SCC and dezincification in environments containing high concentrations of ammonia and hydrogen sulfide. Cracking of admiralty brass tubes has been a recurring problem in a number of refinery heat exchangers during shutdown when ammonia-containing deposits on the tube surfaces are exposed to air. This problem can be overcome by spraying the tube bundle with a very dilute solution of sulfuric acid, immediately after the tube bundle is withdrawn from the shell. Small amounts (0.02%–0.11%) of P, As, or Sb increase resistance to dezincification.

13.21.1.4.5.1 Inhibited Admiralty Brass C44300, C44400, and C44500 exhibit resistance to dezincification and good corrosion resistance in various service environments such as freshwater, seawater, brackish water, steam and steam condensates, and sulfur compounds encountered in refinery operation. However, they may fail in service due to high impingement velocity and ammonia SCC.

13.21.1.4.5.2 Naval Brass—C46400, C46500, C46600, C46700 Addition of 0.75% tin to Muntz metal (60Cu–40Zn) results into naval brass. Naval brass exhibits good resistance to industrial, rural, and marine atmosphere, petroleum products, alcohols, dry gases, and seawater. It has fairly good resistance to weak bases, but generally poor resistance to solutions of cyanides and

ammonium compounds. It resists dezincification and offers good resistance to both fresh- and salt-water. Addition of inhibitor elements P, As, or Sb in small amounts (0.02%–0.11%) to C46400 results in inhibited naval brasses—C46500, C46600, and C46700—which resist dezincification.

13.21.1.4.6 Aluminum Bronzes (Cu–Al–Ni–Fe–Si–Sn), C60600–C64400

Aluminum bronze contains typically 5%–17% aluminum with or without iron, nickel, manganese, and silicon. Typical wrought copper–aluminum alloys are C60800, C61000, C61300, C61400, C61500, C61800, C62300, C63000, and C63200. Alloys range from single-phase composition containing up to about 7% aluminum to complex two-phase alloys containing up to 11% aluminum with additions of iron, nickel, and manganese. They are available in cast and wrought forms. They are generally suitable for service in alkalies, neutral salts, nonoxidizing acid salts, and many organic acids and compounds. They resist corrosion of water—potable, brackish, or seawater. Aluminum bronze and copper–nickel alloys represent the two most important copper alloy groups for seawater applications. Salient characteristic features of aluminum bronzes are thus:

1. Aluminum bronzes resist oxidation and scaling at elevated temperatures due to the formation of aluminum oxide on the surface.
2. Aluminum bronzes offer outstanding strength and resistance to erosion–corrosion.
3. They can be joined by welding and brazing.
4. Susceptible to SCC in moist ammonia and mercurous solution.
5. Resist dealloying but to different degrees depending on alloy composition.
6. The corrosion characteristics are affected by the microstructure of the alloy. A small amount of tin added to C61300 will inhibit intergranular stress corrosion.

Aluminum bronze tubesheets and wrought tubes are extensively used in condensers using seawater. Tubesheets of these alloys are compatible with most condenser tube alloys like C70600, C71500, C68700, and titanium. The cast form (C95400, C95500, C95800) is used as heat exchanger tubesheets and water box.

13.21.1.4.7 Silicon Bronzes (Cu–Si–Ag), C64700–C66100

C65100 silicon bronze B (98.5Cu–1.5Si) and C65500 silicon bronze A (97Cu–3Si) are notable in this group. These alloys contain about 3% silicon and manganese at about 1%. They are known for excellent mechanical properties, workability (both cold working and hot forming), good joinability, and corrosion resistance, particularly corrosion fatigue.

13.21.1.4.8 Aluminum Brass

Aluminum brass owes its resistance to impingement attack in high-velocity seawater and brackish water to a strong tenacious oxide film on its surfaces. It is prone to dezincification; however, this is overcome by inhibiting with arsenic (0.02%–1%). The inhibited arsenical aluminum brass (C68700) finds extensive use in fossil power-plant condensers, boiler feedwater heaters, and shipboard condensers. It is an alternative to inhibited admiralty brass, where cooling-water velocity is high.

13.21.1.4.9 Copper–Nickels (Cu–Ni–Fe), C70000–C79900

Copper–nickels or cupronickels, C70400, C70600, C71000, C71500, and C72200, are single-phase solid solution alloys, with nickel as the principal alloying element. Alloys containing 10% and 30% nickel are important from the heat exchanger construction point of view. They are resistant to fresh-, brackish, and seawater. Copper–nickel alloys with the addition of iron and sometimes manganese are resistant to erosion–corrosion and SCC. Iron enhances the resistance to impingement attack of these alloys, if it is in solid solution. The presence of iron in small microprecipitates can be detrimental to corrosion resistance. Copper–nickels are an alternative to inhibited admiralty metal tubes where cooling-water velocity is high. General corrosion rates for C70600 and C71500 in seawater

are about 1 mpy. Maximum design velocities for condenser tubes are 3.6 m/s (12 ft/s) for C70600 and 4.6 m/s (15 ft/s) for C71500.

At elevated temperatures, the creep strength of cupronickels is greater than that of copper and brasses. Therefore, they find use in high-temperature and high-pressure feedwater heaters and heat exchangers [187]. The cupronickels are highly resistant to SCC. Of all the copper alloys, they are the most resistant to SCC in ammonia environments. Therefore, they are sometimes installed in the air removal sections of large-surface condensers.

They are prone to nonuniform and pitting corrosion, if sulfide is present, for instance, during intermittent service [109]. Dealloying has rarely been seen in the cupronickels.

The 10% copper–nickel (90Cu–10Ni), C70600, finds applications in heat exchangers and condensers in seawater applications, feedwater heaters, and refinery heat exchangers.

The 30% copper–nickel (70Cu–30Ni), C71500, is also known as chromium copper–nickel (67.2Cu–30Ni–2.8Cr). Among all the copper alloys, this alloy exhibits excellent resistance to impingement attack, SCC, and corrosion of most acids and waters and steam condensates. It is used in applications involving severe corrosion problems such as power-plant condensers, feedwater heaters, shipboard heat exchangers and condensers, refinery heat exchangers like overhead condensers and coolers, and aftercoolers. Because of its lower thermal conductivity than brass, some designers provide 5%–10% more heat transfer area [187].

13.21.1.4.10 Designation of Copper and Copper Alloys Used as Heat Exchanger Materials

A detailed list of copper and its alloys and the nominal compositions used in various types of heat exchangers is given in Table 13.38 [188].

13.21.1.5 Product Forms

Copper alloys are available in shapes like plates, sheet and strip, heat exchanger tubes (bare and integral fin), and ferrule stock. ASTM designations for heat exchanger tubes are shown in Table 13.39, and for plates, sheets, and strips in Table 13.40.

13.21.2 COPPER CORROSION

13.21.2.1 Corrosion Resistance

Copper is classed as a noble metal, and therefore copper is corrosion resistant. The formation of a thin protective layer on the surface is the reason for the corrosion resistance of the copper alloys, such as brass, copper–nickel, and bronze. The presence of oxygen or other oxidizing agent is essential for corrosion to take place. Copper alloys are resistant to neutral and slightly alkaline solutions with the exception of those containing ammonia, which causes SCC [131]. They are resistant to urban, marine, and industrial atmospheres. Copper and most of the copper alloys are sensitive to velocity effects. They are resistant to water and find use in domestic and industrial systems and in seawater applications. They are attacked by oxidizing acids, NH_4OH plus O_2 can cause SCC, and hydrogen sulfide, sulfur, and its other compounds attack [189]. Important sources on corrosion of copper are Ref. [183] and Cieslewicz and Schweitzer [190].

13.21.2.2 Galvanic Corrosion

Copper and copper alloys occupy a mid position in the galvanic series. Copper is cathodic to aluminum and SS, yet anodic to passive SS, high-nickel alloys, and titanium. In seawater applications, tubes made of cupronickels, SS, and titanium are more noble than tubesheets made of Muntz and aluminum bronze. Therefore, there will be a galvanic corrosion of tubesheets made of the latter alloys when the tubes are made of the former materials. Galvanic corrosion will also take place between tube inserts and tubes when the SS inserts are fitted into copper tubes to overcome erosion–corrosion.

TABLE 13.38
Copper and Its Alloys Used in Heat Exchangers

UNS No.	Common Name	Composition
C10100 (OFE)	Oxygen-free electrolytic (electronic) copper	99.99% Cu min
C10200 (OF)	Oxygen-free copper without residual deoxidants	99.95% Cu min
C10300	Oxygen-free extra-low-phosphorus copper	99.95% Cu min
C10400	Oxygen-free copper with silver	99.95% Cu min
C10500		
C10700		
C10800	Oxygen-free low-phosphorus copper	99.95% Cu min
C11000	Electrolytic tough-pitch copper	99.95% Cu min
C11300	Silver-bearing tough-pitch copper	99.95% Cu min
C11400		
C11500		
C11600		
C12000 (DLP)	Phosphorus-deoxidized copper (low-residual copper)	99.9% Cu min
C12200 (DHP)	Phosphorus-deoxidized copper (high-residual copper)	99.9% Cu min
C12300 (DHP)	Phosphorus-deoxidized copper (high-residual copper)	99.9% Cu min
C12500	Fire-refined copper	99.88% Cu min, remainder Ag, As, Sb, and others
C12700		
C12800		
C12900		
C13000		
C14200	Phosphorized, arsenical copper	99.94% Cu min, 0.1%–0.5% As, 0.015%–0.04% P
C19200	Phosphorized copper with 1% iron	98.97% Cu, 1.0% Fe, 0.03% P
C19400	High-strength modified copper	97.4% Cu, 2.4% Fe, 0.13% Zn, 0.04% P
C23000	Red brass	84%–86% Cu, remainder Zn
C26000	Cartridge brass	70% Cu, 30% Zn
C26800	Yellow brass	65% Cu, 35% Zn
C27000		
C28000	Muntz metal	60% Cu, 40% Zn
C36500	Leaded Muntz metal, uninhibited	58%–61% Cu, 0.4%–0.9% Pb, 0.25% Sn max, remainder Zn
C36600	Arsenical inhibited leaded Muntz metal	58%–61% Cu, 0.4%–0.9% Pb, 0.25% Sn max, remainder Zn
C36700	Antimonial inhibited	
C36800	Phosphorus inhibited	
C44300	Admiralty brass	70%–73% Cu, 0.9%–1.2% Sn, remainder Zn
C44300	Arsenical inhibited admiralty brass	
C44400	Antimonial inhibited admiralty brass	
C44500	Phosphor inhibited admiralty brass	
C46400	Uninhibited naval brass	59%–62% Cu, 0.5%–1.0% Sn, remainder Zn
C46500	Arsenical inhibited naval brass	
C46600	Antimonial inhibited	
C46700	Phosphorus inhibited	
C60800	Aluminum bronze	95% Cu, 5% Al
C61300	Aluminum bronze, 7%	90% Cu, 6%–7.5% Al, 0.15% Ni, 2%–3% Fe

(continued)

TABLE 13.38 (continued)
Copper and Its Alloys Used in Heat Exchangers

UNS No.	Common Name	Composition
C61400	Aluminum bronze D	91% Cu, 7% Al, 2% Fe
C63000	10% Aluminum–nickel bronze	82% Cu, 10% Al, 5% Ni, 3% Fe
C63200	9% Aluminum–nickel bronze	82% Cu, 9% Al, 5% Ni, 4% Fe
C65100	Low-Si bronze B	98.5% Cu, 1.5%–2.0% Si, 0.7% max Mn
C65500	High-Si bronze A	97% Cu, 3% Si
C68700	Aluminum brass D, arsenical inhibited	77.5% Cu, 20.5% Zn, 2% Al
C70400	Copper–nickel, 5%	95% Cu, 5% Ni
C70600	Copper–nickel, 10%	90% Cu, 10% Ni
C71000	Copper–nickel, 20%	80% Cu, 20% Ni
C71500	Copper–nickel, 30%	70% Cu, 30% Ni
C71640	Copper–nickel–iron–manganese	29%–32% Ni, 1.7%–2.3% Fe, 1.5%–2.5% Mn
C71900	Chromium copper–nickel	67.2% Cu, 30% Ni, 2.8% Cr
C72200	Chromium copper–nickel	83% Cu, 16.5% Ni, 0.5% Cr

Source: Compiled from ASM, Copper, in *Metals Handbook, Vol. 2, Nonferrous Metals*, 9th edn., American Society for Metals, Metals Park, OH, 1979.

TABLE 13.39
ASTM Specifications for Copper Alloy Heat Exchanger Tubes

ASTM Spec.	Description	Alloys UNS No.
B111	Copper and copper alloy seamless condenser tubes and ferrule stock	C10100, C10200, C10300, C10800, C12000, C12200, C14200, C44500, C60800, C61300, C61400, C68700, C70400, C70600, C71000, C71500, C71640, C72200
B359	Copper and copper alloy seamless condenser and heat exchanger tubes with integral fins	C10100, C10200, C10300, C10800, C12000, C12200, C14200, C19200, C23000, C44300, C44400, C44500, C60800, C68700, C70400, C70600, C71000, C71500, C72200
B395	U-bend seamless copper and copper alloy heat exchanger and condenser tubes	C10200, C10300, C10800, C12000, C12200, C14200, C19200, C23000, C44300, C44400, C44500, C60800, C68700, C70400, C70600, C71000, C71500, C72200
B543	Welded copper and copper alloy heat exchanger tube	C10800, C12200, C19400, C23000, C44300, C44400, C44500, C68700, C70400, C70600, C71000, C71500, C71640, C72200
B552	Seamless and welded copper–nickel tubes for water desalting plants	C70600, C71500, C71640, C72200

13.21.2.3 Pitting Corrosion

The main drawback of copper alloys is their susceptibility to pitting corrosion in water containing the combination of oxygen and sulfide. Hence, copper is not suitable for coastal water applications. However, alloys C70600 and C71500 display excellent resistance to pitting in seawater.

13.21.2.4 Intergranular Corrosion

The most susceptible alloys for this form of corrosion are Muntz metal, admiralty metal, aluminum brasses, and silicon bronzes.

TABLE 13.40
Copper Alloy Plates, Sheets, and Strips

ASTM Spec.	Description	Alloys UNS No.
B171	Copper alloy plate and sheet for pressure vessels, condensers, and heat exchangers	C36500, C36600, C36700, C36800, C44300, C44400, C44500, C46600, C46700, C61300, C61400, C63000, C63200, C70600, C71500, C72200
B569	Brass strip in narrow widths and light gage for heat exchanger tubing	C26000
B96	Copper–silicon alloy plate, sheet, strip, and rolled bar for general purposes and pressure vessels	C65100, C65400, C65500, C65800

13.21.2.5 Dealloying (Dezincification)

Various forms of dealloying, including dezincification, have been covered in Chapter 12. Dealloying of copper-base materials is briefly discussed here. Brasses containing more than 15% Zn, such as leaded Muntz metal, admiralty brass, and naval brass, are susceptible to dealloying when subjected to prolonged contact with slow-moving water or mildly acidic water. Details of trends of dezincification, SCC, and impingement attack with increasing zinc content in copper–zinc alloys are discussed in Ref. [81]. A few methods to control dezincification are thus:

1. Copper alloys with copper contents more than 85% resist dezincification. Sensitivity to SCC increases with increasing amount of zinc. Resistance to impingement attack increases with decreasing zinc content.
2. Small amounts (0.02%–0.11%) of As, Sb, or P added to admiralty brass (C44300) impart high resistance to dezincification, and the inhibited alloys are called arsenical admiralty brass, antimonial admiralty brass, and phosphorous admiralty brass. Similarly, the addition of As, Sb, or P tends to inhibit dezincification in leaded Muntz metal C36500 and in naval brass (C46400). The uninhibited alloys and the corresponding inhibited alloys are given in Table 13.41.

13.21.2.5.1 Dealuminification

Dealuminification in the 5%–8% aluminum bronzes is occasionally reported, but it is not a significant problem until aluminum reaches the 9%–11% range [191]. The microstructure is particularly important in the dealloying resistance of the alloys. Dealloying is rarely seen in all alpha, single-phase alloys such as aluminum bronzes C60800, C61300, and C61400, and when seen, conditions of low pH and high temperatures are usually present. But duplex structures are more prone to dealloying. Proper heat treatment can control dealloying in the duplex alloys.

TABLE 13.41
Uninhibited and Inhibited Alloys

Uninhibited Alloys	Inhibited Alloys
C36500 Leaded Muntz metal	C36600, C36700, C36800—As, Sb, P inhibited leaded Muntz metal, respectively
C44300 Uninhibited admiralty brass	C44300, C44400, C44500—As, Sb, P inhibited admiralty brass, respectively
C46400 Uninhibited naval brass	C46500, C46600, C46700—As, Sb, P inhibited naval brass, respectively

13.21.2.5.2 Denickelification

Denickelification is occasionally reported in the higher nickel copper–nickel alloys, 70Cu–30Ni (C71500), in feedwater pressure tubes at temperatures over 212°F (100°C), in low-flow conditions, and in high local heat flux [135], and in refinery overhead condensers, where hydrocarbon streams condense at temperatures above 300°F (149°C) [191]. According to Tuthill [191], denickelification problem appears to be associated with hot spots that develop in the tubing as a result of fouling and thermogalvanic differences that arise.

13.21.2.6 Erosion–Corrosion

Erosion–corrosion is the common tubeside phenomenon in copper and some copper alloys with water on the tubeside as a result of excessively high velocity and turbulence. To improve resistance to erosion–corrosion, copper is alloyed with iron, chromium, and titanium [109]. Aluminum brass and copper–nickels are highly resistant to erosion–corrosion. Remedial measures to overcome erosion–corrosion include (1) proper design and sizing of the system so that maximum velocity is kept about 4–5 ft/s, (2) redesigning the waterbox or install vanes and diffusers to reduce turbulence in the inlet region, (3) installing cathodic protection system in the waterbox, (4) installing tube inserts made of SS or plastics, and (5) using chromium-modified copper–nickel alloys or copper–nickel–iron alloys.

13.21.2.7 Stress Corrosion Cracking

Pure copper is immune to SCC, but the higher zinc content brasses with Zn content in the range of 20%–40% are subject to SCC. Susceptibility increases as zinc content increases from 20% to 40%. Prominent copper alloys susceptible to SCC include C23000, C26000, C26800, C27000, C28000, C36500, C44300 (uninhibited), and C46400. Copper–nickels and pure copper are more resistant.

The combined action of at least three substances usually is necessary to produce SCC in stressed copper-base alloys [191]: (1) ammonia or ammonia-producing material (organic and inorganic substances containing nitrogen), (2) moisture (or water), and (3) oxygen. It is rarely encountered in feedwater heaters and condensers because of their low oxygen content. To keep the oxygen level to the lowest amount, air in-leakage during downtime periods should be minimized. Environments like sulfates, nitrites, and nitrates under certain circumstances also cause SCC of copper alloys. SCC in copper alloys is usually intergranular, whereas admiralty and aluminum brass almost invariably crack transgranularly and so does brass [192]. Cracks can be detected by eddy current inspection. Relative resistance of the various copper alloys to SCC is as follows [190,192]:

Low resistance

Brass containing over 20% zinc

Brass containing over 20% zinc and small amounts of lead, tin, or aluminum such as leaded high brass, naval brass, admiralty and aluminum brass

Medium resistance

Brasses containing less than 20% zinc, such as red brass

Aluminum bronze

Phosphorus bronze

High resistance

Silicon bronze

Phosphorized copper

Very high resistance

Cupronickel

Tough-pitch copper

Commercially pure copper

SCC can be controlled by

1. Selecting copper alloys with less than 15% Zn. Brasses containing less than 15% Zn are resistant SCC. DHP copper and tough-pitch copper are generally immune to SCC.
2. Reducing the stress to a safe level by stress relieving or annealing.
3. Controlling the aggressiveness of the environment by addition of inhibitors.
4. By keeping the tubes free from deposits (since the waterside SCC is often associated with surface deposits).

13.21.2.7.1 *Steam-Side Stress Corrosion Cracking*

Among the copper alloys typically used for condenser tubes, the brasses (copper–zinc) are the most susceptible to SCC in environments containing ammonia. Other susceptible materials include arsenical aluminum brass and admiralty brass. The environmental conditions leading to SCC on the steam-side of copper alloy condenser tubes are ammoniacal solutions containing dissolved oxygen. The ammonia is derived from the water treatment compounds used for boiler feedwater, which decompose due to thermal effects in the boiler [193–195]. The ammonia concentration is particularly high in the air removal section, and this location suffers SCC most often. The high ammonia concentrations develop because the baffles locally shield the tubes and prevent the condensate in this area from being continually washed away by condensate falling from above. The other necessary ingredient for SCC to occur, oxygen, comes from the air drawn into the condenser through leaking joints, valve packing glands, etc. In addition to usual methods, some methods of controlling SCC in condenser tubes include the following [193]:

1. Use alloys resistant to SCC. Brass tubes may be replaced by cupronickel, SS, or titanium tubes, particularly in the air removal section where steam-side environments can be quite aggressive.
2. Reduce or minimize the addition of ammonia and ammonia-producing additives to the boiler feedwater.
3. Ammonia concentrations in the air removal section can be reduced by modifying the design to eliminate horizontal baffles or by installing a water showering system to dilute the ammoniacal condensates.
4. If SCC is due to ammonia liberated from putrefying organisms during shutdown periods, flush the system with freshwater for a short period every day.
5. Eliminate oxygen from the system. All potential sources of air leakages should be attended and rectified.

Test for SCC—ASTM B154: ASTM B154, mercurous nitrate test, is a standard test method for detecting SCC of copper and copper alloys. This test method is an accelerated test for detecting the presence of residual (internal) stress that might result in SCC of individual parts in storage or in service.

13.21.2.8 **Condensate Corrosion**

Copper alloy tubes, particularly brass, can withstand the action of steam condensate in a very satisfactory manner except where the steam condensate contains high concentrations of ammonia and oxygen [194]. Condensate corrosion, also known as “ammonia attack,” on the steam side of condensers, generally takes place in the air removal section where ammonia and oxygen concentrations are particularly high. Many of the methods of preventing ammonia SCC are also helpful to prevent condensate attack.

13.21.2.9 **Deposit Attack**

Deposit attack on condenser tubes occurs under conditions of stagnant or low water velocities, generally less than 3.1 ft/s (1 m/s). Deposition of waterborne particles on tube surfaces leads to

differential aeration and anodic dissolution of the tube material [196]. Deposit attack is overcome by the following measures [194]:

Maintain tubeside water velocity above 1 m/s and avoid stagnant conditions in aggressive media by flushing with treated water during shutdown

Use more resistant materials like 70/30 and 90/10 copper–nickels and titanium

13.21.2.10 Hot-Spot Corrosion

Hot-spot corrosion is a localized form of pitting corrosion that takes place at “hot spots” on the condenser tube wall due to low water velocity and/or high heat flux [196]. These conditions can be caused by poor steam distribution or the absence of water on the cooling-water side of the tube. This form of corrosion rarely takes place in main steam condensers.

13.21.2.11 Snake Skin Formation

Snake skin formation is the result of deposition of copper corrosion product carried from low-pressure feedwaters employing admiralty brass tubes or high-pressure feedwater heater tubes made of Monel 400 or 70Cu–30Ni. The deposition results in thin flaky skin formation similar in appearance to skin shed by snake. This snake skin falls from the tubes when dried [194].

13.21.2.12 Corrosion Fatigue

Copper and copper alloys such as beryllium copper, cupronickels, phosphorus bronzes, and aluminum bronzes exhibit resistance to corrosion fatigue in many environments involving corrosiveness and applied stress.

13.21.2.13 Biofouling

Copper and copper alloys including copper–nickel exhibit excellent resistance to marine biofouling such as barnacles, mussels, and marine invertebrates.

13.21.2.14 Cooling-Water Applications

The principal constituents of water that affect the performance of copper alloys are dissolved oxygen, nutrients, bacteria, organisms, biofouling, sediment, and residual chlorine from the chlorination practice [191]. Inhibited admiralty brass, aluminum brass, and cupronickels exhibit excellent resistance in seawater and show erosion–corrosion and biofouling resistance. Hence, these alloys are now extensively used in fossil power-plant heat exchangers.

13.21.2.15 Resistance to Seawater Corrosion

Corrosion resistance of copper and copper alloys in seawater is determined by the nature of the naturally occurring and protective corrosion product film [191]. The main drawback of copper alloys is their susceptibility to pitting corrosion in sulfide-bearing seawater in the presence of oxygen. This is especially true with polluted coastal water. Sulfide attack is further discussed next.

13.21.2.16 Sulfide Attack

Sulfide attack is the accelerated corrosion of copper alloys that occurs when the cooling water, most often brackish water or seawater, is polluted with sulfides, polysulfides, or elemental sulfur, and no copper alloy is resistant to sulfide attack [194]. Various sources of sulfides include (1) the natural sulfates present in seawater and (2) the putrefaction of organic sulfur compounds from decaying plant and animal matter during periods of extended shutdown [193]. The major effect of the sulfide is to destroy the existing protective surface oxide film, if any. It can greatly increase general corrosion, and it can induce or accelerate dealloying, pitting, and

erosion–corrosion [194]. The corrosion attack is enhanced in the presence of oxygen. The following remedial measures will overcome sulfide attack [193].

1. If sulfide forms during periods of extended shutdown due to the putrefication of organic sulfur compounds, it can be removed daily by flushing the system using freshwater.
2. Precondition the copper alloy surfaces by ferrous sulfate dosing to make them more corrosion resistant.
3. Use alternative materials such as SS and titanium tubes in place of copper.

13.21.2.17 Exfoliation

Copper–nickel alloy feedwater heater tubes are subjected to exfoliation [189,197]. Exfoliation is due to pronounced schistous oxidation of the materials, and the resulting loss in strength of the feedheater tubes, which is no longer sufficient to withstand the water pressure and hence burst. The factors that cause exfoliation are (1) cyclic and peak loads, that is where the plant was frequently started up and shutdown, and (2) the presence of oxygen, water vapor, and water. Among the copper–nickels, 70:30 copper–nickel was the most susceptible, but 80:20 and 90:10 are better. Monel alloy 400, Inconel alloy 600, and titanium retain their “as-installed” appearance under test conditions [197].

13.21.2.18 Copper and Aquatic Life

Copper is declared poisonous to aquatic life. Hence its discharge into the source of cooling water is prohibited by laws and environmental regulations.

13.21.3 COPPER WELDING

Copper and its alloys are welded by SMAW, GTAW, PAW, SAW, and OAW. Of these, GTAW and GMAW are the most popular, with argon, helium, or nitrogen gas shielding. The primary criteria for choosing between GMAW and GTAW are thickness of the metal to be welded and amount of welding to be performed. GMAW is generally preferred for thicknesses greater than about 1/4 in. (6.4 mm). The GMAW process provides intense heat generated by the arc, high deposition, dense deposits, low preheat and interpass temperatures, good properties, and minimum distortion [184]. GTAW is used for thickness less than about 0.08 in. (2 mm). Generally, welding is carried out using DCSP with a 3:1 mix of helium and argon. For thickness between 2 and 6 mm, both processes can be used. Other joining methods include resistance welding and induction welding, brazing, and soldering. Welding of copper and its alloys is discussed in detail by Gaffoglio [184], in Ref. [198], by Dawson [199–201], by McDonald Sketly [202], and in Ref. [203].

13.21.3.1 Weldability

In all welding processes, the dominant factor in establishing weldability is thermal conductivity of the base metal. When welding copper, allowances are necessary for the chilling of the welds because of the very high thermal conductivity of the metal. Preheating is often required. Considerable distortion is possible in coppers because of the higher thermal expansion than other commercial metals. These characteristics pose difficulties that must be overcome for satisfactory welding.

13.21.3.1.1 Factors Affecting Weldability

Other than the elements that comprise a specific alloy, the principal factors that influence weldability are (1) thermal conductivity, (2) preheating, (3) thermal expansion, (4) alloying elements, (5) surface cleanliness and surface oxide, (6) shielding gas, (7) joint design, (8) welding position, (9) consideration for precipitation-hardenable (PH) copper alloys, (10) hot cracking, and (11) porosity.

13.21.3.1.1.1 Thermal Conductivity The high thermal conductivities of copper and certain high-copper alloys such as aluminum bronze, commercial bronze (90%), and red brass (85%) pose problems for satisfactory welds. Unless adequate measures are taken to counteract the rapid heat-sink effect, it is not possible to establish the fully fluid weld pool necessary for good fusion, adequate joint penetration, and deoxidation [184,203]. Therefore, the type of current and the shielding gas must be selected for maximum heat input to counteract the rapid heat dissipation from the weld region. Make all joint preparation with wide root gaps and tack frequently.

13.21.3.1.1.2 Preheating The relatively high thermal conductivities of copper and most copper alloys result in the rapid conduction of heat from the weld joint to the surrounding base metal. Preheating copper is generally necessary for thicknesses above about 1/8 in. (3 mm) when using argon shielding [203]. Preheating of these alloys will reduce welding heat requirements for fusion. Recommended preheat temperature varies from 302°F to 1292°F (150°C to 700°C) depending on the thickness, shielding gas, welding current, and process used. To reduce the preheat requirement, substitute helium for argon in the shielding and make heavy root passes in all multipass welds to insure deoxidation and to prevent cracking [184]. The interpass temperature should be the same as that for preheating.

13.21.3.1.1.3 Thermal Expansion The high thermal expansion causes root gaps to close as welding proceeds, and due allowance must be made when fixturing the assembly for welding. The effect of high contraction stresses on the weld metal during solidification must also be taken into account and may require reduction of cooling rate by some means to give sufficient time for these stresses to be accommodated.

13.21.3.1.1.4 Effects of Alloying Elements on Welding Alloying elements have pronounced effects on the welding behavior of copper alloys. Small amounts of volatile, toxic alloying elements are often present in copper and its alloys, and, as a result, the use of an effective ventilation system to protect the welder or welding machine operator is necessary.

13.21.3.1.1.5 Precleaning and Surface Preparation The joint faces and adjacent surfaces should be clean. Oil, grease, dirt, paint, oxides, and mill scale should be removed by degreasing followed by suitable chemical or mechanical cleaning.

Surface oxides: Surface oxides must be removed from the work surfaces before welding. Surface oxide can cause a serious problem of nonwetting of filler metal during welding, brazing, and soldering. The oxides on beryllium copper, chromium copper, aluminum bronze, and silicon bronze are difficult to remove. Wire brushing is not effective for copper alloys that develop a tenacious surface oxide. These alloys should be cleaned by appropriate chemical or abrasive methods. Mill scale on copper-nickels must be removed by grinding or pickling, since wire brushing is ineffective.

13.21.3.1.1.6 Shielding Gas Argon or a mixture of argon and helium at 25%–70% is normally used for welding.

13.21.3.1.1.7 Joint Design Joint design and fixturing should minimize restraint and residual stresses and provide allowance for the high coefficient of thermal expansion to prevent hot cracking. Backing strips are extensively used on the highly fluid coppers and high-copper alloys. Joint design for copper and copper alloy is shown in Figure 13.22.

13.21.3.1.1.8 Welding Position Because of high fluidity of copper and copper alloys, the flat horizontal position is used whenever possible.

13.21.3.1.1.9 Problems with Precipitation-Hardenable Alloys For PH copper alloys with Be, Cr, Bo, Ni, Si, and Zr, take care to avoid oxidation and incomplete fusion. Weld in the annealed condition and the weldment should be given a precipitation-hardening heat treatment.

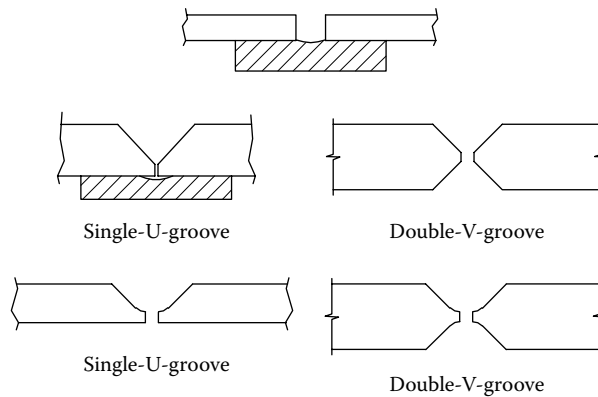


FIGURE 13.22 Typical joint design for welding of copper and copper alloys.

13.21.3.1.1.10 Hot Cracking Copper alloys with wide liquidus-to-solidus temperature ranges, such as copper–tin and copper–nickel, are susceptible to hot cracking. Low-melting interdendritic liquid solidifies at a temperature lower than the bulk dendrite. Shrinkage stresses produce interdendritic cracking during solidification. Hot cracking can be minimized by reducing restraint on the weldment, preheating to slow the cooling rate, reducing the magnitude of the welding stresses, reducing the root opening, and increasing the size of the root pass.

13.21.3.1.1.11 Porosity Elements such as zinc, lead, cadmium, and phosphorus have low boiling points. Vaporization of these elements during welding will result in porosity. Porosity can be minimized by fast weld speeds and use of filler metal low in these elements.

13.21.3.2 Alloy Classification from Weldability Considerations

Copper and its alloys are considered from the welding viewpoint under the following general headings:

1. Copper with small additions: copper–cadmium and PH alloys (copper–beryllium, copper–chromium, copper–zirconium); oxygen-free copper, tough-pitch copper, phosphorus-deoxidized copper
2. High-copper alloys
3. Copper alloys:
 - a. Brasses—admiralty brass, naval brass, aluminum brass
 - b. Silicon bronzes
 - c. Tin bronzes
 - d. Aluminum bronzes
 - e. Copper–nickels

13.21.3.2.1 Copper

Oxygen-free and tough-pitch coppers: For welding oxygen-free copper (C10200) or electrolytic tough-pitch copper (C11000) in thickness to about 1/2 in. (12.7 mm), GTAW is preferred to GMAW, or other processes generating less localized heat input.

Deoxidized copper: Up to about 1.5 in. (38 mm), heavy-walled components made from phosphorus-deoxidized copper are normally welded by GMAW. To ensure high heat input, welding current and preheat temperatures are usually high.

13.21.3.2.2 High-Copper Alloys

Because these alloys have lower thermal conductivities than pure copper, they require lower preheats and welding current. Generally, except for beryllium coppers, the welding procedures are similar to deoxidized copper.

13.21.3.2.3 Copper Alloys

The most notable feature distinguishing the welding of most copper alloys from the welding of pure copper is the reduction of heat input and preheating requirements due to low thermal conductivities of the copper alloys compared to the pure metal. Copper alloys commonly welded, notably brasses, aluminum bronzes, and cupronickels, are readily weldable by all gas-shielded arc welding processes. Metallurgical and welding features that may require particular attention are discussed under the individual alloys.

13.21.3.2.3.1 Brasses Alloying elements lower conductivity. The alloys most commonly welded are naval brass, admiralty brass, and aluminum brass. Compared to the coppers, brasses require much less preheat and less current to weld. Copper's problems with hydrogen and oxygen reactions are absent when welding brasses, because brasses have low-hydrogen solubility limits and zinc deoxidizes [184]. Lead contributes to hot cracking. Evolution of zinc fume causes suffocation to the welder and obstructs the view of the welding. Zinc fume makes welds porous and unacceptable, particularly in autogenous welding [200]. The gas-shielded arc processes provide a means of reducing problems associated with zinc volatilization to a minimum, and due consideration should be given to the possibility of using a nonmatching filler metal like silicon bronze or aluminum bronze, which will reduce the evolution of zinc fumes by forming a surface film on the weld pool [200,203]. When using argon-shielded TIG welding, alternating current is essential, and for direct current working, helium is preferred [203].

13.21.3.2.3.2 Silicon Bronzes Silicon bronzes are the most weldable of the copper alloys. Adding as little as 1.5% silicon reduces conductivity to 15% of that of copper. As a result, preheating is not essential, and little heat input is required so that welding speeds can be high [184]. Silicon bronzes are fluid when molten, but fluxes are needed to penetrate the viscous silica that covers weld metal pool. Both TIG and MIG processes are suited to silicon bronzes. TIG welding is used on thin to moderately thick nonlead silicon bronzes. With TIG welding, employ DCSP with argon or helium shielding. Sometimes, alternating current with argon is preferred because it facilitates the removal of the tenacious oxide surface film, but at the cost of arc stability [203]. For thickness above 1/2 in. (12.7 mm), MIG is often preferred due to higher deposition, though TIG is also suitable.

Silicon bronze is hot short in the temperature range of 1472°F–1742°F (800°C–950°C), and cooling through this critical temperature range should be as rapid as possible, especially when the welded structure is restrained. This is particularly faced when using the MIG welding process, known for high welding speeds and high deposition rates. However, with rapid cooling, there is a possibility of forming brittle, nonequilibrium phases in the weld metal, which, under conditions of restraint, can cause weldment cracking [200].

13.21.3.2.3.3 Copper–Aluminum Alloys (Aluminum Bronzes) Due to relatively high thermal conductivity and the ease with which refractory oxide films form on its surface, aluminum bronzes require a highly concentrated heat source with full shielding of the weld pool [204]. The high gas solubility and affinity of oxygen for molten aluminum bronze, its higher thermal expansion and contraction, and its susceptibility for hot shortness, particularly single-phase aluminum bronzes that contain less than 7% Al, should be considered. Clean welding conditions, a proper weld design and joint preparation, and a welding procedure to accommodate thermal stresses and reduce the tendency for weld metal cracking are suggested [204].

Single-phase aluminum bronzes that contain less than 7% Al are difficult to weld, whereas single-phase alloys with more than 7% Al and two-phase alloys are weldable by GTAW or GMAW techniques, using procedures designed to avoid hot cracking [184]. GTAW produces high-quality welds. When welding, use argon and alternating current to remove tenacious aluminum oxide surface films. For greater success, use DCRP in helium [203]. Porosity is minimized by the presence of iron, manganese, or nickel in the filler metal or base metal, or in both. Preheating should be avoided

whenever possible, and interpass temperatures kept to a minimum to avoid a buildup of temperature in the structure, which may give rise to loss of ductility and associated cracking problems. OAW is not recommended due to the problem with fluxing of aluminum oxide from the weld metal.

13.21.3.2.3.4 Copper–Nickel or Cupronickel Alloys Thermal and electrical conductivities approximate those of carbon steels. These properties facilitate welding without preheating, and the interpass temperature during welding should not exceed 150°F (66°C). The chief problems faced in the welding of copper–nickels are the following:

1. Since resistance to erosion–corrosion requires that the iron be in solid solution, welding of the alloy must be done in a manner that does not cause precipitation of iron compounds.
2. Like nickel-base alloys, the copper–nickel alloys are susceptible to lead, phosphorus, or sulfur embrittlement. Restrict the phosphorus to 0.01% and the sulfur level to a maximum of 0.02%. Maintain surface cleanliness and avoid surface contamination by any of them [184].
3. Copper–nickels have high affinity for the absorption of oxygen, hydrogen, or nitrogen into the molten weld metal, which gives rise to porosity. This problem is overcome by using filler metals containing suitable deoxidants. Titanium, together with manganese, is at present the major deoxidant in the standard filler alloys for the cupronickels. For this reason, the autogenous welding of copper–nickel alloys will leave porous welds.
4. Protection of the weld metal and the underside of the weld by inert gas shielding may be desirable to avoid contamination from oxygen, hydrogen, etc. [203].
5. Both TIG and MIG techniques are used with filler metals containing suitable deoxidants. Welding speeds should never be high enough to cause breakdown of the gas shielding and subsequent oxygen and hydrogen pickup by weld metal, leading to porosity problems.

Cupronickels can be joined by GMAW, gas-shielded arc welding, and OAW. Copper–nickel filler metal of 70Cu–30Ni composition is normally used for welding all of the cupronickel alloys. Filler metals of matching composition may be used in special cases. Mostly, argon is preferred for shielding because it gives easy arc control and uniform weld appearance. Helium is preferred for welding thicker sections, because it gives improved welding conditions. A direct-current, electrode-negative arc is used for GTAW with helium and argon gas shielding. Since the lower copper–nickel alloys are higher in conductivity, they require higher current. A short arc is generally recommended [184]. Use slow welding speeds for GMAW, laying beads with slight weaves, shield with argon, or argon plus helium.

13.21.3.3 PWHT

Copper alloys are not frequently postweld heat-treated, but they may require controlled cooling to minimize residual stress and hot shortness. After welding, the HAZ will be softer and weaker than the adjacent base metal. For copper–zinc alloys, postweld stress-relief heat treatment at 482°F–572°F (250°C–300°C) is advisable from SCC point of view [203].

13.21.3.4 Dissimilar Metal Welding

The requirement to join copper and copper alloys to other copper alloys or to other nonferrous or ferrous alloys is frequently encountered. A few examples for these combinations are given next.

13.21.3.4.1 Copper to Steel

Copper materials may fulfill the design function of corrosion resistance or conductivity, whereas ferrous materials may give structural strength on an economical basis.

13.21.3.4.2 Copper to Aluminum Bronze

Frequently, the main shell of the assembly is of copper, and the welding of the aluminum bronze branches and various fittings to the shell must be accomplished.

13.21.3.4.3 Aluminum Bronze to Cupronickel

Heat exchanger shells made of cupronickel alloys, both 90:10 and 70:30, may involve welds with aluminum bronze castings for branches and tubesheets.

13.21.3.4.4 Cupronickels to Steel

Cupronickels of 90:10 and 70:30 are increasingly being used for heat exchanger shells. Mild steel supports and flanges are attached by welding. Cupronickel tubes are commonly welded into steel tubesheets.

13.21.3.4.5 Factors Influencing the Dissimilar Metal Weld

Important factors to be considered when welding dissimilar metals include the following [201]: interalloying, electrochemical corrosion, differential expansion, and weld metal dilution.

1. *Interalloying*: Where the materials to be joined are metallurgically incompatible, the binary phase diagram gives some indication as to the ultimate weld metal's composition and structure.
2. *Galvanic or electrochemical corrosion*: In a dissimilar joint, the possibility of electrochemical corrosion of the weld metal can be prevented by ensuring that it is cathodic to the base metals.
3. *Differential thermal expansion*: In a welded joint between dissimilar metals, additional stresses are set up due to differential thermal expansion and contraction. Joint design and fixturing must allow for the effect of expansion, which will tend to close the root gap and generally distort the structure as welding proceeds. Problems due to differential thermal expansion are overcome by the following means [201]: (a) select a filler alloy having expansion characteristics midway between the two parent metals and (b) accommodate the metallurgical stresses by the structure as a whole by preheating or postheating the joint area to reduce the cooling rate sufficiently. This is particularly important with inert-gas arc welding where heating is often localized and cooling rates are very high.
4. *Weld metal dilution*: Another important consideration when welding copper to steel is to minimize dilution of iron in the weld metal and the penetration of copper into the steel. Standard techniques to overcome weld metal dilution include the following [201]:
 - a. Buttering, by laying down an overlay of copper filler alloy on to the steel joint face.
 - b. Select a filler metal compatible with both parent metals.
 - c. In dissimilar metal joints with copper, use the cupronickel rather than the copper filler alloys to minimize the risk of porosity.
 - d. While joining copper–nickel to steel, dilution is controlled by attaining low penetration using globular transfer, which occurs at subthreshold welding currents, for the initial overlay on the steel face area.

13.21.3.4.6 Filler Alloys Selection

Filler metal standards are usually specified by codes and standards, but if not specified, alloys of parent metal composition are generally used [203].

13.22 NICKEL AND NICKEL-BASE ALLOYS METALLURGY AND PROPERTIES

Nickel is a hard, tough, and malleable white metal. Nickel exhibits unique properties of high-temperature strength, toughness, wear resistance, and resistance to corrosion and oxidation. Nickel alloys were developed to withstand corrosives found in the chemical, petrochemical power, marine,

and pulp and paper industries. Nickel readily forms alloys with ferrous and nonferrous metals like Fe, Cr, Cu, and Co. The properties that favor the nickel and nickel-base alloys for construction of process equipment include the following:

1. Ability to withstand a wide variety of severe operating conditions involving high temperature, high stresses, corrosive environments, and a combination of these factors.
2. Nickel-base superalloys exhibit good resistance to corrosion, creep-rupture, fatigue, thermal fatigue, thermal shock, and impact.
3. Resistance to elevated-temperature oxidation, sulfidation, and carburization.
4. Used as an alternative material in place of austenitic SS to combat SCC. For all practical purposes, nickel alloys containing more than 30% nickel are immune to SCC.
5. Ability to be formed by conventional methods and to be joined by most conventional welding process such as GTAW, GMAW, and SMAW using coated electrodes.
6. Purity and nontoxic character are exploited in food processing and fine chemical industries.
7. *Low-temperature applications:* Nickel is an fcc metal that retains good ductility and toughness at subzero temperatures. Among the nickel alloys, Monel K-450, Hastelloy B, Hastelloy C, Inconel alloy 600, Inconel alloy 706, Inconel alloy 718, Invar-36, and Inconel X-700 exhibit excellent combinations of strength, ductility, and toughness up to -263°C [205].

13.22.1 CLASSIFICATION OF NICKEL ALLOYS

Nickel alloys are in general classified into the following groups:

1. Commercially pure nickel
2. Nickel–copper alloys and copper–nickel alloys
3. Nickel–chromium alloys
4. Nickel–iron–chromium alloys

Important sources on material properties of various nickel, nickel–copper, Inconel, and Incoloy alloys include Refs. [206–208].

13.22.1.1 Commercially Pure Nickel

Alloys 200 and 201 are the major examples of this class. Because of its corrosion resistance, nickel is used to maintain product purity in the processing of foods and synthetic fibers. Nickel is highly resistant to various reducing chemicals and is unexcelled in resistance to caustic alkalies. A major area for use of alloys 200 and 201 is in caustic evaporators because of their outstanding resistance to hot alkalies. Thermal conductivity of nickel is relatively high. In reducing environments, such as dilute sulfuric acid, nickel is more corrosion resistant than iron but not as resistant as copper or nickel–copper alloys. Annealed nickel has a low hardness and good ductility and malleability. These attributes, combined with good weldability, make the metal highly fabricable.

Nickel 200 (UNS No. 02200) is a commercially pure (99.6%) wrought nickel with good mechanical properties and resistance to a range of corrosive media. It is especially useful in handling caustic alkalies and has good thermal, electrical, and magnetostrictive properties. It is used for a variety of processing equipment, particularly to maintain product purity in handling foods, synthetic fibers, and alkalies.

Nickel 201 (UNS No. 02201) is the low-carbon version of alloy 200. The low carbon content prevents embrittlement by intergranular carbon at temperatures over 600°F (315°C). Lower carbon content also reduces hardness, making Nickel 201 particularly suitable for cold forming.

13.22.1.2 Nickel–Copper Alloys and Copper–Nickel Alloys

Nickel and copper are completely soluble in each other so that a series of alloys has been available. Nickel–copper alloys are known as Monel alloys. Monel alloy 400, Monel alloy R-405, Monel alloy 450, and Monel alloy K-500 offer somewhat higher strength than unalloyed nickel without loss of ductility. Monel alloys resist corrosion in a broader range of environments. Monels exceed nickel in resistance to sulfuric acid, hydrofluoric acid, brines, and water. The thermal conductivity of Monel alloys, although lower than that of nickel, is significantly higher than that of nickel alloys containing substantial amounts of chromium or iron. Monel alloys have essentially the same high level of formability and weldability as nickel.

Monel 400 (UNS 04400): Alloying of 30%–32% copper with nickel produces Monel alloy 400, which shares many of the characteristics of commercially pure nickel but improves on others. It has high strength and excellent corrosion resistance in seawater, hydrofluoric acid, sulfuric acid, and alkalis. Water handling, including brackish and seawaters, is the major area of application. It gives excellent service under high-velocity conditions, as in condenser and feedwater heater tubes. Addition of iron improves resistance to cavitation and erosion–corrosion. Monel 400, like some other high-nickel alloys, is susceptible to SCC in moist aerated hydrofluoric acid. Cracking may not take place if the metal is completely immersed in the acid. Monel 400 also exhibits SCC in high temperature, in concentrated caustic, and in mercury. It is used for marine engineering, chemical, and hydrocarbon processing equipment.

MONEL alloy R-405 (UNS 04405) is similar to MONEL alloy 400. Controlled sulfur is added for improved machining characteristics. Other characteristics are essentially the same as those of MONEL alloy 400.

MONEL alloy 450 (UNS C71500) is a copper–nickel alloy of the 70-30 type having superior weldability. It is resistant to corrosion and biofouling in seawater, has good fatigue strength, and has relatively high thermal conductivity. It is used for seawater condensers, condenser tubesheets, distiller tubes, evaporator and heat exchanger tubes, and saltwater piping.

13.22.1.2.1 90-10 and 70-30 Copper–Nickel Alloys

There are two main copper–nickel alloy grades used in marine service that are generally available in most product forms. These are copper-base alloys with either 10% or 30% nickel and are described as 90-10 and 70-30 copper–nickel, respectively. Both alloys contain small additions of iron and manganese that have been chosen to provide the best combination of resistance to flowing seawater and overall corrosion resistance. The 30% nickel alloy is stronger and can withstand higher seawater velocities, but for most applications, the 90-10 alloy provides good service at a lower cost.

MONEL alloy K-500 (UNS 05500) is a PH nickel–copper alloy that combines the corrosion resistance of MONEL alloy 400 with greater strength and hardness.

The nominal composition of commercial pure nickel and Monel (nickel–copper) is given in Table 13.42 and their products form in Table 13.43.

13.22.1.3 Inconel and Inco Alloy

Inconel includes nickel–chromium alloys and Inco nickel–chromium alloys. The combination of nickel and chromium in the alloys provides resistance to both reducing and oxidizing corrosive solutions. The nickel–chromium alloys resist oxidation, carburization, and other forms of high-temperature deterioration. The alloys do not become brittle at cryogenic temperatures, have good tensile and fatigue strengths at moderate temperatures, and display excellent creep-rupture properties at high temperatures.

In most of the Inconel and Inco alloys, the valuable basic characteristics of the nickel–chromium system are augmented by the addition of other elements. Some of the alloys are strengthened by aluminum, titanium, and niobium (columbium). Others contain cobalt, copper, molybdenum, or

TABLE 13.42**Nominal Composition of Major Alloying Elements of Pure Nickel and MONEL (Nickel–Copper Alloys)**

Alloy Name	UNS Designation	Ni	Cu	Fe (max)	Mn (max)	Others
Nickel 200	N02200	99.0 (min)	0.25	0.40	0.35	C0.08
Nickel 201	N02201	99.0 (min)	0.25	0.40	0.35	C0.02
Monel 400	N04400	66.0	30.0	1.5	2.0	C0.12
Monel R-405	N04405	66.0	31.0	1.2	2.0	C0.15
Monel 450	N044...	31.0	68.0	0.7	—	—
Monel K-500	N05500	66.5	30.0	1.0	0.8	Al 2.8 C0.1

TABLE 13.43**ASTM Spec. for Various Product Forms of Pure Nickel and Monel Alloys (Nickel–Copper Alloys)**

Alloy Name	UNS Designation	Sheet/Plate	Tube	Pipe	Forgings	Fittings	Bar
Nickel 200	N02200	B/SB 162	B/SB163	B/SB161, 725	B/SB160, 564	B/SB366	B166
Nickel 201	N02201	B/SB160, 162	B/SB163	B/SB161, 725	B/SB564	B/SB366	B164
Monel alloy 400	N04400	B127/SB127	B/SB163	B/SB165, 725	B/SB564	B/SB366	B/SB164

tungsten to enhance specific strength or corrosion resistance attributes. The alloys also contain iron in amounts ranging from about 1% to over 20%. In most cases, however, elements other than iron have dominant effects on properties.

Inconel alloy 600 (UNS 06600) is a nickel–chromium alloy with good oxidation resistance at high temperatures and resistance to chloride SCC, corrosion by high-purity water, and caustic corrosion. Alloy 600 is almost entirely resistant to attack by solutions of ammonia over the complete range of temperatures and concentrations. The absence of molybdenum in the alloy restricts its use in applications for which pitting corrosion is the primary concern. Alloy 600 is subject to SCC in high-temperature and high-concentration alkalies. Hence, the alloy should be stress relieved before use, and the operating stresses kept at a minimum.

Inconel alloy 601 (UNS 06601) is a nickel–chromium alloy with an addition of aluminum for high resistance to oxidation and other forms of high-temperature corrosion. It also has high mechanical properties at elevated temperatures. It resists oxidation up to 2300°F and has good resistance to sulfidizing atmospheres.

Inconel alloy 617 (UNS 06617), a nickel–chromium–cobalt–molybdenum alloy, exhibits an exceptional combination of metallurgical stability, strength, and oxidation resistance and carburization resistance at high temperatures. Resistance to oxidation is enhanced by aluminum addition. This alloy resists a wide range of corrosive aqueous environments.

Inconel alloy 625 (UNS 06625) is a nickel–chromium–molybdenum alloy with an addition of niobium that acts with the molybdenum to stiffen the alloy's matrix and thereby provides high strength without a strengthening heat treatment. Its high strength allows the use of more thin-walled vessels and tubing than that is possible with many other materials, thereby saving weight

and improving heat transfer. It exhibits strength and toughness from cryogenic temperatures to 1800°F (980°C). It exhibits good oxidation resistance, fatigue strength, and corrosion resistance. The alloy resists a wide range of severe corrosive environments and is especially resistant to pitting and crevice corrosion.

Inconel alloy 718 (UNS 07718) is a PH nickel–chromium alloy containing significant amounts of iron, niobium, and molybdenum along with lesser amounts of aluminum and titanium. It combines corrosion resistance and high strength with outstanding weldability including resistance to postweld cracking. The alloy has excellent strength from –423°F to 1300°F (–253°C to 705°C). Oxidation resistance is up to 1800°F (980°C).

Inconel alloy X-750 (UNS 07750) is a nickel–chromium alloy similar to Inconel alloy 600 but made PH by additions of aluminum and titanium. The alloy has good resistance to corrosion and oxidation along with high tensile and creep-rupture properties at temperatures to about 1300°F (700°C).

Inco alloy G-3 (UNS 06985) is a nickel–chromium–iron alloy with additions of molybdenum and copper. It has good weldability and resistance to intergranular corrosion in the welded condition. The low carbon content helps prevent sensitization and subsequent intergranular corrosion of the weld HAZs. It is used for flue gas scrubbers and for handling phosphoric and sulfuric acids.

Inco alloy C-276 (UNS 10276) is a nickel–molybdenum–chromium alloy with an addition of tungsten, having excellent corrosion resistance in a wide range of severe environments. The high molybdenum content makes this alloy especially resistant to pitting and crevice corrosion. The low carbon content minimizes carbide precipitation during welding to maintain corrosion resistance in as-welded conditions. It is used in pollution control, chemical processing, pulp and paper production, and waste treatment.

Inco alloy HX (UNS 06002) is a nickel–chromium–iron–molybdenum alloy with outstanding strength and oxidation resistance at temperatures to 2200°F (1200°C). Matrix stiffening provided by the molybdenum content results in high strength in a solid-solution alloy having good fabrication characteristics.

13.22.1.4 Nickel–Iron–Chromium Alloys and Inco Nickel–Iron–Chromium Alloys for High-Temperature Applications

The Incoloy alloys are based predominantly on the nickel–iron–chromium ternary system. Some alloys contain molybdenum and copper for enhanced corrosion resistance, and aluminum, titanium, or niobium for strengthening by heat treatment. The Incoloy alloys are characterized by good corrosion resistance in aqueous environments and by excellent strength and oxidation resistance to high-temperature atmospheres. At high temperatures, the substantial chromium content provides resistance to oxidizing environments, and the combination of nickel, iron, and chromium results in good creep-rupture strength. The high nickel content makes the alloys superior to SSs in resisting corrosion, especially chloride SCC.

Incoloy alloy 800 (UNS 08800) is a nickel–iron–chromium alloy known for its strength, and its excellent resistance to oxidation and carburization in high-temperature applications. The alloy maintains a stable, austenitic structure during prolonged exposure to high temperatures. It is particularly useful for high-temperature equipment in the petrochemical industry because the alloy does not form the embrittling sigma phase after long exposures at 1200°F–1600°F (649°C–871°C). It is used for process piping, heat exchangers, and nuclear steam generator tubing. High creep and rupture strengths are other factors that contribute to its performance in many applications.

Incoloy alloy 800HT (UNS 08811) is a nickel–iron–chromium alloy having the same basic composition as Incoloy alloy 800 but with significantly higher creep-rupture strength in the

TABLE 13.44
Nominal Composition (%) of Major Alloying Elements of Inconel
and Inco Alloys

Alloy Name	UNS Designation	Ni	Cr	Fe	Mo	Others
Inconel alloy 600	N06600	76	15.5	8.0		Ni. 58 (min) , Mn 1 (max)
Inconel alloy 601	N06601	60.5	23.0	14.0		Al 1.4
Inconel alloy 625	N06625	61.0	21.5	2.5	9.0	Nb + Ti 3.6 Nb 3.6
Incoloy alloy 800	N08810	32.5	21.5	45.0		C0.1(max), Al + Ti 0.75
Incoloy alloy 800H	N08810	32.5	21.0	45.0		C 0.07, Al + Ti 0.75
Incoloy alloy 800HT	N08811	32.5	21.0	45.0		C 0.08, Al + Ti 1.0
Incoloy alloy 825	N08825	42.0	21.5	30.0	3.0	Cu 2.2, Ti 1.0
Inco alloy 904L	N08904	25.5	21.0	45.0	4.7	Cu 1.5, Co 0.2
Inco alloy C-276	N10276	57.0	16.0	6.0	16.0	W4.0

1100°F–1800°F (595°C–980°C) range. The higher strength results from close control of the carbon, aluminum, and titanium contents in conjunction with a high-temperature anneal. It is used in chemical and petrochemical processing and in power plants for superheater and reheater tubing.

Incoloy alloy 825 (UNS 08825) is a nickel–iron–chromium alloy with additions of molybdenum and copper and stabilized with titanium. It has excellent resistance to both reducing and oxidizing acids and seawater. It exhibits good resistance to SCC and intergranular corrosion. The alloy is especially resistant to sulfuric, nitric, and phosphoric acids. It is used in evaporators, heat-treating, and chemical-handling equipment and propeller shafts, and for chemical processing, pollution control equipment, nuclear fuel reprocessing, acid production, and pickling equipments. Nominal compositions of major elements of Inco alloys for high-temperature applications are given in Table 13.44. Alloy description, product forms, and ASTM/ASME Code references for Inconel (Nickel—Alloy) and Incoloy Alloy are given in Table 13.45. The ASTM specifications for nickel-base tubular products are given in Table 13.46.

13.22.1.5 Magnetic Properties and Differentiation of Nickels

Nickel, like steel, is strongly magnetic at room temperature. When the Curie temperature (i.e., the temperature at which the metal loses its magnetic properties) is known, a simple magnetic test can be used to differentiate the nickel alloys. For nickel, the Curie temperature is about 680°F (360°C); nickel–copper alloy is slightly magnetic at room temperature and has a Curie temperature of 110°F–140°F (43°C–61.7°C); nickel–chromium alloy is nonmagnetic at room temperature and has a Curie temperature of –40°F (–40°C).

13.22.2 NICKEL AND NICKEL-BASE ALLOYS: CORROSION RESISTANCE

Nickel and nickel-base alloys exhibit resistance to general corrosion in aqueous solution, localized attack, SCC, and erosion–corrosion.

13.22.2.1 Galvanic Corrosion

The element nickel (passive) is nobler than iron and copper in the electrochemical series.

TABLE 13.45**Inconel (Nickel—Alloy) and Incoloy Alloy Product Forms and Specifications**

Alloy Name	UNS Designation	Plate, Sheet, and Strip	Tube	Pipe	Forgings	Fittings	Rod/Bar
Inconel alloy 600	N06600	B/SB168	B/SB163	B/SB167, B/SB829, B/SB775, B/SB163, B516, B/SB751	B/SB564, 516, 517	B/SB366	B/SB166
Inconel alloy 601	N06601	B/SB168	B/SB163	B/SB167	—	B/SB366	B/SB166
Inconel alloy 625	N06625	B/SB443	B 163	B444, B704, B705, B751, B775, B829	B564	B/SB366	B446
Incoloy alloy 800	N08800	A/SA240,	B/SB163	B/SB514,	B/SB564	B/SB366	B/SB408
Incoloy alloy 800H	N08810	480, B/		515,			
Incoloy alloy 800HT	N08811	SB409, 906		407,751, 775,829			
Incoloy alloy 825	N08825	B/SB424, B/SB906	B/SB163	B/SB423, B/SB704, B/SB705, B/SB751, B/SB775, B/SB829	B/SB425, B/SB 564	B/SB366	B/SB 425, B/SB564
Inco alloy 904L	N08904	B/SB625	B/SB163	B/SB673, 674, 677	B/SB649	B/SB366	
Inco alloy C-276	N10276	B/SB575	B/SB163	B/SB619, 622	B/SB564, 574	B366	

13.22.2.2 Pitting Resistance*

The pitting and crevice corrosion resistance of a nickel-based corrosion resistant alloy (e.g. Incoloy 825, Inconel G-3, 622, 625, 686, and C-276) is primarily a function of the steel composition, with chromium, molybdenum tungsten and niobium playing the major roles. The PRE_N is an index used to rank the resistance of individual steels to pitting and crevice corrosion. The PRE_N for selected nickel–chromium–molybdenum alloy is given in Table 13.47. Nickel base alloys provide outstanding resistance to specific chemicals. Nickel alloys are among the few materials able to withstand hot hydrofluoric acid, a chemical that is very corrosive to the reactive metals (titanium, zirconium, niobium, tantalum).

13.22.2.3 Intergranular Corrosion

Nickel–chromium alloys with carbon content above 0.2% exposed to temperatures between 1100°F and 1500°F (593°C–816°C) will be sensitized, resulting in chromium carbide precipitation in

* Source: Rebak, R.B. and Crook, P., Nickel alloys for corrosive environments, *Adv. Mater. Process.*, Haynes International Inc., Kokomo, IN, February 2000.

TABLE 13.46
ASTM Specification for Nickel Alloy Tubular Products

ASTM Spec.	Description	UNS No.
B751	General requirements for nickel and nickel alloy seamless and welded tubes	—
B163	Specification for seamless nickel and nickel alloy condenser and heat exchanger tubes	N02200, N02201, N04400, N06600, N06690, N08800, N08810, N08825
B468	Welded chromium–nickel–iron–molybdenum–copper, columbium-stabilized alloy tubes	N08028, N08024, N08026
B515	Welded nickel–iron–chromium alloy tubes for general corrosion resisting and low- or high-temperature service	N08800, N08810
B516	Welded nickel–iron–chromium alloy tubes for general corrosive service and heat-resisting applications	N06600
B626	Welded nickel and nickel cobalt alloy tube	N10001, N10665, N10276, N06455, N06007, N06975, N08320, N06985, N06002, N06022, N06030, N06059, N08031, N30556, N06230
B720	Seamless cold-worked tubes of nickel alloy for use in condenser and heat exchanger service	N08310

TABLE 13.47
Pitting Resistance Number for Selected
Nickel–Chromium–Molybdenum Alloy

Alloy	UNS Designation	Composition Required to Calculate PRE _N				PRE _N ^a
		Cr	Mo	W	Nb	
Inconel alloy 625	N06625	21.5	9.0	—	3.6	40.4
Incoloy alloy 825	N08825	21.5	3.0	—	—	26.0
Inco alloy 904L	N08904	21.0	4.7	—	—	28.0
Inco alloy C-276	N10276	16.0	16.0	4.0	—	46.0

^a PRE_N = %Cr + 1.5 (%Mo + %W + %Nb).

grain boundaries. This leaves areas adjacent to the boundaries low in chromium and susceptible to intergranular corrosion. Such corrosion can be counteracted in three ways [209]:

1. Select low-carbon alloy and consumables.
2. Select titanium- and columbium-alloyed base metal and welding consumables.
3. Solution anneal the weldment at 2000°F–2200°F (1093°C–1204°C) to dissolve precipitated carbides.

13.22.2.4 Stress Corrosion Cracking

There is a possibility that welded joints in nickel-rich alloys will suffer SCC if in contact with strong caustic soda, fluorosilicates, and certain mercury salts [79]. Nevertheless, nickel alloys have very good resistance to SCC in alkalies and solutions containing chloride ions, definitely much better than the austenitic SSs. Important information on SCC of nickel and nickel-base alloys includes [177] the following: (1) low-carbon nickel (0.02% C max) is recommended for use in contact with caustics if

the service temperature is above 850°F (455°C), (2) nickel–iron alloys and nickel–chromium–iron alloys containing up to 40% nickel can fail by SCC on exposure to hot chloride solutions, (3) sensitized Ni–Cr–Fe alloys containing higher amounts of nickel may be subjected to polythionic acid SCC at ambient temperature, (4) aqueous solutions of mercury salts are found to produce cracking in highly stressed Ni–Cu alloys, (5) high-nickel alloys are susceptible to SCC in aerated hydrofluoric acid vapors and in hydrofluorosilicic acid, and (6) in addition to normal measures, complete annealing of nickel welds and annealing Monel 400 at 1100°F–1200°F (595°C–650°C) are recommended as a means of eliminating residual stresses that could cause SCC. In hydrofluoric acid service, stressed alloy 400 should not be exposed to aerated acid vapors.

13.22.3 NICKEL AND NICKEL-BASE ALLOYS: WELDING

The solid-solution-strengthened (non-age-hardenable) wrought nickel and its alloys can be arc welded under conditions similar to those used in the arc welding of austenitic SSs.

The PH alloys like Monel K-500, Inconel 700, Alloy 718, and Inconel X-750 require special welding procedures because of their susceptibility to cracking. Residual welding stress and stress induced by precipitation cause cracking in the base metal or HAZ on aging or in service, at temperatures above the aging temperature. If PH alloys undergo any operation that introduces high-residual stresses, welding should be done after annealing.

13.22.3.1 Considerations while Welding Nickel

While welding nickel and nickel-base alloys, greater care such as precleaning and cleanliness is required to prevent contamination-induced cracking or porosity, or embrittlement due to sulfur and lead [209,210]. As nickel content increases, the weld puddle viscosity increases; the coefficient of expansion decreases, as does weld penetration [209]. Additional considerations should include effect of minor elements on weldability, susceptibility to cracking in the weld bead caused by high heat input or excessive welding speeds, and SCC of certain welded structures in service. These welding considerations are discussed next.

13.22.3.1.1 *Effects of Minor Elements on Weldability*

Calcium and cerium are used as deoxidizers. Small additions of aluminum and titanium also serve as deoxidizers. These elements tend to contribute to the formation of oxide films and slag spots on the weld surface. In multipass welding, such tenacious slag films should be removed between passes to avoid weld defects.

13.22.3.1.2 *Precleaning and Surface Preparation*

Cleanliness is the single most important requirement for successful joining of nickel alloys [210]. Welding, brazing, soldering, and any postheating must be performed only on base metal that is clean and completely free of surface contaminations. Surface contaminations due to manufacturing processes, like grease, oil, paint or lacquers, cutting fluids, machine lubricants, marking crayons and inks, and shop dirt, must be removed completely either by chemical or by vapor degreasing. Vapor degreasing or swabbing with perchloroethylene or other suitable solvents can remove oil- or grease-base shop dirt. Paint and other materials not soluble in degreasing solvents may be removed by methylene chloride, or alkaline cleaners. Alkaline cleaners that contain sodium sesquisilicate or sodium carbonate must be removed prior to welding. Wire brushing will not remove the residue completely. The best method is spraying or scrubbing with hot water.

13.22.3.1.3 *Surface Oxide Removal*

Nickel oxide melts at a higher temperature than the base metal. Therefore, oxides should be thoroughly removed from the surfaces to be welded because they can inhibit wetting and result in lack of fusion. Oxides are normally removed by grinding with an aluminum oxide or silicon carbide

wheel or a carbide burr, machining, abrasive blasting, or pickling. Any cleaning tools, including wire brushes and carbide burrs, should be clean and free from metals that may be transferred to the base metal. Wire brushes used for cleaning should be made of austenitic SS. However, they will not remove tenacious surface oxides from welds. It merely polishes the oxide.

13.22.3.1.4 Weld Metal Porosity

Surface contaminations, poor welding techniques, improper shielding, and the presence of hydrogen, carbon dioxide, nitrogen, and oxygen gases often cause porosity in nickel weldments. To overcome this problem, electrodes/filler metals containing deoxidizers are a necessity. The deoxidizers combine chemically in the molten weld with inorganic compounds, which then float on the surface.

13.22.3.1.5 Joint Designs

Molten nickel-alloy weld metals do not flow and wet the base metal as readily as do carbon-steel and stainless-steel weld metals. The operator must place the metal at the proper location in the joint. Therefore, the joint must be sufficiently open to permit proper manipulation of the electrode and deposition of the weld beads. Suggested joint designs for butt joints in nickel alloys are shown in Figure 13.23.

13.22.3.1.6 Preheat and Interpass Temperatures

Guidelines on preheat and interpass temperatures are as follows:

1. In general, preheat is not required for welding nickel-base alloys. However, the area to be welded should not be below about 60°F (16°C) to avoid moisture condensate that could produce weld metal porosity.
2. The interpass temperature may be limited to 200°F (93°C). Cooling mediums used to reduce interpass temperature should not introduce contaminants that will cause weld discontinuities. Examples are traces of oil in compressed air and mineral deposits from the water spray.

13.22.3.1.7 Heat Input

High heat input during welding may result in constitutional liquation, carbide precipitation, or other metallurgical phenomena. Some degree of annealing and grain growth can take place in the HAZ. These, in turn, may cause cracking or loss of corrosion resistance, or both.

13.22.3.1.8 Hot Cracking

Weldments of nickel-base alloys are susceptible to liquation cracking or hot cracking. This takes place particularly when welding conditions of high restraint are present, as in circumferential welds that are self-restraining. Therefore, all weld bead surfaces should be slightly convex. Convex beads are virtually immune to centerline cracking; flat and concave beads are particularly susceptible to

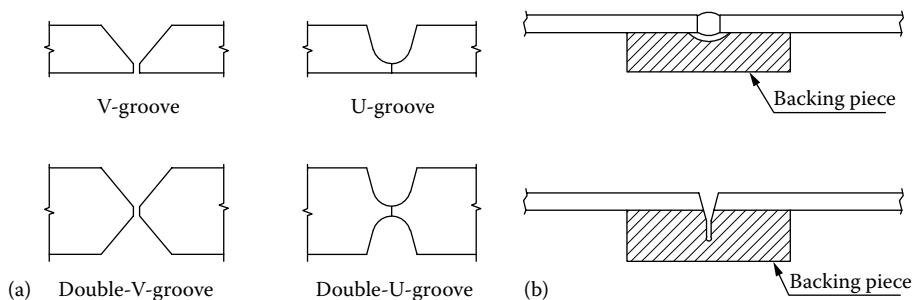


FIGURE 13.23 Nickel welding: (a) joint design and (b) groove in backup bar.

centerline cracking. Excessive width-to-depth or depth-to-width ratio can also result in cracking. Measures to overcome hot cracking include the following: (1) limit heat input during welding, (2) obtain fairly small grain sizes in the microstructures, and (3) minimize the amount of deleterious minor elements such as sulfur and phosphorus that are known to cause hot cracking.

13.22.3.1.9 Sulfur Embrittlement

Nickel combines with sulfur at elevated temperature to form a brittle sulfide. This phenomenon takes place preferentially at the grain boundaries and is exhibited when the material is stressed or bent. Nickel is the most affected, nickel–copper less, and nickel–chromium–iron the least. Prior to carrying out any operation involving high-temperature operations such as welding, brazing, hot forming, PWHT, etc., the surfaces should be cleaned thoroughly and should be free from sulfur-bearing substances. For more details, refer to ASME Code Section VIII, Div. 1, NF-14.

13.22.3.1.10 Lead Embrittlement

Lead causes embrittlement in all nickel-base alloys in much the same manner as sulfur. Therefore, lead-containing fluids or lubricants should be removed from the surfaces.

13.22.3.1.11 Design for Penetration

Nickel alloys give lower weld penetration than ferrous materials. Increasing amperage beyond the recommended range will not significantly increase the penetration of the arc, but it will cause harm. The harmful effects due to over-amperages are [210] the following: (1) overheating of the electrode and the resulting flux flaking off as heat breaks down the binder and (2) puddling of the molten weld metal and resultant loss of deoxidizers, leading to porous welds.

13.22.3.1.12 Welding Fixtures

Proper fixturing and clamping is required to hold the workpieces firmly in place, minimize buckling, maintain alignment, and, when needed, provide compressive stress in the weld metal. A backing bar or any portion of a fixture that might be contacted by the arc should be made of copper. Since copper has high thermal conductivity, an inadvertent arc touch on the copper will not result in fusion of the bar to the weldment. A groove in the backup or chill bar allows weld metal penetration and avoids entrapment of gas or flux at the weld root [210].

13.22.3.1.13 Good Bead Shape

Increased puddle viscosity can cause poor wetting and lack of fusion along bead edges. With low penetration in materials of high nickel content, the angle between the base metal and the weld bead edge should be greater than 100° to facilitate good tie-ins with subsequent beads [209]. Nickel alloy beads should be slightly convex. Avoid flat and concave beads. Susceptibility to centerline cracking during solidification increases as flat or concave beads become stressed in root passes [210].

13.22.3.1.14 Carbide Precipitation

Like some austenitic SSs, nickel–chromium and nickel–iron–chromium alloys with carbon content above 0.2% exposed to temperatures between 1100°F and 1500°F (593°C–816°C) will be sensitized due to carbide precipitation in the weld HAZ. Such sensitization does not result in accelerated attack in most environment. In general, carbide precipitation is overcome by the following measures [209]:

1. Use low-carbon-base alloy and consumables.
2. Select titanium- or columbium-stabilized alloy base metal and consumable.
3. Solution anneal the weldment at 2000°F–2200°F (1093°C–1204°C) to dissolve carbide precipitate.

13.22.3.1.15 *Pitting Corrosion of Weldments*

To resist pitting and crevice corrosion, weldments must have smooth surfaces and be chemically homogeneous on a microscopic level. Molybdenum imparts pitting resistance to nickel–chromium alloys. Use filler metal with sufficient molybdenum; even in the event of iron dilution, enough molybdenum will impart greater resistance to weld metal than that of base metal.

For this reason, many base metals with 4% or 6% Mo have been welded with filler metal such as Inconel 112 (60% Ni) electrode and Inconel 625 filler metal, both containing 9% Mo [209].

13.22.3.1.16 *Strain Age Cracking*

Most of the PH alloys are susceptible to strain age cracking. Alloys containing columbium have a better resistance to cracking because of the slower hardening response of the columbium precipitate than the aluminum or titanium precipitate.

13.22.3.2 **Welding Methods**

Typical arc welding processes employed for welding nickel and nickel-base alloys are GTAW, GMAW, and SMAW. SAW and PAW have limited applicability. The GTAW process is preferred for welding the PH alloys, although GMAW and SMAW can also be used. Reference [211] details the welding of nickel and nickel-base alloys.

13.22.3.2.1 *Gas Tungsten Arc Welding*

GTAW is widely used for joining thin sections of nickel alloys, for the root pass of pipe welds, and where flux residues are harmful. This process is the principal welding method for PH alloys. Argon, helium, or a mixture of the two are the recommended shielding gases. Since presence of oxygen, carbon dioxide, or nitrogen cause porosity in the weld metal, they should be avoided. GTAW usually requires shielding of the weld root. If a complete penetration weld is made in the open, the weld metal exposed on the underside of the bead will be oxidized. Various shielding methods employed to protect the rootside include, grooved backup bars, inert gas backup shielding, and a backing flux.

13.22.3.2.2 *Shielded Metal Arc Welding*

SMAW is primarily used for welding commercially pure nickel and solution-strengthened nickel alloys 1/16 in. (1.6 mm) thick and over. The PH alloys are seldom welded with SMAW process, because the alloying elements that contribute to PH are difficult to transfer across the arc.

13.22.3.2.3 *Gas Metal Arc Welding*

GMAW is used to weld the solution-strengthened nickel alloys except high-silicon casting alloys. Many PH alloys may also be welded. Spray, pulsed spray, globular, or short-circuiting filler metal transfer may be used. The protective shielding gas is usually argon or argon mixed with helium. Use DCRP for all methods of metal transfer with GMAW.

13.22.3.2.4 *Submerged Arc Welding*

SAW can be used for joining solid-solution-strengthened nickel alloys. Monel 400 is mostly welded by this process. It is especially useful for welding thick sections. SAW uses DC with SP or RP. SAW process cannot be used for welding the PH alloys.

13.22.3.2.5 *Oxyacetylene Welding*

The oxyacetylene flame is the only gas flame that burns hot enough, 5000°F–6300°F (2760°C–3482°C), to join nickel alloys. OAW gives good results in all welding positions. It is a cheap process. To weld nickel-base alloys, use a slightly reducing flame. A strongly reducing flame is not recommended when welding nickel alloys containing chromium, to avoid carbon pickup in

the weld. Oxidizing flame is not recommended to weld (1) nickel–copper alloys, because the oxidizing flame forms cuprous oxide, which dissolves in the molten metal, which causes weld brittleness and reduces corrosion resistance, and (2) high-chromium alloys, because an oxidizing flame produces chromium oxide that is not readily soluble in the flux [211].

13.22.3.3 Postweld Heat Treatment

Nickel and nickel-base alloys generally do not experience any metallurgical changes, either in the weld metal or in the HAZ, which affect normal corrosion resistance. Hence, no PWHT is normally required. However, heat treatment may be necessary in circumstances such as (1) to meet specification requirements or (2) for stress relief of a welded structure to avoid age hardening or SCC of the weldment used to contain hydrofluoric acid vapor or caustic soda. If welding induces moderate-to-high residual stresses, the PH alloys require a stress-relief anneal after welding and before aging.

13.22.4 HASTELLOY®

The Hastelloy family of corrosion-resistant alloys include B-3®, C-4, C-22®, C-276, C-2000®, C-22HS®, G-30®, G-35®, G-50®, etc. Standard forms are bar, billet, plate, sheet, strip, coils, seamless or welded pipe & tubing, pipe fittings, flanges, fittings, welding wire, and coated electrodes. For general guidelines for welding, brazing, hot and cold forming, heat treating, pickling and finishing, refer to Hastelloy—corrosion-resistant alloy, Haynes Corrosion-Resistant Alloys International, Global Headquarters, Indiana, USA.

13.23 TITANIUM: PROPERTIES AND METALLURGY

Titanium is a reactive, nontoxic, and low-density metal (density, $\rho = 4.4$ g/cc, whereas the density of steel is 7.8 g/cc). Titanium and its alloys are used in major applications for which their inherent properties justify their selection: (1) for corrosion resistance and (2) where specific strength is of major advantage. Titanium “bridges the design gap” between aluminum and steel and offers a combination of many of the most desirable properties of each. Its lightweight with specific gravity lying between aluminum and steel (approx. 60% of steel) gives a high strength-to-weight ratio. For example, the strength-to-weight ratio for annealed Ti–6Al–4V (Grade 5) is about 7.81 (density is 0.160 lb/in.³ and yield strength is 125 ksi), whereas it is about 1.25 for annealed SSs. Increases in strength, as with other materials, are achieved by the addition of alloying elements such as Al, Cu, Mo, Si, V, and Zr. It is known for its excellent corrosion resistance due to a stable, tenacious oxide film formed on its surface. Corrosion failures with titanium are rare and usually associated with weld defects. All titanium alloys contain minute amount of interstitial elements such as carbon, oxygen, nitrogen, and hydrogen.

13.23.1 PROPERTIES THAT FAVOR HEAT EXCHANGER APPLICATIONS

The combination of high strength, stiffness, good toughness at cryogenic temperature, immunity to corrosion in wet chlorine, excellent corrosion resistance to many chemicals, and erosion resistance allows widespread use of titanium and titanium alloys from cryogenic -253°C (-423°F) to moderately high temperature 600°C (1000°F). Titanium is used as heat exchanger material in chemical industries, refinery, absorption refrigeration and air conditioning, refinery heat exchangers, brine heat exchangers, desalination plants, power-plant surface condensers, and auxiliary exchangers. Titanium finds its widest use in chemical process industries as process equipment, wet scrubbers, heat exchangers, valves, pumps, and piping systems. Almost all nuclear stations the world over have standardized on the use of titanium as tube material. It is available in various product forms including sheets, plates, clad plates, pipes, tubes, including U-bend, and enhanced tubes (integral fin tube, applied fin tube, and corrugated and rope tube).

The arguments against titanium are its high price, high-quality standards, sensitivity to fouling, corrosion fatigue, and possibility of hydrogen embrittlement if cathodic protection in excess is applied [109]. For fixed-baffle spacing, titanium tube heat exchangers are susceptible to flow-induced vibration due to its low modulus of elasticity and the use of thin-walled sections for cost considerations. However, this can be overcome by reducing the baffle spacing.

13.23.2 ALLOY SPECIFICATION

Titanium specification and grades include Grade 1, Grade 2, Grade 3, Grade 4, Grade 5, Grade 6, Grade 7, Grade 9, Grade 11, and Grade 12. Grades 1, 2, 3, and 4 apply to commercially pure titanium (98.5%–99.5%) and differ in the amounts of interstitials like oxygen, nitrogen, carbon, and iron. By varying these interstitial elements, the unalloyed titanium grades can be strengthened. The higher the grade, the greater is the amount of oxygen and the greater is the metal's strength. Grades 5, 7, 11, and 12 are titanium alloys. Various ASTM grades, alloy designations, compositions, and metallurgical phases present are given in Table 13.48; characteristics and application areas are given in Table 13.49. An important source book on titanium is the *Titanium Handbook* [212]; also see Schutz and Thomas [213].

13.23.3 TITANIUM GRADES AND ALLOYS

13.23.3.1 Unalloyed Grades

Pure titanium has low tensile strength and is extremely ductile. Dissolved oxygen and nitrogen markedly strengthen the metal, and carbon and iron to a lesser extent. Grade 1 is purer and therefore more ductile and finds use where severe forming is required; unalloyed titanium mill products of Grade 2, most widely used and more ductile, find use where severe forming is required; this grade has outstanding resistance to general and other forms of corrosion in many environments, but it is not resistant to crevice corrosion [105]. Grade 3 provides slightly higher strength due to its higher percentage of interstitial elements [215].

TABLE 13.48
Titanium Grades, Composition,
and Structure

Grade	UNS No.	Description	Phase
Grade 1	R 50250	Unalloyed titanium	A
Grade 2	R 50400	Unalloyed titanium	A
Grade 3	R 50550	Unalloyed titanium	A
Grade 4	R 50700	Unalloyed titanium	A
Grade 5	R 56400	Ti–6Al–4V	α – β
Grade 5	R 56401	Ti–6Al–4V ELI ^a	α – β
Grade 6	R 54520	Ti–5Al–2.5Sn	A
Grade 6	R 54521	Ti–5Al–2.5Sn ELI ^a	A
Grade 7	R 52400	Ti–0.20 Pd	A
Grade 9	R 56320	Ti–3Al–2.5V	Near α
Grade 11	R 52250	Ti–0.20 Pd	A
Grade 12	R 53400	Ti–0.3Mo–0.8Ni	Near α

^a Extra-low interstitials grade. R 52550 and R 52700 are titanium alloy castings.

TABLE 13.49**General Characteristics of Titanium Alloys and Applications**

Alloy	General Characteristics	Applications
Grade 1 (R 50250)	Highest purity, relatively low strength and high ductility; good corrosion resistance among the four ASTM unalloyed grades due to low interstitials	Used in continuous service up to 425°C (800°F). Used for PHEs
Grade 2 (R 50400)	The pure titanium; work horse material, i.e., most used. Exhibits the best combination of strength, ductility, weldability, and corrosion resistance. Minimum yield strength of 275 MPa, which is comparable to those of annealed austenitic stainless steels	Used in continuous service up to 425°C (800°F) Piping, pressure vessels, and heat exchangers
Grade 3 (R 50550)	Unalloyed titanium, high-strength and medium oxygen	Main use in shell and tube heat exchanger
Grade 4 (R 50700)	Highest strength of the pure unalloyed grades. High oxygen. Moderate formability, outstanding corrosion, and fatigue resistance in saltwater	Piping, pressure vessels, and heat exchangers
Grades 7 and 11 (R 52400 and R 52250)	Unalloyed titanium plus 0.12% to 0.25% Pd. Medium strength, normal oxygen content. Good corrosion resistance in reducing and oxidizing environments. (Note: Grade 11 is with low oxygen, low strength.)	Piping, pressure vessels, and heat exchangers and PHEs
Grade 12 (R 53400)	Stronger and more resistant to crevice corrosion at higher temperatures than unalloyed Titanium grades. Less expensive than Grades 7 and 11	Pressure vessels and heat exchangers

13.23.3.2 Alloy Grades

1. Titanium is not as widely used in the alloyed form in chemical process industries, the exception being titanium–0.2% palladium alloy (Grade 7) to enhance corrosion resistance in mildly reducing solutions and high-temperature chloride solutions. Typical applications extend to hydrochloric, phosphoric, and sulfuric acid solutions and areas of service where the operating conditions vary between oxidizing and mildly reducing conditions [214,216]. The presence of palladium has no other significant effect on the physical or mechanical properties of titanium and it makes titanium costlier.
2. To overcome the cost disadvantage of Grade 7, a new alloy designated Grade 12 with 0.8% Ni and 0.3% Mo has been developed for increased corrosion resistance in specific media [217].
3. Lower alloy Grade 9 (3% Al and 2.5% V) is used for pressure vessel applications.
4. For cryogenic applications, the basic titanium alloy Ti–6Al–4V or Ti–5Al–2.5Sn–ELI (extra-low interstitial) is used.

13.23.3.3 ASTM and ASME Specifications for Mill Product Forms

ASTM and ASME specifications that govern unalloyed titanium and alloyed titanium in various mill product forms such as strip, sheet and plate, seamless and welded pipe, seamless and welded tube for condensers and heat exchangers, bars and billets, and forgings in various grades are given in Table 13.50. For these alloys, the design temperatures should be less than approximately 806°F (430°C) to avoid excessive oxidation and oxygen embrittlement in continuous service.

Industry uses titanium in sheet and plate form in addition to tubes and plate used in heat exchangers. Construction can be solid titanium, titanium-clad steel, or with titanium linings. Solid titanium construction is generally more cost-effective than clad construction when vessel wall thickness is below approximately 1–1.5 in. (25.4–38.1 mm). Commonly used tubesheet materials and their properties are given in the table.

TABLE 13.50**Titanium Product Shapes, Grades, and ASTM/ASME Specifications**

Product Description	Grades*	ASTM/ASME
Strip, sheet, and plate	Grades 1, 2, 3, 4, 5, 7, 9, 11, 12	B265/SB265
Seamless and welded pipe	Grades 1, 2, 3, 4, 7, 9, 11, 12	B861/SB861
Seamless and welded tube for condensers and heat exchangers	Grades 1, 2, 3, 4, 6, 7, 9, 11, 12	B338/SB338
Bars and billets	Grades 1, 2, 3, 4, 5, 6, 7, 11, 12	B348/SB348
Forgings	Grades 1, 2, 3, 4, 5, 6, 7, 11, 12	B381/SB381

* Partially given. For full details refer to the relevant standard.

13.23.4 TITANIUM CORROSION RESISTANCE

13.23.4.1 Surface Oxide Film

Titanium exhibits excellent corrosion resistance to general corrosion, pitting, erosion–corrosion, and galvanic corrosion. The superior corrosion resistance of titanium alloys is derived from the formation of a highly stable, tenacious, protective oxide film on its surface. This film, typically 50–200 Å thick, is primarily titanium dioxide (TiO_2) in rutile (highly crystalline) and/or anatase (somewhat amorphous) form [218]. Even if the oxide film is damaged, being a reactive metal and with a high affinity for oxygen, the protective oxide films form spontaneously and instantaneously whenever fresh metal surfaces are exposed to traces of oxygen or moisture [213]. Film growth is also accelerated under strongly oxidizing conditions such as in HNO_3 and CrO_3 media [219]. Another desirable feature is that at low temperatures, this surface oxide film provides a barrier for penetration of hydrogen into titanium surfaces. Conversely, titanium is severely corroded in a reducing environment wherein it is not readily repassivated. Once the breakdown of the passive film occurs, the corrosion process is unhindered. Loss of oxide film could occur due to abrasion, chemical reduction of the oxide, or surface contamination, notably by iron oxide [220].

13.23.4.2 General Corrosion

The oxide film on titanium is attacked only by a few media, including hot concentrated reducing acids, most notably hydrofluoric acid. Anhydrous conditions in the absence of oxygen should be avoided since the protective film may not be regenerated if damaged. General methods to improve corrosion resistance of titanium in a reducing environment are suggested by Schutz and Thomas [213]. Such measures include the following:

Alloying with metals such as palladium, nickel, and/or molybdenum.

Addition of inhibitor to the environment, such as oxidizing metal cations, oxidizing anions, precious metal ions, oxidizing organic compounds: adding oxidizing species (inhibitors) to the reducing environment is to permit oxide film stabilization; additions of minute amounts of water to certain anhydrous environments is to maintain passivity.

Precious metal surface treatments: This includes precious metals such as platinum and palladium that have been ion implanted, ion plated, or diffused thermally.

Anodizing and thermal oxidation: As stated earlier, titanium relies on the presence of an inert surface oxide film for its corrosion resistance, especially where hydrogen uptake is of concern. Therefore, surface treatment processes such as anodizing and thermal oxide treatment are practiced to thicken and toughen the oxide film, which in turn will improve the metal's corrosion resistance.

Anodic protection by impressed current or galvanic coupling with a more noble metal in order to maintain the surface oxide film: Anodic protection has proven to be quite effective in suppressing corrosion of titanium in many acid solutions.

Surface pickling in HNO_3 -HF solution to remove smeared surface iron.

Metallic coatings.

Noble alloy contact or by the applications of their oxides such as Ni, Cu, Fe, and Mo on titanium alloy surfaces, which is effective for crevice corrosion.

13.23.4.3 Resistance to Chemicals and Solutions

Titanium resists corrosion in seawater, brines, aqueous chlorides, organic and oxidizing acids, and neutral and inhibited reducing conditions better than other metals. Titanium is unique in its resistance to chlorides. Titanium, being immune to corrosion in wet chlorine, would face little maintenance problems. Since the heat transfer rates of titanium are so much better than glass, the titanium coolers require only about 12%–15% the space to do the same job as glass exchangers for chlorine applications. High corrosion resistance to oxidizing and chloride solution led to widespread use in marine, chemical process industries, power plants, and petrochemical industries.

Titanium alloys are attacked severally by red fuming nitric acid or nitrogen tetroxide. Titanium and its alloys are sensitive to reducing acids, and the breakdown of the surface oxide films can take place when the temperature and/or concentration of pure acid exceed certain values. Typical reducing acids include hydrochloric, hydrobromic, hydroiodic, hydrofluoric, phosphoric, sulfuric, and sulfamic acids. In some acids that do attack titanium, the addition of small amounts of an oxidizing acid such as nitric or salts (such as copper sulfate) inhibits attack.

13.23.4.4 Resistance to Waters

Titanium exhibits good corrosion resistance to freshwater, industrial cooling waters including raw seawater, brackish estuary water, and polluted water. Titanium (like many other metals) is subject to the formation of mineral scales when water temperatures are excessive [220]. It resists all forms of corrosive attack by freshwater and steam to temperatures as high as 600°F (316°C) and corrosion by seawater to temperatures as high as 500°F (260°C) [219]. The presence of sulfides in seawater does not affect the corrosion resistance.

13.23.4.5 Forms of Corrosion

13.23.4.5.1 Galvanic Corrosion

From its position in the galvanic series, titanium is highly immune to galvanic corrosion but tends to accelerate the corrosion of the other metal of the galvanic couple. The exception is in highly reducing acid environments where titanium may not passivate. Under these conditions, it has a potential similar to aluminum and will undergo accelerated corrosion when coupled to other more noble metals [219]. While using titanium tubes, extreme care should be taken to avoid galvanic corrosion of tubesheets and water boxes of a condenser, which have different corrosion potential. Solid titanium or titanium-clad tubesheets are preferred in order to eliminate galvanic corrosion of a tubesheet of an anodic material, such as a copper alloy or carbon steel. Water boxes should be coated for protection. If a titanium-clad tubesheet is used (a minimum of 3/16 in. or 4.5 mm thick cladding is required), the tube-to-tubesheet joints should be welded, but if a solid tubesheet is used, roller expansion can be performed.

13.23.4.5.2 Hydrogen Embrittlement

In a galvanic couple, if titanium is the cathodic member, hydrogen may be evolved on its surface. Normally, the surface oxide film on titanium acts as an effective barrier to penetration by hydrogen. By specification, hydrogen is limited to 150 ppm maximum in all the common tube metal grades [220]. Within the range of pH 3–12, the oxide film is stable and presents a good barrier

to penetration by hydrogen [219]. Under certain conditions, titanium can absorb hydrogen and become embrittled:

1. Dry, nonoxidizing hydrocarbon, or hydrogen stream—the oxide films break down since there is no mechanism for replacing oxygen lost to the process stream.
2. Disruption of the oxide film allows easy penetration by hydrogen.
3. If the temperature is above 176°F (80°C), hydrogen may diffuse into the metal and cause hydrogen embrittlement.

Even the risk of failure due to hydrogen embrittlement can be greatly reduced if care is taken to maintain the potential of the tubes/tubesheets in the range -0.5 to -0.07 V on the saturated calomel electrode (SCE) scale [193]. TIMET's recommendation for the limiting temperature for titanium usage in hydrogen environments is 71°C (160°F) [219]. This temperature is based on the barrier effect or near-zero diffusion rate of hydrogen at that temperature [220].

13.23.4.5.3 Crevice Corrosion

Titanium alloy as well as commercially pure titanium will be subjected to localized attack in tight crevices exposed to hot ($>158^{\circ}\text{F}/70^{\circ}\text{C}$) aqueous solutions, or chloride, bromide, iodide, or fluoride solutions. Crevice corrosion of unalloyed titanium may occur in seawater at temperatures above the boiling point. One major exception is the alloys containing 0.2% palladium [221]. Titanium alloy Grade 12 and Ti–Pd (Grades 7 and 11) offer resistance to crevice corrosion in seawater at temperatures up to 500°F (260°C) [219]. Both alloys also provide improved resistance to reducing acid conditions, and Grade 12 offers increased strength particularly as the temperature is increased. Where corrosion of titanium is a problem under deposits, molybdenum-bearing titanium grade-Grade 12, R53400 (Ti–0.3Mo–0.8Ni), should be used.

13.23.4.5.4 Erosion–Corrosion

An important property of titanium is its excellent resistance to erosion–corrosion and its various forms such as cavitation and impingement attack. Titanium is considered one of the best cavitation-resistant materials available for seawater service. Titanium has the ability to resist erosion due to high-velocity seawater up to 30 m/s [218].

13.23.4.5.5 Stress Corrosion Cracking

SCC of commercial titanium and titanium alloys may occur in red fuming nitric acid at room temperatures. The possibilities of SCC in natural seawater can be reduced by alloy selection and heat treatment. The presence of defects combined with an unfavorable stress condition can account for almost instantaneous failure of welded structures in contact with trichloroethylene [79].

13.23.4.5.6 Corrosion Fatigue

Titanium, unlike many other materials, does not suffer a significant loss of fatigue properties in seawater. In fatigue-limited applications, ASME Code Criteria or actual in situ fatigue should be considered.

13.23.4.5.7 MIC

Titanium is highly resistant to MIC. More than 30 years of extensive titanium alloy use in biologically active process and raw cooling waters, especially seawater, appears to substantiate titanium's resistance to MIC [218].

13.23.4.6 Thermal Performance

With its low fouling resistance values in combination with thinner tube walls, the overall heat transfer coefficient has been more than adequate in all installations. Titanium's resistance to erosion–corrosion permits high flow velocity up to 38 m/s (120 ft/s) if pressure drop

considerations permit. High velocity means higher heat transfer rates and lower fouling factors. Experience has shown that titanium exchangers handling seawater can be designed with a fouling factor as low as $0.0005 \text{ h} \cdot \text{ft}^2 \cdot ^\circ\text{F}/\text{BTU}$ [219].

13.23.4.7 Fouling

As titanium is perfectly passivated, its surface has no biostatic action and would be fouled biologically. Fouling, mussels, and barnacles are a problem in a power station installed on the seashore. Therefore, tubes must be kept clean by an online tube cleaning system such as a sponge rubber ball system, or by a correct system cooling water velocity, or by chlorination treatment.

13.23.4.8 Applications

13.23.4.8.1 Titanium Tubing for Surface Condensers

Titanium tubing in steam condensers has proven to be the most reliable of all tubing materials. It is immune to corrosion from chlorides. It returns no harmful metal ions to the environment or to the condensate feedwater stream. Titanium overcomes the problems of random tube failure caused by erosion–corrosion at tube inlets due to turbulence or partial blockage by shells, mussels, debris, and ammonia condensate and is highly resistant to erosion attack by steam impingement. In addition to fresh tubing, titanium tubings are used for retubing the leaky tubes. When retubing an existing condenser that has been designed for use with tubes other than titanium, there are six areas to consider [219]. They are as follows: (1) Titanium tube heat exchangers require shorter baffle spacings to accommodate thinner tubes and low Young’s modulus to overcome FIV problems; (2) tubesheet material for a possible galvanic couple with titanium as cathodic material (titanium can essentially be welded only to titanium, so that the tubesheets must also be made of titanium or be overlaid with titanium if a welded joint is desired); (3) effect of reduced weight due to the use of thin-walled tubes and low density; (4) effect of reduced water velocity since the inner diameter has increased due to thin-walled tubes; (5) fouling; and (6) if there is already a cathodic protection system in operation, make it compatible with titanium; such measures/cautions include that hydriding can take place at potentials greater than -0.75 V (SCE) —do not exceed -0.90 V (SCE) —that the system must have an automatic potential control and that sacrificial anodes should not be placed closer than 30 in. from the tubesheet.

13.23.4.8.2 Refinery and Chemical Processing: Service Experience

The primary reason for titanium’s expanded application in the refinery industries, particularly in the condenser service, is due to its superior resistance to handle refinery process streams containing hydrogen sulfide, chlorides, dilute hydrochloric acid, ammonia, and hydrogen [220,222]. Titanium Grade 2 tubes are used in overhead coolers and condensers. Figure 13.24 shows titanium Grade 2 brine cooler heat exchanger. Titanium for refinery services is limited to operating temperature of 260°C . If hydrogen is present, temperature should not exceed 175°C (350°F) to prevent hydrogen embrittlement.



FIGURE 13.24 Titanium Grade 2 brine cooler heat exchanger. (Courtesy of Titan Metal Fabricators Inc., Camarillo, CA.)

13.23.4.8.3 *Chemical Processing*

The primary basis for titanium's expanded application in the chemical processing industries has been its superior resistance to the aggressive, mildly reducing, oxidizing, and/or chloride-containing process streams.

13.23.4.8.4 *PHE*

Due to its inherent corrosion resistance, titanium is used as a PHE material in corrosive applications.

13.23.5 TITANIUM FABRICATION

13.23.5.1 **Welding Titanium**

Unalloyed titanium and all alpha-titanium alloys are weldable. Alpha-beta alloys, alloy Ti-6Al-4V, and weakly beta-stabilized alloys are also weldable. Beta-phase alloys and strongly stabilized alpha-beta-phase alloys are difficult to weld and they will embrittle.

13.23.5.1.1 *Welding Methods*

Commercially pure titanium and weldable alloys can be arc welded successfully by the manual gas tungsten arc, plasma arc, and gas metal arc processes. If economically justified by thickness, run length, or repetitive work, automatic hot wire TIG with special trailing shields is used. Procedures and equipment are generally similar to those used for welding austenitic SS or aluminum, with two important exceptions [215]: (1) Titanium requires greater cleanliness—wear cotton gloves when heating the parts, store parts in a clean dry area; and (2) it requires auxiliary gas shielding. In general, fluxes are not used due to the high-temperature reactivity of titanium.

13.23.5.1.2 *Weldability Considerations*

When heated in air, titanium oxidizes rapidly, and at temperatures near its melting point 1800°C (3272°F), (1) molten titanium reacts with most materials, which embrittles the weldment and reduces the corrosion resistance; and (2) it dissolves its own oxide, leaving inclusions in welds. In its solid state, titanium above 1200°F absorbs oxygen, nitrogen, and hydrogen from the atmosphere. Even small amounts of these elements can cause embrittlement in the weld and loss of corrosion resistance [223]. Hydrogen in concentrations exceeding 150 ppm can embrittle the pure metal and also the various commercial alloys available [224]. Consequently, to assure a successful titanium weld, air must be excluded from both the face and the back of the weld metal, and a secondary inert-gas shield must protect the weld area until it cools to 600°F–800°F (315°C–425°C).

13.23.5.1.2.1 *Shielding Gases* In arc welding, this is accomplished by replacing the air surrounding the weld area by argon or helium with argon. No other gases can be used.

When titanium parts are heated to more than 500°F (260°C), contact with adhesive tapes, papers, marking crayons, etc., containing more than 50 ppm chlorine or other halogen compounds should be avoided [225].

13.23.5.1.2.2 *Welding of Titanium to Dissimilar Metals* Satisfactory fusion-welding of titanium to dissimilar metals, except with vanadium and silver, is not possible because of the formation of brittle intermetallic compounds. Therefore, interconnections between dissimilar metals are made by mechanical means such as by bolting. Lining vessels with titanium cannot be accomplished directly by fusion-welding. In some instances, silver filler metal is used for seal welds [217].

13.23.5.1.2.3 *Manufacturing Facilities* While it is not always possible to fabricate large titanium assemblies in a closed clean room as demanded for a clean environment, designating areas of the heavy workshop area to be screened off, paying great attention to preventing weld contamination with shop dirt/dust by screening, and stringent solvent cleaning of weld preparations and filler wire before welding are necessary to achieve the proper weld metal characteristics and corrosion resistance.

13.23.5.1.3 *Edge Preparation*

Prepare joints by sawing, machining, or grinding. Joint surfaces should be smooth and free of crevices, roughness, and overlaps that can trap dirt and cleaning solution. If burrs should occur, remove them with a clean, sharp hand file or rotary file. Dirty shearing equipment is likely to contaminate sheared or slit edges and ultimately cause weld metal porosity.

13.23.5.1.4 *Joint Design*

Joint designs for titanium welding are essentially the same as those found in the inert-gas arc welding of other metals. The joint design should allow for full shielding of both sides or permit the exclusion of air from parts of the joint reaching temperatures of 1000°F (538°C) or greater [226]. For example, argon purge holes are provided in vessel shell nozzle reinforcing plates and tubular stiffeners. Special configurations are necessary on titanium-clad tubesheet joints to give adequate back shielding.

13.23.5.1.5 *Precleaning and Surface Preparation*

A good titanium weld begins with cleanliness, both in the immediate weld area and in the shop floor. Do not store parts unless they are wrapped and sealed from the atmosphere. Foreign matters that contaminate the weld lead to porosity and low mechanical properties. Consequently, surface residues such as scale, oxide, grease, dust, grinding wheel grit, etc., must be removed before welding. The surface oxide and scale resulting from normal hot-forming operations can be removed mechanically or chemically.

13.23.5.1.5.1 *Cleaning Titanium* Titanium can be cleaned by steam cleaning, alkaline cleaning, vapor degreasing, and solvent cleaning methods. Cleaning solutions for titanium must maintain passivity and avoid possible hydrogen uptake by the titanium. Titanium cleaning is discussed by Chevalier [225], and ASTM Specification B600 details procedure for descaling and cleaning titanium and its alloys.

13.23.5.1.5.2 *Degreasing* Titanium parts that are free of scale or oxide require only degreasing. Light or medium contamination is degreased by immersion in hot alkaline solutions or by spraying. Heavy contamination is degreased by cleaning in alkaline solution in two stages, preferably after degreasing. Use nonchlorinated degreasing solvents, reagent methanol, acetone, or MEK to degrease or remove machining oil. Avoid using chlorinated solvents such as trichloroethylene vapor, alcohols, and methanol in particular [226]. Deposits remaining from solvents of this type may cause cracking in high-strength alloys if the metal is subsequently heated in stress relief or actual service.

13.23.5.1.5.3 *Descaling or Oxide Removal* Light oxides may be removed by brushing with an SS wire brush, sand blasting, or draw filing. Steel wool or abrasives should never be used because of the danger of contamination. If grinding is required, the use of silicon carbide is preferred. Heavy oxide scales may be removed by grinding, machining, liquid abrasive blasting, salt-bath descaling, or alkaline cleaning. To remove oxide scale formed at temperatures below 1150°F, a pickling solution is used that consists of 25%–30% nitric acid and 2%–3% hydrofluoric acid by weight mixed with water. To remove oxide scale formed at temperatures above 1150°F, sandblasting or solutions of sodium hydride, Virgo, Kolene, or similar salt baths followed by acid pickling are required [226]. Proper inhibition is most critical when reducing acids, such as HCl, H₂SO₄, sulfamic, or oxalic acids, are used to remove scaling. Since rapid titanium attack may occur, hydrofluoric acid cleaning solutions are not to be used for scale removal.

13.23.5.1.5.4 *Rinsing* Water rinsing after degreasing or acid pickling must be carried out with deionized water having a resistivity of more than 50,000 ohm/cc when intending to do an operation such as heat treatment, welding, etc., above 500°F (260°C) [225].

13.23.5.1.5.5 Handling of Cleaned Components Handling of cleaned components before being welded must be with clean gloves to avoid fingerprints; during waiting periods, the parts must be stored in a packed condition and protected from external contamination.

13.23.5.1.6 Fitup

Uniform fitup avoids burn-through, controls underbead contour, and simplifies backup shielding or purging.

13.23.5.1.7 Preheating

Titanium welding does not normally require preheating [215]. For very low ambient temperature and low humidity conditions, preheating to 100°F–150°F (37°C–65°C) helps moisture removal.

13.23.5.1.8 Filler Metal

Thirteen titanium and titanium alloy filler metal (or electrode) classifications are given in AWS A5.16-90. A partial list is shown in Table 13.51. Maximums are set on carbon, oxygen, hydrogen, and nitrogen contents. Filler metal composition is usually matched to the grade of titanium being welded. ERTi-2 and ERTi-0.2Pd are good overall choices. ERTi-2 can be used on Grades 1, 2, and 3 base metal [215]. Recommended filler wire grades and the base-metal grades are given in Table 13.52.

TABLE 13.51
AWS A5.16 Classifications of Titanium
Filler Metal

AWS Classifications	Composition
ERTi-1	Ti–0.50O
ERTi-2	Ti–0.05O
ERTi-3	Ti–0.13O
ERTi-4	Ti–0.20O
ERTi-5	Ti–6Al–4V
ERTi-5ELI	Ti–6Al–4V
ERTi-6	Ti–5Al–2.5Sn
ERTi-6ELI	Ti–5Al–2.5Sn
ERTi-7	Ti–0.05O–0.2Pd
ERTi-9	Ti–3Al–2.5V
ERTi-9ELI	Ti–3Al–2.5V
ERTi-12	Ti–0.3Mo–0.8Ni

TABLE 13.52
Recommended Titanium Filler Metals

Filler Grade	Base Metal Grade
ERTi-1	1
ERTi-2	2
ERTi-3	3
ERTi-4	4
ERTi-6	6
ERTi-7	7
ERTi-9	9
ERTi-11	11
ERTi-5ELI	23

13.23.5.1.9 Welding Procedures

13.23.5.1.9.1 Gas Tungsten Arc Welding Due to the inert-gas shielding characteristics and the high degree of arc control, GTAW is ideally suited for titanium. Use a drooping-characteristic power supply and DCSP. Titanium can be successfully welded with GTAW in thickness ranging from several thousands of an inch to more than several inches. Use the same techniques as for welding of SS. To avoid contamination, weld joint and wire must be clean, and the shielding gas, usually argon, must be free from moisture and impurities. A facility to ignite the arc is required that prevents contamination of the titanium with tungsten inclusions from the electrode. AWS D10.6, *Gas Tungsten Arc Welding of Titanium Piping and Tubing*, covers various aspects of GTAW of titanium.

13.23.5.1.9.2 Shielding Inert-gas shielding (either by argon or by helium) of the weld area is accomplished by the following methods:

1. A vacuum chamber or special inert-gas-filled chamber, which eliminates the need for elaborate jigs and other fixtures that normally would be required to adequately shield complex assemblies in air; it is generally considered that the highest weld quality is obtained by employing vacuum or argon purged chamber welding.
2. A backup gas shielding with trailing shield by welding in open air.
3. Argon is generally used in preference to helium for primary shielding at the torch because better arc stability is achieved. Argon–helium mixture can be used if higher voltage, hotter arc, and greater penetration are desired.
4. Though Argon is costlier compared to helium, the former is preferred for use in trailing shields and backup devices, because it is denser.

A section of AWS D10.6 on gas shielding offers several alternatives for shielding, including work-mounted trailing shields and torch-mounted trailing shields.

13.23.5.1.9.3 Welding Titanium in an Open-Air Environment with Three Shielding Gases Techniques Although historically titanium has been welded in chambers that are either vacuum or argon purged, increased usage of open-atmosphere welding is taking place in the chemical industries and marine sectors with proper shielding techniques. The shielding for welding titanium in an open atmosphere can be accomplished by using a combination of three shielding gases techniques. They are as follows [227]:

1. The primary shielding is provided by the welding torch.
2. The primary shielding is supplemented by a trailing shield, which is known as the secondary shielding; the trailing shield permits cooling of the weld deposit and the adjacent HAZ under a blanket of argon gas.
3. The back shielding protects the backside of the weld and its adjacent HAZ.

Typical gas shielding for tube-to-tubesheet welding is shown in Figure 13.25.

13.23.5.1.9.4 Narrow-Groove Welding of Titanium Using the Hot Wire Gas Tungsten Arc Process Though narrow-groove welding has been dominated by the submerged arc and the GMAW processes, the use of narrow-groove joint designs with the automatic GTAW process is promising for welding of titanium. The automatic hot wire GTAW process with narrow-groove joint designs combines the advantages of automatic hot wire GTAW (high deposition rates, excellent shielding characteristics) with narrow-groove welding (high groove fill rate, reduced weld distortion) [227]. As is true with all of the narrow-groove welding processes, a problem that must be addressed is inadequate control of face fusion.

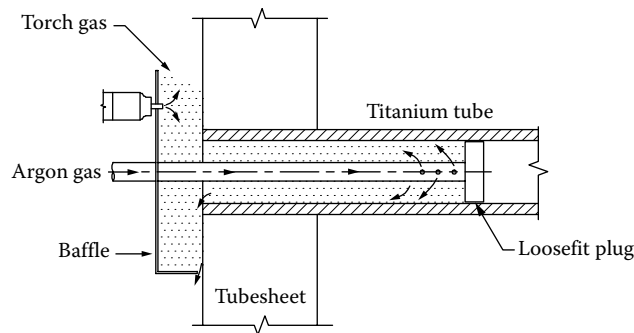


FIGURE 13.25 Gas shielding for titanium tube-to-tubesheet welding.

13.23.5.1.9.5 MIG Welding The MIG process employs a direct current supply and reverse polarity. The power supply generally consists of a constant-potential rectifier, although a power supply with a drooping load characteristic is also applicable.

13.23.5.2 In-Process Quality Control and Weld Tests

13.23.5.2.1 Method to Evaluate the Gas Shielding

Since titanium readily reacts with air at elevated temperatures to form oxides that exhibit specific colors, the oxide color of the weld surface can be used as an effective method to evaluate the inert-gas shielding. Welds made with proper shielding will exhibit a bright, metallic, shiny silvery weld color; the change in color represents increasing amounts of weld contamination, which usually takes place due to faulty or inadequate trailing shielding [227]. Table 13.53 differentiates the acceptance criteria and required disposition for each oxide color category.

13.23.5.2.2 Hardness

A clean weld should not be more than 30 points BHN higher than the base metal. A greater increase indicates contamination [215].

13.23.5.2.3 Bend Test

Make a simple test by butt welding two narrow strips of titanium together and bending the piece over a mandrel with a radius of about three to four times the thickness of the sheet held in a vice. Welds with satisfactory ductility will bend over the following radii without cracking [215]:

Grades 1, 2, 7, and 12	4T
Grade 3	5T

TABLE 13.53
Weld Colors and Their Meanings (Visual Color Acceptance Criteria)

Color of Weld Zone	Interpretation
Silver	Correct shielding. Satisfactory weld
Light straw to dark straw	Slight contamination (Action: Remove surface oxide by brushing and ensure correct shielding)
Dark blue	Heavier contamination, may be acceptable depending on service
Light blue, green	Heavier contamination, unlikely to be acceptable
Gray, white	Very heavy contamination, unacceptable (Action: Remove by grinding, repair, then weld again)

13.23.5.2.4 *Weld Defects*

1. Titanium and its alloys are not prone to solidification cracking. However, under conditions of severe restraint, solidification cracking has been observed sometimes [229].
2. Weld metal porosity is probably the most frequently encountered weld defect in titanium weld metals [228]. Porosity is generally caused by hydrogen, which may originate from gas entrapment, filler metal, or base metal. Careful shielding of the weld metal and cleaning of the surfaces will help to reduce the weld metal porosity. Welding at low speeds gives extra time for gas escape, and quality of cut edges also affects the incidence of porosity.
3. Contamination cracking will occur when substantial pickup of interstitial elements occurs. This problem can be solved by careful cleaning of the surfaces and the weld joint area, and proper shielding.

13.23.5.3 **Heat Treatment**

13.23.5.3.1 *Annealing*

Titanium and its alloys are annealed to improve ductility, dimensional or thermal stability, fracture toughness, and creep resistance. Since improvement in one or more properties is usually obtained at the expense of some other property, the material producer should be consulted for heat-treatment considerations.

13.23.5.3.2 *Stress Relief*

Welding generally increases strength and reduces ductility. PWHT can be helpful to improve mechanical properties and to reduce residual welding stress, and the stabilization of the microstructure for elevated-temperature applications [228]. Ordinarily, low-strength alloys require no stress relief. It is often required in high-strength alloys, especially when constructing elaborate titanium welds. Alpha alloys, which include the commercially pure grades of titanium, can be stress relieved at 1000°F (540°C), 1 h/in. of thickness, in 1/2 to 4 h. Alpha-beta alloys welded in the annealed condition but not subsequently heat-treated can be stress relieved in the same manner [225,226].

13.23.5.4 **Forming of Titanium-Clad Steel Plate**

Titanium reacts with iron at elevated temperatures to form a brittle compound. This alloying may take place when the clad material is subjected to high temperatures while rolling, hot forming, stress relieving, welding, and the like. If the bond deteriorates to a great enough degree, the titanium layer may actually fall off the backing plate.

13.24 **ZIRCONIUM**

13.24.1 **PROPERTIES AND METALLURGY**

Zirconium is a nontoxic, reactive metal. It is very similar in characteristics to titanium except that its density (6.45 g/cm³ or 0.235 lb/in.³) is about 50% higher. The mechanical properties of zirconium are intermediate to those of aluminum and mild steel. It is inert to many chemicals, and it has very low corrosion rates in many corrosive environments. The metal has good ductility and strength and hence can be fabricated in most forms common to other metals. It can be welded comparatively easily and can be used as a structural material in corrosive applications. References [230–234] provide either specific or general information on zirconium.

13.24.1.1 **Alloy Classification**

Zirconium and its alloys are available in two general categories: (1) commercial-grade zirconium, containing hafnium as an impurity—this includes R60702 (unalloyed zirconium), R60703, R60704 (zirconium–tin alloy), R60705 (zirconium–niobium alloy), and R60706; and (2) alloys of zirconium

essentially free of hafnium, for nuclear application, commonly called Zircalloys. These include R60001, R60802 (Zircaloy-2), R60804 (Zircaloy-4), and R60901 (Zr-2.5Nb). The purpose of alloying in zirconium is to improve elevated-temperature strength and corrosion resistance while maintaining low neutron absorption.

13.24.1.1.1 Product Forms

Zirconium and its alloys are available in plate, sheet, bar, rod, and tubing to a variety of material specifications. ASTM B550 covers four commercial grades of zirconium ingots: R60702, R60704, R60705, and R60706. ASTM B523 covers three grades of zirconium and zirconium alloy (R60702, R60704, R60705) seamless and welded tubes for condensers and heat exchangers.

13.24.1.1.2 Applications

Zirconium finds its applications in the nuclear industry and chemical process industries. The properties that favor its use as a structural material in nuclear reactors include its remarkably low thermal neutron absorption cross section, a high melting point, fair strength, and good corrosion resistance in water and liquid metals [231]. Because of its inertness, it is an excellent material for equipment used in food processing and pharmaceutical preparations. In chemical industries, it is used in process equipment, heat exchangers, piping, reactor vessels, etc. Figure 13.26 shows zirconium pull through tube bundle. Zirconium-cladded components are used in heat exchangers exposed to seawater.

13.24.1.2 Limitations of Zirconium

The design of zirconium alloys for elevated-temperature applications is hindered by two factors: (1) the transformation of zirconium from the hexagonal close-packed (hcp) structure to a bcc structure at approximately 1585°F (863°C), and (2) the problem of low corrosion resistance in contact with high-temperature steam.

13.24.2 CORROSION RESISTANCE

Zirconium is a reactive metal. It has a high affinity for oxygen. Its surface is covered with a protective oxide film, which is self-healing in nature. This surface film protects the base metal from corrosion attack. Whenever any fresh zirconium surface is exposed to an oxygen-bearing environment, an adherent protective oxide film forms on its surface instantaneously.

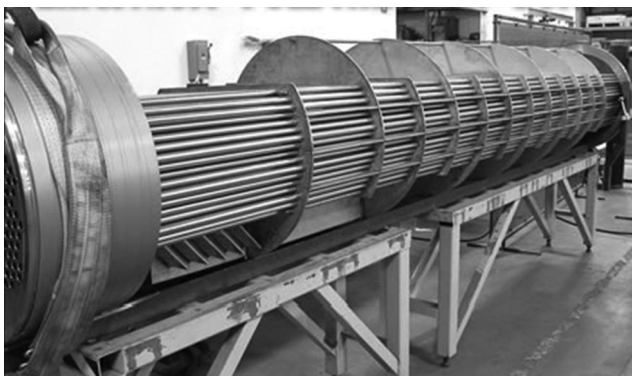


FIGURE 13.26 Zirconium pull through tube bundle. (Courtesy of Titan Metal Fabricators Inc., Camarillo, CA.)

13.24.2.1 Resistance to Chemicals

Zirconium resists corrosion in almost all alkalis, either fused or in solution. Its resistance to alkalis is better than that of tantalum, titanium, and 18:8 SS [232]. It has an excellent resistance to HCl, boiling H_2SO_4 up to 70%, boiling HNO_3 up to 90%, most organics, and all alkaline solutions to boiling temperature, but is attacked by HF. Zirconium is corroded severely in wet chlorine, brine, dilute hydrochloric acid, and seawater that contains chlorine. Zirconium, while resistant to most chloride solutions, is not resistant to ferric and cupric chlorides above 1% [235]. Among the organic acids, trichloroacetic acid appears to be the only one corrosive to zirconium. In sulfuric acid at concentrations from 0% to 70% at boiling temperatures and above, corrosion resistance of zirconium compares favorably with that of tantalum, glass, and graphite. Consequently, zirconium has replaced these materials in many applications as the cost of tantalum is higher and glass and graphite are subject to failure from thermal and/or mechanical shock [233].

13.24.2.2 Forms of Corrosion

Galvanic corrosion: Zirconium is treated as a noble metal. Therefore, galvanic corrosion of a less noble metal is possible when it is in contact with zirconium.

Pitting: Zirconium has a susceptibility to pitting in all halide solutions except fluoride.

Crevice corrosion: Of all the corrosion-resistant metals, zirconium and tantalum are the most resistant to crevice corrosion. In low-pH chloride solutions or chlorine gas, zirconium is not subjected to crevice attack.

Stress corrosion cracking: Zirconium service failures resulting from SCC are few in chemical applications. The environments known to cause SCC include FeCl_3 , and CuCl_2 solutions, concentrated HNO_3 , mixtures of methanol and HCl, and liquid mercury. Apart from the standard practices known for control of SCC, the following additional methods can prevent SCC in zirconium alloys:

1. Maintaining a high-quality surface film; the film should be low in impurities, free from defects, and mechanical damage.
2. Using electrochemical protection techniques.

13.24.2.2.1 Methods to Improve Corrosion Resistance

The corrosion resistance of zirconium is further improved by corrosion protection methods like oxide film formation, anodizing, autoclave film formation, film formation in air, and electrochemical protection.

13.24.3 FABRICATION

Zirconium and its alloys are ductile and workable. In fabrication of zirconium, there are some general considerations that must be taken into account [231]: (1) the purity or composition of the zirconium being fabricated, and (2) its tendency to gale under sliding contact with other metals—hence, while machining zirconium, tools must be kept sharp and avoid light and interrupted cuttings. Zirconium is extremely stable in contact with most common gases at room temperature, but at temperatures of a few hundred degree centigrade, it reacts readily with oxygen, nitrogen, and hydrogen, resulting in embrittlement. Therefore, welding and brazing zirconium requires high-purity inert-gas shielding of weld puddle and hot bead from air.

13.24.3.1 Welding Method

Zirconium and zirconium alloys are most commonly welded using the GTAW process. Other arc welding processes are not used because most zirconium alloys are used in applications that require very high weld metal purity and integrity. Electron beam welding can be used for

welding thick sections. As the most promising commercial property of zirconium is its high resistance to corrosion, it is essential that the welding should not reduce corrosion resistance [234]. Zirconium has a low coefficient of thermal expansion, which contributes to a low distortion during welding.

13.24.3.2 Weld Metal Shielding

At high temperatures, zirconium is extremely reactive. Therefore, the weld metal and the surrounding area must be carefully shielded from air to avoid reaction of weld metal with atmospheric gases and the resulting embrittlement. Shielding by a standard tungsten arc torch is insufficient to provide adequate protection. Critical nuclear welds are made in controlled atmosphere boxes or chambers. For industrial applications, trailing shield torches and gas backup should be adequate along with a temporary purge chamber or box. The shielding gas should be highly pure argon, helium, or a mixture of these two gases. Moisture, oxygen, hydrogen, nitrogen, or carbon dioxide in the shielding gas will be absorbed by the molten metal and will result in weld embrittlement.

13.24.3.3 Weld Preparation

The edges to be joined should be draw filed or wire brushed with an SS brush immediately before welding. This should be followed by a thorough cleaning with alcohol or acetone to ensure a clean area for welding; avoid chlorinated solvents.

13.24.3.4 Surface Cleaning

ASTM Specification B614, Standard Practice for Descaling and Cleaning Zirconium and Zirconium Alloy Surfaces, covers the cleaning and descaling procedure of zirconium and zirconium alloys for the removal of shop dirt, oxides, and scales resulting from heat-treatment operations and surface contaminants, by employing one of these methods or a combination of them: (1) alkaline or emulsion soak-type cleaners, (2) ultrasonic cleaning, (3) acetone or trichloroethylene solvent washing or vapor degreasing, and (4) electrolytic alkaline cleaning system.

13.24.3.5 Filler Metals

Zirconium and zirconium alloy electrodes are covered under AWS A5.24-79.

13.24.3.6 Weld Inspection

As for titanium, a clean, bright weld is obtained through the use of a proper shielding system. White deposits or a black color in the weld area is not acceptable. A bend test is probably the best test to determine weld acceptability.

13.24.3.7 Welding of Dissimilar Metals

Zirconium cannot be welded directly to most other structural metals; the exceptions are titanium, vanadium, and niobium. Hence, it is necessary to line/butter the compatible metals with a zirconium coat.

13.25 TANTALUM

Tantalum is a high-density (16.6 g/cm^3), inherently soft, fabricable metal. It has a high melting point 5432°F (3000°C). It is categorized as a refractory metal. Tantalum and its alloys (Ta-2.5W and Ta-10W) resist the broadest range of environments, making it a preferred corrosion-resistant material. The outstanding corrosion resistance of tantalum in aqueous media is attributed to the spontaneous formation of a thin, amorphous, passive oxide film on the surface of the metal. The passive film forms in almost all environments, even in ones of extremely low oxidizing tendency, except for fluorides including HF, strong caustic, and oleum [235]. Tantalum often competes with zirconium,

niobium, and titanium, whose corrosion resistance also depends upon an amorphous oxide film. It is inert to practically all organic and inorganic compounds at temperatures under 302°F (150°C). The only exceptions to this are hydrofluoric acid and fuming sulfuric acid. Equipment made of tantalum includes heat exchangers, condensers, spiral coils, U-tubes, side-arm reboilers, and distillation columns. Figure 13.27 shows a tantalum pharmaceutical heat exchanger. References [235–242] provide either specific or general information on tantalum.

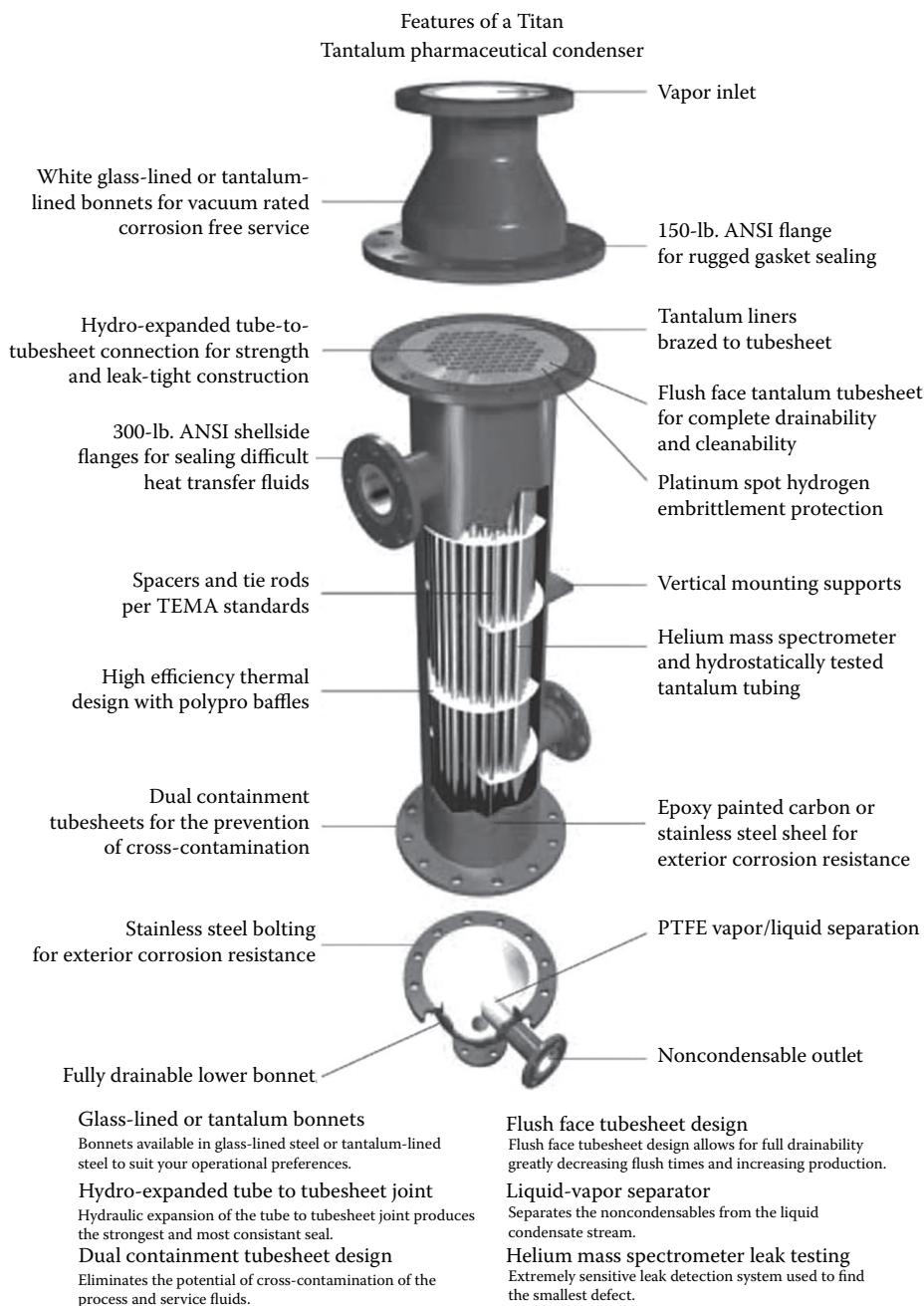


FIGURE 13.27 Tantalum pharmaceutical heat exchanger. (Courtesy of Titan Metal Fabricators Inc., Camarillo, CA.)

13.25.1 CORROSION RESISTANCE

Tantalum exhibits excellent resistance to most forms of corrosion. Its general corrosion rate is extremely low. The passive oxide film virtually prevents pitting, crevice and intergranular corrosion, and SCC. Tantalum is cathodic in a galvanic cell with all construction metals and liberates hydrogen. Hydrogen is rapidly absorbed by tantalum with resulting embrittlement. Hydrogen embrittlement is the single most important cause of failure of tantalum [235]. Therefore, it is of utmost importance to avoid applications in which there may be a cathodic reaction [242]. Hydrogen embrittlement of tantalum is discussed next in detail.

13.25.1.1 Hydrogen Embrittlement

Even though tantalum does not react with molecular hydrogen below 662°F (350°C), it can absorb atomic hydrogen under persistently aggressive conditions, causing embrittlement and failure even when the corrosion rate is low. To protect equipment from exposure to atomic hydrogen, tantalum should be electrically insulated from all other metals. General practice to prevent hydrogen embrittlement is to attach a small amount of platinum (1:1000) to tantalum by spot welding, electroplating, or rubbing with platinum wool. Platinum is effective because it is cathodic to tantalum [238].

13.25.1.2 Resistance to Chemicals

Tantalum has excellent corrosion resistance to a wide variety of acids, alcohols, chlorides, sulfates, and other chemicals. Tantalum should be used for equipment handling hot concentrated hydrochloric, sulfuric, or phosphoric acid. The metal oxidizes in air above about 570°F (299°C), and it is attacked by hydrofluoric, phosphoric, and sulfuric acids, and by chlorine and fluorine gases above 300°F.

13.25.2 PRODUCT FORMS AND COST

Tantalum and its alloys are available in all common product forms, including foil, strip, sheet, plate, wire, rod, bar, ingot tubes and welded tubes, and clad plates.

The initial material cost is higher than that for glass, graphite, fluorocarbons, or other metals. However, when lifetime cost is considered, tantalum is economical, primarily due to its longer life, maintenance-free performance, and considerably reduced downtime. Primarily due to its high initial cost, tantalum is used most often only where other materials fail or will not perform at all or where very high product purity is to be maintained, as in the processing of pharmaceuticals and the preparation of cosmetics, soaps, perfumes, etc. [235].

13.25.3 PERFORMANCE VERSUS OTHER MATERIALS

Tantalum is often compared to glass in regard to corrosion resistance. Of all the metals, tantalum is considered most like glass in corrosion resistance, and due to this property, it is used in glass and glass-lined equipment [242]. However, unlike glass, tantalum has good resistance to brittle fracture and failure due to vibration and shock. Its strength and rigidity are similar to that of steel, while its machinability and formability are similar to copper.

13.25.4 HEAT TRANSFER

Tantalum and its alloys are ideal for heat exchangers because of their high thermal conductivity (thermal conductivity of tantalum is higher than Zr, titanium, 304/316 SS, alloys 600 and 625, and Hastelloys C-276 and B-2), their ability to be used in thin-walled tubes, and nonfouling characteristics. The wall thickness of tantalum tubes, typically 0.015–0.20 in. (0.381–5.08 mm), had become an engineering standard. This compares with 0.035 in. (0.889 mm) for titanium and zirconium,

since allowances have to be made for corrosion [235]. The heat transfer rate of tantalum does not change with time, due to the absence of corrosion and deposits.

13.25.5 WELDING

Similar to titanium and zirconium, tantalum readily reacts with carbon, hydrogen, oxygen, and nitrogen at temperatures above 600°F (315°C). When dissolved interstitially in tantalum, these elements increase the strength properties, but reduce the ductility. Therefore, any fusion-welding must be performed in air-free atmosphere. This is achieved either by vacuum or by inert-gas shielding.

13.26 GRAPHITE, GLASS, TEFLON, AND CERAMICS

To solve the corrosion problem, users are turning in increasing numbers from heat exchangers of metal to graphite, glass, and Teflon fluorocarbon resins. Ceramics are preferred for high-temperature applications, particularly for waste heat recovery. All these nonmetals are characterized by inertness to chemical attack and nonductile nature. Cost and chemical inertness are usually the primary factors in a decision to use a brittle material instead of a metal [243]. Salient features that favor these materials for heat exchanger construction are discussed next.

13.27 GRAPHITE

Graphite is a unique material; it has the most valuable combination of properties. It has properties common to both metals and nonmetals. Impervious graphite is used as a heat exchanger material. It is made by impregnating graphite with a phenolic or furfuryl alcohol resin. Graphite is an allotropic form of carbon. It is used as a heat exchanger material due to the following valuable properties:

1. High thermal conductivity
2. Resistance to corrosive fluids
3. Stable over wide range of temperature
4. Ability to withstand thermal shock
5. Low coefficient of friction
6. Ability to be fabricated to the desired (a) strength, (b) porosity, (c) density and compactness, (d) grain structure and fineness, and (e) surface finish
7. Good machining characteristics and possibility to machine it into desired shapes
8. Due to smooth surface finish, the fouling is minimum, and hence there is less deterioration in thermal performance
9. Ordered crystal structure

References [243–246] provide either specific or general information on graphite.

13.27.1 APPLICATIONS OF IMPERVIOUS GRAPHITE HEAT EXCHANGERS

Impervious graphite resists a wide variety of inorganic and organic chemicals. But strong oxidizing acids such as nitric acid, concentrated sulfuric acid, and wet chlorine cannot be handled [245]. Heat exchangers with improved resistance to oxidizing agents are being developed. Unlike the ceramic, graphite can handle hydrofluoric acid up to 60% and hot caustics [243]. Graphite heat exchangers are employed as boilers and condensers in the distillation by evaporation of hydrochloric acid and in the concentration of weak sulfuric acid and of rare earth chloride solutions.

13.27.2 DRAWBACKS ASSOCIATED WITH GRAPHITE

Drawbacks associated with graphite are the following:

1. The principal limitation in the application of graphite lies in the synthetic resins used for both impregnation and laminate. The resins undergo decomposition at temperatures above 356°F (180°C) and hence graphite heat exchangers are limited to this temperature [245].
2. Porosity and permeability pose problems for liquids and gases, and the other problem is poor tensile strength. However, the porosity problem is overcome by impregnation with synthetic resin.
3. Brittleness (poor impact strength), poor abrasion resistance, and low tensile strength are problems; the poor tensile strength is overcome by modifying the design and fabrication.
4. Not recommended for fine chemical industries like pharmaceutical, brewing, and food processing industries.

13.27.3 FORMS OF GRAPHITE HEAT EXCHANGERS

The principal forms of graphite heat exchangers are the following:

1. Shell-and-tube heat exchanger
2. Cubic or rectangular block heat exchanger
3. Modular block cylindrical exchanger
4. Plate heat exchanger

Graphite heat exchanger construction details are discussed by Hills [244,247] and Schley [246].

13.27.4 SHELL-AND-TUBE HEAT EXCHANGER

The shell-and-tube design consists of graphite tubes and tubesheets to exploit its noncorrosive property on the tubeside. Graphite tube bundle is shown in Figure 13.28; the tube bank is enclosed in a shell made of steel, cast iron, copper, aluminum, or lead, with or without corrosion-resistant linings. The baffles may be of soft metal or plastic (polytetrafluoroethylene [PTFE]). Due to poor strength of graphite, the operating temperature and pressure are limited to 356°F (180°C) and



FIGURE 13.28 Graphite shell-and-tube heat exchanger: (a) graphite tube bundle and (b) heat exchanger unit. (Courtesy of Mersen, Paris La Défense, France.)

5 bar, respectively. The graphite shell-and-tube heat exchanger occupies a very large space, and hence these units are not suitable to handle large throughput of chemicals like fertilizers, synthetic fibers, and heavy chemicals [244].

13.27.5 GRAPHITE PLATE EXCHANGER

The Diabon F graphite PHE is a heat exchanger with graphite plates developed for use with media normally too corrosive for exotic metals and alloys. For details on this type of heat exchanger, refer to Chapter 7.

13.28 GLASS

Low coefficient of thermal expansion, lightweight, inertness to many chemicals, and high compressive strength are the important factors that favor the use of glass. Glass heat transfer equipment finds excellent applications whenever one or more of the following are required:

1. Corrosion resistance
2. Product purity
3. Visibility
4. Low maintenance

References [247–251] provide either specific or general information on glass.

13.28.1 APPLICATIONS

Because of its excellent corrosion resistance and visibility, glass heat transfer equipment proves very desirable in pilot-plant applications in all industries. Its transparency permits fast and accurate troubleshooting if a flow problem arises [243]. The industries that employ glass heat transfer equipments include [247] the following:

1. Chemical and petrochemical (corrosion resistance)
2. Pharmaceutical (corrosion resistance and product purity)
3. Food and beverage (product purity and inertness)
4. Dyestuff (visibility and smooth surface)

13.28.2 MECHANICAL PROPERTIES AND RESISTANCE TO CHEMICALS

Borosilicate glass has a relatively low coefficient of thermal expansion compared to other glasses. It is subject to thermal shock and is weak in impact strength, although this is improved by thermal tempering [243]. Glass heat transfer equipment can operate at temperatures up to 392°F (200°C). This temperature is limited by the gasket material employed and not by the glass material. The permissible internal operating pressure is a function of diameter. As diameter increases, permissible operating pressure decreases. The permissible operating pressure may be about 4 bar.

The chemical stability and catalytic inertness of borosilicate glass are more comprehensive than for any other known material of construction. Only hydrofluoric acid, concentrated phosphoric acid, and strong alkalis at high temperatures can appreciably attack the glass surface.

13.28.3 CONSTRUCTION TYPES

There are three types of glass heat exchangers used today. They are [247] as follows:

1. Shell-and-tube heat exchangers
2. Coil heat exchangers
3. Hybrid heat exchangers

13.28.3.1 Shell-and-Tube Heat Exchangers

The tubes are individually sealed in a PTFE tubesheet with pliable PTFE packing and a PTFE packing grommet. The shell is constructed from standard glass pipe sections and fittings. Shell-and-tube units are available from 2.5 to 25.0 m² of heat transfer area; nominal shell diameters range from 6 to 12 in. (152.4–304.8 mm).

13.28.3.2 Coil Heat Exchangers

Glass coil exchangers have a coil fused to the shell to make a one-piece unit. This prevents leakage between the coil and shellside fluids. The units are manufactured to eliminate any stress concentration at the point of fusion. Maximum operating pressure in the coil is 3 bar, while it is a function of diameter in the shell. Heat transfer areas range from 0.3 to 15.0 m² in these units.

13.28.3.3 Hybrid Heat Exchangers

Hybrid exchangers utilizing glass and some other material of construction have been developed. These include [247] the following:

1. Glass shells with metal bayonet, basket, or immersion coil heaters
2. Glass tubes and end caps with shells fabricated from fiberglass, steel, SS, or other alloys

These units are used when higher pressures or other factors prohibit the use of an all-glass unit.

13.28.3.4 Glass-Lined Steel

Process equipment made of glass-lined steel offers the corrosion resistance of glass and the structural strength of steel.

13.28.3.5 Drawbacks of Glass Material

The parameters that restrict the use of glass as a heat exchanger material are the following:

1. Glass is sensitive to mechanical shock, thermal shock, thermal stresses, abrasion, and over-stressing of nozzles [251].
2. Corrosion: Glass is not completely inert; acids, alkalies, and even water can corrode glass in varying forms and degrees, but very slowly.

13.29 TEFLON

With the introduction of Teflon in 1965, E. I. du Pont de Nemours & Co. Inc. made a significant technical contribution with the design and production of heat exchangers with flexible and non-corroding tubes of Teflon fluorocarbon. Teflon (PTFE), a highly chemically inert, noncorroding material, is well suited for the corrosive applications that have long been a problem in industry. The nonsticking smooth surface of Teflon tubes resists fouling and scale buildup. Exchangers made of Teflon have replaced many exchangers in corrosive services that use construction materials such as SS, impervious graphite, glass, zirconium, titanium, Hastelloy, and tantalum [252]. Shell-and-tube heat exchangers and immersion coils made of Teflon are used successfully for corrosion-free heating, cooling, and condensing of many corrosive fluids found in chemical processing, steel, and plating industries. Part of the information on Teflon has been drawn from Ref. [253].

13.29.1 TEFLON AS HEAT EXCHANGER MATERIAL

The reasons that favor Teflon as a candidate heat exchanger material are [253] as follows:

Noncorrosive: Inert to essentially all industrial chemicals, Teflon is an ideal material for handling corrosives.

Resistant to fouling: The well-known nonstick properties of Teflon help to keep the heat exchanger tubes clean, minimizing the fouling and scaling, and thus limit downtime and maintenance costs.

Resistant to shock: Heat exchangers of Teflon are less subject to damage from thermal or mechanical shock than those of glass or graphite.

Noncontaminating: Since it is chemically inert, Teflon will not produce corrosion products that can contaminate process solutions. Unlike graphite, it contains no binders that can leach out in corrosive solutions. Heat exchangers of Teflon are being used to replace metal and graphite exchangers to achieve increased product purity.

Low maintenance: Inherent resistance to corrosion and fouling minimizes downtime for unscheduled maintenance. Units are easily cleaned with chemical solutions that could damage metal and graphite exchangers.

Size reduction: The compact flexible tube bundle requires less space than a comparable metal exchanger.

Temperature and pressure resistance: Heat exchangers of Teflon can handle corrosives up to 400°F (204°C) and pressures up to 125 psig (862 kPag), depending on temperature.

Good electrical resistance: The electrical resistance of Teflon enhances applications in the plating industry.

13.29.2 HEAT EXCHANGERS OF TEFLON IN THE CHEMICAL PROCESSING INDUSTRY

Two different types of heat transfer equipment are being produced. They are shell-and-tube units and exposed tube bundles.

Shell-and-tube heat exchanger: Shell-and-tube units with tubing of Teflon are used for heating, cooling, or condensing chemically aggressive process streams. These include sulfuric, hydrofluoric, nitric, hydrochloric, and other acids, caustic and other alkalies, halogenated compounds, salt solutions, and organic compounds [253]. The units are single-pass exchangers containing flexible tubes of Teflon fused at both ends into an integrated honeycomb structure. All surfaces exposed to the corrosive process stream are made of Teflon. Units are available with Teflon-lined shells for heat exchange between two corrosive streams.

13.29.3 DESIGN CONSIDERATIONS

Teflon tubing exhibits relatively low thermal conductivity, that is 0.11 BTU/h ft² °F, and this shortcoming is overcome by increasing the heat transfer area and decreasing the wall thickness of the tubing. With small-bore tubing, a large surface area is obtained for a given volume. Practical and economic optimization led to the establishment of 0.1 in. outer diameter tubing as the smallest standard product for coils [252].

13.29.4 SIZE/CONSTRUCTION

For shell-and-tube units, shell diameters range from 3 to 10 in. (76.2–254 mm) for standard units. Nominal tube length is 24–288 in. (610–7315 mm), and shells are made of carbon or SS, fiberglass, or other materials. Tubing sizes range from 0.10 to 0.375 in. (2.54–9.4 mm) for either FEP or Q-series. The heat transfer area is 5.1–1104 ft² (0.5–103 m²) in standard units [253].

13.29.5 HEAT EXCHANGER FABRICATION TECHNOLOGY

In a unique honeycomb process, the ends of individual tubes of Teflon are fused into an integrated tubesheet. This construction provides the user with an extremely large heat transfer area in a relatively compact unit at a low cost.

Reactor coils: Reactor coils are designed for immersion into agitated vessels or storage tanks to heat or cool corrosive fluids.

13.29.6 FLUOROPOLYMER RESIN DEVELOPMENT

Exchangers based on Teflon FEP can be used to 30 psig (207 kPa) at 300°F (149°C), maximum, and these limits have been extended to 50 psig (9345 kPa) at 400°F (204°C) in exchangers made with Q-series fluoropolymer tubes [253]. Substantially higher-pressure capabilities are available at lower than maximum temperatures.

13.30 CERAMICS

For high-temperature heat exchangers, material temperature limits are a major constraining factor. For metallic materials in use above 649°C (1200°F), the choice is essentially limited to SSs, nickel- and cobalt-base superalloys, and heat-resistant cast alloys. Structural ceramics are used to provide mechanical strength at elevated temperatures, usually in the range of 600°C–1600°C (1110°F–2910°F) [254]. Ceramic materials such as silicon carbide and silicon nitride exhibit excellent high-temperature mechanical strength and are used for high-temperature heat exchanger applications. Advanced-technology materials such as carbon-bonded carbon-filament composites have adequate elevated-temperature mechanical properties, but their applications are limited because they are not usable in the presence of oxygen [255].

13.30.1 SUITABILITY OF CERAMICS FOR HEAT EXCHANGER CONSTRUCTION

Because of their high-temperature capability and oxidation resistance, ceramics are obvious materials for high-temperature heat exchangers, particularly in energy and resource conservation. The following are the important factors that favor the ceramics as heat exchanger material [255]:

1. Resistance to high-temperature corrosion and oxidation
2. Stability at elevated temperature
3. Good thermal shock resistance
4. Low cost compared to heat-resistant superalloys
5. Low coefficient of thermal expansion
6. Commercial availability
7. Ability to be fabricated in practical geometries
8. Chemical durability
9. Low porosity

The drawbacks of ceramics for high-temperature applications are

1. Brittleness
2. Permeability
3. Unsuitable for fabrication by joining techniques
4. Irreparability

13.30.2 CLASSIFICATION OF ENGINEERING CERAMICS

There are three major classifications of engineering ceramics [255] as follows:

1. Ceramic oxides such as alumina, beryllia, and zirconia
2. Glass ceramics
3. Ceramic carbides and ceramic nitrides

13.30.3 TYPES OF CERAMIC HEAT EXCHANGER CONSTRUCTION

Tubular construction: Applications for tubular ceramic units include [255] the following:

1. Waste heat recovery in metals industries
2. Chemical plant waste heat recovery
3. Incinerators
4. Closed-cycle gas turbine heat-source exchangers
5. Open-cycle gas turbines (exhaust-heated cycle)
6. Fluidized-bed heat exchangers
7. Gas-to-gas heat recovery units
8. Nuclear process heat intermediate heat exchangers

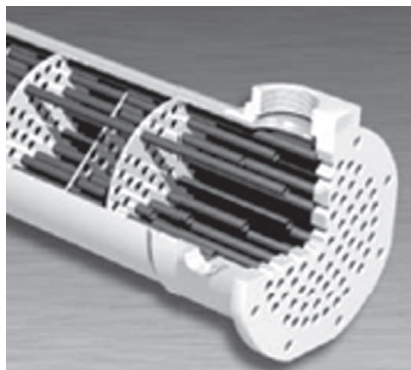
Plate fin construction: Applications for ceramic plate fin units include [255] the following:

1. Vehicular gas turbine recuperators
2. Industrial gas turbine recuperators
3. Stirling engine heat exchangers
4. High-temperature gas-to-gas heat exchangers
5. Rotary generators
6. Applications requiring very compact, small-volume heat exchangers

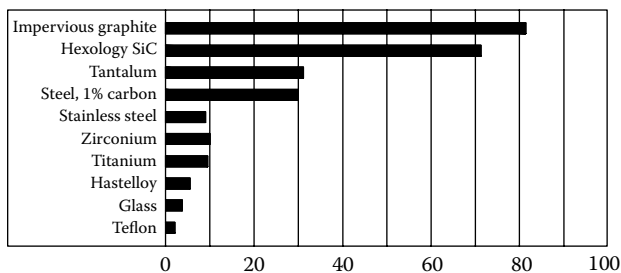
13.31 HEXOLOY® SILICON CARBIDE HEAT EXCHANGER TUBE

An alternative to metals, glass, and other tube materials for enhanced heat transfer, uptime, and reliability for high corrosive environment is Hexoloy silicon carbide (SiC) heat exchanger tubes supplied by Saint-Gobain. Hexoloy silicon carbide heat exchanger is shown in Figure 13.29a. Hexoloy SiC's thermal conductivity is almost equal to that of commonly used graphite tubes. Its thermal conductivity is 2 times that of tantalum, 5 times that of SS, 10 times that of Hastelloy, and 15 times that of glass. The result is higher efficiency while requiring less heat transfer area. Figure 13.29b shows the comparison of thermal conductivity of Hexoloy SiC with few heat exchanger tube materials.

1. High corrosion resistance: Hexoloy SiC tubes have been proven for years in HF, bromine, high concentration nitric acids, mixed acids, bases, oxidants, and chlorinated organics.



(a)



(b)

FIGURE 13.29 Hexoloy heat exchanger tube- (a) Hexoloy silicon carbide heat exchanger unit and (b) comparison of thermal conductivity of Hexoloy SiC with few heat exchanger tube materials. (Courtesy of Saint-Gobain Advanced Ceramics, Niagara Falls, NY.)

2. Extreme hardness and high strength: Hexoloy SiC is one of the hardest high-performance materials available for heat exchanger tubes.

13.32 ALLOYS FOR SUBZERO TEMPERATURES

Steels and nonferrous materials are used for containment, handling, and transporting of liquefied gas and liquefaction of gases. Other applications include stationary structures and mobile equipment exposed to adverse climates or operating conditions or both. Temperatures below -150°C (-238°F) often are identified as cryogenic temperatures. Temperatures for liquefying commonly used types of gases are below 100°C . The temperatures are approximately -162°C for LNG and approximately -184°C for liquefied ethylene gas. The motive for utilizing low-temperature technology is that at cryogenic temperatures, liquid gases occupy much less volume than their pressurized gaseous state. Therefore, the containment vessels for liquid gases may be smaller, thinner (because of lower pressure), and less costly [256].

Material properties relevant at cryogenic temperatures: The most important cryogenic material properties are the following: (1) toughness, (2) DBTT, impact strength, (3) yield strength, (4) plastic deformation, (5) corrosion, (6) thermal conductivity, (7) thermal expansion, (8) specific heat, (9) fatigue behavior, (10) creep behavior, (11) magnetic properties, etc.

13.32.1 DUCTILE–BRITTLE TRANSITION TEMPERATURE

Some metals display a marked loss of ductility in a narrow temperature range below room temperature. This is called the DBTT. The application of steels below their NDT is avoided because of the danger created by brittle crack propagation that could lead to the catastrophic failure of a component or entire system [16]. Below the NDT, very little energy is required for crack propagation [114]. The following factors can improve the toughness of steels [17]: (1) ASTM grain size has a strong effect on a given steel's NDT. As the grain size number increases (i.e., the grains become smaller), the NDT drops. Therefore, fine-grained steels usually are used for low-temperature applications. (2) Proper heat treatment can be very effective in increasing a steel's fracture toughness. Quenching and tempering is an effective heat treatment for improving toughness. (3) Among alloying elements, nickel, titanium, and manganese tend to increase steel's toughness. (4) Another variable that affects DBTT is thickness.

13.32.2 CRYSTAL STRUCTURE DETERMINES LOW-TEMPERATURE BEHAVIOR

Below ambient temperatures, a metal's behavior is characterized somewhat by crystal structure [256]:

1. The yield and tensile strength of bcc structure metals depend greatly on temperature and generally display a marked loss of ductility in a narrow temperature range below room temperature (e.g., iron and molybdenum).
2. fcc structure metals such as aluminum, copper, nickel, and austenitic SS often increase in ductility as temperatures decrease, and their tensile strength is more temperature dependent than their yield strength.
3. The tensile and yield strengths of hcp structure metals are more temperature dependent, and they usually suffer a severe loss of ductility at subzero temperatures (e.g., zinc, titanium, some alpha-titanium alloys); however, they have good ductility down to cryogenic temperatures.
4. Plastic deformation and cryogenic temperature can cause a normally ductile and tough SS such as 301, 302, 304, and 321 to partially transform to a bcc structure, thus affecting ductility and toughness.

5. Impact strength is sensitive to grain structure. A close compact and fine-grained structure offers better impact strength than rough, coarse-grained structure.
6. Minor variations in composition can affect ductility in certain materials. For example, an increase in oxygen from 0.10% to 0.20% in a ductile titanium alloy can lower ductility at -423°F (-253°F) from 15% to almost 0%.

13.32.3 REQUIREMENTS OF MATERIALS FOR LOW-TEMPERATURE APPLICATIONS

A major requirement of materials for liquefaction equipment and for containment and transport of liquefied gases is toughness at the handling temperatures of the liquid. Additional requirements include minimum weight, weldability characteristics to resist hot cracking, cold cracking, and embrittlement of HAZs, high strength and toughness of the welded joints, and corrosion resistance, low thermal expansion to minimize dimensional changes due to temperature difference between the ambient and service temperature, relatively low specific heats, low thermal conductivity to minimize thermal conduction, etc. Carbon steels have only limited corrosion resistance and must be replaced with corrosion-resistant alloys when metal loss becomes severe.

13.32.4 NOTCH TOUGHNESS

Notch toughness is defined as the ability to resist brittle fracture at high stresses, such as that can be caused by impact loading. Notch toughness is measured by various means. The favored method recommended by the American Petroleum Institute as well as the ASTM and ASME is the Charpy V-notch test. It is considered the most appropriate because a part or structure will generally fail due to a notch or other stress concentration [257] or a defect such as a gouge, weld crack, arc strike, or a sharp discontinuity [258]. Using the Charpy V-notch test, one can determine the TT at which a material becomes brittle. This information helps the designer to choose a steel that will remain ductile through the range of temperatures or stresses it will be subjected to in service.

13.32.4.1 Notch Toughness: ASME Code Requirements

The ASME Code should be consulted for allowable stress at low temperatures and for the testing required of the material to ascertain that it is suitable for low-temperature service. The ASME Code stress tables designate -20°F as the beginning of low temperature.

13.32.5 SELECTION OF MATERIAL FOR LOW-TEMPERATURE APPLICATIONS

Selecting materials for low-temperature and cryogenic applications calls for thorough understanding of the application and knowledge of the mechanical properties that each grade of metal provides. Since various low-temperature materials are available, the designer must consider the merits of each material according to the application. Some factors suggested by Marshall [257] include cost by strength ratio, welding, and fabricating costs, and where extra high strength and good impact properties to below -75°F (-59.4°C) are called for, an alloy steel should be chosen.

13.32.6 MATERIALS FOR LOW-TEMPERATURE AND CRYOGENIC APPLICATIONS

Aluminum, copper, titanium, nickel-base alloys, ferritic steels including 9% Ni steels, and SSs offer designers a wide choice and have been used successfully for liquefaction, containment, and transport of liquefied gases. The selection of aluminum, copper, nickel- and cobalt-base alloys, titanium, low-alloy ferritic steels including 9% Ni steels, and SSs is discussed next. Table 13.54 shows a list of materials for low-temperature application along with the minimum temperature applicability.

TABLE 13.54
Materials for Low-Temperature Application

Alloy Designation	Specification	Approximate Lowest Temperature
Low-carbon steel	A 442, A 516	−50°F (−46°C)
	A 537	−75°F (−59°C)
	A 662, A 724	—
Alloy steel	A517	−75°F (−59°C)
	A203, Gr. A and B, 2.25% Ni	−90°F (−68°C)
	A203, Gr. D, E, and F, 3.50% Ni	−150°F (−101°C)
	A645, 5.0% Ni	−320°F (−196°C)
	A353	−320°F (−196°C)
	A553, Type II 8% Ni	−275°F (−170°C)
	A553, Type I 9% Ni	−320°F (−196°C)
	A543	−180°F (−118°C)
	A736	−50°F (−46°C)
	A844 (9% Ni)	−320°F (−196°C)
Stainless steel	304, 304L, 316, 316L, 347	−452°F (−269°C)
Aluminum	1100, 2014 to 2024, 2219-T87, 3003, 5083-O, 5456, 6061-Tb, 7005	−452°F (−269°C)
Copper	C10200, C12200 (DHP), C17200, C22000, C26000, C51000, C70600, C71500	−325°F (−198°C)
Nickel	Monel-K, Hastelloy B, Hastelloy C, Inconel alloy 600,	−452°F (−269°C)
	706, Inconel alloy 718, Invar-36, Inconel alloy	−441°F (−263°C)
	X-700	
Titanium	Ti-5Al-2.5Sn, Ti-6Al-4V (ELI)	−320°F (−196°C)
	Ti-5Al-2.5Sn (ELI)	−423°F (−253°C)

Note: Refer to ASTM Standards or National Codes for applicable lowest temperature.

13.32.6.1 Aluminum for Cryogenic Applications

Aluminum and aluminum alloys have fcc crystal structures and retain good ductility at subzero temperatures. Aluminum can be strengthened by alloying and heat treatment while still retaining good ductility along with adequate toughness at subzero temperatures. Among the aluminum and aluminum alloys, 1100, 2014 to 2024, 2195, 2219-T87, 3003, 5052, 5083-O, 5086 and 5456, 6061-Tb, 7005, 7075, 7079, and 7178 are recommended for cryogenic applications.

The salient features of these alloys are discussed next. Before that, the factors that favor aluminum use in cryogenics are listed [259] in the following:

1. Unlike other metals, aluminum has no DBT transition regardless of the direction of stress.
2. Inertness to cryogenics like methane, ethylene, argon, helium, neon, O₂, N₂, H₂.
3. Absence of corrosion at cryogenic temperatures: Protective coatings are rarely necessary, but the designer should be cautious of galvanic couple.
4. The tensile strength increases proportionately more than yield strength in the cryogenics, so heavily stressed tanks can warp more at cold than at room temperature without failing.
5. Tear resistance, another measure of toughness, is the energy needed to propagate a crack. Tear resistance of 5083-O and its welds is as high at −196°C as it is at room temperature.
6. Emissivity and reflectivity: Aluminum's low emissivity improves the effectiveness of insulation systems [260].
7. Weldable aluminum alloys provide excellent mechanical properties in the as-welded condition.

2000 series: Aluminum alloys such as 1100, 2014 to 2024, 2195, and 2219-T87.

3000 series: Aluminum alloy 3003 is used in the fabrication of brazed PFHEs and other equipment in gas liquefaction plants. It is available as tubing (including finned tubing), pipe, sheet, and plate. It is readily joined by brazing or welding. Alloy 3003 meets the requirements of the ASME Boiler and Pressure Vessel Code for working temperatures up to -321°F (-196°C).

5000 series: Alloys such as 5052, 5053, 5083, 5086, and 5456 exhibit a combination of properties that make them popular for most applications. Their moderate strength, good toughness, and good weldability have resulted in their selection for oceangoing tankers for carrying oxygen, LNG, and other cryogenic gases, and for tank trailers, stationary storage containers, and processing equipment. For PFHEs, 5083-O is used.

6000 series: Alloy 6061 offers the advantage listed for 5000 series alloys except that in the as-welded condition, its strength is low.

7000 series: Alloys such as 7005, 7039, 7075, 7079, and 7178 display the highest strength of all aluminum alloys. But they lose toughness below -320°F (-196°C). They are generally nonweldable and found only in limited application. Two newer alloys, 7039 and X7007, show promise for cryogenic service because they are readily welded and retain adequate toughness at all temperatures [256].

13.32.6.2 Copper and Copper Alloys

Copper and copper alloys have fcc crystal structures similar to those of aluminum and retain a high degree of ductility and toughness at subzero temperatures, down to -423°F (-253°C). Copper alloys that might be considered for use at subzero temperatures are C10200 oxygen-free copper, C12200 (DHP), C17200, C22000, C26000, C51000, C70600, and C71500 [205]. The development of light-weight brazed aluminum heat exchangers for cryogenic applications caused copper to be replaced by aluminum for many of these components.

13.32.6.3 Titanium and Titanium Alloys

Commercially pure titanium may be used for tubing and small-scale cryogenic applications that involve only low stresses in service. For temperatures down to -320°F (-196°C), the normal interstitial-grade alloys Ti-5Al-2.5Sn and Ti-6Al-4V are suitable. Interstitial impurities such as iron, oxygen, carbon, nitrogen, and hydrogen reduce the toughness of these alloys at both room and subzero temperatures. For temperatures below -196°C , ELI grades of Ti-5Al-2.5Sn and Ti-6Al-4V are used [205]. The lower strength, all alpha Ti-5Al-2.5Sn ELI is used down to -423°F (-253°C), the temperature of liquid hydrogen. Titanium and titanium alloys are not recommended for containment or other use with either liquid or gaseous oxygen in cryogenic service, because any fresh surface caused due to abrasion or impact exposed to oxygen will cause ignition and hence possible explosion.

13.32.6.4 Nickel and High-Nickel Alloys

Nickel is an fcc metal that retains good ductility and toughness at subzero temperatures. Unalloyed nickel is low in strength and has only limited applications at subzero temperatures. However, several nickel-base alloys, including some superalloys, exhibit excellent combinations of strength, ductility, and toughness up to -441°F (-263°C). Typical nickel-base alloys for cryogenic applications include Monel K-450, Hastelloy B, Hastelloy C, Inconel alloy 600, Inconel alloy 706, Inconel alloy 718, Inconel X-700, and Invar-36 (36% Ni-iron) [205].

13.32.6.5 Carbon Steels and Alloy Plate Steels

ASTM specifications A203, A353, A442, A516, A517, A537, A553, A612, A645, A662, and A724 describe steel plates with minimum Charpy V-notch energy or lateral expansion requirements at testing temperatures from -15°F to -320°F (-26°C to -196°C).

13.32.6.5.1 Carbon Steels

Carbon steels provide service to -75°F . Less costly than alloy steels, they combine better weldability with low coefficients of thermal expansion and thermal conductivity. In carbon steels, the principal means of improving notch toughness is through changes in composition of C, Mn, Si, and Al contents. Carbon lowers toughness, whereas Mn increases it. Si and Al are added as deoxidizers. Silicon-killed steel has slightly better notch toughness than semikilled steel, and silicon–aluminum-killed steel has still higher toughness [258].

ASTM A516: The major advantage of A516 steels is their low initial cost. But they feature the lowest ASME stresses, 13,750–17,500 psi. Thus, a given design strength requires heavier gauges than are needed with high-strength steels. A516 steel is used widely in air liquefaction plants, refrigerating plants, transport equipment, and containment vessels operating down to -50°F (-46°C) [257]. For these applications, the steel is normally made to meet impact test requirements of ASTM A300 Class 1 specification, which calls for plates to be normalized and to meet a Charpy keyhole minimum of 15 ft-lb at -50°F .

13.32.6.5.2 A517

Of the low-temperature alloy steels, A517 Grade F has the highest allowable stresses. At -50°F , its impact strength (Charpy V-notch) is 40 ft-lb, and its notch and crack resistance are sufficient to encourage wide usage.

13.32.6.5.3 ASTM A537 Grades

Higher strength with good notch toughness is available in carbon steels such as the two classes listed in ASTM A537 grades, normalized (Class A) or quenched and tempered (Class B), which provides 60,000 min psi yield strength plus 15 ft-lb of impact strength (Charpy V-notch) at -75°F .

13.32.6.5.4 2.25% Nickel Steels

ASTM specification A203 Grades A and B are used in service down to -90°F (-68°C). The low-temperature requirements are given in ASTM specification A300.

13.32.6.5.5 3.5% Nickel Steels

ASTM specification A203 Grades D and E are used in service down to -148°F (-100°C). Forgings and bolting materials are also covered in ASTM specifications. The low-temperature requirements are given in ASTM specification A300.

13.32.6.5.6 5% Nickel Steel

This is used as a wrought material for service down to approximately -185°F (-120°C), for the fabrication of welded vessels for handling and storage of liquid ethylene in land-based plant and marine tankers. Quenched, temperized, and reversion annealed ASTM A645 specifies 5% nickel steel designed for LNG service. Armco Cryonic 5 is covered by ASTM A645.

13.32.6.5.7 ASTM A553 Alloy Steel

This is one grade 9% Ni steel, normalized and tempered for subzero use. Yield strength is 75 ksi; specification for longitudinal and transverse impact (Charpy V-notch) energy is 20 ft-lb minimum at -320°F (-196°C).

ASTM A553 steels contain 8% or 9% nickel and are essentially quenched and tempered to 85 ksi yield strength (minimum). Impact energy minimum is 25 ft-lb (longitudinal) and 20 ft-lb (transverse) at -196°C (-320°F) for Type I, 9% Ni, or -170°C (-275°F) for 8% Ni steel (Type II). The welding considerations are the same for both types of steel regardless of heat treatment. The 9% nickel steels have long been used for ethylene, methane, LNG, oxygen, and nitrogen applications. One of the benefits of nickel steels in design of LNG vessels is volume and weight savings due to their relatively high strengths. Selection criteria and fabrication aspect of 9% nickel steel are discussed in detail later.

13.32.6.5.8 36% Ni-Iron Alloy

Low expansion 36% nickel–iron alloy is marketed under various trade names, including Invar 36, Nilo 36, and Dilavar. It is used principally for sea transportation and land-based storage of liquefied gases. It is also used at service temperatures down to that of liquid helium -269°C (-452°F). The nickel–iron alloy plate for pressure vessels is covered in ASTM A658.

13.32.6.6 Products Other than Plate

A partial list of ASTM specifications for other than plate steel products for subzero service is in the following:

- A333 Seamless and welded steel pipe
- A334 Seamless and welded carbon and alloy steel tubes
- A350 Forged or rolled carbon and alloy steel flanges, fittings, and valves
- A352 Ferritic steel castings
- A420 Piping and fittings of wrought carbon steel and alloy steel
- A522 Forged or rolled 8% and 9% nickel steel flanges, fittings, and valves
- A671 Electric fusion-welded steel pipe
- A757 Carbon and alloy steel castings

In addition to the steels listed, a number of proprietary ferritic steels have been developed by several steel producers to meet certain requirements for service at subzero temperatures.

13.32.6.7 Austenitic Stainless Steel

In the last decade, there has been a considerable increase in the use of austenitic SSs for cryogenic services at temperatures between -240°F and -452°F (-151°C and -268.9°C). They play an important role in LNG ships for containment tanks, storage tanks, cargo piping systems, and a variety of ancillary equipment.

The AISI 300 type steels such as 304, 304L, 310S, 316, 316L, 321, and 347 offer a fine combination of toughness and weldability for service down to -452°F (-269°C). Among these alloys, Types 304 and 304L are the most commonly used alloys. Consequently, they have the largest service experience and coverage in design codes. These grades have moderate strength and excellent toughness, and they are selected for their formability, fabricability, and ready availability in a variety of product forms [14,261].

Among the modified varieties, nitrogen-containing, high-proof-strength stainless (e.g., Types 304N, 316L + N) is used for cryogenic processing plants and in liquid oxygen and nitrogen storage and transportation applications. The addition of 0.2% N raises the proof strength by about 40% and moderately increases the tensile strength without sacrificing ductility or fracture toughness [14].

13.32.7 FABRICATION OF CRYOGENIC VESSELS AND HEAT EXCHANGERS

Most of the cryogenic materials are formable and weldable. Most of the units are welded. Brazing is limited to the manufacture of PFHE [256]. Important considerations for fabrication of cryogenic plants are discussed in detail in Ref. [262]. Some of the considerations are the following:

1. All raw materials and consumables should undergo rigorous quality and specification tests.
2. Edge preparation is considered to be of the utmost importance for all types of welding, and clear specifications should be laid down and strictly adhered to for all joints.
3. Welding plants should be checked for proper functioning.
4. It is essential that the weld metal and HAZ achieve a fracture toughness greater than or equal to that of the base metal. The weldment should resist hot and cold cracking and embrittlement of the HAZ.

13.32.8 9% NICKEL STEEL

Low-carbon 9% nickel steel was developed in the United States by the International Nickel Company, Inc. The fundamental mechanical properties of 9% Ni steel must meet the minimum requirements of ASTM 353 or ASTM 553 Type I specifications. The steel is used for vessels and plant for processing, transportation, and storage of liquefied gases down to -196°C . The excellent low-temperature toughness of this steel results from the alloying addition of approximately 9% nickel and the presence of stable retained austenite at cryogenic temperature. Nickel also suppresses the formation of ferrite/pearlite high-temperature transformation products; thus, a microstructure is produced that is higher in strength and notch toughness [263].

13.32.8.1 Merits of 9% Nickel Steel

Materials previously used, such as copper and austenitic corrosion-resistant steels, presented no particular difficulties in construction, but the cost of these materials was high [264]. The use of 9% nickel steel has increased because it is a cheaper material than those materials previously used for operation down to -321°F (-196°C). The higher strength of this steel compared with aluminum, copper, or even austenitic steels makes possible the use of higher design stresses and hence offers high strength-to-weight ratio. The major factors that favor 9% nickel steel include [14] the following:

1. High design stress coupled with good fracture toughness characteristics.
2. Relatively low thermal expansion compared with austenitic SS and aluminum alloys.
3. High melting point and retention of strength at elevated temperatures; this property is important for the structural integrity under shipboard fire conditions.
4. Chemically resistant to liquid oxygen and nitrogen, producing no corrosion products that would hamper the operation of valves and meters or cause unsafe conditions [265].
5. Low thermal conductivity.
6. Good weldability by a variety of processes, including shielded metal arc, gas metal arc, and SAW [266].

13.32.8.2 Forming of 9% Nickel Steel

The material is readily machinable and may be hot or cold formed. After hot forming, however, the steel must be heat-treated by double normalizing and tempering unless the hot-forming temperature approximates the first normalizing temperature, when the first normalizing treatment can be omitted.

13.32.8.3 Surface Preparation and Scale Removal for Welding

Prior to the welding operation, all extraneous material and surface oxides should be removed from the weld joint area by wire brushing. Grinding is a more effective procedure. Residual scale can cause porosity in succeeding layers of weld metal. As an alternative to grinding, it has been found possible to remove the scale from 9% nickel steel by flame cleaning, using conventional oxyacetylene equipment [267].

13.32.8.4 Edge Preparation

The edges should preferably be machined or cut by employing flame cutting. The shape should be such as to afford easily full penetration. Normally, the V bevel with open root or an asymmetrical double V bevel is used [268]. If the edge is prepared by flame cutting, it will be necessary to grind it, to remove the surface oxide formed and to eliminate the underlying layer where the carbon content has become higher.

13.32.8.5 Welding Procedures

The welding procedures most widely used are MMA welding with covered electrodes, automatic or semiautomatic SAW with continuous wire, MIG welding, cored wire welding, and for the root

pass TIG welding and PAW. Employ MIG welding with a spray mode of metal transfer to overcome lack of fusion problems, to obtain clean welds while keeping the heat input to relatively low levels [269].

13.32.8.6 Electrodes

The electrodes that have been used for 9% nickel steel can be considered in the following three classes [270]:

1. Nickel-based electrodes of the Inconel or Hastelloy type; the trade names are Inco weld A, Inconel 192, and Inconel 182.
2. Chromium–nickel SS electrodes to a very limited extent.
3. Low-alloy ferritic electrodes.

13.32.8.7 Guidelines for Welding of 9% Ni Steel

As is well known, 9% Ni steel derives its properties through double normalizing and tempering or quenching and tempering. The welding processes and the weld metal must be such as not to alter, beyond acceptable limits, the structural characteristics of the parent metal in the HAZ. To ensure tensile strength and toughness in the fusion zone, and to avoid welding flaws, a few practical rules are suggested by Pozzolini [268]:

1. Use low-hydrogen electrodes with a diameter less than 4 mm and wires with a diameter less than 3.2 mm.
2. Lay narrow beads in a number of passes rather than large beads partially overlapping.
3. Preferably weld in the horizontal position; avoid the vertical position.
4. Do not preheat unless absolutely necessary.
5. Use relatively low heat inputs (9–16 kJ/cm, according to the welding process) and current settings to keep the dilution to a minimum.
6. Use welding processes with high cooling rates and avoid keeping the material at temperatures exceeding the lowest critical point of transformation.
7. Avoid any stress-relief heat treatment. If really necessary, it should be carried out at temperatures below the lowest critical point of transformation.
8. All the welding materials should be dried prior to welding, and the shielding gases should be of controlled purity.
9. Nine percent nickel steel is not susceptible to underbead cracking or excessive hardening in the HAZ.
10. While welding, 9% nickel steel arc blow will be encountered. AC welding is therefore often preferred with, but dc may also be used. If the maximum magnetism in the plate exceeds 60 Gauss, very unstable arc conditions will result and the plates may need to be demagnetized.
11. The weld metal should contain low nitrogen, low ferrite, low carbon and high nickel.
12. Keep the carbon in the range <0.03%. Low carbon provides superior toughness.

Suggestions for welding 9% nickel steel are also given by Thorneycroft and Heath [267] and include the following:

1. For thicknesses less than 1 in. (25.4 mm), a single-V included joint angle of 75°–80° is recommended. This practice should also be followed for double-V joints in heavier plate.
2. The use of chill bars as backup plates is not recommended. The underside of the root run should be cooled in air.
3. It is recommended that the root run size be larger than normal.

4. The welding gun should be inclined so as to lead the welding arc in the welding direction in order to properly shield the molten deposited weld metal from the atmosphere.
5. Use electrodes with lime–fluorspar coatings, properly dried to ensure low-hydrogen contents in the weld zone.

13.32.8.8 Welding Problems with 9% Ni Steel

Conventionally, welding of 9% Ni steel is made using high-nickel alloy of the austenitic type. This process presents some critical problems [271]:

1. The yield strength of the weld metal is low compared with that of the base metal.
2. During welding, there is a high susceptibility to various forms of hot cracking such as longitudinal bead cracking and crater cracking of the weld metal.
3. The high-alloy filler material is relatively expensive and results in higher construction cost.

13.32.8.9 Postweld Heat Treatment

Since the 9% nickel steel retains its toughness after welding, there is no need for postweld stress-relieving treatment. In October 1960 (see *Operation Cryogenics*), a number of welded pressure vessels in 9% nickel steel were tested to destruction in the United States in the as-welded condition to illustrate that the 9% steel would behave in a tough and ductile manner at -196°C without stress relief [272]. ASME Code Case 1308-S allows use of the steel in the as-welded condition in thicknesses up to 2 in. (50.8 mm). Fabricators of vessels for some chemical applications may for sections above a certain thickness, typically above 50 mm, wish to apply a stress-relieving operation at a temperature of 1050°F . Further, in some instances, it may be necessary to produce large components by welding the plate to required size followed by hot forming; in such work, a double-normalizing and tempering treatment will normally be required on the welded and formed material [273]. Temperatures for PWHT should be kept below the plate tempering temperature to prevent the formation of excessive amounts of austenite, which would affect the toughness, and very slow cooling rates should not be used; ASME Code specifies cooling rates in excess of $166^{\circ}\text{C}/\text{min}$ down to 320°C to minimize the possibility of “temper embrittlement” [266].

13.32.9 WELDING OF AUSTENITIC STAINLESS STEELS FOR CRYOGENIC APPLICATION

The austenitic SSs with or without nitrogen strengthening are readily welded by all of the common welding processes, provided appropriate procedures and consumables are used. The welding processes include SMAW, TIG, and MIG welding processes. The GTAW process in conjunction with ER308L or ER316L wire produces the cleanest weld metal and excellent toughness even at -196°C (-320°F).

Flux-shielded processes: The three flux-shielded processes—SMAW/MMA welding, FCAW, and SAW—do not achieve such low oxygen content, low inclusion content in weld metal, and hence give lower impact properties than the gas-shielded processes. Guidelines on welding of SSs for cryogenic applications are discussed in Ref. [261]. “Guide to the Welding and Weldability of Cryogenic Steels” (IIS/IIW-844-87), issued by the IIW, is principally devoted to the consideration of welding of fine-grain aluminum-killed steels and nickel-alloyed ferritic steels up to 9% nickel.

13.32.9.1 Charpy V-Notch Impact Properties

Due to service conditions, the selection of welding consumables is guided by the mechanical property requirements for the weld metal. The most important mechanical property is Charpy V-notch impact at -450°F (-268°C); the minimum energy absorption is 20 ft-lb, and lateral expansion is 0.015 in minimum.

13.32.9.2 Problems in Welding

The following four main factors affect the strength and toughness of the as-deposited weld metal and take on added significance at cryogenic temperatures [274]:

1. Sensitization
2. Ferrite content
3. Nitrogen pickup
4. Oxide inclusions

These four phenomena are discussed in detail in Ref. [261]. The following discussion is based on that reference.

13.32.9.2.1 Sensitization

The grain boundary precipitation of chromium carbides reduces weld metal toughness at low temperatures. Weld metal toughness can be improved by using very low carbon fillers such as 308L (0.04% C max) and 316L (0.03% C max). For SSs with carbon content higher than 0.03%, annealing of the welds at temperatures greater than 950°C, followed by rapid cooling, dissolves the carbides and improves the toughness.

13.32.9.2.2 Ferrite Content

To avoid microfissuring, for a wide range of SS, the weld metal is usually balanced to provide 4–8 FN. However, for cryogenic service, higher ferrite reduces toughness at –196°C and lower temperature. To obtain a good combination of strength and toughness of the weld, ferrite content should be maintained in the range of 0–2 FN [275].

13.32.9.2.3 Nitrogen Pickup

Nitrogen increases the yield strength and decreases the toughness of SS weld metals [275,276]. When GTAW and GMAW processes are followed, careful gas coverage should be provided to avoid nitrogen pickup in the weld metal. While employing SMAW, lime coatings of the electrode generally give better coverage and less nitrogen pickup than titanium coatings.

13.32.9.2.4 Oxide Inclusion Content

Oxide inclusions form sites for the initiation of microvoids. The toughness at cryogenic temperatures increases with decreasing inclusion contents [276]. To reduce inclusions, use basic-coated electrodes, since they generally provide better toughness than rutile ones, due to lower oxygen content and oxide inclusions than the rutile coatings [277].

13.32.10 SAFETY IN CRYOGENICS

13.2.10.1 Checklist

The following list is a brief compilation of various principles and measures for safety in cryogenics. It can be used as a reminder when designing cryogenic equipment [278].

1. A thorough knowledge of the chemical, physical, and toxic properties of the cryogenics to be used.
2. Knowledge of the construction material properties especially embrittlement, hydrogen embrittlement, and combustibility. Materials susceptible to hydrogen attack and hydrogen embrittlement such as titanium must not be used in hydrogen service.
3. Knowledge of the heat transfer mechanisms.
4. Knowledge of the possible low-temperature effects.
5. Design adequacies and manufacturing techniques.
6. Maintaining safe distance for adjacent structures.

7. Testing of each component and safety device before commissioning.
8. Directives such as onsite emergency plan, clear definitions of work tasks, operation manuals for all possible operating conditions as well as for all possible accident conditions.
9. Training of the operation staff in order to minimize the risk of incidents and accidents.
10. Safety precautions—oxygen monitoring, safety garments, and ventilation.

13.33 CLADDING

Many applications require resistance to corrosive media. It is well known that various grades of austenitic SSs of Types 304, 304L, 308, 316, and 347, nickel, Monel, Inconel, cupronickel, aluminum, zirconium, and titanium exhibit excellent corrosion resistance in many corrosive environments. However, the construction of large assemblies such as pressure vessels and heat exchangers in corrosion-resistant metal involves costs. Consequently, increasing use is being made of clad materials to achieve the optimum balance of strength and surface properties to overcome corrosion by an economical means. The potential for severe corrosion in various coal combustion and incineration environments has renewed interest in cladding technology for both code-approved and enhanced strength developmental alloys [21]. Apart from cladding, the other methods of protecting the base metals are lining, which refers to sheet or strip attached internally to the component by mechanical or intermittent fusion techniques, and sheathing by external attachment.

13.33.1 CLAD PLATE

A clad plate is a composite plate consisting of a base metal and a cladding of corrosion-resistant or heat-resistant metal or a plastic (polyvinyl chloride plastic-clad steel plate is a newly announced development by Lukens Steel Co., USA) on one or both sides. In effect, the joint obtained represents the welding or bonding of a different metal over a large surface area. Often the base material is being selected for economic reasons and strength purposes and the cladding layer for one or a combination of the following: corrosion and erosion resistance. Cryogenic properties, elevated-temperature properties, and wear-resistance properties. The base plate is generally carbon steel, and the cladding metal may consist of a corrosion-resistant material as mentioned earlier.

13.33.2 CLADDING THICKNESS

The thickness of the clad layer required is usually small relative to that of the base material, because the latter is designed to take the majority of the load. The thickness of the clad material may vary from 10% to 50% of the base plate thickness, but normally it is held in the range of 10%–20%. The clad steels are available in the form of sheet, plate, strip, etc.

13.33.3 METHODS OF CLADDING

The term *cladding* covers a wide range of processes including the following:

1. Loose lining
2. Resistance cladding
3. Lining using plug welding
4. Thermal spray cladding
5. Hot roll bonding
6. Weld overlay cladding
7. Explosive bonding
8. Centricast pipe
9. Coextruded pipe or duplex tubing
10. Hot isostatic process
11. Explosive cladding plus roll cladding [279]

Loose linings improve either new or existing structures. Cladding by weld overlay and thermal spraying works for new and existing components. Hot roll bonding and explosive bonding offer corrosion resistance to new construction. Centricast pipe involves centrifugal casting of cladding on the base metal. Duplex tubings are coextruded. All cladding methods have some limitation, either economic or practical. These cladding processes, except hot isostatic process, are discussed next. Duplex tubing has been explained in Chapter 12.

13.33.3.1 Loose Lining

Loose lining refers to the installation of a thin corrosion resistance lining inside a process vessel. The cladding liner is about 0.3–2.0 mm thickness. Early titanium cladding attempts were based on loose lining. Use of thin titanium layers loose clad to steel is limited to process systems where [280]:

1. Heat transfer between the shell and process medium is not critical.
2. Loss of pressure or vacuum will not collapse the liner.
3. Temperatures are low.
4. There is no problem in suspending vessel internals on the lining.

If these four factors are not critical, a loose-clad vessel may be economically practical.

13.33.3.2 Resistance Cladding

In this process, resistance spot welding is employed with proprietary intermediate materials to bond thin-gauge corrosion-resistant material to the base metal. Resistance cladding provides a means of applying a lining to a base metal regardless of whether or not the base metal and the liner material are metallurgically compatible. The Inco method involves intermittently spot welding a thin (0.6–2.0 mm) copper–nickel lining with an MIG torch and wire feed.

13.33.3.3 Lining Using Plug Welding

A variation of resistance cladding is lining using plug welding. Plug welding involves the attachment of relatively thin corrosion-resistant sheet to steel surfaces at predetermined locations by fusion-welding. For example, two techniques are considered for the attachment of copper alloy sheet to steel, and both are inert-gas processes, MIG and TIG welding [281]. In the MIG technique (intermittent spot welding) by triggering the gun as for normal welding operations, the filler wire moves forward and arcs on the clad layer, producing penetration of the clad layer and the base metal to a predetermined depth, then retracting continuously while filling molten metal into the cavity created by arcing until a solid plug weld is completed.

13.33.3.4 Thermal Spraying

Thermal spraying is accomplished by heating the cladding metal to a molten state and spraying it on the prepared surface of the base metal. The thickness normally ranges from 0.2 to 2.5 mm. One of the advantages of this process is that the temperature of the base metal normally does not exceed 302°F–392°F (150°C–200°C), which normally does not affect the base metal. Various methods of cladding by lining are given in Figures 13.30 and 13.31.

13.33.3.5 Weld Overlaying or Weld Surfacing

For fabrications that involve large clad surfaces or the use of plate material exceeding 3–4 in. (76.2–101.6 mm) thickness, the only practicable method of cladding is by weld deposition. The process consists of application of corrosion-resistant thin sheets or deposition of weld metal by various arc welding process, as opposed to making a joint. The surface to be overlaid must be cleaned of oxide and dirt. Weld overlaying by a fusion process may be applied only when the base metal and the weld metal deposit are compatible. While weld surfacing, an important consideration is weld dilution, which is discussed next.

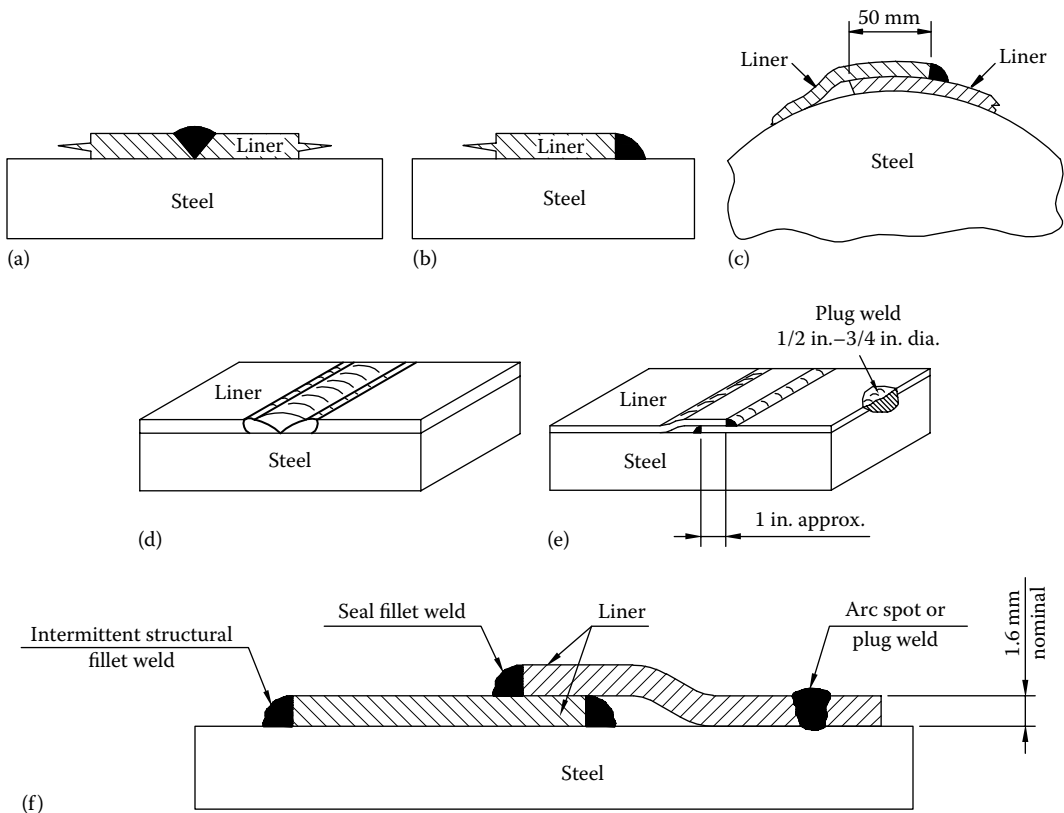


FIGURE 13.30 Various clad lining techniques for plates.

13.33.3.5.1 Weld Dilution

To ensure an overlay of specified composition for the intended purpose, the filler metal must be enriched sufficiently to compensate for dilution. For any given filler metal composition, changes in welding procedures such as maintaining approximately 50% bead overlap, use of small-diameter electrodes, low heat input, and directing the arc onto the previously deposited bead minimize dilution. The welding procedure specification should contain the acceptable limits of chemical composition of the deposit. Methods of calculating weld dilution and the approximate weld metal content of any element 3 shown in Figure 13.32.

13.33.3.5.2 Weld Overlay Cladding Methods

Various methods are employed for overlay cladding. Some of the methods include the following:

- GMAW
- FCAW spray transfer
- Manual TIG
- TIG hot wire
- TIG cold wire (mechanized)
- Plasma hot wire
- SMAW
- Electroslag strip welding
- Submerged arc—single or multiple wire
- Submerged arc strip cladding

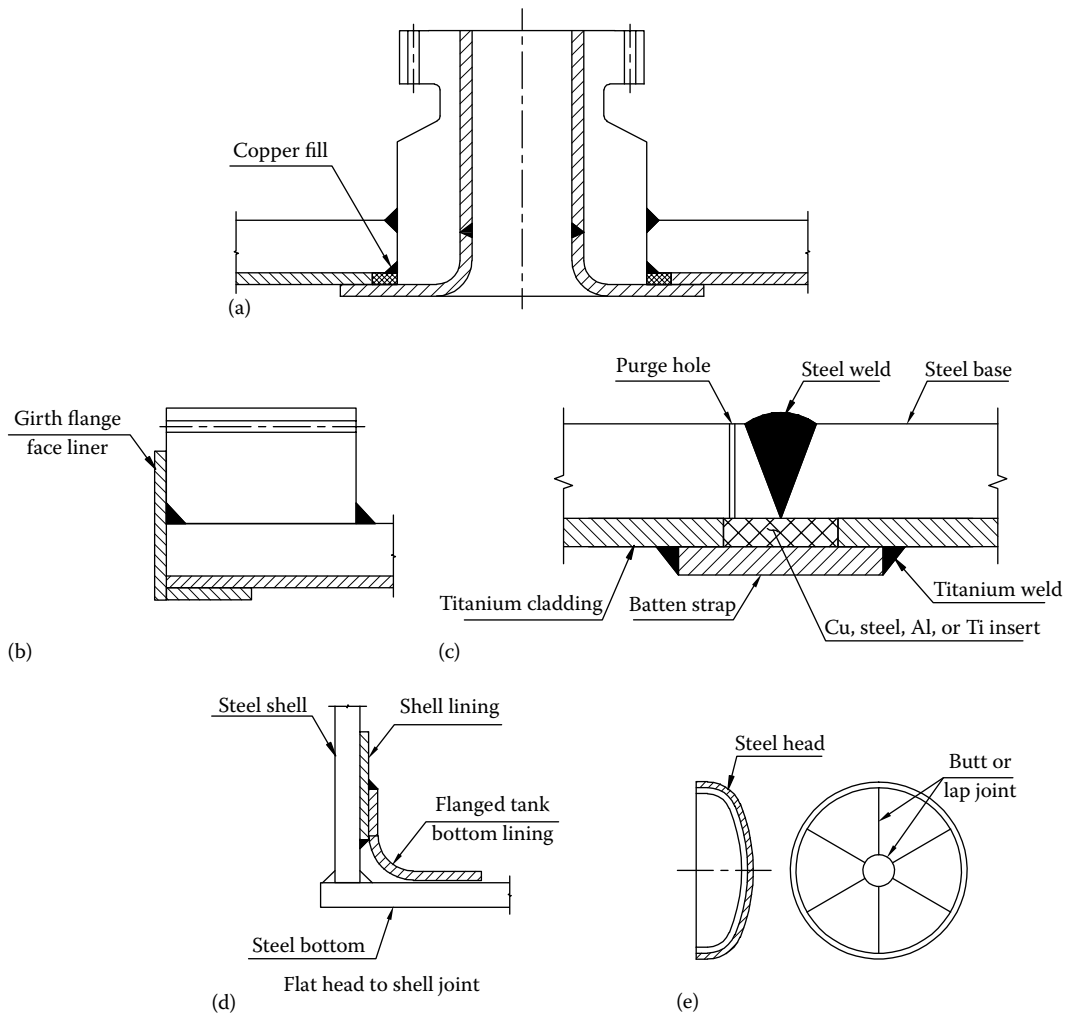


FIGURE 13.31 Various clad lining techniques for vessel components.

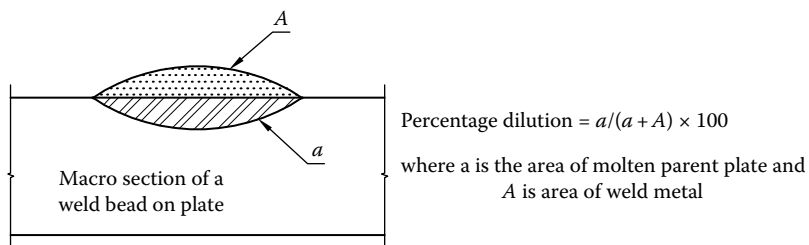


FIGURE 13.32 Estimation of weld metal dilution (schematic).

Of these, (1) MMA process, (2) GMAW or MIG spot welding, (3) strip cladding process, (4) electroslag strip cladding process, and (5) submerged strip cladding process are discussed next. AWS specification for various corrosion-resistant weld-surfacing alloys is covered by, for SS, AWS A5.4, A5.9, and A5.22; for copper base, A5.6 and A5.7; for nickel-base surfacing alloys, AWS A5.11 and A5.14; and for cobalt base, AWS A5.13.

MMA process: The MMA process represents the most flexible means of weld overlaying. This process is economical for small areas and uneconomical for large areas. Submerged arc and electroslag welding are proven economical methods for large areas.

GMAW or MIG spot welding: GMAW process with spray transfer, pulse transfer, or spot welding is normally used. The Inco method involves intermittently spot welding a thin (0.6–2.0 mm) copper–nickel lining to the head with an MIG torch and a wire fed [282].

Strip cladding process: In the strip cladding process, a strip is substituted for a solid wire. Advantages claimed for the process are relatively high deposition rates, low dilution and flexibility, 100% bonding, and good surface finishing [283]. Several variations of the strip cladding process exist, mainly subdivided into single- and double-strip techniques.

Submerged strip cladding methods: The high deposition rates achieved by SAW are well suited to large area surfacing applications. Both single and multiple electrode SAW methods are used for surfacing. The productivity of this process can be improved further by the use of higher welding currents and wider strips. The associated problems are arc blow, increased penetration and poor bead characteristics, and dilution. Magnetic steering reduces penetration, and hence dilution and arc blow control [284].

Electroslag strip cladding process: Electroslag surfacing (ESS) with strip electrodes is a highly cost-effective cladding process that has been used extensively in industry. Compared to conventional cladding processes, such as pulsed GMAW (GMAW-P) and strip submerged arc surfacing, the ESS process is known to provide both high deposition rate and low dilution [285].

13.33.3.5.3 Stainless Steel Strip Cladding

Consideration for stainless steel strip cladding: When it is required to clad a thick-walled carbon steel vessel with an austenitic steel by the strip cladding process, three factors must be considered [283,286]. These are the following:

1. Dilution: In general, the effects of dilution have been overcome either by depositing more than one layer or by using a dual-strip process. The dual-strip process incorporates a cold noncurrent carrying strip as a “barrier layer” on the parent metal surface.
2. A guaranteed minimum thickness of cladding.
3. Suitable deposit microstructure and mechanical properties (e.g., 4%–10% free ferrite in an austenitic matrix and sufficient ductility at the clad metal interface to satisfy a 3T side bend test).

Metal powder additions to control ferrite: A serious problem when strip cladding SS on carbon steel base metal is the absence of ferrite in the cladding near the interface between the cladding and the base metal. The absence of the ferrite content in this transition zone decreases the resistance to hot cracking. Ferrite-stabilizing metal powders are used to control the ferrite content of the cladding and transition zone [287]. Metal powder additions have already been used to enhance deposition rates in many conventional welding processes. According to Oh and Devletian [287], the other benefits of metal powder additions include good control over weld penetration, HAZ size, and improved fracture toughness of the weld.

13.33.3.5.4 Procedure and Welder Qualification

The general requirements for the qualification of cladding are in accordance with the ASME Code, Section IX. Both procedure and welder qualifications are described simultaneously under the outline for corrosion-resistant overlays as recommended in Section IX.

13.33.3.5.5 Heat-Treatment Considerations

Stress relieving of clad vessels is fairly common to relieve fabrication stresses, which under a given combination of conditions might lead to SCC. While heat treating, one might consider the base metal properties, which may be adversely affected due to heat treatment.

13.33.3.5.6 Inspection of Overlays

Soundness of cladding is usually tested by these methods [283]: (1) liquid penetrant to reveal any pinhole porosity; (2) ultrasonic inspection for lack of fusion and to detect large slag inclusions; (3) soundness of bond and ductility by side bend tests—excessive iron dilution or irregular penetration patterns usually fail bend tests; (4) corrosion test for resistance to corrosion; (5) chemical analysis to assure the specified composition; (6) metallography for studying the microstructure; and (7) hardness profile across the overlays. For SS, additional tests include the measurement of delta ferrite in the weld metal.

13.33.3.5.7 Inspection of Stainless Steel Cladding

Clad qualities are evaluated by the following tests [284]:

1. Corrosion test according to ASTM A262
2. Side bend test (ASTM E 190) for the ductility of clad metal and for fusion between clad and base metal
3. Ferrite content test to ensure resistance to hot cracking or microfissuring
4. Microprobe analysis to determine the distribution of Cr and Ni across the depth of cladding
5. Microstructure examination

13.33.3.5.8 Nickel Alloy Cladding

Submerged arc process, GMAW spray transfer, and SMAW are the preferred processes. Nickel alloy weld metals are readily applied as overlays on carbon and low-alloy steels and other materials. Inconel or Monel cladding can be applied to the tubesheet with inert-gas metal arc (MIG) process. These overlays provide excellent chemical and mechanical properties, and ductility to the tube-to-tubesheet joint. In overlaying, avoid excessive dilution with iron and irregular penetration. Large surfaces can be lined by the Inco method. The Inco method involves intermittently spot welding a thin (0.6–2.0 mm) copper–nickel lining with an MIG torch and wire feed.

13.33.3.6 Roll Cladding

Roll cladding involves metallurgically fusing and rolling of corrosion-resistant thin plate to the base metal at the rolling mill, as shown in Figure 13.33. The bond formed is part mechanical and part metallurgical; consequently, metallurgically incompatible materials normally cannot be produced. In the roll cladding process, a rectangular plate pack of compatible base and cladding metals is assembled. The plate pack consists, in this order, of (1) base metal, (2) a layer of cladding metal,

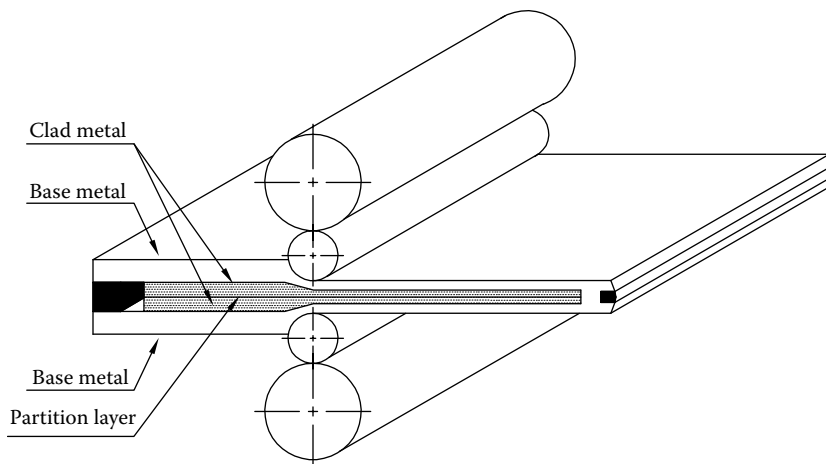


FIGURE 13.33 Roll cladding principle.

(3) a parting compound, (4) a layer of cladding metal, and (5) base metal. The facing surfaces of cladding and base metal are precleaned, and surface oxides are removed. The edges of the pack are welded together to maintain the relative positions of the assembly and it is rolled. As the thickness of the entire pack is reduced, the cladding metal forge welds to the base metal. When the amount of reduction is appropriate, the plate pack is parted, the surfaces are conditioned, and the clad plates are heat treated and cleaned. Sometimes explosive clad plates are rolled to improve the bonding integrity and to straighten the plates.

13.33.3.7 Explosive Cladding

The explosive cladding process utilizes explosive energy to create a metallurgical bond and to produce clad plate of both conventional and unique metal combinations. In this process, the cladding plate is accelerated by means of an explosive charge to a high velocity of the order of 1000 ft/s (322 m/s), before impacting the base plate. This process makes available a range of metal combinations and many materials that are normally considered incompatible and hence cannot be produced by conventional methods. For example, titanium can be bonded to mild steel, copper to SS, SS to brass, and many other combinations. Explosive welding is principally associated with the fabrication of large clad plates, shells, tubes, nozzles, the fabrication of tube-to-tubesheet joints, and the plugging of defective tube joints of shell-and-tube heat exchangers. Most of the clad tubesheet applications have consisted of nickel and nickel alloys, copper and copper alloys, and SS clad on SA 516-70 [288]. Table 13.55 presents a list of alloys commonly supplied as explosion clad [289].

13.33.3.7.1 Welding Geometries

Explosive welding geometries are mostly (1) parallel cladding and (2) angular cladding. Large-area clad plates for fabrication of plates are made using the parallel arrangements. Figure 13.34 illustrates the principles of parallel explosion cladding. Figure 13.35 shows a clad head and Figure 13.36 shows the photomicrograph of a typical explosion weld.

13.33.3.7.2 Angular Geometry

In angular geometry arrangement (Figure 13.37), the two surfaces to be welded are at an angle to each other, and explosive is sited on the reverse side of one of the components. On initiation of the explosion, the two plates are forced together, colliding intimately to form a junction. Small-area cladding such as tube-to-tubesheet joint expansion (and plugging of leaking tubes (Figure 13.37)) is made using the angular arrangements. This setup is appropriate in view of the short bond lengths of approximately 1 in. that are normally required [290]. Metal combinations that are welded commercially include carbon steel to carbon steel, titanium to SS, and 90-30 copper-nickels. The principle of geometry applied for tube-to-tubesheet joint expansion and plugging of leaking tubes is explained next.

TABLE 13.55
List of Clad Alloys and Base Metals

Cladding Metals	Base Metals
SS alloys: A410S, A304/304L,	A 203, A387Gr 11 Cl2, A 516-70
A316/316L, A317/317L, A321, A347	A 387Gr 12 Cl2;
Nickel and nickel alloys: 200, 201, 400, 600,	A 516 Gr 60, 65, 70;
625 800, 904L, 825, 625, C22, C4,	A537 Cl 1, Cl 2;
Titanium	} A553 Type 1, A 738 Gr A, B
Zirconium	
Tantalum	

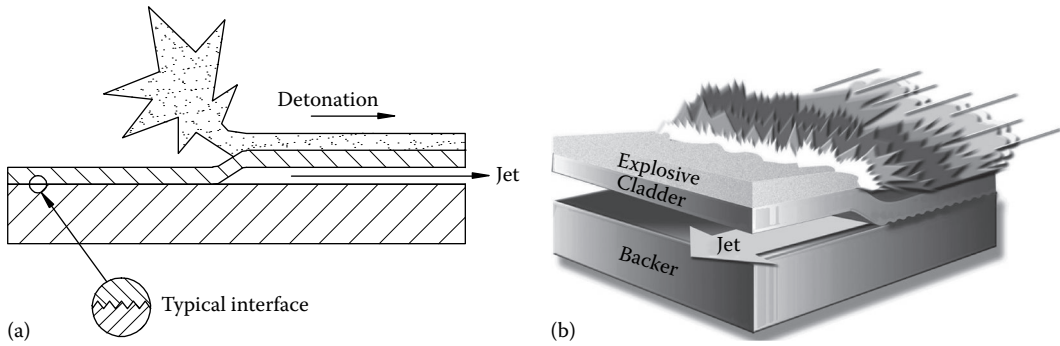


FIGURE 13.34 Explosive cladding principle. (Courtesy of Dynamic Materials Corporation, CO.)



FIGURE 13.35 Clad head. (Courtesy of Dynamic Materials Corporation, CO.)

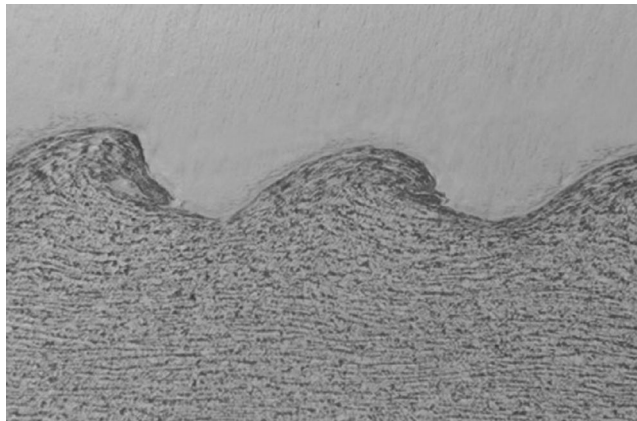


FIGURE 13.36 Photomicrograph of a typical explosion weld. (Courtesy of Dynamic Materials Corporation, CO.)

13.33.3.7.3 Tube-to-Tubesheet Welding

In most instances, the weld is located near the front of the tubesheet and has a length of approximately 0.5 in. (12.7 mm) or three to five times the tube wall thickness [291]. Most applications of explosion welding in tube-to-tubesheet joints involve tube diameters of 0.5–1.5 in. (12.7–38.1 mm). The angular disposition of the component surfaces is achieved in this instance by machining a countersink at the outer end of the tubesheet hole. The countersink depth is usually 0.5–0.6 in. at

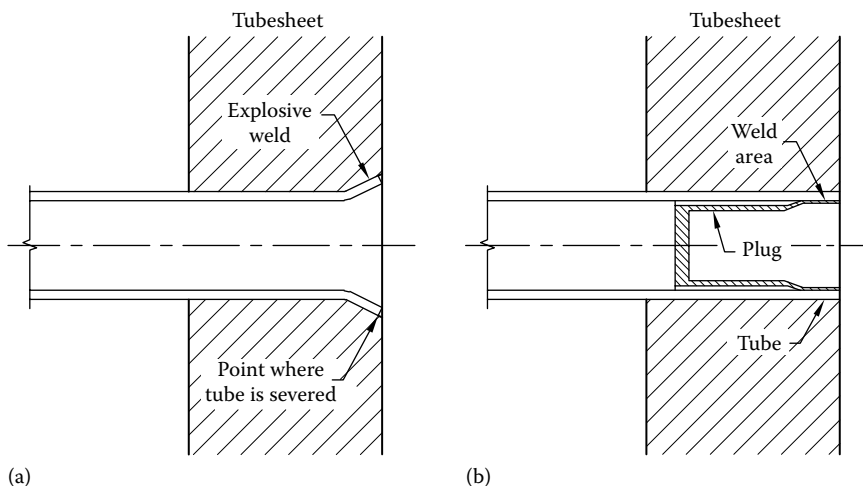


FIGURE 13.37 Angular geometry explosion cladding: (a) tube-to-tubesheet expansion and (b) plugging of leaking tube—Dynaflux[®] explosively welded plug.

an included angle between 10° and 20° [292]. The detonator is placed in the bore of a polyethylene insert to form a composite cartridge, which is placed within the tube hole. On ignition, the shock waves emanating from the detonator are transmitted by the polyethylene insert to the tube, thus imparting to it the required radial velocity. Tubes may be welded individually or in groups. While determining the choice of explosive welding for tube-to-tubesheet joining, one should consider (1) the thickness of the tubesheet, (2) ligament width, and (3) tube diameter and wall thickness [291].

End effect: Because of energy losses at the end of the tube, the velocity at the tube extremity is lower than elsewhere in the system, thereby producing an end effect [290]. This area may well have a velocity below that required for welding. The tube is therefore initially positioned with its end projecting some short distance from the face of the tubesheet. The end effect area thus lies outside the tubesheet, and a reasonably uniform tube velocity is thereby achieved over the intended weld zone along the machined angle, as shown in Figure 13.37.

13.33.3.7.4 Plug Welding

Explosive welding of plugs in leaking tubes is an effective technique for conventional heat exchangers and nuclear heat exchangers where there is a problem of nuclear radiation [293]. These areas may be inaccessible due to hotness, corrosiveness, radiation, etc. Plug welding, being a maintenance operation, is usually carried out on-site. The only operation that remains to be carried out within the confines of the exchanger tubesheet is machining of a countersink, similar to tube-to-tubesheet explosion welding.

13.33.3.7.5 Inspection of Joint Quality

The usual methods of testing explosive welds are discussed in Refs. [291,292]. Typical inspection methods in addition to visual inspection include the following: (1) pulse-echo ultrasonic technique (ASTM A578) to assess the bond integrity—an ultrasonic frequency in the range of 2.5–10 MHz usually is adequate; (2) radiography applicable to welds between metals with significant density variation and an interface with a large wavy pattern; (3) metallographic examination of the weld interface on a plane parallel to the detonation front and normal to the surface—a well-formed wave pattern without porosity generally is indicative of a good joint; and (4) the bond strength by various destructive tests like chisel test, tension-shear test, and tension test. For critical applications, checking the integrity of tube-to-tubesheet joints, helium leak testing can be applied to the fusion zone of an explosive weld.

13.33.4 PROCESSING OF CLAD PLATES

Clad plates usually are distorted somewhat during explosion cladding. This requires straightening to meet standard flatness requirements. Also it is customary to supply explosion-clad plate in the as-cladded condition because the hardening that occurs immediately adjacent to the interface usually does not significantly affect the bulk properties of the base plate. If some service requirements demand PWHT, this requirement may be complied with. Clad steels are always flame-cut from the backing side. While hot forming, extreme care should be taken to ensure there is no danger of sulfur pickup from furnace atmosphere. To overcome this problem, an electric furnace is preferred.

13.33.4.1 Forming of Clad Steel Plates

Pressure vessel heads, shells, tubesheets, and other components can be made from explosion-clad plates by conventional hot- or cold-forming techniques. A differently stressed condition exists at the bond interface, and this governs the thicknesses and diameters that can be successfully bent [294].

Hot forming, welding, or heat treatment must take into account the metallurgical properties of the materials, grain growth, and the possibility of undesirable diffusion that may occur at the interface [291,292]. Hot forming of compatible materials of stainless clad steel plates does not produce any intermetallic compound at the interface, whereas the incompatible clad plate with base metal, like titanium clad to SS, should be hot formed at not more than 1400°F (760°C) to prevent undesirable formation of intermetallic compounds. Cold forming of clad plates poses little difficulty, provided that the largest possible radius is used to avoid excessive work hardening of the cladding. To retain the corrosion resistance property, forming tools should be free from iron oxide scale and surface contaminants. Use of lubricant is not recommended because of the possibility of sulfur and carbon pickup during subsequent hot-working or thermal cycles. Various precautions to be taken while fabricating clad plates are discussed by Ellis [295].

13.33.4.1.1 Welding of Stainless Steel Clad Steels

When welding clad steels, the dilution effects should be given consideration. The backing steel should be welded first; however, if the welding does not present any great difficulty, the clad layer can be welded first with a suitable electrode (i.e., a 33-alloy electrode), back chipped, and the base plate then welded [291,295]. Joint preparation for clad steels is shown in Figure 13.38. A typical welding procedure for Hastelloy clad steel plate is shown in Figure 13.39. Joining clad steel to

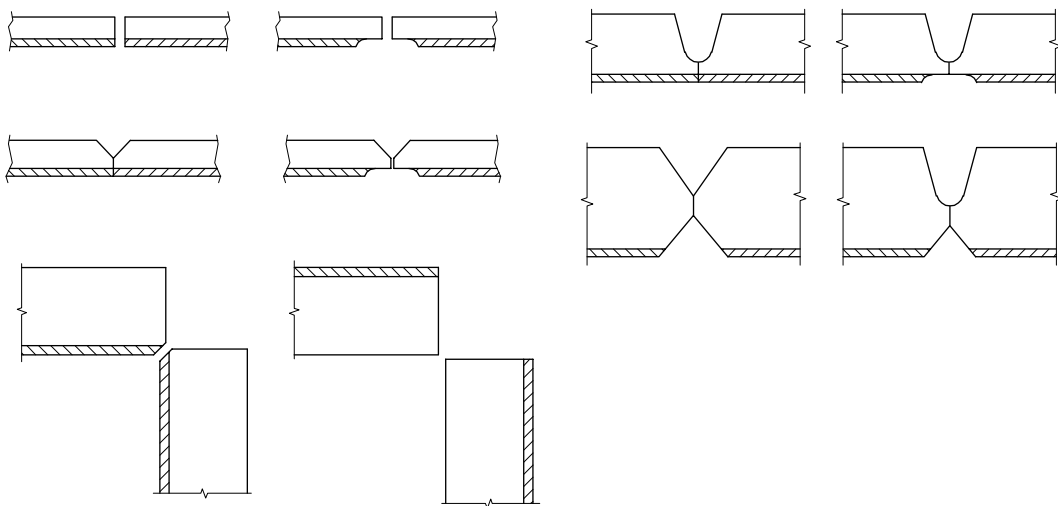


FIGURE 13.38 Joint design for welding of clad steel plate. (Adapted from Kearns, W.H. (ed.), *Welding Handbook, Vol.4, Metals and Their Weldability*, 7th edn., AWS, Miami, FL, 1982, Chapter 12.)

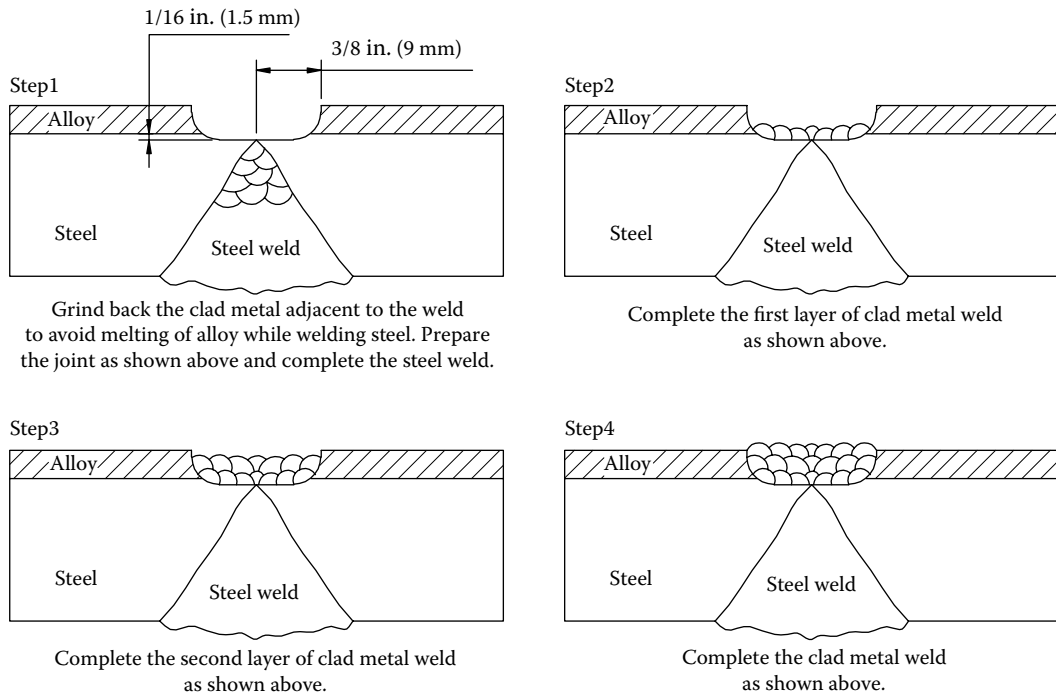


FIGURE 13.39 Method of welding of steel plate clad with Hastelloy.

unclad steel sections normally requires making the butt weld and restoring the clad section in a fashion similar to joining two clad plates. Other considerations for welding SS clads are carbide precipitation, sigma-phase precipitation, and delta ferrite content.

Selection of filler metals: Stainless-steel-clad carbon or low-alloy steel plates are sometimes welded with SS filler metal throughout the whole plate thickness. But it is enough to use carbon or low-alloy steel filler metal on the unclad side, followed by removal of a portion of the cladding and completion of the joint with stainless filler metal. For the clad side, Type 309L filler metal could be used for base metal such as Types 405, 410, 430, 304, and 304L; Type 309 Cb for 321 or 347; and 309 Mo for 316. The user should consider the manufacturer's recommendations in choosing filler metals. Reference [296] gives guidance for selection of filler metals for welding clad metals of austenitic SSs, ferritic SS, nickel alloys, and copper alloys, and guidance for the butt joint designs for welding clad steels from both sides, respectively.

PWHT: If stress-relief annealing is required, use either stabilized or low-carbon SSs to avoid carbide precipitation. Care should be taken to ensure absence of sigma-phase precipitation. Differential thermal expansion between mild steel backing and SS cladding will induce stresses in the cladding.

13.33.4.1.2 Welding of Plain Chromium or Ferritic Stainless Steel Clad Steels

In the welding of plain chromium clad steels of the order of 12%–16% Cr and 0.80% C, precautions must be taken to prevent (1) embrittlement above 1150°C, (2) 475°C embrittlement, (3) brittleness due to sigma phase, and (4) notch sensitivity pronounced at room temperature [295].

13.33.4.1.3 Welding of Nickel-Clad Steels

Iron dilution is a major problem. This problem is overcome by proper choice of electrode and welding techniques. Remove the top surface of the previous run before further welding and adopt a stringer bead technique. Carbon content of the nickel used for clad steels should be less than 0.05% to avoid the intergranular precipitate of graphite that forms at about 1202°F (650°C) [295].

13.33.4.1.4 Welding of Monel-Clad Steels

Iron dilution is a major problem. Iron dilution is overcome by using a root run (from the clad side) of a nickel electrode and using a low-carbon Monel electrode. If an 80-20 nickel-chromium electrode is used, dilution problems are negligible.

13.33.5 FAILURE OF CLAD MATERIAL

Failure of clad material can occur due to cracks in the clad metal or in the welds in the clad plate, or due to a bulged-out clad plate that has separated from the base material.

13.33.6 ASME CODE REQUIREMENTS IN USING CLAD MATERIAL

ASME Code Section VIII, Div. 1, places the responsibility on the owners and users for determining cladding material that will be suitable for the intended service. Salient features of code rules for clad materials are as follows:

Bond strength: The bond strength between the cladding and the backing plate must meet shear strength requirements of the code to prevent separation of the cladding from the backing plate. This shear strength must be a minimum of 20,000 lb/in.²

Spot radiography: All welds on clad vessels using the combined-thickness approach per code rules must have at least spot radiography examinations.

Suitability for service: Suitability for service includes adequate corrosion resistance and the retention of expected mechanical properties for the planned service life.

Telltale hole for detecting corrosion: Telltale holes are required on clad pressure vessels in order to warn the user when the CRC has been penetrated. Telltale holes shall not be provided in vessels that are to contain lethal substances, except as permitted by ULW-76 for vent holes in layered construction.

Welding requirement: Welds that are used on cladding material must have a corrosion resistance at least equal to that of the cladding.

13.34 POSTWELD HEAT TREATMENT OF WELDED JOINTS IN STEEL PRESSURE VESSELS AND HEAT EXCHANGERS

Though many welded structures and components perform satisfactorily without PWHT, there are certain well-established conditions where application of PWHT is either mandatory or traditional [297]. For example,

1. Heavy thickness metals and alloy steels as specified in applicable fabrication code and customer requirement.
2. PWHT of pressure vessel and heat exchanger is mandatory for certain applications (e.g., lethal service).
3. With some welding processes like electroslag and electrogas, PWHT is required. The high heat input and the long thermal cycle inherent in the electroslag welding process produce a large HAZ, which is subject to grain coarsening and a loss of fracture toughness. The coarse-grained weld metal should be refined by a normalizing heat treatment to develop required properties [298, 299]. Normalizing removes nearly all traces of the cast structure of the weld metal and nearly equalizes the properties of the weld metal and the base metal.

4. It is important to note that vessels operating under creep conditions should be stress relieved before being put into service. If the vessels are not stress relieved, residual stresses may be superimposed on the applied stress, and this may lead to premature creep failure.

13.34.1 OBJECTIVES OF HEAT TREATMENT

PWHT is intended to relieve the residual stresses generated by thermal contraction after welding and thereby to minimize the risk of subsequent distortion or cracking or to produce improvements in metallurgical structure or properties of the weld metal. PWHT provides the following features in the welded structure:

1. Relieving of residual stresses
2. Reduction of the risk of failure by brittle fracture
3. More ductility in the weld metal and a lowering of hardness
4. Improved resistance to SCC
5. Improved dimensional stability
6. Improved machinability
7. Improved fatigue performance

13.34.2 TYPES OF HEAT TREATMENT

Annealing is normally applied to material before cold working or before welding (air-hardenable materials). Annealing consists of heating the steel either in or near its critical temperature range, followed by an extended slow furnace cooling. A full anneal is said to be done when the steel is heated above its critical temperature range, which for carbon and alloy steels is in the range of 1550°F–1675°F, depending on the type of steel, and the steel is slowly cooled: 1200°F for carbon steel and 1000°F for low-alloy steels. The resulting structure will give a very soft material.

Normalizing is used to restore the original microstructure after hot forming and severe cold working. It provides uniform grain structure and improves toughness, which is important in machining and roll forming or bending. In normalizing, the material is air cooled after heating to temperatures above the upper critical temperature or A_3 temperature. The normalizing temperature for carbon and alloy steels is in the range of 1600°F–1800°F, depending on the type of steel.

Quench and temper: Steel is rapidly cooled from above its upper critical temperature or A_3 temperature to a temperature far below this range. Water or oil is used to accelerate the cooling. In the as-quenched condition, the product is not suitable for most commercial applications because of its lower ductility and high hardness. Therefore, steel must be tempered in order to soften to improve its ductility and toughness and relieve internal stresses. Tempering is a reheating treatment done at lower temperatures, usually in the range between 400°F and 1300°F.

SHT or quench annealing: This is normally adopted for sensitized austenitic SS. Sensitization causes precipitation of chromium carbide in the HAZ. This precipitation causes the steel to lose chromium below 11% and makes the zone susceptible to corrosion. Also during cold work, SS work hardens to a very high degree. In order to dissolve the carbides in case of welding and to bring down the hardness in cold working, austenitic steels are heated above 1050°C and quenched in water. SHT or quench annealing is also employed to heat treat 6Mo supraustenitics.

Stress relieving is a heat treatment designed to relieve residual stresses in the metal structure. The residual stresses may result from cold-working operations, from machining, or from welding. The treatment consists of slowly heating the part to about 1150°F–1350°F and, after holding at this

temperature for a period of time, slowly cooling the steel in the furnace or still air. With ferritic steels, the treatment preferably consists of heating the complete unit in a furnace to a temperature of 600°C–700°C. This heat treatment is sometimes called process anneal, subcritical anneal, or post heat treatment after welding [300]. Stress relieving of welded assemblies may be necessary for one or more of the following reasons [301]:

1. To prevent distortion or cracking when externally applied stresses are added to the residual stresses.
2. To reduce the risk of brittle fracture. The brittle fracture may be initiated at weld defects by residual stresses combined with service stresses.
3. To reduce the risk of fatigue failure. The safe range of fatigue stress may be reduced by the presence of residual stresses.
4. To reduce the risk of service-oriented problems such as SCC and corrosion fatigue.
5. To reduce the risk of cracking under creep conditions.

13.34.3 EFFECTS OF CHANGES IN STEEL QUALITY AND PWHT

IIW experience [297] shows that steels that are microalloyed with any element (or combination) of Al, Ti, Nb, or V and that have a CE value $\leq 0.41\%$ and carbon content value $\leq 0.15\%$ are susceptible both to HAZs and to degradation of the weld zone by plastic strains and hence can better accommodate the presence of residual stresses induced in the weld zone.

Under certain conditions, use of a suitable filler metal and proper welding procedures can result in satisfactory weld joints without the application of PWHT, provided there is no mandatory code requirement for PWHT. If stress-relief treatment is still required, it may be possible to achieve this with mechanical stress relief or with lower stress-relief temperatures than that are usually required.

The carbon content in steel should be lowered to meet the HAZ hardness requirements, if PWHT is not employed [302].

13.34.4 ASME CODE REQUIREMENTS FOR PWHT

The requirements for PWHT are dictated by most of the codes as a function of base metal composition and thickness. The ASME Code Div. 1 [303] requires specific heating rates, holding times, temperatures, and cooling rates.

13.34.4.1 Charts for Heat Treatment as per ASME Code

As an aid to determining requirements for PWHT in accordance with the ASME Code, Section VIII, Divisions 1 and 2, Carpenter [304] developed charts in the form of decision trees. The proper use of these charts should remove most of the decision-making problems that arise when using the tables in the ASME Code. These charts should be used only as an aid in determining PWHT requirements. They do not contain all requirements.

13.34.5 PWHT CYCLE

When a PWHT is specified, the operations should be monitored and documented by an inspector. Items of importance in heat treatment may include the following:

1. Area to be heated
2. Heating and cooling rates
3. Holding temperature and time
4. Temperature measurements and distribution
5. Equipment calibration

Alloy steels in general require more severe heat treatment than mild steel, but temperature is usually kept below the critical range, i.e., below about 700°C, unless normalizing at a temperature around 900°C is adopted [301].

The rate of heating varies with the quality, specification, geometry, and size of jobs and will be as low as 100°C/h/in. for the case of high-alloy steel and 220°C/h/in. for the case of medium carbon steel. Soaking temperature, soaking time, and rate of cooling depend upon the grade and specifications of materials. Refer to UCS 56 tables of ASME Section VIII, Div. 1.

13.34.6 QUALITY CONTROL DURING HEAT TREATMENT

Heat-treatment schedules should be based on the code, welding procedure specification, and material specification requirements. The heat treatment must be carried out in accordance with the approved procedures. Such heat-treatment procedures should indicate the following:

1. Rate of heating
2. Soaking time and temperature
3. Rate of cooling
4. Location of thermocouple
5. For local heat treatment, the heating band width

For every heat-treatment cycle, a coupon test plate should be made. While heat treating, metals temperature must be measured and recorded. Thermocouple location and number of thermocouples are to be provided as per fabrication code and approved procedure. The time–temperature cycle for heat treatment is recorded on a continuous recorder, which is made available to the authorized inspector for verification. The time–temperature chart and heating diagram are the records of the heat-treatment operation. All thermocouple and temperature measuring and recording instruments are calibrated periodically. For all instruments and gauges, a serial number is allotted. Maintain records giving the following particulars:

1. Type of instrument/gauge
2. Method of calibration
3. Last date of calibration
4. Frequency of calibration/due date for recalibration
5. Initial date of acceptance
6. Standard/specification to which the acceptance is made
7. Place at which calibration has been done

The details of the heat treatment, such as PWHT or heat treatment after cold forming, local heat treatments, and annealing on a job site or part/partial annealing—but not the heat treatment of purchased parts (materials, dished heads)—for the equipment or its parts should be prepared as given in Table 13.56.

13.34.7 METHODS OF PWHT

The methods of PWHT include furnace heating, in situ heating, and local heating. If the whole assembly is to be heat treated, this is usually carried out in a gas-fired or oil-fired furnace. While heat treating in a furnace, care has to be taken to ensure that the entire exchanger is brought uniformly to the holding temperature to avoid introducing unnecessary thermal stresses. This is ensured by the use of thermocouples on the vessel interior as well as the exterior to verify adequate through-wall heating [39]. When local heat treatment is carried out, electric resistance heating with resistance elements or braided heaters or induction heating or gas burners may be used.

TABLE 13.56
Heat Treatment Details

Part	Heat Treatment	Temp.	Holding Time	Holding Rate	Cooling Rate	Remarks
------	----------------	-------	--------------	--------------	--------------	---------

13.34.8 EFFECTIVENESS OF HEAT TREATMENT

The level of residual stress after PWHT depends on the material composition, stress-relieving temperature and duration, and stress level before heat treatment. The efficiency of stress relieving can be determined by [301] the following:

1. Bent bar tests
2. Tests of creep relaxation type
3. Determination of stresses in welds

13.34.9 DEFECTS DUE TO HEAT TREATMENT

1. Overheating, which will cause scaling and surface reaction.
2. Distortion due to poor PWHT cycle temperature program.
3. Sagging of the tube bundle or the shell due to inadequate support or because the existing supports are widely spaced.
4. For weld overlays on steel plates, prolonged overheating will cause carbon diffusion from the base metal into the overlay and will weaken the base metal, and this may cause intergranular corrosion in corrosive environments. Carbide-forming elements like Mo, V, and Cr slow down diffusion. Other effects include sensitization and sigma-phase precipitation if the heat-treatment temperature is high.

13.34.10 POSSIBLE WELDING-RELATED FAILURES

These are possible welding-related failures during stress-relief annealing [76]:

1. Temperature-induced embrittlement
2. Elongation-induced embrittlement
3. SRC or RC

13.34.11 NDT AFTER PWHT

Certain materials are prone to cracking during PWHT. This is known as RC or SRC. HAZs of welds of such materials are to be subjected to NDT after PWHT.

REFERENCES

1. Henthorne, M., Understanding corrosion, *Chem. Eng.*, Deskbook Issue, 4 December, 19–33 (1972).
2. Kobrin, G., Materials selection, in *Metals Handbook*, Korj, L. J. and Olson, D. L., (eds.), vol. 13, Corrosion, 9th edn., American Society for Metals, Metals Park, OH, 1987, pp. 321–337.
3. Moore, R. E., Selecting materials to meet environmental conditions, in *Materials Engineering T. Selecting Materials for Process Equipment* (K. J. McNaughton, ed.), McGraw-Hill, New York, 1980, pp. 31–33.
4. Hildebrand, E. L., Materials selection for petroleum refineries and petrochemical plants, *Mater. Protect. Perform.*, July, 19–22 (1972).

5. Elliott, P., Design details to minimize corrosion, in *Metals Handbook, Vol. 13, Corrosion*, 9th edn., American Society for Metals, Metals Park, OH, 1987, pp. 338–343.
6. Guide to selecting engineered materials, metals, polymers ceramics, composites, *Adv. Mater. Process.*, 137(6), (1990).
7. Designing and fabricating aluminum weldments, *Weld. Design Fabr.*, February, 53–62 (1977).
8. Daemen, R., Welding heavy gauge high tensile steels, *Brown Boveri. Rev.*, 52, 512–524 (1965).
9. Langer, B. F. and Harding, W. L., Material requirements for long life pressure vessels, *Trans. ASME, J. Eng. Power*, October, 403–410 (1964).
10. Hattangadi, A. D. and Seth, B. B., Lamellar tearing in fillet weldments of pressure vessel fabrication, *Weld. J.*, April, 89-s–96-s (1983).
11. Frew, J. A., Lloyd's approach to quality assurance of welded structures, *Weld. Metal Fabr.*, July–August, 256–260 (1974).
12. Clarke, J. S. and Northup, M. S., Design of vessels for petroleum refining and petrochemicals service, *ASME J. Eng. Power*, October, 411–418 (1964).
13. Bravenec, E. V., Why steel fracture, *Chem. Eng.*, July 10, 100–108 (1972).
14. Swales, G. L. and Haynes, G. A., Nickel steels in LNG tankers, in *Source Book on Materials Selection*, Vol. 1, (R. B. Guina, compiler), ASM, Metals Park, OH, 1977, pp. 469–474.
15. Climax Molybdenum Co. Ltd., *Guide to the Choice and Fabrication of Pressure Vessel Steel* (an affiliate of AMAX American Metal Climax, Inc.), Climax Molybdenum Co. Ltd., London, U.K.
16. Schillmoller, C. M. and Craig, B. D., Nickel steels in Arctic service, *Mater. Perform.*, October, 46–49 (1987).
17. Benzer, W. C., Trends in materials application: Steels, *Chem. Eng.*, Deskbook Issue, October 12, 101–110 (1970).
18. Nippon Steel Corporation, Low alloy steel plates for high temperature service, Nippon Steel Corporation, Cat. No. EXE 396, April 1976.
19. Schade, J. P. and Ross, R. W., Control corrosion with nickel base alloys, *Adv. Mater. Process.*, 7, 37–40 (1994).
20. Jana, S. R. and Honavar, D. S., A study in designing of weld metals for high austenitic stainless steels, in *Stainless Steels—Processing and Metallurgy, Proceedings of the International Conference on Stainless Steels* (P. Krishna Rao, M. K. Asundi, N. B. Ballal, and H. S. Gadiyar, eds.), INCOS-89, Bombay, Omega Scientific Publishers, New Delhi, India, 1989, pp. 149–158.
21. Swindeman, R. W. and Gold, M., Developments in ferrous alloy technology for high-temperature service, *ASME J. Pressure Vessel Technol.*, 113, 133–140 (1991).
22. Kane, R. D. and Cayard, M. S., Improve corrosion control in refining processes, *Hydrocarb. Process.*, November, 129–142 (1995).
23. NACE, *Corrosion Abstracts*, National Association of Corrosion Engineers, Houston, TX.
24. NACE, *Corrosion Data Survey—Metals Section*, 6th edn., 1985, and *Corrosion Data Survey—Nonmetals Section*, 1975; National Association of Corrosion Engineers, Houston, TX.
25. Warren, D., Hydrogen effects on steel, *Mater. Perform.*, January, 38–46 (1987).
26. Richardson, H. T., Application of welding requirements and standards for oil refinery equipment, *Weld. Metal Fabr.*, October, 367–374 (1968).
27. Kar, R. J. and Todd, J. A., Alloy modification of thick section 2.25Cr-1Mo steel, in *Application of 2.25 Cr-1 Mo Steel for Thick Wall Pressure Vessels, ASTM STP 755* (G. S. Sangdahl and M. Semchyshen, eds.), American Society for Testing and Materials, Philadelphia, PA, 1982, pp. 228–252.
28. Wilten, H. M., Microscope speeds diagnosis of refinery corrosion, *Hydrocarb. Process. Petrol. Refiner.*, 40, 151–280 (1961).
29. Hagel, W. C. and Miska, K. H., How to select alloy steels for pressure vessels—I, *Chem. Eng.*, July 28, 89–91 (1980).
30. API, Steels for hydrogen service at elevated temperatures and pressures in petroleum refineries and petrochemical plants, API Publication 941, Washington, DC, 1997.
31. Kirchner, W. L., Innovations in vessel fabrication, *Mater. Protect. Perform.*, December, 20–22 (1972).
32. Hoffman, H. C., Pressure vessel primer, *Mach. Design*, October 9, 168–171 (1980).
33. Sattler, F. J., Forrer, G. R., and Parker, W. O., Jr., Inservice inspection of nuclear plants, *Mater. Eval.*, November, 18A–22A, 27A–29A (1972).
34. Landrum, R. J., Designing equipment for corrosion resistance, *Chem. Eng.*, Deskbook Issue, October 12, 75–82 (1970).
35. NACE, Equipment service life factors, *Mater. Perform.*, September, 79 (1988); R. J. Landrum, *Fundamentals of Designing for Corrosion Control*, National Association of Corrosion Engineers, Houston, TX.

36. ASTM, *Annual Book of ASTM Standards for Metal Products, Test Methods and Analytical Procedures. Section 1—Iron and Steel Products; Section 2—Nonferrous Metal Products; Section 3—Metal Test Methods and Analytical Procedures*, ASTM, Philadelphia, PA, 1992.
- 36a. ASTM, *Annual Book of ASTM Standards, Section 1—Iron and Steel, Steel-Piping, Tubing, and Fittings*, Vol. 01.01, ASTM, Philadelphia, PA, 1992.
- 36b. ASTM, *Annual Book of ASTM Standards, Section 1—Iron and Steel: Plate, Sheet, Strip, and Wire*, Vol. 01.03, ASTM, Philadelphia, PA, 1992.
- 36c. ASTM, *Annual Book of ASTM Standards, Section 1—Iron and Steel: Bars, Forging, Bearing, Chain, and Springs*, Vol. 01.04, ASTM, Philadelphia, PA, 1992.
- 36d. ASTM, *Annual Book of ASTM Standards, Section 1—Iron and Steel: Structural, Reinforcing, Pressure Vessel, Railway*, Vol. 01.05, ASTM, Philadelphia, PA, 1992.
- 36e. ASTM, *Annual Book of ASTM Standards, Section 2—Copper and Copper Alloys: Plate/Sheet/Strip Rolled Brass (Cu-Si Alloy) for General Purpose/Pressure Vessels*, Vol. 02.01, ASTM, Philadelphia, PA, 1992.
- 36f. ASTM, *Annual Book of ASTM Standards, Section 2—Aluminum and Magnesium Alloys, and Diecast Metals*, Vol. 02.02, ASTM, Philadelphia, PA, 1992.
- 36g. ASTM, *Annual Book of ASTM Standards, Section 2—Nonferrous Metals: Nickel, Lead, Tin, Zinc, Cadmium Alloys, Precious, Primary, and Reactive Metals*, Vol. 02.04, ASTM, Philadelphia, PA, 1992.
37. Hudgell, R. J. and Tickle, H., Current practices for ultrasonic and radiographic examination of tubes, tubeplates and tubeplate welds of tube bundles in heat exchangers, in *Developments in Pressure Vessel Technology—2, Inspection and Testing*, Applied Science Publishers, London, U.K., 1979, pp. 77–100.
38. Orlando, J. S. and Ballantine, W., Materials for corrosion resistant fasteners, in *Metals Handbook*, desk edition, American Society for Metals, Metals Park, OH, 1985, pp. 15.29–15.30.
39. Danis, J. I., Material selection, fabrication and inspection of refinery heat exchangers, *Weld. J.*, June, 25–30 (1986).
40. Schlunder, E. U. (Editor-in-chief), Mechanical design codes: Expansion joints, in *Heat Exchanger Design Handbook*, Hemisphere, Washington, DC, 1983, Section 4.16.
41. Yokell, S., *A Working Guide to Shell and Tube Heat Exchangers*, McGraw-Hill, New York, 1990.
42. Weymueller, C. R., ASTM specs guide users of plate steels I—Structural steels, *Weld. Design Fabr.*, February, 42–48 (1992).
43. Weymueller, C. R., ASTM specs guide users of plate steels II—Pressure vessel steels, *Weld. Design Fabr.*, March, 47–52 (1992).
44. Smallwood, R. E., Heat exchanger tubing reliability, *Mater. Perform.*, February, 27–32 (1977).
45. BSI, Specification for steel tubes for heat exchanger, BS 3606:1978, British Standards Institution, London, U.K., pp. 1–14.
46. Foxall, D. H. and Gilbert, P. T., Selecting tubes for CPI heat exchangers—III, in *Materials Engineering I: Selecting Materials for Process Equipment* (K. J. McNaughton, ed.), McGraw-Hill, New York, 1980, pp. 172–174.
47. Engle, J. P., Chemical cleaning of feedwater heaters, *Mater. Perform.*, July, 30–33 (1974).
48. Brosilow, R., Weldability—What it means to fabricators, *Weld. Design Fabr.*, June, 74–80 (1978).
49. Nippes, E. F. (ed.), Principles of joining metallurgy, in *Metals Handbook, Vol. 6, Welding, Brazing, and Soldering*, 9th edn., American Society for Metals, Metals Park, OH, 1983, pp. 21–49.
50. Nippes, E. F. (ed.), Arc welding of carbon steels: Shielded metal arc welding, in *Metals Handbook, Vol. 6, Welding, Brazing, and Soldering*, 9th edn., American Society for Metals, Metals Park, OH, 1983, pp. 75–95.
51. Nippes, E. F. (ed.), Arc welding of carbon steels: Submerged arc welding, in *Metals Handbook, Vol. 6, Welding, Brazing, and Soldering*, 9th edn., American Society for Metals, Metals Park, OH, 1983, pp. 114–151.
52. Nippes, E. F. (ed.), Gas metal arc welding (MIG welding), in *Metals Handbook, Vol. 6, Welding, Brazing, and Soldering*, 9th edn., American Society for Metals, Metals Park, OH, 1983, pp. 152–213.
53. Nippes, E. F. (ed.), Plasma arc welding, in *Metals Handbook, Vol. 6, Welding, Brazing, and Soldering*, 9th edn., American Society for Metals, Metals Park, OH, 1983, pp. 214–224.
54. Nippes, E. F. (ed.), Electroslag welding, in *Metals Handbook, Vol. 6, Welding, Brazing, and Soldering*, 9th edn., American Society for Metals, Metals Park, OH, 1983, pp. 225–237.
55. Nippes, E. F. (ed.), Electrogas welding, in *Metals Handbook, Vol. 6, Welding, Brazing, and Soldering*, 9th edn., American Society for Metals, Metals Park, OH, 1983, pp. 238–244.

56. Nippes, E. F. (ed.), Arc welding of low alloy steels and other ferrous metals, in *Metals Handbook, Vol. 6, Welding, Brazing, and Soldering*, 9th edn., American Society for Metals, Metals Park, OH, 1983, pp. 245–370.
57. Nippes, E. F. (ed.), Weld discontinuities, in *Metals Handbook, Vol. 6, Welding, Brazing, and Soldering*, 9th edn., American Society for Metals, Metals Park, OH, 1983, pp. 829–855.
58. Brosilow, R., How can fabricators control weld properties? *Weld. Design Fabr.*, March, 46–50 (1985).
59. Bailey, N., The establishment of safe welding procedures for four low alloy steels, *Weld. J.*, 51, 169s–177s (1972), Welding Research Supplement.
60. Yurioka, N., Suzuki, H., Ohshita, S., and Saito, S., Determination of necessary preheating temperature in steel welding, *Weld. J.*, June, 147-s–153-s (1983).
61. Gross, J. H., Pressure vessel steels: Promise and problems, in *Source Book on Materials Selection*, Vol. 1 (R. B. Guina, compiler), American Society for Metals, Metals Park, OH, 1977, pp. 271–276.
62. Farrar, J. C. M. and Dolby, R. E., *Lamellar Tearing in Welded Steel Fabrication*, Welding Institute, Abington Hall, Abington, Cambridge, U.K., 1972.
63. Wormington, H., Lamellar tearing in silicon-killed boiler plate, *Weld. Metal Fabr.*, September, 370–373 (1967).
64. Gross-Wordemann, J. and Dittrich, S., Prevention of temper embrittlement in 2.25 Cr-1Mo weld metal by metallurgical actions, *Weld. J.*, May, 123-s–128-s (1983).
65. Complementary information test for lamellar tearing, *Weld. World*, 19, 47–53 (1981).
66. Lippold, J. C. and Savage, W. F., Solidification of austenitic stainless steel weldments: Part III—The effect of solidification behaviour on hot cracking susceptibility, *Weld. J.*, December, 388-s–396-s (1982).
67. Goodwin, G. M., Hot cracking, measurement, mechanisms and modelling, *Weld. J.*, February, 26–31 (1990).
68. Lin, W., Lippold, J. C., and Baseslack, W. A., III, An evaluation of heat affected zone liquation cracking susceptibility, Part I: Development of a method for quantification, *Weld. J.*, April, 135-s–153-s (1993).
69. Dhooge, A. and Vinckier, A., Reheat cracking—Review of recent studies (1984–1990), *Weld. World*, 30, 44–71 (1992).
70. Nakamura, H., Naiki, T., and Okahayashi, H., Fracture in the process of stress relaxation under constant strain, in *Proceedings of the First International Conference on Fracture*, Vol. 2., Sendai, Japan, September 12–17, pp. 863–878, and Stress Relief Cracking in HAZ, IIW-IX-648–69 and IIW-X-531–69.
71. Onodera, S., Improved quality of heavy steels and their welds as related to the integrity of reactor pressure components, *Nucl. Ener. Design*, 85(3), 305–313, (1985).
72. Lippold, J. C., Baeslack, W. A. III., and Varol, I., Heat affected zone liquation cracking in austenitic and duplex stainless steels, *Weld. J.*, January, 1-s–5-s (1992).
73. Lin, S. and Indacochea, J. E., Weldability of steels, in *Metals Handbook, Vol. 1, Properties and Selection; Iron, Steels, and High Performance Alloys*, 10th edn., American Society for Metals, Metals Park, OH, 1990, pp. 603–613.
74. Connor, L. P. (ed.), *Welding Hand Book, Vol. 1, Welding Technology*, 8th edn., 1987, pp. 102–121.
75. Datasheet No. 111b, Weldability testing—Weld cracking tests, *Weld. J.*, February, 73 (1990).
76. Kautz, H. R. and Herbert, E. D., Modern welding techniques and component performance, *Weld. World*, 30, 337–341 (1992).
77. U. S. Steel Group, *U. S. Steel Handbook of Plate Products*, U. S. Steel Group, Pittsburgh, PA.
78. Lohmeier, A. and Reynolds, S. D., Jr., Carbon steel tube-to-tubesheet joints for high pressure feedwater heaters, *Westinghouse Eng.*, September, 138–143 (1966).
79. Jarman, R. A. and Shreir, L. L., Corrosion of jointed structures—Part II, *Weld. Metal Fabr.*, November/December, 445–449 (1987).
80. Kirby, G. N., Corrosion performance of carbon steel, in *Materials Engineering I: Selecting Materials for Process, Chemical Engineering*, March 12, 1979, pp. 72–84.
81. Uhlig, H. H., *Corrosion and Corrosion Control*, John Wiley & Son, Inc., New York, 1963.
82. Campbell, H. C., The ABCs of welding metallurgy for plain carbon steels, *Weld. J.*, August, 55–57 (1994).
83. Nippes, E. F. (ed.), *Metals Handbook, Vol. 6, Welding, Brazing, and Soldering*, 9th edn., American Society for Metals, Metals Park, OH, 1983, pp. 238–244.
84. Bargett, W. E. and Reeve, L., High strength weldable steel, *Iron Steel*, October/November, pp. 277–294, (1954).
85. Irvine, K. J., The development of high strength structural steels, in *Proceedings of the ISI/BISR, Joint Conference*, ISI Publication 104, ISI, London, U.K., 1967.
86. Kearns, W. H. (ed.), Carbon and low-alloy steels, in *Welding Handbook, Vol. 4, Metals and Their Weldability*, 7th edn., American Welding Society, Miami, FL, 1982, pp. 2–74.

87. Gutzeit, T., Corrosion in petroleum refining and petrochemical operations, in *Metals Handbook, Vol. 13, Corrosion*, 9th edn., American Society for Metals, Metals Park, OH, 1987, pp. 1262–1287.
88. Wordemann, G. J. and Dittrich, S., Prevention of temper embrittlement in 2.25Cr-1Mo weld metal by metallurgical actions, *Weld. J.*, May, 123-s–128-s (1983).
89. Craig, W. R., Refineries test their metals, *Weld. Design Fabr.*, April, 81–85 (1977).
90. Wilson, A. D., Tougher steels improve pressure vessel performance, *Adv. Mater. Process.*, 4, 39–42 (1993).
91. Murakami, Y., Nomura, T., and Watnabe, J., Heavy section 2¼ Cr-1Mo steel for hydrogenation reactors, in *Application of 2.25 Cr–Mo Steel for Thick Wall Pressure Vessels, ASTM STP 755* (G. S. Sangdahl and M. Semchyshen, eds.), American Society for Testing and Materials, Philadelphia, PA, 1982, pp. 383–417.
92. Baumert, K. L. and Polk, C. J., Temper embrittlement studies on 2.25Cr–Mo steel, *Mater. Perform.*, September, 39–45 (1976).
93. Swift, R. A., Effects of composition and heat treatment on the mechanical properties of 300 mm gage 2.25 Cr-1Mo steel plate, in *Application of 2.25 Cr–1Mo Steel for Thick Wall Pressure Vessels, ASTM STP 755* (G. S. Sangdahl and M. Semchyshen, eds.), American Society for Testing and Materials, Philadelphia, PA, 1982, pp. 166–188.
94. Imgram, A. G. and Swift, R. A., Pressure vessel, piping and welding needs for coal conversion systems, *J. Mater. Ener. Syst.*, December, 212–221 (1985).
95. Lukens Steel Company, *Lukens Plate Steel Specification Guide*, Lukens Steel Company, Coatesville, PA, 1993.
96. Yamamoto, S. and Natsume, S., Improvement of toughness of Cr-Mo steel weld metal at low temperature, *Weld. Metal Fabr.*, April, 110–115 (1986).
97. Climax Molybdenum Company, Modified 9 Cr-1 Mo steel for power plants, *Molybdenum Mosaic*, 6, 17, (1982), Climax Molybdenum Company of Michigan.
98. Ritche, R. O., Parker, E. R., Spencer, P. N., and Todd, J. A., A new series of advanced 3Cr-Mo-Ni steels for thick section pressure vessels in high temperature and pressure hydrogen service, *J. Mater. Ener. Syst.*, December, 151–162 (1964).
99. Brown, R. S., How to select the right stainless steel, *Adv. Mater. Process.*, 4, 20–24 (1994).
100. Debold, T. A., Select the right stainless steel, *Chem. Eng. Prog.*, November, 38–43 (1991).
101. Redmond, J. D. and Miska, K. H., The basics of stainless steels, *Chem. Eng.*, October, 89(10), 79–93 (1982).
102. Linstroth, R. L., Check for atmospheric corrosion when using stainless steels, *Chem. Eng. Prog.*, July, 49–51 (1991).
103. Metallurgy of fusion welding, Pt 3: Stainless steels, *Weld. Metal Fabr.*, October, 376–378 (1994).
104. Llewellyn, D. T., *Steels, Metallurgy and Applications*, Butterworth-Heinemann, Oxford, U.K., 1992.
105. AL-6XN[®] Alloy, Allegheny Ludlum Steel Corporation, Pittsburgh, PA, 2002, pp. 1–56.
106. Kearns, J. R. and Deverell, H. R., The use of nitrogen to improve the corrosion resistance of FeCrNiMo alloys for the chemical process industries, *Mater. Perform.*, June, 18–28 (1987).
107. Davison, R. M., Corrosion of stainless steel, in *Metals Handbook, Vol. 13, Corrosion*, 9th edn., American Society for Metals, Metals Park, OH, 1987, pp. 546–575.
108. Davison, R. M., Rahoi, D. W., and Gemmel, G., Stainless steels for heat exchanger service, in *Industrial Heat Exchangers Conference Proceedings* (A. J. Hayes, W. W. Liang, S. L. Richlen, and E. S. Tabb, eds.), American Society for Metals, Metals Park, OH, 1985, pp. 371–380.
109. Forchhammer, P., Results of damage research on corrosion failures in heat exchangers, *Heat Trans. Eng.*, 5, 19–32 (1984).
110. Paul Mueller Company, Product Literature, Mueller Accu-Therm Plate Heat Exchangers, Paul Mueller Company, Springfield, MO, 2006.
111. Blom, K. J. and Degerbeck, J., Low manganese austenitic stainless steels has improved resistance to pitting and crevice corrosion, *Mater. Perform.*, July, 52–54 (1983).
112. Slaughter, G. M., Franco-Ferreira, E. A., and Patriarca, P., Welding and brazing of high temperature radiators and heat exchangers, *Weld. J.*, January, 15–22 (1968).
113. Redmond, D. J. and Miska, K. H., High performance stainless steels for high chloride service—Part I, *Chem. Eng.*, July 25, 93–96 (1983).
114. Schillmoller, C. M. and Althoff, J. H., How to avoid failures of stainless steels, *Chem. Eng.*, May, 119–122 (1984).
115. Pollock, W. I., What's hot in metal alloys, *Chem. Eng.*, October, 78–88 (1992).
116. Kane, R. D., Super stainless steels resist hostile environments, *Adv. Mater. Process.*, 7, 16–20 (1993).
117. Borenstein, S. W., Microbiologically influenced corrosion failures of austenitic stainless steel welds, *Mater. Perform.*, August, 62–66 (1988).

118. Odegard, L., Welding of stainless steels, corrosion in welds, effect of oxides, slag and weld defects on the pitting resistance, *Weld. World*, 36, 153–160 (1995).
119. Brosilow, R., Can you weld to avoid corrosion, *Weld. Design Fabr.*, September, 67–74 (1982).
120. Standard Recommended Practice for Examination and Evaluation of Pitting Corrosion, G 46, *Annual Book of ASTM Standards*, American Society Testing and Materials, Philadelphia, PA, G46-94, 2005.
121. Garner, A., Materials selection, for bleached pulp washers, *Pulp Paper Canada*, 82, 1 (1981).
122. Bandy, R., Lu, Y. C., Newman, R. C., and Clayton, C. R., Roles of nitrogen in improving the resistance to localised corrosion in austenitic stainless steels, in *Equilibrium Diagrams and Localised Corrosion*, Electrochemical Society, New Orleans, LA, 1984, p. 471.
123. Dexter, C. S., Localized corrosion, in *Metals Handbook, Vol. 13, Corrosion*, 9th edn., American Society for Metals, Metals Park, OH, 1987, pp. 104–122.
124. Uhlig, H. H., Environmental effects on properties of materials, *Mater. Protect. Perform.*, July, 23–27 (1972).
125. Gooch, T. G., Stress corrosion cracking of welded austenitic stainless steel, *Weld. World*, 22, 64–76 (1984).
126. Copson, H. R., Effects of composition on stress corrosion cracking of some alloys containing nickel, in *Physical Metallurgy of Stress Corrosion Fracture*, Interscience, New York, 1959, p. 247.
127. Pitcher, J. H., Trends in CPI materials—Steels, *Chem. Eng.*, Deskbook Issue, December 4, 39–42 (1972).
128. Espy, R. H., Coping with stress corrosion in stainless steel welds, *Weld. Design Fabr.*, October, 82–84 (1977).
129. Nishida, H., Nakamura, K., and Takahashi, H., Intergranular stress corrosion cracking of sensitized 321 SS tube exposed to polythionic acid, *Mater. Perform.*, April, 38–41 (1984).
130. NACE, Protection of austenitic stainless steels in refineries against stress corrosion cracking by use of neutralizing solutions during shutdown, NACE RP-01-70, National Association of Corrosion Engineers, Houston, TX.
131. Fontana, M. G. and Greene, N. D., *Corrosion Engineering*, 2nd edn., McGraw-Hill, New York, 1978.
132. Bangs, S., Gas turbine regenerator uses TIG, laser beam, *Weld. Design Fabr.*, March, 81–88 (1981).
133. Jones, R. L., Prevention of stress corrosion cracking in boiling water reactors, *Mater. Perform.*, February, 70–75 (1991).
134. Gooch, T. G. and Willingham, D. C., Weld decay in austenitic stainless steels, Welding Institute, Abington Hall, Abington, Cambridge, U.K., 1975.
135. Steigerwald, R., Metallurgically influenced corrosion, in *Metals Handbook, Vol. 13, Corrosion*, 9th edn., American Society for Metals, Metals Park, OH, 1987, pp. 123–135.
136. Fenn, R., Welding metallurgy of stainless steel, *Weld. Metal Fabr.*, October, 382–386 (1987).
137. Banks, B., Process selection and filler materials for welding stainless steels, *Weld. Metal Fabr.*, March, 107–110 (1969).
138. Allen, J. S., Fabrication of heat exchangers and specialised vessels, *Weld. Metal Fabr.*, July, 240–245 (1968).
139. Weymueller, C. R., Welding the austenitic steels, *Weld. Design Fabr.*, June, 82–87 (1978).
140. Beigay, J. M. and Lovejoy, P. T., How to arc weld the stainless steels, *Weld. Design Fabr.*, August, 57–63 (1981).
141. Dulicu, D., Practical welding aspects of welding stainless steel, *Weld. Metal Fabr.*, July, 277–280 (1995).
142. Castro, R. and DeCadenet, J. J., *Welding Metallurgy of Stainless and Heat Resisting Steels*, Cambridge University Press, London, U.K., 1975.
143. Castner, H. R., What you should know about austenitic stainless steels, *Weld. J.*, April, 53–59 (1993).
144. Smith, D. V., A practical approach to ferrite in stainless steel weld metal, *Weld. J.*, May, 57–60 (1989).
145. Lundin, C. D., Lee, C. H., Menon, R., and Osorio, V., Weldability evaluation of modern 316 and 347 austenitic stainless steels: Part I—Preliminary results, *Weld. J.*, 35-s–46-s (1988).
146. Kotecki, D. J., Standards and industrial methods for ferrite measurement, *Weld. World*, 36, 161–169 (1995).
- 147a. Schaeffler, A. L., Constitution diagram for stainless steel weld metal, *Metal Prog.*, 56(11), 68 (1949).
- 147b. DeLong, W. T., Ferrite in austenitic stainless steel weld metal, *Weld. J.*, 53(7), 273-s–286-s (1974).
- 147c. Kotecki, D. J. and Siewet, T. A., WRC–1992 constitution diagram for stainless steel weld metals: A modification of the WRC–1988 diagram, *Weld. J.*, May, 171-s–178-s (1992).
148. The Welding Institute, Datasheet no. 82a, Effects of residual, impurity, and microalloying elements on weldability and weld properties, *Weld. J.*, December, 53–54 (1986). Excerpted from *Effects of Residual, Impurity, and Microalloying Elements on Weldability and Weld Properties*, The Welding Institute, 1985; adapted by Hallock C. Campbell.

149. Polland, B., The effects of minor elements on the welding characteristics of stainless steel, *Weld. J.*, 67(9), 202-s–213-s (1988).
150. Vackar, B. K., Satisfying the codes, clean dry materials, good techniques & right chemistry, *Weld. Design Fabr.*, June, 86–87 (1977).
151. Lula, R. A., Introduction, in *Source Book on the Ferritic Stainless Steels* (R. A. Lula, compiler), American Society for Metals, Metals Park, OH, 1982, pp. ix–xii.
152. Nichol, T. J., Franson, I. A., and Moller, G. E., Applications of new high chromium ferritic stainless steels in the chemical process industries, in *Corrosion/81*, Paper No. 117, NACE, 1981, pp. 357–401.
153. Wock, W. C., Selecting steel tubing for high temperature service, in *Materials Engineering I: Selecting Materials for Process Equipment* (K. J. McNaughton, ed.), McGraw-Hill, New York, 1980, pp. 252–255.
154. Davison, R. M. and Steigerwald, R. F., The new ferritic stainless steels, *Metal Prog.*, 116(6), 40–46 (1979).
155. Kaltenhauser, R. H., Improving the engineering properties of ferritic stainless steels, *Amer. Soc. Metals, Metals Eng. Q.*, 11(2), 41–47 (1971).
156. Demo, J. J., *Structure, Constitution, and General Characteristics of Wrought Ferritic Stainless Steels*, ASTM STP 619, McGraw-Hill, New York, 1977.
157. Paul Bond, A., Mechanisms of intergranular corrosion in ferritic stainless steels, *Trans. Metall. Soc. AIME*, 245(8), 2127–2134 (1969).
158. Nichol, T. J. and Davis, J. A., *Intergranular Corrosion Testing and Sensitization of Two High Chromium Ferritic Stainless Steels*, ASTM STP 656, American Society for Testing and Materials, Philadelphia, PA, 1978, pp. 179–196.
159. Walker, R., Duplex and high alloy stainless steels—Corrosion resistance and weldability, *Mater. Sci. Technol.*, 4, 78–84 (1988).
160. Rayner, R. E., Better metallurgy for process equipment, *Hydrocarb. Process.*, January, 53–60 (1994).
161. Stephenson, N., Welding status of duplex stainless steels for offshore application—Part I & II, *Weld. Metal Fabr.*, June, 159–164, and July, 235–238 (1987).
162. Farrar, J. C. M., Developments in stainless steel welding consumables, *Weld. Metal Fabr.*, January, 27–32 (1990).
163. Faucher, D. and Gilbert, D., in *Proceedings of the International Conference on Duplex Stainless Steels '86*, Netherlands Institute voor lastechniek, The Hague, the Netherlands, October 1986.
164. Tuthill, A. H., Usage and performance of nickel-containing stainless steels in both saline and natural waters and brines, *Mater. Perform.*, July, 47–50 (1988).
165. Mats, L., Development of superaustenitic stainless steels, *Weld. World*, 36, 55–63 (1995).
166. Rabensteiner, G., The welding of fully austenitic stainless steels with high molybdenum contents, *Weld. World*, 27, 2–13 (1989).
167. Davison, R. M. and Redmond, J. D., Practical guide to using 6 Mo austenitic stainless steels, *Mater. Perform.*, December, 39–43 (1988).
- 168a. Cary, H. B., Modern welding technology, in *Welding the Nonferrous Metals*, Prentice-Hall, Engle Wood Cliffs, NJ, 1979, pp. 431–460.
- 168b. Kaiser Aluminum and Chemical Sales, Inc., *Welding Kaiser Aluminum*, Kaiser Aluminum and Chemical Sales, Inc., Kaiser Center, Oakland, CA, 1967.
- 168c. Aluminum Company of America, *Welding Alcoa Aluminum*, Aluminum Company of America, Pittsburgh, PA, 1967.
- 168d. Reynolds Metals Company, *Welding, Soldering and Brazing*, Reynolds Metals Company, Richmond, VA, 1958.
169. Swaney, W., Trace, D. E., and Winterbottom, W. L., Brazing aluminum automotive heat exchangers in vacuum: Process and materials, *Weld. J.*, May, 49–57 (1986).
170. Taylor, M. A. (ed.), *Plate-Fin Heat Exchangers, Guide to Their Specification and Use*, HTFS (Harwell Laboratory), Oxon, U.K., 1980.
171. Aluminum Association, *Aluminum Brazing Handbook*, 4th edn., Aluminum Association, Washington, DC, 1990.
172. Irving, B., Welding the four most popular aluminum alloys, *Weld. J.*, February, 51–55 (1994).
173. ASM, Corrosion behaviour, in *Aluminum: Properties and Physical Metallurgy* (J. E. Hatch, ed.), American Society for Metals, Metals Park, OH, 1984, pp. 242–319.
174. Pourbaix, M., *Atlas of Electrochemical Equilibria in Aqueous Solution*, National Association of Corrosion Engineers, Houston, TX, 1974.
175. ASM, Corrosion of aluminum and aluminum alloys, in *Metals Handbook, Vol. 13, Corrosion*, 9th edn., American Society for Metals, Metals Park, OH, 1987, pp. 583–609.

176. Lancaster, J. F., Fabrication of aluminum pressure vessels, *Weld. Metal Fabr.*, December, 455–459 (1958).
177. Logan, H. L., *The Stress Corrosion Cracking of Metals*, John Wiley & Sons, New York, 1966.
178. Henthorne, M., Metals selection for corrosion control, *Chem. Eng.*, March 6, 113–118 (1972).
179. Darden, J. W., Triebel, C. A., Maes, J. P., and VanNeste, W., Monoacid/diacid combination as corrosion inhibitors in antifreeze formulations, SAE 900804, pp. 135–139, (1990).
180. Schwerdtfeger, W. J., Effects of cathodic protection on the corrosion of an aluminum alloy, *J. Res. Nat. Bureau Stand.*, 68C, 283 (1964).
181. McGill, W. A. and Weinbaum, M. J., Aluminum vapour diffused steels resist refinery corrosion, *Mater. Protect. Perform.*, July, 28–32 (1972).
182. Young, J. G., Quality control in aluminum welding, *Weld. Metal Fabr.*, January, 10–14, 62–67 (1964).
183. ASM, Corrosion of copper and copper alloys, in *Metals Handbook, Vol. 13, Corrosion*, 9th edn., American Society for Metals, Metals Park, OH, 1987, pp. 610–640.
184. Gaffoglio, C. J., Copper takes a lot of heat, *Weld. Design Fabr.*, October, 90–99 (1979).
185. Copper Development Association, Inc., *Standards Handbook*, Wrought Products, Alloy Data/2, Copper Development Association, Inc., Greenwich, CT, 1985.
186. Peters, D. T. and Kundig, K. J. A., Selecting copper and copper alloys—Part I: Wrought products & Part II: Cast products, *Adv. Mater. Process.*, 2, 26–32, and 6, 20–26 (1994).
187. Bridgeport Brass Company, *Condenser Tube Handbook*, Bridgeport Brass Company, U.K.
188. ASM, Copper in *Metals Handbook, Vol. 2, Nonferrous Metals*, 9th edn., American Society for Metals, Metals Park, OH, 1979.
189. Baumann, G., Materials for tubes used in the manufacture of high pressure feed heaters, *Brown Boveri Rev.*, 54, 700–702 (1967).
190. Cieslewicz, J. M. and Schweitzer, P. A., Copper and copper and copper alloys, in *Corrosion and Corrosion Protection Handbook*, 2nd edn. (P. A. Schweitzer, ed.), Marcel Dekker, New York, 1983, pp. 125–152.
191. Tuthill, A. H., Guidelines for the use of copper alloys in seawater, *Mater. Perform.*, September, 12–22 (1987).
192. Thompson, D. H., How to prevent stress-corrosion cracking of copper alloys, *Chem. Eng.*, February, 130–134 (1961).
193. Syrett, B. C. and Coit, R. L., Causes and prevention of power plant condenser tube failures, *Mater. Perform.*, February, 44–49 (1983).
194. Syrett, B. C. et al., Corrosion in fossil fuel power plants, in *Metals Handbook, Vol. 13, Corrosion*, 9th edn., American Society for Metals, Metals Park, OH, 1987, pp. 985–1010.
195. Spencer, E., The effect of material choice on heat transfer in steam surface condensers, *Mater. Perform.*, March, 29–32 (1979).
196. Woodward, A. R., Howard, D. L., and Andrews, E. F. C., Condensers, pumps and cooling water plant, chapter 4, in *Modern Power Station Practice, Vol. C, Turbines, Generators, and Associated Plant* (D. J. Littler, E. J. Davies, H. E. Johnson, F. Kirkby, P. B. Myerscough, and W. Wright, eds.), Pergamon Press, New York, 1991.
197. Hopkinson, B. E., Copper-nickel alloys for feedwater heater service, ASME Publication No. 62-WA.294, ASME, New York.
198. Kearns, (ed.), Copper alloys, in *Welding Handbook, Vol. 4, Metals and Their Weldability*, 7th edn., American Welding Society, Miami, FL, 1982, pp. 270–316.
199. Dawson, R. J. C., Inert gas shielded arc welding of copper and copper alloy—Dissimilar metal joint, *Weld. Metal Fabr.*, February, 60–66 (1968).
200. Dawson, R. J. C., Inert gas shielded arc welding of copper and copper alloys, Part 2, *Weld. Metal Fabr.*, February, 59–63 (1967).
201. Dawson, R. J. C., *Fusion Welding and Brazing of Copper and Copper Alloys*, Newness-Butterworths, London, U.K., 1973.
202. McDonald Sketly, L., Arc welding of copper and copper alloys, in *Metals Handbook, Vol. 6, Welding, Brazing, and Soldering*, 9th edn., (E. F. Nippes, ed.), American Society for Metals, Metals Park, OH, 1983, pp. 400–426.
203. Callcut, V. and Brown, L., Joining copper and copper alloys, *Weld. Metal Fabr.*, June, 232–236 (1996).
204. Modern methods for vessel fabrication—Developments at the Works of Daniel Adamson, *Weld. Metal Fabr.*, January, 4–15 (1963).
205. Campbell, E. J., Alloys for structural applications at subzero temperatures, in *Metals Handbook, Vol. 3, Properties and Selection: Stainless Steels, Tool Materials and Special Purpose Metals*, 9th edn., American Society for Metals, Metals Park, OH, 1980.

206. Inco Alloys International, Inc., *Product Handbook*, Publication No. IAI-38, 4th edn., Inco Alloys International, Inc., Huntington, W. VA, 1988.
207. Inco Alloys International, Inc., *Quick Reference Guide to Nickel and High Nickel Alloys*, Inco Alloys International, Inc., Huntington, W. VA.
208. Inco Alloys International, Inc., *High Performance Alloys for Thermal Processing*, Publication No. IAI-48-1, 4th edn., Inco Alloys International, Inc., Huntington, W. VA, 1988.
209. Kiser, S. D., Sound welds in nickel alloys, *Weld. Design Fabr.*, October, 86–88 (1988).
210. Conaway, H. R., Welding the nickel alloys, Part 1: Cleaning and joint design, *Weld. Design Fabr.*, February, 73–75 (1977).
211. Conaway, H. R., Welding the nickel alloys, Part 2: SMAW and GMAW, Part 3: GTAW, SAW and OAW, Part 4: Plasma welding, nickel overlays, *Weld. Design Fabr.*, March, 75–79; April, 106–109; May, 70–73 (1977).
212. ASM, *Material Properties Handbook: Titanium Alloys*, ASM International, Materials Park, OH.
213. Schutz, R. W. and Thomas, E. D., Corrosion of titanium and titanium alloys, in *Metals Handbook, Vol. 13, Corrosion*, 9th edn., American Society for Metals, Metals Park, OH, 1987, pp. 669–706.
214. Data sheet, summary table of titanium alloys, *Adv. Mater. Process.*, 6, 123–126 (1994).
215. Inskeep, J., McMaster, J. A., and Trumbell, C. A., Move over for titanium, *Weld. Design Fabr.*, April, 88–94 (1977).
216. Seagle, S. R. and Bruce, B. P., Titanium: Its properties and uses, *Chem. Eng.*, March 8, 111–113 (1982).
217. *Titanium Fabricators Ltd.—A Profile, Welding and Metal Fabrication*, October 1988, pp. 346–349.
218. Schutz, R. W., A case for titanium's resistance to microbiologically influenced corrosion, *Mater. Perform.*, January, 58–61 (1991).
219. TIMET, *TIMET CodeWedl® Titanium Tubing*, TIMET, Denver, CO.
220. Jacobs, R. L. and McMaster, J. A., Titanium tubing: Economical solution to heat exchanger corrosion, *Mater. Protect. Perform.*, July, 33–38 (1972).
221. Gleekman, L. W., Trends in CPI materials: Nonferrous metals—II, *Chem. Eng.*, Deskbook Issue, December 4, 47–49 (1972).
222. McMaster, J. A., Selection of titanium for petroleum refinery components, *Mater. Perform.*, April, 28–33 (1979).
223. Cooley, J., How to weld titanium without a trailing shield, *Weld. Design Fabr.*, March, 65–66 (1982).
224. Hull, W. G., Fusion welding of titanium and its alloys, *Weld. Metal Fabr.*, January, 24–28 (1961).
225. Chevalier, R., General methods for cleaning titanium, *Weld. Metal Fabr.*, April, 134 (1974).
226. RMI Titanium Company, *Facts about Welding Titanium*, RMI Titanium Company, Niles, OH.
227. Crement, D. J., Narrow groove welding of titanium using the hot-wire gas tungsten arc process, *Weld. J.*, April, 71–76 (1993).
228. Ellis, M. B. D. and Gittos, M. F., Tungsten inert gas welding of titanium and its alloy, *Weld. Metal Fabr.*, January, 9–12 (1995).
229. Baeslack, W. A. and Decker, D. W., Substructural characteristics in titanium alloy weldments, *Metal Trans.*, 11A, 605–612 (1980).
230. Yau, T.-L., Zirconium, in *Corrosion and Corrosion Protection Handbook*, 2nd edn. (P. A. Schweitzer, ed.), Marcel Dekker, New York, 1983, pp. 231–282.
231. Lacy, C. E. and Keeler, J. H., Zirconium—Fabrication techniques and alloys development, *Mech. Eng.*, October, 875–878 (1955).
232. Cox, F. G., Zirconium, *Weld. Metal Fabr.*, October, 358–365 (1958).
233. Webster, R. T. and Yau, T.-L., Zirconium in sulfuric acid applications, *Mater. Perform.*, February, 21–25 (1986).
234. Rollason, E. C., Welding of zirconium, *Weld. Metal Fabr.*, July, 230–234 (1956).
235. Burns, R. H. and Prabhat, K., Conquer corrosion in harsh environments with tantalum, *Chem. Eng. Prog.*, March, 32–35 (1996).
236. Schweitzer, P. A., Tantalum, in *Corrosion and Corrosion Protection Handbook*, 2nd edn. (P. A. Schweitzer, ed.), Marcel Dekker, New York, 1983, pp. 213–230.
237. Keeler, J. H., Four refractory metals—W, Ta, Nb and Mo, *Mech. Eng.*, November, 41–45 (1965).
238. Bishop, C. R. and Stern, M., Hydrogen embrittlement of tantalum in aqueous media, *Corrosion*, 17, 379–385 (1961).
239. Schussier, M., Tantalum—Its properties and applications for the chemical industry, *Refractory Hard Metals*, June (1983).
240. Hampel, C. A., Corrosion resistance of titanium, zirconium and tantalum used for chemical equipment, *Corrosion*, 17, 9–17 (1961).

241. Yan, T.-L. and Bird, K. W., Know which reactive and refractory metals work for you, *Chem. Eng. Prog.*, 88(2), 65–69 (1992).
242. Gleekman, L. W., Trends in CPI materials: Nonferrous metals—I, *Chem. Eng.*, Deskbook Issue, October 12, 111–118 (1970).
243. Sayers, J. A., Trends in CPI materials: Brittle materials, *Chem. Eng.*, Deskbook Issue, December 4, 51–56 (1972).
244. Hills, D. E. G., Graphite heat exchangers—I, *Chem. Eng.*, December 23, 80–83 (1974).
245. Hills, D. E. G., Graphite heat exchangers—II, *Chem. Eng.*, January 20, 116–119 (1975).
246. Schley, J. R., Impervious graphite for process equipment, *Chem. Eng.*, February 18, 144–150 (1974).
247. Muoio, J. M., Glass as a material of construction for heat transfer equipment, in *Industrial Heat Exchangers Conference Proceedings* (A. J. Hayes, W. W. Liang, S. L. Richlen, and E. S. Tabb, eds.), American Society for Metals, Metals Park, OH, 1985, pp. 385–390.
248. Perry, R. H. and Chilton, C. H., *Chemical Engineering Handbook*, 5th edn., McGraw-Hill, New York, 1973.
249. Mejzak, G. J., An introduction of glass for the chemical process industries, in *ASME National Congress on Pressure Vessel and Piping Technology*, 1983.
250. Heat exchangers, in QVF2002, QVF Process system GmbH, a member of De Dietrich Process Systems GmbH, Hattenbergstraße 36, Mainz, Germany, pp. 5.1–5.25 (2007). (http://www.qvf.com/en/Company_5/index.shtml)
251. Lederman, S., Types and prevention of glass lined equipment failures, *Mater. Perform.*, March, 34–41 (1983).
252. Wenner, C. W., Jr., Corrosion-free heating and cooling using Teflon heat exchangers, *Mater. Perform.*, September, 55–58 (1988).
253. Ametek Heat Exchangers of Teflon, M/s. Ametek, Haveg Division, USA.
254. Lehman, R. L., Premier on engineering ceramics, *Adv. Mater. Process.*, June, 31–41 (1992).
255. McDonald, C. F., The role of the ceramic heat exchanger in energy and resource conservation, *Trans. ASME, J. Eng. Power*, 102, 303–315 (1980).
256. Schwartzberg, R. F., Selecting structural materials for cryogenic service, in *Source Book on Materials Selection*, Vol. 1 (R. B. Guina, compiler), ASM, Metals Park, OH, 1977, pp. 25–30.
257. Marshall, E. G., Steels for low temperature service, in *Source Book on Materials Selection*, Vol. 1 (R. B. Guina, compiler), ASM, Metals Park, OH, 1977, pp. 216–220.
258. Vanderbeck, R. W., Special carbon steels—Tough ductile at subzero temperature, *Chem. Eng.*, May, 103–106 (1960).
259. Aluminum in hot pursuit of cryogenics, *Weld. Design Fabr.*, September, 45–49 (1974).
260. Johnson, E. W., Aluminum alloys, *Chem. Eng.*, August 8, 133–135 (1960).
261. Welding of stainless steels for cryogenic application, *Weld. World*, 30, 100–107 (1992).
262. Fabrication of cryogenic plant, *Weld. Metal Fabr.*, March, 84–89 (1969).
263. Nippes, E. F. and Balaguer, J. P., A study of weld heat affected zone toughness of 9% nickel steel, *Weld. J.*, September, 237-s–243-s (1986).
264. Fieldhouse, A. B., New electrode for welding 9% nickel steel, *Weld. Metal Fabr.*, April, 149–150 (1964).
265. Johnson, R. J., Nickel steel alloys for liquids at 320°F, *Chem. Eng.*, July, 115–118 (1960).
266. Tharby, R. H., Welding consumables for 9% nickel steel, *Weld. Metal Fabr.*, February, 51–61 (1973).
267. Thorncroft, D. R. and Heath, D. J., Further aspects of the welding of 9% nickel steel, *Weld. Metal Fabr.*, February, 59–70 (1963).
268. Pozzolini, P. F., The role of 9% nickel steel in the transport of LNG, *Weld. Metal Fabr.*, February, 40–46 (1973).
269. Coulson, K. J., Shop manufacturing experience with 9% nickel steel, *Weld. Metal Fabr.*, February, 47–50 (1973).
270. Machin, R., Welding aspects of 9% nickel steel, *Weld. Metal Fabr.*, July, 266–269 (1966).
271. Watanabe, M., Tanaka, J., and Watanabe, I., Ferritic filter for gas shielded metal arc welding 9% nickel steel, *Weld. Metal Fabr.*, May, 167–176 (1973).
272. *Operation Cryogenics-9% nickel steel vessels burst and impact tests*, International Nickel Co., Inc., Chicago Bridge & Iron Co., and United Steels Corp, Publication AUDCO A-61 (1961). Destructive tests of 9% nickel steel vessels at –320°F, ASME-62-273, Engineering division, ASME annual meeting, New York, Nov. 25–30 (1960).
273. Jordan, D. E., High strength filler material for welding 9% nickel steel, *Weld. Metal Fabr.*, August, 335–339 (1967).
274. McHenry, H. T., The properties of austenitic stainless steels at cryogenic temperatures, in *Austenitic Steels at Low Temperature*, Plenum Press, New York, 1983.

275. Ogawa, T. and Koseki, T., Weldability of newly developed austenitic alloys for cryogenic service: Part II. High nitrogen stainless steel weld metal, *Weld. J.*, 67, 8-s–17-s (1988).
276. Ogawa, T. and Koseki, T., Weldability of newly developed austenitic alloys for cryogenic service: Part I. Up-to-date overview of welding technology, *Weld. J.*, 66, 332-s–341-s (1987).
277. Lancaster, J. F., *The Metallurgy of Welding, Brazing and Soldering*, American Elsevier, New York, 1965.
278. Perinic, G., A small course on safety in cryogenics, 2003. http://cem.ch/gperinic/kryokurs/en/kryok_99.htm
279. Charles, J., Gagnepain, J. C., Dupoirion, F., Jobard, D., and Soullignac, P., Austenitic-ferritic stainless steels and clad plates: Properties and applications to pressure vessels, *WRC Bull.*, 374, pp. 25–37.
280. Gleekman, L. W., Trends in CPI materials: Nonferrous metals—II, in *Materials Engineering I: Selecting Materials for Process Equipment* (K. J. McNaughton, ed.), McGraw-Hill, New York, 1980, pp. 92–94.
281. Newcombe, G., The bimetal concept, *Weld. Metal Fabr.*, November, 379–406 (1974).
282. Firth, K. and Heath, D. J., Nickel alloys provide protective lining and overlays, *Weld. Metal Fabr.*, April, 195–203 (1980).
283. Bush, A. F. and Cohin, P., The successful application of the strip cladding process with austenitic strips, *Weld. Metal Fabr.*, June, 234–241 (1969).
284. Mallya, U. D. and Srinivas, H. S., Effect of magnetic steering of the arc on clad quality in submerged arc strip cladding, *Weld. J.*, July, 289-s–293-s (1993).
285. Devletian, J. H., Koch, A., and Buckley, E. N., Unique application introduces electrosag cladding to US industry, *Weld. J.*, January, 57–60 (1992).
286. Marshall, A. B., Jordan, M. F., and Aston, J. L., Stainless steel strip cladding, *Weld. Metal Fabr.*, August, 292–293 (1973).
287. Oh, Y. K. and Devletian, J. H., Electrosag strip cladding of stainless steel with metal powder additions, *Weld. J.*, January, 37–44 (1992).
288. Hix Hugh, B., Explosion bonded metals offer diversification in vessel design, *Mater. Protect. Perform.*, December, 28–31 (1972).
289. Banker, J. G., Try explosion clad steel for corrosion protection, *Chem. Eng. Prog.*, July, 40–44 (1996).
290. Hardwick, R., Methods for fabricating and plugging of tube to tubesheet joint by explosion welding, *Weld. J.*, April, 238–244 (1975).
291. Linse, V. D. and Temple, P. I., Explosion welding, in *Welding Hand Book*, Vol. 2, 8th edn., 1991, pp. 766–781.
292. Nippes, E. F. (ed.), Explosion welding, in *Metals Handbook*, Vol. 6, *Welding, Brazing, and Soldering*, 9th edn., American Society for Metals, Metals Park, OH, 1983, pp. 705–718.
293. Johnson, W. R., Explosive welding: Plugs into heat exchanger tubes, *Weld. J.*, January, 22–32 (1971).
294. Peacock, G. A., Fabrication of thick plates, *Weld. Metal Fabr.*, June, 242–252 (1963).
295. Ellis, D., Fabrication in clad steels, *Weld. Metal Fabr.*, September, 359–365 (1967).
296. Kearns, W. H. (ed.), *Welding Handbook*, Vol. 4, *Metals and Their Weldability*, 7th edn., AWS, Miami, FL, 1982, Chapter 12.
297. Recommendation of PWHT of welded joints in steel pressure vessels and other heavy duty structures, by Joint Working Group, IIW Commissions IX and X, *Weld. World*, 29, 341–362 (1991).
298. Ellis, D. J. and Gifford, A. F., Application of electrosag and consumable guide welding, *Weld. Metal Fabr.*, April, 112–119 (1973).
299. Ricci, W. S. and Eagar, T. W., A parametric study of the electrosag welding process, *Weld. J.*, December, 397-s–405-s (1982).
300. Carpenter, O. R. and Floyd, C., Heat treatment of carbon and low alloy pressure vessel steel, *Weld. J.*, (1957).
301. Watson, S. J., Post weld treatment of welded units for the relief of stress, *Weld. Metal Fabr.*, September, 318–327 (1958).
302. Ohshita, S., Yurioka, N., Mori, N., and Kimura, T., Prevention of solidification cracking in very low carbon steel welds, *Weld. J.*, June, 129-s–136-s (1983).
303. ASME, Boiler and pressure vessel code, Section VIII, Division 1, Pressure vessels, The American Society of Mechanical Engineers, New York, 1992.
304. Carpenter, D. D., A guide for determining post weld heat treatment requirements for ASME Code Section VIII pressure vessels, *Trans. ASME, J. Pressure Vessel Technol.*, 106, 115–123 (1984).

BIBLIOGRAPHY

- ASM, Corrosion of nickelbase alloys, in *Metals Handbook, Vol. 13, Corrosion*, 9th edn., American Society for Metals, Metals Park, OH, 1987, pp. 641–657.
- ASM, Weldments, brazed assemblies, and soldered joints, in *Metals Handbook, Vol. 17, Nondestructive Evaluation and Quality Control*, 9th edn., American Society for Metals, Metals Park, OH, 1989, pp. 582–609.
- ASM, *Metals Handbook, Vol. 1, Properties and Selection: Iron, Steels, and High Performance Alloys*, 10th edn., American Society for Metals, Metals Park, OH, 1990.
- ASM, *Metals Handbook, Vol. 2, Properties and Selection: Nonferrous Alloys, and Special Purpose Materials*, 10th edn., American Society for Metals, Metals Park, OH, 1992.
- Cary, H. B., *Modern Welding Technology*, Prentice Hall, Englewood Cliffs, NJ, 1979.
- Connor, L. P. (ed.), *Welding Handbook, Vol. 1, Welding Technology, Vol. 2, Welding Processes, Vol. 3, Materials and Application*, 8th edn., American Welding Society, Miami, FL, 1987.
- McNaughton, K. J. (ed.), *Materials Engineering, Part I: Selecting Materials for Process Equipment; Part II: Controlling Corrosion in Process Equipment*, McGraw-Hill, New York, 1980.

14 Quality Control and Quality Assurance, Inspection, and Nondestructive Testing

14.1 QUALITY CONTROL AND QUALITY ASSURANCE

Quality, the compliance of a product with the customer's specifications and requirements, has become the buzzword of industry in many parts of the world during the last two decades. Buyers want it; manufacturers claim to strive for it. Competitiveness in the market, safety and the consequences of product failure, and the developing legislation related to product liability known as consumer protection acts have become important factors in the pursuit of high quality. For heat exchangers and pressure vessels, the overriding reasons are to avoid the consequences of failure, which can be catastrophic in human, monetary, and environmental terms. Flaws in critical components may increase the likelihood of failure.

14.1.1 QUALITY MANAGEMENT IN INDUSTRY

It has often been said that quality cannot be inspected into a component; it must be built into it. This is certainly true in heat exchanger fabrication also [1,2]. In the past, quality control (QC) processes relied on separate QC staff to undertake inspection of the finished products, accepting those that conformed to the specification and rejecting the others. Under this method, higher quality is equated with higher cost. This method is also known for the high rejection of finished products, since control was not exercised at all vital stages of the manufacturing process. Because of this, management faced a conflict between improving quality of the product and reducing product cost. Therefore, a new concept of addressing a more total control of quality of a product/process became known as quality assurance programs (QAPs) and provided systems that could cover all aspects, from raw material to finished product, including design, planning, material selection, purchasing, fabrication, and dispatch. With the introduction of QAP, the traditional "final inspection and test" approach, particularly that involving third-party inspection, has shifted toward total quality assurance (QA); in which responsibility for quality is placed firmly with the fabricator [2].

14.1.2 QUALITY AND QUALITY CONTROL

The term *quality* can be defined as conformance of a material or finished product to specifications and drawings. The definition for quality from ISO 8402-1994 is "The totality of characteristics of an entity (product or service) that bear on its ability to satisfy stated and implied needs."

Some of the definitions of *quality control* (QC) are as follows:

1. The process of inspection to ensure that the material or finished product meets the specifications and drawings.
2. Operational techniques and activities that are used to fulfill the requirements for quality (the definition from ISO 8402-1994).

3. “A management system for programming and coordinating the quality maintenance improvement efforts of the various groups in the design and/or manufacturing organization so as to enable products at the most economic levels which allow for full customer satisfaction” (official definition provided by the European Organization for Quality Control).
4. The QC of a product is the degree to which it meets the requirements of the customer. With manufactured products, it is a combination of both quality of design and quality of manufacture [3].

14.1.2.1 Aim of Quality Control

The aim of QC is to provide quality that is satisfactory, adequate, reliable, and economical. The overall quality system involves integrating the quality aspects of several related steps, including the proper specification, fabrication, and inspection [4]. In order to achieve the quality, a planned and systematic QAP has been established.

14.1.3 QUALITY ASSURANCE

Quality assurance (QA) is the establishment of a QC system to guarantee the desired quality level of a product from design raw materials through fabrication, final assembly, and dispatch. QA comprises two aspects [5]: (1) QC and (2) quality administration. The term quality control was defined already. Rao [5] defines *quality administration* as the systematic organizational effort to effectively implement the quality standards by trained and qualified personnel and to establish documents as proof of quality achieved.

14.1.3.1 Need for QA

It is accepted that inspection and nondestructive testing (NDT) applied at appropriate stages during manufacture constitutes an integral and vital part of QC. There are a number of disadvantages in using inspection to control quality. (1) It is costly; (2) it is operator dependent; (3) it is too late; and (4) it only concentrates on the product, and not the processes. However, there is a growing recognition that quality characteristics and reliability cannot be guaranteed by inspection and tests alone. Such features must be “designed into” and then “built into” the products [2]. QA techniques have been developed to ensure that critical activities such as material procurement, design, and manufacturing activities such as welding and heat treatment are properly controlled.

14.1.3.2 Essential Elements of Quality Assurance Program

A good QAP consists of five basic elements [6]: (1) prevention, (2) control, (3) assurance, (4) corrective action, and (5) quality audit.

QA is based on systematic planning, testing, analysis, and documentation in all phases during the manufacture of a product. It begins with the formulation of the specifications and extends through planning, design, development, production, review, testing, commissioning, after-sales service, and evaluation of the product's performance [7].

In a well-organized company with an established QA system, each manager in the organization knows his or her responsibility and has the required competence.

14.1.3.3 Requirements of QA Programs for Success

To be effective, QA programs should be sufficiently flexible to cater not only for “high-quality” products but also to avoid the unnecessary imposition of high-quality standards on “low-quality” products. This will enhance the quality cost. Without such flexibility, a company cannot remain competitive [2].

14.1.3.4 Quality Assurance in Fabrication of Heat Exchangers and Pressure Vessels

Much of the QA literature is concerned with high-volume mass production industries with emphasis on statistical QC, quality circles, total quality management (TQM), automation, etc., aimed

principally at reducing the rejection, scrap, and rework, and hence at minimizing the product cost [8]. As pressure vessels, boilers, and heat exchangers are usually manufactured for a specific purpose on a “one-off” basis, statistical methods of QC are not usual, although this applied where justified. Most of the QA literature on fabrication of pressure vessels and heat exchangers lie in standards, codes, and the technical literature of the individual industry.

14.1.3.5 Contents of QAP for Pressure Vessels and Heat Exchangers

The QA in fabrication of pressure vessels comprises certain activities to be carried out by the pressure vessel manufacturer to assure the quality of design and construction for the safety and reliability of the pressure vessel. The activities that form the QAP for pressure vessels and heat exchangers are discussed in Refs. [2] and [4].

1. Codes and interpretation
2. Approval of designs by the client/third party/consultant
3. Material control, both procurement and receipt
4. Calibration of testing and inspection equipments
5. Qualification of welding procedures and welder performance
6. Qualification of welding inspectors and NDT personnel
7. Production methods and production control
8. QC during forming and shaping of components
9. QC during assembly of parts
10. QC during production welding
11. NDT of welds
12. Directing and expediting nonconformance reports (NCRs)
13. QC during postweld heat treatment (PWHT)
14. NDT after PWHT
15. Leak testing (LT) of pressure vessels
16. Hydraulic testing or proof testing of pressure vessels
17. Documentation
18. Auditing
19. Periodic preparation of budget reports on inspection costs

14.1.4 QUALITY SYSTEM

To assure that the manufacturer has the ability and integrity to build pressure vessels and heat exchangers that meet the code requirement, it should have and demonstrate a QC system [9]. This system must include a written description, known as a *quality manual*. To be effective, the QC system must have managerial direction, technical support, and resources that are made available for its implementation. Basics of QC system for pressure vessel manufacture are discussed in detail by Chusur [9]. Elements of the QC system as given earlier.

The salient features of QC system for manufacture of pressure vessels/heat exchangers are hereunder [9]:

1. *Authority and responsibility*: The authority and responsibility of the QC manager shall be clearly established through management’s statement of authority, signed by competent authority in the top management. The QC manager shall have sufficient and well-defined responsibility, authority, and organizational freedom to identify QC and QA problems and provide solutions to these problems.
2. *Organization*: An organization chart showing the relationship between management, engineering, purchasing, manufacturing, QC, and inspection shall be presented.

- Define responsibilities, authorities, and lines of communication to perform and verify the activities that affect quality and for the verification of quality; ensure personnel have sufficient freedom from pressure of production. Because a QC program often crosses departmental boundaries within an organization, a company must fix responsibility for the program [11].
3. *Design specifications, drawings, design calculations:* This system provides for the preparation, issue, maintenance, and subsequent revision of drawings, material specifications to meet code requirements, and procedures for design assessment, verification, and review.
 4. *Material procurement control:* This system covers material requirements, indenting, and purchasing. Only code-permitted materials shall be indented. Materials such as plate, tubing, pipes, castings, forgings, and consumables, including NDT consumables, are to be procured only from vendors approved by the QA department. Concise and clearly written specifications should be provided to the material supplier to ensure the proper material supply. For parts like pipe fittings bought from the trade, the purchase order shall meet code requirements. The manufacturer is responsible for surveying and qualifying vendor quality system and control of material at source.
 5. *Material control:* This system covers material receipt, inspection, and identification of materials, storage, and issue, including welding consumables and vendor evaluation. Procedures shall be established for examination of incoming materials like plates, pipes, forgings, etc.
 6. *Process control, examination, and inspection:* This system ensures that the various stages of fabrication are carried out under controlled conditions and defines work instructions that include criteria for workmanship, requirements for equipment, and inspection after each work operation affecting quality. The system establishes written procedures for controlling fabrication and testing, welding, hot forming, NDT, LT, PWHT, hydrostatic testing, etc. At appropriate manufacturing stages, hold points are established so that inspections can be made on the material before commencing the next operation. QC personnel are involved in inspection at hold points, including nondestructive tests and interpretation of these tests.
 7. *Correction of nonconformities:* This system covers control and disposal of nonconforming materials and components (i.e., items not conforming to code requirements) and ensures conditions adverse to quality are identified and corrected. When a nonconformity is noticed, the component or subassembly shall be segregated by a quarantine tag or sticker and an NCR prepared. For repair or rework to be carried out, a supplementary QC plan, process sheet, and checklist with relevant procedures or reference to rework procedures shall be prepared. These shall be referenced in the main process sheet.
 8. *Welding QA:* This system covers the quality of welding of components with specific reference to welding process parameters design, like precleaning and surface preparation, joint design, edge preparation and fit-up, base metal preheat, maintenance of interpass temperature and postheating, gas shielding, filler metal selection and preheating welding electrodes, welding procedures, and qualification of welders and welding machine operators. Specify methods to monitor welding before, during, and after welding. Welds must conform to Section IX of the ASME code [10b]. Welding consumables must be stored as per Section II, Part C of the Code [10c]. Documents must cover issue and return of consumable. Proper choice of materials, welding process, qualified personnel, etc., is necessary to ensure building the quality in the product.
 9. *Nondestructive examination:* This system covers nondestructive examination and inspection carried out in all stages of manufacture, written procedures for various NDT techniques as per Code [10d] requirements, and qualification of personnel, and provides documentary evidence that all code requirements are met.

10. *Heat treatment*: This system covers the requirements of heat treatment and calibration of temperature measuring and recording instruments. The QC system on heat treatment of components, heat exchangers, and vessels shall cover the following:
 - a. Specify when preheating is required and explain procedures for preheating, control of interpass temperature, postheating, and PWHT
 - b. Preheating and PWHT means/devices like use of gas burners, electrical heating elements, or furnace
 - c. Describe how furnace is loaded, placement and location of thermocouples, and recording system for time and temperature
 - d. Methods of heating and cooling, and how temperature is controlled to achieve uniform temperature
 - e. Support of vessel and components during heating to avoid distortion
 - f. Methods to control scaling and oxidation of metal surfaces
11. *Maintenance and calibration of measuring instruments*: This system ensures that inspection and test equipment and gauges are calibrated and maintained properly. Maintain records documenting the accuracy, calibration methods, and history of equipment and standards used for final acceptance. Establish calibration standards and frequency of calibration.
12. *Documentation*: An extensive system of documentation is required to provide QC data records. Send written procedures that define responsibility and assign specific responsibilities to the management, supervisors, and QC staff. Keep records showing that each has done his or her work for follow-up when necessary [11].
13. *Authorized inspector*: Authorized inspectors, or third-party inspection agencies are involved in design approval and materials selection, followed by inspection and testing during various stages of fabrication.
14. *Retention of records*: This system covers the preservation and retention of records of the product manufactured to meet the code requirement. Such records include mill test reports, NDT reports, radiographs, impact test results, heat-treatment charts, etc.
15. *Audits*: An audit is an independent examination of quality to provide information; it is carried out by an independent organization called an audit team [12]. The aim of the audit is to establish that the procedures of the company's quality manual are being followed. Management should establish a schedule for audits and adjust it on the basis of previous results.

14.1.4.1 ASME Code: Quality Control System

Comprehensive QA requirements were included in the first issue of ASME Section III in 1970. Mandatory "QC system" requirements are stated in Appendix 10 of ASME Code Section VIII, Div. 1 [10a]. As per ASME Code, the manufacturer or assembler shall have and maintain a QC system that will establish that all code requirements, including those for material, design, fabrication, examination of vessels and vessel parts, and inspection, will be met. The QC system shall cover the following features: (1) authority and responsibility, (2) organization, (3) drawings, design calculations, and specification control, (4) material control, (5) examination and inspection program, (6) correction of nonconformities, (7) welding, (8) NDT, (9) heat treatment, (10) calibration of measuring and test equipment, (11) records retention, (12) sample forms, (13) inspection of vessels and vessel parts, and (14) inspection of pressure relief valves.

14.1.5 QUALITY MANUAL

To meet the requirements of the codes and standards, the manufacturers develop a quality system and a QAP, which is explained in the company's quality manual or QA manual. It states the company's quality policy and details the quality systems, organization, and the responsibilities of the interrelated functions to meet the objectives of the QA program. The quality manual will form the

basis for the documentation systems developed for QC. It will be reviewed by the inspection agency, and the manual will serve as the basis for continuous auditing of the quality system. It contains all the sample documents (forms and formats) used in the quality management systems and procedures.

14.1.5.1 Details of QA Manuals

The QA manual gives the following details [13]:

- The company's quality policy
- Organizational charts
- Duties of QA personnel, supervisors, and technicians
- Disposition of drawings, documents, and facsimile record-keeping forms
- Material control
- Testing, inspection, and QC procedures
- Qualification of welding procedures and qualification of welding personnel
- Training and qualification of NDT personnel
- Marking of nonconforming products
- Heat-treatment procedures
- Calibration of measuring and testing equipment
- Documentation
- Possession and use of the code stamp

14.1.6 MAIN DOCUMENTS OF THE QUALITY SYSTEM

The main documents used to control the fabrication, examination, and inspection are the QC plan, process sheet, and checklist. These documents are discussed next.

14.1.6.1 Quality Assurance Program

Based on approved drawings and material registration issued by the client, a QAP will be prepared that shall indicate

- Stages of manufacture at which examination and inspection are to be carried out
- Details of examination to be carried out
- Reference documents and acceptance standards
- Witness/hold points for client/third party
- Records to be maintained

Before the commencement of manufacture, the QC plan shall be made available to the authorized inspector, who shall review the same and indicate the approval.

14.1.6.2 Operation Process Sheet

Based upon the QC plan, approved drawings, and the hold points indicated by the authorized inspector, the production engineering department in consultation with the QA section shall prepare the operation process sheet) for various components. The operation process sheet will

1. Describe the stages of manufacture and list them sequentially.
2. Indicate procedures such as welding procedure specification (WPS), heat treatment, etc., to be used for that operation at appropriate columns and contain special instructions to the operator wherever required.
3. Provide space to record and make reference to reports such as NDT, NCR, etc.
4. Provide space for signature by the QC inspector after carrying out necessary examination.
5. Provide space for indicating the hold points and witness points as specified on the QC plan.

Operation process sheets for various operations are given later.

14.1.6.3 Checklist

Based upon the QC plan with the hold and witness points indicated by the authorized inspector, approved drawing, and process sheet, prepare a checklist detailing the examination and inspection to be carried out during the various operations. Provision shall be made for the signature of the authorized inspector. Hold and witness points indicated in the QC plan shall be transferred to the checklist and submitted to the authorized inspector for verification.

14.1.7 ECONOMICS OF QUALITY ASSURANCE

Quality cost may at first seem high due to NDT equipment, measuring instruments, supplies, training, and qualified personnel/labor. Reduced quality may result in low reliability, rework, rejections, downtime, which may give rise to complaints, failures, losses, and hazards to human beings and the environment [7,14]. On the other hand, if the requirements for quality, reliability, safety, and availability are too high, product costs will be unnecessarily high. One of the basic management duties is to strike an optimum balance between the various costs of QA. Elements of quality cost and quality cost model are shown in Figure 14.1 [15]. Production costs rise disproportionately as designers tighten tolerances. One way to decide where tolerances should be tight is to make a Pareto analysis of the dimensions and tolerances of the work [11]. This method classifies the elements of a total unit in the order of their importance to the performance of that unit. Such a classification of dimensions includes functionally critical, significant, and significant only for good appearance and for good workmanship. Veith [11] cites the Pareto analysis of 5000 dimensions of a pressure vessel, which showed that only 5% of the dimensions are critical, 18% are significant, and the remaining 77% dimensions require only good workmanship and acceptable appearance. Keeping in mind that under a QC system, every out-of-tolerance dimension is considered non-conforming, decide just exactly which dimensions are critical to the vessel operation and be more selective in assigning tolerances.

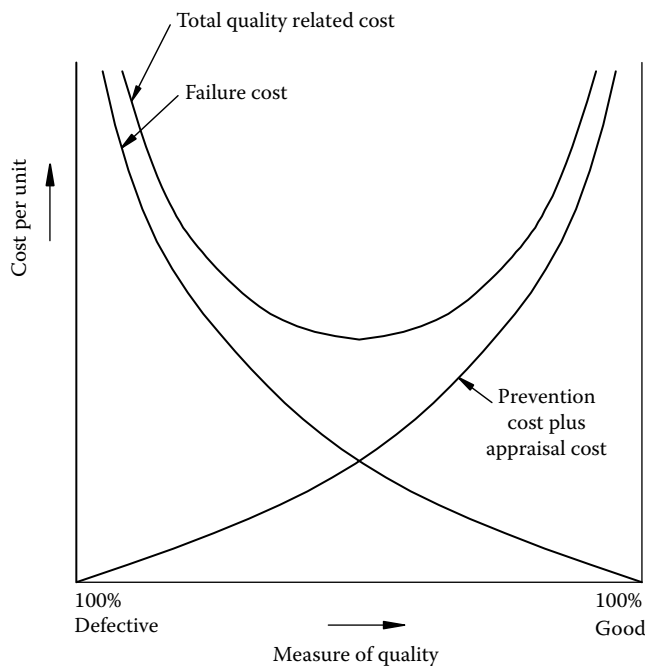


FIGURE 14.1 Quality cost.

14.1.8 REVIEW AND EVALUATION PROCEDURES

Review is an important activity in a quality system to ensure that compliance with a set of procedures and agreed standards takes place all the time at all stages of the production process. Reviews must be methodical, and depending on the nature of the organization, they may take the form of (1) management audits, (2) system audits, or (3) project or product audits. Reviews are carried out periodically.

14.1.8.1 Auditing

Audits should be conducted at specified intervals in accordance with written procedures and a checklist, to verify by investigation that applicable elements of the quality system and QAPs have been effectively implemented and documented.

14.1.8.2 Auditing Procedure

There are four major steps in conducting an internal audit. These same steps apply to audits of all types of activities: engineering, purchasing, manufacturing, and marketing. Only the avenues of inquiry and the specific questions used are different for the various audits. The four steps in conducting audit are [16] (1) planning and preparation, (2) performing the audit, (3) reporting the results, and (4) follow-up and closeout.

14.1.8.3 Contents of an Audit Plan

To carry out an audit adequately, proper planning is essential and auditing procedures should be prepared. The audit structure will take the formal pattern: arrangement, meeting, audit, review, report, and reaudit. The auditing procedure will define the following points [12]:

- Scope of the audit
- Names of audit team members and their organizational affiliation
- Name of the group to be audited
- Listing of areas or activities to be audited
- List of applicable documents
- Equipment to be used
- Auditing method
- Report
- Acceptance criteria

14.1.9 DOCUMENTATION

The quality system requires extensive and minute documentation of every procedure related to the manufacture of a product. The documentation serves as a proof of the activities carried out and the quality achieved by the manufacturer. The following certificates and records should be documented where applicable, and a copy of these should be sent to the customer:

1. Customer's order
2. Vessel detail drawing together with a materials list
3. Material certificates of chemical and physical properties
4. WPS and procedure qualification records (PQRs)
5. Welder qualification records
6. Records of welding consumables used
7. Certificate of radiography and other NDT operations
8. Reports of nonconformities
9. Heat-treatment charts
10. LT report

11. Hydrostatic test report
12. Reproduction of vessel markings and stamping
13. Manufacturer's data report and associated partial data report, if any

14.1.10 ISO 9000

ISO is the International Standards Organization, headquartered at Geneva, Switzerland. One of its purposes is to develop and promote worldwide quality standards.

14.1.10.1 What Is the ISO 9000 Series?

The ISO 9000 series of quality standards defines the basic management systems that a manufacturer should have to ensure that the end product consistently conforms to the order requirements. ISO 9000 places great emphasis on documentation of all the elements/features of quality systems (in manuals and procedures), implemented, audited, and reviewed.

14.1.10.2 Principles of ISO 9000

ISO 9000 is a quality system applicable to any industry and describes what to do, but not how to do. The guiding principles are document, establish, implement, and maintain. In simple terms,

1. Say what you do—procedures and documents
2. Do what you say—implementation
3. Demonstrate that you do what you say—documents and record keeping

14.1.10.3 Why ISO 9000?

Most of the organizations applying for registration under the ISO 9000 standards are doing so to comply with customer and third-party requirements, and to achieve a climate of competitiveness. Over the years, countries with focus on international trade as diverse as the United States, Japan, European Community countries, Russia, Australia, Canada, New Zealand, India, and Mexico have accepted ISO 9000. Various countries have established national schemes to audit and accredit the certification organizations that audit companies to ISO 9000. More countries are basing their quality systems on the ISO 9000 series.

14.1.10.4 Benefits of ISO 9000

The main improvement in the quality system since implementation of ISO 9000 is the continuous improvement of quality, customer confidence in a company's quality system, and efforts targeted toward corrective actions to ensure that the same problems are not repeated. Major benefits of ISO 9000 are the following:

- It introduces a systems concept.
- It brings about changes that are organizational, procedural, and operational.
- It focuses on prevention of nonconformities.
- It improves communication in the system.
- It satisfies quality levels and facilitates improvements.

14.1.10.5 Listing of Selected ISO 9000 Quality Standards

ISO 9000:2005: Quality Management Systems—Fundamentals and vocabulary

ISO 9001:2008: Quality Management Systems—Requirements

ISO 9004:2000: Quality Management Systems—Guidelines for performance improvements

14.1.10.6 Total Quality Management

TQM is often defined as the establishment of a customer–supplier chain. The ISO 9000 standard is an important tool that can be used to develop links with suppliers and establish long-term partnerships.

14.2 INSPECTION

14.2.1 DEFINITIONS

The term *inspection* can be defined as the process of examination of a material or a finished product using sensory organs, tools, equipments, instruments, and gauges to assess the quality of a product.

The term *inspection*, as far as ASME Code Section V [10d] and other referencing Code sections are concerned, applies to the functions performed by the authorized inspector, whereas the term *examination* applies to the QC functions performed as stipulated in the quality manual by QC staff of the company or the manufacturer.

14.2.2 OBJECTIVES OF INSPECTION

During manufacture, inspection has three principal objectives [17]:

1. To provide assurance that there are no defects, indicating manufacturing was above the standard required in the specification
2. To provide assurance that no defects are present that could impede subsequent processing inspections
3. To provide assurance that no defects are present in the completed component that will pose safety problem

14.2.3 DESIGN AND INSPECTION

In the preliminary design stage, performance criteria and material selection should be made compatible with NDT, and the aim should be to provide maximum accessibility for inspection both during fabrication and in service. The design should include inspection in critical areas where the fabrication process is likely to introduce defects or where service conditions will impose critical stresses [6].

14.2.4 INSPECTION GUIDELINES

Some general rules for organization of inspection are as follows:

1. Prepare inspection briefs in clear and concise formats. Assemble and incorporate into the inspection brief the setting plan, assembly drawings, tools, and instruments required for inspection [18].
2. Collect the required documents.
3. Define the techniques of inspection.
4. Establish the sequence of inspections.
5. Specify inspection of materials and components as soon as possible.
6. Establish safety regulations for inspections.

14.2.5 SCOPE OF INSPECTION OF HEAT EXCHANGERS

During the various stages of production process, inspectors examine work and document their observations. The scope of inspection of heat exchangers is briefly listed as follows:

Raw material identification and inspection.
Approve welding procedures by test plates as required.
Approve welders to be employed.
Edge preparation for welding, including visual check penetrant test for laminations.
Inspect weld preparations and setup for welding.

- Inspection of back-gouged welded joints such as set-in nozzles, which are not readily radiographed following welding.
- Inspection of cladding by dye penetrant examination (PT); verify chemistry following completion of the cladding; measure ferrite content.
- Alignment of longitudinal and circumferential seams.
- Tolerances on individual shell section.
- Alignment of sections and components.
- Root pass clearance before welding.
- Examine soundness and general contour of welds.
- Inspect prefabricated parts/trade items.
- Check radiographic or other weld inspection technique.
- Thinning of formed heads after forming.
- Checking of tubesheet and baffle holes after drilling.
- Tubesheet to shell setup prior to welding operation.
- Check dimensions after PWHT.
- Witnessing of LT or hydrostatic test.
- Dimensional examination after hydrostatic test.
- Stamping of the vessel and issue of certificates.
- Packing and dispatch.

(A typical stagewise inspection chart is shown in Figure 15.1d). Various stages of inspection should be selected to avoid heavy reworks at a later stage. But it should not lead to too many stages of inspection, which only lead to delays and rushing by workmanship to compensate for such delays, resulting in poor quality.

14.2.5.1 Material Control and Raw Material Inspection

One of the important duties of inspectors is to inspect the raw materials like plates, forgings, and tubes, and certify that they are as per purchase order and free from defects. The code requires goods to be accompanied by documents that detail the mill test reports and certifications. A designated receiver should have the receiving procedure, the purchase order, and a checklist covering component dimensions, and examine for laminations, surface defects, transshipment damage, identification and verification of heat numbers, and test records supplied by vendors [11]. A sound QC program will rely on more than just a review of the mill test reports that accompany the incoming material. Such a program should include chemistry verification by spot NDT or destructive testing techniques. This may involve in situ x-ray examination, or laboratory wet-chemical or energy-dispersive evaluation [1]. An easy way to avoid using the wrong materials in parts is to check composition using a portable spectroscope, which quickly identifies all major elements [19]. The receiver signs in acceptable material for storage, and tags and segregates nonconforming materials, followed by identification, which includes a job number, serial number, and heat number, if relevant. Throughout production, identification follows the material or component, assuring traceability. All this work is carried out according to the QC procedures laid down in the quality manual [13].

For all high-pressure applications, ultrasonic testing (UT) must be carried out to check for lamination and nonmetallic inclusion. Plate edges are to be examined by magnetic or dye PT. Similarly, thicker forging must be ultrasonically examined.

14.2.5.2 Positive Material Identification

Positive material identification (PMI) is a process used to determine the elemental composition of materials. The test identifies the alloys that make up a particular material. The purpose of alloy verification is to ensure that only materials that are specified as part of the design requirement are supplied and used. PMI is typically a field testing method with portable analyzer. Measurements results are shown either in form of elemental concentration and/or by specific alloy name.

14.2.6 DETAILED CHECKLIST FOR COMPONENTS

Before conducting the inspection, prepare a checklist of what, how, and when to inspect. Instruct the inspector to record deviations and their resolutions in an inspector's log [18]. Checklists detail steps in inspection of shell, channel, tubesheet, flanges, expansion joint, tube bundles, final assemblies, etc. A typical checklist for tubesheet, taken from a manufacturer's work, is given next.

14.2.6.1 Checklist for Tubesheet

- Outer diameter of the tubesheet
- Diameter of the raised face shellside
- Depth of the raised face shellside
- Diameter of the raised face channel side
- Depth of the raised face channel side
- Thickness of the tubesheet
- Width of the pass partition groove
- Depth of the pass partition groove
- Number and orientation of pass partitions
- Size of the tube holes
- Number and layout of tube holes
- Outermost tube periphery diameter
- Ligament
 - Nominal ligament
 - Number of holes below nominal ligament (4% of holes can be lower than TEMA minimum ligament)
- Minimum ligament near pass partition
- Depth of the welding groove
- Expansion groove
 - Width
 - Depth
 - Location
- Number of pulling eyes and sizes
- Number of tie rods and sizing
- Number of bolt holes and sizes
- Neutral line marking

14.2.7 TEMA STANDARD FOR INSPECTION

TEMA [20] inspection policy is specified in paragraph G-2. G-2.1 specifies manufacturer's inspection, and G-2.2 specifies the purchaser's inspection.

14.2.8 MASTER TRAVELER

During fabrication, a traveler that accompanies the part or component is sometimes the easiest way to carry out QC procedure. A drawing with all the welds numbered and marked with the points to be examined is a convenient and careful way to handle QC of welds. This document is known as a master traveler [11,21]. The traveler tabulates operations for manufacture of any part or component. The traveler can continue to cover the complete vessel. From a production standpoint, however, it is often better to divide a complex vessel into components, with a traveler for every component and a separate sheet for the final assembly.

14.2.9 SCOPE OF THIRD-PARTY INSPECTION

In addition to firm's own QAP, acceptance inspection is carried out by specialists and experts from various international inspection organizations (known as third-party inspection) such as

- TUV Nord
- Lloyd's Register
- Stoomwezen
- ISPESL
- Bureau Veritas Quality International
- Det Norske Veritas

Third-party inspection agencies such as Lloyd's Register and Bureau Veritas Quality International, among others, normally stipulate an involvement starting with approval of design, materials, and fabrication, followed by inspection and testing. In general, the scope of third-party inspection includes the following:

1. Approval of design and fabrication drawings to ensure that materials and fabrication details meet code requirements
2. Material clearance for pressure parts
3. Verification of WPS/PQR and welder performance qualification tests and heat treatment
4. Inspection during various stages of fabrication, principally by checkpoints/hold points/witness points, indicated by (R) review of record of inspection by third party; (H) hold further process till review of record of inspection by third party; and (W) witness of process by third party to ensure compliance with code requirements
5. Examination of radiographs and auditing of other nondestructive tests and heat-treatment procedures as required by the code
6. Dimensional examination of the completed vessel
7. Witnessing of leak, hydrostatic, or any other special test as required by the code
8. Stamping of the vessel and issue of certificates

Lloyd's approach to QA of welded structures is discussed by Frew [22]. The approach is briefly described here. Appraisal at the design stage includes the calculation of thickness and an assessment of materials to be used, together with manufacturing and welding processes to be employed, the effect of fabrication, and welding and heat-treatment processes on the materials used. Service conditions are taken into consideration. The efficacy of the fabricator's quality system is evaluated, and suitable NDT methods are considered in relation to the joint geometries involved. Approval of fabrication takes into consideration the welding quality design, welder procedure qualification and production tests, PWHT, etc.

14.2.9.1 Hold Points and Witness Points

Consideration should be given to the establishment of hold points and witness points, where an examination is to occur prior to the accomplishment of any further fabrication steps [23]. This is of vital importance for fabrication of pressure vessels and heat exchangers as per code and/or standard. Through hold points and witness points, authorized code inspectors exercise control over the activities such as design calculations, drawings, receipt of materials and welding consumables, qualification of welding procedures and welders, joint design, work preparation before welding, examination during welding and after welding, NDT, NCR, PWHT, hydrostatic tests, etc. A typical scheme for hold points/witness points and verification points is given in Table 14.1.

TABLE 14.1
Hold Point (H) and Witness Point (W)

Number	Stages of Manufacture	H	W
1.	Drawing and design calculations approved	X	—
2.	Raw material for pressure parts clearance	X	—
3.	WPS/POR/welder qualifications	X	—
4.	Forming dimensions for shell and dished ends	X	—
5.	U-bends, qualification report	—	X
6.	Heat-treatment chart for forming (if applicable)	—	X
7.	Fit up of pr. welds incl. attachments on pr. parts	X	—
8.	Air test for RF pads	—	X
9.	Shell ID check by template	—	X
11.	Radiography for pressure part welds	X	—
12.	MT/PT of nozzle and pressure parts attachment welds	—	X
13.	PWHT (if applicable) clearance for pressure part assembly	X	—
14.	Review of heat-treatment charts	—	X
15.	NDT after heat treatment if applicable	X	—
16.	Destructive testing of production test plate	X	—
17.	Tubesheet and baffle inspection after drilling	—	X
18.	Tube bundle skeleton before tubing	—	X
19.	Tube-to-tubesheet joints, NDT/LT	—	X
20.	Pneumatic and hydro test for tube-to-tubesheet joints	—	X
21.	Shellside and tubeside hydrostatic test	X	—
22.	NCR clearance	X	—
23.	Painting of unit satisfactory	X	—
24.	Stamping and document folder clearance	X	—

Note: H, hold and witness; W, verification of records; X, applicable.

14.3 WELDING DESIGN

14.3.1 PARAMETERS AFFECTING WELDING QUALITY

Three important parameters (Figure 14.2) that contribute to the quality of a welded product are [17] the following:

1. Material—composition, product form, and mechanical properties
2. Welding—procedures, welders, equipment, and supervision
3. Inspection—stage inspection and NDT

Elements of welding design for building quality into the product are discussed in this part.

14.3.2 WELDING QUALITY DESIGN

The highest standards of weld quality demand QC or NDT or both. Not all welds can be inspected by common NDT methods. The achievement of consistent high-quality welds made by manual or automated welding processes requires the following [11,17]:

1. Well-established and qualified welding procedures.
2. Strict implementation of all the weld procedures.
3. Trained and qualified welders, and welding machine operators.

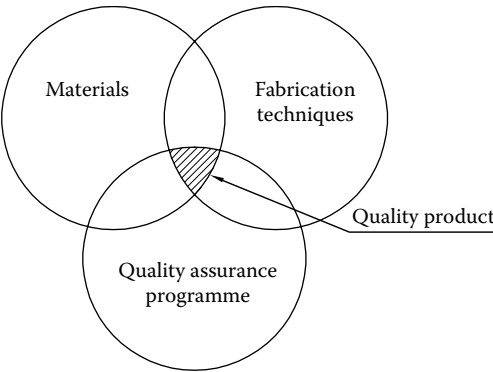


FIGURE 14.2 Components of fabrication assessment.

TABLE 14.2
Welding Parameters for Better Control of Weld Quality

Joint No.	Figure No.	Base Materials	Thickness (mm)	Welding Process	No. Weld Runs	Filler Material	Shld. Gas/Flux	Preheating (°C)	PQR No.	WPS No.	PTP
<i>Note:</i> If necessary, several tables of this form may be used, having the same revision number. A blank space below the table may be left for notes such as weld details and for numbered sketches of the joint.											

- 4. Well-maintained and calibrated equipments, instruments, and gauges.
- 5. Proper supervision and control of welding operations.
- 6. Recording of all information and measurements during welding.
- 7. Detailed NDT.
- 8. Welding consumables must be stored as per Section II, Part C, of the code or as per quality manual.
- 9. Documents must cover issue and return of consumables.

In addition to these, more attention must be paid to the already proven techniques of QC particularly in the following areas [3]:

- Component design—eliminate sites for fatigue or brittle fracture, improve access for welding and inspection
- Weld detail design—use butt welds, rather than fillets or seal welds
- Material selection—weldability considerations
- Operator selection—test the ability of the welder or welding machine
- Supervision and production control—adequate supervision or monitoring in the case of machines

For better control of weld quality of major and critical joints, tabulate the various welding parameters as shown in Table 14.2.

14.3.2.1 Variables Affecting Welding Quality

A wide range of welding variables affect the weld quality. They include [17] welding process, weld preparation, weld bead sequence, parent material compositions, weld metal composition, fluxes, electrodes and filler wires, preheat and interpass temperature, welding speed, heat input, cleaning between passes, PWHT, postweld cleaning, and surface treatment.

14.3.3 SCHEME OF SYMBOLS FOR WELDING

Symbols described in any standard provide the means of placing on drawings information such as the type, size, positions, etc., of the welds in the welded joints. To avoid confusion and misunderstanding, it is essential that only standard symbols are used by all designers and fabricators. However, all information required for welding cannot be conveyed by the symbols alone. AWS welding symbols are used in many countries. [Refer to Standard Symbols for Welding, Brazing and Nondestructive Examination, ANSI/AWS A2.4-93.]

14.3.4 STANDARD FOR WELDING AND WELDING DESIGN

Welding and welding design shall be as per ASME Code Section IX [9]. The scope of Section IX is given here.

14.3.4.1 ASME Code Section IX

Section IX of the ASME code specifies the rules for all manual and machine welding processes and rules for the preparation of WPSs, and the qualification of welding procedures, welders, and welding operators. There are, in addition, tables of P-numbers that have been assigned to each material specification, so that the various examinations can be classified together. Similarly, F-numbers are assigned to electrodes and welding rods to utilize coverage of several different electrodes or welding rods within one qualification test. This section also includes tables for each process listing essential, supplemental essential, and nonessential variables, welding factors that can be altered.

14.3.5 SELECTION OF CONSUMABLES

While selecting the consumables, the requirements for hydrogen control must be satisfied to avoid hydrogen-induced cold cracking. Electrodes and fluxes must be heated before use to ensure low hydrogen contents.

14.3.6 P NUMBERS

All materials used for pressure vessel manufacture have been grouped under different P numbers. The P number grouping of materials is based essentially on comparable metal characteristics such as composition, weldability, and mechanical properties. The object of grouping the base materials is to reduce the number of qualifications required. Thus a single qualification may be adequate for several material specifications. The P number groupings are given in Table 14.3.

14.3.7 FILLER METALS

The filler metals are grouped under both F numbers and A numbers.

TABLE 14.3
P Number and F Number Groupings

Ferrous metals	P1–P11	F1–6
Aluminum and its alloys	P21–P25	F21–24
Copper and its alloys	P31–P35	F31–36
Nickel and its alloys	P41–P45	F41–44
Unalloyed titanium	P51–P52	F51

14.3.7.1 F Numbers

All the electrodes and fillers are grouped under different F numbers. The F number grouping is based essentially on their usability characteristics, and the object of the grouping is to reduce the number of welding procedures and performance qualifications. The F number grouping is given in Table 14.3.

14.3.7.2 A Numbers

As well as classifying the filler metals under F numbers, they are classified under A numbers. The A number classifications of the filler metals are based on the weld metal composition, whereas the F number classifications are based on the usability characteristics.

14.3.8 WELDING PROCEDURE QUALIFICATION: WELDING PROCEDURE SPECIFICATION AND PROCEDURE QUALIFICATION RECORD

The code says that all the details of the welding procedure should be listed in a document known as the WPS. Each of the WPSs shall be qualified by the welding of the test coupons and the testing of specimens as required by the code. The type and the number of tests are selected to provide sufficient information on strength, ductility, toughness, or other properties of the joint. The welding data for the test coupons and the results of the tests shall be recorded in a document called PQR. A WPS may require the support of one or more PQRs, whereas one PQR may support a number of WPS. A WPS will be applicable equally for plate, pipe, and tube joints.

The WPS and the PQR are required to prove that the weldment has desired properties and not to prove the skill of the welder or the welding machine operator. The welder or operator performance qualification is to prove the ability of the welder to deposit good weld metal; the welding operator performance qualification is to show if the operator can operate the welding equipment.

14.3.8.1 Welding Procedure Specification

14.3.8.1.1 Welding Variables

Depending on their influence on obtaining a desired weldment, the welding parameters are classified and listed. Some of them are listed as *essential variables*, some of them as *supplementary essential variables*, and the others as *nonessential variables*.

Essential variables when changed beyond the allowable limits alter the weld properties and requalification is required. Still, there are a number of variables that are declared essential in case a procedure qualification is applied, e.g., a weldment meant for high notch toughness applications. These are called supplementary essential variables.

Nonessential variables when changed (within logical limits) during welding do not alter the desired weld properties, and they are entered in the PQR without qualifying the same. Production welds with such altered variables could be continued without any need for requalification of the welding procedure.

14.3.8.1.2 Contents of Welding Procedure Specification

A WPS shall describe all of the essential/nonessential and supplementary essential variables (when required) for each process used. It will contain information regarding joint details, joint preparation, base metals, type and size of filler metal, welding position, electrical characteristics (type of current, range of current, and voltage), welding techniques, shielding gas, preheat, PWHT, interpass temperature, not preparation prior to welding from second side, welding speed, etc.

14.3.8.1.3 Qualification of a Welding Procedure

The basic steps in the qualification of a welding procedure are as follows:

1. Prepare a preliminary WPS.
2. Prepare a test piece and carry out welding using parameters given in the WPS.

3. Conduct the required tests.
4. Evaluate results of the tests.
5. Document results on PQR.
6. If results are not satisfactory, alter the variables in the WPS and repeat steps 2–6, until test results are satisfactory.
7. Issue approved PQR.
8. Issue approved WPS.

14.3.8.2 Procedure Qualification Record

A PQR is a record of the range of welding parameters used to qualify a welding procedure.

14.3.8.2.1 Contents of the PQR

The completed PQR shall contain all essential and supplementary essential variables (when required) for each welding process used for welding the test coupon and the test results in compliance with code requirements.

14.3.8.3 Welder's Performance Qualification

The object of the welder's performance qualification is to determine the ability of the welders to make sound welds. The welders may be qualified based on the results of the mechanical tests or by radiographic examination (RT) of the test coupon. For qualifying welders, only the essential variables (as applicable to welders' skill) are considered. Any change in those variables requires requalifying the welder. In the case of welding machine operator qualifications, ability to operate the welding machine is tested. A welding machine operator is usually qualified along with a procedure test.

14.3.8.4 Welder Requalification

Some of the welding parameters that will require welder requalification whenever a change is made in WPS are as follows:

1. If a welder had qualified for a WPS with a backing strip and if the backing is removed, then the welder has to requalify. However, if a welder had qualified for a WPS without backing, then that welder is qualified for a WPS with backing also.
2. If the range of thickness has to be increased or there is a change of base metal from one P number to another P number, a new WPS should be prepared and specified by a PQR.
3. A change in F number or A number shall require a new WPS and PQR; a change in the diameter of the electrode also requires a new WPS but need not be qualified by a test.
4. Any change in temperature and duration of the PWHT shall require requalification.

14.3.8.5 Welding Positions and Qualifications

ASME Code has classified five welding positions for qualifications: flat, horizontal, vertical, overhead, and horizontal fixed. Some positions are shown in Figure 14.3 with designated notations for groove and fillet welds.

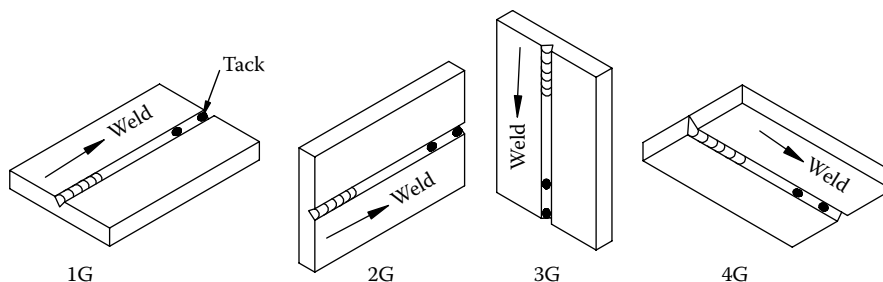


FIGURE 14.3 Welding positions for qualification—fillet weld in plate.

14.3.9 WELD DEFECTS AND INSPECTION OF WELD QUALITY

14.3.9.1 Weld Defects (Discontinuities)

In the correct sense of the word, defect is a rejectable discontinuity or a flaw of rejectable nature. A defect is definitely a discontinuity, but a discontinuity need not necessarily be a defect. Technically, discontinuities are not defects unless they exceed the limits set by the codes or standards have specified [24]. Discontinuities may be found in weld metal, heat-affected zones, and base metal.

14.3.9.2 Causes of Discontinuities

Defects are caused due to inferior design, poor workmanship, wrong welding procedure, poor weldability of the materials, etc.

14.3.9.3 General Types of Defects and Their Significance

Defects in weldments in general can be classified as follows:

1. *Welding process defect*: lack of fusion, incomplete penetration, porosity, slag, etc.
2. *Foreign inclusions*: slag, copper, oxide films, tungsten, etc.
3. *Geometric defects*: overlap, undercut, excessive reinforcement, burnthrough or excessive penetration, distortion, improper weld profile, etc.
4. *Metallurgical defects*: cracks, gas porosity, embrittlement, structural notches, hydrogen-induced cold cracking, liquation cracking, solidification cracking, ductility-dip cracking, stress relief cracking, lamellar tearing, low-delta ferrite, etc.

Planar defects, that is two-dimensional (2D) defects, like cracks, lack of fusion, lack of penetration, severe undercut, etc., are critical in nature, involve lack of bonding, and are not tolerated. Three-dimensional (3D) defects, like slag inclusion, cavities, and pores, are tolerated to a certain extent, depending on the length of the inclusion and product class. Notches are not allowed for low-temperature and cryogenic applications. Sharp notches, which act as stress raisers, are smoothed out wherever accessible to avoid stress concentration. Some weld defects that are schematically shown in Figures 14.4 and 14.5 show radiographic interpretation of welding defects.

Faults in fusion welds, causes, and detection are given later.

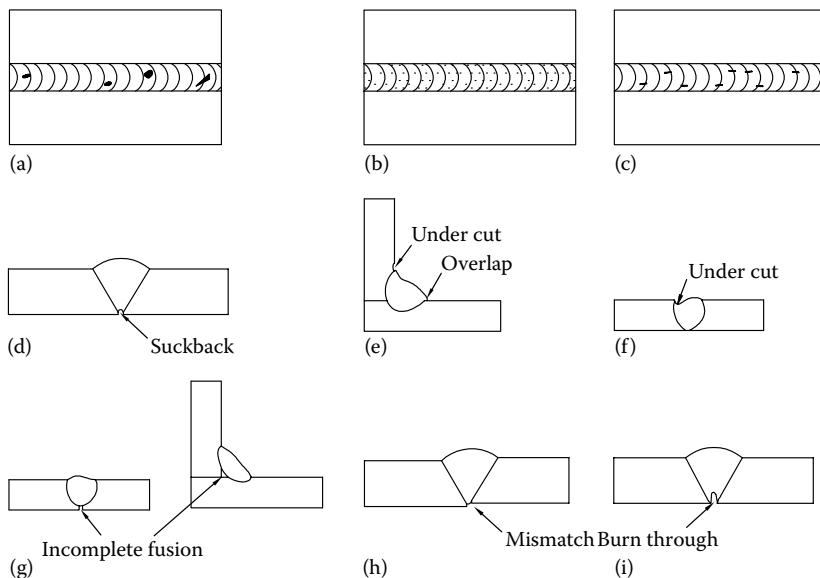


FIGURE 14.4 Weld defects—schematic. (Note: (a) gas porosity or worm holes, (b) distributed porosities, and (c) slag inclusion. Others are defined in the figure itself.)

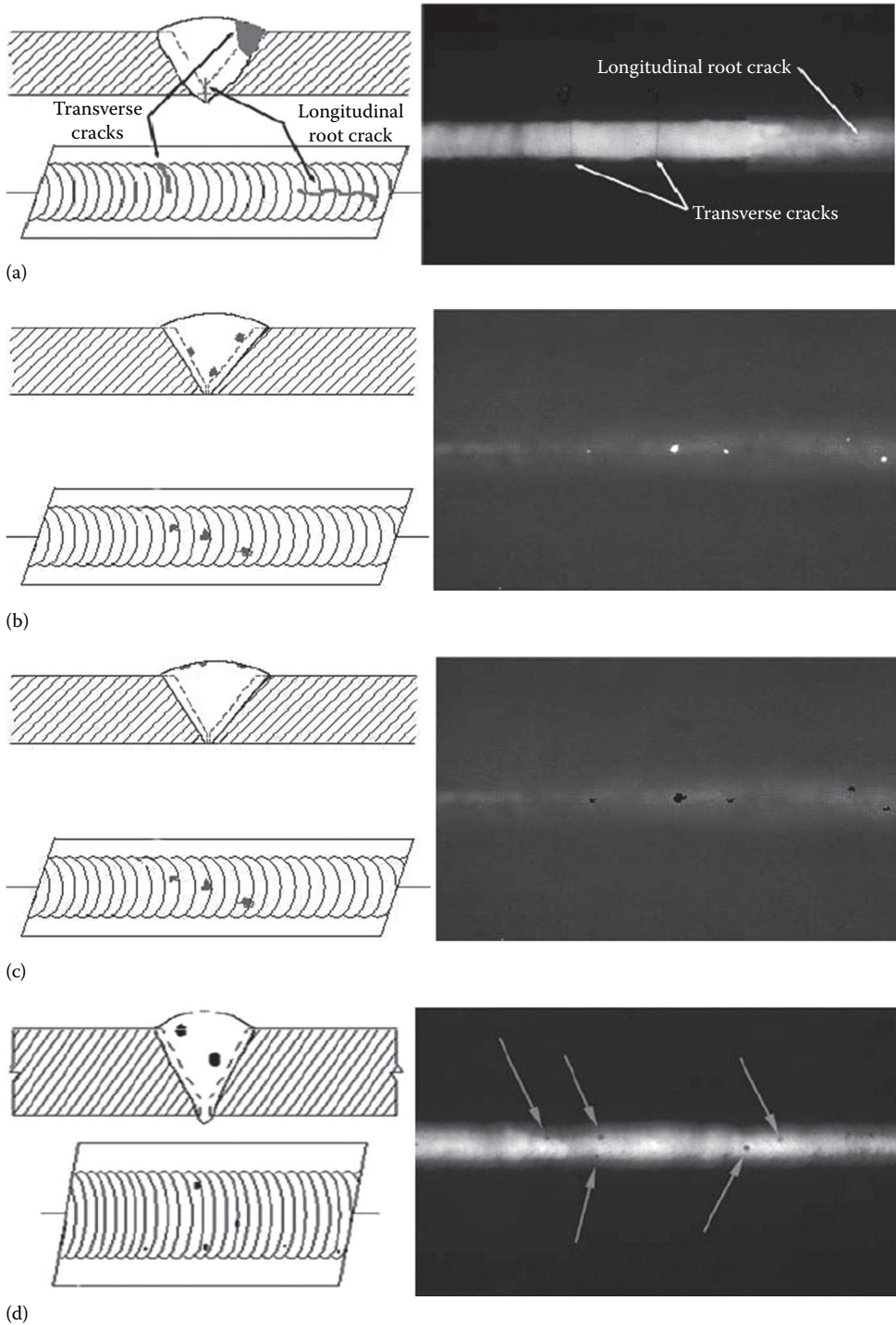


FIGURE 14.5 Radiographic interpretation of welding defects: (a) transverse/longitudinal root crack, (b) slag inclusion, (c) oxide inclusion and (d) porosity. (From NDT Education Resource Center, Developed by the Collaboration for NDT Education, Brian, F.L., ed., Center for Nondestructive Evaluation, Iowa State University, Ames, IA.)

14.3.9.3.1 Faults in Fusion Welds in Constructional Steels

1. Cracks: Solidification cracking, hydrogen-induced HAZ cracking, lamellar tearing, and reheat cracking; longitudinal, transverse, throat, crater, toe, and roof cracks.
2. Porosities: Porosities include uniformly scattered porosity, cluster porosity, linear porosity, elongated porosity, or piping porosity, and wormhole porosity.
 - a. *Worm holes* result from the entrapment of gas between solidifying dendrites of weld metal.
Causes: Gas may arise from contamination of surface to be welded or prevented from beneath weld by joints.
 - b. *Uniformly distributed porosity* results from the entrapment of gas in solidified weld metal. Other forms of porosity are restart porosity and surface porosity.
 - c. *Surface porosity* is caused by excessive contamination from grease, dampness, or atmosphere entrainment. It is occasionally caused by excessive sulfur in consumables or parent metal.
 - d. *Crater pipes* result from shrinkage at the end of weld run where the source of heat is removed. They are caused by incorrect manipulative technique or current decay to allow for crater shrinkage.
3. Solid inclusions: Solid inclusions include linear slag inclusions and isolated slag inclusions, tungsten inclusions, or infused filler metal.
4. Lack of fusion and penetration: This type of defect tends to the subsurface and is therefore detectable only by ultrasonic or x-ray methods. Lack of side wall diffusion, which penetrates the surfaces, could be detected using magnetic particle or dye/fluorescent penetrant inspection.
5. Imperfect shape. Detection: All shape defects are detectable by visual examination (VT). Some of the forms of imperfect shape are as follows:
 - a. *Linear misalignment* is caused by the incorrect assembly and/or distortion during fabrication.
 - b. *Excessive penetration* is caused by the incorrect edge preparation providing insufficient support at the weld root incorrect weld conditions. The provisions of backing strip can alleviate this problem in defective circumstances.
6. Arc strike: Accidental contact of electrode or weld torch with plate surface remote from weld. These usually result in simulated hard spots just beneath the surface, which tend to corrode and thus should be avoided.
7. Miscellaneous faults.
 - a. *Splatter* is caused by the incorrect weld conditions or contaminated consumable or preparations to explosive conditions. Globules of molten metal are thrown out from the weld pool and adhere to the parent metal.
 - b. *Copper pickup* is the melting of copper duct tube in the MIG weld due to incorrect conditions. In general, detection is possible only by x-ray or ultrasonic techniques.

14.3.9.4 Approach to Weld Defect Acceptance Levels

Two quality levels are proposed for weld defect acceptance [25]:

1. The first, the fitness-for-purpose level, is such that larger defects might cause failure of the structure and they must, therefore, be repaired. Suitable fitness-for-purpose analyzes the true significance of the defects in place of the old acceptance levels. Fracture mechanics assessment can be used to demonstrate that many defects are not significant in terms of service conditions and that continued safe operation can be assured [26].
2. The second is a QC level. Repairs are not attended out where welds fall below this, but the cause of the loss of quality is examined so that it may be maintained well above the fitness for purpose level.

14.4 NONDESTRUCTIVE TESTING METHODS

NDT, also referred as nondestructive evaluation (NDE), is an integral and the most important constituent of the QA program of any industry. NDT techniques measure and evaluate the effectiveness of procedure, materials—before, during, and after fabrication—and the overall integrity of assemblies and subassemblies. NDT principally involves surface examination and volumetric examination, material identification and composition, quality characteristics of castings and forgings, welding defects such as cracks, voids, and inclusions, porosities, lack of penetration, lack of fusion, lack of bond, undercut, laminations in rolling and forging, laminar inclusions, and delamination in components, and environmental-assisted cracking such as hydrogen-induced cracking and stress corrosion cracking, etc., can be evaluated by NDT methods. Without effective means of NDT, it would probably be impossible to build many of the major high-integrity structures [26].

The most commonly used NDT methods are VT, dye penetrant testing (PT), magnetic particle testing (MT), radiography testing (RT), UT, acoustic emission testing (AET), eddy current testing (ET), and LT. Besides these, there are other NDT methods, such as radioscopy, thermal imaging, computer tomography, and holography, which are employed for special applications.

14.4.1 SELECTION OF NDT METHODS

There are five main parameters to be considered when selecting an inspection method: (1) capabilities and limitations of the inspection method, (2) acceptance standards, (3) cost, (4) personnel, and (5) equipment.

14.4.1.1 Capabilities and Limitations of Nondestructive Testing Methods

In fabrication of heat exchangers and pressure vessels, NDT is commonly used for the detection of flaws in welds, forgings, castings, plates, tubes, etc. Each NDT method has its own flaw detection characteristics, and therefore no individual NDT method can replace another one. No single test or series of tests will give 100% assurance of quality. To use NDT technique effectively, one must be aware of the limitations of the different methods. NDT selection, applications, advantages, and limitations are tabulated in Refs. [6,27–30], among others, and a typical example is given in Table 14.4.

14.4.1.2 Acceptance Criteria

For each NDT technique, acceptance criteria are an integral part of most codes and standards. Acceptance criteria define different types of discontinuities and whether particular types of discontinuities are acceptable. Discontinuities are rejected if they exceed specification requirements. Acceptance or rejection of flaws is based on different factors, and a vital few are (1) accessibility for repair and cost of repair, (2) safety, with hazards and consequences of failure, (3) desired life, (4) type of materials used, (5) material thickness, (6) design stress, and (7) nature of service environment (corrosive or noncorrosive).

14.4.1.3 Cost

Different NDT methods have different costs in any particular situation. Two basic cost factors that should be considered in the selection of an NDT method are the initial equipment cost and the cost of performing the inspection [28]. The cost of performing NDT tests includes the labor cost, training cost, and cost of consumables such as radiographic film, dyes, magnetic particles, etc. VT is almost always the least expensive; however, this may not be true sometimes while using the latest optical devices such as borescopes, videoprobes, etc., used to aid the VT. In general, the costs of radiographic, ultrasonic, and eddy current inspections are greater than those of visual, magnetic particle, and liquid penetrant techniques.

TABLE 14.4
Common NDE Methods

Method	Principle	Applications	Advantages	Limitations
Visual inspection	Visual inspection is normally performed by using naked eyes. Its effectiveness may be improved with the aid of special tools. Tools include fiberscopes, borescopes, magnifying glasses, and mirrors	To determine such things as the surface condition of the part, reinforcement, and undercutting of welds, alignment of mating surfaces, shape, or evidence of leaking	Cheapest NDT method, applicable at all stages of construction or manufacturing, do not require extensive training, capable of giving instantaneous results	Limited to only surface inspection Require good lighting Require good eyesight
Liquid penetrant	Liquid penetrant is drawn into surface defects by capillary action. Visible or fluorescent dye reveals flaws	Used for the detection of surface discontinuities such as cracks, seams, laps, cold shuts, laminations, and porosity that are open to surface	Inexpensive, portable. Very sensitive. Independent of magnetic and electrical properties of material. Simple to perform	Limited to detection of surface breaking discontinuity Not applicable to porous material, require access for pre- and postcleaning, irregular surface may cause the presence of nonrelevant indication, penetrant must wet surface
Magnetic particle	Detect surface and subsurface flaws and discontinuities which distort applied magnetic field, causing leakage fields that attract iron powder on surface. Flaws upto 1/4 in. beneath a surface can be detected	Cracks, laps, voids, porosity, and inclusions and other discontinuities on or near surface of ferromagnetic materials	Inexpensive, equipments are portable, suitable for large, immovable objects. Equipment easy to operate Provide instantaneous results, sensitive to surface and subsurface discontinuities	Applicable only to ferromagnetic materials. The sensitivity of this method decreases rapidly with depths below the surface being examined. Insensitive to internal defects. Require magnetization and demagnetization of materials to be inspected. Require power supply for magnetization. Coating may mask indication. Material may be burned during magnetization

(continued)

TABLE 14.4 (continued)
Common NDE Methods

Method	Principle	Applications	Advantages	Limitations
Ultrasonic	Flaws reflect sound waves traveling through material; elapsed time before echo is received determines locations of flaw	Applicable for thickness measurement, detection of discontinuity, cracks, voids, porosity, inclusions, laminations, and delaminations, lack of bonding between dissimilar materials, etc., with principal plane perpendicular to sound source and determination of material properties, the depth and exact size of the defect can be determined by the use of the proper technique	Capable of detecting internal defect, not hazardous, can provide the size of discontinuity detected, very sensitive to planar type discontinuity, suitable for automation, equipment are mostly portable and suitable for field inspection, applicable for thick materials, immediate results. Computerized equipment can produce images of flaws (C-scan)	Trained inspectors required, reference standards required. Require the use of couplant to enhance sound transmission. Require calibration blocks and reference standards. Require highly skillful and experience operator/inspector. Not so reliable for surface and subsurface discontinuity due to interference between initial pulse and signal due to discontinuity
Radiographic	Metals absorb x-rays and gamma rays. Flaws and thin sections absorb less, so that more radiation strikes film. Flaws appear as dark shadows	Can detect internal discontinuities such as voids, porosity, inclusions, and cracks in castings and weldments in a wide range of materials, sizes, and shapes. Welding defects like lack of fusion, lack of penetration, cracks, undercuts, weld concavity, convexity, thinning, porosity, etc	Capable of detecting surface, subsurface, and internal discontinuities. Permanent record including evidence of proper test procedures. Defects flaws at any depth. Applicable to almost all materials. Many equipments are portable	Radiation is hazardous to workers. Expensive method, incapable of detecting laminar discontinuities, some equipment are bulky, it needs electricity, require both film side and source side accessibility, results of film RT are not instantaneous—it requires film processing, interpretation, and evaluation. Requires highly trained personnel in the subject of radiography, radiation safety, and interpretation of weld defects.

TABLE 14.4 (continued)
Common NDE Methods

Method	Principle	Applications	Advantages	Limitations
Eddy current	An alternating current is made to flow in a coil (probe), which, when brought into close proximity of the conducting surface of the material to be inspected, induces an eddy current flow in the material. Any discontinuity that appreciably alters the normal flow of eddy current can be detected by eddy current inspection	Conductive materials with constant cross section; especially pipe/tube inspection. Defects variations in metal type and microstructure as well as flaws	The inspection system can easily be automated, it is a noncontact method, equipment are portable and suitable for field application, some equipment are made dedicated for specific measurement (e.g., conductivity, crack depth, etc.). Fast enough for continuous online inspection	Often too sensitive to unimportant parameters or minor dimensional fluctuations, applicable only to conducting materials. If it is to be used for ferromagnetic material, the item must be magnetically saturated to minimize effect from permeability Require highly skilled and experienced operator
AE	Materials and structures/ components emit acoustic energy during crack growth and plastic deformation. Sensor detects noises crack growth	Online monitoring of pressure vessels. Monitoring of weld overlays and thermal shock. Aircraft structures. Creeps. Welds defects. Stress corrosion cracking	Pressurized-vessel flaws are detected before failure. All loaded areas are tested, regardless of sensor location. AE monitoring on production lines is faster than ultrasonic because its sensors need not be moved over the entire surface being inspected.	Plastic deformation during tests is irreversible; test is therefore unrepeatable. Test cannot pinpoint source of emission

14.4.1.4 Personnel

NDT tends to be rather dependent for its effectiveness on the capabilities of the persons performing it. The first requirement for good NDT is the properly trained and experienced personnel. NDT personnel must be able to evaluate and record test results with accuracy and consistency. Poorly run tests or incorrect interpretation of the results leads to rejection of good parts and acceptance of defective parts [31]. Other requirements for personnel involved in NDT examinations include the following: good eyesight, well-developed powers of observation and concentration, high personal integrity, good judgment, and familiarity with codes and standards being practiced.

14.4.1.4.1 NDT Personnel Qualifications

In order to promote uniformity in performing and interpreting NDT tests, the American Society for Nondestructive Testing has drawn up some minimum qualification requirements for personnel, who are graded as Level I, Level II, and Level III. An NDT Level I person must have experience or

training in the performance of the required inspections and tests, and he or she shall receive the necessary instruction or supervision from a certified NDT Level II or III person. Level II shall be able to prepare written instructions, to organize test, and to report the results on NDT tests. A Level III person should be capable of planning and supervising inspections and tests, reviewing and approving procedures, and organizing and reporting results and certifying their validity. This person is also authorized for training, qualifying, and certifying NDT personnel.

Personnel involved in the performance, evaluation, or supervision of NDT examinations, including RT, UT, PT, MT, and ET methods, must meet the Level III qualification requirements, and for gas LT methods, they must meet Level II qualification requirements as specified in SNT-TC-1A of American Society for Nondestructive Testing.

14.4.1.4.2 Training of NDT Personnel

The manufacturer may conduct a training program to meet the requirements of SNT-TC-1A through a designated employee who meets Level III requirements. Qualification and training of NDT personnel are discussed in detail in Ref. [9].

14.4.2 INSPECTION EQUIPMENT

Only high-performance flaw-detecting equipment should be used. NDT equipment is to be handled properly in order to assure continued accuracy of examination. The measuring instruments, tools, and gauges are to be calibrated periodically with reference standards.

14.4.3 REFERENCE CODES AND STANDARDS

ASME Code Section V [10d] is the most widely used code for NDT throughout the world. The basic coverage of ASME Code Section V on nondestructive examination is given here.

14.4.3.1 ASME Code Section V: Nondestructive Examination

This section contains requirements and methods for nondestructive examination, which are referenced and required by other code sections. Also included are manufacturer's examination responsibilities, duties of authorized inspectors, and requirements for qualification of personnel, inspection, and examination. Methods of making the nondestructive examinations are given for the following:

1. RT
2. Ultrasonic examination (UT)
3. Liquid PT
4. Magnetic particle examination (MP)
5. ET for tubular products
6. VT
7. LT

14.4.4 NDT SYMBOLS

Figure 14.6 depicts the AWS symbols for NDT examination.

14.4.5 WRITTEN PROCEDURES

NDT should be carried out in accordance with written procedures to achieve consistency and accuracy. Without a written procedure, there is no guarantee as to the effectiveness or repeatability of the test. Detailed NDT procedures/instructions are essential for several reasons

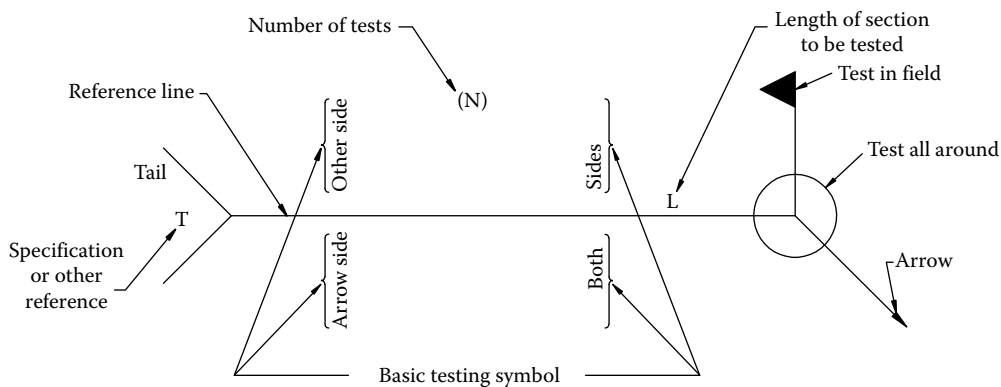


FIGURE 14.6 AWS symbols for NDT examination and standard location of elements.

[2]: (1) they demonstrate that a fabricator fully understands code and standard, and contractual requirements; (2) they provide comprehensive instructions at the place of test and mitigate against difficulties arising from different operator/inspection authority interpretation; and (3) facilitate surveillance and constitute a record of how testing was carried out. The procedure should state the qualifications of personnel operating the equipment and interpreting the results. In general, the procedure must be approved by the buyer or third-party inspection agency. When written procedures are not available, inspectors are asked to work as per codes and specifications.

14.4.5.1 Content of NDT Procedures

NDT should be carried out in accordance with written procedures irrespective of whether or not it is a code requirement [2]. A procedure usually specifies items given in Table 14.5 [32].

14.4.5.2 General Details of Requirements in the NDT Procedure Document

NDT procedures should not be allowed to become lengthy “training manuals” for inexperienced personnel or “educational texts” for the benefit of the customer [2]. However, they must contain sufficient detail to ensure effective examination of the material or component under consideration.

TABLE 14.5
Content of NDT Procedures

1. Scope
2. Applicable documents such as codes and standards
3. Inspecting personnel
4. Inspection equipment—calibration and reference standards
5. Surface preparation
6. Test method/techniques
7. Evaluation of indications and reporting
8. Acceptance criteria
9. Report
10. Records

Source: Adapted from Hamlet, R.A. and Lavender, D.H.,
Br. J. NDT, 359, 1986.

The general details of requirements of NDT procedure are listed and discussed by Hamlett et al. [32], and they are summarized here:

1. The procedure should be on company-headed paper so as to clearly demonstrate its origin.
2. The procedure should specify applicable code and standard.
3. The procedure should be approved and signed by a competent authority.
4. The procedure should have a formal specific title.
5. Each page of the procedure should be numbered and should carry the unique procedure code number.
6. Each section should be numbered and each paragraph should be given a subsection number.
7. The first page of the procedure should be an amendment sheet explaining the latest additions or amendments since the original procedure was issued.

14.4.5.3 Deficiencies in NDT Procedures

The most common deficiencies in NDT procedures fall into three main categories [2]:

1. They lack detail and simply state “refer to” BS Specifications, ASME Code, and so on, in relation to calibration standards, acceptance standards, etc. They fail to identify which of the options contained in the specifications or codes apply to the component under inspection.
2. The method is identified correctly, but the techniques and test parameters specified are not specifically tailored to the actual part to be examined.
3. They omit technical requirements specific to the particular procedure.

Typical NDT procedure deficiencies in RT, UT, MT, and PT are discussed in Ref. [2], and they are listed in the discussion of these NDT techniques.

14.4.6 VISUAL EXAMINATION

VT is the primary evaluative method of inspection, and it is the oldest method of NDT. Visual methods are of necessity restricted to surface examination, but they may sometimes be useful for a detailed examination of an imperfection after other methods have determined its position [33]. In addition to locating surface defects and raw material identification, VT can be an excellent process control technique during various stages of fabrication and can identify subsequent problems revealed during PWHT and hydrostatic testing/LT.

14.4.6.1 Principle of VT

The basic principle used in visual NDT is to illuminate the specimen with light, usually in the visible region. The specimen is then examined with the eye under adequate illumination, either naturally or by light-sensitive devices such as photocells and phototubes. The VT is classified as direct vision technique and remote VT.

14.4.6.1.1 Direct Vision Examination

Direct vision technique is applicable when access is sufficient to place the eye within 24 in. (609.6 mm) of the surface to be examined and at an angle not less than 30° to the surface to be examined. Mirrors as well as aids such as magnifying lens may be used to assist examination.

14.4.6.1.2 Remote Visual Examination

Remote VT is conducted with aids such as mirrors, telescopes, borescopes, fiber optics, cameras, and other suitable equipment. These optical aids supplement direct vision.

14.4.6.2 Merits of Visual Examination

VT is easily applied, quick, and often requires no special equipment other than good eyesight and some relatively simple and inexpensive equipment.

14.4.6.3 VT Written Procedure

Written procedure for VT is detailed in ASME Code Section V. The written procedure should contain at a minimum the following:

1. How VT is to be performed
2. Surface condition and criteria for surface cleaning
3. Surface cleaning procedures
4. Method or tool for surface preparation, if any
5. Whether direct or remote viewing is used
6. Special illumination or optical devices to be used, if any
7. Sequence of performing examination when applicable
8. Data to be tabulated, if any
9. Reports or general statements to be completed

14.4.6.4 Reference Document

Codes and standards or the purchaser's specification is needed. An important document for visual inspectors is the *AWS Guidebook on Visual Examination* [23].

14.4.6.5 Visual Examination: Prerequisites

As with any other nondestructive inspection method, there are various prerequisites that should be considered to perform VT. Some of the more common attributes to consider are [23] the following:

1. The visual examiner should have sufficient visual acuity to perform an adequate inspection.
2. Visual inspectors should have sufficient knowledge on welding procedures and safety practices. There are many potential safety hazards present.

Additionally, the inspector should have adequate illumination, either natural or artificial.

14.4.6.6 Visual Examination Equipment

Certain tools are sometimes necessary for some aspects of visual weld inspection. These tools are specified in Refs. [23,34]. Some of the tools and gauges most frequently used in visual welding inspection are the following:

1. Ammeters to measure current during welding or inspection by MT
2. Temperature-sensitive crayons for surface markings
3. Surface contact thermometers and pyrometers
4. Weld gauges, measuring scales, fillet gauges, and devices
5. Multipurpose gauges capable of performing many measurements such as measuring convex and concave fillet welds, weld reinforcement, and root opening
6. Taper gauge to measure root opening (gap)
7. Hi-lo gauge, also known as a mismatch gauge, to measure the internal alignment of a pipe joint
8. Fiber-optic devices such as borescopes, fiberscopes, etc., and video probes
9. Ferrite gauges

14.4.6.7 NDT of Raw Materials

VT of the base materials, such as plates, tubes, pipes, forging, and castings, prior to fabrication can detect scabs, seams, loose rusts, scale, or other harmful surface conditions that tend to cause

weld defects. Plate laminations may be observed on cut edges. Dimensions should be confirmed by measurements. Base metal should be identified by type, grade, and heat number. Even though plates and forged pressure parts are ultrasonically tested by material suppliers, these products for critical applications warrant ultrasonic inspection in the manufacturer's premises.

6.8 Visual Examination during Various Stages of Fabrication by Welding

The effectiveness of visual inspections is improved when a QC system is instituted that provides for coverage at all phases of the welding process—before, during, and after welding. Visual inspection used before, during, and after welding finds 90% of defects that would be detected later using more costly methods such as UT or radiography [35]. The items to be checked by visual inspection prior to welding, during welding, and after welding are detailed in Refs. [23,28]. Some of the important points are given next.

Visual examination before welding

1. Review drawing and specifications.
2. Check machine settings.
3. Qualification of welding procedures and personnel.
4. Joint preparations, dimensions, cleanliness, and surface preparation.
5. Review welding process and consumables to be used.
6. Establish checkpoints.
7. Check fit and alignment of weld joints: groove angle, root openings, joint alignment, etc.

Visual examination during welding

1. Treatment of tack welds
2. Quality of the root pass and the succeeding weld layers
3. Joint root preparation prior to welding the second side
4. Preheat and interpass temperatures
5. Sequences of weld passes
6. Interpass cleaning
7. Checking the welding procedure parameters, that is voltage, amperage, and speed
8. Parameters pertaining to shielding gases
9. Distortion

Visual examination after welding

This covers final weld inspection like (1) weld size, appearance, color, contour, and surface roughness; (2) extent of welding; (3) dimensions; (4) distortion; and (5) visible external weld defects such as cracks, undercut, overlap, exposed porosity and slag inclusions, unacceptable weld profile, arc strike, weld spatter, reinforcement, concavity, and burnthrough.

14.4.6.9 Developments in Visual Examination Optical Instruments

14.4.6.9.1 Remote Visual Inspection

Remote visual inspection, or RVI, is a technique that permits inspection of an area that has no direct visual access. A slim and often flexible viewing device or “scope” is inserted into the area through a small opening, providing an image for the operator to examine. Many optical aids are currently available that supplement direct vision. Skill and experience are necessary to handle such optical aids. Recent developments in the optical field include the use of television and also of fiber optics to inspect remote and inaccessible areas. Special TV cameras are available that can be inserted into openings as small as 1.5 in. (38.1 mm) diameter [36], and a closed-circuit

transmission system can then be arranged to give an image of the internal surface of butt welds in pipelines and bores [33]. The three basic remote VT aids are borescopes, fiberscopes, and video borescopes. One of the leading visual inspection equipments/aids providers is Olympus NDT Inc., Waltham, MA (<http://www.olympus-ims.com/en/rvi-products/>).

14.4.6.9.2 Borescopes

As the name implies, a borescope is an optical instrument designed to enable an observer to inspect the inaccessible areas such as inside of a narrow tube, bore, or a chamber. One can insert them into very small openings, extending the vision to welds far inside the darkest recess in process piping, heat exchangers, pressure vessels, and other equipment. Illuminating the weld and magnifying it 3× or 4×, borescopes are easy to use, relatively inexpensive, and extremely effective [37].

Basics of borescopes: These instruments use thin glass fibers to transmit light to illuminate the test area and to permit viewing or recording. The brightest images are obtained with borescopes of large diameters and short length. As the length of the borescope is increased, the image becomes less brilliant because of light losses. Likewise, the closer the viewing lens is to the weld, the larger the image.

Flexible fiberscopes: Flexible fiberscopes, in contrast to the stiff borescope, can be inserted into curved pipes and cavities. The light in the fiberscopes is transmitted via a bunch of ultrathin optical fibers with a diameter as small as 7 μm (0.007 mm). A photo of industrial fiberscope is shown in Figure 14.7a.

Stiff borescopes: The stiff borescope can be compared to a periscope, where the objective is placed quite near the object under examination, while the ocular is placed at the desired distance from the objective. The objective and the ocular are connected by means of one or more removable extension tubes. The borescope's length can thus be varied as required. Where straight-line access is available, rigid borescope offer many advantages over fiberscopes, most notably in resolution, image brightness, design flexibility, and price. A photo of rigid borescope is shown in Figure 14.7b.

14.4.6.9.3 Videoimagescopes

Videoimagescopes employ video technology for RVI. At the tip of the flexible videoimagescope probe is a miniature charge-coupled device (CCD) sensor (like a tiny video camera), which sends high-resolution images in full, natural color to be displayed on a TV monitor. Diameters of probes are as small as 8 mm; lengths range from 1.5 to 22 m. A photo of industrial videoscope is shown in Figure 14.7c.

14.4.6.9.4 Video Microscopes

Handheld or fixtured video microscopes see where traditional microscopes cannot. They feature high-resolution CCD image sensors, fiber-optic self-illumination, special objective lenses or HI-Mag borescopic lenses, shutter speeds to 1/10,000 s, freeze frame, and memory, with multiwindow display of 4, 9, 16, or 25 images simultaneously. They can overlay images for comparison or even measurement. Nominal magnifications are from 20× to 1000×.

14.4.6.9.5 Combining Computers and Visual Inspection

Combining visual inspection with computer analysis eases job tracking and planning by storing information and radiographs in databases. Computers that collect and analyze data, update standards, and expand certification programs enable the visual inspector to concentrate on data collection, leaving tedious calculations to the computer [35].



FIGURE 14.7 Remote VT aids. (a) Industrial fiberscope, (b) rigid borescope, and (c) industrial videoscope. (Courtesy of Olympus NDT Inc., Waltham, MA.)

14.4.6.9.6 High-Speed Video

High-speed video uses digital cameras that capture events too fast for the eye to see by recording a very large number of images within a short period of time and then playing them back slowly.

14.4.7 LIQUID PENETRANT INSPECTION

14.4.7.1 Principle

Liquid penetrant inspection (PT) is a means to find discontinuities that are open to the surfaces by bleedout of liquid penetrant medium that is applied over the test surface. The penetrant enters the discontinuities under the influence of capillary action. If the discontinuity is significant, penetrant will be held in the cavity when the excess is removed from the surface. Upon application of a developer, blotter action draws the penetrant from the discontinuity to provide a contrasting indication on the surface, indicating the presence and location of discontinuities. The indications are examined either in natural daylight or in adequate artificial illumination or ultraviolet light, depending on

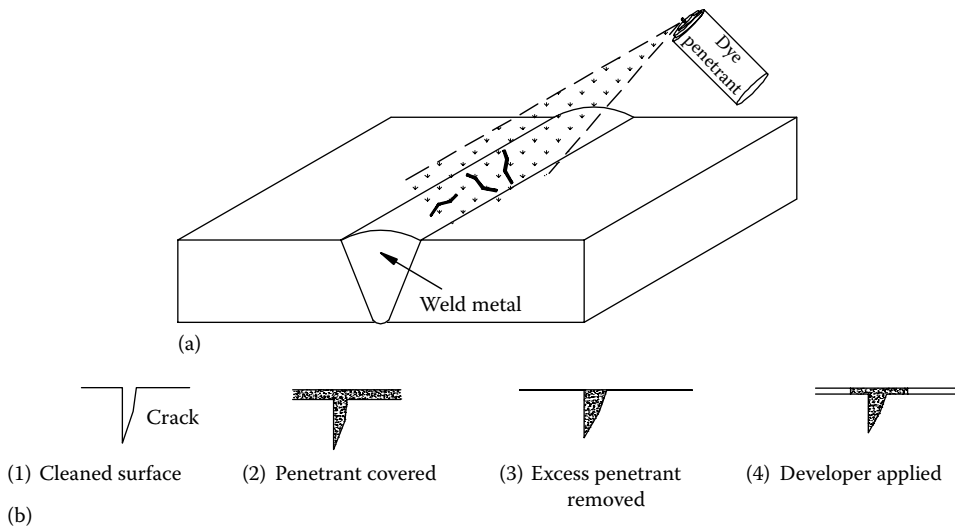


FIGURE 14.8 PT. (a) Schematic and (b) stages of PT.

colored or fluorescent penetrant particles used. Various stages of the PT process are depicted in Figure 14.8. For generic information on PT examination refer to Ref. [38].

14.4.7.2 Applications

Liquid penetrant inspection can be effectively used to detect surface discontinuities such as cracks, porosity, seams, laps, cold shuts, laminations, or lack of bond on nonporous metallic materials, both ferrous and nonferrous, and on nonporous nonmetallic materials such as plastics and glass. The method is particularly useful on nonmagnetic materials, since magnetic particle inspection (MT) cannot be applied to test them.

14.4.7.3 Merits of PT

Its simplicity and low cost make it a popular test. If properly used, it readily detects minute surface openings. The basic steps involved in the application of the test method are relatively simple. Except for VT, it is perhaps the most commonly used nondestructive test for surface examination. Penetrant inspection is reasonably fast. The method is easy to learn and can be applied properly.

14.4.7.4 Limitations

The success of penetrant inspection, like most other inspection methods, depends on the visual acuity of the inspector [28]. The parts must be thoroughly cleaned to allow the penetrant to enter flaw openings, and flaws must be open to the surface [39]. Experience has shown that very slight variations in performing the penetrant process and subsequent inspection can invalidate the findings by failing to indicate all flaws [40]. Therefore, it has become accepted practice that all penetrant inspections be carried out exclusively by trained and certified personnel. It is not suitable for inspecting porous materials.

14.4.7.5 Written Procedure

A written procedure for PT examination is given in Table 14.6.

Liquid penetrant examination procedure deficiencies

Incorrect penetrant material selection, excessive penetrant removal, and incorrect developer application [2].

TABLE 14.6
PT Written Procedure

1.0	Scope: materials, shapes, and sizes to be examined
2.0	Reference document
3.0	Extent of examination
4.0	Approved method and material: type of penetrant, penetrant removal, emulsifier, and developer
5.0	Surface preparation
6.0	Test environment and lighting condition
7.0	Procedure
7.1	Penetrant application, dwell time, and the testing of the surface and penetrant during the examination if outside is 60°F–125°F
7.2	Excess penetrant removal
7.3	Developer application
7.4	Examination
8.0	Acceptance criteria
9.0	Personnel certification
10.0	List of approved penetrant materials

14.4.7.6 Standards

ASTM E 165—Recommended practice for PT

ASTM E 270—Definition of terms relating to PT

ASTM E433—Reference photographs for PT

ASME Sec. V, Articles 6 and 24 ASME Sec. VIII, 1 Div., Appendix 8

14.4.7.7 Test Procedure

Six basic steps make up the liquid penetrant inspection procedure. They are [41] the following:

1. Precleaning the part to be inspected with a solvent and drying
2. Application of the penetrant to the part to form a film over the surface and allowing sufficient time for it to enter into the opening
3. Removal of excess penetrant with water wash, solvent, or emulsifier and drying
4. Application of a thin coating of developer over the surface under observation
5. VT under adequate light and interpretation of indications
6. Post inspection cleaning

14.4.7.8 Penetrants

The penetrants are mixtures of organic solvents, which are characterized by their ability to wet materials, spread rapidly, and penetrate into minute defects and dissolve dyes, so that the indications produce a definite red color as contrasted to the white background of the developer.

14.4.7.8.1 Types of Penetrants

Depending upon the type of dye used, penetrants are divided into *visible penetrants*, which are usually red in color to provide a contrast against the white background from the developer under white light, and *fluorescent penetrants*, which provide a greenish yellow indication against a dark background when viewed under a black light (ultraviolet). The fluorescent penetrants are most generally used for the detection of fine cracks, but these are not recommended for use on rough surfaces because of the difficulty in removing the excess penetrant. While selecting chemicals, only those chemicals that are compatible with the base material are to be chosen.

According to the manner in which the excess penetrants are removed from the surface, that is the rinse process, they are classified into three classes: (1) water washable, (2) solvent removable, and (3) postemulsifiable, which are not in themselves water washable, but are made so by applying an emulsifier after the penetration is completed.

14.4.7.9 Method

There are two varieties of penetrant method, both using a similar principle: the visible dye method and the fluorescent dye method.

14.4.7.10 Selection of Developer

The developer is applied to get the penetrant in the discontinuities back to the surface so that it can form an indication of the discontinuity. The penetrant is drawn out by the capillary action but in the reverse direction. It also serves as a color contrast background for dye material.

14.4.7.11 Penetrant Application

The penetrant should be applied by brushing or spraying. The surface temperature of the part should be between 60°F and 125°F (16°C and 52°C).

7.11.1 Penetration Time or Dwell Time

The period of time during which the penetrant is permitted to remain on the specimen is a vital part of the test. The minimum time required for the penetrant to enter into the discontinuity is called the *dwell time*. The recommended dwell times are as follows:

For carbon steel 10–20 min

For alloy and stainless steel 15–20 min

During the dwell time, the penetrant shall not be allowed to dry up, and fresh penetrant shall be applied as often as required.

14.4.7.11.2 Approved Material

Penetrant must be odorless, nontoxic, nonflammable, and stable in storage. The developer should be wet and nonaqueous. The penetrant and developer must be compatible with each other and should be procured from the same manufacturer. For the examination of nickel-based alloys, sulfur content in the penetrant shall not exceed 1% of the residue by weight, whereas for the examination of the austenitic stainless steels or titanium, the chlorides shall not exceed 1% of the residue by weight.

14.4.7.12 Surface Preparation

The surface to be inspected shall be clean and free from oil, grease, sand, rust or scale, welding flux and spatter, etc. The presence of surface contaminants prevents spreading of the penetrant and affects penetrability mechanical operations such as shot peening, machining, buffing, and sand blasting are strictly prohibited prior to the examination to avoid closing of discontinuities. Weld surface shall be ground free of ripples that might mask the indications of unacceptable discontinuities. Sufficient air circulation is necessary during testing.

14.4.7.13 Excess Penetrant Removal

Excess solvent-removable penetrants shall be removed by wiping with a cloth or absorbent paper, repeating the operation until most traces of penetrant have been removed. The remaining traces shall be removed by lightly wiping the surface with cloth or absorbent paper moistened with solvent. To minimize removal of penetrant from discontinuities, care shall be taken to avoid the use of excess solvent.

14.4.7.14 Standardization of Light Levels for Penetrant and Magnetic Inspection

Proper illumination of indications from PT and MT is essential if an acceptable level of probability of detection is to be achieved with either test method. In order to control the illumination for inspection of workpieces, four separate types of measurement must be specified precisely [42]. These are

1. White light illumination for color contrast processes
2. Ultraviolet illumination for fluorescent processes
3. Ambient visible light in darkened inspection rooms
4. Visible light from ultraviolet sources

The fluorescent light is more sensitive, due to the fact that the human eye can more easily discern a fluorescent indication.

14.4.7.15 Evaluation of Indications

Prior to the evaluation of test results, it is necessary to interpret the indications. Identifying indications requires much practice. Indications can be classified as (1) false indications, (2) nonrelevant indications, and (3) true or relevant indications. False indications are due to improper cleaning, rough surfaces, contaminations due to penetrants on the hands of operator, etc. Nonrelevant indications are caused by surface irregularities. All nonrelevant indications shall be regarded as a defect until the indication either is eliminated by surface conditioning or is evaluated by other NDT methods and proved to be nonrelevant. True indications are those caused by discontinuities in the specimen. Only those indications are to be studied while evaluating the results of the examination.

14.4.7.16 Acceptance Standards

For welds and materials as per ASME Section VIII Div. 1, Appendix 8, all surfaces to be examined shall be free of (1) relevant linear indications, (2) relevant rounded indications greater than $\frac{3}{16}$ in. (4.8 mm), and (3) four or more relevant rounded indications in a line separated by $\frac{1}{16}$ in. (1.6 mm) or less edge to edge.

14.4.7.17 Postcleaning

Penetrants are difficult to remove completely from discontinuities, and if they are corrosive to the material, or otherwise not compatible with the product application, they should be avoided.

14.4.7.18 Recent Developments in PT

PT accessories are available from Magnaflux, a Division of ITW, Inc., USA. They include Ni–Cr test panels (Japanese) and TAM panels. Ni–Cr test panels are used for evaluating penetrant system performance and sensitivity; they are available in four types of flaw depths, 10, 20, 30, or 50 μm . A TAM panel is a fast and reliable means of monitoring the proper functioning of a liquid penetrant system. A stainless-steel panel with five star-shaped flaws of decreasing size is on one half, with a rough sand-blasted surface on other half, for checking sensitivity and removability of penetrants.

14.4.8 MAGNETIC PARTICLE INSPECTION

MT is an NDT technique to locate surface and subsurface discontinuities such as cracks, inclusions, pores, shrinkages, laps, folds, seams, etc., arising out of manufacturing operations and service constraints in ferromagnetic materials. Ferromagnetic materials include most of the iron, nickel, and cobalt alloys. Nonmagnetic metals such as aluminum alloys, copper and its alloys, titanium and its alloys, and austenitic stainless steels and cladding of these metals cannot be inspected by this method.

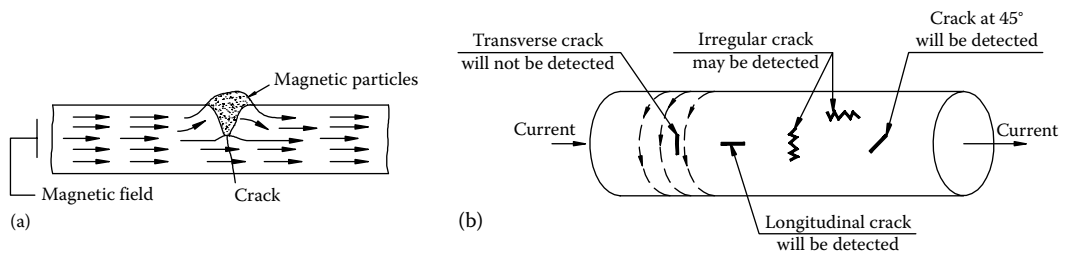


FIGURE 14.9 MT principle—(a) disruption of local flux leakage at the surface over discontinuity and (b) magnetising current and crack detectability.

14.4.8.1 Principle

MT is based on the principle that if a ferromagnetic object is magnetized, the surface or subsurface discontinuities lying at an angle to the magnetic lines of force cause an abrupt change in the path of magnetic flux flowing through the object (Figure 14.9). This results in local flux leakage at the surface over the discontinuity. When finely divided ferromagnetic particles are applied over the surface, some of the particles will be attracted to the regions of leakage field and will pile up and bridge the discontinuity. The piling up of magnetic particles along the discontinuity indicates its location, shape, and extent (Figure 14.9a). While using this method, it should be seen that the magnetic field must be in a direction that will intercept the principal plane of the discontinuity (Figure 14.9b).

14.4.8.2 Applications

MT is used for testing of weld preparations, weld cutbacks on double-sided welds, roots of welds made from one side only, stub, branch, and nozzle welds and attachment welds to shell, load-carrying nonpressure parts like supports and lifting lugs, and areas where temporary attachments have been removed. The latter areas are particularly vulnerable to cracking [43].

14.4.8.3 Reference Documents

ASTM specifications

E 109—Dry powder MT

E 138—Wet powder MT

E 125—MT inspection of ferrous castings

E 269—Definitions of terms related to MT

E 275—MT inspection of steel forgings

E 340—Definition of terms, symbols, and conversion factors relating to MT

ASME Section V, Article 7, and ASME Section VIII, Div. 1, Appendix 6 and 7 (for steel castings) are also used.

14.4.8.4 Test Procedure

There are several basic steps in applying MT:

1. Surface preparation
2. Magnetization of the test object under evaluation
3. Application of magnetic particles
4. Inspect for indications, interpretations of the patterns formed
5. If required, demagnetization of the items being tested

14.4.8.5 Factors Affecting the Formation and Appearance of the Magnetic Particles Pattern

There are many factors that can affect the formation and the appearance of the magnetic particles on the surface of the component being tested. The most common include [41,44] (1) discontinuity size, shape, distance below the surface, and its orientation; (2) direction and strength of the magnetic

field; (3) method of magnetization employed; (4) intensity of current used; (5) size, shape and mobility of the magnetic particle and the method of application; and (6) shape of the component.

14.4.8.6 Merits of Magnetic Particle Inspection

For detection of surface defects, liquid PT and MP are being very widely used. In the case of ferromagnetic materials, magnetic particle technique will also detect subsurface flaws that are not open to surface. Important advantages of the MT method are [41] (1) it is rapid and simple to operate, (2) indications are produced directly on the surface of the component, and (3) a skilled operator can make a reasonable estimate of crack depth with suitable magnetic powders and proper technique.

14.4.8.7 Limitations of the Method

MT has certain limitations, like (1) the method is not applicable for nonmagnetic metal, (2) the sensitivity to detect subsurface flaw decreases exponentially with distance below the surface, (3) exceedingly heavy currents are required at times to examine very large units, and (4) current imparted by electrodes to induce magnetic fields can cause burns, which must be avoided because they can be a source of corrosion attack.

14.4.8.8 Written Procedure

The written procedure should contain the items given in Table 14.7 as minimum requirement.

14.4.8.8.1 Magnetic Particle Examination Procedure Deficiencies

Deficiencies may include (1) incorrect method, e.g., coil method specified for specimens having L/D ratios less than 2, (2) incorrect magnetizing currents, (3) failure to perform examination at more than one current on complex sections, and (4) incorrect sequence of examination or failure to demagnetize when the second operation produces a lower flux density than the first [2].

14.4.8.9 Magnetizing Current

One of the primary requirements for detecting a defect in a ferromagnetic material is that the magnetic field induced in the part must intercept the defect at 45°–90° angle. Flaws that are normal to magnetic field will produce the strongest indications because they disrupt more of the magnet flux. For the purpose of magnetizing parts for MT, either alternating current (which has relatively little penetrating power and hence is good for surface flaw detection) or direct current (good for

TABLE 14.7
Written Procedure for MT

1.0 Scope: materials, shapes, and sizes to be examined
2.0 Reference document
3.0 Magnetizing technique
4.0 Examination equipment
5.0 Surface preparation
6.0 Examination medium: type of ferromagnetic particles to be used, manufacturer, color, wet or dry powder, etc.
7.0 Magnetization current (type and amperage)
7.1 Magnetizing field adequacy
8.0 Application of examination medium
9.0 Evaluation of indication
10.0 Acceptance criteria
11.0 Demagnetization
12.0 Reports
13.0 Records

the detection of subsurface discontinuities) or half-wave rectified alternating current, which has the merits of DC and AC, is widely used. Since it is difficult to correlate the results obtained with AC with the result obtained using DC, it is important to mention in the specifications or drawings whether AC or DC is to be used. In the event that this is not specified, DC shall be used.

14.4.8.10 Equipment for Magnetic Particle Inspection

The magnetic particle test equipment essentially consists of (1) a means to magnetize the component, (2) a device for application of magnetic particles, and (3) demagnetization of components (if required) after inspection.

14.4.8.11 Magnetizing Technique

There are numerous methods of magnetization. Some of the methods include (1) coil magnetization (Figure 14.10a), (2) prod magnetization (Figure 14.10b), and (3) yoke magnetization (Figure 14.10c).

14.4.8.11.1 Coil Magnetization

The use of *coils* and *solenoids* is one of the methods of indirect magnetization. When the length of a component is several times larger than its diameter, a longitudinal magnetic field can be established in the component by use of a coil or solenoid. The component is placed longitudinally in the concentrated magnetic field that fills the center of a coil or solenoid. This magnetization technique is often referred to as coil magnetization.

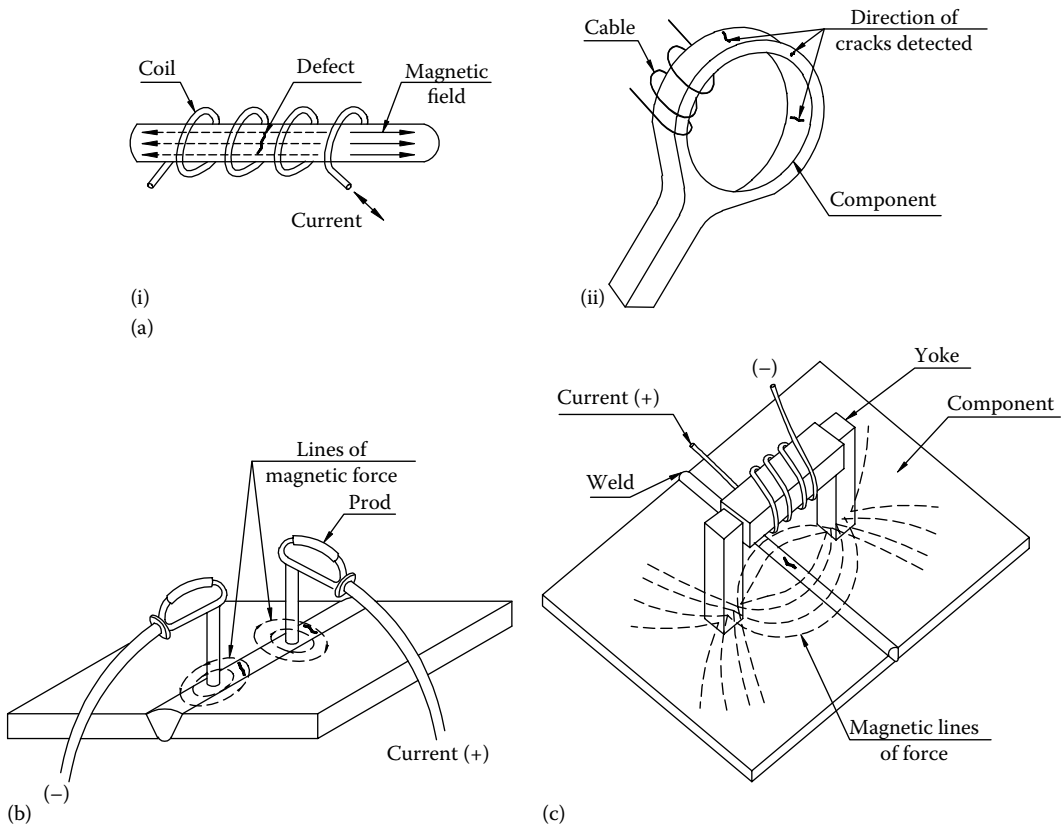


FIGURE 14.10 Magnetizing techniques. (a) Coil magnetization, (b) prod magnetization, and (c) yoke magnetization.

14.4.8.11.2 *Prod Magnetization*

Prod magnetization produces a circular magnetic field. This will detect defects that are lengthwise in the test piece. Prods are portable current-carrying copper conductors, which are used to magnetize localized areas as shown in Figure 14.10b. Magnetization is accomplished by pressing the prods against the surface area to be examined. When current flows through the prods, a circular magnetic field is created in the test part. The magnetic flux is perpendicular to the line joining the two prods, and the flux density is greatest along this line. During prod magnetization, the prods are spaced 150–200 mm apart and in line with the suspected discontinuities. AC, DC, or half-wave DC (HWDC) can be used to suit the job requirement. Mostly, HWDC magnetization is used for prod magnetization. Normally 100–120 A current per inch of prod spacing would be required. If proper contact is not maintained between the prods and the component surface, electrical arcing can occur and cause damage to the component. To avoid arcing, a remote control switch is built into the prod handles to permit the current to be turned on after the prods have been properly positioned.

14.4.8.11.2.1 *Direction of Magnetization* At least two separate examinations shall be performed on each area. During the second examination, the lines of magnetic flux shall be approximately perpendicular to those used during the first examination. Examination shall be done by the continuous method.

14.4.8.11.2.2 *Prod Spacing* Prod spacing should not exceed 8 in. (203.2 mm). Shorter spacing may be used to accommodate the geometric limitations of the area being examined or to increase the sensitivity, but not less than 3 in. (76.2 mm).

14.4.8.11.3 *Yoke Magnetization*

Yoke magnetization introduces a longitudinal field to show up defects perpendicular to the flaw, or across the surface of the part. Both permanent and electromagnetic yokes are used. Permanent magnetic yokes have magnetic strength limitations but are most useful for spot inspection of welds. They can be used when electricity is not available. Electromagnetic yokes are U-shaped with a coil to carry current as illustrated in Figure 14.10c. Longitudinal magnetic fields are set up in the test specimen when the coil is energized by either AC or DC current. Alternating current electromagnetic yokes should have a lifting power of at least 10 lb at the maximum pole spacing. Directions of magnetization should be the same as that for the prod technique. Pole spacing should be limited to 2–8 in. (50.4–203.2 mm).

14.4.8.11.4 *Examination Coverage*

All the examinations should be conducted with sufficient overlap to ensure 100% coverage at the required sensitivity.

14.4.8.12 **Inspection Medium (Magnetic Particles)**

The inspection medium shall consist of finely divided ferromagnetic particles. They must have good mobility, very fine size and shape, high permeability, and low retentivity. The particles may be in dry powder form (for the dry method) or suspended in a suitable liquid medium such as water or kerosene (for the wet method). The size of the dry particles is about 60 μm , and a blend of elongated and spherical particles is used to attain good sensitivity and mobility. The wet particle size is about 40–60 μm .

14.4.8.12.1 *Application of Examination Medium*

The magnetic particles should be applied in such a manner that a thin uniform dust-like coating settles upon the surface of the test part while the part is being magnetized. Specially designed powder blowers are used for this purpose.

14.4.8.13 Inspection Method

According to the condition of the magnetic particles used for inspection, the inspection techniques are known as the dry method and the wet method.

14.4.8.13.1 Dry Method

In the dry method, dry magnetic particles are used for examination. The dry powder method is preferred for surface and subsurface defects [44]. The powders are available in colors that will contrast with the background of the part being examined. Inspection by the dry method is carried out with portable magnetizing equipment.

14.4.8.13.2 Wet Method

In the wet method, the magnetic particles are suspended in a liquid base of oil or water. The magnetic particles used in this method are finer than those used for the dry method, which makes the wet method more sensitive to detection of fine surface defects. Two types of wet magnetic particles are used. They are (1) visible magnetic particles, either reddish or black, observed under normal white light, and (2) fluorescent magnetic particles, which fluoresce when exposed to near-ultraviolet (black) light. The inspection bath is mostly flowed, sprayed, or brushed over the specimen surface. Most MT by the wet method is done with stationary-type equipment, although portable equipment may be used.

14.4.8.13.3 Comparison of Dry Method and Wet Method

Dry method

1. The dry powder method is more sensitive than the wet powder method for the detection of near-surface discontinuities but not as sensitive as wet method in detecting fine discontinuities.
2. The dry method is convenient to use in conjunction with portable equipment for the inspection of large components or for field inspection, whereas the wet method is used with stationary-type equipment.

Wet method

1. All of the surfaces of the component can be quickly and easily covered with a relatively uniform layer of particles.
2. Wet inspection is considered better for detecting very small discontinuities on smooth surfaces.
3. However, on rough surfaces, the particles (which are much smaller in wet suspension) can settle in the surface valleys and lose mobility, rendering them less effective than dry powders under these conditions.

14.4.8.14 Surface Preparation

Surfaces to be inspected shall be clear and free from oil, grease, sand, loose rust, scale, ripples, welding spatters, or any other surface contaminants that could interfere with the interpretation of the magnetic particle indications. Surface preparation by grinding or machining may be necessary where surface irregularities could mask indications due to discontinuities. Magnetic particle test shall not be performed if the surface temperature of the part exceeds 600°F.

1. Preclean inspection area.
2. Place yoke on test piece perpendicular to direction of suspected cracks.
3. Energize yoke to form a magnetic field.
4. Apply magnetic powder or prepared bath while yoke is energized and indications will form immediately.

14.4.8.15 Evaluation of Indications

The types of indications obtained by MT due to “piling up” of the magnetic particles at the lines of flaws are as follows:

1. Relevant indications are those that result from mechanical discontinuities.
2. Linear indications are those indications in which the length is greater than three times the width.
3. Rounded indications are circular or elliptical with the length equal to or less than three times the width.
4. Nonrelevant indications may arise due to metallurgical discontinuities and magnetic permeability variations. These nonrelevant indications shall be reexamined by other suitable NDT methods such as PT and ET.

14.4.8.16 Demagnetization

When the residual magnetism in the part could interfere with subsequent processing or usage, the part shall be demagnetized after completion of the test.

14.4.8.17 Record of Test Data

The information such as material, method used (dry or wet), type of magnetization, type of current, amount of current, and nature of defects should be recorded at the time of each test for future reference.

14.4.8.18 Interpretation

1. Surface defects appear sharp and distinct
2. Subsurface flaws appear rough and fuzzy
3. Width of surface flaw indication varies with depth

14.4.8.19 Acceptance Standards

For pressure vessels, heat exchangers, fittings, and components manufactured to ASME Section VIII Div. 1, as per Appendix 6, all surfaces to be examined shall be free of (1) relevant linear indications, (2) relevant rounded indications greater than $\frac{3}{16}$ in. (4.8 mm), and (3) four or more relevant rounded indications in a line separated by $\frac{1}{16}$ in. (1.6 mm) or less edge to edge.

14.4.8.20 MT Accessories

Various MT accessories are marketed by M/s Magnaflux, a Division of ITW, Inc., USA, and by others. They include residual field indicators, ASME field indicators, quantitative quality indicators, centrifuge tube and stand for ascertaining bath concentration, easy-to-use puffer bulb for applying dry method powders, copper braided pads to prevent burning by ensuring good electrical contact between test part and contact plates, test bar with artificial surface and subsurface discontinuities for testing with yoke method, and test block with subsurface discontinuities for testing with the prod method and coil method. For testing the magnetic particles, a Betz ring is used. The Betz ring has holes drilled at different depths. As a magnetic field is induced in the Betz ring, magnetic particles are sprinkled to the surface. The number of visible line indications determines the sensitivity of the particles. Typically, specifications require visual detection of the fifth hole, which produces a broad indication [39].

14.4.9 RADIOGRAPHIC TESTING

The term *radiography* usually implies a radiographic process that produces a permanent image on a film. RT technique using x-rays and gamma rays is one of the important methods of NDT and has developed, as it is applied today, into a very reliable technique. The technique utilizes

electromagnetic radiation to penetrate an object to reveal information about its internal conditions, particularly internal flaws and surface flaws/discontinuities.

14.4.9.1 Principle of Radiography

When a radiation beam passes through a specimen, some of the radiation energy is absorbed and the intensity of the beam is reduced. To make an RT of the object, the intensities of the radiation that pass through the specimen must be recorded and compared. Variations in beam intensity are seen as difference in shading that are typical of the types and sizes of the flaw present. The recording is being achieved either by letting the rays strike a photographic film (Figure 14.11) or by letting the rays fall on a fluorescent screen that absorbs some of the radiation and converts it to visible light, thus producing a visible image known as fluoroscopy.

14.4.9.2 Application

Surface flaws that are detectable by radiography include undercuts, concavity at the weld root, incomplete filling of the grooves, excessive reinforcements, overlaps and electrode spatter, and internal flaws such as blow holes, gas inclusions, porosity, piping, slag inclusion, cracks, incomplete penetration, incomplete fusion, and tungsten inclusions. More information on flaw-detecting capabilities is discussed later in this section.

14.4.9.3 Radiation Sources (X-Rays and Gamma Rays)

Two types of radiation sources are commonly used in weld inspection. They are x-ray machines and radioactive isotopes. X-rays are produced by machines that range from portable, low-energy units in the range of 50–400 kV used for inspection of relatively thin objects, say, metal thickness up to 7.5 cm steel equivalents, to betatrons and linear accelerators up to 30 MeV, capable of radiography of thick objects up to 20 in. (508 mm) of steel.

Gamma-ray radiation is emitted by radioisotopes, the two most common being cobalt-60 and iridium-192. Cobalt-60 will effectively penetrate a thickness up to approximately 8 in. (203 mm) of steel, whereas iridium-192 is effectively limited to a steel thickness of about 3 in. (76.2 mm). The minimum thickness of steel on which x-rays may be normally used is up to and including 19.05 mm, and gamma-ray sources may normally be used for thicknesses greater than 19.05 mm.

14.4.9.3.1 Comparison of X-Ray and Gamma-Ray Radiography

Most industrial radiography is performed with x-rays. It is highly effective and versatile, and with modern techniques, it is very accurate. The principal advantage of gamma-ray radiography is lower

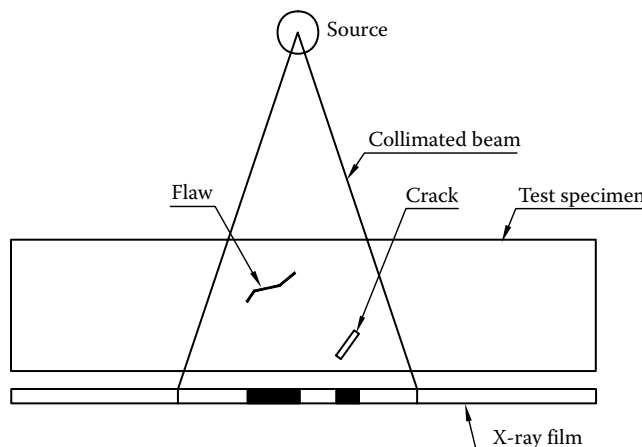


FIGURE 14.11 Radiographic testing principle.

cost, the source can be very small so that transportability is easy, and it is economical for low-volume test pieces. However, gamma rays are not as sensitive to small defects as are x-rays in thickness less than 1 in. (25.4 mm), cracks are the most difficult to detect and generally require a longer exposure time than with x-rays, and they do not provide as sharp a definition [43].

14.4.9.4 Merits and Limitations

Merits: Radiography has been the standard for volumetric inspection of weldments for decades. In spite of high cost, hazards, and the time-consuming nature of the process, radiography stands out as the NDT method that gives a permanent record of test results. Among other advantages, it has surface and subsurface inspection capability, and radiographic images aid in characterizing (identifying type) discontinuities [28].

Limitations: A significant limitation of radiography is that discontinuities must be favorably aligned with the radiation beam. This is usually not a problem for discontinuities round in cross section, such as slag inclusions and porosity [28,33]. On the other hand, cracks and planar defects that diverge considerably from the direction of the radiation beam would nearly miss detection, and therefore ultrasonics is sometimes employed in addition to radiography when very critical examination of a weld is required [33]. Angular notch-type discontinuities such as lack of fusion, incomplete penetration, and cracks must be oriented to the radiation beam so as to show up on the x-rays film [45]. Coarse grain structure, especially in large-pass welding, can cause problem due to diffraction mottling effects [46].

14.4.9.5 Radiographic Test Written Procedure

The radiographic test written procedure is given in Table 14.8.

Radiographic examination procedure deficiencies

These may include incorrect exposure geometry, film placement, source selection, penetrameter selection, incomplete film identification, and failure to submit a technique sheet with sketch [2].

TABLE 14.8
Radiographic Test Written Procedure

1.0 Scope
2.0 Techniques
3.0 Surface preparation
4.0 Identification system
5.0 Location markers
6.0 Radiation sources
7.0 Film
8.0 Screens
9.0 Focus to film or source to film distance
10.0 Penetrameter
10.2 Number of penetrameters
10.3 Placement of penetrameter
11.0 Density
12.0 Sensitivity
13.0 Processing of films
14.0 Processing technique
15.0 Personnel certification
16.0 Evaluation of radiographs
17.0 Reporting
18.0 Retention of radiographs

14.4.9.6 Requirements of Radiography

Essential requirements for producing a radiograph are [28] the following:

1. A source of radiation
2. X-ray film
3. A trained person for operating the equipment
4. A means of processing the exposed film
5. A trained person capable of interpreting the radiographic images

14.4.9.7 General Procedure in Radiography

The steps of performing an RT are as follows:

1. Surface preparation
2. Selection of radiation source, depending upon the thickness of the part and location of the component/assembly
3. Selection of film and exposure parameters for desired quality (i.e., sensitivity, density) and selection of intensifying screens
4. Processing of exposed films
5. Interpretation of radiographs
6. Record keeping and preservation of radiographs

14.4.9.8 Reference Documents

Radiography is one of the most widely established methods for the detection of internal as well as surface defects and has been written into many national codes and standards. ASTM standards E94, E142, E155, E272, E390, E592, E586, and E747 cover RT. ASME Code Section V and VIII, Div. 1, Appendix 4, covers RT.

14.4.9.9 Safety

One of the most important considerations in x-ray or gamma-ray work is the exercise of adequate safeguards for personnel.

14.4.9.10 Identification Marks

The identification marks such as pressure vessel number, job number, seam number, segment number, or spot number, date, and manufacturer's symbol should appear in each film as radiographic images.

14.4.9.11 Location Markers

Location markers should appear as radiographic images and should be placed on the part, and their locations shall be hard stamped or engraved on the surface of the part being radiographed. Lead marker accessories containing sets of alphabets and numbers including arrow and oblique are available in the market.

14.4.9.12 Processing of X-Ray Films

All the radiographs should be free from fogging and processing defects. While processing, radiograph details should not be lost due to scratches, finger marks, etc. The Welding Engineer Data Sheet provides guidance for troubleshooting radiographs [47].

14.4.9.13 Surface Preparation

Weld surfaces should be ground free of ripples so that the resulting radiographic image cannot mask or be confused with the image of discontinuities. Prior dressing of the weld surface ensures

interpretation of films with a minimum amount of referring back to the welds themselves. In the case of submerged arc welding, no surface preparation is required provided the weld bead is smooth and free from valleys or ridges.

14.4.9.14 Radiographic Techniques for Weldments of Pressure Vessels

The common techniques used for the radiography of welds in cylindrical shapes are (1) single-wall, single-image (unidirectional) (Figure 14.12a), (2) single-wall, single-image (panoramic), (3) double-wall, single-image for pipe welds greater than 88.9 mm, and (4) double-wall, double-image for pipe welds with OD less than or equal to 88.9 mm (Figure 14.12b). Whenever possible, single-wall technique is preferred. This technique is employed for plates, shell welds, and castings of larger sizes. In panoramic technique, the radiation source is positioned at the centre of cylindrical component such as a pipe or vessel with the film wrapped around the surface of the weld so that the entire length of circumferential weld joint can be examined with one exposure. Common techniques for various fillet welds are shown in Figure 14.13. A diagrammatic representation of the film and source is shown in Figure 14.14.

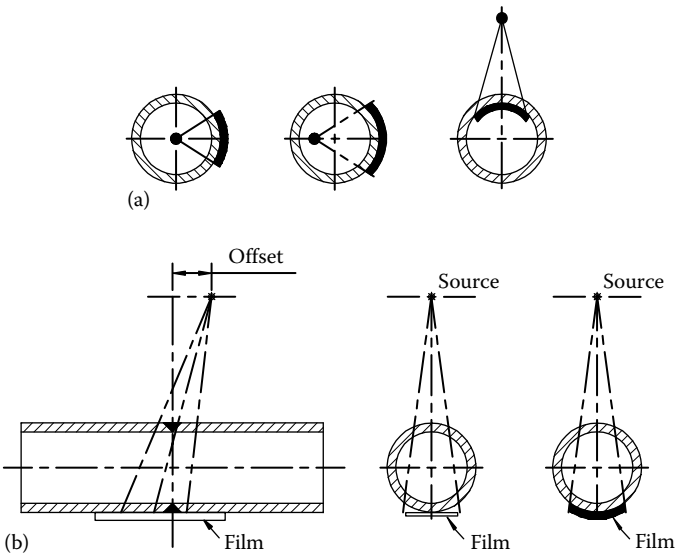


FIGURE 14.12 Radiographic techniques for cylindrical shape testing. (a) Single-wall, single-image (unidirectional), (b) double-wall, double-image.

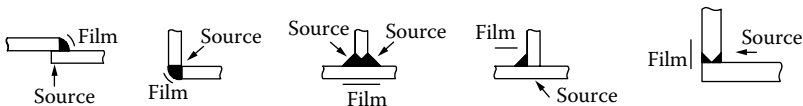


FIGURE 14.13 Common RT techniques for corner fillet welds.

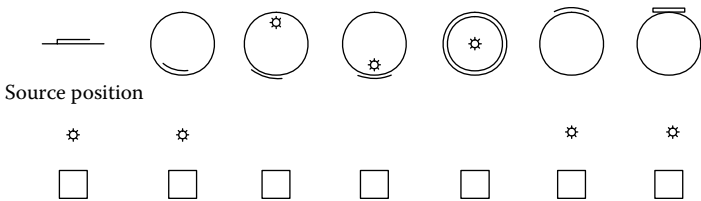


FIGURE 14.14 Diagrammatic representation of the film and source.

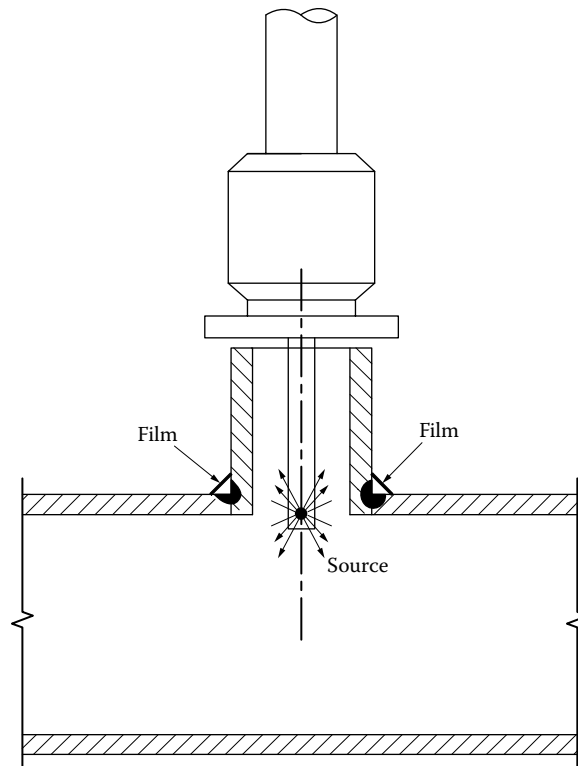


FIGURE 14.15 Gamma ray technique for branch welds.

14.4.9.14.1 Panoramic Radiography with Isotopes

One of the important advantages using isotopes is that by a single exposure, the entire circumference of a weld can be radiographed, provided there is accessibility to keep the source at the center of the pipe [48].

Gamma-ray technique

A gamma-ray technique for branch welds is shown in Figure 14.15.

14.4.9.15 Full Radiography

ASME Code Section VIII, Div. 1, UW-11 lists the conditions for which the full RT for the welded joint is mandatory. Some of these conditions are as follows:

1. All butt welds in the shell and heads of vessels used to contain lethal substances
2. All butt welds in vessels in which the least nominal thickness at the welded joint exceeds 1.5 in. (38.1 mm)
3. All butt welds in the shell and heads of unfired steam boilers having design pressures exceeding 50 psi
4. All butt welds in nozzles, communicating chambers, etc., attached to vessel sections or heads that are required to be fully radiographed under parts 1 or 3

14.4.9.15.1 Spot Radiography

Spot radiography should be in accordance with ASME Code Sec. VIII, Div. 1, UW-52. Spot radiography means that one spot is examined on each vessel for each 50 ft increment of the weld or part thereof for which a joint efficiency from column (b) of Table UW-12 is selected. For vessels with less

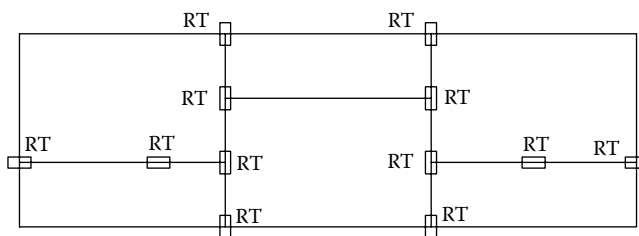


FIGURE 14.16 Spot radiography.

than 50 ft of weld, 50 ft increments of weld may be represented by one spot examination. Length of each radiography shall be at least 6 in. (152.4 mm). Further, all T joints must be radiographed, and at least one shot must be taken on each longitudinal and circumferential seam (Figure 14.16).

14.4.9.16 Radiographic Quality

The quality of the radiographs that decides the efficiency of flaw detection is determined by two factors: sensitivity and density.

14.4.9.16.1 Radiographic Sensitivity

The effectiveness of a radiographic technique to bring out the smallest details in a given thickness of an object is referred to as *radiographic sensitivity*. The more the exactness, the better is the sensitivity. Radiographic sensitivity is affected by two factors: (1) contrast—the magnitude of change in density produced on the film because the defect and sound material absorb different amounts of radiation—and (2) definition—the amount of blurring of the projected shape of the defect produced on the film. The terms and definitions that best represent (1) and (2) are thickness sensitivity and unsharpness, respectively [49]. In quantitative terms, sensitivity is expressed as a percentage ratio of the smallest size of an artificially produced defect shown on the radiograph to the thickness of the object under examination. The smaller the numerical value of sensitivity, the better is the radiographic sensitivity. The artificial defect in the form of a hole, step, or wire of various dimensions is called as image quality indicator (IQI) or *penetrameter*.

14.4.9.16.2 Density of Radiographs

The *density* of a radiograph refers to its darkness. Areas exposed to relatively large amounts of radiation are known as areas of high density, and areas exposed to less radiation are known as areas of light density. The density of the radiograph should be minimum of 1.8 for x-rays and 2.0 for gamma rays. When the density of the radiation varies by more than -15% or $+30\%$ from the density through the body of the penetrameter, additional penetrameters should be placed in the exceptional areas.

14.4.9.16.3 Image Quality Indicators

An IQI, also called a penetrameter (or penny), is a simple geometric form used to judge the quality of a radiograph. It is made of the same material as or a similar material to the component being examined. The dimensions of the IQI bear some numerical relation to the thickness of the part being examined. They are placed on the test piece during setup and are radiographed at the same time as the test piece. IQIs are preferably located in regions of maximum test piece thickness and greatest test piece to film distance, and near the outer edge of the central beam of radiation. The degree to which the image of the IQI is visible in the developed image is a measure of the quality of that image.

IQI designs: A number of IQI designs are used by different authorities. There are American standards, British standards, and French and German standards. Three basic types of IQI are available. They are the wire type, step-wedge type, and strip-hole type.

The most widely used *wire-type* IQI is of the DIN type (German), conforming to DIN 54109 Fe, Cu, and Al. It specifies a set of three parameters, each containing seven equidistant wires.

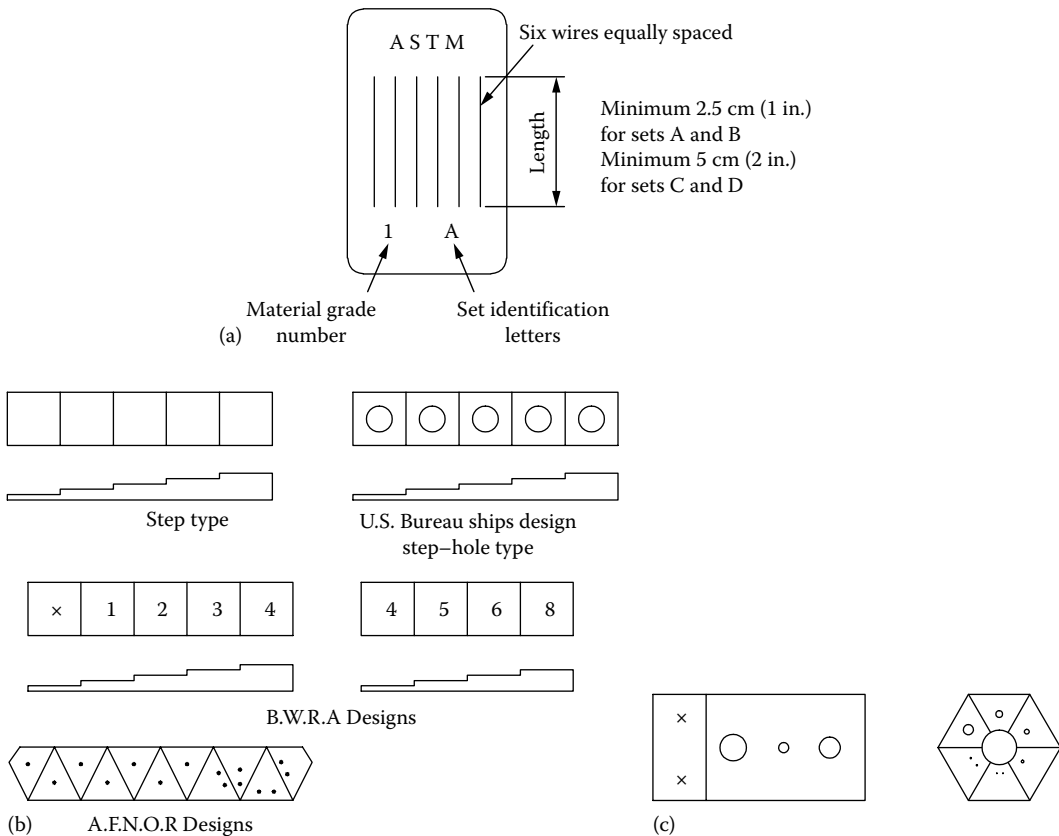


FIGURE 14.17 IQI types. (a) Wire; (b) step wedge; and (c) strip hole.

The diameter of the wires varies in geometric progression. Each diameter is represented by a whole number. The three sets are 1–7, 6–12, and 10–16. The ASTM standard for wire-type IQI is E747 Fe, Cu, and Al. Wire-type IQI is shown in Figure 14.17a.

The *step-wedge type* is the simplest IQI. This type of penetrameter is commonly used in UK-BS 3971, and in France-AFNOR Code. It consists of small steps, whose thickness (0.5%–5% of specimen thickness) increases in geometric progression. Step-wedge-type IQI is shown in Figure 14.17b. Step-hole type is step-wedge type with holes.

For the *strip-hole type* IQI, the most common and widely used version is the ASTM or ASME penny. Strip-hole IQI is also known as plaque-type IQI, whose thickness is about 2% of the specimen thickness. This consists of a small rectangular piece of metal with appropriate material with three holes. The diameters of the holes are multiples of thickness: 1T, 2T, and 4T, where T is the thickness of IQI. Plaque type IQIs are described in ASTM E 142/ASME SE 142 Fe, Cu, Al, Monel, and Ti. Strip-hole type IQI is shown in Figure 14.17c.

14.4.9.16.4 Number of IQIs

One IQI should be used for each radiograph, generally. In case of radiography using a panoramic exposure, three IQIs placed at 120° apart are accepted.

14.4.9.16.5 How to Calculate IQI Sensitivity

An IQI is used to indicate the quality of radiographic technique and not to measure the size of a defect that is shown.

Sensitivity for wire-type IQI is based on the smallest size of wire diameter visible, and for strip-hole type IQI, it is based on diameter of the smallest hole:

$$\text{Percent of sensitivity} = \frac{\text{smallest size of penny visible}}{\text{thickness of the object}} \times 100$$

For the strip-hole type or plaque-type IQIs, the IQI image and the specified hole are the essential indications of sensitivity. The thickness of the IQI and the hole diameter to be seen are generally specified in the code. The following are the different sensitivity levels of inspection with strip-hole type pennies:

1-1T	2-1T	4-1T
1-2T	2-2T	4-2T
1-4T	2-4T	4-4T

Normally, the image of 2-2T hole should be visible in the radiograph. Critical components require a level of 1-2T or 1-1T, and less critical components may need only a quality level of 2-4T or 4-4T.

14.4.9.16.6 Examination of Radiographs

The examination of radiographs of welds should be made on the original films using a viewing device of suitable illuminating power. The standard of acceptance shall be made with respect to the reference chart of x-rays given in ASME Code Section VIII, Div. 1, Appendix 4.

14.4.9.16.7 X-Ray Clues to Welding Discontinuities

When interpreting radiographs of weldments, one must look for different types of discontinuities (undercut, porosity, lack of fusion, etc.). All discontinuities, however, must be considered before deciding to accept or reject and to correct welding practices. Some of the common weld defects and their typical radiographic appearances are given in Table 14.9.

14.4.9.16.8 Acceptance Criteria

For porosity, radiographs are often compared with charts showing arbitrary arrays of pores. The charts are intended to limit the porosity to a certain percentage of the area on the radiograph. Slag inclusions are usually accepted on the basis of length (the only dimension readily measured by radiographs). Planar defects (cracks, lack of fusion, etc.) are normally not permitted [49,50]. An interpretation is complete and a better conclusion is arrived at only after a thorough VT of the part.

For acceptance criteria regarding image density, relevant indications, maximum size of rounded indications, aligned rounded indications, spacing, clustered indications, etc., refer to ASME Code Section VIII, Div. 1, Appendix 4, and Section V, or the International Institute of Welding (IIW) collection of reference radiographs.

14.4.9.16.9 Documentation

When reporting and documenting the results of radiographic film interpretation, complete and accurate information must accompany the radiographs. This is required for subsequent customer review, and possibly regulatory agency review. As per ASME Code Section V, the films shall be retained up to 5 years, by the manufacturers.

14.4.9.17 Recent Developments in Radiography

Over the last few years, several new radiographic techniques have been developed. Important developments in the field of radiography are discussed in Ref. [27] and Hellier [51]. Some of the developments follow.

TABLE 14.9
Weld Defects and Radiographic Appearances

Defect	Image
Crack	Cracks can be detected in a radiograph only when they are propagating in a direction that produces a change in thickness that is parallel to the x-ray beam. Appears as a fine, dark, zig zag irregular line, may be branched
Lack of fusion	Very narrow, straight dark line or lines oriented in the direction of the weld seam along the weld preparation or joining area
Lack of penetration (LOP)	Continuous or intermittent dark straight line at the center of the weldment. Also known as incomplete penetration (IP)
Tungsten inclusions	Since tungsten has a higher atomic number than the iron or aluminum, the radiographic indications are white or lighter area with a distinct outline on the radiograph
Void	Looks rounded and black, and readily recognized with well-defined outlines
Slag inclusions	Nonmetallic solid material entrapped in weld metal. Look less distinct than voids. Dark indications and irregular shapes. May appear singly or be linearly distributed or scattered within the weld or along the weld joint areas
Porosity or gas inclusion or blow hole	Comes in clusters or in random fashion. The image will be normally dark round (since all porosity is void) or irregular spots or specks appearing singularly, in clusters, or in rows
Wormhole porosity	Sometimes porosity is elongated and may appear to have a tail. This is the result of gas attempting to escape while the metal is still in a liquid state
Whisker	“Wire like” indications
Burn-through	Dark spots, which are often surrounded by light globular areas (icicles)
Oxide inclusions	Oxide inclusions are less dense than the surrounding material and, therefore, appear as dark irregularly shaped discontinuities in the radiograph

Source: Adapted from Bryant, L.E. and McIntire, P., eds., *Nondestructive Testing Handbook*, 2nd edn., Vol. 3, Radiography and Radiographic Testing, American Society for Nondestructive Testing, Columbus, OH; Garrett, W.R., *Welding & Design Fabrication*, 77, 1979.

14.4.9.17.1 Computed Tomography

Computed tomography (CT) in radiography is either a 2D or a 3D inspection technique that can be applied for various kinds of objects and materials. This method was adapted from the medical computerized axial tomography scanner. The method involves the repeated scanning of a specimen with a narrow beam of radiation in a series of steps around the specimen. The radiation impinges on a linear array of detectors whose output is digitized and provides a reconstruction of an image or slice, which allows a view of the specimen perpendicular to the direction of the radiation [52]. The principal advantage of this method is that it produces an image of a thin slice of the specimen under examination. This slice is parallel to the path of the x-ray beam as it passes through the specimen as contrast to the image produced by classical radiography, where the image is formed on a plane perpendicular to the path of the x-ray beam on passage through the specimen. The CT image is computed from x-ray intensity data and does not contain information from planes outside the thin slice.

14.4.9.17.2 Microfocus Radiography

Microfocus radiography or the use of fine focus x-ray tubes is finding an important role in industrial radiography. The microfocus x-ray source can produce extremely sharp radiographs at exceedingly short film-to-focus distances. The reason for this is that microfocus x-ray machines with focal spots as small as 1 mm can provide an enhanced flaw detection capability with greater reliability than it is attainable with conventional radiographic equipment. An outstanding application is the radiography of bore-side tube-to-tubesheet weld of steam generators [27]. The rod anode tube heads range in diameters from 4 to 18 mm and available in various lengths up to 1500 mm.

Advantages of using microfocus x-ray equipment include the following:

1. Reduction in film cost due to the use of large grain film and use of higher speed film: such as Kodak AA 400 rollpack and without lead screens
2. One of few methods to do NDT examination on tube-to-tubesheet welds
3. Inspection of microscopic defects with geometric enlargement of over 100 times
4. Showing geometric unsharpness near zero
5. Reduced scatter on film radioactivity (films without lead screens can be used)
6. Reduction in screen unsharpness due to scintillator coating size

Disadvantages

The disadvantages include the following:

1. The application is limited to workshop conditions.
2. Magnetic fields affect the microfocus x-ray beam and can sometimes cause reshoots of films, that is welding machines close to unit.

14.4.9.17.3 Neutron Radiography

This refers to radiographic inspection using neutrons rather than electromagnetic radiation. Neutrons bring out information that is not revealed by x-rays or gamma rays, because the absorption mechanism of neutrons is different from that of x-rays and gamma rays.

14.4.9.17.4 Radioscopy

Radioscopy is similar to radiography; the only difference is that an image receptor replaces the radiographic film. The receptor is an image intensifier coupled to a low-light-level camera. The image shows up on a high-resolution monitor. An operator views the image when it appears on the screen; no film processing is involved. This feature provides online examination of longitudinal and circumferential pipe and shell welds. Radioscopy is nearly 10 times as fast as film radiography, considering time to develop film and interpret radiographs, and the image can be recorded on videotape [53]. Radioscopy is included in ASME Code Section V.

14.4.9.17.5 X-Ray Fluoroscopy

X-ray images can be made visible instantaneously by use of a fluorescent screen instead of a photographic film. Thus, this provides a process of real-time image viewing. For permanent records, fluoroscopy images can be photographed (fluorography).

14.4.9.17.6 Gammascopy

Gammascopy systems with image processing facility are now commercially available for inspection of thick structural parts with iridium-192 or cobalt-60 sources. The sensitivity and resolution obtainable in the gammascopy are inferior to those of film radiography.

14.4.9.17.7 Digitization of Radiographs and Laser Scanner System

Although radiographic film remains the main image capture medium in many applications, it has disadvantages in long-term storage of images because of the possibility of image quality loss over time, difficulty of access and retrieval, and strict storage environment requirements [51]. NDT Scan, a recent development of DuPont NDT Systems, converts high-quality film radiographs from analog to digitized form, which offers the prospects of image storage in a digital format on optical media, analysis, recall, and simultaneously providing solutions to the problems associated with film.

14.4.9.17.8 Imaging Plate

This is a high-sensitivity imaging plate that essentially replaces conventional radiographic film while utilizing standard radiographic equipment. It is estimated that the imaging plate can be reused about 40,000 times [51].

14.4.9.17.9 High-Energy Radiography

Radiation sources such as synchrotrons and betatrons are available.

14.4.9.17.10 Gamma Radiography

The development of modern gamma cameras permits safe and reliable remote operations. Apart from the commonly used isotopes, a number of other sources as europium, ytterbium, etc., are finding increasing applications [27].

14.4.10 ULTRASONIC TESTING

UT is one of the most widely used methods of nondestructive inspection. This method uses sound waves having frequencies in the megahertz range. In UT technique, high-frequency sound waves are transmitted through the material being inspected. The sound waves travel through the material with some loss of energy (attenuation) and are reflected at interfaces or discontinuities such as cracks, flaws, inclusions, and seams[29,54]. The reflected sound beam from the flaws or interface is detected and analyzed to define the presence and location of discontinuities or the thickness of the material. It is also especially suited for determining characteristics of engineering materials such as elastic moduli, study of metallurgical structure, grain size, and density variation. Figure 14.18 shows conventional UT method and Figure 14.19 shows phased array technique.

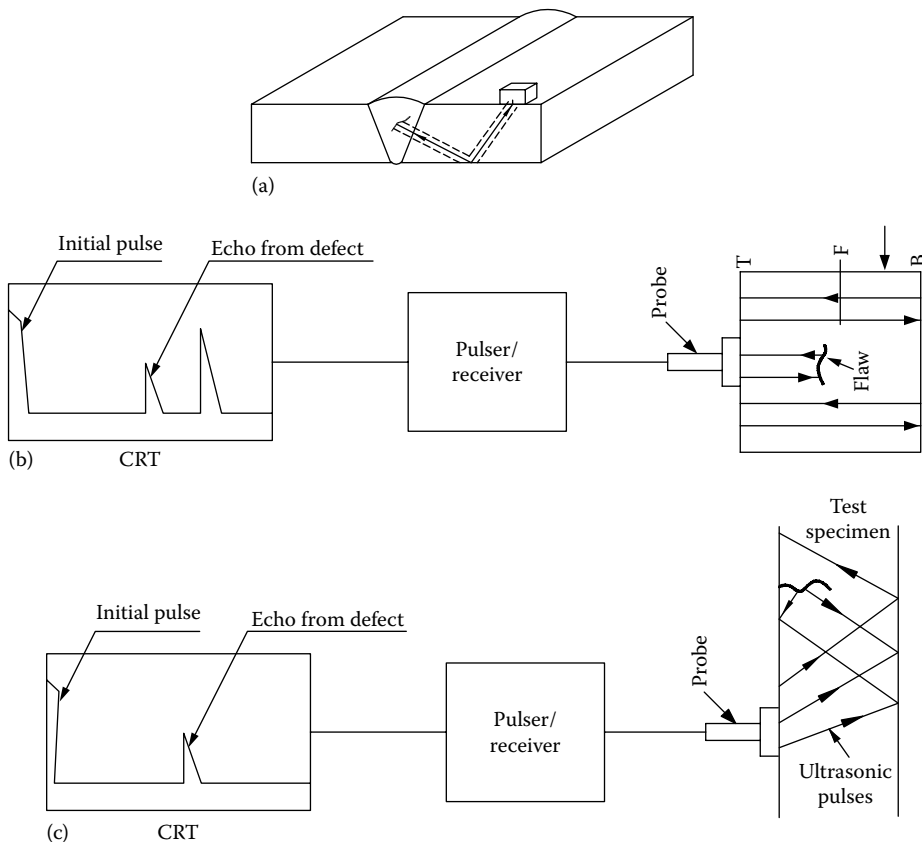


FIGURE 14.18 UT principle—conventional method.

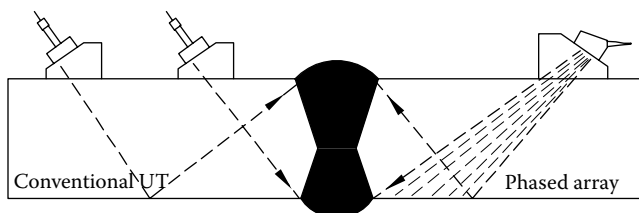


FIGURE 14.19 UT principle—phased array technique compared with conventional method.

14.4.10.1 Test Method

The primary UT techniques and their applications are [55] the following:

1. Pulse echo: most effective for cracks, inclusions, and thickness measurements
2. Through transmission: most effective for porosity, grain size, and density measurements
3. Resonance: most effective for detection of thickness and laminar discontinuities

There are three modes of ultrasonic vibrations that are frequently used in UT of materials. These are (1) longitudinal waves, (2) transverse waves, and (3) surface or Rayleigh waves.

Most ultrasonic weld testing is done manually by an operator manipulating an ultrasonic probe over the test object and visually monitoring the screen of an oscilloscope. The pulse-echo method with A-scan data presentation is most commonly used for inspecting welds. This system utilizes a cathode ray tube (CRT) screen to display the test information.

14.4.10.2 Application of Ultrasonic Technique in Pressure Vessel Industry

This technique's primary application is the detection and characterization of internal discontinuities [28]. It is also used to determine effectiveness of weld overlay bonding/cladding and to measure thickness [33]. The information possible to obtain from the UT data includes defect location, orientation, size, and type. Only ultrasonics and radiography can substantially reveal subsurface flaws. UT includes phased array for weld inspection, manual UT-shear wave, thickness measurement, etc. The inspection is done to detect defects in the welds and to assure that the weld meets the applicable code. The applicable codes for weld inspection are ASME Section V, Article 4, UT of Welds, ASME Section I, Boilers, ASME Section VIII, Pressure Vessels, ASME B31.1, Power Piping, ASME B31.3, Petrochemical Piping, and AWS D1.1 Structural Steel.

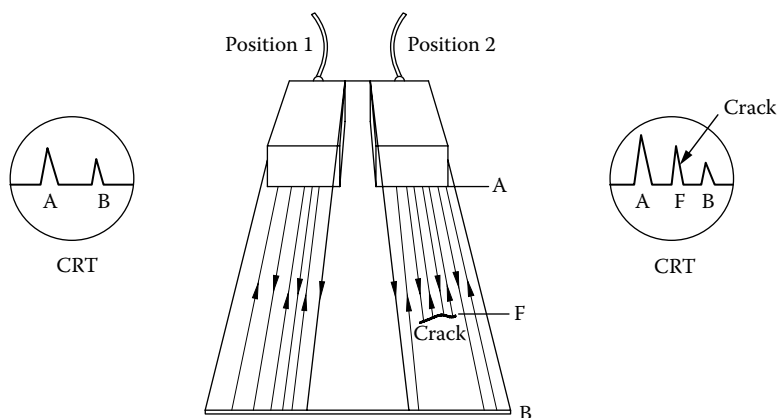


FIGURE 14.20 Ultrasonic plate tester.

Ultrasonic plate tester: Ultrasonic plate testers (Figure 14.20) are available to perform edge-to-edge testing before cutting or welding operations in order to check quickly the presence of laminations, gross internal discontinuities such as pipes, ruptures, or slag inclusions. Shell plate areas on which the branches are to be welded are checked ultrasonically to ensure that the steel is free from cluster inclusions. This is to avoid any likelihood of lamellar tearing due to stress introduced by welding [43].

Ultrasonic examination of nozzle welds: Ultrasonics is of prime importance for examining the attachment welds of nozzles and branches where the wall thickness involved is in the order of 25 mm or greater [43]. Various automated and semiautomated equipment has been developed for double-fillet type through nozzles. The branch weld is normally subject to 100% examination before and after weld heat treatment. The equipment almost invariably employs a longitudinal wave probe operated from the bore of the nozzle.

14.4.10.3 Written Procedure

Minimum information required for written procedure for UT is detailed in ASME Code Section V. A partial list of information to be contained in a UT written procedure is given here:

1. Scope: materials and product form (casting, forging, plate, etc.), weld types, thickness, etc.
2. Surface preparation
3. Couplant
4. Technique (straight beam or angle beam, contact or immersion)
5. Angles and mode(s) of wave propagation in the material
6. Search unit details
7. Ultrasonic instrument details like frequency, screen height, amplitude control linearity
8. Calibration and reference blocks
9. Extent of scanning, maximum scan speed, and scanning pattern
10. Description of the demonstration or qualification of the procedure used to detect and size flaws
11. Evaluation
12. Acceptance criteria
13. Postcleaning
14. Reporting

14.4.10.3.1 Ultrasonic Examination Procedure Deficiencies

These may include insufficient examination, incorrect scanning sensitivity versus calibration sensitivity, failure to describe recalibration, recording, and failure to verify instrument linearity [2].

14.4.10.4 Code Coverage

ASME Code Section V/ASTM Specifications are as follows: (a) SA 388/ASTM, A 388/A 388 M, (b) SA 435/SA 435 M, identical to ASTM A 435/A 435 M, (c) SA 577/SA 577 M, identical to ASTM A 577/A 577 M, (d) SA 578/SA 578 M, identical to ASTM A 578/A 578 M, and (e) SA 609, identical to ASTM A 609/A 609 M except for some deletions.

14.4.10.5 Advantages of Ultrasonic Inspection

The conventional ultrasonic flaw detector is well known for its portability, simplicity of operation, superior penetrating power, and high sensitivity, and allows testing from one surface. The method provides almost instantaneous indications of discontinuities. Ultrasonic method is particularly sensitive for the detection of 2D defects such as fine cracks and laminar-type defects, which are not easily found by other methods including radiography [33,56]. UT is sometimes employed in addition to radiography when critical examination of a weld is required [33]. The greater ability of UT techniques to describe the shape and size of a flaw is basic for fracture mechanics analysis, which

has led to a growing need for UT inspection in pressure vessel industries [21]. With some electronic systems, a permanent record of inspection results can be made for future reference. By combining angulation, amplitude, signal character, signal movement, signal shape, and frequency analysis, it is possible to accurately determine the discontinuity type [45]. UT presents no health hazards such as radiation or chemical hazard.

14.4.10.6 Limitations of Ultrasonic Inspection

Some important limitations of this method include the following:

1. Accuracy and reproducibility of this method depends largely on the skill of the operator to interpret results since perceptible image is not seen, whereas radiography readily gives the image of the discontinuity.
2. All results are based on subjective evaluation, and objective records are not possible to obtain. However, recently various ultrasonic instruments have been developed that automatically scan the weld and also give permanent record on defect indications, thus eliminating one of the main criticisms of manual UT examination that no permanent record is available [33].
3. Discontinuities that are present in a shallow layer immediately beneath the surface may not be detectable.
4. Misleading signals due to grain size. For example, the columnar grain structure of stainless-steel welds generally makes UT impracticable, although UT of stainless steel plate presents no problems [43].
5. The ultrasonic signal background that arises from the clad/metal interface of a clad plate can make it difficult to detect defects up to 10 mm deep just below the clad surface and therefore for critical applications machine clad faces [21].
6. Unfavorable joint geometry and backing bars sometimes create false or nonrelevant indications that can be confused with a defective weld.
7. Weld root conditions pose problems. For example, weldment containing internal concavity and an improperly located counterbore, improper weld capping, sharp reentrant angles, and high-low conditions of vertical fusion zones can cause radiation diffraction and diametrical shrinkage [57].
8. Reference standards made from a similar material as that being tested are required for calibration.
9. UT is less suitable than RT for determining porosity in welds, because round gas pores respond to UTs as a series of single-point reflectors [29].

According to Watson [57], simple modifications to the welding procedures and techniques can reduce problems associated with UT and RT. UT detects more angularly oriented discontinuities and misses some rounded, globular-shaped discontinuities [45]. For more details on UT limitations, consult Refs. [21,43,45,57].

14.4.10.7 Examination Procedure

14.4.10.7.1 Pulse-Echo Technique

This system is the most versatile and the most employed for inspection. In pulse-echo technique, flaws are detected by measuring the amplitude of signals reflected from a flaw and also the time required for these signals to travel between specific surface and the flaw. It is necessary that an internal flaw reflects at least part of the sound energy onto the receiving transducer for such depth measurements to be made. Depending on test piece shape and inspection objectives, pulse-echo technique can be accomplished with longitudinal, shear, or surface waves, and with straight beam or angle beam techniques. Since it is important to intercept the discontinuity at or near 90°, it is common for more than one angle search unit to be used to inspect a particular weld [28]. Data can

be analyzed in terms of type, size, location, and orientation of defects, or any combination of these factors. The basic components of a UT instrument include the following:

1. An electronic signal generator or pulser
2. An electronic clock
3. A transmitting transducer or search unit
4. Couplant to transfer acoustic energy to specimen and back to the receiver
5. A receiving transducer
6. An echo signal amplifier
7. A display device

14.4.10.7.2 Techniques

Two different techniques are employed in UT inspection: (1) contact technique and (2) immersion technique. In the contact technique, the probe is in direct contact with the test object with a thin layer of couplant, whereas in the immersion technique, the sound waves are generally passed through water and are transmitted to the test object. Contact technique is further divided according to the mode of transmission—normal probe technique, angle beam technique, and surface wave technique. The contact method is most commonly used and readily accepted to field testing, and the immersion method is generally limited to the laboratory.

14.4.10.7.2.1 Angle Beam Technique Cracks or other discontinuities perpendicular to the surface of a test piece, or tilted with respect to that surface, are usually invisible with straight beam test techniques because of their orientation with respect to the sound beam. Perpendicular cracks do not reflect any significant amount of sound energy from a straight beam because the beam is looking at a thin edge that is much smaller than the wavelength, and tilted cracks may not reflect any energy back in the direction of the transducer. This situation can occur in many types of welds, in structural metal parts, and in many other critical components. An angle beam assembly directs sound energy into the test piece at a selected angle. A perpendicular crack will reflect angled sound energy along a path that is commonly referred to as a corner trap, as seen in the illustration Figure 14.21. The angled sound beam is highly sensitive to cracks perpendicular to the far surface of the test piece (first leg test)—Figure 14.21a—or, after bouncing off the far side, to cracks perpendicular to the coupling surface (second leg test) as shown in Figure 14.21b. A variety of specific beam angles and probe positions are used to accommodate different part geometries and flaw types. In the case of angled discontinuities, a properly selected angle beam assembly can direct sound at a favorable angle for reflection back to the transducer. Angle beam technique uses shear waves.

14.4.10.7.2.2 Surface Wave Technique To detect defects that are very close to the surface, surface waves are used. For its effectiveness, the surface condition should be good.

14.4.10.7.3 Presentation

A-scan: Mostly A-Scan presentation is used in NDT for detecting discontinuities. In the A-scan presentation, the horizontal baseline on the CRT indicates elapsed time (from left to right), and the vertical deflection shows response amplitude of the reflected waves. The signal amplitude represents the intensities of transmitted or reflected beams. This may be related to flaw size, sample attenuation, or other factors.

B-scan: The B-Scan representation generally applies to the medical applications and is not used in NDT.

C-scan: This presentation offers a plane view of the defect in the part. A good estimate of the size and shape of the flaw is obtained, but only a poor estimate of flaw depth. A combination of the B-Scan and C-Scan will give a 3D image of the defect.

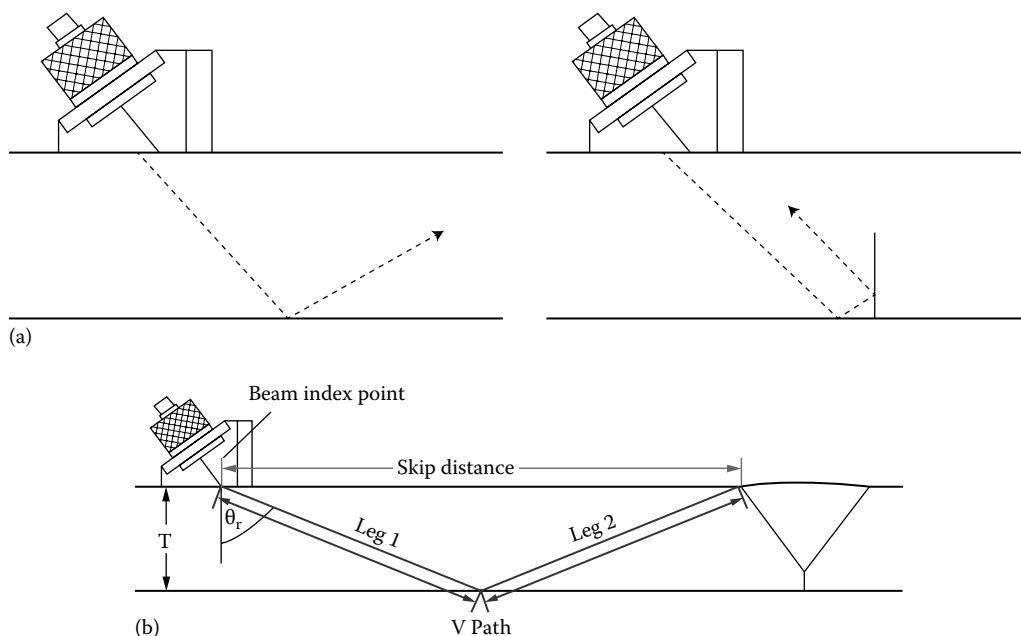


FIGURE 14.21 Angle beam technique. (a) First leg test shows a perpendicular crack reflecting sound wave and (b) second leg test—the angled sound beam after bouncing off the far side, to cracks perpendicular to the coupling surface (second leg test). (Courtesy of Olympus NDT Inc., Waltham, MA.)

14.4.10.8 Surface Preparation

The material surfaces to be used for the ultrasonic scanning must be smooth to allow the free movement of the probes and provide satisfactory conditions for the transmission of the ultrasonic waves. The surface should be free, on each side of the weld for a minimum of one skip distance, from weld spatter, loose rust and scale, grinding particles, dirt, paint, or other foreign matter. It may also be necessary to remove gross weld surface irregularities, undercut, sharp ridges, or valleys that will interfere with the interpretation of the test.

14.4.10.9 Probes

Generation and detection of ultrasonic waves for inspection are accomplished by means of a transducer element, which is contained within a device known as a search unit or a probe. The active element in a search unit is a piezoelectric crystal.

14.4.10.10 Couplant

Where the probes are in direct contact with the sample, a thin layer of viscous medium is used as a couplant between the sample and the probe. Couplants are needed to provide for effective transfer of ultrasonics between search units and parts being inspected. It may be a viscous material, liquid, semiliquid, or paste. Couplant having good wetting characteristics, such as SAE 30, machine oil, grease, gel, or water, should be used. The couplant should be noncorrosive and nontoxic. Couplants may not be comparable to one another, and the same couplant should be used for calibration and examination.

14.4.10.11 Ultrasonic Testing of Welds

14.4.10.11.1 Procedure for Defect Detection in Butt Welds

To detect all possible defects, the weld is to be examined over its entire cross section and along the length specified. In fixed position, the ultrasonic beam is directed at only a part of the weld;

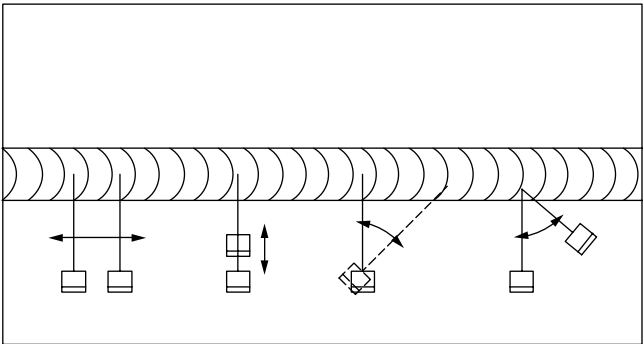


FIGURE 14.22 UT scanning pattern.

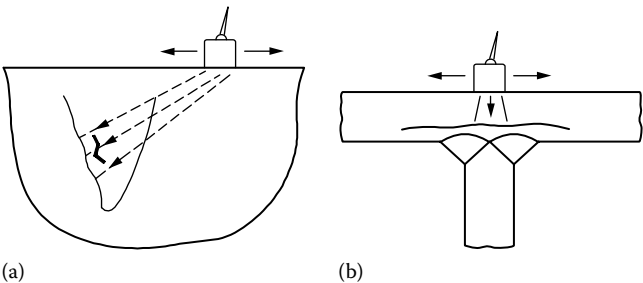


FIGURE 14.23 UT techniques for some defects.

to examine the entire weld, the probe is moved over the scanning zone (Figure 14.22) in the following ways:

- 1. Lateral motion
- 2. Traversing motion
- 3. Swiveling motion
- 4. Orbital motion

Use frequencies of at least 2 MHz. Some UT schemes are shown in Figure 14.23 [58].

14.4.10.11.2 Plate Thickness and Angle of Probe Recommended

The angles of probe recommended for different plate thickness are as follows:

Plate Thickness (mm)	Angle of Probe Recommended
5–15	80°
15–30	70°
30–60	60°
Greater than 60	45°

Thickness over 100 mm: When using a single-probe technique, the path length for a full skip distance in thickness over 100 mm (approx. 4 in.) becomes too great to examine the entire cross section of the weld from one surface. In this case, the weld should be scanned from four sides, that is from both sides of the weld on each surface of the plate.

Applications to Butt-welded curved surfaces: While inspecting the curved surface, the probe may be suitably adopted to match the curved surface so as to comply with this requirement.

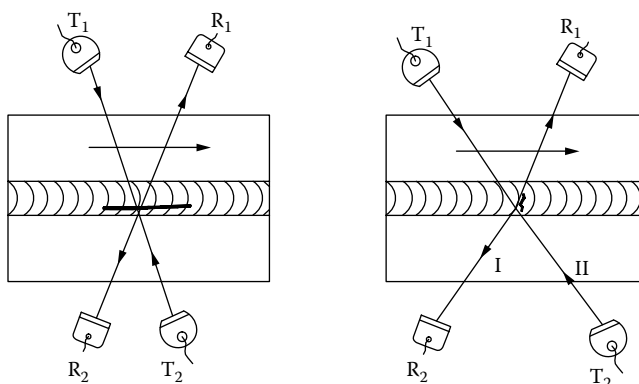


FIGURE 14.24 Position of probes for inspection of Butt welded surfaces—tandem technique.

The examination should be carried out with shear wave probes at a frequency of 2 MHz. At least two different probe angles (45° and 60° or 70°) should be used. Tandem technique scan should be made with 45° probes from the four sides of the weld. Figure 14.24 shows the arrangement of transmitter–receiver probes for detection of longitudinally and transversely oriented defects in welds of butt-welded curved surfaces.

14.4.10.11.3 Defect Location

The accurate determination of the position of a defect in a welded joint is important to carry out repairs or from fracture mechanics point of view. The distance and the depth can be easily calculated from the path length, probe angle, and thickness.

14.4.10.11.4 Sensitivity and Resolution

Defect detectability is dependent on the sensitivity, resolution, and noise discrimination of the equipment. Sensitivity is the ability of the equipment to detect the minute amount of sound energy reflected from a defect. Resolution measures the ability to separate the indication resulting from multiple defects that are close together.

14.4.10.12 Examination Coverage

The test object shall be examined by moving the search unit over the examination surface so as to scan the entire examination volume. As a minimum, each pass of the search unit shall overlap a minimum of 10% of the transducer dimension perpendicular to the direction of the scan.

14.4.10.13 UT Calculators

To determine locations of subsurface indications, inspectors rely on ultrasonic calculators. Calculators come in models for common inspection angles, 45° , 60° , and 70° , used to determine sound path, depth, or surface distance when one variable is known.

14.4.10.14 Acceptance Criteria

According to ASME Code Section VIII, Div. 1, Appendix 12, imperfections that produce a response greater than 20% of the reference level shall be investigated and evaluated in terms of the acceptance standards. Indications characterized as cracks, lack of fusion, or incomplete penetration are unacceptable regardless of length. For additional acceptance criteria, consult the referencing code section.

14.4.10.15 Reference Blocks

Reference blocks are needed for calibrating the UT equipment. The standard reference flaws in calibration blocks serve as a base of comparison for real flaws. The standard flaws are cylindrical holes, flat-bottom holes, grooves, or edges [59]. The most widely used reference blocks are IIW reference

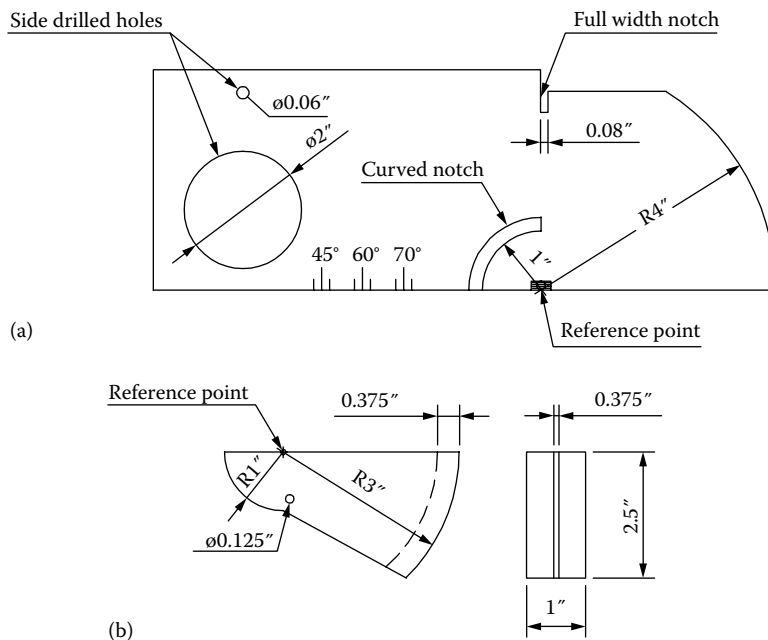


FIGURE 14.25 UT reference block. (a) DSC block and (b) ASME block.

block and the distance sensitivity calibration (DSC) block (Figure 14.25a). There are other types of reference blocks, like the ASME block (Figure 14.25b), BWRA block, Dutch block, Sulzer's block, ASTM block, miniature angle beam block, etc.

14.4.10.16 Calibration

The calibration of the instrument is done to check parameters such as time base, linearity, resolution, sensitivity, beam spread, beam angle, probe index, etc. The ultrasonic probes must be calibrated accurately for angle of propagation, probe index, and beam form.

14.4.10.17 Phased Array Ultrasonic Testing

Phased array testing, or PA, is a specialized type of UT that uses multielement array transducers and powerful software to steer high-frequency sound beams through the test piece and map returning echoes, producing detailed images of internal structures.

Conventional ultrasonic transducers for NDT commonly consist of either a single active element that both generates and receives high-frequency sound waves, or two paired elements, one for transmitting and one for receiving. Phased array probes, on the other hand, typically consist of a transducer assembly with from 16 to as many as 256 small individual elements that can each be pulsed separately in a programmed pattern. These elements are pulsed in such a way as to cause multiple beam components to combine with each other and form a single wave front traveling in the desired direction. Similarly, the receiver function combines the input from multiple elements into a single presentation. These may be arranged in a strip (linear array), a ring (annular array), a circular matrix (circular array), or a more complex shape. As is the case with conventional transducers, phased array probes may be designed for direct contact use, as part of an angle beam assembly with a wedge, or for immersion use with sound coupling through a water path. Transducer frequencies are most commonly in the range from 2 to 10 MHz. A phased array system will also include a sophisticated computer-based instrument that is capable of driving the multielement probe, receiving and digitizing the returning echoes, and plotting that echo information in various standard formats. Unlike conventional flaw detectors, phased array systems can sweep a sound beam through a range

of refracted angles or along a linear path, or dynamically focus at a number of different depths, thus increasing both flexibility and capability in inspection setups. This NDT technology is also referred as swept beam UT. Figure 14.26 displays the concept of phased arrays, principle of testing weld, and example of defect image detected in welds. Time delays to the eight elements control focusing and beam sweep. Focal spot size is controlled by beam spread. Checking of phased array probe resolution is shown in Figure 14.27.

14.4.10.17.1 Merits of PAUT

Unlike conventional and automated UT, which is performed for fixed angles of 45°, 60°, and 70°, phased array testing can cover all angles in this range. This is significant as a single phased array inspection can cover all angles from 40° to 75° and displays the image in real time. The benefits of phased array technology over conventional UT come from its ability to use multiple elements to steer, focus, and scan beams with a single transducer assembly and ability to display the image in real time for the swept angles. Focusing can significantly improve signal-to-noise ratio in challenging applications, and electronic scanning across many groups of elements allows for C-Scan images to be produced very rapidly.

The ability to test welds with multiple angles from a single probe greatly increases the probability of detection of anomalies. Electronic focusing permits optimizing the beam shape and size at

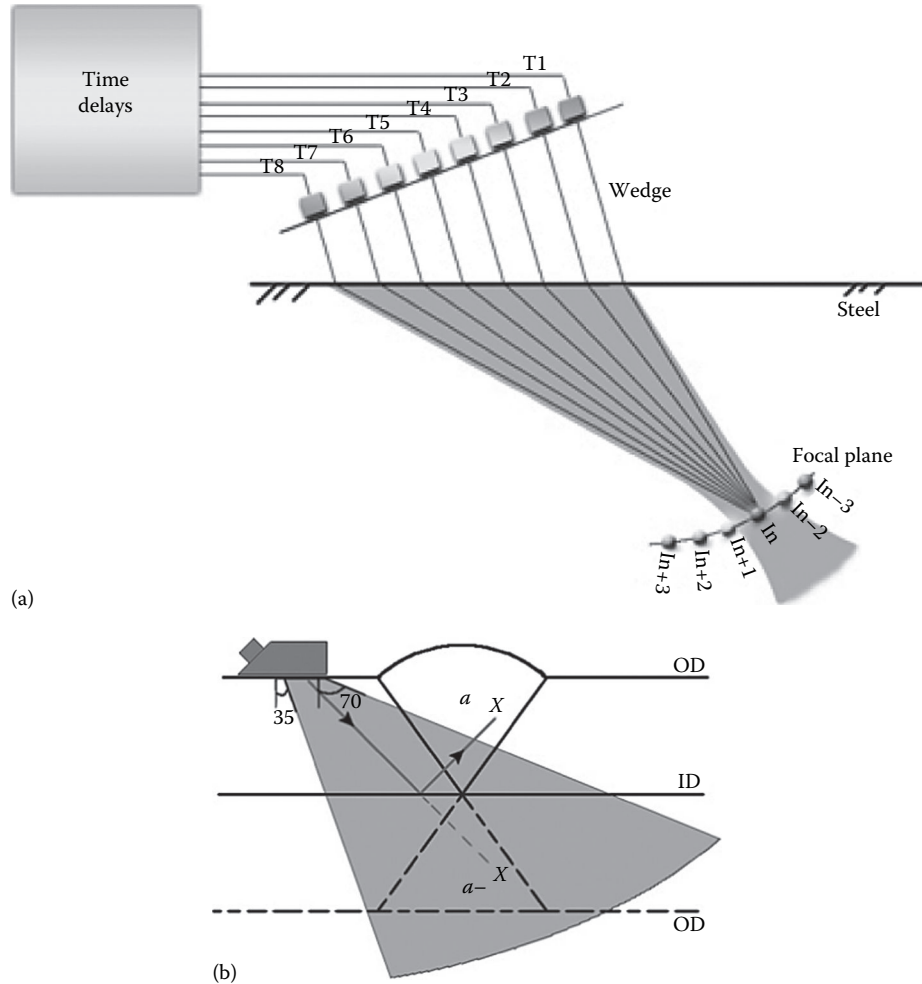


FIGURE 14.26 Phased array technique. (a) Principle and (b) technique for welds.

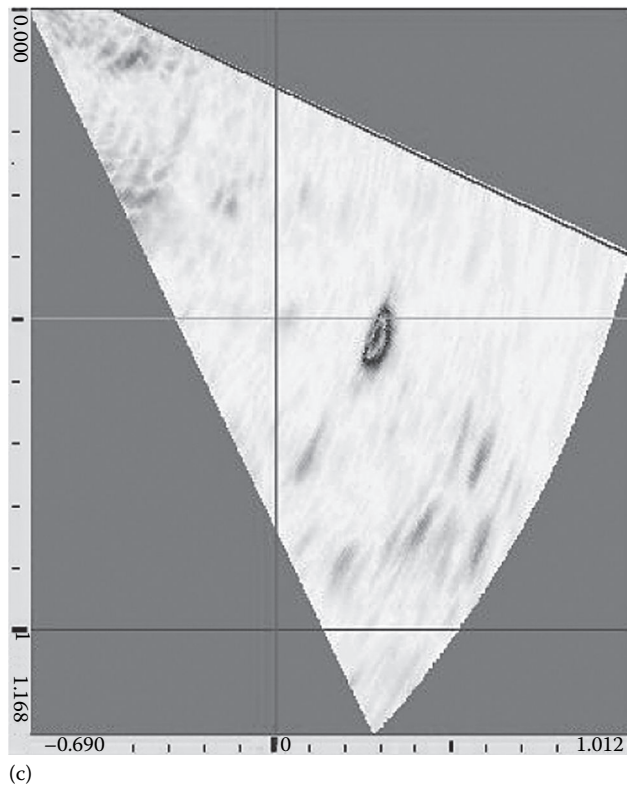


FIGURE 14.26 (continued) Phased array technique. (c) example of defect image detected in welds. (Courtesy of Anmol Birring, Houston, TX.)

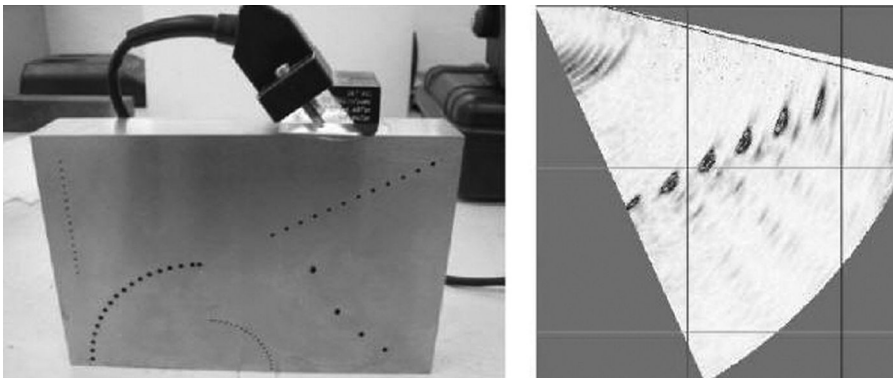


FIGURE 14.27 Checking phased array probe resolution. (Courtesy of Anmol Birring, Houston, TX.)

the expected defect location, thus further optimizing probability of detection. The ability to focus at multiple depths also improves the ability for sizing critical defects for volumetric inspections. Focusing can significantly improve signal-to-noise ratio in challenging applications, and electronic scanning across many groups of elements allows for C-Scan images to be produced very rapidly. The programmed pulsing sequence selected by the instrument's operating software launches a number of individual wave fronts in the test material. These wave fronts in turn combine constructively and destructively into a single primary wave front that travels through the test material and reflects off cracks, discontinuities, back walls, and other material boundaries like any conventional

ultrasonic wave. The beam can be dynamically steered through various angles, focal distances, and focal spot sizes in such a way that a single probe assembly is capable of examining the test material across a range of different perspectives. This beam steering happens very quickly, so that a scan from multiple angles or with multiple focal depths can be performed in a small fraction of sound.

14.4.10.17.2 What Do the Images Look Like?

In most typical flaw detection and thickness gauging applications, the UT data will be based on time and amplitude information derived from processed RF waveforms. These waveforms and the information extracted from them will commonly be presented in one or more of four formats: A-scans, B-scans, C-scans, and S-scans. This section shows some examples of image presentations from both conventional flaw detectors and phased array systems. A phased array system will display similar A-scan waveforms for reference; however, in most cases, they will be supplemented by B-scans, C-scans, or S-scans.

14.4.10.17.3 A-Scan Displays

A-scan is a simple RF waveform presentation showing the time and the amplitude of an ultrasonic signal, as commonly provided by conventional ultrasonic flaw detectors and waveform display thickness gauges. An A-scan waveform represents the reflections from one sound beam position in the test piece. Generalized beam profile and direction of motion and image showing hole/defect position by angle beam UT method as per A-scan is shown in Figure 14.28.

14.4.10.17.4 B-Scan Displays

B-scan is an image showing a cross-sectional profile through one vertical slice of the test piece, showing the depth of reflectors with respect to their linear position. B-scan imaging requires that the sound beam be scanned along the selected axis of the test piece, either mechanically or electronically, while storing relevant data. Generalized beam profile and direction of motion and image showing hole/defect position by conventional UT method as per B-scan is shown in Figure 14.29.

14.4.10.17.5 C-Scan Displays

C-scan is a 2D presentation of data displayed as a top or planar view of a test piece, similar in its graphic perspective to an x-ray image, where color represents the gated signal amplitude at each point in the test piece mapped to its x - y position. Generalized beam profile and direction of motion and image showing hole/defect position by conventional UT method as per C-scan is shown in

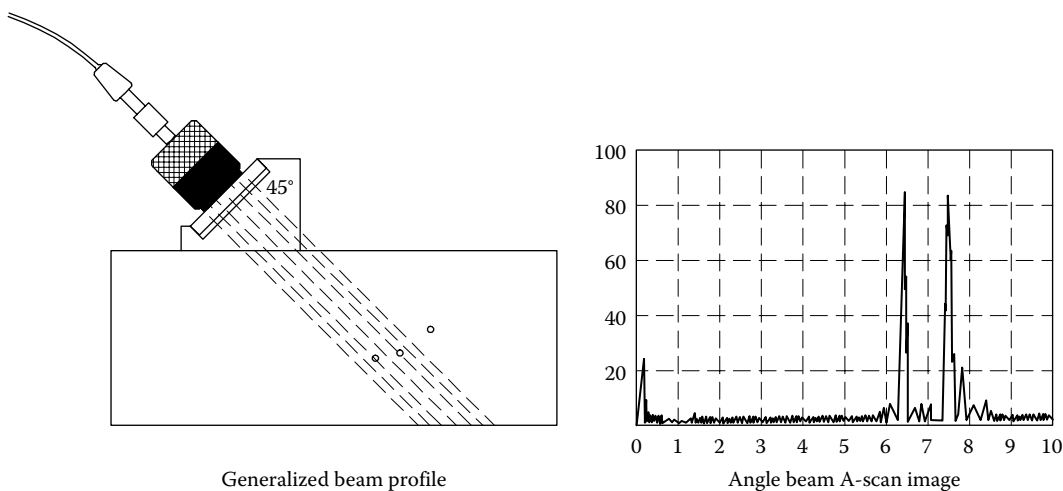


FIGURE 14.28 Generalized beam profile and direction of motion and image showing hole/defect position by angle beam UT method as per A-scan displays. (Courtesy of Olympus NDT Inc., Waltham, MA.)

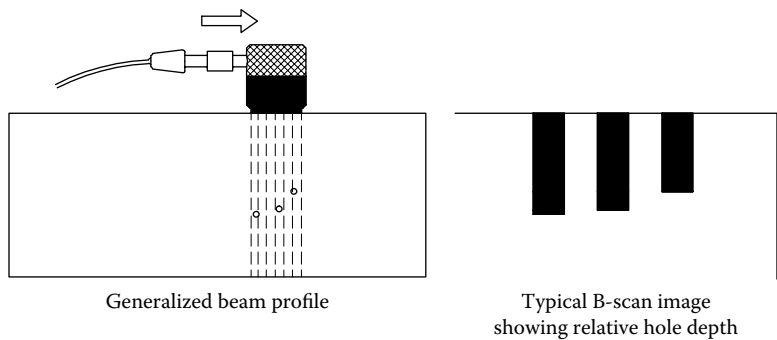


FIGURE 14.29 Generalized beam profile and direction of motion and image showing hole/defect position as per B-scan displays. (Courtesy of Olympus NDT Inc., Waltham, MA.)

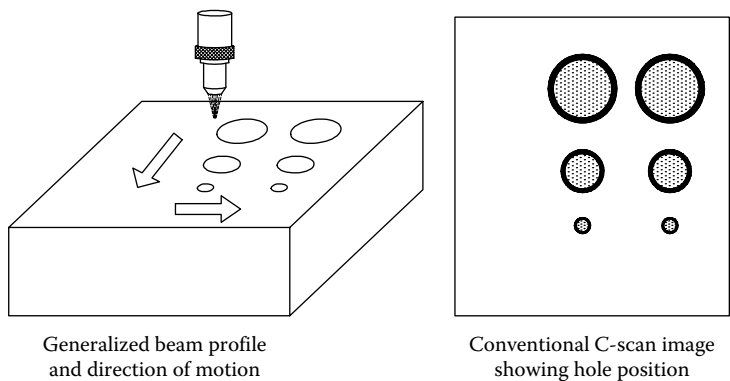


FIGURE 14.30 Generalized beam profile and direction of motion and image showing hole/defect position by conventional C-scan displays. (Courtesy of Olympus NDT Inc., Waltham, MA.)

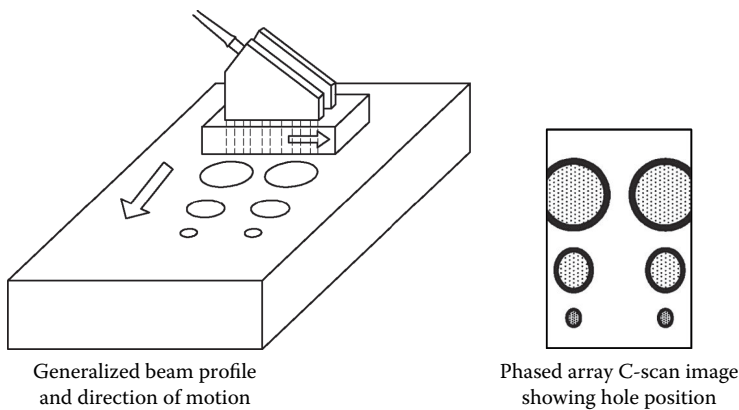


FIGURE 14.31 Generalized beam profile and direction of motion and image showing hole/defect position as per phased array C-scan displays. (Courtesy of Olympus NDT Inc., Waltham, MA.)

Figure 14.30, and generalized beam profile and direction of motion and image showing hole/defect position by phased array method as per C-scan is shown in Figure 14.31.

14.4.10.18 Fracture Mechanics

The basic premise of fracture mechanics is that every structural component, including pressure vessels, contains defects or discontinuities. Three major factors influence the performance of a fabricated

product: stress, material, and defects [60]. Design of the product takes into account the stresses and specifies the material, so that these two factors are fairly known and controllable to some extent. Modern design theories make use of the concept that welds with defects can be accepted if sufficient and accurate data are available about the detail of the defects and residual stresses present [49]. Fracture mechanics allows calculation of the critical defect size, that is the limiting size between failure and no failure of the product. If the defect is larger than the critical defect size, then the failure is likely to occur. If the defect is smaller than the critical defect size, then the risk of failure is small. Before attempting any remedial action, particularly with thick welds, it is essential that the depth of any imperfection be determined so as to assess its importance and to assist in its removal, should that be considered necessary [33].

14.4.10.18.1 Crack Evaluation

Fracture mechanics analysis requires a knowledge of both the length and the extent in depth of a crack, with the latter being the more important factor. Radiography cannot easily indicate crack depth, since this requires continuous density measurement (with a light beam of the order of 10^{-2} mm wide) across the crack image [49]. However, the well-established radiographic tube shift method may be used for depth location [33]. The UT technique provides actual defect size and position, which are then treated mathematically to determine under what service conditions failure may occur or the discontinuities need to be repaired. Alternately, AET can provide the location of the defect and UT can be used to determine its size. However, fracture mechanics and AET have limits to their uses, especially for tough, low-strength steels.

14.4.10.19 What Is New in UT?

Some important developments in the field of UT examination in the recent years are the following:

1. An ultrasonic probe, installed and left in place or attached to a moving fixture, provides a continuous scan of a test part.
2. Automated ultrasonic inspection of weld defects. Computer-based ultrasonic imaging system and automatic scanners for automated inspection of defects give permanent record, postprocessing of signal for detailed analysis, online imaging, and 3D imaging of defects, display of defects in plan, side, end, and isometric views, compare the test with previous tests, and, where differences are noted, reinspect the area- and operator-independent evaluation.
3. Ultrasonic plus eddy current. Southwest Research Institute, San Antonio, TX, has successfully combined UT and eddy current in order to simultaneously inspect the surface of a reactor vessel. It is capable of precise location of small cracks [51].
4. Weld scan probes: Several new weld scan probes were developed whose benefits include instant results that couplant is not necessary, the effects of probe liftoff that permeability variations and natural conductivity variations are minimized, and that whether welds have reinforcement, flush ground, or are of dissimilar metal, there is a probe type for the application [51].
5. Portable UT equipment is available with digital operation and microprocessor controls. They can be interfaced with computers and can provide hard copy printouts on video monitoring and recording.
6. *UT shear wave in lieu of radiography for weld inspection.*

Radiography is commonly used to inspect welds that are fabricated as per a specific ASME code. Radiography is a reliable method, but it has one major limitation. All work in the inspection area has to be stopped and the workers vacated to avoid exposure. This can impair work progress and delay the job. UT shear wave in lieu of radiography is quite attractive as it does not affect any work being done in the vicinity. Some major companies have chosen UT phased array shear wave in lieu of radiography.

14.4.11 ACOUSTICAL HOLOGRAPHY

Acoustical holography is an NDT technique that uses ultrasound to evaluate the interior integrity of a weld or a test object. Holography is basically a two-step process for creating a whole image. In the first step, the amplitude and phase of any type of coherent waves reflected from the object are recorded in a suitable medium by using the principle of interferometry. This record is called a *sound hologram*. In the second step, the wave motion is reconstructed from the hologram by a coherent laser beam, by using the principle of diffraction, which results in the regeneration of a 3D image of the interior of the test object. Ehlman [61] describes the principle and applications of acoustical holography. Acoustical holography is mainly used for thick materials used for pressure vessels, castings, forging, etc., and inspection of welds in thick and thin materials, contouring of the surfaces, and inspection of nozzle welds. At present, two types of acoustical hologram systems are available: the liquid surface type and the scanning type. Scanning-type equipment is mostly used.

14.4.11.1 Merits and Comparison of Acoustical Holography with Radiography and Ultrasonic Testing

In conventional UT, it is difficult to obtain exact information concerning the location, shape, and size of the flaws. Using acoustical holography, a single scanning operation provides top, side, and 3D images that completely characterize weld defects [61]. Ehlman [61] lists the following advantages of acoustical holography over radiography/UT:

1. Standard radiography and UT have limited resolution capability for inspection of thick material due to the widening effect of x-rays and of the ultrasonic beam. Acoustical holography uses focused-beam transducers, which offer good resolution, even on thick material.
2. Acoustical imaging can show a thin horizontal crack that radiography may miss. It is less sensitive to defect orientation than radiography.

14.4.11.2 Holographic and Speckle Interferometry

Advanced NDT techniques such as laser holography interferometry and speckle interferometry have demonstrated their usefulness for inspecting nuclear pressure vessels and piping. The techniques are suited to measuring deformation resulting from residual stresses or mechanical behavior of materials or fatigue.

14.4.12 ACOUSTIC EMISSION TESTING

AET offers a new method for analyzing various physical phenomena and behavior of materials, and for performing NDT of materials, manufacturing processes, and structural components [62]. As an NDT technique, it is used to detect when a flaw or crack occurs and sometimes where it occurs in a wide variety of structures and materials, such as metals, wood, plastic, fiberglass, and concrete. However, the determination of the kind of flaw is normally left to the other methods.

14.4.12.1 Principle of Acoustic Emission

Acoustic emission (AE) is the phenomenon of transient elastic wave generation due to a rapid release of strain energy caused by a structural alteration in a solid material. The release of AE is illustrated in Figure 14.32. When a discontinuity approaches a critical size, the AE count rate increases markedly, warning of impending instability and failure. The emission of transient elastic waves or sound waves can be detected by placing a sensor on the surface of the material. The amplitude of an AE is proportional to local strain in the base material at the AE site. A time–amplitude noise signature generated during the crack growth can be used to indicate the failure process likely to emanate from the site. Since AE reveals its existence during its growth, this leads to one of the advantages of the method: real-time monitoring.

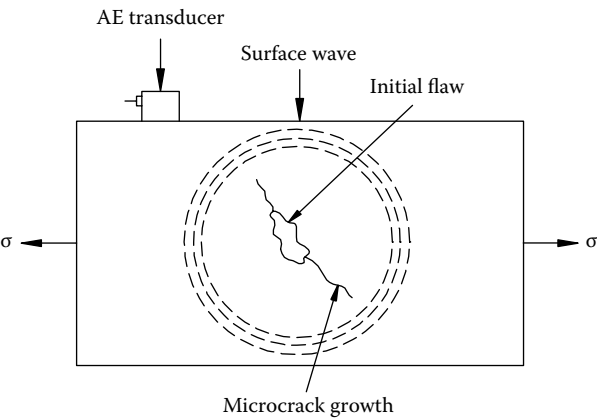


FIGURE 14.32 Release and propagation of AE in a material and the principle of AET. (Adapted from Lenain, J.-C., *Mater. Eval.*, 1000, 1981.)

14.4.12.1.1 Source of Acoustic Emission

Generally, the structural alterations are the results of either internally generated or externally applied load or due to various physical or failure modes. Physical phenomena and failure modes that can release AE are described in Refs. [62,63] and are given in Table 14.10.

14.4.12.2 Emission Types and Characteristics

Basically, the AE signals have been classified into two different types [64]: burst type and continuous type. The characteristics of these wave forms are discussed by Baldev Raj et al. [65]. Both the emission types are generated by discrete processes. The difference between these two types is in the average repetition rate. Some of the differences of these two emission types are as follows [63]: (1) Small releases of strain energy cause burst emissions. The superposition of many repetitive bursts gives the appearance of continuous emission. (2) The amplitude and frequency of continuous emission are usually lower than those of burst emission. (3) In metals and alloys, continuous emission is thought to be associated with the dislocation movements, whereas burst-type emissions are generated by twinning, microfolding, excessive porosity, inclusions, and the development of microcracks.

14.4.12.3 Kaiser Effect

An important feature of AE is its irreversibility. If a material is loaded to a given stress level and then unloaded, usually no AE will be released upon immediate/reloading until the previous load has been exceeded. This is known as the *Kaiser effect*. This property has an important practical

TABLE 14.10
Physical Phenomena That Can Release AE

Plastic deformation (dislocation movement, grain boundary slip, twinning, etc.)
Creep, stress rupture
Ductile/brittle transition temperature
Phase transformations
Seismic activity in geological materials
Leakage of a fluid from a pressure component
Crack growth
Corrosion, including stress corrosion cracking, corrosion fatigue, and hydrogen embrittlement
Metallurgical changes like yielding and crystal dislocations
Fiber breakage and delamination in composites and overlays

implication because it can be used in the detection of subcritical growth of flaws, such as stress corrosion cracking, fatigue crack growth, and hydrogen embrittlement.

14.4.12.4 Reference Code

ASME Code Section V covers AE examination of metal vessels and fiber-reinforced vessels. Section VIII, Division 1, does not include AE for inspection vessels made as per this section.

14.4.12.5 Written Procedure

The written procedure to be applied during an AE examination usually specifies [63] (1) the equipment to be used; (2) the couplant, sensor type, frequency, and the location/placement of AE sensors; (3) the process for stressing the component; (4) the data to be recorded and reported; (5) the qualifications of the personnel operating the equipment and interpreting the results; and (6) system calibration.

14.4.12.6 AE Testing Instrument

The important items of the instrumentation are as follows: (1) a sensor (piezoelectric crystal device) with frequency response between 20 and 600 kHz, (2) a preamplifier to convert signals from 10 μV to 1–10 V DC, (3) high-pass or bandpass filters to eliminate mechanical and electromagnetic noises, (4) an amplifier, (5) a threshold detector, and (6) a counter.

14.4.12.7 Signal Analysis

To use AE monitoring, the noise generated by the flaw growth should be picked and the extraneous background noise should be suppressed. One can sort out sound by three characteristics: frequency, amplitude, and rate of occurrence [66]. There are several ways to process the AE signal. The following are the more common ways by which signals are processed: ring-down counting analysis, energy analysis, amplitude distribution analysis, and frequency analysis [62]. However, the most widely used method for the analysis of AE signals is ring-down counting, which involves the counting of the number of threshold crossings, called counts. Ring-down counting has the major advantages of simplicity and practical effectiveness. An AE signal is characterized by parameters like [62] (1) peak amplitude, (2) signal duration, (3) number of counts per event, (4) rise time, and (5) energy.

14.4.12.8 Factors Influencing AE Data

The factors that influence AE data include [65] source characteristics, structural characteristics of the medium, frequency passband, and gain of amplifiers and threshold level.

14.4.12.9 Applications: Role of AE in Inspection and Quality Control of Pressure Vessels and Heat Exchangers

AE techniques can be successfully used for the following applications [63]:

1. NDT of pressure vessels
2. Online monitoring of pressure vessels
3. Monitoring of welds
4. Detecting of environmental cracking and environmental degradation
5. Monitoring of thermal shock
6. Monitoring of weld overlays
7. Detection of creep failures at welds [67]
8. LT of pressure vessels [34,68]

Proof testing of pressure vessels and heat exchangers: Pressure vessel testing has been one of the most successful areas of application of AE technique. This method is used extensively for

preservice proof testing, periodic requalification testing, and continuous online monitoring of pressure vessels [63]. When discontinuity approaches critical size, the AE count rate increases markedly, warning of impending instability and failure.

Online monitoring: AE is produced when the component undergoes a dynamic change such as deformation, crack growth, phase change, or leakage of a fluid from a pressurized compartment. Hence, continuous online monitoring is possible [68].

Monitoring of welds: AE can monitor and detect failure modes that generate AE, such as phase transformations, lack of fusion, lack of penetration, voids and porosity, inclusions and contamination, and cracking. The technique offers great promise for preliminary weld screening prior to NDT and for welder training [66].

Environmental cracking: AE is used for detecting environmental cracking phenomena such as corrosion fatigue, hydrogen embrittlement, and stress corrosion cracking.

Thermal shock: Frequently, vessels subject to thermal stress cycles are monitored during temperature cycling, during start-up, or during shutdown.

Weld overlays: AE can monitor separation and delamination of weld overlays.

Detection of creep failure at welds: AE has been used to study reheat cracking, a form of brittle creep rupture that occurs in the heat-affected zones of welds during stress relief [67].

Leak detection: Leak detection by AE testing method provides rapid quantitative information. The method is as follows: In the absence of any leak, the AE activity will only be a minimum, caused by the background noise. In the presence of a leak, pressure release from inside the vessel results in the generation of AE that can be detected by the sensor.

14.4.12.10 Merits of Acoustic Emission Testing

The advantages of AET are discussed in Ref. [63]. Some of the advantages are as follows:

1. In AE monitoring, there is no input energy to the structural system/material as in the case of UT or radiography.
2. AE has the capacity to locate and evaluate discontinuities in the entire structure at one time, rather than selectively testing localized regions.
3. AET may be used as a means for confirming the location and concentration of discontinuities determined by techniques such as RT and UT.
4. The use of AET with fracture mechanics and UT may allow the complete characterization of a pressure vessel and its life can be predicted.
5. It requires only limited access and downtime for the requalification of in-service structures.
6. AE monitoring on production lines is faster than ultrasonics because its sensors need not be moved over the entire surface being inspected.

14.4.13 EDDY CURRENT TESTING

ET is a noncontact method widely used for the NDT of tubular products. The basis of ET is the detection of quality problems by observation of the interaction between electromagnetic fields and metals. In this method, a small electric current, known as an eddy current, is induced in a material, and any changes in the flow of this current due to a flaw or inhomogeneities in the material are detected by a nearby coil and subsequently processed electronically. Basically, any discontinuity that appreciably alters the normal flow of eddy current can be detected by eddy current inspection.

Conventional eddy current and remote field eddy current are the two commonly used techniques for heater tube inspections. Nonferromagnetic tubes such as austenitic stainless steel, copper–nickel

alloys, brass are inspected by conventional eddy current method. Ferromagnetic materials are inspected by the remote field eddy current method.

In heat exchanger and pressure vessel applications, the areas of applications of ET are

1. Production-line inspection of tubular products during manufacture to detect seams, laps, cracks, voids, inclusions, etc., on conductive metal surfaces
2. In-service inspection of tubes for service-induced defects such as loss of tube wall thickness due to corrosion, erosion, pitting, fretting wear, baffle cuts, and growth of manufacturing defects
3. For surface, and in some cases subsurface, inspection of welds for discontinuities
4. Material sorting
5. Clad overlay measurement
6. Paint thickness measurement
7. Coating thickness measurement

14.4.13.1 Principles of Eddy Current Testing

In ET, an alternating current is made to flow in a coil (probe), which, when brought into close proximity of the conducting surface of the material to be inspected, induces an eddy current flow in the material (Figure 14.33a). The presence of a defect, a discontinuity, or a metallic object other than the specimen

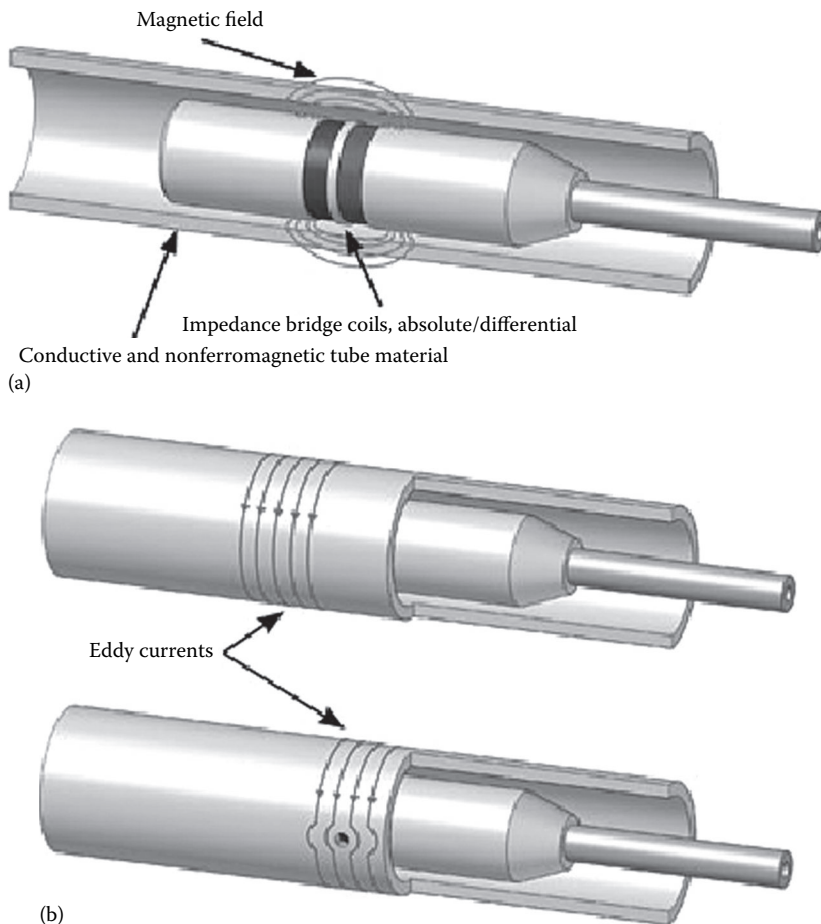


FIGURE 14.33 Principle of ET of tube. (a) Interaction between electromagnetic fields and metals and (b) flow of eddy currents on a normal tube and around a defect. (Courtesy of Olympus NDT Inc., Waltham, MA.)

under test disturbs the eddy current flow (Figure 14.33b). These eddy currents in turn generate an alternating magnetic field, which will cut the windings of the coil and try to produce a reverse current. This reverse current may be detected either as a voltage across a secondary coil or by the perturbation of the impedance of the original coil. This impedance change can be measured and correlated with the presence and the extent of the defect, discontinuity, or metallic object. The test coil is placed in a unit called a measuring probe. The process lends itself to automated production-line testing. ECT signals are interpreted using the ASME depth curve to determine their depth. The ASME depth curve is based on the phase of the ECT signal. Signals with a phase angle in the 0° – 40° range represents inner diameter defects while signals with a phase angle of greater than 40° represent outer diameter defect. The signal from a hole is set to 40° . The ET principle explained in this section is based on Granville [69] and Ref. [70].

14.4.13.2 Written Procedure

ASME Code Section V furnishes the minimum information necessary in the written procedure. A partial list includes the following:

1. Scope of examination: for tubing examination, tube material, diameter, and wall thickness
2. Size and type of probes
3. Examination frequencies
4. Eddy current equipment model and manufacturer
5. Scanning direction and speed during examination
6. Inspection technique, e.g., hand probe, mechanized probe, remote-control fixtures
7. Calibration procedure and standards
8. Description of data-recording equipment and procedure
9. Signal processing and acceptance criteria
10. Reporting results

14.4.13.3 ASTM Specifications

- E 426 for electromagnetic (eddy current) testing of seamless and welded tubular products of austenitic stainless steel and similar alloys
- E 215 for testing of aluminum alloy tubes
- E 309 for steel tubular products with magnetic saturation
- E 243 for seamless copper and copper alloy tubes

14.4.13.4 Probes

Probes can be classified into four categories [34,71]:

1. Surface probes, which are used for crack detection and corrosion measurements.
2. Encircling probes, which are used primarily for production control of wire or tubular products (Figure 14.34a).
3. Internal bobbin probes, which are used to check tubings (Figure 14.34a).
4. Rotating scanning probe, also known as ID surface riding “pancake coil” (RPC) as shown in Figure 14.34c; it can locate very small defects and determine their exact location on the circumference.

14.4.13.4.1 Probe Configuration

Two basic probe coil configurations are used for tube inspection. They are (1) the absolute probe configuration that consists of a single coil as shown in Figure 14.35a, and its test setup is shown in Figure 14.35b and (2) differential probe configuration, which consists of two coils connected in opposition as shown in Figure 14.35c. (*Note:* coil winding pattern is not shown). Figure 14.35 shows differential probe with single encircling coil. The absolute probe is sensitive to gradual changes in tube dimensions such as gradual tube thinning, but relatively poorly sensitive for small, sharp

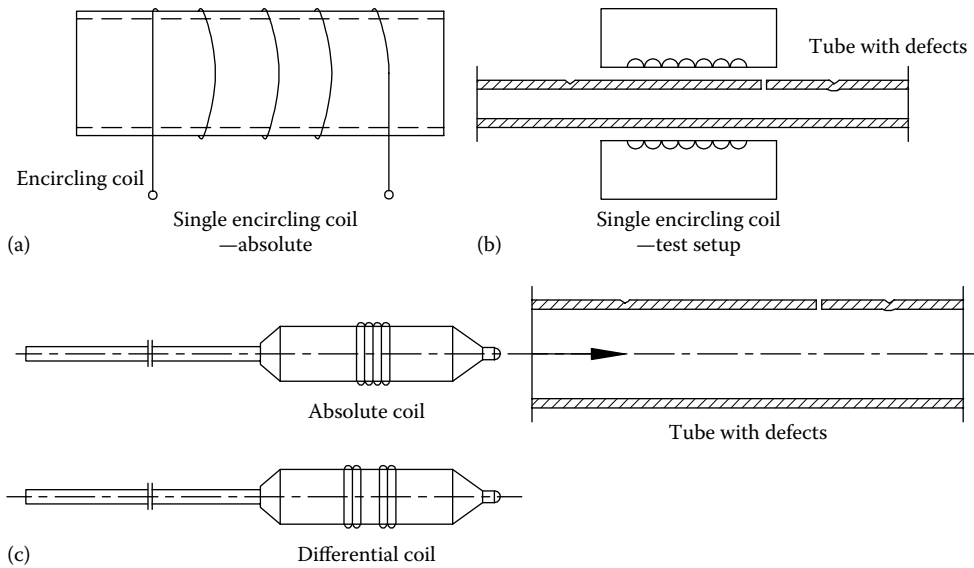


FIGURE 14.34 ET probes: (a) single coil encircling probes, (b) typical test setup with single coil probe, and (c) internal bobbin probes.

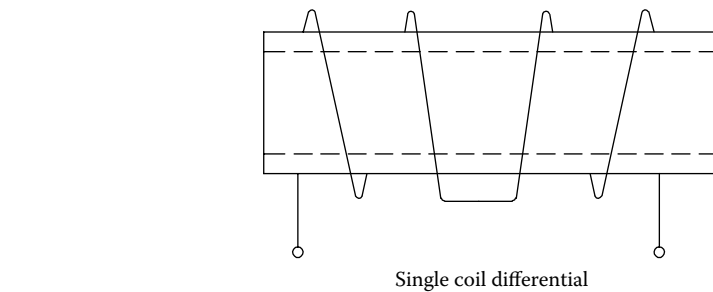


FIGURE 14.35 Eddy current differential probe configuration.

defects such as pitting. In differential probe configuration, the net induced voltage is canceled out when the coils experience identical conditions. Because of this, differential probes are highly sensitive to sharp defects such as pitting, but not sensitive to defects such as gradual tube thinning [69].

14.4.13.5 Eddy Current Test Equipment

Eddy current test equipment covers a range from simple units to fully automatic systems. In general, the eddy current equipments will incorporate these elements:

1. A source to provide an alternating current of required frequency to excite the test coil
2. A modulating device consisting of a test coil and test object combination, which brings out desired information in the form of an electrical signal
3. Signal processing
4. Signal display

14.4.13.6 Signal Processing

Eddy current signals are vector quantities and have both amplitude and direction (phase). The amplitude and phase of the signals can be displayed on a cathode-ray oscilloscope. In the case of tube inspection, the phase of the signal can give information regarding the depth and defect origin [69].

14.4.13.7 Inspection or Test Frequency and Its Effect on Flaw Detectability

Generally, test frequencies used in eddy current inspection range from 200 Hz to 6 MHz or more. Frequency has a direct bearing on the ability to penetrate the component wall thickness. At lower frequencies, penetration is greater, but the sensitivity to flaw detection decreases, whereas at high frequencies, the depth of penetration is lower, and small flaws remain undetected as the depth increases. An optimum frequency should be selected so that the penetration is sufficient to reach any subsurface flaw. When detecting flaws at some considerable depth below the surface, that is a thicker part, very low frequencies must be used and sensitivity is sacrificed [70].

14.4.13.8 Operating Variables

The principal operating variables associated with eddy current inspection include coil impedance, electrical conductivity, magnetic permeability, liftoff and fill factors, edge effect, and skin effect. Fill factor, edge effect, skin effect, depth of penetration, and frequency are discussed next.

14.4.13.8.1 Depth of Penetration and Frequency

The depth of penetration of eddy current is a critical factor. For example, in the case of tube inspection, if the eddy currents do not penetrate the wall thickness, then it will miss the defects. The depth of penetration of eddy current (τ) is given by the following equation [69]:

$$\tau = \frac{500}{\sqrt{\sigma\mu f}}$$

where

σ is the conductivity ($\text{m}/\Omega \cdot \text{mm}^2$)

μ is the magnetic permeability (1 for nonmagnetic materials)

f is the test frequency (Hz)

The standard depth of penetration is generally taken to be that depth at which the eddy current field intensity drops to 37% of the intensity at the conductor surface. For tube inspection, the test frequency is often the frequency at which the depth of penetration is equal to the tube wall thickness. This is given by the equation [69]

$$f = \frac{250}{\sigma t^2} \text{ kHz}$$

where t is the tube wall thickness (mm).

When phase analysis is being applied, the f_{90} frequency, that is the frequency at which there is a 90° phase difference between signals from the inside wall of the tube and signals from the outside wall, will be used. The f_{90} frequency is given by the equation [69]

$$f_{90} = \frac{3\rho}{t^2} \text{ kHz}$$

where ρ is the resistivity ($\mu\text{ohm} \cdot \text{cm}$).

14.4.13.8.2 Fill Factor and Probe Size Requirements

The probe size requirements for eddy current tube testing are determined by the “fill factor,” given by the expression [69]

$$\text{Fill factor} = \left[\frac{d_1}{d_2} \right]^2$$

where

d_1 is the diameter of the probe

d_2 the inside diameter of the tube

For an internal or bobbin-type coil, the fill factor indicates how well the inspection coil fills the inside of the tube being inspected. Ideally, the fill factor should be close to 1.0. A fill factor of 1.0 will not allow smooth travel of the probe inside the tube. Therefore, as a thumb rule, the optimum fill factor for tube testing can be about 0.70 [69]. This allows reasonable sensitivity to be achieved while still maintaining adequate clearance when dirt or dents may be present in the tube.

14.4.13.8.3 Edge Effect

When an inspection coil approaches the end or edge of a part being inspected, the eddy currents are distorted, because they are unable to flow beyond the edge of the part. The distortion of eddy current results in an indication known as “edge effect.” In general, it is not advisable to inspect any closer than $\frac{1}{18}$ in. (3.2 mm) from the edge of a part [70].

14.4.13.8.4 Skin Effect

Eddy currents are not uniformly distributed throughout a part being inspected. They are densest at the surface immediately beneath the coil and become progressively less dense with increasing distance below the surface. This phenomenon is known as “skin effect.” At some distance below the surface of a thick wall, there will be essentially no current flowing.

14.4.13.9 Inspection Method for Tube Interior

The probe, usually an internal bobbin type, is introduced into the tube under test and passed along the length of the tube to the far end, usually not only by means of compressed air, but also by other means. It is then withdrawn from the tube at a constant speed, typically in the range of 0.5–1.0 m/s, using a winch unit [34,69]. During the probe withdrawal, the eddy current signals are recorded on a chart and analyzed further.

14.4.13.9.1 Inspection of Ferromagnetic Tubes

The highly ferromagnetic nature of carbon steel and ferritic stainless steels severely limits the application of standard eddy current technique. Nonferromagnetic materials have a relative permeability of approximately 1, whereas ferromagnetic materials have typical relative permeabilities of 500–2000. Since the higher the permeability is, the lower is the depth of penetration, eddy currents in ferromagnetic materials are concentrated at the surface and hence buried or back-wall defects remain undetected. Also small variations in permeability give rise to relatively high noise levels [69]. This limitation is overcome by saturating the ferromagnetic tubes magnetically with a direct current, so that the material reacts as a nonmagnetic material when inspecting [34] or by remote field slit eddy current (RFEC) technique. The drawbacks of these two methods are discussed by Bergander [72]. Such drawbacks are as follows: (1) Since magnetic saturation uses high-amperage

current for saturation, there is a need for probe cooling, the possibility of false indications due to variations in permeability, difficulty in detecting gradual tube thinning, and complicated probe design. (2) To make the RFEC technique sensitive to gradual wall thinning, the probes have to be complex. To overcome these difficulties, Bergander [72] suggests using a magnetic flux leakage (MFL) method to examine ferritic tubes.

14.4.13.10 Tube Inspection with Magnetic Flux Leakage

MFL is a fast inspection technique suitable for measuring wall loss and detecting sharp defects such as pitting, grooving, and circumferential cracks. MFL is effective for aluminum-finned carbon steel tubes because the magnetic field is almost completely unaffected by the presence of such fins. The principle of MFL as applied to ferrous heat exchanger tubing is illustrated in Figure 14.36a and b.

14.4.13.11 Remote Field Eddy Current Testing

The RFEC inspection technique is similar to the ET method, which uses low-frequency alternating current and through-wall transmission to inspect pipes and tubes from the inside. The method is most preferred to apply to ferromagnetic materials because conventional ET techniques are not suitable for detecting opposite-wall defects in such materials unless the material is saturated [73]. The exciter coil generates eddy currents at low frequency in the circumferential direction. The electromagnetic field transmits through the thickness and travels on the outer diameter. A receiver coil that is placed in the remote field zone of the exciter picks up this field. In this zone, the wall current source dominates the primary field directly from the exciter. The separation between the two coils is between two and five times the tube ID. Remote field testing (RFET) is being used to successfully inspect ferromagnetic tubing such as carbon steel or ferritic stainless steel. This technology offers good sensitivity when detecting and measuring volumetric defects resulting from erosion, corrosion, wear, and baffle cuts.

Principle: The principle of RFEC is explained in Ref. [73] and by Atherton et al. [74] and the same is illustrated schematically in Figure 14.37a and b. The probe uses a relatively large internal exciter coil, which is driven with a low-frequency alternating current. A detector coil is placed near the inside of the pipe wall, but axially displaced from the exciter coil by about two pipe diameters. Two distinct coupling paths exist between the exciter and the detector coils: (1) the direct path inside the tube, which is attenuated rapidly by circumferential eddy currents induced in the tube wall, and (2) the indirect coupling path that originates in fields that diffuse outward through the pipe wall in the vicinity of the exciter. Anomalies anywhere in this indirect path cause changes in the magnitude and phase of the received signal, and can therefore be used to indicate defects. This method has been used primarily for inspecting well casing, small-diameter boiler tubes, and heat exchanger tubes.

Merits and demerits: An important advantage of this method is that the method has higher sensitivity to axially and circumferentially oriented flaws in ferromagnetic materials. This allows detecting corrosion damage due to erosion–corrosion, tube wall thinning, pitting, and stress corrosion cracking [73]. The major disadvantage is that when applied to nonferromagnetic material, it is not generally as sensitive or accurate as conventional ET method.

14.4.13.12 Tube Inspection with Near Field Testing

The near field testing (NFT) technology is a rapid method intended specifically for fin-fan carbon steel tubing inspection. This new technology relies on a simple driver-pickup eddy current probe design (Figure 14.38) providing very simple signal analysis. NFT is specifically suited for the detection of internal corrosion, erosion, or pitting on the inside of carbon steel tubing. The NFT

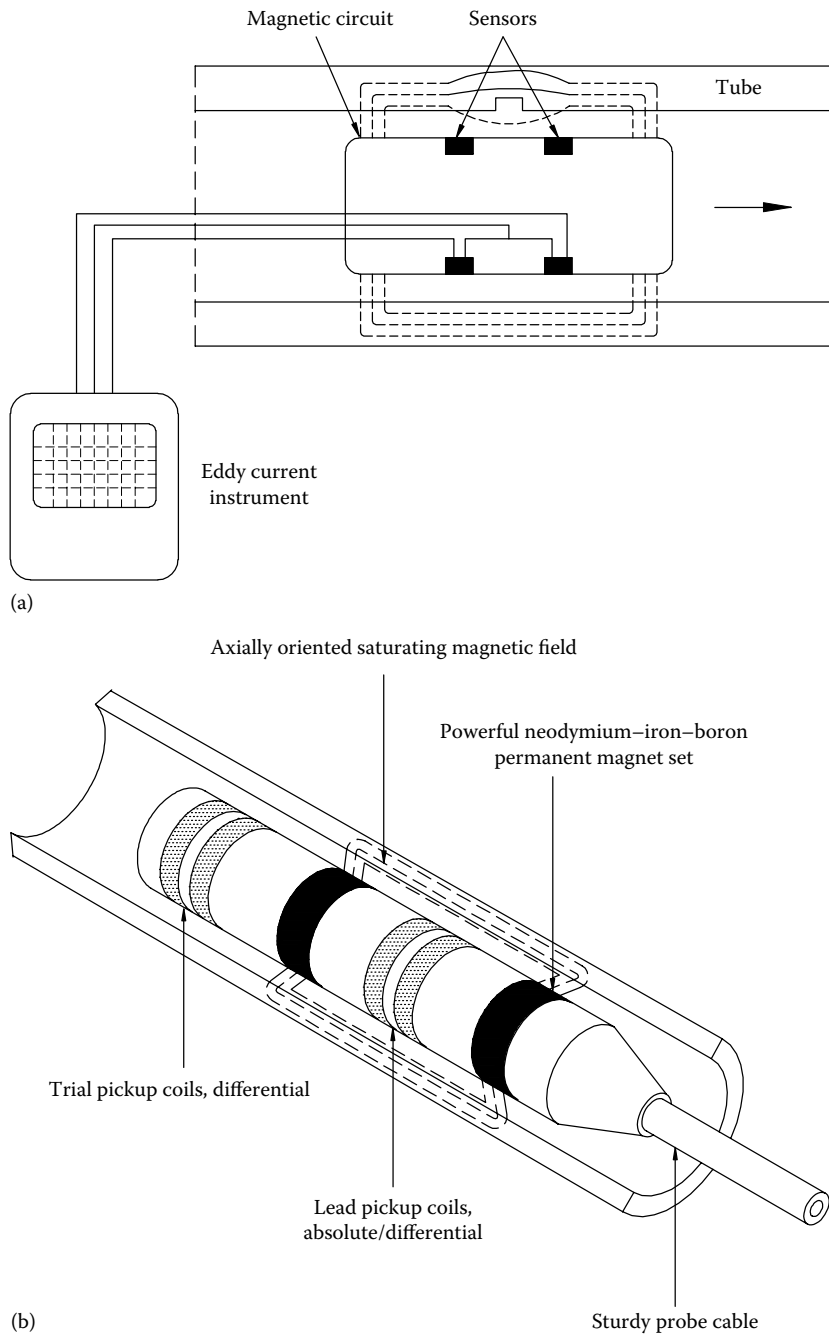


FIGURE 14.36 (a) Principle of MFL inspection of ferrous tube and (b) MFL probe and flow of eddy currents. (Courtesy of Olympus NDT Inc., Waltham, MA.)

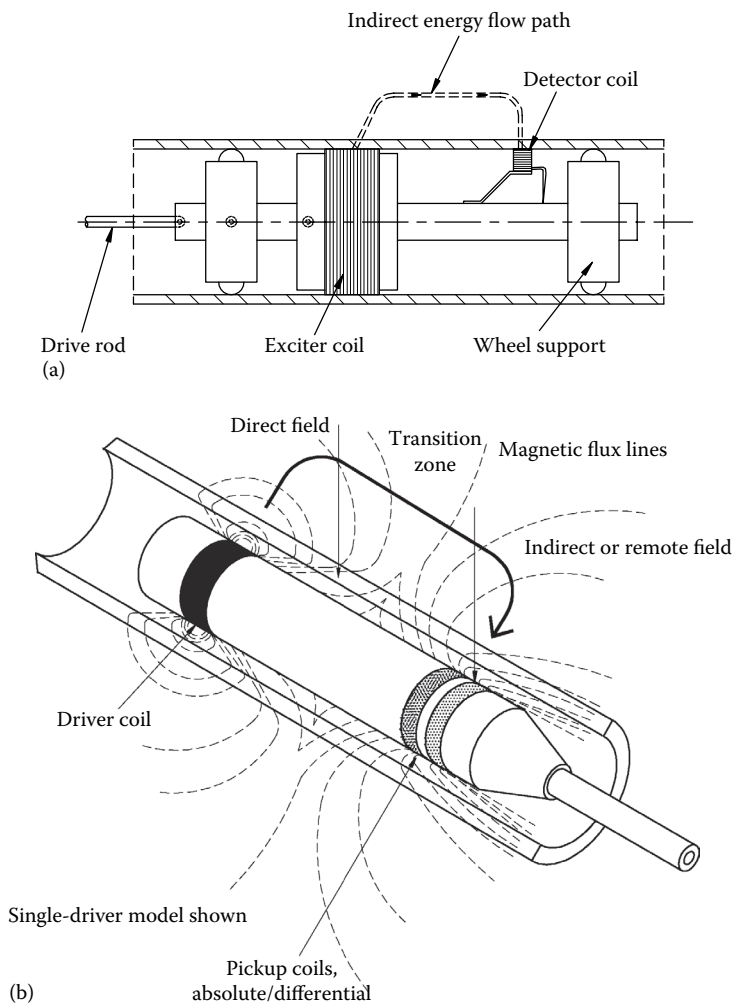


FIGURE 14.37 (a) Tube inspection with remote field ET technique (REFC or RFT) and (b) RFT probe and flow of eddy currents. (Courtesy of Olympus NDT Inc., Waltham, MA.)

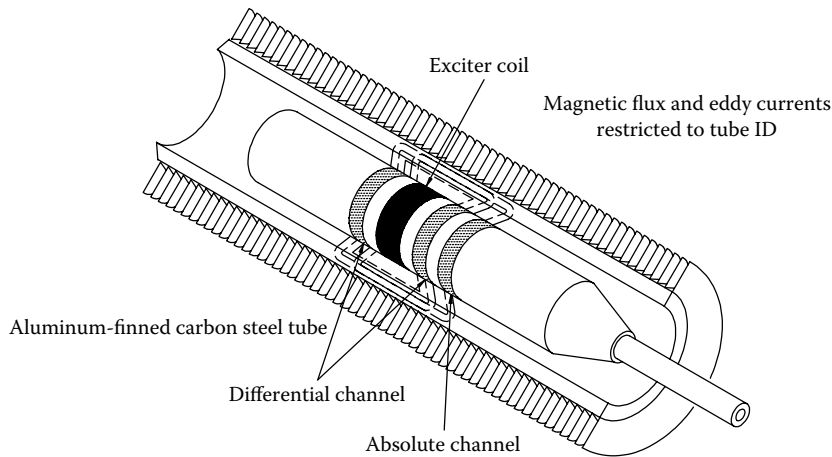


FIGURE 14.38 Tube inspection with eddy current NDT. (Courtesy of Olympus NDT Inc., Waltham, MA.)

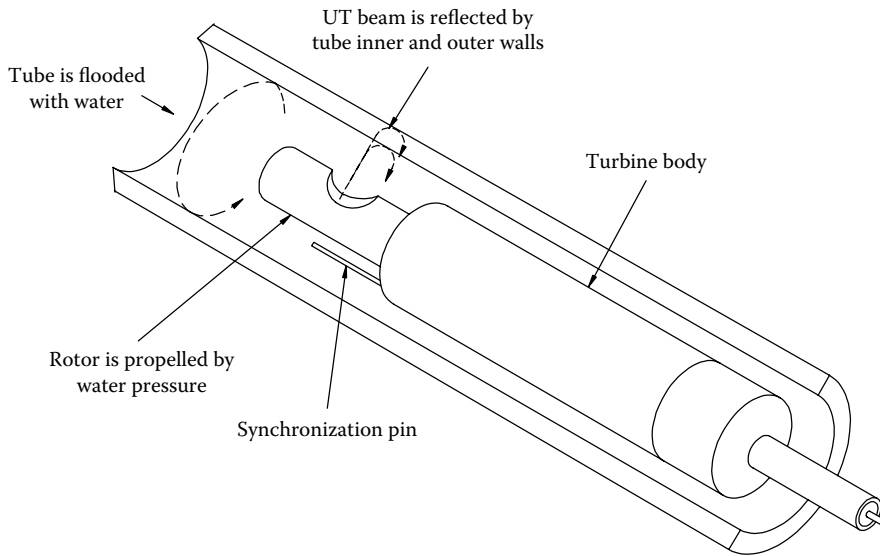


FIGURE 14.39 Tube inspection with IRIS for ferrous and nonferrous materials. (Courtesy of Olympus NDT Inc., Waltham, MA.)

probes measure lift-off or “fill factor” and convert it to amplitude-based signals (no phase analysis). Because the eddy current penetration is limited to the inner surface of the tube, NFT probes are not affected by the fin geometry on the outside of the tubes.

14.4.13.13 Tube Inspection with Internal Rotating Inspection System for Ferrous and Nonferrous Materials

The ultrasonic internal rotating inspection system (IRIS) option is used to inspect a wide range of materials including ferrous, nonferrous, and nonmetallic tubing. This technique (Figure 14.39) detects and sizes wall loss resulting from corrosion, erosion, wear, pitting, cracking, and baffle cuts. Olympus digital IRIS inspection technology is used extensively as a prove-up technique for remote field testing (RFT), MFL, and eddy current inspections.

14.4.13.14 Instrumentation

Olympus MultiScan MS5800 is a multi-technology system offering the technologies such as (a) eddy current, (b) MFL, (c) remote field, and (d) IRIS ultrasound for tube inspection and instrument as shown in Figure 14.40.

14.4.13.15 Testing of Weldments

Because of the circumferential orientation of eddy current flow, this method is effective in detecting most types of longitudinal weld discontinuities such as open welds and weld cracks. On the other hand, difficulty arises for the detection of a thin planar discontinuity that is oriented substantially perpendicular to the axis of the cylinder.

14.4.13.16 Calibration

In order to provide accurate and repeatable results, artificial defects of known size are introduced into a specimen piece of tube of the same material and dimensions as the tubes to be inspected.



FIGURE 14.40 MultiScan MS5800 for tube inspection. (Courtesy of Olympus NDT Inc., Waltham, MA.)

Reference defects can be of various types. The most commonly used reference standard consists of a number of through holes in a tube along with their signal pattern [75].

14.4.13.17 Merits of ET and Comparison with Other Methods

ET is attractive because it offers both very high sensitivity and relatively high scanning speeds. Direct contact with the test material is not required and a coupling medium is not necessary; the process is repeatable, the test method is relatively fast, and it can be easily automated.

14.4.13.18 Limitations of Eddy Current Testing

The major limitations of ET are the following:

1. Skin effects usually restrict the depth of inspection. It is generally limited to 0.25 in. (6.4 mm) for nonferromagnetic materials and 0.010 in. (0.25 mm) for ferromagnetic materials [28]. The limitation due to high permeabilities of ferromagnetic materials may be significantly overcome by magnetic saturation of the area being inspected or by flux leakage method.
2. Since many variables, namely, permeability, conductivity, probe position, and weld contour, can affect an eddy current signal, an accurate measurement of one property requires the ability to eliminate or at least considerably reduce interference from other properties [76]. Multifrequency techniques are used in practice to increase the information content of signals [75]. A classical solution, due to recent developments in ET, which can reduce but not eliminate this problem, is the application of different ET probes [71]. Other limitations include [69] the following: The signal is more closely related to volume of material lost than to wall thickness lost. Defects at the tubesheet, and at the tube and baffle plate interface, can be difficult to detect. For critical applications, results may need to be verified by an alternative technique.

14.4.13.19 Recent Advances in Eddy Current Testing

The development of computer interfacing for data collection, analysis, and display has led to multiple-frequency testing, eddy current imaging, multiple-element eddy current probes, and automated data interpretation systems that significantly enhance both the capabilities and the reliability of the eddy current inspection [71].

14.4.13.19.1 Eddy Current Array

Eddy current array technology provides the ability to electronically drive and read several eddy current coils positioned side by side in the same probe assembly. Data acquisition is possible through multiplexing, which avoids mutual inductance between coils.

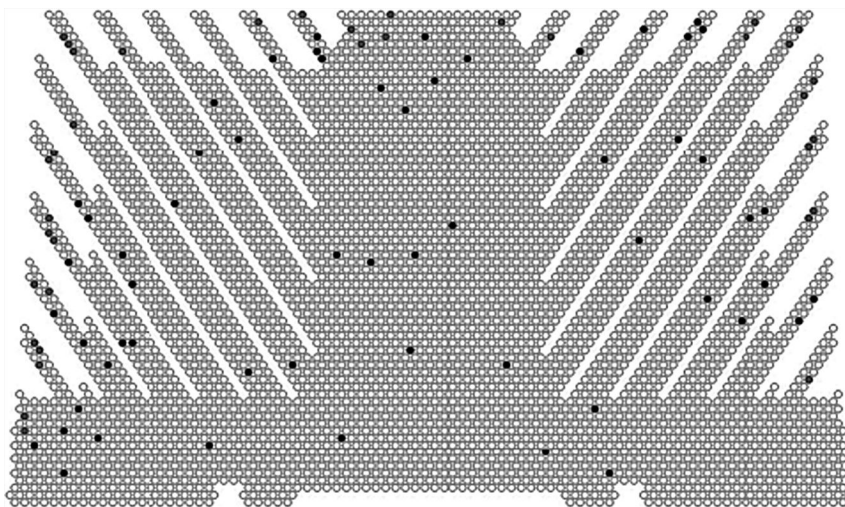


FIGURE 14.41 Tubesheet mapping diagram. (Courtesy of Powerfect, Brick, NJ.)

14.4.13.20 Tubesheet Diagram for Windows

The tubesheet diagram (TSD) for Windows is a computer software intended for use by inspection groups in the oil, gas, and power industries to inspect tubes periodically in heat exchangers, boilers, steam generators, chillers, air conditioners, and similar multitube equipment and to award a classification based on user-defined criteria such as corrosion severity, material type, defect position, etc. [77]. TSD is shown in Figure 14.41.

14.4.13.20.1 Automated Tube Inspection System

Automated tube inspection system (ATIS) is a software package that carries out automated analysis of the data from eddy current and electromagnetic in-service tube inspection systems in real time [78]. The system discriminates between baffle support plate signals and defect signals and can be utilized on a wide variety of tube materials. The results are classified in terms of defect severity and stored in a hard disk, from which they can be retrieved and summarized at any time. TSD can accept manual input from the keyboard or the mouse and can also import results from the silverwing ATIS data files.

14.4.14 LEAK TESTING

LT is an NDT technique used for the detection and location of leaks and for the measurement of fluid leakage in either pressurized or evacuated vessels and components [77]. A leak may be a crack, fissure, hole, or passage that admits any fluid or lets fluid escape. The operational reliability and serviceability of many devices under pressure or vacuum is greatly reduced if sufficiently large leaks exist. LT is performed for three basic purposes:

1. To prevent material leakage loss
2. To prevent environmental contamination or hazards, particularly ones that involve handling of radioactive or lethal fluids
3. To detect unreliable components

For pressure vessels and heat exchangers, LT is used to ensure the leak-tightness of various welded joints, flanged joints, tube-to-tubesheet joints, mechanical joints, enclosures, etc.

14.4.14.1 Written Procedure

LT procedures should encompass one or a combination of the following [78]:

- Locating leaks
- Determining the leakage rate
- Monitoring for leakage

ASME Code Section V specifies the minimum information to be provided for the LT procedure, which include the following:

1. Scope and extent of the examination
2. Type of equipment to be used for detecting leaks or measuring rate of leakage
3. Surface cleanliness and surface preparation
4. LT method
5. Temperature, pressure, gas, and percentage concentration to be used

14.4.14.2 Methods of Leak Testing

The basic principle of LT involves identification and location of the leaks or the measure of the flow of fluid or the testing medium quantitatively through the leak. This could be the actual flow rate, drop in pressure or vacuum level, etc. Various LT methods are detailed in Refs. [77,78], ASME Code Section V, and Yokell [18]. The following are the different LT methods available, arranged in a rough order of increasing sensitivity.

1. Ultrasonic detection
2. Bubble test—direct pressure technique or immersion technique, or vacuum box method
3. Gas leak lake testing
4. Pressure change test
5. Halogen diode detector probe test
6. Helium mass spectrometer detector (sniffer) probe technique
7. Helium mass spectrometer tracer probe technique
8. Helium mass spectrometer hood method

Tests for gross leaks involve direct visual inspection for signs of tracers or leakage products, or scanning of leaking systems with an ultrasonic leak detector to locate the sources of hissing sounds. Small leaks can be detected by sophisticated LT methods utilizing tracer gases such as halogen vapors and helium with detectors such as the heated anode halogen detector and the helium mass spectrometer, respectively. LT methods listed in items 1–8 are discussed next. Yet another method of LT is AET, and this method is explained in the section on AE.

14.4.14.2.1 Ultrasonic Leak Detection

The leakage of a gas through small openings, even for small pressure differences, generates noise in the ultrasonic range. Therefore, it is possible to detect the leaks by listening for them using an ultrasonic listening device, which can record low noise levels produced in the high frequencies (40–50 kHz) that occur due to turbulent flow [34].

14.4.14.2.2 Bubble Testing

Bubble testing can be performed by the direct pressure technique or vacuum box technique. The direct pressure technique using bubble solution is the more common one.

Bubble testing, direct pressure technique: The objective of the direct pressure technique is to locate leaks in a pressurized component by application of a solution or by immersion in liquid that will form bubbles as the leakage gas passes through it. To perform this test, pressurize the shell with inert gas or air; the required pressure differential can be from 1 kg/cm² to 1.25 times the design

pressure of the vessel but less than 20 kg/cm². After sufficient pressure soak time, apply a soap solution over the joints. Generally, the surfaces must be in the temperature range of 40°F–125°F (4.5°C–52°C). This method can detect leaks of the order of 10⁻⁵ pa m³/s when the test objects are immersed in detection liquids.

Bubble testing, vacuum box technique: The objective of the vacuum box technique is to locate leaks in a pressure boundary that cannot be directly pressurized. In this method, on one side of the test joint after application of soap solution, vacuum is created, and if there are any through leaks, atmospheric air from the other side will come out to the vacuum side and will be observed as the formation of a bubble.

14.4.14.2.3 Gas Leak Lake Testing

For this method, pressurize the shellside of the heat exchanger with air or nitrogen to the maximum allowable working pressure at room temperature, set the unit vertically. With a ring of about 2 in. height (50.8 mm), make a dam on the tubesheet face. Fill the tubeside with water to the level of the dam and observe for bubbles.

14.4.14.2.4 Pressure Change Test

This test method describes the technique for detecting the leakage rate of the boundaries of a closed compartment or the vessel at a specific pressure or vacuum by indicating pressure or vacuum change over the given time period.

14.4.14.2.5 Halogen Diode Detector Testing

Principle: A detector or a sniffer sucks a mixture of air and leaking tracer gas through a tubular probe into an instrument that is sensitive to small amounts of tracer gas. The tracer gas can be a halide gas (Refrigerant 12) to a maximum of 25% of the design pressure. A heated platinum element (anode) in the detector ionizes the halogen vapor, and the ions are collected on a cathode plate. A current proportional to the rate of ion formation is measured.

Leak testing method: Traverse the tube ends with a probe at a distance of about 1/8 in. (3.2 mm) and at a predetermined scanning rate using a standard leak. Also insert the probe into the tube ends for about 1/4 in. (6.35 mm). Check for cracked tube ends by inserting the probe into each tube end to a minimum depth of 3/4 in. (19 mm) and holding it there for about 3 s. If the tubes are welded to the tubesheet, check the welds by encapsulating each tube end with a funnel connected to the probe [11]. When the tubes are too small to allow the probe to enter and too close to each other for effective scanning, use the halogen sniffer in a bag test system. The halogen diode detector LT method is a semiquantitative method to detect and locate leakages and should not be considered quantitative. The sensitivity of this method is 10⁻⁶ Pa · m³/s.

14.4.14.2.6 Helium Leak Detection Methods

Principle: For the manufacture of nuclear components, LT using helium as a tracer gas is one of the mandatory code and customer requirements. Helium leak detection can be done either by pressurizing the vessel with helium and sniffing (detector) the welds or joints from outside or by evacuating the vessel and spraying helium on the welds from outside by a tracer probe or enclosed in a vacuum mask. In each case, the helium atoms passing through a leak are collected to a mass spectrometer, where they are ionized. The current proportional to the quantum of ions is amplified and measured as the leak rate.

Helium mass spectrometer test: The basic methods of helium leak detection include [77] the following:

1. Detector probe technique
2. Tracer probe method
3. Vacuum technique or hood method

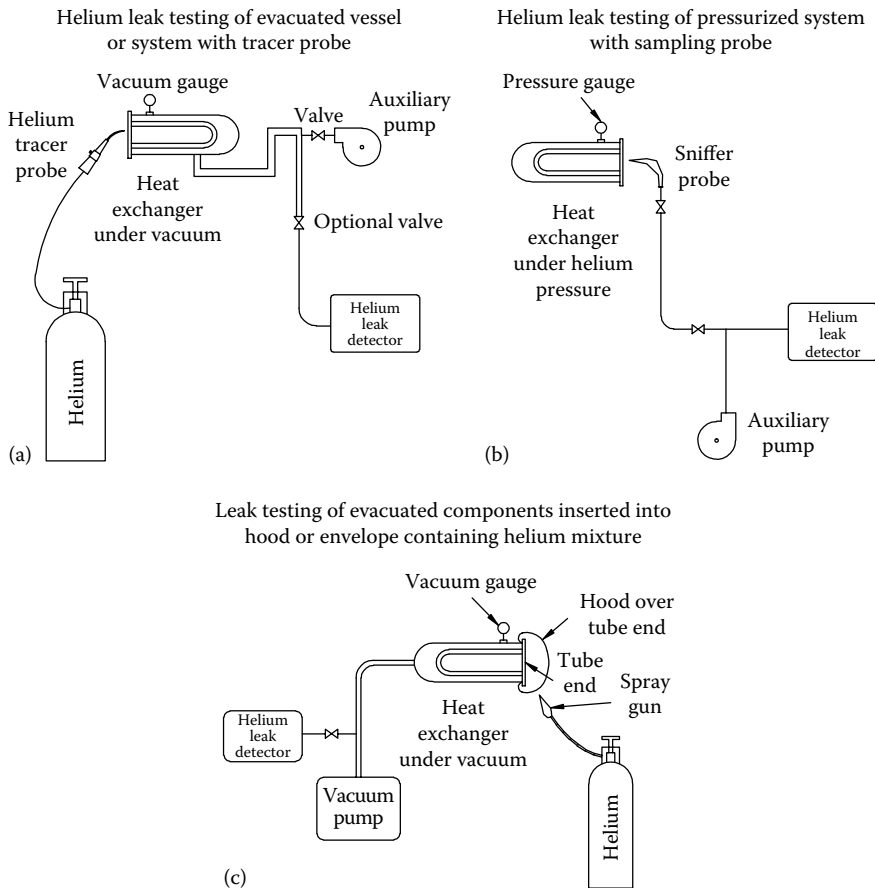


FIGURE 14.42 Helium mass spectrometer testing. (a) Tracer probe technique, (b) detector probe technique, and (c) vacuum technique or hood method. (Adapted from McMaster, R.C., ed., *Nondestructive Testing Handbook, Vol. 1, Leak Testing*, 2nd edn., American Society for Nondestructive Testing and American Society for Metals, Columbus, OH.)

Detector probe technique: The detector probe technique, as shown schematically in Figure 14.42a, involves pressurizing the vessel to be leak tested with certain percentage of pure helium and sensing the leaking helium using the detector probe, which is moved at a definite speed over all the joints to be tested. Any leakage from the pressurized system is detected by the mass spectrometer leak detector. The detector probe is a semiquantitative technique to detect and locate leakages and should not be considered quantitative. The sensitivity of this method is of the order of $10^{-7} \text{ Pa} \cdot \text{m}^3/\text{s}$.

Tracer probe method: In the helium tracer probe method as shown in Figure 14.42b, the mass spectrometer leak detector is connected to the internal volume of an evacuated vessel or heat exchanger while helium is sprayed from the probe at each joint and is moved over the external surface to detect the specific locations of leaks. Any leakage into the vacuum side is detected by the mass spectrometer leak detector. The tracer probe is a semiquantitative technique to detect and locate leakages and should not be considered quantitative.

Vacuum technique or hood method: The vacuum technique or hood method involves evacuating the vessel to be tested and filling with almost 100% helium or air–helium mixture in the enclosing mask and detecting the inflow of helium to the vessel under vacuum through leaks if any, using the instrumentation as shown schematically in Figure 14.42c. This is a quantitative measurement

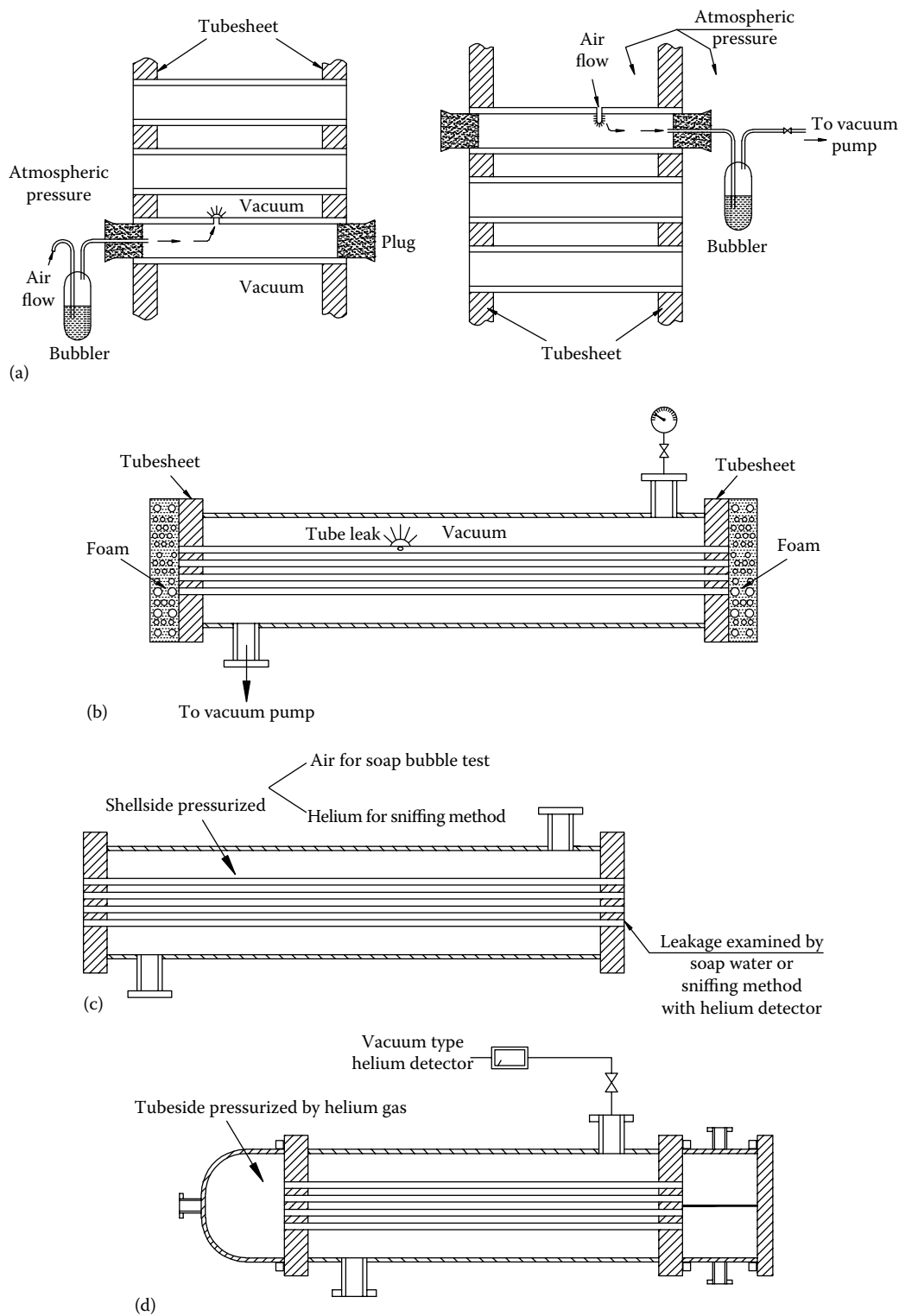


FIGURE 14.43 In-service examination of leaks: (a) by vacuum technique using bubbler and (b) by vacuum technique using soap foam, (c) pressure testing using soap water by sniffing method with helium detector and (d) pressure testing with vacuum type helium detector.

technique. The high sensitivity of the hood technique makes possible the detection and measurement of total helium gas flow from the high pressure side. The sensitivity of this method ranges from 10^{-7} to 10^{-11} Pa·m³/s. ASME Code Section V accepts only the helium hood method (vacuum technique) as quantitative. A typical test setup is shown in Figure 14.42d.

14.4.14.2.7 In-Service Examination of Heat Exchangers for Detection of Leaks

In-service examination of leaks, using either pressurized air or vacuum technique or bubbler, is shown schematically in Figure 14.43. Fractured tubes at the interior section can be plugged using tube stabilizers (Figure 14.44), marketed by M/s Expando Seal Tools. Additionally, individual tube can be tested by the following two methods:

1. Individual near end tube testing plugs/kits as shown in Figure 14.45
2. Individual through the tube testing method as shown in Figure 14.46

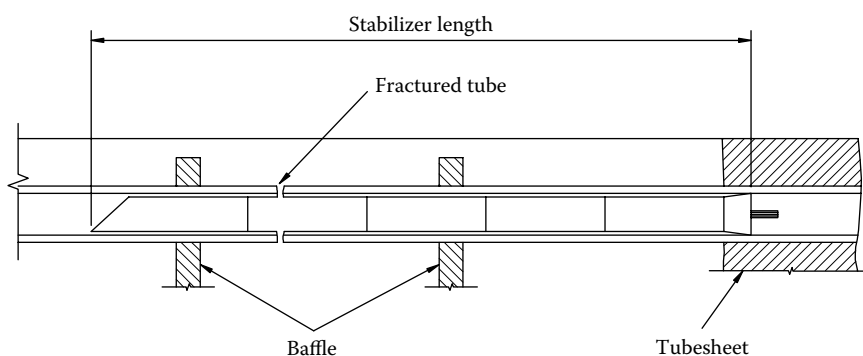


FIGURE 14.44 Plugging fractured tube using tube stabilizer.

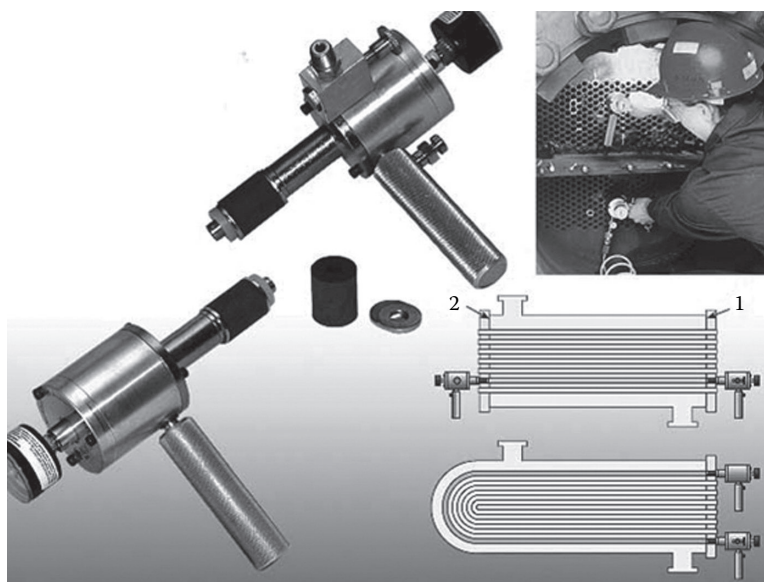


FIGURE 14.45 Individual near end tube testing plugs/kits. (Courtesy of Maus Italia F. Agostino & C.s.a.s., Bagnolo Cremasco (Cr), Italy.)

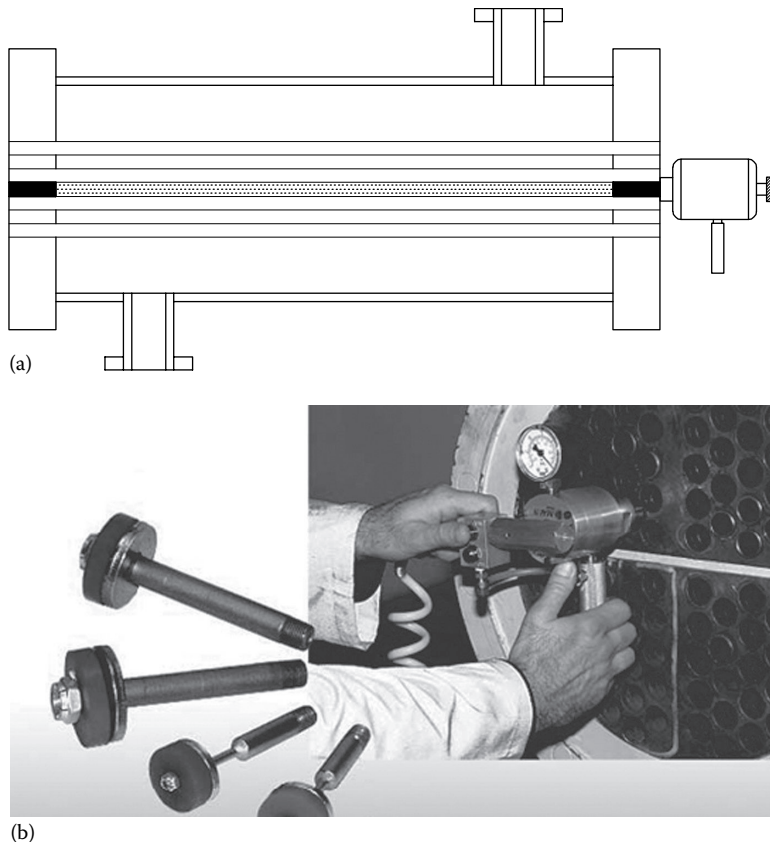


FIGURE 14.46 Individual through the tube testing. (Courtesy of Maus Italia F. Agostino & C.s.a.s., Bagnolo Cremasco (Cr), Italy.)

REFERENCES

1. Danis, J. I., Material selection, fabrication and inspection of refinery heat exchangers, *Welding J.*, June, 25–30 (1986).
2. Nicholson, S., The role of NDT within Q. A. programmes applied to pressure vessels and other process plant, *Br. J. NDT*, May, 121–127 (1982).
3. Burgess, N. T., Quality control—What's it all about? *Weld. Metal Fabr.*, December, 464–468 (1966).
4. Silk, M. G., Developments in ultrasonics for sizing and flaw characterisation, in *Developments in Pressure Vessel Technology—2, Inspection and Testing* (R. W. Nichols, ed.), Applied Science Publishers, London, U.K., 1979, pp. 101–139.
5. Rao, B. S. C., Quality assurance in fabrication of pressure vessels, in *Welding Engineering Handbook*, Vol. I (S. Sundarajan, S. Vijaya Bhaskar, and G. C. Amarnath Kumar, eds.), Welding Research Group, Radiant Publications, Secunderabad, India (1990).
6. Bryant, L. E. and McIntire, P., eds., *Nondestructive Testing Handbook*, 2nd edn., Vol. 3, Radiography and Radiographic Testing, American Society for Nondestructive Testing, Columbus, OH, 1985.
7. Blatter, H. and Frey, H., System effectiveness and quality assurance of electronic systems. *Brown Boveri Rev.*, 11–78, 739–743.
8. Dale, B. G. and Plunkett, J. J., A study of audits, inspection and quality costs in the pressure vessel fabrication sector of the process plant industry, *Proc. Inst. Mech. Eng.*, 198B, 49–54.
9. Chuse, R., *Pressure Vessels, the ASME Code Simplified*, McGraw-Hill, New York, 1984.
10. (a) ASME Boiler and Pressure Vessel Code, Section VIII, Division 1, *Pressure Vessels*, American Society of Mechanical Engineers, New York, 2010; (b) ASME Boiler and Pressure Vessel Code, Section IX, *Welding and Brazing Qualifications*, American Society of Mechanical Engineers, New York, 2010; (c) ASME Boiler and Pressure Vessel Code, Section II, *Material Specifications, Part A—Ferrous Materials*.

- Part—B Nonferrous Materials, Part—C Welding Rods, Electrodes and Filler Metals, Part—D Material Properties*, American Society of Mechanical Engineers, New York, 2007; (d) ASME Boiler and Pressure Vessel Code, Section V. *Nondestructive Examination*, American Society of Mechanical Engineers, New York, 2010.
11. Veith, C. J., Developing a quality control program, *Welding Design Fabr.*, September, 71–73 (1975).
 12. Lavender, D. H. and Lavender, J. D., An NDT audit—What to expect, *Br. J. NDT*, July, 264–265 (1987).
 13. Weymueller, C. R., NDT builds safety into a nuclear plant, *Welding Design Fabr.*, September, 54–57 (1982).
 14. NDT feature-testing triggers big savings, *Welding Design Fabr.*, February, 31–39 (1975).
 15. BS 6143-1:1992, Guide to the economics of quality—Process cost model, British Standards Institution, 1992.
 16. Zairi, M., *Total Quality Management for Engineers*, Aditya Books, New Delhi, India, 1992.
 17. Nicholson, R. D. and Hemsworth, B., Assessment of nuclear reactor fabrication: A regulatory view, *Weld. World*, 30, 126–129 (1992).
 18. Yokell, S., *A Working Guide to Shell-and-Tube Heat Exchangers*, McGraw-Hill, New York, 1990.
 19. Craig, W. R., Refineries test their metals, *Welding Design Fabr.*, April, 81–85 (1977).
 20. TEMA, *Standards of Tubular Exchanger Manufacturers Association*, 9th edn., Tubular Exchanger Manufacturers Association, Tarrytown, NY, 2007.
 21. Nichols, R. W., Golden rules for nondestructive examination, *Metal Constr.* 12, May (1980).
 22. Frew, J. A., Lloyd's approach to quality assurance of welded structures, *Welding Metal Fabr.*, August, 256–260 (1974).
 23. *Guide for the Visual Inspection of Welds*, ANSI/AWS B1.11:2000, American Welding Society, Miami, FL, 2000, p. 30.
 24. Vackar, B. K., Satisfying codes, *Welding Design Fabr.*, June, 86–87 (1977).
 25. Harrison, J. D. and Young, J. G., A rational approach to weld defect acceptance levels and quality control, *Welding Metal Fabr.*, October, 367–371 (1973).
 26. Mercer, W. L., NDT—A vital force in engineering, *Br. J. NDT*, January, 11–14 (1987).
 27. Raj, B. and Subramanian, C. V., Nondestructive testing—Welding industry, in *Welding Engineering Handbook*, Vol. I (S. Sundarajan, S. Vijaya Bhaskar, and G. C. Amarnath Kumar, eds.), Welding Research Group, Radiant Publications, Secunderabad, India (1990).
 28. *Guide for the Nondestructive Inspection of Welds*, ANSI/AWS B1.10–99, American Welding Society, Miami, FL, 1999.
 29. Hayes, C., The ABC's of nondestructive weld examination, *Welding J.*, May, 46–51 (1997).
 30. Robert, R. L. and Crane, W. D., Nondestructive inspection, Chapter 24, in *Handbook of Materials Selection* (M. Kutz, ed.), John Wiley & Sons, Inc., New York, 2002.
 31. Dunn, F. W., Magnetic particle inspection fundamentals, *Mater. Eval.*, December, 42–47 (1977).
 32. Hamlet, R. A. and Lavender, D. H., Standardisation within the writing of the NDT procedure, *Br. J. NDT*, 359–360 (1986).
 33. Litting, B. G., N.D.T. methods and assessment of weld defects, *Welding Metal Fabr.*, 435–440 (1967).
 34. Boving, K. G., ed., *NDE Handbook, Nondestructive Examination Methods for Condition Monitoring*, Butterworths, London, U.K.
 35. Bauer, L., Visual inspection: Looking ahead, *Welding Design Fabr.*, September, 31–32 (1991).
 36. Miller, J. S., Inspect tubes and pipes with mini-TV cameras, *Welding Design Fabr.*, October, 84–86 (1979).
 37. Lang, W. J., Eyeballing welds with a borescope, *Welding J.*, June, 61–62 (1990).
 38. Betz, C. E., *Principles of Penetrants*, Magnaflux Corp., Chicago, IL, 1963.
 39. Selner, R., Dye penetrant and magnetic particle inspection, *Welding J.*, February, 28–31 (1982).
 40. (a) Kevin, W., Guide to liquid penetrant testing, *Welding J.* (Suppl), Nondestructive Examination, October, 21–23 (1997); (b) Lebowitz, C. A., A primer on nondestructive examination methods for weld inspection, *Welding J.* (Suppl), Nondestructive Examination, October, 29–31 (1997).
 41. Heine, H. J., Liquid penetrant and magnetic particle inspection, *Foundry Manage. Technol.*, July, 36–39 (1991).
 42. Lovejoy, D. J., Standardisation of light levels for magnetic and penetrant inspection, *Br. J. NDT*, 36, 8–9 (1994).
 43. Brown, F. and Howes, I., NDT methods and equipment for the quality fabrication shop, *Welding Metal Fabr.*, 611–618 (1977).
 44. Jefferson, T. B., Welder certification: What does it mean? *Welding Design Fabr.*, June, 66–68 (1981).

45. Hellier, C. J., What's new in nondestructive testing of welds and heat affected zones? *Welding J.*, March, 39–43 (1993).
46. Banks, B., Problems of quality control in the manufacture of pressure vessels, *Welding Metal Fabr.*, July, 241–246 (1972).
47. Welding Engineer Data Sheet, No. 468—Troubleshooting guide for radiographs, *Welding Design Fabr.*, September, 79 (1979).
48. Litting, B. G., Quality control of welded components, *Welding Metal Fabr.*, July, 294–297 (1967).
49. Carson, H. L. and Feaver, M. J., An improved means for the measurement of weld radiograph image quality, *Welding Metal Fabr.*, January, 29–36 (1973).
50. Garrett, W. R., Reading radiographs takes time and patience, *Welding Design Fabr.*, September, 77–79 (1979).
51. Hellier, C., Weld inspection—Today and tomorrow, *Welding Design Fabr.*, September, 78–81 (1977).
52. Murray, S. H., Computed tomography used in weld inspections at NASA, *Welding J.*, February, 33–36 (1990).
53. Whritnour, R., Radioscopy speeds inspection, *Welding Design Fabr.*, September, 24–25 (1992).
54. Carl, R. W., Ultrasonic testing for the fabricator, *Welding Design Fabr.*, October, 25–33 (1994).
55. Anjard, R. P., Fundamentals of ultrasonic testing, *Heat Treating*, April, 34–38 (1978).
56. Fortunko, C. M. and Schramm, R. E., Ultrasonic nondestructive evaluations of butt welds using electromagnetic-acoustic transducers, *Welding J.*, February, 39–46 (1982).
57. Watson P. D., Design for welding examination, *Welding J.*, February, 32–35 (1982).
58. Ultrasonic signals, document no. 11S/11W-850–86, The Welding Institute, Abington, Cambridge, U.K.
59. Meyer, H.-J., Estimating flaw size in pressure vessel welds, *Welding Design Fabr.*, November, 78–81 (1977).
60. Hansen, B., A rational approach to NDT of welds, *Welding Design Fabr.*, May, 64–67 (1977).
61. Ehlman, W. G., Acoustical holography looks through welds, *Welding Design Fabr.*, February, 68–70 (1977).
62. Lenain, J.-C., General principles of acoustic emission, *Mater. Eval.*, October, 1000–1002 (1981).
63. Miller, R. K. and McIntire, P., eds., *Nondestructive Testing Handbook, Vol. 5, Acoustic Emission Testing*, 2nd edn., American Society for Nondestructive Testing, Columbus, OH, 1987.
64. Debel, C. P., *Proceedings of the Fifth Riso International Symposium on Metallurgy and Material Science*, Riso National Laboratory, Roskilde, Denmark, 1984, p. 19.
65. Raj, B. and Jha, B. B., Fundamentals of acoustic emission, *Br. J. NDT*, 36, 16–23 (1994).
66. Prine, D. W., Inspect as you go with acoustic emission, *Welding Design Fabr.*, January, 74–77 (1977).
67. Clark, J. N., The detection of creep failure at welds by acoustic emission, Part 1: Brittle creep rupture, *Br. J. NDT*, January, 9–21 (1982).
68. Kalyansundaram, P., Raj, B., Kasiviswanathan, K. V., Jayakumar, T., and Murthy, C. R. L., Leak detection in pressure tubes of a pressurised heavy water reactor by acoustic emission technique, *Br. J. NDT*, 34(11), 539–544 (1992).
69. Granville, R. K., In-service eddy current examination of nonferrous industrial heat exchanger tubing, *Br. J. NDT*, 33, 403–409 (1991).
70. Cecco, V. S., Franklin, E. M., Houser, H. E., Kincaid, T. G., Pellicer, J., Hagemier, D., Eddy current inspection, Lampman, S. R. and Zorc, T. B., (eds.), in *Metals Handbook, Vol. 17, Nondestructive Evaluation and Quality Control*, 9th edn., ASM, Metals Park, OH, 1989, pp. 164–194.
71. Clark, W. G., Multiple-element eddy current probes for enhanced inspection, *Mater. Eval.*, July, 794–802 (1993).
72. Bergander, M. J., Flux leakage examination of ferrous heat exchanger tubing, *Mater. Eval.*, June, 811–812 (1986).
73. Fisher, J. L., Remote field eddy current inspection, in *Metals Handbook, Vol. 17, Nondestructive Evaluation and Quality Control*, 9th edn., American Society for Metals, Metals Park, OH, 1989, pp. 195–201.
74. Atherton, D. L., Frey, P., and Guo, X., Remote field slit defect responses, *Br. J. NDT*, 36, 4–7 (1994).
75. Neumaier, P., Testing heat exchanger tubes using eddy current techniques with computerised signal analysis, *Br. J. NDT*, September, 233–237 (1983).
76. Stepinski, T. and Maszi, N., Conjugate spectrum filters for eddy current signal processing, *Mater. Eval.*, July, 839–844 (1993).
77. McMaster, R. C., ed., *Nondestructive Testing Handbook, Vol. 1, Leak Testing*, 2nd edn., American Society for Nondestructive Testing and American Society for Metals, Columbus, OH.
78. Anderson, G. L., Leak testing, in *Metal Handbook, Vol. 17, Nondestructive Evaluation and Quality Control*, 9th edn., American Society for Metals, Metals Park, OH, 1989, pp. 57–70.

BIBLIOGRAPHY

BSI Handbook 22: 1983 Quality Assurance, British Standards Institution, London, U.K.

Connor, L. P., ed., Chapter 11, Weld quality, Chapter 12, Testing for evaluation of welded joints, Chapter 13, Codes and standards, in *Welding Handbook, Vol. 1, Welding Technology*, 8th edn., American Welding Society, Miami, FL, 1987.

Emerson, W. F., Technology reinvents visual inspection, *Welding Design Fabr.*, May, 31–32 (1995).

Erickson, K. D., Defining the role of a certified visual inspector, *Welding J. Suppl. Nondestruct. Examination*, October, 17–19 (1997).

Hingwe, A. K., Compiler, *Quality Control Source Book—Application of QC to Ferrous Metalworking*, American Society for Metals, Metals Park, OH.

Betz, C. E., *Principles of Magnetic Particle Testing*, Magnaflux Corp, Chicago, IL, 1966.

Jackson, D., ISO 9000: Key to Europe's door, *Welding Design Fabr.*, April, 59–60 (1992).

Kirwillian, A., The true cost of quality, *Welding Metal Fabr.*, January/February, 5–8 (1987).

Krautkramer, J. and Krautkramer, H., *Ultrasonic Testing of Materials*, Section 8.6, 4th edn., Springer-Verlag, New York, 1990.

Lebowitz, C. A., A primer on nondestructive examination methods for weld inspection, *Welding J. Suppl. Nondestruct. Examination*, October, 29–31 (1997).

Libby, H. L., *Introduction to Electromagnetic Nondestructive Test Methods*, Wiley-Interscience, New York, 1971.

McGonnagle, W. J., *Nondestructive Testing*, McGraw-Hill, New York, 1961.

Mikulak, J., Viewpoints on quality, codes, conversions, and pipelines, *Welding Design Fabr.*, March, 70–73 (1977).

Radiography in Modern Industry, 4th edn., Eastman Kodak Co., Rochester, NY, 1980.

Richardson, H. D., *Industrial Radiography Manual*, Government Printing Office, Washington, DC, 1968. Reprinted in 1979 by the American Society for Nondestructive Testing.

Ultrasonic inspection, in *Metals Handbook, Vol. 17, Nondestructive Evaluation and Quality Control*, 9th edn., American Society for Metals, Metals Park, OH, pp. 231–277, 1989.

Waker, K., Guide to liquid penetrant testing, *Welding J. Suppl. Nondestruct. Examination*, October, 21–23 (1997).

Welding Engineer Data Sheet No. 414—Effectiveness of nondestructive testing methods, *Welding Design Fabr.*, February, 41 (1975).

Weldments, brazed assemblies, and soldered joints, in *Metals Handbook, Vol. 17, Nondestructive Evaluation and Quality Control*, 9th edn., American Society for Metals, Metals Park, OH, pp. 582–609, 1989.

Weymueller, C. R., Ultrasonic testing for the fabricator, *Welding Design Fabr.*, October, 25–33 (1994).

15 Heat Exchanger Fabrication

15.1 INTRODUCTION TO FABRICATION OF THE SHELL AND TUBE HEAT EXCHANGER

With advances in material and welding technology, fabrication processes today call for high standards of understanding and workmanship. Equipment made with materials of correct choice and quality and adequate design may fail in service if the workmanship is sacrificed during fabrication [1]. It is needless to say that failure of any heat exchanger in service due to bad manufacturing practices, apart from causing loss of production, may cause accidents and damage to the equipment and property. Therefore, in industries where heat exchangers are to be made as per code, it is essential that the product quality be controlled at all stages of its manufacture.

The detailed methods of shop floor practices are left to the discretion of the manufacturer in conformity with TEMA Standards [2]. The applicable construction code is ASME Code Section VIII, Div. 1 [3]. The manufacturer shall submit for purchaser's approval three prints of an outline drawing showing overall dimensions, nozzle sizes and locations, supports, and weight. The purchaser's approval of drawings does not relieve the manufacturer of responsibility for compliance with TEMA Standard and applicable code.

In any type of manufacturing, the general fabrication methods used are forming, drawing, stretching, rolling, bending, shearing, welding, brazing, grinding, etc. All these methods can introduce residual stresses, which may impair the service life of the component or system during operation. Hence good engineering practices are to be used to keep the residual stress to the minimum. This section details standard shop floor practices for fabrication of heat exchangers.

15.2 DETAILS OF MANUFACTURING DRAWING

Manufacturing drawings for heat exchanger fabrication should contain some additional details than any other engineering drawing. Such additional details for the fabrication of heat exchangers are listed by Rao [4]. Some of the details pertaining to welding and testing plan are [4] as follows:

1. Name plate location and details
2. Weld line orientations and locations, weld profiles, and sizes
3. Testing plan indicating the tests to be conducted on welds, and assemblies such as NDT test, destructive tests, hydrostatic testing/pneumatic testing, etc.
4. Welding plan to show WPS reference to each weld
5. Technical delivery conditions of materials
6. Edge preparation and method employed
7. Electrodes with equivalent AWS specifications
8. Welding methods to be employed
9. Code certification and stamping requirements as indicated in the purchase order
10. Maximum allowable working pressure (MAWP)
11. Design pressure

12. Hydrostatic test pressure
13. Operating temperature
14. Design temperature
15. Minimum design metal temperature

15.2.1 ADDITIONAL NECESSARY ENTRIES

Rao [4] recommends the following additional entries in the drawing:

- Code requirements
- Volume of pressure chambers
- Special loadings
- Corrosion allowance
- Joint efficiency
- Joining method other than welding (e.g., brazing, adhesive bonding, rolling-in of tubes)
- Surface treatment (e.g., painting, pickling, coating, lining)
- Inspection authority
- Instructions for the jobsite (e.g., assembly weld)

15.3 STAGES OF HEAT EXCHANGER FABRICATION

The main stages of heat exchanger manufacture are as follows [1]:

1. Identification of materials
2. Edge preparation and rolling of shell sections, tack welding, and alignment for welding of longitudinal seams (LSs)
3. Welding of shells, checking the dimensions, and subjecting pieces to radiography
4. Checking the circularity and the assembly fit ups, including nozzles
5. Tubesheets and baffles drilling
6. Tube bundle assembly and insertion of the assembly into the shell
7. Tubesheet to shell welding
8. Tube-to-tubesheet joining by rolling/welding
9. Assembly of channel with shell assembly
10. Hydrostatic testing and stamping
11. Preparation for shipment
12. Preparation of data folder

A flowchart (Figure 15.1a), assembly sequence (Figure 15.1b), inspection plan for heat exchanger components (Figure 15.1c) for the manufacture of a fixed tubesheet heat exchanger is shown in Figure 15.1. Stage-wise inspection plan (i.e., quality assurance program) is given in Appendix. (Refer to Section 14.1.6 for more details on operation process sheet of shell and tube heat exchanger manufacture.)

15.3.1 IDENTIFICATION OF MATERIALS

Identification includes a job number, serial number, and heat number, if relevant. Throughout production, identification follows the material or component, assuring traceability [5]. The certified plates fall into two categories. One type certifies the physical and chemical properties, while the other type, in addition to chemical and physical properties, also certifies soundness of material by ultrasonic tests. Ultrasonic tests are used to detect defects such as lamination, porosity, and slag inclusions.

15.3.2 EDGE PREPARATION AND ROLLING OF SHELL SECTIONS, TACK WELDING, AND ALIGNMENT FOR WELDING OF LONGITUDINAL SEAMS

15.3.2.1 General Discussion on Forming of Plates

In general, the forming of plates in the pressure vessel industry covers the bending of plates into shell courses/belts and spinning and pressing of circular plates to form vessel heads. The most critical factors governing the cold forming of a shell course in a given material are (1) the plate thickness and (2) the final diameter of the finished cylinder. Therefore, the radius of bending is limited to a maximum percentage strain in the outer fiber in the range of 3%–4.5% without an intermediate annealing or stress relief [6]. According to Peacock [6], since local straining during cold bending may cause higher values of strain in localized areas, in practice, a factor of safety is

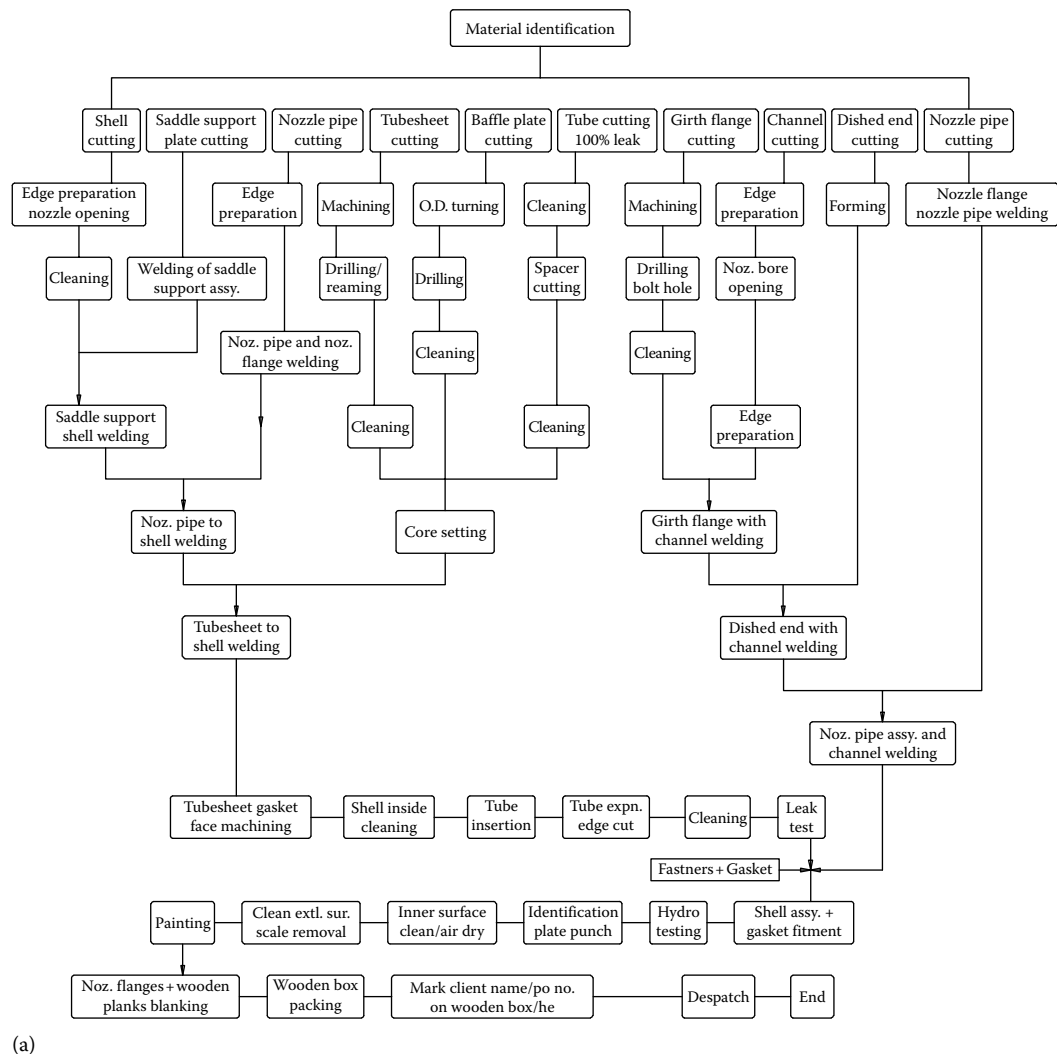


FIGURE 15.1 Manufacture of fixed tubesheet shell and tube heat exchanger. (a) Flowchart (Courtesy of Universal Heat Exchangers Ltd., Coimbatore, India)

(continued)

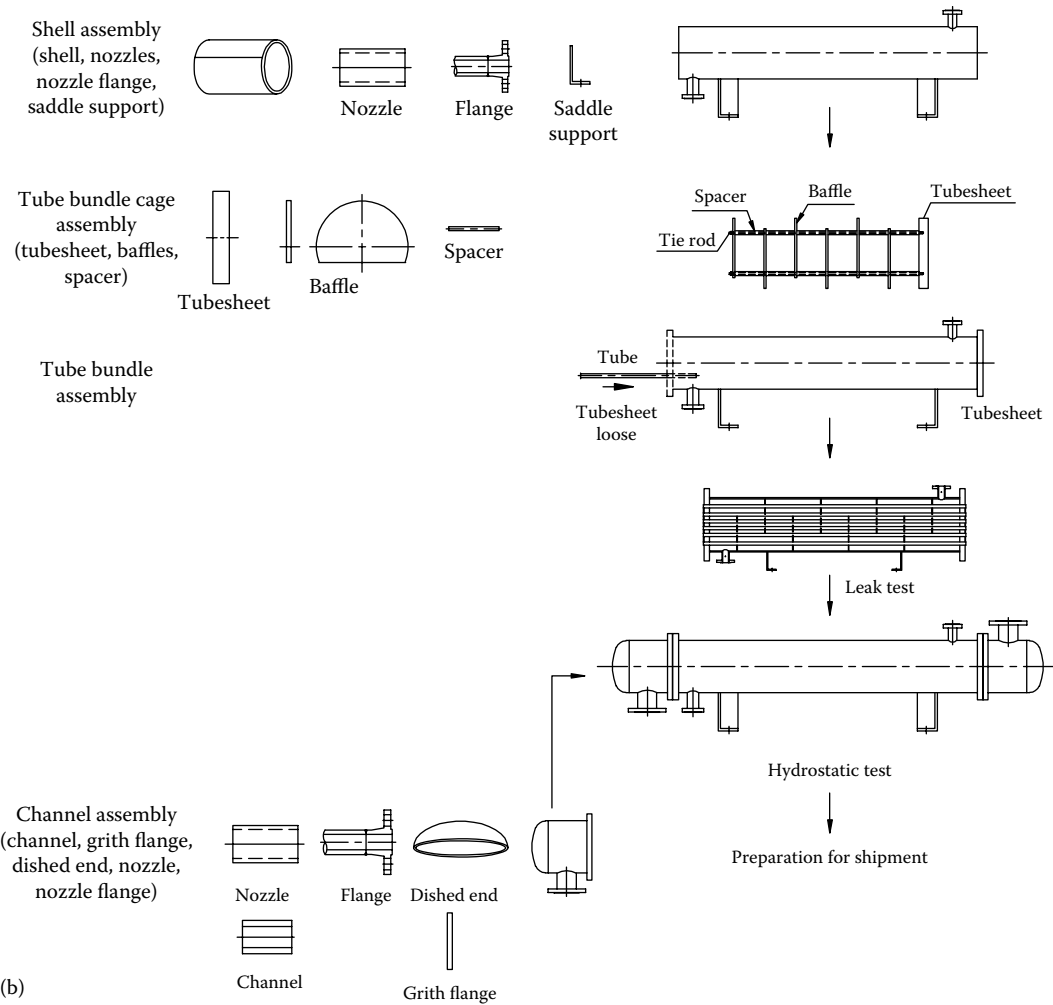


FIGURE 15.1 (continued) Manufacture of fixed tubesheet shell and tube heat exchanger. (b) assembly sequence

adopted to limit the strain in the outer fibers to 2%–2.25%. The strain ϵ on the outer fibers of the shell has been calculated by Carpenter and Floyd [7] as follows:

$$\epsilon = \frac{R_1 R_2 - 0.5 R_1 t}{R_1 R_2 - 0.5 R_2 t} - 1 \tag{15.1}$$

where

- R_1 is the final radius
- R_2 is the initial radius (for a flat plate use a value of 1000 in.)
- t is the thickness of plate

After forming the shell/dished ends, the manufacturer should examine them to make certain that they conform to the prescribed shape/contour and meet the thickness requirements after forming.

INSPECTION & TEST REQUIREMENT FOR VESSELS & HEAT EXCHANGERS

NOMENCLATURE @-Required RT – Radiographic UT – Ultrasonic ET – Eddy Current MT – Magnetic Particle PT – Liquid Penetrant		Heat Exchanger/Vessel Parts								Weld joint categories				
		Major parts						Accessories		A	B	C	D	E
		Plates	forgings	Pipes & tubing	Bolts & nuts	gaskets	Bottom\Support plate	Parts welded to shell/head	Foundation bolts	Others				
Materials	Insp & test as per code/standard, PMI ¹													
	High temp. tensile test at design temp													
	Impact test													
	Hardness test													
	UT													
	ET													
	MT													
PT														
Transfer of identification marks														
Welding procedure qualification test	Transverse tensile test													
	All weld metal tensile test													
	High temp. tensile test at design temp													
	Bending test													
	Impact test													
	Hardness test													
	Macro test													
Micro test														
Production weld test	Transverse tensile test													
	All weld metal tensile test													
	High temp. tensile test at design temp													
	Bending test													
	Impact test													
	Hardness test													
	Macro test													
	Micro test													
Prewelding	Weld preparation													
	Fit up for butt weld													
	After back gauging													
Inspection on the weld	Visual inspection													
	RT													
	UT													
	MT													
	PT													
	Hardness test													
Vacuum box test														
Completed eqpt	Visual inspection													
	Dimensional inspection													
	Hydrostatic test													
	Leakage test													
Note:														
¹ PMI–positive metal identification.														

FIGURE 15.1 (continued) Manufacture of fixed tubesheet shell and tube heat exchanger. (c) inspection plan for heat exchanger components.

15.3.2.2 Fabrication of Shell

As per TEMA section RCB-3, the heat exchanger shell should be fabricated from either commercially available seamless or welded wrought pipe or from plate rolled into a longitudinally fusion-welded cylinder. In the case of rolled shells, the certified plates are put into inspection after marking the sizes as per drawing requirements. The inspector will stamp the plates with a monogram and allow for cutting.

The cutting process includes machining or gas cut or plasma arc cut. Aluminum alloy plates are mechanically cut, using midsaw, bandsaws, portable handsaws, or guillotines; stainless steel is either sawn, guillotined, or cut by the plasma cutting process. Gas-cut plate edges are then machined for weld preparation. After cutting the plates to size and edge preparation, the edges of plates should be examined for defects like cracks and lamination. The plates are then rolled to the required dimensions. Edge preparation is a critical factor in the production of high-quality joints and in the making of sound welds. Inadequate preparation, resulting in irregular plate edge or rough Vformation, prevents close fit, which is essential for quality joints and makes the task of the welder more difficult [8].

Rolling of plates should be in the transverse direction of the plates (as shown in Figure 13.4). The direction should be marked on the plates. A typical rolling of shell plate is shown in Figure 15.2.

For LS welding, the rolled section is held in position by tack welding. The width, length, and thickness of the tack welds are critical. A very thin tack has an effect similar to arc strike, and this local position will reveal cracks from high carbon martensite due to rapid cooling [1]. Therefore, tacks should have sufficient metal deposition. For satisfactory welding, cleanliness of the edges to be welded is essential.

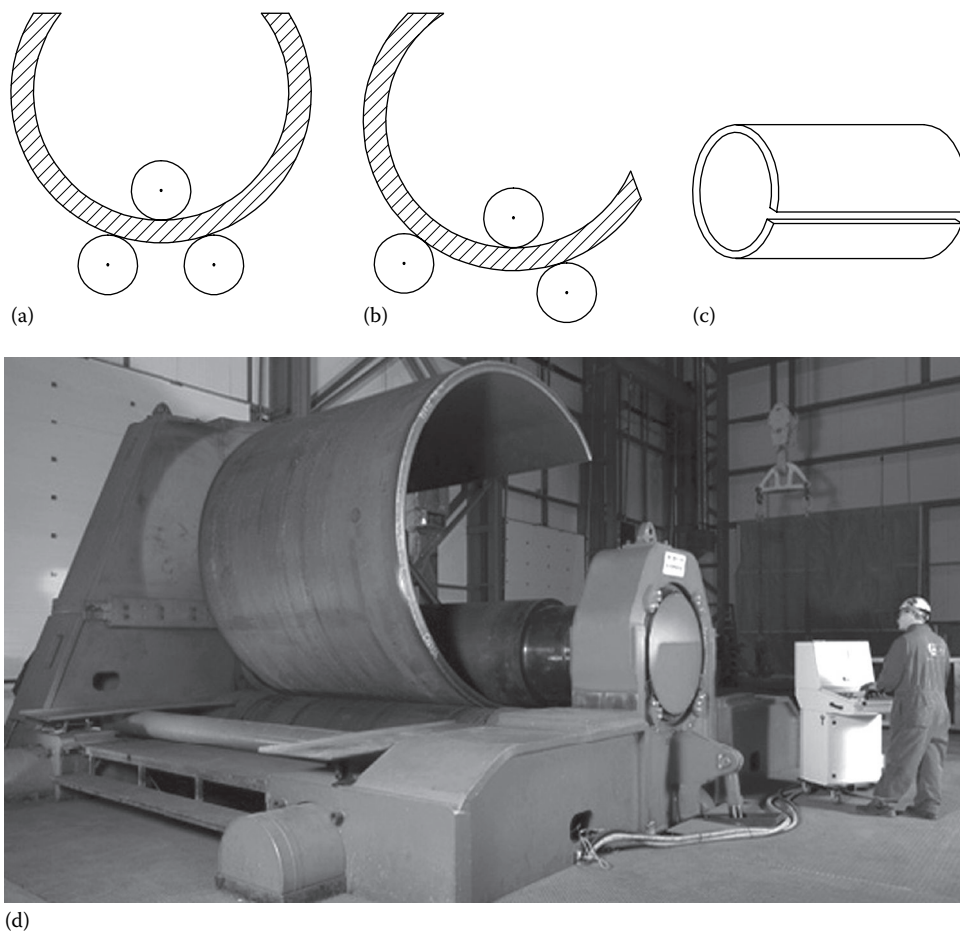


FIGURE 15.2 (a–c) Rolling of shell plate (schematic). (d) Rolling of shell plate. (Courtesy of Edmonton Exchanger & Manufacturing Ltd, Edmonton, Alberta, Canada.)

15.3.3 PLATE BENDING MACHINES, PWHT, AND MANIPULATIVE EQUIPMENT

15.3.3.1 Roll Bending Machine

Mechanical and hydraulic three-roll plate bending machines are appropriate for the hot rolling of heavy plate. A four-roll bending machine offers production advantages, although it is not particularly suited to hot work [9].

15.3.3.2 Vertical Plate Bending Machine

The vertical plate bending machine can be used for all ASME Code pressure vessel work, and results are claimed to be as good as or better than those obtained with horizontal plate bending rolls. Some of the advantages claimed for vertical roll bending include the following [9]: (1) absence of camber in the rolled shell, (2) higher capacity and hence thicker plates can be rolled, (3) less power consumption, (4) the weight of the plate has very little effect on the bending accuracy, and (5) the mill scale experienced on many plates drops clear during the bending operation, whereas in horizontal machines it tends to get rolled into the plate surface.

15.3.3.3 PWHT of Shells

Use spider bracing for adequate support during the stress-relieving operation, and thermocouples are fastened to the vessel internally and externally. Temperatures are closely monitored and controlled during the period of temperature raising, soaking, and relaxing. Test plates inserted both inside and outside the vessel during stress relieving are later tested to ensure that the plate has been returned to its proper ductility and tensile strength [10].

15.3.3.4 Manipulative Equipment

In the fabrication of heat exchangers, rotator sets or turning rolls are utilized to manipulate the shell for various welding positions. They ensure smoother welds. Circumferential welding is carried out by providing for the components to be rotated on the roller manipulator on the support bed. Basically, these comprise two types [11]: (1) self-aligning rotators and (2) conventional rotators. Self-aligning rotators consist of rubber-tired wheels that automatically align themselves to the change from one diameter of vessel to another. In the case of conventional rotators, the rolls have to be manually positioned across the frames to suit the diameter of the vessel.

15.3.4 WELDING OF SHELLS, CHECKING THE DIMENSIONS, AND SUBJECTING PIECES TO RADIOGRAPHY

After tack welding, the shell section is ready for LS welding. During shell welding, spiders are tacked internally to avoid distortion of the shell. The welding is first done from one side. The other side is back chipped or gouged and offered for inspection. The inspector examines the area for the weld metal penetration, oxidized metal removal, and the weld free from weld defects. In very large or thick-walled vessels, the shell course may be fabricated from two or more curved plates and joined by several LS welds (Figure 15.3) [12]. Before the assembly of circumferential joints, each shell course should be checked for shell thickness, inside diameter, and circularity, and shell sections may be rerolled if necessary. If any rerolling is required, it should be done before radiography, and all LSs should be dye penetrant tested after rerolling. Check the curvature using a sweep board. Circumferential welding is carried out by providing for the components to be rotated on the roller manipulator. While welding two shell sections circumferentially, the LSs of the adjacent shell courses should not be aligned. After welding the various shell courses, the circumferential seams are subjected to radiography. If any portion of the weld is found defective, it should be repaired and inspected. (Girth, longitudinal, and nozzle attachment welds in exchanger shall be full penetration weld.)

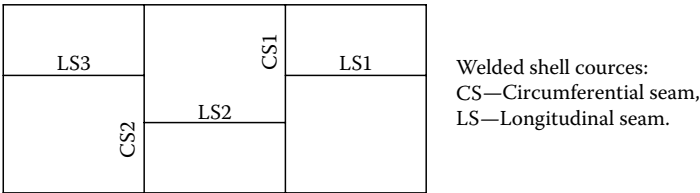


FIGURE 15.3 Welded shell courses (CS, circumferential seam and LS, longitudinal seam).

15.3.5 CHECKING THE CIRCULARITY OF THE SHELL AND THE ASSEMBLY
FIT, INCLUDING NOZZLES AND EXPANSION JOINTS

The ovality of the shell should be kept as low as possible, and the shell should be free from flat spots and projections from weld seams and nozzles. Check the positions of connections, supports, expansion joints, and all appurtenances relative to the working points [13]. The clearance between the baffles and the shell shall be as specified in the drawings. Excessive clearances would decrease the heat transfer efficiency of the exchanger; inadequate clearance will pose a problem when inserting tube bundle. Measure the shell length at the quarter points and the nozzle and support base distances to the shell centerline. To avoid difficulty in insertion of the bundle, a pull-through gauge as shown in Figure 15.4 is passed through the shell [14].

Certain advance preparation is necessary while fabricating the shell. For correcting the ovality and weld distortion, and for baffle gauge checking, suitable fixtures, spiders, and innovative devices

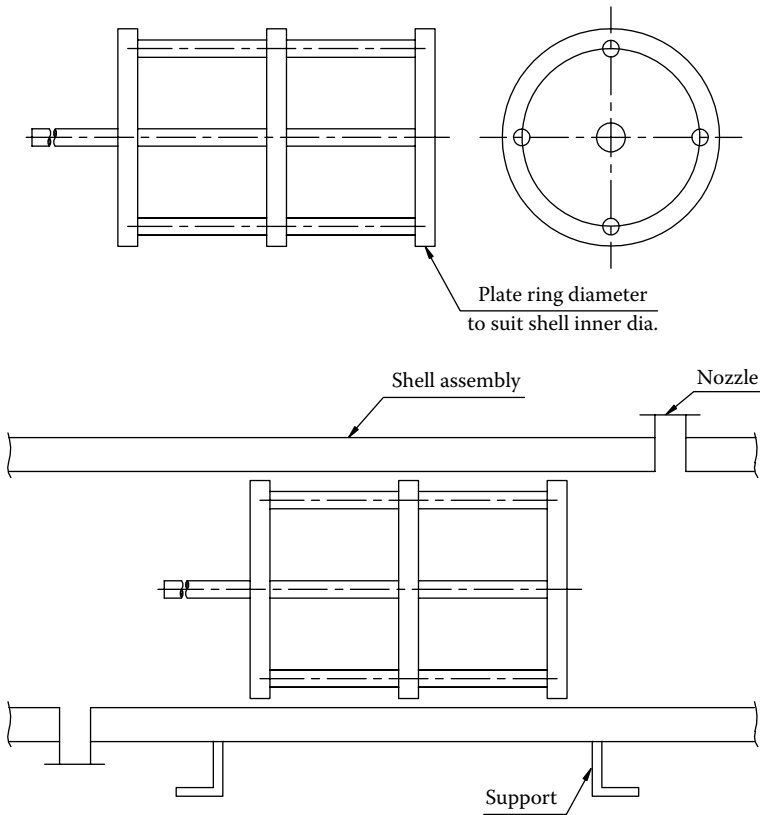


FIGURE 15.4 Pull-through gauge to check the circularity of heat exchanger shell. (a) Schematic and (b) gauge passing through the shell assembly.

for specific type of exchanger are to be developed and kept in advance to avoid unnecessary hammering, heating, and grinding, which reduce the quality of material and weldment. In a big company manufacturing large numbers of exchangers and pressure vessels, standardization of components like elbows, flanges, nozzles, reinforcement (RF) pad designs, and edge preparation is required. This leads to smooth flow of material.

15.3.5.1 Welding of Nozzles

After completion of the shell, mark the shell for the nozzle locations, cut open, prepare edges, fit the RF pad and the nozzle, weld and subject the welds of RF pad for leak test, and examine by penetrant/magnetic particle test. Inspection of back-gouged welded joints by magnetic particle or liquid penetrant examination techniques is especially important for joints of set-in nozzles, which are not readily radiographed following welding. Most shops use a special-purpose submerged arc welding machine. The welding is through the entire thickness of the shell plate. If the component to which nozzles are attached is subsequently stress relieved, it is the fabricator's responsibility to maintain true gasket faces by machining or otherwise. A typical welding of a set-through nozzle is shown in Figure 15.5.

15.3.5.2 Supports

Supports for horizontal exchangers shall comply with the standard drawing attached or as shown in the equipment drawing. When it is important, the consignee will indicate which support shall be fixed and which support shall be sliding, otherwise the vendor shall indicate this on his proposal drawing supports welded to the heat exchanger shall not interfere with inspection of heat exchanger circumferential seams.

15.3.5.3 Attachment of Expansion Joints

Fabrication, inspection and pressure test, stamping, and reports for flanged-and-flued or flanged expansion joints shall conform to the requirements of Part UG and those of (a) through (g) of Appendix CC of ASME Code Section VIII, Div. 1. Some of the ASME Code requirements for the attachment of expansion joint are the following:

1. Flexible elements shall be attached by full-penetration circumferential welds.
2. Attachments such as nozzles and backing strips shall not be located in highly stressed areas such as inner and outer tori, and annular plate of the expansion joint, unless the welds are ground flush and fully radiographed.
3. The circumferential attachment welds between the expansion joint and the shell shall be examined 100% on both sides by penetrant/magnetic particle test.

Welding of an expansion joint and its inspection are shown in Figure 15.6.

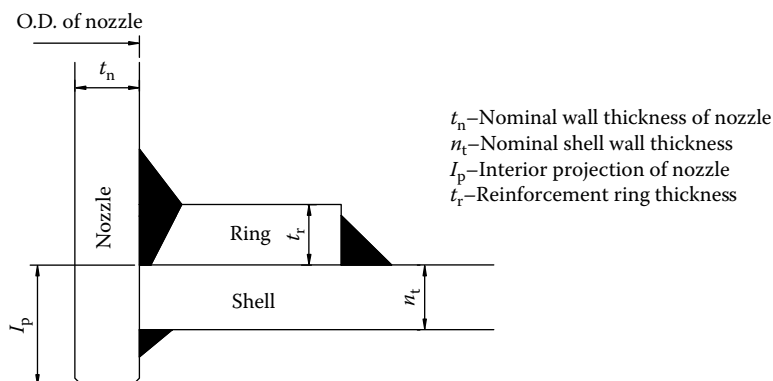


FIGURE 15.5 Welded set-through nozzle.



(a)



(b)



(c)

FIGURE 15.6 Welding of expansion joint with a heat exchanger shell. (a) Closer view (Courtesy of Mueller, Springfield, MO), (b) welding of the expansion joint after insertion of tube bundle (Courtesy of U.S. Bellows, Inc., Houston, TX, www.usbellows.com), and (c) inspection of expansion joint weld with heat exchanger shell. (Courtesy of U.S. Bellows, Inc, Houston, TX, www.usbellows.com.)

15.3.6 TUBESHEET AND BAFFLE DRILLING

15.3.6.1 Tubesheet Drilling

One of the major time-consuming factors in fabrication of heat exchanger lies in the marking out, drilling, reaming, and counterboring the holes in the tubesheets [15]. Most of the fabricators still use radial drilling machines for drilling of tubesheets and baffles. To avoid delays in this process and to achieve better tolerances on hole sizes and ligaments, use of numerical control drilling machine is recommended. Lubricating the holes is sometimes not allowed because the lubricant contaminates the tube-to-tubesheet joint. Holes must be reamed to get smooth finish. After reaming, examine the tubesheets for the tube count, pitch, and the tube layout pattern, which should match the drawings. Tube hole diameters and tolerances shall conform to TEMA Table RCB-7.41. Permissible tubesheet ligaments, drill drift, for the heaviest tube wall thicknesses shall conform to TEMA Table RCB-7-42.

15.3.6.2 Tube Hole Finish

The TEMA Standard (RCB-7.43) and other manufacturers' standards specify a "workman-like" finish for the inside surface of tubesheet holes. In general, tube hole finish ranges from somewhat smoother than 32 rms to the roughest permissible finish. The range of commercially supplied feedwater heater, heat exchanger, and condenser tubing surface finishes is usually 60–100 rms [13]. Inspect the holes using a high-intensity light and a magnifying lens. The surfaces of the holes should be uniform throughout and free of scores, longitudinal scratches,

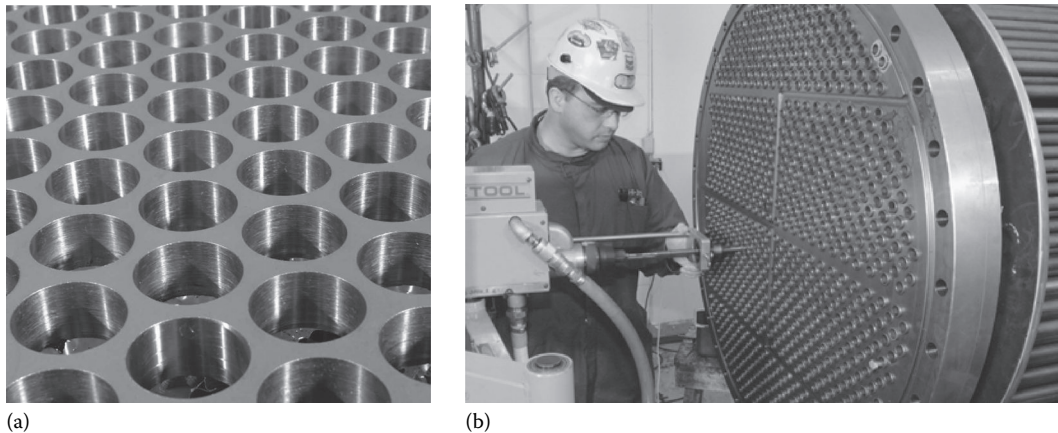


FIGURE 15.7 Drilled tubesheet. (a) A section of drilled tubesheet and (b) a tubesheet under tube rolling-in progress. (Courtesy of Edmonton Exchanger & Manufacturing Ltd, Edmonton, Alberta, Canada.)

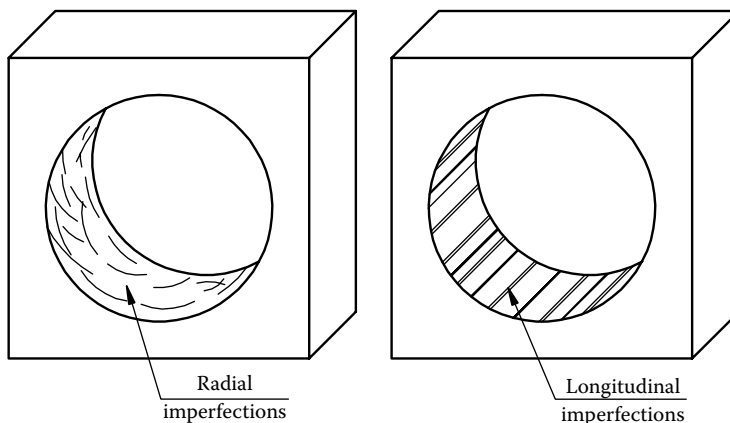


FIGURE 15.8 Surface imperfections in machined tubesheet. (Courtesy of Elliott Tool Technologies Ltd, Dayton, OH.)

spiral, annular, or axial tool marks. The inside edges of tube holes should be free from burrs to prevent cutting of tubes. A drilled tubesheet for shell and tube heat exchanger is shown in Figure 5.7. Schematic of tubesheet holes with radial and longitudinal imperfections is shown in Figure 15.8.

15.3.6.3 Drilling of Baffles

The complete set of baffles is bundled, and the bunch is held tightly with the help of clamps or by other suitable means. The holes in baffles are drilled as per TEMA Standards, that is 0.8 mm over outer diameter of tube for maximum unsupported length of 900 mm or less. Tube holes are drilled 0.4 mm over outer diameter of tubes for unsupported lengths more than 900 mm. After drilling the baffles, examine baffle holes carefully for burrs and projections on the back face created by the penetration of the drill. These must be removed. It is very important to note that no undersized holes are permitted, since retubing will be very difficult. Reject baffles in which more than 2% of the holes exceed the size limits of the standard [13]. Oversized holes can enhance fretting and wear due to flow-induced vibration and can also reduce the thermal performance. Make sure that the cuts match the drawing dimensions and are free from burrs.

15.3.7 TUBE BUNDLE ASSEMBLY

Tube bundle assembly consists of tubes, baffles, spacers, and tie rods. Before insertion, the ends of the tubes must be fine sandblasted to remove all traces of oxide and scale. Tube ends are trued by cutting and deburring of the excess length. The tubes must be degreased by a strong solvent for a distance of 1.5 times the thickness of the tubesheet [16]. For a fixed tubesheet exchanger, the tube bundle assembly is carried out by two methods: (1) assembly of tube bundle outside the exchanger shell and (2) assembly of tube bundle inside the shell. These methods are discussed next.

15.3.7.1 Assembly of Tube Bundle outside the Exchanger Shell

The sequences of operations are discussed in Chapter 14 with quality control, inspection, and NDT. Assembly of tube bundle outside the shell has better control on tie rod and baffles setup, and it is easy to insert the tubes. The drawback of this method is that tubes in the bundle are likely to be damaged while lifting and inserting. The assembly consisting of baffles, tie rods, and spacers with sealing strips, if any, is known as baffle cage assembly (Figure 15.9). A typical baffle cage assembly of Helixchanger® is shown in Figure 15.9a. Figure 15.10 shows a heat exchanger under tube

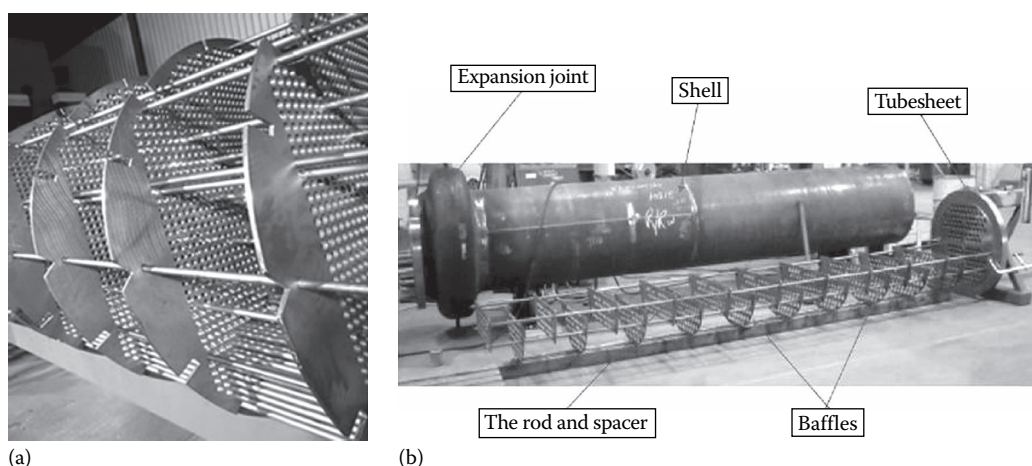


FIGURE 15.9 Heat exchanger assembly. (a) Helixchanger baffle cage assembly (Courtesy of Vermeer Eemhaven B.V., Rotterdam, the Netherlands) and (b) shell and tube heat exchanger under fabrication—baffle assembly is shown adjoining shell. (Courtesy of Festival City Fabricators, div. of CSTI, Stratford, Ontario, Canada.)

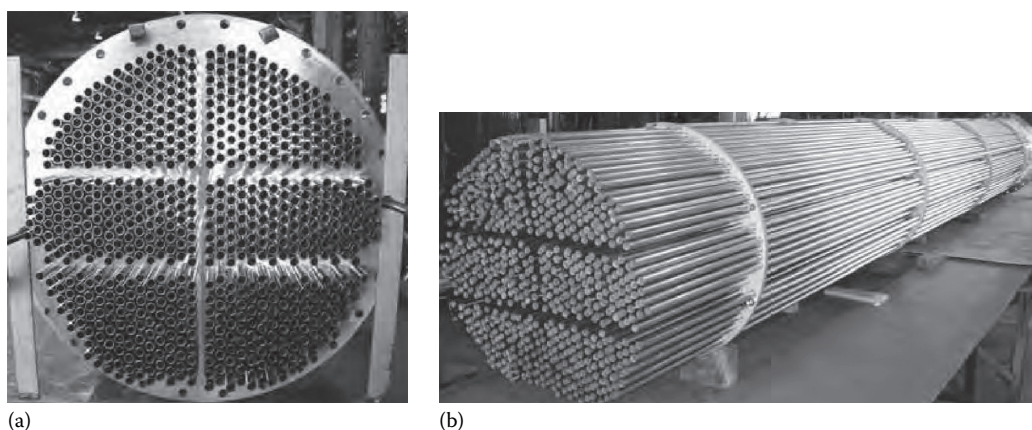


FIGURE 15.10 Tube bundle assembly. (a) Insertion of straight tubes through tubesheet and (b) tube bundle ready for insertion into the shell. (Photo courtesy of Mueller, Springfield, MO.)

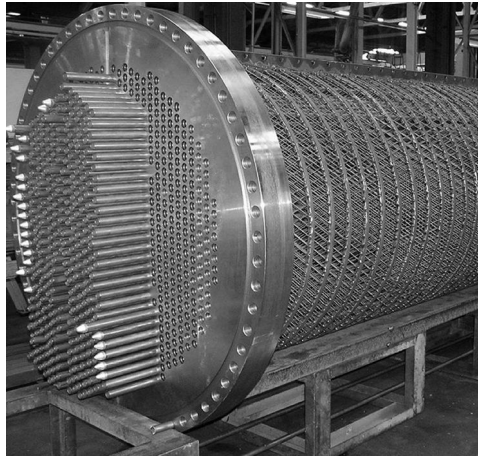
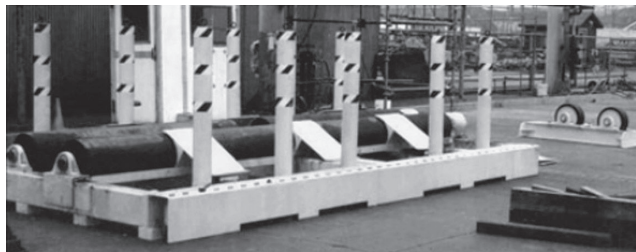


FIGURE 15.11 EMbaffle® tube bundle under assembly. The figure shows tubes with pilots. (Courtesy of Bronswerk Heat Transfer B.V., Nijkerk, the Netherlands. EMbaffle® is a registered trademark of EMbaffle B.V., Alphen a/d Rijn, the Netherlands. EMbaffle® Technology was developed by Shell Global Solutions International B.V. and since July 2012 owned by Brembana & Rolle S.p.A. (www.embaffle.com)).



(a)



(b)

FIGURE 15.12 Tube bundle handling devices. (a) Tube bundle rolls and (b) tube bundle lifter. (Courtesy of Powermaster Ltd, Mumbai, India.)

insertion and a completed tube bundle ready for insertion into a shell. Guide bullets in the leading end of the tube (as shown in EMbaffle heat exchanger, Figure 15.11) greatly assist the tubing operation [13,17]. Assembly of the tube bundle is carried out on a fixture, or tube rolls and/or the tube bundle is lifted using bundle lifter as shown in Figure 15.12 before insertion into a shell. Many times, the tube bundle is moved on trolley (or rolls) before inserting into a shell (Figure 15.13). If the tube bundle is heavy, about 10% of the tubes are inserted on the periphery of the tubesheet to make the baffle assembly true vertical, and the partially assembled tube bundle is inserted into the shell. Remaining tubes are inserted after welding the tubesheet to the shell. For easy insertion of

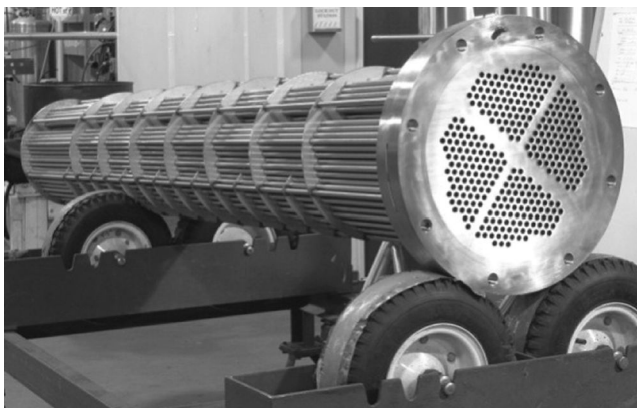


FIGURE 15.13 Completed tube bundle assembly placed on rolls/trolley. (Courtesy of Allegheny Bradford Corporation, Bradford, PA.)

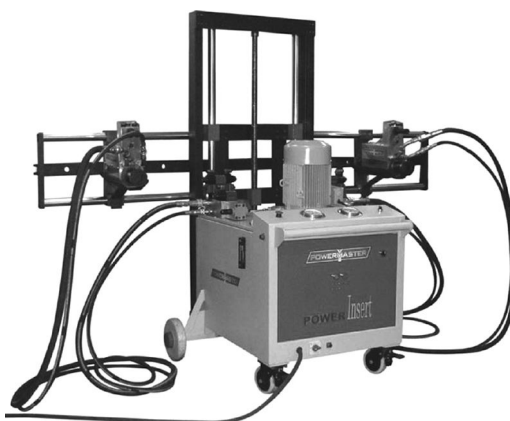


FIGURE 15.14 Tube bundle inserter for heat exchanger. (Courtesy of Powermaster Ltd, Mumbai, India.)

tube bundle inside the shell, devices such as tube bundle inserter are readily available in the market. Typical tube bundle inserter is shown in Figure 15.14.

15.3.7.1.1 Impingement Baffles

When impingement baffles are welded to tie rod or spacers, they shall be supported by at least two tie rods or spacers. Minimum thickness of impingement baffles shall be 6 mm for carbon and low-alloy steel and 3 mm for high-alloy steel and nonferrous or as per standard.

15.3.7.2 Assembly of Tube Bundle inside the Shell

To avoid the risk of tubes getting damaged in the case of the bundle assembled outside, some fabricators prefer to assemble tubes inside the shell. Normally, this method is possible when the shell inside diameter is sufficiently large for a person to go inside and arrange tie rods with tubesheet and baffles. The assembly procedure is shown schematically in Figure 15.15, and the sequence of operations is [14] as follows:

1. The operator will go inside the shell and arrange the baffle assembly by fixing the tie rods with the tubesheet. Insert a few tubes on the periphery to true up the baffle assembly.
2. Inspect the assembly and tack the nuts wherever required.

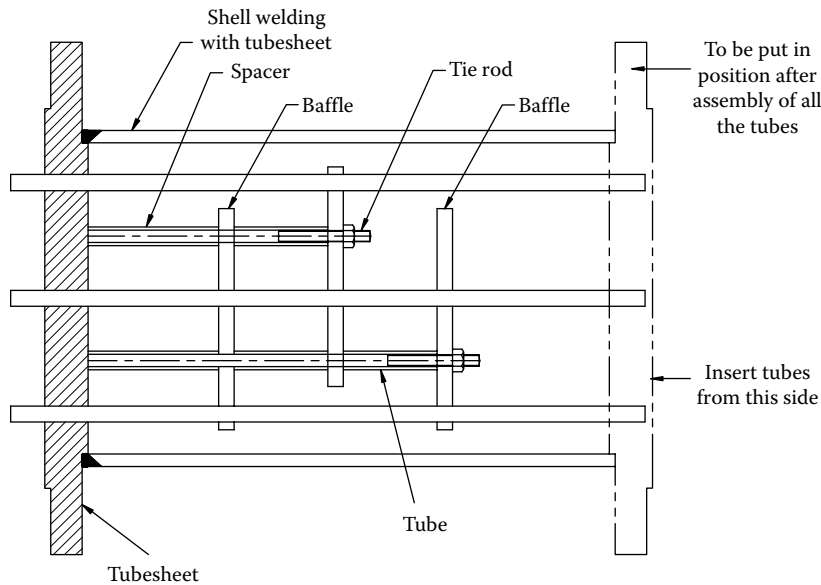


FIGURE 15.15 Scheme for assembly of tube bundle inside the shell.

3. Insert more tubes on the periphery of the baffles to make these true vertical and insert remaining tubes by starting from bottom to top. Use pilots initially to guide the tubes.
4. After insertion of all tubes, the other tubesheet is fixed in its position. Push a few tubes out at the center and at the peripheral ends of the tubesheet and check the projection of the tubes before tacking and welding of the tubesheet with shell.

15.3.7.3 Tube Nest Assembly of Large Steam Condensers

Clean conditions are established within the condenser shell prior to the commencement of tubing. Tubing is usually started at the bottom rows, working progressively upward. This allows personnel to exit easily.

15.3.7.4 Cautions to Exercise while Inserting Tubes

Install the tubes carefully such that the tubes do not suffer any damage. When tubes are at their upper size tolerance and tubesheet holes are at their lower size tolerance, it is difficult to insert tubes. Misalignment of baffles and supports increases the difficulty. It is most important to set as a hold point the beginning of the tube loading and to witness this operation [13].

15.3.7.5 Assembly of U-Tube Bundle

Assembly of a U-tube bundle is always done outside the shell. The following procedure is normally adopted:

1. Insert the innermost row of the tubes through the baffle and tie rod assembly with the tubesheet.
2. After getting the inner row inspected, tubes are tacked or slightly expanded into the tubesheet or tightly held into position by any other means.
3. Insert tubes from the center toward the outside and get each row inspected before proceeding to the next row.
4. After all tubes are inserted, the bundle is carefully lifted with cradles and inserted inside the shell.

Figure 15.16 shows U-tube assembly outside the heat exchanger shell and completed U-tube bundle assemblies.

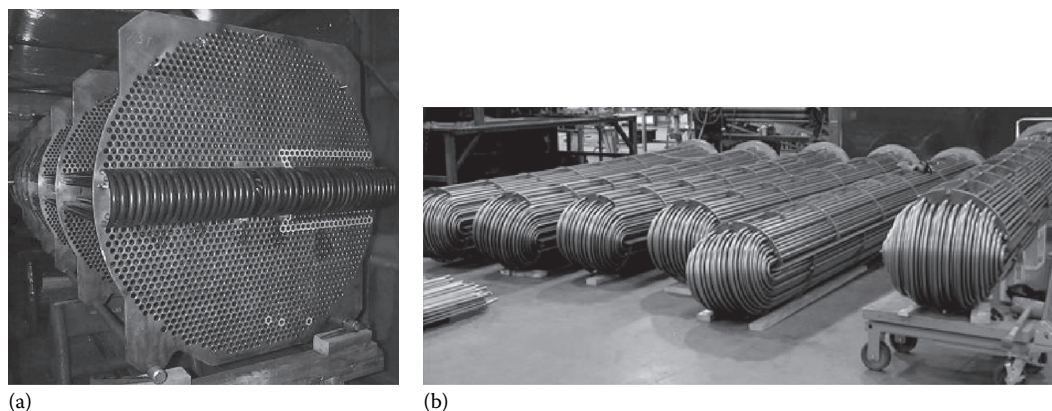


FIGURE 15.16 (a) Insertion of U-tubes through tubesheet (Courtesy of Powerfect, Brick, NJ) and (b) U-tube bundle heat exchangers—on the extreme right, tube bundle is on a movable trolley. (Courtesy of Titan Metal Fabricators Inc, Camarillo, CA.)

15.3.8 TUBESHEET TO SHELL WELDING

Tubesheets are welded to the shell by various methods [13,18,19]. Some configurations of tubesheet to shell welding are shown in Figure 15.17. Welding of tubesheet to shell causes distortion of the tubesheet. The distortion will increase the distance between two tubesheets at some places and reduce at some other places. This will buckle the tubes, and the effect is more prominent in stainless steel material because of its higher thermal expansion coefficient and poor thermal conductivity. Additionally, the distortion will not give a true gasket seating surface, thus causing the joint to leak unless the surface is machined for its trueness. Also, the pass partition plate has to be machined as per the bow to get proper seating [13]. If the tubesheet is to be machined to suit pass partition, the effective thickness of the tubesheet will be reduced by the amount of the bow. A number of methods are used to control distortion of tubesheets as follows:

1. Put a few long tie rods through the tubes and hold the tubesheets at various positions.
2. Put a thick plate at the face of tubesheet and tighten it. Weld this joint well with a trained and qualified welder.
3. Weld the tubesheet with shell while keeping the exchanger vertical. The tubesheet is clamped to the bed plate on which exchanger is resting.

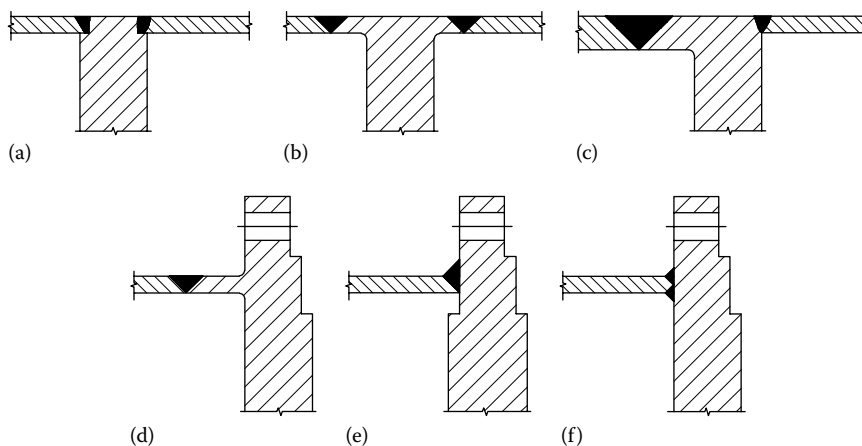


FIGURE 15.17 Configurations of tubesheet to shell welding—(a–c) both shell and channel welded to tubesheet, (d) tubesheet with a stub is welded to shell and (e–f) tubesheet is welded to shell and channel side in bolted design.

4. Use of hubbed tubesheets with a method of joining is known as lip welding (Figure 15.17d).
5. Bolt with a channel or closure to be assembled with it.
6. Use an end ring.

The end ring method is explained next.

Use of an end ring: In this method, an end ring of about 50 mm width is welded on the tubesheet step. Suitable restraint is applied to reduce welding distortion on the tubesheet. Whatever distortion appears on the tubesheet and on the end ring will be machined prior to drilling operation. Figure 15.18 shows the tubesheet with end ring welded, before machining and after machining.

Caution while welding shell to the tubesheet: Before putting the welder on the actual job, some mock-up test piece should be welded and root fusion should be checked by macroetching. It is a common practice of good fabricators to give a root run by the TIG process as shown in Figure 15.19 after purging the exchanger with argon gas [20]. The TIG process gives better root fusion and penetration. In all cases, after welding the tubesheet with the shell, the joint is inspected for welding defects by RT/UT.

15.3.9 TUBE-TO-TUBESHEET JOINT FABRICATION

The usual methods for joining tubes to tubesheets are roller expanding, welding, a combination of roller expanding and welding, and roller expanding and heading or flaring the tube ends, followed by welding. In few cases, a ferrule or similar device is interposed as a packing or seal in the gap between the tube and the tube hole.

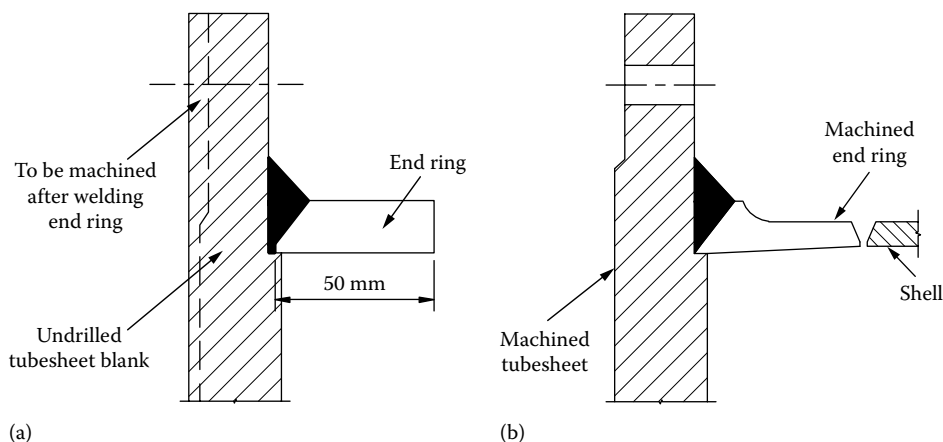


FIGURE 15.18 Tubesheet with end ring welded. (a) Before machining and (b) after machining.

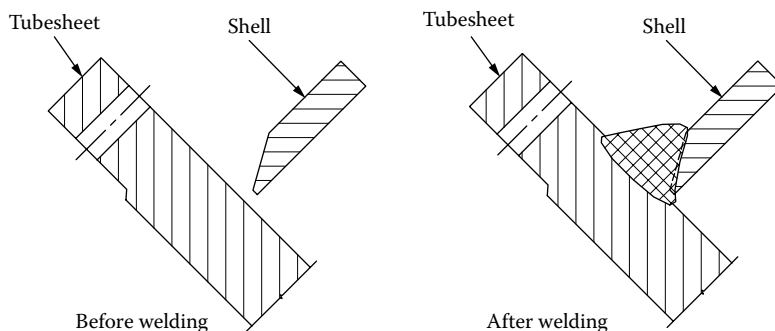


FIGURE 15.19 Tubesheet to shell welding—root run by TIG welding.

15.3.9.1 Quality Assurance Program for Tube-to-Tubesheet Joint

The tube-to-tubesheet joint quality assurance program shall include (1) tube-to-tubesheet mock-up (approval), (2) welder qualifications, (3) welding procedures qualification, (4) tube hole and tube end cleaning procedures, (5) procedure for tube-to-tubesheet joint welding, (6) procedure for tube-to-tubesheet joint roller expansion (known as tube-expanding procedure specification as per ASME Code Sec. VIII, Div. 1), (7) checking of tube-to-tubesheet joint leak tightness, and (8) reference to TEMA Table RCB-7.41 for tube hole tolerances or any other standards or codes as stipulated by the vendor [20].

15.3.9.2 Mock-Up Test

Before undertaking the actual tube expansion work, a mock-up model as shown in Figure 15.20 is made using the same material and the design that is proposed for the full-size heat exchanger and tested for the reliability of the tube-to-tubesheet joints. The test specimens are full-size tube and a test block that models the tubesheets. Process parameters were established by mock-up trials. The joining process was qualified by dye penetrant (DP) test, helium or pneumatic leak test, pullout test, and microetching tests of the welds to ascertain minimum leak path. The test measures tube-to-tubesheet joint strength, that is pullout or pushout (shear load) strength and leak tightness, and anchorage for grooved tubesheets. Pullout strength is the axial force required to break the “bond” between the tube and the tubesheet. The shear load test subjects the specimens to axial loads until

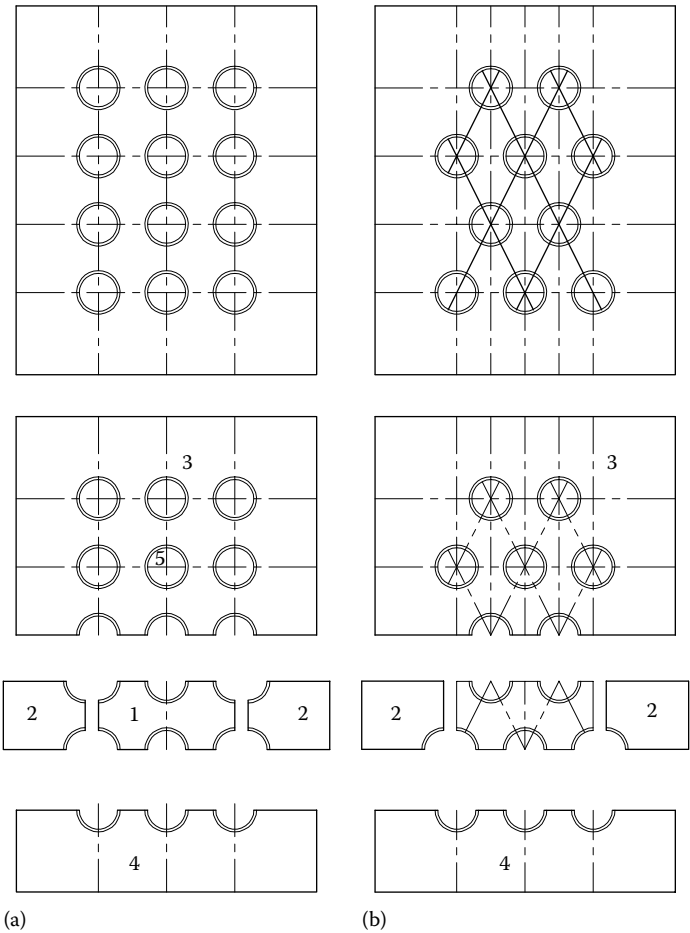


FIGURE 15.20 Mock-up model for tube-to-tubesheet expansion. (a) Square layout and (b) 60° layout.

either the tube or the joint fails. Control unit settings of the expanding unit, which show the amount of torque applied, are noted for individual cases. The best possible torque giving the leak tightness of the joints is then used on actual exchanger.

15.3.9.2.1 *Roller Expanded Joints*

A mechanically expanded joint by roller expansion may be acceptable when

- a. Service temperatures are below 200°C
- b. Tubesheet is sufficiently thick to allow rolling-in a suitable length of tube
- c. Design pressures are relatively low

15.3.9.3 **Tube Expansion**

15.3.9.3.1 *Expanded Tube-to-Tubesheet Joints*

The reliability of a shell and tube heat exchanger depends upon the integrity of all tube-to-tubesheet joints, each of which must be virtually free from defects. An effective tube-to-tubesheet joint must be leak-tight under the operating conditions of expansion and contraction, pressure or vacuum, and corrosion attack. The tubes of most tubular exchangers are connected to the tubesheets by only expanding or by welding and expanding. There are several techniques for expanding tubes into the tubesheets. Three main techniques used for tube expansion are (1) rolling-in, (2) explosive joining, and (3) hydraulic expansion.

15.3.9.4 **Requirements for Expanded Tube-to-Tubesheet Joints**

The connection of the tubes to the tubesheets is a critical operation. The requirements for creating the desired interfacial pressure at the tube-to-tubesheet joints are as follows [21]: (1) the tube deformation must be fully plastic; (2) the surrounding tubesheet must deflect under the pressure that the tube applies; and (3) upon pressure release, tubesheet recovery must be greater than tube recovery. Expanding pressure beyond that required for the tube-to-hole contact must be applied to meet these conditions.

15.3.9.5 **Tube-to-Tubesheet Expansion Methods**

Explosive joining: Explosive joining has been successfully used to expand tubes into tubesheets by detonating a carefully sized explosive charge inside each tube hole, causing it to impact with the tubesheet and make a metal-to-metal joint with the tubesheet. Details of explosive joining have been covered in Chapter 13 with material selection and fabrication and in the section on cladding.

Hydraulic expansion: Hydraulic forming is a relatively new method for tube-to-tubesheet joints in heat exchangers. Hydraulic expansion of tubes into tubesheets can be done by either the bladder or the O-ring technique (also known as direct hydraulic expanding technique) [22]. In the bladder technique (Canadian Patent 1152876), a bladder is inserted into the tube and then pressurized hydraulically to expand the tube. In the O-ring technique, a mandrel with two O-rings at appropriate locations is inserted into the tube. Hydraulic pressure applied between the O-rings causes the tube in that region to expand. Compared to rolled joints, hydraulically expanded joints are weaker than rolled joints, and they are further weakened by thermal cycling [22]. Hydraulic tube expansion process is further discussed later.

Rolling-in process: Rolling is by far the most commonly used technique. Tube expanding, known also as tube rolling or “rolling” of tubes, is the art of cold-working (plastic deformation) the ends of tubes into intimate contact with the walls of tubesheet holes, and the nature of deformation is shown schematically in Figure 15.21. If properly executed, the rolling-in process produces pressure-tight joints to ensure strength and stability. Tube rolling-in has been explained in detail by Sharma [1], Syal [14], Yokell [21], Fisher and Brown [23], Sonnenmoser [24], Dudley [25], and Yokell [26].

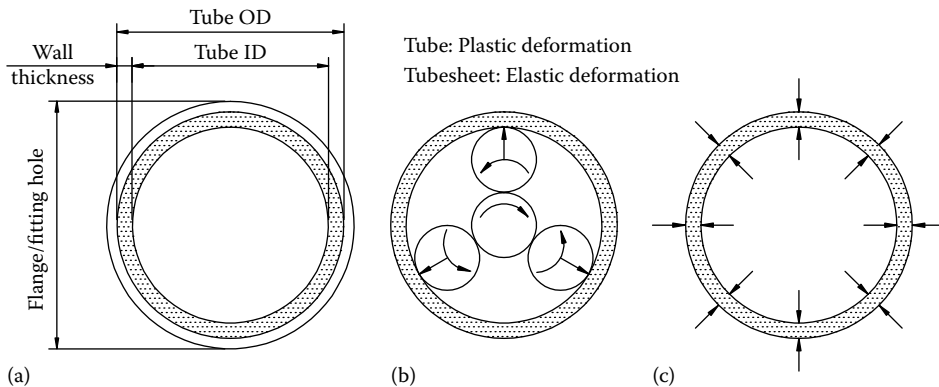


FIGURE 15.21 Cold-working principle of tube expanding. (a) Tube positioned in the tubesheet hole, (b) roller expansion in progress, and (c) expansion completed. (Tube deforms plastically where as tubesheet ligaments deform elastically.) (Courtesy of Elliott Tool Technologies Ltd, Dayton, OH.)

15.3.9.6 Rolling Equipment

A range of electric, electronic, pneumatic, or hydraulically driven torque controlled tube-expanding machines are used for the expansion of heat exchanger tubes. There are several standard types of expanders, as well as expanders built for specific purpose, each of which may be of different size and roller length. However, all work on the same principle and all have three essential parts, namely, a tapered central mandrel or pin; three, four, or five rollers of suitable length spaced equally around the mandrel; and a cylindrical roller cage that constrains the loosely held rollers in their respective positions. Most expanders are self-feeding type. The roller cage may be fitted with a collar mounted on a ball bearing to prevent it from being drawn into the tube. Pneumatic tube-expanding machines are shown in Figures 15.22 and 15.23. A pneumatic driven torque controlled tube-expanding machine and an electric driven torque controlled tube-expanding process in action are shown in Figure 15.24. In addition to the basic tube expander, a few similar tube expanders such as tack rolling tube expander, step-by-step tube expander for thick tubesheet, tube expander for thin tubesheet, step expander designed to avoid destructive axial stress in welded joints, etc., are used on shop floor. A list of different types of tube expanders used on the shop floor for tube-expanding purposes is shown in Figure 15.25.

For successful roller expansion, in addition to tube expanders, a large number of accessories such as tubesheet hole brush, tube guide, serrating/grooving tool, tube end facer, internal tube cutter, special tool for flaring tube ends, standard reversible thrust collar, tube end beveling machine, drift to remove stub, hydraulic ram for gripper-type tube puller, hydraulic operated gripper-type tube puller for condenser tubes and hydraulic ram for spear-type tube puller, tube leak testing gun set, hole gauge, and internal measuring gauge on the shop floor are shown in Figures 15.26 through 15.30. An automatic grooving double-axis working center is shown in Figure 15.31.

15.3.9.7 Basic Rolling Process

When rolling tubes, an expander as shown in Figure 15.22 is inserted into the tube end and the tapered mandrel is rotated. Feeding the mandrel inward causes the expander rollers to be forced apart; by rolling over the inside tube surface, cold-work the tube metal. When the tube hole is enlarged and contacts the tubesheet hole surface, the tubesheet acts as a restraint barrier, and further



FIGURE 15.22 Tube expander. (Courtesy of Elliott Tool Technologies Ltd, Dayton, OH.)

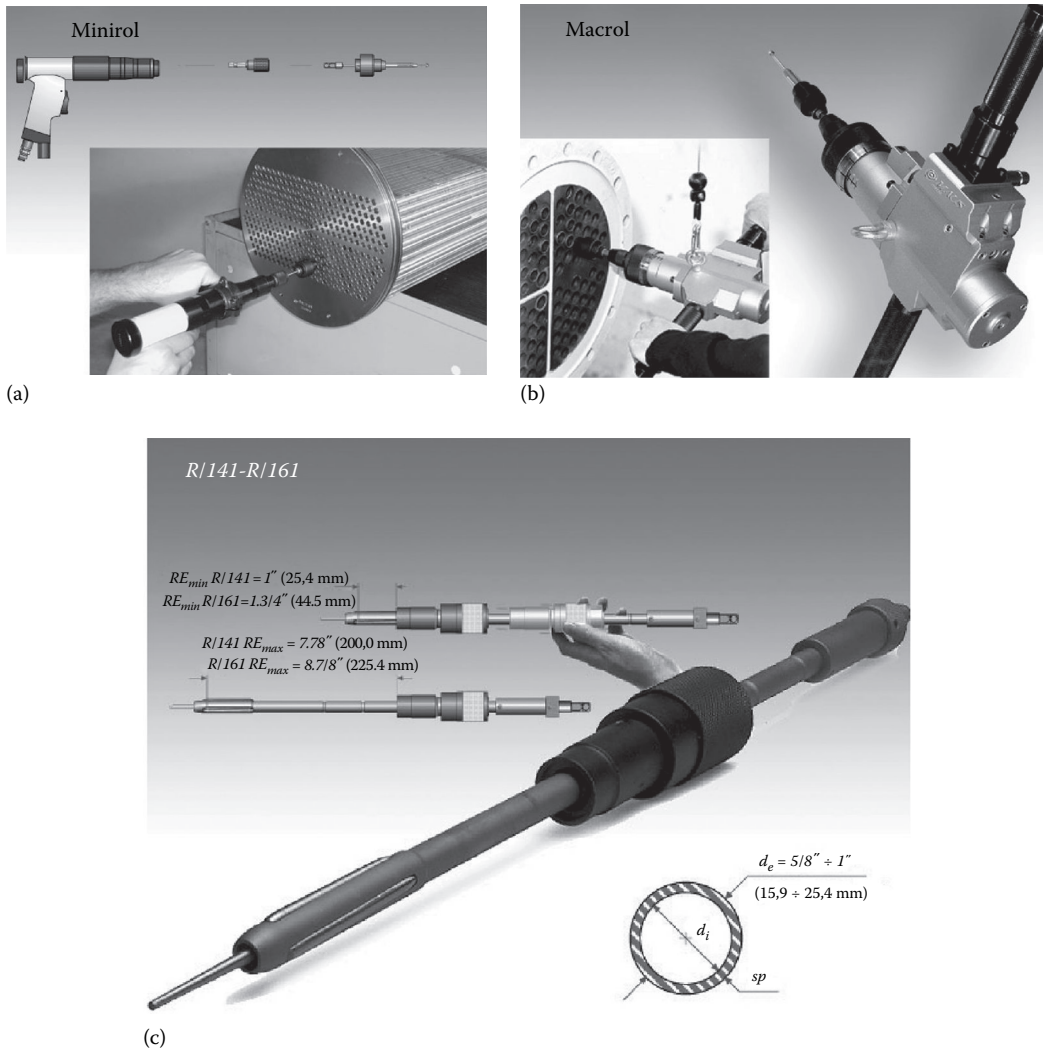


FIGURE 15.23 Pneumatic tube-to-tubesheet rolling machines. (a) Mini torque controlled pneumatic rolling machines for tubes diameter 6.3–15.9 mm (1/4”–5/8”), (b) Macrol—torque controlled pneumatic rolling machines for tube diameters 12.7–50.8 mm (1/2”–2”), and (c) step-by-step expander for thick tubesheet. (Courtesy of Maus Italia F. Agostino & C.s.a.s., Bagnolo Cremasco (Cr), Italy.)

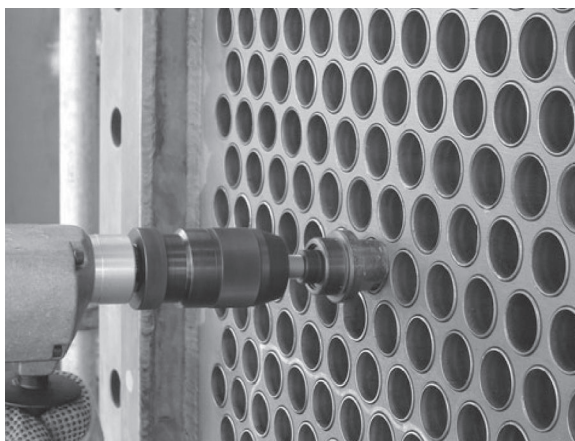
expanding deforms the tube metal and forces it into more intimate contact with the tubesheet metal (Figure 15.32). Since not all displaced tube metal can escape radially, it flows from the center to each end of the rolled joint. The tubesheet metal is also affected and the hole is slightly enlarged [23]. The net result of the expanding operation is a joint condition similar to shrink-fitted shaft coupling.

15.3.9.8 Optimum Degree of Expansion

The most important task on any tube rolling job is to determine the optimum degree of expansion for a particular tube and tubesheet material combination. With the introduction of new materials and higher pressures and temperatures, the need for a control method for the rolling-in of the tubes becomes more apparent [25]. The technique used for expanding the tubes should be one that, to the greatest possible degree, avoids both under- and overrolling [26]. Underrolling results in inadequate plastic flow at the tube–tubesheet interface. This will result in leaks and require rerolling. On the other hand, overrolling will distort the tubesheet, leading to unseating of adjacent tubes and



(a)



(b)

FIGURE 15.24 (a) Pneumatic tube expansion drive and (b) electrical expansion system with torque controller and a telescopic shaft. (Courtesy of Powermaster Ltd, Mumbai, India.)

excessive tubesheet radial expansion and/or over hardening of tubes. The effect of overrolling is shown schematically in Figure 15.33. Therefore, it is important to roll every joint uniformly to the optimum degree. To achieve this, the rolling technique must be one that utilizes automatic control of the tube expansion rather than depending on the skill of the operator.

15.3.9.9 Methods to Check the Degree of Expansion

The methods employed for checking the desired degree of expansion had been achieved are these [23]. One is based on measuring the changes in tube dimensions like reduction in tube wall thickness, or methods that limit or measure the mandrel travel or simulating wall reduction by interference or pullout strength versus torque curve. In order to avoid the undesirable features inherent in rolling methods that employ empirical formulas or that measure changes induced by the tube rolling process, many designers prefer methods that measure the torque applied to the expander mandrel. Various rolling methods based on measure of torque employ methods like the manual “feel” method, mechanical feel method, controlled feel rolling methods, elongation or extrusion measurement, etc. Rolling by “feel” may be the most practical method of retubing, since there will generally be considerable variation in the existing tube holes [27].

15.3.9.10 Criterion for Rolling-in Adequacy

There are many tools designed to actuate the expanding equipment, most with torque controlled by feed and speed limits and some with infinite variable controls. Optimum tube rolls may be predetermined by calculation on the basis of tube wall reduction.

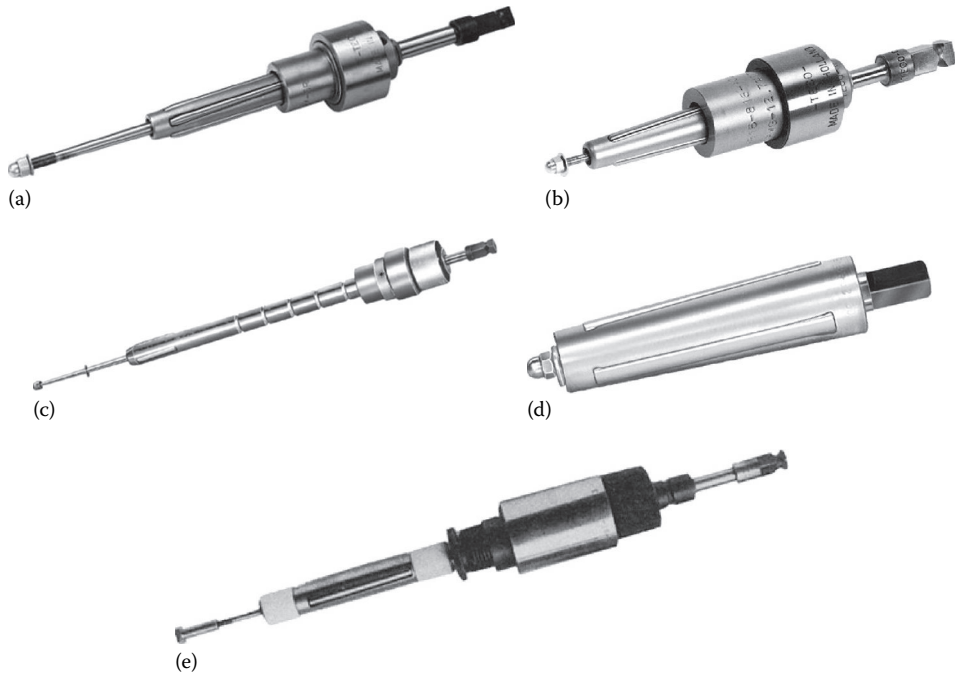


FIGURE 15.25 Tube expanders. (a) Five roll tube expander, (b) TACK rolling tube expander (conical expander), (c) step-by-step tube expander for thick tubesheet, (d) tube expander for thin tubesheet, and (e) step expander designed to avoid destructive axial stress in welded joints. (Courtesy of Teco Tube Expanders Company, Leiderdorp, the Netherlands.)

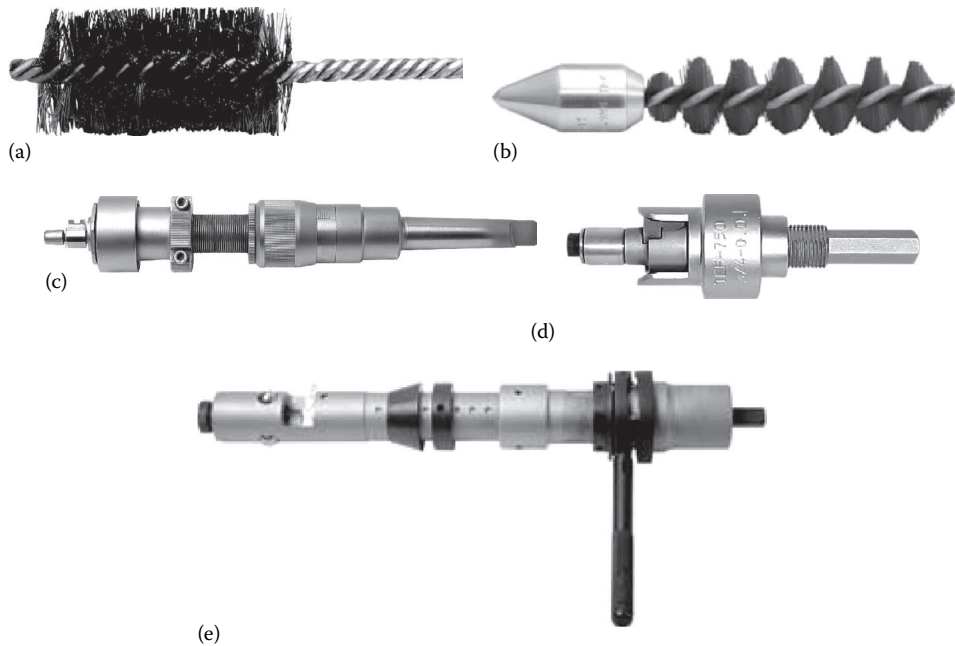


FIGURE 15.26 Accessories for tube expansion. (a) Tubesheet hole brush, (b) tube guide, (c) serrating/grooving tool, (d) tube end facer, and (e) internal tube cutter. (Courtesy of Powermaster Ltd, Mumbai, India.)

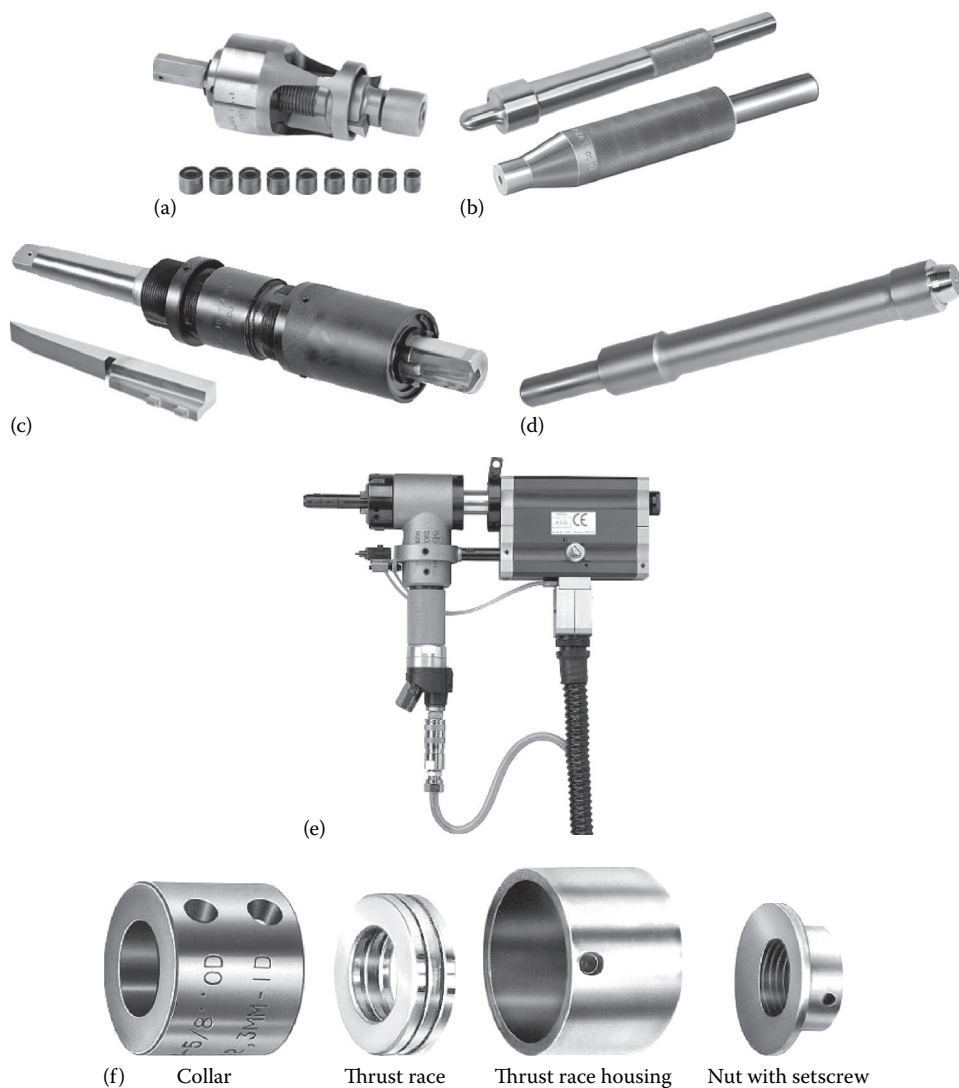


FIGURE 15.27 Accessories for tube expansion. (a) Tube end facers, (b) special tool for flaring tube ends, (c) grooving tool, (d) standard reversible thrust collar, (e) tube end beveling machine, and (f) drift to remove stub. (Courtesy of TECO Tube Expanders Company, Leiderdorp, the Netherlands.)

15.3.9.10.1 Wall Reduction as the Criterion of Rolling-in Adequacy

The amount of wall reduction is estimated by measuring hole and tube dimensions before rolling and tube internal diameter after rolling. The following equation may be used for calculating the percent wall reduction [13]:

$$\text{Percent} = \frac{[d'_i - (d_i + \text{clearance})]100}{2(\text{measured unrolled tube wall thickness, } t)} \quad (15.2)$$

where

d'_i is the tube internal diameter after rolling

d_i is the tube internal diameter before rolling

d is the measured tube outside diameter, and clearance the measured tubesheet hole diameter D minus d

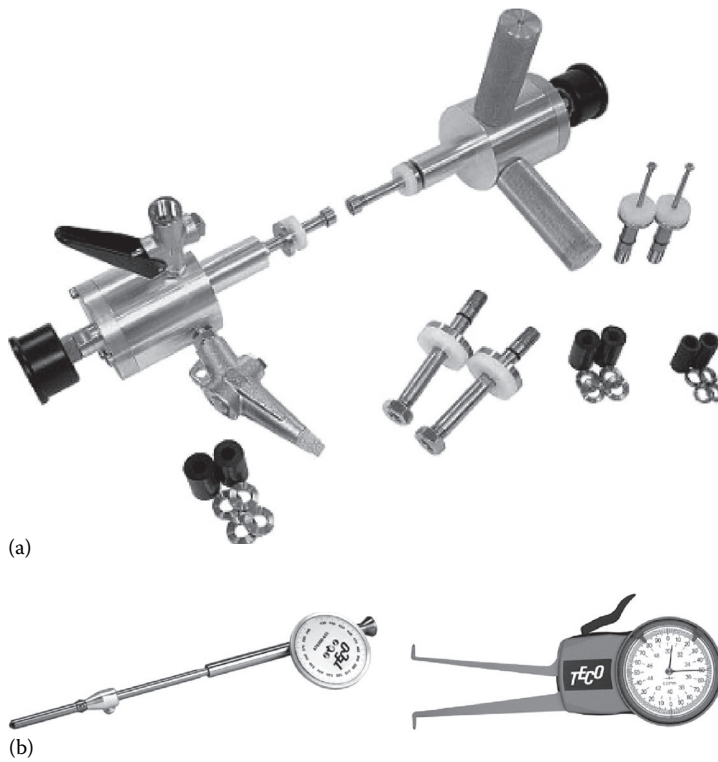


FIGURE 15.28 Accessories for inspection of rolled tube. (a) Tube testing gun set and (b) gauges used for checking holes—hole gauge and internal measuring gauge. (Courtesy of TECO Tube Expanders Company, Leiderdorp, the Netherlands.)

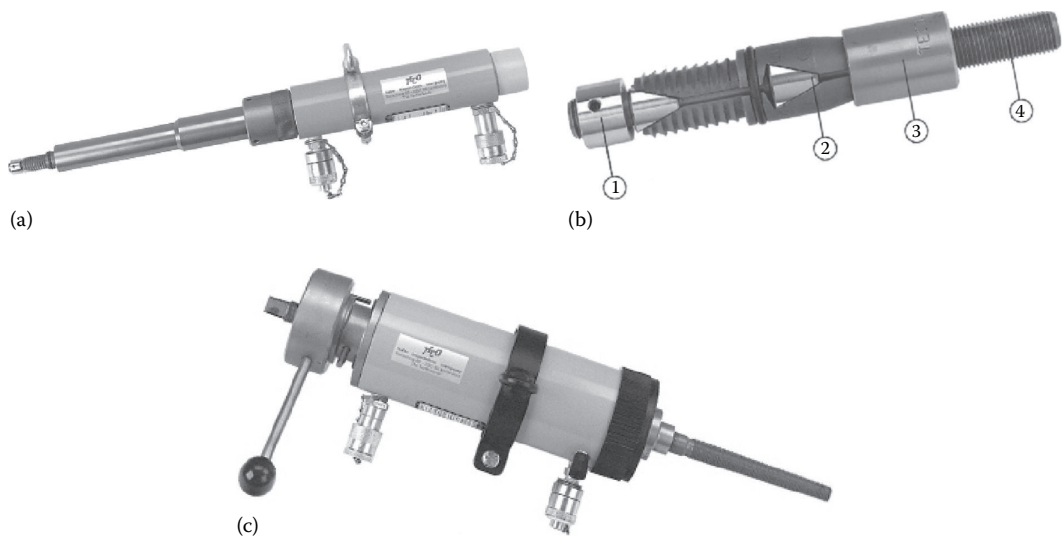


FIGURE 15.29 Tube puller. (a) Hydraulic ram for gripper-type tube puller, (b) hydraulic operated gripper-type tube puller for condenser tubes, and (c) hydraulic ram for spear-type tube puller. (Courtesy of TECO Tube Expanders Company, Leiderdorp, the Netherlands.)

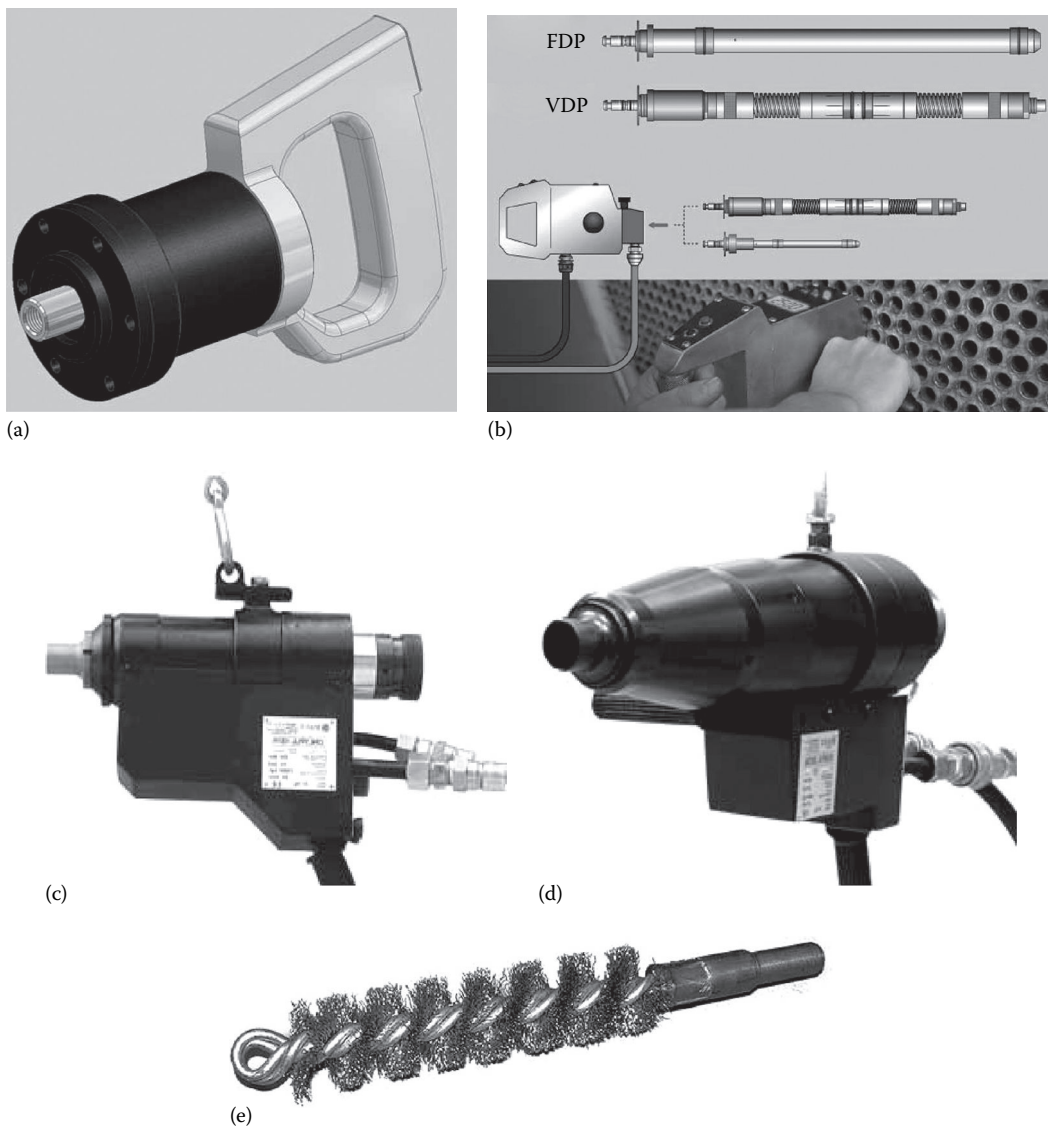


FIGURE 15.30 Tube rolling-in accessories. (a) Mafix system dedicated gun for tube locking. (b) probes FDP and VDP with quick-release coupling, (c) semiautomatic continuous hydraulic tube puller, (d) automatic continuous hydraulic tube puller, and (e) flue brushes for tubesheet holes cleaning. (Courtesy of Maus Italia F. Agostino & C.s.a.s., Bagnolo Cremasco (Cr), Italy.)

From Equation 15.2, the desired tube inside diameter after rolling is given by

$$d'_i = D - 2t(1 - x) \quad (15.3)$$

where

- d'_i is the tube inside diameter after rolling
- D is the diameter of the hole in the tubesheet
- t is the unrolled tube wall thickness
- x is the percent of tube wall thinning



FIGURE 15.31 Automatic grooving double-axis working center. (Courtesy of Maus Italia F. Agostino & C.s.a.s., Bagnolo Cremasco (Cr), Italy.)

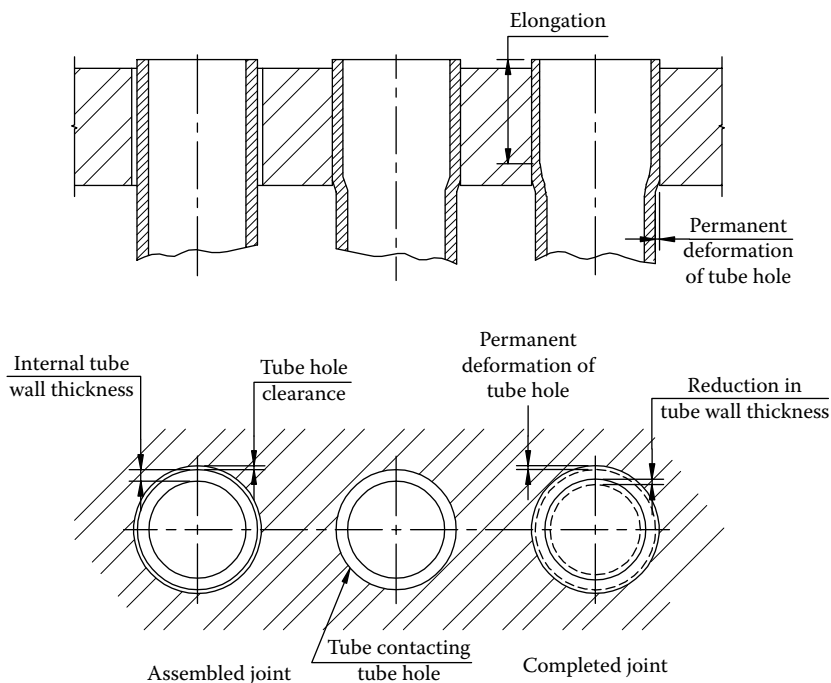


FIGURE 15.32 Basics of tube rolling process. (a) A tube inside the tubesheet hole, (b) tube contacting the tubesheet, and (c) permanent deformation of tube completed joint. (After Fisher, F.F. and Brown, G.J., *Trans. ASME*, 565, 1954.)

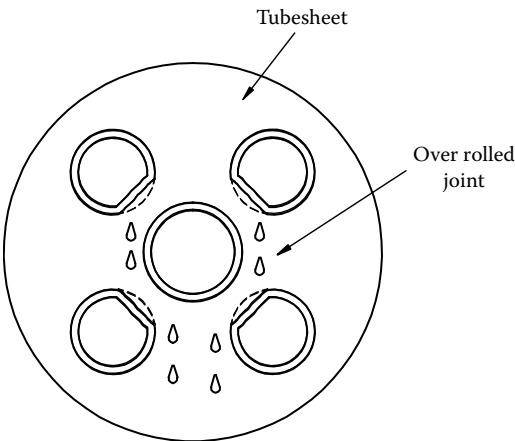


FIGURE 15.33 Effect of overrolling of tube on adjoining tubes—schematic. (Courtesy of Elliott Tool Technologies Ltd, Dayton, OH.)

In other words, expanded tube ID is given by

- 1. Hole diameter in tubesheet- $\text{Tube OD} = \text{Play between tubesheet and tube}$
- 2. $\text{Play between tubesheet and tube} + \text{Tube ID} + \text{Percentage of tube wall reduction} = \text{Expanded tube ID}$

A go and no-go gauge is made to ascertain that the tubes are properly expanded. While calculating tube dimensions after expansion, tolerances on tube outer diameter and tubesheet hole diameter and tube wall thickness must be taken into account.

15.3.9.10.2 Amount of Thinning of Tubes

The amount of thinning of the tubes for full expansion after metal-to-metal contact depends upon the tube and tubesheet material. Percentages of thinning for a few common tube materials are the following:

Carbon steel	5%–8%
Stainless steel	3%–5%
Alloy steel	4%–6%
Titanium	4%–5%
Copper alloy	4%–8%
Admiralty brass	7%–8%
3003/4004 aluminum	5% maximum
6061T aluminum	10%–12%

The setting of the torque control unit is established on a mock-up model.

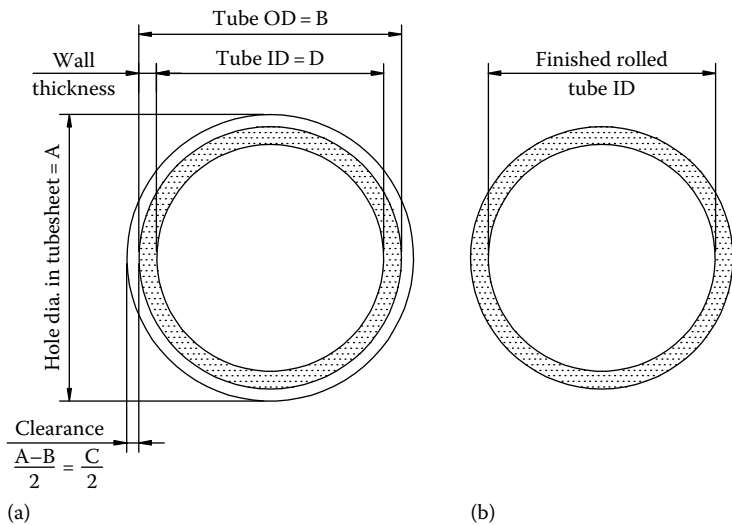
15.3.9.10.3 Correct Tube Wall Reduction

Tube expanding is the art of reducing a tube wall by compressing the OD of the tube against a fixed container such as rolling tubes into tubesheets, ferrules, etc. To assure a proper tube joint, the tube wall must be reduced by a predetermined percentage. The following chart as recommended by Elliott Tool Technologies Ltd, Dayton, OH, can be used for determining the correct

tube wall reduction. This chart shows a typical 3/4”–16 gauge tube. Before rolling this tube, find the proper rolling dimension as follows:

- 1. First determine the tube hole size.
- 2. Then determine the tube outside diameter.
- 3. Subtract the tube outside diameter from the tube hole dimension.
- 4. With a tube gauge, determine the inside diameter of the tube before rolling.
- 5. By adding the dimension found in “4” to the clearance between the tube OD and the tube hole, find out tube’s inside diameter at metal-to-metal contact.
- 6. Roll the tube-to-tubesheet and check the ID of the tube with a tube gauge.
- 7. By subtracting “5” from the rolled diameter, determine the actual amount of expansion (tube wall reduction) on the inside diameter of the tube.

This chart can be used for predetermining both the % of wall reduction required and the actual inside diameter that should be rolled. Since the amount of wall reduction greatly determines the quality of the tube joint, one should arrive at the % required for the application prior to tube rolling. By subtracting the tube inside diameter “4” from “2,” you determine actual wall thickness. Dial setting test chart for determining proper amount of tube expansion with automatic torque control unit is shown in Figure 15.34.



Tube example: 3/4”, 16 Gauge Brass tube

Step	Step Description	Example	1	2	3
A	Measure hole dia. in tubesheet	0.760			
B	Measure tube O.D.	0.750			
C	Calculate clearance (A–B)	0.010			
D	Measure tube I.D.	0.620			
E	Calculate total tube wall thickness (B–D)	0.130			
F	Calculate wall reduction (7% for brass tube)	0.009			
G	Calculate finished rolled tube I.D. (C+D+F)	0.639			

FIGURE 15.34 Rolled tube inner diameter calculation procedure. (a) A tube positioned inside the tubesheet hole and (b) expanded tube. (Courtesy of Elliott Tool Technologies Ltd, Dayton, OH.)

15.3.9.10.4 Determining 3, 4, or 5 Roll Expander Design

Generally, a 3 roll expander is well suited but 4 or 5 roll expander is needed in the following applications:

- Tube material: Stainless steel, titanium, work hardening materials, minimum 4-roll design is desired.
- Wall thickness: 20 gauge (0.035") and thinner
For stainless steel or titanium—5 roll preferred; and carbon steel, brass, copper, aluminum—4 roll preferred.
- Tube pitch: Tubesheets with thin ligaments in a triangular tube pitch pattern may be disrupted using a standard 3 roll expander.

15.3.9.11 Length of Tube Expansion

According to TEMA, for R and B classes, tubes may be expanded into the tubesheets for a length not less than 2 in. (50.8 mm) or the tubesheet thickness minus $\frac{1}{8}$ in. (3.2 mm), whichever is smaller, and for C class, the length not less than 2 tube diameters or 2 in. (50.8 mm) or the tubesheet thickness minus $\frac{1}{8}$ in. (3.2 mm), whichever is smallest.

15.3.9.11.1 Importance of Sealing Full Length of Tubesheet

Seal the full length of tubesheet as shown in Figure 15.35. (1) If less than full length, medium is condensed and trapped between tube and tubesheet, and this will lead to premature joint deterioration and tube decay. (2) If tube is expanded beyond tubesheet thickness, tube bulging creates a sharp edge that weakens the tube.

How a mechanical bond is formed?

- Tube joint is formed by compressing the tube into a fixed container (i.e., tubesheet). Ideally, rolled joint is created when the tube undergoes plastic deformation and is contained by the tubesheet's elastic properties (fully recovers). This has to occur right before the tubesheet turns to a plastic state.
- Underrolling occurs when the tube is not compressed enough and remains at an elastic stage. Bond is not created as yield of material is not compressed enough to turn tubesheet to elastic.
- Overrolling occurs when tube surpasses the elastic property of tubesheet and therefore the ligaments between tubesheet holes are shifted causing adjacent tubes to leak.

15.3.9.11.2 Common Causes of Tube Joint Failure

- Not enough tube expansion (underrolling)
- Too much tube expansion (overrolling)
- Dirty, scratched tubes or tubesheets
- Dents or other imperfections of the tube

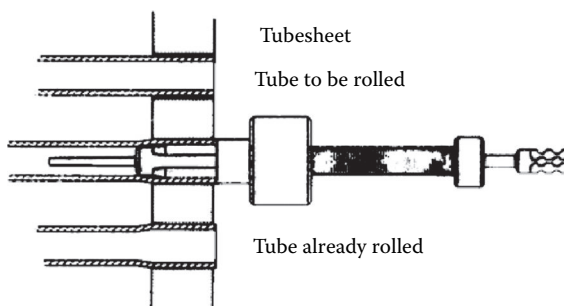


FIGURE 15.35 Sealing full length of tubesheet. (Courtesy of Elliott Tool Technologies Ltd, Dayton, OH.)

15.3.9.12 Full-Depth Rolling

Full-depth rolling on thicker tubesheets may be desirable to close the clearance between the tube and the tubesheet hole; however, in some cases, this may tend to weaken the joint due to differential thermal expansion. For most stringent conditions, welding and rolling may be desirable. When this is considered necessary, the holes should be grooved near the weld face to minimize differential thermal expansion effects [27].

15.3.9.12.1 Joint Cleanliness

Cleanliness is one of the basic requirements for making good joints. Both tube holes and tube ends should be well cleaned from scale, rust, and dirt before assembly, and care should be taken to keep oil, soap, and other lubricants out of the unrolled joint.

15.3.9.12.2 Phenomenon of Tube End Growth during Rolling and the Sequence of Tube Expansion

While rolling, the rolls are always pushing a wave of metal ahead of them. As with the uniform pressure model, any pressure greater than $(2/\sqrt{3})\sigma_1$, where σ_1 is the tube yield strengths at the manufacturing temperature will cause tube end extrusion. This is the reason for the well-known phenomenon of “tube end growth during rolling” [21]. The length of elongation of the rolled tubes is of the order of a few thousandths of an inch to 1/16 in. (3.2 mm) or more, depending on the size, material, and tube wall thickness, as well as the length of the joint to be rolled [23].

Tube end growth of fixed tubesheet exchanger: When rolling U-tubes or tubes having sufficient flexibility to absorb the elongation, no difficulty will be experienced when rolling the second or closing end of the tubes. They should, however, be rolled uniformly in order to maintain the proper tube alignment. However, this is not true for rolling the second end of the tubes that connect second tubesheet of a fixed tubesheet exchanger. If the tubes are expanded sequentially, the tube extrusion can cause a tubesheet to bow and tilt out of perpendicularity. This problem in the fixed tubesheet exchanger is overcome by judiciously spacing and rolling in a sufficient number of so-called tack tubes consisting of a few tubes at six or eight equally spaced at the peripheral locations and at the center as shown in Figure 15.36 [25,26]. On a finished bundle, bowed and dished tubesheets may indicate faulty tube expanding.

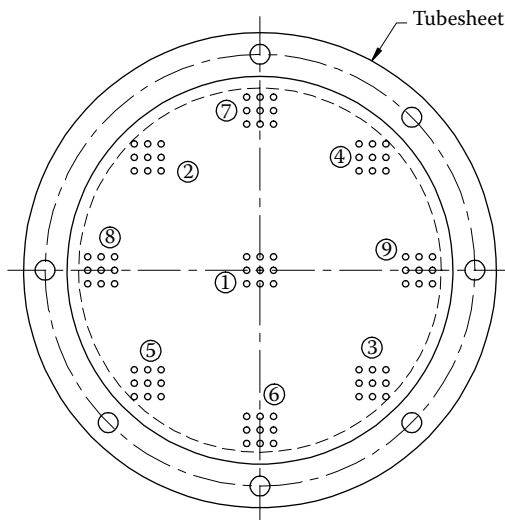


FIGURE 15.36 Sequence of tube rolling. Tack tubes.

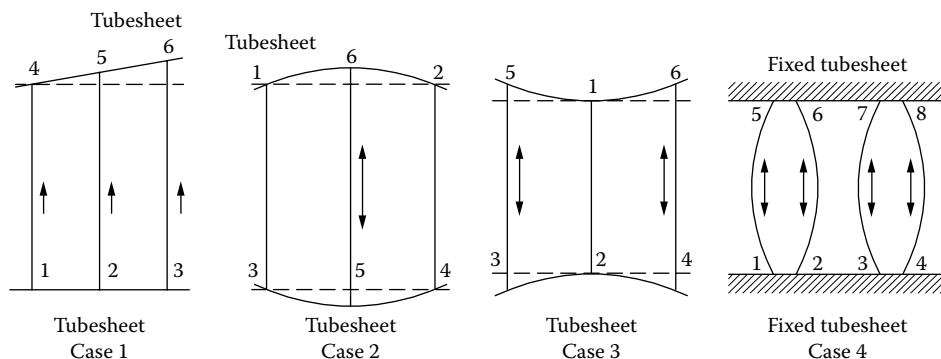


FIGURE 15.37 Effects of rolling sequence on tubesheet and tubes. (From Fisher, F.F. and Brown, G.J., *Trans. ASME*, 565, 1954.)

Figure 15.37, taken from Fisher et al. [23], depicts in a somewhat exaggerated form the effects of elongation created by various rolling sequences. Figure 15.37a shows the effect without tack tubes or other restraining means when rolling operations are carried on successively across the tubesheet. Figure 15.37b and c illustrate the stress conditions created by the rolling sequenced as enumerated. Figure 15.37d depicts the behavior of slender tubes when rolled into two fixed tubesheets. The bow shown, to a certain extent, relieves the load on the tubesheets.

15.3.9.13 Size of Tube Holes

The clearance between tube and tube hole has a definite influence on the tube-expanding operation. Excess clearance lengthens the expanding operation considerably and increases the plastic deformation and work hardening of the tube material, although the actual joint forming time remains the same [23,24]. Minimum play before rolling is to advantage. Tube hole diameters and tolerances are specified in TEMA Standard paragraph RCB-7.4.

15.3.9.13.1 Hydraulic Expansion

Hydraulic expansion is the direct application of a high internal hydraulic pressure within a tube or sleeve in order to form a tight joint between the tube and the tubesheet or a tight seal between the sleeve and the tube. Specifically, high-pressure water is injected inside a tube but within the tubesheet. As pressure increases, the tube goes into plastic deformation until it makes contact with the tube hole. Additional pressure stresses the ligament but always within the ligament's elastic range. When pressure is released, the result is a tight interfacial fit between the OD of the tube and the ID of the hole. Figure 15.38 shows sequences of tube expanding by HydroSwage® system (Figure 15.39). Figure 15.40 shows Hydrex-hydraulic tube expansion system and Figure 15.41 shows hydraulic system for tack expanding unit.

The main benefits of hydroexpanding are the following.

1. No step expanding—Any thickness of tubesheet can be expanded in one operation.
2. Minimal work hardening of the tube material during expansion; even difficult tube materials such as titanium or superduplex stainless can be easily expanded.
3. Less wall reduction and less stress concentration from the expanded to the unexpanded portion of the tube which results in longer tube life.

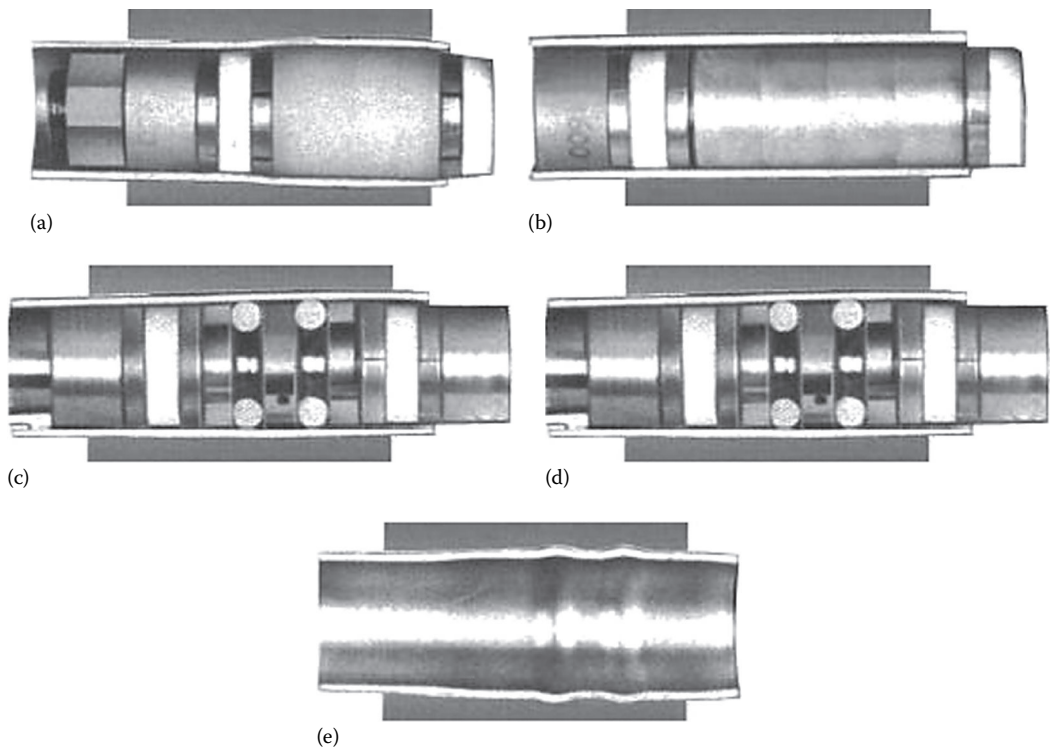


FIGURE 15.38 Sequences of tube expanding. (a) Tube-Loc™ drawbar in tube, (b) drawbar pulls, positions, and sets tube in place, (c) HydroSwage mandrel in tube, (d) high pressure expansion of tube, and (e) smooth transition from expanded to unexpanded areas groove. (Courtesy of Haskell International, Inc., Burbank, CA. All rights reserved.)

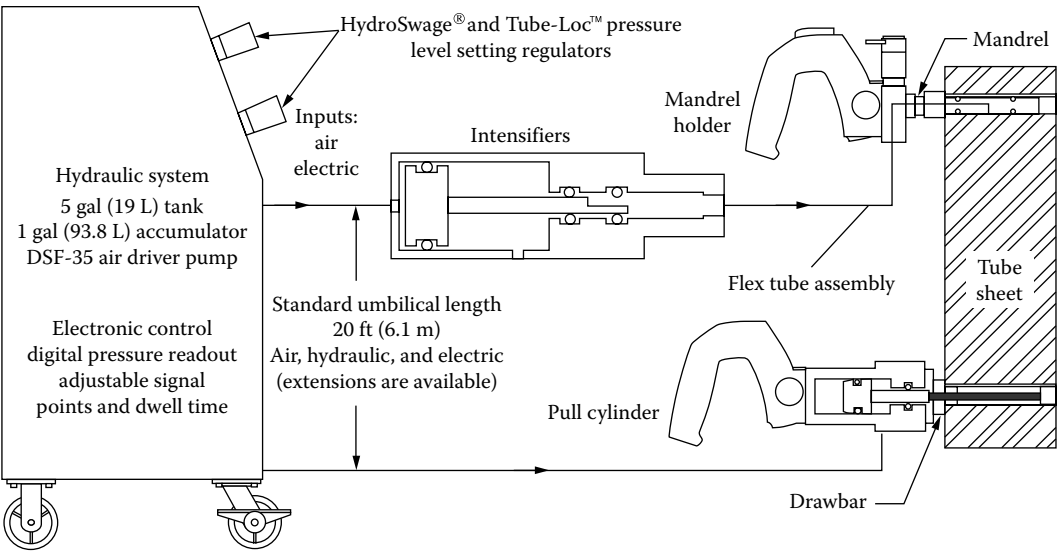


FIGURE 15.39 Mark V HydroSwage system for tube expanding. (Courtesy of Haskell International, Inc., Burbank, CA. All rights reserved.)



FIGURE 15.40 Hydex hydraulic tube expansion system. (Courtesy of Powermaster Ltd, Mumbai, India.)



FIGURE 15.41 Hydraulic system for tack expanding. (Courtesy of Teco Tube Expanders Company, Leiderdorp, the Netherlands.)

15.3.9.14 Factors Affecting Rolling Process

The factors that affect the quality of the rolling process are discussed in detail by Fisher et al. [23]. Some of the important factors are the following:

1. Cleanliness of the tube, tubesheet, and rollers
2. Conditions of the cage, rollers, and mandrel
3. Lubrication and cooling
4. Tube and hole dimensions
5. Torque cutoff control monitoring and maintenance
6. Rolling technique, roller rotation speed, number of rolls, angle of rolls relative to the tube axis, shape of the rolls
7. Worker fatigue

It is best to avoid the use of any lubricant during the roller expansion. But if, because of undue wear or heating of the rolls, lubrication is thought necessary, then it must be applied with discretion [28]. On completion of assembly and expansion, the localized areas around the tube-to-tubesheet joint should be cleaned again with the solvent so as to remove the final traces of lubricant.

15.3.9.15 Strength and Leak Tightness of Rolled Joints

In general, the joint strength and leak tightness of tubes expanded into bare holes, that is without grooves, are functions of the surface area in contact between the tube and the hole, residual interfacial pressure at the tube-to-tubesheet interface produced by the expansion process, static coefficient of friction, and Poisson's ratio [23]. Individual factors that affect the joint strength are discussed next.

Expanders' condition: Well-made/maintained expanders having hardened and ground mandrels and rollers are essential for making good rolled joints [27]. Expanders having rollers with sharp or improperly shaped entrance ends are believed responsible for many joint failures [23].

Feed and speed: In general, faster machine rolling produces better results but with a tendency to greater tube hole deformation, while slower rolling tends to increase tube wall thinning [27].

Length of tube expansion: The strength of a rolled joint increases with an increase (not proportional) in length and an increase in the tube wall thickness [23]. Excessive joint length is more expensive and may cause premature failure if the tube and tubesheet materials have a high difference in coefficients of thermal expansion as, for example, copper tubes and steel tubesheets. Short joint lengths in thick tubesheets have an advantage; that is in case of joint failure or leaks, the unrolled portion of the joint may be utilized.

Tube and tubesheet materials: Ideally, the tubesheet material should match the mechanical properties of the tubes. As the ratio of elastic limits of tube and tubesheet materials rises, the strength of the joint decreases. Therefore, the elastic limit of the tube material should be relatively low [24]. A tube and tubesheet combination consisting of steel tube and steel tubesheet produces joints having a high holding strength, whereas a steel tube rolled into a copper tubesheet would have low strength. Experience has shown that for the best overall results, the hardness of the tube should be less than that of the tubesheet material. A reversed condition usually results in distorted or greatly enlarged tube holes [23]. For materials with limited ductility, like ferritic stainless steel tubes, rolling should be done carefully.

Friction: Expanded joints are primarily friction joints. Thus, all other factors being equal, increase in friction or resistance to sliding will tend to increase the strength of a rolled joint.

Wall reduction: Rolled joint pullout strength increases approximately linearly with wall reduction, but rolling must not proceed to the point at which adjacent holes are distorted and tubes dislodged.

Factors that decide the optimum tube wall reduction: Factors that decide the optimum tube wall reduction for an expanded tube-to-tubesheet joint are specified in TEMA section RGP-RCB-7.5.

15.3.9.15.1 Joint Leak Tightness

Joint leak tightness depends on factors such as quality of tube, tube ends, and tube hole condition in tubesheets, tube wall thickness, and joint RFs by tube hole annular grooves.

Quality of tube holes (tube hole ovality and finish): It must always be remembered that strength of joint alone is not enough to guarantee a good joint. Consideration must be given to joint leak tightness, which is influenced greatly by the degree of roughness of the joint interfaces [23] and tube hole ovality [24]. In general, a leak-tight joint can be made much more easily if the contacting surfaces of tube and tubesheet hole are smooth, but such a joint has, because of this smoothness, a lower joint strength whereas rough tube holes make strong joints. For tubes whose hardness is roughly equal to that of the tubesheet material, as in boiler and refinery heat exchangers, the conventional “drill and ream” tube hole finish is in order [23]. Spiral machining marks and lateral grooves have a detrimental effect on the quality of the joint. This can be avoided by paying proper attention while drilling/reaming the bore [24]. The effect of tube hole finish on the mechanical strength and leak tightness of an expanded tube-to-tubesheet joint is discussed in TEMA section RGP-RCB-7.43.

Baffles, tube ends, and tube hole condition: Baffle holes and tubesheet holes shall be free from burrs to avoid longitudinal scratches on tube ends which is one of the main causes for leaky expanded tube-to-tubesheet joints. Should such scratches or tool marks occur, they should be removed completely by grinding. All tube holes should be truly circular and of cylindrical shape.

Tube wall thickness: The thicker the tube wall, the better is the seal, because of the increase in the difference in mean tangential plastic strain. It is shown that within certain limits, thick-walled tubes are more readily sealed by expansion [24].

Joint reinforcements by tube hole annular grooves: In order to meet the demands of higher pressures, most tube joints are strengthened by the machining of suitably shaped circumferential grooves into the walls of the tubesheet hole (Figure 15.42). During the rolling-in process, a portion of the tube metal is extruded into these grooves. In this manner, additional anchorage and shear strength are provided for the rolled joint, hence increasing the pullout strength. Rectangular grooves are commonly used for RF purposes, and they increase the holding strength and stability of rolled joints by more than 40%–50% [26].

Discussion of tube hole annular grooves provision in TEMA: TEMA RB Class require at least two grooves, each approximately $\frac{1}{8}$ in. wide by $\frac{1}{64}$ in. deep (3.2 mm wide \times 0.4 mm deep). TEMA C class requires grooving for $\frac{5}{8}$ in (15.875 mm) and larger diameter tubes for design pressures over 300 psi (2068 kPa) and/or temperatures in excess of 350°F (176.7°C). When integrally clad or applied tubesheet facings are used, all grooves should be in the base material unless otherwise specified by the purchaser.

When an exchanger is built with small-diameter tubes and with grooving in the tubesheet, the designer should consider [13] (1) the percentage of ligament width removed by the grooving and (2) the percentage of tubesheet thickness that the grooves occupy. For such tubes, better results might be achieved by using a coarse tube hole finish in the range of 250 rms or grooves similar to those desired for thin, high-strength tubes.

More than two annular grooves: The two $\frac{1}{8}$ in. wide \times $\frac{1}{64}$ in. deep (3.2 mm wide \times 0.4 mm deep) grooves of the TEMA are adequate for most rolled joints. However, for thin-walled, high-strength tubes, a series of smaller, shallower grooves of the same total width are also followed.

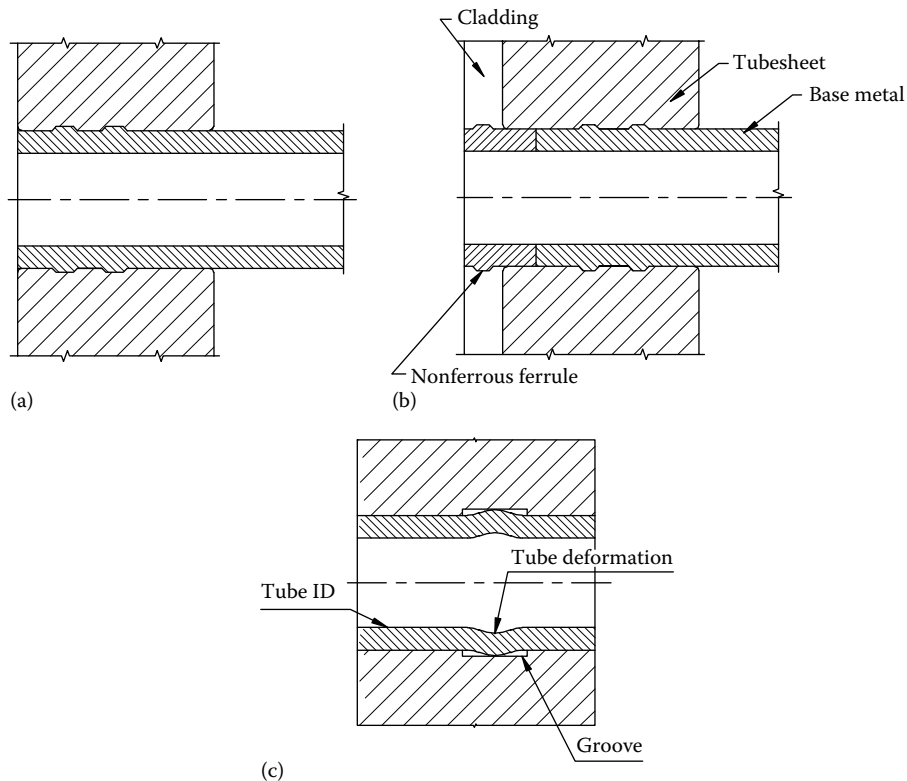


FIGURE 15.42 Tube-to-tubesheet joint RFs by annular groove. (a) Tubesheet with double grooves, (b) duplex tube and clad tubesheet, and (c) tubesheet with single groove.

15.3.9.15.2 Step Rolling

In general, the maximum length of tube that can be roller expanded in one rolling tool application is about 2 in. (50.8 mm). For larger joint lengths, rolling is done in steps with overlapped rolled lengths. If the step-rolled lengths do not overlap, there is a series of transitions between the rolled and unrolled lengths [23].

15.3.9.15.3 Roller Expander for Tube Extending beyond the Tubesheet

For tubes that extend beyond the open face of the tubesheet, a thrust collar that fits over the tube must be used. The thrust collar positioned against the tubesheet face will accurately locate the expanding rolls within the tubesheet hole.

15.3.9.16 Expanding in Double Tubesheets

The recommended sequence of expanding for the double-tubesheet exchangers can be adopted, starting with number 1 as shown in Figure 15.43 [25]. Tube expansion is carried out at the inlet end inner tubesheet first. Particular care is taken in setting up the expanders to ensure that expansion beyond the edge of the tubesheet does not occur.

15.3.9.17 Leak Testing

This is discussed in a later section.

15.3.9.18 Residual Stresses in Tube-to-Tubesheet Joints

All tube-expanding methods leave residual stresses in the tube wall. If these stresses are tensile and above 100 MPa, the tube is susceptible to stress corrosion cracking. Some steam generator manufacturers do

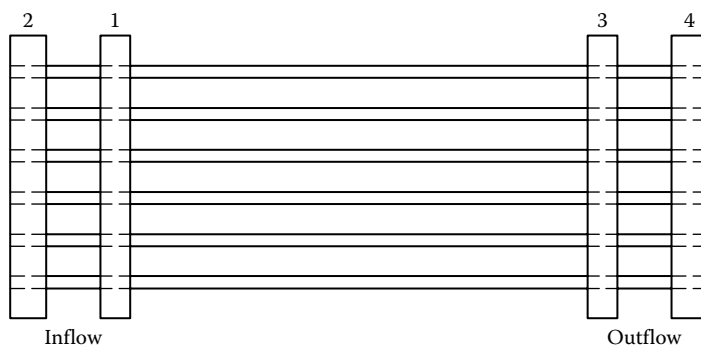


FIGURE 15.43 Recommended sequence of tube expansion for the double-tubesheet exchanger. (After Dudley, F.E., *Trans. ASME*, 76, 577, 1954.)

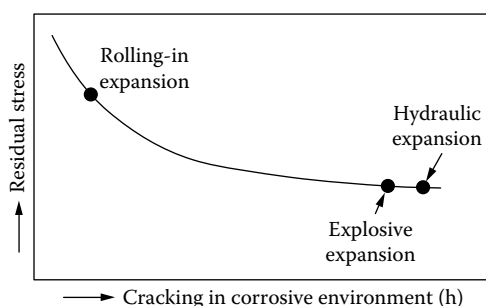


FIGURE 15.44 Stress corrosion due to residual stresses in the tube of tube-to-tubesheet joint. (Adapted from Kong, C.-S., Lee, B.-I., and Shin, S.-H., *Transactions of the 15th International Conference on Structural Mechanics in Reactor Technology (SMiRT-15)*, Seoul, Korea, August 15–20, 1999, pp. IV-81–IV-87.)

a thermal stress relief after expansion to reduce these residual tensile stresses. However, in some situations, this is impractical if not impossible [22]. Compared to rolled joint and explosively expanded joint, hydraulically expanded joint is weaker. The level of residual stress is maximum in roller expanded and minimum in hydraulically expanded joint [29]. The susceptibility of tube-to-tubesheet joints formed by these three methods to stress corrosion cracking is shown in Figure 15.44 [29].

15.3.10 TUBE-TO-TUBESHEET JOINT WELDING

Expanded joints are adequate for many applications and are still used extensively where pressure differences are not high enough to cause leakage. However, higher temperature and pressure requirements on heat exchangers make expanded joints inadequate, and for certain services, the mixing of the shellside and tubeside fluids is prohibited. For these conditions, welding of tube-to-tubesheet joints must be carried out. At high operating temperatures, the expanded joint undergoes stress relief. The interfacial joint stresses, which give the joint its strength, are relaxed, the tube wall contracts, and leakage develops [30]. Weld joints have no such limits at high temperatures. According to Brosilow [30], tube-to-tubesheet welding is preferred for the following circumstances:

1. Tube pitch is too small to permit an expanded joint.
2. Thermal cycling is severe and operating temperatures are relatively high.
3. In critical applications where the danger of corrosion is high. The expanded joint is not continuous, since crevices between tube wall and tubesheet lead to crevice corrosion.
4. When access for maintenance is limited, as in nuclear and in some chemical process exchangers.

If welding is used, either it serves as a seal (known as a seal-welded joint) or the weld is used as the principal means of load-bearing connection (known as a strength-welded joint).

15.3.10.1 Various Methods of Tube-to-Tubesheet Joint Welding

The following means of tube-to-tubesheet welded joints are generally followed, depending on the service involved:

1. Expand in plain holes and seal welding
2. Expand in grooved holes with seal welding
3. Expand in plain holes and strength welding

All compatible weldable materials, namely, tubes, tubesheet, and weld filler metal, may be joined at tube-to-tubesheet joints with conventional arc welding methods and gas tungsten arc (TIG) welding.

15.3.10.2 Tube-to-Tubesheet Joint Configuration

In general, the tube-to-tubesheet connections have been made by passing the tubes through the tubesheet and fillet welding on the face side, recess welding, and internal bore welding using one of the joint geometries as discussed later.

1. Figure 15.45 shows most commonly adopted tube-to-tubesheet joint configuration for welding.

Note:

- a. Figure 15.45c, incorporating a trepan in the tubesheet. It is used for materials in which the welds may be subjected to cracking when made under conditions of restraint. A trepanned joint is more expensive to machine, and the ligament length between tubes is a governing factor in use of such a joint [31].
- b. In Figure 15.45d, a recessed welded type is employed for avoiding stagnation of the fluid on the tubesheet and to reduce turbulence on the tubeside.
- c. Figure 15.45 g shows tube end bell-mouthed and fused.
- d. In Figure 15.45b, projection of 1 mm is preferred because it allows better welding and is suitable for welding without filler metal.
- e. Added ring weld type—Figure 15.45f shows fillet welds of the tube-to-tubesheet joint with a ring of special alloy placed on the protruding end and melted by an argon arc process.

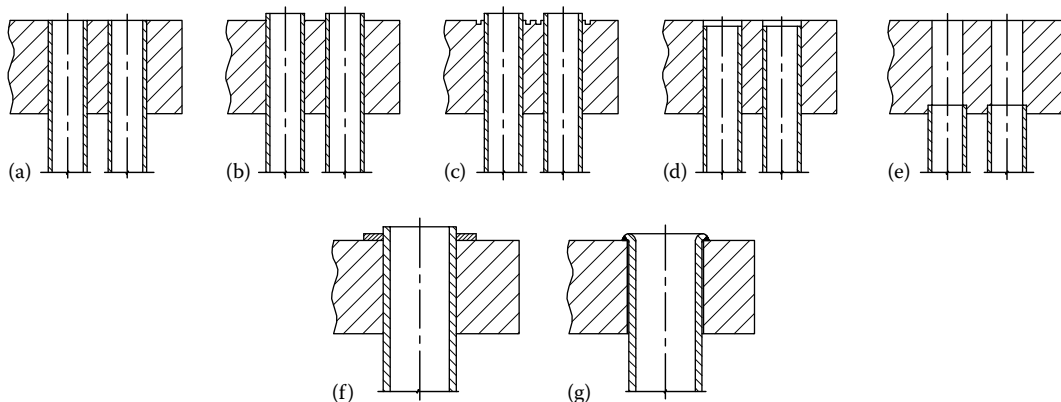


FIGURE 15.45 Commonly adopted tube-to-tubesheet joint configuration for welding. Note: (a) Tube flush with the tubesheet, (b) projecting tube, (c) trepanned tubesheet, (d) recessed tube, (e) rear side welding, (f) added ring weld type, and (g) bell-mouthed and fused welding. (Courtesy of Polysoude, S.A.S, Nantes, France.)

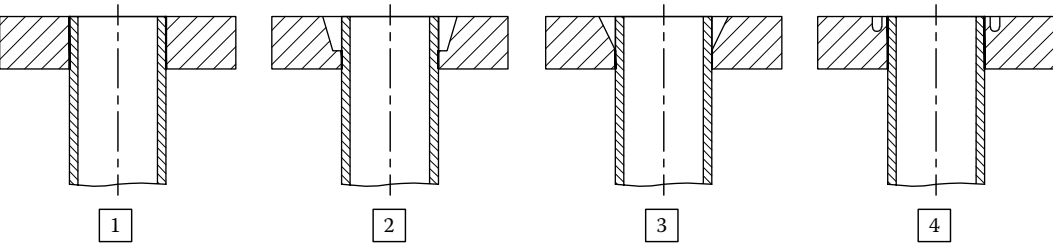


FIGURE 15.46 Tube-to-tubesheet joint configuration for welding of flush tube. (Courtesy of Polysoude S.A.S, Nantes, France.)

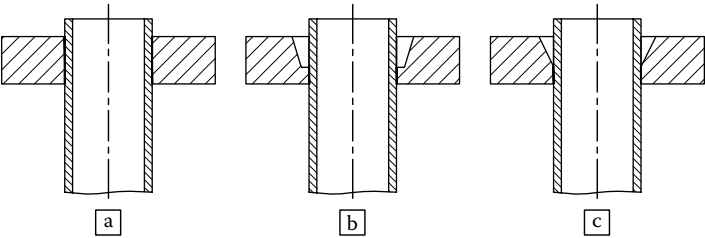


FIGURE 15.47 Tube-to-tubesheet joint configuration for welding of protruding tube.

- 2. Figure 15.46 shows various forms of tube-to-tubesheet joint configuration for welding of flush tubes.
- 3. Figure 15.47 shows various forms of tube-to-tubesheet joint configuration for welding of protruding tubes.
- 4. Figure 15.48 shows forms of tube-to-tubesheet joint configuration for recessed tubesheet welding.

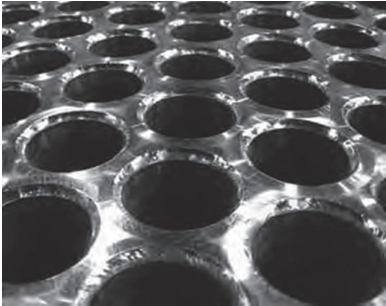
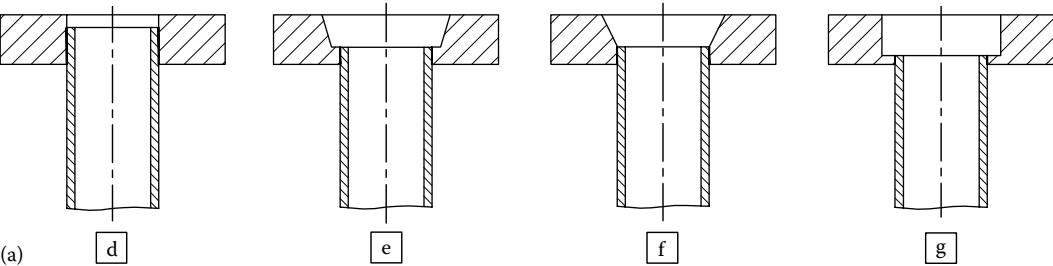


FIGURE 15.48 (a) Tube-to-tubesheet joint configuration for welding of recessed tubesheet. (Courtesy of Polysoude S.A.S, Nantes, France.) (b) Recess welded joint. (Courtesy of Mueller, Springfield, MO.)

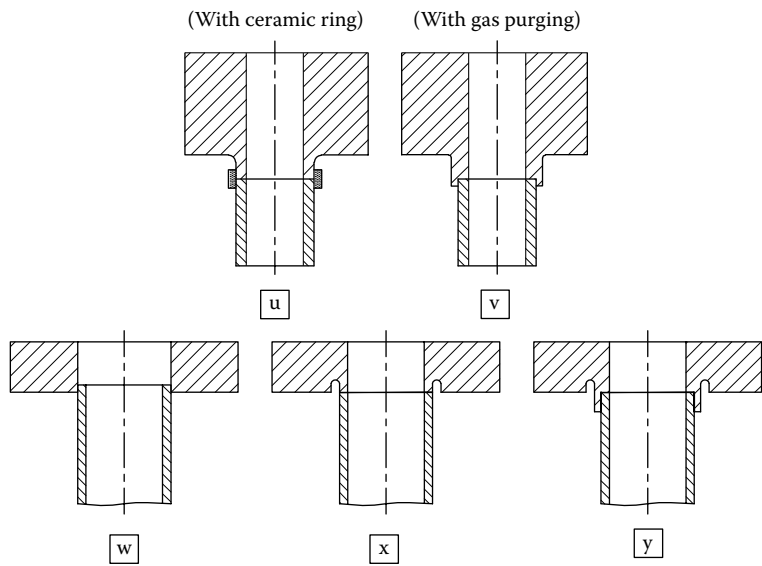


FIGURE 15.49 Tube-to-tubesheet joint configuration for internal bore welding behind the tubesheet. (Courtesy of Polysoude S.A.S, Nantes, France.)

- 5. Figure 15.49 shows various forms of tube-to-tubesheet joint configuration for internal bore welding behind the tubesheet.
- 6. Figure 15.50 shows various forms of tube-to-tubesheet joint configuration for welding of clad tubesheet.

Successful tube-to-tubesheet welding depends critically on the accurate machining of holes, joint preparation of the tubesheet, and cleaning of all surfaces prior to welding. The tubesheet should be

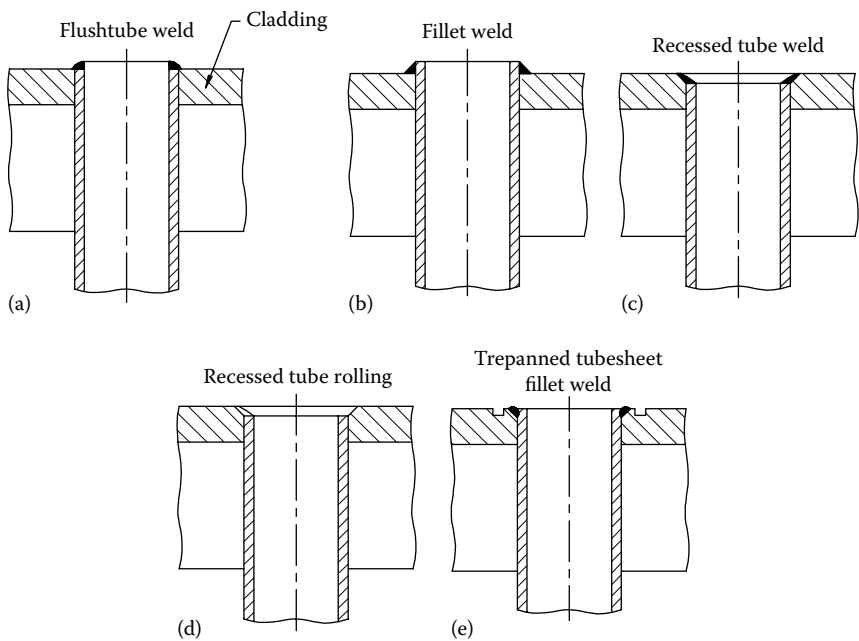


FIGURE 15.50 Tube-to-tubesheet joint configuration for welding of clad tubesheet.

cleaned immediately after drilling, and compressed air should not be used to blow off the cleaning solution. Dry nitrogen is suggested in place of compressed air.

Recessed tube cladding fusion: The recessed tube cladding fusion technique makes possible mechanical cleaning of all surfaces to be fused (Figure 15.50c). This technique requires no addition of filler metal because the cladding provides the filler, and it melts only the corner of the clad hole and fuses only to the top of the tube [32].

15.3.10.2.1 Welding Process

GTAW of tube-to-tubesheet welding: The TIG welding process is used extensively for the welding of nonferrous and austenitic tubes and to a limited extent for carbon steel tubes. This process is particularly useful in the welding of small-diameter tubes where the small ligaments are not suited to the metal arc process [28]. The joint is either autogenous or made with wire feed. Much of the joining of tube-to-tubesheet is done manually, especially on small units, and automatic equipment has been developed for use in large heat exchangers where thousands of tubes are used.

Manual TIG welding: Manual welding requires accurate control over torch movement, especially when the tubes used for weldments have thin walls and small diameters. Although the welds are acceptable, they may lack uniformity and production rate is low; weld size and contour depend largely on the skill of the operator in rotating the torch at a constant speed for proper fusion of the filler wire.

Orbital/automatic TIG welding: Using fully automatic equipment, it is possible to obtain uniform high-quality welds with good reproducibility, and production rate is high. Defects that require rework are few. The automatic GTAW equipment consists of orbital welding setup, in which the welding head is automatically rotated. These orbital welding machines often use a mandrel for self-alignment on the tube to be welded. Once locked into position, a GTAW torch rotates around the face of the tube and joins it to the tubesheet, frequently without the addition of supplemental filler material. Figures 15.51 and 15.52 show the automatic TIG welding heads in action, and Figure 15.53 shows a CNC controlled automatic tube-to-tubesheet welding machine.

Figure 15.54 shows tube-to-tubesheet TIG orbital welding automatic positioning system for tube bundles of tubes from 1/4" to 2" (9.5–50.8 mm), automatic rolling, facing, and welding double-axis working center and a TIG orbital welding head that are manufactured by MAUS ITALIA F. AGOSTINO & C.s.a.s., 26010 Bagnolo Cremasco (Cr), Italy.

In a cold wire method, a cold filler wire is fed to the arc from a spool, through a wire feed drive and an adjustable wire guide tip, all of which rotate with the welding head. Argon shielding gas is automatically fed to the orbiting head. In the actual welding sequence, welding at each end of the



FIGURE 15.51 Tube-to-tubesheet joint welding head. (a) Magnatech welding head and (b) multi welding heads in action. (Courtesy of Magnatech Limited Partnership, East Granby, CT.)

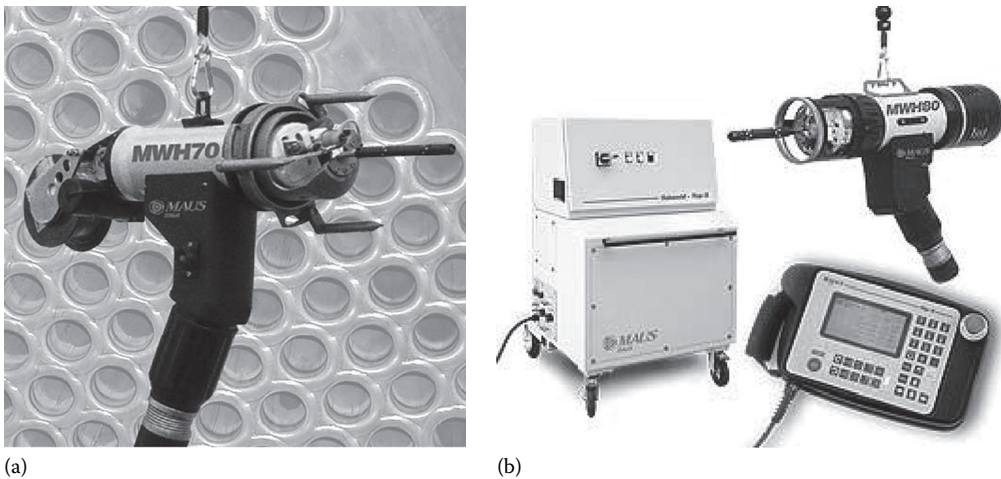


FIGURE 15.52 Tube-to-tubesheet TIG orbital welding head. (a) Weld head and (b) power source and teach pendant. (Courtesy of Maus Italia F. Agostino & C.s.a.s., Bagnolo Cremasco (Cr), Italy.)

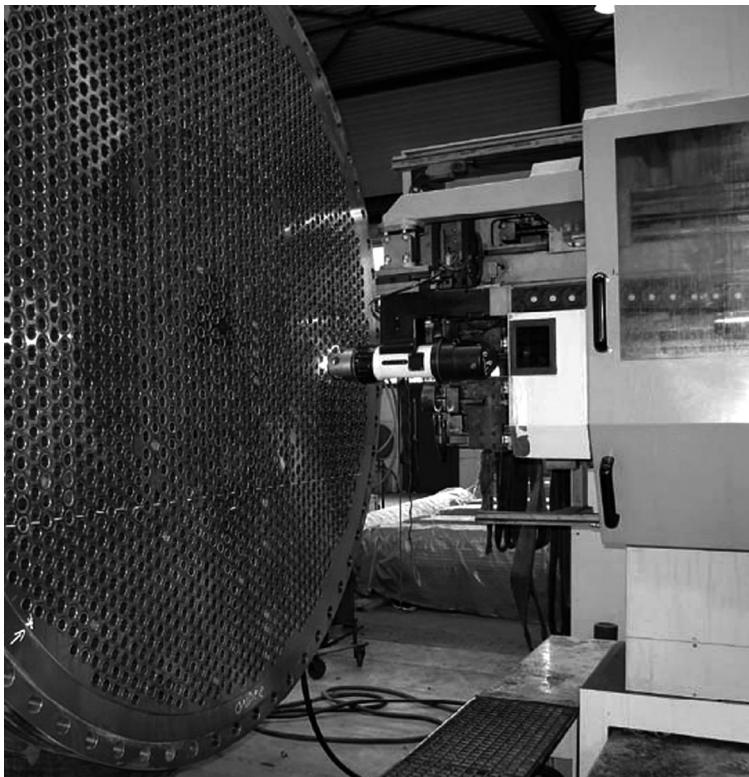


FIGURE 15.53 CNC controlled automatic tube-to-tubesheet welding. (Courtesy of Vermeer Eemhaven B.V. Bunschotenweg, Rotterdam, the Netherlands.)

tube is staggered to ensure that gas leak rate and pressure are not affected by both ends of the tubes being sealed simultaneously [33].

If TIG welding is to be used, the tube wall should be expanded to intimate contact with the tube hole. This may be done by roller expanding or pinning with a tapered pin; however, the tapered pin method is preferred for two reasons [27]: (1) The tube will be exposed to a minimum chance

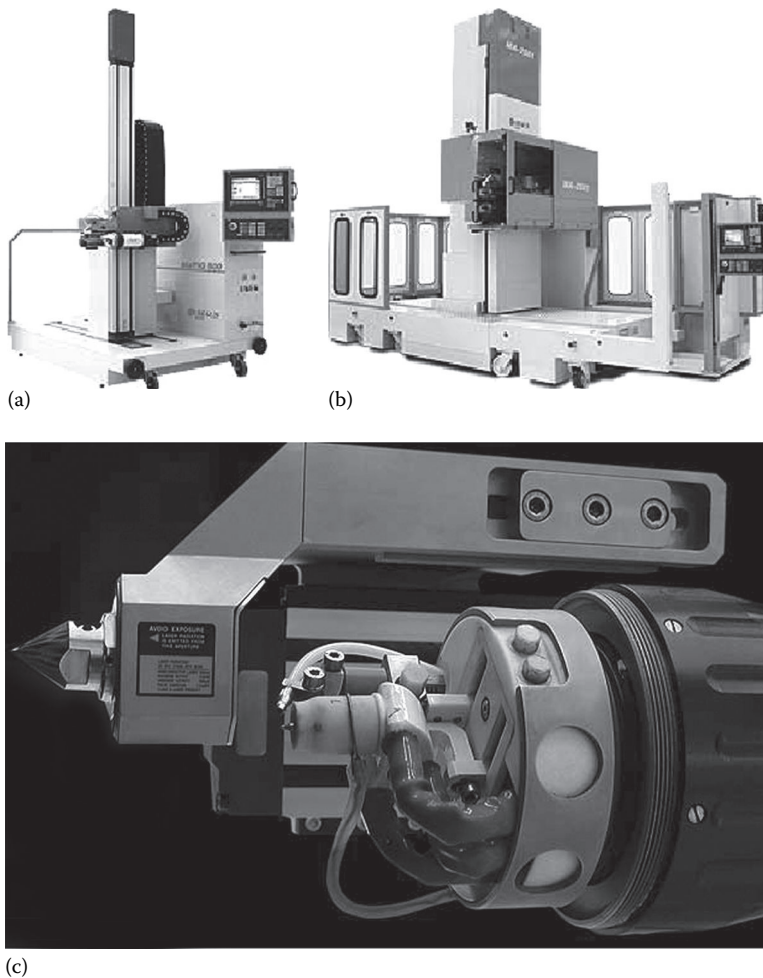


FIGURE 15.54 (a) Tube-to-tubesheet TIG orbital welding automatic positioning system for tube bundles of tubes from 1/4 to 2 in. (9.5 to 50.8 mm), (b) automatic rolling, facing, and welding double-axis working center, and (c) tube-to-tubesheet TIG orbital welding head. (Courtesy of Maus Italia F. Agostino & C.s.a.s., Bagnolo Cremasco (Cr), Italy.)

of contamination, and (2) there will be only a line contact around the periphery of the tube-to-tube hole. This allows the gases generated during welding to escape behind the weld puddle, reducing weld porosity, and the incidence of blow holes as joints are completed.

If preheating and postweld heat treating are required, gas heating can be used or modern equipment is available to carry out the operation in situ. The equipment consists of a computer-controlled temperature monitor and clamp-on cartridge heating elements [33]. Good-quality welds between tube and tubesheet require a high degree of operator skill and concentration. Cleanliness at the joint is always desirable.

15.3.10.2.2 Orbital Welding

Whenever high-quality results are required, orbital welding is the first choice for the joining of tubes. The welding torch—in most cases, the TIG welding process is used—travels around the tubes to be joined, guided by a mechanical system. The name orbital welding comes from the circular movement of the welding tool around the workpiece. Generally, orbital welding technique covers two main fields of application: (1) tube-to-tube/pipe-to-pipe joining and (2) Tube-to-tubesheet welding. Two kinds of current are applied in the TIG welding technique: (1) direct current (DC) is most

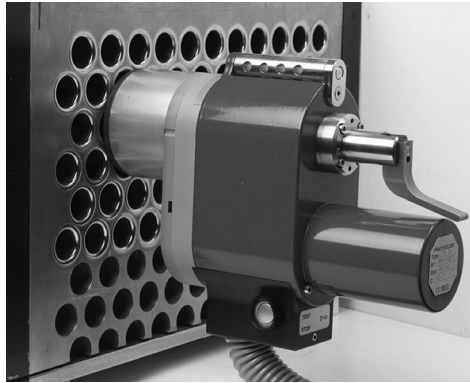


FIGURE 15.55 Orbital TIG welding head—welding of recessed tube-to-tubesheet. (Courtesy of Polysoude S.A.S, Nantes, France.)

frequently used to weld nearly all types of materials and (2) alternating current (AC) is preferred to weld aluminum and aluminum alloys.

15.3.10.2.3 Enclosed Orbital Tube-to-Tubesheet Welding Heads without Filler Wire

Welding head shown in Figure 15.55 is designed for TIG welding (GTAW) of tube-to-tubesheet applications, if they can be accomplished without filler wire. With these weld heads, flush or slightly protruding tubes with a minimum internal diameter of 9.5 mm (3/8") can be welded, the maximum diameter being 33.7 mm (1 1/3"). The weld is carried out in an inert atmosphere inside a welding gas chamber, providing very good protection against oxidation. For clamping, a mandrel is inserted into the tube to be welded and expanded mechanically.

15.3.10.2.4 Open Tube-to-Tubesheet Welding Heads with or without Filler Wire

Open orbital tube-to-tubesheet weld heads that can be used with filler wire cover the whole range of applications from tubes with an ID of 10 mm (13/32") up to tubes with a maximum OD of 60 mm. The TIG torch travels around the tubes, which can be protruding, flush, or recessed. The welding heads are equipped with a TIG torch with gas diffuser (Figure 15.56). A sufficient gas protection is achieved only at the zone around the torch that is covered by the shielding gas streaming out of the gas lens. If oxygen-sensitive materials need to be welded, the gas protection can be improved by installing a gas chamber.

The welding heads can be equipped with an integrated wire feeder. A pneumatic clamping device can be used to hold the weld head in working position on the tube plate, enabling several welding heads to be operated by just one person. Welding lances allow the operator to carry out internal bore welding with gapless joints behind a tubesheet or a double tubesheet.

15.3.10.2.5 Arc Voltage Control Options

As for most orbital welding applications, a pulsed current is applied.

15.3.10.2.6 Welding Equipments

In most cases, the welding equipment used for tube-to-tubesheet welding is strictly adapted to the kind of application and the desired level of automation:

1. Welding equipment featuring three controlled axes (gas, current, rotation) is composed of a stationary installed power source and an enclosed welding head. This equipment allows for the execution of fusion welding without addition of filler wire.
2. The welding equipment, including four controlled axes (gas, current, rotation, wire), is composed of a stationary installed power source and an open welding head. The equipment is suitable for single-pass welding; two passes must be welded in two separate steps.

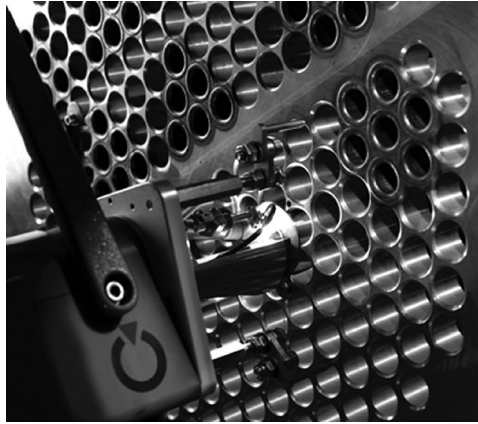


FIGURE 15.56 Orbital TIG welding head—welding of flush tube-to-tubesheet joint using a welding head with tube locking arrangement. (Courtesy of Polysoude S.A.S, Nantes, France.)

3. The welding equipment fitted with five controlled axes (gas, current, rotation, wire, arc voltage control (AVC)) is composed of a power source designed to control six axes and a welding head of the type TS 2000 or TS 60 with AVC configuration. The equipment allows the chaining of two passes with filler wire; the raising of the torch between the first and the second pass can also be programmed and is carried out without interruption of the weld cycle.
4. Welding equipment furnished with six controlled axes (gas, current, rotation, wire, AVC, oscillation), comprises a PC power source and a welding head of the type 20/160. The equipment allows multi-pass welding (two or more passes); the torch can be displaced in radial direction. (This text is based on Polysoude: The art of welding, *The Orbital Welding Handbook*, Polysoude S.A.S, Nantes, France.)

15.3.10.2.7 Specific Requirements of Tubes and Weld Preparations

Compared to manual welding, the planning of the orbital tube-to-tubesheet welding requires some more specific attention:

1. The tubes have to be seamless (or with flattened weld); concentricity faults between the inner and the outer diameter must be limited to a minimum to allow the repeatability of the electrode positioning. With standard applications (flush, protruding, or recessed tubes), the torch is aligned at the inside of the tube whereas the welding is carried out at the external diameter. Concentricity faults would cause unacceptable variations of the distance between workpiece and electrode and thus directly affect the arc length.
2. As with V-joints, it is virtually impossible to ensure reliable melting of the base of the tube edge, especially in the vertically down position (fusion defects are to be seen on micrographic sections); these joints have to be replaced by J-preparations.

15.3.10.2.8 Welding of Flush Tubes

Depending on the application, orbital welding of flush tubes with or without filler metal is possible. Different joint designs are shown as follows:

1. Standard preparations
2. J-preparations
3. V-preparations
4. Relief groove

15.3.10.2.9 *Welding of Flush Tubes with Addition of Filler Wire*

Welding equipment fitted with four or five controlled axes can be used for this application; the open tube-to-tubesheet welding head should be configured with devices adapted to the requirements:

1. Integrated or external wire feeder
2. With or without AVC
3. With or without shielding gas chamber (for the welding of titanium or zirconium)
4. Torch angle of 0° or 15°

Depending on the dimensions, and the required weld thickness, one or two passes are necessary. One pass of the torch is always applied on the first pass for tightness; layers needed for mechanical strength and wear resistance will often require a second pass.

15.3.10.2.10 *Welding of Protruding Tubes*

Protruding tubes are always welded with addition of filler wire, but in some cases, the weld is beginning with a fusion pass. As shown in Figure 15.47, different joint designs are possible.

- a. Standard preparation without groove
- b. J-preparations
- c. V-preparations

Welding equipment fitted with four or five controlled axes can be used for this application. Depending on the pitch and the protruding distance, the torch inclination may be varied. Standard torch angle is 15° or 30°.

15.3.10.2.11 *Welding of Recessed Tubes*

Different joint designs—(d) standard preparation without groove, (e) J-preparation, (f) V-preparation, and (g) welding the tubesheet—are shown in Figure 15.48.

The preparation of the type g is frequently used in the petrochemical industry; welding equipment with six controlled axes and a 20/160 welding head with separate clamping device have to be used. This type of application generally requires a specific project to study the best adaptation of clamping tools and welding procedures. Depending on the dimensions, and the required weld thickness, one or two passes are necessary. One pass of the torch is always applied on the first pass for tightness; layers needed for mechanical strength and wear resistance will often require a second pass.

15.3.10.2.12 *Internal Bore Welding*

Face-side welding techniques shown in Figure 15.46 are economical and generally reliable, but they produce a weld that is difficult to inspect by radiography, and they introduce a long crevice between the tube and the tubesheet [33]. Localized corrosion may start in this crevice. Even if the width of the crevice is made as small as possible by expansion of the tube, inside hole cracks or corrosion still poses a danger. These problems are overcome by internal bore welding methods. In the internal weld joint shown in Figure 15.49b and e, the tube does not pass through the tubesheet. It is welded to a short stub machined on the shell side of the tubesheet. This joint has the important advantages of easy inspectability by radiography and eliminating the crevice. However, it is much more difficult to weld than the face-side design because of the proximity of the tubes. There is no room for an orbiting arc welding head on the outside of the tube. The weld in an internal bore weld is made by welding from the bore side of the tube.

15.3.10.2.13 *Internal Bore Welding behind the Tubesheet*

To avoid crevice corrosion between the tube and the tubesheet, gapless joints are welded from the inside of the tubes at the backside of the plate as shown in Figure 15.57. This type of application requires extended accuracy of the workpiece preparation and welding. Some possible joint designs are x. standard without groove; y. preparation with relief groove, without recess; and z. preparation with relief groove, with recess.



FIGURE 15.57 Internal bore welding behind the tubesheet by TIG welding. (Courtesy of Polysoude S.A.S, Nantes, France.)

Unlike conventional tube-to-tubesheet applications, the internal bore welding operations behind the tubesheet require a gas protection of the root (at the outside of the tube). Only with a preparation of the type x, where the tube end is positioned sufficiently deep in the bore (e.g., half of tube wall thickness), a root protection is not necessary. The protection can be provided by flooding the entire apparatus with inert gas or if the backside of the tubesheet is accessible by a local protection applied tube after tube.

With a tube ID of more than about 35 mm, the use of welding tools with filler metal is possible. If relatively thick-walled tubes of 3–3.6 mm (depending on the base material) are to be welded, a horizontal weld position with the plate at the bottom with the weld head also, horizontally positioned, is recommended. Since the operator cannot see the torch position inside the tube, the distance from the face of the tubesheet to the welding joint must be very precise. Welding equipment fitted with three or four controlled axes can be used for this application; in the case of a joint preparation of type x, five controlled axes are necessary. The welding heads must be equipped with a peculiar lance for internal bore welding. By means of a weld lance that mounted at the front of the weld head, internal bore welding can be carried out at tube ID between 10 and 33.7 mm (13/32" and 1 1/3").

15.3.10.3 Welding of Sections of Unequal Thickness

In SMAW, as in other welding processes, special techniques are required while welding a thick member to a very thin member due to large difference in heat-dissipating capacities. An application involving components of unequal section thicknesses, namely, the welding of heat exchanger tubes having 0.093 in. (3 mm) wall thickness to a tubesheet as thick as 10 in. (254 mm), is discussed in Ref. [34]. In this situation, the welding current needed to obtain good penetration into the thick tubesheet is sometimes very high for the thin tube wall and results in undercutting of the tube and a poor weld. If an adequate amount of current for the tube is used, the heat is not sufficient to provide adequate fusion in the thick tubesheet and again results in a poor weld. Industrial practices to minimize heat-sink differential are [34] as follows:

1. The usual method of avoiding difficulty is to cut a 0.25 in. (6.35 mm) deep circular groove in the upper surface of the tubesheet around the tube hole (Figure 15.45c); the groove restricts heat transfer.
2. To place a copper backing block against the thin member during welding. The block serves as a chill, or heat sink, for the thin member.

Yet another method is to preheat the thick member. Normally, 150°C is preferred for carbon steel tubesheets; for stainless steel, it is not required since the thermal conductivity is very much lower.

Aluminum tubesheet-to-tube welding: For good heat balance, trepan a groove in the tubesheet, making a welding lip of the same thickness as the tube wall, and then edge weld the lip and the wall. Better still, extend the tube one wall thickness beyond the lip to improve melting and fusing [35].

15.3.10.4 Seal-Welded and Strength-Welded Joints

Tube welds at the tubesheet front face are classified as either seal welding or strength welding.

Seal welds: Seal welds are used to prevent fluid leakage between the shellside and the tubeside. Although seal welds confer additional strength on the weld joint, the incremental capacity of the joints to withstand pressure and temperature imposed by loads is neglected in calculating the load-carrying capacity of the joint [21]. Nevertheless, the code requires a qualified welding procedure to be used. Seal-welded joints are normally used for service pressure up to 80 kg/cm² (g) and temperature up to 350°C. It is recommended to expand tubes in grooved holes for better holding strength for higher service pressures.

Strength-welded joints: Strength-welded joints in lieu of full expansion and seal welding are adopted for higher temperatures and pressures, as expanded joints lose their leak tightness at higher temperatures. Tube-to-tubesheet strength welds are used to transfer all longitudinal mechanical and/or thermal loads from the tubes to the tubesheet. The suggested definition of strength weld leads to the following considerations [21]: (1) Using the joint efficiencies specified in the Paragraph UW-15 (c) of ASME Code Section VIII, Div. 1, the total weld cross-sectional area times the joint efficiency must equal the tube cross-sectional area; (2) weld strength must be based upon the lower of the tube or tubesheet allowable stress; and (3) differential thermal expansion between the tube, tubesheet, and weld metal must be considered. The strength weld, which usually has the weld throat 1.4 times the tube wall, is considered to be superior to other joint types in both mechanical strength and sealing ability. When the tube wall thickness is thinner than 1.6 mm (1/16 in.), special weld-groove geometry and welding technique is required. Almost all such strength welds are fillet welds, either at the front face of the tubesheet or within the hole; or, in a very few cases, the tube holes may be drilled to match the tube inside diameter and the tubes butt-welded to the tubesheet secondary face (Figure 15.49u, v and y), known as internal bore welding. Figure 15.58 shows tubes under insertion and tubes welded to tubesheet. Typical strength-welded joints are shown in Figure 15.59 and few acceptable seal welded and strength welded joints as per ASME Code Section VIII, Div. 1 criteria are shown in Figure 15.60.

Joint strength: ASME Code procedure to determine joint strength is discussed in Chapter 11 with mechanical design of shell and tube heat exchangers.

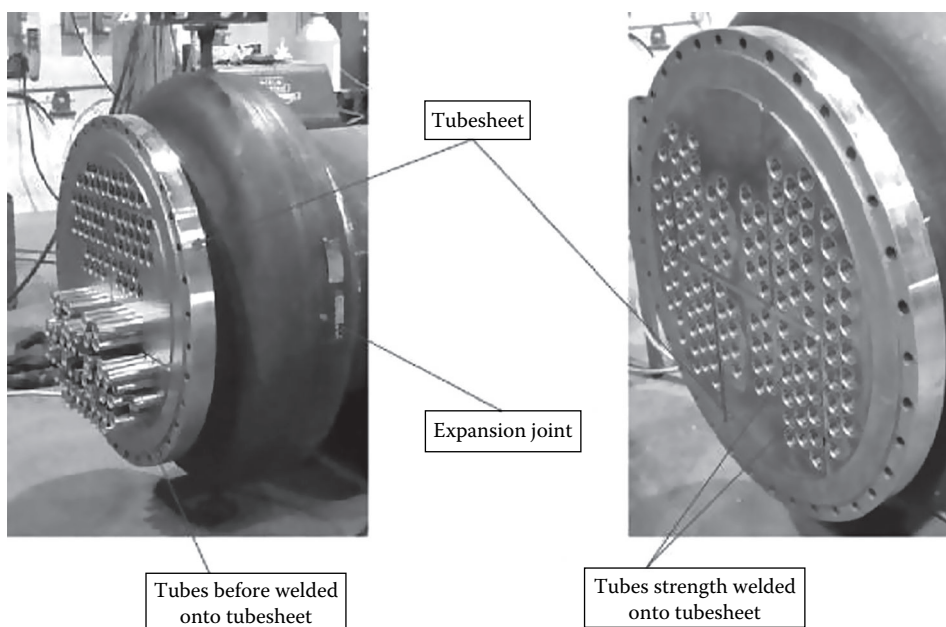


FIGURE 15.58 Tube-to-tubesheet joint—tubes under insertion and tubes welded to tubesheet. (Courtesy of Festival City Fabricators, div. of CSTI, Stratford, Ontario, Canada.)



FIGURE 15.59 Tube-to-tubesheet strength welded joint. (Courtesy of Vermeer Eemhaven B.V., Rotterdam, the Netherlands.)

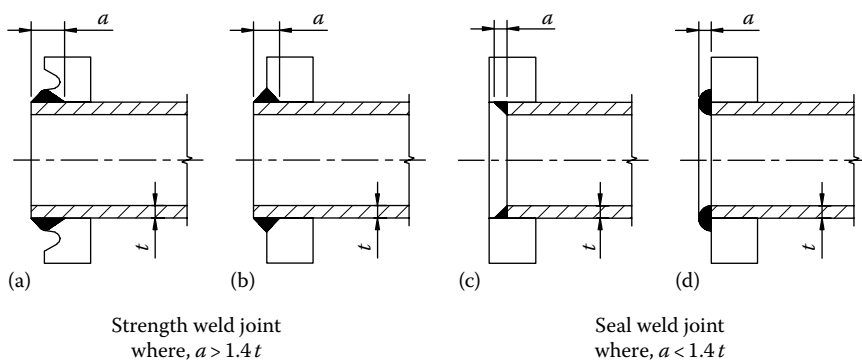


FIGURE 15.60 Some acceptable weld geometries as per ASME Code Section VIII, Div. 1. (a and b) Strength weld joints and (c and d) seal weld joints.

15.3.10.5 Considerations in Tube-to-Tubesheet Welding

There are certain factors to be considered when planning a tube-to-tubesheet joint [36]:

1. Is the tubesheet an air-hardening material that will require PWHT?
2. Are the tube ends and the tubesheet holes clean?
3. Welding before expansion or expansion before welding?

Other factors to be considered include the following [21]:

4. Granular structure
5. The coefficient of thermal expansion of the tubes and tubesheet materials must be close enough

These factors are discussed next.

Is the tubesheet an air-hardening material that will require PWHT? While PWHT is possible under shop conditions, it is often difficult to accomplish under field maintenance conditions. This difficulty is overcome by these measures: (1) Frequently, a non-air-hardening austenitic or Inconel overlay can be specified for the tubesheet [32], thus eliminating the need for PWHT. (2) If an austenitic overlay is not possible due to corrosion problems, the tubesheet can often be overlaid with a low-carbon filler metal of the same nominal composition as the tubesheet. While PWHT would likely be required after overlaying to decrease the HAZ hardness, the lower carbon content of the overlay would not harden as readily during tube-to-tubesheet welding, often eliminating the need for a subsequent PWHT [36]. This aspect is discussed with reference to a feedwater heater with carbon steel tubes welded to carbon steel forging tubesheet in Ref. [32].

Are the tube ends and the tubesheet holes clean? To achieve an absolute seal with good mechanical properties, the welded joint must be free of voids. The tubes, holes, and weld rings should be carefully cleaned to eliminate the danger of voids forming due to evaporation of surface contaminants such as grease, oil, and cutting fluids. It may be necessary to solvent clean the tube ends, the tubesheet should be thoroughly degreased, and the tubesheet holes should be steam cleaned or sand-blasted to remove any scale or dirt that could interfere with the tube-to-tubesheet joints. Titanium tube holes and tubesheets should be cleaned with a solvent such as acetone or methyl ethyl ketone. Methanol or chlorinated solvents such as trichloroethylene should not be used [37]. After cleaning, both the tube ends and tubesheet holes should be visually examined for longitudinal scratches, which could create a leakage path.

Welding before expansion or expansion before welding? A third consideration for achieving successful tube-to-tubesheet joints is the proper application of rolling. To this day, there is ongoing controversy about whether to expand first or weld first [21]. Basically, three different sequences are possible for making tube-to-tubesheet joint. They are the following:

1. Expansion of the tubes followed by welding of tubes
2. Welding of the tube ends followed by expansion
3. Light expansion followed by seal welding and followed by full expansion

The sequence for making a tube-to-tubesheet joint is determined by the following factors [21]: (1) the requirement that the surfaces be very clean; (2) the need for a path of escape of welding-generated gases—otherwise the gases will cause porosity in the weld; (3) the maximum desirable root gap for the material being welded; and (4) the need to repair welds that have failed in service.

Many purchasers recommend to do seal welding first and then roll the joint. The reason that seal welding is done first is to allow the welding gases behind the weld to escape along the tube and to avoid the situation where the presence of oil and fluids used during expansion do not have the opportunity to contaminate the weld pool. If significant rolling is performed prior to welding, a sealed annular space between the tube and the tubesheet is formed. The air in this annular region will expand due to welding heat. Since the gas cannot escape, it expands into the tube-to-tubesheet weld, creating pinhole porosity. Except for joining thin-walled titanium tubes to titanium tubesheets, these requirements indicate that tubes should be welded to the tubesheets prior to expanding [21].

Light expansion followed by seal welding and followed by full expansion is most preferred, since it has the merits of the two sequences just discussed. Prior to tube-to-tubesheet welding, it is often desirable to expand the tube into the tubesheet by a “light roll” to ensure that the tube is centered in the hole for good tracking in automatic welding. A “hard roll” prior to welding increases the chance of producing a weld defect from escaping gas as the weld is being made. Experience has shown that the best welding results are obtained when tubes are only anchored into the tubesheet prior to welding by these means [21,36]: (1) center punching, (2) a tapered drift pin, and (3) a light expansion (presumably to create tube/hole contact that is not hydraulically tight). Another method,

suggested by Yokell [21], is to use one of the commercially available expanders that compresses a polymer in the tube end to produce radial pressure. These can be set to lock the tube in place without creating a hydraulically tight seal.

While performing rolling operation, lubricant should not be used, to avoid contamination. However, without lubricant, there is a possibility that heat due to friction will cause some of the hardened roller and cage material to flake off [21].

Proper rolling techniques following welding are required. Some fabricators have found it necessary to start rolling at least 12.5 mm (0.5 in.) away from the weld, proceeding toward the shellside of the tubesheet [36]. Such a procedure minimizes the amount of mechanical loading on the weld. As indicated by TEMA, rolling should not progress closer than 3.2 mm ($\frac{1}{8}$ in.) to the shellside of the tubesheet.

Granular structure: Tubesheets must have a granular structure fine enough to permit consistently uniform weld metal deposits. Carbon steel tubesheets should always be grain refined [21].

Coefficient of thermal expansion of the tubes and tubesheet materials: Consider, for example, an austenitic stainless steel tube, TIG welded to a carbon steel tubesheet with high-alloy filler metal. The coefficient of thermal expansion of the austenitic stainless steels (17.8×10^{-6} cm/cm $^{\circ}$ C) is about 50% greater than that of the carbon steel (12.1×10^{-6} cm/cm $^{\circ}$ C). The fusion temperature is in the range of 2800 $^{\circ}$ F (1730 $^{\circ}$ C). As the welds solidify rapidly, the difference in the rates of expansion engenders high levels of thermal stress [21]. Stresses due to operating pressure superimposed on the thermal stresses may cause premature failures.

The clearance between the tube and tubesheet hole: When the tube-to-tubesheet hole clearance is excessive, the required root penetration cannot be achieved and the weld root will fracture.

15.3.10.6 Welding of Titanium Tubes to Tubesheet

For highly reliable leak tightness, many nuclear and fossil plant heat exchangers demand welded tube joints. Since titanium cannot be successfully welded to other materials, a titanium tubesheet, either solid or explosively clad titanium, is required. For cladding, at least 3 $\frac{1}{16}$ thick is preferred. Also, the thermal expansion coefficient of titanium (8.9×10^{-6} cm/cm $^{\circ}$ C) is much smaller than those of carbon steel (12.1×10^{-6} cm/cm $^{\circ}$ C) and stainless steel (17.8×10^{-6} cm/cm $^{\circ}$ C), which are commonly used as the base metals of tubesheet. The tube should be roller expanded before welding. Either a light tack roll or a full expansion can be performed. The expansion is required to keep air from the back face from contaminating the weld and to prevent vibration of the tube that could result in weld cracking. i.e., the contact roll eliminating the clearance between the tube and tube hole is a very important operation in obtaining a sound weld. This operation is applicable for other reactive metals like zirconium (whose thermal expansion coefficient is 5.8×10^{-6} cm/cm $^{\circ}$ C). If full expansion is carried out after welding, then tube expansion should start at least 3.1 mm (1/8") back from the weld. Both the tube holes and the tube ends should be cleaned with a solvent such as acetone before welding. Methanol or chlorinated solvents such as trichloroethylene should not be used [37]. Figure 15.61 shows welding of titanium tube-to-titanium clad tubesheet. Since the extrusion of the tube during conventional rolling would lead to problems with a clad-type tubesheet potentially causing the clad layer and interstitial layers to separate, it is suggested that the tubes are hydroswaged as the extrusion forces are deemed to be lower with this application.

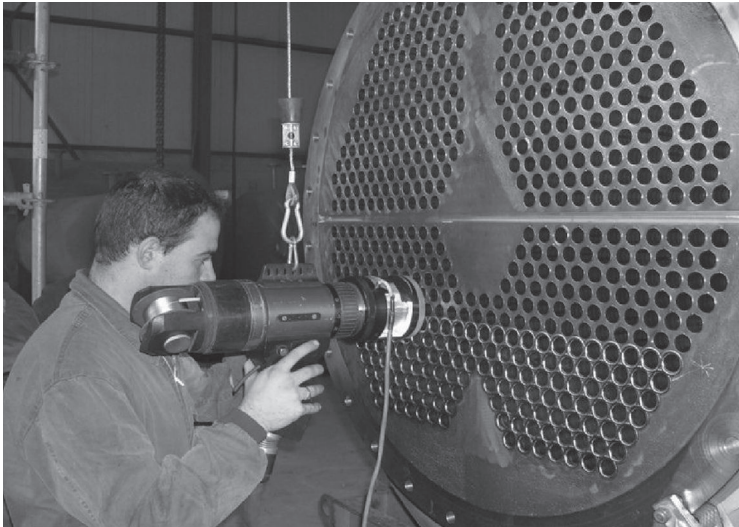
15.3.10.7 Merits of Sequence of Completion of Expanded and Welded Joints

Merits and demerits of these methods are as follows.

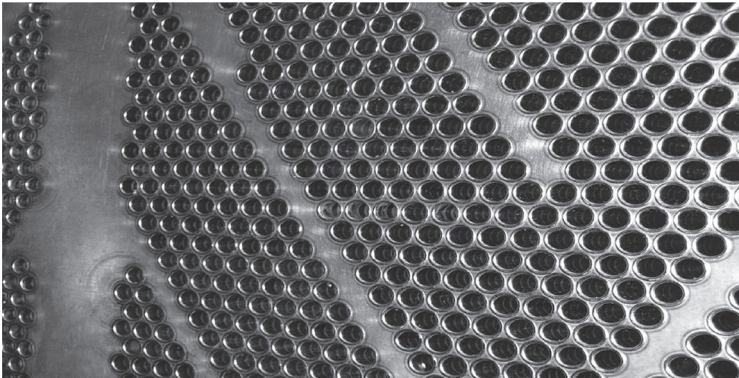
First expansion followed by welding.

Merits

1. Welds are free from strains induced by rolling operation.
2. The integrity of the tube expansion can be tested.



(a)



(b)

FIGURE 15.61 Titanium tube-to-titanium clad tubesheet welding. (a) Tube welding and (b) welded tubesheet. (Courtesy of GEA Iberica S.A., Vizcaya, Spain.)

Demerits

1. Welds may contain porosity due to the presence of lubricants used during expansion, if cleaning is not done properly.
2. Expansion may get loosened under the influence of heat during welding. Such tubes would require rerolling.

First welding followed by expansion.

Merits

1. Welds are free from porosity due to the absence of lubricants.
2. If the tube-to-tubesheet joint requires PWHT, there is no point in expanding first. The heat treatment will relax the tubes.
3. Tube projection for welding is uniform.

Demerits

1. Welds may be damaged due to strain caused by expansion.
2. There is no foolproof check for the leak tightness of the expansion carried out, as the seal welds may help in shadowing the underexpansion of the tubes.
3. Weld shrinkage may reduce the tube inner diameter so that it is difficult to insert expanders. This problem is overcome by reaming.

Ebert [38] discusses four types of tube-to-tubesheet joints (i) expanding with grooves, (ii) expanding without grooves, (iii) expanding with grooves and seal welding, and (iv) strength welding. Characteristics of such joints are hereunder:

1. Roll or expand only (without grooves)
 - Strength is poor
 - Leak resistance is poor
 - Tube replacement is very easy
 - Application is limited (i.e., low-pressure water or air)
2. Roll or expand only (with grooves)
 - Strength is limited (can be improved by explosive expansion)
 - Leak resistance is limited (can be improved by explosive expansion)
 - Tube replacement is easy
 - Applicable for low stresses and low consequences of leakage
3. Roll or expand and seal weld (with grooves)
 - Commonly used by the oil industry
 - Strength is limited (can be improved by explosive expansion)
 - Leak resistance is good (can be improved by explosive expansion)
 - Fabrication problems are faced
 - Tube replacement is more difficult
 - Applicable where stresses are not too high and where risks of leakage is low
4. Strength weld (no grooves required)
 - Full strength
 - Leak resistance is good (maximum leak resistance can be achieved if two pass welds are used)
 - Some fabrication problems, especially if there are grooves
 - Tube replacement is more difficult, especially if there are grooves
 - Applicable where mechanical and thermal stresses are high and leakage is unacceptable

Sequences to be followed in the case of welding tube ends and then expand [39]:

1. Clean the tubesheet holes
2. Clean and deburr the tube ends
3. Insert tubes into tubesheet
4. Tack weld some tubes on tubesheet at four places
5. Weld tube ends
6. Air leak test welds; repair as needed
7. Expand the tube ends
8. Penetrant test welds; repair as needed
9. Leak test welds using helium

Sequences to be followed in the case of expand tubes and then weld [39]:

1. Clean the tubesheet holes and deburr the ends
2. Clean and deburr the tube ends
3. Insert tubes into tubesheet
4. Expand tubes
5. Leak test the rolled joints; re-expand as needed
6. Weld tube ends (weld tube ends in a random order to avoid concentration of heat in a localized area)
7. Perform helium leak test of the welded joints

15.3.10.8 Full-Depth, Full-Strength Expanding after Welding

When the tube welding is to be done at or near the tubesheet front face, it is desirable to expand the tubes to full strength for approximately the whole tubesheet thickness for the following reasons [21]:

1. Expanding the tubes into the holes isolates the welds from the effects of tube vibration.
2. Contact between the tube and the hole permits heat to flow between the tube and tubesheet.
3. For full-strength expanded tubes, the ligament efficiency is much greater than when there is no contact as given by the formulas. For example, the expression for minimum ligament efficiency μ is given by [40]:

$$\mu = \frac{p-d}{p} \quad \text{for tubes welded to the tubesheet}$$

$$\mu = \frac{p-(d-t)}{d} \quad \text{for tubes expanded more than 90% of the tube sheet thickness} \quad (15.4)$$

where

d is the tube outer diameter

p is the tube pitch

t is the tube wall thickness

15.3.10.9 Ductility of Welded Joint in Feedwater Heaters

For applications such as feedwater heaters, the tubesheets are subjected mainly to bending stresses due to high feedwater pressure, which may be as high as 5000 psi in modern plant cycles. The tube-to-tubesheet joints must remain impervious to water under this high pressure while sustaining the cyclic stresses due to tubesheet flexure, and temperature variations between the tube and tubesheet caused by such operating conditions as start-up, load shedding, shutdown, and possible abnormal transient operations [32]. According to Lohmeir et al. [32], due to these reasons, the flexural and thermal stresses can be sufficiently large, even exceeding the elastic limit, to propagate leakage paths from weld metal flaws. In order to cope with such high stresses without suffering damage, the welds must have consistent mechanical properties and high ductility. The main factors to be controlled to ensure the ductility of the joints are [41] the following:

1. Combination of tube and tubesheet materials
2. Welding parameters
3. Heat treatment

The carbon content of the basic material and welding alloy (less significant factor).

The following factors ensure welded joints of even quality and high ductility [41]:

1. Tubes and tubesheets are always of the same material, with a maximum carbon content of 0.20%. The filler is of a special alloy whose main feature is an extremely low percentage of carbon.
2. All joints and the electrode are preheated before welding.
3. When all welding is completed, the entire tubesheet is stress relieved.

15.3.10.10 Welded Mock-Ups

To determine correct welding parameters, use mock-ups to scrutinize tube-to-tubesheet weldments. Welded mock-ups are sectioned and prepared for review of the root area and dimension checks of the weld. Examinations of welded mock-ups are discussed in detail by Syal [14]. An expanded and welded tube-to-tubesheet mock-up is examined by the following methods:

1. Radiography examination: The weld shall be free from porosity, cracks, or other defects that would result in leakage in service.
2. Micro- and macro-examination: to detect defects, metal flow in the annular grooves (if grooves are present in the tubesheet), fusion, penetration, etc.
3. Minimum leak path: For strength-welded joints, the minimum leak path shall be the tubesheet thickness, and for seal-welded joints 0.7 times the tubesheet thickness.
4. Hardness examination: tubesheet, tube, weld, and HAZ; normal hardness limits are for carbon steel 220 HV, low-alloy steel 260 HV, and stainless steels 250 HV or as specified in the specification [14].
5. Tear test for strength welded joint.
6. Pulling test: Tubes shall be pulled on a tensile testing machine with a pulling load not less than $0.1 \times L \times d \times 3000$ (kgf) for expanded tubes without seal welding, where L is the length of expansion joint (cm) and d tube outer diameter (cm) [14].
7. For welded mock-up, pressure test as shown in Figure 15.62.

15.3.10.11 Inspection of Tube-to-Tubesheet Joint Weld

1. The completed tube-to-tubesheet joint weld should be inspected visually for defects. Use magnifying glasses to check and mark cracks, pinholes, etc.
2. A dye penetrant inspection is also adopted.
3. In some tube-to-tubesheet joints, a radiographic inspection can be made of selected areas.

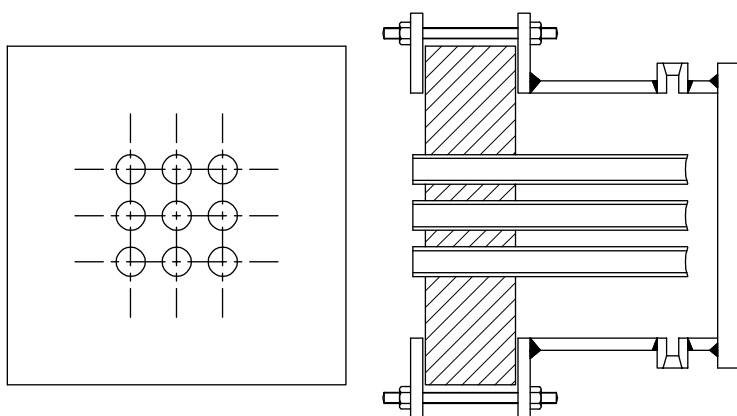


FIGURE 15.62 Welded tube-to-tubesheet model pressure test setup.

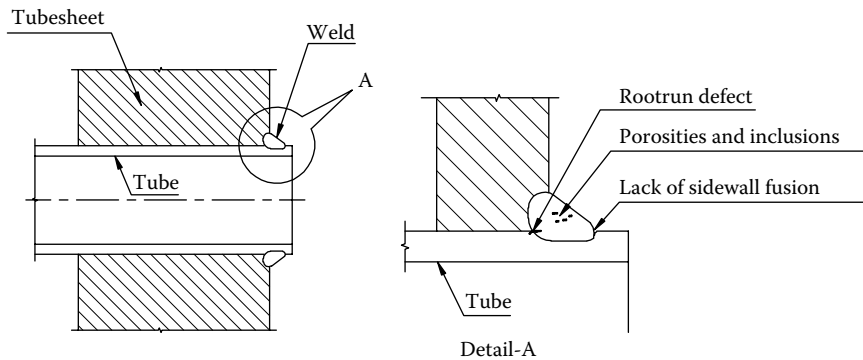


FIGURE 15.63 UT inspection of tube-to-tubesheet joint welds.

4. Defects such as cracks or porosity should be ground out and repaired by GTAW with filler metal.
5. UT inspection of tube-to-tubesheet joint welds. UT inspection on GTAW tube-to-tubesheet welds for critical applications is well established to verify the weld leg length and throat thickness and to investigate the welds for typical defects (Figure 15.63), Ref. [42].
6. Radiographic inspection of tube-to-tubesheet joint welds. For very critical applications, the acceptance standards for tube-to-tubesheet welds like the seal, spigot, and butt/fillet weld are generally based on high-definition panoramic radiography. The small size of the welds and their shape necessitate a very short source to film distance [43]. This requires a highly specialized equipment such as the microfocus rod anode set and miniature low-energy gamma sources, a unique film cassette for use on small-diameter welds to implement radiography on these welds [43,44]. Figure 15.64 illustrates the principles of the radiographic testing technique to test tube-to-tubesheet weld.

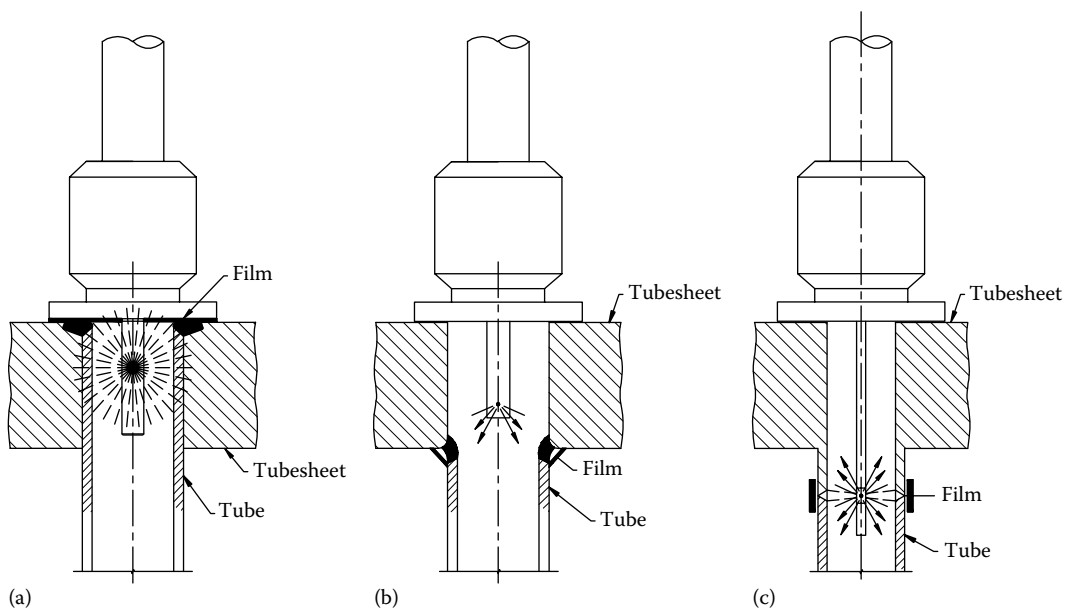


FIGURE 15.64 Radiographic inspection of tube-to-tubesheet weld joint by Microfocus rod anode x-rays set. (a) Front end, (b) rear side fillet weld, and (c) spigot weld.

15.3.10.12 Leak Testing of Tube-to-Tubesheet Joint

Leak testing of exchangers will allow one to determine if tubes have been adequately rolled or welded into the exchanger tubesheets. The simplest and inexpensive test is gas bubble testing also known as soap bubble testing. Such testing can be accomplished by pressurizing the shellside with air to a pressure of 1.0–1.25 ksc (gauge) and “soaping” the face of the tubesheet and looking for bubbles, or by filling the shell with water, pressurizing the channel with air, and looking for bubbles through the shellside nozzle. Various leak testing methods are discussed in Chapter 14 on quality control, inspection, and NDT. Figure 15.65 shows a vacuum gun for rolled joint leak testing gun.

15.3.10.12.1 TEMA Standards on Testing of Tube-to-Tubesheet Joints

As per paragraph RGP-RCB-7.6, tube-to-tubesheet welds are to be tested using the manufacturer’s standard method. Any special testing using halogens or helium will be performed by agreement between manufacturer and purchaser.

If there is a potential hazard due to a leak in service or when the tubeside design pressure is substantially higher than that of the shellside, it is desired to specify halogen or helium sniffer leak testing to satisfy no-leak requirements. For high-pressure feedwater, small leaks through the tube-to-tubesheet joints lead to wire drawing (worm holing), which can be extremely expensive to repair while in service [26]. Hence, typical feedwater heater procurement specifications require helium leak sniffer testing (mass spectrometer method) of the tube-to-tubesheet joints. For tubes welded to the tubesheet and subsequently expanded, in addition to such leak testing, the welds should be examined by dye penetrant test or UT or RT.

15.3.10.13 Brazing Method for Tube-to-Tubesheet Joints

Brazing is used for tube-to-tubesheet joints that are free from stress concentration and crevice corrosion problems. For the fabrication of heat exchangers, three methods of brazing are in common use: torch brazing, furnace brazing, and dip brazing. ASME Code Section VIII, Div. 1, prohibits brazed joints for lethal service and for unfired steam boilers.

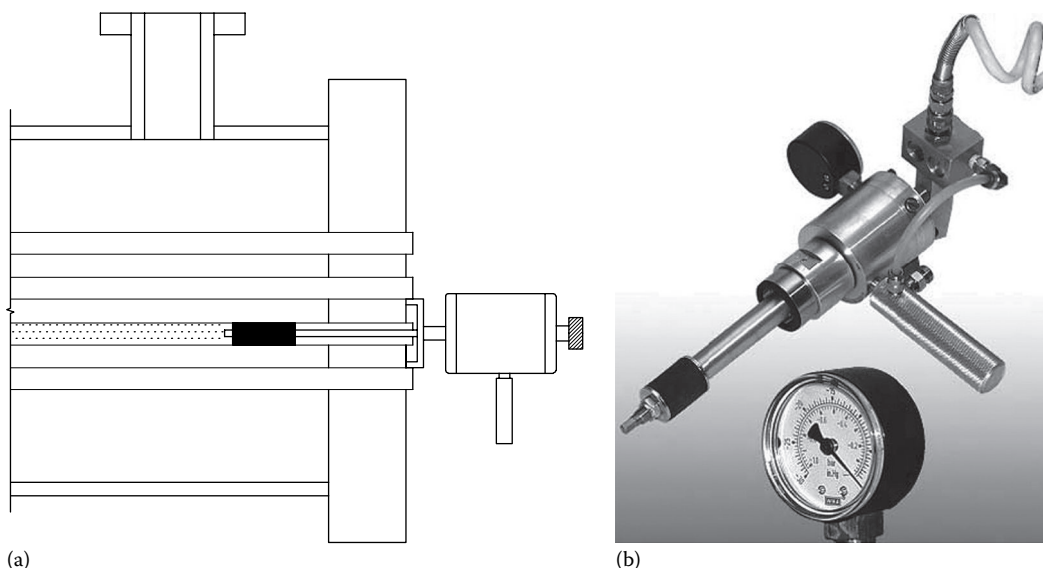


FIGURE 15.65 (a and b) Rolled tube-to-tubesheet joint testing vacuum gun. (Courtesy of Maus Italia F. Agostino & C.s.a.s., Bagnolo Cremasco (Cr), Italy.)

15.3.11 HEAT TREATMENT

Heat treatment of fixed tubesheet exchangers may be done by either of these methods:

1. With tubes welded in one tubesheet and left free in the holes of other tubesheet
2. Both ends of the tubes welded with tubesheets

Salient features of these methods are discussed next.

15.3.11.1 With Tubes Welded in One Tubesheet and Left Free in the Other Tubesheet

The procedure adopted is as follows:

1. After welding the tubes on one tubesheet, stress relieve the joints by leaving the tubes free in the second tubesheet.
2. Weld the tubes to the second tubesheet and stress relieve the second tubesheet by placing only part of the exchanger in the furnace: however, this stress relieving may be waived if proper welding procedure with suitable preheating can control the hardness of the weld metal and HAZ within acceptable limit, provided that PWHT is not a mandatory requirement [14].

15.3.11.2 Both Ends of the Tubes Welded with Tubesheets

During heat treatment, the rate of heating and cooling should not exceed 30°C per hour. The temperature gradient between the outer skin of the shell and the innermost tube should be narrowed down to an acceptable limit by soaking the exchanger during the heating stages.

15.3.11.3 Heat Treatment: General Requirements

Prior to PWHT, the exchanger should be thoroughly examined by visual inspection and NDT methods to avoid welding repair after completion of heat treatment. Consider the following points while heat treating heat exchangers:

1. The complete exchanger should be thoroughly cleaned before charging into the furnace. Any scale formation on the tubesheet and tubes, when tubes are kept free on one side, is avoided by the circulation of nitrogen. Alternately, tube ends may be plugged with ceramic fiber plugs, which will not permit the hot gases from entering the tubes, thereby preventing oxidation.
2. Exchangers must be heat treated in a furnace that is heated electrically or by gas burners. The furnace must be of such a design as to prevent direct impingement of flame on the exchanger. Flame selection, that is oxidizing, reducing, slightly oxidizing, etc., is important to avoid excessive scaling and oxidation.
3. Sufficient numbers of thermocouples should be provided on the exchanger to verify uniform heating; their locations are also important.
4. Rate of heating, holding temperature, and rate of cooling are generally governed by material used and the construction code. PWHT requirements for welds between dissimilar metals shall conform to the requirements of the material having the more stringent requirements.
5. Ensure that the tubes are adequately supported to prevent sagging of the tube bundle. Similarly, during PWHT of the exchanger, it may be necessary to support the shell, if its supports are widely spaced and sagging is likely.
6. Heat treatment should always be done before hydrostatic test. If for any reason tube end welding, however small, is carried out after heat treatment, it is recommended to repeat the heat treatment when PWHT has been specified as requirement.
7. After heat treatment, the tubesheet and tubes shall be examined to ensure that its surfaces are free from scale, oxidation, decarburization, fine cracks, distortion, dimensional accuracy, etc.

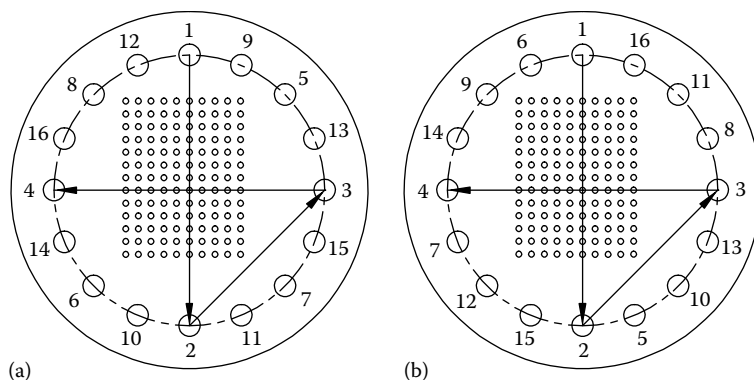


FIGURE 15.66 (a and b) Two types of bolt tightening sequence. (Courtesy of Lummus Technology Heat Transfer, A Division of Lummus Technology Inc., Bloomfield, NJ.)

Details on QC during PWHT of welded components are discussed in Chapter 13 on material selection and fabrication.

15.3.12 ASSEMBLY OF CHANNELS/END CLOSURES

Where a fully pressed end is required, the end closure is purchased from the trade as a pressing or can be fabricated from a series of petals on the shop floor. (Forming of various types of heads are discussed later.) Assemble the channels/end closures with the shell assembly and measure the flatness. Measure tubesheet flatness across the diameter of the gasket ring for conformity with the specifications. Inspect fixed tubesheets extended as flanges for deformation due to weld shrinkage.

15.3.12.1 Bolt Tightening

After the heat exchanger assembly, tighten the bolts in a controlled sequence crisscross pattern similar to that shown in Figure 15.66a or Figure 15.66b except for special high-pressure closures when the instructions of the manufacturer should be followed. It is important that all the flange bolts carry approximately equal load. For exchangers in critical services where it is essential to avoid leakage, use the ultrasonic bolt tensioning devices to ensure that the bolts are tightened uniformly [36].

15.3.13 HYDROSTATIC TESTING

The hydrostatic test shall be carried out after PWHT and complete assembly and all NDT performed, prior to applying painting, insulation, coating, and packing, under the supervision of a QC engineer and/or third-party inspection, by observing the state and local pressure vessel code. Care has to be taken for safe supporting and complete venting of the pressure vessel. Welded joints are to be cleaned prior to testing the exchanger to permit proper inspection during the test.

15.3.13.1 ASME CODE Requirement

As per the ASME Boiler and Pressure Vessel Code Section VIII Division 1, UG99 requires testing the integrity of pressure vessels by subjecting them to a hydrostatic pressure of 1.3 times the MAWP corrected for the difference between allowable stress at the temperature and the design temperature. To compute the hydrostatic test pressure, the following options are available:

- Pressure per UG 99b = $1.3 * \text{MAWP} * \text{Sa/S}$
- Pressure per UG 99b(34) = $1.3 * \text{Design pressure} * \text{Sa/S}$
- Pressure per UG 99c = $1.3 * \text{MAP} - \text{hydraulic head}$
- Pressure per UG 100 = $1.1 * \text{MAWP} * \text{Sa/S}$

where

MAWP is the maximum allowable working pressure in operating condition (temperature and corrosion considered)

MAP is the maximum allowable pressure in new and cold condition

15.3.13.2 TEMA Standard Requirement

For the shell and tube heat exchanger built to the TEMA Standard, as per paragraph RCB 1.31, “The exchanger shall be hydrostatically tested with water. The minimum hydrostatic test pressure at room temperature shall be 1.5 times the design pressure, corrected for temperature, except where other code requirements govern.” The test pressure shall be held for at least 30 min. The shellside and the tubeside are to be tested separately in such a manner that leaks at the tube-to-tubesheet joints can be detected from one side. When the tubeside design pressure is higher than the shellside pressure, the tube bundle shall be tested outside of the shell only if specified by the purchaser and the construction permits. In case of stacked assembly, these tests will be done in the stacked condition.

15.3.13.3 Hydrostatic Testing: Prerequisites

A survey of the entire system to ensure that system is built as per design and code. Ensure that there are no open ends, and all joints are properly made. The equipment shall be supported adequately, and where necessary, additional temporary supports shall be provided to take care of the additional load. Isolate other equipments that are not designed for the test pressure. A relief valve must be included in the pumping circuit to prevent overpressurization. Vents should be provided to release air from high points of the system. Drain should be provided at the lowest point to drain the liquid after test.

When exchanger is tested for the differential pressure, testing shall be done to each side simultaneously with final raising of shell to top pressure with tubes at top pressure or tube to top pressure with shell at top pressure, as the case may be. (Note: Supplier shall provide a conspicuously visible caution plate near to or as a part of the nameplate, indicating that the internals of the exchanger have been designed for differential pressure and that any operating conditions of testing conditions must not be allowed to exceed this differential.)

If any of the pressure part is found to be damaged after a successful test, the exchanger shall be retested after repairs.

15.3.13.3.1 Hydrostatic Testing Procedure

Air lock plays a very important role. Make sure that air is removed completely before conducting the hydrostatic test, and the overflow is witnessed by the inspector before closing the nozzle. The pressure has to be measured with two calibrated pressure gauges, connected independently of each other. The indication range must not exceed 150% of the test pressure. Keep a watch on the pressure gauge dial to spot drop in pressure that indicates leaks. The test pressure shall be held for at least 30 min while looking for water oozing from welds, gaskets, and other potential sources for leaks. For the pressure test, in addition to inspecting the expansion joint for leaks, the expansion joints shall be inspected before, during, or after the pressure test for visible permanent distortion. If leaks are detected, they should be repaired and test repeated until no leakage is detected. The hydrostatic test may be complemented by the application of acoustic emission test with the objective of trying to detect any crack growth that may be generated during the test.

15.3.13.3.2 Hydrostatic Test Fluid

The hydrostatic pressure test is in general carried out with drinking-quality water free from any corrosive and suspended substances, especially, chlorides and microorganisms. In the case of bad water quality, temperatures higher than 30°C combined with longer holding time may cause corrosion. If required, suitable corrosion inhibitors may be used. Do not test austenitic stainless steel exchangers with water that has a chloride ion concentration high enough to cause stress corrosion cracking. Because most potable water supplies are chlorinated, it is necessary to check the chloride levels.

The chloride level in testing water is limited to 25 ppm for austenitic stainless steel types 304, 310, and 321, Incoloy 800, and for aluminum, and 100 ppm for Cr–Ni–Mo austenitic steel types 316 and 317. Alternatively, use conditioned demineralized or distilled water for hydrostatic testing.

15.3.13.3.3 *Use of Fluorescent or Visible Tracer Dyes in Hydrostatic Test Fluids*

Fluorescing dye indicators can be added to the water used in hydrostatic pressure tests for improving the visibility for locating leaks.

15.3.13.3.4 *Cyclic Hydrostatic Testing of Feedwater Heater*

When the tubeside design pressure is very high in the order of 1500 lb/in.² and above as in the case of closed feedwater heater, it is suggested for cyclic testing. High-pressure feedwater heater requires to bring the tubeside to the hydrostatic test pressure followed by dropping the pressure to atmospheric pressure for each cycle, and the cycle is to be repeated for 10 cycles. Such testing has beneficial effects on the structure in addition to possibly opening subsurface porosity bubbles and disclosing cracks in the welds [21].

15.3.13.4 Improved Method for Hydrostatic Testing of Welded Tube-to-Tubesheet Joint of Feedwater Heaters

The integrity of tube-to-tubesheet joints is judged by hydrostatic tests and leak testing techniques. The basic limitations in these tests are that they reveal only those defects that provide, at the time of testing, a flow path completely through the weld. Experience with carbon steel tubesheet welds has shown that the leaks that can occur after service operation give no indication of leakage during shop floor leak testing or hydrostatic testing [32]. One method that has been successful in detecting subsurface defects involves cycling the heat exchanger to hydrostatic test pressure a number of times and providing a thermal shock to the tubesheet weld surface in the shop floor. The high tube-to-tubesheet joint stresses due to pressure cycling have been particularly successful in completing the potential leakage paths that require a short propagation distance.

15.3.13.5 **HydroProof™**

HydroProof is the easiest, most advanced system for the hydrostatic testing of individual tube-to-tubesheet joints for boilers, condensers, feedwater heaters, heat exchangers, and air heaters. Using water under pressure, this lightweight and durable tool can hydrotest up to 2000 psi for sizes from 5/8" to 2.5" OD. With the addition of the full tube length HydroProof, it is now possible to test the integrity of a tube along its entire length, with the same ease of use and setup offered by the standard HydroProof. HydroProof unit is shown in Figure 15.67.

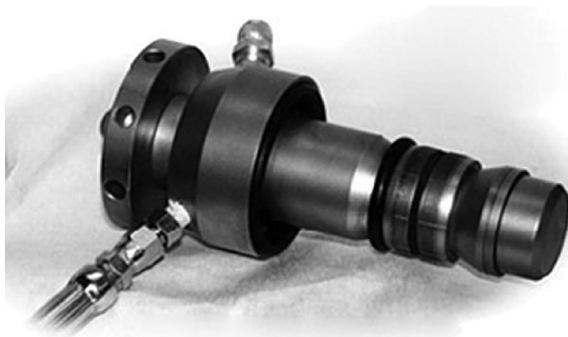


FIGURE 15.67 Hydroproof for the hydrostatic testing of individual tube-to-tubesheet joint. (Courtesy of HydroPro, Inc., San Jose, CA.)

15.3.13.5.1 *Pneumatic Tests*

As per ASME Code paragraph UG-100, vessels that cannot be filled with water or cannot be readily dried and where traces of water are not tolerated can be tested pneumatically at 1.25 times the MAWP to be stamped on the vessel multiplied by the ratio of the stress values of the test temperature of the vessel to the stress value *s* of the design temperature, except where other code requirements govern.

Additionally, pneumatic test shall be carried out for the following:

- 1. To check the leak tightness of tube-to-tubesheet joint, pneumatic test shall be conducted from shellside. Test pressure shall as per applicable code.
- 2. Reinforcement pads, slip-on flanges, and linings at a pressure of 2 bar(g).

15.3.13.5.2 *Pneumatic Testing Procedure*

Pneumatic testing is hazardous and should be used with caution under the following conditions:

- 1. Test pressure shall not exceed 1.25 times the design pressure as per ASME Code Section VIII, Div. 1; the maximum test pressure shall not exceed 150 psig.
- 2. The pressure shall be increased gradually and in increments of 10 psig, which enables detection of any major leaks in the system. The pressure should be held for 10 min.
- 3. A safety valve should be installed to prevent overpressurization.

15.3.13.5.3 *Stamping*

The vessel shall be stamped as follows:

Shellside design Pr	Tubeside design Pr.
Shellside design temp.	Tubeside design temp.
Shellside hydrotest Pr.	Tubeside hydro test Pr.
Serial no.	Inspection by
Hydrotested on	

15.3.13.6 **Plate-Fin Heat Exchanger**

15.3.13.6.1 *Pressure Test*

The brazed aluminum plate-fin heat exchanger (PFHE) must be pressure tested in accordance with the applicable design code. This may be carried out by either of the following methods:

15.3.13.6.2 *Hydrostatic Test*

The heat exchanger is hydrostatically tested with water. Each individual chamber is to be pressurized up to its test pressure. The minimum hydrostatic test pressure at room temperature shall be 1.3 times the design pressure, except where code requirements rule otherwise.

15.3.13.6.3 *Pneumatic Test*

The heat exchanger is subjected to a pneumatic test, where each individual chamber is pressurized up to its test pressure. The pneumatic test pressure shall be in accordance with code requirements.

15.3.13.6.4 *Leak Test*

In order to ascertain the absence of leak from one chamber toward any other chamber or into the atmosphere, a leak test is necessary. The two methods normally followed are (i) air test and (ii) helium test for external leak test and inter-stream leak test.

15.3.14 PREPARATION OF HEAT EXCHANGERS FOR SHIPMENT

During plant manufacture, storage, transport to site, and site erection, special precautions are to be taken to ensure that all the components remain clean and reasonably protected:

1. Internal and external surfaces are to be free from loose scale and other foreign matter that are readily removable.
2. Oil, water, or other liquids used for cleaning and hydrostatic testing should be drained before shipment. The shellside may be dried out by vacuum pump and the tubeside by blowing through with hot air.
3. All exposed machined contact surfaces shall be coated with a removable rust preventive and protected by suitable cover against damage. Rust-preventive compounds must be regarded as contaminants to be removed before the heat exchanger is put into service [44].
4. All threaded connections are to be suitably plugged.
5. The exchanger and any spare parts are to be suitably protected to prevent damage during shipment.
6. All telltale holes shall be packed with hard grease. In the event of alloy material, the grease shall be low lead and should not contaminate the material.

Exchangers which are to be stacked in service shall be stacked in the shop and pressure tested as a combined equipment.

General guidelines for the preparation of heat exchangers for shipment are discussed in TEMA, paragraph G-6.

15.3.14.1 Painting

External surfaces shall be painted as per drawings/specifications. Use paint that will withstand the surface temperature while in operation. Stainless steels do not require painting.

15.3.14.2 Nitrogen Filling

If desired by the purchaser, the heat exchanger internals may be filled with dry nitrogen to protect the internal parts against corrosion.

15.3.15 MAKING UP CERTIFICATES

The following documents may be enclosed in a folder along with the heat exchanger:

1. Vessel detail drawing together with a materials list
2. Material certificates of chemical and physical properties for each vessel item
3. Welding procedure specification and procedure qualification records
4. Welder qualification records
5. Records of welding consumables used and their properties
6. Certificate of radiography and other nondestructive testing methods
7. Heat treatment charts
8. Hydrostatic test report
9. Job inspection report
10. Stagewise inspection chart
11. Final inspection report
12. Guarantee certificate

15.3.15.1 Foundation Loading Diagrams/Drawings

Foundation loading diagrams/drawings shall show the following:

1. Empty weight, operating weight including all possible loads and weight full of the possible content of the equipment
2. Forces and moments due to seismic and wind loads (if applicable)
3. Dimensions of base/support plate and sliding plate (if applicable) complete with diameter, number and location of hold down bolts or anchors, and thickness of metal through which bolts must pass through

15.3.15.2 Schematics or Flow Diagrams

Where a vendor supplies equipment which includes any instrumentation, instrument connections, valves, safety devices, or control schemes, these components shall be shown on a schematic diagram identifying vendor and type and listing respective operating conditions or settings.

15.3.15.3 Installation, Maintenance, and Operating Instructions

When specified on “Vendor Data Requirements” form, the instructions shall be in a completely self-contained manual including the following as a minimum:

1. Equipment description with outline, cross section and details
2. Installation instructions
3. Pre-commissioning check list
4. Details of periodical maintenance and repair procedure

15.4 FORMING OF HEADS AND CLOSURES

15.4.1 FORMING METHODS

For thin plates, the cheapest method is by cold spinning and hot spinning of greater thickness. For still greater thickness, a forming press is used. Where the dimensions of the head are such that a single forming operation is not possible, several plates are pressed to the required contour and then welded together to a cap. This is known as the crown-and-segment technique.

Blank diameter, D_b , for the pressure vessel heads as shown in Figure 11.6a can be determined from the welding engineer data sheet nomograph [45] or from the formula given therein:

$$D_b = 2\sqrt{RH_s + 1.33R^2} \quad (15.5)$$

where

R is internal radius ($D/2$)

H_s is the straight portion of the head.

15.4.2 SPINNING

Spinning of ends is applied to a wide range of materials. The forming is done by either hot or cold spinning. Salient features of spinning of various materials are discussed by Peacock [4] and include the following:

1. Mild steel ends up to $\frac{1}{8}$ in. (3.2 mm) thick are cold spun with intermediate anneals, and ends greater than this thickness are hot spun at 1150°C.
2. Low-alloy steels are successfully hot spun.

- 3. For stainless steels with ends up to 5⁄8 in. (15.9 mm) thickness, cold spinning with intermediate annealing at 1050°C is preferred. Ends greater than this thickness are satisfactorily hot spun in the temperature range 900°C–1200°C; due care is to be taken to avoid carbide precipitation.
- 4. Ends can be made from explosion-clad plates by conventional hot or cold forming techniques. For more details on forming of clad plates, refer to the section on cladding in Chapter 13 on material selection and fabrication.

The spun heads will have a constant thickness in the hoop direction but will vary in the meridional direction. The thickness will be a maximum at the crown and a minimum in the knuckle region. The amount of thinning in the knuckle can be as high as 20%–30%. Under internal pressure, the direct hoop stresses are compressive and hence the heads are susceptible to buckling [46].

15.4.3 PRESSING

Pressing, either hot or cold, is usually employed for the smaller diameter ends and is not as flexible in operation as spinning, because slight changes in end dimension require an alteration to the ring and pressing die. The majority of ends are hot pressed for two main reasons [6]: (1) The metal to be pressed undergoes less work hardening and is less prone to cracking, and (2) the load needed to press the material to the required dimensions is less.

For forming of heads by pressing, two major kinds of equipment are required. They are (1) the cold forming and dishing press and (2) the flanging and knuckling machine [47]. Initially, the plate is manipulated into position beneath the ram and progressively rotated and tilted as successive ram strokes form the required shape. After dishing, the formed head is transferred to the knuckling machine for forming the edge to a more accurate radius. The manufacturing process of heat exchanger heads is shown in Table 15.1.

Figures 15.68 and 15.69 show hot forming of heads, Figure 15.70 shows cold pressing of a head, and Figure 15.71 shows flanging of a head.

TABLE 15.1
Sequence of Manufacturing of Vessel Heads

1. Blank cutting	1. Blank cutting
2. Edge preparation and welding of blanks (for multipiece construction)	2. Edge preparation and welding of blanks (for multipiece construction)
3. Preheating of blank	3. Preheating of blank
4. Cold or hot pressing by means of deep drawing	4. Cold or hot dishing by means of cold step pressing and cold or hot flanging/spinning
5. Multipiece head: Combined cold spinning of crown radius (roll stretch method) and flanging of knuckle area	
6. Heat treatment	
7. Edge preparation	
8. 3D CNC roboter hole cutting and beveling	
9. Mechanical testing (hardness, tensile test, impact test) and nondestructive examinations (PT,MT,UT, RT, PMI)	
10. Descaling (pickling and shot blasting) and polishing	
11. Dimensional control and visual inspection	
12. Dispatch	

Source: König + Co., GmbH, Netphen, Germany, [www. Koenig-co.de](http://www.Koenig-co.de).

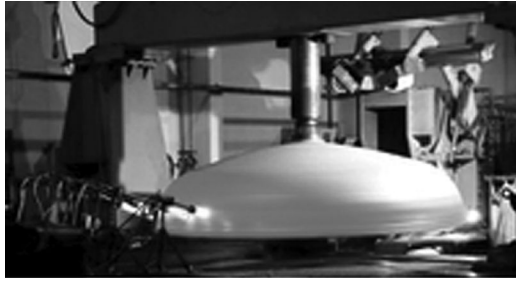


FIGURE 15.68 Hot forming of a head—hot spinning of an elliptical head, $\text{Ø}i4500 \times 80 + 4$ made of SA-516 Gr. 70 + 316L. (Courtesy of König + Co., GmbH, Netphen, Germany.)

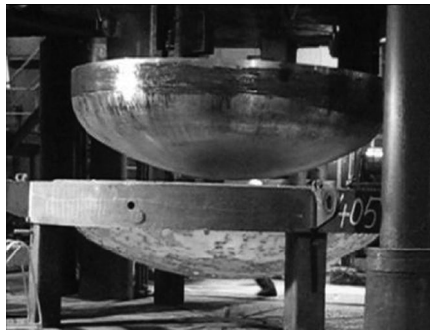


FIGURE 15.69 Hot forming of an ellipsoidal head. (Courtesy of Voestalpine Grobblech GmbH, Linz, Austria.)

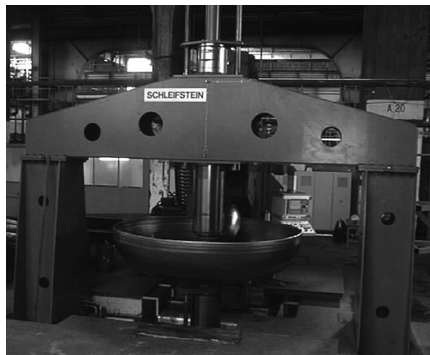


FIGURE 15.70 Cold forming of a head. (Courtesy of Voestalpine Grobblech GmbH, Linz, Austria.)



FIGURE 15.71 Fabrication of a head—flanging. (Courtesy of Edmonton Exchanger & Manufacturing Ltd Edmonton, Alberta, Canada.)

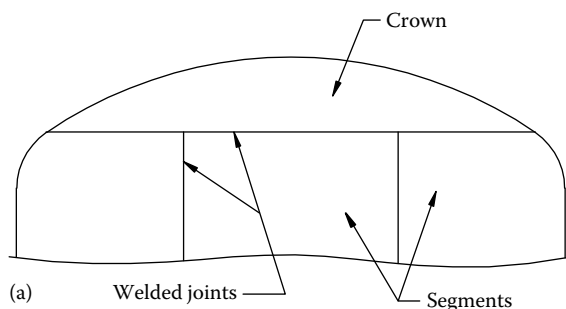
15.4.4 CROWN-AND-SEGMENT (C AND S) TECHNIQUE

Large hemispherical heads and torispherical heads are fabricated by the crown-and-segment (C and S) technique as shown in Figure 15.72a. Hemispherical vessel heads are fabricated from a series of hemispherical orange-peel sections and one dish-shaped section to form a hemisphere, whereas the torisphere is fabricated by welding a spherical cap to a toroidal portion made of several segments (or gores) that have been welded together. Two methods are followed for making the petals [47]. In one method, the required form is marked around the template on the flat plate; the petal is flame cut and then hot formed. In the more common method, the plate is rolled to the required petal shape, and a template made to the form of the finished petal is used to mark out the lines to be cut. Then flame cutting is carried out manually, and the edges are beveled and examined. All the plates are assembled on a supporting structure and welded. Caps for the hemispheres/torispheres are welded into position using suitable welding methods. At the various welds, there may be local variations in geometry, although these will be reduced in magnitude by hammering and spinning after the welding operation. The thickness in the C and S heads will be essentially the same as that of the base plate material [46]. Figures 15.72b and 15.73 show fabrication of heads and cones by C and S technique.

15.4.5 PWHT OF DISHED ENDS

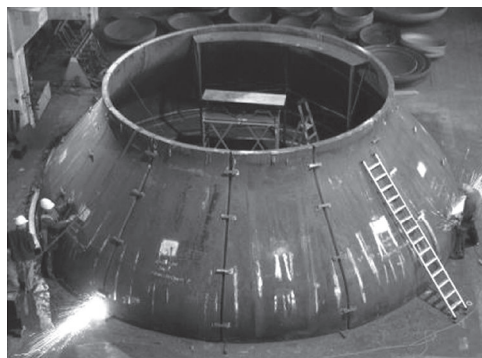
Heat treatment is carried out according to material used for manufacture of heads as shown in the following:

1. Normalizing (N) at a temperature of 850°C–980°C—carbon steel
2. Normalizing and quenching followed by tempering (N + T)—SA 387 Gr 22 or SA 537 Cl



(b)

(i)



(ii)

FIGURE 15.72 (a) Multipiece head (fabrication by crown-and-segment technique). (b) Multipiece head and cone under fabrication by crown-and-segment technique. (Courtesy of Voestalpine Grobblech GmbH, Linz, Austria.)

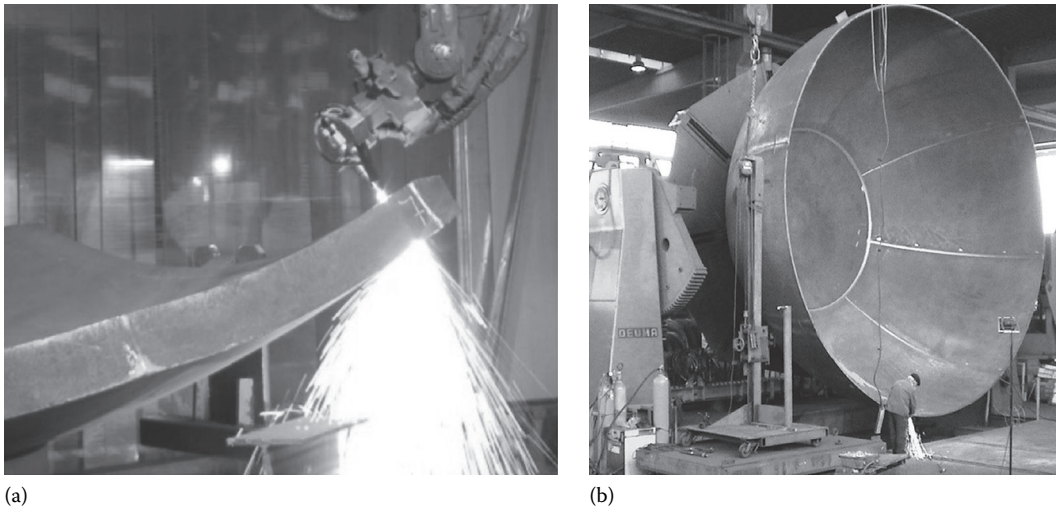


FIGURE 15.73 Crown and petal head fabrication. (a) A petal is under fabrication and (b) a head at finishing stage. (Courtesy of König + Co., GmbH, Netphen, Germany.)

3. Tempering (T) at a temperature of 650°C – 750°C
4. Stress relieving at a temperature of 595°C – 720°C
5. Solution annealing at a temperature of 1000°C – 1180°C —stainless steel, duplex stainless steel, and nickel alloys with subsequent quenching in water bath
6. Soft annealing—aluminum alloys, titanium, and zirconium
7. Quenched and tempered (Q + T)

Dished ends shall be stress relieved if cold formed, and normalized if hot formed. A stress-relieving/normalizing chart duly certified by an inspection agency shall be furnished. For hot-formed dished ends, mechanical properties shall be proved on a test coupon after subjecting the coupon to the same heat treatment as of the dished end, including the final normalizing. Problems faced during heat treatment of heads include [48] the following: (1) When the head is quenched, reasonable escaping of gases and steam should be provided to avoid origination of a steam cushion hindering uniform cooling, and (2) the heat treatment is associated with the risk of distortion. A head under heat treatment is shown in Figure 15.74.



FIGURE 15.74 Heat treatment of a head. (Courtesy of Voestalpine Grobblech GmbH, Linz, Austria.)



FIGURE 15.75 Shape control by automatic laser measurement. (Courtesy of Voestalpine Grobblech GmbH, Linz, Austria.)

15.4.6 DIMENSIONAL CHECK OF HEADS

Heads distorted during the operations after pressing out have to be checked for reduction or enlargement of diameter, ovality, and increase in height [48]. Use of laser for checking of dimensions of formed head is shown in Figure 15.75.

15.4.7 PURCHASED END CLOSURES

Purchased end closures should be accompanied by the following certificates:

- Mill certificates of raw material and test coupons
- Process of manufacture
- Raw material plate thickness used for pressing
- Minimum thickness achieved after pressing
- Type of heat treatment carried out
- Stress-relieving/normalizing chart (time and temperature chart)
- As-built dimensions of dished end
- Mechanical test results on test coupons
- NDT reports

15.5 BRAZING

15.5.1 DEFINITION AND GENERAL DESCRIPTION OF BRAZING

One of the more important processes of fabrication for complex assemblies is brazing. Most of the PFHEs, some tube-fin exchangers, especially automobile radiators, and some highly compact metal rotary regenerators are brazed. Brazing joins two similar or dissimilar metals/nonmetals by heating them in the presence of a filler metal having a liquidus temperature above 840°F (450°C) but below the solidus temperature of the base materials. Heating may be provided by a variety of processes. The molten filler metal distributes itself between the closely fitted surfaces of the joint by capillary action. Brazing differs from soldering in that soldering filler metals have a liquidus temperature below 840°F (450°C).

15.5.2 BRAZING ADVANTAGES

Brazing has the advantages of greater flexibility and scope. Strong, uniform, leak-proof joints are made rapidly, inexpensively, and even several joints simultaneously. It is unrivaled for assembling

thin or delicate components or assemblies that are being produced in large quantities with the facility to produce many joints simultaneously [49,50]. Precise joining is comparatively easy without the application of intense local heat to small areas. There is no heat-affected zone in brazing. Brazing requires little operator skill. Since the base materials do not melt at the brazing temperature, practically any two materials can be joined together in spite of a difference in composition, melting point, or thermal expansion. This includes similar and dissimilar metals. However, not all combinations of dissimilar metals can be brazed.

15.5.3 DISADVANTAGES OF BRAZING

The brazing process is often considered an art today [51]. According to Shah, brazing requires considerable expenditure and capital cost, as well as development time, before ideal brazed joints can be manufactured, particularly for complicated assemblies. If there is any change in any one of the brazing process variables, such as flux, filler metals, temperature, brazing atmosphere including vacuum, or equipment and fixture, in general one needs to redefine the brazing process to obtain ideal joints.

The objective of this section is to provide comprehensive details on the fundamentals of brazing, brazing processes, and brazing of important heat exchanger materials including aluminum, stainless steel, and nickel. References [49–58] provide general and specific information on brazing.

15.6 ELEMENTS OF BRAZING

The proper use of brazing for a given application requires that due consideration be given to several factors:

1. Joint design
2. Filler metal selection
3. Precleaning and surface preparation
4. Fluxing
5. Fixturing
6. Heating method
7. Postbrazing treatment and removing flux residues

These factors are discussed in detail next.

15.6.1 JOINT DESIGN

Joint design should consider the following factors:

1. Joint clearance: Joint clearance determines capillary force. The capillary force draws the molten filler metal deeply into every joint clearance. The joint clearance must be within specified limits. Suggested joint clearances as per joint width for various brazing processes are tabulated in Ref. [49].
2. Avoid flux entrapment: Entrapped flux may make the brazed joints susceptible to in-service corrosion. Too tight joint clearance restricts filler metal flow, whereas too wide joint clearance allows filler metal flow around flux. Flux trapped in the joint may also falsify leak test indications.
3. When joining different metals, their differing coefficients of thermal expansion become vitally important.
4. When brazing foil is used, the mating surfaces should be held in contact. The foil thickness will then determine the joint clearance.
5. The brazing symbol on the engineering drawing designates the location, class, and configuration of the brazed joint. Such symbols shall be as per ANSI/AWS A2.4, Standard Symbols for Welding, Brazing, and Nondestructive Examination.

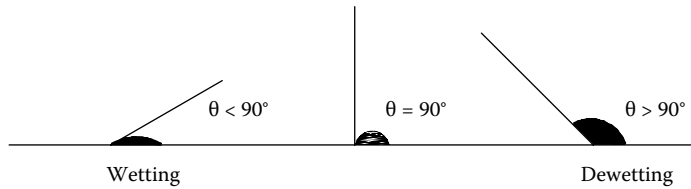


FIGURE 15.76 Molten filler metal contact angle.

15.6.1.1 Joint Types

In common with all forms of brazing, lap joints should be used in preference to butt joints. Joint types can be butt, lap, and T.

15.6.2 BRAZING FILLER METALS

Brazing filler is a nonferrous metal or alloy that melts at a temperature lower than that of the melting point of the base metal. Most filler metals are alloys, so they melt through a range of temperatures. When molten, the filler metal must wet the base metals, flow, and spread into joints to form brazed joints. The desired characteristics of molten filler metal are a low contact angle (Figure 15.76), high liquid surface tension, and low viscosity.

15.6.2.1 Composition of Filler Metals

The American Welding Society lists in AWS 5.8-81 the specifications for brazing filler metal. Conventional fillers that find use in brazing of heat exchangers are in general based on aluminum, copper, nickel, cobalt, silver, and gold. Vacuum-grade fillers are silver-based, gold–palladium, aluminum–silicon, and copper-based alloys. The selection of filler metals is discussed by Weymuller [59] and Birchfield [60].

15.6.2.2 Aluminum Filler Metals

Aluminum filler metals (BA1Si series) are used for brazing aluminum. To reduce the possibility of galvanic corrosion, brazing filler metals are aluminum alloys rather than dissimilar metals [61]. Most of the brazing alloys are based in the aluminum–silicon eutectic system, containing between 7% and 12% silicon with a melting point of 1070°F (577°C). Occasionally, other elements are added. They are available as filler metal or as clad brazing sheet. They are used to joint the wrought grades such as 1100, 3003, 3004, 3005, 5005, 5050, 5052, 6053, 6061, 6062, 6063, 6951, and 7005 [53,59]. Figure 15.77 shows maximum permissible brazing temperatures for various aluminum alloys [49].

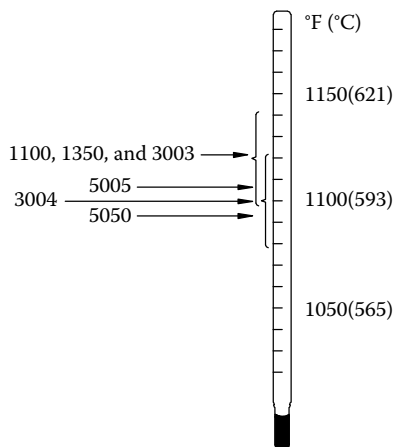


FIGURE 15.77 Maximum permissible brazing temperatures for various aluminum alloys.

15.6.2.3 Copper Fillers

Copper filler (BCu) metal is used to braze ferrous and nickel-based alloys.

Copper–phosphorus fillers (BCuP series) apply mostly for joining copper and its alloys and stainless steel. Avoid using these fillers on ferrous alloys, nickel-based alloys, and copper alloys containing more than 10% nickel [53,59]. These fillers are relatively low in cost, since they lack silver or gold. Copper-based filler alloys are not compatible with sulfur-bearing fuels [59,62].

Copper–zinc fillers (BCuZn series) are used to braze steels, stainless steels, copper and its alloys, and nickel-based alloys.

15.6.2.4 Nickel-Based Filler Metals

Nickel-based filler (BNi series) metals are used primarily to braze heat- and corrosion-resistant alloys, most commonly nickel- and cobalt-based alloys and the AISI 300 and 400 series stainless steels. These filler metals provide joints that have excellent corrosion resistance and high-temperature strength [63]. Since they require relatively high melting temperature, their use is generally restricted to furnace brazing in a controlled atmosphere including vacuum. Also nickel fillers tend to be sluggish in the fluid state; therefore, joint design, filler metal selection, and brazing temperature should be carefully considered [53].

15.6.2.5 Silver-Based Filler Metals

Silver-based brazing alloys (BAg series) find a multitude of uses, because they cover a wide range of brazing temperatures, 1145°F–1900°F. They are used to join ferrous and nonferrous metals and alloys, except low-melting metals such as aluminum, magnesium, and their alloys [59]. Their advantages are free flow, relatively low brazing temperature, and that they make ductile and smooth joints [53].

15.6.2.6 Gold-Based Fillers

Gold-based fillers (BAu series) are preferred for specialized applications such as aerospace heat exchangers to braze stainless steel, nickel, and cobalt-based alloys that require oxidation and corrosion resistance at elevated temperatures, and compatibility with sulfur-bearing fuel. These fillers are primarily used in furnace brazing applications. Because gold interacts little with base metals, gold-based fillers will not alter properties of the base metal [59]. Various filler metals and their applications are given in Table 15.2.

TABLE 15.2
Typical Filler Metal Applications

Primary Metal in Filler	Base Materials
Aluminum	Aluminum-based alloys
Copper	Copper-based alloys, ferrous metals, nickel-based alloys
Copper–phosphorus	Copper-based alloys; avoid using on ferrous alloys, nickel-based alloys, and copper alloys containing more than 10% nickel
Copper–zinc	Steels, stainless steels, copper and its alloys, and nickel-based alloys
Nickel	SS types 300 and 400, nickel-based, and cobalt-based alloys
Silver	Ferrous; nonferrous except aluminum and magnesium and their alloys, which melt at low temperatures
Gold	Thin sections of SS, nickel-based, or cobalt-based alloys requiring high corrosion and oxidation resistance

15.6.2.7 Forms of Filler Metal

To control the amount of filler metal requirement, the filler metals are available in predetermined amounts and shapes known as preforms. Various preforms are wire, strip, sheet, rod, powder, and shapes that fit specific joints. Preforms suit well with automatic brazing. Aluminum brazing sheet is a standard, commercial product. The constructional features and metallurgy of aluminum brazing sheets are explained next.

15.6.2.8 Placement of Filler Metal

Placement of filler metal is an important design factor. Usually, the filler material is preplaced near the joints to be brazed. Either the braze metal is metallurgically clad to a thin flat structural member known as a brazing sheet, sandwiched between the parts to be joined, or base metal is coated with a slurry of braze alloy powder and binder.

15.6.2.9 ASME Code Specification for Filler Metals

Pressure vessel braze metals conform to ASME Section II, Part C. Tables in Part C identify filler metal specifications that are identical to AWS filler metal specifications. The code addresses fluxes or brazing atmospheres indirectly through its requirements to successfully qualify a brazing procedure.

15.6.3 PRECLEANING AND SURFACE PREPARATION

15.6.3.1 Precleaning

Clean, oxide-free surfaces are essential to ensure sound brazed joints. Grease, oil, dirt, marking crayons, and oxides prevent the wetting, uniform flow, and bonding of the brazing filler metal, and they impair fluxing action, resulting in voids and inclusions. Precleaning of components may be accomplished by degreasing with organic solvents or vapors or by a mild chemical etch, such as dilute caustic soda solution [49]. Cleaning should always be carried out before assembly. Otherwise, if an assembled component is immersed in a chemical cleaner, residues will inevitably be trapped in the joints [64].

15.6.3.2 Scale and Oxide Removal

Good performance, which characterizes the soundness (leak tightness, joint strength, and fillet shape) and integrity of the brazed joint, is possible only when the surface oxide film on the metal surface is dispersed sufficiently for wetting and flow of filler metal to occur.

Chemical cleaning: Scale and oxide removal can be accomplished mechanically or chemically. Descaling can be done with any of the following solutions [53]:

1. Acid cleaning
2. Acid pickling—sulfuric, nitric, and hydrochloric acid
3. Salt bath pickling

Prior to descaling, degreasing is recommended.

Mechanical cleaning: Mechanical cleaning is usually confined to those metals with heavy tenacious oxide films. Mechanical methods include abrasive grinding, grit blasting, filing, or wire brushing using stainless steel bristles. Grit blasting should be done with clean blasting material such as silica sand or alumina sand. Care must be taken that the mechanical cleaning materials are not embedded in the metals to be brazed. After mechanical cleaning, air blasting or ultrasonic cleaning should be used to remove all traces of loosened oxides or blasting medium.

15.6.3.3 Protection of Precleaned Parts

After cleaning, the cleaned parts should be assembled and brazed without delay to avoid oxidation and buildup of contamination. The cleaned surfaces should not be hand touched after cleaning. They should be stored and transported to the braze preparation areas in dry, clean containers, such as plastic bags.

15.6.4 FLUXING

Conventional brazing processes performed in air or other oxygen-bearing atmosphere require fluxing. In other words, vacuum brazing does not require flux, and furnace brazing performed in inert or strongly reducing atmosphere usually does not require flux. Fluxes are necessary to displace the oxide layers at the bonding sites and to allow the wetting by the molten filler metal. Without flux, molten filler forms a ball even though the surface it contacts is clean and the temperature is high. Additionally, the flux protects the bonding sites against reoxidation of the cleaned surface during brazing. However, fluxes are not intended to perform the primary function of removal of oxides, scales, coatings, and surface contaminants. Fluxes come as paste, powder, slurry, or liquid.

15.6.4.1 Selection of a Flux

Flux selection is influenced by the following factors [53,63]: base material, filler metal, brazing process, joint configurations, and flux dispensing methods such as brush, dip, syringe, spray, etc., which determine flux forms and ease of cleaning.

15.6.4.2 Composition of the Flux

Fluxes contain one or more heavy metal chlorides in addition to active fluoride salts along with other chemicals. Fluxes are generally mixed with water to form a thick slurry, which is applied to the precleaned parts to be brazed.

15.6.4.3 Demerits of Brazing Using Corrosive Fluxes

Though several advantages can be claimed for the brazing techniques using fluxes [65], brazing fluxes are chemically active, and their residues are highly corrosive, especially in the presence of moisture. Therefore, after brazing, flux residuals must be removed by a cleaning process to avoid both corrosion and contamination problems. Other problems associated with fluxes include [61] the following: (1) Postbrazing cleaning is costly; (2) for complex structures with closed tortuous passage ways, the elimination of flux residuals can require long cleaning cycles; and (3) disposal of spent cleaning solutions can become costly with ever tighter control of plant effluent.

15.6.5 FIXTURING

As far as possible, components to be brazed should be self-fixturing. Fixtures, being in contact with the part, extend the heating time to bring the components up to the brazing temperature. Slow heating due to attachment of fixturing will change the characteristics of the filler metal [64]. Examples of self-fixturing construction include aluminum screws, rivets, resistance welds, argon arc tack welds, piercing, and tagging. For external fixtures, austenitic stainless steels or heat-resisting nickel alloys are recommended. Mild steel can also be used for low-volume production. Use clean and dry fixtures to avoid pumpdown delays.

15.6.6 BRAZING METHODS

Brazing processes are classified according to the sources or methods of heating. There are numerous brazing methods, including the following:

1. Torch brazing
2. Dip brazing
3. Furnace brazing
4. Vacuum and controlled-atmosphere brazing (CAB)
5. Induction brazing
6. Resistance brazing
7. Infrared brazing

All these brazing methods include the same brazing procedures. The prime difference lies in the way the parts are heated and the way flux and filler metals are applied. Except for vacuum and controlled-atmosphere brazing, all methods require flux. In this section, the first four brazing methods are discussed.

To braze, surfaces must be cleaned, free of excess oxide, coated with flux, and spaced a few thousandths of an inch apart. Brazing filler is placed in or near the joint to be formed, assembled, and fixtured. When heat is applied, the flux displaces oxide and shields the metal from air. As the filler flows, it displaces flux and wets the base metal, adapting to submicroscopic irregularities and dissolving the small high points it encounters.

15.6.6.1 Torch Brazing

Any joint that can be reached by a torch and brought to brazing temperature can be readily brazed by this technique. Torch brazing can be either handheld or automatic. Handheld manual torch brazing is most frequently used for repairs, one-of-a-kind brazing jobs, short production runs, and as an alternative to gas or arc welding. For example, repairs or low-production copper-to-copper joints in return bends of an evaporator or a condenser of an air conditioner are preformed by torch brazing. Most commercial torch brazing is carried out by use of oxyacetylene flame in which the torch is adjusted to produce slightly reducing flame for most application. In automatic torch brazing, the assembly is moved automatically in relation to the torch, or vice versa. It is used for mass production.

15.6.6.2 Dip Brazing

In the dip brazing process, often referred to as salt-bath brazing, the part or assembly being joined is held together and immersed in a bath of molten salt, which flows into the joints when the parts reach a temperature approaching that of the bath. The molten flux, at a temperature slightly above the liquidus of the filler metal, serves as a heat source and partially supports the submerged metal parts. In addition to providing the heat for brazing, many of the salts have fluxing properties. Dip brazing has been extensively used in industry for daily production of aluminum and other alloy parts. It has the unique advantages that [48] (1) the time required for heating is about one-fourth that required for furnace brazing, (2) distortion due to self-weight is less due to buoyancy, and (3) the parts reach the brazing temperature uniformly.

Choice of flux: Commercial dip brazing fluxes are generally similar to fluxes used with other brazing methods. Their main ingredients include the combinations of sodium chloride, potassium chloride, aluminum fluoride, and lithium chloride. Dip brazing requires water-free flux to avoid spattering of moisture from the bath.

Dip bath heating means: Heating may be by gas for lower temperature systems or by one of the two forms of electrical heating: either resistance elements mounted around the pot or electrodes immersed in the molten salt bath.

Flux pot: Flux pots comprise steel-reinforced vessels lined with high-alumina, acid-proof fire brick. Pot covers are well insulated. Large covers may be mounted on rollers and power operated.

TABLE 15.3
Dip and Furnace Brazing Steps

Dip Brazing	Furnace Brazing
Precleaning and surface preparation	Precleaning and surface preparation
Preparation of flux bath	Flux preparation and application ^a
Assembly and fixturing	Assembly and fixturing
Preheating	
Brazing in flux bath	Brazing in furnace
Cooling or quenching	Cooling or quenching
Hot water washing	Hot water washing ^a
Flux removal	Flux removal ^a
Finishing and inspection	Finishing and inspection

^a Not applicable for vacuum brazing.

Preheating the assemblies: Dip brazing generally requires preheating. This helps in a flux pre-placed joint, dries the flux, and vaporizes moisture from the assembly before being immersed into the salt bath and thereby prevents accidents from steam explosions. It also can reduce brazing time, minimize the salt residue that forms on the part, and reduce distortion, as well as reduce bath size [53]. Preheating is achieved either by the flue gases or by electrical heating in a suitable furnace to a temperature 50°F–100°F (30°C–60°C) below the solidus temperature of the brazing filler metal until the entire assembly has attained this temperature. For aluminum brazing, the assembly is pre-heated to approximately 1000°F (538°C).

Dip-brazing procedure: The dip brazing steps (along with furnace brazing steps) are given in Table 15.3.

Immersion time: The time needed to form the joints depends on the mass of the assembly and its temperature at the moment it enters the molten salt bath. Dip time varies from as little as a few seconds to as long as 10 or 20 min. There is no formula to arrive at the immersion time, but it is arrived by trial-and-error practice [49].

Maintaining the flux bath: A properly maintained flux bath will produce a workpiece that is bright and shiny, with fillets well formed and complete [53]. To achieve these properties, the bath should be relatively free of sludge and surface film, slightly acidic with a pH between 6.4 and 7.0 (for aluminum, a pH between 5.3 and 6.9), and relatively constant chemical composition. The bath is periodically checked for moisture, acidity, chemical composition, temperature, and other physical characteristics by the laboratory and corrective action made as required.

Scum and sludge removal: Contaminants in and on top of the hot flux interfere with the quality of brazing. Contaminants that float to the surface are called scum, and they are readily removed by skimming the bath’s surface with a sheet of aluminum. There are a number of commercial preparations that, when added to the bath, cause the particles to coagulate, making their removal easier [49]. Contaminants that sink to the bottom of the pot are called sludge. The sludge is removed periodically by ladling with a perforated tool.

Ventilation: Salt-bath dip brazing can emit toxic or noxious gas, fumes, and dust. Ventilation to remove air emissions from above the bath is a must.

Limitations of dip brazing: Some of the limitations of dip brazing are as follows:

1. Dip brazing generally requires preheating to prevent accidents from steam explosions.
2. The shape of the part must be designed to avoid trapping air or salt and to be drained completely.
3. Maintenance problem due to power shutdown for internally electric-heated salt bath.
4. A different salt will probably be required for the next application if either the parent metals or the brazing alloy has been changed; frequent changing is not economical.

15.6.6.3 Furnace Brazing

The term *furnace brazing* can be applied to any brazing process where a furnace is used as the heat source to raise the parts to be joined to their brazing temperature. Furnace brazing is extensively used in industry for brazing heat exchangers and joining complex parts. It offers uniform heating, and hence accurate temperature control is possible. The finished product has excellent quality. The process is economically attractive for brazing heavy assemblies in which multiple brazed joints are to be formed simultaneously or many assemblies are to be joined simultaneously.

Furnace heating: The furnaces may be heated by gas, oil, or electricity, and provided with temperature controls. Fluxes or specially controlled atmosphere that performs fluxing functions must be provided. Filler metal must be preplaced in the form of sheet, wire, rings, powder, or other suitable forms.

Atmospheres: Furnace brazing takes place in a vacuum or in a controlled atmosphere of high-purity inert or reducing gas. Both reduce the amount of flux needed or in some cases eliminate the need for flux completely, and prevent oxidation and scaling during heating. There are, however, examples of this type of furnace being used with an atmosphere of normal air or ultradry air in association with flux. These aspects are discussed later. The brazing atmosphere, whether gaseous or vacuum, should be free from harmful constituents such as sulfur, oxygen, and water vapor. When brazing in a gaseous atmosphere, it is a common practice to monitor the water vapor content of the atmosphere as a function of dew point. In general, a furnace atmosphere having a dew point less than about -60°C (-75°F) produces better quality.

Brazing furnaces: In general, brazing furnaces are classified as (1) batch furnace, (2) semicontinuous or locked furnace, or (3) continuous furnace. Single-chambered, batch-type units are used for low-volume production, while multichambered semicontinuous or continuous furnaces are employed for high-volume production applications. Selection of a particular type of production furnace depends on the size and geometry of the parts to be brazed, as well as production rates required.

Classification of batch furnaces: Batch furnaces are classified as follows [53,66]:

1. Direct-combustion furnaces
2. Muffle furnaces or hot-wall furnaces
3. Retort-bell-type combustion furnaces
4. Vacuum brazing furnaces: single-pumped retort furnaces, double-pumped retort furnace, batch-type vacuum furnace (hot or cold wall design)

These furnace types are briefly discussed next. For more details, see Refs. [53,66].

Direct combustion furnace: The simplest and least expensive furnaces are the direct-combustion type, in which combustion products pass through the brazing zone and hence come into contact with the workpiece. As moisture is always a by-product of combustion and as moisture is a hindrance to good brazing, the direct-combustion furnace will not offer optimum quality joints.

Muffle furnace or hot-wall furnaces: A gas-fired muffle furnace will normally incorporate a refractory chamber so that the flames pass around the outside of the chamber, which ensures that the products of combustion do not come into contact with the workpiece. Because of this, the furnace offers optimum quality joints. For still better quality, employ electric resistance or radiant-tube furnaces, or furnaces that combine resistance and combustion heating.

Retort-bell-type combustion furnaces: The retort-bell-type combustion furnaces have been developed for high-temperature brazing applications. For brazing in a purified hydrogen atmosphere, there is an inner container of a heat-resistant alloy sealed from outside air and the products of combustion. The workpiece is placed into this container; the container is purged with dry hydrogen and then lowered into a pit-type furnace. Hydrogen flows through the container during preheating, brazing, and cooling.

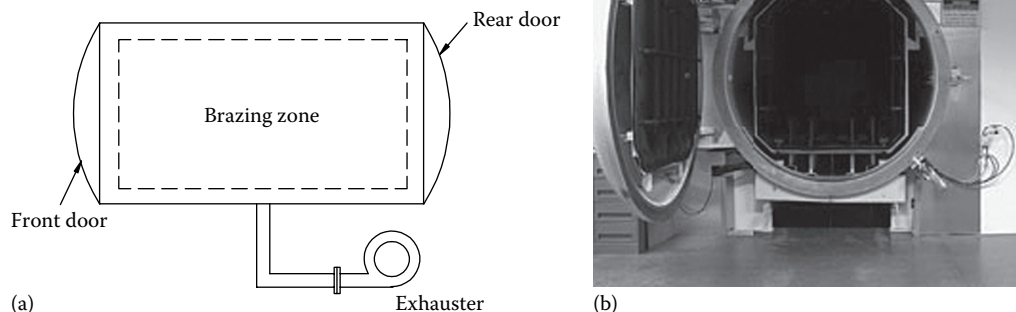


FIGURE 15.78 Vacuum-type batch furnace. (a) Vacuum-type batch furnace (Adapted and modified from Patrick, E.P., *Weld. J.*, October, 159, 1983) and (b) vacuum brazing furnace. (Courtesy of Lytron Inc. Woburn, MA.)

Vacuum brazing furnaces: Vacuum brazing can be of these types: (1) single-pumped retort, (2) double-pumped retort, (3) batch-type furnace, and (4) continuous furnace.

The *single-pumped retort* is loaded with the brazement, evacuated, and heated externally by a resistance or by gas or by oil combustion.

The *double-pumped retort* is for higher temperature brazing. Manufacturers can employ a double-wall retort; the workload sits in a high-vacuum (10^{-2} torr or lower) container that is placed in a rough-vacuum (1–10 torr) chamber.

The *batch-type vacuum furnace* consists of a chamber with doors at one or both ends and is typically equipped with mechanical roughing and oil vapor diffusion pumps. Batch-type vacuum furnaces can be hot- or cold-walled design; cold-wall furnaces are more popular. The term *cold wall* design refers to the fact that the chamber walls are water cooled and that conventional refractory insulation is not present between the hot zone and chamber walls. A typical batch vacuum furnace is shown in Figure 15.78. Depending on the geometry of the workpiece and the desired production rate, the hot zone size can be in the range of 1–600 ft³ (0.028–17 m³). The hot zone can be rectangular or cylindrical in shape. Batch furnace cycle times can vary few minutes to longer than a day. Large components such as cryogenic heat exchanger cores have cycle times of many hours.

In a *semicontinuous vacuum furnace*, the brazing chamber is divided into two or more heating stations so that part movement from station to station brings about the braze. The number of hot zones is determined by the parts to be brazed and the desired production rate. For example, in a three-zone brazing chamber, the braze is completed in three stages, and three carriers of parts, each at a different heating station, are contained in the brazing chamber environment at all times. Cycle times for a three-zone chamber are approximately one-third that for the batch process [67]. A semicontinuous or locked furnace is shown schematically in Figure 15.79. It is developed to avoid contamination while loading or unloading work [68]. The entrance vestibule is generally used to preheat and outgas the parts prior to transfer into the brazing zone. The exit vestibule is used for the initial phase of cooling and filler metal solidification under an inert or dry air environment [67]. For more details on batch-type and continuous-type vacuum furnaces, see Ref. [68].

Procedure: Furnace brazing steps are listed in Table 15.3.

Brazing processes without corrosive flux: Various processes have been developed for reducing or eliminating corrosive flux in the brazing of heat exchangers. Three industrial processes are followed to overcome the requirement of corrosive flux. They are

1. Controlled-atmosphere brazing
2. Use of noncorrosive flux under the trade name Noclock
3. Vacuum brazing

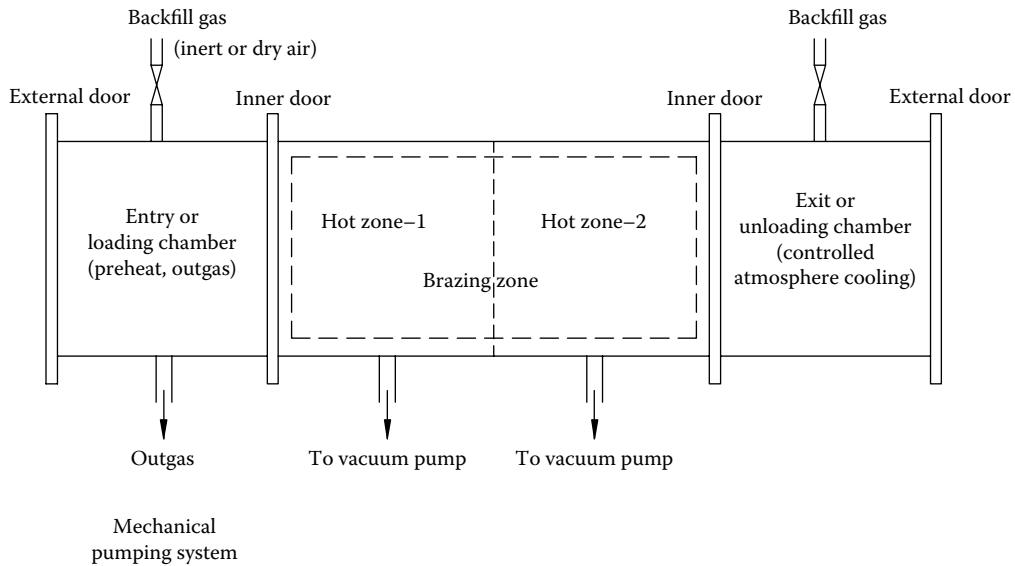


FIGURE 15.79 Semicontinuous or locked furnace.

All three methods are commercially used for the manufacture of heat exchangers and high-volume automotive heat exchangers, such as radiators, air-conditioning evaporators, heater cores, and turbo air coolers. In general, the fluxless processes require furnace atmosphere having a dew point less than about -60°C (-75°F) to produce better quality.

Controlled-atmosphere brazing: In controlled-atmosphere brazing (excluding a vacuum atmosphere), a continuous flow of a certain gas is maintained in the work zone to avoid contamination from outgassing of the metal parts and dissociation of oxides. Controlled atmospheres for furnace brazing include combusted fuel gas, dissociated ammonia, cryogenic or purified $\text{N}_2 + \text{H}_2$, deoxygenated and dried hydrogen, and purified inert gas as specified by AWS designations. The controlled atmosphere such as pure dry hydrogen or inert gases inhibits the oxidation and scaling of the surfaces. Inert gases, such as helium and argon, do not form compounds with metals and inhibit vaporization of volatile elements. A dry-nitrogen atmosphere is excellent for production volume brazing with a fluoride flux. With controlled-atmosphere brazing, the need for a flux is eliminated or the flux requirement is considerably reduced.

The merits of controlled-atmosphere brazing include the following: (1) The need for a flux is eliminated or the flux requirement is considerably reduced; (2) there is more rapid and uniform heating than brazing under vacuum, due to convective heating of the component by the circulated gas; and (3) it prevents oxide and scale formation on the parts being brazed and reduces evaporation of volatile elements. Due to these reasons, the assembled components remain clean and bright after brazing, postbrazing cleaning is generally not necessary, and there are lower maintenance requirements related to buildup of volatile alloying elements [69]. However, controlled atmospheres are not intended to perform the primary cleaning operation and surface oxide removal.

Use of noncorrosive flux under the trade name Nocolock: Use of noncorrosive flux under the trade name Nocolock pertains to aluminum brazing. Therefore, it is covered in the next part, while discussing aluminum brazing.

15.6.6.4 Vacuum Brazing

Vacuum brazing is a form of furnace-brazing process for brazing assemblies in a vacuum environment without the use of flux. Vacuum brazing is being used commercially to produce automotive and aircraft heat exchangers. Large prototype industrial heat exchangers and massive cryogenic heat exchangers have been successfully vacuum brazed. Commercial vacuum brazing generally is

done at pressures varying from 10^{-5} to 10^{-1} torr, depending on the materials brazed and the filler metals being used. A vacuum braze furnace is shown in Figure 15.78.

Parent metals brazed: Vacuum brazing is most suitable to brazing aluminum alloys, stainless steels, superalloys, titanium alloys, zirconium, or other reactive elements with particularly stable oxides.

Merits of vacuum brazing: Merits of vacuum brazing are as follows:

1. The method eliminates the need for fluxes and postbrazing cleaning.
2. It is nonpolluting and possesses high braze performance capabilities.
3. Vacuum prevents oxidation of metals by removing air from around the assembly and also removes volatile impurities and gases from the metals.
4. The method imparts a high standard of cleanliness to the work that could not be achieved by any other method.
5. The overall production time is minimized since there is no fluxing action and subsequent postbrazing cleaning.

15.6.7 POSTBRAZE CLEANING

Brazing fluxes are chemically active, and their residues are highly corrosive, especially in the presence of moisture. Therefore, after brazing, flux residuals must be removed to avoid both corrosion and contamination problems. Use boiling water, which usually removes chloride-type flux residue, or a strong acid such as nitric, followed by water rinsing. Oxidized areas adjacent to the brazed joint can be cleaned by pickling, wire brushing, or blast cleaning.

15.6.7.1 Braze Stopoffs

When filler metal flow must be restricted to definite areas, “stopoffs” are employed to outline the areas that are not to be brazed. Braze stopoff materials, if used, must be compatible with base metal, filler metal, fluxes, and furnace atmosphere [70]. Stopoff residue must be removed from the joint after brazing. Wire brush, air blast, or water flush will remove the stopoff residue.

15.7 FUNDAMENTALS OF BRAZING PROCESS CONTROL

It is generally accepted that the most important variables involved in the brazing process include the brazing temperature, time at temperature, brazing atmosphere, and the rate and mode of heating. Some of these factors are discussed next.

15.7.1 HEATING RATE

Geometry and the distribution of mass within the part, heating element configuration relative to part location, and vacuum environment characteristics will determine the heating rates needed to realize a good braze.

15.7.2 BRAZING TEMPERATURE

Brazing temperature is mostly governed by the base metal characteristics and the type of filler metal. In general, the filler metals with the higher melting points correlate with higher strength joints. Various base metals with their melting and brazing temperatures are shown in Table 15.4.

15.7.3 BRAZING TIME

Brazing time will depend somewhat on the mass/thickness of the parts and the amount of fixturing necessary to hold them. It has become industry practice to minimize the holding time at brazing

TABLE 15.4
Base Metals and Their Melting Temperature Range
and Brazing Temperature Range

Base Metal	Melting Temperature	Brazing Temperature
Aluminum and aluminum	588°C–657°C	571°C–621°C
Alloys	(1090°F–1215°F)	(1060°F–1150°F)
Stainless steels	1370°C–1532°C	618°C–1232°C
	(2500°F–2790°F)	(1145°F–2250°F)

temperatures to minimize excessive filler metal flow and/or erosion, evaporation, and oxidation. Brazing times in the order of less than a minute are common.

15.7.4 TEMPERATURE UNIFORMITY

Producing consistent braze joint quality throughout the part/furnace load/temperature uniformity in all of the workpieces depends on the configuration of the work, its placement, how it interrelates with the hot zone, etc.

15.7.5 CONTROL OF DISTORTION DURING THE FURNACE CYCLE

Control of distortion is vitally important for successful furnace brazing, particularly complex parts. Distortion can result from fast heating, fast cooling, stresses that develop during heating, residual stresses in a workpiece, phase transformation, and properties of dissimilar base materials [71]. According to Tennenhouse [71], distortion can be minimized or eliminated by measures like uniform heating and cooling of the part, reduced and controlled heating rates, use of dummy weights, heat shields and lightened fixtures, and adequate supports to the parts.

15.8 BRAZING OF ALUMINUM

Brazed aluminum assemblies are all aluminum with excellent corrosion resistance when properly cleaned of any residual corrosive flux. Brazed aluminum assemblies conduct heat uniformly. Therefore, brazed aluminum heat exchangers are long-lasting and highly efficient.

Techniques for brazing aluminum are similar to those used for brazing other metals. Commercially, the same equipment is often used. But there are some important differences between aluminum and other brazeable metals that affect the standard brazing techniques. These differences stem from the refractory nature of the surface oxide film on aluminum, from the oxide that forms on aluminum having a high melting point (3722°F), and from the low melting point of aluminum [61]. Other characteristic features of aluminum relevant for brazing include the following: It conducts heat quickly, surface oxides form rapidly, thermal expansion is greater than many other common metals, and it does not change color as its temperature changes [49].

15.8.1 NEED FOR CLOSER TEMPERATURE CONTROL

Aluminum alloys are brazed with aluminum filler metals that are similar to the base metals. Filler metals have liquidus temperatures closer to the solidus temperature of the parent metals, and hence close temperature control is very important [50]. This can be easily understood from Table 15.3. The brazing atmosphere should be approximately 70°F (39°C) below the solidus temperature of the base metal, but if temperature is accurately controlled and the brazing cycle is short, the difference can be as close as 10°F (5.5°C) [58].

15.8.2 ALUMINUM ALLOYS THAT CAN BE BRAZED

A majority of the non-heat-treatable aluminum alloys like 1100, 3003, 3004, and 5005 and many of the heat-treatable alloys like 6053, 6061, 6063, 6951, 7005, and 7072 can be brazed. Aluminum alloys containing more than 2.5% magnesium are difficult to braze. Common brazeable wrought alloys, their composition, and approximate melting range. Approximate brazing temperatures for common aluminum alloys are shown in Figure 15.77. In addition to these, aluminum can be brazed to many dissimilar metals and alloys. A partial list includes the ferrous alloys, nickel, titanium, Monel, and Inconel [49].

15.8.3 ELEMENTS OF ALUMINUM BRAZING

15.8.3.1 Joint Clearance

The joint clearances established for aluminum brazing are furnished in Ref. [49].

15.8.3.2 Precleaning

Brazing aluminum requires that the metal be free from surface contaminants and its oxide layer thin enough to be displaced by the brazing flux. Surface contaminants such as greases, oil, fatty acids, and marking crayons can be removed by vapor degreasing using inhibited trichloroethylene or ultrasonic degreasing.

15.8.3.3 Surface Oxide Removal

As highly reactive material, aluminum and its alloys are covered with an oxide. This oxide can be an important hinderant in brazing process, where the oxide film acts as a barrier to the wetting and flow of filler metal [67]. Hence, oxide barrier dispersal is a prerequisite for successful brazing. For non-heat-treatable aluminum alloys, vapor degreasing or ultrasonic degreasing is adequate [64]. Overly thick oxide layers on heat-treatable alloys can be reduced by either mechanical means or chemical means [49]. Chemical means will consist of a degreasing either in trichloroethylene or a chemical cleaner followed by an acid or alkaline etch. The parts will normally need desmuting in nitric acid, after which they are washed in clean water and dried [64]. Chemical cleaning is not recommended for fluxless vacuum brazing [58].

15.8.3.4 Aluminum Filler Metals

In the case of aluminum, the major elements in the filler metal are the same as the base metal except for some additional melting-point depressants. Complex parts can be formed and assembled using clad brazing sheet to eliminate the need for separate filler wire or shim. Various flux brazing filler alloys, vacuum brazing filler alloys, and clad aluminum flux brazing sheet are dealt with in Ref. [49].

Aluminum brazing sheet: Aluminum brazing sheet consists of a base metal core (typically 3003 or 6951 alloy) and a filler metal, typically either Al-7.5Si (4343) or Al-10Si (4045), clad roll bonded to either one or both sides as illustrated in Figure 15.80. The core provides structural integrity, while the clad plays the role of filler metal. An oxide surface layer is depicted to emphasize the importance of this barrier to the wetting and flow of the filler metal and the requirement that the barrier be dispersed for a successful braze [72].

15.8.3.5 Fluxing

Except for vacuum brazing or controlled-atmosphere (without oxygen) brazing, or salt-bath brazing processes where the salt bath itself consists of flux, all surfaces must be fluxed to break down the oxide film on the surface of the work and to promote wetting, and the filler itself must be fluxed. Fluxes for aluminum brazing contain fluorides and chlorides of the alkali metals. To the base are added “activators” such as fluorides, lithium compounds, and sometimes zinc chloride [61].

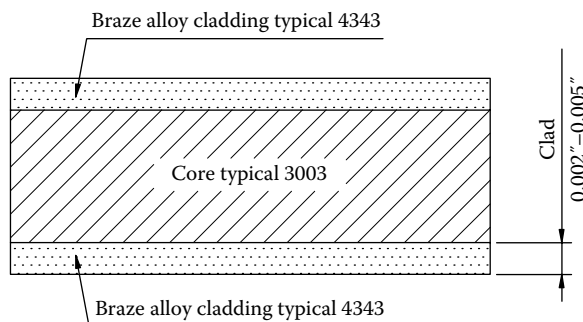


FIGURE 15.80 Clad aluminum brazing sheet.

15.8.4 BRAZING METHODS

The main processes used commercially to braze aluminum heat exchangers are

1. Torch brazing
2. Furnace brazing
 - a. Controlled-atmosphere brazing
 - b. Vacuum brazing
3. Flux dip brazing

Torch brazing and dip brazing employ a flux to break down the oxide film on the surface of the work and promote wetting. Furnace brazing with controlled-gas atmosphere requires less flux or no flux, whereas vacuum brazing does not require a flux and the mechanism of oxide breakdown is quite different.

15.8.4.1 Aluminum Dip Brazing

Aluminum dip brazing has been practiced commercially for many years. The molten salt bath contains chemically active salts that promote brazing. These help to displace the adherent oxide film on aluminum surfaces so that the molten filler metal wets the surfaces and forms the brazed joints. Because of the stability of surface oxide film, and because of low brazing temperatures that have to be used, a highly active flux is required for brazing aluminum. Important parameters pertaining to dip brazing aluminum, includes (1) bath compositions such as AlF , NaCl , KCl , etc., (2) bath melting point, 900°C – 1000°F (482°C – 538°C), (3) preheating temperature (approx.), 1000°F (538°C), and (4) brazing temperature 1030°F – 1190°F (555°C – 643°C) [53]. Manufacturing procedure for dip brazing of PFHE is shown in Figure 15.81.

15.8.4.2 Furnace Brazing

Furnace brazing is the second most popular method of brazing aluminum in use today. Furnace brazing's popularity derives from the comparatively low cost of equipment, from the ease with which the existing furnaces can be adapted to aluminum brazing, and from the minimal fixturing required [49].

15.8.4.2.1 Inert-Gas or Controlled-Atmosphere Brazing of Aluminum

For inert-gas brazing of aluminum, the process variables that affect moisture and oxygen levels in the brazing chamber must be controlled. This requires that the workpiece along with the fixture and the carrier be adequately outgassed to remove adsorbed moisture and oxygen prior to entering the inert-gas chamber. This is achieved by either repeated heating and evacuations, or a vacuum heating of aluminum with magnesium brazing filler metal clad to getter the contaminants.

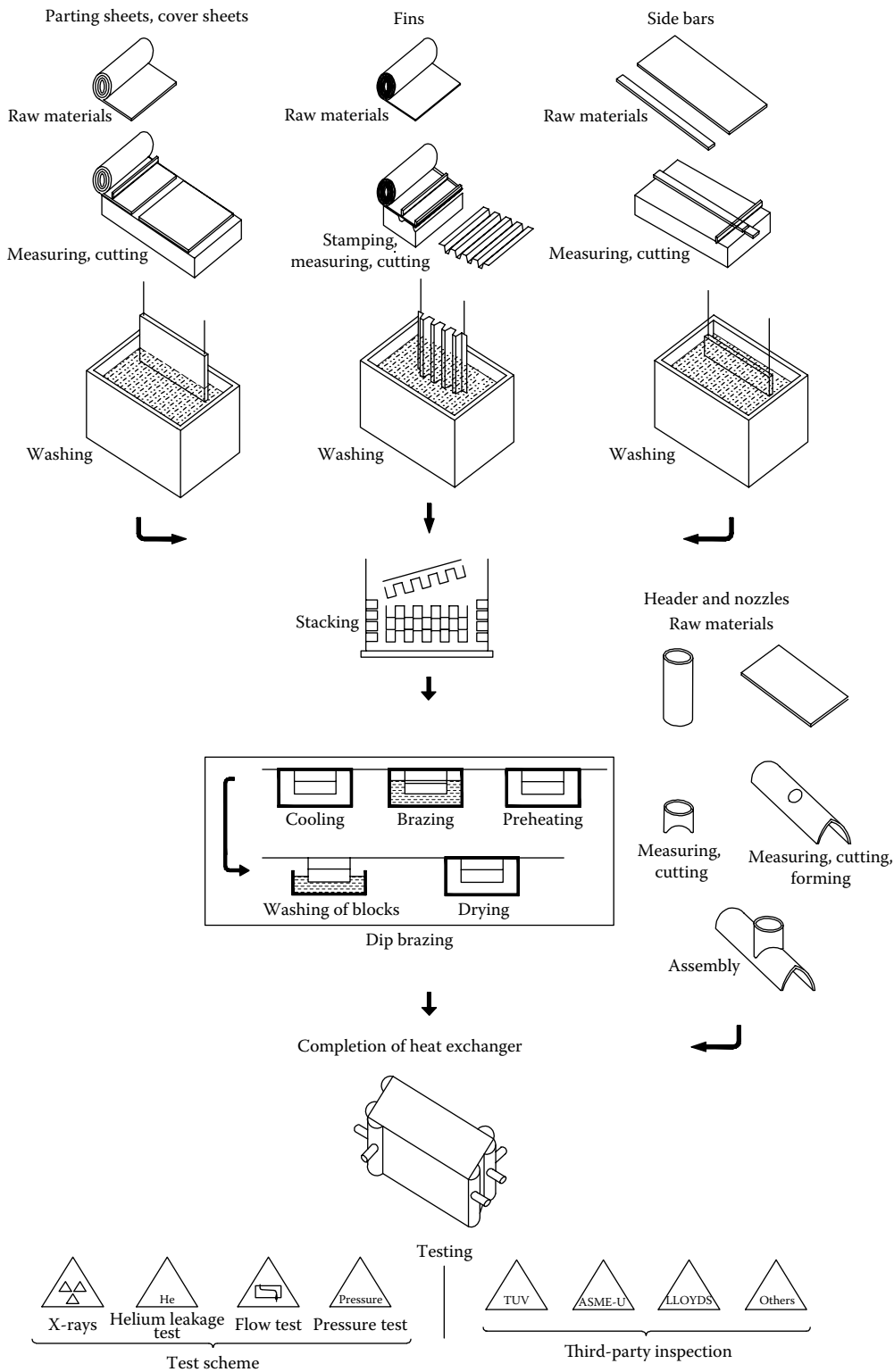


FIGURE 15.81 Manufacturing procedure of dip brazing with flux.

15.8.4.2.2 *Controlled Dry Air Brazing*

The amount of moisture in the brazing atmosphere influences the amount of flux required for successful brazing. When the moisture is not controlled, thick flux slurries, about 50%–75% by weight, are required. Only a small amount of flux serves the intended purpose, and much of it becomes ineffective because it is hydrolyzed by reaction with moisture present in the air, before the brazing alloy melts [73]. In a dry-air atmosphere of -40°F (-40°C) dew point or lower, thin slurries containing 20%–25% flux will serve the purpose. This brazing process also eases the postbrazing cleaning requirements.

15.8.4.2.3 *Controlled-Atmosphere Brazing Process*

CAB of aluminum using a noncorrosive flux is the preferred process for manufacturing aluminum heat exchangers. The process involves brazing in a dry and inert-gas atmosphere. Mostly nitrogen is used. Argon and helium can also be used, but they are more expensive. The gas is introduced into the critical brazing section of the furnace flows toward the entrance and exit. This prevents contamination of the atmosphere in the braze section. The process sequence of CAB depends on the type of heat exchanger being manufactured.

15.8.4.3 **Brazing Process**

For heat exchanger such as radiators and condensers, the most common process sequence is shown as follows as these sequences minimize handling of fluxed components and therefore flux drop-off:

- a. Core assembly.
- b. Fixturing.
- c. Degreasing/cleaning.
- d. Fluxing: The appropriate flux is applied, usually by means of spray nozzles that ensure a homogeneous distribution of the flux on the heat exchangers.
- e. Blowing: Excessive flux is blown off the heat exchanger.
- f. Drying: The temperature is increased to around 250°C in order to dry the heat exchanger.
- g. Heating: The temperature of the heat exchanger moving through the heating section is raised uniformly to the target braze temperature (around 600°C).
- h. Brazing: The flux melts and dissolves the oxide film on the aluminum just prior to the filler metal melting and forming their joints.
- i. Cooling: Solidification of flux and filler metal occurs. The flux residue forms a thin, adherent film.

Due to relatively high investment costs and relative limited flexibility in running production, CAB is most suitable for large quantity manufacturing.

15.8.4.3.1 *CAB Process Advantages*

CAB's advantages include the following:

1. Accepts a less demanding dimensional fit-up
2. Flux is noncorrosive, requiring no postbrazing cleaning
3. Less capital intensive compared to vacuum brazing
4. Continuous flow for high-volume throughput

15.8.4.3.2 *CAB Furnaces*

The CAB process uses a noncorrosive flux to reduce the tenacious aluminum oxide over layer that forms on the heat exchanger aluminum surface. For example, Seco/Warwick, USA, CAB furnaces provide the pure nitrogen atmosphere and temperature profile necessary to promote the formation of braze fillets between the fin and tubes and the tube-to-header joints of aluminum heat

exchangers. The following furnace designs are available to produce a variety of parts in large- or small-volume production runs:

- Radiation CAB furnace
- Convection/radiation CAB furnace
- Convection CAB furnace
- Active Only® CAB furnace
- Vacuum purge furnace

A radiation braze CAB furnace is an ideal method for brazing similar-sized products in a continuous flow environment. When the brazing needs are more diverse, a combination of convection preheating and radiation brazing furnace system is needed. The addition of convection preheating improves the furnace's overall flexibility, enabling manufacturers to run product of different mass and dimension in the same cycle. A pure convection heat-controlled atmosphere furnace system is the most efficient means to braze a wide variety of products in the shortest possible cycle time.

A fully configured CAB furnace system includes an aqueous washer or thermal degreaser, a fluxer unit, a dry off oven, and the CAB furnace with heating, brazing, and cooling zone. A schematic of typical radiation CAB furnace system is shown in Figure 15.82. These systems can be configured in an in-line, a continuous rectangular line as shown in Figure 15.83, or a U-shaped line to meet your plant's installation space requirements.

Furnace brazing of aluminum with a noncorrosive flux—Nocolock flux (Nocolock owned by Alcan Aluminum Ltd): It was discovered that a brazing method using a nonhygroscopic, noncorrosive, potassium fluo-aluminate flux material offered the benefits of flux brazing without a requisite postbrazing cleaning. When used in an inert-gas atmosphere, it has a significant tolerance to impurities in the furnace atmosphere [74]. The flux is active only at or near the brazing temperature and is completely inactive at lower temperatures, which allows the flux residue to be left on the work without any danger of subsequent corrosion. The trade name for the noncorrosive flux

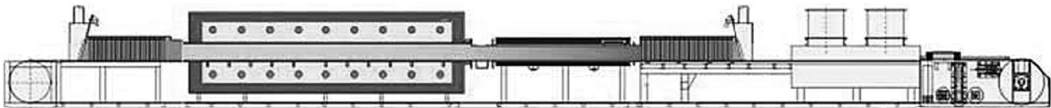


FIGURE 15.82 Radiation CAB furnace (schematic) (entrance chamber, braze chamber, water jacket cooling chamber, exit chamber, air blast drive table). (Courtesy of Seco/Warwick Corporation, Meadville, PA.)



FIGURE 15.83 CAB brazing furnace system. (Courtesy of Seco/Warwick Corporation, Meadville, PA.)

is known as Nocolock. Heat exchangers such as automotive radiators, heater cores, condensers, evaporators, oil coolers, and charge air coolers are being mass produced using the Nocolock flux brazing process [75]. The flux is a fine white powder mixture of potassium fluo-aluminates. It is mixed with water to form a dilute slurry, applied by spray or other methods to cleaned aluminum assemblies, and dried. Parts are normally brazed in a nitrogen atmosphere tunnel furnace. Brazing temperatures of 590°C–620°C (1095°F–1150°F) are suitable.

Postbrazing treatments: Generally speaking, no postbrazing treatments are required. The flux residue is noncorrosive, strongly adherent to the aluminum surface, and provides good corrosion protection. However, in recent years, there continues to be a demand for air-oxidized or blackened-surface radiators and condensers [75]. These are based on the controlled introduction of dry air for surface oxidation or carbon dioxide for surface blackening into an inert atmosphere brazing furnace soon after the completion of the braze. These after-treatments are required to improve corrosion resistance of aluminum heat exchangers.

15.8.4.4 Vacuum Brazing of Aluminum

In vacuum brazing, aluminum assemblies are heated in a vacuum environment by radiation.

The principal differences between vacuum brazing and furnace brazing are that (1) the brazing is done in a vacuum of the order of 10^{-4} to 10^{-6} torr, (2) no flux is used, (3) clad brazing sheet and other forms of filler materials usually contain 0.1%–2.0% magnesium as braze promoter, and (4) heating is by radiation rather than convection.

Typical procedures for vacuum brazing aluminum heat exchanger: These include the following:

1. Precleaning of components
2. Assembly and fixturing
3. Heat/braze in vacuum
4. Back-fill the furnace: Dry nitrogen is often used, although dry air can be used under some circumstances
5. Remove the brazed assemblies, which should be air quenched with a fan or allowed to stand until cool

Typical manufacturing procedure for vacuum brazing of PFHE is shown in Figure 15.84.

Important parameters for vacuum brazing aluminum. Important process parameters that control brazing and braze quality are (1) vacuum environment, (2) brazing assembly temperature and temperature uniformity, (3) oxide dispersion and wetting, (4) special vacuum brazing filler and brazing sheet alloy, and (5) vacuum brazing furnace parameters. Some or all of these parameters are discussed in Refs. [67,68,72].

Vacuum environment: The most important and difficult to control parameter is the vacuum itself. Pressure is generally monitored for most brazing processes, with the total pressure being the sum of the partial pressure of all the gases present. It is particularly important to monitor and control the partial pressure of contaminants such as oxygen and water vapor [68]. Typical commercial furnaces designed for vacuum brazing operate in the 10^{-4} to 10^{-6} torr pressure range. Mechanical roughing and oil diffusion pumps are used to achieve the vacuum.

Temperature control: The brazing assembly temperature and temperature uniformity are important processing factors in brazing under vacuum. In designing the temperature programming for the brazing process, several objectives must be borne in mind [67]: minimization of (1) the time for reaction with vapor-phase contaminants, (2) the temperature gradients within the brazed assembly, and (3) the time at brazing temperature, to reduce erosion and other unwanted core and cladding interactions in the brazing sheet. Braze performance is degraded when the interactions cause a reduction in the available filler metal and/or erosion of the core. Vaporization losses of volatile solute from the molten clad can cause similar problems [72]. The adverse effects of silicon diffusion

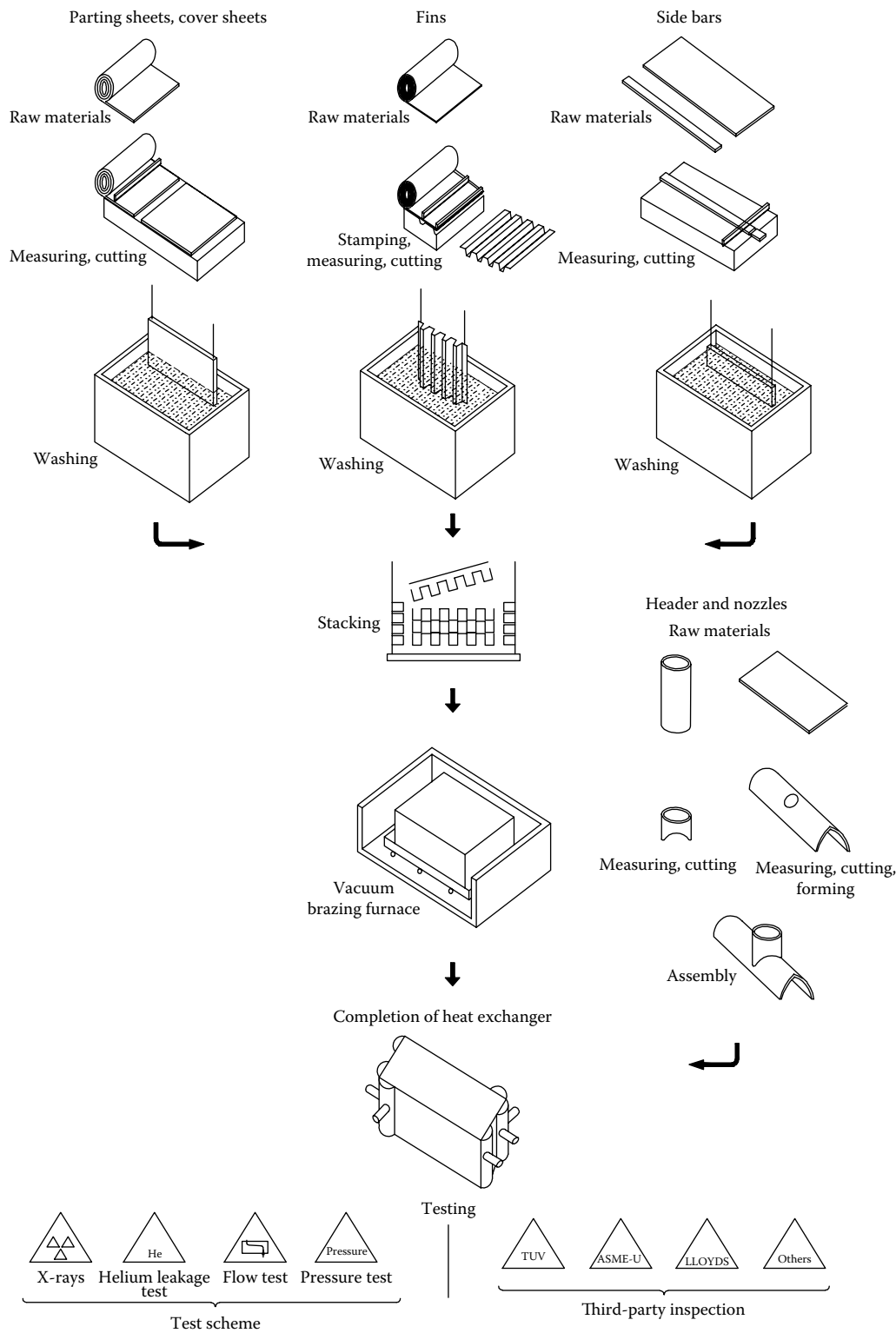


FIGURE 15.84 Manufacturing procedure of flux-free brazing in a vacuum. (From Linde AG, Engineering Division. With permission.)

from core alloy to the braze alloy and vaporization of zinc from base metal on corrosion performance of braze are discussed later.

Oxide dispersion and wetting: It is well known that oxygen and water vapor are the important process contaminants. In fluxless vacuum brazing, the presence of a promoter, either a metal or reactive gas, is needed to getter oxygen and water vapor from the furnace and to suppress reoxidation of the aluminum at the joints, once the oxide film is removed. The fluxless processes use either elemental magnesium, magnesium containing filler metal, or magnesium bearing base metals to getter oxygen [70]. Alternatively, brazing also can be achieved in a high vacuum by prolonged exposure at elevated temperatures without using metal activators [73].

Magnesium as a braze promoter: Many metals can fulfill the function of a braze promoter, but magnesium is the best, because magnesium has the highest vapor pressure of the metals that promote vacuum brazing [73], ease of alloying with aluminum, and low cost [68].

Vacuum brazing filler metals: Generally, vacuum brazing filler metals and brazing sheets are aluminum alloys containing 7.5%–12% silicon and up to 1.5%–2.5% magnesium [59]. Since gravity adversely affects vertical capillary filler metal flow in vacuum brazing, preplace filler metal in vertical joints or use a brazing sheet. Alloys of the 1xxx, 3xxx, 5xxx, 6xxx, and 7xxx series can be vacuum brazed using No. 7, 8, 13, and 14 brazing sheets.

Vacuum brazing furnaces: Vacuum furnaces capable of reaching at least $1200^{\circ}\text{F} \pm 5^{\circ}\text{F}$ ($650^{\circ}\text{C} \pm 3^{\circ}\text{C}$) temperature uniformity in the normal brazing range of 1080°F – 1140°F (582°F – 616°F) are suitable for brazing aluminum [68]. Systems for vacuum brazing of aluminum are discussed in detail in Ref. [67] and Ashburn [76]. Vacuum furnaces are invariably heated by electricity, in any one of a number of forms. A typical electric-heated vacuum furnace has the heating system surrounded by radiation shields and mounted within a water-cooled steel shell, which is known as cold-wall design. Vacuum furnaces for brazing aluminum are equipped with mechanical roughing and oil vapor diffusion pumps to achieve the required 10^{-4} to 10^{-6} torr vacuum.

Nonuniform mass and temperature uniformity: PFHEs are relatively uniform in mass and usually present no particular problems in heating to brazing temperature in a furnace atmosphere. However, tube-fin exchangers such as the automotive radiator, with different thicknesses of parts like fins, tubes, header sheet, and side supports, require special consideration due to their non-uniform mass distribution. This type of radiator can be heated uniformly using one of these two methods [68]: (1) use of heat shields to slow heating of the core area and (2) orienting the radiator in the furnace with heavier sections facing the heating elements. While both methods provide $\pm 5^{\circ}\text{F}$ temperature uniformity, the latter method is more amenable to production use.

Postbrazing cleaning and finishing: The brazed aluminum alloys should be free from residual flux to avoid corrosion during service. The postbrazing cleaning methods include ultrasonic means or using chemical solutions, or using one of the chemical brighteners.

Cleaning of a chloride-type flux

1. The most rapid and efficient method of removing the chloride-type flux is by hot water cleaning, that is by the immersion of the still hot part into boiling water. A chloride flux is highly soluble, and boiling water will quickly remove most of it.
2. Ultrasonic cleaning with proprietary cleaning solutions.
3. Chemical cleaning.

Cleaning of a fluoride-type flux: Even though residual fluoride flux is noncorrosive, for aesthetic reasons and for surface coating, the fluoride flux is cleaned using a caustic etch or chemical brighteners, since fluoride fluxes are not water washable [49].

Finishing: When a brazing fillet has been properly formed, no finishing is required except flux removal by postbrazing cleaning. If necessary, the fillet, like the brazed metal, may be ground, filed, or polished. Caution: The brazed assembly should not be cleaned in caustic solution.

15.9 BRAZING OF HEAT-RESISTANT ALLOYS AND STAINLESS STEEL

Heat-resistant superalloys are either nickel-based or cobalt-based alloys, with the alloying elements chromium, iron, tungsten, and molybdenum. These alloys exhibit strength, oxidation resistance, and resistance to corrosion at elevated temperatures (1200°F–2200°F). Some of the nickel-based wrought alloys used as heat exchanger materials are Hastelloy X, Inconel 625, and Inconel 718, and cobalt-based alloy Haynes 188 [48]. Elements of brazing of nickel-based and cobalt-based alloys are discussed in this section.

15.9.1 BRAZING OF NICKEL-BASED ALLOYS

Requirements for brazing of nickel-based alloys

The success of brazing of nickel-based alloys depends on the careful consideration of the following parameters [77]:

1. Physical metallurgy of the alloys
2. Surface preparation
3. Thermal cycles
4. Brazing atmosphere

Physical metallurgy of the alloys: The surfaces of precipitation-hardenable alloys containing more than 1% Al and Ti are covered with hard, tenacious oxide films. These surface films hinder the wetting of molten filler metal, and the films are in general impossible to reduce, either in a controlled atmosphere or in a vacuum brazing atmosphere. However, these difficulties are not normally encountered with solid-solution-strengthened alloys.

Surface preparation: Successful brazing requires removal of surface oxide films. To improve the wettability by filler metals, additional surface treatment followed by precleaning may be required. The surface treatment consists of electroplating of nickel on the surfaces, known as nickel flashing.

Thermal cycles: The effects of high-temperature thermal cycles are [77] as follows: (1) Brazing temperature above their hardening temperatures of 1100°F–1500°F may alter the alloy properties; (2) at the high brazing temperature of 1850°F, the precipitation-hardenable alloys may be subjected to grain growth and decrease in stress rupture properties, which cannot be recovered by subsequent heat treatment; and (3) the liquid metal is subjected to embrittlement when the molten metal is under the influence of tensile stress. Hence, the residual or applied tensile stress should be relieved before brazing.

Brazing atmospheres: For successful brazing of nickel-based alloys, either a dry, oxygen-free reducing atmosphere or a vacuum is preferred. The effects of various controlled atmospheres have been covered earlier. Vacuum brazing in the range of 10^{-4} torr has proved adequate for brazing most of the nickel-based alloys. The brazing atmosphere, whether gaseous or vacuum, should be free from harmful constituents such as sulfur, oxygen, and water vapor. In general, a gaseous atmosphere having a dew point less than about -60°C (-75°F) will produce better quality.

15.9.1.1 Brazing Filler Metals

Generally, nickel-based alloys are brazed with nickel-based alloys containing boron and/or silicon, which serve as melting-point depressants. Phosphorous is another effective melting-point depressant, and it also aids good flow in applications of low stress; their temperatures do not exceed 1400°F (760°C). Sometimes, chromium is present to provide oxidation and corrosion resistance. Other filler metals include copper and silver brazing alloys for low-temperature applications and proprietary filler metals for service temperature above 1800°F (982°C).

15.9.2 BRAZING OF COBALT-BASED ALLOYS

Brazing of cobalt-based alloys can be accomplished by adopting the same techniques used for brazing of nickel-based alloys but with less stringent brazing requirements [77]. This is due to the absence of appreciable amounts of aluminum and titanium in the base metals. The filler metals are usually cobalt based, nickel based, or gold–palladium compositions. Most cobalt-based filler metals contain boron and/or silicon as melting-point depressants and Cr, Ni, and W for improved strength, corrosion, and oxidation resistance.

15.9.3 BRAZING OF STAINLESS STEEL

In recent years, there has been a demand, particularly from the aircraft and nuclear energy industries, for complex heat exchangers that operate under arduous conditions of temperature and pressure and adverse environments. To meet these requirements, heat exchangers have been fabricated from stainless steel, usually the 18:8 type stabilized with titanium. Other wrought stainless steels such as of AISI types 316, 316L, 347, and 430 are also extensively used as heat exchanger materials for high-temperature applications. Many aircraft heat exchangers are of modular construction [78]. Typical brazed forms of stainless steel heat exchangers include PFHEs, shell and tube heat exchangers, and regenerators. To save weight in aircraft and for greater efficiency in heat transfer, the heat exchangers have been made from thin sheet and thin-wall tubing; typical sizes are sheet 0.005 in thick and tubing of 0.006 in wall thickness. One of the problems in fabricating structures from these thin materials has been to make completely sound joints without any distortion in the heat exchanger matrix.

15.9.3.1 Brazeability of Stainless Steel

Brazing of stainless steels is carried out at high temperatures (see Table 15.4). Among the various factors, the quality of stainless steel brazing depends on the following [62]:

1. Ability to create a proper brazing atmosphere to eliminate oxidation, scaling, and surface reaction that forms sulfides and nitrides on its surface. Brazing either in a controlled atmosphere or in vacuum eliminates the oxidation of the base metal, is effective in reducing the oxides, and promotes the flow of filler metal.
2. Ability to arrest the sensitization of austenitic stainless steel during brazing or proper solution treatment of sensitized steels to restore their corrosion resistance.

Brazing process: Stainless steel can be brazed by all conventional brazing processes including torch, furnace, dip, and induction brazing. Stainless steel heat exchangers are mostly furnace brazed, either in a controlled reducing atmosphere such as dry hydrogen, dissociated ammonia, or argon, or in vacuum.

Furnace brazing in dry hydrogen: Dry hydrogen is the most preferred for brazing of stainless steel since it eliminates the oxidation of the base metal and is effective in reducing the oxides. The principal disadvantages are high cost; difficulty in getting hydrogen in dry condition, free from oxygen and other oxidants; and handling and storage problems [64].

Furnace brazing in dry dissociated ammonia: Stainless steels are brazed in a dry dissociated ammonia, that is with the composition of H_2 and N_2 . Even small traces of NH_3 will nitride stainless steel and dissolve in water if traces of moisture are present.

Vacuum brazing: For high-temperature service applications, vacuum brazing can offer excellent heat and corrosion resistance. A vacuum of 10^{-2} torr of mercury is sufficient to braze most stainless steels. Many structures that could not be brazed in hydrogen have been brazed successfully in vacuum furnaces [64].

Filler metals: In addition to brazeability, for most applications, filler metals are selected for mechanical properties, corrosion resistance, service temperature, and compatibility with process fluids. Filler metals for brazing stainless steels include copper alloys, silver alloys, gold and gold–palladium alloys, and nickel alloys. Nickel-based filler metals alloy with stainless steel and form secondary phases with two undesirable characteristics [77]: (1) low ductility and hence susceptibility to hot cracking and (2) higher melting point than the base metal and hence likely to freeze and retard the filler metal flow. To achieve flow in deep joints, diametral clearances of as much as 0.004–0.008 in. (0.1–0.2 mm) are necessary. Selection of brazing filler metals for brazing stainless steels is also discussed by Amato et al. [79]. For guidance on selection of brazing filler metals for stainless steels brazing, Welding Engineer Data Sheet No. 493 [80] is useful.

Fluxes: Brazing of stainless steel in a controlled atmosphere or in vacuum does not require flux. In some furnace-brazing applications, flux is necessary. But flux is required for torch brazing, dip brazing, or any other conventional brazing process carried out in an uncontrolled atmosphere.

15.10 QUALITY CONTROL, INSPECTION, AND NDT OF BRAZED HEAT EXCHANGERS

The principles of QC, quality assurance, inspection, and NDT techniques have been dealt with in Chapter 14. Even though the focus in that chapter was shell and tube heat exchangers, the underlying principle is relevant for any type of heat exchanger and for any manufacturing process. With this in mind, QC and inspection pertaining to brazing are discussed here. Quality assurance for aluminum brazing is discussed in ANSI/AWS C3.7-93, Specification for Aluminum Brazing [70]. Salient features of quality systems for brazing are as follows:

1. Data cards. An essential part of the quality system is the use of data cards for each job to record brazing parameters. The data cards contain such information as materials used, joint configuration, brazing alloy, thermal cycle, furnace load configuration, and inspection and NDT requirements.
2. Responsibility for inspection. Unless otherwise specified in the contract or purchase order, the manufacturer is responsible for the performance of all inspections during various stages of brazing operation.
3. Sequence of inspection and manufacturing operations. Brazed joints may be inspected at the assembly or subassembly stage, and after postbrazing heat treatment. Flux residue testing shall be performed after completion of all operations of the brazed joint.
4. Temperature measuring devices. All furnaces and molten salt baths used in the brazing shall have automatic temperature controlling and recording devices in proper working order. Periodically calibrate temperature measuring devices, furnace atmosphere controlling instruments, and vacuum measuring devices.
5. Integrity of vacuum furnaces: A critical step for vacuum furnace is to ensure a sound furnace atmosphere through regular, scheduled leak testing.
6. Elements of QC for dip brazing: QC aspects should cover maintenance of flux composition, temperature, pH, removal of scum and sludge, preheating the assembly, etc., as discussed earlier in the section on the dip brazing process.
7. Flux removal test: All components brazed using corrosive flux shall be tested for the presence of residual flux after postbrazing cleaning. The silver nitrate test is popular for determining the presence of flux either in the wash water or remaining on the workpiece after it has been washed and dried. Evidence of any precipitate or cloudy appearance indicates incomplete cleaning, and the piece should be cleaned further or may be rejected. Other test methods may be used as alternates with the written approval of the buyer.

15.10.1 QUALITY OF THE BRAZED JOINTS

The quality of brazed joint shall be such that the brazed assemblies are suitable for the intended purpose and that surfaces are free of excess braze filler material. Quality problems of brazed joints of aluminum heat exchangers are discussed by Shah [51]. Some of these problems may also be common to other metals. A good brazed joint has large smooth fillets, absence of discontinuities and voids, and the width of the joint is sufficient as shown in Figure 15.85. Imperfect brazed joints include the following [51]:

1. Poor fillets: a braze joint with narrow-width fillets, due to insufficient time at the braze temperature.
2. Partial joint (underbrazing): due to low brazing temperature, low amount of melting-point temperature depressant elements in filler metal, or improper heating rate.
3. Overbrazing: a braze joint that is a result of too high brazing temperature or the brazing time; filler metal may dissolve the base metal and reduce its strength.

15.10.1.1 Discontinuities

Discontinuities result in all brazing processes. Some may be process specific. Discontinuities may be associated with structural discontinuities or associated with the braze metal or the brazed joint. Typical discontinuities include [49,52,53] the following: (1) lack of fill, (2) flux entrapment, (3) intermittent bond, (4) noncontinuous fillets, (5) voids, (6) porosity, (7) cracks, (8) base metal erosion, (9) unsatisfactory surface appearance, (10) discoloration, and (11) distortion.

All discontinuities reduce joint strength. Acceptance limits for discontinuities must identify shape, orientation, location in the brazement, and relationship to other discontinuities.

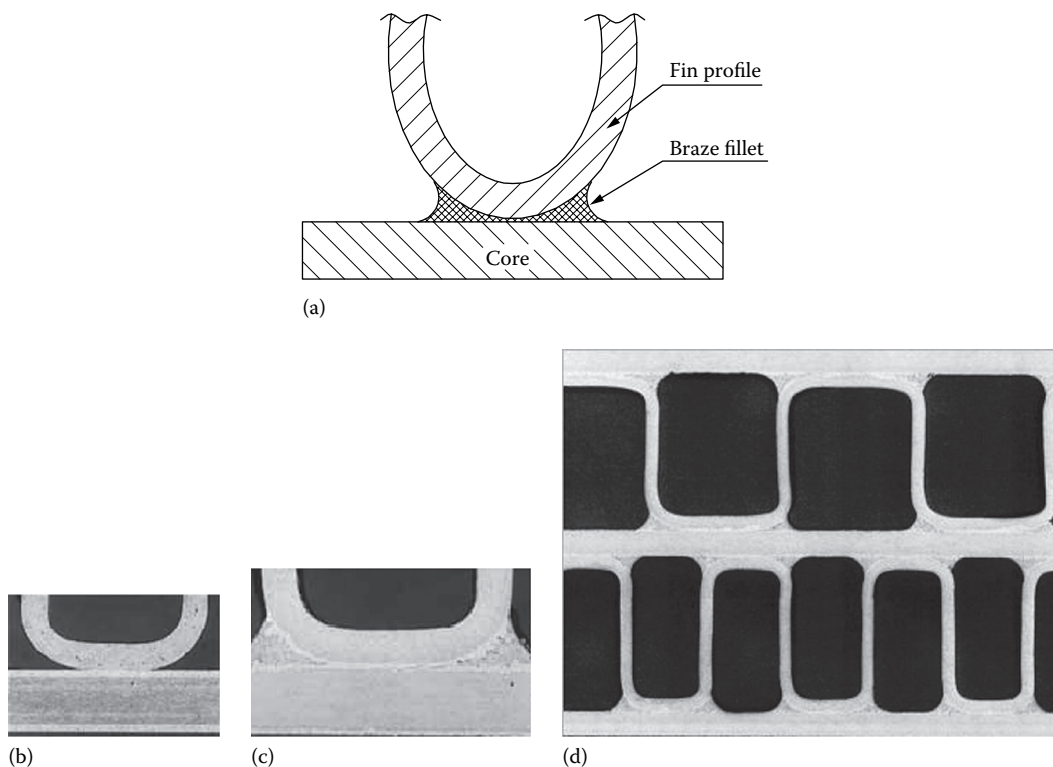


FIGURE 15.85 Plate fin heat exchanger brazing joint details. (a) Schematic, (b) before brazing, (c) after brazing for single fin passage, and (d) after brazing for two layers of fin stack. (Courtesy of Fives Cryo, Golbey, France.)

15.10.2 INSPECTION

Inspection of brazed joints may be conducted on test specimens or by tests of the finished brazed assembly. The tests may be nondestructive or destructive methods, such as peel tests, tension or shear tests, fatigue test, impact tests, torsion tests, and metallographic examination or proof testing. Various NDT methods include PT, RT, and UT. The scheme of NDT techniques is shown in Figures 15.81 and 15.84.

15.10.2.1 Visual Examination

Visual examination is the most commonly used means for rapidly assessing brazed joint quality, dimensions, and distortion, if any. If the fillet is fully formed and smoothly curvilinear, the joint may be accepted as being reasonably sound pending further, more detailed examination [49]. Visual inspection is unsuitable for the detection of flux entrapment.

15.10.2.2 Leak Testing

To make certain no leaks exist, heat exchangers are leak tested. The choice of pressure medium will depend to some extent upon the maximum acceptable leak aperture. Thin oil such as kerosene, heated oil, water, air, or Freon may be used. For critical services, where it is necessary to identify the presence of very minute leaks, helium mass spectrometer leak detection technique may be employed.

15.10.3 BRAZING CODES AND STANDARDS

AWS brazing and soldering documents

B R H	Brazing hand book
S M	Soldering manual
A 2.4	Standard symbols for welding, brazing, and nondestructive testing
A 5.8	Specification for filler metals for brazing, A5.01, filler metal procurement guidelines
B 2.2	Standard for brazing procedures and performance qualification
C 3.2	Standard method for evaluating the strength of brazed joints in shear
C 3.3	Recommended practice for design manufacture and inspection of critical brazed components
C 3.4	Specification for torch brazing
C 3.5	Specification for induction brazing
C 3.6	Specification for furnace brazing
C 3.7	Specification for aluminum brazing
C 3.8	Recommended practices for ultrasonic inspection ASME Code Section II, Part C

15.11 SOLDERING OF HEAT EXCHANGERS

Soldering is defined as a process of joining two similar or dissimilar metals with a filler metal in molten state. Soldering joins materials by heating them in the presence of a filler metal having a liquidus temperature below 840°F (450°C). The filler metal is called *solder*. Heating may be provided by a variety of processes. The filler metal distributes itself between the closely fitted surfaces of the joint.

15.11.1 ELEMENTS OF SOLDERING

Most of the elements of soldering, such as joint design, solder selection, fluxing, precleaning and surface treatment, cleaning after soldering, and inspection, have lot of similarities with brazing process. Therefore, without going deep into these aspects, only salient features of certain

elements relevant to radiator design are described here. Subsequently, two versions of the soldering process are described. One involves the conventional soldering of automobile or locomotive radiators, and the other involves the fluxless ultrasonic soldering of all-aluminum core for room air conditioners.

15.11.1.1 Joint Design

Soldered radiator joints are required to perform in a severe environment. They are subjected to fluctuating temperatures, mechanical vibration, immersion under a water-based fluid, and contact with dissimilar metals. Added to that is the frequent neglect of the quantity and quality of coolant solution [81].

15.11.1.2 Tube Joints

Conventionally, brass flat plates are solder coated and formed into tubes, lock-seam jointed in a soldering machine. Recently, tubes with a butt-welded joint have been used for the construction of tubes. This type of radiator tube is stronger and more leakproof than the conventional roll-formed brass lock-seam product and provides a material savings of about 25% through elimination of the lock seam [82].

15.11.1.3 Tube-to-Header Solder Joints

Solder alloys generally have lower strength properties than the base materials. Joints between the tubes and the header plates are essentially shear loaded in both directions as the radiator is heated, pressurized, and subsequently cooled [83]. Failure of the tube-to-header solder joint occurs because of a variety of problems [84]: weak solder joints due to poor mechanical assembly and fit-up problems, brittle fracture, creep and fatigue, and external or internal corrosion. Possible approaches for increasing the durability of the tube–header solder joints are discussed by Webb et al. [84].

15.11.1.4 Solders

Solders generally have melting points or melting ranges generally below 800°F (425°C). There is a wide range of commercially available solders designed to work with most industrial metals and alloys. Tin–lead solders, improved tin–lead solders, and zinc–aluminum solders are discussed in the following section and their composition is shown in Table 15.5. More details on solder selection can be found in Ref. [52].

Lead-based solders: Tin–lead solders are most widely used in the joining of metals, particularly conventional automotive radiators. Most commercial fluxes, cleaning methods, and soldering processes may be used with tin–lead solders.

TABLE 15.5
Solder Compositions

Sn–Pb		Sn–Pb–Ag			Zn–Al–Cu		
Sn	Pb	Sn	Pb	Ag	Zn	Al	Cu
5	95	5.5	94.0	0.5	95	5	—
10	90	5.0	94.5	0.5	89	7	4
15	85	3.8	95.0	1.2			
20	80	2.5	95.0	1.2			
25	75	1.0	97.5	1.5			
30	70						

Mechanical properties: The requirements of a lead-based solder for tube-to-header radiator joints include the following [81]:

1. It must have a minimum amount of tin so that sufficient tin oxide film is formed to passivate the surface.
2. It must have excellent mechanical properties, particularly with regard to creep resistance, to minimize damage to the protective film.
3. It must have good solderability properties.
4. It must be cost-competitive with alternate joining materials.

All lead-based solders have a very low yield point. Under almost any load, they are subjected to some plastic deformation. These alloys are particularly sensitive to creep deformation.

Improved lead–tin solder alloy: For years, the standard radiator solder had been 70:30 lead/tin. The 70:30 solder is relatively brittle and prone to stress cracking as a result of vibrational stresses built up in the radiators. This led to solder-joint failures. This solder has been replaced almost entirely by high-lead solders containing up to 97% lead [85]. This solder, called soft solder, could better withstand engine vibration; it has the following approximate composition: 97% lead, 1.5%–2.5% tin, and 0.5%–1.5% silver. The tin content was reduced both to save money and to improve mechanical properties. Solders containing less tin will form less eutectic, which will improve the solder's high-temperature mechanical properties [81]. At the same time, a certain concentration of tin in the solder is necessary. If sufficient tin is present in the solder, a tenacious and stable oxide film forms over the solder, which improves the corrosion resistance of the solder joint. Hence, it is necessary that the solder contain a minimum of 5% tin. In high-lead solders, where mechanical strength is considered very important, for example, for tube-to-header joints, silver is added. Typical of these high-lead solders are 95Pb–5Sn and 97.0Pb–0.5Ag–2.5Sn (Modine).

Zinc-based solders: Zinc–aluminum solder, the most standard grade 95Zn–5Al is specifically used for ultrasonic soldering of aluminum. It develops joints with high strength and good corrosion resistance.

15.11.1.5 Cleaning and Descaling

An unclean surface prevents the solder from flowing and makes soldering difficult or impossible. Solvent or alkaline degreasing is recommended for cleaning oily or greasy surfaces. For removing rust or scale, pickling or mechanical cleaning may be used.

15.11.1.6 Soldering Fluxes

With flux soldering, the flux helps to break up the tenacious oxide layer on the base metal, by reacting with or otherwise loosening that film from the base metal surface. Without the action of the flux, the molten solder cannot wet the surface. Soldering fluxes are divided into three main groups based on their residues [83]: corrosive, intermediate, and noncorrosive. Whenever possible, use the least corrosive flux to eliminate the potential postsoldering corrosion problems stemming from the residual flux. Various compositions of fluxes for copper/brass radiator manufacture include the following:

Zinc chloride, ammonium chloride, and water to make

Zinc chloride, sodium chloride, ammonium chloride, hydrochloric acid, and water to make

Zinc chloride, ammonium chloride, petroleum jelly, and water to make

15.11.1.7 Soldering Processes

Soldering processes or the heating methods available for heat exchanger manufacture are as follows:

Flame or torch soldering: Handheld manual torch soldering is most frequently used for repairs to tube-to-tube-plate joints.

Furnace or oven soldering: Furnace soldering is considered when an entire assembly (e.g., radiator) is to be brought to the soldering temperature and when the assembly is complicated in nature, making other heating methods impractical.

Dip soldering: The dip soldering method uses a molten bath of solder to supply both the heat and the solder necessary to join the workpieces. Tube-to-header joints of radiators are made by this process.

Ultrasonic soldering: Ultrasonic soldering can be considered a form of dip soldering, in which the workpiece is immersed in a tank of molten solder. Ultrasonic soldering is discussed separately.

Infrared soldering: This involves focusing infrared light (radiant energy) by means of an optical system. Typical applications include soldering pretinned interference fit return bends by Reynolds interference fit.

15.11.1.7.1 *Various Stages of Radiator Manufacture by Conventional Soldering Process*

In the soldered design, a radiator core is formed by soldering the plain fins or corrugated fins to flattened heat exchanger tubes, and the core is connected to the upper and the lower tanks via a pair of header plates. Radiator tubes are normally made by fabricating a lock seam and joining this seam continuously in a soldering machine. Then the core is formed in a fixture, wherein the fins are stacked and inserted with flat tubes. To insert tubes into the fins stack, a piercing tool is used. The header plates are inserted and pressed onto tubes for making tube-to-header joints. These stages are listed in detail as follows:

1. Tube forming (lock seam), fluxing, solder coating, and cutting to size
2. Burr removal at the tube ends
3. Fin rolling
4. Fin assembly in a fixture
5. Insertion of tubes
6. Fitment of header plates
7. Precleaning
8. Backing in a furnace
9. Squaring of the core assembly and straightening of the blunt fins in the hot condition
10. Expanding the tube ends using a chisel or a blunt formed tool
11. Dip soldering of header plate with tubes
12. Blowing off with air to clear blockages
13. Hot water cleaning and rinsing
14. Leakage test with a dummy water tank
15. Fitment of the metal water tanks and soldering with a tube plate or fitment of plastic/metal water tank and crimping with the tube plate; soldering of inlet, outlet, drain connections, etc.
16. Fitment/soldering of side mounting/side sheet assembly
17. Checking the overall dimensions of the assembly
18. Leak testing
19. Drying and painting
20. Packing and dispatching

15.11.1.8 **Flux Residue Removal**

Zinc chloride-based flux residue is best removed by hot water washing containing 2% of concentrated hydrochloric acid, followed by hot water rinse. The silver nitrate test can be used to determine whether all of the salts have been removed [52]. Additional tests are discussed later.

15.11.2 **ULTRASONIC SOLDERING OF ALUMINUM HEAT EXCHANGERS**

All-aluminum coils for the air-conditioning industry have been fabricated by flux soldering for many years. Use of flux requires flux cleaning equipment and wastewater treatment facilities. Potential problems from incomplete flux removal and new environmental legislation necessitated

development of a fluxless joining process [86], which uses ultrasonic waves to agitate the soldering bath. As ultrasonic waves produce cavitation in the molten bath, they cause a scrubbing action that removes the surface oxide film, thus permitting the solder to wet the aluminum surfaces [87]. Being a fluxless process, ultrasonic soldering is becoming more widely used for the fabrication of all-aluminum coils for the air-conditioning industry. Detailed discussions on the subject can be found from [88–90].

15.11.2.1 Material That Can Be Ultrasonically Soldered

By this method, hard-to-wet metals can be successfully soldered in a very few seconds. Aluminum combined with various other materials, stainless steel, and even ceramic materials has been wetted rapidly and successfully [89]. The ultrasonic soldering process has been used for joining 1100, 1200, 3003, 6061, 6063, Alclad 7072/3003, and some 2xxx aluminum alloys.

15.11.2.2 Basic Processes for Soldering All-Aluminum Coils

Two basic processes that make use of ultrasonic soldering are (1) the “dip” or Alcoa 571 process and (2) the Reynolds interference fit process. Of the two, the Alcoa process is widely used, while the Reynolds method shows promise [90].

Alcoa 571 process: The Alcoa 571 process is a fluxless ultrasonic soldering process specifically developed for the tubular joints in all-aluminum tube-fin air conditioner coils. In simplest terms, the process requires (1) a heated solder, (2) immersion of the part to be soldered, and (3) cavitation of the solder by ultrasonics. The requirements are met by the following four main components of the ultrasonic equipment [90]: (1) an ultrasonic power supply, (2) a set of transducers, (3) a heated vessel, and (4) a heat control console. More details on Alcoa 571 process are furnished by Denslow [90].

Soldering procedure: The operations for fabrication and soldering of a coil can be divided into four general areas [88]: (1) coil preparation, (2) coil transport, (3) coil preheat, and (4) coil soldering. The coil preparation includes precleaning the return bends and the tube ends, preferably by ultrasonic vapor degreasing.

The coils or core is made by assembling U-tubes and fins and expanding the tubes in the conventional fashion. The ends of the U-tubes are flared to a prescribed socket geometry (Figure 15.86) to provide a joint and a friction fit for the inserted return bends [88]. After vapor degreasing the return bends and core tubes ends, the return bends are simply tapped into position. The joints are preheated to soldering temperature in the inverted position by hot air or gas flame. The coil is then quickly transferred and lowered into a molten bath of 95% Zn–5% Al solder and exposed for a few seconds to ultrasonic cavitation. The actual soldering of a coil requires only a few seconds of ultrasonic exposure. The sequence of operations is depicted in Figure 15.87.

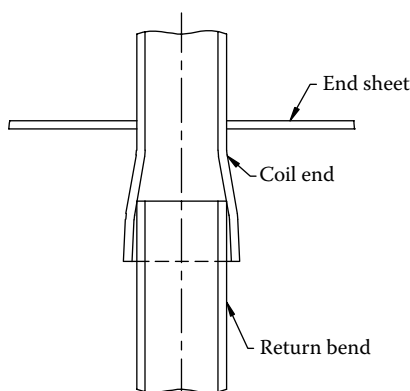


FIGURE 15.86 Heat exchanger coil socket configuration.

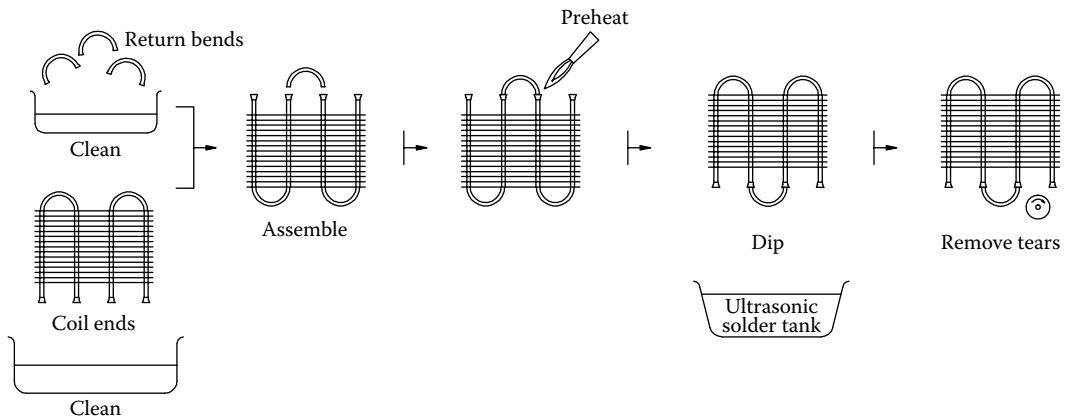


FIGURE 15.87 Fluxless ultrasonic soldering by the Alcoa 571 process. (Adapted from Jenkins, W.B., *Weld. J.*, January, 28, 1976.)

Solder composition and maintenance of soldering bath: The solder composition recommended is 95Zn–5Al, which is maintained at a temperature of 780°F–800°F. Since each coil processed through the soldering bath takes out some solder with it, the bath should be replenished with fresh solder to maintain its depth. During the tinning process, some aluminum will be eroded off the parts [91]. Therefore, the replenisher is slightly lean in aluminum, typically 98Zn–2Al, to keep the bath at 5% Al [87].

Process control: There are four factors that have significant effects on the joint quality [88]: (1) ultrasonic solder pot design, (2) socket design, (3) preheat, and (4) depth of immersion. Another important factor is the soldering time.

Ultrasonic soldering pot: The heart of the Alcoa 571 process is the ultrasonic soldering pot, which is the container for the molten zinc-based solder [89]. Generally, the pot is made from AISI 304-type stainless steel. These pots come in rectangular (flat bottom), circular, or contoured shape. Bottoms of rectangular pots usually have one or two rows of transducers. Circular and contoured pots are better for soldering large coils because they have room for more transducers [87]. Figure 15.88 shows a sketch of the ultrasonic pot. In general, rectangular tanks have not performed satisfactorily when compared to round tanks [90].

Socket design: Joints of tube sockets are designed for strength and resistance to corrosion. The ends of the U-tubes are flared to a prescribed socket geometry (Figure 15.89) to provide a joint area and a friction fit for the inserted return bends. Solder penetrates the annular space between the return bend and the socket, wets the surfaces, and completes the joint.

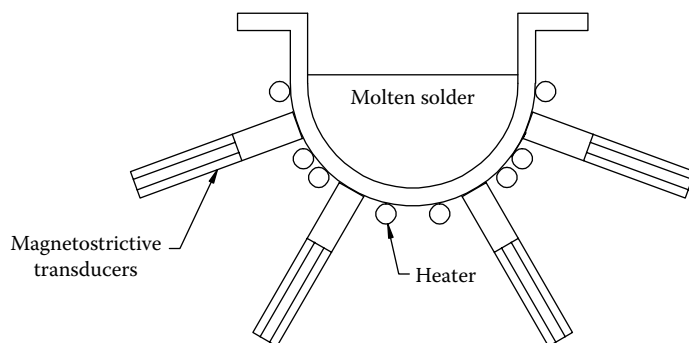


FIGURE 15.88 Ultrasonic pot—round bottom. (Adapted from Hunnicke, R.L., *Weld. J.*, March, 191, 1976.)

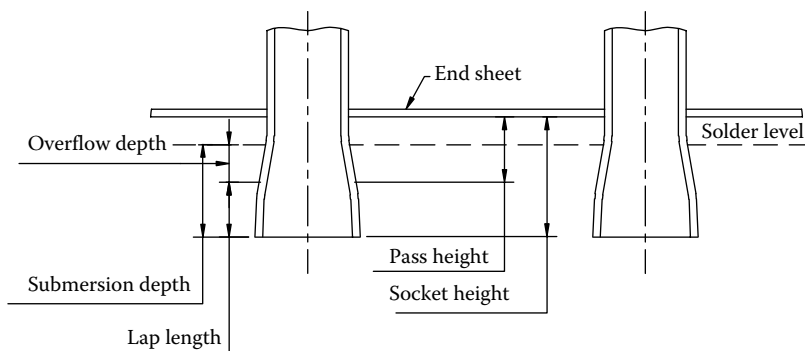


FIGURE 15.89 Socket geometry of heating/cooling coils for ultrasonic cleaning. (Adapted from Schuster, J.L. and Chilko, R.J., *Weld. J.*, October, 711, 1975.)

Preheat temperature: The assembled coil must be preheated before it is dipped in the molten solder, to drive out all the moisture. Preheating reduces the pot size and the soldering time. The preheating should be uniform to ensure that all sockets are above the solder temperature. Preheating time should be minimum to reduce the amount of oxidation. Excessive oxide formation due to longer preheating time makes it difficult for the cavitating solder to break up the oxide film [86,87]. At the same time, the preheating temperature must be high enough to keep the solder from solidifying on parts entering the ultrasonic bath. Preheating sockets at 840°F–950°F (450°C–510°C) ensure that all are above the soldering temperature of 780°F (415°C) without being overheated. For preheating, oscillating spear flame burners are used on nearly every production.

Depth of immersion: In an ultrasonic soldering process, the most important factor is the depth to which the joint is submerged [88], which is shown schematically in Figure 15.89. Soldering does not take place until the joint goes deep enough for its interior surfaces to become wet, even though its outer surfaces may start to wet at shallower depths. From the laws of acoustic physics, it is known that the bath develops a gradient of cavitation intensity, reaching a maximum of 1.5–2 in. (38.50–50.8 mm) beneath the bath surface [87].

Soldering time: Aluminum parts to be tinned are preheated to 800°F, inserted in the solder pot, and the ultrasonics is activated for approximately 3–6 s, depending on the solder temperature, coil complexity, and solder pot characteristics [87]. At least 3 s is usually required for good joints. For copper and steel, the time should be increased to 5–8 s. Longer duration of soldering time lengthens the joint length, but causes erosion of return bends.

Reynolds process: The Reynolds Metals Company process (U.S. Patent 3,633,266) or interference process comprises four basic steps [91]:

1. Ultrasonic tinning: Pretinning of the ends of return bends by immersion in a molten solder bath, which is agitated by ultrasonic energy
2. Assembly of the bare and pretinned tubular components
3. Heating of the preassembled tubular components to melt the solder film
4. Final assembly by the mechanical pressing of the “cork-fit” tube joints together to disrupt the oxide on the bare member and thereby provide a metallurgically bonded leak-free joint

The sequence of the Reynolds process is depicted in Figure 15.90.

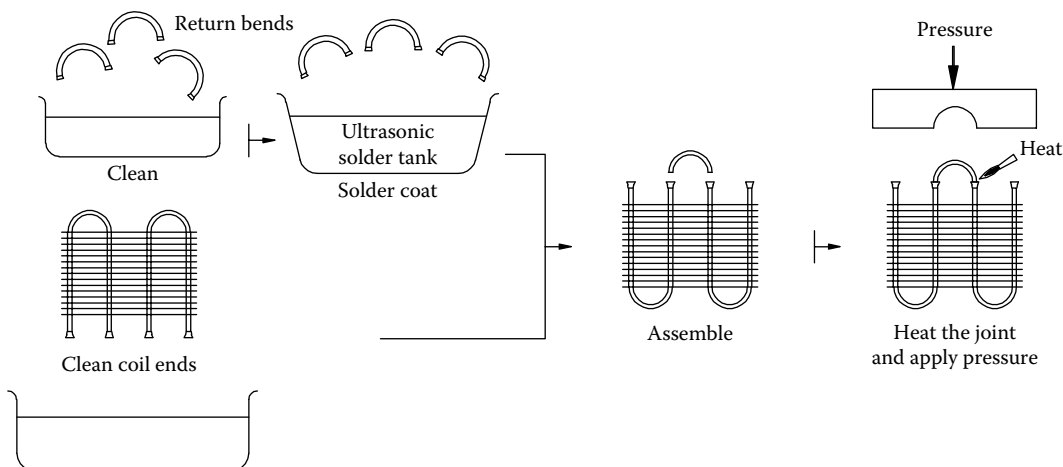


FIGURE 15.90 Sequence of ultrasonic soldering of heat exchanger coils by Reynolds process. (Adapted from Jenkins, W.B., *Weld. J.*, January, 28, 1976.)

Merits of the Reynolds process: Because only the return bend ends need tinning, large ultrasonic pots are not required, and the ultrasonic equipment cost is also very much less. Depth of insertion of parts to be tinned in the pot is not critical [91].

15.11.3 QUALITY CONTROL, INSPECTION, AND TESTING

In this section, QC, inspection, and testing of soldered heat exchangers are discussed. Some or most of the part of the discussion may not be relevant for ultrasonically soldered heat exchangers. QC during various stages of flux-soldered radiator manufacture should consider at a minimum the following points:

1. Fin and tube dimensions, thickness of solder coating
2. Solder bath temperature and composition
3. Tube washing tank temperature and pH
4. Soldering furnace temperature
5. Core washing tank pH
6. Leak testing and recording the number of leakages in tank, pipe, plate, tube, and others
7. Core dimensions

15.11.4 NONDESTRUCTIVE TESTING

15.11.4.1 Visual Inspection

Nearly all soldered joints are visually inspected for defects. A soldered joint surface should be shiny, smooth, and free from cracks, porosity, or holes. Ordinarily, no flux residues should remain.

15.11.4.2 Discontinuities

Some types of discontinuities common for soldering are dewetting, nonwetting, and dull or rough solder.

15.11.4.3 Removal of Residual Flux

Corrosivity of residual flux deposits is important. A water extract method of measuring corrosivity through conductivity has been developed. Extracts from flux residues can also be evaluated. The three basic methods of flux residue detection are radioactive tracers, standard chemical analysis, and fluorescent dye evaluation [83]. Minute amounts of dye in the remaining flux readily fluoresce under ultraviolet light.

15.11.4.4 Pressure and Leak Testing

Pressure testing and leak testing can be used to check the integrity of the soldered joints.

15.11.4.5 Destructive Testing

Destructive testing involves sectioning of soldered joints for determining the quality of joints in the interior. Normal destructive testing techniques include mechanical tests, corrosion evaluation, and metallographic examination.

15.12 CORROSION OF BRAZED AND SOLDERED JOINTS

Brazing involves joining of two similar or dissimilar metal pieces by a filler metal with composition different from the base metals or the same as the base metals. Therefore, galvanic corrosion is a possibility. In addition to galvanic corrosion, corrosion attack is possible due to entrapment of residual corrosive flux. Similar to soldered radiators, brazed radiator joints are required to perform in a severe environment. They are subjected to fluctuating temperatures, mechanical vibration, immersion under engine cooling water, and in contact with dissimilar metals, engine exhaust gases, etc. Added to that is the frequent neglect of the quantity and quality of coolant solution [81].

15.12.1 FACTORS AFFECTING CORROSION OF BRAZED JOINTS

All forms of corrosion can take place in brazed joints. Parameters that contribute to the corrosion of brazed joints are the following:

1. Galvanic couple between the base metal and the filler metal
2. Joint design
3. Brazing method and brazing environment
4. Brazing filler metal
5. Flux material
6. Postbrazing cleaning
7. Thermal stresses induced during brazing

In this section, the corrosion of aluminum brazed joints related to galvanic couple, filler metal, and brazing process and solder bloom corrosion (SBC) of a copper/brass radiator are discussed. The influence of corrosive flux and the importance of postbrazing cleaning were discussed earlier.

15.12.2 CORROSION OF THE ALUMINUM BRAZED JOINT

15.12.2.1 Galvanic Corrosion Resistance

The corrosion resistance of a brazed aluminum joint, completely free of corrosive flux, is directly related to the solution potential difference that may exist between the alloys in contact. The lower the potential difference, the lower is the rate of corrosion. Potential differences of less than 0.013 V are usually considered insignificant [49,58]. Since the aluminum brazing fillers are aluminum alloys rather than dissimilar metals, they have very slight potential differences. Therefore, the possibility of galvanic corrosion is low. This is explained by referring to the solution potential of certain aluminum alloys given in Table 15.5.

The common filler alloys 4343, 4045, and 4047 produce a solution potential of -0.82 V in the standard test solution and commonly brazed alloys 1100, 3003, 6061, and 6063 show -0.83 V. The difference in solution potential between these two groups of alloy is 0.01 V, which is insignificant, and this is responsible for the excellent corrosion resistance of the brazed joint.

15.12.2.2 Influence of Brazing Process

It was proposed by Naruki et al. [92] that the furnace-brazed radiator was superior to the vacuum-brazed radiator, as far as corrosion resistance is concerned, since the former incorporated a zinc diffusion layer in its surface, which afforded the sacrificial corrosion. This aspect is further discussed next, and suggestions are given to overcome the problem.

Zinc retention: Pitting corrosion property of vacuum-brazed 7072 clad aluminum alloy: To attain high pitting corrosion resistance, aluminum heat exchanger tubes in cooling water system are made of 7072 clad aluminum alloy, which contains a nominal concentration of 1% zinc. The 7072 clad is designed to preferentially corrode and thereby delay or prevent pitting attack on the core metal [69]. In the vacuum brazing process, the 7072 clad tube loses its alloying element zinc by vaporization and diffusion [93]. As a result, pitting resistance properties may be changed following vacuum brazing. This is especially true for lighter gauges, 0.02 in. (0.5 mm) or less. However, for heavier gauges, 0.05 in. (1.3 mm), there is sufficient retained zinc in the postbrazed composite [94]. In inert-gas brazing, the evaporation of the zinc is minimized [69]. Four factors influence the degree of zinc loss in the vacuum brazing process [95]:

1. Initial zinc content in the cladding
2. Cladding thickness
3. Furnace thermal cycles and vacuum level
4. Part geometry

The loss of zinc due to evaporation is overcome by the following measures [95]:

1. The zinc content of the cladding may be increased to 2%–3% from the 1% level in 7072 to achieve a higher net zinc content in the cladding, after brazing.
2. Clad thickness may be increased, as the zinc must diffuse through a greater distance to the surface, where it is lost.
3. In the brazing operation, shorter furnace cycle times and a “softer” vacuum will retard the loss of zinc, but adjustment of these factors is severely constrained by the primary necessity of producing sound brazed joints.
4. Development of K805: Kaiser Aluminum Co. developed a new cladding alloy, one in which the active alloying element would be nonvolatile in the vacuum brazing process. This cladding alloy has been designated K805.

A multilayer-clad aluminum material with improved brazing properties [96]: Radiator parts are manufactured from clad braze materials with 3003 or 6063 as the core alloy and 4004 as the cladding. At brazing temperature, silicon from the cladding will to some extent diffuse into the core material. With a non-heat-treatable core of the 3000 series, which has low silicon content and a high and narrow melting range, the penetration is reduced and causes no problem. However, using a heat-treatable core alloy of the 6000 series, the silicon diffusion is more pronounced due to higher silicon content in the core and lower and wider melting range. As silicon diffusion takes place preferentially at the grain boundaries, there are apprehensions that corrosion resistance and strength can be adversely influenced, reducing the amount of filler metal available for flow. To improve the brazing and reliability of the heat-treatable alloys, a multilayer-clad aluminum material known as Multiclad was developed. Multiclad consists of a normal heat-treatable core alloy of the 6000 type clad with commonly used braze cladding of the 4000 type. As an intermediate layer between the core and the braze cladding is an alloy of either pure aluminum or aluminum–manganese such as 3003, as shown schematically in Figure 15.91. This intermediate layer acts as a diffusion barrier and significantly reduces silicon penetration into the core during brazing, with reduced risk of intergranular corrosion. The melting range of the interlayer is higher than that of the core material.

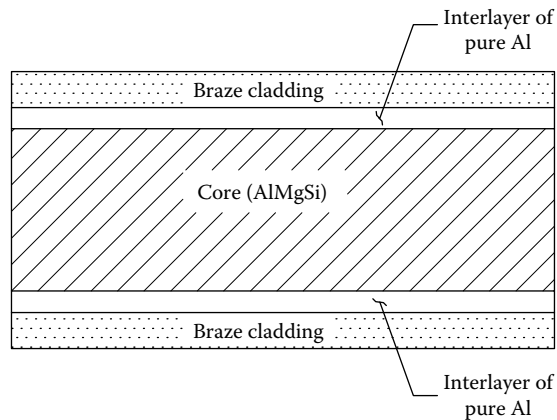


FIGURE 15.91 Multilayer clad aluminum brazing sheet.

15.12.3 CORROSION OF SOLDERED JOINTS

The basic corrosion mechanism on high lead solder in a radiator is galvanic. With a galvanic attack, solder is the more active metal and hence corrodes, whereas the more noble metal, the brass, acts as the cathode. Corrosion resistance of various solders in automobile coolant systems is compared by Falke et al. [97].

15.12.3.1 Solder Bloom Corrosion

SBC can be defined as a corrosion mode of the copper/brass automotive radiator's internal solder joints [98]. Park [98] uses the term *bloom* to describe the flowering appearance of corrosion by products. SBC, in general, leads to the blockage of radiator tube passages when the internal surface is solder coated or of tube openings when the tube outer surfaces are solder coated. Two different field repair methods are employed to clean the blocked tubes. They are (1) roding by utilizing small-size ice picks and thin steel rods and (2) caustic rinse. Roding involves removal of corrosion products.

15.12.3.2 Manufacturing Procedures to Control Solder Bloom Corrosion

To reduce the SBC potential of copper/brass radiators, the radiator materials and manufacturing process can be adjusted as recommended [98]:

- Introduce air blow-off operation immediately after solder dip to minimize the solder buildup at the opening and inside surfaces of the tube ends.
- Change the header dip process to the air-side soldering process to minimize the solder coating inside the tube surface.
- Use low-lead solders (Pb below 90%), in place of high-lead solders like 97/2.5/0.5 (Pb/Sn/Ag), 94/5.5/0.5 (Pb/Sn/Ag).
- Avoid solder coating inside tube surface.
- Use a properly inhibited coolant.
- Use an appropriate radiator rinse cleaning system.

15.13 EVALUATION OF DESIGN AND MATERIALS OF AUTOMOTIVE RADIATORS

In general, mechanically assembled aluminum radiators, vacuum-brazed aluminum radiators, and copper/brass radiators are evaluated by a number of accelerated tests designed to build confidence in design before large-scale fleet trials. Some of these tests are designed to represent worst field conditions [99]. These tests are primarily used to assess (1) the mechanical durability and (2) the internal

and external corrosion resistance, inhibitors evaluation, etc. The mechanical durability tests and corrosion evaluation tests carried out for the development and field service history of Ford automotive aluminum radiators are discussed by Barkely et al. [99]. Some of these tests are briefly discussed here.

15.13.1 MECHANICAL DURABILITY TESTS

Some of the tests developed to evaluate the mechanical durability of the aluminum radiator are given in the following:

1. Combined pressure cycle and vibration test: Radiators were subjected to higher than normal system pressure pulsating at 145 kPa (21 psi) versus 110 kPa (16 psi) while being vibrated at common engine frequencies.
2. Vibration test: Radiator assemblies were mounted on a simulated vehicle front end, filled with coolant, pressurized, and vibrated at their resonant frequencies to failure.
3. Coolant fill test: Radiator assemblies were subjected to several evacuation and coolant fill cycles, similar to those encountered in auto assembly plants.
4. Thermal shock test: Radiator assemblies were subjected to thermal shocks while mounted to a simulated vehicle front end in an environmental chamber.
5. Vehicle durability test: This test involves the vehicle operation with pressure surges, vibrations, thermally induced loading, and severe vehicle front end torsion and bending.

15.13.2 TESTS FOR CORROSION RESISTANCE

15.13.2.1 External Corrosion Tests

The aluminum radiator is susceptible to two major types of external corrosion: galvanic and localized pitting. In general, uniform corrosion is not an important durability problem for the aluminum radiator, since it results from exposure to very high or very low pH solutions in the absence of inhibitors [99]. Some of the laboratory tests for evaluating external corrosion resistance are the following:

1. Salt spray (fog) test—ASTM Salt Spray (fog) Testing B-117: This involves internally pressurizing the radiators to 145 kPa (21 psig) and then subjecting them to 1000 h of salt spray testing.
2. Humidity test: Several thousand hours of testing in a noncondensing humidity chamber, maintained at 38°C (100°F) and approximately 95% relative humidity.
3. SWAAT test: This is a severe acidified seawater fog corrosion test designed to induce rapid attack.

15.13.2.2 Internal Corrosion Tests

The major internal corrosion concerns are the possibility of intergranular corrosion, erosion-corrosion, crevice corrosion, and pitting attack. Internal corrosion tests used to evaluate materials and coolants are as follows:

1. Laboratory glassware corrosion tests like static pitting tests and polarization diagrams
2. Simulated service circulation test

The solders were used to bind copper fins to brass tubes and brass tubes to headers, which are the essential steps in the radiator assembly. These methods are still widely employed today to make heavy-duty radiators for truck and off-road applications. The basic process consists of melting, flowing, and solidifying the solder at the joint, typically forming a metallic bond with the soldered surfaces (or parent metals). Typically, the filler metal flows into the joint gap by capillary force, solidifies, and forms a bond.

15.14 CUPROBRAZE HEAT EXCHANGER

For decades, copper–brass (flat rectangular fin with flat tube made by lock-seam method) soldered radiators were used in heavy-duty diesel engines to avoid annealing effects if brazing is adopted to manufacture radiators. Brass and copper alloys offer high strength as well as excellent retention of strength at elevated operating temperatures. They can withstand high-temperature brazing processes without a substantial loss in strength. They would be more durable than soldered serpentine-fin designs, and compared to aluminum, they would hold the advantage of greater cooling efficiency as well as being more rugged. Other features that favour CuproBrazed radiators include better corrosion resistance, repairability, higher shock and vibration withstanding capacity. Manufacturing processes are now being applied globally in the manufacture of advanced heat exchangers using the new brazing process, known as CuproBrazed. Brazing furnaces have been developed for all levels of production including batch, three-chamber (semicontinuous), and continuous furnaces. CuproBrazed heat exchangers are made using special anneal-resistant alloys of copper and brass. Tubes are fabricated from brass strip and coated with a brazing filler material. The copper fins, coated tubes, headers and sidesupports made of brass are fitted together into a core assembly, which is then brazed in a furnace. CuproBrazed technology is flexible and scalable. The International Copper Association licenses CuproBrazed technology free of charge to heat exchanger manufacturers.

15.14.1 ROUND TUBE VERSUS FLAT TUBE

Conventional soldered copper–brass radiators use flat tube. Though round tubes provide a strong joint at the header plates, because of their low surface-to-volume ratios, round tubes are inefficient at transferring heat from the tubeside fluid. The surface-to-volume ratio can be dramatically increased using flat tubes. Again, the best size and shape of tubes depend on the heat exchanger design and on the fluid, including whether it is a liquid or a gas, and the pressure, temperature, and flow rate of the fluid. Young Touchstone, USA/UK, offers its patented Flat-Round technology. It uses brass tubes that are flat in the core and round at the headers. This Flat-Round design combines the superior air-flow and heat transfer characteristics of flat tubes with reliable tube-to-header mechanical bonding for exceptional durability [100].

15.14.1.1 Tube Fabrication

Several types of brass tubes can be used to manufacture CuproBrazed heat exchangers. These tubes are uniformly made from brass strip to ensure lightweight and efficient heat exchange. Tube fabrication requires that the edges of the strip be reliably bonded together. The tube seams can be sealed during the brazing process, or they can be welded prior to the brazing process. High-frequency (HF) welded tubes are convenient to use for CuproBrazed heat exchangers because their contoured shape is uninterrupted around the circumference of the tube. The most common folded tube uses the lock-seam fold. The drawback of the lock-seam fold is that the seam becomes an irregularity on the tube surface, which makes it difficult to achieve a uniform gap in brazing the tube to the header. New tube designs offer advantage over the lock-seam design. The overfold design (called snap-over) and B-fold design are just two of many folds being tested for CuproBrazed heat exchangers [100].

15.14.1.2 High-Performance Coatings

An uncoated radiator has approximately 30% longer lifetime than a cosmetically spray-coated radiator. Electrophoretic coating is the best technical solution to increase corrosion resistance. It increases the lifetime by 2.5–3 times compared to an uncoated radiator. A new option is powder coating that gives good results with respect to corrosion resistance and thermal performance and has a lower cost compared to an electrophoretic coating [100].

15.A APPENDIX

Quality Assurance Program/Stage Wise Inspection Chart for Heat Exchanger Manufacture									
M/s XYZ Engineering, Company. QA Department			Job No:		XYZ MK:		QAP No:		
					Sheet No.		REV Date		
Prepared by:			Reviewed by:		Drg. No.		Issued by:		REV: Page:
Sl No	Component/ Operation	Characteristics	Check Visual/ Dimensional	Ref. Document (Code, Standard, Drawing, Spec.)	Acceptance Norm-Code, Standard/ Drawing	Format of Record	Examination by	Inspection by Authorized Inspector/Inspecting Authority Hold Point Witness Point Department	
1.0	Review of drawing	—							
2.0	Review of quality assurance program	—							
3.0	Review of WPS, PQR and WPQR	—							
4.0	Material receipt inspection (including bought outs)	As per material specification and technical delivery condition							
5.0	Examination of marking of materials	Dimensions							
6.0	Material attestation	Verification of transferred identification							

7.0	Examination of cutting—by flame for carbon steel and by plasma for others/ nonferrous material	Preheating to 149°C for carbon steel of thickness above 32 mm
8.0	Examination of prepared edges	Bevel preparation
9.0	Cold forming of shell, rolled neck, dished head and RF pad	Profile
10.0	Stress relieving of cold formed rolled neck	Stress relieving cycle: Specify rate of heating, soaking temperature, soaking time and rate of cooling
11.0	Normalizing of cold formed dished heads	Normalizing cycle (with coupon test plate): Specify soaking temperature, soaking time and cooling in still air
11.1	Testing of coupon test plate	a. Tensile b. Micro

(continued)

(continued)

- 15.0

Long seam/
circular seam/
seam in test
flange, floating
head to flange
welding, seam in
rolled neck

a. Set up

b. I side welding as
per WPS

c. II side welding
groove

d. II side welding
as per WPS

e. Spot radiography
(at least 10% of
total weld length
must be radio
graphed, length of
each RT be 250
mm)—except for
floating head to
flange welds, test
flange seams

f. PT/MT on
floating head to
flange weld
- 16.0

Nozzle neck to
WNRF flange

a. Set up

b. I side welding as
per WPS (PT on
root run for single
side welding)

c. II side welding
groove if
accessible

d. II side welding
as per WPS

e. Spot radiography
for nozzle
connection 10
inch and above

(continued)

M/s XYZ Engineering,
Company, QA
Department

Quality Assurance
Program/Stage
Wise Inspection
Chart for Heat
Exchanger
Manufacture

Job No:

XYZ MK:

QAP No:

Sheet No.

REV

Date

Page:

Prepared by:

Reviewed by:

Drg. No.

Issued by:

REV:

Acceptance
Norm-Code,
Standard/
Drawing

Ref. Document
(Code, Standard,
Drawing, Spec.)

Check
Visual/
Dimensional

Format
of
Record

Examination
by

Inspection by Authorized
Inspector/Inspecting
Authority

Hold Point

Witness Point

Department

SI No	Component/ Operation	Characteristics	Marking Cutting Bevel preparation Set up I side welding as per WPS(PT on root run for single side welding) II side welding groove (if accessible) II side welding as per WPS PT/MT on welds Air leak test on reinforcement pad at a pressure of 1.25 kg/cm ² (g)
17.0	Nozzle opening on shell, nozzle		
18.0	Nozzle on shell/ nozzle (with reinforcement pad—wherever applicable)		

19.0	External/internals	a. Set up b. Welding as per WPS
20.0	Tube sheet/baffle holes marking	a. Hole diameter b. Pitch c. Number of holes d. The tie rod holes in baffle e. Tie rod/pulling eye/sliding strip fixing hole in tube sheet
21.0	Examination of drilled tube sheet	a. Outer tube limit, facing, bolt circle dia., ligament, etc. b. Hole diameter using go/no go gauge c. Taped hole for the rod/pulling eye/slot for sliding strip d. Pass partition grooves e. Expansion grooves (if any)
22.0	Examination of drilled baffles	a. No. of holes and hole diameter using go/no go gauge b. Tie rod holes c. Slots for sliding strip

(continued)

(continued)

Quality Assurance
Program/Stage
Wise Inspection
Chart for Heat
Exchanger
Manufacture

M/s XYZ Engineering,
Company, QA
Department

Job No:

XYZ MK:

QAP No:

Sheet No.

REV

Date

Issued by:

REV:

Page:

Prepared by:

Reviewed by:

Drg. No.

Characteristics

Check
Visual/
Dimensional

Ref. Document
(Code, Standard,
Drawing, Spec.)

Acceptance
Norm-Code,
Standard/
Drawing

Format
of
Record

Examination
by

Inspection by Authorized
Inspector/Inspecting
Authority

Hold Point

Witness Point

Department

Sl
No

Component/
Operation

23.0

Assembly of tube
bundle

a. Tie rod fixing

b. Baffle,
supporting plate
and spacer tube
arrangement

c. Sliding strip to
supporting plate/
baffle welding as
per WPS

24.0

Tube-to-tubesheet
joint

d. Tube insertion

a. Tube projection

b. Tube expansion/
welding

25.0

Examination of
shell before
bundle insertion

Out of roundness
checking using
pull through gauge

a. Minimum two
calibrated pressure
gauges shall be
used.

b. Leak lightness

26.0

Pneumatic test at
a pressure of
1.25 kg/cm² g or
as per code

27.0	Examination before hydrostatic test	<div><div>a. Verification of NDE reports</div><div>b. Overall dimension</div></div>
28.0	Hydrostatic test at a pressure of <div>1. Shell side;</div> <div>2. Tube side;</div>	<div><div>a. Minimum two calibrated pressure gauge shall be used</div><div>b. Leak tightness</div><div>c. Water used for hydrostatic shall have approx 2% (by volume) of an approved wetting agent in addition to 0.2% of sodium nitrate or any other corrosion inhibitor</div></div>
29.0	Examination after hydrostatic test	Visible and dimensional
30.0	Cleaning	<div><div>a. Equipment shall be dried by passing dry air</div><div>b. Equipment shall be purged by dry nitrogen of three times the volume or as specified in the specification</div></div>
31.0	Painting	As per drawing

(continued)

(continued)

M/s XYZ Engineering,
Company, QA
Department

Quality Assurance
Program/Stage
Wise Inspection
Chart for Heat
Exchanger
Manufacture

Job No:

XYZ MK:

QAP No:

Sheet No.

REV

Date

Page:

Prepared by:

Reviewed by:

Drg. No.

Issued by:

REV:

Inspection by Authorized
Inspector/Inspecting
Authority

Hold Point

Witness Point

Department

SI No	Component/ Operation	Characteristics	Check Visual/ Dimensional	Ref. Document (Code, Standard, Drawing, Spec.)	Acceptance Norm-Code, Standard/ Drawing	Format of Record	Examination by
32.0	Marking	a. Tangent lines/ main axis b. Owners name and address c. Item no and PO No. d. Inspection by					
33.0	Final examination	a. Inspection of equipment b. Verification of documents, spares and loose items c. Blanking and rust prevention d. Test hole plugging by hard grease a. Inspectors stamp b. Rub off of details c. Dry N ₂ filling at 0.25 bar					
34.0	Stamping and shipping						

35.0	Documents	
35.1	To be retained by vendor	<div>a. Material test certificates</div> <div>b. Material and data report</div> <div>c. Time temp chart</div> <div>d. NDE and non-conformity report</div> <div>e. Pressure test reports</div> <div>f. Rub off of name plate</div> <div>g. Final dimensional report</div> <div>h. As made drawing</div>
35.2	To be sent to customer	<div>a. Inspection certificates</div> <div>b. Material and data report</div> <div>c. Heat treatment chart</div> <div>d. NDE report</div> <div>e. Pressure test reports</div> <div>f. Rub off of name plate and stamping details</div> <div>g. Final dimensional report</div> <div>h. As made drawing</div> <div>i. Others</div>
<i>Note:</i> RF, pad-reinforcement pad; RT, radiographic; MT, magnetic particle; PT, liquid penetrant; PQR, procedure qualification record and WPS, welding procedure specification.		

REFERENCES

1. Sharma, D. D., Heat exchanger fabrication techniques, Lecture Notes of Course No. 490-SPL, Energy Efficient Heat Exchangers Design, Continuing Education Department, University of Roorke, Roorke, India, 1990.
2. TEMA, *Standards of Tubular Exchanger Manufacturers Association*, 9th edn., Tubular Exchanger Manufacturers Association, Inc., Tarrytown, NY, 2007.
3. *ASME Boiler and Pressure Vessel Code*, Section VIII, Division 1, Pressure Vessels, American Society of Mechanical Engineers, New York, 2010.
4. Rao, B. S. C., Quality assurance in fabrication of pressure vessels, in *Welding Engineering Hand-book—Vol. 1* (S. Sundarrajan, S. Vijaya Bhaskar, and G. C. Amarnath Kumar, eds.), Welding Research Group, Radiant Publications, Secunderabad, India.
5. Weymueller, C. R., NDT builds safety into a nuclear plant, *Weld. Design Fabr.*, September, 54–57 (1982).
6. Peacock, G. A., Fabrication of thick plates, *Weld. Metal Fabr.*, June, 242–252 (1963).
7. Carpenter, O. R. and Floyd, C., Heat treatment of carbon and low alloy pressure vessel steel, Research Suppl., *J. Am. Soc. Naval Eng.*, 69(3), 515–526, (August 1957).
8. Davies, S., Equipment for boiler fabrication, *Weld. Metal Fabr.*, August, 306–309 (1969).
9. Aldridge, M., Plate bending and forming, the choice between 3-roll and 4-roll bending rolls, *Weld. Metal Fabr.*, November, 555–566 (1977).
10. Trawsfynydd Power Station, Part 1: Heat exchanger fabrication, *Weld Metal Fabr.*, September, 350–361 (1961).
11. Bode, C. F., Manipulators and positioners for welding, *Weld. Metal Fabr.*, January/February, 26–30 (1987).
12. Ellis, D. J. and Gifford, A. F., Application of electroslag and consumable guide welding, *Weld. Metal Fabr.*, April, 112–119 (1973).
13. Yokell, S., *A Working Guide to Shell and Tube Heat Exchangers*, McGraw-Hill, New York, 1990.
14. Syal, P. K., *Fabrication of Heat Exchangers*, Specialised Publication, Cooperative Industries, Mumbai, India.
15. Allen, J. S., Fabrication of heat exchangers and specialised vessels, *Weld. Metal Fabr.*, July, 240–245 (1968).
16. Luthy, A., The role of welding in the fabrication of machines and equipment, *Brown Boveri Rev.*, 52, 495–511 (1965).
17. Woodward, A. R., Howard, D. L., and Andrews, E. F. C., Condensers, pumps and cooling water plant, Chapter 4, in *Modern Power Station Practice, Vol. C, Turbines, Generators, and Associated Plant* (D. J. Littler, E. J. Davies, H. E. Johnson, F. Kirkby, P. B. Myerscough, and W. Wright, eds.), 3rd edn., Pergamon Press, New York, 1991.
18. Singh, K. P. and Soler, A. I., *Mechanical Design of Heat Exchangers and Pressure Vessel Components*, Arcturus, Cherry Hill, NJ, 1984.
19. Bevevino, J. W., Tube-to-tubesheet welding techniques, *Chem. Eng. Prog.*, 70, 71–73 (1974).
20. Olson, D. L., Chaney, E., Dallam, C. B., Hellner, R. L., Jones, J. E., Liu, S., North T. H., Sabo, R. S., and Sims, J. E., Submerged arc welding, in *Metals Handbook, Vol. 6, Welding, Brazing, and Soldering*, 9th edn., (E. F. Nippes, ed.), American Society for Metals, Metals Park, OH, 1983, pp. 114–151.
21. Yokell, S., Expanded, and welded-and-expanded tube-to-tubesheet joints, *Trans. ASME J. Pressure Vessel Technol.*, 114, 157–165 (1992).
22. Scott, D. A., Wolgemuth, G. A., and Aikin, J. A., Hydraulically expanded tube-to-tubesheet joints, *Trans. ASME J. Pressure Vessel Technol.*, 106, 104–109 (1984).
23. Fisher, F. F. and Brown, G. J., Tube expanding and related subjects, *Trans. ASME*, 76(4), 565–575 (1954).
24. Sonnenmoser, A., Expanded joints for austenitic steel tubes in feedheaters for BWR nuclear power station, *Brown Boveri Rev.*, 7/8–73, 360–370 (19).
25. Dudley, F. E., Electronic control method for the precision expanding of tubes, *Trans. ASME*, 76, 577–584, (1954).
26. Yokell, S., Heat exchanger tube-to-tubesheet connections, in *The Chemical Engineering Guide to Heat Transfer, Volume 1: Plant Principles* (K. J. McNaughton, ed.), Hemisphere Publishing Corporation, McGraw-Hill Publications Co., New York, 1986, pp. 76–92.
27. Spencer, T. C., Mechanical design and fabrication exchangers in the United States, *Heat Transfer Eng.*, 8, 58–61 (1987).
28. Cotton, H., Seal welding of heat exchanger tubulars by the metal arc process, *Br. Weld. J.*, May, 250–257 (1963).

29. Kong, C.-S., Lee, B.-I., and Shim, S.-H., The characteristics and application of explosive joint on the tubes-to-tubesheet in the heat exchangers of power plants, *Transactions of the 15th International Conference on Structural Mechanics in Reactor Technology (SMiRT-15)*, Seoul, Korea, August 15–20, 1999, pp. IV-81–IV-87.
30. Brosilow, R., Making the most of tube-tubesheet joints, *Weld. Design Fabr.*, May, 54–56 (1976).
31. Slaughter, G. M., *Welding and Brazing of Nuclear Reactor Components*, AEC Monograph, Row-man and Littlefield, New York, 1964.
32. Lohmeier, A. and Reynolds, S. D., Jr., Carbon steel tube-to-tubesheet joints for high pressure feedwater heaters, *Westinghouse Eng.*, September, 138–143 (1966).
33. Viri, D. P. and Iceland, W. F., Clinch River modular steam generator tube-to-tubesheet and shell closure welding, *Weld. J.*, July, 18–21 (1984).
34. Serangeli, G. L., Bebernitz, A. R., Hemzacek, R. T., and Lesnewich, A., Arc welding of carbon steels: Shielded metal arc welding, in *Metals Handbook, Vol. 6, Welding, Brazing, and Soldering*, 9th edn. (E. F. Nippes, ed.), American Society for Metals, Metals Park, OH, 1983, pp. 73–244.
35. Designing and fabricating aluminum weldments, *Weld. Design Fabr.*, February, 53–62 (1977).
36. Danis, J. I., Material selection, fabrication and inspection of refinery heat exchangers, *Weld. J.*, June, 25–30 (1986).
37. TIMET CodeWeld® Titanium Tubing, TIMET(now Valtimet, Inc.), Denver, CO, 1984.
38. Ebert, H. W., Improving the reliability of tube-to-tubesheet joints, *Welding J. Am. Welding Soc.*, 79(9), 47–49 (2000).
39. Sanders, B. J., Tube-to-tubesheet joints: The many choices, ATI Wah Chang, www.atimetals.com/businesses/business-units/.../2001011.pdf, pp. 111–118.
40. CODAP: *French Code for the Construction of Pressure Vessels*, A SNCT, 1985.
41. Sonnenmoser, A., Design and operation of large high pressure feedheaters, *Brown Boveri Rev.*, 7/8–73, 352–359.
42. Marino, A. and Carminati, M., Enhanced inspection of tube-to-tubesheet welds in heat exchanger and JFTA for defect characterization, ECNDT 2006-Tu.3.8.3, Berlin, Germany, 2006, pp. 1–5.
43. Hudgell, R. J. and Tickle, H., Current practices for ultrasonic and radiographic examination of tubes, tubeplates, and tubeplate welds of tube bundles in heat exchangers, in *Developments in Pressure Vessel Technology—2, Inspection and Testing* (R. W. Nichols, ed.), Applied Science Publishers, London, U.K., 1979, pp. 77–100.
44. Engle, J. P., Chemical cleaning of feedwater heaters, *Mater. Perform.*, July, 30–33 (1974).
45. Ganapathy, Welding engineer data sheet, *Weld. Design Fabr.*, October, 104–105 (1979).
46. Galletly, G. D., Plastic buckling of torispherical and ellipsoidal shells subjected to internal pressure, *Proc. Inst. Mech Eng.*, 195, 329–345 (1981).
47. Vessel fabrication at Old Park, *Weld. Metal Fabr.*, November, 392–397 (1991).
48. Jilek, L., Technology of pressing large heads, *Weld. Metal Fabr.*, March, 50–53 (1987).
49. Aluminum Association, *Aluminum Brazing Handbook*, 4th edn., Aluminum Association, Washington, DC, 1990.
50. Jones, N. H., Brazing: Its contribution to modern industry, *Weld. Metal Fabr.*, January, 4–9 (1964).
51. Shah, R. K., Brazing of compact heat exchangers, in *Compact Heat Exchangers—A Festschrift for A. L. London* (R. K. Shah, A. D. Kraus, and D. Metzger, eds.), Hemisphere, Washington, DC, 1990, pp. 491–529.
52. Lucas, M. J., Peaske, R. L., Commen, W. H., and Tomsic, M. J., Brazing, in *Welding Hand Book*, Vol. 2, 8th edn., American Welding Society, Miami, FL, 1991, pp. 279–422.
53. Brazing, Reference Issue, *Weld. Design and Fabr.*, 66(6), 15–71, June (1993).
54. Schwartz, M. M., *Brazing*, ASM International, Metals Park, OH, 1987.
55. Shah, R. K., The art of brazing, in *Thermophysical Aspects of Manufacturing and Materials Processing* (R. K. Shah et al. eds.), Hemisphere Publishing Corporation, Washington, DC, 1992, pp. 193–213.
56. Brooker, H. R. and Beatson, E. V., *Industrial Brazing*, Newnes-Butterworths, London, U.K., 1975.
57. Taylor, M. A., ed., *Plate-Fin Heat Exchangers, Guide to Their Specification and Use*, HTFS (Harwell Laboratory), Oxon, U.K., 1980.
58. Lentz, A. H., Brazing of aluminum alloys, in *Metals Handbook, Vol. 6, Welding, Brazing, and Soldering*, 9th edn. (E. F. Nippes, ed.), American Society for Metals, Metals Park, OH, 1983, pp. 1022–1032.
59. Weymuller, C. R., How to choose filler metals, *Weld. Design Fabr.*, July, 33–39 (1984).
60. Birchfield, J. R., Paste fillers, automation take pain out of brazing, *Weld. Design Fabr.*, June, 78–80 (1980).

61. Singleton, O. R., A look at the brazing of aluminum—Particularly fluxless brazing, *Weld. J.*, November, 843–849 (1970).
62. Moorhead, A. J. and Whalen, S. J., Brazing of stainless steels, in *Metals Handbook, Vol. 6, Welding, Brazing, and Soldering*, 9th edn. (E. F. Nippes, ed.), American Society for Metals, Metals Park, OH, 1983, pp. 1001–1013.
63. Miller, F. M., How to choose nickel base filler metals for vacuum brazing, *Weld. Design Fabr.*, October, 87–88 (1977).
64. Harvey, J., The brazing of aluminum: Part 1, *Weld. Metal Fabr.*, September, 454–457 (1977).
65. Schultze, W. and Schoer, H., Fluxless brazing of aluminum using protective gas, *Weld. J.*, October, 644–651 (1973).
66. (a) Boughton, J. D. and Roberts, P. M., Furnace brazing, a survey of modern processes and plant, *Weld. Metal Fabr.*, March, 85–92 (1973); (b) Boughton, J. D. and Roberts, P. M., Furnace brazing—2, A survey of modern process and plant, *Weld. Metal Fabr.*, April, 121–138 (1973).
67. Winterbottom, W. L., Process control criteria for brazing aluminum under vacuum, *Weld. J.*, October, 33–39 (1984).
68. Patrick, E. P., Vacuum brazing of aluminum, *Weld. J.*, October, 159–162 (1983).
69. Schmatz, D. J. and Winterbottom, W. L., A fluxless process for brazing aluminum heat exchangers in inert gas, *Weld. J.*, October, 31–38 (1983).
70. ANSI/AWS C3.7–93, *Specification for Aluminum Brazing*, American Welding Society, Miami, FL, 1993.
71. Tennenshouse, C. C., Control of distortion during the furnace cycle, *Weld. J.*, October, 701–704 (1971).
72. Swaney, W., Trace, D. E., and Winterbottom, W. L., Brazing aluminum automotive heat exchangers in vacuum: Process and materials, *Weld. J.*, May, 49–57 (1986).
73. Terrill, J. R., Cochran, C. N., Stokes, J. J., and Haupin, W. E., Understanding the mechanisms of aluminum brazing, *Weld. J.*, December, 833–839 (1971).
74. Cooke, W. E., Wright, T. E., and Hirschfield, J. A., Furnace brazing of aluminum with a noncorrosive flux, *Weld. J.*, December, 23–28 (1978).
75. McCubbin, J. and Lemay, R., A modification of the NOCOLOK™ flux brazing process to produce superior corrosion resistance or black surfaces, SAE-900408, pp. 416–425.
76. Ashburn, L. L., Furnace design considerations for aluminum brazing under vacuum, *Weld. J.*, October, 45–54 (1983).
77. Kelly, T. J., Andreano, G. A., Cove, E. J., Flynn, J., Gerken, J. M., Ryan, E. J., and Sponaugle, J. C., Brazing of heat resistant alloys, in *Metals Handbook, Vol. 6, Welding, Brazing, and Soldering*, 9th edn. (E. F. Nippes, ed.), American Society for Metals, Metals Park, OH, 1983, pp. 1014–1021.
78. Lindsay, L. B. and Wireman, D. F., Continuous hydrogen furnace brazing of aircraft heat exchangers, *Weld. J.*, October, 737–739 (1975).
79. Amato, I., Cappelli, P. G., and Fenoglio, G., Brazing of stainless steel heat exchangers for gas turbine applications, *Weld. J.*, October, 338–s–343-s (1975).
80. Welding Engineer Data Sheet No. 493—Selection guide for brazing filler metals, *Weld. Design Fabr.*, March, 82 (1982).
81. Lane, J. W. and Brennan, D. T., Improved solder alloy enhances auto radiators, *Weld. J.*, October, 41–45 (1984).
82. Mill welds thin wall aluminum radiator tubes at 600 fpm, *Weld. J.*, October, 52 (1982).
83. Beal R. E., Bud, P. J., Smith J. F., and White, C.E.T., Soldering, in *Metals Handbook, Vol. 6, Welding, Brazing, and Soldering*, 9th edn. (E. F. Nippes, ed.), American Society for Metals, Metals Park, OH, 1983, pp. 1071–1101.
84. Webb, R. L. and Farrell, P. A., Improved thermal and mechanical design of copper/brass radiators, SAE-900724, 1990, pp. 737–748.
85. Mitchell, W. A., Statistical treatment of laboratory data for ASTM D 1384–70, using soft solder, in *Engine Coolant Testing: Slate of the Art, ASTM STP 705* (W. H. Ailor, ed.), American Society for Testing and Materials, Philadelphia, PA, 1980, pp. 220–232.
86. Haddon, R. C., Ultrasonics dispenses with need for soldering flux, *Weld. Metal Fabr.*, January/February, 50–54 (1979).
87. Gunkel, R. W., Solder aluminum joints ultrasonically, *Weld. Design Fabr.*, September, 90–95 (1979).
88. Schuster, J. L. and Chilko, R. J., Ultrasonic soldering of aluminum heat exchangers, *Weld. J.*, October, 711–717 (1975).
89. Hunicke, R. L., Ultrasonic soldering pots for fluxless production soldering, *Weld. J.*, March, 191–194 (1976).

90. Denslow, C. A., Ultrasonic soldering equipment for aluminum heat exchangers, *Weld. J.*, February, 101–107 (1976).
91. Jenkins, W. B., Fluxless soldering of aluminum heat exchangers, *Weld. J.*, January, 28–35 (1976).
92. Naruki, K. and Hasegawa, Y., Corrosion testing of furnace and vacuum brazed aluminum radiators, in *Engine Coolant Testing: State, of the Art, ASTM STP 705* (W. H. Ailor, ed.), American Society for Testing and Materials, Philadelphia, PA, 1980, pp. 109–132.
93. Hattori, T. and Sakamoto, A., Pitting corrosion property of vacuum brazed 7072 clad aluminum alloy, *Weld. J.*, October, 339-s–342-s (1982).
94. McNamara, P. and Singleton, O. R., Zinc distribution in vacuum brazed Alclad brazing sheet, *Weld. J.*, January, 7-s–11-s (1979).
95. Scott, C. A., A new cladding alloy for coolantside corrosion protection of vacuum brazed aluminum radiators, in *Engine Coolant Testing: Second Symposium, ASTM STP 887* (R. E. Beal, ed.), American Society for Testing and Materials, Philadelphia, PA, 1986, pp. 27–43.
96. Engstrom, H. and Gullman, L. O., A multilayer clad aluminum material with improved brazing properties, *Weld. J.*, October, 222-s–226-s (1988).
97. Falke, W. L., Schwaneke, A. E., and Lee, A. Y., Corrosion of solders in automobile coolant systems, *Weld. J.*, October, 460-s–465-s (1973).
98. Park, K. H., Solder bloom corrosion analysis based on field survey data, potential causes, and resolution, in *Engine Coolant Testing: Second Symposium, ASTM STP 887* (R. E. Beal, ed.), American Society for Testing and Materials, Philadelphia, PA, 1986, pp. 123–143.
99. Barkley, J. M., Wiggle, R. R., and Winterbottom, W. L., The development and field service history of Ford automotive aluminum radiators, in *Engine Coolant Testing: Second Symposium, ASTM STP 887* (R. E. Beal, ed.), American Society for Testing and Materials, Philadelphia, PA, 1986, pp. 11–26.
100. Executive Report, High efficiency and extreme durability result from ICA's CuproBraz technology and Young Touchstone's FLATROUND technology, International Copper Association, Ltd, New York.

SUGGESTED READING

- Cold spinning dished ends, *Weld. Metal Fabr.*, January, 30–32 (1969).
- Dawson, R. J., Silver brazing copper and its alloys, *Weld. Metal Fabr.*, February, 54–59 (1971).
- Douglass, M., Feedwater heating systems, in *Modern Power Station Practice, Vol. C, Turbines, Generators, and Associated Plant* (D. J. Littler, E. J. Davies, H. E. Johnson, F. Kirkby, P. B. Myerscough, and W. Wright, eds.), Pergamon Press, New York, Chapter 3.
- Franklin, H. N., Roper, D. R., and Thomas, D. R., Internal bore welding method repairs condenser leaks, *Weld. J.*, December, 49–51 (1986).
- Foster, B. E. and McClung, R. W., Study of x-ray and isotopic techniques for boreside radiography of tube-to-tubesheet welds, *Mater. Eval.*, American Society for Nondestructive Testing, July 1977, pp. 43–51.
- Haslinger, K. H. and Hewitt, E. D., Leak tight, high strength joints for corrosion resistant condenser tubing, ASME Paper No. 83-JPGC-Pwr39, ASME, New York.
- Hatch, J. E., Properties of Commercial Wrought Alloys, in *Aluminum: Properties and Physical Metallurgy*, American Society for Metals, Metals Park, OH, 1984, pp. 354–355.
- Hidemasa, I., Consideration on tube-to-tubesheet joint of zirconium and titanium tubular heat exchangers, The ATI Wah Chang, www.atimetals.com/businesses/business-units/.../1999011.pdf
- Illingworth, A., Testing and inspection, in *Heat Exchanger Design Handbook*, Vol. 4 (E. U. Schlunder, editor-in-chief), Hemisphere, Washington, DC, 1983, Section 4.7.
- Koman, P. and Thiemal, K., Heat exchanger in industry, *3rd International Symposium on Orbital Welding in Heat Exchanger Industry, Organized by Polysoude*, Paris, France, 1999, pp. 1–20.
- McGill, W. A. and Weinbaum, M. J., Alonized heat exchanger tubes give good high temperature service, *Mater. Perform.*, January, 16, 18–20 (1978).
- McIntyre, D. R., How to prevent stress corrosion cracking in stainless steels—Part I, in *The Chemical Engineering Guide to Corrosion Control in the Process Industries* (R. W. Greene, ed.), McGraw-Hill Publications Co., New York, 1986, pp. 4–7.
- Moorehead, A. J. and Red, R. W., Internal bore welding of 2.25Cr-1Mo steel tube-to-tubesheet joints, *Weld. J.*, January, 26–36 (1980).

16 Heat Exchanger Installation, Operation, and Maintenance

The major problems faced with heat exchangers in service are inadequate heat transfer and excessive pressure drop. Common reasons for inadequate heat transfer are that the plant is operating at enhanced capacity, gradual fouling buildup, variation in inlet temperatures of process fluids, air or gas binding resulting from improper piping installation or lack of suitable vents, operating conditions differing from design conditions, maldistribution of flow in the unit, fabrication defects like excessive clearances between the baffles and shell and/or tubes, poor orientation of baffle, wrong fitment of gaskets, excessive corrosion, blocked tubes/nozzles, leakage due to tube wall rupture and tube-to-tubesheet joint failures, lack of performance monitoring, improper maintenance procedures, lack of preventative maintenance schedules, etc. As a result, the existing heat exchanger equipment cannot achieve the desired heat duty. To ensure the designed performance level and to prevent leaks and failures, the heat exchanger installation, operation, maintenance, and periodical inspection must be carried out as per the manufacturer's operation and maintenance manual such as Ref. [1] or by experienced service providers or skilled personnel. Various issues involved, procedures for installation and commissioning, safe operation, and maintenance of heat exchangers are discussed later.

16.1 STORAGE

If the heat exchanger is not used immediately, take the precautions as follows:

Short-time storage

1. Keep the heat exchanger in a clean and dry room.
2. If its storage is outdoor or where humidity is high, seal the heat exchanger and wrap it with a vinyl sheet or the like.

Long-time storage

The heat exchanger is normally shipped with its inside surfaces coated with rust-preventive oil. The rust-preventive coating normally stays active for a period of 2–3 months in a dry room. If the heat exchanger is to be stored longer, open its ports and apply the same type of rust-preventive oil where necessary every 2 or 3 months. If the storage is for more than a year, test the heat exchanger at its maximum service pressure and make sure it is in working order prior to operation.

PHE

If the heat exchanger is to be placed in long-term storage, the following steps should be taken:

- a. Store heat exchanger in a closed room at 60°F–70°F.
- b. The heat exchanger tightening bolts and plate pack shall be completely un-tightened and stress free.
- c. The heat exchanger should be totally covered in black plastic to prevent light and dirt from adversely affecting the gaskets.
- d. Avoid heat, ultraviolet, and welding light.
- e. Apply a rust preventative.

16.2 INSTALLATION

1. When transporting the heat exchanger, take precautions to prevent it from tumbling or falling.
2. Fit the anchor bolts securely, taking into account the heat exchanger's weight.
3. When lifting the heat exchanger, use the two hooks on top of the main body or attach rope to the main body securely.
4. Ensure that the ropes are attached properly to prevent the heat exchanger from falling. Roping and hoisting should be carried out only by qualified personnel.
5. Install the heat exchanger on a level floor. Taking into account the heat exchanger's weight during operation, secure it using the specified anchor bolts.
6. Ensure that sufficient space is provided for removal of the drain plug.
7. Avoid applying excessive force to the nozzle when making connections. If subjected to excessive force, it may break.
8. Ensure that there is sufficient space around the heat exchanger for maintenance. It is particularly important to provide space for removal of the tube bundle for inspection, cleaning, and to carry out repairs.
9. Connect all nozzles, making sure that the inlet and outlet connections are made correctly. Ensure that all pipe joints are completely leakproof.
10. *U-tube heat exchangers*: For U-tube heat exchangers, with removable bundles, clear at the stationary head end to permit withdrawal of the tube bundle, or at the opposite end to permit removal of the shell.
11. *Foundations*: Foundations must be adequate so that exchangers will not settle and impose excessive strains on the exchanger.
12. *Foundation bolts*: Foundation bolts should be loosened at one end of unit to allow free expansion of shells. Slotted holes in supports are provided for this purpose when saddles are provided.
13. *Fittings and piping*: It may be desirable to provide valves and bypasses in the piping systems to permit inspection and repairs.
14. *Vents*: Proper venting is a start-up necessity. Improper venting usually occurs on start up and is recognized by poor heat transfer and a high pressure drop. Vent valves should be provided so units can be purged to prevent vapor or gas binding. Special consideration must be given to the discharge of hazardous or toxic fluids.
15. *Drains*: Drains may discharge to atmosphere, if permissible, or into a vessel at lower pressure.
16. *Pulsation and vibration*: In all installations, care should be taken to eliminate or minimize the transmission of fluid pulsations and mechanical vibrations to the heat exchangers.
17. *Safety relief devices*: The ASME Code defines the requirements for safety relief devices. When specified by the purchaser, the manufacturer will provide the necessary connections for the safety relief devices. The purchaser will provide and install the required relief devices.

16.3 OPERATION

1. While starting, ensure that all operating conditions conform to the heat exchanger's specifications.
2. Do not use seawater with a heat exchanger that is designed for use with freshwater or vice versa.
3. On both sides, the fluid stream flow rate must be maintained within the specified limits.
4. The heat exchanger operating pressures must not exceed the specified values.
5. *Design and operating conditions*: Equipment must not be operated at conditions that exceed the design parameters.

6. *Operating procedures:* Before placing any exchanger in operation, reference should be made to the exchanger drawings, specification sheet(s), and name plate(s) for any special instructions. Local safety and health regulations must be considered. Improper start-up or shutdown sequences may cause leaking of tube-to-tubesheet joint and/or bolted flanged joints.
7. *Start-up operation:* Shell and tube exchanger fluids must be introduced in such a manner as to minimize differential expansion between the shell and tubes. The exchanger may be placed into service by first filling the colder medium, followed by gradual introduction of the hotter medium. During start-up, all vent valves should be opened and left open until all passages have been purged of air and completely filled with fluid.
8. *Shutdown operation:* The unit must be shut down in a manner to minimize differential thermal expansion between shell and tubes. Exchangers may be shut down by first gradually stopping the flow of the hotter medium, then the flow of the colder medium through the unit. After shutting down the system, all units should be drained completely, especially when there is a likelihood of freezing or prone for corrosion. To guard against water hammer, condensate should be drained from steam heaters and similar apparatus during start-up or shutdown. To reduce water retention after drainage, the tubeside of the exchanger should be blown out with air.

16.4 MAINTENANCE

1. *Daily check:* Check for oil or water or process fluid leaks if any in the sealed areas of the heat exchanger.
2. *Periodical maintenance:* Ensure that the corrosion/fouling control is in place. Overhaul the heat exchanger and clean parts as per schedule. At the same time, check for visible cracks, if any, of heat exchanger components, integrity of liners, insulation, etc.
3. Disassembly
 - a. Check that all pipings are sealed/disconnected prior to disassembly.
 - b. Stop the hydraulic pump and check that the heat exchanger's internal pressure is zero before disassembling the heat exchanger.
 - c. Before disassembly, the user must assure himself that the unit has been depressurized, vented and drained, neutralized, and/or purged of hazardous material.
4. Other than the instructions on maintenance, a log of all plant operational events, start-ups, shutdowns, and malfunctions that affect the heat exchanger performance should be kept.

16.5 PERIODICAL INSPECTION OF UNIT

At regular intervals and as frequently as experience indicates, an examination should be made of the interior and exterior conditions of the unit. Negligence in keeping all tubes clean may result in complete or structural damage to other components. Sacrificial anodes, when provided, should be inspected to determine whether they should be cleaned or replaced.

16.6 INDICATIONS OF FOULING

Exchangers subject to fouling or scaling should be cleaned periodically. A light sludge or scale coating on the tube greatly reduces its efficiency. A marked increase in pressure drop and/or reduction in thermal performance usually indicate that cleaning is necessary. The unit should first be checked for air or vapor binding to confirm that this is not the cause for the reduction in performance. Since the difficulty of cleaning increases rapidly as the scale thickness or deposit increases, the intervals between cleanings should be optimum.

16.7 DETERIORATION OF HEAT EXCHANGER PERFORMANCE

In the following sections, the analysis of the performance deterioration of air-cooled heat exchanger (ACHE), shell and tube heat exchanger, and compact heat exchanger and remedial measures to improve the performance are briefly dealt.

16.7.1 AIR-COOLED HEAT EXCHANGERS

Many older ACHEs in service perform poorly compared to their original specified design due to several factors such as age, poor design, hot air recirculation, higher process fluid flow rates, deterioration of fin tubes, loss of thermal contact between fins and tubes, fouling both on the tubeside and airside, missing air seals, poor air distribution and/or airflow bypassing through bundle, etc. [2]. A step-by-step economical method by which an end user can systematically improve the heat transfer performance of the existing equipment is explained by Giammaruti [3], and the method is briefly mentioned here.

16.7.1.1 Determine the Original Design Performance Data of the ACHE

Have an overview of the basic thermal and mechanical design data, materials of construction, and control information and compare the same against the current process parameters.

16.7.1.2 Inspect the Heat Exchanger Unit

Inspect tube bundle, tensioning device, integrity of frame header, tube support, fins, wiggle strips, header, condition of air seals, leaks at the plugs or cover plate gaskets, corrosion of fin tubes, etc. Based on the condition of the parts, measures should be taken as necessary to bring the ACHE back to its as-built condition.

16.7.1.3 Determine the Current ACHE Performance and Set Baseline

Measure the airflow and associated temperature rise across the bundle and hence calculate the amount of heat rejected to the air. The calculated airside heat transfer duty should then be compared to the design duty to determine how much more cooling is needed.

16.7.1.4 Install Upgrades

The following are the typical steps that can be taken in order to improve the tube bundle performance [3]:

Fans

1. In most applications, one of the quickest ways to obtain more duty out of the ACHE is to increase the airflow rate either by increasing the fan blade pitch or by increasing the fan speed so long as the fan does not stall and enough motor horsepower is available to meet the increased airflow rate.
2. Reset tip clearances.
3. Install inlet bells.
4. Install fan seal disk.
5. *Install high-efficiency fans:* Older ACHEs will usually have straight chord aluminum fan blades whose efficiency will be around 35%–55%. Today's more modern fans made of fiberglass or aluminum are more aerodynamic with a tapered chord and increasing pitch or twist from the blade tip to the fan hub with significantly greater efficiency of about 75%–85%. It is possible to obtain about 25%–40% more airflow with high-efficiency fans at the same or slightly more motor horsepower.

16.7.1.5 Tube Bundle

The heart of the ACHE is the tube bundle, and to improve its performance, the following measures are suggested: (1) Clean the finned tube bundle—both airside and tubeside, (2) if a small number of fin tubes have been degraded due to overheating or excessive corrosion, retube the bundle with equivalent or high-performance fin tubes. Integral fin tubes typically have the maximum heat transfer ability over a sustained period of time. Overall, about 10%–50% increase in ACHE duty can be achieved depending on the level of fin tube deterioration. If major part of the tube bundle is deteriorated, replace the bundle by a high-performance unit. Test the unit to confirm the increase in ACHE thermal duty achieved.

16.7.2 SHELL AND TUBE HEAT EXCHANGER

16.7.2.1 Quality Auditing of Existing Heat Exchanger

First step in conducting performance auditing is to collect information about the present thermal performance of the heat exchanger and compare it with design conditions, Gulley [4]. The performance auditing of existing heat exchanger normally covers the following: (1) Assess the present operating conditions and compare it with the design conditions; review the operations data sheet; (2) observe actual performance test data; (3) observe for terminal temperatures and flow rates of shellside and tubeside fluids; (4) examine the periodic maintenance procedure; review the methods of cleaning and results of heat exchanger performance after cleaning; (5) examine the in situ water treatment programs for adequacy of corrosion control (inadequate monitoring can result in calcium deposit on hot heat exchanger tube; Langelier index is a common water quality chemistry analysis that can be used to reduce the likelihood of scaling due to calcium deposits); (6) observe for the existing biofouling control mechanism and its adequacy; (7) verify that the firm had evaluated the potential for water hammer in susceptible heat exchangers and undertaken appropriate measure to address it; (8) verify that the number of plugged tubes is within permitted limit based on thermal duty; (9) examine, if available, the eddy current test and visual inspection records to determine the structural integrity of the heat exchanger (also review the records of online monitoring of structural integrity of vessels or heat exchangers by acoustic emission if in place); (10) verify that adequate controls on flow and operational limits are in place to prevent heat exchanger degradation due to excessive flow-induced vibration during operation; (11) observe tube-to-tubesheet joints for leaks, and shell and channel for cracks; and (12) perform weep-hole inspection for any telltale signs of leaks as discussed later.

16.7.2.2 Leak Detection: Weep-Hole Inspection

Pressure vessels that involve multilayer shells or a single shell with a liner, and that are designed to Section VIII of the ASME Boiler and Pressure Vessel Code, generally are provided with weep holes. The purpose of the weep holes is to allow the detection of any leak that develops in the inner liner of the vessel. Thus, during any vessel inspection, perform weep-hole inspections as given later [5]:

1. Check for moistness.
2. Perform soap bubble test.
3. Examine the weep hole with lighting source; if diameter of weep holes is sufficiently large, borescopic examination can be conducted.
4. Utilization of special tubular bore scrapers to collect deposits for determining if the deposits are the result of external corrosion or corrosion products resulting from leakage from the inside of vessel.
5. Analysis of deposits collected for the determination of source of deposits (external or internal leakage).

16.7.2.3 Tube Bundle Removal and Handling

To avoid possible damage during the removal of a tube bundle from a shell, a pulling device should be attached to eyebolts screwed into the tubesheet. If the tubesheet does not have tapped holes for eyebolts, steel rods or cables inserted through tubes and attached to bearing plates may be used. The bundle should be supported on the tube baffles supports, or tubesheets and handled carefully to avoid damage to the tube bundle. Gasket and packing contact surfaces should be protected. Large number of models of tube bundle pulling kits and devices, tube bundle handling devices, and/or band saw for the dismantling and refurbishment of heat exchanger tubesheets are available from heat exchanger service providers and/or tube-to-tubesheet rolling/welding equipment manufactures like Maus, Italia, Powermaster, India, Teco Tube Expanders, the Netherlands, etc. Two types of tube bundle pulling devices are shown in Figure 16.1a through c, transportation unit is shown in Figure 16.2, and heat exchanger tube bundle gripper is shown in Figure 16.3.

16.7.2.3.1 Cleaning Tube Bundles

16.7.2.3.1.1 Cleaning Methods The heat transfer surfaces of heat exchangers should be kept reasonably clean to assure satisfactory performance. Convenient means for cleaning should be made available. Heat exchangers may be cleaned either online or off-line by chemical or mechanical methods. Various cleaning methods had been dealt with in Chapter 9. Additionally, automatic high-pressure external cleaning robot and multiple nozzle carrier robot for the automatic internal cleaning of tube bundles are shown in Figure 16.4, and pneumatic shafting tube cleaners for tube bundle heat exchangers of Maus, Italia, make are shown in Figure 16.5.

16.7.2.3.1.2 Locating Tube Leaks Shellside leak testing by hydrostatic method is the preferred method to locate perforated or split tubes and leaking tube-to-tubesheet joint. In most cases, the entire front face of each tubesheet will be accessible for inspection. The point where water escapes indicates a defective tube or tube-to-tubesheet joint.

16.7.2.3.2 Gasket Replacement

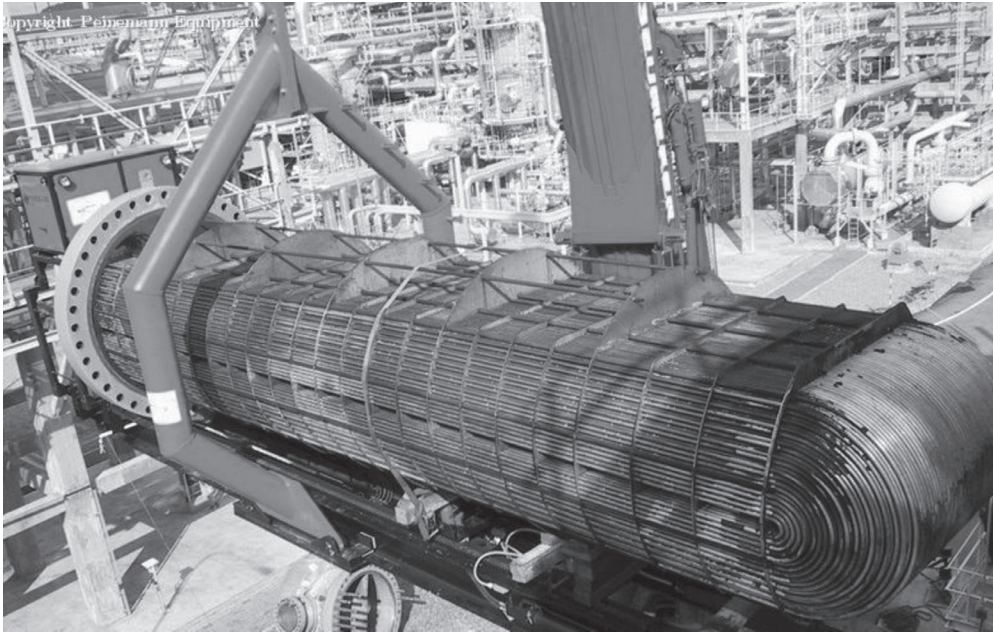
Gaskets and gasket surfaces should be thoroughly cleaned and should be free of scratches and other defects. Gaskets should be properly positioned before attempting to tighten bolts. It is recommended that when a heat exchanger is dismantled for any cause, it be reassembled with new gaskets. Bolted joints and flanges are designed for use with the particular type of gasket specified. Substitution of a gasket of different construction or improper dimensions may result in leakage and damage to the gasket surfaces. Therefore, any gasket substitutions should be of compatible design. Any leakage at a gasketed joint should be rectified to avoid damage to the gasket surfaces.

16.7.2.3.3 Heat Exchanger Tube Failures

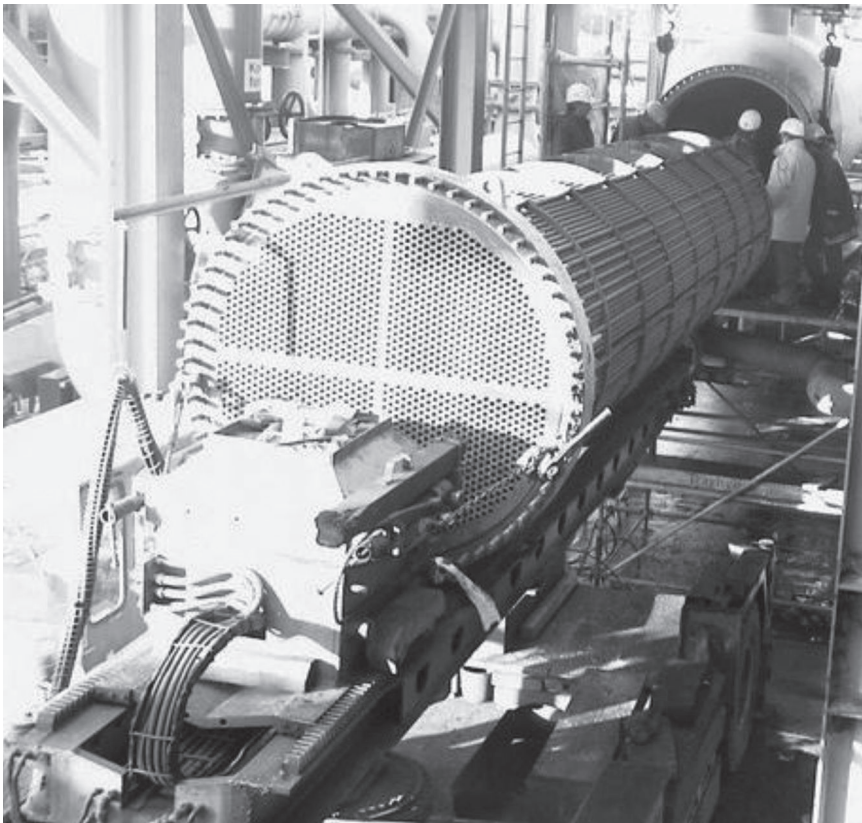
Tube-to-tubesheet joint failure and flow-induced vibration are leading causes of leaks. These issues are best dealt with through careful thermal design, performing flow-induced vibration analysis using state-of-the-art software, mechanical design, selection of the proper materials of construction, appropriate construction of the equipment, including careful inspection during fabrication and to carry out necessary heat treatment process of components at appropriate stages of construction, etc.

16.7.2.3.4 Heat Exchanger Tube Plugging

Individual tubes that have been found to be leaking can be plugged by pop-a-plug device or replaced with solid rods in place of tubes. Sometimes gradual patterns of tube leaks develop,



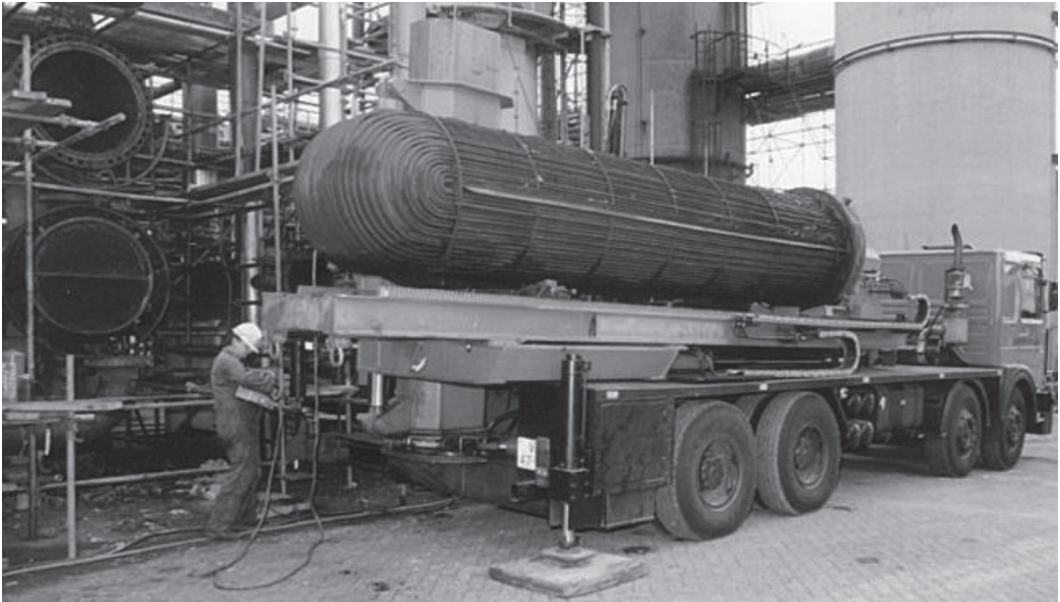
(a)



(b)

FIGURE 16.1 (a) Aerial tube bundle extractor—45 ton capacity and (b) Self-propelled bundle extractor.

(continued)



(c)

FIGURE 16.1 (continued) (c) Truck mounted bundle extractor. (Courtesy of Peinemann Equipment, Hoogvliet, the Netherlands.)



FIGURE 16.2 On-site self-propelled tube bundle transporter. (Courtesy of Maus Italia F. Agostino & C.s.a.s., Bagnolo Cremasco (Cr), Italy.)



FIGURE 16.3 Bundle gripper. (Courtesy of Peinemann Equipment, Hoogvliet, the Netherlands.)

which can suggest plugging the tubes for entire rows or regions within the heat exchanger. As a practical guideline, plugged tube count can be about 10% of the tube count. Plug and seal materials are available for shell and tube exchangers such as *feedwater heaters, condensers, air coolers, steam boilers, process heat exchangers, chillers, etc.* Sizes suitable for inner diameter range from 10 to 51 mm (0.400–2.000 in.). Figures 16.6 through 16.10 show various tube plug models readily available in the market. These plugs are installed by either pulling the taper pin of the plug or by the application of torque. Figure 16.11 shows tube plugs welded at the tube ends. Another option is the replacement of part of or all of an existing heat exchanger's tubes. In some instances, it will be best to design and procure a new heat exchanger for the current and projected plant requirement.

16.7.2.3.4.1 Tube Plug Sleeve

Most heat exchangers are designed with a certain amount of extra tube capacity to allow a percentage of tubes to be plugged during the life of the exchanger. Two primary causes of tube failure, which often result in tubes being plugged or replaced, are erosion and corrosion. In fact, heat exchangers are often completely retubed to repair tube failures that occur only at the tube ends. The HydroSwage® Strain Control Sleeve System 43101, offers a method of installing sleeves (ferrules) as shown in Figure 16.12 to restore lost tube material or as sacrificial barriers to the damaging elements that cause the tube loss. Strain control is a two-stage process that pre-expands

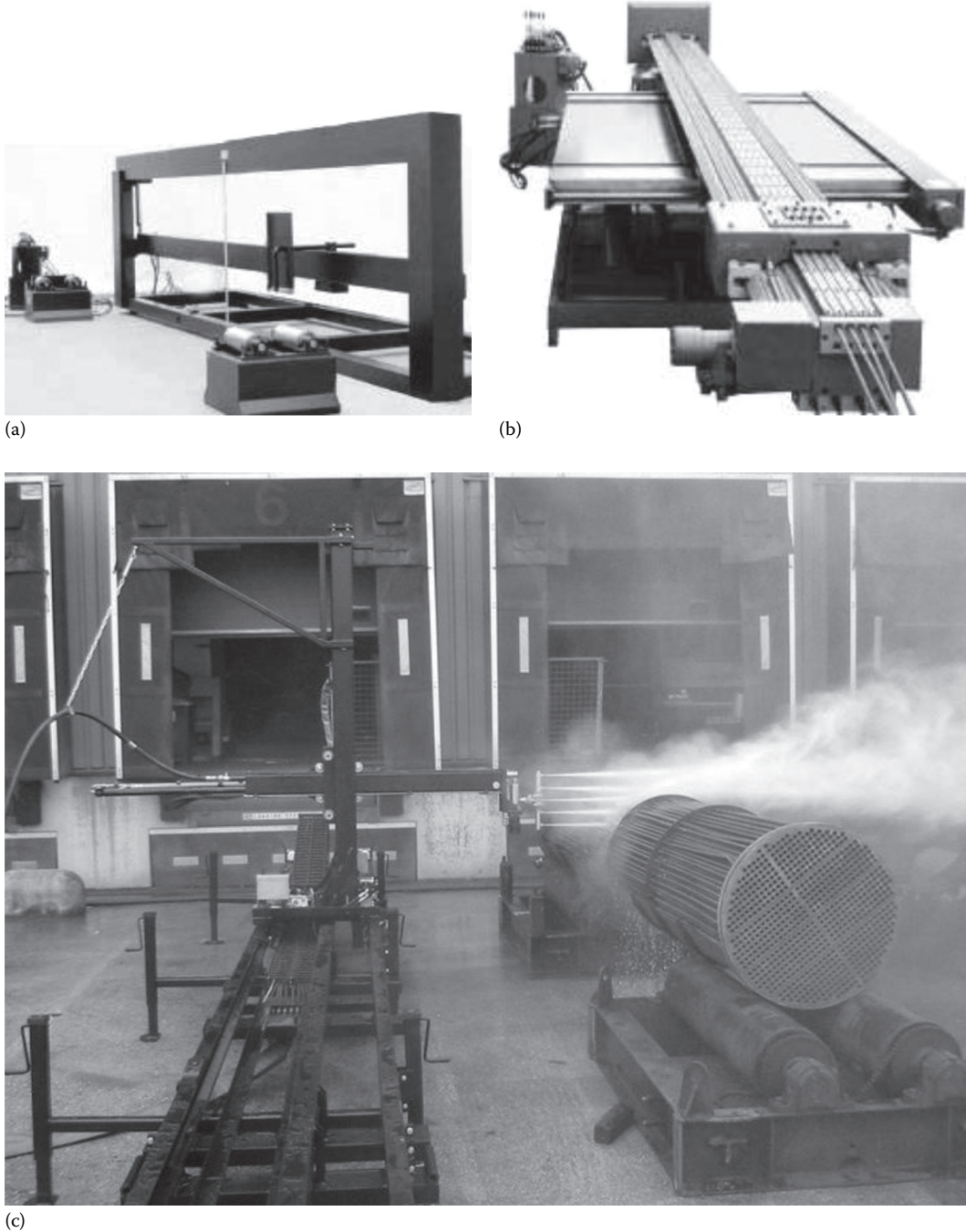


FIGURE 16.4 (a and b) Automatic high-pressure external cleaning robot and multiple nozzle carrier robot for the automatic internal cleaning of tube bundles. (Courtesy of Maus Italia F. Agostino & C.s.a.s., Bagnolo Cremasco (Cr), Italy.) (c) Outside tube bundle cleaners. (Courtesy of Peinemann Equipment, Hoogvliet, the Netherlands.)

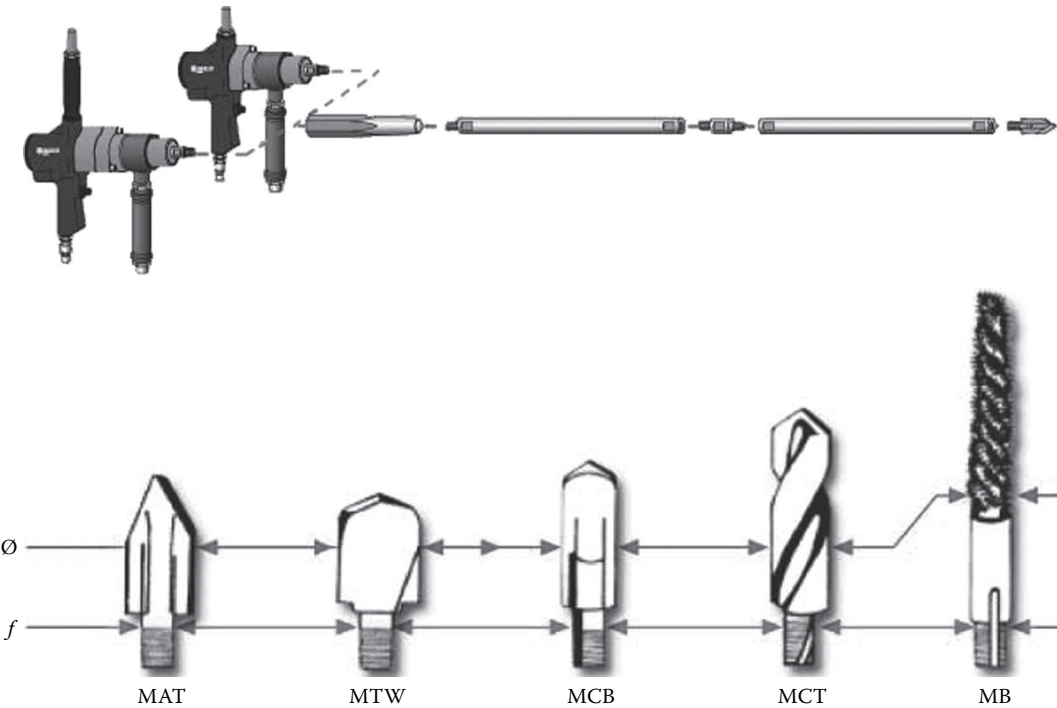


FIGURE 16.5 Pneumatic shafting tube cleaners for tube bundle heat exchangers. (Courtesy of Maus Italia F. Agostino & C.s.a.s., Bagnolo Cremasco (Cr), Italy.)

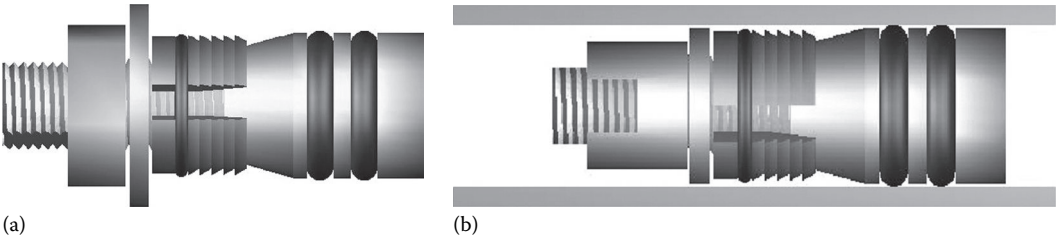


FIGURE 16.6 Mechanical seal plug. (a) Schematic and (b) plug installed in a tube. (Courtesy of Powerfect, Brick, NJ.)

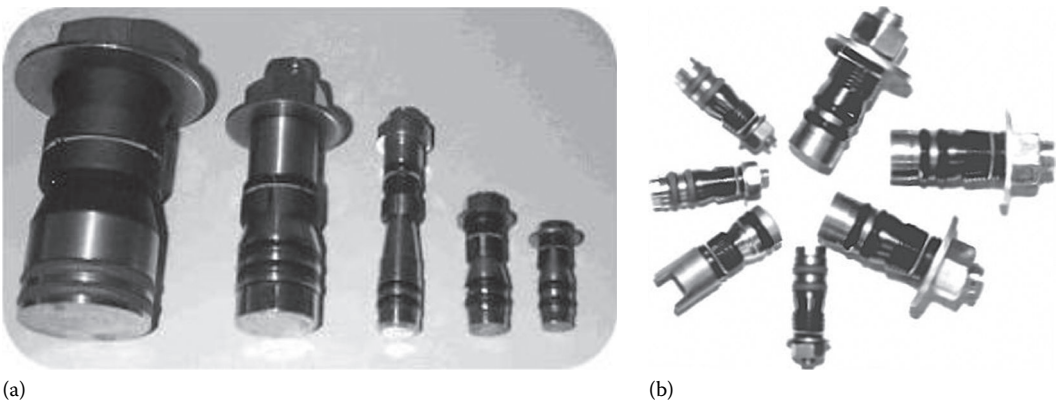


FIGURE 16.7 (a–b) Mechanical seal plugs. (Courtesy of Powerfect, Brick, NJ.)

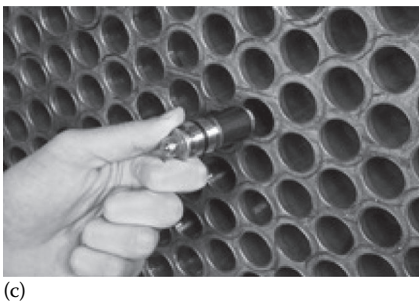
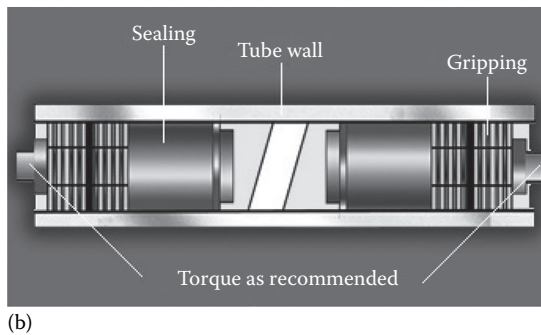


FIGURE 16.8 Plugging of tube holes. (a) Tube plugs, (b) tube plugs installed inside a tube (schematic), (c) insertion of tube plug into a tube, and (d) mechanism of installation of tube plug. (Courtesy of Conco Systems, Inc., Verona, PA.)

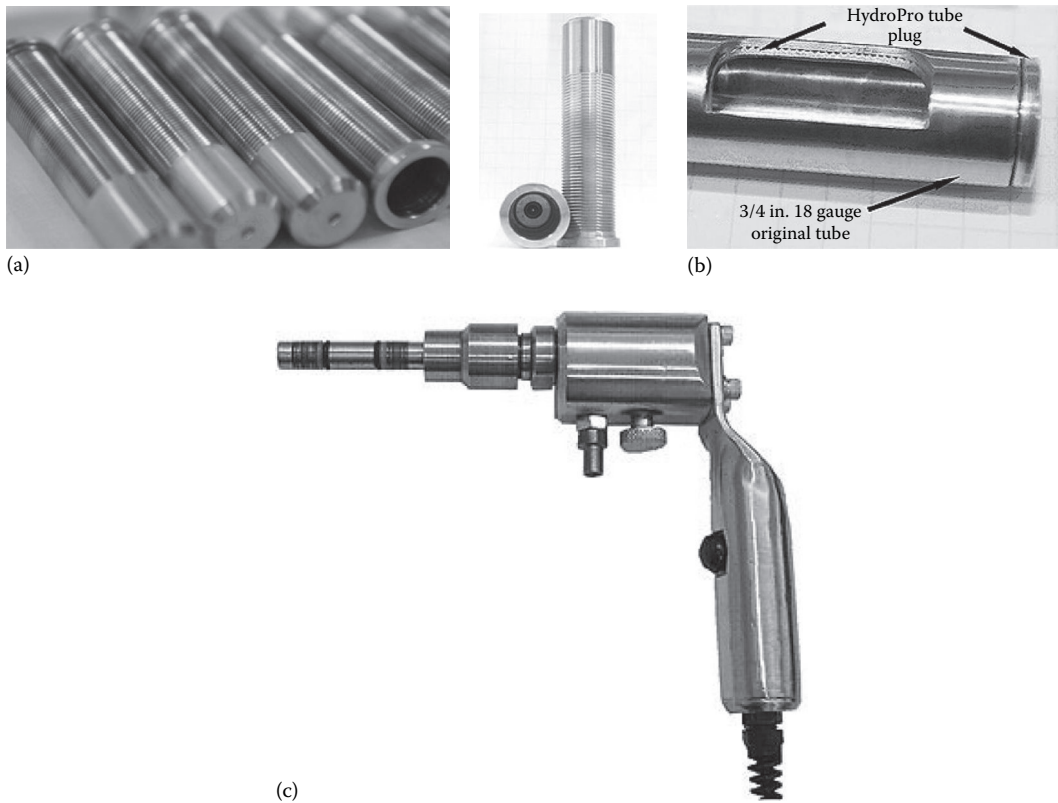


FIGURE 16.9 Tube plugs. (a) Unexpanded tube plugs, (b) cutaway showing a HydroPro tube plug in place in a 3/4 in. 18 gauge original tube, and (c) HydroPro Tube Plug Installation Mandrel Assembly and Mandrel Holder (Gun). (Courtesy of HydroPro, Inc., San Jose, CA.)

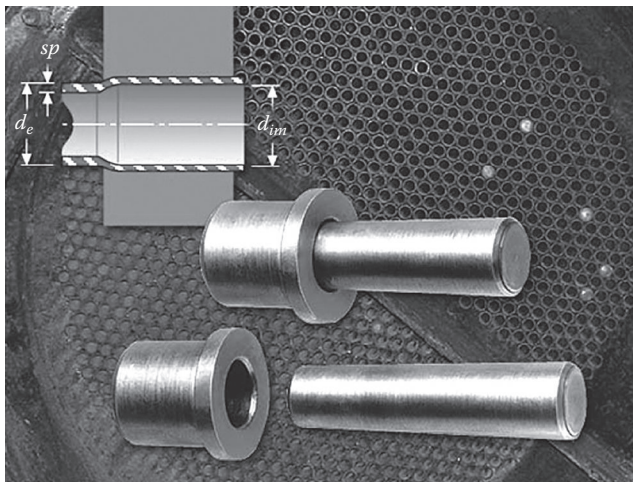


FIGURE 16.10 Tube plugs showing ring and a tapered pin. (Courtesy of Maus Italia F. Agostino & C.s.a.s., Bagnolo Cremasco (Cr), Italy.)

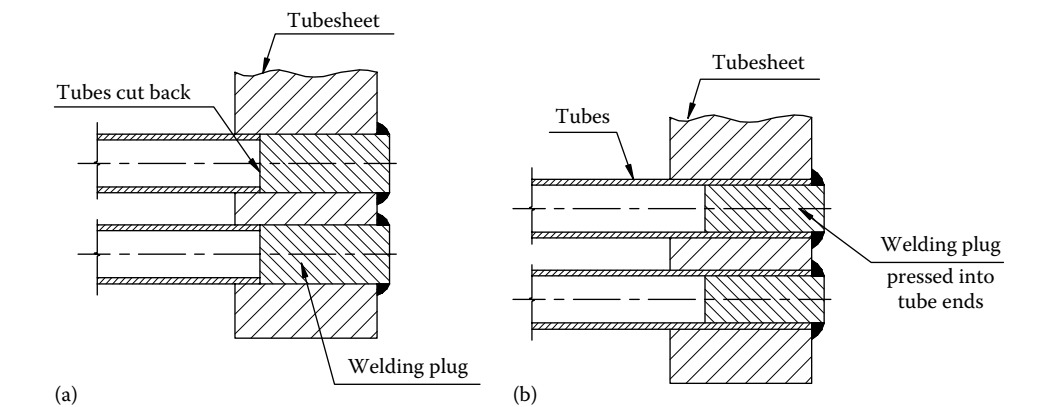


FIGURE 16.11 (a–b) Tube plugs welded at the tube ends.

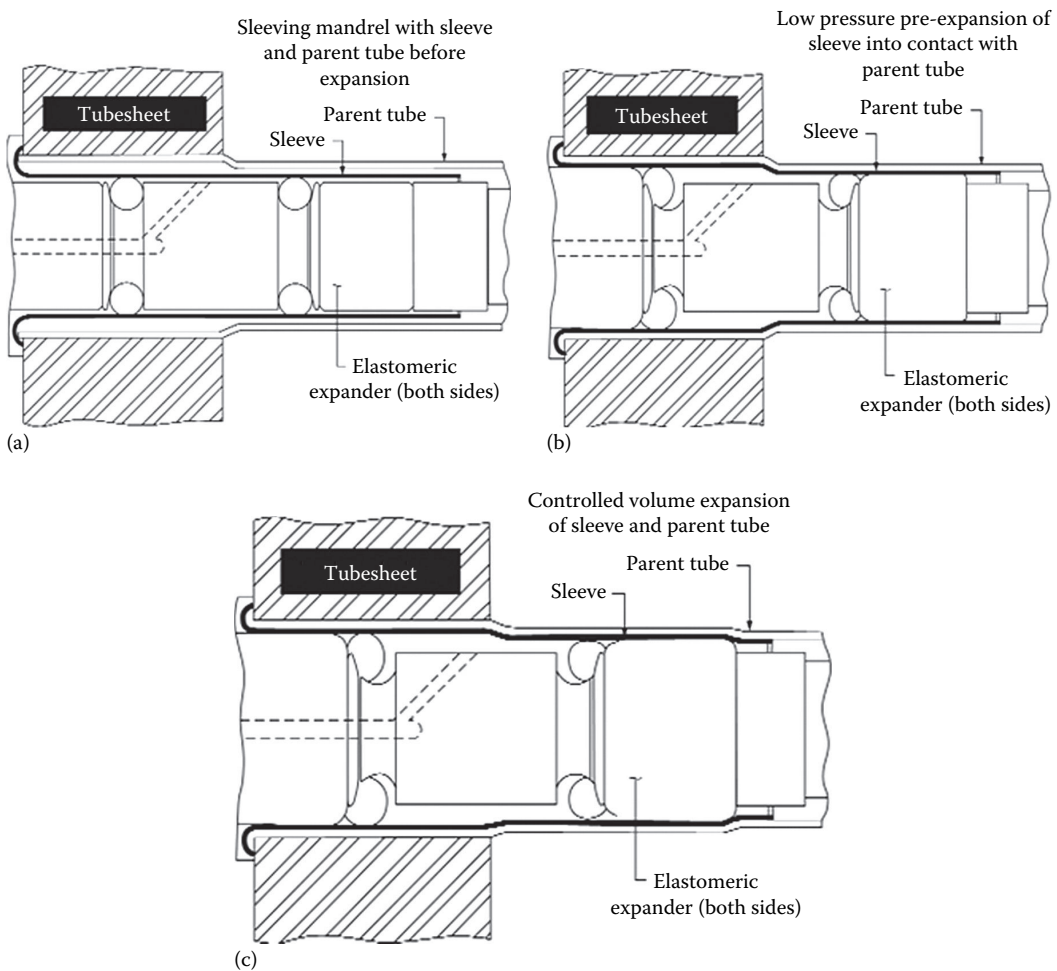


FIGURE 16.12 (a–c) HydroSwage Strain Control Sleeving System. (Courtesy of Haskell International, Inc., Burbank, CA. All rights reserved.)

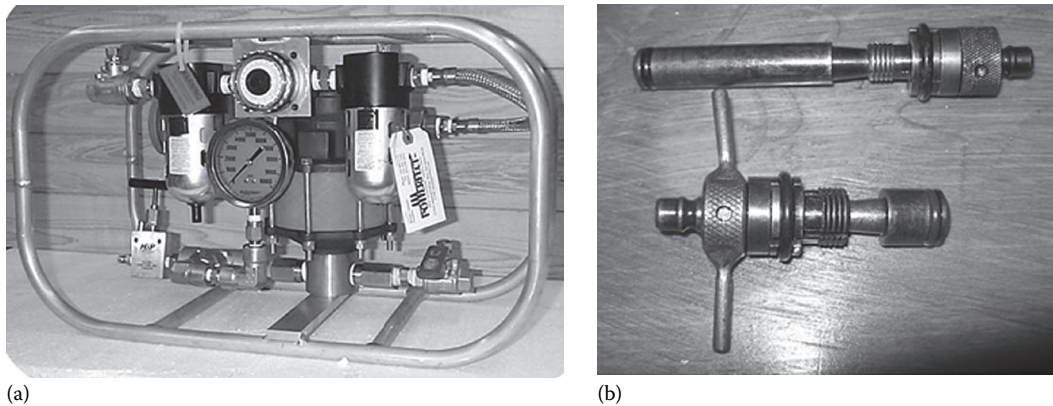


FIGURE 16.13 Individual tube hydrostatic testing equipment kit. (a) Equipment and (b) hydrostatic test plugs. (Courtesy of Powerfect, Brick, NJ.)

a prepared metal sleeve into the damaged or failing section of the tube. The first stage expands the sleeve at a pre-calculated hydraulic pressure beyond the sleeve yield strength, but less than combined yield strength of the sleeve and parent tube. The second-stage expansion is controlled by injecting (at a higher pressure) a predetermined volume of water to control the radial expansion of the sleeve and parent tube to produce a constant interference fit between the sleeve and the parent tube.

Hydrostatic testing equipment

Hydrostatic testing equipment makes possible the testing of individual tubes inside any shell and tube heat exchanger to a pressure within the tube design ASME code limits and provides a positive means of determining the integrity of each tube. Weak tubes will fail during the test, rather than when the unit is placed back in service, thus avoiding expensive forced outages. A typical individual hydrostatic tube testing equipment kit and test plugs are shown in Figure 16.13.

16.7.3 BRAZED ALUMINUM PLATE-FIN HEAT EXCHANGER

Problems with brazed aluminum plate-fin heat exchangers are rare. However, if problems develop, advice should be sought from the manufacturer.

16.7.3.1 Leak Detection

External leaks will be evident by the appearance of localized freeze spots or vapor cloud on the outer casing of the insulation. Or the smell or sound of the escaping fluid may also be discernible. When a leak is suspected, it should be investigated fully and immediately, and the manufacturer's repair procedure be put in action as soon as practicable.

16.7.3.2 Repair of Leaks

Detected external leaks such as cracked pipe welds may be repaired by rewelding using an approved weld procedure and by a qualified aluminum alloy welder. Should the need arise to locate and repair a leak associated with the brazed aluminum plate-fin heat exchanger, then the manufacturer is to be consulted [6].

16.8 NDT METHODS TO INSPECT AND ASSESS THE CONDITION OF HEAT EXCHANGER AND PRESSURE VESSEL COMPONENTS

16.8.1 ULTRASONIC INTERNAL ROTARY INSPECTION SYSTEM

Ultrasonic internal rotary inspection system (IRIS) is based on the principle of measuring thickness using ultrasonic waves. The IRIS probe consists of an ultrasonic transducer that is lined up in the centerline of the tube and incident on a rotating mirror. The mirror reflects the beam in the radial direction as it rotates in the tube. The IRIS probe scans the entire circumference of the tube as it is pulled out of the tube. The IRIS display includes the cross section of the tube and a C-scan of the tube. The IRIS method is mostly used for inspection of carbon steel tubes. The method is very accurate for thickness measurement as well as for detecting internal and external pits. IRIS can, however, miss pinholes, and this method is not recommended for the detection of cracks [7].

16.8.2 REMOTE FIELD EDDY CURRENT TESTING

The remote field eddy current testing (RFECT) is generally used for the detection of wall loss in carbon steel tubes. Pits can be detected using differential coils; however, the reliability for pit detection is limited. Pinholes can be missed by RFECT. Pit detection sensitivity can be improved by reducing the pull speed. The inspection speed with RFECT is significantly lower than conventional ECT. While conventional ECT can easily be performed at a speed up to 6 ft/s, RFECT is limited to about 10 in./s. Higher pull speeds will miss small defects and increase background noise. Flaw sizing with RFECT is done using the voltage–plane curves. These curves are used to size tube wall loss. The curves relate flaw depth, flaw length, and the flaw circumference to the phase of the remote field signal in the absolute channel [7].

16.8.3 EDDY CURRENT TESTING

Both the conventional eddy current testing (ECT) and remote field ECT are used for inspection. Conventional ECT is used for inspection of nonferromagnetic tubing such as stainless steel, copper–nickel alloys, titanium, etc. Remote field ECT is applicable for inspection of ferromagnetic tubing such as carbon steel and nickel. A specialized version of conventional ECT is full saturation ECT. This technique is applicable for thin ferromagnetic tubes such as Seacure in condenser tubes and partially ferromagnetic tubing materials such as Monel and Alloy 2205 [7].

Vessels in petrochemical plants: The two major applications of ECT in vessel inspection are crack detection and clad thickness measurement. The technique is used as an alternate to penetrant testing (PT) as it can detect tight cracks, and the technique is significantly faster than PT. Clad measurement is performed on vessels with carbon steel shell and stainless steel clad. NDE Associates, Inc., uses the Hocking Phasec 2200 and the Nortec 1000 for such inspection.

Piping systems: Stainless steel is susceptible to stress corrosion cracking. ECT is a highly effective technique for the detection of SCC cracking on the OD surface of SS piping. The technique detects tight cracks that can be missed by dye PT. ECT will also detect cracks that are just below the surface but within the eddy current skin depth.

Bolt hole inspection: Bolt holes are to be inspected for cracks. Cracks in bolt holes can be caused by fatigue and corrosion. Inspection is done with a bolt hole scanner interfaced to an ECT machine.

Bellows: ECT is applied on bellows for crack detection. Cracks in bellows are caused by stress corrosion. Both stainless steel and Inconel bellows are inspected for the detection of ID and OD surface cracks.

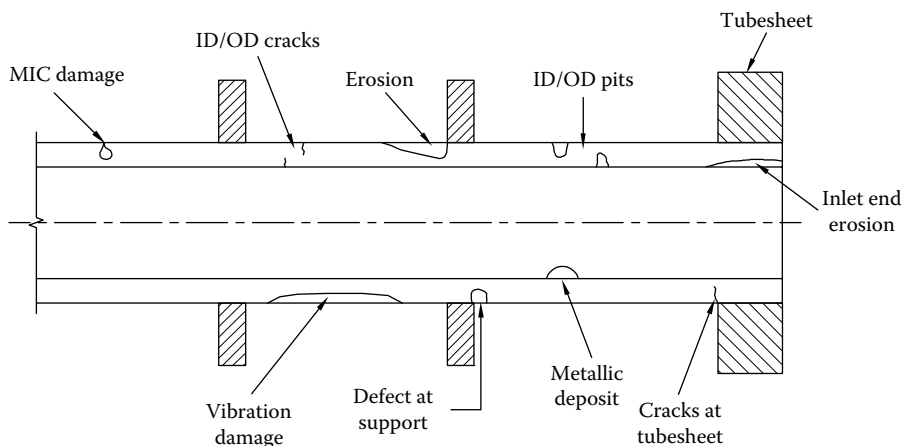


FIGURE 16.14 Typical heat exchanger tube defects (in service). (Courtesy of Anmol Birring, Houston, TX.)

16.8.4 TUBES

Failure of high pressure (HP) feedwater heater tubes is one of the major causes of forced outages in fossil fired power plants. Deterioration of tubes occurs because of either poor design or improper heater operation. The location of damage across the tubesheet and along the tube length depends on the cause of damage. Tube inspections identify damaged tubes and location of damage along tube length. The problem areas in the feedwater heaters include [8,9] (1) normal and abnormal operating conditions (maximum); (2) tube plugging due to leaks; (3) drain cooler zone-level control; (4) steam impingement desuperheat zone, condensing zone; (5) tube vibration; (6) inlet end erosion; (7) loss of impingement plates, etc. Schematic of typical tube defects is shown in Figure 16.14.

16.9 RESIDUAL LIFE ASSESSMENT OF HEAT EXCHANGERS BY NDT TECHNIQUES

The presence of flaws in critical components will affect its structural integrity and increase the likelihood of failure. In-service NDT can detect and quantify the damage and provide input for remedial actions. Also the residual life can be assessed. It has been shown that the sound attenuation in steel or any other construction material can be used to quantify the level of degradation of the material's mechanical properties. Knowing this, the remaining life of an affected plant can be estimated. There are a number of inspection methods available. Some of the methods based on ultrasonics are [10] as follows:

1. Ultrasonic echo attenuation method
2. Amplitude-based backscatter method
3. Creep waves (i.e., time-of-flight measurement)
4. Pitch-catch mode shear wave velocity
5. Ultrasonic method based on backscatter and velocity ratio measurement
6. Advanced ultrasonic backscatter techniques (AUBT)
7. Method based on thickness mapping, backscatter, and velocity ratio (TOFD)
8. Photon-induced positron annihilation (PIPA) and distributed source positron annihilation (DSPA)
9. In situ metallographic replicas

Other methods are based on radiography, replication technique, etc. Basic principles of some of the methods are mentioned later.

16.9.1 CREEP WAVES

This technique uses ultrasonic waves that travel along the surface of a component. As it propagates, it converts to a mode that travels into the component at an angle to the surface. The latter wave will convert back to a surface wave if it hits a surface parallel to the surface on which it originated.

16.9.2 ULTRASONIC METHOD BASED ON BACKSCATTER AND VELOCITY RATIO MEASUREMENT

Both the base metal and weld HAZ should be inspected for hydrogen attack. Base metal attack is detected by using a combination of ultrasonic backscatter and velocity measurements [6]. Hydrogen attack increases the ultrasonic backscatter and reduces the ultrasonic velocity in the material. The backscatter and velocity ratio measurements are applied to detect hydrogen attack. Application of ultrasonic backscatter for the detection of high-temperature hydrogen attack is shown in Figure 16.15. The ultrasonic backscatter technique was developed by Birring [7].

16.9.3 PULSED EDDY CURRENTS

This is a technique for detecting corrosion and erosion and measuring average remaining wall thickness.

16.9.4 FLASH RADIOGRAPHY

Originally developed to image rapidly moving dynamic object, flash radiography has found application in the detection of corrosion on pipe outside diameter under insulation.

16.9.5 LOW-FREQUENCY ELECTROMAGNETIC TEST

Low-frequency electromagnetic test (LFET) is a technique by which changes in the wall thickness of carbon steel storage tank floor plates can be detected. The technique involves passing a low-frequency magnetic field into the plate and using scanner-mounted pickup coils to detect the induced AC magnetic field in the plate material. In the presence of wall thickness loss and pitting, a measurable distortion is induced in the field that can be detected.

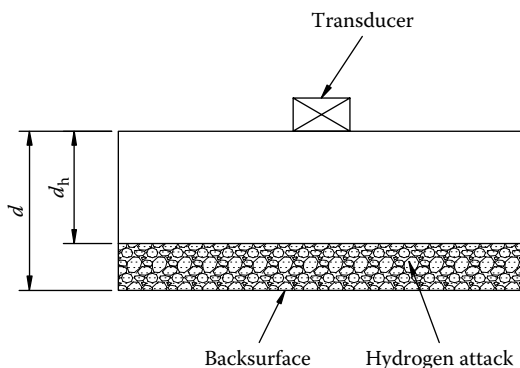


FIGURE 16.15 Application of ultrasonic backscatter for the detection of high-temperature hydrogen attack. (Adopted and modified from Birring, A. S., Selection of NDT techniques for inspection of heat exchangers, Presented at the ASNT International Conference on Petroleum Industry Inspection Conference, Houston, TX, June 1999.)

16.9.6 PHOTON-INDUCED POSITRON ANNIHILATION AND DISTRIBUTED SOURCE POSITRON ANNIHILATION

PIPA and DSPA technologies detect fatigue, embrittlement, and other forms of structural damage in materials at the atomic level. These techniques can determine the remaining life of various materials precisely.

16.9.6.1 Replication Techniques

When a component is subject to localized overheating, as a result of either a fire or an upset operating condition, severe damage can result. Or it may also involve metallurgical changes to the component that, in the worst case, will result in failure. Generally, the most effective method of evaluating the effects of these conditions is in situ metallurgical examination (known as replication technique) in conjunction with hardness testing. In the replication technique, a small area on the surface of the subject vessel is ground sufficiently, and a replica of the ground spot is taken and the microstructure is studied with a reference standard [5].

16.9.6.2 Creep Determinations by Nondestructive Testing Method

Conditions of creep occur in many pressure vessels, heat exchangers, boilers, etc. Because of a number of catastrophic failures, detection of creep by nondestructive examination techniques has become increasingly important. In recent years, creep has been measured by metallurgical techniques referred as replication technique. These methods generally are costly in that they require removal of insulation and cooling of the equipment to room temperature to see the location where creep is suspected. A more effective nondestructive examination technique that recently has been developed involves direct creep measurements with capacitive strain gauges attached to the surface of the pressure vessel or heat exchanger [5].

16.10 PRESSURE VESSEL FAILURE

Pressure vessels, heat exchangers, and pressure pipings used in refineries, chemical processing plants, water treatment systems of boilers, etc., fail due to design errors, specifying or using improper materials, inadequacies in fabrication and welding, inadequacies in quality assurance program, discontinuities, stress raisers, improper heat treatment, damage during shipment, storage and erection and commissioning, excess pressure and temperature, corrosion, caustic embrittlement, erosion and improper maintenance, etc. The most common heat exchanger failure is a tube leak causing contamination, deteriorated thermal performance, and plant capacity loss. Safety considerations associated with rupture or leakage failures are blast effects, fire, fragmentation damage, explosion, suffocation, chemical burns, poisoning, thermal burns, environmental degradation, etc. [11].

16.10.1 FAILURE MODES

Heat exchangers can fail for a wide variety of reasons. Brittle fracture, cracking, explosion, rupture, leakage, stress corrosion cracking, thermal shock, fatigue, erosion, creep, stress rupture, and hydrogen embrittlement are among some of the common failure modes found in pressure vessel components [11]. Failure analysis can identify the causes that have contributed to pressure vessel failure.

16.11 PROFESSIONAL SERVICE PROVIDERS FOR HEAT EXCHANGERS

A number of professional service providers are available in the open market. Such service providers include among others, Westinghouse Electric Company, PA, Powerfect, Brick, NJ, American Power Services Inc, Erlanger, KY, and NDE Associates, Inc., Webster, TX. They can provide professional assistance in the areas of performance assessment, residual life assessment, condition monitoring

of condenser, heat exchanger and feed water heater, and their repair. Typical service offered by them include tube plugging and sleeving, leak testing, tube removal, on-site troubleshooting, visual inspection and nondestructive testing such as eddy current tube testing/remote field tube testing, ultrasonic testing, magnetic particle testing, metallurgical analysis, hydrostatic testing, etc.

REFERENCES

1. Sanitary shell and tube heat exchanger specification, *Installation Instructions, Operation Instructions and Maintenance Procedures*, Allegheny Bradford Corporation, Bradford, PA.
2. Ellmer, M., *A Practical Guide for Identifying and Solving Air-Cooled Heat Exchanger Performance Problems in the Field*, Reprinted from *Hydrocarb. Eng.*, pp. 1–6, April 2008.
3. Giammaruti, R., Performance improvement to existing air-cooled heat exchangers, Paper No. TP04-13, Dry cooling, Presented at the *Cooling Technology Institute Annual Conference*, Houston, TX, February 2–11, 2004, pp. 1–16.
4. Gulley, D., Troubleshooting shell and tube heat exchangers, *Hydrocarb. Process.*, 75(9), 91–98 (1996).
5. JobShop.com, Nondestructive testing techniques on plant reliability, Technical Information, 1996. www.jobshop.com
6. ALPEMA Standard, *The Brazed Aluminium Plate-Fin Heat Exchanger Manufacturer's Association*, 3rd edn., Didcot, Oxon, U.K., 2010, www.alpema.org
- 7a. Birring, A. S., Selection of NDT techniques for inspection of heat exchangers, Presented at the *ASNT International Conference on Petroleum Industry Inspection Conference*, Houston, TX, June 1999.
- 7b. Birring, A. S. and Kawano, K., Ultrasonic detection of hydrogen attack in steels, *Corrosion*, March, 1989.
8. Electric Power Research Institute, Feedwater heater survey, Palo Alto, CA, August 1991, GS 7417.
9. Electric Power Research Institute, High-reliability feedwater heater study, Palo Alto, CA, June 1988, CS-5856.
10. Kot, R., Hydrogen attack, detection, assessment and evaluation, *10th Asia-Pacific Conference on Non-Destructive Testing*, September 2001, Brisbane, Queensland, Australia.
11. Metallurgical Consultants, Pressure vessel failure, Altamonte Springs, FL, 2009, pp. 1–2, www.materialsengineer.com/DA-Pressure-Vessel.htm

“One of the most important strengths I noticed after reading Chapter 1 was the detailed description about the different kinds of heat exchangers. This kind of description is ideal for students and industry professionals. ... Looking at the contents and title, the author has made efforts to cover all aspects of heat exchanger design related to concepts, materials, geometry, fabrication, quality control, and maintenance. I found it extremely useful as a design reference guide for industry professionals or course textbook for engineering students.”

– RAJEEV MADAZHY, Engineering Manager, Taper-Lok, Sugar Land, TX

Completely revised and updated to reflect current advances in heat exchanger technology, **Heat Exchanger Design Handbook, Second Edition** includes enhanced figures and thermal effectiveness charts, tables, a new chapter, and additional topics—all while keeping the qualities that made the first edition a centerpiece of information for practicing engineers, research, engineers, academicians, designers, and manufacturers involved in heat exchange between two or more fluids.

See What's New in the Second Edition:

- Updated information on pressure vessel codes, manufacturer's association standards.
- A new chapter on heat exchanger installation, operation, and maintenance practices.
- Classification chapter now includes coverage of scrapped surface, graphite, coil wound, microscale, and printed circuit heat exchangers.
- Thorough revision of fabrication of shell and tube heat exchangers, heat transfer augmentation methods, fouling control concepts and inclusion of recent advances in PHEs.

New topics like EMbaffle[®], Helixchanger[®], and Twisted Tube[®] heat exchanger, feedwater heater, steam surface condenser, rotary regenerators for HVAC applications, CAB brazing and cupro-braze radiators.

Without proper heat exchanger design, efficiency of cooling/heating system of plants and machineries, industrial processes and energy systems can be compromised, and energy wasted. This thoroughly revised handbook offers comprehensive coverage of single-phase heat exchangers—selection, thermal design, mechanical design, corrosion and fouling, FIV, material selection and their fabrication issues, fabrication of heat exchangers, operation, and maintenance of heat exchangers—all in one volume.



CRC Press

Taylor & Francis Group
an informa business

www.taylorandfrancisgroup.com

6000 Broken Sound Parkway, NW
Suite 300, Boca Raton, FL 33487
711 Third Avenue
New York, NY 10017
2 Park Square, Milton Park
Abingdon, Oxon OX14 4RN, UK

K11966

ISBN: 978-1-4398-4212-6



9 781439 842126

www.crcpress.com